OXFORD

OXFORD TEXTBOOKS IN SURGERY

Oxford Textbook of Neurological Surgery

EDITED BY

Ramez W. Kirollos
Adel Helmy
Simon Thomson
Peter J.A. Hutchinson

ALL CONTENT AVAILABLE AT OXFORDMEDICINE.COM

Oxford Textbook of

Neurological Surgery

Oxford Textbooks in Surgery

SERIES EDITOR

Professor Sir Peter J. Morris Nuffield Professor of Surgery Emeritus, and former Chairman of the Department of Surgery and Director of the Oxford Transplant Centre, University of Oxford and Oxford Radcliffe Hospitals, UK

PUBLISHED

Oxford Textbook of Trauma and Orthopaedics 2e edited by Christopher Bulstrode, James Wilson-MacDonald, Deborah M. Eastwood, John McMaster, Jeremy Fairbank, Parminder J. Singh, Sandeep Bawa, Panagoitis D. Gikas, Tim Bunker, Grey Giddins, Mark Blyth, and David Stanley

Oxford Textbook of Fundamentals of Surgery edited by William E. G. Thomas, Malcolm W. R. Reed, and Michael G. Wyatt

Oxford Textbook of Vascular Surgery edited by Matthew M. Thompson, Robert Fitridge, Jon Boyle, Matt Thompson, Karim Brohi, Robert J. Hinchliffe, Nick Cheshire, A. Ross Naylor, Ian Loftus, and Alun H. Davies

Oxford Textbook of Urological Surgery edited by Freddie C. Hamdy and Ian Eardley

Oxford Textbook of Neurological Surgery edited by Ramez W. Kirollos, Adel Helmy, Simon Thomson, and Peter J.A. Hutchinson

IN PRESS

Oxford Textbook of Plastic and Reconstructive Surgery edited by Simon Kay, Daniel Wilks, and David McCombe

Oxford Textbook of Paediatric Surgery edited by Paul Johnson, Eleri Cusick, and Spencer Beasley

Oxford Textbook of

Neurological Surgery

Ramez W. Kirollos

Consultant Neurosurgeon, Addenbrooke's Hospital, Cambridge, UK

Adel Helmy

University Lecturer Neurosurgery, University of Cambridge, UK/Honorary Consultant Neurosurgeon, Addenbrooke's Hospital, Cambridge, UK

Simon Thomson

Consultant Neurosurgeon, Leeds Teaching Hospitals NHS Trust, Leeds, UK

Peter J.A. Hutchinson

Professor of Neurosurgery, University of Cambridge, UK

OXFORD
UNIVERSITY PRESS

OXFORD
UNIVERSITY PRESS

Great Clarendon Street, Oxford, OX2 6DP,
United Kingdom

Oxford University Press is a department of the University of Oxford.
It furthers the University's objective of excellence in research, scholarship,
and education by publishing worldwide. Oxford is a registered trade mark of
Oxford University Press in the UK and in certain other countries

© Oxford University Press 2019

The moral rights of the authors have been asserted

First Edition Published in 2019

Impression: 1

All rights reserved. No part of this publication may be reproduced, stored in
a retrieval system, or transmitted, in any form or by any means, without the
prior permission in writing of Oxford University Press, or as expressly permitted
by law, by licence or under terms agreed with the appropriate reprographics
rights organization. Enquiries concerning reproduction outside the scope of the
above should be sent to the Rights Department, Oxford University Press, at the
address above

You must not circulate this work in any other form
and you must impose this same condition on any acquirer

Published in the United States of America by Oxford University Press
198 Madison Avenue, New York, NY 10016, United States of America

British Library Cataloguing in Publication Data

Data available

Library of Congress Control Number: 2019946066

ISBN 978–0–19–874670–6

Printed in Great Britain by
Bell & Bain Ltd., Glasgow

Oxford University Press makes no representation, express or implied, that the
drug dosages in this book are correct. Readers must therefore always check
the product information and clinical procedures with the most up-to-date
published product information and data sheets provided by the manufacturers
and the most recent codes of conduct and safety regulations. The authors and
the publishers do not accept responsibility or legal liability for any errors in the
text or for the misuse or misapplication of material in this work. Except where
otherwise stated, drug dosages and recommendations are for the non-pregnant
adult who is not breast-feeding

Links to third party websites are provided by Oxford in good faith and
for information only. Oxford disclaims any responsibility for the materials
contained in any third party website referenced in this work.

Series Preface

This is a new development in surgical publishing; the first two editions of the Oxford Textbook of Surgery are to be replaced by a series of specialty-specific textbooks in surgery. This change was precipitated by the ever-increasing size of a single textbook of surgery which embraced all specialties (the second edition of the Oxford Textbook of Surgery was three volumes), and a decision to adapt the textbooks to meet the needs of the audience; firstly, to suit the requirements of Higher Surgical trainees and, secondly, to make it available online.

Thus, we have produced a key book to deal with the fundamentals of surgery, such as Anatomy, Physiology, Biochemistry, Evaluation of Evidence, and so forth. Then there are to be separate volumes covering individual specialties, each appearing as an independent textbook and available on Oxford Medicine Online.

It is planned that each textbook in each specialty will be independent although there obviously will be an overlap between different specialties and, of course, the core book on Fundamentals of Surgery will underpin the required scientific knowledge and practice in each of the other specialties.

This ambitious programme will be spread over several years, and the use of the online platform will allow for regular updates of the different textbooks.

Each textbook will include the proposed requirements for training and learning as defined by the specialist committees (SACs) of surgery recognized by the four Colleges of Surgery in Great Britain and Ireland, and will continue to be applicable to a global audience.

This ambitious programme will be spread over several years, and the use of the online platform will allow for regular updates of the different textbooks.

When completed, the Oxford Textbooks in Surgery series will set standards for a long time to come.

Professor Sir Peter J. Morris
Nuffield Professor of Surgery Emeritus, and former Chairman of the Department of Surgery and Director of the Oxford Transplant Centre, University of Oxford and Oxford Radcliffe Hospitals, UK

Forewords

The *Oxford Textbook of Neurological Surgery* is a new book complementing the Oxford Textbooks in Surgery series. It is arguably the first British-led comprehensive textbook covering the breadth of neurological surgery since *Northfield's Surgery of the Central Nervous System*.

Although the book was conceived and led from the United Kingdom, it has an extensive international contribution and will be of value to specialists from all countries.

The book bridges the gap between short handbook-type texts and the large encyclopaedic multivolume tomes. It is suited to junior and senior neurosurgical trainees and consultants, and will also be useful to specialists from other disciplines. In addition, it will be of immense benefit to those studying for the UK Intercollegiate Neurosurgical Examination, the European examination, and equivalent examinations in other continents. It is written in such way as to emphasize the clinical implications of the science.

The book is divided into 20 main sections with 99 chapters, 1000 pages in print, and over 1000 figures and tables. The chapters are carefully arranged such that it can be read from cover to cover or used as a reference for specific topics, given the comprehensive index. Each chapter follows a uniform format with abstract and key words, followed by comprehensive coverage of the topic illustrated by clear multicoloured figures.

The hard-copy print edition is complemented by an online version, which provides an alternative format to enabling instant access to specific topics.

The ability to update at the proof stage means the book is up-to-date in covering recent advances; for example, the results of clinical trials.

I congratulate the authors on bringing together experts from all neurosurgical subspecialties and from all across the globe to deliver a book that is clearly laid out, readable, and well-illustrated. I am sure it will find its place as a reference book on the bookshelves of neurosurgeons across the globe.

Franco Servadei

The past four decades have seen advances on a scale and pace that have made the practice of neurosurgery almost unrecognizable in comparison to the specialty in which I trained. The dawning in the 1970s of microsurgery and cross-sectional imaging, along with advances in pre- and perioperative care, sparked technological and technical developments that reinvented concepts of what is possible several times over. Specialization became necessary to take full advantage of the new opportunities to advance patients' outcomes and neurosurgeons were spurred to accumulate the dedicated, detailed knowledge, skills, and experience that drove the specialty forward and made it increasingly complex and diverse.

The editors of the *Oxford Textbook of Neurological Surgery* have taken on a substantial challenge: to provide, in a single, comprehensive volume, the knowledge that spans the practice of modern neurosurgery. Alongside this sheer breadth are integrated two critical perspectives: a rigorous understanding of basic science and the subtlety of neurosurgical operative practice.

It succeeds in filling a gap in the neurosurgical literature: a single volume that provides a thorough review of neurological surgery for trainee and trained surgeons alike. Its approach is forward-looking, highlighting the importance of basic and clinical research and evidence-based medicine. Safe and successful neurosurgery will increasingly require deep anatomical knowledge, clinical judgement, and high levels of technical skill, tied to an ability to synthesize an ever-growing and complex literature into reasoned practice.

UK neurosurgery has a proud history. Modern neurological surgery dawned in Scotland (Glasgow) in 1879 and the Society of British Neurological Surgeons is one of the oldest national societies in the world. But its perspective has been and remains broad, engaging colleagues in the worldwide community of neurosurgeons that transcends shifting national, political boundaries. Reflecting this, although the book is undoubtedly grounded in UK neurosurgery, the editors have successfully drawn in some of the most prolific and experienced surgeons and insightful scientists from around the world. As a result, the *Oxford Textbook of Neurological Surgery* provides an invaluable companion to neurosurgeons, from their earliest years of training into subspecialty experience and consultant practice. It will become the definitive single volume textbook for those who treat surgical disorders of the nervous system in the United Kingdom and around the world.

Sir Graham Teasdale

Contents

Symbols and abbrevations xv
List of contributors xxi

SECTION 1
Principles of neurological surgery

1. **The history of neurosurgery** 3
   Eleni Maratos and Henry Marsh
2. **Clinical assessment** 11
   Peter Bodkin and Elizabeth Visser
3. **Overview of neuroimaging** 31
   Tomasz Matys, Daniel. J. Scoffings, and Tilak Das
4. **The operating theatre environment** 45
   Neil Kitchen and Jonathan Shapey
5. **Perioperative care of the neurosurgical patient** 57
   Karol P. Budohoski, Alessandro Scudellari, Sylvia Karcheva, and Derek Duane

SECTION 2
Tumours and skull base-intrinsic tumour

6. **Low-grade glioma** 75
   Thomas Santarius, Lorenzo Bello, and Hugues Duffau
7. **High-grade gliomas and molecular biology of neurosurgical oncology** 89
   Stephen J. Price, Harry Bulstrode, and Richard Mair
8. **Intracranial metastasis** 107
   Andrew Brodbelt and Rashed Zakaria
9. **Primary central nervous system lymphoma** 117
   Boon Leong Quah, Thangaraj Munusamy, and Colin Watts
10. **Glioneuronal and other epilepsy-associated tumours** 129
    Matthias Simon and Alexander Grote
11. **Radiotherapy and radiosurgery for brain tumours** 141
    Susan Short
12. **Chemotherapy for brain tumours** 149
    Nicholas F. Brown, Daniel Krell, and Paul Mulholland
13. **Surgical techniques in the management of intrinsic tumours** 163
    Shawn Hervey-Jumper and Mitchel Berger

SECTION 3
Tumours and skull base—extra-axial and skull lesions

14. **Meningiomas and haemangiopericytoma (HPC): solitary fibrous tumour (SFT)** 175
    Harjus S. Birk, Seunggu J. Han, Ramez W. Kirollos, Thomas Santarius, and Michael W. McDermott
15. **Chordomas and chondrosarcomas of the skull base** 189
    Rami O. Almefty and Ossama Al-Mefty
16. **Dermoid and epidermoid cysts** 197
    Andrew McEvoy
17. **Esthesioneuroblastoma** 205
    Georgios Klironomos, Lior Gonen, and Fred Gentili
18. **Malignant skull base tumours** 213
    Benedict Panizza and Adel Helmy
19. **Surgical management of tumours of the orbit** 221
    Joseph D. Chabot, S. Tonya Stefko, and Paul Gardner
20. **Skull lesions** 229
    Giorgio Gioffre and Ivan Tmofeev
21. **Surgical management of anterolateral skull base lesions** 241
    Michael D. Cusimano and Michael P. Meier

SECTION 4
Tumours and skull base—CP angle lesions

22. **Schwannomas** 255
Tiit Mathiesen, Petter Förander, and David Pettersson

23. **Glomus tumours** 271
Omar Pathmanaban and Andrew King

24. **Surgical management of cerebellopontine angle and petrous lesions** 281
Nicholas Hall, Yuval Sufaro, and Andrew H. Kaye

SECTION 5
Tumours and skull base—sellar and suprasellar tumours

25. **Pituitary tumours** 299
Kanna Gnanalingham, Zsolt Zador, Tara Kearney, Federico Roncaroli, and H. Rao Gattamaneni

26. **Craniopharyngioma and Rathke's cleft cysts** 321
Rudolf Fahlbusch, V. Gerganov, and H. Metwali

27. **Surgical management of sellar and suprasellar tumours** 339
Jayson A. Neil and William T. Couldwell

SECTION 6
Tumours and skull base—posterior fossa

28. **Medulloblastoma** 353
James Rutka

29. **Ependymoma** 361
Christopher Chandler

30. **Haemangioblastoma** 367
Ammar Natalwala and Donald MacArthur

31. **Surgical approaches to posterior fossa tumours** 375
Jacques J. Morcos, Osaama H. Khan, and Ashish H. Shah

SECTION 7
Tumours and skull base—intraventricular

32. **Intraventricular tumours** 385
Paul Grundy and Vasileios Apostolopoulos

33. **Colloid cyst** 393
Asim Sheikh and Paul Chumas

34. **Choroid plexus tumours** 403
Jonathan Roth, Rina Dvir, and Shlomi Constantini

35. **Surgical management of intraventricular lesions** 411
Eduardo C. Ribas, Guilherme C. Ribas, and Ramez W. Kirollos

SECTION 8
Tumours and skull base—pineal

36. **Pineal tumours** 427
Mueez Waqar, Samantha Mills, Conor L. Mallucci, and Michael D. Jenkinson

37. **Surgical management of pineal region lesions** 439
Christoph M. Woernle, René L. Bernays, and Nicolas de Tribolet

SECTION 9
Tumours and skull base—tumour syndromes

38. **Neurophakomatoses** 449
Fay Greenway, Frances Elmslie, and Timothy Jones

39. **Uncommon brain lesions** 461
Yizhou Wan, Hani J. Marcus, and Thomas Santarius

SECTION 10
Neurotrauma and intensive care

40. **Epidemiology of head injury and outcome after head injury** 475
Nabeel Alshafai and Andrew Maas

41. **Pathophysiology of traumatic brain injury** 483
John K. Yue, Hansen Deng, Ethan A. Winkler, John F. Burke, Catherine G. Suen, and Geoffrey T. Manley

42. **Intensive care management of head injury** 497
Matthew A. Kirkman and Martin Smith

43. **Surgical management of head injury** 509
Hadie Adams, Angelos G. Kolias, Adel Helmy, Peter J.A. Hutchinson, and Randall M. Chesnut

44. **Complications of head injury** 521
Fardad T. Afshari, Antonio Belli, and Peter C. Whitfield

45. **Concussion and sports-related head injury** 531
Mark Wilson

SECTION 11
Vascular neurosurgery

46. **Normal cerebrovascular physiology and vascular anatomy** 539
Diederik O. Bulters and Andrew Durnford

47. **The pathophysiology of aneurysms** 559
Federico Cagnazzo, Giuseppe Lanzino, and Neal F. Kassell

48. **The pathophysiology of subarachnoid haemorrhage** 567
Jason McMillen

49. **Management of subarachnoid haemorrhage** 575
Roberto Rodriguez Rubio, Brian P. Walcott, and Michael T. Lawton

50. **Cerebral arteriovenous malformation and dural arteriovenous fistulae** 591
Michael Morgan

51. **Carotid artery disease and cerebral ischaemia** 615
Kieron Sweeney, A. O'Hare, and Mohsen Javadpour

52. **Extracranial-intracranial bypass for cerebral ischaemia** 627
Mathew R. Guilfoyle and Peter J. Kirkpatrick

53. **Giant aneurysms and bypass surgery** 633
Mario Teo, Omar Choudhri, and Michael Lawton

54. **Spontaneous intracranial haematoma** 643
Berk Orakcioglu and Andreas W. Unterberg

55. **Cavernomata and angiographically occult lesions** 651
Janneke van Beijnum and Hiren Patel

SECTION 12
Spinal surgery—principles

56. **Surgical principles in spinal surgery** 661
Simon Thomson, Chris Derham, and Senthil Selvanathan

57. **Spinal stability** 669
Peter R. Loughenbury and Richard M. Hall

58. **Spinal physiology** 679
Sadaquate Khan, Kevin Tsang, and Lamia Nayeb

59. **Medical pathologies of the spinal cord** 687
Chris McGuigan, Karen O'Connell, Eavan McGovern, and Iain McGurgan

SECTION 13
Spinal surgery

60. **Cervical spinal disease** 697
Navin Furtado, Georgios Tsermoulas, and Adikarige Haritha Dulanka Silva

61. **Thoracic spinal disease** 711
Kieron Sweeney, Catherine Moran, and Ciaran Bolger

62. **Lumbar spinal disease** 719
Christopher G. Kellett and Matthew J. Crocker

63. **Spinal tumours** 733
John Brecknell and Boon Leong Quah

64. **Vascular lesions of the spinal cord** 751
Daniel Walsh

65. **Spinal cerebrospinal fluid dynamics** 761
Graham Flint

66. **Scoliosis and spinal deformity** 769
Nigel Gummerson

SECTION 14
Spinal trauma

67. **Managing spinal cord trauma** 781
Saksith Smithason, Bryan S. Lee, and Edward C. Benzel

68. **Cervical spine injuries** 789
Calan Mathieson, Chris Barrett, and Likhith Alakandy

69. **Thoracic and lumbar spine injuries** 801
Bedansh Roy Chaudhary and Shiong Wen Low

70. **Spinal cord injury rehabilitation** 813
Fahim Anwar, Wail Ahmed, Tamara Tajsic, Damiano G. Barone, and Harry Mee

SECTION 15
Peripheral nerve surgery

71. **Electrodiagnostics** 827
Alan Forster and Robert Morris

72. **Entrapment syndromes** 839
Grainne Bourke and Mobin Syed

73. **Supraclavicular brachial plexus and peripheral nerve injuries** 847
Jonathan Perera and Marco Sinisi

74. **Peripheral nerve tumours** 855
Rikin Trivedi and Vincent Nga

SECTION 16
Functional neurosurgery

75. **Principles of deep brain stimulation** 865
Erlick A. C. Pereira, Alexander L. Green, and Tipu Z. Aziz

76. **Movement disorders** 873
Keyoumars Ashkan and Ismail Ughratdar

77. **Spasticity** 885
John Goodden, Catherine Hernon, and Brian Scott

78. **Pain pathophysiology and surgical management** 895
Richard Mannion and Rokas Tamosauskas

79. **Cranial nerve vascular compression syndromes** 909
Marc Sindou and George Georgoulis

80. **Neurosurgical interventions for psychiatric disorders** 929
Chris Bervoets, Bart Nuttin, and Loes Gabriëls

SECTION 17
Epilepsy

81. **Classification of seizures and epilepsy** 935
Andrew McEvoy, Tim Wehner, and Victoria Wykes

82. **Epilepsy—diagnosis and assessment** 945
Richard Selway

83. **Surgical management of epilepsy** 957
Johannes Schramm

SECTION 18
Paediatrics

84. **Developmental disorders of the brain** 971
Colin Ferrie, Daniel Warren, and Atul Tyagi

85. **Spinal development and spinal dysraphism** 983
Dominic Thompson

86. **Craniofaciosynostosis: Syndromic and non-syndromic craniofacial anomalies** 993
Federico Di Rocco, Pierre-Aurelien Beuriat, and Eric Arnaud

87. **Special considerations in paediatric head and spinal trauma** 999
Andrew Kay, Desiderio Rodrigues, Melanie Sharp, and Guirish Solanki

88. **Paediatric brain tumours** 1009
Jonathan Roth and Shlomi Constantini

89. **Paediatric hydrocephalus** 1023
Matt Bailey, Chris Parks, and Conor L. Malucci

90. **Paediatric neurovascular disorders** 1037
Helen G. McCullagh,Tufail Patankar, Tony Goddard, and Atul Tyagi

91. **Paediatric epilepsy** 1047
Sophia Varadkar and Martin Tisdall

SECTION 19
CSF disorders

92. **Hydrocephalus and normal CSF dynamics** 1057
Alexander Gamble and Harold Rekate

93. **Shunt technology and endoscopic ventricular surgery** 1071
Ian K. Pople and William Singleton

94. **Normal pressure hydrocephalus** 1083
Nicole C. Keong

95. **Pseudotumour cerebri syndrome** 1093
John D. Pickard and Nicholas Higgins

96. **Arachnoid cysts** 1101
Ruichong Ma and Stana Bojanic

SECTION 20
Infection

97. **Microbiology** 1109
Walter A. Hall

98. **Cranial infections** 1117
Thangaraj Munusamy, Boon Hoe Tan, and Eugene Yang

99. **Spinal infection** 1129
Nicholas Haden and Edward White

Index 1137

Symbols and abbreviations

Ω	omega
α	alpha
β	beta
δ	gamma
μg	micrograms
AAA	asleep-awake-asleep
AAICH	anticoagulation-associated intracerebral haemorrhage
AANS	acute and chronic settings
ABC	aneurysmal bone cyst
ABI	auditory brainstem implants
ABR	auditory brainstem responses
AC	anterior and posterior commissure (also arachnoid cyst)
ACA	anterior cerebral artery
ACD	anterior cervical discectomy
ACPP	atypical choroid plexus papilloma
ADC	apparent diffusion coefficient
ADI	atlantodental interval
ADL	activities of daily living
ADNFLE	autosomal-dominant nocturnal frontal lobe epilepsy
ADPKD	autosomal dominant polycystic kidney disease
AED	antiepileptic drug
AF	atrial fibrillation
AGNIR	Advisory Group on Non-ionising Radiation
AICA	anterior inferior cerebellar artery
AIDS	acquired immunodeficiency syndrome
AIP	aryl hydrocarbon receptor-interacting protein
AIS	Abbreviation Injury Score (*also* ASIA Impairment Scale)
ALI	acute lung injury
ALIF	anterior lumbar interbody fusion
ALL	acute lymphatic leukaemia
ALL	anterior longitudinal ligament
AP	anteroposterior
ASA	American Society of Anesthesiologists
ASA	anterior spinal artery
ASIA	American Spinal Injuries Association
ASPECTS	Alberta Stroke Programme Early CT Score
AT	anaplastic transformation
ATA	anterior temporal artery
ATIII	antithrombin III
ATLS	advance trauma life support
ATRT	atypical teratoid rhabdoid tumour
AVF	arteriovenous fistula
AVM	arteriovenous malformation
AZ	Annulus of Zinn
BAEP	brainstem auditory evoked potentials
BBB	blood–brain barrier
BECTS	benign epilepsy with centrotemporal spikes
BIS	bispectral index
BMD	bone mineral density
BMI	body mass index
BOLD	blood oxygen level dependent
BP	blood pressure
BRAT	Barrow Ruptured Aneurysm Trial
BTF	Brain Trauma Foundation
CA	cerebral autoregulation
CAA	cerebral amyloid angiopathy
CAD	coronary artery disease
CAMS	cerebrofacial metameric arteriovenous syndromes
CAPECTH	craniectomy-associated progressive extra-axial collections with treated hydrocephalus
CAR	cerebral autoregulation
CAS	carotid angioplasty and stenting
CBF	cerebral blood flow
CBV	cerebral blood volume
CCA	common carotid artery
CCM	cerebral cavernous malformations
CDC	Centers for Disease Control
CDK	cyclin dependent kinases
CFAM	cerebral function analysing monitor
CHF	congestive heart failure
CHLA	Children's Hospital Los Angeles
CISS	Constructive Interference in Steady State
CM	cavernous malformations
CM	central myelin
CMAP	compound motor action potential
$CMRO_2$	cerebral metabolic rate of oxygen consumption
CN	cranial nerve
CNS	central nervous system (also Congress of Neurological Surgeons)
COPD	chronic obstructive pulmonary disease
COSS	Carotid Occlusion Surgery Study
CPA	cerebellopontine angle
CPC	choroid plexus carcinoma
CPH	choroid plexus hyperplasia
CPP	cerebral perfusion pressure (also choroid plexus papilloma)
CPP	choroid plexus papilloma
CPT	choroid plexus tumour

CRF	corticotrophin factor
CRH	corticotrophin-releasing hormone
CRP	C-reactive protein
CRPS	complex regional pain syndrome
CRW	Cosman-Roberts-Wells
CSF	cerebrospinal fluid
CSW	cerebral salt wasting
CSWS	cerebral salt wasting syndrome
CT	computed tomographic
CTA	computed tomography angiography
CTP	cerebellar tonsillar prolapse
CTS	carpal tunnel syndrome
CTV	clinical target volume
CUSA	cavitron ultrasonic surgical aspirator
DBS	deep brain stimulation
DEBS	direct electrical brain stimulation
DES	drug-eluting stents
DESD	detrusor external sphincter dyssynergia
DEXA	dual-energy X-ray absorptiometry
DI	diabetes insipidus
DIND	delayed ischaemic neurological deficits
DISH	diffuse idiopathic skeletal hyperostosis
DLGG	diffuse low-grade gliomas
DNP	dynamic nuclear polarization
DNT	dysembryoplastic neuroepithelial tumours
DPG	diffuse pontine glioma
DRG	dorsal root ganglion
DRIFT	Drainage, Irrigation and Fibrinolytic Therapy
DSA	digital subtraction angiography
DSB	double-strand break
DTI	diffusion tensor imaging
DVA	deep venous anomaly
DVA	developmental venous anomaly
DVT	deep vein thrombosis
DWI	diffusion-weighted imaging
DWMH	deep white matter hyperintensities
DXA	dual X-ray absorbitometery
ECA	external carotid artery
ECG	electrocardiogram
ECoG	electrocorticography
EDF	elongation derotation flexion
EDL	extensor digitorum longus
EEA	endoscopic endonasal approach
EEG	electroencephalography
EGFR	epidermal growth factor receptor
EIEE	early infantile onset epileptic encephalopathies
ELISA	enzyme-linked immunosorbent assay
EMA	epithelial membrane antigen
EMG	electromyography
ENT	ear, nose, and throat
EOIS	early onset idiopathic scoliosis
EOR	extent of resection
EORTC	European Organization for Research and Treatment of Cancer
EP	evoked potential
EPC	epilepsia partialis continua
ES	ethmoid sinus
ERG	Electroretinogram
ES	Ewing's sarcoma
ESO	European Stroke Organisation
ESR	erythrocyte sedimentation rate
ET	essential tremor
ETT	endotracheal tube
ETV	endoscopic third ventriculostomy
EVD	external ventricular drain
EZ	epileptogenic zone
FA	fractional anisotropy
FCD	focal cortical dysplasias
FCU	flexor carpi ulnaris
FD	fibrous dysplasia
FDA	Food and Drug Administration
FEF	frontal eye field
FES	functional electric stimulation
FFP	fresh frozen plasma
FGN	French Glioma Network
FIESTA	fast imaging in steady state
FIPA	familial isolated pituitary adenoma
FLAIR	fluid attenuated inversion recovery
FLE	frontal lobe epilepsy
FM	Foramen of Monro
FSH	follicle-stimulating hormone
FSU	functional spinal unit
FTT	failure to thrive
FV	flow velocities
FZS	fronto-zygomatic suture
GABA	gamma aminobutyric acid
GAF	Global Assessment of Function
GCS	Glasgow Coma Scale
GCT	germ cell tumours (*also* granular cell tumour)
GFAP	glial fibrillary acid protein
GFR	glomerular filtration rate
GH	growth hormone
GHIH	growth hormone-inhibiting hormone
GHRH	growth hormone release hormone
GI	gastrointestinal
GMFM	Gross Motor Function Measure
GSPN	greater superficial petrosal nerve
GTCS	generalized tonic-clonic seizures
GTR	gross total resection
GTV	gross tumour volume
GW	gliadel wafers
H&E	haematoxylin and eosin
HBO	hyperbaric oxygen
HDDST	high-dose dexamethasone suppression tests
HGG	high-grade glioma
HHT	hereditary haemorrhagic telangiectasia
HIF	hypoxia inducible factor
HIFU	high-intensity focused ultrasound
HIV	human immunodeficiency virus
HLA	human leukocyte antigen
HMSN	hereditary motor, and sensory neuropathy
HO	heterotrophic ossification
HPA	hypothalamic-pituitary axis
HPC	haemangiopericytoma
HR	homologous recombination

HRQOL	health-related quality of life
HS	hippocampal sclerosis
HS	hypertonic saline
HSV	herpes simplex virus
HU	Hounsfield units
IA	intra-arterial
IAC	internal auditory canal
IAM	internal auditory meatus
IBE	International Bureau for Epilepsy
ICA	inferior cerebellar artery (also internal carotid artery)
ICA	internal carotid arteries
ICBP	infraclavicular brachial plexus
ICE	ifosfamide, carboplatin, and etoposide
ICH	intracerebral haemorrhage
ICP	intracranial pressure
ICU	intensive care unit
IFOF	inferior fronto-occipital fasciculus
IJV	internal jugular vein
ILAE	International League Against Epilepsy
IO	inferior oblique
IOF	inferior orbital fissure
IOM	Intraoperative monitoring
IPG	implantable pulse generator
IPG	implanted battery-operated pulse generators
IPSS	inferior petrosal vein sampling
IR	inferior rectus
IR	iterative reconstruction
ISAT	International Subarachnoid Aneurysm Trial
ISCoS	International Spinal Cord Society
ISNCSCI	International Standards for Neurological Classification of Spinal Cord Injury
ITB	intrathecal baclofen
IVC	inferior vena cava
IVP	intraventricular pressure
JET	Japanese EC-IC Bypass Trial
KOLT	Kendrick object learning test
kPa	kilopascal
KPS	Karnofsky Performance Status
LCH	Langerhans cell histiocytosis
LDD	L'hermitte-Duclos disease
LDDST	low-dose dexamethasone suppression test
LDL	low-density lipoprotein
LDM	limited dorsal myeloschisis
LFS	Li-Fraumeni syndrome
LG	lacrimal gland
LGG	low-grade glioma
LH	luteinizing hormone
LINAC	linear accelerator
LMN	lower motor neuron
LMWH	low molecular weight heparin
LOC	level of consciousness
LOH	loss of heterozygosity
LOIS	late onset idiopathic scoliosis
LOR	line of response
LOVA	longstanding overt ventriculomegaly in adults
LP	levator palpebrae
LP	lumbar puncture
LR	lateral rectus
LR	Lindegaard ratio
LSO	lumbar sacral orthosis
LSR	lateral spread responses
MAC	minimal alveolar concentration
MAP	mean arterial pressure
MC	Meckel cave
MCA	middle cerebral artery
MCD	malformation of cortical development
MDT	multidisciplinary team
MEG	magnetoencephalography
MEP	minimally endoscopic procedures
MEP	motor evoked potential
MHC	major histocompatibility complex
MI	myocardial infarction
MIP	maximum intensity projection
MIT	minimally invasive techniques
MLF	medial longitudinal fasciculus
MM	multiple myeloma
MMD	moya moya disease
MMS	moya moya syndrome
MMSE	mini-mental state examination
MND	motor neurone disease
MOG	myelin oligodendrocyte glycoprotein
MPBT	malignant paediatric brain tumours
MPNST	malignant peripheral nerve sheath tumours
MR	magnetic resonance
MR	medial rectus
MRA	magnetic resonance angiography
MRA	MR-angio
MRC	Medical Research Council
MRI	magnetic resonance imaging
MRM	magnetic resonance myelography
MRN	magnetic resonance neurography
MRS	magnetic resonance spectroscopy
MRSA	methicillin-resistant Staphylococcus aureus
MRV	magnetic resonance venography
MS	multiple sclerosis
MSH	melanocyte-stimulating hormone
MTG	middle temporal gyrus
MTLE	mesial temporal lobe epilepsy
MTT	mean transit time
MUAP	motor unit action potential
MVA	motor vehicle accidents
MVC	motor vehicle collisions
MVD	microsurgical vascular decompression
Na+	sodium
NAA	N-acetyl aspartate
NASCIS	National Acute Spinal Cord Injury Studies
NCS	nerve conduction studies
NeuN	neuronal nuclei
NFPA	non-functioning pituitary adenomas
NHEJ	non-homologous end-joining
NHL	non-Hodgkin's lymphoma
NICE	National Institute of Clinical Excellence
NIRS	near infrared spectroscopy
NLI	neurological level of injury
NMDA	N-methyl-D-aspartate
NMS	non-motor symptoms

NOAC	new oral anticoagulants
NOS	not otherwise specified
NPH	normal pressure hydrocephalus
NPSA	National Patient Safety Agency
NPUAP	National Pressure Ulcer Advisory Panel
NSAID	non-steroidal anti-inflammatory drug
OC	optic canal
OCR	optico-carotid recesses
OCT	optical coherence tomography
ODI	Oswestry Disability Index
OEF	oxygen extraction fraction
OLE	occipital lobe epilepsy
OLF	ossification of the ligamentum flavum
ON	optic nerve
OPG	optic pathway glioma
OPLL	ossification of the posterior longitudinal ligament
OS	overall survival
OSA	obstructive sleep apnoea
PA	pilocytic astrocytoma
PAR	protease-activated receptors
PBI	penetrating brain injury
PBT	paediatric brain tumour
PCA	posterior cerebral artery
PCC	prothrombin complex concentrate
PCNSL	primary central nervous system lymphoma
PCR	polymerase chain reaction
PCV	procarbazine, CCNU, vincristine
PD	Parkinson's disease (also proton density)
PDGFR	platelet-derived growth factor receptor
PE	preoperative embolization
PE	pulmonary embolism
PEDI	Pediatric Evaluation of Disability Inventory
PEEK	poly-ether-ether-ketone
PEEP	positive end-expiratory pressure
PEG	percutaneous endoscopic gastrostomy
PET	positron emission tomography
PFO	patent foramen ovale
PFS	progression-free survival
PI	pelvic incidence
PICA	posterior inferior cerebellar artery
PIH	prolactin-inhibiting hormone
PIOL	primary intraocular lymphoma
PLL	posterior longitudinal ligament
PML	progressive multifocal leukoencephalopathy
PNET	primitive neuroectodermal tumour
PONV	postoperative nausea and vomiting
PPTID	pineal parenchymal tumours of intermediate differentiation
PRH	prolactin-releasing hormone
PSA	posterior spinal arteries
PSO	pedicle subtraction osteotomy
PT	pelvic tilt (*also* prothrombin time)
PTA	pure-tone audiogram
PTH	post-traumatic hydrocephalus
PTPR	papillary tumour of the pineal region
PTS	post-traumatic seizures
PTSD	post-traumatic stress disorder
PTT	partial thromboplastin time
PTV	planning target volume
PVA	poly-vinyl-alcohol
QoL	quality of life
QOLIBRI	Quality of Life after Brain Injury
RA	rheumatoid arthritis
RANKL	receptor activator of NF-KB ligand
RANO	Response Assessment in Neuro-Oncology
RAPD	relative afferent pupil defect
RCC	renal cell carcinoma
RCN	Rare Cancer Network
RCT	randomized clinical trials
REM	rapid eye movement
REZ	root entry zone
RF	rheumatoid factor
RNFL	retinal nerve fibre layer
RT	radiation therapy
RT	resistance in the tube
RVAD	rib-vertebral-angle difference
SAH	subarachnoid haemorrhage
SARS	sacral anterior nerve root stimulator
SBP	supraclavicular brachial plexus
SCA	superior cerebellar artery
SCA	superior cerebellar artery
SCAVM	spinal cord arteriovenous malformations
SCI	spinal cord injury
SCID	severe-combined immunodeficiency disease
SCM	strap muscles
SCO	spindle cell oncocytoma
SCPP	spinal cord perfusion pressure
SDAVF	spinal dural arteriovenous fistula
SDR	selective dorsal rhizotomy
SDS	speech discrimination score
SEA	spinal epidural abscess
SEEG	stereoencephalography
SEER	Surveillance Epidemiology and End Results
SEGA	subependymal giant cell astrocytomas
SEP	Somatosensory evoked potential
SESH	spontaneous epidural spinal haemorrhage
SFT	solitary fibrous tumour
SGCT	subependymal giant cell tumour
SIADH	syndrome of inappropriate antidiuretic hormone
SIVMS	Scottish Intracranial Vascular Malformation Study
SLE	systemic lupus erythematous
SLF	superior longitudinal fasciculus
SMA	supplementary motor area
SNAP	sensory nerve action potential
SNO	Society for NeuroOncology
SNUC	sinonasal undifferentiated carcinoma
SO	superior oblique
SOF	superior orbital fissure
SOM	spheno-orbital meningiomas
SOV	superior ophthalmic vein
SPECT	single photon emission computed tomography
SPES	single pulse electrical stimulation
SPN	selective peripheral neurotomy
SPV	superior petrosal venous
SR	superior rectus

SSFP	steady state free precession
SSI	surgical site infection
SSMA	supplementary sensorimotor area
SSS	superior sagittal sinus
SST	Short Synacthen Test
STA	superficial temporal artery (*also* superior thyroid artery)
STASCIS	Surgical Treatment of Acute Spinal Cord Injury Study
STG	superior temporal gyrus
STIR	short tau inversion recovery
STR	subtotal resection
SUDEP	sudden unexplained death in epilepsy
SUNCT	short-lived, unilateral neuralgic headache with conjunctival injection and tearing
SVA	sagittal vertical axis
SVM	spinal vascular malformation
SWI	susceptibility weighted imaging
TBI	traumatic brain injury
TCD	transcranial Doppler
TCGA	The Cancer Genome Atlas
TF	tissue factor
TFPI	tissue factor pathway inhibitor
TIVA	total intravenous anaesthesia
TLE	temporal lobe epilepsy
TLSO	thoracolumbar sacral orthosis
TMG	transmural pressure gradient
TMS	tumefactive multiple sclerosis
TN	trigeminal neuralgia
TOF	time of flight
TORCH	Toxoplasmosis, Other (syphilis, varicella-zoster, parvovirus B19), Rubella, Cytomegalovirus (CMV), and Herpes infections
TREZ	trigeminal root entry zone
TRH	thyroid-releasing hormone (*also* thyrotropin-releasing hormone)
TSC	tuberous sclerosis complex
TSH	thyroid-stimulating hormone
TT	thrombin time
TTM	targeted temperature management
TTP	time to peak
TZ	transitional zone
UH	unfractionated heparin
UMN	upper motor neuron
UMNL	upper motor neurone lesions
VA	vertebral artery
VAD	ventricular access device
VAE	venous air embolism
VASO	vascular space occupancy
VBA	vertebrobasilar artery
VDE	velocity of diametric expansion
VEGF	vascular endothelial growth factor
VEP	visual evoked potential
VGAM	vein of Galen malformations
VGPN	vago-glossopharyngeal neuralgia
VHL	Von Hippel-Lindau
VMAT	volumetric modulated arc therapy
VNS	vagus nerve stimulation
VP	vancomycin powder
VP	ventriculoperitoneal
VRE	vancomycin-resistant enterococci
VS	vestibular schwannoma (also ventral striatum)
VTE	venous thromboembolism
vWF	von Willebrand factor
WBC	white blood cell
WBRT	whole-brain radiation therapy
WFNS	World Federation of Neurosurgical Societies
WFSBP	World Federation of Societies of Biological Psychiatry
WHO	World Health Organization
YBOCS	Yale-Brown Obsessive-Compulsive Scale

Contributors

Hadie Adams Cambridge University Hospitals NHS Foundation Trust, Cambridge, UK
43: Surgical management of head injury

Fardad T. Afshari Cambridge University Hospitals NHS Foundation Trust, Cambridge, UK
44: Complications of head injury

Wail Ahmed Consultant, Spinal Cord Injuries in Stoke Mandeville Hospital, Aylesbury, Buckinghamshire, UK
70: Spinal cord injury rehabilitation

Likhith Alakandy Consultant Neurosurgeon, Southern General Hospital, Glasgow, UK
68: Cervical spine injuries

Kieren Allinson Department of Pathology, Addenbrooke's Hospital, Cambridge, UK

Ossama Al-Mefty UAMS Medical Center, Little Rock, AK, USA; and Department of Neurosurgery, Brigham and Women's Hospital, Boston MA, USA
15: Chordomas and chondrosarcomas of the skull base

Rami O. Almefty Department of Neurosurgery, Temple University, Philadelphia, PA, USA
15: Chordomas and chondrosarcomas of the skull base

Nabeel Alshafai Assistant Professor, Neurosurgery, Antwerp, Belgium
40: Epidemiology of head injury and outcome after head injury

Fahim Anwar Consultant in Rehabilitation Medicine, Department of Rehabilitation Medicine, Cambridge University Hospital NHS, Foundation Trust, Cambridge, UK
70: Spinal cord injury rehabilitation

Vasileios Apostolopoulos University Hospital Southampton NHS Foundation Trust, Southampton, UK
32: Intraventricular tumours

Eric Arnaud Department of Pediatric Neurosurgery, Necker-Enfants Malades Hospital, Paris, France
86: Spinal development and spinal dysraphism

Keyoumars Ashkan Kings College Hospital, London, UK
76: Movement disorders

Tipu Aziz The Nuffield Department of Clinical Neurosciences, University of Oxford, Oxford, UK
75: Principles of deep brain stimulation

Matt Bailey Consultant Neurosurgeon, Salford Royal NHS Foundation Trust, Salford, UK
89: Paediatric hydrocephalus

Damiano G. Barone Department of Neurosurgery, Addenbrooke's Hospital, Cambridge, UK
70: Spinal cord injury rehabilitation

Chris Barrett Consultant Neurosurgeon, Southern General Hospital, Glasgow, UK
68: Cervical spine injuries

Janneke van Beijnum Salford Royal NHS Foundation Trust, Salford, UK
55: Cavernoma and angiographically occult lesions

Antonio Belli Reader in Neurotrauma, School of Clinical and Experimental Medicine, College of Medical and Dental Sciences, University of Birmingham, Birmingham, UK
44: Complications of head injury

Lorenzo Bello Associate Professor Neurosurgery, University of Milan, Italy
6: Low-grade glioma

Edward Benzel Chairman and Spinal Surgeon, Cleveland Clinic, OH, USA
67: Managing spinal cord trauma

Mitchel Berger Department of Neurological Surgery, University of California, San Francisco, CA, USA
13: Surgical techniques in the management of intrinsic tumours

René Bernays Department of Neurosurgery, Klinik Hirslanden, Zurich, Switzerland
37: Surgical management of pineal region lesions

Chris Bervoets Psychiatrist, UZ Leuven, Leuven, Belgium
80: Neurosurgical interventions for psychiatric disorders

Pierre-Aurelien Beuriat Hopital Chu de Lyon, Lyon, France
86: Spinal development and spinal dysraphism

Harjus Birk Department of Neurological Surgery, University of California, San Francisco, CA, USA
14: Meningiomas and haemangiopericytoma (HPC)—solitary fibrous tumour (SFT)

Peter Bodkin Aberdeen Royal Infirmary, Scotland, UK
2: Clinical assessment

Stana Bojanic Department of Neurosurgery, Oxford University Hospitals NHS Foundation Trust, Oxford, UK
96: Arachnoid cysts

Ciaran Bolger College of Surgeons, Dublin, Ireland
61: Thoracic spinal disease

Grainne Bourke Leeds General Infirmary, Clarendon Way, Leeds, UK
72: Entrapment syndromes

John Brecknell Queen's Hospital, Romford, London, UK
63: Spinal tumours

Andrew Brodbelt The Walton Centre NHS Foundation Trust, Liverpool, UK
8: Intracranial metastasis

Nicholas Brown University College Hospitals, London, UK
12: Chemotherapy for brain tumours

Karol P. Budohoski Neurosurgical Specialist Registrar, Cambridge University Hospital NHS Trust, Department of Neurosurgery, Addenbrooke's Hospital, Cambridge University Hospitals, Cambridge, UK
5: Perioperative care of the neurosurgical patient

Harry Bulstrode Clinical Lecturer in Neurosurgery, Neurosurgery Division, Department of Clinical Neurosciences, Cambridge Biomedical Campus, Cambridge, UK
7: High-grade gliomas and molecular biology of neurosurgical oncology

Diederik O. Bulters Department of Neurosurgery, Wessex Neurological Centre, Southampton General Hospital, Southampton, UK
46: Normal cerebrovascular physiology and vascular anatomy

John F. Burke Resident Physician, Department of Neurological Surgery, University of California, San Francisco, CA, USA
41: Pathophysiology of traumatic brain injury

Federico Cagnazzo Università di Pisa, Pisa, Italy
47: The pathophysiology of aneurysms

Joseph D. Chabot Department of Neurological Surgery, University of Pittsburgh, PA, USA
19: Surgical management of tumours of the orbit

Christopher Chandler Consultant Adult and Paediatric Neurosurgeon, King's College Hospital, London, UK
29: Ependymoma

Bedansh Roy Chaudhary Cambridge University Hospitals NHS Foundation Trust, Cambridge, UK
69: Thoracic and lumbar spine injuries

Randall M. Chesnut Professor, Neurological Surgery; Professor, Orthopedics and Adjunct Professor, Global Health, Harborview Medical Center, Department of Neurosurgery, Seattle, WA, USA
43: Surgical management of head injury

Omar Choudhri Assistant Professor, Department of Neurosurgery, University of Pennsylvania, PA, USA
53: Giant aneurysms and bypass surgery

Paul Chumas Consultant in Neurosurgery, Leeds Teaching Hospitals, Leeds, UK
33: Colloid cyst

Shlomi Constantini Director, Department of Pediatric Neurosurgery, Dana Children's Hospital, Tel Aviv Sourasky Medical Center, Sackler Faculty of Medicine, Tel Aviv University, Tel Aviv, Israel
34: Choroid plexus tumours; 88: Paediatric brain tumours

William T. Couldwell Professor, Neurosurgery, University of Utah, UT, USA
27: Surgical management of sellar and suprasellar tumours

Matt Crocker Consultant Neurosurgeon, St George's Hospital, London, UK
62: Lumbar spinal disease

Michael D. Cusimano Division of Neurosurgery, University of Toronto, ON, Canada; Keenan Research Centre for Biomedical Science, The Li Ka Shing Knowledge Institute, St. Michael's Hospital, Toronto, ON, Canada
21: Surgical management of anterolateral skull base lesions

Tilak Das Addenbrooke's Hospital, Cambridge University Hospitals, Cambridge, UK
3: Overview of neuroimaging

Hansen Deng Resident Physician, Department of Neurological Surgery, University of Pittsburgh Medical Center, Pittsburgh, PA, USA
41: Pathophysiology of traumatic brain injury

Chris Derham Consultant Neurosurgeon, Leeds General Infirmary, Leeds, UK
56: Surgical principles in spinal surgery

Federico Di Rocco The Hôpital Necker Enfants Malades, Paris, France
86: Spinal development and spinal dysraphism

Derek Duane Consultant in Neuroanaesthesia and Neurointensive Care, Cambridge University Hospital NHS Trust, Department of Anaesthesia, Addenbrooke's Hospital, Cambridge, UK
5: Perioperative care of the neurosurgical patient

Hugues Duffau Institute for Neurosciences of Montpellie, France
6: Low-grade glioma

Andrew Durnford Department of Neurosurgery, Wessex Neurological Centre, Southampton General Hospital, Southampton, UK
46: Normal cerebrovascular physiology and vascular anatomy

Rina Dvir Department of Pediatric Hemato-Oncology, Dana Children's Hospital, Tel-Aviv Medical Center, Tel-Aviv University, Tel-Aviv, Israel
34: Choroid plexus tumours

Frances Elmslie South West Thames Regional Genetics Service, St George's University Hospitals NHS Foundation Trust, London, UK
38: Neurophakomatoses

Rudolf Fahlbusch International Neuroscience Institute (INI), Hannover, Germany
26: Craniopharyngioma and Rathke's cleft cysts

Colin Ferrie Department of Paediatric Neurology, Leeds General Infirmary, Leeds, UK
84: Developmental disorders of the brain

Graham Flint Consultant Neurosurgeon, Queen Elizabeth Hospital, Birmingham, UK
65: Spinal cerebrospinal fluid dynamics

Petter Förander Karolinska Institute, Stockholm, Sweden
22: Schwannomas

Alan Forster Consultant Clinical Neurophysiologist, Aberdeen Royal Infirmary, Scotland, UK
71: Electrodiagnostics

Navin Furtado Queen Elizabeth Hospital, Birmingham, UK
60: Cervical spinal disease

Alexander Gamble Bedford, New Hampshire, USA
92: Hydrocephalus and normal CSF dynamics

Paul Gardner Department of Neurological Surgery, University of Pittsburgh, PA, USA
19: Surgical management of tumours of the orbit

H. Rao Gattamaneni Consultant in Clinical oncology, Christie Foundation Trust, Manchester, UK
25: Pituitary tumours

Fred Gentili Division of Neurosurgery, University of Toronto, ON, Canada
17: Esthesioneuroblastoma

George Georgoulis Department of Neurosurgery, General Hospital of Athens "Gennimatas", Athens, Greece
79: Cranial nerve vascular compression syndromes

V. Gerganov Consultant Neurosurgeon, Department of Neurosurgery, International Neuroscience Institute, Hannover; and Associate Professor, Hannover Medical School, Germany
26: Craniopharyngioma and Rathke's cleft cysts

Giorgio Gioffre Treviso, Italy
20: Skull lesions

Kanna Gnanalingham Salford Royal NHS Foundation Trust, UK
25: Pituitary tumours

Tony Goddard Consultant Interventional Neuroradiologist, Leeds General Infirmary, Leeds, UK
90: Paediatric neurovascular disorders

Lior Gonen Division of Neurosurgery, Department of Surgery, University of Toronto, Canada. Department of Neurosurgery, Aurora Neuroscience Innovation Institute, Aurora St. Luke's Medical Center, Milwaukee, Wisconsin
17: Esthesioneuroblastoma

John Goodden Consultant Neurosurgeon (Adult & Paediatric), Leeds General Infirmary, Leeds, UK
77: Spasticity

Alex Green The Nuffield Department of Clinical Neurosciences, University of Oxford, UK
75: Principles of deep brain stimulation

Fay Greenway Atkinson Morley Department of Neurosurgery, St George's University Hospitals NHS Foundation Trust, London, UK
38: Neurophakomatoses

Alexander Grote Department of Neurology, University of Bonn, Bonn, Germany
10: Glioneuronal and other epilepsy-associated tumours

Paul Grundy Department of Neurosurgery, Wessex Neurological Centre, University Hospital Southampton NHS Foundation trust, UK
32: Intraventricular tumours

Mathew Guilfoyle Department of Neurosurgery, Addenbrookes's NHS Trust, Cambridge, UK
52: Extracranial-intracranial bypass for cerebral ischaemia

Nigel Gummerson Consultant in Orthopaedic Trauma, Leeds General Infirmary, Leeds, UK
66: Scoliosis and spinal deformity

Nicholas Haden Plymouth Hospitals NHS Trust, Plymouth, UK
99: Spinal infection

Nicholas Hall Surgeon, Royal Melbourne Hospital Academic Centre, Parkville, VIC, Australia
24: Surgical management of cerebellopontine angle and petrous lesions

Richard M. Hall Professor of Spinal Biomechanics, School of Mechanical Engineering, University of Leeds, Leeds, UK
57: Spinal stability

Walter Hall Professor of Neurosurgery, Upstate Medical University, Syracuse, NY, USA
97: Microbiology

Seunggu J. Han Department of Neurological Surgery, University of California, San Francisco, CA, USA
14: Meningiomas and haemangiopericytoma (HPC)—solitary fibrous tumour (SFT)

Adel Helmy University Lecturer Neurosurgery, University of Cambridge, UK/Honorary Consultant Neurosurgeon, Addenbrooke's Hospital, Cambridge, UK
18: Malignant skull base tumours; 43: Surgical management of head injury

Catherine Hernon Consultant in Plastic & Reconstructive Surgery, Leeds General Infirmary, Leeds, UK
77: Spasticity

Shawn Hervey-Jumper Associate Professor, Neurosurgery, University of California San Francisco, USA
13: Surgical techniques in the management of intrinsic tumours

Nicholas Higgins Department of Radiology, Addenbrooke's Hospital, Cambridge, UK
95: Pseudotumour cerebri syndrome

Peter J.A. Hutchinson Professor of Neurosurgery, University of Cambridge, Cambridge, UK
43: Surgical management of head injury

Mohsen Javadpour Beaumont Hospital, Dublin, Ireland
51: Carotid artery disease and cerebral ischaemia

Michael D. Jenkinson Department of Neurosurgery, University of Liverpool, Liverpool, UK
36: Pineal tumours

Timothy Jones Department of Neurosurgery, St George's University Hospital Foundation Trust, London, UK
38: Neurophakomatoses

Sylvia Karcheva Consultant in Neuroanaesthesia, Cambridge University Hospital NHS Trust, Department of Anaesthesia, Addenbrooke's Hospital, Cambridge University Hospitals, Cambridge, UK
5: Perioperative care of the neurosurgical patient

Neal Kassell University of Virginia School of Medicine, Charlottesville, VA, USA
47: The pathophysiology of aneurysms

Andrew Kay Consultant Paediatric Neurosurgery, Queen Elizabeth Hospital, Birmingham, UK
87: Special considerations in paediatric head and spinal trauma

Andrew H. Kaye Surgeon, Royal Melbourne Hospital Academic Centre, Parkville, VIC, Australia
24: Surgical management of cerebellopontine angle and petrous lesions

Tara Kearney Salford Royal NHS Foundation Trust, UK
25: Pituitary tumours

Chris Kellett University College London Hospitals, London, UK
62: Lumbar spinal disease

Nicole C. Keong Consultant Neurosurgeon, National Neuroscience Institute and Duke-NUS Medical School, Singapore
94: Normal pressure hydrocephalus

Osaama H. Khan Department of Neurological Surgery, Northwestern University
31: Surgical approaches to posterior fossa tumours

Sadaquate Khan Department of Clinical Neurosciences, Western General Hospital, Edinburgh, Scotland, UK
58: Spinal physiology

Andrew King Manchester Skull Base Unit, Department of Neurosurgery, Manchester Centre for Clinical Neurosciences, Salford Royal Hospital, University of Manchester, Manchester, UK
23: Glomus tumours

Matthew A. Kirkman Specialty Registrar in Neurosurgery and Honorary Fellow in Neurocritical Care; and The National Hospital for Neurology and Neurosurgery, University College London Hospitals NHS Foundation Trust, Queen Square, London, UK
42: Intensive care management of head injury

Peter Kirkpatrick Department of Neurosurgery, Addenbrookes's NHS Trust, Cambridge, UK
52: Extracranial-intracranial bypass for cerebral ischaemia

Ramez W. Kirollos Consultant Neurosurgeon, Addenbrooke's Hospital, Cambridge, UK; Department of Neurological Surgery, University of California, San Francisco, CA, USA
14: Meningiomas and haemangiopericytoma (HPC)—solitary fibrous tumour (SFT); 35: Surgical management of intraventricular lesions

Neil Kitchen National Hospital for Neurology and Neurosurgery, University College London Hospital NHS Foundation Trust, London, UK
4: The operating theatre environment

Georgios Klironomos Division of Neurosurgery, Department of Surgery, University of Toronto, Canada
17: Esthesioneuroblastoma

Angelos G. Kolias Clinical Lecturer Neurosurgery, Addenbrooke's Hospital, Cambridge, UK
43: Surgical management of head injury

Daniel Krell University College Hospitals, London, UK
12: Chemotherapy for brain tumours

Giuseppe Lanzino Mayo Clinic, Rochester, MN, USA
47: The pathophysiology of aneurysms

Michael Lawton Department of Neurosurgery, Barrow Neurological Institute, Phoenix, AZ, USA
49: Management of subarachnoid haemorrhage; 53: Giant aneurysms and bypass surgery

Bryan Lee Neurosurgeon, Barrow Neurological Institute, Phoenix, AZ
67: Managing spinal cord trauma

Boon Leong Quah Department of Neurosurgery, Queen's Hospital, Romford, London, UK and Division of Neurosurgery, Khoo Teck Puat Hospital, Singapore
9: Primary central nervous system lymphoma; 63: Spinal tumours

Shiong Wen Low Consultant Neurosurgeon, National University Hospital and Ng Teng Fong General Hospital, Singapore; and Associate Professor, Department of Surgery, National University of Singapore
69: Thoracic and lumbar spine injuries

Peter Loughenbury Leeds Teaching Hospital NHS Trust, Leeds, UK
57: Spinal stability

Ruichong Ma Department of Neurosurgery, Oxford University Hospitals NHS Foundation Trust, Oxford, UK
96: Arachnoid cysts

Andrew Maas University of Antwerp and Antwerp University Hospital, Department of Neurosurgery, Antwerp, Belgium
40: Epidemiology of head injury and outcome after head injury

Richard Mair Clinical Lecturer in Neurosurgery, Neurosurgery Division, Department of Clinical Neurosciences, Cambridge Biomedical Campus, Cambridge, UK
7: High-grade gliomas and molecular biology of neurosurgical oncology

Conor L. Mallucci Department of Paediatric Neurosurgery, Alder Hey Children's Hospital, Liverpool, UK
36: Pineal tumours; 89: Paediatric hydrocephalus

Geoffrey T. Manley Professor and Vice Chair, Department of Neurological Surgery, University of California San Francisco, San Francisco, CA, USA
41: Pathophysiology of traumatic brain injury

Richard Mannion Department of Neurosurgery, Addenbrooke's Hospital, Cambridge, UK
78: Pain pathophysiology and surgical management

Hani Marcus Faculty of Medicine, Department of Surgery and Cancer, Imperial College London, London, UK
39: Uncommon brain lesions

Henry Marsh Senior Consultant Neurosurgeon, St George's Hospital, London, UK
1: The History of Neurosurgery

Eleni Maratos Consultant Neurosurgeon, King's College Hospital, London, UK
1: The History of Neurosurgery

Tiit Mathiesen Department of Clinical Neuroscience, Karolinska Institutet, Stockholm, Sweden; and University of Copenhagen & Rigshospitalet, Copenhagen, Denmark
22: Schwannomas

Calan Mathieson Consultant Neurosurgeon, Southern General Hospital, Glasgow, UK
68: Cervical spine injuries

Tomasz Matys University Lecturer and Honorary Consultant Neuroradiologist, Department of Radiology, University of Cambridge, Cambridge, UK
3: Overview of neuroimaging

Donald McArthur Consultant Adult and Paediatric Neurosurgeon, Nottingham University Hospitals NHS Trust, Nottingham, UK
30: Haemangioblastoma

Helen McCullagh Leeds General Infirmary, Leeds, UK
90: Paediatric neurovascular disorders

Michael McDermott Department of Neurological Surgery, University of California, San Francisco, USA
14: Meningiomas and haemangiopericytoma (HPC)—solitary fibrous tumour (SFT)

Andrew McEvoy National Hospital for Neurology and Neurosurgery, University College London Hospitals NHS Foundation Trust, UK
16: Dermoid and epidermoid cysts; 82: Classification of seizures and epilepsy

Eavan McGovern University College Dublin and St. Vincent's University Hospital, Dublin, Ireland
59: Medical pathologies of the spinal cord

Chris McGuigan University College Dublin and St. Vincent's University Hospital, Dublin, Ireland
59: Medical pathologies of the spinal cord

Iain McGurgan University College Dublin and St. Vincent's University Hospital, Dublin, Ireland
59: Medical pathologies of the spinal cord

Jason McMillen Consultant Neurosurgeon, Royal Brisbane and Women's Hospital, Brisbane, Queensland, Australia
48: The pathophysiology of subarachnoid haemorrhage

Harry Mee Department of Rehabilitation Medicine, Cambridge University Hospital NHS Foundation Trust, Cambridge, UK
70: Spinal cord injury rehabilitation

Michael P. Meier Department of Surgery, Division of Neurosurgery, St. Michael's Hospital, University of Toronto, ON, Canada
21: Surgical management of anterolateral skull base lesions

H. Metwali International Neuroscience Institute (INI), Hannover, Germany
26: Craniopharyngioma and Rathke's cleft cysts

Samantha Mills Department of Neuroradiology, The Walton Centre NHS Foundation Trust, Liverpool, UK
36: Pineal tumours

Catherine Moran College of Surgeons, Dublin, Ireland
61: Thoracic spinal disease

Jacques J. Morcos Department of Neurological Surgery, University of Miami Miller School of Medicine, FL, USA
31: Surgical approaches to posterior fossa tumours

Michael Morgan Cerebrovascular Neurosurgeon, Macquarie University Hospital, Sydney, NSW, Australia
50: Cerebral arteriovenous malformation and dural arteriovenous fistulae

Robert Morris Consultant Neurosurgeon, Addenbrooke's Hospital, Cambridge, UK
71: Electrodiagnostics

Paul Mulholland University College Hospitals, London, UK
12: Chemotherapy for brain tumours

Thangaraj Munusamy Department of Neurosurgery, Addenbrooke's Hospital, Cambridge, UK; and Division of Neurosurgery, Khoo Teck Puat Hospital, Singapore
9: Primary central nervous system lymphoma; 98: Cranial infections

Ammar Natalwala Specialist Registrar in Neurosurgery, Queen's Medical Centre, Nottingham, UK
30: Haemangioblastoma

Lamia Nayeb South Thames Foundation Trust, London, UK
58: Spinal physiology

Jayson A. Neil Midwest Neurosurgery Associates, Kansas City, MO, USA
27: Surgical management of sellar and suprasellar tumours

Vincent Nga Consultant Neurosurgeon, National University Hospital Singapore, Singapore
74: Peripheral nerve tumours

Bart Nuttin Neurosurgeon, UZ Leuven, Leuven, Belgium
80: Neurosurgical interventions for psychiatric disorders

Karen O'Connell University College Dublin and St. Vincent's University Hospital, Dublin, Ireland
59: Medical pathologies of the spinal cord

A. O'Hare Beaumont Hospital, Dublin, Ireland
51: Carotid artery disease and cerebral ischaemia

Berk Orakcioglu Ethianum, Heidelberg, Germany; and Department of Neurosurgery, University of Heidelberg, Heidelberg, Germany
54: Spontaneous intracranial haematoma

Brian P. Walcott Department of Neurosurgery, University of Southern California, Los Angeles, USA
49: Management of subarachnoid haemorrhage

Benedict Panizza University of Queensland, Princess Alexandra Hospital, QLD, Australia
18: Malignant skull base tumours

Chris Parks Department of Paediatric Neurosurgery, Alder Hey Children's Hospital, Liverpool, UK
89: Paediatric hydrocephalus

Tufail Patankar Consultant Interventional Neuroradiologist, Leeds General Infirmary, Leeds, UK
90: Paediatric neurovascular disorders

Hiren Patel Salford Royal NHS Foundation Trust, Salford, UK
55: Cavernoma and angiographically occult lesions

Omar Pathmanaban Manchester Skull Base Unit, Department of Neurosurgery, Manchester Centre for Clinical Neurosciences, Salford Royal Hospital, University of Manchester, Manchester, UK
23: Glomus tumours

Erlick Pereira Senior Lecturer and Honorary Consultant at St George's, London, UK
75: Principles of deep brain stimulation

Jonathan Perera Guy's and St. Thomas' NHS Foundation Trust, London, UK
73: Supraclavicular brachial plexus and peripheral nerve injuries

David Pettersson Karolinska Institute, Stockholm, Sweden
22: Schwannomas

John D. Pickard Division of Neurosurgery, Department of Clinical Neurosciences, University of Cambridge, Cambridge, UK
95: Pseudotumour cerebri syndrome

Ian K. Pople Department of Neurosurgery, Southmead Hospital, Bristol, UK
93: Shunt technology and endoscopic ventricular surgery

Stephen Price Addenbrooke's Hospital, Cambridge University Hospitals, Cambridge, UK
7: High-grade gliomas and molecular biology of neurosurgical oncology

Harold Rekate Hofstra University, Hempstead, NY, USA
92: Hydrocephalus and normal CSF dynamics

Eduardo C. Ribas Division of Neurosurgery, University of São Paulo Medical School, and Albert Einstein Hospital, São Paulo, Brazil
35: Surgical management of intraventricular lesions

Guilherme C. Ribas Professor of Surgery, Department of Surgery, University of São Paulo Medical School, Department of Surgery and Neurosurgeon, Albert Einstein Hospital, São Paulo, Brazil
35: Surgical management of intraventricular lesions

Desiderio Rodrigues Consultant Paediatric Neurosurgeon, Queen Elizabeth Hospital, Birmingham, UK
87: Special considerations in paediatric head and spinal trauma

Roberto Rodriguez Rubio Department of Neurological Surgery, University of California, San Francisco, USA
49: Management of subarachnoid haemorrhage

Federico Roncaroli Clinical Reader in Neuropathology, University of Manchester, Manchester, UK
25: Pituitary tumours

Jonathan Roth Department of Pediatric Neurosurgery, Dana Children's Hospital Tel-Aviv Sourasky Medical Center, Tel Aviv University, Israel
34: Choroid plexus tumours; 88: Paediatric brain tumours

James Rutka Neurosurgeon and Senior Scientist, The Hospital for Sick Children (SickKids), Toronto, ON, Canada
28: Medulloblastoma

Thomas Santarius Department of Neurosurgery, Addenbrooke's Hospital, Cambridge, Cambridge, UK
6: Low-grade glioma; 14: Meningiomas and haemangiopericytoma (HPC)—solitary fibrous tumour (SFT); 39: Uncommon brain lesions

Johannes Schramm Department of Neurosurgery, University of Bonn, Bonn, Germany
83: Surgical management of epilepsy

Daniel. J. Scoffings Addenbrooke's Hospital, Cambridge University Hospitals, Cambridge, UK
3: Overview of neuroimaging

Brian Scott Consultant Paediatric Orthopaedic Surgeon, Leeds General Infirmary, Leeds, UK
77: Spasticity

Alessandro Scudellari Consultant in Neuroanaesthesia, Addenbrooke's Hospital, Cambridge University Hospitals, Cambridge, UK
5: Perioperative care of the neurosurgical patient

Senthil Selvanathan Consultant Neurosurgeon, Leeds Teaching Hospital NHS Trust, Leeds, UK
56: Surgical principles in spinal surgery

Richard Selway King's College Hospital NHS Foundation Trust, London, UK
81: Diagnosis and assessment

Ashish H. Shah Department of Neurological Surgery, University of Miami Miller School of Medicine, FL, USA
31: Surgical approaches to posterior fossa tumours

Jonathan Shapey The National Institute of Neurology and Neurosurgery, London, UK
4: The operating theatre environment

Melanie Sharp Consultant Paediatric Neurosurgeon, Queen Elizabeth Hospital, Birmingham, UK
87: Special considerations in paediatric head and spinal trauma

Asim Sheikh Consultant Neurosurgeon, Leeds General Infirmary, Leeds, UK
33: Colloid cyst

Susan Short Professor of Clinical Oncology and Neuro-Oncology, Leeds Institute of Cancer and Pathology, Leeds, UK
11: Radiotherapy and radiosurgery for brain tumours

Adikarige Haritha Dulanka Silva Queen Elizabeth Hospital, Birmingham, UK
60: Cervical spinal disease

Matthias Simon Department of Neurology, University of Bonn, Bonn, Germany
10: Glioneuronal and other epilepsy-associated tumours

Marc Sindou Department of Neurosurgery, University of Lyon 1, Hôpital Neurologique P. Wertheimer, Groupement Hospitalier Lyon, Lyon, France
79: Cranial nerve vascular compression syndromes

William Singleton Department of Neurosurgery, Southmead Hospital, Bristol, UK
93: Shunt technology and endoscopic ventricular surgery

Marco Sinisi Consultant Surgeon, Guy's and St Thomas' NHS Foundation Trust, London, UK
73: Supraclavicular brachial plexus and peripheral nerve injuries

Martin Smith Martin Consultant in Neuroanaesthesia and Neurocritical Care, National Hospital for Neurology and Neurosurgery, University College London Hospitals, UK
42: Intensive care management of head injury

Saksith Smithason Cleveland Clinic, OH, USA
67: Managing spinal cord trauma

Guirish Solanki Consultant Paediatric Neurosurgeon, Queen Elizabeth Hospital, Birmingham, UK
87: Special considerations in paediatric head and spinal trauma

S. Tonya Stefko Department of Ophthalmology, University of Pittsburgh, PA, USA
19: Surgical management of tumours of the orbit

Catherine Suen Department of Neurology, University of Utah School of Medicine, UT, USA
41: Pathophysiology of traumatic brain injury

Yuval Sufaro Skull Base Fellow, Royal Melbourne Hospital, Australia
24: Surgical management of cerebellopontine angle and petrous lesions

Kieron Sweeney Department of Paediatric Neurosurgery, Children's University Hospital, Dublin, Ireland
51: Carotid artery disease and cerebral ischaemia; 61: Thoracic spinal disease

Mobin Syed Consultant Plastic surgeon Guys and St Thomas Hospital, London
Mobinsyed@doctors.org.uk

Tamara Tajsic Department of Neurosurgery, Cambridge University Hospital NHS Foundation Trust, Cambridge UK
70: Spinal cord injury rehabilitation

Rokas Tamosauskas Consultant in Anaesthesia and Pain Medicine, Cambridge University Hospitals NHS Foundation Trust, Department of Pain Medicine, Addenbrooke's Hospital, Cambridge, UK
78: Pain pathophysiology and surgical management

Boon Hoe Tan Division of Neurosurgery, Khoo Teck Puat Hospital, Singapore
98: Cranial infections

Mario Teo Consultant Neurosurgeon, Bristol Institute of Clinical Neuroscience, UK
53: Giant aneurysms and bypass surgery

Dominic Thompson Consultant in Paediatric Neurosurgery, Great Ormond Street Hospital, London, UK
85: Spinal development and spinal dysraphism

Simon Thomson Leeds Teaching Hospital NHS Trust, Leeds, UK
56: Surgical principles in spinal surgery

Martin Tisdall Consultant Paediatric Neurosurgeon, Great Ormond Street Hospital, London, UK
91: Paediatric epilepsy

Ivan Tmofeev Department of Neurosurgery, Addenbrookes's NHS Trust, Cambridge, UK
20: Skull lesions

Nicolas de Tribolet Professor of Neurosurgery, University of Lausanne, Switzerland
37: Surgical management of pineal region lesions

Rikin Trivedi Department of Neurosurgery, Addenbrooke's Hospital, Cambridge, UK
74: Peripheral nerve tumours

Kevin Tsang Consultant Neurosurgeon, Imperial College NHS Trust, London, UK
58: Spinal physiology

Georgios Tsermoulas Queen Elizabeth Hospital, Birmingham, UK
60: Cervical spinal disease

Atul Tyagi Consultant Neurosurgeon (Adult & Paediatric), Leeds General Infirmary, Leeds, UK
84: Developmental disorders of the brain; 90: Paediatric neurovascular disorders

Ismail Ughratdar University Hospitals Birmingham NHS Foundation Trust, Birmingham, UK
76: Movement disorders

Andreas W. Unterberg Department of Neurosurgery, University of Heidelberg, Heidelberg, Germany
54: Spontaneous intracranial haematoma

Sophia Varadkar Consultant Paediatric Neurologist, Great Ormond Street Hospital, London, UK
91: Paediatric epilepsy

Elizabeth Visser Aberdeen Royal Infirmary, Scotland, UK
2: Clinical assessment

Daniel Walsh Consultant Neurosurgeon, Kings College Hospital, London, UK
64: Vascular lesions of the spinal cord

Yizhou Wan Resident Physician, Department of Neurosurgery, Oxford University Hospitals, Oxford, UK
39: Uncommon brain lesions

Mueez Waqar Department of Neurosurgery, The Walton Centre NHS Foundation Trust, Liverpool, UK
36: Pineal tumours

Daniel Warren Consultant Neuroradiologist, Leeds General Infirmary, Leeds, UK
84: Developmental disorders of the brain

Colin Watts Professor of Neurosurgery/Honorary Consultant Neurosurgeon, University of Birmingham
9: Primary central nervous system lymphoma

Tim Wehner Formerly Department of Clinical Neurophysiology, National Hospital for Neurology and Neurosurgery, Department of Clinical and Experimental Epilepsy, Institute of Neurology, University College London, London, UK
82: Classification of seizures and epilepsy

Edward White Consultant Neurosurgeon, University Hospitals Birmingham, UK
99: Spinal infection

Peter C. Whitfield University Hospitals Plymouth, Derriford Road, Plymouth, UK
44: Complications of head injury

Mark Wilson St Mary's Hospital, London, UK
45: Concussion and sports-related head injury

Ethan A. Winkler Resident Physician, Department of Neurological Surgery, University of California, San Francisco, CA, USA
41: Pathophysiology of traumatic brain injury

Christoph M. Woernle Department of Neurosurgery, Klinik Hirslanden, Zurich, Switzerland
37: Surgical management of pineal region lesions

Victoria Wykes Department of Neurosurgery, National Hospital for Neurology and Neurosurgery, University College London, London, UK
82: Classification of seizures and epilepsy

Eugene Yang Division of Neurosurgery, Khoo Teck Puat Hospital, Singapore
98: Cranial infections

John K. Yue Resident Physician, Department of Neurological Surgery, University of California, San Francisco, CA, USA
41: Pathophysiology of traumatic brain injury

Zsolt Zador NIHR Academic Clinical Lecturer and Specialty Registrar in Neurosurgery, Department of Neurosurgery, Salford Royal NHS Foundation Trust, University of Manchester, Manchester, United Kingdom
25: Pituitary tumours

Rashed Zakaria The Walton Centre NHS Foundation Trust, Liverpool, UK
8: Intracranial metastasis

SECTION 1

Principles of neurological surgery

1. **The history of neurosurgery** 3
   Eleni Maratos and Henry Marsh
2. **Clinical assessment** 11
   Peter Bodkin and Elizabeth Visser
3. **Overview of neuroimaging** 31
   Tomasz Matys, Daniel. J. Scoffings, and Tilak Das
4. **The operating theatre environment** 45
   Neil Kitchen and Jonathan Shapey
5. **Perioperative care of the neurosurgical patient** 57
   Karol P. Budohoski, Alessandro Scudellari, Sylvia Karcheva, and Derek Duane

1

The history of neurosurgery

Eleni Maratos and Henry Marsh

Introduction

The history of neurosurgery falls naturally into the premodern era, where it is essentially the history of surgery to the skull and of head injuries, and the modern era, where it is the history of surgery to the brain itself, made possible by cerebral localization theory, antisepsis, and anaesthesia, all of which developed in the nineteenth century.

The first known neurosurgical procedures were skull trephines, seemingly carried out on both the living and the dead. It is unclear whether these were performed for therapeutic or ritualistic reasons. There are many trepanned skulls dating back thousands of years to the Neolithic era, and perhaps to even earlier, from sites all over the world.

Ancient Egypt

The earliest neurosurgical writings can be traced to Ancient Egypt and have been preserved in the Edwin Smith Papyrus that dates from *c.*1600 BC. This is the first time that the management of head injuries was based on rational scientific method rather than magic. In a style that is highly reminiscent of modern case reports, the first ten cases focus on head wounds and also contain the earliest known reference to the brain itself (as opposed to the skull), which describes a 'convoluted structure like ripples that happen in copper through smelting'. The cases vividly describe a methodical approach—first ascertaining the depth of the injury and whether there is an underlying skull fracture or exposed brain, and then advocating different management strategies according to the findings. The papyrus has been translated and reproduced by the National Institutes of Health and can be studied online (https://ceb.nlm.nih.gov). As well as the earliest known advice on head injury management, the Edwin Smith Papyrus also contains the first references to spinal immobilization in order to prevent further injury.

Ancient Greece and Byzantium

Hippocrates (460–370 BC) wrote extensively on head injuries in *De capitis vulneribus* (*On Head Wounds*). His management strategy was almost exclusively based on classifying the fracture rather than on the clinical state of the patient. He described five categories of skull fracture, including contre-coup injuries. On head injuries, he wrote *'nullum capitis vulnus contemnendum est'* (no head injury should be considered trivial). His writings were not confined to head injury and he is also credited with the first description of a subarachnoid haemorrhage:

> . . . when persons in good health are suddenly seized with pains in the head and straight away are laid down speechless and breath with stertor they die in seven days unless fever comes on.

He also described contralateral convulsions associated with brain injury; he can therefore perhaps be credited with being the first doctor to describe cerebral localization.

The Alexandrian school introduced formal anatomy dissection in approximately 300 BC. It was at this time that Herophilus began to develop the anatomic nomenclature that we use today (see **Fig. 1.1**). He identified that nerves and tendons were indeed different structures, contrary to what the Egyptians had thought, and he also was the first to describe the anatomy of the ventricles and the venous sinuses. The confluence of the sinuses, of course, still bears his name 'torcula (wine press) Herophili'. He also described the pen nib or 'calamus scriptorius' at the base of the fourth ventricle 'αναγλυφη της χαλαμης' and the choroid plexus (named after its resemblance to the vessels of the placenta).

Celsus, who lived from 25 BC to 50 AD, was the first to describe inflammation (*rubor, dolor, tumor*) and also wrote about extradural haemorrhage, hydrocephalus, trigeminal neuralgia, and spinal fractures. He advocated craniotomy only as a last resort in head injury and described the technique of drilling holes and connecting them up with a hammer and chisel with a protective blade. In another early account of cerebral localization, he advised operating on the side with the greatest pain.

Galen 129–200 AD

With Galen came the encephalocentric model of science and medicine, where the brain was recognized as the seat of intelligence and voluntary movement. He identified the pia (as different from the dura mater), the corpus callosum, the ventricles (alongside Herophilus), and the pineal and pituitary glands. He described the aqueduct of

Fig. 1.1 Herophilus of Chalcedon (*c.* 330–260 BC), a Greek doctor who practised in Alexandria. Here he is seen depicted in discussion with Erasistratus of Ceos.
Wellcome Collection

Sylvius and the foramen of Monro before the anatomists whose names they now possess. He made other significant contributions to neuroscience by identifying that transecting the spinal cord leads to loss of function below the level of the lesion, and he also described what we now call Brown-Séquard syndrome. In addition, he noted that recurrent laryngeal nerve injuries led to hoarse 'voices' in his experimental dogs. He also advocated elevating depressed skull fractures and using irrigation to reduce the heat created by trephining. His teachings were accepted, largely unquestioned, for 1500 years.

During mediaeval times (750–1200 AD) most innovative medical writing came from the Islamic and Arabic worlds, which also kept the Hippocratic and Galenic teachings alive. It was during this time that traditional bedside teaching was established.

The beginning of the scientific era

The sixteenth and seventeenth centuries were remarkable for the advances in all aspects of science and philosophy. Anatomical dissection of cadavers was already practised in mediaeval Europe before Vesalius, but he was more extensive and systematic in his dissections and was the first to challenge the teachings of Galen and Aristotle. William Harvey (1578–1657) published his seminal work on the function of the heart and circulation of blood *de motu Cordis et Sanguinis in Animalibus* (1628). Willis (1621–1675) applied this knowledge to his understanding of cerebral anatomy and showed that occluding parts of his eponymous circle did not compromise flow, thereby confirming their anastomotic nature.

Surgery continued to develop in all areas, although neurosurgery remained confined to trauma. In a challenge to orthodoxy, Yonge (1646–1721) stated that mortality was 'not inevitable' once the dura had been breached. Percival Pott not only worked on tuberculosis (TB) of the spine (which has made a recent resurgence in neurosurgical practice) but also made significant advances in our understanding of head injuries. He asserted that in head injury, trepanning could relieve the pressure from extravasated fluid, thus providing a rationale for the oldest neurosurgical operation. At the same time, Jean Louis Petit (1674–1750) described the classic 'lucid interval' associated with an extradural haematoma as a brief loss of consciousness followed by a gradual deterioration due to accumulation of blood compressing the brain. The importance of brain injury rather than head injury began to be recognized. Bell (Edinburgh 1749–1806) described the loss of pupillary reaction to light and recognized this as an indication to perform a 'rapid and prompt evacuation' of an extradural haematoma. Bell is also credited with identifying that hydrocephalus can be associated with spina bifida.

Although the majority of operations were still for trauma, one key exception was the successful extirpation by Morand (1697–1773) of a temporal abscess following otitis media and mastoiditis. He describes exploring it with his finger and washing out the cavity before placing a silver tube which was slowly withdrawn—a method which resonates today, where silver is once again finding a medical role for its bactericidal properties.

Cotugno (1736–1822) further characterized the cerebrospinal fluid (CSF) pathways and described the 'nervous origins' of sciatica for the first time. He also described hydrocephalus *ex vacuo* as being secondary to cerebral atrophy.

The surgeon/anatomist John Hunter (1728–1793) was a student of Pott's and made major contributions to general surgery and neurosurgery. His extensive anatomy collection houses the Irish giant (Cushing's original acromegalic) and can still be seen at the Hunterian Museum at the Royal College of Surgeons, London.

However, during this time neurosurgical operations were still plagued by infection and the lack of anaesthetic agents meant that operations had to be rapid and not always accurate. The clinical skill of cerebral localization was also yet to be described, so surgery was confined to lesions that had external manifestations.

Early modern to nineteenth century

The modern practice of neurosurgery as we know it today began in the nineteenth century. The parallel advances in anaesthesia and antisepsis allowed mortality rates to fall to acceptable levels and the ability to localize cerebral lesions by clinical examination alone allowed surgeons to tackle occult lesions, thereby dramatically broadening the scope of the specialty. These advances ultimately led to the creation of neurosurgery as a specialty in its own right.

Parallel advances

Anaesthesia

The introduction of ether in the 1840s allowed surgery to be performed in a pain-free manner without the surgeon being rushed or restraints being used. The dentist William Morton persuaded Dr Warren to use ether to excise a submaxillary tumour in 1846 at the Massachusetts General Hospital. Shortly after this, in 1847, Marie Jean Pierre Flourens successfully used chloroform anaesthesia. It was not without risk, but the advantages to both surgeons and patients were clear. As anaesthesia became safer, so the range of pathologies that could be tackled grew and complex surgical approaches could be developed.

Antisepsis

Before antisepsis, neurosurgery was almost inevitably fatal due to 'suppuration'. Louis Pasteur (1822–1895) developed his germ theory and radically changed current opinion as to the origins of

infection. He postulated that meat putrefaction and fermentation were not due to 'spontaneous' degeneration but to living microscopic organisms. Joseph Lister (1827–1912), who was Professor of Surgery at the University of Glasgow, applied Pasteur's germ theory to surgery and in particular to wound infections. He began using carbolic acid and commented that his wounds healed without pus. The mortality from amputations was dramatically cut from 45% to 15%. Meanwhile, in America William Keen (1837–1932) adopted Lister's principles in his operating theatre, applying them to the surgeon, the patient, and to the theatre environment; principles that are still being pursued today. He insisted all surfaces were cleaned with carbolic and carpets and furniture were removed. The surgeon's hands were washed with soap, alcohol, and sublimate, and the patients were also prepped for the first time with a head shave, soap and water, ether, and wet sublimate dressings as well as mercuric chloride washings.

Handwashing was also shown to radically reduce infections in obstetrics and gynaecology by Holmes Semmelweiss. Keen boiled his surgical instruments for 2 hours in a precursor to heat sterilization, which was introduced in 1891 by Ernst von Bergman. In 1883 Neuber began to use sterile gowns and caps, but it was not until William Stewart Halsted (1852–1922) commissioned Goodyear to make some rubber gloves in 1890 to protect his nurse's hands from the mercuric chloride that gloves were routinely used in surgery (see Fig. 1.2). Mikulicz subsequently introduced masks in 1897.

Cushing himself stated in 1915 that 'certainly infections cannot be attributed to the intervention of the devil but must be laid at the surgeon's door'. He published his series of 130 cases with only a single infection—an infection rate of less than 1%, which remains enviable today. A Centre for Disease Control and prevention (CDC) audit on craniotomy infection rates from 1992 to 2003 reported rates between 0.86% for low risk cases and 2.32% for the high risk. Cushing also reported a perfectly respectable 8.4% mortality in the same series (Cushing, 1915). In the 1940s antibiotic prophylaxis was introduced to reduce postoperative infection.

Cerebral localization

In the 1860s the correlation of neurological symptoms and signs with the cerebral location of a lesion began to transform the scope of neurosurgery. The neurological examination is so ingrained in our current practice that it is difficult to imagine a time before cerebral localization. At the beginning of the nineteenth century, localization theory had been associated with the discredited pseudo-science of phrenology. Paul Broca (1824–1880) then showed that speech was localized in the brain's left hemisphere and John Hughlings Jackson (1835–1911) described what came to be known as the 'Jacksonian march' of focal motor activity 'in which parts of the body are affected one after another'. He also correctly identified that a third cranial nerve palsy lateralizes the haematoma to the side of the fixed and dilated pupil. He directed Sir Jonathan Hutchinson (1828–1913) to perform surgeries based on his localizations and ipsilateral pupillary dilatation carries the eponym 'Hutchinson's pupil'.

It was during the same period that David Ferrier (1843–1928) was using Faradic current stimulation in animals including primates to create one of the first cortical maps, including the correct location of the motor cortex. He credited Hughlings Jackson with predicting the outcome of his animal studies. Fritz and Hitzig were using similar cortical stimulation techniques to map the cortex in dogs during the same time period.

Dr Alexander Hughes Bennett (1848–1901) is credited with being the first neurologist to direct the removal of a tumour by cerebral localization alone. In 1885 he directed Sir Rickman Godlee (1849–1925) to remove a motor strip tumour from a patient who had presented with contralateral focal motor seizures and subsequent progressive hemiparesis. The operation was successful, but the patient later died of infection, as was so often the case (Bennett and Godlee, 1965; Kerr et al., 2005).

Fig. 1.2 Photograph of Harvey Cushing and William Halsted in the operating room. Note the rubber gloves, made by Goodyear, that Halsted was the first to use routinely in surgery.

Haemostasis

The development of effective neurosurgery required new methods to deal with the torrential haemorrhage often associated with craniotomy. William Bovie (1882–1958) developed the method of electrocautery for haemostasis and it was first used by Cushing in 1926. The development of blood transfusion in the early years of the twentieth century was also of importance. Until then, craniotomies would sometimes be done as staged procedures, with an interval between the operations to allow the patient's own haematopoeisis to replace the blood lost on opening the scalp and skull.

Early pioneers

These major technical advances in anaesthesia, antisepsis, cerebral localization, and haemostasis set the scene for the early pioneers of neurosurgery to establish neurosurgery as a specialty in its own right.

Victor Horsley 1857–1916

Sir Victor Horsley (1857–1916) was a clinician, researcher, and surgeon, and was therefore ideally qualified to make significant advances in cerebral localization. He published works on the topography of the motor cortex and 'the arrangement of the internal capsule', as well as relating surface anatomy to underlying cortical features in 'topographical relations of the cranium and surface of the cerebrum'. In 1888 he was the first to successfully remove a spinal cord tumour (localized by William Gowers, neurologist, 1845–1915). He was not the first to remove a brain tumour—that was William Macewen (1848–1924)—but he is credited with performing several pioneering operations, including craniosynostosis surgery for raised intracranial pressure and sectioning of the posterior root of the trigeminal nerve for neuralgia; he was also the first to operate on the pituitary. His technical advances included the development of antiseptic beeswax for bone bleeding (still used today) and the Horsley-Clark stereotactic frame. He was a general surgeon himself, but was at the forefront of developing neurosurgery as a specialty and was given the first specifically neurosurgical appointment while at Queen Square. He died in the First World War from desert fever.

William Macewen 1848–1924

William Macewen (1848–1924) was born in Port Bannatyne on the Isle of Bute, Scotland. He was Regius Professor of Surgery at Glasgow University from 1892 to 1924 and was knighted in 1909 when he became Surgeon to the King. His major contributions to surgery were in orthopaedics, establishing bone graft surgery, and setting up the Princess Louise Scottish Hospital for Limbless Soldiers and Sailors where he also designed the Erskine artificial limb. He is credited with performing the first brain tumour operation when he successfully removed a presumed meningioma from a 14-year-old girl in 1879. He did not require the then-novel technique of cerebral localization as there was hyperostosis overlying the meningioma, which directed his surgery. She had indeed presented with cosmetic deformity, and subsequently had refractory seizures contralateral to the lesion, which provided Macewen with the indication to attempt the resection. He was a strong believer in sterile surgical techniques and she survived a further 8 years, and was able to work, before dying of other causes. The low mortality of his operations for cerebral abscess bears comparison with modern series.

William W. Keen 1837–1924

The first American neurosurgeon was William Williams Keen Jr. He studied at Jefferson Medical College and was President of the Philadelphia School of Anatomy. As was commonplace at that time he toured Europe during his education, spending time in Paris and Berlin. He is credited with introducing the Gigli saw to America. He pioneered CSF drainage for hydrocephalus, describing the eponymous parietal burr hole still often used for ventriculoperitoneal shunt insertion 3 cm posterior and superior to the pinna. Although not the first to remove a brain tumour, he was noted for removing some large tumours successfully.

Harvey Williams Cushing 1869–1939

Harvey Williams Cushing is often seen as the father of modern neurosurgery (see **Figs. 1.3** and **1.4**). Arriving on the scene at just the right time when antisepsis, anaesthesia, and cerebral localization

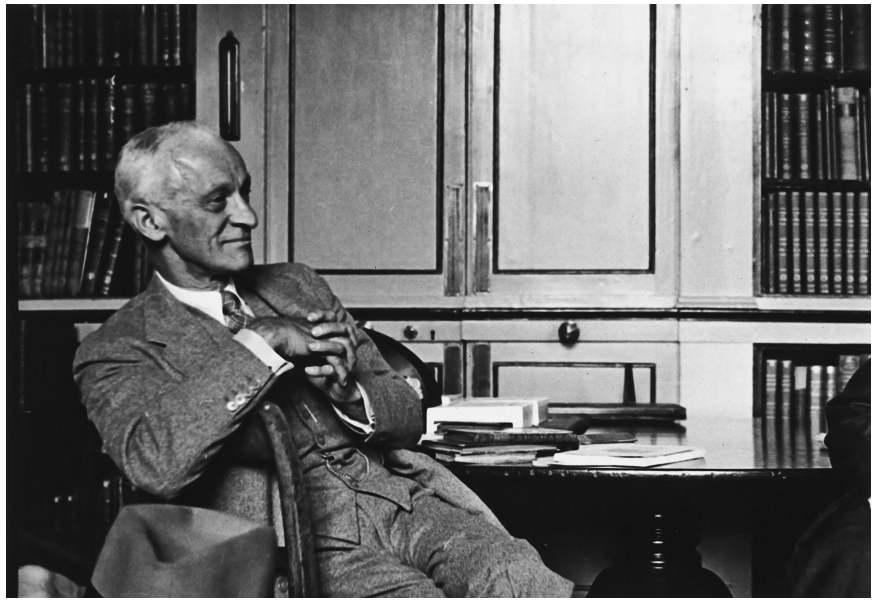

Fig. 1.3 Harvey Cushing, the father of modern neurosurgery.

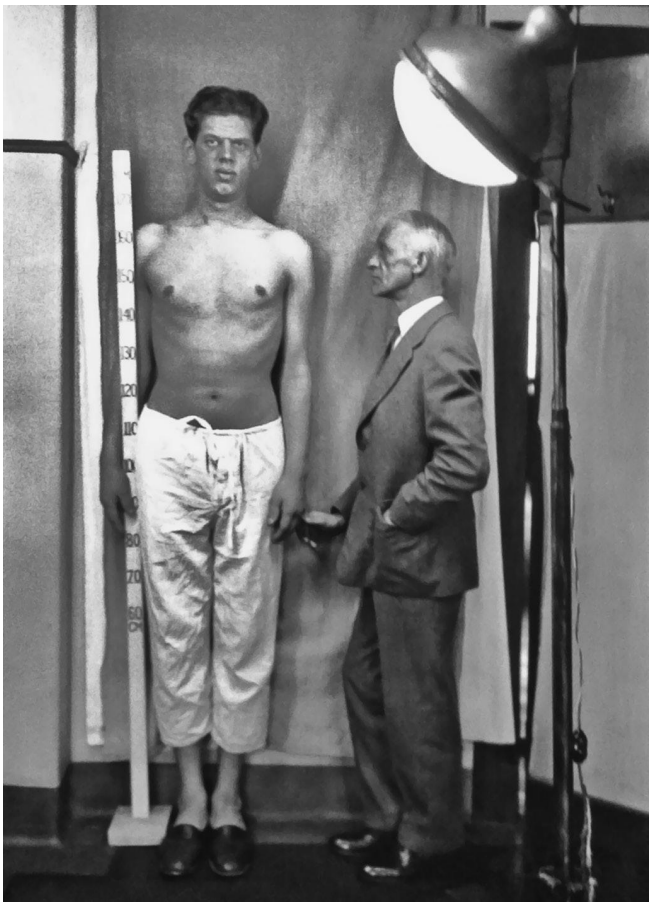

Fig. 1.4 Harvey Cushing stands by a patient with gigantism.
Reproduced from Shin P. Harvey Cushing's Ghosts: Death and Hauntings in Modern Medicine. Yale J Biol Med. 2011;84(2):91–101

were now established, Cushing was well positioned to make his contribution to the specialty.

He was trained in general surgery by Halsted himself, who was Professor of Surgery at the time, and who is credited for teaching Cushing his meticulous surgical technique. Another great influence on Cushing was Sir William Osler (1849–1919), who encouraged him in the more philosophical aspects of medicine including the study of the history of medicine. Cushing was one of Osler's 'latchkeyers', students who lived next door to Osler and were given the 'latchkey' to his extensive library.

In those days it was common for American doctors to spend some time visiting their counterparts in Europe, and Osler encouraged Cushing to do the same. Cushing visited Horsley in London and by his own account was 'a little disappointed' in him. A meticulous surgeon himself, Cushing described Horsley's technique as 'execrable' and commented that he must have many 'septic wounds'. Indeed, at that time Horsley accepted mortality rates of 30–50% from 'brain fungation' (i.e. infection).

Cushing then travelled to France and Switzerland where he worked with Kocher in Bern. In contrast to what he writes about Horsley, he comments that Kocher's technique was 'detailed' and 'tedious' with 'absolute haemostasis'. Cushing's seminal work on intracranial pressure began at this time in the lab of Kronecker. It was here that he made the discovery that 'an increase in intracranial tension occasions a rise of BP which tends to find a level slightly above that exerted against the medulla'—now known as the Cushing reflex. His travels then took him to Italy where he was so impressed with the blood pressure monitor designed by Scipione Riva-Rocci that he brought it back to America with him.

This era from 1901 to 1910 was a key decade for neurosurgery. Cushing recognized the importance of raised intracranial pressure and of meticulous surgical technique. He was responsible for the introduction of intraoperative blood pressure monitoring and following his own experience of a death on the operating table, he also introduced anaesthetic charts to record pulse and respirations during a procedure. With Percival Bailey (1892–1973) and Louise Eisenhardt (1891–1967) he coauthored the standard works on gliomas and meningiomas, and was responsible for pioneering work on the diagnosis and treatment of pituitary disorders.

Walter Dandy 1886–1946

Walter Edward Dandy studied medicine and subsequently spent his whole career at Johns Hopkins Hospital (see **Fig. 1.5**). He was of the same Halsted surgical dynasty as Cushing and was Cushing's research assistant at the Hunterian laboratory that Cushing had established at Johns Hopkins. His work on the production and absorption of CSF acknowledged the importance of the choroid plexus and made advances in our understanding of hydrocephalus of infancy.

His work on 'pneumoventriculography' (1918) radically changed neurosurgery for the next 60 years. In 1913 Luckett had described the radiological appearances of pneumocephalus but Dandy developed the technique by which air ventriculography (or pneumoencephalography as it was known) allowed the interpreter to infer the location of intra-axial masses by the distortion they created in the ventricles. Along with cerebral angiography (discovered by

Fig. 1.5 Walter Dandy, a student of Cushing's and later his rival, made several key contributions to neurosurgery.

Moniz in 1927) this became the mainstay of diagnostic imaging until the advent of the computed tomography (CT) scanner in the 1970s. Previously Cushing and others had used X-rays to identify extra-axial masses such as sellar lesions but until the technique of pneumoencephalography was introduced, intra-axial lesions could only be diagnosed by the clinical skill of cerebral localization. He was the first surgeon to operate for a colloid cyst in 1921.

He advocated total resection of an acoustic neuroma as opposed to Cushing's more conservative subtotal removal, sectioning the fifth cranial nerve for trigeminal neuralgia and developed a transcallosal approach to the pineal. He also identified a ruptured intervertebral disc as a cause of cauda equina syndrome and bilateral sciatica in 1929.

Late twentieth century to today

In recent decades, progress has largely been driven by advances in technology, with the sometimes slightly paradoxical effect of changing management away from neurosurgery, with developments such as interventional radiology for aneurysms and stereotactic radiosurgery for small vestibular schwannomas.

Technological advances

Diagnostic imaging

The development of diagnostic imaging techniques has revolutionized neurological diagnosis (and introduced the modern problem of the incidental finding). Following Dandy's pneumoencephalography the next major advance in imaging techniques was cerebral angiography. This was developed by Antonio Caetano de Egas Moniz (1874–1935) who was subsequently awarded the Nobel Prize in 1949 for the more dubious invention of frontal leucotomy for psychosis (and was also shot and rendered paraplegic by one of his patients). Myelography was introduced by Jean Athanase Sicard (1872–1919) and allowed mass lesions of the spine to be identified.

Parallel advances in X-rays and computing allowed the development of the CT scanner by Godfrey Hounsfield (1919–2004) at EMI. The first CT scan of a patient was in 1971 at the Atkinson Morley Hospital, London, confirming a right frontal lobe tumour. The development of positron emission tomography (PET) and magnetic resonance imaging (MRI) swiftly followed in the 1980s.

Operative microscope

Gunnar Holmgren in Stockholm in 1927 was one of the pioneers of the binocular microscope and its first clinical use was by oto-rhinolaryngologists for the management of otitis media. Several refinements were made to the apparatus, largely led by ears, nose, and throat (ENT) surgeons themselves. Perhaps surprisingly it was not until 1957 that the microscope was first used in neurosurgery. Theodor Kurze, apparently inspired by a film of the ENT surgeon William House using the operative microscope, used it for the removal of a neurilemoma in a 5-year-old.

There are innumerable other advances in the field of neurosurgery. The adoption of the endoscope, for example, has transformed skull base surgery and the introduction of ventriculoperitoneal shunts has radically changed our management of hydrocephalus. These technologies are still, relatively speaking, in their infancy and will continue to develop throughout this century at least.

History of spinal neurosurgery

Although this chapter mainly focuses on the history of cranial neurosurgery, the development of spinal surgery should not be overlooked. Once more, the Edwin Smith Papyrus gives us vivid descriptions of the way spinal trauma was managed in Ancient Egypt. The ability of the Ancient Egyptians, and in particular Imhotep (thought to be the world's first physician) to tie in the clinical picture with the management plan and the prognosis was remarkable. Case 31 clearly describes a complete spinal cord injury secondary to a cervical vertebra dislocation—centuries before Brown-Séquard's treatise on spinal localisation in 1858.

The Hippocratic School in Ancient Greece described the first traction device, advocating correction of an acquired kyphosis following trauma. Hippocrates recognized compression of 'spinal marrow' by displaced vertebrae as the cause of paralysis. As in Ancient Egypt, no treatment was advised if the patient was paralysed. Celsus and Galen did not advocate surgery either, recognizing the poor outcomes associated with spinal cord damage, especially once urinary dysfunction had occurred. Celsus recognized that high cervical lesions were associated with quadriparesis and respiratory compromise while thoracic lesions led to paraparesis. Galen (131–201 AD) coined the terms kyphosis, lordosis, and scoliosis. It is worth noting that he also was the first to describe tuberculous spinal disease (a few hundred years before Percival Pott 1713–1788) and, having conducted experiments where he demonstrated that spinal cord transection led to loss of function below the level of the lesion, he also contributed to the conceptual advance of the brain as the source of voluntary action with signals being passed along the spinal cord. Paulus of Aegina (624–690 AD) was the first to advocate surgery on the spine, removing bony fragments in injured patients with paralysis. Interestingly, in an early reference to 'informed consent' he describes his surgery as being carried out 'after warning of the dangers'.

Very little progress was made in the mediaeval period and the 'dark ages' in Europe. The seat of medicine was transferred to the Arabic world. Previously acquired knowledge from the Alexandrian and Hippocratic schools was preserved by translating the Latin documents into Arabic, but not advanced in any significant way. One notable exception is the Turkish physician Sabunuoglu (*b.*1385) who provides us with the first description of treating sciatica—the first description of degenerative rather than traumatic spinal disease. It was not until 1764 that Cotugno postulated that neural compression was the source of sciatica, a model that was later added to by the French neurologists Lasegue, Dejerine, and Sicard.

During the eighteenth and nineteenth centuries, the Age of Enlightenment in Europe, the foundations for modern spinal surgery were built. Percival Pott (1713–1788) described his now eponymous tuberculous spinal disease and washed out a paravertebral abscess with some success. John Bell (1763–1826) described the flaccid and spastic paralysis and sphincter disturbance associated with spinal cord injury and, with regards to spinal surgery, is quoted as saying 'the cutting into a vertebra is a dream' in 1799. Mr Cline Jr, a surgeon at St Thomas' Hospital, London, is credited with the first 'trepanation' of the spine in 1814 on a paralysed man who was paraplegic after falling from a balcony. He performed a laminectomy and removed the facet joints to reduce the dislocation, but the patient died. There are reports from military history of surgeon Louis operating

on Captain Villedon, who had sustained a spinal cord injury from a thoracic gunshot wound and reportedly regained some distal function postoperatively.

Surgery remained controversial due to its high mortality and morbidity until the advent of antisepsis (Lister 1882–1912 and Semmelweiss 1818–1865) and safe general anaesthesia. Spinal cord localization mirrored cerebral localization with the early work being carried out by Blesius in 1666 (he described the grey-white matter differentiation) and the anterior-posterior spinal nerve roots. The decussation of the pyramids was described by Mistichelli in 1709 and Huber described the denticulate ligaments in 1739. The substantia gelatinosa was described by Rolando in 1809 and Brown-Séquard's description of the decussation of the sensory tracts was published in 1846. Brown-Séquard was a strong advocate of surgery for spinal cord injury. His contribution to spinal cord localization and his description of the spinal cord tracts is immortalized in his eponymous syndrome of hemisection of the cord. Further work on biomechanics of the spine was carried out *in vivo* and *in vitro* by Rauber, Weber, and Messerer in the 1800s.

In the late 1800s, spinal surgery was still mostly confined to trauma and infection (TB). Almost two centuries after Cotugno described the neural compression in sciatica, Oppenheim and Kruse described the first surgery for disc herniation (1909). Mixter and Barr fully described the pathogenesis of disc herniation in 1933 and advocated a 'transdural' approach to the disc. In 1977 Caspar and Yasargil described the microsurgical intralaminar extradural approach that is practised today. Critical to these developments had been Roentgen's discovery of X-rays in 1895, radically improving the diagnosis of spinal fractures. Previously spinal fractures were thought to be almost invariably associated with neurological deficit (90%). Sudeck developed the systematic interpretation of X-rays and established that most fractures in intact patients were missed and that therefore the true rate of paralysis was more like 15–20%. The advent of imaging modalities such as CT (1970s) and MR (1980s) had an equally great impact on the development of surgery for degenerative spinal disease.

Although a few key spinal operative 'firsts' are attributed to nineteenth-century surgeons, it has been the twentieth century where advances in imaging and materials science has allowed the field of spinal surgery to expand into spinal fixation. Anterior, posterior, and lateral approaches to all regions of the spine were developed. The cervical spine has particular challenges due to its poor biomechanical strength and the proximity of important neural and vascular structures. During the last 50–100 years, we have seen the progression from the first anterior cervical surgery of Bailey and Badgley in the 1950s who described the anterior cervical discectomy (ACD) without any graft, to the ACD and fusion (ACDF) advocated by Cloward in 1958 and then by Smith and Robinson. The first anterior cervical plate was designed by Orozco and Lovet and required bicortical screws, which are technically challenging to place. Technological and biomechanical advances allowed the introduction of the unicortical locking screw and then the dynamic load-sharing plates with variable angle screws which was introduced in 2000. Throughout this time, posterior approaches to the subaxial spine have also benefited from advances in materials science with stronger, lower profile screws and posterior cervical fixation has moved forward from the silver wire used in the first posterior c-spine fixation in 1891 via interspinous wires (1942 by Rogers), sublaminar wires (1970), facet wires, and eventually Roy-Camille's lateral mass screws in the 1980s. The history of spinal fixation warrants a chapter in itself. Key advances took forward the principles of open reduction and internal fixation used by orthopaedic surgeons for long bone fractures and applied them to the spine. In 1953 Holdsworth and Hardy described a system of plates and screws. Transpedicular screw fixation was described by King in 1944 but not implemented until 1959 by Boucher. In 1958 Harrington described his system of dorsal instrumentation to correct scoliosis—initially due to polio and then applied to idiopathic. Ventral scoliosis surgery was first described in 1964 by Dwyer. The early focus in disc surgery was to preserve motion and avoid stiffness; this was challenged subsequently when the pathology of disc herniation was found to be secondary to instability and the drive towards fusion became popular. Contrary to this belief, others have focused on developing motion-preserving disc replacements first proposed by Fernstrom in 1966 and patented (although never implanted) by Froning in 1975. The charité intervertebral disc is now the most commonly used artificial disc.

Intradural spinal tumour surgery has progressed along similar lines to cranial surgery, with the first successful removal of an intradural tumour being credited to Horsley in 1887. Elsberg performed the first successful removal of an intramedullary tumour in 1907 and described a two-stage technique for myelotomy and then tumour removal at a second sitting. The technique of pneumoencephalography developed by Dandy was also useful in the spine and, of course, the introduction of the operating microscope greatly improved the success of intradural and intramedullary resections.

Technological advances continue at a rapid pace in spinal surgery. Recent advances in minimal access surgery, image guided screw placement, and endoscopic approaches have all developed in the last 30 years. The thoracoscopic discectomy and fusion of the 1990s has progressed to the treatment of scoliosis and corpectomies using minimal access. Laparoscopic discectomies also developed at a similar time. The father of endoscopy Desormenaux in 1853 could not have foreseen its current myriad applications. Spinal surgery continues to be a rapidly expanding field and the current population demographics mean there will be no shortage of demand for the treatment of spinal trauma, infection or, of course, the degenerative spine.

The future of neurosurgery

The last 100 years have brought dramatic advances in the practice of neurosurgery. The future is likely to see a further move away from open cranial surgery to minimally invasive, endoscopic, and radiologically guided interventional techniques.

REFERENCES

Bennett, A.H. & Godlee, R.J. (1965). Case of cerebral tumour. In: Wilkins R.H. (ed.) *Neurosurgical Classics*, pp. 361–71. New York/London: Johnson Reprint Corp.

Cushing, H. (1915). Concerning the results of operations for brain tumor. *JAMA*, **64**, 189–95.

Kerr, P.B., Caputy, A.J., & Horwitz, N.H. (2005). A history of cerebral localization. *Neurosurg Focus*, **18**(4), e1.

2

Clinical assessment

Peter Bodkin and Elizabeth Visser

Introduction

The practical process of clinical assessment in modern neurosurgery is slightly different to the traditional model. The ground rules of history taking and examination set down by William Osler and the other forefathers of clinical method rightly remain core to our approach, but we must also take into account the realities of the patient journey before the first encounter with a neurosurgeon. Whether by the bedside or in the outpatient setting, it would be rare nowadays for us not to have already been presented with pertinent background information—and indeed, often we will have seen high-quality imaging detailing the patient's pathology with great anatomical detail. The referring physician will most likely have provided a potential list of differential diagnoses. In other words, the patient has usually been neatly packaged well before we ever get to meet them.

Our job, however, is more than simply to supply a surgical fix to a given problem. We are not merely technicians. Although we must take into account the information given to us, we must never take it on face value. All sorts of errors in assessment and incorrect conclusions may have been made along the way. Likewise, imaging is very useful but should never be viewed outside the clinical context. An MRI scan will localize a lesion with more confidence than the best clinician, but technology cannot make us consider a diagnosis of acromegaly from a spongy handshake or common peroneal palsy from the sound of a slapping foot coming to the clinic door.

As we gather and make sense of this information there is an equally, if not more, important process at work. By putting the patient's symptoms into the context of their daily life we begin to develop a relationship with the patient, starting to establish trust and mutual understanding. The rapport built here will be the basis of how a patient measures the success or failure of our interventions.

The traditional neurological clinical assessment described in most textbooks has other subtle differences to those required of the neurosurgeon. This chapter aims to cover that broad spectrum of clinical method for the practising neurosurgeon and those in training.

The neurosurgical history

The main aim of the neurosurgical history is to gain sufficient information to estimate the anatomical location of the problem and to get an impression of the pathological process at work. In particular, the time course and severity of the symptoms will be important guides as to whether surgical intervention is required and how quickly.

As with any important task, being well prepared will provide a good first impression and will save time in the long run. Referral letters, clinical notes, imaging, and other investigations should have been carefully reviewed. Prior discussions with relevant team members may also be useful.

In the clinic, calling the patient from the waiting room yourself can be very valuable. An impression of their social support may be gained by seeing who is with the patient and how attentive they are. Anaesthetic fitness can be crudely assessed by how long it takes to get up and into the clinic room or how out of breath they might be. It is also an opportune moment to make an assessment of gait and a note of walking aids, and so on.

Thought should be given to the physical environment for the meeting. This should be arranged such that the patient and doctor are on as level a playing field as possible. One should be aware that being at a higher eye level or sitting behind a desk may have an intimidating effect and will detract from getting the most out of the encounter. When dealing with digital images, viewing platforms should already be opened with relevant images downloaded.

Introductions should be clear, giving your name and position. Significant others should be welcomed and acknowledged but it should be made clear that the patient is the focus of discussions.

How you open the consultation is important. One should start with open questions, 'So what's been the trouble?', or 'How can I help you?' The referral letter or consultation request has a tendency to emphasize the symptoms that will lure you into seeing the patient in the first place. It is wise, therefore, to avoid saying things like, 'So your doctor has asked me to see you about your facial pain?' Assumptions can be misleading and may encourage patients to tell you what you are expecting to hear.

Once you have encouraged the patient to tell their story, it may be necessary to fill in some gaps. The patient may have painted a picture but there could be large areas missing or fundamental details that are only sketchy. When it comes to the information that is going to influence your decision on treatment keep delving until you feel there is satisfactory detail for a conclusion to be drawn. In the course of this it is important to remember to find out the occupation of the patient and often handedness is pertinent. It is not enough to say a patient

is 'retired'. A retired university professor will have quite different expectations in life compared to a retired ship builder.

The history taking needs to cover time course, anatomical location of symptoms, variability, and character. One must refine questioning with the aim of localizing the lesion or getting clues as to the underlying pathological process. If a patient is not volunteering a symptom, one must consider symptoms that might be associated and ask about them directly. For example, when assessing a patient presenting with spatial disorientation due to a right parietal tumour one needs to remember to ask about problems with their visual fields in case of involvement of the optic radiation, and so on.

The most vital part of the story is often the impact that the condition is having on the patient's way of life. It may seem an unnecessary intrusion to pursue this but most patients are happy to let you know their problems and the knock-on effects on their home, work, and family life. By establishing that you are not solely interested in dealing with their particular pathological entity but rather you want to help them get back to doing the things they enjoy, you turn a medical interview into a more meaningful conversation. The patient will understand that you are treating them and not just their tumour or slipped disc.

Pick up cues. Have an ear for the incongruous. If what you hear doesn't make sense, explore it. Don't let it pass unmentioned. It is also useful to find out what has been done so far to address the problem: pain killers, physio, injections, visits to other physicians, and so on. Is the patient fit for an anaesthetic? Are there drugs that need to be stopped prior to surgery? Could an unhealthy lifestyle be contributing to the problem?

Drawing the history to a conclusion, the patient should feel that their issues have been adequately addressed. 'Is there anything else you'd like to discuss?' is a useful way of allowing any additional information to be voiced. The patient will hopefully be in a more relaxed and open frame of mind by this stage of the interview and might reveal underlying motivations and concerns. Finally, it may be useful to agree on a brief summary and have a final effort to clarify any lingering grey areas or inconsistencies.

The neurosurgical examination

Examination of the unconscious patient

The approach to the patient who has altered conscious level is obviously limited by the inability of the patient to comply with given instructions and to provide verbal feedback. We are therefore restricted to rather crude and basic bedside tests (i.e. examination of pupillary response to light and the Glasgow Coma Score). Often high-stake decisions are made on the basis of these assessments and it is therefore crucial that they are performed with utmost care, being mindful of possible confounding factors (Table 2.1).

Impairments of pupillary response may be due to damage at a number of locations along the afferent and efferent pathways. Direct trauma to the orbit may cause rupture of the pupil sphincter muscles and produce a traumatic mydriasis. Traumatic optic neuropathy may be due to direct disruption due to penetrating injury or indirectly by shearing forces in blunt head trauma. Lesions in the region of the pretectal nuclei or Edinger–Westphal nuclei in the rostral midbrain will also cause mydriasis. There are complex regulatory pathways from various sources including the ipsilateral hypothalamus that drives sympathetic pupillary tone and indeed poorly understood descending control from the cortex that results in ipsilateral or contralateral mydriasis or miosis following a seizure (Plum and Posner, 2007). Therefore, damage in many brain regions may result in pupillary abnormalities (Fig. 2.1). Compression of the parasympathetic fibres along the third cranial nerve by the herniating uncus is a common cause of pupillary abnormality in neurosurgical practice.

Table 2.1 Confounding factors in assessment of GCS

Glasgow Coma Score	Confounding factors
Eye opening (4 = spontaneous, 3 = to speech, 2 = to pain, 1 = do not open)	Orbital injuries Ecchymosis Photophobia
Verbal response (5 = oriented, 4 = confused, 3 = inappropriate words, 2 = incomprehensible sounds, 1 = no sound)	Non-native speakers Maxillofacial injury Endotracheal intubation/tracheostomy Deafness
Motor response (6 = obeys commands, 5 = localizes to pain, 4 = flexion/withdrawal to pain, 3 = abnormal flexion to pain, 2 = extension to pain, 1 = no movement)	Spinal cord injury Upper limb fractures, casts, and fixation

Reprinted from *The Lancet*, Vol 304, Issue 7872, Graham Teasdale, Bryan Jennett, Assessment of Coma and Impaired Consciousness A Practical Scale, pp. 81–4, Copyright (1974), with permission from Elsevier.

The Glasgow Coma Score brings together diverse clinical features to provide a guide to global brain function. Of the three divisions (eye opening, verbal response, and motor response) the motor response is most likely to differentiate the severity of injury. Lesions above the red nucleus produce decorticate posturing (flexion of upper limbs and extension of lower, rubrospinal tract function) and those below produce decerebrate posturing (extension in upper and lower limbs, vestibulospinal tract function). Normal flexion (M4) constitutes flexion with supination; abnormal flexion (M3) constitutes flexion with pronation analogous to decorticate posturing and release of rubrospinal tract function as just described; and extension (M2) is analogous to decerebrate posturing and release of vestibulospinal tract function. It is best to apply painful stimuli to trigeminal territories in case of spinal cord injury causing peripheral numbness. Pressure over the supraorbital notch is sufficient.

Rising blood pressure, falling heart rate, and altered respiratory pattern (Cushing's triad) is a classical response to raised intracranial pressure but is usually a very late, agonal feature.

Examination of language and speech disorders

It is important to appreciate any abnormalities of speech and language as this can impact on the history taking, neurological examination, and assessment of higher function and thus alter the outcome of the consultation in general. The ability to correctly identify disorders of speech can aid in localization of neurological pathology. In order for us to communicate through speech and language, hearing, understanding, voice production, articulation, consciousness, thought, and word finding must be intact. Language is a complex

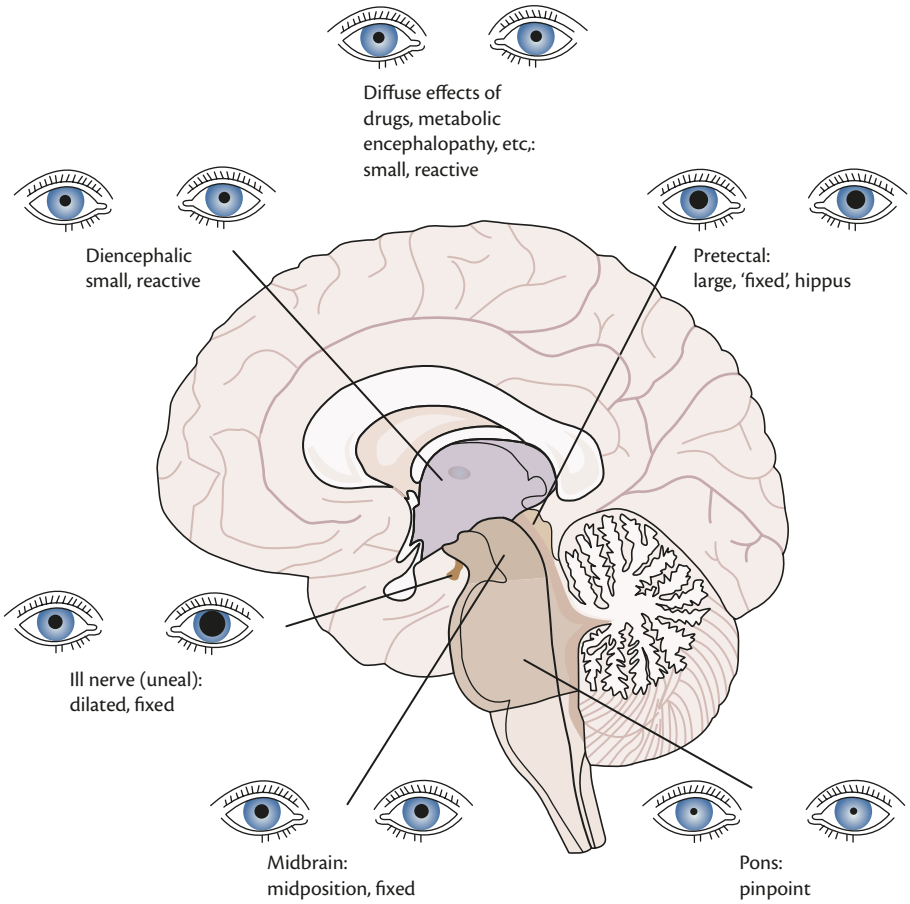
Diffuse effects of drugs, metabolic encephalopathy, etc,: small, reactive
Diencephalic small, reactive
Pretectal: large, 'fixed', hippus
Ill nerve (uneal): dilated, fixed
Midbrain: midposition, fixed
Pons: pinpoint

Fig. 2.1 Typical pupillary abnormalities associated with anatomical location of damage.
Reproduced with permission from Kandel et al., *Principles of Neural Science*, Fifth Edition, McGraw Hill, New York, Copyright © 2000.

interaction of combinations of sounds, writing, and meaning often linked to a cultural background.

To assess understanding start by engaging the patient in normal conversation and asking simple questions: 'What is your name? What is or was your occupation? How did you get here today?' Ensure that the patient can hear you properly and enquire as to what their first language is. Establish if the patient is left- or right-handed. As a rule of thumb, 99% of right-handed individuals have language dominance in their left hemisphere; 60% of left-handed patients will be left hemisphere dominant; 20% bilateral; and 20% right hemisphere dominant.

Now consider the different disorders of language defined here:

1. Aphasia—this is defined as a disorder of spoken language. It is divided into subcategories as follows:
   - **1.1** Non-fluent aphasia (anterior, motor, or Broca's);
   - **1.2** Fluent aphasia (posterior, sensory, or Wernicke's);
   - **1.3** Conduction aphasia;
   - **1.4** Transcortical aphasia (sensory and motor).
2. Alexia or dyslexia is a disorder of acquired reading ability.
3. Agraphia or dysgraphia is defined as disorders of written language.
4. Dysarthria is a disorder of articulation or speech production.
5. Dysphonia is defined as an abnormality of noise production by expired air over vibrating vocal cords.

Further examinations of these disorders include assessment of spontaneous speech, fluency, naming, repetition, articulation, speech volume, reading, and writing, and will help to localize the pathology.

1. Assessment for aphasia

Assess spontaneous speech, fluency, and if the patient uses the wrong words (paraphasia). Ask the patient to name animals or words beginning with 'F' in a minute. This tests word finding ability. Also ask them to name familiar objects: a pen, a watch, a tie, and so on. Now ask the patient to repeat phrases. Table 2.2 summarize the findings on examination and localization.

2. To assess for alexia or dyslexia, ask the patient to read a sentence or obey a written command.
3. Agraphia or dysgraphia can be examined by asking the patient to write a sentence; this can only be assessed if there is no motor disability.
4. Dysarthria is examined by asking the patient to repeat a phrase; for example, 'red lorry, yellow lorry' requires intact lingual function and 'baby hippopotamus' requires intact labial function. Listen for slurring and rhythm of speech. Dysarthria can be described as spastic (caused by pseudobulbar palsy as in motor neuron disease), extrapyramidal (associated with Parkinsonian syndromes, often associated with dysphonia), cerebellar dysarthria (associated

Table 2.2 Assessment of aphasia (Clark, 2009; Fuller, 2013)

	Comprehension	Fluency	Naming	Repetition	Other features	Localization
Non-fluent aphasia	Intact	Non-fluent	Impaired	Impaired	Right hemiplegia, depressed	Left frontal lobe (inferior and temporal insula), Broca's area
Fluent aphasia	Impaired	Fluent	Can be intact	Impaired	Neologisms, meaningless speech, paranoid, could have a visual field defect	Posterior superior temporal lobe, Wernicke's area
Conduction aphasia	Intact	Fluent	Impaired	Impaired	Depressed, cortical sensory loss right arm	Parietal operculum/ arcuate fasciculus
Global aphasia	Impaired	Non-fluent	Impaired	Impaired	Right hemiparesis worst in arm	Peri-Sylvian, both Wernicke's and Broca's areas
Nominal aphasia		Non-fluent	Impaired			Angular gyrus
Transcortical motor aphasia	Intact	Fluent	Impaired	Intact	Halting, effortful speech	Left anterior superior frontal area
Transcortical sensory aphasia	Impaired	Fluent	Can be intact	Intact	Semantic paraphasia	Posterior temporo-occipital-parietal area
Transcortical mixed aphasia	Impaired	Non-fluent	Impaired	Intact		Both Wernicke's and Broca's areas

Data from Clarke, C; Howard, R; Rossor, M; Shorvon, S. (2009) *Neurology: A Queen Square Textbook*. Wiley-Blackwell (p. 252–4), Fuller, G. (2004) Neurological Examination Made Easy, 3e. Churchill Livingstone. (p. 17–25).

with multiple sclerosis, alcohol intoxication, or inherited ataxia), and lower motor neuron dysarthria (this is caused by lesions affecting palatal movement causing nasal speech, tongue movements causing patients to struggle with the letters 'T' and 'S' and facial movement resulting in difficulty with the letters 'B', 'P', 'M', and 'W' and often involves the lower cranial nerves).

5. Finally listen to the volume of speech; if this is reduced it is described a dysphonic speech.

The lobar examination

The examination of the functions of the individual lobes of the brain should be a familiar and fluent part of the neurosurgeon's assessment. One should be aware of the somewhat arbitrary divisions between the lobes, however, and it may well be that one should test more than one lobe if the lesion is on or near a dividing sulcus. Anatomically, Yasargil's seven lobe system is most satisfactory (frontal, central, parietal, occipital, temporal, insular, and limbic; see Ribas, 2010) but here we will use frontal, parietal, temporal, occipital, and cerebellum.

Frontal lobe

As one might expect, as it is the largest lobe, frontal examination has the most components and complexity (Box 2.1). Anatomically, it is useful to consider four distinct regions—the precentral gyrus, the dorsolateral cortex, the orbitofrontal cortex, and medial cortex (Fig. 2.2).

The assessment of the function of the primary motor cortex requires testing for upper motor neurone signs on the opposite side. The patient may adopt postures typical of pyramidal weakness (i.e. flexors stronger than extensors in the upper limbs and vice versa in the lower limbs). Pronator drift is perhaps the archetypal neurosurgical test and is extremely useful in bringing out subtle weakness. Lying anterior to the primary motor cortex lies an area known laterally as the premotor cortex and medially as the supplementary motor area (SMA). The functions of these areas are complex but act in conjunction with the primary motor cortex. The cortical area immediately anterior to the primary motor cortex (Brodmann's Area 6) comprises of the lateral premotor area on the lateral aspect and the SMA on the medial and interhemispheric aspect. The lateral premotor area has reciprocal connections with the cerebellum and is involved with refinement of movements with external sensory cues. The SMA has reciprocal connections with the basal ganglia and is involved with initiation of movements from internal sensory cues. In contrast to the primary motor cortex homunculus (leg medial, upper limb, face, and tongue lateral) the SMA homunculus is arranged horizontally (leg posterior adjacent to the paracentral lobule and primary motor area for leg, upper limb, then face and tongue more anteriorly). The SMA has roles in postural stability in walking, initiating and sequencing movements, and coordination of both sides of the body. Frontal lobe ataxia causes a characteristic magnetic gait as if stuck to the floor (Brun's apraxia). This has similarities to Parkinsonian gait, but does not have the lack of arm swing. It is part of the clinical triad of normal pressure hydrocephalus (disturbance of gait, continence, and cognition). This reflects the anatomical proximity of the micturition inhibitory area (just inferior to

Box 2.1 Scheme for frontal lobe assessment

- Ask about handedness and assess speech
- Observe behaviour—abulia, inappropriate dress, verbal dysdecorum
- Posture/gait—decorticate, 'magnetic'
- Pyramidal weakness
- Saccadic eye movements
- Primitive reflexes
- Look for urinary catheter
- Anosmia and Foster Kennedy syndrome
- Neuropsychological tests—echopraxia, perseveration, conceptualization, working memory

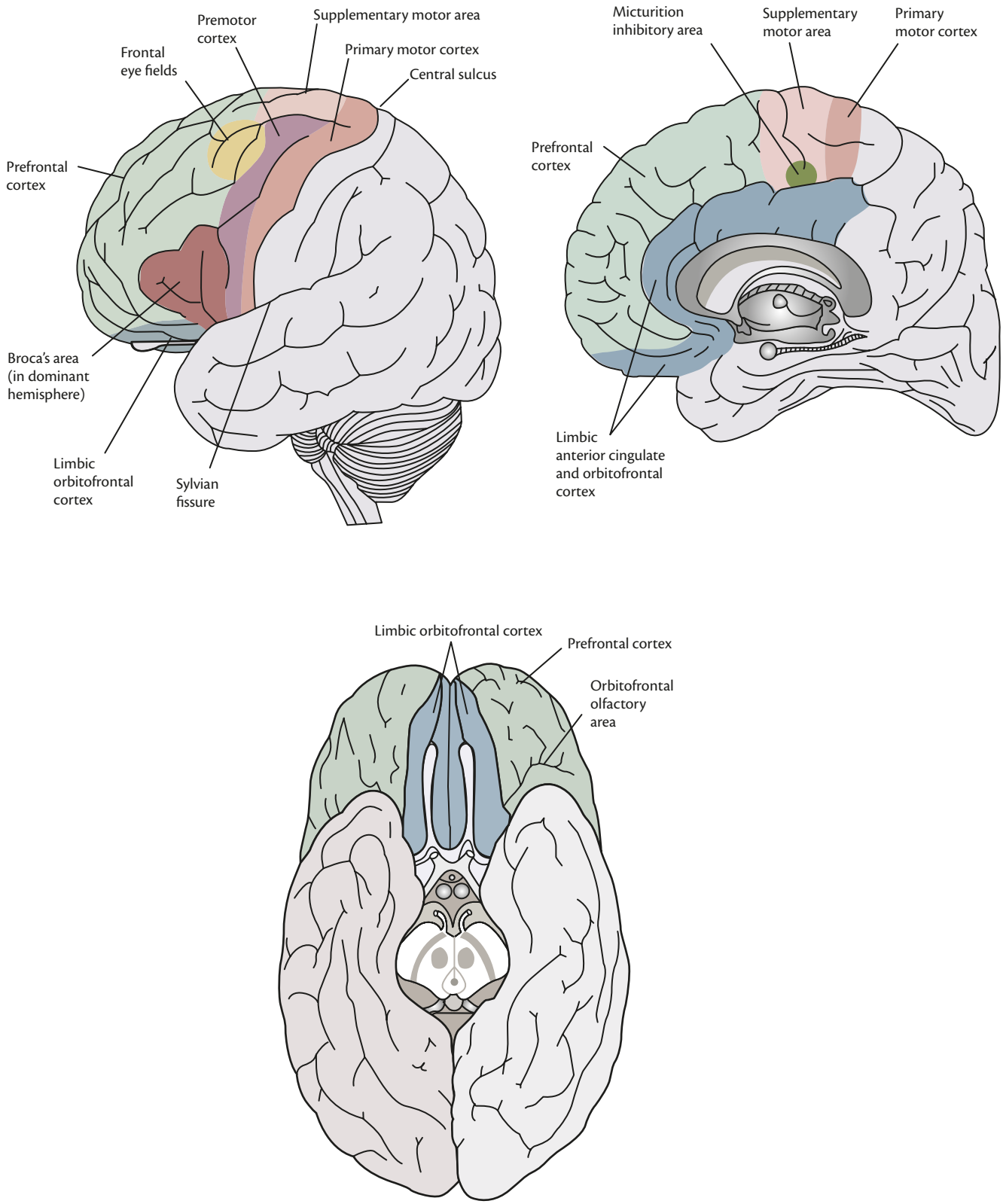

Fig. 2.2 The frontal lobe.
Neuroanatomy through Clinical Cases, 1st Edition by Blumenfeld (2002) Fig.19.11 p. 848. By permission of Oxford University Press, USA.

the SMA) and the more diffuse role of the frontal lobe in cognition. Frontal lobe dysfunction may also cause gegenhalten—the resistance to passive movement.

The frontal eye fields (FEFs, Brodmann's Area 8) lie in the posterior part of the middle frontal gyrus and adjacent precentral sulcus. A mass lesion here may result in horizontal conjugate gaze deviation

towards the side of the lesion (Prévost or Vulpian sign). Seizures will result in looking away from the lesion. Saccadic eye movement should be tested by asking the patient to look between two fixed points (e.g. a fist and a finger) while keeping the head still. Damage to the FEF may result in impaired saccades away from the lesion.

Re-emergence of primitive reflexes or 'frontal release signs' may also be demonstrated. The grasp reflex is assessed by gently passing a finger across the palm. It is most reliably done by distracting the patient by asking them to count backwards from ten. The palmomental reflex is a brief contraction of the ipsilateral mentalis muscle in response to stroking the palm. The snouting reflex is seen when the lips purse in response to tapping the upper lip or the sucking reflex when pressing an object to the lips. Glabellar tap may also cause persistent blinking, whereas in the normal individual it attenuates. It should be remembered that these reflexes may well be seen in normal individuals, particularly in older people (25% of normal adults have the palmomental reflex; see Brazis et al., 2011).

The prefrontal area contains a large volume of brain that has complex roles in control of behaviour. One may divide these into restraint (the restriction of behaviour to that which is socially and culturally acceptable), initiative (motivation to put thoughts into action), and order (to sequence tasks appropriately; see Blumenfeld, 2002). Simply observing and talking with the patient will give insights into this. Apparently quite contradictory behaviours may be encountered, some patients lacking any kind of 'get up and go' compared to others for whom it is difficult to stop talking, or who are overfamiliar or tactless. In general, abulia is more frequently seen in lesions of the dorsolateral convexity whereas disinhibition is often an orbitofrontal feature. There are many neuropsychological tests that are pertinent to examining the frontal lobes (**Box 2.2**).

Parietal lobe

The parietal lobe (**Fig. 2.3**) may be divided into the postcentral gyrus, posteriorly is the superior parietal lobule and inferior parietal lobule (angular and supramarginal gyrus). Processing of somatic sensations and perceptions occurs in the postcentral gyrus (monomodal); the posterior parts are polymodal assimilating inputs from somatic, visual, and other sensory modalities mostly for the control of movement especially the hand and upper limb (Kolb and Whishaw, 2009). The left inferior parietal lobule has a role in language and is considered under that heading. Disorders of the parietal lobe will impair sensation. However, as much of somatic sensation is processed in the thalamus there will not be complete numbness but rather more subtle impairments. These may be tested looking for sensory extinction, astereoagnosia, dysgraphasthesia, and two-point discrimination (**Box 2.3**).

Lesions of the dominant parietal lobe have been associated with a collection of signs known as Gerstmann's syndrome. Although rare in combination, it is still useful to have these four signs in mind for completeness of examination (**Box 2.4**). For the non-dominant parietal lobe (**Box 2.5**) there is a preponderance for there to be contralateral neglect. This may be noted from the patient's appearance with lack of grooming on one side. Other features may become apparent such as loss of geographical orientation (getting lost in familiar places), dressing apraxia, and anosognosia (lack of awareness of illness).

Box 2.2 Neuropsychological tests of frontal lobe function

Luria's three-step test
This tests motor sequencing. Tell the patient you are going to show him a series of hand movements. Without verbal prompting show a sequence of fist, edge, palm, and repeat five times. Ask the patient to do the same. The patient may demonstrate perseveration with repetition of the same movement or be quite unable to do the sequence in order.

Go/no-go test
This tests ability to shift set. Hold two fingers out palm down—'put out one finger when I do this', hold down one finger—'put out two fingers when I do this'. Do this several times. Then change the instructions. Place two fingers—'put out one finger when I do this'. Place one finger—'do nothing when I do this'. The inability to follow the second set of instructions implies a deficit.

Verbal fluency
Produce as many words beginning with a particular letter in one minute, proper nouns not allowed. Normally 12 or more.

Tower of Hanoi
A game moving discs between stacks aiming to achieve goal in as few moves as possible

Wisconsin card sorting test
This is a card matching test testing executive function.

Stroop test
Read out a list of coloured words (i.e. the word green spelt out in yellow text). Test of restraint.

Temporal lobe

The temporal lobes have roles in processing auditory information (Heschl's gyrus), visual information (inferotemporal cortex), emotion (amygdala), and memory and spatial navigation (hippocampus). Its role in language is important especially in the vocalization (dominant) and perception of (non-dominant) emotion in language (emotional prosody). It should be recalled that Meyer's loop passes over the roof of the temporal horn and lesions may, therefore, cause a 'pie in the sky' quadrantanopia. Apart from simple tests of memory, speech, and visual fields there are limited bedside tests for the temporal lobe. Neuropsychologists may perform dichotic listening tests where different recordings are presented to either ear of a pair of headphones to assess selective auditory attention or may carry out advanced tests of verbal and non-verbal memory.

Occipital lobe

Vision and its interpretation is the primary function of the occipital lobe and is dealt with in that section.

Cerebellum

The cerebellum coordinates smooth, planned motor actions by analysing extensive sensory inputs from the brain and spinal cord. The midline structures (the vermis and flocculonodular lobes) control coordination of trunk and eye movement. The cerebellar hemispheres maintain control of limb movement and aid motor planning. Because cerebellar outputs remain ipsilateral or cross twice, lesions of a cerebellar hemisphere will cause an ipsilateral deficit. Ataxia is a characteristic sign of cerebellar dysfunction. Movements are clumsy due to poor coordination between agonist and antagonist muscle groups. There is imprecision of trajectory though space (dysmetria) and also in timing of movements. Truncal ataxia may make even sitting up in bed very difficult. Gait may be wide-based and staggering. Appendicular ataxia may be tested by asking the patient to repeat rapid alternating movements of the limbs (e.g. supinating/pronating one hand on the other). When abnormal this is known as dysdiadochokinesia. One can also ask the patient to outstretch their arm, then touch their nose, or to touch the examiner's finger and back to their nose. An intention tremor may be also elicited. Holmes

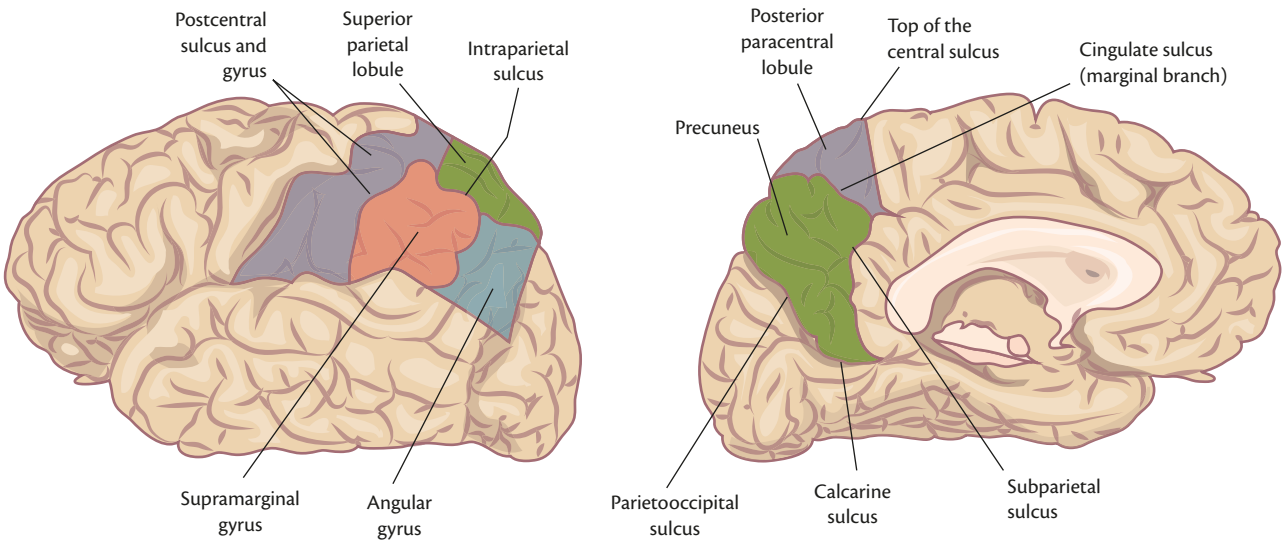

Fig. 2.3 Parietal lobe.

This article was published in Gross Anatomy and General Organization of the Central Nervous System in Nolte's *The Human Brain*, John Nolte, Copyright Elsevier (2009).

rebound test demonstrates overshooting. For example, with arms outstretched and eyes closed, the examiner pushes one arm downward. On release the patient's arm shoots up higher than originally placed. There is ipsilateral hypotonia and a pendular knee jerk may be found. The cerebellum has a role in articulation and when damaged will cause dysarthria with laboured, slurred speech. Mutism is a well-recognized problem following surgical resections in the midline, well documented in children following medulloblastoma resection. The anatomical basis is from disruption of a dentato-rubro-thalamo-cortical pathway such that bilateral dentate nucleus injury causes mutism. This explains why dominant hemisphere SMA injury, bilateral thalamotomies and mesencephalic strokes (red nucleus) can result in the same syndrome. Cerebellar mutism was originally, mistakenly, attributed to approaches that split the vermis given the close proximity of the dentate nuclei to the midline.

Nystagmus may also be present with the fast phase towards the abnormal side. Vertical nystagmus (e.g. downbeat nystagmus may be seen in Chiari malformation). Head tilt may occur in children with posterior fossa lesions. Cognitive-affective symptoms are increasingly being recognized in cerebellar disorders.

Box 2.3 Examination of parietal lobe function (either hemisphere)

Sensory extinction
Ask patient to hold out arms with eyes shut. Touch either one or both sides of the corresponding part of the body and ask where he has been touched. Extinction occurs when the patient says that only one side is being touched when in fact it is both.

Stereognosis
With the patient's eyes closed, place a familiar object in their hand and ask them to identify it. Coins of different denominations may be used.

Graphesthesia
Ask the patient to identify the number or letter that you trace on their palm. It should be agreed which way is up before starting.

Two-point discrimination
Using callipers or a bent paper clip, ask the patient if they can feel one or two points. On the fingertips one should be able to recognize two separate points to about 2–4 mm apart, on the palm 8–15 mm.

Visual fields
Examine for homonymous inferior quadrantanopia.

Constructional apraxia
Ask patient to copy a 3D drawing.

Box 2.4 Parietal lobe examination—dominant hemisphere (Gerstmann's syndrome)

Dyscalculia
Ask the patient to subtract 7 from 100 and continue subtracting 7 sequentially.

Agraphia
Ask the patient to write a simple sentence.

Finger anomia and left-right disorientation
These two can be examined together by crossing your hands and asking, 'Which finger am I wiggling?' (Fig. 2.4) or alternatively asking the patient to touch their right ear with their left ring finger. Remember to also assess speech (see earlier).

Fig. 2.4 Testing finger anomia and left-right disorientation: 'Which finger am I wiggling?' Correct answer: 'Your left ring finger.'

Box 2.5 Parietal lobe examination—non-dominant hemisphere

Unilateral spatial neglect

Ask the patient to mark the middle of a horizontal line. Displacement of the centre towards the side of the brain lesion (generally right hemisphere) indicates neglect. Target cancellation tests can also be used. This is where a patient is asked to circle every 'a' on a page or something similar. Only one side of the page will be attended to.

Crossed response test

Ask patient to move the limb opposite the one that is touched (motor neglect).

Dressing apraxia

Ask the patient to take off a jumper or other item of clothing. Turn it inside out and ask the patient to put it back on the right way.

Paper cutting

Ask patient to use a pair of scissors to cut out a shape from a piece of paper.

The visual system examination

This section will detail the examination of the eye and cranial nerves II, III, IV, and VI. A thorough history is necessary to understand the patient's range of visual symptoms. These may include drooping eyelids, blurred vision, double vision, 'seeing things', visual loss (transient or persistent, partial, or complete), abnormal movements of the visualized world, eye pain, headache, or orbital pain. In this section we will provide an examination example that avoids missing the most important eye signs.

The neuro-ophthalmological examination should include:

1. *Visual acuity*

   Optic nerve, chiasmal, optic tract lesions, and ocular pathology can all influence visual acuity. This is assessed with corrected vision or refractive vision, like the patient's own glasses or a pin hole. The standard is the Snellen chart that measures vision at a distance of 6 metres. This is expressed as a fraction (distance in metres from chart/distance in metres at which letters should be seen). If the acuity is reduced but is correctable with refraction; this is due to an ocular defect. If the acuity is not correctable, then it signifies a problem in the visual pathway. If the patient is unable to see the largest print, the chart can be brought closer or assessed by finger counting, perception of hand movements, or perception of light.

2. *Colour vision*

   This is most useful for assessing the optic nerve function. It is assessed by using Ishihara plates and scored in each eye individually by the number of plates correctly identified. The speed of identifying the plate should also be considered when comparing the eyes. Remember that 8% of males and 0.5% of females may have X-linked recessive congenital colour deficiency or dyschromatopsia. In these patients the loss of colour vision will be bilateral with normal visual acuity and fields. A cruder method of assessing colour vision is to ask the patient to look at a coloured target like a red cap and in the affected eye it may seem faded or 'washed out'.

3. *Visual field testing*

   Visual fields are tested to direct confrontation and each eye is assessed individually. The patient should fixate on the examiner's nose and cover each eye in turn. This test can detect hemianopia, quadrantanopia, altitudinal, and central field defects. With the eye covered ask the patient if all the parts of the examiner's face are clear, or if there are parts that are blurred or missing. Ask the patient to count fingers in each quadrant.

   Peripheral fields are best assessed with a white hat pin, whereas central fields and blind spots should be tested with a red hat pin. The latter is assessed against the examiner's blind spot by moving the pin. Visual field defects are mapped out according to the patient's description. Abnormalities are illustrated as follows (see Fig. 2.5) and can localize the defect in the visual pathway All patients with a suspected visual field

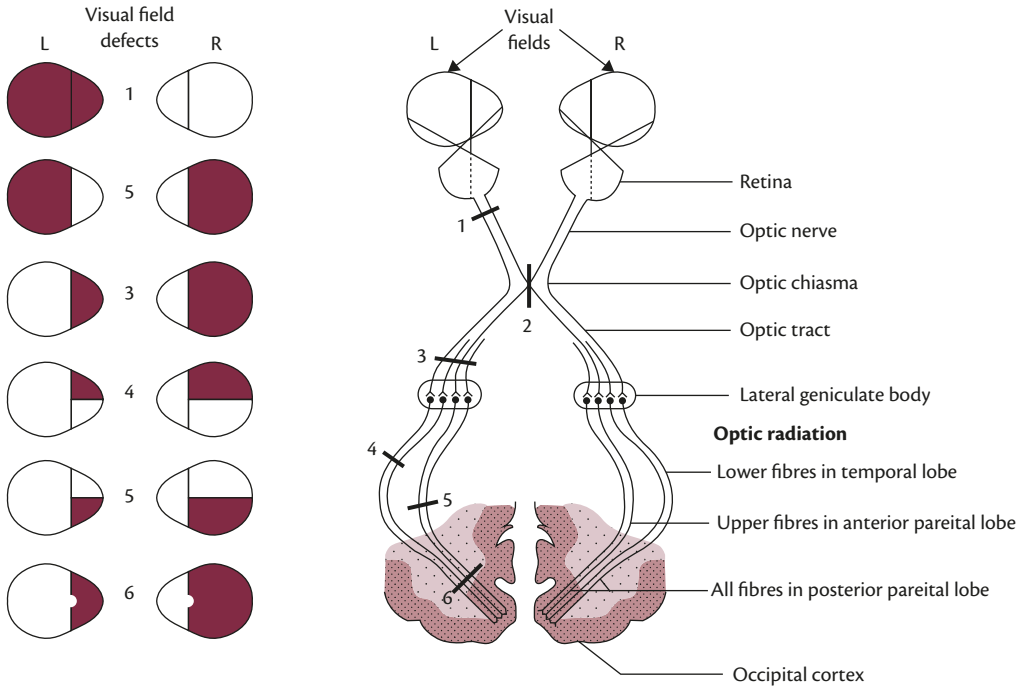

Fig. 2.5 Assessment of visual fields and localization of defects.
From: *Macleod's Clinical Examination*, Ninth edition figure 7.8 page 211, J. Munro and C.R.W. Edwards.

Box 2.6 Parinaud's syndrome

- Impairment of upgaze
- Large irregular pupils that do not react to light but can accommodate (light-near dissociation)
- Eyelid abnormalities—lid retraction or ptosis
- Impaired convergence
- Nystagmus retractorius

defect should have formal perimetry for accurate localization and monitoring. Macular sparing with ischaemic occipital lobe lesions relates to the dual blood supply to the occipital pole from both the middle cerebral artery as well as the posterior cerebral artery.

4. *Pupils*

The pupillary light reaction pathways include the optic nerve (afferent) and the parasympathetic component of the third cranial nerve (efferent). Accommodation arises from the frontal lobes (afferent) and the parasympathetic component of cranial nerve III (efferent).

Inspect first for anisocoria, and then ask the patient to fixate on a distant target and then test the direct and indirect light reflexes, the pupillary reactions to accommodation and finally perform the swinging light test.

4.1 *Size*

The examination of the pupils should first be conducted in room light, if the anisocoria is greater in light than in dark, the parasympathetic system is abnormal, and the larger pupil is abnormal. A cranial nerve III paresis, Adie's pupil, or damaged iris sphincter are examples of the parasympathetic pathway. Then examine for anisocoria in dim light, if this is greater in dim light, a sympathetic dysfunction is present and the smaller pupil is abnormal. Horner's syndrome is a manifestation of a sympathetic disorder. If the anisocoria is the same under both conditions, it is not indicative of a neurological problem.

Conditions that impair light response but do not affect accommodation (light-near dissociation) include Parinaud's syndrome (Box 2.6), neuro-syphilis, diabetes mellitus, Adie's pupil, bilateral optic neuropathy, and aberrant regeneration of cranial nerve III.

4.2 *Light response (direct and indirect)*

Shine a bright light in each eye, and observe the pupils for speed and magnitude of constriction (see Fig. 2.6). If the pupil does not react normally to light, examine the response by viewing a near target. Again, check for speed and magnitude of constriction to a near target and the speed of dilatation when looking at a distant target.

4.3 *Swinging light test*

To perform this test the lights should be dimmed while the patient should fixate on a target in the distance. Swing the light from eye to eye for about a second at a time. Look for the initial movement in each pupil (normally constriction). To diagnose a relative afferent pupil defect (RAPD), one pupil should consistently dilate rather than constrict. The presence of a RAPD is indicative of optic neuropathy (Table 2.3).

5. *Ophthalmoscopy*

For the purposes of this chapter we advise that ophthalmoscopy should be performed on all patients to examine for papilloedema that can suggest raised intracranial pressure and optic pallor suggestive of optic atrophy. Systematically examine the optic disc, the bloods vessels, and then the retinal background.

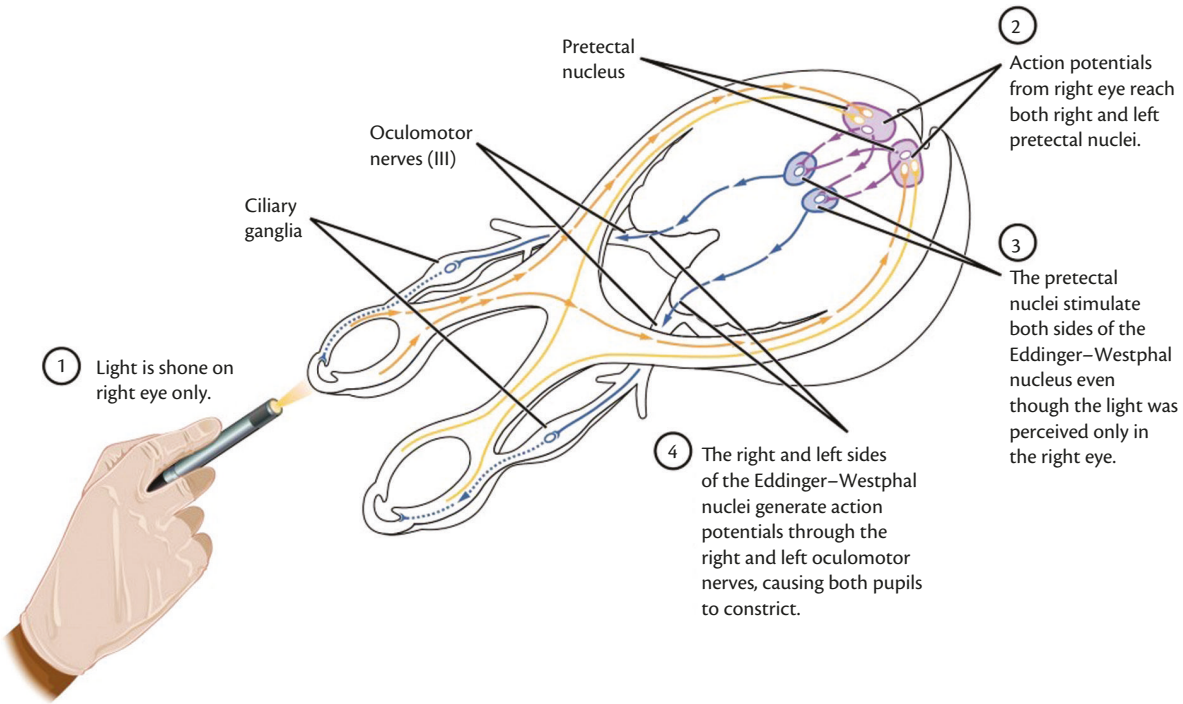
Pretectal nucleus
2
Action potentials from right eye reach both right and left pretectal nuclei.
Oculomotor nerves (III)
Ciliary ganglia
3
The pretectal nuclei stimulate both sides of the Eddinger–Westphal nucleus even though the light was perceived only in the right eye.
1
Light is shone on right eye only.
4
The right and left sides of the Eddinger–Westphal nuclei generate action potentials through the right and left oculomotor nerves, causing both pupils to constrict.

Fig. 2.6 The light reflex.

Authored by: OpenStax College. Provided by: Rice University. Project: Anatomy & Physiology. http://cnx.org/content/col11496/latest/

Table 2.3 Relative afferent pupil defect (Pane, 2007)

Normal pupil		
Light stimulus	**Right pupil**	**Left pupil**
None	•	•
Left	•	•
Right	•	•
Left relative afferent pupil defect		
Light stimulus	**Right pupil**	**Left pupil**
None	•	•
Left	•	•
Right	•	•

This article was published in *The Neuro-ophthalmology Survival Guide*, A Pane, p 379, Copyright Elsevier (2007).

Table 2.4 summarizes some findings that can aid in the localization of lesions that present with visual symptoms using the techniques described so far.

6. *Eye movements*

6.1 *Fixation, nystagmus, and saccades*

Disorders of fixation include nystagmus and saccadic intrusions. The examination will stem from a history of involuntary eye movements or oscillopsia. Congenital fixation disorders are usually asymptomatic and incidentally noticed.

Nystagmus is the rhythmic oscillation of the eyes. Start the examination with eyes in the primary position, then different positions of gaze. Note the fast phase of the nystagmus and the direction or if it is pendular. Also note if the nystagmus is similar in both eyes and if there is a latent component or increased nystagmus with one eye covered. Different types of nystagmus can aid in localization of pathology as summarized in Table 2.5.

Assessing how rapidly and accurately patients can fixate on an eccentric target by testing saccades can expose a subtle internuclear ophthalmoplegia or sixth cranial nerve palsy. It is tested by asking the patient to look at two different objects on either side of the patient's head. The patient is asked to alternate gaze between the objects. Note saccadic initiation, velocity, and accuracy. This can be either too small (hypometric) or too large (hypermetric).

6.2 *Eye movements and cranial nerves III, IV, and VI*

Eye movements include saccades controlled by the frontal lobe, pursuit (the slow movement that facilitate fixation on a moving object) that is controlled by the occipital lobe, the vestibulo-ocular reflex (that allows compensation of eye position for movement of the body or head) controlled by the cerebellar vestibular nuclei and convergence (fixating on an object close to the face) that is controlled by the midbrain. Input from the different control centres have to be integrated to allow synchronous eye movement. The medial longitudinal fasciculus (MLF) in the midbrain runs between the nuclei of cranial nerves III and IV in the midbrain and VI in the pons. The eye muscles are the lateral rectus controlled by cranial nerve VI, the superior oblique controlled by cranial nerve IV, and all the rest are controlled by cranial nerve III.

6.2.1 *Cranial nerve III palsy (oculomotor nerve)*

A complete palsy is a triad of ptosis, a large and unreactive pupil, and the eye position of 'down and out' (Fig. 2.7). Pupil sparing implies that the deeper nerve fibres have been affected most likely from ischaemia. The parasympathetic fibres lie circumferentially on the outside of the nerve and are more commonly affected by compressive causes, classically a posterior communicating artery aneurysm.

Internuclear ophthalmoplegia is the result of a lesion of the MLF. The patient has dysconjugate eye movements; there is incomplete adduction of one eye and jerky nystagmus of the other eye on abduction when testing lateral gaze. It is described as left-sided when there is failure of left adduction when looking to the right (Fig. 2.8). The horizontal conjugate gaze centre resides in the paramedian pontine reticular formation at the level of the fifth cranial nerve nucleus. On an attempt to move the eyes in a horizontal direction, the abducting eye is able to move (VI) but the signal to the third nerve is unable to pass through the MLF to the third nerve is nucleus and there is a failure of adduction. The resulting diplopia may underlie the nystagmus in the abducting eye as there is an attempt to overcome this. The vertical gaze centre resides in the rostral interstitial nucleus of the MLF (riMLF) at the level of the third nerve/superior colliculus.

Table 2.4 Localization of lesions in the visual system (see Beck and Smith, 1988)

	Optic nerve	Optic chiasm	Optic tract	Temporal lobe	Parietal lobe	Occipital lobe
Visual acuity	Normal or reduced	Normal or reduced	Normal or reduced	Normal	Normal	Normal
Colour vision	Normal or reduced	Normal or reduced	Normal or reduced	Normal	Normal	Normal
Visual field	Central scotoma	Bitemporal	Homonymous incongruous	Homonymous superior	Homonymous inferior or complete	Homonymous exquisitely congruous
Relative afferent pupil defect	Present	Present or absent	Present or absent	Absent	Absent	Absent
Disc pallor	Present or absent	Present or absent	Present or absent	Absent	Absent	Absent

Beck & Smith, *Neuro-Ophthalmology: A Problem-Oriented Approach*, 1e, Little Brown & Co, USA, Copyright © 1987.

Table 2.5 Types of nystagmus and neurological localization

Type of nystagmus	Localization
Down beat	Craniocervical junction
Periodic alternating	Craniocervical junction
Gaze-evoked	Vestibular, cerebellum
Up beat	Cerebellum, medulla
Seesaw	Diencephalon, mesencephalon
Torsional	Central vestibular
Convergence–retraction	Dorsal midbrain
Rebound	Cerebellum

Beck & Smith, *Neuro-Ophthalmology: A Problem-Oriented Approach*, 1e, Little Brown & Co, USA, Copyright © 1987.

6.2.2 *Cranial nerve IV palsy (Trochlear nerve)*

This presents with diplopia on looking down and head tilt away from the side of the palsy with no clear squint (Fig. 2.9). The pupil of the affected eye may lie slightly higher than the normal eye, but this is not obvious.

On suspecting a fourth nerve palsy, it is useful to ask the patient to look at a horizontal object (e.g. the top of the door frame alternately with each eye). A trochlear palsy will produce two images angled towards the abnormal side (Fig. 2.10).

6.2.3 *Cranial nerve VI palsy (Abducens nerve)*

This presents with diplopia with two images with horizontal separation (Fig. 2.11). There is a squint, diplopia away from the weak muscle. The pupil is normal.

7. *Lid position*

Inspect for the eyelid position, contour, and measure the palpebral fissures keeping the eyes in the primary position. The upper lid usually covers 1 mm of the cornea, more than that indicates ptosis. Also examine for variable ptosis in different directions of gaze as seen in congenital ptosis and Duane's syndrome. Fatigable ptosis (>2 mm after 2 minutes) on up gaze is suggestive of neuromuscular weakness such as myasthenia gravis.

8. *Orbits*

Finally, during inspection of the orbits one should look for proptosis, enophthalmos, or ocular injection. One should stand behind the patient to assess proptosis looking down over the forehead. A Hertel exophthalmometer provides a more accurate measurement. It may be useful to auscultate over the closed eyelid for a bruit that could signify a carotid-cavernous fistula.

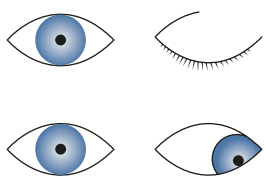

Fig. 2.7 Left third nerve palsy.
From Fuller, G. (2004) *Neurological Examination Made Easy*, 3e, Churchill Livingstone, p. 88, Fig 9.4.

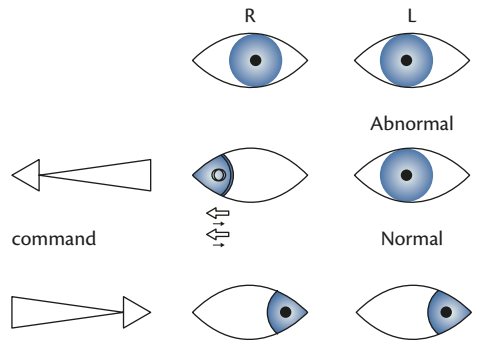

Fig. 2.8 Left internuclear ophthalmoplegia.
From Fuller, G. (2004) *Neurological Examination Made Easy*, 3e. Churchill Livingstone, p. 88, Fig 9.6.

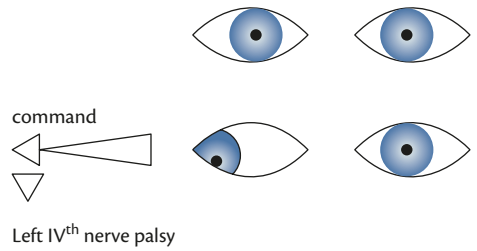

Fig. 2.9 Left fourth nerve palsy.
From Fuller, G. (2004) *Neurological Examination Made Easy*, 3e. Churchill Livingstone, p. 88, Fig 9.4.

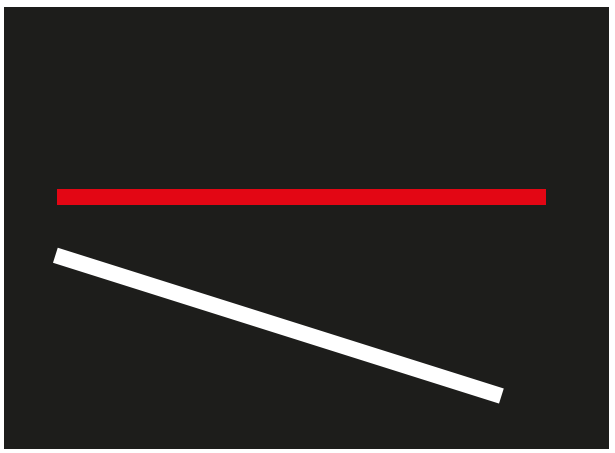

Fig. 2.10 'Door frame' test of patient with left fourth nerve palsy—two images pointing to abnormal side.

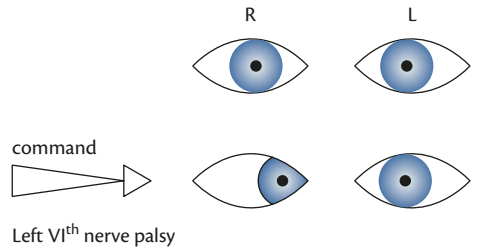

Fig. 2.11 Left sixth nerve palsy.
From Fuller, G. (2004) *Neurological Examination Made Easy*, 3e. Churchill Livingstone, p. 88, Fig 9.4.

Examination of the cranial nerves

This section will include the examination of the cranial nerves not discussed in the section on eye examination.

1. Cranial nerve I (olfaction). Ask if the patient has noticed any change in smell. Examine with two different smells (e.g. coffee or orange). Olfactory test kits are available.
2. Cranial nerve II (typically acuity, fields, and pupillary function). A complete examination would also include fundoscopy, assessment of blind spot, and colour vision.
3. Cranial nerves III, IV, and VI (eye movements).
4. Cranial nerve V (sensation to the face and muscles of mastication). The trigeminal nerve has both motor and sensory components: the maxillary division is the nerve of the first branchial arch derivatives. The motor examination is performed by palpating the muscles of mastication when the patient clenches the jaw and look for jaw movement when asked to open the mouth against resistance. Also tap the jaw jerk. The sensory examination is performed by testing all three divisions of the trigeminal nerve (ophthalmic, maxillary, and mandibular divisions) with light touch. Lastly, perform the corneal reflex (afferent limb Va, efferent limb VII) by gently touching the cornea with a small piece of cotton wool. The approach to the cornea should be lateral to the field of vision. An alternative method is to gently blow in the eye and assess response. Also note the normal conjunctival reaction of lacrimation and injection.
5. Cranial nerve VII (facial expression and taste to anterior two-thirds of the tongue). The facial nerve innervates the muscles of facial expression, stylohyoid, stapedius, and the posterior belly of the digastric muscle, and is the nerve of the second branchial arch (Fig. 2.12). When facial weakness occurs it is important to decide if the weakness is upper (UMN) or lower motor neuron

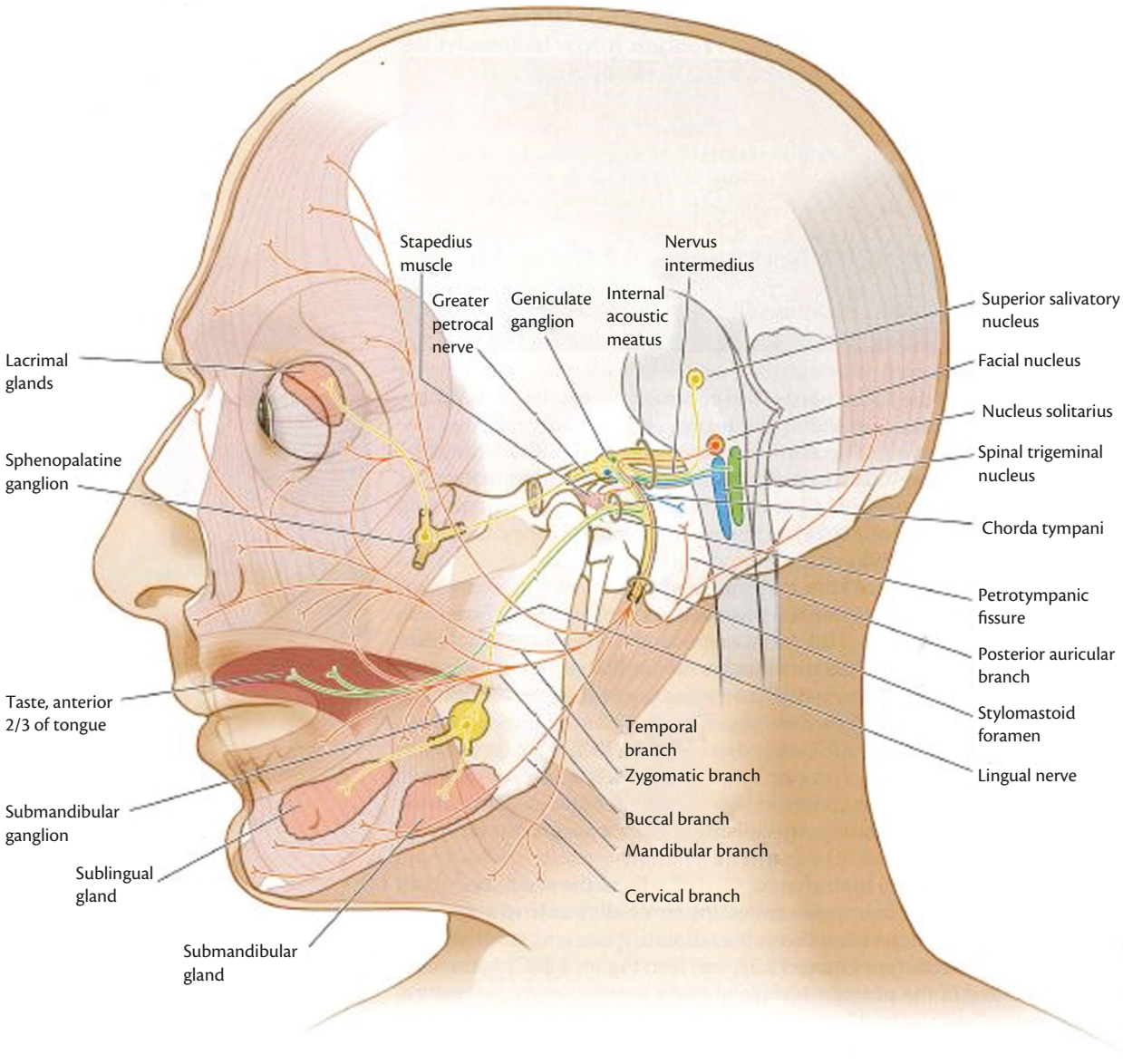

Fig. 2.12 Facial nerve—motor, parasympathetic, and special sense innervation.
Blumenfeld, Hal. (2002) *Neuroanatomy through Clinical Cases*. Sunderland, Massachusetts: Sinauer. Fig 12.10, chapter 12 p. 480.

(LMN). The different clinical features are explained by the bilateral innervation from the nuclei of the facial nerve supplying the superior facial muscles. Firstly, look for asymmetry in facial movement, which can be very subtle: just a hint of incomplete eye closure, slow blinking, or delay in a grin. Then ask the patient to raise the eyebrows (frontalis, temporal branch), close the eyes tightly (orbicularis oculi, zygomatic branch), blow out the cheeks (buccinators) or whistle (orbicularis oris, both buccal branch), show your teeth (zygomaticus major, buccal or marginal mandibular branch), wrinkle the chin (mentalis, marginal mandibular branch), and wrinkle the neck (platysma, cervical branch). The severity of facial palsy is classified using the House–Brackmann scale (see Chapter 24 on the surgical management of cerebellopontine angle lesions).

In UMN weakness the forehead is seen to be stronger than the lower face, also called sparing of the forehead. Unilateral weakness can be due to vascular lesions, demyelination, tumours, or brain stem lesions. Bilateral weakness can be due to pseudobulbar palsy or motor neuron disease.

In LMN weakness, the lower face is seen to be as weak as the forehead. Bell's palsy is a common cause of this and is usually worst within 12 hours from the onset and can be associated with pain around the mastoid, loss of taste, and hyperacusis. Other causes of LMN facial weakness are pontine lesions, cerebellopontine angle lesions, and parotid tumours. Causes of bilateral LMN facial weakness are disorders of the neuromuscular junction like myasthenia gravis, motor neuron disease, myopathies, neurosarcoidosis, or Guillain–Barré syndrome.

6. Cranial nerve VIII (auditory and vestibular nerves). The auditory examination is conducted by testing each ear individually. Cover the ear on the opposite side of the ear being tested. Test the hearing by rubbing your fingers together or whispering. If there is reduced hearing, perform Rinne's and Weber's tests. For these tests you will need a 512 Hz tuning fork. Rinne's test compares bone versus air conduction. The tuning fork is struck and the base is placed on the mastoid process (bone conduction). When the tone disappears, the tuning fork prongs are placed over the external auditory meatus (air conduction). The normal response is for the tone to reappear when the tuning fork is moved in front of the external auditory meatus (i.e. air conduction is better than bone conduction, AC>BC). This reflects the amplification provided by the tympanum and middle ear ossicles. Weber's test involves striking the tuning fork and placing the base over the midline over the forehead. The tone should be heard equally in both ears. If it localizes to one side this can reflect a sensorineural hearing deficit on the contralateral side, or a conductive hearing loss on the ipsilateral side with an increased sensitivity in that ear. These tests can be difficult to interpret and the formal investigation is pure tone audiometry, and with sensorineural hearing loss imaging of the internal auditory canal.

   To examine vestibular function, examine the gait and look for nystagmus. Other tests of value are the Hallpike's test used in patients with positional vertigo. This is performed with the patient sitting up, then turning the head to one side, lie the patient back quickly with their head extended, the examiner should support the patient's head. Observe for nystagmus, associated delay, and also if it fatigues. Ask if the patient experiences vertigo. Repeat this on both sides. If the nystagmus is fatigable and delayed, this is in keeping with peripheral vestibular disturbance such as benign paroxysmal positional vertigo. If not fatigable, this is caused by a central abnormality. Unterberger's test is performed by asking the patient to stand facing the examiner with their arms stretched out in front of him. Ask the patient to close their eyes and march on the spot. Watch for any rotation. Patients turn to the side of vestibular pathology. Only perform this if the patient is able to stand safely. Romberg's test is to assess proprioceptive loss, not specifically balance or vestibular function.

7. Cranial nerve IX and X (palatal movement, swallow, and gag reflex). The glossopharyngeal and vagus nerves are examined together. Firstly, listen to the voice quality for evidence of bulbar weakness, then ask the patient to cough. Inspect the position of the uvula and then ask the patient to say 'Aah'. If there is weakness, the uvula will deviate away from the side of the lesion. The gag reflex is rarely performed and should not be performed if there is any doubt about their safety to swallow as there is potential for aspiration. Video fluoroscopy is safer in such patients.
8. Cranial nerve XI (power to sternocleidomastoid and trapezius). The accessory nerve is examined by testing the power of the trapezius muscles by asking the patient to shrug their shoulders, noting any asymmetry in the initial movement and on inspection. Winging of the scapula may be seen with weakness of trapezius (although serratus anterior palsy from damage to the long thoracic nerve is more common). Test the power and bulk of the sternocleidomastoid muscles by asking the patient to rotate the head to the opposite side against resistance.
9. Cranial nerve XII (tongue power and movements). Examination of the hypoglossal nerve should start with inspection of the tongue lying in the floor of the mouth. Note any wasting or fasciculations. When the patient is asked to protrude the tongue, it will deviate towards the weak side or the side of the unilateral lesion. The speed and fluidity of the movement will be affected in bilateral pyramidal lesions. Power is assessed by asking the patient to press against resistance from the examiner's finger on the outside of the cheek by pressing the tongue firmly on the inside of the same cheek.

Examination of autonomic function and dysfunction

An understanding of how the autonomic system is organized is required to interpret clinical signs that may be encountered during head and neck examination.

Sympathetic fibres arise from the preganglionic cell bodies of the lateral horns of T1–4, form the sympathetic chain and distribute postganglionic fibres via the inferior (to vertebral artery, C7–8), middle (to inferior thyroid artery and C5–6), and superior cervical ganglia (to carotid artery and C1–4). This chain lies posteromedial to the carotid sheath and anterior to the longus muscles. The postganglionic fibres then ride along the external carotid to supply the ciliary ganglion and hence the dilator of the pupil, and the external carotid to supply the submandibular ganglion (submandibular and sublingual glands) and the otic ganglion (parotid gland). A lesion to first, second, or third-order sympathetics will result in Horner's syndrome where there is pupil constriction, partial ptosis, and loss of hemifacial sweating (**Fig. 2.13** and **Box 2.7**). The remainder of the sympathetic

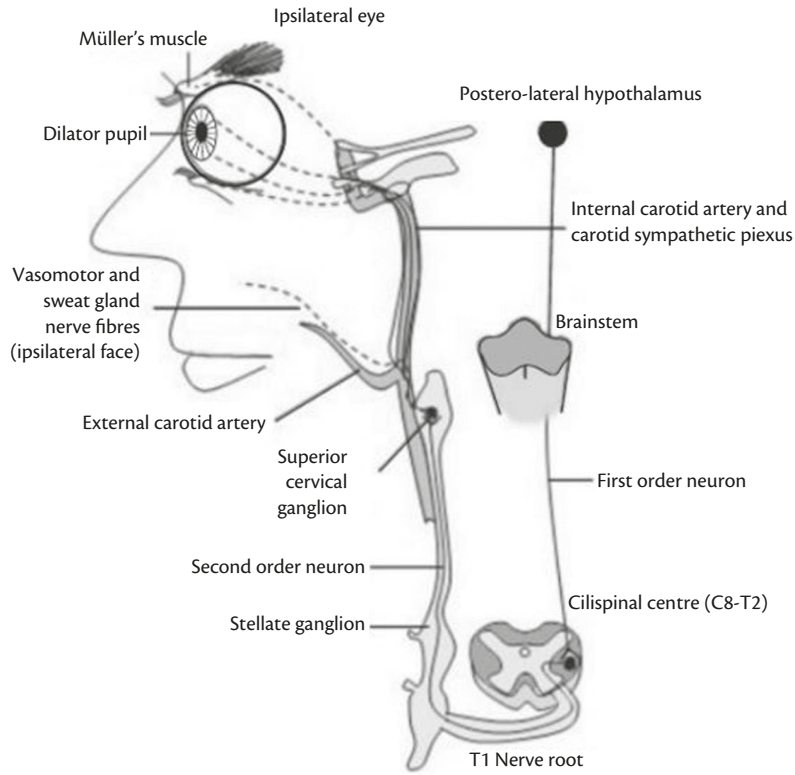

Fig. 2.13 The sympathetic supply of the pupil and causes of Horner's syndrome (Kong, 2007).

Reproduced with permission from Kong, YX, Wright, G, Pesudovs, K, O'Day J, Wainer Z, Weisinger H, Horner syndrome, *Clinical and Experimental Optometry*, volume 90 issue 5, pp. 336–44. Copyright ©2007 Optometrists Association of Australia and John Wiley & Sons.

supply to the head and neck travels with the internal carotid artery: the deep cervical nerve forms over the petrous segment of the carotid, continues into the middle fossa through the foramen lacerum, and joins the parasympathetic greater superficial petrosal nerve (GSPN) to form the Vidian nerve. The Vidian nerve passes through its own canal to supply autonomic fibres to the pterygopalatine ganglion and distribute parasympathetics with branches of the maxillary division of the trigeminal nerve.

Parasympathetic fibres are carried by four cranial nerves: III, VII, IX, and X. There are four equivalent brainstem parasympathetic nuclei: Edinger Westphal nucleus (III); superior salivatory nucleus (VII); inferior salivatory nucleus (IX); and the dorsal vagal nucleus (X). The vagus provides no cranial parasympathetic supply but provides supply to all the viscera of the thorax and abdomen as far as the midgut (two-thirds of the transverse colon). The preganglionic parasympathetic fibres of the remaining three cranial nerves synapse in four ganglia: ciliary ganglion (III via nerve to inferior oblique); pterygopalatine ganglion (VII via the GSPN); submandibular ganglion (VII via the chorda tympani); and otic ganglion (IX via lesser superficial petrosal nerve). Thus, the facial nerve has two parasympathetic branches that originate at the brainstem level within the nervus intermedius (Fig. 2.12). Crocodile tears syndrome is an uncommon consequence of damage to the facial nerve where there is misdirection of regenerating gustatory fibres to the lacrimal gland resulting in tearing when presented with food.

The postganglionic parasympathetic fibres are then delivered to the target glands by a branch of the trigeminal nerve. Fibres from the ciliary ganglion pass along the short ciliary nerves (branch of nasociliary nerve, Va) to control pupillary constriction and accommodation. Fibres from the pterygopalatine ganglion pass to the lacrimal gland via the zygomaticotemporal (Vb) and lacrimal (Va) nerves. The remainder of the fibres from the pterygopalatine ganglion supply the nose, palate, and nasopharynx sinuses via branches of the maxillary division of the trigeminal nerve. The fibres from the submandibular ganglion supply submandibular and sublingual glands via the lingual nerve (Vc).

Finally, the fibres from the otic ganglion supply the parotid gland via the auriculotemporal nerve (Vc).

Examination of the peripheral nervous system: Upper and lower limbs

The neurological examination of the extremities is based on inspection, assessment of tone, power, reflexes, coordination, and sensation. Having been directed by the history further localization will rely on key examination findings (e.g. confirmation of long tract signs in the patient with suspected myelopathy, correlating deficits in corresponding myotomes and dermatomes in radiculopathy, testing spinothalamic versus dorsal column function in possible syringomyelia, differentiating signs of peripheral neuropathy versus radiculopathy in brachialgia or sciatica, and so on). Understanding the differences between upper and lower motor neurone signs is of course crucial. With this in mind there should be a logical process of elimination, the order of which is open to personal choice and circumstances.

Box 2.7 Differential diagnoses for Horner syndrome

First-order neuron lesions

Arnold–Chairi malformation
Basal meningitis (e.g. syphilis)
Basal skull tumours
Cerebrovascular accident/lateral medullary syndrome
Demyelinating disease (e.g. multiple sclerosis)
Intrapontine haemorrhage
Neck trauma
Pituitary tumour
Syringomyelia

Second-order neuron lesions

Pancoast tumour
Birth trauma with injury to lower brachial plexus
Cervical rib
Aneurysm/dissection of aorta, subclavian, or common carotid artery
Central venous catheterization
Trauma/surgical injury (radical neck dissection, thyroidectomy, carotid angiography, coronary artery bypass graft, upper spine chiropractic manipulation)
Chest tube insertion
Lymphadenopathy (e.g. Hodgkin's disease, leukaemia, tuberculosis, mediastinal tumours)
Mandibular tooth abscess
Lesions of the middle ear (e.g. acute otitis media)
Neuroblastoma
Lumbar epidural anaesthesia

Third-order neuron lesions

Internal carotid artery dissection
Cluster/migraine headaches
Carotid artery thrombosis
Carotid-cavernous fistula
Herpes zoster
Orbital apex tumour
Idiopathic

Reproduced with permission from Kong, YX, Wright, G, Pesudovs, K, O'Day J, Wainer Z, Weisinger H, *Horner Syndrome, Clinical and Experimental Optometry,* volume 90 issue 5, pp. 336–44. Copyright ©2007 Optometrists Association of Australia and John Wiley & Sons.

Box 2.8 Gait abnormalities

- Hemiplegic—spastic leg traces a semicircle due to fixed plantarflexion and extension at the knee
- Diplegic—narrow-based, scissoring gait often due to cerebral palsy
- Myelopathic—broad-based clumsy gait
- Equine—high stepping gait seen in patients with foot drop due to L5 radiculopathy or common peroneal palsy
- Myopathic—waddling gait with pelvis dropping on alternating sides
- Parkinsonian—slow little steps *marche à petits pas*
- Cerebellar—veering uncontrolled gait
- Magnetic—feet seem to be stuck to the floor, seen in normal pressure hydrocephalus

Inspection

There should be an initial general inspection noting features such as abnormal posturing, or preferential use of one limb over another. Stigmata of related systemic disease such as rheumatoid arthritis may be apparent. Assessment of gait may be done at this point. Characteristic pathological gaits point to particular neuroanatomical disorders (Box 2.8). Heel-toe (tandem) walking and Romberg's test are useful adjuncts. Classically, Romberg's test is positive only with disorders of proprioception. Notably, this is not a test of cerebellar function as ataxia would be present with or without closing the eyes with cerebellar disorders. Inspection should continue with examination for atrophy of muscle groups, fasciculations, tremors, and scars such as previous carpal tunnel decompression.

Tone and reflexes

The resistance of muscle groups across a joint is a result of a complex system involving feedback from muscle spindles and Golgi tendon organs, monosynaptic reflexes with agonist and antagonist alpha motor fibres, inhibitory supraspinal control, and processing via the cerebellum. Tone can be decreased (hypotonia) or increased (spasticity or rigidity). Spasticity is a velocity dependent increase in muscle tone in response to a passive stretch, with exaggerated tendon jerks, in association with other features of the upper motor neurone syndrome (Lance, 1980). At the end of range of movement there is often a characteristic 'give' (clasp knife). Rigidity is not velocity or force dependent and lacks any 'give'. Spasticity is more often associated with corticospinal damage whereas rigidity is generally extrapyramidal in origin. Assessment may be by gentle internal and external rolling of the leg, brisk raising of the knee, or pronation/supination at the wrist.

The deep tendon reflexes are tests of a monosynaptic arc. The afferent neurone is stimulated by activity of a Golgi tendon organ; the efferent neurone is an alpha motor neurone. The most frequently tested reflexes are the biceps (C5), supinator (C6), triceps (C7), knee (L3/4), and ankle (S1) jerks. The patient should be in a relaxed posture. A tendon hammer should be used to briskly strike the tendon. If absent, reinforcement can be used by asking the patient to clench the teeth or by interlocking the fingers against resistance.

Specific tests of upper neurone dysfunction include Hoffmann's sign, the plantar response, and clonus. A positive Hoffmann's sign is when quickly flicking the distal phalanx of the middle finger downwards causes flexion of the thumb. Clonus should be tested with the knee flexed, and anything more than five beats of the ankle is pathological.

Power

Muscle groups may be tested in several ways. One can ask the patient to maximally contract the muscle and then attempt to counteract it (isometric). Alternatively, one can attempt to counteract the muscle group through a range of motion (isotonic). The Medical Research Council (MRC) scale provides a reproducible grading system (see Table 2.6). The emphasis placed on examining different muscle groups will depend if one is looking for pyramidal weakness, long tract disease, radiculopathy, or a peripheral nerve problem. When

Table 2.6 MRC grading of power

Grade 5	Normal power
Grade 4	Submaximal movement against resistance
Grade 3	Movement against gravity but not against resistance
Grade 2	Movement with gravity eliminated
Grade 1	Flicker of movement
Grade 0	No movement

Used with the permission of the Medical Research Council.

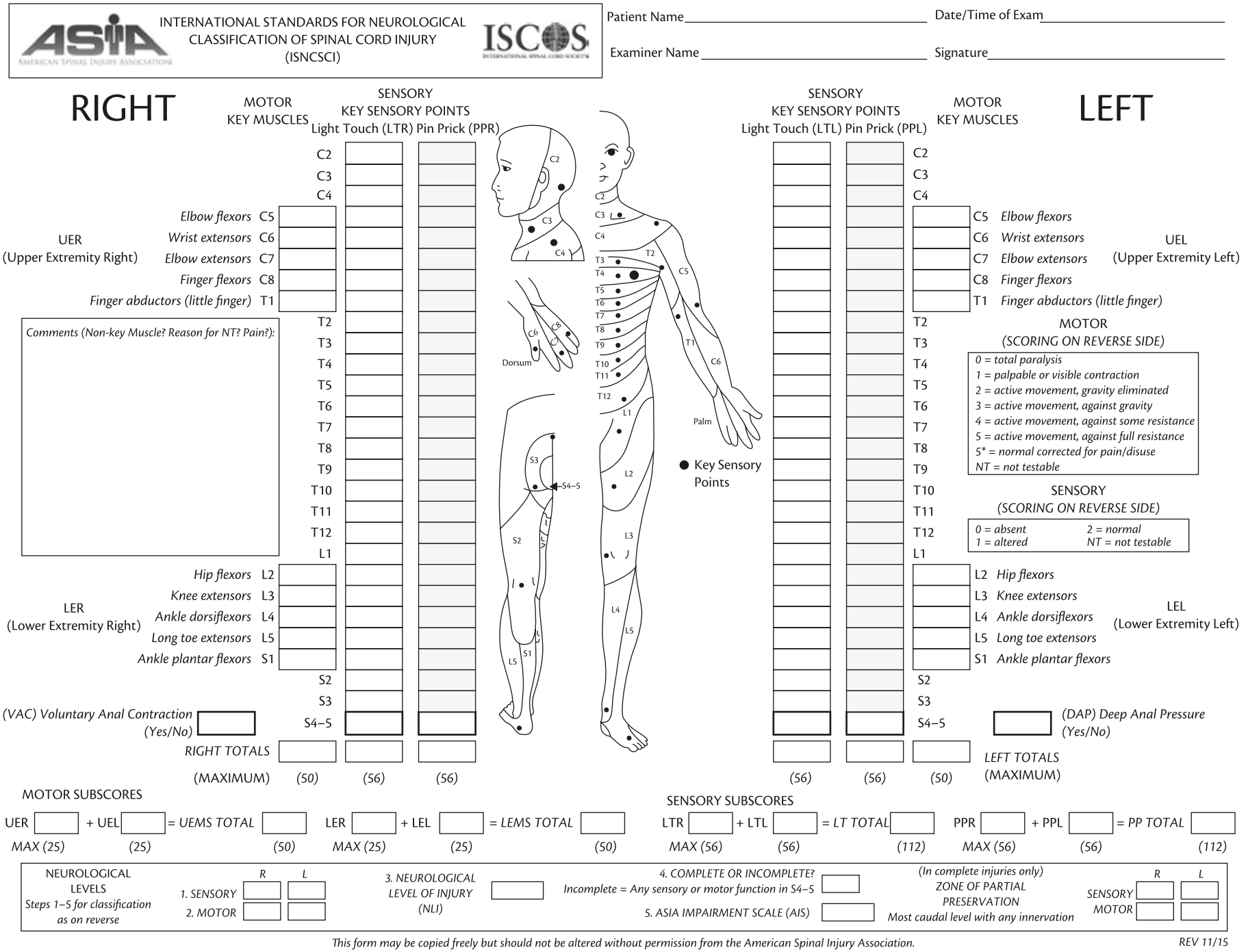
INTERNATIONAL STANDARDS FOR NEUROLOGICAL CLASSIFICATION OF SPINAL CORD INJURY (ISNCSCI)
Patient Name
Date/Time of Exam
Examiner Name
Signature
RIGHT
LEFT
MOTOR KEY MUSCLES
SENSORY KEY SENSORY POINTS
Light Touch (LTR) Pin Prick (PPR)
Light Touch (LTL) Pin Prick (PPL)
UER (Upper Extremity Right)
UEL (Upper Extremity Left)
LER (Lower Extremity Right)
LEL (Lower Extremity Left)
Elbow flexors C5
Wrist extensors C6
Elbow extensors C7
Finger flexors C8
Finger abductors (little finger) T1
Hip flexors L2
Knee extensors L3
Ankle dorsiflexors L4
Long toe extensors L5
Ankle plantar flexors S1
Comments (Non-key Muscle? Reason for NT? Pain?):
(VAC) Voluntary Anal Contraction (Yes/No)
(DAP) Deep Anal Pressure (Yes/No)
RIGHT TOTALS
LEFT TOTALS
(MAXIMUM)
Key Sensory Points
MOTOR (SCORING ON REVERSE SIDE)
0 = total paralysis
1 = palpable or visible contraction
2 = active movement, gravity eliminated
3 = active movement, against gravity
4 = active movement, against some resistance
5 = active movement, against full resistance
5* = normal corrected for pain/disuse
NT = not testable
SENSORY (SCORING ON REVERSE SIDE)
0 = absent
1 = altered
2 = normal
NT = not testable
MOTOR SUBSCORES
UER + UEL = UEMS TOTAL
LER + LEL = LEMS TOTAL
SENSORY SUBSCORES
LTR + LTL = LT TOTAL
PPR + PPL = PP TOTAL
NEUROLOGICAL LEVELS
Steps 1–5 for classification as on reverse
1. SENSORY
2. MOTOR
3. NEUROLOGICAL LEVEL OF INJURY (NLI)
4. COMPLETE OR INCOMPLETE?
Incomplete = Any sensory or motor function in S4–5
5. ASIA IMPAIRMENT SCALE (AIS)
(In complete injuries only)
ZONE OF PARTIAL PRESERVATION
Most caudal level with any innervation
This form may be copied freely but should not be altered without permission from the American Spinal Injury Association.
REV 11/15

Fig. 2.14 International standards for neurological classification of spinal cord injury workbook.

testing the nerve roots or level of cord dysfunction, the American Spinal Injuries Association workbook (ASIA, 2015) provides an excellent, logical schema (Fig. 2.14). For each level, a particular action is specified to test individual nerve roots.

Sensation

As for the motor examination, sensation should be tested either in a radicular manner or according to peripheral nerve distribution (Fig. 2.15). In addition to peripheral localization, there are different modalities to be considered. Importantly, one should remember that discriminative light touch, proprioception, vibration, and two-point discrimination are conducted through large fast-conducting fibres in the dorsal columns. Pinprick (superficial pain), and temperature are conducted through smaller, slower fibres in the spinothalamic tracts. Again, the ASIA chart is an invaluable guide as to the optimal points for testing sensation. An exact point on the skin is indicated where light touch and pin prick should be tested. It is vital to compare one side against the other as one proceeds. Areas of hypoaesthesia or hyperaesthesia should be carefully mapped out. Asking the patient to close their eyes may provide additional objectivity.

On testing joint position sense, it is important to remember that the patient may be able to tell the direction of motion by how pressure is exerted on a digit. One should, therefore, ensure that the thumb or the great toe are held side to side rather than above and below. Should proprioception be lost, one should test the next proximal joint.

Examination techniques for some common peripheral neuropathies are detailed in Boxes 2.9, 2.10 and Table 2.7.

Putting it all together

As one progresses with the history and examination the information should constantly be distilled, therefore refining the line of questioning and narrowing the focus of examination. Eventually, one has to draw these disparate pieces of information together, make sense of them, and attempt to identify the most likely anatomical source of the patient's complaint and potential pathological processes that may have caused it. Once this point has been reached, it is necessary to decide on whether further investigations are required and what they might consist of.

In the course of this decision-making process, one needs to be rigorous in ensuring strictest objectivity.

> Doctors … are more interested in patients they can help, and diseases they can cure, than the ones they can't. There is, therefore, a tendency for them to make the diagnosis fit their skills or even . . . to have a vested interest in inventing illnesses which they can cure. (Handy, 1990)

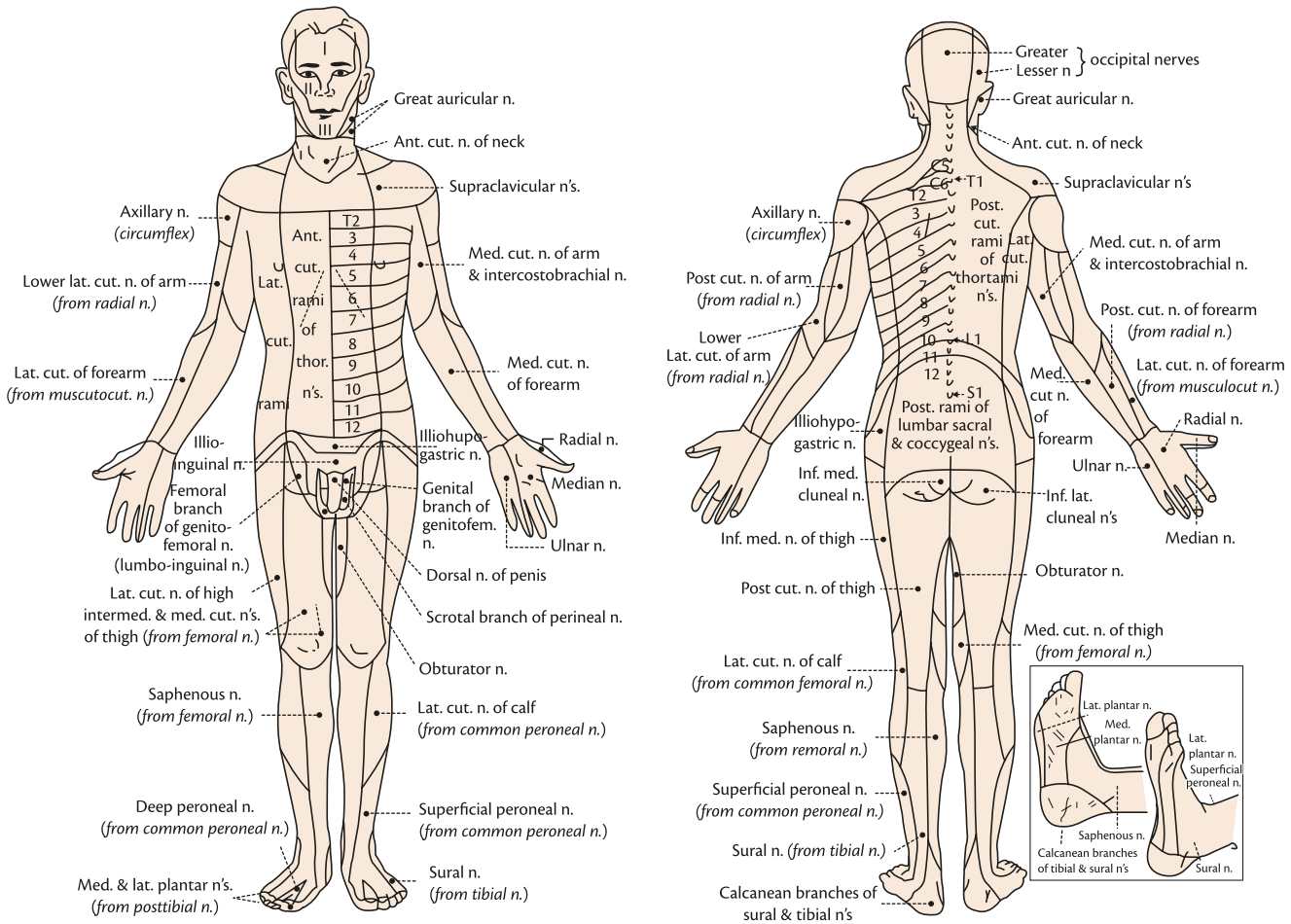
Great auricular n.
Ant. cut. n. of neck
Supraclavicular n's.
Axillary n. (circumflex)
Lower lat. cut. n. of arm (from radial n.)
Lat. cut. of forearm (from muscutocut. n.)
Med. cut. n. of arm & intercostobrachial n.
Med. cut. n. of forearm
Ant. cut. rami of thor. n's.
Lat. cut. rami of thor. n's.
Illio-inguinal n.
Femoral branch of genito-femoral n. (lumbo-inguinal n.)
Lat. cut. n. of high intermed. & med. cut. n's. of thigh (from femoral n.)
Saphenous n. (from femoral n.)
Deep peroneal n. (from common peroneal n.)
Med. & lat. plantar n's. (from posttibial n.)
Illiohypo-gastric n.
Genital branch of genitofem. n.
Dorsal n. of penis
Scrotal branch of perineal n.
Obturator n.
Lat. cut. n. of calf (from common peroneal n.)
Superficial peroneal n. (from common peroneal n.)
Sural n. (from tibial n.)
Radial n.
Median n.
Ulnar n.
Greater Lesser n occipital nerves
Great auricular n.
Ant. cut. n. of neck
Supraclavicular n's
Axillary n. (circumflex)
Post cut. n. of arm (from radial n.)
Lower Lat. cut. of arm (from radial n.)
Post. cut. rami of thor. n's.
Lat. cut. rami of thor. n's.
Post. rami of lumbar sacral & coccygeal n's.
Med. cut. n. of arm & intercostobrachial n.
Post. cut. n. of forearm (from radial n.)
Lat. cut. n. of forearm (from musculocut n.)
Med. cut n. of forearm
Radial n.
Ulnar n.
Median n.
Illiohypo-gastric n.
Inf. med. cluneal n.
Inf. lat. cluneal n's
Inf. med. n. of thigh
Obturator n.
Post cut. n. of thigh
Med. cut. n. of thigh (from femoral n.)
Lat. cut. n. of calf (from common femoral n.)
Saphenous n. (from remoral n.)
Superficial peroneal n. (from common peroneal n.)
Sural n. (from tibial n.)
Calcanean branches of sural & tibial n's
Lat. plantar n.
Med. plantar n.
Lat. plantar n.
Superficial peroneal n.
Saphenous n.
Calcanean branches of tibial & sural n's
Sural n.

Fig. 2.15 Cutaneous distribution of peripheral nerves (Harrison and Kasper, 2015).

Box 2.9 Examining for carpal tunnel syndrome

- Atrophy of thenar eminence
- Test opposition of thumb by making an O sign
- Test abduction of thumb, lay back of hand down and point thumb upwards
- Splitting of sensation of the ring finger—more sensation on ulnar side
- No loss of sensation in central palm as the palmar cutaneous branch runs above flexor retinaculum
- Phalen's sign (good predictive value)
- Tinel's sign (poor predictive value)
- Absence of benediction sign (attempts to make fist, but thumb and index finger remain extended)—this is due to more proximal compression of median nerve

Box 2.10 Examining for ulnar neuropathy at the elbow

- Wasting of first dorsal interosseous muscle and hypothenar eminence
- Wartenberg's sign—little finger remains abducted, has a tendency to catch on pockets
- Test finger abduction
- Ulnar paradox—ulnar claw hand seen with ulnar nerve damage at the wrist, not present with more proximal lesion at the elbow
- Froment's test—test of adductor pollicis, the only muscle supplied by the ulnar nerve in the thenar eminence. With hands supine ask patient to hold onto piece of paper. Flexion of the thumb on withdrawing the paper indicates positive test
- Tender and enlarged ulnar nerve in the ulnar groove, positive Tinel's test
- Splitting of sensation of the ring finger—more sensation on radial side
- Remember to rule out C8 radiculopathy, Pancoast's tumour, and thoracic outlet syndromes (look for Horner's syndrome to help differentiate)

Table 2.7 Clinical features differentiating L5 radiculopathy and common peroneal palsy[a,b]

	L5 radiculopathy	Common peroneal palsy
Pattern of weakness	Foot inversion (tibialis posterior, the foot invertor, supplied by L4 and L5 via tibial nerve, *not* the peroneal nerve) Hip abduction (gluteus medius and minimus supplied by L4/L5/S1 via superior gluteal nerve)	Foot eversion
Nerve root tension signs	On hip flexion	On ankle inversion
Tinel's test at fibular neck	Negative	Positive

[a] Always remember central causes for foot drop, especially a parafalcine meningioma pressing on the motor cortex.

[b] For peripheral causes the frequencies are as follows: peroneal neuropathy (46%); lumbar radiculopathy (15%); sciatic nerve disorder (5%) (Jeon, 2013).

In considering a patient for an operation there is always a balance to be struck. What are the risks of surgery versus the risk of doing nothing? A clear understanding of natural history is required just as much as the potential complications of a particular operation.

The history and examination provide the foundation stones of patient management. What one does with this information must be guided by our knowledge of neurosurgical conditions. This is described in subsequent chapters.

FURTHER READING

Blumenfeld, H. (2002). *Neuroanatomy Through Clinical Cases*. Sunderland, MA: Sinauer Associates.

Brazis, P.W., Masdeu J.C., & Biller J. (2011). *Localization in Clinical Neurology*, 6th edition. Philadelphia PA: Wolters Kluwer/Lippincott Williams & Wilkins Health.

Fuller, G. (2013). *Neurological Examination Made Easy*, 5th edition. Edinburgh, UK: Churchill Livingstone.

Kolb, B. & Whishaw, I.Q. (2009). *Fundamentals of Human Neuropsychology*. New York: Worth Publishers.

Pane, A. (2007). *The Neuro-ophthalmology Survival Guide*, 1st edition. London, UK: Mosby Elsevier, p. 379.

REFERENCES

American Spinal Injuries Association (ASIA) (2015). *International Standards for Neurological Classification of Spinal Cord Injury*. https://asia-spinalinjury.org/information/downloads/

Beck, R. & Smith, C. (1988). *Neuro-ophthalmology: A Problem-orientated Approach*, 1st edition. Boston, MA: Little, Brown and Company, p. 14.

Blumenfeld, H. (2002). *Neuroanatomy Through Clinical Cases*. Sunderland, MA: Sinauer Associates, p. 848.

Brazis, P., Biller, J., & Masdeu, J. (2011). *Localization in Clinical Neurology*. Philadelphia PA: Wolters Kluwer/Lippincott Williams & Wilkins Health, p. 535.

Clarke, C. (2009). *Neurology*, 1st edition. Chichester, UK: Wiley, pp. 252–4.

Handy, C. (1990). *Inside Organizations*, 1st edition. London, UK: BBC Books.

Harrison, T. & Kasper, D. (2015). *Harrison's Principles of Internal Medicine*, 19th edition. New York [u.a.]: McGraw-Hill Medical, p. 160.

Jeon, C., Chung, N., Lee, Y., Son, K., & Kim, J. (2013). Assessment of hip abductor power in patients with foot drop. *Spine*, **38**(3), 257–63.

Kolb, B. & Whishaw, I. (2009). *Fundamentals of Human Neuropsychology*. New York: Worth Publishers.

Kong, Y.X., Wright, G., & Pesudovs, K., et al. (2007). Horner syndrome. *Clin Exp Optom*, **90**(5), 336–44.

Lance, J.M. (1980). Pathophysiology of spasticity and clinical experience with baclofen. In: Lance, J.W., Feldman, R.G., Young, R.R., Koella, W.P. (eds.) *Spasticity: Disordered Motor Control*, pp. 185–204. Chicago, IL: Year Book Medical Publishers.

Plum, F. & Posner, J. (2007). *Plum and Posner's Diagnosis of Stupor and Coma*, 1st edition. Oxford, UK: Oxford University Press, p. 58.

Ribas, G. (2010). The cerebral sulci and gyri. *Neurosurg Focus*, **28**(2), 1–24.

RELATED LINKS TO EBRAIN

An Approach to the Cognitively-impaired Adult. https://learning.ebrain.net/course/view.php?id=37

Examination of the Limbs. https://learning.ebrain.net/course/view.php?id=49

Examining Patients in Coma. https://learning.ebrain.net/course/view.php?id=44

Neurological Assessment: Movement Disorders. https://learning.ebrain.net/course/view.php?id=38

Neurological Assessment: Weakness and Sensory Loss. https://learning.ebrain.net/course/view.php?id=36

Neurological Examination: Cranial Nerves. https://learning.ebrain.net/course/view.php?id=51

Neurological Examination: Gait. https://learning.ebrain.net/course/view.php?id=47

Neurological Examination: Speech. https://learning.ebrain.net/course/view.php?id=45

Neurological Examination: Visual Function. https://learning.ebrain.net/course/view.php?id=50

Neurological History: General Approach and Common Pitfalls. https://learning.ebrain.net/course/view.php?id=39

Neuromuscular Assessment. https://learning.ebrain.net/course/view.php?id=41

Principles of Neurological Investigation. https://learning.ebrain.net/course/view.php?id=43

3

Overview of neuroimaging

Tomasz Matys, Daniel. J. Scoffings, and Tilak Das

Introduction

The development of computed tomography (CT) (Hounsfield, 1995) and magnetic resonance imaging (MRI) (Mansfield and Maudsley, 1977; Lauterbur, 1989) in the last 40 years has revolutionized neuroimaging, overcoming the limitations of previously used methods that relied on the demonstration of displacement of intracranial vessels or ventricles, and instead allowing the direct visualization of intracranial pathology (Hoeffner et al., 2012). The first clinical CT examination was performed on a patient with a brain tumour and it could be argued that no other field of medicine has benefited more from the further development of cross-sectional imaging techniques than neuroscience. Refinement of MRI and nuclear medicine methods, with the introduction of positron emission tomography (PET) in particular, has allowed for imaging of selected aspects of central nervous system function, such as blood flow, tissue microenvironment, and metabolism. Future progress will no doubt include continuing improvement in the spatial and soft tissue resolution of anatomical imaging and extending the application of functional methods, but also hopefully clinical translation of the full scope of molecular imaging, allowing visualization of specific cellular and molecular events underlying the disease process in addition to its pathological and functional sequelae (Hoffman and Gambhir, 2007; Massoud and Gambhir, 2007).

In this chapter we discuss current neuroradiology imaging modalities that are useful in neurosurgical practice. Due to space constraints, information regarding the underlying physical principles is limited to the basics, while more comprehensive descriptions can be found elsewhere (Allisy-Roberts and Williams, 2007). We focus here on the general usefulness and limitations of neuroradiological methods rather than the imaging manifestations of individual disease processes, which are discussed elsewhere in the relevant chapters of this book. The interested reader can find further information in dedicated neuroradiology monographs (see Nadgir and Yousem, 2016).

Principles of imaging

Radiographs and fluoroscopy

Radiographs ('plain X-rays') are produced by passing a collimated beam of X-rays through a patient onto an image receptor, traditionally a cassette containing combination of a fluoroscopic screen and radiographic film, but in modern practice a digital detector is typically used. The tissues in the patient's body attenuate the X-ray beam to differing degrees so that the intensity of the X-rays reaching the detector varies across its surface. In this way radiographs can distinguish between air (black), fat (dark grey), soft tissue and water (light grey), and bone (white). The radiographic image is also a two-dimensional representation of a three-dimensional structure and it is typically necessary to obtain images in different (often orthogonal) projections to infer the position of a given abnormality within the patient.

With the increasing availability of CT and MRI, the role of conventional radiographs in the assessment of patients with neurosurgical disease has reduced, but they retain a role in certain circumstances. The advantages of radiographs include their ease of acquisition, low cost, widespread availability, the ability to obtain images at the bedside, and also to obtain a degree of dynamic information by acquiring radiographs with the patient in different positions (e.g. standing, in flexion, and extension of the spine). Although they have high spatial resolution, a major disadvantage of radiographs is their limited soft tissue resolution. Indications for radiographs include assessment of the continuity of the extracranial components of ventricular shunts, the position and integrity of spinal implants and prostheses, and the follow-up of patients with spinal fractures in whom loss of normal alignment or progression of vertebral body compression is suspected. Radiographs are less sensitive than CT in the detection of spinal fractures and have a very limited role in the primary assessment of suspected spinal injury. Flexion-extension radiographs are often used in evaluation of potential instability in patients with degenerative or spondylolytic spondylolisthesis.

Fluoroscopy provides real-time images of the area of anatomical interest by passing a continuous or pulsed X-ray beam through the patient onto an image-intensifier, most commonly using a C-arm apparatus which can be rotated and positioned around the patient to provide the desired view. Uses of fluoroscopy include the identification of the correct level for spine surgery, monitoring the placement of spinal fixation devices or prostheses, and the performance of lumbar puncture in patients in whom bedside lumbar puncture (LP) has been unsuccessful due to obesity or degenerative changes.

Computed tomography

CT basics and techniques

Introduced into clinical practice in 1973, CT was the first diagnostic imaging modality to enable direct visualization of the brain (Wolpert, 2000). Similar to plain film radiography, CT is based on a differential attenuation of X-rays by tissues, but uses a differently collimated beam sweeping around the patient in a circular fashion and reaching a large number of individual detectors; the image is then created using mathematical reconstruction algorithms. In brief, when an X-ray photon travels along a particular line through the patient's body, it experiences energy loss that depends on attenuation coefficients of tissues it encounters on its path. By measuring photon energy from multiple directions around the object, it is possible to calculate the attenuation coefficients for each voxel (volume element) within the examined volume. Attenuation coefficient values are then converted into more convenient-to-use radiodensity values ('CT numbers') calculated in relation to water and air, and expressed in Hounsfield units (HU). The scale of CT numbers ranges from –1000 HU (air) to over 3000 HU (cortical bone), with 0 HU being the attenuation of distilled water. Typical values for different central nervous system (CNS) tissues are given in **Table 3.1**.

The way in which the multidirectional information is obtained and the speed of acquisition have dramatically changed with technological advances, from a pencil-like X-ray beam translating along a slice in the original machine to a fan-shaped beam and increasing number of detectors along the circumference of the gantry and across multiple rows (Ginat and Gupta, 2014). An important development in CT scanning technology was the advent of helical or spiral CT, where the data is obtained in continuous fashion while the patient moves smoothly through the gantry and the X-ray tube rotates, continuously tracing a spiral trajectory around the body. While this mode of acquisition allowed significant improvements in body CT scanning, it introduces unwanted 'windmill artefacts' (Barrett and Keat, 2004), and sequential CT may still be preferable for head imaging. In neuroradiological applications, helical CT does allow excellent quality CT angiography for the evaluation of neck and intracranial vessels, as well as isotropic resolution volumetric reconstructions that can be visualized in any arbitrary plane.

To convert raw CT data into a useful image, the matrix of radiodensities is displayed as shades of grey. From the range of the Hounsfield scale, possible CT numbers span up to 4000 levels of radiodensity, yet the human observer can theoretically perceive approximately 720 shades of grey in optimal conditions (Kimpe and Tuytschaever, 2007) and this is much lower in practice. It is therefore not possible to map the entire dynamic range of CT numbers to greyscale at the same time, necessitating the use of a 'window' centred at a certain level and of particular width to display a suitable fragment of this range. Values of radiodensities within the window are displayed as shades of grey, while values below and above the window boundaries are displayed as black and white, respectively. Because most tissues of interest in the brain lie in the range of 0 to 100 HU, these are optimally depicted using a window centred at a level of around 40 HU and width of 80 HU (Fig. 3.1A). As the radiodensity of acute haemorrhage lies close to the upper limit of the standard window, haemorrhage appears bright and is readily apparent; it is however difficult to appreciate blood immediately adjacent to bone. Using 'subdural windows' with at a slightly higher level and a larger width (e.g. L/W 70/200) makes acute blood better distinguishable from the adjacent bone (**Fig. 3.1B**). Setting the window level to negative values allows differentiation of fat from air. To interrogate bone detail, the window needs to be set to a higher level and width (e.g. L/W 500/3000, **Fig. 3.2**).

One of the most important parameters that affect image quality is the kind of mathematical reconstruction algorithm, also referred to as a reconstruction kernel or filter. Use of different kernels changes the balance between spatial resolution and image noise. A smooth kernel generates images with lower noise and better low-contrast detectability more suited to brain examinations, at a cost of reduced spatial resolution. A sharp kernel generates images with high spatial

Table 3.1 Attenuation values of the main tissues/materials in neuroimaging

Material	Hounsfield units
Acute blood	56 to 76
Air	–1000
Bone	1000 to 3000
Calcification	140 to 200
Cerebrospinal fluid	0
Fat	–30 to –100
Grey matter	32 to 41
White matter (centrum semiovale)	23 to 34

This table was adapted from *Neuroradiology: The Requisites*, David Yousem, Robert Zimmerman, Robert Grossman, Copyright Elsevier (2010).

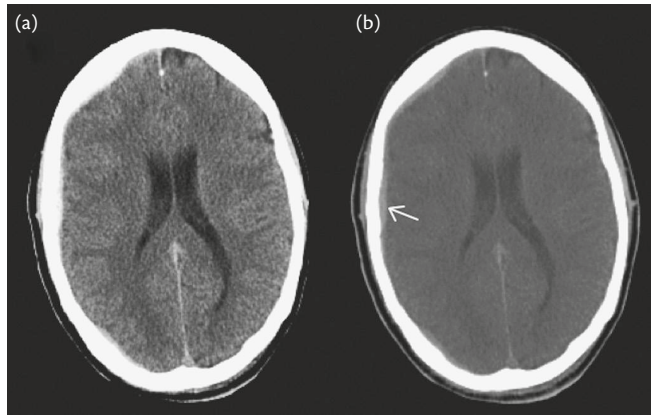

Fig. 3.1 Standard window (A, level/width 40:80) provides good differentiation of the grey and white matter but high-density haemorrhage adjacent to the skull is difficult to appreciate. Widening the window (B, 'subdural window' 70:200) makes the thin right sided subdural haemorrhage (arrow) more conspicuous.

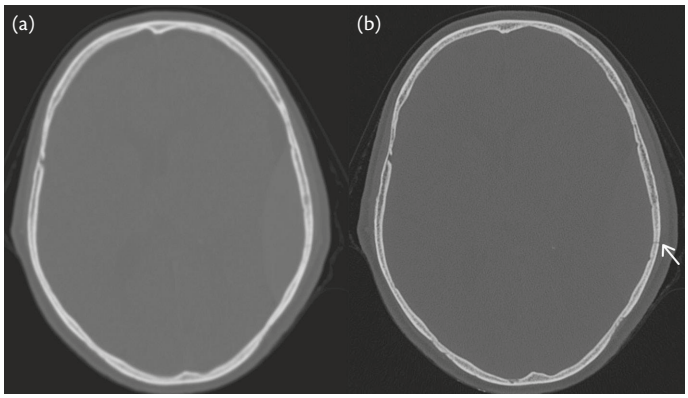

Fig. 3.2 Image of the skull seen on bone window (L/W 500:3000) reconstructed using standard (A) and bone (B) kernel. Hairline fracture of the left squamous temporal bone is much more conspicuous using bone kernel reconstruction (arrow).

resolution better suited to the assessment of bony structures. Use of bone kernel is essential for detection of fractures (Fig. 3.2) and should be a part of any CT performed in the context of trauma, as well as sinonasal and temporal bone examinations.

CT contrast media and risks

Iodinated contrast media have historically been the contrast agent of choice for X-ray and CT applications due to high attenuation of iodine compounds thanks to its high atomic number (Lusic and Grinstaff, 2013). In CT brain imaging, contrast media are used to detect areas of blood-brain barrier breakdown, where contrast medium leaks into parenchyma, or to opacify blood vessels in CT angiography, including venography.

The risks of iodinated contrast media include allergic reactions and contrast-induced acute kidney injury. To minimize this, it is important to identify susceptible individuals (Box 3.1) and take appropriate preventative steps (Iodinated Contrast Media Guideline, Royal Australian and New Zealand College of Radiologists).

The current standard is to use non-ionic, low osmolarity compounds. The incidence of severe reactions with this type of media is 0.04% and for very serious reactions is 0.004% (Hunt et al., 2009). A typical adult dose of intravenous contrast medium for head CT is 50 ml of a compound containing 300 mg/ml iodine. Larger amounts are used in angiographic applications. Contrast medium can also be administered intrathecally through a lumbar, cervical, cisternal, or ventricular approach (Nadgir and Yousem, 2016); this may require lower concentration compound approved for intrathecal use, especially in children.

Box 3.1 Risk factors for contrast-induced acute kidney injury (CI-AKI) and allergic reaction to contrast media

Risk factors for CI-AKI

Known kidney disease (including kidney transplant)
Presence of diabetes
Metformin (risk of lactic acidosis)

Risk factors for allergic reaction to contrast media

Previous allergic reaction to iodinated contrast media
Previous significant allergic reactions to other substances or history of eczema
History of asthma
Use of beta blockers

The Royal Australian and New Zealand College of Radiologists. Iodinated Contrast Media Guideline. Sydney: RANZCR; 2018.

Advantages and disadvantages of CT

CT plays an extremely important role in neuroimaging, particularly in the emergency and neurosurgical settings (Nadgir and Yousem, 2016). It is a rapid, easily accessible, and efficient modality for screening patients with major traumatic injury. It has high sensitivity to haemorrhage, particularly in the first 24 hours compared to MRI, and can demonstrate features of raised intracranial pressure and brain herniation, allowing for rapid decision-making in early stages of traumatic injury. For the detection of subarachnoid haemorrhage (SAH), it remains the initial imaging study of choice in suspected cases and can be rapidly followed by CT angiography when SAH is identified. Similarly, it remains a useful technique for assessment of cerebral infarction and, in conjunction with CT angiography and CT perfusion, for guiding thrombolytic therapy in patients with suspected ischaemic stroke (Kidwell and Wintermark, 2010).

For postoperative examinations in both brain and spine, CT is useful in evaluating for complications (such as haemorrhage, infarct, or hydrocephalus), and the position of ventricular drains or other adjuncts. Portable head CT scanners are now available allowing examination at a neurocritical care bed without the need for transporting an unstable patient.

CT venography can often be used as an alternative to MR venography or help with troubleshooting in the case of confounding artefacts on MRI.

CT is the best modality for assessing bone lesions and is essential for the evaluation of skull, skull base, facial, and spine fractures. It is also the technique of choice for primary evaluation of the temporal bones and paranasal sinuses.

CT sensitivity for calcification is helpful with the diagnosis of calcium-containing CNS tumours (e.g. meningioma, oligodendroglioma, craniopharyngioma), metabolic disorders (e.g. hyperparathyroidism), and congenital lesions (e.g. TORCH infections, tuberous sclerosis). Finally, CT myelography is a viable alternative to MR in spine imaging in patients with absolute contraindications to MR imaging.

The use of radiation remains a drawback for CT technology. For a head CT, the average effective dose is approximately 2 millisievert (mSv), compared to an annual background radiation of 2–5 mSv. Other neuroradiological examinations incur higher doses (Table 3.2). Possible effects of radiation can be divided into deterministic (predictable and depending on cumulative radiation dose, for example, cataract due to lens irradiation), and stochastic (chance-like, for example, induction of malignancy) (Allisy-Roberts and Williams, 2007). The risk of cataract should be taken into account, especially in children (Michel et al., 2012).

In pregnancy, the dose to the fetus from head and neck CT is low and the risk of inducing childhood cancer is thought to be < 1 in 1 000 000. Examinations with direct exposure of the fetus (e.g. spinal CT) result in higher risk (1 in 1000–10 000) and should be avoided (The Royal College of Radiologists, 2009). The administration of iodinated contrast agents carries a theoretical risk of fetal thyroid suppression and thyroid function should be checked in the first week after birth.

Table 3.2 Typical radiation dose in neuroradiological CT-based examinations (Cohnen et al., 2006; Mettler et al., 2008)

Examination	Average dose (range)
CT head	1.7 mSv
CT angiogram head	1.9 mSv
CT angiogram neck	2.8 mSv
CT perfusion cerebral	1.1–5.0 mSv
Comprehensive stroke protocol	Up to 9.5 mSV
CT spine	6 mSV

Data from Cohnen, M et al., Radiation exposure of patients in comprehensive computed tomography of the head in acute stroke, *AJNR. American Journal of Neuroradiology*, volume 27, issue 8, pp. 1741–5. 2006, and Mettler, F.A et al., Effective doses in radiology and diagnostic nuclear medicine: a catalog, *Radiology*, volume 248, issue 1, pp. 254–63. 2008.

Advances in CT technology include attempts to reduce the necessary radiation dose while maintaining acceptable image quality, particularly important for paediatric imaging. The main way of reducing radiation exposure is adapting the dose by changing the tube voltage and current (and therefore X-ray photon energy and beam intensity) according to the patient's size, weight, and specific imaging application. A different method that allows scanning with a lower dose while maintaining image quality is replacement of the conventional reconstruction technique, known as filtered back projection, with iterative reconstruction (IR) which requires additional computation time but generates images with lower noise and higher spatial resolution, as well as reduced beam hardening and metal artefacts. Although the effects are more pronounced in body imaging, dose reductions have also been demonstrated for head imaging (Kilic et al., 2011; Mirro et al., 2016). The images appear subjectively different between the two reconstruction techniques and IR is therefore still under clinical evaluation.

Magnetic resonance imaging (MRI)

MRI basics and techniques

MRI takes advantage of the phenomenon of nuclear magnetic resonance, inherent to nuclei that have a magnetic moment due to an uneven number of protons or neutrons; in practice this mainly involves imaging of hydrogen nuclei (^{1}H) containing a single proton. MRI is based on a radiofrequency signal that is emitted when protons aligned with a strong magnetic field are tipped out of alignment by an externally applied radiofrequency pulse and then return to equilibrium (**Fig. 3.3**). The emitted signals are read out in a spatially ordered fashion and reconstructed into an image reflecting the magnitude of signal in a given voxel. The type of excitation pulse, time at which the signal is read out, and interval between excitations can be varied resulting in a different contrast in the final image (Allisy-Roberts and Williams, 2007). Two principal MRI sequences provide image weighting that depends on T_1 or T_2 relaxation times of the tissue (**Table 3.3**); appearances of the brain on the most commonly used sequences are shown in **Figure 3.4**. Images weighted according to proton density (PD) can be obtained together with T_2-weighted images with no additional scanning time required; they provide good contrast between the grey and white matter, and are of value in certain situations, but are not universally used in neuroradiology. Water has high signal on T_2-weighted sequences, and because most pathological processes are associated with increased water content (oedema), they appear hyperintense on T_2 weighted images. Fat is hyperintense on T_2-weighted images but unlike water it shows high T_1 signal. Besides fat, T_1 hyperintensity can also be due to melanin, protein-rich fluid, calcification, and gadolinium-chelate contrast agents (see later). Haemorrhage has complex appearances on MRI with combination of signal intensities dependent on the degradation phase of blood products (**Table 3.4**).

Signal in MRI can be produced using spin echo or gradient recalled echo sequences (Bitar et al., 2006; Allisy-Roberts and Williams, 2007). Spin echo provides better signal-to-noise ratio and is generally preferable, but slower than gradient echo. Acquisition of large volumetric datasets, required for example by neurosurgical navigation systems, is therefore performed using a variant of the gradient echo sequence. An important feature of gradient echo sequences is the lack of compensation of magnetic field inhomogeneities, resulting in its sensitivity to local susceptibility effects. This is used in practice for detection of haemorrhage, as the local susceptibility effect caused by iron in haemosiderin results in a very low signal with 'blooming' on gradient echo sequences. Even better depiction of haemosiderin, for example, microhaemorrhages in the setting of traumatic brain injury, is achieved with susceptibility weighted imaging (SWI), a high-resolution 3D velocity-compensated long echo time gradient echo sequence (Di Ieva et al., 2015). Gradient echo sequences are also used in other situations in which image contrast depends on susceptibility effects such as dynamic susceptibility contrast perfusion imaging and blood-oxygenation level dependent methods.

Image contrast in MRI can be varied using suppression techniques designed to null signal from a specific tissue. In the brain, this is used in fluid-attenuated inversion recovery (FLAIR), which nulls the cerebrospinal fluid signal; it is routinely used with T_2-weighting to make parenchymal T_2 hyperintensity more conspicuous (T_2-FLAIR, usually referred to simply as FLAIR). This should not be confused with a less common T_1-FLAIR sequence, which is used for example to improve grey-white matter contrast that is otherwise reduced at higher magnetic field strengths.

Fat suppression techniques increase conspicuity of fluid signal on T_2-weighted images or contrast enhancement on T_1-weighted images in situations where they could be masked by the presence of fat (such as detection of oedema in the vertebral column or paraspinal soft tissues, or contrast enhancement at the skull base, respectively). Fat suppression can be achieved by short tau inversion recovery (STIR) or spectral saturation. STIR is useful near bone-containing structures (orbit, skull base, sinuses), metallic foreign bodies, and across large fields of view, for example, in spine imaging. STIR is however problematic when combined with contrast medium, when spectral fat saturation is used instead.

Balanced steady state free precession (SSFP) sequences provide high resolution and excellent signal-to-noise ratio with a mixed T_2/T_1-weighting. In neuroimaging, these sequences are usually performed with a heavy T_2-weighting delivering high contrast resolution between cerebrospinal fluid and contained structures, such as the cisternal segments of the cranial nerves and adjacent blood vessels. Balanced SSFP techniques such as fast imaging in steady state (FIESTA) or constructive interference in steady state are therefore useful in investigation of vascular loops as the cause underlying trigeminal neuralgia or hemifacial spasm, as well as in screening for cerebellopontine angle tumours. Other uses include the evaluation of inner ear structures, and identification of cerebrospinal fluid leaks (Saindane, 2015).

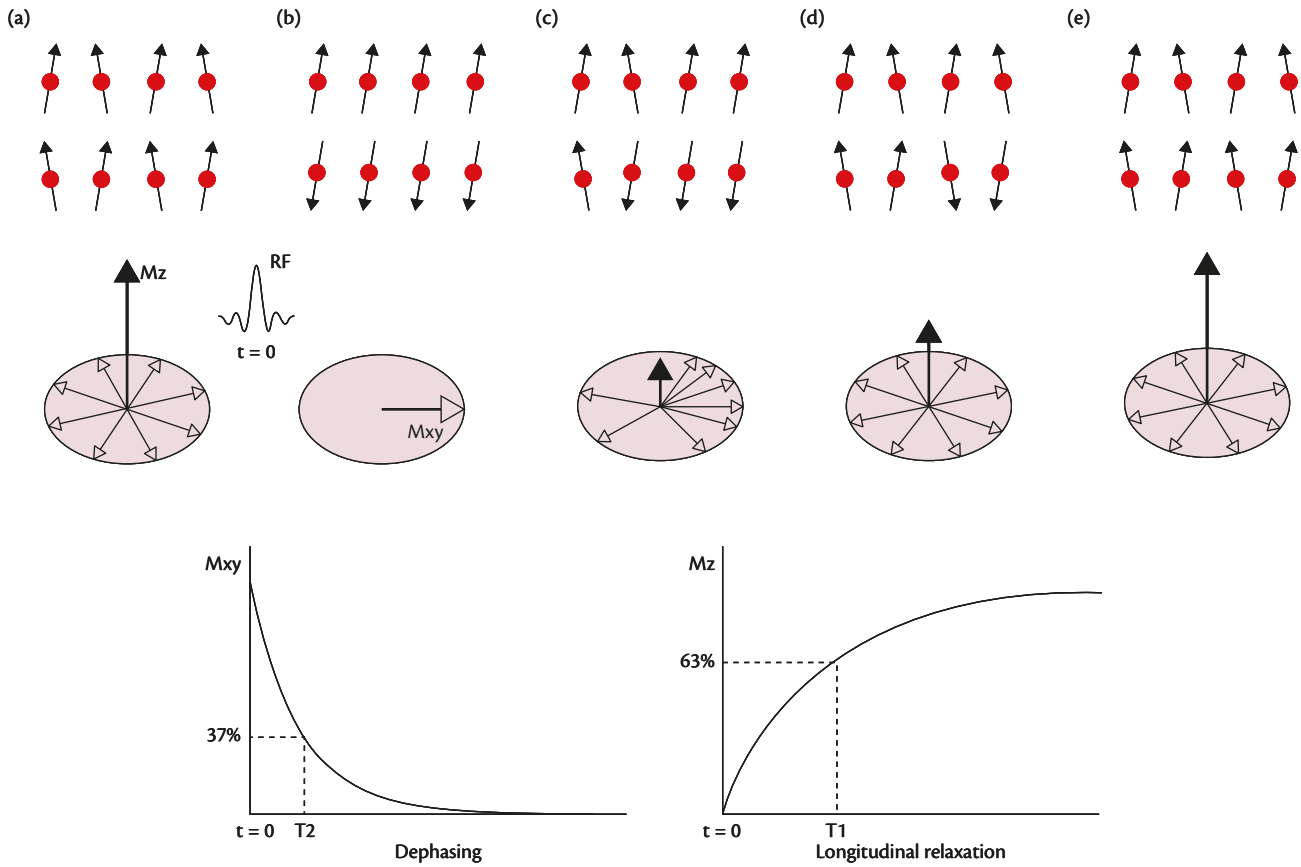

Fig. 3.3 Due to having a charge and spin, protons display magnetic properties and behave like magnetic dipoles. Outside of a magnetic field, the dipoles are randomly distributed and the net magnetization is zero in any direction in space. When placed in a magnetic field, the magnetic dipoles align with the field, either parallel ('spin up') or antiparallel ('spin down') to it, and start to precess (wobble around their axes) with a frequency dependent on the strength of the magnetic field (Larmor frequency). (A) Because a small excess of dipoles (approximately three per million) point 'spin up' their longitudinal magnetization vectors add up creating net longitudinal magnetization Mz. Due to precession, each dipole also creates a transverse magnetization vector rotating in the transverse plane. However, because the dipoles precess in different phases, their transverse magnetization vectors cancel each other and the net transverse magnetization remains zero. (B) Application of an external radiofrequency (RF) pulse turns some dipoles spin down; a so-called 90°RF pulse turns exactly half of the excess dipoles spin down, so now equal numbers of dipoles point in either direction and the net Mz vector is null. The RF pulse also causes synchronization of the phase of precession, so all the dipoles precess together (they achieve phase coherence) and their transverse magnetization adds up to produce a net transverse magnetization vector Mxy, rotating in the transverse plane. (C–E) After the RF pulse ends, within a short time the protons return to their initial state by losing phase coherence (dephasing, resulting in a loss of transverse magnetization Mxy) and by returning to the spin up orientation (longitudinal relaxation, resulting in 'regrowth' of the longitudinal magnetization vector Mz). These processes happen exponentially with time constants T2 and T1, respectively—T2 indicates the time after which dephasing is complete in 63% (so 37% phase coherence remains), and T1 corresponds to the time at which 63% of the longitudinal magnetization has recovered (bottom panels). T2 is always shorter and dephasing is complete (D) before longitudinal relaxation (E). T1 and T2 times depend on the type of the tissue and determine tissue contrast on T1- and T2-weighted sequences. Tissues with short T1 appear bright on T1-weighted sequence, while long T2 results in low signal on T2-weighted sequence (e.g. fat has high signal on T1- and T2-weighted sequences due to short T1 and relatively long T2).

Table 3.3 Signal intensity of different substances and tissues on T1- and T2-weighted MRI sequences

Substance	T1-weighted sequence	T2-weighted sequence
Water/Cerebrospinal fluid	↓	↑
Fat	↑	↑
Air	↓	↓
Cortical bone	↓	↓
Red bone marrow	=/↑	↑
Yellow bone marrow	↑	↑

Diffusion-weighted imaging (DWI) is sensitive to the movement of water molecules. DWI weighting is usually achieved by applying special diffusion-encoding gradients along the three principal spatial directions, and combining the signal into a trace image. Because the DWI trace image has both diffusion weighting and T_2-weighting, apparent hyperintensity can be due to restricted diffusion, or 'shine-through' phenomenon if the underlying area is T_2-hyperintense. It is therefore essential to review the apparent diffusion coefficient map (ADC), which eliminates the effect of T_2 weighting and demonstrates restricted diffusion as low signal intensity. Restricted diffusion may reflect a reduction in the size of the extracellular space that can be a result of cell swelling (e.g. in ischaemic stroke) or high cellularity (e.g. in lymphoma or

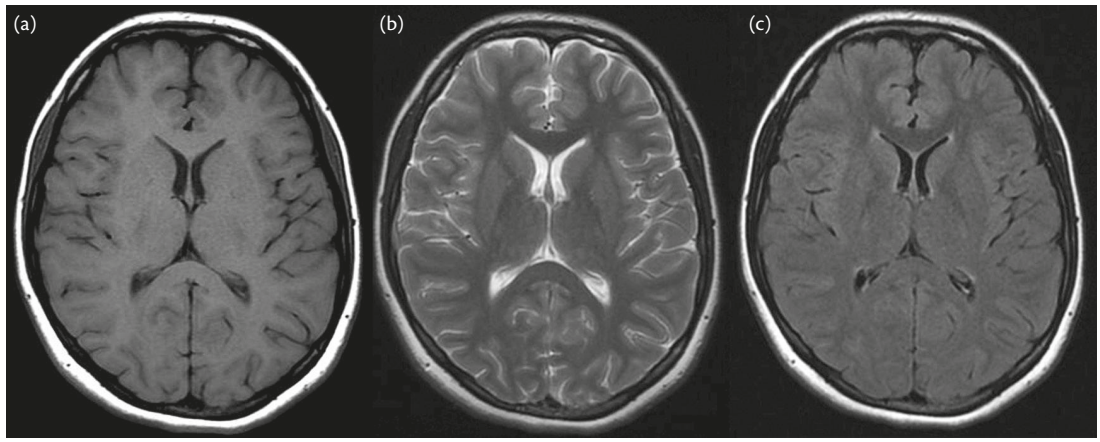

Fig. 3.4 Appearances of the brain on routine MRI sequences. (A) On T_1-weighted image grey matter is darker ('greyer') than white matter. (B) On T_2-weighted image the white matter is darker than grey matter and fluid is hyperintense. (C) T_2-FLAIR show similar contrast between the grey and white matter as T_2-weighted images but the signal from CSF is nulled.

medulloblastoma), as well as in lesions such as cholesteatoma or epidermoid cyst. In neurosurgical practice, the most important application of DWI is differentiation of pyogenic abscess from other ring-enhancing lesions, with the contents of the abscess demonstrating markedly restricted diffusion.

Applying diffusion gradients in at least six different directions underlies diffusion tensor imaging (DTI) which enables calculation of the predominant direction of diffusion in a given voxel. Because the movement of water is relatively unrestricted along the white matter tracts, DTI allows calculation of nerve fibres' direction and reconstruction of white matter tracts (DTI tractography), useful in neurosurgical planning (Waldman et al., 2009; Saindane, 2015). DTI also enables estimation of several measures of diffusion anisotropy with promising results in imaging and prognostication in traumatic brain injury (Hulkower et al., 2013) and high-grade gliomas (Price et al., 2007; Yan et al., 2016).

Functional MRI (fMRI) is based on blood oxygen level dependent (BOLD) effect resulting from different magnetic properties of oxyhaemoglobin (diamagnetic) and deoxyhaemoglobin (paramagnetic). Areas of the cortex with increased neuronal activity demonstrate higher oxygen consumption, but also increased perfusion due to neurovascular coupling; the effect of increased perfusion predominates, and the net result is a relative increase in MRI signal. Different activation paradigms allow the individual mapping of important cortical functions such as sensorimotor cortex and language localization (Stippich and Blatow, 2007).

Table 3.4 Signal intensity of haemorrhage of different stages on T1- and T2-weighted MRI sequences

Haemorrhage stage	Haemoglobin product	T1-weighted sequence	T2-weighted sequence
Hyperacute (<24 hrs)	Oxyhaemoglobin	=	↑
Acute (1–3 days)	Deoxyhaemoglobin	=	↓
Early subacute (3–7 days)	Intracellular methaemoglobin	↑	↓
Late subacute (1–4 weeks)	Extracellular methaemoglobin	↑	↑
Chronic (>1 month)	Haemosiderin	↓	↓↓

Contrast media in MRI

The majority of the contrast media used in MRI are paramagnetic agents based on gadolinium compounds. The pharmacokinetics of these agents are similar to those of iodinated contrast media with rapid passage from the vascular compartment to the interstitial compartment; an exception is gadofosveset, a blood pool agent that binds to albumin and remains in the vascular compartment. Gadolinium compounds do not pass through an intact blood-brain barrier so contrast enhancement is considered reflective of blood-brain barrier breakdown, apart from circumventricular organs, which have an incomplete blood-brain barrier and demonstrate physiological contrast enhancement that should not be mistaken for abnormality (Horsburgh and Massoud, 2013). Contrast enhancement is more conspicuous on MRI than on CT, and is invaluable in characterization of tumours, vascular disease, inflammation, and infection, both in the brain and in the spine.

Gadolinium compounds are generally safe but there are potential side effects associated with the release of unbound gadolinium from its chelates and accumulation in tissues. Nephrogenic systemic fibrosis is a rare but disabling dermopathy resembling scleroderma and eosinophilic fasciitis, first observed in patients on dialysis undergoing gadolinium contrast-enhanced MRI. Most cases were associated with the use of less stable linear agents that are now classified as high risk (Table 3.5). These compounds require renal function monitoring and are contraindicated in patients with glomerular filtration rate (GFR) below 30 ml/min/1.73 m^2, in neonates, and in the perioperative liver transplantation period; breastfeeding should

Table 3.5 Classification of gadolinium-based MRI contrast agents according to the risk of nephrogenic systemic fibrosis

High risk	Medium risk	Low risk
Gadodiamide (Omniscan)	Gadoxetic acid (Primovist)	Gadoteric acid (Dotarem)
Gadoversatamide (OptiMARK)	Gadobenic acid (MultiHance)	Gadoteridol (ProHance)
Gadopentetic acid (Magnevist)	Gadofosveset (Vasovist)	Gadobutrol (Gadovist)

Data from Drug Safety Update Jan 2010, vol 3 issue 6: 3. https://www.gov.uk

be discontinued for at least 24 hours after high-risk agent administration. Similar precautions are recommended but not mandatory for medium- and low-risk agents.

Recently it has been recognized that repeated administration of gadolinium-based contrast agents leads to accumulation of gadolinium in the brain, with the highest concentrations detected in the dentate nucleus and globus pallidus (Kanda et al., 2015b; McDonald et al., 2015). Accumulation of gadolinium is seen in patients receiving the less stable linear, but not macrocyclic compounds (Kanda et al., 2015b), and occurs even in the presence of normal renal function (Kanda et al., 2015a; McDonald et al., 2015). The clinical significance of these findings is however currently unknown.

General application of MRI in neurosurgery

Structural MRI has several advantages over CT and is the investigation of choice in the assessment of intracranial and spinal pathology with the exception of a few specific situations. In structural imaging, MRI provides superior tissue contrast, greater sensitivity to parenchymal abnormalities and contrast enhancement, better demonstration of anatomy, and allows imaging in any plane without using ionizing radiation; further information can be gained by addition of functional sequences. Disadvantages of MRI include long scanning time making it problematic in medically unstable patients and more prone to motion artefacts; therefore CT, with its established value in demonstration of intracranial haemorrhage and fractures, remains the investigation of choice in emergency situations, especially in trauma. CT is also better in demonstrating cortical bone and calcification, and remains more easily available and less costly. Use of MRI can be limited by several safety issues related to the static magnetic field, radiofrequency pulses, and gradient fields. MRI cannot generally be performed in patients with pacemakers, ferromagnetic aneurysm clips, implants, or foreign bodies. Care must be taken when imaging patients with shunt valves, cochlear implants, and heart valves, as well as in pregnancy; departmental practices vary. Finally, claustrophobia may preclude many patients from undergoing the MRI investigation or limit the scan time.

Positron emission tomography (PET)

PET is a nuclear medicine technique that uses tracers labelled with positron-emitting isotopes. The most commonly used radionuclide is fluorine-18 (^{18}F) due to its relatively long half-life that approaches two hours and is sufficiently long to allow transportation from an external cyclotron facility to the imaging centre. Short-lived isotopes require an on-site cyclotron (^{11}C, ^{13}N, ^{15}O) or are produced in a generator (^{68}Ga, ^{82}Rb). In the target organ, positrons emitted by the radionuclides travel a very short distance before interacting with electrons in neighbouring atoms and undergoing annihilation with the emission of two high energy photons that travel in opposite directions, which are detected by a ring array of solid-state scintillator detectors. The image is reconstructed based on the coregistration of pulses between opposite pairs of detectors, allowing placement of the annihilation event along a specific line of response (Fig. 3.5). Time of flight PET (TOF-PET) also measures tiny differences in time of arrival of the two photons to the opposite detectors, allowing more precise placement of the annihilation event to a segment along the line of response. Data needs to be corrected for the attenuation of photons inside the patient; this is achieved by using a rotating radiation source in standalone PET or direct information on attenuation

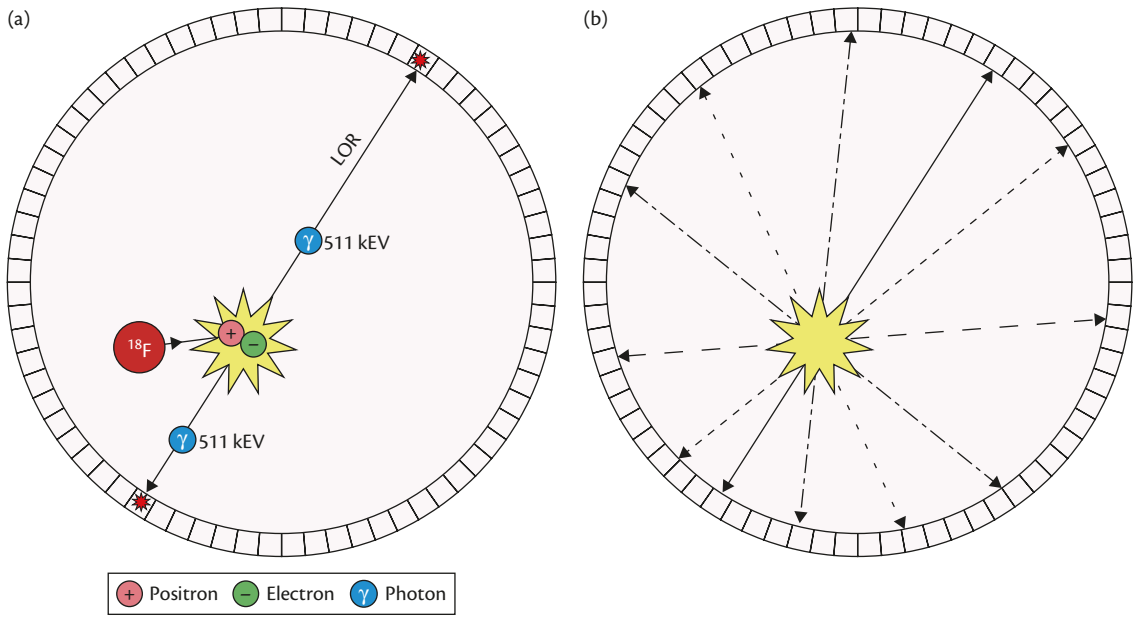

Fig. 3.5 (A) A positron-emitting isotope (most commonly 18F) releases positrons which collide with electrons in the target organ resulting in a series of annihilation events. Each annihilation event results in the emission of two high energy (511 keV) photons travelling in a straight line in opposite directions (at 180° to each other) at the speed of light. The two photons reach a ring of detectors placed around the gantry at the same time (if the annihilation happens in the centre of the gantry) or within a very short time window (if annihilation happens off-centre). The detection of such a coincidence event allows localization of the source of photons somewhere along the line of response (LOR) joining the pair of detectors which registered the photons. In time of flight (TOF) PET the tiny difference in time it takes for each photon to reach the detector for off-centre events is also taken into account, allowing the localization of the annihilation event more precisely along the LOR. (B) As photons produced by a series of annihilation events travel along different lines of response, combining information from multiple detected coincidence events allows localization of the radiation source.

obtained from a CT scan in PET-CT hybrid scanners. Data correction in MRI-PET is more challenging and requires calculation of attenuation values from anatomical MRI images.

PET is extremely sensitive, being able to detect picomolar quantities of tracer labelled with a positron emitter. In theory, any physiologically occurring substance, drug, or receptor ligand can be labelled, making PET the most promising technique for functional and molecular imaging. The most widely used tracer is ^{18}F-fluorodeoxyglucose (^{18}F-FDG), the uptake of which reflects the rate of glucose metabolism. Use of ^{18}F-FDG in the brain is problematic due to high rate of physiologic glucose metabolism; its potential applications include imaging of high-grade brain tumours, anaplastic transformation of low-grade gliomas, differentiation of radiation necrosis from tumour progression, differentiation of lymphoma from toxoplasmosis in immunocompromised patients, as well as detection of focal cortical dysplasia in epilepsy investigation. The armamentarium of PET tracers and range of potential applications in brain imaging is expanding; these are summarized in Table 3.6.

Most PET scanners in clinical use currently are either standalone machines, or PET-CT hybrids. Increasingly, PET-MRI hybrid scanners are becoming available. In view of the superior tissue contrast and resolution of MRI in the brain, integrated PET-MRI has potential advantages in neuroimaging. So far, it has been possible to combine sequential PET and MRI images acquired sequentially on separate scanners but hybrid PET-MRI imaging greatly facilitates such fusion eliminating the need for subsequent coregistration. More importantly, simultaneous acquisition of PET and MRI images could be of value when measuring parameters that undergo temporal changes, such as cerebral perfusion or hypoxia (Catana et al., 2012). These methods are currently largely limited to neuroimaging research, and their clinical usefulness remains to be established.

Other nuclear medicine techniques

Most nuclear medicine techniques use tracers labelled with radioligands emitting gamma radiation. The most commonly used radionuclide is ^{99m}Tc (technetium) due to a combination of optimal half-life, ease of production, and ease of incorporation into radiopharmaceuticals. Other isotopes used in neuroimaging include ^{111}In (indium) and ^{133}Xe (xenon). Emitted gamma rays can be detected using a planar gamma camera or rotating gamma camera in single-photon emission computed tomography (SPECT). Applications of SPECT in neuroradiology include cerebral perfusion measurements with ^{99m}Tc-HMPAO, ^{99m}Tc-ECD, and ^{133}Xe, diagnosis of dementia, identifying seizure focus in epilepsy, dopamine transporter imaging in diagnosis of parkinsonian syndromes, and brain tumour evaluation (McArthur et al., 2011). Planar gamma camera images are obtained in radionuclide cisternography, usually with ^{111}In-DTPA, performed for investigation of hydrocephalus or CSF leaks.

Myelography

Although MRI is the preferred method for examination of most spinal abnormalities, myelography remains indicated in patients who cannot undergo MRI (e.g. because of a pacemaker) and it also has a role in the detection of CSF leak sites in patients with spontaneous intracranial hypotension (Kranz et al., 2016). Iodinated contrast medium is injected into the spinal subarachnoid space, most commonly after lumbar puncture but sometimes after a lateral puncture at C1–2 if lumbar puncture cannot be performed. The puncture is typically done using fluoroscopic guidance and the injection of contrast is monitored by intermitted fluoroscopy to ensure that inadvertent epidural or subdural injection has not occurred. The contrast is then moved along the spinal canal to the appropriate location(s)

Table 3.6 Examples of PET tracers used in neuroimaging

PET tracer	Mechanism of action and applications
^{11}C-methionine, ^{18}F-FET	Transport into the cell via amino acid transporter increased in malignant tumours—characterization of tumour extent, biopsy guidance, treatment planning, response assessment (radiation necrosis, recurrence, pseudoresponse), prognostication; assessment of striatal dopamine pathway (^{18}F-DOPA)
^{18}F-FLT	Uptake correlated with activity of thymidine kinase-1 in proliferating cells—assessment of tumour grade, treatment response, prognostication
^{18}F-FMISO, ^{18}F-FAZA	Accumulation in hypoxic cells—assessment of hypoxia in brain tumours with potential relevance to tumour progression and resistance to treatment
^{11}C-PK11195, ^{18}F-GE180	Binding to translocator protein (TSPO) expressed in activated microglia and cancer cell lines—assessment of microglial activation/inflammation, assessment of tumour grade
^{68}Ga-DOTA-TOC ^{68}Ga-DOTA-TATE	Somatostatin analogues with high uptake in certain intracranial tumours—diagnosis of meningioma, pituitary adenoma, hemangioblastoma, medulloblastoma, PNET
^{11}C-PiB (Pittsburgh compound) ^{18}F-florbetaben, ^{18}F-florbetapir ^{18}F-flutemetamol	Binding to beta-amyloid plaques—diagnosis of Alzheimer disease
^{11}C-PBB3 ^{18}F-FDDNP	Binding to tau protein/neurofibrillary tangles—diagnosis of Alzheimer disease and tauopathies
^{11}C-flumaeznil ^{11}C-diprenorphine ^{11}C-SCH23390 ^{11}C-raclopride	Benzodiazepine receptor ligand—receptor binding studies Opioid receptor ligand—receptor binding studies Dopamine D_1 receptor ligand—receptor binding studies Dopamine D_2 receptor ligand—receptor binding studies
$^{15}O_2$ and [^{15}O] H_2O ^{11}C-leucine, ^{11}C-tyrosine ^{11}C-albumin $^{11}CO_2$, ^{11}C-DMO	Cerebral blood flow, oxygen metabolism Protein synthesis rate Plasma volume pH

by tilting the examination table and radiographs are obtained with the patient supine, prone, and in oblique positions. Myelography is typically then followed by a CT examination of the spine, which provides greater anatomical information than can be obtained from radiographs alone and allows excellent depiction of bony anatomy and spinal nerve roots on the same image.

Contraindications to myelography include allergy to iodinated contrast media, seizure disorders, bleeding disorders, or patients taking anticoagulants or antiplatelet agents, patients with suspected raised intracranial pressure, and uncooperative patients. Complications are uncommon with modern water-soluble iodinated contrast agents but include postdural puncture headache, seizures, bleeding at the puncture site, nerve root injury, and arachnoiditis (Sandow and Donnal, 2005).

Ultrasound

Ultrasound (US) is sound that has a frequency greater than the upper threshold of human hearing, approximately 20 kHz. Ultrasound used for medical imaging typically has a frequency between 2 MHz and 18 MHz. When transmitted from an ultrasound probe into the body, an US beam undergoes reflection and refraction when it passes through changes in tissue density and compressibility. The US probe can detect the returned echoes and determine their depth of origin within the patient based on the time since transmission and the speed of sound in tissue. The intensity of the returned echoes is affected by the reflectivity of the tissue and the degree to which it attenuates the US beam. It is thus possible to construct a two-dimensional greyscale image in which the position and brightness of each pixel corresponds to the site of origin and strength of an echo arising within the patient, so-called B-mode imaging (Allisy-Roberts and Williams, 2007).

Bone and calcified tissues are both highly reflective and attenuating, preventing through transmission of sound, so appear as a bright white interface beyond which there is an 'acoustic shadow' in which no information is obtained. Conversely fluid is of low reflectivity and attenuates the beam weakly, thus appearing as an anechoic area beyond which there is increased through transmission of sound relative to adjacent tissues and resulting in posterior acoustic enhancement.

The attenuation of the US beam by bone limits the utility of B-mode imaging for assessing the brain in adults and children. Transfontanellar US scanning of neonates and infants can be used to assess the size of the ventricles, detect intraventricular and parenchymal haemorrhage in preterm neonates, and evaluate the brain parenchyma in cases of hypoxic ischaemic encephalopathy. Ultrasound of the spine can also be performed in neonates for assessment of suspected cases of dysraphism to assess the position of the conus, presence of diastematomyelia, or associated intraspinal masses.

When US waves are reflected by a moving interface their frequency is changed by the Doppler effect, resulting in an increase in frequency if the interface is moving towards the transducer and a reduction in frequency for a reflector that is moving away. The velocity of reflector motion affects the amount of change in frequency. This effect is exploited by pulsed-wave Doppler US to obtain waveforms from blood vessels that show the velocity and direction of blood flow with respect to the transducer. In colour Doppler imaging the information regarding direction and velocity of blood flow is overlaid on a greyscale B-mode image as a colour-coded map.

Doppler US can be used to detect the presence of carotid artery stenosis in patients with carotid bruits, transient ischaemic attacks, or ischaemic strokes. The degree of carotid stenosis is generally assigned to a percentage range based on the increase in blood flow velocity through area of stenosis. It is also possible to assess the blood flow of major intracranial arteries by transcranial Doppler (TCD). This requires the use of low frequency (2–3 MHz) transducers that can penetrate through the relatively thin bone of the pterion or by scanning through the foramen magnum. TCD can be used to perform bedside monitoring of patients with aneurysmal subarachnoid haemorrhage to look for increases in blood flow velocity that can indicate vasospasm (Marshall et al., 2010). Some institutions also use intraoperative colour Doppler US for the assessment of CSF flow at the foramen magnum in cases of foramen magnum decompression for Chiari I malformation.

Vascular imaging

Digital subtraction angiography

Digital subtraction angiography (DSA) (Wolpert, 1999) remains the reference standard for imaging of vascular disorders of the brain and spine, although with improvements in CT angiography and MR angiography, the indications for DSA as the first-line investigation have decreased. DSA is usually performed under local anaesthesia, although sedation or general anaesthesia may be necessary in uncooperative patients, for interventional neuroradiology procedures and, depending on operator preference, in diagnostic spinal angiography. The usual route of access to the arterial system is through the common femoral artery; where this is not possible then transradial or transbrachial arterial approaches may be used. After puncture with a needle, a soft-tipped guidewire is threaded through the needle into the artery and the needle is then removed and exchanged for a polyethylene catheter. A variety of catheter shapes are available, the selection partly depending on operator preference but also on the degree of arterial tortuosity. Under fluoroscopic guidance the catheter can be positioned in the internal and external carotid arteries and the vertebral arteries as necessitated by the indication for the DSA. Neuroangiography is typically performed using biplane angiography units that have two X-ray tubes and image intensifiers or, increasingly often, flat panel digital detectors. This allows acquisition of images simultaneously from two different projections, reducing the length of the examination and the volume of contrast material that needs to be injected. Images are acquired using pulsed X-rays immediately before (so-called mask images) and then during the injection of contrast material into the artery. By subtracting mask images from those obtained during the injection of contrast, images are produced that eliminate bone and soft tissue detail and show only the contrast within the blood vessels. If the patient moves during image acquisition the mask images will not be correctly registered with the postcontrast images and they may need to be aligned manually. It is also possible to obtain three-dimensional images by rotating the C-arm around the patient's head during the injection of contrast (rotational 3D DSA).

Possible complications of cerebral DSA include those common to all invasive angiographic procedures such as puncture site haematoma (approximately 5%), arterial dissection, and contrast reactions. Manipulation of catheters in the aortic arch and neck arteries

also carries a small risk of neurologic deficits, which are most often transient (approximately 2.5%) but can rarely be permanent (approximately 0.2%). The risk of neurological complications depends on the operator's experience and is increased in older patients and longer procedures.

CT angiography and CT venography

CT angiography (CTA) involves the rapid acquisition of a thin section data set of the area of clinical interest during the first pass of an injected bolus of iodinated contrast material. Acquisition of images during the arterial phase can be achieved by bolus tracking or test bolus methods. Bolus tracking involves triggering the scan acquisition when the attenuation within a chosen vessel, most often the internal carotid artery, reaches a predetermined level after the start of contrast injection. The test bolus method determines the optimum time to start scan acquisition by using a separate injection of a small volume of contrast medium. Although image interpretation always requires review of the axially acquired source images, reconstruction of the 3D data using multiplanar reformats, maximum intensity projection (MIP), and volume-rendered images can facilitate the identification of abnormalities and enhance the appreciation of their relationship to surrounding vessels.

Advantages of CTA over DSA include its non-invasive nature, more widespread availability, and the ease and speed of acquisition. Disadvantages of conventional CTA include its poor temporal resolution—images are essentially a 'snapshot' that do not provide dynamic information, reduced spatial resolution relative to DSA, and potential obscuration of small vascular abnormalities adjacent to bone. Bone-subtracted CTA images can be obtained by acquiring a mask of CT data before injecting contrast and subtracting it from the postcontrast images in a manner analogous to DSA, or by using dual energy X-ray acquisition (although this requires a dedicated dual energy CT scanner).

CT venography is similar in principle to CTA except that the images are acquired when the majority of the injected contrast is in the venous phase. The timing of image acquisition is less critical and can generally be achieved with a fixed scan delay of 40 seconds after the start of contrast injection.

MR angiography (MRA) and venography (MRV)

There are several different methods by which angiographic images can be obtained with MRI. Non-contrast methods rely on signal differences between flowing blood and surrounding stationary tissues (Lim and Koktzoglou, 2015). Time-of-flight magnetic resonance angiography (TOF-MRA) depends on flow-related enhancement, where stationary tissues saturated by repeated radiofrequency pulses display low signal, while non-saturated blood flowing into the imaged slice is hyperintense. Phase-contrast angiography (PC-MRA) uses two bipolar gradients inducing a phase shift in blood flowing along the gradient direction, which is proportional to the flow velocity. By changing the gradient strength, velocity encoding sensitivity (Venc) can be tailored to optimally demonstrate arterial or venous flow. Both TOF-MRA and PC-MRA can be performed using two (2D) or three-dimensional (3D) acquisition. Contrast-enhanced MRA (CE-MRA) is similar in principle to CTA, whereby the vessel visualization depends on intravenously injected contrast agent. In practice, 3D TOF-MRA is the main technique used to image intracranial vasculature, with sensitivity and specificity in aneurysm detection similar to CTA when performed on a three-tesla system (Lim and Koktzoglou, 2015). Large aneurysms or aneurysm with slow flow are better demonstrated with CE-MRA, which can also be performed as time-resolved examination (Saindane, 2015) for evaluation of arteriovenous malformations or dural fistulas. In detection of carotid artery stenosis, TOF-MRA is less sensitive and specific than CE-MRA (Gough, 2011) and tends to overestimate the degree of stenosis. MRV is most often performed using a phase-contrast method, as time of flight can be confounded by hyperintense appearances of a subacute thrombus that can mimic normal flow-related enhancement (Nadgir and Yousem, 2016). MRV can also be performed as contrast-enhanced examination (Sadigh et al., 2016).

Other vascular techniques

As mentioned earlier, high sensitivity of SWI to even small quantities of blood products renders it highly useful for detection of intracranial haemorrhage, for example, microhaemorrhages in cerebral amyloid angiopathy or traumatic brain injury. In addition, due to its sensitivity to paramagnetic properties of deoxyhaemoglobin, SWI allows excellent demonstration of venous structures (Di Ieva et al., 2015). SWI has been shown to be useful in demonstrating venous drainage of arteriovenous malformations (AVMs) and evaluation of the extent of their neurosurgical resection, as well as depiction of micro-AVMs (Mossa-Basha et al., 2012; Saindane, 2015).

In addition to evaluation of the vessel lumen, there has been increasing emphasis on the assessment of the vessel wall. In carotid artery imaging, the main focus is on the evaluation of atherosclerotic plaque, in particular its stability and propensity to rupture (Young et al., 2011). Intracranial vessel wall imaging can be useful in evaluation of intracranial atherosclerosis, moyamoya disease, vasculitis, reversible cerebral vasoconstriction syndrome, and intracranial arterial dissection (Mandell et al., 2017).

Imaging methods to measure cerebral blood flow and metabolism

Imaging of cerebral perfusion and metabolism has a wide variety of research and clinical applications including assessment of acute stroke, hypoxic brain injury, vasospasm, characterization of cerebrovascular reserve, and evaluation of traumatic brain injury (Coles, 2006; Dani and Warach, 2014). Major applications are found in neuro-oncology where different methods are combined to derive information on tumour type and grading, differentiation from non-neoplastic lesions, biopsy guidance, response assessment, and differentiation of chemotherapy and radiotherapy effects from tumour progression (Herholz et al., 2007; Waldman et al., 2009; Kim et al., 2016). Regional differences in blood flow and metabolism also provide additional diagnostic information in dementia and neurodegenerative disease (Schuff, 2013; Ishii, 2014). Space constraints dictate only a brief description of the available modalities; more comprehensive analysis can be found in the references provided, as well as dedicated volumes (Gillard et al., 2010; Barker et al., 2013).

Measuring cerebral blood flow

The imaging methods used to measure cerebral perfusion can be based on inert diffusible tracers or non-diffusible intravascular tracers (Coles, 2006). The former rely on the Fick principle stating that

uptake of any substance by the target organ depends on its arteriovenous concentration gradient and the organ perfusion. Techniques that use diffusible traces include xenon-enhanced CT with non-radioactive ^{131}Xe, and nuclear medicine methods such as SPECT with ^{99m}Tc-HMPAO, ^{99m}Tc-ECD or radioactive ^{133}Xe isotope, and PET with $^{15}O_2$. Quantitative $^{15}O_2$ PET and xenon CT are considered the gold standard for measuring cerebral perfusion, but are not routinely used in clinical imaging (Thompson et al., 2010). Magnetically tagged water molecules in MR perfusion using arterial spin labelling also behave like a diffusible tracer, and this approach is likely to be increasingly applied in a clinical setting (Grade et al., 2015).

Techniques that require intravascular injection of a non-diffusible tracer are more widely available and are increasingly becoming part of routine imaging, especially in stroke and neuro-oncological imaging. The basic principles underlying measurement of perfusion parameters with these methods by CT or MRI are similar and rely on rapid serial imaging during the first pass of an injected bolus of contrast material (Konstas et al., 2009a). In simple terms, the resulting changes in attenuation (CT) and signal intensity (MRI) in the brain depend on the combination of the inherent perfusion characteristics of the tissue and the inflow of contrast from the arteries supplying the voxels of interest (arterial input function), assuming that the contrast agent remains within the vascular space. The area under the contrast concentration curve and the width of the contrast bolus provide estimates of cerebral blood volume (CBV) and mean transit time (MTT), respectively, and the cerebral blood flow (CBF) can be calculated from the central volume theorem (CBF = CBV/MTT). CT perfusion (CTP) is now widely used in the evaluation of the extent of core infarction and ischaemic penumbra in acute stroke (Konstas et al., 2009a; Konstas et al., 2009b) and in diagnosis and management of vasospasm following subarachnoid haemorrhage (Mir et al., 2014). The greatest advantage of CTP is the linear relationship between the concentration of iodine and tissue attenuation, and direct measurement of arterial input and venous output functions, allowing for direct calculation of vascular parameters. A disadvantage of perfusion CT compared with MRI has been the use of ionizing radiation, and its limited craniocaudal coverage, now largely overcome with larger detector array CT scanners and shuttling table techniques.

Perfusion MRI techniques are based either on measuring susceptibility effects of gadolinium contrast agent causing a reduction of T_2* signal (dynamic susceptibility contrast, DSC), or its relaxivity effects reflected by an increase in T_1 signal (dynamic contrast enhancement, DCE). Quantitative assessment of absolute perfusion parameters is more difficult than for CTP and requires mathematical and pharmacokinetic modelling with several assumptions about the behaviour of the injected tracer, and correction accounting for contrast leakage into extravascular space (Jackson, 2004). To simplify comparisons, perfusion parameters derived from DSC can be expressed as relative values, usually normalized against contralateral white matter. DCE allows calculation of several parameters that characterize the microvascular environment, including permeability. The most commonly used indices include estimates of blood flow (F), permeability surface area product per unit mass of tissue (PS), the volume transfer constant (K_{trans}), volumes of the extravascular extracellular space (V_e) and blood plasma (V_b), as well as semiquantitative indices derived from the shape of the enhancement curve (Thompson et al., 2010; Griffith and Jain, 2015).

An emerging technique of cerebral blood volume quantification is vascular space occupancy imaging (VASO), which uses T_1 difference between the blood and tissue to separate the two compartments. VASO MRI can detect changes in CBV with high temporal resolution without the use of injected contrast medium, and provides absolute CBV measurements when also performed with intravenous contrast agent (Lu and Uh, 2013).

Recently there has been renewed interest in measuring brain perfusion using intravoxel incoherent motion imaging (IVIM) which is based on the observation that signal in diffusion weighted MRI depends not only on diffusion itself, but also on blood flow within the capillary bed (pseudo diffusion). By using a range of diffusion gradient strengths and bi-exponential fitting or kurtosis models, the effects of capillary flow and true diffusion can be separated, providing an estimation of perfusion (Federau et al., 2014).

It is also worth mentioning here the methods used to evaluate brain oxygenation, which depends on perfusion and oxygen metabolism. The gold standard technique is $^{15}O_2$ PET which may be supplemented with $[^{15}O]H_2O$ and $[^{15}O]CO$ administration (triple oxygen PET), providing absolute values of cerebral metabolic rate of oxygen ($CRMO_2$) and oxygen extraction fraction, in addition to cerebral perfusion indices. Emerging MRI-based methods include quantitative BOLD, phase- and susceptibility-based imaging, and intravascular T_2-based approaches (Christen et al., 2013).

Measuring cerebral metabolism

The two major imaging modalities currently used for assessment of cerebral metabolism are PET and magnetic resonance spectroscopy (MRS). As described earlier, depending on the tracer PET allows estimation of local or regional glucose metabolism (^{18}FDG-PET) and oxygen metabolism ($^{15}O_2$, triple oxygen). In brain tumours, PET allows estimation of amino acid transport (^{11}C-methionine, ^{18}F-FET), protein synthesis (^{11}C-methionine and ^{11}C-leucine) and DNA synthesis (^{18}F-FLT), as well as tissue-level hypoxia (^{18}F-FMISO and ^{18}F-FAZA).

MRS is based on chemical shift, a specific change in resonance frequency that arises as a result of electron shielding when an atom of interest is chemically bound within a compound. MRS allows probing of the biochemical milieu in a defined voxel of interest (single voxel spectroscopy) or as 2D or 3D magnetic spectroscopic imaging (CSI), mapping the concentration of a given compound across the brain. MRS is generally a challenging technique due to low sensitivity and low signal-to-noise ratio, and requires higher strength and precise shimming of the magnetic field. The most commonly used form of MRS due to relative abundance of the target nucleus is proton spectroscopy (^{1}H-MRS). In the brain, ^{1}H-MRS detects a spectrum of several metabolites considered markers of specific metabolic aspects, in particular N-acetyl aspartate (NAA, a marker of neuronal integrity), choline (Cho, a marker of membrane turnover), creatine, and myoinositol (markers of cellular energy status). Pathologic conditions cause changes in the spectral pattern, or appearance of abnormal metabolite peaks such as lactate (Lac, marker of metabolic acidosis and cell death), or lipids (marker of tissue breakdown); for example, high-grade gliomas demonstrate a reduction in NAA and elevated Cho, accompanied by lipid and lactate peaks (Herholz et al., 2007). More technically challenging ^{31}P-MRS allows estimation of energy metabolism by detecting spectra from phosphorus-containing molecules of ATP, phosphocreatine, and inorganic phosphate, as well as of the neuronal membrane

metabolism by detecting phosphomonoesters and phosphodiesters (Herholz et al., 2007).

Recently there has been intense interest in dynamic nuclear polarization (DNP or hyperpolarization), a technique aiming to address the inherent problem of low sensitivity in spectroscopy by increasing the proportion of nuclei contributing to magnetic resonance signal. Normally, magnetic moments of nuclei polarized in a magnetic field align either parallel (spin up) or antiparallel to the field (spin down); net magnetic resonance signal is attributed to the tiny difference between the number of nuclei pointing each way (with just a few more nuclei per million pointing spin up). DNP is performed by extreme cooling of a sample containing nuclei of interest and free radicals as a source of unpaired electrons in a solid state, and subjecting it to a strong magnetic field. In these conditions, electron spins become highly polarized, and this polarization is partly transferred to nuclear spins by microwave irradiation, resulting in a more than 10 000-fold increase in signal-to-noise ratio (Ardenkjaer-Larsen et al., 2003). Such a treatment cannot of course be performed *in vivo*, but can be used to hyperpolarize a sample containing MRS-detectable nuclei, which can be quickly warmed up, injected into a patient, and imaged with increased signal-to-noise ratio. Systems capable of DNP in humans are now available, and there is intense research effort in this area. The most common metabolite currently used in DNP is [1-^{13}C]pyruvate, which after injection is converted into [1-^{13}C]lactate by lactate dehydrogenase (LDH), [1-^{13}C]alanine by alanine transaminase, and $^{13}CO_2$ by pyruvate dehydrogenase (PDH), the latter further converted into [^{13}C]bicarbonate. Conversion of pyruvate into lactate is increased in malignant tumours, even in the presence of sufficient oxygen (Warburg effect), which is leveraged in cancer diagnosis and assessment of treatment response (Kim et al., 2016). Other promising markers which proved potentially useful in animal models include [1,4-^{13}C]fumarate for detection of cellular necrosis, [^{13}C]bicarbonate for *in vivo* measurement of pH, and [5-^{13}C]glutamine for assessment of tumour metabolism, while [1-^{13}C]urea can be used as a perfusion marker. It is also possible to inject and detect several hyperpolarized substrates simultaneously, provided that their chemical shift is sufficiently different to distinguish them spectroscopically (Brindle et al., 2011).

Future directions

Current conventional radiological methods allow demonstration of anatomical and macroscopic pathological features of disease with excellent sensitivity and resolution. Functional imaging methods that have enabled insight into variety of physiological and pathological phenomena as described earlier, are an important first step beyond anatomical imaging towards more precise characterization of the disease process. These methods however remain generally non-specific, demonstrating changes that are common endpoints of many possible pathological pathways. One avenue towards more specific information is radiomics—conversion of images into higher dimensional data and subsequent feature extraction and data mining in a manner analogous to genomic, proteomic, or metabolomic approaches, with the aim to obtain imaging signatures corresponding to particular features of disease (Gillies et al., 2016). Radiomic features include both semantic measures (e.g. shape, size, or vascularity), and mathematically derived agnostic descriptors (such as histogram skewness or kurtosis, fractal, and texture analysis). Radiomics provides useful additional information for diagnosis, treatment selection, and prognostication, but its inherent limitation is the same as of the original imaging method used to obtain the source data. The ultimate goal would be to obtain information on the cellular and molecular events that precede and underlie the observed anatomical and functional sequelae by using probes specific to a particular molecular target or biochemical pathway. This would lead to better understanding of abnormal biology, enable earlier detection, and provide precise diagnosis and disease staging. Molecular imaging could also provide better endpoint biomarkers in the drug discovery process, allowing rapid assessment of treatment effect on molecular level even before phenotypical response occurs (Massoud and Gambhir, 2007). Arguably, the most important application of such methods will be in neuro-oncology, where there are already several examples of clinical applications of detecting specific receptors, or protein products specific to certain enzyme isoforms (Kim et al., 2016). It is likely that PET and MRI will be used for detection of imaging probes due to limitations of optical, photoacoustic, or ultrasound techniques for intracranial imaging, although these could be used intraoperatively or during endoscopy. Nanoparticles are emerging as an ideal imaging agent (Thakor and Gambhir, 2013) that can be targeted to a specific tissue and labelled for detection by a chosen assay, or even multiple methods, for example, for preoperative imaging by MRI, and intraoperative localization using photoacoustic and optical imaging (Kircher et al., 2012). Concurrent loading of nanoparticles with a therapeutic agent enables combination of diagnostics and therapy—theranostics (Kelkar and Reineke, 2011; Thakor and Gambhir, 2013), in which imaging is paired to the targeted delivery of a chemotherapeutic, gene-silencing agent; or radioactive isotope; or to radiosensitization, photodynamic, or photothermal interventions. In the future, imaging will undoubtedly be the key element of precision medicine, enabling precise diagnosis and individualized therapy tailored for the individual patient and targeted to a particular pathological entity (Kim et al., 2016).

REFERENCES

Allisy-Roberts, P. & Williams, J.R. (2007). *Farr's Physics for Medical Imaging*, illustrated edition. Philadelphia, PA: Elsevier Health Sciences.

Ardenkjaer-Larsen, J.H., Fridlund, B., Gram, A., et al. (2003). Increase in signal-to-noise ratio of > 10,000 times in liquid-state NMR, *Proc Natl Acad Sci U S A*, **100**(18), 10158–63.

Barker, P.B., Golay, X., & Zaharchuk, G. (2013). *Clinical Perfusion MRI Techniques and Applications*. Cambridge, UK: Cambridge University Press.

Barrett, J.F. & Keat, N. (2004). Artifacts in CT: recognition and avoidance. *Radiographics*, **24**(6), 1679–91.

Bitar, R., Leung, G., Perng, R., et al. (2006). MR pulse sequences: what every radiologist wants to know but is afraid to ask. *Radiographics*, **26**(2), 513–37.

Brindle, K.M., Bohndiek, S.E., Gallagher, F.A., & Kettunen, M.I. (2011). Tumor imaging using hyperpolarized 13C magnetic resonance spectroscopy. *Magn Reson Med*, **66**(2), 505–19.

Catana, C., Drzezga, A., Heiss, W.D., & Rosen, B.R. (2012). PET/MRI for neurologic applications. *J Nucl Med*, **53**(12), 1916–25.

Christen, T., Bolar, D.S., & Zaharchuk, G. (2013). Imaging brain oxygenation with MRI using blood oxygenation approaches: methods, validation, and clinical applications. *AJNR*, **34**(6), 1113–23.

Cohnen, M., Wittsack, H.J., Assadi, S., et al. (2006). Radiation exposure of patients in comprehensive computed tomography of the head in acute stroke. *AJNR*, **27**(8), 1741–5.

Coles, J.P. (2006). Imaging of cerebral blood flow and metabolism. *Curr Opin Anaesthesiol*, **19**(5), 473–80.

Dani, K.A. & Warach, S. (2014). Metabolic imaging of ischemic stroke: the present and future. *AJNR*, **35**(6 Suppl), S37–43.

Di Ieva, A., Lam, T., Alcaide-Leon, P., Bharatha, A., Montanera, W., & Cusimano, M.D. (2015). Magnetic resonance susceptibility weighted imaging in neurosurgery: current applications and future perspectives. *J Neurosurg*, **123**(6), 1463–75.

Federau, C., O'Brien, K., Meuli, R., Hagmann, P., & Maeder, P. (2014). Measuring brain perfusion with intravoxel incoherent motion (IVIM): initial clinical experience. *J Magn Reson Imaging*, **39**(3), 624–32.

Gillard, J.H., Waldman, A.D., & Barker, P.B. (2010). *Clinical MR Neuroimaging: Physiological and Functional Techniques*. Cambridge, UK: Cambridge University Press.

Gillies, R.J., Kinahan, P.E., & Hricak, H. (2016). Radiomics: images are more than pictures, they are data. *Radiology*, **278**(2), 563–77.

Ginat, D.T. & Gupta, R. (2014). Advances in computed tomography imaging technology. *Annu Rev Biomed Eng*, **16**, 431–53.

Gough, M.J. (2011). Preprocedural imaging strategies in symptomatic carotid artery stenosis. *J Vasc Surg*, **54**(4), 1215–18.

Grade, M., Hernandez Tamames, J.A., Pizzini, F.B., Achten, E., Golay, X., & Smits, M. (2015). A neuroradiologist's guide to arterial spin labeling MRI in clinical practice. *Neuroradiology*, **57**(12), 1181–202.

Griffith, B. & Jain, R. (2015). Perfusion imaging in neuro-oncology: basic techniques and clinical applications. *Radiol Clin North Am*, **53**(3), 497–511.

Herholz, K., Coope, D., & Jackson, A. (2007). Metabolic and molecular imaging in neuro-oncology. *Lancet Neurol*, **6**(8), 711–24.

Hoeffner, E.G., Mukherji, S.K., Srinivasan, A., & Quint, D.J. (2012). Neuroradiology back to the future: brain imaging, *AJNR*, **33**(1), 5–11.

Hoffman, J.M. & Gambhir, S.S. (2007). Molecular imaging: the vision and opportunity for radiology in the future. *Radiology*, **244**(1), 39–47.

Horsburgh, A. & Massoud, T.F. (2013). The circumventricular organs of the brain: conspicuity on clinical 3 T MRI and a review of functional anatomy. *Surg Radiol Anat*, **35**(4), 343–9.

Hounsfield, G.N. (1995). Computerized transverse axial scanning (tomography): part I. Description of system. 1973. *Br J Radiol*, **68**(815), H166–72.

Hulkower, M.B., Poliak, D.B., Rosenbaum, S.B., Zimmerman, M.E., & Lipton, M.L. (2013). A decade of DTI in traumatic brain injury: 10 years and 100 articles later. *AJNR*, **34**(11), 2064–74.

Hunt, C.H., Hartman, R.P., & Hesley, G.K. (2009). Frequency and severity of adverse effects of iodinated and gadolinium contrast materials: retrospective review of 456,930 doses. *AJR Am J Roentgenol*, **193**(4), 1124–7.

Ishii, K. (2014). PET approaches for diagnosis of dementia. *AJNR*, **35**(11), 2030–8.

Jackson, A. (2004). Analysis of dynamic contrast enhanced MRI. *Br J Radiol*, **77** Spec No 2, S154–66.

Kanda, T., Fukusato, T., Matsuda, M., et al. (2015a). Gadolinium-based contrast agent accumulates in the brain even in subjects without severe renal dysfunction: evaluation of autopsy brain specimens with inductively coupled plasma mass spectroscopy. *Radiology*, **276**(1), 228–32.

Kanda, T., Osawa, M., Oba, H., et al. (2015b). High signal intensity in dentate nucleus on unenhanced T1-weighted MR images: association with linear versus macrocyclic gadolinium chelate administration. *Radiology*, **275**(3), 803–9.

Kelkar, S.S. & Reineke, T.M. (2011). Theranostics: combining imaging and therapy. *Bioconjugate Chem*, **22**(10), 1879–903.

Kidwell, C.S. & Wintermark, M. (2010). The role of CT and MRI in the emergency evaluation of persons with suspected stroke. *Curr Neurol Neurosci Rep*, **10**(1), 21–8.

Kilic, K., Erbas, G., Guryildirim, M., Arac, M., Ilgit, E., & Coskun, B. (2011). Lowering the dose in head CT using adaptive statistical iterative reconstruction. *AJNR*, **32**(9), 1578–82.

Kim, M.M., Parolia, A., Dunphy, M.P., & Venneti, S. (2016). Non-invasive metabolic imaging of brain tumours in the era of precision medicine. *Nat Rev Clin Oncol*, **13**(12), 725–39.

Kimpe, T. & Tuytschaever, T. (2007). Increasing the number of gray shades in medical display systems—how much is enough? *J Digi Imaging*, **20**(4), 422–32.

Kircher, M.F., de la Zerda, A., Jokerst, J.V., et al. (2012). A brain tumor molecular imaging strategy using a new triple-modality MRI-photoacoustic-Raman nanoparticle. *Nat Med*, **18**(5), 829–34.

Konstas, A.A., Goldmakher, G.V., Lee, T.Y., & Lev, M.H. (2009a). Theoretic basis and technical implementations of CT perfusion in acute ischemic stroke, part 1: theoretic basis. *AJNR*, **30**(4), 662–8.

Konstas, A.A., Goldmakher, G.V., Lee, T.Y., & Lev, M.H. (2009b). Theoretic basis and technical implementations of CT perfusion in acute ischemic stroke, part 2: technical implementations. *AJNR*, **30**(5), 885–92.

Kranz, P.G., Luetmer, P.H., Diehn, F.E., Amrhein, T.J., Tanpitukpongse, T.P., & Gray, L. (2016). Myelographic techniques for the detection of spinal CSF leaks in spontaneous intracranial hypotension. *AJR Am J Roentgenol*, **206**(1), 8–19.

Lauterbur, P.C. (1989). Image formation by induced local interactions: examples employing nuclear magnetic resonance. *Clin Orthop Relat Res*, (244), 3–6.

Lim, R.P. & Koktzoglou, I. (2015). Noncontrast magnetic resonance angiography: concepts and clinical applications. *Radiol Clin North Am*, **53**(3), 457–76.

Lu, H. & Uh, J. (2013). Vascular space occupancy (VASO) imaging of cerebral blood volume. In: Barker, P.B., Golay, X., Zaharchuk, G., et al. (eds) *Clinical Perfusion MRI Techniques and Applications*, pp. 89–102. Cambridge, UK: Cambridge University Press.

Lusic, H. & Grinstaff, M.W. (2013). X-ray-computed tomography contrast agents. *Chem Rev*, **113**(3), 1641–66.

Mandell, D.M., et al. & Vessel Wall Imaging Study Group of the American Society of Neuroradiology (2017). Intracranial vessel wall MRI: principles and expert consensus recommendations of the American Society of Neuroradiology. *AJNR Am J Neuroradiol*, **38**(2), 218–29.

Mansfield, P. & Maudsley, A.A. (1977). Medical imaging by NMR. *Br J Radiol*, **50**(591), 188–94.

Marshall, S.A., Nyquist, P., & Ziai, W.C. (2010). The role of transcranial Doppler ultrasonography in the diagnosis and management of vasospasm after aneurysmal subarachnoid hemorrhage. *Neurosurg Clin N Am*, **21**(2), 291–303.

Massoud, T.F. & Gambhir, S.S. (2007). Integrating noninvasive molecular imaging into molecular medicine: an evolving paradigm, *Trends Mol Med*, **13**(5), 183–91.

McArthur, C., Jampana, R., Patterson, J., & Hadley, D. (2011). Applications of cerebral SPECT. *Clin Radiol*, **66**(7), 651–61.

McDonald, R.J., McDonald, J.S., Kallmes, D.F., et al. (2015). Intracranial gadolinium deposition after contrast-enhanced MR imaging. *Radiology*, **275**(3), 772–82.
Mettler, F.A., Huda, W., Yoshizumi, T.T., & Mahesh, M. (2008). Effective doses in radiology and diagnostic nuclear medicine: a catalog. *Radiology*, **248**(1), 254–63.
Michel, M., Jacob, S., Roger, G., et al. (2012). Eye lens radiation exposure and repeated head CT scans: a problem to keep in mind. *Eur J Radiol*, **81**(8), 1896–900.
Mir, D.I., Gupta, A., Dunning, A., et al. (2014). CT perfusion for detection of delayed cerebral ischemia in aneurysmal subarachnoid hemorrhage: a systematic review and meta-analysis. *AJNR*, **35**(5), 866–71.
Mirro, A.E., Brady, S.L., & Kaufman, R.A. (2016). Full dose-reduction potential of statistical iterative reconstruction for head CT protocols in a predominantly pediatric population. *AJNR*, **37**(7), 1199–205.
Mossa-Basha, M., Chen, J., & Gandhi, D. (2012). Imaging of cerebral arteriovenous malformations and dural arteriovenous fistulas. *Neurosurg Clin N Am*, **23**(1), 27–42.
Nadgir, R. & Yousem, D.M. (2016). *Neuroradiology: The Requisites*, 4th edition. Philadelphia, PA: Elsevier.
Price, S.J., Jena, R., Burnet, N.G., Carpenter, T.A., Pickard, J.D., & Gillard, J.H. (2007). Predicting patterns of glioma recurrence using diffusion tensor imaging. *Eur Radiol*, **17**(7), 1675–84.
Sadigh, G., Mullins, M.E., & Saindane, A.M. (2016). Diagnostic performance of MRI sequences for evaluation of dural venous sinus thrombosis. *AJR Am J Roentgenol*, **206**(6), 1298–306.
Saindane, A.M. (2015). Recent advances in brain and spine imaging. *Radiol Clin North Am*, **53**(3), 477–96.
Sandow, B.A. & Donnal, J.F. (2005). Myelography complications and current practice patterns. *AJR Am J Roentgenol*, **185**(3), 768–71.
Schuff, N. (2013). MR perfusion imaging in neurodegenerative disease. In: Barker, P.B., Golay, X., Zaharchuk, G., et al. (eds) *Clinical Perfusion MRI: Techniques and Applications*, pp. 164–178. Cambridge, UK: Cambridge University Press.
Stippich, C. & Blatow, M. (2007). *Clinical Functional MRI: Presurgical Functional Neuroimaging*. Berlin, Germany/New York: Springer.
Thakor, A.S. & Gambhir, S.S. (2013). Nanooncology: the future of cancer diagnosis and therapy. *CA Cancer J Clin*, **63**(6), 395–418.
The Royal Australian and New Zealand College of Radiologists (2016). *RANZCR Iodinated Contrast Guidelines*. https://www.ranzcr.com/search/ranzcr-iodinated-contrast-guidelines
The Royal College of Radiologists (2009). *Protection of Pregnant Patients during Diagnostic Medical Exposures to Ionising Radiation*. https://www.rcr.ac.uk/protection-pregnant-patients-during-diagnostic-medical-exposures-ionising-radiation
Thompson, G., Mills, S.J., Stivaros, S.M., & Jackson, A. (2010). Imaging of brain tumors: perfusion/permeability, *Neuroimaging Clin N Am*, **20**(3), 337–53.
Waldman, A.D., et al. & National Cancer Research Institute Brain Tumour Imaging Subgroup (2009). Quantitative imaging biomarkers in neuro-oncology. *Nat Rev Clin Oncol*, **6**(8), 445–54.
Wolpert, S.M. (1999). Neuroradiology classics. *AJNR*, **20**(9), 1752–3.
Wolpert, S.M. (2000). Neuroradiology classics. *AJNR*, **21**(3), 605–6.
Yan, J.L., van der Hoorn, A., Larkin, T.J., Boonzaier, N.R., Matys, T., & Price, S.J. (2016). Extent of resection of peritumoral diffusion tensor imaging-detected abnormality as a predictor of survival in adult glioblastoma patients. *J Neurosurg*, **126**(1), 1–8.
Young, V.E., Sadat, U., & Gillard, J.H. (2011). Noninvasive carotid artery imaging with a focus on the vulnerable plaque. *Neuroimaging Clinics of North America*, **21**(2), 391–405, xi–xii.

RELATED LINKS TO EBRAIN

CT Based Imaging Techniques. https://learning.ebrain.net/course/view.php?id=692
Digital Subtraction Angiography. https://learning.ebrain.net/course/view.php?id=693
Intraoperative Imaging Techniques. https://learning.ebrain.net/course/view.php?id=89
MR Based Imaging Techniques. https://learning.ebrain.net/course/view.php?id=1029
Nuclear Medicine Based Imaging Techniques. https://learning.ebrain.net/course/view.php?id=701
Principles of Neurological Investigation. https://learning.ebrain.net/course/view.php?id=43
Spinal Myelography. https://learning.ebrain.net/course/view.php?id=702
Ultrasound and Doppler Imaging. https://learning.ebrain.net/course/view.php?id=703
X-ray Development, Physics, Uses, Risks and Regulation. https://learning.ebrain.net/course/view.php?id=704

4

The operating theatre environment

Neil Kitchen and Jonathan Shapey

The neurosurgical operating theatre

Over the last century the neurosurgical operating theatre has evolved with significant improvements in lighting, equipment, air flow, and sterility. Further developments with intraoperative imaging and integrated navigation systems are now beginning to emerge. (**Fig. 4.1**).

Modern standard theatre complexes are divided into zones in order to minimize bacterial contamination. The operating room is an aseptic zone, the anaesthetic room is a clean zone and other areas are dirty zones. Standard theatres have a unidirectional air flow system to reduce the risk of airborne contamination with a minimum of 20 air changes per hour. Air is filtered before it enters the operating theatre and travels from the cleanest areas to the more contaminated ones, but the air flow is disrupted if theatre doors are left open. Smoke tests may be used to assess how air flows through operating theatres. Ultraclean theatres with laminar flow hoods have been developed for use during orthopaedic implant surgery but their use in neurosurgery is problematic because of the difficulties of positioning equipment, especially the operating microscope.

The temperature and humidity of operating theatres are also regulated. An average temperature of 20–22°C is comfortable for most theatre teams but warming blankets and the infusion of warmed intravenous fluids must be used to prevent patient hypothermia.

Special consideration is needed to ensure and maintain sterility during instrumented spine and implant surgery. This may include minimizing the number and entry of theatre personnel and using a 'no-touch technique' skin preparation, equipment sterilization, and intraoperative antibiotic prophylaxis to minimize the risks of infection are considered in detail in Chapter 94.

In 2009 the World Health Organization (WHO) published a landmark study that found that implementing a systemic process of checks can reduced safety incidents by up to a third (Haynes et al., 2009). The National Patient Safety Agency's (NPSA) launched the 'five steps to safer surgery' initiative in 2010 and all NHS healthcare organizations are now obliged to use the WHO Surgical Safety Checklist (**Fig. 4.2**). The aim of the initiative is to reduce harm associated with perioperative care and to support a change in culture within the theatre environment leading to better communication throughout the team. The five steps are: (1) preoperative team briefing; (2) sign in; (3) time out; (4) sign out; and (5) postoperative team briefing.

Surgical patient positioning

The central piece of equipment in the operating theatre is the operating table. Modern neurosurgical operating tables are radiolucent with interchangeable head and leg sections and are set on an offset column base that allows the table top to be moved cranially or caudally and tilted in all planes. Head-up positioning is used for most neurosurgical procedures as it reduces intracranial pressure and venous haemorrhage. Excessive head-up positioning however should normally be avoided because of the risks of air embolus, subdural postoperative pneumocephalus, and watershed infarction. Skull fixation is indicated in most microsurgical procedures to ensure that the head position is fixed in an optimal position with consideration given to the resulting angulation of the skull base, the desired surgical corridor, and the need to minimize brain retraction. Skull fixation is especially important when intraoperative image guidance systems are used, and it is also required for many cervical spine operations.

Skull fixation is achieved by using a pin-fixation device such as the three-point fixation Mayfield clamp. Tension rings of 20, 40, 60, and 80 lbs are marked on the rocker pin with 60 lbs of tension providing secure fixation in an adult. When positioning the pins it is important to avoid the squamous part of the temporal bone, the supraorbital ridge, implanted shunt devices, and large frontal sinuses. Skull fixation should be used with care in paediatric patients and is generally best avoided as it can result in skull perforation and extradural haemorrhage.

Various surgical positions are used in neurosurgery and each surgeon will develop their preferred position for each operation. Common surgical positions include the supine, prone, park-bench, and sitting positions (**Fig. 4.3**). Close collaboration with the anaesthetist is essential in ensuring the patient is placed in the optimal surgical position but every member of the surgical team must remain vigilant to the potential complications of improper positioning. Bony prominences are at risk of pressure damage during surgery and must be well padded, while the patient's eyes must also be covered to protect them from pressure and to avoid injury from alcoholic cleaning solutions. Peripheral nerve injuries may be caused by pressure or traction palsies with the ulnar and common peroneal nerves most at risk, especially when operating in the lateral (park-bench) position. In the sitting position there is an increased

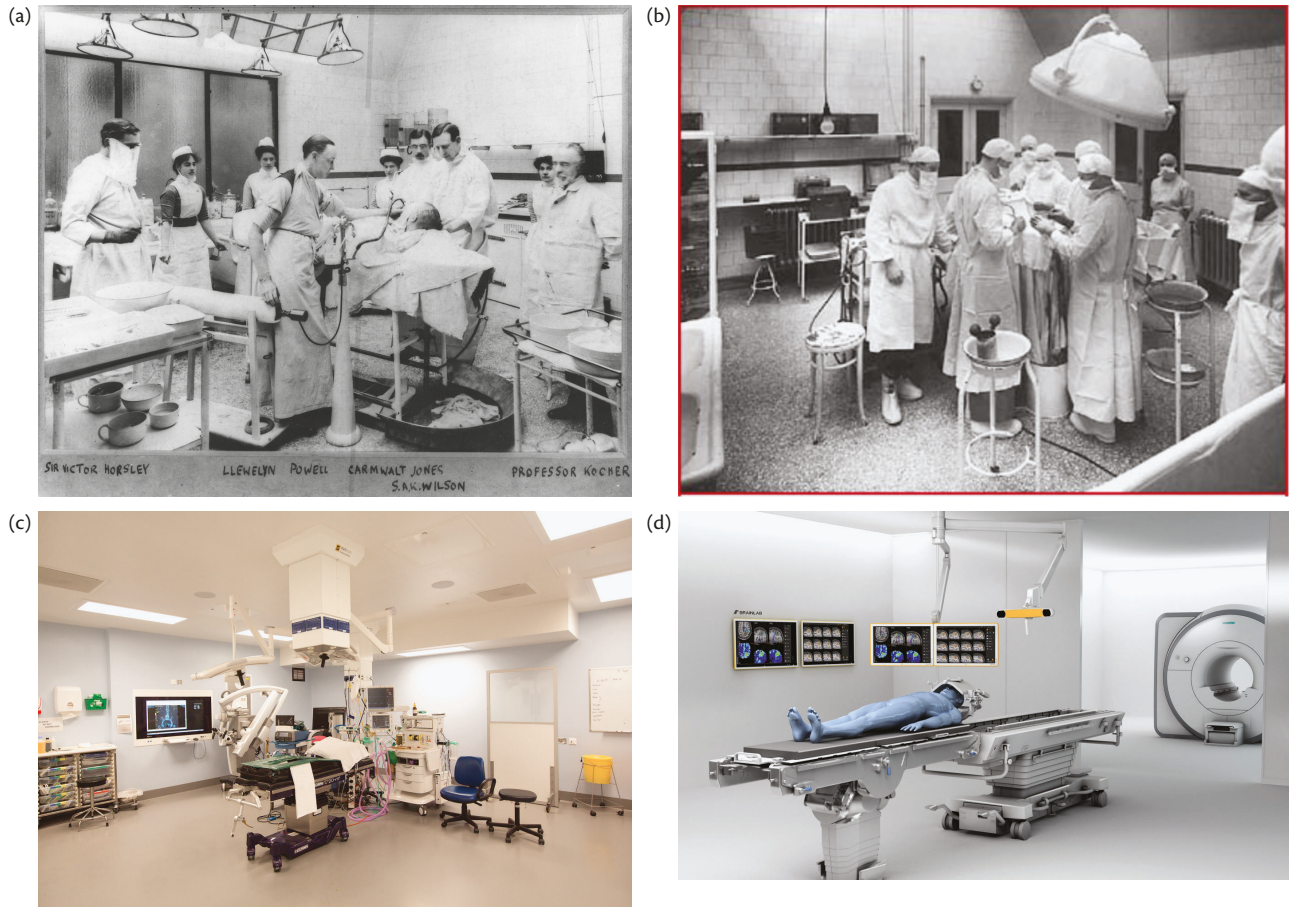

Fig. 4.1 Neurosurgical operating theatres. (A) Victor Horsley in the operating room at Queen Square Hospital, 1906; (B) 1930s operating theatre; (C) The modern neurosurgical operating theatre; (D) intraoperative MRI suite.

risk of air embolism (evidenced most rapidly by a rise in end tidal CO_2), and there is a small risk of blindness associated with surgery performed in the prone position as a result of increased intraocular pressure and reduced optic nerve perfusion pressure. Improper skull fixation can also cause scalp necrosis or local haematomas.

Positioning equipment in theatre to optimize surgical performance

The surgeon needs to consider the position of theatre personnel during a procedure. The surgical assistant should not be positioned between the surgeon and the scrub nurse, excess unused equipment should not be in theatre. Drills, ultrasonic aspirators, and bipolars must be positioned so the surgeon can use them with their dominant hand and without wires crossing the operative field. Image-guidance cameras should be positioned in such a way that the microscope and theatre staff do not obstruct the line of site to the patient. Sound levels in theatre should not be at a level where the surgeon, anaesthetist, and other theatre staff cannot communicate effectively.

Hypoglycaemia, coffee, and a full bladder may all affect a surgeon's ability to conduct microsurgery. Surgeon comfort is not a luxury but a necessity for safe surgery. Some retractor systems and chairs will allow a surgeon to rest their elbows and wrists on a firm surface and this is very useful in minimizing fatigue. Some surgical positions, notably the sitting position require that the surgeon operates with arms elevated in a way that makes fatigue problematic. Long operations may be best performed by surgical teams so that rests can be taken as required.

Theatre equipment

The neurosurgeon needs to be familiar with many types of surgical equipment and to cover all these is beyond the scope of this chapter, but the following equipment merits special consideration.

Operating microscope

There remains considerable controversy regarding who invented the first true microscope, but it is thought to have been developed in the late sixteenth century. It was Carl Zeiss, a German machinist working with the physicist Ernst Abbé who revolutionized lens making and microscope manufacturing. By the early twentieth century, the microscope was an integral part of laboratory medical research but was not used in the operating room until 1921 when Carl Nylén, a Swedish otolaryngologist, used a microscope to operate on a patient with chronic otitis media. Zeiss introduced their first series operating microscope in 1953 and in 1957 Theodore Kurze became the first neurosurgeon to use the microscope on a patient, removing a neurilemmoma of the seventh nerve in a 5-year-old

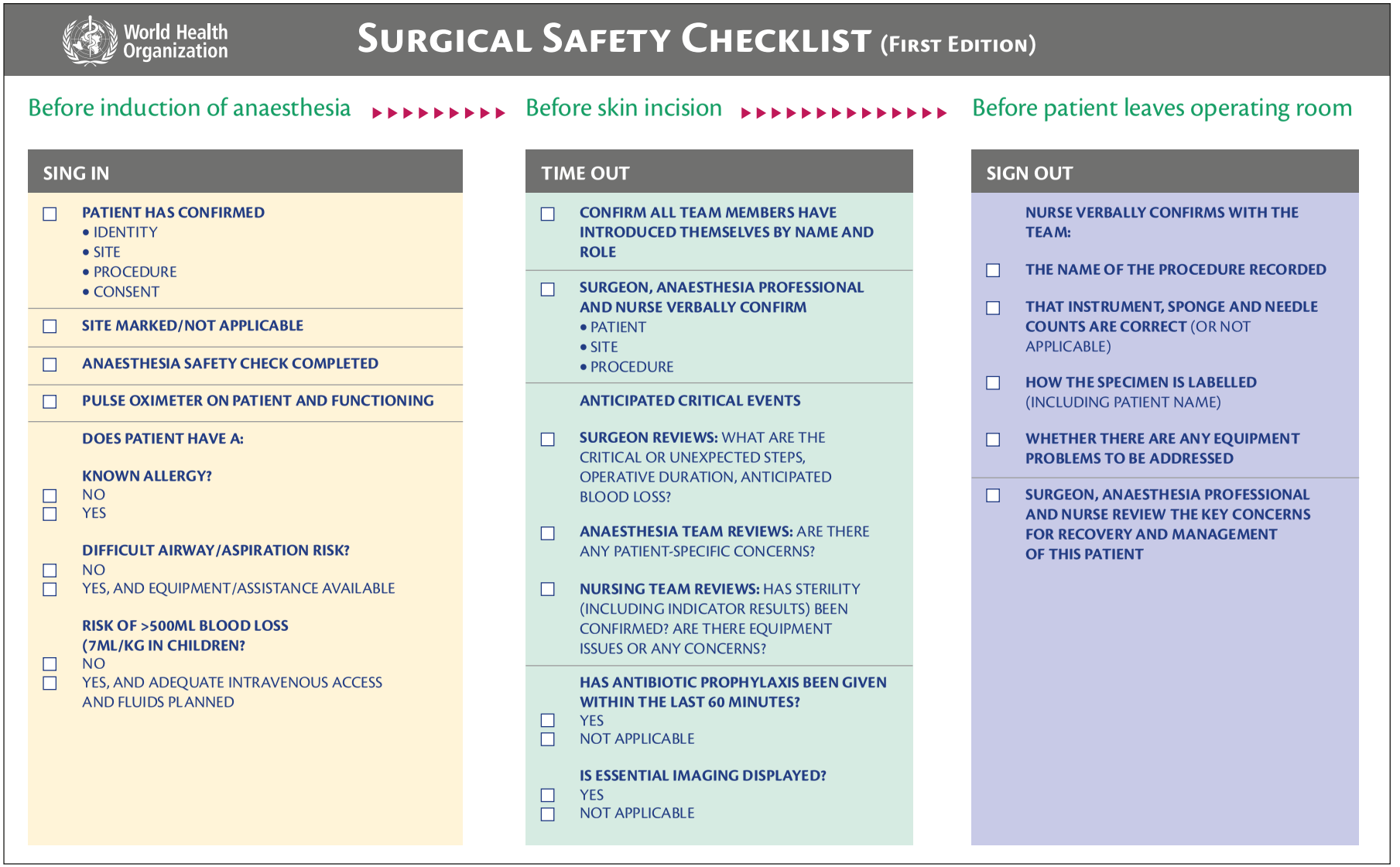
World Health Organization
SURGICAL SAFETY CHECKLIST (FIRST EDITION)
Before induction of anaesthesia
Before skin incision
Before patient leaves operating room
SING IN
PATIENT HAS CONFIRMED
• IDENTITY
• SITE
• PROCEDURE
• CONSENT
SITE MARKED/NOT APPLICABLE
ANAESTHESIA SAFETY CHECK COMPLETED
PULSE OXIMETER ON PATIENT AND FUNCTIONING
DOES PATIENT HAVE A:
KNOWN ALLERGY?
NO
YES
DIFFICULT AIRWAY/ASPIRATION RISK?
NO
YES, AND EQUIPMENT/ASSISTANCE AVAILABLE
RISK OF >500ML BLOOD LOSS (7ML/KG IN CHILDREN?
NO
YES, AND ADEQUATE INTRAVENOUS ACCESS AND FLUIDS PLANNED
TIME OUT
CONFIRM ALL TEAM MEMBERS HAVE INTRODUCED THEMSELVES BY NAME AND ROLE
SURGEON, ANAESTHESIA PROFESSIONAL AND NURSE VERBALLY CONFIRM
• PATIENT
• SITE
• PROCEDURE
ANTICIPATED CRITICAL EVENTS
SURGEON REVIEWS: WHAT ARE THE CRITICAL OR UNEXPECTED STEPS, OPERATIVE DURATION, ANTICIPATED BLOOD LOSS?
ANAESTHESIA TEAM REVIEWS: ARE THERE ANY PATIENT-SPECIFIC CONCERNS?
NURSING TEAM REVIEWS: HAS STERILITY (INCLUDING INDICATOR RESULTS) BEEN CONFIRMED? ARE THERE EQUIPMENT ISSUES OR ANY CONCERNS?
HAS ANTIBIOTIC PROPHYLAXIS BEEN GIVEN WITHIN THE LAST 60 MINUTES?
YES
NOT APPLICABLE
IS ESSENTIAL IMAGING DISPLAYED?
YES
NOT APPLICABLE
SIGN OUT
NURSE VERBALLY CONFIRMS WITH THE TEAM:
THE NAME OF THE PROCEDURE RECORDED
THAT INSTRUMENT, SPONGE AND NEEDLE COUNTS ARE CORRECT (OR NOT APPLICABLE)
HOW THE SPECIMEN IS LABELLED (INCLUDING PATIENT NAME)
WHETHER THERE ARE ANY EQUIPMENT PROBLEMS TO BE ADDRESSED
SURGEON, ANAESTHESIA PROFESSIONAL AND NURSE REVIEW THE KEY CONCERNS FOR RECOVERY AND MANAGEMENT OF THIS PATIENT
THIS CHECKLIST IS NOT INTENDED TO BE COMPREHENSIVE. ADDITIONS AND MODFICATIONS TO FIT LOCAL PRACTICE ARE ENCOURAGED.

Fig. 4.2 WHO surgical safety checklist.

Reproduced with permission from the World Health Organization.

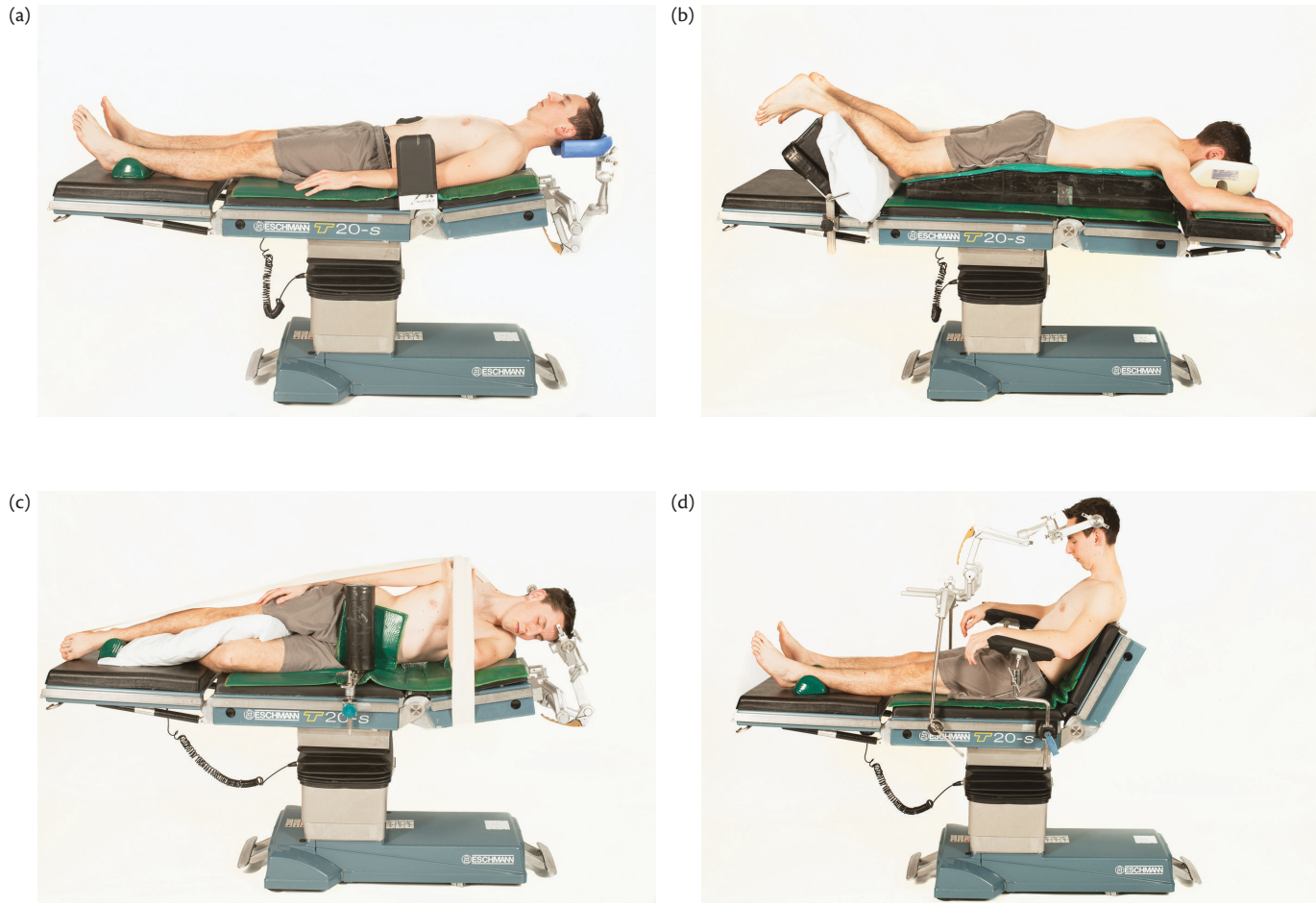

Fig. 4.3 Commonly patient positions for neurosurgery. (A) Supine position: pterional craniotomy (pictured); frontal/subfrontal/supraorbital craniotomy; parietal craniotomy; temporal craniotomy (shoulder roll placed under ipsilateral shoulder); transsphenoidal surgery. (B) Prone position: midline suboccipital craniectomy; spinal surgery (pictured). (C) lateral/park-bench/three-quarter prone position: retrosigmoid/lateral suboccipital craniectomy (pictured); spinal surgery; (D) sitting position: suboccipital craniectomy; cervical spine surgery.

child. The first microneurovascular case was performed in 1960 by Raymond Donaghy. He also established a microsurgical training laboratory in Vermont where a young Gazi Yasgaril was sent to learn this emerging technique. More than anyone else, Yasgaril publicized the advantages of microscopic neurosurgery and made the operating microscope an integral part of modern neurosurgery (Kriss and Kriss, 1998).

The modern microscope enables the operating surgeon to see three dimensional images at high magnification. The main components of a modern microscope are the objective lens, the binocular tube, the light source, a motorized zoom system, and the suspension system. The design of the operating microscope ensures that high-quality lighting runs exactly parallel and very close to the optical path. The two eye fields are also close together, permitting binocular vision can be achieved at the bottom of a deep, narrow wound. The more a microscope is zoomed in the less depth of field the surgeon has so the surgeon should attempt to keep the microscope as close as possible to the patient. However, a good working distance between the microscope and the wound is required to allow instruments to be used without clashing with each other or the microscope. Modern microscopes have electric variable objective lenses with focal lengths from 200 to 500 mm and the focal length is virtually identical to the working distance. Eyepieces are used to re-magnify the intermediate image 10-fold and can be used to compensate for ametropia. In order to allow free movement of the microscope preoperative balancing is essential, and drapes must not restrict microscope movements.

Modern microscopes are also commonly fitted with two additional light sources; an infrared 800 nm light allows visualization of blood flow using intraoperative fluorescence and blue 400 nm light is used for fluorescence-guided tumour surgery.

Surgical endoscope

Neuroendoscopy was first performed in 1910 when urologist Victor Lespinasse used a paediatric cystoscope to treat paediatric hydrocephalus by attempting endoscopic coagulation of the choroid plexus (Abd-El-Barr and Cohen, 2013). Following this, Dandy and Mixter attempted endoscopic fenestration of the third ventricle for the treatment of hydrocephalus in the 1920s but true advances in neuroendoscopy came in the 1970s with technological developments in optics and electronics (Liu et al., 2004).

The amount of intraoperative illumination and vision under the microscope is determined by the surgical approach and may be

significantly limited in cases where the surgical corridor is long and narrow. Modern endoscopes are able to bring increased light intensity into the surgical field and provide an extended viewing angle with better magnification in close-up positions. Other potential advantages of endoscopic surgery include minimal tissue disruption and brain retraction, improved cosmetic results, shorter hospital stay, and reduced surgical morbidity.

Two main types of endoscopes are available; namely, fibreoptic flexible and rigid rod lens systems. Both types of endoscope use a xenon light source that is transmitted via a fibreoptic cable to the endoscope. Fibreoptic flexible endoscopes transmit the image through a group of tightly packed fibreoptic threads and are smaller and more malleable than rigid solid lens endoscopes. Rigid endoscopes are more expensive than fibreoptic endoscopes, but they provide superior image resolution and light transmission through a series of lenses. Some endoscopes have a working channel that allows the insertion of compatible instruments such as microforceps, endoscopic scissors, monopolar diathermy, or Fogarty balloon catheters. Irrigation channels allow the constant irrigation of fluid to clear debris from the lens and bleeding from the surgical field. Endoscopes come with a variety of lens angles (0°, 30°, 70°, and 120°) to allow visualization of hidden parts of the surgical field although intervention is usually only performed using 0° and 30° scopes.

Neuroendoscopic procedures were initially limited to the ventricles of the brain but the endoscope is now used in treating a wide spectrum of neurosurgical pathology. H.D. Jho pioneered the endonasal endoscopic approach for pituitary surgery (Jho and Alfieri, 2001) and its application to other skull base pathologies continues to expand (Paluzzi et al., 2012). The endoscope is also utilized in spinal surgery, particularly for thoracic procedures. It is important to select an appropriate endoscope with the desired characteristics for the procedure being performed. For instance, a non-channelled fibreoptic scope may be appropriate for a diagnostic ventriculostomy but a rigid solid multichannelled lens endoscope is preferable when performing endoscopic endonasal surgery. Despite endoscopy being a rapidly expanding field endoscopic surgery is still not practised routinely by all neurosurgeons and there is consequently a steep learning curve. Appropriate training is essential and collaboration with consultants from other specialties, such as otolaryngology, who are experienced in endoscopy, may shorten the difficult learning phase and reduce operative time and surgical morbidity.

Fluorescent agents

Indocyanine green (ICG)

Indocyanine green (ICG) is the commonest fluorescent agent used for intraoperative angiography. It has a peak spectral absorption at around 800 nm following intraoperative intravenous injection and due to its tight binding to plasma proteins, becomes confined to the vascular system, permitting excellent intraoperative angiography.

5-aminolevulinic acid (5-ALA)

Fluorescence-guided tumour surgery is performed following the oral administration of 5-aminolevulinic acid (5-ALA) approximately 2–4 hours before anaesthesia. Once administered patients should avoid direct sunlight due to the risk of developing a photosensitivity skin reaction. 5-ALA is a natural precursor of protoporphyrin IX (PpIX) in the haem biosynthesis pathway and excess 5-ALA provides selective and abundant accumulation of PpIX in malignant glioma cells but only slight or no accumulation in the normal brain. 5-ALA in itself is not fluorescent but PpIX is a highly fluorescent substance with maximal absorption at 440 nm, thus enabling the surgeon to differentiate between pathological tumour and normal brain intraoperatively.

Fluorescein

Fluorescein is a synthetic organic compound available as a dark orange/red powder. It is soluble in water and is widely used as a fluorescent tracer for many applications. In neurosurgery, intrathecal fluorescein administration has become an important tool in the diagnosis and localization of cerebrospinal fluid (CSF) leak and is used intraoperatively to assist in localizing the site of skull base defects. Current recommendations of fluorescein administration suggest removing 10 ml of the patient's CSF and replacing it with an equivalent injection of a 10 ml dilute solution of fluorescein into the intrathecal space. The dilute solution is bright green in colour and does not usually require visual augmentation; however, a blue light filter can assist in localization of fluorescein-coloured CSF at the skull base in equivocal cases.

Drills

Modern high-speed surgical bone drills may be pneumatically or electrically powered. The rotational speed of a drill is measured in revolutions per minute (rpm) and pneumatic drills can generate up to 100 000 rpm. Electric drills have adjustable speeds from 200 to 75 000 rpm and are smaller, lighter, and more easily manoeuvrable, although they do not provide the same level of power as pneumatic drills.

Various drill bits may be attached to the drill depending on the surgical need. **Table 4.1** illustrates some of the commonly used drill attachments and how they are used in cranial and spinal neurosurgery.

Retractors

The brain retractor was first introduced by Harvey Cushing and Victor Horsley in the early twentieth century and has since been a key neurosurgical instrument. Brain spatulas are either rectangular or tapered and are available in a variety of sizes. Articulated arms, such as the Yasargil Leyla retractor, were designed to stabilize the spatula while in use and various retractor systems have since been developed to provide a solid anchoring platform for retractors (Dujovny et al., 2010).

Inappropriate or prolonged brain retraction has the potential to cause cortical contusions, vessel injury, brain swelling, and neurological deficit and the incidence of brain retraction injury has been observed to be as high as 10% in some series (Spetzler et al., 1992). Other surgeons advocate the avoidance of retractors altogether—and certainly careful patient positioning, so that gravity assists rather than hinders the surgeon, draining cerebral spinal fluid, mannitol infusion, skilled anaesthetics, and surgical patience all contribute to make excessive retraction unnecessary. Judicious and careful use of brain retraction can minimize retraction related complications and such techniques include the placing of surgical linteens under the

Table 4.1 Common drill bits and attachments used in cranial and spinal neurosurgery

Match stick/match head - Side cutting burr, blunt tip improves safety when drilling down		**Footed attachment**	
Cutting burr - Rapid circumferential bone removal		Straight short/large bore attachment	
Diamond burr - Provides extra control when drilling due to slow bone removal - Generates heat for 'hot-drilling' - Can be used safely to drill bone over venous sinuses (e.g. translabyrinthine approach)	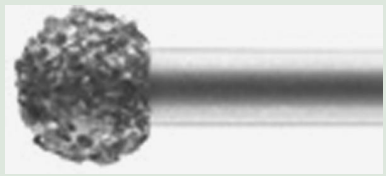	Straight variable exposure attachment (10 mm adjustment)	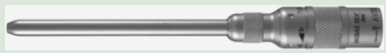
Acorn - Rapid vertical bone removal - Often used for creating 'mini' burr holes as part of turning a craniotomy flap	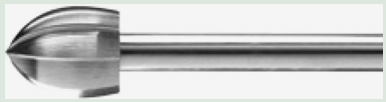	Angled short/large bore attachment	

Medtronic, Midas Rex.

retractors, avoiding firm retraction, and the use of silicon coated retractor blades.

Diathermy

Diathermy is used for cutting tissues and haemostasis. Heat is generated by the passage of high-frequency alternating current through body tissues. Currents of up to 500 mA are safe at frequencies of 400 kHz to 10 MHz and locally concentrated high-density currents can generate temperatures of up to 1000°C. There is no stimulation of neuromuscular tissue at frequencies above 50 kHz.

There are two distinct types of diathermy.

Monopolar diathermy

Monopolar diathermy uses a high-power unit (400 W) to generate high-frequency alternating current that passes from a tipped electrode (high current density), via a ground plate (with a low current density) back to the generator. The voltage used changes the mode of diathermy. Cutting diathermy uses continuous low voltage output (500–1000 V) to generate high local temperature that causes superficial tissue disruption and water vaporization but minimal vessel coagulation and haemostasis. The alternative coagulation setting generates pulsed high voltage output (up to 6000 V) of high-frequency current at short intervals resulting in tissue water vaporization and vessel coagulation. Many diathermy machines will also allow a blend of cutting and coagulation.

Monopolar diathermy does not work in a wet field and can cause heat to spread, damaging the surrounding (1–2 cm) tissues. Incorrect placement of the patient electrode plate is the most common cause of accidental diathermy burns. To minimize the risk of complications the patient electrode plate should have a surface area of at least 70 cm^2 and be placed with good contact on dry, shaved skin away from bony prominences, metal prostheses (e.g. hip replacements) and scar tissue.

Monopolar diathermy should be used with caution in patients with a history of arrhythmias and cannot be used in patients with a cardiac pacemaker due to the risk of causing cardiac arrest. There are case reports of alcoholic skin prep catching fire if not left to dry before diathermy is used.

Bipolar diathermy

Bipolar diathermy uses lower power (50 W) to generate high-frequency alternating current that passes between the two tips of diathermy forceps. It uses a 1 MHz waveform for both cutting and coagulation and because it only uses 140 V it can be used in patients with pacemakers and defibrillators. There is no need to use a patient electrode plate and bipolar diathermy can be used effectively in a wet environment.

Forceps vary in length and tip sharpness. Coagulated, charred tissue can stick to the forceps and they must be kept clean to avoid this risk. Modifications available include irrigating bipolar forceps and cooler tipped forceps that make this risk less likely.

Ultrasonic aspirators

Ultrasonic aspirators are vibrating surgical instruments which utilize ultrasound as a physical energy to fragment (cavitate), emulsify, and remove unwanted tissue. Examples of ultrasonic aspirators used in neurosurgery include the Cavitron Ultrasonic Surgical Aspirator (CUSA) (Integra) and Sonopet (Stryker). The hollow titanium tip vibrates along its longitudinal axis generating an ultrasound frequency of 20–60 kHz and all models allow the surgeon to specify the level of vibration, irrigation, and suction in order to achieve maximal control during tissue dissection. The CUSA includes a supplementary Tissue Select function that further regulates the relative

tissue fragmentation rate and some aspirators (e.g. Sonopet) permit fine bone dissection by coupling longitudinal vibration with torsional vibration.

Ultrasonic surgical aspirators provide ultrasonic cavitation, irrigation and aspiration in a single hand-held unit which helps to limit instrument traffic within the surgical field and improve the surgeon's view. The selective fragmentation of target neural tissues also reduces the risk of vessel injury, but one must be mindful of causing collateral damage from thermal injury and the risk of developing indistinct 'false' tissue planes.

Haemostatic agents

Achieving and maintaining haemostasis in neurosurgery is critical to the outcome. Various haemostatic agents have been developed and target different elements of the clotting cascade (Fig. 4.4 and Table 4.2) (Grant, 2007). Some of these agents may swell in the postoperative period and care should be taken to avoid leaving haemostatic agents in places where swelling will cause neurological compression. This is especially relevant in the spine. Some haemostatic agents may result in MR artefacts making postoperative assessment of residual tumour difficult.

Problematic bleeding can also be controlled by changing the patient position, tranexamic acid, haemostatic clips, or muscle patches. Bees wax was developed for use in neurosurgery by Victor Horsley, and is now widely used to stop bleeding from bone edges.

Neuronavigation

Imaging techniques have revolutionized the practice of neurosurgery and have become essential in guiding diagnosis, preoperative planning, and intraoperative navigation. In particular, image-guided surgery has become an indispensable modern neurosurgical technique and is applicable to numerous neurosurgical procedures including neuro-oncology, vascular, and functional neurosurgery.

The aim of stereotactic surgery is to register the anatomical or imaging space to the surgical or physical space in which the patient is located and in which surgery is to take place. Image guidance allows for smaller more precisely positioned incisions and accurate localization of lesions. Stereotactic neurosurgery may be frame-based or frameless.

Frame-based stereotactic neurosurgery

The concept of stereotactic localization was first applied in 1908 in the device of Victor Horsley and Robert Clark although the apparatus was only developed for work on small to medium sized experimental animals (Fig. 4.5A). The first successful cranial application of stereotactic surgery in humans is credited to the team of Ernest Speigel and Henry Wycis in 1947 but it was Lars Leksell, a Swedish neurosurgeon, who developed the arc-centred stereotactic frame system following a visit to Wycis in Philadelphia in 1949. Leksell's frame consisted of a rectangular base ring attached to the skull

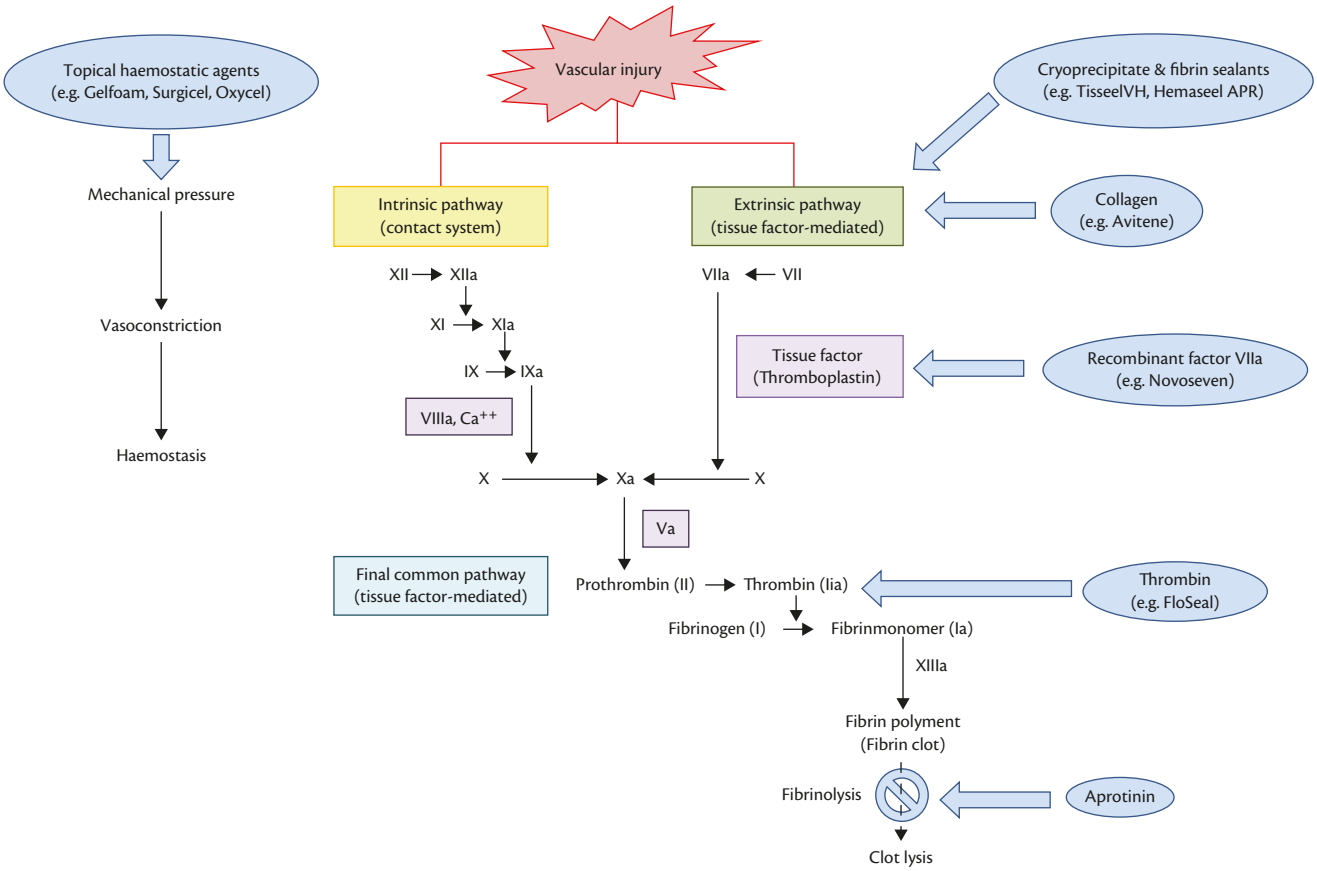

Fig. 4.4 Haemostatic adjuncts and their mechanism of action.
Adapted from *Surgery*, Volume 142, issue 4, Gerald A. Grant, Update on hemostasis: neurosurgery, pp. S55–S60, Copyright (2007), with permission from Elsevier.

Table 4.2 Haemostatic adjuncts and their mechanism of action

Haemostatic adjunct	Trade name	Active component
Topical haemostatic agents	Gelfoam	Gelatine sponge
	Surgical	Oxidized regenerated cellulose
	Oxycel	Oxidized cellulose
Collagen	Avitene	Microcrystalline collagen (reacts with platelets)
Fibrin sealants	Tisseel Haemaseel APR	Fibrinogen/factor XIII concentrate (cryoprecipitate) and thrombin mixture
Thrombin	FloSeal	Gelatine matrix and thrombin mixture
Aprotinin		Fibrinolytic inhibitor of plasmin (inhibits fibrinolysis)

Adapted from *Surgery*, Volume 142, issue 4, Gerald A. Grant, Update on hemostasis: neurosurgery, pp. S55–S60, Copyright (2007), with permission from Elsevier.

with four pins and used three polar coordinates (angle, depth, and anterior–posterior location). The three coordinates always indicate the centre of the arc, representing the target, and the arc-centred device allows maximum flexibility in choosing the probe entry point and trajectory. The frame has been modified over the ensuing years, but remarkably remains very similar in function and appearance to the original 1949 device (**Fig. 4.5B**).

Another commonly used frame system is the Cosman-Roberts-Wells (CRW) Precision™Arc System (**Fig. 4.5C**). It has an N-shaped 'picket-fence' localizer ring and the lesion is placed at the centre of a stereotactic sphere with a fixed radius that allows free selection of an unlimited number of entry points. The CRW Precision™ Arc System also has a phantom base that can be used to confirm the target before applying the settings to the patient. Computed tomography (CT) and MRI compatible models of both Leksell and CRW Precision™ Arc Systems are available.

The advent of high-resolution MR imaging has transformed stereotactic surgical planning. Stereotaxy is no longer reliant on anatomical atlases and is usually performed on a computer workstation that allows the planning of targets and trajectories on a computer-generated 3D model. Frame-based stereotaxy has the highest degree of precision and, although largely superseded in general intracranial practice by frameless stereotactic techniques, continues to be used for cases where target placement is critical including, for example, functional lesioning and electrode or catheter placement, biopsy of small or deep lesions, and gamma knife stereotactic radiosurgery.

Frameless stereotactic neurosurgery

Frameless stereotaxy involves the use of bony landmarks, facial features, or fiducial markers to coregister the patient's skull relative to a 3D volumetric image obtained prior to surgery. Fiducials are adhesive markers, visible on both CT and MRI, and are placed on a patient's head, covering as much of the geometry of the head as possible but centred on the target lesion. For optical registration, the patient's head is fixed using a pin-fixation device and infrared reflective spheres arranged in a predetermined geometrical configuration and anchored to the same fixation device. An infrared camera detects light reflected from the spheres.

Registration is performed by the surgeon and computer software correlates the imaging studies with the defined anatomical landmarks of the patient's head. Registration remains accurate so long as the patient's head remains in same position relative to the reflectors. Registration accuracy can be enhanced by collecting as many registration points as possible, by using fiducials and by spreading anatomical registration points around the head as much as possible.

Electromagnetic (EM) registration involves generating an electromagnetic field around the patient's head in order to triangulate the position of instruments and intraoperative tools. EM navigation does not require the head to be fixed and is especially useful when the head cannot be fixed easily (e.g. shunt or paediatric surgery). EM systems track the tip of the surgical instrument and can therefore be used to track the tip of a flexible endoscope.

A registration error is a computer-generated number that denotes the degree of deviation from the ideal image-to-patient correlation. Acceptable registration accuracy depends on the size of the target lesion. Volumetric registration enables the surgeon to view images in three orthogonal planes and once registered, instruments fitted with reflective spheres may be used by the surgeon to relate the position of the instrument to the images in real time. Additional image sequences such as functional imaging and tractography can also be merged with the volumetric data enabling the surgeon to view these intraoperatively. Image-guidance systems have also been adapted for use in spinal instrumentation surgery and can be linked to operating microscopes so that the focal point of the microscope is used as the image-guidance pointer and so that image-guidance data can be overlaid in the operators view down the microscope.

Frameless image-guidance systems are a significant technological advance and an essential piece of modern neurosurgical equipment however one must be aware of their limitations. Inaccuracies in registration may occur as a result of intraoperative brain shift following loss of cerebrospinal fluid or tumour resection, because of movement of the patient, the reference frame, or fiducials, and because of a loss of line of sight between the camera and infrared reflectors. In cases where submillimetre accuracy is required and a fixed trajectory is acceptable, a frame-based system is preferable.

Intraoperative imaging

X-ray

Mobile X-ray image intensifiers are commonly used in the neurosurgical operating theatre for a variety of applications, including localization of the correct anatomical level during spinal surgery, imaging during spinal instrumentation, and for localizing other bony anatomy such as skull base foraminae or the pituitary fossa.

Mobile image intensifiers typically consist of a single unit with a low intensity X-ray source and an image intensifier positioned directly opposite each other on a mount. The mount, often referred to as a C-arm, may be rotated and translated around the patient as required. Mobile image intensifiers can provide good spatial resolution of bony anatomy and are quick and cheap to use, although the image quality is dependent on operator experience and the patient's body habitus.

Imaging during spinal instrumentation helps to ensure that the desired anatomical alignment is achieved and assists in the accurate

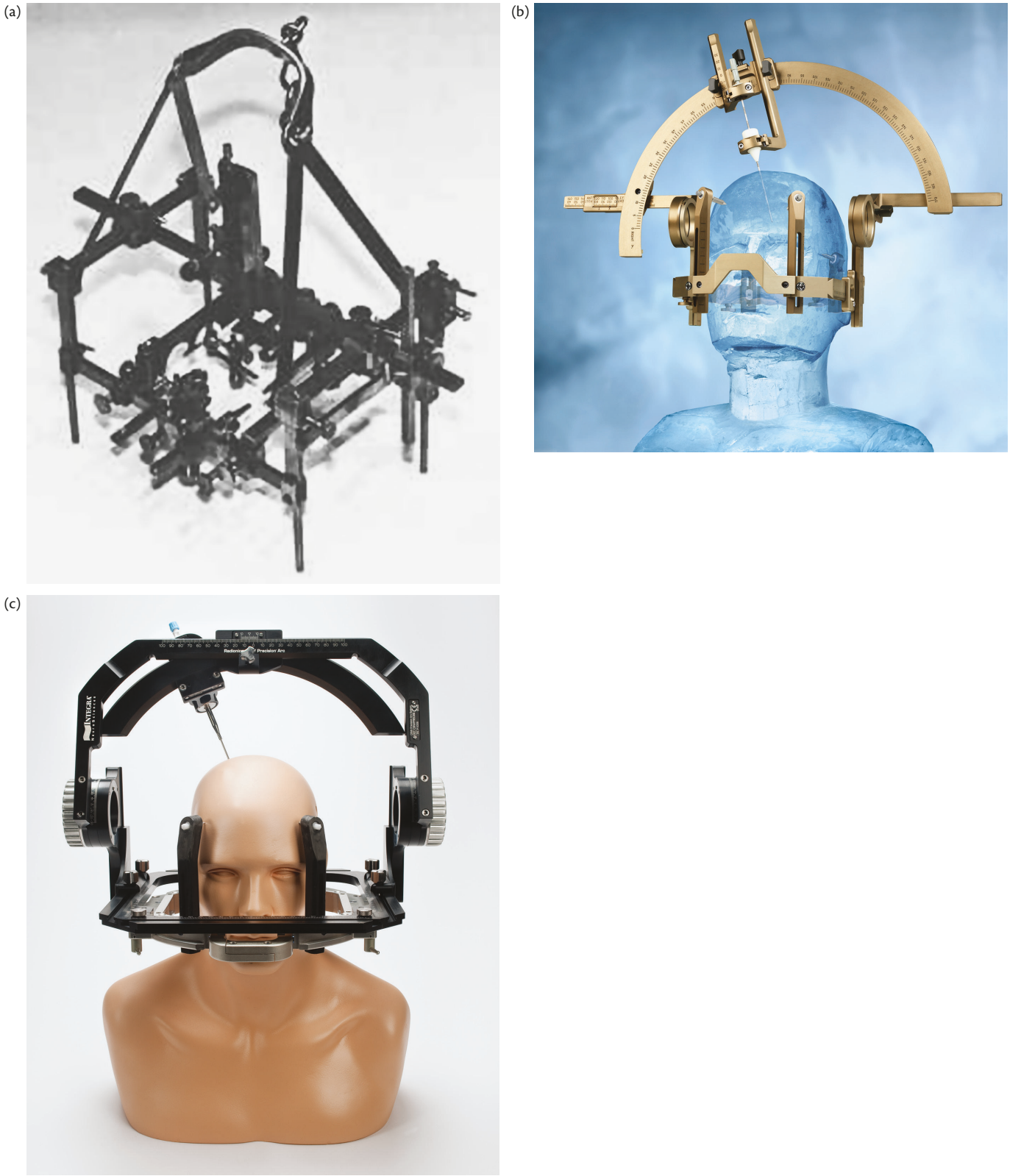

Fig. 4.5 Stereotactic frames: (A) Horsley-Clarke stereotactic frame (1908); (B) Leksell stereotactic frame; (C) CRW Precision™Arc System.

placement of implanted metalwork, such as pedicle screws. A radiolucent operating table should be used if fluoroscopic imaging is to be used intraoperatively to permit anterior–posterior views in addition to lateral views. Ensuring accurate screw positioning from 2D imaging can be difficult, particularly where there is abnormal anatomy or where complex instrumentation is used. Newer imaging

techniques are being introduced to overcome this difficulty including dedicated 3D equipment such as '3D C-arms' or the 'O-arm', and neuronavigation techniques incorporating registered fluoroscopic images with preoperative 3D CT scans.

Ultrasound

Intraoperative ultrasound is a relatively inexpensive technique that has the potential to provide surgeons with fast, real-time imaging. Ultrasound imaging relies on the use of high-frequency sound waves to image tissues. Sound is defined as mechanical energy travelling through matter as longitudinal waves producing alternating zones of compression and rarefaction. Intraoperative ultrasound uses a transducer to transmit ultrasonic waves in the range of 5–10 MHz into tissues.

Where there are interfaces of different tissue density, energy is reflected back by the tissue towards the transducer as 'echoes'. The amount of energy reflected depends on a tissue's acoustic impedance, which is proportional to the density of the tissue propagating the sound wave. Echo vibrations are then converted to electrical pulses and used to produce representative images. Greyscale or Brightness (B-mode) is the mainstay of anatomical ultrasound imaging and provides 2D greyscale images of tissues based on their relative echogenicity. Doppler ultrasound can also be incorporated into intraoperative ultrasound. The doppler effect describes a change in the frequency of sound when a sound wave encounters a moving interface, such as blood within an artery and blood flow may be mapped in colour on real-time ultrasound images.

Intraoperative ultrasound is very operator dependent and image interpretation is associated with a learning curve as most surgeons are unfamiliar with this imaging modality. Ultrasound is unable to penetrate through bone and so cannot be used for planning a craniotomy and it has limited penetration through to deeper structures meaning that careful case selection is required. Intraoperative ultrasound has been used in treating a variety of pathologies but is most frequently used during glioma surgery. Some navigation machines are now also capable of coregistering the ultrasound pictures with a reconstructed plane from the pre-op MR scan. Intraoperative doppler ultrasound has a role in neurovascular surgery and some surgeons also use ultrasound to demonstrate adequate CSF flow following foramen magnum decompression.

Intraoperative MRI (iMRI)

Neurosurgeons have become increasingly dependent on image guidance to perform optimal, safe, and efficient surgery. Routine neuronavigation systems do not allow the neurosurgeon to adjust for intraoperative brain shift and this consideration led to the development of intraoperative MRI systems (Fig. 4.1D) (Hall and Truwit, 2008). The principal feature of iMRI systems is the ability to acquire contemporaneous imaging during surgery to inform surgeons on the extent of resection achieved in order to guide further surgical decision making and most iMRI systems also allow the new images to be registered onto the neuronavigation system.

iMRI systems may be vertically or horizontally open. In vertically open systems the patient remains within a fixed position and the surgeon works within the confines of the scanner. All surgical instruments must be MR compatible and various levels of shielding of other equipment must be maintained. Images can be easily and quickly acquired at any point during the procedure without moving the patient or the magnet however vertically open systems are typically low field scanners (0.3–0.5 T) so the standard of the images obtained are not of the same quality as those generated by standard diagnostic imaging techniques.

Horizontally open iMRI systems include a high-field magnet (1.5–3.0 T) located within an integrated operating theatre (Fig. 4.1D). The table can slide or pivot out of a marked magnetic field line (5-Gauss line), allowing surgery to be performed in the usual manner using standard instruments and equipment until a scan is required. New high-field horizontally open iMRI scanners produce higher quality images allowing greater versatility and acquisition of functional MRI, MR angiography, MR venography, MR spectroscopy, and tractography. The disadvantages of this system include the significant cost required to build the intraoperative suite and the increased time spent intraoperatively manoeuvring the patient in and out of the scanner.

Intraoperative neurophysiological monitoring

Intraoperative neurophysiological monitoring offers a real-time, continuous assessment of the nervous system integrity and is considered essential for various types of neurosurgical procedure (Gonzalez et al., 2009). It is vital to consult with an expert neurophysiologist before the procedure to ensure that the most appropriate modality is selected and results must always be interpreted in the context of the surgical procedure being performed. For this reason, it is helpful to have a neurophysiologist in the operating theatre during surgery. Intraoperative monitoring can be significantly affected by anaesthetic agents so close collaboration with the anaesthetist is also essential.

Sensory evoked potentials

The visual, auditory, and somatosensory systems can be stimulated and evoked potentials can record the biofeedback response of the nervous system to these external stimuli. The recordings give information on the sensory pathway from the peripheral nerve to the level of the cortex.

Somatosensory evoked potentials (SSEP)

Somatosensory evoked potentials (SSEPs) are produced by short (0.1–1.0 msec) electrical stimulation (1–5 Hz) of a peripheral nerve and the generated responses are recorded over a proximal part of the nerve or sensory pathway. Recording electrodes are placed in named, reproducible locations. Each location is designated by a letter; N (negative deflection) or P (positive deflection) and a number that corresponds to the latency of wave. The median or tibial nerve is usually stimulated and SSEPs are monitored in terms of latency and amplitude.

The SSEP waveform is often quite variable and should therefore be monitored before surgery begins and throughout the procedure. To separate the SSEP signal from background noise a technique called signal averaging is used to combine a large number of SSEP signals. The time required to perform signal averaging means that SSEP changes may not be seen until a few minutes after the neurological injury has occurred. A decrease of about 50% in amplitude or a 10% increase in latency of the SSEP waveform is considered to be significant. Inhalational anaesthetic agents, fluctuations in blood pressure,

hypothermia, and oxygenation can all affect SSEPs to varying degrees so close consultation with the anaesthetist is needed beforehand to ensure stable anaesthesia is achieved. In thoracic spinal surgery, the upper limb SSEP signal can be used as a control. Continuous SSEP monitoring of the dorsal columns is commonly used during spinal cord and complex spine surgery and is considered essential for scoliosis surgery (Thirumala et al., 2014). Cortical mapping with SSEPs can also be used in epilepsy surgery or sensorimotor and insular cortex tumour surgery.

Visual evoked potentials (VEP) and brainstem auditory evoked potentials (BAEP)

Intraoperative visual evoked potentials (VEPs) and brainstem auditory evoked potentials (BAEPs) are less commonly used. VEPs can be evoked by patterned or unpatterned stimuli and may be used during surgery around the optic chiasm or optic tract however results under anaesthesia are not reliable. BAEPs record a waveform composed of seven discrete waves after an auditory stimulus is delivered to the external auditory canal. Each wave corresponds to a specific locus of the auditory system from the organ of Corti to the auditory cortex. BAEPs may be used during hearing preservation vestibular schwannoma surgery or during microvascular decompression for hemifacial spasm.

Motor evoked potentials

Motor evoked potentials (MEPs) are generated by stimulating the motor cortex, spinal cord, or a peripheral nerve with an electrical or magnetic stimulus. Transcranial magnetic stimulation is preferred in preoperative mapping because it is less invasive but transcranial electric stimulation using corkscrew or needle electrodes is usually performed intraoperatively. Neurogenic MEPs are recorded directly from the spinal cord or from peripheral nerves. Neurogenic MEPs generate two types of wave: direct propagation of the stimulus along the corticospinal tract generates direct waves (D waves), while indirect waves (I waves) are caused by activation of adjacent cortex. Myogenic MEPs record the muscle response (M response) of a specified muscle by using electromyography (EMG) recording. The M response reflects the motor unit action potential (MUAP) and represents the summated action potentials of the muscle fibres of one motor unit.

Inhalation anaesthetics have a significant effect on MEPs, in particular I wave responses. D waves are not affected by inhalation anaesthetics, but the α-motor neurone is blocked at higher doses, even when stimulated by transcranial electric stimulation. Intravenous anaesthetics only have a mild effect on MEPs and total IV anaesthetic using propofol and etomidate is typically preferred when using MEPs as they are less suppressive than gases at similar depths of anaesthesia. However, excessively high doses of propofol may be similarly suppressive to inhalation agents. Benzodiazepines are usually avoided because they eliminate MEP responses. Neuromuscular blocking agents do not affect neurophysiological monitoring and can actually enhance I wave recordings but MUAPs cannot be recorded when the neuromuscular transmission of acetylcholine is completely blocked. The anaesthetist observes the M-responses to evaluate the degree of neuromuscular blockade.

MEPs can monitor the dorsolateral and ventral spinal cord tracts during spinal cord and complex spine surgery and complements SSEP monitoring of the dorsal columns (Schwartz et al., 2007). Monitoring of pudendal MEPs and sacral EMG recording from the anal sphincter is used when performing selective dorsal rhizotomy for the treatment of spasticity and helps identify nerve rootlets that can be selectively sectioned.

Unlike SSEPs, MEPs are not usually monitored continuously as the patient may move following a stimulation. The surgeon and neurophysiologist also need to work together to ensure frequent MEPs are obtained without disrupting the surgery.

Electromyography

A recording electrode is placed inside a needle and inserted into a muscle to record the MUAP of that muscle. Signals are then converted into sound to demonstrate muscle activity. Evoked EMG uses electrical stimulation to identify specific nerves whereas free-running EMG is used to identify any interruptions to the nerve's normal electrical discharge. Spontaneous benign discharges produce short non-sustained discharges (likened to the sound of 'popcorn') and indicate proximity of the stimulus to the nerve whereas a neurotonic discharge is prolonged and indicates ongoing nerve injury.

Facial nerve monitoring is the commonest type of intraoperative EMG used in cranial neurosurgery whereby recording electrodes are placed in the orbicularis oris and orbicularis oculis muscles. Muscle activity is recorded either during a surgeon's intentional stimulation of the nerve or by inadvertent nerve stimulation during manipulation, mechanical, or thermal injury. Optimal facial nerve EMG recordings are obtained when neuromuscular blockade is avoided but facial muscles appear relatively resistant to the effects of muscle relaxants. Hartman's solution irrigation should be used instead of saline irrigation to avoid stimulation of the facial nerve. EMGs are also used to monitor muscle group activity during selective dorsal root rhizotomy for spasticity and spinal root monitoring is considered a key component of multimodality spinal monitoring used during spinal instrumentation.

Intraoperative cortical mapping (brain mapping)

Intraoperative brain mapping is typically used to locate the motor, sensory, or speech cortex during epilepsy or tumour surgery in and around eloquent areas. Phase reversal SSEPs may be utilized in anaesthetised patients to localize the primary sensory or motor cortex whereby a strip grid is placed on the surface of the brain perpendicular to the anticipated orientation of the central sulcus. A phase reversal of the N20/P20 peak indicates that those electrodes straddle the central sulcus. In awake patients, direct cortical stimulation may be used to map the motor cortex.

For speech mapping in the temporal lobe, a recording electrode strip is placed on the brain surface and the cortex is then stimulated using a bipolar cortical stimulator. The stimulating current is increased in small 2 mA increments, up to a maximum of 10 mA, while observing for any after discharges (akin to focal seizures). Once the patient's threshold for after discharges has been established, patients are asked to name objects shown on picture cards while the cortex continues to be stimulated and any paraphasic errors or speech arrest are noted. The aforementioned steps are then repeated so that the patient's speech area may be mapped out on the brain's surface. Awake craniotomy is usually required for brain mapping, especially for the speech areas.

The key to a successful awake procedure is patient preparation. Good patient cooperation is required, and careful patient selection

is needed to ensure the patient fully understands what will happen during surgery. Various anaesthetic and surgical techniques have been described in the context of performing awake craniotomy but a successful procedure mandates anticipation of specific problems and clinical vigilance (Erickson and Cole, 2012). Fully awake surgery is performed after the infiltration of local anaesthetic into the scalp or following regional nerve block of the scalp. The asleep-awake-asleep (AAA) technique uses general anaesthesia, with or without the use of an airway, during the opening and closing portions with emergence of patients from anaesthesia in the interim. However, the more commonly advocated anaesthesia technique for the opening and closing portions is termed monitored anaesthesia care (also called conscious sedation). The same medications used in the AAA technique are given (propofol and fentanyl) but they are given in pulses and at lower doses with the goal of providing a smooth transition to alertness and obviating the difficulties of airway intervention (Erickson and Cole, 2012).

FURTHER READING

Abd-El-Barr, M.M. & Cohen, A.R. (2013). The origin and evolution of neuroendoscopy. *Childs Nerv Syst*, **29**, 727–37.

Gonzalez, A.A., Jeyanandarajsan, D., Hansen, C., Zada, G. &, Hsieh, P.C. (2009). Intraoperative neurophysiological monitoring during spine surgery: a review. *Neurosurg Focus*, **27**(4), E6.

Hall, W.A. & Truwit, C.L. (2008). Intraoperative MR-guided neurosurgery. *J Magn Reson Imaging*, **27**, 368–75.

Haynes, A.B., et al.; Safe Surgery Saves Lives Study Group (2009). A surgical safety checklist to reduce morbidity and mortality in a global population. *N Engl J Med*, **360**(5), 491–9.

Kriss, T.C. & Kriss, V.M. (1998). History of the operating microscope: from magnifying glass to microneurosurgery. *Neurosurgery*, **42**(4), 899–907.

REFERENCES

Abd-El-Barr, M.M. & Cohen, A.R. (2013). The origin and evolution of neuroendoscopy. *Childs Nerv Syst*, **29**, 727–37.

Dujovny, M., Ibe, O., Perlin, A., & Ryder, T. (2010). Brain retractor systems. *Neurol Res*, **32**(7), 675–83.

Erickson, K.M. & Cole, D.J. (2012). Anesthetic considerations for awake craniotomy for epilepsy and functional neurosurgery. *Anesthesiol Clin*, **30**(2), 241–68.

Gonzalez, A.A., Jeyanandarajan, D., Hansen, C., Zada, G., & Hsieh, P.C. (2009). Intraoperative neurophysiological monitoring during spine surgery: a review. *Neurosurg Focus*, **27**(4), E6.

Grant, A.G. (2007). Update on hemostasis: neurosurgery. *Surgery*, **142**(4 Suppl), S55–60.

Hall, W.A. & Truwit, C.L. (2008). Intraoperative MR-guided neurosurgery. *J Magn Reson Imaging*, **27**, 368–75.

Haynes A.B., et al.; Safe Surgery Saves Lives Study Group. (2009). A surgical safety checklist to reduce morbidity and mortality in a global population. *N Engl J Med*, **360**(5), 491–9.

Jho, H.D. & Alfieri, A. (2001). Endoscopic endonasal pituitary surgery: evolution of surgical technique and equipment. *Minim Invasive Neurosurg*, **44**(1), 1–12.

Kriss, T.C. & Kriss, V.M. (1998). History of the operating microscope: from magnifying glass to microneurosurgery. *Neurosurgery*, **42**(4), 899–907.

Liu, C.Y., Wang, M.Y., & Apuzzo, M.L.J. (2004). The physics of image formation in the neuroendoscope. *Childs Nerv Syst*, **20**, 777–82.

Paluzzi, A., Gardner, P., Fernandez-Miranda, J.C., & Snyderman C. (2012). The expanding role of endoscopic skull base surgery. *Br J Neurosurg*, **26**(5), 649–61.

Schwartz, D.M., Auerbach, J.D., Dormans, J.P., et al. (2007). Neurophysiological detection of impending spinal cord injury during scoliosis surgery. *J Bone Joint Surg Am*, **89**(11), 2440–9.

Spetzler, R.F., Daspit, C.P., & Pappas, C.T. (1992). The combined supra- and infratentorial approach for lesions of the petrous and clival regions: experience with 46 cases. *J Neurosurg*, **76**, 588–99.

Thirumala, P.D., Bodily, L., Tint, D., et al. (2014). Somatosensory-evoked potential monitoring during instrumented scoliosis corrective procedures: validity revisited. *Spine J*, **14**(8), 1572–80.

RELATED LINKS TO EBRAIN

Advanced Microsurgical Skills. https://learning.ebrain.net/course/view.php?id=93

Image-guided Neurosurgery. https://learning.ebrain.net/course/view.php?id=92

Intraoperative Imaging Techniques. https://learning.ebrain.net/course/view.php?id=89

Intraoperative Neurosurgical Electrophysiological Monitoring. https://learning.ebrain.net/course/view.php?id=489

Preparing the Operative Site. https://learning.ebrain.net/course/view.php?id=96

Principles of Awake Craniotomy. https://learning.ebrain.net/course/view.php?id=496

Surgery in Children. https://learning.ebrain.net/course/view.php?id=73

The Modern Theatre Environment. https://learning.ebrain.net/course/view.php?id=97

The Operating Microscope. https://learning.ebrain.net/course/view.php?id=94

Use of an Endoscope. https://learning.ebrain.net/course/view.php?id=91

Use of Standard Neurosurgical Equipment. https://learning.ebrain.net/course/view.php?id=70

5

Perioperative care of the neurosurgical patient

Karol P. Budohoski, Alessandro Scudellari, Sylvia Karcheva, and Derek Duane

Introduction

Multidisciplinary involvement in the care and planning of patients for neurosurgical procedures is now a common and necessary requirement to limit complications and promote better neurological outcomes. In the perioperative period, failings in clinical management can be devastating and cause severe disability or death (Wacker and Staender, 2014). The shared goal of the neurosurgeon along with the neuroanaesthetist acting as perioperative physician, is to facilitate optimization of the patient's clinical and psychological readiness for the operative intervention and subsequent recovery while preventing avoidable harm. To enable this, an established perioperative pathway is followed that includes performing a preoperative evaluation, completing appropriate investigations, communicating risk, complying with patient safety measures, promoting teamwork, and pursuing specific intra- and postoperative management strategies. These processes will be discussed in detail in the following sections, while highlighting their importance in the preservation of normal neurological function.

Preoperative anaesthetic evaluation

The purpose of the preoperative assessment is to optimize a patient's comorbidities and formulate a perioperative management plan. This review should follow the time-honoured tradition of history taking, examination, deciding on necessary investigations, risk assessment analysis, information sharing, and seeking informed consent. When assessing patients preoperatively, use is made of the American Society of Anesthesiologists (ASA) physical status classification system. This is one accepted method used for the stratification of a patient's pre-existing health status (**Table 5.1**).

Airway

Airway difficulty resulting in hypoxia and hypercarbia is the single most important cause of anaesthesia related morbidity and mortality. Therefore, it is vital to conduct a comprehensive examination of the airway preoperatively. Many tests to predict a difficult airway assess parameters such as mouth opening with grading of pharyngeal structures, neck mobility, and anatomical oropharyngeal measurements but none has the desired specificity and positive predictive value to be consistently useful. In the neurosurgical population, patients with cervical spine disease leading to limited movement, instability requiring a cervical collar or traction weights and those with acromegaly can all cause potential airway difficulty for the anaesthetist. To ensure adequate preoperative hydration and to help avoid gastric contents aspiration during intubation, recent guidelines encourage anaesthetists to allow adults and children to drink clear fluids up to 2 hours before elective surgery, while solid food should be prohibited for 6 hours (Smith et al., 2011).

Respiratory system

Optimizing pulmonary function is important to ensure the patient can be adequately oxygenated and ventilated intraoperatively, thus permitting respiratory manipulation of cerebrovascular physiology. Patients with neurological disorders have a higher risk of suffering aspiration pneumonia and neurogenic pulmonary oedema, both of which can adversely affect neurological outcome and survival.

Patients with a smoking habit should stop at least 6–8 weeks prior to surgery allowing for improvement in lung function and a better perioperative outcome. Acute exacerbations of infective or inflammatory airway diseases will need treatment and deferment of anaesthesia for up to 6 weeks to permit airway sensitivity to resolve. Chronic pulmonary diseases should be assessed clinically and where there is evidence of worsening impairment, further imaging and functional testing will sometimes be necessary to help clarify the risk of complications which can include postoperative ventilation. Patients who suffer from obstructive sleep apnoea especially those with acromegaly or Cushing's disease are often very sensitive to opioid analgesics and sedative agents. These patients can develop impaired respiratory gas exchange, atelectasis, and pulmonary infections without the routine use of continuous positive airway pressure prior to surgery.

Cardiovascular system

The prevalence of heart disease is common in neurosurgical patients and a careful assessment of the functional state of the cardiovascular system is necessary to reliably predict perioperative and long-term

Table 5.1 American Society of Anesthesiologists (ASA) physical status classification system

ASA grade	Definition
I	A healthy patient with no systemic disease
II	Mild to moderate systemic disease
III	Severe systemic disease imposing functional limitation on patient
IV	Severe systemic disease which is a constant threat to life
V	Moribund patient who is not expected to survive with or without the operation
VI	A declared brain-dead patient whose organs are being removed for donor purposes
	For emergency cases the suffix 'E' is used

ASA Physical Status Classification System is reprinted with permission of the American Society of Anesthesiologists, 1061 American Lane, Schaumburg, Illinois 60173–4973.

cardiac complications (Fleisher et al., 2014). In patients with the usual risk factors and a history of shortness of breath, fatigue, or chest pain while performing daily living activities, usually have poor cardiovascular reserve requiring further investigation. The revised cardiac risk index (Table 5.2) using six independent variables is helpful in assessing the neurosurgical patient's risk of cardiac complications and mortality (Ford et al., 2010).

Poorly controlled hypertension (systolic >180 mmHg and mean arterial pressure (MAP) over 110 mmHg) increases cerebrovascular resistance and causes a right shift of the cerebral blood flow autoregulatory curve resulting in poor tolerance to acute hypotension. If surgery can be postponed, weeks to months of treatment may be needed to adequately control the blood pressure otherwise perioperative management by intravenous agents can be instituted for emergency surgery albeit with increased risk of complications.

Patients who have had a recent myocardial infarction or coronary stent intervention are at a higher risk of further myocardial damage if operated on within six months. Heart failure, in particular, is a significant risk for perioperative morbidity and mortality and requires optimal treatment prior to surgery in line with international guidelines and local cardiology advice to ensure a good outcome (Yancy et al., 2013).

Patients with a newly suspected heart valve lesion need echocardiography evaluation to quantify its severity. Some patients may need a valvular intervention before their elective neurosurgical procedure to reduce their perioperative cardiac risk. In general, knowing the severity of the valvular heart disease allows choice of the appropriate anaesthetic technique as well as deciding on the best perioperative monitoring and level of postoperative care for the patient.

Cardiac dysrhythmias and conduction disorders occur more frequently with increasing age such that all patients over the age of 55 years should have a routine electrocardiograph prior to surgery. The presence of a dysrhythmia in the preoperative setting should prompt investigations into the underlying cause. Atrial fibrillation (AF) is the most common tachydysrhythmia. Patients with rate-controlled AF who are clinically stable generally do not require special evaluation in the perioperative period other than adjustment of anticoagulation. Patients who develop conduction abnormalities leading to bradydysrhythmias, or episodes of supraventricular or ventricular tachycardias require referral to a cardiologist for further evaluation and possible cardioversion to sinus rhythm or insertion of a permanent transvenous pacing device. Those patients who present for neurosurgery with implanted cardiac pacemakers or defibrillators will need their device checked for any signs of malfunction after surgery if electrocoagulation is used during the procedure.

Table 5.2 Revised Cardiac Risk Index

Revised Cardiac Risk Index	
1	High risk type of surgery
2	Ischaemic heart disease (includes any of the following: history of MI, positive exercise test, current chest pain, nitrate use, or electrocardiography with Q waves)
3	Congestive heart failure
4	History of cerebrovascular disease
5	Preoperative treatment with insulin
6	Preoperative serum creatinine >2.0 mg/dl

Reproduced with permission from Thomas H. Lee et al., Derivation and Prospective Validation of a Simple Index for Prediction of Cardiac Risk of Major Noncardiac Surgery, *Circulation*, Volume 100, Issue 1, Copyright © 1999 Wolters Kluwer Health, Inc.

Neurological system

A preoperative record of the patient's neurological state using the Glasgow Coma Scale (GCS) score should be made to identify pre-existing deficits. Pupil size and reaction to light should be noted. Assessment of cranial nerve integrity is important to establish problems with bulbar function along with gag and cough reflexes. Examination of sensory and motor function will establish the presence of any anomalies. This baseline neurological examination is essential to allow comparison with a patient's postoperative state for detection of any possible deterioration in function.

Other medical conditions

Other medical disorders affecting the endocrine, renal, hepatic, neuromuscular, and metabolic systems will need to be optimized prior to neurosurgery. Electrolytes, (especially sodium and potassium) and water disturbances resulting from conditions such as cerebral salt wasting (CSW) syndrome, or inappropriate antidiuretic hormone secretion (SIADH) and diabetes insipidus (DI) will need appropriate management preoperatively to ensure anaesthesia can be administered safely. Hyperglycaemia, a commonly encountered problem in neurosurgical patients mainly due to corticosteroid treatment, has well documented adverse effects on injured brain tissue (Kramer et al., 2012). Insulin therapy instituted preoperatively according to local guidelines may be necessary to achieve adequate glycaemic control.

Prehospital medications and allergy status

The continuation of a patient's prehospital medications is usual up to the day of surgery. However, depending on neurosurgical advice, specific recommendations in relation to corticosteroids, and anticonvulsants are often made. Most antihypertensive agents and analgesic drugs for chronic pain should also be continued. Diabetic patients can sometimes omit oral hypoglycaemic agents but to optimize their blood glucose they may need an insulin sliding-scale regimen preoperatively. Anticoagulant and antiplatelet agents should be stopped at the appropriate time to allow clotting and platelet function to return to normal. This decision should be informed by haematology

or cardiology advice and based on a consideration of procedure urgency, along with the risks associated with the potential for haemorrhage and thrombosis.

A patient's history of drug allergies should be documented prior to anaesthesia. Any record of anaphylaxis, facial swelling, bronchospasm, hypotension, or profound cutaneous erythema related to a particular agent are all highly significant and warrant avoidance. Drug allergies are often readily documented to antibiotics, intravenous contrast, and anaesthetic agents but enquiry should also be made about reactions due to latex, iodine, chlorhexidine, adhesive tapes, and other substances used during the surgical procedure.

Preoperative investigations

Guidelines from both the ASA and the National Institute for Health and Care excellence (NICE) do not advocate routine preoperative investigations but rather tests based on the type of procedure (minor to complex major) and the functional impairment imposed by comorbidities. Biochemical, haematological, and electrophysiological testing along with imaging evaluate the degree of pathology and dysfunction of a particular organ system thus providing information on physiological reserve and the potential response to anaesthetic agents.

A risk factor assessment based on a patient's history and examination should indicate the need to check the haemoglobin level preoperatively. When significant blood loss is anticipated, blood group type and cross-matching will be required. Establishing a history of familial bleeding disorders or other risk factors for coagulopathy necessitates preoperative coagulation testing. However, there is little evidence that abnormal tests are predictive of perioperative haemorrhage (Seicean et al., 2012).

Comorbidities affecting the renal and hepatic systems either directly or indirectly require testing for sodium, potassium, creatinine, urea, estimated glomerular filtration rate, and liver enzyme levels. In patients with convulsive disorders, assessment of magnesium, calcium, and anticonvulsant drug levels may be appropriate. When endocrine abnormalities are suspected, baseline investigation of the hypothalamic-pituitary-end-organ axis should be established. Other blood investigations should be guided by the severity of a patient's comorbidities and the associated functional impairment.

An electrocardiogram is useful as a baseline investigation in patients with signs and symptoms of ischaemic heart disease. It may highlight hypertensive heart disease, rhythm abnormalities, or occult ischaemia. Further investigation of the cardiovascular status of the patient using a combination of exercise stress testing, echocardiography, nuclear imaging studies, and coronary angiography is usually indicated with findings of exertional dyspnoea and chest pain. Preoperative chest radiographs and pulmonary function testing are necessary only in patients whose symptoms and underlying lung disease is progressive.

Intraoperative anaesthetic management

Induction and maintenance of anaesthesia

The basic principles of neuroanaesthesia for cranial neurosurgery are essentially twofold; (1) the provision of a relaxed brain to enable good operative surgical conditions, and (2) the maintenance of cerebral perfusion pressure (CPP) and cerebral oxygenation. Controversy remains regarding the best practice to enable these overall goals such that interventions are often empirical rather than evidence-based.

Venous access

Once a patient is deemed fit for surgery their pathway from induction to emergence follows specific anaesthetic interventions. An inhalational induction is more usual in children and uncooperative or needle phobic adult patients but more commonly, an intravenous induction is used after initial venous access has been obtained. In general, both arterial and venous access can be achieved under local or general anaesthesia. Depending on the type of surgery and the severity of the patient's comorbidities, a central venous catheter is sometimes indicated.

Type of induction and drugs used

Intravenous induction of anaesthesia is commonly performed using short-acting agents such as propofol, thiopentone, etomidate, or ketamine (see **Table 5.3** and **Fig. 5.1**). Each agent has their own benefits and drawbacks but there is little to choose between them. In general, propofol and thiopentone are fast-acting but cause significant hypotension. Etomidate and ketamine cause less haemodynamic instability but the former agent can suppress adrenocortical activity for many hours and the later drug can cause postoperative hallucinations and nightmares. If intravenous access is not initially possible, there is concern over possible airway control or if the patient is a child, then an inhalational induction with a volatile agent and a mixture of oxygen and air is performed (see **Table 5.4**). This form of induction generally takes longer, is associated with excitatory phenomena, and if airway issues arise there is no immediate intravenous access to allow the administration of neuromuscular blocking agents.

Airway management

After induction of anaesthesia, intubation or the insertion of a supraglottic airway device is facilitated using a non-depolarizing neuromuscular blocking agent such as atracurium or rocuronium. Depending on the dose, these agents can take 1–3 minutes to reach peak effect and they are more commonly implicated in causing histamine release or rarely anaphylaxis. Securing the airway with a plain or reinforced cuffed endotracheal tube (ETT) is commonplace for most neurosurgical procedures. The ETT should be taped with care to avoid inadvertent dislodgement, especially for patients in the prone position. If a difficult airway is predicted from the scoring systems used in the preoperative assessment and the patient has cervical spine pathology, then a fibreoptic-assisted awake or asleep intubation may be required. An unpredicted difficult airway is no more common than in the general surgical population and the standard management algorithms for this clinical scenario should be followed. After intubation, patients are ventilated using an air/oxygen mixture of gases and an inhalational agent is added if required.

In emergency situations, a rapid sequence ('crash') induction is commonly performed. This involves using 100% oxygen for up to 5 minutes to preoxygenate the patient, the administration of a short-acting intravenous sedative agent (e.g. propofol or thiopentone) and simultaneous application of cricoid pressure to help avoid aspiration of the contents of a presumed full stomach. Once the patient is unconscious, a rapid administration of a depolarizing neuromuscular

Table 5.3 Effects of intravenous anaesthetic agents on cerebrovascular, respiratory, and cardiovascular parameters

	Target receptor	ICP	CBF	$CMRO_2$	CO_2 reactivity	Auto-regulation	Respiratory depression	Cardiovascular depression	Indication
Propofol	GABA	↓↓	↓	↓↓	→	→	++	++	Induction and maintenance of anaesthesia
Thiopental	GABA	↓↓	↓	↓↓	→	→	++	+	Induction of anaesthesia; Deep barbiturate coma
Etomidate	GABA	↓↓	↓	↓↓	→	→	++	-/+	Induction of anaesthesia (cardiovascularly unstable patients)
Ketamine	NMDA	↑/↓	↑	↑	→	→	-	-	Hypovolemic trauma patient
Dexmedetomidine	α_2 adrenoceptor	↓	↓	↓	→	→	-	Concentration dependent	Functional neurosurgery
Benzodiazepine	GABA	↓	↓	↓	→	→	+	+	Sedative premedication; ICU sedation

↓ decrease: ↑ increase: → unchanged

a) Reproduced with permission from Srejic, U., 'Volatile Anesthetic Agents', pp. 62–6, in R. Adapa, D. Duane, A. Gelb, & A. Gupta (Eds.), *Gupta and Gelb's Essentials of Neuroanesthesia and Neurointensive Care*, 2018 © Cambridge University Press.

b) This article was adapted from *Cottrell and Young's Neuroanesthesia*, James Cottrell William Young, Effects of Anesthetic Agents and other Drugs on Cerebral Blood Flow, Metabolism and Intracranial Pressure, pp. 78–95, Copyright Elsevier (2010).

blocking agent (e.g. suxamethonium) or a higher dose of a non-depolarizing agent is given. The time to adequate intubating conditions is usually 90-seconds following this regimen.

Monitoring

Standard physiological parameters are monitored during neuroanaesthesia. These include: heart rate; three or five lead electrocardiography; pulse oximetry; non-invasive or invasive blood pressure; respiratory rate; end tidal carbon dioxide; nasopharyngeal temperature; and the concentrations of oxygen and inhalational agent. Ventilation parameters (i.e. tidal volume, peak inspiratory pressure, and positive end-expiratory pressure (PEEP)) are adjusted to achieve an arterial oxygen level of greater than 13 kPa and a carbon dioxide level of between 4.5 and 5 kPa. A urinary catheter is

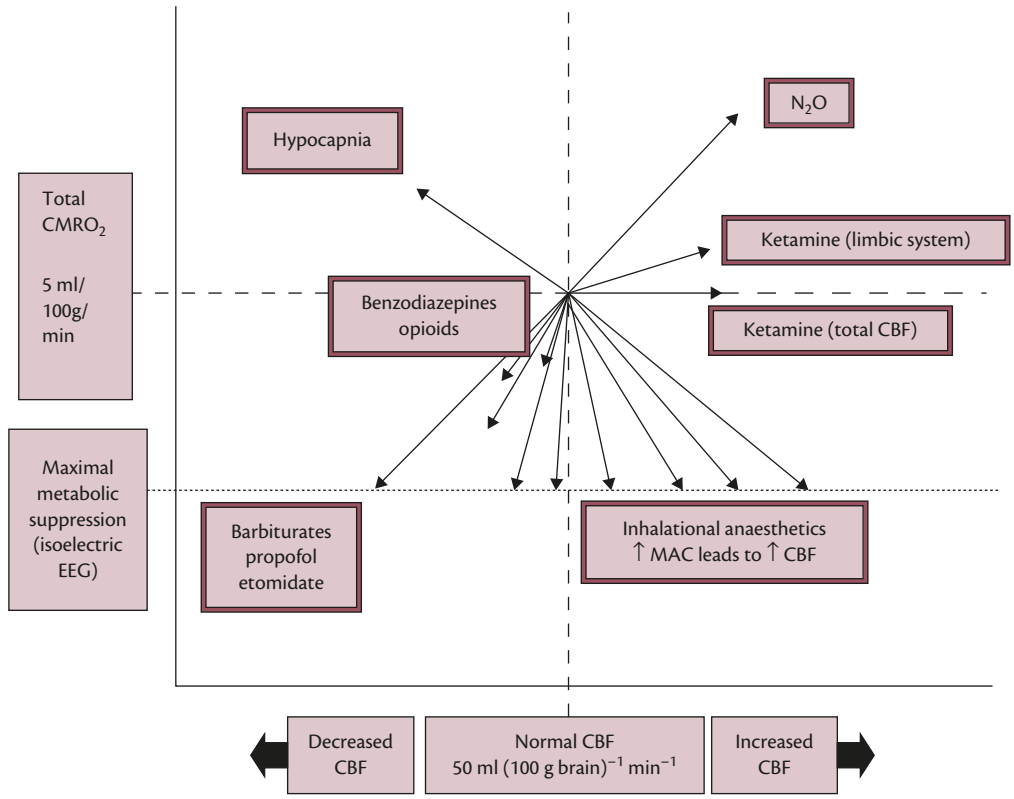

Fig. 5.1 Effects of intravenous anaesthetic agents on cerebrovascular, respiratory, and cardiovascular parameters.

Table 5.4 The effects of inhalational anaesthetics on cerebrovascular parameters

	ICP	CBF	$CMRO_2$	CO_2 reactivity	Autoregulation	Cardiovascular depression
Sevoflurane	→ or ↑	↑ or →	↓↓	Dose related ↓	Dose related ↓	+
Desflurane	↑ or →	↑ or ↓	↓↓	Dose related ↓	Dose related ↓	+
Isoflurane	→ or ↑	↑ or →	↓↓	Dose related ↓	Dose related ↓	+

Reproduced with permission from Srejic, U., "Volatile Anesthetic Agents", pp. 62–6, in R. Adapa, D. Duane, A. Gelb, & A. Gupta (Eds.), *Gupta and Gelb's Essentials of Neuroanesthesia and Neurointensive Care*, 2018 © Cambridge University Press.

sometimes inserted to measure renal output during protracted surgery, for anticipated significant blood loss or where hyperosmolar therapy is used. Neuromuscular junction monitoring is essential in all cases where muscle paralysis is maintained throughout anaesthesia.

In certain circumstances, electroencephalography (EEG), electrophysiological monitoring of cranial nerves, and the measurement of motor or sensory evoked potentials can help prevent postoperative neurological deficits. Processed EEG-based depth of anaesthesia monitoring using the bispectral index or spectral entropy is recommended as an option in patients undergoing total intravenous anaesthesia (TIVA) with muscle relaxants, deep anaesthesia without the use of muscle relaxants and those at a higher risk of unintended awareness (Escallier et al., 2014).

Positioning

After induction of anaesthesia, potent stimuli resulting from laryngoscopy, insertion of a bladder or central vascular catheter, the application of skull pins, and positioning can cause a hypertensive response that must be obtunded to avoid an unexpected rise in intracranial pressure. This complication may also arise in patients positioned without a 15- to 30-degree head elevation, when the neck is flexed or turned resulting in obstruction to cerebral venous outflow, when PEEP greater than 10 cm H_2O is used and in the prone position which obstructs adequate ventilation. Hyperflexion of the neck should also be avoided as it may result in tongue and airway oedema thus preventing safe extubation at the end of surgery.

The sitting position is well known for its complications of hypotension, venous air embolism (VAE), macroglossia, pneumocephalus, and nerve injuries. Despite this, if a strict team protocol is followed the position is generally well tolerated and excellent operative conditions are ensured. In prone positioning, it is the responsibility of both surgical and anaesthetic teams to adopt strategies to minimize the risk of organ system pressure-injuries, myocutaneous necrosis, peripheral neuropathies, and ophthalmic complications (DePasse et al., 2015).

Maintenance of anaesthesia

General anaesthesia comprises a triad of hypnosis, analgesia, and muscle relaxation. In general, intravenous anaesthetic agents couple the reduction in cerebral metabolic rate of oxygen consumption ($CMRO_2$) and cerebral blood flow (CBF), preserve cerebral autoregulation (CAR) and carbon dioxide reactivity while reportedly inhibiting excitotoxicity and free radical-mediated lipid peroxidation. However, they can lower the MAP and CPP with resulting potentially harmful effects on cerebral oxygenation and intracranial pressure (ICP). In comparison, inhalational agents, to a varying degree, suppress $CMRO_2$ in a dose-dependent manner but cause cerebral vasodilatation (desflurane ~ isoflurane > sevoflurane) which may promote an increase in CBF and hence ICP unless compensated by hypocapnia induced vasoconstriction. These agents also cause a dose-dependent decrease in CPP, CAR, and carbon dioxide reactivity.

Despite the difference in the effects of both intravenous and inhalational agents on cerebral haemodynamics, there is not yet a consensus as to the best anaesthetic technique for neurosurgical procedures (Chui et al., 2014). However, in patients with known intracranial hypertension, intravenous-maintained anaesthesia would seem to have the theoretical advantage while inhalational agents should be used by those more experienced. In procedures where electrophysiological monitoring of the brain and spinal cord are undertaken, TIVA, rather than inhalational agents, has only a minimal influence on measured potential. During operations on the vertebral column and spinal cord, the anaesthetic considerations should be the same as for cranial interventions.

Intraoperative events and anaesthetic emergence

Respiratory and cardiovascular

The ability to control arterial oxygen and carbon dioxide levels by altering the patient's ventilation is essential in the management of intracranial hypertension. Important causes that can prevent adequate ventilation and require immediate remedy include: (1) inadvertent endobronchial intubation; (2) sputum blocking or kinking of the ETT; (3) bronchospasm; (4) faulty prone positioning; and (5) an unrecognized pneumothorax after central venous access or tunnelling during a cerebrospinal fluid (CSF) diversion procedure.

Intraoperative arterial hypotension (systolic blood pressure <90 mmHg), known to be associated with a poor outcome in patients with traumatic brain injury (TBI) often requires a reduction in anaesthesia dosing as well as fluid and inotropic support. Cardiac rhythm disturbances can be evoked by ICP-mediated vagus nerve stimulation, trigeminal cardiac reflex activation, brainstem manipulation, and lidocaine toxicity. Cessation of the stimulus is usually sufficient to terminate the disturbance or restoration to sinus rhythm may be pharmacologically assisted. In the event of a cardiac arrest during neurosurgery the usual advanced life support protocols should be followed, as well as consideration given to early removal of the patient from the head-fixation clamp and adoption of the supine position (Resuscitation Council (UK), 2014).

Intraoperative fluid management

In general, maintenance intraoperative fluids should be kept to a minimum unless there is significant bleeding or haemodynamic instability. Glucose-free iso-osmolar crystalloid fluids are most often used. Fluid and electrolyte balance can be significantly affected by the use of hyperosmolar agents and other diuretics and aggressive replacement to avoid metabolic derangement is sometimes needed.

Perioperative blood loss during neurosurgery can be unpredictable and significant resulting in hypotension, reduced cerebral oxygenation, coagulopathy, and anaemia. Prompt restoration of blood volume is mandatory using crystalloid fluids and blood products. Coagulation testing and haematology advice should guide the administration of clotting factors. The optimal haemoglobin trigger for transfusion is contentious. Reports from several studies have shown both anaemia and red blood cell transfusion to be associated with worsening patient outcomes (Alan et al., 2014; Gruenbaum and Ruskin, 2014).

Other unexpected events

Catastrophic unexpected events can occur during neurosurgical procedures requiring action to be taken collaboratively by both surgeon and anaesthetist. Such events include; anaphylaxis, seizures, acute brain swelling, aneurysm rupture, and VAE. The underlying principles in the management of these critical events include identification and removal of the cause followed by treatment to prevent or limit any adverse outcome for the patient. In all events, efforts are directed towards (1) optimizing cerebral oxygenation by restoring CPP using fluids and inotropic agents; (2) attempting a neuroprotection strategy by reducing $CMRO_2$ with anaesthetic drugs, anticonvulsants, and hypothermia; and (3) lowering ICP with hyperosmolar agents and short-term hyperventilation.

Prophylactic antiepileptic medication has been variably recommended for use during neurosurgical, especially neuroncology procedures. The incidence if seizures in the first postoperative week is reduced by approximately 40–50%, but with little or no effect on the incidence of late seizures (Temkin, 2002).

Anaesthetic emergence

Emergence from anaesthesia at the end of surgery should be a managed process. The aim is to preserve haemodynamic stability, avoid excessive coughing and bucking on the ETT while achieving a rapid and smooth transition to normal cognitive function. This allows a prompt neurological assessment and early detection of deficits that may require urgent intervention. There is no difference in the timing of return to normal cognition when either intravenous or inhalational anaesthesia is used for neurosurgery (Chui et al., 2014).

A poorly managed emergence may result in haemodynamic instability and possibly cause intracranial bleeding, cerebral hyperperfusion syndrome, or ischaemic myocardial dysfunction. Antihypertensive agents may be needed to control the systolic blood pressure to below 160 mmHg usually. In general, most patients should be delivered to the postanaesthesia care unit without the need for airway support, breathing spontaneously, haemodynamically stable, conscious, alert, normothermic, and comfortable.

Postoperative anaesthetic care and complications

Respiratory

At the end of surgery, patients are usually extubated in the operating room or in a high-dependency care area. Early postoperative respiratory complications following cranial procedures have an incidence of up to 20% (Ali, 2015). They manifest as hypoxia and hypercarbia secondary to a pneumothorax, atelectasis, sputum retention, aspiration pneumonia, bronchospasm, or neurogenic pulmonary oedema. Supplementary oxygen, physiotherapy, antibiotics, bronchodilators, diuretics, non-invasive ventilation, and tube thoracostomy after imaging may be required as treatment options. If measured arterial oxygen and carbon dioxide levels continue to deteriorate, early reintubation and ventilation to avoid secondary brain injury should be instituted without delay.

Cardiovascular

Transient hypertension on extubation is not uncommon but it may persist into the postoperative period. Treating postoperative pain may be sufficient to lower blood pressure to within the patient's normal range. However, persistent systolic hypertension can lead to intracerebral bleeding or a cerebral hyperperfusion syndrome and may require prompt treatment with short-acting antihypertensive agents. Overaggressive management should be avoided as it can risk cerebral ischaemia. Hypotension in the postoperative period usually responds to fluid management unless myocardial dysfunction is suspected when further investigations are required.

Delayed neurological recovery

A delayed neurological recovery may be related to the residual depressant effect of anaesthetic drugs, inadequate reversal of muscle relaxants, hypoglycaemia, or hypothermia. Patients who have a depressed conscious level or signs of abnormal neurology on examination within a reasonable period after stopping anaesthesia, warrant a computer tomography (CT) brain scan. Pneumocephalus may be revealed as the cause and treatment with high oxygen concentration for up to 12 hours will usually bring about improvement. In the absence of any abnormality on the scan to account for a delayed recovery, a diagnosis of a subclinical seizure by exclusion is often made. Patients should be loaded with intravenous anticonvulsants and investigated further with electroencephalography. In all cases and especially where seizure activity accounts for the altered state of consciousness, there may be a need to provide ventilatory support and admit the patient to the neurocritical care unit.

Postoperative nausea and vomiting

The incidence of postoperative nausea and vomiting (PONV) after surgery is about 30–50% exceeding 70% in high risk patients. Persistent PONV after a neurosurgical procedure may cause intracranial bleeding and brain swelling. Risk factors include female gender, younger age, previous history, intracranial pathology, infratentorial surgery, use of nitrous oxide, sensitivity to opioids, and postoperative hypotension. Various antiemetics ranging from anticholinergics, antihistamines, dopamine receptor antagonists, 5-HT3 antagonists, steroids, and neurokinin-1 receptor antagonists have all been studied but no one agent is favoured over another.

Most anaesthetists take a multimodal approach using two or three agents when attempting to prevent or treat PONV (Kranke, 2015).

Pain management

Two-thirds of patients experience moderate to severe pain in the first 24–48 hours after a neurosurgical procedure. There are no large-scale studies to provide level one evidence for any particular postoperative analgesic regimen in these patients due perhaps to the multiple postulated pain mechanisms involved. A multimodal approach to pain management is necessary with the goal of targeting several of these pain-signalling pathways. Opioids are the main stay of treatment for moderate to severe pain after either cranial or spinal procedures. Fear of use related to the side effects of increased PONV, urinary retention, pupillary changes, sedation, and respiratory depression must be balanced against the patient's pain scores, agitation, altered cerebral haemodynamics, and raised intracranial pressure as a result of inadequate analgesia.

Codeine-based agents, paracetamol, non-steroidal anti-inflammatory drugs (NSAIDs), gabapentinoids, centrally acting alpha-2 agonists, ketamine, lidocaine infusions, and magnesium are less effective as monotherapy but more successful in opioid sparing and providing pain relief when used within a multimodal treatment protocol (Devin and McGirt, 2015). The use of NSAIDs must be considered against the risk of haemorrhage, gastric ulceration, renal toxicity, impaired bone fusion, and coronary vascular thrombosis. Ketamine may cause hallucinations, sedation, and diplopia while gabapentin is associated with sedation, dizziness, headache, and visual disturbances. Infratentorial surgery is often associated with more pain and the efficacy of patient-controlled analgesia has been shown is some studies.

Scalp infiltration with local anaesthetic agents in the form of a regional scalp block should be considered in all patients undergoing a craniotomy procedure. Evidence exists for reduced opioid requirements and postoperative pain scores are lower in the first 24 hours (Guilfoyle et al., 2013). Epidural and intrathecal neuraxial analgesia using a combination of drugs has its advocates for postsurgical pain relief after spinal operations. However, the literature provides little evidence with respect to the optimum route or dose of agent to use in relation to the type of surgery (Sharma et al., 2012).

Fluid and electrolyte management

Most patients who have undergone an uneventful neurosurgical procedure do not require regular intravenous postoperative fluid replacement. Clinical problems that may necessitate a postoperative fluid prescription to maintain normovolaemia include; a delayed return to consciousness, cerebral vasospasm, disturbed bulbar function, persistent PONV, significant blood loss during surgery, large volume diuresis from hyperosmolar therapy, haemodynamic instability, and endocrine issues such as diabetes mellitus, DI, and CSW syndrome. Iso-osmolar crystalloid fluids sometimes supplemented with potassium chloride are generally used. Glucose containing fluids may exacerbate neurological damage and increase brain free-water content.

Disorders of water balance causing hypo- or hypernatraemia (136 mmol/litre >Na^+ >150 mmol/litre) are common in patients after subarachnoid haemorrhage, traumatic brain injury, intracranial tumours, and pituitary surgery. Patients with these conditions usually benefit from measuring urine output and serum sodium for 24–48 hours postoperatively. A rising plasma sodium in the presence of hypotonic polyuria is robust evidence of acute DI and warrants decisive action usually in the form of desmopressin and fluid resuscitation guided by endocrinology advice.

Hyponatraemia is more common in neurosurgical patients caused by SIADH or cerebral salt wasting syndrome (CSWS). The diagnosis of SIADH can be considered if the plasma sodium and urea are falling in a euvolaemic patient with a low urine output after the exclusion of hypoadrenalism and hypothyroidism. Where there is hyponatraemia, an increase in urine volume, hypovolaemia, a fall in blood pressure, and a rise in blood urea (in the absence of diuretic therapy), the diagnosis of CSWS should be considered. Total 24-hour urinary sodium loss may help distinguish between SIADH and CSWS.

Treatment for CSWS involves sufficient intravenous sodium chloride to keep pace with urine losses and fludrocortisone in refractory cases. However, SIADH in the neurosurgical setting should involve expert advice on the limits of fluid restriction and the use of hypertonic saline, demeclocycline, and selective vasopressin-2 receptor antagonists. The rapidity of correction of hyponatraemia must be carefully monitored, to avoid neurological complications such as central pontine myelinolysis. A rate of correction no more than 12 millimoles/litre/day is generally considered safe.

Neurosurgical patients often present with disorders of potassium homeostasis because of perioperative osmotic therapy, associated renal failure, or trauma. Hypokalaemia (K^+<3.5 mmol/litre) and hyperkalaemia (K^+>5.5 mmol/litre) should be treated promptly to avoid life-threatening arrhythmias and haemodynamic instability.

Postoperative care facilities

It is crucially important that all neurosurgical patients are cared for postoperatively in an area dedicated to the monitoring, assessment, and recognition of neurosurgical complications. Expertise is required for a multitude of tasks that include; continuous neurological assessment, the maintenance of haemodynamic targets, interpretation of gas exchange parameters, observation for wound haematomas, the management of external ventricular drains, timely administration of medications for extrapyramidal disorders and the administration of antithrombotic agents after neuroradiological interventional procedures. Evidence suggests that as well as being cost-effective, the care of elective neurosurgical patients in these postoperative care areas rather than on a neurointensive care unit is safe (Smith, 2015).

Anaesthesia for specific neurosurgical interventions

Traumatic brain injury

The main role of the anaesthetist during surgery for traumatic brain injury is to protect the brain from further secondary injuries. Intraoperative management involves maintenance of an adequate cerebral perfusion pressure, while keeping oxygen and carbon dioxide levels, along with temperature and glucose, within normal range.

Many patients are the victims of accidents resulting in polytrauma and may already be intubated and ventilated when received in the

operating room. Life-threatening injuries are managed as a priority for cardiopulmonary stability before neurosurgical intervention. Every attempt should be made to assess and document GCS score, pupil size, reactivity, pre-existing neurological deficits, axial spine stability, and any other available relevant medico-social history. Aside from routine biochemical and haematological tests, analysis of clotting function and the availability of blood products must be ensured prior to any intervention.

Induction of anaesthesia is usually with propofol or thiopentone, as both significantly reduce $CMRO_2$ and therefore ICP. However, most anaesthetic agents, except ketamine and etomidate, cause a degree of hypotension which can be offset with vasopressors. Suxamethonium, a depolarizing neuromuscular blocking agent, is often used to facilitate airway management as part of a rapid sequence induction. Neither depolarizing or non-depolarizing agents have significant effects on ICP. Intubation can be difficult in neurotrauma patients who require a cervical collar and manual in-line stabilization for possible cervical spine injury. It is essential to have a backup plan for a failed intubation to avoid any rise in ICP due to hypoxia and hypercapnia.

During surgery, standard monitoring is augmented with measurements of temperature, urine output, and neuromuscular function. Invasive arterial blood pressure monitoring is essential and it allows regular blood gas measurements. Large-bore peripheral venous access is sufficient in most cases while central venous access, unless essential, should not delay surgery.

Total intravenous anaesthesia using infusions of propofol and remifentanil is a widely used technique for the maintenance of anaesthesia in brain injured patients. Inhalational agents can be used but in low concentrations (<1MAC) and nitrous oxide should be avoided. A PaO_2 of more than 11 kPa achieved using PEEP less than 8 cmH_2O and a $PaCO_2$ of 4–4.5 kPa is preferred. Prolonged hypocapnia can cause cerebral ischaemia and should be avoided. In adults, a CPP of more than 60 mmHg is maintained with fluids (blood products or glucose-free crystalloids) and vasopressors, as needed. Hyperosmolar therapy in the form of mannitol (0.25–1 g kg^{-1}) and/or hypertonic saline (5%, 2–3 ml kg^{-1}) is used to reduce brain swelling. Otherwise, patients are maintained normoglycaemic, normothermic, euvolaemic, electrolytes within normal range, and metabolically stable.

Postoperatively, severely injured patients will have ICP monitoring sited and require a period of sedation and ventilation on a neuro-critical care unit. Some patients may be suitable for extubation and require high-dependency, level II care for neurological observation, analgesia, as well as fluid and electrolyte management. Anticonvulsive therapy and pharmacological thromboprophylaxis should be administered on the advice of the neurosurgical team.

Brain swelling and neuroprotection

The aetiology of severe intraoperative brain swelling is multifactorial and is a recognized complication during surgery for TBI. In many cases, medical treatment is unsatisfactory and without immediate effect such that bone replacement is impossible and urgent scalp closure over the herniating brain is required. Implementing measures to manipulate basic neurophysiological parameters will eventually yield some benefit. CPP should be optimized with the use of fluids or vasopressors, hypoxia corrected and mild transient hypercapnia (4–4.5 kPa) instituted. Patients should be placed in a 30° head-up tilt, anaesthetic depth increased with boluses of propofol, thiopentone, or opiates, neuromuscular blockade established, and hyperosmolar or diuretic therapy started. Hyperthermia should be treated aggressively by ambient air cooling and cold intravenous crystalloid fluids while consideration should be given to instituting mild hypothermia (35–36°C). Intravenous insulin will be required for hyperglycaemia and anticonvulsant agents can be useful if seizure activity is a precipitating cause. A thiopentone infusion to achieve EEG burst suppression and surgical CSF drainage may add some benefit to the treatment regimen.

Cerebral aneurysm surgery

In the perioperative period, anaesthetic management for patients undergoing neurovascular surgery aims to optimize outcomes which are defined by the risks associated with neurological, systemic, anaesthetic, and neurosurgical complications.

A comprehensive preoperative assessment for emergency neurovascular surgery is often not possible. However, it is essential to establish baseline neurological function and optimize the patient's condition in relation to complications associated with hydrocephalus, cardiopulmonary dysfunction, and electrolyte abnormalities. This may involve treatment of dysrhythmias, hypovolemia, hypotension, hypoxia resulting from neurogenic pulmonary oedema, and dysnatraemias caused by SIADH or CSW. Baseline investigations should include a complete blood count, electrolyte studies, cardiac troponin levels, coagulation profile, blood group determination, 12-lead electrocardiograph, echocardiography when indicated, and a chest radiograph. Medical therapy for coexisting conditions should be continued along with nimodipine and anticonvulsant medications. For elective neurovascular surgery, a comprehensive preoperative assessment is performed focusing on associated comorbid conditions. Prior to surgery, a review of anticoagulant and antiplatelet medications should help formulate a management plan in consultation with haematological advice.

During anaesthesia, in addition to routine cardiac, respiratory, urine output, and nasopharyngeal temperature monitoring, more specialized haemodynamic assessment of cardiac output may be necessary to guide vascular filling, especially if myocardial dysfunction is suspected. Central venous access may be necessary for the delivery of vasoactive agents. Intravenous induction of anaesthesia should aim to avoid wide swings in mean arterial and intracranial pressures which may alter the transmural pressure gradient (TPG = MAP-ICP) across the aneurysm and cause it to rupture. Laryngoscopy, intubation, and the application of skull pins are potent hypertensive stimuli which should be anticipated and prevented. MAP should then be maintained within 20% of the patient's normal preoperative level to achieve an adequate CPP.

Cerebral aneurysm surgery can be performed under inhalational anaesthesia or TIVA. Short-acting intravenous drugs such as propofol, fentanyl, remifentanil, or sufentanil are commonly used. Volatiles agents, if used, should not exceed a minimum alveolar concentration of one (MAC <1) because of their potential to cause cerebral vasodilatation thus increasing cerebral blood volume and therefore ICP. Short-acting neuromuscular blocking agents can be used to help facilitate adequate ventilation. Hypercapnia should be avoided and the $PaCO_2$ should be kept between 4.5 and 5 kPa. A PaO_2 of more than 11 kPa should be maintained along with normothermia and normoglycaemia. Hyperosmolar agents such as

mannitol (0.5–1 g/kg) or hypertonic saline (2 ml/kg of 5% NaCl), should be initiated slowly and, ideally, delayed until the dura is open.

During surgery, more than 15–20 min of temporary arterial occlusion risks ischaemia and therefore the MAP is usually augmented to improve collateral circulation. Unfortunately, good evidence is lacking for the use of inhalational agents, hypothermia, barbiturates, propofol, and extra doses of mannitol to safely extend the duration of occlusion. Once the aneurysm has been clipped, mild to moderate hypertension using metaraminol, norepinephrine, or phenylephrine, is permitted to improve cerebral perfusion. At the end of uneventful aneurysm surgery, patients should be extubated with minimal coughing and haemodynamic fluctuations and a rapid return of consciousness allows for early neurological assessment. Neurovascular patients should be managed in a neurosurgical high-dependency or intensive care unit to ensure appropriate analgesia, continued haemodynamic monitoring, adequate oxygenation, optimum fluid and electrolyte management, and early detection of complications.

Management of intraoperative aneurysm rupture

The incidence of intraoperative aneurysm rupture for urgent cases is between 5% and 10%. The patient's survival depends on rapidly controlling the bleeding while maintaining adequate cerebral perfusion. Effective communication with the neurosurgical team is essential. The patient should be ventilated with 100% oxygen. Adenosine-induced transient asystole or short-term hypotension using anaesthetic agents or vasoactive drugs may allow surgical control of the bleeding. Restoration of intravascular volume with blood, clotting products, and crystalloid solutions should enable maintenance of a safe minimum CPP. Further doses of propofol, thiopental or etomidate can be used to achieve electroencephalographic burst suppression thereby reducing cerebral metabolic rate to a minimum. Cerebral oedema can be treated with hyperosmolar agents and inducing mild hyperthermia (34–35°C) may be considered, although without good evidence. Once the aneurysm is secured, CPP should be restored to normal levels.

Posterior fossa surgery

The risk of arrhythmias, complications associated with positioning and the potential occurrence of a VAE are fundamental considerations in the perioperative management of patients undergoing posterior fossa surgery.

In addition to the usual preoperative assessment, a detailed neurological examination is crucial to plan perioperative management. In particular, signs of raised intracranial pressure and dysfunction associated with pathology of the brain stem, cranial nerves, and cerebellum should be sought. Relevant imaging should be discussed with the neurosurgeon and a plan formulated for positioning, CSF drainage, neurophysiological monitoring, and any potential significant complications.

In addition to standard monitoring, an intra-arterial catheter is recommended while insertion of a central venous catheter may prove useful in the event of a VAE. Electrophysiological monitoring should be tailored to the site of surgery and the location of the lesion. Use of the sitting position for posterior fossa surgery has declined due to the increased risks of haemodynamic instability, VAE, and spinal cord compression from severe neck flexion. Surgery is now commonly performed in the prone or semi-prone positions which requires careful attention to avoid complications associated with airway oedema along with skin, peripheral nerve, and abdominal organ damage.

There is no evidence for improved outcomes in relation to a specific anaesthetic technique for posterior fossa surgery. The general goals of adequate anaesthesia, analgesia, maintenance of CPP, haemodynamic stability, and avoidance of coughing remain self-evident. Brain stem manipulation can cause cardiac dysrhythmias, particularly bradycardia as well as ventricular and supraventricular tachycardias. Most terminate with cessation of surgical stimulation and it is rare for pharmacological intervention or rarer still, for external cardiac massage, to be required. Stimulation of the trigeminocardiac reflex can also cause marked intraoperative hypertension which can be treated by deepening anaesthesia.

As with all neurosurgery, early postoperative neurological evaluation of the patient is essential. However, after prolonged surgery in the prone position, some anaesthetists perform a 'leak test' on the endotracheal tube with the cuff deflated to check if airway oedema will delay extubation. If this is the case, or airway reflexes are slow to return, patients may be kept intubated and require ventilation on the intensive care unit until extubation can be safely completed. Hypertension should be avoided in the early postoperative period to limit the risks of brain oedema and intracranial haemorrhage.

Venous air embolism

The incidence of haemodynamically significant VAE in posterior fossa surgery is 8% to 15% in the sitting position and 3% to 5% in the prone or park-bench position. Risk factors include operative site above the level of the heart and the presence of non-collapsible veins. Almost 25% of the adult population have a patent foramen ovale which increases the risk for paradoxical air embolism that can lead to myocardial and cerebral ischaemia. The intraoperative clinical presentation for a VAE can vary between minimal air entrainment with low morbidity to sudden cardiac arrest and death with larger air volumes.

The pathophysiology of a VAE involves; impaired right ventricular outflow, mechanical obstruction of pulmonary capillaries, increased intrapulmonary shunting leading to hypoxia and hypercarbia, raised pulmonary artery pressure, bronchoconstriction, a decrease in cardiac output, hypotension, arrhythmias, myocardial failure, and cardiac arrest. Precordial doppler ultrasound and capnography remain the recommended monitors for VAE during posterior fossa surgery and will allow detection before clinical signs occur. In the event of a VAE, inform the surgeon to prevent further air entrainment by flooding the wound with saline. Compressing the jugular vein can temporarily increase venous pressure and allow localization and repair of the site of entrainment. Decrease the gradient between the heart and the operative site. Administer 100% oxygen and stop nitrous oxide. Attempt to aspirate air through a central venous catheter and provide haemodynamic support if required. If the patient remains in a precarious cardiopulmonary state, surgery may need to be abandoned, the patient turned supine, and further resuscitation measures instituted as necessary.

Neurosurgical oncology

Preoperative assessment of patients presenting with primary or metastatic brain tumours involves an assessment of symptoms, history of seizures, an evaluation of premorbid conditions and a review of preadmission medication. Patients should be examined for level

of consciousness, peripheral neurological deficits, in addition to speech and language abnormalities. Laboratory tests should rule out significant biochemical, haematological, and coagulation disorders. Imaging of the primary cerebral lesion is checked for site, size, signs of raised ICP, and vascularity while the spread of metastatic disease in those with secondary tumours needs careful evaluation. Up to 4 hours before induction of anaesthesia 5-aminolevulinic acid (5-ALA), which improves the likelihood of complete tumour resection, is sometimes administered. At this stage, a postoperative plan to manage the patient in a high-dependency or critical care setting should be considered if needed.

Induction of general anaesthesia usually proceeds with an intravenous agent combined with an opiate and a non-depolarizing muscle relaxant. Obtunding haemodynamic responses to laryngoscopy and head-pin insertion will help maintain a stable CPP and avoid excessive rises in ICP. Along with standard monitoring, an intra-arterial catheter, central venous access, temperature, and urine output measurement, in addition to more advanced methods to assess haemodynamic function, may be required for prolonged complex procedures or when comorbidities dictate. In specific circumstances, electrophysiological monitoring is required. Patients may receive hyperosmolar agents during the craniotomy procedure and subsequent blood analysis for monitoring of electrolyte imbalances. Appropriate head-up positioning and avoidance of venous obstruction during positioning can limit elevations in ICP, while minimizing neck flexion will help avoid airway oedema postoperatively.

Anaesthesia is usually maintained by a total intravenous or inhalational technique, supplemented with opiates and sometimes neuromuscular blocking agents. Propofol reduces cerebral blood volume (CBV) and preserves autoregulation and CO_2 reactivity, while volatile agents can increase ICP because they cause cerebral vasodilatation. When electrophysiological monitoring is employed, intravenous anaesthesia interferes less with signal characteristics. Glucose-free iso-osmolar crystalloid solutions should be administered during surgery unless blood loss requires a transfusion to maintain haemodynamic stability and adequate brain oxygenation. In general, the principal aims during anaesthesia for craniotomy procedures is to avoid hypoxia, hypercapnia, hypothermia, hypoglycaemia, ICP rises, and maintain CPP while improving brain compliance. The management of complications related to neurosurgical oncology can involve blood products and clotting factors for acute haemorrhage, intravenous anaesthetic, and anticonvulsant medication for seizure control and imaging with possible evacuation of blood clot for postoperative haemorrhage. The treatment of VAE and acute cerebral oedema have been referred to in other sections.

Emergence from anaesthesia with minimal coughing and straining avoids an increase in ICP. Early neurological assessment is facilitated by a prompt return to consciousness if cessation of anaesthesia is timed appropriately. Pneumocephalus, if significant, can delay wake-up and benefits from early recognition to allow treatment with high oxygen concentrations. Hypertension in the postoperative period is usually treated to a MAP less than 160 mmHg with short-acting beta-blockers. The analgesic effects of strong opiates need to be balanced against their sedative properties, but less use of these drugs may be required if a local anaesthetic block of scalp nerves is performed prior to waking the patient.

Anaesthesia for awake craniotomy

Developments in neurosurgery have placed a greater focus on awake procedures which are now routinely used in epilepsy surgery and for removal of lesions involving eloquent brain areas. These procedures can be performed awake under local anaesthetic with or without sedation, under general anaesthesia initially (intubated or use of supraglottic airway device), then awake (asleep-awake), or reanaesthetized (asleep-awake-asleep). Patients need to be carefully chosen, counselled, and fully consented to ensure success of these procedures. The role of the anaesthetist is crucial to ensure; (1) maintenance of airway patency and ventilation, (2) haemodynamic stability, (3) adequate analgesia and sedation as required, (4) patient cooperation for continuous neurological assessment and (5) timely treatment of any seizure activity. Constant anaesthetic presence and vigilance is essential to help avoid potential complications injuring the brain and risking the patient's life.

Spinal surgery

Anaesthesia for spinal surgery involves consideration of a combination of specific issues to ensure a good outcome. These include, managing a potential airway problem due to traumatic or degenerative cervical spine disease, dealing with the complications of the prone position, adapting anaesthetic techniques to facilitate accurate neurophysiological monitoring, dealing with blood loss and coagulation matters and providing effective multimodal postoperative analgesia to enable early mobilization and hospital discharge (Bajwa and Halder, 2015).

Due to the age range of people presenting for spinal surgery, only a systematic approach to the preoperative assessment will ensure the identification of any pre-existing focal neurology or altered physiological reserve resulting from recent trauma or chronic comorbid diseases. Procedures required to manage a difficult airway are not uncommon in patients needing cervical or upper thoracic surgery. Previous cervical fixation surgery or arthritis leading to limited neck movement, cervical spine instability, and cord compression will often necessitate an awake or asleep fibreoptic intubation or the use of other videolaryngoscopy instruments to permit intubation without causing further damage to the spinal cord. Respiratory function (e.g. reduced volume and compliance parameters) can be compromised in patients needing surgery for scoliosis or other neuromuscular conditions. Chest trauma, resulting in multiple rib fractures, flail segments, pneumothoraces, and pulmonary contusions, can make adequate oxygenation and ventilation problematic intraoperatively, especially in those patients positioned prone who may also need further postoperative critical care management.

Patients presenting for spinal surgery to stabilize a spinal cord injury can be haemodynamically unstable due to spinal shock or autonomic dysreflexia and require vasoactive agents to ensure an adequate heart rate and MAP. Patients with cardiac disease but limited mobility due to degenerative spinal conditions often need stress echocardiography prior to surgery. Acquired coagulation abnormalities due to medications or trauma need to be normalized to avoid bleeding and haematoma formation potentially causing spinal cord compression. Blood loss should be anticipated in major spinal surgery such that blood and coagulation factors are made readily available while cell salvage and the use of tranexamic acid help reduce homologous transfusion requirements (Cheriyan et al., 2015).

The principal anaesthetic objective during spinal surgery is maintaining adequate spinal cord perfusion at all times. The conduct of anaesthesia usually involves (1) large-bore venous access; (2) standard monitoring; (3) measurements of invasive arterial and/or central venous pressures, temperature, and urinary output; (4) intravenous induction; (5) appropriate airway management with the use of a double-lumen endotracheal tube if transthoracic procedures are planned; (6) maintenance with an inhalational agent or total intravenous anaesthesia if neurophysiological monitoring is used to avoid amplitude reduction in the evoked potential signals; (7) use of a forced-air warming device; and (8) cell salvage usage if major blood loss is anticipated.

Emergence from anaesthesia should be planned and attention paid to identifying airway oedema after prolonged prone positioning. Patients should be turned carefully supine, placed more than 30° head-up and extubated with minimal coughing and when responding to command. Blood pressure should be expectantly managed avoiding systolic hypertension more than 160 mmHg with beta-blockers or another vasoactive agent. Any new motor deficit requires immediate neurosurgical review, urgent imaging, and possibly exploratory surgery. Pain management should be multimodal involving the use of epidurals, patient-controlled analgesia, intermittent intravenous or oral opioid analgesics, non-steroidal anti-inflammatory drugs, gabapentinoids, alpha-2-agonists (e.g. clonidine), and ketamine.

Prone positioning

Prone positioning requires the correct equipment and sufficient staff for moving and handling the patient. A minimum of six people is required for log-rolling to maintain spinal alignment. Patients can be positioned on various frames (e.g. Wilson, Allen), tables (e.g. Jackson) and mattresses (e.g. Montreal). There should be no constriction of the abdomen thus allowing free excursion of the diaphragm, permitting ventilation with the lowest possible intrathoracic pressures, and avoiding venous congestion which can cause a bloody surgical field. Abdominal organ ischaemia, resulting in an unexplained metabolic acidosis can result from poor positioning. Due to diminished preload, cardiac output usually falls on turning prone which often requires fluids and vasopressor agents to restore haemodynamic stability. The head and neck should be in a neutral position either in a Mayfield clamp or a foam cushion. There should be no pressure on the eyes which are usually taped and padded. The arms should be kept at the patient's side or abducted to no greater than 90 degrees. All extremities and pressure points need to be padded to avoid injuries to the brachial plexus, ulnar, median, lateral cutaneous, common peroneal and sciatic nerves. The incidence of visual loss after spinal surgery is 1 in 30 000 and is likely due to ischaemic optic atrophy, cortical ischaemia, or central retinal artery occlusion. Factors involved in the aetiology of this complication include, surgery more than 6 hours duration, significant intraoperative blood loss and hypotension, non-neutral head positioning, and incorrect use of head supports, and other possible patient-related factors (Shmygalev and Heller, 2011).

Pituitary surgery

The management of the consequences of pituitary pathology in relation to raised ICP, mass effects, and disruption of hormonal secretion is the focus of perioperative assessment for these patients. Preoperatively, imaging defines the extent of the lesion while other tests identify if patients have developed electrolyte disturbances, abnormal hormone secretion syndromes, reduced cardiopulmonary reserve, and dysfunction of upper airway structures.

Acromegaly, caused by hypersecretion of growth hormone from a functioning pituitary macroadenoma, can cause anaesthetic concerns in relation to upper airway changes. These include prognathism, macroglossia, tissue hypertrophy reducing glottic opening and hoarseness from possible recurrent laryngeal nerve injury. This disease is also associated with obstructive sleep apnoea (OSA), hypertension, cardiac muscle and conduction abnormalities, diabetes mellitus, kyphoscoliosis, and proximal myopathy. These patients may need preoperative transthoracic echocardiography to assess left ventricular function, respiratory function testing, and consideration given to performing an awake fibreoptic intubation for a potentially difficult airway.

Hypersecretion of adreno-corticotropic hormone from a pituitary adenoma resulting in excess glucocorticoid is called Cushing's disease. Patients often have truncal obesity, moon facies, thin extremities, OSA, cardiac dysfunction, coagulation abnormalities, osteoporosis, thin skin, and diabetes mellitus. With this condition, anaesthetic concerns include possible airway difficulties and intraoperative cardiorespiratory instability.

Hyperthyroidism caused by thyroid stimulating hormone producing adenomas will require treatment as indicated before surgery with somatostatin analogues, antithyroid medications, and beta-blockers. Certain patients will need steroid supplementation at induction to cover the metabolic stress of anaesthesia and surgery.

The most important anaesthetic concerns in patients presenting for pituitary surgery are related to airway management and haemodynamic instability. Expertise in a variety of intubation techniques, including video laryngoscopy and awake fibreoptic intubation, should be available. Reinforced or south-facing oral endotracheal tubes are frequently used for endonasal pituitary surgery. The oropharynx if usually packed with gauze to help prevent blood entering the airways and it must be removed prior to extubation. Cardiovascular disease is common in patients presenting with hormone-secreting tumours. Intraoperative haemodynamic instability from hypertension, dysrhythmias, myocardial ischaemia, and ventricular dysfunction may require invasive arterial monitoring and vasoactive agents to maintain an adequate cerebral perfusion pressure.

The anaesthetic technique for this surgery can be either intravenous or inhalational. Standard monitoring supplemented with measurements of invasive arterial pressure, temperature, and urine output is customary. Painful stimulation, resulting in hypertension, is common during nasal/transsphenoidal dissection but minimal during surgery on the sellar lesion itself. Haemodynamic parameters can be further adversely affected by application of adrenaline-containing local anaesthetic to the nasal mucosa. The use of remifentanil, short-acting beta-blockers, and vasodilators are used to preserve cardiovascular stability. Controlled hypercapnia and temporary increases in ICP via a lumbar intrathecal catheter can be used to push the tumour into the surgical field. Fluid loss is replaced with glucose-free crystalloid solutions to maintain a neutral balance while avoiding electrolyte disturbances. Blood loss is usually minimal unless there is injury to the cavernous sinus when transfusion if often required. A sellar CSF leak, sometimes identified by a Valsalva manoeuvre, is usually surgically sealed with autologous abdominal or thigh fat and facia.

Prior to emergence from anaesthesia, the oropharynx is suctioned and any gauze pack removed. Smooth emergence prevents dislodgement of surgically-placed nasal packs. Patients with known airway difficulties should be positioned with head-up tilt and safely extubated when responding to commands. Myopathic patients may be too weak to extubate and require a period of postoperative ventilation on a critical care unit. Adequate analgesia and antiemetics should be prescribed for all patients during their stay on the postanaesthesia care unit. When discharged to the ward, combined care with endocrinologists provides guidance on further steroid and hormone replacement therapy in addition to assisting the early recognition and treatment of other neuroendocrine complications.

Coagulation disorders and venous thromboembolic disease

Pathophysiology of coagulation

Cascade model

The concept of coagulation as a proteolytic enzyme cascade was described by two groups in 1964 (Davie and Ratnoff, 1964; Macfarlane, 1964). Schematically, the coagulation pathway can be divided into the extrinsic and intrinsic pathways (Fig. 5.2). The extrinsic pathway is activated when blood comes into contact with tissue factor (TF) on the surface of extravascular cells (e.g. fibroblasts within the vascular wall). The role of the intrinsic pathway is less clear *in vivo*. It is activated with internal damage to vessel wall and when mechanical devices come into contact with blood. Nevertheless, both the extrinsic and intrinsic pathways are extremely useful in understanding the biochemical reactions underpinning common coagulation assays, such as the prothrombin time (PT) and partial thromboplastin time (Table 5.5).

Both the extrinsic and intrinsic pathway ultimately lead to the conversion of factor X to Xa (factor X being the first factor of the common pathway), which is an essential component of the prothrombinase complex. This consists of factors Xa and Va bound together on a phospholipid membrane by calcium ions. The prothrombinase complex acts to convert prothrombin (factor II) to thrombin (factor IIa), which in turn activates factor XIII. This allows stabilization of the clot by creating covalent cross-links between fibrin molecules.

Cell-based model

While the classical model explains the function of laboratory assays of coagulation and the interactions between specific clotting factors, it is not sufficient to allow a full understanding of coagulation *in vivo*. The cell-based model has been developed to fill that niche and better describe some of the coagulation disorders seen clinically, such as the failure of the extrinsic pathway to compensate for factor deficiencies of the intrinsic pathway observed in haemophilia (Hoffman and Monroe, 2001; Hoffman, 2003).

The new model places emphasis on specific cells and their cell surface receptors in the process of coagulation which occurs in three overlapping stages of initiation, amplification, and propagation. Initiation occurs on TF-containing cells (e.g. stromal fibroblasts, which normally lie outside the vasculature), blood mononuclear cells, or endothelial cells in states of inflammation. A breach in the vessel wall exposes TF-containing cells to plasma. Factor VII binds to TF on the cell surface and is then activated to factor VIIa. The VIIa/TF complex activates factor X and factor IX. When confined to the cell surface, factor Xa binds with factor Va and leads to the production of thrombin from prothrombin, beginning the amplification process. Importantly, factor Xa is rapidly inhibited when dissociated from the cell surface by tissue factor pathway inhibitor and antithrombin III (ATIII).

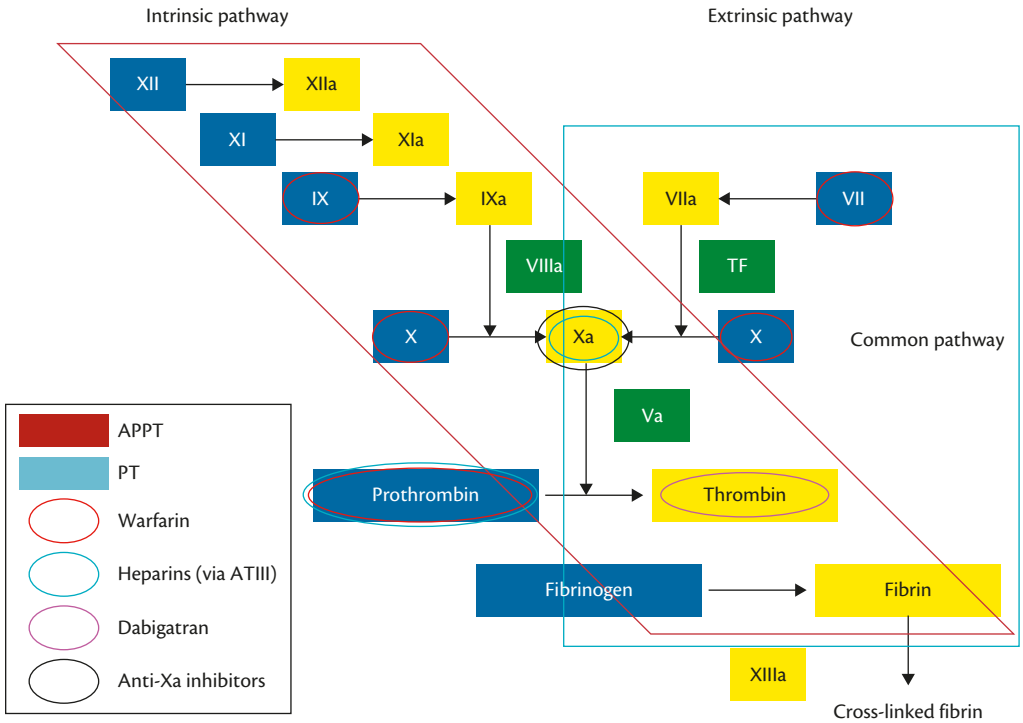

Fig. 5.2 Coagulation cascade pathways including mechanisms of action of commonly used anticoagulants.

Table 5.5 Coagulation assays, related clotting factors, and clinical use

Test	Inherited	Acquired	Pathway	Clinical
aPTT	vWF, VIII, IX, XI, XII factor deficiencies (haemophilia)	Heparin; antiphospholipid antibodies	Intrinsic, and common pathway	Factor deficiency about 20–40% before abnormality seen; monitoring heparin therapy
PT	VII deficiency	Warfarin; factor VII inhibitor; Vit K deficiency; liver disease;	Extrinsic and common pathway	Screen for factor VII deficiency; Screen for factor X, V II, I (together with aPTT); monitor warfarin use (INR); INR not appropriate for liver disease
TEG			Whole process of coagulation including platelet function	Used differentiate surgical bleeding from coagulation disorder

Thrombin produced on TF-containing cells and acting via protease-activated receptors, leads to platelets activation, which in states of tissue damage are already adherent to extravascular matrix. These activated platelets, lead to the production of activated factors V and VIII. Factor Va is released from platelet alpha granules while factor VIIIa is released from the von Willebrand factor (vWF). Together these lead to large-scale thrombin production, which constitutes the amplification phase of coagulation. The propagation phases relate to formation of a stable fibrin clot with the help of enzymatic complexes on the surface of activated platelets. Instrumental in this is the factor VIIIa/IXa complex, which activates factor Xa.

In the cell-based model of coagulation, platelet cell surface is essential in the amplification and propagation phases of coagulation. The special function of platelets is related to their ability to adhere to injured surfaces using multiple receptors and pathways. Platelets express glycoprotein Ib/IX and vWF, which help localize platelets to the site of injury. It is important that the initiating and propagating steps of anticoagulation are normally sequestered to different cell surfaces to limit the undesired activation of coagulation. Table 5.5 demonstrates the mechanism of action of commonly used anticoagulants.

Management of deranged coagulation prior to neurosurgery

Deranged coagulation in neurosurgery is frequently related to the preoperative use of antiplatelet or anticoagulant medications for the prevention of primary or secondary cardiovascular disease. In addition, the use of fibrinolytic agents for the management of cerebrovascular and cardiovascular emergencies, increases the incidence of intracranial haemorrhage which may necessitate neurosurgical intervention.

Elective neurosurgery

In elective cases, suspected or known coagulation disorders should be adequately diagnosed and treated with the appropriate factor replacement. Coagulation dysfunction related to preoperative administration of antiplatelet or anticoagulant medications should be normalized by stopping these agents before surgery (Table 5.6). In dealing with perioperative anticoagulation, a balance must be had between the risk of surgical bleeding, the likelihood of any pre- and postoperative venous thromboembolism (VTE) event and the shortest and safest time interval for the discontinuation and recommencement of anticoagulant agents.

Antiplatelet agents are given orally or intravenously for the prevention of cerebral, coronary, or carotid thromboembolic disease, and reversibly or irreversibly inhibit cyclooxigenase-1 (COX-1) and thromboxane A2 (subscript) synthesis and the P2Y12 receptor affecting platelet function for up to ten days. To allow regeneration of the platelets prior to surgery, antiplatelet medication should be stopped until new platelets can be made (typically 20 000 platelet as made per day, i.e. 5 days are required to generate 100 000 new platelets). Certain neurosurgical procedures are commonly performed without discontinuation of antiplatelet medication (e.g. carotid endarterectomy or low flow extracranial-to-intracranial bypass) to minimize the risk of perioperative stroke and/or vessel occlusion.

In relation to cardiovascular disease, most guidelines agree that the risk of thrombosis is at its highest for up to six weeks after insertion of a bare metal cardiac stent, six months for a drug-eluting stent and three months after a myocardial infarction, stroke, or deep venous thrombosis (DVT) (Rabbitts et al., 2008). The risk diminishes considerably after 12 months. In these patients, even short periods without dual antiplatelet therapy increases the risk of instent thrombosis and cardiac events. Therefore, any elective surgery should be postponed in this group of patients. Patients whose thrombotic risk is high, such as those with mechanical heart valves, require discontinuation of warfarin 3 days prior to surgery. Bridging therapy using therapeutic doses of low molecular weight heparin (LMWH) until 12–24 hours before the operation is usually needed. Recommencement of antithrombotic medication should usually begin within 24–48 hours postoperatively.

Table 5.6 Duration of cessation for antiplatelets and anticoagulants before elective surgery

Drug	Time	Pre-op tests	T1/2
Aspirin	5 days		20 K platelets produced per day. 5 days = 100 K platelets
Clopidogrel	5–7 days		20 K platelets produced per day. 5 days = 100 K platelets
Warfarin	3–5 days	INR day of operation	36–42 h
LMWH	12 h	Anti Xa assay	4 h
UH	4 h	Check APTT ratio	1 h
NOAC	2 days		9–17 h (approx. 12 h)

LMWH, low molecular weight heparin; NOAC, new oral anticoagulants; UH, unfractionated heparin.

Emergency neurosurgery

The management of coagulopathies, either iatrogenic or disease-related, in patients undergoing emergency neurosurgery has minimal good evidence to support best practice. Rarely, urgent operations may need to be performed despite a coagulopathy, but in general, there is usually time for patient assessment, laboratory testing, and the institution of appropriate treatments.

Anticoagulation-associated intracerebral haemorrhage

The need for neurosurgical interventions is sometimes the result of prior anticoagulation and antiplatelet medication use. The most common problem encountered is anticoagulation-associated intracerebral haemorrhage (AAICH). The use of oral anticoagulants such as vitamin K inhibitors has increased the incidence of AAICH to 15% of all ICH while these patients have an 11-fold higher risk of developing this complication (Wintzen et al., 1984; Flaherty et al., 2007). Furthermore, patients on oral anticoagulants are at significantly higher risk of haematoma expansion and worse outcomes (Flibotte et al., 2004). Management of AAICH is based on four principals: the need to stabilize the bleed (i.e. prevent expansion); addressing the safety of performing any intervention; emergency reversal of anticoagulation; and monitoring the effect and prevention of thromboembolic complications.

Prevention of haematoma expansion is mainly achieved through strict systolic blood pressure management. A recent meta-analysis of four large randomized trials evaluating blood pressure targets for management of ICH (rapid blood pressure reduction in acute intracerebral haemorrhage; INTERACT; ICH ADAPT; INTERACT2) demonstrated that lowering the systolic blood pressure target to less than 140 mmHg was associated with reduced haematoma growth in the first 24 hours and improved outcomes at 3 months (Tsivgoulis et al., 2014). Therefore, current guidelines recommend systolic blood pressure targets of less than 140 mmHg (Hemphill et al., 2015).

Reversing anticoagulants and antiplatelet agents

Urgent reversal of anticoagulation is frequently difficult to achieve with certainty, takes time to implement, and usually requires transfusion of specific blood products. There is limited evidence regarding the efficacy of specific interventions, nevertheless certain principals are widely accepted. **Table 5.7** summarizes the strategies used to reverse commonly used anticoagulants and antiplatelet agents.

Warfarin

Warfarin is the commonest agent implicated in AAICH. In patients with an international normalized ratio (INR) more than 1.4, vitamin K should be administered. Importantly, vitamin K can take up to 24 h to full effect and therefore, additional measures should be taken. Current recommendations include, transfusion of fresh frozen plasma (FFP) or prothrombin complex concentrate (PCC). FFP contains all clotting factors, however, it requires time to cross-match and large transfusion volumes may lead to lung injury, volume overload as well as allergic reactions. Three (II, IX, and X) and four (II, IX, X, and VII) factor PCC are available. In a study of 202 patients with warfarin-associated bleeding, PCC was shown to normalize the INR within 30 min in approximately 60% of cases, as opposed to 10% of cases who received FFP (Sarode et al., 2013), making PCC the treatment of choice in most centres.

Table 5.7 Emergency reversal of anticoagulation in neurosurgery

Agent	Test	Treatment
Aspirin	PFA-100	1–2 U of platelets; DDAVP 0.4 mcg/kg over 30 min
Clopidogrel	Platelet aggregation test	1–2 U of platelets; DDAVP 0.4 mcg/kg over 30 min
Ticagrelor		1–2 U of platelets; DDAVP 0.4 mcg/kg over 30 min
UH	APTT ratio	Protamine 1 mg per 100 U of UH in last 2–3 h (repeat dose of 0.5 mg per 100 U of UH if APTT remains elevated)
LMWH	Anti-Xa assay	protamine 1 mg per 1 mg (enoxaparin) 100 U (dalteparin). Half dose if >8 h since LMWH administration
Pentasaccharides	Anti-Xa assay	4 factor PCC 20 U/kg; rfVIIa 90 mcg/kg
Warfarin	INR	Vit K 5–10 mg; FFP 15 ml/kg; 4 factor PCC 20 U/kg; rfVIIa
Direct thrombin inhibitors	APTT/TT	Dabigatran—idarucizumab 5 mg in two doses every 15 min; haemodialysis; TXA, 4 factor PCC activated charcoal 50 g if taken within 2 h
Factor Xa inhibitors	Anti-Xa assay	Four-factor PCC 50 U/kg; activated charcoal 50 g if taken within 2 h

LMWH, low molecular weight heparin; NOAC, new oral anticoagulants; PCC, prothrombin complex concentrate; TXA, tranexamic acid; UH, unfractionated heparin.

New anticoagulants

Non-vitamin K oral anticoagulants (NOACs) - also referred to as DOACs (direct oral anticoagulants), are a diverse group of medications which include factor Xa inhibitors (rivaroxaban, apixaban, edoxaban) and direct thrombin (factor IIa) inhibitors (dabigatran). These agents have a rapid onset of action, a close dose-dependent effect, shorter half-lives (average: 5–15 hours), undergo renal and hepatic metabolism, and have a more predictable pharmacokinetic profile. Therefore, the major advantage is a much lower requirement for routine drug monitoring. If a patient is on a NOAC agent, has normal renal and liver function, and there is a low surgical bleeding-risk compared to a VTE event, then a discontinuation for 2–3 half-lives of the drug would suffice or 4–5 half-lives when the bleeding-risk is high. On average, the half-life of NOACs is 12 hours, therefore, it is thought that discontinuation for 48 hours allows for safe surgery. Once haemostasis is deemed stable postoperatively, NOACs should be restarted as soon as possible.

However, with the exception of dabigatran, there is no specific antidote for these medications. Idarucizumab, a monoclonal antibody against dabigatran is now licensed for rapid reversal of bleeding associated with its use. In the emergency situation or when no antidote is available, expert opinion recommends the use of activated four-factor prothrombin complex concentrate, activated recombinant factor VII, the possible use of oral activated charcoal (patient presents within 2 hours of NOAC ingestion) and haemodialysis. It is important to acknowledge that the commonly measured laboratory assessments of haemostasis are either prolonged or unaffected by NOACs and that normal values may not exclude a clinically relevant concentration of

the drugs. Anti-Xa assays, diluted thrombin time (TT) tests, ecarin clotting times, and NOAC antidotes are currently being assessed in clinical trials to enable the development of evidenced-based guidelines for NOAC reversal (Gehrie and Tormey, 2015).

Heparin

Unfractionated heparin (UH) treatment is associated with ICH in only 0.1% of patients. Emergency reversal involves stopping the infusion and administering protamine. Monitoring APTT is mandatory as repeated doses of protamine may be indicated. LMWH inhibits factor Xa via antithrombin, but has a limited effect on thrombin. Protamine (1 mg per 1 mg of enoxaparin or 100 U of dalteparin) only partially reverses LMWH and any residual effect should be monitored using, an anti-factor Xa assay.

Antiplatelet agents

The association of antiplatelet agents with ICH is controversial and unconfirmed in recent literature (Sansing et al., 2009). In general, antiplatelet drugs should be discontinued when ICH is diagnosed. Interestingly, the PATCH study (Baharoglu et al., 2016) which was the first randomized trial of platelet transfusion for ICH associated with antiplatelet use, demonstrated a shift towards unfavourable outcome in the transfusion group. Although evidence is not conclusive, platelet transfusion is not recommended unless surgical intervention is planned (Frontera et al., 2016). DDAVP was shown in a small study to improve platelet function and may be considered for patients on aspirin, ADP receptor inhibitors or for COX-1 inhibitor associated ICH (Kapapa et al., 2014; Naidech et al., 2014; Frontera et al., 2016).

Venous thromboembolic disease in neurosurgery

Incidence

The development of a DVT of the lower or upper limbs is believed to be the source of up to 90% of pulmonary emboli. The term venous thromboembolism refers to both phenomena. It is the potential for embolization of the blood clot to the lung, associated with a mortality rate of 50–60%, which is of critical importance in relation to preventable death. In the neurosurgical population, the main risk factors for VTE include, neurological malignancy, traumatic brain injury, spinal cord injury, cerebrovascular disease, prolonged surgery, steroids, sepsis, and decreased mobility. Using only mechanical devices, the estimated risk of developing a DVT after a neurosurgical procedure is about 16%. When LMWH is added to the prophylactic regimen within 24 hours after surgery, the risk is reduced to 9%. The risk of a pulmonary embolism (PE) is generally acknowledged to be about 1.5–5%. Recent studies in neurosurgical interventions confirm a reduction in the number of symptomatic VTEs over bleeding episodes by the early use of LMWH (Rolston et al., 2014).

Prophylactic treatment

Craniotomy for brain tumours

Kimmell and Jahromi (2015) showed in their cohort of over 4000 patients undergoing a craniotomy procedure that the rate of VTE was higher than for other neurosurgical patients. Further analysis demonstrated that neuro-oncological surgery, medical comorbidities, age greater than 60 years, use of steroids, surgical time greater than four hours, and postoperative complications significantly increased the risk of VTE. In a systematic review by Salmaggi et al. (2013) it was concluded that all patients undergoing neuro-oncological surgery should have mechanical prophylaxis for VTE instituted preoperatively and continued until discharge, while patients considered to be at a low risk for major bleeding should have LMWH added 24 hours after surgery. However, in practice all patients after craniotomy for tumour, unless specifically instructed not to, should have LMWH DVT prophylaxis from post operative day 1.

Spinal surgery

The incidence of VTE in patients undergoing spinal surgery can vary according to the spinal level operated on, extent of the surgery, and the degree of perioperative mobility. Patients having thoracolumbar surgery with instrumentation and fusion appear to be at a higher risk of VTE. While some form of intraoperative mechanical prophylaxis is considered a minimum, postoperative chemoprophylaxis should be considered for patients undergoing complex spinal surgery of long duration, anterior-posterior approaches, and those with known thromboembolic risk factors such as spinal cord injury, malignancy, and hypercoagulable states. In view of the known and definable risks of neurological deterioration from epidural haematoma formation along with bleeding, transfusion and wound complications, individual risk–benefit analysis for chemoprophylaxis is required on all patients undergoing spinal surgery.

Traumatic brain injury

The incidence of DVT in TBI without prophylaxis can be as high as 54% (Foreman et al., 2014). Using mechanical prophylaxis, studies have shown a fall in rates to 30% for DVTs and 3% for PEs. Chemoprophylaxis in this setting is controversial because of concern over the expansion of the intracranial haemorrhage. Several studies have shown rates of around 3% progression in the setting of a stable intracranial injury (low risk TBI) leading to the generation of protocols (e.g. Parkland protocol) suggesting a stable repeat CT of the head within 24 hours from admission of a TBI can permit the safe administration of LMWH (Phelan, 2012). Where patients have multiple contusions, epidural, subdural, subarachnoid, or intraventricular blood, they are deemed a moderate risk TBI and LMWH is only instituted when a CT scan performed after 72 hours shows a stable lesion. Patients requiring a craniotomy or external ventricular drain for a high risk TBI pattern should be considered for insertion of an inferior vena cava (IVC) filter which has been shown to help reduce PEs but may increase DVT recurrence.

FURTHER READING

American Society of Anesthesiologists: Standards and Guidelines. http://www.asahq.org/quality-and-practice-management/standards-and-guidelines

Association of Anaesthetists Safety Guidelines. http://www.aagbi.org/publications/publications-guidelines

National Clinical Guideline Centre. http://www.ngc.ac.uk/Guidelines/Published/120

REFERENCES

Alan, N., Seicean, A., Seicean, S., Neuhauser, D., & Weil, R.J. (2014). Impact of preoperative anemia on outcomes in patients undergoing elective cranial surgery. *J Neurosurg*, **120**(3), 764–72.

Ali, Z. (2015). Early postoperative respiratory complications following elective craniotomies. *J Neuroanaesthesiol & Crit Care*, **2**(2), 85–7.

Baharoglu, M.I., Cordonnier, C., Al-Shahi Salman, R., et al. (2016). Platelet transfusion versus standard care after acute stroke due to spontaneous cerebral haemorrhage associated with antiplatelet therapy (PATCH): a randomised, open-label, phase 3 trial. *Lancet*, **387**(10038), 2605–13.

Bajwa, S.J.S. & Halder, R. (2015). Pain management following spinal surgeries: an appraisal of the available options. *J Cranioverter Junction Spine*, **6**(3), 105–10.

Cheriyan, T., Maier, S.P., Bianco, K., et al. (2015). Efficacy of tranexamic acid on surgical bleeding in spine surgery: a meta-analysis. *Spine J*, **15**(4), 725–61.

Chui, J., Mariappan, R., Mehta, J., Manninen, P., & Venkatraghavan, L. (2014). Comparison of propofol and volatile agents for maintenance of anesthesia during elective craniotomy procedures. *CJA*, **61**(4), 347–56.

Davie, E.W. & Ratnoff, O.D. (1964). Waterfall sequence for intrinsic blood clotting. *Science (New York, N.Y.)*, **145**(3638), 1310–12.

DePasse, J.M., Palumbo, M.A., Haque, M., Eberson, C.P., & Daniels, A.H. (2015). Complications associated with prone positioning in elective spinal surgery. *World J Orthop*, **6**(3), 351–9.

Devin, C.J. & McGirt, M.J. (2015). Best evidence in multimodal pain management in spine surgery and means of assessing postoperative pain and functional outcomes. *J Clin Neurosci*, **22**(6), 930–8.

Escallier, K.E., Nadelson, M.R., Zhou, D., & Avidan, M.S. (2014). Monitoring the brain. *Anaesthesia*, **69**(8), 899–910.

Flaherty, M.L., Kissela, B., Woo, D., et al. (2007). The increasing incidence of anticoagulant-associated intracerebral hemorrhage. *Neurology*, **68**(2), 116–21.

Fleisher, L.A., Fleischmann, K.E., Auerbach, A.D., et al. (2014). ACC/AHA 2014 guidelines on perioperative cardiovascular evaluation and care for noncardiac surgery. *J Am Coll Cardiol*, **64**(22), 2373–405.

Flibotte, J.J., Hagan, N., O'Donnell, J., Greenberg, S.M., & Rosand, J. (2004). Warfarin, hematoma expansion, and outcome of intracerebral hemorrhage. *Neurology*, **63**(6), 1059–64.

Ford, M.K., Beattie, S.W., & Wijeysundera, D.N. (2010). Prediction of perioperative cardiac complications and mortality by the revised cardiac risk index. *Ann Intern Med*, **152**, 26–35.

Foreman, P.M., Schmalz, P.G., & Griessenauer, C.J. (2014). Chemoprophylaxis for venous thromboembolism in traumatic brain injury. *Clin Neurol Neurosurg*, **123**, 109–16.

Frontera, J.A., Lewin, J.J. 3rd, Rabinstein, A.A., et al. (2016). Guideline for reversal of antithrombotics in intracranial hemorrhage: executive summary. A statement for healthcare professionals from the Neurocritical Care Society and the Society of Critical Care Medicine. *Neurocrit Care*, **44**(12), 2251–7.

Gehrie, E. & Tormey, C. (2015). Novel oral anticoagulants. *Arch Pathol Lab Med*, **139**(5), 687–92.

Gruenbaum, S.E. & Ruskin, K.J. (2014). Red blood cell transfusion in neurosurgical patients. *Curr Opin Anaesthesiol*, **27**(5), 470–3.

Guilfoyle, M.R., Helmy, A., Duane, D., & Hutchinson, P.J. (2013). Regional scalp block for postcraniotomy analgesia. *Anaes Analg*, **116**(5), 1093–102.

Hemphill, J.C. 3rd, Greenberg, S.M., Anderson, C.S., et al. (2015). Guidelines for the management of spontaneous intracerebral hemorrhage: a guideline for healthcare professionals from the American Heart Association/American Stroke Association. *Stroke*, **46**(7), 2032–60.

Hoffman, M. & Monroe, D.M. 3rd (2001). A cell-based model of hemostasis. *Thromb Haemost*, **85**(6), 958–65.

Hoffman, M. (2003). A cell-based model of coagulation and the role of factor VIIa. *Blood Rev*, **17** Suppl 1, S1–5.

Kapapa, T., Röhrer, S., Struve, S., et al. (2014). Desmopressin acetate in intracranial haemorrhage. *Neurol Res Int*, **2014**, 298767.

Kimmell, K.T. & Jahromi, B.S. (2015). Clinical factors associated with venous thrombo-embolism risk in patients undergoing craniotomy. *J Neurosurg*, **122**(5), 1004–11.

Kramer, A.H., Roberts, D.J., & Zygun, D.A., 2012. Optimal glycemic control in neurocritical care patients. *Crit Care*, **16**(5), R203.

Kranke, P. (2015). General multimodal or scheduled risk-adapted postoperative nausea and vomiting prevention. *BJA*, **114**(2), 190–3.

Macfarlane, R.G. (1964). An enzyme cascade in the blood clotting mechanism, and its function as a biochemical amplifier. *Nature*, **202**, 498–9.

Naidech, A.M., Maas, M.B., Levasseur-Franklin, K.E., et al. (2014). Desmopressin improves platelet activity in acute intracerebral hemorrhage. *Stroke*, **45**(8), 2451–3.

Phelan, H.A. (2012). Pharmacologic venous thromboembolism prophylaxis after traumatic brain injury. *J Neurotrauma*, **29**(10), 1821–8.

Rabbitts, J.A., Nuttall, G.A., Brown, M.J., et al. (2008). Cardiac risk of noncardiac surgery after percutaneous coronary intervention with drug-eluting stents. *Anesthesiology*, **109**(4), 596–604.

Resuscitation Council (UK) (2014). *Management of Cardiac Arrest During Neurosurgery in Adults*. https://www.resus.org.uk/publications

Rolston, J.D., Han, S.J., Bloch, O., & Parsa, A.T. (2014). What clinical factors predict the incidence of deep venous thrombosis and pulmonary embolism in neurosurgical patients? *J Neurosurg*, **121**(4), 908–18.

Salmaggi, A., Simonetti, G., Trevisan, E., et al. (2013). Perioperative thromboprophylaxis in patients with craniotomy for brain tumours. *J Neurooncol*, **113**(2), 293–303.

Sansing, L.H., Messe, S R., Cucchiara, B.L., et al. (2009). Prior antiplatelet use does not affect hemorrhage growth or outcome after ICH. *Neurology*, **72**(16), 1397–402.

Sarode, R., Milling, T.J. Jr, Refaai, M.A., et al. (2013). Efficacy and safety of a 4-factor prothrombin complex concentrate in patients on vitamin K antagonists presenting with major bleeding: a randomized, plasma-controlled, phase IIIb study. *Circulation*, **128**(11), 1234–43.

Seicean, A., Schiltz, N.K., Seicean, S., Alan, N., Neuhauser, D., & Weil, R.J. (2012). Use and utility of preoperative hemostatic screening and patient history in adult neurosurgical patients. *J Neurosurg*, **116**(5), 1097–105.

Sharma, S., Balireddy, R.K., Vorenkamp, K.E., & Durieux, M.E. (2012). Beyond opioid patient-controlled analgesia: a systematic review of analgesia after major spine surgery. *Reg Anesth Pain Med*, **37**(1), 79–98.

Shmygalev, S. & Heller, A.R. (2011). Perioperative visual loss after nonocular surgery. *Anaesthesist*, **60**(7), 683–94.

Smith, I., Kranke, P., Murat, I., et al. (2011). Perioperative fasting in adults and children: guidelines from the European Society of Anaesthesiology. *Eur J Anaesthesiol*, **28**(8), 556–69.

Smith, M. (2015). Postoperative care after elective endovascular treatment of unruptured intracranial aneurysms. *Anesth Analg*, **121**(1), 17–19.

Temkin, N.R. (2002). Prophylactic anticonvulsants after neurosurgery. *Epilepsy Curr*, **2**(4), 105–7.

Tsivgoulis, G., Katsanos, A.H., Butcher, K.S., et al. (2014). Intensive blood pressure reduction in acute intracerebral hemorrhage: a meta-analysis. *Neurology*, **83**(17), 1523–9.

Wacker, J. & Staender, S. (2014). The role of the anesthesiologist in perioperative patient safety. *Curr Opin Anaesthesiol*, **27**(6), 649–56.

Wintzen, A.R., de Jonge, H., Loeliger, E.A., & Bots, G.T. (1984). The risk of intracerebral hemorrhage during oral anticoagulant treatment: a population study. *Ann Neurol*, **16**(5), 553–8.

Yancy, C.W., Jessup, M., Bozkurt, B., et al. (2013). ACCF/AHA 2013 guidelines for the management of heart failure. *J Am Coll Cardiol*, **62**(16), e147–239.

SECTION 2

Tumours and skull base-intrinsic tumour

6. **Low-grade glioma** *75*
   Thomas Santarius, Lorenzo Bello, and Hugues Duffau
7. **High-grade gliomas and molecular biology of neurosurgical oncology** *89*
   Stephen J. Price, Harry Bulstrode, and Richard Mair
8. **Intracranial metastases** *107*
   Andrew Brodbelt and Rashed Zakaria
9. **Primary central nervous system lymphoma** *117*
   Boon Leong Quah, Thangaraj Munusamy, and Colin Watts
10. **Glioneuronal and other epilepsy-associated tumours** *129*
    Matthias Simon and Alexander Grote
11. **Radiotherapy and radiosurgery for brain tumours** *141*
    Susan Short
12. **Chemotherapy for brain tumours** *149*
    Nicholas F. Brown, Daniel Krell, and Paul Mulholland
13. **Surgical techniques in the management of intrinsic tumours** *163*
    Shawn Hervey-Jumper and Mitchel Berger

6

Low-grade glioma

Thomas Santarius, Lorenzo Bello, and Hugues Duffau

Introduction

The term 'low-grade glioma' generally means glioma of a grade lower than anaplastic according to the WHO Classification of Tumours of the Central Nervous System, last revised in 2016 (see Louis et al., 2016). In this chapter we are going to focus on the management of adult patients with supratentorial WHO grade 2 diffuse low-grade gliomas (DLGG), that is, astrocytomas and oligodendrogliomas. It is becoming increasingly clear that these histological diagnoses do not describe uniform entities, but rather a heterogeneous spectrum of neoplastic diseases with a diverse biological and clinical behaviour. At the same time, radiological and molecular markers are being identified, gradually improving the prognostic accuracy.

It was once generally believed that low-grade gliomas are static in terms of their biology, but now we know that these tumours, like most other neoplasias, undergo evolution into biologically more aggressive entities, eventually satisfying histological criteria for WHO grade 3 or 4. This is often referred to as malignant or anaplastic transformation (AT), a change from a non-malignant to a malignant entity. Although such change can be sudden and dramatic in some cases, especially from the clinical point of view, it is likely to be more incremental at the biological level in most patients. In other words, DLGGs rather than being a disease, constitute a period, a stage in the evolution of a disease.

Last decades have brought major technical and conceptual advancements in cognitive neurosciences, imaging, and genetics, leading to the emergence of seminal concepts of DLGG as a brain disease and individualized treatment. It is wrong to think of DLGG as a tumour mass within the brain. Instead, it should be thought of as a progressive, invasive, and chronic disease of the central nervous system. The effects of the disease on the brain and consequently on the patient are specific to the individual patient and have a dynamic dimension. Because of brain function is so fundamental to the definition of an individual, his/her role in family and wider society, even the most subtle impairment and alterations can have profound influence on patient's quality of life and social function. The management of patients with DLGG has therefore moved away from the classical, rigid order of therapeutic modalities (surgery followed by irradiation in the case of incomplete resection, followed by chemotherapy at recurrence) without any attempt to tailor the sequence of treatments to the individual patient. Here we present a modern view of the management of patients with long-term, multimodal, individualized, and dynamic planning with built-in flexibility to respond to the feedback provided by clinical, radiological, and histomolecular data with the aim to maximize the length and quality of life of each individual patient.

Incidence

Based on the data from Europe and the United States, the incidence of DLGG is approximately 1–1.5/100 000 patients/year (astrocytic low-grade glioma (LGG), 0.6–1.2/100 000 patients/year; oligodendroglial LGG, 0.3/100 000 patients/year), accounting for 10–15% of all primary brain tumours (Crocetti et al., 2012; Ostrom et al., 2014). At the time of diagnosis, patients with DLGG are typically between 30 to 45 years of age (Capelle et al., 2013). In the French study of 1295 DLGGs, 47 cases were incidental. The age at radiological diagnosis of the incidental DLGGs was found to be slightly lower as compared symptomatic DLGGs (median of 35.5 vs. 37.0 years; Pallud et al., 2010b). The incidence of GLGGs will likely increase with growing access to brain imaging worldwide.

DLGGs show predilection for eloquent areas, such as the insula or the supplementary motor area (Duffau and Capelle, 2004). This preferential location may be, at least partially, due to the fact that the threshold for triggering symptoms is lower in these areas of the brain (Pallud et al., 2010b). This is consistent with the observation that incidentally found DLGGs occur less likely in eloquent areas (Pallud et al., 2010b; Potts et al., 2012; Zhang et al., 2014).

Males constitute approximately 60% of patients in most DLGG series (McGirt et al., 2008; Schomas et al., 2009; Pallud et al., 2010a). This slight male preponderance was found to be inverted in the incidental DLGG cohort (58% females) analysed by Pallud et al. and later confirmed by Potts et al. (Pallud et al., 2010b; Potts et al., 2012). The reason for the gender distributions of symptomatic and incidental DLGGs is unclear. Based on the finding that headaches were listed as the most common reason for requesting an MRI, the authors hypothesized that the gender representation difference between symptomatic and asymptomatic cohorts (P <0.001) may be related to higher incidence of headaches in women (Pallud et al., 2010b) or women generally being more likely to seek medical attention than men (Potts et al., 2012).

Clinical presentation

More than 80% of patients will DLGGs present with seizures. Others present with focal deficits, altered mental state, or increased intracranial pressure (Pallud et al., 2010b; Pallud et al., 2014). Epileptic seizures are more frequently associated with cortically based tumours, particularly in frontal, temporal, and insular and central locations and with oligodendroglial tumours (Pallud et al., 2014).

Patients presenting with neurological deficit have always formed a minority, but they are getting even rarer. In a retrospective review of hospital records of 852 adult patients, Youland et al. compared clinical presentations of two historical cohorts, 1960–1989 and 1990–2011 (Youland et al., 2013). The authors found that in the earlier cohort more patients presented with multiple symptoms at diagnosis than in the more recent cohort (51% vs. 24%; P <0.0001)—see also **Table 6.1**.

The relative scarcity of neurological deficit as well the existence of time lag of months or even years before development of seizures in the presence of DLGGs may be somewhat surprising, especially as these tumours are frequently located within eloquent brain areas (Duffau and Capelle, 2004). This stands in clear contrast to the presentation of higher-grade gliomas, especially glioblastoma multiforme, and is due to several factors, including the lack, or only a minimum of cerebral oedema, and the slow-growing nature of DLGG. The latter allows relocation of invaded cerebral functional circuits, in other words remapping of brain function, a phenomenon known as brain plasticity (Duffau, 2005). Increasingly more DLGGs are diagnosed as a result of scanning for reasons other than suspected glioma. In the aforementioned 1960–1989 cohort of Youland et al. there were no incidental DLGGs, while there were 11 in 1990–2011 cohort (Youland et al., 2013).

Although 'gross neurological deficit' such as dysphasia and hemiparesis are rare at presentation of DLGGs, more subtle cognitive deficits are often observed when objective neuropsychological assessments are performed at the time of diagnosis. Disorders of executive functions, attention, concentration, working memory, or emotion are frequently detected (Klein et al., 2012; Duffau, 2013; van Loon et al., 2015; Racine et al., 2015). These deficits can be attributed to the tumour itself, to seizures, and to antiepileptic medications. A systematic assessment of higher mental functions and health-related quality of life is now recommended before oncological treatment. This serves several important purposes: (1) detection of subtle neuropsychological deficits; (2) tailoring of the therapeutic strategy for a given individual (e.g. choosing neoadjuvant chemotherapy rather than surgery first in cases of very diffuse DLGG with cognitive disturbances); (3) devising of surgical strategy according to the detected deficit and location of the tumour (i.e. selection the optimal neurological tests that should be administrated during awake surgery); (4) establishing of a pretreatment baseline that will allow detection of post-treatment deficit and facilitate planning of specific functional rehabilitation following surgery.

Radiological diagnosis

MRI is the main tool for diagnosing and assessing DLGGs. DLGGs are hypointense on T1 and hyperintense of T2. The extent of the tumour was shown to best correspond to FLAIR hyperintensity (Price, 2010). However, it is important to remember that DLGG is a diffuse neoplastic disease and that glioma cells have been shown to be present beyond the FLAIR signal abnormality as far as 2 cm (Pallud et al., 2010c).

Generally, the lack of enhancement results in a radiological diagnosis of 'low-grade glioma', while contrast uptake by the tumours raises suspicion of tumour being of grade 3 or 4. Although this is true for the majority, more than 30% of cases with no contrast enhancement will be reclassified as grade 3 or 4 and, conversely, some 15–30% of DLGGs enhance (Cavaliere et al., 2005). The likelihood of histological grade being higher than grade 2 in non-enhancing gliomas increases with age (Barker et al., 1997).

Among DLGGs, enhancement is more common in oligodendrogliomas (~20–50%), making the presence of enhancement a feature relatively less grade-specific in oligodendroglial tumours, whose anaplastic counterpart shows enhancement in 62–72% cases (White et al., 2005). Haemorrhage and calcifications are also more common in oligodendrogliomas. Approximately one-quarter of oligodendrogliomas show calcifications, which can be best observed on CT scans (Khalid et al., 2012). Calcifications are twice as common in anaplastic oligodendrogliomas, consistent with their progression from low to higher grade over time (Khalid et al., 2012).

Diffuse low-grade gliomas have characteristic shape, location, and spread along white matter tracts. The MRI appearance or DLGG is not uniform, but instead constitute a range from apparently well-circumscribed tumour at one end, to *gliomatosis cerebri* at the other end of the spectrum (**Fig. 6.1**). Making a diagnosis of DLGG on imaging is usually possible in the context of the clinical picture and by repeating the scan, typically in 3 months or earlier, depending on the degree of suspicion of pathology other than DLGGs and

Table 6.1 Presentation of patients with DLGGs in two historical cohorts, 1960–1989 and 1990–2011

Symptom	Overall N = 852 (%)	1960–1981 N = 281(%)	1990–2011 N = 571(%)	P value
Seizures	610 (72)	218 (78)	392 (69)	0.008
Headaches	258 (30)	130 (46)	128 (23)	<0.0001
Speech	61 (7)	26 (9)	35 (6)	0.12
Sensory/motor symptom	271 (32)	113 (40)	158 (28)	0.003

Reproduced with permission from Youland, Ryan S.; Schomas, David A.
Changes in presentation, treatment, and outcomes of adult low-grade gliomas over the past fifty years, *Neuro-Oncology*, Volume 15, Issue 8, pp. 1102–10. Copyright © 2013 Oxford University Press and the Society for NeuroOncology (SNO).

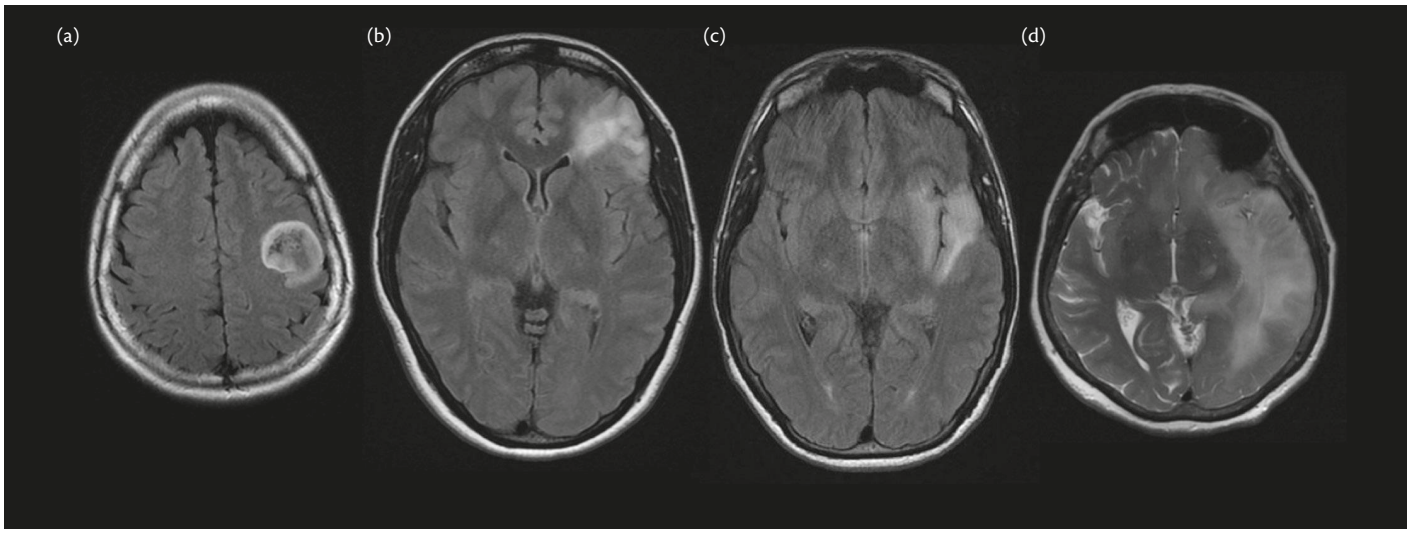

Fig. 6.1 Spectrum of the diffuse nature of DLGG, from relatively circumscribed (A), through more diffuse, but contained within one lobe (B), spread into adjacent lobes (C) to *gliomatosis cerebri* (D).
Courtesy of Dr Kieren Allinson, Department of Pathology, Addenbrooke's Hospital, Cambridge.

the likelihood of harmful consequences of delayed diagnosis. The radiological differential diagnosis includes: encephalitis, cerebral ischaemia/infarction, and other intrinsic low-grade tumours (e.g. DNET, ganglioglioma) or gliomas of higher grades. However, in the context of good clinical history, the diagnosis of a glioma is rarely in doubt and a biopsy to differentiate this from another process (e.g. Rasmussen encephalitis) is rarely necessary. Needle biopsy is only performed if the alternative diagnosis is more likely and needs to be confirmed histologically (Fig. 6.2). An interval MRI scan, when appropriate, not only helps with differential diagnosis, but is important for patient management as the speed of growth is an established DLGG prognostic factor (see more details later on; see also Pallud et al., 2013). MR spectroscopy can also be useful in differentiating between neoplastic and non-neoplastic lesions (Oz et al., 2014).

Anaplastic transformation represents the principal lethal factor in these patients, as demonstrated by the parallel linearity of the survival and anaplastic curves in a series by Capelle et al. (Capelle et al., 2013). It is therefore important to monitor for this to occur. Positron emission tomography (PET) is not only useful in refining differential diagnosis, especially in the context of radiation-treated gliomas, but can be helpful in identifying potential anaplastic loci (Ewelt et al., 2011; la Fougère et al., 2011; Thon et al. 2015). However, for routine monitoring and detection of AT, perfusion MRI measuring the relative cerebral blood volume (rCBV) is more practical, especially if frequent (e.g. three-monthly) surveillance is required (Danchaivijitr et al., 2008; Hu et al., 2012).

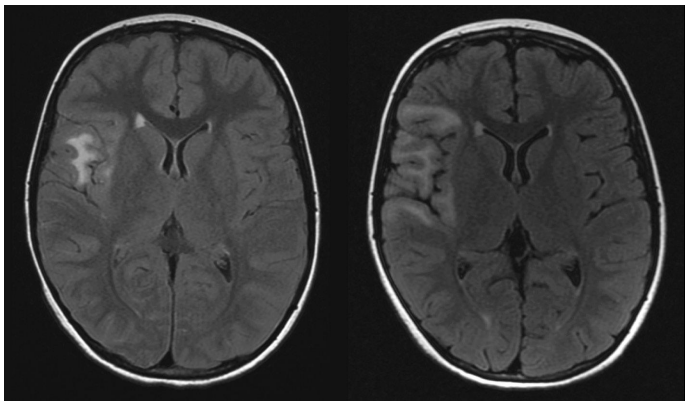

Fig. 6.2 The differential diagnosis of DLGG includes autoimmune encephalitis. This 14-year-old presented with progressive intractable seizures. The scans were taken one month apart.

Management after radiological diagnosis

Establishing radiological diagnosis of DLGG spells a beginning of a journey, whose course is determined by the cancer, the brain, and the choices the patient makes in collaboration with his/her treating team. Yet another level of complexity is added by the long OS and the constant evolution of our understanding of the nature of DLGGs and the effects of treatments on it. Nevertheless, at present, DLGGs remain incurable and over several years they relentlessly progress via serial anaplastic transformations towards the unequivocal endpoint, mortality. In the process the disease volume will increase, distorting and invading the surrounding brain, and will gradually interfere more and more with brain's normal function. The patient journey is complex and the treating team needs, together with the patient, devise a strategy that will maximize the patient's survival while preserving his or her quality of life (QoL). As applies for each patient, so each tumour is individual and both need individualized approach (i.e. personalized treatment).

In Table 6.2 are listed most important variables (prognostic factors) associated with outcome of patients with DLGGs (overall survival and time to anaplastic progression). Their individual and combined influence on the natural history of the disease and QoL need to be taken into. It is vital that patients understand as much as possible about these variables, including the uncertainties associated with each of them. Essentially, some variables are given (clinical, radiological, histological, and molecular prognostic factors) and others can be modified (volume of the tumour) or deployed (treatment: surgery, chemotherapy, and radiotherapy). These are

Table 6.2 Factors associated with outcome (overall survival, OS; time to anaplastic transformation, TAT) in patients with DLGGs

Variable	OS	TAT	Reference
Age	✓		(Leighton et al., 1997; Bauman et al., 1999; Pignatti et al., 2002; Capelle et al., 2013; Jakola et al., 2013)
KPS	✓		(Leighton et al., 1997; Capelle et al., 2013; Jakola et al., 2013)
Presence of neurological deficits	✓		(Pignatti et al., 2002)
Presenting with seizures	✓		(Leighton et al., 1997; Pignatti et al., 2002)
Tumour volume	✓		(Berger et al., 1994; Lote et al., 1997; Pignatti et al., 2002; Shaw et al., 2002; Chang et al., 2008; Capelle et al., 2013; Smith et al., 2008; Jakola et al., 2013)
Tumour crossing midline	✓		(Pignatti et al., 2002; van den Bent et al., 2005)
Tumour location—frontal	✓		(Capelle et al., 2013)
Speed of growth	✓	✓	(Pallud et al., 2013)
rCBV	✓		(Bisdas et al., 2009; Caseiras et al., 2010)
Histology: astrocytoma rather than oligodendroglioma	✓		(Leighton et al., 1997; Pignatti et al., 2002; Mehta et al., 2014)
1p19q codeletion	✓	✓	(Kaloshi et al., 2007; Cancer Genome Atlas Research Network et al., 2015; Eckel-Passow et al., 2015)
IDH mutations	✓	✓	(Cancer Genome Atlas Research Network et al., 2015; Eckel-Passow et al., 2015)
TERT mutation	✓	✓	(Cancer Genome Atlas Research Network et al., 2015; Eckel-Passow et al., 2015)
Degree of resection	✓	✓	(Leighton et al., 1997; Smith et al., 2008; Jakola et al., 2012; Capelle et al., 2013)

discussed in following five sections. In the last section we will describe the typical management paths used in our institutions.

Clinical prognostic parameters

Patient age has been a long-established prognostic factor in DLGGs (Bauman et al., 1999; Pignatti et al., 2002; Capelle et al., 2013; Jakola et al., 2013). Interestingly, age has also been associated with higher frequency of anaplasia in non-enhancing gliomas (Barker et al., 1997).

Age, presence of neurological deficits or absence of seizures at onset, and low performance status (KPS <70%) are associated with a poorer outcome (Leighton et al., 1997; Pignatti et al. 2002; Jakola et al., 2012; Capelle et al., 2013).

Radiological prognostic parameters

The negative association between tumour volume and OS has been seen in number of studies (Berger et al., 1994; Lote et al., 1997; Pignatti et al., 2002; Shaw et al., 2002; Chang et al., 2008).

Mass effect, focal deficits, and/or intracranial hypertension leading to a poorer functional status are significant factors on univariate analysis but not on multivariate analysis, probably because they are related to tumour volume. Larger tumour size limits therapeutic possibilities and increases the risk of treatment-related complications (Shaw et al., 2002; Smith et al., 2008). Similarly, extension to or location in eloquent areas is associated with shorter OS, presumably because of the functional limitations to the extent of resection and, possibly, because of earlier development of neurological dysfunction (Chang et al., 2008).

Speed of growth, expressed as velocity of diametric expansion (VDE), a measurement reflecting both the initial tumour volume and the increase in volume (Pallud et al., 2012), was found to be an independent prognostic factor for OS and malignant PFS, regardless of histopathological findings and molecular status (Pallud et al., 2013). One of the strengths of VDE as a predictor and a monitoring tool is its relative immunity to a sampling bias as it takes into account the tumour as a whole. In addition, the method is non-invasive, simple, reproducible, and relatively cheap.

PET, MR spectroscopy, and high cerebral blood volume measured by MRI (rCBV) can detect signs of malignant transformation and correlate with shorter OS (Bisdas et al., 2009; Caseiras et al., 2010), while the presence of lactates and lipids on MR spectroscopy is related to more aggressive behaviour (Guillevin et al., 2012). The choline-to-creatine ratio (Cho/Cr) known to be correlated with tumour cell proliferation (Herminghaus et al., 2002). Cho/Cr as well as NAA (N-acetylaspartate)/Cr ratio can help differentiating between low-grade and high-grade gliomas with sensitivity and specificity in an approximate range of 80–85% (Server et al., 2011; Zou et al., 2011; Collet et al., 2015) including differentiation between grade 2 and grade 3 (Collet et al., 2015). MR spectroscopy detected elevated 2-hydroxyglutarate (2HG) levels in gliomas with *IDH1* mutations compared with wild type in a study of 27 patients with gliomas ($P = 0.003$; see Pope et al., 2012).

Floeth et al. prospectively followed 21 patients with small non-enhancing T2-hyperintense incidental lesions with serial MRI scans and 18F-FET PET (Floeth et al., 2008). Two patients had lesions that demonstrated slow growth and negative 18F-FET PET studies. Subsequent tissue diagnosis revealed WHO grade 2 astrocytomas. A second group of patients had rapid growth with positive 18F-FET PET findings and were found to have high-grade gliomas. However, for routine monitoring and detection of anaplastic transformation, perfusion MRI measuring rCBV is more practical, especially if frequent (e.g. 3-monthly) surveillance is required (Danchaivijitr et al., 2008; Hu et al., 2012).

Functional MR, DTI tractography, and magnetoencephalography (MEG) can be helpful in preoperative planning, but discussion of their role in management of DLGGs is beyond the scope of this chapter (Ottenhausen et al., 2015).

Histological and molecular prognostic parameters

Based on histological examination, gliomas are graded according to the 2016 WHO Classification of Tumours of the Central Nervous System (Louis et al., 2016) into four grades; the higher the grade, the worse the prognosis (Table 6.3). Grade 1 astrocytomas, such as pilocytic astrocytomas and giant cell astrocytomas, for example, constitute an entirely different group of diseases and will not be considered here. Although grade 2 diffuse supratentorial gliomas (astrocytoma and oligodendroglioma; Fig. 6.3) are the subject of this chapter, these cannot be discussed without reference to grade 3 and grade 4 gliomas, not least because grades 2–4 are a continuum rather than discrete categories and, perhaps even more importantly, grade 2 tumours invariably progress to higher grades. Therefore, a grade 2 glioma is a stage of a disease rather than disease itself.

Although overall survival broadly correlates with each histological diagnosis (Table 6.3) there is extensive evidence that tumours from individual patients who share the same histological diagnosis do not necessarily share the same biology and their outcomes may vary widely (Gravendeel et al., 2009; Gorovets et al., 2012). There is a number of reasons for this, but perhaps the two most important being the possibility of erroneous grading and the inherent dynamism of the disease.

The two main sources of diagnostic error are sampling and interobserver variability. The latter is related to the descriptive and ambiguous nature of some of the classification criteria, especially criteria for discriminating between grade 2 and 3 tumours (Louis et al., 2007). For example, the criterion for grade 3 designation of astrocytomas ('brisk mitotic activity') does not clearly specify any mitotic cut-off and is, therefore, subjective and often based on the pathologist's individual experience and bias. In a large study investigating the rate of diagnosis disagreement after expert neuropathology review, approximately 40% of case reviews had some type of disagreement with the original diagnosis, of which approximately 9% were serious with immediate effect on treatment (Bruner et al., 1997). Similarly, the criteria for the mixed oligoastrocytoma category ('recognition of neoplastic glial cells with convincing astrocytic oligodendroglial phenotypes') present in the 2007 edition of the Classification was felt to be highly subjective and this diagnostic category was practically eliminated from the 2016 revision (see more later in this chapter; also see Louis et al., 2016).

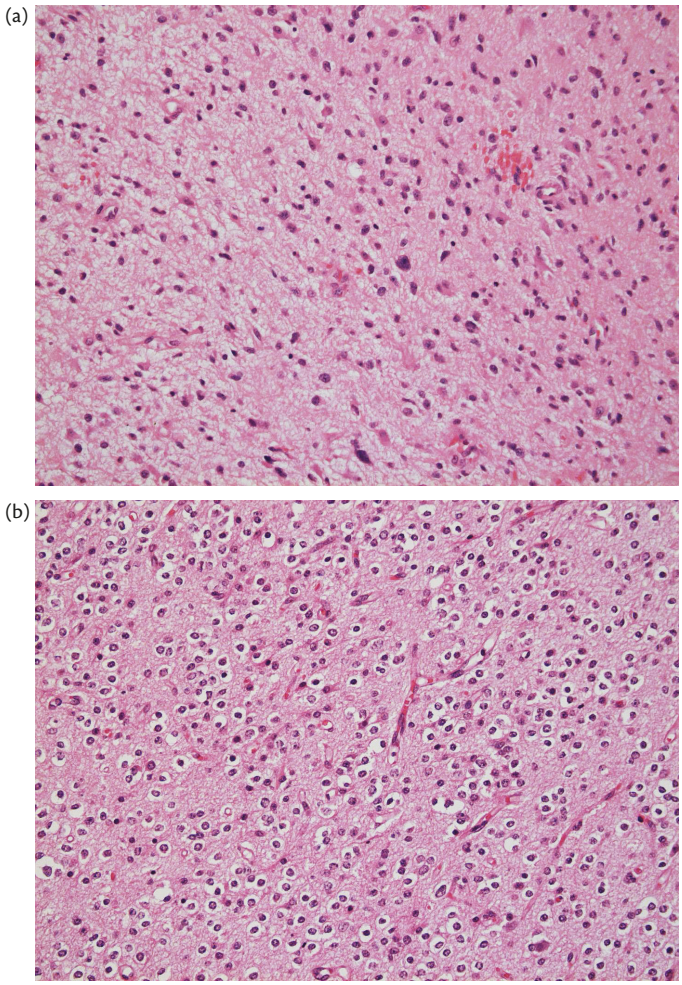

Fig. 6.3 Histological appearance of diffuse low-grade gliomas: astrocytoma (A) and oligodendroglioma (B) (haematoxylin and eosin staining, 20× magnification).

(A) Aastrocytomas are hypercellular area as compared to the normal white matter. There is nuclear pleomorphism and small microcysts. There are no vascular proliferation and no necrosis. (B) Oligodendrogliomas are composed of monomorphic cells with uniform round nuclei and perinuclear halos ('fried egg' or 'honeycomb' appearance). The perinuclear halo is artefact due to fixation, and is not present in frozen sections. Another typical feature seen on this slide is the arborizing thin capillaries often described as 'chicken wire pattern'.

Courtesy Dr Kieren Allinson, Consultant Neuropathologist, Addenbrooke's Hospital, Cambridge.

Table 6.3 Five- and ten-year survival rates for diffuse gliomas grades 2–4

Diffuse glioma (WHO grade)	5-year relative survival rate (%)	10-year relative survival rate (%)
Oligodendroglioma (2)	79.5	62.8
Anaplastic oligodendroglioma (3)	52.2	39.3
Astrocytoma (2)	47.4	37.0
Anaplastic astrocytoma (3)	27.3	19.0
Glioblastoma (4)	5.0	2.6

Reproduced with permission from Ostrom, Quinn T.; Gittleman, Haley, CBTRUS Statistical Report: Primary Brain and Central Nervous System Tumors Diagnosed in the United States in 2007–2011, *Neuro-Oncology*, Volume 16, suppl 4, pp. 1–63. Copyright © 2014 Oxford University Press and the Society for NeuroOncology (SNO).

Histological grade intratumoural heterogeneity and consequent sampling error is another important source of possible misdiagnosis. Kunz et al. have found anaplastic foci to be between 0.6 and 8.7 ml in volume and covering 4–44% of the entire visible tumour volume (Kunz et al., 2011) Inadequate sampling (especially with needle biopsy and subtotal resections), failure to process, and histologically examine the entire specimen, could lead to overlooking anaplastic foci and so result in an erroneous diagnosis, usually undergrading of the disease. Sampling accuracy can be improved with the use of PET-directed guidance, both in the case of needle biopsy and resection (Kunz et al., 2011; Thon et al., 2015). The addition of 5-ALA may also help with intraoperative identification of the hotspot(s) demonstrated on preoperative PET (Ewelt et al., 2011). These facts need to be taken into account when interpreting old studies in which diagnosis was established based on needle biopsy alone.

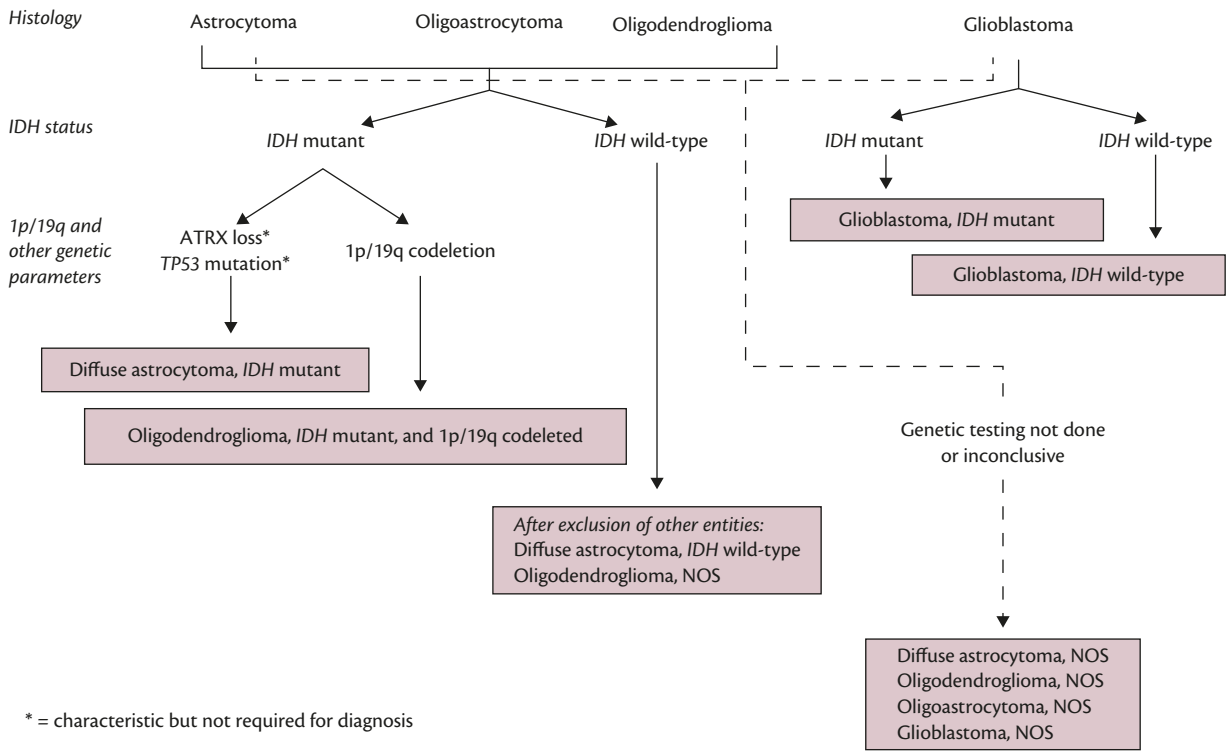

Fig. 6.4 A simplified algorithm for classification of the diffuse gliomas based on histological and genetic features.
Data from Louis, D.N. et al., *WHO classification of tumours of the central nervous system*, IARC Press. 2016.

The limitations of histological diagnosis are a major driver for searching for more accurate, objective, and clinically relevant markers for stratifying patients with DLGGs. As cancer is essentially a genetic disease (Vogelstein and Kinzler, 2004), undoubtedly it will be molecular biology that will deliver many of such markers. Indeed, a number of glioma-relevant molecular markers have been discovered and seem to be superior to histology in predicting outcome (Gorovets et al., 2012). These include the presence of mutations or *IDH1* or *IDH2, ATRX*, and *TERT* genes, and the loss of 1p/19q chromosomal arms and have been incorporated, for the first time, in the latest WHO classification (Louis et al., 2016). In fact, if the tumour bears the molecular characteristics of an oligodendroglioma (IDH-mutant and 1p/19q-codeleted) it is diagnosed as oligodendroglioma, even if histologically it was to look like an astrocytoma. Similarly, if the tumour was to look like an oligodendroglioma under the microscope, but was found to have mutated IDH, ATRX, and TP53, but intact 1p/19q it will be diagnosed as diffuse astrocytoma (see also **Fig. 6.4**). This will leave the rather vague category of oligoastrocytoma reserved for cases where cell population with demonstrated oligodendroglial and astrocytic molecular features, respectively, are demonstrated or where histologically (phenotypically) both oligodendroglial and astrocytic tumour cells are present. The latter applies only to situations where molecular diagnostic tests are not available.

An inactivating mutation of a gene coding for isocitrate dehydrogenase 1 or 2 (IDH-1 and 2) occurs in approximately 75% of grade 2 and 3 diffuse gliomas and 80% of secondary glioblastomas, which themselves constitute only a minority of glioblastomas (~10%). IDH mutations are very rare (<5%) in secondary glioblastomas. These facts are consistent with the notion that IDH mutations are early events in the evolution of gliomas. There appear to be a separate, mutually exclusive with IDH-mutated DLGGs, lineages of development of DLGGs, characterized by ATRX and p53 or TERT mutations (Eckel-Passow et al., 2015). These lineages are associated with an astrocytic phenotype. 1p19q codeletion is associated with oligodendroglial phenotype.

Recently, two major molecular studies by the Cancer Genome Atlas (TCGA) group (Cancer Genome Atlas Research Network et al., 2015) and the Mayo Clinic-University of California San Francisco (Mayo-UCSF; Eckel-Passow et al., 2015) collaborative were published. In the TCGA study, diffuse grade 2 and 3 tumours displaying IDH mutation and 1p/19q codeletion (1p/19q-del) had the best prognosis, followed by those with IDH mutation and no 1p/19q-del. IDH wild-type tumours had the same survival as glioblastomas (Cancer Genome Atlas Research Network et al., 2015). In the Mayo-UCSF study, diffuse grade 2 and 3 tumours were classified into five glioma molecular groups using three alterations: mutations in the TERT promoter and in IDH, and 1p/19q codeletion (Eckel-Passow et al., 2015). *IDH mutation only* tumours were found to be the most common (45%) and bear intermediate prognosis. They account for half of all patients who have gliomas with an oligodendroglial component and two-thirds of those who have grade II or III astrocytomas. These tumours almost always acquire mutations in TP53 and ATRX. *Triple-positive* (IDH- and TERT-mutated, 1p/19q-del) tumours were the second most common (29%) and were found to have good prognosis. They have few additional acquired alterations and are strongly associated with the oligodendroglial histological type. IDH- and TERT-mutated without 1p/19q-del have similar prognosis, but are rare (5%). Triple negative tumours occur with similar frequency (7%) and have poor prognosis. The

associated mutations occur in *EGFR, PTEN*, and *NF1* genes. The worst prognosis is associated with TERT-only mutation (wild-type IDH, no 1p/19q-del). These tumours made up 10% of the grade 2 and 3 cohort. Similarly to the triple negative group, they had numerous other gene mutations, including *EGFR, EGFRvIII, PTEN, NF1, RB1*, and *PIK3CA* or *PIK3R1*.

The classification of tumours is an evolving process. The discovery of molecular markers and better understanding of the biology of gliomas will undoubtedly accelerate and further change the way gliomas are classified today.

Surgery

The value of surgery in the management of DLGGs had been controversial. Over the last two decades, however, it has become increasingly clear that surgical resection can be a major positive factor influencing the natural history of patients with DLGG. Both, improved data collection and refined surgical techniques based on better understanding of the brain and tumour/brain interaction facilitated these developments.

The classical low-grade glioma literature suffers from several shortcomings related to data collection, including lack of stringent reporting of histological diagnosis, length, and quality of follow-up and measurement of the extent of resection, which was largely based on the surgeon's intraoperative impression (Sanai and Berger, 2008). If postoperative imaging was used at all, it was not used in a systematic manner and lacked uniformity (Sanai and Berger, 2008). Due to the invasive nature of DLGG, the extent of residual tumour was underestimated in numerous studies, resulting in erroneous conclusions about the benefit of surgery. Today, FLAIR MRI is the gold standard for objective calculation of postoperative residual volume.

In all recent series with objective postoperative evaluation of the extent of resection (EOR) based on volumetric assessment of FLAIR MRI (reviewed later on), the degree of resection predicted a significant improvement in OS. When no signal abnormality was visible on postoperative MRI (complete resection), patients had a significantly longer OS compared with patients having any residual abnormality. Moreover, even with incomplete resection patients with greater degree of resection had a significantly longer OS. This is due to the fact that surgery delayed 'histological upgrading', because the volume of residual tumour serves as a predictor of AT (Berger et al., 1994). The likely underlying mechanism of this effect is removal of all or many of anaplastic foci, which could result in immediate histological upgrading and the case being excluded from the 'low-grade cohort' or true biological downgrading of the tumour. In fact, such downgrading is not a binary event, but rather graded reduction of the anaplastic potential of the residual tumour, which is reflected by continuous character of the inverse relationship between OS and the residual tumour volume.

In 156 DLGGs, Claus et al. (2005) reported that patients who underwent incomplete resection had 4.9 times the risk of death compared with those who underwent total resection.

Yeh et al. (2005) demonstrated that EOR and postoperative KPS showed independent prognostic significance for OS using multivariate analysis of 93 consecutive DLGGs.

Comparing two historical cohorts one of 100 DLGG resections without (1985–1996) and one of 122 resections with functional mapping (1996–2003), Duffau et al. (2005) found that 20.6% of patients with more than 10 cc of residue died, while only 8% of patients with less than 10 cc of residue died and no patients with complete resection died ($P = 0.02$).

In the series by Smith et al. (2008) with 216 DLGGs, after adjusting for the effects of age, KPS, tumour location, and tumour subtype, EOR remained a significant predictor of malignant PFS ($P = 0.005$) and OS ($P = 0.001$), with an 8-year OS of 98% of patients who underwent complete resection. Moreover, the survival was significantly better with at least 90% EOR compared with less than 90% EOR, whereas EOR of at least 80% also remained a significant predictor of OS.

McGirt et al. (2008) observed that gross total resection (complete resection of the preoperative FLAIR signal abnormality) versus subtotal resection was independently associated with increased OS ($P = 0.017$). In 191 consecutive DLGGs, the same team also showed that gross total resection was an independent factor associated with anaplastic transformation ($P = 0.05$; see Chaichana et al., 2010).

In 130 DLGGs studied by Ahmadi et al. (2009), using multivariate analysis the authors identified more than 90% resection to be associated with prolonged OS.

In a study of 314 DLGG patients with 13.6-year follow-up, Schomas et al. (2009) identified by multivariate analysis that less than subtotal resection was an adverse prognostic factor for OS. The same team has also recently confirmed that gross total resection and subtotal resection were factors associated with improved OS in a series with 852 DLGGs (Youland et al., 2013).

Based on a review of 190 cases of DLGGs, Ius et al. (2012) demonstrated that patients with an EOR equal to or more than 90% had an estimated 5-year OS of 93%, those with EOR between 70% and 89% had a 5-year OS of 84%, and those with EOR less than 70% had a 5-year OS of 41% ($P = 0.001$).

Jakola et al. (2012) investigated survival in population-based parallel cohorts of DLGGs from two hospitals with different surgical strategies. Treatment at a centre that favoured early surgical resection was associated with better OS (median survival was not reached) than treatment at a centre that favoured biopsy and watchful waiting (median survival, 5.9 years).

Finally, the French Glioma Network (FGN) published the largest surgical series of DLGG ever reported (1097 patients), showing that EOR and postsurgical residual volume were independent prognostic factors significantly associated with longer OS (Capelle et al., 2013). The same group has also found surgical resection being an independent prognostic factor associated with increased malignant PFS ($P = 0.001$) and OS ($P = 0.016$), based on a series of 1509 DLGGs (Pallud et al., 2014), In this series, the OS was almost 15 years, that is, about double of the OS reported in classical studies in which no attempt was made to perform extensive resection (Karim et al., 2002; Pignatti et al., 2002; van den Bent et al., 2005; De Witt Hamer et al., 2012) or in series with only a biopsy (Jakola et al., 2012).

The modern literature has thus provided ample evidence about the oncological benefit of radical resection of DLGGs. This oncological benefit has to be, however, balanced against the risk of functional deficit that may arise from radical surgery (onco-functional balance). The advances in the understanding of the brain, tumour, brain-tumour interaction as well as popularization of awake surgeries and direct electrical brain stimulation (DEBS) techniques led to improvement of surgical techniques and consequent reduction of permanent neurological deficit to below 5% (Keles et al., 2004; Duffau et al., 2008; McGirt et al., 2008; Smith et al., 2008; Capelle

et al., 2013), thus gaining oncological advantage while controlling the functional risks. Some of the factors that have driven improvements in surgical outcomes, both technical and conceptual, will be discussed next.

A great deal of progress has been made in understanding of brain function, moving from the concept of 'cortical areas' with specific functions to the concept of functional networks, also known as the hodotopical model (hodos—pathway, topos—place; see Duffau, 2015). As gyri and sulci are readily recognizable at surgery, surgeons have traditionally focused on recognizing and preserving cortex known to be associated with certain function, such as precentral gyrus housing neurons of the corticospinal tract. White matter, on the other hand appears amorphous and was, therefore, largely ignored with the consequences of either very conservative degree of resection or uncontrolled risk of neurological deficit or both.

Another important concept is that of brain plasticity, that is, the ability of brain functions to relocate from one anatomical location to another ('brain rewiring'). Brain plasticity is the underlying reason why neurological deficits are rare in patients with DLGG, even if these tumours are frequently located within eloquent areas (Duffau and Capelle, 2004). The slow-growing nature of these tumours allows functional remapping of the brain to take place, thus allowing broad surgical resection of brain regions traditionally deemed to be inoperable (Desmurget et al., 2007; Duffau, 2014). For example, extensive removal of diffuse tumour invading the classical 'Broca's area' in the left hemisphere has been carried out without causing permanent neurological deficit. (Benzagmout et al., 2007; Lubrano et al., 2010). In addition, resection of the pars opercularis and/or pars triangularis of the left inferior frontal gyrus is possible without risking aphasia, for two reasons. First, in a networking model of the human brain based on a probabilistic map of critical regions built from 771 stimulation sites, it has recently been demonstrated that Broca's area is not the speech output region (Tate et al., 2014; Tate et al., 2015). Second, tissue loss in this area can be compensated for by recruitment of adjacent regions, primarily the ventral premotor cortex (the crucial epicentre for speech articulation), and the pars orbitalis of the inferior frontal gyrus, the dorsolateral prefrontal cortex, or the insula as well as by remote areas, such as the contralateral homologous region (Benzagmout et al., 2007; Duffau, 2012a).

Even if some DLGGs may appear as 'well-circumscribed', they all infiltrate brain along the white matter tracts and, as such, tumour and tissues are intermingled. Aiming primarily 'to remove tumour' will either carry out an uncontrolled risk of neurological deficit or will result in lower than possible degree of resection. Instead, it is helpful to think of DLGG surgery as surgery on the brain rather than tumour surgery. The limit of resection should not be the 'tumour boundary' but rather brain functional boundary. Therefore, although image navigation is useful, it is the identification of critical brain 'hodos' and 'topos' through the combination DEBS and suitable neurophysiological and clinical feedback tools (Coello et al., 2013; Bello et al., 2014). It is therefore not surprising that the use of intraoperative DEBS has been found to be associated with greater degree of resection (gross total resection of 75% vs. 58%) and lower rate of permanent neurological deficit than in surgeries without DEBS (3.4% vs. 8.2%; see De Witt Hamer et al., 2012). Awake surgery is another important tool in the armamentarium for surgery for DLGGs and is absolutely essential for gaining functional feedback in cases infiltrating or adjacent to regions of the brain involved in speech. A prospective study of 105 patients conducted by the European Low Grade Glioma Network has found awake surgery to be well-tolerated and safe (Beez et al., 2013). Resection probability maps, a quality assessment tool of resective glioma surgery, was developed by De Witt Hamer et al. (2013) The technical details of surgery for DLGG are beyond the scope of this chapter and are covered elsewhere in this textbook.

The concept of functional boundaries being the limit of resection enables, in some cases, performing a supratotal resection (i.e. resection extending beyond the MRI signal abnormalities). A recent series reported that a supratotal resection performed in patients with a DLGG within non-eloquent brain regions avoided AT at a mean follow-up of 35.7 months and maximum follow-up of 135 months (Yordanova et al., 2011). This series was compared with a control group having only complete resection for a DLGG. AT was observed in seven patients in the control group but not in any of the patients who underwent supratotal resection ($P = 0.037$). Furthermore, adjuvant treatment was administrated to ten patients in the control group versus only one patient with supracomplete resection ($P = 0.043$).

In addition to the oncological benefit, surgical resection can often result in symptomatic improvement (Teixidor et al., 2007; Duffau et al., 2009). This is especially true for patients suffering from epilepsy, the most common and often debilitating symptom of patients with DLGGs. Gross total resection was found to be predictive of seizure freedom in two institutional studies (Englot et al., 2011; You et al., 2012). In a large series (N = 1509) by the FGN not only total, but also subtotal resections were found to be predictive of postoperative seizure control (Pallud et al., 2014).

Reoperation should be considered not only at recurrence, but right at the outset as a part of a long-term, multimodal treatment plan for a patient with DLGG. In the FGN series using multivariate analysis, subsequent surgical resection was an independent prognostic factor significantly associated with longer OS (Capelle et al., 2013). As with primary surgery the degree of resection influences OS (Ramakrishna et al., 2015). Reoperation should be considered in all recurrent tumours, including those located in eloquent areas as greater degree of resection can be achieved. In the series by Martino et al., total or subtotal resection was achieved in 73.7% of patients during the reoperation, despite involvement of functional areas (Martino et al., 2009). In this series, the median time between surgeries was 4.1 years. As the rate of anaplastic transformation found at reoperation is high (42–58%; see Schmidt et al., 2003; Martino et al., 2009; Ramakrishna et al., 2015) and because transformed tumours had longer time to second operation (49 compared to 22.5 months; Schmidt et al., 2003), it was proposed to overindicate early reintervention rather than perform late surgery after AT had already occurred (Martino et al., 2010).

Such a multistage surgical approach—beginning with initial function-guided resection, followed by a period of several years, and then a second surgery with optimization of EOR while preserving QoL—is possible, thanks to brain plasticity (Duffau, 2005; Duffau, 2014). Cerebral remapping can be induced by the first surgery itself, the postsurgical functional rehabilitation, and the slow-growing nature of DLGG (Duffau, 2011). Regular neurocognitive assessments and serial functional neuroimaging can provide helpful data for predicting EOR of a second or even third or fourth surgery. (Duffau, 2013; Duffau, 2014). Thus, the optimal onco-functional balance of

multiple surgeries can be found for each patient only if the relationship between the growth of DLGG and brain adaptation are taken into account (Duffau, 2012c).

However, a significant oncological benefit of surgery was demonstrated only when the resections were at least subtotal. Therefore, when the glioma is very diffuse, especially with wide invasion of the cortico-subcortical structures that cannot be removed due to limitations of cerebral plastic potential (Duffau and Taillandier, 2015) and/or with bihemispheric infiltration, one can predict that surgical removal will be only partial (Duffau, 2011; De Witt Hamer et al., 2013). In these cases, there is no indication to perform (re-) operations except in patients with intractable epilepsy because even partial resection may result in a relief of seizures. This is particularly true for tumours located within the insula or mesiotemporal structures. Rarely, planned subtotal resection maybe indicated for existing or anticipated radiation treatment-induced focal symptomatic mass effect or raised intracranial pressure. In cases with intractable epilepsy, chemotherapy (ChT) and/or radiation therapy (RT) should also be considered.

Although the vast majority of GLGGs present with seizures, increasingly more DLGGs are discovered when cranial imaging is ordered for reasons other than suspected glioma, the most common reasons being headaches and trauma (see also the section on incidence; Pallud et al., 2010b; Potts et al., 2012; Zhang et al., 2014). Incidental compared to symptomatic DLGGs are less likely to be located in eloquent areas of the brain, have lower preoperative volume, greater likelihood of total resection and longer OS (Pallud et al., 2010b; Potts et al., 2012; Zhang et al., 2014). Incidental discovery was found to be associated with a significant survival benefit ($P = 0.04$) (Pallud et al., 2010b). As EOR is a major predictor of OS, PFS, and AT, and because of gross total and supratotal resections are more likely achievable in incidental DLGGs, early and radical surgical resection has been proposed (Duffau, 2012b) and arguments are now being put forward for screening for DLGGs (Mandonnet et al., 2014).

Chemotherapy

The usefulness of chemotherapy for patients progressing after surgery and RT is well established (Soffietti et al., 2010). PCV (procarbazine, lomustine (also known as CCNU), vincristine) and temozolomide (TMZ) yield similar objective response rates on MRI (45–62%) and duration of response (10–24 months). However, the toxicity profile favours TMZ because of its better tolerability (especially reduced myelotoxicity) and resulting QoL (Soffietti et al., 1998; van den Bent et al., 1998; Quinn et al., 2003; van den Bent et al., 2003; van den Bent et al., 2012; Fisher et al., 2015). ChT may also result in improvement of QoL, especially for patients responding radiologically and some patients with stable disease, thanks to reduction of seizures and neurological deficits. (Quinn et al., 2003; Koekkoek et al., 2015).

ChT as initial treatment after surgery has also been investigated in DLGG patients with incomplete resection, persisting seizures, or rapid progression on follow-up MRIs (Hoang-Xuan et al., 2004). In most cases, a response was observed by objectively calculating the growth rate on repeated MRIs with at least minor, or even partial, shrinkage of the tumour (Ricard et al., 2007). The reduction in volume can occur with a latency of as much as 24–30 months and may persist once ChT has been terminated, even though this is not the case for the majority of patients. Most patients with seizures have clinical benefit, even in the absence of a radiological change (Koekkoek et al., 2015). Patients with oligodendroglial tumours are more likely to respond, but those with mixed or astrocytic tumours also may respond (Koekkoek et al., 2015). Although the vast majority of DLGGs exhibit some response to TMZ treatment, the response rate is significantly higher and the duration of response is longer and resulted in longer PFS and OS for patients with 1p/19q loss than for those with 1p/19q intact (Kaloshi et al., 2007; Kesari et al., 2009). Although patients with methylated MGMT promoter had a longer OS when treated with TMZ, protracted low doses of TMZ when compared with standard TMZ regimen have resulted in prolonged OS and PFS even in patients with unmethylated MGMT promoters (Kesari et al., 2009). However, this was associated with increase in TMZ-related toxicity.

Johnson et al. (2014) have described occurrence of multiple mutations in DLGG patients treated with TMZ. Six out of their ten patients treated with TMZ recurred as high-grade gliomas. However, the study cohort (N = 23) is not representative of DLGGs as a whole as only one case was an oligodendroglioma with all samples having either *ATRX* or p53 or both genes mutated and nearly three-quarters of the tumours recurred as high-grade gliomas. At present it is unclear whether this TMZ-induced hypermutation genotype found in this study is a phenomenon occurring in DLGGs across the board and it is even less clear whether the hypermutation genotype influences outcome in DLGGs. As such these findings should be regarded only as a laboratory finding (van den Bent, 2014).

Radiotherapy

Two phase III randomized trials have demonstrated no advantage for high versus low radiation doses and reported increased toxicity in higher doses (Karim et al., 1996; Shaw et al., 2002). Regarding the timing of radiotherapy (RT), the European Organization for Research and Treatment of Cancer (EORTC) 22845 phase III randomized trial has shown that early RT had no impact on OS, despite an increase in PFS (Karim et al., 2002; van den Bent et al., 2005). Although RT may be beneficial for seizure control, patients who had neuropsychological follow-up at a mean of 12 years and were free of tumour progression maintained their cognitive status if not irradiated, whereas patients who received RT experienced worsening of their attentional and executive functioning as well as their information-processing speed (Douw et al., 2009). It is nonetheless important to acknowledge some limitations in this study: the lack of baseline testing, the inherent selection bias of patients who received radiotherapy having more aggressive disease, and the use of out-dated techniques such as whole brain radiotherapy.

Results from RTOG 9802 trial (18–39-year-olds with less than total resection or biopsy or 40-year-olds and older with any extent of resection) presented at the 2014 meeting of the American Society of Clinical Oncology showed improved OS when upfront RT and PCV were given compared RT alone (13.3 vs. 7.8 years, $P = 0.03$; see Mehta et al., 2014). The upfront RT and PCV also conferred advantage over RT alone in PFS (10.4 vs. 4.0 years, $P = 0.002$). This study is frequently misinterpreted as demonstrating benefit of early use of radio- and chemotherapy. Instead, it demonstrates benefit of early use of chemotherapy. Because of its potentially delayed neurotoxicity and the equivalent results in terms of OS whatever the timing of treatment (early or late), RT is being increasingly reserved to high-risk patients with unresectable tumours or tumours that cannot be

reoperated and in cases of progression after ChT, but not as a first therapeutic option (Youland et al., 2013).

Multimodal and multistaged treatments strategies used at our institutions

In this section we present a brief summary of our current approach to the treatment of patients with DLGGs (Fig. 6.5). It is a constantly evolving process depending on our understanding of the condition, which in turn, is determined by published data and, inadvertently, by our personal experience.

In the first instance, a proper assessment of patient and the disease has to be carried out. This includes calculation of the tumour volume and its growth (at least two scans with at least two-month interval are needed) and extensive neuropsychological assessment. The imaging and clinical information is used to discuss the specific aims and risks of surgery as well as to select specific tools for intraoperative mapping that will help minimize the risks of permanent neurological deficit and maximize the extent of resection (Coello et al., 2013).

As alluded to before, the treatment plan should be developed together with the patient. He or she should be appropriately informed about the chronic and incurable nature of the disease and that multiple therapeutic interventions will be required in the coming years, the type and timing of which will depend on the evolution of each individual disease. It is important that immediate, medium-, and long-term benefits and risks of available interventions are discussed and, considering the relatively long OS, the possibility of new therapies also taken into account.

Early and maximal surgical resection is the first therapeutic option to consider in DLGG, as recommended by the European guidelines published in 2010 (Soffietti et al., 2010). The role of needle biopsy is limited to patients who do not want or who are not able to undergo resection for medical reasons. Biopsy can be mainly considered for diffuse lesions, such as gliomatosis, when a subtotal resection is not a priori possible.

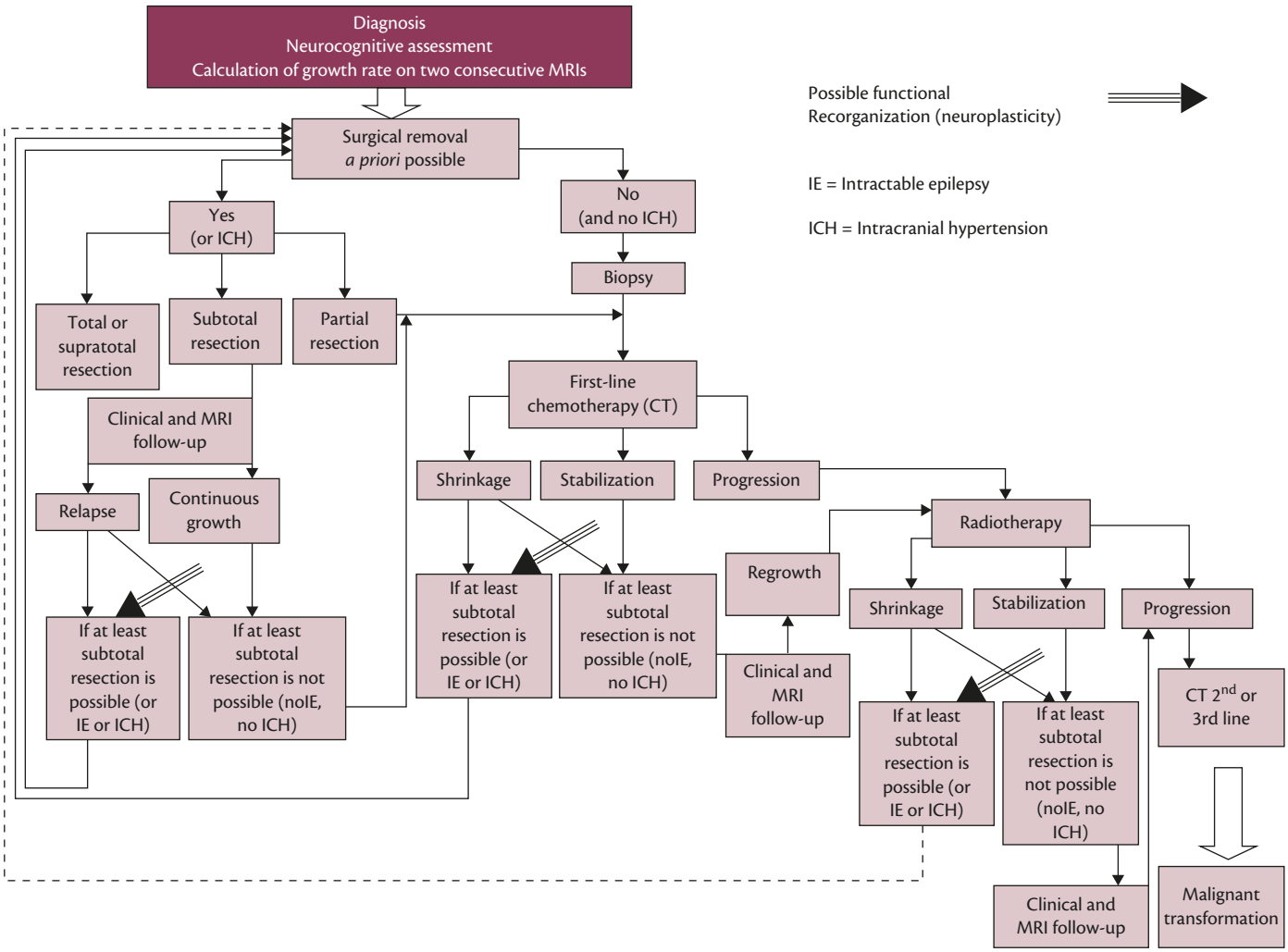

Fig. 6.5 Schematic depiction of the treatment algorithm used in our institutions.

(A) Reproduced with permission from Duffau, Hugues; Taillandier, Luc, New concepts in the management of diffuse low-grade glioma: Proposal of a multistage and individualized therapeutic approach, *Neuro-Oncology*, Volume 17, Issue 3, Copyright © 2015 Oxford University Press and the Society for NeuroOncology (SNO).

(B) Adapted from Reproduced with permission from Duffau H., Surgery of low-grade gliomas: towards a functional neurooncology, *Current Opinion in Oncology*, Volume 21, Issue 6, pp. 543–9. Copyright © 2009 Wolters Kluwer Health, Inc.

Once histological diagnosis has been established, certain clinical parameters need to be taken into account to decide whether adjuvant therapy should be instituted. The following clinical characteristics would make recommendation of adjuvant treatment more likely: aged more than 40, partial resection/residual more than 10 ml, astrocytoma histology, triple negative, or TERT mutation status, rapid growth, difficult to control seizures. The threshold for radiotherapy will probably be lower in the case of astrocytoma, TERT, and triple negative tumours, considering their poorer OS and the poor response to ChT. However, the significance of the molecular markers ought to be considered with a degree of caution, especially as they await wider validation.

REFERENCES

Ahmadi, R., Dictus, C., Hartmann, C., et al. (2009). Long-term outcome and survival of surgically treated supratentorial low-grade glioma in adult patients. *Acta Neurochir*, **151**(11), 1359–65.

Barker, F.G., Chang, S.M., Huhn, S.L., et al. (1997). Age and the risk of anaplasia in magnetic resonance-nonenhancing supratentorial cerebral tumors. *Cancer*, **80**(5), 936–41.

Bauman, G., Lote, K., Larson, D., et al. (1999). Pretreatment factors predict overall survival for patients with low-grade glioma: a recursive partitioning analysis. *Int J Radiat Oncol Biol Phys*, **45**(4), 923–9.

Beez, T., Boge, K., Wager, M., et al. (2013). Tolerance of awake surgery for glioma: a prospective European Low Grade Glioma Network multicenter study. *Acta Neurochir*, **155**(7), 1301–8.

Bello, L., Riva, M., Fava, E., et al. (2014). Tailoring neurophysiological strategies with clinical context enhances resection and safety and expands indications in gliomas involving motor pathways. *Neuro-Oncology*, **16**(8), 1110–28.

Benzagmout, M., Gatignol, P., & Duffau, H. (2007). Resection of World Health Organization Grade II gliomas involving Broca's area: methodological and functional considerations. *Neurosurgery*, **61**(4), 741–52– discussion 752–3.

Berger, M.S. Deliganis, A.V., Dobbins, J., & Keles, G.E. (1994). The effect of extent of resection on recurrence in patients with low grade cerebral hemisphere gliomas. *Cancer*, **74**(6), 1784–91.

Bisdas, S., Kirkpatrick, M., Giglio, P., Welsh, C., Spampinato, M.V., & Rumboldt, Z. (2009). Cerebral blood volume measurements by perfusion-weighted MR imaging in gliomas: ready for prime time in predicting short-term outcome and recurrent disease? *AJNR Am J Neuroradiol*, **30**(4), 681–8.

Bruner, J.M., Inouye, L., Fuller, G.N., & Langford, L.A. (1997). Diagnostic discrepancies and their clinical impact in a neuropathology referral practice. *Cancer*, **79**(4), 796–803.

Cancer Genome Atlas Research Network, Brat, D.J., Verhaak, R.G., et al. (2015). Comprehensive, integrative genomic analysis of diffuse lower-grade gliomas. *New Engl J Med*, **372**(26), 2481–98.

Capelle, L., Fontaine, D., Mandonnet, E., et al. (2013). Spontaneous and therapeutic prognostic factors in adult hemispheric World Health Organization Grade II gliomas: a series of 1097 cases. *J Neurosurg*, **118**(6), 1157–68.

Caseiras, G.B., Chheang, S., Babb, J., et al. (2010). Relative cerebral blood volume measurements of low-grade gliomas predict patient outcome in a multi-institution setting. *Eur J Radiol*, **73**(2), 215–20.

Cavaliere, R., Lopes, M.B.S., & Schiff, D. (2005). Low-grade gliomas: an update on pathology and therapy. *Lancet Neurol*, **4**(11), 760–70.

Chaichana, K.L., McGirt, M.J., Laterra, J., Olivi, A., & Quiñones-Hinojosa, A. (2010). Recurrence and malignant degeneration after resection of adult hemispheric low-grade gliomas. *J Neurosurg*, **112**(1), 10–17.

Chang, E.F., Smith, J.S., Chang, S.M., et al. (2008). Preoperative prognostic classification system for hemispheric low-grade gliomas in adults. *J Neurosurg*, **109**(5), 817–24.

Claus, E.B., Horlacher, A., Hsu, L., et al. (2005). Survival rates in patients with low-grade glioma after intraoperative magnetic resonance image guidance. *Cancer*, **103**(6), 1227–33.

Coello, A.F. Moritz-Gasser, S., Martino, J., Martinoni, M., Matsuda, R., & Duffau, H. (2013). Selection of intraoperative tasks for awake mapping based on relationships between tumor location and functional networks. *J Neurosurg*, **119**(6), 1380–94.

Collet, S., Valable, S., Constans, J.M., et al. (2015). [(18)F]-fluoro-l-thymidine PET and advanced MRI for preoperative grading of gliomas. *Neuroimage Clin*, **8**, 448–54.

Crocetti, E., Trama, A., Stiller, C., et al. (2012). Epidemiology of glial and non-glial brain tumours in Europe. *Eur J Cancer*, **48**(10), 1532–42.

Danchaivijitr, N., Waldman, A.D., Tozer, D.J., et al. (2008). Low-grade gliomas: do changes in rCBV measurements at longitudinal perfusion-weighted MR imaging predict malignant transformation? *Radiology*, **247**(1), 170–8.

De Witt Hamer, P.C., Robles, S.G., Zwinderman, A.H., Duffau, H., & Berger, M.S. (2012). Impact of intraoperative stimulation brain mapping on glioma surgery outcome: a meta-analysis. *J Clin Oncol*, **30**(20), 2559–65.

De Witt Hamer, P.C., Hendriks, E.J., Mandonnet, E., Barkhof, F., Zwinderman, A.H., & Duffau, H. (2013). Resection probability maps for quality assessment of glioma surgery without brain location bias. *PloS One*, **8**(9), p.e73353.

Desmurget, M., Bonnetblanc, F., & Duffau, H. (2007). Contrasting acute and slow-growing lesions: a new door to brain plasticity. *Brain*, **130**(Pt 4), 898–914.

Douw, L., Klein, M., Fagel, S.S., et al. (2009). Cognitive and radiological effects of radiotherapy in patients with low-grade glioma: long-term follow-up. *Lancet Neurol*, **8**(9), 810–18.

Duffau, H. & Capelle, L. (2004). Preferential brain locations of low-grade gliomas. *Cancer*, **100**(12), 2622–6.

Duffau, H. (2005). Lessons from brain mapping in surgery for low-grade glioma: insights into associations between tumour and brain plasticity. *Lancet Neurol*, **4**(8), 476–86.

Duffau, H. (2011). *Brain Mapping: From Neural Basis of Cognition to Surgical Applications*, 1st edition. Wien/New York: Springer.

Duffau, H. (2012a). The "frontal syndrome" revisited: lessons from electrostimulation mapping studies. *Cortex*, **48**, 120–31.

Duffau, H. (2012b). Awake surgery for incidental WHO grade II gliomas involving eloquent areas. *Acta Neurochir*, **154**(4), 575–84; discussion 584.

Duffau, H. (2012c). The challenge to remove diffuse low-grade gliomas while preserving brain functions. *Acta Neurochir*, **154**(4), 69–74.

Duffau, H. (2013). Cognitive assessment in glioma patients. *J Neurosurg*, **119**(5), 1348–9.

Duffau, H. (2014). The huge plastic potential of adult brain and the role of connectomics: new insights provided by serial mappings in glioma surgery. *Cortex*, **58**, 325–37.

Duffau, H. & Taillandier, L. (2015). New concepts in the management of diffuse low-grade glioma: proposal of a multistage and individualized therapeutic approach. *Neuro Oncol*, **17**(3), 332–42.

Duffau, H. (2015). Stimulation mapping of white matter tracts to study brain functional connectivity. *Nature Rev Neurol*, **11**(5), 255–65.

Duffau, H., Lopes, M., Arthuis, F., et al. (2005). Contribution of intraoperative electrical stimulations in surgery of low-grade

gliomas: a comparative study between two series without (1985–96) and with (1996–2003) functional mapping in the same institution. *J Neurol Neurosurg Psychiatry*, **76**(6), 845–51.

Duffau, H., Peggy Gatignol, S.T., Mandonnet, E., Capelle, L., & Taillandier, L. (2008). Intraoperative subcortical stimulation mapping of language pathways in a consecutive series of 115 patients with grade II glioma in the left dominant hemisphere. *J Neurosurg*, **109**(3), 461–71.

Duffau, H., Moritz-Gasser, S., & Gatignol, P. (2009). Functional outcome after language mapping for insular World Health Organization Grade II gliomas in the dominant hemisphere: experience with 24 patients. *Neurosurgical Focus*, **27**(2), E7.

Eckel-Passow, J.E., Lachance, D.H., Molinaro, A.M., et al. (2015). Glioma groups based on 1p/19q, IDH, and TERT promoter mutations in tumors. *N Engl J Med*, **372**(26), 2499–08.

Englot, D.J., Berger, M.S., Barbaro, N.M., & Chang, E.F. (2011). Predictors of seizure freedom after resection of supratentorial low-grade gliomas. *J Neurosurg,* **115**(2), 240–4.

Ewelt, C., Floeth, F.W., Felsberg, J., et al. (2011). Finding the anaplastic focus in diffuse gliomas: the value of Gd-DTPA enhanced MRI, FET-PET, and intraoperative, ALA-derived tissue fluorescence. *Clin Neurol Neurosurg*, **113**(7), 541–7.

Fisher, B.J., Hu, C., Macdonald, D.R., et al. (2015). Phase 2 study of temozolomide-based chemoradiation therapy for high-risk low-grade gliomas: preliminary results of Radiation Therapy Oncology Group 0424. *Int J Radiat Oncol Biol Phys*, **91**(3), 497–504.

Floeth, F.W., Sabel, M., Stoffels, G., et al. (2008). Prognostic value of 18F-fluoroethyl-L-tyrosine PET and MRI in small nonspecific incidental brain lesions. *J Nucl Med*, **49**(5), 730–7.

Gorovets, D., Kannan, K., Shen, R., et al. (2012). IDH mutation and neuroglial developmental features define clinically distinct subclasses of lower grade diffuse astrocytic glioma. *Clin Cancer Res*, **18**(9), 2490–501.

Gravendeel, L.A.M., Kouwenhoven, M.C., Gevaert, O., et al. (2009). Intrinsic gene expression profiles of gliomas are a better predictor of survival than histology. *Cancer Res*, **69**(23), 9065–72.

Guillevin, R., Menuel, C., Abud, L., et al. (2012). Proton MR spectroscopy in predicting the increase of perfusion MR imaging for WHO grade II gliomas. *J Magn Reson Imaging*, **35**(3), 543–50.

Herminghaus, S., Pilatus, U., Möller-Hartmann, W., et al. (2002). Increased choline levels coincide with enhanced proliferative activity of human neuroepithelial brain tumors. *NMR Biomed*, **15**(6), 385–92.

Hoang-Xuan, K., Capelle, L., Kujas, M., et al. (2004). Temozolomide as initial treatment for adults with low-grade oligodendrogliomas or oligoastrocytomas and correlation with chromosome 1p deletions. *J Clin Oncol*, **22**(15), 3133–8.

Hu, L.S., Eschbacher, J.M., Dueck, A.C., et al. (2012). Correlations between perfusion MR imaging cerebral blood volume, microvessel quantification, and clinical outcome using stereotactic analysis in recurrent high-grade glioma. *AJNR Am J Neuroradiol*, **33**(1), 69–76.

Ius, T., Isola, M., Budai, R., et al. (2012). Low-grade glioma surgery in eloquent areas: volumetric analysis of extent of resection and its impact on overall survival. A single-institution experience in 190 patients: clinical article. *J Neurosurg*, **117**(6), 1039–52.

Jakola, A.S., Myrmel, K.S., Kloster, R., et al. (2012). Comparison of a strategy favoring early surgical resection vs a strategy favoring watchful waiting in low-grade gliomas. *JAMA*, **308**(18), 1881–8.

Jakola, A.S., Unsgård, G., Myrmel, K.S., et al. (2013). Surgical strategy in grade II astrocytoma: a population-based analysis of survival and morbidity with a strategy of early resection as compared to watchful waiting. *Acta Neurochir*, **155**(12), 2227–35.

Johnson, B.E., Mazor, T., Hong, C., et al. (2014). Mutational analysis reveals the origin and therapy-driven evolution of recurrent glioma. *Science*, **343**(6167), 189–93.

Kaloshi, G., Benouaich-Amiel, A., Diakite, F., et al. (2007). Temozolomide for low-grade gliomas: predictive impact of 1p/19q loss on response and outcome. *Neurology*, **68**(21), 1831–6.

Karim, A.B., Maat, B., Hatlevoll, R., et al. (1996). A randomized trial on dose-response in radiation therapy of low-grade cerebral glioma: European Organization for Research and Treatment of Cancer (EORTC) Study 22844. *Int J Radiat Oncol Biol Phys*, **36**(3), 549–56.

Karim, A.B.M.F., Afra, D., Cornu, P., et al. (2002). Randomized trial on the efficacy of radiotherapy for cerebral low-grade glioma in the adult: European Organization for Research and Treatment of Cancer Study 22845 with the Medical Research Council study BRO4: an interim analysis. *Int J Radiat Oncol Biol Phys*, **52**(2), 316–24.

Keles, G.E., Lundin, D.A., Lamborn, K.R., Chang, E.F., Ojemann, G., & Berger, M.S. (2004). Intraoperative subcortical stimulation mapping for hemispherical perirolandic gliomas located within or adjacent to the descending motor pathways: evaluation of morbidity and assessment of functional outcome in 294 patients. *J Neurosurg*, **100**(3), 369–75.

Kesari, S., Schiff, D., Drappatz, J., et al. (2009). Phase II study of protracted daily temozolomide for low-grade gliomas in adults. *Clin Cancer Res*, **15**(1), 330–7.

Khalid, L., Carone, M., Dumrongpisutikul, N., et al. (2012). Imaging characteristics of oligodendrogliomas that predict grade. *AJNR Am J Neuroradiol*, **33**(5), 852–7.

Klein, M., Duffau, H., & De Witt Hamer, P.C. (2012). Cognition and resective surgery for diffuse infiltrative glioma: an overview. *J Neurooncol*, **108**(2), 309–18.

Koekkoek, J.A.F., Dirven, L., Heimans, J.J., et al. (2015). Seizure reduction in a low-grade glioma: more than a beneficial side effect of temozolomide. *J Neurol Neurosurg Psychiatry*, **86**(4), 366–73.

Kunz, M., Thon, N., Eigenbrod, S., et al. (2011). Hot spots in dynamic (18)FET-PET delineate malignant tumor parts within suspected WHO grade II gliomas. *Neurooncology*, **13**(3), 307–16.

la Fougère, C., Suchorska, B., Bartenstein, P., Kreth, F.W., & Tonn, J.C. (2011). Molecular imaging of gliomas with PET: opportunities and limitations. *Neuro Oncol*, **13**(8), 806–19.

Leighton, C., Fisher, B., Bauman, G., et al. (1997). Supratentorial low-grade glioma in adults: an analysis of prognostic factors and timing of radiation. *J Clin Oncol*, **15**(4), 1294–301.

Lote, K., Egeland, T., Hager, B., et al. (1997). Survival, prognostic factors, and therapeutic efficacy in low-grade glioma: a retrospective study in 379 patients. *J Clin Oncol*, **15**(9), 3129–40.

Louis, D.N., Ohgaki, H., Wiestler, O.D., et al. (eds.) (2007). *WHO Classification of Tumours of the Central Nervous System*. Lyon, France: IARC.

Louis, D.N., Perry, A., Reifenberger, G., et al. (eds.) (2016). *WHO Classification of Tumours of the Central Nervous System*. Lyon, France: IARC.

Lubrano, V., Draper, L., & Roux, F.-E. (2010). What makes surgical tumor resection feasible in Broca's area? Insights into intraoperative brain mapping. *Neurosurgery*, **66**(5), 868–75; discussion 875.

Mandonnet, E., de Witt Hamer, P., Pallud, J., Bauchet, L., Whittle, I., & Duffau, H. (2014). Silent diffuse low-grade glioma: toward screening and preventive treatment? *Cancer*, **120**(12), 1758–62.

Martino, J., Taillandier, L., Moritz-Gasser, S., Gatignol, P., & Duffau, H. (2009). Re-operation is a safe and effective therapeutic strategy in recurrent WHO grade II gliomas within eloquent areas. *Acta Neurochir*, **151**(5), 427–36; discussion 436.

Martino, J., Brogna, C., Robles, S.G., Vergani, F., & Duffau, H. (2010). Anatomic dissection of the inferior fronto-occipital fasciculus revisited in the lights of brain stimulation data. *Cortex*, **46**(5), 691–9.

McGirt, M.J., Chaichana, K.L., Attenello, F.J., et al. (2008). Extent of surgical resection is independently associated with survival in patients with hemispheric infiltrating low-grade gliomas. *Neurosurgery*, **63**(4), 700–7; author reply 707–8.

Mehta, M.P., Won, M., Shaw, E.G., et al. (2014). Mature survival data from RTOG 9802: a phase III study of radiation therapy (RT) with or without procarbazine, CCNU, and vincristine (PCV) for adult patients with high-risk low-grade glioma (LGG). *Int J Radiat Oncol Biol Phys*, **90**(1) Suppl, S37–8.

Ostrom, Q.T., Gittleman, H., Liao, P., et al. (2014). CBTRUS statistical report: primary brain and central nervous system tumors diagnosed in the United States in 2007–2011. *Neuro Oncol*, **16** Suppl 4, iv1–63.

Ottenhausen, M., Krieg, S.M., Meyer, B., & Ringel, F. (2015). Functional preoperative and intraoperative mapping and monitoring: increasing safety and efficacy in glioma surgery. *Neurosurg Focus*, **38**(1), E3.

Oz, G., Alger, J.R., Barker, P.B., et al. (2014). Clinical proton MR spectroscopy in central nervous system disorders. *Radiology*, **270**(3), 658–79.

Pallud, J., Capelle, L., & Mandonnet, E. (2010a). Comment on parameters of low-grade glioma as predictors. *Radiology*, **256**(3), 1014.

Pallud, J., Fontaine, D., Duffau, H., et al. (2010b). Natural history of incidental World Health Organization grade II gliomas. *Ann Neurol*, **68**(5), 727–33.

Pallud, J., Varlet, P., Devaux, B., et al. (2010c). Diffuse low-grade oligodendrogliomas extend beyond MRI-defined abnormalities. *Neurology*, **74**(21), 1724–31.

Pallud, J., Taillandier, L., Capelle, L., et al. (2012). Quantitative morphological magnetic resonance imaging follow-up of low-grade glioma: a plea for systematic measurement of growth rates. *Neurosurgery*, **71**(3), 729–39; discussion 739–40.

Pallud, J., Blonski, M., Mandonnet, E., et al. (2013). Velocity of tumor spontaneous expansion predicts long-term outcomes for diffuse low-grade gliomas. *Neuro Oncol*, **15**(5), 595–606.

Pallud, J., Audureau, E., Blonski, M., et al. (2014). Epileptic seizures in diffuse low-grade gliomas in adults. *Brain*, **137**(Pt 2), 449–62.

Pignatti, F., van den Bent, M., Curran, D., et al. (2002). Prognostic factors for survival in adult patients with cerebral low-grade glioma. *J Clin Oncol*, **20**(8), 2076–84.

Pope, W.B., Prins, R.M., Albert Thomas, M., et al. (2012). Non-invasive detection of 2-hydroxyglutarate and other metabolites in IDH1 mutant glioma patients using magnetic resonance spectroscopy. *J Neuro Oncol*, **107**(1), 197–205.

Potts, M.B., Smith, J.S., Molinaro, A.M., & Berger, M.S. (2012). Natural history and surgical management of incidentally discovered low-grade gliomas. *J Neurosurg*, **116**(2), 365–72.

Price, S.J. (2010). Advances in imaging low-grade gliomas. *Adv Tech Stand Neurosurg*, **35**, 1–34.

Quinn, J.A., Reardon, D.A., Friedman, A.H., et al. (2003). Phase II trial of temozolomide in patients with progressive low-grade glioma. *J Clin Oncol*, **21**(4), 646–51.

Racine, C.A., Li, J., Molinaro, A.M., Butowski, N., & Berger, M.S. (2015). Neurocognitive function in newly diagnosed low-grade glioma patients undergoing surgical resection with awake mapping techniques. *Neurosurgery*, **77**(3), 371–9.

Ramakrishna, R., Hebb, A., Barber, J., Rostomily, R., & Silbergeld, D. (2015). Outcomes in reoperated low-grade gliomas. *Neurosurgery*, **77**(2), 175–84.

Ricard, D., Kaloshi, G., Amiel-Benouaich, A., et al. (2007). Dynamic history of low-grade gliomas before and after temozolomide treatment. *Ann Neurol*, **61**(5), 484–90.

Sanai, N. & Berger, M.S. (2008). Glioma extent of resection and its impact on patient outcome. *Neurosurgery*, **62**(4), 753–64; discussion 264–6.

Schmidt, M.H., Berger, M.S., Lamborn, K.R., et al. (2003). Repeated operations for infiltrative low-grade gliomas without intervening therapy. *J Neurosurg*, **98**(6), 1165–9.

Schomas, D.A., Laack, N.N., Rao, R.D., et al. (2009). Intracranial low-grade gliomas in adults: 30-year experience with long-term follow-up at Mayo Clinic. *Neuro Oncol*, **11**(4), 437–45.

Server, A., Kulle, B., Gadmar, Ø.B., Josefsen, R., Kumar, T., & Nakstad PH (2011). Measurements of diagnostic examination performance using quantitative apparent diffusion coefficient and proton MR spectroscopic imaging in the preoperative evaluation of tumor grade in cerebral gliomas. *Eur J Radiol*, **80**(2), 462–70.

Shaw, E., Arusell, R., Scheithauer, B., et al. (2002). Prospective randomized trial of low- versus high-dose radiation therapy in adults with supratentorial low-grade glioma: initial report of a North Central Cancer Treatment Group/Radiation Therapy Oncology Group/Eastern Cooperative Oncology Group study. *J Clin Oncol*, **20**(9), 2267–76.

Smith, J.S., Chang, E.F., Lamborn, K.R., et al. (2008). Role of extent of resection in the long-term outcome of low-grade hemispheric gliomas. *J Clin Oncol*, **26**(8), 1338–45.

Soffietti, R., Rudà, R., Bradac, G.B., & Schiffer, D. (1998). PCV chemotherapy for recurrent oligodendrogliomas and oligoastrocytomas. *Neurosurgery*, **43**(5), 1066–73.

Soffietti, R., Baumert, B.G., Bello, L., et al. (2010). Guidelines on management of low-grade gliomas: report of an EFNS-EANO Task Force. *Eur J Neurol*, **17**(9), 1124–33.

Tate, M.C., Herbet, G., Moritz-Gasser, S., Tate, J.E., & Duffau, H. (2014). Probabilistic map of critical functional regions of the human cerebral cortex: Broca's area revisited. *Brain*, **137**(Pt 10), 2773–82.

Tate, M.C., Herbet, G., Moritz-Gasser, S., Tate, J.E., & Duffau, H. (2015). Reply: probabilistic map of language regions: challenge and implication. *Brain*, **138**(Pt 3), p.e338.

Teixidor, P., Gatignol, P., Leroy, M., Masuet-Aumatell, C., Capelle, L., & Duffau, H. (2007). Assessment of verbal working memory before and after surgery for low-grade glioma. *J Neurooncol*, **81**(3), 305–13.

Thon, N., Kunz, M., Lemke, L., et al. (2015). Dynamic 18F-FET PET in suspected WHO grade II gliomas defines distinct biological subgroups with different clinical courses. *Int J Cancer*, **136**(9), 2132–45.

van den Bent, M.J., Kros, J.M., Heimans, J.J., et al. (1998). Response rate and prognostic factors of recurrent oligodendroglioma treated with procarbazine, CCNU, and vincristine chemotherapy. Dutch Neuro-oncology Group. *Neurology*, **51**(4), 1140–5.

van den Bent, M.J., Taphoorn, M.J., Brandes, A.A., et al. (2003). Phase II study of first-line chemotherapy with temozolomide in recurrent oligodendroglial tumors: the European Organization for Research and Treatment of Cancer Brain Tumor Group Study 26971. *J Clin Oncol*, **21**(13), 2525–8.

van den Bent, M.J., Afra, D., de Witte, O., et al. (2005). Long-term efficacy of early versus delayed radiotherapy for low-grade astrocytoma and oligodendroglioma in adults: the EORTC 22845 randomised trial. *Lancet*, **366**(9490), 985–90.

van den Bent, M.J., Snijders, T.J., & Bromberg, J.E.C. (2012). Current treatment of low-grade gliomas. *Memo*, **5**(3), 223–7.

van den Bent, M.J. (2014). Practice changing mature results of RTOG study 9802: another positive PCV trial makes adjuvant

chemotherapy part of standard of care in low-grade glioma. *Neuro Oncol*, **16**(12), 1570–4.
van Loon, E.M.P., Heijenbrok-Kal, M.H., van Loon, W.S., et al. (2015). Assessment methods and prevalence of cognitive dysfunction in patients with low-grade glioma: a systematic review. *J Rehabil Med*, **47**(6), 481–8.
Vogelstein, B. & Kinzler, K.W. (2004). Cancer genes and the pathways they control. *Nat Med*, **10**(8), 789–99.
White, M.L., Zhang, Y., Kirby, P., & Ryken, T.C. (2005). Can tumor contrast enhancement be used as a criterion for differentiating tumor grades of oligodendrogliomas? *AJNR Am J Neuroradiol*, **26**(4), 784–90.
Yeh, S.-A., Ho, J.T., Lui, C.C., Huang, Y.J., Hsiung, C.Y., & Huang, E.Y. (2005). Treatment outcomes and prognostic factors in patients with supratentorial low-grade gliomas. *Br J Radiol*, **78**(927), 230–5.
Yordanova, Y.N., Moritz-Gasser, S., & Duffau, H. (2011). Awake surgery for WHO Grade II gliomas within 'noneloquent' areas in the left dominant hemisphere: toward a 'supratotal' resection. *J Neurosurg*, **115**(2), 232–9.
You, G., Sha, Z-.Y., Yan, W., et al. (2012). Seizure characteristics and outcomes in 508 Chinese adult patients undergoing primary resection of low-grade gliomas: a clinicopathological study. *Neuro Oncol*, **14**(2), 230–41.
Youland, R.S., Schomas, D.A., Brown, P.D., et al. (2013). Changes in presentation, treatment, and outcomes of adult low-grade gliomas over the past fifty years. *Neuro Oncol*, **15**(8), 1102–10.
Zhang, Z.-Y., Ka-Yin Chan, A., Ng, H-.K., et al. (2014). Surgically treated incidentally discovered low-grade gliomas are mostly IDH mutated and 1p19q co-deleted with favorable prognosis. *Int J Clin Exp Pathol*, **7**(12), 8627–36.
Zou, Q.-G., Xu, H.B., Liu, F., Guo, W., Kong, X.C., & Wu, Y. (2011). In the assessment of supratentorial glioma grade: the combined role of multivoxel proton MR spectroscopy and diffusion tensor imaging. *Clin Radiol*, **66**(10), 953–60.

RELATED LINKS TO EBRAIN

Assessment of the Patient with a Brain Tumour. https://learning.ebrain.net/course/view.php?id=1247
Clinical Presentation of Patients with Brain Tumours. https://learning.ebrain.net/course/view.php?id=1249
CNS Tumours: Basic Histology WHO Grading System. https://learning.ebrain.net/course/view.php?id=1250
Diagnostic Imaging in Brain Tumours. https://learning.ebrain.net/course/view.php?id=931
Histological and Molecular Diagnostics of Brain Tumours. https://learning.ebrain.net/course/view.php?id=1390
Histology and Molecular Pathology of IDH Wild Type Gliomas. https://learning.ebrain.net/course/view.php?id=1393
Histology and Molecular Pathology of LGG incl Pilocytic Astrocytoma and Glioneuronal Tumours. https://learning.ebrain.net/course/view.php?id=1394
Molecular and Cell Biology in CNS Tumours. https://learning.ebrain.net/course/view.php?id=510
Molecular Pathology and Histology of IDH Mutant Gliomas. https://learning.ebrain.net/course/view.php?id=1392
Non-surgical management of Low Grade Gliomas. https://learning.ebrain.net/course/view.php?id=446
Surgical Management of Low Grade Glioma. https://learning.ebrain.net/course/view.php?id=585

7

High-grade gliomas and molecular biology of neurosurgical oncology

Stephen J. Price, Harry Bulstrode, and Richard Mair

The molecular basis of neurosurgical oncology

Normal human cells develop into cancer cells through a stepwise accumulation of genomic and epigenomic alterations. These alterations, in the context of a permissive tissue microenvironment, cooperate to drive deregulated cell growth, proliferation, and survival, leading to tumour development. Recent conceptual developments frame tumours not as balls of cells proliferating uncontrollably, but rather as complex tissues in their own right: tumour initiation, maintenance, and progression then represent complex emergent products of deregulated mechanisms of tissue maintenance and renewal.

Fundamentals of cancer genomics

Somatic mutation

Over the past decade it has become technically feasible to understand the cancer genomic landscape. This has largely been enabled by the development of, and refinements made to, next-generation sequencing (reviewed in Goodwin et al., 2016). Tumours contain an average of 33–66 mutations that affect protein production, but this figure varies depending upon the cancer aetiology and the age of the patient at cancer onset (Vogelstein et al., 2013). Brain tumours contain relatively few mutations when compared to tumours arising in proliferating tissues in response to mutagens. For example, glioblastomas (GBM) average 35 non-synonymous mutations (i.e. mutations that lead to amino acid sequence change) per tumour, compared to an average 135 mutations in melanomas arising in response to UV radiation and average 163 mutations in small cell lung cancers resulting from cigarette smoke exposure (Meyerson et al., 2010). Mutations that confer selective growth advantage and are encountered repeatedly across examples of a given tumour type are termed 'driver' mutations. Driver mutations can be subdivided into *oncogenes*, whose mutational product drives tumour generation (e.g. KRAS), and *tumour suppressor genes*, by whose loss-of-function tumours progress (e.g. NF2). A typical GBM cell will have 2–5 driver mutations. Oncogenes and tumour suppressors exhibit markedly distinct patterns of mutation in gliomas (Vogelstein et al., 2013). Oncogenes typically exhibit missense point mutations at key locations: these single base substitutions in the DNA code introduce a specific functional change in the amino acid sequence, resulting in initiation of oncogene activity. Specific mutations at specific locations are necessary to achieve this effect, but mutation of a single allele is sufficient to drive cancer formation. Alternatively, chromosomal rearrangements can result in the expression of fusion proteins with oncogenic activity. By contrast, tumour suppressors are subject to inactivation by any mutation resulting in the incidence of a stop codon within the reading frame, including insertions, deletions, and even single base substitutions occurring throughout the coding sequence. Typically, loss of both tumour suppressor alleles is necessary for cancer development, either by somatic mutation of both alleles, or else somatic mutation of a single allele in the context of a germline mutation in the other—for example, in phakomatoses such as neurofibromatosis and von-Hippel Lindau disease.

Although individual tumour cell clones typically demonstrate just a handful of driver mutations, genetic instability means that a wide range of additional driver mutations exist at low frequency in subclones of a few cells within the tumour bulk. Therefore, targeted treatments directed at specific mutations often demonstrate a dramatic initial response, followed by treatment failure as a pre-existing resistant subclone grows up to replace the lost cells. Tumours also possess many mutations that do not offer a growth advantage. These 'passenger' mutations represent an accidental payload, which varies between and within tumours, and can be used to map tumour evolution.

Chromosomal alteration

Chromosomal changes in cancer cells are common with aneuploidy consistently observed in cancers from a variety of origins. Copy number variation is prevalent in cancer cells with amplification of gene expression, through simply the increased number of gene copies per cell; for example, epidermal growth factor receptor (EGFR), occurring alongside deletions of genomic regions, where tumour suppressor genes are lost (e.g. phosphatase and tensin homolog (PTEN), resulting in a decrease or absence of their expression (Cancer Genome Atlas Research, 2008)). A non-balanced translocation affecting chromosome arms 1p and 19q with subsequent loss of one of the derivative chromosomes is the molecular classifier for oligodendroglioma and of predictive significance (Cairncross et al., 1998). This is described in more detail later.

Chromosomes can also undergo fusion events whereby breakage of DNA and subsequent mal-reconstitution lead to the generation of an oncogenic target, for example, C11orf95-RELA in supratentorial ependymoma (Parker et al., 2014). These rearrangements can be interchromosomal, intrachromosomal, or intragenic, and lead to aligning disparate regions of the genome erroneously.

Capabilities of a cancer

Mutagenesis has downstream effects on 12 intracellular signalling pathways, which enable cancer cells to develop a neoplastic phenotype. This occurs through the development of eight 'hallmark' capabilities, famously described by Hanahan and Weinberg (Hanahan and Weinberg, 2011) and relate back to the three fundamental cellular processes of cell fate, cell survival, and genome maintenance.

Sustained signalling

Cells respond to their external environment through the development of signalling pathways. Cancer subverts these pathways through several mechanisms such as the upregulation of receptor proteins, autocrine proliferative signalling, constitutive receptor activation (i.e. activation even if no ligand is present, e.g. EGFRvIII amplification in GBM) and disruption of intracellular negative feedback loops (PTEN loss).

Evading growth suppressors

Normal cell cycle regulatory proteins are commonly mutated in cancer. Uncontrolled flux through the cell cycle occurs following mutation of retinoblastoma (Rb) via the loss of intracellular transduction of extracellular inhibitory signals and through mutation of TP53, which detects intracellular stress and induces apoptosis accordingly.

Evading contact inhibition

Cell contact inhibition is often bypassed in cancer. Mutation of NF2 affects the production of merlin (schwannomin), a cytoskeletal protein that limits mitogenic signalling through intracellular tyrosine kinase binding. Thus loss of this inhibition results in cellular proliferation under conditions in which it would usually be suppressed (Okada et al., 2005). Over half of meningiomas contain NF2 tumour suppressor gene mutations. Through clustering of this and other somatic mutations in meningioma, the mutation of NF2 and deletion of chromosome 22 correlated with a hemispheric origin of the meningioma (Arnold et al., 2013).

Genomic instability, mutation, and avoiding cell death

TP53 induces apoptosis following DNA strand break and chromosomal injury (e.g. following cell stress or during cell division). Loss of p53 protein thus enables the cell to evade programmed cell death and continue to proliferate. Concomitantly cells with mutations in TP53 thus have an ongoing increased rate of mutation due to the loss of this checkpoint. Mismatch repair gene mutation, occurring following temozolomide treatment in LGG, has also been shown to lead to the development of a hypermutated phenotype (Turcan et al., 2012). Interestingly, the loss of apoptosis within cells does not always lead to continued cell proliferation. Cells often become non-viable and although unable to undergo apoptosis, they undergo necrosis. This is potentially protumourigenic as it induces a pro-inflammatory microenvironment that stimulates cytokine secretion that induces angiogenesis and promotes tumour cell invasion and proliferation (Grivennikov et al., 2010).

Enabling replicative immortality

Normal cells can undertake only a limited number of cell divisions: the loss of genetic material at the ends of chromosomes inherent to the division process results in replicative senescence after ~50 divisions, the Hayflick limit. Various mutations associated with elongation and maintenance of telomeric DNA exist within neuro-oncology. Two common mutations to affect this process that are commonly mutated within glioma are ATRX and TERT. These are both described later as molecular biomarkers.

Inducing angiogenesis

Angiogenesis is a key factor in the instigation, sustenance, and progression of a variety of neoplastic processes both local to and distant to the primary tumour, it has been shown to be an independent predictor of poor prognosis in GBM (Jain et al., 2007). GBM has been shown to display the highest degree of vascular proliferation and endothelial cell hyperplasia of any solid tumour (Folkman, 1972).

Gliomas need to develop a blood supply to promote tumour growth. The initial phase involves vascular co-option where the tumour takes over normal brain vessels. The next phase involves angiogenesis where new vessels start sprouting. vascular endothelial growth factor (VEGF) is a key driver of tumour angiogenesis, and the VEGF receptor inhibitor bevacizumab has a potent but short-lived effect on tumour growth although it may also promote tumour invasion.

Deregulating cellular energetics

The development of abnormal cellular metabolism plays a fundamental role in tumour development as it fuels the energy requirements of upregulated cellular proliferation as well as generating the biosynthetic precursors required for rapid cell turnover (Vander Heiden et al., 2009). Isocitrate dehydrogenase is an intracellular enzyme that catalyses the oxidative decarboxylation of isocitrate forming a-ketoglutarate and CO_2. It has three isoforms: IDH1, which is cytosolic as well as IDH2 and 3 which are located within the mitochondria. Mutation of either IDH1 or IDH2 alters the enzymatic function, through altered substrate specificity, and thus leads to the erroneous production of 2-hydroxyglutaric acid (Dang et al., 2009). This 'oncometabolite' affects dioxygenase activity within the cell. Ten-eleven translocation (TET) enzyme (amongst others) are inhibited resulting in the hypermethylated phenotype identified in low-grade glioma (glioma CpG island methylated phenotype or G-CIMP) and leads to tumour formation (Turcan et al., 2012). Finally, cancer cell to stromal cell metabolic symbiosis has been demonstrated whereby lactate generating stromal cells 'feed' lactate utilizing cancer cells in an analogous fashion to the glial and neuronal relationship within the central nervous system (Feron, 2009).

Tumour-promoting inflammation

As discussed earlier, genomic instability, in isolation is unlikely to be sufficient for tumour maintenance. A supportive microenvironment is also required to drive tumour progression. The complex interplay between a tumour and the immune system results in the expression of both suppressive cytokines as well as chemokines (Qian and Pollard, 2010). Studies within GBM have suggested a correlation between GBM

subtype and immune characteristics. The correlation between immune cell infiltration and differing underlying mutational landscapes alongside the ability of prominent cytokines (e.g. TGF-b) to regulate proliferation, migration, and tumorigenicity in mesenchymal GBM further defines the role of the immune microenvironment in GBM.

Epigenomics

Epigenomics refers to DNA modifications that result in gene expression changes that do not alter the base pair sequence. For example, methylation of the MGMT promoter is an epigenomic modification resulting in reduced expression of this DNA repair gene, thereby conferring increased sensitivity of GBM to alkylating chemotherapy. In practice, tumourigenesis involves a process of genomic and epigenomic evolution converging on traits which confer selective advantage and hence malignancy, for example unconstrained cell division. Genomic mutations can also drive epigenomic progression: unbiased genome-sequencing based approaches have repeatedly and unexpectedly identified examples of driver mutations in genes concerned with cellular regulation of gene expression including histone proteins responsible for DNA packaging in paediatric GBM (H3K27M and H3G34R/V mutations) (Wu et al., 2012), and IDH mutations driving production of the oncometabolite 2-hydroxyglutarate which inhibits DNA methylation turnover in diffuse glioma (Dang et al., 2009).

Glioma stem cells

Stem cells are defined by their ability to self-renew: the ability to divide indefinitely giving rise to more cells of the same type, multipotency: the capacity to differentiate into multiple lineages, for example, glia and neurons and their ability to generate tumours *in vivo*.

GBM and medulloblastoma are two prototypical examples of tumours with a stem cell fraction that can be isolated and transplanted into mice to form tumours with high efficiency, while the bulk of the tumour cell population does not have this property. Cancer stem cells and bulk tumour progeny share the same mutations, so it follows that these mutations are necessary but not sufficient to specify stem cell identity, with gene expression and genome configuration (epigenomics) as well as microenvironment also playing key roles. In practice, the cancer stem cells found in GBM consistently demonstrate gene expression patterns associated with neural stem and progenitor populations in the embryonic brain. This is perhaps to be expected given that these cell programmes have evolved to support rapid proliferation in the specific central nervous system (CNS) niche, and given that the cell-of-origin for these stem cells is likely to be a CNS progenitor, or a cell derived from one. Seminal experiments demonstrated that surface markers of neural stem cells including CD133 and CD15/SSEA-1 also select for brain tumour stem cells (Singh et al., 2004). These brain tumour stem cells may be selectively resistant to radiotherapy and chemotherapy (Bao et al., 2006).

Stem cells in medulloblastomas

Medulloblastoma provides an excellent example of how co-option of neural stem cell pathways may drive brain tumour stem cell proliferation. Distinct medulloblastoma subgroups demonstrate gene mutations in either the sonic hedgehog pathway, or the Wnt/B-catenin pathway. These pathways demonstrate a degree of functional redundancy, converging to drive tumour stem cell self-renewal proliferation and medulloblastoma histology. Key differences in biology and prognosis are reflected in the incorporation of molecular subtyping in the World Health Organization (WHO) 2016 CNS classification (Louis et al., 2016). Medulloblastoma, WNT-activated (typically exhibiting CTNNB1 mutations) and medulloblastoma, Shh-activated (typically PTCH1, SMO, SUFU mutations), are recognized alongside Group 3 and Group 4 medulloblastoma, less well characterized, and conferring generally poorer prognosis. Medulloblastoma classification typifies a new generation of molecular tumour classification systems, which promise to capture the association of mutation and gene expression profiles, grounded in mechanistic understanding. While the classification described here is based on gene expression, identification of concurrent genomic mutation within subgroups further delineates prognostic groups (e.g. TP53 mutation within the SHH group predicts a poorer prognosis). Likewise, in meningioma, SMO mutation resulting in activation of the Sonic Hedgehog pathway has been associated with tumours arising from the anterior skull base. Mutations within meningioma have also been correlated to histological subtype. For other tumours, including GBM, expression-based classification systems exist. The Cancer Genome Atlas classification (summarized in **Table 7.1**) is perhaps the best-known molecular classification system of glioblastoma to date, but is by no means definitive (Verhaak et al., 2010). The proneural group showed improved survival, but interestingly showed no survival advantage with chemoradiotherapy vs. radiotherapy alone. Further work is underway to understand the significance of this classification for individual patients. Analysis of trials of antiangiogenic drugs suggest that this proneural group may gain benefit from antiangiogenic therapy (Sandmann et al., 2015).

Table 7.1 Cancer Genome Atlas classification of GBM subtypes

Subtype	Characteristic mutations	Expression signature
Proneural	*TP53, PDGFRA, PI3K, IDH1*	*OLIG2, NKX2-2*
Neural	*TP53, EGFR*	*MBP, SYT1*
Classical	*EGFR, Chr10, PDGFRA*	*EGFR, AKT2*
Mesenchymal	*NFkB, NF1*	*CD44, YKL40*

Reprinted from *Cancer Cell*, Vol 17, issue 1, Roel G.W. Verhaak et al., Integrated Genomic Analysis Identifies Clinically Relevant Subtypes of Glioblastoma Characterized by Abnormalities in PDGFRA, IDH1, EGFR, and NF1, pp. 98–110, Copyright (2010), with permission from Elsevier.

High-grade gliomas

The term high-grade glioma (HGG) encompasses several histological entities that are considered by the WHO Classification as WHO Grade III and IV tumours. They have traditionally been considered as having similar behaviour and had been treated in a similar manner. Recent advances in our understanding of tumour biology, however, have led to the identification of molecular markers that are now central to the classification of these tumours. This has led to us thinking of these tumours as molecularly distinct subtypes that will behave differently and should be managed in a particular way.

Classification of high-grade gliomas

High-grade gliomas arise from supporting glial cells in the brain. The predominant cell type determines the pathological classification.

Tumours are graded on appearances seen on light microscopy, according to the WHO grading system (Grade I to IV). HGGs comprise of WHO grade III (anaplastic astrocytoma and anaplastic oligoastrocytoma) and IV tumours (glioblastoma, glioblastoma with oligodendrocyte component, and gliosarcoma). The 2016 version of the WHO grading system removed the mixed gliomas (i.e. oligoastrocytomas)—these are now classified according to their molecular classification.

Histologically, grade III tumours are diffusely infiltrating gliomas with focal or dispersed anaplasia and a marked proliferative potential with increased cellularity, distinct nuclear atypia, and high mitotic activity. Grade IV tumours show cellular polymorphism, nuclear atypia, brisk mitotic activity, vascular thrombosis, microvascular proliferation, and necrosis. Examples are shown in **Figure 7.1**.

Tumours are graded on the most malignant part of the tumour. For that reason, adequate sampling to determine the proper grade is essential—especially in biopsy procedures.

Epidemiology

High-grade gliomas are the commonest primary intrinsic brain tumour accounting for 85% of all newly diagnosed primary malignant brain tumours. The incidence of these tumours is often reported as approximately 5/100 000 person-years in Europe and North America. Recent data on glioblastomas from the UK Tumour Registries found a similar overall national age standardized incidence of 4.64/100 000/year, with an average of over 2100 cases per year (Brodbelt et al., 2015). These figures are likely to underestimate the true numbers as a fifth are not admitted to hospital (Pobereskin and Chadduck, 2000).

Of all high-grade gliomas, glioblastomas account for 60–70%, anaplastic astrocytomas for 10–15%, anaplastic oligodendrogliomas for about 10%, while anaplastic ependymoma and anaplastic ganglioglioma make up the rest.

There has been a recent increase in incidence of HGGs in the Western world, particularly in the elderly population. This probably reflects the easy availability of improved diagnostic imaging (Wen and Kesari, 2008). Incidence of glioblastomas increases with age, with a peak between 65 and 75 years of age (Brodbelt et al., 2015). Men have an incidence 1.66 that of women (Brodbelt et al., 2015).

Aetiology of high-grade gliomas

In most cases, no causative factors can be attributed. However, exposure to ionizing radiation, such as from treatment of previous cancer is an established risk factor (Walter et al., 1998). Many other factors have been studied including head injury, foods with N-nitrose compounds, electromagnetic fields, smoking, and most recently usage of mobile phones, none of these have been shown to

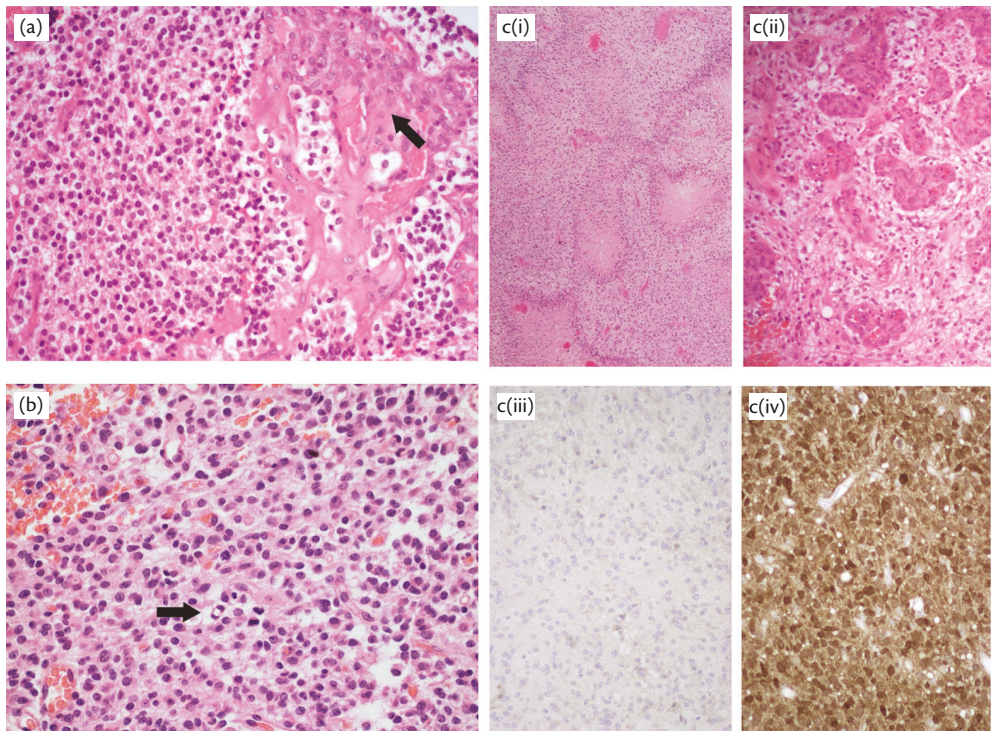

Fig. 7.1 (A) Anaplastic oligodendroglioma (grade III): round nuclei with perinuclear haloes indicate oligodendroglial lineage; microvascular proliferation (arrow), necrosis, and brisk mitotic activity are high-grade features. This histological diagnosis is strongly associated with IDH mutation and 1p/19q codeletion. (B) Anaplastic astrocytoma (grade III): high cellularity, nuclear pleomorphism, and the presence of mitotic figures (arrow) are high-grade features. Necrosis and microvascular proliferation, present in glioblastoma grade IV, are absent. (C) Glioblastoma (Grade IV) (i) A hypercellular band of tumour cells highlights the borders of the necrotic tumour in what is known as palisading (or pseudopalisading) necrosis. This is a classic histological feature of glioblastoma. (ii) Microvascular proliferation, forming these glomeruloid structures, is another classic histological feature of glioblastoma. Immunostaining for the IDH1 R132H mutation distinguishes IDH wild-type (iii) and IDH mutant (iv) tumours.
Courtesy of Dr Kieren Allinson, Department of Pathology, Addenbrooke's Hospital, Cambridge.

be a risk factor for the development of HGG (Inskip et al., 2001; Kleinerman et al., 2005; Holick et al., 2007).

There does appear to be some genetic risk to developing gliomas. The risk of an individual with a family member with a glioblastoma developing a GBM appears to be double that of people without a family history (Schwartzbaum et al., 2006). Approximately 5% of patients with HGG have a family history of gliomas (Bondy et al., 1994). Some of these are familial and associated with genetic syndromes such as neurofibromatosis types 1 and 2, Li-Fraumeni syndrome, and Turcot's syndrome. Studies have also shown links between DNA repair genes and tumour aggressiveness (Bhowmick et al., 2004; Okcu et al., 2004; Simon et al., 2006). Mutations of the telomere shelterin gene complex, in particular POT1, have been recently associated with these familial glioma syndromes (Bainbridge et al., 2015). At present there are no clear guidelines on screening for familial gliomas.

Role of cytomegalovirus in glioblastoma aetiology

There has been much interest in the possibility that viral infections are involved in the multistep development of gliomas. When one study found cytomegalovirus (CMV) gene products in 100% of glioblastoma samples but failed to identify it in normal tissues (Cobbs et al., 2002), there was great interest that this could be an important cause of gliomas. But other studies failed to replicate these results (Dey et al., 2015). A randomized, double-blind trial of valganciclovir, an anti-CMV therapy used in addition to chemoradiotherapy (the VIGAS Study), failed to show any survival benefit (Stragliotto et al., 2013). A subsequent letter to the *New England Journal of Medicine* by the same group, however, created much publicity (Stragliotto et al., 2013). They reported that in a retrospective analysis of a subset of their patients treated with valganciclovir both as part of the trial and on compassionate grounds had an improved survival compared to contemporary controls. This study has several flaws, and currently the consensus statement concluded that current literature supports an oncomodulatory role for CMV in malignant gliomas, but future studies are needed to focus on determining the role of CMV as a glioma-initiating event (Dziurzynski et al., 2012).

Atopic diseases may be protective

One unusual finding is that atopic diseases (e.g. asthma, eczema, or allergies) are 'protective' factors for developing gliomas. Patients with gliomas have fewer atopic symptoms compared to control subjects. As atopy may be a marker of immune dysfunction it may indicate a role for immunologic factors in glioma causation.

Pathology and pathogenesis of high-grade glioma

Molecular biology of high-grade gliomas

The introduction of the World Health Organization (WHO) Classification of Tumours of the Central Nervous System has resulted in broad changes for the categorization of high-grade glioma (Louis et al., 2016). The definition of molecular subgroups has grossly divided glial-origin tumours into isocitrate dehydrogenase (IDH) wild-type, IDH mutated, and IDH not specified (i.e. where IDH mutation has not been sought; see Louis et al., 2016). Within this classification (and with the inclusion of 1p 19q chromosomal codeletion for oligodendroglioma) diffuse glioma, oligodendroglioma, anaplastic astrocytoma, anaplastic oligodendroglioma, and glioblastoma have all now been defined.

Mutations and intratumoural heterogeneity in glioblastomas

Mutations that do occur tend to converge upon three intracellular signalling pathways: Specifically, PI3K, TP53 and Rb (Cancer Genome Atlas Research, 2008). Typical 'hits' include activating mutations of the growth signalling receptors *EGFR, PDGFR*, and *MET*, and their downstream targets *PI3K, AKT, MTOR*, and *RAS*. Equally tumour suppressors responsible for regulating these cascades are subject to loss-of-function mutations in GBM—these include *PTEN, NF-1, RB1*, and *TP53*. These pathways are summarized in **Figure 7.2**.

Despite this convergence, inter and intratumoural heterogeneity is seen in GBM and has been proposed as a major source of treatment failure and disease relapse. Gene expression-based classification systems exist for GBM, but have so far proved less reliable (Verhaak et al., 2010) and widespread coexistence of different groups within single tumours have been identified (Sottoriva et al., 2013).

Development and progression of high-grade gliomas

Glioblastomas develop either as primary tumours or arise from pre-existing low-grade gliomas. These primary and secondary GBMs constitute separate and distinct disease entities. They affect different epidemiological groups and carry different prognoses.

Primary gliomas usually are of *de novo* manifestation involving older patients with a shorter clinical history. On the other hand, secondary gliomas are usual part of a malignant progression from low grade to high grade involving younger patients with a variable interval between one to ten years.

Spread and progression in high-grade gliomas

Tumour invasion

Local white matter invasion is a key pathological hallmark of gliomas, and a major cause of treatment failure. This extent of invasion varies between individuals. Histological studies looking at the extremes of invasion show that between 20% and 27% of GBM have limited invasion defined as less than 1 cm spread (Scherer, 1940; Burger et al., 1988) while about 20% have diffuse invasion defined as greater than 3 cm spread (Burger et al., 1988).

Invading cells show changes in gene expression with upregulation of genes that promote migration and reduced expression of proapoptotic genes (Hoelzinger et al., 2005). The invasion process itself has three stages, firstly there is expression of cell adhesion molecules allowing glioma cells to attach to components of the extracellular matrix (especially tenascin-C), secondly there is production of proteases (e.g. metalloproteinases) which degrade the matrix removing the barriers to cell movement. In gliomas the production of metalloproteinases (MMP)—especially the secreted MMP-2, MMP-9 and the tissue bound MT1-MMP appear critical to invasion (Lampert et al., 1998; Beliveau et al., 1999). The secreted MMPs are regulated by their tissue inhibitors TIMP-1 and TIMP-2 which are down regulated in gliomas (Beliveau et al., 1999) Finally the cells migrate into the region of the matrix degraded by protease

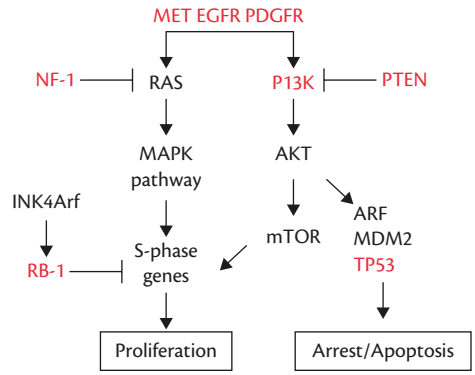

Fig. 7.2 Metabolic pathways that are involved in gliomagenesis. Commonly mutated components of these pathways are highlighted in red in the figure.

activity. This is promoted by the increased secretion of the chemokine CXCL12 (Zhang et al., 2005) that binds to the CXCR4 receptor that is upregulated in invasive glioma cells.

Recently glioblastomas have been shown to contain a small population of cells capable of self-renewal and tumour formation. The cells have been shown to be representative of the parent tumour at the molecular genetic level. They are highly motile *in vitro* and show extensive host invasion *in vivo*. Preliminary gene expression analysis shows that they express several markers associated with invasion and migration including membrane–bound proteins such as MT1-MMP, NG2, and B1-integrin, and soluble factors including plasminogen, MMP2, and MMP9.

Glioma dissemination and metastasis

As mentioned in the previous section, high-grade gliomas mostly progress by invasion of white matter tracts. Scherer described other mechanisms of tumour growth (Scherer, 1938) including subpial growth along the pial surface and subependymal growth along the ventricular surface. This can lead to the occasional 'drop metastasis' into the spine.

Metastasis of HGG is very rare but has been described. It is mostly related to spread along ventriculoperitoneal shunts into the peritoneal cavity or into the scalp, especially where the bone flap is missing. There have been cases of developing HGG metastases in patients who have been transplanted organs from HGG patients, suggesting that suppression of the immune system is required for these cells to grow.

The 'hypoxic switch' in glioma progression

The invasive cells that are growing into white matter tracts have different biology and behaviour to central tumour cells. These cells are more motile, but do not divide (Giese et al., 1996). As their number increases, they challenge for the available metabolites. In the rapidly dividing areas of high-grade gliomas this competition will lead to the development of hypoxia. This 'hypoxic switch' leads to three major behavioural changes within these tumours (Bjerkvig et al., 2009), hypoxia promotes cancer stem cell division, it promotes angiogenesis due to production of factors such as VEGF, and finally it promotes invasion by up regulating invasive factors.

As the degree of malignancy increases this hypoxia will lead to eventual necrosis and microvascular proliferation—both histological features of glioblastomas.

Hypoxia is central for the dichotomized behaviour of glioma stem cells where they either 'go or grow' (Giese et al., 1996). In hypoxic conditions the tendency is to migrate and invade, while at higher oxygen tensions proliferation is favoured: neither phenotype is clinically desirable.

Molecular biomarkers in high-grade gliomas

Several molecular biomarkers of tumourigenesis can be identified. A biomarker is a characteristic that is objectively measured and evaluated as an indicator of normal biological or pathogenic processes or pharmaceutical response to a therapeutic intervention. These biomarkers can be diagnostic, prognostic, or predictive of response to therapy. In high-grade gliomas, a number of these have been identified, and are now being used to better classify these tumours.

Isocitrate dehydrogenase (IDH) mutations

Isocitrate dehydrogenase (IDH) gene encodes a cytosolic enzyme that converts isocitrate to α-ketoglutarate. Mutation of this gene causes a tenfold increase in the production of 2-hydroxyglutarate instead of α-ketoglutarate (Dang et al., 2009). Mutation of IDH-1 gene was found in 5.6–12% of GBM patients and seems to confer a better progression-free survival and median survival, (3.7 years vs. 1.1 years) (Parsons et al., 2008; Weller et al., 2009) suggesting that IDH mutations are prognostic rather than just predictive (van den Bent et al., 2010). Most mutations are a point mutation involving arginine 132—the R132H mutation. This allows an immunohistochemistry test on paraffin embedded tissue and has been shown to have 88–99% concordance with DNA sequencing (Zou et al., 2015). An example of IDH R132H mutation with immunohistochemistry is shown in Figure 7.1C. The other mutations can involve either other point mutations of IDH-1 or mutations of the mitochondrial IDH-2.

What is becoming clear is that low-grade gliomas without mutation have a very poor prognosis (Eckel-Passow et al., 2015). It suggests that the division between high- and low-grade gliomas should now be based on IDH mutation status rather than histology (Brandner and von Deimling, 2015).

Deletion of chromosome 1p/19q

In the WHO 2016 classification loss of heterogeneity of 1p19q in IDH mutated tumours is diagnostic of oligodendroglioma or anaplastic oligodendroglioma. This mutation has an improved survival with chemotherapy and was originally thought to be predictive of chemosensitivity. Results from a trial of radiotherapy versus chemoradiotherapy showed the radiotherapy only arm with 1p19q loss did better than the chemoradiotherapy arm without loss of 1p19q suggesting again the prognostic nature of these molecular markers (van den Bent et al., 2006). Long-term follow-up of two similar studies, however, have now clearly showed a survival advantage for 1p19q deleted tumours treated with radiotherapy and chemotherapy suggesting that this should be part of our standard care for these tumours (van den Bent et al., 2013, Cairncross et al., 2013).

Epigenetic methylation of O-6-methylguanine-DNA methyltransferase (MGMT)

The MGMT gene encodes O-6-methylguanine-DNA methyltransferase enzyme—a DNA repair enzyme that removes alkyl groups from the O-6 position of guanine, an important site of DNA alkylation. MGMT methylation status has been used to prognosticate response to alkylating chemotherapeutic agents like temozolomide. In the methylated form, it is non-functional (i.e. the enzyme is not produced thus limiting DNA repair). MGMT methylation occurs in up to 45% of cases of GBM (Hegi et al., 2005; Stupp et al., 2005), and is associated with improvements in median survival which is significantly longer after radiotherapy with temozolomide than radiotherapy alone (Hegi et al., 2005; Weller et al., 2009). In comparison, the difference in survival in the unmethylated group was insignificant, but there was a survival tail in the cohort treated with chemoradiotherapy (Stupp et al., 2005). As the methylated group with radiotherapy alone has better survival than either unmethylated groups, it suggests MGMT methylation functions as a prognostic marker rather than a predictive marker.

Assessment of MGMT methylation status is not without its technical problems. Multiple sites for mutation have been identified making this marker difficult to assess. In addition, the results are semiquantitative with no clear cut off to define positive or negative status, resulting in no clear clinical standard test for interpretation of results.

TERT promoter mutations

Mutations of TERT, a gene that encodes for telomerase has been found to be present in some brain tumours. Interestingly mutations have been found in both GBM and low-grade gliomas. This suggests maintenance of the telomere may be important for the formation of gliomas (Killela et al., 2013; Vinagre et al., 2014).

Histone H3 mutations

Mutations of histone H3 family 3A (H3F3A) have been identified in paediatric brain stem and midline glioblastomas (Wu et al., 2014). These are point mutations between glycine-to-arginine/valine alteration at codon 34 (G34R/V) within H3F3A. In adults they occur in 3.4% of all glioblastomas (Yoshimoto et al., 2017). These tend to be midline tumours in younger adults.

Controversy: Should we classify high-grade gliomas by histology or molecular markers?

It is now very clear that tumour diagnoses based on histological criteria encompass several different subclasses of tumour and that molecular markers will be essential in our subclassifications of HGG. The current question is how much should these molecular markers play in our classification of these tumours?

Studies combining three markers—namely IDH mutations, 1p19q codeletions and TERT mutations have been able to identify five molecular subclasses of gliomas (Eckel-Passow et al., 2015; summarized in **Table 7.2**). In WHO Grade II/III tumours, most have either mutations of all markers (triple positive), TERT and IDH, or IDH alone. These mutations have a favourable prognosis. Around 17% of tumours however have either mutations of TERT alone or no abnormalities, and these have a similar outcome to glioblastomas. The recent International Society of Neuropathology Consensus of Haarlem (Louis et al., 2014) has highlighted the importance of including these molecular markers in diagnosis.

The latest WHO 2016 Classification System has now incorporated molecular diagnostics to provide a layered diagnosis. This layered diagnosis ensures the classification can be used in resource-limited countries where molecular diagnostics are not available. The integrated diagnosis allows incorporation of molecular information and tissue-based diagnosis to provide a specific *identity*. Where molecular diagnostics are not available tumours are classified as not otherwise specified (NOS). These layers are:

Layer 1: Integrated diagnosis (incorporating all tissue-based information)
Layer 2: Histological classification
Layer 3: WHO grade (reflecting natural history)
Layer 4: Molecular information

Table 7.2 Molecular subclassification of gliomas based on three molecular markers

	Triple-positive	TERT and IDH	IDH alone	Triple-negative	TERT only
Grouping alterations	IDH-1, 1p/19q and TERT mutations	TERT and IDH mutations	IDH mutation	-	TERT mutation
Common acquired mutations	CIC, FUBP1, NOTCH1, and PIK3CA, or PIK3R1	TP53 and ATRX	TP53 and ATRX	EGFR, PTEN, and NF1	EGFR, EGFRvIII, PTEN, NF1, RB1, and PIK3CA, or PIK3R1
Average age	44 years	46 years	37 years	50 years	59 years
TGCA subtype	Proneural	Mesenchymal, neural, proneural	Proneural	Classical, mesenchymal, neural, and proneural	Classical and mesenchymal
Common histology	Oligodendroglioma	Astrocytoma–WHO Grade II or III	Astrocytoma–WHO Grade II or III	67% GBM	90% GBM 10% Grade II or III

Source data from Eckel-Passow, J., Lachance, D., Molinaro, A., et al., Glioma groups based on 1p/19q, IDH, and TERT Promoter Mutations in Tumors, *N Engl J Med* 2015; 372: 2499–508. DOI:10.1056/NEJMoa1407279.

Table 7.3 Examples of the layered diagnosis in the WHO 2016 Classification

	Glioblastoma	Anaplastic astrocytoma	Anaplastic oligodendroglioma
LAYER 1: Integrated diagnosis	Glioblastoma—IDH wild-type	Anaplastic astrocytoma—IDH mutated, 1p19q non-codeleted	Anaplastic oligodendroglioma—IDH mutated, 1p19q codeleted
LAYER 2: Histological Diagnosis	Glioblastoma	Anaplastic astrocytoma	Anaplastic oligodendroglioma
LAYER 3: Grading	IV	III	III
LAYER 4: Molecular information	IDH wild-type TERT mutated MGMT methylated	IDH mutated 1p19q non-codeleted	IDH mutated 1p19q codeleted
DIAGNOSIS WITHOUT MOLECULAR INFORMATION	Glioblastoma NOS	Anaplastic astrocytoma NOS	Anaplastic oligodendroglioma NOS

An example is shown in Table 7.3.

Clinical presentation

Many patients with HGG present with signs and symptoms of raised intracranial pressure from mass effect, oedema, or haemorrhage. These frequently manifest as headaches, nausea, and vomiting, reduced visual acuity, diplopia, drowsiness, and confusion. Other presentations include focal neurological deficits, symptoms which are dependent on the location of the tumour such as aphasia, limb weakness, altered sensation and neurocognitive defects including disinhibition and personality changes (Tucha et al., 2000). Approximately 50% of grade III and 25% of Grade IV tumours presented with seizures compared to 80% of low-grade gliomas.

Imaging high-grade gliomas

The initial imaging modality is usually a contrast-enhanced computed tomography (CT) scan, however, magnetic resonance imaging (MRI) is more sensitive and is now the imaging modality of choice for all patients with brain tumours.

HGG typically appears as an irregular, ill-defined mass with associated vasogenic oedema on both CT and MRI. Enhancement typically is around the rim of the mass with a central area of non-enhancing tissue. Enhancement *per se*, cannot be taken as a diagnostic feature as between 30% and 50% of anaplastic tumours fail to enhance on CT (Chamberlain et al., 1988), and 16% fail to enhance on MRI (Al Okaili et al., 2007). In addition, 20% of low-grade gliomas (typically oligodendrogliomas) enhance on CT (Chamberlain et al., 1988) and 35% enhance on MRI (Al Okaili et al., 2007).

The location of these tumours is mostly in the supratentorial component. The frontal lobe is the most common site (24.9%), followed by temporal lobe (21.8%), parietal lobe (16.7%), occipital lobe (4.8%), cerebellum (0.5%), brain stem (0.4%), or was not specified/other (30.9%) (Brodbelt et al., 2015).

One of the major problems with using imaging for treatment planning is that anatomical imaging is unable to identify tumour margins. Both post-mortem and biopsy studies have shown that the tumour extends beyond the margin on CT (Lilja et al., 1981; Selker et al., 1982; Burger et al., 1983; Kelly et al., 1987), contrast-enhanced T_1-weighted MRI (Lunsford et al., 1986; Kelly et al., 1987; Price et al., 2006), and T_2-weighted MRI (Lunsford et al., 1986; Kelly et al., 1987; Johnson et al., 1989; Watanabe et al., 1992; Price et al., 2006). These techniques cannot determine the margin or the invasiveness of these tumours. Advanced imaging methods have been developed for assessment of these tumours. These are being used in clinical practice and are summarized elsewhere (Price, 2007).

Postoperative MRI is the only method of objectively assessing the extent of resection. Studies have shown it identifies more cases of incomplete resection compared to the judgement of the surgeon (Albert et al., 1994). Imaging within 72 hours avoids the postoperative changes that occur later.

Advanced MRI for HGG

Some advanced MR methods are now in routine practice to assess tumours and provide information on tumour physiology and pathology and are summarized next and elsewhere (Price et al., 2007; see Fig. 7.3).

Diffusion imaging is a method sensitive to diffusion of protons within an image. Areas where there are trapped protons, such as in areas of ischaemic cytotoxic oedema, epidermoid cysts or abscesses appear bright on diffusion-weighted imaging (DWI). As DWI has a component of T2-weighted signal DWI cannot be used as a quantitative measure. The apparent diffusion coefficient (ADC) is used as a quantitative measure that relates to how far protons can diffuse. In areas of free diffusion (e.g. CSF spaces) the ADC is large. Where there is restricted diffusion the ADC is low. In HGG due to increased water from oedema the ADC is larger than normal brain, but as the cellularity increases the ADC reduces. As a result, lower-grade gliomas have a lower ADC than high-grade gliomas (Sugahara et al., 1999).

Diffusion tensor imaging is an extension of DWI imaging that is sensitive to directional diffusion of water molecules. It is used to assess disruption of white matter tracts and the location of tracts close to the tumour.

Perfusion MRI assesses blood flow. Higher grade tumours tend to have higher perfusion and there is some evidence that perfusion may be able to identify anaplastic foci within low-grade gliomas (Danchaivijitr et al., 2008).

MRI Spectroscopy can identify tumour metabolites in a volume of interest. High-grade gliomas have a spectral pattern with reduced N-acetylaspartate (a marker of white matter integrity), increased total choline (a marker of membrane turnover) and signals for lipids and lactate (due to necrosis).

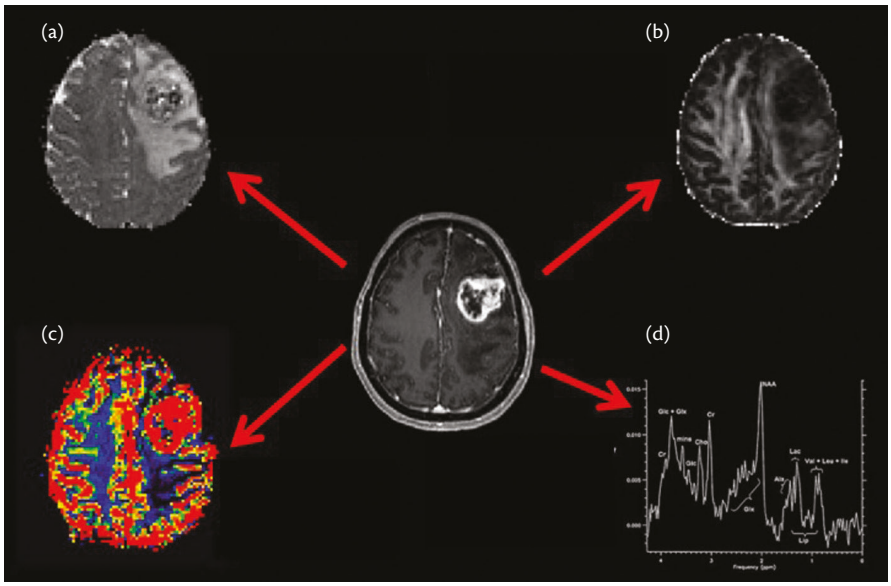

Fig. 7.3 Advanced imaging of the tumour. This contrast enhancing glioblastoma can be evaluated using other imaging techniques. (A) Shows an apparent diffusion coefficient (ADC) image from diffusion-weighted MRI. Decreased ADC can be due to increased tumour cellularity. There is a general reduction in ADC within the tumour due to the increased tumour cellularity. (B) Shows a fractional anisotropy (FA) image from diffusion tensor MRI (DTI)—this shows disruption of white matter tracts and can be used to tract white matter tracts and see how they relate to the tumour. (C) Is perfusion imaging and shows a map of relative cerebral blood volume (rCBV)—a measure of vascularity and angiogenesis. (D) MR proton spectroscopy can be used to look for metabolic profile of high-grade glioma. In this case the spectra shown is of normal brain.

Positron-emission tomography (PET) imaging of HGG

On PET imaging high-grade gliomas tend to be hypermetabolic compared to normal cortex. In FDG PET the tumour may be difficult to differentiate from functioning cortex. In addition, increased FDG uptake is not specific to tumour and can be seen in inflammatory regions. Amino acid PET using either [11C]-methionine (MET PET) or [18F]-ethyl tyrosine (FET PET) is more specific for tumour and appears to better delineate the tumour extent (Pirotte et al., 2006).

Studies that have used PET to direct image-guided biopsies have shown that it improves diagnostic yield from biopsies (Levivier et al., 1995) and can help identify the region for surgical resection (Pirotte et al., 2009)

Management of high-grade gliomas

HGGs are best managed with a multidisciplinary team (MDT) approach. Options for management span the spectrum from conservative treatment to surgery and adjuvant therapy. The main thrust of management is diagnosis and prolongation of progression-free survival.

Dexamethasone is vitally important in controlling cerebral oedema associated with tumours. The response to steroids can be extremely rapid. Failure to improve with steroids suggests radical surgical resection may cause a worsening neurological deficit (Stummer et al., 2011a). The role of steroids, their complications and dosing in neuro-oncology has been reviewed elsewhere (Ryan et al., 2012).

Conservative management is a valid option in patients with a poor prognosis as identified by age and poor performance status—especially for tumours that are considered unresectable. In this situation good palliative and supportive care is important.

Changes in behaviour and personality are very common in patients with brain tumours—often due to the location of the tumour and the effect of treatment. Support of psychosocial function is important and a neuropsychologist should be involved. Major depression in patients with HGG is much more common than in the normal population and impacts on quality of life.

Surgery for HGG

The aims of surgery are to obtain a representative tissue sample of the tumour for histological and molecular marker assessment, to safely remove tumour with the aim of improving pressure symptoms, improving efficacy of adjuvant therapy, delaying deterioration, and improving survival and finally there is the potential of delivering surgically delivered treatments.

Image-guided tumour biopsy

Biopsies are minimally invasive, well tolerated, and suitable for lesions at any site or of any size but are usually only considered when the risks of resection outweigh the benefits. Biopsy is best utilized in cases where the initial diagnosis may influence subsequent management. It has pitfalls, however, in the form of sampling error especially in small or heterogeneous samples as well as complications due to haemorrhage. Image-guidance is now normally used to reduce the risk of non-diagnostic biopsies.

Sampling error is a problem when biopsying HGGs; when the diagnoses are compared between series of patients undergoing biopsy with those undergoing resection, there are discrepancies. In patients undergoing resection, 82% had glioblastomas and 18% had anaplastic astrocytomas, whereas in patients undergoing biopsy 49% had glioblastomas and 51% had anaplastic astrocytomas

(Glantz et al., 1991). In patients who underwent an initial biopsy before a subsequent resection the diagnosis changes in 39–49% of cases (Jackson et al., 2001; McGirt et al., 2003).

Tumour resection

Debulking surgery is beneficial in reducing the tumour load and thus the side effects of raised intracranial pressure and providing a more representative histological sample. The aim of surgery for glioblastomas is to remove as much of the tumour as possible without damaging the surrounding normal brain. Estimates suggest that 50% of patients are suitable for radical resection (Schucht et al., 2012). Whether it provides an improvement in survival has been controversial. The Cochrane review of the literature has highlighted the lack of quality studies in this area (Hart et al., 2000). Retrospective studies have suggested that gross total resection as defined by postoperative MRI findings of more than 98% tumour resection, has shown better quality of life and progression-free survival (Lacroix et al., 2001). The median survival, according to one study, improved from 8 months for subtotal resection to 13 months after gross total resection (McGirt et al., 2009b). This was reconfirmed by a study involving an RPA analysis that showed the survival benefit was greatest in patients with more severe baseline disease based on age, performance status, neurology, and mental status (Pichlmeier et al., 2008). When combined with chemotherapy and radiotherapy, complete resection of contrast enhancement is associated with a prolonged survival (Stummer et al., 2012). This improvement was not seen where any residual enhancing tumour remained. The results of three major randomized controlled studies also confirm improvement in survival with radical resection (Stummer et al., 2011b).

The difficulty with these cohort studies is that there is an inherent resectability bias. Patients with good prognostic features (i.e. those that are young, with good performance status, with smaller tumours in non-eloquent areas) are more likely to have a gross total resection than older patients with poorer performance status and larger tumours in eloquent regions (Stummer et al., 2008). In addition, most surgeons would now consider it unethical to randomize their patients into partial resection.

The difficulty in performing gross total resections (i.e. complete resection of the contrast enhancing component of the tumour on early postoperative imaging; see Vogelbaum et al., 2012) of these tumours is identifying the limits of resection within these tumours. As there is a poor margin between tumour and normal brain most studies suggest that a gross total resection is performed in less than 30% of patients (Wood et al., 1988; Vecht et al., 1990; Albert et al., 1994; Barker et al., 1996; Kowalczuk et al., 1997). A variety of tools have been developed to improve this resection rate.

Image-guidance is essential for planning craniotomies, but unpredictable brain shift limits its use in identifying the tumour limits.

Intraoperative ultrasound is a useful method, but user dependent. Assessment of the tumour border with biopsies, preresection shows a high specificity and sensitivity of 95%, but this deteriorates during resection (sensitivity 87% and specificity 42%) (Rygh et al., 2008).

Intraoperative MRI provides the most accurate method, but is very expensive and does add time to tumour resections. Cohort studies suggest that maximal resection using intraoperative MRI improves survival (Mehdorn et al., 2011).

5-aminolevulinic acid fluorescence guidance (5-ALA) provides a method that can be used in all neurosurgical centres and helps identify tumour (Fig. 7.4). 5-ALA is a new surgical adjuvant used to identify glioma tissue under blue (400 nm) light. 5-ALA is taken up and is converted in the normal haem biosynthesis pathway. In tumours there is a deficiency of the ferrochelatase enzyme that leads to the accumulation of the fluorophore protoporphyrin IX that fluoresces under blue light. The use of 5-ALA enables more complete resections of contrast enhancing tumour, leading to improved progression-free survival in patients with malignant glioma. Stummer et al. showed a 29% increase in complete resections rates in the 5-ALA group as opposed to the white light group. The 5-ALA group also had a higher 6-month progression-free survival than the white light group (41% vs. 21.1%) (Stummer et al., 2006).

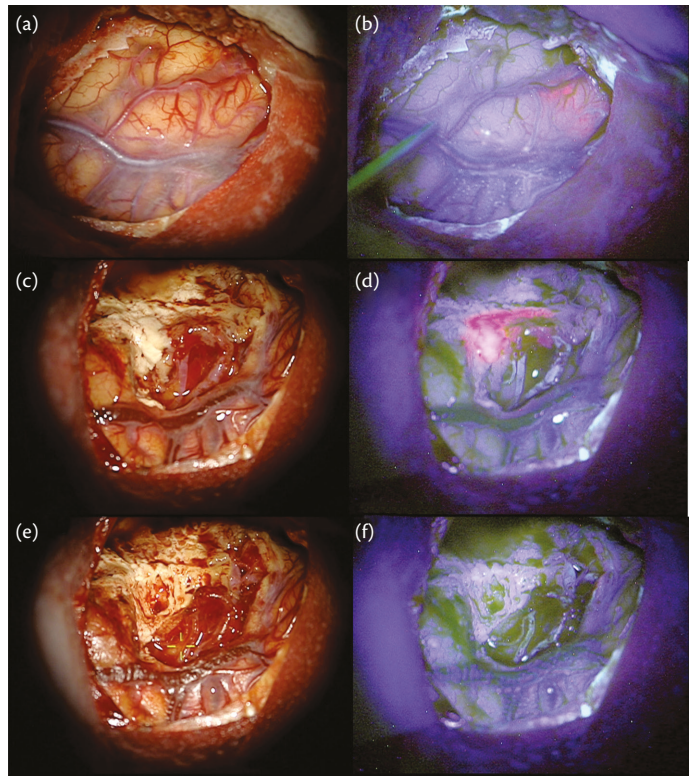

Fig. 7.4 Resection cavity and 5-ALA. Precorticotomy view of the cerebral cortex under white light (A) and 5-ALA fluorescence (B). This shows fluorescent tumour visible in the posterior part of the tumour. The next row shows intraoperative view under white light (C) and 5-ALA (D). The fluorescent area appears normal under white light. At the end of resection there is complete resection of fluorescent tumour (E—white light, f—5-ALA), providing a suitable endpoint to the resection.

The key issue for the surgical neuro-oncologist is to maximize the extent of resection but avoid causing neurological deterioration. It is clear that causing motor and language deficits not only impacts quality of life but also is associated with worse survival (McGirt et al., 2009a). Intraoperative mapping of function using cortical and subcortical mapping (De Witt Hamer et al., 2012) can half the incidence of postoperative neurological deficits.

Radiotherapy for HGG

Radiotherapy has been the mainstay of adjuvant therapy for high-grade gliomas. Multiple studies from the 1970s showed a survival benefit (Walker et al., 1978). Attempts to improve on the initial benefits by increasing the dosage of radiation have failed. Unfortunately,

the therapeutic window for radiotherapy to the brain is narrow and there is an increasing incidence of radiation necrosis with increasing radiation dose. Part of the reason for this is the inability of conventional imaging to identify infiltrating tumour. As a result, radiotherapy planning outlines the obvious tumour as the gross tumour volume (GTV). A 2.5 cm margin is then applied to form the clinical target volume (CTV). A 0.5 cm margin is added to account for set up errors and patient movement to form the planning target volume (PTV). In other words, a 3 cm margin is applied around the tumour that will contain normal brain. To reduce the risk of radiation necrosis the dose is therefore limited.

There are two radiotherapy regimes normally used in HGG. Radical radiotherapy gives a 60 Gray dose over 30 daily fractions while short course or palliative radiotherapy gives 30 Gray over two weeks in 6 fractions. There is less planning required for palliative radiotherapy so patients can start treatment very quickly and it is well tolerated. It is useful where patients are acutely deteriorating.

Chemotherapy for HGG

Procarbazine, lomustine, and vincristine (PCV) was the standard adjuvant chemotherapeutic regime in use before the advent of temozolomide. This nitrosourea-based chemotherapy provided a small survival benefit; a 5% increase in 2-year survival rates (Stewart, 2002). The treatment involves a 10-day oral course of procarbazine, a single oral dose of CCNU (lomustine), and a single intravenous infusion of vincristine given in six weekly cycles.

The introduction of temozolomide has provided some improvement in survival. It is given orally over five days every 28-day cycle. Leucopenia and thrombocytopenia are commonly associated side effects of this treatment. The combination of radical radiotherapy and daily, concomitant temozolomide followed by six cycles of adjuvant temozolomide has significantly altered the prognosis of GBM. Stupp et al. in a multicentre trial showed that at a median follow-up of 28 months, the median survival was 14.6 months in the radiotherapy plus temozolomide group as compared to 12.1 months with radiotherapy alone. The 2-year survival rate was 26.5% versus 10.4% (Stupp et al., 2005) while a 5-year review of the same population has revealed 9.8% survival at 5 years in the temozolomide group compared to 1.9% in the radiotherapy group (Stupp et al., 2009). This represents a significant advance over previous survival statistics in high-grade glioma. The MGMT status was found to be the single most important predictive factor for a favourable outcome.

It is now well recognized that MR appearances immediately after chemoradiotherapy can show apparent progression of disease, 22% of patients in the study reported by Stupp et al. (2009) did not receive adjuvant chemotherapy phase due to presumed tumour progression. Subsequent imaging shows that this either stabilizes or improves. This *pseudo progression* is more commonly seen in patients with methylated MGMT and is thought to represent a good prognostic sign of response to therapy.

Local chemotherapy

Another adjuvant to surgery has been local therapy with BCNU loaded wafers. These wafers provide a method of local delivery of high concentration chemotherapeutic agent bypassing the blood-brain barrier. A placebo-controlled study in patients at progression showed a significant improvement in median survival (31 weeks vs. 23 weeks) and six-month survival (44% dead at 6 months vs. 64%) compared to placebo (Brem et al., 1995). A further study in newly diagnosed HGG also showed a survival advantage

The use of these agents remains controversial though, as questions have been raised about their efficacy as well as side effects including CNS and wound infection rates as high as 28% (Engelhard, 2000; McGovern et al., 2003). However, there is substantial evidence for the use of BCNU wafers in adjuvant treatment. A retrospective review on BCNU wafer implantation in combination with temozolomide and radiotherapy in newly diagnosed GBM revealed a median survival of 20.7 months with a 2-year median survival of 36% (McGirt et al., 2009b). It is clear that more extensive resection (>90%) is required to obtain benefit (Stummer et al., 2012).

Targeted molecular therapies

Targeted molecular therapies are an exciting new therapeutic option, presently at various stages of research and development. These are drugs that target the oncogenic pathways in gliomas either by interacting with receptors or affecting a downstream target. Clinical trials of drugs blocking the EGFR, platelet-derived growth factor receptor (PDGFR), phosphatidylinositol 3-kinase (PI3K), and related pathways and the SRC-related pathways have so far been disappointing. It is clear that monotherapy will have little effect and trials combining these are now underway as summarized by Wick et al. (2011). The reason for this poor response is thought to be the fact that multiple receptor tyrosine kinases are activated in the development of a glioma, so blocking one receptor has little effect on the overall pathway (Stommel et al., 2007). Combinations of targeted therapies are likely to be the way forward.

Antiangiogenic therapies

One targeted therapy of particular interest blocks the vascular endothelial growth factor pathway involved in tumour angiogenesis. A small, non-randomized phase 2 study of bevacizumab at recurrence showed a high response rate (PFS at 6 months 46%; OS at 6 months 77%) (Vredenburgh et al., 2007). This trial paved the way for an FDA approval. But the non-randomized nature of the study and non-standard endpoints has made the European Medicines Agency (EMEA) reject its use in Europe. One of the problems with studies using antiangiogenic agents is the marked decrease in enhancement due to closure of the blood-brain barrier. This so called *pseudoresponse* does not predict the response to these agents, and subsequent progression can occur with no apparent contrast enhancement (Norden et al., 2008).

Two large, phase III studies—the European AVAGlio study (Chinot et al., 2014) and the North American RTOG 0825 study (Gilbert et al., 2014) have both failed to show any survival advantage from adding bevacizumab to standard treatment. The studies found differing findings on quality of life—RTOG 0825 found patients deteriorated on bevacizumab treatment whereas the AVAGlio study showed stable quality of life until tumour progression (Taphoorn et al., 2015).

Immunotherapy

The brain is often considered an immune-privileged organ due to its lack of lymphatics, a blood-brain barrier blocking the passage of cytokines and cells into the brain, low baseline expression of major histocompatibility complex proteins (MHC) and high levels of immunoregulatory cells that decrease baseline function.

These assumptions have been refuted in recent years. Nevertheless, brain tumours further evade and suppress the immune response by their very low expression of MHC proteins, reduction of monocyte phagocytic function and antigen presentation, reduced T-cell activation, and expressing markers that promote immune cell apoptosis. Overcoming these mechanisms would allow specific identification and destruction of tumour cells without injuring normal brain. Immunotherapy would seem an ideal treatment to deal with invasive cells that are distributed within normal brain. Immunotherapy is an exciting method of targeting individual tumour cells without injuring normal tissue and is independent of whether the cell is in cycle (as is the problem with cytotoxic therapies).

Three methods for overcoming tumour-induced immunosuppression have been suggested.

Cytokine therapy—this is based on activating the immune system by these potent immunoregulators. The difficulty has been delivery across the blood-brain barrier and attempts have been made with injection and infusion of cytokines or gene therapy to promote cytokine expression. Certain early phase studies have shown that this is safe but with variable efficacy and these methods might provide a useful adjunct to other therapies.

Passive immunotherapies—including serotherapy—whereby monoclonal antibodies are directed to tumour-specific antigens to deliver toxins or radioactive substances to selectively kill cells. Targets such as tenascin or the mutated EGFR-Viii form that is found in gliomas have been used, but results of early phase studies have been disappointing. Adoptive immunotherapy attempts have largely aimed to augment the tumour response by using IL-2 to stimulate harvested lymphocytes to produce lymphokine-activated killing cells. The results of early studies have shown a small benefit, but are limited by toxicity from IL-2 induced cerebral oedema.

Active immunotherapies—these methods have involved priming the immune response by vaccination against tumour-specific antigens. The difficulty with such methods is the poor antigen presentation ability within the brain. Interest has recently focused on dendritic cells which, when stimulated by an antigen, can activate T-lymphocytes to proliferate and destroy these cells. Approaches have involved taking autologous dendritic cells from either blood or bone marrow, stimulating them with antigens, and then delivering them back to the patient as a subdermal injection. The antigens used have either been common ones found within tumour or individualized from the patient's tumour. Early phase studies have shown promise and minimal toxicity, thus allowing some of these methods to enter phase III studies (Hdeib and Sloan, 2015).

Dietary therapy

The role of diet in managing neurological disease is well established. Ketogenic diets to control medically refractory epilepsy have been used for many years. As gliomas preferentially metabolize glucose and do not metabolize ketone bodies well, inducing a state of ketosis using high fat, low carbohydrate diets. Preclinical studies have shown the antitumor, proapoptotic, and antiangiogenic effects of interrupting these glycolytic pathways in cancer cell lines including gliomas. It is clear that ketogenic diets will not be tolerable for most patients, so a modified Atkin's diet has been suggested. Studies of varying quality have so far failed to show clear efficacy.

Tumour treating fields

Tumour treating fields are a novel device for treating brain tumours. Preclinical studies showed that using a low intensity and intermediate frequency electrical field can disrupt mitosis without causing heating or depolarizing neurons. A recently reported phase III study shows there is a significant survival advantage when used during the adjuvant phase of chemotherapy (Stupp et al., 2015). There is now a move that this should be considered as standard of care (Mehta et al., 2017), although the costs may prohibit routine use at present.

Managing HGG in older people

With an increasingly aged population, gliomas in older people are becoming more of a common problem. The elderly tend to have a more aggressive phenotype and, often due to frailty and other comorbidities, respond poorly to treatments. They tend to be excluded from clinical trials. As a result, patients over the age of 60 are less likely to receive the most radical treatment (Brodbelt et al., 2015).

Radical surgery for these tumours appears to be a useful treatment with improved outcome (Ewelt et al., 2011). Two large studies have shown that in elderly patients who have MGMT methylated glioblastomas there is better survival with temozolomide alone than with radiotherapy (Malmström et al., 2012; Wick et al., 2012).

Treatment at tumour progression

Despite the best management, virtually all patients with HGG will develop recurrence of tumour at some point. Salvage therapies may be considered at this point depending on the patient's clinical condition.

Surgery: Reoperation is associated with higher morbidity and mortality than for the original operation. It is, however, an option in patients with a long progression-free survival who have tumour that is maximally resectable. Insertion of carmustine wafers at this stage has been shown to improve survival (Brem et al., 1995).

Radiotherapy: There has been some suggestion that the toxicity of re-irradiation has been overestimated. Re-irradiation is an increasingly used option with precise fractionated radiotherapy being the most optimal technique. There has also been some suggestion that for accurate, focal radiotherapy to a recurrent tumour, radiosurgery may be considered. On average, time to secondary progression is in the range of several months.

Cytotoxic chemotherapy: Conventional chemotherapy regimens also improve time to secondary progression, but the efficacy is only modest and treatment related toxicities like myelosuppression occur very frequently (Niyazi et al., 2011). Recent phase III trials have failed to show that temozolomide has a survival advantage over PCV regimes (Brada et al., 2010). Recent data suggests that MGMT methylation is a prognostic biomarker for dose-intense temozolomide rechallenge (Weller et al., 2015).

At present there is little data to support routine use of targeted therapies. These should therefore be considered only as part of a clinical trial.

Prognosis

Despite many advances in management, a diagnosis of HGG still carries a dismal prognosis. The median survival without any treatment is less than 6 months, but with treatment, this increases up to 18 months. Poor survival is associated with increasing age, poor initial neurology, poor general condition as evidenced by Karnofsky Performance score (KPS) and absence of MGMT methylation. Patients who undergo surgery and chemoradiotherapy have shown better long-term benefits. Why certain group of patients survive longer than others is still unknown. Death is usually due to cerebral oedema and raised intracranial pressure.

FURTHER READING

Hegi, M.E., Diserens, A.C., Gorlia, T., et al. (2005). *MGMT* gene silencing and benefit from temozolomide in glioblastoma. *N Engl J Med*, **352**(10), 997–1003.

Parsons, D.W., Jones, S.N., Zhang, X., et al. (2008). An integrated genomic analysis of human glioblastoma multiforme. *Science*, **321**(5897), 1807–12.

Stummer, W., Pichlmeier, U., Meinel, T., Wiestler, O.D., Zanella, F., & Reulen, H.-J. (2006). Fluorescence-guided surgery with 5-aminolevulinic acid for resection of malignant glioma: a randomised controlled multicentre phase III trial. *Lancet Oncol*, **7**(5), 392–401.

Stupp, R., Mason, W.P., van den Bent, M.J., et al. (2005). Radiotherapy plus concomitant and adjuvant temozolomide for glioblastoma. *N Engl J Med*, **352**(10), 987–96.

Wick, W., Platten, M., Meisner, C., et al. (2012). Temozolomide chemotherapy alone versus radiotherapy alone for malignant astrocytoma in the elderly: the NOA-08 randomised, phase 3 trial. *Lancet Oncol*, **13**(7), 707–15.

REFERENCES

Al Okaili, R.N., Krejza, J., Woo, J.H., et al. (2007). Intraaxial brain masses: MR imaging-based diagnostic strategy—initial experience. *Radiology*, **243**, 539–50.

Albert, F.K., Forsting, M., Sartor, K., Adams, H.P., & Kunze, S. (1994). Early postoperative magnetic resonance imaging after resection of malignant glioma: objective evaluation of residual tumor and its influence on regrowth and prognosis. *Neurosurgery*, **34**, 45–60.

Arnold, C.D., Gerlach, D., Stelzer, C., Boryn, L.M., Rath, M., & Stark, A. (2013). Genome-wide quantitative enhancer activity maps identified by STARR-seq. *Science*, **339**, 1074–7.

Bainbridge, M.N., Armstrong, G.N., Gramatges, M.M., et al. (2015). Germline mutations in shelterin complex genes are associated with familial glioma. *J Natl Cancer Inst*, **107**, 384.

Bao, S., Wu, Q., Mclendon, R.E., et al. (2006). Glioma stem cells promote radioresistance by preferential activation of the DNA damage response. *Nature*, **444**, 756–60.

Barker, F.G., 2nd, Prados, M.D., Chang, S.M., et al. (1996). Radiation response and survival time in patients with glioblastoma multiforme. *J Neurosurg*, **84**, 442–8.

Beliveau, R., Delbecchi, L., Beaulieu, E., et al. (1999). Expression of matrix metalloproteinases and their inhibitors in human brain tumors. *Ann New York Acad Sci*, **886**, 236–9.

Bhowmick, D.A., Zhuang, Z., Wait, S.D., & Weil, R. J. (2004). A functional polymorphism in the EGF gene is found with increased frequency in glioblastoma multiforme patients and is associated with more aggressive disease. *Cancer Res*, **64**, 1220–3.

Bjerkvig, R., Johansson, M., Miletic, H., & Niclou, S.P. (2009). Cancer stem cells and angiogenesis. *Semin Cancer Biol*, **19**, 279–84.

Bondy, M., Wiencke, J., Wrensch, M., & Kyritsis, A.P. (1994). Genetics of primary brain tumors: a review. *J Neurooncol*, **18**, 69–81.

Brada, M., Stenning, S., Gabe, R., et al. (2010). Temozolomide versus procarbazine, lomustine, and vincristine in recurrent high-grade glioma. *J Clin Oncol*, **28**, 4601–8.

Brandner, S. & Von Deimling, A. (2015). Diagnostic, prognostic and predictive relevance of molecular markers in gliomas. *Neuropathol Appl Neurobiol*, **41**, 694–720.

Brem, H., Piantadosi, S., Burger, P.C., et al. (1995). Placebo-controlled trial of safety and efficacy of intraoperative controlled delivery by biodegradable polymers of chemotherapy for recurrent gliomas. The Polymer-brain Tumor Treatment Group. *Lancet*, **345**, 1008–12.

Brodbelt, A., Greenberg, D., Winters, T., Williams, M., Vernon, S., Collins, V.P., & National Cancer Information Network Brain Tumour, G. (2015). Glioblastoma in England: 2007–2011. *Eur J Cancer*, **51**, 533–42.

Burger, P.C., Dubois, P.J., Schold, S.C., Jr., et al. (1983). Computerized tomographic and pathologic studies of the untreated, quiescent, and recurrent glioblastoma multiforme. *J Neurosurg*, **58**, 159–69.

Burger, P. C., Heinz, E. R., Shibata, T., & Kleihues, P. (1988). Topographic anatomy and CT correlations in the untreated glioblastoma multiforme. *J Neurosurg*, **68**, 698–704.

Cairncross, G., Wang, M., Shaw, E., et al. (2013). Phase III trial of chemoradiotherapy for anaplastic oligodendroglioma: long-term results of RTOG 9402. *J Clin Oncol*, **31**, 337–43.

Cairncross, J. G., Ueki, K., Zlatescu, M.C., et al. (1998). Specific genetic predictors of chemotherapeutic response and survival in patients with anaplastic oligodendrogliomas. *J Natl Cancer Inst*, **90**, 1473–9.

Cancer Genome Atlas Research Network (2008). Comprehensive genomic characterization defines human glioblastoma genes and core pathways. *Nature*, **455**, 1061–8.

Chamberlain, M.C., Murovic, J.A., & Levin, V.A. (1988). Absence of contrast enhancement on CT brain scans of patients with supratentorial malignant gliomas. *Neurology*, **38**, 1371–4.

Chinot, O.L., Wick, W., Mason, W., et al. (2014). Bevacizumab plus radiotherapy-temozolomide for newly diagnosed glioblastoma. *N Engl J Med*, **370**, 709–22.

Cobbs, C. S., Harkins, L., Samanta, M., et al. (2002). Human cytomegalovirus infection and expression in human malignant glioma. *Cancer Res*, **62**, 3347–50.

Danchaivijitr, N., Waldman, A.D., Tozer, D.J., et al. (2008). Low-grade gliomas: do changes in rCBV measurements at longitudinal perfusion-weighted MR imaging predict malignant transformation? *Radiology*, **247**, 170–8.

Dang, L., White, D. W., Gross, S., et al. (2009). Cancer-associated IDH1 mutations produce 2-hydroxyglutarate. *Nature*, **462**, 739–44.

De Witt Hamer, P.C., Robles, S.G., Zwinderman, A.H., Duffau, H., & Berger, M.S. (2012). Impact of intraoperative stimulation brain mapping on glioma surgery outcome: a meta-analysis. *J Clin Oncol*, **30**, 2559–65.

Dey, M., Ahmed, A.U., & Lesniak, M.S. (2015). Cytomegalovirus and glioma: putting the cart before the horse. *J Neurol Neurosurg Psychiatry*, **86**, 191–9.

Dziurzynski, K., Chang, S.M., Heimberger, A.B., et al. (2012). Consensus on the role of human cytomegalovirus in glioblastoma. *Neuro Oncol*, **14**, 246–55.

Eckel-Passow, J.E., Lachance, D.H., Molinaro, A.M., et al. (2015). Glioma groups based on 1p/19q, IDH, and TERT promoter mutations in tumors. *N Engl J Med*, **372**, 2499–508.

Engelhard, H.H. (2000). The role of interstitial BCNU chemotherapy in the treatment of malignant glioma. *Surg Neurol*, **53**, 458–64.

Ewelt, C., Goeppert, M., Rapp, M., Steiger, H.J., Stummer, W., & Sabel, M. (2011). Glioblastoma multiforme of the elderly: the prognostic effect of resection on survival. *J Neurooncol*, **103**, 611–18.

Feron, O. (2009). Pyruvate into lactate and back: from the Warburg effect to symbiotic energy fuel exchange in cancer cells. *Radiother Oncol*, **92**, 329–33.

Folkman, J. (1972). Anti-angiogenesis: new concept for therapy of solid tumors. *Ann Surg*, **175**, 409–16.

Giese, A., Loo, M.A., Tran, N., Haskett, D., Coons, S.W., & Berens, M.E. (1996). Dichotomy of astrocytoma migration and proliferation. *Int.J Cancer*, **67**, 275–82.

Gilbert, M. R., Dignam, J. J., Armstrong, T. S., et al. (2014). A randomized trial of bevacizumab for newly diagnosed glioblastoma. *N Engl J Med*, **370**, 699–708.

Glantz, M.J., Burger, P.C., Herndon, J.E., et al. (1991). Influence of the type of surgery on the histologic diagnosis in patients with anaplastic gliomas. *Neurology*, **41**, 1741–4.

Goodwin, S., McPherson, J.D., & McCombie, W.R. (2016). Coming of age: ten years of next-generation sequencing technologies. *Nat Rev Genet*, **17**, 333–51.

Grivennikov, S.I., Greten, F.R., & Karin, M. (2010). Immunity, inflammation, and cancer. *Cell*, **140**, 883–99.

Hanahan, D. & Weinberg, R.A. (2011). Hallmarks of cancer: the next generation. *Cell*, **144**, 646–74.

Hart, M. G., Grant, R., & Metcalfe, S.E. (2000). Biopsy versus resection for high grade glioma. *Cochrane Database Syst Rev*, **2**, CD002034.

Hdeib, A. & Sloan, A.E. (2015). Dendritic cell immunotherapy for solid tumors: evaluation of the DCVax(R) platform in the treatment of glioblastoma multiforme. *CNS Oncol*, **4**, 63–9.

Hegi, M.E., Diserens, A.C., Gorlia, T., et al. (2005). MGMT gene silencing and benefit from temozolomide in glioblastoma. *N Engl J Med*, **352**, 997–1003.

Hoelzinger, D.B., Mariani, L., Weis, J., et al. (2005). Gene expression profile of glioblastoma multiforme invasive phenotype points to new therapeutic targets. *Neoplasia*, **7**, 7–16.

Holick, C.N., Giovannucci, E.L., Rosner, B., Stampfer, M.J., & Michaud, D.S. (2007). Prospective study of cigarette smoking and adult glioma: dosage, duration, and latency. *Neuro Oncol*, **9**, 326–34.

Inskip, P.D., Tarone, R.E., Hatch, E.E., et al. (2001). Cellular-telephone use and brain tumors. *N Engl J Med*, **344**, 79–86.

Jackson, R.J., Fuller, G.N., Abi-Said, D., et al. (2001). Limitations of stereotactic biopsy in the initial management of gliomas. *Neuro Oncol*, **3**, 193–200.

Jain, R.K., Di Tomaso, E., Duda, D.G., Loeffler, J.S., Sorensen, A.G., & Batchelor, T.T. (2007). Angiogenesis in brain tumours. *Nat Rev Neurosci*, **8**, 610–22.

Johnson, P.C., Hunt, S.J., & Drayer, B.P. (1989). Human cerebral gliomas: correlation of postmortem MR imaging and neuropathologic findings. *Radiology*, **170**, 211–17.

Kelly, P.J., Daumas-Duport, C., Kispert, D.B., Kall, B.A., Scheithauer, B.W., & Illig, J.J. (1987). Imaging-based stereotaxic serial biopsies in untreated intracranial glial neoplasms. *J Neurosurg*, **66**, 865–74.

Killela, P. J., Reitman, Z. J., Jiao, Y., et al. (2013). TERT promoter mutations occur frequently in gliomas and a subset of tumors derived from cells with low rates of self-renewal. *Proc Natl Acad Sci U S A*, **110**, 6021–6.

Kleinerman, R.A., Linet, M.S., Hatch, E.E., et al. (2005). Self-reported electrical appliance use and risk of adult brain tumors. *Am J Epidemiol*, **161**, 136–46.

Kowalczuk, A., Macdonald, R.L., Amidei, C., et al. (1997). Quantitative imaging study of extent of surgical resection and prognosis of malignant astrocytomas. *Neurosurgery*, **41**, 1028–36.

Lacroix, M., Abi-Said, D., Fourney, D.R., et al. (2001). A multivariate analysis of 416 patients with glioblastoma multiforme: prognosis, extent of resection, and survival. *J Neurosurg*, **95**, 190–8.

Lampert, K., Machein, U., Machein, M.R., Conca, W., Peter, H.H., & Volk, B. (1998). Expression of matrix metalloproteinases and their tissue inhibitors in human brain tumors. *Am J Pathol*, **153**, 429–37.

Levivier, M., Goldman, S., Pirotte, B., et al. (1995). Diagnostic yield of stereotactic brain biopsy guided by positron emission tomography with [18F]fluorodeoxyglucose. *J Neurosurg*, **82**, 445–52.

Lilja, A., Bergstrom, K., Spannare, B., & Olsson, Y. (1981). Reliability of computed tomography in assessing histopathological features of malignant supratentorial gliomas. *J Comput Assist Tomogr*, **5**, 625–36.

Louis, D.N., Perry, A., Burger, P., et al. (2014). International Society of Neuropathology—Haarlem consensus guidelines for nervous system tumor classification and grading. *Brain Pathol*, **24**, 429–35.

Louis, D.N. Perry, A., Reifenberger, G., et al. (eds.) (2016). *WHO Classification of Tumours of the Central Nervous System*. Lyon, France: IARC Press.

Lunsford, L.D., Martinez, A.J., & Latchaw, R.E. (1986). Magnetic resonance imaging does not define tumor boundaries. *Acta Radiol Suppl*, **369**, 154–6.

Malmström, A., Grønberg, B.H., Marosi, C., et al. (2012). Temozolomide versus standard 6-week radiotherapy versus hypofractionated radiotherapy in patients older than 60 years with glioblastoma: the Nordic randomised, phase 3 trial. *Lancet Oncol*, **13**, 916–26.

Mcgirt, M.J., Mukherjee, D., Chaichana, K.L., Than, K.D., Weingart, J.D., & Quinones-Hinojosa, A. (2009a). Association of surgically acquired motor and language deficits on overall survival after resection of glioblastoma multiforme. *Neurosurgery*, **65**, 463–9; discussion 469–70.

Mcgirt, M.J., Than, K.D., Weingart, J.D., et al. (2009b). Gliadel (BCNU) wafer plus concomitant temozolomide therapy after primary resection of glioblastoma multiforme. *J Neurosurg*, **110**, 583–8.

McGirt, M.J., Villavicencio, A.T., Bulsara, K.R., & Friedman, A.H. (2003). MRI-guided stereotactic biopsy in the diagnosis of glioma: comparison of biopsy and surgical resection specimen. *Surg Neurol*, **59**, 277–81.

McGovern, P.C., Lautenbach, E., Brennan, P.J., Lustig, R.A., & Fishman, N.O. (2003). Risk factors for postcraniotomy surgical site infection after 1,3-bis (2-chloroethyl)-1-nitrosourea (Gliadel) wafer placement. *Clin Infect Dis*, **36**, 759–65.

Mehdorn, H.M., Schwartz, F., Dawirs, S., Hedderich, J., Dorner, L., & Nabavi, A. (2011). High-field iMRI in glioblastoma surgery: improvement of resection radicality and survival for the patient? *Acta Neurochir Suppl*, **109**, 103–6.

Mehta, M., Wen, P., Nishikawa, R., Reardon, D., & Peters, K. (2017). Critical review of the addition of tumor treating fields (TTFields) to the existing standard of care for newly diagnosed glioblastoma patients. *Crit Rev Oncol Hematol*, **111**, 60–5.

Meyerson, M., Gabriel, S., & Getz, G. (2010). Advances in understanding cancer genomes through second-generation sequencing. *Nat Rev Genet*, **11**, 685–96.

Niyazi, M., Siefert, A., Schwarz, S.B., et al. (2011). Therapeutic options for recurrent malignant glioma. *Radiother Oncol*, **98**, 1–14.

Norden, A.D., Young, G.S., Setayesh, K., et al. (2008). Bevacizumab for recurrent malignant gliomas: efficacy, toxicity, and patterns of recurrence. *Neurology*, **70**, 779–87.

Okada, T., Lopez-Lago, M., & Giancotti, F.G. (2005). Merlin/NF-2 mediates contact inhibition of growth by suppressing recruitment of Rac to the plasma membrane. *J Cell Biol*, **171**, 361–71.

Okcu, M.F., Selvan, M., Wang, L.E., et al. (2004). Glutathione S-transferase polymorphisms and survival in primary malignant glioma. *Clin Cancer Res*, **10**, 2618–25.

Parker, M., Mohankumar, K.M., Punchihewa, C., et al. (2014). C11orf95-RELA fusions drive oncogenic NF-kappaB signalling in ependymoma. *Nature*, **506**, 451–5.

Parsons, D.W., Jones, S.N., Zhang, X., et al. (2008). An integrated genomic analysis of human glioblastoma multiforme. *Science*, **321**, 1807–12.

Pichlmeier, U., Bink, A., Schackert, G., & Stummer, W. (2008). Resection and survival in glioblastoma multiforme: an RTOG recursive partitioning analysis of ALA study patients. *Neuro Oncol*, **10**, 1025–34.

Pirotte, B., Goldman, S., Dewitte, O., et al. (2006). Integrated positron emission tomography and magnetic resonance imaging-guided resection of brain tumors: a report of 103 consecutive procedures. *J Neurosurg*, **104**, 238–53.

Pirotte, B. J., Levivier, M., Goldman, S., et al. (2009). Positron emission tomography-guided volumetric resection of supratentorial high-grade gliomas: a survival analysis in 66 consecutive patients. *Neurosurgery*, **64**, 471–81; discussion 481.

Pobereskin, L.H. & Chadduck, J.B. (2000). Incidence of brain tumours in two English counties: a population-based study. *J Neurol Neurosurg Psychiatry*, **69**, 464–71.

Price, S.J. (2007). The role of advanced MR imaging in understanding brain tumour pathology. *Br J Neurosurg*, **21**, 562–75.

Price, S., Jena, R., Burnet, N., Carpenter, T., Pickard, J., & Gillard, J. (2007). Predicting patterns of glioma recurrence using diffusion tensor imaging. *Eur Radiol*, **17**, 1675–84.

Price, S., Jena, R., Burnet, N., et al. (2006). Improved delineation of glioma margins and regions of infiltration with the use of diffusion tensor imaging: an image-guided biopsy study. *AJNR Am J Neuroradiol*, **27**, 1969–74.

Qian, B.Z. & Pollard, J.W. (2010). Macrophage diversity enhances tumor progression and metastasis. *Cell*, **141**, 39–51.

Ryan, R., Booth, S., & Price, S. (2012). Corticosteroid-use in primary and secondary brain tumour patients: a review. *J Neurooncol*, **106**, 449–59.

Rygh, O.M., Selbekk, T., Torp, S.H., Lydersen, S., Hernes, T.A., & Unsgaard, G. (2008). Comparison of navigated 3D ultrasound findings with histopathology in subsequent phases of glioblastoma resection. *Acta Neurochir (Wien)*, **150**, 1033–41.

Sandmann, T., Bourgon, R., Garcia, J., et al. (2015). Patients with proneural glioblastoma may derive overall survival benefit from the addition of bevacizumab to first-line radiotherapy and temozolomide: retrospective analysis of the AVAglio trial. *J Clin Oncol*, **33**(25), 2735–44.

Scherer, H.J. (1938). Structural development in gliomas. *Am J Cancer*, **34**, 333–51.

Scherer, H.J. (1940). The forms of growth in gliomas and their practical significance. *Brain*, **63**, 1–35.

Schucht, P., Beck, J., Abu-Isa, J., et al. (2012). Gross total resection rates in contemporary glioblastoma surgery: results of an institutional protocol combining 5-aminolevulinic acid intraoperative fluorescence imaging and brain mapping. *Neurosurgery*, **71**, 927–35; discussion 935–6.

Schwartzbaum, J.A., Fisher, J.L., Aldape, K.D., & Wrensch, M. (2006). Epidemiology and molecular pathology of glioma. *Nat Clin Pract Neurol*, **2**, 494–503; quiz 1 p following 516.

Selker, R.G., Mendelow, H., Walker, M., Sheptak, P.E., & Phillips, J.G. (1982). Pathological correlation of CT ring in recurrent, previously treated gliomas. *Surg Neurol*, **17**, 251–4.

Simon, M., Ludwig, M., Fimmers, R., et al. (2006). Variant of the *CHEK2* gene as a prognostic marker in glioblastoma multiforme. *Neurosurgery*, **59**, 1078–85; discussion 1085.

Singh, S.K., Hawkins, C., Clarke, I.D., et al. (2004). Identification of human brain tumour initiating cells. *Nature*, **432**, 396–401.

Sottoriva, A., Spiteri, I., Piccirillo, S.G., et al. (2013). Intratumor heterogeneity in human glioblastoma reflects cancer evolutionary dynamics. *Proc Natl Acad Sci U S A*, **110**, 4009–14.

Stewart, L.A. (2002). Chemotherapy in adult high-grade glioma: a systematic review and meta-analysis of individual patient data from 12 randomised trials. *Lancet*, **359**, 1011–18.

Stommel, J.M., Kimmelman, A.C., Ying, H., et al. (2007). Coactivation of receptor tyrosine kinases affects the response of tumor cells to targeted therapies. *Science*, **318**, 287–90.

Stragliotto, G., Rahbar, A., Solberg, N.W., et al. (2013). Effects of valganciclovir as an add-on therapy in patients with cytomegalovirus-positive glioblastoma: a randomized, double-blind, hypothesis-generating study. *Int J Cancer*, **133**, 1204–13.

Stummer, W., Meinel, T., Ewelt, C., et al. (2012). Prospective cohort study of radiotherapy with concomitant and adjuvant temozolomide chemotherapy for glioblastoma patients with no or minimal residual enhancing tumor load after surgery. *J Neurooncology*, **108**, 89–97.

Stummer, W., Pichlmeier, U., Meinel, T., Wiestler, O.D., Zanella, F., & Reulen, H.-J. (2006). Fluorescence-guided surgery with 5-aminolevulinic acid for resection of malignant glioma: a randomised controlled multicentre phase III trial. *Lancet Oncol*, **7**, 392–401.

Stummer, W., Reulen, H.J., Meinel, T., et al. (2008). Extent of resection and survival in glioblastoma multiforme: identification of and adjustment for bias. *Neurosurgery*, **62**, 564–76.

Stummer, W., Tonn, J.C., Mehdorn, H.M., et al. (2011a). Counterbalancing risks and gains from extended resections in malignant glioma surgery: a supplemental analysis from the randomized 5-aminolevulinic acid glioma resection study. Clinical article. *J Neurosurg*, **114**, 613–23.

Stummer, W., Van Den Bent, M.J., & Westphal, M. (2011b). Cytoreductive surgery of glioblastoma as the key to successful adjuvant therapies: new arguments in an old discussion. *Acta Neurochir (Wien)*, **153**, 1211–18.

Stupp, R., Hegi, M. E., Mason, W. P., et al. (2009). Effects of radiotherapy with concomitant and adjuvant temozolomide versus radiotherapy alone on survival in glioblastoma in a randomised phase III study: 5-year analysis of the EORTC-NCIC trial. *Lancet Oncol*, **10**, 459–66.

Stupp, R., Mason, W.P., Van Den Bent, M.J., et al. (2005). Radiotherapy plus Concomitant and Adjuvant Temozolomide for Glioblastoma. *New Engl J Med*, **352**, 987–96.

Stupp, R., Taillibert, S., Kanner, A. A., et al. (2015). maintenance therapy with tumor-treating fields plus temozolomide vs temozolomide alone for glioblastoma: a randomized clinical trial. *JAMA*, **314**, 2535–43.

Sugahara, T., Korogi, Y., Kochi, M., et al. (1999). Usefulness of diffusion-weighted MRI with echo-planar technique in the evaluation of cellularity in gliomas. *J Magn Reson Imaging*, **9**, 53–60.

Taphoorn, M.J., Henriksson, R., Bottomley, A., et al. (2015). Health-related quality of life in a randomized phase III study of bevacizumab, temozolomide, and radiotherapy in newly diagnosed glioblastoma. *J Clin Oncol*, **33**(19), 2166–75.

Tucha, O., Smely, C., Preier, M., & Lange, K.W. (2000). Cognitive deficits before treatment among patients with brain tumors. *Neurosurgery*, **47**, 324–33; discussion 333–4.

Turcan, S., Rohle, D., Goenka, A., et al. (2012). IDH1 mutation is sufficient to establish the glioma hypermethylator phenotype. *Nature*, **483**, 479–83.

Van Den Bent, M.J., Brandes, A.A., Taphoorn, M.J., et al. (2013). Adjuvant procarbazine, lomustine, and vincristine chemotherapy in newly diagnosed anaplastic oligodendroglioma: long-term follow-up of EORTC brain tumor group study 26951. *J Clin Oncol*, **31**, 344–50.

Van Den Bent, M.J., Carpentier, A.F., Brandes, A.A., et al. (2006). Adjuvant procarbazine, lomustine, and vincristine improves progression-free survival but not overall survival in newly diagnosed anaplastic oligodendrogliomas and oligoastrocytomas: a randomized European Organisation for Research and Treatment of Cancer phase III trial. *J Clin Oncol*, **24**, 2715–22.

Van Den Bent, M. J., Dubbink, H. J., Marie, Y., et al. (2010). IDH1 and IDH2 mutations are prognostic but not predictive for outcome in anaplastic oligodendroglial tumors: a report of the European Organization for Research and Treatment of Cancer Brain Tumor Group. *Clin Cancer Res*, **16**, 1597–604.

Vander Heiden, M.G., Cantley, L.C., & Thompson, C.B. (2009). Understanding the Warburg effect: the metabolic requirements of cell proliferation. *Science*, **324**, 1029–33.

Vecht, C.J., Avezaat, C.J., Van Putten, W.L., Eijkenboom, W.M., & Stefanko, S.Z. (1990). The influence of the extent of surgery on the neurological function and survival in malignant glioma. A retrospective analysis in 243 patients. *J Neurol Neurosurg Psychiatry*, **53**, 466–71.

Verhaak, R.G., Hoadley, K.A., Purdom, E., et al. (2010). Integrated genomic analysis identifies clinically relevant subtypes of glioblastoma characterized by abnormalities in *PDGFRA, IDH1, EGFR*, and *NF1*. *Cancer Cell*, **17**, 98–110.

Vinagre, J., Pinto, V., Celestino, R., et al. (2014). Telomerase promoter mutations in cancer: an emerging molecular biomarker? *Virchows Arch*, **465**, 119–33.

Vogelbaum, M.A., Jost, S., Aghi, M.K., et al. (2012). Application of novel response/progression measures for surgically delivered therapies for gliomas: Response Assessment in Neuro-Oncology (RANO) Working Group. *Neurosurgery*, **70**, 234–43; discussion 243–4.

Vogelstein, B., Papadopoulos, N., Velculescu, V.E., Zhou, S., Diaz, L.A., Jr., & Kinzler, K.W. (2013). Cancer genome landscapes. *Science*, **339**, 1546–58.

Vredenburgh, J.J., Desjardins, A., Herndon, J.E., et al. (2007). Bevacizumab plus irinotecan in recurrent glioblastoma multiforme. *J Clin Oncol*, **25**, 4722–9.

Walker, M.D., Alexander, E., Jr., Hunt, W.E., et al. (1978). Evaluation of BCNU and/or radiotherapy in the treatment of anaplastic gliomas. A cooperative clinical trial. *J Neurosurg*, **49**, 333–43.

Walter, A.W., Hancock, M.L., Pui, C.H., et al. (1998). Secondary brain tumors in children treated for acute lymphoblastic leukemia at St Jude Children's Research Hospital. *J Clin Oncol*, **16**, 3761–7.

Watanabe, M., Tanaka, R., & Takeda, N. (1992). Magnetic resonance imaging and histopathology of cerebral gliomas. *Neuroradiology*, **34**, 463–9.

Weller, M., Felsberg, J., Hartmann, C., et al. (2009). Molecular predictors of progression-free and overall survival in patients with newly diagnosed glioblastoma: a prospective translational study of the German glioma network. *J Clin Oncol*, **27**, 5743–50.

Weller, M., Tabatabai, G., Kastner, B., et al. (2015). MGMT promoter methylation is a strong prognostic biomarker for benefit from dose-intensified temozolomide rechallenge in progressive glioblastoma: the DIRECTOR trial. *Clin Cancer Res*, **21**, 2057–64.

Wen, P.Y. & Kesari, S. (2008). Malignant gliomas in adults. *N Engl J Med*, **359**, 492–507.

Wick, W., Platten, M., Meisner, C., et al. (2012). Temozolomide chemotherapy alone versus radiotherapy alone for malignant astrocytoma in the elderly: the NOA-08 randomised, phase 3 trial. *Lancet Oncol*, **13**, 707–15.

Wick, W., Weller, M., Weiler, M., Batchelor, T., Yung, A.W., & Platten, M. (2011). Pathway inhibition: emerging molecular targets for treating glioblastoma. *Neuro Oncol*, **13**, 566–79.

Wood, J.R., Green, S.B., & Shapiro, W.R. (1988). The prognostic importance of tumor size in malignant gliomas: a computed tomographic scan study by the Brain Tumor Cooperative Group. *J Clin Oncol*, **6**, 338–43.

Wu, G., Broniscer, A., McEeachron, T.A., et al. (2012). Somatic histone H3 alterations in pediatric diffuse intrinsic pontine gliomas and non-brainstem glioblastomas. *Nat Genet*, **44**, 251–3.

Wu, G., Diaz, A.K., Paugh, B.S., et al. (2014). The genomic landscape of diffuse intrinsic pontine glioma and pediatric non-brainstem high-grade glioma. *Nat Genet*, **46**, 444–50.

Yoshimoto, K., Hatae, R., Sangatsuda, Y., et al. (2017). Prevalence and clinicopathological features of H3.3 G34-mutant high-grade gliomas: a retrospective study of 411 consecutive glioma cases in a single institution. *Brain Tumor Pathol*, **34**(3), 103–12.

Zhang, J., Sarkar, S., & Yong, V.W. (2005). The chemokine stromal cell derived factor-1 (CXCL12) promotes glioma invasiveness through MT2-matrix metalloproteinase. *Carcinogenesis*, **26**, 2069–77.

Zou, Y., Bai, H.X., Wang, Z., & Yang, L. (2015). Comparison of immunohistochemistry and DNA sequencing for the detection of IDH1 mutations in gliomas. *Neuro Oncol*, **17**, 477–8.

RELATED LINKS TO EBRAIN

Assessment of the Patient with a Brain Tumour. https://learning.ebrain.net/course/view.php?id=1247

Clinical Presentation of Patients with Brain Tumours. https://learning.ebrain.net/course/view.php?id=1249

CNS Tumours: Basic Histology WHO Grading System. https://learning.ebrain.net/course/view.php?id=1250

Diagnostic Imaging in Brain Tumours. https://learning.ebrain.net/course/view.php?id=931

Histological and Molecular Diagnostics of Brain Tumours. https://learning.ebrain.net/course/view.php?id=1390

Histology and Molecular Pathology of IDH Wild Type Gliomas. https://learning.ebrain.net/course/view.php?id=1393
Intraoperative Chemotherapy and Radiotherapy. https://learning.ebrain.net/course/view.php?id=1241
Molecular Pathology and Histology of IDH Mutant Gliomas. https://learning.ebrain.net/course/view.php?id=1392
Palliative Care and End of Life in Brain Tumour Patients. https://learning.ebrain.net/course/view.php?id=483
Referral and Management Guidelines for Patients with Brain Tumours. https://learning.ebrain.net/course/view.php?id=507
Surgical Management of High Grade Gliomas. https://learning.ebrain.net/course/view.php?id=450
The Treatment of High Grade Gliomas. https://learning.ebrain.net/course/view.php?id=448

8

Intracranial metastases

Andrew Brodbelt and Rasheed Zakaria

Introduction

See **Box 8.1** for the principles of the management of patients with metastases.

Epidemiology

Intracranial metastases are among the most common intracranial tumours. Western population-based studies describe annual age adjusted incidence rates of 7–14 per 100 000 (Fox et al., 2011) compared to 4.6 for glioblastoma and 7.6 for meningioma (Ostrom et al., 2014; Brodbelt et al., 2015). Autopsy studies suggest a brain metastasis may be found in up to 24% of patients with a solid organ cancer, although only 6% of patients will develop symptomatic intracranial metastases in the course of their disease (Posner and Chernik, 1978). The incidence is increasing, due, in part, to improved survival from better systemic cancer treatments and more sensitive detection methods (Fox et al., 2011). The effects of age and gender on brain metastasis incidence are dependent on the primary cancer. Female patients with lung and breast cancers are more likely to develop brain metastasis than their male counterparts but the reverse is true for melanoma, renal and colorectal cancer (Davis et al., 2012). While younger patients (<40 years) with breast and lung cancer are approximately twice as likely to develop brain metastasis as those over 70 years, the increased prevalence of cancer in older patients means that overall more metastases are still seen in older patients. Clinicians should not therefore consider any patients with suspicious symptoms to be 'too young' to develop brain metastases.

Approximately one-third of patients present with a solitary lesion, one-third oligometastatic (2–3 lesions), and a third polymetastatic (>4 lesions; see Norden et al., 2005). Metastasis rates vary with tumour type, with up to 20% of lung cancer patients developing brain disease, compared to less than 1% of thyroid, prostate, stomach, or ovarian cancer patients (National Cancer Institute, 2015). Some 30–60% of patients with brain metastases will have lung cancer (Fox et al., 2011) and of those non-small cell lung cancer (NSCLC) is the most prevalent (Delattre et al., 1988). Other common tumour primary sites include breast, melanoma, renal and colorectal cancers (Delattre et al., 1988). The median time between diagnosis of the primary cancer to presentation of brain metastasis is approximately 12 months but ranges from 3 (NSCLC) to 46 months (ovarian carcinoma) (Nussbaum et al., 1996; Kolomainen et al., 2002). Certain genetic subtypes can also favour brain spread, for example in breast cancer, both triple negative (oestrogen receptor, progesterone receptor, and HER2 receptor negative) and HER receptor positive subtypes are associated with a higher risk of brain metastasis (Pestalozzi et al., 2006).

A brain tumour in a patient with a known cancer does not always mean a brain metastasis. In one small series, 4 out of 21 patients with previous systemic malignancy were misdiagnosed as having brain metastases and received WBRT when they actually had a new primary malignant brain tumour (Maluf et al., 2002). Suspicion of a second malignancy should be aroused when there is a lack of active systemic disease (particularly in lung cancer), a long disease-free interval, a primary tumour type that rarely metastasizes to the brain (e.g. prostate carcinoma), or prior exposure to cranial radiation. One-third of patients with a new brain metastasis will have no history of systemic cancer. In these cases, the primary will usually be found within 2 months (synchronous presentation) but 5–10% will not. Patients with cancer of unknown primary do badly and may not always benefit from traditional chemo and radiotherapy strategies (Norden et al., 2005; NICE, 2010).

Pathology

In contrast to primary brain tumours, brain metastases arise from the haematogenous spread of cancer cells and are therefore found in areas of high relative cerebral perfusion. Eighty percent of metastases are seen in the cerebral hemispheres, 15% in the cerebellum, and 5% in the brainstem (Delattre et al., 1988). In the cerebrum, the metastatic cells preferentially adhere at the narrow vascular branch points found in the watershed zone at the grey white interface (Louis et al., 2007). The capillaries around brain metastases have an abnormal microstructure and leaky gap junctions which, coupled with the local release of cytokines, make them permeable to large molecules and water then follows by osmosis. This intense vasogenic oedema contains few tumour cells, and is reduced with steroids or metastectomy.

The metastatic cascade, describing cancer cell movement from primary site to the brain, is a complex and inefficient process

Box 8.1 Principles of the management of patients with metastases

Treatment is not curative. The aim is extension of quality life.
The patient's performance score is crucial to outcome.
Increasing age is associated with worsening outcomes.
Minimum staging includes an MRI brain with either CT or CT PET of chest/abdomen/pelvis.
The whole patient and their cancer load must be considered, not just the brain metastasis
If the treatment is not working, consider malignant meningitis.
In patients with a history of cancer, a new brain lesion can still be a different cancer or an abscess.

(Fig. 8.1). Each stage is a potential drug or therapeutic target. For example, detection of early metastases with labelled iron particles attached to the cell adhesion molecule VCAM-1, before they are seen on conventional contrast-enhanced magnetic resonance imaging (MRI), offers future treatment development opportunities (Serres et al., 2012).

The macroscopic appearance of metastases may be firm or rubbery, with necrotic areas in the core. They are usually yellow or tan in colour, although melanoma metastases are often black due to melanin. Blood products may be present, altering the colour. Haemorrhage is most commonly reported in renal, melanoma, choriocarcinoma, thyroid, and hepatocellular metastases. The tumour frequently appears well demarcated and compresses the adjacent glial tissue forming a pseudocapsule (Fig. 8.2).

Despite an apparent macroscopic plane, there is increasing evidence of local invasion in brain metastases with implications for both treatment and prognosis (Fig. 8.2). More infiltration is associated with poorer survival (Siam et al., 2015). Diffusion MRI changes at the tumour-brain interface are predictive of local recurrence, and could be used to aid treatment planning, including increased resection margins, or stereotactic radiosurgery (SRS) treatment field (Zakaria et al., 2014).

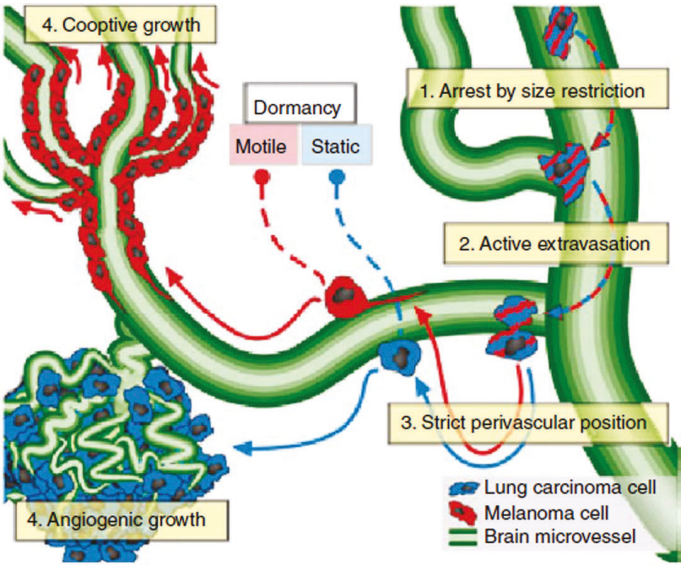

Fig. 8.1 The metastatic cascade: a solid organ cancer cell transitions from a static 'epithelial' to a more mobile 'mesenchymal' cell phenotype, driven by growth factors including TGF-β, IGF, and EGF, detaches from its neighbours, and invades the local extracellular matrix requiring cadherin breakage, and proteolytic enzymes, such as matrix metalloproteinases. Intravasation (entering the bloodstream) is facilitated by the formation of invadopodia, actin rich protrusions of the plasma membrane that guide the cell through its microenvironment, coupled with tissue plasminogen activator release. 1. Once in the circulation, the cells must survive intense sheer forces and immune attack, which involves a strengthened cytoskeleton. The cells attach to the endothelium at branch points and narrowings. 2. Crossing the blood–brain barrier requires integrin and cell adhesion molecule mediation. 3. Metastatic cancer cells remain adjacent to the blood vessels. 4. Brain invasion is tumour specific, with melanoma cells growing along blood vessels (co-optive growth) whereas lung cancer cells generate new blood vessels (neoangiogenesis).

Reproduced with permission from Yvonne Kienast et al., Real-time imaging reveals the single steps of brain metastasis formation, *Nature Medicine*, Volume 16, Issue 1, Copyright © 2009 Springer Nature.

Symptoms and signs

Patients with metastases present with symptoms and signs of raised intracranial pressure, CSF pathway obstruction, neurological mass effect, and in the untreated situation, coning and death. Irritation of the cortex may lead to focal or generalized seizure presentation in 15–20% of patients, but more so (50%) in those with melanoma (Taillibert and Delattre, 2005). Solitary or oligometastatic disease presents with headache (80%), focal neurological deficit (30–40%), and visual disturbance (6%) while polymetastatic disease may present as an encephalopathic or acute confusional state (Gaspar et al., 1997). Any of these features in a patient with known cancer should lead to suspicion of intracranial metastases, although one series found 40% of patients with lung cancer and brain metastases were asymptomatic (Ohana et al., 2014).

Investigations

The first step is to take a history and perform a clinical examination. This should include an enquiry for indicators of cancer (weight loss, change in bowel habit, smoking), any previous cancer history, other medical problems, and breast or rectal examinations. The performance score should be calculated and recorded. The World Health Organization (WHO), European Organisation for the Research and Treatment of Cancer (EORTC), and Karnofsky performance scores are all used, but the main determinate of outcome relates to the need of the patient for any help with daily activities. This is indicated by a score of 2 or over (WHO, EORTC), or less than 70 (Karnofsky).

Initial radiological investigations include a CT scan of the head, which is often enough to suggest the diagnosis. MRI is essential for diagnosis and treatment planning (Fig. 8.3). MRI detects smaller tumours than CT, although the exact size depends on slice thickness. Double and triple contrast dosing improves detection rates, but risks nephrotoxicity and increases false positives.

Questions the imaging should help answer include whether this is a brain metastasis; that is, can infection, high-grade glioma, lymphoma, and other lesions including multiple sclerosis or toxoplasmosis be excluded? How many and what size/volume are the metastases? Where is the primary cancer and how extensive is the extracranial disease? How safe is surgery?

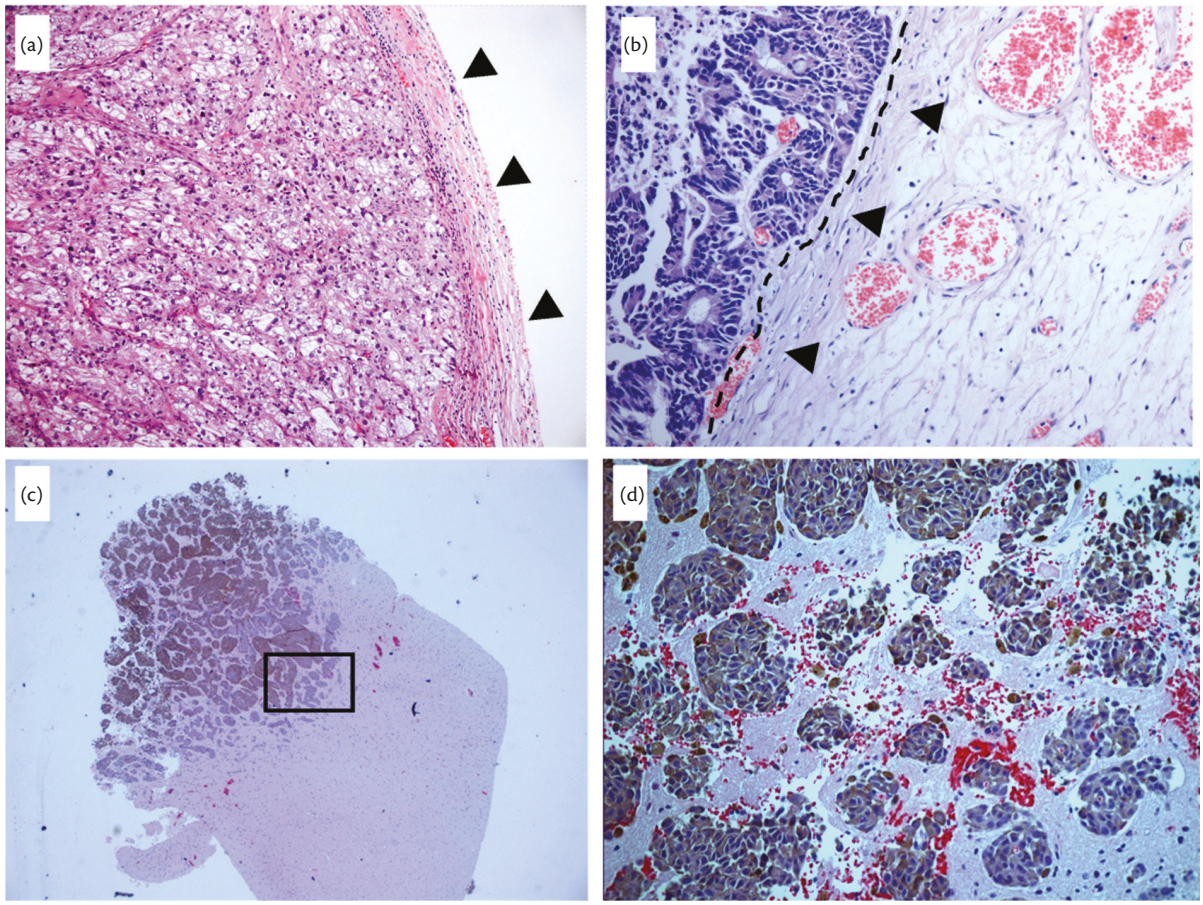

Fig. 8.2 (A) and (B) Brain metastases may appear to have a definite plane with the surrounding brain. Renal (A, ×100) and lung adenocarcinoma (B, ×200) metastases demonstrate the pseudocapsule of compressed white matter (arrowheads) with a clear boundary between brain and tumour (dashed line). (C) and (D) A diffusely invasive edge is found in up to a third of metastases (Neves et al., 2001; Berghoff et al., 2013). C (×50), D (×200) melanoma metastasis showing microscopic islands of tumour in the surrounding brain parenchyma.

Multimodal MRI has been used to aid in differentiating metastases from other imaging abnormalities. Metastases may show lower peritumoral perfusion and higher diffusion than infiltrating gliomas, while the MR spectroscopic signature can help differentiate meningioma or lymphoma. In practice, the best guide remains the presence of surrounding vasogenic oedema and the appearance of the lesion on standard T1, T2, and gadolinium-enhanced T1 weighted MRI sequences. Diffusion-weighted imaging (DWI) and apparent diffusion coefficient (ADC) MRI maps are rapid to obtain and can show an abscess by restricted water movement, although restricted diffusion can also occur in mucinous metastases (Fig. 8.4; see also Ebisu et al., 1996). Cranial [18F] FDG-PET appears to be a sensitive way of detecting brain metastases in patients with known or suspected solid organ cancers, and may distinguish brain metastases from lymphoma but not high-grade glioma. Poor spatial resolution mandates a clinical assessment and MRI to complete the evaluation.

Quality of life after treatment impacts on survival, and advanced techniques such as functional MRI and tractography are being increasingly used in metastasis surgery (Fig. 8.5).

Staging aids in treatment decisions, and a full blood count, urea, and electrolytes, clotting profile, and liver function tests can all help assess systemic cancer effects. Specific tumour staging requires whole-body positron emission tomography (PET) CT or contrast CT of the chest, abdomen, and pelvis. In patients with synchronous or unknown primaries, tumour markers may be considered which include human chorionic gonadotrophin (ßHCG) for germ cell tumours, alpha fetoprotein (αFP) for hepatocellular carcinoma, carcinoembryonic antigen for gastrointestinal, lung, and breast cancers, and CA125 for ovarian tumours. Further radiological assessments include a skeletal survey, mammography, ultrasound, and MRI where indicated. Rapid, appropriate staging within 2–7 days aids efficient decision-making and avoids clinically relevant tumour progression which might reduce treatment options.

Treatment

Oral or intravenous corticosteroid therapy (dexamethasone) can dramatically reduce the symptoms caused by a tumour's vasogenic oedema. The initial dexamethasone dose is 16 mg per day in two or four divided doses but should be tapered as fast as tolerated. The side effects of dexamethasone include, but are not limited to, peptic ulceration, insomnia, myopathy, weight gain, psychosis, skin thinning, Cushing's syndrome, adrenal suppression, and increased risk

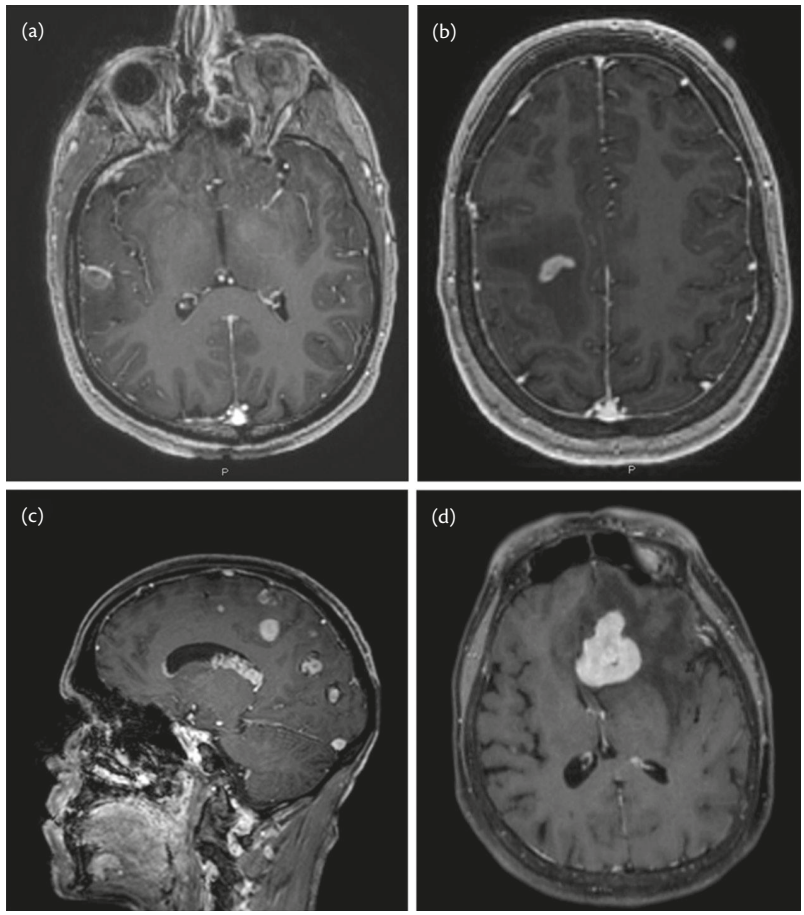

Fig. 8.3 Differential diagnoses of an enhancing mass on T1 + gadolinium MRI. (A) A 55-year-old, with negative staging and no history of primary cancer, was found on resection to have a high-grade glioma. (B) A 22-year-old with a short history of left-sided numbness and weakness, and normal whole-body CT, had an inflammatory picture on LP, and a diagnosis of a multiple sclerosis plaque was made. (C) A 42-year-old HIV positive male with a history of melanoma required a biopsy to prove toxoplasmosis. (D) A 70-year-old smoker presented with confusion and a hilar mass on chest CT which could not be sampled by the thoracic surgeons. Biopsy revealed lymphoma.

of infection. These effects support routine, synchronous gastric protection with a proton pump inhibitor and the use of as low a dose of dexamethasone for as short a time as possible.

Individual treatment options can be divided into focal (Surgery, SRS, interstitial laser therapy, and focused ultrasound treatment) and whole brain or body techniques (whole-brain radiotherapy (WBRT), chemotherapy and targeted or immune therapies). The aim of the final treatment plan, using therapy options individually or in combination, is to improve local control, extend life, and prevent further neurological complications.

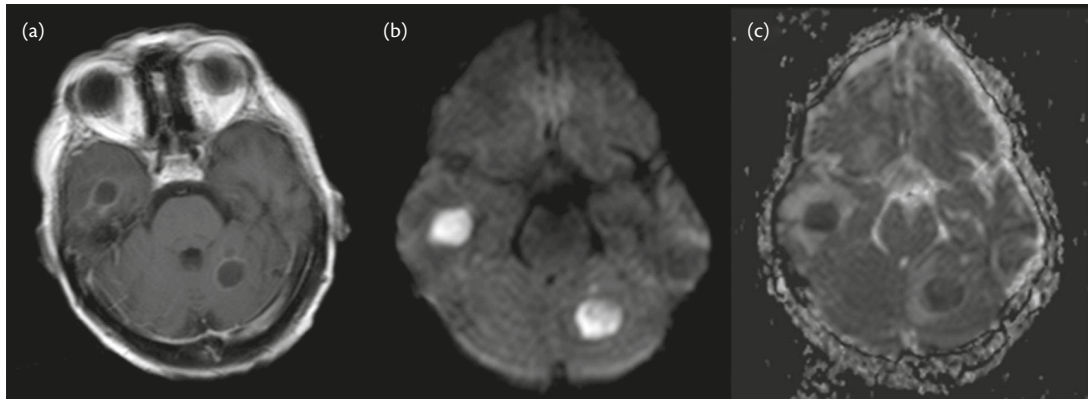

Fig. 8.4 A 53-year-old male with a history of head and neck cancer, presented with low grade fever and confusion. A T1-weighted MRI scan with gadolinium (A) indicated multiple enhancing lesions. Diffusion-weighted MRI (B) and apparent diffusion coefficient map (C) showed restricted diffusion. Aspiration demonstrated pus (*Streptococcus)* and investigation found endocarditis. After prolonged IV antibiotic therapy there was complete resolution.

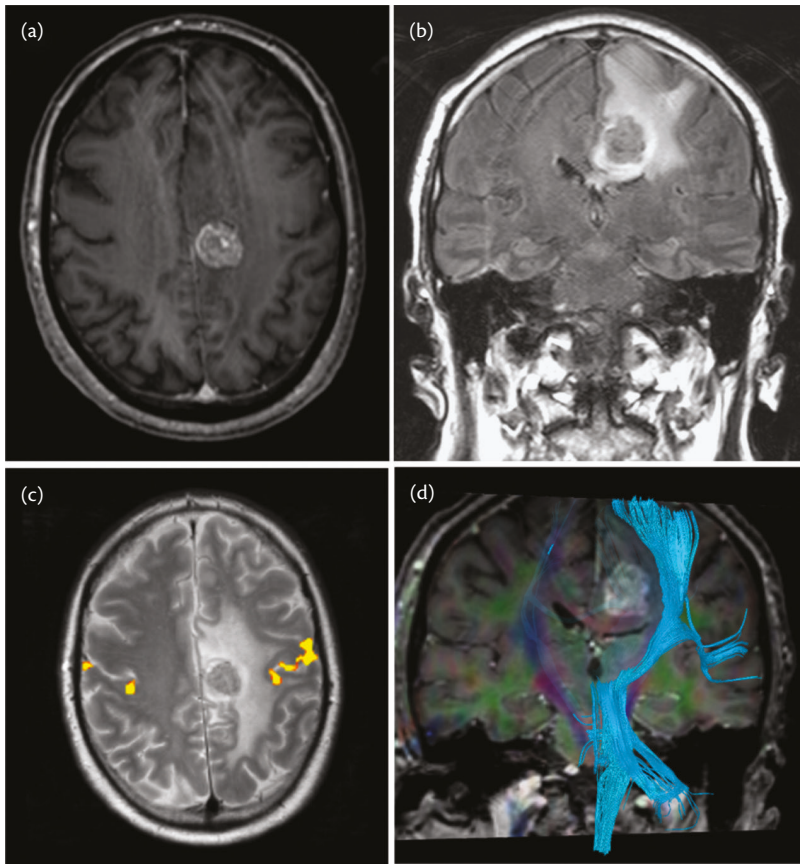

Fig. 8.5 A 58-year-old man presented with right sided hemiparesis, which improved with steroids, and a suspected brain metastasis. (A) Postcontrast T1-weighted MRI demonstrated an enhancing mass. (B) Sagittal FLAIR confirmed a cingulate location with oedema. The patient was a heavy smoker and CT staging identified a small hilar mass. Hilar biopsy and bronchial washings were unsuccessful. (C) Functional MRI using a finger tapping paradigm localized the primary motor cortex. (D). Seeded tractography with diffusion tensor imaging (DTI) showed the corticospinal tracts displaced laterally. An interhemispheric resection removed an adenocarcinoma, with no increase in neurological morbidity and following treatment he survived almost a year with good performance status before succumbing to the primary tumour.

Surgery for intracranial metastases provides diagnostic tissue, relieves mass effect, and is considered for solitary or oligometastatic disease. Meta-analysis of randomized controlled trials has shown surgery improves survival and functional status compared to WBRT alone (Hart et al., 2005). The disadvantages, even with modern microneurosurgical techniques that include awake surgery, integrated multimodal MRI studies, and image guidance (Fig. 8.4), remain the risk to life, infection, and neurological disability. Surgical techniques originally used in cancer resections in other organ systems, including *en bloc* and supramarginal methods are being used in brain metastectomies to reduce local recurrence rates and leptomeningeal spread (Yoo et al., 2009; Patel et al., 2010). Surgery remains the method of choice for large tumours with mass effect, cystic, or radioresistant tumours, if diagnostic tissue is required, and when SRS is not available.

Stereotactic radiosurgery describes a form of ionizing radiation therapy that focuses high-powered energy on a small target in a single or a few fractions. The advantages of SRS include that it can be done as a day case, can use a thermoplastic mask rather than a frame, avoids any surgical procedure, can target multiple lesions in deep or eloquent cortex, and has results comparable to surgical series. Limitations exist and not all tumours are suitable, as lesions need to be typically 4 cm (or less) or 20 cc, those abutting the optic nerves or brainstem risk local radionecrosis while cystic and radioresistant tumour (commonly renal and melanoma) lesions respond less well. Tumours can swell after treatment leading to extended steroid treatment and concomitant side effects which make SRS less suitable for certain post fossa metastases. No tissue is taken for diagnosis. There are no certain efficacy or safety differences between the different platforms available (gamma knife, cyberknife, and linear accelerator). Radiation necrosis rates increase with increasing tumour volume irradiated and hypofractionated regimes for lesions larger than 20 cc may be used.

WBRT improves survival and tumour control in the brain, but current concerns relate to cognitive harm. Ninety percent of patients with brain metastases have impaired neurocognitive function at diagnosis and up to two-thirds will show further decline within 2–6 months of WBRT (Pinkham et al., 2015). Omitting whole-brain radiotherapy after local therapy increases the time until cognitive decline and improves verbal memory but it is argued that progression and the associated salvage treatments outweigh any benefit that has been gained. Recent evidence suggests WBRT does not improve survival in all patients and notably in those older patients with NSCLC, and poor performance score, simple steroid treatment and good palliative care may be more appropriate (Mulvenna et al., 2016). New fractionated radiotherapy strategies may reduce

cognitive harm by hippocampal sparing, using reduced whole brain fields while boosting the tumour bed, or by using neuroprotective agents such as memantine (Brown et al., 2013).

Recent developments have challenged the view that systemic drug therapy is not effective in treating brain metastases. Areas under investigation include identifying antimetastasis effects among agents that cross the blood–brain barrier (BBB), developing agents that act systemically to prevent brain metastases occurring and facilitating traditional chemotherapy agents to cross the blood–brain barrier. In melanoma pretreatment with the immunotherapy agent ipilimumab improved the effects of surgery (Jones et al., 2015) and in the half of patients with a B-Raf Proto-oncogene (BRAF) mutation, inhibiting the pathway can extend overall survival (> 7 months) for patients with untreated brain metastases (Goyal et al., 2015). A new UK study (CAMBT1) of a tyrosine kinase inhibitor for patients undergoing resection of lung or breast metastases is testing whether low-dose, targeted radiotherapy to the metastasis preoperatively improves drug penetration.

Novel treatments include interstitial laser thermal therapy which passes a laser through a burr hole to heat up tumours, controlled by almost real-time MR thermography (Hawasli et al., 2013). MR-guided focused ultrasound (MRgFUS) uses ultrasound, controlled with MR thermography, to target deep seated lesions. Initially used for fibroids, MRgFUS is starting to be used for cranial lesions (Coluccia et al., 2014). Carmustine wafers (Gliadel) implanted in the cavity following surgery have been reported to reduce local recurrence (Abel et al., 2013) but are rarely used.

As treatment for brain metastases is unlikely to lead to a cure, patients and their families will require ongoing supportive and symptomatic care whatever management plan is agreed. Specific problems include cognitive decline, poor mobility, thromboembolism, pain, reduced self-care, anxiety, depression, and epilepsy (Taillibert and Delattre, 2005). Early involvement of palliative care teams is essential to maximize a patient's quality of life.

Treatment selection

Regular multidisciplinary team (MDT or tumour board) meetings have been developed to optimize the efficient review of a patient's planned management. Experienced neuroradiological review, discussion between oncologists, neurosurgeons, pathologists, specialist nurses, and palliative care teams ensures modern treatment practices are followed and improves recruitment into clinical trials. The final treatment choice remains the responsibility of the treating clinician and the patient.

There are a number of possible treatment combinations. Traditionally surgery was followed by WBRT. WBRT is used following local treatments to reduce the local recurrence rates, and control disease elsewhere in the brain, but concerns remain regarding the associated cognitive decline. In a randomized controlled trial comparing surgery plus WBRT (n = 49) to surgery alone (n = 46), the addition of WBRT improved intracranial control from 30% to 82% (Patchell et al., 1998). However overall survival and quality of life (in the form of time spent in good performance status) were only secondary measures and neither showed improvement. These results have been used to justify omitting WBRT after surgery. However, local recurrence in this study was associated with increased neurological death, which was more common in the surgery only group. A large European trial (Kocher et al., 2011) randomized patients who had undergone surgery to observation or WBRT. WBRT reduced the frequency of recurrence in the resection bed from 60% to less than 30% but with only a modest increase in progression-free survival and no change in overall survival. Quality of life data from this trial found that WBRT caused poorer physical functioning and fatigue at 8 weeks, worsening global health status at 9 months, and deteriorating cognitive functioning.

If SRS is used, it can be followed by WBRT. A large trial (Kocher et al., 2011) randomized patients who had received SRS for between one and three brain metastases to observation or WBRT. There was no difference in overall survival from adding WBRT but intracranial progression causing death was reduced from 44% to 28% and fewer salvage therapies were required. A meta-analysis concluded that adding WBRT to SRS improves local control but not overall survival, but then recommended omitting WBRT due to the deleterious cognitive effects (Tsao et al., 2012).

Surgery followed by SRS is one way of improved local control with less cognitive side effects. A randomized controlled trial suggested SRS to the surgical cavity gave comparable survival rates to surgery followed by WBRT but with improved cognitive outcomes (Brown et al., 2017) and this paradigm is gaining popularity. Advanced MRI (e.g. DWI) prediction of microscopic infiltration and tumour residual could be used in the future to try to improve SRS planning and treatment selection.

Although WBRT remains the standard of care for patients with polymetastatic brain disease, improved planning algorithms have allowed the use of SRS for these patients. A prospective observational study of 1194 patients with up to ten metastases (total volume <15 ml) and a performance score of 70 or over treated with SRS alone, showed no difference between those patients with 2–4 and those with 5–10 metastases with respect to overall survival, complications, and local recurrence (Yamamoto et al., 2014). There is no randomized controlled trial comparing SRS with WBRT for polymetastatic disease. SRS delivers a lower dose to normal brain tissue, is deliverable as a day case, and appears to provide promising outcomes in this patient group.

Principles in treatment selection are vital (**Box 8.2**). In solitary or oligometastatic disease, a patient who can still look after themselves (KPS >70, WHO ≤2), and a systemic disease load allowing at least a 3–6-month prognosis, should be considered for aggressive treatment. Surgery where appropriate or SRS provides local control, may improve neurological function, and will extend life. The addition of WBRT reduces local and distal recurrence and hence neurological deterioration and death. SRS to the cavity following surgery aids local control. Avoiding WBRT reduces the risk of cognitive decline but necessitates continued surveillance and further salvage treatments. In polymetastatic disease, WBRT remains the treatment of choice, but SRS is becoming more important. As personalized systemic chemotherapy and immunotherapy develops, new alternatives to surgery or radiation and novel combination treatments are likely. A close discussion between the patient, neurosurgeon, and treating oncologist is required to balance the risks and benefits of the therapies available (see **Box 8.2**).

Malignant meningitis

Five percent of brain metastasis patients will develop malignant meningitis (carcinomatous meningitis, leptomeningeal metastasis), and may present with cranial neuropathies, unexplained hydrocephalus,

Box 8.2 Principles of treatment decision-making

Treatment is not curative; the aim is extension of quality life.
The psychological and supportive care of the patient is as important as the treatment of the metastasis.
If a patient is unable to look after themselves, they are unlikely to benefit from treatment.
WBRT is the standard of care to improve intracranial control following surgery but the risks of associated neurocognitive decline should be considered.
Local treatments (surgery and SRS) increase quality life expectancy and improve local control.
Local treatments given alone have less cognitive side effects than WBRT, but require continued monitoring to control distal neurological disease.
Systemic cancer treatments are evolving. A discussion with an oncologist may offer alternatives to radiation treatments and surgery.

or confusion (Le Rhun et al., 2013). Perineural spread of tumour cells along the subarachnoid spaces may be detected on contrast-enhanced T1 and FLAIR MRI or at lumbar puncture (LP). Repeated large volume LPs, processed immediately can reveal the diagnosis in 80% (Le Rhun et al., 2013). Open biopsy for larger deposits is problematic, and surgical CSF diversion risks tumour seeding into the abdomen, although both may have a role. Craniospinal radiation and intrathecal chemotherapy via a CSF reservoir are the mainstays of treatment, although outcomes remain poor (6 weeks untreated).

Prognosis

Multiple prognostic scoring systems exist (Table 8.1). These systems emphasize the importance of the patient's performance score

Table 8.1 The prognosis of patients with brain metastases may be estimated by scoring systems of increasing complexity. The Recursive Partitioning Analysis (RPA) paper statistically examined a series of patients treated with radiotherapy and described a three-class system, with no benefit found from treating patients with a poor performance score. The graded prognostic assessment (GPA) included patients from various trials treated with different strategies, and split each feature and included the number of metastases, while the diagnosis-specific GPA included different primary cancer types. The one factor that is common to every scoring system and disease is the Karnofsky performance score.

Scoring system	Category	Factors				Outcomes (median overall survival)						
RPA	Class I	Age <65, KPS ≥ 70, Controlled primary tumour, no extracranial metastases				7.1 months						
	Class II	All patients not in Class I or III				4.2 months						
	Class III	KPS <70				2.3 months						
GPA	0 points	Age >60	KPS <70	>3 mets	Extracranial metastases	GPA 0–1		2.6 months				
	0.5 points	Age 50–59	KPS 70–80	2–3 mets		GPS 1.5–2.5		3.8 months				
	1 point	Age <50	KPS 90–100	1 met	No extracranial metastases	GPA 3		6.9 months				
						GPA 3.5–4.0		11.0 months				
DS-GPA	**Primary cancer** NSCLC/SCLC	**Points**	**0**	**0.5**	**1**	–	–	**DS-GPA**	**0–1**	**1.5–2.5**	**3**	**3.5–4**
		Age	>60	50–60	<50	–	–	NSCLC	3.0	6.5	11.3	14.8
		KPS	<70	70–80	90–100	–	–					
		ECM	Present	–	Absent	–	–	SCLC	2.8	5.3	9.6	17.0
		No. of mets	>3	2–3	1	–	–					
	Melanoma/ renal cell cancer	**Points**	**0**	**1**	**2**	–	–	Melanoma	3.4	4.7	8.8	13.2
		KPS	<70	70–80	90–100	–	–	RCC	3.3	7.4	11.3	14.8
		No. of mets	>3	2–3	1							
	Breast cancer	**Points**	**0**	**0.5**	**1**	**1.5**	**2**	Breast	3.4	7.7	15.1	25.3
		KPS	≤50	60	70–80	90–100	–					
		Subtype	Basal	–	LumA	HER2	LumB					
		Age	≥60	<60	–	–	–					
	GI cancers	**Points**	**0**	**1**	**2**	**3**	**4**	GI cancer	3.1	4.4	6.9	13.5
		KPS	<70	70	80	90	100					

RPA, recursive partitioning analysis; GPA, graded prognostic assessment; DS, disease specific; KPS, Karnofsky performance score; ECM, extracranial metastases; NSCLC, non-small cell lung cancer; SCLC, small cell lung cancer; GI, gastrointestinal; RCC, renal cell cancer.

Data from Gaspar et al., Recursive partitioning analysis (RPA) of prognostic factors in three Radiation Therapy Oncology Group (RTOG) brain metastases trials, *International Journal of Radiation Oncology, Biology, Physics*, Volume 37, pp. 745–51, 1997; Sperduto PW, Berkey B, Gaspar LE, Mehta M, Curran WJ, A new prognostic index and comparison to three other indices for patients with brain metastases: An analysis of 1960 patients in the RTOG database, *International Journal of Radiation Oncology, Biology, Physics*, Volume 70, pp. 510–14, 2008; Sperduto PW, Chao ST, Sneed P, et al., Diagnosis-specific prognostic factors, indices and treatment outcomes for patients with newly diagnosed brain metastases: a multi-institutional analysis of 4259 patients, *International Journal of Radiation Oncology, Biology, Physics*, Volume 77, Issue 3, pp. 655–61, 2010.

in treatment decisions. The only exception for the poor performance score patient is when surgery improves functioning by reducing mass effect or treating hydrocephalus. More recent scoring systems incorporate tumour subtypes, biochemical parameters, and imaging data (Sperduto et al., 2010). Currently, screening of asymptomatic patients does not appear to improve survival.

Landmark papers

Patchell and colleagues ran two landmark studies in the 1990s which defined the modern treatment of intracranial metastases. They asked two questions:

Should we take out intracranial metastases?

In the first study they randomized 48 patients with a solitary brain metastasis to tumour removal or biopsy followed by WBRT (Patchell et al., 1990). Recurrence at the site of the original metastasis was less frequent in the surgical group than in the radiation group (5 of 25 [20%] vs. 12 of 23 [52%]; P <0.02). Survival was significantly longer in the surgical group (median, 40 weeks vs. 15 weeks; P <0.01), and the patients treated with surgery remained functionally independent longer (median, 38 weeks vs. 8 weeks; P <0.005).

If we completely take out a metastasis, should we give radiotherapy postoperatively?

Ninety-five patients were randomized to WBRT or no further treatment after resection of their tumour. Patients underwent a postoperative brain MRI to confirm complete resection (Patchell et al., 1998). Patients treated with radiation were less likely to show recurrence in the brain or die of neurological causes.

Controversies: SRS or neurosurgery?

Debate continues on whether SRS or surgery provides better local treatment but there has never been a direct, controlled trial comparing surgery and SRS. A retrospective case series found no difference between SRS or surgery, when both were followed by WBRT (Schöggl et al., 2000). In a separate study, SRS alone was compared to surgery and WBRT, and showed no difference at 6 months (Muacevic et al., 2008). In UK clinical practice, SRS is reserved for treating 1–3 smaller tumours (with an upper limit of 20 cc or 30 mm diameter), where there is little oedema or mass effect and the patient is expected to survive 6 months. SRS is undoubtedly quicker and less invasive than neurosurgery alone, but some tumour types are known to be relatively radioresistant (e.g. melanoma, renal cell carcinoma). In patients fit enough for anaesthesia, neurosurgery has the advantage of removing mass effect and relieving oedema, thus potentially improving CSF flow and neurological deficits, particularly in the posterior fossa or with larger, non-eloquent supratentorial lesions. Crucially, surgery also provides tissue for diagnosis in those without a known primary cancer. For patients with cystic metastases, a combined approach with surgical cyst drainage and SRS has proved effective (Franzin et al., 2008). In the future, hybrid approaches with combinations of surgery for the larger tumour plus SRS, interstitial laser thermal therapy, or MRgFUS., for smaller inaccessible lesions could become standard unless significant improvements in chemotherapy and immunotherapy occur.

Conclusions

Intracranial metastases are becoming more common, the management of these patients can be challenging and crosses multiple subspecialties. Treatments are developing, although surgery, SRS, and WBRT remain the core options. The patient's performance score is central to outcome, and care must be taken to maximize quality of life. Progress in the management of cancer is beginning to lead to better outcomes for this patient group.

FURTHER READING

Gaspar, L., Scott, C., Rotman, M., et al. (1997). Recursive partitioning analysis (RPA) of prognostic factors in three Radiation Therapy Oncology Group (RTOG) brain metastases trials. *Int J Radiat Oncol Biol Phys*, **37**, 745–51.

Patchell, R.A., Tibbs, P.A., Regine, W.F., et al. (1998). Postoperative radiotherapy in the treatment of single metastases to the brain: a randomized trial. *JAMA*, **280**, 1485–9.

Patchell, R.A., Tibbs, P.A., Walsh, J.W., et al. (1990). A randomized trial of surgery in the treatment of single metastases to the brain. *N Engl J Med*, **322**, 494–500.

Sperduto, P.W., Chao, S.T., Sneed, P.K., et al. (2010). Diagnosis-specific prognostic factors, indexes, and treatment outcomes for patients with newly diagnosed brain metastases: a multi-institutional analysis of 4,259 patients. *Int J Radiat Oncol Biol Phys*, **77**(3), 655–61.

Tsao, M., Xu, W., Sahgal, A., et al. (2012). A meta-analysis evaluating stereotactic radiosurgery, whole-brain radiotherapy, or both for patients presenting with a limited number of brain metastases: meta-analysis for brain metastases. *Cancer*, **118**, 2486.

REFERENCES

Abel, T.J., Ryken, T., Lesniak, M.S., & Gabikian, P. (2013). Gliadel for brain metastasis. *Surg Neurol Int*, **4**, S289–93.

Berghoff, A.S., Rajky, O., Winkler, F., et al. (2013). Invasion patterns in brain metastases of solid cancers. *Neuro Oncol*, **15**, 1664–72.

Brodbelt, A., Greenberg, D., Winters, T., Williams, M., Vernon, S., & Collins, V. P. (2015). Glioblastoma in England: 2007–2011. *Eur J Cancer*, **51**, 533–42.

Brown, P.D., Pugh, S., Laack, N.N., et al. (2013). Memantine for the prevention of cognitive dysfunction in patients receiving whole-brain radiotherapy: a randomized, double-blind, placebo-controlled trial. *Neuro Oncol*, **15**, 1429–37.

Brown, P.D., Ballman, K.V., Cerhan, J.H., et al. (2017). Postoperative stereotactic radiosurgery compared with whole brain radiotherapy for resected metastatic brain disease (NCCTG N107C/CEC·3): a multicentre, randomised, controlled, phase 3 trial. *Lancet Oncol*, **18**(8), 1049–60.

Coluccia, D., Fandino, J., Schwyzer, L., et al. (2014). First noninvasive thermal ablation of a brain tumor with MR-guided focused ultrasound. *J Ther Ultrasound*, **2**, 17.

Davis, F.G., Dolecek, T.A., McCarthy, B.J., & Villano, J.L. (2012). Toward determining the lifetime occurrence of metastatic brain tumors estimated from 2007 United States cancer incidence data. *Neuro Oncol*, **14**, 1171–7.

Delattre, J.Y., Krol, G., Thaler, H.T., & Posner, J.B. (1988). Distribution of brain metastases. *Arch Neurol*, **45**, 741–4.

Ebisu, T., Tanaka, C., Umeda, M., et al. (1996). Discrimination of brain abscess from necrotic or cystic tumors by diffusion-weighted echo planar imaging. *Magn Reson Imaging*, **14**, 1113–16.

Fox, B.D., Cheung, V.J., Patel, A.J., Suki, D., & Rao, G. (2011). Epidemiology of metastatic brain tumors. *Neurosurg Clin N Am*, **22**, 1–6, v.

Franzin, A., Vimercati, A., Picozzi, P., et al. (2008). Stereotactic drainage and Gamma Knife radiosurgery of cystic brain metastasis. *J Neurosurg*, **109**, 259–67.

Gaspar, L., Scott, C., Rotman, M., et al. (1997). Recursive partitioning analysis (RPA) of prognostic factors in three Radiation Therapy Oncology Group (RTOG) brain metastases trials. *Int J Radiat Oncol Biol Phys*, **37**, 745–51.

Goyal, S., Silk, A.W., Tian, S., et al. (2015). Clinical management of multiple melanoma brain metastases: a systematic review. *JAMA Oncol*, **1**, 668–76.

Hart, M.G., Grant, R., Walker, M., & Dickinson, H. (2005). Surgical resection and whole brain radiation therapy versus whole brain radiation therapy alone for single brain metastases. *Cochrane Database Syst Rev*, **1**, CD003292.

Hawasli, A.H., Bagade, S., Shimony, J.S., Miller-Thomas, M., & Leuthardt, E.C. (2013). Magnetic resonance imaging-guided focused laser interstitial thermal therapy for intracranial lesions: single-institution series. *Neurosurgery*, **73**, 1007–17.

Jones, P.S., Cahill, D.P., Brastianos, P.K., Flaherty, K.T., & Curry, W.T. (2015). Ipilimumab and craniotomy in patients with melanoma and brain metastases: a case series. *Neurosurg Focus*, **38**, E5.

Kocher, M., Soffietti, R., Abacioglu, U., et al. (2011). Adjuvant whole-brain radiotherapy versus observation after radiosurgery or surgical resection of one to three cerebral metastases: results of the EORTC 22952-26001 study. *J Clin Oncol*, **29**, 134–41.

Kolomainen, D.F., Larkin, J.M., Badran, M., et al. (2002). Epithelial ovarian cancer metastasizing to the brain: a late manifestation of the disease with an increasing incidence. *J Clin Oncol*, **20**, 982–6.

Le Rhun, E., Taillibert, S., & Chamberlain, M.C. (2013). Carcinomatous meningitis: leptomeningeal metastases in solid tumors. *Surg Neurol Int*, **4**, S265–88.

Louis, D.N., Ohgaki, H., Wiestler, O.D., et al. (2007). The 2007 WHO classification of tumours of the central nervous system. *Acta Neuropathol*, **114**, 97–109.

Maluf, F.C., Deangelis, L.M., Raizer, J.J., & Abrey, L.E. (2002). High-grade gliomas in patients with prior systemic malignancies. *Cancer*, **94**, 3219–24.

Muacevic, A., Wowra, B., Siefert, A., Tonn, J.-C., Steiger, H.-J., & Kreth, F. (2008). Microsurgery plus whole brain irradiation versus Gamma Knife surgery alone for treatment of single metastases to the brain: a randomized controlled multicentre phase III trial. *J Neurooncology*, **87**, 299–307.

Mulvenna, P., Nankivell, M., Barton, R., et al. (2016). Dexamethasone and supportive care with or without whole brain radiotherapy in treating patients with non-small cell lung cancer with brain metastases unsuitable for resection or stereotactic radiotherapy (QUARTZ): results from a phase 3, non-inferiority, randomised trial. *Lancet*, **388**(10055), 2004–14.

National Cancer Institute, Surveillance Research Program, Surveillance Systems Branch (2015). *Surveillance, Epidemiology, and End Results (SEER) Program Populations (1969–2013) released January 2015*. http://seer.cancer.gov/data/

Neves, S., Mazal, P.R., Wanschitz, J., et al. (2001). Pseudogliomatous growth pattern of anaplastic small cell carcinomas metastatic to the brain. *Clin Neuropathol*, **20**, 38–42.

NICE (2010). *Metastatic Malignant Disease of Unknown Primary Origin: Diagnosis and management*. https://www.nice.org.uk/guidance/cg104

Norden, A.D., Wen, P.Y., & Kesari, S. (2005). Brain metastases. *Curr Opin Neurol*, **18**, 654–61.

Nussbaum, E.S., Djalilian, H.R., Cho, K.H., & Hall, W.A. (1996). Brain metastases. Histology, multiplicity, surgery, and survival. *Cancer*, **78**, 1781–8.

Ohana, M., Jeung, M.Y., Bazille, G., & Roy, C. (2014). Cerebral staging of lung cancer: is one single contrast-enhanced T1-weighted three-dimensional gradient-echo sequence sufficient? *Neuroradiology*, **56**, 621–7.

Ostrom, Q. T., Gittleman, H., Liao, P., et al. (2014). CBTRUS statistical report: primary brain and central nervous system tumors diagnosed in the United States in 2007–2011. *Neuro Oncol*, **16** Suppl 4, iv1–63.

Patchell, R.A., Tibbs, P.A., Regine, W.F., et al. (1998). Postoperative radiotherapy in the treatment of single metastases to the brain: a randomized trial. *JAMA*, **280**, 1485–9.

Patchell, R.A., Tibbs, P.A., Walsh, J.W., et al. (1990). A randomized trial of surgery in the treatment of single metastases to the brain. *N Engl J Med*, **322**, 494–500.

Patel, A.J., Suki, D., Hatiboglu, M.A., et al. (2010). Factors influencing the risk of local recurrence after resection of a single brain metastasis. *J Neurosurg*, **113**, 181–9.

Pestalozzi, B.C., Zahrieh, D., Price, K.N., et al. (2006). Identifying breast cancer patients at risk for Central Nervous System (CNS) metastases in trials of the International Breast Cancer Study Group (IBCSG). *Ann Oncol*, **17**, 935–44.

Pinkham, M.B., Sanghera, P., Wall, G.K., Dawson, B.D., & Whitfield, G.A. (2015). Neurocognitive effects following cranial irradiation for brain metastases. *Clin Oncol (R Coll Radiol)*, **27**(11), 630–9.

Posner, J.B. & Chernik, N.L. (1978). Intracranial metastases from systemic cancer. *Adv Neurol*, **19**, 579–92.

Schöggl, A., Kitz, K., Reddy, M., et al. (2000). Defining the role of stereotactic radiosurgery versus microsurgery in the treatment of single brain metastases. *Acta Neurochirurgica*, **142**, 621–6.

Serres, S., Soto, M.S., Hamilton, A., et al. (2012). Molecular MRI enables early and sensitive detection of brain metastases. *Proc Natl Acad Sci U S A*, **109**, 6674–9.

Siam, L., Bleckmann, A., Chaung, H.N., et al. (2015). The metastatic infiltration at the metastasis/brain parenchyma-interface is very heterogeneous and has a significant impact on survival in a prospective study. *Oncotarget*, **6**(30), 29254–67.

Sperduto, P.W., Chao, S.T., Sneed, P., et al. (2010). Diagnosis-specific prognostic factors, indices and treatment outcomes for patients with newly diagnosed brain metastases: a multi-institutional analysis of 4259 patients. *Int J Radiat Oncol Biol Phys*, **77**(3), 655–61.

Taillibert, S. & Delattre, J.Y. (2005). Palliative care in patients with brain metastases. *Curr Opin Oncol*, **17**, 588–92.

Tsao, M., Xu, W., Sahgal, A., et al. (2012). A meta-analysis evaluating stereotactic radiosurgery, whole-brain radiotherapy, or both for patients presenting with a limited number of brain metastases: meta-analysis for brain metastases. *Cancer*, **118**, 2486.

Yamamoto, M., Serizawa, T., Shuto, T., et al. (2014). Stereotactic radiosurgery for patients with multiple brain metastases (JLGK0901): a multi-institutional prospective observational study. *Lancet Oncol*, **15**, 387–95.

Yoo, H., Kim, Y.Z., Nam, B.H., et al. (2009). Reduced local recurrence of a single brain metastasis through microscopic total resection. *J Neurosurg*, **110**, 730–6.
Zakaria, R., Das, K., Radon, M., et al. (2014). Diffusion-weighted MRI characteristics of the cerebral metastasis to brain boundary predicts patient outcomes. *BMC Med Imaging*, **14**, 26.

RELATED LINKS TO EBRAIN

Assessment of the Patient with a Brain Tumour. https://learning.ebrain.net/course/view.php?id=1247
Clinical Presentation of Patients with Brain Tumours. https://learning.ebrain.net/course/view.php?id=1249
Intracranial Metastases Imaging and Differential Diagnosis. https://learning.ebrain.net/course/view.php?id=1240
Malignant Meningitis. https://learning.ebrain.net/course/view.php?id=502
Management Principles for Metastases. https://learning.ebrain.net/course/view.php?id=437
Palliative Care and End of Life in Brain Tumour Patients. https://learning.ebrain.net/course/view.php?id=483
Referral and Management Guidelines for Patients with Brain Tumours. https://learning.ebrain.net/course/view.php?id=507

9

Primary central nervous system lymphoma

Boon Leong Quah, Thangaraj Munusamy, and Colin Watts

Introduction

Primary central nervous system lymphoma (PCNSL) is a rare form of non-Hodgkin's lymphoma (NHL) confined to the central nervous system, which continues to be a challenging malignancy to treat. The reason behind this lies in the fact that its systemic counterpart carries a more favourable prognosis with a cure rate of approximately 70%, whereas the prognosis of PCNSL remains poor in the immunocompetent and even poorer in HIV-associated PCNSL. Fortunately, the median overall survival has nearly doubled since the 1970s reflecting a better understanding, and more effective management of this disease. In this chapter, we will explore the many reasons behind this increased survival as well as current management options from a neurosurgical perspective.

Epidemiology

Primary central nervous system lymphoma (PCNSL) is a rare tumour affecting approximately 0.48 in 100 000, comprising approximately 2–3% of primary central nervous system (CNS) tumours, they are aggressive and high grade. PCNSLs are non-Hodgkin's lymphomas, and account for approximately 2% of all cases of NHL. The vast majority of PCNSL's are the diffuse large B-cell type (DLBCL). In the immunocompetent, the peak incidence occurs in the 60-year and above age group whereas the median age of presentation is 37 years in HIV-associated PCNSL (Norden et al., 2011). HIV-associated PCNSL is almost always associated with Epstein–Barr virus (EBV), which is in contrast to only 20% of systemic AIDS-related lymphomas (Wang et al., 2014). The male to female ratio is 1.2–1.7:1 in immunocompetent patients, in contrast to a male predominance for the immunocompromised group (**Table 9.1**).

Epidemiological data has also shown an increase in the frequency of PCNSL cases in immunocompetent patients from the 1990s onwards, especially in those above 65 years old. Conversely, the frequency of cases has dropped in HIV-associated PCNSL, not surprisingly due to the widespread availability and access to highly effective antiretroviral treatment.

Clinical presentation

PCNSL is defined by involvement of the brain, leptomeninges, cranial nerves, spinal cord, cerebrospinal fluid (CSF) or eyes, without evidence of systemic disease. Patients usually present with neurological symptoms that reflect the neuroanatomical location of the lesion(s). The majority of patients have constitutional, cognitive, neuropsychiatric, or motor symptoms, 20% present with seizures. Leptomeningeal disease occurs in 15–20% of patients and may present with multiple cranial nerve palsies. Approximately 20–30% of patients have ocular involvement at the time of diagnosis, often affecting both eyes causing non-specific symptoms such as pain, redness, photophobia, blurred vision, and reduced visual acuity. HIV-associated PCNSL is an AIDS-defining illness associated with low CD4 counts and Epstein–Barr virus (EBV) infection, and is more likely to present with encephalopathy and a history of other concurrent infections. Temporal progression of disease is variable among patients. Some exhibit chronic symptoms that precede diagnosis by years, while for others disease progression is rapid and aggressive.

Diagnosis

Radiological

The common sites affected by PCNSL are the periventricular region, basal ganglia, corpus callosum, and deep white matter. The frontal lobe is the most frequently affected, followed in order by the parietal, temporal, and occipital lobes. MR imaging characteristically shows an avid, homogenously contrast-enhancing lesion (**Table 9.1**).

However, 10% of immunocompetent patients will harbour non-enhancing lesions, particularly seen at recurrence. Multiplicity is seen in approximately 70% of AIDS patients, in which heterogenous ring-enhancing lesions are more commonly seen. PCNSL is characteristically seen tracking along Virchow-Robinson perivascular spaces. Calcification, haemorrhage, and necrosis are rarely present but are more commonly seen following treatment. MR spectroscopy (MRS) commonly demonstrates much higher choline to creatine ratio compared to gliomas. Also, large lipid peaks on single-voxel proton MRS are characteristic (Yamasaki et al., 2015).

Table 9.1 Comparison between immunocompetent and immunocompromised patients with PCNSL

PCNSL		Immunocompetent	Immunocompromised
	Age (years)	60s (median 56)	30s (median 35)
	Time to diagnosis	3 months	2 months
Symptoms		Neurological deficits (extent dictated by location of tumour) Seizures and cranial nerve palsies less common	Neurological deficits (extent dictated by location of tumour) Commonly presents with seizures, encephalopathy, and cranial nerve palsies
Location in CNS	Adults	Solitary (70%), supratentorial (85%), periventricular (60%), corpus callosum (12%)	Multiple (50%), supratentorial
	Paediatrics	Solitary Parietal and frontal lobes, cerebellum, pituitary stalk, hypothalamus Leptomeningeal spread commoner (18%)	
Differential diagnosis		High-grade gliomas Multiple sclerosis Metastasis Neurosarcoidosis	Toxoplasmosis Abscess Progressive multifocal leukoencephalopathy
Radiological features	CT	Hyperdense to grey matter Enhances homogenously with contrast	Heterogenous, ring enhancing
	MRI	Hypointense on T1WI, hyperintense on T2WI, homogenously enhancing	Heterogenous, ring enhancing (also commonly seen in paediatric population)
Subtyping		Ranges from low grade to high grade 95% DLBCL Association with EBV: rare	Almost always EBV-positive Mostly high-grade, DLBCL, immunoblastic type (features similar in both AIDS and transplant patients)

Abbreviations: AIDS, acquired immunodeficiency disease; BCL-6, B-cell lymphoma 6 protein; CNS, central nervous system; CT, computed tomography; DLBCL, diffuse large B-cell lymphoma; DWI/ADC, diffusion-weighted imaging/apparent diffusion coefficient map; EBV, Epstein–Barr virus; MRI, magnetic resonance imaging; MRS, magnetic resonance spectroscopy; PCNSL, primary central nervous system lymphoma; T1WI, T1-weighted imaging; T2WI: T2-weighted imaging.

PCNSL lesions are hypermetabolic when imaged by positron emission tomography (PET) and single-photon emission computed tomography (SPECT). This is useful in differentiating it from the hypometabolic toxoplasmosis lesions in patients with AIDS. Figures 9.1 and 9.2 give radiological examples of cases of PCNSL and other differential diagnoses.

Eye examination (slit lamp, vitrectomy)

All patients suspected of having PCNSL must undergo a complete ophthalmic examination and CSF analysis, if no contraindication exists. Approximately 25% of patients with PCNSL develop ocular involvement, and conversely, up to 90% of patients with primary intraocular lymphoma (PIOL) go on to develop PCNSL (Gündüz et al., 2003). Abnormalities consistent with PCNSL on the slit-lamp examination would prompt a biopsy with either a fine-needle aspiration to obtain a vitreous sample or a diagnostic vitrectomy in the eye where vision or disease is worse. Vitrectomy can also improve vision by removing the cellular debris that is responsible for the blurred vision and floaters. This procedure is less invasive than a brain biopsy and could potentially clinch the diagnosis in about 25% of patients without having to subject them to the hazards of a stereotactic brain biopsy.

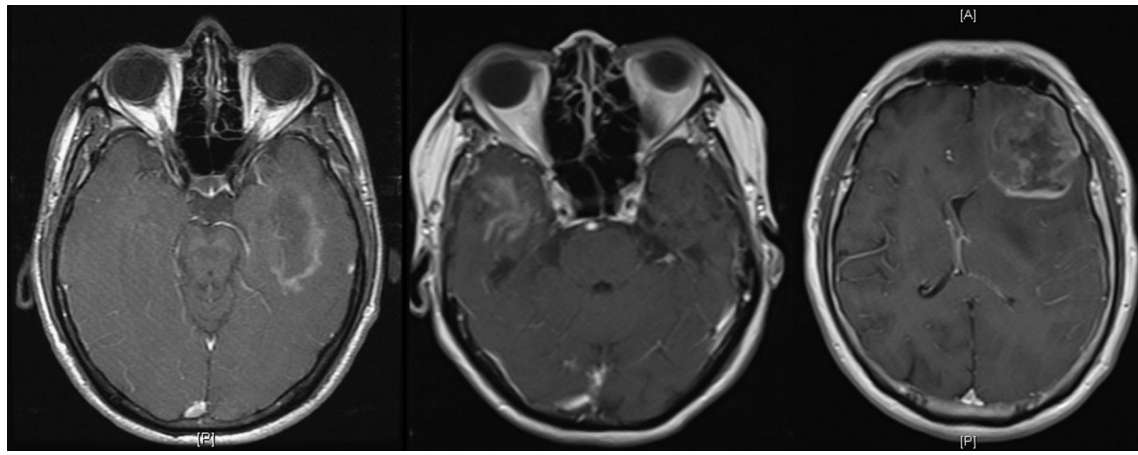

Fig. 9.1 Similarity of contrast-enhanced MR imaging of PCNSL to other pathologies. Left: Left temporal tumefactive multiple sclerosis. Middle: Right temporal DLBCL type PCNSL. Right: Left frontal glioblastoma WHO Grade IV.

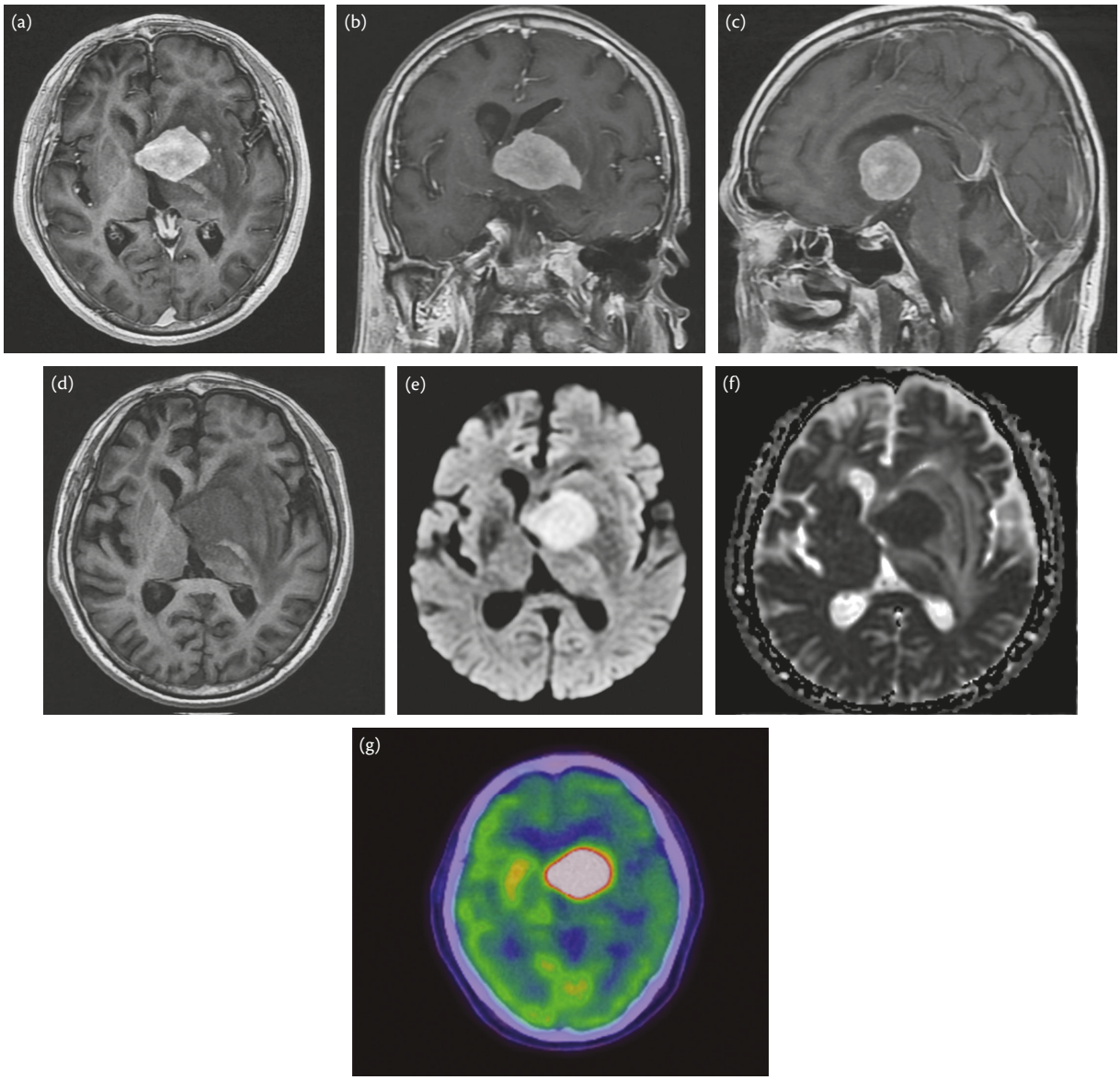

Fig. 9.2 MR images of a patient with PCNSL involving left basal ganglia and the internal capsule.
(A) Homogenous and avidly enhancing axial (B) and (C) coronal and sagittal T1-weighted images with gadolinium. (D) Non-contrasted axial T1-weighted image demonstrating a hypointense lesion. (E) and (F) Restricted diffusion on DWI and ADC images. (G) PET scan revealing a hypermetabolic PCNSL lesion.

CSF examination (cytology, flow cytometry, PCR)

Multimodal CSF analysis utilizing cytology, flow cytometry, and polymerase chain reaction (PCR) investigations are important additional investigative tools that complement each other, and aid in the diagnosis of PCNSL in the presence of suspicious radiological findings. Positive CSF cytology nearly always represents leptomeningeal involvement but has limited sensitivity in specimens with low cellularity. CSF flow cytometry on the other hand, does not suffer from this limitation and has demonstrated good sensitivity and specificity in the detection of PNCSL (Craig et al., 2011). Demonstration of monoclonality of lymphocytes in the CSF by PCR can establish the diagnosis, and this technique can also be used in vitrectomy specimens to diagnose PIOL. CSF examination is particularly useful and important in the setting of AIDS associated PCNSL by demonstrating EBV DNA and obviating the need for a stereotactic brain biopsy.

Histopathology

It cannot be overemphasized that the gold standard for diagnosis of PCNSL is a positive tissue biopsy and histology. The WHO 2016 revision of the 2007 Classification of CNS Malignancies has expanded and clarified the tumour entities included, aligning them with the 2008 WHO Classification of Haematopoietic and Lymphoid Tissues (Louis et al., 2016). Diffuse large B-cell lymphoma of the CNS or primary CNS lymphoma (PCNSL) is strictly defined as a large B-cell lymphoma confined to the CNS at presentation. PCNSL is a distinct mature B-cell lymphoma that corresponds to late germinal-centre exit B cells with blocked terminal B-cell differentiation. They show

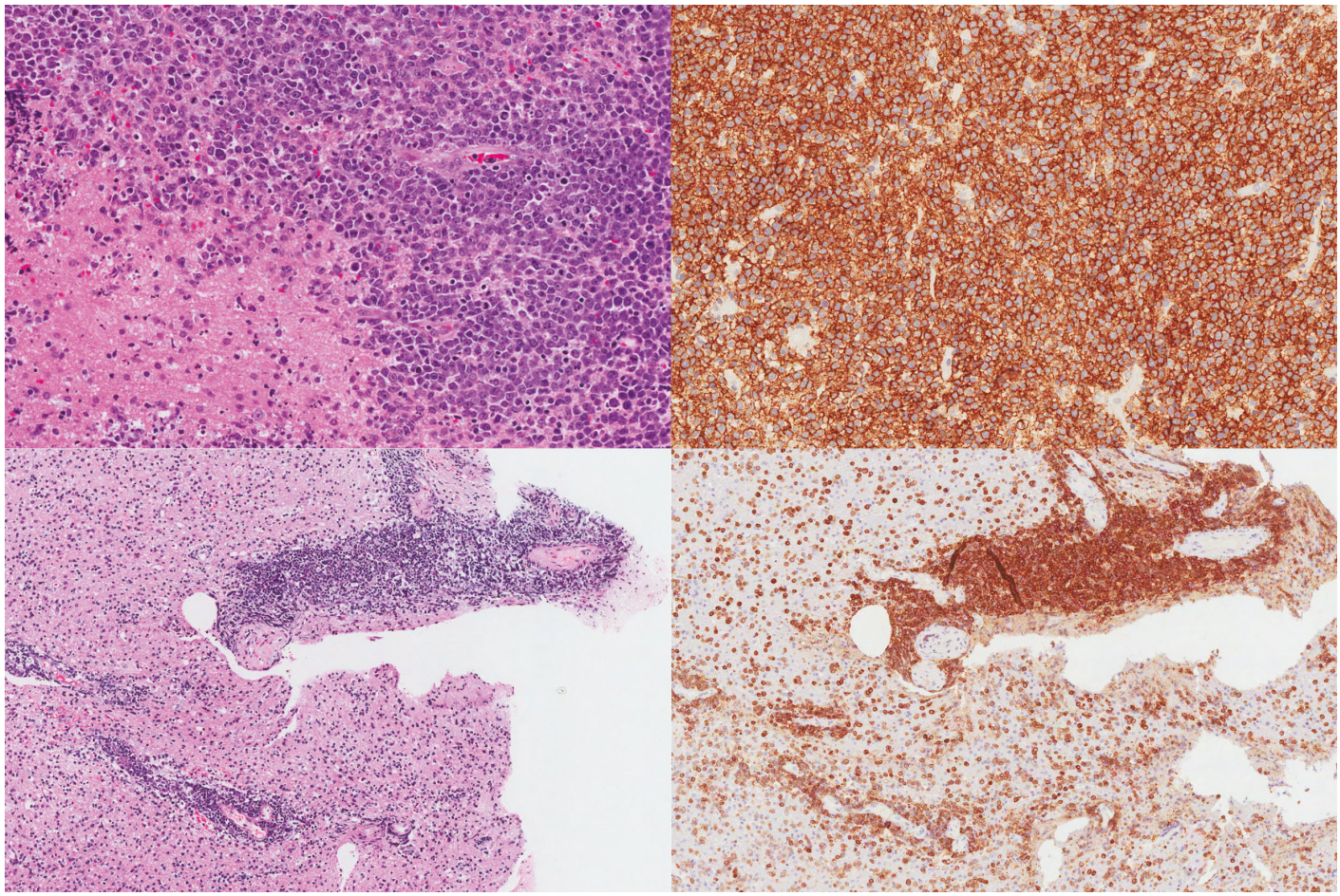

Fig. 9.3 Two examples of diffuse large B-cell lymphoma. Top left: Brain biopsy showing diffuse large B-cell lymphoma with viable tumour in the upper right region and necrosis in lower left region (H&E, original magnification ×20). Top right: CD20 immunohistochemistry.
Bottom left: Brain biopsy from the edge of a different lymphoma, which is tracking along perivascular spaces (H&E, original magnification ×10). Bottom right: CD79A immunohistochemistry.

CD20 (as well as CD79a, PAX5) immunopositivity, mostly BCL6 (60–80%) and MUM1/RF4 (90%) positivity, and only rarely CD10 expression (<10%). They carry rearranged and somatically mutated immunoglobulin (IG) genes with evidence of ongoing somatic hypermutation.

PCNSL is distinct from other lymphomas, which can also present primarily in the CNS, including lymphomas arising from the dura, intravascular large B-cell lymphoma, and lymphoma of T-cell or NK-cell lineage. It is also distinct from immunodeficiency-associated primary CNS lymphomas, which include immunodeficiency-associated CNS lymphoma (inherited or acquired), AIDS-related diffuse large B-cell lymphoma, EBV-positive diffuse large B-cell lymphoma, NOS (of elderly), and lymphomatoid granulomatosis.

Histologically, PCNSL resembles its systemic counterpart with cytoarchitectural features of diffuse parenchymal infiltration and angiocentric growth pattern (Mrugala et al., 2009). Small and medium-sized blood vessels are surrounded by cuffs of malignant lymphocytes and some may invade the blood vessel wall contributing to blood–brain barrier (BBB) disruption. These lymphoma cells lack intercellular cohesion and do not form glands or other structures (**Figs. 9.3 and 9.4**). They have prominent nucleoli surrounded by a scanty rim of basophilic cytoplasm. Confluent areas may show the presence of apoptotic cells or necrosis. In addition, there are varying numbers of reactive T-cells and astrocytes, mimicking the appearance of encephalitis.

Immunocompromised

The immunocompromised have an elevated risk of developing PCNSL compared to their immunocompetent counterparts, and can be separated into three distinct groups: acquired (HIV-associated), iatrogenic (transplant recipients), and congenital immunodeficient states (**Table 9.2**). The incidence and prognosis differ significantly between these groups. However, the principles of management are essentially the same—aim to reinstate immune competence.

Diagnosing PCNSL in the immunocompromised is no different from the current set of recommendations for the immunocompetent, where a tissue diagnosis remains the gold standard (**Fig. 9.3**). However, the potential morbidity faced by the patient and the potential risks towards the healthcare workers justifies pursuing a less invasive work-up for this group of patients in the first instance. A positive CSF polymerase chain reaction (PCR) for EBV DNA in the setting of typical MR features of PCNSL, coupled with demonstration of a hypermetabolic lesion on PET is highly likely

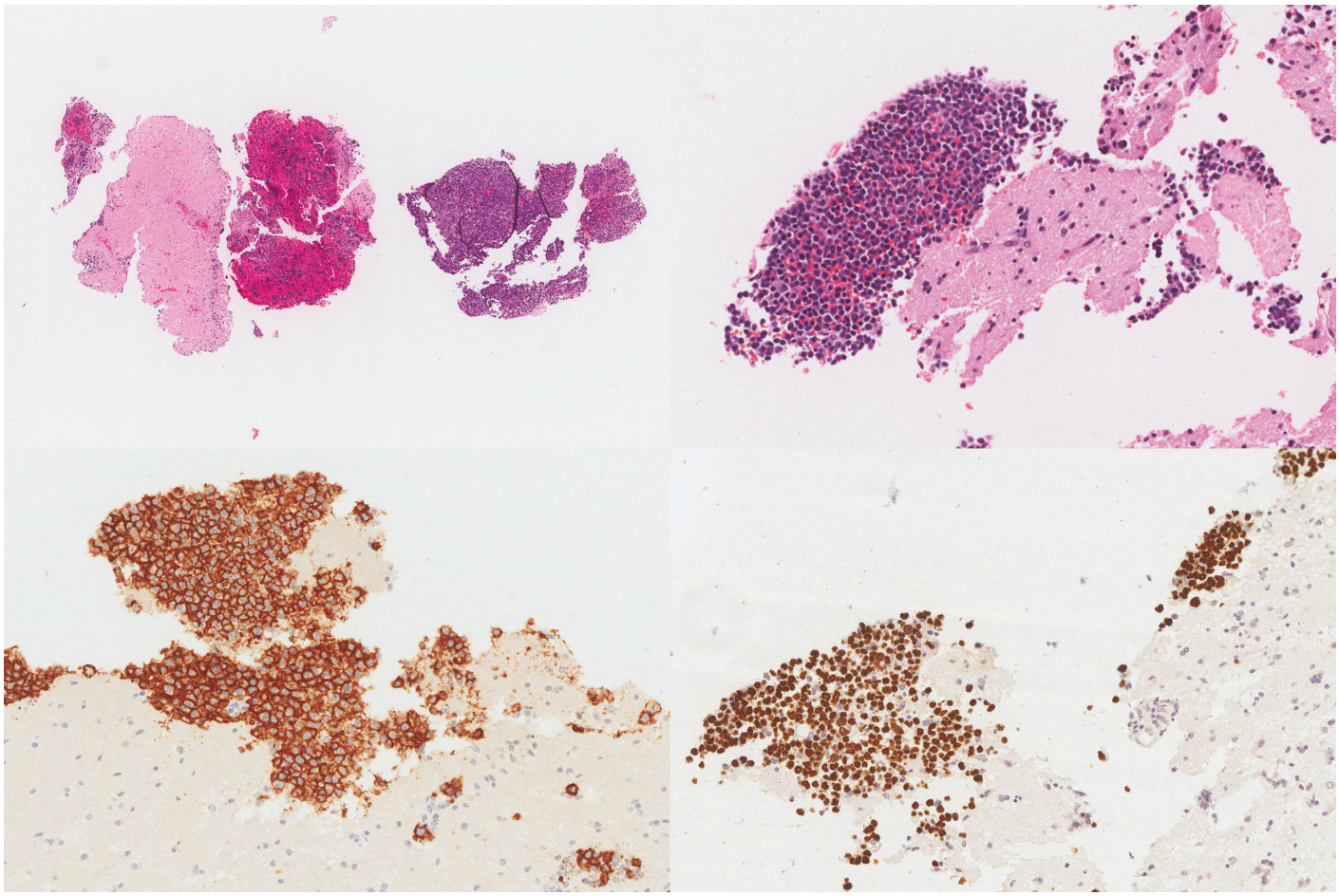

Fig. 9.4 Diffuse large B-cell lymphoma, EBV-positive. Top left: Low power image of three fragments of tumour showing, from left to right, necrosis, haemorrhage, and viable tumour (H&E, original magnification ×4). Top right: Separate area of viable tumour with adjacent brain tissue (H&E, original magnification ×20). Lower left: CD20 immunohistochemistry. Lower right: EBER *in-situ* hybridization.

to represent PCNSL. Alternatively, a negative response to a trial of antitoxoplasmosis treatment is suggestive of PCNSL but there are opponents to this approach for a few reasons. Firstly, a definitive histological diagnosis is not obtained. Secondly, the diagnosis is delayed and further neurological deterioration is common. Lastly, both toxoplasmosis and PCNSL may coexist.

Molecular tumour cell biology

Normal B cells arise from haematopoietic stem cells and emerge from the bone marrow as mature but naïve B cells. They subsequently undergo somatic hypermutation and affinity maturation upon encountering an antigen in peripheral lymphoid tissue and terminally differentiate into plasma cells or memory B cells (Fig. 9.5).

It has been hypothesized that the molecular pathogenesis of B-cell lymphomas is related to perturbation of the normal B-cell development pathway such as alterations to the genes critical to B-cell development or physiology. These alterations may occur at any stage of the differentiation process described earlier. Some of the important genes and mediators in PCNSL and their roles are summarized in Table 9.3. 10% of tumours express CD10, 50–90% express BCL2 and BCL6 (Braaten et al., 2003), and more than 95% stain positive for MUM1 (Camilleri-Broët et al., 2006), which means that these B cells are on the verge of exiting the germinal centre. However, as the brain is devoid of germinal centres, it is not known whether the malignant

Table 9.2 Risk of PCNSL in immune competent and compromised states

Immune status	Groups	Disorders/syndromes	Incidence/risk of PCNSL
Competent			~ 0.5 in 100 000
Compromised	Acquired	HIV-associated (AIDS)	2–6% incidence in HIV infected
	Iatrogenic (PTLD)	Renal, cardiac, lung, liver transplant	1–7% of transplant recipients
	Congenital	SCID, Wiskott–Aldrich syndrome, ataxia-telangiectasia	4% risk

AIDS, acquired immunodeficiency syndrome; HIV, human immunodeficiency virus; PTLD, post-transplant lymphoproliferative disorder; SCID, severe-combined immunodeficiency disease.

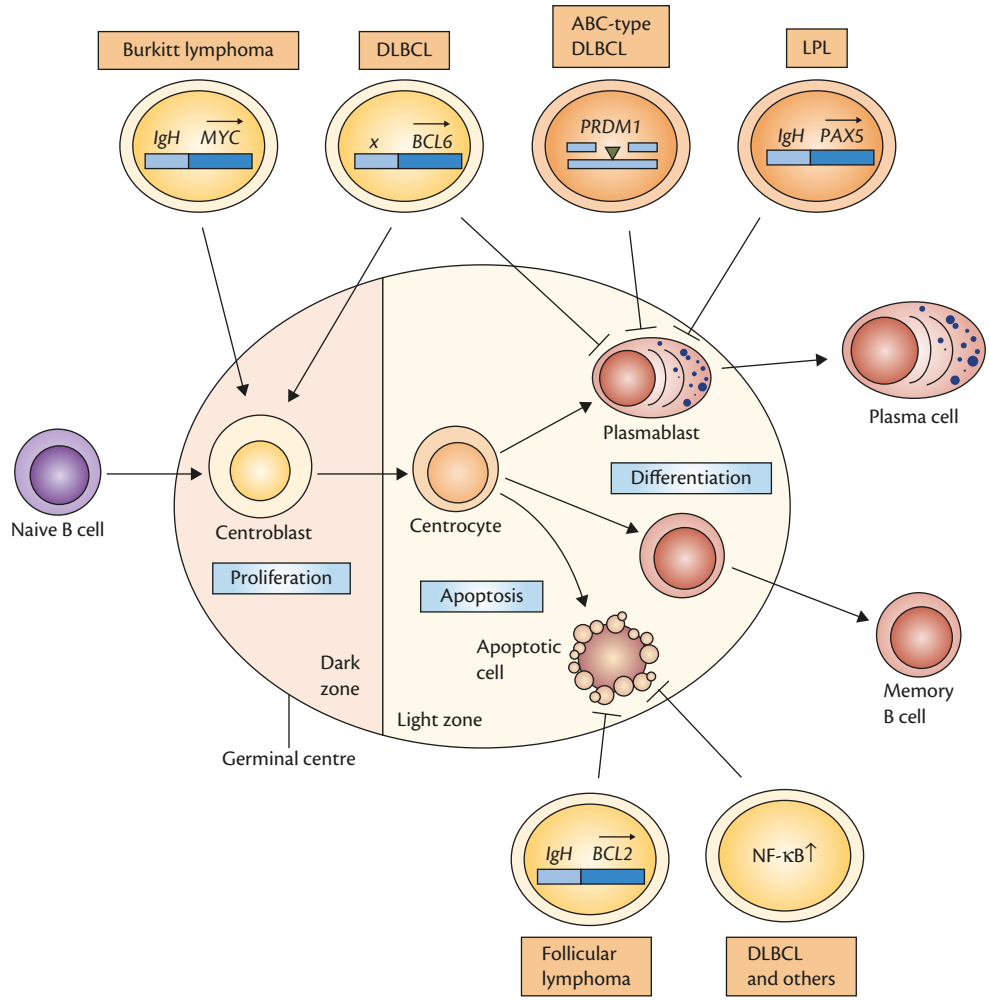

Fig. 9.5 Normal B-cell development (Klein and Dalla-Favera, 2008).

Reproduced with permission from Ulf Klein, Riccardo Dalla-Favera, Germinal centres: role in B-cell physiology and malignancy, *Nature Reviews Immunology*, Volume 8, Issue 1, pp. 22–33. Copyright © 2008 Springer Nature.

Table 9.3 The role of genes and regulators in PCNSL

Gene/Mediator	Role	Authors
HLA (6p21)	Antigen processing, signalling pathway	Cady et al., 2008
PRDM1 (6q21)	Regulate B-cell differentiation into plasma cell	Courts et al., 2008
PTPRK	Cell adhesion	Cady et al., 2008
TNFAIP3	Regulator of nuclear factor NFKB signalling	Paik et al., 2013
MALT1	Activation of NFKB pathway	Schwindt et al., 2009
TBL1XR1	Transcriptional regulation of NFKB pathway	Nakamura et al., 2004
MYD88	Activation of NFKB pathway and JAK/STATb pathways	Nakamura et al., 2016
CD79B	B-cell receptor signalling pathway	Nakamura et al., 2016
CDKN2A	Cell cycle regulator	Schwindt et al., 2009
MYC	Transcription regulation	Rubenstein et al., 2006; Cady et al., 2008
IL4	Up-regulation promotes cell survival via JAK/STAT pathway	Rubenstein et al., 2006

CD, cluster of differentiation; CDKN, cyclin-dependent kinase inhibitor; HLA, human leucocyte antigen; IL, interleukin; JAK, janus kinase; PRDM, positive regulatory domain; PTPRK, protein tyrosine phosphatase receptor type K; MALT, mucosa-associated lymphoid tissue lymphoma translocation; MYC, myelocytomatosis; MYD, myeloid differentiation; NFKB, nuclear factor kappaB; STAT, signal transducer and activator of transcription; TBL1XR1, transducin (beta)-like 1 X-linked receptor 1; TNFAIP3, tumour necrosis factor alpha-induced protein 3.

Data from Wang CC, Carnevale J, Rubenstein JL. Progress in central nervous system lymphomas. *British Journal of Haematology*, volume 166, issue 3, pp. 311–25, Copyright © 2014 John Wiley & Sons; Nakamura M, Shimada K, Ishida E, Konishi N. Histopathology, pathogenesis and molecular genetics in primary central nervous system lymphomas. Histology and Histopathology, volume 19, pp. 211–9, Copyright © 2004.

transformation of B cells in PCNSL occurs prior to migration into the CNS.

The microenvironment plays a fundamental role in the pathogenesis of PCNSL where it contains chemokines that act as neurotropic or survival factors. Detection of these factors within CSF allows their utilization as biomarkers of PCNSL, aiding diagnosis and monitoring treatment response. Elevated levels of CXCL13 and IL-10 in CSF were found to be 99.3% specific for PCNSL, with good sensitivity (Rubenstein et al., 2013). The benefits of testing for these biomarkers may be more pronounced for high-risk patients, and in those with a potentially low-yield biopsy.

High levels of EBV DNA were detected in the CSF of almost 100% of HIV-positive patients with PCNSL in a study by Knowles (2003). The pathogenesis of AIDS-related PCNSL appears to occur when the CD4 + lymphocyte count falls below 100 cells/μl, and has been hypothesized to be different from its immunocompetent counterpart. It is perhaps due to impaired T-cell responses and malignant transformation of activated B cells.

Treatment

Clinical outcomes and survival rates have improved significantly since the advent of chemoradiation protocols, incorporating high-dose methotrexate (HD-MTX) and whole-brain radiation therapy (WBRT) were developed in the 1980s. However, disease relapse and neurotoxicity continued to pose major treatment challenges. The current paradigm shift in treatment focuses on accurate radiological, clinical, and molecular diagnosis and effective treatment regimens comprising novel cytotoxic combinations, monoclonal antibody therapy, and stem cell therapy in an attempt to improve disease control while reducing adverse neurocognitive side effects.

Steroids

Dexamethasone is cytotoxic to PCNSL cells and reduces vasogenic oedema by stabilizing the BBB. These effects are invariably short-lived and are responsible for certain cases of negative biopsies, with some cases demonstrating a dramatic decrease in enhancement and size of the lesions. It is therefore preferable for steroids to be withheld wherever possible until the diagnosis of PCNSL is established or refuted. Additionally, dexamethasone reduces the permeability of the BBB to chemotherapy and thus may impair the therapeutic benefit of this treatment.

Surgery

Biopsy

Stereotactic biopsy remains the gold standard for diagnosing and subtyping PCNSL. Biopsies are usually well tolerated and can be performed relatively quickly with minimal risk. The option of performing the procedure under local anaesthetic exists, and there is a theoretical reduction in the risk of tumour seeding along the path of the biopsy. It is important to target the centre of the suspected PCNSL lesion to reduce the chances of a negative biopsy. The adequacy of samples can be verified and the preliminary diagnosis can be made intraoperatively by a neuropathologist.

Debulking and excisional procedures

Anything more invasive than a biopsy is thought to risk neurological deficits while failing to improve overall survival (Bierman, 2014). However, additional analysis of the data from the German PCNSL Study Group-1 (G-PCNSL-SG-1) found that patients who underwent gross-total or subtotal resection were more likely to be in complete remission six months after surgery. Interestingly, patients harbouring single, surgically accessible lesions were more likely to undergo resection than biopsy (31% and 19%, respectively). The advantage of overall survival was lost after adjusting for the number of lesions despite having a better progression-free survival. The authors of this subanalysis concluded that surgery for PCNSL should be reconsidered especially for patients with single lesions that might be safely resected (Weller et al., 2012).

The patient with a rapidly deteriorating neurological status secondary to mass effect by PCNSL poses a unique challenge for a neurosurgeon. High-dose dexamethasone and mannitol are usually commenced, and a rapid decision to take the patient to the operating theatre could prove life-saving. An excisional or debulking procedure is invariably performed in such emergencies as the initial radiological features usually favour a glioma or metastasis. Interestingly, Lee et al. (2014) have described a case where surgery was avoided in a patient with rapid neurological deterioration using medical treatment with hyperosmolar therapy, dexamethasone, and chemotherapy. This resulted in a marked reduction of peritumoural oedema, the size of the tumour, and consequently mass effect.

Chemotherapy and radiotherapy

The current evidence favours a shift in treatment strategy away from WBRT or HD-MTX monotherapy to HD-MTX based combination chemotherapy regimens. This current standard of care has been accompanied by improved overall survival rates (OS), compared to results obtained by treatment with WBRT alone, or single-agent HD-MTX chemotherapy (**Table 9.4**).

Treatment is divided into two phases: induction and consolidation. HD-MTX based chemotherapy regimens constitute the induction phase, which are aimed at controlling the disease and inducing remission. Ongoing trials are assessing the role of concurrent immunotherapy using rituximab, an anti-CD20 monoclonal antibody (IELSG-32 and HOVON105 PCNSL/ALLG NHL24 trials). Intrathecal MTX was previously in fashion to treat PCNSL with evidence of disseminated meningeal disease and spinal involvement. However, the benefit of intrathecal chemotherapy is not clear, given that therapeutic concentrations of MTX are readily achieved via the intravenous route. The concept of BBB disruption followed by chemotherapy was a novel approach developed with the hope of improving effects of chemotherapy but has been limited to research centres equipped with appropriate facilities and technical capabilities (see *International Blood-Brain Barrier Disruption Consortium*). Using this technique, McAllister et al. (2000) showed comparable results to that of other studies utilizing HD-MTX-based regimens but reported four deaths, and increased seizure, TIAs, and stroke rates. While this treatment approach appears promising by potentially enhancing chemotherapy effectiveness and reducing chemotherapy doses, it requires further evaluation.

Table 9.4 Various combined modality regimens and survival rates

Year	Reference	Regimen	No. of patients	Median follow-up (months)	OS (%)	Median OS (months)	2-year PFS (%)	Median PFS (months)
2002	DeAngelis et al. (2002)	MTX, PCB, Vincristine, IT-MTX, WBRT	98	56	NA	37	NA	24
2006	Illerhaus et al. (2006)	MTX, ASCT, WBRT	30	63	(3 y OS) 68.5	NA	NA	NA
2007	Montemurro et al. (2007)	MTX, thiotepa, ASCT, WBRT	28	15	(2 y OS) 48	48	45	45
2009	Ferreri et al. (2009)	MTX, ARA-C, WBRT	79	30	(3 y OS) 46	NA	NA	NA
2012	Wieduwilt et al. (2012)	MTX, TMZ, rituximab, etoposide, ARA-C	31	79	NA	66	79	24
2013	Morris et al. (2013)	MTX, rituximab, vincristine, PCB, ARA-C, rd-WBRT	52	70	(5 y OS) 80	79	77	39
2015	Omuro et al. (2015)	MTX, rituximab, vincristine, PCB, ASCT	33	45	(2 y OS) 81	NR	79	NR

ARA-C, cytarabine; ASCT, autologous stem cell transplantation; IT, intrathecal; NA, not available; NR, not reached; OS, overall survival; MTX, methotrexate; PCB, procarbazine; PFS, progression-free survival; TMZ, temozolomide.

Adapted with permission from Chia-Ching Wang, Julia Carnevale, James L. Rubenstein, Progress in central nervous system lymphomas, *British Journal of Haematology*, Volume 166, Issue 3, pp. 311–25, Copyright © 2014 John Wiley and Sons.

Data from Omuro A, Correa DD, DeAngelis LM, et al., R-MPV followed by high-dose chemotherapy with TBC and autologous stem-cell transplant for newly diagnosed primary CNS lymphoma, *Blood*, Volume 125, Issue 9, pp. 1403–10, Copyright © 2015 American Society of Hematology.

The rationale for the consolidation phase of treatment is to eradicate residual disease following induction chemotherapy. This commonly takes the form of WBRT and/or chemotherapy. In the younger and fitter patients, high-dose chemotherapy and autologous stem cell transplantation (HDT-ASCT) may be considered as an alternative treatment (Schorb et al., 2013).

The current treatment options have not proven to be robust in producing durable results by producing sustained complete remission or cure. Disease recurrence is almost inevitable and a particularly challenging area as no standard treatment approach exists. Options available are radiotherapy, if not already utilized as part of consolidation treatment, and second-line chemotherapy regimens.

Prognosis

Understandably, there is paucity of data in the literature regarding prognosis of treatment naïve patients with PCNSL as most of the data captured reflects the OS and PFS of treated patients. It is conceivable that the prognosis without treatment is dismal for this rare tumour, perhaps in the range of weeks to months. Henry et al. (1974) reported a survival of 3.3 months with supportive care alone. Norden et al. (2011) analysed data from the Surveillance, Epidemiology, and End Results (SEER) database and found that the median survival was 7.5 months for patients diagnosed in the 1970s. It also showed that the median survival following treatment for the immunocompetent patient is approximately 14 months, and a dismal 2 months for the HIV-associated PCNSL. Another population-based study in Korea that analysed data from 688 patients between 1999 and 2007 had a median survival of 21 months (Shin S-H et al., 2015) but did not specify the immune status of their subjects. Nevertheless, this data offers a realistic representation of the current survival pattern of patients with PCNSL.

Trial data, on the other hand, reports figures that are substantially better than epidemiology data (Table 9.4). This is mainly due to patient selection criteria. All trials on PCNSL treatment typically exclude immunocompromised patients and patients with diffuse involvement, while others would only include patients with localized disease. While selection criteria are necessary to ensure a uniform study population and in order to obtain meaningful results, the population studied is not always a true representation of PCNSL patients as a whole. Nevertheless, current data is encouraging, with improved survival rates following treatment.

Immunocompromised patients

By and large, HIV-associated PCNSL is uniformly fatal with a median survival of approximately 3 months. Commencement of HAART (Highly Active Anti-Retroviral Therapy) in the treatment naïve patients, or a change in the drug combination, has been associated with an improvement in disease control and overall survival. The treatment of the acquired and congenitally immunosuppressed associated PCNSL follows the same principle—improvement or elimination of the immunosuppressive state. This needs to be carefully balanced with the risks of transplant rejection and disease progression. Corticosteroids and WBRT form the mainstay of treatment. Other forms of treatment such as chemotherapy and reduced-dose WBRT (rdWBRT), although promising, should only be offered as part of investigational studies in appropriate tertiary centres. Jacomet et al. (1997) studied HD-MTX as sole therapy in HIV-associated PCNSL and demonstrated improved survival rates of 9.7 months. Ideal patients for this form of treatment are those in good neurological condition and without active opportunistic infection. CSF EBV DNA levels act as a surrogate tumour marker to measure response to chemotherapy.

Controversy: The role of radiotherapy in treatment of PCNSL

The case against radiotherapy

WBRT was historically utilized as the main treatment modality for PCNSL and despite the profound initial immediate response, Nelson et al. (1992) found that more than 60% of patients receiving WBRT as the sole form of treatment had progression within the radiation field. The median overall survival was only 11.6 months in this same group. With the introduction of HD-MTX, more encouraging outcomes were demonstrated when used in combination with WBRT. However, data from the G-PCNSL-SG-1 (Thiel et al., 2010) demonstrated that overall survival was not compromised with omission of WBRT from first-line chemotherapy. Additionally, patients with a sustained complete response to treatment suffered from significant delayed neurotoxicity with increased mortality and morbidity (Doolittle et al., 2013). Patients more than 60 years of age were particularly susceptible, and survivors often required custodial care. In an attempt to reduce this complication, the concept of rdWBRT as consolidation treatment was trialled but was met with mixed results. Bessell et al. (2002) reported inferior results for rdWBRT (at 30.6Gy) following combination chemotherapy. Morris et al. (2013), on the other hand, demonstrated encouraging results using combination chemotherapy followed by 23.4Gy radiotherapy but the subgroup older than 60 years had a significantly inferior outcome. A review by Wang et al. (2014) summarized three important limitations with WBRT: inadequate local control, dissemination of radiologically occult lymphoma cells outside of the radiation field, and deleterious effects of radiation on brain function.

The case for radiotherapy

The rationale for consolidation radiotherapy following combination chemotherapy regimens lies in the fact that PCNSL is a diffuse disease, and consolidation WBRT has been associated with increased PFS and OS. The G-PCNSL-SG-1 trial provided evidence of modest improvement in PFS with inclusion of WBRT but failed to demonstrate any significant improvement in OS. This study was criticized due to several flaws in its execution: failure in meeting its primary endpoint, protocol violations, and a high risk of bias. The Cochrane Collaboration published a review regarding the role of additional radiotherapy in treatment of PCNSL. The authors found insufficient data to draw any definitive conclusion that combination chemo-radiotherapy compared to chemotherapy alone have similar effects on OS. Also, the review judged the evidence for the outcome of PFS to be low (Zacher et al., 2014). Ferreri et al. (2009) compared chemotherapeutic modalities (HD-MTX vs. HD-MTX in combination with cytarabine) followed by WBRT. Although the effects of WBRT were not studied as a primary outcome, WBRT following either regime was accompanied by complete remission rates of 64% in the intervention arm, compared to 30% in the control arm. Prica et al. (2012) published results from a decision analysis study that suggested improvements in survival and quality adjusted life years for patients less than 60 years old who had received chemotherapy followed by consolidation WBRT.

Further studies and considerations

Three studies evaluating the role of WBRT in the treatment of PCNSL are ongoing at the time of writing of this chapter. PRECIS is a prospective randomized phase 2 study in France that aims to compare HD-MTX combined with WBRT to HD-MTX and haematopoietic stem cell rescue. The British initiated IELSG32 is a randomized phase 2 trial evaluating three different chemotherapy regimens, in which patients achieving complete remission undergo either WBRT or autologous stem cell transplantation. RTOG-1114 is a randomized phase 2 clinical trial in the United States evaluating treatment with R-MVP chemotherapy regime followed by either cytarabine alone, or cytarabine plus WBRT.

In the search for more effective treatment of PCNSL that gives similar results to the treatment of systemic NHL, it is foreseeable that radiotherapy will continue to play an important role. The role of radiotherapy with the availability of effective chemotherapy regimens remains unclear with data obtained from the G-PCNSL-SG-1 trial. But until higher quality evidence becomes available, the arguments 'for' and 'against' WBRT require careful consideration.

In patients under the age of 60 years, WBRT provides the attractive potential of improved remission rates, and lengthened PFS and OS when combined with effective chemotherapy regimens. However, the benefits need to be carefully weighed against the potentially devastating effects of delayed neurotoxicity, especially in patients over the age of 60 years. Furthermore, salvage WBRT is potential option as a treatment of disease relapse in WBRT-naïve individuals. Patient expectations and the potential impact of any form of treatment on the patient's quality of life must be factored in.

Acknowledgements

A substantial portion of the section on 'Histopathology' was contributed by Dr Pieter Wesseling, Consultant Neuropathologist, Radboud University Nijmegen.

The pathology images (Figs. 9.3 and 9.4) were contributed by Dr Seet Ju Ee, Senior Consultant, Department of Pathology, National University Hospital, Singapore. The cases are from the departmental archive.

REFERENCES

Bessell, E.M., López-Guillermo, A., Villá, S., et al. (2002). Importance of radiotherapy in the outcome of patients with primary CNS lymphoma: an analysis of the CHOD/BVAM regimen followed by two different radiotherapy treatments. *J Clin Oncol*, **20**(1), 231–6.

Bierman, P.J. (2014). Surgery for primary central nervous system lymphoma: is it time for reevaluation? *Oncology (Williston Park)*, **28**(7), 632–7.

Braaten, K.M., Betensky, R.A., de Leval, L., et al. (2003). BCL-6 expression predicts improved survival in patients with primary central nervous system lymphoma. *Clin Cancer Res*, **9**(3), 1063–9.

Cady, F.M., O'Neill, B.P., Law, M.E., et al. (2008). Del(6)(q22) and BCL6 rearrangements in primary CNS lymphoma are indicators of an aggressive clinical course. *J Clin Oncol*, **26**(29), 4814–19.

Camilleri-Broët, S., Crinière, E., Broët, P., et al. (2006). A uniform activated B-cell-like immunophenotype might explain the poor

prognosis of primary central nervous system lymphomas: analysis of 83 cases. *Blood*, **107**(1), 190–6.
Courts, C., Montesinos-Rongen, M., Brunn, A., et al. (2008). Recurrent inactivation of the PRDM1 gene in primary central nervous system lymphoma. *J Neuropathol Exp Neurol*, **67**(7), 720–7.
Craig, F.E., Ohori, N.P., Gorrill, T.S., & Swerdlow, S.H. (2011). Flow cytometric immunophenotyping of cerebrospinal fluid specimens. *Am J Clin Pathol*, **135**(1), 22–34.
DeAngelis, L.M., Seiferheld, W., Schold, S.C., et al. (2002). Combination chemotherapy and radiotherapy for primary central nervous system lymphoma: Radiation Therapy Oncology Group Study 93–10. *J Clin Oncol*, **20**, 4643–8.
Doolittle, N.D., Korfel, A., Lubow, M.A., et al. (2013). Long-term cognitive function, neuroimaging, and quality of life in primary CNS lymphoma. *Neurology*, **81**(1), 84–92.
Ferreri, A.J., Reni, M., Foppoli, M., et al. (2009). High-dose cytarabine plus high-dose methotrexate versus high-dose methotrexate alone in patients with primary CNS lymphoma: a randomised phase 2 trial. *Lancet*, **374**, 1512–20.
Gündüz, K., Shields, C.L., Günalp, I., & Shields, J.A. (2003). Magnetic resonance imaging of unilateral lacrimal gland lesions. *Graefes Arch Clin Exp Ophthalmol*, **241**, 907–13.
Henry, J.M., Heffner, R.R. Jr, Dillard, S.H., Earle, K.M., & Davis, R.L. (1974). Primary malignant lymphomas of the central nervous system. *Cancer*, **34**(4), 1293–302.
Illerhaus, G., Marks, R., Ihorst, G., et al. (2006). High-dose chemotherapy with autologous stem-cell transplantation and hyperfractionated radiotherapy as first-line treatment of primary CNS lymphoma. *J Clin Oncol*, **24**(24), 3865–70.
Jacomet, C., Girard, P.M., Lebrette, M.G., Farese, V.L., Monfort, L., & Rozenbaum, W. (1997). Intravenous methotrexate for primary central nervous system non-Hodgkin's lymphoma in AIDS. *AIDS*, **11**(14), 1725–30.
Klein, U. & Dalla-Favera, R. (2008). Germinal centres: role in B-cell physiology and malignancy. *Nat Rev Immunol*, **8**(1), 22–33.
Knowles, D.M. (2003). Etiology and pathogenesis of AIDS-related non-Hodgkin's lymphoma. *Hematol Oncol Clin North Am*, **17**, 785–820.
Lee, B.S., Juthani, R.G., Healy, A.T., Peereboom, D.M., & Recinos, V.M. (2014). Hyperosmolar and methotrexate therapy avoiding surgery in the acute presentation of primary central nervous system lymphoma. *Surg Neurol Int*, **5**(Suppl 4), S175–80.
Louis, D.N., Ohgaki, H., Wiestler, O.D., & Cavenee, W.K. (2016). *World Health Organization: Histological Classification of Tumours of the Central Nervous System*. Paris, France: IARC.
McAllister, L.D., Doolittle, N.D., Guastadisegni, P.E., et al. (2000). Cognitive outcomes and long-term follow-up results after enhanced chemotherapy delivery for primary central nervous system lymphoma. *Neurosurgery*, **46**(1), 51–60.
Montemurro, M., Kiefer, T., Schüler F, et al. (2007). Primary central nervous system lymphoma treated with high-dose methotrexate, high-dose busulfan/thiotepa, autologous stem-cell transplantation and response-adapted whole-brain radiotherapy: results of the multicenter Ostdeutsche Studiengruppe Hamato-Onkologie OSHO-53 phase II study. *Ann Oncol*, **18**(4), 665–71.
Morris, P.G., Correa, D.D., Yahalom, J., et al. (2013). Rituximab, methotrexate, procarbazine, and vincristine followed by consolidation reduced-dose whole-brain radiotherapy and cytarabine in newly diagnosed primary CNS lymphoma: final results and long-term outcome. *J Clin Oncol*, **31**(31), 3971–9.
Mrugala, M.M., Rubenstein, J.L., Ponzoni, M., & Batchelor, T.T. (2009). Insights into the biology of primary central nervous system lymphoma. *Curr Oncol Rep*, **11**, 73–80.
Nakamura, M., Shimada, K., Ishida, E., & Konishi, N. (2004). Histopathology, pathogenesis and molecular genetics in primary central nervous system lymphomas. *Histol Histopathol*, **19**, 211–19.
Nakamura, T., Tateishi, K., Niwa, T., et al. (2016). Recurrent mutations of CD79B and MYD88 are the hallmark of primary central nervous system lymphomas. *Neuropathol Appl Neurobiol*, **42**(3), 279–90.
Nelson, D.F., Martz, K.L., Bonner, H., et al. (1992). Non-Hodgkin's lymphoma of the brain: can high dose, large volume radiation therapy improve survival? Report on a prospective trial by the Radiation Therapy Oncology Group (RTOG): RTOG 8315. *Int J Radiat Oncol Biol Phys*, **23**, 9–17.
Norden, A.D., Drappatz, J., Wen, P.Y., & Claus, E.B. (2011). Survival among patients with primary central nervous system lymphoma, 1973–2004. *J Neurooncol*, **101**(3), 487–93.
Omuro, A., Correa, D.D., DeAngelis, L.M., et al. (2015). R-MPV followed by high-dose chemotherapy with TBC and autologous stem-cell transplant for newly diagnosed primary CNS lymphoma. *Blood*, **125**(9), 1403–10.
Paik, J.H., Go, H., Nam, S.J., et al. (2013). Clinicopathologic implication of A20/TNFAIP3 deletion in diffuse large B-cell lymphoma: an analysis according to immunohistochemical subgroups and rituximab treatment. *Leuk Lymphoma*, **54**(9), 1934–41.
Prica, A., Chan, K., & Cheung, M.C. (2012). Combined modality therapy versus chemotherapy alone as an induction regimen for primary central nervous system lymphoma: a decision analysis. *Br J Haematol*, **158**(5), 600–7.
Rubenstein, J.L., Fridlyand, J., Shen, A., et al. (2006). Gene expression and angiotropism in primary CNS lymphoma. *Blood*, **107**(9), 3716–23.
Rubenstein, J.L., Wong, V.S., Kadoch, C., et al. (2013). CXCL13 plus interleukin 10 is highly specific for the diagnosis of CNS lymphoma. *Blood*, **121**(23), 4740–8.
Schorb, E., Kasenda, B., Atta, J., et al. (2013). Prognosis of patients with primary central nervous system lymphoma after high-dose chemotherapy followed by autologous stem cell transplantation. *Haematologica*, **98**(5), 765–70.
Schwindt, H., Vater, I., Kreuz, M., et al. (2009). Chromosomal imbalances and partial uniparental disomies in primary central nervous system lymphoma. *Leukemia*, **23**(10), 1875–84.
Thiel, E., Korfel, A., Martus, P., et al. (2010). High-dose methotrexate with or without whole brain radiotherapy for primary CNS lymphoma (G-PCNSL-SG-1): a phase 3, randomised, non-inferiority trial. *Lancet Oncol*, **11**(11), 1036–47.
Wang, C.C., Carnevale, J., & Rubenstein, J.L. (2014). Progress in central nervous system lymphomas. *Br J Haematol*, **166**(3), 311–25.
Weller, M.,. Martus, P., Roth, P., Thiel, E., Korfel, A.; German PCNSL Study Group (2012). Surgery for primary CNS lymphoma? Challenging a paradigm. *Neuro Oncol*, **14**(12), 1481–4.
Wieduwilt, M.J., Valles, F., Issa, S., et al. (2012). Immunochemotherapy with intensive consolidation for primary CNS lymphoma: a pilot study and prognostic assessment by diffusion-weighted MRI. *Clin Cancer Res*, **18**, 1146–55.
Yamasaki, F., Takayasu, T., Nosaka, R., et al. (2015). Magnetic resonance spectroscopy detection of high lipid levels in intraaxial tumors without central necrosis: a characteristic of malignant lymphoma. *J Neurosurg*, **122**(6), 1370–9.

Zacher, J., Kasenda, B., Engert, A., & Skoetz, N. (2014). The role of additional radiotherapy for primary central nervous system lymphoma. *Cochrane Database Syst Rev*, **6**, CD009211.

RELATED LINKS TO EBRAIN

Aetiology and Pathophysiology of CNS Lymphoma. https://learning.ebrain.net/course/view.php?id=1243

Assessment of the Patient with a Brain Tumour. https://learning.ebrain.net/course/view.php?id=1247

Clinical Presentation of Patients with Brain Tumours. https://learning.ebrain.net/course/view.php?id=1249

Histopathology of CNS Lymphomas. https://learning.ebrain.net/course/view.php?id=1253

Imaging Features of Central Nervous System Lymphomas. https://learning.ebrain.net/course/view.php?id=1261

Management of Primary CNS Lymphoma. https://learning.ebrain.net/course/view.php?id=439

Palliative Care and End of Life in Brain Tumour Patients. https://learning.ebrain.net/course/view.php?id=483

Referral and Management Guidelines for Patients with Brain Tumours. https://learning.ebrain.net/course/view.php?id=507

10

Glioneuronal and other epilepsy-associated tumours

Matthias Simon and Alexander Grote

Introduction

Neuronal and glioneuronal tumours account for less than 5% of all intracranial neoplasms. The most common variants, that is, *gangliogliomas* and *dysembryoplastic neuroepithelial tumours* (DNT), are frequently encountered in the setting of surgery for pharmacoresistant epilepsy. While any brain tumour can cause seizures, a rather specific subset of tumour types is associated with chronic or pharmacoresistant epilepsy. In addition to the already mentioned gangliogliomas and DNTs, this includes *pilocytic* and *pleomorphic astrocytomas*, the more recently described *angiocentric glioma* (ANET), and some *diffuse gliomas* of the WHO grades II and III. Together, these tumour entities have been referred to as LEATs (longstanding or long-term epilepsy-associated tumours), or more recently 'low-grade epilepsy-associated neuroepithelial tumours', since most cases undergo surgery before the criterion historically used to define 'long-term' epilepsy (>2 years) has been met (Blumcke et al., 2016).

The somewhat stereotypical clinical presentation with chronic or refractory epilepsy, the usually very benign clinical course, and the description of mixed (glioneuronal) tumours point to a true biological link between the various histological LEAT variants (Blumcke et al., 2014). However, most of the available molecular genetic and immunohistochemical studies suggest otherwise. Of note, oncological outcomes can be considerably worse in patients with a LEAT histology treated outside the epilepsy surgery context. This has important clinical implications. In our view, presumed LEAT patients with incidental findings or tumours diagnosed following (e.g. a single seizure) should be offered early surgery rather than simple neuroimaging follow-up. It is not clear if such cases will go on to develop long-term epilepsy and have a very benign clinical course, or if the tumour will behave a lot more like a true oncological disease.

The present chapter attempts to review the clinical, pathological, and imaging characteristics of neuronal and glioneuronal tumours as well as the non-glioneuronal LEAT variants. We describe the relatively common gangliogliomas and DNTs and a characteristic central nervous system (CNS) manifestation of a rare familial hamartoma syndrome (*dysplastic cerebellar gangliocytoma, Lhermitte-Duclos disease*). We also provide information on the other, much rarer (glio)neuronal tumour variants included in the current WHO classification (*papillary glioneuronal tumour, rosette-forming glioneuronal tumour of the fourth ventricle, desmoplastic infantile ganglioglioma/astrocytoma, extraventricular neurocytoma* and *cerebellar liponeurocytoma*) and on the non-glioneuronal LEATs. Finally, we include a brief discussion of the pros and cons of hippocampal resections when operating on temporal epilepsy-associated tumours.

Gangliogliomas

Gangliogliomas are most often diagnosed in children and young adults. Their incidence has been quoted as 0.3–5.2% in adult and up to 14% in paediatric brain tumour cohorts. The most common tumour location is the temporal followed by the frontal lobe. Rare but somewhat typical locations include the supratentorial midline, basal ganglia and thalamus, the cerebellum, brainstem, and spinal cord.

Histologically, gangliogliomas are composed of dysplastic ganglion cells and neoplastic glial elements (**Fig. 10.1**). The respective proportion may vary considerably resulting in a morphological spectrum ranging from tumours with a very prominent neuronal cell population (gangliocytoma) to lesions with a predominantly glial phenotype. The vast majority of gangliogliomas are assigned to the WHO grade I. Anaplastic (WHO grade III) tumours account for only 1–2.6% of all gangliogliomas. While the current WHO classification no longer recognizes an intermediate (i.e. non-benign non-anaplastic) 'atypical' grade II ganglioglioma, there is some clinical evidence to suggest a three rather than a two-tiered grading system. Gangliogliomas may evolve into outright glioblastomas. We have seen secondary glioblastomas in 5 of 11 patients undergoing surgery for recurrent ganglioglioma at our institution (Luyken et al., 2004; Majores et al., 2008). Specific BRAF oncogene mutations (BRAF *c.*1799T >A/ BRAF V600E) occur in possibly more than 50% of GG cases (Koelsche et al., 2013). BRAF V600E mutations may carry a negative prognostic impact (Dahiya et al., 2013). Gangliogliomas may very rarely harbour IDH1 mutations.

The typical ganglioglioma patient presents with symptomatic epilepsy. A non-epileptic presentation in a case with a presumed ganglioglioma should alert the treating clinician to the possibility of a non-benign clinical course. Deep-seated (**Fig. 10.2**), cerebellar, brainstem, or spinal gangliogliomas will present with location-dependent signs and symptoms. Gangliogliomas are hyperintense

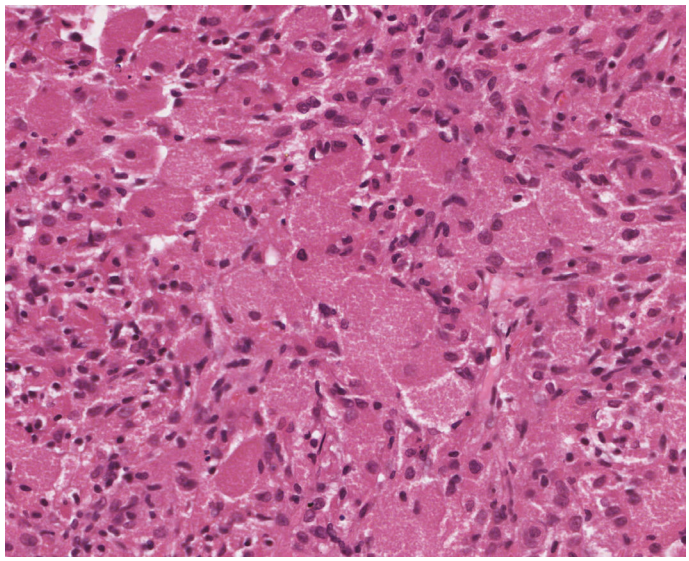

Fig. 10.1 Nests of abnormal ganglion cells are a feature of ganglion cell tumours, which may also have a neoplastic glial element. Less specific features include eosinophilic granular bodies and perivascular lymphocytes.

Courtesy of Dr Kieren Allinson, Department of Pathology, Addenbrooke's Hospital, Cambridge.

on T2 and FLAIR, and hypo- to isointense on T1-weighted MR images. Tumour cysts and contrast enhancement ranging from patchy to nodular are common (**Figs. 10.4A** and **10.12A**). Calcifications are not infrequent. Anaplastic tumours typically have an uncharacteristic MRI appearance, while the atypical variants usually resemble benign gangliogliomas.

The treatment of choice for gangliogliomas is surgery. Complication rates are usually low and reflect tumour location and the generally young age and good general condition of most ganglioglioma patients. The epileptological results following surgical treatment are also very good. We have seen Engel class I outcomes (seizure-free or only occasional non-disabling seizures) in approximately 80% of LEAT cases during a 10 yrs. follow-up in a cohort of 207 patients (including 86 gangliogliomas) undergoing surgery for drug-resistant epilepsy of more than 2 years at our institution (Luyken et al., 2003). In our experience, a complete tumour resection will cure all but the very occasional patient with a ganglioglioma WHO grade I (Luyken et al., 2004). Quite in contrast, 5 yr. progression-free survival was only approximately 70% and 30% in our patients with atypical and anaplastic gangliogliomas, respectively. Presentation with long-term or refractory epilepsy is an immensely important clinical prognostic marker (Majores et al., 2008). Oncological results are substantially worse in centres, which see a higher proportion of cases outside the context of chronic epilepsy and epilepsy surgery. A recent report of

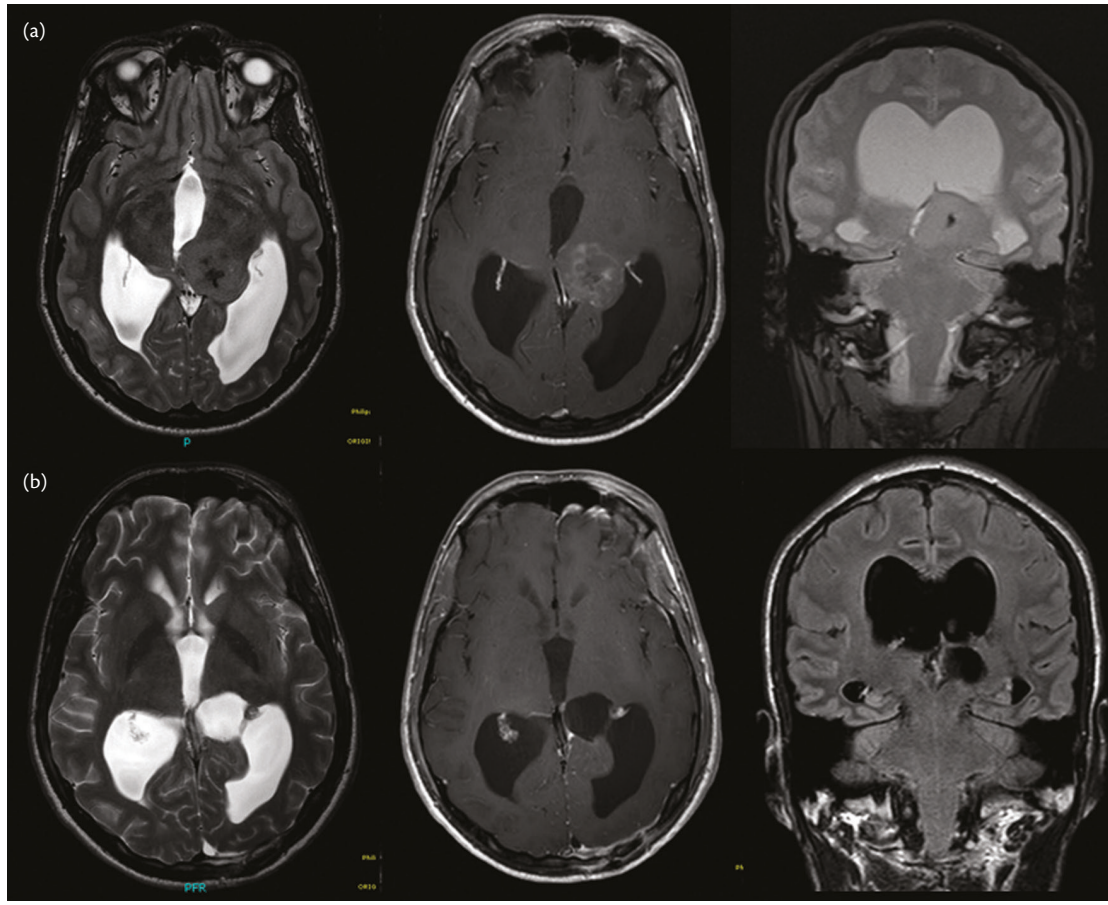

Fig. 10.2 Ganglioglioma WHO grade I of the left thalamus in a 26-year-old male who presented with signs and symptoms of obstructive hydrocephalus. The patient was operated through a parietal transventricular approach and recovered from surgery without neurological deficit. (A) Preoperative and (B) postoperative MR images.

88 such cases detailed a 5 yrs. progression-free survival rate of only 58% following surgery (Compton et al., 2012).

Given the relatively adverse prognosis of patients with anaplastic gangliogliomas WHO grade III radiotherapy should probably be routinely prescribed in such cases in analogy to other anaplastic gliomas even if this recommendation is not based on very substantial evidence. Radiotherapy may be an option in recurrent, unresectable, or incompletely resected tumours with histological signs of atypia, which do not fulfil the criteria for the diagnosis of a WHO grade III tumour. The evidence for the use of chemotherapy is anecdotal at best.

Dysembryoplastic neuroepithelial tumours (DNTs)

DNTs are the second most common glioneuronal tumour variant encountered in clinical practice. They seem to be slightly more frequent in males and patients usually come to medical attention in their second or third decade of life. Paediatric patients account for a substantial percentage of the cases. The most common tumour location is the temporal lobe, but DNTs can also grow in any other part of the supratentorial cortex. Deep-seated supratentorial (caudate nucleus, septum) and posterior fossa (brainstem, cerebellum) lesions have also been described.

DNTs are histologically characterized by a multinodular appearance and by the specific glioneuronal element, an admixture of oligodendrocyte-like cells arranged in columns perpendicular to the cortical surface and non-dysplastic neurons (**Fig. 10.3**). They are assigned to the WHO grade I. The WHO classification distinguishes between simple and complex subtypes. The existence of a diffuse variant is more controversial and may reflect the not uncommon difficulty to distinguish a DNT from a diffuse low-grade glioma. Mixed DNTs/gangliogliomas have also been described (Thom et al., 2011). We found neither BRAF V600E nor IDH1 mutations in a collection of 32 DNTs (Grote and Simon, 2015). There are some reports of rare LOH 1p/19q or IDH1 mutations in DNTs (Thom et al., 2011). Some DNT series report coexisting cortical dysplasias (FCDs) in up to 70–80% of cases. The pathogenetic relationship of FCDs to the actual tumour is not well understood. One hypothesis regards these changes as the remainder of a pretumorous bed which has partially transformed into the actual LEAT. More likely, FCDs coexisting with LEATs develop in synchronicity or secondary to the growth of the neoplasm (Thom et al., 2012).

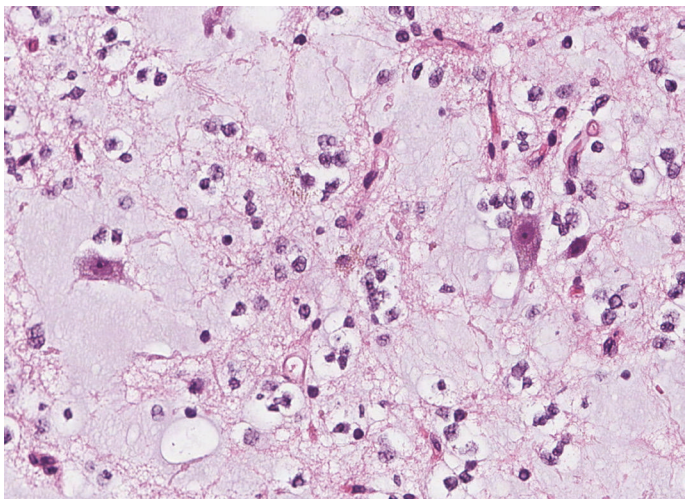

Fig. 10.3 Dysembryoplastic neuroepithelial tumour (H&E ×400). These neoplasms are often characterized by large pyramidal neurons 'floating' in pools of mucin. This feature is unusual in oligodendroglioma, the main histological differential diagnosis.

Courtesy of Dr Kieren Allinson, Department of Pathology, Addenbrooke's Hospital, Cambridge.

DNTs most commonly present with (drug-resistant) epilepsy. We have not seen patients with neurological deficits related to tumour growth. DNT growing in eloquent cortical areas may lead to substantial functional reorganization, which can render them resectable despite their location. In our experience, incidental DNTs are not rare. MR imaging typically shows a multicystic tumour with little mass effect or oedema, which is hyperintense on T2 and FLAIR and hypointense on T1 weighted images. Contrast enhancement and calcifications are not infrequent (15–20%). Erosions of the adjacent skull have been variably described in 20–70%. The primary differential diagnosis is that of a ganglioglioma or other LEAT followed by a diffuse glioma. Some DNTs have been preoperatively misdiagnosed as cavernomas (**Figs. 10.4B** and **10.12B**).

DNTs should be treated by surgery. Complication rates are low similar to ganglioglioma patients. The epileptological results are gratifying with Engel class I outcomes of approximately 80% even in cases with refractory epilepsy which remain stable over many years (Luyken et al., 2003). Incomplete resections and the presence of an FCD are the main predictors of epilepsy persistence or recurrence. From an oncological perspective DNTs are most often extremely benign. We have only seen a single case of tumour recurrence (or rather growth of residual tumour following an incomplete resection of a complex DNT) in our cohort. Nevertheless, a small but growing number of cases are on record with recurrent tumour even after what was thought to be a complete resection, or with malignant transformation (Thom et al., 2011). It therefore seems wise to recommend serial imaging follow-up to DNT patients in particular in cases with residual tumour and following partial resections. There is no evidence to support radio- or chemotherapy for DNTs. Of note, adjuvant therapy has been associated with malignant transformation.

Dysplastic cerebellar gangliocytoma (L'Hermitte-Duclos disease)

The dysplastic cerebellar gangliocytoma (L'Hermitte-Duclos disease, LDD) is the major CNS manifestation of Cowden disease. Cowden disease (OMIM entry 158350) is an autosomal dominant disorder most often caused by PTEN germline mutations. LDD in the setting of Cowden syndrome may also be due to a PIK3CA mutation. The clinical spectrum is characterized by multiple hamartomas derived from all three germ cell layers classically including trichilemmomas and an increased risk for breast, non-medullary thyroid, and endometrial cancer. The lifetime risk for PTEN mutation carriers to contract breast, thyroid and endometrial cancer may be as high as 85%, 38% and 28%, respectively. Isolated and sporadic LDD may also occur and has been attributed to somatic PTEN mutations. No PTEN mutations have been identified in the rare cases with paediatric LDD (Pilarski et al., 2013).

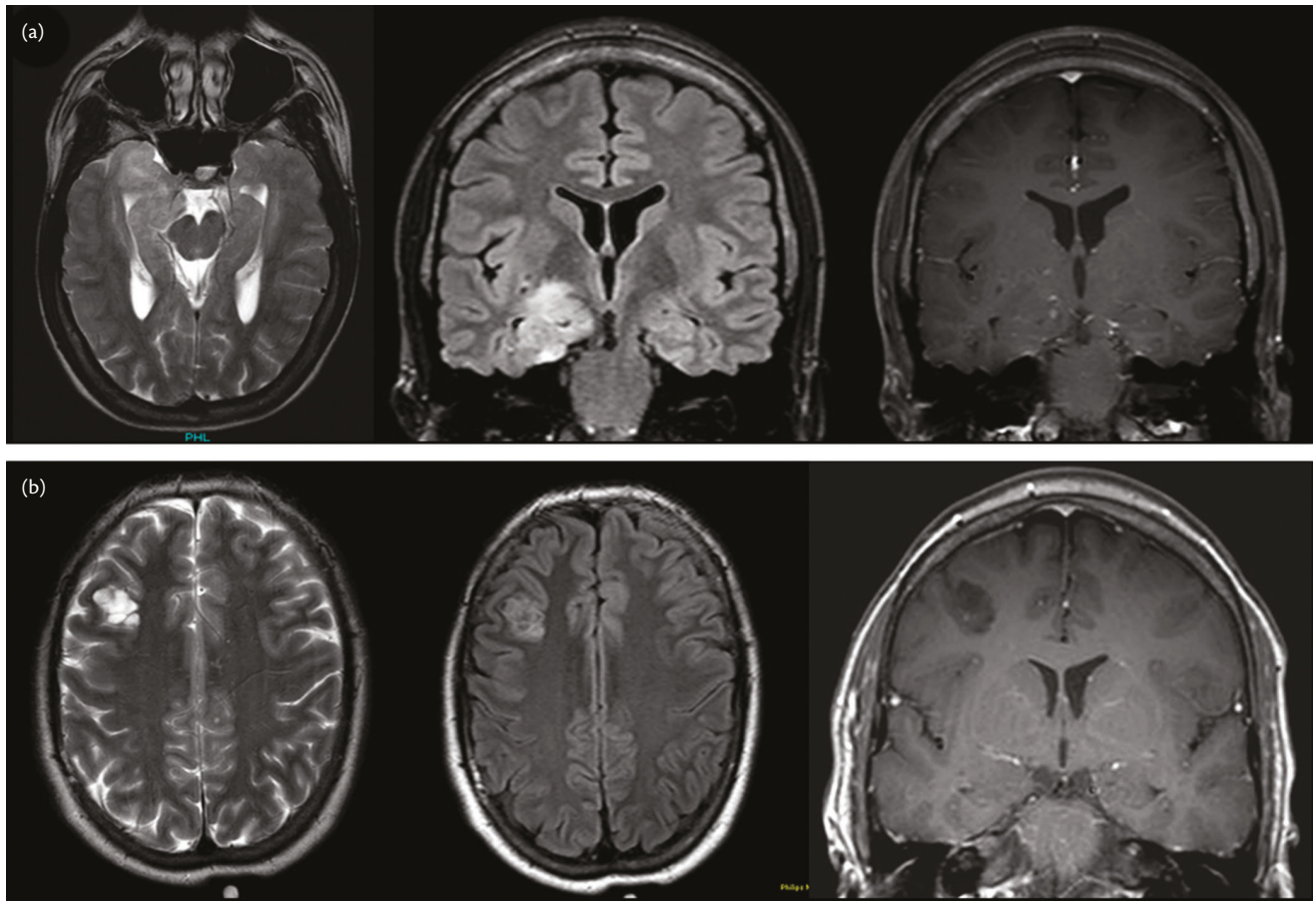

Fig. 10.4 Long-term epilepsy-associated gangliogliomas and dysembryoplastic neuroepithelial tumours (DNTs). (A) Left 'holo'-temporomesial ganglioglioma WHO grade I in a 19-year-old male with pharmacoresistant epilepsy since his first year of life. The tumour grows in the mesial temporal pole, the uncus, the amygdalum, the hippocampus, and parahippocampus, and extends posteriorly well beyond the level of the dorsal midbrain. (B) Right frontal dysembryoplastic neuroepithelial tumour (DNT) WHO grade I in a 22-year-old male with a 6-year history of eventually refractory epilepsy.

Dysplastic cerebellar gangliogliomas cause an enlargement of the molecular and the internal granular layers of the cerebellum filled with dysplastic ganglionic cells (Fig. 10.5). Macroscopically this results in thickened and dysmorphic cerebellar foliae.

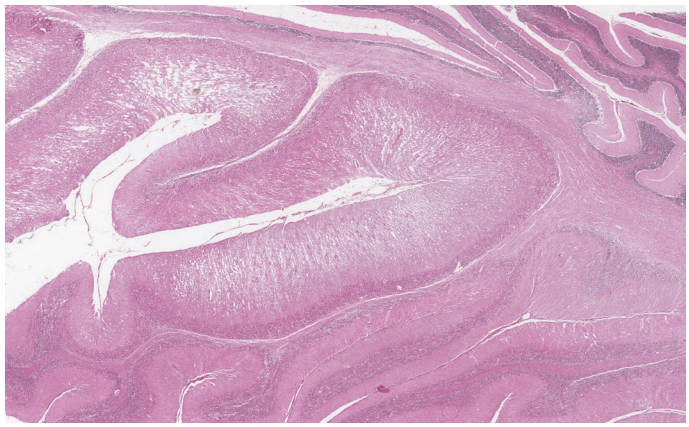

Fig. 10.5 Lhermitte-Duclos disease (dysplastic gangliocytoma of the cerebellum) is best appreciated at low magnification where the thickening of the affected cerebellar cortex and loss of the darkly-staining granular layer is most apparent. Compare with the normal cortex in the top right of the image.
Courtesy of Dr Kieren Allinson, Department of Pathology, Addenbrooke's Hospital, Cambridge.

Correspondingly, MR imaging shows a characteristic 'tiger-striped' pattern on T2 weighted images. Patchy contrast enhancement may occur. The MRI features are often so characteristic as to obviate the need for a tissue diagnosis in many cases (Fig. 10.6). LDD may be accompanied by hydrocephalus, megalencephaly, syringomyelia, meningiomata, cavernomas, and venous angiomas. It is unclear if LDD is hamartomatous or truly neoplastic in nature. Some patients have been diagnosed with true glioneuronal tumours growing against the background of what was thought to be LDD. The clinical presentation of LDD may be that of an incidental finding or an expanding cerebellar mass. Decompressive surgery is the treatment of choice in the latter cases with poorly defined borders of the lesion being the major technical issue during the operation, and results in long-term survival. Radiotherapy has resulted in symptomatic stabilization, but also in progressive neurological deterioration (Prestor, 2006).

Non-glioneuronal LEATs

Diffuse astrocytomas and oligodendroglial tumours are not infrequently encountered in the epilepsy surgery setting. In a recent series from our institution 26/158 (16.5%) of cases could be assigned to this category (Grote and Simon, 2015). Histologically,

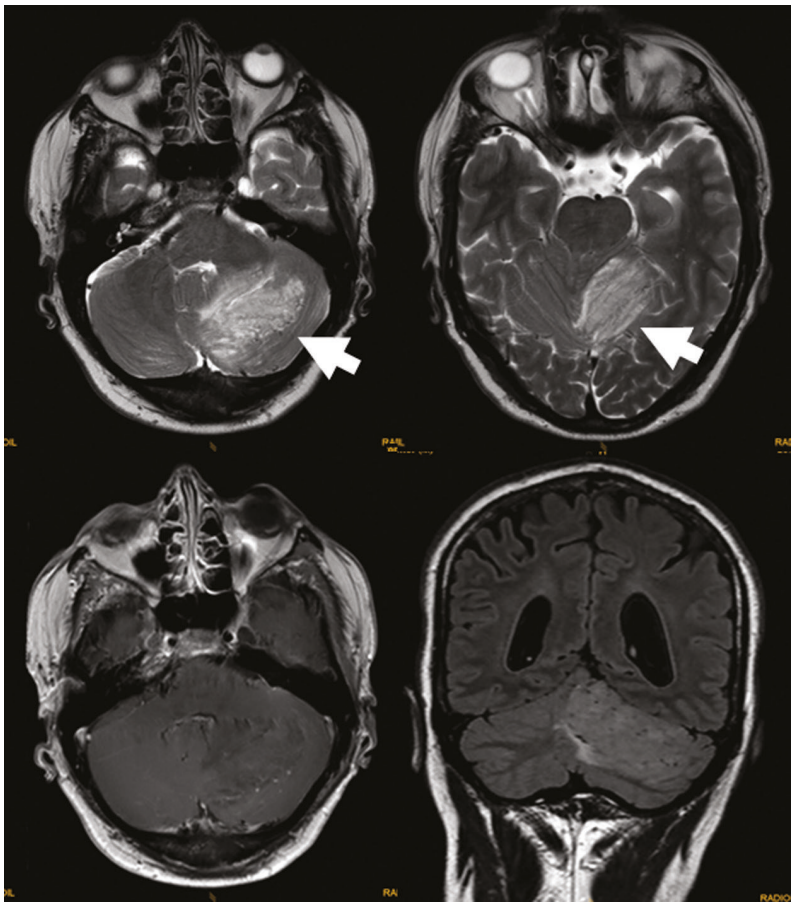

Fig. 10.6 Presumed dysplastic cerebellar gangliocytoma (L'Hermitte-Duclos disease) in a 50 yrs. old male with Cowden syndrome caused by a PTEN mutation. Note the characteristic striated appearance of the thickened cerebellar foliae (arrows).

these tumours can be classified as astrocytomas, mixed gliomas and oligodendrogliomas, and assigned to the WHO grades II and III. They frequently carry IDH1 mutations (39% in our series), however, this figure is markedly lower than the 60–90% IDH1 mutation rate found in unselected diffuse glioma series. This may point to a specific LEAT biology of these tumours. Tumours occur predominantly in the temporal and frontal lobe, but also in the paralimbic system (i.e. the insula). Imaging findings do not differ between LEAT and non-LEAT diffuse gliomas. The oncological as well as the epileptological prognosis is surprisingly good—calculated as 10 years progression-free with overall survival at 75% and 90%, respectively, in a series of 35 WHO grade II and 3 grade III astrocytomas undergoing surgery for their tumours and refractory epilepsy at our institution (Luyken et al., 2003). Around 70% were seizure-free one year after surgery. The *isomorphic astrocytoma* is a very rare diffuse astrocytoma variant with an exceedingly benign clinical course (Schramm et al., 2004).

Pilocytic astrocytomas account for 2.5% to more than 10% of cases in epilepsy surgery series. They are characterized by a biphasic growth pattern consisting of bipolar astrocytes and so-called Rosenthal fibres. The differential diagnosis between pilocytic astrocytomas and gangliogliomas may be difficult, which may in part explain the relatively variable incidence in published clinical cohorts. Pilocytic astrocytomas are associated with mitogen-activated protein kinase (MAPK) pathway alterations. Extracerebellar pilocytic astrocytomas harbour BRAF:KIAA1549 fusions and duplications (in approximately 60% of cases) or BRAF V600E, FGFR1, KRAS, NF1, and PTPN11 mutations or NTRK2 fusions (Jones et al., 2013). Epileptogenic pilocytic astrocytomas usually grow in the temporal lobe. MR imaging often shows cystic changes and evidence of recent haemorrhage. The classical picture is that of a large tumour cyst with a contrast enhancing wall and mural nodules. Contrast enhancement can range from strong to patchy and (rarely) none at all (**Fig. 10.7**). Oncological as well as epileptological outcomes for epilepsy surgery patients are generally very good and parallel the figures for gangliogliomas. This is not necessarily the case in patients encountered outside this setting. We found 5 yrs. PFS and OS rates of only 72% and 87%, respectively, in a series of 44 adult patients diagnosed with pilocytic astrocytomas. Histologically, 14% of cases displayed atypical and 6% anaplastic features. Patients benefited from a complete vs. a subtotal resection/biopsy, and we obtained some anecdotal evidence in favour of radio- and chemotherapy for aggressive tumours (Stuer et al., 2007).

Pleomorphic xanthoastrocytomas (PXA) most commonly affect children and young adults. The histological appearance is quite variable ('pleomorphic'). Spindly elements are intermingled with mono-and multinucleated giant astrocytes and xanthomatous cells ('xanthoastrocytoma') (**Fig. 10.8**). MR imaging shows an often-cystic mass with focal contrast enhancement and superficial cortico-leptomeningeal growth (**Fig. 10.9**). The vast majority of the tumours are found in the supratentorial compartment and in particular in the

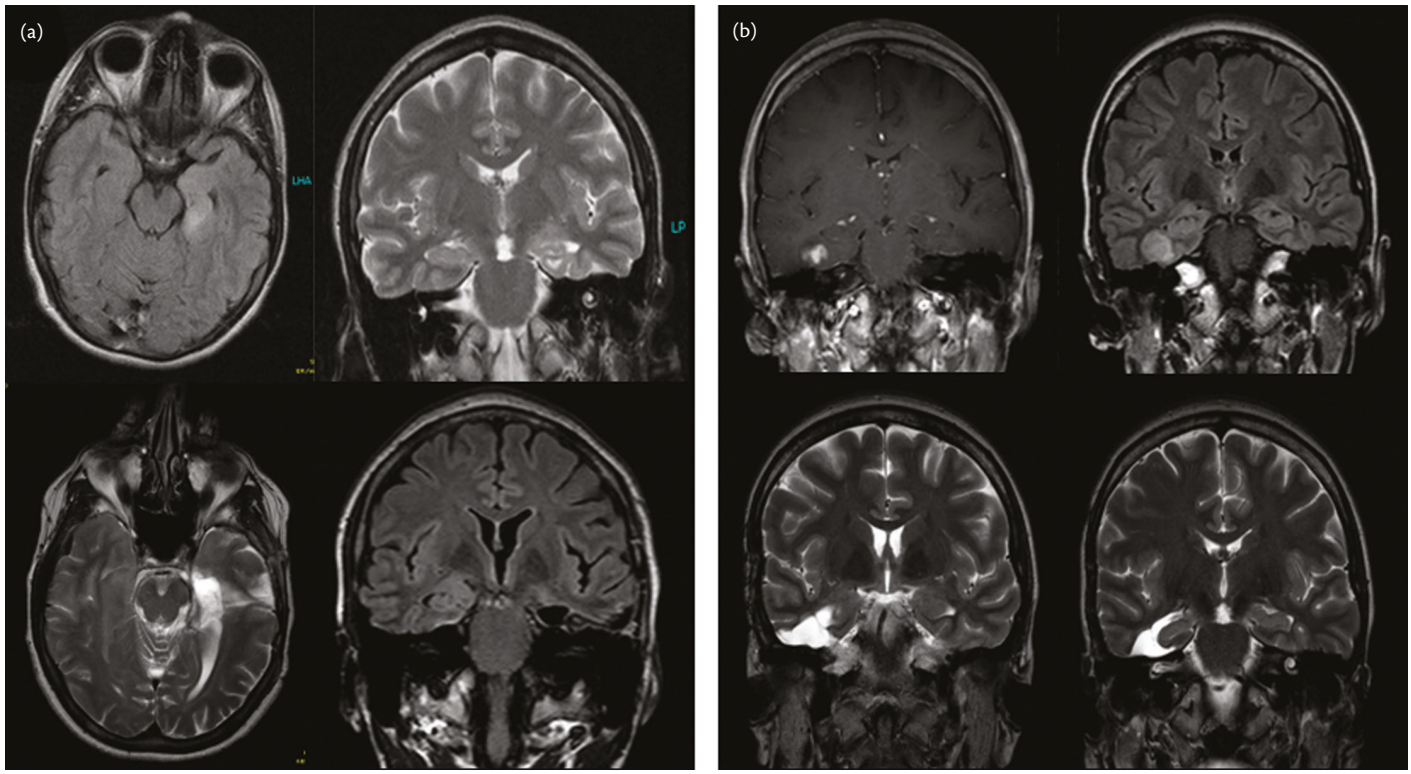

Fig. 10.7 (A) Right temporal pilocytic astrocytoma WHO grade I diagnosed and operated following a first generalized seizure in a 17-year-old female. (B) Upper panel: pilocytic astrocytoma WHO grade I of the dorsal amygdalum/basal ganglia. This 55-year-old female patient presented with cephalgias and other unspecific symptoms. Lower panel: postoperative MR images show no residual tumour. There was no new postoperative neurodeficit.

temporal lobe. The majority of PXAs are assigned to the WHO grade II. Lesions with anaplastic features and increased mitotic activity (>5 mitoses/10 HPF) account for approximately a third of cases. PXAs frequently (65–80%) harbour BRAF V600E but no IDH1 mutations. BRAF V600E mutations are more frequent in grade II than in anaplastic tumours, and correlate with a temporal tumour location and possibly younger age. Patients mostly present with seizures (>60–80%) and PXA may comprise more than 5% of tumours in epilepsy surgery series (Luyken et al., 2003; Ida et al., 2014; Grote and Simon, 2015). Surgery is the treatment of choice for PXAs and PXA associated epilepsy. None of the five PXA cases in the epilepsy surgery series reported by Luyken et al. recurred after a median follow-up of 8 years in the overall cohort (Luyken et al., 2003). The prognosis in unselected cohorts (i.e. including cases without long-term epilepsy) is worse: 5 years progression-free and overall survival for PXAs WHO grade II in a recent study was reported as 71% and 90%, respectively. The corresponding figures for anaplastic PXA were 49% and 57% only. A gross total resection seems to confer a significant survival benefit when compared to STR/biopsy cases (Ida et al., 2014). There are some data to support radiotherapy and treatment with alkylating chemotherapy for anaplastic PXA. The BRAF inhibitor vemurafenib has been used in a few cases with otherwise treatment resistant PXA.

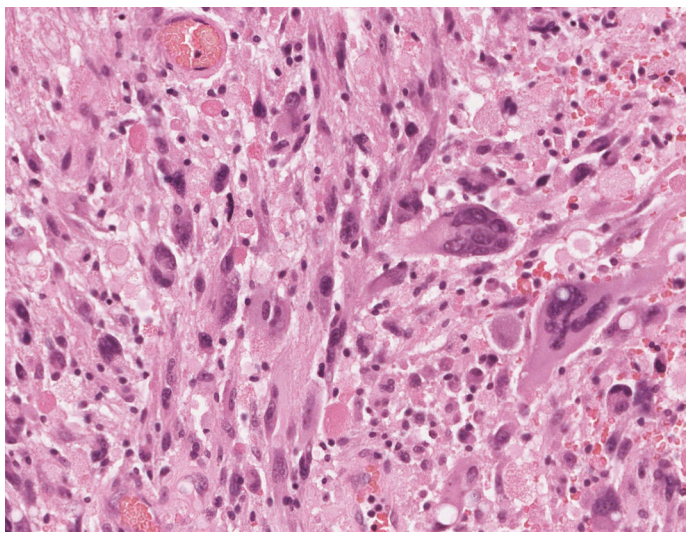

Fig. 10.8 Pleomorphic xanthoastrocytomas combine spindle shaped astrocytes and large, multinucleated, pleomorphic cells. Lipid vacuoles, eosinophilic granular bodies, and perivascular lymphocytes are also common features.

Courtesy of Dr Kieren Allinson, Department of Pathology, Addenbrooke's Hospital, Cambridge.

Angiocentric gliomas (ANETs) accounted for 5/158 (3.1%) of cases in a recent series of epilepsy-associated tumours from our institution (Grote and Simon, 2015). ANETs typically occur in children and (young) adults and patients almost exclusively present with refractory epilepsy. Histologically, ANETs are characterized by an angiocentric growth pattern of bipolar cells, and ependymoma-like features such as pseudorosettes, and they are assigned to the WHO grade I. Tumours are found predominantly in the frontal and temporal lobe (Chen et al., 2014). We found no BRAF V600E or IDH1 mutation in five cases from our institution. MYB or MYBl1

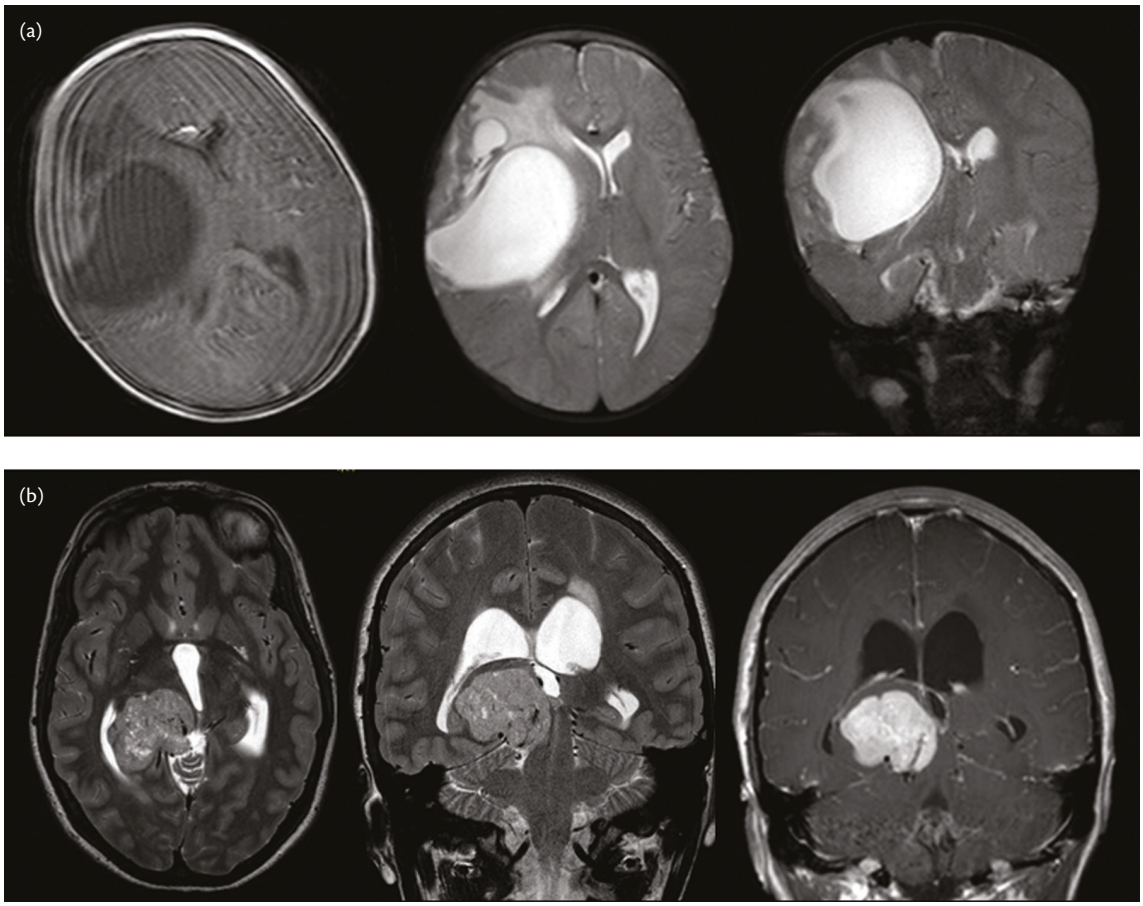

Fig. 10.9 (A) Temporopolar pleomorphic xanthoastrocytoma WHO grade II in a 20-year-old female with an 18-year epilepsy history. (B) Pleomorphic xanthoastrocytoma WHO grade II of the dorsal middle temporooccipital gyrus in a 19-year-old male diagnosed following a first complex-partial seizure. Note the prominent cortical leptomeningeal growth of both tumours (arrow).
Courtesy of Dr Kieren Allinson, Department of Pathology, Addenbrooke's Hospital, Cambridge.

abnormalities have been detected in several ANETs (Zhang et al., 2013b). LOH 1p/19q has not been described in these tumours. Neuroimaging usually reveals a non-enhancing cortical lesion involving the subcortical white matter (Fig. 10.10). Reported oncological outcomes are very good, but a few cases with anaplastic features (and tumour recurrence) are on record (Chen et al., 2014).

Other glioneuronal tumours

The *papillary glioneuronal tumour* (PGNT) has been recognized as a very rare separate tumour type of mostly young adults only very recently. Histologically, these tumours are characterized by prominent pseudopapillary growth and interpapillary sheets or focal collections of neuronal cells. MR and CT imaging features resemble those of gangliogliomas, however, rim-like contrast enhancement is not uncommon, and in comparison to gangliogliomas they are not as frequently located in the temporal lobe, while periventricular growth is rather common. A FGFR1 mutation has been found in one tumour (Gessi et al., 2014a). Prognosis after a complete resection is good. However, even though PGNTs are assigned to the WHO grade I tumour recurrence is not uncommon. A recent review analysed 71 cases and found an 82% 2 yrs. PFS rate. Even a case with primary metastatic dissemination is on record. A few patients (mostly cases with residual tumour) have undergone radiotherapy (Schlamann et al., 2014).

The *rosette-forming glioneuronal tumour of the fourth ventricle* (RGNT) has been initially described as DNT of the cerebellum, but is now included as a specific disease in the WHO classification. It is assigned to the WHO grade I. Approximately 20% of cases are located outside the posterior fossa, often close to the third ventricle and even in the spine. The histological picture is that of a biphasic neoplasm with uniform neurocytes forming rosettes and perivascular pseudorosettes on the one hand, and an astrocytic component resembling a pilocytic astrocytoma on the other. FGFR1 mutations were found in two of eight tumours tested (Gessi et al., 2014b). MR imaging usually reveals a mixed cystic/solid and not always contrast enhancing mass. Treatment is usually surgical and aims a complete resection, however, different views are also held, and a recent series of 41 cases failed to show the superiority of a gross total over a subtotal resection (Zhang et al., 2013a). Surgery may be difficult because of tumour location and adherence and/or infiltration of adjacent structures resulting in relatively high rate of new postoperative deficits. Metastatic dissemination has been seen in as many as 7% of cases in a 2014 review. 6% of the assessable patients in this review reportedly died during follow-up (Schlamann et al., 2014).

Desmoplastic infantile gangliogliomas (DIG) and *astrocytomas* (DIA) are very rare frontoparietal meningocerebral WHO grade

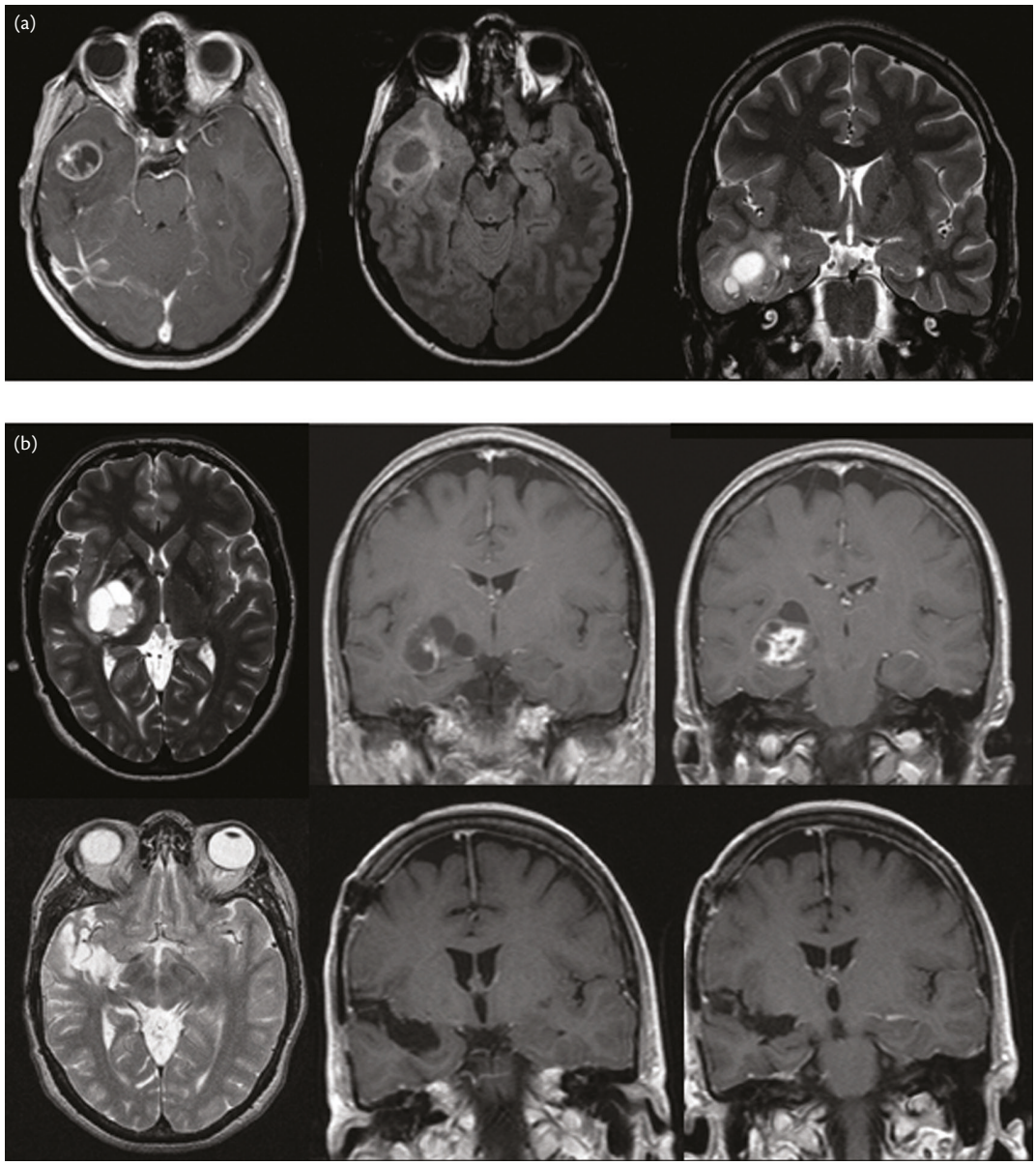

Fig. 10.10 Right parietal angiocentric glioma (ANET) in a 20-year-old male with a 3-year history of medically refractory epilepsy. Courtesy of Dr Kieren Allinson, Department of Pathology, Addenbrooke's Hospital, Cambridge.

I tumours of infancy. Most cases have been diagnosed within the first year of life. They are slightly more common in males. Histological investigation typically reveals a prominent desmoplastic stroma with intermingled neoplastic astrocytes, a variable component of neuronal cells, and aggregates of undifferentiated cells. A subset of DIG/DIA contains BRAF V600E mutations (Koelsche et al., 2014). Neuroimaging usually shows a large, dura-based, cystic, and often septated mass (**Fig. 10.11A**). The solid tumour typically appears attached to the cortex and dura. Contrast enhancement can be intense and is commonly restricted to the solid part of the tumour. Patients usually present with signs of increased intracranial pressure. Treatment is surgical, and may be quite challenging because of tumour size and location. Complete resection often results in long-term tumour control. However, up to 40% of cases may require adjuvant chemotherapy and possibly radiotherapy in older children. Patients with disseminated disease are not altogether uncommon (Hummel et al., 2012).

The WHO classification lists several tumour variants, which are histologically characterized by small, isomorphic neuronal cells, and therefore termed *neurocytomas. Central neurocytomas* are covered elsewhere in this text. Tumours with a similar histology but growing without association with the ventricular system are termed *extraventricular neurocytomas* (EVN). They occur throughout the cerebrum, but may also grow outside the cranial vault. EVN are usually assigned to the WHO grade II. Imaging findings include cysts, heterogenous contrast enhancement, mass effect and oedema (**Fig. 10.11B**). Atypical histological features and/or increased mitotic activity (i.e. MIB-1 index >3%) are seen in approximately a quarter of the patients. Patients with atypical EVN appear to have a substantially worse prognosis than those with typical tumours. A recent literature review reported 5 yrs. recurrence rates of 36% and 68% for cases with atypical and typical EVNs, respectively (Kane et al., 2012). Complete resections are helpful in controlling EVNs, but may be difficult to achieve because of tumour size or location.

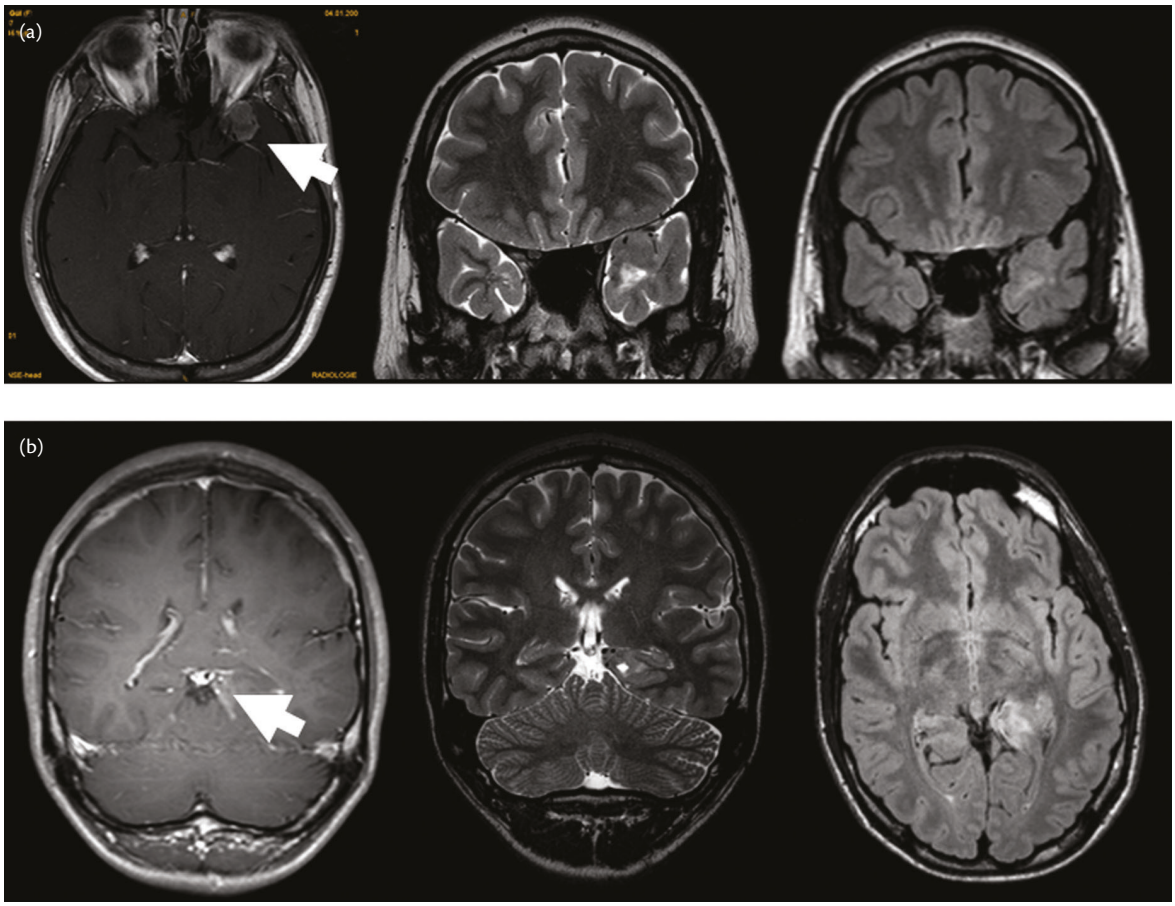

Fig. 10.11 (A) Right frontoparietal desmoplastic infantile gangliogliomas (DIG) in an 8 months female infant. (B) Atypical extraventricular neurocytoma WHO grade II growing in the dorsal thalamus and middle temporooccipital gyrus. The tumour occurred in a 25-year-old female with hydrocephalic symptoms.
Courtesy of Dr Kieren Allinson, Department of Pathology, Addenbrooke's Hospital, Cambridge.

Radiotherapy may compensate to some extent for an incomplete resection with respect to progression-free survival.

Many *cerebellar liponeurocytomas* are typical posterior fossa tumours. They usually originate from the vermis or the cerebellar hemispheres. Growth in or onto the cisterns has been observed. Tumours consist of isomorphic neuronal cells ('neurocytoma') with focal lipomatous differentiation and are assigned to the WHO grade II. MR imaging features reflect the distribution and proportion of lipidized tissue. The tumours usually show heterogenous contrast enhancement. The main differential diagnoses both for the neuroradiologist and the neuropathologist are medulloblastoma and ependymoma. Indeed these tumours have initially been referred to as lipidized medulloblastomas. Cerebellar liponeurocytomas seem to carry a rather substantial recurrence rate and reduced overall survival. A review of 19 published cases reported a 5 yrs. survival rate of only 48% and the literature contains several case reports describing an aggressive clinical behaviour and/or histologically anaplastic variants. Extracerebellar supratentorial liponeurocytomas have been described. Surgery is considered the treatment of choice (Chakraborti et al., 2011). The role of radiotherapy is debatable.

Controversies

Surgical management of temporal LEATs—with or without hippocampectomy?

Operative treatment for LEATs usually aims more at controlling tumour-related epilepsy than tumour growth. To this end various surgical strategies have been employed ranging from simple tumour removal or 'lesionectomy' to tumour resections together with a surrounding rim of cortex ('extended lesionectomy') and resections including an additional corticectomy or removal of temporomesial structures in order to excise an extended epileptogenic zone (Zaghloul and Schramm, 2011). This latter approach necessitates a formal and at times even invasive preoperative epileptological work-up or intraoperative electroencephalograph (EEG) recordings (ECoG).

If and when resections involving more than the tumour itself are indicated remains a contentious and controversial issue. The first argument in favour of simple lesionectomies is the often good epileptological outcome seen after such surgery. According to a recent literature review almost 80% of patients with temporal low-grade tumours and epilepsy will become seizure-free following gross total tumour resections (Englot et al., 2012). The second argument is the preservation of neurological function. Even in experienced hands temporomesial resections carry a quite low but nevertheless measurable risk of hemiparesis, dysphasia, and significant visual field cuts. Neuropsychological outcomes following surgery for temporal lobe epilepsy may be better following more restricted resections when compared to temporal lobectomies (Schramm, 2008). Resection of MR imaging and histopathologically negative hippocampal tissue carries a significant risk for memory impairment (especially if the dominant hemisphere is involved), while patients

with a diseased hippocampus have deficits usually already before surgery and memory deterioration is less frequent (Helmstaedter et al., 2011). Interestingly, more extensive hippocampal resections did not result in better epileptological outcomes in a randomized trial of 207 patient with mesial temporal lobe epilepsy (>95% due to mesial temporal lobe sclerosis) (Schramm et al., 2011).

However, a case can also be made for an additional temporomesial resection during surgery for a temporal LEAT. Firstly, more patients may become seizure-free if a hippocampectomy and/or corticectomy in addition to a gross total resection is performed (86–87% as compared to 79% according to a recent survey) (Englot et al., 2012). Of note, these figures likely underestimate the impact of extended resections on seizure outcomes, since cases with more difficult epilepsy will probably more often undergo more extensive surgeries. Secondly, the appropriate surgical strategy will have to take into account the pathophysiology of the epilepsy. Patients with pharmacoresistant epilepsy and glioneuronal LEATs not uncommonly harbour additional epileptogenic pathologies. As detailed earlier, cortical dysplasias can be found in association with up to a quarter of gangliogliomas and are even more frequently together with DNTs (Thom et al., 2012). Additional hippocampal sclerosis may be seen in LEAT cases (Fig. 10.12A). Also, tumours may not only cause seizures through pressure on and irritation of surrounding brain (the rationale behind the concept of a simple lesionectomy). Tumour-associated seizures may commonly originate in the border zone (sometimes termed 'collision zone') between the tumour and surrounding normal brain, as well as distant brain areas as evidenced, for example, by ECoG recordings (Zaghloul and Schramm, 2011).

Our policy has always been to perform 'extended' lesionectomies for extratemporal and temporolateral LEATs causing neocortical temporal lobe epilepsy (i.e. gross total tumour resections with removal of a 0.5–1 cm rim of surrounding cortical tissues). If the lesion lies within or borders eloquent cortex, we restrict ourselves to simple lesionectomies. Appropriate preoperative neuroimaging is vitally important in order to identify additional epileptogenic lesions (i.e. to properly delineate the epileptogenic vs. tumorous lesion). Tumours involving the temporomesial structures should be resected together with any abnormal hippocampus/parahippocampus and a rim of adjoining temporomesial tissues (**Fig. 10.12**). The results of preoperative depth electrode recordings or ECoG recordings may suggest taking the resection more dorsally if the epileptological

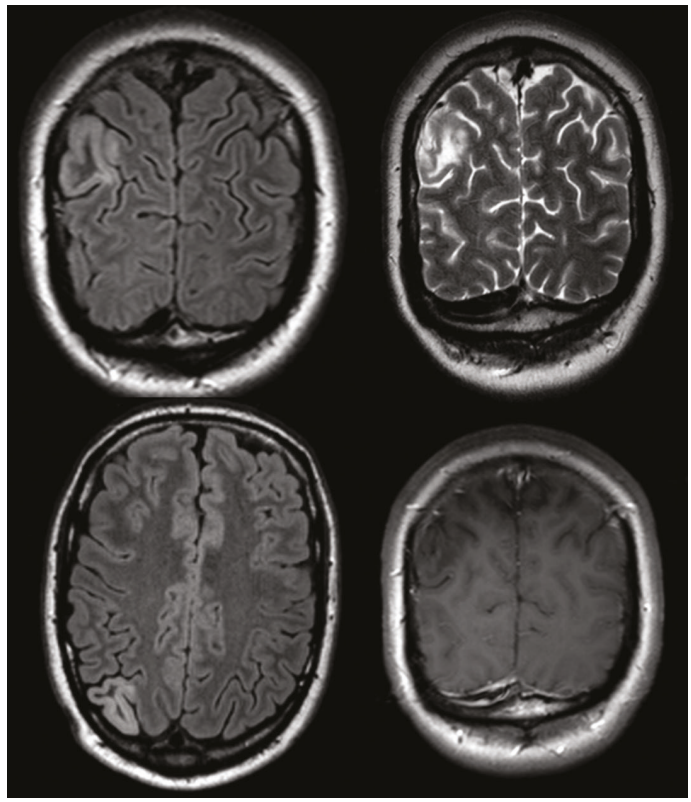

Fig. 10.12 Surgical treatment for temporo-mesio-basal long-term epilepsy-associated tumours—with and without hippocampectomy. (A) Upper panel: left parahippocampal ganglioglioma WHO grade I in a 36-year-old female with a 32-year history of epilepsy. The tumour either also involves part of the hippocampus or there is associated hippocampal sclerosis. Lower panel: we performed an extended lesionectomy including amygdalohippocampectomy. The patient has been completely seizure-free for three years and is working full-time as a kindergarten teacher. Resection of diseased hippocampus is required for epilepsy control in such cases and not associated with adverse neuropsychological sequelae. (B) Upper panel: dysembryoplastic neuroepithelial tumour (DNT) WHO grade I of the lateral temporo-occipital gyrus. The tumour was diagnosed in a 34-year-old female following a 5-year seizure history. Lower panel: an extended lesionectomy *sparing the hippocampus and amygdalum* was performed, since neither neuroimaging nor seizure semiology or EEG recordings suggested a hippocampal seizure origin. The patient has been completely seizure-free for the last three years.

Courtesy of Dr Kieren Allinson, Department of Pathology, Addenbrooke's Hospital, Cambridge.

benefit is felt to outweigh the potentially adverse neuropsychological sequelae. Experience suggests that dominant hippocampal surgery may carry higher risks for neurocognitive deterioration (e.g. memory deficits).

FURTHER READING

Englot, D.J., Han, S.J., Berger, M.S., Barbaro, N.M., & Chang, E.F. (2012). Extent of surgical resection predicts seizure freedom in low-grade temporal lobe brain tumors. *Neurosurgery*, **70**, 921–8; discussion 928.

Luyken, C., Blumcke, I., Fimmers, R., et al. (2003). The spectrum of long-term epilepsy-associated tumors: long-term seizure and tumor outcome and neurosurgical aspects. *Epilepsia*, **44**, 822–30.

Majores, M., Von Lehe, M., Fassunke, J., Schramm, J., Becker, A.J., & Simon, M. (2008). Tumor recurrence and malignant progression of gangliogliomas. *Cancer*, **113**, 3355–63.

Thom, M., Blumcke, I. & Aronica, E. (2012). Long-term epilepsy-associated tumors. *Brain Pathol*, **22**, 350–79.

Zaghloul, K. A. & Schramm, J. (2011). Surgical management of glioneuronal tumors with drug-resistant epilepsy. *Acta Neurochir (Wien)*, **153**, 1551–9.

REFERENCES

Blumke, I., Aronica, E., Becker, A., et al. (2016). Low-grade epilepsy-associated neuroepithelial tumours—the 2016 WHO classification. *Nat Rev Neurol*, **12**(12), 732–40.

Blumcke, I., Aronica, E., Urbach, H., Alexopoulos, A., & Gonzalez-Martinez, J.A. (2014). A neuropathology-based approach to epilepsy surgery in brain tumors and proposal for a new terminology use for long-term epilepsy-associated brain tumors. *Acta Neuropathol*, **128**, 39–54.

Chakraborti, S., Mahadevan, A., Govindan, A., et al. (2011). Supratentorial and cerebellar liponeurocytomas: report of four cases with review of literature. *J Neurooncol*, **103**, 121–7.

Chen, G., Wang, L., Wu, J., Jin, Y. & Wang, X. (2014). Intractable epilepsy due to angiocentric glioma: a case report and minireview. *Exp Ther Med*, **7**, 61–5.

Compton, J.J., Laack, N.N., Eckel, L.J., Schomas, D.A., Giannini, C., & Meyer, F.B. (2012). Long-term outcomes for low-grade intracranial ganglioglioma: 30-year experience from the Mayo Clinic. *J Neurosurg*, **117**, 825–30.

Dahiya, S., Haydon, D.H., Alvarado, D., Gurnett, C.A., Gutmann, D.H., & Leonard, J. R. (2013). BRAF(V600E) mutation is a negative prognosticator in pediatric ganglioglioma. *Acta Neuropathol*, **125**, 901–10.

Englot, D.J., Han, S.J., Berger, M.S., Barbaro, N.M., & Chang, E.F. (2012). Extent of surgical resection predicts seizure freedom in low-grade temporal lobe brain tumors. *Neurosurgery*, **70**, 921–8; discussion 928.

Gessi, M., Abdel Moneim, Y., Hammes, J., Waha, A., & Pietsch, T. (2014a). FGFR1 N546K mutation in a case of papillary glioneuronal tumor (PGNT). *Acta Neuropathol*, **127**, 935–6.

Gessi, M., Moneim, Y.A., Hammes, J., et al. (2014b). FGFR1 mutations in Rosette-forming glioneuronal tumors of the fourth ventricle. *J Neuropathol Exp Neurol*, **73**, 580–4.

Grote, A. & Simon, M. (2015). Unpublished.

Helmstaedter, C., Petzold, I., & Bien, C.G. (2011). The cognitive consequence of resecting nonlesional tissues in epilepsy surgery—results from MRI—and histopathology-negative patients with temporal lobe epilepsy. *Epilepsia*, **52**, 1402–8.

Hummel, T.R., Miles, L., Mangano, F.T., Jones, B.V., & Geller, J.I. (2012). Clinical heterogeneity of desmoplastic infantile ganglioglioma: a case series and literature review. *J Pediatr Hematol Oncol*, **34**, e232–6.

Ida, C.M., Rodriguez, F.J., Burger, P.C., et al. (2014). Pleomorphic xanthoastrocytoma: natural history and long-term follow-up. *Brain Pathol*, **25**(5), 575–86.

Jones, D. T., Hutter, B., Jager, N., et al. (2013). Recurrent somatic alterations of FGFR1 and NTRK2 in pilocytic astrocytoma. *Nat Genet*, **45**, 927–32.

Kane, A.J., Sughrue, M.E., Rutkowski, M.J., et al. (2012). Atypia predicting prognosis for intracranial extraventricular neurocytomas. *J Neurosurg*, **116**, 349–54.

Koelsche, C., Wohrer, A., Jeibmann, A., et al. (2013). Mutant BRAF V600E protein in ganglioglioma is predominantly expressed by neuronal tumor cells. *Acta Neuropathol*, **125**, 891–900.

Koelsche, C., Sahm, F., Paulus, W., et al. (2014). BRAF V600E expression and distribution in desmoplastic infantile astrocytoma/ganglioglioma. *Neuropathol Appl Neurobiol*, **40**, 337–44.

Luyken, C., Blumcke, I., Fimmers, R., et al. (2003). The spectrum of long-term epilepsy-associated tumors: long-term seizure and tumor outcome and neurosurgical aspects. *Epilepsia*, **44**, 822–30.

Luyken, C., Blumcke, I., Fimmers, R., Urbach, H., Wiestler, O.D., & Schramm, J. (2004). Supratentorial gangliogliomas: histopathologic grading and tumor recurrence in 184 patients with a median follow-up of 8 years. *Cancer*, **101**, 146–55.

Majores, M., Von Lehe, M., Fassunke, J., Schramm, J., Becker, A.J., & Simon, M. (2008). Tumor recurrence and malignant progression of gangliogliomas. *Cancer*, **113**, 3355–63.

Pilarski, R., Burt, R., Kohlman, W., Pho, L., Shannon, K.M., & Swisher, E. (2013). Cowden syndrome and the PTEN hamartoma tumor syndrome: systematic review and revised diagnostic criteria. *J Natl Cancer Inst*, **105**, 1607–16.

Prestor, B. (2006). Dysplastic gangliocytoma of the cerebellum (Lhermitte-Duclos disease). *J Clin Neurosci*, **13**, 877–81.

Schlamann, A., Von Bueren, A.O., Hagel, C., et al. (2014). An individual patient data meta-analysis on characteristics and outcome of patients with papillary glioneuronal tumor, rosette glioneuronal tumor with neuropil-like islands and rosette forming glioneuronal tumor of the fourth ventricle. *PLoS One*, **9**, e101211.

Schramm, J., Luyken, C., Urbach, H., Fimmers, R., & Blumcke, I. (2004). Evidence for a clinically distinct new subtype of grade II astrocytomas in patients with long-term epilepsy. *Neurosurgery*, **55**, 340–7; discussion 347–8.

Schramm, J. (2008). Temporal lobe epilepsy surgery and the quest for optimal extent of resection: a review. *Epilepsia*, **49**, 1296–307.

Schramm, J., Lehmann, T.N., Zentner, J., et al. (2011). Randomized controlled trial of 2.5-cm versus 3.5-cm mesial temporal resection in temporal lobe epilepsy—Part 1: intent-to-treat analysis. *Acta Neurochir (Wien)*, **153**, 209–19.

Stuer, C., Vilz, B., Majores, M., Becker, A., Schramm, J., & Simon, M. (2007). Frequent recurrence and progression in pilocytic astrocytoma in adults. *Cancer*, **110**, 2799–808.

Thom, M., Blumcke, I., & Aronica, E. (2012). Long-term epilepsy-associated tumors. *Brain Pathol*, **22**, 350–79.

Thom, M., Toma, A., An, S., et al. (2011). One hundred and one dysembryoplastic neuroepithelial tumors: an adult epilepsy series with immunohistochemical, molecular genetic, and clinical correlations and a review of the literature. *J Neuropathol Exp Neurol*, **70**, 859–78.

Zaghloul, K.A. & Schramm, J. (2011). Surgical management of glioneuronal tumors with drug-resistant epilepsy. *Acta Neurochir (Wien)*, **153**, 1551–9.

Zhang, J., Babu, R., Mclendon, R.E., Friedman, A.H., & Adamson, C. (2013a). A comprehensive analysis of 41 patients with rosette-forming glioneuronal tumors of the fourth ventricle. *J Clin Neurosci*, **20**, 335–41.

Zhang, J., Wu, G., Miller, C.P., et al. (2013b). Whole-genome sequencing identifies genetic alterations in pediatric low-grade gliomas. *Nat Genet*, **45**, 602–12.

11

Radiotherapy and radiosurgery for brain tumours

Susan Short

Case history: Management and work-up of patients with malignant brain tumours

All patients with suspected brain tumours should be reviewed and managed through a multidisciplinary team comprising all relevant clinical and allied healthcare specialists. Prior to discussion the clinical history and relevant imaging needs to be available and in most instances, this is a contrast-enhanced MRI brain scan.

In most cases, surgery is first-line management. This serves to provide material for histological diagnosis as well as remove tumour tissue, which may be beneficial for relieving mass effect and other symptoms. Since these tumours are typically highly invasive, surgery cannot address subclinical microscopic disease and is rarely curative in isolation. Nevertheless, in the majority of malignant tumours there is a well-described positive correlation between extent of surgery and overall outcome although randomized studies to address the value of different extents of surgery directly have not been undertaken and would be ethically challenging.

Recent data addressing the utility of using fluorescence-guided or image-guided resection with 5-aminolevulinic acid (5-ALA) or intraoperative MRI have supported the role of maximal safe resection (Schatlo et al., 2015). Following surgery, the histopathology in context of the clinical history and radiology is presented and discussed at a multidisciplinary meeting where decisions on likely recommendations for additional treatment can be made and appropriate referral expedited. In most cases this will involve referral for adjuvant radiotherapy and/or chemotherapy, the details of which depends on the tumour histology as well as clinical factors including patient age and performance status. This is also an important opportunity to consider eligibility for clinical studies to test the effect of new treatment approaches.

Following surgery, radiotherapy remains the most effective treatment for primary brain tumours and its contribution in grade III and IV gliomas has been confirmed in meta-analyses of outcome data. In GBM, the commonest adult glioma, the standard of care was established in a landmark EORTC study in 2005, in which six weeks of radiotherapy (60 Gy total dose, given as 30 2 Gy fractions Monday to Friday) with concomitant temozolomide chemotherapy, was shown to be superior to radiotherapy alone (Stupp et al., 2005). The median survival after combined treatment was 14 months.

In anaplastic astrocytoma (WHO Grade III astrocytoma), maximal surgery followed by external beam radiotherapy using a similar dose regime remains standard treatment. Whether combined modality treatment will improve outcome further, as it has in GBM remains to be seen and relevant studies are ongoing (EORTC 26053-22054). In grade III oligodendrogliomas, radiotherapy is also a central component of treatment. Long-term follow up data from two trials (EORTC 26951, RTOG 9402) comparing radiotherapy with and without adjuvant chemotherapy (procarbazine, CCNU, Vincristine (PCV)) demonstrate very favourable survival outcomes (greater than 10 years) with combination treatment postsurgery.

In low-grade gliomas the role of radiotherapy remains more open to debate. Radiotherapy remains the standard approach in patients deemed to need treatment and who are not suitable for radical surgery, for example, due to high-risk clinical features. A recent Phase III European study (EORTC 22033-26033) has addressed whether chemotherapy with temozolomide is as effective as radiotherapy as first line treatment in these patients, these data suggest that the two approaches are similar in terms of progression-free survival, additional data pertaining to subgroups of tumours defined by molecular pathology are awaited (Baumert et al., 2016). The limitations of radiotherapy in this patient group is often the extensive nature of these tumours, meaning that large volumes of brain need to be treated at the relatively young age at which these patients present. It is not established that these tumours require such high doses as those used in high-grade tumours and large studies have not demonstrated a dose response between 45 and 60 Gy. Low-grade oligodendrogliomas, defined using integrated molecular pathology as described in WHO 2016 (Louis et al., 2016), with 1p 19q chromosomal loss appear to respond particularly well to combined radiotherapy and PCV chemotherapy in line with their higher-grade counterparts.

Basic science of radiotherapy

Principles of radiobiology

Radiation causes cellular damage when it interacts with cells and is an effective treatment because cancer cells are less tolerant of damage than normal cells and are therefore selectively killed. The

principle toxic lesion following irradiation of nucleated cells is a double-strand break (DSB) in the DNA double helix and all cells have a complex series of mechanisms to recognize and attempt to repair these lesions. The two major DNA DSB repair pathways in mammalian cells are non-homologous end-joining (NHEJ) and homologous recombination (HR). NHEJ is active throughout the cell cycle, whereas HR functions in S and G2 phases when a sister chromatid is present to act as a template for repair of the damaged strand, however the balance of repair carried out by each pathway can be influenced by the kinetics of initial repair and the presence of other proteins that affect chromatin structure. An important difference between these repair pathways is that HR is generally error free since a normal template is used to regenerate damaged DNA, whereas NHEJ is error prone since DNA sequence can be lost between re-joined strand ends. Repair by NHEJ may therefore be mutagenic and contribute to radiation-induced malignancy. The signalling events and major effector proteins in each pathway are summarized in **Figure 11.1A**.

In principle the cytotoxic effects of radiation can be augmented specifically in cancer cells by targeting repair pathways unique to them or pathways on which they exhibit overreliance compared to normal cells. The concept of synthetic lethality is an example of this approach, in which a repair inhibitor is targeted at the specific repair processes that are active in tumour cells with abnormal repair capacity. In glioma, although combination treatment with radiotherapy and temozolomide chemotherapy has been shown to significantly improve outcome in patients with GBM (Stupp et al., 2005; Stupp et al., 2009), there is little evidence to support that this is directly due to radiosensitization, with most preclinical data suggesting an additive effect when these two agents are combined. The detailed molecular biology of DNA repair is still being investigated, and this work is likely to identify new targets for treatment that may be effective radio and chemosensitizers.

The effects of radiation on cells can be assessed in a variety of ways, including visualization of protein relocalization at sites of damaged DNA using immunofluorescent (IF) staining. IF for the phosphorylated histone protein H2AX has proven extremely useful since this protein is rapidly phosphorylated at sites of DNA DSB and dephosphorylated when DSB are repaired. Individual foci of phosphorylated protein can be visualized in nuclei and the number of these are linearly related to induced DNA DSB, allowing quantification of damage and analysis of repair kinetics. Foci numbers visualized early after radiation can also be used as an indirect measurement of radiation dose. A representative image using this approach is shown in **Figure 11.1B**.

Cellular survival following radiation has a more complex relationship to dose, reflecting the varying capacity of cells to repair damage. For most cells exposed to X-rays the dose–response relationship for survival, for example, measured using a clonogenic survival assay is linear-quadratic, with an inflection of the survival curve at a dose above which cells become more sensitive per unit dose. This inflection point varies between cell types, but tends to be lower in normal tissue than in tumour cells. This leads to the important and long-established radiobiological principle that large total radiation doses are better tolerated when delivered as a series of small doses given 5 days per week. This allows normal tissue, which is less able to tolerate large single doses, to repair and regenerate following treatment. Hence a standard radiotherapy regime is given as daily doses (fractions) of around 2 Gy and a radical dose (around 60 Gy) is achieved during a 6-week treatment course. In circumstances where normal tissue is excluded from the treatment field, larger doses per day or single large doses, known as radiosurgery may be tolerated.

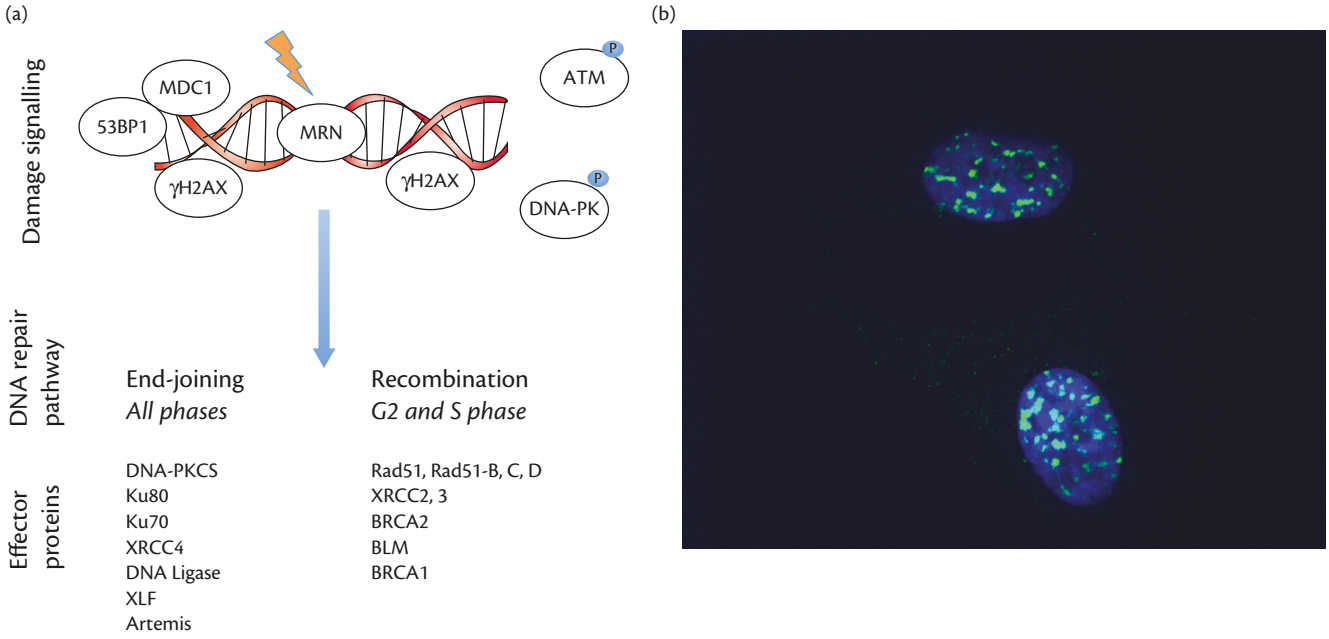

Fig. 11.1 (A) A summary of the two major DNA damage repair pathways in mammalian cells that are activated after DNA double-strand breaks caused by radiation and the major signalling and effector proteins involved. (B) Representative image of glioma cells stained for the repair protein γH2AX following exposure to radiation. Nucleus stained with 4′,6-diamidino-2-phenylindole (DAPI) (blue) and phosphorylated protein foci stained green.

Physics of radiotherapy

Modern radiotherapy makes optimal use of the physics of high energy (kilovoltage range) X-rays to deliver treatment. Clinical beams are most commonly generated in linear accelerators in which an electron beam is accelerated to a metal target, producing secondary X-rays which are then filtered and collimated to produce a homogenous beam of a set energy range and shape. The beam energy determines the depth in tissue where most of the beam energy and therefore cellular damage is deposited. For high energy beams, this is in the range of several centimetres. In order to produce a high-energy deposition region at depth, multiple beams from different directions are focused on the tumour target, permitting dose build up where the beams cross and reducing dose to non-target tissue in the beam entry paths. A treatment plan is designed in 3D space to place the target at the intersection of the beams where the additive dose is highest and to spare normal tissue, which lies outside this region, and so will receive a lower dose. Further differential sparing of normal tissue can be achieved by increasing the number of incident beams or by delivering treatment in a dynamic manner so that a smaller volume of normal tissue is exposed for any given tumour dose.

Radiotherapy techniques

Conformal external beam radiotherapy

Conventional conformal radiotherapy utilizes three-dimensional diagnostic imaging, usually from a combination of MRI and computed tomography (CT). Importantly one of these data sets (usually CT) is derived when the patient is in the intended treatment position, so that the anatomy can be cross-reference to the treatment situation. The secondary imaging data set (usually MRI, or sometimes positron emission tomography (PET)) is then digitally superimposed on the CT image. The patient is immobilized in a personalized plastic mask for both CT imaging and for subsequent treatment, permitting accurate, conformal, and reproducible treatment for many tumour types. The treatment beams are then designed as described earlier to deliver a high dose to the tumour target and avoid as much normal tissue exposure as possible. In this approach 3 or 4 static beams are generally used and the dose is delivered proportionately from each beam direction sequentially. The limitations of this approach are apparent when complex 3D targets are defined or when radiosensitive organs at risk of radiation damage are located in concavities close to the tumour. 3D-conformal treatment cannot then deliver high doses to the tumour while sparing normal tissue. In the central nervous system (CNS) this is particularly relevant in regions close to the posterior orbit and the skull base.

Intensity-modulated radiotherapy

Intensity-modulated radiotherapy (IMRT) delivers treatment using dynamic modulation of the radiation beam. This is achieved by using multileaf collimators that are moved within the beam path as it exits the machine head so that the beam is modulated in 3D before it reaches the patient. This permits much more complex shapes to be treated in a highly conformal way and specifically enables dose to be delivered around concave structures.

The applicability of IMRT for treatment of brain cancers has been evaluated in clinical and dosimetric studies, which show that it can be used to target these tumours effectively (Khoo et al., 1999; Narayana et al., 2006). Further developments in technology including approaches in which IMRT is delivered more rapidly in an arc-mode have optimized IMRT delivery by reducing the beam 'on time' to reduce the period that the patient needs to be on the treatment couch. This approach also lowers the total body dose due to internal scatter which can be high when multiple beam directions are used. A comparison of 3D conformal and IMRT plans for a glioma patient is shown in Figure 11.2.

Stereotactic radiosurgery

Radiosurgery is used to describe delivery of highly focused radiotherapy given as a single dose with the aim of producing local tumour ablation. As discussed earlier, normal tissue has a limited capacity to recover from large single radiation doses, which means that this approach is generally limited to small, well-defined targets where local normal tissue can be excluded from the irradiated

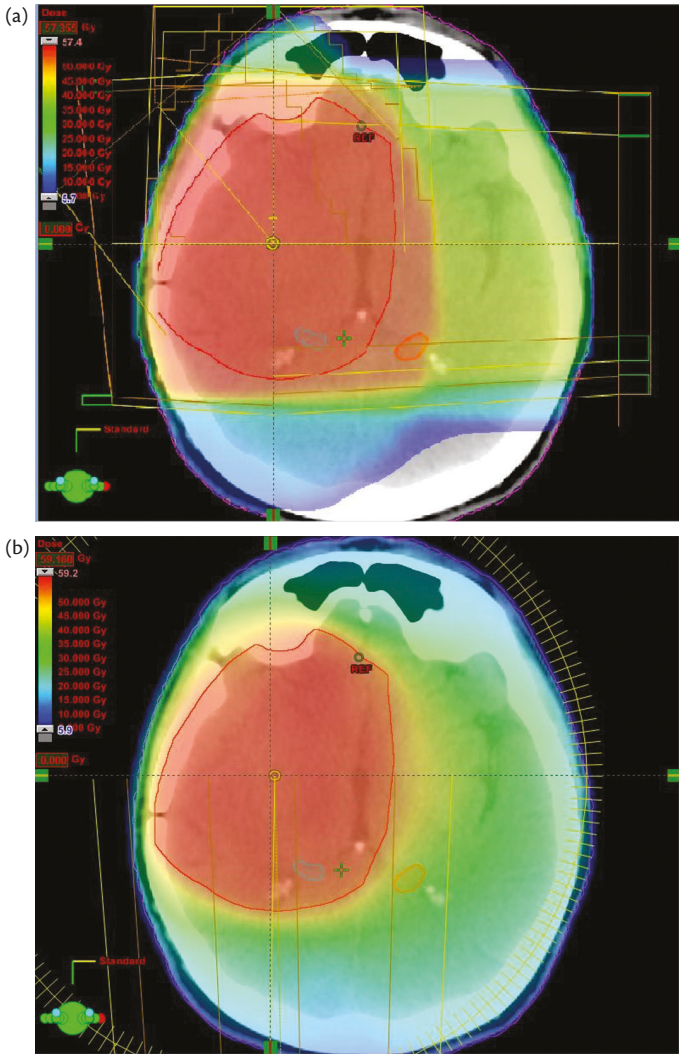

Fig. 11.2 An axial image of a 3D conformal radiotherapy plan for a patient with glioma, showing isodose lines in different colours superimposed on the CT (A) and the same target volume treated using IMRT (B). The target volume is shown outlined in red. High-dose volume is shown as red colour wash. Blue colour wash represents the low-dose (<30%) region outside the tumour target. Hippocampus is outlined separately as an organ at risk (left, orange outline, right, blue outline).

volume. Historically, radiosurgery has been most commonly delivered using cobalt-based technology (Gamma Knife) in which multiple sources are targeted at a single point, producing a very high dose at the intersection of the radiation beams (isocentre) with a steep dose fall off beyond. In this approach patients are immobilized in a head-frame to ensure accurate delivery in 3D space. Equivalent treatments can also be achieved using other technologies, for example the Cyber Knife, which uses image guidance to deliver radiosurgery through a robotic gantry without the need for an immobilization frame.

For most malignant brain tumours, radiosurgery is not useful as the tumour volume is large and rather poorly defined due to the infiltrating nature of the disease. Clinical studies that have used radiosurgery to deliver a boost dose to high-grade gliomas by targeting smaller subregions for a higher total dose have not demonstrated any advantage (Baumert et al., 2003; Baumert et al., 2008). However, radiosurgery is now a standard approach for treating brain metastases as these are frequently small, well defined lesions (Fig. 11.3).

Brachytherapy

Brachytherapy refers to treatment in which a radioactive source is placed directly in contact with the tumour or tumour bed target. In the brain this is not a commonly used method although there are a significant number of historical studies which have used different brachytherapy techniques, most often in an attempt to deliver high local doses to poor prognosis tumours. Overall the response to this approach has been disappointing with few studies demonstrating good local tumour control, but most demonstrating an increased risk of radionecrosis. More recently brachytherapy has been explored as an alternative to surgery for tumours at eloquent sites, however confirmation of the utility of this approach awaits assessment in randomized studies (Ruge et al., 2013).

Boron neutron capture therapy

Boron neutron capture therapy is based on the principle of local enhancement of radiation dose. This is achieved by delivering a boron-containing compound (usually a boronated amino acid such as phenylalanine) to the tumour then delivering a local low-dose neutron beam to activate emission of alpha particles from boron. Since tumour cells selectively uptake boron-amino acid compounds due to enhanced amino acid membrane transport systems, this approach can selectively sensitize tumour cells to neutron irradiation. In principle this will also apply to scattered invading cells anywhere in the irradiated volume, making this an appealing approach. The challenges inherent in this model include effective delivery of boronated compounds in sufficient quantities for efficacy at the time of irradiation and the specialist equipment required to produce and target the low energy neutron beam. Several groups worldwide are investigating this technique, but it is not yet widely available and has not been formally compared to conventional radiotherapy in clinical studies (Miyatake et al., 2009).

Proton beam therapy

Proton beam radiotherapy utilizes charged proton particles in place of X-rays for the treatment beam. The advantage of this approach comes from the specific dose profile of charged particles in tissue. There is a small range over which the proton energy is deposited called the Bragg peak, which is dependent on the energy of the beam and the tissue that the beam traverses. This can be used to target a beam that delivers high-energy irradiation at a very specific point with practically no effect on deeper tissues. This is advantageous in situations in which normal tissue sits very close to a tumour target, or where large volumes of radiosensitive tissue lie in the exit path of the beam. Proton beam radiotherapy can therefore be used in situations where conventional X-ray beam treatment would lead to an unacceptably high risk of normal tissue toxicity, for example at the

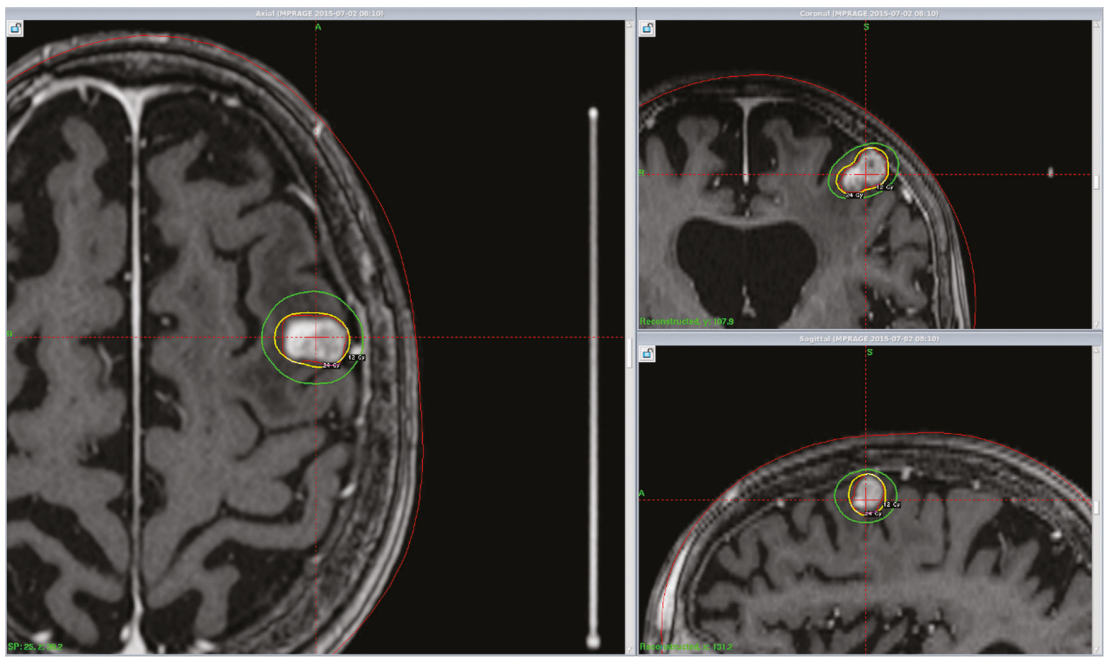

Fig. 11.3 A representative panel of images (axial, coronal, sagittal) of a radiosurgery treatment plan for a patient with brain metastases. The high-dose target is outlined in yellow and high-dose envelope in green, showing steep dose fall off in all planes beyond the tumour.

skull base, close to the optic pathway and brain stem or close to the spinal cord. It is also an advantage for many paediatric tumours, where developing normal tissue is particularly sensitive to radiation exposure so removing the exit beam dose reduces long-term toxicity risks significantly. Figure 11.4 is a representation of the dose deposition in tissue using proton beam (A) and a proton beam treatment plan for a patient with a base of skull tumour (B).

Limitations and side effects of radiotherapy

Despite optimization of complex radiotherapy delivery methods, non-tumour tissue can rarely be totally excluded from exposure to radiation during treatment. In the CNS, the relevant normal tissues are the skin and hair on the scalp, non-involved eloquent brain, the optic and auditory apparatuses, the pituitary gland, and the cerebral vasculature. All of these tissues show dose-dependent toxicity, expressed over a time course that depends on the tissue involved. Side effects are conventionally grouped according to the time at which they are expressed, early effects in weeks, and late effects in months to years. An additional effect may occur at an intermediate time, manifesting as a somnolence syndrome (Powell et al., 2011). Common early toxicities include hair loss and skin erythema, within 3–4 weeks of commencing treatment. Late effects include pituitary hormone failure, damage to visual and auditory pathways, and cognitive deficit. A set of data describing the acute side effects of radiotherapy and their time course is shown in Figure 11.5.

An important radiation-induced pathology in normal brain expressed as normal tissue necrosis, can occur between 6 months and several years after treatment. The incidence of this complication is related to the total dose, fraction size, and the volume of normal brain irradiated. Radionecrosis may be asymptomatic but can cause raised intracranial pressure or focal neurological symptoms. The best estimates of incidence suggest that this occurs in less than 5% of patients treated with conventional fractionation regimes, but a higher proportion when large doses per fraction are used and when larger volumes of normal brain are included. This is most relevant after radiosurgery where the incidence of radionecrosis has been documented as up to 25%. The major diagnostic challenge in this context is differentiating between radionecrosis and high-grade tumour progression on standard MRI scans. Radionecrosis typically

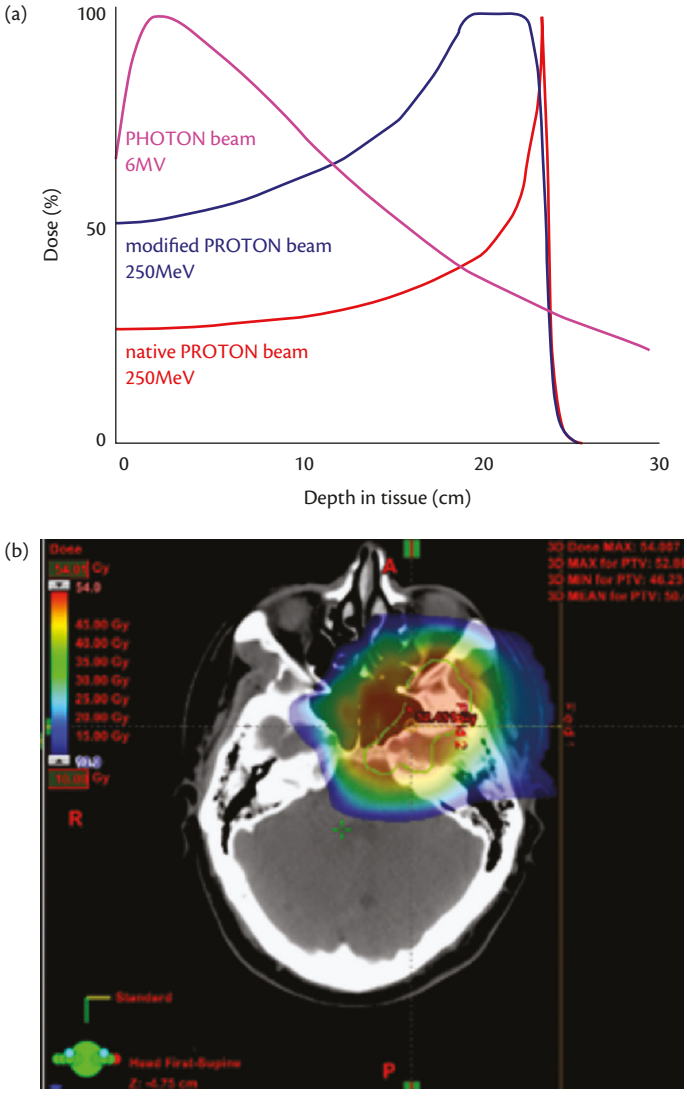

Fig. 11.4 (A) A graphic representing the different dose deposition in tissue using a photon beam, with the maximal dose near the surface and significant dose beyond the tissue maximum (pink line). In comparison a proton beam deposits dose over a narrow range of depth in tissue at the Bragg peak, with a steep dose fall off beyond (native proton beam, red line). This can be modified to spread the Bragg peak over a wider range in tissue (modified proton beam, blue line) at the cost of some increased dose closer to the surface. (B) A representative image from a proton beam plan for a patient undergoing treatment for a skull base tumour. The blue isodose line represents the low-dose region, which falls off very steeply beyond the tumour target.

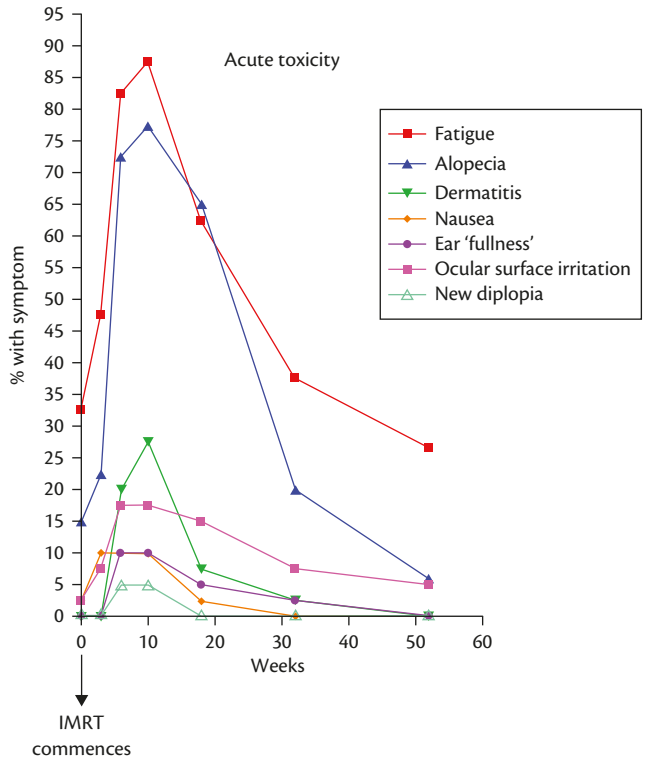

Fig. 11.5 A graphical representation of the time course and incidence of acute radiotherapy side effects in a series of patients (N = 50) undergoing intensity-modulated radiotherapy to the skull base.
Reproduced by agreement with Dr J. Maclean.

appears as an enhancing area due to disruption of the blood–brain barrier which is indistinguishable from active tumour and occurs at a time when there is a significant risk of tumour recurrence. Developing imaging protocols that can reliably distinguish between radiation necrosis and tumour recurrence using PET, SPECT, or advanced MRI techniques is an active area of research. In cases where management decisions would be critically altered by the presence of active tumour, biopsy remains the only definitive way to distinguish between these two conditions.

In most cases management of suspected radionecrosis is supportive, using steroid medication to reduce accompanying oedema, antiseizure medication as required with close clinical and radiological surveillance. There is a developing literature on the use of vascular endothelial growth factor (VEGF) inhibition in this context and several small studies have reported good outcomes using Bevacizumab, a humanized anti-VEGF monoclonal antibody in patients with symptomatic radionecrosis who do not respond to steroids. Small series have also reported favourable outcomes using hyperbaric oxygen therapy (HBO), the rationale for this being that enhancing oxygen delivery to damaged tissue by increasing plasma oxygen carriage enhances recovery. A course of HBO sessions is usually recommended which may require up to 20 attendances. This is not widely available, and HBO is generally reserved for patients with limited other treatment options. In cases presenting with mass effect that does not respond to steroid treatment or other medical management, consideration should be given to surgical removal of the lesion.

The phenomenon of 'pseudoprogression' in patients who have received surgery and adjuvant radiotherapy or radiochemotherapy is thought to be a related issue. MR imaging appears to show an increased enhancing tumour volume at early follow up, 1–2 months postradiotherapy, which is often asymptomatic and resolves without specific intervention. This suggests that the underlying cause is a treatment induced effect on blood–brain barrier permeability associated with neural or vascular tissue damage. The current recommendation for treatment is for supportive management and re-evaluation after 4–6 weeks, when pseudoprogression is likely to begin to resolve.

Over much longer time frames, of many years, radiation-induced tumours, most commonly meningiomas, but rarely also radiation-induced malignant tumours including gliomas and sarcomas occur (Brada et al., 1992; Minniti et al., 2005). The incidence of true radiation-induced malignancy is difficult to determine, particularly in a population with rather short median survival. Data from paediatric populations implies a significant risk following brain irradiation, probably 5–10-fold higher than non-irradiated cohorts, although younger age at exposure is also recognized as an important factor that inflates risk for a given dose. Epidemiologic data, for example A-bomb survival data confirm a malignancy risk that is proportional to dose, but these whole-body doses are challenging to convert to risk estimates in patients who have been exposed to high-dose treatment to only partial organ volumes, in whom risk is likely to be lower. However, the established mutagenic potential of radiation and available data, particularly in survivors of childhood cancer make it clear that mitigating risk of radiation-induced malignancy is an important challenge as treatment efficacy improves. Modern radiotherapy techniques contribute to this since they deliver dose more accurately to tumour volumes and reduce high-dose exposure to surrounding normal tissue. However some of these techniques, including IMRT, may also increase the volume of normal tissue that is exposed to very low-dose radiation and the contribution of this dose component to overall long-term risk is unknown. To date no studies have reported on second cancer risk after brain radiotherapy using IMRT or proton beam therapy.

Mechanisms of late toxicity are related to damage to the endothelial as well as the glial compartment in the CNS (Benczik et al., 2002; Otsuka et al., 2006). The majority of cells within the CNS are postmitotic and therefore not expected to exhibit sensitivity to radiation. The most sensitive differentiated cell type in the CNS is the oligodendrocyte population, and demyelination occurs following relatively low radiation doses (Panagiotakos et al., 2007). Current models of late toxicity following radiotherapy to the brain include the effects of loss of a population of stem-like cells that inhabit specific anatomic and biological niches including the subventricular zones and hippocampi. In rodent models, loss of these cells is associated with cognitive deficit and studies are ongoing to address whether specifically excluding stem-cell-rich areas from radiation may reduce these long-term side effects. It is a concern that clinical data sets suggest that stem cell populations are sensitive to very low radiation doses (Marsh et al., 2010). These data have led to radiotherapy planning approaches that specifically exclude these brain regions from high-dose exposure during treatment if this is compatible with delivering high dose to the tumour volume. Hippocampal sparing approaches have been shown to be deliverable using IMRT techniques, in which the hippocampus is defined as an avoidance structure, but as yet no prospective randomized data on the impact of this approach on neurocognitive outcomes are available. An alternative approach is to use drugs that may act as neuroprotectants for example memantine, during radiotherapy. The randomized studies that have reported this approach have not thus far shown significant benefit.

Case history

A 70-year-old patient presented to his general practitioner with episodes of confusion when driving. On examination the patient had reduced motor power on the left as well as left sided inattention. Investigations including an MRI brain were arranged and representative images are shown in **Figure 11.6**. The right frontal lesion was biopsied and found to be a grade III oligodendroglioma with loss of heterozygosity (LOH) of 1p19q.

Standard treatment for grade III gliomas is external beam radiotherapy with additional chemotherapy for those with 1p19q LOH. This approach has not been assessed in randomized studies in patients over the age of 70. For multifocal disease, as in this case, radiotherapy can be challenging to deliver since the total tumour volume is large and multiple organs at risk may be in close proximity. In this case the concern was how to encompass the whole tumour volume, which includes multiple lobes, and is close to the optic chiasm. An alternative approach in these cases can be to treat with chemotherapy to attempt to reduce the tumour volume, which may then be encompassable in a radiotherapy field with lower risks of toxicity. Not all of these tumours respond to chemotherapy but most cases with 1p19q loss of heterozygosity are thought to be chemosensitive.

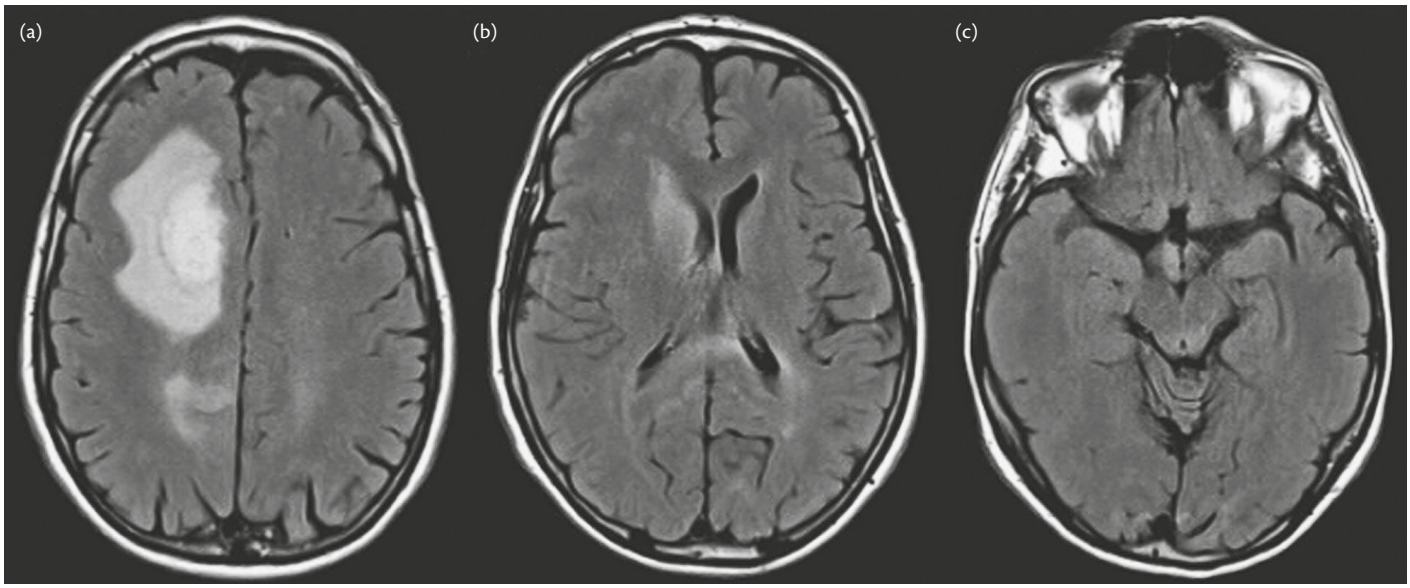

Fig. 11.6 MRI images including fluid-attenuated inversion recovery (FLAIR) images showing multifocal signal hyperintensity change in the right frontal and bilateral parietal lobes (A), right head of caudate and splenium of the corpus callosum (B) and, right fornix and right mammillary body (C).

FURTHER READING

Baumert, B.G., Hegi, M.E., van den Bent, M.J., et al. (2016). et al. temozolomide chemotherapy versus radiotherapy in high-risk low-grade glioma (EORTC 22033-26033): a randomised, open-label, phase 3 intergroup study. *Lancet*, **17**, 1521–32.

Brada, M., Ford, D., Ashley, S., et al. (1992). Risk of second brain tumour after conservative surgery and radiotherapy for pituitary adenoma. *BMJ*, **304**(6838), 1343–6.

Louis, D.N., Perry, A., Reifenberger, G., et al. (2016). The 2016 World Health Organisation classification of tumours of the central nervous system: a summary. *Acta Neuropathol*, **131**, 803–20.

Stupp, R., Hegi, M.E., Mason, W.P., et al. (2009). Effects of radiotherapy with concomitant and adjuvant temozolomide versus radiotherapy alone on survival in glioblastoma in a randomised phase III study: 5-year analysis of the EORTC-NCIC trial. *Lancet Oncol*, **10**(5), 459–66.

Stupp, R., Mason, W.P., van den Bent, M.J., et al. (2005). Radiotherapy plus concomitant and adjuvant temozolomide for glioblastoma. *N Engl J Med*, **352**(10), 987–96.

REFERENCES

Baumert, B.G., Hegi, M.E., van den Bent, M.J., et al. (2016). Temozolomide chemotherapy versus radiotherapy in high-risk low-grade glioma (EORTC 22033-26033): a randomised, open-label, phase 3 intergroup study. *Lancet*, **17**, 1521–32.

Baumert, B.G., Brada, M., Bernier, J., et al. (2008). EORTC 22972–26991/MRC BR10 trial: fractionated stereotactic boost following conventional radiotherapy of high-grade gliomas. Clinical and quality-assurance results of the stereotactic boost arm. *Radiother Oncol*, **88**(2), 163–72.

Baumert, B.G., Lutterbach, J., Bernays, R., Davis, J.B., & Heppner, F.L. (2003). Fractionated stereotactic radiotherapy boost after post-operative radiotherapy in patients with high-grade gliomas. *Radiother Oncol*, **67**(2), 183–90.

Benczik, J., Tenhunen, M., Snellman, M., et al. (2002). Late radiation effects in the dog brain: correlation of MRI and histological changes. *Radiother Oncol*, **63**(1), 107–20.

Brada, M., Ford, D., Ashley, S., et al. (1992). Risk of second brain tumour after conservative surgery and radiotherapy for pituitary adenoma. *BMJ*, **304**(6838), 1343–6.

Khoo, V.S., Oldham, M., Adams, E.J., Bedford, J.L., Webb, S., & Brada, M. (1999). Comparison of intensity-modulated tomotherapy with stereotactically guided conformal radiotherapy for brain tumors. *Int J Radiat Oncol Biol Phys*, **45**(2), 415–25.

Louis, D.N., Perry, A., Reifenberger, G., et al. (2016). The 2016 World Health Organisation classification of tumours of the central nervous system: a summary. *Acta Neuropathol*, **131**, 803–20.

Marsh, J.C., Godbole, R.H., Herskovic, A.M., Gielda, B.T., & Turian, J.V. (2010). Sparing of the neural stem cell compartment during whole-brain radiation therapy: a dosimetric study using helical tomotherapy. *Int J Radiat Oncol Biol Phys*, **78**(3), 946–54.

Minniti, G., Traish, D., Ashley, S., Gonsalves, A., & Brada, M. (2005). Risk of second brain tumor after conservative surgery and radiotherapy for pituitary adenoma: update after an additional 10 years. *J Clin Endocrinol Metab*, **90**(2), 800–4.

Miyatake, S., Kawabata, S., Yokoyama, K., et al. (2009). Survival benefit of boron neutron capture therapy for recurrent malignant gliomas. *Appl Radiat Isot*, **67** (7–8 Suppl), S22–4.

Narayana, A., Yamada, J., Berry, S., et al. (2006). Intensity-modulated radiotherapy in high-grade gliomas: clinical and dosimetric results. *Int J Radiat Oncol Biol Phys*, **64**(3), 892–7.

Otsuka, S., Coderre, J.A., Micca, P.L., et al. (2006). Depletion of neural precursor cells after local brain irradiation is due to radiation dose to the parenchyma, not the vasculature. *Radiat Res*, **165**(5), 582–91.

Panagiotakos, G., Alshamy, G., Chan, B., et al. (2007). Long-term impact of radiation on the stem cell and oligodendrocyte precursors in the brain. *PLoS One*, **2**(7), e588.

Powell, C., Guerrero, D., Sardell, S., et al. (2011). Somnolence syndrome in patients receiving radical radiotherapy for primary brain tumours: a prospective study. *Radiother Oncol*, 2011, **100**(1), 131–6.

Ruge, M.I., Kickingereder, P., Stefan Grau, S., et al. (2013). Stereotactic iodine-125 brachytherapy for the treatment of WHO grades II and III gliomas located in the central sulcus region. *Neuro Oncol*, **15**(12), 1721–31.

Schatlo, B., Fandino, J., Smoll, N.R., et al. (2015). Outcomes after combined use of intraoperative MRI and 5-aminolevulinic acid in high-grade glioma surgery. *Neuro Oncol*, **17**(12), 1560–7.

Stupp, R., Hegi, M.E., Mason, W.P., et al. (2009). Effects of radiotherapy with concomitant and adjuvant temozolomide versus radiotherapy alone on survival in glioblastoma in a randomised phase III study: 5-year analysis of the EORTC-NCIC trial. *Lancet Oncol*, **10**(5), 459–66.

Stupp, R., Mason, W.P., van den Bent, M.J., et al. (2005). Radiotherapy plus concomitant and adjuvant temozolomide for glioblastoma. *N Engl J Med*, **352**(10), 987–96.

RELATED LINKS TO EBRAIN

Intraoperative Chemotherapy and Radiotherapy. https://learning.ebrain.net/course/view.php?id=1241

Long-term Complications of Radiotherapy and Chemotherapy for CNS Disease. https://learning.ebrain.net/course/view.php?id=484

Principles of Radiotherapy and Radiosurgery. https://learning.ebrain.net/course/view.php?id=488

12

Chemotherapy for brain tumours

Nicholas F. Brown, Daniel Krell, and Paul Mulholland

Introduction

Surgical resection is the cornerstone of the initial management of brain tumours. However, the infiltrative and invasive nature of malignant brain tumours means that complete resection is unattainable, and so while the extent of surgical resection improves prognosis (Lacroix et al., 2001), it must be balanced against the potential for disabling neurological deficits. Furthermore, recurrence after initial therapy is frequently due to malignant cells migrating into normal brain tissue, which are not amenable to other focal treatments such as radiotherapy. Thus chemotherapy offers an additional treatment to prolong survival and maintain the functional status of patients with brain tumours.

The role of chemotherapy in brain tumours is currently fairly limited in comparison to cancers originating outside the brain. The poor prognosis and lack of effective treatments for high-grade tumours means that novel therapies are required. Several innovative chemotherapeutics are currently in clinical trials and may provide the basis for future treatment.

In this chapter, we outline the basic concepts of chemotherapy, the use of molecular markers, how response to treatment is monitored, the pharmacology of chemotherapeutics used in neuro-oncology, the evidence for chemotherapy in gliomas, and potential future treatments. The use of chemotherapy in non-glioma primary brain tumours and the treatment of metastatic disease in the brain is not discussed.

Concepts in chemotherapy

Aims

The rationale for chemotherapy in treating cancer is based upon our understanding of how a single transformed cell develops into a malignant tissue through an accumulation of genetic instability and mutations. These acquired 'hallmark' characteristics of cancer include: developing sustained proliferative signalling; evading growth suppressors; immunosuppression; preventing cell death; enabling replicative immortality; and inducing angiogenesis, invasion, and metastasis (Hanahan and Weinberg, 2011). Each of these hallmarks represent targets for current and potential future treatments.

The aim of chemotherapy in brain tumours is to prolong survival or control symptoms (*palliative*). It is often used as an adjunct to increase the effectiveness of other therapies (*adjuvant*). There is no proven role in brain tumours for administering chemotherapy prior to surgery (*neoadjuvant*) or with the aim of cure (*curative*), although chemotherapy has this role in other tumour locations.

Mechanisms of action

Cytotoxic drugs target processes of cellular division, killing cells through blocking crucial stages in the synthesis of DNA or its nucleotide precursors, or by assaulting the structural integrity of DNA. The rationale for their use in cancer is that cancer cells are more likely to be replicating. However, normal tissues contain dividing cells, and so cytotoxic agents are non-selective, which accounts for the common and widespread toxicities associated with chemotherapy, notably myelosuppression, gastrointestinal symptoms, fatigue, neuropathy, infertility, teratogenicity, cognitive symptoms, and alopecia. Similarly, cancer cells that are quiescent within the resting phase of the cell cycle (G0) when chemotherapy is delivered will not be targeted by cytotoxic chemotherapy and can be recruited into the next cell cycle to cause tumour growth (Chabner and Loeffler, 2015).

Principles of use

Exposing tumours to a defined dose of chemotherapy for a defined time period, results in a constant fraction of tumour cells killed, independent of the size of tumour, termed 'fractional kill' (Berenbaum, 1972). Poor tumour penetration reduces the fraction killed, and systemic toxicities reduce the dose that can be delivered. Thus current regimens deliver chemotherapy in repeated 'cycles' with the aim of eliminating the cancer cell population through successive fractional kills. The dose delivered is typically the maximum tolerated dose, with the interval between dosing sufficient to allow recovery from toxicities. These parameters are determined in early phase trials. Chemotherapeutics are often delivered as combinations of drugs in order to increase efficacy (additive or synergistic) through different mechanisms of action, with minimal overlapping toxicities. Practically, the dose limiting toxicity of most chemotherapeutics is myelosuppression, and this is the most frequent limitation of combination dosing.

Limitations

There are several limitations to chemotherapy. Intrinsic or acquired resistance can limit the effect of chemotherapy. Resistance mechanisms include the development of efflux pumps on cancer cell surfaces, gene amplification, or modification of chemotherapy targets, defects in apoptotic pathways, and upregulation of DNA repair genes. Intratumour genetic heterogeneity reduces the likelihood of killing all cancer cells within a tumour, and further 'spatial' genetic heterogeneity between tumours in different locations and 'temporal' heterogeneity as the tumour evolves with time further compounds this. Disruption of the normal vascular architecture can limit the access to the tumour of systemically delivered drugs. With brain tumours the blood–brain barrier presents a unique barrier to chemotherapy, although it is disrupted to a variable extend by the tumour itself. Tight junctions between capillaries in the blood–brain barrier can prevent transport of large and hydrophilic molecules, and efflux pumps can remove drugs from the brain into the cerebrospinal fluid, limiting the access of potential efficacious chemotherapeutic agents. While most chemotherapeutics are delivered systemically through intravenous or oral administration, the blood–brain barrier has resulted in the development of alternate methods of delivery in the treatment of brain tumours, including topical administration at surgery and experimental techniques such as convection enhanced delivery.

Other chemotherapies

Non-cytotoxic drugs that are variably considered chemotherapy include targeted therapies and immunotherapy. Targeted therapies use small molecules or monoclonal antibodies against intracellular proteins or cell surface receptors that are either mutated or overexpressed in tumour cells, with the aim of increasing cancer cell kill with fewer systemic toxicities. Immunotherapy aims to use the innate and adaptive immune systems to target cancer cells, and is discussed in more detail later in this chapter.

Clinical trials

Novel chemotherapeutics and innovative combinations are in constant development. Clinical trials form the basis for the introduction of new treatment. *Good Clinical Practice* (GCP) is an international quality standard that provides a framework to ensure that human trials are conducted in a regulated, ethical, and scientifically robust fashion.

- In phase 1 trials the primary objective is to assess the safety and toxicity of a new compound, with determination of a maximum tolerated dose through a dose escalation design. Secondary objectives will include pharmacokinetic data, and clinical activity and efficacy.
- A phase 2 trial assesses the activity of the compound, as well as continuing to assess safety and tolerability. These may be randomized, often against placebo.
- Phase 3 trials establish efficacy compared with the current standard of treatment. This forms the basis for licensing of drugs by regulatory authorities (Medicines and Healthcare Regulatory Agency in the United Kingdom, Food and Drug Administration in the United States, and the European Medicines Agency in the European Union).

Glioblastoma is the most common intrinsic brain tumour and so is the most frequently studied tumour within clinical trials. Short life-expectancy means that a primary endpoint of survival is attainable more efficiently than with other tumour types. Data from glioblastoma trials is often extrapolated for use on the basis for clinical trials in other brain tumours. Stratification of patients using molecular markers allows identification of subgroups who do or do not benefit from treatment.

Chemotherapeutics

The decision to start chemotherapy is typically made by an oncologist with the written consent of the patient, following discussion of the rationale and intention of treatment, and common and serious toxicities. The regimen and dose will be calculated and adjusted according to the patients' weight or body surface area (BSA), performance status, organ function (particularly bone marrow, kidney, liver), comorbidities, and toxicities experienced during previous chemotherapy. These parameters are monitored frequently during the treatment, with delay or reduction of dose as required. High-frequency toxicities are pre-empted with prophylactic supportive medication. Patients are monitored closely by physicians and nurses who are specifically trained in chemotherapy administration, and toxicities are treated actively to avoid dose-delays, omissions, or reductions where possible. Blood tests are monitored before each cycle, and at prespecified time points within cycles. Patients have 24-hour telephone access to chemotherapy trained nurses to discuss management of toxicities, and are advised to monitor themselves for signs of infection which may require urgent hospital admission and commencement of intravenous antibiotics. Response to therapy is monitored with imaging at prespecified time points.

Table 12.1 provides a summary of the pharmacology of the most frequently used chemotherapeutics licensed for use in gliomas, with their frequently occurring side effects. Comprehensive details can be found in each drug's summary of product characteristics available online from the European Medicines Agency (EMA), or the U.S. Food and Drug Administrating (FDA). Evidence for their use is discussed later in this chapter.

Molecular markers and chemotherapy

Molecular markers are used routinely in oncology as diagnostic and prognostic indicators. Concordance between local diagnosis and central neuropathology is as low as 50% (Stupp et al., 2014) and so molecular markers aid accurate diagnosis which is vital in predicting likely benefit from chemotherapy. Furthermore, molecular markers can be independently prognostic of a response to chemotherapy, and so can be used to identify whether individual patients are more or less likely to respond to chemotherapy. Markers that aid chemotherapy treatment decisions are discussed next. Other useful diagnostics markers (e.g. ATRX, TERT) that aid diagnosis, but are not independently linked to chemotherapy response are not discussed. The 2016 WHO Classification of Tumours of the Central Nervous System has incorporated molecular markers into the diagnostic algorithms for gliomas (Louis et al., 2016). All gliomas are now defined

Table 12.1 Chemotherapeutics commonly used in the treatment of gliomas

Mechanism of action	Characteristics	Regimen	Side effects
Temozolomide			
An oral derivative of dacarbazine. Both are pro-drugs of the alkylating agent 3-methyl-(triazene-1-yl)imidazole-4-carboxamide (MTIC). Alkylating agents irreversibly attach an alkyl group to guanine base on DNA disrupting DNA replication and leading to arrest of cell replication and induction of apoptosis.	It is a relatively small lipophilic molecule (194 Da), is highly bioavailable, and crosses the blood–brain barrier where it spontaneously hydrolyses to its active metabolite. Generally well tolerated.	In glioblastoma it is delivered orally in combination with radiotherapy at 75 mg/m² BSA per day for 42 days, and then as maintenance therapy for six cycles at 150–200 mg/m² BSA for days one to five of a 28-day cycle. Prophylactic antibiotics are given to prevent pneumocystis jirovecii pneumonia (PCP).	Very common (>10%): anorexia, constipation, nausea, vomiting, rash, dry skin, infertility, alopecia, fatigue. Common (1–10%): anaemia, leucopoenia, thrombocytopenia, abnormal liver function tests, oral candidiasis, dysphagia, stomatitis, hyperglycaemia, dysgeusia, cough, dyspnoea, musculoskeletal pain, myasthenia, fatigue, urinary incontinence, oedema, DVT, blurred vision, hearing impairment, tinnitus, anxiety, depression, insomnia, headache, convulsions. Azoospermia is reported.
Lomustine (CCNU, 1-(2-Chloroethyl)-3-cyclohexyl-1-nitrosourea)			
An alkylating nitrosourea. Nitrosoureas are compounds that contain both a nitroso (R-NO) group and a urea. Non-enzymatic degradation of nitrosoureas yield products with alkylating and carbamoylating activities that lead to intra- or interstrand cross links of DNA and mitotic arrest.	Lipophilic, therefore can cross the blood–brain barrier.	In gliomas is used as monotherapy, or in the PCV regimen in combination with procarbazine and vincristine. It is delivered by capsule orally, and is usually given as a single dose on the first day of each cycle (every six to eight weeks) for six cycles.	Very common: (>10%) rash, dry skin, diarrhoea, abnormal liver function, thrombocytopenia (relatively late nadir at four weeks post dose), and leucopoenia (nadir at five to six weeks). Common (1–10%): fatigue, nausea, vomiting, anorexia, loss of fertility, and anaemia. Other significant side effects include liver and renal impairment, lung infiltrates, coordination difficulties, and confusion.
Carmustine (BiCNU, bis-chloroethylnitrosourea)			
A mustard-gas related nitrosourea alkylating agent (see Lomustine).	Can be given intravenously, but also available as a gel wafer (Gliadel®) licensed in the UK in glioblastoma (Arbor Pharmaceuticals, 2014).	Following surgical tumour resection up to eight wafers can be implanted into the cavity floor and deliver a controlled release of carmustine over approximately five days with the aim of avoiding systemic toxicities.	Gliadel® wafers: new or worsening seizures (54%), cerebral oedema (23%), delayed wound healing (16%), and meningitis (4%). Tonsillar herniation and wafer migration causing obstructive hydrocephalus have been reported.
PCV			
A chemotherapy regimen combining procarbazine, lomustine (CCNU), and vincristine.		Typically given in a 42-day cycle for six cycles. On day one patients receive intravenous vincristine and oral lomustine, and a 10-day course of oral procarbazine is commenced on day 1 or 2.	
Procarbazine			
An alkylating agent (see temozolomide) whose individual mechanism of action is not fully understood.	A cytochrome P450 inhibitor with multiple drug interactions, and a monoamine oxidase (MAO) inhibitor and thus can produce a disulfiram-like reaction with alcohol.		Very common (>10%): nausea, vomiting, and anorexia. Common (1–10%): leucopoenia, anaemia, thrombocytopenia, fatigue, flu-like symptoms, depression, insomnia, neuropathy, amenorrhea, and loss of fertility. Hypersensitivity and tyramine reactions can occur, thus tyramine containing foods should be avoided, and patients should be provided with a list of foods to avoid.
Vincristine			
A vinca alkaloid derived from the Madagascar periwinkle. It binds to tubulin dimers inhibiting microtubule structure and thus arresting mitosis in metaphase.	It is for intravenous use only and designated; **FATAL IF GIVEN INTRATHECALLY** due to neurotoxicity. Multiple deaths have occurred due to inadvertent intrathecal administration.		Very common (>10%): neuropathy, fatigue, severe constipation, abdominal pain, nausea, vomiting, and alopecia. Common (1–10%): leucopoenia, infection, myasthenia, injections site reactions, urinary retention, allergic reactions, mouth ulcers, jaw pain, paralytic ileus, and rash.
Bevacizumab			
A recombinant humanized monoclonal antibody to vascular endothelial growth factor A (VEGF-A). Angiogenesis is common in glioblastoma. Hypoxia is the principle driver and leads to tumour expression of proangiogenic factors including VEGF that stimulate endothelial cell proliferation, migration, and invasion. Antiangiogenics cause vascular normalization and decrease the permeability of the blood–brain barrier (Friedman et al., 2009).		Intravenously every two to three weeks.	Very common (>10%): hypertension, nausea, vomiting, fatigue, leucopoenia, neuropathy, anorexia, constipation, and headaches. Common (1–10%): proteinuria, deep-vein thrombosis, bowel perforation, bleeding, fistula, impaired healing, posterior leukoencephalopathy, cardiac failure, and arrhythmia.

by their IDH status. Tumours that were previously considered 'oligoastrocytoma' due to mixed histological features are now classified as either oligodendrogliomas or astrocytomas depending on the respective presence or absence of 1p19q codeletion. However, tumour heterogeneity (Forshew et al., 2013) confounds interpreting the clinical consequences of any molecular marker results, and leads to clinically insignificant positive results if the molecular marker is present in the area of tumour biopsied but not elsewhere, and similarly may lead to false-negative results.

Chromosome 1p/19q codeletion

Genetic loss on chromosomes 1p and 19q with codeletion or loss of heterozygosity occurs due to an unbalanced translocation of chromosomes 1p and 19q (Cairncross et al., 2013). It is a distinct tumour entity whose pathological consequences are as yet unclear, but indicates an oligodendroglioma and is uncommon in glioblastomas (<5%) (present in 15% of grade II diffuse astrocytomas, 30–60% of grade II oligodendroglioma/oligoastrocytomas, 15% of grade III anaplastic astrocytoma, and 50–80% or oligodendroglioma/oligoastrocytomas) (Stupp et al., 2014). It is associated with an increased sensitivity to chemotherapy and survival (Cairncross et al., 2013).

6-methylguanine-DNA methyl transferase (MGMT) promoter methylation

The primary cytotoxic effect of temozolomide is due to DNA methylation at the O6 position of guanine. MGMT is a ubiquitous DNA repair enzyme that removes methyl groups from the O6 position of guanine and thus reverses alkylation and inhibits the cytotoxic effect of temozolomide. Methylation of the promotor that initiates transcription leads to epigenetic silencing of MGMT which increases susceptibility of tumours to alkylating agents such as temozolomide (Weller et al., 2010). Methylation-specific polymerase chain reaction (MSP) is used to determine MGMT-promotor methylation, due to lack of standardization with immunohistochemistry. It is present in 40–50% of grade II diffuse astrocytomas, 60–80% of grade II oligodendroglioma/oligoastrocytoma, 50% of grade III anaplastic astrocytomas, 70% of anaplastic oligodendrogliomas, and 35% of glioblastoma (Stupp et al., 2014). It is a positive prognostic marker in anaplastic glioma and glioblastoma and is correlated with an improved prognosis in anaplastic gliomas treated with alkylating chemotherapeutics. It confers increased likelihood of response to chemotherapy, discussed in detail below.

Isocitrate dehydrogenase (IDH) 1 and 2 mutations

Mutations in IDH 1 or 2 lead to production of an abnormal metabolite, 2-hydroxyglutarate, which produces epigenetic changes through hypermethylation. IDH 1 and 2 mutations are hallmarks of low-grade glioma and if found in high-grade tumour suggest transformation from a low-grade precursor. IDH mutations are found in 70–80% of grade II diffuse astrocytomas and oligodendrogliomas, 50–80% of astrocytomas and anaplastic oligodendrogliomas, but only 5–10% of glioblastomas. Around 90% of mutations are the R132H mutation on IDH1 and can be visualized on immunohistochemistry. If negative gene sequencing can be performed to exclude IDH2 and IDH1 mutations at other sites (Stupp et al., 2014). IDH mutation is a positive prognostic marker, and has been shown to predict response to temozolomide in anaplastic oligodendroglioma (van den Bent et al., 2013). Furthermore, IDH is being investigated as a therapeutic target for inhibitors (AG-221), in immunotherapy, and 2-hydroxyglutarate can be detected by magnetic resonance spectroscopy offering a potential imaging molecular marker (Kang and Adamson, 2015).

Epidermal growth factor receptor (EGFR)

EFGR amplification/mutation is found in multiple tumour types, with targeted therapies as standard practice in colorectal, lung, and head and neck cancers. Half of glioblastomas have EGFR amplification or mutation, with half of these being EGFRvIII mutation, which confers a negative prognosis. It is unusual in other gliomas, found in only 9% of anaplastic astrocytomas (Kang and Adamson, 2015). It is a promising therapeutic target and although no phase 3 trial of EGFR targeted agents have shown survival benefit, several EGFR targeted agents remain in development and are being evaluated in clinical trials.

BRAFV600

BRAF mutations have been identified as key drivers of oncogenesis in several cancers. Over 95% are missense mutations with substitution of valine to glutamate at amino acid position 600E (BRAFV600E). While overall BRAF mutations are uncommon in glioma, there are more frequently observed in pleomorphic xanthoastrocytoma, and pilocytic astrocytomas (9%) (Schindler et al., 2011). The 2016 WHO Classification of CNS tumours includes a new variant of IDH wild type glioblastoma, epithelioid glioblastoma, that frequently harbours a BRAF mutation (Louis et al., 2016). Patients with BRAFV600 mutant tumours can be treated with small molecule inhibitors of mutated BRAFV600E.

Monitoring for response

The most frequent reported measures of response are median overall survival (mOS), progression free survival (PFS), and objective response (OR). Overall survival (OS) and PFS are frequently reported at time points (e.g. 6 or 12 months) after treatment initiation. Cognitive function, quality of life, symptoms, functional independence, and the requirement for steroids are used as additional markers of clinical response (Lin et al., 2013).

Radiological outcomes are categorized into complete response (CR), partial response (PR, 30% unidimensional or 50% bidimensional shrinkage), stable disease (SD, not meeting the criteria for response or progression), and progressive disease (PD, 20–25% increase).

The Response Evaluation Criteria in Solid Tumour (RECIST) guidelines are the standard evaluation for tumours originating outside of the CNS and categorize response based on change in target lesion size (Eisenhauer et al., 2009). The Macdonald criteria for supratentorial malignant glioma (Macdonald et al., 1990) allowed for objective radiological assessment of tumour response to be classified with recognition of glioma specific considerations such as steroid use and clinical symptoms. While designed for computerized tomography, it was extrapolated for use with MRI. The Response Assessment in Neuro-Oncology working group (RANO) criteria (Table 12.2) were developed to resolve perceived limitations

Table 12.2 RANO and iRANO criteria. iRANO recommends confirming disease progression with repeat imaging three months after initial radiological progression if it is six months or less from commencing immunotherapy if there are no new or substantially worsened neurological deficits that are not due to comorbid events or concurrent medication.

	Malignant glioma	Low-grade glioma
Complete response	Disappearance of all enhancing disease for ≥4 weeks; no new lesions; stable or improved T2/FLAIR; no more than physiological steroids; clinically stable or improved	Disappearance of all enhancing and T2/FLAIR disease for ≥4 weeks; no new lesions; no more than physiological steroids; clinically stable or improved
Partial response	≥50% decrease in the sum of biperpendicular diameters of enhancing disease for ≥4 weeks; no new lesions; stable or improved T2/FLAIR; stable or decreased steroid dose; clinically stable or improved	≥50% decrease in the sum of biperpendicular diameter of T2/FLAIR disease for ≥4 weeks; no new lesions; stable or decreased steroid dose; clinically stable or improved
Minor response	Not applicable	25–49% decrease in the sum of biperpendicular diameters of T2/FLAIR disease for ≥4 weeks; no new lesions; clinically stable or improved
Stable disease	Does not qualify for complete response, partial response, or progressive disease; no new lesions; stable or improved T2/FLAIR; stable or decreased steroid dose; clinically stable or improved	Does not qualify for complete response, partial response, or progressive disease; no new lesions; stable or improved T2/FLAIR; stable or decreased steroid dose; clinically stable or improved
Progressive disease	≥25% decrease in the sum of biperpendicular diameters of enhancing disease; or new lesions; or substantial worsened T2/FLAIR; or substantial clinical decline	≥25% decrease in the sum of biperpendicular diameters of T2/FLAIR disease; or new lesions; or substantial clinical decline

Reprinted from *The Lancet Oncology*, Volume 16, issue 15, Okada et al., Immunotherapy response assessment in neuro-oncology: a report of the RANO working group, pp. e534–42, Copyright (2015), with permission from Elsevier.

Data from Wen PY, Macdonald DR, Reardon DA, et al. Updated response assessment criteria for high-grade gliomas: response assessment in neuro-oncology working group, *Journal of Clinical Oncology*, Volume 28, issue 11, pp. 1963–72, 2010.

Data from van den Bent M, Wefel J, Schiff D, et al. Response assessment in neuro-oncology (a report of the RANO group): assessment of outcome in trials of diff use low-grade gliomas. *Lancet Oncology*, volume 12, issue 6, pp. 583–93, 2011.

of the Macdonald criteria including the lack of assessment of non-enhancing components and the use of increased contrast enhancement as a surrogate for tumour growth.

Contrast enhancement reflects the passage of contrast across the blood-tumour barrier, and changes may reflect non-tumoural processes such as inflammation, radiation necrosis, seizures, steroid dose, and antiangiogenics. 'Pseudoprogression' is a non-tumoural increase in imaging lesions that may actually reflect response to treatment and occurs in 20–30% of patients treated with temozolomide chemoradiotherapy (Wen et al., 2010). 'Pseudoresponses' are non-tumoural decrease in lesions, that may reflect decrease permeability of the blood-tumour barrier to contrast, such as with antiangiogenics. To account for these occurrences, the RANO criteria requires repeated imaging for any responses within 12 weeks after the completion of therapy, unless progression is outside of the radiotherapy field or pathologically confirmed. In patients with potential pseudoprogression, treatment should continue until response is clarified with subsequent imaging.

Immunotherapy, currently in clinical trials in gliomas, presents several new challenges for determining response. Due to the time required to develop an immunological response, tumour progression may occur first, which may itself be masked by the inflammatory changes. These have been addressed with the immunotherapy iRANO criteria (Table 12.2) (Okada et al., 2015).

Glioblastoma (WHO grade IV)

Carmustine was the first chemotherapeutic to become standard therapy in addition to surgery and radiotherapy following the RTOG-8302 trial in 1980. This randomized trial in patients with malignant glioma demonstrated improved survival with carmustine and radiotherapy combined versus radiotherapy or chemotherapy alone (Walker et al., 1980). Nitrosourea chemotherapy use was substantiated with a systematic review of 12 randomized trials involving 3004 patients with high-grade glioma (grade III and IV) that confirmed a modest increase in survival in patients receiving chemoradiotherapy versus radiotherapy alone [Hazard radio (HR) 0.85, 95% confidence interval (CI) 0.78–0.91, P <0.0001] with OS at 1 year increasing from 40 to 46% and at 2 years from 15 to 20%, and a significant 17% reduction in the risk of progression or death (HR 0.83; 95%CI 0.75–0.91, P <0.0001) (Stewart, 2002).

The current standard of treatment following surgery in glioblastoma is chemoradiotherapy with 60 Gray in 30 fractions of radiotherapy with concurrent daily temozolomide for six weeks, followed by a four-week break, and then up to six cycles of adjuvant temozolomide. This was introduced following the EORTC-NCIC trial in 2005. This was a phase 3 trial in 573 patients with glioblastoma randomized to temozolomide chemoradiotherapy versus radiotherapy monotherapy. It demonstrated a significantly improved median OS with chemoradiotherapy of 14.6 months vs. 12.1 months (HR 0.63, 95%CI 0.52–0.75, P <0.001) (Fig. 12.1) and an improvement in 2-year survival with chemoradiotherapy from 10.4 to 26.5%. MGMT-promotor methylation was a favourable prognostic factor for OS both independently (HR 0.45, 95%CI 0.32–0.61, P <0.001) and also as predictor of response to chemotherapy with an increase in OS from 15.3 months (95%CI 13–20 months) in the unmethylated patients to 21.7 months (95%CI 17.4 to 30.4) in those with methylated promotors (P = 0.007). In the absence of methylation there was a smaller and non-significant difference in survival between the two treatment groups (Stupp et al., 2005).

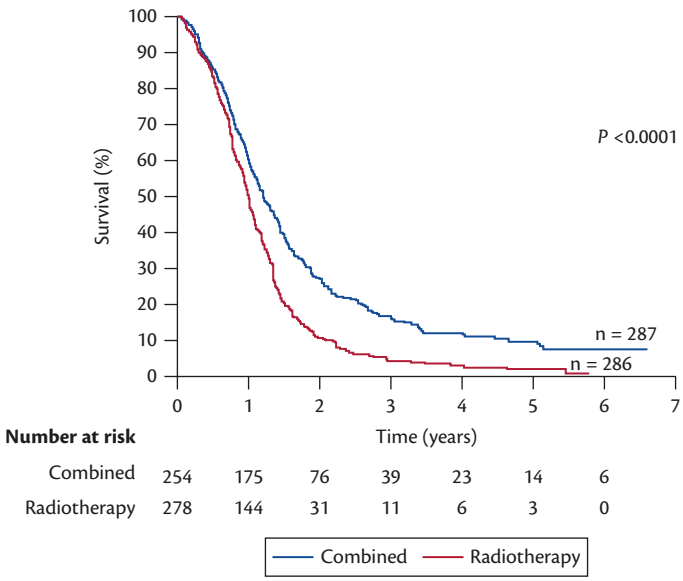

Fig. 12.1 Overall survival in radiotherapy with concomitant and adjuvant temozolomide versus radiotherapy alone in glioblastoma.
Reprinted from *The Lancet Oncology*, Volume 10, issue 5, Stupp et al., Effects of radiotherapy with concomitant and adjuvant temozolomide versus radiotherapy alone on survival in glioblastoma in a randomised phase III study: 5-year analysis of the EORTC-NCIC trial, pp. 459–66, Copyright (2009), with permission from Elsevier.

Dose-dense temozolomide (dosing on days 1–21 of a 28-day cycle) leads to prolonged depletion of MGMT. However, in a phase 3 randomized trial in 833 patients with GBM it was not superior to standard adjuvant therapy (days 1–5) regardless of MGMT status (OS 14.9 vs. 16.6 months (HR 1.03 $P = 0.63$); PFS 6.7 vs. 5.5 months HR 0.87 $P = 0.06$), and was associated with increased severe toxicities (34 vs. 53%; $P < 0.01$) (Gilbert et al., 2013).

The landmark chemoradiotherapy trial excluded patients over 70 years of age, but reported decreased benefit from chemotherapy in patients over 60 (Stupp R. et al., 2009). However, while elderly patients have a poorer performance status and are more prone to toxicities from chemotherapy, clinical trials in older patients have demonstrated survival benefits of chemotherapy. The NOA-08 phase 3 trial randomized 373 patients older than 65 years with high-grade glioma (89% glioblastoma) to temozolomide or radiotherapy with crossover salvage therapy as appropriate at progression (Wick et al., 2012). This trial reported temozolomide as non-inferior to radiotherapy with median OS of 8.6 months in the temozolomide group and 9.6 months in the radiotherapy group (HR 1.09, 95%CI 0.84–1.42, $p_{\text{non-inferiority}}=0.0330$). Event free survival was longer in patients with MGMT-promotor methylation in the chemotherapy group (8.4 months (95%CI 5.5–11.7) vs. 4.6 (4.2–5.0)), with the opposite in patients without MGMT-promotor methylation (3.3 months (3.0–3.5) vs. 4.6 months (3.7–6.3)). The Nordic phase 3 trial randomized 291 patients older than 60 years with glioblastoma to temozolomide or radiotherapy (hypofractionated or standard) (Malmström et al., 2012). mOS was significantly longer with temozolomide than with standard radiotherapy (8.3 vs. 6.0 months HR 0.7; 95%CI 0.52–0.93, $P = 0.01$). Survival between patients treated with hypofractionated radiotherapy and temozolomide was similar. Patients treated with temozolomide with MGMT methylated tumours had significantly longer survival than those without methylation (9.7 vs. 6.8 months, HR 0.56 95%CI 0.34–0.93 $P = 0.02$), but no difference was noted in patients in the radiotherapy group (HR 0.97 95%CI 0.69–1.38 $P = 0.81$). Thus, while these trials support temozolomide use in elderly patients with MGMT-promotor methylated tumours, benefit in unmethylated tumours is unclear with some evidence suggesting inferiority. The EORTC 26062-22061 phase III trial randomized 562 elderly patients (>65 years) with newly diagnosed glioblastoma to short-course radiotherapy (40 Gy in 15 fractions) with or without concomitant and adjuvant temozolomide (Perry et al., 2016). The addition of temozolomide was well tolerated and increased mOS from 7.6 to 9.3 months (HR 0.67 (95%CI 0.56–0.8) $P < 0.0001$). mOS almost doubled in patients with MGMT methylation (13.5 vs. 7 months; HR 0.53 (0.38–0.73) $P = 0.0001$), but was not statistically significant in patients with MGMT unmethylated tumours (10 vs. 7.9 months, HR 0.75 (0.56–1.01, $P = 0.055$).

Thus in patients unlikely to tolerate chemoradiotherapy, such as the elderly, a potential treatment strategy is to consider temozolomide in those with MGMT-promotor methylated tumours, and radiotherapy in those with unmethylated tumours.

Recurrence

There is no standard treatment for recurrent disease and clinical trials have failed to establish significant clinical benefit, although lomustine or PCV (Table 12.1) are most frequently used. Investigational clinical trials are appropriate if patients have already received chemotherapy.

Modest benefit of single-agent lomustine has been confirmed following use as a control group in several trials. For example, the REGAL phase 3 trial investigated cediranib (a VEGF inhibitor) with or without lomustine versus lomustine monotherapy. The mOS was 9.8 months and PFS was 82 days, with no additional benefit in cediranib containing arms (Batchelor et al., 2013).

Controversies

Bevacizumab

Use of bevacizumab as standard therapy varies. Bevacizumab is licensed for recurrent disease in the United States. However, it failed to meet the requirements for licensing in the EU. A non-comparative randomized phase 2 trial of bevacizumab monotherapy versus combination with irinotecan in 167 patients with recurrent glioblastoma (Friedman et al., 2009) demonstrated a 6-month PFS of 42.6% with bevacizumab versus 50.3% in combination with irinotecan, compared with a stated historical control of 15%. The primary endpoint of radiographic response was 28.2% with bevacizumab and 37.8% in combination, compared with a stated historical control of 5–10%. There was no difference in overall survival. It is difficult to determine the clinical significance of these imaging-based end-points due to the potential for pseudoresponse. However, there was a trend for patients taking corticosteroids to take stable or decreasing doses over time. The only reported study including a control arm without bevacizumab is the BELOB phase 2 trial of single-agent bevacizumab or lomustine versus a combination in 153 patients with recurrent glioblastoma. This trial did not show a survival benefit with bevacizumab monotherapy versus lomustine, although an OS at 9 months of 63% (95%CI 49–75) with bevacizumab in combination with lomustine (versus 43% (29–57) with lomustine alone, and 38% (25–51) with bevacizumab alone), met the prespecified criteria for the phase 3 study which is ongoing (Taal et al., 2014).

Two phase 3 trials have studied the use of bevacizumab in addition to temozolomide chemoradiotherapy in newly diagnosed glioblastoma. The AVAGlio study randomized 921 patients to receive either bevacizumab or placebo until progression (Chinot et al., 2014). The RTOG0825 trial randomized 637 patients to either bevacizumab or placebo for up to 12 cycles (Gilbert et al., 2014). Both trials showed no difference in OS with bevacizumab but a significant increase in PFS (10.5 vs. 6.2 months in AVAGlio (HR 0.64 95%CI 0.55–0.74 P <0.001); 10.7 vs. 7.3 months in RTOG0825 (HR 0.79 95%CI 0.66–0.94 P = 0.007)). Given the uncertainty with pseudo-response, quality of life assessment was included as a secondary endpoint in both trials, with contradictory results. While the AVAGlio study reported longer maintenance of baseline health-related quality of life, performance status, and reduced use of glucocorticoids with bevacizumab, the RTOG0825 study found an increased symptom burden and worsened quality of life with bevacizumab. Thus, the use of bevacizumab in newly diagnosed glioblastoma remains unclear.

Carmustine wafers (Gliadel®)

There have not been any prospective trials comparing interstitial carmustine wafers (Gliadel®) to the current standard of temozolomide chemoradiotherapy. Surgery with or without Gliadel® wafer insertion followed by temozolomide chemoradiotherapy was evaluated in a single retrospective study of 65 patients with high-grade glioma and found no difference in median relapse free survival in those with Gliadel® insertion versus those without (12.9 vs. 14 months P = 0.89) (Noël et al., 2012). A Cochrane systematic review studied the clinical effectiveness in newly diagnosed high-grade gliomas of Gliadel® versus placebo wafers, in combination with adjuvant radiotherapy (Hart et al., 2011). Two randomized controlled trials meeting the inclusion criteria were identified (n = 32 and 240). Overall, Gliadel® increased OS (14 vs. 11.5 months HR 0.65, 95%CI 0.48–0.86, P = 0.003) with no significant increase in side effects apart from increased intracranial hypertension in one study (P = 0.019). Although reporting improvements in OS similar to temozolomide chemoradiotherapy these should be interpreted with caution. In the larger trial grade III tumours (associated with both increased survival and response to chemotherapy) were more frequent in the Gliadel® group (16 vs. 12%). In a subgroup analysis of glioblastoma patients the treatment benefits of Gliadel® were not statistically significant (P = 0.1), although became significant (P = 0.04) if adjusted for baseline prognostic factors (age, performance status).

No survival benefit of Gliadel® wafer use at recurrence was found by the Cochrane review in a single identified trial which randomized 222 patients with recurrence of high-grade glioma treated with surgery and radiotherapy to Gliadel® wafers or placebo (mOS 31 vs. 23 weeks HR 0.83 95%CI 0.62–1.10 P = 0.19), although the authors reported a significant treatment effect if prognostic factors were considered (Brem et al., 1995).

Thus the benefit of Gliadel® wafer insertion is unclear and use varies between different centres. See **Box 12.1**.

WHO grade III glioma

Anaplastic oligodendroglioma (IDH mutant, 1p19q codeleted), anaplastic astrocytoma (IDH mutant), and anaplastic astrocytoma (IDH wild type) are the most common grade III gliomas in the 2016 WHO Classification of CNS Tumours (Louis et al., 2016). Traditionally, grade III tumours were treated with surgery followed by adjuvant radiotherapy, with chemotherapy given at relapse. However, there is accumulating evidence that the addition of chemotherapy to radiotherapy improves survival, particularly in molecularly favourable subgroups.

The EORTC-26951 trial compared radiotherapy with or without PCV chemotherapy in 368 patients with anaplastic oligodendroglioma (van den Bent et al., 2013) and demonstrated improved overall survival with the addition of chemotherapy (42.3 vs. 30.6 months HR 0.75 95%CI 0.6–0.95). In a subgroup analysis of 80 cases where 1p19q codeletion status could be tested, increased benefit from the addition of chemotherapy was found in patients with codeleted tumours (mOS not reached vs. 112 months, HR 0.56 (0.31–1.03)) compared to those without codeleted tumours (mOS 25 vs. 21 months, HR 0.83 (0.6–1.10)). The RTOG9402 phase 3 trial further compared radiotherapy with or without PCV chemotherapy in 289 patients with anaplastic oligodendroglioma (Cairncross et al., 2013). Although overall the increase in survival with PCV was not statistically significant (4.6 vs. 4.7 years HR 0.79 95%CI 0.61–1.04 P = 0.1), the median survival in patients with 1p/19q codeleted tumours receiving PCV-RT was twice that receiving RT alone (14.7 vs. 7.3 years HR 0.59 95%CI 0.37–0.95 P = 0.03), with no difference found in non-codeleted tumours. Subsequent analysis identified that patients with IDH mutated tumours also derived benefit from the addition of PCV (mOS 9.4 vs. 5.7 years HR 0.59 95%CI 0.40–0.86 P = 0.006) (Cairncross et al., 2013). Of note, survival benefit only became apparent after long-term follow-up, both trials initially reported no increase in survival with chemotherapy.

The addition of temozolomide to radiotherapy, improved survival in the published interim analysis of the CATNON trial which enrolled 748 patients with anaplastic gliomas without 1p19q codeletion (HR 0.645 (95%CI 0.45–0.926), P = 0.0014) (Van Den Bent et al., 2016).

The current practice in grade III tumours is surgery with radiotherapy. Additionally, patients with 1p/19q codeleted tumours receive adjuvant PCV chemotherapy. Those without 1p/19q codeletion receive temozolomide, and the final results from the CATNON trial are awaited. The clinical outcomes of patients with IDH wild type anaplastic astrocytoma are similar to glioblastoma, and many clinicians therefore feel it is appropriate to treat these patients with the same regimens used in glioblastoma. This approach is being investigated in the CATNON trial, with three chemotherapy subgroups: RT with concurrent temozolomide, RT followed by adjuvant temozolomide, and RT with both concurrent and adjuvant temozolomide.

See **Box 12.2**.

Low-grade glioma (WHO grades I and II)

Grade I tumours are considered benign, with no identified role for chemotherapy. While traditionally grade II tumours were not treated with chemotherapy until relapse, there is accumulating evidence that earlier chemotherapy improves survival.

The RTOG-9802 phase 3 randomized trial in 254 patients with high-risk grade II gliomas found an improvement in mOS from 7.8

Box 12.1 Case study 1

The patient in **Figure 12.2** was diagnosed with glioblastoma multiforme (Panel A) after presenting with dysphasia. He had surgical debulking in October 2011 followed by adjuvant chemoradiotherapy and six cycles of maintenance temozolomide, completed in August 2012 (B). Following tumour progression in February 2014 (C) he had a second surgical debulking with three cycles of adjuvant temozolomide. After a further recurrence in May 2014 (D), he commenced a combination of lomustine, bevacizumab, and valganciclovir, followed by ipilimumab. He had a clear response to treatment (E), but relapsed in February 2015. He subsequently commenced further therapies. He died in September 2015.

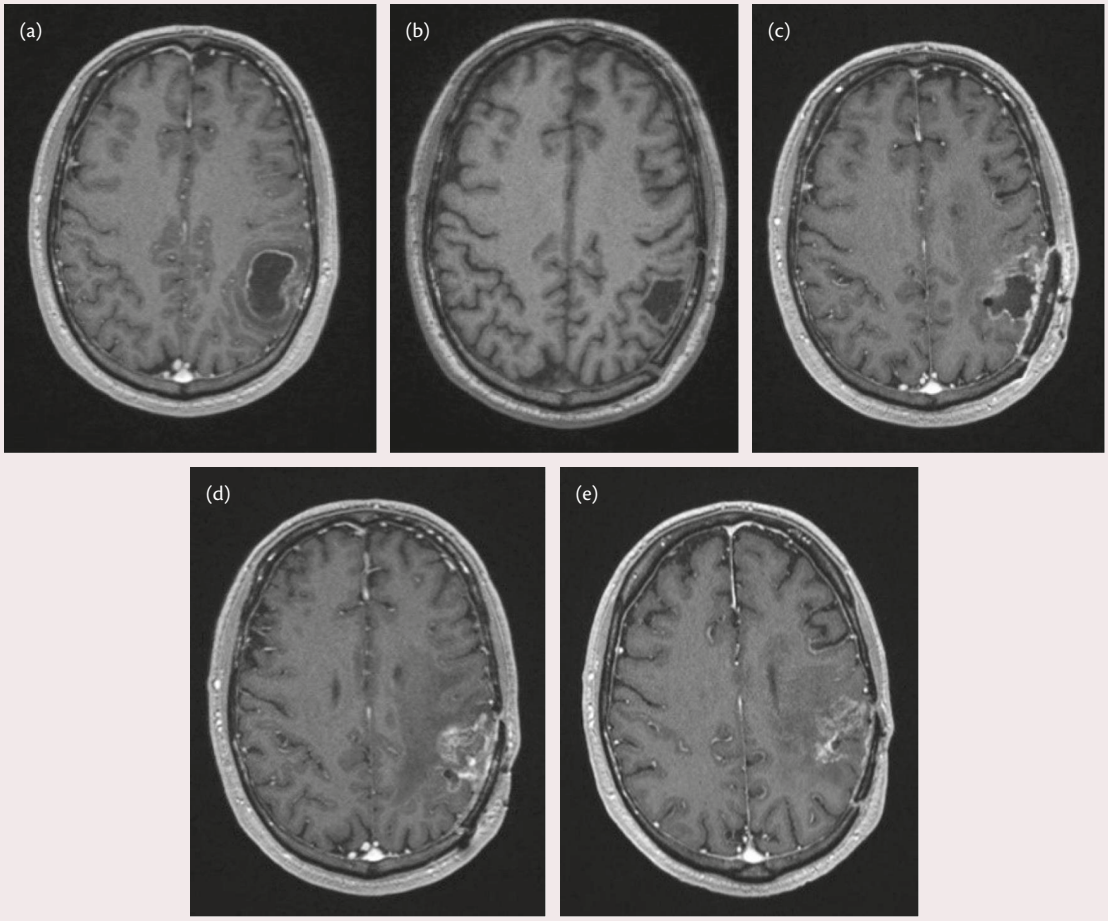

Fig. 12.2 MRI brain (T1 + gadolinium).

to 13.3 years (HR 0.59 $P = 0.03$) and PFS from 4 to 10.4 years (HR 0.5 $P = 0.002$) with radiotherapy followed by PCV chemotherapy compared with radiotherapy alone, with increase in 10 year survival to 60% from 40% (Buckner et al., 2016). Oligodendrogliomas were the most sensitive to chemotherapy, with non-significant benefit in astrocytomas. Patients with IDH mutated tumours had significant survival benefit from the addition of PCV (HR 0.42 (0.2–0.86) $P = 0.02$) but conclusions were not drawn for patients with IDH wild type or 1p19q codeleted tumours.

Chemotherapy alone versus radiotherapy alone is under investigation in the EORTC-22033 phase 3 randomized trial of temozolomide chemotherapy versus radiotherapy in 477 patients with progressive, symptomatic, or high-risk low-grade glioma. Preliminary analysis has shown no difference in progression free survival, with a trend for a reduced PFS in patients without 1p deletion treated with temozolomide and a possible increased OS in patients with 1p-deletion treated with temozolomide (Baumert et al., 2013).

In relapsed disease, the EORTC-26972 prospective phase 2 trial demonstrated the clinical efficacy of temozolomide in 28 patients with oligodendroglioma who had relapsed after initial treatment with PCV (van den Bent et al., 2003). Some 25% of patients had an objective response (95%CI 11–45%) with a 6- and 12-month PFS of 19 and 11%, respectively, and a median time to progression for responding patients of 8 months.

Patients with low-grade tumours that are deemed low-risk adopt a 'watch-and-wait' approach and do not receive adjuvant chemotherapy or radiation. However, there are no standard criteria to determine risk. Subtotal resection, age over 40 years, and new or worsening symptoms were among inclusion criteria for the aforementioned trials in an attempt to stratify patients as high risk. Molecular profiling of tumours can assist in identifying those at

Box 12.2 Case study 2

Following diagnosis with an anaplastic oligodendroglioma (WHO grade III, 1p/19q deletion), the patient in **Figure 12.3** had a left craniotomy and debulking in February 2006 followed by adjuvant chemoradiotherapy and maintenance temozolomide chemotherapy. The patient remained clinically stable despite subtle incremental growth on serial imaging until September 2014 when she developed focal seizures and weakness in her right arm (MRI, A), She received six cycles of PCV chemotherapy with almost complete resolution of the tumour (B).

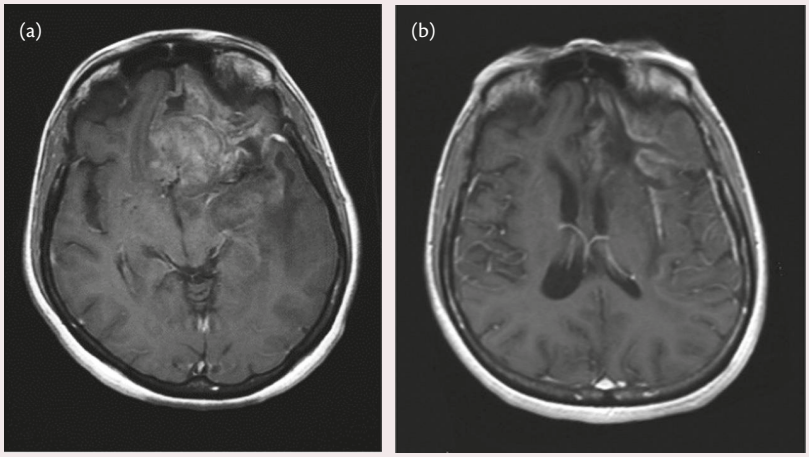

Fig. 12.3 MRI brain (T1 + gadolinium) prior (A) and following (B) PCV chemotherapy with almost complete resolution of the midline mass

high risk with poor prognosis, and those more likely to respond to chemotherapy.

Novel chemotherapeutics

The poor prognosis in patients with high-grade gliomas and limited benefit from current therapies, particularly in the recurrent setting, necessitate the development of novel therapies. The expansion of our understanding of molecular markers, gene expression, and epigenetics should afford multiple new targets for therapies. It will be vital to accurately determine individual patients that are likely to benefit from novel therapeutics to gain access to otherwise prohibitively expensive new medications.

Alternative delivery mechanisms are also in development to expose tumours to therapies that are unable to penetrate the blood–brain barrier. Examples include nanoparticles which increase blood–brain barrier penetration through reduced adhesive interactions, and convection enhanced delivery which administers chemotherapy directly into a resection cavity through intraparenchymal catheters inserted at surgery.

Targeted therapy

Despite identification of suitable molecular targets with efficacy in other tumour types, results from clinical trials of targeted therapies in brain tumours have been disappointing.

For example, EGFR is overexpressed in approximately 40% of glioblastomas, and EGFR targeted therapies are used routinely in lung, head, neck, and colorectal cancers. Despite promising activity in earlier trials, phase 3 trials of the EGFR targeted monoclonal antibody nimotuzumab and EGFRvIII targeted vaccine rindopepimut failed to show any survival benefit. While first generation tyrosine kinase inhibitors (e.g. erlotinib, gefitinib, lapatinib) have been ineffective in glioblastoma, second generation inhibitors are currently in clinical trials (Kang and Adamson, 2015).

Antiangiogenics are the only targeted therapies to demonstrate even limited benefit in clinical trials, as described earlier with bevacizumab. Other agents that target angiogenesis and invasion, such as cilengitide (an integrin inhibitor) have failed in clinical trials (CENTRIC, Stupp et al., 2014), although other therapies that target this pathway are being investigated in early phase clinical trials (e.g. the FAK inhibitor GSK2256098).

BRAF inhibitors such as dabrafenib and vemurafenib have revolutionized the treatment of BRAFV600 mutated tumours, with enhanced efficacy with the addition of the MEK inhibitor trametinib to overcome BRAF resistance (Robert et al., 2015). Case studies and 'basket' clinical trials have reported efficacy in progressive BRAFV600 mutated gliomas following treatment with radiotherapy and cytotoxic chemotherapy (Hyman et al., 2015; Brown et al., 2016). However, it is unclear whether patients would receive increased benefit from earlier use of BRAF inhibitors.

There are several reasons for the repeated failures to demonstrate efficacy in clinical trials despite promising preclinical activity. In order to be an effective target for therapy, targets must be present in all malignant cells, and the target must be critical for growth or invasion of the tumour. Despite an increased understanding of the molecular profiles of gliomas, no molecular driver has yet been established (Kang and Adamson, 2015). Are failures inevitable because the colossal mutational load within brain tumours creates tumour heterogeneity with no single driver mutation to target, or have we simply not yet identified a potential therapeutic target? Could potentially beneficial drugs be hidden within unsuccessful trials, as they were administered to overly-heterogeneous patient groups, hiding a cohort of patients that may benefit if an appropriate molecular marker is identified (note **Box 12.3**)?

Box 12.3 Case study 3

The patient in **Figure 12.4** had primary surgical resection of a right parietal glioblastoma multiforme in October 2008, with adjuvant chemoradiotherapy and maintenance temozolomide. She subsequently relapsed and had surgical debulking in June 2009, but relapsed shortly after (MRI, A) and started cilengitide. She remained clinically stable with a significant reduction in enhancing disease for over 3 years (MRI, B). Her tumour progressed and she stopped cilengitide in December 2012. She subsequently started carboplatin chemotherapy in February 2013 with no objective response and died three months later.

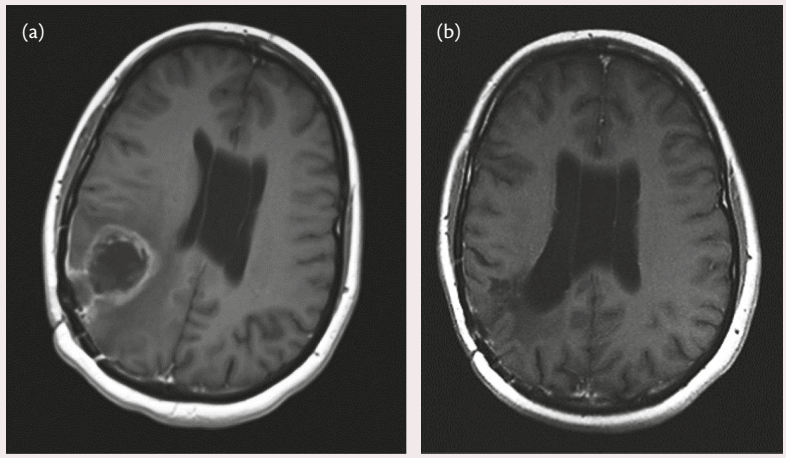

Fig. 12.4 MRI brain (T1 + gadolinium) prior to starting cilengitide (June 2009, A) and during treatment (March 2011, B) showing significant reduction in tumour enhancement

Immunotherapy

The immune system can potentially identify and selectively target specific tumour antigens and lead to durable response through immunological memory. It is thus an attractive therapeutic strategy that has led to breakthroughs in the management of melanoma and lung cancer, and is an exciting research area in other tumour types including brain tumours. Despite having active T cells against tumour antigens, most patients do not produce an adequate immunological response to destroy tumour cells. Cancer cells induce an immunosuppressive micro-environment through MHC down-regulation, production of inhibitory cytokines, regulatory T-cell infiltration, and increased expression of immune checkpoint receptors. This leads to tolerance and evasion from cells capable of inducing an effective immune response such as dendritic cells, natural-killer cells, and effector T cells. The CNS was historically considered an immunoprivileged site, distinct from the systemic immune system, due to the perceived inability of leucocytes to penetrate the blood–brain barrier, an absence of native T cells within the CNS, and no overt lymphatic drainage. However, there is disruption of the blood–brain barrier in gliomas, and it is now recognized that the CNS fully interacts with the systemic immune system. Lymphatic drainage from the CNS has been found in deep cervical lymph nodes (Reardon et al., 2014). Immunotherapy aims to modulate the immunosuppressive tumour micro-environment (*passive*) or stimulate tumour-specific immunity (*active*). A limited selection of examples are outlined next.

Passive immunotherapy

Programmed-death 1 (PD-1) is a protein receptor expressed on the surface of T cells and pro-B cells. When bound to its ligands (PD-L1/PD-L2), it dampens the immune response, through promoting apoptosis in antigen specific T cells and reducing apoptosis in regulatory T cells. It functions as an *immune checkpoint*: promoting self-tolerance and preventing autoimmunity. Cytotoxic T-lymphocyte-associated protein 4 (CTLA-4) is a further immune checkpoint that down-regulates immune responses when bound to CD80 or CD86 on antigen-presenting cells. Increased tumour expression of checkpoint receptors contributes to tolerance of tumours by the immune system. Nivolumab and ipilimumab are monoclonal antibodies against anti-PD-1 and CTLA-4 (*checkpoint* inhibitors) licensed for use in melanoma and squamous-cell lung cancer, with trials underway in brain tumours. Non-specific T-cell proliferation in patients using these drugs can lead to toxicities including colitis, hepatitis, diffuse rash, ocular changes, and endocrine dysregulation (Reardon et al., 2014). The Checkmate-143 trial is evaluating nivolumab with or without ipilimumab in recurrent glioblastoma. Published preliminary data in 20 patients report an encouraging OS at 6 months of 75% (Sampson et al., 2015).

Other potential immunomodulators under investigation include the use of cytokines such as interferon interleukin-1 to generate a pro-inflammatory state, and the suppression of regulatory T cells through inhibitors such as basiliximab against CD25 and IL-2 (Kang and Adamson, 2015).

Active immunotherapy

Peptide therapy involves the use of vaccines against tumour-specific or tumour-associated antigens. IMA-950 is a vaccine containing 11 HLA-binding tumour-associated peptides identified on human leukocyte antigen (HLA) surface receptors in primary human glioblastoma tissue. A phase 1 trial of 45 patients reported promising results with a 6-month PFS of 74% (Halford et al., 2014).

Adoptive therapies activate immune cells ex-vivo. Dendritic cells (DCs) are the most potent antigen-presenting cells and can mediate

long-lasting immunity, but are not frequently activated against tumour antigens due to the immunosuppressive tumour microenvironment. Several dendritic cell vaccine therapies are in development to overcome this local immunosuppression. With DCVax-L (currently in phase 3 trials), dendritic cells are isolated from the patient by leukapheresis, exposed to tumour antigens from a lysate taken at surgery, and then re-administered to the patient (Northwest Biotherapeutics, 2014).

Chimeric antigen receptors insert receptors for tumour-associated antigens onto effector T cells. Several targets are currently under investigation in clinical trials in glioblastoma, including HER-2 (overexpressed in 80% of glioblastoma) (NCT01109095) and EGFRvIII (NCT01454596).

Key points

- Chemotherapy can improve survival of patients with brain tumours
- Temozolomide chemoradiotherapy is the current standard of care in newly diagnosed glioblastoma following surgery. In elderly patients unlikely to tolerate chemoradiotherapy with a MGMT-promotor methylated tumour receive more benefit from chemotherapy than radiotherapy
- Gliadel® wafer use has not been prospectively tested against temozolomide chemoradiotherapy
- At recurrence of glioblastoma, there is modest benefit from lomustine or temozolomide re-challenge. Bevacizumab may prolong PFS and decrease use of corticosteroids
- Anaplastic oligodendrogliomas (WHO grade III) with 1p/19q codeletions are treated with PCV chemotherapy following radiotherapy
- 'High-risk' low-grade gliomas, particularly with 1p/19q codeletion should be treated with chemotherapy
- Targeted therapies and immunotherapy may form the basis of future treatment regimens.

Landmark papers

1. Stupp, R., Hegi, M.E., Mason, W.P., et al. (2009). Effects of radiotherapy with concomitant and adjuvant temozolomide versus radiotherapy alone on survival in glioblastoma in a randomized phase III study: 5-year analysis of the EORTC-NCIC trial. *Lancet Oncol*, **10**(5), 459–66.
2. Malmström, A., Grønberg, B., Marosi, C., et al. (2012). Temozolomide versus standard 6-week radiotherapy versus hypofractionated radiotherapy in patients older than 60 years with glioblastoma: the Nordic randomized, phase 3 trial. *Lancet Oncol*, **13**(9), 916–26.
3. Cairncross, G., Wang, M., Shaw, E., et al. (2013). Phase III trial of chemoradiotherapy for anaplastic oligodendroglioma: long-term results of RTOG 9402. *J Clin Oncol*, **31**(3), 337–43.
4. van den Bent, M.J., Brandes, A.A., Taphoorn, M.J., et al. (2013). Adjuvant procarbazine, lomustine, and vincristine chemotherapy in newly diagnosed anaplastic oligodendroglioma: long-term follow-up of EORTC Brain Tumor Group Study 26951. *J Clin Oncol*, **31**(3), 344–50.
5. Buckner, J., Shaw, E., Pugh, S., et al. (2016). Radiation plus procarbazine, CCNU, and vincristine in low-grade glioma. *N Engl J Med*, **374**(14), 1344–55.

FURTHER READING

Buckner, J., Shaw, E., Pugh, S., et al. (2016). Radiation plus procarbazine, CCNU, and vincristine in low-grade glioma. *N Engl J Med*, **374**(14), 1344–55.

Cairncross, G., Wang, M., Shaw, E., et al. (2013). Phase III trial of chemoradiotherapy for anaplastic oligodendroglioma: long-term results of RTOG 9402. *J Clin Oncol*, **31**(3), 337–43.

Malmström, A., Grønberg, B., Marosi, C., et al. (2012). Temozolomide versus standard 6-week radiotherapy versus hypofractionated radiotherapy in patients older than 60 years with glioblastoma: the Nordic randomised, phase 3 trial. *Lancet Oncol*, **13**(9), 916–26.

Stupp, R., Hegi, M.E., Mason, W.P., et al. (2009). Effects of radiotherapy with concomitant and adjuvant temozolomide versus radiotherapy alone on survival in glioblastoma in a randomised phase III study: 5-year analysis of the EORTC-NCIC trial. *Lancet Oncol*, **10**(5), 459–66.

Van Den Bent, M.J., Erridge, S., Vogelbaum, M., et al., 2013. Adjuvant procarbazine, lomustine, and vincristine chemotherapy in newly diagnosed anaplastic oligodendroglioma: long-term follow-up of EORTC brain tumor group study 26951. *J Clin Oncol*, **31**(3), 344–50.

REFERENCES

Arbor Pharmaceuticals (2014). *Gliadel Wafer (Carmustine Implant)*. http://gliadel.com/hcp

Batchelor, T., Mulholland, P., Neyns, B., et al. (2013). Phase III randomized trial comparing the efficacy of cediranib as monotherapy, and in combination with lomustine, versus lomustine alone in patients with recurrent glioblastoma. *J Clin Oncol*, **31**(26), 3212–18.

Baumert, B., Mason, W., Ryan, G., Bromberg, J., & Van Den Bent, M. (2013). Temozolomide chemotherapy versus radiotherapy in molecularly characterized (1p loss) low-grade glioma: a randomized phase III intergroup study by the EORTC/NCIC-CTG/TROG/MRC-CTU (EORTC 22033-26033). *J Clin Oncol*, **31**(suppl; abstr 2007).

Berenbaum, M.C. (1972). *In vivo* determination of the fractional kill of human tumor cells by chemotherapeutic agents. *Cancer Chemotherapy Reports*, **56**(5), 563–71.

Brem, H., Piantadosi, S., Burger, P., Walker, M., Selker, R., & Vick, N. (1995). Placebo-controlled trial of safety and efficacy of intraoperative controlled delivery by biodegradable polymers of chemotherapy for recurrent gliomas. The Polymer-brain Tumor Treatment Group. *Lancet*, **345**(8956), 1008–12.

Brown, N., Carter, T., & Mulholland, P. (2016). Dabrafenib in BRAFV600-mutated anaplastic pleomorphic xanthoastrocytoma. *CNS Oncol*, **6**(1), 5–9.

Buckner, J., Shaw, E., Pugh, S., et al. (2016). Radiation plus procarbazine, CCNU, and vincristine in low-grade glioma. *N Engl J Med*, **374**(14), 1344–55.

Cairncross, G., Wang, M., Shaw, E., et al. (2013). Phase III trial of chemoradiotherapy for anaplastic oligodendroglioma: long-term results of RTOG 9402. *J Clin Oncol*, **31**(3), 337–43.

Chabner, B.A. & Loeffler, J. (2015). Cancer chemotherapy and radiation therapy. In: Warrell, D.A., Cox, T.M., & Firth, J.D. (eds.) *Oxford Textbook of Medicine*, 5th edition, pp. 396–404. Oxford: Oxford University Press.

Chinot, O., Wick, W., Mason, W., & Henriksson, R. (2014). Bevacizumab plus radiotherapy-temozolomide for newly diagnosed glioblastoma. *N Engl J Med*, **379**(8), 709–22.

Eisenhauer, E.A., Therasse, P., Bogaerts, J., et al. (2009). New Response Evaluation Criteria in Solid Tumours: revised RECIST guideline (version 1.1). *Eur J Cancer*, **45**(2), 228–47.

European Medicines Agency. (n.d.). *European Public Assessment Reports*. https://www.ema.europa.eu/en/medicines/download-medicine-data#european-public-assessment-reports-(epar)-section

Forshew, T., Lewis, P., Waldman, A., et al. (2013). Three different brain tumours evolving from a common origin. *Oncogenesis*, **2**, e41.

Friedman, H.S., Prados, M.D., Wen, P.Y., et al. (2009). Bevacizumab alone and in combination with irinotecan in recurrent glioblastoma. *J Clin Oncol*, **27**(28), 4733–40.

Gilbert, M., Dignam, J., Armstrong, T., et al. (2014). A randomized trial of bevacizumab for newly diagnosed glioblastoma. *N Engl J Med*, **370**(8), 699–708.

Gilbert, M., Wang, M., Aldape, K., et al. (2013). Dose-dense temozolomide for newly diagnosed glioblastoma: a randomized phase III clinical trial. *J Clin Oncol*, **31**(32), 4085–91.

Halford, S., Rampling, R., James, A., et al. (2014). Final results from a Cancer Research UK first in man phase I trial of IMA950 (a novel multi peptide vaccine) plus GM-CSF in patients with newly diagnosed glioblastoma. *Ann Oncol*, **25**(Suppl 4), iv361–72.

Hanahan, D. & Weinberg, R.A. (2011). Hallmarks of cancer: the next generation. *Cell*, **144**(5), 646–74.

Hart, M., Garside, R., Rogers, G., Somerville, M., Stein, K., & Grant, R. (2011). Chemotherapy wafers for high grade glioma. *Cochrane Database Syst Rev*, **3**, CD007294.

Hyman, D., Puzanov, I., Subbiah, V., et al. (2015). Vemurafenib in multiple nonmelanoma cancers with BRAF V600 mutations. *N Engl J Med*, **373**(8), 726–36.

Kang, J. & Adamson, C. (2015). Novel chemotherapeutics and other therapies for treating high-grade glioma. *Expert Opin Investig Drugs*, **24**(10), 1361–79.

Lacroix, M., Abi-Said, D., Fourney, D., et al. (2001). A multivariate analysis of 416 patients with glioblastoma multiforme: prognosis. *J Neurosurg*, **95**(2), 190–8.

Lin, N.U., Wefel, J.S., Lee, E.Q., et al. (2013). Challenges relating to solid tumour brain metastases in clinical trials, part 2: neurocognitive, neurological, and quality-of-life outcomes. A report from the RANO group. *Lancet Oncol*, **14**(10), e407–16.

Louis, D., Perry, A., Reifenberger, G., et al. (2016). The 2016 World Health Organization classification of tumors of the central nervous system: a summary. *Acata Neuropathol*, **131**(6), 803–20.

Macdonald, D., Cascino, T., Schold Jr, S.C., & Cairncross, J. G. (1990). Response criteria for phase II studies of supratentorial malignant glioma. *J Clin Oncol*, **8**, 1277–80.

Malmström, A., Grønberg, B., Marosi, C., et al. (2012). Temozolomide versus standard 6-week radiotherapy versus hypofractionated radiotherapy in patients older than 60 years with glioblastoma: the Nordic randomised, phase 3 trial. *Lancet Oncol*, **13**(9), 916–26.

Noël, G., Schott, R., Froelich, S., et al. (2012). Retrospective comparison of chemoradiotherapy followed by adjuvant chemotherapy, with or without prior gliadel implantation (carmustine) after initial surgery in patients with newly diagnosed high-grade gliomas. *Int J Radiat Oncol Biol Phys*, **82**(2), 749–55.

Northwest Biotherapeutics (2014). *DCVax®—L*. http://www.nwbio.com/dcvax-l/

Okada, H., Weller, M., Huang, R., et al. (2015). Immunotherapy response assessment in neuro-oncology: a report of the RANO working group. *Lancet Oncol*, **16**(15), e534–42.

Perry, J., Laperriere, N., O'Callaghan, J., et al. (2016). A phase III randomized controlled trial of short-course radiotherapy with or without concomitant and adjuvant temozolomide in elderly patients with glioblastoma (CCTG CE.6, EORTC 26062-22061, TROG 08.02, NCT00482677). *J Clin Oncol*, **34**(suppl; abstr LBA2).

Reardon, D., Freeman, G., Wu, C., et al. (2014). Immunotherapy advances for glioblastoma. *Neuro Oncol*, **16**(11), 1441–58.

Robert, C., Karaszewska, B., Schachter, J., et al. (2015). Improved overall survival in melanoma with combined dabrafenib and trametinib. *N Engl J Med*, **372**(1), 30–9.

Sampson, J., Vlahovic, G., Sahebjam, S.O., & Baehring, J. (2015). Preliminary safety and activity of nivolumab and its combination with ipilimumab in recurrent glioblastoma (GBM): CHECKMATE-143. *J Clin Oncol*, **33**(15 suppl), 3010.

Schindler, G., Capper, D., Meyer, J., et al. (2011). Analysis of BRAF V600E mutation in 1,320 nervous system tumors reveals high mutation frequencies in pleomorphic xanthoastrocytoma, ganglioglioma and extra-cerebellar pilocytic astrocytoma. *Acta Neuropathol*, **121**(3), 397–405.

Stewart, L.A. (2002). Hemotherapy in adult high-grade glioma: a systematic review and meta-analysis of individual patient data from 12 randomised trials. *Lancet*, **359**(9311), 1011–18.

Stupp, R., Brada, M., van den Bent, M. J., Tonn, J. C., Pentheroudakis, G., & ESMO Guidelines Working Group (2014). ESMO Guidelines Working Group. High-grade glioma: ESMO Clinical Practice Guidelines for diagnosis, treatment and follow-up. *Ann Oncol*, **25**(Supplement 3), iii93–iiii101.

Stupp, R., Hegi, M.E., Mason, W.P., et al. (2009). Effects of radiotherapy with concomitant and adjuvant temozolomide versus radiotherapy alone on survival in glioblastoma in a randomised phase III study: 5-year analysis of the EORTC-NCIC trial. *Lancet Oncol*, **10**(5), 459–66.

Stupp, R., Hegi, M., Gorlia, T., et al. (2014). Cilengitide combined with standard treatment for patients with newly diagnosed glioblastoma with methylated MGMT promoter (CENTRIC EORTC 26071-22072 study): a multicentre, randomised, open-label, phase 3 trial. *Lancet Oncol*, **15**(10), 1100–8.

Stupp, R., Mason, W., van den Bent, M., et al. (2005). Radiotherapy plus concomitant and adjuvant temozolomide for glioblastoma. *N Engl J Med*, ***552***(10), 987–96.

Taal, W., Oosterkamp, H., Walenkamp, A., et al. (2014). Single-agent bevacizumab or lomustine versus a combination of bevacizumab plus lomustine in patients with recurrent glioblastoma (BELOB trial): a randomised controlled phase 2 trial. *Lancet Oncol*, **15**(9), 943–53.

Van Den Bent, M.J., Brandes, A.A., Taphoorn, M.J., et al. (2013). Adjuvant procarbazine, lomustine, and vincristine chemotherapy in newly diagnosed anaplastic oligodendroglioma: long-term follow-up of EORTC Brain Tumor Group Study 26951. *J Clin Oncol*, **31**(3), 344–50.

Van Den Bent, M., Chinot, O., Boogerd, W., Bravo Marques, J., Taphoorn, M., & Kros, J. (2003). Second-line chemotherapy with temozolomide in recurrent oligodendroglioma after PCV

(procarbazine, lomustine and vincristine) chemotherapy: EORTC Brain Tumor Group phase II study 26972. *Ann Oncol*, **14**(4), 599–602.

Van Den Bent, M., Erridge, S., Vogelbaum, M., et al. (2016). Results of the interim analysis of the EORTC randomized phase III CATNON trial on concurrent and adjuvant temozolomide in anaplastic glioma without 1p/19q co-deletion: an intergroup trial. *J Clin Oncol*, **34**(suppl; abstr LBA2000).

Walker, M.D., Green, S.B., Byar, D.P., et al. (1980). Randomized comparisons of radiotherapy and nitrosoureas for the treatment of malignant glioma after surgery. *N Engl J Med*, **303**(23), 1323–9.

Weller, M., Stupp, R., Reifenberger, G., et al. (2010). MGMT promoter methylation in malignant gliomas: ready for personalized medicine? *Nat Rev Neurol*, **6**(1), 39–51.

Wen, P., Macdonald, D.R., Reardon, D.A., et al. (2010). Updated response assessment criteria for high-grade gliomas: response assessment in neuro-oncology working group. *J Clin Oncol*, **28**(11), 1963–72.

Wick, W., Platten, M., Meisner, C., et al. (2012). Temozolomide chemotherapy alone versus radiotherapy alone for malignant astrocytoma in the elderly: the NOA-08 randomised, phase 3 trial. *Lancet Oncol*, **13**(7), 707–15.

RELATED LINKS TO EBRAIN

Intraoperative Chemotherapy and Radiotherapy. https://learning.ebrain.net/course/view.php?id=1241

Long-term Complications of Radiotherapy and Chemotherapy for CNS Disease. https://learning.ebrain.net/course/view.php?id=484

Principles of Chemotherapy. https://learning.ebrain.net/course/view.php?id=485

13

Surgical techniques in the management of intrinsic tumours

Shawn Hervey-Jumper and Mitchel Berger

Introduction

Surgical resection plays a central role in the management of intrinsic brain tumours, and there is a growing body of evidence concerning the value of extent of resection to improve patient outcome and quality of life. Maximal resection can be difficult to achieve due to tumour proximity to eloquent structures and uncertainty as to tumour margins. Direct stimulation mapping, functional neuronavigation, intraoperative MRI, and fluorescence-guided surgery are all useful tools to improve the extent of tumour resection while minimizing morbidity. Current evidence suggests that a more extensive surgical resection is associated with longer survival and improved quality of life for patients with either low- or high-grade gliomas. This chapter emphasizes the evidence supporting the role of surgery for intrinsic brain tumours, their surgical neuroanatomy, and techniques to maximize the extent of resection while minimizing morbidity.

Surgical neuroanatomy

Cerebral hemispheres and cranio-cerebral relationship

(See Fig. 2.2, Chapter 2.)

The adult cerebrum is divided into two hemispheres containing frontal, parietal, central, temporal, occipital lobes, and the insula. There are six principal sulci, which are continuous: the Sylvian, callosal, parieto-occipital, collateral, central, and calcarine sulci. There are two interrupted sulci: the precentral and inferior temporal sulci.

The frontal lobe is separated by two main sulci: the superior and inferior frontal sulci, which divide the lateral surface of the frontal lobe into the superior, middle, and inferior frontal gyri. These extend from the precentral sulcus and are oriented in the anterior-posterior direction. Running parallel to the central sulcus is the precentral sulcus, which lies at the posterior end of the frontal lobe. The inferior frontal gyrus is further divided by the anterior ascending, and the posterior rami of the Sylvian fissure into the pars orbitalis, triangularis, and opercularis. A readily recognizable landmark seen at the intercepting point between the superior frontal and precentral sulci is the hand region of the motor cortex, which has the morphology of the Greek letter 'Ω' (omega).

Boundaries of the parietal lobe include the interhemispheric fissure medially, the Sylvian fissure and temporal-occipital line inferiorly, the central sulcus anteriorly, and the lateral parietal-temporal line posteriorly. There are two main sulci in the parietal lobe: postcentral and intraparietal sulci. The intraparietal sulcus divides the surface of the parietal lobe into the superior and inferior parietal lobules. The superior parietal lobule is superomedial and smaller and continues as the precuneus medially, whereas the inferior parietal lobule comprises the supramarginal and angular gyri. The supramarginal gyrus is the posterior continuation of the superior temporal gyrus, and the angular gyrus is the posterior continuation of the middle temporal gyrus.

The superior limitation of the temporal lobe is the Sylvian fissure. The temporal lobe has the superior and inferior temporal sulci, which divide the temporal lobe into superior, middle, and inferior temporal gyri. These three temporal gyri converge anteriorly to form the temporal pole. Boundaries of the occipital lobe include the calcarine sulcus medially and the parietal-temporal line laterally. The occipital lobe is composed of several short horizontal sulci, which divide the lateral occipital lobe into superior and inferior occipital gyri.

Separating the frontal, parietal, and temporal lobes is the Sylvian fissure, which is composed of a deep and a superficial portion. Deep to the Sylvian fissure lies the insula. The superficial portion of the Sylvian fissure contains a stem and three rami. The stem extends medially from the uncus to the lateral end of the sphenoid wing, where it divides into the anterior horizontal, anterior ascending, and posterior rami. The deep portion of the Sylvian fissure is divided into sphenoidal and operculoinsular compartments (Ribas et al., 2015). The sphenoidal compartment arises anteriorly in the region of the limen insula and extends laterally towards the anterior perforated substance. The operculoinsular compartment is formed by an opercular cleft (between the opposing lips of the frontoparietal and temporal operculae) and an insular cleft (with a superior limb located between the insula and frontoparietal opercula, and an inferior limb between the insula and temporal operculum) (Ribas et al., 2015). At

the threshold between the carotid cistern medially and the Sylvian fissure laterally is the limen insula. The central sulcus of the insula divides the lateral surface of the insula into an anterior zone, which is divided into three short gyri and a posterior zone formed by the anterior and posterior long gyri (Ribas et al., 2015). Encircling the insula is the circular sulcus, which separates it from the overlying opercula.

White matter tracts

(See Fig. 35.5, Chapter 35.)

The contemporary view of human brain function has shifted from a rigid organization to a more dynamic view of brain processing. Large-scale subcortical white matter networks facilitate complex functions such as language, movement, and cognition. Association fibres connect cortical areas of different lobes in the same hemisphere and can be divided into short and long association fibres. Short association fibres connect adjacent gyri, whereas the long association fibres (also known as fasciculi) connect distant gyri and form distinct compact bundles. The primary fasciculi of clinical importance are (1) the superior longitudinal fasciculus, (2) uncinate fasciculus, (3) inferior fronto-occipital fasciculus, and (4) the cingulum. The superior longitudinal fasciculus curves around the insula and connects the frontal, parietal, and temporal lobes. The uncinate fasciculus lies within the anterior insula along the limen insulae, and connects the basal frontal lobe with the temporal lobe. The cingulum resides below the rostrum of the corpus callosum to the parahippocampal gyrus. Connecting the frontal and occipital lobes, as well as the posterior portion of the temporal and parietal lobes, is the inferior fronto-occipital fasciculus (IFOF). The IFOF converges from the frontal lobe just lateral to the basal ganglia, before running alongside the uncinate fasciculus.

Perhaps the most relevant white matter tracts of importance from a neurosurgical perspective are those related to language function. Early models of language organization were derived from language deficits after cortical lesions. In 1861 Jean-Baptiste Bouillaud published a series of patients with long-term speech loss after frontal lobe lesions. These findings were followed by Broca's observation that speech arrest was separate from motor language activations, but represented a distinct inability to articulate language (Chang et al., 2015). Several years later Karl Wernicke described lesions in the posterior superior temporal lobe which caused impaired repetition, naming, and comprehension but intact fluency. Aphasia, or the impairment of language affecting the production or comprehension of speech, can be classified as global aphasia, Broca's aphasia, Wernicke's aphasia, mixed non-fluent aphasia, or anomic aphasia.

Global aphasia is the most severe form of aphasia and describes patients who can produce very few recognizable words and comprehend only occasional spoken language. Patients with global aphasia can therefore neither read nor write. Broca's aphasia have reduced laborious and clumsy speech output marked by shorter sentences including less than four words. Patients with Broca's aphasia typically comprehend speech and maintain their ability to read, but are unable to write.

The hallmark of Wernicke's aphasia is impaired comprehension while speech fluency is preserved. Reading and writing are often impaired with Wernicke's aphasia. Mixed non-fluent aphasia is classified scant, effortful speech similar to severe Broca's aphasia however patients have limited comprehension resulting in difficulties reading and writing. Patients with anomic aphasia have an inability to name nouns and verbs, which results in relatively normal fluency but speech content is vague as patients have difficulty finding words.

Current models of language organization are based on dorsal and ventral stream processing (Chang et al., 2015). The dorsal stream is located primarily within the dominant hemisphere and critical for sensorimotor integration while the ventral stream is bilateral and essential for language comprehension. Using subcortical electrical stimulation mapping we now have an evolving but more complete understanding of the functional networks essential for language processing. The superior longitudinal fasciculus (SLF) is composed of four major components (SLF I, II, III, and SLF-temporoparietal (tp)) (Chang et al., 2015). While SLF I is not involved in language processing, SLF II connects the premotor cortex to the angular gyrus, SLF III connects the ventral prefrontal cortex with the supramarginal gyrus and SLF-tp connects the inferior parietal lobule with the posterior superior temporal lobe. Stimulation mapping of the SLF II and III causes dysarthria while stimulation of both SLF III and SLF-tp causes errors or language repetition. The arcuate fasciculus was classically thought to connect Broca's and Wernicke's areas. It is now understood that the arcuate fasciculus connects fronto-opercular and posterior temporal cortical sites in a much more diverse fashion then originally appreciated. Stimulation of the arcuate fasciculus causes anomia and phonemic paraphasias, while lesions to this subcortical pathway results in conduction aphasia (intact comprehension, fluent speech production but poor repetition; see Chang et al., 2015).

Neurological deficits

Neurological deficits from intrinsic brain tumours are highly variable depending on tumour location and the extent of disease. Non-specific physical findings can occur with elevated intracranial pressure, including papilloedema (oedema of the head of the optic nerve associated with engorgement of retinal veins) and oculomotor palsy (due to uncal herniation). Frontal tumours may result in impaired gait, abulia, personality changes, and hemiparesis. Aphasia suggests involvement with cortical language centres located in the dominant frontal or temporal lobes. Temporal lobe tumours may also result in memory loss, impaired auditory discrimination, seizures, or contralateral superior quadrantanopia. Parietal lobe tumours may lead to impaired sensory function, distractibility, contralateral inferior quadrantanopia, aphasia, or anosognosia. Occipital lobe tumours result in visual deficits, while brainstem tumours may impair cranial nerves and lead to long-tract signs. Pineal tumours that compress the midbrain tectum result in Parinaud's syndrome, which includes upgaze palsy, eyelid retraction (Collier's sign) or ptosis, loss of pupillary light reflex (light-near dissociation where the pupil does not respond to light but constricts on accommodation), and retraction-convergence nystagmus.

Headaches are the most common symptom in brain tumour patients, occurring in at least 50% of patients at some point. Classically, brain tumour patients present with headaches that are worse upon waking in the morning and may often be severe enough to wake a patient from sleep.

Headaches are thought to occur as a result of temporary increases in intracranial pressure caused by recumbency and elevations in the partial pressure of carbon dioxide (PCO_2) during sleep. The combination of elevated intracranial pressure due to mass effect from

the presence of tumour and cerebral vasodilation due to increased pCO_2 causes additive increases in intracranial pressure, ultimately resulting in headache.

Preoperative surgical management

Preoperative planning

Preoperative clinical evaluation should include baseline sensorimotor and language assessment performed 24–48 hours prior to surgery (Hervey-Jumper et al., 2015).

Preoperative imaging includes brain MRI with and without gadolinium enhancement, DTI of white matter pathways (including the corticospinal tract, superior longitudinal fasciculus, arcuate fasciculus, uncinate fasciculus, and interior orbitofrontal fasciculus), task-based functional brain MRI (fMRI) (Deng et al., 2015; Ille et al., 2015) (Fig. 13.1) and perfusion MRI.

Preoperative anatomical imaging provides information regarding tumour location, vascularity, mass effect, peritumoural oedema, and proximity to areas of potential functional significance. Additionally, these anatomical studies can be reconstructed to create three-dimensional models that can be used during surgery (neuronavigation). DTI defines the integrity of white matter tracts surrounding a tumour and is commonly used in the planning of both surgical and radiation therapy (Alexander et al., 2007; Berman et al., 2007; Bello et al., 2008). Task-based fMRI uses the blood oxygenation level dependent (BOLD) signal to identify cortical and subcortical regions of activation to create an operative corridor or plan for resection that minimizes risk to eloquent surrounding structures (Bogomolny et al., 2004; Nimsky et al., 2004). Finally perfusion MRI is useful for evaluating tumour angiogenesis, endothelial permeability, and response to treatment.

In combination anatomical MRI, functional MRI, DTI tractography, and perfusion MRI enable clinicians to make more accurate preoperative diagnoses and provide information regarding the interface of tumour tissue with the adjacent functional cortical and subcortical pathways.

Medical management

The management of intrinsic brain tumours begins with surgery aimed at establishing the pathological diagnosis and maximizing safe resection. Preoperative medical management and surgical planning are critical to the success of any surgical intervention. Corticosteroids are commonly used preoperatively to reduce symptoms of mass effect and peritumoural vasogenic oedema. Though timing and dose of corticosteroids vary by surgeon preference, a common regimen for adults is 4–6 mg of dexamethasone intravenously or by mouth every six hours.

Patients presenting with seizures should be initiated on an anticonvulsant. However, with few exceptions, there is no data to suggest that the prophylactic use of anticonvulsants reduces the risk of new onset seizures in patients with intrinsic brain tumours (Chang et al., 2005; Chang et al., 2008; de Oliveira Lima, 2015). Even so, in cases of tumour involvement in highly epileptogenic areas such as the motor cortex, patients with low-grade gliomas, multiple metastatic tumours with large amounts of vasogenic oedema, or leptomeningeal disease are often treated with prophylactic seizure medications. Phenytoin was historically the first-line antiepileptic agent; however, phenytoin levels must be monitored to ensure a therapeutic serum drug concentration. Levetiracetam is now commonly used due to its low toxicity, minimal side-effect profile, and lack of need to monitor serum levels.

Intraoperative surgical management

Biopsy and extent of resection

In recent years, a number of studies have enhanced our understanding of the impact of tumour resection on progression-free overall survival in patients with intrinsic brain tumours (Hervey-Jumper and Berger, 2014). However, the initial goal of surgery is to establish a definitive histological diagnosis. The decision to offer surgical resection versus biopsy depends on tumour location and size, patient age, and performance status. One must balance the natural history of the tumour and its propensity to transform and grow over

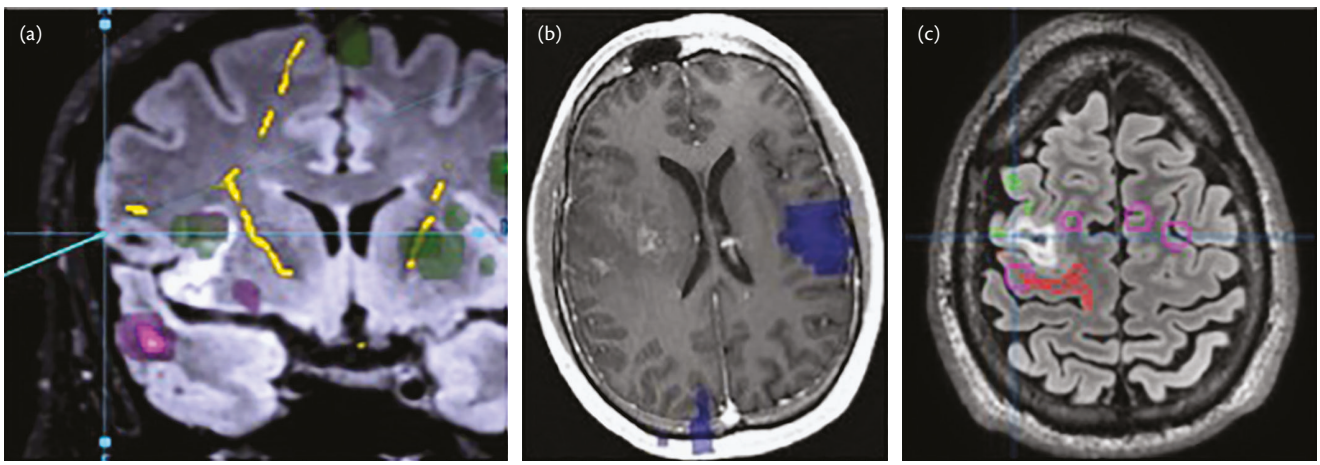

Fig. 13.1 Imaging modalities such as fMRI, MEG, and DTI provide valuable information for both preoperative and intraoperative use. (A) fMRI reveals language activation sites in purple. (B) MEG similarly identifies activation of verb generation in blue. (C) DTI identifies corticospinal fibres running posterior and superior to longitudinal fasciculus fibres lateral to the glioma.

time. Recent data places maximal safe surgical resection alongside patient age, tumour histology, tumour performance status, and molecular markers as predictive of long-term outcome (Hervey-Jumper and Berger, 2014). For this reason, maximal safe resection is preferred over biopsy.

The value of surgical resection for intrinsic brain tumours (particularly low-grade glioma) has been validated by a number of studies illustrating a survival benefit of 60–90 months with greater than 90% resection (Smith et al., 2008). In a large population-based series of Norwegian patients, early maximal resection was superior to biopsy and watchful waiting with respective 5-year survival rates of 74% and 60%, illustrating the advantage of resection over watchful waiting (Jakola et al., 2012). Additionally, 90% extent of resection in low-grade gliomas delays and reduces malignant transformation and improves survival. Seizure control is also enhanced after gross total resection of intrinsic brain tumours (Chang et al., 2008).

Image-guidance

For the brain tumour surgeon, functional and anatomic image-guidance is an essential part of determining the risks associated with surgery and for consulting patients about potential postoperative neurological outcomes. Image-guidance also allows for a generalized preoperative impression of where a functional pathway might be displaced by a space-occupying lesion. Neuronavigation is widely used in brain tumour surgery and can be integrated with DTI tractography, magnetoencephalograpy (MEG), or fMRI (commonly referred to as 'functional neuronavigation') to identify cortical and subcortical areas of potential sensory, motor, language, and visual significance (Trinh et al., 2014) (**Fig. 13.1**). Neuronavigation can therefore generate individualized maps of functional areas and their relationship with mass lesions within the brain. Variability in individual neuroanatomy, distortion due to mass lesions, and functional re-organization caused by plasticity make classic anatomic identification of functional areas insufficient (Thiel et al., 2001; Duffau, 2006). Compared with direct cortical stimulation, fMRI has a sensitivity and specificity of 91% and 64% for identification of Broca's area, 93% and 18% for identification of Wernicke's area, and 100% and 100% in motor areas, respectively (Bizzi et al., 2008).

Resting state coherence measured with MEG or MRI is capable of mapping functional connectivity of the brain. Intrinsic brain tumours with decreased resting state connectivity have a relatively low risk of postoperative neurological deficits, while those with increased resting state connectivity are associated with higher risk of postoperative neurological deficits (Guggisberg et al., 2008). These studies are helpful for determining the risks associated with surgery, the optimal surgical approach, and advising patients about potential postoperative neurological outcomes. Identification of subcortical pathways is critical in preventing injury to white matter pathways and preserving function (Sarubbo et al., 2015). While the current gold standard for assessing functional tissue in the cortex and subcortically is intraoperative stimulation testing, it is advantageous to preoperatively and intraoperatively 'visualize' white matter tracts and their spatial relationship to the brain tumour.

Awake craniotomy and neurophysiological monitoring

First employed by Wilder Penfield, direct cortical stimulation mapping allows for the identification of language, motor, and sensory function during surgery for removal of intrinsic brain tumours (Hervey-Jumper et al., 2015). Individual variability and pathway distortion from intrinsic brain tumours makes neuronavigation less reliable. Speech arrest, anomia, and alexia are often located far outside the anatomic boundaries of Broca's area (Sanai et al., 2008). Direct stimulation mapping is the gold standard for identification and preservation of functional areas.

Cortical stimulation depolarizes a focal area of brain, which excites local neurons via diffusion of current using both orthodromic and antidromic propagation. Bipolar stimulation using a 2-mm tip with 5 mm of separation allows for local diffusion and more precise mapping (Nathan et al., 1993). Early mapping techniques utilized large craniotomies with the goal of identifying positive functional sites; however, one can also use smaller exposures with reliance on negative mapping (Sanai et al., 2008). Negative mapping strategies represent a shift in mapping techniques, keeping eloquent areas untouched and free from exposure. The tumour surgeon must balance the goal of maximal resection with preservation of motor and language functional sites.

Specialized neuroanaesthesia is critical for completion of a safe awake craniotomy (Taylor and Bernstein, 1999). Clear communication between neurosurgeon, anaesthesiologist, speech pathologist, and other members of the mapping team ensures accuracy and patient safety. Surgery commences with the application of patient monitors (axillary temperature probe, blood pressure cuff, arterial line) and premedicating with midazolam, fentanyl, or dexmedetomidine prior to positioning (Hervey-Jumper et al., 2015). Sedation is achieved with propofol (up to 100 μg/kg/min) or dexmedetomidine (up to 1 μg/kg/min) and remifentanil (0.07–2.0 μg/kg/hr) (Herrick et al., 1997; Bekker et al., 2001; Olsen, 2008). Sedation continues during Foley catheter insertion and Mayfield head holder pin placement. A scalp block using a mixture of 1% lidocaine with 1:100 000 epinephrine, 0.5% bupivacaine, plus 8.4% sodium bicarbonate is applied by the neurosurgeon. The optimal head positioning that allows for ease of operation, patient comfort, and potential insertion of a laryngeal mask airway must be discussed by neurosurgery and anaesthesia. After skin incision and removal of the bone flap, all sedatives are stopped, after which the patient is asked to take multiple deep breaths to decrease hypercapnia before dural opening. A dedicated intravenous line is filled with a 1 mg per kg bolus of propofol if needed for suppression of an intraoperative grand mal seizure. Topical ice-cold Ringers lactate solution is available on the surgical field at all times for seizure suppression.

Mapping begins with a stimulation current of 1.5–2 mA and increases to a maximum of 6 mA if necessary. A constant current generator delivers 1.25 millisecond biphasic square waves in 4 second trains at 60 Hz. Numerical markers are placed on the surgical field spaced 1 cm apart (**Fig. 13.2**). Continuous electrocorticography is used to improve mapping accuracy, monitor for subclinical seizure activity, and detect after-discharge potentials. All language testing is repeated at least three times per cortical site, and a positive site is defined as the inability to count, name objects, or read words during stimulation at least two out of three times. Language mapping seeks to identify sites responsible for speech arrest, anomia, and alexia with stimulation testing. Speech arrest is defined as discontinuation in number counting without simultaneous motor response. Dysarthria can be distinguished from speech arrest by an absence of involuntary muscle contractions affecting speech (Sanai et al., 2008).

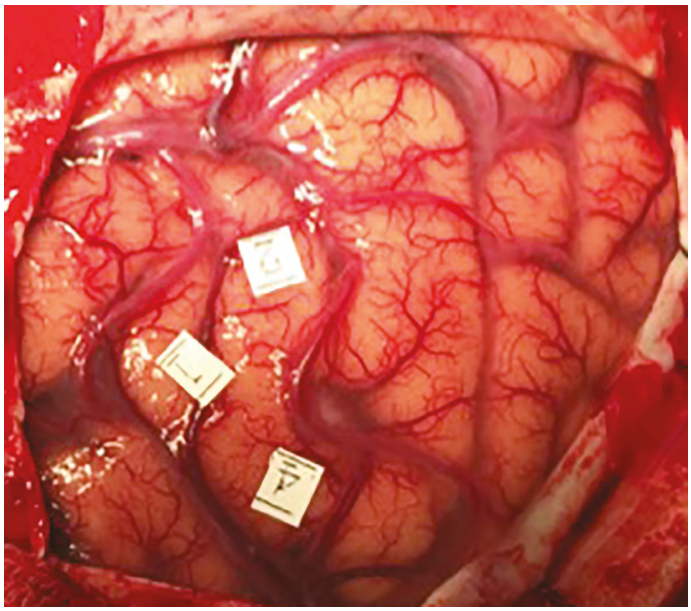

Fig. 13.2 Direct cortical and subcortical stimulation mapping is the gold standard for identification of functional language and sensorimotor areas. Cortical mapping uses numbered markers placed at 1-cm intervals to test regions overlying and directly adjacent to tumour.

5-aminolevulinic acid (5-ALA)

Gross total resection of intrinsic brain tumours can be challenging and it has been well-established that the majority of tumour recurrences occur within a centimetre of the prior resection cavity. Most neurosurgeons overestimate the degree of resection they are able to achieve. 5-ALA is a non-fluorescent amino acid precursor that produces an accumulation of fluorescent porphyrins (mainly protoporphyrin IX) in high-grade gliomas (Stummer et al., 2006). Exogenous 5-ALA results in accumulation of intracellular fluorescent protoporphyrins in malignant glioma, which peak six hours after administration and remain elevated for 12 hours (Stummer et al., 2003). Protoporphyrin IX has an absorption band strongest in the 380 +/- 420 nm spectrum, emitting red fluorescence at 635 nm and 704 nm in the brain. The most common established protocol is 5-ALA administration orally 3 hours before surgery with a goal of tumour removal 4 to 5 hours after 5-ALA administration. A long-pass filter mounted to the surgical microscope allows for tumour visualization as the operator switches between white and violet light (Fig. 13.3).

Several studies have examined the efficacy of 5-ALA to improve the extent of resection and prolong survival for patients with malignant glioma. Complete removal of all fluorescent material ('5-ALA complete resection') offers greater six-month and overall survival in malignant glioma without an increase in postoperative neurological deficits (Stummer et al., 2006). A phase III clinical trial of patients with suspected malignant glioma receiving either conventional white light microsurgery or fluorescence-guided surgery assisted with 5-ALA found 65% of 5-ALA patients received a gross total resection compared with 36% of patients treated with conventional white light microsurgery. Study patients therefore experienced a 50% improvement in six-month progression-free survival (41.0% vs. 21.1%) (Stummer et al., 2006).

Gliadel wafers

Carmustine wafers, also known as Gliadel wafers (GW) (Arbor Pharmaceuticals, LLC, Atlanta, GA) are approved for treatment of newly diagnosed and recurrent high-grade glioma (WHO grades III and IV). Carmustine is an alkylating agent that interferes with DNA synthesis and repair. GWs are biodegradable polymers containing 3.85% carmustine. These polymers are implanted into the resection cavity following surgery for tumour resection, releasing 7.7 mg of drug for roughly 5 days. Widespread use has been limited for several reasons. The safety and efficacy of GW has been an issue of debate, with some published reports illustrating excellent patient tolerance and improved survival, while others have found no improvement in survival by adding carmustine wafers to standard therapies (Xing et al., 2015). Currently the use of carmustine wafers is limited in most settings, given concern regarding wound healing and the likelihood that it will preclude enrolment in subsequent clinical trials.

Deep-seated tumours

Deep-seated tumours remain challenging to treat due to their proximity to important vascular structures and location around

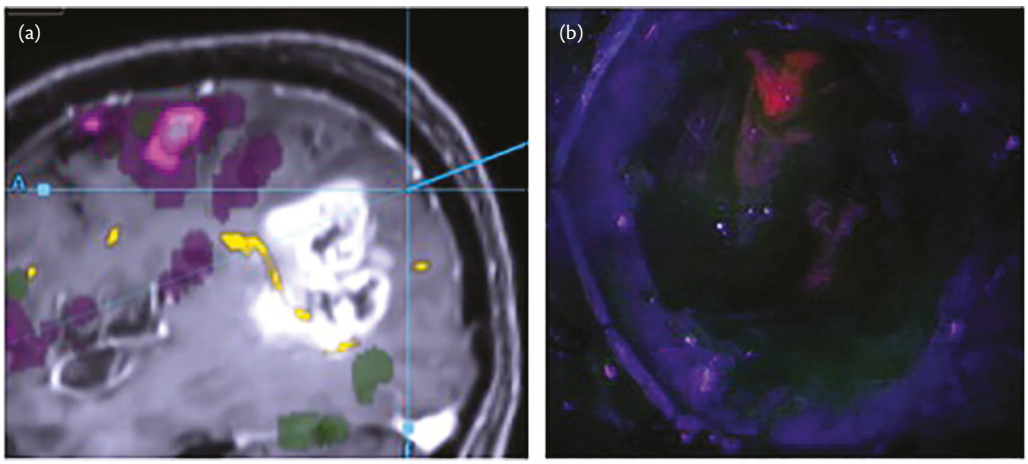

Fig. 13.3 5-ALA administered 2 to 5 hours prior to surgery allows intracellular uptake of fluorescent porphyrins. Functional neuronavigation shows a cortical approach to the tumour (A), which is confirmed under violet-blue light as pink in colour (B).

functional areas. Lesions within the insula, cingulate, and thalamus were previously considered inoperable due to the high risk of perioperative complications. A combination of improved neuroanaesthesia, advanced structural and functional imaging, and microsurgical techniques have allowed greater access to many deep-seated tumours. The surgical approaches and technical considerations for deep-seated tumours within the insula, cingulate, and thalamus will be discussed in greater detail next.

Insular lesions

Insular tumours are among the most challenging neurosurgical lesions to manage. Tumour location and hemisphere of language dominance determines whether a transcortical or trans-Sylvian approach should be considered (Benet et al., 2015). Patients are positioned semi-lateral with the head parallel to the floor (Sanai et al., 2010). For tumours located predominately above or below the Sylvian fissure the vertex of the head is positioned 15 degrees towards the ceiling or floor (respectively). A craniotomy is tailored based on the tumour's location and involvement of the overlying frontal or temporal opercula. Cortical and subcortical sensorimotor and language mapping may be utilized. Once functional areas have been identified transcortical windows superior and inferior to the Sylvian fissure are created through non-functional areas between insular arteries ('cortical windows'). Surgical resection then continues as the vessels of the Sylvian fissure are skeletonized. The resection continues by working under the Sylvian fissure along the uncinate fasciculus. The supra-Sylvian lenticulostriate arteries must be identified and preserved and subcortical motor mapping of the corticospinal tract marks the medial border of the resection. Early identification of the long lenticulostriate perforating branches to the internal capsule and corona radiata and avoidance of excessive manipulation, which may induce vasospasm, minimizes ischaemic complications. The horizontal fibres of the superior longitudinal fasciculus are adjacent to the superior peri-insular sulcus while the uncinate fasciculus is adjacent to the inferior peri-insular sulcus. The IFOF at the level of the external capsule is identified by inducing semantic paraphasia through subcortical stimulations.

Cingulate lesions

The cingulate gyrus covers the corpus callosum and is positioned immediately below the falx cerebri. The cingulate is subdivided into anterior and posterior regions and is covered by the callosomarginal artery, which runs along its medial surface. Due to their location deep within the interhemispheric fissure, tumours within the anterior and posterior cingulate gyrus are difficult to access surgically. Patients are positioned either supine or in a sitting position, for a unilateral or bilateral craniotomy according to the tumour location, size, vascularity, and pathology. Preoperative imaging should be carefully inspected for bridging veins, which may influence the surgical approach. The dura should be opened cautiously to avoid injury to the superior sagittal sinus or proximal draining veins. The surgical approach begins by creating a surgical corridor followed by tumour devascularization, and identification of the callosomarginal and pericallosal arteries. The choice between an interhemispheric approach, superior frontal gyrus resection, or superior parietal lobule resection is made on surrounding functional areas, vascularity, tumour size and location (Talacchi et al., 2010).

Thalamic lesions

Thalamic tumours are relatively rare representing 1–5% of all brain tumours (Sai Kiran et al., 2013). While lesions in this location have historically been treated with stereotactic biopsy and radiotherapy alone, advanced structural imaging and microsurgical techniques have allowed for surgical resection with minimal postoperative morbidity. Surgical resection is reserved for contrast enhancing tumours with clear margins on preoperative imaging. Non-enhancing tumours with poorly defined margins should be managed with a biopsy. Surgical approach is based on tumour location (anterior or posterior within the thalamus) and proximity to the posterior limb of the internal capsule. The majority of deep-seated intrinsic tumours cause anterolateral displacement of posterior limb of the internal capsule making the middle temporal gyrus corridor the common approach. After a temporal corticectomy the tumour is approached through the lateral ventricle along the posterolateral margin of the tumour. Upon reaching the temporal horn of the lateral ventricle the tumour is approached through the choroidal fissure. This approach ensures an entry corridor inferior to the insula and posterior to the internal capsule.

If located anteriorly and presenting into the lateral ventricle especially if the ventricle is enlarged, a transcallosal approach is suitable but is limited by the lateral extension of larger lesions. Care is needed to avoid damage to the crus of the fornix overlying the thalamus or the choriodal fissure in cases where there is medial extension to the third ventricle. A posterior interhemispheric or infratentorial supracerebellar approach may be used to access those lesions located posteriorly in the pulvinar. Visual tract fibres are at risk as a number of these are closely associated with the pulvinar adjacent to the lateral geniculate body.

Postoperative surgical management

In the immediate postoperative period, patients are observed closely in the setting of an intensive care unit, where serial neurological examinations are carried out (Chang et al., 2005). Depending on the tumour location and extent of resection, corticosteroids may be tapered over the days following surgery. Anticonvulsants are continued in patients who have a history of seizures and for tumours in areas known to have a propensity to cause seizures. The long-term use of seizure medications for prophylaxis remains controversial. Given the prognostic significance of the extent of resection for glioma patients and the difficulty in detecting residual tumour during surgery, it is becoming standard practice for surgeons to obtain postoperative MRIs with enhancement to look for residual tumour within 24 hours of resection.

Complications

Surgery for intrinsic brain tumours carries the risk of developing postoperative medical as well as surgical complications. Neurologic complications may produce visual field, motor, sensory, cognitive, or language deficits (Chang et al., 2005). They result from violation of functional cortical and subcortical pathways, cerebral oedema, haematoma, or vascular injury. In most series, the risk of a new neurologic deficit after craniotomy for resection of an intrinsic brain tumour ranges from 10 to 25%. These risks increase with older age,

deeper tumour location, tumour proximity to functional regions, and a low performance score. Neurological complications can be minimized by individualizing the surgical approach planned based on anatomic and functional imaging, cortical mapping techniques, minimizing excessive brain retraction, meticulous haemostasis, and early identification of major vascular structures.

Additional complications are related to the surgical wound and surrounding brain parenchyma. These include surgical wound infections, pneumocephalus, cerebrospinal fluid (CSF) leaks, hydrocephalus, seizure, brain abscess, cerebritis, meningitis, and pseudomeningocele. These complications occur in 1–5% of patients undergoing craniotomy for resection of an intrinsic brain tumour, and happen more readily in elderly patients and those undergoing re-operation. The posterior fossa location and re-operations are associated with a higher rate of pseudomeningocele, CSF fistula, hydrocephalus, and wound infections. Postoperative wound infections and cellulitis occur in 1–2% of patients after supratentorial craniotomy. They typically result from bacterial contamination from the skin by *Staphylococcus aureus* or *Staphylococcus epidermidis*. The risk of postoperative seizures following supratentorial craniotomy is 0.5–5%. Prophylactic antiepileptic drugs can be routinely used in the postoperative period; however, their dose and duration remain controversial.

Systemic complications include adverse events such as deep vein thrombosis (DVT), pulmonary embolus, pneumonia, urinary tract infections, myocardial infarction, and sepsis. These medical complications occur in 5–10% of patients undergoing craniotomy for removal of an intrinsic brain tumour and are more prevalent in older patients and neurologically impaired patients with poor performance status. DVT is the most common complication, occurring in 1–10% of patients within the first month after a craniotomy. Patients with systemic cancer, glioblastoma multiforme, hemiplegia, extended periods of bed rest, and prolonged surgery are at particularly increased risk of developing a DVT or pulmonary embolus. Early postoperative mobilization, intermittent compression devices, and postoperative anticoagulation with low molecular weight heparin may decrease the incidence of postoperative DVT.

Craniotomy for resection of intrinsic brain tumours can be performed safely and most complications can be prevented with careful preoperative planning, meticulous surgical technique, and attentive postoperative care.

Controversy

Awake craniotomy vs. intraoperative MRI (iMRI)

MRI-guided brain tumour surgery has been shown to enhance the extent of glioma resection and patient survival. Numerous studies have attempted to quantify the effect of iMRI on extent of tumour resection (Knauth et al., 1999; Wirtz et al., 2000). Both iMRI and awake craniotomy are tools to maximize the extent of resection while limiting neurological deficits. The main rationale for the use of iMRI combined with conventional neuronavigation-guided resection is the avoidance of brain shift due to CSF loss and tissue oedema (Nimsky et al., 2002). Neuronavigation becomes less reliable as surgery progresses. Intraoperative MRI has been shown to increase both the extent of the resection and survival in patients with low- or high-grade glioma (Black et al., 1999). With no differences in postoperative neurological deficits following surgery, iMRI resulted in a significant improvement in extent of tumour resection. This enhanced extent of resection is supported by a modestly enhanced survival in a number of series involving patients with high-grade glioma (Schneider et al., 2005).

Controversies exist over the use of awake mapping procedures and iMRI-guided procedures. Awake procedures allow real time language and sensorimotor mapping and monitoring, which may be combined with functional and structural imaging (functional neuronavigation). While this is the optimal approach for identification of functional areas, the extent of resection in functional and non-functional areas might be limited. The primary advantage of iMRI is the ability to acquire updated imaging throughout the procedure. Many patients are not ideal candidates for either approach based on their weight and body habitus (awake craniotomy) or cardiac comorbidities (iMRI). It is increasingly acceptable to use awake mapping with MRI-guided surgery within an iMRI suite, which for properly selected patients optimizes the extent of the resection and patient safety.

FURTHER READING

Hervey-Jumper, S.L., Li, J., Lau, D., et al. (2015). Awake craniotomy to maximize glioma resection: methods and technical nuances over a 27-year period. *J Neurosurg*, **24**, 1–15.

Jakola, A.S., Myrmel, K.S., Kloster, R., et al. (2012). Comparison of a strategy favoring early surgical resection vs. a strategy favoring watchful waiting in low-grade gliomas. *JAMA*, **308**(18), 1881–8.

Sanai, N., Mirzadeh, Z., & Berger, M.S. (2008). Functional outcome after language mapping for glioma resection. *N Engl J Med*, **358**(1), 18–27.

Smith, J.S., Chang, E.F., Lamborn, K.R., et al. (2008). Role of extent of resection in the long-term outcome of low-grade hemispheric gliomas. *J Clin Oncol*, **26**(8), 1338–45.

Stummer, W., Pichlmeier, U., Meinel, T., et al. (2006). Fluorescence-guided surgery with 5-aminolevulinic acid for resection of malignant glioma: a randomised controlled multicentre phase III trial. *Lancet Oncol*, **7**(5), 392–401.

REFERENCES

Alexander, A.L., Lee, J.E., Lazar, M., & Field, A.S. (2007). Diffusion tensor imaging of the brain. *Neurotherapeutics*, **4**(3), 316–29.

Bekker, A.Y., Kaufman, B., Samir, H., & Doyle, W. (2001). The use of dexmedetomidine infusion for awake craniotomy. *Anesthesia & Analgesia*, **92**(5), 1251–3.

Bello, L., Gambini, A., Castellano, A., et al. (2008). Motor and language DTI fiber tracking combined with intraoperative subcortical mapping for surgical removal of gliomas. *Neuroimage*, **39**(1), 369–82.

Benet, A., Hervey-Jumper, S.L., Sánchez, J.J., Lawton, M.T., & Berger, M.S. (2015). Surgical assessment of the insula. Part 1: surgicla anatomy and mosphometric analysis of the transsylvian and transcortical approaches to the insula. *J Neurosurg*, **124**(2), 469–81.

Berman, J.I., Berger, M.S., Chung, S.W., Nagarajan, S.S., & Henry, R.G. (2007). Accuracy of diffusion tensor magnetic resonance imaging tractography assessed using intraoperative subcortical stimulation mapping and magnetic source imaging. *J Neurosurg*, **107**(3), 488–94.

Bizzi, A., Blasi, V., Falini, A., et al. (2008). Presurgical functional MR imaging of language and motor functions: validation with intraoperative electrocortical mapping. *Radiology*, **248**(2), 579–89.
Black, P.M., Alexander, E. 3rd, Martin, C., et al. (1999). Craniotomy for tumour treatment in an intraoperative magnetic resonance imaging unit. *Neurosurgery*, **45**(3), 423–31.
Bogomolny, D.L., et al. (2004). Functional MRI in the brain tumour patient. *Top Magn Reson Imaging*, **15**(5), 325–35.
Chang, E.F., Potts, M.B., Keles, G.E., et al. (2008). Seizure characteristics and control following resection in 332 patients with low-grade gliomas. *J Neurosurg*, **108**(2), 227–35.
Chang, E.F., Raygor, K.P., Berger, M.S., et al. (2015). Contemporary model of language organization: an overview for neurosurgeons. *J Neurosurg*, **122**, 250–61.
Chang, S.M., Parney, I.F., Huang, W., et al. (2005). Patterns of care for adults with newly diagnosed malignant glioma. *JAMA*, **293**(5), 557–64.
De Oliveira Lima, G.L. & Duffau, H. (2015). Is there a risk of seizures in 'preventive' awake surgery for incidental diffuse low-grade gliomas? *J Neurosurg*, **122**(6), 1397–405.
Deng, X., Zhang, Y., Xu, L., et al. (2015). Comparison of language cortex reorganization patterns between cerebral arteriovenous malformations and gliomas: a functional MRI study. *J Neurosurg*, **122**(5), 996–1003.
Duffau, H. (2006). New concepts in surgery of WHO grade II gliomas: functional brain mapping, connectionism and plasticity—a review. *J Neurooncol*, **79**(1), 77–115.
Guggisberg, A.G., Honma, S.M., Findlay, A.M., et al. (2008). Mapping functional connectivity in patients with brain lesions. *Ann Neurol*, **63**(2), 193–203.
Herrick, I.A., Craen, R.A., Gelb, A.W., & Miller, L.A. (1997). Propofol sedation during awake craniotomy for seizures: patient-controlled administration versus neurolept analgesia. *Anesthesia & Analgesia*, **84**(6), 1285–91.
Hervey-Jumper, S.L. & Berger, M.S. (2014). Role of surgical resection in low- and high-grade gliomas. *Curr Treat Options Neurol*, **16**(4), 284.
Hervey-Jumper, S.L., Li, J., Lau, D., et al. (2015). Awake craniotomy to maximize glioma resection: methods and technical nuances over a 27-year period. *J Neurosurg*, **24**, 1–15.
Ille, S., Sollmann, N., Hauck, T., et al. (2015). Combined noninvasive language mapping by navigated transcranial magnetic stimulation and functional MRI and its comparison with direct cortical stimulation. *J Neurosurg*, **123**(1), 212–25.
Jakola, A.S., Myrmel, K.S., Kloster, R., et al. (2012). Comparison of a strategy favoring early surgical resection vs. a strategy favoring watchful waiting in low-grade gliomas. *JAMA*, **308**(18), 1881–8.
Knauth, M., Wirtz, C.R., Tronnier, V.M., Aras, N., Kunze, S., & Sartor, K. (1999). Intraoperative MR imaging increases the extent of tumour resection in patients with high-grade gliomas. *AJNR Am J Neuroradiol*, **20**(9), 1642–6.
Nathan, S.S., Sinha, S.R., Gordon, B., Lesser, R.P., & Thakor, N.V. (1993). Determination of current density distributions generated by electrical stimulation of the human cerebral cortex. *Electroencephalogr Clin Neurophysiol*, **86**(3), 183–92.
Nimsky, C., Ganslandt, O., Tomandl, B., Buchfelder, M., & Fahlbusch, R. (2002). Low-field magnetic resonance imaging for intraoperative use in neurosurgery: a 5-year experience. *Eur Radiol*, **12**(11), 2690–703.
Nimsky, C., Ganslandt, O., Von Keller, B., Romstock, J., & Fahlbusch, R. (2004). Intraoperative high-field-strength MR imaging: implementation and experience in 200 patients. *Radiology*, **233**(1), 67–78.
Olsen, K.S. (2008). The asleep-awake technique using propofol-remifentanil anaesthesia for awake craniotomy for cerebral tumours. *Eur J Anaesthesiol*, **25**(8), 662–9.
Ribas, E.C., Yagmurlu, K., Wen, H.T., & Rhoton, A.L., Jr. (2015). Microsurgical anatomy of the inferior limiting insular sulcus and the temporal stem. *J Neurosurg*, **122**(6), 1263–73.
Sai Kiran, N.A., Thakar, S., Dadlani, R., et al. (2013). Surgical management of thalamic gliomas: case selection, technical considerations, and review of literature. *Neurosurg Rev*, **36**(3), 383–93.
Sanai, N., Mirzadeh, Z., & Berger, M.S. (2008). Functional outcome after language mapping for glioma resection. *N Engl J Med*, **358**(1), 18–27.
Sanai, N., Polley, M.Y., & Berger, M.S. (2010). Insular glioma resection: assessment of patient morbidity, survival, and tumour progression. *J Neurosurg*, **112**(1), 1–9.
Sarubbo, S., De Benedictis, A., Merler, S., et al. (2015). Towards a functional atlas of human white matter. *Hum Brain Mapp*, **36**(8), 3117–36.
Schneider, J.P., Trantakis, C., Rubach, M., et al. (2005). Intraoperative MRI to guide the resection of primary supratentorial glioblastoma multiforme—a quantitative radiological analysis. *Neuroradiology*, **47**(7), 489–500.
Smith, J.S., Chang, E.F., Lamborn, K.R., et al. (2008). Role of extent of resection in the long-term outcome of low-grade hemispheric gliomas. *J Clin Oncol*, **26**(8), 1338–45.
Stummer, W., Reulen, H.J., Novotny, A., Stepp, H., & Tonn, J.C. (2003). Fluorescence-guided resections of malignant gliomas--an overview. *Acta Neurochir Suppl*, **88**, 9–12.
Stummer, W., Pichlmeier, U., Meinel, T., et al. (2006). Fluorescence-guided surgery with 5-aminolevulinic acid for resection of malignant glioma: a randomised controlled multicentre phase III trial. *Lancet Oncol*, **7**(5), 392–401.
Talacchi, A., Corsini, F., & Gerosa, M. (2010). Surgical approaches to tumours of the anterior gyrus cinguli. *Neurosurgery*, **66**(6), 245–51.
Taylor, M.D. & Bernstein, M. (1999). Awake craniotomy with brain mapping as the routine surgical approach to treating patients with supratentorial intraaxial tumours: a prospective trial of 200 cases. *J Neurosurg*, **90**(1), 35–41.
Thiel, A., Herholz, K., Koyuncu, A., et al. (2001). Plasticity of language networks in patients with brain tumours: a positron emission tomography activation study. *Ann Neurol*, **50**(5), 620–9.
Trinh, V.T., Fahim, D.K., Maldaun, M.V., et al. (2014). Impact of pre-operative functional magnetic resonance imaging during awake craniotomy procedures for intraoperative guidance and complication avoidance. *Stereotact Funct Neurosurg*, **92**(5), 315–22.
Wirtz, C.R., Knauth, M., Staubert, A., et al. (2000). Clinical evaluation and follow-up results for intraoperative magnetic resonance imaging in neurosurgery. *Neurosurgery*, **46**(5), 1112–20.
Xing, W.K., Shao, C., Qi, Z.Y., Yang, C., & Wang, Z. (2015). The role of Gliadel wafers in the treatment of newly diagnosed GBM: a meta-analysis. *Drug Des Devel Ther*, **9**, 3341–8.

RELATED LINKS TO EBRAIN

Anaesthetic Management of Supratentorial Tumours. https://learning.ebrain.net/course/view.php?id=1246
Assessment of the Patient with a Brain Tumour. https://learning.ebrain.net/course/view.php?id=1247

Clinical Presentation of Patients with Brain Tumours. https://learning.ebrain.net/course/view.php?id=1249

Diagnostic Imaging in Brain Tumours. https://learning.ebrain.net/course/view.php?id=931

How to Do an Image-guided Biopsy. https://learning.ebrain.net/course/view.php?id=1258

How to Do an Image-guided Craniotomy. https://learning.ebrain.net/course/view.php?id=1259

Intraoperative Chemotherapy and Radiotherapy. https://learning.ebrain.net/course/view.php?id=1241

Intraoperative Surgical Adjuncts. https://learning.ebrain.net/course/view.php?id=495

Surgical Management of High-grade Gliomas. https://learning.ebrain.net/course/view.php?id=450

Surgical Management of Low-grade Gliomas. https://learning.ebrain.net/course/view.php?id=585

SECTION 3

Tumours and skull base—extra-axial and skull lesions

14. **Meningiomas and haemangiopericytoma (HPC): solitary fibrous tumour (SFT)** *175*
Harjus S. Birk, Seunggu J. Han, Ramez W. Kirollos, Thomas Santarius, and Michael W. McDermott

15. **Chordomas and chondrosarcomas of the skull base** *189*
Rami O. Almefty and Ossama Al-Mefty

16. **Dermoid and epidermoid cysts** *197*
Andrew McEvoy

17. **Esthesioneuroblastoma** *205*
Georgios Klironomos, Lior Gonen, and Fred Gentili

18. **Malignant skull base tumours** *213*
Benedict Panizza and Adel Helmy

19. **Surgical management of tumours of the orbit** *221*
Joseph D. Chabot, S. Tonya Stefko, and Paul Gardner

20. **Skull lesions** *229*
Giorgio Gioffre and Ivan Timofeev

21. **Surgical management of anterolateral skull base lesions** *241*
Michael D. Cusimano and Michael P. Meier

14

Meningiomas and haemangiopericytoma (HPC)

Solitary fibrous tumour (SFT)

Harjus S. Birk, Seunggu J. Han, Ramez W. Kirollos, Thomas Santarius, and Michael W. McDermott

Introduction

Meningiomas were first described by Harvey Cushing in 1922 and have since been recognized as the most common intracranial non-glial tumour (Ostrom et al., 2016). These slow-growing tumours arise contiguously to the meninges and originate from arachnoidal cap cells of the leptomeninges. They have the potential of exerting pressure or, less commonly, invade the brain, spinal cord, and cranial and peripheral nerves, resulting in neurological deficits.

Depending on the location, meningiomas can produce a wide array of symptoms. Symptoms and signs can be related directly to compression of adjacent neural structures or secondary to the effects of elevated intracranial pressure. For example, if the tumour is located on the medial part of the sphenoid wing, decreased vision and eye movement paralysis may be commonplace, whereas a tumour at the posterior fossa may result in a different constellation of symptoms including hydrocephalus and dysphonia.

Epidemiology

Meningiomas account for 36.7% of all primary intracranial neoplasms (Ostrom et al., 2016). Taking into account population increases in the United States, 150 000 people currently may have a diagnosis of meningioma, with an incidence rate of 3–3.5 per 100 000 (Claus et al., 2005). Increasing meningioma incidence rates are being reported, with a more pronounced rise in elderly age groups (Klaeboe et al., 2005). This increase can be explained by the introduction of advanced imaging techniques that have allowed for thorough patient examinations, upon which incidental meningiomas are now commonly detected. Incidental findings on brain MRI are common and the prevalence largely increases with age (Morris et al., 2009). This trend is likely to continue in the future.

The risk of developing meningiomas increases with age, with the most affected age range being 40–70 years. There is a predilection for women, with a female-to-male ratio of 1.8:1 for all meningiomas and a slightly higher ratio of 2.3:1 for symptomatic meningiomas (Radhakrishnan et al., 1995). The female-to-male ratio is different for WHO grade 1 versus grade 2 and 3 meningiomas: 2.3, 1.2 and 1.1, respectively (Ostrom et al., 2016). Meningiomas are rather uncommon in children, accounting for only 1.5% of the total, and are extremely rare in infants (Kotecha et al., 2011). Interestingly, childhood meningiomas are slightly more common in males than in females, with a 1.3:1 ratio (Kotecha et al., 2011). Up to 15–25% of childhood meningioma cases are associated with neurofibromatosis type 1 (*NF2*) or type (*NF2*) (Baumgartner and Sorenson, 1996; Kotecha et al., 2011). These cases tend to occur in younger individuals with an equal female-to-male ratio.

Radiation-induced meningiomas

The risk of radiation-induced meningiomas depends upon the radiation dose and field, possible genetic predisposition and, most importantly, the follow-up given the latency period. These meningiomas include different grades and over 10% of these are multiple. The average latency period is 22.9 ± 11.4 years with shorter latency period for those of higher grades (Yamanaka et al., 2017). In one study of childhood cancer survivors receiving cranial radiotherapy, the cumulative incidence of a subsequent meningioma by the age of 40 years was 5.6% with a median interval from primary cancer to meningioma diagnosis of 22 years and increased risk correlating with increased radiation dose (Bowers et al., 2017).

Pathology

Meningiomas are thought to arise from meningothelial cells (also known as arachnoidal cap cells). Meningothelial cells are most abundant on the surface of arachnoid villi around major sinuses,

large cerebral veins, basilar plexus, crista galli, and over the basilar venous plexus, but are also found in the arachnoid membrane in all its locations and other parts of the central nervous system (Haines and Frederickson, 1991). Although frequently repeated, this is, however, only a hypothesis based on observations of striking similarity between meningothelial and meningioma cells, and of the relationship between high concentration of meningothelial cells and common locations of meningiomas (Riemenschneider et al., 2006). Very rare extradural meningiomas are thought to arise either as an entrapment of meningothelial cells or from some other 'stem-like' cell (Lang et al., 2000).

Like other brain tumours, meningiomas are graded based on their histological appearance according to the WHO Classification of the Tumours of the Central Nervous System (WHO Classification), with its last modification published in 2016 (Louis et al., 2016). The histological criteria indicating a more aggressive behaviour and an increase in the malignancy grade include frequent mitoses, regions of hypercellularity, sheet-like growth, high nuclear–cytoplasmic ratio, prominent nucleoli, and spontaneous necrosis.

Meningiomas expand and displace, but generally do not infiltrate adjacent brain or spinal cord. Invasion of the dura and skull does occur and has no significance for malignancy grading. Invasion of the skull may elicit an osteoblastic reaction. Brain invasion can occur in meningiomas of all malignancy grades and indicates a greater likelihood of recurrence, but was not considered a sufficient criterion alone to increase the malignancy grade until the 2016 edition of the WHO Classification (Louis et al., 2016; Jenkinson et al., 2017). Nevertheless, many pathologists classified meningiomas with brain invasion as atypical following the 2007 edition of the WHO Classification.

Prior to the 2000 classification meningioma grade 1 constituted approximately 90% of all meningiomas, while atypical (grade 2) approximately 5% and anaplastic (grade 3) 1–2%. Following the adoption of the 2000 WHO Classification, the proportion of grade 2 meningiomas increased to 15–35% of diagnosed meningiomas (Claus et al., 2005; Riemenschneider et al., 2006; Pearson et al., 2008). In the 2007 Classification, meningiomas with otherwise grade 1 histological features but microscopic brain invasion could be classified as atypical, which led to yet further increased proportion of atypical meningiomas (Backer-Grøndahl et al., 2012). In the population-based study by Kshettry et al., the annual incidence (per 100 000) of atypical meningiomas increased from 26–28% (2004–2006) to 30–32% (2008–2010) (Kshettry et al., 2015). Interestingly, atypical meningiomas are more common in the non-skull base locations (Backer-Grøndahl et al., 2012).

WHO grade 3 meningiomas, also sometimes referred to as malignant meningiomas are defined either by high mitotic index (more than 20 mitoses per 10 high-power fields) or by their histological appearance resembling a carcinoma, sarcoma, or a melanoma. They are the rarest grade of meningiomas, encompassing only 1–2% of newly diagnosed meningiomas (Kshettry et al., 2015). The median overall survival for patients with these tumours averages between 2 and 3 years (Sughrue et al., 2010; Perry, 2013; Champeaux et al., 2015). Even with aggressive management that likely consists of surgery and radiotherapy, local control is often unattainable and extracranial metastases may occur.

The relative frequencies of benign meningioma subtypes (**Fig. 14.1**), as reported by Backer-Grøndahl et al. (2012), are listed in **Table 14.1**. These are similar to other reported series (Perry et al., 1999; Willis et al., 2005). Distinguishing between benign subtypes of meningiomas is of little prognostic importance, however, it is helpful in differentiating meningiomas from other tumours, especially metastases. Secretory subtype can often be predicted from imaging, as these meningiomas are associated with substantial amount of oedema, which can be life-threatening (Regelsberger et al., 2009). Meningiomas may progress to a higher histological grade (approximately 50% anaplastic meningiomas progressed from lower-grade meningiomas) (Champeaux et al., 2015) and should therefore be thoroughly sampled not to miss potential areas with a more aggressive histology.

Diagnosis of atypical (**Fig. 14.2**) and anaplastic meningiomas is made primarily based on mitotic count and other 'softer' criteria listed in **Table 14.2**. However, some rare meningioma subtypes, characterized by particular tumour cell phenotypes, are associated with more frequent recurrence and are automatically (regardless of the presence of aforementioned histological 'features of malignancy') graded as WHO grade 2 (chordoid and clear cell) or WHO grade 3 (papillary and rhabdoid) meningiomas. However, rhabdoid meningiomas are no longer automatically classified as grade 3, but instead those that lack malignant histological features should be classified as any other meningiomas as they seem to be running a course resembling the normal meningioma grades (Louis et al., 2016).

Molecular tumour cell biology

Meningiomas were one of the first solid tumours in humans to be shown to have consistent chromosomal abnormalities and the loss of one copy of chromosome 22 was identified as early as 1972 (Mark et al., 1972). The fact that the second most common tumour in neurofibromatosis type 2 (*NF2*) patients was meningioma, pointed to the *NF2* gene as a target on chromosome 22 (Rouleau et al., 1993; Trofatter et al., 1993). *NF2* is a textbook example of a tumour suppressor gene following Knudson's two-hit hypothesis, where the first hit (loss of one allele) is usually a loss of heterozygosity and second hit is either a loss (deletion) or inactivating (usually a missense) point mutation. *NF2* gene was subsequently found to be mutated in 40–60% of sporadic meningiomas (Ruttledge et al., 1994; Riemenschneider et al., 2006). The *NF2* gene codes for merlin, also known as neurofibromin 2, a membrane cytoskeleton protein. This protein has been shown to be involved in the control of cell growth and motility in culture (Shaw, 2001; Lallemand, 2003). Genetically engineered mice with only one wild-type allele have been shown to develop many tumour forms (McClatchey et al., 1998) while tissue specific inactivation in Schwann cells or leptomeningeal cells resulted in schwannoma or meningioma formation, respectively (Giovannini et al., 2000; Kalamarides et al., 2002).

Numerous reports have been published confirming the important role of *NF2* mutation in meningioma. Using new generation sequencing techniques, three papers published in January 2013 discovered several other genes that are likely important in meningiomas, especially those with wild-type *NF2* (Brastianos et al., 2013; Clark et al., 2013; Reuss et al., 2013). The Clark et al. (2013) and Brastianos et al. (2013) studies have identified mutations in two well-known cancer genes, *SMO* and *AKT1*, both of which were mutually exclusive and exclusive of *NF2* mutations. The frequencies of *SMO* and *AKT1* mutations were, 5% and 10–15%, respectively. Clark et al

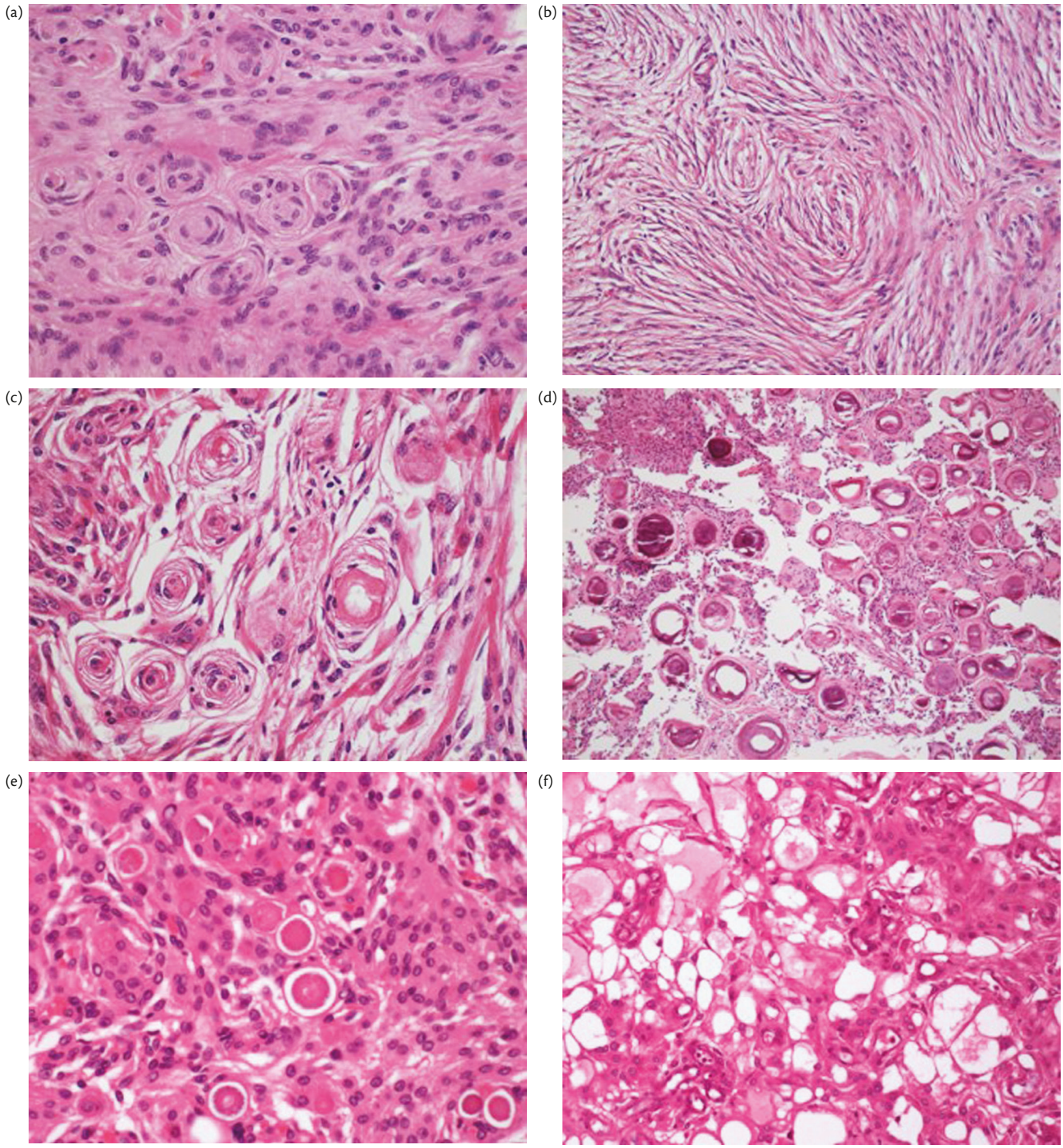

Fig. 14.1 Grade I meningioma–examples of histological subtypes. (A) Meningiotheliomatous meningioma—oval nuclei, a pseudosyncytial cytoplasm, and frequent whorls characterize the meningiotheliomatous meningioma.
(B) Fibroblastic meningioma—spindle-shaped cells arranged in fascicles, often with intervening collagen, are features of fibroblastic meningioma.
(C) Transitional meningioma—perhaps most meningiomas display an admixture of meningothelial and fibroblastic patterns: the so-called transitional meningioma.
(D) Psammamatous meningioma—although present in the vast majority of meningiomas, spherical laminated calcified concretions, known as psammoma bodies, dominate the histology of this subtype that is often encountered in the region of the thoracic spinal cord.
(E) Secretory meningioma—numerous round, eosinophilic 'secretory bodies' characterize this grade I subtype that is often associated with large amounts of cerebral oedema on MRI.
(F) Microcystic meningioma—a cobweb-like, microcystic architecture exemplifies this grade I subtype, which, like the secretory subtype, can be associated with disproportionate cerebral oedema. The glistening cut surface of this subtype gave the entity its old-fashioned name of 'humid meningioma'.
Courtesy of Dr Kieren Allinson, Department of Pathology, Addenbrooke's Hospital, Cambridge.

Table 14.1 Relative frequencies of meningioma subtypes

WHO grade	Histological subtype	Approximate proportion (%)
Benign (70–80%)		
	• Meningothelial	17
	• Fibrous (fibroblastic)	7
	• Transitional (mixed)	40
	• Psammomatous	1
	• Angiomatous	1
	• Microcystic	1
	• Secretory	1
	• Lymphoplasmacyte-rich	1
	• Metaplastic	1
Atypical (20–30%)	20–30	
	• Atypical	29
	• Chordoid	
	• Clear Cell	1
Malignant (1–2%)	1–2	
	• Anaplastic	1
	• Papillary	
	• Rhabdoid	

Reproduced with permission from Thomas Backer-Grondahl, Bjornar H Moen, Sverre H Torp, The Histopathological Spectrum of Human Meningiomas. *International Journal of Clinical and Experimental Pathology*, Volume 5, Issue 3, pp. 231–42. Copyright © 2012.

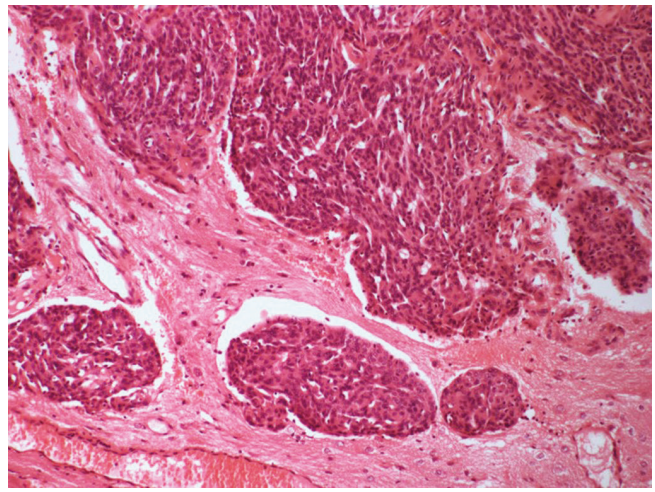

Fig. 14.2 Atypical meningioma—invasion of the meningioma into brain tissue, as seen here, would qualify this meningioma as atypical and therefore WHO grade II. Other features associated with grade II meningioma include necrosis and increased mitotic activity.

Courtesy of Dr Kieren Allinson, Department of Pathology, Addenbrooke's Hospital, Cambridge.

also reported mutations of TRAF7, which has previously not been linked to cancers (24% of all tumours), and in 10% of *KLF4*, a gene that promotes reprogramming of pluripotent stem cells from terminally differentiated somatic cells (Clark et al., 2013). These investigators also reported that *AKT1* mutations can co-occur with those of TRAF7, but not with those of *KLF4*. *NF2*-mutated meningiomas were found to have more genomic rearrangement than *NF2*-wild type, suggesting that there is greater genomic instability in tumours with *NF2* mutations.

Mutations in all these genes appear to segregate with different histological subtypes and tumour locations. Reuss et al. have observed *KLF4* mutation in 30/30 and TRAF7 mutation in 29/30 secretory meningiomas (Reuss et al., 2013). While *KLF4* mutations were exclusively seen in secretory meningiomas, TRAF7 mutations were also seen in 8% of non-secretory meningiomas. Meningiomas that occur due to *NF2* mutations tend to be transitional or fibroblastic, while those with SMO and *AKT1* mutations tend to be predominantly of meningothelial subtype (Brastianos et al., 2013; Sahm et al., 2013). Little is known about the genetic bases of meningioma progression to more malignant grades. It seems, however, that higher-grade meningiomas have a greater number of mutations, probably stemming from higher genomic instability (Weber et al., 1997; Brastianos et al., 2013; Clark et al., 2013). When skull base meningiomas were considered, SMO- and *AKT1*/TRAF7-mutated meningiomas were found located in the midline, with KLF/TRAF7 meningiomas, in addition to midline, also occupying more lateral middle cranial fossa. *NF2*-mutated meningiomas were generally more posterior and lateral (Clark et al., 2013). Meningiomas occurring in association with Schwannomatosis disease, which is caused by germline SMARCB1 mutations, are predominantly found in the falx cerebri (van den Munckhof et al., 2012).

Cases with more than one meningioma, but no other clinical features of *NF2* or Schwannomatosis, may arise because of independent sporadic tumours (Butti et al., 1989), mosaic *NF2* with no mutation identified in the blood (Evans et al., 2005), or clonal spread of a single sporadic tumour (Larson et al., 1995; Stangl et al., 1997). The identification of different *NF2* mutations in each tumour indicates that the tumours arose independently. Identical, biallelic *NF2* mutations in each tumour indicates mosaic *NF2* or clonal spread. Identical somatic mutations in other genes or X-inactivation of the same X chromosome (Evans et al., 2005) indicates clonal spread of a single tumour. Rare families also exist with a history of meningiomas, inherited in an autosomal dominant fashion, outside of the context of *NF2* disease (Aavikko et al., 2012; Smith et al., 2013).

Table 14.2 Comparison of World Health Organization (WHO) grade II and III meningioma criteria

Grade 2	Atypical	4–19 mitotic figures/10 HPF or	**Brain invasion or 3 of the following histologic features:** - Increased cellularity - Small cells w/high N/C ratio - Large, prominent nucleoli - Patternless, sheet-like growth - Foci of geographic necrosis
Grade 3	Anaplastic	20 or more mitotic figures/10HPF or	- Frank sarcomatous or carcinomatous histology

Meningioma receptors

Meningioma growth rates are known to be influenced by sex hormones levels such as during pregnancy and with exogenous agents such as the antiandrogen cyproterone acetate. Although progesterone receptors are expressed in up to 70% of meningiomas, attempts of controlling these by antiprogesterone agents, such as mifepristone (RU 486), have not so far proven effective in clinical practice (Cossu et al., 2015; Ji et al., 2015). Currently other agents, such as somatostatin analogues and antiangiogenesis factors, are being investigated to determine their therapeutic role. Octreotide, a somatostatin analogue, targeting the expression of somatostatin receptor subtype 2 (SST2) resulted in decreased proliferation rates in meningiomas *in vitro* but did not induce apoptosis (Graillon et al., 2017).

Simpson grading

An original scheme for grading of the degree of resection of meningiomas was described by Donald Simpson in 1957 (Simpson, 1957). This scale consists of five grades and correlates degree of surgical resection with recurrence of symptoms (Table 14.3). The completeness of surgical removal has consistently been identified as an important prognostic feature (Kallio et al., 1992; Condra et al., 1997; Stafford et al., 1998; Pollock et al., 2012; Heald et al., 2014) although its relevance has been questioned (Sughrue et al., 2010; Rogers et al., 2015). Clearly, the aim of complete resection has to be balanced against the risks of mortality and morbidity and its effects on quality of life of individual patients.

Treatment: Roles of surgery and radiotherapy

When considering treatment for meningiomas, factors to be taken into account include the presence of symptoms, growth pattern, and proximity to sensitive neurovascular structures. Compression, invasion, or oedema of these structures caused or likely to be caused by the tumour and its time frame on one hand and the damage to these structure by the available treatment options on the other are balanced against each other. As recommended by the National Comprehensive Cancer Network guidelines, incidental, asymptomatic meningiomas behave with less aggression and may be managed with observation (Sughrue et al., 2010; Chamoun et al., 2011). With larger, symptomatic meningiomas it is important to consider surgery or other definitive management options, including radiotherapy, once tumour grade is determined. For patients seeking definitive therapy the standard treatment is complete resection, although numerous subsets of patients have not been successfully maintained by surgery alone. In addition, resection by itself is often not feasible if the meningioma is not separable from eloquent anatomy. It is well known that the potential for recurrence exists whether following subtotal resection (STR) or gross-total resection (GTR), and therefore the utilization of multimodal therapy for meningioma treatment has been explored extensively (Stafford et al., 2001; Soyuer et al., 2004).

Table 14.3 Original Simpson grading scheme for meningiomas

Grade 1	GTR, dural attachment excision	9% symptomatic recurrence at 10 years
Grade 2	GTR, dural attachment coagulation	19% symptomatic recurrence at 10 years
Grade 3	GTR, w/o resection or coagulation of dural attachments	29% symptomatic recurrence at 10 years
Grade 4	Partial tumour resection	44% symptomatic recurrence at 10 years
Grade 5	Simple decompression, with or w/o biopsy	100% symptomatic recurrence at 10 years

Reproduced with permission from Donald Simpson, The Recurrence of Intracranial Meningiomas After Surgical Treatment, *Journal of Neurology, Neurosurgery & Psychiatry*, Volume 20, Issue 1, pp. 22–39, Copyright © 1957 BMJ Publishing Group Ltd.

Among grade 1 meningiomas, gross-total resection remains the surgical objective and has been achieved in one-half to two-thirds of patients in surgical series (Mirimanoff et al., 1985; Pollock et al., 2012). Among benign meningiomas, subtotal resection carries higher rates of progression. For instance, one study revealed that patients who underwent STR alone for benign meningiomas experienced a 15-year survival rate of 51%, much inferior to the 88% for patients who had a GTR (Condra et al., 1997). Radiation therapy for grade 1 meningiomas is commonly supported as an adjunct to STR as a preventative measure against recurrence, specifically in cases in which tumour location is near the optic nerve sheath or cavernous sinus where surgically accessibility may be limited. Reoperation for all but the larger recurrent tumours in these areas can be a difficult, if not an impossible task to complete, with considerable risks and the low likelihood of complete resection. The senior author has abandoned the idea of reoperation for small recurrences around the optic apparatus (anterior clinoid process, tuberculum, diaphragm). Studies revealed that in these cases radiation therapy achieved long-term control in 68% to 100% of WHO grade 1 meningiomas at 5 and 10 years postoperatively (Pollock et al., 2012; Santacroce et al., 2012).

For grade 2 meningiomas, there is consensus among neurosurgeons that STR alone is insufficient treatment. One study reported a 10-year local control rate of only 17% following STR of atypical meningiomas (Goyal et al., 2000). It is recommended that after STR radiotherapy or stereotactic radiosurgery (SRS) be performed to manage residual tumour for grade 2 meningiomas. In a systematic analysis of 619 subtotally resected atypical meningiomas, the 5-year recurrence rate was 53.3% for those receiving adjuvant SRS vs. 89.9% with serial surveillance only, a significant difference suggesting the potential benefit of adjuvant therapy (Lagman et al., 2017). Currently most North American and British neurosurgeons observe atypical meningiomas after Simpson grade 1 and 2 GTR. However, it has to be taken to consideration that the clinical impact of recurrence in grade 2 meningioma is usually more significant than in grade 1 meningiomas (Marcus et al., 2008). Various forms of radiation therapy may be implemented for grade 2 meningiomas following STR, such as SRS and fractionated external beam radiation therapy (EBRT). Studies have indicated that the timing of radiotherapy may play a key role in improving local control. For example, Choi et al. revealed that SRS within 6 months after STR dramatically improved local tumour control (Choi et al., 2010). Multisession SRS is also

recommended for atypical meningiomas, especially for sensitively located tumours (Choi et al., 2010). Kaur et al performed a systematic review examining the role radiotherapy in grade 2 and grade 3 meningiomas (Kaur et al., 2014). Although they have observed the trend towards clinical benefit with adjuvant radiation therapy, the lack of statistical significance is likely a result of small sample sizes, limiting the statistical power to detect any differences between groups. Trials to further clarify the role of radiotherapy in the treatment of meningioma grade 2 meningiomas are being conducted (Jenkinson et al., 2015).

For patients with recurrent meningiomas or newly diagnosed WHO grade 3 (malignant) meningiomas, surgery followed by high-dose EBRT is the first-line therapy. Recurrence has been shown to correspond with extent of resection, and therefore aggressive GTR surgery is often pursued for these malignant tumours when a clear plane between tumour and normal surrounding tissue is identified (Sughrue et al., 2010; Sughrue, Sanai, et al., 2010). A recent paper retrospectively analysed 37 patients who were treated for anaplastic meningiomas and concluded that aggressive GTR conferred an overall survival advantage (Moliterno et al., 2015). Although no randomized trials exist documenting the efficacy of surgery and radiotherapy in malignant meningiomas, retrospective studies have reported measurable benefits of multimodal therapy for grade 3 meningiomas (Moliterno et al., 2015). Furthermore, among these tumour types it has been shown that if radiotherapy is used, higher doses may significantly improve local tumour control (Milosevic et al., 1996; Rogers et al., 2015). Magill et al have reported their experience with ^{125}I brachytherapy treatment of 14 atypical and 28 malignant meningiomas after all other means of treatment were exhausted (Magill et al., 2016). The median survival after the diagnosis was 11.1 and 9.1 years for the respective histological types. Despite associated complications that included radionecrosis (16%), wound breakdown (12%) and infection (6%), these results compare favourably with historical cohorts, and constitute a valid treatment option for patients with high-grade meningiomas.

Special considerations for specific meningiomas

The common locations for meningiomas are parasagittal, sphenoid wing, and the convexity.

Parasagittal meningiomas

Parasagittal meningioma arise from the dura of the superior sagittal sinus (SSS). They are the most prevalent group, making approximately a quarter of all intracranial meningiomas. The middle third of the SSS harbours over 50% of parasagittal meningiomas, while the anterior third somewhat more than the posterior third. The incidence of meningiomas by location most probably reflects the distribution of density of arachnoid cap cells within the body.

The understanding of the anatomy and flow dynamics of SSS, bridging veins, emissary veins, and their collaterals is fundamental to management of and surgery in patients with parasagittal meningiomas. Therefore, not only static structural imaging, but often digital subtraction angiography is required. The consequences of venous compromise caused by surgery range from temporary asymptomatic through symptomatic cerebral oedema, reversible neurological deficit caused by venous infarction, haemorrhagic transformation of venous infarction to malignant brain swelling with the potential of severe permanent neurological deficit and mortality. In some cases, it may be appropriate to treat symptoms and signs associated with obstruction of venous outflow by venous stenting (Higgins et al., 2008; Ganesan et al., 2008).

Similarly to patients with meningiomas in other location, management of patients with parasagittal meningiomas ought to be based on considerations related to the patient (e.g. social functions, occupation, hobbies, age), the tumour (e.g. anatomical location, size, speed of growth, presence of calcifications) and its effect on the surrounding tissues (e.g. brain oedema, SSS narrowing/occlusion, presence of venous collaterals), as well as all other available treatment options (surgery, fractionated radiotherapy, SRS, and venous stenting).

Most commonly Simpson grade 2 is achieved, but in some cases residual tumour invading the wall or lumen of the SSS may have to be left behind. For these, adjuvant radiation treatment either at the outset or after progression on radiological surveillance should be considered on an individual basis. Although opening of the SSS to remove intraluminal meningioma extension followed by suturing or patching is possible, it is liable to failure with thrombosis and has serious consequences, particularly if attempted on the posterior third of the SSS. Most surgeons, including the authors, advocate resection of the SSS only in the presence of completely occluded SSS with well-established collaterals. These may include venous channels in the falx and tentorium as well as emissary veins. Careful preoperative studies of these collaterals and their preservation at surgery is essential. Regrowth or recurrence that results in gradual and eventually total occlusion of the SSS would be amenable to a more radical resection at the second surgery.

Falcine meningiomas

Some 9% of intracranial meningiomas arise from the falx. Unlike parasagittal meningiomas, which tend to have bridging veins running deep to them, some falcine meningiomas extend deep into the hemispheres with compression of the pericallosal arteries and the corpus callosum and have bridging veins running over them. In fact, in the majority of cases upon opening of the dura the tumour is not visible, instead one can see the convexity brain overlying it. Falcine meningiomas can be unilateral or bilateral with varying proportions of tumour bulk on respective sides. For complete surgical removal, when indicated, resection of the falcine origin is recommended, but preservation of important dural venous channels needs to be ensured, especially if the SSS is also compromised. Given that these tumours tend to grow 'into the brain', it may, in some unilateral cases, be advantageous to approach them from the contralateral side to avoid excessive brain retraction and manipulations, disturb the overlying bridging veins and gain early control of the falcine blood supply. Patients with tumours adjacent to the supplementary motor cortex may suffer transient postoperative hemiparesis and mutism.

Convexity meningiomas

Fifteen per cent of intracranial meningiomas arise from the convexity. They compress adjacent brain and their blood supply comes primarily via meningeal arteries. Like in other locations, large, rapidly growing, grade II and III and secretory type meningiomas

are usually associated with perilesional oedema, which usually indicates disruption of the pial surface. These tumours tend to recruit additional cortical blood supply (Alvernia and Sindou, 1994). Venous flow obstruction by stretching adjacent cortical veins can, in its own right, be the cause of, or contribute to the surrounding oedema.

On postcontrast imaging, the majority of meningiomas are seen to have a 'dural tail', a tapered extension of contrast along the meninges away from their attachment. Clusters of meningiotheliomatous cell aggregates were shown to extend onto the surrounding dura at varying distances from the main meningioma attachment (Borovich and Doron, 1986). As recurrences tend to appear at the resection margins, Kinjo et al. advocated grade 0 resection where an additional cuff of 2 cm of circumferential dura is excised around the tumour (Kinjo et al., 1993). Given the relative ease of achieving Simpson grade 1 or even grade 0 resection in the high proportion of convexity meningiomas, surgical cure is more likely in this group of meningiomas than those in other locations. However, this does not mean that each convexity meningioma ought to be treated surgically at first presentation. For example, small incidental meningiomas in older people frequently become static and non-progressive and do not require treatment.

Sphenoid wing meningiomas

Sphenoid wing meningiomas (SWM) make up 10–20% of intracranial meningiomas. They are often discussed as either lateral (LSWM) or medial sphenoid wing meningiomas (MSWM) and there are quite different considerations associated with each group, especially as surgery and prognosis is concerned. A special group of meningiomas with predominantly intraosseous component involving the greater sphenoid wing, called spheno-orbital meningiomas (SOM), will be discussed separately.

Lateral sphenoid wing meningiomas

Management and surgery of meningiomas arising from the lateral sphenoid wing are similar to that of convexity meningiomas. Bone involvement and *en plaque* tumours seem to be relatively common in this group of meningiomas and require special considerations. Some have wide *en plaque* extension along the middle fossa which can be challenging to excise, especially in the proximity of the skull base neural exit foramina. Underlying hyperostotic bone has been shown in most cases to contain tumour cells within the bone lamellae and to achieve complete resection the inner table or the entire bone width, of if the outer table is also affected, should be drilled extradurally at the beginning of the resection. To minimize the risk of recurrence very large craniotomy flaps are required and affected meninges ought to be resected.

Medial sphenoid wing and clinoidal meningiomas

As a group, medial SWMs are more challenging to manage, especially because of their proximity and potential involvement with neurovascular structures as well as invasion of the cavernous sinus. Extension into the middle cranial fossa can sometimes continue extracranially to the infratemporal fossa through the neural foraminae and skull base. Cavernous sinus involvement varies from being in the lateral wall to being extensively within the sinus ('holocavernous'). To avoid surgical morbidity these residual extensions are best dealt with SRS, if indicated (i.e. to ameliorate symptoms or to progressive growth). In some cases a more extensive skull base approaches, such as the fronto-temporal-orbitozygomatic approach, are needed. (See also Chapters 21 and 27 for operative approaches.)

Meningiomas with predominant origin at the anterior clinoid process (ACP) termed clinoidal meningiomas may extend to the suprasellar region and/or through the anterior tentorial hiatus to the prepontine and ambient cisterns. They have a tendency to encase the origin of the internal carotid artery. In most cases an arachnoidal plane is present between the tumour and surrounding neurovascular structures, but some meningiomas are adherent to the adventitia and some residual tumour may have to be left behind. Similarly, other structures, such as the internal carotid artery (ICA) branches, proximal A1 and M1 segments of the anterior and middle cerebral arteries, optic nerve, and chiasm, oculomotor nerve, and the pituitary stalk can be fused with the meningioma and, rarely, even course within the tumour. In these cases identification of the distal middle cerebral artery branches at the superior pole of the meningioma by widely splitting of the Sylvian fissure would safely identify in a retrograde fashion the course of the arteries. It is important to consider and spare the lenticulostriate branches as these are the most vulnerable. Frequently there is extension into the superolateral segment of the optic canal which should be explored in cases with visual compromise even if not readily visible on preoperative imaging. If the ipsilateral optic nerve and chiasm is surrounded by tumour, a subfrontal trajectory to identify the contralateral optic nerve, again, helps decompression of the chiasm and optic nerve in a retrograde fashion thus facilitating the preservation of its blood supply which is predominantly via the superior hypophyseal arteries.

Spheno-orbital meningiomas

SOMs make up around 5% of intracranial meningiomas, but the numbers published in the literature are very much dependent on the exact definition of this group. SOMs are frequently indolent and do not require intervention if vision is preserved, are not growing, or severe visual compromise with optic atrophy has already been established. The major indications for surgery are potential or incipient optic nerve compromise, proptosis, or for cosmetic reasons.

Although the extent of the tumour varies widely, they tend to be confined to the sphenoid bone with its greater wing forming a large part of the lateral orbital wall and extend to the floor of the middle fossa and its foraminae (rotundum, ovale, and spinosum) as well as the superior orbital fissure. This is located between the lesser and greater wing and is separated medially from the optic canal by the optic strut linking the ACP to the body of the sphenoid bone. The squamous temporal bone can also be involved. The soft tissue component can involve the intracranial compartment as well as the orbit and can grow down to the infratemporal fossa or deep to the temporalis muscle. The intracranial component is variable, ranging from an *en plaque* extension to a distinct intracranial mass. Image-guidance on bone window settings facilitates radical resection of involved bone (Marcus et al., 2013). The stages of resection are extradural followed by intradural excision. The aim is to decompress the optic canal and orbit whenever involved and this may require a 'tailored' clinoidectomy. Residual tumours in the orbital apex or involving the cavernous sinus may require radiation treatment if progressive.

Anterior cranial fossa meningiomas

Olfactory groove meningiomas

10–15% of intracranial meningiomas are classified as olfactory groove meningiomas (OGM). They originate in the midline between the crista galli and the fronto-sphenoid suture behind which the anterior fossa floor continues as planum sphenoidale. OGMs can reach large sizes at the time of diagnosis with the majority of patients being anosmic and exhibiting varying degrees of cognitive dysfunction. Occasionally they may present with a classic Foster–Kennedy syndrome consisting of anosmia, optic atrophy in one eye and papilloedema in the other. For large lesions, a frontal transbasal approach with a supraorbital osteotomy or its modifications allows early control of its blood supply which is predominantly from the anterior ethmoidal artery and the placement of a pericranial flap to repair the skull base after cranialization of the frontal sinus and drilling of the hyperostotic bone at their origin. Frontolateral approaches allow early identification and protection of posterior neurovascular structures, such as anterior cerebral arteries and optic nerves. (See also Chapters 21 and 27 for operative approaches.)

Planum sphenoidale and tuberculum sellae meningiomas

Between 5 and 10% of intracranial meningiomas are classified as planum sphenoidale (PSM) or tuberculum sellae meningiomas (TSM). Arbitrarily, the tumours originating anteriorly to the limbus sphenoidale are termed PSMs, whereas those originating posteriorly to the limbus are called TSMs. The origin of TSM may be at the tuberculum sellae itself, the chiasmatic sulcus, or the diaphragma sellae, the latter sometimes referred to separately as diaphragma sellae meningiomas. The exact origin of large meningiomas in this region cannot always be established, but given the relationship between their site of origin and the optic apparatus, TSMs tend to elevate, while PSMs depress the optic chiasm. The location of hyperostosis on the computed tomography (CT) scan can also hint the site of origin.

The main indication for surgery is visual preservation. Despite the close proximity to the pituitary gland and stalk, pituitary function is almost always preserved preoperatively, which is in contrast to other lesions in that region. It is important to appreciate the frequency of extension into the optic canals regardless of the preoperative radiological appearance (Sughrue et al., 2015; Nimmannitya et al., 2016). Lesions that are small or extending into the sphenoid sinus with absence of vascular encasement on MRI and not extending laterally to the carotid may be considered for extended endoscopic endonasal approaches, especially if they are of soft consistency. This may, to an extent, be predicted by a bright signal on T2-weighted MRI sequence. The pterional approach allows to deal with further extensions into the interpeduncular cistern and around the internal carotid artery, but will likely involve a degree of manipulation of the ipsilateral optic nerve and the area medial to the nerve could be a blind spot. The anterior interhemispheric approach rather than subfrontal can preserve olfaction more readily and avoid manipulations of the optic nerves, but a retroclival extension, especially with a prefixed chiasm, is a blind spot. (See also operative approaches in Chapters 21 and 27.)

Tentorial meningiomas

Different surgical approaches are required based on the wide-ranging locations and extensions of meningiomas arising from the tentorium. Resection of the tentorial attachment is desirable whenever possible to achieve complete resection, but one has to bear in mind potentially vital venous drainage from the deep brain structures and its variability.

This is especially important around the falcotentorial junction and the torcular (see next). Anteriorly located supratentorial meningiomas are approached via the trans-Sylvian or subtemporal approaches trying to minimize brain retraction. Early opening of the cisterns and cerebrospinal fluid egress is desirable, but it may not be readily achievable at the very start of the exposure. Insertion of a lumbar drain is generally not safe, especially for large lesions with brain oedema. Particular attention should be given to preserving the integrity of the trochlear nerve at the tentorial hiatus.

The occipital interhemispheric approach exposes falcotentorial tumours and the occipital transtentorial approach is used for those extending to the pineal region and posterior central tentorial hiatus. (See also Chapter 37 for operative approaches.) Large lesions may require a combined supra- and infratentorial approaches with preservation of the transverse sinus whenever possible. Preservation of patent straight sinus and the deep veins is most important and may necessitate leaving residual tumour. Posterior fossa lesions which are supracerebellar and may extend to the cerebellopontine angle as well as petrotentorial meningiomas are approached via a suboccipital craniotomy. They tend to displace rather than directly involve the cranial nerves.

Petroclival meningiomas

Albeit relatively rare (approximately 2% of intracranial meningiomas) these are one of the most challenging lesions to manage. Several of these meningiomas are static or demonstrate slow growth rate, especially in older age, and most of those with no or minimal symptoms are best observed, with surgery advocated only if progressive. The origin of the petroclival meningiomas is centred at the petroclival junction medial to the internal auditory meatus and posteriorly to the Meckel's cave. True clival meningiomas arise from medial to the sixth nerve and may extend to the cavernous sinus.

Both clival and petroclival meningiomas can grow into a substantial volume before becoming symptomatic. At this stage they often extend to the cavernous sinus and tentorium with invasion of the Meckel's cave. The morbidity of radical resection is related to cranial nerve dysfunction with the sixth nerve being particularly vulnerable. A signal change in the brainstem on FLAIR sequences of preoperative MRI indicates disruption of the pial surface. In these cases adhesion to the brainstem and its vascular supply is to be expected, and subtotal resection is advised. The serious nature of the neurological deficits that may arise from the cranial nerves, vessels and brainstem has shifted the practice towards more conservative surgery aiming to minimize neurological deficit and maintaining quality of life. (See also Chapter 24 for operative approaches.)

Foramen magnum meningiomas

Foramen magnum meningiomas (FMM) are rare and constitute only some 2% of all intracranial meningiomas. The most popular definition places their origin from meninges between the upper border of the arch of C2 and the junction of the lower and the middle

third of clivus, laterally extending to the jugular tubercle. Early presentation with neurological deficits from neural compression is usual, although diagnosis is commonly delayed. This is mostly because of similarity with symptoms of commoner conditions affecting musculoskeletal and nervous system in this region. Cruciate paresis, also known as hemiplegia cruciata, is often mentioned in the context of more anteriorly placed FMMs, but in practice it is rarely encountered.

The location of the meningioma, circumferentially (posterior *vs.* posterolateral *vs.* anterolateral *vs.* anterior) as well cranio-caudally (intracranial extension *vs.* spinal extension), dictates the surgical approach. For the more anterior locations a far lateral approach is ideal. However, the need and degree of the condylar resection (transcondylar approach) should be tailored to the location and size of the lesion. Even modestly sized meningiomas often create a sufficient surgical corridor by displacing the medulla and spinal cord thus obviating the need for condylar resection. However, transcondylar approach may be necessary for a small anterior lesion. For those extending mainly to the upper cervical canal and foramen magnum at the level of the C1 tubercle, condylar resection is not needed. Tumours with superior extension up to the jugular foramen often have the jugular tubercle obscuring the view of the tumour. The attachment just medial to the dural entry of the vertebral artery (VA) poses another difficulty with the VA obscuring this attachment. Releasing the first denticulate ligament which separates the spinal accessory nerve from VA as it enters the intradural space, opens the surgical window wider onto the anteriorly placed meningiomas. In many cases where the dural origin is not resected a persistent enhancing dural base on postoperative MRIs tend to be stable in the long term. *(see also Chapter 31 for operative approaches).*

Intraventricular meningiomas

Intraventricular meningiomas are very rare, constituting 1–3% of all intracranial meningiomas. They are thought to originate from meningeal cell rests within the choroid plexus. Many of the rarely reported paediatric meningiomas are intraventricular. They are discussed in Chapter 35.

Calvarial meningiomas

Although these meningiomas can be purely intraosseous, many have intracranial extensions as minor durally based lesions. The indications for surgery are usually cosmetic and diagnostic (to differentiate from other pathologies, such as metastases). An intraoperatively tailored or a preformed image-guided cranioplasty is usually completed at the time of resection. Calvarial meningiomas located over the sinuses, such as the superior sagittal sinus, could be challenging.

Multiple meningiomas

These can be seen in 1–9% of meningiomas, occurring more frequently in females and do not necessarily indicate association with *NF2* syndrome (Terrier and François, 2016). They can arise at different times. Multiple lesions may be seen with radiation-induced meningiomas.

Case for and against preoperative embolization of meningiomas

During the past few decades, rapid technological advancements in microcatheters and embolization treatments have led to the adoption of these techniques for preoperative management of meningiomas with the goal of a safer resection. Currently this is a controversial issue, and analysis of the published literature makes the case for and against preoperative embolization of meningiomas.

The first-line treatment for symptomatic meningiomas growing over time is surgical resection. However, resection may be hindered by tumour location if proximal to eloquent brain regions or structures as well as limited accessibility. Other factors that may prevent adequate tumour removal include tumour hypervascularity and dural venous sinus involvement. Embolization can reduce the tumour blood supply and ease resection by curtailing operative time and intraoperative blood loss (Gruber et al., 2000; Dowd et al., 2003). However, some surgeons believe that the benefits of preoperative embolization do not outweigh the risks. For instance, reports exist of excessive blood loss, subarachnoid haemorrhage, and retinal emboli following embolization of meningiomas (Hayashi et al., 1987; Raper et al., 2014). Other potential complications include inadvertent embolization of cerebral arteries through anastomoses of the ECA branches to the ICA (Raper et al., 2014). In 2000 a group compared two groups of 30 patients each, one who underwent preoperative embolization and the second group who did not (Bendszus et al., 2000). It was concluded that there was no effect on blood loss nor haemostasis during resection, and there was one permanent neurological deficit caused by the embolization.

Limited consensus has been reached defining the role of preoperative embolization for intracranial meningiomas. A recent systematic review in 2013 analysed 36 studies comprising 459 patients who had undergone this procedure prior to meningioma resection. Among these patients, 4.6% (21/459) had reported complications that were a direct result of the embolization. Incidence of major complications among these 21 patients was 4.8% (1/21), with the mortality rate double that at 9.5% (2/21). Therefore, it can be stated that preoperative embolization for meningiomas carries risks of significant morbidity and mortality. However, these risks can be limited with meticulous selection of patients in whom this procedure would be of the most benefit. Further prospective studies that analyse the role of preoperative embolization will likely elucidate the benefits and risks of this procedure among certain meningioma types.

Prognosis

Residual tumour, histological grade and, likely, biological (genome, transcriptome and methylome) factors determine the risk of recurrence. When considering prognosis of meningiomas, it is crucial to analyse the WHO grade of the tumour as well as what mode of therapy was undertaken, and whether surgery alone was performed or also radiotherapy. Benign meningiomas are slow-growing and have a 5% 5-year recurrence rate following gross-total resection

(Riemenschneider et al., 2006). Atypical meningiomas have a 5-year recurrence rate of 40%. Anaplastic WHO grade 3 meningiomas have a recurrence rate of 80%, double that of grade 2 and 16-fold greater than that of grade 1 meningiomas (Choy et al., 2011). Among patients who underwent multimodal treatment, the 5- and 10-year survival rates for atypical and anaplastic meningiomas were 95% and 79%, and 64% and 35%, respectively (Palma, 1997). A major clinical factor in recurrence is extent of resection. Patient age, location, and other tumour factors will influence the decisions related to the degree of resection. Again, depending on age and a number of other factors the decision between radiological surveillance or adjuvant radiation, including SRS for localized residual or recurrence, is made on individual basis.

Controversy: Management and follow-up of incidental meningiomas

Decision-making in the management of incidental meningiomas depends on multiple factors such as age, size, location, potential morbidity of the treatment and its effectiveness at the time of discovery and later on, as well as the psychological impact of knowledge of the diagnosis on the patient. The indications ought to be considered on an individual basis and guidelines, despite of good intentions, may be a step backwards by offering coarse treatment packages rather than bespoke, refined, and flexible personal treatment plans. For example, the proximity of the tumour to important structures, such as cranial nerves, may an important factor to indicate treatment prior to the onset of potentially irreversible deficit in one patient, but it may be a reason to adopt conservative management in another patient to whom the potential morbidity from surgery is not acceptable at that time. The growth rate is variable and on many occasions is non-linear. Therefore, for those managed with radiological follow-up a robust, ideally, volumetric assessment over time should be adopted.

Haemangiopericytoma (HPC)-solitary fibrous tumour (SFT)

Although not a meningioma, haemangiopericytoma-solitary fibrous tumour (HPC-SFT) is discussed in this chapter as these tumours resemble meningiomas and for that reason, in the past, some of them were classified as meningiomas and haemangiopericytomas (HPCs). In fact, HPCs were generally classified as angioblastic meningiomas until 1954 when Begg and Garret reported the first meningeal HPC (Begg and Garret, 1954). In other parts of the body HPCs were increasingly classified as solitary fibrous tumours (SFTs), however until recently in the CNS they were kept separate, not least because different prognosis. Since 2013 edition of the WHO Classification of Tumours of Soft Tissue and Bone (Fletcher et al., 2013), HPC and SFTs are considered one entity. The term HPC has been abandoned and both entities are now called SFT. This is because they share the same *NAB2-STAT6* fusion gene. Molecular studies on HPCs of the dura/meninges have found similar genetic aberrations and the most recent WHO Classification of Tumours of the CNS (Louis et al., 2016) also considers haemangiopericytoma-solitary fibrous tumour as the same entity (Fig. 14.3).

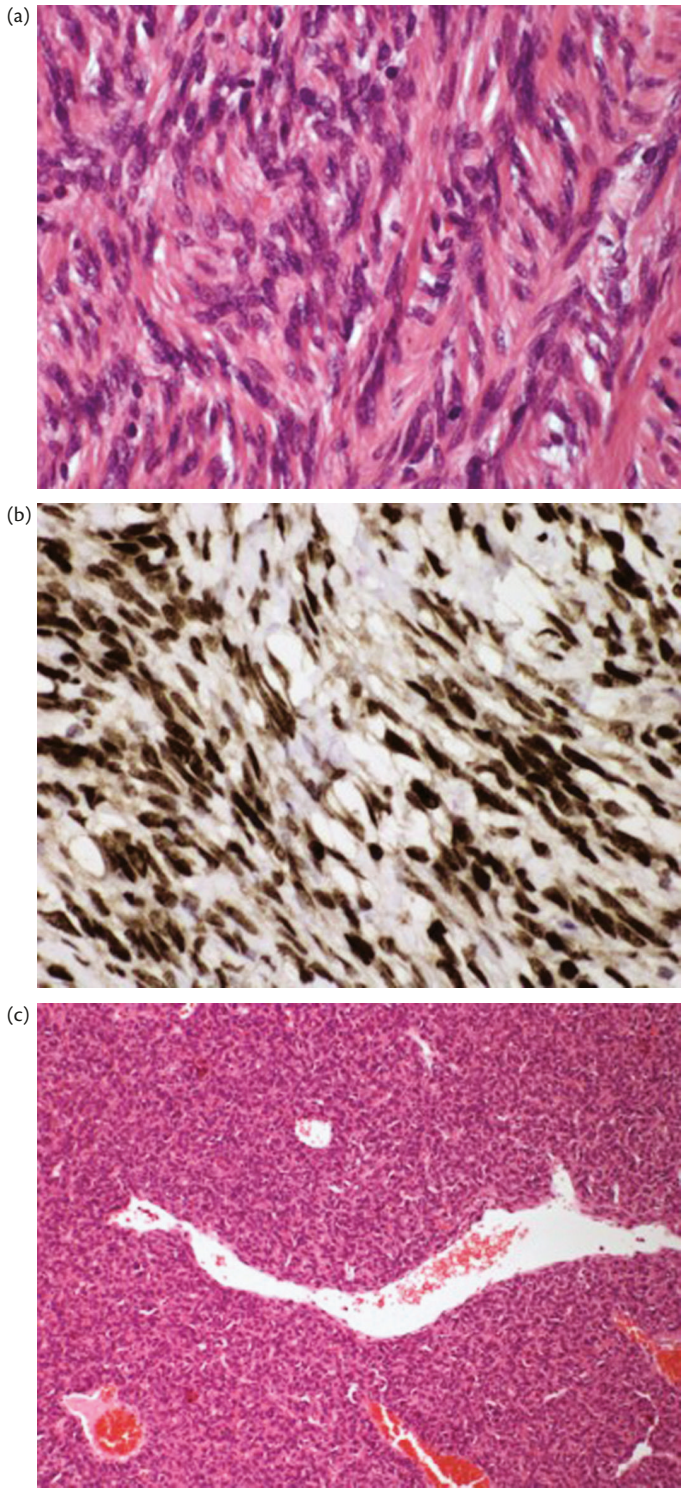

Fig. 14.3 (A) Solitary fibrous tumour—fascicles of spindle cells characterize this tumour that often mimics meningioma radiologically. The histology of this neoplasm can be mistaken for fibroblastic meningioma or schwannoma. Immunohistochemistry will resolve this differential.
(B) Solitary fibrous tumour *STAT6* immunoreactivity—the central and (to date) specific genetic abnormality in SFT and the related tumour, haemangiopericytoma, is a fusion between the *NAB2* and *STAT6* genes. This results in the nuclear localization of *STAT6* which is well-demonstrated by immunohistochemistry.
(C) Haemangiopericytoma—a highly cellular tumour composed of patternless sheets of spindle cells with characteristic dilated, thin-walled vessels. As with the related solitary fibrous tumour, nuclear expression of *STAT6* would be expected immunohistochemically.
Courtesy of Dr Kieren Allinson, Department of Pathology, Addenbrooke's Hospital, Cambridge.

SFTs commonly affects the pleura, peritoneum, meninges, and lower extremities, but they can be found in any body site. Approximately 12–22% are found to be malignant (DeVito et al., 2015). Meningeal SFTs are nearly always benign, but very rare malignant variant exists. HPCs are generally of WHO grade 2 and grade 3. Although meningeal HPCs and SFTs are generally distinct from each other, an overlap exists. Overall, it is probably most practical to think of meningeal HPCs and SFTs as a part of the same disease spectrum. Although the ultimate diagnostic test is identification of the *NAB2-STAT6* fusion gene, this is not practical as the first step. Instead, identification of nuclear staining of STAT6 using immunohistochemistry is a good surrogate test (Schweizer et al., 2013).

The radiological appearances are similar to those of meningioma, both in terms of location and signal characteristics. The features that make the diagnosis of SFT/HPC more likely include: heterogeneous signal intensity on T2-weighted images; the presence of areas of low T2 signal intensity that strongly enhance after gadolinium injection; the absence of dural tail adjacent to the tumour; the absence of skull bone thickening; and, on MR spectroscopy, an elevated myo-inositol peak (Clarençon et al., 2011). Few have no dural attachment with intraparenchymal or rarely intraventricular (Bisceglia et al., 2011).

The initial management of HPC-SFT is pretty much the same as treatment of meningiomas, with resection and tissue diagnosis. If the diagnosis is of HPC, body staging is done as the frequency of systemic metastases is high (25–50%). The main potential difficulty at surgery can be excessive bleeding as many HPCs are very vascular.

The recurrence of HPC after surgery is 60–75% and 5-year overall survival probabilities vary between 65 and 95% with median overall survival between 7 and 16 years (Guthrie et al., 1989; Kim et al., 2003; Rutkowski et al., 2012; Melone et al., 2014). Malignant transformation may occur with further recurrences (Apra et al., 2017). Despite the latest WHO Classification unification of SFTs and HPCs, there is a clear distinction between the clinical outcomes of these historically distinct conditions. Champeaux et al have analysed SFTs and HPCs together, but in a multivariate analysis histological type (SFT vs. HCP) came out as one of the independent prognostic factors (Champeaux et al., 2017). Other significant prognostic factors in the same analysis included venous sinus invasion and completeness of resection. The impact of radiotherapy on overall survival is unclear (Trifiletti et al., 2017). Given the high recurrence rate and metastatic potential, postoperative radiotherapy is uniformly used in HCPs.

Conclusions

Meningiomas are the most common form of primary brain tumour over the age of 30 and continue to challenge modern surgical and medical techniques in achieving cure or long-lasting tumour control. While the natural history of benign meningiomas is one of slow growth, and understanding that every intervention carries risk, patients should be aware of the risks associated with observation and their likely distribution over time. Many tumours that ultimately grow may have been amenable to surgical cure with lower perioperative medical and neurological morbidity if operated at an earlier age when the tumour was at its smallest size. Physical forms of treatment with surgery and radiotherapy have probably reached their peak and we look forward to advances in targeted medical therapies and immunotherapy to help us prolong and improve the lives of patients, especially those with recurrent meningiomas.

Haemangiopericytomas (HPC) are now considered one entity with solitary fibrous tumours (SFT). HPC-SFT thus form a pathological entity with a range of behaviour from benign to malignant with tendency to recur and forming distant metastases.

REFERENCES

Aavikko, M., Li, S.P., Saarinen, S., et al. (2012). Loss of SUFU function in familial multiple meningioma. *Am J Human Genet*, **91**(3), 520–6.

Alvernia J.E. & Sindou M.P. (2009). Parasagittal meningiomas. In: Lee J.H. (eds) *Meningiomas*, pp. 309–17. London, UK: Springer.

Apra, C., Mokhtari, K., Cornu, P., Peyre, M., & Kalamarides, M. (2017). Intracranial solitary fibrous tumors/hemangiopericytomas: first report of malignant progression. *J Neurosurg*, **128**, 1–6.

Backer-Grøndahl, T., Moen, B.H., & Torp, S.H. (2012). The histopathological spectrum of human meningiomas. *Int J Clin Exp Pathol*, **5**(3), 231–42.

Baumgartner, J.E. & Sorenson, J.M. (1996). Meningioma in the pediatric population. *J Neurooncol*, **29**(3), 223–8.

Begg, C.F. & Garret, R. (1954). Hemangiopericytoma occurring in the meninges: case report. *Cancer*, **7**(3), 602–6.

Bendszus, M., Rao, G., Burger, R., et al. (2000). Is there a benefit of preoperative meningioma embolization? *Neurosurgery*, **47**(6), 1306–11– discussion 1311–12.

Bisceglia, M., Galliani, C., Giannatempo, G., et al. (2011). Solitary fibrous tumor of the central nervous system: a 15-year literature survey of 220 cases (August 1996–July 2011). *Adv Anat Pathol*, **18**(5), 356–92.

Borovich, B. & Doron, Y. (1986). Recurrence of intracranial meningiomas: the role played by regional multicentricity. *J Neurosurg*, **64**(1), 58–63.

Bowers, D.C., Moskowitz, C.S., Chou, J.F., et al. (2017). Morbidity and mortality associated with meningioma after cranial radiotherapy: a report from the Childhood Cancer Survivor Study. *J Clin Oncol*, **35**(14), 1570–6.

Brastianos, P.K., Horowitz, P.M., Santagata, S., et al. (2013). Genomic sequencing of meningiomas identifies oncogenic SMO and *AKT1* mutations. *Nat Genet*, **45**(3), 285–9.

Butti, G., Assietti, R., Casalone, R., & Paoletti, P. (1989). Multiple meningiomas: a clinical, surgical, and cytogenetic analysis. *Surg Neurol*, **31**(4), 255–60.

Chamoun, R., Krisht, K.M., & Couldwell, W.T. (2011). Incidental meningiomas. *Neurosurgical FOCUS*, **31**(6), E19.

Champeaux, C., Wilson, E., Brandner, S., Shieff, C., & Thorne, L. (2015). World Health Organization grade III meningiomas. A retrospective study for outcome and prognostic factors assessment. *Br J Neurosurg*, **29**(5), 693–8.

Champeaux, C., Khan, A.A., Wilson, E., Thorne, L., & Dunn, L. (2017). Meningeal haemangiopericytoma and solitary fibrous tumour: a retrospective bi centre study for outcome and prognostic factor assessment. *J Neurooncol*, **134**(2), 387–95.

Choi, C.Y.H., Soltys, S.G., Gibbs, I.C., et al. (2010). Cyberknife stereotactic radiosurgery for treatment of atypical (WHO grade II) cranial meningiomas. *Neurosurgery*, **67**(5), 1180–8.

Choy, W., Kim, W., Nagasawa, D., et al. (2011). The molecular genetics and tumor pathogenesis of meningiomas and the future directions of meningioma treatments. *Neurosurg Focus*, **30**(5), E6.

Clarençon, F., Bonneville, F., Rousseau, A., et al. (2011). Intracranial solitary fibrous tumor: imaging findings. *Eur J Radiol*, **80**(2), 387–94.

Clark, V.E., Erson-Omay, E.Z., Serin, A., et al. (2013). Genomic analysis of non-*NF2* meningiomas reveals mutations in TRAF7, *KLF4, AKT1*, and SMO. *Science*, **339**(6123), 1077–80.

Claus, E.B., Bondy, M.L., Schildkraut, J.M., Wiemels, J.L., Wrensch, M., & Black, P.M. (2005). Epidemiology of intracranial meningioma. *Neurosurgery*, **57**(6), 1088–95.

Condra, K.S., Buatti, J.M., Mendenhall, W.M., Friedman, W.A., Marcus, R.B. Jr, & Rhoton, A.L. (1997). Benign meningiomas: primary treatment selection affects survival. *Int J Radiat Oncol Biol Phys*, **39**(2), 427–36.

Cossu, G., Levivier, M., Daniel, R.T., & Messerer, M. (2015). The role of mifepristone in meningiomas management: a systematic review of the literature. *BioMed Res Int*, **2015**(4), 267831.

DeVito, N., Henderson, E., Han, G., et al. (2015). Clinical characteristics and outcomes for solitary fibrous tumor (SFT): a single center experience. *PloS One*, **10**(10), e0140362.

Dowd, C.F., Halbach, V.V., & Higashida, R.T. (2003). Meningiomas: the role of preoperative angiography and embolization. *Neurosurgical Focus*, **15**(1), E10.

Evans, D.G.R., Watson, C., King, A., Wallace, A., & Baser, M. (2005). Multiple meningiomas: differential involvement of the *NF2* gene in children and adults. *J Med Genet*, **42**(1), 45–8.

Fletcher, C., Unni, K.K., & Mertens, F. (2013). *World Health Organization Classification of Tumours of Soft Tissue and Bone*, 4th edition. Geneva, Switzerland: WHO.

Ganesan, D., Higgins, J.N., Harrower, T., et al. (2008). Stent placement for management of a small parasagittal meningioma. Technical note. *J Neurosurg*, **108**(2), 377–81.

Giovannini, M., Robanus-Maandag, E., van der Valk, M., et al. (2000). Conditional biallelic *NF2* mutation in the mouse promotes manifestations of human neurofibromatosis type 2. *Genes Dev*, **14**(13), 1617–30.

Goyal, L.K., Suh, J.H., Mohan, D.S., Prayson, R.A., Lee, J., & Barnett, G.H. (2000). Local control and overall survival in atypical meningioma: a retrospective study. *Int J Radiat Oncol Biol Phys*, **46**(1), 57–61.

Graillon, T., Romano, D., Defilles, C., et al. (2017). Octreotide therapy in meningiomas: *in vitro* study, clinical correlation, and literature review. *J Neurosurg*, **127**(3), 660–9.

Gruber, A., Killer, M., Mazal, P., et al. (2000). Preoperative embolization of intracranial meningiomas: a 17-years single center experience. *Minim Invasive Neurosur*, **43**(1), 18–29.

Guthrie, B.L., Ebersold, M.J., Scheithauer, B.W., & Shaw, E.G. (1989). Meningeal hemangiopericytoma: histopathological features, treatment, and long-term follow-up of 44 cases. *Neurosurgery*, **25**(4), 514–22.

Haines, D.E. & Frederickson, R.G. (1991). The meninges. In: Al-Mefty, O. (ed.) *Meningiomas*, pp. 9–25. New York: Raven Press.

Hayashi, T., Shojima, K., Utsunomiya, H., Moritaka, K., & Honda, E. (1987). Subarachnoid hemorrhage after preoperative embolization of a cystic meningioma. *Surg Neurol*, **27**(3), 295–300.

Heald, J.B., Carroll, T.A., & Mair, R.J. (2014). Simpson grade: an opportunity to reassess the need for complete resection of meningiomas. *Acta Neurochirurg*, **156**(2), 383–8.

Higgins, J.N.P., Burnet, N.G., Schwindack, C.F., & Waters, A. (2008). Severe brain edema caused by a meningioma obstructing cerebral venous outflow and treated with venous sinus stenting. Case report. *J Neurosurg*, **108**(2), 372–6.

Jenkinson, M.D., Javadpour, M., Haylock, B.J., et al. (2015). The ROAM/EORTC-1308 trial: radiation versus observation following surgical resection of atypical meningioma: study protocol for a randomised controlled trial. *Trials*, **16**(1), 519.

Jenkinson, M.D., Santarius, T., Zadeh, G., & Aldape, K.D. (2017). Atypical meningioma—is it time to standardize surgical sampling techniques? *Neuro Oncol*, **19**(3), 453–4.

Ji, Y., Rankin, C., Grunberg, S., et al. (2015). Double-blind phase III randomized trial of the antiprogestin agent mifepristone in the treatment of unresectable meningioma: SWOG S9005. *J Clin Oncol*, **33**(34), 4093–8.

Kalamarides, M., Niwa-Kawakita, M., Leblois, H., et al. (2002). *Nf2* gene inactivation in arachnoidal cells is rate-limiting for meningioma development in the mouse. *Genes Dev*, **16**(9), 1060–5.

Kallio, M., Sankila, R., Hakulinen, T., & Jääskeläinen, J. (1992). Factors affecting operative and excess long-term mortality in 935 patients with intracranial meningioma. *Neurosurgery*, **31**(1), 2–12.

Kaur, G., Sayegh, E.T., Larson, A., et al. (2014). Adjuvant radiotherapy for atypical and malignant meningiomas: a systematic review. *Neuro Oncol*, **16**(5), 628–36.

Kim, J.H., Jung, H.W., Kim, Y.S., et al. (2003). Meningeal hemangiopericytomas: long-term outcome and biological behavior. *Surg Neurol*, **59**(1), 47–53; discussion 53–4.

Kinjo, T., Al-Mefty, O., & Kanaan, I. (1993). Grade zero removal of supratentorial convexity meningiomas. *Neurosurgery*, **33**(3), 394–9; discussion 399.

Klaeboe, L., Lonn, S., Scheie, D., et al. (2005). Incidence of intracranial meningiomas in Denmark, Finland, Norway and Sweden, 1968–1997. *Int J Cancer*, **117**(6), 996–1001.

Kotecha, R.S., Pascoe, E.M., Rushing, E.J., et al. (2011). Meningiomas in children and adolescents: a meta-analysis of individual patient data. *Lancet Oncol*, **12**(13), 1229–39.

Kshettry, V.R., Ostrom, Q.T., Kruchko, C., Al-Mefty, O., Barnett, G.H., & Barnholtz-Sloan, J.S. (2015). Descriptive epidemiology of World Health Organization grades II and III intracranial meningiomas in the United States. *Neuro Oncol*, **17**(8), 1166–73.

Lagman, C., Bhatt, N.S., Lee, S.J., et al. (2017). Adjuvant radiosurgery versus serial surveillance following subtotal resection of atypical meningioma: a systematic analysis. *World Neurosurg*, **98**, 339–46.

Lallemand, D., Curto, M., Saotome, I., Giovannini, M., & McClatchey, A.I. (2003). NF2 deficiency promotes tumorigenesis and metastasis by destabilizing adherens junctions. *Genes Dev*, **17**(9), 1090–100.

Lang, F.F., Macdonald, O.K., Fuller, G.N., & DeMonte, F. (2000). Primary extradural meningiomas: a report on nine cases and review of the literature from the era of computerized tomography scanning. *J Neurosurg*, **93**(6), 940–50.

Larson, J.J., Tew, J.M. Jr, Simon, M., & Menon, A.G. (1995). Evidence for clonal spread in the development of multiple meningiomas. *J Neurosurg*, **83**(4), 705–9.

Louis, D.N. Perry, A., Reifenberger, G., et al. (eds.) (2016). *WHO Classification of Tumours of the Central Nervous System*. Lyon, France: IARC.

Magill, S.T., Lau, D., Raleigh, D.R., Sneed, P.K., Fogh, S.E., & McDermott, M.W. (2016). Surgical resection and interstitial iodine-125 brachytherapy for high-grade meningiomas. *Neurosurgery*, **80**(3), 1–8.

Marcus, H., Schwindack, C., Santarius, T., Mannion, R., & Kirollos, R. (2013). Image-guided resection of spheno-orbital skull-base meningiomas with predominant intraosseous component. *Acta Neurochirurg*, **155**(6), 981–8.

Marcus, H.J., Price, S.J., Wilby, M., Santarius, T., & Kirollos, R.W. (2008). Radiotherapy as an adjuvant in the management of intracranial meningiomas: are we practising evidence-based medicine? *Br J Neurosurg*, **22**(4), 520–8.

Mark, J., Levan, G., & Mitelman, F. (1972). Identification by fluorescence of the G chromosome lost in human meningomas. *Hereditas*, **71**(1), 163–8.

McClatchey, A.I., Saotome, I., Mercer, K., et al. (1998). Mice heterozygous for a mutation at the *NF2* tumor suppressor locus develop a range of highly metastatic tumors. *Genes Dev*, **12**(8), 1121–33.

Melone, A.G., D'Elia, A., Santoro, F., et al. (2014). Intracranial hemangiopericytoma—our experience in 30 years: a series of 43 cases and review of the literature. *World Neurosurg*, **81**(3–4), 556–62.

Milosevic, M.F., Frost, P.J., Laperriere, N.J., Wong, C.S., & Simpson, W.J. (1996). Radiotherapy for atypical or malignant intracranial meningioma. *Radiat Oncol Biol*, **34**(4), 817–22.

Mirimanoff, R.O., Dosoretz, D.E., Linggood, R.M., Ojemann, R.G., & Martuza, R.L. (1985). Meningioma: analysis of recurrence and progression following neurosurgical resection. *J Neurosurg*, **62**(1), 18–24.

Moliterno, J., Cope, W.P., Vartanian, E.D., et al. (2015). Survival in patients treated for anaplastic meningioma. *J Neurosurg*, **123**(1), 23–30.

Morris, Z., Whiteley, W.N., Longstreth, W.T. Jr, et al. (2009). Incidental findings on brain magnetic resonance imaging: systematic review and meta-analysis. *BMJ*, **339**, b3016.

Nimmannitya, P., Goto, T., Terakawa, Y., et al. (2016). Characteristic of optic canal invasion in 31 consecutive cases with tuberculum sellae meningioma. *Neurosurg Rev*, **39**(4), 691–7.

Ostrom, Q.T., Gittleman, H., Xu, J., et al. (2016). CBTRUS statistical report: primary brain and other central nervous system tumors diagnosed in the United States in 2009–2013. *Neuro Oncol*, **18**(suppl 5), v1–v75.

Palma, L., Celli, P., Franco, C., Cervoni, L., & Cantore, G. (1997). Long-term prognosis for atypical and malignant meningiomas: a study of 71 surgical cases. *J Neurosurg*, **86**(5), 793–800.

Pearson, B.E., Markert, J.M., Fisher, W.S., et al. (2008). Hitting a moving target: evolution of a treatment paradigm for atypical meningiomas amid changing diagnostic criteria. *Neurosurgical Focus*, **24**(5), E3.

Perry, A. (2013). Meningiomas. In: *Russell & Rubinstein's Pathology of Tumors of the Nervous System*, 7th edition, pp. 427–74. Boca Raton, FL: CRC Press.

Perry, A., Scheithauer, B.W., Stafford, S.L., Lohse, C.M., & Wollan, P.C. (1999). 'Malignancy' in meningiomas: a clinicopathologic study of 116 patients, with grading implications. *Cancer*, **85**(9), 2046–56.

Pollock, B.E., Stafford, S.L., Link, M.J., Garces, Y.I., & Foote, R.L. (2012). Single-fraction radiosurgery for presumed intracranial meningiomas: efficacy and complications from a 22-year experience. *Int J Radiat Oncol Biol Phys*, **83**(5), 1414–18.

Radhakrishnan, K., Mokri, B., Parisi, J.E., O'Fallon, W.M., Sunku, J., & Kurland, L.T. (1995). The trends in incidence of primary brain tumors in the population of Rochester, Minnesota. *Ann Neurol*, **37**(1), 67–73.

Raper, D.M.S., Starke, R.M., Henderson, F. Jr, et al. (2014). Preoperative embolization of intracranial meningiomas: efficacy, technical considerations, and complications. *AJNR Am J Neuroradiol*, **35**(9), 1798–804.

Regelsberger, J., Hagel, C., Emami, P., Ries, T., Heese, O., & Westphal, M. (2009). Secretory meningiomas: a benign subgroup causing life-threatening complications. *Neuro Oncol*, **11**(6), 819–24.

Reuss, D.E., Piro, R.M., Jones, D.T., et al. (2013). Secretory meningiomas are defined by combined *KLF4* K409Q and TRAF7 mutations. *Acta Neuropathol*, **125**(3), 351–8.

Riemenschneider, M.J., Perry, A., & Reifenberger, G. (2006). Histological classification and molecular genetics of meningiomas. *Lancet Neurol*, **5**(12), 1045–54.

Rogers, L., Barani, I., Chamberlain, M., et al. (2015). Meningiomas: knowledge base, treatment outcomes, and uncertainties. A RANO review. J Neurosurg, **122**(1), 4–23.

Rouleau, G.A., Merel, P., Lutchman, M., et al. (1993). Alteration in a new gene encoding a putative membrane-organizing protein causes neuro-fibromatosis type 2. *Nature*, **363**(6429), 515–21.

Rutkowski, M.J., Jian, B.J., Bloch, O., et al. (2012). Intracranial hemangiopericytoma: clinical experience and treatment considerations in a modern series of 40 adult patients. *Cancer*, **118**(6), 1628–36.

Ruttledge, M.H., Sarrazin, J., Rangaratnam, S., et al. (1994). Evidence for the complete inactivation of the *NF2* gene in the majority of sporadic meningiomas. *Nat Genet*, **6**(2), 180–4.

Sahm, F., Bissel, J., Koelsche, C., et al. (2013). *AKT1*E17K mutations cluster with meningothelial and transitional meningiomas and can be detected by SFRP1 immunohistochemistry. *Acta Neuropathol*, **126**(5), 757–62.

Santacroce, A., Walier, M., Régis, J., et al. (2012). Long-term tumor control of benign intracranial meningiomas after radiosurgery in a series of 4565 patients. *Neurosurgery*, **70**(1), 32–9; discussion 39.

Schweizer, L., Koelsche, C., Sahm, F., et al. (2013). Meningeal hemangiopericytoma and solitary fibrous tumors carry the *NAB2-STAT6* fusion and can be diagnosed by nuclear expression of STAT6 protein. *Acta Neuropathologica*, **125**(5), 651–8.

Shaw, R., Paez, J.G., Curto, M., et al. (2001). The Nf2 tumor suppressor, merlin, functions in Rac-dependent signaling. *Dev Cell*, **1**(1), 63–72.

Simpson, D. (1957). The recurrence of intracranial meningiomas after surgical treatment. *J Neurol Neurosurg Psychiatry*, **20**(1), 22–39.

Smith, M.J., O'Sullivan, J., Bhaskar, S.S., et al. (2013). Loss-of-function mutations in SMARCE1 cause an inherited disorder of multiple spinal meningiomas. *Nat Genet*, **45**(3), 295–8.

Soyuer, S., Chang, E.L., Selek, U., Shi, W., Maor, M.H., & DeMonte, F. (2004). Radiotherapy after surgery for benign cerebral meningioma. *Radiother Oncol*, **71**(1), 85–90.

Stafford, S.L., Perry, A., Suman, V.J., et al. (1998). Primarily resected meningiomas: outcome and prognostic factors in 581 Mayo Clinic patients, 1978 through 1988. *Mayo Clinic Proc*, **73**(10), 936–42.

Stafford, S.L., Pollock, B.E., Foote, R.L., et al. (2001). Meningioma radiosurgery: tumor control, outcomes, and complications among 190 consecutive patients. *Neurosurgery*, **49**(5), 1029–37; discussion 1037–8.

Stangl, A.P., Wellenreuther, R., Lenartz, D., et al. (1997). Clonality of multiple meningiomas. *J Neurosurg*, **86**(5), 853–8.

Sughrue, M., Kane, A., Rutkowski, M.J., Berger, M.S., & McDermott, M.W. (2015). Meningiomas of the anterior clinoid process: is it wise to drill out the optic canal? *Cureus*, **7**(9), e321.

Sughrue, M.E., Kane, A.J., Shangari, G., et al. (2010). The relevance of Simpson grade I and II resection in modern neurosurgical treatment of World Health Organization grade I meningiomas. *J Neurosurg*, **113**(5), 1029–35.

Sughrue, M.E., Rutkowski, M.J., Aranda, D., Barani, I.J., McDermott, M.W., & Parsa, A.T. (2010). Treatment decision making based on the published natural history and growth rate of small meningiomas. *J Neurosurg*, **113**(5), 1036–42.

Sughrue, M.E., Sanai, N., Shangari, G., Parsa, A.T., Berger, M.S., & McDermott, M.W. (2010). Outcome and survival following primary and repeat surgery for World Health Organization Grade III meningiomas. *J Neurosurg*, **113**(2), 202–9.

Terrier, L.-M. & François, P. (2016). [Multiple meningiomas]. *Neuro-Chirurgie*, **62**(3), 128–35.

Trifiletti, D.M., Mehta, G.U., Grover, S., & Sheehan, J.P. (2017). Clinical management and survival of patients with central nervous system hemangiopericytoma in the National Cancer Database. *J Clin Neurosci*, **44**, 169–74.

Trofatter, J.A., MacCollin, M.M., Rutter, J.L., et al. (1993). A novel moesin-, ezrin-, radixin-like gene is a candidate for the neurofibromatosis 2 tumor suppressor. *Cell*, **72**(5), 791–800.

van den Munckhof, P., Christiaans, I., Kenter, S.B., Baas, F., & Hulsebos, T.J. (2012). Germline SMARCB1 mutation predisposes to multiple meningiomas and schwannomas with preferential location of cranial meningiomas at the falx cerebri. *Neurogenetics*, **13**(1), 1–7.

Weber, R.G., Boström, J., Wolter, M., et al. (1997). Analysis of genomic alterations in benign, atypical, and anaplastic meningiomas: toward a genetic model of meningioma progression. *Proc Natl Acad Sci*, **94**(26), 14719–24.

Willis, J., Smith, C., Ironside, J.W., Erridge, S., Whittle, I.R., & Everington, D. (2005). The accuracy of meningioma grading: a 10-year retrospective audit. *Neuropathol Appl Neurobiol*, **31**(2), 141–9.

Yamanaka, R., Hayano, A., & Kanayama, T. (2017). Radiation-induced meningiomas: an exhaustive review of the literature. *World Neurosurg*, **97**, 635–44.e8.

RELATED LINKS TO EBRAIN

Aetiology and Pathophysiology of Intracranial Meningiomas. https://learning.ebrain.net/course/view.php?id=1244

Characteristic Appearance and Differential Diagnosis of Meningiomas. https://learning.ebrain.net/course/view.php?id=1248

Histopathology of Meningiomas. https://learning.ebrain.net/course/view.php?id=1254

Management of Meningiomas. https://learning.ebrain.net/course/view.php?id=473

15

Chordomas and chondrosarcomas of the skull base

Rami O. Almefty and Ossama Al-Mefty

Introduction

Chordomas and chondrosarcomas are often paired together because of their similarities in anatomical location, clinical presentation, and radiographic findings. However, they represent two distinct pathologies with starkly different clinical outcomes. This chapter reviews both entities and highlights the key distinctions between them.

Epidemiology

Chordomas and chondrosarcomas of the skull base are rare tumours. Together, they make up 0.1% of all brain tumours and have a combined incidence of 0.02 per 100 000 (CBTRUS, 2012). Chondrosarcomas are even more rare than chordomas.

Chordomas are located in the skull base, mobile spine, or sacrum. McMaster and others used the Surveillance, Epidemiology, and End Results (SEER) programme of the National Cancer Institute to calculate a population-based incidence of 0.8 per 100 000. In their study chordomas occurred nearly equally among the skull base (32%), spine (33%) and sacrum (29%) (McMaster et al., 2001). Heffelfinger et al. published the Mayo Clinic's experience of 155 chordomas, 76 (49%) occurred in the sacrum, 55 (35%) in the skull base, and 24 (15%) in the mobile spine (Heffelfinger et al., 1973). Since this study is based on an institutional experience rather than population based, it may be affected by the institutions' expertise and referral patterns.

Chordomas in general have a male predominance, perhaps as high as 2:1 (Heffelfinger et al., 1973; McMaster et al., 2001), however; this does not hold true for cranial chordomas where there is a near equal incidence (McMaster et al., 2001; Almefty et al., 2007). Cranial chordomas also present at an earlier age than chordomas at other sites. According to McMaster et al., the median age at presentation for cranial tumours is 49 years with a quarter of patients presenting prior to 35 years of age (McMaster et al., 2001). In the senior author's (OA) published series of 89 cranial chordomas, the mean age was 37.7 years (Almefty et al., 2007). Chordomas are even rarer in the paediatric population and especially rare in those younger than five years old. In a cross-sectional national database analysis, Chambers et al. reported that of 594 cranial chordomas, 30 cases occurred in patients 10–19 years old and 26 in those less than ten years old (Chambers et al., 2014). At the time of their report, Borba et al. found 21 of the 76 reported paediatric cases to be in those younger than five years old (Borba et al., 1996). Chordomas are exceedingly rare in African-Americans (McMaster et al., 2001; Almefty et al., 2007).

Pathology

Chordomas arise from primitive notochord remnants at the sphenooccipital synchondrosis (**Fig. 15.1**). They are typically described as slow growing but this belies their malignant and invasive behaviour (**Fig. 15.2**). They form a grey, gelatinous, lobulated mass with an encapsulated soft tissue component but with infiltrative bone involvement. Microscopically, they contain uniform physaliferous cells which are small, oval cells with eccentric nuclei with dense chromatin and numerous cytoplasmic vacuoles. A pseudocapsule appearance is created by fibrous strands forming thick hyalinized septae or lobules with thin septations. The lobules can have the appearance of sheets of physaliferous cells or a pool of mucin. The sheets of cells contain a varying degree of intracytoplasmic mucin (Heffelfinger et al., 1973). Heffelfinger et al. described the chondroid variant of chordoma which also has a cartilaginous component (Heffelfinger et al., 1973). The distinction between chondroid chordoma and chondrosarcoma can be difficult histologically, highlighting the need for immunohistochemistry in differentiating the two, as chondroid chordoma behaves the same as non-variant chordomas and must be treated as such (Rosenberg et al., 1994; Almefty et al., 2007). In addition to the classic and chondroid types, the final subtype of chordoma is the de-differentiated or atypical type. Atypical chordoma is rare, even among chordomas, and has a more aggressive cytology and clinical course.

Chondrosarcomas originate from primitive mesenchymal cells or from embryologic rests in the cranium of the cartilaginous matrix. They typically occur in the long bones and pelvis and are rare in the cranium. Grossly, they are composed of multiple, interconnecting globules of chondroid or myxoid consistency. These tumours can be

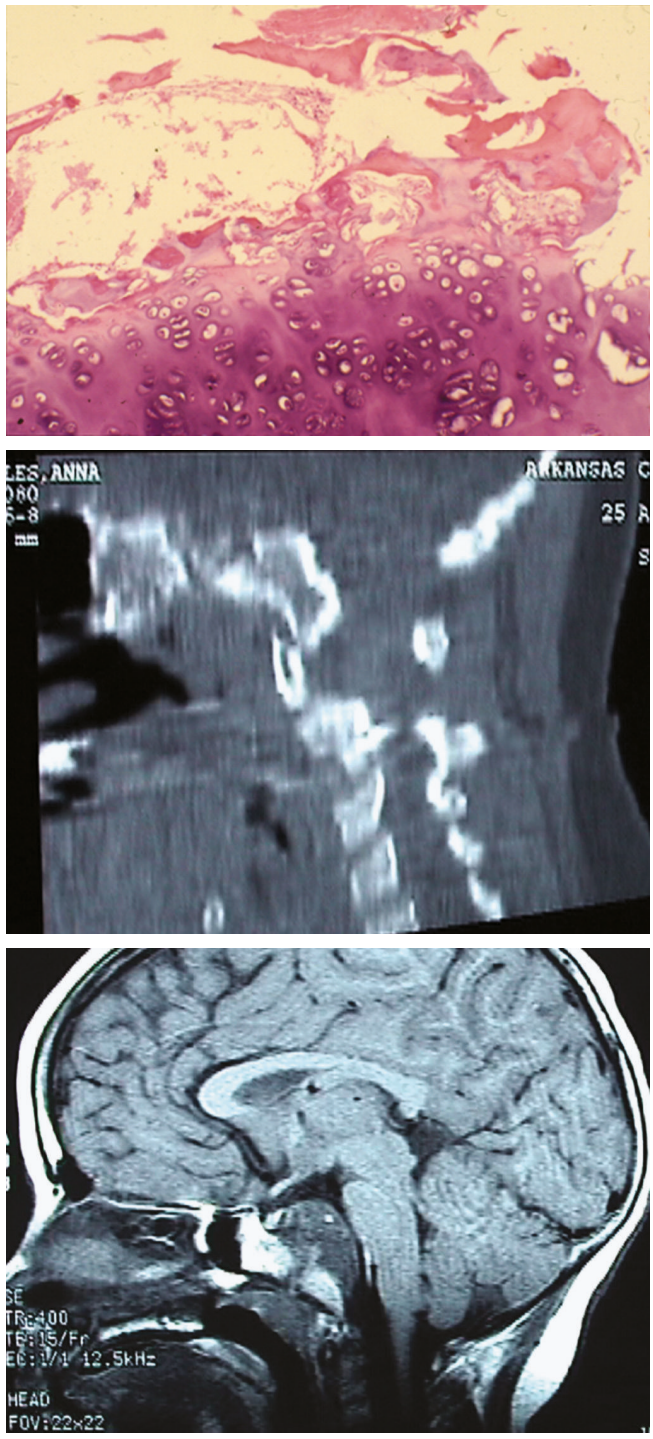

Fig. 15.1 H and E stain (A), bone window sagital CT scan (B), and sagital MRI (C) showing the origin of chordoma from the sphenooccipital synchondrosis.

grouped into classic, mesenchymal, and myxoid. The classic form is most common and contains large cells with single or multiple nuclei in a variable chondroid matrix. Classic chondrosarcomas are divided into grades I, II, or III depending on mitotic rates, cellularity, and nuclear size. The chondroid matrix in higher grade tumours have increased mitosis and less chondroid matrix (Evans et al., 1977). The mesenchymal type contains areas of relatively well differentiated cartilage and undifferentiated round or spindle shaped cells, whereas the myxoid type has a myxoid matrix with strings of round cells (Korten et al., 1998).

The key pathological distinction between the two entities that must be studied is their immunohistochemical profile (see Fig. 15.3). Chordomas are positive for cytokeratin, EMA, S-100, and vimentin, including the chondroid variant. Chondrosarcomas, however, are negative for cytokeratin and EMA but are positive for S-100 and vimentin (Rosenberg et al., 1994). Brachyury is a nuclear transcription factor additionally helpful in the diagnosis of chordoma and distinction from chondrosarcoma. Brachyury staining is rare outside of chordoma and not present in the lesions typically considered in the differential diagnosis. When included with an immunohistochemical panel of S-100 and epithelial markers a sensitivity of 100% can be achieved (Oakley et al., 2008; Jo et al., 2014).

Genetics

The sum results of studies to date have characterized chordoma as a genetically heterogenous tumour with frequent imbalances of large chromosomal regions without recurrent structural rearrangements (Hallor et al., 2008). Scheil-Bertram et al. demonstrated the genetic heterogeneity when they found 166 unique aberrations in a study of 33 cases (Scheil-Bertram et al., 2014). When chordoma karyotypes are abnormal, whole or partial loss of chromosomes 1, 3, 4, 9, 10, 13, 18 gains in chromosomes 7 and 20 and the formation of isochromosome 1q have been shown (DeBoer et al., 1992; Bridge et al., 1994; Sawyer et al., 2001; Scheil et al., 2001; Tallini et al., 2002; Sandberg and Bridge, 2003; Kuzniacka et al., 2004; Brandal et al., 2005; Bayrakli et al., 2007). 1p36 has been purported as a tumour suppressor gene locus in sporadic chordomas (Dalpra et al., 1999; Miozzo et al., 2000; Riva et al., 2003) as 7q33 has for familial cases (Kelley et al., 2001). Hallor et al. used array comparative genomic hybridization (aCGH) to show the absence of CDKN2A and CDKN2B in 70% of cases (Hallor et al., 2008). More advanced techniques such as aCHG and whole-genome single—nucleotide polymorphism microarray analysis (SNP) have revealed chromosal abnormalities in 91–100% of chordomas (Scheil et al., 2001; Hallor et al., 2008; Le et al., 2011; Kitamura et al., 2013; Scheil-Bertram et al., 2014).

Al-Mefty et al. were able to define the clinical significance of cytogenetic abnormalities in chordomas. Chordomas with normal karyotypes were found to have a recurrence rate of 3% in *de novo* cases. *De novo* tumours with an abnormal karyotype, on the other hand, had a recurrence rate of 45%. They found an abnormal karyotype in 75% of recurrent cases in comparison to 24% of *de novo* cases. Tumours with aberrant chromosomes 3, 4, 12, 13, and 14 showed frequent recurrences and decreased survival. Abnormalities in chromosome 13 had the highest odds ratio for progression (OR 24), and a median recurrence-free survival rate of only 4.5 months, significantly shorter than tumours with aberrant karyotypes not involving chromosome 13. It should be noted that karyotyping was done using the G banding technique and comparative genomic hybridization may reveal abnormalities not detected with the G banding technique (Almefty et al., 2009). Other authors have found gain of 2p (Kitamura et al., 2013), deletion of 9p21 (Horbinski et al., 2010), and p53 overexpression (Naka et al., 1996) to be associated with poorer prognosis. Loss of the SMARCB1 locus has been associated with

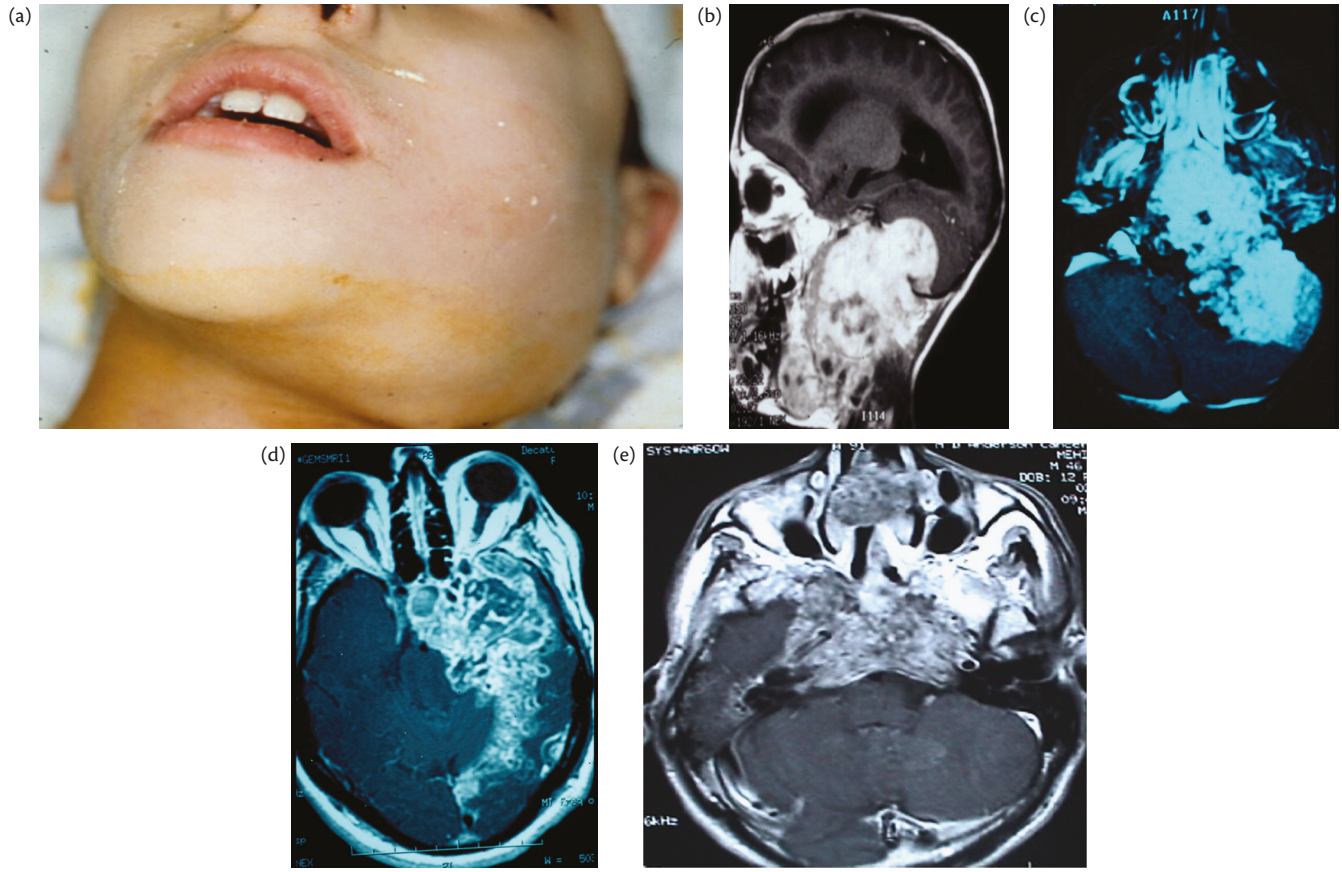

Fig. 15.2 (A, B) Axial enhanced MRI scan and patient photograph showing a chordoma extensively invading the skull base and neck. (C, D, E) Additional examples of axial enhanced MRI scans showing the invasive nature of chordomas.

poorly differentiated cases (Mobley et al., 2010) and homozygous loss of CDKN2A and CDKN2B has been linked to metastatic cases (Hallor et al., 2008). Chordomas demonstrate the classic theory of tumour progression where the accumulation of additional genetic mutations correlates with more aggressive clinical behaviour.

Preoperative work-up and planning

The preoperative assessment of patients with chordoma should include MRI, CT, and vascular imaging. A thorough review of all available imaging is critical in understanding the tumours extension and relationship to critical neurovascular structures and to best plan radical resection and postoperative radiotherapy. On CT imaging, chordoma appears as a centrally located, well circumscribed, primarily hyperdense mass arising from the clivus. CT is most valuable in showing the extensive lytic bone involvement that can spread throughout the skull base and must be removed for a truly radical resection. Intratumoural calcification that most likely represents sequestered bone may be present. Chordoma enhances with iodinated contrast. MRI is complimentary to CT as it better delineates the soft tissue tumour extent with excellent anatomical detail. Typically chordoma appears as low to intermediate

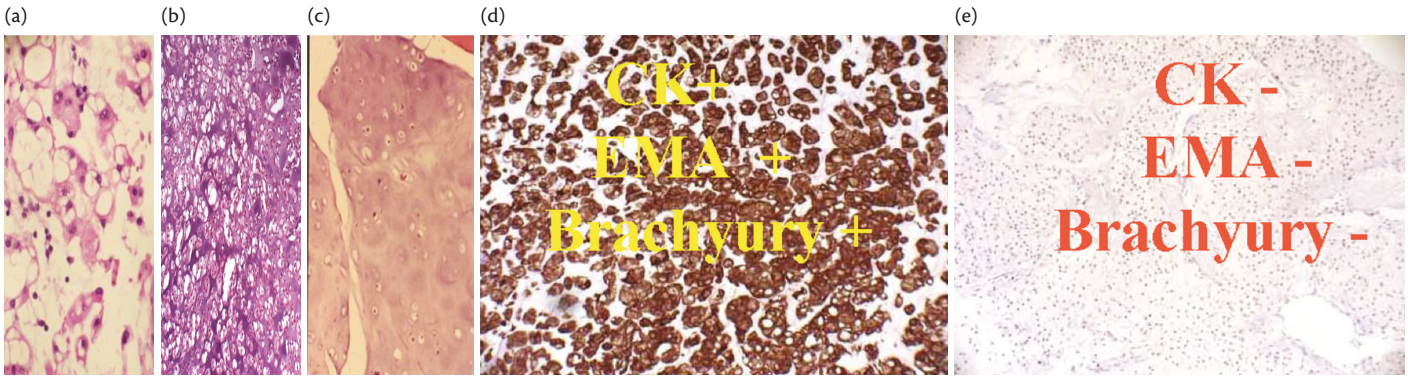

Fig. 15.3 H&E stain of chordoma, chondroid chordoma, and chondrosarcoma; and immunohistochemical staining of chordoma and chondrosarcoma.

intensity on T1-weighted imaging, hyperintense on T2-weighted imaging, and is moderate to markedly enhancing. In the event of necrosis or a large amount of mucinous material, the enhancement may be diminished or absent. Vascular imaging is also obtained to delineate tumoural encasement or displacement of cerebral vessels and to study the venous anatomy for approach planning (Erdem et al., 2003). This can typically be accomplished with non-invasive imaging and we have found dynamic CT angiography to be particularly helpful (Bi et al., 2015). On occasion, catheter angiography is needed if vessel narrowing is severe, to assess collateral flow, or in the event of prior radiation to assess for radiation induced angiopathy, which can make any dissection around the artery hazardous.

Additional studies beneficial in the preoperative assessment are pituitary function testing and neuro-ophthalmological testing. As chordomas frequently involve the sellar area, hypopituitarism can occur and should be diagnosed and corrected. Many patients with chordomas present with visual complaints and the tumours often spread to involve the optic apparatus. Baseline testing is important in following these patients.

Treatment

It is critical to understand chordoma behaviour and natural history in order to optimally manage a patient's disease. Though they are histologically benign, their natural history and aggressive behaviour is *malignant*. They have a short life expectancy without treatment, a high recurrence rate (Forsyth et al., 1993; Gay et al., 1995; Al-Mefty and Borba, 1997; Ammirati and Bernardo, 1999), and a propensity to metastasize (Markwalder et al., 1979; Fagundes et al., 1995), and surgically implant (Arnautovic and Al-Mefty, 2001; Fagundes et al., 1995). Considering the malignant behaviour of chordoma, the need for early, aggressive treatment is unambiguous. Chordomas must be treated at the time of diagnosis without a period of observation.

Long-term survival has been reported where treatment has consisted of radical removal followed by high-dose radiation to the tumour bed at the onset of diagnosis (Al-Mefty and Borba, 1997; Almefty et al., 2007). Anything less is doomed to recur. Following recurrence, chordoma has a dismal prognosis with 3- and 5-year survival rates of 43 and 7% (Fagundes et al., 1995). To this end, everything must be done to control chordoma at the time of initial treatment.

The extent of surgical removal to recurrence-free survival has been well-established (Forsyth et al., 1993; Fagundes et al., 1995; Gay et al., 1995; Al-Mefty and Borba, 1997; Colli and Al-Mefty, 2001; Tamura et al., 2015). The advancements in skull base and microsurgery have made radical removal of skull base chordomas safe. Several considerations must be made when discussing the surgical removal of chordomas. Key among them is the fact that chordoma exists as islands in the surrounding bone and not just the clearly visible soft tissue mass. Therefore, to achieve radical resection, extensive drilling of the surrounding bone must be performed in addition to complete removal of the soft tissue mass. Preoperative CT imaging must be thoroughly reviewed to understand the bony involvement and plan surgery accordingly, as chordoma has a tendency to spread throughout the skull base.

We have characterized this phenomenon by dividing chordomas into three types based on their extension into skull base compartments. Type 1 tumours are rare cases limited to one compartment confined to a single anatomical area. Type II tumours extend to two or more contiguous areas that can be radically resected through a single approach, and Type III tumours extend to several compartments and require multiple approaches. We have found 60% of tumours to involve the cavernous sinus, 50% the petrous apex, 25% the occipital condyle and 50% to have extended intradurally (al-Mefty and Borba, 1997). These extensions must be anticipated, studied, and planned for in the operative approach or approaches. Indeed, multiple skull base approaches are often needed to achieve radical removal of chordomas and provide the best chance of long-term control.

All approaches to chordomas should be planned to allow for the fact that chordomas begin as extradural tumours, so extradural approaches should be used in the first instance. If the tumour has not yet spread intradurally, then every effort should be made to keep the operation extradural. If the tumour has extended intradurally then it can be followed intradurally from an extradural approach.

Since most chordomas extensively involve the clivus, an anterior midline approach is typically needed. We have found the sublabial transmaxillary, transphenoidal and anterior clivectomy approach to provide an excellent exposure (Al-Mefty et al., 2008). The entire length of the clivus can be exposed and it offers a wide working area suitable for both microscopic and endoscopic techniques. We prefer to use the microscope for the drilling of the clivus as it offers critical three-dimensional vision. The endoscope is an extremely valuable adjunct that allows visualization of areas hidden from the microscopic view. The combined use of the microscope and endoscope is an excellent strategy that we have found useful for all tumour types (Abolfotoh et al., 2015). All skull base surgeons should have expertise in both techniques as they are complementary.

Given the frequent involvement of the cavernous sinus, radical resection of chordomas includes removal of the cavernous sinus component and this can be done safely from the middle fossa approach (Al-Mefty, 1998). When the occipital condyle is involved as frequently occurs, a transcondylar approach is needed and this may necessitate occipito-cervical fusion, which can be accomplished during the same exposure (Al-Mefty, 1998). Since the radical resection of chordomas involves extensive skull base removal and the tumours often extend intradurally, cerebrospinal leak is a concern that must be planned for, in advance, with preparation of a vascularized flap of temporalis muscle or pericranium.

Given the extreme importance of radical resection, we do everything possible to ensure the maximal possible resection has been achieved. As a part of this strategy, we feel intraoperative imaging is essential. We prefer to perform all chordoma resections in the Advanced Multimodality Image Guided Operating (AMIGO) suite. The suite is equipped with intraoperative MRI, CT scan, PET CT, ultrasound, and angiography allowing one to leave the operating room knowing all possible tumour has been resected (**Figs. 15.4A–C**).

Another operative consideration in the treatment of chordomas is their propensity for surgical implantation (Figs. 15.5A–C). All efforts must be taken intraoperatively to avoid potential seeding. First, preoperative planning of all clival lesions should allow for the possibility of a chordoma. If chordoma is considered, approaches and techniques must be employed that minimize the risk of seeding. An approach that provides a contained surgical field is optimal. After the approach is completed but before the tumour resection commences, the field and operative tunnel are coated with fibrin glue and cotton patties. Following complete removal of the tumour, the glue and patties are removed prior to introducing clean grafts. Prior to initiating the closure, all contaminated drapes and towels are

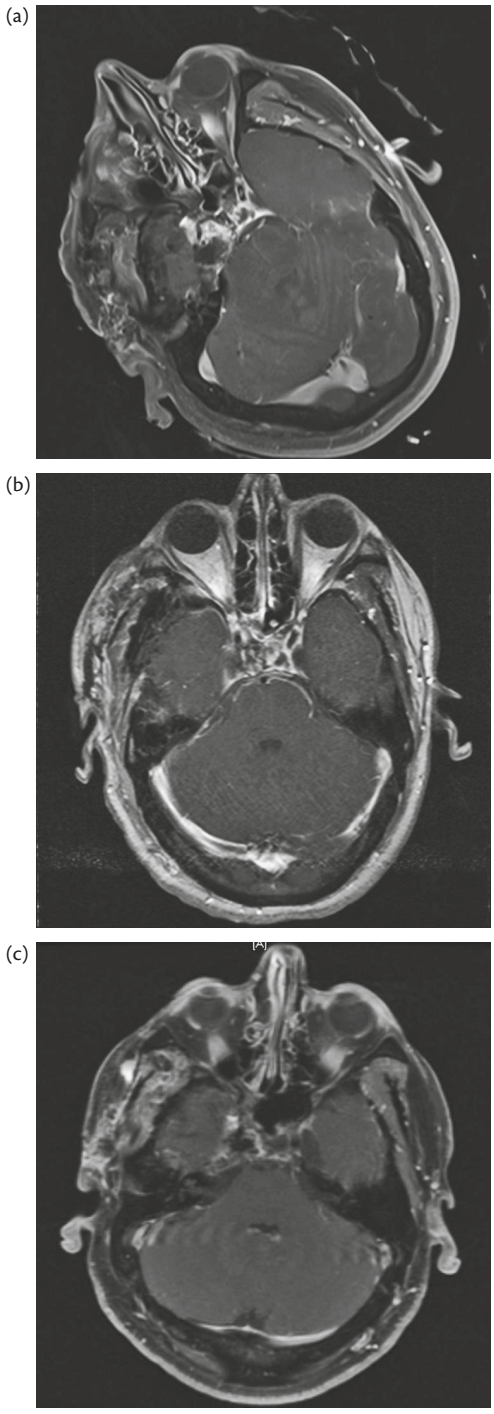

Fig. 15.4 (A) Intraoperative MRI showing residual chordoma; (B) postoperative MRI showing no residual chordoma after additional resection; (C) 3-month follow-up MRI showing no residual chordoma.

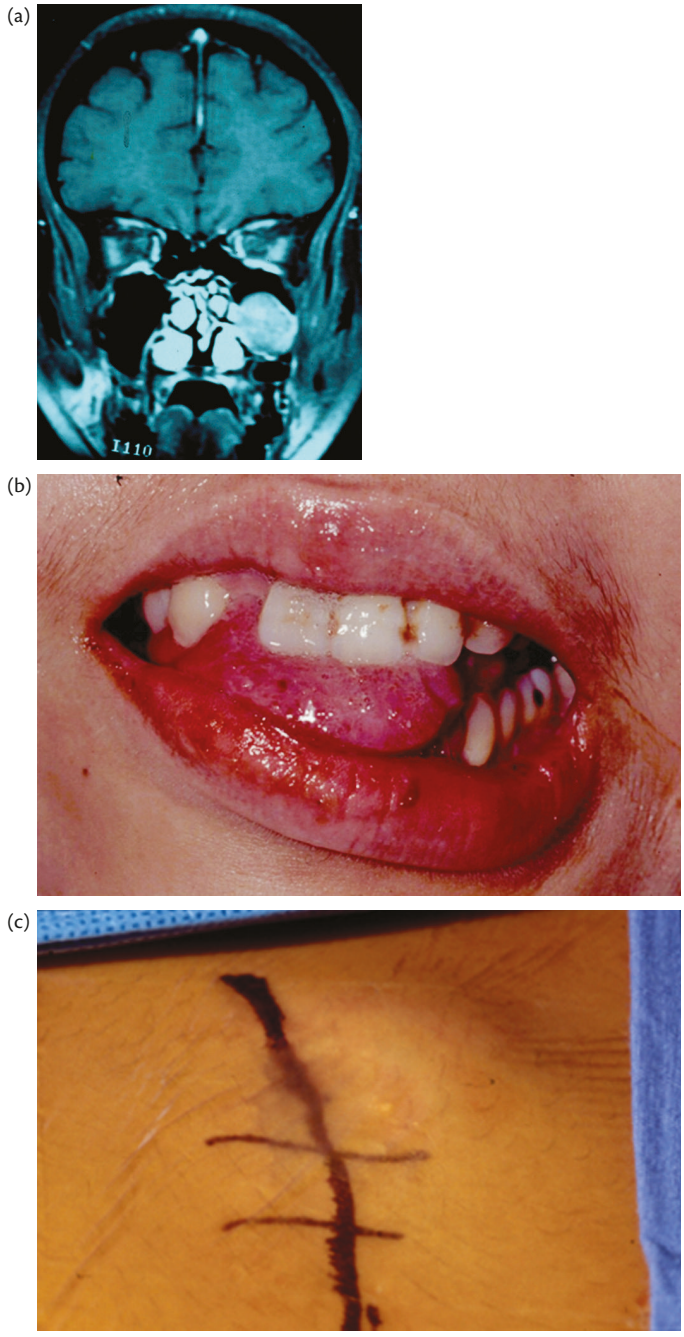

Fig. 15.5 Examples of surgical seeding of chordoma. (A) Coronal MRI showing chordoma seeding of the maxilla following a transmaxillary approach. (B) Patient photograph demonstrating chordoma seeding the gingiva following a sublabial exposure. (C) Patient photograph showing seeding of the abdomen at the site of the abdominal fat graft.

replaced, and clean instruments and gloves are used. If fat or fascia is harvested from other sites, clean instruments and gloves are used and a clean field recreated (Arnautovic and Al-Mefty, 2001).

In keeping with the idea that chordomas act malignantly and given the dismal prognosis following recurrence, the best chance for long-term control is maximal treatment at presentation. Therefore, radical resection should be followed with high-dose radiotherapy. Chordomas are relatively radiation resistant tumours, however, high-dose radiation such as is possible with particle-based therapy has been shown to offer improved local control and survival (Hug et al., 1999; Munzenrider and Liebsch, 1999; Igaki et al., 2004; Noel et al., 2005; Weber et al., 2005). Due to the high rate of local recurrence and infiltrative nature of chordoma and propensity for seeding, it is important that the radiation field includes the entire operative bed, surgical corridor, and anatomical compartment.

In contrast to chordoma, chondrosarcoma has an excellent prognosis. Radical removal of chondrosacromas offers the potential for long-term control and possible cure and should be pursued with zeal. Radiation therapy has been proven to be effective in providing

long-term control, but this may reflect the less aggressive nature of this tumour and may not, therefore, be necessary after complete resection. We advocate radical removal without adjuvant radiation therapy and radiological surveillance of any small residual.

Prognosis

Several factors affect the prognosis of chordomas including age, histologic subtype, and treatment received. The impact of gender will not be discussed in detail, other than to say conflicting results have been reported. Unfortunately, due to their rarity, the frequent mixing with chondrosarcomas, and the lack of uniform treatment, the true prognosis of patients with chordomas is difficult to determine. However, we will address how each of these factors affect prognosis and emphasize that the best chance for long-term control is with radical resection including the involved bony islands followed by high-dose radiation at the time of initial diagnosis.

The effect of age on prognosis has revealed conflicting results with the exception of the particularly aggressive course of chordomas in those less than five years old. In children less than five years old, 65% of tumours are atypical and those with the classical subtype are more cellular. Furthermore, nearly 60% of patients less than five years old suffer from metastases (Borba et al., 1996). However, in general with the paediatric population, we have been pleased to see a number of long-term disease-free survivors using the strategy of radical resection and high-dose radiation (unpublished data).

Atypical chordomas have a worse prognosis than the classic or chondroid type (Ouyang et al., 2014; Yakkioui et al., 2014). In their seminal work on chordoma and chondrosarcoma in which they introduced the chondroid subtype, Heffelfinger et al. suggested that the chrondroid variant had a more benign course and other authors have supported that claim (Heffelfinger et al., 1973; Rich et al., 1985). Debate over the prognostic significance of this type has ensued, however, we have convincingly shown in a study of 109 patients all with pathology confirmed with immunohistochemical staining that chondroid tumour is indeed a subtype of chordoma with no difference in outcome and that both chordoma subtypes have a significantly worse outcome than chondrosarcoma (Almefty et al., 2007). Other studies have supported this finding (Forsyth et al., 1993; Colli and Al-Mefty, 2001; Bohman et al., 2014). These findings highlight the importance of confirming the pathologic diagnosis with immunohistochemical staining.

The combination of radical surgical resection and high-dose radiation treatment has proven to be the optimal treatment strategy for patients with skull base chordoma. However, this management path is not uniformly followed, so the survival of patients with chordoma may be underestimated in some publications. Two critical points are evident, firstly that treatment with anything less than an aggressive approach is doomed to recurrence and short life expectancy following recurrence. Secondly, that radical resection with up-front high-dose radiotherapy offers a chance for prolonged control. Indeed, when complete tumour removal is achieved and adjuvant proton beam therapy utilized, we have seen a recurrence-free survival rate of 74%, whereas, this falls to 40% when residual tumour is present (Almefty et al., 2007).

Although, often grouped together, chondrosarcomas have been repeatedly shown to have a much better prognosis than chordoma. In our study of 20 patients with chondrosarcoma, none suffered a recurrence or died from their disease. Half of these patients received proton beam therapy (Almefty et al., 2007). Proton beam therapy has been proven to have excellent control rates with five- and ten-year survival rates in the 90–100% range (Hug et al., 1999; Munzenrider and Liebsch, 1999; Ares et al., 2009). However, it is quite likely that these excellent control rates are more indicative of the tumours favourable biology. Therefore, it is our practice to attempt complete resection of chondrosarcomas and avoid radiation therapy. Small residual chondrosarcomas can be followed.

Controversies

Optimal radiation modality for chordomas

We have stated throughout this chapter the benefit of high-dose radiation for chordomas. Particle-based therapy, in which the largest experience is with protons, has been shown superior to conventional photon based treatment (Cummings et al., 1983; Fuller and Bloom, 1988; Catton et al., 1996; Hug et al., 1999; Munzenrider and Liebsch, 1999; Zorlu et al., 2000; Igaki et al., 2004; Noel et al., 2005; Weber et al., 2005; Ares et al., 2009). The radiation treatment of chordomas must consider that chordomas are intimately associated with vital structures, are relatively radioresistant, and require high radiation doses, have a high rate of local recurrence, have a high rate of surgical seeding, disperse as islands of microscopic tumour throughout the skull base, and local control is a critical part in overall survival. Given these features, proton-based therapy offers many advantages that are ideally suited for skull base chordomas. Key among the advantages in proton-based therapy is that it does not have an exit dose, making the volume of normal tissue receiving radiation smaller than with photons. The properties of chordoma also create a clear advantage for fractionated proton therapy over single-fraction radiosurgery. Single-fraction radiosurgery typically targets gross tumour volume and only limited microscopic volume. Any microscopic tumour beyond the target will receive a sharp fall-off in the dose. In contrast, as Hug et al. describe, proton irradiation for chordomas uses the concept of a clinical target volume defined as 'any area of risk for microscopic disease, in general including the entire operative bed and anatomical compartment of initial extension' (Hug, 2001). The clinical target volume has a distinctly different shape and size than the gross tumour volume and for chordoma is one that is not ideally suited for single-fraction radiotherapy.

The use of carbon ions as particle therapy radiation is a developing technology that has garnered enthusiasm from some authors (Schulz-Ertner et al., 2007; Takahashi et al., 2009). Carbon ions offer some of the same advantages as proton therapy in that they have a steep dose fall-off but are said to have a higher biological equivalent dose. The higher biological equivalent dose and ability for intensity modulation may allow the same tumour effect at lower dose potentially reducing the toxicity. Schulz-Ertner et al. reported 3- and 5-year local control rates of 80% and 70% and overall survival of 92% and 89% treated with surgery plus carbon ion therapy (Schulz-Ertner et al., 2007). Takahashi et al. reported 3- and 5-year recurrence-free survival rates of 70% and 70%, although only nine patients were included (Takahashi et al., 2009). Carbon ion therapy has the potential to be an attractive option for the adjuvant treatment of chordomas

but additional studies with more patients and longer follow-up are needed.

Endonasal resection of chordomas

With the development and growing popularity of endonasal approaches to the anterior skull base, this technique is being increasingly used in the treatment of chordomas. We have already mentioned the virtues of the endoscopic techniques and the importance of surgeons learning this skill. The controversy regarding the endonasal approach for resection of chordomas is not its utilization but rather its use as the sole surgical modality. Given that chordomas are extradural tumours arising from the clivus, anterior midline approaches are typically needed. However, chordoma is not limited to the visible soft tissue mass but exists as islands in the surrounding bone. Therefore, radical resection of chordomas requires removal of this bone. Frequently, to accomplish this goal, multiple approaches are needed and an endonasal approach alone in these cases will not achieve the sought-after radical removal. Additionally, the clivus is typically widely involved and extensive drilling is required. In order to drill in such a critical area, the three-dimensional view provided by an operative microscope is preferable. Finally, chordomas have a propensity for surgical seeding and the endoscope may increase the risk of implantation because to maintain a sense of depth of field constant movement with the endoscope is necessary and instruments are constantly passed through an uncontained field.

REFERENCES

Abolfotoh, M., Bi, W.L., Hong, C.K., et al. (2015). The combined microscopic-endoscopic technique for radical resection of cerebellopontine angle tumors. *J Neurosurg*, **123**, 1301–11.

Al-Mefty, O. (1998). *Operative Atlas of Meningiomas*, Philadelphia, PA: Lippincott-Raven.

Al-Mefty, O. & Borba, L.A. (1997). Skull base chordomas: a management challenge. *J Neurosurg*, **86**, 182–9.

Al-Mefty, O., Kadri, P.A., Hasan, D.M., Isolan, G.R., & Pravdenkova, S. (2008). Anterior clivectomy: surgical technique and clinical applications. *J Neurosurg*, **109**, 783–93.

Almefty, K., Pravdenkova, S., Colli, B.O., Al-Mefty, O., & Gokden, M. (2007). Chordoma and chondrosarcoma: similar, but quite different, skull base tumors. *Cancer*, **110**, 2457–67.

Almefty, K.K., Pravdenkova, S., Sawyer, J., & Al-Mefty, O. (2009). Impact of cytogenetic abnormalities on the management of skull base chordomas. *J Neurosurg*, **110**, 715–24.

Ammirati, M. & Bernardo, A. (1999). Management of skull base chordoma. *Crit Rev Neurosurg*, **9**, 63–9.

Ares, C., Hug, E.B., Lomax, A.J., et al. (2009). Effectiveness and safety of spot scanning proton radiation therapy for chordomas and chondrosarcomas of the skull base: first long-term report. *Int J Radiat Oncol Biol Phys*, **75**, 1111–18.

Arnautovic, K.I. & Al-Mefty, O. (2001). Surgical seeding of chordomas. *Neurosurg Focus*, **10**, E7.

Bayrakli, F., Guney, I., Kilic, T., Ozek, M., & Pamir, M.N. (2007). New candidate chromosomal regions for chordoma development. *Surg Neurol*, **68**, 425–30; discussion 430.

Bi, W.L., Brown, P.A., Abolfotoh, M., Al-Mefty, O., Mukundan, S., Jr., & Dunn, I.F. (2015). Utility of dynamic computed tomography angiography in the preoperative evaluation of skull base tumors. *J Neurosurg*, **123**, 1–8.

Bohman, L.E., Koch, M., Bailey, R.L., Alonso-Basanta, M., & Lee, J.Y. (2014). Skull base chordoma and chondrosarcoma: influence of clinical and demographic factors on prognosis: a SEER analysis. *World Neurosurg*, **82**, 806–14.

Borba, L.A., Al-Mefty, O., Mrak, R.E., & Suen, J. (1996). Cranial chordomas in children and adolescents. *J Neurosurg*, **84**, 584–91.

Brandal, P., Bjerkehagen, B., Danielsen, H., & Heim, S. (2005). Chromosome 7 abnormalities are common in chordomas. *Cancer Genet Cytogenet*, **160**, 15–21.

Bridge, J.A., Pickering, D., & Neff, J.R. (1994). Cytogenetic and molecular cytogenetic analysis of sacral chordoma. *Cancer Genet Cytogenet*, **75**, 23–5.

Catton, C., O'Sullivan, B., Bell, R., et al. (1996). Chordoma: long-term follow-up after radical photon irradiation. *Radiother Oncol*, **41**, 67–72.

CBTRUS (2012). *CBTRUS Statistical Report: Primary Brain and Central Nervous System Tumors Diagnosed in the United States in 2004–2008*. Hinsdale, IL: Central Brain Tumor Registry of the United States.

Chambers, K.J., Lin, D.T., Meier, J., Remenschneider, A., Herr, M., & Gray, S.T. (2014). Incidence and survival patterns of cranial chordoma in the United States. *Laryngoscope*, **124**, 1097–102.

Colli, B. & Al-Mefty, O. (2001). Chordomas of the craniocervical junction: follow-up review and prognostic factors. *J Neurosurg*, **95**, 933–43.

Cummings, B.J., Hodson, D.I., & Bush, R.S. (1983). Chordoma: the results of megavoltage radiation therapy. *Int J Radiat Oncol Biol Phys*, **9**, 633–42.

Dalpra, L., Malgara, R., Miozzo, M., et al. (1999). First cytogenetic study of a recurrent familial chordoma of the clivus. *Int J Cancer*, **81**, 24–30.

Deboer, J.M., Neff, J.R., & Bridge, J.A. (1992). Cytogenetics of sacral chordoma. *Cancer Genet Cytogenet*, **64**, 95–6.

Erdem, E., Angtuaco, E.C., Van Hemert, R., Park, J.S., & Al-Mefty, O. (2003). Comprehensive review of intracranial chordoma. *Radiographics*, **23**, 995–1009.

Evans, H.L., Ayala, A.G., & Romsdahl, M.M. (1977). Prognostic factors in chondrosarcoma of bone: a clinicopathologic analysis with emphasis on histologic grading. *Cancer*, **40**, 818–31.

Fagundes, M.A., Hug, E.B., Liebsch, N.J., Daly, W., Efird, J., & Munzenrider, J.E. (1995). Radiation therapy for chordomas of the base of skull and cervical spine: patterns of failure and outcome after relapse. *Int J Radiat Oncol Biol Phys*, **33**, 579–84.

Forsyth, P.A., Cascino, T.L., Shaw, E.G., et al. (1993). Intracranial chordomas: a clinicopathological and prognostic study of 51 cases. *J Neurosurg*, **78**, 741–7.

Fuller, D.B. & Bloom, J.G. (1988). Radiotherapy for chordoma. *Int J Radiat Oncol Biol Phys*, **15**, 331–9.

Gay, E., Sekhar, L.N., Rubinstein, E., et al. (1995). Chordomas and chondrosarcomas of the cranial base: results and follow-up of 60 patients. *Neurosurgery*, **36**, 887–96; discussion 896–7.

Hallor, K.H., Staaf, J., Jonsson, G., et al. (2008). Frequent deletion of the CDKN2A locus in chordoma: analysis of chromosomal imbalances using array comparative genomic hybridisation. *Br J Cancer*, **98**, 434–42.

Heffelfinger, M.J., Dahlin, D.C., MacCarty, C.S., & Beabout, J.W. (1973). Chordomas and cartilaginous tumors at the skull base. *Cancer*, **32**, 410–20.

Horbinski, C., Oakley, G.J., Cieply, K., et al. (2010). The prognostic value of Ki-67, p53, epidermal growth factor receptor, 1p36, 9p21, 10q23, and 17p13 in skull base chordomas. *Arch Pathol Lab Med*, **134**, 1170–6.

Hug, E.B. (2001). Review of skull base chordomas: prognostic factors and long-term results of proton-beam radiotherapy. *Neurosurg Focus*, **10**, E11.

Hug, E.B., Loredo, L.N., Slater, J.D., et al. (1999). Proton radiation therapy for chordomas and chondrosarcomas of the skull base. *J Neurosurg*, **91**, 432–9.

Igaki, H., Tokuuye, K., Okumura, T., et al. (2004). Clinical results of proton beam therapy for skull base chordoma. *Int J Radiat Oncol Biol Phys*, **60**, 1120–6.

Jo, V.Y., Hornick, J.L., & Qian, X. (2014). Utility of brachyury in distinction of chordoma from cytomorphologic mimics in fine-needle aspiration and core needle biopsy. *Diagn Cytopathol*, **42**, 647–52.

Kelley, M.J., Korczak, J.F., Sheridan, E., Yang, X., Goldstein, A.M., & Parry, D.M. (2001). Familial chordoma, a tumor of notochordal remnants, is linked to chromosome 7q33. *Am J Hum Genet*, **69**, 454–60.

Kitamura, Y., Sasaki, H., Kimura, T., et al. (2013). Molecular and clinical risk factors for recurrence of skull base chordomas: gain on chromosome 2p, expression of brachyury, and lack of irradiation negatively correlate with patient prognosis. *J Neuropathol Exp Neurol*, **72**, 816–23.

Korten, A.G., Ter Berg, H.J., Spincemaille, G.H., Van Der Laan, R.T., & Van De Wel, A.M. (1998). Intracranial chondrosarcoma: review of the literature and report of 15 cases. *J Neurol Neurosurg Psychiatry*, **65**, 88–92.

Kuzniacka, A., Mertens, F., Strombeck, B., Wiegant, J., & Mandahl, N. (2004). Combined binary ratio labeling fluorescence in situ hybridization analysis of chordoma. *Cancer Genet Cytogenet*, **151**, 178–81.

Le, L.P., Nielsen, G.P., Rosenberg, A.E., et al. (2011). Recurrent chromosomal copy number alterations in sporadic chordomas. *PLoS One*, **6**, e18846.

Markwalder, T.M., Markwalder, R.V., Robert, J.L., & Krneta, A. (1979). Metastatic chordoma. *Surg Neurol*, **12**, 473–8.

McMaster, M.L., Goldstein, A.M., Bromley, C.M., Ishibe, N., & Parry, D.M. (2001). Chordoma: incidence and survival patterns in the United States, 1973–1995. *Cancer Causes Control*, **12**, 1–11.

Miozzo, M., Dalpra, L., Riva, P., et al. (2000). A tumor suppressor locus in familial and sporadic chordoma maps to 1p36. *Int J Cancer*, **87**, 68–72.

Mobley, B.C., Mckenney, J.K., Bangs, C.D., et al. (2010). Loss of SMARCB1/INI1 expression in poorly differentiated chordomas. *Acta Neuropathol*, **120**, 745–53.

Munzenrider, J.E. & Liebsch, N.J. (1999). Proton therapy for tumors of the skull base. *Strahlenther Onkol*, **175** Suppl 2, 57–63.

Naka, T., Fukuda, T., Chuman, H., et al. (1996). Proliferative activities in conventional chordoma: a clinicopathologic, DNA flow cytometric, and immunohistochemical analysis of 17 specimens with special reference to anaplastic chordoma showing a diffuse proliferation and nuclear atypia. *Hum Pathol*, **27**, 381–8.

Noel, G., Feuvret, L., Calugaru, V., et al. (2005). Chordomas of the base of the skull and upper cervical spine. One hundred patients irradiated by a 3D conformal technique combining photon and proton beams. *Acta Oncol*, **44**, 700–8.

Oakley, G.J., Fuhrer, K., & Seethala, R.R. (2008). Brachyury, SOX-9, and podoplanin, new markers in the skull base chordoma vs. chondrosarcoma differential: a tissue microarray-based comparative analysis. *Mod Pathol*, **21**, 1461–9.

Ouyang, T., Zhang, N., Zhang, Y., et al. (2014). Clinical characteristics, immunohistochemistry, and outcomes of 77 patients with skull base chordomas. *World Neurosurg*, **81**, 790–7.

Rich, T.A., Schiller, A., Suit, H.D., & Mankin, H.J. (1985). Clinical and pathologic review of 48 cases of chordoma. *Cancer*, **56**, 182–7.

Riva, P., Crosti, F., Orzan, F., et al. (2003). Mapping of candidate region for chordoma development to 1p36.13 by LOH analysis. *Int J Cancer*, **107**, 493–7.

Rosenberg, A.E., Brown, G.A., Bhan, A.K., & Lee, J.M. (1994). Chondroid chordoma--a variant of chordoma. A morphologic and immunohistochemical study. *Am J Clin Pathol*, **101**, 36–41.

Sandberg, A.A. & Bridge, J.A. (2003). Updates on the cytogenetics and molecular genetics of bone and soft tissue tumors: osteosarcoma and related tumors. *Cancer Genet Cytogenet*, **145**, 1–30.

Sawyer, J.R., Husain, M., & Al-Mefty, O. (2001). Identification of isochromosome 1q as a recurring chromosome aberration in skull base chordomas: a new marker for aggressive tumors? *Neurosurg Focus*, **10**, E6.

Scheil, S., Bruderlein, S., Liehr, T., et al. (2001). Genome-wide analysis of sixteen chordomas by comparative genomic hybridization and cytogenetics of the first human chordoma cell line, U-CH1. *Genes Chromosomes Cancer*, **32**, 203–11.

Scheil-Bertram, S., Kappler, R., Von Baer, A., et al. (2014). Molecular profiling of chordoma. *Int J Oncol*, **44**, 1041–55.

Schulz-Ertner, D., Karger, C.P., Feuerhake, A., et al. (2007). Effectiveness of carbon ion radiotherapy in the treatment of skull-base chordomas. *Int J Radiat Oncol Biol Phys*, **68**, 449–57.

Takahashi, S., Kawase, T., Yoshida, K., Hasegawa, A., & Mizoe, J.E. (2009). Skull base chordomas: efficacy of surgery followed by carbon ion radiotherapy. *Acta Neurochir (Wien)*, **151**, 759–69.

Tallini, G., Dorfman, H., Brys, P., et al. (2002). Correlation between clinicopathological features and karyotype in 100 cartilaginous and chordoid tumours. A report from the Chromosomes and Morphology (CHAMP) Collaborative Study Group. *J Pathol*, **196**, 194–203.

Tamura, T., Sato, T., Kishida, Y., et al. (2015). Outcome of clival chordomas after skull base surgeries with mean follow-up of 10 years. *Fukushima J Med Sci*, **61**(2), 131–40.

Weber, D.C., Rutz, H.P., Pedroni, E.S., et al. (2005). Results of spot-scanning proton radiation therapy for chordoma and chondrosarcoma of the skull base: the Paul Scherrer Institut experience. *Int J Radiat Oncol Biol Phys*, **63**, 401–9.

Yakkioui, Y., Temel, Y., Creytens, D., et al. (2014). A comparison of cell-cycle markers in skull base and sacral chordomas. *World Neurosurg*, **82**, e311–18.

Zorlu, F., Gurkaynak, M., Yildiz, F., Oge, K., & Atahan, I.L. (2000). Conventional external radiotherapy in the management of clivus chordomas with overt residual disease. *Neurol Sci*, **21**, 203–7.

16

Dermoid and epidermoid cysts

Andrew McEvoy

Introduction

Dermoid and epidermoid cysts are important intracranial developmental lesions. They are commonly derived from retained surface ectoderm trapped by two fusing neuroectodermal surfaces during neural tube closure, and are also termed congenital ectodermal inclusion cysts. There is some debate as to whether they arise from a primary failure of neural tube closure in the third to fifth week of embryogenesis, or an earlier primary failure of gastrulation that would explain the associated mesodermal abnormalities (Dias and Walker, 1992). Occasionally epidermoid cysts are acquired lesions derived from iatrogenic implantation of surface ectoderm (termed implantation dermoids).

Epidemiology

Dermoid cysts are rare, making up 0.3% of intracranial tumours, while intracranial epidermoid cysts are approximately four times as common, making up 0.5–1.5% of intracranial tumours (MacCarty et al., 1959; Gormley et al., 1994). Both exhibit slow, linear growth, but dermoid cysts typically present at an earlier age with a shorter duration of symptoms.

Pathology

Dermoid cysts have a tendency to occur near the midline. The most common intracranial sites are near the anterior fontanelle extradurally, and in the sellar, parasellar, and intraventricular regions intradurally. The most common intraspinal site is near the cauda equina, and can be associated with a dermal sinus tract and subsequent increased risk of bacterial infection.

Dermoid cysts are composed of epithelial cell debris and keratin, and also include elements of dermis such as hair follicles, sebaceous glands and sweat glands (**Fig. 16.1**). The active secretion of glandular fluid and subsequent growth and rupture is postulated as a possible cause for their earlier presentation (Osborn and Preece, 2006).

Macroscopically dermoid cysts are well-defined, lobulated, pearly masses with thick partially calcifiesd capsules. The contents of the cyst may include the yellow, odious fluid that results from glandular secretion, and may also contain hair and teeth. Histologically dermoid cysts exhibit both dermal and epidermal elements, although the epithelial cell lining may be less well differentiated compared with epidermoid cysts.

Epidermoid cysts are mainly intracranial, and are found away from the midline. The most common location is the cerebellopontine angle (40–50%), where they make up the third most common lesion in adults after vestibular schwannomas and meningiomas. They are also found in the fourth ventricle, the sellar and parasellar regions, the cerebral hemispheres, and the brainstem. Epidermoid cysts are less common but do occur in the spine, with a predilection for the thoracic spine.

Epidermoid cysts are composed of only epithelial cell debris, including cholesterol and keratin, with no dermal involvement, that is laid down in a lamellar pattern (**Fig. 16.1**). This gives rise to a more irregular and lobulated mass, with a sheeny surface that grows to encase surrounding nerves and vessels along cleavage planes. The cyst contains soft keratohyalin material that results from progressive epithelial desquamation, and is often described as having a classic 'candle wax' appearance intraoperatively.

Epidermoid and dermoid cysts can broadly present in two ways. Firstly there is local mass effect, which is dependent on tumour location and insidious by nature on account of the slow, linear growth rate. Cysts in the middle cranial fossa are often asymptomatic, and can grow relatively large before detection, with atypical presentations such as trigeminal numbness.

Secondly there is a more acute presentation, secondary to cyst rupture (**Fig. 16.2**). Aetiology may be traumatic, iatrogenic, or spontaneous, with a consequent leakage of cyst contents into the subarachnoid space and associated chemical meningitis. This should be distinguished from the septic meningitis seen in intraspinal dermoid cysts, caused by the presence of a dermal sinus tract. Cyst rupture can lead to several neurological sequelae, including headache, seizures, vasospasm, neurological deficit, and death.

Finally, dermoid cysts can be associated with other congenital abnormalities that may account for the initial presentation. An association with Klippel-Feil syndrome has been reported for both intraspinal (McLaughlin et al., 2013) and intracranial (Pai et al., 2007) dermoid cysts. The presence of associated mesenchymal abnormalities supports the notion put forward by Dias and Walker that the key embryological event for the development of dermoid cysts occurs prior to neural tube closure, around the time of the formation

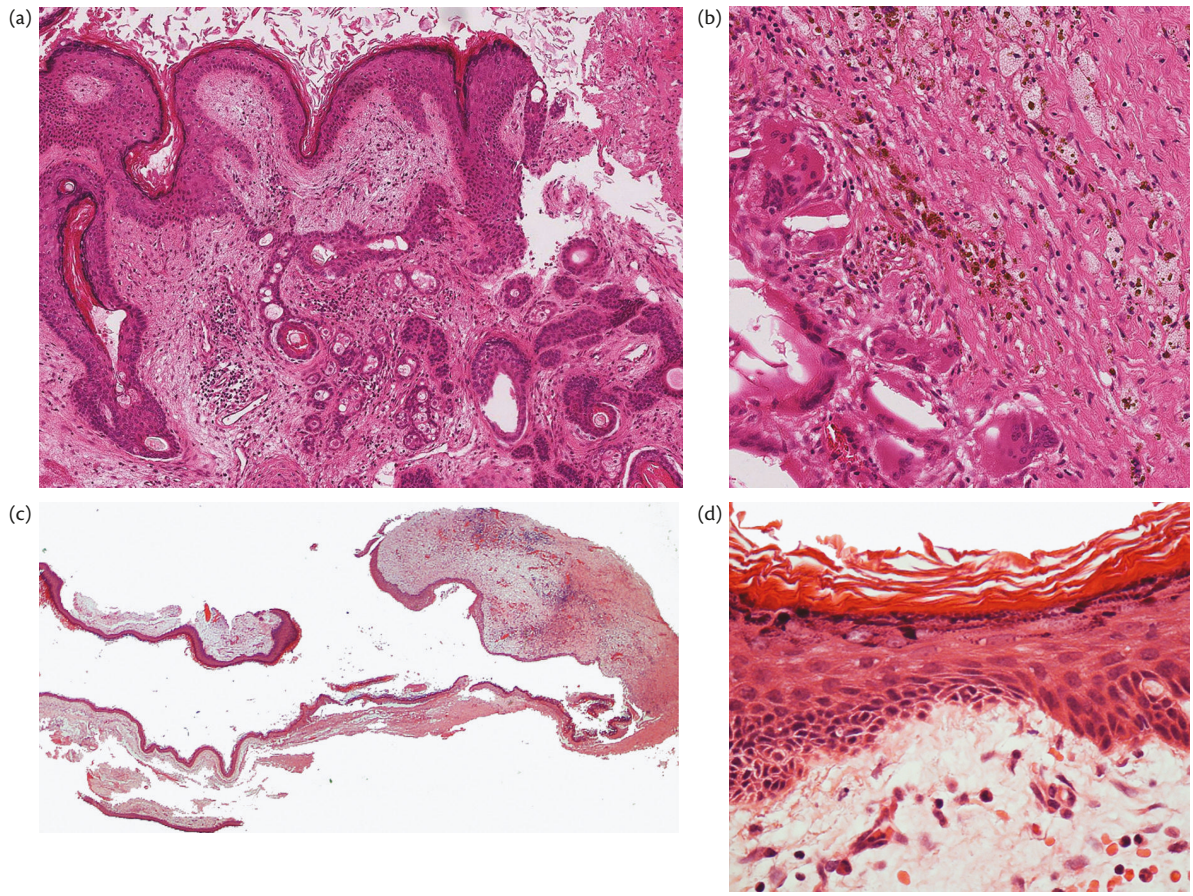

Fig. 16.1 Histopathology of dermoid and epidermoid cysts
(A) Wall of a dermoid cyst with a lining of stratified squamous epithelium with prominent surface keratinization. The wall of the cyst shows mature adnexal structures including pilosebaceous glands, which classify this as a dermoid. (B) A focal foreign body giant cell reaction with macrophages and haemosiderin pigment is seen indicative of previous cyst rupture. (C) Epidermoid cyst at low power magnification showing a simple unilocular cyst with a squamous epithelial lining and fibrocollagenous wall but no adnexal structures. (D) The epithelial lining is simple stratified squamous epithelium with keratinization.

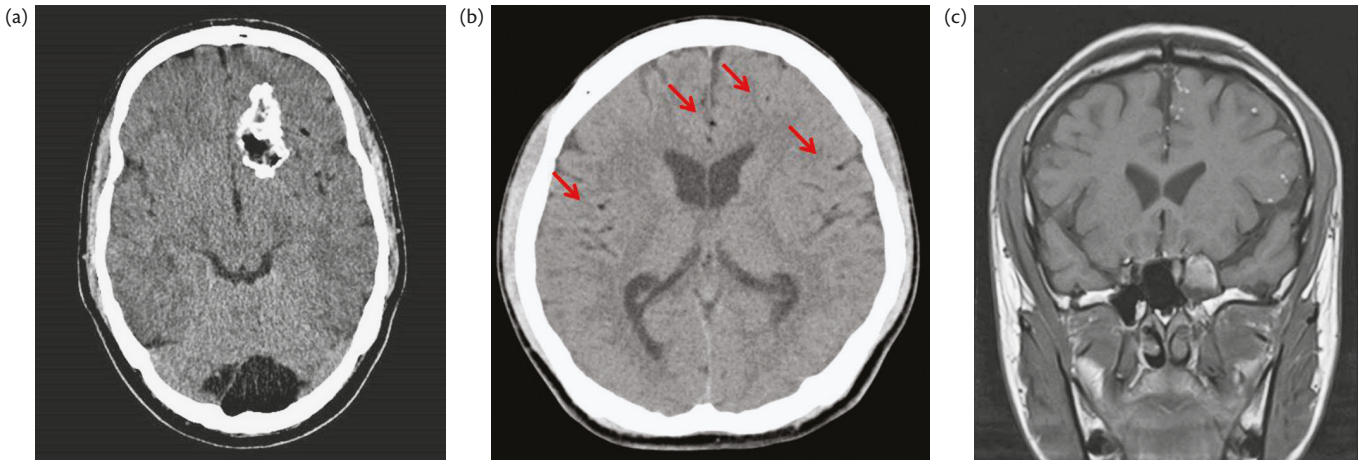

Fig. 16.2 Ruptured dermoid cyst. (A) CT showing ruptured left frontal calcified dermoid cyst. (B) CT showing disseminated locules of fat in the subarachnoid space. (C) Coronal T1W MRI showing ruptured left parasellar dermoid cyst.

Table 16.1 Features of dermoid and epidermoid cysts

	Dermoid	Epidermoid
Frequency	Rare	More common
Location	Midline	Off midline
Presentation	Earlier	Later
Contents	Dermal elements	No dermal elements
Rupture	More common	Less common
Associated abnormalities	May be present	Absent
Surgical resection	Less difficult	Difficult

of the trilaminar plate (Dias and Walker, 1992). Table 16.1 presents the features of dermoid and epidermoid cysts.

Radiological features

The typical radiological findings of epidermoid and dermoid cysts are shown in Table 16.2.

Fluid attenuated inversion recovery (FLAIR) and diffusion MRI (DWI) are useful to distinguish epidermoid cysts from arachnoid cysts. In contrast to epidermoid cysts, arachnoid cysts exhibit signal drop-out with FLAIR and free diffusion with DWI (Fig. 16.4).

Dermoid cysts (Fig. 16.5) can have a variable appearance on MRI, dependent on the balance of their contents which may include fat, hair, sebum, and teeth. They differ from lipomas by not consistently following fat densities on all sequences. Haemorrhage within the cyst can lead to hyperdensity on CT, and can occasionally mask the underlying lesion (Sanchez-Mejia et al., 2006).

Surgery

Indications

The aim of resective surgery for any space-occupying lesion is threefold, diagnostic, treatment of symptoms, and improvement in outcome. With the range of MRI sequences outlined surgery is rarely indicated to make a diagnosis in these cases. Therefore, the main indication for surgery is to treat current symptomatology, which is usually secondary to the mass effect. The risk of future morbidity can be difficult to predict, and a broader discussion on the advantages and disadvantages of conservative management follows in a later section.

Preoperative

Patients should undergo comprehensive MR diagnostic imaging, with the input of an experienced neuroradiologist. For posterior fossa cysts, particular attention should be paid to the presence of associated abnormalities at the craniocervical junction, including occipitalization of C1, basilar invagination, atlantoaxial subluxation, Klippel-Feil syndrome and Chiari malformations (Chandra et al., 2005).

All patients should be examined for signs of a dermal sinus tract, which may predispose to bacterial infection. In these cases, excision of the tract should be incorporated with the surgical resection of the cyst.

The slow, linear growth of these cysts means there is little surrounding vasogenic oedema, and a preoperative course of corticosteroids is rarely necessary. However, corticosteroids are indicated following cyst rupture or postoperatively when cyst contents are spilled, when they are thought to reduce the severity and duration of chemical meningitis.

Surgical rationale

The ideal goal of surgery is complete resection of the cyst including the epithelial lining, providing curative treatment and removing the risk of recurrence. However, surgery can be technically demanding on account of the deep, critical location of the tumours and the relationship of the tumours to surrounding neurovascular structures. Since this is a benign condition, a form of subtotal resection with functional preservation is always preferable to gross total resection when there is a high risk of causing neurological deficits.

There are few large case series on account of the rarity of the tumours. In Yasargil's series of 43 patients treated at a single centre (consisting of 35 epidermoid and eight dermoid cysts), compete resection was achieved in 41 cases (34 epidermoid cysts and seven dermoid cysts) with excellent results, using strict microsurgical

Table 16.2 Radiological features of dermoid and epidermoid cysts

Imaging modality	Dermoid	Epidermoid
CT	Hypodense, very similar to CSF Lobulated margins Fine linear strands No enhancement	Hypodense, slightly greater than CSF Bone erosion in 33% No enhancement
T1W MRI	Typically hyperintense, same as fat No enhancement	Isointense, same as CSF Occasionally hyperintense around periphery, No enhancement
T2W MRI	Variable	Isointense or hyperintense, same as CSF
FLAIR	Variable	Hyperintense to CSF
DWI	Restricted diffusion, hyperintense to CSF	Restricted diffusion, hyperintense to CSF
Fat saturation sequence	High signal drops out	Unchanged
Local findings	More mass effect Associated abnormalities (i.e. Klippel-Feil, dermal sinus tract)	Insinuates between neurovascular structures

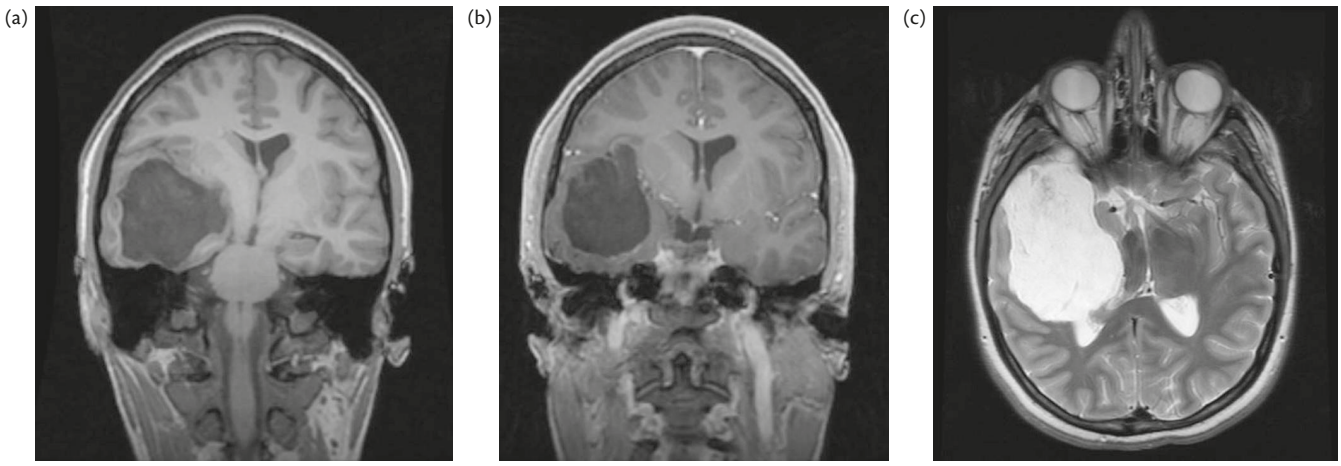

Fig. 16.3 Epidermoid cyst. (A and B) Coronal T1W MRI without and with gadolinium showing right perisylvian epidermoid cyst. (C) Axial T2W MRI showing right perisylvian epidermoid cyst.

skull base surgery approaches (Yasargil et al., 1989). In this series total resection was defined as complete removal of cyst contents and capsule. Most other series report lower rates of total resection ranging from 0% to 75% (Lynch et al., 2014). This reflects the technical difficulties of surgery and emphasizes the need to avoid causing functional deficits. The development of minimally invasive skull base techniques may change the way these tumours are approached (Chivukula et al., 2013), although it remains to be seen whether this will improve the rates of gross total resection.

Independent of the surgical approach resection can be technically demanding for several reasons. Tumour adhesions to adjacent structures on the skull base and also to surrounding brain

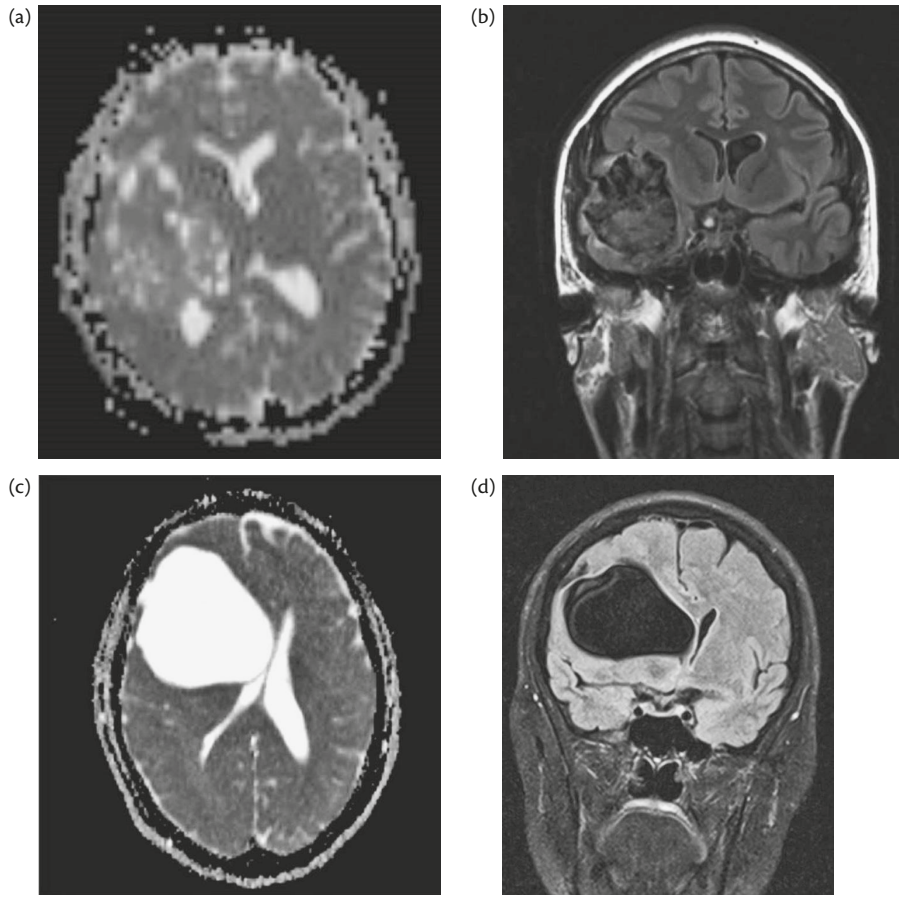

Fig. 16.4 Differentiating epidermoid (A and B) from arachnoid cyst (C and D).
(A) ADC map shows restricted diffusion of epidermoid cyst; (B) coronal FLAIR shows persistence of high signal in epidermoid cyst; (C) ADC map shows free diffusion of arachnoid cyst; (D) coronal FLAIR shows signal drop out in arachnoid cyst.

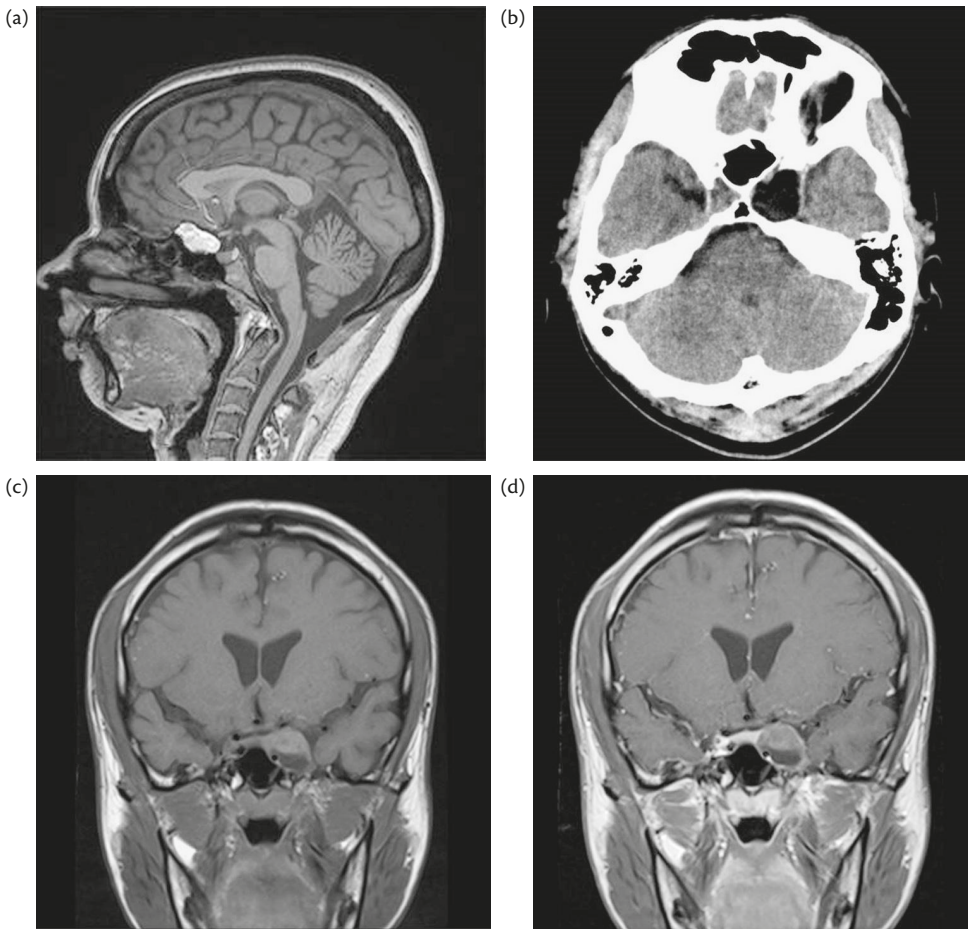

Fig. 16.5 Dermoid cyst. (A) Sagittal T1W MRI showing parasellar dermoid cyst; (B) axial CT scan showing parasellar dermoid cyst; (C and D) coronal T1W MRI pre- and postcontrast showing parasellar dermoid cyst.

parenchyma are common. This is most pronounced with dermoid cysts, which tend to cause a greater granulomatous reaction with the arachnoid mater and occasionally the pia mater. Additionally, the cyst can extend between different anatomical compartments. This is most pronounced with epidermoid cysts, which are soft and pliable and have a tendency to 'flow' into the available subarachnoid space. Finally, prolonged linear growth of tumours can lead to substantial distortion of the surrounding anatomy, such as displacement of the basilar artery from the ventral surface of the brainstem. A strict microsurgical technique should be employed at all times, with wide exposure, minimal retraction, preservation of surrounding arachnoid planes and meticulous haemostasis. The principles of resection involve using the ultrasonic aspirator to achieve a primary intracapsular debulking followed by removal of the capsule by the development of a plane between capsule and overlying arachnoid. The cyst contents should not be allowed to spill into the subarachnoid space as they are intensely irritant and can cause a chemical meningitis. This requires meticulous layering of the surrounding normal structures with linteens before the cyst is opened and the contents accessed. In cases where the capsule is adherent to the brain or important neurovascular structures, it may be necessary to leave residual capsule behind. This carries the risk of tumour recurrence in the future, and possibly commits the patient to long-term surveillance imaging and follow-up. However, this approach avoids damage to neurovascular structures that may be disastrous for the patient.

Most series that report surgical outcomes group epidermoid and dermoid cysts together, making it difficult to discern differences between groups. There is no evidence that outcomes are worse for epidermoid cysts compared with dermoid cysts. Dermoid cysts may present more of a challenge in the development of a plane between capsule and arachnoid in areas of granulomatous reaction, while epidermoid cysts may be more challenging in their anatomical location and extension.

There is currently no role for radiotherapy or chemotherapy in the treatment of dermoid or epidermoid cysts with the exception of malignant transformation.

Complications

A well-recognized complication from surgical resection of both dermoid and epidermoid cysts is the 'spilling' of the contents of the cyst into the surrounding CSF, which can occur with intraoperative handling. This results in the dissemination of fat droplets throughout the subarachnoid and intraventricular space, setting up a chemical inflammation of the meninges (Fig. 16.2). The clinical sequelae are variable, and include no adverse effects (Carvalho et al., 2000), headaches, seizures, and hydrocephalus (Liu et al., 2008). The risk of intraoperative spillage can be reduced by sharp dissection of the

capsule, copious irrigation in the surgical field and protection of the surrounding brain with cotton pads. Treatment is largely conservative, although steroids are indicated for chemical meningitis, and hydrocephalus should be treated with appropriate CSF diversion.

Recurrence

Complete tumour resection is desirable to minimize the risk of future morbidity from tumour recurrence, and the first resection is usually the best opportunity to achieve this. The recurrence rate for dermoid and epidermoid cysts is likely to be dependent on the volume of residual tumour left following subtotal resection. However, growth is linear, leading to long periods of patients being asymptomatic. In one series of 29 patients who underwent resection of epidermoid cysts with long-term follow-up, primary recurrence occurred in seven patients after a mean period of 8 years and 10 months, and secondary recurrence (recurrence following re-do surgery) occurred after a mean period of 12 years 6 months from their first resection (Yamakawa et al., 1989). Re-do resections present new difficulties, with the added presence of intradural adhesions as a result of previous surgery. However, in symptomatic patients with tumour recurrence re-operation is often indicated.

Risk of malignant transformation

Malignant transformation of dermoid and epidermoid cysts is a rare but recognized cause of intracranial squamous cell carcinoma, after metastases and extension from the cranial base. A review found 52 cases of malignant transformation of cysts in the literature, with a median survival of 9 months (Hamlat et al., 2005). Radiotherapy is considered to confer a modest survival benefit (median survival 26 vs. 3 months, $P = 0.077$). Leptomeningeal carcinomatosis has only been seen with malignant transformation of epidermoid cysts and is associated with a particularly poor prognosis. Although extremely rare, malignant transformation should be considered in any patient who does not recover as expected from surgery and who deteriorates in the absence of hydrocephalus with rapid recurrence of the tumour or where imaging shows enhancement at the tumour site.

Controversies with follow-up imaging: The case for and against

Routine surveillance imaging may follow initial diagnosis as part of a conservative strategy, and may also follow a subtotal or gross total resection.

The benefits of surveillance imaging are that tumour growth and recurrence may be closely monitored so that both patient and surgeon will have a good understanding of the tumour's behaviour. This may be especially important if the tumour begins to encroach on vital structures or straddle anatomical compartments, making total resection more difficult to achieve. There is also a theoretical advantage of improving detection of malignant transformation, although this is a very rare event with few documented cases in the literature (Hamlat et al., 2005).

The main disadvantage for the patient is that follow-up imaging may add to the psychological burden. Radiological progression in the absence of symptoms is rarely an indication for surgery. A pragmatic approach would therefore be to repeat imaging when the patient presents with new symptoms or signs.

There are currently no clear guidelines on how this patient group should be followed up. From the surgeon's point of view, an immediate postoperative MRI is essential to establish a baseline of residual tumour, and some staged follow-up imaging can prove useful in providing patient information on the risk of future morbidity or surgery. Occasionally patients with no new symptoms may be suitable for surgery if there is clear radiological progression with impending neurological deficit. However, in all cases the frequency of follow-up imaging should be discussed with the patient, and tailored to fit their own expectations and practical circumstances.

FURTHER READING

Chivukula, S., Koutourousiou, M., Snyderman, C.H., Fernandez-Miranda, J.C., Gardner, P.A., & Tyler-Kabara, E.C. (2013). Endoscopic endonasal skull base surgery in the pediatric population. *J Neurosurg Pediatr*, **11**, 227–41.

Dias, M.S. & Walker, M.L. (1992). The embryogenesis of complex dysraphic malformations: a disorder of gastrulation? *Pediatr Neurosurg*, **18**, 229–53.

Liu, J.K., Gottfried, O.N., Salzman, K.L., Schmidt, R.H., & Couldwell, W.T. (2008). Ruptured intracranial dermoid cysts: clinical, radiographic, and surgical features. *Neurosurgery*, **62**, 377–84; discussion 384.

Lynch, J.C., Aversa, A., Pereira, C., Nogueira, J., Goncalves, M., & Lopes, H. (2014). Surgical strategy for intracranial dermoid and epidermoid tumors: an experience with 33 patients. *Surg Neurol Int*, **5**, 163.

Yasargil, M.G., Abernathey, C.D., & Sarioglu, A.C. (1989). Microneurosurgical treatment of intracranial dermoid and epidermoid tumors. *Neurosurgery*, **24**, 561–7.

REFERENCES

Carvalho, G.A., Cervio, A., Matthies, C., & Samii, M. (2000). Subarachnoid fat dissemination after resection of a cerebellopontine angle dysontogenic cyst: case report and review of the literature. *Neurosurgery*, **47**, 760–3; discussion 763–4.

Chandra, P.S., Gupta, A., Mishra, N.K., & Mehta, V.S. (2005). Association of craniovertebral and upper cervical anomalies with dermoid and epidermoid cysts: report of four cases. *Neurosurgery*, **56**, E1155; discussion E1155.

Chivukula, S., Koutourousiou, M., Snyderman, C.H., Fernandez-Miranda, J.C., Gardner, P.A., & Tyler-Kabara, E.C. (2013). Endoscopic endonasal skull base surgery in the pediatric population. *J Neurosurg Pediatr*, **11**, 227–41.

Dias, M.S. & Walker, M.L. (1992). The embryogenesis of complex dysraphic malformations: a disorder of gastrulation? *Pediatr Neurosurg*, **18**, 229–53.

Gormley, W.B., Tomecek, F.J., Qureshi, N., & Malik, G.M. (1994). Craniocerebral epidermoid and dermoid tumours: a review of 32 cases. *Acta Neurochir (Wien)*, **128**, 115–21.

Hamlat, A., Hua, Z.F., Saikali, S., et al. (2005). Malignant transformation of intra-cranial epithelial cysts: systematic article review. *J Neurooncol*, **74**, 187–94.

Liu, J.K., Gottfried, O.N., Salzman, K.L., Schmidt, R.H., & Couldwell, W.T. (2008). Ruptured intracranial dermoid cysts: clinical, radiographic, and surgical features. *Neurosurgery*, **62**, 377–84; discussion 384.

Lynch, J.C., Aversa, A., Pereira, C., Nogueira, J., Goncalves, M., & Lopes, H. (2014). Surgical strategy for intracranial dermoid and epidermoid tumors: an experience with 33 patients. *Surg Neurol Int*, **5**, 163.

MacCarty, C.S., Leavens, M.E., Love, J.G., & Kernohan, J.W. (1959). Dermoid and epidermoid tumors in the central nervous system of adults. *Surg Gynecol Obstet*, **108**, 191–8.

Mclaughlin, N., Weil, A.G., Demers, J., & Shedid, D. (2013). Klippel-Feil syndrome associated with a craniocervico-thoracic dermoid cyst. *Surg Neurol Int*, **4**, S61–6.

Osborn, A.G. & Preece, M.T. (2006). Intracranial cysts: radiologic-pathologic correlation and imaging approach. *Radiology*, **239**, 650–64.

Pai, V.V., Lowe, L.H., Castillo, M., Huang, B.Y., & Shao, L. (2007). Posterior fossa dermoid cysts in association with Klippel-Feil syndrome: report of three cases. *AJNR Am J Neuroradiol*, **28**, 1926–8.

Sanchez-Mejia, R.O., Limbo, M., Tihan, T., Galvez, M.G., Woodward, M.V., & Gupta, N. (2006). Intracranial dermoid cyst mimicking hemorrhage. Case report and review of the literature. *J Neurosurg*, **105**, 311–14.

Yamakawa, K., Shitara, N., Genka, S., Manaka, S., & Takakura, K. (1989). Clinical course and surgical prognosis of 33 cases of intracranial epidermoid tumors. *Neurosurgery*, **24**, 568–73.

Yasargil, M.G., Abernathey, C.D., & Sarioglu, A.C. (1989). Microneurosurgical treatment of intracranial dermoid and epidermoid tumors. *Neurosurgery*, **24**, 561–7.

RELATED LINKS TO EBRAIN

Pathology and Management of Dermoids and Epidermoids. https://learning.ebrain.net/course/view.php?id=478

Radiology of Dermoids and Epidermoids. https://learning.ebrain.net/course/view.php?id=479

17

Esthesioneuroblastoma

Georgios Klironomos, Lior Gonen, and Fred Gentili

Introduction

Esthesioneuroblastoma (ENB) is a rare, malignant tumour of neuroectodermal origin, arising in the upper nasal cavity. First described in 1924 by Berger and Richard, several names have subsequently been assigned to this tumour but currently the most common terms are 'esthesioneuroblastoma' and 'olfactory neuroblastoma'. Histological and molecular studies indicate that the most likely cells of origin are the basal cells of the olfactory epithelium located at the area of cribriform plate, the upper third of the nasal septum and the superior nasal turbinate. In humans the olfactory epithelium retains the capacity to regenerate through division and differentiation of the basal cells. ENB is an aggressive tumour with a variable tendency to metastasize. It can extend or recur intracranially by local extension through the cribriform plate. It may be difficult to differentiate this tumor from other neoplasms arising in the nasal cavity and paranasal sinuses.

Epidemiology and clinical presentation

ENB represents 0.3% of all cancers of the upper digestive tract and approximately 3–6% of all intranasal malignant tumours of the nasal cavity (Broich et al., 1997). There is a slight male predominance (male 55%, female 45%), and it affects several ethnicities. In the literature a bimodal age distribution has been suggested with one peak around 20 years of age and a second peak in the fifth decade (Klepin et al., 2005). However recent reviews indicate that the incidence of ENB has a unimodal distribution with a peak in the fifth and sixth decade (Platek et al., 2011). No predisposing factors have been described for ENB.

The clinical presentation of patients with ENB is insidious, nonspecific, and mimics benign processes and other nasal malignancies. A large number of patients with small tumours may be asymptomatic and diagnosed incidentally. Nasal obstruction followed by unilateral epistaxis are the most common presenting symptoms and may be present from 6 to 12 months before the ENB diagnosis is made. Other symptoms may be present depending on the tumour's size and the presence of extension to adjacent structures. Symptoms may include headache, facial pain, sinusitis, anosmia/hyposmia, visual changes, diplopia, and proptosis if orbital involvement occurs. Neurological symptoms may be present in cases of intracranial extension including nausea and vomiting due to intracranial hypertension, hormonal disturbances secondary to pituitary gland and hypothalamic involvement and visual changes due to the involvement of the visual apparatus. Paraneoplastic syndromes related to ENB have been reported, most commonly related to antidiuretic hormone (SIADH) and adrenocorticotrophic hormone secretion (Gabbay et al., 2013). Ectopic ENBs have been described in the sphenoid sinus, the oral cavity, maxillary sinus and intracranially (Purochit et al., 2015). Symptoms of ENB are in most cases non-specific and may mimic benign sinonasal pathologies. For this reason, a high index of suspicion is very important for the early detection of these lesions.

Diagnostic evaluation

Any patient with persistent nasal symptomatology should have a thorough evaluation from an ear, nose, and throat (ENT) specialist. Apart from detailed physical and cranial nerves examination, nasal examination with a flexible endoscope permits a thorough inspection of the nasal cavity and nasopharynx. ENB may appear as a fleshy, reddish-yellow mass filling the nasal cavity to a varying extent, covered by mucosa with possible ulceration.

After tumour identification radiological evaluation should be undertaken including a high resolution (3 mm section) computed tomography (CT) scan of the skull base, paranasal sinus, and neck with and without contrast. The tumour appears hyperintense on non-contrast CT because of the high cellularity and it heterogeneously enhances with contrast administration. The major advantage of a CT scan is the evaluation of bony structures. Thin coronal and sagittal sections can reveal destruction of the cribriform plate, lamina papyracea and sphenoid sinus walls (**Fig. 17.1**). A neck CT scan should be obtained in all patients with ENB in order to evaluate possible regional lymph node spread.

MRI is another imaging modality that is recommended for the evaluation of tumour extension as it has a better resolution in soft tissue imaging. The tumour typically displays lower signal compared with grey matter on T1 and enhances heterogeneously after gadolinium administration. On T2-weighted images, the ENB appears slightly hyperintense. T2 sequences demonstrate the cystic components of the tumour better and are useful in differentiating

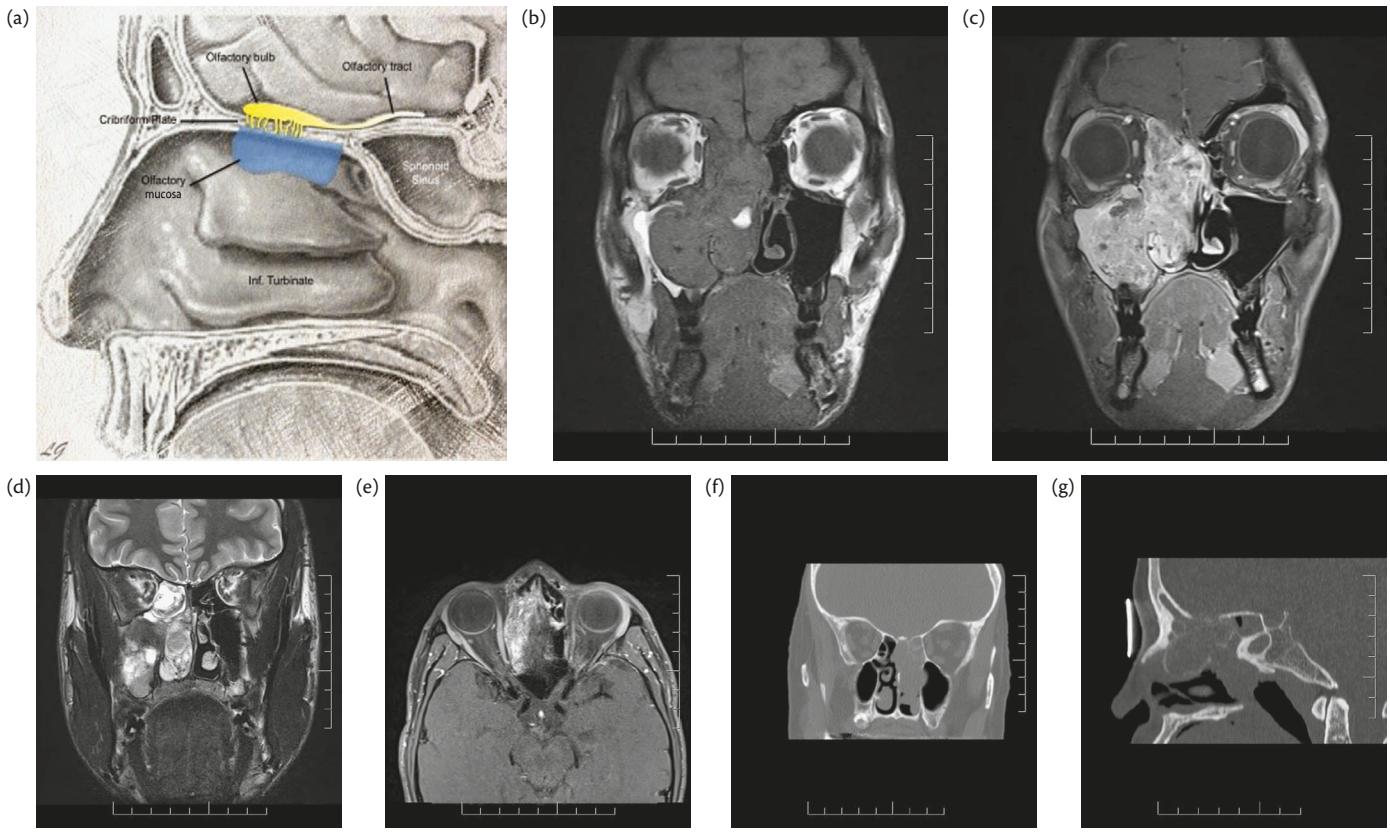

Fig. 17.1 (A) The olfactory mucosa at the upper part of nasal cavity is the area of ENB development. (B) Coronal T1 MRI without gadolinium of a 21-year-old male who presented with nasal obstruction and epistaxis for 6 months. (C) Heterogeneous enhancement after gadolinium administration. (D) Coronal T2 reveals a high signal lesion and intact dura of the frontal base. (E) Axial T1 with gadolinium showing compression of the lamina papyracea. (F) Coronal thin cut CT showing that the lamina papyracea and the cribriform plate are intact. (G) Cribriform plate erosion in another case of ENB in a 55-year-old female with anosmia and nasal blockage.

mucus retention inside the sinuses from true tumour invasion. MRI is the best modality for evaluation of periorbital invasion as well as for dural involvement and intracranial extension. ENBs, especially those of higher grade, appear restricted on diffusion-weighted imaging (DWI) due to increased cellularity.

Angiography is not routinely recommended as a diagnostic modality for ENB. However, in some cases it may be useful to delineate the relationship of the tumour to the carotid artery as well as the vascularity of the tumour. In cases of significant tumour vascularity preoperative embolization may be useful.

The next step in the diagnostic workup for ENB after radiographic evaluation is biopsy of the lesion. We recommend biopsy inside the operative room under general anaesthetic because of the high vascularity of the tumour.

If metastatic disease is suspected a neck CT is recommended as well as PET CT.

Staging

ENB may appear as a purely intranasal mass originating from the olfactory mucosa (Fig. 17.1) at the time of diagnosis or more commonly can invade the paranasal sinuses or extend towards the orbit or intracranial space. Cervical lymph node metastases have been reported in about 10% of the patients at the time of diagnosis. Remote, haematogenous metastases are rare at the first presentation but may occur at recurrence. The usual locations for metastases are the lungs, bones, and brain while rare delayed distal dural metastasis have also been reported. Defining the exact extent of the tumour is very important for choosing the appropriate treatment modality and for the overall prognostic evaluation. Several staging systems have been proposed for ENB. The first and most commonly used, was described by Kadish et al. in 1976 (Kadish et al., 1976). According to the Kadish staging system tumours that involve only the nasal cavity are classified as Kadish A, tumours that extend to the paranasal sinuses are classified as Kadish B and those that extend outside the paranasal sinus are classified as Kadish C. This system does not classify regional and remote metastases. Morita, in 1993 modified the Kadish staging system by designating D tumours with nodal and remote metastases (Morita et al., 1993).

The second most common grading system used for ENB is that proposed by Dulguerov (Dulguerov and Calcaterra, 1992) (Table 17.1). The Dulguerov staging system is a more detailed classification that differentiates between involvement of the nasal cavity, sinuses, and cribriform plate, as well as extension of disease to the anterior fossa, dura, and brain. Moreover, it provides information concerning regional and distant involvement and separates disease extent by the traditional T, N, and M categories.

It remains unclear which staging system is the most accurate and useful for evaluation of treatment efficacy and patient outcome.

Table 17.1 Dulguerov and Biller staging systems

	Dulguerov staging system	Biller staging system
T1	Tumour inside nasal cavity and/or paranasal sinuses but spares sphenoid sinus and superior ethmoid cells	Tumour inside nasal cavity/paranasal sinuses but not the sphenoid
T2	Tumour involves sphenoid and/or cribriform plate	Tumour extents into the orbit and/or cranial cavity
T3	Tumour extents into the orbit or into the anterior cranial fossa without dural invasion	Tumour involves the brain but deemed resectable
T4	Tumour involves the brain	Tumour involves the brain extensively and deemed unresectable
N0	No lymph nodes involvement	No lymph nodes involvement
N1	Lymph nodes involvement	Lymph nodes involvement
M0	No distant metastasis	No distant metastasis
M1	Distant metastasis	Distant metastasis

Source data from Pavel Dulguerov, Thomas Calcaterra, Esthesioneuroblastoma: The UCLA experience 1970–1990, *The Laryngoscope*, volume 102, issue 8, pp. 843–9, 1992 and Hugh F. Biller, William Lawson, Ved P. Sachdev, et al. Esthesioneuroblastoma: Surgical treatment without radiation, *The Laryngoscope*, volume 100, issue 3, pp. 1199–201, 1990.

A retrospective study of 261 patients with ENB performed by Jethanam et al. showed significant differences in patient outcome in the four different stages of the modified Kadish system. Patients with lymph nodes and remote metastases displayed a poor outcome. It is obvious that the presence of regional and distal metastatic disease negatively affects a patient's outcome and this needs to be considered when choosing a staging system.

Gross appearance, histology, and grading system

The tumour appears grossly as a nasal mass covered by intact or occasionally, in undifferentiated tumours, ulcerated respiratory mucosa. A cut surface will appear fleshy and reddish because of the abundant vascularized stroma.

Histologically ENB displays cells with nesting or sheet-like appearances in the submucosa. The tumour nests are separated by abundant hyalinized, fibrous, highly vascularized, or inflammatory stroma. In some cases, focal or complete sheet-like appearances of tumour cells and minimal stroma may be seen. The sheet-like formation is more common but not exclusive to higher grade tumours. The nuclei of ENB cells are usually small, round and with 'salt and pepper' appearance and small nucleoli. Nuclear pleomorphism is usually mild but occasionally larger cells with a prominent nucleolus resembling a ganglion cell may be seen. The cytoplasm may be minimal like in 'small round blue cell tumours' or lightly eosinophilic or amphiphilic like carcinoid or pituitary adenoma cells. Mitotic activity is generally low, but high-grade undifferentiated tumours are characterized by high mitotic rate, excessive nuclear pleomorphism, little stroma, and necrotic areas. The tumour stroma is mostly made of interdigitating cellular processes that appear eosinophilic and fibrillary (neuropil) and a vascular bed of plexiform or glomeruloid capillaries. Tumour cells may surround stroma areas creating a palisade structure forming pseudorosettes of Homer-Wright type which are characteristic of well differentiated tumours.

Pseudorosettes are almost pathognomonic for ENB when they surround true neuropil and are encountered in biopsies of intranasal lesions. True rosettes of Flexner-Wintersteiner type, where the tumour cells form gland like structures, may be apparent in low-differentiated tumours. Perivascular rosettes also may be seen. Some ENB cases may display calcifications, necrosis in higher grade tumours, cysts, and areas of squamous or glandular epithelium surrounded by tumour cells. Rarely ENB may exhibit divergent differentiation to melanocytes, myogenic cells, or display focal glandular configuration making the differential diagnosis challenging.

The most commonly used grading system for ENB was developed by Hyams (Hyams et al., 1998). This system is based on the architecture of tumour development, amount of neuropil, frequency and type of rosettes, mitotic activity, the presence of necrosis, and the extent of nuclear pleomorphism (Table 17.2). There are several studies

Table 17.2 Hyams grading system

Grade	Lobular architecture	Mitotic index	Nuclear pleomorphism	Necrosis	Rosettes	Fibrillary stroma
I	+	none	–	–	HW	++
II	+	low	+/–	–	HW	+
III	+/-	moderate	+	rare	FW	+/-
IV	+/-	high	++	common	none	-

HW, Homer Wright; FW, Flexner-Wintersteiner.

Source data from Hyams et al., *Tumours of the upper respiratory tract and ear*, 2nd edition. Washington: Armed forces institute of Pathology; Copyright (c) 1998.

showing a good correlation of the Hyam grading system with outcome (Miyamoto et al., 2000; Dulguerov et al., 2001).

Immunohistochemical characteristics

Immunohistochemistry is performed in all cases of suspected ENB. The differential diagnosis is very critical as it can direct the therapeutic strategy and also determine the patient's prognosis. Care should be taken when dealing with recurrent tumours as the immunohistochemical profile may have changed. ENBs often express non-specific enolase, chromogranin, and synaptophysin. The diagnosis of ENB requires that either synaptophysin or chromogranin be positive in a high percentage of cells. Other neuroendocrine or neuronal markers such as CD56 and CD57 are also positive. S-100 staining can be seen at the periphery of tumour cell nests in the sustentacular cells which have a supportive role to the olfactory cells in normal epithelium and have a Schwann-like ultrastructure. Their presence as s-100 positive cells is very helpful for an ENB diagnosis and this tumour should not be confused with a melanoma. These cells are not found in high-grade lesions. Very rarely tumour cells can be s-100 positive. Glial fibrillary acidic protein (GFAP), b-tubulin, and microtubule-associated protein staining is variable. About 30–40% of ENBs display regional staining for keratins and low molecular weight keratins. Epithelial markers are typically negative in ENBs, although in some cases diffuse positive staining may be seen. Staining for mesenchymal markers such as desmin, myogenin, vimentin, and actin is negative as well. Melanocytic markers such as HMB-45 are negative despite some reports of melanocytic differentiation and melanin pigmentation. Ewing's sarcoma and PNET markers such as MIC2 (CD99), FLI1 are negative. Common leukocyte antigen and other haemopoietic markers are negative as well. See **Figure 17.2**.

Differential diagnosis

The differential diagnosis of ENB is broad and must be considered in all cases presenting with a sinonasal mass. ENB must be differentiated from other tumours of neuroectodermal origin with epithelial differentiation (neuroendocrine tumours) such as poorly differentiated small cell or non-small cell tumours (sinonasal undifferentiated carcinoma, or SNUC). Tumours of neuroectodermal origin with neural differentiation such as paraganglioma, malignant melanoma, Ewing sarcoma/PNET, neurofibroma, and schwannoma must also be in the differential diagnosis. Other pathologies that must be considered are lymphoma, rhabdomyosarcoma, adenocarcinoma, adenoid cyst carcinoma, sinonasal squamous carcinoma, nasopharyngeal carcinoma, osteosarcoma, and chondrosarcoma. Benign neoplasms that may develop in this area include inverted papilloma and pituitary adenoma.

The differential diagnosis is critical for the appropriate treatment modality, the follow-up schedule of the patient and the overall prognosis. Neuroendocrine tumours tend to behave more aggressively with higher risk of local and distal failure. High-grade ENB may be difficult to differentiate from neuroendocrine tumours. Typically, SNUC have a higher mitotic index. Cytokeratin staining is positive for neuroendocrine carcinoma but typically negative for ENB. S-100 staining is absent in neuroendocrine carcinoma but has a characteristic pattern in ENB.

Treatment

Surgery, radiation, and chemotherapy alone or in different combinations are the treatment modalities that have been used in the treatment of ENB. The most common treatment strategy is a combination of surgery with postoperative radiation for resectable tumours and the addition of chemotherapy for more advanced, metastatic, or non-operative cases.

The main goal of surgery is the achievement of gross total resection with clear resection margins. The traditional surgical approach is the anterior craniofacial resection using a bifrontal craniotomy and lateral rhinotomy, Weber-Ferguson fascial flap, or fascial degloving approach. The transglabellar subcranial approach is an alternative traditional approach. Tumours that reach the dura require resection of the dura and olfactory tracts. In cases of brain invasion safe brain resection may be necessary in order to achieve clear margins. The resection through the facial approach can involve partial or extensive maxillectomies with or without orbital exenteration.

Endoscopic endonasal approaches have advanced significantly in the last two decades and have been used alone and in combination with open transcranial approaches for the treatment of ENBs. Tumours of Kadish stage A or B and stage C without significant lateral extension are the best candidates for a purely endoscopic resection where clear margins can be achieved. Published studies describe satisfactory results with pure endoscopic resection of ENB (Hanna et al., 2009). The accumulating experience and the increasing sophistication of endoscopic skull base reconstruction techniques has decreased the complication rates. In carefully selected patients the endoscopic approach is an excellent, less invasive surgical alternative for ENB treatment.

Radiation is an important treatment modality for ENB. It can be used alone, accompany surgery in a preoperative or postoperative manner or be used in combination with chemotherapy. Radiation as a monotherapy or in combination with chemotherapy may be used for cases with local or regional involvement where complete resection is impossible or surgery is not an option. Several studies have shown that surgical resection followed by radiation has better results than either surgery or radiation alone (Jethanamest et al., 2007). The goal of postoperative radiation is to treat microscopic residual diseases and is usually given as intensity modulated radiation treatment (IMRT) in a schedule of 1.8–2 Gys up to total dose of 70 Gys. The option of preoperative radiation has been evaluated in several studies. The goal of preoperative radiation is to reduce the tumour volume and increase the tumour resectability. The report of Bachar et al. showed that there is no difference in patient survival and recurrence between groups receiving preoperative versus postoperative radiation (Bachar et al., 2008).

There is limited data supporting the role of chemotherapy in ENB and its use is based on the experience reported from treating other head and neck malignancies. Generally, chemotherapy is used either preoperatively or postoperatively together with radiation. The use of chemotherapy has been proposed in locally or distantly advanced disease.

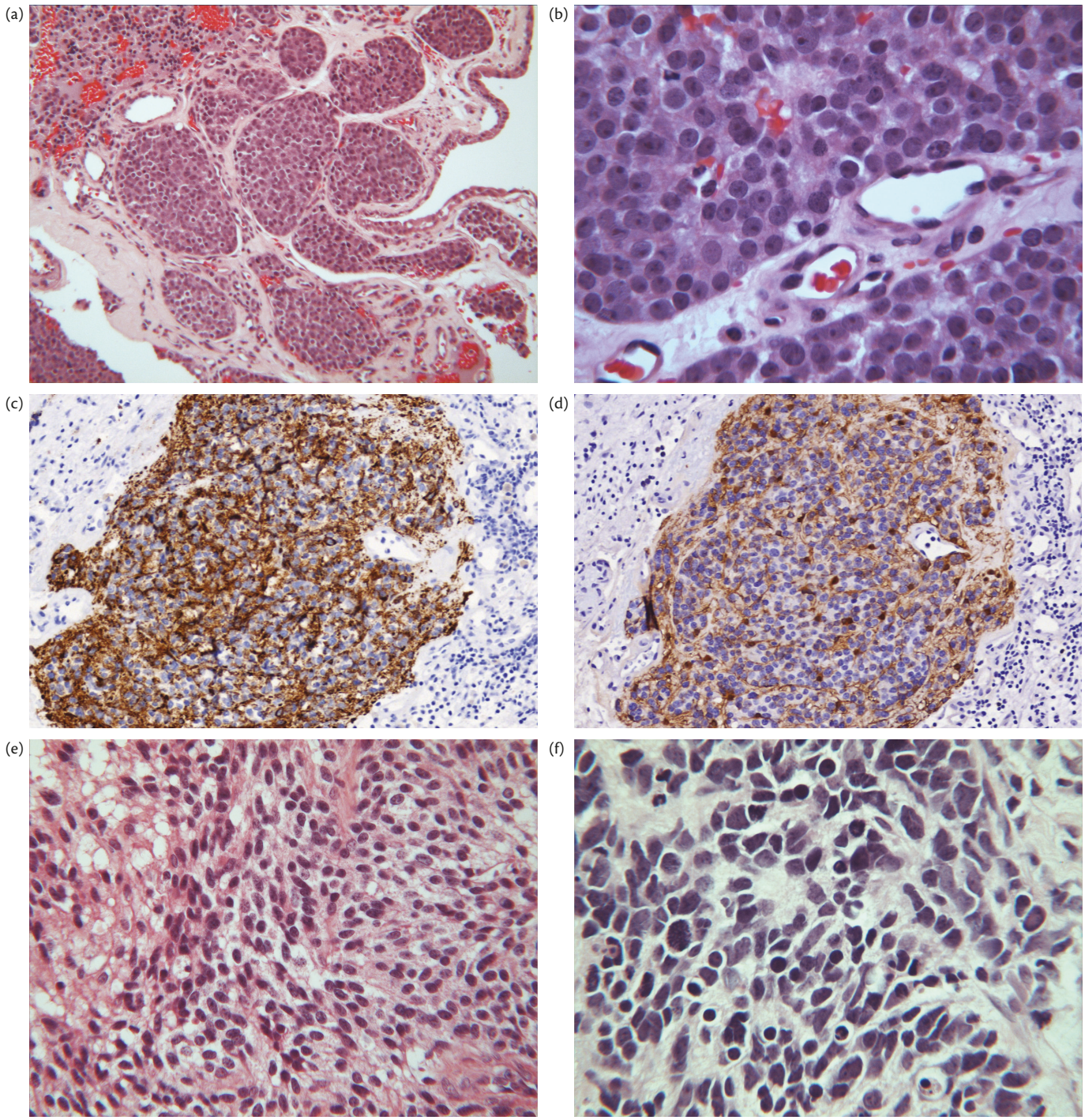

Fig. 17.2 (A) H&E stain, lower magnification view showing the typical lobular growth of a grade I ENB. Note the intact covering nasal mucosa. (B) H&E, high magnification of a grade I ENB showing the neoplastic cells with relatively uniform, round-to-oval nuclei, and finely granular cytoplasm surrounded by neurofibrillary matrix. Homer Wright pseudorosettes are seen. (C) ENB positive for chromogranin. (D) s-100 staining of the sustentacular cells. This is the characteristic pattern in ENB. (E, F) Grade IV ENB, H&E staining. Note the high nuclear pleomorphism and mitotic figures.

Prognosis and recurrent disease

The rate of local recurrence of ENB depends on the primary treatment. The study of Demiroz et al. (2011) showed that the rate of local recurrence was 71% in 5 years for patients treated with surgery alone and 17% in 6 years for patients treated with surgery followed by radiation. The success of salvage treatments to control the recurrent disease depends on the extent of recurrence and for this reason close follow-up with nasal endoscopy and MRI is important. Local recurrence is usually manageable, with further surgery, endoscopic or open, plus salvage radiation if possible. A metanalysis of 33 articles revealed that 20.2% of patients developed neck metastasis

and in 61.7% of those, metastases occurred 6 months after initial treatment. Salvage rates for these recurrences (defined as 1 year of disease-free survival) was 31.2% and this was higher with combined surgery and radiation compare with either treatment alone (Gore and Zanation, 2009). Distant metastases developed in up to 10% of patients and indicate a poor prognosis. Despite the poor prognosis salvage treatment can offer palliation of symptoms and extend survival. Cisplatin based treatment was shown to be active in advanced disease in a report of McElroy et al. (1998).

Conclusion

Esthesioneuroblastoma is a rare and aggressive tumour that continues to pose challenging management problem. The use of uniform staging systems has helped correlate survival and recurrence. A multimodality, multidisciplinary treatment approach is the preferred treatment for most lesions. While very small tumours located below the cribriform plate can be considered for resection without additional radiotherapy the great majority of patients require surgery with adjuvant radiation. Recurrent metastatic lesions may require chemotherapy. Recurrence in ENB is frequent and can occur many years after initial treatment thus necessitating close long-term follow-up of patients.

The introduction of endoscopy for the treatment of esthesioneuroblastomas, in either a purely endonasal or combined cranionasal approach has been a very positive addition to the surgical management and early results are favourable demonstrating outcomes in selected patients that are better than with standard approaches.

Controversies

The management of neck lymph node metastatic disease in ENB is not well established. Published data suggest that the incidence of lymph node involvement at presentation may be around 10% but eventually 20–30% of patients will develop lymph node metastasis. Patients with clinical or radiographic lymph node metastases at presentation or during the follow-up period are candidates for neck dissection and postoperative neck radiation. The extent of neck dissection is usually guided by the level of lymph node involvement. Elective or prophylactic neck dissection is not standard and there are no reports showing clear benefit. Elective neck irradiation has not been shown to reduce the incidence of lymph node recurrence (Noh et al., 2011) despite other data supporting the elective irradiation of neck lymph nodes (Monroe et al., 2003). Despite this the neck area is commonly included prophylactically in the radiation field for patients who receive radiation as an adjuvant treatment.

FURTHER READING

Broich, G., Pagliari, A., & Ottaviani, F. (1997). Esthesioneuroblastoma: a general review of the cases published since the discovery of the tumour in 1924. *Anticancer Res*, **17**, 2683–706.

Dulguerov, P., Allal, A.S., & Calcaterra, T.C. (2001). Esthesioneuroblastoma: a metanalysis and review. *Lancet Oncol*, **2**, 683–90.

Hanna, E., DeMonte, F., Ibrahim, S., Roberts, D., Levine, N., & Kupferman, M. (2009). Endoscopic resection of sinonasal cancer with and without craniotomy: oncologic results. *Arc Otolaryngol Head and Neck Surg*, **135**(12), 1219–24.

Hyams, V.J., Batsakis, J.G., & Michaels, L. (1998). *Tumors of the Upper Respiratory Tract and Ear*, 2nd edition Washington, DC: Armed Forces Institute of Pathology.

Jethanamest, D., Morris, L.G., Sikora, A.G., & Kutler, D.I. (2007). Esthesioneuroblastoma: a population-based analysis of survival and prognostic factors. *Arc Otolaryngol Head Neck Surg*, **133**(3), 276–80.

Miyamoto, R.C., Gleich, L.L., Biddinger, P.W., & Gluckman, J.L. (2000). Esthesioneuroblastoma and sinonasal undifferentiated carcinoma: impact of histological grading and clinical staging on survival and prognosis. *Laryngoscope*, **110**, 1262–5.

Noh, O.K., Lee, S.W., Yoon, S.M., et al. (2011). Radiotherapy for esthesioneuroblastoma: is elective nodal radiation warranted in the multimodality treatment approach? *Int J Radiat Oncol Biol Phys*, **79**(2), 443–9.

REFERENCES

Bachar, G., Goldstein, D.P., Shah, M., et al. (2008). Esthesioneuroblastoma: the Princess Margaret Hospital experience. *Head and Neck*, **30**(12), 1607–14.

Broich, G., Pagliari, A., & Ottaviani, F. (1997). Esthesioneuroblastoma: a general review of the cases published since the discovery of the tumour in 1924. *Anticancer Res*, **17**, 2683–706.

Demiroz, C., Gutfeld, O., Aboziada, M., Brown, D., Marentette, L.J., & Eisbruch, A. (2011). Esthesioneuroblastoma: is there a need for elective neck dissection? *Int J Radiat Onvol Biol Phys*, **81**(4), e255–61.

Dulguerov, P. & Calcaterra, T. (1992). Esthesioneuroblastoma: the UCLA experience 1970–1990. *Laryngoscope*, **102**, 843–9.

Dulguerov, P., Allal, A.S., & Calcaterra, T.C. (2001). Esthesioneuroblastoma: a metanalysis and review. *Lancet Oncol*, **2**, 683–90.

Gabbay, U., Leider-Trejo, L., Marshak, G., Gabbay, M., & Fliss, D.M. (2013). A case and a series of public cases of esthesioneuroblastoma (ENB) in which long standing paraneoplastic SIADH had preceded ENB diagnosis. *Ear Nose Throat J*, **92**(10–11), E6.

Gore, M.R. & Zanation, A.M. (2009). Salvage treatment of late neck metastasis in esthesioblastoma. *Arch Otolaryngol Head Neck Surg*, **135**(10), 1030–4.

Hanna, E., DeMonte, F., Ibrahim, S., Roberts, D., Levine, N., & Kupferman, M. (2009). Endoscopic resection of sinonasal cancer with and without craniotomy: oncologic results. *Arc Otolaryngol Head and Neck Surg*, **135**(12), 1219–24.

Hyams, V.J., Batsakis, J.G., & Michaels, L. (1998). *Tumors of the Upper Respiratory Tract and Ear*, 2nd edition Washington, DC: Armed Forces Institute of Pathology.

Jethanamest, D., Morris, L.G., Sikora, A.G., & Kutler, D.I. (2007). Esthesioneuroblastoma: a population-based analysis of survival and prognostic factors. *Arc Otolaryngol Head Neck Surg*, **133**(3), 276–80.

Kadish, S., Goodman, M., & Wang, C.C. (1976). Olfactory neuroblastoma. A clinical analysis of 17 cases. *Cancer*, **37**(3), 1571–6.

Klepin, H.D., McMullen, K.P., & Lesser, G.J. (2005). Esthesioneuroblastoma. *Curr Treat Opin Oncol*, **6**(6), 509–18.

McElroy, E.A. Jr., Buckner, J.C., & Lewis, J.E. (1998). Chemotherapy for advanced esthesioneuroblastoma: the Mayo Clinic experience. *Neurosurgery*, **42**(5), 1203–7.

Miyamoto, R.C., Gleich, L.L., Biddinger, P.W., & Gluckman, J.L. (2000). Esthesioneuroblastoma and sinonasal undifferentiated carcinoma: impact of histological grading and clinical staging on survival and prognosis. *Laryngoscope*, **110**, 1262–5.

Monroe, A.T., Hinerman, R.W., Amdur, R.J., Morris, C.G., & Mendenhall, W.M. (2003). Radiation therapy for esthesioneuroblastoma. Rational for elective neck irradiation. *Head and Neck*, **25**(7), 529–34.

Morita, A., Ebersold, M.J., Olsen, K.D., Foote, R.L., Lewis, J.E., & Quast, L.M. (1993). Esthesioneuroblastoma: prognosis and management. *Neurosurgery*, **32**, 706–15.

Noh, O.K., Lee, S.W., Yoon, S.M., et al. (2011). Radiotherapy for esthesioneuroblastoma: is elective nodal radiation warranted in the multimodality treatment approach? *Int J Radiat Oncol Biol Phys*, **79**(2), 443–9.

Platek, M.E., Merzianu, M., Mashtare, T.L., et al. (2011). Improved survival following surgery and radiation for olfactory neuroblastoma: analysis of the SEER data base. *Radiat Oncol*, **6**, 41.

Purochit, B., Winder, T., Maggio, E.M., & Kollioas, S.S. (2015). Aggressive primary olfactory neuroblastoma of the sphenoclival region. A case report and literature review. *Laryngoscope*, **125**, 822–5.

18

Malignant skull base tumours

Benedict Panizza and Adel Helmy

Introduction

The majority of tumours encountered in skull base neurosurgery are histologically benign. The philosophy for treating those tumours is based around choosing an appropriate surgical corridor (e.g. endoscopic endonasal, anterior, lateral, midline posterior), protecting surrounding neurovascular structures, internal debulking, and extracapsular dissection. Malignant skull base tumours (MSBT) however, are a much rarer and more histologically diverse group of tumours that are more complex to treat and require a distinct set of management principles. For this reason they are grouped together despite a wide variation in pathology, outcome, and prognosis. In order to deliver the highest standards of care a truly multidisciplinary approach is required that bridges the surgical specialties (neurosurgery, head and neck, otology, plastic and reconstructive), radiology, and oncology. Several of the more common MSBT, such as chordoma, chondrosarcoma, and esthesioneuroblastoma, are considered in separate chapters and will not be discussed in detail here.

A remarkable range of histological entities can be found at the skull base, that reflect the anatomical complexity of the boundary between the head and neck and the intracranial cavity. These tumours can arise from skin, mucous membranes, salivary gland, cartilage, bone, or muscle. The most useful clinical distinction is into anterior skull base and lateral skull base tumours (**Table 18.1**). Alternatively, one can classify tumours from the pathological perspective as primarily arising at the skull base, invading from surrounding tissues (e.g. from nasal cavity or infratemporal fossa, and distant metastasis).

There is little definitive epidemiological data on these tumour types when the subset that involve the skull base is considered. However, they are all rare entities with even the commonest histological subtype, squamous cell carcinoma (SCC), rare at 0.5–1/1 000 000 per annum usually arising in the sinonasal cavity and spreading to the anterior skull base. These tumours are more common in Japan, Indonesia, and some parts of Asia. Primary temporal SCCs are estimated to occur in 6/1 000 000 per annum, although in 90% cases where temporal bone resection is carried out, the original pathology is cutaneous malignancy with secondary spread to the temporal bone.

In principle, the optimal treatment for MSBT is extensive resection *en bloc* with histologically negative tumour margins. Piecemeal resection of tumours risks seeding of tumour cells within the surgical cavity and compromising clearance at the surgical margin. In some cases, *en bloc* resection is not possible, for example, large tumours that occlude access to the deep margin or those adjacent to critical structures, such as the jugular foramen or in the region of the internal carotid artery, where *en bloc* resections would carry high morbidity. In these cases, piecemeal resection with macroscopic clearance is utilized. This often requires extensive craniofacial resections with the associated challenges of dural repair, to avoid CSF leak and pneumocephalus, and plastic surgical input to ensure soft tissue coverage.

Adjuvant treatment most commonly includes radiotherapy to involved tumour margins, although in specific pathologies, chemotherapy is taking an increasing role.

The American Joint Committee of Cancer Staging (AJCC) have published specific staging systems for several extracranial tumours that encompass three domains: T (tumour extent); N (regional lymph node involvement); and M (metastasis remote to regional lymph nodes). Although not all tumour types have the full range of values, the outline of the system is described in **Table 18.2**. The TNM system is used as a method for prognostication as well as determining treatment paradigms related to curative versus palliative surgery, and the need for coexistent management of the head and neck lymph node basin. The National Comprehensive Cancer Network (NCCN) provides detailed algorithms for treatment of head and neck malignancies based on the TNM staging system (Network, 2019).

Anterior skull base

Clinical assessment

Anterior skull base malignancies most commonly present to the ear nose throat (ENT) surgeon with combinations of anosmia, ageusia (loss of taste), pain, nasal blockage, nasal discharge, and epistaxis. In more locally advanced tumours, ocular symptoms from cavernous sinus involvement precipitating diplopia or ophthalmoplegia, direct involvement of the orbit causing proptosis, chemosis, or pain and direct compression of the optic nerve pathway causing visual field or acuity deficits. Seizure from direct invasion of the frontal lobes and

Table 18.1 Common histological subtypes malignant skull base tumours

Anterior skull base	Lateral skull base
Squamous cell carcinoma	
Salivary gland malignancies (adenocarcinoma, adenoid cystic, acinic)	
Sarcoma (e.g. osteosarcoma, fibrosarcoma, rhabdomyosarcoma, liposarcoma, Ewing's)	
Malignant melanoma	Basal cell carcinoma
Sinonasal undifferentiated carcinoma	
Olfactory neuroblastoma	

headache from raised intracranial pressure (ICP) are rarely the first presentation.

Clinical examination in the outpatient clinic, combined with nasal endoscopy, can sometimes identify the tumour within the nasal cavity; however, MRI with gadolinium contrast is regarded as the first line investigation for diagnosis and to determine the anatomical extent of the tumour. A concomitant fine-cut (<1 mm cuts) bony computed tomography (CT) scan with multiplanar reconstruction provides detailed information on the bony extent of tumour invasion and is critical in surgical planning, especially to determine the extent and need for skull base reconstruction.

Any newly diagnosed, presumed malignant, skull base tumour requires staging in line with the TNM system, with clinical examination of the cervical lymph nodes and systemic imaging to assess lymph node dissemination and metastatic disease, as necessary.

Depending on the size and extent of the lesion, formal ophthalmological or dental assessments may also be needed alongside those from the head and neck surgeon.

Following the necessary clinical assessments, determining a histological diagnosis is a key determinant of the management paradigm and will require transnasal biopsy before definitive treatment planning, except for vascular tumours such as suspected juvenile nasopharyngeal angiofibroma.

Location and histology

Although there are a wide range of histological entities, the degree of aggressiveness of the tumour and the extent of invasion determine the management plan. Intermediate grade malignancies such as low-grade adenoid cystic carcinoma, chondrosarcoma, and olfactory neuroblastoma can be managed with less aggressive resections to avoid neurological morbidity on the understanding that adjuvant radiotherapy can control residual disease. For more aggressive histological entities such as squamous cell carcinoma, melanoma, or high-grade sarcomas that have not spread systemically, a more extensive resection with macroscopic excision should be considered to achieve potential cure. These are difficult decisions to make and depend on the patient's wishes, comorbidities, and the treating surgical team's expertise.

Table 18.2 Outline of TNM system for extracranial tumours

T: Tumour extent	N: Lymph node involvement	M: Metastasis
Tx: Cannot be evaluated	Nx Cannot be evaluated	
Tis: Carcinoma *in situ*	N0: No regional nodes	M0: No distant metastasis
T0: No sign of primary tumour	N1: Proximate regional nodes	M1: Distant metastasis
T1–4: Size and or extension tumour	N2–3: Progressive involvement of more numerous or distant nodes	

Source data from *AJCC Cancer Staging Manual*.

Surgical management

Over the past 10 years, there has been a dramatic increase in endonasal endoscopic techniques for the full range of anterior skull base pathology. However, other than in the case of esthesioneuroblastoma, the current evidence base does not support the use of endoscopic techniques for definitive treatment of MSBT (Rawal et al., 2012). The endoscope is simply a tool for delivering surgical goals and if equivalence in oncological control can be demonstrated, it is envisaged that combined and independent endoscopic approaches will become more popular as they have significantly less morbidity than traditional craniofacial approaches (Castelnuovo et al., 2014).

Radiotherapy

Postoperative radiotherapy is an essential adjunct to surgical resections with both palliative and curative intent. In practice, the location of these tumours ensures that surgical margins are always close and patients should be routinely counselled as to the need for postoperative radiotherapy. This is typically delivered by LINAC-based systems rather than radiosurgery as a large treatment volume is required in the region of critical neurovascular structures. Fractionation is used to minimize dosage to normal structures, for example, 60 Gy in 30 fractions.

Other adjuvant therapy

Adjuvant chemotherapy also has a role in MSBT when postoperative margins are histologically involved or there is extranodal tumour spread. However, there are exceptions to this. On one hand, sinonasal undifferentiated carcinoma is treated definitively in many head and neck cancer units with chemotherapy and radiotherapy without surgical intervention with equivalent results. Alternatively, there is currently no evidence for chemotherapy in the treatment of perineural spread of cutaneous malignancies.

Outcomes

There is a wide spectrum of malignant tumours that present at the skull base, however, overall the outcome for craniofacial resection at 5 years is 60% disease-specific survival and 53% recurrence specific survival. One-third of patients will have a postoperative complication with wound problems being the most common. Perioperative mortality is in the order of 4% (Patel et al., 2003). Specifically, in melanoma, perioperative complication rates are similar, but the longer-term prognosis is poorer with a 3-year disease-specific survival of 30% and recurrence-free survival of 26% (Ganly et al., 2006). Endoscopic techniques are able to provide similar disease control with reduced perioperative morbidity. As for all head and neck malignancies, clear margins confer a survival advantage.

Lateral skull base

Clinical assessment

Lateral skull base pathology most commonly involves the temporal bone, however, tumours can also extend into the middle fossa from the infratemporal fossa. Clinical presentations are diverse but most commonly arise from cutaneous primaries either as a first presentation or following partial treatment. As tumours spread deeply a wide range of symptoms can develop including hearing loss, otalgia, facial weakness, and imbalance from temporal bone involvement, diplopia and facial numbness from cavernous sinus/petrous apex involvement, lower cranial nerve, and brainstem symptoms, as well as trismus from temporomandibular joint involvement.

The primary site of the tumour should be identified in the first instance, as either from the skin or, more rarely, from infratemporal fossa pathologies such as salivary gland malignancy or a primary mesenchymal tumour. Clinical assessment must include examination of the relevant lymph node basins. MR and CT imaging is essential in defining the site and extent of the tumour as for anterior skull base malignancies.

Location and histology

The commonest pathology to require neurosurgical involvement is a squamous cell carcinoma invading the temporal bone. These are aggressive malignancies that initially arise in the skin of the external auditory meatus or, in 5% of cases, from the middle ear lining. In addition, it is common to require a temporal bone excision to enable clear margins with tumours extending to the temporal bone usually from cutaneous malignancy and involving the preauricular temporomandibular sulcus region. In one series, T4 tumours (invading medial petrous structures or extensive soft tissue involvement) were most commonly located in the preauricular region and this region carried a worse prognosis (Essig et al., 2013). Other histological subtypes of tumour include basal cell carcinoma (most common tumour on the pinna), salivary gland malignancies (adeno, adenoid cystic, acinic carcinomas from the parotid gland) and sarcomas. The complexity of temporal bone anatomy allows several potential routes for tumour spread once the middle ear is breached including anteriorly to the carotid canal and Eustachian tube, medially into the vestibule, cochlea, and internal auditory meatus, inferiorly to the jugular bulb and lower cranial nerves and finally superiorly through the tegmen tympani into the middle fossa.

Several staging systems have been described for SCC of the temporal bone with some variations however whichever system is used the following factors are recognized as conferring a poor prognosis: bone invasion, middle ear invasion, facial paralysis, dural involvement, perineural spread of tumour, and regional lymphadenopathy.

Surgical management

Lateral skull base malignancies mandate *en bloc* resection to attain optimal outcomes even more so than in the anterior skull base. Biopsy or resection in the nasal cavity is at an air/tumour interface and intact mucosa over normal tissue provides a barrier to seeding of the malignant cells. However, in lateral skull base pathology the deep resection margin provides a well vascularized bed that can accommodate tumour implantation especially as a result of use of a high-speed drill.

Figure 18.1 shows imaging and operative photographs from a patient with an invasive temporal bone SCC presenting with a House-Brackmann 6 facial palsy. Several methods of temporal bone resection (TBR) have been described for SCC, that all incorporate a superficial parotidectomy. Lateral TBR incorporates resection of the external auditory meatus with its bony margin as far as the tympanic annulus, leaving the facial nerve intact. Subtotal TBR additionally includes resection of the mesotympanum and internal auditory meatus nerves leaving only the petrous apex and carotid intact. Total TBR also includes resection of the carotid artery and petrous apex risking additional damage to the cavernous sinus and is rarely used. In this case, a radical parotidectomy, mandibulectomy, and lateral TBR was combined with a temporal craniotomy and resection of the radiologically involved dura. Resection of dura potentially increases the risk of seeding of malignant cells into the CSF space and should be avoided unless it is demonstrably involved and the tumour can be completely removed. Leaving the dura intact not only acts as a barrier to spread but also allows for a more focussed radiotherapy field.

Various methods have been suggested to minimize the risk of carotid sacrifice, however, these still carry significant morbidity. Preoperative test balloon occlusion (TBO) is used in many settings to predict ischaemic complications following occlusion of the carotid artery but the predictive accuracy varies with a 2–16% risk of stroke (van Rooij et al., 2005; Whisenant et al., 2015) and with thrombo-embolism and hypoperfusion both contributing to morbidity. For this reason, the senior author recommends preservation of the carotid artery in most cases (e.g. **Figs. 18.2** and **18.3**) as the morbidity of total TBR cannot be justified given the option of adjuvant radiotherapy.

Following surgery for invasive tumours where the adventitia of the carotid has been used as a margin, angiographic follow-up is carried out at 2–3 days and 2–3 weeks postoperatively to exclude vascular injury, dissection, or pseudoaneurysm formation. Similarly, involvement of the jugular foramen implies a poor prognosis and the morbidity of jugular bulb resection and lower cranial nerve palsy is regarded as unacceptable. In these cases, near total resection combined with adjuvant therapy is preferred.

Temporal bone resections require involvement of plastic and reconstructive surgeons in order to provide soft tissue coverage. This most commonly requires a free flap reconstruction with vascular supply from the external carotid. This has implications for planning concomitant cervical lymph node dissection.

Radiotherapy

Postoperative radiotherapy combined with histologically clear margins provide the best outcomes. With positive margins, postoperative radiotherapy is also recommended to deal with residual disease. In select cases with advanced disease such as jugular or carotid involvement, a decision may be made to avoid the morbidity of extensive surgery and carry out a palliative resection with adjuvant radiotherapy.

Other adjuvant therapy

Immunotherapeutic agents such as PD-1 and PDL-1 inhibitors may lead to dramatic changes in how we deal with advanced cutaneous malignancy. Early impressive and short term sustainable (1-2 years) results have been obtained in residual and recurrent cases of advanced cutaneous SCC. How these novel agents fit in to current treatments will require ongoing clinical trials.

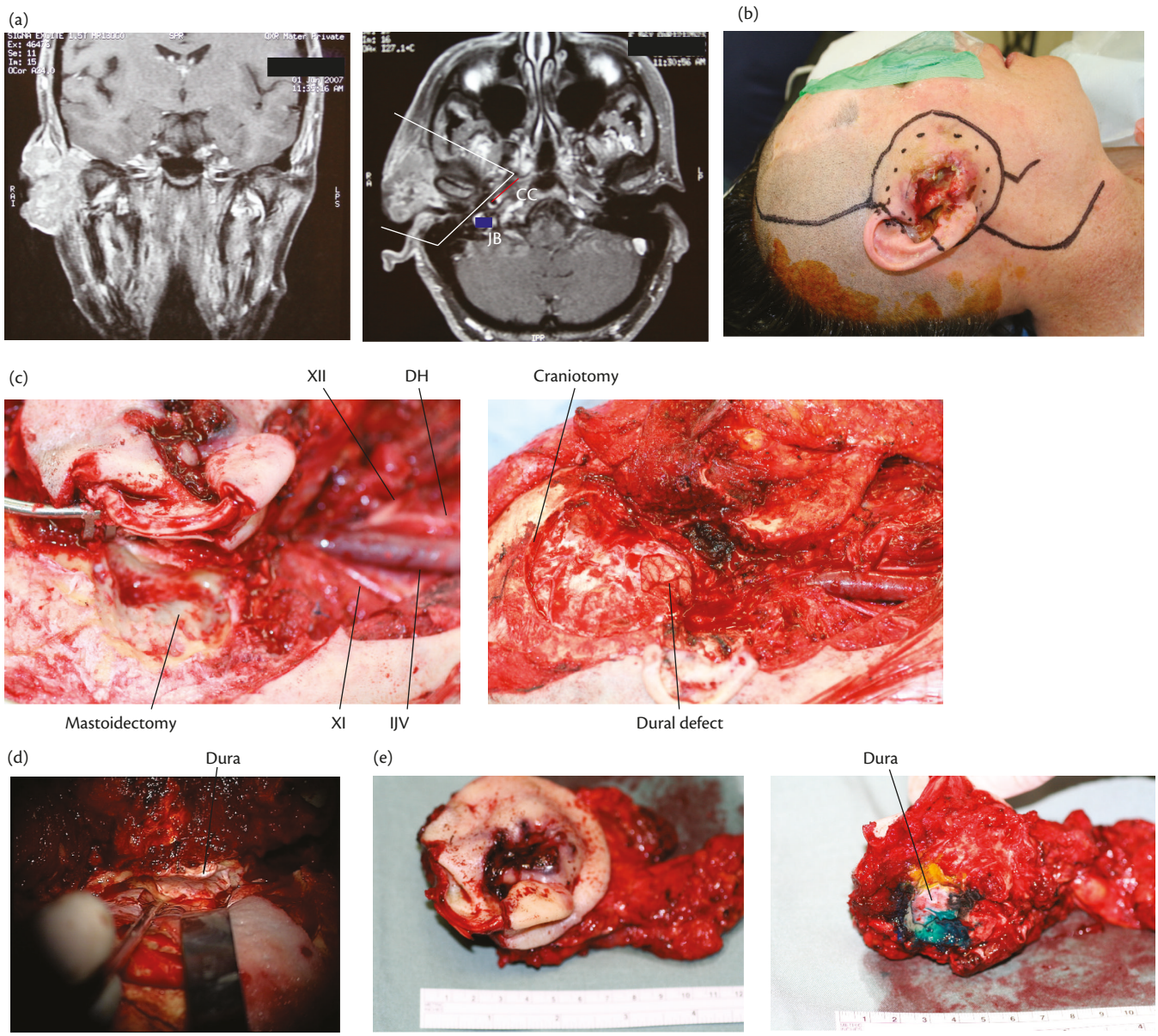

Fig. 18.1 Temporal bone squamous cell carcinoma. This patient presented with an ulcerating lesion anterior to the pinna. (A) Preoperative T1 weighted MRI with gadolinium contrast in sagittal and axial planes. The limits of the surgical resection are demonstrated on the axial image in white alongside the position of the carotid canal (CC) and jugular bulb (JB). (B) Operative planning incorporating part of pinna with extension of excision to allow access for craniotomy, infratemporal fossa, and neck dissection. (C) Macroscopic operative stills showing mobilization of tumour from the infratemporal fossa, temporal craniotomy, disconnection of deep margin of tumour and removal of the affected dura. (D) Intraoperative microscope views of disconnection of the deep margin of the specimen, craniotomy, and attachment of middle fossa dura to the bone which is circumferentially drilled to allow an en bloc removal. (E) Superficial and deep (inked dura) margins of tumour. (XI, spinal accessory nerve; XII, hypoglossal nerve; IJV, internal jugular vein; DH, descendens hypoglossi.)

Outcomes

For lateral temporal bone resection, the senior author's outcomes are 5-year disease-specific survival 62% and disease-free survival 59%.

Controversies

Perineural involvement of cutaneous malignancies are a particularly complex surgical problem. A subset of tumours has an aggressive neurotropic phenotype that involves divisions of the trigeminal or facial nerves (Panizza et al., 2014; Warren et al., 2016b). These patients present with numbness or formication in a trigeminal nerve branch or weakness in a facial nerve branch. Tumour can extend centrally towards the brainstem and, via branch points, into adjacent nerves. As tumour spread is extensive on presentation surgical management requires extensive resection. The alternative approach is radiotherapy to the involved nerves with palliative intent, but avoiding the risks of surgery. However high-volume centres have described good outcomes (70% curative resection) in patients without brainstem involvement (Warren et al., 2016a).

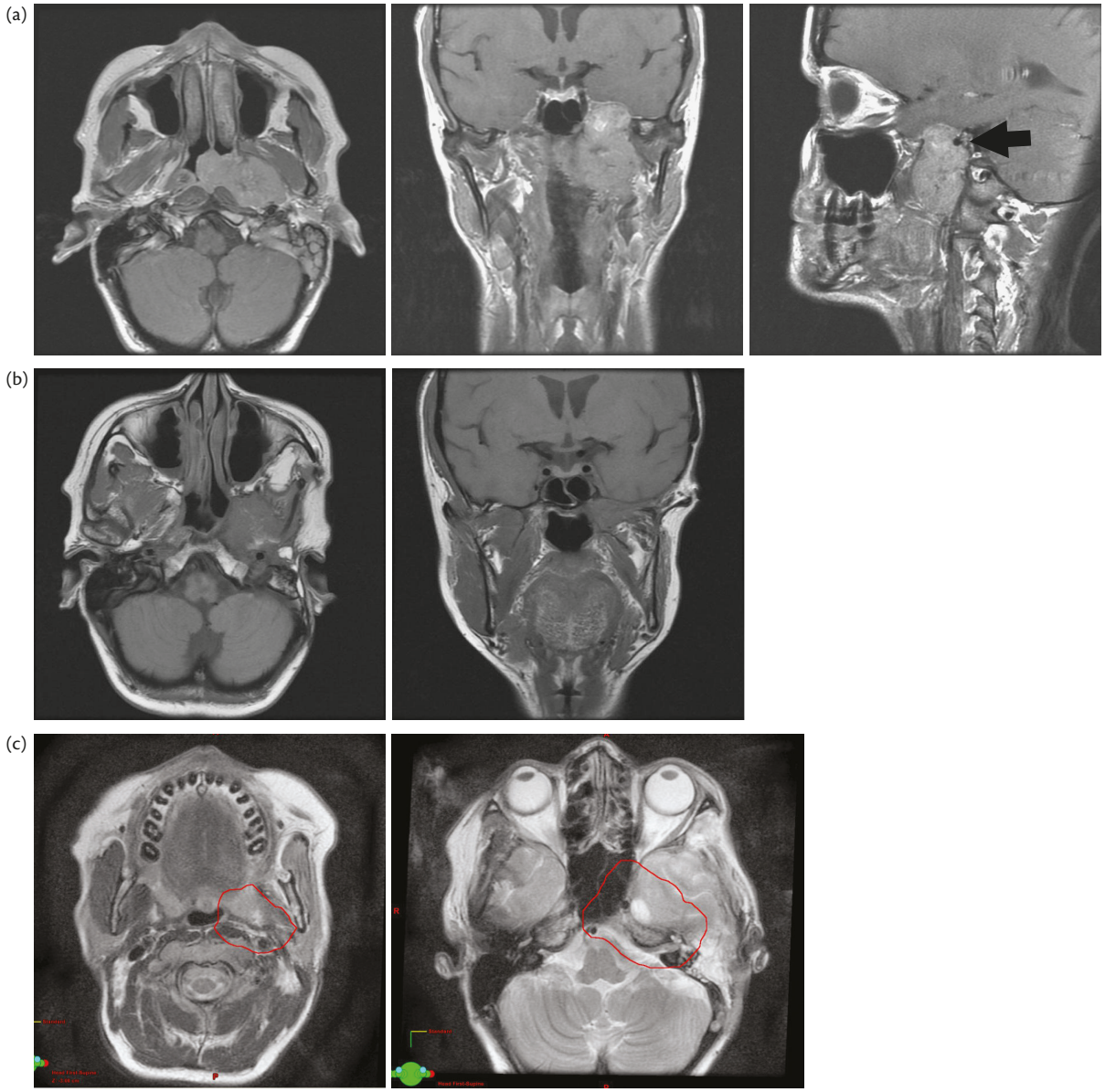

Fig. 18.2 Low-grade adenocarcinoma. This 52-year-old woman presented with deafness from a left middle ear effusion with a smooth vascular swelling identified in the posterior nasal space on endoscopy. Biopsy revealed a low-grade adenocarcinoma. The patient underwent an infratemporal fossa clearance and a middle fossa craniotomy in order to clear disease. Postoperative radiotherapy consisted of 60 Gy in 30 fractions. (A) Preoperative T1-weighted imaging with gadolinium contrast in axial, coronal, and sagittal planes. Carotid encasement by tumour is seen on the sagittal cut (arrowed) (B) Corresponding postoperative axial and sagittal cuts on T1-weighted MRI. (C) Illustrative radiotherapy plans encompassing the previous extent of the tumour.

Figure 18.4 shows pre- and postoperative imaging for a 55-year-old patient presenting with pain and sensory loss in the mandibular division (V3) of the trigeminal nerve. Biopsy confirmed adenoid cystic carcinoma and preoperative T1 weighted MRI with gadolinium contrast demonstrated contiguous extension of the tumour mass through the foramen ovale into the Gasserian ganglion. When confronted with an extensive tumour of this sort, the first consideration is whether the tumour is wholly resectable and whether a macroscopic clearance would provide acceptable tumour control if combined with postoperative radiation. If an extensive resection is considered the potential benefits to the patient will only be accrued if the tumour can be wholly excised and this would need to encompass resection of the proximal portion of V3 at the Gasserian ganglion as well as the peripheral branches of the nerve in the infratemporal fossa. The details of surgical management are outside the scope of this chapter, but the interested reader can find additional details in the literature (Redmond and Panizza, 2016; Solares et al., 2016).

The potential morbidity from an *en bloc* resection of the infratemporal fossa and hemi-mandible in addition to ocular morbidity from denervation of the ophthalmic division of the trigeminal nerve at the Gasserian ganglion must be balanced against the survival advantage of complete surgical resection with the potential for curative resection.

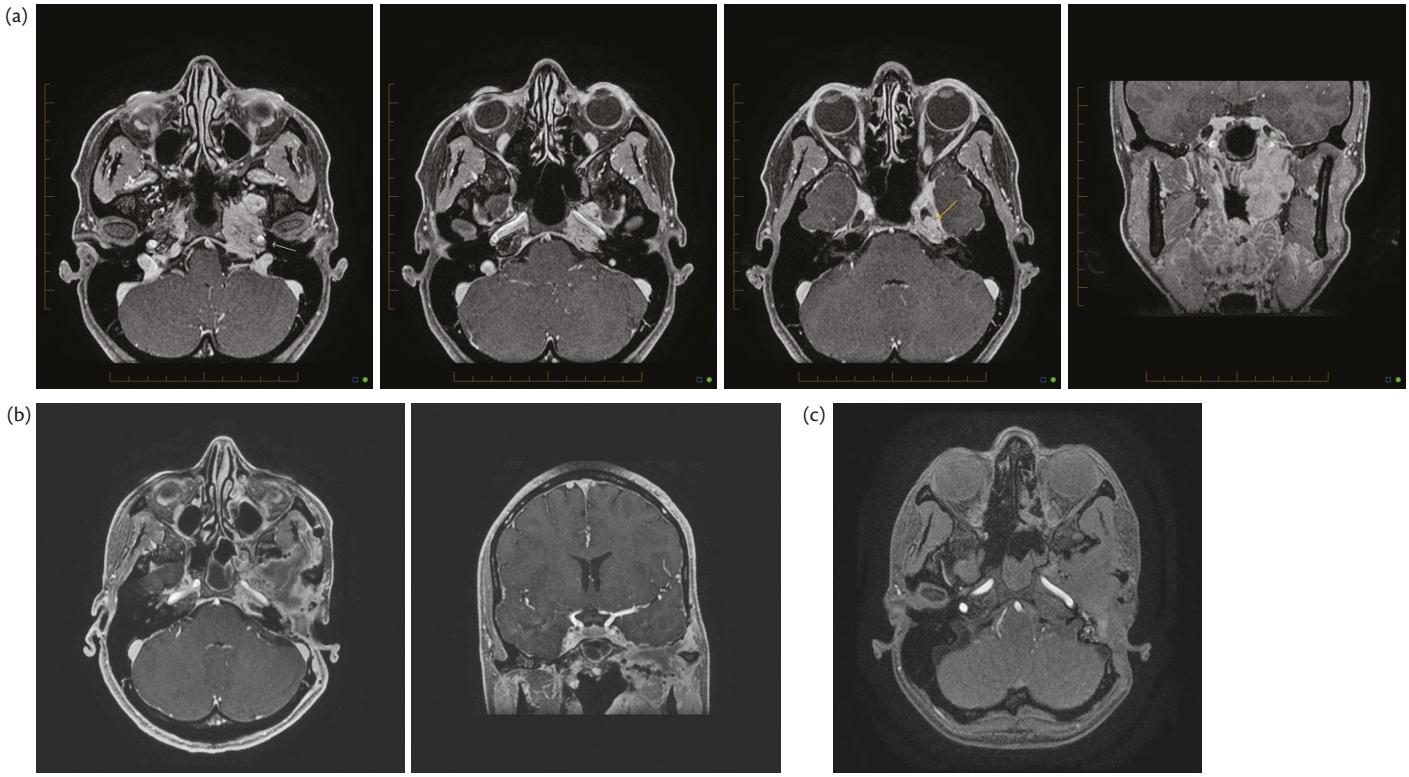

Fig. 18.3 Adenoid cystic carcinoma. This 37-year-old lady presented with 18 months of left-sided earache and Eustachian tube dysfunction. Biopsy demonstrated adenoid cystic carcinoma. The patient underwent a nasoendoscopic mobilization of the nasopharyngeal margin, transoral approach to the inferior oropharyngeal margin, an infratemporal fossa approach, and middle and posterior cranial fossa craniotomies. (A) Axial and coronal preoperative T1-weighted MRI with gadolinium contrast. The tumour is seen abutting the cavernous sinus and surrounding the petrous carotid artery (arrowed). (B) Postoperative T1 weighted MRI with gadolinium contrast. (C) Postoperative time of flight MRI angiogram to confirm carotid patency.

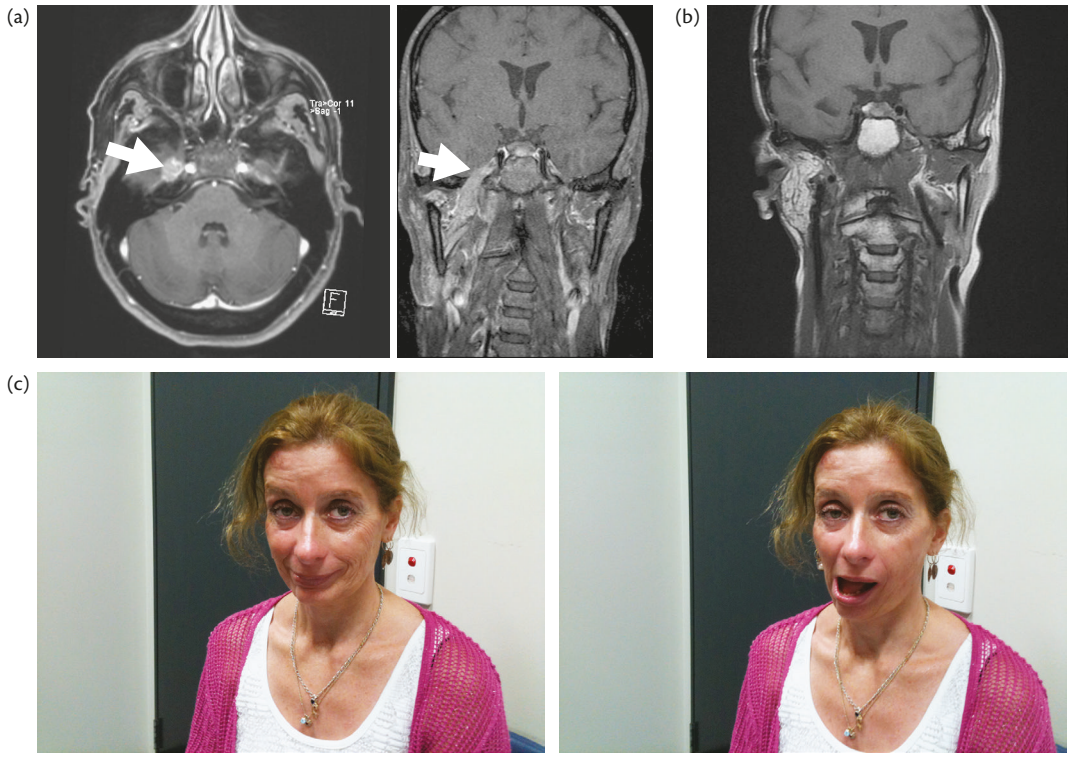

Fig. 18.4 Adenoid cystic carcinoma with perineural spread. This patient presented with formication and paraesthesia in the mandibular division of the trigeminal nerve. (A) Axial and coronal preoperative T1-weighted MRI with gadolinium contrast demonstrating infratemporal fossa mass with bulky contiguous enhancing extension into the cavernous sinus via the foramen ovale (arrowed). (B) Coronal 7-year postoperative T1-weighted MRI with gadolinium contrast demonstrating removal of the mandibular division of the trigeminal nerve. (C) Postoperative examination. In the left image the patient has been asked to 'smile' and 'raise their eyebrows' demonstrating intact facial nerve function. In the right image the patient has been asked to protrude the jaw with jaw deviation to the affected side from infratemporal fossa and mandibular bone resection.

Given the good premorbid state of the patient, and following discussion of the treatment options, the patient elected to have macroscopic resection of the tumour. A subtemporal preauricular approach was taken to the infratemporal fossa and combined with a hemimandibulectomy in order to remove the inferior alveolar nerve in its entirety within its bony canal. This was performed deep to the masseter muscle in order to preserve the facial nerve and combined with a subtemporal craniotomy and extradural approach to the Gasserian ganglion. The foramen rotundum and ovale were first exposed from the inferior aspect before a subtemporal craniotomy was performed to allow extradural access from within the intracranial cavity allowing retraction of the temporal lobe and incision and splitting of the two dural leaves between V2 and V3. Progressive dissection of this plane exposed the cavernous sinus, analogous to the Dolenc approach. It is key to preserve V1 to prevent the morbidity of an insensate cornea and the upper portion of V2 is used to delineate the upper border of the Gasserian ganglion resection. Once the nerve fibres are divided a frozen section was sent from the foramen rotundum portion of V2 to confirm a clear margin and allowing it to be safely divided and dissected out with V3 thus permitting the intradural dissection to be removed *en bloc* with the infratemporal fossa specimen. Positive margins at V2 would necessitate further drilling of the more distal portion of the nerve into the pterygopalatine fossa. Preoperative planning based on the radiological appearance minimizes the chances of encountering unexpectedly positive margins.

Figure 18.4C shows the patient's postoperative outcome with preserved facial nerve function and loss of mandibular nerve function. The patient remains alive and well 7 years postresection. Careful planning and a combination of skull base and neurosurgical expertise can deliver good outcomes even in these challenging tumours.

FURTHER READING

Castelnuovo, P., Battaglia, P., Turri-Zanoni, M., et al. (2014). Endoscopic endonasal surgery for malignancies of the anterior cranial base. *World Neurosurg*, **82**, S22–31.

Essig, G.F., Kitipornchai, L., Adams, F., et al. (2013). Lateral temporal bone resection in advanced cutaneous squamous cell carcinoma: report of 35 patients. *J Neurol Surg B Skull Base*, **74**, 54–9.

Network, N.C.C. (2014). *NCCN Clinical Practice Guidelines in Oncology: Head and Neck Cancers*. http://www.nccn.org/professionals/physician_gls/f_guidelines.asp

Panizza, B., Warren, T.A., Solares, C.A., Boyle, G.M., Lambie, D., & Brown, I. (2014). Histopathological features of clinical perineural invasion of cutaneous squamous cell carcinoma of the head and neck and the potential implications for treatment. *Head Neck*, **36**, 1611–18.

Warren, T.A., Panizza, B., Porceddu, S.V., et al. (2016a). Outcomes after surgery and postoperative radiotherapy for perineural spread of head and neck cutaneous squamous cell carcinoma. *Head Neck*, **38**, 824–31.

REFERENCES

Castelnuovo, P., Battaglia, P., Turri-Zanoni, M., et al. (2014). Endoscopic endonasal surgery for malignancies of the anterior cranial base. *World Neurosurg*, **82**, S22–31.

Essig, G.F., Kitipornchai, L., Adams, F., et al. (2013). Lateral temporal bone resection in advanced cutaneous squamous cell carcinoma: report of 35 patients. *J Neurol Surg B Skull Base*, **74**, 54–9.

Ganly, I., Patel, S.G., Singh, B., et al. (2006). Craniofacial resection for malignant melanoma of the skull base: report of an international collaborative study. *Arch Otolaryngol Head Neck Surg*, **132**, 73–8.

Network, N.C.C. (2019). *NCCN Clinical Practice Guidelines in Oncology: Head and Neck Cancers*. http://www.nccn.org/professionals/physician_gls/f_guidelines.asp

Panizza, B., Warren, T.A., Solares, C.A., Boyle, G.M., Lambie, D., & Brown, I. (2014). Histopathological features of clinical perineural invasion of cutaneous squamous cell carcinoma of the head and neck and the potential implications for treatment. *Head Neck*, **36**, 1611–18.

Patel, S.G., Singh, B., Polluri, A., et al. (2003). Craniofacial surgery for malignant skull base tumors: report of an international collaborative study. *Cancer*, **98**, 1179–87.

Rawal, R.B., Gore, M.R., Harvey, R.J., & Zanation, A.M. (2012). Evidence-based practice: endoscopic skull base resection for malignancy. *Otolaryngol Clin North Am*, **45**, 1127–42.

Redmond, M.J. & Panizza, B.J. (2016). Intracranial management of perineural spread in the trigeminal nerve. *J Neurol Surg B Skull Base*, **77**, 150–60.

Solares, C.A., Mason, E., & Panizza, B.J. (2016). Surgical management of perineural spread of head and neck cancers. *J Neurol Surg B Skull Base*, **77**, 140–9.

Van Rooij, W.J., Sluzewski, M., Slob, M.J., & Rinkel, G.J. (2005). Predictive value of angiographic testing for tolerance to therapeutic occlusion of the carotid artery. *AJNR Am J Neuroradiol*, **26**, 175–8.

Warren, T.A., Panizza, B., Porceddu, S.V., et al. (2016a). Outcomes after surgery and postoperative radiotherapy for perineural spread of head and neck cutaneous squamous cell carcinoma. *Head Neck*, **38**, 824–31.

Warren, T.A., Whiteman, D.C., Porceddu, S.V., & Panizza, B.J. (2016b). Insight into the epidemiology of cutaneous squamous cell carcinoma with perineural spread. *Head Neck*, **38**, 1416–20.

Whisenant, J.T., Kadkhodayan, Y., Cross, D.T., 3rd, Moran, C.J., & Derdeyn, C.P. (2015). Incidence and mechanisms of stroke after permanent carotid artery occlusion following temporary occlusion testing. *J Neurointerv Surg*, **7**, 395–401.

19

Surgical management of tumours of the orbit

Joseph D. Chabot, S. Tonya Stefko, and Paul Gardner

Introduction

The orbit can harbour a variety of lesions and their approach and treatment should be dictated by anatomical location and pathology. The proximity of the orbit to the sinonasal cavity and anterior and middle cranial fossae make it an ideal location for collaboration among neurosurgeons, otolaryngologists, and ophthalmologists.

Traditional orbitotomy, microsurgical transcranial, and endoscopic endonasal approaches (EEA) provide 360-degree access for biopsy or resection of both primary intraorbital lesions and those involving the structures surrounding the orbits.

This chapter outlines the anatomy, clinical presentation, and techniques that guide surgeons in management of these lesions.

Anatomy

In his description of orbital anatomy, Dr Albert Rhoton describes a 'rule of sevens', seven nerves, and seven muscles inside a pyramid made of seven bones (Martins et al., 2011). The base of the pyramid is the anterior surface of the eye and lids, the space tapers posteromedially to the orbital apex. The volume of this pyramid is approximately 30 cc, consisting of fat, muscle, nerves, blood vessels, glands, connective tissue, and the globe (approximately 7 cc).

The seven bones that make up the orbit are the frontal, ethmoid, lacrimal, palatine, sphenoid, maxilla, and zygoma. The orbital roof consists mostly of the frontal bone separating the orbit from the frontal lobe anteriorly, and the lesser wing of the sphenoid demarcating the parasellar regions posteriorly.

The frontal bone joins inferiorly and medially with the ethmoid bone which forms the mass of the medial wall. The body of the sphenoid posteriorly and the lacrimal bones and maxilla anteriorly join the ethmoid and frontal bones to form the medial wall of the orbit, which separate the orbit from the nasal cavity.

Inferiorly, the orbital process of the palatine bone and the orbital surface of the maxillary bone create the triangular orbital floor, which ends laterally at the inferior orbital fissure. This wall separates the orbit from the pterygopalatine fissure and the maxillary sinus.

As the zygoma sweeps superiorly, it meets with the greater wing of the sphenoid creating the lateral wall of the orbit. This separates the orbit from the temporalis muscle and temporal lobe.

Seven nerves pass through two openings in the orbital apex. Medially, the optic canal (OC), a 4.5 mm wide, 5–10 mm long, bony channel through the lesser wing of the sphenoid, transmits the optic nerve (ON) and ophthalmic artery. A fold of dura called the falciform ligament covers its proximal opening. The intracranial dura passes through the OC and splits into two layers, the optic nerve sheath and the periorbita. The artery enters the OC lateral and inferior to the ON and terminates intraorbitally as the central retinal artery. It is the main blood supply to the retina, while perforators from the ICA perfuse the prechiasmatic and intracanalicular optic nerve (Hendrix et al., 2014).

The other six nerves, oculomotor, trochlear, abducens and the lacrimal, frontal, and nasociliary branches of the ophthalmic division of the trigeminal nerve, pass through the superior orbital fissure (SOF), which is separated from the optic canal by the optic strut.

At the exit of the optic canal, the four rectus muscles originate from the Annulus of Zinn and form a cone, topped by the globe, with the ON in the centre (**Fig. 19.1**). The superior oblique muscle originates high and posterior on the medial wall. The levator palpebrae arises from the roof of the orbit, and the inferior oblique from the anteromedial floor of the orbit.

The superior ophthalmic vein (SOV), the dominant drainage pathway, forms from several medial tributaries, while the inferior orbital vein forms from lateral tributaries. These veins anastomose with the facial and angular veins at the anterior orbit (base of the pyramid), and the SOV continues posteriorly via the SOF to join the cavernous sinus.

Clinical presentation

Symptoms of orbital lesions correspond to their relationship to the 'cone' of extraocular muscles and ON. Extraconal lesions may be outside (extraorbital) or inside (intraorbital) the periorbita. Proptosis and diplopia occur early, while visual impairment is a later finding as the lesion deforms the globe and optic nerve. Intraconal lesions lie

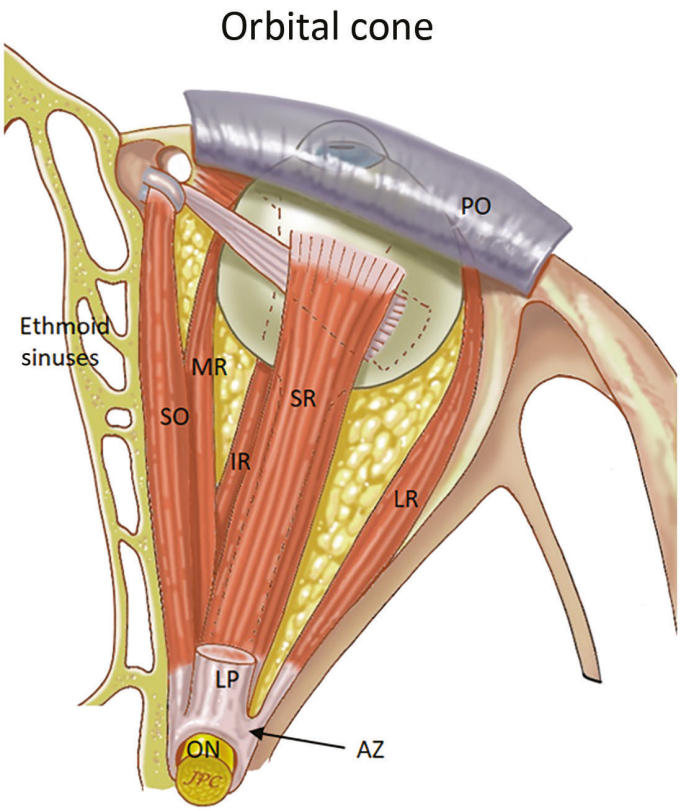

Fig. 19.1 Orbital cone: A view of the orbit from superior with the orbital roof resected, and the periorbita (PO) reflected anteriorly. The levator palpebrae (LP) has been truncated at its origin. The muscles originating from the Annulus of Zinn (AZ) and comprising the orbital 'cone' are the superior rectus (SR), lateral rectus (LR), inferior rectus (IR). The superior oblique (SO) runs superomedially. The inferior oblique muscle is not pictured. The optic nerve (ON) is in the centre of the cone.
©Jon Coulter, MA, CM1.

between the rectus muscles and ON. They present with early vision loss, axial proptosis, and diplopia, usually involving multiple fields of gaze.

Intracanalicular (optic canal) lesions present with early vision loss, optic nerve head oedema, and optociliary shunt vessels, but infrequently with diplopia or proptosis.

Tumours of the orbit can be divided into two major groups: those arising from the orbit, and those extending to the orbit from the surrounding cranium or sinonasal cavities. The most common tumours extending into the orbit are meningiomas and sinonasal carcinomas (Gardner and Stefko, 2014). Primary lesions and their locations can be found in Table 19.1 (Tailor et al., 2013).

Surgical planning

The orbit can be viewed as a clock with the optic nerve in the centre (Fig. 19.2). The safest surgical approach avoids crossing the ON, and can be determined by the lesion's location around the clock face (Paluzzi et al., 2015). For our purposes here, the remainder of the chapter will describe a right orbit. The mirror image would be used for the left orbit.

Table 19.1 Common locations of orbital masses

Intraconal	Extraconal
Cavernoma[a]	Hemangiopericytoma[b]
Optic nerve glioma	Lymphoid hyperplasia[b]
Optic nerve sheath meningioma	Atypical Hyperplasia[b]
Primary orbital melanoma	Lymphoma[b]
Metastasis	Pleomorphic adenoma
	Adenoid cystic carcinoma
	Lacrimal gland lymphoma
	Schwannoma[b]
	Neurofibroma[b]
	Metastasis

[a] less frequently extraconal

[b] less frequently intraconal

Data from Tailor, T.D., Gupta, D., Dalley, R.W., Keene, C.D., & Anzai, Y., Orbital neoplasms in adults: clinical, radiologic, and pathologic review, *Radiographics*, Volume 33, pp. 1739–58, Copyright © 2013

Lateral corridor approaches

Frontotemporal craniotomy (9:00–1:00), with orbitozygomatic osteotomy (6:00–1:00) for more extensive lesions

For lesions in the superolateral orbit posterior to the globe, a standard pterional incision, and elevation of a frontotemporal craniotomy may be used. This approach can be modified, for lesions inferior and lateral in the orbit (McDermott et al., 1990).

For an orbitozygomatic approach, the skin incision should be either bicoronal or three-quarter-coronal, extending from the ipsilateral tragus to at least the contralateral superior temporal line. Use interfascial dissection anteriorly to preserve the frontalis nerve. A straight line drawn from one end of the incision to the other should cross the targeted region. Dissection of the temporalis from the orbital rim is sufficient to reach the lateral orbit. If more extensive exposure is necessary, the temporalis can be mobilized completely from the temporal bone.

After performing a frontotemporal craniotomy, the frontal and temporal dura can then be dissected from the roof and the lateral wall of the orbit. The periorbita is dissected carefully from the inferior orbital fissure (IOF) to the supraorbital notch. A reciprocating saw is used to make a cut through the orbital roof at or just lateral to the supraorbital notch and through the body of the zygoma at the level of the IOF, protecting the periorbita and dura with malleable retractors. The cuts are connected using a high-speed drill, and the orbital roof and rim are then removed.

If necessary, an extradural clinoidectomy may be performed to decompress the optic canal. Drilling directly over the OC should be done using an 'eggshelling' technique with a diamond drill and copious irrigation. The bone can then be gently curetted from the underlying optic nerve sheath.

Bone removal posteriorly to the SOF and division of the meningo-orbital fold allows access to the parasellar regions and cavernous sinus.

Intraorbital lesions can be identified with palpation, ultrasound, or image-guidance. The periorbita is opened anterior to posterior,

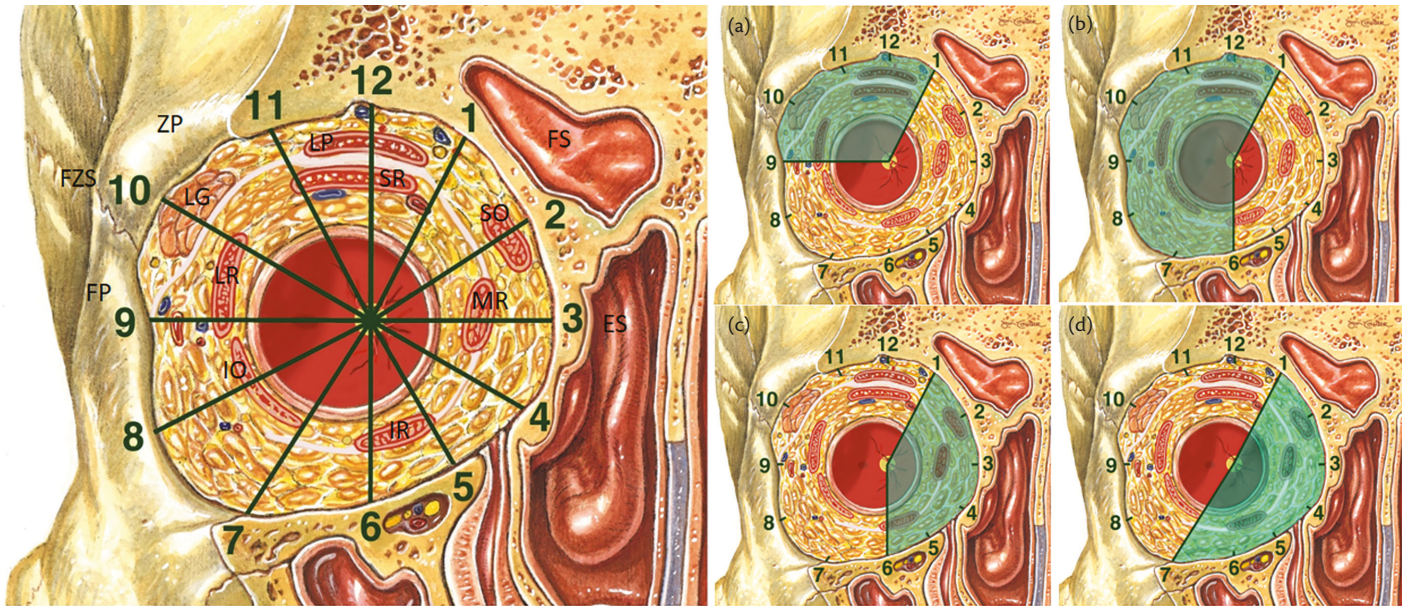

Fig. 19.2 Surgical planning: The 'clockface' centred on the optic nerve. Pertinent anatomic structures are the levator palpebrae (LP), superior rectus (SR), superior oblique (SO), medial rectus (MR), inferior rectus (IR), inferior oblique (IO), and lateral rectus (LR). The lacrimal gland (LG) is located superolaterally. The ethmoid sinus (ES) and frontal (FS) sinuses are located medially. The zygomatic process of the frontal bone (FP) joins to the frontal process of the zygoma at the fronto-zygomatic suture (FZS). The shaded portions of the clockfaces show the regions of the orbit exposed by the medial and lateral approaches. A frontotemporal craniotomy (A) can be combined with an orbitozygomatic osteotomy for more inferior lesions (B). A medial micro-orbitotomy (C) is the approach of choice for lesions anterior to the anterior ethmoidal artery from 1:00 to 6:00. Lesions posterior to the anterior ethmoidal artery in this location may be accessed using an endoscopic endonasal approach (D), or a combination of the two approaches.
©Jon Coulter, MA, CM1.

and the orbital fat is manipulated with cottonoids, q-tips, or an irrigating bipolar.

Fronto-orbital approach (9:00–1:00)

A less-invasive option for lesions in the superolateral orbit makes use of an incision made along the eyebrow from the supraorbital notch to the lateral edge of the cilia. A U-shaped pericranial flap based along the superior orbital rim is elevated preserving its inferomedial pedicle.

After limited dissection of the temporalis, a lateral burr hole is made at the keyhole, and the frontal dura dissected. A frontal craniotomy is then made from the burr hole extending as far superiorly as the skin incision allows and inferiorly along the orbital rim and roof. Drilling the posterior table of the frontal bone flush with the orbital roof, or removal of the orbital rim, maximizes access in this approach. An eyelid crease incision can also be used to provide a slightly more inferior trajectory with greater lateral access, though this limits the removal of the lateral and superior rims and requires bone removal from inside the orbit outwards.

For both of the aforementioned approaches, the removed bone can be replaced using titanium plates and screws or hydroxyapatite, with care taken to avoid entrapment of the extraocular muscles.

Lateral orbitotomy (8:00–10:00)

This is a classical approach for lateral orbital tumours (Maroon and Kennerdel, 1976). We favour an incision along an existing skin crease through the lateral commissure with lateral cantholysis. The aperture between the upper and lower eyelids becomes part of the effective incision providing exposure of the lateral orbital rim without a cosmetically unappealing incision in the mid-face.

The temporalis muscle is subperiosteally dissected and retracted laterally and the periorbita medially. Bony cuts are then made through the lateral orbital wall at the level of the IOF inferiorly and the frontozygomatic suture superiorly before the lateral wall is outfractured.

Using a retractor to protect the orbital contents, the greater wing of the sphenoid is then drilled to reach the orbital apex. Removal of the adjacent temporal bone allows the temporal dura to be dissected and the greater wing of the sphenoid to be drilled flush with the middle fossa floor.

To create a surgical corridor for intraorbital tumours, an incision through the periorbita is made parallel to the lateral rectus muscle, which can be retracted with a suture or vessel loop. Using microsurgical techniques of internal debulking and extracapsular dissection, the tumour can be safely removed.

Medial corridor approaches

Anterior medial micro-orbitotomy and transconjunctival approach (1:00–6:00)

After performing a conjunctival peritomy around the cornea, the medial rectus muscle is mobilized on a double-armed absorbable suture from its insertion site. A ribbon retractor displaces the globe laterally. If more lateral retraction is required, a lateral orbitotomy can be performed. After tumour removal, the medial rectus and inferior rectus can be reattached and the conjunctiva closed. While useful for lesions anterior in the orbit, the amount of retraction required for lesions posterior to the globe makes the endonasal approach preferable.

The transcaruncular approach is an approach to extraconal pathologies in these meridians. An incision is made between the caruncle and the plica semilunaris. The avascular plane between the lacrimal sac and periorbita is bluntly dissected posteromedially to the posterior lacrimal crest. The anterior and posterior ethmoidal arteries must be identified and coagulated in this approach to prevent sight-threatening orbital haemorrhage. Periorbita can be opened anterior to posterior if necessary.

Endonasal approaches (1:00–7:00)

The endoscopic endonasal approach (EEA) is well-suited for lesions displacing the optic nerve superiorly and laterally (Berhouma et al., 2014; Signorelli et al., 2015). Key to success with this approach to the orbit is a team including an ENT and neurosurgeon for every case, and an oculoplastic surgeon for intraconal tumours.

A uninarial approach consists of an uncinectomy, maxillary antrostomy, anterior and posterior ethmoidectomies, and sphenoidotomy to entirely expose the medial orbital wall. For intraconal, large, or orbital apex lesions, a binarial approach allows better manoeuvrability of the instruments posteriorly. This requires removal of the ipsilateral middle turbinate, wide opening of the sphenoid sinus, and posterior septectomy. If cerebrospinal fluid (CSF) is expected to be encountered during the surgery, a vascularized nasoseptal flap should be raised before the septectomy, usually from the contralateral side.

Important bony landmarks in the posterior sphenoid sinus and the structures they signify are as follows: carotid protuberance (cavernous carotid artery), lateral optico-carotid recess (optic strut), and medial optico-carotid recess (intersection of ON and carotid artery). Further superior and anterolateral bony removal exposes the ON, SOF, and orbital apex.

In most cases, fibrin glue, allograft, or fat graft is sufficient for reconstruction. If CSF is encountered, a vascularized nasoseptal flap can be used to decrease the incidence of postoperative CSF leaks (Hadad et al., 2006). Since it is not possible to suture the periorbita, the nasoseptal flap may be used to reconstruct the medial wall and prevent scarring of the rectus muscles.

Medial-inferior extraconal (1:00–5:00)

This approach can be used for orbital apex and ON lesions and for resection of medial tumours without intraconal extension. After performing the aforementioned steps, the lamina papyracea can be gently outfractured from anterior to posterior to expose the underlying peri-orbita. The bone overlying the orbital apex and ON can then be drilled with irrigation and gently elevated. For intraorbital tumours, the periorbita is opened over the lesion, which can then be removed with careful dissection. For tuberculum sella and planum meningiomas, the tumour can be removed from the OC by dividing the medial falciform ligament and opening the dura from medial to lateral over the superior aspect of the ON as it enters the canal. Recent studies have shown excellent visual outcomes with this technique (Gardner et al., 2008; Dehdashti et al., 2009).

Transmaxillary extraconal (1:00–7:00)

By anterior extension of the medial maxillectomy and removal of part of the pyriform aperture, more lateral extension can be obtained inferiorly along the floor of the orbit. With this approach, the pterygopalatine fossa and its contents can be dissected. By identifying V2 at the foramen rotundum, just deep to the infraorbital fissure, the infraorbital nerve can be identified and followed to the infraorbital canal.

This approach can be used for tumours that involve the middle fossa, orbit, infratemporal fossa, pterygopalatine fossa, or maxillary sinus (e.g. schwannomas, juvenile nasal angiofibromas). This approach requires knowledge of the course of the trigeminal nerve and the parapharyngeal segment of the internal carotid artery in order to avoid injury.

Medial intraconal (4:00–7:00)

For inferomedial intraconal lesions too posterior for the medial micro-orbitotomy (behind the globe), an external transconjunctival approach can be added to an inferior medial approach. A vessel loop is passed around the medial and inferior rectus muscles to aid in endoscopic identification and retraction. For wider access, the medial rectus can be tagged with a suture, detached from the globe, and displaced posteromedially while remaining attached to the Annulus of Zinn.

The tumour is first dissected along its lateral margin to avoid damage to the optic nerve, which is superior and lateral in this approach, as well as the ophthalmic and central retinal arteries which lie medial to the optic nerve in the orbit. Although bipolar cautery can be used to shrink the periorbital fat, it should be used sparingly to avoid damage to the intraconal nerves and blood supply to the optic nerve. After resection, the muscle can then be reattached to the globe. Closure is with the nasoseptal flap as mentioned earlier.

Superomedial modification (1:00 to 4:00)

If access superior to the medial rectus muscle is required, a superomedial orbitotomy may be added to this approach by removing the lamina papyracea, retracting the orbital contents, and drilling the medial roof of the orbit. This opens a narrow corridor between the medial rectus and superior oblique muscles. This approach is limited by the ophthalmic artery medially and by the ethmoidal arteries superiorly.

Fibrous dysplasia

Fibrous dysplasia (FD) is a congenital disorder in which immature bone and fibrous tissue replaces cancellous bone. Cranio-orbital dysplasia is a common manifestation, causing orbitofacial deformity, exophthalmos, ocular dysmotility, and visual impairment as it progresses (Amit et al., 2011).

On imaging, there are three types of FD: sclerotic (35%), cystic (25%), and mixed (40%). On MRI, these can appear quite extensive. The bony portions usually have very low signal on T2-weighted MRI, and the cystic portions and associated mucoceles show high T2 signals. Computed tomography (CT) scans show a 'ground glass' appearance and are essential for assessing the involvement of skull base foramina (Fig. 19.3) as well as guiding postoperative reconstruction.

Since FD generally progresses indolently and almost never in adulthood, observation may be the preferred course. Radiotherapy is contraindicated due to the high incidence of malignant

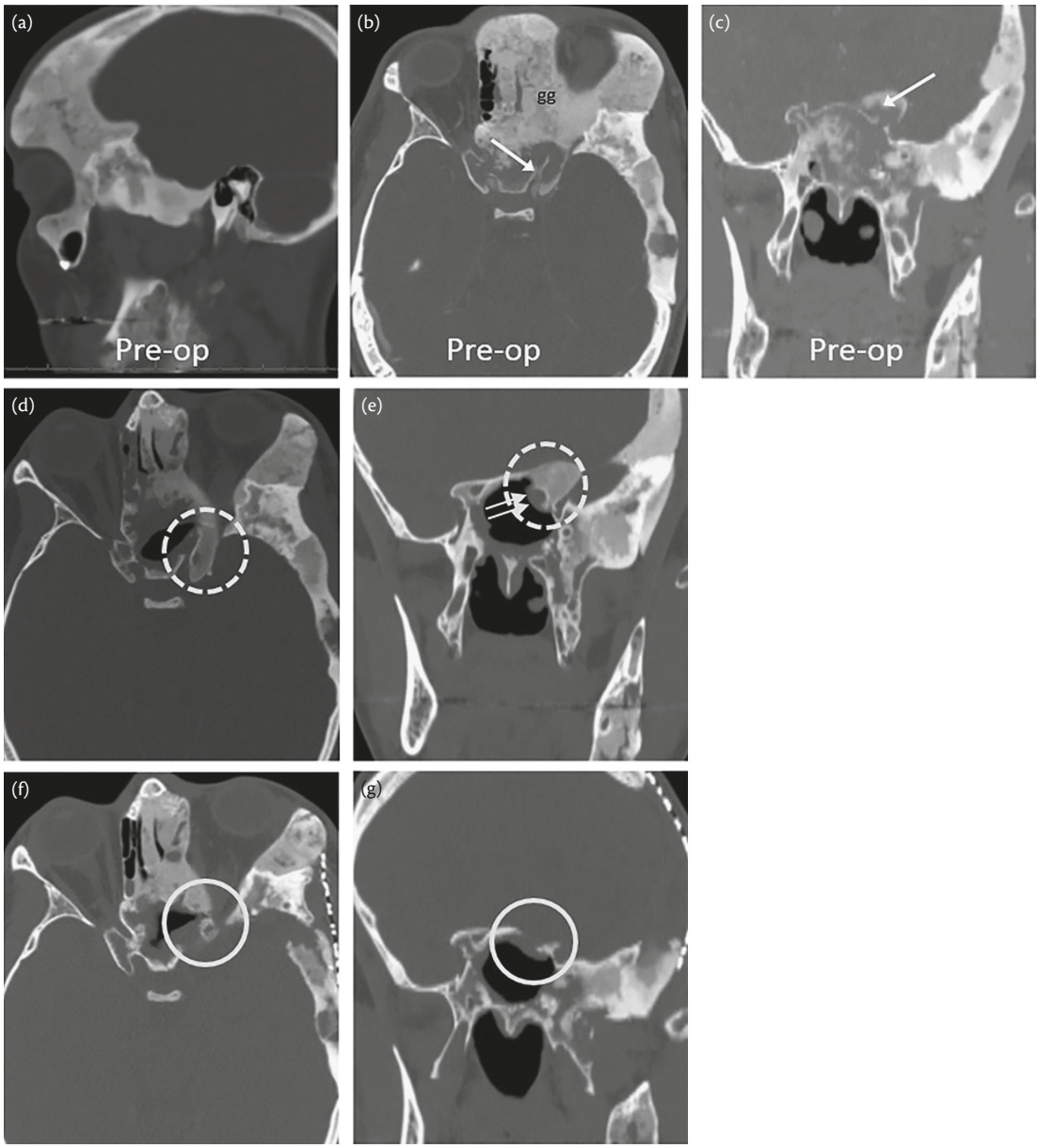

Fig. 19.3 Fibrous dysplasia: 22-year-old male with fibrous dysplasia involving the maxilla, mandible, temporal bone, frontal bone, and sphenoid bone on the left side. Bone algorithms of preoperative fine-cut CT (A, B, C) show the pathognomonic ground glass (gg) appearance. White arrows (B, C) demonstrate compression of the optic canal. The patient underwent endoscopic endonasal decompression of his left optic canal after developing progressive visual loss and optic neuropathy. This allowed an excellent medial decompression (double white arrows, E) and symptomatic improvement. 9 months later, he developed a superior visual field defect from his enlarged anterior clinoid (dashed circle, D, E). He underwent a left frontotemporal craniectomy and clinoidectomy for lateral and superior decompression of the optic canal (solid white circle, F, G). The patient's vision has been stable, but he has required additional operations for decompression of his infraorbital nerve and debulking of his mandible and maxilla.

transformation. Various medications have been used with inconclusive results.

For patients with cosmetic deformities, orbital reconstruction ranges from simple bone removal to a larger cranio-orbital approach with complete allograft reconstruction. ON decompression should be performed on patients with acute or progressive vision loss, while it is of questionable benefit for those with a chronically stable deficit. The choice of approach depends on the aetiology of the visual loss and may require more than medial decompression if there is cystic degeneration of the anterior clinoid process (Chen et al., 1997; Dumont et al., 2001).

Complications

Complications from orbital surgery are few but can be critical. Retrobulbar haematomas from medial approaches are avoided by coagulating the ethmoidal arteries. For tumours directly involving the ON and its meninges, preservation of the delicate pial blood supply is necessary to prevent visual loss. The risk of a postoperative hematoma is much greater for intraconal tumours.

An intraoperative CSF leak can be managed endoscopically with a vascularized nasoseptal flap to prevent meningitis. Microsurgical procedures may be required with a layered closure, fat graft, and

lumbar drain if a watertight seal is not possible. New diplopia following orbital surgery, related to oedema in the periorbital tissues, is usually temporary.

Controversies

The lateral orbitotomy and supraorbital 'keyhole' approach have increased in popularity as a direct 'minimally invasive' approach to lesions in the anterior and middle cranial fossa (Fig. 19.4). The disadvantage of these approaches is the narrow size of the surgical corridor due to the limited ability to displace the orbital contents. This makes vascular control and manipulation of larger tumours difficult. In addition, a clear understanding of the anatomy via a standard approach is critical before attempting these approaches. As yet, there is no consensus on the size or extent of the tumour that limits the use of these approaches as opposed to a full craniotomy.

Medial endoscopic endonasal decompression of the optic nerve in cases of compressive lesions of the optic canal and orbital apex, is also controversial. In cases of spheno-orbital meningiomas which often cause compression by hyperostosis, or in fibrous dysplasia, the endoscopic approach can provide safe decompression of more than 180-degrees of the optic nerve with minimal morbidity.

Results

The data at our institution is very encouraging regarding the endonasal approach for optic nerve decompression. In a series of 81 EEAs for 77 patients from 2003 to 2015 with decreased visual acuity from intraorbital lesions compressing the optic nerve, there were only two patients whose vision was worse after the surgery. Vision was improved in 31 eyes, and stable in 48.

We have also found that the lateral orbitotomy approach can be used to access lesions involving the middle fossa. Over a two-year period, we have performed 11 such operations, 6 of which were for spheno-orbital meningiomas (unpublished data). Proptosis and diplopia improved in these patients, and there were no new visual deficits. A watertight dural closure was difficult for those patients from whom affected dura was resected, which led to CSF leak in high-risk patients such as the obese and those with inhibited healing.

Conclusion

The anatomical location of the orbits adjacent to the middle and anterior cranial fossae and sinonasal cavity allows for a variety of approaches. The most appropriate surgical corridor will avoid crossing the vertical plane of the optic nerve and will also avoid excess

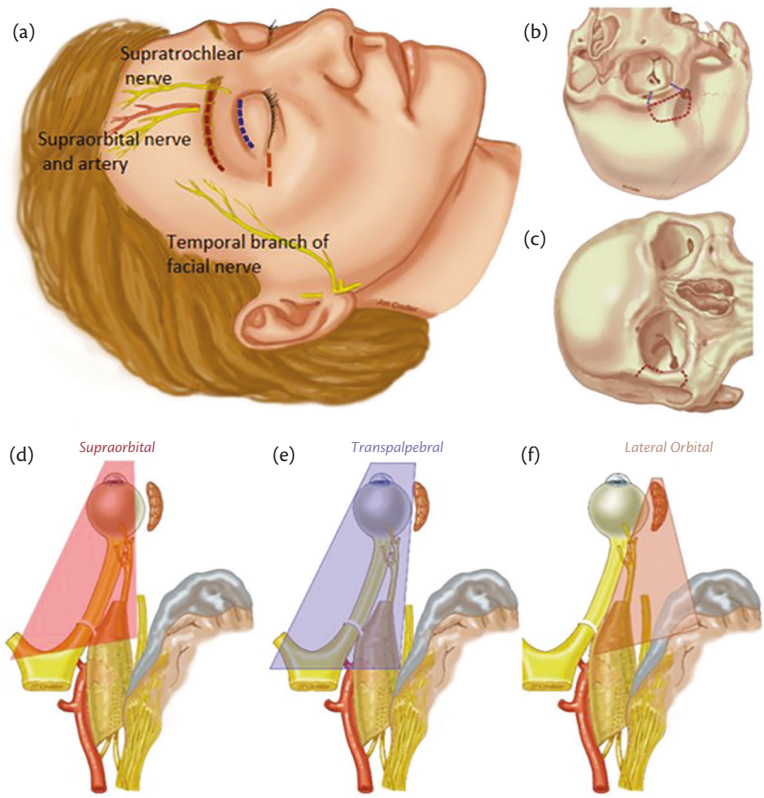

Fig. 19.4 Transorbital surgical corridors: panel A shows minimally invasive incisions for orbital approaches: supraorbital (dark red), transpalpebral (blue), lateral orbital (orange). A standard pterional or preauricular incision (not pictured) may also be used. Panel B outlines the bony cuts for the frontal craniotomy (red) with and removal of orbital rim (blue). Panel C shows the bony cuts in the lateral orbital rim. Panels G, H, and I show the potential intracranial structures that can be reached via transorbital approaches.

©Jon Coulter, MA, CM1.

retraction of the globe. A multidisciplinary team with all available specialties is therefore ideal for management of orbital lesions.

FURTHER READING

Amit, M., Fliss, D.M., & Gil, Z. (2011). Fibrous dysplasia of the sphenoid and skull base. *Otolaryngol Clin North Am*, **44**, 891–902, vii–viii.

Berhouma, M., Jacquesson, T., Abouaf, L., Vighetto, A., & Jouanneau, E. (2014). Endoscopic endonasal optic nerve and orbital apex decompression for nontraumatic optic neuropathy: surgical nuances and review of the literature. *Neurosurg Focus*, **37**, E19.

Maroon, J.C. & Kennerdel, J.S. (1976). Lateral microsurgical approach to intraorbital tumors. *J Neurosurg*, **44**, 556–61.

Martins, C., Costa, E.S.I.E., Campero, A., et al. (2011). Microsurgical anatomy of the orbit: the rule of seven. *Anat Res Int*, **2011**, 468727.

Paluzzi, A., Gardner, P.A., Fernandez-Miranda, J.C., et al. (2015). 'Round-the-clock' surgical access to the orbit. *J Neurol Surg B Skull Base*, **76**, 12–24.

REFERENCES

Amit, M., Fliss, D.M., & Gil, Z. (2011). Fibrous dysplasia of the sphenoid and skull base. *Otolaryngol Clin North Am*, **44**, 891–902, vii–viii.

Berhouma, M., Jacquesson, T., Abouaf, L., Vighetto, A., & Jouanneau, E. (2014). Endoscopic endonasal optic nerve and orbital apex decompression for nontraumatic optic neuropathy: surgical nuances and review of the literature. *Neurosurg Focus*, **37**, E19.

Chen, Y.R., Breidahl, A., & Chang, C.N. (1997). Optic nerve decompression in fibrous dysplasia: indications, efficacy, and safety. *Plast Reconstr Surg*, **99**, 22–30; discussion 31–3.

Dehdashti, A.R., Ganna, A., Witterick, I., & Gentili, F. (2009). Expanded endoscopic endonasal approach for anterior cranial base and suprasellar lesions: indications and limitations. *Neurosurgery*, **64**, 677–87; discussion 687–9.

Dumont, A.S., Boulos, P.T., Jane, J.A., Jr., Ellegala, D.B., Newman, S.A., & Jane, J.A., Sr. (2001). Cranioorbital fibrous dysplasia: with emphasis on visual impairment and current surgical management. *Neurosurg Focus*, **10**, E6.

Gardner, P.A., Kassam, A.B., Thomas, A., et al. (2008). Endoscopic endonasal resection of anterior cranial base meningiomas. *Neurosurgery*, **63**, 36–52; discussion 52–4.

Gardner, P.M. & Stefko, S.T. (2014). Tumors of the Orbit. *In:* Winn, H.R. (ed.) *Youmans Neurological Surgery*, 7th edition. Philadelphia, PA, USA: Elsevier Saunders.

Hadad, G., Bassagasteguy, L., Carrau, R.L., et al. (2006). A novel reconstructive technique after endoscopic expanded endonasal approaches: vascular pedicle nasoseptal flap. *Laryngoscope*, **116**, 1882–6.

Hendrix, P., Griessenauer, C.J., Foreman, P., Shoja, M.M., Loukas, M., & Tubbs, R.S. (2014). Arterial supply of the upper cranial nerves: a comprehensive review. *Clin Anat*, **27**, 1159–66.

Maroon, J.C. & Kennerdel, J.S. (1976). Lateral microsurgical approach to intraorbital tumors. *J Neurosurg*, **44**, 556–61.

Martins, C., Costa,, Campero, A., et al. (2011). Microsurgical anatomy of the orbit: the rule of seven. *Anat Res Int*, **2011**, 468727.

McDermott, M.W., Durity, F.A., Rootman, J., & Woodhurst, W.B. (1990). Combined frontotemporal-orbitozygomatic approach for tumors of the sphenoid wing and orbit. *Neurosurgery*, **26**, 107–16.

Paluzzi, A., Gardner, P.A., Fernandez-Miranda, J.C., et al. (2015). 'Round-the-clock' surgical access to the orbit. *J Neurol Surg B Skull Base*, **76**, 12–24.

Signorelli, F., Anile, C., Rigante, M., Paludetti, G., Pompucci, A., & Mangiola, A. (2015). Endoscopic treatment of orbital tumors. *World J Clin Cases*, **3**, 270–4.

Tailor, T.D., Gupta, D., Dalley, R.W., Keene, C.D., & Anzai, Y. (2013). Orbital neoplasms in adults: clinical, radiologic, and pathologic review. *Radiographics*, **33**, 1739–58.

RELATED LINKS TO EBRAIN

Orbital and Cavernous Sinus Disorders. https://learning.ebrain.net/course/view.php?id=1216

Special Considerations for Skull Base Tumours. https://learning.ebrain.net/course/view.php?id=493

20

Skull lesions

Giorgio Gioffre and Ivan Timofeev

Introduction

Skull vault lesions are rare and represent 1–2% of all bone masses. They are commonly an incidental finding or may be discovered during staging work-up for other diseases.

Different classification systems can be employed in order to categorize such lesions: primary (benign and malignant) or secondary as well as neoplastic and non-neoplastic (inflammatory and proliferative).

For many of these lesions the clinical and radiological features are often non-specific making the diagnosis cumbersome. Rather than being defined clinical entities, they frequently form part of a spectrum of disease where ruling out an unfavourable progression is of paramount importance.

Combining a basic knowledge of the epidemiology, clinical presentation, imaging findings, and histopathology is essential to differentiate these pathologies.

The aim of this chapter is to define the important features of each lesion, to offer an overview of the investigations and treatment, and to provide guidance for the differential diagnosis based on imaging. Therefore, pathological entities with similar radiological appearances are grouped together.

Predominantly lytic lesions

Metastasis

Metastases from extracranial primary neoplasms are the most common skull tumours, in 60% of cases origination from carcinomas of breast and lung (Colas et al., 2015). Other primary tumours that can metastasize to the skull are carcinomas of prostate, kidney, uterus, colon, liver, ovary, thyroid as well as other non-epithelial and bone tumours, while sarcoma and neuroblastoma are the most common primary causes in children (Mitsuya et al., 2011). Furthermore, the presence of a skull metastasis is associated with a secondary deposit in other bones in 90% of cases, and with brain metastasis in 30% of cases.

The prevalence of skull metastases is higher during the sixth and seventh decades of life. The majority of metastatic lesions appear as lytic, usually solitary and destroying either the inner or the outer table of the skull with invasion of the intra- or extracranial tissues.

Conventional radiography and computed tomography (CT) show single or multiple lytic lesions, typically lacking a sclerotic border, with indistinct margins, invading and infiltrating the adjacent soft tissues (**Fig. 20.1**).

Contrast-enhanced MRI is more sensitive than CT and radionuclide imaging in the characterization of skull metastases, allowing detection of dural and soft tissue invasion. The typical appearance is T1-hypointense, variable T2 signal changes, and variable contrast enhancement. When present, the enhancing pattern can be homogeneous, ring-like, or heterogeneous (Mitsuya et al., 2011). Bone scan and 18FDG PET show intense uptake, and may detect smaller calvarial metastatic deposits.

Blastic lesions are most commonly associated with primary carcinoma of the breast, prostate, colon, and bone. Their main feature is a bilateral symmetrical expansion of the diploe, with infiltrative borders and marrow replacement. Mixed radiological appearances are also possible.

From a clinical standpoint, they can be asymptomatic and often diagnosed in the context of staging of a known primary tumour, while less often they are the initial manifestation of an unknown malignancy. When symptomatic, painless, or painful swelling and headache are the most common symptoms (Stark et al., 2003; Mitsuya et al., 2011). Other symptoms are related to the primary disease or may be related to the presence of intracranial extension (neurological deficits, seizures, and other symptoms).

Differential diagnosis is with multiple myeloma, other skull lesions, postsurgical, or post-traumatic defects.

Treatment and prognosis are dictated by the nature and the clinical course of the primary tumour (**Fig. 20.2**).

Conventional fractionated radiation therapy remains the primary treatment. Radiosurgery can provide good tumour control in selected cases (Mitsuya et al., 2011), while bisphosphonates can be used in the palliative treatment of painful lesions (Mitsuya et al., 2011).

Indications for surgical treatment are: decompression of neurovascular structures, painful lesions, extensive infiltration of surrounding tissues and dura, obtaining tissue for histology (Mansfield, 1977; Stark et al., 2003).

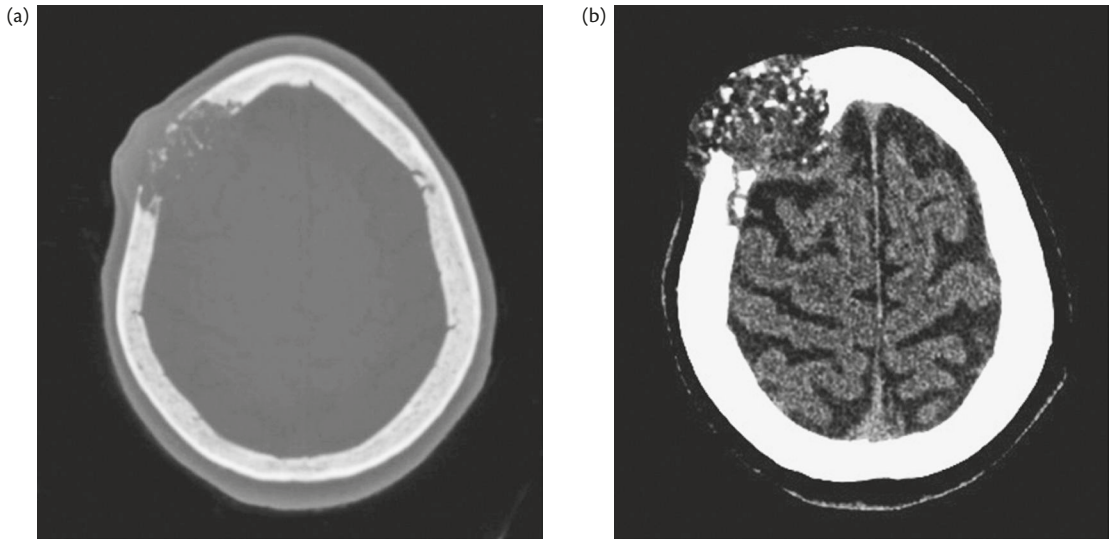

Fig. 20.1 Lytic lesions lacking a sclerotic border, with irregular margins, invading and infiltrating the adjacent soft tissues, representing metastasis.

Multiple myeloma

Multiple myeloma (MM) is a malignant disseminated disease of the bone marrow, characterized by a monoclonal proliferation of terminally differentiated plasma cells, replacing the normal marrow, and producing monoclonal immunoglobulins (Colas et al., 2015). MM is the most common primary malignant bone lesion (el Quessar et al., 1997) with a peak of incidence falling on the eight's decade. The aetiology is as yet unknown and it is possibly multifactorial, including genetic and environmental factors. It is associated with cytogenetic abnormalities in 80–90% of cases, the most common being chromosome 13 deletion.

Lesions are usually disseminated throughout the axial skeleton, and multiple skull lesions are found in more than 60% of patients with multiple myeloma. They usually arise in the diploe, sparing the inner table and deforming the periosteum, with a macroscopic appearance of a gelatinous red-brown tissue replacing the bone marrow.

Clinical presentation is in keeping with destruction of bone marrow and with the presence of abnormal circulating immunoglobulins. Skull involvement is usually asymptomatic, and detected during staging. However, symptoms may arise from skull base involvement with cranial neuropathies and proptosis, should orbital involvement occur. Serum and urine electrophoresis are part of the initial diagnostic workout. Diagnosis is confirmed by a bone marrow biopsy (Senapati et al., 2013).

MM can also present as a solitary lesion, representing a localized form of the disease (plasmacytoma) with no systemic manifestation. This is extremely rare in the skull (Senapati et al., 2013) and is thought to be a very early stage of MM, preceding the disseminated disease by several years (Kaur Gill et al., 2013).

In such cases, diagnosis is possible only after complete bone survey, bone marrow aspirate and after serum and urine electrophoresis have ruled out disseminated disease (Senapati et al., 2013).

X-ray and CT appearances are characteristic of multiple, well-demarcated, round, or oval osteolytic skull lesions. It can also present with diffuse sclerosis of the diploe and, less frequently, with skull osteopenia. MRI is useful in delineating meningeal disease and adjacent soft tissue involvement. Myeloma-related signal is mainly T1-hypointense and T2-hyperintense. Lesions tend to enhance with contrast on CT and MRI. Scintigraphy is insensitive given the exclusive osteolytic nature of the lesions.

Differential diagnosis is with postsurgical defects, metastases, haemangioma, brown tumours of hyperparathyroidism.

The mainstay of treatment is medical, through the combination of chemotherapy and focal radiation therapy. The reported rate

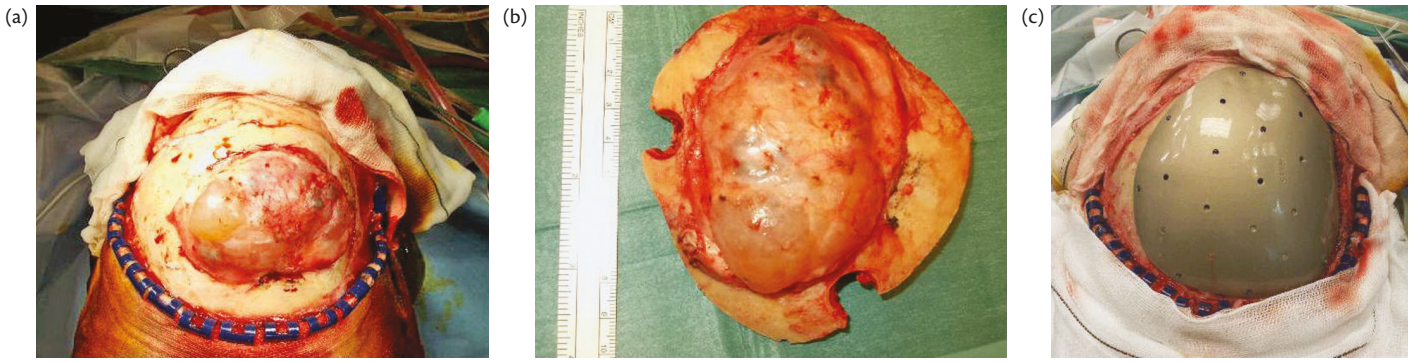

Fig. 20.2 Intraoperative findings—resection of calvarial metastasis with simultaneous titanium cranioplasty.

of 5 years survival is 20%, with a median survival of 3 years with conventional treatment protocols, and 6 months if left untreated. Chromosome 13 or 11q deletions are predictors of poor prognosis.

Plasmacytomas may be treated with surgical excision followed by radiation therapy (Kaur Gill et al., 2013; Senapati et al., 2013).

Haemangioma

Haemangiomas are a benign, mesenchymal, slow-growing intraosseous vascular tumour with predominantly vascular components.

Haemangioma is the second most common primary skull neoplasm, accounting for approximately 7–10% of primary skull tumours. It is three times as common in women as in men, and usually presents in the fourth decade of life. It is typically unifocal (Khanam et al., 2001) but can be multiple in up to 15% of cases. It is mostly found in the vertebral bodies, but when it arises in the skull is mainly found in parietal, temporal and frontal bones (Khanam et al., 2001). It mostly occurs as a sporadic solitary lesion, even though can arise as part of congenital angiomatosis. In some cases, it may be related to previous trauma.

Macroscopic features are those of subperiosteal, brownish-red lesions. They are often asymptomatic and found incidentally, can present with headache and a localized, slowly progressing, painful, and tender swelling, sometimes associated with a pulsatile sensation. Signs of seventh and eighth nerve compression can occur, for temporal bone localizations (Khanam et al., 2001; Colas et al., 2015).

Typically, the overlying skin is freely mobile. Soft tissues are rarely involved with the exception of infants. The occurrence of bruits or thrills can suggest the presence of an associated vascular malformation.

Skull radiography shows a well-circumscribed round or oval lesion with radiolucent honeycomb or trabecular pattern surrounded by a thin sclerotic rim. The classic 'sunburst' appearance is not frequently seen (Khanam et al., 2001).

CT usually shows a sharply marginated, well-circumscribed intradiploic osteolytic lesion with a thin peripheral sclerotic rim. In a third of cases, trabecular thickening with radiating spicules and hyperdense soft tissue contents can be present (Khanam et al., 2001; Colas et al., 2015). On MRI these lesions appear isointense on a T1- and hyperintense on a T2-weighted sequences. Usually no flow voids are displayed due to a very slow flow within the lesion and their small size. Haemangiomas are usually intensely contrast-enhancing.

Angiography can demonstrate hypervascular lesions, with a delayed persistent blush with a 'cluster of grapes' appearance mainly fed by the middle meningeal or superficial temporal arteries (Khanam et al., 2001).

Differential diagnosis for solitary haemangiomas is mainly with normal anatomic variant (vascular channel, foramen, emissary vein), postsurgical defects, dermoid, eosinophilic granuloma, metastases, cephaolocele, intradiploic arachnoid cyst, intradiploic meningioma, sarcomas (Khanam et al., 2001). Differential for multiple lesions is with lymphoma, osteoporosis, hyperparathyroidism.

Haemangiomas are a benign and slow-growing neoplasm that rarely requires treatment. Indications for surgery include correction of mass effect, cosmesis, and haemorrhage control. Surgery is the definitive treatment, with en-bloc removal together with a rim of normal bone. Curettage may lead to excessive bleeding and recurrence (Khanam et al., 2001). Unresectable lesions, deeply invading and permeating the surrounding tissues, may be treated with radiotherapy or super-selective embolization (Khanam et al., 2001). Malignant sarcomatous transformation is exceedingly rare.

Langerhans cell histiocytosis

Langerhans cell histiocytosis (LCH) is a multisystemic, idiopathic (Ralston et al., 2008) granuloma-forming proliferative disorder characterized by a spectrum of abnormal proliferation of Langerhans cells in various tissues and comprises a related group of three histiocytic disorders (Ralston et al., 2008; Colas et al., 2015): eosinophilic granuloma (70%), the localized benign form, characterized by a focal infiltration of histiocytes, with the calvarium involved in most cases (De Angulo et al., 2013); Hand-Schuller-Christian syndrome (20%), which is the multifocal chronic disseminated form; and Letter-Siwe syndrome (10%), the acute, malignant, disseminated type (Ralston et al., 2008).

LCH most commonly affects young people with 70% of patients under 20 years of age, and is most frequent in white males (90%). The specific incidence of eosinophilic granuloma, the localized form of the disease, is 0.4/100 000.

It predominantly involves the axial skeleton, where the neurocranium is frequently affected, especially in the frontal and parietal regions (Colas et al., 2015), followed by the mastoid, mandible, and facial bones.

While eosinophilic granuloma is a self-limiting, gradually enlarging, tender, unifocal calvarial mass, usually with a history of several months, Hand-Schuller-Christian and Letter-Siwe syndrome have a multisystemic involvement, with a more severe prognosis.

In eosinophilic granuloma, conventional radiographic imaging and CT show a sharply marginated 'punched out' lesion with scarce surrounding sclerosis and bevelled edges, involving both inner and outer tables (**Fig. 20.3**; also see Ralston et al., 2008). Mastoid localizations are characterized by marked bone destruction. The soft tissue within the lytic defect often displays contrast enhancement. MRI findings are those of a focal lytic T2-hyperintense soft tissue mass, often with extracortical extension, with a 'champagne cork' or a 'collar button' appearance, depending on their mono or bicortical extension. 18-FDG PET shows increased uptake in proliferating lesions (Ralston et al., 2008). Differential diagnosis is with other causes of lytic calvarial lesions (epidermoid, dermoid, postsurgical defect, metastases, skull tuberculosis). Lesions involving temporal bone have to be differentiated from a severe mastoiditis and rhabdomyosarcoma.

The natural history is variable, depending on factors such as age of onset, extent of involvement, presence of multiorgan dysfunction, and relapse. Mortality reaches 18% in multifocal disease. Treatment depends on the extent of disease; eosinophilic granuloma may spontaneously regress, but recurrence is reported in 30% of cases, often in a different site, mostly in children. Simple observation (De Angulo et al., 2013), local surgical resection, radiotherapy to treat recurrences, and combined irradiation and chemotherapy in case of multifocal calvarial involvement have been described.

Ewing's sarcoma

Primary Ewing's sarcoma (ES) of the skull is very uncommon (less than 4% of all cases), while the secondary haematogenous spread from other localizations is far more frequent (Salunke et al., 2011). The peak of incidence is between 15 and 25 years, predominantly in

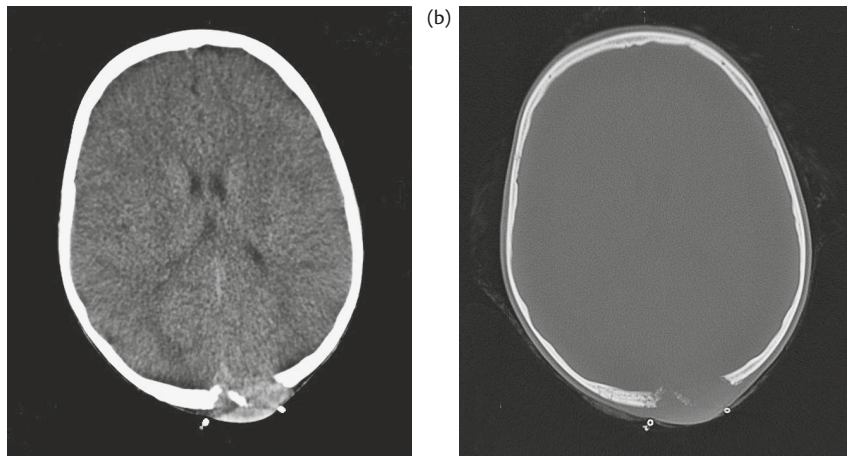

Fig. 20.3 LCH—'punched out' lesion with sharp margins, absence of significant sclerosis, and faint soft tissue enhancement.

males (Desai et al., 2000; Salunke et al., 2011) It usually involves the parietal and frontal bones, while very rarely affects the skull base (Desai et al., 2000; Salunke et al., 2011).

The histogenesis is uncertain, with likely origin from mesenchymal stem cells (Desai et al., 2000; Salunke et al., 2011).

The main macroscopic feature is a pattern of bone destruction associated with abnormal subperiosteal bone deposition.

Clinical presentation includes local swelling and signs and symptoms of raised intracranial pressure with focal neurological deficits (Desai et al., 2000).

Metastases tend to occur in 80% of cases in the first 2 years, mainly to lungs and other bones (Desai et al., 2000) even though cranial primary tumours seem to display a far less aggressive behaviour (Salunke et al., 2011).

The typical radiographic features of 'onion-skin' or 'sunburst' lesion might not be present. Most commonly ES of the skull presents as a non-specific lytic lesion with periosteal reaction and a contrast-enhancing content, best characterized by MRI, where the soft tissue components can have variable signal intensities (Desai et al., 2000).

Differential diagnosis is mainly with osteogenic sarcoma, primitive neuroectodermal tumours, rhabdomyosarcomas, metastatic neuroblastomas, and lymphomas (Desai et al., 2000).

Primary skull locations tend to have a better prognosis, compared with the axial skeleton.

The prognosis for patients with local recurrent disease is poor, with a 5-year survival following recurrence of 10–15% (Salunke et al., 2011).

Radical surgical resection followed by radiation and chemotherapy allows a 2-year disease-free survival rate of 55–60% (Desai et al., 2000).

Osteogenic sarcoma

Osteogenic sarcoma is a non-meningotheliomatous malignant mesenchymal neoplasm arising from multipotent mesenchymal cells of perivascular sheaths.

It is exceedingly rare in the skull, despite being the second most common overall primary bone malignancy after multiple myeloma. It most commonly occurs in males from the second to the fourth decade, and is often secondary to previous irradiation, Paget's disease, fibrous dysplasia, giant cell tumour, and chronic osteomyelitis (el Quessar et al., 1997). Macroscopic features are consistent with haemorrhagic soft tissue with necrosis and calcifications.

It typically presents as a rapidly growing mass, which is often painful (el Quessar et al., 1997). The associated clinical features are highly variable and depend on tumour location. A highly aggressive course is unfortunately common with rapid development of distant metastases predominantly in the lungs.

Plain X-ray and CT show a radiolucent, ill-defined lesion lacking adjacent sclerosis (no periosteal reaction) often with both intra- and extra-axial components, mostly enhancing. MRI displays a T1-hypointense, T2-heterogeneously hyperintense signal change, with intense enhancement after gadolinium. Imaging features depend on the histological type. The osteoblastic type can present with a typical 'sunburst' appearance, extending into the soft tissues, with associated thickened cortex although it can also display features of a non-specific enhancing lytic lesion with thickening of the surrounding bone and scattered calcifications. Differential diagnosis includes metastases, chondrosarcoma, osteochondroma, and benign and malignant meningothelial tumours (el Quessar et al., 1997).

Gross total resection with wide margins to achieve local control of disease is the goal of surgical treatment and is combined with irradiation and chemotherapy, in order to decrease local recurrence and metastatic spread (el Quessar et al., 1997). Despite treatment, the prognosis is poor with only a minority of patients achieving long-term survival.

Fibrosarcoma

Fibrosarcoma is a non-meningotheliomatous malignant mesenchymal neoplasm, which originates from the connective tissue in the bone marrow. It is a rare tumour, which mostly occurs secondary to a Paget's disease of the bone, prior irradiation, fibrous dysplasia, giant cell tumour, bone infarction or chronic osteomyelitis, and usually affects middle-aged adults (Mansfield, 1977). Skull involvement is often the consequence of the invasion from a nearby primary site (paranasal sinuses, face, scalp, dura).

Clinically it presents as a rapidly growing lesion, locally aggressive, and rapidly metastasizing to lungs and bones.

On plain X-ray and CT fibrosarcoma presents as an ill-defined non-specific lytic lesion with variably enhancing soft tissue content (Mansfield, 1977). MRI displays a T1-hypointense and

T2-heterogeneously hyperintense signal change with intense contrast enhancement. The differential diagnosis is largely with metastases and benign and malignant meningothelial tumours.

Gross total resection with wide margins to achieve local control of the disease is the goal of surgical treatment, combined with irradiation and chemotherapy.

Osteoclastoma (giant cell tumour)

Believed to originate from mononuclear cells of macrophage origin, is a very rare tumour of the calvarium, and typically arises at the epiphyses of long bones (Leonard et al., 2001; Harris et al., 2004).

It usually develops in the third and fourth decade of life, with a female preponderance (Harris et al., 2004). Rarely, it can present secondarily to Paget's disease: such cases are usually associated with the polyostotic form of the tumour, which commonly involves craniofacial bones, presents in an older age group, and tends to have a more favourable course compared to primary lesions (Leonard et al., 2001).

When located at the skull, osteoclastoma has a predilection for temporal and sphenoidal bones (Leonard et al., 2001; Harris et al., 2004).

Osteoclastoma tends to present as painful, progressively enlarging mass, which may occasionally be related to previous trauma.

Malignant degeneration occurs in 5–10% of cases (Leonard et al., 2001) while a pseudomalignant behaviour is not uncommon and is associated with pulmonary metastases (Harris et al., 2004).

Radiological features are those of a non-specific lytic lesion (Harris et al., 2004) with homogenously enhancing soft tissue content. Multilocular lesions can simulate an aneurysmal bone cyst or brown tumours in hyperparathyroidism. Unilocular lesion can radiologically resemble a giant cell granuloma, chondroblastoma and chondromyxoid fibroma (Harris et al., 2004). Also, imaging can also be indistinguishable from lytic metastases or direct invasion of a submucosal nasopharyngeal carcinoma.

Radical surgical resection is the gold standard, however not always achievable because of the location and infiltrative pattern. Preoperative arterial embolization can be considered to limit intraoperative bleeding. When partially resected these tumours have a tendency to recur within a relatively short time frame (1–2 years).

Giant cell tumours are generally radio-resistant and may undergo malignant transformation when irradiated (Harris et al., 2004). Radiation therapy has been advocated only for inaccessible non-resectable recurrence and when a clearly malignant behaviour is displayed. The receptor activator of NF-KB ligand (RANKL) signalling pathway that regulates osteoclast differentiation and activation has recently been shown to play a key role in the pathogenesis giant cell tumours and represents a promising therapeutic target, when surgical intervention is not feasible.

Aneurysmal bone cyst

Aneurysmal bone cyst (ABC) is a lesion composed of numerous thin-walled vascular spaces, separated by fibrous and mineralized tissue trabeculae, lacking normal endothelium.

Very rarely it occurs in the skull vault (1–6% of skull lesion cases) (Colas et al., 2015) with only 60 cases reported in the literature. It has equal sex distribution and usually affects patients younger than 20 years. It is also evenly distributed along the skull vault bones, involving symmetrically both inner and outer tables.

The pathophysiology of ABC is unclear, and there is debate whether it actually represents a neoplastic lesion. Local haemodynamic disturbances have been advocated to explain its occurrence.

ABC usually presents as a palpable tender mass, even though a form involving a predominantly intracranial growth, presenting with intracranial haemorrhage, has been described. It can also present in association with and secondary to fibrous dysplasia, giant cell tumours, and osteoblastomas.

Conventional radiography and CT imaging demonstrate a sharply defined lytic lesion with soap-bubble appearance with multilocular, scarcely enhancing spaces surrounded by thin inner and outer tables. MRI findings are consistent with a multiseptated lesion with fluid–fluid levels and blood degradation products. Angiography shows a hypervascular lesion. Findings consistent with a solid component may suggest a metastatic cause (Colas et al., 2015).

The neoplastic nature of an ABC is debated and its progression is often unpredictable and variable. Complete surgical excision is curative. In this regard, curettage and subtotal excision are associated with haemorrhage and high recurrence rates. Preoperative selective arterial embolization to avoid excessive blood loss might be considered.

If deemed non-resectable because of location or risk of haemorrhage, radiation therapy has been recommended. Cryosurgery and alcohol embolization have also been suggested to decrease recurrence rates of partially resected lesions.

Intraosseous lipoma

Intradiploic lipoma is one of the rarest bone tumours known (Kaneko et al., 2011), with only few case reports in the literature. It is a benign lesion, consisting of mature adipocytes in a matrix of thin bony trabeculae, originating from errors in the differentiation of mesenchymal stem cells covering the mature brain (Kaneko et al., 2011). They present clinically as a slowly growing lesion that spares the periosteum.

Imaging is in keeping with a fat filled cavity in the bone with no features of enhancement, infiltration, or erosion of a surrounding bone.

The differential diagnosis is with dermoid cysts, which appear more hyperdense, and from the reparative process after fracture or bone infarction, in which permeation of surrounding bone is seen. Fibrous dysplasia and meningiomata should also be taken into consideration.

Recurrence has not been reported and malignant transformation is exceptional. In view of benign clinical history radical resection is probably unjustified and in asymptomatic cases continued observation is acceptable (Kaneko et al., 2011).

Intradiploic epidermoid and dermoid cysts

These are benign calvarial lesions, which histologically represent inclusion cysts that result from entrapment of ectodermal or dermal elements during neural tube closure in embryonic development or rarely as a result of traumatic implantation. Epidermoid cysts contain only epidermal tissue and keratinized debris, whereas dermoids may contain dermal elements, such as hair follicles, skin glands, and teeth.

While most commonly diagnosed in children within a first decade of life these cysts can also be found in older children and adults, can affect both calvarial bones and skull base. They are generally less common than intradural lesions. Clinically they present as a

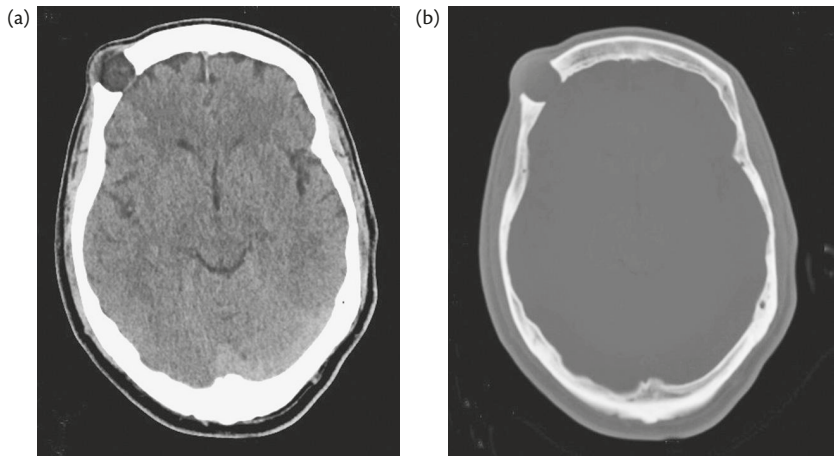

Fig. 20.4 Non-enhancing hypodense lesion with sharply defined bony margins characteristic of epidermoid cyst.

painless firm non-mobile slow-growing masses. Typically dermoid cysts have predilection to midline as well as sutures next to anterior fontanelle and epidermoids are commonly found in parietal, frontal, occipital bone, or next to the orbit. The cysts can affect outer or inner table or both. CT imaging demonstrates non-enhancing hypodense lesions with well-demarcated and often calcified margins and other zones of calcifications (Fig. 20.4). On T1 MRI the lesions are slightly hyperintense to CSF, on T2 isointense, on FLAR hyperintense, and on DWI demonstrate restricted diffusion. Ultrasound can also be utilized to diagnose and monitor both epidermoid and dermoid cysts (Riebel et al., 2008). Surgical treatment often considered for cosmetic reasons and to prevent the potential but rare complication of intracranial rupture of contents is usually associated with larger and more rapidly growing cysts involving the inner table. Operative options include open and endoscopic resection and curettage.

Overall prognosis is excellent and spontaneous regression can occur even with non-operative management.

Table 20.1 summarizes predominantly lytic lesions.

Predominantly blastic lesions

Osteoma and benign osteoblastic lesions

Osteoma is a benign mesenchymal tumour, macroscopically resembling mature lamellar bone. It originates from mature cortical bone and grows outward to form a solid dome-shaped mass, mainly in regions developing from membranous ossification. It is the most common primary calvarial tumour (Haddad et al., 1997), constituting up to 30% of craniofacial bone neoplasms, with a prevalence of 0.4% in the general population, and more frequently presenting in females with a F:M ratio of approximately 3:1, and a peak between the fourth and fifth decade of life (Colas et al., 2015). Usually located in the paranasal sinuses, it less frequently involves the calvaria and the mandible. When doing so it usually arises in the frontal bone, but can occur anywhere in the skull. It often involves the outer table of the skull (Haddad et al., 1997), but can arise from the diploe or from an inner table and are frequently found in proximity to the sutures, which are however normally spared (Colas et al., 2015).

Table 20.1 Predominantly lytic lesions

Metastasis	Metastatic cell infiltrates displaying the features of the primary lesion
Multiple myeloma	Pleomorphic, enlarged plasma cells, often in sheets with oval, eccentric nuclei, clumped chromatin, perinuclear halo, and cytoplasmatic inclusions ('Russell bodies')
Haemangioma	*Cavernous*: most common subtype in the calvaria, constituted by a mass of blood-filled sinusoidal channels lined with endothelial cells, set within a structure of fibrous septi and bony trabaculae as a result of bony remodelling *Capillary*: most common subtype in the vertebral bodies, consists of clumps of capillaries with associated necrosis *Venous*: consists of thick-walled venous channels, with reactive bone formation in a radiating pattern due to trabecular thickening
Langerhans histiocytosis	Monoclonal proliferation of Langerhans cells, with the characteristic presence of Birbeck granules, 'tennis-racket'-shaped cytoplasmic organelles with a central linear density and a striated appearance
Ewing's sarcoma	Sheets of cells with small, round hyperchromasic nuclei, scant cytoplasm, high nuclear/cytoplasmatic ratio, often forming pseudorosettes
Osteogenic sarcoma	*Osteoblastic*: 50% of cases, characterized by single or multinucleated atypical polygonal cells, with marked anaplasia and high mitotic figures in abundant immature osteoid. Other subtypes: *chondroblastic*, *fibroblastic*, *telangiectatic*
Fibrosarcoma	High cellularity with malignant collagen-producing fibroblasts, organized in sheets or fascicles with a 'herring bone' pattern with spindle-shaped nuclei, mild hyperchromasia, and high mitotic activity
Osteoclastoma	Vascular stroma with polyhedral and multinucleated giant cells, with prominent nucleolus. Areas with round mononuclear cells and spindle-shaped stromal cells usually coexist
Epidermoid and dermoid cysts	Inclusion cysts containing keratinized and stratified squamous epithelium. In dermoid cysts dermal elements (sebaceous and sweat glands, hair follicles, and so on) can be also present

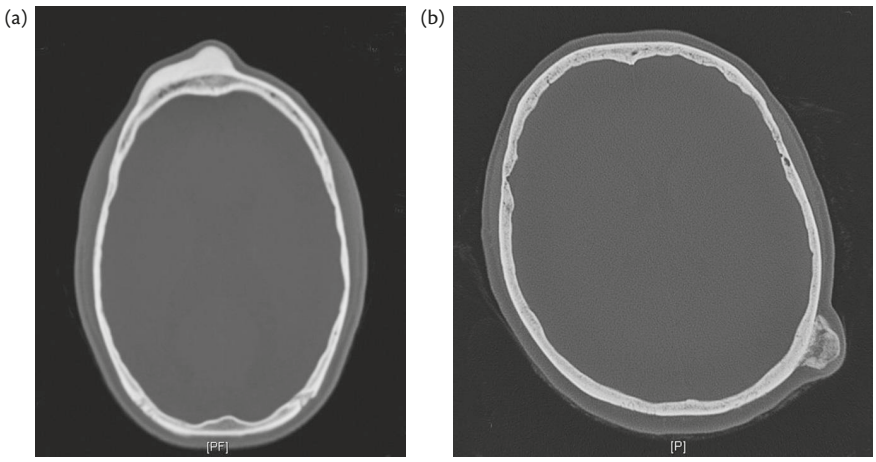

Fig. 20.5 Osteoclastic lesions—osteoma (A) and osteochondroma (B).

Most frequently asymptomatic, it presents as a solitary, painless, slow-growing, solitary, hard calvarial lesion, often only noticed as a cosmetic problem.

If multiple lesions are present, the possible diagnosis of Gardner's syndrome (autosomal dominant form of gastrointestinal polyposis characterized by the association of benign soft tissues neoplasms, thyroid cancer, and multiple osteomas of the skull and mandible) should be considered.

On X-ray and CT imaging osteoma usually appears as a dense, not enhancing, well defined lesion with variable central inhomogeneity (Fig. 20.5). MRI findings consist of homogeneous hypointense T1-weighted signal and variable signal on T2-weighted images, without involvement of the surrounding soft tissue or bone, and with no enhancement (Colas et al., 2015). Bone scan can show variable uptake, depending on the bone-synthesis phase of the lesion. When considering a differential diagnosis intraosseous benign and malignant meningothelial tumours (Fig. 20.6), and malignant non-meningothelial tumours ought to be considered.

Complete excision is the goal of treatment (Haddad et al., 1997) and is mainly undertaken for cosmetic reasons. If the lesion is small and arising from the outer table, it can be removed sparing the inner table by drilling or curettage. Formal craniotomy might be required for larger lesions or for those arising from the inner table, with subsequent simultaneous cranial reconstruction.

Other benign osteoblastic lesions are:

- Osteoid osteoma: benign osteoblastic neoplasm, uncommon in the calvaria as it most frequently arises from the long bones. Classically presents with pain occurring at night and relieved by aspirin.
- Osteoblastoma (also known as osteogenic fibroma): extremely rare in the skull with only sphenoidal location described. Similar to osteoid osteoma, but does not usually cause pain. The lesions tend to be more vascular than osteoid osteoma and sarcomatous change, although very rare, has been described (Figarella-Branger et al., 1991).

Osteoid osteoma and osteoblastoma are histologically undistinguishable, and conventional differentiation is based on the size of the former, measuring less than 1 cm and osteoblastomas being bigger lesions, which can cause tissue compression.

Chondroma (osteochondroma)

Chondroma is a benign osseocartilaginous tumour, macroscopically resembling cartilage, or ossified cartilage. It is the most common benign skeletal osseocartilaginous tumour, accounting for 9–10% of all bone tumours. It is mainly seen in women, from the second to the fifth decade of life, and usually occurs in bone formed by enchondral ossification, and given the almost exclusive intramembranous origin of craniofacial bones—in opposition

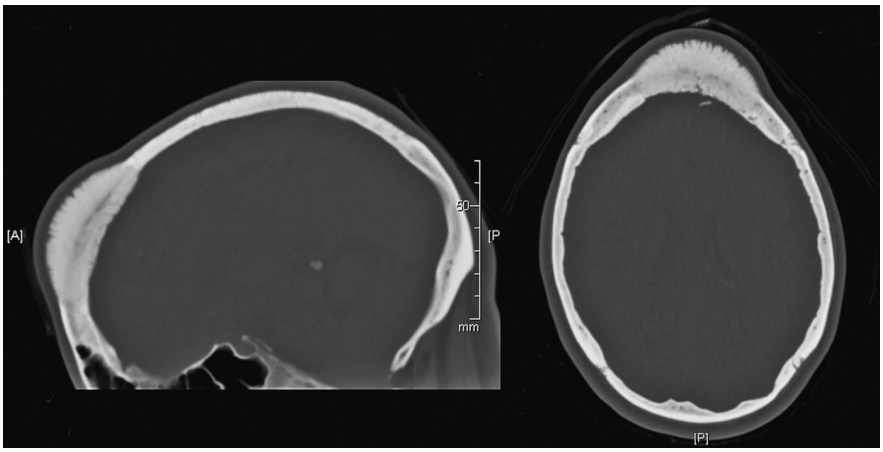

Fig. 20.6 Intraosseous meningioma—osteoblastic expansile lesion.

to the clivus and skull base, which develop by endochondral ossification—it is very rare in the neurocranium, representing less than 0.5% of intracranial tumours (Rathore et al., 2005). It therefore mainly arises in the skull base in the sphenoid (spheno-occipital synchondrosis), occipital (petro-occipital synchondrosis), and ethmoid (spheno-ethmoidal synchondrosis) areas. It has also been reported to occur in the choroid plexus and meninges, and when not arising in the skull base, the fronto-parietal skull is the most common location (Rathore et al., 2005).

It macroscopically appears as a non-pedunculated chondroid mass, or as a sessile exostosis, with or without a cartilage cap, depending on the ratio between osteoid and chondroid elements.

Clinically it presents as a slow-growing calvarial lump. When arising in the skull base, can give symptoms related to cranial nerves compression. Multiple lesions may be associated with Ollier's disease (multiple enchondromatosis) or Maffucci's syndrome (multiple enchondromatosis with subcutaneous haemangiomatosis) (Fountas et al., 2008).

These lesions share radiological features of a lobulated soft tissue mass, containing curvilinear matrix calcifications with scalloped endosteal bone resorption (Fountas et al., 2008). They appear moderately hyperdense on CT scan (Fig. 20.5) and hyperintense on T1-weighted MRI with a variegated pattern, depending on the amount of fat, fibrous tissue, vessels, and mineralized bone present. The cartilage cap can be slightly enhancing. Bone scan can demonstrate a variable uptake depending on the bone synthetic phase. The differential diagnosis is mainly with benign and malignant meningothelial tumours, intraosseous or with osseous invasion, and with malignant non-meningothelial tumours (sarcomas).

The mainstay of treatment is surgical, with complete excision (Fountas et al., 2008). When not completely resectable, decompression of the neural structures should be the primary aim. Transformation into chondrosarcoma is rare (1%), but more likely in the context of syndromic enchondromatosis (25–30%).

Hyperostosis frontalis interna

This condition consists of an irregular thickening of the inner table, diploe, and frontal squama, due to idiopathic deposition of new bone, typically in a nodular pattern. It tends to be bilateral, sparing the midline at the insertion of the falx (She and Szakacs, 2004). The incidence in the general population is 1.4–5%, and is most common in elderly white females, with a F:M ratio as high as 9:1 (She and Szakacs, 2004).

Its pathologic significance is debated, and it is almost always asymptomatic.

The aetiology of this condition remains unknown, but an associated endocrine imbalance may play a role. It is generally found in association with endocrinologic abnormalities (acromegaly, hyperprolactinemia), metabolic abnormalities (obesity, DM), hypertension, headache, CN deficits, seizures, dementia, and depression, and shows a very slowly progressive growth over the years (She and Szakacs, 2004).

CT and MRI show a nodular, symmetrical thickening of the frontal inner tables, which can reach a thickness up to 4 cm. There is little evidence in the literature regarding the surgical treatment of this condition, with lack of significant case series.

Table 20.2 summarizes predominantly blastic lesions.

Table 20.2 Predominantly blastic lesions

Osteoma	*Compact*: resembling cortical bone, with little fibrous tissue, almost exclusively arising from an outer table *Cancellous* (or trabecular): includes compact, trabecular, fibrous, and fat components, and usually originates from the diploe or the inner table *Fibrous*: made of lamellar bone, with a more cellular stroma usually eventually evolving into a 'compact' type
Osteochondroma	*Chondroma*: benign chondrocytes in scattered lacunae within an abundant hyaline cartilage matrix and with immunohistochemical positivity for s100 and vimentin *Osteochondroma:* benign chondrocytes capping an exostosis with cortex, trabeculae, and a normal marrow

Mixed lytic-blastic lesions

Neuroblastoma

Neuroblastoma is a tumour originating from the neural crest cells, whose development has been arrested in the neuroblast stage prior to becoming sympathetic ganglia cells. This explains its tendency to metastasize to the craniofacial skeleton, which shares the same neuroectodermal origin (D'Ambrosio et al., 2010a). It is the most common skull metastasis in children (D'Ambrosio et al., 2010a). The primary lesions arise from the adrenal medulla in 50% of cases with the remainder affecting the sympathetic chain.

It is most common during the first decade of life it does not show gender predominance.

Metastases occur in 50% of patients, and are typically blood-borne mainly to the liver, lungs, and bones. Metastatic involvement of the skull has been found in up to 25% of cases (D'Ambrosio et al., 2010b). When the craniofacial skeleton is involved, common presentations include easy facial bruising and exophthalmos in the case of orbital spread, or rapidly enlarging solitary or multiple masses of the calvaria, which can be associated with cranial nerve deficits (D'Ambrosio et al., 2010b). Skull base involvement and intracranial extension can also occur although generally the meninges act as a barrier to brain invasion.

Metastatic involvement of the skull can generate several different radiographic findings, including thickened bone, 'hair-on-end' periosteal reaction, lytic defects, and separation of sutures. CT usually shows a moderately hyperdense lesion, associated with permeative changes in the adjacent bone. MRI shows a T2-hypointense and T1-hyperintense signal change, with soft tissue infiltration often displaying a thick, 'plaque-like' peridural extension. Most lesions are contrast-enhancing.

The differential diagnosis is mainly with rhabdomyosarcoma, Langerhans cell histiocytosis, Ewing's sarcoma, and osteogenic sarcoma (D'Ambrosio et al., 2010b).

Radiation therapy is the mainstay of treatment, given the radiosensitive nature of the disease, and is used in combination with chemotherapy, and surgery, if focal compression of the neurovascular structures is present.

Paget's disease of bone

Paget's disease of bone is a chronic metabolic disorder characterized by abnormally excessive bone turnover (Ralston et al., 2008),

localized to a single bone or extending to the contiguous segments. It entails abnormal osteoclast activation, causing increased rate of bone resorption, with reactive osteoblastic hyperactivity and production of weaker, woven bone (Ralston et al., 2008). Paget's disease ranges from active lytic phases to reparative/quiescent ones; these may or may not coexist, with individual sites progressing at variable rates.

Incidence increases with age, reaching a prevalence of 3% in adults older than 40 years of age, and 10% in older than 80 years. There is equal sex distribution, and is most common in Caucasians and Ashkenazi Jews.

Skull involvement is present in 30–65% of cases, mostly in the frontal and occipital bones (Colas et al., 2015).

The aetiology is unknown. A genetic link exists with HLA DR2, with increased expression of genes that inhibits apoptosis, the most important being SQSTM1, which is a scaffold protein in the nuclear factor κB (NFκB)—ligand signalling pathway (Ralston et al., 2008).

Frequently asymptomatic, it is often discovered after an incidental finding of raised serum phosphatase alkaline (Ralston et al., 2008; Colas et al., 2015). It can also present as a painful, diffuse calvarial thickening. Entrapment neuropathies can occur if exit formaninae are narrowed, most frequently involving the eighth nerve with pulsatile tinnitus and hearing loss (pure sensorineural or mixed). Platybasia, associated or not with basilar impression, occurs in approximately 33% of patients, with potential brainstem compression, mostly in women. Depending on the extent of the disease, high output heart failure and secondary hyperparathyroidism can ensue, due to high vascularity and aggressive bone remodelling of the lesions. Sarcomatous transformation is reported to occur in less than 1% of cases (Hansen et al., 2006), mainly to osteosarcoma (50–60%), fibrosarcoma (20–25%), and chondrosarcoma (10%). Giant cell tumours are also associated with Paget's, and are frequently multiple in the context of polyostotic disease, with almost exclusive involvement of the craniofacial bones. These present at older ages compared to primary osteoclastomas, and tend to have a less aggressive behaviour (Leonard et al., 2001).

Three radiological forms are described, depending on the phase of the disease: an early destructive phase, which is characterized by osteolytic, radiolucent lesions ('osteoporosis circumscripta cranii', when involvement of the frontal bone prevails). Intense contrast enhancement reflects the increased vascularity of this phase. An intermediate-transition phase, which presents coexistence of lysis and sclerosis. Conventional radiography at this stage shows well-circumscribed areas of 'mottled' bone, and CT displays a 'cotton wool' like enlargement of the diploe. A late phase in which a sclerotic pattern prevails, resulting in a uniform thickening of the cortical bone and trabeculae.

MRI finding are T2-hyperintensity in the osteolytic phase, and variable T1 hyperintensity in the sclerotic stage, in relation to the status of the bone marrow replacement (Colas et al., 2015).

Bone scan shows radionuclide pick up, in relation to the osteoblastic hyperactivity.

A persistently lytic focus, not changing to sclerosis over time, with an enhancing content with no periosteal reaction is a suspicious finding for sarcomatous or giant cell tumour transformation.

The differential diagnosis is with skull metastases, osteosclerotic (prostate, breast, lymphoma) or osteolytic (lung, renal, thyroid), fibrous dysplasia, and all the causes of calvarial thickening (hyperostosis frontalis interna, meningioma). The mainstay of treatment is medical, with the goal of pain control, mainly achieved with osteoclast inhibitors. Close monitoring of the disease phases and imaging follow-up to detect malignant degeneration are warranted. Surgical treatment may be challenging because of the hypervascular nature of the disease, and profuse bleeding is common.

Fibrous dysplasia

Fibrous dysplasia is a congenital non-hereditary benign disorder of the mesenchymal precursor of bone. It is a consequence of the mutation of Gs alpha protein—encoded by GNAS gene—in osteoblastic progenitors' cells, resulting in an abnormal osteoblastic differentiation and maturation, with progressive replacement of normal bone by immature woven bone (Colas et al., 2015) mixed with fibrous connective tissue (Bowers et al., 2014; Wu et al., 2014).

It represents 2.5% of all bone tumours (Bowers et al., 2014), with an incidence of 1:4000–1:10 000. Males and females are equally affected, usually before the third decade of life.

It is monostotic in 75–80% of cases, but more commonly polyostotic in younger patients. Skull involvement is more common in the polyostotic form mainly involving the sphenoid, frontal, ethmoid, maxillary, occipital, and temporal bones (Bowers et al., 2014).

Clinical presentations include: painless localized bone swelling in the orbito-cranial territories, proptosis, entrapment cranial neuropathies (commonly the optic nerve), headache, seizures, spontaneous scalp haemorrhages (Bowers et al., 2014). In the polyostotic form, these findings come in association with long bones fractures and deformities.

Malignant degeneration is rare, seen in less than 1% of cases. The risk is greater in mono-ostotic locations, especially of the maxilla and mandible as well as following radiation therapy (Bowers et al., 2014). Osteosarcoma is the most common associated malignancy followed by fibrosarcoma and chondrosarcoma.

Lesions usually grow during childhood, and do not progress beyond puberty (Colas et al., 2015), with the end of skeletal maturation (Wu et al., 2014).

The polyostotic form of the disease can be part of McCune–Albright syndrome, characterized by the triad: polyostotic disease, café au lait spots, multiple endocrine dysfunction.

Three main radiological presentations have been described: pagetoid (35% of cases), characterized by alternating sclerotic and lytic features, with the sclerotic mainly involving the skull base, whereas the lytic lesions affect the cranial vault with a 'worm-eaten' appearance (**Fig. 20.7**). A sclerotic 'compact' form (50% of cases), characterized by homogeneous thickening of the bone, thought to represent the least active form. CT shows a ground-glass appearance (Bowers et al., 2014) mainly at the skull base. A cystic or 'lytic' (15% of cases) type, thought to represent the most active form, showing a non-homogeneous pattern of expanded bone on CT with radiolucent lesions surrounded by a thin sclerotic area resembling an eggshell. The cystic changes appear hyperintense on T2-weighted MRI, whereas areas of sclerosis show marked hypointensity (Bowers et al., 2014). The lesions are variably and inconsistently enhancing after gadolinium administration.

Differential diagnosis is with a wide range of conditions, given the polymorphic nature of the disease including Paget's, neurocutaneous

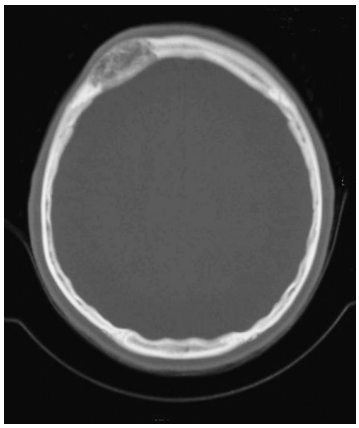

Fig. 20.7 Fibrous dysplasia exhibits a non-homogeneous pattern of expanded bone with radiolucent lesions surrounded by a thin sclerotic areas.

disorders, meningioma, brown tumours, osteopetrosis, hyperostosis frontalis interna, thalassemia, and craniometaphyseal dysplasia.

Surgical indications depend on the presence of progressive neurological impairment, the extent of the disease, and the age of the patient. When indicated, complete surgical resection is the goal of treatment. If not feasible, the aim is to achieve decompression of the neural structures (Bowers et al., 2014). Single stage bone reconstruction may be necessary. The lesions are radio- and chemo-resistant and radiotherapy has been reported to increase the risk of sarcomatous transformation.

Table 20.3 summarizes mixed lytic-blastic lesions.

Traumatic and congenital lesions

Sinus pericranii

This condition consists of a venous transdiploic venous channel, connecting the intracranial venous system with an epicranial or subgaleal vein (Bouali et al., 2015). It is a very rare finding, usually diagnosed from childhood to the third decade.

Sinus pericranii is mainly located along the sagittal sinus, in the midline frontal region, but can occur also more laterally. Two types are described: 'closed' type, where the flow comes from and drains into a dural sinus, and 'drainer' type, where blood drains transdiploe (Bouali et al., 2015).

Clinical presentation is of a soft, reducible mass in proximity of the midline, fluctuating with Valsalva manoeuvre and with changes in head position (Bouali et al., 2015). Neurological impairment is uncommon, but the disturbance of flow along the superior sagittal sinus has been thought to be the potential cause for non-specific symptoms such as headache, vomiting, and bradycardia (Bouali et al., 2015). Different aetiologies have been proposed: congenital, in association with other vascular anomalies, especially Von Hippel–Lindau syndrome; mixed congenital-traumatic, implying the presence of a large number of emissary veins which are torn by transient increases of ICP (coughing, straining), eventually allowing the formation of a blood varix progressively eroding the skull; traumatic, when an emissary vein or a dural sinus are torn by a skull fracture, causing a venous epidural haematoma.

Arteriography shows an enhancing transdiploic vascular channel, communicating with the intracranial veins, that may be anomalous and slowly filling.

The differential diagnosis includes vascular malformations of the scalp (cavernous haemangioma), ruled out by CT and MRI angiography, which show the lack of involvement of the intracranial circulation. Also pseudomeningocele, cranioschisis, growing skull fracture, scalp dermoid cyst should be considered (Bouali et al., 2015).

Surgical correction is indicated mainly for cosmesis, prevention of massive intracranial haemorrhage, and risk of air embolism, and is achieved mainly through craniotomy/craniectomy, closure of the communication between the extracranial veins and the intracranial venous sinus, and excision of the extracranial component with subsequent cranioplasty. Endovascular closure has also been described (Bouali et al., 2015). The prognosis of this condition is generally good.

Cephalohematoma

This consists of a subperiosteal haemorrhage, by definition stopping at the sutures. It occurs as a result of birth trauma, in 1% of live births, but can be also non-traumatic, if coagulopathy coexists. It is most common in in the parietal convexity, and may become apparent 24–48 hours after birth; it progresses over a few days, and usually resolves within 4 weeks, even if it can take longer (Kaufman et al., 1993). If it does not resolve after a month, calcification may occur in the site where the periosteum was lifted, with remodelling of the outer table.

The differential diagnosis is with caput succedaneum, which crosses the sutures and resolves after a few days, and with subgaleal haemorrhage, which similarly crosses the sutures and may extend towards the neck. CT imaging may be required to rule out depressed skull fracture and meningocele.

Head wrapping has been described, and may promote resorption. Needle aspiration of the fluid prior to wrapping is debated, since it may introduce infection. Surgical removal by drilling may be required if calcification occur, mainly for cosmetic reasons (Kaufman et al., 1993).

Table 20.3 Mixed lytic-blastic lesions

Paget's disease	Microscopic features vary between the different phases of the disease; in the early lytic-destructive phase giant multinucleated osteoclasts prevail, causing aggressive resorption and marrow substitution by fibrovascular tissue; the transition to the late sclerotic phase comprises an intermediate phase, with an increase in osteoblastic activity, leading to a final stage of decrease in osteoblastic activity with disappearance of the vascular stroma leaving a sclerotic, brittle bone with an atrophic marrow. Such sclerotic bone, made up of thickened trabecular, lacks structural strength ('pumice bone')
Fibrous dysplasia	Whorls of fibroblasts, immature woven bone, and cartilage—with bone trabeculae floating within a fibrous stroma forming 'Chinese letter' shapes

Leptomeningeal cyst

This is an intradiploic pseudocyst, without epithelial lining, occurring almost exclusively as a consequence of a skull fracture mainly in children under the age of three. When not related to a skull fracture, an epithelial lining is usually present ('true intradiploic leptomeningeal cyst') and the aetiology may be congenital or might involve a post-traumatic enlargement of Pacchioni's granulations (Menkü et al., 2004). It is most common (50%) in the parietal region, followed by frontal and occipital.

Such finding is usually associated with a blow to the calvaria, and can be thought as a retained form of growing fracture, with rupture of the inner table and intact outer table incorporating a dural and arachnoidal tear, associated or not with parenchymal injury and herniation through the meningeal breach. This is followed by subsequent enlargement of the fracture to form an intraosseous defect, due to the pulsation of the arachnoid and brain through the defect itself (Açikgöz and Tekkök, 2002) causing remodelling of the bony edges (Menkü et al., 2004). Growing fracture are associated instead with mechanical failure of both the inner and outer tables, and a cyst might develop trans- and beyond the diploe, forming a leptomeningeal pseudocyst (pseudomeningocele) (Açikgöz and Tekkök, 2002).

It presents as a soft, pulsating, fluctuant mass, more prominent with the patient supine, occurring in 50% of cases within a year of the original injury, and is occasionally associated with seizures or focal neurological deficits.

CT and MRI show the herniated meninges and brain. MRI has higher specificity to assess the involvement of brain parenchyma and the status of the dura. Differential diagnosis is mainly with epidermoid and congenital arachnoid intradiploic cyst (Menkü et al., 2004).

Surgical treatment consists in the resection of the cyst, with or without amputation of the herniated brain. Closure of the dural defect is necessary to prevent recurrence (Açikgöz and Tekkök, 2002). Cranial reconstruction is often needed.

REFERENCES

Açikgöz, B. & Tekkök, I.H. (2002). Post-traumatic intradiploic leptomeningeal fistula and cyst. *J Clin Neurosci*, **9**(4), 468–73.

Bouali, S., Maamri, K., Abderrahmen, K., Asma, B., Boubaker, A. & Hafedh, J. (2015). Clinical and imaging findings in a rare case of sinus pericranii. *Child's Nerv Syst*, **31**(9), 1429–32.

Bowers, C.A., Taussky, P., & Couldwell, W.T. (2014). Surgical treatment of craniofacial fibrous dysplasia in adults. *Neurosurg Rev*, **37**(1), 47–53.

Colas, L., Caron, S., & Cotten, A. (2015). Skull vault lesions: a review. *Am J Roentgenol*, **205**(4), 840–7.

D'Ambrosio, N., Lyo, J., Young, R.J., Haque, S.S., & Karimi, S. (2010a). Common and unusual craniofacial manifestations of metastatic neuroblastoma. *Neuroradiology*, **52**(6), 549–53.

D'Ambrosio, N., Lyo, J.K., Young, R.J., Haque, S.S., & Karimi, S. (2010b). Imaging of metastatic CNS neuroblastoma. *AJR Am J Roentgenol*, **194**(5), 1223–9.

De Angulo, G., Nair, S., Lee, V., et al. (2013). Nonoperative management of solitary eosinophilic granulomas of the calvaria. *J Neurosurg*, **12**(1), 1–5.

Desai, K.I., Nadkarni, T.D., Goel, A., Muzumdar, D.P., Naresh, K.N., & Nair, C.N. (2000). Primary Ewing's sarcoma of the cranium. *Neurosurgery*, **46**(1), 62–9.

Figarella-Branger, D., Perez-Castillo, M., Garbe, L., Grisoli, F., Gambarelli, D., & Hassoun, J. (1991). Malignant transformation of an osteoblastoma of the skull: an exceptional occurrence. Case report. *J Neurosurg*, **75**, 138–42.

Fountas, K.N., Stamatiou, S., Barbanis, S., & Kourtopoulos, H. (2008). Intracranial falx chondroma: literature review and a case report. *Clin Neurol Neurosurg*, **110**(1), 8–13.

Haddad, F.S., Haddad, G.F., & Zaatari, G. (1997). Cranial osteomas: their classification and management: report on a giant osteoma and review of the literature. *Surg Neurol*, **48**(2), 143–7.

Hansen, M.F., Seton, M., & Merchant, A. (2006). Osteosarcoma in Paget's disease of bone. *J Bone Min Res*, **21**(S2), P58–63.

Harris, A.E., Beckner, M.E., Barnes, L., Kassam, A., & Horowitz, M. (2004). Giant cell tumor of the skull: a case report and review of the literature. *Surg Neurol*, **61**(3), 274–7.

Kaneko, Y., Hokao, K., Ogasawara, N., Nakano, S., & Masuda, T. (2011). A case of intraosseous lipoma in the frontal bone. *Neurol Surg*, **39**(10), 975–80.

Kaufman, H.H., Hochberg, J., Anderson, R.P., Schochet, S.S. Jr., & Simmons, G.M. Jr. (1993). Treatment of calcified cephalohematoma. *Neurosurgery*, **32**(June), 1037–40.

Kaur Gill, M., Makkar, M., & Singh Bains, S.P. (2013). Solitary plasmacytoma of skull: a rare cytological diagnosis. *J Clin Diagn Res*, **7**(8), 1702–3.

Khanam, H., Lipper, M.H., Wolff, C.L., & Lopes, M.B. (2001). Calvarial hemangiomas: report of two cases and review of the literature. *Surg Neurol*, **55**(1), 63–7; discussion 67.

Leonard, J., Gökden, M., Kyriakos, M., Derdeyn, C.P., & Rich, K.M. (2001). Malignant giant-cell tumor of the parietal bone: case report and review of the literature. *Neurosurgery*, **48**(2), 424–9.

Mansfield, J.B. (1977). Primary fibrosarcoma of the skull. Case report. *J Neurosurg*, **47**, 785–7.

Menkü, A., Koç, R.K., Tucer, B., & Akdemir, H. (2004). Is skull fracture necessary for developing an intradiploic pseudomeningocele as a complication of head injury in adulthood? *Acta Neurochirurgica*, **146**(6), 623–7.

Mitsuya, K., Nakasu, Y., Horiguchi, S., et al. (2011). Metastatic skull tumors: MRI features and a new conventional classification. *J Neurooncol*, **104**(1), 239–45.

el Quessar, A., Boumedin, H., Chakir, N., el Hassani, M.R., Jiddane, M., & Boukhrissi, N. (1997). Primary osteosarcoma of the skull. *J Neuroradiol*, **24**, 70–4.

Ralston, S.H., Langston, A.L., & Reid, I.R. (2008). Pathogenesis and management of Paget's disease of bone. *Lancet*, **372**(9633), 155–63.

Rathore, P.K., Mandal, S., Meher, R., Subhalakshmi, R., Chauhan, V., & Singh, S. (2005). Giant ossifying chondroma of skull. *Int J Pediatr Otorhinolaryngol*, **69**(12), 1709–11.

Riebel, T., David, S., & Thomale, U.W. (2008). Calvarial dermoids and epidermoids in infants and children: sonographic spectrum and follow-up. *Childs Nerv Syst*, **24**(11), 1327–32.

Salunke, P.S., Gupta, K., Malik, V., et al. (2011). Primary Ewing's sarcoma of cranial bones: analysis of ten patients. *Acta Neurochir (Wien)*, **153**(7), 1477–85.

Senapati, S.B., Mishra, S.S., Dhir, M.K., Das, S., & Tripathy, K. (2013). A case of multiple myeloma presenting as scalp swelling with intracranial extension. *J Neurosci Rural Pract*, **4**(4), 445–8.

She, R. & Szakacs, J. (2004). Hyperostosis frontalis interna: case report and review of literature. *Ann Clin Laborat Sci*, **34**(2), 206–8.

Stark, A.M., Eichmann, T., & Mehdorn, H.M. (2003). Skull metastases: clinical features, differential diagnosis, and review of the literature. *Surg Neurol*, **60**(3), 219–25.

Wu, H., Yang, L., Li, S., et al. (2014). Clinical characteristics of craniomaxillofacial fibrous dysplasia. *J Craniomaxillofac Surg*, **42**(7), 1450–5.

RELATED LINK TO EBRAIN

Skull Lesions. https://learning.ebrain.net/course/view.php?id=481

21

Surgical management of anterolateral skull base lesions

Michael D. Cusimano and Michael P. Meier

Introduction

The following section outlines major considerations in the treatment of anterolateral skull base lesions. The essential anatomy, including the nasosinal region and anterior fossa, is presented. The challenge of choosing the appropriate surgical approach is highlighted. We report on the principles of preoperative investigations and explain the perisurgical treatment of patients with lesions of the anterolateral skull base.

The chapter focuses on surgical decision-making and the techniques used in managing anterolateral lesions. Detailed descriptions of the anterior interhemispheric approach, supraorbital minicraniotomy, extended endoscopic endonasal approach, orbitozygomatic approach, and the Fisch approaches are provided. Ultimately we present and discuss the surgically relevant nuances of four selected cases to highlight and illustrate the decision-making and controversies when applying certain approaches.

Neuroanatomy

Neurosurgeons must be masters of surgical anatomy. Not only must they understand the anatomy for the localization of lesions for diagnosis, but they also must master relational anatomy and the anatomy of the surgical corridors to lesions inside and outside the brain. In terms of the anterolateral approaches to skull base lesions, surgeons must understand the relational anatomy above, below, and across the anterolateral skull base. In terms of surgical corridors, this means understanding nasal and orbital anatomy, as well as cranial and transcranial anatomy.

The key to understanding the whole central skull base is the sphenoid bone, with its central body, lesser and greater wings, and the pterygoid plates, perforated by multiple foramina and bounding several fissures and the sphenoid sinus. The sphenoid provides passage to the internal carotid arteries, the middle meningeal arteries and presides over cranial nerves (CN) I-VI. Neurosurgeons must appreciate its anatomy from the primary different perspectives of anterior to posterior, posterior to anterior, lateral to medial, medial to lateral, superior to inferior, and inferior to superior in addition to rotated views that correspond to different head positions. It forms the core of the middle fossa and combines with the frontal bone and bones of the orbit and nasal complex to complete the anterior fossa and the structures above and below those regions.

The frontal bone provides the major structure of the anterior fossa. The frontal sinuses are extremely variable in size and position involving the lateral supraorbital ridge and orbital roofs. The frontal, sphenoid and ethmoid sinuses must be carefully studied on preoperative imaging, and should the surgical corridor necessitate transgressing these sinuses, appropriate reconstruction should be planned. The orbital roof is generally very thin, corrugated, and can be simply removed with an osteotomy. When combined with tenting of the dura inferiorly across a broad base, the subfrontal corridor is widely opened without the need for frontal lobe retraction.

The sphenoid and frontal bone make a good portion of the orbit, but the other bones of the orbit including the zygoma are critical in understanding lesions that transgress this area and the anterolateral approaches.

Folds of dura form the falx cerebri, and a division of the meningeal layers of the lateral wall of the cavernous sinus provide a home for cranial nerves III, IV, VI, and V2, before they transgress the superior orbital fissure and foramen rotundum (V2).

Preoperative

Workup of anterolateral skull base lesions

A detailed clinical history will shed light on the pathology of the lesion and help decide whether surgery is indicated and define the urgency of any procedures. A full neurological assessment should include an ophthalmological exam with visual acuity, pupillary reflexes, and a search for relative afferent pupillary defects, colour vision, and the perfusion of the disc with fundoscopy. A standardized cognitive assessment such as the Montreal Cognitive assessment (Nasreddine et al., 2005) can be extremely useful in monitoring a patient's progress. Since frontal lesions may not present with localized motor symptoms, special attention to these factors will be important in addition to testing olfaction. We routinely have patients assessed by a multidisciplinary team including a neurosurgeon, neuro-ophthalmologist, endocrinologist, and ear nose throat (ENT) surgeon. If needed, formal visual fields, optical coherence tomography, baseline hormonal blood work, and others thereafter complete

the specialist's examinations. If necessary, preoperative discussion with otorhinolaryngology, medical oncology, neuroradiology, and radiation oncology within a multidisciplinary setting may be helpful in planning optimum care.

Imaging

We routinely use computed tomography (CT) to help image bony anatomy and pathoanatomy (e.g. hyperostosis), paranasal sinus landmarks (e.g. sphenoid septae) and, if required, vascular anatomy with CT angiography (CTA). Three-plane volumetric MRI T1- and T2-weighted scans without and with contrast are also routinely used in defining the relationship of the tumour to the brain, skull base transgression, orbital contents, vessels, and other local structures. Special attention to the arachnoid plane or to focal peritumoral oedema, which may represent a breach of the arachnoid plane, is important in terms of treatment and prognosis.

We rarely resort to conventional digital subtraction angiography for neoplastic lesions but it is routinely used to clarify ambiguous CTA results or vascular lesions. We infrequently use preoperative embolization of highly vascularized lesions, for example in juvenile nasopharyngeal angiofibromas. In cases where metastatic spread from another organ malignancy is suspected, full body CT or even a positron emission tomography (PET) scan may be performed.

Differential diagnosis

A history in which symptoms are rapidly progressive, particularly with multiple cranial neuropathies, without a long prodrome should raise suspicion of an infection or a malignant entity. Lesions of the anterolateral skull base will vary depending on the region of the world and the endemic conditions in those regions. A useful memory aid in defining the differential diagnosis is that of 'Tumour, Pus, or Blood'. Tumours may be primary benign (e.g. meningioma, pituitary adenoma, craniopharyngioma) or primary malignant (e.g. esthesioneuroblastoma, chordoma, chondrosarcoma) or secondary (e.g. direct spread of sinus cancer or haematogenous spread of a distant metastasis), infectious (e.g. fungal, bacterial, tuberculous, or other) or inflammatory lesions, and vascular lesions such as aneurysms. Tumours may also be classified based on the presumed cell type of origin (e.g. bone, cartilage, meninges, nerves, endothelial cells).

Planning for surgery

Major considerations prior to surgery should include diagnosis (i.e. history and physical examination), special investigations to confirm or refute the clinical diagnosis, and making a decision on whether to treat or observe. In slow growing lesions, or debilitated, elderly patients, surgery may not be the primary treatment. Physically fit patients should be considered for surgery if the patient requires a tissue diagnosis, oncologic cytoreduction, or decompression of neural structures (e.g. visual loss or raised intracranial pressure). Major considerations including the anticipated pathology, and whether the lesion is likely to be completely resected. Other options, for some tumours are subtotal resection plus radiation, or biopsy alone followed by radiation or chemotherapy as adjuvant treatments. Maintaining functionality with optimum long-term outcome including survival and quality of life are key. In accordance with the above-mentioned, the surgical approach is naturally selected on considering the tumour location, but also on the surgeon's experience and familiarity.

The surgeon should visualize every step of the operation prior to beginning the procedure. The astute surgeon who seeks expertise will do the same after surgery and reflect on the factors for or against success encountered with each patient and make careful documentation of each case. Preoperatively briefing the surgical team can be useful. Surgical steps entail presurgical and anaesthetic preparation (e.g. blood component preparation, anticonvulsants for epileptogenic lesions), patient positioning, the approach respectively tissue preparation, tumour resection, and reconstruction. Surgeons need to be aware of each step, the associated risks, and the required equipment. Preparation of the particular equipment such as neuronavigation, neurophysiologic monitoring with selection of the specific modalities, ultrasound, microinstruments, cavitron ultrasonic surgical aspirator, endoscope with choice of appropriate optics, fibrin glue, and others. The anaesthesiologist needs to be informed about the expected surgical time, blood loss, particular dangerous surgical phases as well as required extra drugs. It is recommended to mention any need for antibiotics, corticosteroids, or means to lower intracerebral pressure such as mannitol, hyperventilation, and positioning before the skin incision.

Naturally if a lumbar drain needs to be inserted, it has to be performed before the final patient positioning. We use this routinely if there is an expected large cerebrospinal fluid (CSF) leak due to widely opened basal cisterns to the nasal cavity to reduce CSF pulsation pressure against a multilayer closure. We also use drains routinely for extradural or intradural procedures where less brain retraction is desired and there is minimal risk of brain herniation.

When the choice concerning the surgical approach has been made, further considerations include patient positioning and preparation techniques. The patient is always positioned and all pressure points are carefully protected. While in a comfortable position, the patient is securely strapped onto the operating table so as to allow safe rotation in such a way that gravity widens access to deep anatomy without brain retraction. The patient is positioned with the head above the body to ensure venous drainage. Depending on the location of the pathology the head is held neutral or rotated and fixed in a three- or four-point head holder. We always try to avoid brain retraction by removing sufficient bone and by using gravity to allow the brain to fall away from the surgical access path. The neck needs to be extended in order to achieve a sufficient surgical view.

Reconstruction of any defect should be considered when deciding on the surgical approach. Allogenic tissue such as fascia lata and fat is often ideal while synthetic or animal-based products, although sometimes acceptable are often more costly. We try to preserve cranial periosteum at all costs unless we need a vascularized flap such as to repair a widely opened defect with exposure to the aerodigestive tract. We have seen many cases where pericranium was sacrificed to repair a simple dural defect when a fascia lata or synthetic graft would have done as well or better. Subsequently, the patient has required repeat surgery or radiation or both, only to have the compromised scalp be the source of healing problems, which have even, on occasion, been fatal. In general, if one is not planning to use the pericranium as a vascularized flap (e.g. to cover the nasal cavity), the best place to leave it is with the scalp. Leaving it on the bone and then de-vascularizing or denervating it should be avoided whenever possible.

In cases where a frontotemporal craniotomy is included, we regularly perform an interfascial dissection. The superficial layer of the

temporalis fascia is dissected together with the superficial temporalis fascia and kept on the scalp flap. The dissection is continued anteriorly on the deep facial plane deep to the fat pad and superficial to the deep temporalis fascia to prevent injuries to the frontalis branch of the facial nerve.

Patient selection and decision-making

General treatment options in skull base surgery include conservative treatment, surgery, and radiation therapy as well as the combination of these. In the management of anterolateral skull base lesions benign tumours causing symptoms due to tissue displacement rather than invasion and amenable to complete resection will be surgical candidates. Malignant radiosensitive skull base lesions and lesions in moribund patients are recommended for radiation treatment. Occasionally, atypical lesions should be biopsied and further management decided based on tissue diagnosis. Asymptomatic lesions where imaging characteristics suggest benign behaviour may be observed with periodic imaging. However, the final treatment decision has to be made by the patient supported by a competent neurosurgical consultation.

Anterolateral approaches entail various advantages including good basal access, a wide working range in different angles, space to look up as well as down, ideal conditions for reconstruction (e.g. of the frontal sinus) and minimization of brain retraction.

Two issues should be considered in deciding on an approach, the anatomy of the lesion and the most likely pathology of the lesion.

Anatomical indications for the anterolateral and orbitozygomatic approaches include lesions involving the orbit (superior orbital fissure, superior or lateral optic canal, posterior, superior, and lateral wall), sphenoid bone, parasellar space, tentorial incisura, basal cisterns, optic nerve, optic chiasm, circle of Willis, mesial temporal lobe, basal frontal lobe, anterolateral midbrain, and infratemporal fossa.

Pathological indications for anterolateral and orbitozygomatic approaches include vascular lesions like aneurysms of the anterior communicating artery, proximal internal carotid artery, posterior communicating artery, or the upper basilar artery and tumours including meningiomas, schwannomas, craniopharyngiomas, pituitary adenomas, chordomas, chondrosarcomas, different types of bone tumours, and secondary meningeal-based tumours. Skull base infections for example aspergillosis are also indications. Lesions requiring resection or decompression rather than biopsy should be approached this way.

Surgical approaches

Frontal anterior interhemispheric approach

The anterior interhemispheric approach is a common and frequently used technique for lesions at the anterior skull base. This approach is best for midline lesions without a large lateral extension. Lesions at the lower frontal skull base, not presenting on the surface or interhemispheric fissure are reached by a superiorly placed approach, whereas suprasellar lesions require a lower skull opening. Similarly, deep-seated lesions can be well accessed by a contralateral paramedian craniotomy.

Position: Supine with the back elevated so as to raise the head above the heart and the head fixed either neutral or slightly extended for lesions at or below the skull base so as to allow gravity to permit the frontal lobes to fall away from the skull base or slightly flexed for those above the skull base.

Incision: Usually along the coronal suture bilaterally to the top of the pinna or to the tragus. Be sure not to shorten the potential pericranial flap by using the so-called 'soutar' style incision, which in our opinion has no advantages. We generally do not make low frontal scalp incisions so as not to sacrifice the vascularized pericranium, as noted earlier. However, for very small lesions or those very unlikely to require pericranial salvage, a straight incision behind the frontal hairline or at one forehead wrinkle might be appropriate. For unilateral lesions, particularly those requiring some temporal fossa exposure, a reverse question-mark type incision is appropriate. The skin flap including the galea and the periosteum is elevated in a single layer wherever possible to assure appropriate moisture and blood supply during the procedure. If a vascularized pericranial flap is planned for reconstruction, we prefer to leave the periosteum on the skull and to elevate it separately from the other layers of the scalp and keep it vascularized and innervated at its base.

Craniotomy: Two or more burr holes are drilled on the midline, then the superior sagittal sinus (SSS) is stripped from the skull to avoid damage. A keyhole burr hole is also placed at the keyhole unilaterally. The craniotomy can be bifrontal or carried out such that the skull flap extends about 1 to 1.5 cm to the contralateral side facilitating access on both sides of the falx cerebri.

Dura and intradural: The dural opening depends on what access is required. Often the SSS is suture ligatured at its base and the remaining falx cerebri divided to give full midline access, as for example with an anterior communicating artery aneurysm or midline meningioma. Alternatively, a semicircular unilateral opening with the base towards the superior sagittal sinus or a unilateral cruciate opening or a semicircular flap with the base on the orbital rim are all potential options depending on what access is required. In general, we like to have a sufficient corridor and if possible, to keep the dura on the brain to avoid dehydration and facilitate normal dural closure. Bridging veins draining into the superior sagittal sinus are now exposed and efforts should be taken to preserve these. After approaching the anterior interhemispheric fissure sufficient CSF is drained to reduce the retraction required later once the surgical target has been reached.

Reconstruction: After finishing the intracranial procedure and before skin closure the burr holes should be sealed with a bridge cranioplasty technique (Cusimano et al., 2012) or alternatively with the more expensive titanium MRI compatible, low profile miniplates to improve the cosmetic result of the forehead craniotomy. If the frontal sinus is opened, watertight dural closure, vascularized coverage, or frontal sinusectomy with defunctioning is required. In the event of frontal sinus opening, methylmethacrylate, silastic, and other similar artificial reconstructive materials should be avoided, given the high risk of infection.

Supraorbital craniotomy and minicraniotomy

The supraorbital subfrontal approach facilitates good exposure to the ipsilateral anterior skull base, the suprasellar and parasellar region, and in rare cases can even allow access to anatomical structures of the contralateral and retroclinoid area. Since Fedor Krause (Krause, 1908) first reported the approach in 1908, many modifications have been described resulting in smaller craniotomies with acceptable cosmetic results. The Perneczky group (van Lindert et al.,

1998; Reisch et al., 2003) reported the surgical technique of the supraorbital keyhole craniotomy through an eyebrow skin incision which benefits from minimal brain retraction with optimal access to deep-seated skull base lesions.

Position: To utilize the advantages of this approach, the patient's head needs to be rotated and extended to accurately reach the surgical target. For ipsilateral lesions, the head is rotated to 15° whereas contralateral lesions require an angle of up to 30° to 60°.

Incision: Considering the individual anatomy of the frontal paranasal sinus the skin incision is placed lateral to the supraorbital foramen running within the eyebrow and extending a few millimetres laterally.

Craniotomy: Following retraction of the orbicular and the occipitofrontal muscles a small burr hole is placed posterior to the temporal line after detaching the anterior edge the muscle. Once the anterior fossa is reached a minicraniotomy is initiated by cutting a straight line parallel to the glabella in a lateral to medial direction. Thereafter a C-shaped line is sawn from the burr hole to the medial border of the previous cut. Before the dura is opened it is recommended to drill the inner edge of the bone above the orbital rim to improve intraoperative manoeuvrability.

Dura and intradural: A curved dural incision with a pedicle flap based towards the orbit. The most crucial step to avoid significant brain retraction is the drainage of CSF by opening of the chiasmatic and internal carotid cisterns or by usage of a lumbar drain as described earlier. After the removal of the skull base lesion, closure is performed in reverse order. Note that this approach sacrifices the pericranial flap and if the pathology demands resection of the skull base along with vascularized pericranial reconstruction, another approach should be chosen.

Endoscopic surgery

The advent of the fully endoscopic binasal approach to the skull base began with the work of Cusimano and Fenton, first reported in 1996 (Cusimano and Fenton, 1996). The first approach was performed in 1993 and consisted of a binasal exposure, posterior septotomy, wide exposure of the skull base including sphenoidal, ethmoidal and, if necessary, maxillary sinus opening. It has been frequently presented at scientific conferences and has gained widespread popularity (Di Ieva et al., 2014). As the transsphenoidal approach to the sellar and suprasellar space is covered in a different chapter, the following will address the specific characteristics of the extended endoscopic endonasal approach (EEA) to lesions of the anterior skull base.

Major limitations of the EEA are large, firm lesions, and those that markedly extend beyond the skull base midline or encase important arteries. Opening of the anterior skull base from below is limited due to the necessity of mobilizing the optic nerves. We perform the procedure as a two nostril, four-hand endoscopic procedure, which always requires the support by an ENT surgeon with particular experience in nasal sinus surgery (Cusimano and Fenton, 1996; Cusimano et al., 2012; Cusimano et al., 2013). Furthermore, for extended approaches where we know there will be wide opening of the basal cisterns and a high flow CSF fistula, we routinely insert a lumbar drain preceding the surgical procedure and we always use a vascularized nasoseptal flap. A practice that we have employed since 1996–1997 with very good success.

Preparation and positioning: After placing the lumbar drain the patient is positioned supine with the back elevated 10 degrees. When approaching the sella the head is placed neutral so that the forehead is parallel to the floor and neutrally fixed in a four-point head clamp, whereas for more rostral located lesions the head may need more retroflexion. The abdomen and the right leg are prepared to harvest fat and fascia lata for the skull base reconstruction. The nasal cavity is then temporarily packed with soaked adrenalin 1:100 000 concentration topical pledgets. We apply a 0° endoscope for the nasal phase and 30°, 45°, and 70° endoscopes for the skull base procedure. We routinely prepare neuronavigation and a micro-doppler to safely localize the inferior cerebellar artery (ICA) and anterior cerebral arteries.

Approach: The procedure is initiated by reducing the middle turbinates bilateral and followed by the harvesting of a naso-septal flap, which is usually performed on only one side. For a better overview of the patient's anatomy the natural sphenoid ostium is sought and accessed even if the sphenoidotomy is not required. The septostomy is introduced by fracturing the posterior vomer and perpendicularis plate as required, which is then taken off the sphenoidal rostrum. The bone is stored in bacitracin and will eventually be used for the reconstruction. If desired the sphenoidotomy is now accomplished on either side. For more rostrally located lesions (e.g. at the planum-tuberculum junction or cribriform plate), the posterior (or anterior) cells of the ethmoid sinus are opened and taken down laterally to the lamina papyracea. If the approach is taken far anterior beyond the course of the posterior ethmoid artery olfaction is likely to be impaired. However, as tumours at this location commonly invade the olfactory filaments most of the patients are already anosmic preoperatively and ideally this should be confirmed in the clinic. The anterior fossa floor should be drilled, assisted if necessary with Kerrison rongeur, or lifted away with osteotomes. We routinely preserve the bones with osteotomes, which has the benefit of preserving bone for the reconstruction.

The tumour is initially devascularized with bipolar cautery of feeding vessels like the posterior ethmoidal arteries bilaterally. The dura is opened widely so as to expose the base and anterior, posterior, and possibly lateral edges of the tumour. After a biopsy to confirm the diagnosis, the lesion, depending on its size, is debulked centrally. Once debulked, the margin and adjacent arachnoid plane are carefully accessed. The arachnoid is preserved and 'undressed' from the tumour by working in the cleavage plane between the tumour and the arachnoid. Sequentially debulking and dissection of the margin allows progressive tumour removal. Keeping the arachnoid with the patient allows preservation of critical structures like the anterior cerebral arteries.

Reconstruction: For the avoidance of complications due to postsurgical CSF leaks it is crucial to perform a layer-by-layer reconstruction assisted with lumbar drainage. Therefore, we always use fascia lata and fat graft. Some countries have dural substitutes which can also be used. Fat can be used for dead space occlusion as well as to support a fascia lata duraplasty, which ideally is placed underneath the excised dural edges using an 'in-lay' position (Cusimano and Suhardja, 2000). While the lumbar drain is kept closed until the fascia lata is adequately placed, the drain is then opened, and CSF is continuously drained during the rest of the closure. Next, we apply bone chips that are placed overlapping and wedged with the resection margins of the skull base. This is supported by placement of some tissue glue, which furthermore adheres the vascularized septal mucosal flap. The reconstruction is supported and secured by

packing of the nasal cavity with polyvinyl acetal sponges or pallets packed inside a glove. Nasal silastic trumpets are advanced to the level of the choanae, which enable nose breathing and support the packing. The lumbar drain is clamped on the second postsurgical day and removed the following day.

Orbitozygomatic approach

In the mid-1980s, Pellerin et al. (1984) and Harbuka et al. (1986) first described the orbital-cranial-zygomatic (OCZO) or simply, orbitozygomatic approach (OZY or OZO) to the anterior, middle, and upper part of the posterior cranial fossa. The OZY approach is an extension of the classic frontotemporal craniotomy and combines the advantages of wide skull base access, short working distances with excellent manoeuvrability with minimal brain retraction. We have used the approach extensively since 1991 to approach a wide variety of lesions (van Furth et al., 2006). The anatomical and pathological indications for this very versatile approach have been listed earlier as the indications for anterolateral approaches.

There are multiple variations of the approach. The most common variant is simply the orbito-cranial segment osteotomy, which includes only the superior and lateral orbit with zygomatic bone and not the zygomatic arch. This approach is excellent for pathologies in the anterior cranial fossa and to the level of the oculomotor trigone such as anterior circulation aneurysms. Lesions more posterior than the oculomotor trigone, benefit from removal of the zygomatic arch. For midline structures, we simply perform the osteotomy of the superior orbital rim and roof unilaterally, or if taken across the nasofrontal suture, bilaterally. We routinely perform the craniotomy initially and then the osteotomy of the orbit, the so-called 'two-piece technique', since we find this efficient and safe with visualization of all pertinent anatomy. Alternatively, a one-piece technique that incorporates craniotomy and orbital osteotomy into a single construct as described by Al-Mefty (Al-Mefty, 1987) and others (Jane et al., 1982; Ikeda et al., 1991) is also possible.

Position: Similar to an ordinary frontotemporal craniotomy the patient's head is rotated, depending on the anatomical regions that require access, contralaterally to about 10–45°. The neck is slightly extended to allow gravity to pull down the frontal and temporal lobe.

Incision: Starts anterior to the tragus and is continued up to the hairline near the midline, either curved or in question-mark shape as if for a small trauma flap. Forming the skin flap an interfascial dissection is carried out together with the periosteum, which is mobilized up until the orbital rim. The supraorbital nerve and its accompanying vessel are freed out of the supraorbital foramen with small osteotomes. Careful dissection of the periorbita to a depth of 2.5 to 3 cm, followed by detaching the temporalis muscle from its fossa and the zygomatic arch precede the frontotemporal craniotomy.

Craniotomy and osteotomy: We prefer a bridge cranioplastic technique of craniotomy (Cusimano and Suhardja, 2000) to expose frontal and temporal regions as required by the surgical target. The orbitozygomatic osteotomy is accomplished by five separate sequential bone cuts. One surgeon makes the cuts and the other protects the orbital contents. The anaesthetist is alerted since any manipulation of the orbital contents can induce a profound trigeminal-vagal response with severe bradycardia. The dura is covered with long cottonoid slabs and a brain spatula but without retraction. The first cut is made by the surgeon standing at the head of the bed. The cut starts just lateral to the supraorbital notch and extends posteriorly about 2.5 cm from the inner table of the skull. The surgeon then moves to the side of the head. Starting from the posterior end of the first cut, the second is carried out along the posterior orbital roof approximately half way to the inferior orbital fissure. The third cut is then accessed at the inferior temporal fossa and sawed from the inferior orbital fissure supero-posteriorly to come into the previous cut. For the fourth cut the saw blade is placed into the orbital cavity at the inferolateral edge with the blade in the inferior orbital fissure to direct the cut downwards and outwards along the zygomatic bone or so-called 'malar eminence'. Initially the deeper cut is done with the tip of the blade in the inferior orbital fissure and, subsequently a reciprocating saw is held more posteriorly and superficially up until the midpoint of the zygomatic bone. The saw is now removed and repositioned at the posterior edge of the zygoma to saw back up to end at the previous cut, staying above the zygomaticofacial foramen to avoid opening of the maxillary sinus. The last cut is taken obliquely through the most posterior part of the origin of the zygomatic process. Following these five bone cuts, the orbitozygomatic bone piece is now freed up by tapping the remaining bone bridges with an osteotome. Depending on the need for additional exposure further adjustments can be performed to expose, for example, the petrous internal carotid by removal of the condylar fossa and by inferiorly subluxating the glenoid capsule and head of the mandible. Once the osteotomy is fashioned, if further work such as removing the middle fossa floor to access transbasal or infratemporal lesions is required then this can now be performed.

Dura and intradural: This depends on the primary origin of the lesion and whether the need is greater in the anterior or middle fossa or equal access to both is required. Cavernous sinus and Meckel's cave lesions should be approached extradurally if possible. If intradural access is required, then we most often perform a C-shaped opening of the dura centred on the Sylvian Fissure. The dura is tented upwards to widen the surgical corridor.

Reconstruction: The pathology and surgical resection defines the reconstruction. We generally try to replace dura and always do if the bone of the anterolateral skull base has been removed. In the event of an opening into a paranasal air sinus, we try to de-function the sinus or cover it with vascularized tissue. The osteotomy is carefully replaced into the anatomical position with care taken to avoid any strangulated fat around the edges. We do not try to suture opened periorbita unless they are quite small. The osteotomy is usually fixed with titanium miniplates or with heavy non-absorbable sutures placed through tiny drill holes. The craniotomy is fixated with multipoint fixation to the native skull and to the osteotomy. If possible, the bridge technique is used and burr holes filled with autologous sawed-bone dust after the hole has been stitched across with non-absorbable suture. Alternatively, prefabricated burr-hole covers or some sort of bone substitute can be used if finances permit.

Fisch approaches

Although not anterolateral in approach, the infratemporal fossa approaches can be used to access lesions in the middle fossa up to the back of the orbit. They are among the most challenging surgeries for neurosurgeons as well as otolaryngologists. Fisch et al. (Fisch, 1978; Fisch and Pillsbury, 1979) was the first to describe three different approaches for tumours of the pyramidal tip, clivus, and parasphenoid region that involve essential neurovascular structures such as the carotid artery, jugular vein, and cranial nerves V–XII. These are

inferolateral approaches that work from the skull base and below, looking upward towards the skull base. As such they are ideally suited for lesions in the temporal bone region and as far anterior as the middle fossa floor and pterygomaxillary fissure. Key features of the Fisch A, B, and C approaches are described as follows.

Indications for type A approaches lesions involving the infralabyrinthine and apical compartment of the temporal bone including glomus jugulare tumours, meningiomas, cranial nerve schwannomas, as well as cholesteatomas, and lower clivus chordomas.

Technique: Type A: Initiating a craniotemporo-cervical skin incision the facial nerve is identified and its main branches are exposed. The skin of the external auditory canal along with the tympanic membrane, and the ossicles down to the stapes footplate will have to be removed subsequently. Despite the adverse result of a conductive hearing loss the inner ear function is preserved. A radical mastoidectomy is performed to expose the fallopian canal thereafter. A groove is then created in the anterior epitympanum between the geniculate ganglion and the roof of the zygoma to translocate the CN VII within it. The carotid artery has to be exposed and can, if required and if the patient can sustain it, be ligated distal to the lingual branch. The sigmoid sinus may also require ligation cranial to the tumour that already occludes the sinus (e.g. glomus jugulare) and the temporomandibular joint is displaced anteriorly. A subtotal petrosectomy enables visualization of the carotid wall, the infralabyrinthine bone, the posterior fossa dura, and the inferior sigmoid sinus up to the jugular foramen. Following tumour dissection the Eustachian tube has to be occluded and the external auditory canal is blind sac closed. Dead space occlusion is then carried out with abdominal fat and temporalis muscle.

Type B: Lesions of the clivus, foramen magnum, sphenoid sinus, and epipharynx are preferably managed through *type B approaches*. After a subtotal temporal bone resection, the zygomatic arch, the temporalis muscle, and the facial nerve are reflected inferiorly. The temporomandibular joint is disarticulated and the mandibular condyle is resected to expose the foramina ovale and spinosum. The Eustachian tube, the middle meningeal, and the mandibular division of CN V are obliterated and the petrous carotid artery is skeletonized. Post-tumour resection, blind sac closure of the external auditory canal is performed and the temporalis muscle is reflected with the zygomatic arch, which is reattached with wires.

Type C: The type B approach might be extended to a *type C* approach in order to access the nasopharynx, pterygomaxillary fossa, and the parasellar region. Therefore, the orbital process together with the lateral orbital rim is folded inferiorly and the pterygoid process is resected. The approach furthermore entails the temporary section of some CN VII branches and eventually a V3 section. By lifting the middle cranial fossa dura exposure of the infracavernous carotid segments is achieved which allows the surgeon to approach lesions such as extensive juvenile nasopharyngeal angiofibromas or radiation failure squamous cell carcinomas.

Postoperative

Potential postoperative complications should be carefully considered and discussed with the patient and team prior to any surgical procedure. The surgical plan must be developed with potential complications in mind and should include methods to prevent such complications. The surgeon should rehearse plans personally and with the team and openly discuss methods of prevention. The surgeon should reflect on the surgery postoperatively and provide honest detailed descriptions and do a postoperative discussion with the surgical team.

Maintaining the safety of the patient and so the avoidance of complications should be a key surgical goal. For example, brain retraction is avoided at every opportunity by removing bone that obscures access and by achieving brain relaxation through adequate head-up positioning, hyperventilation, and hyperosmolar agents. We insert lumbar drains preoperatively to improve the surgical corridor and reduce brain retraction. CSF drainage during surgery helps avoid post-op CSF leaks in cases where trespassing of the meninges is planed or considered possible. To avoid postoperative keratitis and ulcers in cases with trigeminal and/or facial nerve involvement, a tarsorrhaphy is performed in selected cases prior to the onset of the major surgical intervention. All patients with periorbital work, trigeminal or facial nerve or greater superficial petrosal nerve involvement should get routine and frequent corneal lubricating ointments every 2–4 hours and ophthalmological assessment.

Perioperative antibiotics repeated every four to six hours intraoperatively associated with meticulous and careful tissue handling and closure help to overcome the risk of infections, especially when nasal air cells have been opened. We suggest continuing antibiotic prophylaxis until the lumbar drain and packing of the nasal air cells has been removed. Whenever possible we prefer to have the patient extubated before the transfer to the intensive care unit to allow for a neurological assessment as early as possible. This permits the team to immediately initialize necessary investigations and adequate treatment in the event of a neurological deficit.

Routine postoperative imaging is performed as a CT scan after a 6–12-hour period, frequently augmented by contrast enhanced scans. In selected cases and in postoperative complications other imaging modalities such as CTA, perfusion scans, or MR imaging are requested. In general MRI scans are of most value when performed in a remote fashion, in particular in benign extra-axial lesions and in cases where the resection cavity has been filled with autologous substances (e.g. fat). Air or blood may obscure tissue planes on MRI in the early postoperative period.

The postoperative assessments are completed at least twice a day by the neurosurgical team and other specialties as required. Nurses contact the patient at home after discharge from hospital. MRI assessment and postoperative clinical assessments are routinely done by all the teams who saw the patient preoperatively, so as to reassess the patient regularly as an outpatient.

Case example(s) and discussion of controversies

Case 1

A case of 31-year-old man with increased ocular pressure and restricted eye movements on the left. A CT head scan revealed a large lesion at the middle cranial fossa, extending into the left orbit with distinct bone remodelling (Fig. 21.1). The neurological exam showed a left proptosis, with his residual eye movement being superior 0%,

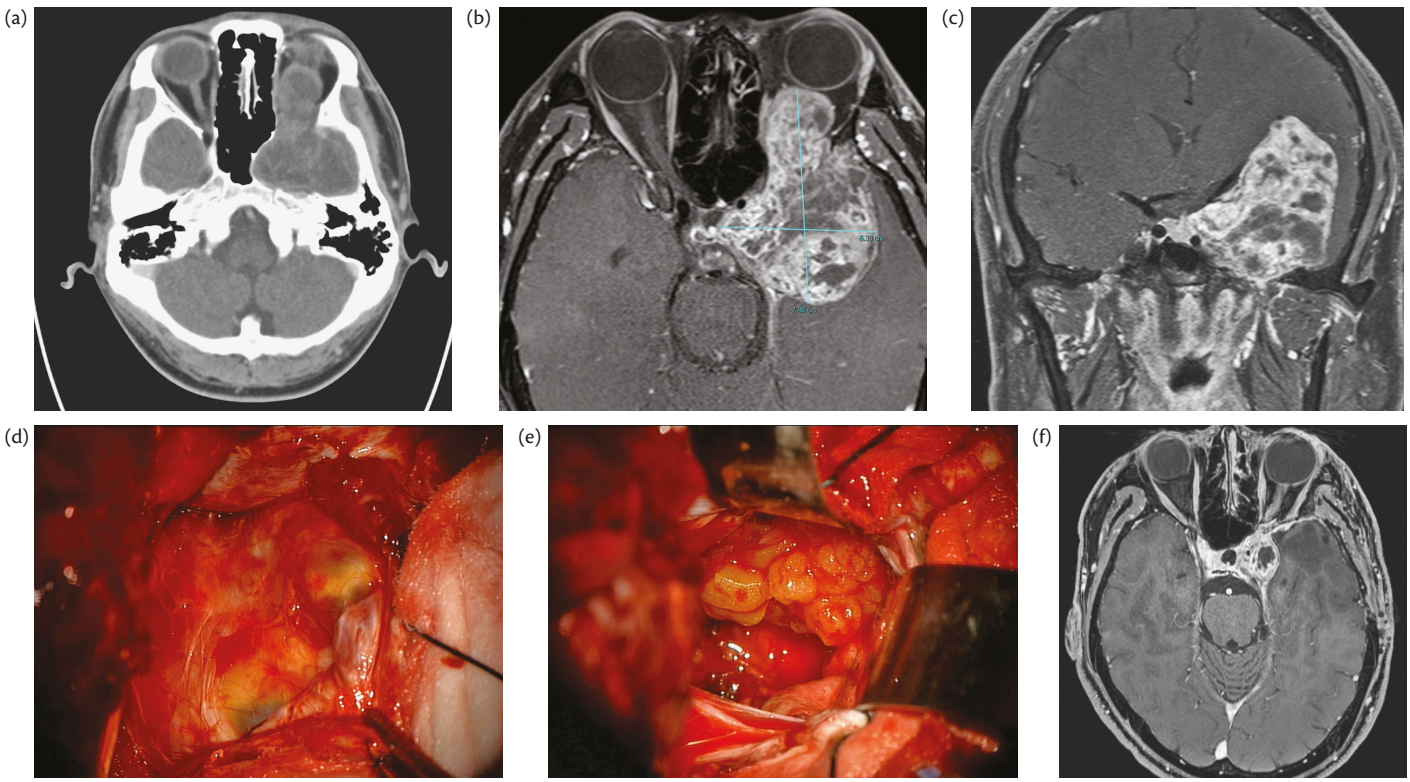

Fig. 21.1 (A) Axial CT head scan showing an extensive skull base lesion with distinct bone remodelling. (B) Axial T1 Gad-enhanced MRI showing the partially solid, partially cystic lesion growing into the orbit and pushing the cavernous sinus to the right.
(C) Coronal T1 Gad-enhanced MRI showing the left ICA dislocated inferomedial and the middle cerebral artery (MCA) pushed upwards.
(D) Intraoperative microscopic view showing the tumour underneath the inner wall of the dura at the cavernous sinus. (E) Intraoperative microscopic view of the fat-like looking tumour. (F) Six-month postsurgical axial T1 Gad-enhanced MRI with the fat graft inside the small residual lesion.

inferior 60%, lateral 80% and medial 90%. He had a mild afferent pupillary defect and a decreased sensation of about 10% in all trigeminal divisions. The MRI scan showed a large 7.4 × 6.6 × 5.3 cm, multicystic, partially solid, inhomogeneous contrast-enhancing lesion of the middle fossa, that was growing into the orbit and pushing down into the infratemporal fossa. It looked like it had grown below the superior rectus muscle, suggesting that it might have arisen from the superior division of CN V3.

We decided to perform a left frontotemporal craniotomy with left orbitozygomatic osteotomy and left subtemporal decompressive craniectomy as described earlier. The procedure was performed after insertion of a lumbar drain, under continuous neurophysiological monitoring with neuronavigation and ultrasound. The second cut of the orbital osteotomy was facilitated due to the widened superior orbital fissure (SOF). After the approach was completed, we could appreciate the bone remodelling of the orbit, the SOF, and the lesser sphenoid wing. We started the extradural dissection to the middle fossa, sacrificing the middle meningeal artery. We performed an interdural approach to the lateral wall of the cavernous sinus starting at the SOF and taking it to the foramen rotundum and then posteriorly, carefully separating the outer dural layer from the inner perineurial layer. We incised the perineurium parallel to the fibres of V2 and exposed the bright yellow looking tumour. The partially suckable tumour was removed as piecemeal. At the anterior part of the cavernous sinus the tumour was stuck to several fibres, which is why we left a small piece here, the posterior part as well as the intraorbital part was good to resect. The resection cavity was finally checked with the ultrasound and the endoscope, confirming extensive tumour resection. The reconstruction was performed with a duraplasty, including fat graft at the orbit and at the left cavernous sinus region, and titanium plate cranioplasty. The final pathology revealed a schwannoma. At 18 months this patient is doing very well, has a Karnofsky score of 100, and without deficit or evidence of recurrence.

Case 2

The second case is a 71-year-old man who had a 6-month history of short-term memory loss, bradyphrenia, and irascible personality change, as well as progressive lethargy. In addition to his cognitive and olfactory deficits, he had normal CN II through XII and no papilledema. Imaging revealed a contrast-enhancing lesion of the anterior skull base suspicious for an olfactory groove meningioma with a small amount of transcranial involvement (Fig. 21.2). The decision was made for an open craniotomy with microsurgical tumour removal. Although the tumour origin is at the midline, due to the size of the lesion, the wide based anterior skull base attachment, and the lateral extension beyond the midpupillary line, in our opinion this lesion would be better and more feasibly managed through a transcranial orbitofrontal approach.

After bicoronal skin incision, a large scalp flap with preservation of the pericranium was carried out. The bifrontal craniotomy was then followed by an orbital cranial osteotomy ('orbital bar removal') to achieve the lowest possible anterior skull base access thus minimizing the need for brain retraction. As the tumour extended more

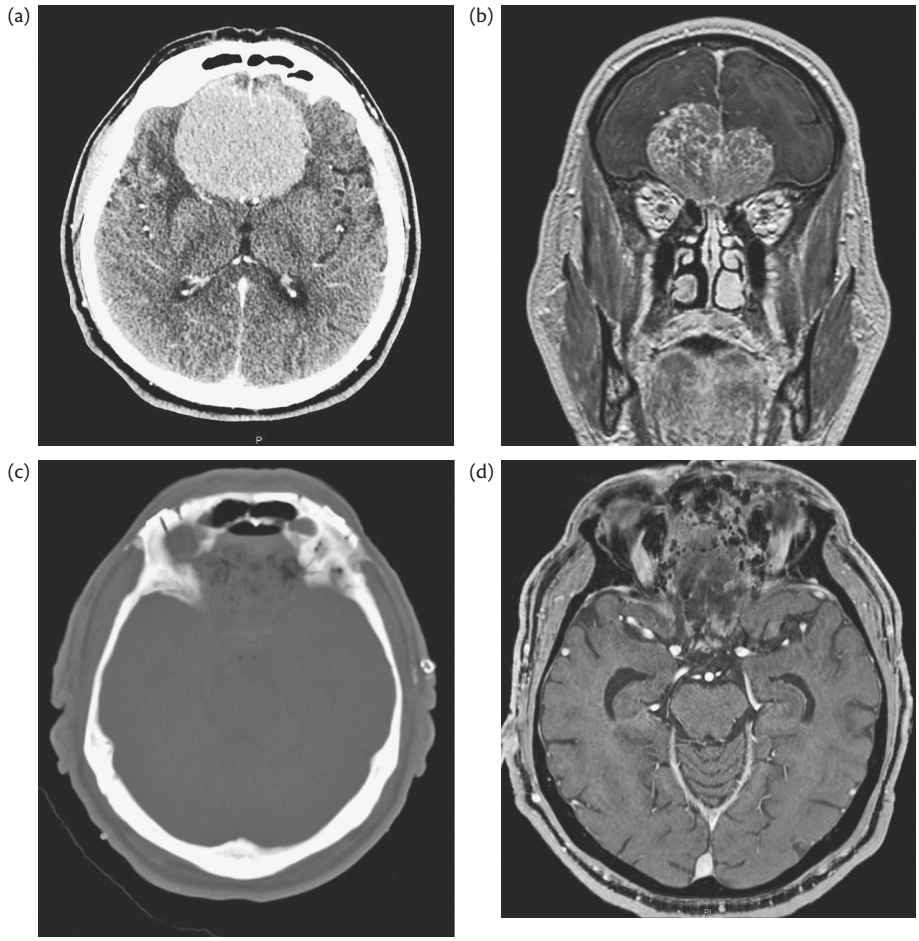

Fig. 21.2 (A) Axial CT head scan showing an anterior skull base lesion homogenously contrast-enhancing with displacement of the bilateral A2 segment posteriorly. (B) Coronal T1 Gad-enhanced MRI showing the lesion attached to the cribriform plate. (C) Postsurgical axial CT bone window showing the skull base reconstruction. Note the low craniotomy at the anterior skull base with removal of the orbital bar. (D) Six-months postsurgical axial T1 Gad-enhanced MRI scan showing complete tumour removal, note the extradural air bubbles at the level of the ethmoid air cells without evidence of residual tumour.

to the right, an orbital osteotomy with removal of the entire orbital roof was performed on the right, whereas the left orbit was only partially exposed. The tumour removal was initiated by an extradural devascularization of the tumour supplying vessels (e.g. anterior and posterior ethmoidal branches), followed by the intradural tumour resection without the need for any brain retraction. We performed a duraplasty with the well-preserved pericranium and sealed the anterior skull base with bone wax and tissue glue. Pathology confirmed a WHO grade 1 meningioma.

This case could have been done by several different approaches, including unilateral and bilateral ones. A minicraniotomy approach would be possible but given the deep cribriform plates and bifrontal exposure as well as the height of the exposure and the potential need to have a pericranial flap reconstruction, we did not choose it as ideal. A true pterional approach would be possible but certainly limited and with few options for skull base reconstruction and therefore a potentially higher risk of residual tumour. A unilateral subfrontal approach using a low craniotomy with or without an orbital cranial osteotomy are also both possible but if there is a need for a bilateral repair of the skull base because of tumour extension, a pericranial flap repair might be limited, particularly if the frontal sinuses are large. The interhemispheric approach with preservation of the pericranial flap could easily access the lesion but dissection of the interhemispheric fissure is likely unnecessary here and would not add much to the exposure, resection, or reconstruction. An EEA is possible for the central part of the lesion but would not be as efficient for complete resection, particularly when this is so easily accessed via an orbital cranial approach without brain retraction. It would also have a large skull base defect that would not be as easily repaired as the pericranial flap. It might also be complicated by significant bleeding and more chance of residual tumour. The bilateral subfrontal-orbitocranial approach we utilized allowed easy and efficient access to, and resection of, all the tumour, involved dura, and bone with no brain retraction and a complete vascularized repair of the skull base defect.

Case 3

A 62-year-old female underwent an MRI head scan five years prior to our visit, due to worsening of her migraines. At that time, a small lesion in the midline of the anterior fossa was identified. Regular follow-up throughout the following years displayed continuous growth of the extra-axial, contrast-enhancing, dural-based lesion

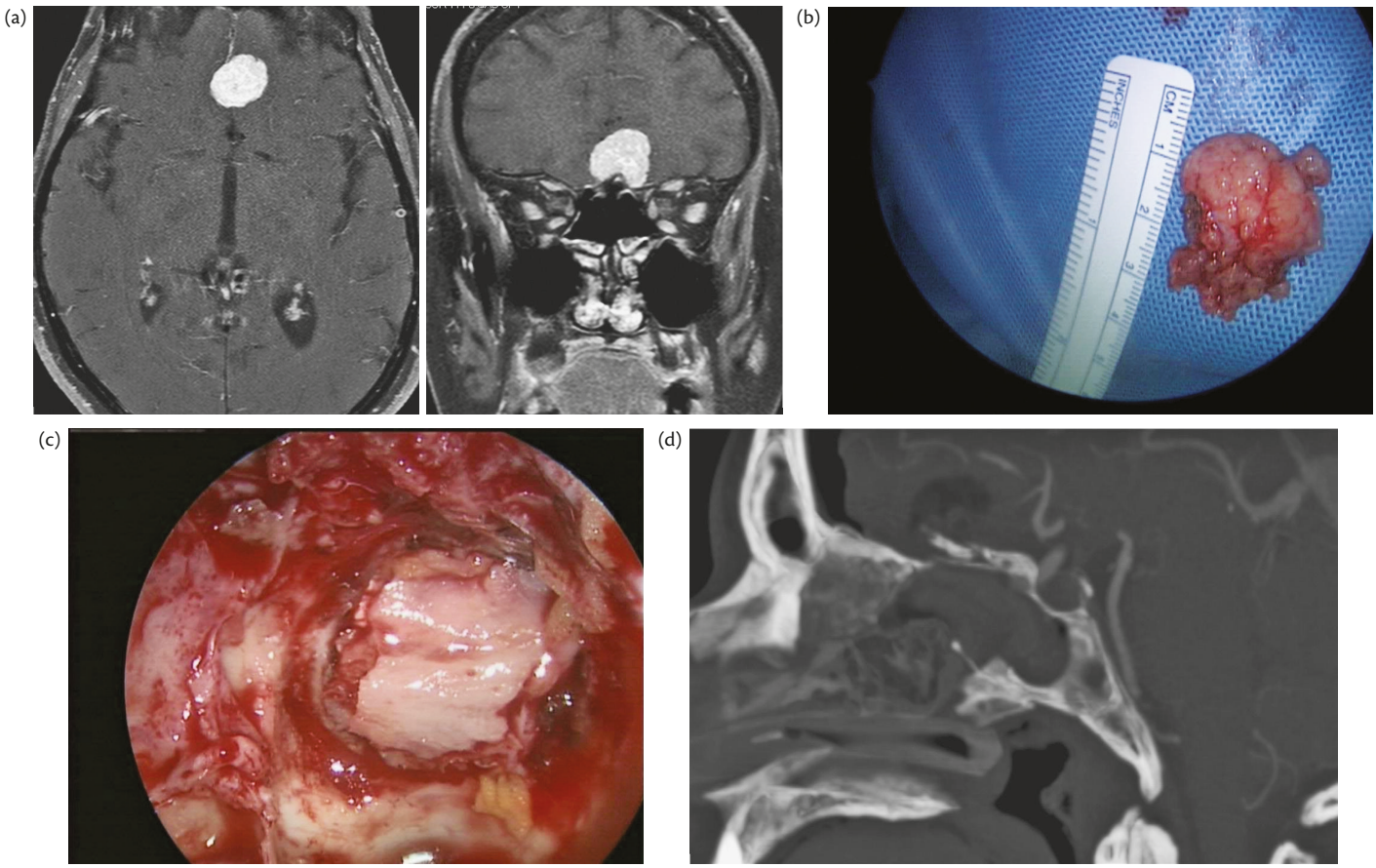

Fig. 21.3 (A) Axial and coronal T1 Gad-enhanced MRI showing the lesion attached to the cribriform plate. (B) Intraoperative picture showing the size of the tumour. (C) Intraoperative microscopic view of the skull base reconstruction before placement of the mucosal flap. (D) Postsurgical sagittal CT showing the anterior skull base reconstruction.

(Fig. 21.3). Eventually, after extensive discussion of all treatment options including observation, gamma knife, and fractionated radiotherapy, the patient requested to undergo surgery for resection of the anterior fossa lesion. We felt the lesion, most likely a cribriform plate meningioma, would be best approached using an extended EEA to resect the tumour. After placing a lumbar drain, the drain was clamped, the patient was positioned, and the EEA was performed. A full sphenoidotomy including exposure of the planum sphenoidale, and the cribriform plate was fashioned under assistance of neuronavigation and endoscopes up to 70 degree. The anterior fossa bone was drilled just below the tumour, and at the level of the dura, a piece of bone was mobilized that showed a punctuate hyperostosis, suggesting it was the origin of the tumour. After confirming sufficient bony opening, the dura was bipolared and incised. Initially internal debulking was carried out and then we gradually dissected around the lesion in the arachnoid cleavage plane. Once the lesion and critical structures were identified and protected, the tumour was delivered from the frontal lobe, leaving the arachnoid intact. The dural edges were bipolared. The right olfactory tract was entirely intact, the left although distorted was still in continuity. The skull base reconstruction was then initiated by opening of the lumbar drain, followed by placing small fat pieces around the dural opening to support the fascia lata graft, which was subsequently placed overlapping and under the edges of the dura. Additionally, the anterior skull base was reconstructed with two small bone pieces, before tissue glue was applied to adhere the vascularized septal mucosal flap. The postsurgical course was unremarkable and pathology confirmed a WHO grade 1 meningioma. At 18 months, the patient remains well with intact right sided olfaction, a Karnofsky score of 100 and no tumour recurrence.

Case 4

A 56-year-old female presented with a Bell's palsy, when a CT head scan incidentally revealed an anterior fossa skull base lesion. Initially the lesion was monitored, as the lesion was felt to be asymptomatic, the MRI scan showed a dural-based contrast-enhancing lesion most consistent with a cribriform plate meningioma, and the patient recovered from the Bell's palsy. However, the tumour showed progressive growth up to the size of 4.0 × 2.5 × 3.5 cm (Fig. 21.4).

After discussion of all treatment options the patient requested to undergo surgical removal of the tumour. Because of the size, but much more due to the superior extent and an anterior bend of the lesion we felt a craniotomy would be the more definitive, efficient, and safer approach.

We placed a lumbar drain; we did a bicoronal skin incision and turned the scalp flap together with the periosteum. A left greater than right frontal craniotomy just across the midline was performed. A frontal sinus mucosa exenteration was necessary. An orbitocranial osteotomy and orbitotomy was performed to achieve the lowest possible anterior skull base access thus minimizing the need for brain

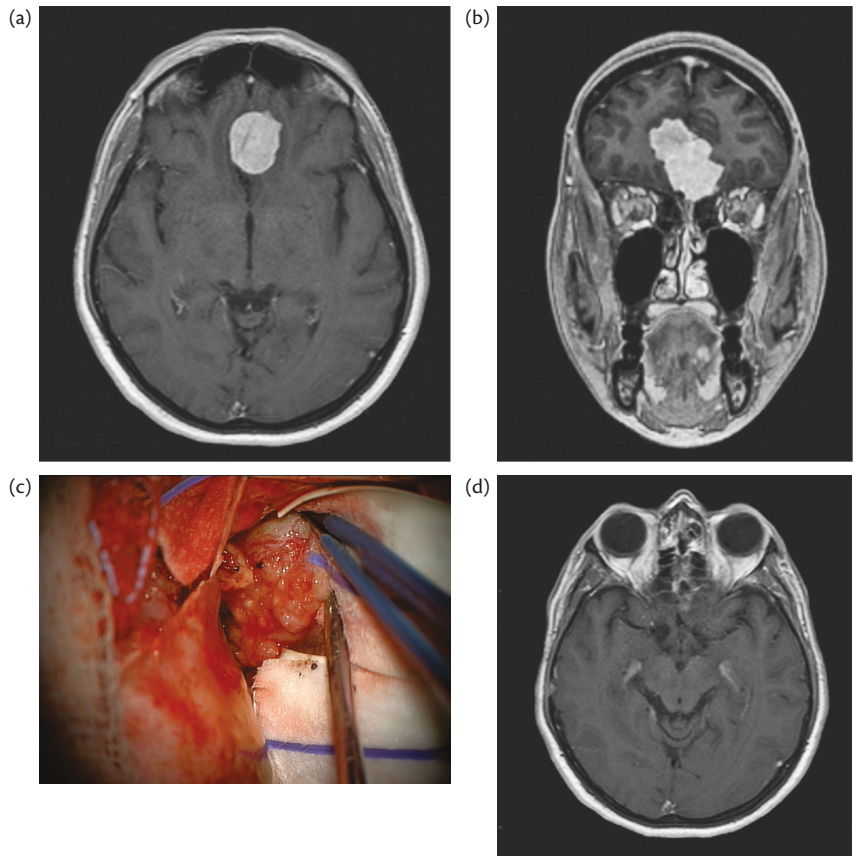

Fig. 21.4 (A) Axial and (B) coronal T1 Gad-enhanced MRI showing a large, multilobulated, anterior fossa lesion originating from the cribriform plate. (C) Intraoperative anterolateral, subfrontal microscopic view of the firm tumour. (D) Postsurgical axial T1 Gad-enhanced MRI showing complete tumour resection.

retraction. The orbital osteotomy with removal of the entire orbital roof was performed on the left, whereas the right orbit was only partially exposed. The midline osteotomy was taken as low as the nasofrontal suture. We took out the crista gali and bipolared the base of the SSS. The tumour removal was initiated by an extradural devascularization of the tumour supplying vessels (e.g. anterior and posterior ethmoidal branches), followed by an intradural tumour resection. We could see the olfactory tract, which was totally infiltrated and distorted by the tumour. The tumour was initially debulked from within and then it was dissected in the arachnoid cleavage plane. The origin was at the posterior aspect of the cribriform plate and the anterior planum sphenoidale, where it had gone through the dura with an area of hyperostosis. The tumour was excised with the involved lower falx, the hyperostotic origin was removed, and the blood supply as well as the anterior skull base was bipolared with removal of all involved bone and dura. We performed a fascia lata and fat graft duraplasty and sealed the anterior skull base with bone wax and tissue glue, which was followed by a cranioplasty. The procedure was performed under ultrasound and neuronavigation guidance, the pathology revealed a WHO grade 1 meningioma. The patient remains well with intact cognition, a Karnofsky score of 100, anosmic but without recurrence after 20 months of follow-up.

Cases 3 and 4 are presented to allow discussion of the capabilities and limitations of EEA. Skull base endoscopy offers various approaches that must be adapted to different kinds of lesions. One major limitation of EEA are lesions with significant lateral extent. Typically the laminae papyracea limits the lateral exposure of the anterior fossa in most cases but in a case where the optic nerve can be mobilized, this may not remain limiting. Although angled endoscopes allow excellent lateral or anterior visualization, instrumentation to operate in extreme positions endoscopically is sometimes limiting and craniotomy becomes much more efficient and complete in terms of tumour resection. Beyond that, the length of available instruments sometimes limits the removal of lesions with broad superior extension. Especially in firm and partially calcified lesions, or highly vascular lesions, such as meningiomas, one cannot expect the lesion to descend after partial debulking from inside the tumour. However, this can partially be provoked by applying a mild Valsalva manoeuvre.

A potential challenge in endoscopic approaches, particularly the ones requiring repeat surgery and those in a radiated bed, is the ability to safely prevent meningitis by adequate reconstruction. In these cases, this was not an issue, but reconstruction should be considered in decision-making in every case. As opposed to large skull base defects the sealing of smaller defects is much easier to manage, especially when applying all the aforementioned means of a layer-by-layer skull base reconstruction. Although we felt that that the lateral extension of the cribriform plate meningioma in case 4 would be amenable through an EEA, we eventually decided to perform a craniotomy because of the extensive superior extension of the lesion.

The outcome was excellent in this case. Ultimately, surgeons should use those approaches with which they can achieve the best overall result for their patient.

REFERENCES

Al-Mefty, O. (1987). Supraorbital-pterional approach to skull base lesions. *Neurosurgery*, **21**, 474–7.

Cusimano, M.D., Di Ieva, A., Lee, J., & Anderson, J. (2013). Canula-assisted endoscopy in bi-portal transphenoidal cranial base surgery: technical note. *Acta Neurochir (Wien)*, **155**, 909–11.

Cusimano, M.D. & Fenton, R.S. (1996). The technique for endoscopic pituitary tumor removal. *Neurosurg Focus*, **1**, e1; discussion 1p following e3.

Cusimano, M. D., Kan, P., Nassiri, F., et al. (2012). Outcomes of surgically treated giant pituitary tumours. *Can J Neurol Sci*, **39**, 446–57.

Cusimano, M.D. & Suhardja, A.S. (2000). Craniotomy revisited: techniques for improved access and reconstruction. *Can J Neurol Sci*, **27**, 44–8.

Di Ieva, A., Tam, M., Tschabitscher, M., & Cusimano, M.D. (2014). A journey into the technical evolution of neuroendoscopy. *World Neurosurg*, **82**, e777–89.

Fisch, U. (1978). Infratemporal fossa approach to tumours of the temporal bone and base of the skull. *J Laryngol Otol*, **92**, 949–67.

Fisch, U. & Pillsbury, H.C. (1979). Infratemporal fossa approach to lesions in the temporal bone and base of the skull. *Arch Otolaryngol*, **105**, 99–107.

Hakuba, A., Liu, S., & Nishimura, S. (1986). The orbitozygomatic infratemporal approach: a new surgical technique. *Surg Neurol*, **26**, 271–6.

Ikeda, K., Yamashita, J., Hashimoto, M., & Futami, K. (1991). Orbitozygomatic temporopolar approach for a high basilar tip aneurysm associated with a short intracranial internal carotid artery: a new surgical approach. *Neurosurgery*, **28**, 105–10.

Jane, J.A., Park, T.S., Pobereskin, L.H., Winn, H.R., & Butler, A.B. (1982). The supraorbital approach: technical note. *Neurosurgery*, **11**, 537–42.

Krause, F. (1908). *Chirurgie des Gehirns und Rückenmarks nach eigenen Erfahrungen*. Berlin, Urban und Schwarzenberg.

Nasreddine, Z. S., Phillips, N. A., Bedirian, V., et al. (2005). The Montreal Cognitive Assessment, MoCA: a brief screening tool for mild cognitive impairment. *J Am Geriatr Soc*, **53**, 695–9.

Pellerin, P., Lesoin, F., Dhellemmes, P., Donazzan, M., & Jomin, M. (1984). Usefulness of the orbitofrontomalar approach associated with bone reconstruction for frontotemporosphenoid meningiomas. *Neurosurgery*, **15**, 715–18.

Reisch, R., Perneczky, A., & Filippi, R. (2003). Surgical technique of the supraorbital key-hole craniotomy. *Surg Neurol*, **59**, 223–7.

Van Furth, W.R., Agur, A.M., Woolridge, N., & Cusimano, M.D. (2006). The orbitozygomatic approach. *Neurosurgery*, **58**, ONS103–7; discussion ONS103–7.

Van Lindert, E., Perneczky, A., Fries, G., & Pierangeli, E. (1998). The supraorbital keyhole approach to supratentorial aneurysms: concept and technique. *Surg Neurol*, **49**, 481–9; discussion 489–90.

SECTION 4

Tumours and skull base—CP angle lesions

22. **Schwannomas** *255*
Tiit Mathiesen, Petter Förander, and David Pettersson

23. **Glomus tumours** *271*
Omar Pathmanaban and Andrew King

24. **Surgical management of cerebellopontine angle and petrous lesions** *281*
Nicholas Hall, Yuval Sufaro, and Andrew H. Kaye

22

Schwannomas

Tiit Mathiesen, Petter Förander, and David Pettersson

Sporadic vestibular schwannoma

Sporadic vestibular schwannoma (VS) is the commonest tumour of the cerebellopontine angle and comprise 6–8% of all intracranial tumours. The inferior branch of the vestibular nerve of the eighth cranial nerve is the origin in approximately 65–75% of all patients. Some authors report it is as high as 90%, with the superior branch in the remainder; cochlear nerve origin is rare (Komatsuzaki and Tsunoda, 2001; Khrais et al., 2008). Vestibular schwannomas were originally thought to originate at the of oligodendrocyte-Schwann cell junction between the central and peripheral nervous system but current data instead suggest an association with the sensory ganglia of the vestibular nerve in the internal auditory canal (Xenellis and Linthicum, 2003; Roosli et al., 2012; Tryggvason et al., 2012).

Historically, only large, life-threatening tumours were diagnosed and treated. In the 1920s, surgical mortality associated with VS removal exceeded 70%. Historical neurosurgical leaders achieved paradigmatic improvements of treatment. Using intracapsular removal Cushing decreased surgical mortality to 30% (Cushing, 1917), but high mortality from recurrent tumours became a problem (Olivecrona, 1950); Dandy again performed radical surgery, at a cost of a higher risk of facial nerve sacrifice (Dandy, 1934). Olivecrona pioneered radical surgery with facial nerve preservation (Olivecrona, 1950). The next developments were microsurgery by House and radiosurgery made possible by Leksell (Norén et al., 1993). Today, mortality from treatment is a rarity. Treatment options include wait and scan, microsurgery, radiosurgery, and radiotherapy. Individual therapeutic choices are made depending on tumour size, symptomatology and expected natural history (**Fig. 22.1**).

Epidemiology of sporadic vestibular schwannomas

A wider indication for work-up and better access to MRI imaging has led to an increased detection of schwannomas. Stangerup and coworkers found a linear relationship between the number of MRI scanners and incidence of vestibular schwannomas in Denmark (Stangerup et al., 2004). In the United States, vestibular schwannomas were diagnosed in 10/million/year in 1991 (National Institutes of Health, 1991). Population studies in autopsy material, however, detected a prevalence ranging between 0.8 and 2.4% which indicated that most schwannomas went undiagnosed (reviewed in Schmidt et al., 2012).

The group of Tos and Thomsen reported a Danish incidence of 3.1/million/year in 1976 which increased to 22.8 in 2004 and fell back to 19.8 in 2008 (Stangerup et al., 2010). Recently, the incidences were estimated to be 12 and 14 cases per million population for the United States (Babu et al., 2013) and United Kingdom (Evans et al., 2005), respectively. The latest Danish incidence estimate was 35/million/year (Sass et al., 2018). The differences between the countries may well reflect local diagnostic routines and registration, but biological differences may exist between populations; American data show a dominance for Caucasians among those registered in The Surveillance Epidemiology and End Results (SEER) database (Gal et al., 2010) (**Fig. 22.2**).

The commonest age at diagnosis has remained in the interval 50–64 years, and the gender distribution is equal. The mean size of schwannomas has decreased and hearing is better at diagnosis in recent decades compared to the 1980s (Gal et al., 2010; Stangerup et al., 2010).

Aetiology, ionizing radiation, and cellular phones.

Schwannomas are benign tumours with WHO grade 1 (**Fig. 22.3**). Malignant nerve sheath tumours are rare, but comprise an important differential diagnosis to all radiologically diagnosed schwannomas. They can be suspected from aggressive clinical behaviour and require histopathological evaluation for diagnosis. The genetical profile of schwannomas has been studied widely. Mutations are usually found in the neurofibromin (*NF2*) gene on chromosome 22q12.2 which is biallelically inactivated in most sporadic vestibular schwannomas as in neurofibromatosis type-2 associated schwannomas. The mutations in sporadic tumours are usually small deletions. The gene product is a 590 amino acid protein named merlin (schwannomin) (Lee et al., 2012; Lassaletta et al., 2013), which is a tumour suppressor gene. Merlin suppresses a large number of different intracellular growth-promoting signals which can explain a tumorigenic effect from a single gene defect (**Fig. 22.4**). Between 5 and 10% of patients with vestibular schwannomas have additions on 9q34 or 17q. Angiogenesis is indispensable for tumour growth, but the relationship between angiogenetic factors and tumour growth is unclear. Small studies have, however, detected some improvement and retarded schwannoma growth with the VEGF-inhibitor bevacizumab.

The only well-established risk factor for sporadic vestibular schwannoma is ionizing radiation (Ron et al., 1988; Preston et al.,

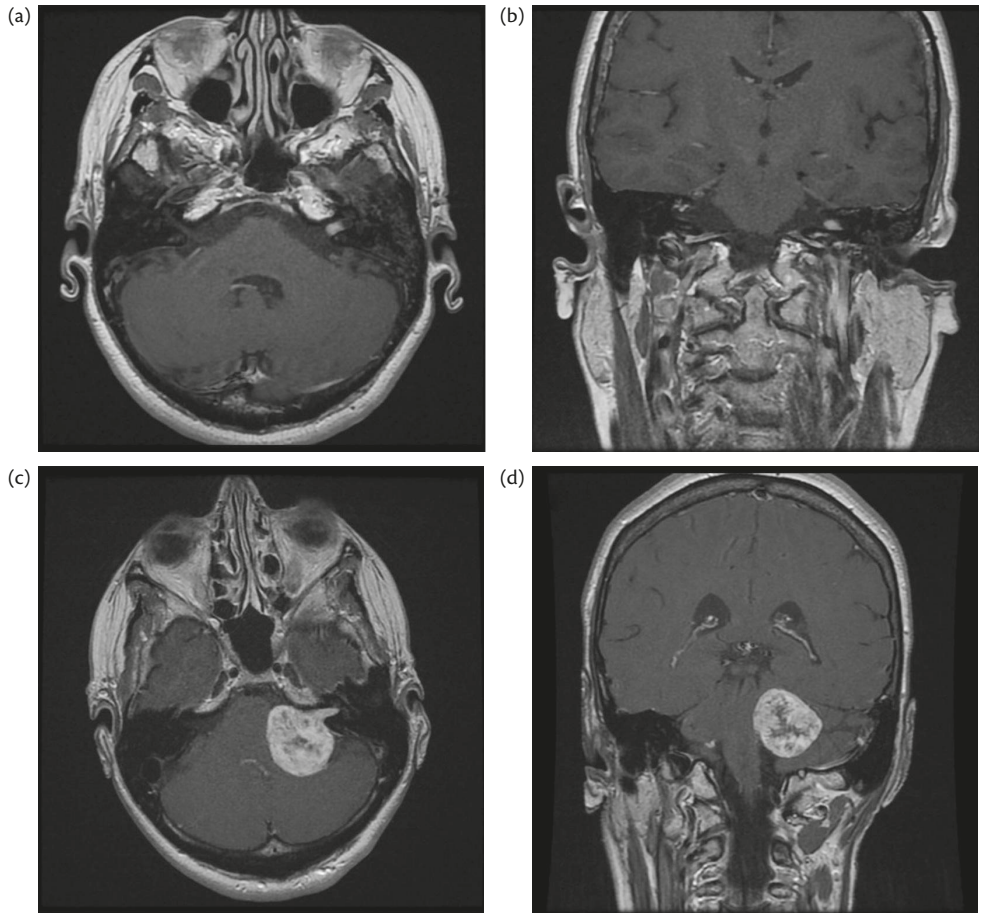

Fig. 22.1 Vestibular schwannoma MRI. Axial (A) and coronal (B) T1-weighted MRI with gadolinium contrast illustrating intracanalicular vestibular schwannoma. Axial (C) and coronal (D) T1-weighted MRI with gadolinium illustrating a large vestibular schwannoma with brainstem compression.

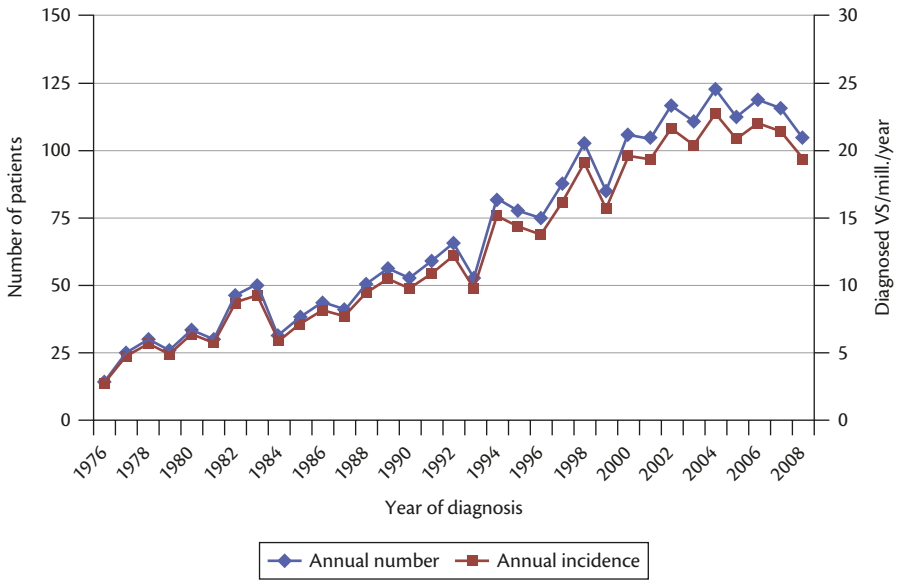

Fig. 22.2 Epidemiology of vestibular schwannoma.
Reprinted from *Otolaryngologic Clinics of North America*, Volume 45, issue 2, Sven-Eric Stangerup, Per Caye-Thomasen, Epidemiology and Natural History of Vestibular Schwannomas, pp. 257–8, Copyright (2012), with permission from Elsevier.

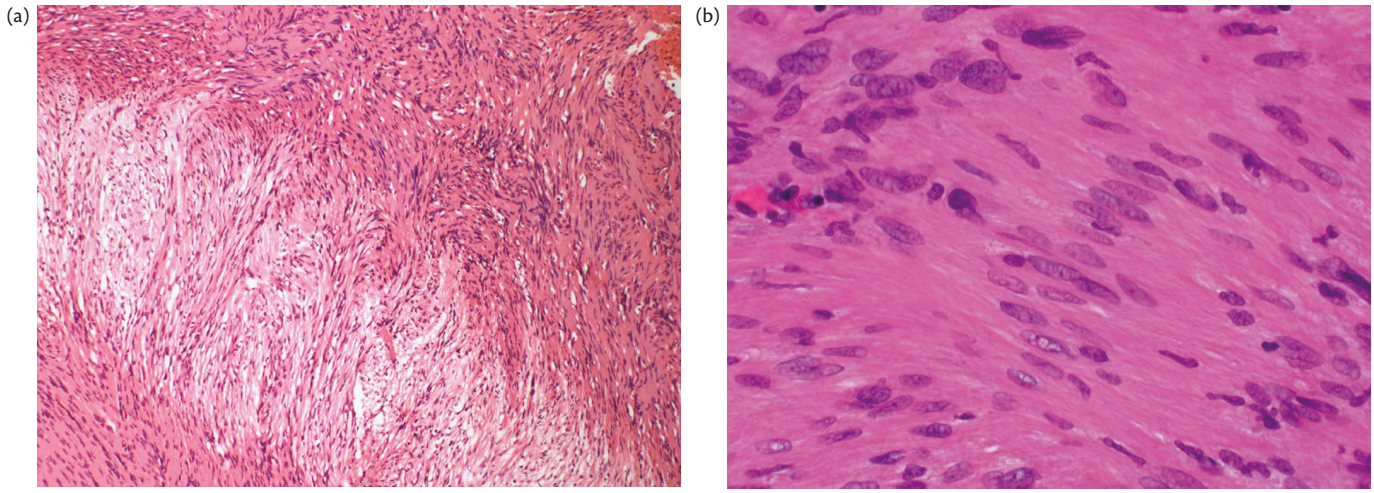

Fig. 22.3 Histopathology vestibular schwannoma. (A) Schwannoma (H&E ×100). Two distinct histological patterns characterize these neoplasms. Compact, hypercellular regions, and pale-staining hypocellular regions are known as Antoni A and Antoni B tissue, respectively. (B) Schwannoma (H&E ×400). The eponymous Verocay body, formed by tumour nuclei lining up in rows, is a particular characteristic of these nerve sheath tumours.

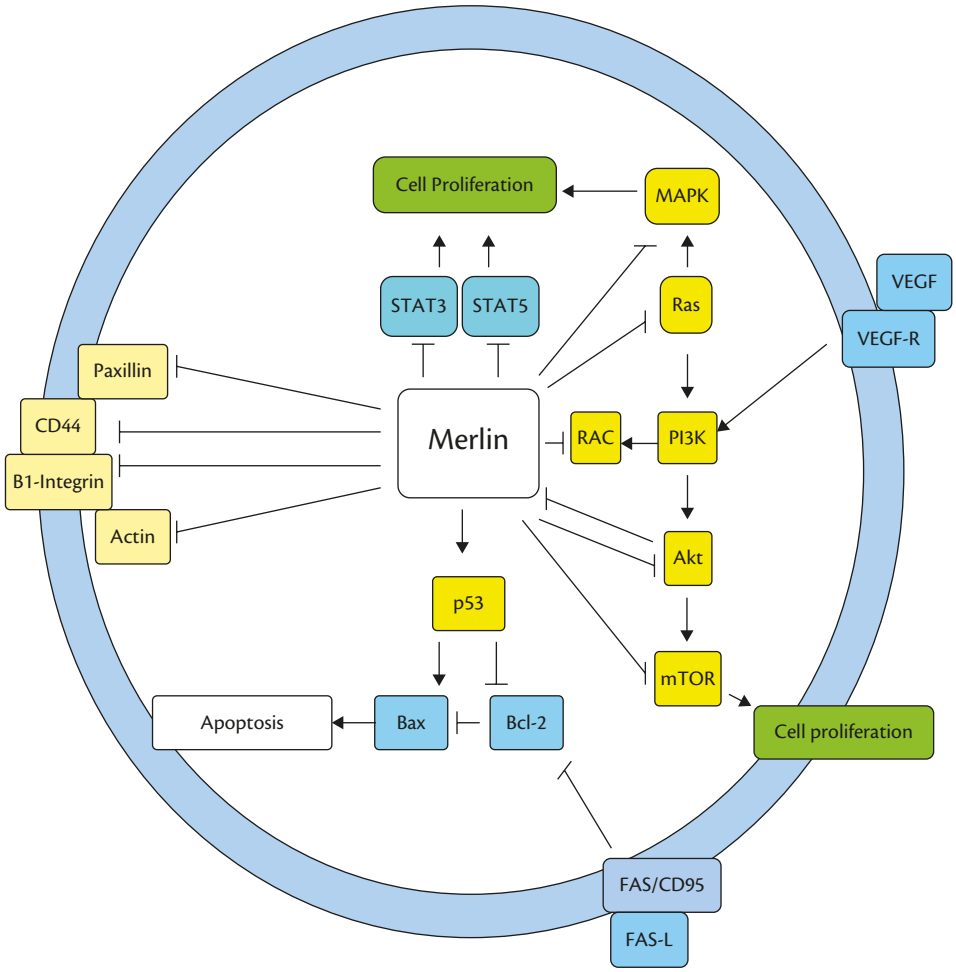

Fig. 22.4 Schematic illustrating known molecular interactions of merlin with intracellular cascades.

Reproduced from Sughrue, M. E., Yeung, A., Rutkowski, M. J., et al., Molecular biology of familial and sporadic vestibular schwannomas: implications for novel therapeutics, *Journal of Neurosurgery*, Vol. 114, No. 2 (2011) with permission from JNS Group.

2002; Schneider et al., 2008), although other environmental and biological factors such as radiofrequency fields, noise, smoking, chemicals, socioeconomic status, parity, and hormone replacement have been studied. Unexpectedly, income and education were associated with tumour diagnoses in two studies (Inskip et al., 2003; Schuz et al., 2010). Parity and hormone replacement therapy were also associated with increased risk of tumours (Schoemaker et al., 2007; Benson et al., 2010b), while current smoking appeared to protect from schwannomas in two case-control and one cohort study (Schoemaker et al., 2007; Benson et al., 2010a; Palmisano et al., 2012). Noise was reported as a causal factor in 1985 (Preston-Martin et al., 1989), but could not be corroborated (Edwards et al., 2006; Fisher et al., 2014). Chemical exposure is difficult to evaluate retrospectively. Asbestos and toluene show conflicting findings but the well-known carcinogen benzene was repeatedly reported to have an association with schwannomas (Pettersson et al., 2014).

Radiofrequency fields and mobile phones fall into a controversial area (Pettersson et al., 2014). The case-control studies conducted by Hardell and colleagues suggested a dose dependent correlation between mobile phone use and risk of vestibular schwannomas (Hardell et al., 1999; Hardell et al., 2005; Hardell et al., 2013). In contrast, larger studies and studies with prospective designs have failed to corroborate any associations between mobile phone use and vestibular schwannomas. The INTERPHONE case-control study (Interphone Study Group, 2011), which is the largest study on mobile phones and vestibular schwannoma still in 2016, found an odds ratio of 0.85 (95% CI: 0.69–1.04) for regular use of mobile phones and 0.76 (95% CI: 0.52–1.11) for ≥ 10 years of mobile phone use. A cohort study conducted in Denmark found a relative risk of 0.87 (95% CI: 0.52–1.46) for mobile phone subscribers of 11 years or more (Schuz et al., 2011). A recently updated UK cohort study (Benson et al., 2013) found a relative risk for any use of mobile phones slightly above one (RR = 1.19, 95% CI: 0.81–1.75), a similar estimate for 10 years' use or longer (RR = 1.17, 95% CI: 0.60–2.27), and the highest risk estimate for 5–9 years of use (RR = 1.46 (95% CI: 0.94–2.27), which agrees with the latest Swedish findings (Pettersson et al., 2014). The latter study also scrutinized laterality of tumours and preferred side of phone use without finding any association above chance. Furthermore, experimental carcinogenic effects from radiofrequency exposures below guideline limits do not occur (AGNIR, 2012). Taken together, there is no support for a strong etiological relationship between cellular phones and vestibular schwannomas.

Natural history

It is no longer believed that all patients with newly diagnosed tumours benefit from surgery. Subsequently, data on natural history during MRI follow-up has become available. Slow or no growth was detected in many patients. A meta-analysis (Yoshimoto, 2005) of 26 studies and 1340 patients showed growth in 46% (95% CI 43–48) and regression in 8% (95%CI 6–10) during a mean follow-up period of 38 months. The mean annual growth rate was 1.2 mm in growing tumours. Many of the progressing tumours grew very slowly and only 40% were treated. Natural history was mostly studied in smaller tumours selected for conservative treatment, but a number of patients with larger tumours were also included; many of these also regressed in older patients. Hence, initial conservative management is possible, preferably in older patients with few symptoms in spite of large size tumours.

Thirty-eight months is a short follow-up time for benign tumours, but studies with longer follow-up are available. Stangerup and Caye-Thomasen (2012) found 29% growth rate and 1% decrease during long-term follow-up of intraextrameatal tumours less than 20 mm (Fig. 22.5). For intracanalicular tumours, Kirchmann et al. (2017) found tumour growth in 37%, 61% of which grew into the posterior fossa, after 9.5 years of follow-up. Neither Stangerup nor Kirchmann found tumour progression after the fifth year of follow-up.

Treatment goals

The slow growth of most vestibular schwannomas and availability of radiological surveillance allows safe management without extensive surgery. The number of surgeries for vestibular schwannomas has decreased. Lately, 17% of registered American patients were followed with scanning and 21% were treated with radiosurgery (Gal

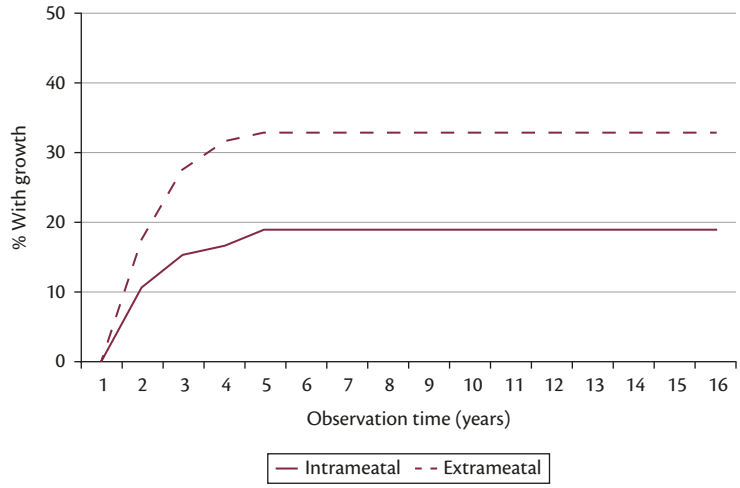

Fig. 22.5 Natural history of intra- and extrameatal vestibular schwannomas.

Reprinted from *Otolaryngologic Clinics of North America*, Volume 45, issue 2, Sven-Eric Stangerup, Per Caye-Thomasen, Epidemiology and Natural History of Vestibular Schwannomas, pp. 257–68, Copyright (2012), with permission from Elsevier.

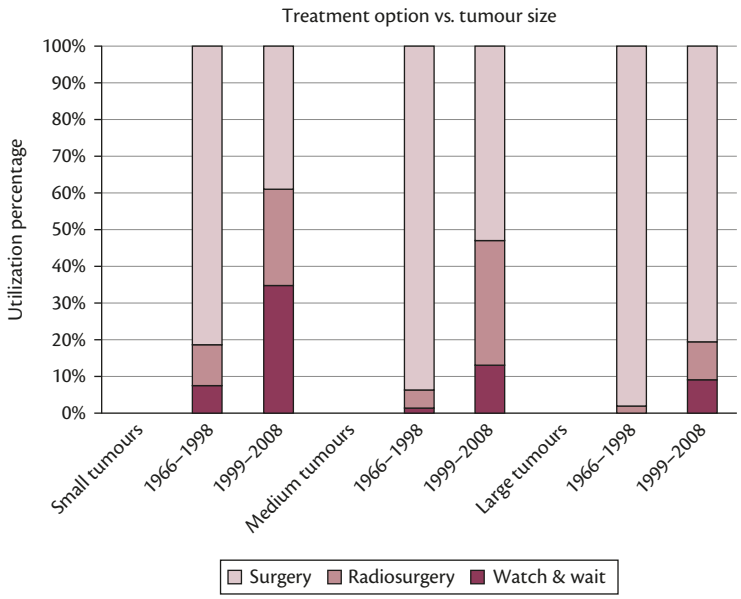

Fig. 22.6 The changing management of vestibular schwannomas. In this figure tumour size is defined as small (<1.5 cm), medium (1.5–2.5 cm), and large (>2.5 cm).

Reproduced with permission from Jaymin Patel, Rohit Vasan, Harry van Loveren, et al, The changing face of acoustic neuroma management in the USA: Analysis of the 1998 and 2008 patient surveys from the acoustic neuroma association, *British Journal of Neurosurgery*, Volume 28, Issue 1, 2014 © The Neurosurgical Foundation, reprinted by permission of Taylor & Francis Ltd, www.tandfonline.com on behalf of The Neurosurgical Foundation.

et al., 2010). The therapeutic goals have changed from radical tumour removal to tumour control and preservation of neurological function (Kemink et al., 1991; Park et al., 2006; Seol et al., 2006). Many small tumours are treated by radiosurgery or followed radiologically to select the fast-growing lesions for treatment. Larger tumours are more often treated with subtotal or partial surgery (Fig. 22.6). Frequently, one goal of surgery is to tailor a residual for gamma knife radiosurgery. Subtotal removal decreases the need to dissect already compromised nerves from the tumour-nerve interface and appears to correlate with better facial nerve outcome (Park et al., 2006; Schwartz et al., 2013). Hearing preservation of larger tumours is also more frequent with subtotal removal (Iwai et al., 2015). Although the proportion of morbidity in all patients with known vestibular schwannomas may have decreased, the actual number of complications has increased (Patel et al., 2013). The paradoxical finding reflects a different case-mix with an increased proportion of large tumours, but also decreased surgical experience. A continued primary focus on neurological outcomes and surgical techniques are important (Rahimpour et al., 2016); an increased proportion of non-radical operations will ensue.

Growth of residual schwannomas

A lower propensity towards radical resection translates into higher frequencies of tumour recurrence. The relationship between extent of removal and risk of recurrence probably depends on surgical techniques, tumour biology, and selection of cases. In addition, follow-up strategies may differ between surgeons and centres. Bloch et al. described 3% recurrences within five years of near total removal and 32% in subtotal (Bloch et al., 2004); Schwartz et al found recurrence rates of 21–22% at a mean follow-up of 3.7–3.9 years (Schwartz et al., 2013). Several later patient series fail to corroborate such a difference between near total and subtotal. Instead they describe 5-year recurrence rates of 7–9% following near total or subtotal removal without a major difference between near- and subtotal (Sughrue et al., 2011; Chen et al., 2014b; Syed et al., 2017) (Fig. 22.7). Retrospective recurrence data are difficult to evaluate also because radiologically demonstrated progression does not necessarily imply a treatment failure to the extent that additional therapy was indicated; in most series only approximately half of all patients with demonstrated regrowth have received additional treatment (Sughrue et al., 2011; Syed et al., 2017). All residuals are not biologically equal. An isolated residual on the brainstem has a lower supply of energy and nourishment than a well vascularized residual in the internal

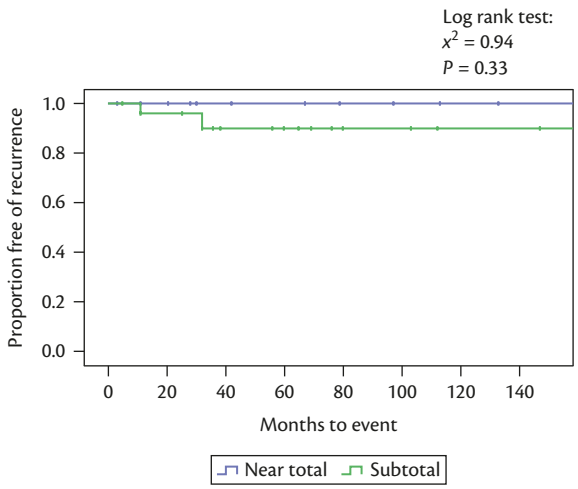

Fig. 22.7 Recurrence following subtotal and near total resection of vestibular schwannoma.

Reproduced with permission from M.I. Syed et al., The behaviour of residual tumour after the intentional incomplete excision of a vestibular schwannoma: is it such a bad thing to leave some behind?, *Clinical Otolaryngology*, Volume 42, Copyright © 2016 John Wiley and Sons.

acoustic meatus, which can influence the potential to recur. In small incidental schwannomas, growth is usually detectable within 3–5 years of conservative treatment (Stangerup and Caye-Thomasen, 2012), but the biology of inert incidental tumours is probably different from residuals of once large lesions. Actual long-term data are lacking and we do not know how recurrence rates will increase with even longer follow-up.

Primary gamma knife radiosurgery and tumour control

Radiosurgery utilizes sharp dose gradients achieved with multiple focused beams, which is geometrically possible only with small treatment volumes. Hence, small tumours are the commonest indication. Initially, tumour shrinkage was the expected treatment effect which was seen in most patients. The first nine cases were treated between 1969 and 1974. In 1993 Norén et al. reported the earliest series of 254 patients (Norén et al., 1993). He found tumour shrinkage in 55%, stable tumours in 33% and 77% hearing preservation, but high incidences of mostly temporary facial and trigeminal nerve deficits. Subsequently, the radiation doses were decreased without detectable loss of tumour control while radiation complications were minimized. The goal of treatment shifted from shrinkage to 'control', which is defined as absence of progression during long-term follow-up after more than 1–2 years. Importantly, successful treatment includes temporary post-treatment tumour swelling in up to 30% of radiosurgically treated patients. Recently patients received marginal doses of approximately 13 Gy and were reported to have tumour control of 97% with a mean follow-up of 6 years (Boari et al., 2014), 92% at a mean follow-up of 9 years (54) and also 92% with a 12.5-year mean (10-year minimum) follow-up (Hasegawa et al., 2013). Régis et al. use 12 Gy to the margin with a reduction to 11 if hearing is serviceable (Régis et al., 2013a). Long-term control rates of 98–99% were found with early retreatment of suspected failures or selection of only Koos grade 1 tumours (Régis et al., 2013a). Koos grading is described in Table 22.1. The control rates in case series do, however, not necessarily reflect a treatment effect. The control rates can be adjusted to express the influence of radiosurgery on control, since natural history does not entail progression for the majority of tumours. Miller et al. (2014) estimated the actual radiosurgically achieved 10-year control rate to 78–87%. It is also discussed whether radiosurgical control differs between tumours that were stable and tumours that grew before treatment. Investigators who have studied the cohorts separately do, however, not find any influence by previous growth rates on long-term tumour control (Meijer et al., 2008; Niu et al., 2014; Wangerid et al., 2014) (Fig. 22.8). Fractionated radiation has been described as a successful for vestibular schwannomas, but selection of cases and limited follow-up makes conclusions regarding long-term efficacy difficult (Combs et al., 2005; Choy et al., 2013; Litre et al., 2013).

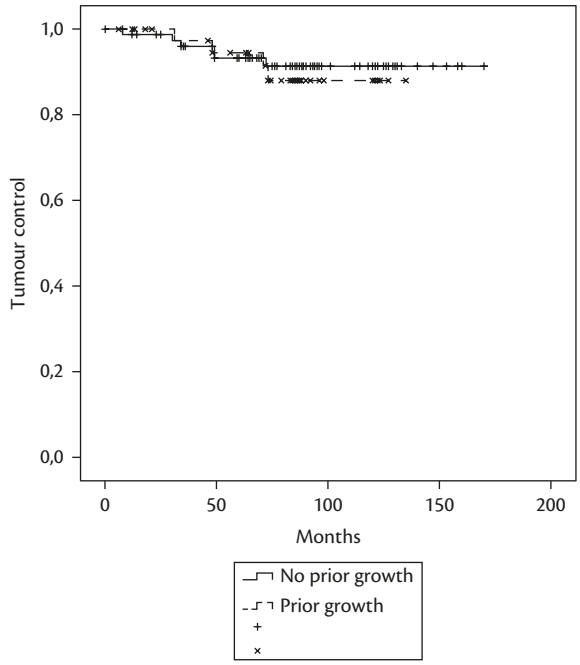

Fig. 22.8 Gamma knife control rates for vestibular schwannoma stratified by prior growth.

Reproduced with permission from Theresa Wangerid, Jiri Bartek, Mikael Svensson et al., Long-term quality of life and tumour control following gamma knife radiosurgery for vestibular schwannoma, *Acta Neurochirurgica*, Volume 156, Issue 2, pp. 389–96, Copyright © 2013 Springer Nature.

Table 22.1 Koos grading scale

Grade	Description
1	Tumour only involves internal auditory canal
2	Tumour extends into cerebellopontine angle but does not encroach onto brainstem
3	Tumour fills the entire cerebellopontine angle
4	Tumour displaces brainstem and adjacent cranial nerves

Source data from Koos, W. T., Day, J., Matula, C., & Levy, D. I. (1998). Neurotopographic considerations in the microsurgical treatment of small acoustic neurinomas, *Journal of Neurosurgery*, 88(3), 506–512.

Combined micro- and radiosurgery, salvage radiosurgery, and tumour control

The rationale for accepting an up to 30% risk of recurrence, after subtotal resection, includes the availability of subsequent radiosurgery and the belief that subsequent radiosurgery provides tumour control. Radiosurgery of a residual, stable, or growing, lead to tumour control in 11/11 treated patients treated by Hori (Hori and Maruyama, 2013) while others have reported control rates around 90%, similar to long-term data on primarily treated schwannomas. Van de Langenberg et al. (2011) reported tumour control 90% after less than 3 years follow-up of intentional subtotal surgery of large schwannomas followed by gamma knife radiosurgery (Rowe et al., 2007) and Iwai et al. (2015) found 10-year tumour control of 86% with 95% House-Brackman 1–2 and 42% hearing preservation. With previously operated schwannomas, larger size (>6 cm^3) was a risk factor for treatment failure which required salvage surgery in a few patients. Ionizing radiation is an established risk factor for tumorigenesis and a number of case reports have described rapidly growing tumours and even gliomas in patients treated by radiosurgery. The absolute risk is, however, very low. Reviews of treated patients and reviews of malignant schwannomas do not support malignant transformation or induction of secondary malignancies at any detectable rate (Demetriades et al., 2010). Residual and recurrent tumours were treated by radiosurgery or microsurgery (Jeltema et al., 2015; Nonaka et al., 2016; Samii et al., 2016b; Wise et al., 2016; Huang et al., 2017).

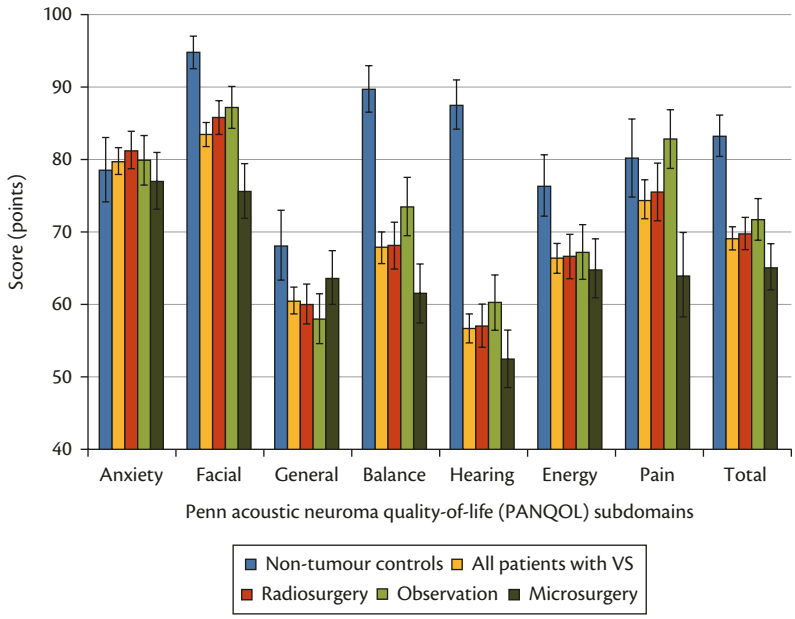

Fig. 22.9 Long-term health-related quality of life using disease specific outcomes in vestibular schwannoma.
Carlson, M., Tveiten, O., and Driscoll, C., et al, Long-term quality of life in patients with vestibular schwannoma: an international multicenter cross-sectional study comparing microsurgery, stereotactic radiosurgery, observation, and nontumor controls, *Journal of Neurosurgery*, Vol. 122, No. 4 (2015) with permission from JNS Group.

Symptoms and quality of life

At diagnosis, most patients have one or more of the typical components of the triad of: hearing deficit, vertigo, and tinnitus. Harun et al. reported the respective frequencies at presentation at 93%, 67%, and 84% in a consecutive series of 1200 patients (Harun et al., 2012). The facial and trigeminal nerves may also be affected, but are more frequently affected by treatment; headache is a possible symptom before treatment but can remain or occur after surgery. Neurological symptoms are central for subjective discomfort and suffering, since only a small fraction of patients are diagnosed with potentially life-threatening tumours. Patients with vestibular schwannomas do report a reduced quality of life compared to a reference population (Harun et al., 2012). Preservation or regained quality of life is the primary management objective which may be difficult to achieve. Broomfield and O'Donoghue recently (2016) surveyed 568 members of members of the British Acoustic Neuroma Association regarding quality of life; they reported that their schwannomas had changed overall quality of life for better in 18%, a little worse in 38% and a lot worse in 19%. 'A little worse' was distributed equally among treated and conservatively followed patients while surgical treatment dominated among those reporting 'a lot worse'. In various studies 61–76% of patients have returned to work 6–12 months after treatment, but the proportions appear to be similar regardless of surgical approach or radiosurgery. Quality of life appears to be slightly better in patients followed conservatively than operated, and appears to be slightly better following radiosurgery than microsurgery (Carlson, Tveiten, et al., 2015; Golfinos et al., 2016). Taken together, treatment effects and differences between treatments are difficult to evaluate. Quality of life is a treacherous term. Physicians care more about health-associated issues, especially those that are affected by the specific disease and its treatment. The commonest instrument, SF-36, actually measures health-associated factors rather than actual quality of life. It is possible to have a low quality of life in spite of good health and minimal treatment morbidity and vice versa. Our reasonable priority is the specific symptoms of disease and their relative health impact (Fig. 22.9). Even so, the topic is complex and influenced by individual coping, permanence of deficit, duration, expectations, and how caregivers actually deal with different symptoms. Textbook knowledge comprises concern for facial nerve function, tinnitus, and unilateral loss of hearing but the prospective studies of Carlson and coworkers instead described dizziness and headaches as the strongest predictors of long-term reduced quality of life (Carlson et al., 2015a; Carlson et al., 2015b). It is possible that comparison of ever-present deficits such as hearing loss and facial nerve function to periodic disabilities such as dizziness and headaches is difficult. Constant symptoms may be ranked as less bothersome as they are predictable and can be adjusted to. It is also possible that the awareness among caregivers is better and that these deficits are dealt with consciously before treatment, avoided during treatment, and rehabilitated after.

Hearing deficit and worsening of hearing with wait and scan, micro-, or radiosurgery

Preserved hearing and useful hearing are usually defined as a pure-tone audiogram (PTA)with less than 50 dB loss and a Speech Discrimination Score (SDS) greater than 50% according to American Association of Otolaryngology-Head and Neck Surgery Classes (AAO-HNS) A or B, and Gardner-Robertson classes I or II. Gardner-Robertson classification is described in Chapter 25. At inclusion in a prospective study on 538 patients, 11% had class A and 12% class B hearing (Tveiten et al., 2015). A subgroup of 128 patients was followed with observation only for a mean of 7 years. Class A hearing decreased from 32% to 22, class B from 32% to 23, class C increased from 8 to 11%, and class D from 30 to 44%. Sughrue found 50% loss of functional hearing during 26–52 months of follow-up (Sughrue et al., 2010) while Stangerup et al. (2008) followed 334 patients with good hearing and speech discrimination more than 70%, suitable for 'wait and scan', for ten years. In those patients,

hearing was preserved in only 31%. However, patients with perfect discrimination (100%) at inclusion had an 88% preservation rate. Intracanalicular schwannomas comprise a subgroup with very small tumours. Without treatment, audiometrically measured serviceable hearing was preserved for a mean of 9.5 years in 34% and speech discrimination is preserved in 58% (Kirchmann et al., 2017). During a mean follow-up of 44 months, Régis (Régis et al., 2013a) found more than 10 dB hearing loss in 38% including 5% who became deaf. The hearing outcomes without treatment are dismal for most patients.

With treatment, microsurgery of cases selected for surgery showed hearing preservation of serviceable hearing in 8–51% of retrospective series (reviewed in Samii et al., 2006; Tveiten et al., 2015) and 14% in the microsurgical subgroup comprising 139 of 539 patients in a prospective cohort study (Tveiten et al., 2015). Microsurgical series have a wide range of outcomes as they reflect different selection of patients and different timing of surgery. Most importantly, however, individual surgical skill and experience in patient selection are crucial for microsurgical results and experienced surgeons consistently report predictable good hearing in selected patients (Samii et al., 2006; Rahimpour et al., 2016). Depending on patient selection, series show 10–70% hearing preservation. Following initially favourable hearing outcomes, however, 15–20% of patients may experience further loss of initially preserved hearing (Wang et al., 2013).

After radiosurgery, further decline of hearing is to be expected with 5.9 dB/year during the two first years and 1.9 dB/year thereafter (Yomo et al., 2012) and sudden deafness may occur. Carlson (Carlson et al., 2013) described 23% preservation of serviceable hearing after 10 years, which is similar to the natural history. Comparative data on a potential benefit of radiosurgery are conflicting. Régis et al. found 60% preserved hearing with radiosurgery compared to 14% in untreated controls after 5 years in an open, prospective comparative study (Régis et al., 2013b) and Boari claimed especially good results in young patients with excellent hearing pretreatment (Boari et al., 2014). In contrast, Tveiten et al. failed to detect a benefit in a two-centre prospective trial. Their radiosurgical cohort comprised 240 patients followed for 7 years; class A decreased from 25 to 7%, class 2 from 22 to 12%, class C from 12 to 11 and class D increased from 41% to 70. Significant difference of hearing preservation between radiosurgery and natural history could not be asserted and outcomes actually appeared worse after radiosurgery (Tveiten et al., 2015). Two ongoing randomized controlled studies comparing initial radiosurgery and initial conservative treatment will hopefully give a more confident answer on a potential hearing preserving effect of radiosurgery (https://www.clinicaltrials.gov: NCT 02249572 and NCT 01938677).

Tinnitus

Tinnitus is speculated to be caused by ephaptic transmission, cochlear dysfunction, loss of efferent vestibular fibres and cortical reorganization. Cortical reorganization is one reason to why sectioning of a cochlear nerve may fail to cure tinnitus. Tinnitus usually has a high frequency pitch and is reported in 70–80% of all patients at diagnosis (Baguley et al., 2006; Tveiten et al., 2015). It is constant in approximately two-thirds and intermittent in the remaining third of patients. David Moffat's group classified tinnitus as mild tinnitus, which is only perceived in silence, moderate which is perceived over ambient background noise and severe tinnitus, which also interfered with sleep (Quaranta et al., 2007). They found moderate tinnitus in 2–26% and severe in 11–24%. The influence of treatment on tinnitus is variable and findings are not sufficiently reproducible. Several authors suggest that tinnitus can be ameliorated by hearing preservation at surgery or cochlear nerve section rather than preserving a non-functioning nerve. Tinnitus outcome is, however, unpredictable, and not statistically different between conservative management, microsurgery, and radiosurgery. During a mean follow-up of 3 years, most patients reported unchanged tinnitus, improved in 6% and worsened in 16% (Quaranta et al., 2007). Tinnitus alone is not an indication for surgical treatment and tinnitus was not found to significantly affect quality of life in larger groups, although individual patients may experience suffering described as catastrophic. Handicap from tinnitus is not directly related to severity. With time, most patients appear to adjust to remaining tinnitus.

Vertigo and dizziness

Dizziness is the most significant audiovestibular predictor of quality of life in patients with vestibular schwannomas and was consistently associated with long-term quality of life reduction in patients with sporadic vestibular schwannomas regardless of conservative or active treatment (Gauden et al., 2011; Jufas et al., 2015). More than 50% of vestibular schwannoma patients experienced dizziness, usually unsteadiness and vertigo only in 8%, still 8 years after diagnosis (Carlson et al., 2014). A prospective cohort study (Andersen et al., 2015) reported spinning vertigo in 11% and severe dizziness in 9% at baseline. Loss of response to caloric testing of the horizontal semicircular canal, 'canal paresis', was detectable in more than 70% of investigated patients. Canal paresis and postural unsteadiness correlated with moderate-severe dizziness while relationship with hearing and tumour size were less clear. Central compensation allows adjustment and subsequently a large group of schwannoma patients do not experience dizziness in spite of vestibular deficits, especially when vestibular loss is gradual. It is probable that larger tumours and stable loss of vestibular function allows better compensation and coping. Dizziness in the absence of large tumour size, growth, or other symptoms is an unusual indication for surgery. Surgery does allow section of the vestibular nerves to discontinue any erratic signalling. Disabling vertigo was resolved in 17/19 patients undergoing hearing preservation surgery for otherwise asymptomatic small vestibular schwannomas (Samii et al., 2016a). The indication is, however, controversial since surgery did not predictably improve dizziness in studies with other patients harbouring larger tumours. Selection of patients and microsurgical refinement may be keys to the good results. Many patients improve spontaneously and vestibular rehabilitation is necessary also after surgery (Thomeer et al., 2015).

Facial nerve function

Facial nerve palsy is consistently ranked, together with hearing deficit, as the most significant impairment after treatment for vestibular schwannoma (Carlson, Tveiten, et al., 2015). The House-Brackmann grading of facial function is described in Table 22.2. Facial nerve dysfunction causes difficulties with corneal protection, eating, drinking, and speaking. In addition, psychological distress can cause decreased self-esteem, anxiety, and depression, which are more important predictors of social disability in patients with facial paralysis (VanSwearingen et al., 1998). Unexpectedly, however,

Table 22.2 House-Brackmann grading

Grade	Gross function	Motion
1 **Normal**	Normal symmetrical function in all areas	
2 **Mild dysfunction**	Slight weakness noticeable on close inspection May have slight synkinesis At rest, normal symmetry	Forehead—moderate to good function Eye—complete closure with minimal effort Mouth—slight asymmetry
3 **Moderate dysfunction**	Obvious but not disfiguring difference between sides Noticeable (but not severe) synkinesis, contracture, or hemifacial spasm At rest, normal symmetry and tone	Forehead—slight to moderate movement Eye—complete closure with effort Mouth—slightly weak with maximum effort
4 **Moderately severe dysfunction**	Obvious weakness and/or disfiguring asymmetry At rest, normal symmetry and tone	Forehead—none Eye—incomplete closure Mouth—asymmetrical with maximal effort
5 **Severe dysfunction**	Only barely perceptible motion At rest, asymmetry	Forehead—none Eye—incomplete closure Mouth—slight movement
6 **Complete paresis**	No movement	

Reproduced with permission from John W. House, Derald E. Brackmann, Facial Nerve Grading System, *Otolaryngology—Head and Neck Surgery*, Volume 93, Issue 2, pp. 146–7, Copyright © 1985 SAGE.

facial nerve deficit had very little bearing on long-term quality of life scores (Carlson et al., 2015b). In agreement, Lassaletta et al. (2013) suggested that the visibility of a facial nerve paresis caused surgeons to put inappropriate emphasis on facial palsies compared to other postoperative symptoms.

Vestibular schwannoma patients rarely (<5%) present with facial nerve deficits and this raises the possibility of a facial nerve schwannoma. The facial nerve is primarily affected in patients with large tumours. Hence, new facial nerve deficits are not expected to occur during follow-up of non-growing lesions. Following microsurgery, facial nerve outcomes reflect surgical skill and goals. The risks vary with tumour size, extent of resection, and surgical experience. Temporary facial weakness is fairly common for larger tumours while permanent deficits occur in up to 20% of radically operated large tumours; considerably less in smaller or subtotally operated tumours. Radiosurgery is performed with low radiation doses, high resolution MRI, and modern dose planning which allow a low incidence of facial nerve deficits; they occur in less than 1% of patients (Yang et al., 2009; Régis et al., 2013a; Wangerid et al., 2014).

Intermedius nerve damage may occur in over 50% of patients operated by microsurgery, but is frequently noticed only if specifically looked for (Yang et al., 2009; Noonan et al., 2016). The symptoms comprise dry eyes and taste alteration. Lack of lacrimation is especially problematic when combined with a sensory deficit or inability to cover the cornea and dysgeusia can affect quality of life severely in persons for whom the sense of taste is important.

Headache

Persistent headaches were reported in 0–77% of participants of retrospective studies (reviewed in Carlson et al., 2015a) and surveys after vestibular schwannoma surgery. The headaches were usually of tension-type. They were frequently severe after three months but declined and became insignificant in many patients during further follow-up. Retrosigmoid craniotomies were associated with most complaints and subsequently speculation of causality has included traction of dura following healing of the incisions, aseptic meningitis correlated with CSF pseudocysts or bone dust from drilling and secondary mildly increased intracranial pressure from stenosis of venous sinuses. Cases that 'prove the concept' of each of the theories have been described and measures that decrease the amount of bone dust by replacing drilling with ultrasonic bone removal decrease the incidence of headaches. Only recently did Carlson et al. study headaches prospectively in patients treated by observation alone, microsurgery or radiosurgery (Carlson et al., 2015a). The incidence at presentation was 60%, which agrees with an estimated life-time prevalence of headaches in the general population. Headaches improved in 10% following observation, 14% following radiosurgery, and 19% following microsurgery; and worsened in 10% with observation, 14% with radiosurgery, and 25% following microsurgery. Long-term outcomes do not show statistically significant differences between the groups, although microsurgery was associated with more headaches during the first year after treatment. Younger age, previous migraine, a previous history of headaches and greater anxiety and depression predicted worse headaches after treatment and are also predictors of headache in the general population. Headaches remain severe after 1 year in 6–9% of all patients regardless of treatment and were then an important cause of decreased quality of life. Patients with conservatively managed vestibular schwannomas had headaches at twice the rate of controls (Breivik et al., 2012).

Non-vestibular schwannomas

Biologically and pathologically, non-vestibular schwannomas are very similar to vestibular schwannomas. They grow slowly and also appear to respond to radiosurgery (Pollock et al., 2002). Epidemiological data are derived from surgical series in specialized centres and may reflect selection bias. It is, however, clear that non-vestibular schwannomas are rare and comprise 6–10% of intracranial schwannomas or less than 1% of all intracranial tumours. The commonest of these are trigeminal nerve schwannomas, followed by jugular foramen schwannomas and facial nerve schwannomas.

Distinctly rare schwannomas are found on the oculomotor, trochlear, hypoglossal, and abducens nerves in that order. Tumours may also occur in the cochlea or vestibule. Occasional schwannomas that were not related to the cranial nerves have been discovered in the third ventricle, pituitary, or frontal base. Schwannomas also occur extracranially in the head and neck areas, intraorbitally, and elsewhere in the body, but will not be covered in this chapter.

Trigeminal schwannomas

Trigeminal schwannomas comprise 1–8% of intracranial schwannomas (MacNally et al., 2008; Chen et al., 2014a) (Fig. 22.10). The commonest presenting symptom is facial hypesthesia, followed by headache, dizziness, and ataxia. The tumours can arise along any portion of the trigeminal root, ganglion, and nerves, although locations centred around the ganglion are commonest. The tumours were originally classified according to their location by Geoffrey Jeffersson (Jefferson, 1953) as A–C, while 'D' was added later (Table 22.3). The commonest location is C, which describes a dumbbell tumour perched *en cheval* on the petrous bone, extending from the middle fossa to the posterior through the porus trigeminus.

Similar to vestibular schwannomas, the focus of management goals has shifted from radical removal to preservation of function and long-term control. Microsurgery for trigeminal schwannomas thus aims at bulk removal with preservation of intact rootlets, unless clinical behaviour or histopathology indicates an aggressive tumour. Nevertheless, microsurgery and cranial base techniques have increased complete removal of trigeminal schwannomas that were rarely radically operated in the premicrosurgical era. Schwannomas predominantly located in the cavernous sinus are preferentially approached frontotemporally with a Dolenc-technique (Dolenc, 1994) that includes extradural removal of the anterior clinoid process and dissection of the temporal dura off the cavernous sinus inner dural membrane. The posterior fossa component can be radically or near radically removed via the widened porus trigeminus in patients with moderate posterior fossa tumour extensions. Larger posterior fossa components require division of the tentorium and drilling of the anterior part of the petrous ridge or a second suboccipital approach (Yoshida and Kawase, 1999). A suboccipital trajectory is sufficient for a posterior fossa tumour and the petrous bone can be drilled intradurally to access Meckel's cave from the posterior fossa. Microsurgical removal of small trigeminal schwannomas is feasible with low morbidity. Small schwannomas are also usually controllable with radiosurgery, while its use can be prohibited by tumour size and close proximity to the optic apparatus. Trigeminal schwannomas that fail radiosurgery have been operated without added morbidity or loss of tumour control by conservative surgery

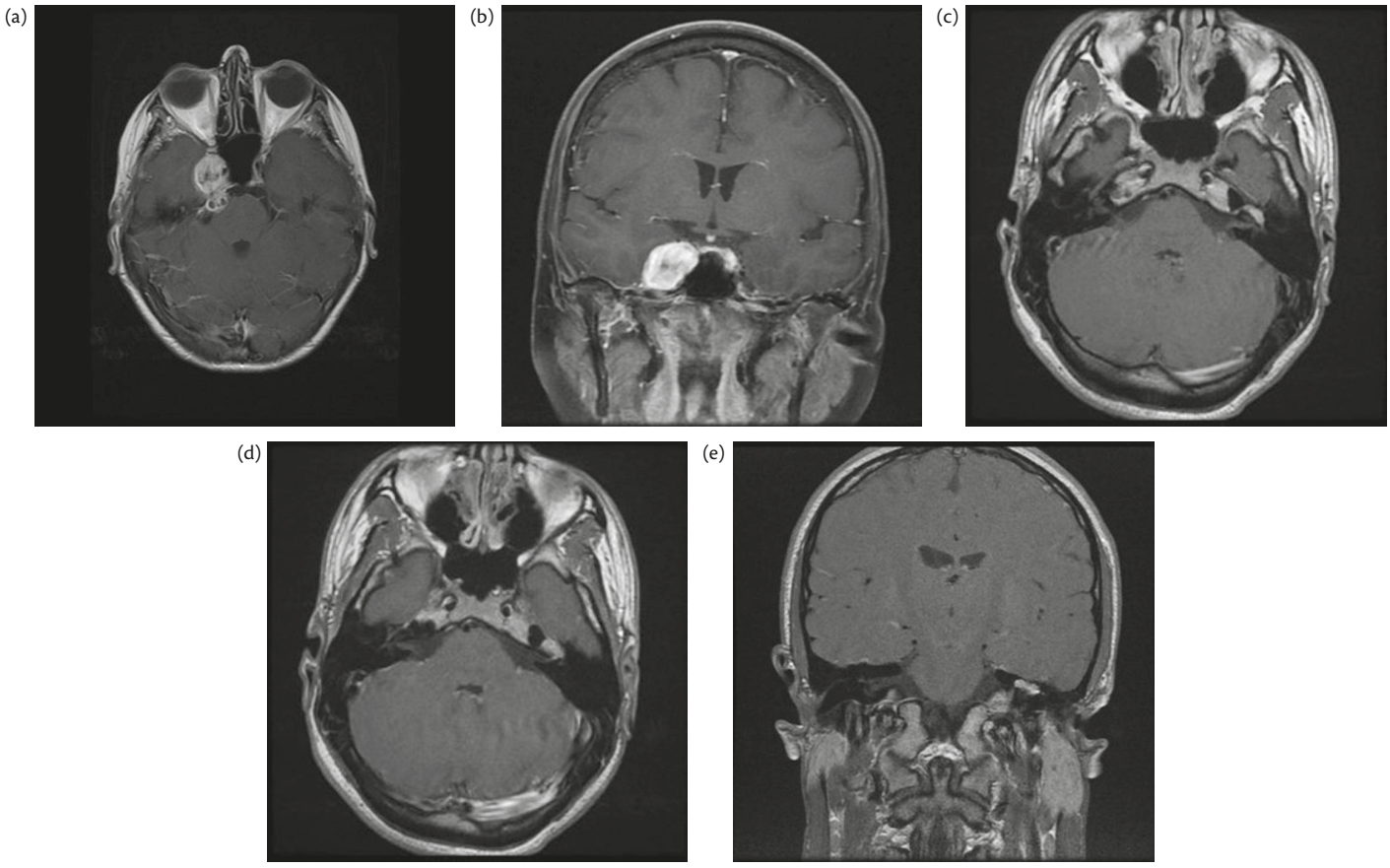

Fig. 22.10 Trigeminal and facial schwannomas. Axial (A) and coronal (B) T1-weighted MRI with gadolinium contrast illustrating a trigeminal schwannoma. The axial image illustrates the characteristic dumbbell shape with one portion extending from Meckel's cave into the posterior fossa and one portion extending from the cavernous sinus into the middle cranial fossa. Axial (C, D) and coronal (E) T1-weighted MRI imaging with gadolinium contrast illustrating the extension of the left-sided contrast-enhancing schwannoma along the labyrinthine and tympanic segments on either side of the geniculate ganglion.

Table 22.3 Modified Jeffersson classification of trigeminal schwannomas

Type	Main location	Frequency
A	Middle fossa	40%
B	Posterior fossa	22%
C	Dumbbell tumour; middle and posterior fossa	32%
D	From postganglionic nerves	6%

Reproduced with permission from S. P. MacNally, S. A. Rutherford, R. T. Ramsden, et al, Trigeminal schwannomas, *British Journal of Neurosurgery*, Volume 22, Issue 6, 2008 © The Neurosurgical Foundation, reprinted by permission of Taylor & Francis Ltd, www.tandfonline.com on behalf of The Neurosurgical Foundation.

and an aim of functional preservation. In those with predominant medial extension in relation to the carotid artery, an extended endoscopic endonasal transpterygoid approach may be considered. Following entrance into the maxillary sinus the posterior wall is drilled to access the pterygopalatine and infratemporal fossae. At the petrous apex, the trigeminal ganglion straddles the horizontal segment of the petrous internal carotid artery.

The surgical outcome regarding trigeminal nerve function depends on technique and management priorities; with meticulous cranial base microsurgical techniques and acceptance of near- or subtotal resection, a high degree of surgical radicality is possible with 10% improvement of sensation and less than 10% deterioration (Chen et al., 2014a) while earlier or more radical series reported higher rates of trigeminal functional loss. Surgery of larger tumours and cavernous sinus extensions may cause diplopia, and mortality occurred in older series. Trigeminal dysfunction can be very bothersome in spite of minimal visible deficits. New trigeminal symptoms were studied in patients operated for skull base meningiomas (Westerlund et al., 2012). Most patients seemed to adjust to numbness or mild neuropathic pain, while ocular symptoms and rare anaesthesia dolorosa are causes of major morbidity.

Third, fourth, and sixth nerve schwannomas

Schwannomas of the third, fourth, and sixth nerves are very rare and most commonly encountered in patients with neurofibromatosis type 2. Sporadic ocular nerve schwannomas comprise less than 1% of intracranial schwannomas and are discovered incidentally or during work-up for headaches or diplopia; partial ocular nerve palsy is the common symptom; available literature comprises reports of a total of 40–100 cases of each kind. They can arise anywhere along the nerves and occur in the intradural compartment, cavernous sinus wall (oculomotor and trochlear), inside the cavernous sinus (abducent) or orbit and have slow growth rates that motivate 'wait and scan' in many patients with minimal symptoms. Symptomatic tumours or growing tumours can be managed by radiosurgery if small and distant from the optic apparatus while microsurgery is feasible for all tumours. Non-radical surgery with a primary goal of preserving functional nerves may need to be combined with subsequent radiosurgery for tumour control. Radical surgery is technically feasible, but not with preservation of neuronal function. Results of nerve grafting have not been reported. Nerve grafting of the smaller nerves (trochlear and abducent) is theoretically possible, while occulomotor functional recovery following grafting is unlikely, as nerve suture has been shown to be futile.

Facial nerve schwannomas

Facial nerve schwannomas comprise less than 2% of intracranial schwannomas. Like other schwannomas, they grow slowly, are sensitive to stereotactic radiosurgery and tumour control is usually feasible. Facial schwannomas can occur anywhere along the nerve. The geniculate and tympanic segments are most commonly affected (**Fig. 22.10**). Three types of tumour can be discerned. One common location is the internal acoustic meatus, where they mimic vestibular schwannomas and extend into the cerebellopontine angle. These tumours are not dissectible from the facial nerve. The second type of tumours grow in the nerve in the fallopian canal and may appear as a contrast enhancing (on MRI), thickened segment of the nerve. A third typical location is around the greater petrosal nerve and the geniculate ganglion, which produces an exophytic extradural tumour on the subtemporal surface of the petrous bone.

Extensive loss of axonal function can occur before facial paresis develops. Hence, many facial nerve schwannomas present with tinnitus and hearing loss if located in the internal acoustic meatus or mass effect if located subtemporally. Schwannomas in the petrous bone usually cause facial nerve dysfunction, unless they are incidental findings. Radical surgery of facial nerve schwannomas comprises complete resection with nerve sacrifice and subsequent grafting. Hence, the surgical goals must be preconceived and transparent. Nerve grafting cannot be expected to provide better facial function than House-Brackman III, and is thus usually reserved for patients with manifest high-grade facial nerve palsy. For patients with large tumours and good facial function, subtotal removal with the prospect of added radiosurgery in case of tumour progression is a good alternative. The subtemporal tumours arising from the geniculate ganglion are removed near totally with a subtemporal epidural approach, which preserves facial function (Ichimura et al., 2010). Small tumours may grow very slowly and can be monitored with radiological surveillance. Gamma knife radiosurgery is feasible for small tumours that progress clinically or radiologically.

Schwannomas of the lower cranial nerves in the jugular foramen

Jugular foramen schwannomas include tumours originating from the glossopharyngeal, vagal, and accessory nerves; they comprise less than 3% of all intracranial schwannomas (**Fig. 22.11**). Glossopharyngeal tumours are probably the commonest, but it is frequently impossible to discern the nerve of origin. Originally, many tumours were detected during work-up for increased intracranial pressure. Such presentation still occurs but specific neurological deficits are more common. A partial or total jugular foramen syndrome and swallowing difficulties are present in approximately half of all patients while 30–60% show vestibulocochlear symptoms.

The tumours can be located anywhere along the nerves. Kaye and Samii proposed a classification of A, B, C, and D depending on origin and growth pattern (Kaye et al., 1984; Samii et al., 1995). Jugular foramen type A schwannomas occupy the cerebellopontine angle, type B are intraforaminal with intradural extension, type C are extracranial (not further covered here), and type D dumbbell shaped intraextra cranial. For radical removal, intracranial type A tumours are approached by the retrosigmoid approach whereas type B and D tumours require a retrosigmoid/transpetrous approach. A transpetrous approach with facial nerve transposition

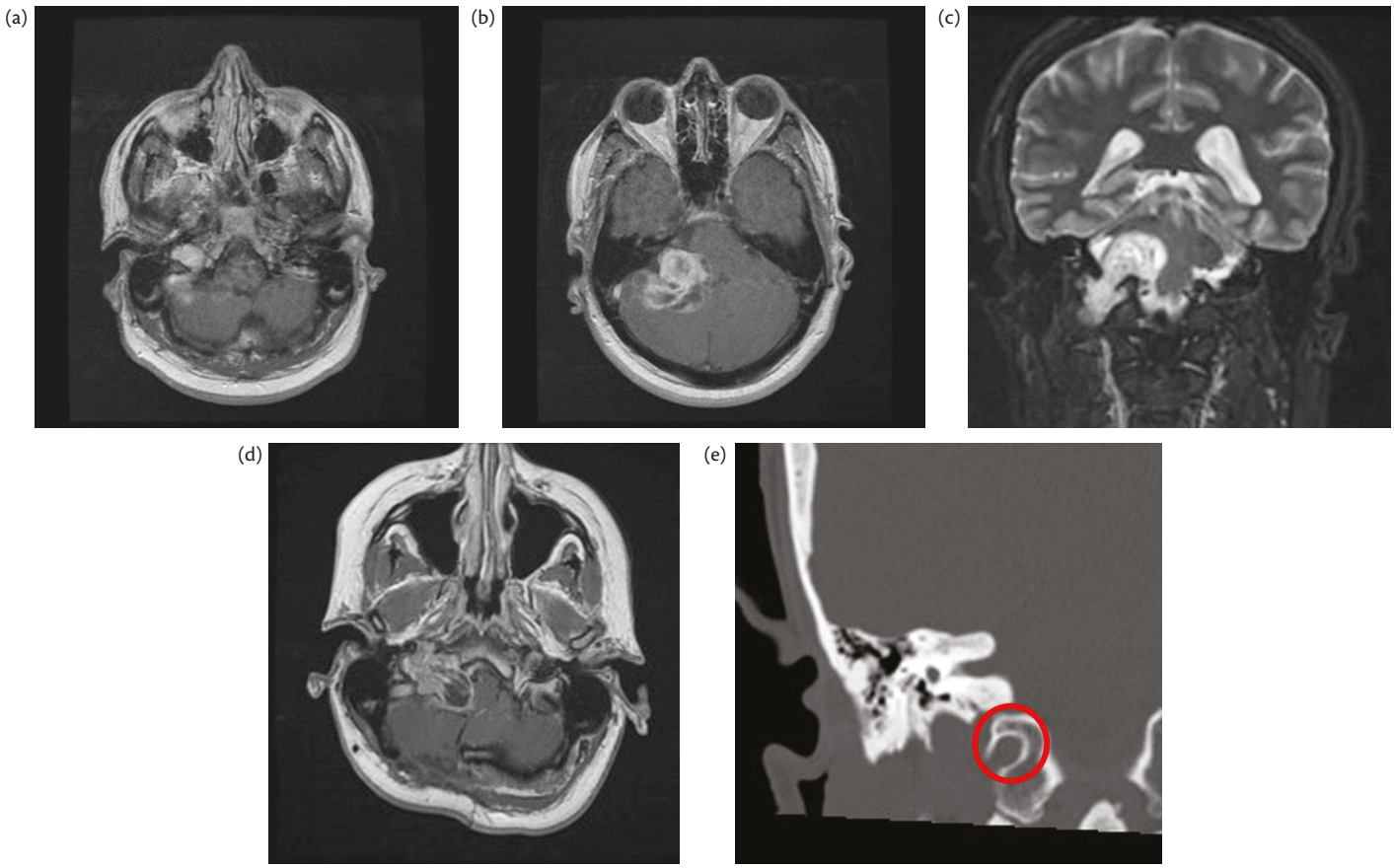

Fig. 22.11 Lower cranial nerve schwannomas. Axial (A, B) T1-weighted MRI with gadolinium contrast and coronal T2 (C) short T1 inversion recovery (STIR) MRI sequences of lower cranial nerve schwannoma. The tumour can be seen exiting the jugular foramen. Recurrent hypoglossal schwannoma (D) on T1-weighted MRI with gadolinium contrast. The hypoglossal canal can be identified easily on coronal computed tomography (CT) scan (E) as the Eagle's beak (circled in red). A hypoglossal schwannoma expands the hypoglossal canal and abolishes the Eagle's beak appearance. This can help to distinguish hypoglossal schwannomas from other lower cranial nerve schwannomas.

was frequently used in the past, but largely abandoned because of resulting facial nerve morbidity. Cranial nerve morbidity following gross total or near total resection has been reported in up to 100% for the lower cranial nerves, facial nerve morbidity in 11–80%, and vestibulocochlear morbidity in 4–45% (Park et al., 2016). Radical surgery of jugular foramen tumours carries a high risk of impaired lower cranial nerve function with ensuing hoarseness, dysphagia, or aspiration. Lower cranial nerve dysfunction may require tube feeding, gastrostomy, or tracheostomy for a shorter or longer period which has a strong negative impact on quality of life (Mathiesen et al., 2007). The tumours grow slowly and functional preservation has become a major objective for jugular foramen tumours. Intradural decompression and tailoring for radiosurgery allows medium term growth control with preservation of glossopharyngeal, vagal, and accessory nerve function (Park et al., 2016). Long-term data more than 10 years have, however, not been assessed or published and the expectation of long-term control reflect generalization of radiosurgical outcomes in vestibular schwannomas. Schwannomas of the spinal accessory nerve are surgically accessible with minimal morbidity other than unilateral spinal accessory paresis.

Hypoglossal schwannomas

Intracranial hypoglossal schwannomas are rare and only described in small clinical series and case reports describing approximately 100 cases. They appear to be more commonly cystic and rapidly progressing or recurring than other schwannomas (Fig. 22.11). Hemiatrophy of the tongue and hypoglossal paresis are typical symptoms. Up to half of all patients with unilateral hypoglossal paresis harbour a benign or malignant tumour around the cranial base. A hypoglossal schwannoma is reached intradurally and in the hypoglossal canal via a lateral, partial transcondylar approach. Hypoglossal function appears to recover rapidly following radical removal of a schwannoma with subsequent grafting (Mathiesen et al., 2009). The functional benefit of grafting and the feasibility of subtotal removal with or without adjuvant radiosurgery have not been sufficiently evaluated. Case reports with limited follow-up suggest that subtotal surgery with adjuvant radiosurgery is feasible also for hypoglossal schwannomas. Unilateral hypoglossal palsy is reported not to affect speech; hence several authors have argued that the handicap would be well tolerated. However, the impact on swallowing and quality of life has not been critically analysed.

Controversy: 'The small incidental acoustic'

The management of small, incidental vestibular schwannomas is subject to controversy. 'Wait and scan' is recommended to many

patients. Small tumours can technically be treated by micro- or radiosurgery, hence many patients choose a treatment. The controversies are should the patient be treated or followed, and which treatment is a better if active treatment is selected.

1. 'Active treatment' is based on the risks of symptomatic progression or growth, added to the uncertainty of pathology. Approximately a third of all patients with good hearing lose functional hearing during 3-year follow-up. A tumour may grow to a size where the risk of facial nerve complications, which is close to negligible for the smallest tumours, becomes a reality. It is also possible that the tumour grows to a size when radiosurgery is not feasible, and the choice becomes obsolete. Finally, early removal is preferable in the unlikely event that the tumour is malignant. Ideally, early treatment offers cure of the tumour and preservation of hearing and facial nerve function.

'It is better to take a higher risk early to gain cure and preserve hearing'

2. 'Wait and scan' is based on the benign natural history. The main arguments are that only one-third of small incidental vestibular schwannomas grow during 5-year follow-up and late growth is possible but not to be expected. It is likely that treatment is futile in patients who have stable tumours, since neither surgery nor radiosurgery can predictably improve hearing, vertigo, or tinnitus. In addition, microsurgery and to a lower extent radiosurgery exposes the patient to inherent treatment discomfort and morbidity in addition to exposing the patient to a stochastic risks of treatment complications. Demonstrated tumour growth or sometimes symptomatic progression are indications for treatment.

'It is better to avoid unnecessary treatment, treatment can be delayed without a statistically worse final outcome', 'The best way to preserve long-term hearing'

2.1 'No active treatment with radiosurgery' is based on (1) the belief that the goal of radiosurgery is 'tumour control', which already is the expected 5-year outcome without any treatment in approximately 70% of the patients. (2) Radiosurgery may have complications. Radiation to the facial and vestibulocochlear nerves may damage function. The treatment risk for facial nerve palsy is 1–2% and hearing is expected to deteriorate slowly during follow-up after radiosurgery, although opposing data have been published. Ionizing radiation is known to carry a risk of chromosomal damage and subsequent tumour induction or malignancy.

'For cure the tumour should be removed and the albeit low but uncontrollable risk of malignancy should be avoided'

2.2 'No active treatment with microsurgery' is based on the belief that (1) surgery requires hospitalization and absence from regular life with inherent morbidity and pain; (2) severe complications including death are, although rare, a real to the few who suffer from these; (3) most surgical series suggest higher rates of facial nerve complications and short-term hearing loss after microsurgery than radiosurgery.

'The tumour should be treated, and the possible acute severe complications of microsurgery are unacceptable' or '*Radiosurgery is the best strategy to preserve long-term hearing'*

The controversy reflects the variation in the medical evidence and individual values. There is general consensus regarding literature data, but large studies and meta-analyses only provide mean-figures for complication rates and outcomes in large populations of different patients and surgeons. Thus, individual treatment risks cannot be blindly extrapolated from large clinical studies. The risks vary with individual surgeon skills and experience; the surgeon and patient can also agree on treatment goals that affect risks of recurrence and morbidity. Ionizing radiation increases tumour incidence on the population level, but has only a marginal effect in individual patients. Rapid growth and malignant histology have been described in a few tumours, but the literature does not describe a sufficiently high risk to avoid radiosurgery. Tumours may grow and hearing may be lost during follow-up, but severe worsening is very rare. The best rationale for radiosurgery is literature support of better long-term hearing outcomes; however, different studies have different results and conclusions. The scientific challenge is to assess whether the patient shares similarities with the population that showed benefit rather than the other subgroups.

Most importantly, individual patient's values regarding outcomes and acceptable risks vary. With a transparent risk assessment, different patients may opt for wait and scan, radiosurgery, or microsurgery for an identical tumour. It is the duty of the surgeon to share knowledge and experience in a transparent way without hiding personal experience and results and also to empower the patient to make a shared decision; the decision should reflect the patient's values and the surgeon's knowledge and professional ethics.

REFERENCES

AGNIR (2012). Health effects from Radiofrequency Electromagnetic Fields. *Documents of the Health Protection Agency, RCE-20*. Chilton, Oxfordshire, UK: The Health Protection Agency's independent Advisory Group on Non-ionising Radiation (AGNIR).

Andersen, J.F., Nilsen, K.S., Vassbotn, F.S., et al. (2015). Predictors of vertigo in patients with untreated vestibular schwannoma. *Otol Neurotol*, **36**(4), 647–52.

Babu, R., Sharma, R., Bagley, J.H., Hatef, J., Friedman, A.H., & Adamson, C. (2013). Vestibular schwannomas in the modern era: epidemiology, treatment trends, and disparities in management. *J Neurosurg*, **119**, 121–30.

Baguley, D.M., Humphriss, R.L., Axon, P.R., & Moffat, D.A. (2006). The clinical characteristics of tinnitus in patients with vestibular schwannoma. *Skull Base*, **16**, 49–58.

Benson, V.S., Green, J., Pirie, K., & Beral, V. (2010a). Cigarette smoking and risk of acoustic neuromas and pituitary tumours in the Million Women Study. *Br J Cancer*, **102**, 1654–6.

Benson, V.S., Pirie, K., Green, J., et al. (2010b). Hormone replacement therapy and incidence of central nervous system tumours in the Million Women Study. *Int J Cancer*, **127**, 1692–8.

Benson, V.S., Pirie, K., Schuz, J., Reeves, G.K., Beral, V., & Green, J. (2013). Mobile phone use and risk of brain neoplasms and other cancers: prospective study. *Int J Epidemiol*, **42**, 792–802.

Bloch, D.C., Oghalai, J.S., Jackler, R.K., et al. (2004). The fate of the tumor remnant after less-than-complete acoustic neuroma resection. *Otolaryngol Head Neck Surg*, **130**, 104–12.

Boari, N., Bailo, M., Gagliardi, F., et al. (2014). Gamma knife radiosurgery for vestibular schwannoma: clinical results at long-term follow-up in a series of 379 patients. *J Neurosurg*, **121** Suppl, 123–42.

Breivik, C.N., Varughese, J.K., Wentzel-Larsen, T., Vassbotn, F., & Lund-Johansen, M. (2012). Conservative management of vestibular schwannoma—a prospective cohort study: treatment, symptoms, and quality of life. *Neurosurgery*, **70**, 1072–80.

Broomfield, S.J. & O'Donoghue, G.M. (2016). Self-reported symptoms and patient experience: a British Acoustic Neuroma Association survey. *Br J Neurosurg*, **30**(3), 294–301.

Carlson, M.L., Jacob, J.T., Pollock, B.E., et al. (2013). Long-term hearing outcomes following stereotactic radiosurgery for vestibular schwannoma: patterns of hearing loss and variables influencing audiometric decline. *J Neurosurg*, **118**, 579–87.

Carlson, M.L., Tveiten, Ø.V., Driscoll, C.L., et al. (2015). Risk factors and analysis of long-term headache in sporadic vestibular schwannoma: a multicenter cross-sectional study. *J Neurosurg*, **123**(5), 1276–86.

Carlson, M.L., Tveiten, O.V., Driscoll, C.L., et al. (2015a). Long-term quality of life in patients with vestibular schwannoma: an international multicenter cross-sectional study comparing microsurgery, stereotactic radiosurgery, observation, and nontumor controls. *J Neurosurg*, **122**(4), 833–42.

Carlson, M.L., Tveiten, Ø.V., Driscoll, C.L., et al. (2015b). What drives quality of life in patients with sporadic vestibular schwannoma? *Laryngoscope*, **125**(7), 1697–702.

Carlson, M.L., Tveiten, Ø.V., Driscoll, C.L., et al. (2014). Long-term dizziness handicap in patients with vestibular schwannoma: a multicenter cross-sectional study. *Otolaryngol Head Neck Surg*, **151**(6), 1028–37.

Chen, L.F., Yang, Y., Yu, X.G., et al. (2014a). Operative management of trigeminal neuromas: an analysis of a surgical experience with 55 cases. *Acta Neurochir*, **156**, 1105–14.

Chen, Z., Prasad, S.C., Di Lella, F., et al. (2014b). The behavior of residual tumors and facial nerve outcomes after incomplete excision of vestibular schwannomas. *J Neurosurg*, **120**(6), 1278–87.

Choy, W., Spasic, M., Pezeshkian, P., et al. (2013). Outcomes of stereotactic radiosurgery and stereotactic radiotherapy for the treatment of vestibular schwannoma. *Neurosurgery*, **60**(Suppl 1), 120–5.

Combs, S.E., Volk, S., Schulz-Ertner, D., Huber, P.E., Thilmann, C., & Debus, J. (2005). Management of acoustic neuromas with fractionated stereotactic radiotherapy (FSRT): long-term results in 106 patients treated in a single institution. *Int J Radiat Oncol Biol Phys*, **63**(1), 75–81.

Cushing, H. (1917). *Tumours of the Nervus Acusticus and the Syndrome of the Cerebellopontine Angle*. Philadelphia, PA: Saunders.

Dandy, W.E. (1934). Removal of cerebellopontine tumours through a unilateral approach. *Arch Surg*, **29**, 337–44.

Demetriades, A.K., Saunders, N., Rose, P., et al. (2010). Malignant transformation of acoustic neuroma/vestibular schwannoma 10 years after gamma knife stereotactic radiosurgery. *Skull Base*, **20**, 381–7.

Dolenc, V.V. (1994). Frontotemporal epidural approach to trigeminal neurinomas. *Acta Neurochir (Wien)*, **130**, 55–65.

Edwards, C.G., Schwartzbaum, J.A., Lonn, S., Ahlbom, A., & Feychting, M. (2006). Exposure to loud noise and risk of acoustic neuroma. *Am J Epidemiol*, **163**, 327–33.

Evans, D.G., Moran, A., King, A., Saeed, S., Gurusinghe, N., & Ramsden, R. (2005). Incidence of vestibular schwannoma and neurofibromatosis 2 in the North West of England over a 10-year period: higher incidence than previously thought. *Otol Neurotol*, **26**, 93–7.

Fisher, J.L., Pettersson, D., Palmisano, S., et al. (2014). Loud noise exposure and acoustic neuroma. *Am J Epidemiol*, **180**(1), 58–67.

Gal, T.J., Shinn, J., & Huang, B. (2010). Current epidemiology and management trends in acoustic neuroma. *Otolaryngol Head Neck Surg*, **142**, 677–81.

Gauden, A., Weir, P., Hawthorne, G., & Kaye, A. (2011). Systematic review of quality of life in the management of vestibular schwannoma. *J Clin Neurosci*, **18**(12), 1573–84.

Golfinos, J.G., Hill, T.C., Rokosh, R., et al. (2016). A matched cohort comparison of clinical outcomes following microsurgical resection or stereotactic radiosurgery for patients with small- and medium-sized vestibular schwannomas. *J Neurosurg*, **1**, 1–11.

Hardell, L., Carlberg, M., & Hansson Mild, K. (2005). Case-control study on cellular and cordless telephones and the risk for acoustic neuroma or meningioma in patients diagnosed 2000–2003. *Neuroepidemiology*, **25**, 120–8.

Hardell, L., Carlberg, M., Soderqvist, F., & Mild, K.H. (2013). Pooled analysis of case-control studies on acoustic neuroma diagnosed 1997–2003 and 2007–2009 and use of mobile and cordless phones. *Int J Oncol*, **43**, 1036–44.

Hardell, L., Nasman, A., Pahlson, A., Hallquist, A., & Hansson Mild, K. (1999). Use of cellular telephones and the risk for brain tumours: a case-control study. *Int J Oncol*, **15**, 113–16.

Harun, A., Agrawal, Y., Tan, M., Niparko, J.K., & Francis, H.W. (2012). Sex and age associations with vestibular schwannoma size and presenting symptoms. *Otol Neurotol*, **33**(9), 1604–10.

Hasegawa, T., Kida, Y., Kato, T., Iizuka, H., Kuramitsu, S., & Yamamoto, T. (2013). Long-term safety and efficacy of stereotactic radiosurgery for vestibular schwannomas: evaluation of 440 patients more than 10 years after treatment with gamma knife surgery. *J Neurosurg*, **118**(3), 557–65.

Hori, T. & Maruyama, T. (2013). Whether gamma knife radiosurgery is really necessary for treatment of patients with vestibular schwannomas. *Acta Neurochir Suppl*, **116**, 19–23.

Huang, M.J., Kano, H., Mousavi, S.H., et al. (2017). Stereotactic radiosurgery for recurrent vestibular schwannoma after previous resection. *J Neurosurg*, **126**(5), 1506–13.

Ichimura, S., Yoshida, K., Sutiono, A.B., Horiguchi, T., Sasaki, H., & Kawase, T. (2010). Greater petrosal nerve schwannomas-analysis of four cases and review of the litterature. *Neurosurg Rev*, **33**(4), 477–82.

Inskip, P.D., Tarone, R.E., Hatch, E.E., et al. (2003). Sociodemographic indicators and risk of brain tumours. *Int J Epidemiol*, **32**, 225–33.

Interphone Study Group (2011). Acoustic neuroma risk in relation to mobile telephone use: results of the INTERPHONE international case-control study. *Cancer Epidemiol*, **35**(5), 453–64.

Iwai, Y., Ishibashi, K., Watanabe, Y., Uemura, G., & Yamanaka, K. (2015). Functional preservation after planned partial resection followed by gamma knife radiosurgery for large vestibular schwannomas. *World Neurosurg*, **84**(2), 292–300.

Jefferson, G. (1953). The trigeminal neurinomas with some remarks on malignant invasion of the gasserian ganglion. *Clin Neurosurg*, **1**, 11–54.

Jeltema, H.R., Bakker, N.A., Bijl, H.P., Wagemakers, M., Metzemaekers, J.D., & van Dijk, J.M. (2015). Near total extirpation of vestibular schwannoma with salvage radiosurgery. *Laryngoscope*, **125**(7), 1703–7.

Jufas, N., Flanagan, S., Biggs, N., Chang, P., & Fagan, P. (2015). Quality of life in vestibular schwannoma patients managed by surgical or conservative approaches. *Otol Neurotol*, **36**(7), 1245–54.

Kaye, A.H., Hahn, J.F., Kinney, S.E., et al. (1984). Jugular foramen schwannomas. *J Neurosurg*, **60**, 1045–53.

Kemink, J.L., Langman, A.W., Niparko, J.K., & Graham, M.D. (1991). Operative management of acoustic neuromas. *Otolaryngol Head Neck Surg*, **104**, 96–9.

Khrais, T., Romano, G., & Sanna, M. (2008). Nerve origin of vestibular schwannoma: a prospective study. *J Laryngol Otol*, **122**, 128–31.

Kirchmann, M., Karnov, K., Hansen, S., Dethloff, T., Stangerup, S.E., & Caye-Thomasen, P. (2017). Ten-year follow-up on tumor growth and hearing in patients observed with an intracanalicular vestibular schwannoma. *Neurosurgery*, **80**, 49–56.

Komatsuzaki, A. & Tsunoda, A. (2001). Nerve origin of the acoustic neuroma. *J Laryngol Otol*, **115**, 376–9.

Lassaletta, L., Torres-Martin, M., Pena-Granero, C., et al. (2013). NF2 genetic alterations in sporadic vestibular schwannomas: clinical implications. *Otol Neurotol*, **34**, 1355–61.

Lee, J.D., Kwon, T.J., Kim, U.K., & Lee, W.S. (2012). Genetic and epigenetic alterations of the NF2 gene in sporadic vestibular schwannomas. *PLoS One*, **7**, e30418.

Litre, F., Rousseaux, P., Jovenin, N., et al. (2013). Fractionated stereotactic radiotherapy for acoustic neuromas: a prospective monocenter study of about 158 cases. *Radiother Oncol*, **106**(2), 169–74.

MacNally, S.P., Rutherford, S.A., Ramsden, R.T., Evans, D.G., & King, A.T. (2008). Trigeminal schwannomas. *Br J Neurosurg*, **22**(6), 729–38.

Mathiesen, T., Gerlich, A., Kihlström, L., Svensson, M., & Bagger-Sjöbäck, D. (2007). Effects of using combined transpetrosal surgical approaches to treat petroclival meningiomas. *Neurosurgery*, **60**, 982–91.

Mathiesen, T., Svensson, M., Lundgren, J., Kihlström, L., Parisotto, R., & Bagger-Sjöbäck, D. (2009). Hypoglossal schwannoma—successful reinnervation and functional recovery of the tongue following tumour removal and nerve grafting. *Acta Neurochir*, **151**, 837–41.

Meijer, O.W., Weijmans, E.J., Knol, D.L., et al. (2008). Tumor-volume changes after radiosurgery for vestibular schwannoma: implications for follow-up MR imaging protocol. *AJNR Am J Neuroradiol*, **29**, 906–10.

Miller, T., Lau, T., Vasan, R., et al. (2014). Reporting success rates in the treatment of vestibular schwannomas: are we accounting for the natural history? *J Clin Neurosci*, **21**(6), 914–18.

National Institutes of Health (1991). Acoustic neuroma. *NIH Consens Statement*, **9**, 1–24.

Niu, N.N., Niemierko, A., Larvie, M., et al. (2014). Pretreatment growth rate predicts radiation response in vestibular schwannomas. *Int J Radiat Oncol Biol Phys*, **89**(1), 113–19.

Nonaka, Y., Fukushima, T., Watanabe, K., Friedman, A.H., Cunningham, C.D. 3rd, & Zomorodi, A.R. (2016). Surgical management of vestibular schwannomas after failed radiation treatment. *Neurosurg Rev*, **39**(2), 303–12.

Noonan, K.Y., Rang, C., Callahan, K., Simmons, N.E., Erkmen, K., & Saunders, J.E. (2016). Nervus intermedius symptoms following surgical or radiation therapy for vestibular schwannoma. *Otolaryngol Head Neck Surg*, **155**(4), 657–62.

Norén, G., Greitz, D., Hirsch, A., & Lax, I. (1993). Gamma knife surgery in acoustic tumours. *Acta Neurochir Suppl (Wien)*, **58**, 104–7.

Olivecrona, H. (1950). Analysis of results of complete and partial removal of acoustic neuromas. *J Neurol Neurosurg Psychiatry*, **13**(4), 271–2.

Palmisano, S., Schwartzbaum, J., Prochazka, M., et al. (2012). Role of tobacco use in the etiology of acoustic neuroma. *Am J Epidemiol*, **175**, 1243–51.

Park, C.K., Jung, H.W., Kim, J.E., et al. (2006). Therapeutic strategy for large vestibular schwannomas. *J Neurooncol*, **77**, 167–71.

Park, E.S., Lee, E.J., Park, J.B., et al. (2016). A single institution retrospective study of jugular foramen schwannoma management. *World Neurosurg*, **88**, 552–62.

Park, E.S., Lee, E.J., Park, J.B., et al. (2016). A single-institution retrospective study of jugular foramen schwannoma management: radical resection through a retrosigmoid suboccipital approach followed by radiosurgery. *World Neurosurg*, **88**, 552–62.

Patel, S., Nuño, M., Mukherjee, D., et al. (2013). Trends in surgical use and associated patient outcomes in the treatment of acoustic neuroma. *World Neurosurg*, **80**, 142–7.

Pettersson, D., Mathiesen, T., Prochazka, M., et al. (2014). Long-term mobile phone use and acoustic neuroma risk. *Epidemiology*, **25**, 233–41.

Pettersson, D., Wiebert, P., Mathiesen, T., et al. (2014). Occupational exposures and acoustic neuroma risk: a Swedish population-based case-control study [Original paper].

Pollock, B.E., Foote, R.L., & Stafford, S.L. (2002). Stereotactic radiosurgery: the preferred treatment for patients with nonvestibular schwannomas? *Int J Radiat Oncol Biol Phys*, **52**, 1002–7.

Preston, D.L., Ron, E., Yonehara, S., et al. (2002). Tumors of the nervous system and pituitary gland associated with atomic bomb radiation exposure. *J Natl Cancer Inst*, **94**, 1555–63.

Preston-Martin, S., Thomas, D.C., Wright, W.E., & Henderson, B.E. (1989). Noise trauma in the aetiology of acoustic neuromas in men in Los Angeles County, 1978–1985. *Br J Cancer*, **59**, 783–6.

Quaranta, N., Baguley, D.M., & Moffat, D.A. (2007). Change in hearing and tinnitus in conservatively managed vestibular schwannomas. *Skull Base*, **17**(4), 223–8.

Rahimpour, S., Friedman, A.H., Fukushima, T. et al. (2016). Microsurgical resection of vestibular schwannomas: complication avoidance. *J Neurooncol*, **130**(2), 367–75.

Régis, J., Carron, R., Delsanti, C., et al. (2013a). Radiosurgery for vestibular schwannomas. *Neurosurg Clin N Am*, **24**(4), 521–30.

Régis, J., Carron, R., Park, M.C., et al. (2013b). Wait-and-see strategy compared with proactive Gamma Knife surgery in patients with intracanalicular vestibular schwannomas: clinical article. *J Neurosurg*, **119** Suppl, 105–11.

Ron, E., Modan, B., Boice, J.D., Jr., et al. (1988). Tumors of the brain and nervous system after radiotherapy in childhood. *N Engl J Med*, **319**, 1033–9.

Roosli, C., Linthicum, F.H., Jr., Cureoglu, S., & Merchant, S.N. (2012). What is the site of origin of cochleovestibular schwannomas? *Audiol Neurootol*, **17**, 121–5.

Rowe, J., Grainger, A., Walton, L., Silcocks, P., Radatz, M., & Kemeny, A. (2007). Risk of malignancy after gamma knife stereotactic radiosurgery. *Neurosurgery*, **60**, 60–5.

Samii, M., Babu, R.P., Tatagiba, M., & Sepehrnia, A. (1995). Surgical treatment of jugular foramen schwannomas. *J Neurosurg*, **82**, 924–32.

Samii, M., Gerganov, V., & Samii, A. (2006). Improved preservation of hearing and facial nerve function in vestibular schwannoma surgery via the retrosigmoid approach in a series of 200 patients. *J Neurosurg*, **105**(4), 527–35.

Samii, M., Metwali, H., & Gerganov, V. (2016a). Efficacy of microsurgical tumor removal for treatment of patients with intracanalicular vestibular schwannoma presenting with disabling vestibular symptoms. *J Neurosurg*, **17**, 1–6.

Samii, M., Metwali, H., & Gerganov, V. (2016b). Microsurgical management of vestibular schwannoma after failed previous surgery. *J Neurosurg*, **15**, 1–6.

Sass HCR, N.M., West, N., Moeller, N.M., & Cayé-Thomassen, P. (2018). Workup and treatment for vestibular schwannoma. *Ugeskr laeger,* **180**: V02180131.

Schmidt, R.F., Boghani, Z., Choudhry, O.J., et al. (2012). Incidental vestibular schwannomas: a review of prevalence, growth rate, and management challenges. *Neurosurg Focus*, **33**(3), E4.
Schneider, A.B., Ron, E., Lubin, J., et al. (2008). Acoustic neuromas following childhood radiation treatment for benign conditions of the head and neck. *Neuro Oncol*, **10**, 73–8.
Schoemaker, M.J., Swerdlow, A.J., Auvinen, A., et al. (2007). Medical history, cigarette smoking and risk of acoustic neuroma: an international case-control study. *Int J Cancer*, **120**, 103–10.
Schuz, J., Steding-Jessen, M., Hansen, S., et al. (2011). Long-term mobile phone use and the risk of vestibular schwannoma: a Danish nationwide cohort study. *Am J Epidemiol*, **174**, 416–22.
Schuz, J., Steding-Jessen, M., Hansen, S., Stangerup, S.E., Caye-Thomasen, P., & Johansen, C. (2010). Sociodemographic factors and vestibular schwannoma: a Danish nationwide cohort study. *Neuro Oncol*, **12**, 1291–9.
Schwartz, M.S., Kari, E., Strickland, B.M., et al. (2013). Evaluation of the increased use of partial resection of large vestibular schwannomas: facial nerve outcomes and recurrence/regrowth rates. *Otol Neurotol*, **34**(8), 1456–64.
Seol, H.J., Kim, C.H., Park, C.K., Kim, C.H., Kim, D.G., & Chung, Y.S. (2006). Optimal extent of resection in vestibular schwannoma surgery: relationship to recurrence and facial nerve preservation. *Neurol Med Chir (Tokyo)*, **46**, 176–81.
Stangerup, S.-E. & Caye-Thomasen, P. (2012). Epidemiology and natural history of vestibular schwannomas. *Otolaryngol Clin North Am*, **45**(2), 257–68.
Stangerup, S.E., Caye-Thomasen, P., Tos, M., & Thomsen, J. (2008). Change in hearing during 'wait and scan' management of patients with vestibular schwannoma. *J Laryngol Otol*, **122**, 673–81.
Stangerup, S.E., Tos, M., Caye-Thomasen, P., Tos, T., Klokker, M., & Thomsen, J. (2004). Increasing annual incidence of vestibular schwannoma and age at diagnosis. *J Laryngol Otol*, **118**, 622–7.
Stangerup, S.E., Tos, M., Thomsen, J., & Caye-Thomasen, P. (2010). True incidence of vestibular schwannoma? *Neurosurgery*, **67**, 1335–40; discussion 40.
Sughrue, M.E., Kaur, R., Rutkowski, M.J., et al. (2011). Extent of resection and the long-term durability of vestibular schwannoma surgery. *J Neurosurg*, **114**, 1218–23.
Sughrue, M.E., Yang, I., Aranda, D., et al. (2010). The natural history of untreated sporadic vestibular schwannomas: a comprehensive review of hearing outcomes. *J Neurosurg*, **112**, 163–7.
Syed, M.I., Wolf, A., Ilan, O., et al. (2017). The behaviour of residual tumor after the intentional incomplete excision of a vestibular schwannoma: is it such a bad thing to leave some behind? *Clin Otolaryngol*, **42**(1), 92–7.
Thomeer, H., Bonnard, D., Franco-Vidal, V., et al. (2015). Prognostic factors of balance quality after transpetrosal vestibular schwannoma microsurgery: an instrumentally and DHI-based prospective cohort study of 48 patients. *Otol Neurotol*, **36**(5), 886–91.
Tryggvason, G., Barnett, A., Kim, J., Soken, H., Maley, J., & Hansen, M.R. (2012). Radiographic association of schwannomas with sensory ganglia. *Otol Neurotol*, **33**, 1276–82.
Tveiten, O.V., Carlson, M.L., Goplen, F., Vassbotn, F., Link, M.J., & Lund-Johansen, M. (2015). Long-term auditory symptoms in patients with sporadic vestibular schwannoma: an international cross-sectional study. *Neurosurgery*, **77**(2), 218–27.
van de Langenberg, R., Hanssens, P.E., van Overbeeke, J.J., et al. (2011). Management of large vestibular schwannoma. Part I. Planned subtotal resection followed by Gamma Knife surgery: radiological and clinical aspects. *J Neurosurg*, **115**(5), 875–84.
VanSwearingen, J.M., Cohn, J.F., Turnbull, J., Mrzai, T., & Johnson, P. (1998). Psychological distress: linking impairment with disability in facial neuromotor disorders. *Otolaryngol Head Neck Surg*, **118**, 790–6.
Wang, A.C., Chinn, S.B., Than, K.D., et al. (2013). Durability of hearing preservation after microsurgical treatment of vestibular schwannoma using the middle cranial fossa approach. *J Neurosurg*, **119**(1), 131–8.
Wangerid, T., Bartek, J. Jr, Svensson, M., & Förander, P. (2014). Long-term quality of life and tumour control following gamma knife radiosurgery for vestibular schwannoma. *Acta Neurochir (Wien)*, **156**(2), 389–96.
Westerlund, U., Linderoth, B., & Mathiesen, T. (2012). Trigeminal complications arising after surgery of cranial base meningiomas. *Neurosurg Rev*, **35**(2), 203–9.
Wise, S.C., Carlson, M.L., Tveiten, Ø.V., et al. (2016). Surgical salvage of recurrent vestibular schwannoma following prior stereotactic radiosurgery. *Laryngoscope*, **126**(11), 2580–6.
Xenellis, J.E. & Linthicum, F.H., Jr. (2003). On the myth of the glial/schwann junction (Obersteiner-Redlich zone): origin of vestibular nerve schwannomas. *Otol* Neurotol, **24**, 1.
Yang, I., Sughrue, M.E., Han, S.J., et al. (2009). Facial nerve preservation after vestibular schwannoma Gamma Knife radiosurgery. *J Neurooncol*, **93**(1), 41–8.
Yomo, S., Carron, R., Thomassin, J.M., et al. (2012). Longitudinal analysis of hearing before and after radiosurgery for vestibular schwannoma. *J Neurosurg*, **117**, 877–85.
Yoshida, K. & Kawase, T. (1999). Trigeminal neurinomas extending into multiple fossae: surgical methods and review of the literature. *J Neurosurg*, **91**, 202–11.
Yoshimoto, Y. (2005). Systematic review of the natural history of vestibular schwannoma. *J Neurosurg*, **103**(1), 59–63.

RELATED LINKS TO EBRAIN

Histopathology of Nerve Sheath Tumours and Schwannomas. https://learning.ebrain.net/course/view.php?id=470
Management of Cerebellopontine Angle Tumours. https://learning.ebrain.net/course/view.php?id=471
Peripheral Nerve Sheath Tumours. https://learning.ebrain.net/course/view.php?id=468
Stereotactic Radiosurgery for Acoustic Neuromas. https://learning.ebrain.net/course/view.php?id=469

23

Glomus tumours

Omar Pathmanaban and Andrew King

Introduction

Glomus tumours are slow-growing, abundantly vascular tumours, which occur in the anatomically complex jugulotympanic region of the lateral skull base. They are usually benign, but locally invasive, and extend into the adjacent petrous bone, as well as cerebellopontine angle (CPA) and neck in some cases. The tumour spreads through low resistance pathways such as air cells, peri- and intravascular spaces, Eustachian tube, and skull base foraminae, as well as by erosion of bone.

Clinical presentation

Glomus tumours are generally indolent and can progress to a significant size before diagnosis due to a lack of symptoms or subtle symptoms, which are not recognized as a cause for concern. When symptoms become apparent, they are representative of the biological hallmarks of glomus tumours, namely hypervascularity, which produces pulsatile tinnitus in 90% of patients, and local invasion, leading to conductive hearing loss in 80% of patients (Fayad et al., 2010). Otalgia and aural fullness occur in around 10% of patients (Fayad et al., 2010). Other anatomically localizing neurological symptoms relate to the path of invasion in the lateral skull base (**Table 23.1**). Vertigo may occur with labyrinthine incursion and sensorineural hearing loss with cochlear involvement. Cranial nerve palsies vary in frequency between published series and neural invasion may occur in the absence of preoperative deficits because of the functional compensation afforded by slow progression (Makek et al., 1990). Dysphagia and/or dysphonia may be evident at presentation due to compromise of the glossopharyngeal and vagal rootlets at the jugular foramen; the location of these lesions makes any of the lower cranial nerve syndromes possible (**Table 23.2**). Facial motor deficits may be evident in a proportion of patients (Fayad et al., 2010; Jackson et al., 1990; Makek et al., 1990). Facial sensory disturbance and diplopia are sometimes seen due to extension into the CP angle through the jugular foramen or along the petrous face with trigeminal and abducent nerve encroachment, respectively. In the case of a significant intracranial tumour component, focal/lateralizing neurological deficits and or obstructive hydrocephalus can also occur due to brainstem compression. Horner's syndrome may be seen with large tumours secondary to brainstem compression or more likely, damage to sympathetic nerves due to internal carotid artery encasement and invasion. Otoscopy classically reveals a red mass (**Fig. 23.1**) in the middle ear in more than 90% of cases and is sometimes described as having the appearance of the setting sun (Fayad et al., 2010).

Clinical anatomy and classification

Glomus tumours of the cranial base can be broadly categorized using three anatomical descriptions:

- Glomus tympanicum—confined to the middle ear
- Glomus jugulare—confined to the jugular foramen
- Glomus jugulotympanicum—involving both jugular foramen and middle ear

Glomus tympanicum tumours arise from paraganglia along the middle ear course of Jacobson's nerve (inferior tympanic branch of cranial nerve IX). Glomus jugulare tumours (**Fig. 23.2**) may arise from paraganglia associated with the jugular bulb adventitia, along Arnold's nerve (auricular branch of cranial nerve X), or the jugular fossa course of Jacobson's nerve (Forbes et al., 2012). The fragile jugular plate of the middle ear floor (thin cortical bone separating the hypotympanum from the jugular bulb inferomedially) is the path of tumour progression between jugular and middle ear compartments and is the defining anatomical landmark with regards to the name attached to the tumour. With large jugulotympanic tumours, the point of origin is academic and can only be inferred. However, determining the anatomical stage of glomus tumours is clinically important, because tumours restricted to the middle ear can be removed by an otologist via a transtympanic approach and minimal morbidity, whereas advanced tumours require more invasive skull base approaches. The two most commonly used radiology staging systems are the Jackson-Glasscock classification (**Table 23.3**) and the Fisch classification (**Table 23.4**) (Jackson et al., 1982; Fisch and Mattox, 1988).

Table 23.1 Anatomically localizing symptoms

Symptom	Anatomical structure involved
Deafness	Middle ear/Cochlea
Dizziness/Vertigo	Labyrinth/CPA—cranial nerve VIII
Dysphonia	Jugular foramen—cranial nerve X
Dysphagia	Jugular foramen—cranial nerves IX/X
Facial weakness	Petrous bone/CPA—cranial nerve VII
Facial numbness	Petrous apex/CPA—cranial nerve V
Double vision	Petrous apex/CPA—cranial nerve VI
Headache	Brainstem/fourth ventricle—hydrocephalus
Tongue wasting	Hypoglossal canal—cranial nerve XII

Imaging

Combined CT and MR imaging are the modalities of choice for diagnosis and staging of glomus tumours of the temporal bone. Axial and coronal thin section CT imaging clearly delineates the extent of bone invasion, which usually has irregular edges. MR further defines the relationship to skull base neurovascular structures and tumour extension into the CPA (Fig. 23.3). T1-weighted and T2-weighted MR images characteristically show mixed signal intensity described as 'salt and pepper' appearance reflecting hypervascular signal voids (high-flow tumour vessels) together with focal areas of high signal intensity due to intratumoural blood products (Rao et al., 1999). T1-weighted gadolinium enhanced images show avid contrast uptake and demonstrate a smooth tumour contour.

Catheter angiography is not usually required diagnostically in the modern era, but is useful in select cases where the diagnosis is not clear and in all surgical cases (where embolization is performed preoperatively—see treatment section later on in this chapter). A dense hypervascular tumour blush is seen (Fig. 23.4) often with early venous filling due to intratumoural arterio-venous shunting and usually multiple external carotid arterial feeders (notably ascending pharyngeal) with further supply from the internal carotid and/or vertebral arteries in large tumours (Rao et al., 1999).

Other investigations and consultations

Audiometry should be performed to determine hearing loss. Laryngoscopy is performed to assess function of the vocal cords. Endocrinology consultation with plasma and 24-hour urine collection for biochemical measurement of metanephrines and catecholamines is performed in all cases, even when there are no symptoms of catecholamine hypersecretion. This is because a minority of cranial base paragangliomas are secretory and there is also the possibility of multifocality with additional undetected secretory paragangliomas. The more recently available test for 3-methoxytyramine (dopamine derivative) should ideally be checked in all patients. It can be used as biomarker for malignancy and recurrence after treatment as well as risk of haemodynamic instability (Eisenhofer et al., 2012). Genetics consultation should be part of routine management and genetic counselling and testing is advised for all cases even in the absence of family history. The purpose of genetic testing is to determine risk for the individual in terms of tumour progression and synchronous and metachronous tumours. It also allows identification of at-risk family members and counselling regarding parenting options including preimplantation diagnosis. Institutional protocols regarding radiological screening for other tumours vary and include MR imaging and ^{123}I-metaiodobenzylguanidine (MIBG) radioisotope imaging. Our preferred modality is whole body MRI including coronal T1-weighted and STIR sequences and axial fat saturation T2-weighted sequences. Somatostatin receptor scintigraphy and positron emission tomography are also used in some centres for screening purposes.

Table 23.2 Lower cranial nerve syndromes

Syndrome	Nerve palsies
Vernet's	IX, X, XI
Collet-Sicard	IX, X, XI, XII
Villaret's	IX, X, XI, XII, sympathetics (Horner's)

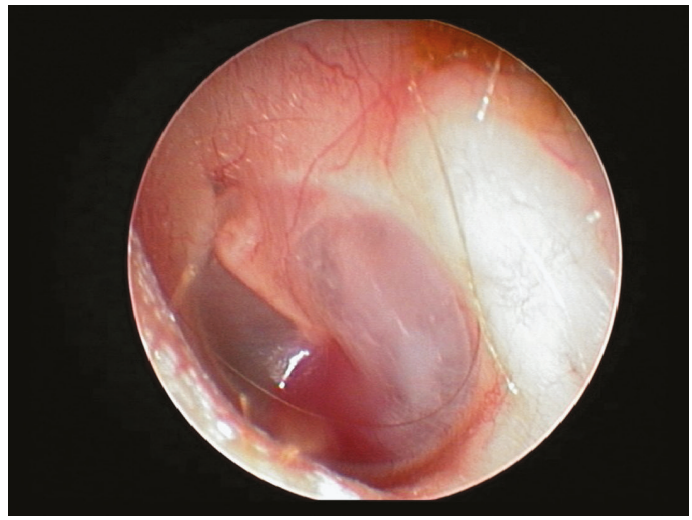

Fig. 23.1 Otoscopic photograph demonstrating the setting sun sign. A characteristic blood red glomus tumour is seen in the middle ear.

Pathology

Origin

Glomus tumours arise from extra-adrenal autonomic paraganglia. Paraganglia have been found to store and secrete catecholamines and are thought to play a homeostatic role, but their physiological purpose in health remains largely unknown (with the notable exception of carotid body oxygen chemoreceptors). They are small neuroendocrine clusters of chief cells derived from the neural crest during embryonic development (Heth, 2004). Neoplasms, including glomus tumours, that are derived from these cells are properly termed paragangliomas and are of the same lineage as phaeochromocytomas; they may retain functional catecholamine production and secretion (DeLellis, 2004). These tumours can be broadly divided into three subgroups:

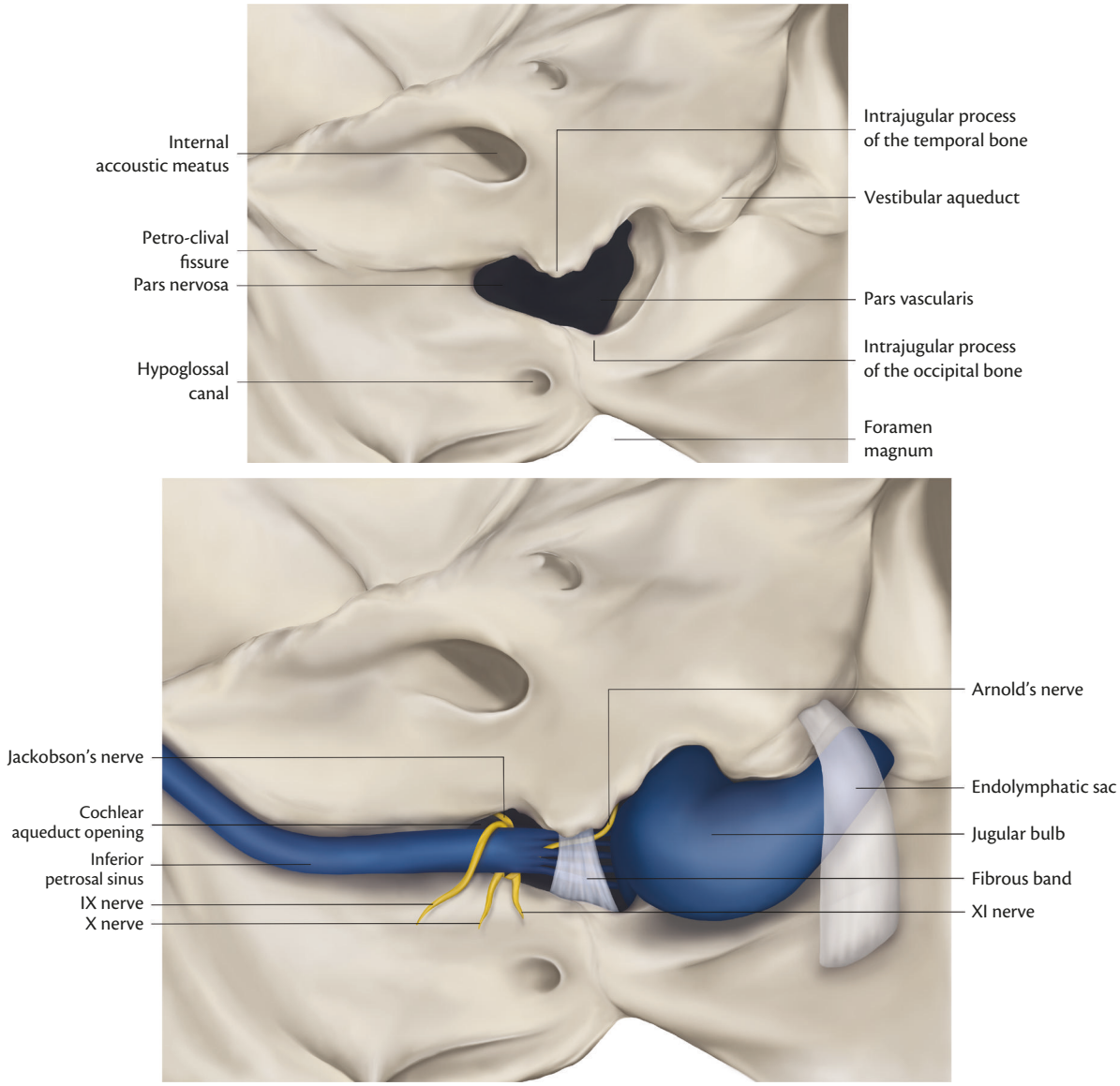

Fig. 23.2 (A) Two classifications exist for the subdivision of the jugular foramen. The traditional division is into pars vascularis containing the sigmoid sinus and CNs X and XI and pars nervosa containing CN IX. Some authors propose an additional subdivision of the pars vascularis into the compartment containing the sigmoid sinus alone lying posteriorly and a further intermediate compartment (the intrajugular compartment) bounded posteriorly by the petro-occipital ligament (a fibrous or osseous band connecting the jugular processes of the occipital and temporal bones) and anteriorly by a dural fold. This intrajugular compartment is described as containing CNs X and XI. There are three compartments of the jugular foramen with the sigmoid part posterolateral and the smaller petrosal anteromedial part harbours the inferior petrosal sinus—'pars vascularis'. The intrajugular processes of the temporal and occipital bones are joined by a fibrous and sometimes osseous band forming the intrajugular septum. The third compartment is intrajugular—'pars nervosa' is between the sigmoid and petrosal parts. [the pars nervosa includes the ninth nerve adjacent to the inferior petrosal sinus while the tenth and eleventh nerves runs with the sigmoid-internal jugular junction in the pars vascularis].
(B) The inferior petrosal sinus joins the sigmoid through openings in the medial wall of the jugular bulb. This connection lies between the ninth nerve anteriorly and the tenth and eleventh nerves posteriorly. These nerves penetrate the dura at the medial margin of the intrajugular process of the temporal bone and pass on the medial aspect of the internal jugular vein. The cochlear aqueduct opening is above the petrosal part near the ninth nerve in the interjugular part. The meningeal branches of the ascending pharyngeal and occipital arteries, the tympanic branch of CN IX 'Jacobson's nerve' entering the tympanic canaliculus to reach the tympanic cavity and the auricular branch of CN X 'Arnold's nerve' entering the mastoid canaliculus located in the anterior wall of the sigmoid part to exit at the tympanomastoid suture are the relevant structures within the jugular foramen with regards to glomus tumours.

- Phaeochromocytomas—intra-adrenal paragangliomas (functional)
- Sympathetic paragangliomas—extra-adrenal arising anywhere along sympathetic chain from cranial base to pelvis (usually functional; also known as chromaffin paragangliomas)
- Parasympathetic paragangliomas—extra-adrenal parasympathetically innervated tumours, which arise at the skull base and in the neck associated with the ninth and tenth cranial nerve branches (rarely functional; also known as non-chromaffin paragangliomas)

Table 23.3 Glasscock–Jackson classification[a]

I	Small tumour involving jugular bulb, middle ear, and mastoid
II	Tumour extending under internal auditory canal; may have intracranial canal extension
III	Tumour extending into petrous apex; may have intracranial canal extension
IV	Tumour extending beyond petrous apex into clivus or intratemporal fossa; may have intracranial canal extension

[a] Adapted from, Glasscock ME 3rd, Jackson CG, Dickins JR, Wiet RJ: Panel discussion: Glomus jugulare tumors of the temporal bone–The surgical management of glomus tumors. *Laryngoscope* 89: 1640–51, 1979 (16) and Willen SN, Einstein DB, Maciunas RJ, Megerian CA: Treatment of glomus jugulare tumors in patients with advanced age: Planned limited surgical resection followed by staged gamma knife radiosurgery—A preliminary report. *Otol Neurotol* 26:1229–34, 2005 (41).

Jugulotympanic glomus tumours belong to the parasympathetic non-chromaffin paraganglioma subgroup.

Histology

Histological sections of paragangliomas (Fig. 23.5) stained with haematoxylin and eosin (H&E) show a thin tumour capsule, a meshwork of fibrovascular stroma rich in thin walled capillary channels surrounding diagnostic nested balls of round or polygonal chief cells (zellballen) and spindle-shaped supporting or sustentacular cells at the periphery. Immunohistochemistry shows positive reaction for antibodies directed against synaptophysin in chief cells and S100 and GFAP in sustentacular cells (Branica et al., 1993). Electron microscopy is not a routine diagnostic investigation, but confirms the presence of neurosecretory granules in the chief cells (Warren et al., 1985). Determination of the grade of tumour is not possible histologically. Sustentacular cells are notably lost in high grade tumours with metastases (Kliewer and Cochran, 1989), but other microscopic features of malignancy such as mitotic figures and necrosis are not reliable and the WHO classification considers metastasis as the only diagnostic criteria for malignancy (DeLellis, 2004).

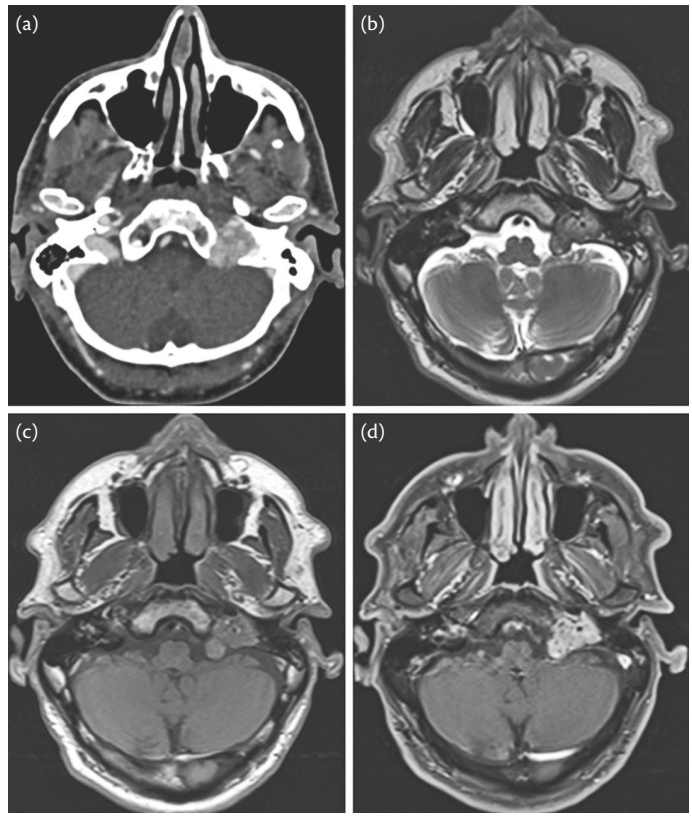

Fig. 23.3 Cross-sectional imaging at the level of the jugular foramen: postcontrast axial CT scan (A), T2-weighted axial MR (B), precontrast T1-weighted axial MR (C), and postcontrast T1-weighted axial MR (D) images demonstrate a typical enhancing glomus jugulare tumour on the left with bone destruction and vascular flow voids.

Table 23.4 Fisch classification

Class	Description
A	Limited to middle ear (glomus tympanicum)
B	Limited to middle ear/mastoid, jugular plate intact, no infralabyrinthine involvement
C	Involving infralabyrinthine part of temporal bone and petrous apex
C1	Carotid foramen involved, but limited vertical carotid canal destruction
C2	Invasion of the vertical section of the carotid canal
C3	Invasion of the horizontal portion of the carotid canal, foramen lacerum spared
C4	Invasion beyond foramen lacerum to cavernous portion of carotid artery
De	Intracranial extradural extension
De1	<2 cm posterior fossa extradural extension
De2	>2 cm posterior fossa extradural extension
Di	Intracranial intradural extension
Di1	<2 cm posterior fossa intradural component
Di2	2–4 cm posterior fossa intradural component
Di3	>4 cm posterior fossa intradural component

From Fisch, U. & Mattox, D. 1988. *Microsurgery of the skull base*, Thieme.

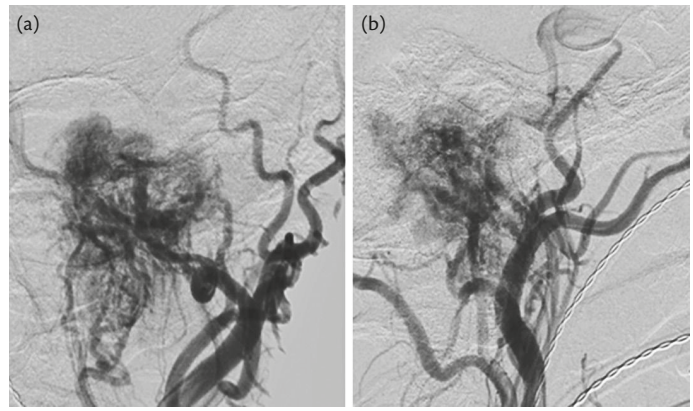

Fig. 23.4 Intra-arterial digital subtraction angiogram: selective catheter angiography of the left external carotid artery demonstrates a glomus jugulare tumour in frontal (A) and lateral (B) projections with a characteristic hypervascular appearance.

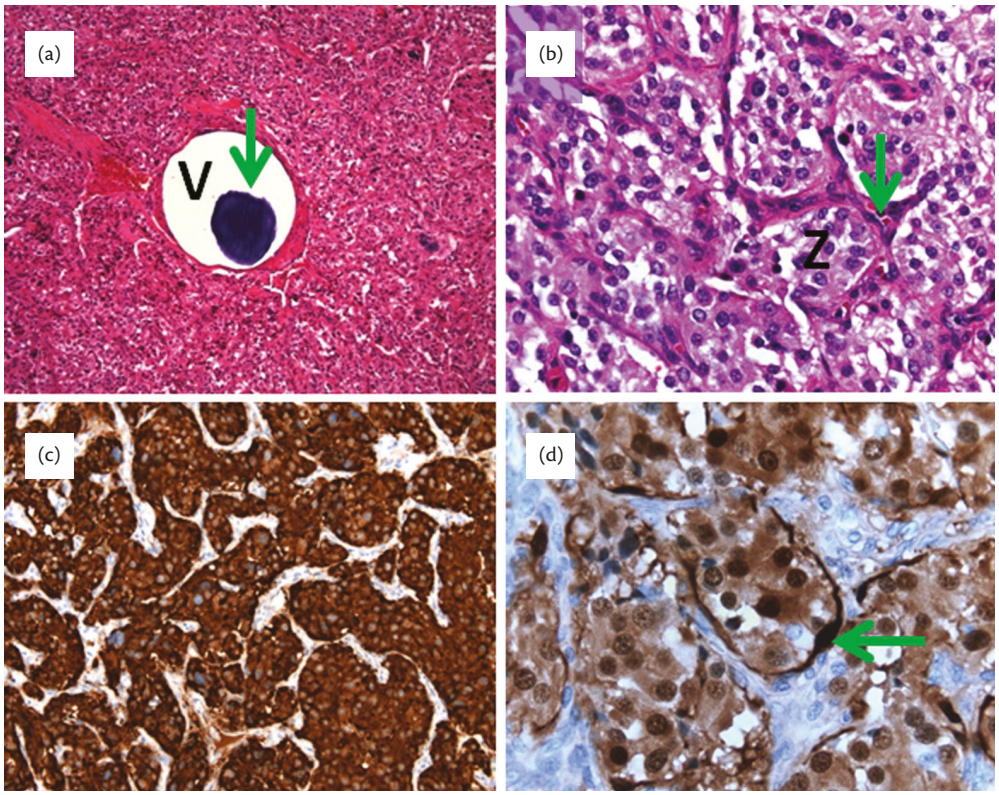

Fig. 23.5 Glomus jugulare histology: H&E stained section from a glomus jugulare tumour (panel A, ×100 original magnification) demonstrating a vessel (V) with endovascular embolization material evident (arrow). A higher power H&E photomicrograph (panel B, ×400 original magnification) showing the 'zellballen' arrangement of tumour cells (Z) with surrounding rich capillary networks (arrow). Immunohistochemistry using antibodies against synaptophysin (panel C, ×200 original magnification) demonstrates diffuse strong immunoreactivity of tumour cells confirming neuroendocrine cell lineage. S100 immunostaining (panel D, ×630 original magnification) demonstrating strong anti-S100 staining of sustentacular support cells surrounding tumour cell nests (nuclear and cytoplasmic staining of tumour cells represents unspecific staining). A bipolar densely staining sustentacular cell (arrow) is clearly seen in association with the centre cell nest as a densely brown staining cell with bipolar projections enveloping the cell ball. Photomicrographs courtesy of Dr Daniel du Plessis.

Epidemiology

These tumours are rare and as such an accurate incidence is not known, despite variable figures found in the published literature. The combined incidence of the phaeochromocytoma-paraganglioma spectrum of neuroendocrine tumours is 0.8 per 100, 000 per year (Beard et al., 1983). Women are affected more often, 4:1 F:M (Reddy et al., 1983). Malignant glomus tumours—defined by systemic metastases—are unusual and it is not clear what the specific incidence is for glomus tumours of the skull base; for paragangliomas at all sites, it has been estimated that the incidence is less than 100 persons per 400 million per year (Welander et al., 2011). Sporadic tumours are often diagnosed in the fifth decade of life, with hereditary disease tending to present earlier.

Risk factors

Environment

It is notable that carotid body hyperplasia is seen at high altitudes and sporadic paragangliomas at this site are more common at high altitudes, particularly in females. Glomus jugulare tumours are also more common in this setting, which may be due to chronic hypoxia, although this remains to be proven (Saldana et al., 1973).

Genetics and hereditary syndromes

Family history of paragangliomas and female sex confer a higher risk of paraganglioma tumorigenesis. Glomus tumours are either sporadic or familial, with recent data suggesting up to 50% of extra-adrenal paragangliomas are familial (Fishbein et al., 2013). In addition, paragangliomas are part of several other genetic syndromes: multiple endocrine neoplasia type 2 (*RET* gene), von Hippel Lindau syndrome (*VHL* gene), neurofibromatosis type 1 (*NF1* gene) and Carney triad/Carney-Stratakis syndrome (Galan and Kann, 2013). Young age, bilateral/multiple tumours, other stigmata of the various syndromes and family history may point to the diagnosis of a genetic syndrome, but it is important that all patients with paragangliomas are referred to a clinical genetics service for comprehensive workup. There are currently at least 15 known susceptibility genes and next-generation sequencing is now the method of choice for genetic testing. A recent consensus document recommends which genes should be included in the test panel (Toledo et al., 2017). Familial paragangliomas are autosomal dominant with variable penetrance and some are exclusively transmitted via paternal mutations due to maternal genetic imprinting. Inherited paragangliomas have been linked to mutations in the genes coding

the subunits of the succinate dehydrogenase (SDH) enzyme, which is important in the Krebs cycle and mitochondrial respiratory chain. There are four genes encoding separate enzyme subunits (*SDHA, SDHB, SDHC, SDHD*) and another coding a protein which flavinates the first subunit (*SDHAF2*). The *SDHx* genes are believed to have tumour suppressor functions. Although the mechanisms and mediators of this are not fully understood, *SDHx* mutations may interfere with cellular oxygen sensing and cause succinate and reactive oxygen ions and peroxides to accumulate, causing stabilization of hypoxia inducible factor-1α and consequent activation of hypoxia signalling cascades (Heth, 2004; Galan and Kann, 2013). Five hereditary *SDHx* paraganglioma syndromes have been discovered to date, each with a different gene mutation (Table 23.5). *SDHD* mutation is the most common and is associated with paraganglioma syndrome 1 (PGL1), which is particularly prevalent in Dutch familial skull base/head and neck paraganglioma patients due to a single founder mutation (Hensen et al., 2011).

Table 23.5 Familial paraganglioma syndromes

Syndrome	Chromosome	Gene	Description
PGL1	11q	*SDHD*	• Paragangliomas / pheochromocytomas • Paragangliomas more common • Multiple in more than half of cases • Usually parasympathetic • Malignancy reported, but uncommon • Paternal transmission (gene maternally imprinted) • High penetrance • Most common familial paraganglioma syndrome
PGL2	11q	*SDHAF2*	• Parasympathetic paragangliomas • Usually multiple • Paternal transmission (gene maternally imprinted) • High penetrance
PGL3	1q	*SDHC*	• Paragangliomas • Mainly parasympathetic • Multiple in a fifth of cases • Malignancy reported, but uncommon • Low penetrance
PGL4	1p	*SDHB*	• Paragangliomas/ pheomochromocytomas • Paragangliomas more common • Multiple in a fifth of cases • Most often sympathetic secreting tumours • Most commonly pelvic/ abdominal/thoracic • Skull base location reported, but unusual • Associated with renal cell carcinoma • Higher risk of malignancy • High penetrance • Relatively young age at diagnosis typical • Relatively poor prognosis • Second most common familial paraganglioma syndrome
PGL5	5P	*SDHA*	• Paragangliomas/ pheochromocytomas • Paragangliomas more common • Sympathetic or parasympathetic • Multiple not described • Malignancy not described • Low penetrance

Treatment and prognosis

Although skull base paragangliomas are generally benign, patients have reduced quality of life (Havekes et al., 2008). Optimal management of glomus tumours is both challenging and controversial (see 'Controversies' section), and requires a personalized approach administered by an experienced multidisciplinary team including neurosurgeons, neuro-otologists, endocrinologists, clinical geneticists, interventional neuroradiologists, radiation oncologists, and pathologists.

Conservative

Glomus tumours are normally slowly progressive and some are static over protracted follow-up. The risks of treatment can therefore exceed the risks of doing nothing in some cases, therefore a watch, wait, and rescan policy is often the first-line management strategy. Initially, a repeat scan at 6 months is performed. Static tumours and slow growing small tumours can be managed conservatively with further interval clinical and imaging review on an annual basis. This surveillance interval is often extended once the indolent behaviour of the tumour is established. A similar approach is sometimes appropriate with larger tumours in older people and those with significant comorbidities. Large tumours, faster growing smaller tumours (particularly in younger patients) and secreting tumours may require treatment with surgery and/or radiation therapy. Established lower cranial nerve deficits ipsilateral to the tumour lower the threshold for treatment, as it reduces the fear of iatrogenic deficits and tends to signal a more invasive tumour phenotype. Treatment decisions have to be made in the context of the patient's genetic status and synchronous tumours. This is most evidently important when there are bilateral tumours with risk of cranial nerve deficits on both sides. In such cases the decision of the team must aim at minimizing the risk of permanent tracheostomy and enteral feeding. The aim is to preserve function, while controlling the tumour.

Surgery

Surgery for glomus tumours has evolved significantly over the last few decades with widespread adoption of multidisciplinary teams, preoperative embolization, intraoperative cranial nerve monitoring, and advanced microsurgical techniques. Glomus tympanicum tumours can be excised totally using neuro-otological transcanal approaches with hearing preservation and minimal morbidity. Therefore, surgery is the treatment of choice in these cases and there is a limited role for radiotherapy. Total excision of glomus jugulare and jugulotympanic tumours can also be attempted via transmastoid-transcervical and infratemporal fossa approaches depending on size and the invaded structures. This is often suitable

when examination (including laryngoscopy) indicates the presence of established lower cranial nerve deficits on the side of the tumour, whereas partial excision (with adjuvant radiation therapy or further observation) is an option to discuss with the patient when lower cranial nerves are functional. The decisions regarding operative approach can be aided by use of the Fisch classification, but each patient is unique and the approach must be tailored. The details of surgical anatomy, approaches, and nuances of technique are dealt with in Chapter 24. These tumours are very vascular and intraoperative haemorrhage can be dramatic, preoperative catheter embolization should therefore be strongly considered in all cases. Carotid balloon occlusion test is indicated where there is internal carotid involvement and study of the contralateral venous sinuses should also be performed, when the jugular venous drainage will need to be sacrificed during surgery. In the hands of an experienced team with all treatment modalities and adjuncts available, there is the possibility of surgical cure, but the risk of postoperative morbidity is high, particularly cranial nerve deficits. Gross total tumour excision is achieved in roughly 80% of patients (even with large tumours) and long-term tumour control can be expected in over 85% of cases. Notably up to 7% of patients reported to have had gross total resection develop recurrence, but less than 1% of patients treated surgically go on to die as a result of tumour progression (Suárez et al., 2013). The most striking drawback to surgery is the high reported rate of new cranial nerve deficits (20–60%, although some will be temporary). Lower cranial nerve palsies can ultimately have fatal consequences, although peri-operative mortality is low, in the region of 1–3% (Makiese et al., 2012). As a result of the cranial nerve morbidity, treatment strategies are moving away from surgery for the majority of patients (excluding glomus tympanicum) and towards radiotherapy in many centres (see 'Controversies' section).

Radiotherapy/radiosurgery

Radiation treatment can be used as primary treatment, adjuvant treatment after partial excision, or as second-line treatment at the point of recurrence or growth of residual tumour. Conformal fractionated radiotherapy, stereotactic radiosurgery, or hypofractionated stereotactic radiotherapy are all used depending on the individual tumour characteristics, patient choice, and available resources. Generally, radiosurgery is suitable for smaller lesions less than 3 cm in diameter and larger lesions require fractionated radiotherapy. The aim of irradiation is to stop growth (control), rather than to eradicate the tumour and in most series, tumour control rates greater than 90% have been observed for all forms of radiation treatment with up to 10 years follow-up in some series. Cranial nerve morbidity is favourable when compared to surgery with some patients even improving after treatment (Tran Ba Huy, 2014). Deaths due to subsequent tumour progression have been reported in around 3% of cases treated with conventional radiotherapy. Treatment-related mortality is also less than 2%. Acute toxicity symptoms are common, but transient, and include headache, nausea, vomiting, mucositis, and weight loss. Long-term xerostomia, dysphagia, and inflammatory otitis media/externa can be problematic for some patients and iatrogenic sensorineural deafness continues to be seen in up to 5% of cases (Suárez et al., 2013; Tran Ba Huy, 2014). Osteonecrosis and brain necrosis were severe complications seen with external beam radiotherapy in the past, but this has been essentially eliminated with newer intensity-modulated conformal and stereotactic methods. Vascular sequelae including carotid stenosis with ischaemic complications can occur, but appear to be unusual, however as younger patients with longer lifespan are now treated, rates of late vascular complications will need to be assessed. Similarly, the rates of late radiation induced malignancy are thought to be low (less than 1/1000), but long-term follow-up, particularly in young patients with many decades to live is required (Tran Ba Huy, 2014).

Drugs

Alpha-blockers are routinely used in patients with secreting tumours, and medication should be commenced several weeks before planned intervention to reduce the risk of dangerous swings in blood pressure and cardiac arrhythmias. Beta-blockers are required less often as these tumours produce nor-adrenaline rather than adrenaline. There is no role for systemic chemotherapy in isolated glomus body tumours, but chemotherapy can induce remission or stability in some cases of metastatic paraganglioma (Patel et al., 1995).

Post-treatment management

All patients, regardless of treatment modality, should be followed up with interval MR scans. Specific post-treatment cranial nerve deficits should be addressed if they are present. Tracheostomy and nasogastric/gastrostomy feeding are usually required temporarily if the lower cranial nerves have been sacrificed. Dysphonia and swallowing problems can improve with speech therapy and where voice problems persist, laryngologists can offer a variety of injection and surgical treatments to help. Facial weakness requires physiotherapy, ophthalmic review, and sometimes reanimation surgery, and is best managed through a specialist facial function clinic. Hearing loss and balance problems can be addressed with hearing aids and vestibular rehabilitation, respectively. Reduced shoulder movement and consequent shoulder pain due to accessory nerve dysfunction should be treated with physiotherapy exercises. Tongue weakness and dysarthria require speech therapy support.

Controversies

There is variability in the management of temporal bone glomus tumours. In particular, the choice of radiation or surgery as the primary treatment has been controversial. Surgery is the mainstay of benign tumour management in essentially all other areas of the body. However, the skull base is unique due to its complex anatomy and delicate neurovascular structures. Despite significant advances in surgery, excision is associated with relatively high cranial nerve morbidity. Cranial nerve function can be protected to some degree by a policy of accepting partial excision, leaving a small amount of tumour over cranial nerves if need be (Wanna et al., 2014). While this was once controversial, this is now seen as a good strategy by most of the skull base community. At the same time, targeted radiotherapy and radiosurgery methodology has evolved to minimize risks, while achieving tumour control in most cases. The severe complications such as osteoradionecrosis and brain necrosis, which used to reinforce the surgical paradigm, are now extremely rarely encountered. As a consequence, radiation treatment has become the

mainstay in many units in recent years. Nevertheless, surgery is still indicated in selected cases:

- Sustained growth after radiotherapy/radiosurgery
- Tumours with CPA or petroclival extension and brainstem compression
- Symptomatic catecholamine secreting tumours (chief cell secretion is radioresistant)

Additionally, there is debate to be had regarding primary treatment modality in the following scenarios:

- Young patients
- Small growing tumours
- Patients with established cranial nerve deficits before treatment

Young patients should therefore be offered the options of surgery or radiosurgery with a discussion about the risks of both including the possibilities of late radiation effects and the lack of quality follow-up data beyond ten years. The risk of cranial nerve injury with surgery is proportional to the size of the tumour (Moe et al., 1999) and so it is also appropriate to have this discussion with patients who have small growing tumours, where the risk of postoperative cranial nerve deficits is likely to be low. Finally, with regards to patients who have established cranial neuropathies before treatment, the main morbidity associated with surgery—cranial nerve injury—is factored out of the equation to some extent, although new deficits such as facial weakness should not be underestimated. Moreover, apparent lower cranial neuropathies found preoperatively are often incomplete and sacrifice during surgery can produce unanticipated swallowing problems by converting to complete impairment. Nevertheless, while a proportion of patients may gain some subjective improvement in nerve function after radiation therapy, most will not and radiation denies them the chance of surgical cure, while still exposing them to the standard risks of radiation. There is undoubtedly therefore still a role for surgery in select cases, but most will be treated with radiation.

It would not be possible to undertake randomized controlled trials to answer these questions because of rarity, need for prolonged follow-up over decades, complex anatomical tumour variability and mixed populations, including older people with comorbidities and patients with and without a variety of germline tumorigenic mutations. Retrospective reviews of published case series, expert opinion and patient choice are therefore all that is available to guide management and it is likely that these complex scenarios will remain controversial for the foreseeable future.

Conclusions

Skull base glomus tumours (paragangliomas) are slow growing benign neuroendocrine tumours, which are locally invasive, but demonstrate low rates of malignant transformation. They are sporadic or familial, in which case *SDHx* mutations are usually implicated. Many patients can be managed with observation and serial imaging alone. When treatment is indicated, radiation and surgery are options, with a recent swing towards radiation treatment for most cases.

REFERENCES

Beard, C.M., Sheps, S.G., Kurland, L.T., Carney, J.A., & Lie, J.T. (1983). Occurrence of pheochromocytoma in Rochester, Minnesota, 1950 through 1979. *Mayo Clin Proc*, **58**, 802–4.

Branica, S., Sprem, N., Danilović, Z., & Seiwerth, S. (1993). Immunohistochemistry of glomus jugulare and tympanicum tumors. *Acta Med Croatica*, **47**, 123–4.

DeLellis, R.A. (2004). *Pathology and Genetics of Tumours of Endocrine Organs*. Paris, France: IARC.

Eisenhofer, G., Lenders, J.W., Siegert, G., et al. (2012). Plasma methoxytyramine: a novel biomarker of metastatic pheochromocytoma and paraganglioma in relation to established risk factors of tumour size, location and SDHB mutation status. *Eur J Cancer*, **48**(11), 1739–49.

Fayad, J.N., Keles, B., & Brackmann, D.E. (2010). Jugular foramen tumors: clinical characteristics and treatment outcomes. *Otol Neurotol*, **31**, 299–305.

Fisch, U. & Mattox, D. (1988). *Microsurgery of the Skull Base*. New York: Thieme.

Fishbein, L., Merrill, S., Fraker, D.L., Cohen, D.L., & Nathanson, K.L. (2013). Inherited mutations in pheochromocytoma and paraganglioma: why all patients should be offered genetic testing. *Ann Surg Oncol*, **20**, 1444–50.

Forbes, J.A., Brock, A.A., Ghiassi, M., Thompson, R.C., Haynes, D.S., & Tsai, B.S. (2012). Jugulotympanic paragangliomas: 75 years of evolution in understanding. *Neurosurg Focus*, **33**, E13.

Galan, S.R. & Kann, P.H. (2013). Genetics and molecular pathogenesis of pheochromocytoma and paraganglioma. *Clin Endocrinol (Oxf)*, **78**, 165–75.

Havekes, B., van der Klaauw, A.A., Hoftijzer, H.C., et al. (2008). Reduced quality of life in patients with head-and-neck paragangliomas. *Eur J Endocrinol*, **158**, 247–53.

Hensen, E.F., Siemers, M.D., Jansen, J.C., et al. (2011). Mutations in SDHD are the major determinants of the clinical characteristics of Dutch head and neck paraganglioma patients. *Clin Endocrinol (Oxf)*, **75**, 650–5.

Heth, J. (2004). The basic science of glomus jugulare tumors. *Neurosurg Focus*, **17**, E2.

Jackson, C.G., Cueva, R.A., Thedinger, B.A., & Glasscock, M.E. (1990). Conservation surgery for glomus jugulare tumors: the value of early diagnosis. *Laryngoscope*, **100**, 1031–6.

Jackson, C.G., Glasscock, M.E., & Harris, P.F. (1982). Glomus tumors. Diagnosis, classification, and management of large lesions. *Arch Otolaryngol*, **108**, 401–10.

Kliewer, K.E. & Cochran, A.J. (1989). A review of the histology, ultrastructure, immunohistology, and molecular biology of extra-adrenal paragangliomas. *Arch Pathol Lab Med*, **113**, 1209–18.

Makek, M., Franklin, D.J., Zhao, J.C., & Fisch, U. (1990). Neural infiltration of glomus temporale tumors. *Am J Otol*, **11**, 1–5.

Makiese, O., Chibbaro, S., Marsella, M., Tran Ba Huy, P., & George, B. (2012). Jugular foramen paragangliomas: management, outcome and avoidance of complications in a series of 75 cases. *Neurosurg Rev*, **35**, 185–94; discussion 194.

Moe, K.S., Li, D., Linder, T.E., Schmid, S., & Fisch, U. (1999). An update on the surgical treatment of temporal bone paraganglioma. *Skull Base Surg*, **9**, 185–94.

Patel, S.R., Winchester, D.J., & Benjamin, R.S. (1995). A 15-year experience with chemotherapy of patients with paraganglioma. *Cancer*, **76**, 1476–80.

Rao, A.B., Koeller, K.K., & Adair, C.F. (1999). From the archives of the AFIP. Paragangliomas of the head and neck: radiologic-pathologic correlation. Armed Forces Institute of Pathology. *Radiographics*, **19**, 1605–32.

Reddy, E.K., Mansfield, C.M., & Hartman, G.V. (1983). Chemodectoma of glomus jugulare. *Cancer*, **52**, 337–40.

Saldana, M.J., Salem, L.E., & Travezan, R. (1973). High altitude hypoxia and chemodectomas. *Hum Pathol*, **4**, 251–63.

Suárez, C., Rodrigo, J.P., Bödeker, C.C., et al. (2013). Jugular and vagal paragangliomas: systematic study of management with surgery and radiotherapy. *Head Neck*, **35**, 1195–204.

Toledo, R.A., Burnichon, N. Cascon, A., et al. (2017). Consensus statement on next-generation sequencing-based diagnostic testing of hereditary phaeochromocytomas and paragangliomas. *Nat Rev Endocrinol*, **13**(4), 233–47.

Tran Ba Huy, P. (2014). Radiotherapy for glomus jugulare paraganglioma. *Eur Ann Otorhinolaryngol Head Neck Dis*, **131**, 223–6.

Wanna, G.B., Sweeney, A.D., Carlson, M.L., et al. (2014). Subtotal resection for management of large jugular paragangliomas with functional lower cranial nerves. *Otolaryngol Head Neck Surg*, **151**, 991–5.

Warren, W.H., Caldarelli, D.D., Javid, H., Lee, I., & Gould, V.E. (1985). Neuroendocrine markers in paragangliomas of the head and neck. *Ann Otol Rhinol Laryngol*, **94**, 555–9.

Welander, J., Söderkvist, P., & Gimm, O. (2011). Genetics and clinical characteristics of hereditary pheochromocytomas and paragangliomas. *Endocr Relat Cancer*, **18**, R253–76.

24

Surgical management of cerebellopontine angle and petrous lesions

Nicholas Hall, Yuval Sufaro, and Andrew H. Kaye

Introduction

At the turn of the twentieth century, Harvey Cushing, the father of neurosurgery, described the cerebellopontine angle (CPA) region of the brain as 'the gloomy corner of neurosurgery', famously comparing this anatomical region with the bloody fence corner of the Gettysburg. With limited magnification and illumination, a modern skull base subspecialist neurosurgeon can understand the huge technical challenges that pioneers such as Cushing would have faced treating large tumours with major pre-existing morbidity in this location. At that stage Cushing advocated subtotal tumour debulking as the only rational strategy, however, shortly after that Dandy began to advocate safe total removal of CP angle tumours.

Since these early days introduction of more sophisticated anaesthesia, perioperative antibiotic prophylaxis, the operating microscope, and cranial nerve monitoring techniques have all resulted in significant advances in CP angle surgery. The concentration of cases in subspecialty centres and the recognition of the importance of experience and meticulous technique has transformed skull base surgery into a subspecialty field with consequent reductions in mortality and morbidity. Although fragile and tenuous anatomical structures, supplying critical function, will always make treatment of pathology in this region a high-risk challenge, frequently, curative outcomes are now achieved with minimal morbidity for patients.

This chapter aims to outline the anatomy and pathology of the CP angle. The chapter describes the presentation of patients and investigations needed to make diagnoses for the different pathologies in this region, and the surgical techniques, approaches, and outcomes that we use to treat these lesions.

Anatomy

An intimate understanding of the complex anatomical relationships, anatomical variants and how the anatomy is distorted by pathological processes is critical to the surgeon's ability to access and treat pathologies located in this beautiful but treacherous angle.

An angular cerebellopontine fissure is formed by the petrosal cerebellar surface folding around the pons and the middle cerebellar peduncle with superior and inferior limbs extending from the angle. Within the angle are three subcompartments: superior, middle, and inferior. Each of the compartments contains an arterial supply, a portion of the brainstem, part of the fissure, and a series of cranial nerves.

The superior compartment contains the superior cerebellar artery (SCA), midbrain surface, cranial nerves III, IV, and V, the superior cerebellar peduncle, and the cerebellomesencephalic fissure. The neurovascular complex runs across the cerebellomesencephalic cistern.

The middle compartment contains the anterior inferior cerebellar artery (AICA), the seventh and eighth nerve complex, the anterolateral surface of the pons, the middle cerebellar peduncle, and the cerebellopontine fissure. At the apex of the middle compartment lies the foramen of Lushka medial to which is the lateral recess of the fourth ventricle. The flocculus of the cerebellum lies rostral and slightly posterior to the lateral recess out of which choroid plexus runs.

The inferior CPA contains the lower cranial nerves IX–XII, the posterior inferior cerebellar artery, and the lateral surface of the medulla, the inferior cerebellar peduncle, and the cerebellomedullary fissure. The sixth cranial nerve runs near the base of the fissure in a line containing the superior and inferior limbs of the fissure. The complex anatomy of the cranial nerves, arteries, veins, and cerebrospinal fluid (CSF) arachnoid cisterns, as well as the anatomical variations of these structures, is described comprehensively by Albert Rhoton (Rhoton, 2007).

The cranial nerves traverse across the arachnoid cisterns to enter their respective foraminae within the skull. The hypoglossal nerve runs from the medulla, in a line continuous with the ventral spine nerve roots and anterior to the olive, to enter the hypoglossal foramen in the occipital condyle. The accessory nerve is formed from both spinal and cranial components from the medulla on the inferior third, anterior to the olive and the upper cervical cord. These multiple rootlets are immediately below the brainstem origin of the inferior rootlets of the vagus, which may be indistinguishable as they all run forwards as multiple rootlets to enter the pars vascularis of the jugular foramen. The glossopharyngeal nerve is composed of one or two more substantial trunks that leave the brainstem posterior to the olive, coursing ventral to the choroid plexus and entering the jugular foramen separately to the vagus and accessory nerves within the

pars nervosa. The facial nerve arises from the brainstem at the lateral end of the pontomedullary sulcus 1–2 mm anterior to where the vestibulocochlear nerve enters the brainstem at the lateral end of the sulcus. At the brainstem, the facial and vestibulocochlear nerves are most widely separated joining and running almost together in the pontocerebellar cistern. The AICA frequently passes below or between the brainstem origin of the VII and VIII nerves. The V cranial nerve arises at the midpoint of the pons and runs obliquely forwards from the lateral pons towards Meckel's cave, sitting in the trigeminal impression on the apex of the petrous temporal bone. There is considerable variability of the rotational axis of the trigeminal nerve as it runs across the cistern in close proximity to the superior cerebellar artery.

Presentation of cerebellopontine angle lesions

The different pathologies and their size result in considerable variability of clinical presentation. Smaller lesions may be found either incidentally, as part of the work up for common ailments such as headache, or with specific symptoms related to the location of the lesion and its surrounding structures such as hearing loss and dysequilibrium in the case of vestibular schwannomas. The tempo of onset and the specific neurological symptoms, respectively, give important clues to the type of pathology and the location of the lesion. Vascular, ischaemic pathology and haemorrhage present with hyperacute symptoms over a period of seconds and minutes. Rapidly growing lesions such as metastasis may cause acute hydrocephalus and typically present over days to weeks, but the vast majority of CP angle lesions are slow growing and present more insidiously over months or even years.

The specific neurological features give important clues to the location and type of pathology. Lesions in the upper CP angle often present with trigeminal hypoaesthesia or occasionally facial pain or diplopia. Anterior petroclival lesions may present with diplopia from sixth nerve palsies. Mid-CP angle lesions present with symptoms affecting the seventh and eighth cranial nerve complex, more commonly with dysequilibrium and hearing loss than facial weakness, which may be a sign of a facial neuroma. Lower CP angle lesions may present with a hoarse voice, cough, or recurrent chest infection from aspiration. Larger lesions present with symptoms consistent with hydrocephalus these ranging from headache, nausea, vomiting, and visual deterioration to memory and gait disturbance. Brainstem and cerebellar compression in the largest lesions may present with progressive gait deterioration, weakness, and spasticity followed ultimately by coma and death.

The most common lesion arising within the CP angle is the acoustic neuroma, accounting, over multiple case series, for between 78 and 85% of CP angle lesions (House, 1964; Moffat and Ballagh, 1995). The second most common tumour in this region is the meningioma accounting in Moffat's 1993 series of 305 tumours from Addenbrookes, Cambridge, for 6.5% of tumours (Moffat et al., 1993) and in Revilla's seminal 1947 series for 6%. The third most common lesion within this region is the epidermoid cyst accounting for 4.6 and 6%, respectively. Other lesions in this location have been described but in total account for only 2.7% of lesions. Rare differentials include glomus jugulare lesions 1.7%; other schwannomas: facial 1%, trigeminal 1%, arachnoid cyst 0.7%, and metastasis 0.7%. Other very rare, differential diagnoses include: aneurysm, arteriovenous malformation, choroid plexus papilloma, lipoma, lymphoma, ependymoma, medulloblastoma, chordoma, chondrosarcoma,

Fig. 24.1 Anatomical representation of posterior fossa components. Colours correlate with Table 24.1.

endolymphatic sac tumour, and cholesterol granuloma. The imaging characteristics on MRI and CT can lend considerable help to differentiation of many of these diagnoses and many of the lesions have characteristic appearances. Bonneville elegantly described a segmental approach to the radiological diagnosis of rare CP angle lesions (Fig. 24.1 and Table 24.1) (Bonneville et al., 2001).

The presenting features of differential diagnosis may lend clues to the type of lesion with sparing of hearing and involvement of facial or trigeminal nerves seen more commonly in both the presentation of meningioma and other cranial nerve schwannomas. Other particularly pertinent imaging characteristics for differentiation of lesions include the expansion and remodelling of the internal auditory meatus (IAM) in schwannomas of the VII/VIII nerve complex, the presence of a dural tail and flat base in meningiomas and the presence of CSF-like signal properties, low T1, high T2, in epidermoid tumours with concurrent gross diffusion restriction (high-signal DWI, low-signal ADC map) (Bonneville et al., 2001).

Presentation of patients with vestibular schwannomas

Although the typical presenting symptoms for acoustic neuroma are unilateral hearing loss, tinnitus, and dysequilibrium, there is emerging an increasing group of patients representing 5–12% of presentations with asymptomatic tumours identified incidentally on MRI (Selesnick et al., 1999).

Hearing loss is the most common presenting symptom with numerous historical case series reporting rates of hearing loss at 94–96% (Tos and Thomsen, 1984; Hardy et al., 1989; Kentala and Pyykkö, 2001). Typically, patients experience difficulty with speech discrimination and high-frequency sensorineural loss (Johnson, 1977). The duration of symptoms prior to presentation has been

Table 24.1 Segmental approach to differential diagnosis of CPA lesions based on site of origin

Cisterns	Epidermoid cyst Dermoid cyst Lipoma Neuroenteric cyst Neuroepithelial cyst	Meninges	Meningioma Arachnoid cyst Metastasis
Arteries	Aneurysm Ectasia	Nerves	Acoustic neuroma Facial neuroma CN V, VI, IX, -XII neuroma
Skull base	Cholesterol granuloma Paraganglioma Petrous apicitis Chordoma Chondrosarcoma Endolymphatic sac tumour Pituitary adenoma	Parenchyma/Ventricle	Pilocytic astrocytoma, glioma, metastasis, haemangioblastoma, ependymoma, medulloblastoma, lymphoma, papilloma, DNET

Reproduced from Bonneville, F., Sarrazin, J.L., Marsot-Dupuch, K., et al, Unusual Lesions of the Cerebellopontine Angle: A Segmental Approach, *RadioGraphics*, Vol. 21, No. 2, March 2001 with permission from RSNA.

reported as 3–8 years (Thomsen et al., 1983). Dysequilibrium or vertigo is another common finding in patients with an acoustic neuroma secondary to involvement of the vestibular nerve. This symptom is reported in 50–77% of patients (Hardy et al., 1989; Kentala and Pyykkö, 2001) though it is unusual for this to be the major presenting feature. 47% of patients experience brief episodes of giddiness lasting between 2 seconds and 5 minutes, while 32% of patients had longer attacks lasting up to a few hours. Subtle abnormalities of balance may be detected in patients using the Unterberger's stepping test. In this test, the patient is asked to stand upright with eyes closed and arms outstretched at 90 degrees to the trunk, and to march on the spot. The result is positive if the patient deviates more than 50 cm or in excess of 30 degrees from the spot. More severe ataxia may be found in association with larger tumours and cerebellar dysfunction.

Tinnitus is another common feature at presentation being found in 57–83% of patients. Tinnitus is rarely found in isolation, accounting as the sole presenting complaint in 3% of patients. In his series of 1000 patients, Samii evaluated the preoperative symptoms and found that tinnitus became less common as tumour size increased from 86% in pure intrameatal tumours to 51% in tumours with brainstem compression (Matthies and Samii, 1997).

Cerebellar dysfunction is a common presenting feature in larger tumours, present in 58% of patients if the tumour is more than 4 cm in diameter. Cerebellar dysfunction is commonly picked up with an abnormal finger to nose test and abnormal gait.

Nystagmus is a common sign at the time of presentation and may be of different types depending on the location of compression. Large tumours causing significant compression of the pontine gaze centre may present with opticokinetic nystagmus or Bruns' nystagmus. Bruns' nystagmus comprises coarse ipsilateral horizontal nystagmus and high-frequency fine nystagmus to contralateral gaze. Vestibular nystagmus in smaller tumours manifests as fine horizontal nystagmus beating away from the lesion (Kaye and Laws, 2012).

Cranial neuropathy is found more rarely presenting with subtle trigeminal hypoesthesia often in the V2 distribution in Samii's series in 18% of patients. Rates increase with larger tumours to up to 32% (Matthies and Samii, 1997). Facial weakness is also unusual but can be identified with absence or delay of the blink reflex. This sign may be found in up to 17% of patients (Matthies and Samii, 1997). Loss of sensation in the posterior aspect of the external auditory meatus is common and is secondary to nervus intermedius involvement.

Headache is another common presenting feature found in 20–85% of patients (Stucken et al., 2012). Headache is often the cause for investigations leading to the finding of an incidental acoustic neuroma on MRI or CT brain scans.

Raised intracranial pressure was common in early reports of acoustic neuroma causing the constellation of symptoms of headache, nausea, vomiting, decreased vision, diplopia, papilloedema, and altered consciousness. In Cushing's 1917 series, 66% of patients were reported to have diplopia (Cushing, 1917) compared to only 3% in a more recent study published from UCSF (Selesnick et al., 1993).

Less commonly (1.8%), the abducent nerve is involved producing lateral gaze diplopia (Matthies and Samii, 1997). Rare cases have been described of trigeminal neuralgia, hemifacial spasm, and sudden hearing loss in relation to acoustic neuroma presentation (Matthies and Samii, 1997).

Further evaluation of cerebellopontine angle lesions

Radiological evaluation

Advances in the radiological tools available to clinicians have undoubtedly changed the landscape of diagnosis of skull base and CP angle lesions. From the early days of the use of plain radiographs to image the 'petrous pyramid' in 1910, through the era of pneumoencephalography and contrast myelography, we have moved on to the combination of CT and MRI as our gold standard tools. In diagnostic terms the sensitivity and specificity of MRI in the diagnosis of acoustic neuroma has been reported to be as high as 100% (Brackmann and Kwartler, 1990; Newton et al., 2010). The addition of gadolinium contrast sequences and fine slice acquisition sequences such as heavily saturated T2 fast spin echo and 3DFT-CISS, allow vestibular schwannomas as small as 3 mm to be detected with sensitivity and specificity rates of 97 and 96% (Stuckey et al., 1996; Naganawa et al., 1998).

The typical MRI appearance of vestibular schwannoma is that of a tumour within and usually expanding the IAM, extending variably into the CP angle. The tumour is low signal on T1 sequences and on T2 is low signal compared to CSF and high signal compared to the

pons. Meningiomas in comparison to schwannomas have a broad dural base, are more likely to be isointense to brain on T1 and T2 images precontrast and vividly enhance with gadolinium. CP angle meningiomas are rarely centred on the IAM and when they are do not usually expand the IAM. The shape of meningiomas is typically said to be more oval in the CP angle than the rounder vestibular schwannoma and the meningioma may also have a dural tail sign, not present with schwannomas. Epidermoid tumours have a characteristic MRI appearance, isointense to CSF on T1 and T2 sequences with no gadolinium enhancement but strong diffusion restriction on DWI and ADC map sequences.

Though not necessary in diagnostic terms, CT scans may be useful in the evaluation of CP angle lesions. Expansion of the IAM is better visualized on CT than MRI and calcification is well identified on CT and seen in approximately 25% of meningiomas. We routinely use CT as an adjunct to surgical planning as it provides valuable information regarding the extent of aeration of the petrous temporal bone, the presence of perimeatal air cells and the bony anatomy of the jugular bulb. We use this information to determine the suitability for the translabyrinthine approach and for the extent of drilling of the lateral internal auditory canal in a retrosigmoid approach for removal of a tumour invaginating the canal. In the presence of CP angle tumours involving the petrous temporal bone such as cholesteatoma or glomus jugulare tumours, anatomical information regarding the bony anatomy of the fallopian canal, the medial wall of the jugular foramen and the middle ear is also crucial for surgical planning during exposure.

Audiometry

Given that vestibular schwannomas represent 75–85% of CP angle lesions and characteristically present with hearing loss, the use of audiometry is an important part of the preoperative evaluation of CP angle lesions. As all CP angle surgery has a risk of hearing deterioration it is also important to have a hearing baseline evaluation. In addition, some approaches which may optimize tumour access and resection such as the translabyrinthine approach, result in unilateral deafness. The improved access and subsequent minimization of operative morbidity may make this a preferred approach but the presence of pre-existing contralateral normal hearing must be determined so as to ensure the approach does not render the patient deaf.

Pure-tone audiogram (PTA) thresholds in patients with acoustic neuroma range from 5 to 130 dB with a mean threshold of 66.5 dB. Some 16% of patients have complete loss of hearing precluding testing. 65% of patients have high-frequency loss and 22% have flat type loss (Johnson, 1977; Stucken et al., 2012). Poor speech discrimination is a typical feature of retrocochlear pathology. In Johnson's 1977 study, 24% of 500 patients with acoustic neuroma had no speech discrimination, while 56% had speech discrimination scores (SDS) of 60% or less.

The combination of PTA and SDS form the basis of several definitions for 'serviceable' and 'salvageable' hearing, which are used to assess patients with acoustic neuroma for potential hearing preservation surgery. The Gardner Robertson scale for hearing function classifies patients into excellent, serviceable, non-serviceable, poor, and non-hearing (Table 24.2) with 0–30 dB on PTA and 70–100% SDS being associated with the best chances of hearing preservation.

Auditory brainstem responses (ABRs) measure the synchronized response of neurons in the lower auditory pathways in response to a stimulus. The ABR became an established tool to screen patients for acoustic neuromas after expansion of their application from a research to clinical application in 1977 by Selters and Brackmann (Selters and Brackmann, 1977). ABR involves generating a stimulus and measuring the evoked response. The most commonly used stimulus is the 100 μs click. The response is recorded from scalp electrodes and is displayed as a predictable series of waves that are labelled waves I to V. Waves I and V are the most predictable and respectively demonstrate activity from the cochlear nerve and the neurons of the inferior colliculus. The most reliable latency between waves is the interaural wave I to V latency difference known as IT5. A test latency difference of more than 0.2 ms is abnormal (Selesnick and Jackler, 1992). The sensitivity of the test for diagnosing acoustic neuromas was initially reported as being excellent, with sensitivity reported between 93 and 100% and specificity of 90% (Stucken et al., 2012). Since the introduction of MRI, these figures have been shown to be less accurate with sensitivity of 63–95%; this is particularly the case with small tumours of less than 1 cm where accuracy rates of 58% are cited (Schmidt et al., 2001). The discovery that ABRs were not as sensitive as previously thought led to the development of stacked ABRs. These represent a measurement of essentially all of the VIII CN fibres not just a part and so does not depend so much on size and location of the tumour. In 2005, Don et al. published a series of 54 patients with small tumours demonstrating 95% sensitivity and 88% specificity (Don et al., 2005).

Facial nerve function

Preoperative evaluation of facial nerve function is an important part of diagnostic evaluation. The presence of subtle weakness in vestibular schwannomas is cited in up to 17% of patients though only

Table 24.2 Gardner Robertson hearing classification

Gardner Robertson class	Description	Speech discrimination score (SDS)	Maximum pure-tone audiogram (PTA)
I	Good	70–100%	0–30 dB
II	Serviceable	50–69%	31–50 dB
III	Non-Serviceable	5–49%	51–90 dB
IV	Poor	1–4%	91 dB to max
V	Non	0%	Not testable

Reproduced with permission from Gardner G, Robertson JH, Hearing preservation in unilateral acoustic neuroma surgery, *Annals of Otology, Rhinology & Laryngology*, Volume 97, pp. 55–66, Copyright © 1988, SAGE.

one-third of patients have awareness of symptoms (Matthies and Samii, 1997). Larger tumours causing displacement of the brainstem and fourth ventricle have reported rates of 26% (Matthies and Samii, 1997). Subtle weakness may be detected as slowing in the efferent arc of the blink reflex, a small proportion of patients will have altered taste and a larger proportion of patients will demonstrate hypoaesthesia in the posterior external auditory meatus.

Pre- and postoperative facial nerve function should be documented and numerous scales exist to assess facial nerve function. The long-recognized system devised by House in 1985 has widespread acceptance and most postoperative outcomes to date have been reported based on this scale (House and Brackmann, 1985; also see Chapter 22). This scale though has received widespread criticism as it does not allow individual assessment of each area of the face. Of the 19 validated facial nerve assessment tools, only the Sunnybrook system (Ross et al., 1996) scores each facial nerve territory, examines static and dynamic activity and synkinesis with good interobserver reliability (Fattah et al., 2015).

Patients with significant preoperative facial weakness and a CP angle lesion may be suspected of having a facial neuroma. Facial neuromas typically extend laterally beyond the internal auditory meatus and into or beyond the fundus of the IAM.

Operative treatment of CP angle lesions

The complex algorithm for determining the optimal surgical approach for CP angle and petrous lesions must take into account a multitude of factors such as the anatomical location of the lesion, its size, hearing status on the approached side, bony and sinus anatomy of the patient, and the imaging characteristics of the lesion.

The surgical approaches to the posterior fossa can be categorized into the presigmoid and retrosigmoid approaches. While the retrosigmoid approach involves a craniotomy or craniectomy of the occipital bone, the presigmoid approaches mandates drilling out of the petrous bone to allow access to the dura and posterior fossa pathology, anterior to the sigmoid sinus, with minimal brain retraction. The term presigmoid usually refers to posterior petrosal approaches, which are all extensions of the basic mastoidectomy. Included under this category with a progressively increasing extent of petrous bone resection from posterior to anterior are the retrolabyrinthine, translabyrinthine, and the transcochlear approaches. These allow a surgical corridor into the CPA, specifically to the middle and upper thirds of the clivus. The more anterior the petrous bone resection, the wider the surgical corridor into the posterior fossa (Fig. 24.2). The retrolabyrinthine approach, almost never used in isolation, spares the vestibular organ, thus being the least morbid of the three approaches, while the translabyrinthine approach involves its resection therefore inevitably resulting in hearing loss. Further resection of the cochlea requires transposition of the facial nerve and the possibility of at least partial facial nerve injury, thus increasing approach related morbidity significantly. Some modifications to the transpetrosal approaches have been described, aimed to address the high associated cranial nerve morbidity while allowing improved surgical exposure. In the trancrusal approach, selective resection of the posterior and superior semicircular canals from ampulla to common crus, allows for exposure in the range close to that of the translabyrinthine approach while providing a substantial chance of preserving hearing. Hearing preservation outcome reports with this approach are scant, mainly owing to its infrequent use due to the highly specific skills

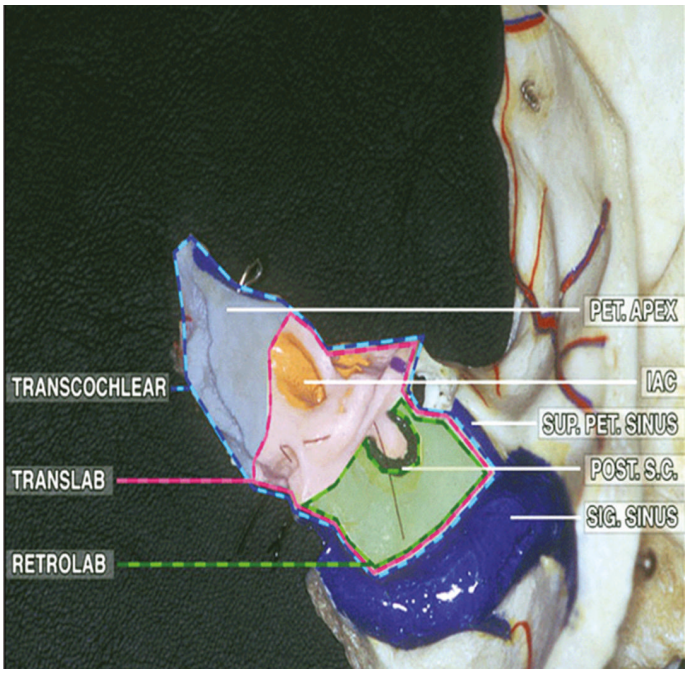

Fig. 24.2 Three-dimensional demonstration of the bone resection for the transpetrosal approaches.

needed. However, it is reported to be 58–100% (Sekhar et al., 1999; Horgan et al., 2001; Kaylie et al., 2004; Brandt et al., 2010). In the transotic approach, the otic capsule is entered with complete removal of the semicircular canals and skeletonization of the facial nerve. As in the transcochlear approach, hearing is lost but facial nerve morbidity is reduced. Similarly to the transcrusal approach, outcome data for the transotic approach is not robust. The reporting of facial nerve functional outcome is often equivocal. Most of the studies available refer to HB I–II as good facial functional outcome. Reports of HB I-II at long-term follow-up vary from 27% to 90%. The type of pathology also plays a role. When the transotic approach was applied for resection of petroclival meningiomas, functional results of the facial nerve differed to a greater degree (De la Cruz and Teufert, 2009; Gurgel et al., 2012; Miller et al., 2015).

In general terms the retrosigmoid approach offers wide access to the CP angle. With this approach lesions are resectable across the whole of the CP angle from tentorium to foramen magnum. If smaller lesions lie medial to the petro-occipital synchondrosis the retrosigmoid approach allows limited access without unacceptable morbidity from brainstem retraction. Larger clival and petroclival lesions enable anterior access as the tumour has effectively opened a dissection corridor by displacing the brainstem during its slow growth. The retrosigmoid approach is limited superiorly by the tentorium and lesions that extend above the tentorial hiatus or beyond the petrous apex into the middle fossa are difficult to resect completely using this approach alone. In this circumstance either a staged or combined middle fossa–presigmoid approach allows access above the tentorium and the petrous apex.

In larger lesions centred around the IAM such as large vestibular schwannomas we prefer to utilize the translabyrinthine approach. This has the advantage of minimizing cerebellar retraction by rotating the angle of approach to the tumour buried into the cerebellar hemisphere, it also shortens the working distance between surgeon

and tumour allowing greater instrument control. With adequate exposure by an experienced surgeon the translabyrinthine approach allows even the largest schwannomas to be removed. Anatomical factors that may make this approach less desirable include a high dominant jugular bulb, a poorly pneumatized mastoid, and an anteriorly placed sigmoid sinus. These factors all reduce the working space within this approach and reduce the angle available for visualization particularly of the inferior and brainstem aspects of a larger tumour.

A combined presigmoid middle fossa approach gives excellent exposure for lesions located anterior to the cranial nerves, but with increased morbidity related to the approach. The commonest is the combined retrolabyrinthine middle fossa craniotomy which allows visualization of tumours antero-lateral to the upper pons and lower midbrain especially if there is extension into the middle fossa.

For lesions predominantly at the petrous apex and within the middle fossa, such as many trigeminal schwannomas, the widest access for optimal resection would usually be provided via a predominantly middle fossa, subtemporal approach with the possibility of further petrous apex removal via approaches such as the Kawase approach. The borders of the Kawase triangle are defined by the V3 division of the trigeminal nerve anteriorly, the greater superficial petrosal nerve laterally, the arcuate eminence posteriorly, and the superior petrosal sinus medially. This approach is also referred to as the anterior petrosal approach. In these lesions it is common for much of the bone to be already eroded by the tumour itself. In the case of intracanalicular tumours with minimal CP angle extension and intact hearing a middle fossa approach to the IAM also facilitates removal.

While the anatomical location and size of the lesion play a major part in the decision-making algorithm, temperance must be exercised. In patients with significant comorbidities or advanced age, the optimal choice of approach may be simply the least invasive approach. In this situation the goal of surgery might change from complete excision of the tumour to decompression of the brainstem and cerebellum with a limited debulking procedure via a retrosigmoid approach. The surgeon's hubris for complete tumour excision must be constrained in situations of high morbidity such as in facial or lower cranial nerve schwannomas or in patients with NF2 where hearing preservation is a maxim.

In addition, the expected tumour consistency and vascularity of the lesion play a part in determining the ideal approach. Tumours with high T2 signal might be expected to be less firm and allow intracapsular debulking and mobilization from surrounding neurovascular structures with greater ease. Conversely a tumour with an expected high vascularity or firm consistency may require a more elaborate approach to maximize access and give the operator shorter, better angles for tumour removal.

In some cases, particularly where a tumour extends widely from anterior to posterior cranial fossae multiple staged approaches are required.

Retrosigmoid approach

The retrosigmoid approach is ideal for vestibular schwannomas where hearing preservation is being attempted. We also favour this approach for many other tumours centred on the petrous temporal bone. This approach also lends itself to access larger more anterior lesions such as petroclival meningiomas, and is especially useful in the older and more medically frail population where extended anaesthetic duration or temporal lobe manipulation may be less well tolerated. For the majority of epidermoid tumours this approach allows safe removal of the tumour and the angled endoscope can facilitate complete removal.

Positioning: Although numerous positions are described for this approach, we favour the lateral or park-bench position. The patient is placed laterally on the operating table with the operative side up. The contralateral axilla with an axillary roll is at the uppermost end of the table with the contralateral arm held in a sling attached to the arm gutter for the ipsilateral arm. Both legs are flexed and two pillows placed transversely between them. The hips are taped to the table and a back support placed mid-torso to which the ipsilateral shoulder is taped gently. The head is held in a three-pin head holder, and flexed and rotated 10–15° towards the floor. At this time, a lumbar CSF drain is usually placed. Continuous electrophysiological monitoring for facial nerve function during the operation is essential. For tumours low within the CP angle we also favour monitoring of lower cranial nerves using an endotracheal tube with vocal cord monitoring, a soft palate electrode, and trapezius electrode. We occasionally utilize the semi-sitting position for large patients with short necks.

Incision and exposure. A slightly sigmoid incision is made 1 cm posterior to the mastoid from approximately 2.5 cm above the transverse sigmoid junction to below the level of the mastoid tip. The inferior end of the incision is curved away from the mastoid tip so as to avoid the deeply placed vertebral artery coursing around the transverse process of C1 (**Fig. 24.3**). The muscles and fascia are reflected from the suboccipital region, lateral to the digastric groove. A burr hole is then made at the level of the asterion and the hole widened to expose the transverse sigmoid junction. Further burr holes are made posteriorly to expose the transverse sinus and inferiorly over the thin occipital bone and the craniotomy is completed. Care must be taken to preserve the dura and ensure the more superficially placed sinuses are not damaged during exposure and that the frequently placed mastoid emissary vein is skeletonized away from the sinus and coagulated and divided away from the sinus wall. We find the use of a 5 mm coarse diamond burr helpful to safely skeletonize the sinus. The dura is opened in an asymmetrical Y shape, basing the edges of the opening on the sigmoid and transverse sinuses. Prior to opening the dura 5–10 ml of CSF is drained via the lumbar catheter. This relaxes the dura and the contents of the posterior fossa. The presence of a very large tumour with untreated hydrocephalus would be a contraindication to a spinal drain, in which case the cisterna magna needs to be accessed for CSF drainage through a small durotomy. After opening dura, the basal cisterns can be accessed utilizing the operating microscope for further drainage of CSF.

At this stage, a Greenberg retractor system is attached and the retractor blade may, only if necessary, be used to very gently retract the cerebellum. Following identification of the tumour, the arachnoid plane overlying the posterior capsule is identified and opened. This greatly facilitates dissection of the tumour capsule away from surrounding structures all of which must be preserved. Inferiorly, the CN IX–XI complex and loop of AICA are identified and preserved. Branches of AICA are frequently associated with the posterior capsule of vestibular schwannomas and tumours in the mid-CP angle, and these must be preserved. However, smaller branches that are seen to enter the tumour capsule may be coagulated and divided.

Fig. 24.3 Positioning and incision for retrosigmoid craniotomy. (A) Skin incision; (B) lateral positioning; (C) lateral positioning noting the arrangement of axillary roll, contralateral slung arm, and ipsilateral arm gutter.

Superiorly, CN V and IV are identified along with the superior petrosal vein of Dandy. The vein is preserved if possible but occasionally may need to be coagulated and divided, especially if thought to be at risk of being avulsed from the superior petrosal sinus. Care should be taken to ensure no branches of the SCA are inadvertently coagulated at this time, which may account for some of the reports of morbidity associated with coagulation of this vein.

In most CP angle tumours, it is possible to enter the arachnoid plane between tumour capsule and cerebellum and dissect the plane to visualize the brainstem and respective cranial nerves at their root entry zones. In larger tumours, with more gross brainstem compression, internal debulking of the tumour must precede this step utilizing a combination of bipolar coagulation, sharp dissection, and a suction aspirator to perform internal debulking. The bipolar forceps must be used at the lowest voltage settings to minimize the risk of heat transmission and injury to the nerves. In the case of vestibular schwannomas, following internal debulking, the tumour can be further mobilized inferiorly allowing dissection of CN V from the superior tumour capsule, and laterally allowing full visualization of the eighth nerve root entry zone and AICA. If hearing preservation is not being attempted, the vestibular and cochlear fibres can be divided sharply with care taken to ensure that CN VII lying immediately adjacent is preserved. Frequently, AICA runs between the two nerves. The facial nerve may also be identified by its white colour and close proximity to the root entry zone of the glossopharyngeal nerve and confirmed by gentle electrical stimulation. Following identification of the VII CN, the tumour can then be further debulked and the tumour brainstem interface sharply and carefully opened. The VII nerve is dissected from the capsule meticulously using microscissors or a sharp arachnoid knife in a side-to-side direction. Where hearing preservation is a goal, the cochlear nerve is not divided but similarly dissected free of the tumour capsule with a meticulous sharp technique.

In the case of other CP angle tumours, the principles remain the same, with internal debulking creating room for the tumour capsule to be rolled away from surrounding vessels and cranial nerves as well as the cerebellum and brainstem. The layering of the arachnoid planes around a vestibular schwannoma mean that the facial nerve lies stretched, directly on the surface of the tumour capsule. In contrast meningiomas usually demonstrate a layer of arachnoid between the capsule and the overlying neurovascular structures which facilitate the identification of meticulous dissection planes. Where tumours extend into the IAM or jugular foramen, further bone removal may be necessary to remove this tumour bulk safely. Once the dura of the IAM has been opened and arachnoid dissected between the tumour capsule and the margins of the IAM the tumour may be further debulked to allow mobilization. Following excision of the lesion, the lateral extent of the IAM is inspected using a 70° endoscope to ensure that no small volume tumour residual remains beyond the lateral extent of the drilled canal.

Translabyrinthine approach

This approach sacrifices hearing so particularly lends itself to treatment of larger vestibular schwannomas where hearing is already diminished. It is particularly useful for these tumours as the exposure

opens the posterior and superior walls of the IAM allowing exposure of the facial nerve at the fundus of the IAM, thus allowing good visualization of the most lateral part of the tumour for gross total resection. In addition, the exposure provides a more direct approach to the CP angle and negates the need for cerebellar retraction. The approach when combined with a middle fossa craniotomy and division of the tentorium also provides panoramic access to anteriorly located tumours high within the CP angle and extending into the middle fossa. Care must be taken during this approach to evaluate and preserve the insertion of the vein of Labbe and to minimize elevation of the temporal lobe, damage to either of these structures can result in significant morbidity.

In a typical translabyrinthine approach, the posterior fossa dura is opened in Trautmann's triangle bounded by the sigmoid sinus, jugular bulb, and superior petrosal sinus. The presence of an anteriorly placed sigmoid sinus or superiorly placed jugular bulb may restrict the access of this approach. The high-riding jugular bulb may be found in 9–18% of temporal bones and is predicted by poor pneumatization of the temporal bone.

We perform most CP angle surgery requiring skull base specialist exposure as a skull base team together with highly experienced and skilled neuro-otologists. We prefer to use the supine position for this procedure with the head placed in three-pin fixation and rotated to approximately 45°. Lateral flexion should be used to widen the angle between the shoulder and the exposure to better visualize the tentorium in larger superior lesions. The head of the table should be raised to 30 degrees to improve venous return and the neck should slightly extended so the fallopian canal is parallel to the floor. Fat is harvested from the abdomen and if tentorial reconstruction is needed fat and fascia lata are harvested from the lateral thigh. We use a generous C-shaped incision, placed well behind the mastoid and sigmoid sinus. Following elevation of a scalp flap, fibroperiosteal flaps are elevated after performing a T-shaped incision exposing the cortical mastoid bone. The neuro-otologist then performs an extensive cortical mastoidectomy.

The lateral cortical mastoidectomy is completed exposing anteriorly the thinned bone overlying the external auditory canal. Superiorly the dura of the middle fossa and superior petrosal sinus is exposed and posteriorly the sigmoid sinus is exposed and the mastoid decorticated to show the digastric notch and followed towards the jugular bulb. The mastoid antrum and aditus is opened and the incus removed to demonstrate the lateral semicircular canal on the medial wall of the epitympanic recess, deep and anterior to which lies the horizontal portion of the facial nerve. The semicircular canals are then identified and opened, removing the lateral canal to open the vestibule and the posterior and superior canals to demonstrate the common crus deep to which lies the second genu of the facial nerve. The fallopian canal is skeletonized. Deep to the vestibule the internal auditory canal (IAC) is then opened to 270° and laterally to the fundus where the transverse crest is identified. CSF can usually be partially drained via the cochlear aqueduct to allow some cerebellar relaxation. Technical aspects we consider to be particularly pertinent with this approach include removing occipital bone approximately 1 cm behind the sigmoid sinus to allow posterior retraction of the sinus thus increasing exposure. We also take pains to minimize compression of the sigmoid sinus or aggressive lowering of a high-riding jugular bulb in the case of a dominant venous sinus complex. In some circumstances this influences the decision to perform this approach versus a retrosigmoid approach. We also consider maximal exposure of the IAM helpful, particularly in larger, more anterior tumours where 270° opening of the IAM achieves improved access to this portion of the tumour (**Fig. 24.4**).

In cases of vestibular schwannoma, the IAC dura is opened allowing identification and stimulation of the facial, vestibular, and cochlea nerves at the fundus. In our team the neurosurgeon then opens the dura, releases CSF, and identifies the arachnoid planes surrounding the tumour. The tumour capsule is stimulated and safely opened, allowing internal debulking of the lesion using scissors, suction, and cavitronic suction aspiration. This debulking allows the edges to be rolled away from the cerebellum, superior petrosal vein, lower cranial nerves, and traversing SCA branches. Once the tumour is debulked enough to identify CN VIII and VII at the brainstem, the lesion is further debulked and rolled off these nerves laterally. Arachnoid dissection and removal of the thinned capsule usually allows lateral displacement and resection of the tumour until the nerve becomes more adherent towards the porous of the IAM. Where the nerve spreads widely and becomes attenuated in calibre the most meticulous dissection must occur to preserve facial function. The IAM component of the tumour is often reduced until just this part remains. We then remove this and the IAM component in a medial to lateral direction with the aim to achieve complete tumour extirpation. If the facial nerve is particularly adherent and thinned, we may elect to leave a small volume of residual capsule at this point alone, though this is rarely necessary. Constant electromyography (EMG) monitoring during tumour debulking and facial nerve dissection is essential to reduce injury to the nerve. Proximal stimulation can be used to assess functional integrity both during dissection and at the completion of the tumour removal.

Following meticulous haemostasis, the opened dura is closed under magnification to the dura of the porus acusticus. The middle ear cavity is then packed with a combination of small pieces of fat and muscle, and after filling the CP angle with irrigation solution an antibiotic fat graft is placed in the mastoid cavity. The temporalis fascia is closed in a watertight fashion and the skin closed in layers with a mastoid bandage and dressing to reinforce the closure.

Retrolabyrinthine approach

The retrolabyrinthine approach allows access to middle clival region. On its own, the amount of petroclival region and CPA exposure is limited. However, in patients with serviceable hearing, as part of a combined transtentorial, middle fossa approach, this technique has an important role in the resection of lesions spanning the posterior and middle fossae. A detailed description of the approach can be found in the surgical literature (Brackmann, 1979; McElveen et al., 1988; Glasscock et al., 1991; Ortiz Armenta, 1992). Positioning of the patient is similar to that described for the translabyrinthine approach. After completing the mastoidectomy, further medial resection of the temporal bone is performed using the high-speed drill in order to expose Trautmann's triangle, which corresponds to the area of cerebellar dura limited by the jugular bulb inferiorly, the middle fossa dura superiorly, the superior petrosal sinus and sigmoid sinus posteriorly, and the otic capsule anteriorly. The endolymphatic sac can be seen along the inferior portion of Trautmann's triangle, inferior to the posterior semicircular canal. Great care should be taken not to dissect the endolymphatic sac or drilling into the semicircular canals as this may well result in permanent hearing loss. The dural

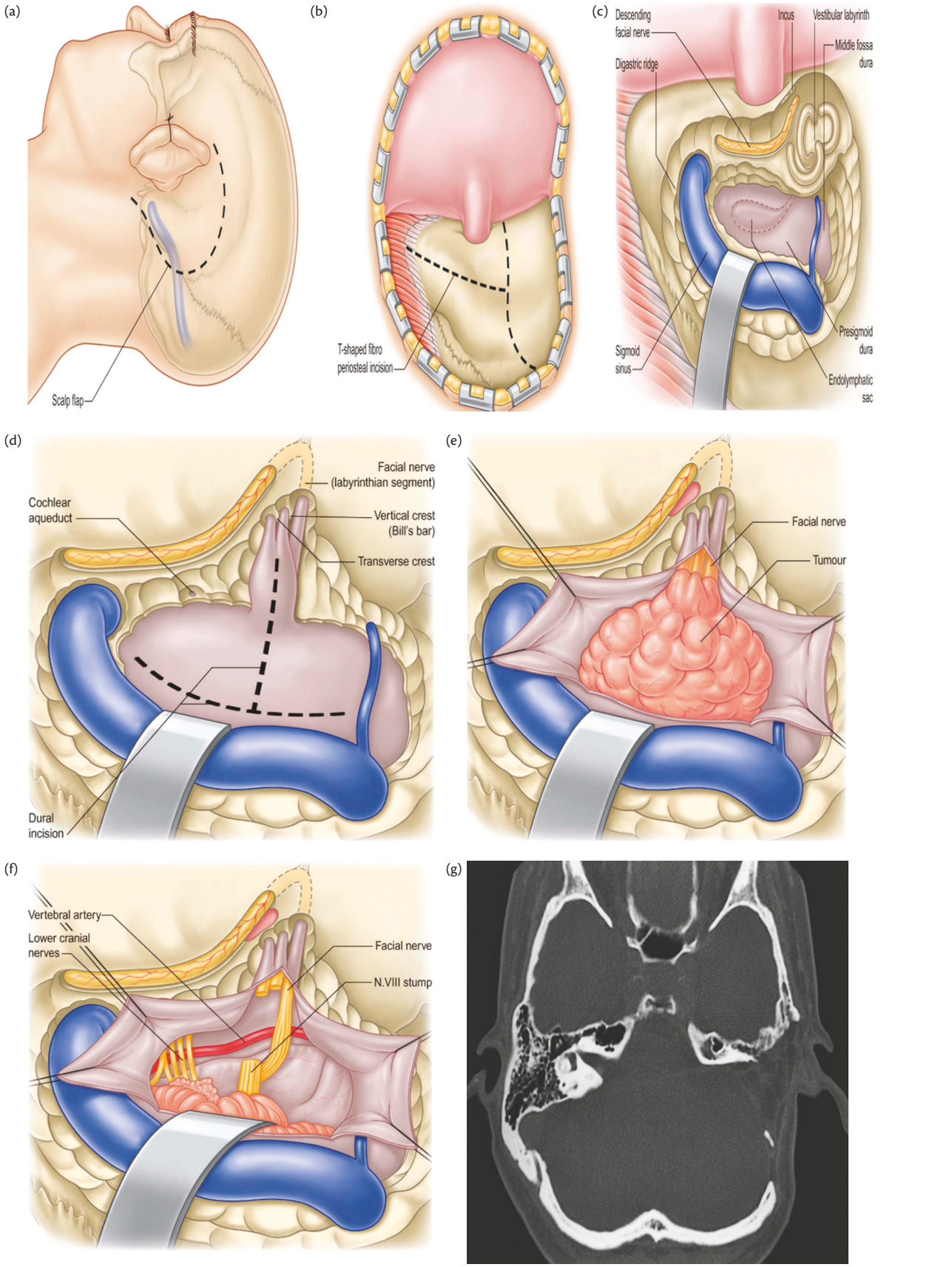

Fig. 24.4 (A) Skin incision for the translabyrinthine operation. (B) Fibroperiosteal incisions to expose mastoid cortex. (C) Extended mastoidectomy completed with skeletonization of the semicircular canals and descending facial nerve. (D) Temporal bone and internal auditory canal dissection complete: lines for dural incision shown. (E) Initial tumour exposure following dural incision and retraction. (F) The tumour bed at completion of the resection. The facial nerve is shown in its most usual position displaced medially and upwards. (G) Postoperative CT demonstrating the left temporal bone defect following translabyrinthine removal of a large acoustic neurinoma. Exposure of the cerebellopontine angle and internal auditory meatus is more direct than via a suboccipital approach.

(A–F) This article was published in *Brain Tumors: An Encyclopedic Approach*, Third edition, Kaye, Andrew H. II. Laws, Edward R., pp. 535 to 553, 614, Copyright Elsevier 2012.

flap is then elevated with an anterior base in parallel with the otic capsule.

Transcochlear approach

Of the posterior transpetrosal approaches, this provides the maximum amount of petrous bone removal and the most anterior exposure. It offers a wide corridor to the middle and upper thirds of the clivus as well as to the anterior brainstem. This approach is not very useful for the resection of acoustic neuromas and is associated with intrinsic associated morbidity, such as facial paralysis and potential CSF leakage. There is a transotic variation where the bony facial canal is left intact and remains as a bridge within the approach field. There are two variations of the transcochlear approach. The original, as described by House and Hitselberger, involves facial nerve transposition (Hitselberger, 1966; House and Luetje, 1979). It involves complete skeletonization of the facial nerve to mobilize the nerve posteriorly and to obtain a flat exposure. The greater superficial petrosal nerve is cut where it emerges from the geniculate ganglion so that the facial nerve can be released and mobilized. Once the facial nerve is mobilized posteriorly, the cochlea is entered. In the transotic approach described by Fisch, the facial nerve is not mobilized, but the external auditory canal is occluded and resected. Drilling continues to the petrous apex along the inferior petrosal sinus. The petrous portion of the internal carotid artery constitutes the lateral aspect of the exposure.

Combined middle fossa and transpetrosal approach

Tumours involving the petroclival region with extension into the perimesencephalic or peripontine structures can be approached using the petrosal approach. For more extensive lesions extending anteriorly to the clinoidal and carotid cisterns, the extended petrosal approach should be considered. To access these regions, the petrosal approach offers a number of advantages. The surgeon's operative distance to these regions is shorter than with the retrosigmoid approaches, there is minimal retraction of the cerebellum and temporal lobe, the neural structures (i.e. cranial nerves VII and VIII) are preserved, the otologic structures (i.e. cochlea, labyrinth, and semicircular canals) are preserved, the major venous sinuses (i.e. transverse and sigmoid), along with the vein of Labbe and other temporal and basal veins, are preserved.

The patient is positioned in much the same manner as for a translabyrinthine approach. The incision starts at the zygoma, anterior to the tragus, and extends posteriorly approximately 2–3 cm above and encircling the ear, where it descends behind the mastoid process. The skin flap is sharply dissected from the underlying pericranium and fascia. The temporalis fascia is reflected sharply and is kept in continuity with the sternocleidomastoid muscle then the temporalis muscle itself is sharply dissected off the bone and reflected anteriorly and inferiorly. Four burr holes, two on each side of the transverse sinus, are made. The first burr hole is placed just medial and inferior to the asterion, which is located at the inferior junction of the transverse and sigmoid sinuses. The second burr hole is placed at the squamous and mastoid junction of the temporal bone, along the projection of the superior temporal line, which opens into the supratentorial compartment. The final two holes are placed approximately 2–3 cm more medially and closer together on either side of the transverse sinus. A temporoparietal craniotomy and lateral occipital craniotomy are performed without connecting the burr holes across the sinus. The holes across the sinus are then connected. After meticulous separation of the wall of the sinus from the flap, the bone plate is elevated. The surgeon next performs a posterior petrous temporal bone removal, either retrolabyrinthine or translabyrinthine depending on the extent of tumour and the patient's preoperative hearing status. Once the bone removal has been completed, the dura of the posterior fossa is opened. Superiorly, the dura overlying the temporal lobe is also opened and these are joined ligating the superior petrosal sinus anterior to the insertion of the vein of Labbe, which must be preserved. The tentorium is then divided under microscopic visualization with a loosely placed retractor sitting under the temporal lobe for support. At the tentorial hiatus deep retraction sutures are placed before careful completion of the medial tentorial division posterior to the point where the IV CN enters the medial aspect of the tentorium. The IV can be seen traversing the perimesencephalic cistern beneath the arachnoid prior to this step. The dural edges are retracted forwards revealing this panoramic exposure. (Fig. 24.5).

Surgical outcomes for CP angle lesions

Vestibular schwannoma

For the purposes of assessing efficacy of removal of vestibular schwannomas both the retrosigmoid and translabyrinthine approaches have comparable outcomes. There are advantages and disadvantages of either approach and in practical terms most teams develop an approach that they are most familiar and comfortable with.

The single biggest determinant of outcome in terms of mortality, facial nerve function, and hearing preservation has been documented across multiple series as the size of the tumour (King and Morrison, 1980; Ruth et al., 1985; Hardy et al., 1989; Anderson et al., 2005; Samii et al., 2010; Sughrue et al., 2011). Though debate continues regarding the approach associated with the least morbidity,

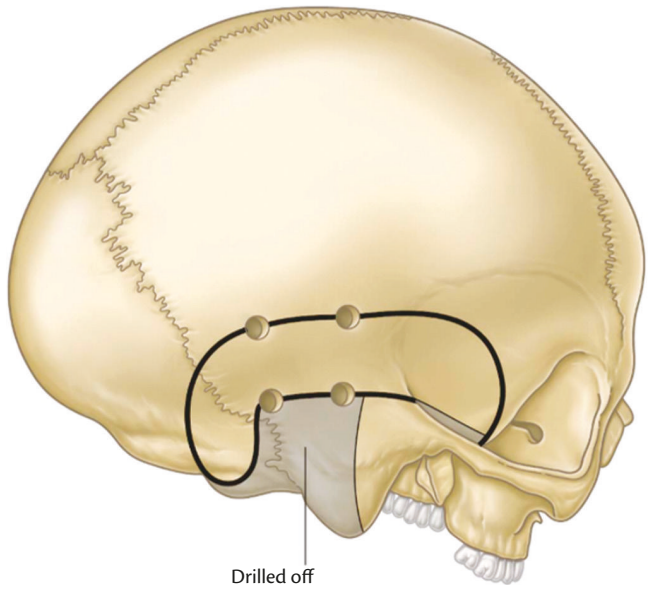

Fig. 24.5 Craniotomy for combined presigmoid middle fossa approach.
This article was published in *Brain Tumors: An Encyclopedic Approach*, Third edition, Kaye, Andrew H. II. Laws, Edward R., pp. 535 to 553, 614, Copyright Elsevier 2012.

there have been many studies highlighting good results for each of the approaches.

When considering the choice of approach for a given lesion, we consider that other than in the case of bilateral tumours or pre-existing contralateral hearing loss, most patients' primary concerns are the issues of postoperative facial weakness and completeness of resection of the lesion, rather than preservation of hearing (Kaye and Laws, 2012). The psychological impact of facial weakness in terms of a patient's perceptions of outcome should not be underestimated and is a major determinant of postoperative quality of life (Ryzenman et al., 2005; Nicoucar et al., 2006; Browne et al., 2008).

Sughrue from UCSF recently comprehensively reviewed the outcome of facial nerve preservation across the acoustic neuroma literature evaluating 296 studies with 25 000 patients and reporting on 11 873 patients across 79 studies (Sughrue et al., 2010b). This analysis defined facial nerve preservation as an outcome of House–Brackmann score of I or II, and demonstrated outcomes of 85% via the middle fossa approach, 81% via the translabyrinthine approach, and 78% for the retrosigmoid approach. Patients with tumours less than 2 cm had facial preservation rates of 90% versus 67% in tumours more than 2 cm. Patients less than 65 years old had lower facial preservation rates 71% versus 84% and intraoperative monitoring was associated with improved facial nerve outcomes. The presence of preoperative facial weakness is an independent predictor of postoperative facial weakness with rates being as high as 33%. Preoperative facial weakness is associated with large tumours and may also be associated with involvement of tumour invested within the nerve rather than displacing it (Lye et al., 1982).

If gross weakness exists preoperatively, or if the facial nerve is severed during surgery, consideration should be given to facial nerve reconstruction options intraoperatively. Facial nerve cable grafting using sural or greater auricular nerve grafts have been shown to have outcome rates of House–Brackmann III or better in 45–75% of cases (Fisch et al., 1987; Stephanian et al., 1992; Gidley et al., 1999; Bacciu et al., 2009). In this event microsurgical repair follows standard microsurgical techniques, with delicate and minimal nerve handling and tensionless apposition of the epineurium.

Auditory monitoring techniques: As surgical techniques have developed and the rates of functional and anatomical preservation of the CN VII have improved, attention has been focussed towards the goal of hearing preservation surgery. Adjuncts developed to assist in the monitoring and preservation of VIII nerve function are based on either 'far field' or 'near field' techniques. Far field intraoperative auditory monitoring techniques were first used and described in 1978 by Levine (Levine et al., 1988). There are several techniques currently used to monitor auditory function.

Brainstem auditory evoked potentials (BAEPs) represent the bioelectric neural activity that occurs in response to the stimulation of the vestibulocochlear nerve. This is produced by placing scalp and ear electrodes, and monitoring averaged responses from an auditory stimulator placed in the operated ear. The BAEPs have to be distinguished from background noise requiring averaging of several thousand responses and thus have a significant time lag. This delay in response of seconds to minutes means it may be difficult to determine the cause of a change in waveform. The prognostic significance of BAEPs is based solely on the preservation of waves and is thus of limited value (Oh et al., 2012). Setting up and monitoring intraoperatively requires expertise and should be performed by an expert technician.

The electrocochleogram (EcoG) and direct compound near action potentials (dCNAPs) record electrical response close to the origin of stimulus on the cochlear nerve. This means that the averaging needed to detect a stimulus is reduced and a more rapid assessment of nerve function is achieved. In this technique, reference and ground electrodes are placed on the ipsilateral earlobe forehead, respectively. A foam ear plug not only holds the electrode in place but also reduces external sound interference. The stimulating electrode administers click impulses and responses are averaged for a wave pattern to emerge. In dCNAP, the action potential is measured directly from the acoustic nerve itself after placing an electrode on the nerve proximal to the tumour. These near-field techniques have the advantage of being more rapidly attained and thus more reflective of an intraoperative change. The utility of dCNAP is also increased by its higher predictive value in postoperative function with improved sensitivity and specificity (Yamakami et al., 2009). The near-field techniques do have specific disadvantages with EcoG providing only functional information about the lateral part of the auditory pathway. A proximal division of the nerve may not be identified using this technique (Colletti et al., 1998). dCNAP recording may also present technical difficulties with placement of the CN VIII electrode made difficult in moderate or large sized tumours, thus, generally limiting the use of this technique to removal of smaller tumours where some groups have reported improved outcomes in terms of hearing preservation (Danner et al., 2004) at rates of up to 71% in small tumours.

Hearing preservation outcomes: Results relating to the efficacy of performing surgery with hearing preservation as a goal have been widely reported and the success rates of this approach are significantly different across the board. Quotes range from 17–100% with regards to hearing preservation and a clear relationship between the size of the tumour and hearing preservation rates. Although many authors would argue that hearing preservation rates are negligible in larger tumours, some authors have published data showing hearing preservation rates of 43% in very large tumours (Matthies and Samii, 2002). Sughrue recently reviewed the literature regarding hearing preservation rates and identified 123 studies, 49 of which detailed data that could be extracted (Sughrue et al., 2010a). Of 998 patients included in their analysis, hearing preservation was most significantly dependent upon the size of the tumour, preoperative hearing levels, and the age of the patient. Overall hearing rates were 52% over a follow-up period of 6 months to 7 years. Hearing rates in patients less than 30 years of age were 53% versus 29% in patients more than 60 years. Tumours smaller than 1 cm had hearing preservation rates of 64% compared to 32% in tumours larger than 3 cm.

Long-term durability of hearing preservation surgery also remains a contentious issue with the House group reporting delayed hearing loss in 56% of their patients (Shelton et al., 1990). Theories for the mechanism of delayed hearing loss include scar tissue formation around the cochlear or microvascular injury to the cochlear blood supply (Chee et al., 2003). Since then, a number of other studies have shown ongoing durability of long-term hearing preservation with maintenance of rates of 85–96% (Betchen et al., 2005; Woodson et al., 2010; Mazzoni et al., 2012).

Acute hearing loss in the contralateral ear has been reported as a complication of acoustic neuroma surgery, and mild hearing

loss is common following posterior fossa surgery. The mechanism behind this phenomenon is poorly understood but may relate to low CSF pressure in the perilymph and perilymphatic hypotonia. This may also improve spontaneously (Clemis et al., 1982; Walsted et al., 1991).

Brainstem and cochlear implants

The presence of an intact and functional cochlear nerve and cochlear allows placement of a cochlear implant. In the case of vestibular neuroma surgery this may be utilized if a translabyrinthine approach is used for technical considerations and the cochlear nerve is preserved.

Auditory brainstem implants (ABI) are typically used in a situation where hearing is threatened bilaterally. This situation arises most commonly in patients with Neurofibromatosis type 2 (NF-2) where the patient has bilateral vestibular schwannomas. The implant can be placed either following first tumour removal where a gross total removal is expected as hearing on this side has already significantly diminished or been lost, or after removal of a second schwannoma where hearing has been lost. Patients with preserved hearing gain little benefit from an ABI as it is rare to get more hearing quality than environmental sounds and closed-set words. If an ABI is placed at first side surgery with hearing intact it is not usually used until hearing on the contralateral side has been lost. Although detailed discussion is beyond the scope of this chapter, if possible, we favour debulking of tumours in patients with NF-2 with attempt to preserve hearing and minimize the morbidity of deafness. Placement of an ABI is feasible with either a retrosigmoid or translabyrinthine approach. The surgical technique is well described (Toh and Luxford, 2008) but essentially involves placement of an electrode on the ventral cochlear nucleus. This is not visible directly and so must be placed using indirect surface landmarks within the lateral recess adjacent to the dorsal nucleus and the inferior aspect of the ventral nucleus between the roots of the facial and glossopharyngeal nerves. Once placed, an electrode array is used to test the response of the implant and adjacent nerves and structures. The array is secured using Teflon or fat within the opening of the lateral recess and the electrode lead positioned in the mastoid cavity and the ground electrode under the temporalis muscle.

Results for the ABIs indicate that 85% of patients receive auditory sensations. Combined with lip reading, 93% of patients demonstrated improved sentence understanding at 3–6 months. Most patients have awareness of environmental sounds as well as closed-set words, consonants, and vowels. Results continue to improve for 8 years (Ebinger et al., 2000; Maini et al., 2009).

Petroclival meningioma

Petroclival meningiomas arise from the upper two-thirds of the clivus, medial to the fifth cranial nerve. These tumours typically displace the brain stem, but may displace or engulf the basilar artery, cranial nerves III–XI as well as extend into Meckel's cave, the cavernous sinus, Dorello's canal, the internal auditory meatus, or the jugular foramen. Surgical removal is frequently challenging and as such, operative morbidity may be correspondingly significant.

Published series examining extent and morbidity of resection have varied greatly, mainly being influenced by the philosophy of the treating team. The substantial morbidity of petroclival meningioma resection certainly urges weighing aggressiveness versus outcome. Factors including improvements in microscope technology, preoperative imaging, and the development of radiosurgical techniques have resulted in improved patient outcomes. In larger tumours microsurgery remains the only viable treatment option. The resection of these tumours is undoubtedly associated with significant morbidity. Feng Xu et al. reviewed 840 cases of patients that underwent surgical resection for petroclival meningioma. Mortality ranged from 0 to 9%, new cranial nerves deficits ranged from 20.3% to 76%. Gross total resection was 28–85% (Xu et al., 2013). Almefty et al. reported the results of 64 patients of whom 54 had long-term follow-up, 39% had persistent cranial nerve deficits, mainly cranial nerves V–VIII. Notably CN V and VIII were more likely to improve from preoperative status while CN VI is the most at risk for permanent deficit (Almefty et al., 2014). Brain stem compression is frequent with large tumours. Dissection of tumours that have brainstem pial or basilar artery encasement may lead to catastrophic brain stem infarct. Preoperative indicators that may be helpful to identify are tumour consistency as measured by T2 signal, presence of a CSF cleft between tumour and brainstem on MRI, or MRI evidence of brainstem oedema, which suggests increased adhesiveness to the brain stem (Uede et al., 1996; Carvalho et al., 2000).

Extent of resection does play a role in recurrence rate. Following gross total resection, recurrence rates of 6–9.8% have been reported. Following subtotal resection recurrence is reported to be as high as 26–41% (Seifert, 2010; Li et al., 2013; Almefty et al., 2014). In patients where GTR is precluded by expected severe neurological morbidity, radiation therapy may be initiated following evidence of progression of tumour growth.

Trigeminal schwannoma

With modern microsurgical techniques mortalities have been drastically reduced. Chen's review of 459 patients described five operative deaths and a mortality rate of 1% (Chen et al., 2014). Additional morbidity includes cranial nerve injury, CSF leak, meningitis, and hydrocephalus. Many patients will be left with some degree of permanent trigeminal dysfunction, most commonly the persistence of trigeminal hypoesthesia (Fukaya et al., 2010), which patients should be informed may never resolve. The combination of this with facial nerve injury often necessitates eyelid closure techniques to prevent neurotropic keratitis. New onset postoperative cranial nerve dysfunction, such as abducens and oculomotor palsies, usually resolve within 4 months. Some preoperative neurologic deficits, such as cerebellar and brainstem compression syndromes, diplopia, facial pain and weakness, and hearing loss may improve postoperatively. CSF leak and/or hydrocephalus may require shunt placement.

Jugular foramen schwannoma

Complications following surgical removal of these tumours potentially include dysphagia, hoarseness, aspiration, and stridor. Most recent reports have demonstrated a remarkably low incidence of serious dysphagia and aspiration (Bakar, 2008; Bulsara et al., 2008; Cavalcanti et al., 2011). In some persistent cases of serious dysphagia, tracheostomy or vocal cord medialization techniques may be needed. Many patients though can be managed with temporary nasogastric feeding and meticulous pulmonary toilet in order to reduce the chance of aspiration pneumonia. Most will eventually adapt and tolerate a regular diet.

Dermoid and epidermoid tumours

With the development of microsurgery, the mortality and morbidity of dermoid and epidermoid tumour surgery have dropped dramatically. Yaşargil et al. were able to obtain an improvement in 86% of their patients, with a 9% neurologic morbidity and 5% mortality. In this same series the rate of meningitis (including chemical) was described to be 19%, and hydrocephalus was present in 19% of the patients (Yaşargil et al., 1989).

The primary complications from management of these lesions are aseptic meningitis, septic meningitis, hydrocephalus, and neurological dysfunction related to the position of the lesion. The neurological deficits of concern follow involvement of the lower cranial nerves and subsequent difficulty with swallowing, aspiration pneumonia, and death.

Both dermoid and epidermoid cysts can recur after many years, although symptomatic recurrence is rare. The recurrence potential is related to the volume of capsule that remains unresected. This capsule will produce cells at the normal rate of cell transformation (Alvord, 1977) and thus a symptomatic recurrence is uncommon. A recurrent tumour is still likely to be benign though malignant change has been reported in both dermoid and epidermoid cysts.

Dissemination can only occur if there has been rupture of the cyst contents into the CSF spaces. Maravilla (1977) described this pattern of dissemination associated with multiple secondary satellites nodule.

Controversies

The management of small vestibular schwannomas: Observation vs. stereotactic radiosurgery vs. microsurgical excision

For many lesions smaller than 1.5 cm in middle aged and older patients, initial management with observation and close radiological and clinical follow-up is appropriate. Growth in these patients should trigger intervention.

The treatment of tumours less than 2 cm in size can be either microsurgery or radiosurgery. Surgery for small tumours performed in high volume subspecialty centres offers excellent rates of gross total resection with rates of good facial nerve outcome typically more than 90%. Radiosurgery offers a viable alternative in small tumours, with good control of growth and typically excellent, low rates of facial nerve dysfunction. Salvage microsurgery following failed radiosurgery is typically associated with more challenging nerve dissection and higher rates of facial nerve morbidity.

Radiosurgery in anticoagulated patients is relatively contraindicated with a significantly increased rate of intratumoural haemorrhage.

The timing and extent of intervention and tumour excision in patients with NF-2

Given the high priority in this patient group of hearing preservation, the management of vestibular schwannomas is inherently more conservative. Growing tumours associated with poor hearing or a deaf ear should be managed with microsurgical excision. While hearing remains intact we adopt a strategy of maximal debulking while placing the intraoperative priority on preservation of the cochlear nerve. This situation frequently means that residual tumour remains and patients may require multiple retrosigmoid craniotomies. We typically reserve treatment in patients with NF-2 until the size of the lesion is compressive on the cerebellum. Radiosurgery in this patient group is less effective at controlling growth and is typically not advised except as a salvage strategy.

The choice of approach in patients with large tumours and serviceable hearing

Excepting the NF-2 patient population, and the small proportion of idiopathic patients with poor hearing on the side contralateral to the tumour, we would generally advocate that in the case of a large tumour the primary goal of surgery remains safety to both the brainstem and cerebellum. We feel that minimizing cerebellar retraction and maximizing the angle for safe brainstem dissection of the tumour with a translabyrinthine approach optimizes the surgical outcome for the patient. In large tumours we believe that the possibility of useful hearing preservation is low in any approach and thus our choice is typically translabyrinthine.

FURTHER READING

Almefty, R., Dunn, I.F., Pravdenkova, S., Abolfotoh, M., & Al-Mefty, O. (2014). True petroclival meningiomas: results of surgical management. *J Neurosurg*, **120**, 40–51.

House, J.W. & Brackmann, D.E. (1985). Facial nerve grading system. *Otolaryngol Head Neck Surg*, **93**, 146–7.

Rhoton, A.L. (2007). *Rhoton's Cranial Anatomy and Surgical Approaches*. Philadelphia, PA: Wolters Kluwer, Chapter 8.

Samii, M., Gerganov, V.M., & Samii, A. (2010). Functional outcome after complete surgical removal of giant vestibular schwannomas. *J Neurosurg*, **112**, 860–7.

Yaşargil, M.G., Abernathey, C.D., & Sarioglu, A.C. (1989). Microneurosurgical treatment of intracranial dermoid and epidermoid tumors. *Neurosurgery*, **24**, 561–7.

REFERENCES

Almefty, R., Dunn, I.F., Pravdenkova, S., Abolfotoh, M., & Al-Mefty, O. (2014). True petroclival meningiomas: results of surgical management. *J Neurosurg*, **120**, 40–51.

Alvord, E.C., Jr. (1977). Growth rates of epidermoid tumours. *Ann Neurol*, **2**, 367–70.

Anderson, D.E., Leonetti, J., Wind, J.J., Cribari, D., & Fahey, K. (2005). Resection of large vestibular schwannomas: facial nerve preservation in the context of surgical approach and patient-assessed outcome. *J Neurosurg*, **102**, 643–9.

Bacciu, A., Falcioni, M., Pasanisi, E., et al. (2009). Intracranial facial nerve grafting after removal of vestibular schwannoma. *Am J Otolaryngol*, **30**, 83–8.

Bakar, B. (2008). The jugular foramen schwannomas: review of the large surgical series. *J Korean Neurosurg Soc*, **44**, 285–94.

Betchen, S.A., Walsh, J., & Post, K.D. (2005). Long-term hearing preservation after surgery for vestibular schwannoma. *J Neurosurg*, **102**, 6–9.

Bonneville, F., Sarrazin, J.L., Marsot-Dupuch, K., et al. (2001). Unusual lesions of the cerebellopontine angle: a segmental approach. *Radiographics*, **21**, 419–38.

Brackmann, D.E. (1979). The retrolabyrinthine approach. *Rev Laryngol Otol Rhinol (Bord)*, **100**, 331–4.
Brackmann, D.E. & Kwartler, J.A. (1990). A review of acoustic tumours: 1983–1988. *Am J Otol*, **11**, 216–32.
Brandt, M.G., Poirier, J., Hughes, B., Lownie, S.P., & Parnes, L.S. (2010). The transcrusal approach—a 10-year experience at one Canadian center. *Neurosurgery*, **66**(5), 1017–22.
Browne, S., Distel, E., Morton, R.P., & Petrie, K.J. (2008). Patients' quality of life, reported difficulties, and benefits following surgery for acoustic neuroma. *J Otolaryngol Head Neck Surg*, **37**, 417–22.
Bulsara, K.R., Sameshima, T., Friedman, A.H., & Fukushima, T. (2008). Microsurgical management of 53 jugular foramen schwannomas: lessons learned incorporated into a modified grading system. *J Neurosurg*, **109**, 794–803.
Carvalho, G.A., Matthies, C., Tatagiba, M., Eghbal, R., & Samii, M. (2000). Impact of computed tomographic and magnetic resonance imaging findings on surgical outcome in petroclival meningiomas. *Neurosurgery*, **47**, 1287–94; discussion 1294–5.
Cavalcanti, D.D., Martirosyan, N.L., Verma, K., et al. (2011). Surgical management and outcome of schwannomas in the craniocervical region. *J Neurosurg*, **114**, 1257–67.
Chee, G.H., Nedzelski, J.M., & Rowed, D. (2003). Acoustic neuroma surgery: the results of long-term hearing preservation. *Otol Neurotol*, **24**, 672–6.
Chen, L.F., Yang, Y., Yu, X.G., et al. (2014). Operative management of trigeminal neuromas: an analysis of a surgical experience with 55 cases. *Acta Neurochir (Wien)*, **156**, 1105–14.
Clemis, J.D., Mastricola, P.G., & Schuler-Vogler, M. (1982). Sudden hearing loss in the contralateral ear in postoperative acoustic tumour: three case reports. *Laryngoscope*, **92**, 76–9.
Colletti, V., Fiorino, F.G., Mocella, S., & Policante, Z. (1998). ECochG, CNAP and ABR monitoring during vestibular Schwannoma surgery. *Audiology*, **37**, 27–37.
Cushing, H. (1917). *Tumors of the Nervus Acusticus and the Syndrome of the Cerebellopontile Angle*. Philadelphia, PA: W.B. Saunders.
Danner, C., Mastrodimos, B., & Cueva, R.A. (2004). A comparison of direct eighth nerve monitoring and auditory brainstem response in hearing preservation surgery for vestibular schwannoma. *Otol Neurotol*, **25**, 826–32.
De La Cruz, A. & Teufert, K.B. (2009). Transcochlear approach to cerebellopontine angle and clivus lesions: indications, results, and complications. *Otol Neurotol*, **30**, 373–80.
Don, M., Kwong, B., Tanaka, C., Brackmann, D., & Nelson, R. (2005). The stacked ABR: a sensitive and specific screening tool for detecting small acoustic tumours. *Audiol Neurootol*, **10**, 274–90.
Ebinger, K., Otto, S., Arcaroli, J., Staller, S., & Arndt, P. (2000). Multichannel auditory brainstem implant: US clinical trial results. *J Laryngol Otol Suppl*, **27**, 50–3.
Fattah, A.Y., Gurusinghe, A.D., Gavilan, J., et al. (2015). Facial nerve grading instruments: systematic review of the literature and suggestion for uniformity. *Plast Reconstr Surg*, **135**, 569–79.
Fisch, U., Dobie, R. A., Gmur, A., & Felix, H. (1987). Intracranial facial nerve anastomosis. *Am J Otol*, **8**, 23–9.
Fukaya, R., Yoshida, K., Ohira, T., & Kawase, T. (2010). Trigeminal schwannomas: experience with 57 cases and a review of the literature. *Neurosurg Rev*, **34**, 159–71.
Gidley, P.W., Gantz, B.J., & Rubinstein, J.T. (1999). Facial nerve grafts: from cerebellopontine angle and beyond. *Am J Otol*, **20**, 781–8.
Glasscock, M.E., Thedinger, B.A., Cueva, R.A., & Jackson, C.G. (1991). An analysis of the retrolabyrinthine vs. the retrosigmoid vestibular nerve section. *Otolaryngol Head Neck Surg*, **104**, 88–95.
Gurgel, R.K., Dogru, S., Amdur, R.L., & Monfared, A. (2012). Facial nerve outcomes after surgery for large vestibular schwannomas: do surgical approach and extent of resection matter? *Neurosurg Focus*, **33**, e16.
Hardy, D.G., Macfarlane, R., Baguley, D., & Moffat, D.A. (1989). Surgery for acoustic neurinoma. An analysis of 100 translabyrinthine operations. *J Neurosurg*, **71**, 799–804.
Hitselberger, W.E. (1966). External auditory canal hypesthesia: an early sign of acoustic neurilemoma. *Am Surg*, **32**, 741–3.
Horgan, M.A., Delashaw, J.B., Schwartz, M.S., Kellogg, J.X., Spektor, S., & Mcmenomey, S.O. (2001). Transcrusal approach to the petroclival region with hearing preservation. Technical note and illustrative cases. *J Neurosurg*, **94**, 660–6.
House, J.W. & Brackmann, D.E. (1985). Facial nerve grading system. *Otolaryngol Head Neck Surg*, **93**, 146–7.
House, W.F. (1964). Differential diagnosis of cerebellopontine angle lesions. *Laryngoscope*, **74**, 1283–90.
House, W.F. & Luetje, C.M. (1979). *Acoustic Tumours*. Baltimore, MD: University Park Press.
Johnson, E.W. (1977). Auditory test results in 500 cases of acoustic neuroma. *Arch Otolaryngol*, **103**(3), 152–8.
Kaye, A.H. & Laws, E.R. (2012). *Brain Tumours: An Encyclopedic Approach*. Edinburgh/New York: Saunders/Elsevier.
Kaylie, D.M., Horgan, M.A., Delashaw, J.B., & McMenomey, S.O. (2004). Hearing preservation with the transcrusal approach to the petroclival region. *Otology & Neurotology*, **25**, 594–8.
Kentala, E. & Pyykkö, I. (2001). Clinical picture of vestibular schwannoma. *Auris Nasus Larynx*, **28**(1), 15–22.
King, T.T. & Morrison, A.W. (1980). Translabyrinthine and transtentorial removal of acoustic nerve tumours. Results in 150 cases. *J Neurosurg*, **52**, 210–16.
Levine, R.A., Liederman, J., & Riley, P. (1988). The brainstem auditory evoked potential asymmetry is replicable and reliable. *Neuropsychologia*, **26**, 603–14.
Li, D., Hao, S.Y., Wang, L., et al. (2013). Surgical management and outcomes of petroclival meningiomas: a single-center case series of 259 patients. *Acta Neurochir (Wien)*, **155**, 1367–83.
Lye, R.H., Dutton, J., Ramsden, R.T., Occleshaw, J.V., Ferguson, I.T., & Taylor, I. (1982). Facial nerve preservation during surgery for removal of acoustic nerve tumours. *J Neurosurg*, **57**, 739–46.
Maini, S., Cohen, M.A., Hollow, R., & Briggs, R. (2009). Update on long-term results with auditory brainstem implants in NF2 patients. *Cochlear Implants Int*, **10** Suppl 1, 33–7.
Maravilla, K.R. (1977). Intraventricular fat-fluid level secondary to rupture of an intracranial dermoid cyst. *AJR Am J Roentgenol*, **128**, 500–1.
Matthies, C. & Samii, M. (1997). Management of 1000 vestibular schwannomas (acoustic neuromas): clinical presentation. *Neurosurgery*, **40**, 1–9; discussion 9–10.
Matthies, C. & Samii, M. (2002). Vestibular schwannomas and auditory function: options in large T3 and T4 tumours? *Neurochirurgie*, **48**, 461–70.
Mazzoni, A., Zanoletti, E., & Calabrese, V. (2012). Hearing preservation surgery in acoustic neuroma: long-term results. *Acta Otorhinolaryngol Ital*, **32**, 98–102.
Mcelveen, J.T., Shelton, C., Hitselberger, W.E., & Brackmann, D.E. (1988). Retrolabyrinthine vestibular neurectomy: a reevaluation. *Laryngoscope*, **98**, 502–6.
Miller, M.E., Mastrodimos, B., & Cueva, R.A. (2015). Facial nerve function after the extended translabyrinthine approach. *J Neurol Surg B Skull Base*, **76**, 1–6.

Moffat, D.A. & Ballagh, R.H. (1995). Rare tumours of the cerebellopontine angle. *Clin Oncol (R Coll Radiol)*, **7**, 28–41.

Moffat, D.A., Saunders, J.E., Mcelveen, J.T., Jr., Mcferran, D.J., & Hardy, D.G. (1993). Unusual cerebello-pontine angle tumours. *J Laryngol Otol*, **107**, 1087–98.

Naganawa, S., Ito, T., Fukatsu, H., et al. (1998). MR imaging of the inner ear: comparison of a three-dimensional fast spin-echo sequence with use of a dedicated quadrature-surface coil with a gadolinium-enhanced spoiled gradient-recalled sequence. *Radiology*, **208**, 679–85.

Newton, J.R., Shakeel, M., Flatman, S., Beattie, C., & Ram, B. (2010). Magnetic resonance imaging screening in acoustic neuroma. *Am J Otolaryngol*, **31**, 217–20.

Nicoucar, K., Momjian, S., Vader, J.P., & De Tribolet, N. (2006). Surgery for large vestibular schwannomas: how patients and surgeons perceive quality of life. *J Neurosurg*, **105**, 205–12.

Oh, T., Nagasawa, D.T., Fong, B.M., et al. (2012). Intraoperative neuromonitoring techniques in the surgical management of acoustic neuromas. *Neurosurg Focus*, **33**, e6.

Ortiz Armenta, A. (1992). Retrolabyrinthine vestibular neurectomy. 10 years' experience. *Rev Laryngol Otol Rhinol (Bord)*, **113**, 413–17.

Rhoton, A.L. (2007). *Rhoton's Cranial Anatomy and Surgical Approaches*. Philadelphia, PA: Wolters Kluwer, Chapter 8.

Ross, B.G., Fradet, G., & Nedzelski, J.M. (1996). Development of a sensitive clinical facial grading system. *Otolaryngol Head Neck Surg*, **114**, 380–6.

Ruth, H.R., Luetje, C.M., & Whittaker, C.K. (1985). Acoustic tumours: preoperative measurement and correlation with postoperative facial nerve function. *Otolaryngol Head Neck Surg*, **93**, 160–3.

Ryzenman, J.M., Pensak, M.L., & Tew, J.M., Jr. (2005). Facial paralysis and surgical rehabilitation: a quality of life analysis in a cohort of 1,595 patients after acoustic neuroma surgery. *Otol Neurotol*, **26**, 516–21; discussion 521.

Samii, M., Gerganov, V.M., & Samii, A. (2010). Functional outcome after complete surgical removal of giant vestibular schwannomas. *J Neurosurg*, **112**, 860–7.

Schmidt, R.J., Sataloff, R.T., Newman, J., Spiegel, J.R., & Myers, D.L. (2001). The sensitivity of auditory brainstem response testing for the diagnosis of acoustic neuromas. *Arch Otolaryngol Head Neck Surg*, **127**, 19–22.

Seifert, V. (2010). Clinical management of petroclival meningiomas and the eternal quest for preservation of quality of life: personal experiences over a period of 20 years. *Acta Neurochir (Wien)*, **152**, 1099–116.

Sekhar, L.N., Schessel, D.A., Bucur, S.D., Raso, J.L., & Wright, D.C. (1999). Partial labyrinthectomy petrous apicectomy approach to neoplastic and vascular lesions of the petroclival area. *Neurosurgery*, **44**, 537–50; discussion 550–2.

Selesnick, S.H. & Jackler, R.K. (1992). Clinical manifestations and audiologic diagnosis of acoustic neuromas. *Otolaryngol Clin North Am*, **25**, 521–51.

Selesnick SH, Jackler, R.K., & Pitts, L.W. (1993). The changing clinical presentation of acoustic tumors in the MRI era. *Laryngoscope*, **103**(4 Pt 1), 431–6.

Selesnick S.H., Deora, M., Drotman, M.B., et al. (1999). Incidental discovery of acoustic neuromas. *Otolaryngol Head Neck Surg*, **120**, (6), 815–18.

Selters, W.A. & Brackmann, D.E. (1977). Acoustic tumor detection with brain stem electric response audiometry. *Arch Otolaryngol*, **103**(4), 181–7.

Shelton, C., Hitselberger, W.E., House, W.F., & Brackmann, D.E. (1990). Hearing preservation after acoustic tumour removal: long-term results. *Laryngoscope*, **100**, 115–19.

Stephanian, E., Sekhar, L.N., Janecka, I.P., & Hirsch, B. (1992). Facial nerve repair by interposition nerve graft: results in 22 patients. *Neurosurgery*, **31**, 73–6; discussion 77.

Stucken, E.Z., Brown, K., & Selesnick, S.H. (2012). Clinical and diagnostic evaluation of acoustic neuromas. *Otolaryngol Clin North Am*, **45**, 269–84, vii.

Stuckey, S.L., Harris, A.J., & Mannolini, S.M. (1996). Detection of acoustic schwannoma: use of constructive interference in the steady state three-dimensional MR. *AJNR Am J Neuroradiol*, **17**, 1219–25.

Sughrue, M.E., Kaur, R., Rutkowski, M.J., et al. (2011). Extent of resection and the long-term durability of vestibular schwannoma surgery. *J Neurosurg*, **114**, 1218–23.

Sughrue, M.E., Yang, I., Aranda, D., Kane, A.J., & Parsa, A.T. (2010a). Hearing preservation rates after microsurgical resection of vestibular schwannoma. *J Clin Neurosci*, **17**, 1126–9.

Sughrue, M.E., Yang, I., Rutkowski, M.J., Aranda, D., & Parsa, A.T. (2010b). Preservation of facial nerve function after resection of vestibular schwannoma. *Br J Neurosurg*, **24**, 666–71.

Thomsen, J., Terkildsen, K., & Tos, M. (1983). Acoustic neuromas. Progression of hearing impairment and function of the eighth cranial nerve. *Am J Otol*, **5**(1), 20–33.

Toh, E.H. & Luxford, W.M. (2008). Cochlear and brainstem implantation. 2002. *Neurosurg Clin N Am*, **19**, 317–29, vii.

Tos, M. & Thomsen, J. (1984). Epidemiology of acoustic neuromas. *J Laryngol Otol*, **98**(7), 685–92.

Uede, T., Wanibuchi, M., Nonaka, T., Ohtaki, M., & Hashi, K. (1996). [Distinctions of petroclival meningioma with perifocal edema on adjacent brain stem]. *No Shinkei Geka*, **24**, 841–7.

Walsted, A., Salomon, G., & Olsen, K.S. (1991). Low-frequency hearing loss after spinal anesthesia. Perilymphatic hypotonia? *Scand Audiol*, **20**, 211–15.

Woodson, E.A., Dempewolf, R.D., Gubbels, S.P., et al. (2010). Long-term hearing preservation after microsurgical excision of vestibular schwannoma. *Otol Neurotol*, **31**, 1144–52.

Xu, F., Karampelas, I., Megerian, C.A., Selman, W.R., & Bambakidis, N.C. (2013). Petroclival meningiomas: an update on surgical approaches, decision making, and treatment results. *Neurosurg Focus*, **35**, e11.

Yamakami, I., Yoshinori, H., Saeki, N., Wada, M., & Oka, N. (2009). Hearing preservation and intraoperative auditory brainstem response and cochlear nerve compound action potential monitoring in the removal of small acoustic neurinoma via the retrosigmoid approach. *J Neurol Neurosurg Psychiatry*, **80**, 218–27.

Yaşargil, M.G., Abernathey, C.D., & Sarioglu, A.C. (1989). Microneurosurgical treatment of intracranial dermoid and epidermoid tumors. *Neurosurgery*, **24**, 561–7.

RELATED LINKS TO EBRAIN

Performing a Retrosigmoid Craniotomy. https://learning.ebrain.net/course/view.php?id=77

The Translabyrinthine Approach to the Cerebellopontine Angle. https://learning.ebrain.net/course/view.php?id=75

SECTION 5

Tumours and skull base—sellar and suprasellar tumours

25. **Pituitary tumours** *299*
Kanna Gnanalingham, Zsolt Zador, Tara Kearney, Federico Roncaroli, and H. Rao Gattamaneni

26. **Craniopharyngioma and Rathke's cleft cysts** *321*
Rudolf Fahlbusch, V. Gerganov, and H. Metwali

27. **Surgical management of sellar and suprasellar tumours** *339*
Jayson A. Neil and William T. Couldwell

25

Pituitary tumours

Kanna Gnanalingham, Zsolt Zador, Tara Kearney, Federico Roncaroli, and H. Rao Gattamaneni

The pituitary gland: Essential anatomy

The pituitary gland occupies the sella turcica, approximately 5 cm posterior to the tip of the nose in the midline of the skull base (Fig. 25.1A). It is closely related to the hypothalamus and third ventricle superiorly, chiasm and lamina terminalis antero-superiorly, sphenoid sinus antero-inferiorly, cavernous sinus and cavernous segment of the carotid artery laterally, the posterior clinoids and clivus posteriorly.

There are two distinct components to the pituitary gland, the anterior and posterior lobe, which are derived from the ectoderm and neuroectoderm respectively (Fig. 25.1B). The anterior pituitary constitutes 80% of the gland mass and in the horizontal plane it is distributed into two lateral wings. The hormones produced by the anterior pituitary are adrenocorticotropic hormone (ACTH), prolactin (PRL), growth hormone (GH), thyroid-stimulating hormone (TSH), follicle-stimulating hormone (FSH), and luteinizing hormone (LH). The normal endocrine cells have a distinct distribution with GH and PRL producing cells being abundant in the anterior and posterior parts of the lateral wings respectively; TSH and ACTH producing cells most represented in the anterior and posterior part of the central wedge respectively and gonadotropin cells being scattered throughout the anterior lobe (Fig. 25.1C).

Blood supply to the pituitary is integral to its hormone-producing function (Fig. 25.1D). The superior and inferior hypophyseal arteries, direct branches of the supraclinoid and cavernous carotid, respectively, supply the pituitary gland and ventral hypothalamus. The superior hypophyseal artery forms the hypophyseal portal system by branching into the primary plexus circumventing the ventral hypothalamus and the pituitary stalk. This plexus drains towards the anterior lobe via the hypophyseal portal veins to form the secondary plexus around the anterior lobe. This second plexus is then collected in the anterior hypophyseal veins and drains into the cavernous sinus. The importance of this plexus is that it couples the trophic factors released from the arcuate nucleus of the hypothalamus to the anterior lobe to control its hormone secretion. The posterior lobe is supplied by the inferior hypophyseal artery and drained towards the posterior hypophyseal veins. The gland is connected to the hypothalamus superiorly via the pituitary stalk, which harbours the axons of the paraventricular and supraoptic nuclei. These axons transport oxytocin and vasopressin into the posterior pituitary and are released into the posterior hypophyseal vein (Fig. 25.1).

Epidemiology of pituitary tumours

Pituitary gland abnormalities are relatively common, the majority being pituitary adenomas. Their estimated prevalence as an incidental finding is approximately 17% according to a meta-analysis from radiological and post-mortem studies with no gender predilection (Ezzat et al., 2004). However, most these pituitary lesions are very small, incidental, and do not require clinical intervention.

Symptomatic pituitary adenomas have an incidence of 19–28/million/year which peaks between the third and sixth decade of life with an overall predominance in premenopausal women. The exact prevalence varies based on the study population; surgical series are biased by focus on lesions causing mass effect, whereas medical series may capture more of functioning adenomas such as prolactin-secreting adenomas that are typically medically managed. Up to 20% of pituitary adenomas, depending on series are discovered incidentally and many remain asymptomatic.

Pituitary adenomas requiring intervention represent 10–15% of all intracranial tumours, ranking them the third most common tumours after gliomas and meningiomas. Their classification is based on pathological and immunohistochemical features. Seven types and 13 subtypes are currently recognized in the WHO Classification of Tumours to Endocrine Organs (WHO, 2017). The types include a predominant lactotroph (prolactin immunostaining, 39%), gonadotroph (LH/FSH immunostaining, 27%), somatotroph (GH immunostaining, 16%), corticotroph (ACTH immunostaining, 16%) and thyrotroph (TSH immunostaining, 1%) cell type, and the rest include null cell and plurihormonal adenomas (WHO, 2017).

Pituitary adenomas in children are about ten times less common than adults contributing to 2–6% of all intracranial paediatric tumours (Keil and Stratakis, 2008). Only 3.5–8.5% of pituitary adenomas are diagnosed before the age of 20. Paediatric adenomas can have a dramatic impact on the critical period of development in childhood.

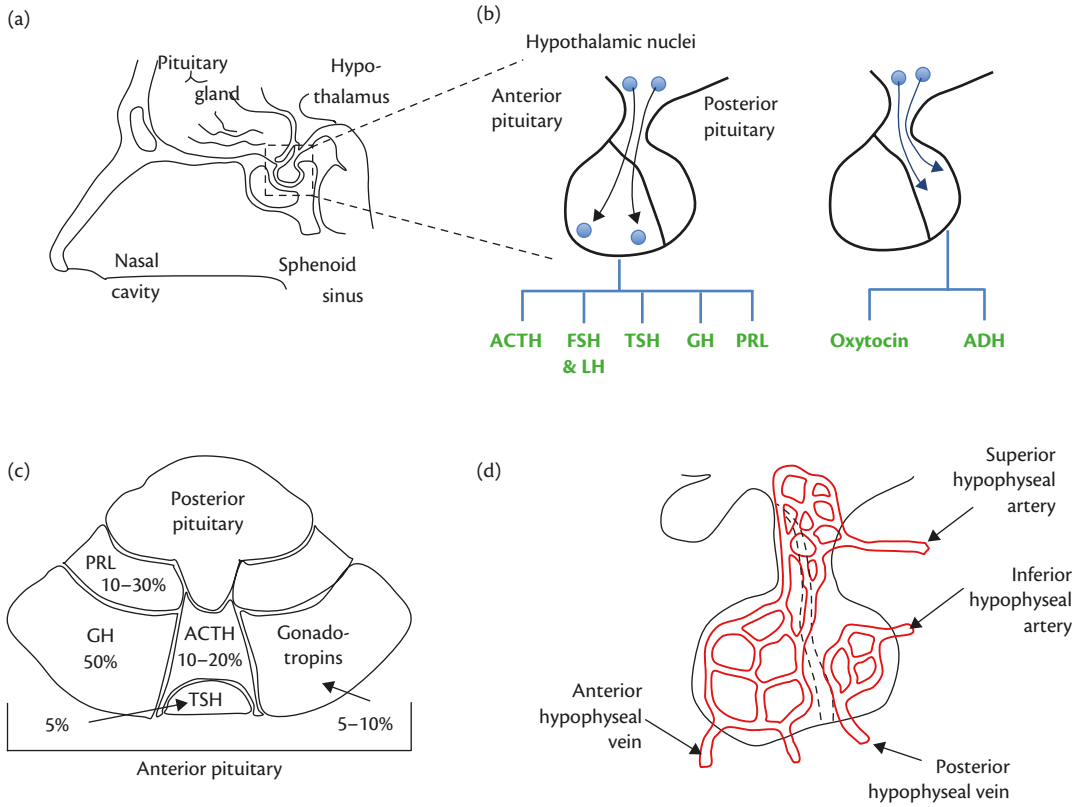

Fig. 25.1 Panel A: regional anatomy of the pituitary gland, panel B: pituitary gland structures and hormonal secretion panel C: topographic distribution of hormone-producing cells within the pituitary gland. Panel D: pituitary blood supply, the hypophyseal portal system.

Genetics

The classical concept of disruption in the oncogene proto-oncogene balance that regulates cell proliferation and leads to clonal expansion of tumour cells may provide some explanation, but the pathogenesis of pituitary adenomas remains unclear (Daly et al., 2009; Marques and Korbonits, 2017). Several lines of evidence support the monoclonality of pituitary tumours, however there are also evidence for multiple foci of monoclonal expansion.

The majority of pituitary tumours are sporadic (95%). A small minority are familial (5%) and occur either as isolated (i.e. familial isolated pituitary adenomas, FIPA), or as part of a familial genetic syndromes, including multiple endocrine neoplasia type 1 (MEN 1), MEN type 4, McCune–Albright syndrome, Carney complex (CNC), X-linked acrogigantism (XLAG syndrome), SDH mutations, and mutations of *DICER* gene (Vandeva et al., 2010; Marques and Korbonits, 2017).

Sporadic pituitary adenomas

There are multiple oncogenes identified to promote pituitary tumour formation (Daly et al., 2009; Marques and Korbonits, 2017). One of the first identified was the *gsp* oncogene, where a gain of function mutation is detectable in 40% of somatotrophinomas. *Gsp* codes the $G\alpha_s$ subunit of a GTPase and the mutation results in persistently elevated cAMP levels. This constitutes a constant stimulation from the growth hormone release hormone (GHRH) and may lead to the development of somatotrophinomas. Other relatively common mutational events involve the genes encoding USP8 (ubiquitin-specific protease 8) and P13K (phosphatidylinositol 3-kinase). Altered expression of cell cycle protein abnormalities have been noted in up to 80% of pituitary adenomas and these include the cyclin-dependent kinases (CDK), pituitary tumour transforming gene 1 (*PTTG1*), and various growth factors.

Familial pituitary adenomas

Familial isolated pituitary adenoma (FIPA): This condition was defined as the occurrence of two or more cases of pituitary adenomas in a family, but not associated with other tumours. The majority (~60%) of FIPA are macroadenomas with somatotroph and lactotroph adenomas being the dominant tumour types. Mutations in the aryl hydrocarbon receptor-interacting protein gene (*AIP*) have been identified as the cause in 15–30% of FIPA families (Marques and Korbonits, 2017). The *AIP* gene is located at chromosomal region 11q13.2 and it is suggested that in *AIP*-mutated FIPA, *AIP* loses its ability to bind its partners, and therefore, loses its activity as a tumour suppressor. The penetrance of pituitary adenomas among AIP mutation-positive carriers is around 12–30%.

MEN1 (Multiple endocrine neoplasia): The estimated incidence of MEN1 is 1–10/100 000/year. The syndrome is caused by a loss of function mutation in the *MEN 1* tumour suppressor gene on chromosome 11q13 (Balogh et al., 2006; Daly et al., 2009; Marques and Korbonits, 2017). The mutation is dominantly inherited with a penetrance of up to 90%. *MEN1* gene encodes

Menin, which has a complex regulatory interaction with a series of further proteins and gene expression. The spectrum of the condition includes primary hyperparathyroidism, pancreatic neuroendocrine tumours, and pituitary adenomas. The latter develop in 40% of cases. The distribution of histotypes is similar to sporadic adenomas. Lactotroph adenomas in *MEN1* show much lower response rate to dopamine agonist (approximately 40% normalization rate) and tend to be more invasive. The majority of *MEN1*-related pituitary tumours are macroadenomas. These patients therefore present twice as frequently with mass effect (approximately 80% vs. 40% in sporadic cases) compared to non-*MEN1* cases.

MEN4 (multiple endocrine neoplasia): This is a very rare inherited syndrome with autosomal dominant transmission and caused by mutations in the *CDKN1B* gene encoding the cyclin dependent inhibitor p27. The syndrome was first identified in rats with a frameshift mutation causing the synthesis of an unstable protein (MENX) (Pellegata et al., 2006). Both homozygous and heterozygous animals develop gonadotroph adenomas and phaeochromocytoma with 100% penetrance. Patients can present with acromegaly, primary hyperparathyroidism, renal angiomyolipoma, testicular cancer, and cervical carcinoid tumour.

McCune–Albright syndrome: This syndrome first described in 1937 is characterized by café-au-lait spots, fibrous dysplasia, hormonal abnormalities such as precocious puberty, excess GH production and prolactin hypersecretion (Albright et al., 1937; McCune and Bruch, 1937). It is caused by postzygotic somatic mutations in the *GNAS1* gene (guanine nucleotide binding protein, alpha-stimulating activity polypeptide 1) on chromosome 20q13.2-q13.3. Such postzygotic mutations lead to the mosaic-like phenotype typical of the disease and cause a variable clinical picture, which depend on the cell lineage affected. The specific tissue types affected are the pituitary gland, notably GH and prolactin-producing adenomas, skin, proximal femur, and facial bones.

Carney complex (CNC): This rare syndrome was first described in 1985 and consists of myxomas (cutaneous and cardiac), spotty pigmentations and endocrine overactivity, including pituitary adenomas (Casey et al., 1998). Pituitary adenomas are part of the phenotype in only 10% of cases with 75% of patients having subclinical elevation of GH, IGF-1, and prolactin. The genetic basis of Carney complex is heterogeneous. Associated germline mutations include CNC1 loci at 17q22-24, which encodes protein kinase A regulatory subunit Ia (PRKAR1A) and a site at 2p16, proposed to code the CNC2 gene.

X-linked acrogigantism: Sporadic and germline microduplications of the GPR101 on Xq26.3 account for about 10% of cases of gigantism. Abnormal growth occurs by the first four years of life. Mammosomatotroph hyperplasia and mixed lactrotroph/somatotroph adenomas are the underlying pathology in XLAG patients. The clinical features are striking but genetic diagnosis can be challenging, particularly in patients with somatic mosaicism. Surgery can be curative (Marques and Korbonits, 2017).

Mutations of succinate dehydrogenases: Patients with mutations in one of four subunits of SDH and its associated assembly factor can develop pituitary macroadenomas, which occur more commonly in familial cases, tend to be more aggressive than their sporadic counterpart and to be resistant to treatment (Marques and Korbonits, 2017).

DICER1: Heterozygous germline mutation in the *DICER1* gene cause pleuro-pulmonary blastoma familial tumour and dysplasia syndrome that is characterized by the occurrence of several tumours including cystic nephroma, Sertoli-Leydig cell tumours, goitre, and sarcomas. Children with *DICER1* mutations can also develop pituitary blastoma at very low penetrance

Radiology

Skull X-ray

X-rays are now mostly of historical interest (Fig. 25.2A). Prior to the advent of computed tomography (CT) and MR, plain X-rays were useful in detecting enlarged sella, erosion of the posterior clinoid or clivus for craniopharyngiomas, enlarged sphenoid sinus with tuberculum sella meningiomas and a 'J' shaped sella for optic nerve gliomas. Abnormal thickening of the skull is a feature of acromegaly.

CT head

CT scan can reveal an enlarged sellar and the associated pituitary mass (Fig. 25.2B). CT is also useful to identify calcification, which is more commonly seen in craniopharyngiomas and tuberculum sellar meningiomas. Pituitary apoplexy may be first seen on CT brain as a hyperdense lesion within the sella. The vascular relations of the pituitary can be assessed with contrast enhanced CT or CT angiogram. The most widely used application of CT however is for assessment of sinus characteristics as part of operative planning and/or intraoperative neuronavigation for endonasal approaches. Coronal and sagittal reconstructions are used to assess skull base/sinus anatomy.

MRI head

This is the standard modality for evaluating the tumour size, enhancement characteristics and neurovascular relationships of pituitary lesions in different planes (Fig. 25.2 C, D). The pituitary gland enhances compared to normal brain after administration of gadolinium due to the absence of the blood brain barrier (Fig. 25.2D). The posterior lobe accumulates contrast first followed by the anterior gland.

There are age- and sex-dependent variations in the size of the normal pituitary gland with an upper limit of 9–10 mm. However, it is important to be aware that physiological enlargement can occur at puberty and pregnancy resulting in a bulbous appearance on coronal MRI and dimensions of up to 12 mm.

On T1-weighted imaging, the posterior pituitary shows high signal also referred to as the 'bright spot'. Relations to adjacent neurovascular structures are better assessed with MRI than CT. Of particular importance are the relations of the optic apparatus and internal carotid artery to the pituitary tumour. Pituitary microadenomas can cause unilateral enlargement of the gland, with displacement of the pituitary stalk to the contralateral side.

Dynamic MR

Most pituitary adenomas can be detected by conventional imaging. However, small adenomas may be less obvious. Dynamic MRI

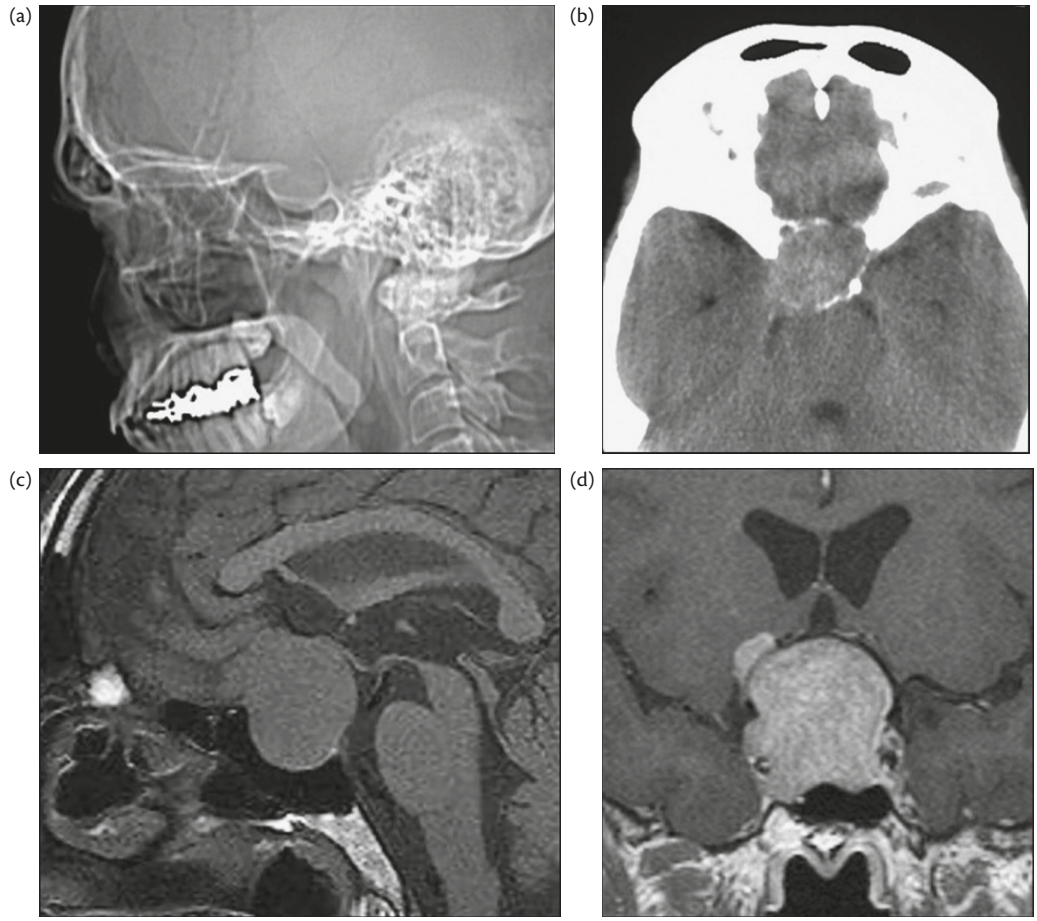

Fig. 25.2 Lateral skull X-ray (A) depicting an expanded pituitary fossa secondary to the adenoma. Axial CT scan (B) depicting a pituitary mass. Sagittal T1-weighted MR (C) and coronal T1-weighted MR with enhancement (D) reveal a pituitary macroadenoma with chiasmal compression.

imaging relies upon the altered contrast enhancement of pituitary microadenomas in relation to the normal gland (Figs. 25.3A–C). The technique involves intravenous administration of gadolinium followed by sequential rapid acquisition of T1-weighted MRI images for approximately 2–3 minutes from the time of contrast administration. Tumours usually enhance at a later (or sometimes earlier) time point compared to the normal pituitary gland. The timing correlates with tumour size, vascularity, integrity of blood brain barrier and also physical consistency (Kanou et al., 2002).

Other specialised MR sequences such as the spoiled gradient recalled acquisition in the steady state (SPGR) may also have value in identifying small microadenomas not seen with conventional MR sequences.

Inferior petrosal vein sampling (IPSS)

This is a useful test in determining the site of ACTH overproduction in Cushing disease (Deipolyi et al., 2011) (Figs. 25.3D, E). It is an invasive procedure with small risks of stroke, haemorrhage, and puncture site haematomas, and therefore currently used as an adjunct to the remaining diagnostics. The procedure involves guiding an intravenous catheter into the petrosal veins and measuring ACTH levels directly from the venous aspirate before and/or after corticotrophin factor (CRF) administration. Hormonal levels from within the inferior petrosal sinuses are interpreted in conjunction to peripheral samples. Sensitivity of IPSS reaches 80–90%, but IPSS is more useful in confirming the central (ie pituitary) origin of ACTH rather than the laterality of the microadenoma within the pituitary fossa.

Grading systems for pituitary adenomas

Grading systems of pituitary adenomas are typically based on anatomical and imaging information. The most widespread classification is the distinction between maximum tumour diameter above 1 cm (macroadenomas) or diameter below 1 cm (microadenomas).

Sophisticated classifications were developed to describe the involvement of adjacent structures such as extension into the para- or suprasellar area with the degree of spread into the sella floor, sphenoid, and distant spread. The main aim of these classifications was to assess difficulty of excision, probability of residual tumour, predict recurrence, and hormonal remission.

The initial radiological concept of grading pituitary adenomas was established by Hardy and Wilson in the 1970s (Hardy and Vezina, 1976; Fig. 25.4). In this scheme pituitary adenomas that do not breach the sella floor are classified as non-invasive, whereas sellar destruction qualifies the adenoma as invasive (Fig. 25.4A). The second feature is suprasellar extension of the tumour with distinction between intradural lesions and extradural spread (Fig. 25.4B).

The Knosp classification (Knosp et al., 1993) primarily assesses the extent tumour extending across into the cavernous sinus with focus on relations to the cavernous carotid (Fig. 25.5)

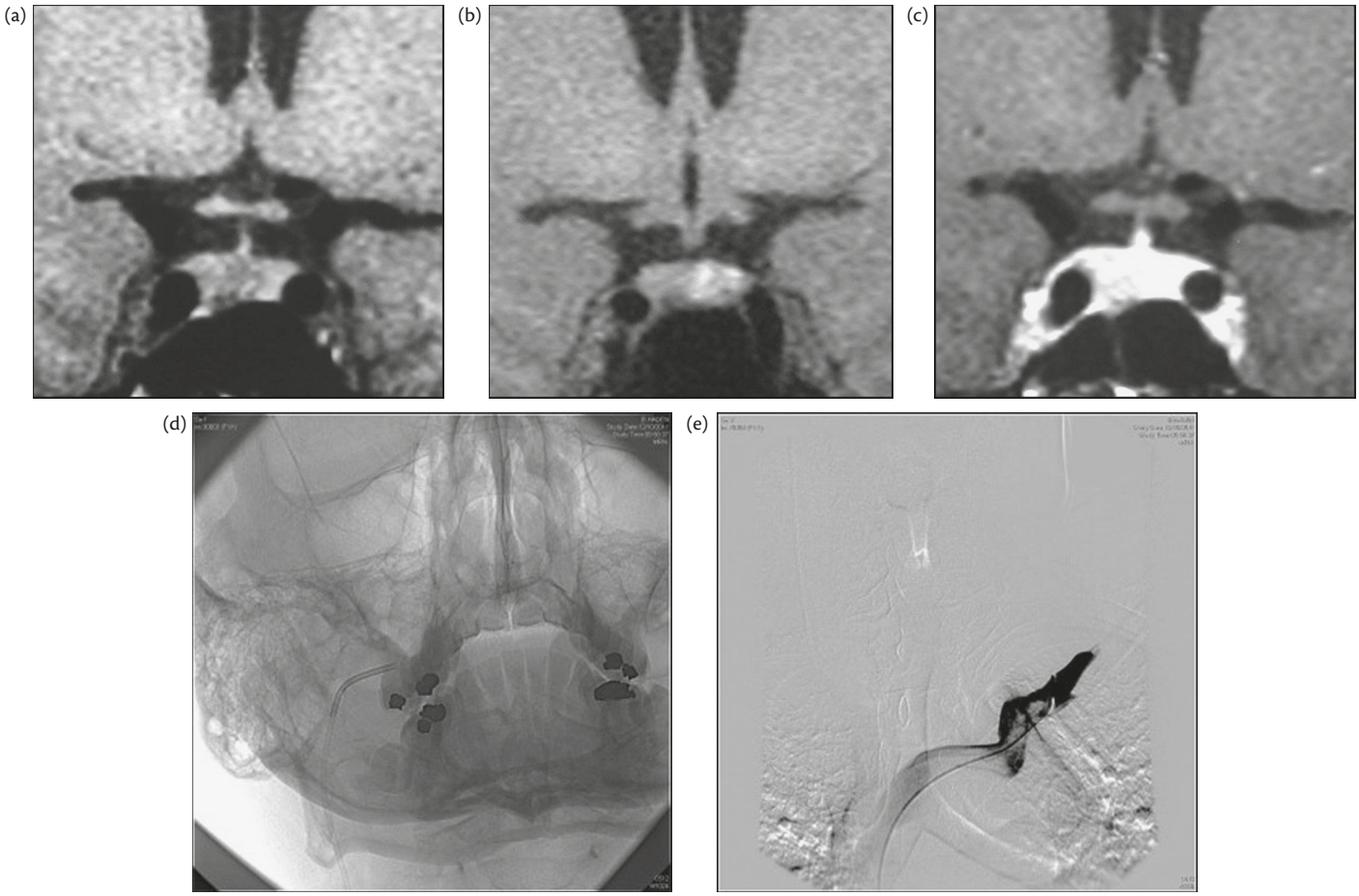

Fig. 25.3 Different phases of the dynamic MRI scan (A–C) demonstrating a right sided microadenoma, that shows less enhancement than the normal pituitary gland to the left at 5 seconds (B), but not later at 3 mins (C) in a patient with Cushing's disease. Anteroposterior (AP) skull X-rays showing endovascular catheter (arrow, D) placed into the right petrosal sinus that is then out lined by contrast (E).

Pathology

Histopathology

Historically pituitary tumours were classified according to the tintorial properties of their cytoplasm into acidophil, basophil and chromophobe (Kernohan and Sayre, 1956). Staining properties correlate with adenoma function: acidophil tumours are generally GH producing and linked with gigantism and acromegaly, basophil tumours were more likely to secrete ACTH, and chromophobe adenomas were thought to be hormonally inactive (Fig. 25.6). The introduction of electron microscopy has improved the classification and allowed the identification of subtypes such as densely and sparsely granulated somatotroph adenomas, but it was with the advent of immunohistochemistry that the spectrum of types and subtypes was recognized (Kovacs et al., 2001).

Morpho-functional classification

The current classification of pituitary adenoma includes seven major morphological and functional types (WHO, 2017) each of which is divided into subtypes with distinct histological and ultrastructural features, immune-phenotype, and function. Immunohistochemistry for pituitary hormones is the mainstream technique for the classification of adenomas; immunohistochemical stains for cytokeratins and transcription factors SF1, pit-1, and T-pit are also helpful to further define adenomas. Much less commonly, adenoma can be stained with antibodies directed against epidermal growth factor receptor (EGFR), oestrogen receptor, e-cadherin, VEGF, and mitochondria. A broader panel of antibodies is used when light microscopic features of a sellar tumour are not typical of adenoma and the lesion has to be differentiated from other primary, non-adenomatous tumours, or metastatic deposits.

Pathological features must always be correlated with clinical phenotype and biochemical evidence of hormone overproduction. Adenomas that are immunohistochemically positive for one or more pituitary hormones in the absence of clinical features of hormone hypersecretion are defined as clinical silent or clinically non-functioning. The lack of function may depend on several factors including defect in hormone release or synthesis of a biologically inactive hormone. In fact, immunohistochemistry detects the hormonal storage within the tumour cell cytoplasm and is not an indicator of secretory activity. Finally, adenomas such as lactotroph and gonadotroph adenomas can release active hormones but occur in postmenopausal women and therefore appear as clinically non-functioning and present with signs and symptoms of mass effect.

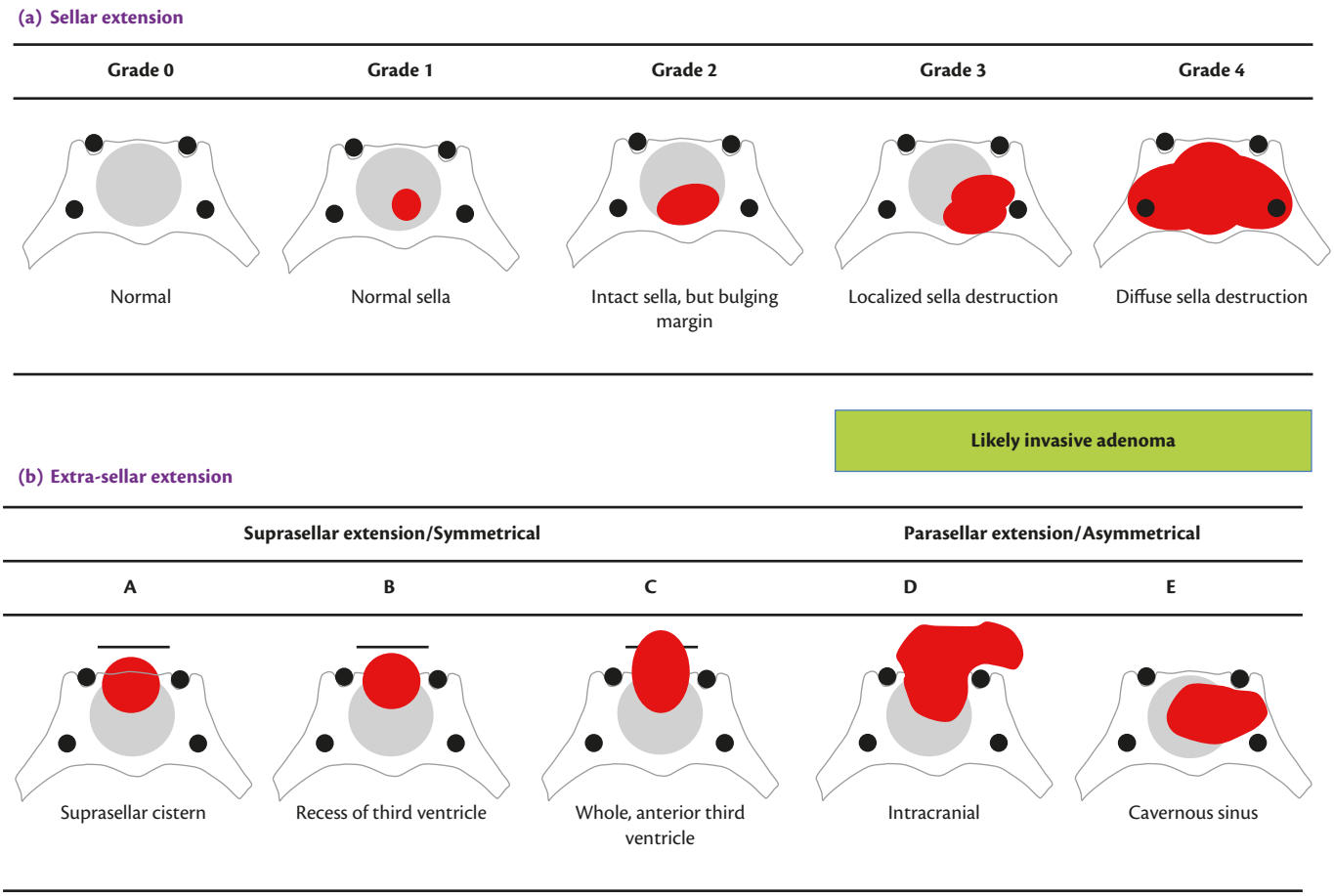

Fig. 25.4 Modified Hardy grading for pituitary adenomas. Grades 3, 4, D, and E reflect likely cavernous sinus invasion.
Hardy J, Vezina JL: Transsphenoidal neurosurgery of intracranial neoplasm, in Tompson RA, Green JR (eds): *Advances in Neurology*. New York, Raven Press, 1976, vol 15, pp 261–75.

The application of electron microscopy is limited to rare cases where light microscopic features and immunophenotype are not diagnostic. Ultrastructural features such as number, location, and size of secretory granules, location and aggregation of intermediate filaments, and presence of nuclear inclusions are those usually considered in the diagnosis.

Prediction of behaviour and response to treatment

Histotype, proliferative activity and tumour invasiveness are predictors of outcome for pituitary adenomas. The recent European Society of Endocrinology guidelines propose an integrated clinico-pathological approach to define aggressive adenomas that includes invasion, rapid growth, lack of response to treatment and

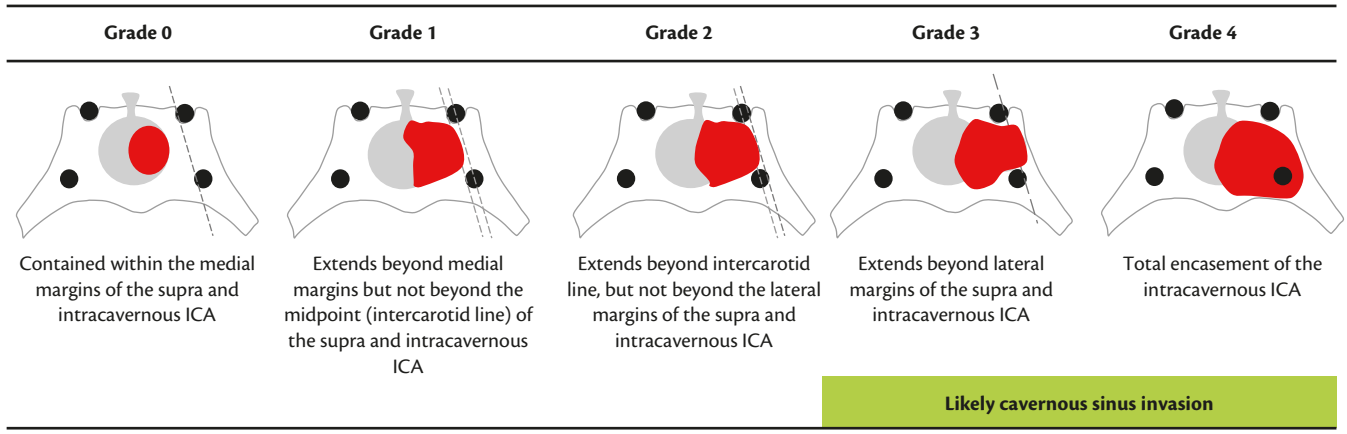
Grade 0
Grade 1
Grade 2
Grade 3
Grade 4
Contained within the medial margins of the supra and intracavernous ICA
Extends beyond medial margins but not beyond the midpoint (intercarotid line) of the supra and intracavernous ICA
Extends beyond intercarotid line, but not beyond the lateral margins of the supra and intracavernous ICA
Extends beyond lateral margins of the supra and intracavernous ICA
Total encasement of the intracavernous ICA
Likely cavernous sinus invasion

Fig. 25.5 Knosp grading for pituitary adenomas. Grades 3 and 4 reflect cavernous sinus invasion.
Reproduced with permission from Knosp, Engelbert; Steiner, Erich, Pituitary Adenomas with Invasion of the Cavernous Sinus Space: A Magnetic Resonance Imaging Classification Compared with Surgical Findings, *Neurosurgery*, Volume 33, Issue 4, pp. 610–17; discussion 617–18. Copyright © 1993 Oxford University Press and the Congress of Neurological Surgeons (CNS).

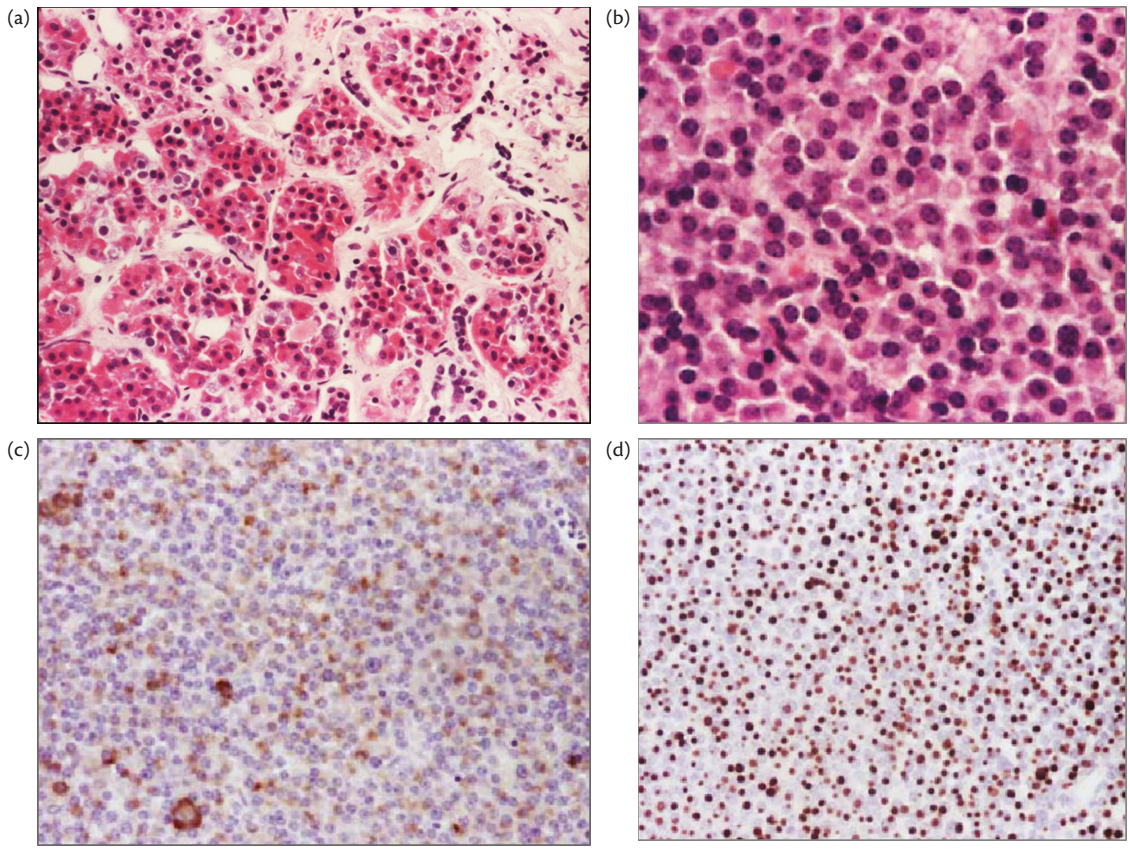

Fig. 25.6 Haematoxylin and eosin stain of the normal pituitary gland (A, ×10). Sparsely granulated somatotroph adenoma (B–D), showing haematoxylin-eosin (B, ×20), growth hormone (C, ×10) and cytokeratin immunostaining (D, CAM5.2, ×10).

increased proliferation (Raverot et al., 2018). The definition of atypical adenoma that was introduced in the 2004 version of the WHO classification is no longer contemplated in the 2017 edition (WHO, 2017).

Assessment of mitotic activity can be helpful to predict recurrence, particularly in adenomas that extend outside the sella and where complete excision is not possible.

The prognostic value of Ki-67 proliferation index is not universally accepted given the interlaboratory variability of immunostains and the lack of a consensus for quantification. Nevertheless Ki 67 values ≥3% should raise concerns as they may predict aggressive behaviour.

Expression of the enzyme O6-methyl-guanine-DNA methyltransferase (MGMT) can routinely be assessed by immunohistochemistry to help predict the response to temozolomide (TMZ). Low-level MGMT immunoexpression was correlated with a favourable response but MGMT immunoexpression is not always concordant with methylation of the MGMT gene promoter. Nuclear expression of the DNA Mismatch Repair Protein (MSH6) seen on immunohistochemistry can also contribute to assess response to chemotherapy.

The value of immunostains for somatostatin receptors 2, 3, and 5 in predicting the response to somatostatin analogues is still under debate.

The definition of pituitary carcinoma is still restricted to a tumour of adenohypophyseal cells that metastasize within and outside the cranio-spinal axis. Pituitary carcinoma is exceedingly rare representing about 0.12% of adenohypophyseal tumours collected in German Pituitary Registry and accounting for 6% of invasive adenomas in the SEER (Surveillance, Epidemiology, and End Results programme) database. Pituitary carcinomas in children are exceptional.

Endocrine aspects

Pituitary hormones and homeostatic feedback loops

Hormone secretion of the pituitary gland is regulated via multiple feedback loops involving the hypothalamus, pituitary gland, and target organs. A summary of these feedback loops is depicted in Figure 25.7.

The arcuate nucleus of the hypothalamus secretes (growth hormone releasing hormone (GHRH) growth hormone-inhibiting hormone (GHIH, usually referred to as somatostatin); thyrotropin-releasing hormone (TRH); gonadotropin-releasing hormone (GnRH); prolactin-releasing hormone (PRH); prolactin-inhibiting hormone (PIH, dopamine); and corticotrophin-releasing hormone (CRH). These factors are secreted into the hypophyseal portal system and transported to the anterior pituitary.

There are six hormones produced by the anterior pituitary: adrenocorticotrophic hormone (ACTH), prolactin (PRL), growth hormone (GH), thyroid stimulating hormone (TSH), follicle stimulating hormone (FSH) and luteinizing hormone (LH) (Figs. 25.1 and 25.7).

Oxytocin and anti-diuretic hormones (ADH, also known as vasopressin) are hormones secreted by the posterior pituitary. They are synthesized by neurons of the paraventricular and

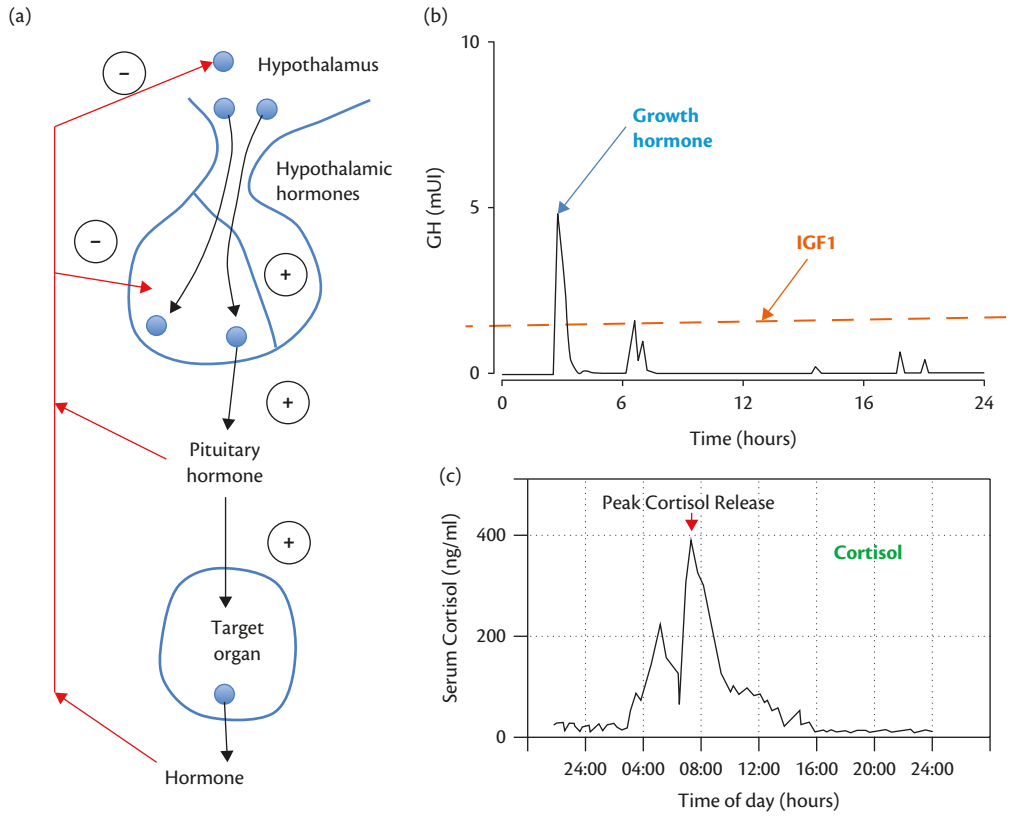

Fig. 25.7 Schematic depicting the hormonal feedback loop (A), pulsatile growth hormone release (B) and the circadian rhythm of serum cortisol release during the day (C).

supraoptic nuclei of the hypothalamus and are transported via the axons coursing through the pituitary stalk in to the posterior lobe.

Several hormones are dynamically secreted and cycles vary over days or months. For example, GH is released in a pulsatile fashion throughout the day. GH stimulates the production of IGF1 in the liver, which has more stable blood levels (Fig. 25.7B). Cortisol release peaks in the morning and reaches a trough by midnight (Fig. 25.7C). Other hormones such as LH and FSH follow a monthly cyclical pattern.

The primary target organs of the pituitary hormones include the adrenal glands (ACTH), thyroid gland (TSH), reproductive organs (FSH and LH) and breasts (PRL). Other hormones such as GH have a more widespread systemic effects, including impact on bone and muscle growth.

Basal, stimulation, and suppression endocrine tests

Pituitary hormone profile can be considered as basal endocrine tests. Basic profile includes prolactin levels, thyroid function, IGF-1, 9am or random cortisol, ACTH, LH, FSH, oestradiol, or testosterone. Prolactin is an important test for the management of patients because prolactin-secreting adenomas can be managed medically in the vast majority and surgery be avoided.

Stimulation tests are used to investigate diminished function of the pituitary or the target organ. A common example is the insulin stress test which is used to assess cortisol or GH deficiency by inducing hypoglycaemia which stimulates glucostatic counter-regulatory hormones ACTH, cortisol, or GH production (Fig. 25.8A). An alternative to this test is the glucagon stress test, which is better tolerated by patients. Glucagon stress test raises glucose to above normal and then the drop in glucose levels back down to normal stimulates glucostatic counter-regulatory hormones GH and ACTH.

Suppression tests investigate hormone overproduction. For example, the dexamethasone suppression test is used to suppress ACTH and cortisol responses and thus confirm Cushing's syndrome (Fig. 25.8B). The oral glucose tolerance test is used to confirm the diagnosis of growth hormone excess. In acromegaly, it demonstrates the lack of GH suppression by the raised serum glucose. The clinical use of these tests is detailed under the specific conditions later.

Occasionally the Short Synacthen Test (SST) can be used as a surrogate marker of ACTH production by the pituitary. Synacthen assesses the adrenal response to exogenous ACTH, but does not confirm that the patient has endogenous ACTH secretion. However, if the patient has been chronically ACTH deficient it is likely that they will have adrenal atrophy and so the SST can be used as an indirect assessment of chronic ACTH deficiency. It cannot be used to assess recent onset ACTH deficiency as inadequate time will have ensued to cause adrenal atrophy and hence they will still respond to exogenous ACTH while being deficient endogenously.

Treatment options

Surgical options

Surgery is undertaken to treat tumour-related mass effect and/or normalize excessive hormonal secretion. A diagnostic biopsy is required in cases where neuroimaging features are not clear.

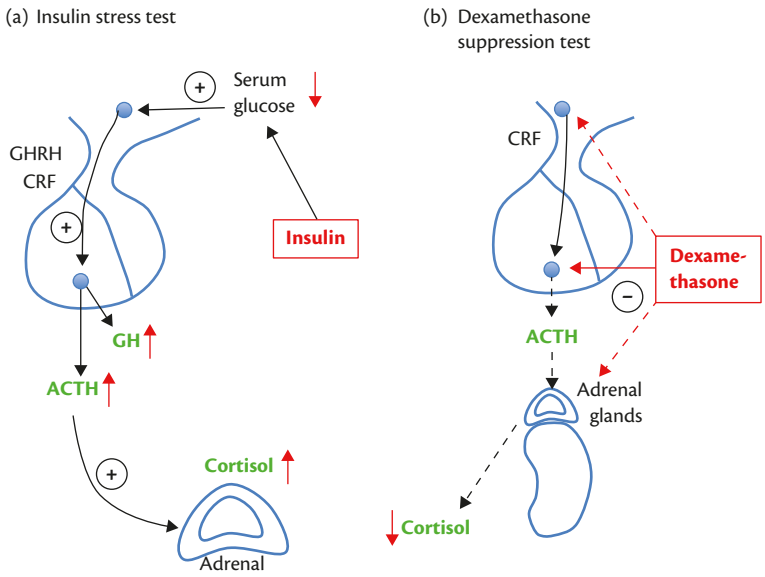

Fig. 25.8 Schematic examples of stimulation (A—insulin stress test) and suppression tests (B—dexamethasone suppression test).

The surgical techniques are described in the accompanying chapters. The general considerations of surgical approaches are dictated by the central location of the pituitary gland. Consequently, there are several approaches to the pituitary region. However, the vast majority of cases are tackled using the endoscopic transnasal approaches. See Figure 25.9.

Medical management

There are several aspects to medical management. At a simple level it involves replacing the missing hormones to treat hormone deficiencies and medically treating excess hormone production by pituitary tumours.

Common causes of hypopituitarism in the case of pituitary tumours are due to (1) tumour mass effect on the normal pituitary tissue; (2) postoperative impairment in pituitary function; and (3) hypopituitarism following radiotherapy. ACTH and ADH deficiency can be life-threatening and require urgent replacement. Other hormones can be replaced at a later date.

Hormone excess and the associated mass effect in some functioning adenomas could be successfully controlled medically. The most frequently encountered example is using dopamine agonists for prolactin-secreting adenomas. For other hormone active tumours medical options also exist although not as effective (e.g. somatostatins for GH-producing adenomas).

Radiotherapy

Radiotherapy is mainly used as an adjuvant therapy to reduce tumour growth in the postsurgical residuum, which could not be removed safely. Very occasionally, it can also be used as a first-line treatment in those patients where surgical intervention is contraindicated or ill advised.

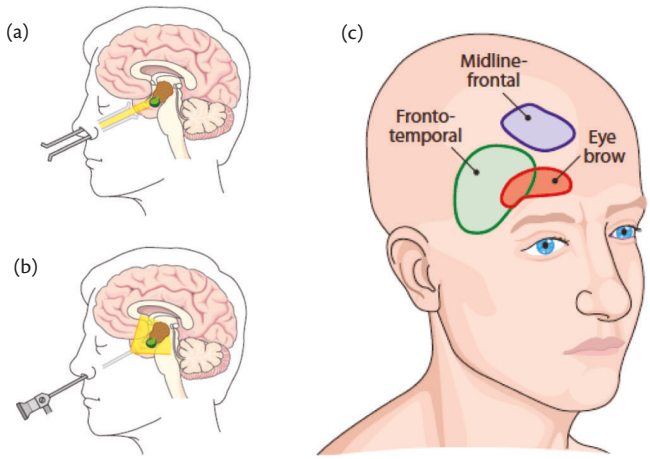

Fig. 25.9 Schematic overview of surgical approaches to pituitary tumours. Endonasal transsphenoidal approach with microscopic (A) and endoscopic (B) techniques. Transcranial options (panel C) include the eyebrow, pterional, and frontal craniotomies.

Modalities of radiotherapy include conventional linear accelerators where radiation is delivered from multiple ports in daily fractions over a period of 5–6 weeks constituting a total dose of 40–50 Gy. Fractionated radiotherapy carries the advantage of allowing adjacent normal neuronal tissue to recover between doses (Kanner et al., 2009). It is reported to be effective at disease control in 93% of cases at 10 years follow-up (Darzy and Shalet, 2009).

Complications include the gradual development of hypopituitarism over the course of several years following treatment. Hypopituitarism following radiotherapy to the sellar region is progressive and irreversible and therefore requires regular monitoring and adjustments in treatment. The risk is influenced by the radiation dose and there is a difference in the susceptibility of each hormonal system (Darzy and Shalet, 2009). Production of GH is the most vulnerable, deficiencies occur even with a radiation dose below 24 Gy and exposures between 40 and 50 Gy cause insufficiency in up to 50–100% of cases. TSH and ACTH production is less susceptible. Gonadotropin deficiency differs among genders: precocious puberty occurs in girls at a dose below 30 Gy and deficiency occurs in both genders at 30–50 Gy. Hyperprolactinaemia due to loss of hypothalamic inhibition is usually subclinical.

Radiotherapy is guided by face mask head fixation and high-resolution three-dimensional MRI to allow more accurate target delineation. Conformal planning with linear accelerators is standard in the modern era **Figures 25.10A & 25.10B**. Intensity-modulated radiotherapy (IMRT) and volumetric modulated arc therapy (VMAT) help plan a steep dose fall outside the target and thus better sparing the normal tissue.

The most frequently used stereotactic radiosurgery systems are Gamma knife and Linear accelerator (LINAC) **Figures 25.10C & 25.10D**. They are either used to deliver a single dose (15–20 Gy) or in 2–5 fractions in some cases. Tumour control rates range from 88–97% and morbidity ranges from 0% to 12% for optic nerve function, and 0% to 41% for the pituitary function.

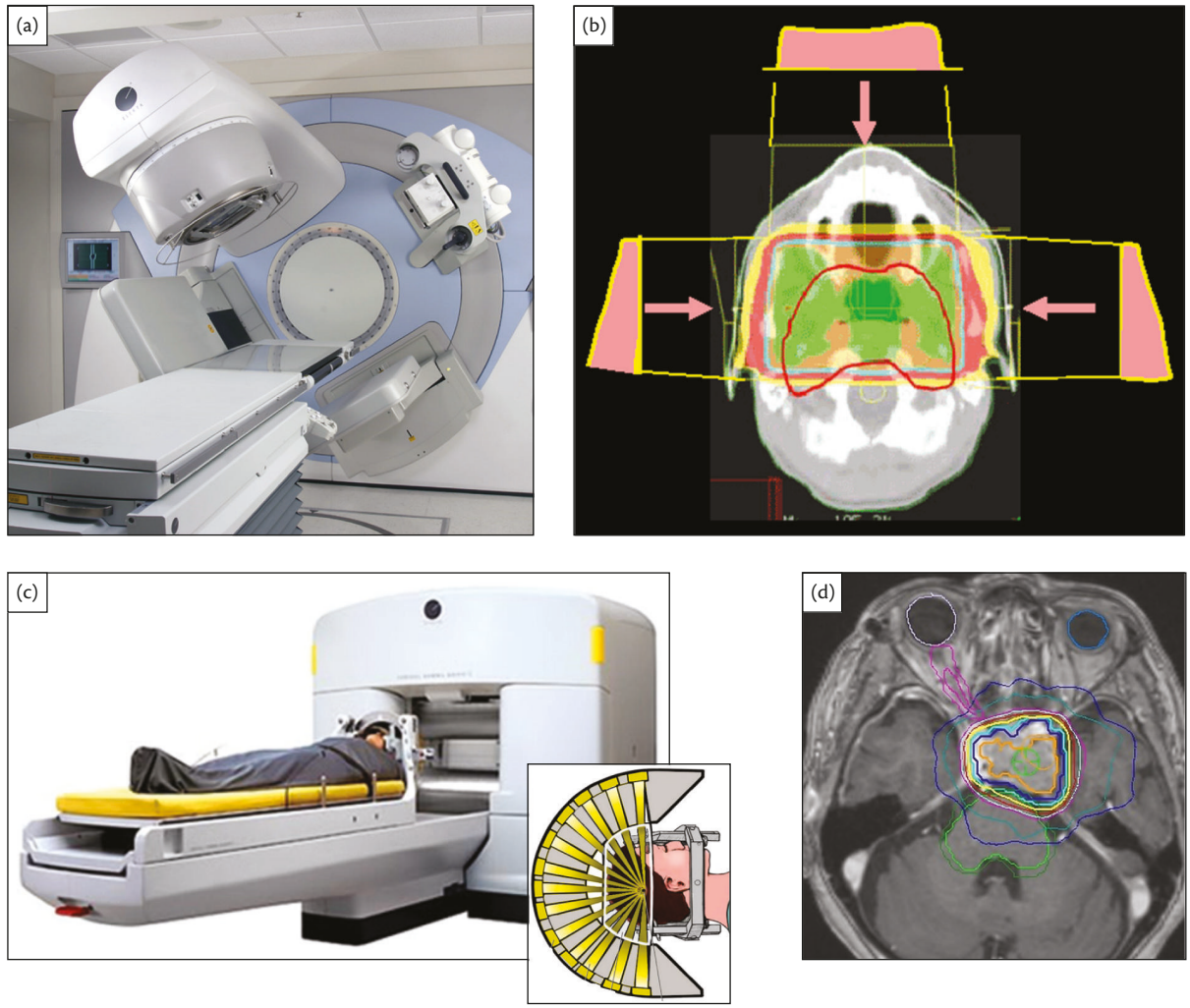

Fig. 25.10 Modalities of radiotherapy. Panel A: conventional radiotherapy with multileaf collimators targeting the beam. Panel B: radiotherapy dose planning. Panel C: stereotactic radiosurgery (Leksell Gamma Knife). Panel D: schematic of radiosurgical planning.

Choice between these modalities depends on the size and shape of residual tumour: stereotactic radiosurgery is recommended for small and focal targets that are more than 3 mm distance from the optic apparatus, whereas larger targets can be candidates for more conventional fractionated radiotherapy.

Proton beam is an emerging option to treat some skull base lesions and carries the advantage of a sharp drop out of radiation (i.e. the 'Bragg-Peak' effect). This enables higher doses of radiotherapy to be administered to the tumour with relative sparing of adjacent normal tissue. Proton beam therapy is not routinely recommended for pituitary adenomas. It is more reserved for treatment of residual skull base chordomas and chondrosarcomas which require a higher dose of radiotherapy with sparing of normal brainstem and optic chiasm.

Chemotherapy

Chemotherapy is rarely used in pituitary tumours except as a salvage treatment for very aggressive pituitary adenomas, where other treatment modalities have been exhausted. Oral temozolomide, a second-generation alkylating agent has been used in the treatment of pituitary adenomas and carcinomas with favourable response (Syro et al., 2011). Results of a Phase I trial suggested a possible role for placement of Gliadel (Carmustine wafers) into the resection cavity of pituitary tumours (Laws et al., 2003).

Management of tumour subtypes

Non-functioning pituitary adenomas (NFPA)

NFPA represent about 20% of all pituitary tumours and are the most frequent tumour type in terms of surgical caseload. About 80% belong to the gonadotroph cell lineage. They usually do not secrete active hormones. As a result, they remain clinically silent and continue to grow until they cause symptoms from mass effect or hypopituitarism by compression of the normal gland. By the same token NFPA are mostly macroadenomas.

These most frequently present with visual field defects, detected in 60–80% of cases. The chiasm is typically compressed from below in the midline, initially affecting the upper temporal quadrant, then progressing to bitemporal hemianopia (Fig. 25.11B). Contralateral homonymous hemianopia is also possible if the lesion is more posterior and with greater compromise of the proximal optic tract and involvement of Wilbrand's knee. Headaches are part of the presentation in up to 70% of cases, endocrine deficit in 8–20% of cases, apoplexy in approximately 2–7%, while cranial nerve palsies are less frequently seen (3%).

With the increasing availability of MRI and CT scans these lesions are also increasingly being discovered as incidental findings. A full set of pituitary function test should be performed as part of the workup.

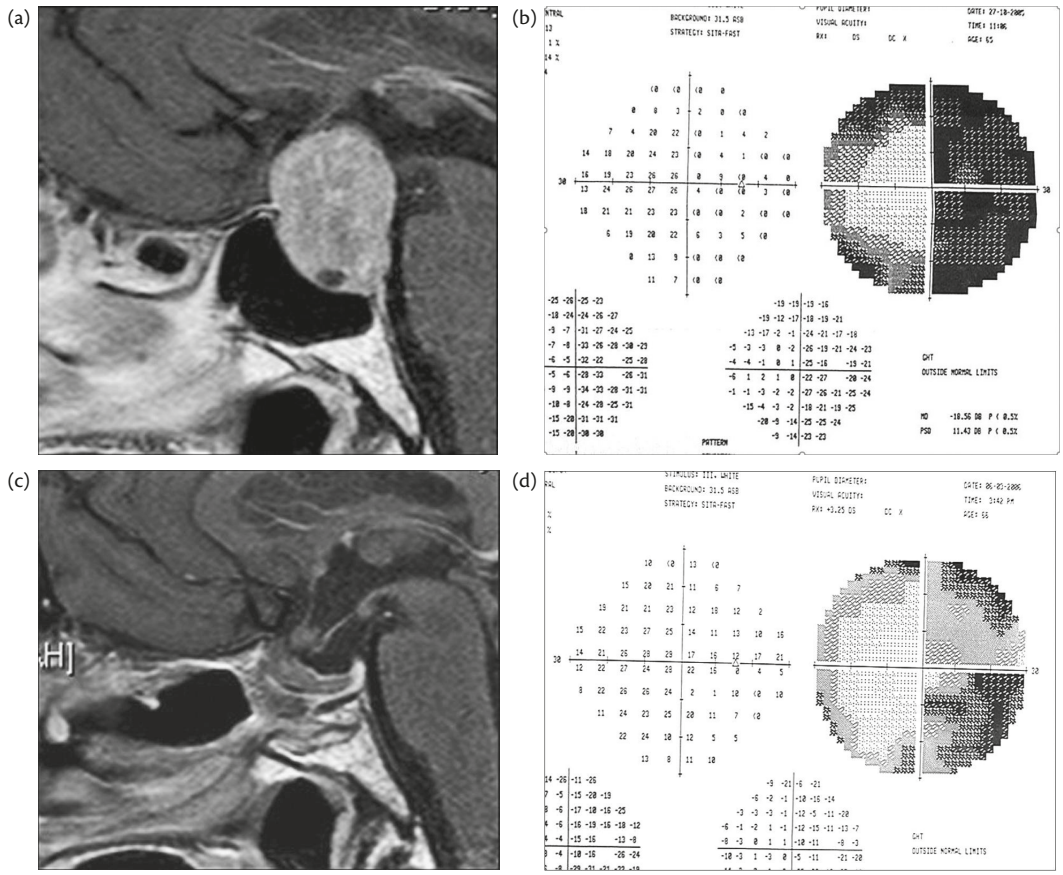

Fig. 25.11 Case example of a NFPA. Panel A: sagittal T1 gadolinium enhanced MRI scan a NFPA, displacing the optic chiasm upwards. Panel B: preoperative visual field assessment of the right eye for the same patient, showing right temporal hemianopia. Panel C: postoperative MRI appearances, with the descent of the optic chiasm following tumour debulking. Panel D: visual field assessment 6 months postoperatively with substantial improvement of the previously demonstrated deficit.

Primary treatment is surgical debulking with the aim to relieve compression on surrounding structures. The most commonly used surgical technique is endoscopic transsphenoidal approach.

Postoperatively vision improves in the majority with return to normal in 35%, partial improvement in 60% and there is no improvement or worsening vision in only around 5% (Gnanalingham et al., 2005). Postoperative visual improvement is typically progressive and over several years, but 50% of the eventual improvement in visual field deficits is apparent within the first 6 months (Fig. 25.11D).

Pituitary tumours being managed non-surgically can show spontaneous regression in about 10% of cases, but 50% of cases will progress and ultimately require surgery. Residual tumours can be targeted with fractionated radiotherapy or stereotactic radiosurgery.

Prolactin-producing adenomas

Incidence of prolactinomas ranges from 6 to 8 million/year. There are gender differences. Microprolactinomas are diagnosed 20 times more frequently in women of childbearing age, presumably because of the impact this has on fertility and the menstrual cycle, which prompts earlier investigation. Macroprolactinomas however occur with equal frequency for both genders. Furthermore, for women suffering from microadenomas, frequent symptoms are oligo or amenorrhoea, infertility, and galactorrhoea due to tumours secretory activity rather than mass effect. Hyperprolactinaemia in men can cause decreased libido, erectile dysfunction, gynaecomastia, and rarely galactorrhoea. See Figure 25.12.

Baseline prolactin levels are the first line of investigation, but several factors can affect serum prolactin levels. For example, the stress of a vein puncture can be associated with raised prolactin and thus blood samples taken from a cannula are preferred. Other extrapituitary causes of hyperprolactinaemia include neurogenic stimulation, drugs such as antidepressants, antipsychotics, and decreased serum clearance secondary to renal or hepatic insufficiency. Non-secreting pituitary lesions can also cause a modest increase in serum prolactin (typically 500–1000 mU/litre) due to pressure on the pituitary stalk. Values during pregnancy and breastfeeding can be around 3000–6000 mU/litre). In general, Prolactin levels greater than 2000 mU/litre are likely to be associated with prolactinomas and there is also a correlation between the prolactin level and the tumour size.

Two biochemical caveats to consider are the hook effect and the presence of macroprolactin. With the hook effect, high levels of prolactin are detected as falsely low due to the signal quenching effect of very high prolactin. This artefact can be corrected using serial sample dilution (St-Jean et al., 1996). Macroprolactin is a physiologically inactive form of prolactin found in a small proportion of people. It is in fact prolactin bound to IgG and some laboratory assays will detect it as prolactin, leading to a falsely elevated result.

The majority of prolactin-secreting adenomas can be managed medically with dopamine agonists such as cabergoline, bromocriptine, or pergolide. These agents are usually effective in approximately 90% of patients in suppressing the serum prolactin levels and inducing tumour shrinkage. Long-term clinical follow-up is recommended in patients managed medically with dopamine agonists. Some studies have reported that the dopamine agonists in some patients may be successfully weaned off longer term when no detectable tumour is seen on MR imaging and prolactin is completely suppressed, although this is not a universal finding (Schlechte, 2007).

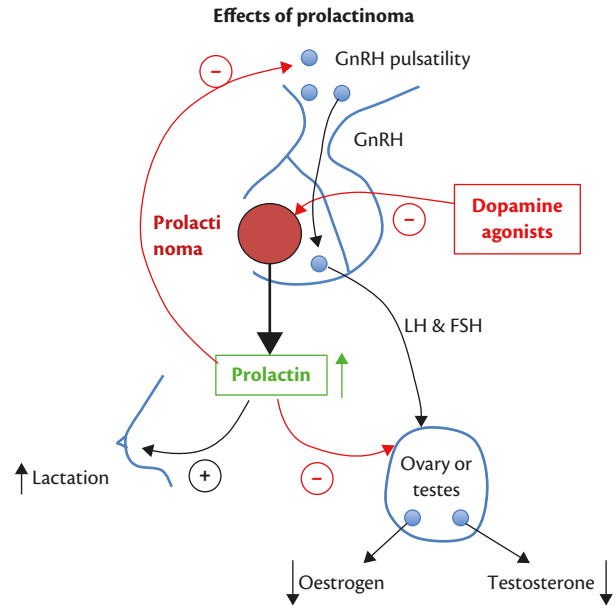

Fig. 25.12 Effect of prolactin-producing adenomas and medial management.

A rare but important side effect of cabergoline is cardiac valve abnormalities, which occurs secondary to fibroblast proliferation within the valve due to dopaminergic stimulation. Therefore, an echocardiogram is recommended prior to starting cabergoline and these patients should be monitored for this side effect. Dopamine agonists, notably cabergoline can be used to treat prolactinomas during pregnancy, with minimal risk of spontaneous abortion and congenital malformations.

About 10% of patients do not respond to treatment or are unable to tolerate the side effects of dopamine agonists such as nausea or depression. Thus only a minority of patients who are unable to tolerate the various dopamine agonists or fail to respond, warrant surgery. Surgical treatment is initially effective in 80–90% of microprolactinomas and in only about 50% of macroprolactinomas. Hyperprolactinaemia can persist and even recur after initial normalization. Radiotherapy can also be considered for inoperable tumours if medical therapy is not an option.

Growth hormone-producing tumours

GH-producing tumours constitute 20% of all pituitary adenomas with an incidence of 3–4 million/year. The source of growth hormone excess is a pituitary adenoma in 99% of cases with ectopic sources being exceptionally rare (Endocrine Society guidelines, Giustina et al., 2010).

Clinical presentation is often a combination of symptoms secondary to GH excess and/or mass effect from the tumour presenting as headaches and visual disturbance (Figs. 25.13B, C). In children and adolescents when the epiphyseal growth plates are active, GH excess causes gigantism, while in adults GH excess causes acromegaly. The constellation of signs and symptoms in acromegaly include swelling of soft tissues and internal organs, and pronounced jaw and frontal protuberances. Furthermore, excess GH production has a broad impact on body physiology affecting the following systems: musculoskeletal

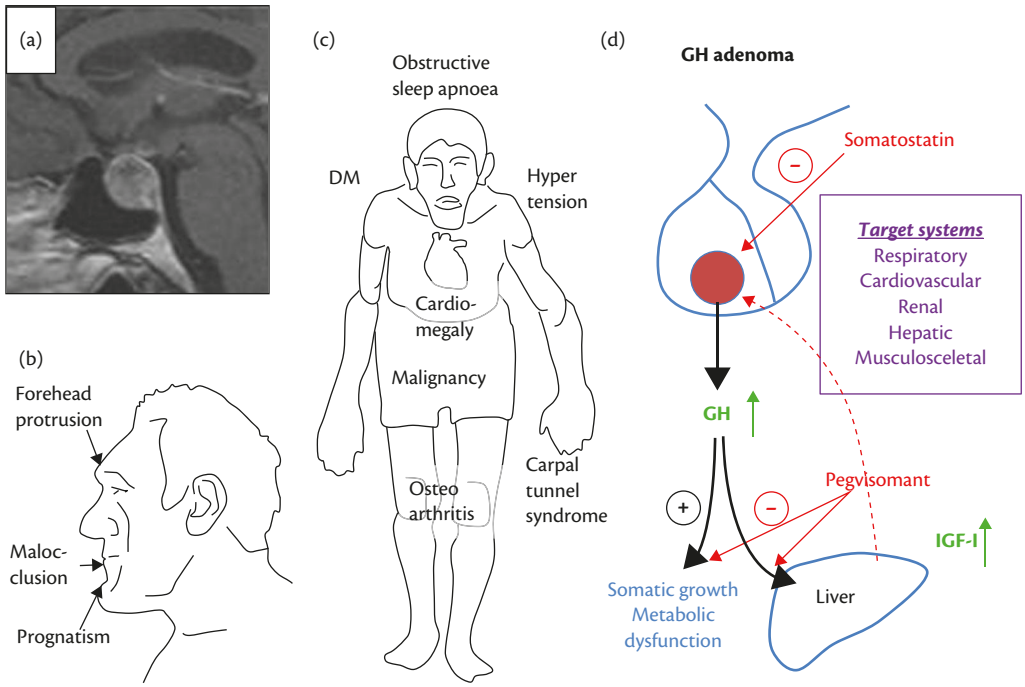

Fig. 25.13 (A) T1-weighted MRI scans of a growth hormone-producing macroadenoma. Presenting features of acromegaly (B) with typical involvement of multiple organ systems (C). Feedback loops and targets of medical management in growth hormone-producing adenomas (D).

in 70% of cases (e.g. arthropathy, degenerative osteoarthritis, vertebral fractures and compression neuropathy), cardiovascular in 60% of cases (e.g. cardiomyopathy, arrhythmia, hypertension and valvular disease) and respiratory in more than 50% of cases (e.g. obstructive sleep apnoea and nasal polyps). There are also pronounced metabolic effects such as diabetes, hypertension, dyslipidaemia and gout. There is a twofold risk of colon cancer in acromegaly. Compared to the general population, overall there is a twofold risk of mortality for untreated acromegaly due to the aforementioned cardiovascular, respiratory, and also neoplastic conditions.

Gender and age adjusted IGF-1 levels are the first line of investigation. As GH levels follow a pulsatile secretion pattern, random GH levels are difficult to interpret. IGF-1 is used as a surrogate marker of GH secretion and is usually raised in people with acromegaly. Confirmation of excessive GH secretion is obtained by the oral glucose tolerance test, which assesses adequate feedback of glucose on serum GH levels. Suppression of GH below 0.4 μg/litre with normal IGF1 levels rules out acromegaly (Giustina et al., 2010). Further confirmation can be obtained by demonstrating a raised mean GH level of greater than 1 μg/litre during a GH day curve. Coproduction of prolactin is also evident in 30–50% of cases.

MRI brain is warranted to delineate the pituitary adenoma prior to surgery. With negative MRI findings extrapituitary sources of GH/GHRH production should be investigated with further imaging (e.g. CT chest and abdomen).

Surgery is the most effective treatment for acromegaly with the goal of normalizing hormonal levels (i.e. both GH and IGF1) and decompressing surrounding structures. Endonasal transsphenoidal surgery generally achieves good outcomes with an average remission rate of 50–90% (Giustina et al., 2010). However, outcome is dependent upon several factors including surgeon experience, tumour size, tumour invasiveness, and preoperative GH levels. Predictors of good outcome include microadenomas (i.e. tumours smaller than 1 cm), non-invasive adenomas on MR and preoperative GH levels below 10 μg/litre. Early re-exploration may be considered for residual tumours and patients who are not in remission by the first operation to minimize surgical scarring.

Medical management consists of somatostatin analogues (eg. octreotide), which are successful at reducing GH levels in about half of the patients and partially shrink tumour size in about 30% of cases (Fig. 25.13D). GH receptor antagonists (e.g. pegvisomant) can reduce IGF1 levels in 95% of cases, but due to relative lack of feedback, there is an increase in adenoma size in about 5% of patients. In GH adenomas cosecreting prolactin, dopamine agonists can also be utilized. In practice, medical treatment serves as a postoperative adjunct in improving hormone levels in those not cured by surgery and for patients who are not medically fit for surgical intervention. Some centres also use pre-op medical treatment to help treat diabetes hypertension and to shrink tumour size.

Radiotherapy and radiosurgery are usually considered for residual tumour and are associated with a remission rate of 40–50, but there is a time delay of several years to achieve this (Castinetti et al., 2009).

Cushing's disease

Cushing's disease is a subtype of the greater category of Cushing's syndrome, which is defined as excess of serum cortisol. The most frequent cause of Cushing's syndrome is iatrogenic, where patients are kept on prolonged course of steroids for chronic conditions such as chronic obstructive pulmonary disease (COPD) or cerebral tumours. In the remaining cases glucocorticoid excess can be due to overproduction of ACTH either from a pituitary adenoma (~85% of cases) or other ectopic sources (~1%). Excess cortisol production by adrenal adenomas account for the remainder (approx. 15%).

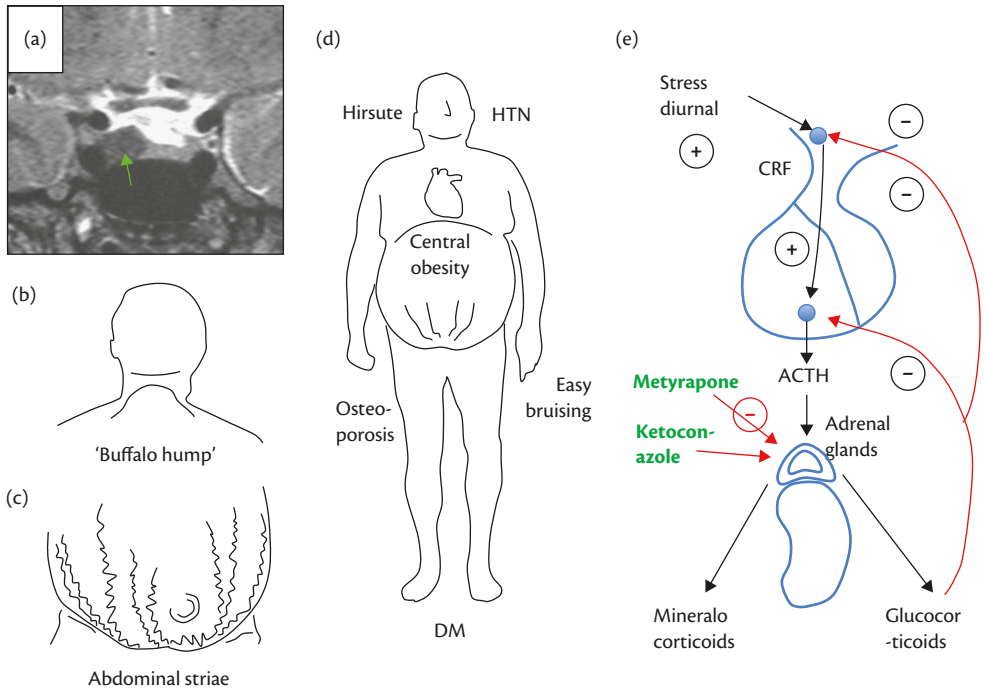

Fig. 25.14 MRI demonstrating right pituitary microadenoma causing Cushing's disease (A). Clinical features of Cushing's disease, including 'buffalo hump' (B), abdominal striate (C) and central obesity and involvement of multiple organ systems (D).

Pituitary adenomas associated with Cushing's disease are rare and carry an incidence of 1–2 million/year. Excessive exposure to glucocorticoids causes symptoms such as central obesity, facial plethora, rounded face, decreased libido, thin skin, decreased linear growth, hypertension, hirsutism, mood disorders, easy bruising, glucose intolerance, weakness, osteopenia, and nephrolithiasis (Figs. 25.14 B–D). Patients are often diagnosed in a delayed fashion, on grounds of the associated conditions such as difficult to control diabetes, hypertension, or obesity after a lengthy clinical journey.

In Cushing's disease the diagnostic pathway can also be complicated as no single diagnostic test has absolute sensitivity and specificity. Serum cortisol levels follow a circadian pattern and are influenced by several factors such as stress, depression, alcoholism, anorexia nervosa, or pregnancy.

Initial screening tests include early morning cortisol and ACTH levels, 24-hour urine free cortisol or midnight and 9am salivary cortisol levels. Late night salivary cortisol measurements have a sensitivity and specificity between 95 and 98% and can be used in the outpatient setting. The overnight dexamethasone suppression test involves giving 1 mg of oral dexamethasone at 23:00 hrs followed by measurement of serum cortisol at 9am the next day. Serum cortisol below 50 nmol/litre excludes Cushing's syndrome. In general, with pituitary and ectopic sources of Cushing's syndrome, both cortisol and ACTH levels are elevated. In Cushing's syndrome secondary to adrenal tumours, the cortisol levels but not the ACTH levels are high (Table 25.1).

Diagnostic dynamic tests are then undertaken and include the low-dose dexamethasone suppression test (LDDST). This involves the administration of dexamethasone (0.5 mg every 6 hours for 48 hours) following which 9am cortisol levels should suppress to below 50 nmol/litre. Failure to do so should be considered diagnostic of Cushing's, however in 3–8% of cases the sensitivity to dexamethasone is retained.

Table 25.1 Comparison of basal serum ACTH and cortisol levels in different causes for Cushing's syndrome. In Cushing's disease the diagnostic pathway can also be complicated as no single diagnostic test has absolute sensitivity and specificity. The typical changes seen with low-dose (LDDST) and high-dose dexamethasone suppression tests (HDDST) are shown

Tumour	ACTH	Cortisol	LDDST	HDDST
Normal	→	→	↓	↓
Pituitary adenoma	↑	↑	↑	→ or ↓
Ectopic ACTH	↑↑	↑	↑	↑
Adrenal tumours	↓	↑	↑	↑

The high dose dexamethasone involves administration of 8 mg of dexamethasone at 23:00 hrs and suppresses cortisol production in 50% of people with pituitary-dependent Cushing's, but its low sensitivity means that it is no longer commonly used (Table 25.1).

A dedicated MRI scan of the pituitary with contrast is used to look for the pituitary adenoma. Cushing's related tumours are largely microadenomas. However, in approximately 20–40% of cases, standard MRI scans fail to identify an adenoma in suspected cases of Cushing's disease. In such cases a dynamic MR scan is the next port of call (see radiology section, earlier on in this chapter).

If the adenoma is not clearly visible on the MR scan and/or if the biochemistry is equivocal then IPSS should be considered (Deipolyi et al., 2011). Despite it being an invasive investigation with potential morbidity, IPSS can help verify if the ACTH source is central (i.e. a CRF stimulated central to peripheral ratio of ACTH more than 3:1 is almost 100% sensitive and specific). Moreover, with IPSS a greater than 1.5-fold difference in CRF stimulated ACTH levels between the left and right sides can correctly identify the side of the lesion in the pituitary gland in approximately 70% of cases.

Suspected cases of ectopic tumours and adrenal adenomas are investigated with CT of the chest, abdomen, and pelvis.

For Cushing's disease secondary to a pituitary adenoma, surgical excision via a transnasal approach remains the most effective form of treatment. For non-invasive tumours selective microadenectomy can produce an initial remission rate of 70–80% but a relapse rate of up to 20% is quoted on longer follow-up. Remission rate is lower for macroadenomas, especially when invasive.

Medical treatment includes agents that inhibit steroid synthesis in the adrenal gland (e.g. metyrapone, ketoconazole, aminoglutethimide, and mitotane) (Fig. 25.14E). Medical therapy is also indicated for preoperative optimization and also reserved for patients where surgical treatment was not successful. Pituitary radiotherapy/radiosurgery is also generally reserved for when pituitary surgery has been unsuccessful.

In patients with ongoing disease after pituitary surgery, bilateral adrenalectomy is a salvage option to eliminate glucocorticoid excess. This treatment can result in Nelson's syndrome where due to the lack of negative feedback from glucocorticoids the increased ACTH production is associated with increase in melanocyte stimulating hormone (MSH), as both ACTH and MSH are derived from the same precursor, pro- opiomelanocortin. Increased MSH levels which stimulates melanocytes and causes excessive skin pigmentation. Furthermore, the remaining pituitary tumour can hypertrophy leading to mass effect.

Clinically 'silent' corticotroph adenomas may also become symptomatic due to mass effect or more rarely with conversion to Cushing`s disease in some patients.

Other functioning tumours

Thyrotropin-releasing pituitary tumours are much rarer and account for about 0.5–1% of all pituitary adenomas with an incidence of 1 per million population per year, limiting our experience to relatively small case series (Sanno et al., 2001). The majority of these tumours are macroadenomas presenting with signs secondary to mass effect and/or symptoms secondary to thyroxine excess including weight loss, palpitations, sleep disorders, and fatigue. TSHomas can be clinically indistinguishable from other causes of thyrotoxicosis.

Elevated serum T4 in association with raised or inappropriately normal TSH levels that do not suppress appropriately are the key biochemical findings. A MR scan to identify a pituitary mass is the other essential test.

Primary treatment is surgical excision, but preoperative medical control of hyperthyroidism is advised using beta-blockers and antithyroid agents (e.g. carbimazole or propylthiouracil). With transsphenoidal surgery, hormonal remission is achieved in about 80% of cases, but the ultimate cure rate is approximately 30%. Second-line treatment is radiotherapy, somatostatin analogues, or dopamine agonists.

Adenomas that produce biologically active gonadotropins (i.e. LH and FSH) are extremely rare. These patients usually present with signs of hypogonadism (e.g. irregular menstrual cycle or low libido), as the circadian rhythm is lost and testosterone levels are low. These patients can get large testes although this is extremely rare. On the other hand LH and FSH immunostaining adenomas that produce biologically inactive form of LH and FSH are common. This is apparent in the vast majority of non-functioning pituitary adenomas (Chaidarun and Klibanski, 2002).

Pituitary apoplexy

Pituitary apoplexy is an acute clinical condition secondary to infarction and/or haemorrhage within a pituitary adenoma (British Endocrine Society guidelines, Rajasekaran et al., 2011). Due to their rich vascular supply, tumours of the pituitary are approximately five times more likely to bleed or infarct than other brain tumours (Fig. 25.15). Overall, about 2–7% of pituitary adenomas can result in pituitary apoplexy. Risk factors include, anticoagulation, dopamine agonist therapy, pregnancy, hypertension, although most cases of apoplexy occur spontaneously.

The rapid expansion of the adenoma causes local mass effect with (1) visual field deficit; (2) endocrine disturbances due to compression of adjacent pituitary gland and hypothalamus; (3) cranial nerve deficits due to cavernous sinus compression; and/or (4) signs of raised intracranial pressure secondary to obstructive hydrocephalus. Headache is the most frequent presenting symptom occurring in 80–90% of cases. Headache is relatively acute in onset mimicking intracerebral or subarachnoid bleeds. Visual deficits, ocular paresis, and vomiting occur in 30–40% of patients. Altered consciousness is noted in approximately 20% of cases while meningism is seen less frequently.

Endocrine disturbances of one or more pituitary hormones are present in most (~80–90%) patients with pituitary apoplexy, with growth hormone and ACTH deficiency being the most common (65–80%). Pituitary apoplexy score (0–10) is based on the hierarchical consideration of deranged conscious level, visual acuity, visual field defect, and ocular paresis (Rajasekaran et al., 2011).

Management of pituitary apoplexy is dependent upon the severity of presenting symptoms. Factors to consider include decreased conscious level, severity of visual impairment, MR findings, endocrine and electrolyte disturbances. The initial medical management includes replacement of steroids (i.e. IV hydrocortisone) and fluid resuscitation.

Urgent surgery is advised in most patients with visual disturbance and corresponding mass effect and chiasmal compromise on MR. Moreover the timing of surgical decompression is subject to ongoing debate. In general, early surgery is considered for patients with severe visual deficits and those with less visual defect being treated conservatively. As a general rule, surgical decompression should take place within 1–2 days and once the patient has been medically stabilized. Transsphenoidal approach is favoured for most patients and the presence of hydrocephalus requires insertion of an external ventricular drain. Visual outcomes generally improve following surgery. However, the majority of patients with hypopituitarism at the outset do not recover from the hormone deficit. Moreover, even with conservative management, studies have shown that tumour shrinkage can happen over time with recovery in visual disturbances.

Craniopharyngioma

Craniopharyngioma is a rare suprasellar tumour with an incidence of 0.5–2.5 million/year. It is an epithelial-squamous, calcified, and cystic tumour arising from remnants of the craniopharyngeal duct and/or Rathke's cleft. Adamantinomatous and papillary variants are recognized histologically and intraoperatively the presence of dark brown 'machine oil' fluid with speckles of calcification and cholesterol clefts are pathognomonic.

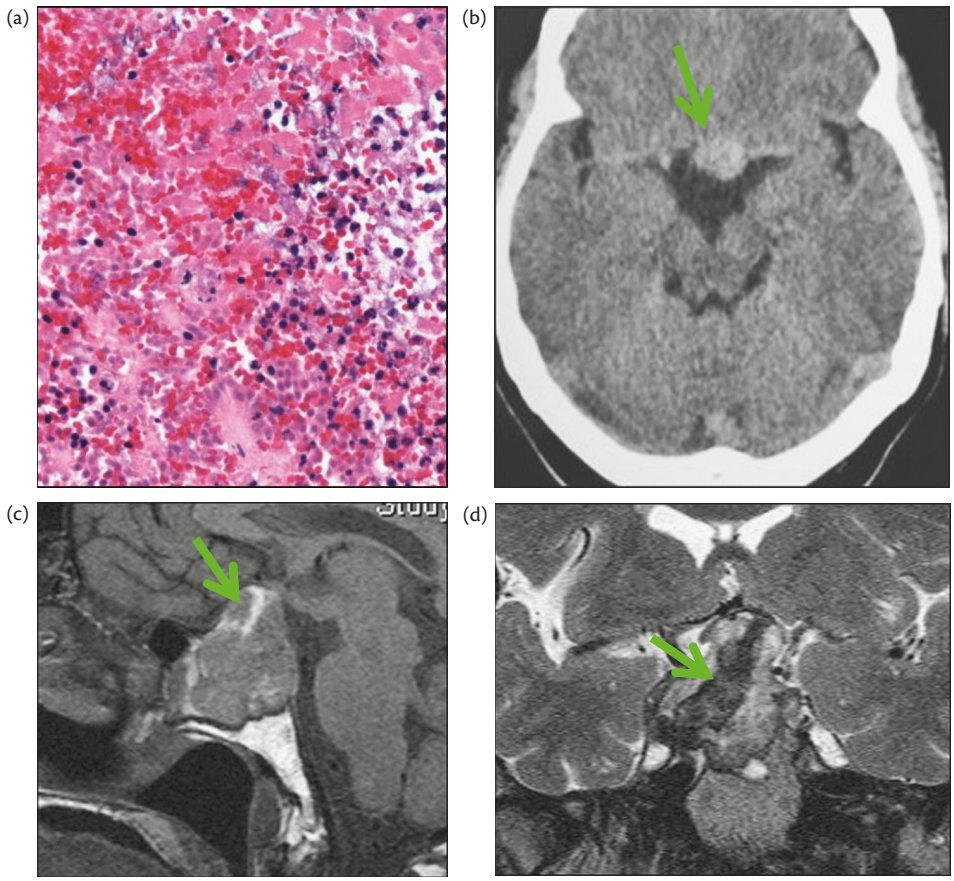

Fig. 25.15 In a case of pituitary apoplexy CT brain (panel B) and sagittal T1 (panel C) and coronal T2-weighted (panel D) MR images demonstrating haemorrhage (arrow) into a pituitary macroadenoma. Haematoxylin and eosin stain confirming evidence of haemorrhage and inflammatory cell infiltrate (A).

Endocrine deficits occur in 80–90% of cases and are associated with signs of mass effect such as visual field defect (20–25%). Diabetes insipidus is seen in 8–35% of cases at presentation.

MR and CT imaging usually differentiates craniopharyngiomas from pituitary adenomas based on the presence of calcification (80–90%), suprasellar position, cystic components, and patchy enhancement (Fig. 25.16A). Lesions can arise from the sellar, stalk, and suprasellar region extending into the third ventricle.

Principles of treatment consist of maximal and safe surgical resection and to decompress the optic chiasm, while taking care to minimize operative morbidity, notably hypothalamic injury. Cystic recurrence can be a troublesome problem and is usually managed by insertion of an Omaya reservoir. Radiotherapy and stereotactic radiosurgery are reserved for residual tumours and for patients who are not fit for surgery. With these measures, tumour control rates can reach up to 80%.

Rathke's cleft cyst

This is a non-neoplastic epithelium-lined cystic lesion arising from the embryologic remnants of Rathke's pouch in the sellar or suprasellar area. The majority of Rathke's cleft cysts are asymptomatic and are incidentally discovered. The cystic content is usually proteinaceous fluid, that appears high signal of T1-weighted MR imaging (Fig. 25.16B).

Management can be conservative if the cystic lesion is small and radiologically shown to be stable. With relatively large lesions or especially if increasing in size, the goal of surgery is drainage of the cyst and consequent decompression of the optic chiasm. Cyst recurrence may require further surgical drainage (e.g. transsphenoidal or transcranial approaches) and/or insertion of an Omaya reservoir to aid future percutaneous drainage in the event of recollections.

Inflammatory conditions

Lymphocytic hypophysitis: This is a rare inflammatory autoimmune condition (incidence 1/million/year). Most frequently it occurs in the peripartum period in women and acute, subacute, and chronic subtypes are recognized. In acute hypophysitis, the most frequent presentation is related to the mass effect from a rapidly expanding inflammatory mass. In the subacute or chronic setting, the symptoms of mass effect and hormonal deficits are more subtle.

This diagnosis can be suspected from clinical history and MRI findings, however if there is uncertainty a surgical biopsy is warranted. On MR imaging there is symmetric enlargement of the gland, with uniform enhancement and thickening of the pituitary stalk (Fig. 25.16C).

Treatment is determined by how fast the symptoms develop: surgical decompression is indicated for cases with acute deterioration and with no response to medical management. Expectant management (including steroids and hormone replacement) where there is little mass effect can be successful with progressive reduction in the size of the lesion (Falorni et al., 2014).

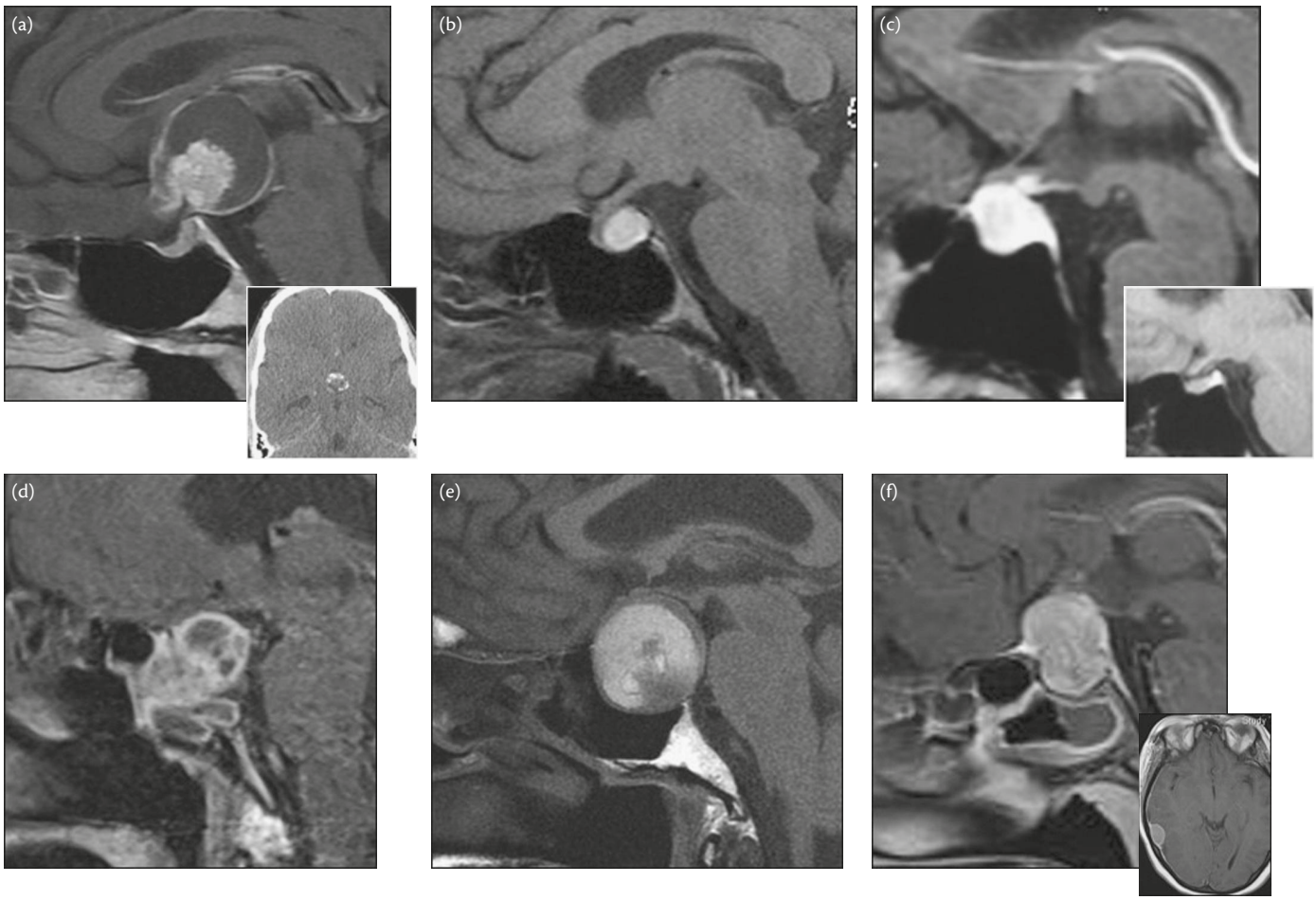

Fig. 25.16 Example of MR images of Craniopharyngioma (A; sagittal T1 with contrast and inset showing calcification on CT), Rathke's cyst (B; sagittal T1 MR), lymphocytic hypophysitis (C; sagittal T1 with contrast and inset showing shrinkage of lesion 8 months later), pituitary abscess (D; sagittal T1 with contrast), pituitary metastasis from adenocarcinoma of bowel (E; sagittal T1 MR) and pituitary carcinoma (F; sagittal T1 with contrast and inset showing right temporal dural metastasis (F).

Neurosarcoidosis: This is a rare presentation of systemic sarcoidosis. It affects the central nervous system in 5–15% of cases with a mortality of 10–20%. Cranial nerves, hypothalamus, meninges, and the pituitary gland are the most frequently affected in the central nervous system. Pituitary sarcoidosis contributes to less than 1% of intrasellar lesions. The most frequently reported hormonal deficit is hypogonadism followed by TSH, ADH deficiency.

Investigations include MRI brain (enhancing sellar and dural lesions), elevated serum ACE levels, and CSF analysis. Surgical biopsy for histological confirmation is usually needed. Medical management consists of hormone replacement, steroids or other immunosuppressants (e.g. prednisolone, methotrexate, cyclophosphamide, and azathioprine) and low-dose radiotherapy. Although MRI abnormalities resolve with steroids, the hormonal deficits persist in the majority of cases (Langrand et al., 2012).

Infections involving the pituitary gland

Infections of the pituitary gland are rare conditions. They can occur on grounds of aseptic necrosis of the gland, haematogenous spread, or direct extension of brain abscesses or tuberculomas (Zhang et al., 2012). Pituitary abscesses constitute approximately 0.5% of pituitary lesions and most common presentations are headaches and visual disturbances. Most frequent organisms are streptococci and staphylococci. Tuberculomas of the pituitary occur in the context of immunosuppressed patients and those with tuberculosis elsewhere.

Imaging findings are classically those of a peripherally enhancing sellar mass with restricted diffusion (Fig. 25.16D). Treatment options include surgical drainage by endonasal transsphenoidal or transcranial routes. Histological and microbiological analysis is paramount to clinch the diagnosis, followed by long-term antibiotics (at least 6 weeks or more) with serial contrast enhanced MRI scans to confirm disease clearance.

Secondary malignancies

The prevalence of metastasis to the pituitary is estimated at between 1% and 3.6% based on autopsy studies (Fassett and Couldwell, 2004). Virtually any tumour can metastasize to the pituitary gland. Spread is usually haematogenous and much less commonly by contiguity from the surrounding bone. The most common primary malignancies are breast and lung (Fig. 25.16E). Pituitary metastasis is only symptomatic in 7% of cases with diabetes insipidus, ophthalmoplegia, headaches, and anterior pituitary deficiency as the most common presentation.

Surgical biopsy/excision is the primary treatment modality combined with postoperative radiotherapy to the tumour bed and systemic oncological treatment depending on the primary malignancy and staging of disease. Most patients have systemic spread of their primary disease by the time the pituitary metastasis is found and therefore prognosis is very poor.

Other parasellar lesions

There are several other lesions such as meningiomas, chordomas, chondrosarcomas, fibrous dysplasia, Langerhans cell histiocytosis, and vascular abnormalities that can occur in the parasellar regions and extend to the sella. Differential diagnosis with pituitary adenomas can at times be challenging but the majority can be identified with reasonable confidence based on the presenting history and imaging (MR/CT) findings. These pathologies are covered elsewhere in this book.

Postoperative endocrine management

Risk of hypopituitarism

The risk of hypopituitarism following surgery varies depending on a number of factors, including the rigorous nature of endocrine tests, degree of compromise of pituitary function preoperatively and the type and size of tumour. Overall the risk of new pituitary hormone deficiency is estimated to be approximately 10–20% after transsphenoidal surgery. However, 50–70% of patients with pituitary adenomas may present with established hypopituitarism, with LH/FSH deficiencies being the commonest (Jahangiri et al., 2014). The risk of transient diabetes insipidus occurs at a rate of 16–25%, although permanent diabetes insipidus is below 5%, again influenced by the type of tumour, with craniopharyngiomas having a relatively high risk.

Steroid replacement protocols

In general patients undergoing pituitary surgery are at risk of hypocortisolaemia, which can be life-threatening. They should receive hydrocortisone on induction of anaesthesia and postoperatively until the endogenous cortisol production is confirmed to be satisfactory.

Peri- and postoperative hydrocortisone replacement protocols vary. A typical example is as follows: 100 mg intravenously in theatre at the time of surgery (and a further dose 8 hrs later), followed by a tapered oral dose of 20 mg (08:00 hrs), 10 mg (12:00 hrs), 10 mg (18:00 hrs) for the next 2 days, and then to a maintenance oral dose of 10 mg (08:00 hrs), 5 mg (12:00 hrs), and 5 mg (18:00 hrs). Two to three weeks later, the patient will need basal (09:00 hrs cortisol levels) and dynamic tests (e.g. insulin or glucagon stress test) to check the need for long-term steroid replacement. Alternatively, with the patient not on steroid supplements, 9am cortisol may be assessed in the days after surgery, with the patient put on steroid replacement when the 9am cortisol levels are low (i.e. <400 nmol/litre). The cortisol axis will also need further tests in the months postoperatively as the pituitary gland function may recover over time. The need for long-term postoperative steroids varies, with the majority of patients not requiring it.

Postoperative hyper- and hyponatraemia

Hypernatraemia: Diabetes insipidus (DI) is the most common cause of postoperative hypernatraemia. Typical biochemical criteria for the diagnosis of DI is polyuria (i.e. urine output >200 ml/hr for 3 or more consecutive hours), associated with hypernatraemia (i.e. serum sodium >145 mmol/litre) and increased serum osmolality together with a decreased urine osmolality. Transient DI immediately after pituitary surgery is frequently seen with prevalence varying between 10 and 30% for transnasal techniques. Permanent DI is much rarer occurring in 0–7% of cases (Schreckinger et al., 2013). DI occurs more often with craniopharyngiomas (especially postoperatively), neurosarcoidosis, and pituitary metastases.

Besides transient and permanent DI, a triphasic pattern can rarely occur (1–3% of postop cases. This consists of an acute phase of DI in the first few days after surgery related to the abrupt discontinuation of ADH release, followed by a surge in ADH from the degenerating hypothalamic nuclei, usually 1–2 weeks postoperatively resulting in low serum sodium (i.e. syndrome of inappropriate ADH release; SIADH). This phase is followed by the relapse to permanent DI phase due to the exhaustion of ADH production.

First line of management in DI is fluid resuscitation (oral or IV as appropriate) with repeat biochemistry at frequent intervals. Depending on the response, DDAVP replacement (IV, oral, or nasal spray formulations available) may be warranted. Gentle correction of serum sodium (i.e. no more than 10 mmol/litre per day) is advisable.

Hyponatraemia Postoperative hyponatraemia is an infrequent complication of pituitary surgery (up to 10–15% of cases) and it can occur in the context of syndrome of inappropriate ADH production (SIADH) or cerebral salt wasting (CSW). Differentiating between these two conditions is essential, as they require different treatments. SIADH is more common that CSW following pituitary surgery. It is characterized by excessive secretion of ADH, which leads to water retention through the distal collective ducts in the kidney. This results in reduced urine output, hyponatraemia, and increased total body water content.

Treatment is with fluid restriction of up to 500–750 ml per day with repeat biochemistry every 24 hours (or more frequently depending on the severity of hyponatraemia) until serum sodium is normal. Gradual correction of sodium is essential (i.e. less than 10 mmol/litre serum sodium per day), to avoid the risk of central pontine myelinolysis. Medical management is occasionally needed with demeclocycline and less commonly hypertonic saline and/or Tolvaptan (a vasopressin receptor 2 antagonist that needs close monitoring).

CSW is less common following pituitary surgery and is more frequently seen after head injury or subarachnoid haemorrhage. It is associated with excessive sodium loss in urine from the kidneys, depleted intravascular volume with raised urine sodium content. Treatment is salt replacement with salt tablets (can be irritant to the stomach), IV saline, and/or fludrocortisone.

Differentiating between SIADH and CSW can be difficult and the most useful differentiating features are assessment of body fluid volume status (eg central venous pressure etc) and response to saline fluid challenge (i.e. hyponatraemia worsens in SIADH and improves in CSW).

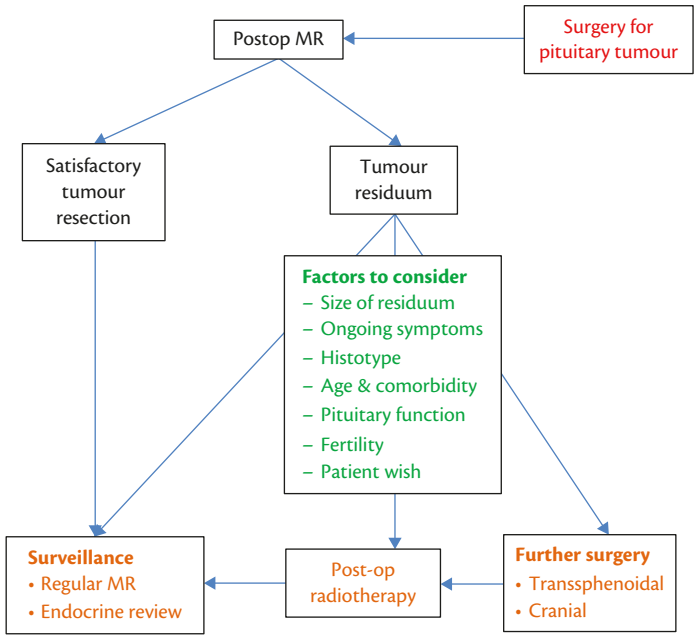

Fig. 25.17 Line diagram depicting clinical decision algorithms for residual tumours.

Topical issues

Management of residual tumour

The management of residual tumours depends on multiple factors and therefore management decisions are best made on a case-by-case basis with involvement of a pituitary multidisciplinary team (MDT; Fig. 25.17).

Most patients have their follow-up MRI scan at 4–6 months after the surgery to allow for blood and other haemostatic materials placed in the tumour bed to be absorbed. The decision on further surgery, radiotherapy, or continued surveillance is influenced by the MR scan findings (e.g. size and invasiveness of tumour residuum) and other factors such as histological features, ongoing tumour-related symptoms (e.g. visual disturbance), age, comorbidity, pituitary function, fertility state (if fertility is desired), and patient wishes.

In general, symptomatic patients with sizeable or progressively enlarging tumours can undergo repeat operation through a transnasal or cranial approach. Radiotherapy and stereotactic radiosurgery are very effective in controlling small residual tumours that are difficult to resect. Early radiotherapy can be favoured in patients with established hypopituitarism and comorbidity. Age is another consideration for radiotherapy as younger patients are more likely to suffer from long term radiation induced complications (e.g. neurocognitive sequelae, development of secondary tumours etc). Suspected small tumour residuum on post-op MR scans without significant associated symptoms can also be observed with regular (mostly annual) MRI scans, with a view to surgically intervening at a later stage. This is especially so in patients with relatively intact pituitary function.

Management of incidentalomas

Pituitary adenomas are being increasingly diagnosed in an incidental fashion due to the greater availability of MR imaging. In adults who underwent cranial imaging for reasons other than pituitary disease, incidentalomas were seen on MRI between 10–38% of patients, although less than 1% are macroadenomas (i.e. >1 cm in maximum diameter).

The general recommendations are that patients presenting with a pituitary incidentaloma undergo an endocrine review, including evaluation for evidence of hypopituitarism and hormone hypersecretion (Freda et al., 2011).

Management of the pituitary incidentaloma will depend on a number of factors, including size of the lesion, endocrine status, visual status, and also taking into account other factors such as patient age, comorbidity, and patient wishes. In general, surgery should be considered in patients with an incidentaloma causing chiasmal compression, visual deficits attributable to the lesion and/or hormone secretion, with the exception of prolactinomas which can invariably be managed medically (Fig. 25.18; Freda et al., 2011).

Patient's with small microadenomas, with no relevant symptoms can be managed conservatively. They usually require annual MR scans for the first 3 years and if the lesion remains radiologically stable then progressively at increasing scanning intervals. Surgery becomes an option if the lesion significantly increases in size during the surveillance period. This is more likely with macroadenomas, which on a recent review increased in 24% of patients, although for all incidentalomas this risk is ~8% per year (Freda et al., 2011). Patients being managed conservatively also need to be warned of the small (~2%) risk of pituitary apoplexy and the potential development of visual symptoms and need for urgent surgical decompression.

Hypopituitarism following traumatic brain injury (TBI) and aneurysmal subarachnoid haemorrhage (SAH)

In recent years there has been increasing recognition of hypopituitarism following TBI or SAH. The incidence of hypopituitarism following TBI is reported to vary between 15% and 68% of cases (an average of 27.5% on a systematic review by Agha et al., 2007; Schneider et al., 2007). Indeed, some of the presenting features of

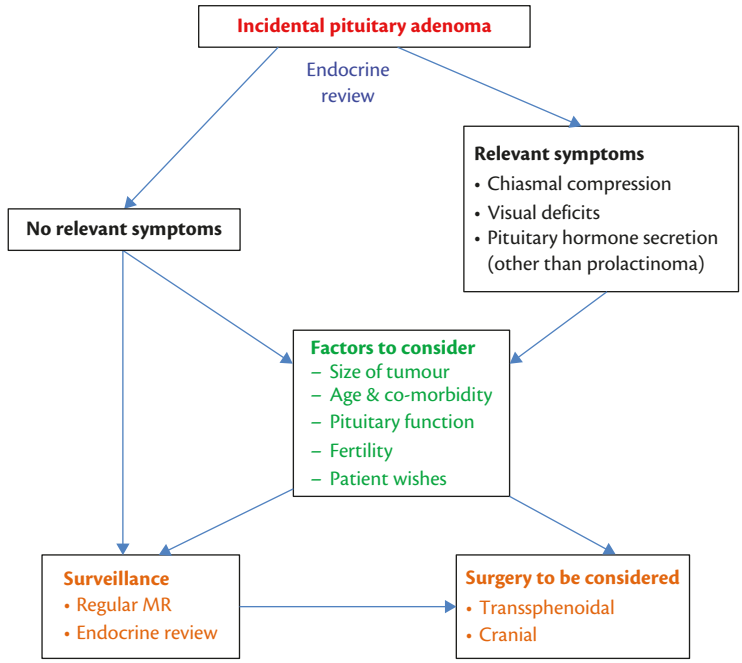

Fig. 25.18 Line diagram depicting clinical decision algorithms for incidental tumours.

hypopituitarism such fatigue, low mood, poor concentration, and other neurocognitive issues are often attributed to the brain injury itself and therefore the impairment of pituitary function remains unrecognized. The reported de novo deficiencies for pituitary hormone production are variable; the most frequently affected hormones are gonadotropins (13%), growth hormone (12%), and ACTH (8%). Spontaneous recovery was seen in 50–70% of cases. Acute phase DI can be present in approximately 20% of cases and in 7% of long-term survivors. Severity of head injury was found to be a possible predictor of hypopituitarism with frequencies of 35%, 11% and 17% for severe, moderate, and mild head injuries respectively (Schneider et al., 2007).

The literature on postop hypopituitarism following SAH is sparse. Acute pituitary dysfunction occurs in about 38–55% of patients (i.e. average of 47% in a systemic review) following aneurysmal subarachnoid haemorrhage but this figure is based on multiple relatively small case series (Schneider et al., 2007). The most frequently affected hormones are gonadotropins (25%) and growth hormone (6%) and ACTH (21%). Moreover, a systemic review of the literature showed a gradual recovery of pituitary function over time with 26% at 6 months post injury and only 7% had pituitary dysfunction after 14 months (Schneider et al., 2007).

Awareness of hypopituitarism in both TBI and SAH is important, because some of the presenting symptoms (fatigue, neuropsychiatric symptoms) can be attributed to the primary pathology rather than a scenario of hormonal deficiency. The benefits of replacing the missing pituitary hormones in managing neurocognitive symptoms are less clear and subject to ongoing studies.

REFERENCES

Agha, A., Phillips, J., & Thompson, C.J. (2007). Hypopituitarism following traumatic brain injury (TBI). *Br J Neurosurg*, **21**(2), 210–16.

Albright, F., Butler, A.M., Hampton, A.O., & Smith, P. (1937). Syndrome characterized by osteitis fibrosa disseminata, areas of pigmentation and endocrine dysfunction, with precocious puberty in females: report of five cases. *New Eng J Med*, **216**(17), 727–46.

Balogh, K., Rácz, K., Patócs, A., & Hunyady, L. (2006). Menin and its interacting proteins: elucidation of menin function. *Trends Endocrinol Metab*, **17**(9), 357–64.

Casey, M., Mah, C., Merliss, A.D., et al. (1998). Identification of a novel genetic locus for familial cardiac myxomas and carney complex. *Circulation*, **98**(23), 2560–6.

Castinetti, F., Morange, I., Dufour, H., Regis, J., & Brue, T. (2009). Radiotherapy and radiosurgery in acromegaly. *Pituitary*, **12**(1), 3–10.

Chaidarun, S.S. & Klibanski, A. (2002). Gonadotropinomas. *Semin Reprod Med*, **20**(4), 339–48.

Daly, A.F., Tichomirowa, M.A., & Beckers, A. (2009). The epidemiology and genetics of pituitary adenomas. *Best Pract Res Clin Endocrinol Metab*, **23**(5), 543–54.

Darzy, K.H. & Shalet, S.M. (2009). Hypopituitarism following radiotherapy. *Pituitary*, **12**(1), 40–50.

Deipolyi, A., Karaosmanoglu, A., Habito, C., et al. (2011). The role of bilateral inferior petrosal sinus sampling in the diagnostic evaluation of Cushing disease. *Diagn Interv Radiol*, **18** (1), 132–8.

Ezzat, S., Asa, S.L., Couldwell, W.T., et al. (2004). The prevalence of pituitary adenomas: a systematic review. *Cancer*, **101**(3), 613–19. Review.

Falorni, A., Minarelli, V., Bartoloni, E., Alunno, A., & Gerli, R. (2014). Diagnosis and classification of autoimmune hypophysitis. *Autoimmun Rev*, **13**(4–5), 412–16.

Fassett, D.R. & Couldwell, W.T. (2004). Metastases to the pituitary gland. *Neurosurg Focus*, **16**(4), E8.

Freda, P.U., Beckers, A.M., Katznelson, L., et al. (2011). Pituitary incidentaloma: an endocrine society clinical practice guideline. *J Clin Endocrinol Metab*, **96**(4), 894–904.

Giustina, A., Chanson, P., Bronstein, M.D., et al. (2010). A consensus on criteria for cure of acromegaly. *J Clin Endocrinol Metab*, **95**, 3141–48.

Gnanalingham, K.K., Bhattacharjee, S., Pennington, R., Ng, J., & Mendoza, N. (2005). The time course of visual field recovery following transphenoidal surgery for pituitary adenomas: predictive factors for a good outcome. *J Neurol Neurosurg Psychiatry*, **76**(3), 415–19.

Hardy, J. & Vezina, J.L. (1976). Transsphenoidal neurosurgery of intracranial neoplasm. In: Tompson, R.A. & Green, J.R. (eds) *Advances in Neurology*, vol. **15**, pp. 261–75. New York: Raven Press.

Jahangiri, A., Wagner, J., Han, S.W., et al. (2014). Morbidity of repeat transsphenoidal surgery assessed in more than 1000 operations. *J Neurosurg*, **121**(1), 67–74.

Kanner, A.A., Corn, B.W., & Greenman, Y. (2009). Radiotherapy of nonfunctioning and gonadotroph adenomas. *Pituitary*, **12**(1), 15–22.

Kanou, Y., Arita, K., Kurisu, K., Tomohide, A., & Iida, K. (2002). Clinical implications of dynamic MRI for pituitary adenomas: clinical and histologic analysis. *J Clin Neurosci*, **9**(6), 659–63.

Kernohan, L.W. & Sayre, G.P. (1956). In: *Tumours of the Pituitary Gland and Infundibulum. Atlas of Tumor Pathology*, Section X-Fascicle 36. Washington, DC: Armed Forces Institute of Pathology.

Knosp, E., Steiner, E., Kitz, K., & Matula, C. (1993). Pituitary adenomas with invasion of the cavernous sinus space: a magnetic resonance imaging classification compared with surgical findings. *Neurosurgery*, **33**(4), 610–17; discussion 617–18.

Kovacs, K., Horvath, E., & Vidal, S. (2001). Classification of pituitary adenomas. *J Neurooncol*, **54**(2), 121–7.

Langrand, C., Bihan, H., Raverot, G., et al. (2012). Hypothalamo-pituitary sarcoidosis: a multicenter study of 24 patients. *QJM*, **105**(10), 981–95.

Laws, E.R. Jr., Morris, A.M., & Maartens, N. (2003). Gliadel for pituitary adenomas and craniopharyngiomas. *Neurosurgery*, **53**(2):255–69; discussion 259–60.

Keil, M.F. & Stratakis, C.A. (2008). Pituitary tumors in childhood: an update in their diagnosis, treatment and molecular genetics. *Expert Rev Neurother*, **8**(4), 563–74.

Marques, P. & Korbonits, M. (2017). Genetic aspects of pituitary adenomas. *Endocrinol Metab Clin N Am*, **46**, 335–74

McCune, D.J. & Bruch, H. (1937). Progress in pediatrics: osteodystrophia fibrosa. *Am J Dis Child*, **54**(4), 806–48.

Pellegata, N.S., Quintanilla-Martinez, L., Siggelkow, H., Samson, E., Bink, K., & Hofler, H. (2006). Germ-line mutations in p27Kip1 cause a multiple endocrine neoplasia syndrome in rats and humans. *Proc Natl Acad Sci U S A*, **103**, 15558–63.

Rajasekaran, S., Vanderpump, M., Baldeweg, S., et al. (2011). UK guidelines for the management of pituitary apoplexy Pituitary Apoplexy Guidelines Development Group: May 2010. *Clin Endocrinol*, **74**(1), 9–20.

Raverot, G., Burman, P., McCormack, A., et al. (2018). European Society of Endocrinology Clinical Practice Guidelines for the management of aggressive pituitary tumours and carcinomas. *Eur J Endocrinol*, 178, G1–G24. https://doi.org/10.1530/EJE-17-0796

Sanno, N., Teramoto, A., & Osamura, R.Y. (2001). Thyrotropin-secreting pituitary adenomas. Clinical and biological heterogeneity and current treatment. *J Neurooncol*, **54**(2), 179–86.

Schlechte, J.A. (2007). Long-term management of prolactinomas. *J Clin Endocrinol Metab*, **92**(8), 2861–5.

Schneider, H.J., Kreitschmann-Andermahr, I., Ghigo, E., Stalla, G.K., & Agha, A. (2007). Hypothalamopituitary dysfunction following traumatic brain injury and aneurysmal subarachnoid hemorrhage: a systematic review. *JAMA*, **298**(12), 1429–38.

Schreckinger, M., Szerlip, N., & Mittal, S. (2013). Diabetes insipidus following resection of pituitary tumors. *Clin Neurol Neurosurg*, **115**(2), 121–6.

St-Jean, E., Blain, F., & Comtois, R. (1996). High prolactin levels may be missed by immunoradiometric assay in patients with macroprolactinomas. *Clin Endocrinol*, **44**, 305–9.

Syro, L.V., Ortiz, L.D., Scheithauer, B.W., et al. (2011). Treatment of pituitary neoplasms with temozolomide: a review. *Cancer*, **117**(3), 454–62.

Vandeva, S., Vasilev, V., Vroonen, L., et al. (2010). Familial pituitary adenomas. *Ann Endocrinol (Paris)*, **71**(6), 479–85.

WHO (2017). *WHO Classification of Tumours of Endocrine Organs. WHO/IARC Classification of Tumours*, 4th edition. Lloyd, R.V., Osamura, R.Y., Klöppel, G., & Rosai, J. (eds). Geneva, Switzerland: WHO.

Zhang, X., Sun, J., Shen, M., et al. (2012). Diagnosis and minimally invasive surgery for the pituitary abscess: a review of twenty-nine cases. *Clin Neurol Neurosurg*, **114**(7), 957–61.

RELATED LINKS TO EBRAIN

Aetiology and Pathophysiology of Pituitary Adenomas. https://learning.ebrain.net/course/view.php?id=1245

Medical Management of Pituitary Adenomas. https://learning.ebrain.net/course/view.php?id=421

Pituitary Apoplexy. https://learning.ebrain.net/course/view.php?id=466

Surgical Management of Pituitary Adenomas. https://learning.ebrain.net/course/view.php?id=465

26

Craniopharyngioma and Rathke's cleft cysts

Rudolf Fahlbusch, V. Gerganov, and H. Metwali

Introduction

Both craniopharyngiomas and Rathke's cysts are rare pituitary lesions of dysembryogenic origin. Their radiological differentiation may be sometimes difficult due to their occasionally similar imaging characteristics. The surgical management of these lesions, especially of craniopharyngiomas, may be very challenging.

Gross total removal of a craniopharyngioma is associated with longer recurrence-free survival but could be associated with higher rate of surgery-related morbidities and pituitary insufficiency. Craniopharyngiomas are considered in most cases to be a 'chronic disease'. A principle difference in the operative management of these two lesions is that in craniopharyngiomas resection of their thicker capsule is mandatory in order to achieve complete removal, whereas it is nearly impossible and not recommended to attempt such cyst wall removal in Rathke's cysts. Emptying of the cyst content is usually sufficient to provide cure in the majority of these patients. Recurrences in Rathke's cyst are only rarely observed in contrast to craniopharyngiomas.

Craniopharyngiomas

Craniopharyngiomas are relatively rare tumours with an overall incidence of 0.13/100 000 neoplasms per year. It has been estimated that approximately 340 new cases should be diagnosed annually in the United States (Bunin et al., 1997). They have a bimodal age distribution, with one peak occurring in the paediatric population between 5 and 14 years of age, and a second peak in adults during the fifth decade of life (Nielsen et al., 2011). In children they account for 5–10% of all primary brain tumours (Hussain et al., 2013). The lesion is so rare that even 'the experts' have between 6 and 10 new patients per year, according to their published surgical series.

Craniopharyngiomas are regarded as histopathologically benign intracranial tumours but may be very adherent to adjacent structures including the pituitary stalk, tuber cinereum, and hypothalamus which makes their complete resection challenging. Nevertheless, resection is possible without major morbidity in most cases, as proven by many recent publications. Alternative treatment strategies include non-radical surgical resection followed by fractionated radiation therapy, cyst aspiration with implantation of an Ommaya reservoir, intracavity radioisotope or chemotherapy instillation, and radiosurgery.

Pathology and pathogenesis of craniopharyngiomas

There are two major subtypes of craniopharyngioma, adamantinomatous and papillary, which differ both clinically and histologically. The papillary subtype (pCR) is more rare and is typical for adults: it comprises 11–14% of all craniopharyngiomas. Papillary CR are thought to arise from metaplastic transformation of anterior pituitary or pituitary stalk epithelial cells (**Fig. 26.1**). Adamantinomatous craniopharyngiomas (aCR) are found predominantly in children but can present at any age. They arise from neoplastic transformation of ectopic embryonic rests during the development and involution of the Rathke pouch. aCR resemble some odontogenic tumours, which indicates a common embryonic origin. Macroscopically adamantinomatous craniopharyngiomas are usually lobular with a sharp irregular interface, frequently adherent to surrounding structures and invasive. Histologically they consist of mature squamous epithelium and pseudopapillae (**Fig. 26.1**). These CR can have solid or cystic components. The cystic contents are usually viscous, from yellow to dark brown or black in colour ('motor-oil' appearance), which reflects the variable cholesterol crystal content. In contrast, pCR are encapsulated, often solid, and do not adhere to surrounding structures. If they have a cystic component, the fluid content is clear (Crotty et al., 1995; Shin et al., 1999; Larkin and Ansorge, 2013).

In addition to the clinical and histopathologically differences, the two subtypes are thought to have distinct genetic origins. The development of CR is driven by mutations in a single well-established oncogene, catenin beta-1 (CTNNB1) in the adamantinomatous form and *BRAF* in the papillary form, independent of age. The CTNNB1 mutation in aCR and *BRAF* mutation in pCR are clonal. No other recurrent mutations or genomic aberrations have been detected in either subtype (Brastianos et al., 2014).

In recent years, the molecular pathogenesis of craniopharyngioma initiation, growth, and recurrence have been extensively studied. Due to advances in molecular biology, such as comparative genomic hybridization, genetic sequencing, targeted genotyping, and development of appropriate genetically engineered animal models, some of the pathogenetical mechanisms of CR development have been elucidated.

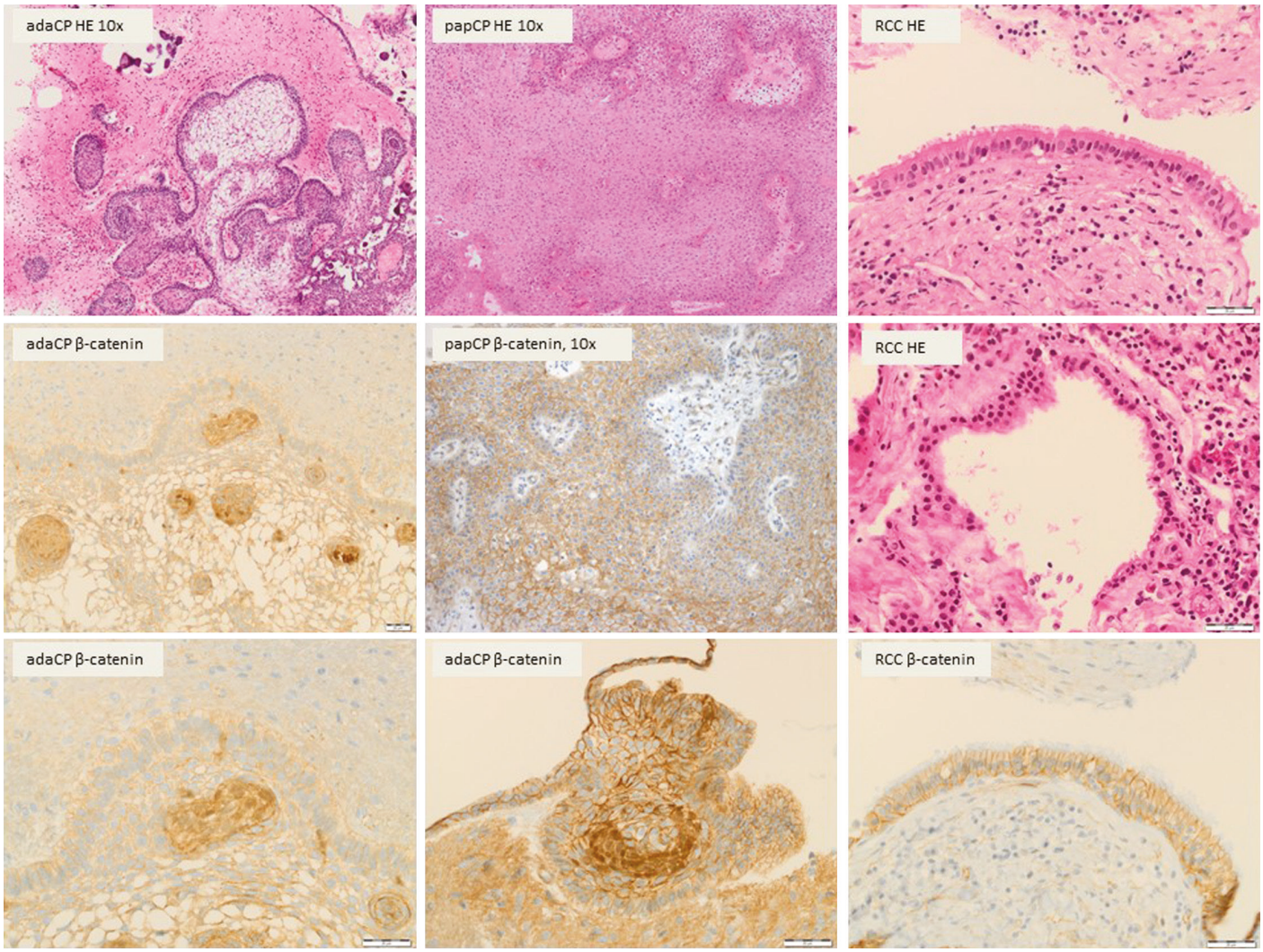

Fig. 26.1 The left column shows the histological features of an adamantinomatous craniopharyngioma, the upper slide was stained with H&E and the middle and lower by β-catenin. In the middle column, the upper two images demonstrate the histological features of a papillomatous craniopharyngioma where the upper slice was stained with H&E, and the middle slices by β-catenin. The lower image of the middle column shows an adamantinomatous craniopharyngioma stained for ß-catenin together with brain tissue. The right column shows the histological features of Rathke's cleft cyst. The upper and the middle slices show the columnar partially pseudostratified lining. The lower slice shows that Rathke's cysts are not stained by β-catenin which is useful in differentiating them from craniopharyngiomas.
Courtesy of Dr Kieren Allinson, Department of Pathology, Addenbrooke's Hospital, Cambridge.

The main abnormality at molecular level or driver in the oncogenesis of the adamantinomatous subtype is related to the Wnt/β-catenin pathway. This signalling pathway is crucial during embryogenesis in forming the dorsoventral axis of the developing neural tube in vertebrates. Adamantinomatous, but not papillary craniopharyngiomas harbour β-catenin mutations (Crotty et al., 1995; Prabhu and Brown, 2005; Holsken et al., 2009; Larkin and Ansorge, 2013).

The CTNNB1 mutations in the β-catenin gene on chromosome 3 and aberrations in β-catenin expression have been implicated in the development of other cancers including colorectal, hepatocellular carcinomas and medulloblastomas (Hussain et al., 2013).

Mutations in CTNNB1 have been found in approximately 70% of adamantinomatous craniopharyngiomas. Recent studies, however, have identified mutations in CTNNB1 in nearly all aCR, 92% when whole exome sequencing is used and 96% with targeted genotyping is used (Brastianos et al., 2014).

Such mutations stabilize b–catenin thus leading to constitutive activation of the Wnt signalling pathway (Holsken et al., 2009; Holsken et al., 2010; Larkin and Ansorge, 2013). It is known that most CTNNB1 mutations occur in exon 3 (Sekine et al., 2002). Experiments with genetically engineered animal models have proven a role for Wnt/β-catenin pathway dysregulation in the pathogenesis of craniopharyngiomas. The tumourigenic anomaly in the remaining aCR tumours, that do not have the CTNNB1 mutations, has not been identified. However, the anomaly is likely to be related to Wnt pathway activation.

Along with the pathogenesis of CR, many studies recently focus on the molecular mechanisms underlying tumour behaviour and relation to surrounding structures. These issues are very relevant from a practical neurosurgical point of view because invasion of adjacent structures is a limiting factor in successful surgical removal of aCR. Interestingly, β-catenin mutations are present in all cells but nuclear location of the β-catenin mutation is found only in small clusters of

cells near the infiltrating edge of the aCR. It has been hypothesized therefore, that Wnt signalling via β-catenin is implicated in the migratory behaviour of aCR. Furthermore, in aCR the concentration of fascin (FSCN1), which is a key cytoskeletal protein related to cell mobility, is increased. The Wnt/β-catenin/TCF pathway is linked to the expression of FSCN1. Down regulation of CTNBB1 reduces levels of fascin and subsequently tumour cell migration (Holsken et al., 2010). EGFR is overexpressed in aCR but in a heterogeneous pattern with the highest levels at the infiltration zone between tumour cells and normal brain tissue. The involvement of b–catenin, fascin and EGFR in the migratory behaviour of aCR cells suggests that the cell clusters with nuclear β-catenin may promote the infiltration of tumour into the surrounding tissues (Holsken et al., 2010; Larkin and Ansorge, 2013).

The molecular mechanisms underlying the development or recurrence of aCR may be related to different gene expression patterns. In recurrent tumours there is an increased expression of growth factors and related receptors which normally regulate cellular proliferation such as the platelet-derived growth factor receptor–a (PDGFR-a) and fibroblast growth factor-2 (FGF-2) (Sun et al., 2010).

We observed very unusual cases of invasive craniopharyngiomas with a high tendency to recur. One of them was a young 12 years old female patient who was operated on for a craniopharyngioma several times within one year with frequent recurrences. The tumour invaded all the suprasellar and the parasellar areas as well as the basal ganglia with a high proliferation rate (MiB 20%). The patient died at the age of 13, 6 months after the last surgery and subsequent radiotherapy.

The mechanism of pCR development at molecular level has been only recently elucidated (Brastianos et al., 2014). Using whole exome sequencing recurrent mutations in *BRAF* (V600E) have been detected in all papillary craniopharyngiomas, while with targeted genotyping this mutation is detected in 95% of tumours.

Better understanding of the molecular pathogenesis of CR has important implications for the diagnosis and may provide targets for future molecular guided medical therapies.

Clinical presentation

In the senior author's series, including 291 patients (83% adults and 17% children) operated in the period 1983–2005, 47% presented with visual compromise, 31% with endocrine deficits, 17% with hydrocephalus and headache, and 5% with neurological deficits. Objective findings at examinations were a chiasmal syndrome in 75% and endocrinological deficits in 77%. Diabetes insipidus was present in 30%.

Adults

Visual disturbance

Craniopharyngiomas can cause different patterns of visual field defects depending on the tumour location and extension. The classical bitemporal hemianopia can develop due to compression of the optic chiasm from below by intrasellar and suprasellar tumours. Other patterns are also possible especially in cases of retrosellar and parasellar tumour development. Subjective visual symptoms at the time of presentation are encountered in approximately 47% of the patients but ophthalmological findings at the time of presentation occur in 75%. Optic pathway dysfunction at the time of presentation is observed in 40–70% of patients. Visual field abnormalities are followed with decreased visual acuity and in later stages with optic atrophy.

Endocrine manifestations

Only 31% of the patients presented with symptomatic endocrine deficiency due to compression of the pituitary stalk or gland. Endocrinological analysis of the diagnosed cases revealed anterior lobe deficiency in 77% and diabetes insipidus (DI) in 30%. Nearly 80% of adults complained of decreased sexual drive, and almost 90% of the male patients complained of impotence. Most women reported amenorrhea. At presentation, 40% of the patients had symptoms related to hypothyroidism. Almost 25% had signs and symptoms of adrenal failure, and 20% had DI. Growth hormone deficiency is a laboratory finding in almost all cases of craniopharyngioma, if adequately tested.

Hypothalamic vegetative manifestations

Change in the sleep-wake rhythm, obesity, abnormal electrolytes, and caloric regulation also occur in patients with craniopharyngiomas. Unfortunately, objective criteria to document vegetative dysfunction are missing. Exclusive pituitary dysfunction of the hypothalamus can also manifest with endocrine disturbance (tertiary pituitary insufficiency).

Neurological manifestations

Headache can be the first presenting symptom of a craniopharyngioma. It is typically in the forehead area and is accentuated in the morning. Headache can be the only indication for surgery, especially in small craniopharyngiomas. The cause of headache may also be developing hydrocephalus due to large tumours that compress the foramina of Monroe or the Sylvian aqueduct.

Oculomotor palsy is seen in cases of parasellar extension of the tumour and compression of the oculomotor nerve. Diminished hearing and trigeminal nerve symptoms can occur in cases with cerebellopontine angle extension. Epilepsy occurs in parasellar craniopharyngiomas that compress the mesial temporal lobe. Short term memory deficits may also be observed and are due to compression of the fornix.

Special findings in children

Visual disturbance

Visual disturbances are recognized late in children. They are frequently unaware of having even significant vision loss but this symptom occurs at presentation in 20–60% of the paediatric patients with craniopharyngioma. The pattern of visual loss depends on the extension of the tumour in relation to the optic pathway. Fundus examination shows papilledema in 20% of cases (Poretti et al., 2004; Yosef et al., 2015).

Endocrine manifestations

Short stature due to growth hormone deficiency and delayed puberty due to gonadotropin deficiency are common clinical presentation in children with craniopharyngioma. They may present with adrenocorticotropin deficiency or hypothyroidism (Poretti et al., 2004; Halac and Zimmerman, 2005). Adiposogonadal syndrome (Fröhlich's syndrome) is a combination of hypogonadism and obesity and is due to hypothalamic pituitary failure.

The presenting symptom in children can be DI, which may be accompanied with absence of thirst (adipsia). This condition is very dangerous due to the excess fluid loss without adequate compensation.

Vegetative symptoms

These include manifestations of hypothalamic failure including obesity, alteration of the sleep rhythm, electrolytes disturbance, and endocrinal deficiencies.

Radiological assessment

The main diagnostic imaging used is magnetic resonance imaging with and without gadolinium enhancement. The imaging allows assessment of the extent of the tumour, as well as its relation to the neurovascular structures. The anatomy of the optic nerve and optic chiasm, the length of the internal carotid artery, the location of the anterior communicating artery, the floor of the third ventricle and the presence of a true intraventricular component should be noted.

Computer tomographic scans can be useful in detecting calcification, which is a typical radiological sign of craniopharyngiomas. A CT scan is also important to define the anatomy of the bone of the skull base, especially if a skull base approach is planned. It also has value as an emergency diagnostic measure where there has been an acute deterioration in the level of consciousness from hydrocephalus.

Classification

There are several classification systems (Yasargil et al., 1990), the following are commonly used.

Depending on the tumour location, craniopharyngioma can be classified into intrasellar and suprasellar. Considering the relation of the tumour to the diaphragma sellae, craniopharyngioma can be classified into supradiaphragmatic and infradiaphragmatic. The tumour can be located anterior to the optic chiasm or posterior to the optic chiasm. The tumour can elevate the floor of the third ventricle but in some cases it will even grow through the floor of the ventricle and have an intraventricular component. The tumour can extend all directions mainly laterally in the parasellar area and posteriorly in the retrosellar space. We have observed ectopic locations of craniopharyngiomas (e.g. in the cerebellopontine angle, sphenoid sinus, or in the pharynx).

Morphologically, the craniopharyngiomas are usually partially solid and partially cystic. Few cases are purely solid or purely cystic. Intensely calcified tumours are also well described.

Preoperative evaluation

Extensive preoperative endocrinological evaluation of the anterior lobe of the pituitary gland is mandatory. This evaluation should include T3, T4, TSH, LH, FSH, testosterone or oestrogen, ACTH, cortisol, prolactin, GH, and IGF-1. Dynamic tests should be performed whenever needed to complete the evaluation. The visual status evaluation should include visual acuity, visual fields, and

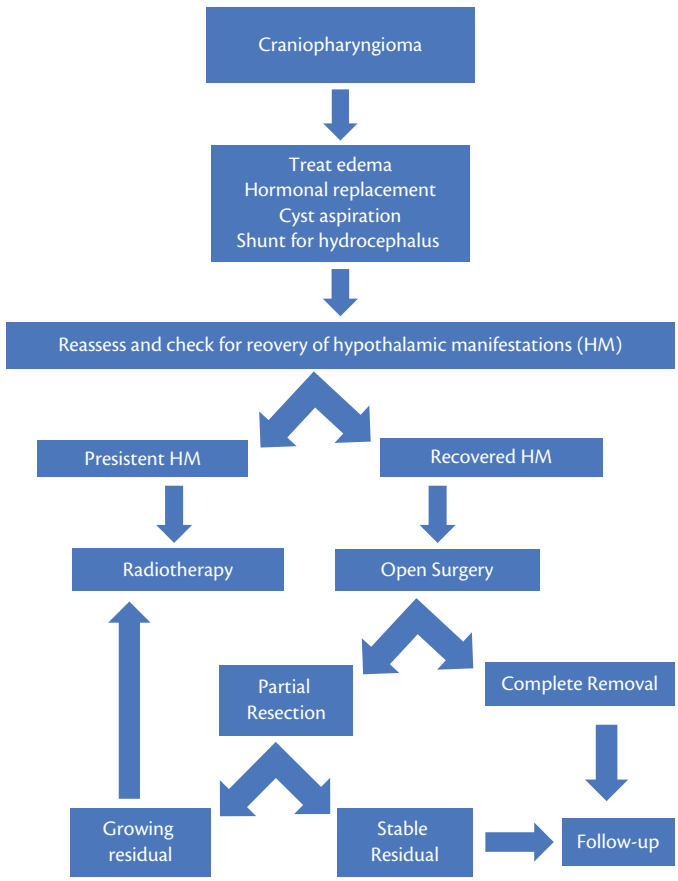

Fig. 26.2 Management algorithm for craniopharyngioma.

fundoscopy. This is important when planning the management and as a baseline for follow-up.

Treatment

The decision on how and when to operate on a patient with a craniopharyngioma depends on many factors, both tumour-related (size, extension, adhesion, or involvement of vital adjacent structures) and patient-related (age, endocrine status) (Fig. 26.2). In some cases prompt surgery is required, while in others the best option might be initial conservative treatment or radiotherapy.

Symptomatic treatment

Insertion of a ventriculoperitoneal shunt may be required in patients with hydrocephalus. Direct treatment of the tumour can be with insertion of cystoventricular shunt or more rarely cystoperitoneal shunt. Tumour debulking may be appropriate in patients with profound vegetative symptoms in whom radical surgery is contraindicated or in those with a progressive chiasm syndrome. Radiotherapy may be indicated.

Indications for surgical intervention

Surgery is indicated to achieve decompression of the pituitary gland and preserve endocrine function, to achieve decompression of the optic chiasm or optic nerves or to decompress the oculomotor nerve. Surgery is absolutely indicated to manage hydrocephalus.

Contraindications to radical resection

Preoperative contraindications include significant peritumoural oedema or bilateral infiltration of the hypothalamus. Patients with irreversible hypothalamic dysfunction manifest clinically with extreme obesity or a change in the sleep/wake rhythm and radiologically with massive hypothalamic compression or the presence of peritumoural oedema. In these cases we recommend treatment with dexamethasone to verify the reversibility of the hypothalamic disturbance. If they are reversible, surgical resection can be performed. However, if they prove to be irreversible, only symptomatic treatment is indicated (see next).

Intraoperative limitations to radical resection include heavily calcified tumours, tumours with an attachment to the hypothalamus or to the small perforator vessels and those demonstrating repeated intraoperative bradycardias.

Surgical treatment

The treatment concept of the senior author has evolved since 1982 but has always aimed to achieve safe and radical resection. In the first period, between 1982 and 1996, 168 patients had surgery, and gross total tumour removal was achieved in 45.7% of the transcranial cases and in 85.7% of the transsphenoidal ones. The main reasons for incomplete removal were attachment to, or infiltration of, the hypothalamus, major calcifications, and attachment to vascular structures (Fahlbusch et al., 1999). Between 1996 and 2005 the author's technique advanced further and the rate of safe radical resection increased, gross total resection was achieved in 88.5% of the transsphenoidal cases and in 79.5% of the transcranially operated ones (Fahlbusch and Hofmann, 2008).

Since 2005, the author has adopted the concept of personalized treatment. Patient selection and planning of therapy depend mostly on the patient's clinical condition with special attention to the endocrine and vegetative statuses.

Clinical examples

A male patient presented with large cystic craniopharyngioma. He complained about a short-term memory deficit without endocrine or visual deficits. A cystoventricular shunt was performed and then the patient was followed. His memory deficits improved and radical surgery was not required.

A female patient presented with a cystic craniopharyngioma. She wished to have a child so a cystoventricular shunt was inserted as a first step. After her successful pregnancy and birth, radical tumour removal was performed.

An 18-year-old male was initially misdiagnosed as having a cannabis psychosis. Neuroimaging, however, revealed severe hydrocephalus caused by a large cystic craniopharyngioma. Considering his pronounced cognitive disturbances, a decision was taken to use a ventriculoperitoneal shunt. Later, a cystoperitoneal shunt had to be inserted. Only when his cognitive function improved did we proceed to radical tumour resection.

Surgical considerations

Hoffmann et al. (1992) and Yasargil et al. (1990) were the first to report the possibility of radical resection of a craniopharyngioma. Following which, total resection of craniopharyngiomas was carried out using various approaches. Especially challenging were the large and giant tumours. Various modifications and combinations of approaches have been used for resection of such craniopharyngiomas with the presumption that sufficient exposure of all parts of the tumour is essential for their safe and complete removal.

The first precondition to resect a craniopharyngioma through a small frontolateral craniotomy is that the slowly growing tumour causes a continuous stable displacement of the neurovascular structures and thus provides a potentially large preformed resection corridor. Importantly, these corridors remain more or less stable during and after tumour resection, which is performed via the subchiasmatic, the opticocarotid, the carotido-occulomotor, and the translamina terminalis pathways. This gives the surgical advantage that the tumour bed does not collapse after the early steps of tumour resection and remains opened, providing access to the deeper parts of the tumour. The first series used a frontal craniotomy confined to one side, but later the size of the craniotomy was reduced to the current frontolateral approach. The main goal is to protect the frontal lobe, which in giant tumours is especially vulnerable. Moreover, the larger opening of the skull did not enhance our ability to remove deep-seated lesions. Once sufficient internal decompression has been achieved, the more peripheral tumour portions can be mobilized and brought into view by slight traction.

A second requirement for any operative approach is that there should not be a high risk of approach related morbidity. The frontolateral approach meets this criteria and is the one favoured by us even in cases of giant craniopharyngiomas (Fig. 26.3), which tend to develop in the suprasellar region and rarely have intrasellar extensions. A subset of craniopharyngiomas, even of large size, can be successfully removed via a transnasal transsphenoidal microscopic, endoscopic, or combined approach.

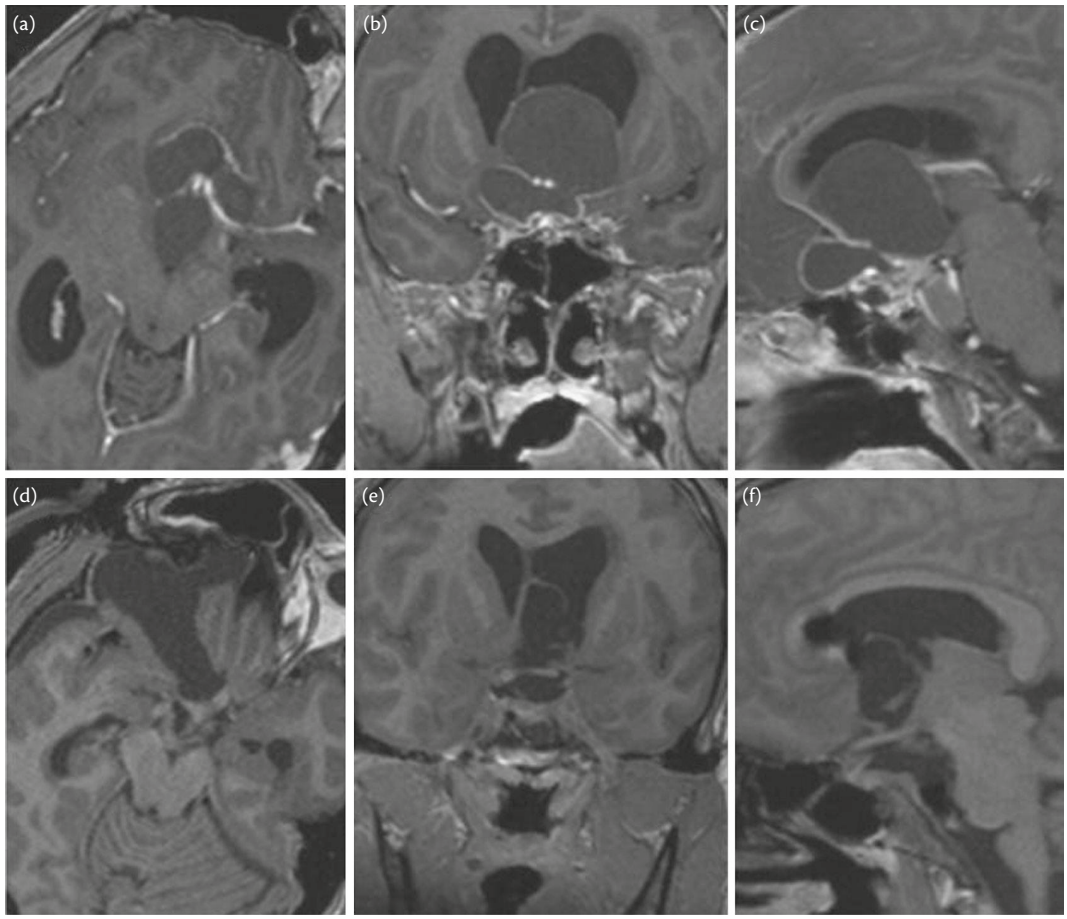

Fig. 26.3 Preoperative (A, B, and C) and postoperative (D, E, and F) MRI showing resection of a large craniopharyngioma via a right frontolateral craniotomy. The patient was operated on using an iMRI.
Source data from Gerganov, et al. *J Neurosurg.* 2014 Feb;120(2):559–70.

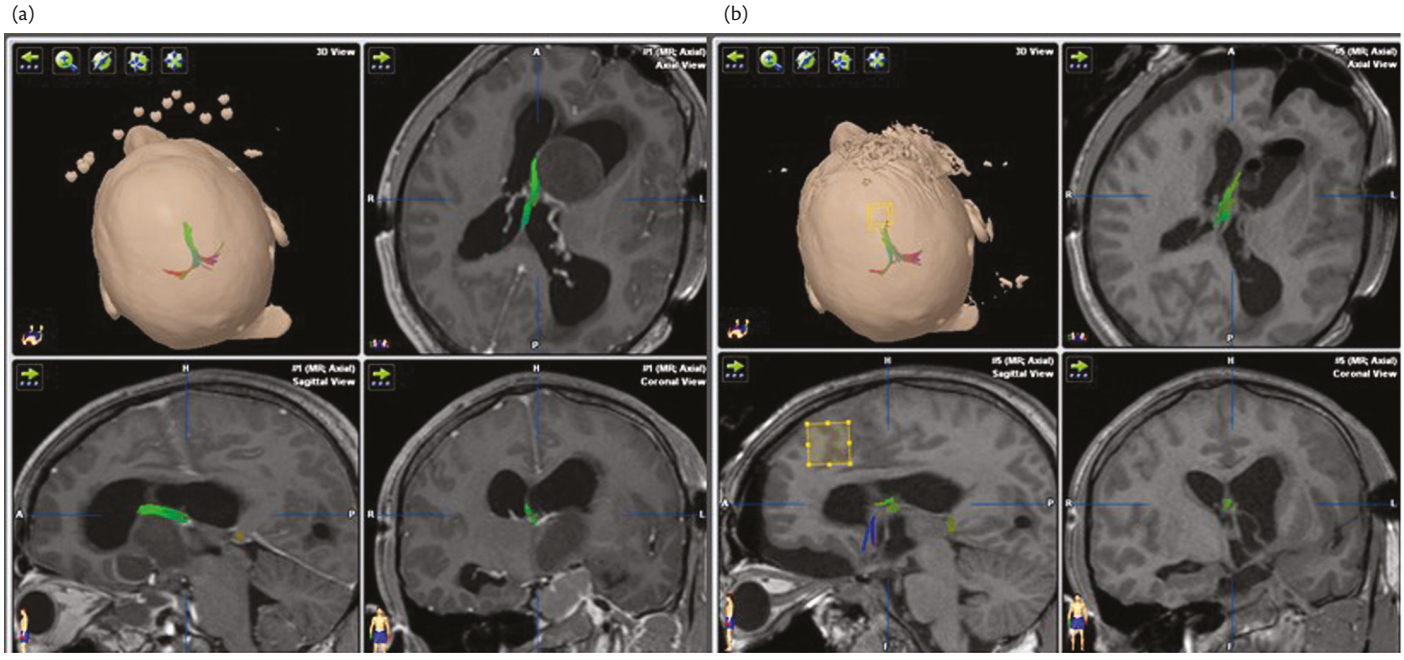

Fig. 26.4 Fibre tracking for localization and navigation of the fornix especially in tumours with a large extension into the third ventricle. (A) shows the fornix preoperatively, while (B) shows the preserved fornix after resection of the craniopharyngioma via a frontolateral approach.
Source data from Gerganov, et al. *J Neurosurg.* 2014 Feb;120(2):559–70.

The intraventricular craniopharyngioma can be approached either through the interhemispheric translamina terminalis approach or the transcallosal approach. The transcallosal approach is restricted to the ventricle and the midline and cannot access craniopharyngiomas with parasellar extension. The interhemispheric translamina terminalis approach can expose both the intraventricular part and, to some extent, the parasellar part.

The size of the parasellar extension can influence the side of the surgical approach. The parasellar component, which is insinuated lateral to the supraclinoidal internal carotid artery and the posterior communicating artery and its perforators, is approached through the carotido-occulomotor space on the same side. Therefore, in cases of parasellar extension the craniotomy should be placed on the ipsilateral side.

In cases where there is a prefixed chiasm or in tumours with large retroclival extensions some authors have described the petrosal approach, accessing the tumour from inferior to superior and from posterior to anterior.

Special attention is given to the course and location of the fornix, especially in tumours with extension into the third ventricle (Fig. 26.4).

Details of the commonly used surgical approaches

Transsphenoidal approach

The classical transsphenoidal approach is indicated in all subdiaphragmatic intra- and suprasellar craniopharyngiomas (Fig. 26.5). In supradiaphragmatically located tumours the extended transsphenoidal approach via the removed tuberculum sellae ('transtubercular') can be used (initially published by Weiss et al). However, limitations for safe total removal are tumour growth outside the arachnoid space and an intimate relation to surrounding brain structures. In cases with small supradiaphragmatic extensions of a mainly intra- but even suprasellar craniopharyngioma, the diaphragma sellae can be split to allow total tumour removal (senior author's experience).

The nasal approach to the sphenoid sinus is usually performed directly pernasal, microscopically, endoscopically, or combining these techniques. The sublabial incision is preferred in small children with tiny nasal openings, rarely in combination with a transmaxillary approach when the tumour is more lateral. Additional help in cases where the sphenoid sinus is not yet or not sufficiently pneumatized or the configuration of the sella turcica is invisible (children <3–4 years) is provided by neuronavigation or the c-arm. Although some authors regard this situation as a contraindication to a transsphenoidal approach experienced pituitary surgeons are able to safely drill and open the sellar floor. In sufficiently pneumatized sinuses the protuberance of the carotid artery serves to provide midline orientation. Special attention should be given when bony septi within the sphenoid sinus insert into the area of the protuberance, as this bony layer over the carotid artery serves as its protector.

After drilling the sellar floor to achieve its maximal wide opening, the normal sella size is 10 × 6 × 8 mm, the dura is opened from the midline laterally, reaching the medial wall of the cavernous sinus. Posteriorly it reaches the posterior intercavernous sinus and anteriorly the connection to the diaphragm sellae. In half of these cases the pituitary gland is located anteriorly (which is in contrast to pituitary adenomas). In such cases the diaphragma has to be split for one or more millimetres before the usually thick wall of the craniopharyngioma capsule is reached.

The tumour content, whether cystic, solid, or calcified is removed first from all parts of the sella. The surgeon should start in the midline or laterally, then move in the suprasellar direction, expecting the descent of the elevated diaphragma sellae.

Removal of the mainly thick tumour capsule, although time-consuming and challenging, is mandatory (in contrast to the thin wall of Rathke's cysts) in order to prevent recurrences. The senior author recommends starting with resection of the easy to identify tumour wall then dissect the posterior part, moving laterally and from anterior to posterior below the diaphragma sellae. The pituitary stalk can normally be preserved. Occasionally firm tumour parts have to be resected sharply at their origin on the pituitary stalk. Where the last piece of tumour is not completely resectable, careful bipolar coagulation is an option.

In some cases, cerebrospinal fluid (CSF) leaks are unavoidable in the attempt to achieve total removal. The leak originates most

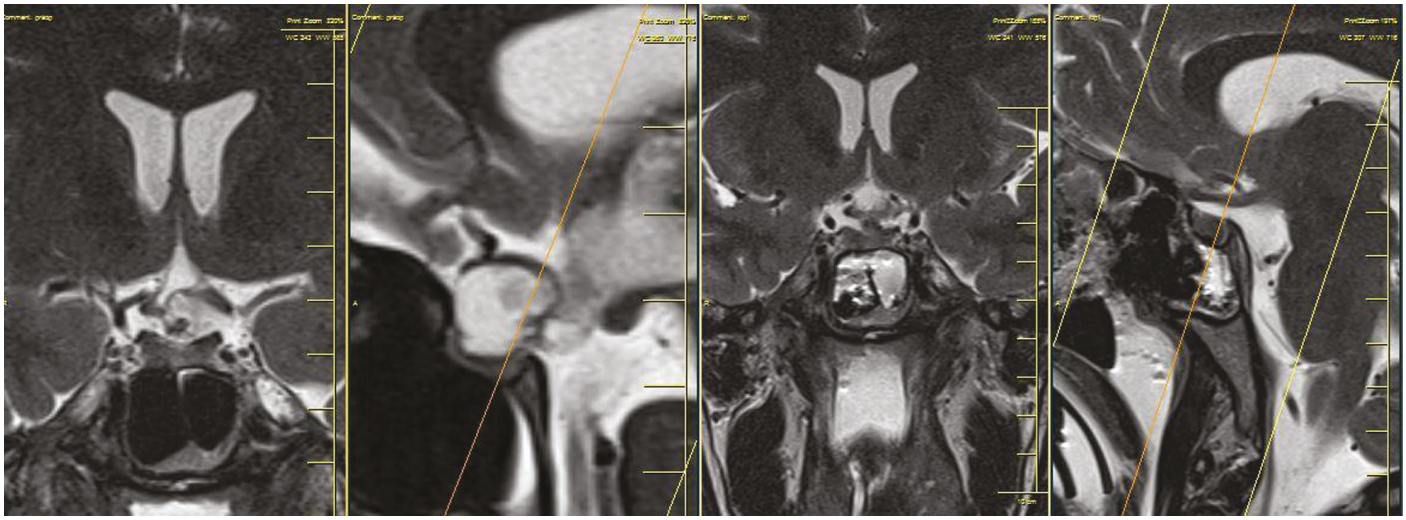

Fig. 26.5 Pre and postoperative MRI after transsphenoidal resection of a craniopharyngioma. The first two images showed the tumour preoperatively. The last MRI shows tumour resection through splitting of the pituitary gland.

frequently from the thinner anterior diaphragma sellae. The leak is repaired using tiny pieces of fat, taken from the upper limb or abdomen that are then sealed with fibrin glue. Some authors prefer more complex reconstructive procedures of the sella floor. In extended transtubercular approaches all patients have a CSF leak, which is a major disadvantage and burden of this kind of approach. Reoperations are reported in up to half of these cases although experienced endoscopic surgeons have reported recent significant improvements in this regard, using a mucosal flap as a covering.

The frontolateral approach

Tumour resection in cases of long optic nerves and a postfixed chiasm

In these cases, the optic chiasm is usually displaced posteriorly and superiorly creating a wide working space to the subchiasmatic and prechiasmatic areas. The surgeon performs gradual internal tumour decompression. The contralateral optic nerve is dissected from the tumour initially from its medial side taking care to preserve the small vessels on the surface of the nerve. Subsequently the central part of the suprasellar portion is removed bringing the contralateral suboptic part into view. The contralateral suboptic part is gradually decompressed and dissected from the inferior surface of the optic nerve, the inferior cerebellar artery (ICA), and the posterior communicating artery. After removal of the suboptic part, the contralateral oculomotor nerve can be seen entering the oculomotor trigone. Moving the microscope to a more central trajectory, the retrosellar compartment can be seen. Due to the commonly preserved membrane of Liliequist in this area, the tumour can be dissected relatively easily from the basilar artery and its branches. Liliequist's membrane is stretched by the tumour and separates the descending part of the tumour in the prepontine and CPA cisterns from the nearby structures although in previously operated cases it is less obvious.

The ipsilateral suboptic part is usually not in the direct line of vision. This portion can be removed by opening the carotid cistern with an incision in the medial carotid membrane and removing the tumour through the created space between the ipsilateral optic nerve and the ICA (the opticocarotid triangle).

Tumour resection in cases of short optic nerves and a prefixed chiasm

The prechiasmatic and the subchiasmatic spaces in these cases are usually very narrow and do not allow access to the tumour in the suprasellar region. In this situation, further arachnoid dissection is required in the lamina terminalis cistern. The A1s and A2s on both sides are exposed. The A1s are dissected from the optic nerves on both sides and from the optic chiasm keeping them attached to the frontal lobe to minimize injury of the perforators. The anterior cerebral artery complex is elevated with the frontal lobe exposing the lamina terminalis. In order to remove the intraventricular part of the tumour, the lamina terminalis is opened in the midline remembering the tumour's relationship to the optic chiasm, the branches of the anterior cerebral and anterior communicating arteries that run to the hypothalamus.

Surgery around the pituitary stalk

Only in cases in which the stalk is extensively involved by the tumour is it justified to resect it for the sake of radicality. In cases in which it is involved to a lesser extent, however, an attempt may be made to preserve its continuity as well as its blood supply by performing partial stalk sectioning (one-third to one-half of its diameter). Medial optic nerve mobilization by opening the roof of the optic canal and resection of the lateral part of the tuberculum sellae can help to better visualize the pituitary stalk.

Resection of the parasellar part

The part of the tumour that extends lateral to the ICA and the posterior communicating artery can be tackled by incising the intracarotid membrane and dissecting between the uncus and the ICA. During resection of this part of the tumour, the course of the anterior choroidal artery should be taken into consideration.

Cyst aspiration

Aspiration of the cyst content is an option that can provide temporary relief of symptoms that are related to mechanical compression of surrounding structures. As the cysts tend to re-accumulate, a viable option is to place an Ommaya or Rickham reservoir in the cyst, which will then allow repeated cyst aspirations. In order to position the catheter optimally, some kind of navigatory control is very helpful. Cyst aspiration is usually indicated in patients presenting in a poor condition as a temporary solution or in recurrent cystic CR that are not suitable for surgical removal.

Craniopharyngiomas in children

The quality of life is frequently impaired in long-term survivors mostly due to endocrine, metabolic, and visual abnormalities. In a series published by an endocrinologist, it was documented that radical resection obtained by differently experienced surgeons reduced the quality of life in almost 50% of long-term survivors (Muller, 2013). Particularly problematic are the disturbances of pubescent development, the overall growth, and morbid hypothalamic obesity. Some authors stress that because of the surgically induced hypothalamic deficits and the high rate of recurrence even after apparently complete resection, planned radical resection in children should not be attempted.

In children above the toddler age an attempt at complete resection with preservation of all functions should be made in order to minimize the risk of recurrence. Children presenting earlier benefit form prolongation of the interval until treatment. In children presenting with a large cystic CR and clinically in poor condition or of a very young age, catheter drainage via an intracystic catheter or implantation of an Ommaya reservoir may be a valuable treatment option. This approach provides pressure relief and symptomatic improvement while the patient matures. The two-staged approach is an alternative strategy in patients with large cysts causing mass effect, cyst drainage to relieve pressure followed soon afterwards by resection (Fahlbusch et al., 1999).

In toddlers, as well as in cases of unfavourable CR extension, for example when the hypothalamus is involved, a planned partial resection might be the optimal temporary treatment option. The tumour, if growing, could be approached later on, when the child matures. Although radiotherapy following incomplete tumour resection is favoured both in adults and children, it should be applied with extreme caution at younger ages. The outcome of irradiation after incomplete resection is under investigation in randomized multinational trials (Muller, 2013).

Postoperative outcome and care

Hormonal

Postoperative hormonal evaluation is mandatory. Patients with preoperative cortisol insufficiency receive high-dose hydrocortisone during and early after surgery. It is then reduced to the normal daily maintenance dose. Assessment of the basal hormonal status is performed usually after 6–10 days. Hormonal deficiencies, if present, should be replaced. Special attention should be given to children and adolescents to support normal growth and puberty (Honegger et al., 1999).

In the first series from the senior author with safe resection operated via the transsphenoidal approach, 10% of cases showed secondary hypothyroidism and 10% adrenocorticotropic deficiency. In patients operated via the transsphenoidal approach using the same concept, 20% suffered from secondary hypothyroidism and 40% from adrenocorticotropic deficiency. The percentages of new endocrine deficiencies were worse in the series with aggressive resection. Around 20% showed secondary hypogonadism, 30% secondary hypothyroidism, and 60% secondary hypocorticism. Endocrine deficiencies are less frequent in cases treated via the transsphenoidal approach.

Electrolytes

The patients after surgical resection of craniopharyngioma are liable to electrolyte disturbance from diabetes insipidus. The rate of DI increases from 16% preoperatively to 59.4% postoperatively (up to 70% in cases of aggressive resection). DI manifests early after surgery or delayed, after 5–7 days. DI is characterized by polyuria, polydipsia, and hypernatraemia. Conscious patients can compensate for the polyuria by drinking and thus the sodium level may stay within the normal range. The management of patients that are not fully conscious or are unable to drink sufficiently is challenging. DI is typically managed with Desmopressin. We start Desmopressin usually on demand depending on the urinary output, the urine-specific gravity, and sodium level. The dose of Desmopressin is then slowly adjusted to the final fixed dose, as required. Some patients develop only transient DI that resolves within 1–2 weeks. We prefer to give the main Desmopressin dose in the evening and in the day, only if needed, which allows the patient a chance of uninterrupted sleep.

Rarely, some patients develop hyponatraemia after surgery. If the cortisol level is normal or well replaced, the patients are managed with fluid restriction. Some patients may require temporary sodium infusions. If hyponatraemia persists, the patient can be given fludrocortisone or even tolvaptan (ADH antagonist) (Ichimura et al., 2015). Correction of sodium should be slow, and the sodium level should not fluctuate. A fluctuating sodium level can cause brain oedema and pontine myelinolysis.

Vision

The visual acuity and the field of vision are tested after surgery. In the published series of the senior author, the chiasm syndrome completely regressed in approximately one-third of the patients after transcranial surgery, and in an additional one-third of the patients in whom vision recovered partially. Visual deterioration was found in 14.7% of patients after transcranial surgery. After transsphenoidal surgery, the chiasm syndrome normalized completely in 46.7% of the patients and partially in another 40%. None of the patients developed visual deterioration after surgery (Fahlbusch et al., 1999).

Cognitive outcome

Cognitive dysfunction can present preoperatively and postoperatively due to compression of the fornix. Some patients show improvement after surgery (5/8). There is also improvement in the reduction of drive (2/4), loss of concentration (2/2), abolished diurnal rhythm (2/2), and loss of attention span (1/1). There was no worsening of cognitive function in our operated series but cognitive development and school performance in children after resection of craniopharyngioma can decline after surgery (Honegger et al., 1998).

Degree of resection

In the first report of the senior author about the first 168 cases (Fahlbusch et al 1999), total tumour removal was achieved in 45.7% of transcranial and 85.7% of transsphenoidal procedures. The rate of recurrence-free survival after GTR was 86.9% at 5 years and 81.3% at 10 years. On the other hand, the 5-year recurrence-free survival rate was 48.8% after subtotal removal, and 41.5% after partial removal. Following primary surgery, the overall survival rate was 92.7% at 10 years, with the best results after GTR. Furthermore, 117 (79%) of 148 patients who underwent primary surgery were independent and without impairment.

Subsequently, the senior author has reported experience with a further 73 cases (Hofmann et al., 2012). GTR was accomplished in 88.5% of cases in whom a transsphenoidal approach was applied and 79.5% of those in whom a transcranial approach was applied. In the total series, GTR was achieved in 83.1% of cases (vs. 49.3% in the authors' former series). The complication rate was 13.8% without any mortality. New endocrine deficits were observed more frequently in patients treated with transcranial approaches (16.3–66.7% vs. 2.6–50.0%) but were less frequent after transsphenoidal approaches (5.2–19.2% vs. 2.9–45.7%).

Surgical complications

After transsphenoidal surgery, CSF leak was observed in 2% of cases. CSF leak should be promptly managed to avoid subsequent meningitis. A lumbar drainage can be inserted as a prophylactic measure immediately after surgery, if there is CSF leak during surgery with evidence of large opening of the arachnoid membrane. Delayed CSF rhinorrhoea can be managed as a first trial with lumbar drainage but in other cases with direct surgical repair.

After transcranial surgery, hypothalamic dysregulation was observed in two cases (from 176 transcranial procedures). Other nonspecific complications like wound infection, epidural hematomas, and seizures have also been reported.

Controversies

Gross total resection versus partial resection

In the recent literature, GTR has been achieved on average in 53% of the cases (Yang et al). It ranges from 13% (Lo et al., 2014) to 83% (Hofmann et al., 2012) in the recently reported large series (**Table 26.1**). GTR can be achieved in 87.5% of giant craniopharyngiomas (Gerganov et al., 2014). Partial resection is indicated when only symptomatic decompression treatment is appropriate and in order to avoid damage to vital structures. Contraindications to GTR

Table 26.1 Key differences between craniopharyngiomas and Rathke's cysts

	Craniopharyngioma	Rathke's cyst
Location		
• Intrasellar	++	+++
• Intra and suprasellar	++	+
• Suprasellar	++	(+)
Clinical feature		
• Hypothalamic disturbance	+++	-
• Visual	+++	+
• Pituitary insufficiency	+	+
• Headache		+++
Radiological features		
• Calcification	+++	(+)
• Cyst formation	++	+++
• Hydrocephalus	++	-
Cyst wall	Thick	Thin
Histology		
• β-catenin	++	-
Surgery		
• Transsphenoidal	++	+++
• Transcranial	+++	(+)
• Shunt	+	-
Wall resection	+++	(+)

include irreversible hypothalamic dysfunction but the rate of GTR also depends on institutional and personal experience.

While GTR is associated with better overall survival and a lower recurrence rate, it is contraindicated in cases of irreversible hypothalamic dysfunction or peritumoural oedema. Preservation of function is one of the main purposes of surgery, if the tumour is adherent to the hypothalamus or small vessels or heavily calcified then GTR should not be attempted. Such patients should be followed until the remnant grows when redo surgery is the favoured management option. Radiotherapy should be recommended if the remnant is considered inoperable due to unacceptably high associated morbidity (**Table 26.2**, **Figs. 26.6**, **26.7**, and **26.8**).

Surgical approaches

We operate on subdiaphragmatic craniopharyngiomas (either intrasellar or intra- and suprasellar) using an endoscopically assisted transsphenoidal approach. Transcranial approaches are reserved for supradiaphragmatic craniopharyngiomas. In such cases the senior author has previously used interhemispheric and pterional approaches. Recently, however, we have favoured the frontolateral approach.

The pure endoscopic extended transsphenoidal approach has been described for resection of supradiaphragmatic craniopharyngiomas. It is associated with high incidence of CSF leak and low rate of GTR. Kassam's group reported a series of 16 patients in 2008 where total resection could be achieved in 50% but with a high incidence of postoperative CSF leak that required reoperation (58%) (Gardner et al., 2008). The reported CSF leak rate in the recent reports by the same group is between 15% and 23%, DI occurred in 48–67% of the patients and hypopituitarism 25–58%. The GTR rate varies between 37% and 69% (Koutourousiou et al., 2013; Cavallo et al., 2014).

Radiotherapy for craniopharyngioma

Fractionated radiotherapy is used in the management of patients with residual or recurrent CR and in cases where complete surgical removal is considered inappropriate due to an unacceptably high associated morbidity. Its use in cases of deliberate incomplete tumour removal is controversial. The rationale for this strategy is the reported high morbidity and mortality of radical surgery if attempted.

Another controversial concept is the use of radiotherapy immediately following CR removal or later on without considering the option of repeat surgery. The rationale once again is the greater surgical difficulty in repeat operations. Some studies have shown that the 10-year CR control rates (75–90%) are superior to the results obtained from incomplete excision alone (30–50%). However, there are no prospective randomized studies comparing the various management options.

The main drawbacks of radiotherapy are the side effects of irradiation in a region, which is composed of highly radiosensitive and vulnerable structures leading to late pituitary insufficiency and epilepsy. In children below 6 years, it can cause cognitive impairment. Even with recent advances in fractionated radiotherapy, which allow for greater precision and a reduction in radiation exposure to the normal brain, the risk of radiation-induced morbidity remains high. Early cystic enlargement, occurring within some months of completion of radiotherapy, while not disease progression, may still cause compression of the optic apparatus and hydrocephalus. The rate of such cystic enlargement in CR is reported to be between 10 and 20%.

The major side effects of irradiation are late and include cerebrovascular disturbance, radiation necrosis, neurocognitive dysfunction, and radiation neuropathy. It has been shown that radiation optic neuropathy occurs in 1–2% patients receiving doses up to 50 Gy. The most frequent late complication is pituitary dysfunction with new hormone deficiencies requiring replacement after a 5–10-year period occurring in 30–50% of the patients (Brada and Thomas, 1993). The clinical results of radiosurgery in CR are less favourable than those after fractionated radiotherapy with worse tumour control and the toxicity is not lower (Aggarwal et al., 2013).

Modern CR microsurgery allows achieving complete tumour removal without high surgical morbidity and almost no mortality (Gerganov et al., 2014). As mentioned elsewhere in the text, the best long-term results in regards to tumour control are observed in patients without residual tumour. Some authors recommend radiation therapy even after complete tumour removal. Surgery after previous radiotherapy is more challenging with higher morbidity. Therefore, in our opinion, radiotherapy should be reserved only for those patients that are not surgical candidates.

In patients, in whom part of the tumour cannot be removed safely and has to be left, we recommend initial follow-up. Modern MRI imaging allows detection of even slight growth in the remnant. If a tumour remnant is seen to progress, the main management option again is surgery. Only in cases where such surgery is impossible due to the particular location or other characteristics of the remnant would radiotherapy be considered.

Intracavitary therapy

Intracavitary delivery of radiation therapy or intracavitary irradiation is a method used to instil a radioisotope into the tumour cyst

Table 26.2 List of selected recent publications of large surgical series of craniopharyngiomas focusing on the percentage of total resection, morbidity, mortality, and rates of recurrence

	Year	No	GTR	Morbidity	Mortality	Recurrence
Van Effenterre & Boch, 2002	2002	122	Total in 59%, subtotal in 29%, and partial in 12%	Excellent in 85%, good in 9%, fair in 5%	2.5%	29/122
Mortini et al., 2011	2011	112	71.6%	Some 8.8% patients were partially or completely dependent on others for daily living activities before surgery	2.7%	24.5%
Karavitaki et al., 2005	2005	121	16/121			38% recurrence-free survival in patients with partial resection vs. 100% in GTR
Zuccaro, 2005	2005	153	69%	After surgery, endocrine status worsened in almost all patients, but visual status improved markedly	N/A	0% in GTR
Caldarelli et al., 2005	2005	52	40/52	At long-term follow-up, all survivors showed good clinical condition, even though approximately 60% relied on hormone replacement, and some patients presented obesity. DI has subsided in about 80% of the cases; visual deficits improved or remained stable, whereas postoperative neurological deficits subsided in all but one patient	2/52 early 1 late	Nine recurrences occurred 1–8 years after surgery (three true recurrences, and six re-growths of incompletely resected tumours) that required reoperation. Twelve patients underwent radiotherapy, six after an initially incomplete tumour resection and six following relapse
Duff et al., 2000	2000	121	69/121	The overall 'good outcome' rate was 60.3%		29 (24%) recurrences
Maira et al., 2004	2004	92	63%	All patients had good clinical results. Postoperative cerebrospinal fluid leakage occurred in ten cases, but only one case required a surgical repair of the sella	2/92	8/92
Puget et al., 2007	2007	66	20%	There have been no new cases of postoperative hyperphagia, morbid obesity, or behavioural dysfunction in this prospective cohort	NA	NA
Shi et al., 2006	2006	284	83.5%	The pituitary stalk was preserved in 176 (62.0%) patients, severed in 52 (18.3%), and unidentified in 56 (19.7%). Normal activities of daily living were regained in 63 (80%) patients, independence in 29 (14.2%), and daily life with assistance in 9 (4.4%)	12 within one month 4 later on	During the follow-up, 23 (14.1%) patients experienced tumour recurrence 1.0–3.5 years (mean, 1.8 +/–1.6) after total tumour removal, and 24 (64.9%) had recurrent tumour 0.25–1.5 years (mean, 0.5 +/– 0.4) after subtotal or partial resection
Yang et al., 2010	2010 (metanalysis)	442	58%		The 5- and 10-year overall survival (OS) rates for the GTR group versus the STR+XRT group were 98 versus 99%, and 98 versus 95%, respectively	The 2- and 5-year PFS rates for the GTR group versus the STR+XRT group were 88 versus 91%, and 67 versus 69%, respectively
Lo et al., 2014	2014	123	15%	Kaplan–Meier rates for visual deterioration, anterior pituitary hormone deficiency, DI, seizure disorder, and cerebrovascular events (CVE) due to treatment, not tumour progression, were 27%, 76%, 45%, 16%, and 11%, respectively	DSS was 88%, and OS was 80%. Primary treatment modality did not affect DSS or OS, while older age was a negative prognostic factor for OS but not DSS	Patients treated with STR+RT or CD+RT had the highest PFS (82% and 83%, respectively). There were no significant differences between PFS after adjuvant versus salvage RT (84% vs. 74%, respectively; $P = 0.6$)
Hofmann et al., 2012	2012	73	83.1%	13.8% New endocrine deficits were observed more frequently in patients treated with transcranial approaches over the years (16.3–66.7% vs. 2.6–50.0%) but were less frequent after transsphenoidal approaches (5.2–19.2% vs. 2.9–45.7%)	0%	NA

DDS, disease-specific survival; DI, diabetes insipidus; GTR, gross total resection; PFS, progression-free survival; OS, overall survival.

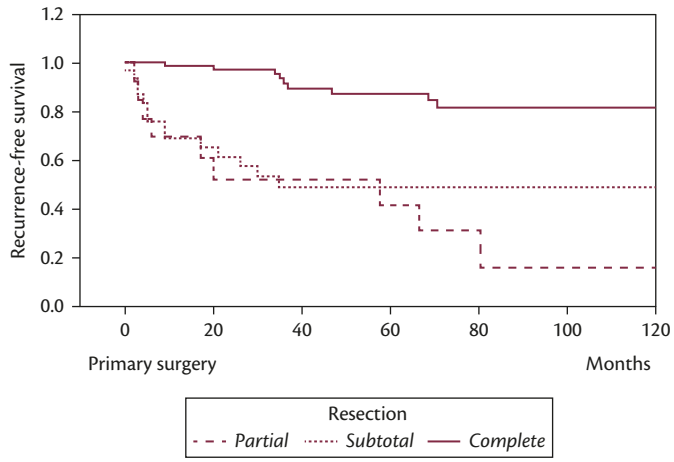

Fig. 26.6 Graph depicting recurrence-free survival times in patients who underwent surgery for craniopharyngioma in relation to the extent of tumour resection (Kaplan–Meier method).
Fahlbusch et al.

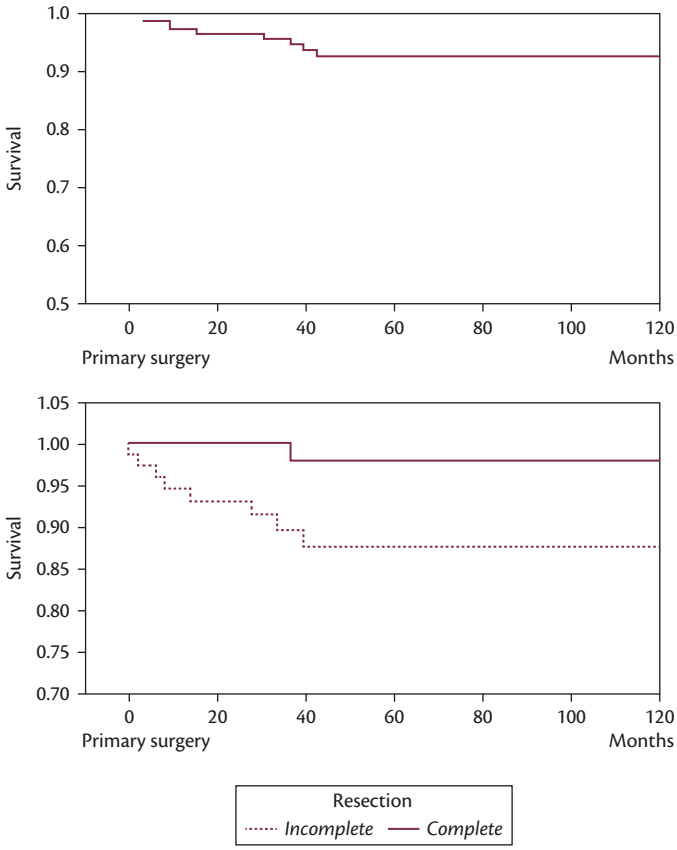

Fig. 26.7 Upper: graph displaying the actuarial survival curve of 148 patients who underwent primary surgery for craniopharyngioma. Lower: graph showing survival times in patients who underwent primary surgery for craniopharyngioma in relation to the extent of tumour resection (Kaplan–Meier method).
Fahlbusch, R., Honegger, J., Paulus, W., Huk, W., & Buchfelder, M. 1999. Surgical treatment of craniopharyngiomas: experience with 168 patients. *J Neurosurg*, 90, 237–50.

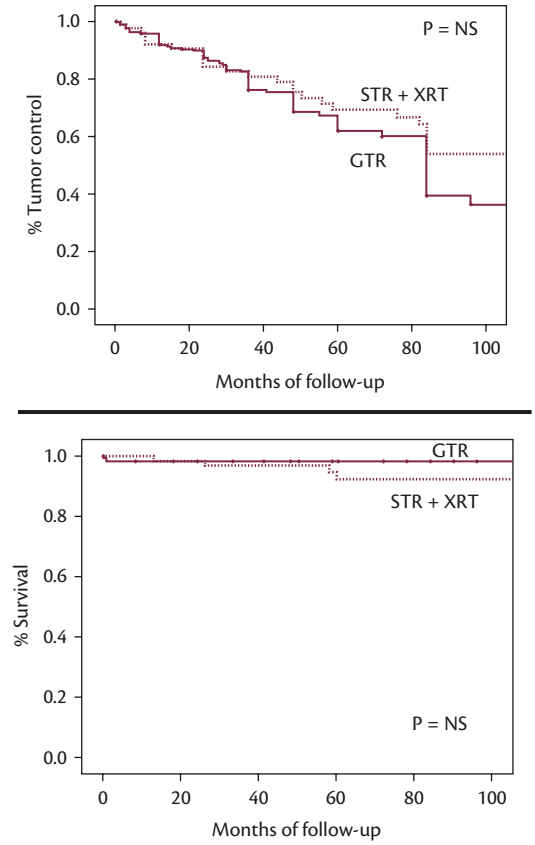

Fig. 26.8 The overall survival and the recurrence rate in comparison between patients operated for gross total resection (GTR) and those for partial resection (PR) followed with radiosurgery.
Reproduced from Yang, I., Sughrue, M. E., Rutkowski, M. J., et al. 2010. Craniopharyngioma: a comparison of tumour control with various treatment strategies. *Neurosurg Focus*, 28, E5, with permission from JNS Group.

cavity and has been used over the last six decades. Radioisotopes emitting short-range beta radiation with a short half-life are used, most frequently 90 yttrium, 32 phosphorus, or 186 rhenium. They are instilled stereotactically following aspiration of the cyst content. The delivery of a very high radiation dose of approximately 150 Gy to the cyst's secretory epithelial lining provides good tumour control (70–96%) (Derrey et al., 2008). On the other hand, it may affect visual function, the endocrine system, or the major surrounding vessels due to the radiation effect over the next 3–3.5 mm beyond the cyst wall. The published morbidity data vary widely in the literature. Therefore, the technique has not been widely accepted.

Another method, favoured in the past is the stereotactic instillation of bleomycin into the cyst cavity (Hukin et al., 2007). The reported response rates vary widely—from 57% to 100% and the risk of injury to surrounding structures due to the effect of bleomycin or its spillage may be high.

Future developments

Future developments for improved therapy for craniopharyngiomas are based on new knowledge of the morphological structure of the hypothalamus, including the nuclei with specific endocrine and vegetative functions. Advanced 7 Tesla MRI techniques may lead to more objective criteria for deciding on surgical treatment.

Conventional treatments could be enhanced by molecular based therapies including antihormonal treatments.

Hypothalamic obesity currently controlled mainly temporally by Baretić therapy remains challenging to treat (Rottembourg et al., 2009). Leptin-oriented approaches are not encouraging (Trivin et al., 2009; Roemmler-Zehrer et al., 2014). Recent trials with diazoxide and metformin should be regarded as preliminary (Aubert et al., 2011; Hamilton et al., 2011; Malin and Kashyap, 2014).

Rathke's cleft cyst

Rathke's cysts are non-neoplastic cystic formations from the glandular rests of the Rathke's cleft in the region of the intermediate lobe of the pituitary gland (Saeger et al., 2007). They are found in the pars distalis or pars intermedia in up to 22% of routine autopsy series (Teramoto et al., 1994). From the 4335 operations in the sellar region performed by the senior author between December 1982 and September 2005, 7% were craniopharyngiomas and only 2% were non-adenomatous cysts, mostly Rathke's cysts. It is a common incidental finding in neuroradiology and most frequently is asymptomatic. The main differential diagnosis is a craniopharyngioma. Surgical intervention is indicated in symptomatic lesions, which present with a typical headache, and in lesions showing growth, particularly when a craniopharyngioma cannot be ruled out. We recommend fenestration of the cyst with evacuation of the cyst contents and discourage aggressive attempts to remove the cyst wall. Attempts at total resection are associated with a high incidence of postoperative endocrine disturbance and are not related to a lower risk of recurrence.

Rathke's cysts are thought to originate during the development of the pituitary gland. It is thought that a rostral outpouching of the stomodeum in the third or fourth week of gestation meets a downward projection from the diencephalon, the infundibulum, forming the two lobes of the pituitary gland. The anterior wall of the pouch then proliferates to form the anterior lobe of the pituitary gland and pars tuberalis. The posterior wall becomes the pars intermedia. In a large percentage of human pituitaries the lumen is obliterated by epithelial infoldings. But after the formation of the adenohypophysis and neurohypophysis, a cleft may remain in the area of the pars intermedia. This cleft has been called the Rathke's cleft. A symptomatic Rathke's cleft cyst develops when this cleft fails to regress and starts to increase in size due to retention of secretions. Other theories of development of these cysts have included an endodermal origin or reverse metaplasia of pituitary cells (Ikeda and Yoshimoto, 2002).

The histopathological diagnosis of a Rathke's cyst has been confused, in some cases, with craniopharyngiomas. Nowadays, maturation of the β-catenin pathway, which is present in craniopharyngiomas, not in Rathke's cysts, facilitates differentiation between the two pathologies (**Fig. 26.1**). Sometimes, especially after drainage of a Rathke's cyst, it may be difficult to obtain a surgical specimen of the cyst wall, which does not permit conclusive histological diagnosis. The cyst has typically simple columnar or cuboidal epithelium, often with ciliated or mucinous goblet cells. Pseudostratified columnar cells are also frequently observed. Squamous metaplasia has been noted in 9–39% of the patients and is associated with higher rates of cyst recurrence. Rarely, the cyst is lined with stratified squamous epithelium and is thought to pose a higher risk of cyst recurrence. Rathke's cleft cysts with squamous metaplasia and transitional features (such as squamous epithelial cells) may resemble cystic craniopharyngiomas on histopathological examination and imaging studies. Some authors have pointed out the possible continuum between Rathke's cysts and craniopharyngiomas. Ikeda et al reviewed 42 patients with Rathke's cysts and found that three cases had squamous epithelium in the cyst wall similar to that observed in craniopharyngiomas (Ikeda and Yoshimoto, 2002).

Rathke's cysts developed usually intrasellarly in the pars intermedia. The cyst may be large and may extend also into the suprasellar cistern. Isolated suprasellar Rathke's cysts are rare. Ectopic Rathke's cysts are even more rare in the nasopharynx, sphenoidal sinus, the clivus, and cerebellopontine angle.

Clinical features

According to the largest published series on Rathke's cysts from the Weiss's group (Aho et al., 2005), approximately 70% of the incidentally discovered Rathke's cysts remain asymptomatic. Around 30% develop symptoms due to local mass effect and compression of the visual pathways and the pituitary gland, causing pituitary insufficiency. The most common symptom is headache. In a small group of patients, patients with Rathke's cysts show clinical evidence of panhypopituitarism, progressive visual loss, and symptoms mimicking meningitis or hypophysitis.

Asymptomatic lesions

Aho et al. (2005) reported on 160 cases of Rathke's cyst. In 42 of them the cyst was incidentally discovered during MRI examination for other reasons, they did not grow or cause endocrine or visual signs and symptoms (Aho et al., 2005). In another series from Teramto's group (Sanno et al., 2003), as few as 5.4% increased in size during the follow-up period (Sanno et al., 2003).

Symptomatic lesions

Symptomatic lesions present most frequently during the fourth or fifth decade of life, with a slight female preponderance. The typical symptoms associated with Rathke's cysts include headache, pituitary insufficiency, and visual disturbance. Headache is present in all symptomatic lesions and could be the only indication for surgery. It is usually felt around the bregma in cases of intrasellar lesions. In lesion with compression of the cavernous sinus, the patient may have periorbital pain.

As examples, a 17-year-old school boy with a Rathke's cyst presented only with severe headache that interfered with his school performance. After surgery, the headache was completely resolved with resumption of successful school activities. A 57-year-old lady presented with intermittent headache, then several weeks of persistent therapy resistant pain and she decided to have surgery. After surgery her headache completely and permanently resolved.

Visual disturbance preoperatively has been reported in 35–50% of patients undergoing surgical intervention. This includes visual field defects as well as declining visual acuity. Jahangiri et al. reported that preoperative hypopituitarism occurred in 41% of adults and 45% of paediatric patients. The most common endocrine findings are hyperprolactinemia and growth hormone deficiency, followed by hypocorticism and hypogonadism. DI has been described as a presenting condition in approximately 7–20% of the patients, less frequent than in craniopharyngioma. Other rare presentations include

chemical meningitis, or intracystic haemorrhage (Harrison et al., 1994; Jahangiri et al., 2011; Neidert et al., 2013). Some cases have presented with a sudden onset of symptoms together with imaging evidence of intracystic bleeding. This condition has been described as Rathke's cleft cyst apoplexy (Neidert et al., 2013).

Radiological features

Magnetic resonance imaging is the main imaging modality for preoperative assessment of Rathke's cysts and for differentiating Rathke's cysts from other cystic sellar lesions like craniopharyngiomas (Zada et al., 2010). The signal intensity of the cyst varies, and could be hypo-, hyper-, or isointense, depending of the composition of its content. Although most of the cysts display homogeneous signal intensity, up to 40% contain an intracystic nodule composed of protein and cellular debris that typically does not enhance following contrast administration (Brassier et al., 1999; Byun et al., 2000; Binning et al., 2005). A thin rim of enhancement can be attributed to inflammation or squamous metaplasia of the cyst wall, or to a circumferential displacement of the pituitary gland (Brassier et al., 1999; Byun et al., 2000; Kim et al., 2004; Zada, 2011). Even if the thin cystic capsule were to enhance, this would be below the resolution capacity of MRI. The pattern and the intensity of contrast enhancement are not constant findings in all cases. This is probably due to an inflammatory reaction in the surrounding tissues, namely the pituitary gland and sometimes the sellar dura, due to occasional leaks of the cyst contents. The pituitary gland is usually displaced by the cyst and in some cases the cyst remains encased inside the gland. The cysts are commonly intrasellar or intra-, para-, or suprasellar. Pure suprasellar cysts are rare.

Computer tomography can be used to detect calcification which appears more in cases of craniopharyngiomas. Nevertheless, Rathke's cysts are reported to exhibit calcifications but rarely and for a lesser extent. Further entities in the differential diagnosis are sellar abscess and lymphocytic hypophysitis.

Management

Asymptomatic Rathke's cysts (usually <1 cm) are followed up with serial MRI imaging, endocrine, and ophthalmic examinations.

A symptomatic Rathke's cyst is an indication for surgical intervention. Headache can be the only symptom. The aim of surgery is local decompression and, if possible, gaining tissue for histological diagnosis. Evacuation of the cyst contents is the most frequently used strategy. In the best operative situation, when the cyst has a superficial location and is directly related to the dura of the sellar floor, it can be fenestrated without incision of the pituitary gland and part of the wall can be taken for histology. The sellar and the intra or suprasellar cysts can be drained, the cyst wall will collapse, and the functions of the pituitary gland are preserved (Fig. 26.9). In some cases the cyst is inside the pituitary gland and the surgeon needs to split the pituitary gland. In this situation, the surgeon can only evacuate the cyst but should not risk taking a biopsy from the cyst wall. An attempt to completely or aggressively remove the cyst wall is associated with a higher incidence of endocrine deficiencies including DI. According to some reports, however, the cyst wall remnant is associated with higher

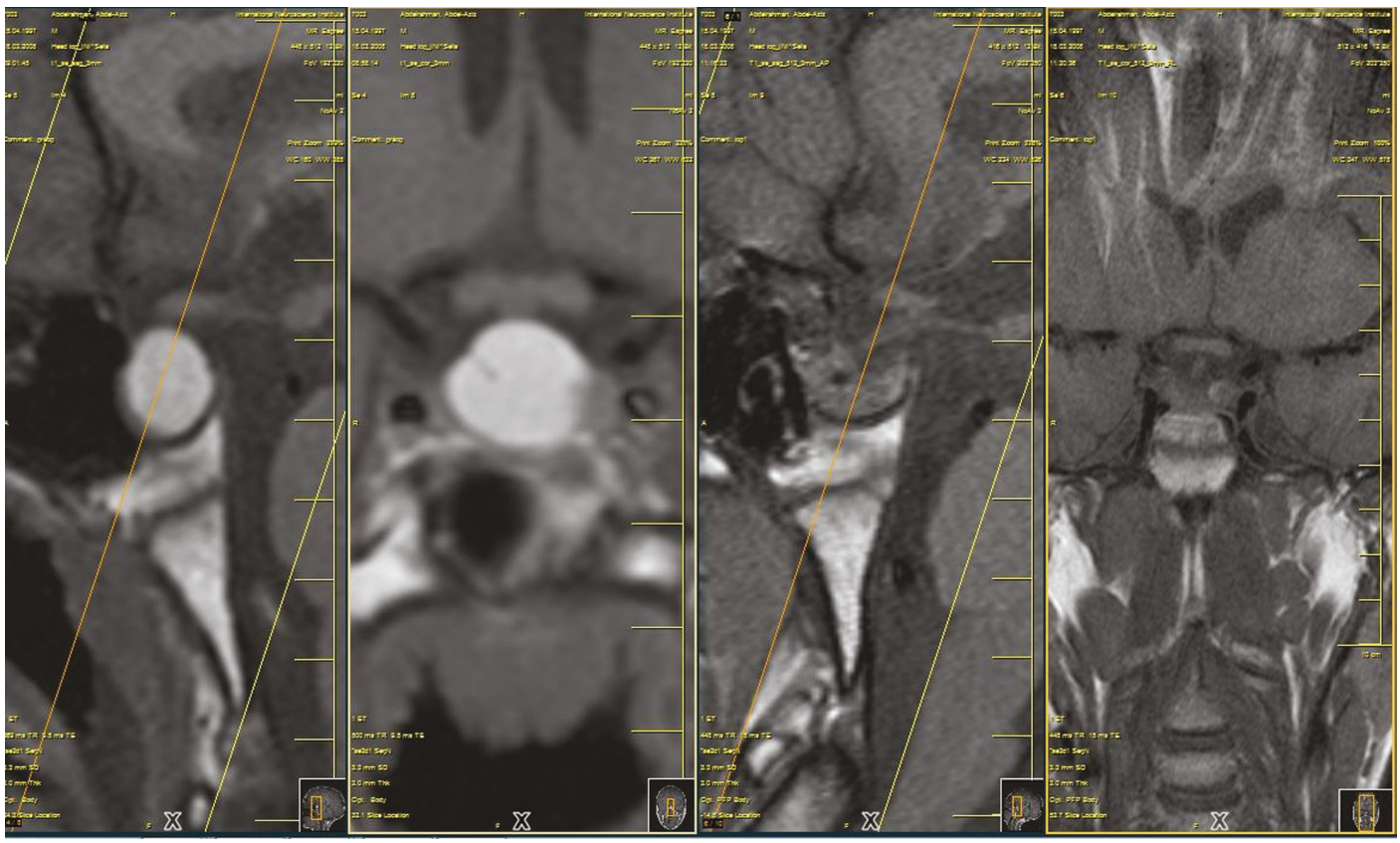

Fig. 26.9 Preoperative and postoperative MRI showing complete drainage of Rathke's cyst via a transsphenoidal approach.

recurrence rates. The experience of the senior author has shown that the potential risk of recurrence does not justify the morbidity risk, associated with aggressive cyst removal.

In pure suprasellar cysts the transcranial approach should be used, especially if a craniopharyngioma cannot be ruled out.

Outcome and follow-up

The rate of resolution of Rathke's cyst on postoperative MRI imaging after drainage is more than 90%. The headache improves immediately after surgery in all cases and visual functions improve in more than 80% after surgical drainage. Weiss's group (Aho et al.) presented a large surgical series of Rathke's cyst in adults, with an initial gross total resection rate of 97% and a recurrence rate of 18% after 5 years follow-up (Aho et al., 2005). Headache, visual symptoms, and hyperprolactinemia usually improve after surgical treatment, but panhypopituitarism and DI are less likely to improve because of the chronic compression of the pituitary gland. DI is more likely to occur after aggressive removal of the cyst wall. We have experienced, in some patients, postoperative temporary hyponatraemia that has been managed with fluid restriction.

Overall long-term recurrence rates after fenestration or resection of Rathke's cysts vary from 3% to 33%. The recurrence risk may correlate with the preoperative enhancement pattern of the cyst wall on imaging studies, the presence of squamous metaplasia, chronic inflammation, or stratified epithelium, the aggressiveness of cyst wall resection, and the insertion of an abdominal fat graft.

After surgical treatment of a Rathke's cyst, MR imaging is recommended after 3 months and then on a yearly basis for 5 years. After that every 2–3 years, if clinically stable, for a further 10 years.

Symptomatic recurrences of the Rathke's cysts are rare and are reported to range between 5 and 18%. Recurrence is usually manifested on the follow-up MRI, with or without reappearance of symptoms. Radiological evidence of recurrence on its own, is not an indication for reoperation. Symptomatic recurrence is an indication for operation to achieve adequate drainage. If the recurrence is asymptomatic, it should be followed with serial MRIs and with serial ophthalmic and endocrine examinations.

Controversies

One of the main points of discussion in the management of Rathke's cyst is how to measure the degree of resection. It is either described as the surgeon's impression or according to the postoperative MRI findings. The surgeon's impression is subjective and it is difficult in many cases to visualize and resect the thin wall of the cyst from the normal tissue of the pituitary gland safely. The cyst wall is normally not visible on the MRI and only the cyst contents give the radiological characteristics of the Rathke's cyst. Postoperative MRI cannot confirm removal of the cyst wall but can show complete evacuation of the cyst content. Accordingly, the term gross total resection of Rathke's cyst is very controversial.

We recommend fenestration and evacuation of the cyst via the transsphenoidal approach. The arachnoid should be kept intact. If there is intraoperative evidence of a CSF leak, we seal it with a small fat graft, taken from the subcutaneous tissue of the thigh or the abdomen. Transcranial approaches can be used in cases of isolated suprasellar symptomatic Rathke's cyst especially if large or when a craniopharyngioma cannot be excluded.

Acknowledgement

The authors would like to thank Professor Dr Rolf Buslei, Neuropathology institute, University of Erlangen, Germany for providing the histological sections.

FURTHER READING

Aho, C.J., Liu, C., Zelman, V., Couldwell, W.T., & Weiss, M.H. (2005). Surgical outcomes in 118 patients with Rathke cleft cysts. *J Neurosurg*, **102**, 189–93.

Fahlbusch, R. & Hofmann, B.M. (2008). Surgical management of giant craniopharyngiomas. *Acta Neurochir (Wien)*, **150**, 1213–26.

Fahlbusch, R., Honegger, J., Paulus, W., Huk, W., & Buchfelder, M. (1999). Surgical treatment of craniopharyngiomas: experience with 168 patients. *J Neurosurg*, **90**, 237–50.

Honegger, J., Buchfelder, M., & Fahlbusch, R. (1999). Surgical treatment of craniopharyngiomas: endocrinological results. *J Neurosurg*, **90**, 251–7.

Larkin, S.J. & Ansorge, O. (2013). Pathology and pathogenesis of craniopharyngiomas. *Pituitary*, **16**, 9–17.

REFERENCES

Aggarwal, A., Fersht, N., & Brada, M. (2013). Radiotherapy for craniopharyngioma. *Pituitary*, **16**, 26–33.

Aho, C.J., Liu, C., Zelman, V., Couldwell, W.T., & Weiss, M.H. (2005). Surgical outcomes in 118 patients with Rathke cleft cysts. *J Neurosurg*, **102**, 189–93.

Aubert, G., Mansuy, V., Voirol, M.J., Pellerin, L., & Pralong, F.P. (2011). The anorexigenic effects of metformin involve increases in hypothalamic leptin receptor expression. *Metabolism*, **60**, 327–34.

Binning, M.J., Gottfried, O.N., Osborn, A.G., & Couldwell, W.T. (2005). Rathke cleft cyst intracystic nodule: a characteristic magnetic resonance imaging finding. *J Neurosurg*, **103**, 837–40.

Brada, M. & Thomas, D.G. (1993). Craniopharyngioma revisited. *Int J Radiat Oncol Biol Phys*, **27**, 471–5.

Brassier, G., Morandi, X., Tayiar, E., et al. (1999). Rathke's cleft cysts: surgical-MRI correlation in 16 symptomatic cases. *J Neuroradiol*, **26**, 162–71.

Brastianos, P.K., Taylor-Weiner, A., Manley, P.E., et al. (2014). Exome sequencing identifies *BRAF* mutations in papillary craniopharyngiomas. *Nat Genet*, **46**, 161–5.

Bunin, G.R., Surawicz, T.S., Witman, P.A., Preston-Martin, S., Davis, F., & Bruner, J. M. (1997). The descriptive epidemiology of craniopharyngioma. *Neurosurg Focus*, **3**, e1.

Byun, W.M., Kim, O.L., & Kim, D. (2000). MR imaging findings of Rathke's cleft cysts: significance of intracystic nodules. *AJNR Am J Neuroradiol*, **21**, 485–8.

Caldarelli, M., Massimi, L., Tamburrini, G., Cappa, M., & Di Rocco, C. (2005). Long-term results of the surgical treatment of craniopharyngioma: the experience at the Policlinico Gemelli, Catholic University, Rome. *Childs Nerv Syst*, **21**, 747–57.

Cavallo, L.M., Solari, D., Esposito, F., Villa, A., Minniti, G., & Cappabianca, P. (2014). The role of the endoscopic endonasal route in the management of craniopharyngiomas. *World Neurosurg*, **82**, S32–40.

Crotty, T.B., Scheithauer, B.W., Young, W.F., Jr., et al. (1995). Papillary craniopharyngioma: a clinicopathological study of 48 cases. *J Neurosurg*, **83**, 206–14.

Derrey, S., Blond, S., Reyns, N., et al. (2008). Management of cystic craniopharyngiomas with stereotactic endocavitary irradiation using colloidal 186Re: a retrospective study of 48 consecutive patients. *Neurosurgery*, **63**, 1045–52; discussion 1052–3.

Duff, J., Meyer, F.B., Ilstrup, D.M., Laws, E.R., Jr., Schleck, C.D., & Scheithauer, B.W. (2000). Long-term outcomes for surgically resected craniopharyngiomas. *Neurosurgery*, **46**, 291–302; discussion 302–5.

Fahlbusch, R. & Hofmann, B.M. (2008). Surgical management of giant craniopharyngiomas. *Acta Neurochir (Wien)*, **150**, 1213–26.

Fahlbusch, R., Honegger, J., Paulus, W., Huk, W., & Buchfelder, M. (1999). Surgical treatment of craniopharyngiomas: experience with 168 patients. *J Neurosurg*, **90**, 237–50.

Gardner, P.A., Kassam, A.B., Snyderman, C.H., et al. (2008). Outcomes following endoscopic, expanded endonasal resection of suprasellar craniopharyngiomas: a case series. *J Neurosurg*, **109**, 6–16.

Gerganov, V., Metwali, H., Samii, A., Fahlbusch, R., & Samii, M. (2014). Microsurgical resection of extensive craniopharyngiomas using a frontolateral approach: operative technique and outcome. *J Neurosurg*, **120**, 559–70.

Halac, I. & Zimmerman, D. (2005). Endocrine manifestations of craniopharyngioma. *Childs Nerv Syst*, **21**, 640–8.

Hamilton, J.K., Conwell, L.S., Syme, C., Ahmet, A., Jeffery, A., & Daneman, D. (2011). Hypothalamic obesity following craniopharyngioma surgery: results of a pilot trial of combined diazoxide and metformin therapy. *Int J Pediatr Endocrinol*, **2011**, 417949.

Harrison, M.J., Morgello, S., & Post, K.D. (1994). Epithelial cystic lesions of the sellar and parasellar region: a continuum of ectodermal derivatives? *J Neurosurg*, **80**, 1018–25.

Hoffman, H.J., De Silva, M., Humphreys, R.P., Drake, J.M., Smith, M.L., & Blaser, S.I. (1992). Aggressive surgical management of craniopharyngiomas in children. *J Neurosurg*, **76**, 47–52.

Hofmann, B.M., Hollig, A., Strauss, C., Buslei, R., Buchfelder, M., & Fahlbusch, R. (2012). Results after treatment of craniopharyngiomas: further experiences with 73 patients since 1997. *J Neurosurg*, **116**, 373–84.

Holsken, A., Buchfelder, M., Fahlbusch, R., Blumcke, I., & Buslei, R. (2010). Tumour cell migration in adamantinomatous craniopharyngiomas is promoted by activated Wnt-signalling. *Acta Neuropathol*, **119**, 631–9.

Holsken, A., Kreutzer, J., Hofmann, B.M., et al. (2009). Target gene activation of the Wnt signaling pathway in nuclear beta-catenin accumulating cells of adamantinomatous craniopharyngiomas. *Brain Pathol*, **19**, 357–64.

Honegger, J., Barocka, A., Sadri, B., & Fahlbusch, R. (1998). Neuropsychological results of craniopharyngioma surgery in adults: a prospective study. *Surg Neurol*, **50**, 19–28; discussion 28–9.

Honegger, J., Buchfelder, M., & Fahlbusch, R. (1999). Surgical treatment of craniopharyngiomas: endocrinological results. *J Neurosurg*, **90**, 251–7.

Hukin, J., Steinbok, P., Lafay-Cousin, L., et al. (2007). Intracystic bleomycin therapy for craniopharyngioma in children: the Canadian experience. *Cancer*, **109**, 2124–31.

Hussain, I., Eloy, J.A., Carmel, P.W., & Liu, J.K. (2013). Molecular oncogenesis of craniopharyngioma: current and future strategies for the development of targeted therapies. *J Neurosurg*, **119**, 106–12.

Ichimura, S., Fahlbusch, R., & Ludemann, W. (2015). Treatment of hyponatremia with tolvaptan in a patient after neurosurgical treatment of a pituitary tumour: case report and review of literature. *J Neurol Surg Rep*, **76**, e279–81.

Ikeda, H. & Yoshimoto, T. (2002). Clinicopathological study of Rathke's cleft cysts. *Clin Neuropathol*, **21**, 82–91.

Jahangiri, A., Molinaro, A.M., Tarapore, P.E., et al. (2011). Rathke cleft cysts in pediatric patients: presentation, surgical management, and postoperative outcomes. *Neurosurg Focus*, **31**, E3.

Karavitaki, N., Brufani, C., Warner, J.T., et al. (2005). Craniopharyngiomas in children and adults: systematic analysis of 121 cases with long-term follow-up. *Clin Endocrinol (Oxf)*, **62**, 397–409.

Kim, J.E., Kim, J.H., Kim, O.L., et al. (2004). Surgical treatment of symptomatic Rathke cleft cysts: clinical features and results with special attention to recurrence. *J Neurosurg*, **100**, 33–40.

Koutourousiou, M., Gardner, P.A., Fernandez-Miranda, J.C., et al. (2013). Endoscopic endonasal surgery for craniopharyngiomas: surgical outcome in 64 patients. *J Neurosurg*, **119**, 1194–207.

Larkin, S.J. & Ansorge, O. (2013). Pathology and pathogenesis of craniopharyngiomas. *Pituitary*, **16**, 9–17.

Lo, A.C., Howard, A.F., Nichol, A., et al. (2014). Long-term outcomes and complications in patients with craniopharyngioma: the British Columbia Cancer Agency experience. *Int J Radiat Oncol Biol Phys*, **88**, 1011–18.

Maira, G., Anile, C., Albanese, A., Cabezas, D., Pardi, F., & Vignati, A. (2004). The role of transsphenoidal surgery in the treatment of craniopharyngiomas. *J Neurosurg*, **100**, 445–51.

Malin, S.K. & Kashyap, S.R. (2014). Effects of metformin on weight loss: potential mechanisms. *Curr Opin Endocrinol Diabetes Obes*, **21**, 323–9.

Mortini, P., Losa, M., Pozzobon, G., et al. (2011). Neurosurgical treatment of craniopharyngioma in adults and children: early and long-term results in a large case series. *J Neurosurg*, **114**, 1350–9.

Muller, H.L. (2013). Childhood craniopharyngioma. *Pituitary*, **16**, 56–67.

Neidert, M.C., Woernle, C.M., Leske, H., et al. (2013). Ruptured Rathke cleft cyst mimicking pituitary apoplexy. *J Neurol Surg A Cent Eur Neurosurg*, **74** Suppl 1, e229–32.

Nielsen, E.H., Feldt-Rasmussen, U., Poulsgaard, L., et al. (2011). Incidence of craniopharyngioma in Denmark (n = 189) and estimated world incidence of craniopharyngioma in children and adults. *J Neurooncol*, **104**, 755–63.

Poretti, A., Grotzer, M.A., Ribi, K., Schonle, E., & Boltshauser, E. (2004). Outcome of craniopharyngioma in children: long-term complications and quality of life. *Dev Med Child Neurol*, **46**, 220–9.

Prabhu, V.C. & Brown, H.G. (2005). The pathogenesis of craniopharyngiomas. *Childs Nerv Syst*, **21**, 622–7.

Puget, S., Garnett, M., Wray, A., et al. (2007). Pediatric craniopharyngiomas: classification and treatment according to the degree of hypothalamic involvement. *J Neurosurg*, **106**, 3–12.

Roemmler-Zehrer, J., Geigenberger, V., Stormann, S., et al. (2014). Food intake regulating hormones in adult craniopharyngioma patients. *Eur J Endocrinol*, **170**, 627–35.

Rottembourg, D., O'Gorman, C.S., Urbach, S., et al. (2009). Outcome after bariatric surgery in two adolescents with hypothalamic obesity following treatment of craniopharyngioma. *J Pediatr Endocrinol Metab*, **22**, 867–72.

Saeger, W., Ludecke, D.K., Buchfelder, M., Fahlbusch, R., Quabbe, H.J., & Petersenn, S. (2007). Pathohistological classification of pituitary tumours: 10 years of experience with the German Pituitary Tumour Registry. *Eur J Endocrinol*, **156**, 203–16.

Sanno, N., Oyama, K., Tahara, S., Teramoto, A., & Kato, Y. (2003). A survey of pituitary incidentaloma in Japan. *Eur J Endocrinol*, **149**, 123–7.

Sekine, S., Shibata, T., Kokubu, A., et al. (2002). Craniopharyngiomas of adamantinomatous type harbor beta-catenin gene mutations. *Am J Pathol*, **161**, 1997–2001.

Shi, X.E., Wu, B., Zhou, Z.Q., Fan, T., & Zhang, Y.L. (2006). Microsurgical treatment of craniopharyngiomas: report of 284 patients. *Chin Med J (Engl)*, **119**, 1653–63.

Shin, J.L., Asa, S.L., Woodhouse, L.J., Smyth, H.S., & Ezzat, S. (1999). Cystic lesions of the pituitary: clinicopathological features distinguishing craniopharyngioma, Rathke's cleft cyst, and arachnoid cyst. *J Clin Endocrinol Metab*, **84**, 3972–82.

Sun, H.I., Akgun, E., Bicer, A., et al. (2010). Expression of angiogenic factors in craniopharyngiomas: implications for tumour recurrence. *Neurosurgery*, **66**, 744–50; discussion 750.

Teramoto, A., Hirakawa, K., Sanno, N., & Osamura, Y. (1994). Incidental pituitary lesions in 1,000 unselected autopsy specimens. *Radiology*, **193**, 161–4.

Trivin, C., Busiah, K., Mahlaoui, N., et al. (2009). Childhood craniopharyngioma: greater hypothalamic involvement before surgery is associated with higher homeostasis model insulin resistance index. *BMC Pediatr*, **9**, 24.

Van Effenterre, R. & Boch, A.L. (2002). Craniopharyngioma in adults and children: a study of 122 surgical cases. *J Neurosurg*, **97**, 3–11.

Yang, I., Sughrue, M.E., Rutkowski, M.J., et al. (2010). Craniopharyngioma: a comparison of tumour control with various treatment strategies. *Neurosurg Focus*, **28**, E5.

Yasargil, M.G., Curcic, M., Kis, M., Siegenthaler, G., Teddy, P.J., & Roth, P. (1990). Total removal of craniopharyngiomas. Approaches and long-term results in 144 patients. *J Neurosurg*, **73**, 3–11.

Yosef, L., Ekkehard, K.M., & Shalom, M. (2015). Giant craniopharyngiomas in children: short- and long-term implications. *Childs Nerv Syst*, **32**(1), 79–88.

Zada, G. (2011). Rathke cleft cysts: a review of clinical and surgical management. *Neurosurg Focus*, **31**, E1.

Zada, G., Lin, N., Ojerholm, E., Ramkissoon, S., & Laws, E.R. (2010). Craniopharyngioma and other cystic epithelial lesions of the sellar region: a review of clinical, imaging, and histopathological relationships. *Neurosurg Focus*, **28**, E4.

Zuccaro, G. (2005). Radical resection of craniopharyngioma. *Childs Nerv Syst*, **21**, 679–90.

RELATED LINKS TO EBRAIN

Management of Craniopharyngiomas. https://learning.ebrain.net/course/view.php?id=463

Tumours of the Central Nervous System: Craniopharyngioma. https://learning.ebrain.net/course/view.php?id=464

27

Surgical management of sellar and suprasellar tumours

Jayson A. Neil and William T. Couldwell

Introduction

Despite their shared location, sellar and suprasellar tumours are an extremely diverse group of lesions with multiple sources of origin. These tumours may be congenital lesions, such as lipomas, Rathke's cleft (pars intermedia) cysts, arachnoid cysts, and hamartomas, or they may develop from any of the surrounding structures, resulting in pituitary adenomas, meningiomas, craniopharyngiomas, chordomas, optic nerve gliomas, among others. Non-neoplastic lesions, such as cavernous malformations, fibrous dysplasia, and inflammatory lesions such as sarcoidosis also present here, and tumours from remote sites are found in the form of metastasis in both the pituitary gland and the cavernous sinus. This extraordinary variety can make management of cases with these tumours more complicated because of the myriad of pathologies encountered.

To add to the complexity of treatment for sellar and suprasellar tumours, there are numerous critical structures in this region, including the pituitary gland, critical vessels, and multiple cranial nerves. Avoiding injury to these important structures is a key component of treatment planning.

In this chapter, we will discuss the anatomy of the sellar and suprasellar region with these factors in mind. We will discuss the workup, management, operative strategy, postoperative care, and complication management of these tumours, then elaborate on controversies related to these issues.

Surgical anatomy

A thorough understanding of the sellar and suprasellar anatomy is critical to an understanding of the pathology and its development and to the planning of any operative approach to this region. To simplify the discussion, we will divide the anatomy into the nasal cavity and sphenoid sinus and the sellar, parasellar, and suprasellar compartments, although much of the pathology in this area will encompass multiple compartments.

Nasal cavity and sphenoid sinus

The nasal cavity is a paired structure that opens anteriorly to the nares and posteriorly to the nasopharynx through the choana. It is bordered medially by the nasal septum. The bony nasal septum is formed by the vomer inferiorly and the perpendicular plate of the ethmoid superiorly with attachments to the rostrum or anterior wall of the sphenoid sinus providing a reliable midline landmark. On the lateral wall are the inferior, middle, and superior conchae and openings for the ethmoidal, frontal, and maxillary sinuses, as well as the nasolacrimal duct. The superior border is the cribriform plate, and the posterior border is the sphenoid bone. In the superior and posterior aspects, the nasal cavity communicates with the sphenoid sinus through the sphenoid ostia just medial and superior to the superior turbinates. The inferior turbinate is a separate bone and is the largest turbinate.

The sphenoid sinus is a single midline structure that communicates anteroinferiorly through the paired sphenoid ostia into the paired nasal cavities. It is encompassed by sphenoid bone and may be divided by multiple and eccentric septi. The blood supply to the sphenoid sinus arises from the sphenopalatine and posterior ethmoid arteries. The posterior septal branch of the sphenopalatine artery provides the pedicle for the nasoseptal flap and courses below the inferior border of the sphenoid ostium and passes anteriorly to supply the septal mucosa. The carotid arteries and optic nerves are closely apposed to the superolateral wall of the sphenoid sinus, and the sinus itself is often contoured around these structures, which may be dehiscent within the sinus. The horizontal petrous carotid continues to the cavernous segment, which in the endoscopic literature is termed the 'paraclival' carotid, and is vertically orientated in the posterolateral sphenoid sinus. This continues as an intracavernous segment which, more distally, loops posterolaterally and is not visible in the sphenoid sinus. It re-emerges on either side of the sella as the 'parasellar' carotid. It is important to recognize that the bone over the parasellar carotid can be thin and dehiscent.

The junctures between the parasellar carotid and the impression of the optic nerve are termed the optico-carotid recesses (OCR). The lateral OCR marks the location of the optic strut and anterior clinoid process and can be aerated and appear as a hollow from an endoscopic view. The medial OCR is in the vicinity of the middle clinoid process and medial cavernous sinus. The sella turcica hangs within the superior and posterior aspect of the sphenoid sinus (**Figs. 27.1** and **27.2**).

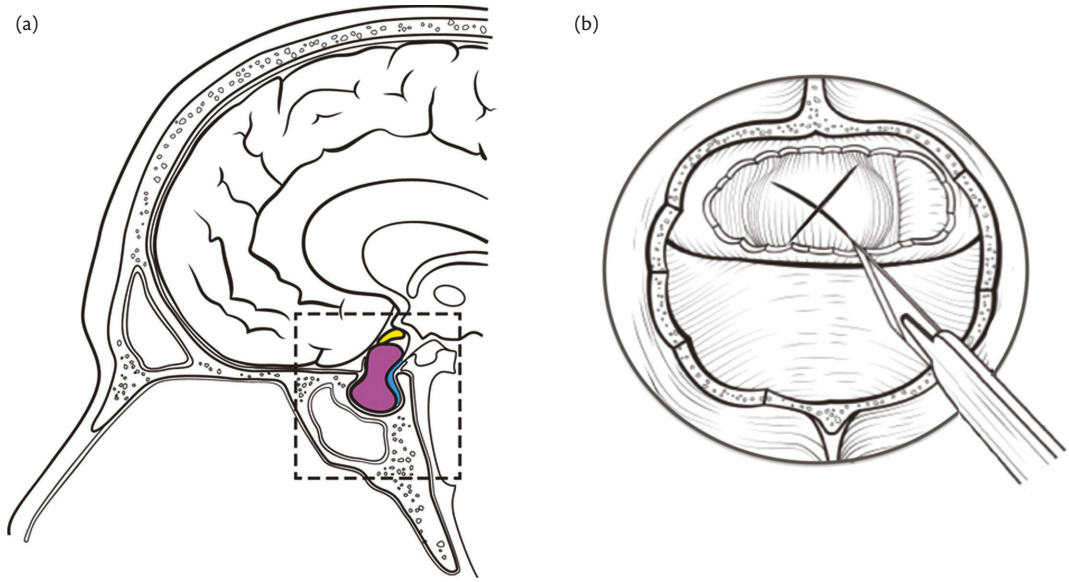

Fig. 27.1 (A) Sagittal view with pituitary adenoma shown in purple filling the sella and projecting into the suprasellar space. The optic chiasm, in yellow, is displaced upward and the normal pituitary gland, in blue, is displaced posteriorly or superiorly. (B) Anterior skull base as viewed from below through a microscope showing the incisions in the dura overlying the sella, which hangs in the posterior and superior aspect of the sphenoid sinus.
Copyright © Department of Neurosurgery, University of Utah, USA. Reproduced with permission.

Sellar compartment

The sella turcica is a saddle-shaped depression in the body of the sphenoid bone. The hypophyseal fossa sits in the centre of the depression and is bordered anterosuperiorly by the tuberculum sellae, posteriorly by the dorsum sellae, laterally by the cavernous sinuses, anteroinferiorly and inferiorly by the sphenoid sinus, and superiorly by the suprasellar diaphragm sellae and suprasellar cistern. The pituitary gland sits in the hypophyseal fossa and is composed of an anterior lobe (adenohypophysis) and posterior lobe (neurohypophysis). The adenohypophysis originates from Rathke's pouch in the stomodeum and ascends along the craniopharyngeal duct into the sella. The neurohypophysis is an invagination of the floor of the third ventricle, which descends into the sella.

Parasellar compartment

The parasellar compartment is composed of the cavernous sinuses bilaterally, which are composed of dilated venous channels through which the cavernous portion of the carotid arteries and cranial nerves III, IV, V1, V2, and VI run. The cavernous sinus is bordered by a single layer of periosteal dura medially; the dura from the floor of the sella turcica, middle fossa floor, and clivus join the periosteal dura, creating a double layer of dura around the rest of the cavernous sinus (Fig. 27.2).

Suprasellar compartment

The suprasellar compartment is composed predominantly of the suprasellar cistern. The suprasellar cistern is a cerebrospinal fluid (CSF) filled space directly above the sella turcica and below the third ventricle. It contains the infundibular stalk, optic chiasm, and circle of Willis (Figs. 27.1 and 27.2). It appears pentagonal in shape on axial imaging.

Preoperative workup

Clinical evaluation

The clinical signs and symptoms with which a patient presents depend on the pathology, size, location, and chronicity of the lesion. A detailed clinical history should be combined with a physical examination including detailed head, neck, and cranial nerve examination, with a special focus on cranial nerves I–VI. Common symptoms include headache, double or blurry vision, loss of vision, and symptoms related to endocrinopathy (galactorrhoea, amenorrhea, acromegaly, Cushing syndrome, hypopituitarism), vascular compromise (e.g. transient ischaemic attack, stroke), and hydrocephalus

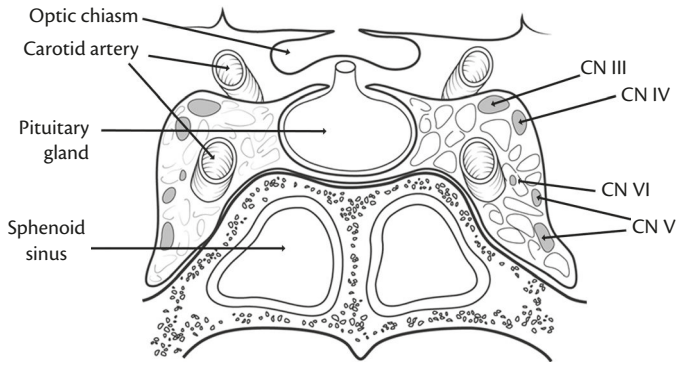

Fig. 27.2 Coronal cross-sectional drawing of the sellar region depicting the sella, bilateral cavernous sinuses (with contents), suprasellar cistern.
Copyright © Department of Neurosurgery, University of Utah, USA. Reproduced with permission.

in very large tumours. If the tumour invades the paranasal sinuses, the patient may present with symptoms related to sinus occlusion (nasal obstruction, sinusitis).

The formal neuro-ophthalmological evaluation should include visual acuity testing, and visual field evaluation, as well as funduscopic examination to evaluate for papilloedema, venous congestion, or other findings indicative of raised intracranial pressure. The funduscopic examination may also provide evidence of optic nerve injury and atrophy. Formal visual fields are necessary to evaluate further nerve injury, which may be indicative of optic nerve compression from suprasellar components of a tumour. Typical bitemporal hemianopsia from chiasmal compromise as well as other forms of compression including within the optic canal can be identified. Optical coherence tomography (OCT) can also be utilized to obtain high-resolution images of the retina to better assess optic nerve atrophy and axonal integrity. If the retinal nerve fibre layer (RNFL) thickness is maintained this is a positive predictor of visual improvement following adequate surgical decompression of the optic nerve pathway.

Laboratory evaluation

Standard laboratory evaluations, including a complete blood count, a basic metabolic panel, and coagulation evaluations, should be completed. Furthermore, if the patient has a history of cancer, lymphoma, infection, or granulomatosis diseases, specific workup pertaining to those entities should be ordered; a lumbar puncture for CSF analysis can be part of this evaluation. A complete endocrinologic workup should also be performed; this is covered in detail in Chapter 25.

Radiographic evaluation

Magnetic resonance imaging (MRI) remains the best study with which to evaluate sellar and suprasellar lesions. In particular, thin-cut T1-weighted MRI with and without contrast enhancement should always be performed (usually done as part of a pituitary protocol). In addition, fat-suppressed imaging and thin-cut T2-imaging with sagittal and coronal reconstructions can be helpful in elucidating the extent of the lesion and its relationship to the cavernous sinus, optic and other cranial nerves, and carotid arteries. Computed tomography (CT) allows visualization of the sella and skull base osseous structures, can assist in evaluating for calcium within the tumour (such as in craniopharyngioma, chordoma, or chondrosarcoma, among others), and may also provide information regarding haemorrhage (e.g. pituitary apoplexy). In addition, it is superior to MRI in determining whether there is bone involvement from the lesion, such as hyperostosis or pneumosinus dilatans with meningioma, or bone erosion with other lesions. If a vascular lesion such as a large aneurysm is included in the differential diagnosis or if there is vascular encasement or compromise, a CT angiogram, or formal angiogram should be performed prior to any intervention.

Surgical planning

Multiple approaches exist for accessing sellar and suprasellar lesions. These include, but are not limited to, the transnasal–transsphenoidal, pterional, and subfrontal approaches and their variations. All of these approaches can be performed with the operative microscope, endoscope, or both, and multiple approaches may be combined to resect particularly large or difficult lesions. The expected pathology, location, and attachment of the lesion should be considered in choosing an approach. Likewise, the direction of displacement of the pituitary gland, stalk, optic nerves, and other cranial nerves are noted to assist in determining the side and nature of the approach. To avoid postoperative complications such as a CSF leak, there should be a clear plan for the surgical resection and closure. The necessary equipment and experience should be available before the procedure is started.

Intraoperative

Transcranial approaches

Pterional

The pterional approach has several advantages, including its familiarity to most neurosurgeons and the early visualization of the optic nerves, chiasm, pituitary stalk, carotid artery, and anterior cerebral artery vasculature. This approach also offers the shortest distance to access the suprasellar cistern and provides the ability to look behind the optic nerves early in the dissection to allow control of the carotid artery and its branches. In addition, there is early access to CSF for brain relaxation and less frequent transgression of the frontal sinus, which reduces the risk of CSF leak or infection. If there is significant anterior skull base involvement or if substantial skull base reconstruction is anticipated, this approach affords less access than a bilateral subfrontal approach.

For the pterional approach, the patient is positioned supine with an ipsilateral shoulder roll, and the operating table is slightly reflexed to position the head above the right atrium of the heart. The head is fixed in a Mayfield 3-pin head holder, rotated 30–40°, and slightly extended. The head may be variably extended to afford a more inferior-to-superior trajectory to access lesions that extend superiorly. Further extension facilitates the superior view and aids in frontal lobe retraction by gravity. The skin incision follows a gentle curve behind the hairline from just anterior to the tragus at the level of the zygoma to the midline at the anterior most aspect of the normal hairline. The temporalis fascia and muscle are incised linearly, and in most instances a combined musculocutaneous flap is elevated and retracted anteroinferiorly (Fig. 27.3). Burr holes are placed at the keyhole, along the posterior superior temporal line, and at the lower temporal fossa. The dura is separated from the calvaria, and a high-speed drill with footplate is used for the craniotomy, which should be customized to the patient and access needed.

The lateral aspect of the lesser wing of the sphenoid bone is removed down to the meningo-orbital artery using bone rongeurs and a high-speed drill. The dura is incised in a C-shaped fashion and retracted anteriorly. Early dissection of the Sylvian fissure allows for brain relaxation by CSF egress and exposes the olfactory, optic, and oculomotor nerves, as well as the carotid and anterior cerebral arteries. At this point, the suprasellar cistern is visualized, and most suprasellar tumours will be visible (Fig. 27.4). Tumour debulking

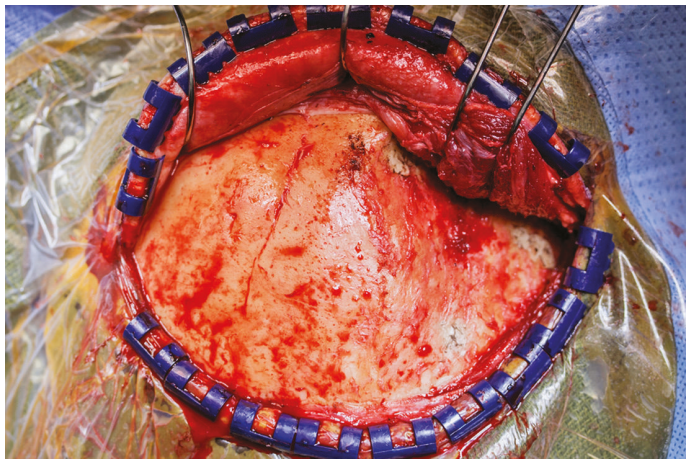

Fig. 27.3 Operative photograph of skin incision, elevation of musculocutaneous flap, and right pterional craniotomy.

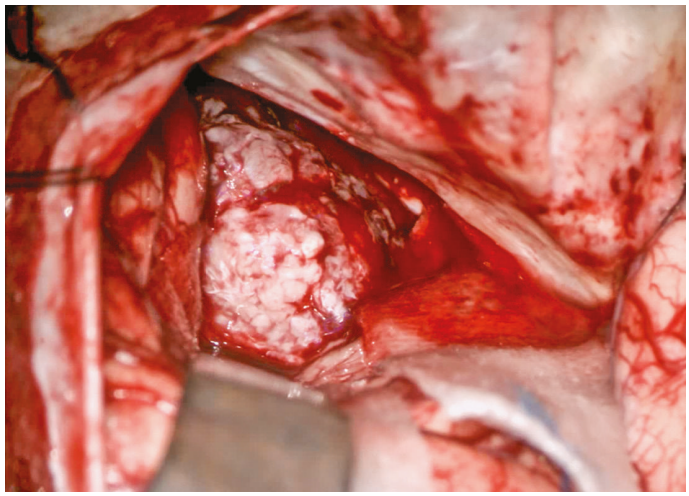

Fig. 27.4 Operative photograph of the occipital grey matter (just superior to the metal retractor) as viewed through a right pterional approach.

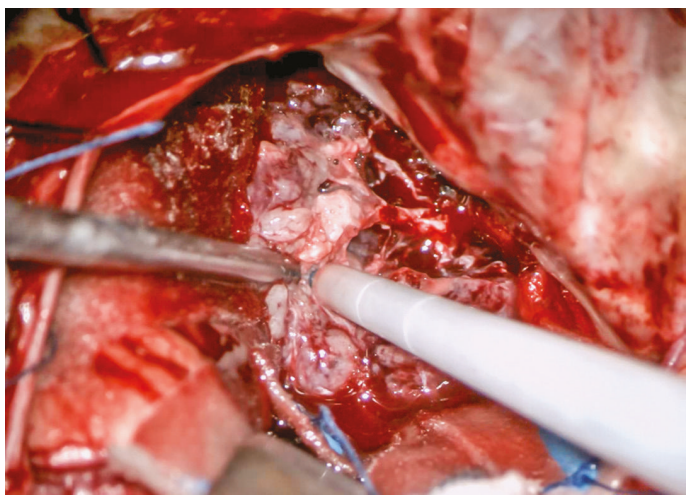

Fig. 27.5 Operative photograph of debulking of occipital grey matter using and ultrasonic aspirator as viewed through a right pterional approach.

will assist in dissection from the surrounding neurovascular structures (Fig. 27.5). The dura is closed primarily in a watertight fashion, and the bone flap is replaced using titanium plates and screws. A cranioplasty over the craniectomized sphenoid wing is performed using Medpor polyethylene implants to offset temporalis wasting. The temporalis muscle and fascia and the overlying soft tissues are closed in a standard fashion. See Box 27.1.

Variations on the frontotemporal approach: Fronto-orbital and orbitozygomatic

The primary indication for extending the standard frontotemporal approach to a fronto-orbital (removal of the orbital rim) or orbitozygomatic approach (removal of the orbital rim and zygoma) is to provide additional inferior-to-superior viewing trajectory while minimizing frontal and temporal lobe retraction. Which of these variants to use depends on the particular tumour. In most instances, the fronto-orbital variant is used, and a segment of the anterior and lateral orbital rim is included in the flap (extending from just lateral to the supraorbital notch to the lateral aspect of the orbital rim). Careful cuts are made to avoid disruption of the periorbita. The orbitozygomatic variant is used when a more extensive superior trajectory is needed. It is performed by eliminating the temporalis muscle by reflecting the muscle down and posteriorly and can be carried out in a one- or two-piece fashion, the technical details of which are covered in other chapters.

Subfrontal

Frontal or subfrontal craniotomies can be performed either unilaterally or bilaterally as needed for access to the lesion, a subcranial extension can be utilized if necessary (Fig. 27.6). For a unilateral subfrontal craniotomy, the patient is positioned similarly to the pterional approach, but with the head turned less, approximately 10–20° from the midline. The bicoronal skin incision generally ends just across the midline or at the contralateral superior temporal line. The scalp flap and periosteum are reflected anteriorly to expose the supraorbital vessels and nerves and to identify the orbital rim. Burr holes are placed, usually at the keyhole (the temporalis muscle is reflected in its anterior region to accommodate this hole). A decision will need to be made whether the sagittal sinus will be exposed, and the holes in the midline will be placed accordingly. The bone flap is brought low, just above the orbital rim. The frontal sinus is invariably entered with this flap. We usually choose to cranialize the sinus (remove the posterior table) and drill out the mucosa. The nasofrontal duct will then be plugged with muscle or fascia. The dura is usually incised in a C-shaped fashion with the base directed inferiorly.

For bilateral subfrontal craniotomy, the patient is positioned strictly supine with the bed reflexed to place the head above the right atrium of the heart. The head is fixed in a Mayfield 3-pin head holder and slightly extended to place the bilateral maxillary process at the highest point to facilitate brain retraction (Fig. 27.7). The skin incision is carried from zygoma to zygoma just anterior to the tragus bilaterally. Dissection is carried anteriorly with care taken to preserve the pericranium for use in reconstruction of the skull base. Minimal temporalis dissection is necessary and primarily only along the superior aspect near the keyhole bilaterally. Burr holes are made at the keyhole, posterior along the superior temporal line, and posteromedially lateral to the superior sagittal sinus (Fig. 27.6). Care must be taken to dissect the superior sagittal sinus from the calvaria, and if the sinus dura is very adherent, a trough can be created by using a drill with a diamond bit or the ridge of bone between the burr holes over the sinus can be removed using a Kerrison's

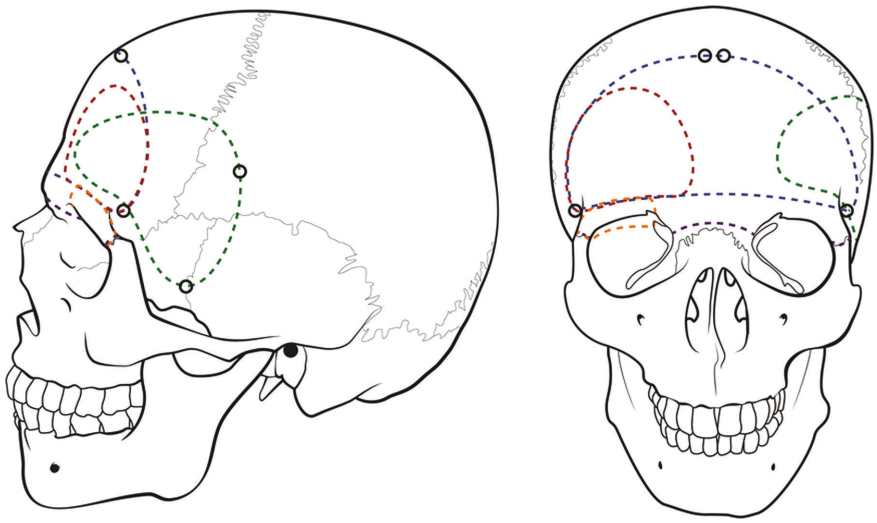

Fig. 27.6 Diagram of craniotomy paths based on operative approach. Displayed are the unilateral frontal (red), pterional (green), and bifrontal (blue) approaches. Additional orbital (orange) and subcranial (purple) cuts may be performed.

Copyright © Department of Neurosurgery, University of Utah, USA. Reproduced with permission.

Fig. 27.7 Operative photographs of patient positioning and marked skin incision.

punch. No burr holes are placed over the forehead. The dura is dissected from the calvaria, and the craniotomy is performed using a high-speed drill with a footplate. The frontal sinus is exenterated and cranialized by removing the posterior wall with a high-speed drill and rongeurs. The mucosa of the frontal sinus is completely removed, and the frontonasal ducts are plugged using fascia and temporalis muscle. The dura is incised lateral to the superior sagittal sinus as far in the anterior direction as is afforded by the pathology (generally well within the anterior third of the sinus). The sinus is ligated using two double loops of 2-0 silk suture through the falx and incised between the sutures.

For both the unilateral and bilateral subfrontal approaches, the brain is gently elevated and the olfactory nerves can be followed back to their crossing with the optic nerves. If possible, the arachnoid over the olfactory bulb and nerves should be released to avoid injury to these nerves. The tumour should be visualized along the anterior skull base or in the suprasellar cistern. Tumour resection is carried out in an anterior-to-posterior fashion. As in any approach, if the tumour base is anchored to the dura (as in meningiomas), early detachment from the base will devascularize the tumour and aid in resection. Internal debulking will assist in tumour dissection from the surrounding neurovascular structures, which is critical in this approach because most of these structures will be located posterolateral to the lesion. The dura is closed primarily in a watertight fashion, and a dural graft may be necessary. If skull base reconstruction is necessary, then the anterior skull base can be packed with autologous fat and fascial grafts. The vascularized pericranial graft harvested at the beginning of the surgery can be used for further reconstruction. The bone is replaced with titanium plates and screws, with care taken to avoid positioning any hardware over the forehead and to allow adequate blood flow to the pericranium to avoid strangulation. The soft tissue is closed in the usual fashion. CSF diversion may be considered to assist in preventing CSF leakage through the wound.

Endoscopic approaches

Endoscopic approaches generally refer to transnasal approaches to the anterior skull base, sphenoid sinus, suprasellar cistern, and parasellar regions, and this section will focus on that approach. Nevertheless, the endoscope may be selected for use with any approach. Both cranial and transnasal approaches can be performed with the microscope, endoscope, or both. Even if the majority of the procedure is performed with the microscope, it can be extremely helpful to inspect the resection cavity with an endoscope using an angled lens to look around structures for residual tumour. Likewise, there is no reason for a surgeon to be restricted to an endoscope for a transnasal surgery, as the tools are complementary and should be utilized as such.

In general, the transnasal approach is ideal for lesions contained within the ethmoid and sphenoid sinuses and sella. For lesions outside the sella, further bone removal along the anterior skull base including opening the dura has been described by Weiss in 1987 (Weiss, 1987). In these cases, the relative merits and drawbacks of this approach (expanded endonasal) compared with a transcranial approach should be considered. The expanded endonasal approach is best utilized for small to medium-sized tumours and tumours that involve the ethmoid and sphenoid sinuses or the sella. The approach is advantageous because there is no evident skin incision, no ligation of the superior sagittal sinus, essentially no brain retraction, and early access to the tumour, and, in anterior skull base meningiomas, their vascular supply. The disadvantages are late visualization of neurovascular structures in suprasellar lesions, higher rates of CSF leak, and potentially lower rates of gross total resection if the tumour extends laterally over the orbits, superiorly and anteriorly against the frontal sinus, or above medialized carotid arteries posteriorly. In particular, meningiomas with a dural tail extending beyond the anterior skull base opening are challenging. Maintaining olfaction when using this approach for anterior skull base meningiomas can also be problematic if the region of the cribriform plate is involved with the tumour or opening.

Immediately prior to surgery, the patient is given decongestant nasal spray and positioned supine with the endotracheal tube taped to the left side. The bed is reflexed to position the head above the right atrium of the heart. The head is fixed in a Mayfield 3-pin head holder slightly extended to the left and rotated right; this allows the surgeon to stand to the patient's right to have a neutral view of

the head. The nasal cavities are packed with decongestant-soaked pledgets, and neuronavigation is registered with monitors for the navigation and endoscope at the head of the bed. The right lower quadrant of the abdomen or the lateral thigh is prepped for fat and fascia graft harvesting.

The packing pledgets are removed, and the nostrils are explored with a zero-degree endoscope to reveal the anatomy of the inferior, middle, and superior turbinates. The septum, choanae, and sphenoid ostia are also visualized. The nasal mucosa may be infiltrated with anaesthetic and epinephrine for haemostasis if needed. Although a deviated septum is more likely than not, a significant angulation ('septal spur') will need to be flattened to allow unobstructed access. It is important to appreciate that while the middle turbinate is attached to the ethmoid bone laterally via a basal horizontal lamella, more anteriorly there is an additional vertical attachment to the cribriform plate. The middle turbinate attachment is vertical anteriorly, before becoming progressively more horizontal and attaching to the palatine bone at its posterior extent. Frequently this turbinate needs to be mobilized (lateralization) if not removed altogether on the side of the surgeon, to expand the access and allow placement of the endoscope. During mobilization of the middle turbinate a crack of the vertical attachment can result in a fracture into the cribriform plate and difficult to treat CSF fistula. In some cases, the middle turbinate harbours air cells ('concha bulosa'), which may be seen on preoperative thin-slice CT, and this can make the middle turbinate bulky and necessitate excision.

Depending on the location of the lesion, a sphenoidectomy and posterior or superior septectomy is performed (especially if binasal access is required). For anterior skull base meningiomas the anterior and posterior ethmoidal arteries can be coagulated to assist in haemostasis and to devascularize the tumour. An important step in endoscopic surgery is the identification of the sphenoid ostia in the sphenoethmoidal recess medial to the superior turbinate. However, on occasions, this is not readily visible as it is covered with mucosa. If a Freer's dissector is passed into the sphenoethmoidal recess ~15 mm posterior to the superoposterior choana, it will enter the sphenoid ostium. Enlargement of the ostia is followed by excising or drilling the anterior wall and opening of the sphenoid sinus. In well-aerated sphenoid sinuses, the sella floor is surrounded with the air cell completely and is termed a 'sellar' type sinus. If it is only partially aerated, anteriorly it is termed 'presellar' and if non-aerated, as in young children (aeration begins from age 3) may persist as the 'conchal' type, which even with image guidance may limit transnasal approaches to the sella. The septations within the sphenoid sinus can be multiple and are rarely midline. The attachment of these septae posteriorly may abut the carotid, and they should therefore be drilled down as a fracture may lacerate the vessel. During the operation, the endoscope is generally in the superior aspect of the field and the suction in the dependent aspect, with microinstruments navigating between the two. If lateral exposure is necessary, the lamina papyracea can be removed but the periorbita is respected. Any bony removal is performed using a high-speed drill with a diamond drill bit. If a dural opening is required, the dura is first coagulated and then incised. Tumour removal is then performed using a standard microsurgical technique including internal debulking and dissection away from neurovascular structures. As the capsule is dissected, care should be taken to avoid traction on the neurovascular structures as these are generally poorly visualized until the end of the procedure.

Many transnasal cases present a significant risk of CSF leak and require a multilayer closure. The dead space created by tumour removal is occasionally packed with Gelfoam or fat graft. An autologous fascia graft or layer of allogenic acellular dermal allograft (AlloDerm) is tucked under the edges of the dura and, rarely, in large defects, reinforced with autologous vomer or septal bone, or Medpor. Lastly, a vascularized nasoseptal flap is rotated over the opening and can be reinforced with fat graft or sealant. The nasoseptal flap is pedicled on the posterior septal branch of the sphenopalatine artery inferior to the sphenoid ostium and is usually raised with monopolar diathermy from the floor of the nose, as far anterior as the nare and superiorly along a line from the superior portion of the sphenoid ostium sparing the olfactory mucosa (which extends 1–1.5 cm over the superior septal mucosa). Injudicious use of diathermy superiorly can also damage this mucosa and impair olfaction. CSF diversion is used in cases with large openings, to aid in graft healing, usually for 2–3 days postoperatively.

Endoscopic endonasal trans-sphenoidal hypophysectomy (EETSH)

Pituitary adenomas are the most common lesions removed by the endoscopic endonasal route. The bone over the sellar floor is drilled to expose the sphenoid sinus. The extent of bony removal depends on the location of the tumour and, although not always necessary, exposure superoinferiorly of the intercavernous sinuses may be required. Similarly, exposure of the cavernous sinuses is not required for large midline tumours but can be achieved by identifying the bluish colour medial to the carotids. An x shaped dural incision of the sellar floor avoiding extension into the venous sinuses and coagulation of the edges of the dural leaves allows good access into the sella.

The vast majority of macroadenomas are soft in consistency and, after obtaining adequate pathological specimens are easily removed by curettes and suction. It is advisable to clear the inferior aspect of the sella first as premature descent of the diaphragm may obscure residual tumour more posteriorly. In some cases the consistency of the adenoma may allow 'extracapsular' resection by circumferentially passing a dissector between the outer edge of the tumour and the dural walls of the sella, starting at the open dural edges. In these cases, care should be exerted at the superior pole to avoid breaching of the arachnoid layer of the diaphragm resulting in CSF leak and disruption of the compressed normal pituitary gland. After clearing of the superior aspect, the diaphragm is expected to descend fully, indicating adequate decompression. The normal pituitary can usually be spared as it is of a firmer consistency than the tumour and its location may be predicted from the direction of deviation of the stalk on the preoperative MRI.

fter debulking, inspection of the cavity using a 30° scope may identify further tumour remnants 'around the corners'. Operating using the 0° endoscope allows visualization in a 'cone' fashion and hence the portion of sellar lesions extending anteriorly on the anterior fossa lies in a blind spot; for full exposure the lip of bone at the tuberculum sellae may need to be drilled. If a wider dural

opening is required, the superior intercavernous sinus is coagulated and the view is supplemented by using the angled lens on an endoscope.

Microadenoma resection requires the identification of the lesion within the surrounding 'normal' pituitary gland. Lateralization of microadenomas is predicted on preoperative scans (both MRI and PET, e.g. C11-methionine) and biochemistry (such as inferior petrosal sinus sampling) but at surgery may be deep within the sella. They are identified by their different colour and softer consistency. Because the commonest indication for microadenoma resection is hypersecreting endocrinopathy complete resection for cure is required, and extension of the resection beyond the soft margins ensures removal of infiltrating tumour cells beyond the 'pseudocapsule'. Some authors recommend 'hemihypophysectomy' to ensure adequate removal.

Intraoperative breaches of the diaphragma sellae resulting in CSF leak can vary from a pinpoint hole to larger defects to the suprasellar cisterns and are repaired accordingly by simple fat or synthetic grafts or using a nasoseptal flap.

Extended endoscopic endonasal transplanum surgery (EEETS)

The favourable factors on MRI for selection of a lesion for an endonasal endoscopic extended transplanum approach for suprasellar lesions include the absence of encasement of blood vessels indicated by a cuff of cortical tissue between tumour and vessel, absence of lateral tumour extension beyond the carotids or beyond the midpupillary line in the coronal plane, and a bright T2-weighted signal indicating a soft consistency. An important consideration is extension of the tumour into the optic canal. From this approach the inferior and medial perimeter of the optic canal can be drilled, opened, and decompressed while the superolateral corner is not readily accessible.

The planum sphenoidale is related to the gyrus rectus on each side, so a transplanum trajectory to the suprasellar cisterns must be directly obliquely from anteroinferior to posterosuperior. Therefore, for lesions such as craniopharyngioma, drilling of the planum does not have to extend too far anteriorly but rather, drilling of the thick bone at the tuberculum sellae and even dividing the superior intercavernous sinus is advantageous.

The OCRs and optic canals are identified, and V-shaped drilling of the planum in between the diverging optic canals is completed. Caution is needed while elevating this bone fragment to avoid tilting of its edges onto the optic nerve by mobilizing it from an anterior to a posterior direction. The superior intracavernous sinus is controlled and may be divided to widen the access.

During intracranial dissection of lesions compressing the chiasma, the supplying branches from the superior hypophyseal arteries, which arise on its inferior aspect and onto the pituitary stalk, should be preserved to avoid ischaemia. Similarly, the ophthalmic artery should be protected during drilling of the optic canal. The endonasal endoscopic approach provides good visualization and a direct corridor to extensions into the third ventricle through its floor. Craniopharyngiomas in a retroinfundibular location are more challenging than those in a preinfundibular position particularly if stalk integrity is to be preserved.

Extended endonasal endoscopic approaches to parasellar lesions

If a transpterygoid endoscopic approach to a parasellar lesions is to be considered, then the first step is entrance into the maxillary antrum via the middle meatus behind the uncinate process after removal of the middle turbinate. The structures in the middle meatus such as the bulla ethmoidalis and hiatus semilunaris are identified, and coagulation of the sphenopalatine artery at its foramen, which overlaps the position of the Vidian nerve may be necessary. If a nasoseptal flap is planned, then this should be based on the other side. Important anatomic landmarks are the location of the Vidian canal in the plane of the floor of the sphenoid sinus laterally and the V2 branch of the trigeminal nerve emerging from the foramen rotundum orientated 45° superolateral to the Vidian canal. The pterygopalatine fossa communicates with the infratemporal fossa through the pterygomaxillary fissure and harbours the terminal maxillary artery. The pterygopalatine ganglion is suspended from V2 and it provides several branches including the greater and lesser palatine nerves, while V2 continues as the infraorbital nerve. Both parasympathetic and sympathetic fibres pass through the Vidian nerve into the pterygopalatine ganglion although only the parasympathetic fibres synapse. The trigeminal ganglion straddles the petrous carotid artery superolaterally in the depths. The ganglion is accessed through the posterior wall of the maxillary sinus. Drilling guided by the Vidian canal leads to the horizontal petrous-vertical cavernous junction of the carotid artery. This route to the petrous apex can be expanded naturally by trigeminal schwannomas eroding the bony corridor. This route is also used for cholesterol granulomas at the petrous apex.

Postoperative

outcomes

Postoperative outcomes vary considerably depending on the pathology and tumour location. For non-functioning pituitary adenomas, a large meta-analysis demonstrated overall mortality, morbidity, and risk of recurrence of less than 1%, 5% or less, and 18%, respectively (Murad et al., 2010). In craniopharyngiomas, a meta-analysis demonstrated new endocrinopathies in 37% of patients after surgical resection, with 2.5 times the rate of new endocrinopathies after gross total resection as compared with subtotal resection with or without radiotherapy (Sughrue et al., 2011). Another recent review noted that subtotal resection followed by radiotherapy demonstrated the best progression-free survival with rates at 5 and 10 years of 93% and 82%, respectively (Lo et al., 2014). For anterior skull base meningiomas, a recent review demonstrated gross total resection was more frequently achieved in open craniotomy (92.8%) than with endoscopic surgery (63.2%), with a higher rate of CSF leak in the endoscopic (31.6%) than the open craniotomy (6%) groups (Komotar et al., 2012).

Complication management

Complications related to transcranial procedures typically relate to encephalomalacia and postoperative seizures, infection,

postoperative hematoma, and cranial nerve or vascular injury. The risk of postoperative encephalomalacia and seizure can be reduced by minimizing brain retraction with adequate bone removal and a meticulous intradural technique. Infection risk is reduced by pre- and intraoperative antibiotic dosing and strict sterile technique. Postoperative hematomas may be prevented through preoperative cessation of medications such as anticoagulants and antiplatelets and good haemostasis; aggressive evacuation of clinically significant postsurgical hematomas is recommended. Lastly, cranial nerve and vascular injury can be avoided by thorough review of the patient's individual anatomy and imaging prior to surgery including vascular imaging if applicable. Internal debulking of the tumour, including the use of an ultrasonic aspirator, can improve visualization and increase the safety of dissection. If major arteries are encased in tumour, leaving a small residual may be preferable to complicated revascularization procedures or vascular injury. Lastly, if vascular injury is suspected, an intra- or postoperative angiogram should be considered.

Complications related to transnasal procedures typically relate to inadequate tumour removal or CSF leak; neurovascular injury

Box 27.1 Case illustration

A 21-year-old man presented with a one-month history of worsening double vision and an inability to abduct his left eye. A detailed neurological examination demonstrated an isolated left VI cranial nerve palsy. An MRI performed with contrast enhancement demonstrated a large sphenoid sinus, sellar, suprasellar, skull base, and left cavernous sinus lesion. Non-contrast CT demonstrated large calcifications within the lesion (**Fig. 27.8**). A left pterional craniotomy was used for an extradural approach to access the cavernous sinus through Parkinson's triangle. The tumour within the cavernous sinus was resected using ultrasonic aspiration, suction, and transsphenoidal ring curettes. Throughout this portion of the procedure, both the microscope and endoscope were used for visualization. In the same operative sitting, a transnasal approach was used to access the tumour within the sphenoid sinus, sella, and skull base. This tumour was resected using suction and transsphenoidal ring curettes, and the skull base was drilled using a diamond bit. Again, both the operative microscope and endoscope were used during this portion of the operation. Autologous fat graft was used to pack the cavernous sinus and sphenoid sinus, fibrin glue was used to seal the sphenoid sinus graft, and an external ventricular drain was placed then clamped and removed after six days. Postoperative MRI demonstrated minimal residual tumour at the posterior superior aspect. There were no complications, and no new deficits. The pathological analysis indicated the tissue was consistent with a chondrosarcoma, and the patient will undergo radiotherapy.

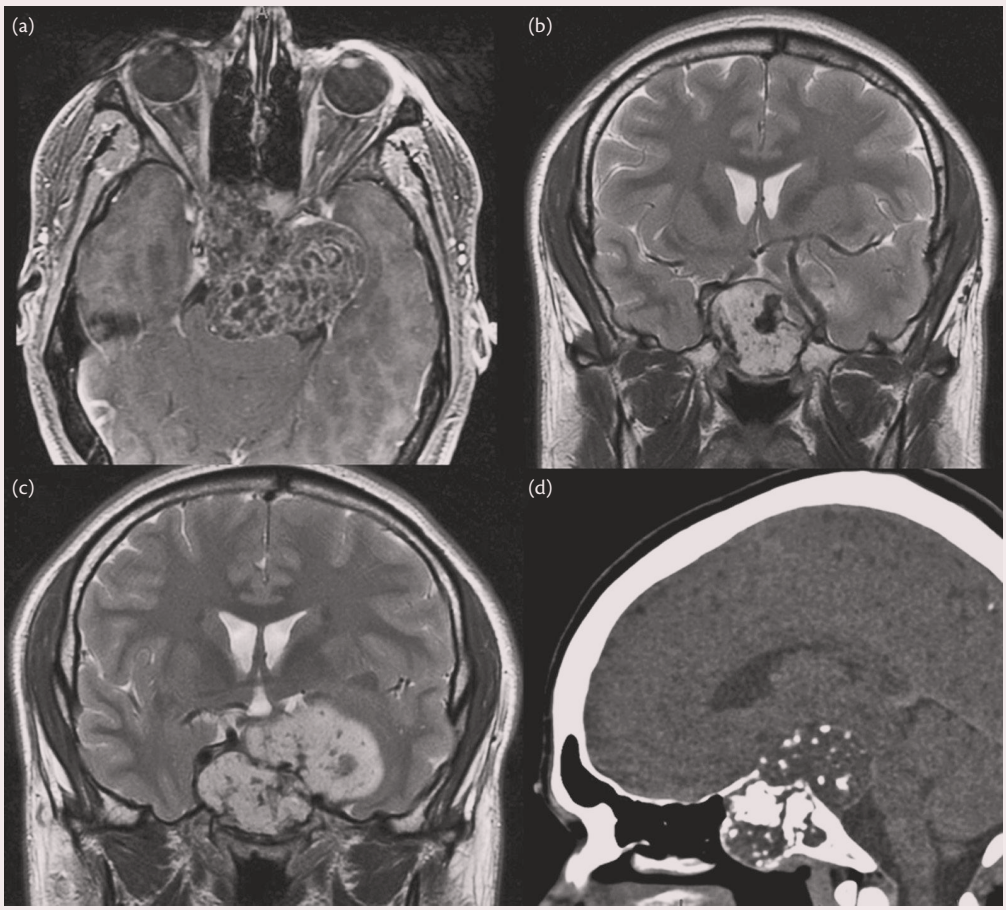

Fig. 27.8 Axial T1-weighted MRI with contrast (A) demonstrating tumour involving the sphenoid sinus, left cavernous sinus, and prepontine cistern. Coronal T2-weighted MRI demonstrating anterior and superior displacement of the left internal carotid artery (A), elevation of the optic chiasm and invasion of the left cavernous sinus (C). A sagittal non-contrast CT demonstrates large calcifications within the lesion filling the sphenoid sinus, sella, and suprasellar regions (D).

is noted occasionally. The risk of inadequate tumour removal can be reduced through careful evaluation of preoperative imaging, and by looking for the extent of the tumour and its attachments. Inadequate tumour removal often stems from inadequate bony removal. The bony opening should be adequate to encompass at least the attachment of the tumour and should not limit the exposure. If this is not possible, then the chosen approach may be inadequate for the lesion. The risk of CSF leak can be reduced using meticulous closure. Multiple techniques have been advocated, but generally a multilayer closure with an inlay of fascia or other dural substitute, fat, nasoseptal flap, and nasal packing is advised. Multilayer closure with inlay combined with 3–7 days of CSF diversion dramatically reduces postoperative CSF leak. Lastly, the risk to neurovascular structures can be reduced by proper preoperative planning and with understanding of the patient's anatomy based on imaging. The surgeon's experience will also play a role with the technique because of the long and narrow working distances. Furthermore, especially with angled endoscope lenses, visualization may be excellent, but access may be limited by working angles or poor microsurgical access. See Box 27.1.

Controversies

Transcranial vs. extended endoscopic approaches for meningiomas

Surgeons should familiarize themselves with both transcranial and extended endoscopic techniques for resection of tumours such as anterior skull base meningiomas, as both techniques are not only useful but required for some tumours such as large esthesioneuroblastomas. Nevertheless, deciding on which approach to use can and should be a very personalized decision based on a number of factors, not least of which is the operating surgeon's comfort and experience.

Transnasal extended or expanded endoscopic transcribriform approaches can confer specific advantages for certain tumours based on location and size. First, the hyperostotic bony attachment on the anterior skull base is directly accessed and resected, and any tumour growth into the paranasal sinuses is much more suited for resection through this approach. Likewise, the tumour is devascularized very early in the procedure and even the anterior and posterior ethmoidal arteries can be coagulated and cut prior to tumour resection. Furthermore, brain retraction and manipulation of neurovascular structures is reduced.

The disadvantages of the aforementioned endoscopic approaches are related to the inherent limitations of the midline exposure and risk of postoperative CSF leak. Tumour or dural tail extension laterally over the medial orbital wall or orbital roof, lateral to the optic canal, or into the sphenoid wing are very difficult to completely resect through the midline exposure and are more readily accessible via a transcranial approach. Neurovascular structures are often visualized later in the endoscopic approach when compared with the transcranial approach and are prone to injury if manipulated. Therefore, tumours that significantly encase the cranial nerves or the carotid, anterior communicating, or anterior cerebral arteries are often best approached through a transcranial approach where they can be visualized (and controlled if necessary) proximally and distally to the lesion. CSF leaks requiring repair can be more common in endoscopic approaches than transcranial approaches because of the increased difficulty in closure from the transnasal route when compared with the transcranial route and because of the increased size of the dependent osteodural defect created using the endoscopic approach. Nevertheless, modern surgical techniques including multilayer closures with the use of substances such as allogenic acellular dermal allograft (AlloDerm) and nasoseptal vascularized flaps combined with CSF diversion may drastically reduce the rate of CSF leak from these procedures.

Conclusion

The sellar and suprasellar tumours remain among the most challenging neurosurgical cases because of the complexity of the surrounding anatomy with a high concentration of important neurovascular structures. Furthermore, the multitude of pathologies results in significant clinical differences in outcome and treatment based on the pathology being addressed; however, continued advancements of surgical technique, including the use of the endoscope and endoscopic techniques in both open craniotomy and transnasal approaches, are consistently providing improved outcomes.

FURTHER READING

Bowers, C.A., Altay, T., & Coulwell, W.T. (2011). Surgical decision-making strategies in tuberculum sellae meningioma resection. *Neurosurg Focus*, **30**(5), E1.

Couldwell, W. & Weiss, M. (1992). Pituitary macroadenomas. In: Apuzzo, M. (ed.), *Brain Surgery: Complication Avoidance and Management*, pp. 295–313. Philadelphia, PA: Churchill Livingstone.

Cushing, H. (1912). *The Pituitary Body and its Disorders*. Philadelphia, PA: J.B. Lippincott.

Elliott, R.E., Jane, J.A. Jr., & Wisoff, J.H. (2011). Surgical management of craniopharyngiomas in children: meta-analysis and comparison of transcranial and transsphenoidal approaches. *Neurosurgery*, **69**, 630–43.

Sekhar, L., Mantovani, A., Mortazavi, M., Schwartz, T., & Couldwell, W.T. (2014). Open vs. endoscopic: when to use which. *Neurosurgery*, **61**(Suppl 1), 84–92.

REFERENCES

Komotar, R.J., Starke, R.M., Raper, D.M., Anand, V.K., & Schwartz, T.H. (2012). Endoscopic endonasal versus open transcranial resection of anterior midline skull base meningiomas. *World Neurosurg*, **77** (5–6), 713–24.

Lo, A.C., Howard, A.F., Nichol, A., et al. (2014). Long-term outcomes and complications in patients with craniopharyngioma: the British Columbia Cancer Agency experience. *Int J Radiat Oncol Biol Phys*, **88** (5), 1011–18.

Murad, M.H., Fernández-Balsells, M.M., Barwise, A., et al. (2010). Outcomes of surgical treatment for nonfunctioning pituitary adenomas: a systematic review and meta-analysis. *Clin Endocrinol (Oxf)*, **73** (6), 777–91.

Sughrue, M.E., Yang, I., Kane, A.J., et al. (2011). Endocrinologic, neurologic, and visual morbidity after treatment for craniopharyngioma. *J Neurooncol*, **101** (3), 463–76.
Weiss, M.H. (1987). Transanasal transsphenoidal approach. In: Apuzzo, M.L.J. (ed.), *Surgery of the Third Ventricle*, pp. 476–94. Baltimore, MD: Williams & Wilkins.

RELATED LINKS TO EBRAIN

Chiasmal Disorders. https://learning.ebrain.net/course/view.php?id=1209
Performing a Pterional Craniotomy. https://learning.ebrain.net/course/view.php?id=86
Performing a Subfrontal Approach. https://learning.ebrain.net/course/view.php?id=83
Performing a Transphenoidal Approach to the Sellar. https://learning.ebrain.net/course/view.php?id=82
Performing an Eyebrow Craniotomy. https://learning.ebrain.net/course/view.php?id=80
Surgical Management of Pituitary Adenomas. https://learning.ebrain.net/course/view.php?id=465

SECTION 6

Tumours and skull base—posterior fossa

28. **Medulloblastoma** *353*
James Rutka

29. **Ependymoma** *361*
Christopher Chandler

30. **Haemangioblastoma** *367*
Ammar Natalwala and Donald MacArthur

31. **Surgical approaches to posterior fossa tumours** *375*
Jacques J. Morcos, Osaama H. Khan, and Ashish H. Shah

28

Medulloblastoma

James Rutka

Introduction

With their seminal work in 1925, Bailey and Cushing described a 'common type of midcerebellar glioma of childhood' which they named *medulloblastoma* (Bailey and Cushing, 1925). They postulated that this tumour originates from embryonic undifferentiated cells in the ependymal lining of the fourth ventricle and described the prominent histological features of increased cellularity and frequent mitoses. It was later noticed that several other supratentorial tumours share these features and a similar grim outcome. The heterogeneous group of '*small, round, blue cells*' tumours was named CNS–primitive neuroectodermal tumours (PNET). According to the 2007 WHO classification (Louis et al., 2007), these are composed of undifferentiated or poorly differentiated neuroepithelial cells. With respect to their most prominent cell line they were described as neuroblastomas, ependymoblastomas, medulloepitheliomas, ganglioneuroblastomas, and pineoblastomas. Medulloblastomas were grouped as the infratentorial PNETs. However, emerging evidence from molecular studies showed that medulloblastoma is a biologically distinct malignancy. In addition, similar analyses showed that a classification of CNS-PNETs based on their biological features is more elegant and realistic, compared to their histopathological classification (Picard et al., 2012).

The recent report from the Central Brain Tumor Registry of the United States (CBTRUS) (Ostrom et al., 2013) utilized the WHO classification for embryonal tumours (medulloblastoma plus CNS–PNET) and showed that the most common brain and CNS histologies at the age group of 0 to 14 years were pilocytic astrocytomas (17.5%) and embryonal tumours (15.7%). The percentage of embryonal tumours at the ages 15–19 years fell to 4.3%. The age-adjusted, pick incidence for medulloblastomas was 0.66/100 000 at the age group 5–9 years. A modest male predominance was again noticed (1.4/1).

Aetiology, pathogenesis, and current classification

Different polyomaviruses have been used to induce tumours with phenotype similar to human medulloblastoma (MB) in rats and hamsters. However, no definite causative factor has been found so far, regarding human embryonal tumours. Some theories describe the external granular layer (EGL) of the developing cerebellum as the cell group from where medulloblastomas originate, while others focus on the ventricular and dorsal brainstem neuronal progenitor zone. Proliferation of precursor neurons in the EGL is controlled by the Sonic Hedgehog (SHH) pathway (Wechsler-Reya and Scott, 1999). Similar insights in the genomics and molecular biology of medulloblastomas have increased our knowledge and understanding of their pathogenesis and behaviour. Currently, it has been shown that at least four distinct variants exist which are genetically and clinically distinct (Taylor et al., 2012). Medulloblastomas are now classified according to these subgroups which show significant prognostic value and prediction of survival.

1. The WNT (Wingless) subgroup shows activation of the WNT pathway from mutations of the *CTNNB1* gene. This results in intranuclear accumulation of β-catenin. Another common finding is monosomy 6. This group represents about 10% of medulloblastoma cases and is frequent in older children and adolescents with a 1:1 sex ratio. Most patients have classical histology and the prognosis is very good.
2. The SHH (Sonic Hedgehog) subgroup shows activation of the SHH pathway and frequently encountered mutations include the *PCTH1, SMO*, and *SUFU* genes, while *GLI2* and *MYCN* amplifications are also observed. Common chromosomal aberrations are 9q and 10q deletions. It represents 30% of all the cases and shows bimodal age distribution, in infants and adults, with a 1:1 sex ratio. Common histological type in this group is the desmoplastic one and infants harbouring this type in the SHH group, have favourable prognosis. Other SHH activated medulloblastomas show intermediate prognosis.
3. Group 3 has not yet revealed a dominant pathway activation. The *MYC* amplification is the hallmark of this group and an important cytogenetic aberration is isochromosome 17q. About 25% of medulloblastomas are group 3 and is frequently found in children and infants, with a slight male predominance. The large cell anaplastic (LCA) histological type is commonly represented and the survival in these patients is dismal.
4. Group 4 is the least understood. Common amplification is the *MYCN* and structural alteration is the *SNCAIP* duplication (subgroup 4α). As in group 3, the majority of patients have isochromosome 17q. It is the commonest subgroup (35%) and patients are typically children with male predominance (3:1). The histology is mainly classical with several LCA cases and the prognosis, as with the SHH group, is heterogeneous.

Table 28.1 Familial syndromes associated with medulloblastomas

Syndrome	Penetrance	Gene	Locus	Other manifestations
Gorlin	AD	*PTCH*	9q31	BCCs, palmar-plantar pits, jaw cysts, dural calcifications, bifid ribs, ovarian fibromas, macrocephaly
Turcot	AD	*APC*	5q21	Multiple colorectal neoplasms, other brain tumours (astrocytomas, ependymomas)
Li-Fraumeni	AD	*TP53*	17p13	Sarcomas, premenopausal breast cancers, acute leukaemias, other brain tumours (astrocytomas, choroid plexus tumours)
Bloom	AR	*BLM1*	15q26.1	Dwarfism, sun sensitivity, facial rash
Fanconi anaemia	AR	several genes		bone marrow failure, leukaemia, solid tumours

AD, autosomal dominant; AR, autosomal recessive; BCC, basal cell carcinoma.

Medulloblastomas are associated with familial cancer syndromes, as shown on Table 28.1. In Gorlin syndrome (Nevoid Cell Carcinoma syndrome) the common MB histology is of desmoplastic type and belongs to the SHH group. In Turcot syndrome, such tumours would present in patients younger than 10 years old, while in Li-Fraumeni syndrome, medulloblastomas can be found in 5% of the cases.

The PNET pathogenesis concept assumed that MBs and supratentorial PNETs derive from subependymal matrix cells which give rise to neuronal and glial cells. It was presumed that a common precursor cell was involved. However, emerging evidence showed different genetic alterations between medulloblastomas (aka infratentorial PNETs) and supratentorial PNETs. Two additional entities described under the umbrella of embryonal tumours are the atypical teratoid rhabdoid tumour (ATRT) and the embryonal tumour with abundant neuropil and true rosettes (ETANTR). The ATRTs are common in young children and distinguishable from medulloblastomas based on *INI1/hSNF5* negative staining. ETANTRs are the previously named 'ependymoblastomas' and have a particularly poor survival rate. An attempt to classify CNS-PNETs based on transcriptional signatures has currently defined three molecular subgroups (Picard et al., 2012):

1. Group 1: Amplification of *C19MC* at 19q13.41-42 and positivity for LIN28. This group enriches for neural stem cell genes and clinically, includes younger patients with midline tumours (cerebellum, brain stem, spinal cord) and dismal prognosis.
2. Group 2: Has more oligoneural markers (positivity for OLIG2—a marker for motor neuron and oligodendrocyte differentiation).
3. Group 3: No definite marker has been proposed so far and is described as LIN28/OLIG2 negative. Genes in this group have mesenchymal differentiation. Patients are more likely to present with metastatic disease, compared to both the other groups, although the overall prognosis is actually better (Adamski et al., 2014).

Histopathology

A typical medulloblastoma arises from the vermis and fills the fourth ventricle as a pink, grey, or purple mass. Small foci of necrosis can be evident. Similar macroscopic appearances present the supratentorial PNETs. The parenchymal tumours may have massive growths with more frequent cysts, haemorrhages, and necroses (Louis et al., 2007). Three main types are described:

1. The classic type (Fig. 28.1A) is the commonest (70%) and is composed of densely packed cells with round to ovoid or more elongated hyperchromatic nuclei, surrounded by scanty cytoplasm. A type of neuroblastic pseudorosette (Homer-Wright) is observed in less than 40%. Neuronal differentiation is common

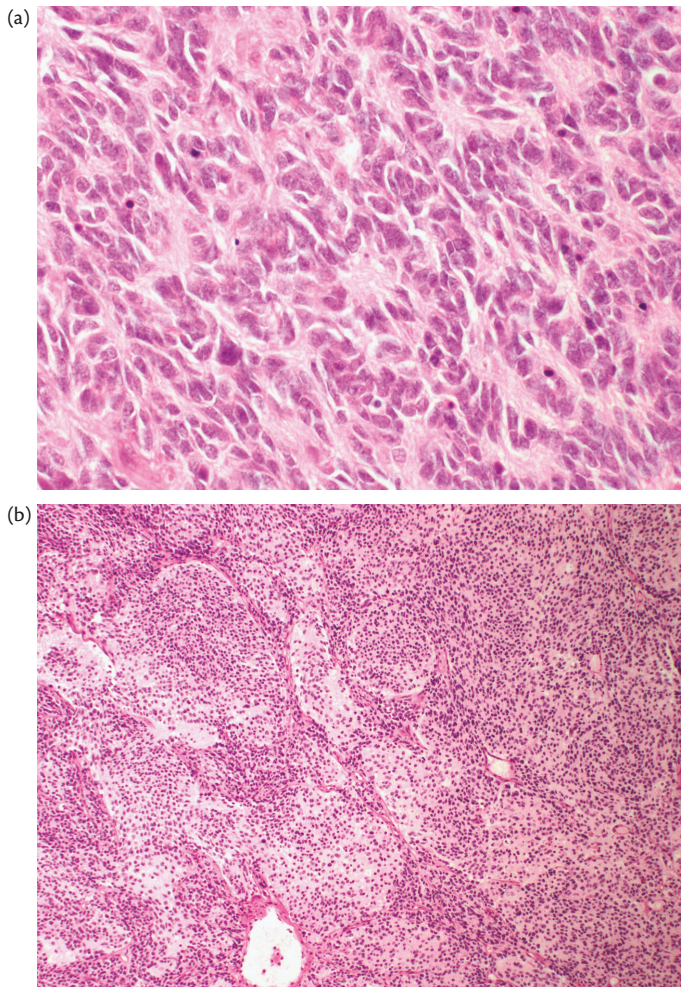

Fig. 28.1 (A) Classical medulloblastoma demonstrating neuroblastic (Homer-Wright) rosettes are an uncommon but highly characteristic feature of this grade IV neoplasm. (B) Desmoplastic/nodular medulloblastoma showing pale nodules of better differentiated tissue is a prognostically favourable feature in medulloblastoma. This histological pattern predominates in the desmoplastic/nodular variant.
Courtesy of Dr Kieren Allinson, Department of Pathology, Addenbrooke's Hospital, Cambridge.

and reveals as immunopositivity for the neuronal marker synaptophysin.

2. The desmoplastic type (Fig. 28.1B) is more common in infants and adults and typically associated with the SHH molecular subgroup. Presents a biphasic pattern with nodular, reticulin-free zones ('pale islands') surrounded by highly proliferative tumour cells with pleomorphic nuclei and a dense intercellular reticulin fibre network. Within the nodules there is synaptophysin positivity, while the outside cells show higher Ki-67 proliferation index and GFAP positivity. A variant of this type is the medulloblastoma with extensive nodularity (MBEN), previously known as cerebellar neuroblastoma. The desmoplastic type has shown favourable prognosis in infants (Rutkowski et al., 2005).
3. The large cell and anaplastic types are currently described in a unified group due to the significant overlapping between them. This variant presents in 4% of medulloblastomas, is more common in molecular group 3 and has the poorest prognosis. The cells lack cohesiveness and show abundant mitotic and apoptotic figures.

Though previously regarded as separate variants, medullomyoblastomas and melanotic medulloblastomas are now described as cases of medulloblastoma with myogenic and melanotic differentiation, respectively.

CNS-PNETs have the same 'small, round, blue cells' microscopic appearance found in embryonal tumours. More precisely, these cells are poorly differentiated with high nucleus/cytoplasm ratios. Neuronal features can be found to better differentiated types. Frequency of Homer-Wright rosettes varies. Calcifications are common and vascular endothelial proliferation may also be seen. The Ki-67 proliferation index varies among groups but generally is high.

Clinical presentation

Presenting signs and symptoms depend on the patient's age. Typically, a posterior fossa midline tumour causes obstructive hydrocephalus and increased intracranial pressure. In infants and toddlers with open sutures, this would result in macrocephaly and bulging fontanel. Poor feeding, irritability, regression of milestones, and vomiting usually follows. Not infrequently, these babies are investigated for milk allergies and gastrointestinal issues. In severe cases, patients present at the emergency department with lethargy, apnoeas, bradycardias, and seizure-like episodes ('hydrocephalic crises' with tonic posturing). Young children with huge PNETs can rapidly deteriorate after intratumoral bleeding and present with herniation phenomena.

Older children typically suffer from morning headaches and vomiting episodes which relieve the headache. Possibly, the accumulation of CO_2 during sleep causes vasodilation and further increase of the intracranial pressure (ICP). The duration of these symptoms varies from few weeks to 2 months. Alarming signs in later stages are strabismus and/or diplopia due to VI nerve paresis. Symptoms from direct mass effect depend on tumour location. Midline lesions cause truncal ataxia and long tract signs, while more lateral locations—as seen in older children and adolescents—present with cranial nerve paresis, vertigo, and appendicular ataxia. Sudden onset of torticollis in a child should prompt further investigations.

About 30–40% of medulloblastomas have metastases on diagnosis but these are mainly found on diagnostic imaging. Groups 3 and 4 are characterized by early disseminated disease. Spinal metastases may present with paraparesis, bladder dysfunction, or radiculopathies.

Imaging features

Head ultrasound can be used as an initial imaging modality for the diagnosis of hydrocephalus caused by posterior fossa tumour in children with open fontanel. *Computed tomography (CT)* would show a midline cerebellar lesion with surrounding vasogenic oedema and obstructive hydrocephalus (Fig. 28.2). Medulloblastomas are hypercellular tumours and they present as hyperdense lesions on CT. Calcifications can be seen in 22% of the cases and cystic formation in 59% (Poretti et al., 2012). All patients

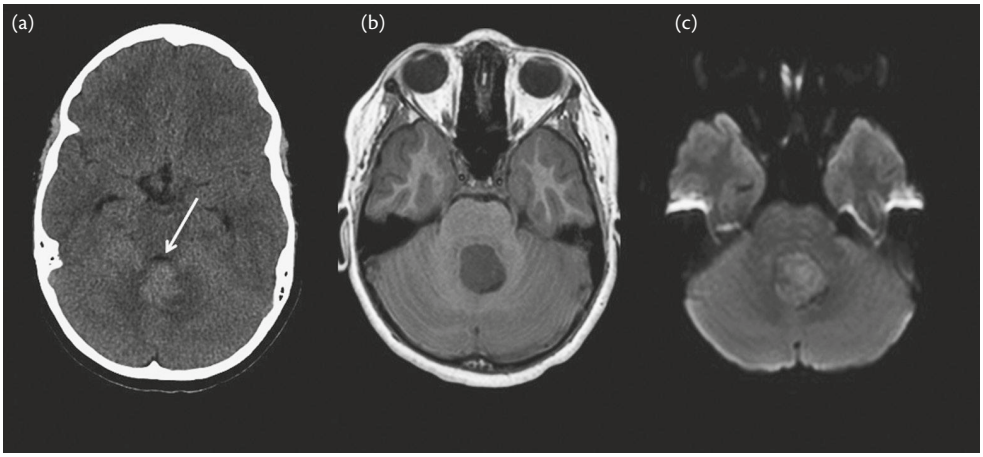

Fig. 28.2 A 12-year-old boy with typical medulloblastoma. (A) Non-contrast CT shows the hyperdense lesion filling the fourth ventricle (arrow) from posteriorly and causing triventricular hydrocephalus. (B) On axial T1-weighted MRI, the tumour has low signal and (C) the DWI imaging shows high signal (restriction). Hyperdensity on CT and restriction on DWI are indicators of hypercellularity and increased malignancy.
Courtesy of Dr Kieren Allinson, Department of Pathology, Addenbrooke's Hospital, Cambridge.

with a posterior fossa tumour should undergo detailed examination of head and spine with magnetic resonance imaging (MRI). Young children would require general anaesthesia for such scanning. If the patient deteriorates rapidly due to increased intracranial pressure, then MRI should not delay adequate neurosurgical management. On T1-weighted images the tumour appears hypo- to isointense compared to the normal brain. On T2-weighted MRI the signal intensity is variable. Hypercellular lesions usually show low signal on T2W. This hypercellularity of high-grade tumours such as medulloblastomas, with high nucleus/cytoplasm ratio, results in reduced free water and gives the high signal (restriction) on diffusion-weighted imaging (DWI) (Jaremko et al., 2010). This can differentiate a medulloblastoma from the other common posterior fossa tumours, the pilocytic astrocytoma (PA) and the ependymoma. In addition, the medulloblastoma typically originates from the roof of the fourth ventricle, while ependymoma from the floor. The later shows a 'plastic' behaviour and can be found extending through the outlet foramina of the fourth ventricle. Such an extension is seen in 14% of medulloblastomas. Disseminated disease with 'drop' metastases into the ventricles or the craniospinal subarachnoid spaces are found in 40% of newly diagnosed medulloblastomas (Fig. 28.3). Ideally the whole neuraxis should be scanned preoperatively with and without gadolinium administration to detect such metastases. Postoperative imaging of the neuraxis for grading purposes should be delayed for 2 weeks, to minimize the false positive findings due to debris and blood degradation products (Meyers et al., 2000).

CNS-PNETs may have similar imaging features. MRI of supratentorial PNETs shows a large complex mass with minimal peritumoral oedema (Fig. 28.4). Enhancement is heterogeneous and commonly they restrict on DWI with low according apparent diffusion coefficient (ADC) values (hypercellularity). Calcifications and intratumoral bleeding are frequent. Both they present as susceptibility areas on gradient imaging (GE). Imaging of the entire neuraxis is mandatory due to the common leptomeningeal spreading of these lesions.

Management

Children with medulloblastomas and CNS-PNETs should be managed by a multidisciplinary approach in experienced paediatric centres. These patients would present with signs and symptoms of increased intracranial pressure from obstructive hydrocephalus. Detailed preoperative evaluation is paramount but only if the clinical status allows such investigations. Usually the symptomatology will improve with intravenous administration of dexamethasone which decreases the vasogenic oedema. Whole neuraxis MRI is done with the appropriate sequences as per each centre ('tumour protocols'). If there is time, evaluation of hearing and renal function is performed for baseline assessment, as the adjuvant chemo- and radiotherapies have known toxicities. The family is consented for the proposed treatment, research enrolments, and blood products transfusions.

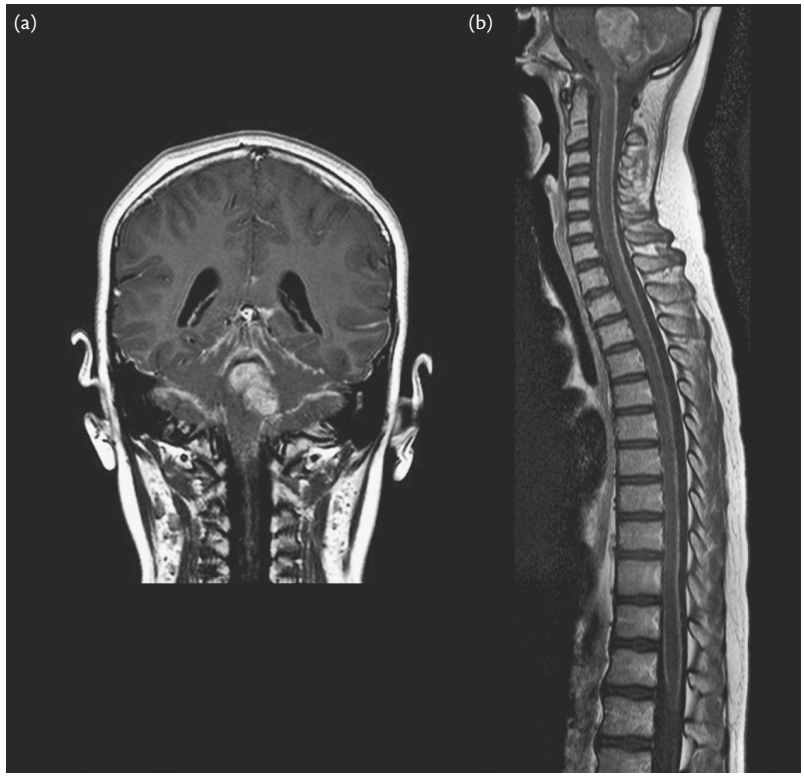

Fig. 28.3 A 10-year-old boy with disseminated medulloblastoma. (A) Coronal T1-weighted MRI postgadolinium administration with homogeneously enhancing fourth ventricular primary tumour and diffuse leptomeningeal enhancement of the cerebellum. (B) Midsagittal T1-weighted MRI postgadolinium of the whole spine shows leptomeningeal enhancement of the entire cord surface laminar, 'sugar-coating' pattern.
Courtesy of Dr Kieren Allinson, Department of Pathology, Addenbrooke's Hospital, Cambridge.

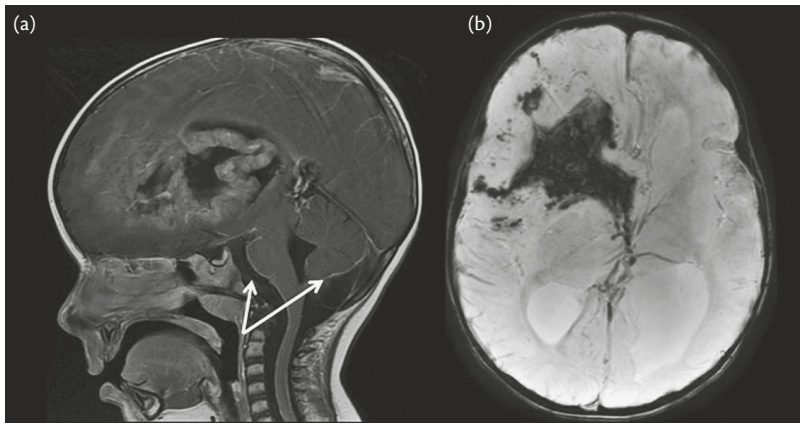

Fig. 28.4 A 2-year-old boy with supratentorial PNET. (A) Midsagittal T1-weighted postgadolinium MRI shows a large, lobulated mass with large cystic component and homogeneous enhancement of the thick peripheral rim. Arrows show the thin leptomeningeal enhancement along the brainstem and the inferior surface of the cerebellum. (B) On axial gradient echo MRI, there is marked susceptibility (dark) centrally located and smaller areas of susceptibility in the periphery (haemorrhages and calcifications).
Courtesy of Dr Kieren Allinson, Department of Pathology, Addenbrooke's Hospital, Cambridge.

Management of hydrocephalus is controversial. If the patient presents in extreme condition, a life-saving insertion of external ventricular drain (EVD) is justified, with extreme care to avoid upward herniation through the tentorial incisura. Routine insertion of ventriculoperitoneal shunts (VPS) should be avoided because only 10–40% of children will eventually require permanent CSF diversion postoperatively and these patients will be exposed to the significant risk for VPS complications throughout their lives (Lee et al., 1994). Risk factors for postoperative need for permanent shunting are young age, severe preoperative hydrocephalus, larger tumour size, and disseminated disease. A study from Paris found that preoperative endoscopic third ventriculostomy (ETV) in such cases, significantly reduced the risk of persistent postoperative hydrocephalus (Sainte-Rose et al., 2001). The authors acknowledged the risk of exposing several patients to an unnecessary procedure, especially in routinely performed ETVs. In any case where CSF is obtained preoperatively, a specimen should be sent for cytology.

Surgical management

Most surgeons prefer the prone position to perform a midline suboccipital craniotomy. Intraoperative neuromonitoring is important. Persistent bleeding usually indicates residual tumour. The endoscope is a useful tool to inspect for remnants 'around the corners'. The target is gross total resection (GTR) under maximum safety. Residual more than 1.5 cm^3, as measured in postoperative MRI, was associated with worst outcome (Zeltzer et al., 1999). If the tumour invades the floor of the fourth ventricle or is firmly attached to the lower cranial nerves, the surgeon should avoid aggressive resection and resulting palsies which significantly decrease the quality of life. Some centres utilize intraoperative MRI scans to achieve GTRs with encouraging results (Avula et al., 2013). Postoperative MRI should be performed within 72 hours or after 2 weeks, to avoid false positive findings due to blood products. Lumbar CSF is obtained for cytology and staging purposes, in conjunction with the whole neuraxis MRI, for increased sensitivity (Fouladi et al., 1999). Lumbar CSF sampling is more reliable compared to EVD or intraoperative CSF sampling (Gajjar et al., 1999).

Non-surgical management

The child's age grossly determines further treatment options after the initial medulloblastoma resection. In children less than 3 years of age, radiation therapy is avoided due to devastating neuro-cognitive sequelae.

Age less than 3 years

Even in cases of disseminated disease, current protocols follow radiation-free approaches (Rutkowski et al., 2005). Commonly, they start with systemic, platinum-based regimens, followed by myeloablative chemotherapy with autologous stem cell support. Systemic chemotherapy is also combined with intraventricular methotrexate. This is administered through a subcutaneous reservoir (Ommaya) or via an already placed VP shunt, with special care to avoid intraperitoneal spreading of methotrexate (e.g. through transient flow occlusion valves). Focal radiation is reserved for relapses and the results, compared to chemotherapy alone, are controversial (Grill et al., 2005; Ashley et al., 2012). Prognosis is poor in this age group with 5-year survival of 50–70%. The desmoplastic histological variant is an exception with almost 90% survival.

Age more than 3 years

Administration in of adjuvant therapies in this age group is stratified into average and high-risk patients, according to clinical criteria (Fig. 28.5). Poor prognosticators are metastatic disease (Chang et al., 1969), tumour residual more than 1.5 cm^3, positive CSF cytology and, for some authors, large cell/anaplastic histology. Children in the high-risk group receive 3600 cGy of craniospinal irradiation with a boost at the tumour bed and to focal metastases. Adjuvant systemic chemotherapy follows. Five-year survival rates are 40–82% (Adamski et al., 2014). Average-risk patients receive reduced craniospinal irradiation (2340 cGy) with a boost to the tumour bed of 5400–5580 cGy. Concomitant chemotherapy with vincristine is typically given. Systemic chemotherapy (cisplatin based) follows and the 5-year survival rates are 85% (Gajjar et al., 2006). Proton radiotherapy delivers the same radiation amount to the target area but is superior to the photon radiotherapy due to the significantly less penetration into the surrounding healthy tissues. Higher costs and

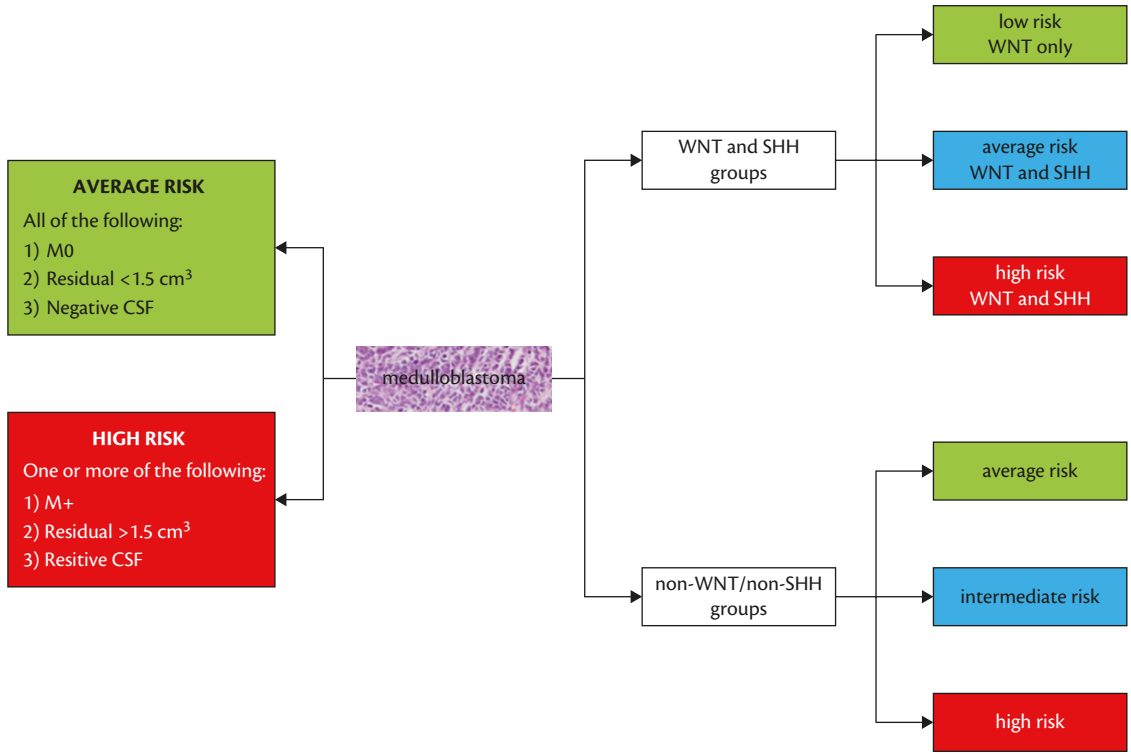

Fig. 28.5 Diagram showing on the left, the current clinical stratification on average and high-risk medulloblastoma for patients aged more than 3 years. On the right, a stratification currently under investigation, based mainly on molecular features—adapted from (Gottardo et al., 2014). Criteria for increased risk are metastatic disease (M+), *MYC* amplification, non-gross/near total resection and large cell/anaplastic histology.

poor availability are currently important drawbacks. Radiotherapy strategies designed to improve outcomes are hyperfractionation and the use of radio-sensitizers. Significant risks of radiotherapy, besides poor cognitive outcome in young children, are ototoxicity, endocrine issues (thyroid dysfunction and growth failure), radiation necrosis, and secondary malignancies. Recurrent disease has very poor outcome with a salvage rate less than 10%. Better chances have localized recurrences amenable to surgical resection, with relative chemosensitivity and if re-irradiation is possible (Pizer et al., 2011).

Current management of CNS-PNETs in infants is based on similar to medulloblastoma protocols. Dose-intensive chemotherapy, including high-dose modalities with autologous stem cell rescue is used in attempts to avoid or delay radiation. Overall survival is dismal, ranging from 0 to 49%. In older children, CNS-PNETs are rare and strong evidence-based management strategies are absent. They are treated as high-risk patients. It is not clear if residual tumour or metastatic disease are strong prognostic factors of poor outcome. Overall survival rates between 15 and 73%, and PNETs localized in the pineal region, tend to have better outcome than other sites (Chintagumpala et al., 2009).

Future management of embryonal tumours is an area of intense investigations. Subgrouping of patients, based on cytogenetic biomarker-driven stratification may predict survival and add information for improved treatment strategies (Shih et al., 2014). The excellent survival rates in the WNT group may suggest overtreatment approaches at these patients (Adamski et al., 2014). In the SHH group, new molecular targeted therapies with the smoothened inhibitors LDE225 and GDC-449 are under investigation with promising results (Kool et al., 2014). Management of metastatic disease may dramatically change after the discovery that metastases are extremely similar to each other but significantly divergent from the matched primary tumour (Wu et al., 2012). Regarding the significance of biology based prognostic factors, currently it has been shown that for medulloblastomas poor outcome is linked to non-WNT/SHH group, *FSTL5* overexpression, *MYC*/*MYCN* amplification and gain of 17q chromosome. For the CNS-PNETs, poor prognosticators are *C19MC* amplification and LIN28 positivity.

Case presentation—controversies

Figure 28.6 presents a case of a 2.5-year-old girl. She was admitted with a 2 week history of worsening weakness of her lower extremities and bladder dysfunction (Fig. 28.6A). Sagittal T1-weighted postgadolinium MRI showed a heterogeneously enhancing fourth ventricular tumour, with triventricular hydrocephalus (Fig. 28.6B). Imaging of her spine revealed multiple nodular metastases causing cord compression at T_2 and T_9 levels and a large mass in her lumbar spine with mass effect on her cauda equina. Note the enlarged bladder. Her treatment required prioritization of three issues: dealing with her neurological deficits, oncological management, and treatment of hydrocephalus. Which one should be dealt with first is a matter of controversy. The multidisciplinary neuro-oncological decision was to operate first on the primary posterior fossa tumour and irradiate the spinal lesions as soon as possible. It was not clear as to which one of the spinal metastases was causing her symptoms so the option to operate on the spine first was rejected. The primary lesion (medulloblastoma) was gross totally

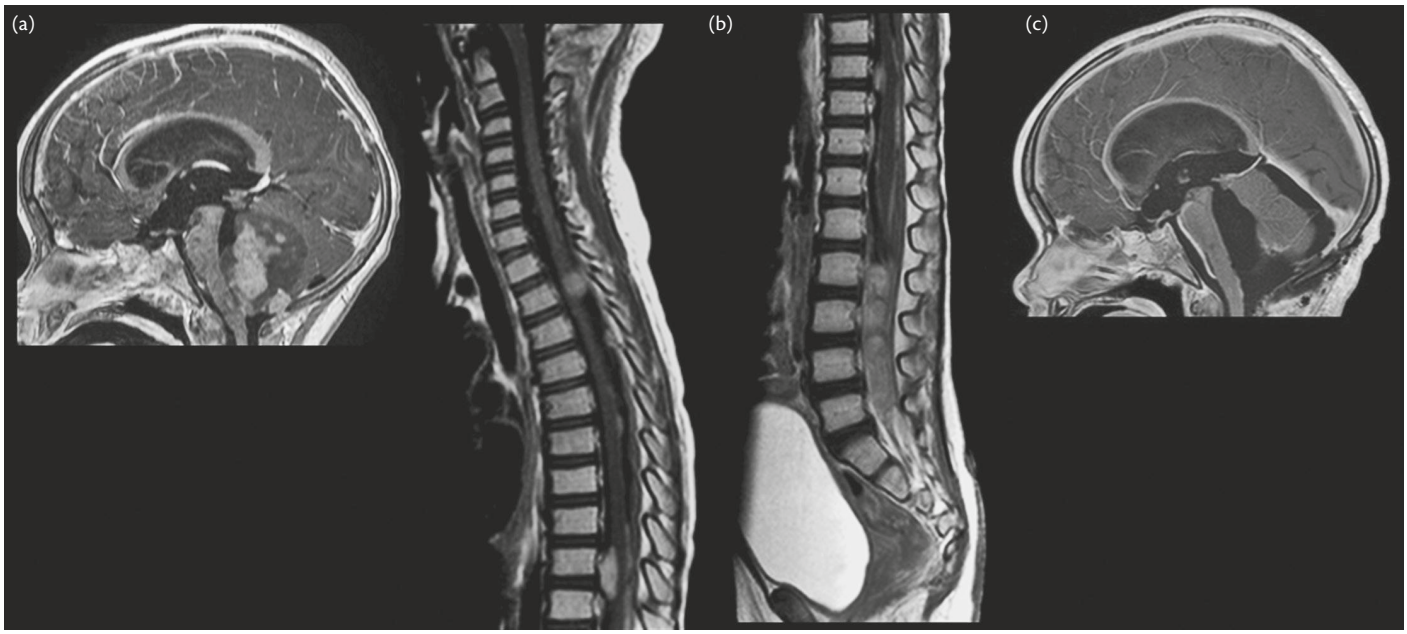

Fig. 28.6 The case of a 2.5-year-old girl.
Courtesy of Dr Kieren Allinson, Department of Pathology, Addenbrooke's Hospital, Cambridge.

removed within 24 hours (Fig. 28.6C) and the first postoperative day the spinal irradiation commenced. In 5 days, she received 2000 cGy locally on the lower thoracic and lumbar region. Her hydrocephalus persisted postoperatively. The management controversy was between ETV and VP shunt insertion. The decision was for VPS based on the urgent necessity for adjuvant treatment and the need to minimize the postoperative complication rate after shunt diversion procedures (Kulkarni et al., 2010). Her weakness improved and she was further managed on a high-risk medulloblastoma protocol.

REFERENCES

Adamski, J., Ramaswamy, V., Huang, A., & Bouffet, E. (2014). Advances in managing medulloblastoma and intracranial primitive neuro-ectodermal tumors. *F1000Prime Rep*, **6**, 56.

Ashley, D.M., Merchant, T.E., Strother, D., et al. (2012). Induction chemotherapy and conformal radiation therapy for very young children with nonmetastatic medulloblastoma: Children's Oncology Group study P9934. *J Clin Oncol*, **30**, 3181–6.

Avula, S., Pettorini, B., Abernethy, L., Pizer, B., Williams, D., & Mallucci, C. (2013). High field strength magnetic resonance imaging in paediatric brain tumour surgery—its role in prevention of early repeat resections. *Childs Nerv Syst*, **29**, 1843–50.

Bailey, P. & Cushing H. (1925). Medulloblastoma cerebelli: a common type of midcerebellar glioma of childhood. *Arch Neurol Psychiatry*, **14**, 192–223.

Chang, C.H., Housepian, E.M., & Herbert, C. Jr. (1969). An operative staging system and a megavoltage technic for cerebellar medulloblastoma. *Radiology*, **93**, 1351–9

Chintagumpala, M., Hassall, T., Palmer, S., et al. (2009). A pilot study of risk-adapted radiotherapy and chemotherapy in patients with supratentorial PNET. *Neuro Oncol*, **11**, 33–40.

Fouladi, M., Gajjar, A., Boyett, J.M., et al. (1999). Comparison of CSF cytology and spinal magnetic resonance imaging in the detection of leptomeningeal disease in pediatric medulloblastoma or primitive neuroectodermal tumor. *J Clin Oncol*, **17**, 3234–7.

Gajjar, A., Chintagumpala, M., Ashley, D., et al. (2006). Risk-adapted craniospinal radiotherapy followed by high-dose chemotherapy and stem-cell rescue in children with newly diagnosed medulloblastoma (St Jude Medulloblastoma-96): long-term results from a prospective, multicentre trial. *Lancet Oncol*, **7**, 813–20.

Gajjar, A., Fouladi, M., Walter, A.W., et al. (1999). Comparison of lumbar and shunt cerebrospinal fluid specimens for cytologic detection of leptomeningeal disease in pediatric patients with brain tumors. *J Clin Oncol*, **17**, 1825–8.

Gottardo, N.G., Hansford, J.R., McGlade, J.P., et al. (2014). Medulloblastoma Down Under 2013: a report from the third annual meeting of the International Medulloblastoma Working Group. *Acta Neuropathol*, **127**, 189–201.

Grill, J., Sainte-Rose, C., Jouvet, A., et al. (2005). Treatment of medulloblastoma with postoperative chemotherapy alone: an SFOP prospective trial in young children. *Lancet Oncol*, **6**, 573–80.

Jaremko, J.L., Jans, L.B., Coleman, L.T., & Ditchfield M.R. (2010). Value and limitations of diffusion-weighted imaging in grading and diagnosis of pediatric posterior fossa tumors. *AJNR Am J Neuroradiol*, **31**, 1613–16.

Kool, M., Jones, D.T., Jäger, N., et al. (2014). Genome sequencing of SHH medulloblastoma predicts genotype-related response to smoothened inhibition. *Cancer Cell*, **25**, 393–405.

Kulkarni, A.V., Drake, J.M., Kestle, J.R., Mallucci, C.L., Sgouros, S., & Constantini, S. (2010). Endoscopic third ventriculostomy vs cerebrospinal fluid shunt in the treatment of hydrocephalus in children: a propensity score-adjusted analysis. *Neurosurgery*, **67**, 588–93.

Lee, M., Wisoff, J.H., Abbott, R., Freed, D., & Epstein, F.J. (1994). Management of hydrocephalus in children with medulloblastoma: prognostic factors for shunting. *Pediatr Neurosurg*, **20**, 240–7.

Louis, D.N., Ohgaki, H., Wiestler, O.D., et al. (eds.) (2007). *WHO Classification of Tumours of the Central Nervous System*. Lyon, France: IARC Press.

Meyers, S.P., Wildenhain, S.L., Chang, J.K., et al. (2000). Postoperative evaluation for disseminated medulloblastoma involving the spine: contrast-enhanced MR findings, CSF cytologic analysis, timing of disease occurrence, and patient outcomes. *AJNR Am J Neuroradiol*, **21**, 1757–65.

Ostrom, Q.T., Gittleman, H., Farah, P., et al. (2013). CBTRUS statistical report: primary brain and central nervous system tumors diagnosed in the United States in 2006–2010. *Neuro Oncol*, **15** Suppl 2, ii1–56.

Picard, D., Miller, S., Hawkins, C.E., et al. (2012). Markers of survival and metastatic potential in childhood CNS primitive neuroectodermal brain tumours: an integrative genomic analysis. *Lancet Oncol*, **13**, 838–48.

Pizer, B., Donachie, P.H., Robinson, K., et al. (2011). Treatment of recurrent central nervous system primitive neuroectodermal tumours in children and adolescents: results of a Children's Cancer and Leukaemia Group study. *Eur J Cancer*, **47**, 1389–97.

Poretti, A., Meoded, A., & Huisman, T.A. (2012). Neuroimaging of pediatric posterior fossa tumors including review of the literature. *J Magn Reson Imaging*, **35**, 32–47.

Rutkowski, S., Bode, U., Deinlein, F., et al. (2005). Treatment of early childhood medulloblastoma by postoperative chemotherapy alone. *N Engl J Med*, **352**, 978–86.

Sainte-Rose, C., Cinalli, G., Roux, F.E., et al. (2001). Management of hydrocephalus in pediatric patients with posterior fossa tumors: the role of endoscopic third ventriculostomy. *J Neurosurg*, **95**, 791–7.

Shih, D.J., Northcott, P.A., Remke, M., et al. (2014). Cytogenetic prognostication within medulloblastoma subgroups. *J Clin Oncol*, **32**, 886–96.

Taylor, M.D., Northcott, P.A., Korshunov, A., et al. (2012). Molecular subgroups of medulloblastoma: the current consensus. *Acta Neuropathol*, **123**, 465–72.

Wechsler-Reya, R.J. & Scott, M.P. (1999). Control of neuronal precursor proliferation in the cerebellum by Sonic Hedgehog. *Neuron*, **22**, 103–14.

Wu X., Northcott, P.A., Dubuc, A., et al. (2012). Clonal selection drives genetic divergence of metastatic medulloblastoma. *Nature*, **482**, 529–33.

Zeltzer, P.M., Boyett, J.M., Finlay, J.L., et al. (1999). Metastasis stage, adjuvant treatment, and residual tumor are prognostic factors for medulloblastoma in children: conclusions from the Children's Cancer Group 921 randomized phase III study. *J Clin Oncol*, **17**, 832–45.

RELATED LINKS TO EBRAIN

Aetiology and Pathogenesis of Embryonal Tumours of the CNS. https://learning.ebrain.net/course/view.php?id=1242

Histopathology of Embryonal Tumours of the CNS. https://learning.ebrain.net/course/view.php?id=1257

Imaging Features of Medulloblastoma and Other PNETs. https://learning.ebrain.net/course/view.php?id=1262

Management of Primitive Neuroectodermal Tumours. https://learning.ebrain.net/course/view.php?id=429

29

Ependymoma

Christopher Chandler

Epidemiology

Ependymomas which include both subependymoma and myxopapillary ependymoma variants are slow growing tumours of glial origin, believed to arise from radial glial stem cells within the ependymal surface within the central nervous system (CNS) and spinal cord. Consequently, they are most commonly found in association with a ventricular surface, primarily within the fourth ventricle. The majority of these tumours occur in children, representing approximately 10% of all paediatric CNS tumours, following astrocytomas and PNET in frequency, and there does not appear to be a gender bias. The majority of paediatric ependymomas are intracranial and about half occur in children less than 5 years old (Foreman et al., 1996). Interestingly in children while the majority (more than two-thirds) of ependymomas are found within the posterior fossa, adults present with an almost equal incidence of intracranial and spinal cord tumours, and in those adults with intracranial ependymomas, an almost equal incidence of supra and infratentorial locations. In adults, ependymomas are much less common; with many arising within the spinal axis, either as intramedullary tumours or as extramedullary tumours in the region of the conus medullaris.

Two rare subtypes of ependymoma are recognized: subependymoma and myxopapillary ependymoma. Subependymomas are benign slow growing indolent tumours and their true incidence is not well characterized as many never cause symptoms and may be discovered incidentally as a post-mortem finding. Those that are symptomatic are found to occur most frequently in middle aged and elderly patients. Like other types of ependymoma, they are found in association with a ventricular surface, predominantly the fourth ventricle followed less commonly by the lateral ventricles. If found incidentally many may not progress nor require removal. Surgical removal is usually curative unless a subtotal resection is performed.

In contrast myxopapillary ependymomas, which are also slow growing, tend to affect young adults, and occur almost exclusively within the spinal canal (extramedullary) in the region of the conus medullaris, though they have been reported within other CNS sites. They may rarely metastasize and surgical resection is, as for subependymoma, usually curative unless a subtotal resection is performed.

Pathology

The older World Health Organization (WHO) grading of ependymomas identified four subtypes of tumour: subependymoma (WHO 1), myxopapillary (WHO 1), classic (WHO 2) and anaplastic (WHO 3). Several morphological variants are also recognized within the classic subtype: cellular, papillary, clear cell, and tanycytic though these variants have no prognostic significance.

Leaving aside the rare subtypes (subependymoma and myxopapillary ependymoma), the vast number of paediatric ependymomas fall into either the Classic or Anaplastic category. In the remainder of this chapter these are the two subtypes of tumour whose features and management will be discussed.

Classic ependymomas (**Fig. 29.1**) are moderately cellular tumours with rare or absent mitoses. The cells are uniform in size with minimal pleomorphism and a high nuclear/cytoplasmic ratio. The typical structural features are perivascular pseudorosettes or much less commonly the appearance of ependymal rosettes. Perivascular pseudorosettes are formed by radial disposition of tumour cells around blood vessels, while true ependymal rosettes are formed by tumour cells arranged in a columnar fashion creating a central lumen defined by the tumour cells themselves. Most ependymomas stain positive for GFAP especially in the fibrillary processes immediately adjacent to the region of the perivascular pseudorosettes. Occasional areas of necrosis may be seen but do not necessarily indicate the presence of the anaplastic subtype of tumour. Though the histological criteria necessary to classify a tumour as an ependymoma are clearly set out, the identification of histological features to definitively classify its subtype, so important in predicting prognosis, has been challenging. Combinations of intratumoural heterogeneity, interobserver variability, variations in definitions, the use of different histological criteria, the uneven application of criteria for anaplasia by review pathologists, and idiosyncratic small patient cohorts have led to significant disagreements in pathological grading. This has presented difficulties in classifying ependymomas, particularly with reference to anaplastic tumours, well documented in excellent works dealing with this subject (Tihan et al., 2008; Ellison et al., 2011).

Anaplastic ependymomas (**Fig. 29.2**) are malignant tumours with a poor overall prognosis. They are highly cellular, show accelerated growth, high mitotic activity, and a tendency towards dissemination.

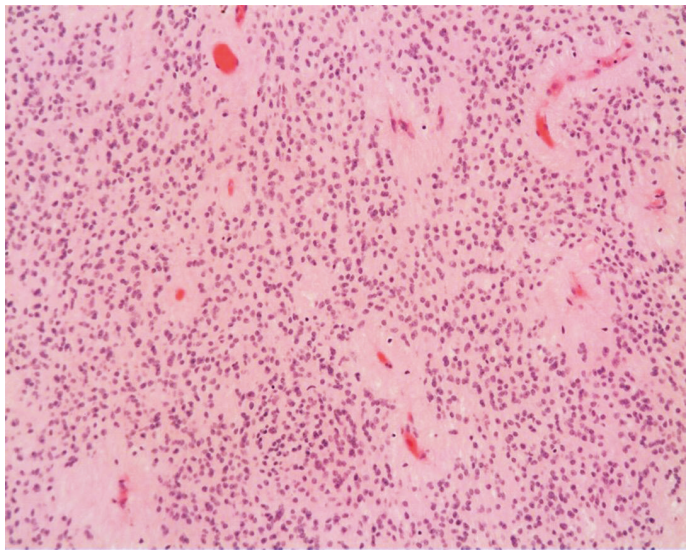

Fig. 29.1 Ependymoma, WHO grade II. Moderate cellularity, vascular pseudorosettes, and infrequent mitosis. Intradural/extramedular lesion in L1, 61-year-old-man. Epithelial membrane antigen (EMA) expressed in paranuclear dot pattern, GFAP positive, Ki67 2%, and RELA negative.
Courtesy of Dr Kieren Allinson, Department of Pathology, Addenbrooke's Hospital, Cambridge.

Histologically they show pseudopalisading necrosis, microvascular proliferation, and perivascular pseudorosettes. Unfortunately, at present there is not a reliable widely accepted neuropathological consensus of criteria for anaplastic ependymoma, though most neuropathologists would accept the importance/significance of mitotic index, Ki67, cellularity, and degree of differentiation. Ki67 proliferation index appears to correlate well with survival with lower survival seen in patients whose tumours have a Ki67 greater than 5%.

This lack of consensus can present serious challenges to clinicians (Robertson et al., 1998) whose treatment paradigms are markedly different between classic and anaplastic ependymoma. It may also result in widely different outcomes and create difficult decisions for clinicians making treatment decisions.

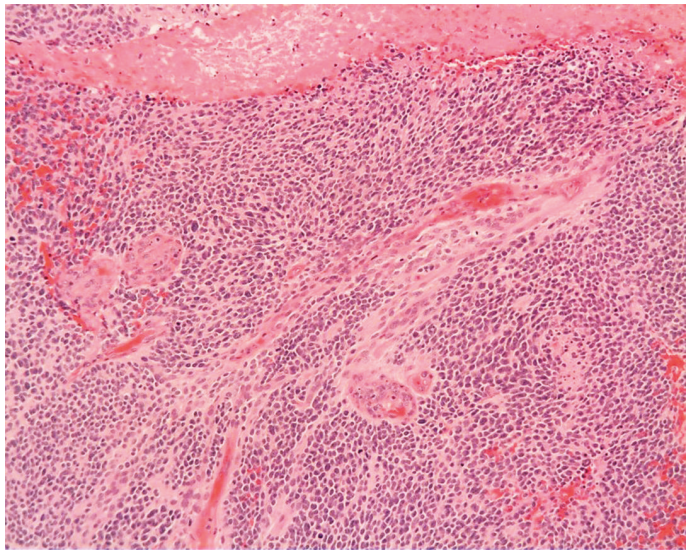

Fig. 29.2 Anaplastic ependymoma, WHO grade III. Hypercellular tumour with necrosis (top), endothelial cell proliferation, and brisk mitosis. Supratentorial tumour in a 5-year-old. EMA expressed in paranuclear dot pattern, GFAP positive, Ki67 40%, and RELA positive.
Courtesy of Dr Kieren Allinson, Department of Pathology, Addenbrooke's Hospital, Cambridge.

Tumour molecular genetics

A range of cytogenetic anomalies is found in ependymomas though there is not yet enough consistency in these changes to influence grading or treatment decisions (Table 29.1). Up to 30% of ependymomas have been found to contain anomalies of chromosome 22, which may include monosomy, deletions, or translocations (Hamilton and Pollock, 1997).

Interestingly and perhaps not surprising is the finding that intramedullary spinal ependymomas are found more frequently in NF-2 patients leading to the belief that the NF-2 gene is somehow involved in ependymoma tumourigenesis (Slavc et al., 1995). Other genetic anomalies include losses in 6q, 9q, 3p, 10q, and 11q. In the clear cell variant, which histologically may resemble oligodendrogliomas there is no 1p 19q codeletion. In the future these cytogenetic changes may very well play a significant role in diagnosis and tailored, biologically driven treatment paradigms.

Biological markers are also the subject of intense scrutiny though to date there has been no significant validation of any current biomarkers (Andreiuolo et al., 2013). The tremendous advance in molecular profiling, which may in future lead to changes in treatment, has led to a newer WHO classification of ependymoma (Box 29.1).

Treatment

Surgery

The role of radiotherapy

Ependymomas are truly surgical tumours. The prognosis in all age groups and all CNS locations has long been recognized to be utterly dependent on the extent of surgical resection (Healey et al., 1991; Perilongo et al., 1997). The terrible dilemma for the neurosurgeon is that due to this tumour's propensity to adhere to the brainstem and cranial nerves in the posterior fossa, to spinal cord tissue/nerve roots (intramedullary and myxopapillary ependymoma), total resection may result in serious and significant neurological morbidity. This aggressive surgical strategy must be carefully weighed up against the poor overall prognosis if a subtotal resection is achieved even with advanced multimodality neuro-oncological treatment (Merchant, 2002; Merchant et al., 2009).

The initial workup of these patients involves full cranio-spinal axis MRI to accurately determine the location of the tumour, its relationship to adjacent structures (brainstem, cranial nerves) and presence or absence of metastases. MRI appearances are not unique to ependymoma but they are most often iso/hypointense on T1 sequences, high signal on T2 sequences, and enhance avidly after contrast (Figs. 29.3 and 29.4). FIESTA (fast imaging employing steady state acquisition) sequences may allow more accurate resolution of cranial nerves and vascular structures, and both diffusion-weighted imaging (DWI) and apparent diffusion coefficient (ADC) mapping are now routinely used to identify high grade tumours. MRS may also be a useful with ependymomas showing a low NAA/Choline ratio somewhere between a PNET and a glioma. Calcification, cyst

Table 29.1 Summary of molecular pathology and genetics of ependymoma subtypes

Anatomic location	Group	Genetics	Histology	Age group
Supratentorial	ST-EPN-RELA	*RELA* fusion gene	Classic/Anaplastic	Infant -> adult
Supratentorial	ST-EPN-YAP1 ST	*YAP1* fusion gene	Classic/Anaplastic	Infant/child
Supratentorial	ST-SE	Balanced genome	Subependymoma	Adult
Posterior fossa	PF-EPN-A	Balanced genome	Classic/Anaplastic	Infant
Posterior fossa	PF-EPN-B	Genome-wide polyploidy	Classic/Anaplastic	Child -> Adult
Posterior fossa	PF-SE	Balanced genome	Subependymoma	Adult
Spinal	SP-EPN	*NF2* mutation	Classic/Anaplastic	Child -> Adult
Spinal	SP-MPE	Genome-wide polyploidy	Myxopapillary	Adult
Spinal	SP-SE	6q deletion	Subependymoma	Adults

formation, and haemorrhages may also be seen. A particular imaging feature, which is strongly suggestive of ependymoma is when the tumour fills the lateral recesses of the fourth ventricle or may even extend out through the Foramina of Luschka and Magendie into the cerebellopontine angle (CPA) and spinal canal, respectively. High dose steroids are highly beneficial in the pre and peri-operative management to reduce brain swelling particularly when hydrocephalus is present. Patients with infratentorial tumours often present with symptomatic hydrocephalus and the initial decision for the surgeon is how to manage this. At present there does not appear to be any significant consensus/advantage over which method is used to treat the hydrocephalus. Endoscopic third ventriculostomy, external ventricular drainage, and shunting all have their proponents, as do surgeons who advocate tumour resection without a preresection cerebrospinal fluid (CSF) drainage procedure. Given only a small percentage of cases will develop postoperative hydrocephalus a preop shunt is the least practised option.

The optimal surgical approach utilized is dependent on the tumour location. Infratentorial tumours may be accessed via a standard midline suboccipital craniotomy/craniectomy and for more lateral tumours a retromastoid craniotomy/craniectomy may be used. If a preresection CSF drainage procedure has not been undertaken the surgeon might initially create a posterior burr hole and insert an external ventricular drain (EVD) immediately before undertaking the craniotomy. Many neurosurgeons use a telo-velar approach to access 4th ventricular tumours to avoid/minimize damage to the vermis, to try and reduce the risk of posterior fossa mutism/syndrome.

The aim is always to achieve gross total resection given its massive importance in prognosis and outcome. Ependymomas are frequently adherent to the brainstem and cranial nerves in the CPA and avoiding damage to these structures can challenge even experienced surgeons. It is therefore no surprise that the use of intraoperative neurophysiology and ultrasound are increasing, in hopes that a more complete resection is achieved and neurological morbidity is minimized. Following the operation it is essential to obtain an MRI scan within 24 hours to accurately document the extent of the resection, as this influences both the treatment paradigm and the outcome. The use of intraoperative MRI helps to immediately identify if residual tumour is present. If resectable tumour is identified on the post-op scans the surgeon should be prepared to re-operate and attempt total resection. The increasingly aggressive surgical strategies employed to achieve total resection of the tumour do come at a price and there are often significant neurological deficits, which may result in the need for tracheostomy and gastrostomy. Despite this aggressive approach less than 50% of all paediatric ependymomas are able to be completely resected.

Consistent treatment paradigms in the management of ependymomas have proven difficult to establish due to several factors: its uncommon occurrence; inconsistencies in pathological tumour grading; and the resultant difficulties of comparing outcomes between different groups of patients. Most studies have been retrospective. This introduces an element of bias, particularly when it involves small numbers of patients accrued over long periods of time, during which treatment modalities and classification criteria may alter. The significant positive elements, which have most influenced ependymoma management, are the importance of the extent of surgical resection, improved surgical treatment, and widespread access to MRI imaging.

The overall management of intracranial ependymoma is controversial but includes surgery combined with radiation and chemotherapy. Poor 5-year survival results leads to a lack of uniformity in treatment protocols. Local relapse is the primary cause of treatment failure. The decision to treat the patient with radiation and or

Box 29.1 Key points

- Ependymomas are primarily tumours of childhood
- The majority occur in the posterior fossa
- Complete surgical resection is the single most important factor in prognosis
- Significant difficulties exist in histological differentiation between classic and anaplastic subtypes
- Conformal adjuvant radiation therapy increases survival after surgery
- Chemotherapy is used primarily in children under 3 to control disease and delay need for radiation therapy
- Most tumours relapse locally
- Overall 5-year survival is 36–64% in children

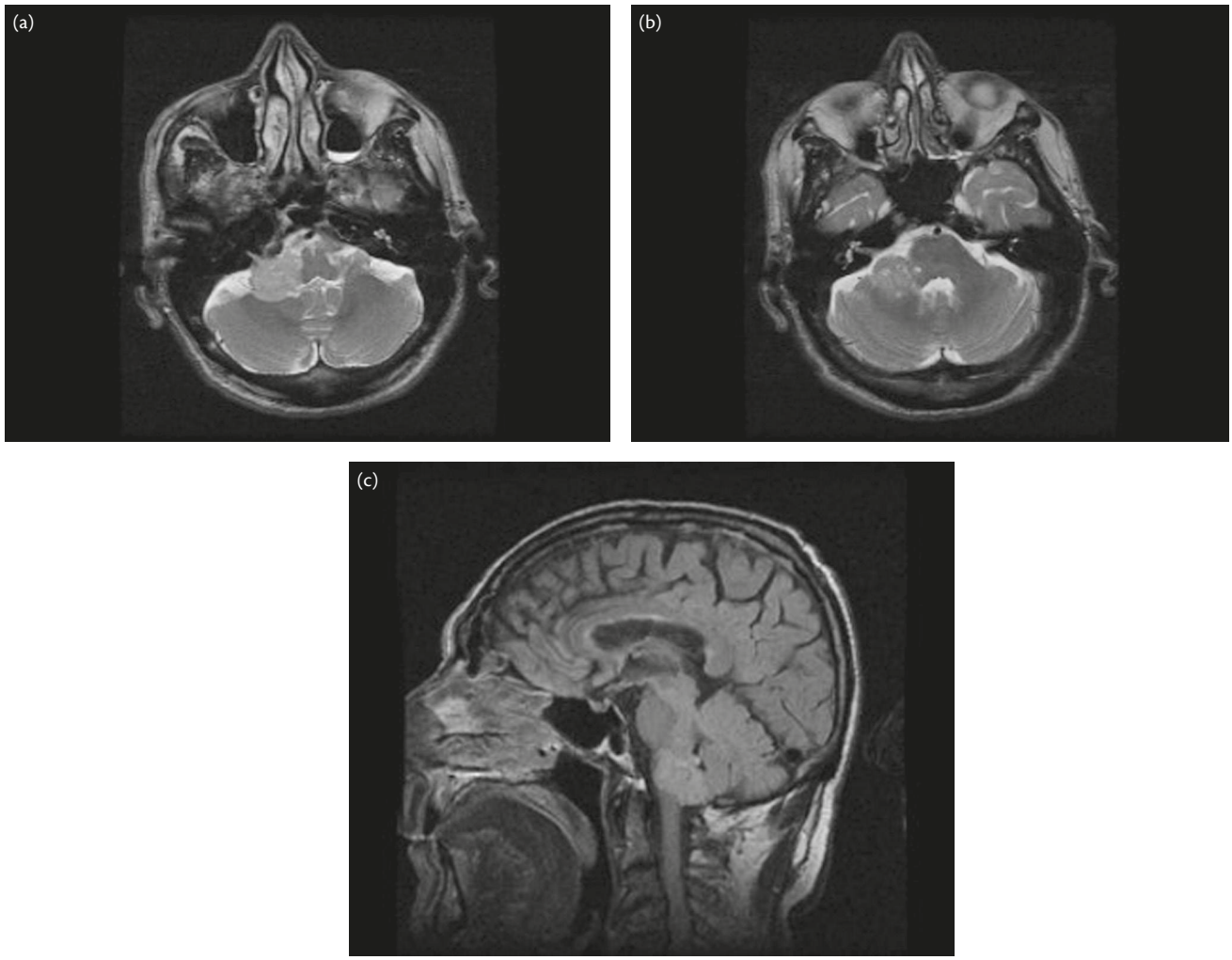

Fig. 29.3 MR imaging of posterior fossa ependymoma extending to the cerebellopontine (CP) angle through the foramen of Lushka mimicking a CP angle schwannoma. (A, B) Axial T2-weighted imaging. (C) Sagittal T1-weighted imaging with gadolinium enhancement.
Courtesy of Dr Kieren Allinson, Department of Pathology, Addenbrooke's Hospital, Cambridge.

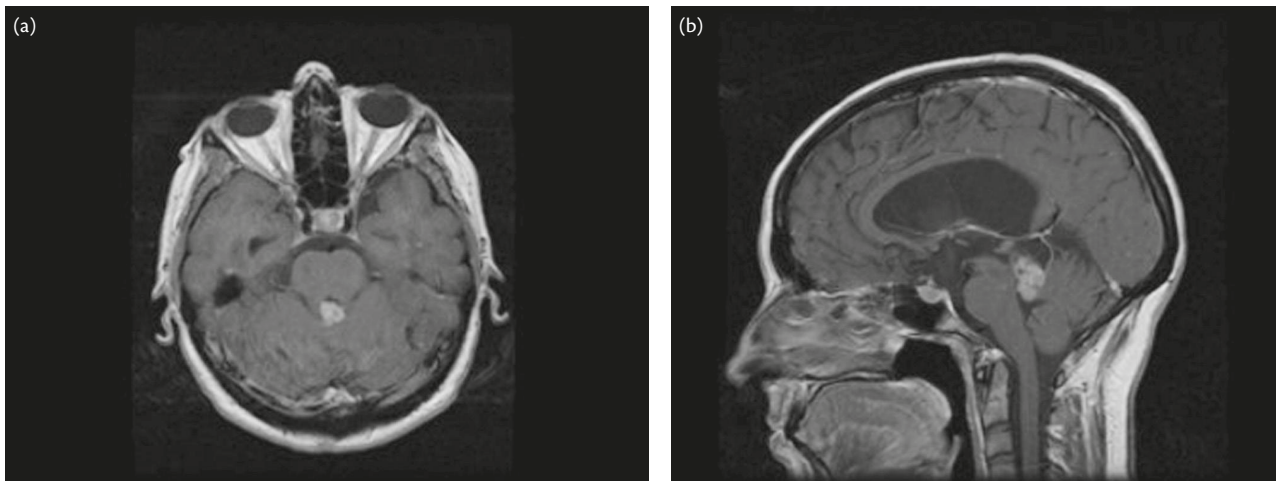

Fig. 29.4 T1-weighted gadolinium enhanced MR imaging of a fourth ventricular ependymoma obstructing the aqueduct of Sylvius. (A) axial; (B) sagittal.
Courtesy of Dr Kieren Allinson, Department of Pathology, Addenbrooke's Hospital, Cambridge.

chemotherapy is based on several factors; age of the patient, tumour grade, extent of resection, and the presence of metastatic disease. There is a consensus that those patients who are treated with radiation therapy have better event free survival than those treated with chemotherapy and therefore radiation therapy is considered to be mandatory adjuvant therapy except in those children less than three years of age (Shuman et al., 1975; Mork and Loken, 1997).

Cranio-spinal radiation (CSI) was, for a considerable period of time, the standard adjuvant therapy as for medulloblastoma until it became apparent that with ependymomas the presence of disseminated disease at presentation and at relapse was much less frequent than originally appreciated. CSI has now been replaced by conformal radiotherapy, which uses 3D imaging and software to optimize dose delivery (Merchant et al., 2004; Merchant et al., 2009) unless metastatic disease is present.

A range of different radiotherapy paradigms is now available which include: hyperfractionated accelerated radiotherapy, IMRT (intensity modulated radiotherapy), LINAC, SRS (stereotactic radiosurgery), and proton beam radiotherapy. Continuing active debate persists as to the optimal format and dose. Newer methods of radiation therapy, particularly proton beam, by reducing the dose to surrounding structures, aims to reduce side effects, which is critical in children while continuing to deliver a lethal dose to the tumour/tumour bed. At the heart of all radiation strategies is minimizing the collateral damage while delivering a lethal dose to the tumour bed to reduce recurrence of the tumour. In children less than 3 years old or those with metastatic disease, a number of different strategies are available, primarily chemotherapy based, to try and control the disease and delay radiation therapy until the child has reached an age where radiation can be considered (Zacharoulis and Moreno, 2009). However, studies looking at radiation therapy in children under 3 years old have shown reasonable progression free survival with good functional outcome and this treatment may be one which becomes more prevalent in the future (Merchant et al., 2004). Radiosurgery is currently only utilized in the context of relapsed disease but may in the future be used together with conventional radiotherapy paradigms.

The role of chemotherapy is much less clear and there are a multitude of different regimens and drugs used (Bouffet and Foreman, 1999). It has not been shown to greatly affect the clinical course of ependymoma either singly or in combination. Its main role is in delaying radiotherapy in small children and it also has a smaller role in facilitating the resection of residual tumour.

Prognosis

The overall prognosis for ependymoma depends on a number of factors the most critical of which is the extent of surgical resection (Healey et al., 1991). Most studies have shown that the prognosis of patients with totally resected tumours is substantially higher in all age groups compared with those patients whose tumours are subtotally resected (Bouffet et al., 1998; Merchant, 2002).

In children, aged below 3, incomplete tumour resection, presence of metastases at presentation and anaplastic histology are all considered to be poor prognostic indicators. In older patients important prognostic factors include age, presence of metastases, location (posterior fossa vs. spinal) and histological subtype (myxopapillary vs. anaplastic). Once relapse occurs there is no hope of a cure and the focus of management is on disease control (Pollack et al., 1995; Robertson et al., 1998).

Multiple further surgical procedures to effect local disease control can be very effective palliative treatment. Reirradiation is also becoming a viable treatment option with marked improvement in short-term survival with suggestions of altered tumour oncological potential (Bouffet et al., 2012).

A range of different strategies of oncological therapy for relapsed ependymoma are also available though there is little evidence that these are effective.

Controversies

Proton beam vs. radiotherapy

The more recent availability and increasing use of proton beam radiotherapy may also yield more improvement in overall outcome. Proton beam radiotherapy delivers an equivalent dose of radiation of equal efficacy to standard photon-based treatment with a lower dose to surrounding structures. The major perceived advantage of proton bean radiation therapy is reduced incidence of radiation-induced side effects, which in the paediatric population may significantly reduce long-term morbidity (MacDonald et al., 2008). Radiosurgery is currently only used in the context of relapsed disease but may, in the future, be used together with conventional radiotherapy paradigms. Unfortunately, both proton beam and radiosurgery are not yet fully assessed with only one significant clinical trial reported which showed reduced systemic complication rates in children treated with craniospinal proton beam radiotherapy (Yock et al., 2016).

REFERENCES

Andreiuolo, F., Ferreira, C., Puget, S., & Grill, J. (2013). Current and evolving knowledge of prognostic factors for pediatric ependymomas. *Future Oncol*, **9**, 183–91.

Bouffet, E. & Foreman, N. (1999). Chemotherapy for intracranial ependymoma. *Childs Nerv System*, **15**, 563–70.

Bouffet, E., Perilongo, G., Canete, A., & Massimino, M. (1998). Intracranial ependymomas in children: a critical review of prognostic factors and a plea for cooperation. *Med Pediatr Oncol*, **30**(6), 319–29; discussion 329–31.

Bouffet, E., Hawkins, C.E., Ballourah, W., et al. (2012). Survival benefit for pediatric patients with recurrent ependymoma treated with reirradiation. *Int J Radiat Oncol Biol Phys*, **83**(5), 1541–8.

Ellison, D.W., Kocak, M., Figarella-Branger, D., et al. (2011). Histopathological grading of pediatric ependymoma: reproducibility and clinical relevance in European trial cohorts. *J Negat Results Biomed*, **10**, 7.

Foreman, N.K., Love, S., & Thorne, R. (1996). Intracranial ependymomas: analysis of prognostic factors in a population-based series. *Pediatr Neurosurg*, **24**(3), 119–25.

Hamilton, R.L. & Pollock, I.F. (1997). The molecular biology of ependymomas. *Brain Pathol*, **7**, 807–22.

Healey, E., Barnes, P., Kupsky, W., et al (1991). The prognostic significance of post-operative residual tumor in ependymoma. *Neurosurgery*, **28**, 666–72.

MacDonald, S.M., Safai, S., Trofimov, A., et al. (2008). Proton radiotherapy for childhood ependymoma: initial clinical outcomes and dose comparisons. *Int J Radiat Oncol Biol Phys*, **71**, 979–86.

Merchant, T. (2002). Current management of childhood ependymoma. *Oncology*, **16**, 629–44.

Merchant, T.E., Mulhern, R.K., Krasin, M.J., Kun, L.E., Williams, T., & Li, C. (2004). Preliminary results from a phase II trial of conformal radiation therapy and evaluation of radiation-related CNS effects for pediatric patients with localized ependymoma. *J Clin Oncol*, **22**(15), 3156–62.

Merchant, T.E., Li, C., Xiong, X., Kun, L.E., Boop, F.A., & Sanford, R.A. (2009). Conformal radiotherapy after surgery for paediatric ependymoma: a prospective study. *Lancet Oncol*, **10**, 258–66.

Mork, S.J. & Loken, A.C. (1997). Ependymoma: a follow-up study of 101 cases. *Cancer*, **40**, 907–15.

Perilongo, G., Massimino, M., Sotti, G., et al (1997). Analyses of prognostic factors in a retrospective review of 92 children with ependymoma: Italian Pediatric Neuro-oncology Group. *Med Pediatr Oncol*, **29**(2), 79–85.

Pollack, I.F., Gerszten, P.C., Martinez, A.J., et al. (1995). Intracranial ependymomas of childhood: long-term outcome and prognostic factors. *Neurosurgery*, **37**(4), 655–66; discussion 666–7.

Robertson, P.L., Zeltzer, P.M., Boyett, J.M., et al. (1998). Survival and prognostic factors following radiation therapy and chemotherapy for ependymomas in children: a report of the Children's Cancer Group. *J Neurosurg*, **88**(4), 695–703.

Shuman, R.M., Alvord, E.C., Leech, R.R., et al (1975). The biology of childhood ependymomas. *Arch Neurol*, **32**, 731–9.

Slavc, I., MacCollin, M.M., Dunn, M., et al. (1995). Exon scanning for exon mutations of the NF-2 gene in pediatric ependymomas, rhabdoid tumors and meningiomas. *Int J Cancer*, **64**(4), 243–7.

Tihan, T., Zhou, T., Holmes, E., Burger, P.C., Ozuysal, S., & Rushing, E.J. (2008). The prognostic value of histological grading of posterior fossa ependymomas in children: a Children's Oncology Group study and a review of prognostic factors. *Mod. Pathol*, **21**, 165–77.

Yock, T.I., Yeap, B.Y., Tarbell, N.J., et al. (2016). Long-term toxic effects of proton radiotherapy for paediatric medulloblastoma: a phase 2 single-arm study. *Lancet Oncol*, **17**(3), 287–98.

Zacharoulis, S. & Moreno, L. (2009). Ependymoma: an update. *J Child Neurol*, **24**, 1431–8.

30

Haemangioblastoma

Ammar Natalwala and Donald MacArthur

History and epidemiology

Haemangioblastomas (HBLs) are uncommon, highly vascular, and benign tumours that account for 1 to 2.5% of all intracranial tumours. This specific tumour entity was first described in 1872 by Hughlings and Jackson, while the term 'haemangioblastoma' itself was coined by Cushing and Bailey in 1928 to describe vascular tumours of the CNS which had previously been known as 'vascular gliomas'. This description differentiated these tumours from CNS telangiectasia or cavernous and venous angiomas (Weil et al., 2003). In 1895 the German ophthalmologist Eugen von Hippel had presented a first case of angiomatosis retinae and in 1926, the Swedish pathologist Arvid Wilhelm Lindau described the clinical syndrome (now known as Von Hippel-Lindau syndrome or VHL) that combined retinal angiomas and cerebellar HBLs. He described CNS haemangioblastomas based on a series of criteria including 'unmistakable neoplasticity' with 'composition of blood vessel elements' and a 'tendency towards cyst formation' (Hussein, 2007).

Approximately 30% of CNS HBL cases are associated with VHL, whereas 70% occur sporadically. VHL disease is clinically heterogenous with the other associated tumours being retinal angiomas, renal cysts, renal cell carcinomas (RCC), pancreatic tumours, phaeochromocytomas, endolymphatic sac tumours of the middle ear, and epididymal cysts (Bründl et al., 2014). CNS HBLs, in association with VHL, are diagnosed at a younger age compared to spontaneous HBLs (i.e. they present in the second and third decade of life versus fourth and fifth decades).

Clinical presentation

Symptomatic tumours usually present due to compressive effects from the tumour or occasionally due to haemorrhage within it or paraneoplastic effects (such as polycythaemia). The mean time to diagnosis has been reported from 7 weeks to 13 months but this can vary depending on the type of HBL and is usually shorter in cases of VHL. These tumours have solid and cystic components and it is generally the cystic HBLs that cause more compressive symptoms. Solid HBLs may grow slowly and patients can remain asymptomatic for many years. Asymptomatic HBLs in patients with VHL are frequently detected by imaging surveillance.

Headache is the main symptom in 95% of cases involving cerebellar and brainstem HBLs. Vomiting, ataxia, vertigo, diplopia, and nystagmus are the next most common symptoms. Less commonly, patients present with neck pain, nausea, dysarthria, or cranial nerve deficits. Patients with spinal HBLs often have long tract signs with pain and associated syringomyelia in 50% of cases (Hussein, 2007). Spinal HBLs are more common in younger men and are usually thoracic and intramedullary. Despite being slow growing tumours, HBLs can cause life-threatening complications (Richard et al., 2000). For example, patients can present with obstructive hydrocephalus depending on the size and location of the tumour and spontaneous massive haemorrhage has been reported.

As a paraneoplastic effect, HBLs are the only brain tumours associated with polycythaemia (seen in 9–20% of intracranial tumours, but not in spinal lesions) due to the unregulated secretion of erythropoietin (EPO) (Hussein, 2007). The molecular genetics involved in this process are discussed later in this chapter.

Pathology

Location

HBLs can occur anywhere in the CNS but have a preponderance towards infratentorial structures and represent 7.5% of all adult posterior fossa tumours and 4% of adult spinal cord tumours (Bründl et al., 2014). **Figure 30.1** outlines the common locations for HBLs overall and in patients with VHL. Infratentorial HBLs are often found at the dorsum cerebelli, obex, and dorsal root entry zone of the spinal cord. Supratentorial HBLs are rare. A systematic review by Mills and colleagues investigated 132 such cases and found 60% had VHL disease (Mills et al., 2012). Other locations for HBLs include spinal nerve roots where the tumour can be intradural extramedullary, extradural, or a combination of these. They often have an intrafascicular origin and thus cannot be completely resected without sacrificing the nerve root. HBLs outside the CNS have also been reported in the literature including within the orbit, intestine, and retroperitoneum.

Radiological and macroscopic appearance

HBLs are usually well circumscribed and do not always have a true capsule. Thus, they can sometimes infiltrate adjacent brain

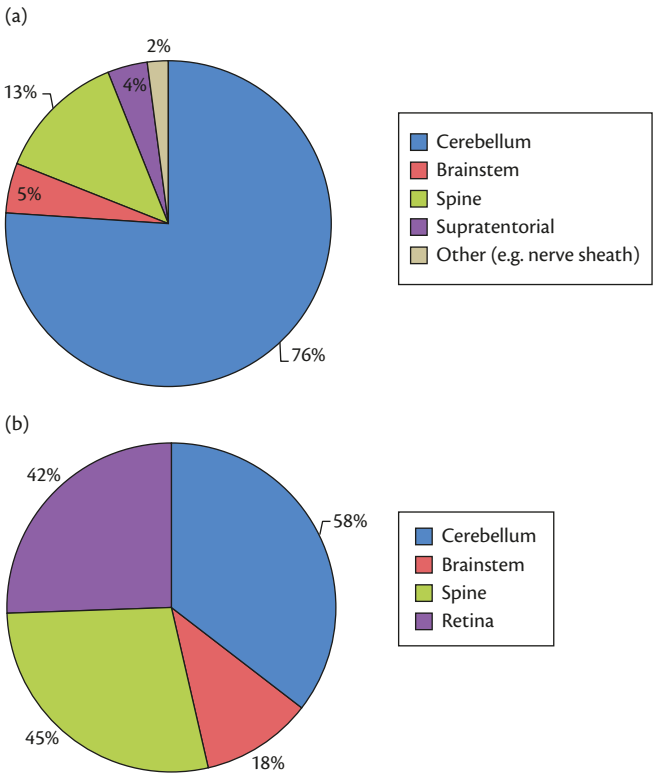

Fig. 30.1 (A) The most common locations of HBLs overall in the CNS and (B) the distribution of HBLs in patients with VHL (tumours often found in more than one location).

Percentages are based on averages from reports in the literature (Ammerman, 2006; Gläsker, 2005; Hussein, 2007; Kanno, 2014; Padhi et al., 2011).

parenchyma. They avidly enhance on postcontrast CT and T1-weighted MRI. T2-weighted images and fluid-attenuated inversion recovery (FLAIR) sequences are used to investigate peritumoural oedema around cysts associated with HBL (Wind and Lonser, 2011). Sun and colleagues report distinct radiologically different groups of HBLs; cystic with an enhancing large cyst and tumour nodule, non-enhancing cyst wall but evenly enhanced tumour nodule, solid HBL comprising of multiple small solid tumours and solid tumour with single or multiple cysts (Sun et al., 2015). These are outlined in Figure 30.2. Knowledge of these subtypes may aid diagnosis based initially on radiological imaging.

Cystic HBLs are often found in the cerebellum and on cross-section they are comprised of yellow xanthochromic or grey proteinaceous fluid and a dense red coloured mural nodule, usually 0.5 to 2.5 cm in diameter (Richard et al., 2000). The formation of cysts in HBL can be intra- or peritumoural (Hussein, 2007). Studies report intratumoural cyst formation occurs mainly due to intratumoural necrosis, whereas peritumoural cysts develop as a result of a tumour interstitial process that generates oedema (Jagannathan et al., 2008). Cystic HBLs without a mural nodule visible are rare, solid HBLs and those with internal cysts are often found in the spinal canal (Richard et al., 2000).

Solid tumours tend to be larger, more vascular, and more commonly involve the brainstem. The main growth pattern for HBL is described as 'saltatory' growth that is characterized by periods of quiescence (2.1 ± 1.6 years) and interspersed periods of rapid growth (1.1 ± 1.3 years). Lonser et al. also reported linear and exponential growth patterns in HBLs associated with VHL (Lonser, 2014).

Histology

HBLs are benign, WHO grade I tumours (Fig. 30.3). They are highly vascular, being composed of a rich capillary network with interspersed large, polyhedric lipid-laden stromal or 'Zwischenzellen' cells (Richard et al., 2000). Based on the relative proportion of these two components, HBLs may be divided into reticular (capillaries predominate) and cellular (stromal cells predominate) subtypes. Recurrence rates are reported to be higher in cellular subtypes (25%) compared to reticular (8%). There may be frequent mast cells (Hussein, 2007). The vascular spaces within the tumour are variably sized and may be poorly developed towards the centre of the lesion. The stromal cells are typically bland but there may be striking nuclear atypia which is thought to be degenerative in nature and is not prognostically important. Mitotic figures are infrequent. Foci of extramedullary haematopoiesis are seen infrequently and are likely to be due to production of EPO by the stroma cells. The brain adjacent to HBLs may show prominent gliosis which may be piloid, containing frequent Rosenthal fibres. This presents a diagnostic pitfall for the unwary, particularly in small biopsies, and should not be interpreted as evidence of a pilocytic astrocytoma.

Stromal cells are not a component of the normal CNS and the histogenesis of HBL remains controversial. They are thought to arise from haemangioblast progenitor cells. Stromal cells lack specific organelles or cell attachments and have been shown to differentiate into erythrocytes and vascular endothelial cells.

Pathologically, the key differential diagnosis of HBL is metastatic renal cell clear cell carcinoma, which is also common in VHL (Hussein, 2007). Other entities that can enter the differential include paraganglioma and angiomatous meningioma. In addition to the morphological differences, a panel of immunohistochemical stains, including CD10, D2–40, epithelial membrane antigen, inhibin-α, and S100, will usually allow a firm diagnosis to be reached.

Molecular tumour genetics and risk factors

VHL is inherited in an autosomal dominant manner (Asthagiri et al., 2010). It has more than 90% penetrance by the age of 65 years. The VHL gene is a tumour suppressor gene located on the short arm of chromosome 3 and widely expressed in fetal and adult tissue. It encodes the VHL protein (pVHL) which is an E3 ubiquitin ligase that targets hypoxia inducible factor alpha (HIF-α) and as such regulates the expression of many hypoxia induced genes including those responsible for angiogenesis (vascular endothelial growth factor or VEGF) and erythropoiesis (EPO). The pVHL can also stabilize other binding proteins leading to HIF-independent activity such as extracellular matrix regulation, apoptosis, microtubule stability, cilia formation and gene transcription and in these respects is considered to be involved in tumour suppression (Hsu, 2012). The expression of VEGF protein induces recruitment of abundant reactive vascular cells into the tumour and therefore seems to be responsible for the hypervascularity of these lesions (Hussein, 2007).

VHL patients harbour germline mutations or deletions of one copy of the VHL gene. It is believed that familial tumours arise from cells where a somatic mutation of the wild-type VHL gene leads to biallelic inactivation (Gläsker, 2005). VHL gene mutations are also found in a fraction of sporadic HBLs (10–44%). Shankar et al found

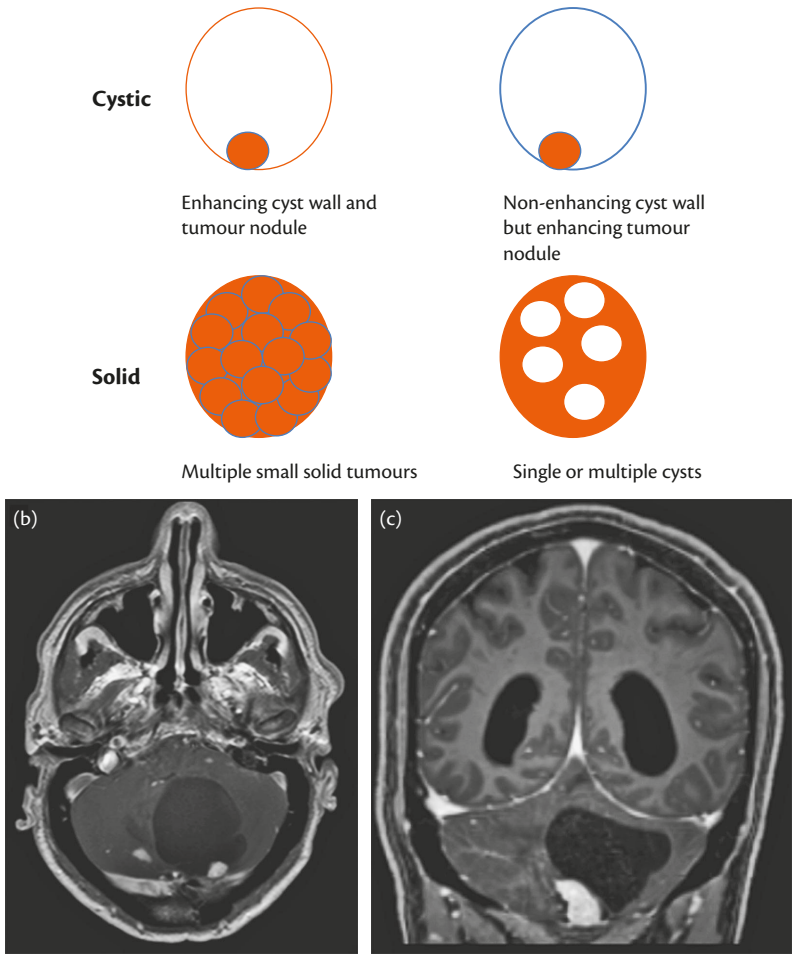

Fig. 30.2 (A) Diagram depicting different morphological subtypes of HBL and appearance on contrast enhanced MRI imaging (based on description reported by Sun et al., 2015). (B and C) Axial and coronal images, respectively, showing typical MRI appearances (T1 postcontrast) of posterior fossa HBLs in a 52-year-old man with known VHL. Image B shows an enhancing mural nodule on the left and associated cyst (non-enhancing cyst wall) as well as a solitary nodule adjacent to this on the right (as well as other smaller nodules).

a markedly high prevalence of recurrent somatic mutations (50%) and loss of heterozygosity (LOH) of the gene locus on chromosome 3p (72%). Together, these alterations accounted for biallelic inactivation of VHL in 47% and an inactivating alteration in at least one allele in 78% of sporadic HBLs (Shankar et al., 2014). Genotype–phenotype studies have identified several different VHL subtypes with different tumour profiles and this is discussed in more detail in a separate chapter.

Treatment

Current treatment options for HBL include surgery to resect the tumour with or without preoperative endovascular embolization, stereotactic radiosurgery (SRS), and radiotherapy. Complete surgical resection is the mainstay of treatment and for accessible tumours can be curative with minimal morbidity and mortality (Hussein, 2007). The optimal timing of treatment is uncertain, however, if there is progression of neurologic symptoms, evidence of tumour or cyst growth, or haemorrhage then intervention is considered by most neurosurgeons.

Surgery

HBLs, in particular the solid type, are often compared to arteriovenous malformations (AVMs) and the surgical principles involved to obtain complete resection without significant bleeding are similar. Surgeons should avoid entering into the tumour or attempting biopsy as piecemeal resection can lead to problematic bleeding (Hussein, 2007). Surgical resection is more straightforward in HBLs following the margins of gliotic tissue, with a wide exposure, circumferential dissection, and *en bloc* removal. As with AVMs, the feeding artery should be occluded prior to occlusion of the draining veins to avoid bleeding secondary to venous outflow obstruction in a hyperdynamic circulation. Multiple feeding arteries are often present as well as more than one abnormally thick draining vein which can make it difficult to differentiate vessels. The mural nodule in cystic HBLs which will usually be identifiable by its reddish or orange colouration must be removed completely in order to prevent recurrence. An attempt may be made to remove an enhancing cyst wall; but Gläsker has suggested that often a non-enhancing cyst wall represents simple reactive gliosis without tumour cells, and it can be left untreated (Gläsker et al., 2010). Depending on location, some solid HBLs may require extended

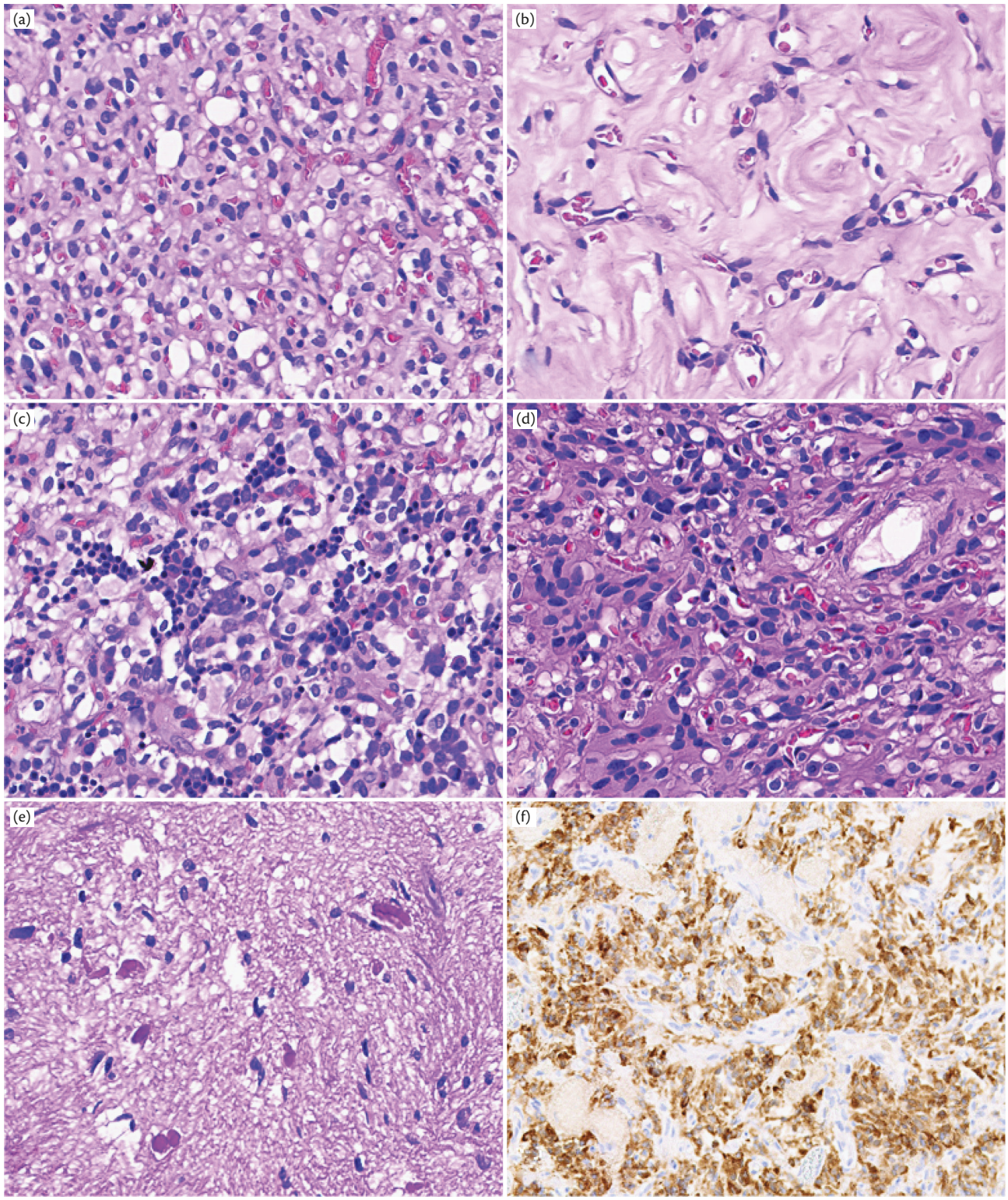

Fig. 30.3 (A) HBL (WHO grade I) is composed of capillaries and stromal cells with variably vacuolated cytoplasm (H&E, objective ×20). (B) The proportion of the two components can vary markedly and it is not unusual to see collagenized, paucicellular areas (H&E, objective ×20). (C) Foci of extramedullary haematopoiesis, thought to be due to production of EPO by the stroma cells, can be seen and may be associated with secondary polycythaemia (H&E, objective ×20). (D) Nuclei atypia, which is presumed to be degenerative, may be striking but is of no prognostic significance (H&E, objective ×20). (E) There may be piloid gliosis, with prominent darkly-stained Rosenthal fibres, in the adjacent brain (H&E, objective ×40). (F) Stromal cell immunoreactivity for inhibin-α is helpful in distinguishing HBL from mimics such as metastatic renal cell carcinoma (anti-inhibin-α immunohistochemistry, ×10). Thank you to Dr Simon Paine (Consultant Neuropathologist, Nottingham University Hospitals) for providing histopathology advice and images.

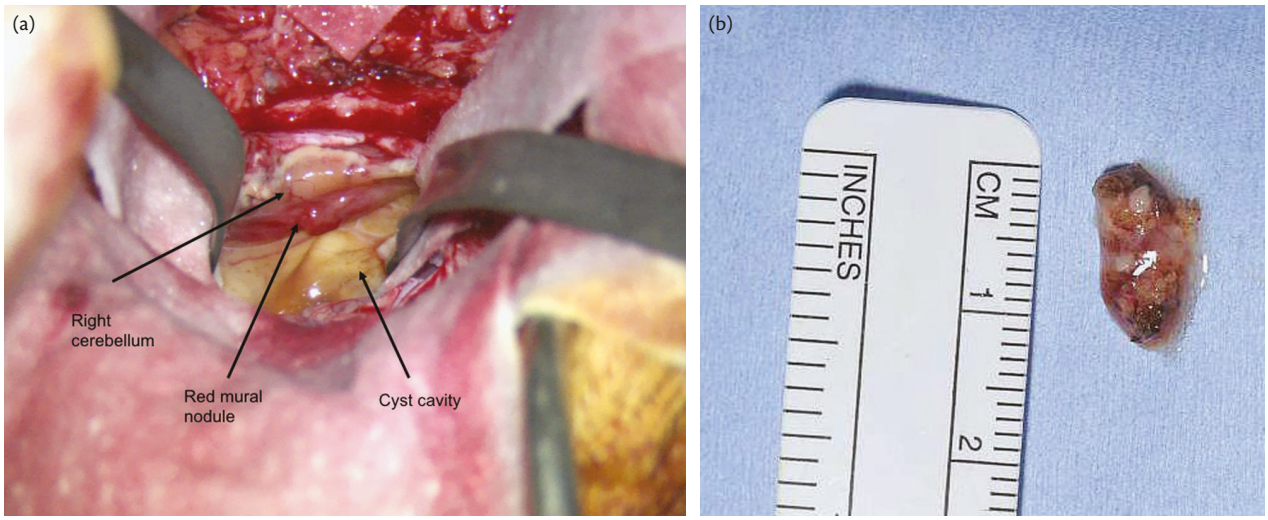

Fig. 30.4 (A) Intraoperative image showing the mural nodule within an opened cyst cavity in the right cerebellum. (B) The mural nodule was resected *en bloc*.

skull base approaches (Dow et al., 2002). The most common surgical approaches include midline suboccipital and retromastoid craniotomies, with or without a C1 laminectomy. Particular care must be taken with brainstem HBLs as they have a subpial attachment and attempts to resect can lead to heavy bleeding and CNS injury (Hussein, 2007). Electrophysiological monitoring may have a role in resection of HBLs of the brainstem, cerebellopontine angle (CPA), and spine. Figure 30.4 shows the intraoperative appearance of HBL.

Some groups advocate preoperative embolization to facilitate surgery by reducing the vascularity of HBLs and subsequent intraoperative bleeding, although these procedures themselves carry a risk of haemorrhage, infarction, and swelling causing secondary hydrocephalus. A range of embolic agents are available but liquid agents such as N-butyl cyanoacrylate (NBCA) and Onyx have the best durability and penetration and are often the methods of choice. However, these agents can migrate and inadvertently cause venous obstruction and thus infarction or haemorrhage (Shin et al., 2014). Cornelius and colleagues report this to be more frequent in cerebellar HBLs (43%) compared to brainstem or spinal HBLs (5.6%) (Cornelius et al., 2007). Figure 30.5 shows pre- and postembolization angiograms of a treated HBL.

Intraoperative indocyanine green videography has been reported as a useful adjunct to surgery by some authors to identify tumour related blood flow and target feeding vessels more easily. Similarly, intraoperative ultrasound has been recommended to help find the

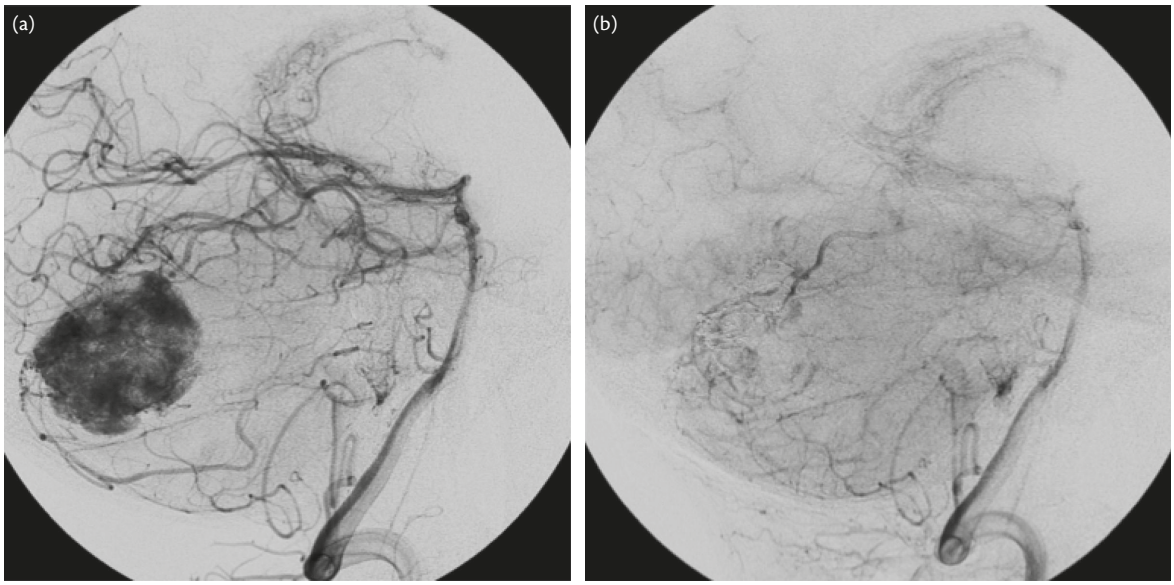

Fig. 30.5 Preoperative endovascular treatment of a left cerebellar HBL in a 53-year-old patient. The medial component of the tumour was supplied by the right posterior inferior cerebellar artery (PICA) and lateral component by left superior cerebellar artery (SCA). (A) A vascular blush is seen postcontrast injection pre-embolization. (B) The distal vermian branch of the right PICA was occluded using NBCA and the postembolization image shows reduced vascularity of the tumour. Thank you to Dr Robert Lenthall (Consultant Interventional Neuroradiologist, Nottingham University Hospitals) for providing interventional radiology advice and images.

plane between tumour and brain parenchyma or the spinal cord particularly in HBLs with a poorly defined outer capsule.

Non-surgical treatment

When surgery is not possible, other treatment options including SRS, radiotherapy, and other salvage systemic treatments may be used.

SRS is generally preferred for recurrent and multiple HBLs or when they are in eloquent or high-risk areas with a low chance of achieving gross total resection. It can often be difficult to know which lesion (if multiple) is causing the symptoms. The presence of a cystic component probably negatively impacts on control rates (Matsunaga et al., 2007). Kano et al. recently reported outcomes for 186 patients with 517 HBLs who underwent SRS across 19 centres in North America and Japan with 15–18 Gray (Gy) dosing (Kano et al., 2015). At a median 5 years follow-up, 20 died of intracranial disease progression and nine of other causes. Factors predicting longer survival were younger age, absence of neurological symptoms, fewer tumours, and higher Karnofsky Performance Status (KPS). Tumour control rates were 89% at 5 years and 79% at 10 years. Some 41% of VHL-associated HBL patients had new tumour recurrences and 16% of the sporadic cases had recurrence at the original tumour site with the specific 5-year recurrence rate being 43% versus 24% in VHL-associated and sporadic HBL, respectively. Thirteen patients (7%) had adverse radiation effects with one patient dying due to this. SRS has also been reported as a preoperative adjunct to significantly reduce vascularity permitting safe resection (Kamitani et al., 2004).

External beam radiotherapy (EBRT) has also been used to treat HBLs. One study investigated the use of EBRT over 20 years in HBL and found local control rates of 57% in fractions totalling 50 Gy versus 33% when less than 50 Gy was delivered (Smalley et al., 1990). Simone et al. explored the effect of infratentorial craniospinal irradiation for advanced HBL associated with VHL; seven patients with 84 HBLs were treated (43.2 Gy in 24 fractions). After treatment, the mean tumour volume was increased by 25% and the total number of tumours also increased to 91 (8.3% more). However, the overall tumour growth rate was lower than reported for the natural history of HBL. Mean follow-up time was 73.8 months (Simone et al., 2011).

Salvage systemic therapy has been tried for patients with recurrence despite surgery and irradiation. Capitanio et al. describe treatments including chemotherapy agents (interferon-alpha-2a or IFN-2a), tyrosine kinase inhibitors, selective VEGF inhibitors, monoclonal antibodies (bevacizumab), and thalidomide. These data are based on case reports and phase II trials, showing stabilization of CNS HBLs and improvement in symptoms but without any change in radiological appearance. Further studies will be needed to elucidate a role for antiangiogenic agents in treatment of HBLs (Capitanio et al., 2013).

Screening for VHL

The presence of more than one haemangioblastoma, early age at diagnosis or the presence of other manifestations of VHL disease should all serve as indications for genetic screening for germline VHL mutations. As well as whole CNS imaging, abdominal ultrasound, or MRI, 24-hour urine for catecholamines, and retinal imaging with ophthalmoscopy and fluorescein angiography is required. The Melmon and Rosen diagnostic criteria for VHL require the presence of one retinal, CNS, or visceral lesion if there is a family history of VHL. Without a family history the requirement includes two CNS HBLs or one CNS HBL and one visceral lesion excluding unilateral papillary cystadenoma of the epididymis and renal cysts which are common findings in the general population or papillary cystadenoma of the broad ligament.

Prognosis

General recurrence rates for HBL are reported between 20% and 33%. The clinicopathological factors that positively correlate with recurrence of these tumours include younger age (<30 years at time of diagnosis), presence of multicentric tumours of the CNS at initial diagnosis, tumours with lower frequencies of cyst formation and lower proportions of lipid-laden stromal cells (Hussein, 2007). Solid HBL tumours also had higher rates of recurrence. VHL patients develop new CNS HBL during follow-up at a rate of having a new tumour every 2.1 years (Conway et al., 2001). Propensity for new tumour growth is far higher in VHL compared to sporadic cases (93% vs. 44%, respectively). While HBLs are considered to be benign tumours, the tumour cells can migrate causing recurrence in distant parts of the brain.

Cerebellar HBL has a good prognosis following complete resection where survival at 5 years is more than 50% (Sun et al., 2015). Following complete resection, it is unlikely HBLs will recur and so chemotherapy and radiotherapy are rarely used postoperatively. Weil et al. in 2003 reported 12 cases of brainstem HBLs that underwent surgical resection and found that fewer preoperative neurological symptoms predicted better postoperative outcome. Tumour and cyst size did not affect outcome. All 12 patients were better or neurologically stable postoperatively and at long-term follow-up (>36 months) only 1 of the 12 had deteriorated.

Surgical outcomes reported by Jagannathan et al. in 2008 for HBL patients with VHL show 88% stability or improvement in symptoms postoperatively with 12% having new cerebellar signs that resolved over an average of 9 days. Long-term follow-up (median 84 months) showed that 7.5% worsened and 10% died. Hydrocephalus resolved in 94% and 6% needed a shunt. Mills and colleagues reported five-year progression-free survival (PFS) for gross total resection (GTR) and subtotal resection (STR) to be 100% and 53%, respectively, for supratentorial HBLs. GTR had been possible in 77% of the cases.

A recent single-centre study focussing on spinal HBLs examined 92 cases over 5 years (60 sporadic and 32 VHL-associated) that underwent 102 operations to resect 116 HBLs. Forty-one per cent were intramedullary tumours and GTR was achieved in 94%. Forty-one per cent had functional improvement, 44% remained stable, and 15% deteriorated. Mean follow-up time was 50 months. The main risk factor predicting outcome was STR. Seventy-seven per cent of patients had an associated syrinx that reduced postoperatively in 83% following tumour resection. Ventral and intramedullary tumours did worse overall in terms of clinical outcome (Deng et al., 2014).

In SRS, 5-year PFS for all CNS HBLs ranged from 63% to 85%. Other studies report 5-year tumour control rates between 71% and 96% for SRS but radiation necrosis can be a serious side effect particularly in the brainstem (Rachinger et al., 2009). Local control rates for SRS drop to 61% at 10 years and 51% at 15 years (Wind and

Lonser, 2011). Kano et al. (2008) report overall survival after SRS to be 94% at 3 years, 90% at 5 years and 74% at 10 years, and local tumour control rates of 92%, 89%, and 79%, respectively. Factors improving local control were VHL-associated HBL, solid and small tumours, and a higher margin dose. Thirteen patients (7%) had adverse radiation effects and one died as a result.

PFS for fractionated radiotherapy for all CNS HBLs ranges from 33% to 90.5% with better outcome attributed to high-dose radiotherapy (57% PFS vs. 33%; fractions ≥50 Gy vs. <50 Gy, respectively) (Mills et al., 2012). Koh et al. report 5-year PFS rates of 80% for VHL-associated HBL and 48% for sporadic HBL in patients received EBRT (Koh et al., 2007).

Reported mortality rates range from 4% to 8% (Conway et al., 2001; Padhi et al., 2011; Bründl et al., 2014). Ten-year outcome data by Bründl and colleagues shows 83% GTR and 17% STR with 75% of these patients having improvement or no change in symptoms after surgery. Their postoperative complications include bleeding (17%), hydrocephalus requiring shunting (4–11%), CSF infection (13%), ischaemia (8%), CSF leak (8%), new diplopia (4%), new hemiparesis (4%), bulbar syndromes, and tetraparesis (8%). Brainstem HBLs have the most unfavourable prognosis (Bründl et al., 2014). San Pedro and colleagues looked at 44 cases of HBL and report that spontaneous macroscopic bleeding is rare compared to asymptomatic microscopic intratumoural haemorrhage. Tumour size, spinal radicular location, and solid subtype of HBLs were associated with higher rates of bleeding. Gläsker et al. report HBLs less than 1.5 cm in diameter to have virtually no risk of bleeding.

Controversy

Age limit for screening for VHL with a single haemangioblastoma

In the absence of an existing family history of VHL, factors favouring a diagnosis of VHL in a patient with a newly diagnosed HBL are younger age of onset (mean age 29 for VHL-associated HBL versus 48 for sporadic HBL; see Maher, 2011), HBL outside the cerebellum (very unusual in sporadic cases but seen in up to 50% of VHL cases), and multiple HBLs (seen in up to 90% of VHL cases, and enabling a clinical diagnosis of VHL).

Some 97% of VHL patients will have presented by age 60 (Maher et al., 1990) but nonetheless, a first diagnosis of VHL has been made at 73 years of age (Kanno et al., 2014). Most authorities now suggest, in keeping with the French VHL study group (Richard et al., 1998), that all patients with apparent sporadic HBL should be investigated for evidence of VHL disease. The frequency of VHL gene mutations in patients presenting with an apparently isolated HBL is reported to be 4–14% (Catapano et al., 2005). However, somatic mosaicism particularly for a patient with a *de novo* mutation may mean that the mutation is not carried in the peripheral blood leukocytes resulting in a false negative genetic test (Butman et al., 2008). On this basis there is a case for keeping early onset HBL patients under close surveillance even if mutation analysis is negative. On the other hand, for older patients (>50 years of age) with negative initial investigations the risk of familial VHL disease appears small (Woodward et al., 2007) but still present.

SRS for haemangioblastomas

In a disease where HBLs are frequently multiple and may occur in the brainstem rather than just the cerebellum there are obvious attractions to a treatment which can avoid the need for multiple neurosurgical interventions and deal with lesions in inaccessible areas. However, the results of studies describing 'tumour control' need to be looked at critically in the context of a tumour which has a well-recognized saltatory growth pattern in the great majority of cases with periods of growth lasting on average 13 months and periods of quiescence lasting 2 or more years (Ammerman et al., 2006).

SRS for HBL is recognized as having a complication rate of 7–20% with adverse effects including worsened headaches due to peritumoural oedema which may necessitate prolonged corticosteroid administration or even surgery to resect the treated lesion (Asthagiri et al., 2010). The apparent early effects of SRS for HBL can be misleading in up to 25% (Asthagiri et al., 2010) with some tumours shrinking initially and then later progressing, while others may enlarge before regressing. The longer-term effects remain uncertain.

In contrast, for accessible lesions conventional surgery appears to offer excellent tumour control and almost immediate symptom control. Symptomatic HBLs should clearly be considered for treatment with surgery or if this does not seem feasible or acceptable to the patient, for SRS. Interventions such as SRS should be used judiciously for asymptomatic lesions found on screening scans. In one 10-year observational study, while 97% of HBLs grew radiologically, only 50% of them required treatment in this time for symptoms (Ammerman et al., 2006), while 45% of the tumours which ultimately became symptomatic over time and required treatment were not present at the time of first scan.

FURTHER READING

Ammerman, J.M., Lonser, R.R., Dambrosia, J., Butman, J.A., & Oldfield, E.H. (2006). Long-term natural history of hemangioblastomas in patients with von Hippel-Lindau disease: implications for treatment. *J Neurosurg*, **105**(2), 248–55.

Hussein, M.R. (2007). Central nervous system capillary haemangioblastoma: the pathologist's viewpoint. *Int J Exp Pathol*, **88**(5), 311–24.

Jagannathan, J., Lonser, R.R., Smith, R., DeVroom, H.L., & Oldfield, E.H. (2008). Surgical management of cerebellar hemangioblastomas in patients with von Hippel-Lindau disease. *J Neurosurg*, **108**(2), 210–22.

Kano, H., Shuto, T., Iwai, Y., et al. (2015). Stereotactic radiosurgery for intracranial hemangioblastomas: a retrospective international outcome study. *J Neurosurg*, **122**(6), 1469–78.

Richard, S., Campello, C., Taillandier, L., Parker, F., & Resche, F. (1998). Haemangioblastoma of the central nervous system in von Hippel-Lindau disease. French VHL Study Group. *J Intern Med*, **243**(6), 547–53.

REFERENCES

Ammerman, J.M., Lonser, R.R., Dambrosia, J., Butman, J.A., & Oldfield, E.H. (2006). Long-term natural history of hemangioblastomas in patients with von Hippel-Lindau disease: implications for treatment. *J Neurosurg*, **105**(2), 248–55.

Asthagiri, A.R., Mehta, G.U., Zach, L., et al. (2010). Prospective evaluation of radiosurgery for hemangioblastomas in von Hippel-Lindau disease. *Neuro Oncol*, **12**(1), 80–6.

Bründl, E., Schödel, P., Ullrich, O.W., Brawanski, A., & Schebesch, K.M. (2014). Surgical resection of sporadic and hereditary hemangioblastoma: our 10-year experience and a literature review. *Surg Neurol Int*, **5**, 138.

Butman, J.A., Linehan, W.M., & Lonser, R.R. (2008). Neurologic manifestations of von Hippel-Lindau disease. *JAMA*, **300**(11), 1334–42.

Capitanio, J.F., Mazza, E., Motta, M., Mortini, P., & Reni, M. (2013). Mechanisms, indications and results of salvage systemic therapy for sporadic and von Hippel-Lindau related hemangioblastomas of the central nervous system. *Crit Rev Oncol Hematol*, **86**(1), 69–84.

Catapano, D., Muscarella, L.A., Guarnieri, V., Zelante, L., D'Angelo, V.A., & D'Agruma, L. (2005). Hemangioblastomas of central nervous system: molecular genetic analysis and clinical management. *Neurosurgery*, **56**(6), 1215–21; discussion 1221.

Conway, J.E., Chou, D., Clatterbuck, R.E., Brem, H., Long, D.M., & Rigamonti, D. (2001). Hemangioblastomas of the central nervous system in von Hippel-Lindau syndrome and sporadic disease. *Neurosurgery*, **48**(1), 55–62; discussion 62–3.

Cornelius, J.F., Saint-Maurice, J.P., Bresson, D., George, B., & Houdart, E. (2007). Hemorrhage after particle embolization of hemangioblastomas: comparison of outcomes in spinal and cerebellar lesions. *J Neurosurg*, **106**(6), 994–8.

Deng, X., Wang, K., Wu, L., et al. (2014). Intraspinal hemangioblastomas: analysis of 92 cases in a single institution: clinical article. *J Neurosurg Spine*, **21**(2), 260–9.

Dow, G.R., Sim, D.W., & O'Sullivan, M.G. (2002). Excision of large solid haemangioblastomas of the cerebellopontine angle by a skull base approach. *Br J Neurosurg*, **16**(2), 168–71.

Gläsker, S. (2005). Central nervous system manifestations in VHL: genetics, pathology and clinical phenotypic features. *Fam Cancer*, **4**(1), 37–42.

Gläsker, S., Klingler, J.H., Müller, K., et al. (2010). Essentials and pitfalls in the treatment of CNS hemangioblastomas and von Hippel-Lindau disease. *Cent Eur Neurosurg*, **71**(2), 80–7.

Hsu, T. (2012). Complex cellular functions of the von Hippel-Lindau tumor suppressor gene: insights from model organisms. *Oncogene*, **31**(18), 2247–57.

Hussein, M.R. (2007). Central nervous system capillary haemangioblastoma: the pathologist's viewpoint. *Int J Exp Pathol*, **88**(5), 311–24.

Jagannathan, J., Lonser, R.R., Smith, R., DeVroom, H.L., & Oldfield, E.H. (2008). Surgical management of cerebellar hemangioblastomas in patients with von Hippel-Lindau disease. *J Neurosurg*, **108**(2), 210–22.

Kamitani, H., Hirano, N., Takigawa, H., et al. (2004). Attenuation of vascularity by preoperative radiosurgery facilitates total removal of a hypervascular hemangioblastoma at the cerebello-pontine angle: case report. *Surg Neurol*, **62**(3), 238–43; discussion 243–4.

Kanno, H., Kobayashi, N., & Nakanowatari, S. (2014). Pathological and clinical features and management of central nervous system hemangioblastomas in von Hippel-Lindau disease. *J Kidney Cancer VHL*, **1**(4), 46–55.

Kano, H., Niranjan, A., Mongia, S., Kondziolka, D., Flickinger, J.C., & Lunsford, L.D. (2008). The role of stereotactic radiosurgery for intracranial hemangioblastomas. *Neurosurgery*, **63**(3), 443–50; discussion 450–1.

Kano, H., Shuto, T., Iwai, Y., et al. (2015). Stereotactic radiosurgery for intracranial hemangioblastomas: a retrospective international outcome study. *J Neurosurg*, **122**(6), 1469–78.

Koh, E.S., Nichol, A., Millar, B.A., Ménard, C., Pond, G., & Laperriere, N.J. (2007). Role of fractionated external beam radiotherapy in hemangioblastoma of the central nervous system. *Int J Radiat Oncol Biol Phys*, **69**(5), 1521–6.

Lonser, R.R. (2014). Surgical management of sporadic spinal cord hemangioblastomas. *World Neurosurg*, **82**(5), 632–3.

Maher E.R., Yates, J.R., Harries, R., et al. (1990). Clinical features and natural history of von Hippel-Lindau disease. *Q J Med*, **77**(283), 1151–63.

Maher, E.R., Neumann, H.P., & Richard, S. (2011). Von Hippel-Lindau disease: a clinical and scientific review. *J Neurooncol*, **103**(1), 155–62.

Matsunaga, S., Shuto, T., Inomori, S., Fujino, H., & Yamamoto, I. (2007). Gamma knife radiosurgery for intracranial haemangioblastomas. *Acta Neurochir (Wien)*, **149**(10), 1007–13; discussion 1013.

Mills, S.A., Oh, M.C., Rutkowski, M.J., Sughrue, M.E., Barani, I.J., & Parsa, A.T. (2012). Supratentorial hemangioblastoma: clinical features, prognosis, and predictive value of location for von Hippel-Lindau disease. *Neuro Oncol*, **14**(8), 1097–104.

Padhi, S., Sarangi, R., Challa, S., Bussary, P., Panigrahi, M.K., & Purohit, A.K. (2011). A 10-year retrospective study of hemangioblastomas of the central nervous system with reference to von Hippel-Lindau (VHL) disease. *J Clin Neurosci*, **18**(7), 939–44.

Rachinger, J., Buslei, R., Prell, J., & Strauss, C. (2009). Solid haemangioblastomas of the CNS: a review of 17 consecutive cases. *Neurosurg Rev*, **32**(1), 37–47; discussion 47–8.

Richard, S., Campello, C., Taillandier, L., Parker, F., & Resche, F. (1998). Haemangioblastoma of the central nervous system in von Hippel-Lindau disease. French VHL Study Group. *J Intern Med*, **243**(6), 547–53.

Richard, S., David, P., Marsot-Dupuch, K., Giraud, S., Béroud, C., & Resche, F. (2000). Central nervous system hemangioblastomas, endolymphatic sac tumors, and von Hippel-Lindau disease. *Neurosurg Rev*, **23**(1), 1–22; discussion 23–4.

Shankar, G.M., Taylor-Weiner, A., Lelic, N., et al. (2014). Sporadic hemangioblastomas are characterized by cryptic VHL inactivation. *Acta Neuropathol Commun*, **2**, 167.

Shin, G.W., Jeong, H.W., Seo, J.H., Kim, S.T., Choo, H.J., & Lee, S.J. (2014). Preoperative embolization of cerebellar hemangioblastoma with onyx: report of three cases. *Neurointervention*, **9**(1), 45–9.

Simone, C.B. 2nd, Lonser, R.R., Ondos, J., Oldfield, E.H., Camphausen, K., & Simone, N.L. (2011). Infratentorial craniospinal irradiation for von Hippel-Lindau: a retrospective study supporting a new treatment for patients with CNS hemangioblastomas. *Neuro Oncol*, **13**(9), 1030–6.

Smalley, S.R., Schomberg, P.J., Earle, J.D., Laws, E.R. Jr., Scheithauer, B.W., O'Fallon, J.R. (1990). Radiotherapeutic considerations in the treatment of hemangioblastomas of the central nervous system. *Int J Radiat Oncol Biol Phys*, **18**(5), 1165–71.

Sun, Z., Yuan, D., Sun, Y., Yan, P., & Zuo, H. (2015). Surgical resection of cerebellar hemangioblastoma with enhanced wall thickness: a report of two cases. *Oncol Lett*, **9**(4), 1597–9.

Weil, R.J., Lonser, R.R., DeVroom, H.L., Wanebo, J.E., & Oldfield, E.H. (2003). Surgical management of brainstem hemangioblastomas in patients with von Hippel-Lindau disease. *J Neurosurg*, **98**(1), 95–105.

Wind, J.J. & Lonser, R.R. (2011). Management of von Hippel-Lindau disease-associated CNS lesions. *Expert Rev Neurother*, **11**(10), 1433–41.

Woodward, E.R., Wall, K., Forsyth, J., Macdonald, F., & Maher, E.R. (2007). VHL mutation analysis in patients with isolated central nervous system haemangioblastoma. *Brain*, **130**(Pt 3), 836–42.

31

Surgical approaches to posterior fossa tumours

Jacques J. Morcos, Osaama H. Khan, and Ashish H. Shah

Introduction

Lesions of the fourth ventricle and foramen magnum can be difficult to manage surgically due to their proximity to critical brainstem structures. Understanding the anatomy of the fourth ventricle, lower cranial nerves, and basilar cisterns remains paramount for deciding surgical approaches to this location. Detailed preoperative workup and planning are necessary to minimize surgical morbidity and maximize tumour resection.

This chapter provides an overview of the relevant anatomy and surgical techniques for lesions in the posterior fossa, specifically the fourth ventricle the foramen magnum. We will split this chapter into two main sections: microsurgical approaches to the fourth ventricle and skull base approaches to the foramen magnum.

Preoperative planning for posterior fossa lesions

When presented with a lesion in the posterior fossa, a detailed understanding of the pathology and involved structures is fundamental. Preoperative imaging (CT/MRI) should be evaluated for proximity to cranial nerves, surgical accessibility, vascular involvement, and the presence of hydrocephalus. Any hydrocephalus may need to be addressed prior to surgery with a ventriculostomy or a ventriculoperitoneal shunt (Tamburrini et al., 2008). A ventriculostomy is placed if the obstructive hydrocephalus is expected to be reversible after tumour resection or if CSF diversion is deemed helpful in relaxing the cerebellum during the surgical approach. A ventriculoperitoneal shunt is selected if the hydrocephalus is unlikely to be reversible. If there is a suspicion of a hemangioblastoma or other vascular lesion, preoperative angiography may also be helpful. For some vascular lesions, to facilitate surgery preoperative embolization may be used, it is uncommon for hemangioblastomas to be amenable to embolization because their arterial feeders may be too fine for selective catheterization (Standard et al., 1994; Sakamoto et al., 2012).

Deciding on a surgical approach depends mainly on the size and location of the lesion. For lesions near the fourth ventricle, two main surgical approaches are used, the suboccipital transvermian and the suboccipital telovelar approach. The transvermian approach is less desirable because of the potential downside of disrupting intercerebellar tracts, and clearly requires a corticotomy in order to access the fourth ventricle. The approach may be preferred to reach the superior pole of the fourth ventricle, when the lesion has not created its own space and surgical corridor (Tanriover et al., 2004). In contrast, the telovelar approach may be more suited to lesions near the foramen of Luschka and Magendie, or in larger more cranially placed lesions that have created their own surgical path.

Anatomy of the fourth ventricle

Lesions within the fourth ventricle are especially challenging for neurosurgeons because there are few structures around the pathology that could be considered non-eloquent (Lassiter et al., 1971; Alvisi et al., 1985; Liu et al., 1998). A thorough understanding of the anatomy of the fourth ventricle is essential to approaching these tumours. Here we highlight some key aspects of the surgical anatomy of this region.

The most common surgical view of lesions in the fourth ventricle is from a midline posterior suboccipital approach. At the superior end of the exposure, the posterior cerebellar incisura forms a cleft between the cerebellar hemispheres, ultimately leading to the vermis. The portion of the vermian surface, dorsal to the roof of the fourth ventricle, is divided into two main portions, the pyramid, and the uvula (which lies in between the cerebellar tonsils). Just deep to the uvula, the fourth ventricle runs from the cerebral aqueduct to the foramen of Magendie. Rhoton divides the roof of the fourth ventricle into two main components, superior and inferior. The inferior portion of the roof of the fourth ventricle is composed of two separate layers (tela choroidea and inferior medullary velum). This inferior portion can be accessed through the superior portion of the cerebellomedullary fissure, a complex cleft that extends between the ventral surface of the cerebellum and the dorsal medulla. The inferior medullary velum forms a thin membrane that extends laterally from the nodule to the flocculus, the inferior medullary velum, and the nodule form the cranial aspect of the inferior half of the fourth ventricular roof, while the tela choroidea forms the

caudal end. The inferior medullary velum is contiguous with the superior medullary velum rostrally and the tela choroidea caudally.

The tela choroidea is an arachnoid membrane that transmits the vessels of the choroid plexus into the fourth ventricle. Both foraminae of Luschka and Magendie fenestrate the tela choroidea in the subarachnoid space. This anatomy becomes especially relevant when discussing the telovelar approach.

Operative technique

Suboccipital craniotomy

The midline suboccipital craniotomy is the mainstay surgical approach to lesions of the fourth ventricle and posterior fossa. We prefer the prone position and only use the sitting position in exceptional circumstances. A Mayfield cranial frame holder is used with the head flexed and translated posteriorly to allow for visualization of the pathology. Careful attention must be paid to ensure that the head is not flexed excessively to block jugular venous outflow. In the prone position, patients should be padded carefully to avoid pressure related injuries during these procedures, and the plane of the table is usually tilted head up approximately 10 degrees to promote venous drainage

Once the midline incision is made, we generally carry it from 2 cm above the inion to the level of the C2 spinous process. We are careful not to disrupt the pericranium above the inion as it may often be used as a dural patch during closure. Dissection in the deep subcutaneous plane is carried out laterally just below the level of the superior nuchal line. This is done with the specific aim of creating space to allow a transverse cut in the superior nuchal line and ensure a watertight muscular closure. The cuff does not need to be wider than 5–10 mm. It is not necessary and counterproductive to extend this separation between the deep subcutaneous tissue and the muscular epimysium all the way inferiorly as this dissection does not improve the eventual exposure and, worse, it creates dead space for a potential pseudomeningocele. Next, we look for the midline fatty avascular midline muscular raphe and incise it down to C1, creating a T-shaped mobilization of the musculature. We then place fishhooks symmetrically, retracting the muscles laterally and, very importantly, downwards. This compresses the muscles and skin edge down, therefore minimizing the depth of the exposure, an advantage that will be appreciated during the microsurgical portion of the case, when the angles of surgical freedom are maximized. Meticulous subperiosteal dissection is carried out along the posterior arch of C1. Monopolar cautery is never used here for the fear of injuring the V3 segment of the vertebral artery in the sulcus arteriosus. This off-midline region is best exposed through a repeating sequence of spreading and cutting the fascia with scissors, or cautiously using gauze at the tip of a periosteal elevator to improve frictional mobilization of the periosteum without shearing the vertebral arteries. Similarly, one needs to make sure prior to working along C1 that there are no congenital anomalies such as a bifid arch, for the fear of traumatizing the cord. The lip of the foramen magnum is then exposed with an angled curette. The craniotomy size and exact location varies with the pathology, but a typical bone flap is midline 3 × 3 cm in size, with additional drilling of the lip of the foramen magnum to each side towards the occipital condyle without reaching them. The bone flap can be created with one or rarely two small holes, or when the dura can be easily dissected, with no initial holes at all, but rather using the lip of the well dissected foramen magnum as a starting position for the foot plate of the drill. After the craniotomy is done, and depending if the lesion extends to below the foramen magnum, the arch of C1 is resected, again with special attention to the vertebral arteries and surrounding venous plexus. Venous bleeding is easily stopped with powdered gelfoam mixed with thrombin. In younger patients with less adherent dura, we generally place tack-up sutures to minimize the risk of a postoperative epidural hematoma. The dura is then open in a Y-shape, with the vertical limb slightly to one side of midline, in order to avoid troublesome bleeding from a sometimes sizeable occipital sinus. The latter can be controlled pre-emptively with vascular clips. CSF is obtained from the cisterna magna and then the microscope is brought into the field.

Telovelar approach

Once haemostasis is obtained and the dura tented, the tonsils may be gently mobilized laterally from the uvula to expose the inferior half of the fourth ventricular roof, the tela choroidea, and inferior medullary velum. This mobilization is not achieved by self-retaining retractors which we feel are generally counterproductive. Rather, the tonsils are freed up through extensive sharp arachnoidal lysis, including preservation and separation of the tonsillar loops of the posterior inferior cerebellar arteries (PICA). Careful dissection from the tela at the level of the foramen of Magendie to the velum allows visualization of nearly the entire fourth ventricle. Additional dissection through the inferior medullary velum superiorly can expose tumours within the superior part of the fourth ventricle and fastigium (Tanriover et al., 2004). The superior and middle cerebellar peduncles are at a high risk of injury when opening the velum superiorly as they form the lateral walls of the fourth ventricle at that level. As the dissection is carried out cranially, small arterial branches (choroidal) from PICA are divided to allow untethering of the cerebellum. The telovelar approach is generally performed on the same side as the larger part of the tumour. Once maximal dissection is carried out, and if necessary, then a self-retaining retractor can be placed to 'hold' (rather than 'create') the exposure attained, with the tonsil held up and laterally. This is also the point during the surgery when appropriate head flexion achieved during positioning is appreciated. **Figure 31.1** demonstrates the telovelar approach.

Transvermian approach

The transvermian approach to the fourth ventricle has been the more traditional approach to this region, involving transecting the inferior vermis. The vermian incision is intended to expose the nodule and underlying telovelar surface. A midline incision can be carried out through both the nodule and tela choroidea medially with careful attention to avoid injuring the telovelotonsillar segments of the PICA bilaterally. Adequate exposure in the transvermian approach allows visualization of the entire surface of the fourth ventricular floor, which is approximately 4 cm from the obex to the Sylvian aqueduct (Tanriover et al., 2004). However, the transvermian approach is limited in its exposure of the lateral recesses and foraminae of Luschka. Additionally, it involves undesirable neural incision.

When comparing the transvermian and telovelar approaches, there is some limitation with the telovelar approach in the operative angle to the rostral end of the exposure but the benefit of preserving critical cerebellar structures outweighs this slight operative nuisance. It has been proposed that the telovelar approach may produce

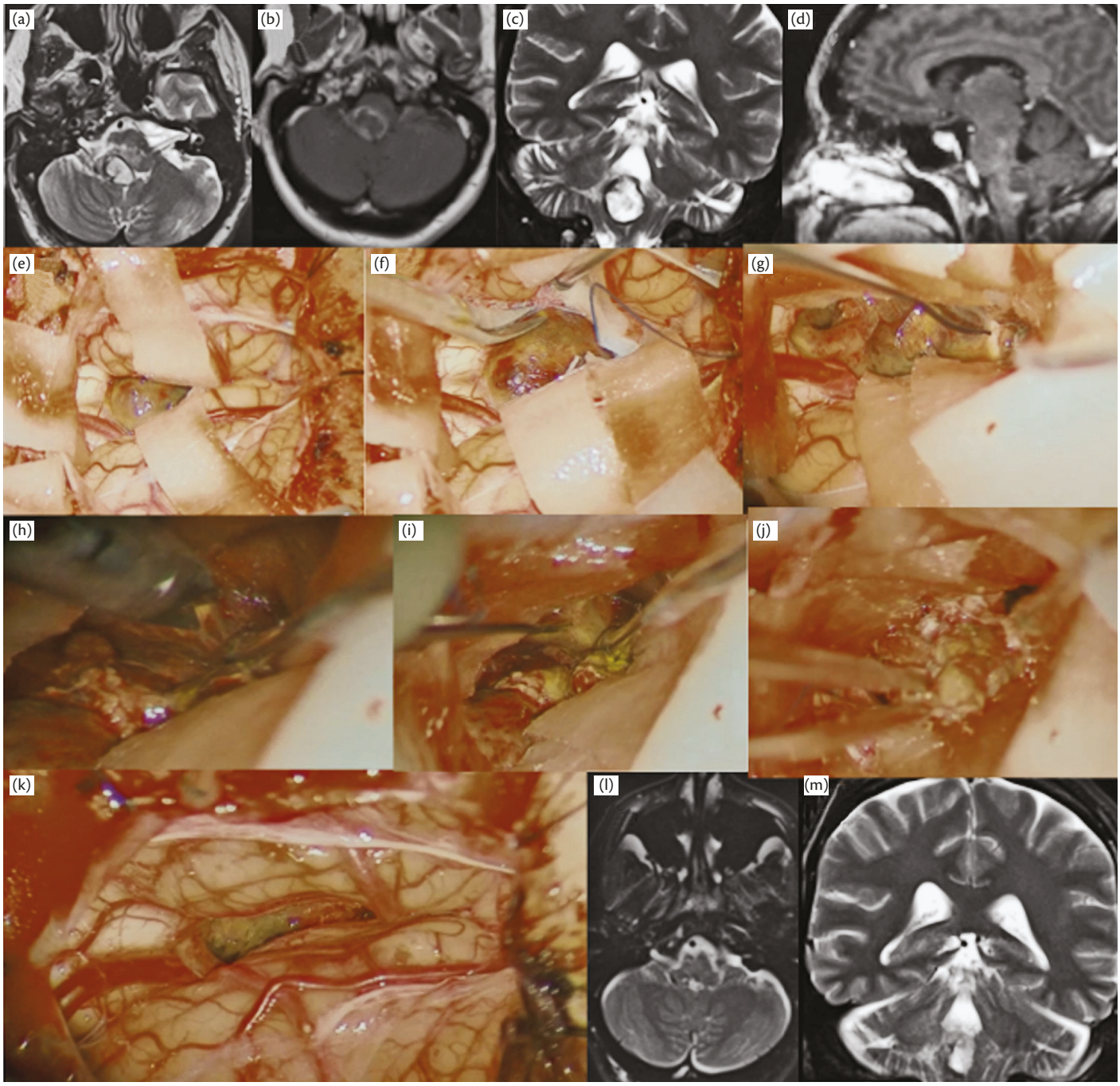

Fig. 31.1 Telovelar approach to a brainstem cavernous malformation. A 35-year-old female presented with a new onset dysphagia, diplopia, and right-sided dysmetria. An MRI (A—axial T2, B—axial T1 with contrast, C—coronal T2, D—sagittal with contrast) reveals a fourth ventricular cavernous malformation. A suboccipital craniotomy with wide dural opening (E) was performed through a right telovelar approach (E). The cavernous malformation can be appreciated protruding between the tonsils. The facial nerve stimulator is used not only to map out the facial colliculus (G) but also as a dissection tool (I). Sharp dissection (H) is used to remove the lesion (J) in its entirety (K). Postoperative axial (L) and coronal (M) MRI confirms complete removal of the malformation.

a lower incidence of cerebellar mutism and ataxia due to the preservation of the vermis and nodule (Tanriover et al., 2004; Deshmukh et al., 2006).

Tumours of the fourth ventricle

The telovelar approach to the fourth ventricle was first described by Matsushima in 1992 to avoid transecting midline cerebellar structures (Matsushima et al., 1992). Since then, the operative approach has become widely adopted to gain access to the lateral recesses and floor of the fourth ventricle. Nevertheless, its efficacy for large fourth ventricular lesions has been brought into question by some authors. Recently, Tomasello et al. reviewed the extent of resection of large fourth ventricular lesions and his group was able to achieve approximately 90% resection for most tumours (Tomasello

et al., 2015). Lesions near the foramen of Luschka and superolateral recesses such as ependymomas and choroid plexus papillomas were especially accessible using the telovelar approach (Lee et al., 2012; Tomasello et al., 2015). In large rostral tumours and those with brainstem involvement the efficacy of the telovelar approach was limited as the working angle was less favourable compared to the transvermian approach. Nevertheless, aggressive surgical resection should be mitigated in circumstances where there is clear brainstem infiltration or high-grade pathology (El-Bahy, 2005). Our philosophy is to use the telovelar approach as a default, and only add a small caudal vermian split if the exposure proves insufficient.

Anatomy of the foramen magnum

The foramen magnum (from the Latin, meaning 'great hole') is located at the base of the skull in the occipital bone. The dura, medulla oblongata, spinal branches of the accessory nerve, vertebral arteries, posterior spinal arteries, and the apical ligament of the dens and tectorial membrane pass through it.

The hypoglossal canal lies inferior and medial to the jugular foramen. Its floor is comprised of the occipital condyles, the anterior-medial wall by the basi-occiput (clivus), the posterior-lateral wall by the squamous portion of the occipital bone, and the roof by the jugular tubercle. This canal transmits the twelfth cranial nerve, a meningeal branch of the ascending pharyngeal artery, and the hypoglossal venous plexus. Foraminae also exist for the mastoid and condylar emissary veins.

The vertebral artery arises from the subclavian artery and has four segments; V1 from its origin to the foramen transversarium of the sixth cervical vertebra, V2 from the C6 to the C2 foramen, V3 from the C2 foramen transversarium to the dural ring, and V4 from the dural ring to the vertebrobasilar junction. The cervical segment runs up and backward between the longus colli and scalenus anterior muscles to reach the transverse foramen of the sixth cervical vertebra. The foraminal segment of the artery ascends through the transverse foramina of the upper six cervical vertebrae, turning upwards and laterally to enter the transverse foramen of the atlas. The Atlantic segment of the vertebral artery curves backward and medially behind the lateral mass of the atlas and onto the upper surface of the posterior arch of the atlas (sulcus arteriosus). This portion is accessible through the suboccipital triangle and is surrounded by a plexus of veins. Branches from this part are to the suboccipital muscles. It then enters the dura below the posterior atlantooccipital membrane. The branches of V4 are the posterior meningeal, anterior spinal, and the posterior inferior cerebellar artery. From a surgical perspective, it is very important to realize that the PICA may arise extradurally (from V3 instead of V4) and therefore be at risk of coagulation injury during the approach.

The V4 segment ascends ventral to the roots of cranial nerves IX, X, XI, and XII. It usually gives off the PICA before joining the contralateral V4 to form the basilar artery at the lower border of the pons. PICA is divided into five main segments from proximal to distal: anterior medullary, lateral medullary, tonsillomedullary, telovelotonsillar, and cortical (Lister et al., 1982). The basilar artery gives rise to the anterior inferior cerebellar arteries (AICA), which pass to the inferior surface of the cerebellum and come into close relationship with cranial nerves VII and VIII in the cerebellopontine angle. The basilar artery then gives rise to the superior cerebellar arteries (SCA) and the posterior cerebral arteries (PCA), which form the posterior axis of the circle of Willis. Other branches are the pontine and, occasionally, labyrinthine arteries.

The orientation of the muscle anatomy of the suboccipital region is important to appreciate when deciding on surgical approaches. This region is protected by strong suboccipital musculature. The sternocleidomastoid and the digastric muscles arise from and deep to the mastoid tip, respectively. The occipital artery runs posteriorly deep to the mastoid tip. The splenius capitis and longissimus capitis lie deep to sternocleidomastoid. Posteriorly, in the midline lies the trapezius and deep to this arises the semispinalis capitis. After these muscles are reflected off the superior nuchal line, the suboccipital triangle is exposed. This triangle is bordered by the obliquus capitis superior and inferior and the rectus capitis posterior major. Within the triangle lie the dorsal ramus of the first cervical nerve and the vertebral artery with its venous plexus. The triangle is crossed by the great occipital nerve.

Dissection in this triangle allows mobilization of the vertebral artery and exposure of the occipital condyle, which can be drilled away to gain access to the foramen magnum and anterior brainstem, if necessary.

Tumours of the foramen magnum

Historically, access to lesions of the anterior cervicomedullary junction was difficult. In the early part of the twentieth century, neurosurgeons failed numerous times to safely excise lesions in this location through mostly posterior-based approaches (Elsberg and Strauss, 1929; Flores et al., 2013). However, in the 1980s, a new surgical technique (far lateral craniotomy) described by Heros and George independently helped facilitate surgical resection of these lesions (Heros, 1986; George et al., 1988). Over the last three decades, the far lateral craniotomy has been a mainstay approach for surgical access to this region.

The far lateral approach is mainly used for foramen magnum meningiomas, and its efficacy for gross total resection has been widely reported. Recent series conclude that a far lateral craniotomy may be able to achieve gross total resection in nearly 60–90% of cases. Komotar et al. recently concluded that the extent of the resection was limited by large tumour size, neural or vascular invasion, firm tumour consistency, and prior radiation (Komotar et al., 2010). Aggressive surgical approaches to the foramen magnum may also increase the risk of operative morbidity. In cases where there is a small residual tumour, gamma knife radiosurgery to the postoperative tumour bed may be a safe adjuvant therapy to prevent tumour progression.

Operative technique

Far lateral approach

The far lateral approach is an ideal approach to extra-axial lesions spanning the level of the lower third of the clivus, foramen magnum, or C1, and when the tumour is located anteriorly or anterolaterally to the neural axis. The approach may also be used in intra-axial lesions located anterolaterally in the medulla and lower pons. **Figure 31.2** demonstrates the far lateral approach.

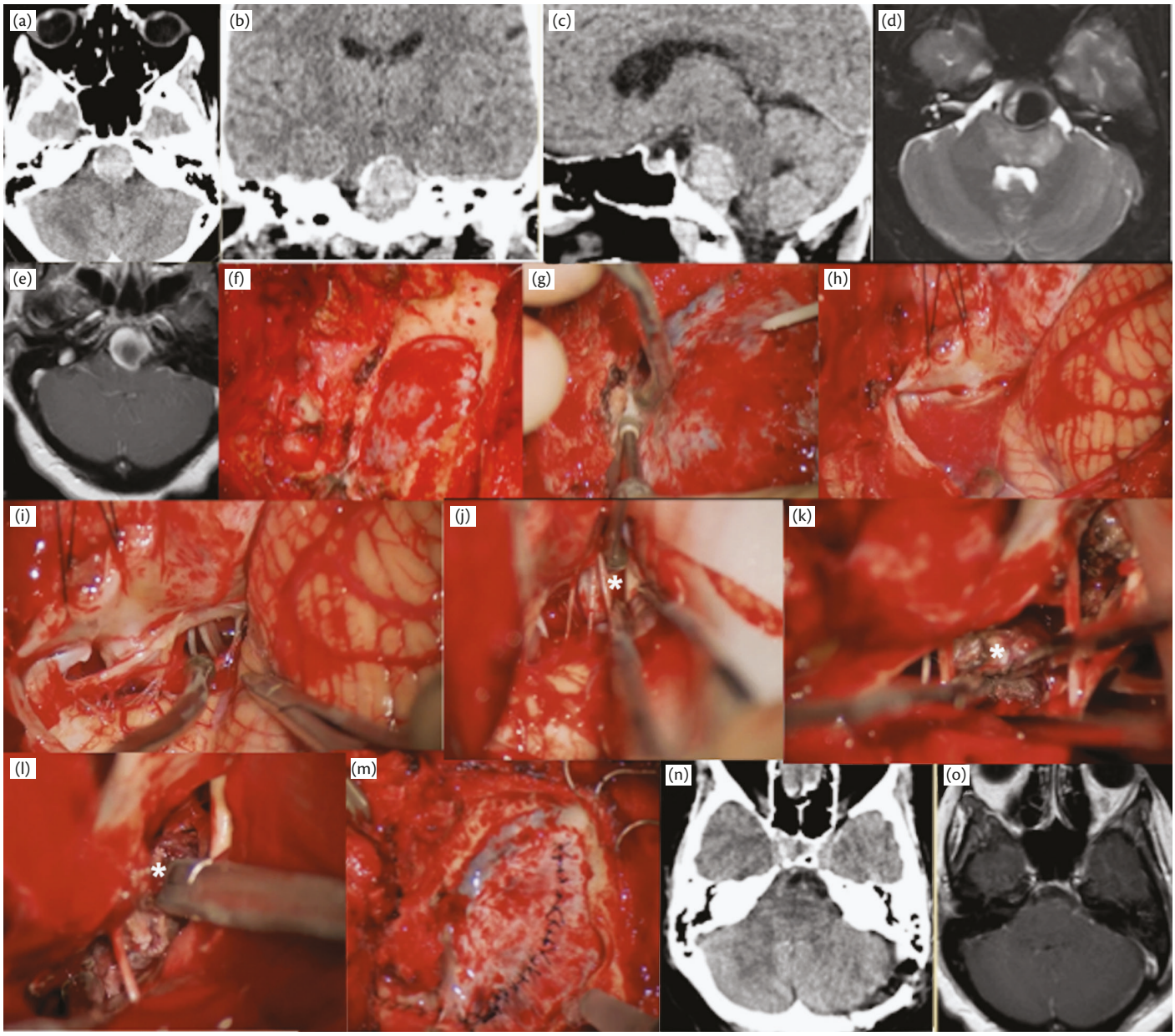

Fig. 31.2 Far lateral approach to jugular tubercle meningioma. Case illustration of a 54-year-old female presenting with a sixth nerve palsy. The CT scan (axial (A), coronal (B), sagittal (C)) shows a partially calcified lesion, the MRI (axial T2 (D) and T1 with contrast (E)) demonstrates a fluid level and enhancement. A retrosigmoid craniotomy (F) was performed with the left side up in a three-quarter prone position with drilling extended into a 'far lateral' craniotomy (G). The dura (H) is held out under traction to optimize visualization and wide arachnoid dissection (I) is performed. The tumour (*) is visualized (J) deep to the lower cranial nerves and debulking of the tumour (K) can be appreciated as well as tumour removal (L) in a piecemeal fashion. A watertight dural closure (M) is performed and a postoperative axial CT (N) and axial MRI with contrast (O) shows complete tumour resection.

Lesions that are posterior or posterolateral do not require this approach as they are more easily resected through a simple suboccipital or retrosigmoid approach. For the far lateral approach, the idea is to come in at an angle that avoids the cerebellum and points medially and often superiorly (Elhammady et al., 2012). This is why we position the patient in the three-quarters prone position with the ipsilateral side up. The head is placed with four movements: neck flexion, rotation towards the floor, tilting towards the floor, and finally upwards or posterior translation. The combination of these four moves achieves an opening of the angle between the shoulder and the head and a partial opening of the occiput to C1 joint, which makes visualizing the condyle easier. This manoeuvre places the ipsilateral cerebellar hemisphere in a position where gravity will help it fall away from the lesion. The incision is hockey stick in shape, starting in the midline from C2 to above the inion, and then curving laterally to the tip of the mastoid. The same soft tissue principles apply here as for the midline suboccipital craniotomy, although the approach here is unilateral. A cuff is preserved at the superior nuchal line for closure. The myocutaneous mass is retracted with fish hooks lateroinferiorly. Generally, the bone flap has a tear drop-like shape because it is narrower at the foramen magnum than at the upper edge. Again, a 3 cm height is usually enough but individual

tailoring can be done. The flap can be taken close to the sigmoid sinus if a retrosigmoid vantage point is also necessary. After the bone flap is lifted, the remaining lip of foramen magnum leading to the juxta-condylar bone is drilled with a matchstick or round drill bit. Since the occipital condyles are located anterior to the transverse equator of the foramen magnum, the drilling of the juxta-condylar bone does not need to extend into the condyle. The 'far lateral' designation of this approach implies that the condyle is not drilled. In exceptional circumstances, such as in lesions infiltrating the condyle, a true 'transcondylar' approach may be necessary. After this thorough drilling, the ipsilateral hemi-arch of C1 needs to be removed, with similar techniques and precautions as were described in the suboccipital approach. The dura is then ready to be opened in a U-shaped flap based laterally and held with traction sutures. A sign of adequate drilling is when there is no bony protrusion seen tenting the dural flap at its base. That base should be as flat as possible, otherwise the microsurgical view will be suboptimal laterally.

One of the main goals once the dura is opened and the brain relaxed with CSF egress, is to correctly identify microanatomical structures including the vertebral artery (VA) as it pierces the dura, the attachments of the first two dentate ligaments and the lower cranial nerves. The spinal contribution of cranial nerve XI is posterior to the dentate ligament. The V3 segment of the vertebral artery pierces the dura at the most superior dentate ligament. The rostral dentate ligaments are divided to allow for better visualization of anteriorly based tumours, such as a foramen magnum meningioma. The arachnoid of the lateral cerebellomedullary fissure is then thoroughly excised to allow untethering of the cerebellar hemisphere. Once the anatomy and tumour are clearly delineated, an effort to devascularize and detach the tumour must be made. It is important to note that foramen magnum meningiomas should be approached based on their relationship to the V3 segment (Flores et al., 2013). If the meningioma arises distal (above) the vertebral artery, then dissection should start rostrally, and likewise if the lesion arises below the VA, the tumour plane should be defined inferiorly. Most of these operations are done with the benefit of intraoperative monitoring of lower cranial nerves, somatosensory evoked potentials, and motor evoked potentials. If there is no developed arachnoid plane between the tumour and vascular structures, it may be best to leave a small carpet of residual tumour. The dura must be closed in a watertight fashion to reduce the risk of a postoperative CSF leak and pseudomeningocele, through the use of an autologous pericranial patch if needed (Flores et al., 2013).

The most common morbidities after the far lateral approach are a cranial nerve palsy, pseudomeningocele, or hydrocephalus. The incidence of lower cranial nerve palsies after a far lateral approach ranges from 30% to 40% depending on the surgical series; however, most (80%) improve within the first few months after surgery (Komotar et al., 2010; Talacchi et al., 2012). Craniocervical instability may also occur in cases where there is significant (>50%) drilling of the occipital condyle. The need for postoperative fusion may be correlated to the degree of bony involvement, location, and size of the lesion. Lastly, development of a pseudomeningocele or CSF leak from the wound may also be potential complications after resection of foramen magnum lesions. Meticulous wound closure and a watertight dural closure can help avoid these complications.

FURTHER READING

Elhammady, M.S., Peterson, E.C., Heros, R.C., & Morcos, J.J. (2012). Far lateral approach and transcondylar and supracondylar extensions for aneurysms of the vertebrobasilar junction. In: Co., W.S. (ed.) *Schmidek & Sweet Operative Neurosurgical Techniques*, 6th edition, pp. 951–7. Philadelphia, PA: Elsevier.

George, B., Dematons, C., & Cophignon, J. (1988). Lateral approach to the anterior portion of the foramen magnum. Application to surgical removal of 14 benign tumors: technical note. *Surg Neurol*, **29**, 484–90.

Heros, R.C. (1986). Lateral suboccipital approach for vertebral and vertebrobasilar artery lesions. *J Neurosurg*, **64**, 559–62.

Matsushima, T., Fukui, M., Inoue, T., Natori, Y., Baba, T., & Fujii, K. (1992). Microsurgical and magnetic resonance imaging anatomy of the cerebello-medullary fissure and its application during fourth ventricle surgery. *Neurosurgery*, **30**, 325–30.

Tanriover, N., Ulm, A.J., Rhoton, A.L., Jr., & Yasuda, A. (2004). Comparison of the transvermian and telovelar approaches to the fourth ventricle. *J Neurosurg*, **101**, 484–98.

REFERENCES

Alvisi, C., Cerisoli, M., & Maccheroni, M.E. (1985). Long-term results of surgically treated brainstem gliomas. *Acta Neurochir (Wien)*, **76**, 12–17.

Deshmukh, V.R., Figueiredo, E.G., Deshmukh, P., Crawford, N.R., Preul, M.C., & Spetzler, R.F. (2006). Quantification and comparison of telovelar and transvermian approaches to the fourth ventricle. *Neurosurgery*, **58**, ONS-202-6; discussion ONS-206–7.

El-Bahy, K. (2005). Telovelar approach to the fourth ventricle: operative findings and results in 16 cases. *Acta Neurochir (Wien)*, **147**, 137–42; discussion 142.

Elhammady, M.S., Peterson, E.C., Heros, R.C., & Morcos, J.J. (2012). Far lateral approach and transcondylar and supracondylar extensions for aneurysms of the vertebrobasilar junction. In: Co., W.S. (ed.) *Schmidek & Sweet Operative Neurosurgical Techniques*, 6th edition, pp. 951–7. Philidelphia, PA: Elsevier.

Elsberg, C.A. & Strauss, I. (1929). Report of a case in which a growth was removed from the ventral and lateral aspects of the medulla oblongata and upper cervical cord. *Arch Neurol Psychiatry*, **21**, 261–73.

Flores, B.C., Boudreaux, B.P., Klinger, D.R., Mickey, B.E., & Barnett, S.L. (2013). The far-lateral approach for foramen magnum meningiomas. *Neurosurg Focus*, **35**, E12.

George, B., Dematons, C., & Cophignon, J. (1988). Lateral approach to the anterior portion of the foramen magnum. Application to surgical removal of 14 benign tumours: technical note. *Surg Neurol*, **29**, 484–90.

Heros, R.C. (1986). Lateral suboccipital approach for vertebral and vertebrobasilar artery lesions. *J Neurosurg*, **64**, 559–62.

Komotar, R.J., Zacharia, B.E., McGovern, R.A., Sisti, M.B., Bruce, J.N., & D'Ambrosio, A.L. (2010). Approaches to anterior and anterolateral foramen magnum lesions: a critical review. *J Craniovertebr Junction Spine*, **1**, 86–99.

Lassiter, K.R., Alexander, E., Jr., Davis, C.H., Jr., & Kelly, D.L., Jr. (1971). Surgical treatment of brain stem gliomas. *J Neurosurg*, **34**, 719–25.

Lee, C.C., Lin, C.F., Yang, T.F., et al. (2012). Telovelar approach for choroid plexus papilloma in the foramen of Luschka: a safe way using a neuromonitor. *Clin Neurol Neurosurg*, **114**, 249–53.

Lister, J.R., Rhoton, A.L., Jr., Matsushima, T., & Peace, D.A. (1982). Microsurgical anatomy of the posterior inferior cerebellar artery. *Neurosurgery*, **10**, 170–99.

Liu, G.T., Phillips, P.C., Molloy, P.T., et al. (1998). Visual impairment associated with mutism after posterior fossa surgery in children. *Neurosurgery*, **42**, 253–6; discussion 256–7.

Matsushima, T., Fukui, M., Inoue, T., Natori, Y., Baba, T., & Fujii, K. (1992). Microsurgical and magnetic resonance imaging anatomy of the cerebello-medullary fissure and its application during fourth ventricle surgery. *Neurosurgery*, **30**, 325–30.

Sakamoto, N., Ishikawa, E., Nakai, Y., et al. (2012). Preoperative endovascular embolization for hemangioblastoma in the posterior fossa. *Neurol Med Chir (Tokyo)*, **52**, 878–84.

Standard, S.C., Ahuja, A., Livingston, K., Guterman, L.R., & Hopkins, L.N. (1994). Endovascular embolization and surgical excision for the treatment of cerebellar and brain stem hemangioblastomas. *Surg Neurol*, **41**, 405–10.

Talacchi, A., Biroli, A., Soda, C., Masotto, B., & Bricolo, A. (2012). Surgical management of ventral and ventrolateral foramen magnum meningiomas: report on a 64-case series and review of the literature. *Neurosurg Rev*, **35**, 359–67; discussion 367–8.

Tamburrini, G., Massimi, L., Caldarelli, M., & Di Rocco, C. (2008). Antibiotic impregnated external ventricular drainage and third ventriculostomy in the management of hydrocephalus associated with posterior cranial fossa tumours. *Acta Neurochir (Wien)*, **150**, 1049–55; discussion 1055–6.

Tanriover, N., Ulm, A.J., Rhoton, A.L., Jr., & Yasuda, A. (2004). Comparison of the transvermian and telovelar approaches to the fourth ventricle. *J Neurosurg*, **101**, 484–98.

Tomasello, F., Conti, A., Cardali, S., La Torre, D., & Angileri, F.F. (2015). Telovelar approach to fourth ventricle tumours: highlights and limitations. *World Neurosurg*, **83**, 1141–7.

RELATED LINKS TO EBRAIN

Performing a Far Lateral Craniotomy. https://learning.ebrain.net/course/view.php?id=76

Performing a Midline Posterior Fossa Craniotomy. https://learning.ebrain.net/course/view.php?id=78

Performing a Retrosigmoid Craniotomy. https://learning.ebrain.net/course/view.php?id=77

SECTION 7

Tumours and skull base—intraventricular

32. **Intraventricular tumours** *385*
Paul Grundy and Vasileios Apostolopoulos

33. **Colloid cysts** *393*
Asim Sheikh and Paul Chumas

34. **Choroid plexus tumours** *403*
Jonathan Roth, Rina Dvir, and Shlomi Constantini

35. **Surgical management of intraventricular lesions** *411*
Eduardo C. Ribas, Guilherme C. Ribas, and Ramez W. Kirollos

32

Intraventricular tumours

Paul Grundy and Vasileios Apostolopoulos

Introduction and general principles of management

Some 1.2% of the primary brain tumours have an intraventricular location, according to the Central Brain Tumour Registry of the US (CBTRUS 2006–2010 statistical report, N = 326 711; Ostrom et al., 2013). They represent a diverse group of tumours of variable histological origin; however, most are low-grade tumours. The radiological differential diagnosis can be challenging but is usually narrowed by considering the imaging features of the tumour, the patient's age, the location of the tumour within the ventricle, the clinical presentation, and associated medical conditions (e.g. tuberous sclerosis). Symptoms suggestive of raised intracranial pressure secondary to hydrocephalus are a common presentation, but increasingly frequently they are being diagnosed as an incidental finding. Characteristic patterns of growth have been observed and are recognized as typical for various types of intraventricular tumours. Depending on their pattern of growth and size intraventricular tumours can be confined in one ventricle or can extend into the adjacent ventricle (e.g. central neurocytoma) or into an adjacent cistern through outflow foramina (e.g. fourth ventricular ependymoma). Large tumours can extend through the ependymal wall out into the parenchyma (e.g. large meningiomas, or choroid plexus tumours). Indeed, for extremely large tumours it can sometimes be difficult to differentiate whether they are parenchymal tumours extending into the ventricle or vice versa (**Fig. 32.1**). The management of intraventricular tumours needs to be tailored to the individual case but as a rule the management of hydrocephalus is the first consideration. For third ventricular tumours, neuro-endoscopy can obtain both cerebrospinal fluid (CSF) diversion (endoscopic third ventriculostomy +/– septostomy) and a biopsy. CSF diversion should be carried out first as the biopsy can cause bleeding from the tumour with reduced visibility. CSF and plasma tumour markers should be sent if germ cell tumours are suspected. Imaging of the whole craniospinal axis is indicated for tumours with known potential of CSF dissemination (**Table 32.1**). All cases should be discussed at a neuro-oncology MDT meeting before definite surgical treatment is planned unless delay would harm a patient. Conservative management with serial imaging follow-up maybe the best option if the patient is asymptomatic, the tumour is not growing, or the patient is not fit for surgery. For older and unfit patients and when tumour is considered low grade with an indolent clinical course, CSF diversion alone maybe the best alternative (e.g. subependymoma of the fourth ventricle in older people).

Classification (anatomic, pathological, topographic)

Different intraventricular tumours tend to occur in specific parts of the ventricular system largely because the cell populations they originate from exist preferentially in certain parts of the ventricular system (**Table 32.1**). This knowledge is helpful to narrow the differential radiological diagnosis. Intraventricular tumours may originate from the ependyma or subependyma lining the walls of the ventricular system, septum pellucidum, or choroid plexus. Colloid cysts are related to misplacement of endodermal elements at the embryonic telencephalon/diencephalon interface. Many apparently intraventricular tumours are intraparenchymal tumours exophytic into the ventricles, for example, large astrocytic tumours can grow into the ventricle from the frontal lobe, the corpus callosum, or thalamus, and brain stem gliomas can be exophytic into the fourth ventricle.

Medulloblastomas are usually vermian tumours (although in young adults they can also grow within the cerebellar hemispheres) but frequently present as large tumours filling much of the fourth ventricle. Not infrequently large sellar and suprasellar tumours grow upwards into the third ventricle. Similarly, pineal region tumours can grow from the pineal region into the posterior third ventricle. More details about tumours growing in specific parts of the ventricles will be provided next.

Anterior body and frontal horn

Tumours here most commonly derive from the ventricular walls (ependymoma, subependymoma) or the septum pellucidum (central neurocytoma). Primary septal tumours (astrocytoma, lymphomas, and germinoma) are extremely rare. Metastatic melanoma of the septum has been also reported (Cipri et al., 2009).

Large intraparenchymal, high grade astrocytic tumours can become exophytic into the ventricles and many obliterate the foramen of Monro, or cut-off the posterior lateral ventricle and cause obstructive

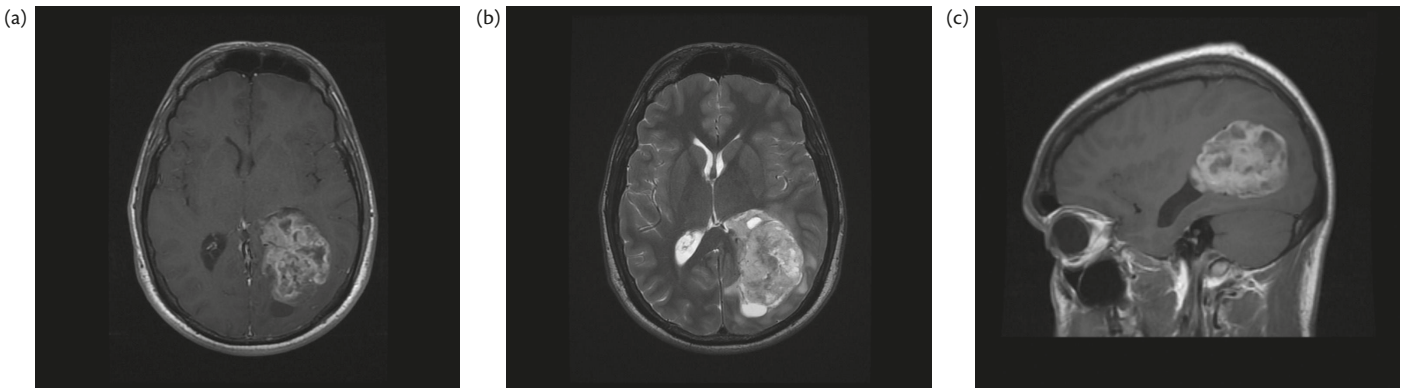

Fig. 32.1 Ganglioglioma with appearances suggestive of intraventricular location, thought preoperatively to be a meningioma. Exophytic intrinsic gliomas may grow into the adjacent ventricles. Axial (A) and sagittal (B) T1 MRI with gadolinium and axial T2 (C).

Table 32.1 Intraventricular tumours—quick review table

Location	Attachment	Cells of origin	Tumour	WHO	MRI features	Commonest location, associated conditions, pt population	CSF seeding, potential of recurrence
Lateral ventricles	Walls of the ventricle	Ependymal cells (glial cells with ependymal differentiation)	**Ependymomas**	II, III	Well defined, lobulated, Heterogeneous +– calcifications, haemorrhage, cysts, Iso@T1, hyper@T2, enhancement	Fourth ventricle if supratentorial can also be extraventricular, NF2,	Possible, can recur if not completely excised
		Subependymal glial cells	**Subependymomas**	I	Well defined, lobulated hypo@T1, hyper@ T2, most are non-enhancing although some enhancement possible	Usually in the fourth ventricle, older pts than with ependymomas	Never, cured if completely excised
		Mixed neuronal and giant cell astrocytes within subependymal nodules in TS	**Subependymal giant cell astrocytomas**	I	Well circumscribed, other subependymal nodules, Hypo-iso@T1, hyper@T2, avid enhancement	Lateral ventricle near the foramen of Monro, children with tuberous sclerosis	Never
	Septum pellucidum	Precursor neuronal cells	**Central neurocytomas**	II, III	Wide attachment on the septum pellucidum, well circumscribed, lobulated, can contain cysts, calcifications, rarely haemorrhages Iso@T1, Iso@T2, heterogeneous enhancement,	Lateral ventricle near the foramen of Monro, young adults	Unlikely, can be cured if completely excised, have higher recurrence rate higher recurrence if atypical
		Astrocytes	**Astrocytomas**	II, III, IV			Unlikely, Likely to recur
	Trigone	Arachnoid cap cells within choroid plexus	**Meningiomas**	I, II	Lobulated, homogeneously enhancing	slightly more common on the left	Unlikely
		Choroid plexus	**Choroid plexus tumours (CPP I, CPP II, CPP III)**	I, II, III	Lobulated avidly enhancing	Trigone, young adults	Rare for CPP I, II. Frequent for CPC III. Whole spine MRI recommended
		Lymphocytes	**Lymphomas**			Rare, usually multiple	Unlikely
Third ventricle	Foramen of Monro	Paraphysis elements from foramen of Monro	**Colloid cyst**	I	Hyper@T1, iso/hypo@T2, no enhancement	Anterior third ventricle, foramen of Monro	Never, cured if completely excised, can recur if incompletely removed
		Choroid plexus	**CPP, CPC**		Hyper@T1, iso/ hypo@T2, no enhancement	Rare	Rare for CPP I, II. Frequent for CPC III. Whole spine MRI recommended

Table 32.1 Continued

Location	Attachment	Cells of origin	Tumour	WHO	MRI features	Commonest location, associated conditions, pt population	CSF seeding, potential of recurrence
		Arachnoid cap cells – Vellum Interpositum	**Meningiomas**			Rare	Never
	Suprasellar	Squamous cells – Rathke's cleft	**Craniophangiomas**		Refer Chapter 26		Unlikely, tend to recur if incompletely removed
		Germ cells	**Germ cell tumours (germinomas and non-germinomas)**		Isointense or slightly hyperintense for T1 and T2 and homogenous enhancement	Pineal/suprasellar, children/young adults	Likely
	Posterior third ventricle	Intra-axial tumours from the thalamus can become exophytic into the posterior third ventricle, but most commonly tumours in this area originate from the pineal region (see relevant chapter). Obstructive hydrocephalus is a usual initial presentation that needs to be treated as a first priority.					
Fourth ventricle	Walls/floor of the ventricle	Ependymal cells	**Ependymomas**	II, III	Well defined, lobulated, Heterogeneous +- calcifications, haemorrhage, cysts, Iso@T1, hyper@T2, enhancement	Fourth ventricle if supratentorial can also be extraventricular, NF2,	Possible, can recur if not completely excised
		Subependymal cells	**Subependymomas**	I	Well defined, lobulated hypo@T1, hyper@ T2, most are non-enhancing although some enhancement possible	Usually in the fourth ventricle, older pts than with ependymomas	Never, cured if completely excised

hydrocephalus for the whole ventricle or cause enlargement of the trapped posterior part of the ventricle (encysted ventricle).

Central neurocytomas originate from precursors of neuronal cells that exist within the septum pellucidum. They are isointense to grey matter on T1 and T2 and show heterogeneous enhancement. Typically, they have a wide attachment on the septum pellucidum and can grow to a significant size within the lateral ventricle (Fig. 32.2). Occasionally they can also grow into the third ventricle through the foramen of Monro. They are well circumscribed, can be lobulated, contain cysts, and have heterogenous signal and flow voids, and they can also contain calcifications. They occasionally encase the columns of Fornix, in which case complete surgical excision maybe contraindicated to preserve memory. Details of this tumour will be discussed later in this chapter.

Subependymomas are well circumscribed non-enhancing benign tumours most frequently seen in the fourth ventricle but they can also be encountered within the lateral ventricle as non-enhancing, or minimally enhancing tumours attached on the lateral wall of the lateral ventricle. Surgical resection is indicated if they become symptomatic or progressive on imaging. Within the lateral ventricle complete excision and surgical cure can be usually achieved. The management of these tumours needs to be tailored to the patient age and general fitness. Conservative management for older and asymptomatic patients is a reasonable management option.

Subependymal giant cell astrocytomas (SEGA) are tumours of mixed glial and neuronal differentiation arising from subependymal nodules and are common in patients with tuberous sclerosis. They appear as iso or hypointense on T1 and hyperintense on T2 and demonstrate avid enhancement. They grow slowly usually in the area of the foramen of Monro, leaving the overlying ependyma intact. If they reach a significant size can cause obstructive hydrocephalus. The usual practice is close surveillance with serial imaging and clinical follow-up, if the patient is asymptomatic. Surgical excision is indicated if continuous growth is demonstrated on serial scans or the patient develops hydrocephalus. Stereotactic radiosurgery for smaller lesions has also been suggested by some authors.

Recurrence of SEGAs after surgery has been found to be low in patients treated with mTOR inhibitors. These medications down regulate the mTOR signalling pathway of the cell cycle found to be overactive in many cancers. In SEGAs these drugs not only reduce the recurrence rate of SEGAs but can also lead to shrinkage of other tumours associated with tuberous sclerosis, such as angiofibromas and angiomyolipomas. However, the benefits of this treatment should be balanced carefully with significant and potentially debilitating side effects including Immunosuppression and recurrent infections, significant anaemia, thrombocytopenia fatigue, nausea, and diarrhoea (Campen and Porter, 2011).

Ependymomas in adults are more frequent in the fourth ventricle (60%), but they can also be seen within the lateral ventricle. They can theoretically grow anywhere in CSF spaces within the craniospinal axis (third ventricle, aqueduct), and they are also one of the commonest intramedullary spinal cord tumours. They are well circumscribed tumours that enhance and frequently contain calcifications. They are usually isointense or hypointense to the white matter on T1 and hyperintense on T2.

Astrocytomas can be exophytic into the ventricles from the surrounding brain parenchyma. However rarely they can grow as primary septal tumours.

Posterior body–trigone

Meningiomas are the commonest intraventricular tumour in the trigone of the lateral ventricle, but only represent 4% of all intracranial

Fig. 32.2 Central neurocytoma of lateral ventricle, axial T2 (A) and coronal T1 (B) with gadolinium showing typical appearances involving septum and fornices and here protrusion into the third ventricle and dilatation of left lateral ventricle.

meningiomas. They are more common in adults with a slight predilection for female patients for reasons not completely understood, also with a slight predilection for the left side. They are thought to originate from arachnoid cap cells trapped within the choroid plexus during embryonal life. They may reach a large size and cause symptoms suggestive of high intracranial pressure but they can also be incidental. They appear as large homogeneously enhancing tumours usually with a significant feeding vessel that on MRI is seen to enter the tumour, usually a branch from one of the choroidal arteries (Fig. 32.3). Intraventricular meningiomas can also occur at a much lower frequency in the posterior third ventricle (arachnoid cap cells from vellum interpositum) or in the fourth ventricle (arachnoid cap cells within the choroid plexus). Treatment options (depending on the size and clinical picture) include surgery, SRS, or surveillance.

Choroid plexus tumours arise from the choroid plexus and located most commonly in the lateral ventricle in children and the fourth ventricle in adults. Most frequently they occur in children younger than 15 years, but can also occur in the first year of life. Histologically they can be choroid plexus papillomas (CPP—WHO I), atypical choroid plexus papillomas (CPP—WHO II) or choroid plexus carcinomas (CPC—WHO III). The radiological appearances for all these types of choroid plexus tumours are similar but the prognosis differs significantly. Most they appear as avidly enhancing tumours with lobulated margins and flow voids and they can frequently reach a large size. When they reach a large size, they can breach through the ependyma into the surrounding parenchyma. They tend to present with hydrocephalus both due to increased CSF production and due to obstruction. The best management regardless the WHO grade of the tumour is gross total resection. Preoperative embolization should be considered as it can reduce intraoperative bleeding which can be catastrophic. Postoperative radiotherapy is used for CPCs but the single most important prognostic factor is the presence or not of residual tumour. The prognosis for CPC is considered generally poor. CPPs can be cured it completely excised. The location, size, and enhancement characteristics of the choroid plexus tumours can occasionally make difficult to differentiate from meningiomas in this area. CSF seeding is rare for the CPP I, II, but individual cases have been reported. CSF seeding is frequent for CPCs. Whole spine MRI before any definite management decision is therefore mandatory.

Third ventricle

Anterior third ventricle

Foramen of Monro

Colloid cysts are the commonest third ventricular tumours. The true incidence of colloid cysts cannot be calculated with accuracy as a

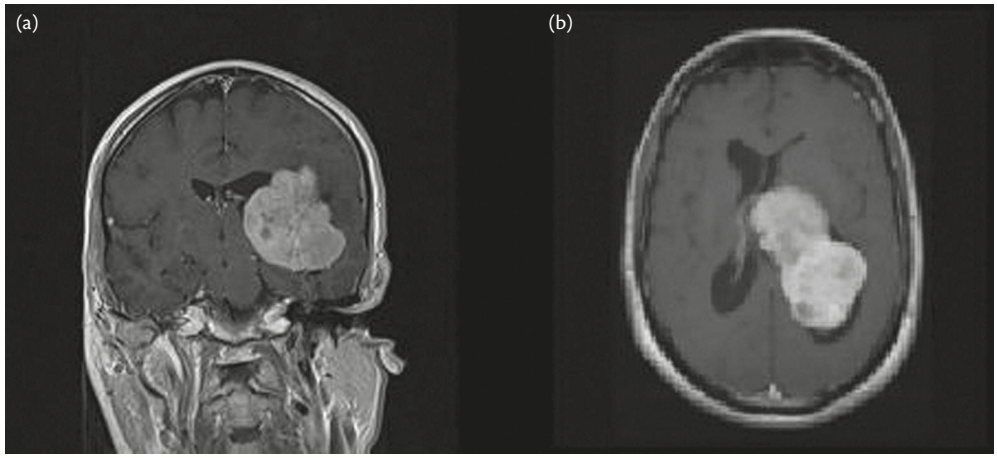

Fig. 32.3 Intraventricular meningioma within trigone of lateral ventricle. T1 weighted MRI in coronal (A) and axial (B) planes.

significant proportion of these tumours are asymptomatic therefore underreported (Pollock and Huston, 1999). They are benign lesions consisting of epithelial-lined cysts filled with gel—density material which contains mucin, cholesterol, and hyaloid substances. The relative proportion of the components of the contained material can vary from case to case causing a wide variety of different appearances on imaging and different consistency at surgery.

On CT they appear typically as hyperdense and less commonly iso or hypodense unilocular lesions filling the anterior third ventricle with or without associated hydrocephalus. On MRI they can be hypo-iso or hyperintense with no enhancement on T1 but most commonly hypointense on T2. They can be diagnosed as an incidental finding or present with acute, intermittent, or chronic obstructive hydrocephalus (intermittent headache, drop attacks). Although the origin of these cysts is not completely elucidated it is thought that they derive from abnormal folding of the primitive neuro-epithelium which in this area separates the telencephalon from the diencephalon. Sudden death is rare but has been reported. While traditionally this was thought to be related to acute obstructive hydrocephalus caused by mobile tumours ('the ball-valve mechanism'), theories of cardiac involvement secondary to acute hypothalamic dysfunction have become more and more prominent (Turillazzi et al., 2012).

As a general principle, symptomatic colloid cysts should be removed. According to level II evidence 98% of asymptomatic colloid cysts will remain clinically silent on long term follow-up (Pollock and Huston, 1999). The risk of observation for asymptomatic cysts was also found to be higher for patients younger than 50 and cysts larger than 1 cm (Pollock et al., 2000).

Surgical options include open surgery via a transcortical or transcallosal approach, endoscopic excision, or frameless stereotactic aspiration. There are pros and cons for each. The open approaches have a higher chance to achieve complete excision of the cyst but may carry a higher risk for seizures or forniceal injury. The size of the ventricles can be a limitation for the endoscopic approach. The viscosity of the cyst content can also be a limiting factor for the stereotactic or endoscopic aspiration. If incompletely aspirated colloid cysts can recur.

Extension of a sellar mass, most likely a large pituitary adenoma, has typical appearance on MRI for pituitary tumours, bitemporal visual field disturbance, and hormone disturbance on endocrine profile.

Suprasellar tumours extending into the ventricles—most commonly craniopharyngioma but also germinoma—please see more details in Chapter 27.

Optic pathway and hypothalamic gliomas—most often affects the paediatric population. More details in Chapters 38 and 88.

Meningiomas from the skull base extending upwards. More details in Chapter 14.

Posterior third ventricle

1. *Pineal region tumours* can grow into the posterior third ventricle. Please refer to the relevant chapter on these tumours.
2. *Meningiomas* from the tentorial edge (included in the differential diagnosis of the pineal region tumours).
3. *Arachnoid cysts*—might be difficult to be spotted easily on first look. They can cause triventricular hydrocephalus. If they are symptomatic, they can be managed with endoscopic fenestration.
4. *Dermoid cysts*—rare.

Fourth ventricle (adults)

1. *Ependymomas*—enhancing lobulated tumours more common in young adults that tend to grow outwards through the foramina of ventricular outflow (Fig. 32.4). The main treatment is surgical but when these tumours originate from the floor of the fourth ventricle radical excision needs to be balanced carefully with the significant risk of lower cranial nerve palsies. In such cases, if a good dissection plane is maintained between the tumour and the floor of the fourth ventricle it is likely that postoperative cranial nerve palsies (likely to occur) are likely to improve gradually over time (although full recovery cannot be guaranteed). All this should be discussed carefully with the patient before the operation. Preoperative imaging of the whole craniospinal axis is mandatory due to the risk of CSF dissemination. The difficulty of correlating histologic grading and clinical significance in ependymomas is well documented. The new WHO CNS tumour classification in 2016 has not elucidated this further. However, a new entity, the RELA fusion-positive ependymoma (common with supratentorial ependymoma in children), was included.

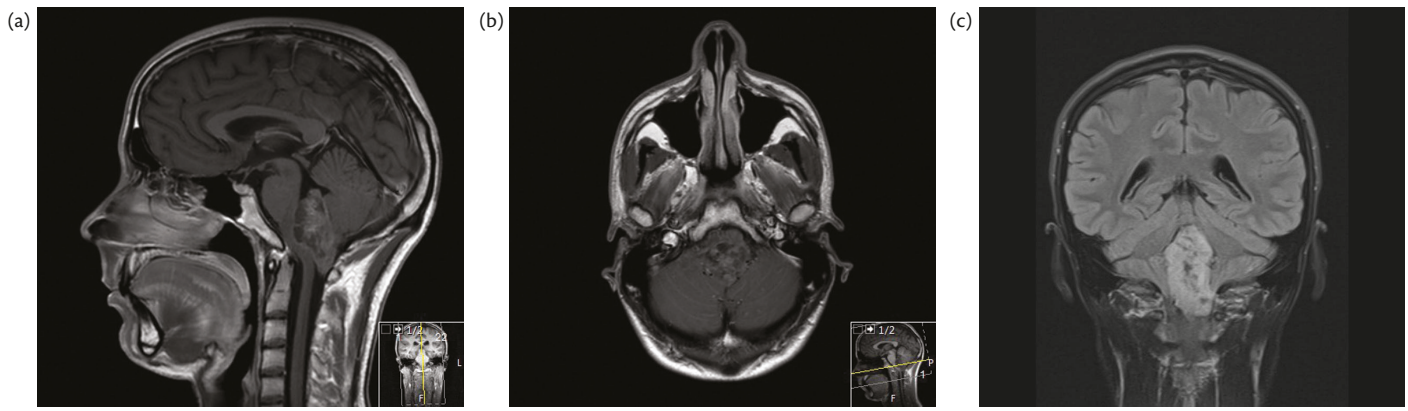

Fig. 32.4 Ependymoma of fourth ventricle, sagittal (A) and axial (B) T1 with gadolinium and coronal (C) FLAIR showing typical appearances with patchy contrast enhancement, compression of brainstem, growth through foramen of Magendie and involvement of posterior inferior cerebellar artery branches.

Also, the previously recognized entity of cellular ependymomas was deleted from the classification as it was considered identical with the standard ependymomas.

2. *Subependymomas*—non-enhancing (or sometimes containing enhancing components) lobulated tumours commoner in middle age and older patients and often is an incidental finding. If small and asymptomatic or if the patient is not fit to undergo surgery, they can be managed conservatively. Occasionally CSF diversion might be necessary, but often patients are managed conservatively due to the indolent clinical course of these tumours. Resection should be considered for younger patients with larger or symptomatic tumours but is often deliberately subtotal to avoid injury to floor of the fourth ventricle.
3. *Medulloblastomas*—originate from the cerebellar vermis and most commonly occur in the paediatric population but can rarely occur in young adults (location in the cerebellar hemisphere possible). They usually present with acute obstructive hydrocephalus. The 2016 WHO CNS tumour classification provides a very useful presentation of the usual combinations of the well-established histological subtypes of these tumours (desmoplastic/nodular, medulloblastoma with extensive nodularity, large cell, and anaplastic) and four now established genetic subtypes (WNT activated, SHH activated, group 3 subtype, and group 4 subtype) (Louis et al., 2016). The management should be prioritized and considered carefully; the management of acute hydrocephalus, imaging of the whole craniospinal axis and CSF sampling, MDT discussion, surgery for the primary tumour (aim for maximal tumour resection, establish histological, and molecular subtype) and further oncological treatment depending on the stage of the disease and the age of the patient. Locally established protocols usually apply. At the time of presentation, a significant percentage of the patients have already secondary deposits in the spine. Secondary deposits or CSF dissemination at the time of presentation, subtotal excision of the primary tumour and younger age are all well recognized factors of poor prognosis (more details in Chapter 28).
4. *Choroid plexus tumours*—the fourth ventricle is an unusual location for these tumours, but they can occur here as avidly enhancing lobulated tumours. The main treatment is surgical. If subtotally resected they can recur.
5. *Exophytic brain stem gliomas*—usually pontine gliomas. More common in children (more details in Chapter 7).
6. *Cysticercosis*—should be included in the differential diagnosis if the patient comes from or travelled in to endemic areas.

Clinical presentation

The clinical presentation of intraventricular tumours depends on their location, size, and progress rate. Rapid progression can cause acute hydrocephalus (severe headache, drowsiness, nausea, and vomiting) that require CSF diversion before the definite management of the tumour. Slow growing tumours however are asymptomatic for a long time before they become symptomatic and usually present with a chronic, NPH-like clinical picture (cognitive decline, gait disturbance, and incontinence). The management of these patients should focus on the surgical management of the tumour as this can also address the resulted hydrocephalus. Incidental diagnosis particularly of low-grade intraventricular tumours has become increasingly frequent nowadays due to the wide availability of imaging. Certain intraventricular tumours can reach a significant size and can cause symptoms from direct mass effect on periventricular neural structures. Large tumours in the left lateral ventricle have been associated with memory and speech disturbance. Large tumours on either side can cause motor deficit, and if they have a significant extraventricular extension into the parenchyma they can also cause epilepsy. Visual disturbance can occur either as a result of the long-standing high intracranial pressure or various visual field deficits can occur due to the direct pressure on the visual pathways. Tumours of the posterior third ventricle and pineal region can also present with Parinaud's syndrome as well as acute hydrocephalus. Large posterior fossa tumours usually present with acute obstructive hydrocephalus and depending on their size and extension with balance disturbance. The slow and gradual onset and progress of symptoms of low-grade tumours can rarely be accelerated by intratumoural haemorrhage, which leads to sudden deterioration (Ogbodo et al., 2012).

Management

If an intraventricular tumour causes obstructive hydrocephalus with deteriorating neurological state CSF diversion should take the priority. For third ventricular tumours, bilateral drainage of the ventricles should be considered if the tumour obstructs both foramina of Monro, although this is not always necessary. The ventricles can be drained by inserting an external ventricular drain, or depending on the working diagnosis, Endoscopic third ventriculostomy can be carried out first followed by endoscopic biopsy of the tumour (e.g. posterior third ventricle/pineal region tumours). Endoscopic third ventriculostomy can potentially be a CSF diversion option for all cases when blockage of the ventricle happens at posterior third ventricle or below.

For patients with slow growing tumours with chronic hydrocephalus, the management of the tumours can take the priority. However, in these cases if a decision is made for the patient to be managed conservatively, a ventriculoperitoneal (VP) shunt can be inserted to treat hydrocephalus. This is a commonly followed management plan for older patients who are diagnosed with lower grade intraventricular lesions and are not fit to undergo excision of the intraventricular tumour.

For tumours with a potential of CSF dissemination (**Table 32.1**), enhanced MRI of the whole spine and CSF sampling preoperatively is mandatory to stage the tumour adequately.

Tumour markers from the blood and CSF should be sent for pineal region tumours. CT of the whole body should be considered if suspected metastases.

Central neurocytoma

Low-grade tumours, most common in young adults. When initially described in 1982 (Hassoun et al., 1982) were graded WHO I tumours but due to the high recurrence rate of some histological subtypes were subsequently upgraded to WHO II tumours. They

usually present with gradual onset of symptoms suggestive of raised intracranial pressure due to hydrocephalus. Apart from headaches a clinical picture of chronic hydrocephalus with cognitive decline, gait disturbance, and incontinence is common. When very large the patients can also present with symptoms due to direct mass effect of the tumour on the periventricular structures. Intratumoural haemorrhage can lead to sudden deterioration of symptoms that leads to diagnosis. They have generally a good prognosis, but if incompletely excised they can recur. They are usually located in the lateral ventricle originating from the septum pellucidum and occasionally extend into the third ventricle. They show mild to moderate enhancement and can contain cysts, calcifications, and flow voids.

Epidemiology

Rare tumours reported in different series to represent up to 0.5% of brain tumours.

Pathology

Well differentiated tumours with neuronal differentiation. Due to their clear cytoplasm, they can mimic other clear cell tumours. The presence of synaptophysin and the neuronal nuclear antigen are used to confirm the diagnosis. Cytoplasmic vacuolations of this tumour give the tumour the 'fried egg' appearance, like that seen in oligodendroglioma.

The MIB-1 labelling index when more than 3% was associated with a worse prognosis for local control and survival (Rades et al., 2004). These tumours are called atypical central neurocytomas.

Despite their usual benign nature, malignant transformation of central neurocytomas has been reported (Amagasa et al., 2008).

Treatment

Due to low occurrence rate of these tumours there is no enough data to support large prospective studies. The highest level of evidence available on the management of central neurocytomas tumours comes from meta-analyses. The largest meta-analysis reported (N = 438) on the management of central neurocytomas concluded that in all cases gross total resection should be attempted if considered safe (Rades and Schild, 2006). In this study the tumours were divided in typical and atypical central neurocytomas based on the MIB-1 labelling index greater than 3% and the presence or not of atypical histological features. In 351 of the patients with typical neurocytomas it was found that the addition of radiotherapy after gross total resection has achieved the same 5-year survival but slightly higher (100% vs. 87%) local control rate. However, taking into consideration the risks of radiotherapy is not generally recommended. Radiotherapy has however proven beneficial in patients with typical neurocytomas who underwent subtotal resection as it improved both the 5-year survival and local control to almost the gross total resection (GTR) levels (see **Box 32.1**).

For the management of atypical central neurocytomas in a meta-analysis for treatments applied for 85 atypical neurocytomas, it was concluded that after GTR five-year survival was slightly lower when compared to typical neurocytomas (93% vs. 100%), but the local control rate was significantly lower (57% vs. 87%). The addition of radiotherapy was not found to improve the survival or local control and therefore is not recommended.

Box 32.1 Management of central neurocytomas (typical and atypical)

Grade 1c recommendations

- Attempt GTR if safely feasible (applies for typical and atypical central neurocytomas)
- STR + RT = GTR control rates/survival—applies for typical central neurocytomas where GTR is considered high risk
- RT after STR of typical neurocytomas is recommended at 50–54 Gy
- RT after GTR of atypical central neurocytomas not recommended
- RT after STR of atypical central neurocytomas is recommended at 55–60 Gy

Grade 2c recommendations

- Do not use RT after GTR in typical central neurocytomas
- Biopsy, CSF diversion, and RT are sometimes effective for typical central neurocytomas

CSF, cerebrospinal fluid; GTR, gross total resection; RT, radiation therapy; STR, subtotal resection.

For subtotal resection the 5-year survival and local control are very low, but improve dramatically with postoperative radiotherapy (survival 43–78% and local control 7–70%).

An interhemispheric-transcallosal or transcortical approach can be employed for the surgical resection of these tumours. The interhemispheric-transcallosal approach provides easy access to the ventricles with no risk of seizures and very low risk of disconnection syndrome.

A summary for the management of central neurocytomas can be seen in **Box 32.1**. See **Figure 32.5** for the histopathological features of typical central neurocytoma.

Prognosis

Much depends on the proliferative potential of the tumour and the degree of resection achieved.

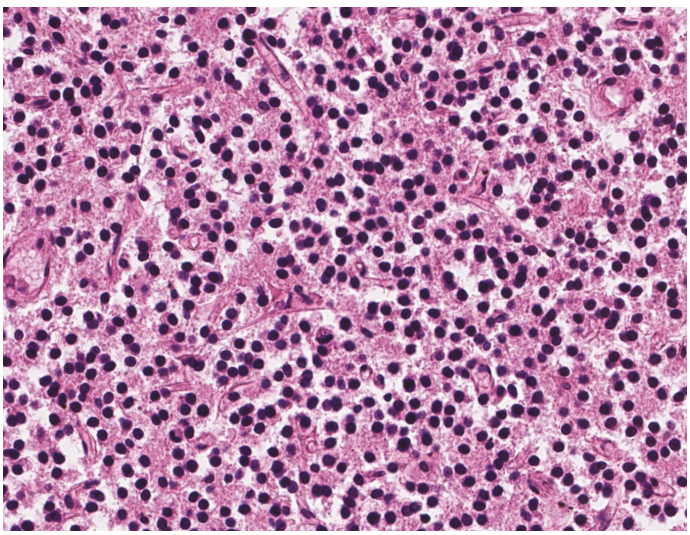

Fig. 32.5 Histopathological features of central neurocytoma. Neurocytic cells with uniformly round nuclei are typical features. Occasional poorly formed rosettes may occur as in this example. Strong immunoreactivity for synaptophysin would be expected.

Courtesy of Dr Kieren Allinson, Department of Pathology, Addenbrooke's Hospital, Cambridge.

REFERENCES

Amagasa, M., Yuda, F., Sato, S., & Kojima, H. (2008). Central neurocytoma with remarkably large rosette formation and rapid malignant progression: a clinicopathological follow-up study with autopsy report. *Clin Neuropathol*, **27**, 252–7.

Campen, C.J. & Porter, B.E. (2011). Subependymal giant cell astrocytoma (SEGA) treatment update. *Curr Treat Options Neurol*, **13**, 380–5.

Cipri, S., Mannino, R., & Cafarelli, F. (2009). Metastatic melanoma of the septum pellucidum mimicking a colloidal cyst of the third ventricle. A novel case. *J Neurosurg Sci*, **53**(3), 125–9.

Hassoun, J., Gambarelli, D., Grisoli, F., et al. (1982). Central neurocytoma. An electron-microscopic study of two cases. *Acta Neuropathol*, **56**, 151–6.

Louis, D.N., Perry, A., Reifenberger, G., et al. (2016). The 2016 World Health Organization Classification of Tumors of the Central Nervous System: a summary. *Acta Neuropathol*, **131**, 803–20.

Ogbodo, E., Kaliaperumal, C., Bermingham, N., & O'Sullivan, M. (2012). Spontaneous haemorrhage and rupture of third ventricular colloid cyst. *BMJ Case Rep*, pii: bcr2012006863.

Ostrom, Q.T., Gittleman, H., Farah, P., et al. (2013). CBTRUS statistical report: primary brain and central nervous system tumors diagnosed in the United States in 2006–2010. *Neuro-Oncology*, **15**, ii1–ii56.

Pollock, B.E. & Huston, J. 3rd. (1999). Natural history of asymptomatic colloid cysts of the third ventricle. *J Neurosurg*, **91**(3), 364–9.

Pollock, B.E., Schreiner, S.A., & Huston, J. 3rd. (2000). A theory on the natural history of colloid cysts of the third ventricle. *Neurosurgery*, **46**, 1077–81; discussion 1081–3.

Rades, D. & Schild, S.E. (2006). Treatment recommendations for the various subgroups of neurocytomas. *J Neurooncol*, **77**, 305–9.

Rades, D., Schild, S.E., & Fehlauer, F. (2004). Prognostic value of the MIB-1 labeling index for central neurocytomas. *Neurology*, **62**, 987–9.

Turillazzi, E., Bello, S., Neri, M., Riezzo, I., & Fineschi, V. (2012). Colloid cyst of the third ventricle, hypothalamus, and heart: a dangerous link for sudden death. *Diagn Pathol*, **7**, 1746–596.

RELATED LINK TO EBRAIN

The Histopathology of Neuronal and Glioneuronal Tumours. https://learning.ebrain.net/course/view.php?id=1394

33

Colloid cysts

Asim Sheikh and Paul Chumas

Introduction

Colloid cysts are benign, mostly intraventricular tumours accounting for 0.5 to 2% of all intracranial mass lesions. They are most commonly found in the anterior portion of third ventricle at the level of foramina of Monro and, if symptomatic, usually present with obstructive hydrocephalus of the lateral ventricles. The original description historically linked them with sudden death in the pre-CT era. They are also known as neuroepithelial cysts (**Figs. 33.1, 33.2, 33.3,** and **33.4**).

Management options include treatment of hydrocephalus alone, aspiration of the cyst contents and removal of the cyst endoscopically or via a microsurgical approach.

Epidemiology

Cushing described an asymptomatic case of a colloid cyst. Interestingly, a colloid cyst was reportedly found on autopsy of Harvey Cushing himself (Fulton, 1946). Due to most colloid cysts being asymptomatic, it is difficult to ascertain the exact incidence of this benign lesion (Fulton, 1946). With the advent and ever-increasing availability of modern imaging techniques, more asymptomatic colloid cysts are being diagnosed. The prevalence is estimated at 1 in 8500 persons based on autopsy as well as MR imaging series (de Witt Hamer et al., 2002). A study in Finland calculated symptomatic colloid cyst incidence at 3.2 per million per year over a 14-year observation period, accounting for 2% of all intracranial tumours (Hernesniemi and Lievo, 1996). Vandertop estimated that one case becomes symptomatic per million-person years (de Witt Hamer et al., 2002). Age at diagnosis ranges from intrauterine until 76 years of age (Gaertner et al., 1993; Romani et al., 2008) but the most common age of diagnosis is between 20 and 50 years old. Although presumed to be congenital, they are rarely reported in children (Macdonald et al., 1994; Maqsood et al., 2006).

Pathogenesis

Colloid cysts are normally located anteriorly in the third ventricle at the level of foramen of Monro in the coronal plane, although they can also be located more posteriorly in the third ventricle, roof, or floor of the third ventricle, the columns of the fornix or in the choroid plexus (Fries and Perneczky, 1994) (**Fig. 33.5**). Other rare locations include the lateral ventricles, the septum pellucidum, fourth ventricle and prepontine region (Ciric and Zivin, 1975; Shima et al., 1976; Jan et al., 1989; Maurice-Williams and Wadley, 1998; Jeffree and Besser, 2001; Killer et al., 2001; Jaskólski et al., 2003). Most are found as an isolated lesion, but multiple cysts have also been described (Maurice-Williams and Wadley, 1998). Their size can range from few millimetres up to 9 cm in diameter (Shuangshoti and Netsky, 1966).

Histologically, cysts are made up of either a single layer of pseudostratified columnar epithelium with or without cilia, or cuboidal low columnar epithelium (Leech et al., 1982) (**Figs. 33.6, 33.7,** and **33.8**). Mucus goblet cells are also commonly seen, with a mucin positive mucicarmine on periodic acid-Schiff staining. The epithelium and surrounding capsule together form the wall of the cyst. The wall can be variable in its thickness, the contents of the cyst are an amorphous material believed to be mucin discharge from epithelial cells and cellular desquamation. The content consistency is also very variable, from liquid to viscous, and may be semisolid or solid. This is an important consideration when planning treatment options (Bosch et al., 1978).

Colloid cysts have historically been referred to by various other names including neuroepithelial cells, neurenteric cysts, and primary actinomycoma (Powers and Dodds, 1977; Graziani et al., 1995). They are thought to arise from neuroepithelial cells including those of the choroid plexus, ependymal and embryonic paraphysis. A more recent hypothesis suggests they may be of non-neural origin (Takahiro et al., 1992). Although most cases are sporadic and isolated, several familial cases have also been described with a suggested autosomal recessive inheritance pattern (Ibrahim et al., 1986; Akins et al., 1996; Nader-Sepahi and Hamlyn, 2000; Joshi et al., 2005). Screening may be of value in cases where two or more family members are affected.

Pathologically, colloid cysts can either enlarge due to production of colloid material, causing obstructive hydrocephalus or have sudden enlargement due to intracystal haemorrhage when they may compress nearby structures. Sjovall in 1910 suggested intermittent blockage of CSF flow at the level of the foramen of Monro may occur due to the pendular attachment of the cyst to the tela choroidae

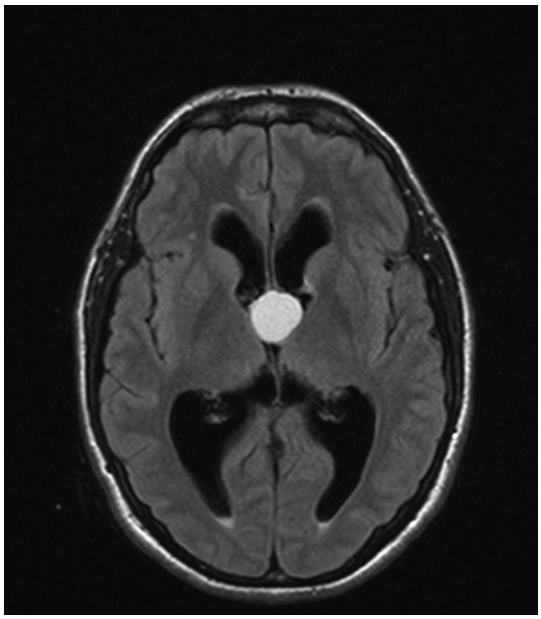

Fig. 33.1 MRI T2W FLAIR image of colloid cyst.

(Sjovall, 1910). Colloid material production can cause both increase in the size of the cyst and local inflammation. A sudden increase in size can be due to acute haemorrhage within the cyst and can produce rapid and often serious neurological deficit (Malik et al., 1980; Beems et al., 2006). Nearby structures can also be compressed by cyst enlargement, for example, local pressure on the fornices can lead to long-term memory problems (Aggleton et al., 2000). Direct compression of the lateral walls of the third ventricle with resultant compromise of the hypothalamic cardiovascular regulatory centres has been postulated as a cause of acute deterioration (de Witt Hamer et al., 2002). A change in posture may cause direct compression of the internal cerebral veins and lead to increased intracranial venous pressure (Hamlat et al., 2004). Acute deterioration may also be seen after a lumbar puncture.

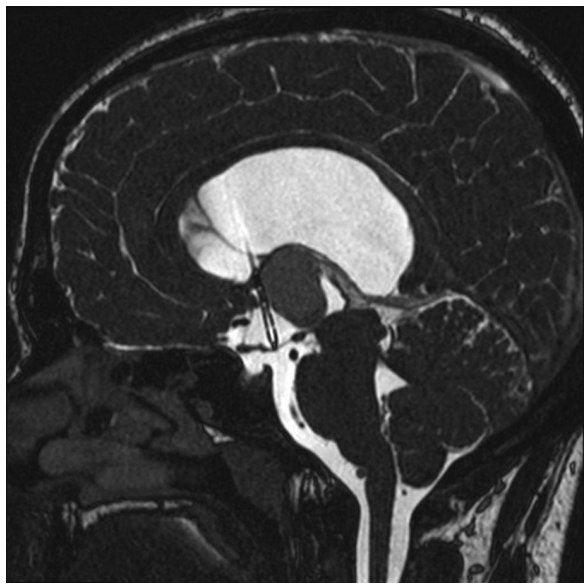

Fig. 33.2 Sagittal T2W CISS sequence of colloid cyst and external ventricular drain.

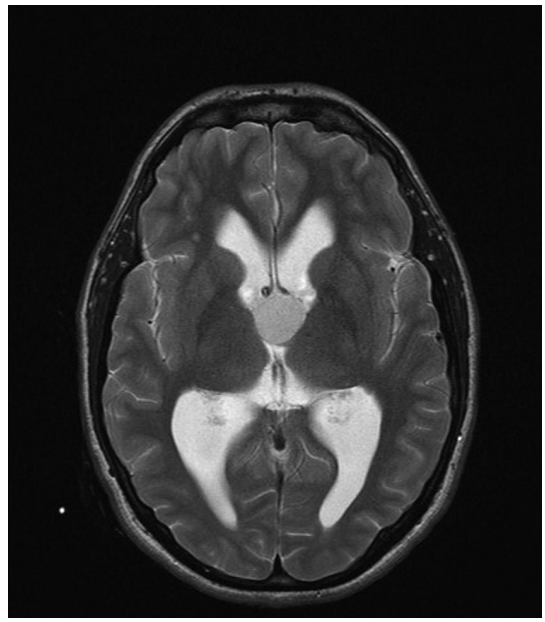

Fig. 33.3 T2W axial image of colloid cyst.

Presentation

There are a wide variety of symptoms that patients may present with, however there are none which are specifically pathognomonic. Symptoms can either be due to acute intermittent raised intracranial pressure, presumed to be from intermittent obstruction to CSF flow from mobile pedunculated cysts or they can be from (permanent) hydrocephalus due to longstanding partial CSF outflow obstruction. There are also a growing number of patients who present with incidentally found cysts.

The commonest symptoms are headaches (68%), gait disturbance (47%) and short-term memory loss (37%). Nausea, vomiting (37%) and blurred vision (24%) are also commonly seen (Little and MacCarty, 1974). The commonest signs are evidence of papilloedema (47%) and gait disturbance (32%). A quarter of

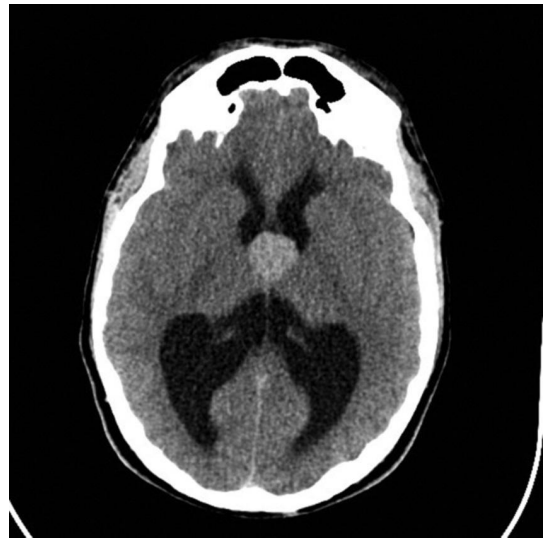

Fig. 33.4 CT axial image of hyperdense colloid cyst.

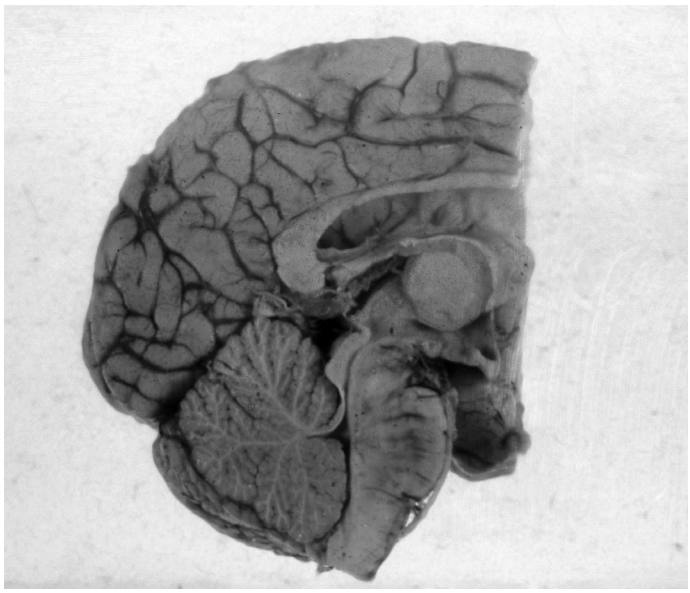

Fig. 33.5 Autopsy findings of colloid cyst in sagittal section.
Acknowledgment: Dr Azzam Ismail, Consultant Histopathologist, Leeds General Infirmary.

patients will have no signs demonstrable on examination (Little and MacCarty, 1974).

Headache duration, location, and character is variable. A recent study aimed to categorize patients into three groups. One, presenting with headache as the main symptom (72%), another with memory loss with or without signs of raised intracranial pressure and the last group with paroxysmal symptoms while being asymptomatic between attacks (Pollock et al., 2000). However, this distinction is difficult and a combination of symptoms is possible.

It is also worth discussing the often-overestimated risk of sudden death associated with colloid cysts. In the pre-CT era, colloid cysts were associated with a high risk of sudden death due to presumed mobility of the cysts causing acute CSF outflow obstruction. This was most likely associated with interventions such as lumbar punctures and ventriculography. It is possible, however, to

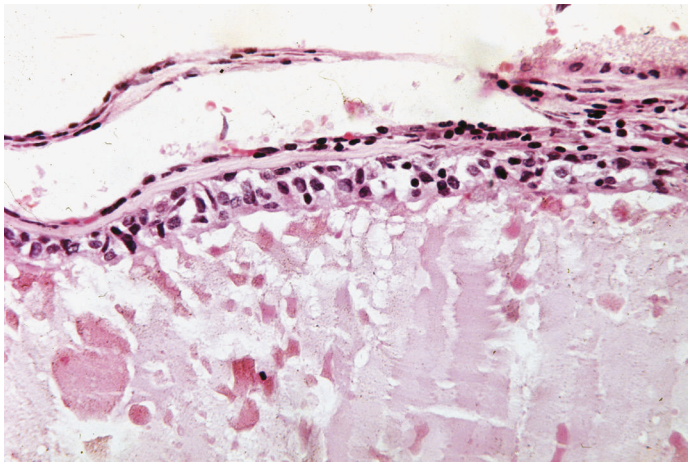

Fig. 33.6 Epithelial lining of a colloid cyst wall.
Acknowledgment: Dr Azzam Ismail, Consultant Histopathologist, Leeds General Infirmary.

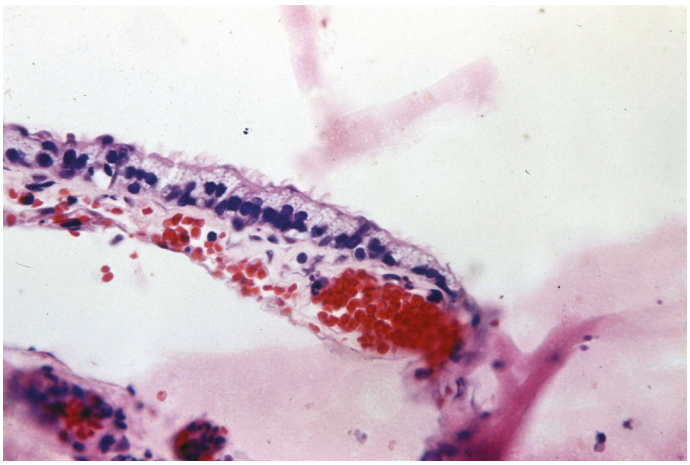

Fig. 33.7 The lining epithelium is simple cuboidal to columnar, ciliated cells, while goblet cells are present and the wall is fibrocollagenous. The stain is haematoxylin and eosin (H&E).
Acknowledgment: Dr Azzam Ismail, Consultant Histopathologist, Leeds General Infirmary.

have decompensation and death occurring in patients with chronic hydrocephalus as well. Hypothalamic cardiovascular centre reflex mechanisms may also be responsible for acute deterioration due to direct pressure from the cyst (de Witt Hamer et al., 2002).

Diagnostic imaging

Historically, pneumoencephalography was the mainstay of diagnosis for third ventricular tumours. The advent of CT and then of MRI has made it easier to diagnose colloid cysts. Isodense lesions on CT can pose diagnostic challenges (Powell et al., 1983).

CT imaging shows colloid cysts to be well circumscribed lesions at the level of the foramen of Monro with associated hydrocephalus and periventricular lucency in acute CSF obstruction. Cysts are commonly hyperdense, but may also be isodense or hypodense (Ganti et al., 1981; Hine and Chui, 1987). Cysts that are hypodense on CT, usually have fluid contents and thus there is an option to treat

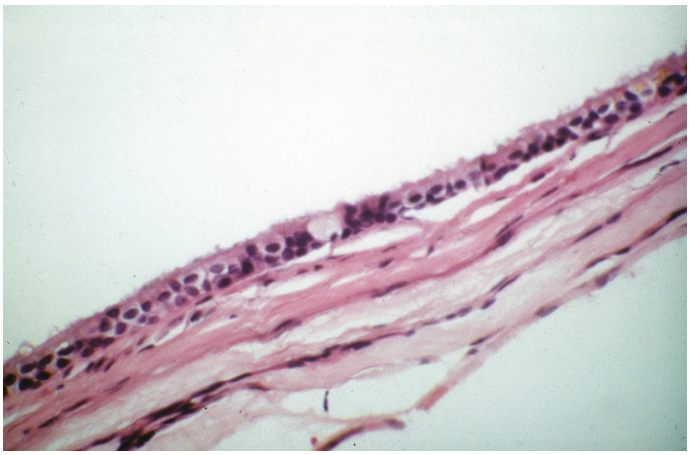

Fig. 33.8 Cuboidal epithelial lining.
Acknowledgment: Dr Azzam Ismail, Consultant Histopathologist, Leeds General Infirmary.

these with aspiration (El Khoury et al., 2000). Some cysts show moderate peripheral enhancement although this is uncommon.

On MRI, most cysts appear homogenously hyperintense on T1-weighted images and hypointense on T2 images (Maeder et al., 1990). Presence of cholesterol esters may cause the central portion to be low in intensity on T2-weighted images. Rarely, inspissated debris may form a dependent nodule that can be seen on CT and MRI scans.

Intraventricular haemorrhage occasionally mimics a colloid cyst on CT scans and MRI. Subependymomas, central neurocytomas, and subependymal giant cell astrocytomas may occur in the same area as a colloid cyst on imaging studies, but these entities can be distinguished by their shape, contrast enhancement, and signal intensity.

Natural history

Colloid cysts account for less than 2% of intracranial lesions (Little and MacCarty, 1974). A long-term follow-up of such rare tumours is therefore not widely available. Pollock published a series of 155 patients spanning 24 years of observation (Pollock et al., 2000). Four factors were found to be positively associated with symptomatic lesions, younger age group (below 44 years), larger cyst size (more than 13 mm), ventricular dilatation, and increased intensity on MRI T2-weighted images.

The natural history of colloid cysts is related to the rate of cyst growth, development of CSF obstruction, and the fact that cyst size becomes stable as patients age. The natural history can be classified into three groups. Firstly, asymptomatic patients where cyst growth stops prior to CSF obstruction and ventricular dilatation. A second group, also asymptomatic, where an initial rapid growth of the cyst causes ventricular dilation but subsequent cyst stability and lack of growth maintains a symptom free course. Lastly, the group where an enlarging cyst causes CSF obstruction and ventricular dilatation, which in turn causes symptoms. This group commonly has hyperintense T2 characteristics on MRI.

Spontaneous rupture of cysts is also known to occur (Motoyama et al., 2002) and they can reduce in size spontaneously (Hattab et al., 1990).

Management

The current practice of the senior author is complete microsurgical excision of colloid cysts in young symptomatic patients. The majority of 'incidental' cysts are actually found after a scan done for headaches. This poses a real dilemma to ascertain whether these are truly incidental or contribute to a symptom complex.

In a small proportion of elderly patients or those not fit for a prolonged anaesthetic, CSF diversion alone may be considered reasonable. While a conservative approach with radiological surveillance may be appropriate for asymptomatic small sized cysts.

We look at the different management options in detail here.

Conservative management

The majority of colloid cysts either present with symptoms or become symptomatic soon after discovery and hence require treatment. For patients to be managed conservatively with colloid cysts, they must have a radiological diagnosis that is clear, no hydrocephalus, no significant symptoms and the size of cyst should not be more than 10 mm in size (de Witt Hamer et al., 2002; Hamlat et al., 2004). Thus, for small incidentally found colloid cysts, a conservative approach to management is reasonable.

CSF diversion procedures and pellucidotomy

Patients presenting acutely with ventricular dilatation and who are otherwise not surgical candidates for microsurgical removal of colloid cysts, may require urgent CSF diversion. This can be undertaken by placement of bilateral external ventricular drain or shunts. Alternatively a unilateral shunt with endoscopic pellucidotomy may be utilized. Placement of a unilateral shunt alone risks contralateral ventricular dilatation and may result in a deteriorating neurological status.

Rarely, colloid cysts located in the posterior third of the third ventricle may result in triventricular dilatation. In these cases, endoscopic third ventriculostomy can be performed (Hopf et al., 1999).

Percutaneous stereotactic aspiration

Percutaneous aspiration of colloid cyst contents remains a valuable treatment option. Historically, Gutierrez-Lara et al reported on free hand aspiration of colloid cysts in 1975 (Gutierrez-Lara et al., 1975). This method was then refined by use of stereotactic frame (Bosch et al., 1978). The simplicity of aspiration has a definite appeal.

The advantages of aspiration include that it is simple and relatively safe to perform, and it can be used in patients with normal or small ventricles from an earlier shunting procedure (Bosch et al., 1978). While there is a higher recurrence rate, total or subtotal aspiration may be the only treatment required in some patients (Mathiesen et al., 1993).

The disadvantages of aspiration includes a higher recurrence rate (Mathiesen et al., 1993) which can occur as late as 6 years after an aspiration procedure. Aspiration is not always possible because the contents may be too viscous, high cyst viscosity is evident from hyperdensity on CT and is seen in two-thirds of cases (Rivas and Lobato, 1985; Kondziolka and Lunsford, 1992). Furthermore, the capsule may be too tough or a small cyst may deflect away from the aspirating needle (Kondziolka and Lunsford, 1992). Early attempts at aspiration had a high morbidity from vascular injury and mechanical trauma. Spillage of contents while aspirating may cause ventriculitis or aqueductal blockage (Antunes et al., 1980). For these reasons, percutaneous aspiration has now been confined to a very limited group of patients.

Endoscopic aspiration

Endoscopic aspiration of cyst contents was first described by Powell et al in 1983. Deinsberger in 1994 showed that endoscopic aspiration of colloid cysts is safe and if the cyst wall is opened widely, has low recurrence rates (Deinsberger et al., 1994).

Endoscopic excision of cysts

Numerous published series advocate the endoscopic excision of colloid cysts.

The advantages of the endoscopic approach over open surgery are shorter operating times (mean 110 minutes vs. mean 206 minutes for microsurgical excision), lower complication rates owing to the

Table 33.1 Comparison of microsurgery and endoscopy as the primary surgical procedure in colloid cyst management

Parameter	Microsurgical	Endoscopic	Significance *P* value
Age (mean in years)	40.0	40.5	
Female: Male	3.1:1	1:1.4	
Cyst size (mm)	13.2	14.3	
Gross total resection	96.8%	58.2%	<0.0001
Recurrence	1.48%	3.91%	0.0003
Mortality	1.4%	0.6%	0.2469
Reoperation	0.38%	3.0%	0.0006
Shunt dependency	6.2%	3.9%	0.1160
Follow-up mean (months)	49.7	36.7	
Follow-up range (months)	11–144	10–76	

Adapted with permission from Ahmed B. Sheikh, Zachary S. Mendelson, James K. Liu., Endoscopic Versus Microsurgical Resection of Colloid Cysts: A Systematic Review and Meta-Analysis of 1278 Patients, *World Neurosurgery*, Volume 82, Issue 6, p. 1187, Copyright © 2014 Elsevier.

smaller cortical incision, and therefore a lower risk of postoperative seizures (Lewis et al., 1994). A 13-year follow-up of endoscopically removed colloid cysts showed a recurrence rate of only 6.3% (Levine et al., 2007). The rate of mortality and shunt dependency is similar in both groups. Hence some centres are offering this technique as the treatment of choice.

However, another recent study reviewed the available literature on endoscopic vs. microsurgical excision of colloid cysts (Sheikh et al., 2014). This study concluded that microsurgical removal of colloid cysts appears to result in a significantly higher rate of complete radical resection, decreased rate of recurrence, and fewer reoperations than endoscopic removal. This may be related to the advantage of performing two-handed microdissection of the cyst wall from critical adherent structures to achieve true gross total resection. Tables 33.1 and 33.2 provide comparative data on the techniques.

The technique of endoscopic excision of a colloid cyst is performed under general endotracheal anaesthesia, the patient is positioned supine with the head supported in a horseshoe head support. A head up position of approximately 15° is used. A linear incision is made just in front of the coronal suture in the mid-pupillary line and a burr hole is made. The dura is opened and ventricular cannulation is carried out with a No.14 French peel away introducer and stylet. Either a rigid or a flexible endoscope is inserted through the peel away catheter. Flexible scopes are useful for colloid cyst excision when the cyst is attached more posteriorly or to inspect the third ventricle and aqueduct for any debris.

The foramen of Monro is identified and usually found to be obstructed by the colloid cyst. The vascular cyst wall is coagulated with endoscopic bipolar or monopolar electrodes. Some centres have also utilized potassium titanyl phosphate (KTP) 600 μc laser fibres to coagulate and perforate the cyst capsule. The contents are then aspirated, adequate irrigation is maintained using lactated ringer's solution in a pulsed or continuous fashion. A pair of 1 mm punch biopsy forceps may be used to remove the cyst capsule and colloid material. The third ventricle and aqueduct are inspected for any debris or blockage at the end of the procedure.

A ventricular access device is left in the tract left by the endoscope and connected to an Ommaya reservoir that can be later converted to a shunt if required. Gel foam is placed at the cortical opening to help prevent a CSF leak.

Microsurgical approaches to cyst removal

Transcortical, transventricular approach

Most colloid cysts are located in the anterior third of the third ventricle and can be removed using a transcortical, transventricular approach as described by Dandy in the 1930s (Dandy, 1933).

Anterior third ventricular lesions are approached via a precoronal suture craniotomy, while more posterior lesions are approached via more frontally based openings allowing a more oblique posterior trajectory through the foramen of Monro. In the 1930s, Dandy resected part of the frontal lobe to access the third ventricle. This is now refined to a mere 10–15 mm cortical opening either transgyral or preferably trans-sulcal. Large tumours can be approached via an ipsilateral approach while smaller cysts can be accessed with a contralateral approach. Although this can be used in patients with normal ventricles, it is ideally used when hydrocephalus is present.

The common postoperative complications include epilepsy (9.3%), meningitis (3.3%), wound infections, and memory problems due to fornix injury. Total removal was possible in 87 of 88 reported cases (98.8%). Charalampaki et al. have described 100% removal of colloid cysts with an endoscopically assisted transcortical-transventricular technique (Charalampaki et al., 2006).

Table 33.2 Postoperative complications comparison

Treatment	Seizures	Memory deficit	Intravent haemorrhage	Venous infarct	Intracerebral haematoma	Subdural haematoma	Arterial infarct	Hemiparesis	Meningitis	Overall
Endoscopy n = 666	0.3%	5.0%	1.2%	0%	0%	0.2%	0.3%	0.9%	2.7%	10.5%
Microsurgery n = 552	4.3%	5.1%	0%	2.1%	0.05%	0.018%	0.07%	1.6%	1.6%	16.3%
Transcallosal n = 446	2.9%	4.9%	0%	2.7%	0%	0.2%	0.9%	1.1%	1.1%	14.4%
Transcortical n = 106	10.4%	5.7%	0%	0%	2.8%	0%	0%	3.8%	3.8%	24.5%

Adapted with permission from Ahmed B. Sheikh, Zachary S. Mendelson, James K. Liu., Endoscopic Versus Microsurgical Resection of Colloid Cysts: A Systematic Review and Meta-Analysis of 1278 Patients, *World Neurosurgery*, Volume 82, Issue 6, p. 1187, Copyright © 2014 Elsevier.

Interhemispheric, transcallosal approach

The advantages of this approach are that it can be utilized in the absence of hydrocephalus, the access is through a relatively atraumatic corridor in the midline and via a small callosotomy, which gives a direct route to the colloid cyst.

However, the technique is technically more demanding and nearby vascular structures are vulnerable to damage. These include the superior sagittal sinus, cortical bridging veins, the anterior cerebral, and pericallosal arteries. Transient hemiparesis can be seen afterwards. A disconnection syndrome can be avoided by keeping the callosotomy less than 2 cm long in the anteroposterior (AP) dimension. Mutism can result from bilateral retraction of the supplementary motor areas within the cingulate gyri and fornix damage causing memory difficulties is a constant risk.

The interhemispheric, transcallosal approach is carried out under general anaesthetic with the head held in pins. The neck should be flexed and the operating table positioned in a 15° head-up position. Neuronavigation is helpful in planning the craniotomy site and trajectory by locating an avascular corridor away from cortical bridging veins. The typical craniotomy flap crosses the midline and is 4 cm anterior and 2 cm posterior to the coronal suture. The approach to the corpus callosum is down the falx and between the cingulate gyri. The Calloso-marginal and pericallosal arteries are identified and taking care to avoid placing a retractor directly on the vessels, may be gently retracted with the ipsilateral hemisphere on each side. An anterior callosotomy of 2 cm or less is made to access the lateral ventricle. The ventricle laterality is determined by the orientation of the choroid plexus, thalamostriate vein, and foramen of Monro before one of the following trajectories is utilized.

A paraforniceal approach may be adopted for smaller lesions presenting through the foramen of Monro that can be directly approached through the foramen and excised without the need to enter the third ventricle.

An interforniceal approach may be used for larger lesions and those located more posteriorly or where there is an associated cavum septum pellucidum. Dissection progresses between the two leaves of the septum pellucidum and the two fornices to access the third ventricle through the velum interpositum between the internal cerebral veins. The biggest disadvantage of this technique is the vulnerability of the fornices to bilateral injury, which can lead to severe antegrade amnesia (Sweet et al., 1959). In patients with larger cysts, the fornices may be splayed open by the cyst, making it easier to access by this route (**Figs. 33.9, 33.10,** and **33.11**).

A subchoroidal approach is used to avoid forniceal damage. The foramen of Monro can be enlarged posteriorly via subchoroidal dissection through the taenia thalami. This was popularized by Lavyne and Patterson (1983). This approach is limited by the terminal portion of the thalamostriate vein and although some authors have described division of the thalamostriate vein this needlessly risks venous infarction within the thalamus and is therefore not recommended.

A transchoroidal approach which similarly is fornix sparing can be adopted by dissecting past the choroid plexus on the medial side through the taenia fornices (Wen et al., 1998). This avoids the thalmostriate vein as it drains into the internal cerebral vein, however, the internal cerebral vein is still at risk within the velum interpositum. The fornix must also be protected with this approach.

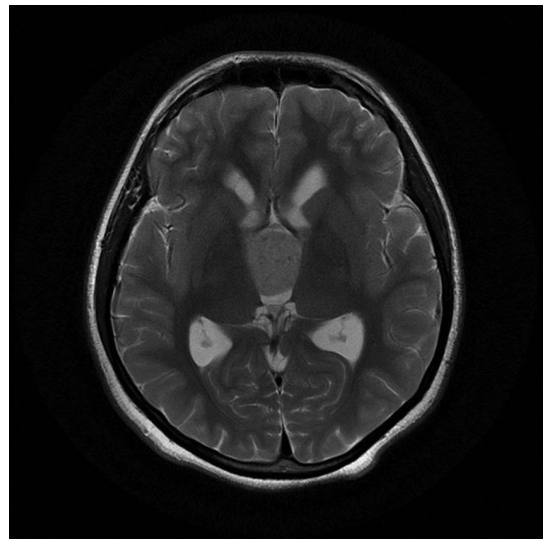

Fig. 33.9 Large colloid cyst with forniceal columns pushed apart.

The main disadvantage of both subchoroidal and transchoroidal approaches is the potential risk to the thalamostriate and internal cerebral veins. However, with large tumours, the choroidal fissure may be splayed by the underlying cyst which facilitates access.

Frontal translamina terminalis approach

This approach utilizes either a subfrontal dissection or paramedian interhemispheric route to the lamina terminalis. It is advantageous to utilize this approach for third ventricular colloid cysts in the anterior third ventricle or those encroaching into the suprachiasmatic recess (Desai et al., 2002).

There is currently no literature available on combining endoscope-assisted cyst excision with an approach through the lamina terminalis, although it has been shown to be feasible in cadaveric studies (Abdou and Cohen, 2000). This may be an area for development in the future.

Fig. 33.10 Sagittal T2-weighted MRI of large colloid cyst.

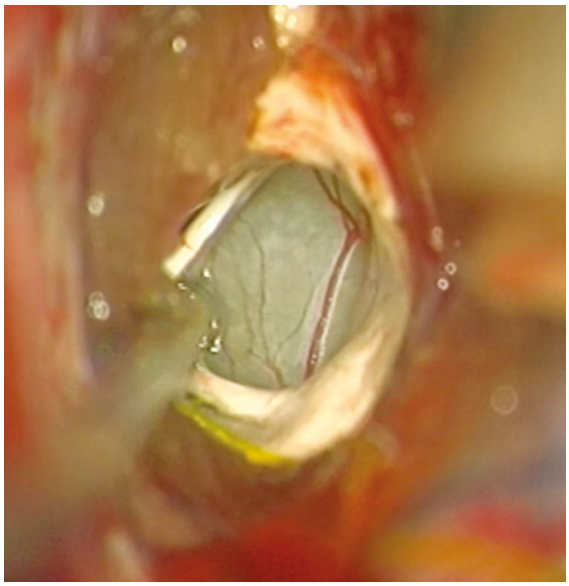

Fig. 33.11 Interhemispheric transforniceal approach. The left lateral ventricle has been accessed and the septum pellucidum then split to view the colloid cyst in this patient, with the preoperative scan findings seen in Figures 33.9 and 33.10. Refer the video in the link: https://drive.google.com/open?id=0B3x_xC0sImigajQxYTBTUWoyZ1E

Controversies in management

Smaller cysts, less than 1 cm in size which are picked up incidentally, pose a clinical dilemma. It can be challenging to determine whether these cysts are truly incidental or not because a vast proportion of the CT scans performed are in fact requested due to episodes of headache. A careful clinical evaluation is required that may sometimes, include a period of intracranial pressure (ICP) monitoring. It may be difficult to counsel patients on the importance of reporting headaches, as a sign of incipient hydrocephalus, when they have had headaches of sufficient severity to warrant neuroimaging in the first place. This may therefore lower the threshold for surgical intervention, depending on the psychological state of the patient.

The frequency of radiological surveillance required for patients with conservatively managed cysts, such as the very small incidental cysts with no symptoms, unrelated headaches, or classic migraine, is not clear.

Choosing between an endoscopic and microsurgical approach is also an area of controversy. Both techniques have their pros and cons as described earlier and in Tables 33.1 and 33.2. While the endoscopic approach offers a smaller craniotomy and cortical tract, it is necessary for the ventricles to be sufficiently enlarged and it may be difficult to remove all the cyst capsule and therefore the recurrence rates are higher. In general terms, the choice of the procedure type (endoscopic vs. microsurgical) comes down to the experience/expertise of the surgeon and his/her frank discussions with the patient. With regards the route for microsurgical approaches (transcortical or transcallosal)—again this largely comes down to surgeon preference. While some surgeons argue the transcortical approach gives a better angle of approach to tackle most colloid cysts, the ventricles need to be sufficiently enlarged and the risk of epilepsy is increased. In contrast, an interhemispheric approach can be used in patients with small or large ventricles. Taking into account patient preference, our unit policy is to offer microsurgery in younger fit patients where there is likely to be more tolerance of a major procedure and where long-term cyst control is of greater importance. Endoscopic approaches being reserved where the cyst anatomy and morphology are favourable and are appropriate in a slightly older age group where the complications of surgery may not be so well tolerated. Finally, cyst aspiration or CSF diversion alone is generally used in the least fit patients or older people where long-term control is a less significant factor. However, the most important factor in the choice of any of these approaches is operator experience.

FURTHER READING

Fulton, J.F. (1946). *Biography of Harvey Cushing*. Springfield IL: Charles C. Thomas.

Levine, N.B., Miller, M.N., & Crone, K.R. (2007). Endoscopic resection of colloid cysts: indications, technique, and results during a 13-year period. *Minim Invasive Neurosurg*, **50**(6), 313–17.

Pollock, B.E., Schreiner, S.A., & Huston, J. 3rd. (2000). A theory on the natural history of colloid cysts of the third ventricle. *Neurosurgery*, **46**(5), 1077–81; discussion 1081–3.

Sheikh, A.B., Mendelson, Z.S., Liu, J.K. (2014). Endoscopic versus microsurgical resection of colloid cysts: a systematic review and meta-analysis of 1,278 patients. *World Neurosurg*, **82**(6), 1187–97.

REFERENCES

Abdou, M.S. & Cohen, A.R. (2000). Endoscopic surgery of the third ventricle: the subfrontal trans-lamina terminalis approach. *Minim Invasive Neurosurg*, **43**(4), 208–11.

Aggleton, J.P., McMackin, D., Carpenter, K., et al. (2000). Differential cognitive effects of colloid cysts in the third ventricle that spare or compromise the fornix. *Brain*, **123**, 800–15.

Akins, P.T., Roberts, R., Coxe, W.S., et al. (1996). Familial colloid cyst of the third ventricle: case report and review of associated conditions. *Neurosurgery*, **38**, 392–5.

Antunes, J.L., Louis, K.M., & Ganti, S.R. (1980). Colloid cysts of the third ventricle. *Neurosurgery*, **7**(5), 450–5.

Beems, T., Menovsky, T., & Lammens, M. (2006). Hemorrhagic colloid cyst: case report and review of the literature. *Surg Neurol*, **65**(1), 84–6.

Bosch, D.A., Rähn, T., & Backlund, E.O. (1978). Treatment of colloid cysts of the third ventricle by stereotactic aspiration. *Surg Neurol*, **9**(1), 15–18.

Charalampaki, P., Filippi, R., Welschehold, S., & Perneczky, A. (2006). Endoscope-assisted removal of colloid cysts of the third ventricle. *Neurosurg Rev*, **29**(1), 72–9.

Ciric, I. & Zivin, I. (1975). Neuroepithelial (colloid) cyst of the septum pellucidum. *J Neurosurg*, **43**, 69–73

Dandy, W.E. (1933). Case reports of colloid cysts in the third ventricle (group I). In: Dandy, W.E. (ed.) *Benign Tumours in the Third Ventricle of the Brain: Diagnosis and Treatment*, pp. 4–37. Baltimore, MD: Williams and Wilkins.

Deinsberger, W., Böker, D.K., & Samii, M. (1994). Flexible endoscopes in treatment of colloid cysts of the third ventricle. *Minim Invasive Neurosurg*, **37**(1), 12–16.

Desai, K.I., Nadkarni, T.D., Muzumdar, D.P., & Goel, A.H. (2002). Surgical management of colloid cyst of the third ventricle—a study of 105 cases. *Surg Neurol*, **57**(5), 295–302.

de Witt Hamer, P.C., Verstegen, M.J., & De Haan, R.J., et al. (2002). High risk of acute deterioration in two patients harbouring symptomatic colloid cysts of third ventricle. *J Neurosurg*, **96**, 1041–5.

El Khoury, C., Brugières, P., Decq, P., et al. (2000). Colloid cysts of the third ventricle: are MR imaging patterns predictive of difficulty with percutaneous treatment? *AJNR Am J Neuroradiol*, **21**(3), 489–92.

Fries, G. & Perneczky, A. (1994). Tumours and cysts of the third ventricle. In: Wilkins, R.H. & Rengachary, S.S. (eds.) *Principles of Neurosurgery*, pp. xx. Philadelphia, PA: Elsevier.

Fulton, J.F. (1946). *Biography of Harvey Cushing*. Springfield IL: Charles C. Thomas.

Gaertner, H.J., Prager, B., & Himkel, G.K. (1993). Colloid Cyst of the third ventricle with XYY syndrome. *J Hirnforsch*, **34**(4), 555–60.

Ganti, S.R., Antunes, J.L., Louis, K.M., & Hilal, S.K. (1981). Computed tomography in the diagnosis of colloid cysts of the third ventricle. *Radiology*, **138**(2), 385–91.

Graziani, N., Dufour, H., Figarella-Branger, D., Donnet, A., Bouillot, P., & Grisoli, F. (1995). Do the suprasellar neurenteric cyst, the Rathke cleft cyst and the colloid cyst constitute a same entity? *Acta Neurochir (Wien)*, **133**(3–4), 174–80.

Gutierrez-Lara, F., Patiño, R., & Hakim, S. (1975). Treatment of tumors of the third ventricle: a new and simple technique. *Surg Neurol*, **3**(6), 323–5.

Hamlat, A., Pasqualini, E., & Askar, B. (2004). Hypothesis about the physiopathology of acute deterioration and sudden death caused by colloid cysts of the third ventricle. *Med Hypotheses*, **63**(6), 1014–17.

Hattab, N., Freger, P., Tadie, M., & Creissard, P. (1990). [Treatment of colloid cysts of the third ventricle by cerebrospinal fluid shunt]. *Neurochirurgie*, **36**(2), 129–31.

Hernesniemi, J. & Lievo, S. (1996). Management outcome in third ventricular colloid cysts in a defined population: a series of 40 patients treated mainly by transcallosal microsurgery. *Surg Neurol*, **45**, 2–14.

Hine, A.L. & Chui, M.S. (1987). Hypodense colloid cyst of the third ventricle. *Can Assoc Radiol J*, **38**(4), 288–91.

Hopf, N.J., Grunert, P., Fries, G., Resch, K.D., & Perneczky, A. (1999). Endoscopic third ventriculostomy: outcome analysis of 100 consecutive procedures. *Neurosurgery*, **44**(4), 795–804.

Ibrahim, A.W., Farag, H., Naguib, M., et al. (1986). Neuroepithelial (colloid) cyst of the third ventricle in identical twins. *J Neurosurg*, **65**, 401–3.

Jan, M., Zeze, V.B., Velut, S. (1989). Colloid cyst of fourth ventricle: diagnostic problems and pathogenic considerations. *Neurosurgery*, **24**(6), 939–42.

Jaskólski, D.J., Wróbel-Wiśniewska, G., Papierz, W., et al. (2003). Colloid-like cyst located in the prepontine region. *Surg Neurol*, **60**, 260–4.

Jeffree, R.L. & Besser, M. (2001). Colloid cyst of the third ventricle: a clinical review of 39 cases. *J Clin Neuroci*, **8**, 328–31.

Joshi, S.M., Gnanalingham, K.K., Mohaghegh, P., Wilson, A., & Elsmore, A. (2005). A case of familial third ventricular colloid cyst. *Emerg Med J*, **22**, 909–10.

Killer, H.E., Flammer, J., Wicki, B., & Laeng, R.H. (2001). Acute asymmetric upper nasal quandrantanopsia caused by a chiasmal colloid cyst in a patient with multiple sclerosis and bilateral retrobulbar neuritis. *Am J Ophthalmol*, **132**(2), 286–8.

Kondziolka, D. & Lunsford, L.D. (1992). Factors predicting successful stereotactic aspiration of colloid cysts. *Stereotact Funct Neurosurg*, **59**(1–4), 135–8.

Lavyne, M.H. & Patterson, R.H. Jr. (1983). Subchoroidal transvelum interpositum approach to mid-third ventricular tumors. *Neurosurgery*, **12**(1), 86–94.

Leech, R.W., Freeman, T., & Johnson, R. (1982). Colloid cyst of the third ventricle. A scanning and transmission electron microscopic study. *J Neurosurg*, **57**(1), 108–13.

Levine, N.B., Miller, M.N., & Crone, K.R. (2007). Endoscopic resection of colloid cysts: indications, technique, and results during a 13-year period. *Minim Invasive Neurosurg*, **50**(6), 313–17.

Lewis, A.I., Crone, K.R., Taha, J., van Loveren, H.R., Yeh, H.S., & Tew, J.M. Jr. (1994). Surgical resection of third ventricle colloid cysts. Preliminary results comparing transcallosal microsurgery with endoscopy. *J Neurosurg*, **81**(2), 174–8.

Little, J.R. & MacCarty, C.S. (1974). Colloid cysts of the third ventricle. *J Neurosurg*, **39**, 230–5.

Macdonald, R.L., Humphreys, R.P., Rutka, J.T., et al. (1994). Colloid cysts in children. *Pediatr Neurosurg*, **20**, 169–77.

Maeder, P.P., Holtås, S.L., Basibüyük, L.N., Salford, L.G., Tapper, U.A., & Brun, A. (1990). Colloid cysts of the third ventricle: correlation of MR and CT findings with histology and chemical analysis. *AJR Am J Roentgenol*, **155**(1), 135–41.

Malik, G.M., Horoupian, D.S., & Boulos, R.S. (1980). Hemorrhagic (colloid) cyst of the third ventricle and episodic neurologic deficits. *Surg Neurol*, **13**(1), 73–7.

Mallucci, C. (2010). *Cerebrospinal Fluid Disorders*. New York, NY: Informa Healthcare.

Maqsood, A.A.R., Devi, I.B., Mohanty, A., et al. (2006). Third ventricular colloid cysts in children. *Pediatr Neurosurg*, **42**, 147–50.

Mathiesen, T., Grane, P., Lindquist, C., & von Holst, H. (1993). High recurrence rate following aspiration of colloid cysts in the third ventricle. *J Neurosurg*, **78**(5), 748–52.

Maurice-Williams, R.S. & Wadley, J.P. (1998). Paired colloid cysts of the third and lateral ventricles. *Br J Neurosurg*, **12**(1), 47–50.

Motoyama, Y., Hashimoto, H., Ishida, Y., & Iida, J. (2002). Spontaneous rupture of a presumed colloid cyst of the third ventricle—case report. *Neurol Med Chir (Tokyo)*, **42**(5), 228–31.

Nader-Sepahi, A. & Hamlyn, P.J. (2000). Familial colloid cysts of the third ventricle: case report. *Neurosurgery*, **46**, 751–3.

Pollock, B.E., Schreiner, S.A., & Huston, J. 3rd. (2000). A theory on the natural history of colloid cysts of the third ventricle. *Neurosurgery*, **46**(5), 1077–81; discussion 1081–3.

Powell, M.P., Torrens, M.J., Thomson, J.L., & Horgan, J.G. (1983). Isodense colloid cysts of the third ventricle: a diagnostic and therapeutic problem. *Neurosurgery*, **13**(3), 234–7.

Powers, J.M. & Dodds, H.M. (1977). Primary actinomycoma of the third ventricle—the colloid cyst. A histochemical and ultrastructural study. *Acta Neuropathol*, **37**(1), 21–6.

Rivas, J.J. & Lobato, R.D. (1985). CT-assisted stereotaxic aspiration of colloid cysts of the third ventricle. *J Neurosurg*, **62**(2), 238–42.

Romani, R., Niemelä, M., Korja, M., et al. (2008). Dizygotic twins with a colloid cyst of the third ventricle: case report. *Neurosurgery*, **63**, E10003.

Sheikh, A.B., Mendelson, Z.S., Liu, J.K. (2014). Endoscopic versus microsurgical resection of colloid cysts: a systematic review and meta-analysis of 1,278 patients. *World Neurosurg*, **82**(6), 1187–97.

Shima, T., Ishikawa, S., Okada, Y., Kajikawa, H., & Kodama, Y. (1976). ['Colloid cyst' of the lateral ventricle--report of a case (author's transl)]. *No Shinkei Geka*, **4**(8), 791–7.

Shuangshoti, S. & Netsky, M.G. (1966). Neuroepithelial (colloid) cysts of the nervous system. Further observations on pathogenesis, location, incidence and histochemistry. *Neurology*, **16**, 887–903.

Sjovall, E. (1910). Über eine Ependymcyste embryonalen Charakters (Paraphyse?) im dritten Hirnventrikel mit lipochromer Veranderungen mit autreten vo Halbondkorperchen. *Beitr Pathol Anat*, **47**, 248.

Sweet, W.H., Talland, G.A., & Ervin, F.R. (1959). Loss of recent memory following section of fornix. *Trans Am Neurol Assoc*, **84**, 76–82.

Takahiro, T., Hruban, R.H., Carson, B.S., et al. (1992). Colloid cysts of the third ventricle: immunohistochemical evidence for nonneuroepithelial differentiation. *Hum Pathol*, **23**, 811–16.

Wen, H.T., Rhoton, A.L. Jr, & de Oliveira, E. (1998). Transchoroidal approach to the third ventricle: an anatomic study of the choroidal fissure and its clinical application. *Neurosurgery*, **42**(6), 1205–17.

RELATED LINKS TO EBRAIN

Pathophysiology and Management of Colloid Cysts. https://learning.ebrain.net/course/view.php?id=422

Radiology of CNS Cysts. https://learning.ebrain.net/course/view.php?id=577

34

Choroid plexus tumours

Jonathan Roth, Rina Dvir, and Shlomi Constantini

Introduction

Choroid plexus tumours (CPT) are rare intraventricular tumours that originate from the choroid plexus epithelium. According to the 2007 and 2016 WHO classification, there are three tumour subtypes (Wrede et al., 2009; Menon et al., 2010; Dudley et al., 2015; Louis et al., 2016):

- Choroid plexus papilloma (CPP), which is benign and compose roughly 40–60% of CPT
- Choroid plexus carcinoma (CPC), which is malignant and compose roughly 30–50% of CPT
- Atypical choroid plexus papilloma (ACPP), which is an intermediate subtype and compose roughly 10–30% of CPT

Typically, CPT are considered more prevalent in the infantile age group; however, CPT may present in adulthood too.

In this chapter, we discuss the main diagnostic, genetic, and treatment-related aspects of CPT.

Epidemiology

CPTs occur mainly in infants before the age of 2 years (Lam et al., 2013); however, it may occur in older children and adults (Turkoglu et al., 2014). Their prevalence, pathology, and anatomical distribution differ between age groups (Lam et al., 2013). CPT represent 2–5% of paediatric brain tumours, as opposed to 0.4–0.8% of adult brain tumours. CPT often present as congenital/neonatal tumours and comprise 10–20% of brain tumours diagnosed during the first year of life (Serowka et al., 2010; Lang et al., 2012; Sun et al., 2014b).

Pathology also differs between age groups. CPC and ACPP are more common in the infantile age group, with a median age for CPC of 3 years old. There is a slight male predominance, possibly linking CPT to an x-linked mutation (Menon et al., 2010; Dudley et al., 2015).

CPT typically occur in the ventricular system since they arise from the choroid plexus. In children, they are typically located in the lateral ventricle, mostly at the atrium (**Fig. 34.1**). Third ventricular CPT are rare, occurring mostly in infants (Gupta et al., 2013) (**Fig. 34.2**). In adults, most CPT occur in the posterior fossa, mostly in the fourth ventricle (Bostrom et al., 2011). While CPPs are almost always confined to the ventricular system, CPCs are not usually limited in that way. CPC may reach very large sizes, often presenting as a large hemispheric tumour in an infant.

CPC is associated with worse overall survival (OS) compared to CPP and ACPP (Lam et al., 2013; Dudley et al., 2015). OS at 5 years for CPP following complete resection ranges between 84% and 100% (Wrede et al., 2009; Lam et al., 2013; Dudley et al., 2015). In contrast, CPC is a highly malignant tumour with a dismal prognosis despite multimodal treatment, with OS at 5 years of about 26–70% (Wrede et al., 2009; Lam et al., 2013; Dudley et al., 2015). Most ACPP have an OS rate similar to CPP, however a small subgroup displays the biological behaviour and prognosis of CPC (Wrede et al., 2009).

Presenting symptoms

CPP are one of two entities leading to overproduction of CSF (the other being choroid plexus hyperplasia (CPH)). CPP may produce up to 5 litres per day (Fujimura et al., 2004; Cataltepe et al., 2010; Nimjee et al., 2010), often with a high protein level. Thus, CPP may lead to hydrocephalus secondary to several causes: CSF overproduction, CSF pathway obstruction, and CSF malabsorption. Many of the patients with CPT present with hydrocephalus (Pencalet et al., 1998; Bettegowda et al., 2012; Sun et al., 2014b) (**Figs. 34.2, 34.3, 34.4,** and **34.7**).

Signs and symptoms of increased intracranial pressure secondary to hydrocephalus in infants include increased head circumference, upward gaze limitation, general hypotonia, bulging fontanel, vomiting, and failure to thrive (FTT). In older children and adults, symptoms often include headaches, nausea/vomiting, visual decline, and focal signs depending on the exact location (Lang et al., 2012).

As CPC are often large invading tumours, they may present with symptoms secondary to a hemispheric mass effect (leading to elevated intracranial pressure and seizures) (**Fig. 34.3**). APCC are more closely related to CPP than to CPC (**Figs. 34.2** and **34.4**). They are often of intermediate size, located in the ventricle, and generally do not invade the surrounding hemisphere. They are more prevalent in the infantile age group, but may present in adulthood too.

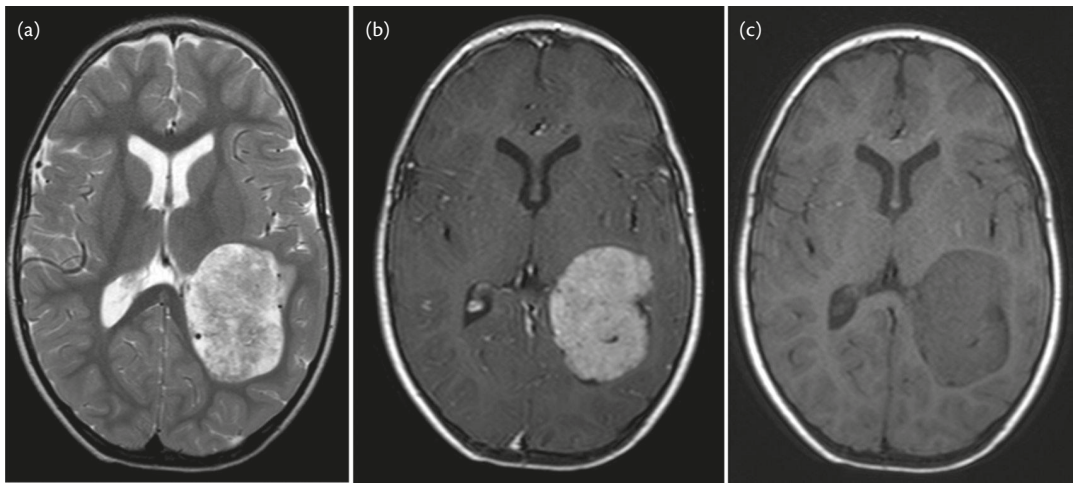

Fig. 34.1 A 2.5-year-old with a CPP. Axial T2 (A), T1-Gad (B), and T1 (C) MRI scans, showing an atrial tumour. The tumour was completely resected.
Courtesy of Dr Kieren Allinson, Department of Pathology, Addenbrooke's Hospital, Cambridge.

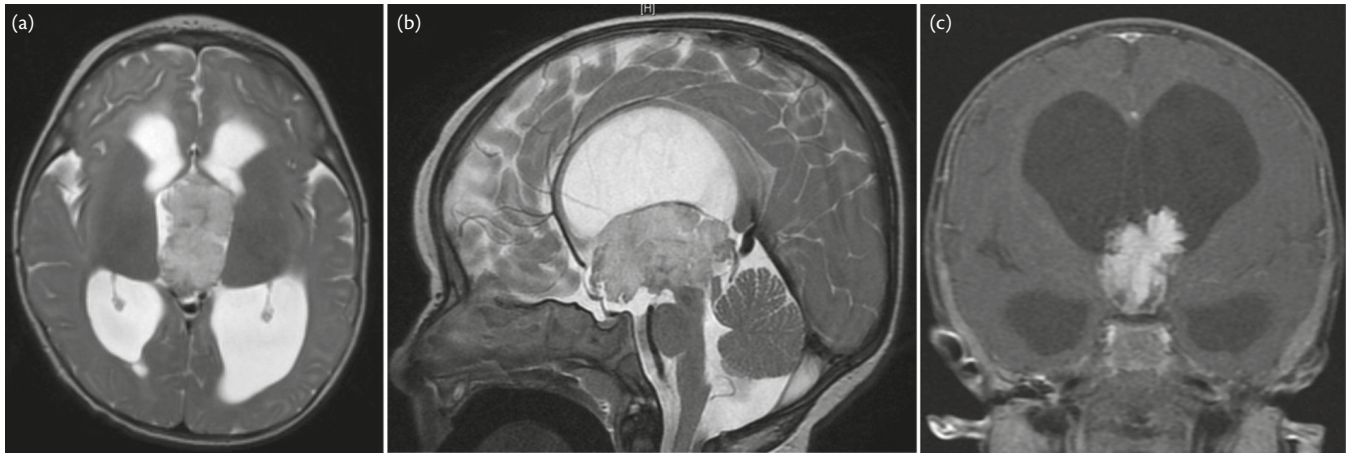

Fig. 34.2 A 5-month-old child with ACPP. Axial T2 (A), Sagittal T2, and coronal T1-Gad (C) MRI scans, showing a third ventricular lesion. The tumour was completely resected and child followed up.
Courtesy of Dr Kieren Allinson, Department of Pathology, Addenbrooke's Hospital, Cambridge.

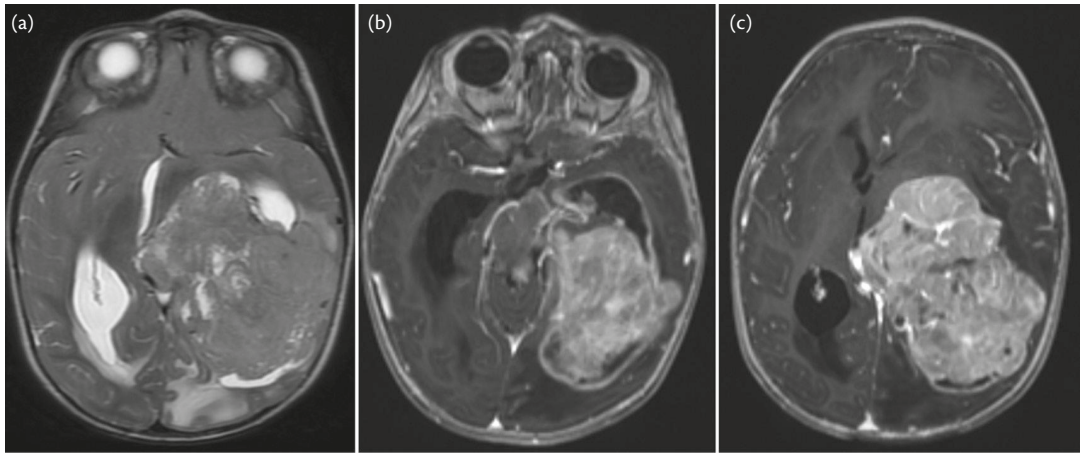

Fig. 34.3 A 20-month-old child with CPC. Axial T2 (A) and T1-Gad (B&C) MRI scans, showing a large ventricular tumour. Note ependymal enhancement. The tumour was completely resected, followed by chemotherapy. The child succumbed to the tumour less than a year after diagnosis.
Courtesy of Dr Kieren Allinson, Department of Pathology, Addenbrooke's Hospital, Cambridge.

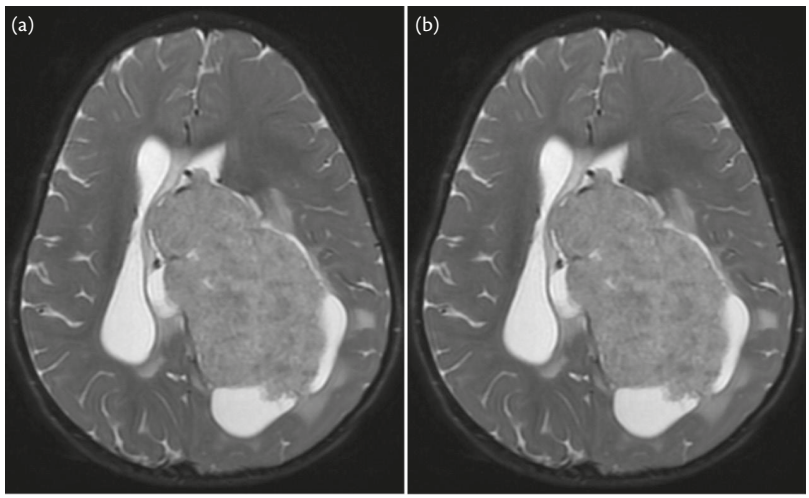

Fig. 34.4 An 11-month-old child with ACPP. Axial T2 (A) and T1-Gad (B) MRI scans, showing a large ventricular tumour. The tumour was completely resected followed by chemotherapy due to tumour recurrence.
Courtesy of Dr Kieren Allinson, Department of Pathology, Addenbrooke's Hospital, Cambridge

Diagnosis

CPTs are located mostly within the ventricular system. As stated earlier, most CPP in the paediatric age group arise in the lateral ventricle, mostly at the atrium, as opposed to CPP in adult patients, which are located most commonly in the fourth ventricle (Figs. 34.1, 34.3, 34.4, 34.6, and 34.7). CPT have been described in the third ventricle (Mishra et al., 2014) and cerebellopontine angle (CPA) (Menon et al., 2010; Prasad et al., 2014), originating from the local choroid plexus (Figs. 34.2 and 34.5). CPP may also occur extraventricularly, in the pineal region (Sasani et al., 2014), brainstem (Xiao et al., 2013), sellar/suprasellar region (Bian et al., 2011), and brain parenchyma (Imai et al., 2011).

The classical radiological appearance of CPP is of a cauliflower-like lesion, isointense on T1, with brisk and homogeneous enhancement (Fig. 34.1). However, in rare instances they may not enhance (Pratheesh et al., 2009). They are often isohyperintense on T2 (Figs. 34.1, 34.5, 34.6, and 34.7). On CT they are usually isodense with mild calcifications. CPP may rarely be cystic with mural nodules (Emami-Naeini et al., 2008). ACPP generally resembles CPP radiologically (Figs. 34.2 and 34.4).

CPC often have a large, non-homogenous enhancing appearance. Leptomeningeal spread (or drop metastasis) is rare in CPP (about 5%). However, it may occur in ACPP and CPC in up to 50% of cases, thus a spinal MRI is indicated (Menon et al., 2010, Wrede et al., 2009) (Fig. 34.3). It is unclear if surgery is a risk factor for drop metastasis (Sun et al., 2014b).

Of major importance is the blood supply. The choroidal vessels are often engorged, leading to large deep-seated veins—including thalamostriate, atrial vein, internal cerebral vein, and vein of Galen. These arteries and veins are usually located on the deep/medial aspect of the tumour. Peripherally located draining ependymal veins are also common, especially in large and high-grade CPT. Digital subtraction angiography (DSA) often shows an early tumour blush, with prominent choroidal arteries.

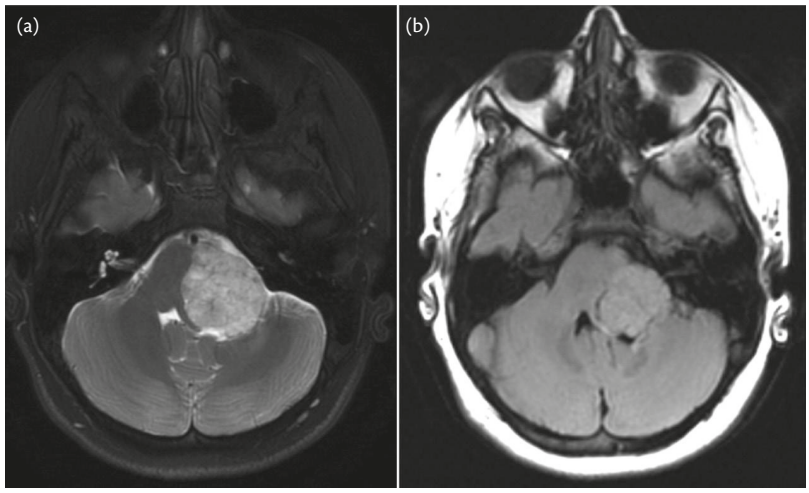

Fig. 34.5 A 12-year-old child with a CPP. Axial T2 (A) and T1 (B) MRI scans, showing a CPA lesion. The lesion was completely resected.
Courtesy of Dr Kieren Allinson, Department of Pathology, Addenbrooke's Hospital, Cambridge

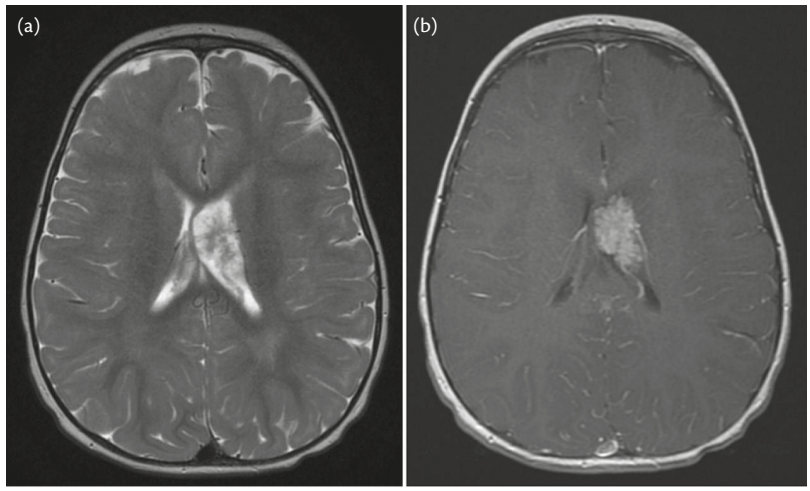

Fig. 34.6 A 15-month-old child with a CPP. Axial T2 (A) and T1-Gad (B) MRI scans, showing a lateral ventricle lesion. The tumour was completely resected.
Courtesy of Dr Kieren Allinson, Department of Pathology, Addenbrooke's Hospital, Cambridge.

Hydrocephalus is commonly seen secondary to the various mechanisms stated here earlier.

Pathology

CPC display the classic histopathological signs of malignancy such as a high mitotic index, cellular atypia, and brain invasion (Fig. 34.8). In contrast, CPP are benign papillary neoplasms resembling non-neoplastic choroid plexus (Fig. 34.9). Nevertheless, despite the obvious histological differences, there is a histological continuum between choroid plexus hyperplasia (CPH), CPP, ACPP, and CPC (D'Ambrosio et al., 2003). However, genetic and molecular studies in CPT are limited. Although rare, malignant transformation of CPP and ACPP to CPC has been described (Jeibmann et al., 2007).

While CPH is a non-tumoural pathology with no growth potential, differentiation between CPH and CPP may be difficult (D'Ambrosio et al., 2003; Cataltepe et al., 2010). Various measures have been used to differentiate between the two pathologies, including MIB-1 proliferative index (in CPH it is close to 0, while in CPP it ranges between 0.2 and 17). Histologically, CPT are differentiated from normal choroid plexus by EAAT-1 expression. EAAT-1 is a glial glutamate transporter that is commonly seen in CPT, and is absent in normal choroid plexus (Beschorner et al., 2009).

Since 2007 (and remaining in the 2016 version), the WHO described an intermediate group—*atypical CPP* (ACPP) (Louis et al., 2016). These tumours resemble CPP but with increased mitotic activity (≥2 mitoses/10HPF) (Jeibmann et al., 2006). ACPP tend to occur in younger patients compared to CPP and CPC (Wrede et al., 2009; Lam et al., 2013). OS for ACPP is similar to OS for CPP in young children, but is considered a poor prognostic factor in children older than 3 years old (Thomas et al., 2015).

CPC is one of the characteristic paediatric tumours of Li-Fraumeni syndrome (LFS), a familial cancer predisposition syndrome characterized by a high frequency of malignant tumours at a young age. TP53 germline mutations are the genetic hallmark of

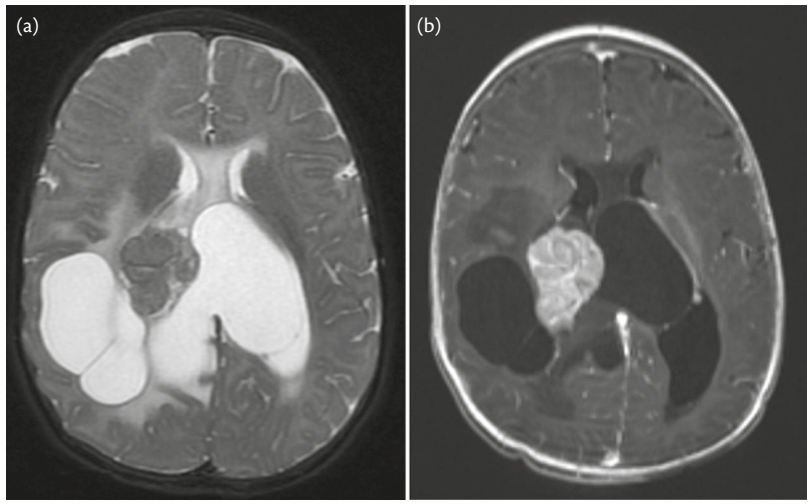

Fig. 34.7 A 5-month-old child with CPP. Axial T2 (A) and T1-Gad (B) MRI scans, showing a ventricular tumour with an accompanying cyst. The tumour was completely resected.
Courtesy of Dr Kieren Allinson, Department of Pathology, Addenbrooke's Hospital, Cambridge.

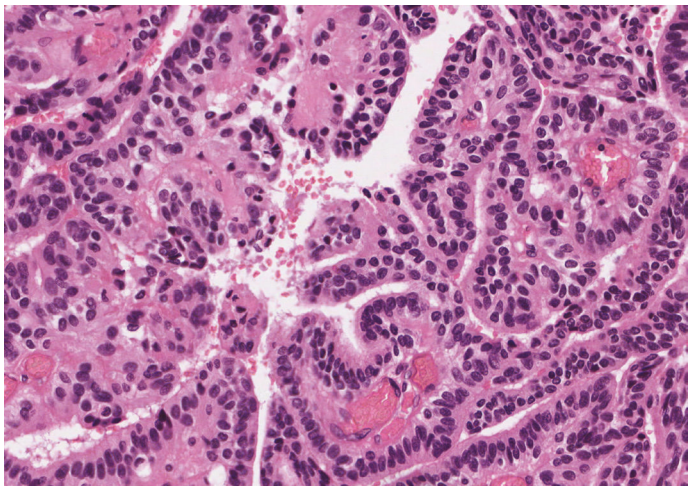

Fig. 34.8 Atypical choroid plexus papilloma—atypical examples such as this display raised mitotic activity and variable loss of the papillary pattern.
Courtesy of Dr Kieren Allinson, Department of Pathology, Addenbrooke's Hospital, Cambridge.

LFS. Patients with CPC should be screened for Li-Fraumeni syndrome (TP53 germline mutations) (Gozali et al., 2012; Giacomazzi et al., 2013).

Genetic and molecular studies have shown similarities between CPP and ACPP (Merino et al., 2015). It has been suggested that ACPP represents an immature variant of CPP, characterized by increased proliferative activity, whereas CPC seem to represent a genetically distinct tumour (Japp et al., 2015). CPC is highly correlated with TP53 mutations, where more copies of mutated TP53 are associated with increased CPC aggressiveness and a worse rate of survival (Merino et al., 2015). These mutations can either be part of a germline LFS or somatic TP53 mutations in the tumour tissue itself.

CPC and ATRT (atypical terato-rhabdoid tumour) may show similar histological appearances. However, INI1 protein staining is positive in CPC and negative in ATRT, differentiating between the two (Stevens et al., 2009; Sun et al., 2014b).

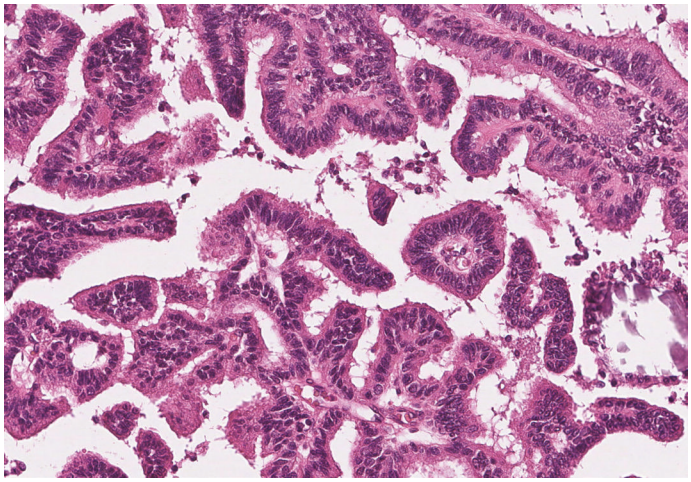

Fig. 34.9 Choroid plexus papilloma—a papillary architecture composed of epithelium overlying fibrovascular cores. Mitotic figures are rare in this grade I example.
Courtesy of Dr Kieren Allinson, Department of Pathology, Addenbrooke's Hospital, Cambridge.

Treatment

Complete surgical resection (gross total resection, GTR) is the cornerstone of treatment for CPP, ACPP, and CPC, in both paediatric and adult patients (Wrede et al., 2009; Safaee et al., 2013; Koh et al., 2014; Sun et al., 2014a; Dudley et al., 2015). Various series have shown a significant correlation between complete resection, overall survival, and progression-free survival (Sun et al., 2014a; Dudley et al., 2015). GTR is more commonly achieved in CPP (80–100%) compared to ACPP (63%) and CPC (47–62%) (Pencalet et al., 1998; Wrede et al., 2009). Tumour recurrence following GTR is estimated at about 30% in ACPP, and about 6% in CPP (Jeibmann et al., 2007).

As CPT are more common among infants and are often extremely vascular, several technical points need to be addressed in order to improve patient safety and decrease blood loss and patient morbidity.

Preoperative embolization

Preoperative embolization (PE) has been described in a small number of series, with encouraging results. Super-selective embolization of the feeding arteries via the anterior or posterior choroidal arteries, using various materials such as microspheres, NBCA, onyx, and histoacryl glue, has been shown to significantly reduce blood loss and improve the surgeon's resection control and extent of resection (Takahashi et al., 2009; Trivelato et al., 2012; Haliasos et al., 2013b; Wang et al., 2013). Interestingly, PE was found to reduce CSF production following surgery; however, it did not reduce the need for permanent CSF diversion (Haliasos et al., 2013a). In a single case report, embolization was performed in a three-month-old baby to treat a third ventricular tumour suggestive of being a CPP (Wind et al., 2010). Following embolization, the tumour completely involuted.

Age was not found to limit the ability to safely enter the feeding vessels and embolize the tumours, with PE performed in babies even in the neonatal period and during first few months of life (Otten et al., 2006; Hartge et al., 2010; Wind et al., 2010).

Surgical resection

Anaesthesia-related factors include preoperative preparation of sufficient blood products. At surgery, large venous access lines (as well as a central line if necessary), and an invasive arterial-line should be placed. Major blood loss and the need for massive transfusions is a major point to be addressed, especially among infants (Piastra et al., 2007).

Positioning of the patient should allow good venous drainage with no compression on the jugular veins. The head should be raised above the level of the heart. The surgical corridor should be comfortable. These cases may be extremely bloody, and a small 'minimal-invasive' approach may restrict the surgeon's comfort as well as the patient's safety.

The surgeon must attempt early identification and control of the feeding vessels. Nevertheless, often, especially in large tumours, the vessels are exposed only after a major debulking of the tumour has been performed. Thus, in such cases, an efficient technique should be applied, including removing parts of the tumour, coupled with blood products as needed, and tamponade every few minutes to reduce blood loss. Continuous surgeon-anaesthesiologist updates are paramount in such cases, to alert the surgeon once hypovolemic

signs arise, and alert the anaesthesiologist regarding any major bleeding. The very large tumours (especially CPC) may necessitate many blood product transfusions. Tranexamic acid (TXA)—an antifibrinolytic agent—has been suggested to reduce operative blood loss in small children with CPT (Phi et al., 2014).

Luckily, most CPP are soft and easily aspirated by suction. Thus, a relatively fast tumour removal may be achieved, exposing the feeding vessels, and allowing for their coagulation and control. It is important to 'protect' the surrounding ventricle (especially the regions of the foraminae of Monro) from blood spillage, to avoid casts of blood in the ventricular system. Following tumour resection, it is important to inflate the ventricular system with irrigation, as following CSF drainage may trigger subdural hematomas and collections (Pencalet et al., 1998). Some surgeons have advocated 'sealing' the corticectomy opening with fibrin glue (Pencalet et al., 1998).

Surgical approaches to the ventricular system depend on the exact location as well as size of the tumour and ventricles, and vascular supply. Generally, lesions located at the atrium are often located posterior-laterally, thus limiting interhemispheric approaches. These may be approached transcortically, via the low parieto-occipital junction, taking into account optic radiation fibres, as well as arcuate fibres (especially on the dominant side), or via superior parietal lobule. Another approach to the atrium is the contralateral interhemispheric translingual approach. Other transtemporal/transparietal approaches depend on dominance and cortical mantle over the tumour. Tumours located at the body of the lateral ventricle may be approached via a transcallosal approach. Third ventricular tumours may be approached via a transforaminal with or without a transchoroidal extension, or via a posterior approach, as though to the pineal region. Recently, endoscopic resections of third ventricular choroid plexus tumours have been described (Santos and Souweidane, 2015; Sufianov et al., 2015). CPA lesions may be approached via a retrosigmoid approach, and a fourth ventricular lesion can be approached via a telovelar approach.

CPT of the fourth ventricle may invade the brainstem (Kumabe et al., 2008). Thus, these cases should be operated while using intraoperative monitoring, possibly performing a subtotal resection and adding adjuvant treatment.

It has been shown that hydrocephalus may persist even following complete tumour resection. This may be secondary to prior compromised absorption, in addition to the reaction to surgical blood products. Obstructive hydrocephalus may arise from local adhesions at the foramen of Monro or aqueduct. Also, secondary to major ventricular involvement and spillage of blood products, postoperative fever is common, and may need to be differentiated from infectious causes. Thus, following tumour resection, the ventricular system needs to be irrigated to remove blood clots. An external ventricular drain (EVD) is often placed to allow clearance of CSF over a few days.

In cases presenting with severe hydrocephalus, an early EVD may control the intracranial pressure prior to resection of the tumour. However, especially in small children, severe electrolyte imbalance may follow (Phi et al., 2011).

Radiation and chemotherapy

CPP is generally considered a benign tumour, which does not require treatment after a gross total resection has been achieved. CPC is a highly proliferative malignant tumour that can metastasize along the neuroaxis and generally has a poor survival outcome. The mainstay of CPC treatment is surgery with adjuvant chemotherapy. In selected cases, neoadjuvant chemotherapy is administered prior to definitive surgery. Older children and adults are often treated with chemo-radiotherapy protocols. Several chemotherapy regimens are employed in CPC, including ICE (ifosfamide, carboplatin, and etoposide) (Berrak et al., 2011) and regimens containing multiagent chemotherapy (carboplatin, cyclophosphamide, etoposide, doxorubicin, and methotrexate) (Passariello et al., 2015). ICE has been used also as a neoadjuvant treatment prior to tumour resection, increasing the rates of GTR and reducing blood loss (Lafay-Cousin et al., 2010; Schneider et al., 2015). Some institutions employ myeloablative high-dose chemotherapy with stem cell support either as upfront treatment (Zaky et al., 2015), or as a salvage treatment for relapsed cases (Mosleh et al., 2013). The 5- and 10-year overall survival for CPC following GTR is 70% and 67%, respectively (Dudley et al., 2015).

The benefit of radiation in CPC treatment remains a matter of debate. In a recent population-based study, radiation failed to improve OS of patients with CPC (Cannon et al., 2015; Dudley et al., 2015). However, in another meta-analysis published in 2014, radiation conferred a survival advantage to patients that underwent complete or incomplete resection of CPC (Sun et al., 2014b). In CPC associated with Li-Fraumeni syndrome, radiation has been associated with poorer OS rates (Bahar et al., 2015).

Stereotactic radiosurgery (SRS) has been selectively applied for refractory tumours (Kim et al., 2008). It may also be applied for small and/or distant tumours that recurred following surgery.

Adjuvant treatment of ACPP is controversial. In younger patients, ACPP is not considered a bad prognostic factor. Complete resection followed by 'watch and see' is the accepted regimen (Thomas et al., 2015). In children older than 3 years of age, a close follow-up after GTR is recommended because of the prognostic impact of ACPP (Thomas et al., 2015).

For incompletely resected ACPP, adjuvant chemotherapy is the accepted treatment. Similar to the CPC treatment protocols, various treatment regimens exist, including high-dose chemotherapy and stem cell rescue (Mosleh et al., 2013; Zaky et al., 2015). This protocol postpones radiotherapy usage, depending on the child's age and status of residual tumour.

Favourable prognostic factors for CPC include supratentorial location, GTR of tumour, no TP53 mutation (either somatic or germline), age older than 3 years of age, no tumour dissemination, no tumour recurrence, and adjuvant treatment (Sun et al., 2014b).

REFERENCES

Bahar, M., Kordes, U., Tekautz, T., & Wolff, J. (2015). Radiation therapy for choroid plexus carcinoma patients with Li-Fraumeni syndrome: advantageous or detrimental? *Anticancer Res*, **35**(5), 3013–17.

Berrak, S.G., Liu, D.D., Wrede, B., & Wolff, J.E. (2011). Which therapy works better in choroid plexus carcinomas? *J Neurooncol*, **103**(1), 155–62.

Beschorner, R., Pantazis, G., Jeibmann, A., et al. (2009). Expression of EAAT-1 distinguishes choroid plexus tumors from normal and reactive choroid plexus epithelium. *Acta Neuropathol*, **117**, 667–75.

Bettegowda, C., Adogwa, O., Mehta, V., et al. (2012). Treatment of choroid plexus tumors: a 20-year single institutional experience. *J Neurosurg Pediatr*, **10**, 398–405.

Bian, L.G., Sun, Q.F., Wu, H.C., Jiang, H., Sun, Y.H., & Shen, J.K. (2011). Primary choroid plexus papilloma in the pituitary fossa: case report and literature review. *Acta Neurochir (Wien)*, **153**, 851–7.

Bostrom, A., Bostrom, J.P., Von Lehe, M., Kandenwein, J.A., Schramm, J., & Simon, M. 2011. Surgical treatment of choroid plexus tumors. *Acta Neurochir (Wien)*, **153**, 371–6.

Cannon, D.M., Mohindra, P., Gondi, V., Kruser, T.J., & Kozak, K.R. (2015). Choroid plexus tumor epidemiology and outcomes: implications for surgical and radiotherapeutic management. *J Neurooncol*, **121**(1), 151–7.

Cataltepe, O., Liptzin, D., Jolley, L., & Smith, T. W. (2010). Diffuse villous hyperplasia of the choroid plexus and its surgical management. *J Neurosurg Pediatr*, **5**, 518–22.

D'Ambrosio, A.L., O'Toole, J.E., Connolly, E.S., Jr., & Feldstein, N.A. (2003). Villous hypertrophy versus choroid plexus papilloma: a case report demonstrating a diagnostic role for the proliferation index. *Pediatr Neurosurg*, **39**, 91–6.

Dudley, R.W., Torok, M.R., Gallegos, D., Liu, A.K., Handler, M.H., & Hankinson, T.C. 2015. Pediatric choroid plexus tumors: epidemiology, treatments, and outcome analysis on 202 children from the SEER database. *J Neurooncol*, **121**, 201–7.

Emami-Naeini, P., Nejat, F., & El Khashab, M. (2008). Cystic choroid plexus papilloma with multiple mural nodules in an infant. *Childs Nerv Syst*, **24**, 629–31.

Fujimura, M., Onuma, T., Kameyama, M., et al. (2004). Hydrocephalus due to cerebrospinal fluid overproduction by bilateral choroid plexus papillomas. *Childs Nerv Syst*, **20**, 485–8.

Giacomazzi, J., Selistre, S.G., Rossi, C., et al. (2013). Li-Fraumeni and Li-Fraumeni-like syndrome among children diagnosed with pediatric cancer in Southern Brazil. *Cancer*, **119**, 4341–9.

Gozali, A. E., Britt, B., Shane, L., et al. (2012). Choroid plexus tumors; management, outcome, and association with the Li-Fraumeni syndrome: the Children's Hospital Los Angeles (CHLA) experience, 1991–2010. *Pediatr Blood Cancer*, **58**, 905–9.

Gupta, P., Sodhi, K.S., Mohindra, S., Saxena, A.K., Das, A., & Khandelwal, N. (2013). Choroid plexus papilloma of the third ventricle: a rare infantile brain tumor. *J Pediatr Neurosci*, **8**, 247–9.

Haliasos, N., Brew, S., Robertson, F., Hayward, R., Thompson, D., & Chakraborty, A. (2013a). Pre-operative embolisation of choroid plexus tumours in children. Part II. Observations on the effects on CSF production. *Childs Nerv Syst*, **29**, 71–6.

Haliasos, N., Brew, S., Robertson, F., Hayward, R., Thompson, D., & Chakraborty, A. (2013b). Preoperative embolisation of choroid plexus tumours in children: part I—does the reduction of perioperative blood loss affect the safety of subsequent surgery? *Childs Nerv Syst*, **29**, 65–70.

Hartge, D.R., Axt-Fliedner, R., & Weichert, J. (2010). Prenatal diagnosis and successful postnatal therapy of an atypical choroid plexus papilloma—case report and review of literature. *J Clin Ultrasound*, **38**, 377–83.

Imai, M., Tominaga, J., & Matsumae, M. (2011). Choroid plexus papilloma originating from the cerebrum parenchyma. *Surg Neurol Int*, **2**, 151.

Japp, A. S., Gessi, M., Messing-Junger, M., et al. (2015). High-resolution genomic analysis does not qualify atypical plexus papilloma as a separate entity among choroid plexus tumors. *J Neuropathol Exp Neurol*, **74**, 110–20.

Jeibmann, A., Hasselblatt, M., Gerss, J., et al. (2006). Prognostic implications of atypical histologic features in choroid plexus papilloma. *J Neuropathol Exp Neurol*, **65**, 1069–73.

Jeibmann, A., Wrede, B., Peters, O., Wolff, J.E., Paulus, W., & Hasselblatt, M. (2007). Malignant progression in choroid plexus papillomas. *J Neurosurg*, **107**, 199–202.

Kim, I.Y., Niranjan, A., Kondziolka, D., Flickinger, J.C., & Lunsford, L.D. (2008). Gamma knife radiosurgery for treatment resistant choroid plexus papillomas. *J Neurooncol*, **90**, 105–10.

Koh, E.J., Wang, K.C., Phi, J.H., et al. (2014). Clinical outcome of pediatric choroid plexus tumors: retrospective analysis from a single institute. *Childs Nerv Syst*, **30**, 217–25.

Kumabe, T., Fujimura, M., Jokura, H., & Tominaga, T. (2008). Surgical treatment for choroid plexus tumors in the fourth ventricle: brain stem infiltration hinders total extirpation. *Neurosurg Rev*, **31**, 165–72; discussion 172.

Lafay-Cousin, L., Mabbott, D.J., Halliday, W., et al. (2010). Use of ifosfamide, carboplatin, and etoposide chemotherapy in choroid plexus carcinoma. *J Neurosurg Pediatr*, **5**, 615–21.

Lam, S., Lin, Y., Cherian, J., et al. (2013). Choroid plexus tumors in children: a population-based study. *Pediatr Neurosurg*, **49**, 331–8.

Lang, S.S., Beslow, L.A., Gabel, B., et al. (2012). Surgical treatment of brain tumors in infants younger than six months of age and review of the literature. *World Neurosurg*, **78**, 137–44.

Louis, D.N., Perry, A., Reifenberger, G., et al. (2016). The 2016 World Health Organization Classification of Tumors of the Central Nervous System: a summary. *Acta Neuropathol*, **131**, 803–20.

Menon, G., Nair, S.N., Baldawa, S.S., Rao, R.B., Krishnakumar, K.P., & Gopalakrishnan, C.V. (2010). Choroid plexus tumors: an institutional series of 25 patients. *Neurol India*, **58**, 429–35.

Merino, D.M., Shlien, A., Villani, A., et al. (2015). Molecular characterization of choroid plexus tumors reveals novel clinically relevant subgroups. *Clin Cancer Res*, **21**, 184–92.

Mishra, A., Ojha, B.K., Chandra, A., Singh, S.K., Chandra, N., & Srivastava, C. (2014). Choroid plexus papilloma of posterior third ventricle: a case report and review of literature. *Asian J Neurosurg*, **9**, 238.

Mosleh, O., Tabori, U., Bartels, U., Huang, A., Schechter, T., & Bouffet, E. (2013). Successful treatment of a recurrent choroid plexus carcinoma with surgery followed by high-dose chemotherapy and stem cell rescue. *Pediatr Hematol Oncol*, **30**, 386–91.

Nimjee, S.M., Powers, C.J., Mclendon, R.E., Grant, G.A., & Fuchs, H.E. (2010). Single-stage bilateral choroid plexectomy for choroid plexus papilloma in a patient presenting with high cerebrospinal fluid output. *J Neurosurg Pediatr*, **5**, 342–5.

Otten, M.L., Riina, H.A., Gobin, Y.P., & Souweidane, M.M. (2006). Preoperative embolization in the treatment of choroid plexus papilloma in an infant. Case report. *J Neurosurg*, **104**, 419–21.

Passariello, A., Tufano, M., Spennato, P., et al. (2015). The role of chemotherapy and surgical removal in the treatment of choroid plexus carcinomas and atypical papillomas. *Childs Nerv Syst*, **31**(7), 1079–88.

Pencalet, P., Sainte-Rose, C., Lellouch-Tubiana, A., et al. (1998). Papillomas and carcinomas of the choroid plexus in children. *J Neurosurg*, **88**, 521–8.

Phi, J.H., Goobie, S.M., Hong, K.H., Dholakia, A., & Smith, E.R. (2014). Use of tranexamic acid in infants undergoing choroid plexus papilloma surgery: a report of two cases. *Paediatr Anaesth*, **24**, 791–3.

Phi, J.H., Shin, C.H., Wang, K.C., Park, S.H., & Kim, S.K. (2011). Catastrophic electrolyte imbalance caused by excessive production

and overdrainage of cerebrospinal fluid in an infant with choroid plexus papilloma. *Childs Nerv Syst*, **27**, 1153–6.
Piastra, M., Di Rocco, C., Tempera, A., et al. (2007). Massive blood transfusion in choroid plexus tumor surgery: 10-years' experience. *J Clin Anesth*, **19**, 192–7.
Prasad, G.L., Kumar, R., & Suri, V. (2014). Primary cerebellopontine angle choroid plexus papilloma in a child: a rare occurrence. *Neurol India*, **62**, 438–9.
Pratheesh, R., Moorthy, R.K., Singh, R., & Rajshekhar, V. (2009). Choroid plexus papilloma presenting as a non-contrast-enhancing fourth ventricular mass in a child. *Neurol India*, **57**, 486–8.
Safaee, M., Oh, M.C., Sughrue, M.E., et al. (2013). The relative patient benefit of gross total resection in adult choroid plexus papillomas. *J Clin Neurosci*, **20**, 808–12.
Santos, M.M. & Souweidane, M.M. (2015). Purely endoscopic resection of a choroid plexus papilloma of the third ventricle: case report. *J Neurosurg Pediatr*, **16**, 54–7.
Sasani, M., Solmaz, B., Oktenoglu, T., & Ozer, A.F. (2014). An unusual location for a choroid plexus papilloma: the pineal region. *Childs Nerv Syst*, **30**, 1307–11.
Schneider, C., Kamaly-Asl, I., Ramaswamy, V., et al. (2015). Neoadjuvant chemotherapy reduces blood loss during the resection of pediatric choroid plexus carcinomas. *J Neurosurg Pediatr*, **16**, 126–33.
Serowka, K., Chiu, Y., Gonzalez, I., et al. 2010. Central nervous system (CNS) tumors in the first six months of life: the Children's Hospital Los Angeles experience, 1979–2005. *Pediatr Hematol Oncol*, **27**, 90–102.
Stevens, E.A., Stanton, C.A., Nichols, K., & Ellis, T.L. (2009). Rare intraparenchymal choroid plexus carcinoma resembling atypical teratoid/rhabdoid tumor diagnosed by immunostaining for INI1 protein. *J Neurosurg Pediatr*, **4**, 368–71.
Sufianov, A.A., Gaibov, S.S., & Sufianov, R.A. (2015). Endoscopic monoportal removal of a choroid plexus papilloma in the posterior third ventricle in a child. *J Neurosurg Pediatr*, **16**, 107–11.
Sun, M.Z., Ivan, M.E., Clark, A.J., et al. (2014a). Gross total resection improves overall survival in children with choroid plexus carcinoma. *J Neurooncol*, **116**, 179–85.
Sun, M.Z., Oh, M.C., Ivan, M.E., et al. (2014b). Current management of choroid plexus carcinomas. *Neurosurg Rev*, **37**, 179–92; discussion 192.
Takahashi, M., Yamamoto, J., Aoyama, Y., Soejima, Y., Akiba, D., & Nishizawa, S. (2009). Efficacy of multi-staged surgery and adjuvant chemotherapy for successful treatment of atypical choroid plexus papilloma in an infant: case report. *Neurol Med Chir (Tokyo)*, **49**, 484–7.
Thomas, C., Ruland, V., Kordes, U., et al. (2015). Pediatric atypical choroid plexus papilloma reconsidered: increased mitotic activity is prognostic only in older children. *Acta Neuropathol*, **129**, 925–7.
Trivelato, F.P., Manzato, L.B., Rezende, M.T., Barroso, P.M., Faleiro, R.M., & Ulhoa, A.C. (2012). Preoperative embolization of choroid plexus papilloma with Onyx via the anterior choroidal artery: technical note. *Childs Nerv Syst*, **28**, 1955–8.
Turkoglu, E., Kertmen, H., Sanli, A.M., et al. (2014). Clinical outcome of adult choroid plexus tumors: retrospective analysis of a single institute. *Acta Neurochir (Wien)*, **156**, 1461–8; discussion 1467–8.
Wang, H.H., Luo, C.B., Guo, W.Y., et al. (2013). Preoperative embolization of hypervascular pediatric brain tumors: evaluation of technical safety and outcome. *Childs Nerv Syst*, **29**, 2043–9.
Wind, J.J., Bell, R.S., Bank, W.O., & Myseros, J.S. (2010). Treatment of third ventricular choroid plexus papilloma in an infant with embolization alone. *J Neurosurg Pediatr*, **6**, 579–82.
Wrede, B., Hasselblatt, M., Peters, O., et al. (2009). Atypical choroid plexus papilloma: clinical experience in the CPT-SIOP-2000 study. *J Neurooncol*, **95**, 383–92.
Xiao, A., Xu, J., He, X., & You, C. (2013). Extraventricular choroid plexus papilloma in the brainstem. *J Neurosurg Pediatr*, **12**, 247–50.
Zaky, W., Dhall, G., Khatua, S., et al. (2015). Choroid plexus carcinoma in children: the head start experience. *Pediatr Blood Cancer*, **62**, 784–9.

RELATED LINK TO EBRAIN

The Histopathology of Choroid Plexus Neoplasms. https://learning.ebrain.net/course/view.php?id=462

35

Surgical management of intraventricular lesions

Eduardo C. Ribas, Guilherme C. Ribas, and Ramez W. Kirollos

Anatomy of the lateral and third ventricles

Anatomy of the lateral ventricles

Deep inside each cerebral hemisphere, the lateral ventricle is found encircling the thalamus, which is characterized as an ovoid mass. The lateral ventricle is subdivided into openly communicating portions that receive different denominations according to their disposition in relation to the thalamus, the frontal horn corresponds to the ventricular portion located anterior to the thalamus, the ventricular body is the portion disposed over the thalamus, the atrium, or ventricular trigone, is located posterior to the thalamus, the temporal horn of the ventricle is placed beneath the thalamus and the occipital horn corresponds to a variable posterior extension of the atrium, which narrows progressively to one end (Timurkaynak et al., 1986; Rhoton, 2003) (**Figs. 35.1, 35.2, 35.3,** and **35.4**). Between the frontal horn and the body of each lateral ventricle, the interventricular foramen of Monro can be found, connecting each lateral ventricle with the third ventricle.

Each of these five portions has a floor, a roof, a lateral and a medial wall, with the frontal and temporal horns, and the atrium, also having an anterior wall (Timurkaynak et al., 1986; Ribas, 1999; Rhoton, 2003). Besides the thalamus, other structures that delimit the lateral ventricle portions are the corpus callosum, caudate nucleus, hippocampus, fornix, amygdala, the stria terminalis, and septum pellucidum.

The hippocampus is composed by Ammon's horn, characterized as an exuberant intraventricular prominence of the parahippocampal gyrus, and by the dentate gyri, disposed medially along the superior, medial, and flat surface of the parahippocampal gyrus called the subiculum (Williams and Warwick, 1980; Wen et al., 1999). The hippocampus is constituted by allocortex, characterized by three layers of cells, and is covered by the alveus which corresponds to the white matter formed by the axons of the neurons of these different cell layers (Williams and Warwick, 1980; Heimer, 1995; Duvernoy, 1998). It is interesting to note that, as other phylogenetically old nervous structures as the cord and brainstem, the white matter of the hippocampus is disposed externally and not internally.

Macroscopically the hippocampus is formed anteriorly by a head and a body which together constitute the medial aspect of the floor of the temporal horn, and by its tail that ends at the medial wall of the ventricular atrium (Timurkaynak et al., 1986; Rhoton, 2003).

The fornix arises along the hippocampus as the convergence of the alveus' fibres that form initially the thin fimbria of the fornix, which constitutes the most medial structure of the floor of the temporal horn. As the fornix continues posteriorly it encircles the most posterior part of the thalamus, called the pulvinar, assuming a form that resembles a tape called crura (the leg) of the fornix. Both crura of the fornices are connected together by the commissure of the fornix or hippocampal commissure, which are then attached to the inferior surface of the splenium of the corpus callosum. The fimbria of the fornix continues anteriorly and medially with the crura of the fornix turning into the body of the fornix, which is juxtaposed to the body of the contralateral fornix. The most anterior segment of the body of the fornix then detaches from the superior thalamic surface moving again away from the contralateral fornix with an anterior-lateral and inferior course becoming the column or pillar of the fornix. Most of its fibres run posteriorly to the anterior commissure, and penetrates the hypothalamic parenchyma to finally reach the ipsilateral mammillary body of the hypothalamus (**Figs. 35.2** and **35.3**). When detaching from the thalamus each column of the fornix becomes the anterior margin of the interventricular foramen of Monro, the posterior margin of which is formed by the most anterior aspect of the ipsilateral thalamus (Timurkaynak et al., 1986; Nagata et al., 1988; Rhoton, 2003). Given their locations, the crura of the fornix corresponds to the most medial aspect of the anterior wall of the atrium, and the body of the fornix to the most medial aspect of the floor of the ventricular body.

The choroidal fissure is the cleft between each thalamus and each fornix and corresponds to the insertion site of the choroid plexus to these two structures along two small ridges (taenia), respectively, the tenia thalami (or choroidea) and the tenia fornices. It extends between the inferior choroidal point, located just next to the transition between the head and body of the hippocampus at the level of the lateral geniculate body, and the interventricular foramen of Monro, which then corresponds to a widening of this cleft as a result from the detachment of the column of the fornix from the thalamus (Nagata et al., 1988; Rhoton, 2003) (**Fig. 35.3**). Since the choroidal fissure encircles the thalamus, there is no choroid plexus in the frontal and occipital horns (Nagata et al., 1988; Wen et al., 1998).

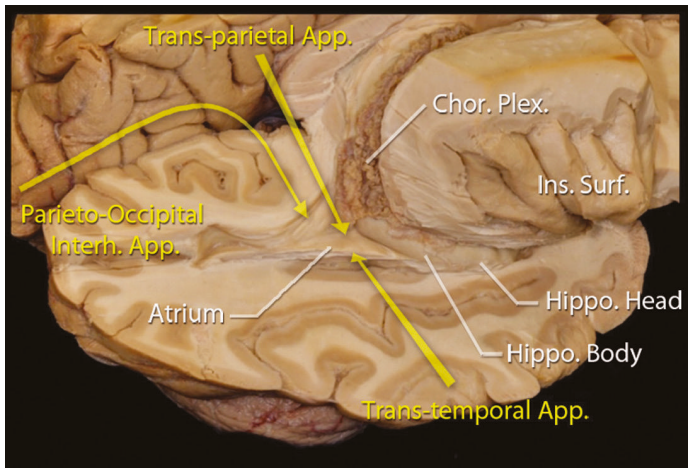

Fig. 35.1 The atrium of the lateral ventricle is exposed by a coronal cut posterior to the thalamus and an axial cut at the level of the temporal horn, and three usual approaches (yellow arrows) to this region are shown.

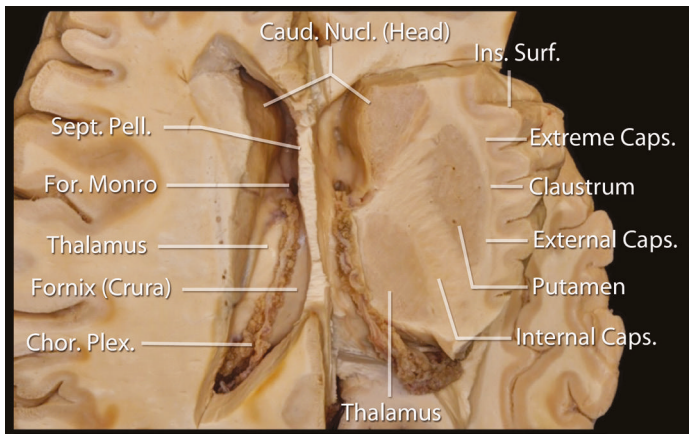

Fig. 35.2 At the left, an axial cut at the level of the roof of the lateral ventricle opens this cavity. At the right, a more caudal axial cut crosses the central core of the brain and reveals its structures: basal ganglia, thalamus, and white matter capsules. Note the proximity of the genu of the internal capsule to the ependymal surface at the level of the foramen of Monro.

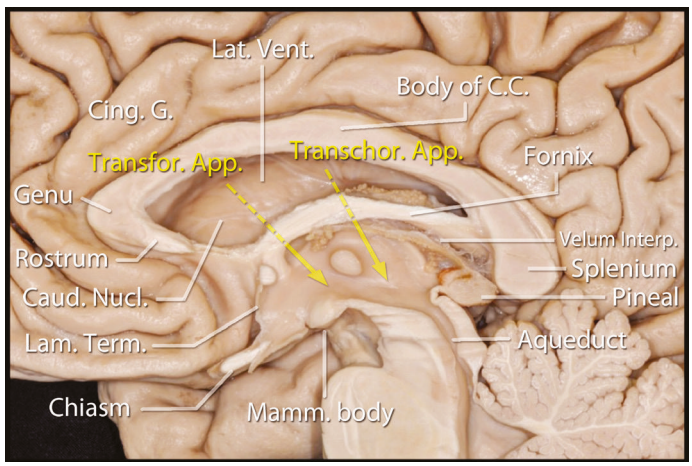

Fig. 35.3 A midline sagittal cut crosses the corpus callosum and exposes the third and lateral ventricle (anterior horn and body). Yellow arrows depict possible surgical approaches to these cavities.

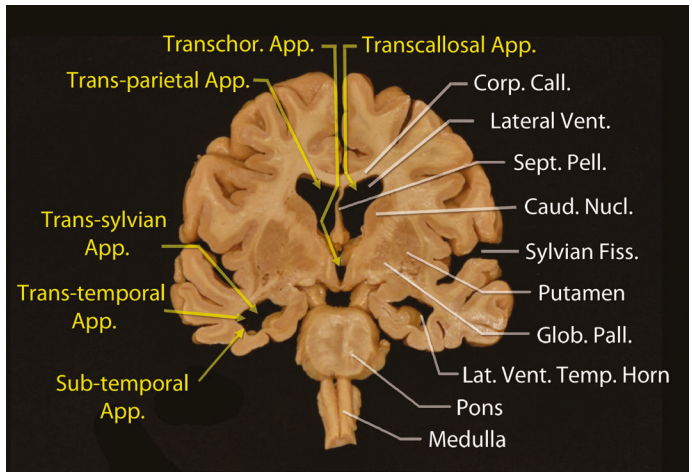

Fig. 35.4 A coronal cut through both hemispheres at the level of the foramen of Monro depicting the various approaches (yellow arrows) to the lateral and third ventricles.

Lateral and parallel to each fornix, the caudate nucleus also encircles the thalamus more laterally, and is constituted by a head, a body, and a tail, which respectively constitute the lateral wall of the frontal horn, the lateral wall of the ventricular body, the most lateral aspect of the anterior wall of the atrium, and the medial aspect of the roof of the temporal horn. The tail of the caudate nucleus ends anteriorly merging with the amygdala, which constitutes the anterior wall of the temporal horn (Wen et al., 1999).

Along the medial side of the caudate nucleus, the stria terminalis is found running over the thalamic-striate sulcus between the thalamus and the caudate nucleus also with a C-shaped configuration. This structure is constituted by a thin bundle of fibres originating at the amygdaloid complex, and ends under the head of the caudate nucleus at a nucleus called 'the bed nucleus of the stria terminalis' (Williams and Warwick, 1980; Heimer, 1995). Within the body of the ventricle the stria terminalis runs underneath the thalamostriate vein.

The upper surface of the thalamus constitutes the floor of the ventricular body, and its posterior surface, called the pulvinar, constitutes the middle portion of the anterior wall of the atrium, between the laterally placed tail of the caudate nucleus and the medially placed crura of the fornix. The medial surfaces of both thalami constitute the lateral walls of the third ventricle (Yamamoto et al., 1981), and their most posterior and inferior surfaces, medial to both choroidal fissures, constitute the roofs of the both sides of the transverse fissure of the brain, which harbour the ambient cisterns and part of the quadrigeminal cistern.

The corpus callosum is distinguished as the largest cerebral commissure, composed of fibres that connect almost all of the cortex in both hemispheres (Fig. 35.3). Exceptions are the anterior portion of the temporal lobes that are connected by the anterior commissure, the primary visual areas, and most of the somatosensory areas which are not interhemispherically connected (Brodal, 1981). Along a midsagittal section the corpus callosum resembles roughly a hook facing forward and downward in relation to the brain. Its anterior portion is thicker and has a curve with an anterior convexity, called the genu of the corpus callosum, which harbours the forceps minor, a bundle of fibres that connects the poles and the anterior aspects of the

frontal lobes. Inferiorly, the genu continues with a thinner horizontal and basal portion known as the rostrum of the corpus callosum, which ends posteriorly at the anterior commissure and interconnects the fronto-orbital surfaces. Posterior to the genu, the body (Heimer, 1995; Rhoton, 2003) or trunk (Williams and Warwick, 1980) of the corpus callosum has an almost horizontal portion with a slight superior curve, and interconnects most frontal and parietal convexities. The trunk of the corpus callosum is continuous with the splenium, the most posterior and thicker portion of the corpus callosum, which harbours the forceps major, a bundle of fibres that connects the posterior parietal and occipital cerebral lobes (Williams and Warwick, 1980).

Morphologically, the corpus callosum can be understood as a set of transverse fibres that cross the midline and fan out in several directions in order to spread throughout both hemispheres. The fibres of the corpus callosum can be seen as a butterfly flapping its wings, where the body of the butterfly corresponds to the midline portion of the corpus callosum and the beat of each wing corresponds to the distribution of its fibres throughout each hemisphere.

Given the morphology of its fibres, the corpus callosum is closely related to the five portions of the lateral ventricles, forming a large part of the walls, lined with ependyma as with other ventricular surfaces.

Anteriorly, the rostrum and genu constitute respectively the floor and anterior wall of both frontal horns, while the trunk constitutes the roof of the frontal horns and of the ventricular bodies.

As the fibres from the splenium of the corpus callosum open up laterally and posteriorly, they constitute on each side the roof and the lateral wall of the atrium and posterior horn. As they extend medially and inferiorly to the atrium and posterior horn, they also constitute the medial and inferior walls of these ventricular portions. Therefore, the fibres of the splenium embrace the whole atrium and posterior horn, encircling them, and participating in the composition of all their walls.

On the medial wall of each atrium, a distinct prominence of the splenium can be seen and is called the bulb of the corpus callosum, and, more posteriorly, already on the medial wall of the posterior horn, another prominence called calcar avis is also usually seen, corresponding to an intraventricular bulging of the deep calcarine fissure.

The septum pellucidum consists of two thin membranes of white matter intermingled with scattered neurons and glial cells that form the medial walls of the ventricular frontal horns and bodies (Williams and Warwick, 1980). In each frontal horn, the respective septum pellucidum membrane is attached superiorly to the upper trunk of the corpus callosum, anteriorly to its genu, and inferiorly along its rostrum. At the ventricular bodies, the septum pellucidum membrane is attached superiorly to the trunk of the corpus callosum and inferiorly to each body of the fornices, which are disposed together medially (**Figs. 35.2** and **35.3**).

Given the rise of the bodies of the fornices as they run posteriorly, to finally end up joining the inferior surface of the splenium, the septum pellucidum progressively decreases in height along the anteroposterior direction, ending thus as a bevel. The posterior end of the septum pellucidum determines the posterior limit of the ventricular bodies and the anterior limit of the atriums (Timurkaynak et al., 1986; Rhoton, 2003).

The floor of each atrium and occipital horn consists of a flat and triangular area called the collateral trigone, the anterior extension of this trigone becomes prominent constituting the collateral eminence that forms the lateral aspect of the floor of the temporal horn. The medial half of the floor of the temporal horn is formed by the hippocampus, which corresponds to the intraventricular bulging of the parahippocampal gyrus, and which posteriorly has its macroscopic insertion on the medial wall of the ventricular atrium (Timurkaynak et al., 1986; Wen et al., 1999; Rhoton, 2003).

Despite the fact that the collateral trigone and eminence correspond to the intraventricular projection of the deep collateral sulcus of the basal surface of the brain, the floor of the atrium and of the temporal horn is placed mostly over the fusiform gyrus. Located medial to the inferior temporal gyrus and laterally to the parahippocampal gyrus, the fusiform gyrus is bounded laterally by the occipitotemporal sulcus and medially by the collateral sulcus (Ono et al., 1990). Between the fusiform gyrus and the floor of the atrium and temporal horn, the inferior longitudinal fasciculus is found.

The main white matter fibre bundles can be identified through fibre dissection (**Fig. 35.5**). The superior longitudinal fascicle is deep to the frontal, parietal, and posterior temporal lobes, and is lateral to the lateral ventricles. The extreme, external, and internal capsules are composed of several white matter pathways which run underneath the insular surface, but as their fibres continue towards the cerebral lobes, pass underneath the insular limiting sulci. The extreme capsule is formed by short association fibres which interconnect adjacent insular gyri and continue towards both opercula. The external capsule is medial to the claustrum and mainly formed by three major fibre bundles (uncinate fascicle, inferior fronto-occipital fascicle, and claustrofugal fibres), and the internal capsule is medial to the putamen and formed by projection fibres (mainly the pyramidal and corticopontocerebellar fibres). The anterior commissure passes underneath the antero-inferior pole of the globus pallidus, and its fibres connect both medial aspects of the temporal lobes.

The white matter that constitutes the lateral wall of the ventricular atrium and temporal horn constitutes the so-called sagittal stratum (Ludwig and Klinger, 1956), which lies underneath the subcortical temporal white matter (u-fibres, temporo-pontine-cerebellar fibres) and which is composed by the inferior fronto-occipital fascicle, anterior commissure fibres, and by the posterior thalamic peduncle which harbours the optic radiation fibres.

The optic radiation fibres originate at the lateral geniculate body region. While its anterior bundle is initially directed anteriorly forming a curve named Meyer's loop (Ebeling and Reulen, 1988) to after bends posteriorly, its central and and posterior bundles have a more straight and posterior course. Finally, these fibres will continue to run posteriorly towards the upper and lower banks of the calcarine fissure (Párraga et al., 2012) (**Fig. 35.5**). Underneath the visual radiation fibres, callosal fibres known as the tapetum (Williams and Warwick, 1980) are found, constituting the more internal and directly related fibres with the ventricular cavity. Fibres of the inferior thalamic peduncle, which is constituted particularly by the auditory radiation (Türe et al., 2000; Williams and Warwick, 1980), are found more anteriorly and superiorly to the temporal horn since they run towards the Heschl gyrus. See **Figure 35.6** for the brain structures related to each lateral ventricle.

Anatomy of the third ventricle

The third ventricle is a single cavity located in the centre of the brain, between the thalami (Yamamoto et al., 1981; Rhoton, 2003). It receives cerebrospinal fluid (CSF) from both lateral ventricles through

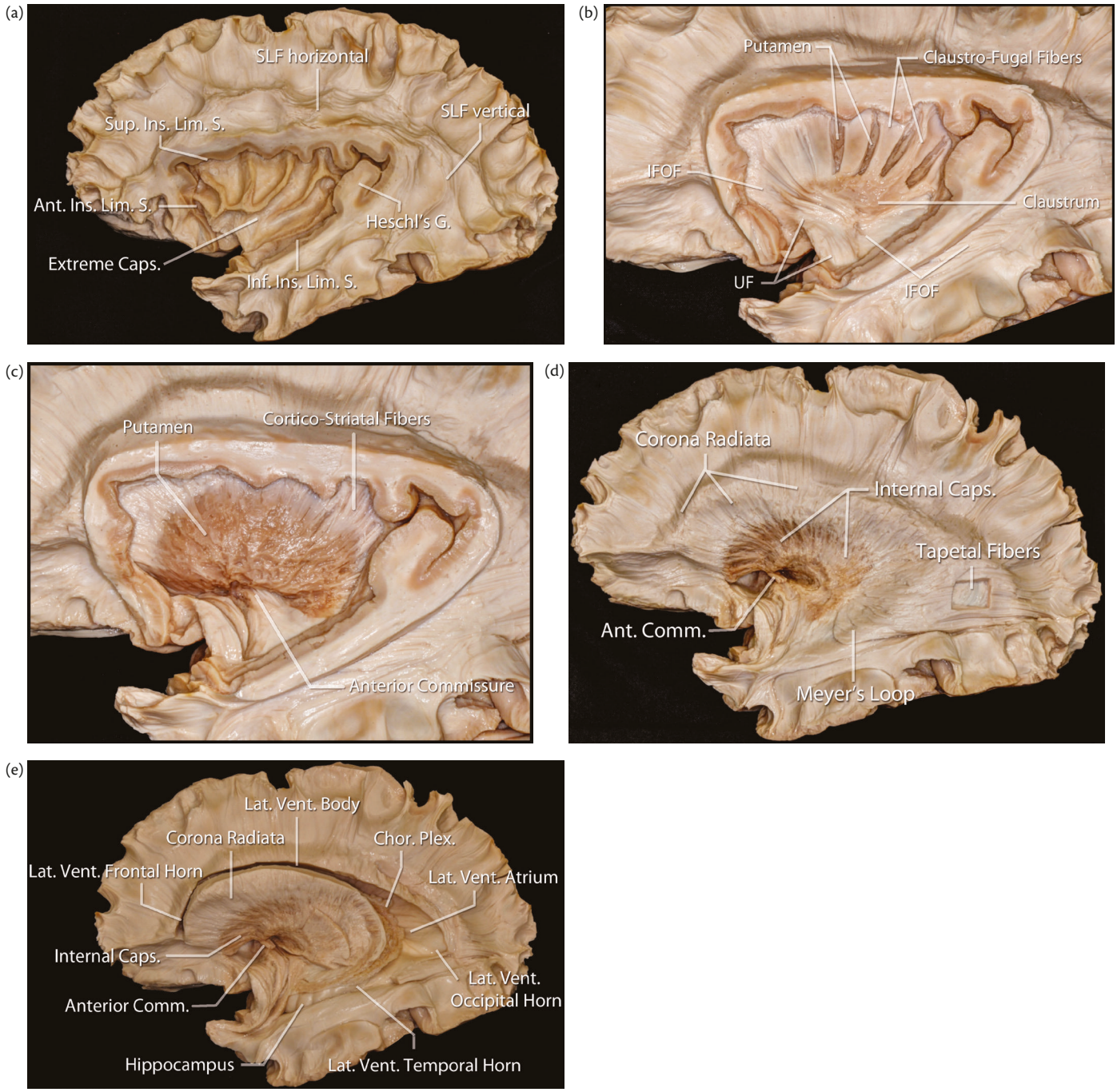

Fig. 35.5 Stepwise lateral fibre dissection of the left cerebral hemisphere demonstrating the insular and peri-insular white mater tracts related to the lateral ventricle. (A) The extreme capsule is made by short association fibres and is exposed after removing the insular cortex. The superior longitudinal fasciculus (SLF) is found outside the insular region, after decortication and removal of the more superficial short association fibres. (B) The inferior fronto-occipital and uncinate fasciculi (IFOF, UF) are found as the dissection progresses at the insular region, and their trajectory to others cerebral lobes can also be identified. (C) The removal of the previous white matter fibres leads to the exposure of the putamen and, inferiorly, anterior commissure fibres. (D) The internal capsule is found after removing the lentiform nucleus; the tapetum is formed by callosal fibres and found deeply, posterior to the insular region. (E) A deep circular cut was made along the outer margin of the insular region, leading to the wide exposure of the lateral ventricular cavity including the frontal horn, body, atrium, occipital horn, and temporal horn.

both foramina of Monro which are located next to each other at the anterior part of its roof, and drains into the fourth ventricle through the aqueduct of Sylvius, the opening of the aqueduct is located in the posterior part of the floor. Some CSF is also produced in this cavity by two small strains of choroid plexus located along the roof.

The anterior wall of the third ventricle is mainly formed by the lamina terminalis, which is a thin membrane that stretches from the anterior commissure (superiorly and posteriorly) to the optic chiasm (inferiorly and anteriorly) that forms a prominence already at the anterior margin of the floor (Yamamoto et al.,

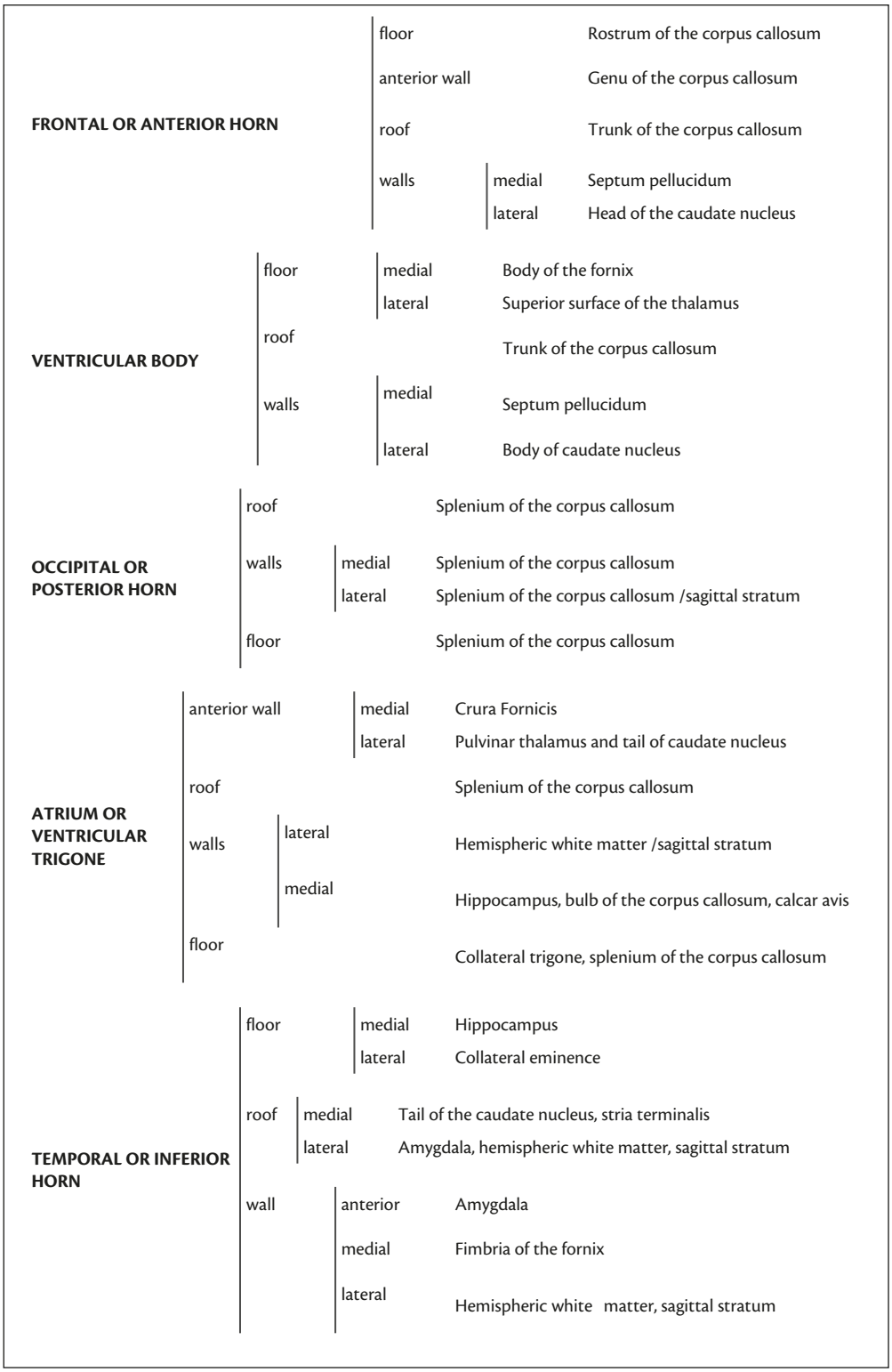

Fig. 35.6 Brain structures related to each lateral ventricle.

1981) (Fig. 35.3). The small recess between the lamina terminalis and the optic chiasm is named the optic recess. While the superior third of the lamina terminalis is hidden posterior to the rostrum of the corpus callosum, the lower two-thirds lie within the lamina terminalis cistern that harbours the anterior communicating artery.

The lateral walls of the third ventricle are mainly constituted by both thalami, with both interventricular foramina of Monro located next to each other at the most anterior and superior aspect of this ventricular cavity.

On each side, the shallow and superiorly concave hypothalamic sulcus extends from the foramen of Monro towards the orifice of the

aqueduct, separating the thalamus from the ipsilateral hypothalamus which is basally continuous with the contralateral hypothalamus, with all these surfaces then assuming a u-shaped configuration. The lateral arms of the u corresponds to the lateral walls, the upper two-thirds, constituted by the thalami, and the lower third by the hypothalamus. The bottom of the u is constituted by the hypothalamus and corresponds to part of the floor of the third ventricle.

The superior limit of each lateral wall is given by the stria medularis thalami which runs along the supero-medial border of each thalamus, from the foramen of Monro to the habenular commissure. This commissure connects both habenulas, which are small eminences located on the dorsomedial surfaces of both thalami, superior to the posterior commissure.

The massa intermedia connects both thalamic medial upper half surfaces, in approximately two-thirds of brains (Yamamoto et al., 1981).

The floor of the third ventricle extends from the optic chiasm to the orifice of the aqueduct of Sylvius, which has the posterior commissure as its superior margin and the mesencephalic tegmentum as its inferior margin, and can be divided into an anterior hypothalamic part and a posterior mesencephalic part. The anterior part is composed, from anterior to posterior, by the optic chiasm, the infundibulum, the tuber cinereum, and the mammillary bodies, while the posterior part already corresponds to the roof of the interpeduncular fossa and is formed by the mesencephalic tegmentum (Fig. 35.3). The infundibulum is continuous with the pituitary stalk, and connects the hypothalamus to the posterior lobe of the pituitary gland (neurohypophysis) through the supraopticoparaventriculo-hypophyseal tract, which transports colloid droplets containing the oxytocin and vasopressin hormones (Nieuwenhuys et al., 2007).

When the floor is seen from above and from inside the ventricle, the infundibular recess can be easily identified between the optic chiasm prominence and the tuber cinereum, and the mammillary bodies appear as two prominences posterior to the infundibular recess. An endoscopic third ventriculostomy should be performed by opening the thin and commonly translucent area between the infundibular recess and the mammillary bodies. Posterior to the mammillary bodies, the floor of the third ventricle has a concave and smooth surface, marked by the triangular-shaped opening of the aqueduct more posteriorly.

When seen from outside within the cerebral basal surface, the floor of the third ventricle is located just posterior to the optic chiasm and between the optic tracts and cerebral peduncles, with the roof of the interpeduncular fossa corresponding to the anterior aspect of the mesencephalic part of the third ventricle floor. While the anterior perforated substance spreads along the basal areas anteriorly to both optic tracts, the posterior perforated substance spreads along all the inferior aspect of the third ventricle floor.

The roof of the third ventricle extends from the foramina of Monro to the habenular commissure, and is formed by four layers of structures, the superior layer comprised by the fornices, then layers consisting of the superior and the inferior tela choroidea, and the space between these two thin membranes which constitutes the velum interpositum cistern.

The superior and neural layer is anteriorly constituted by both bodies of the fornices which run juxtaposed. While the upper sheet of tela choroidea is in intimate contact with the inferior borders of both fornices, the lower sheet of tela choroidea is attached to both stria medullaris that run along the supero-medial thalamic borders.

The velum interpositum cistern in between the tela choroidea layers ends anteriorly at the level of both foramina of Monro, and opens posteriorly into the quadrigeminal or pineal cistern. It harbours the medial posterior choroidal arteries and the internal cerebral veins within small trabeculae (Fig. 35.3).

The internal cerebral veins are formed by the junction of the anterior septal vein and the thalamostriate vein, which usually happens close to their entry point into the vellum interpositum cistern as they pass underneath the fornix through the choroidal fissure, next to the foramen of Monro. The internal cerebral veins exit the velum interpositum cistern posteriorly, over the pineal gland, and join to the basal vein of Rosenthal to form the great vein of Galen.

Two small strands of choroid plexus project downward from the lower sheet of tela choroidea into the third ventricle along both sides of the midline. Each of these choroid plexus strands is continuous along its pedicle with the choroid plexus of the ipsilateral lateral ventricle through the choroidal fissure, which defines the lateral aspect of the third ventricle roof.

The posterior wall extends from the suprapineal recess, located superiorly to the habenular commissure, to the opening of the aqueduct, and includes, from superior to inferior, the suprapineal recess, the habenular commissure, the pineal gland, the pineal recess, and the posterior commissure which is the upper aspect of the opening of the aqueduct (Fig. 35.3).

The pineal gland is found in the quadrigeminal cistern, already outside the third ventricle, and is attached to the posterior wall by a double stalk that projects superiorly to the habenular commissure and inferiorly to the posterior commissure. The pineal recess is anterior to the pineal gland and constitutes an extension of the third ventricle cavity between the upper and lower attachments of the pineal gland. See Table 35.1 for brain structures related with the third ventricle.

Surgery for supratentorial intraventricular tumours

Preoperative planning

Once a diagnosis has been made, decisions to make include whether there is an indication for surgical resection, and if so, whether the goal is gross total resection. Finally, the choice of the appropriate surgical approach can be planned.

Imaging

Preoperative investigations include imaging with MRI to establish the characteristics of the lesion and its anatomical origin and extent. Typical appearances can sometimes be diagnostic such as in colloid cysts of the third ventricle or epidermoids with characteristic restricted diffusion. A high signal on T2-weighted sequences may indicate high-water content and 'soft' consistency while a computed tomography (CT) scan may demonstrate calcification.

For some lesions with propensity for CSF seeding (e.g. primitive neuroectodermal tumours, ependymoma, germ cell tumours), imaging of the entire neuraxis, including the spine, should be completed to plan management.

Table 35.1 Brain structures related with the third ventricle

Anterior wall	Foramina of Monro	
	Pillars or Columns of the fornices	
	Anterior commissure	
	Lamina terminalis	
	Optic recess	
	Optic chiasm	
Lateral walls	Thalami	
	Stria medullaris thalami	
	Hypothalamic Sulcus	
	Hypothalamus	
Floor	Hypothalamus	Optic chiasm
		Infundibular recess
		Infundibulum
		Tuber cinereum
		Mamillary bodies
		Posterior perforated substance
	Mesencephalon	Mesencephalic tegmentum/Roof of interpeduncular fossa
		Posterior perforated substance
		Orifice of aqueduct
Roof	Foramina of Monro	
	Bodies and crura of fornices, hippocampal commissure	
	Superior tela choroidea	
	Velum interpositum cistern (medial posterior choroidal arteries, internal cerebral veins)	
	Inferior tela choroidea	
	Choroid plexus	
	Suprapineal recess	
Posterior wall	Suprapineal recess	
	Habenula	
	Habenular commissure	
	Pineal recess	
	Pineal gland	
	Posterior commissure	

Tumour markers

The detection of positive tumour markers initially in the serum and subsequently in the CSF, if available, dictate further management. For germ cell tumours in the vicinity of the third ventricle elevation of levels of alpha-fetoprotein (AFP) or human chorionic gonadotropin (ß HCG) restrict the diagnosis to only a few categories that are all managed at least initially with radiotherapy or chemotherapy. See Chapter 36.

Endoscopic procedures

Prior to resection of some intraventricular lesions an endoscopic procedure may serve as an urgent treatment to relief CSF obstruction, obtain a biopsy, or fenestrate a cystic lesion. At the same time CSF can be sampled for tumour markers and cytological examination. For lesions obstructing the aqueduct, a third ventriculostomy is recommended. If the lesion infiltrates the floor of the third ventricle and if obstructing the foramina of Monro then an endoscopic septum pellucidotomy and insertion of a single ventriculoperitoneal (VP) shunt can simplify CSF diversion. In cases where an intended endoscopic biopsy is planned in addition to the procedure to relieve obstructive hydrocephalus, it is recommended to carry out the ventriculostomy first as bleeding from the biopsy site may obscure the endoscopic view required to complete the procedure. The use of a flexible endoscope may facilitate both procedures through the same burr hole.

Decision-making

The indication for surgical resection depends upon patient and lesion factors. Patient factors include age, comorbidities, and the anticipated prognosis. The tumour factors take into account the presence of metastatic and CSF spread and the availability of alternative non-surgical treatment such as in cases of lymphoma or germinoma. In some cases, such as germ cell tumours with positive tumour markers, initial treatment with radiotherapy or chemotherapy is instituted, and surgery is reserved to resect any residual thereafter.

Planning of the surgical approach is important and relies upon evaluation of complex and multiple factors. The approach has to be tailored to achieve the predetermined goal of resection and requires knowledge of the anticipated surgical 'blind spots' and potential morbidity of each approach. In general choosing an approach depends on the planned extent of resection which in turn depends on patient factors including the existence of neurological deficits, the type and prognosis of the lesion, and whether effective adjuvant therapies are available to deal with residual disease. Technically, characteristics such as the size, configuration, extent, and consistency of the lesion help to dictate the most appropriate approach.

Surgical approaches to supratentorial intraventricular lesions

Table 35.2 demonstrates the surgical approaches to supratentorial intraventricular lesions.

Approaches to the body and frontal horn

Transcallosal approach

The patient is positioned supine, with some neck flexion and head elevation, which provides a direct trajectory. Either a coronal incision or a laterally based U-flap is fashioned. Classically, a bifrontal craniotomy across the midline is fashioned with one or two burr holes directly on the superior sagittal sinus (SSS) or if preferred on either side of the SSS and extending one-third posterior to and two-thirds anterior to the exposed coronal suture. This is based on the fact that the callosotomy must be placed anteriorly as the fornices underlie the corpus callosum (CC) posteriorly prior to sweeping anteroinferiorly to form the septum pellucidum (Rhoton, 2002). The craniocerebral relationship indicates that the foramina of Monro are coronally at the level of the coronal suture and that the central sulcus is 5 cm posterior to the coronal suture (Ribas et al., 2006), indicating the location of the pre- and postcentral gyri which should be protected from

Table 35.2 Surgical approaches to supratentorial intraventricular lesions

	Lateral ventricle Body + frontal horn	Lateral ventricle Trigone + atrium	Third ventricle	Third ventricle posterior	Third ventricle anterior
Approaches	Transcallosal/transcortical	Transcortical/ Trans-sulcal Superior temporal Intraparietal	Transforaminal Transchoroidal/ Subchoroidal	Supracerebellar Occipital transtentorial	Transcranial translamina terminalis EEETS
Blind spots	Contralateral lateral ventricle roof FM	Apex of vascular pedicle	Roof of third ventricle	Tectum Ipsilateral wall of third ventricle	Roof of third ventricle Interpeduncular cistern (retroinfundibular)
Morbidity of approach	Bridging veins SMA Pericallosal artery	Optic radiation Superior longitudinal/ Arcuate fasciculus	Fornix Thalamus/veins	Deep veins Visual cortex	Olfactory ACoA perforators Pituitary Stalk
Morbidity of resection	Fornix Thalamus/veins	↓	Fornix Deep veins Hypothalamus	Tectum Deep veins	Hypothalamus Fornix

ACoA, anterior communicating artery; EEETS, extended endonasal endoscopic transsphenoidal; FM, foramen of Monro; SMA, supplementary motor area.

manipulation or retraction. The antero-posterior dimensions of the craniotomy should be adequate to allow the surgeon to choose an area devoid of bridging veins allowing an interhemispheric approach without disruption of these key vessels. Although either lateral ventricle can be entered from this approach, it is easier to expose more of the hemisphere for which the corresponding ventricle is to be entered. Some authors advocate detailed imaging preoperatively of the draining veins such as with computed tomography venogram (CTV) or magnetic resonance venogram (MRV) and the approach can then be tailored with image-guidance to avoid the bridging veins.

The interhemispheric approach (**Fig. 35.4**) requires careful dissection preserving the pial surface deeper to the inferior edge of the falx as the medial frontal lobes can be adherent. The trajectory in the sagittal plane is guided by the fact that the surface markings of the foramen of Monro are in a plane corresponding to the coronal suture intersecting with the superior temporal line, and hence the approach is facilitated by inspection of the inclination of the partially exposed coronal suture during the craniotomy and by the use of image-guidance. Although retraction injury occurs with injudicious placement of brain retractors, excessive 'dynamic retraction' is equally detrimental. Therefore, a strategy of brain relaxation and gentle manipulation is required. In the presence of gross hydrocephalus initial placement of a ventricular drain at the start, without totally collapsing the ventricle, facilitates the approach and allows placement of a brain retractor as a 'holder' if the surgeon wishes to do so.

The CC is exposed and identified by its glistening white colour and the surface vascular pattern. It is ideal to identify both pericallosal arteries and these are dissected and mobilized laterally, each with the corresponding hemisphere so as not to disrupt the supplying branches to the pial surface. With experience and especially where there are dilated ventricles a central white septum in the midline sagittal plane at the attachment of the septum pellucidum can be identified. This allows placing the callosotomy lateral enough to enter the desired lateral ventricle. A large callosotomy is generally not required provided that the trajectory to visualize the intraventricular lesion is correct. The location rather than the size of the callosotomy is important to avoid damaging the fornices. Separation of the fibres of the CC reveals the underlying purple coloured ependyma which once punctured allows CSF egress.

Orientation once the ventricular cavity is entered requires identification of the choroid plexus which is followed to the foramen of Monro. Once the thalamostriate vein is identified the laterality of the ventricle is established (Rhoton, 2002). If no choroid plexus is visible it is likely that this is the frontal horn and if changing the trajectory more posteriorly still shows that the cavity is devoid of choroid plexus, then entry into a cavum septum pellucidum should be suspected.

It is best to perform a septum pellucidotomy avoiding bleeding from the septal vein especially with lesions obstructing the foramina of Monro as a single catheter for CSF diversion may be used later if CSF flow is not re-established. In many cases the lesion may be obstructing the view of interventricular landmarks and hence it is possible to inspect the contralateral ventricle through the pellucidotomy and use this as a reference to establish the relative depth and location of the fornices and deep veins.

Prior to resecting the lesion either identify the location of the fornix and important veins or at least be aware of their relative location. If possible, establish the origin of the lesion aided by preoperative imaging. The lesion may predominantly arise from the septum pellucidum such as a central neurocytoma and some subependymomas, from the choroid plexus such as papillomas or meningiomas or from the ependymal wall such as gliomas or giant cell astrocytomas. The anatomical origin may not be possible to determine in large or bilateral lesions. If accessible, first coagulate and separate the choroid plexus from the surface of the lesion to control a possible source of blood supply. Proceed to piecemeal resection with suction or CUSA surgical aspiration depending on the consistency of the lesion with intermittent haemostasis, as excessive bleeding will preclude visualization within the ventricle. The extent of resection takes into account patient factors such as age, the nature of the lesion and whether adjuvant therapy is available and the preoperative presence of neurological deficits. This may necessitate leaving a small residual adjacent to the fornices or adherent to the major veins. For those lesions arising in the brain parenchyma and which are exophytic into the ventricle care must be taken not to extend the resection in such a way as to injure the surrounding caudate nucleus, thalamus, or the genu of the internal capsule which lies at a level adjacent to that of the foramina of Monro.

In most cases leaving an external ventricular drain for a few days until the CSF clears is advised. It can be placed either at the outset or at the end of the procedure through the callosotomy and tunnelled through the dura and away from the incision. This is followed by meticulous dural closure, replacement of the bone flap with burr hole covers and wound closure.

The pitfalls of this approach include SSS compression by retractors which, if prolonged may lead to thrombosis. Sacrifice of major bridging veins may lead to venous infarction and postoperative epilepsy and a trajectory followed too posteriorly in the sagittal plane risks damage to the fornices. Cingulate gyrus damage may occur if this structure is mistaken for the CC, the area between the pericallosal and callosomarginal vessels is entered rather than the corridor between the two pericallosal arteries, contusion and surrounding swelling of the cingulate gyrus may then result in a postoperative supplementary motor area (SMA) syndrome. Pericallosal artery injury or disruption of its branches to the corresponding hemisphere may cause hemiparesis especially affecting the lower limb. Entering a cavum septum pellucidum rather than the lateral ventricular and confusing which ventricle has been entered can lead to serious damage for example attempted septostomy damaging the caudate or thalamus. Forniceal damage through the approach or during resection should be avoided, if the lesion is adherent or partially infiltrating the fornix, then a subtotal resection is advocated. Finally a pellucidotomy without clear vision and orientation can result in bleeding from a septal vein and if inferiorly placed can damage part of the fornix.

Blind spots of this approach where tumours may be accidentally left include the roof of the contralateral lateral ventricle. It should be noted that for large intraventricular lesions, the foramen of Monro, the fornix, and thalamostriate vein may initially be obscured by the lesion.

Transcortical approach

Alternatively, the body and frontal horn can be approached through a frontal transcortical approach (Rhoton, 2002). The superior frontal sulcus is frequently deep and an initial trans-sulcal approach or an approach through the middle frontal gyrus can provide a trajectory to the ventricle. This approach is facilitated in cases with hydrocephalus. Image-guidance helps to plan the trajectory through the white matter tracts (Szmuda et al. 2014).

Once the ventricle is entered the subsequent operative steps are similar to those just described but bearing in mind the orientation of the operative view from a more lateral to medial trajectory.

Approaches to the atrium of the lateral ventricle

Although the bodies of the lateral ventricles are near the midline, the atria or trigones are off midline cavities located behind both thalami and consequently their access requires off midline approaches. A key anatomical feature to have in mind regarding the atria is that while the most posterior aspect of the splenium within the midline ends covering the pineal or quadrigeminal cistern, its lateral extensions open bilaterally and posteriorly covering both thalamic pulvinars and encircling both atrial cavities and their variable posterior extensions that constitute the occipital horns, already inside the brain parenchyma and hence posterior to the most posterior aspect of the splenium seen along the midline.

Given this anatomical location, only the most superior and anterior tumours of the atrium can be reached through the anterior transcallosal approaches already described to access the frontal horn and the body of each lateral ventricle, with other atrial tumours requiring different transcortical approaches according to their main location, extension, and vascular supply. The principal approaches to the ventricular atrium are the transparietal, the transtemporal, and the alternative parieto-occipito interhemispheric (**Fig. 35.1**).

Planning the trajectory has to take into account not only the cortical entry site avoiding eloquent cortex, but also the trajectory through the white matter tracts. Neurological deficits from cortical injury often recover due to neuronal plasticity, however white matter tract disruption results in a permanent deficit. It is imperative to state that the safest rather than the shortest trajectory should be adopted. The use of image-guidance is very useful in optimizing the orientation of the trajectory to the target but the surgeon should resist the temptation to choose the shortest route through a seemingly thin but eloquent neural mantle.

Transparietal approach

Although sometimes interrupted the intraparietal sulcus is a very evident sulcus that transverses the superolateral surface of the parietal lobe and which, usually, is continuous with the inferior and downward segment of the postcentral sulcus. The actual or projected meeting or transition point of these sulci constitutes the nearest point of the parietal surface to the atrium (Harkey et al., 1989; Ebeling and Steinmetz, 1995; Ribas et al., 2006). Nevertheless, the transparietal microneurosurgical approach to the atrium (**Fig. 35.4**) has to be mandatorily initiated through the transitional site between these two sulci, moving more posteriorly along the intraparietal sulcus allows access to the more posterior part of the atrium, particularly if this cavity is not enlarged.

For this approach the patient should ideally be in the semi-sitting position, and the craniotomy should be done having as its centre the projection of the actual or projected transition point of the intraparietal and postcentral sulci, which is located approximately 6 cm superior to the lambda along the sagittal suture and 5 cm lateral to it (Ribas et al., 2006).

Preoperatively both the shape and interruptions of both sulci, as well as their joining site, can be estimated through careful study of 3D-rendered MRI images, the projection of their joining site on the skull surface can be better estimated with fusion of the CT and MRI images.

Intraoperatively, after identifying the locations of the intraparietal and the postcentral sulci visible segments considering their usual or known courses as carefully seen on the MR images, the identification of their actual or projected meeting or transition point can usually be identified as a variable enlargement of the subarachnoid space, and should also be confirmed with the aid of neuronavigation if available. It is frequent to find veins running along or immediately next to both sulci.

The transparietal approach to the atrium can be done trans-sulcal, subpial, or transgyral, but always considering that the transition site between the postcentral and the intraparietal sulci constitutes the nearest and easiest surface site to more securely reach the atrium, the surgical route has to follow the sulcal orientation which always leads towards the nearest ventricular cavity (Harkey et al., 1989; Ebeling

and Steinmetz, 1995; Ribas et al., 2006) and the approach has to be along a 30° posteriorly oblique radial approach (Ribas et al., 2006). Both neuronavigation and intraoperative ultrasound can be very helpful to confirm the route towards the atrium.

A wide sulcal opening is often needed to expose and allow piecemeal delivery of firm lesions and hence it is advantageous to be able to plan the use of a deep sulcus on preoperative imaging and to anatomically localize this at surgery.

Once the ventricular cavity is encountered the surgical corridor can be enlarged, if necessary, by removing more brain tissue posteriorly along the intraparietal sulcus orientation and preferably medially from the superior parietal lobule, in order to avoid further damage to the superior longitudinal and arcuate fascicles which run mostly laterally to the intraparietal sulcus within the inferior parietal lobule.

The transparietal approach to the atrium just posterior to the postcentral sulcus and along the level of the intraparietal sulcus, hence posterior to the somatosensory cortex, will always cause damage to the parietal u-fibres, the parietal projection fibres (mostly parietopontocerebellar fibres), and the most superior fibres of the optic radiation which cover the atrium and run towards the cuneal margin of the calcarine fissure causing a contralateral homonymous lower quadrantinopia.

While non-dominant parietal damage is more particularly related with left hemi-neglect and anosognosia, spatial disorientation, construction, and dressing apraxias, dominant parietal damage can cause dysphasias, dyslexia, dyscalculia, apraxia, tactile agnosia, and possibly Gerstmann's syndrome (dysgraphia, dyscalculia, finger agnosia and right/left disorientation).

Posterior temporal approach

The approach to the atrium through the distal part of the superior temporal sulcus (Harkey et al., 1989; Ebeling and Steinmetz, 1995; Ribas et al., 2006) is appropriate for more inferior atrial tumours, particularly when these lesions extend towards the temporal horn or receive a significant blood supply from the anterior choroidal artery. This approach can damage the optic radiation that runs along the lateral wall of the atrium. The Wernicke area with its underlying language related fibres is also at risk where it lies predominantly within the posterior aspect of the superior temporal gyrus and within the supramarginal gyrus, in the dominant hemisphere. Awake craniotomy, when feasible, can minimize these risks.

The most distal point of the superior temporal sulcus, prior to its usual trifurcation, lies about 2–3 cm posterior and inferior to the posterior Sylvian point (end of the Sylvian fissure) (Ribas et al., 2006). For craniotomy purposes, this area is located about 3 cm vertically above the meeting point of the horizontal parieto-mastoid suture and the ascending posterior aspect of the squamous suture, which is a site that can usually be palpated as a slight depression over the superior aspect of the mastoid process (Ribas et al., 2006; Ribas and Rodrigues, 2007). Once the horizontal sulcal segment just inferior and posterior to the end of the Sylvian fissure has been identified, an adjoining transparenchymal approach can be performed transsulcal, subpial, or transgyral, 30–40° anteriorly and radially oriented (Ribas, 2005; Ribas et al., 2006) (Fig. 35.1). The ventricular route can be enhanced by the use of neuronavigation and intraoperative ultrasound. Further removal of brain tissue can be performed as necessary to obtain adequate exposure.

Since the Heschl gyrus bounds anteriorly and obliquely the triangular temporal plane, with its inner apex immediately next to the atrium, the opening of the most posterior aspect of the Sylvian fissure can also lead to the atrium. Nevertheless, this opening is technically difficult due to the flatness of the fissure at this level. This approach obliquely requires further removal of the superior temporal intraopercular surface (auditory primary cortical area), and the base of the supramarginal gyrus.

There is a blind spot in large lesions where the vascular pedicle at the attachment of the choroid plexus may not be exposed prior to reducing some of the bulk of the tumour mass.

Alternative approaches

Anatomical operative approaches to the body and trigone of the lateral ventricle which totally avoid the visual white matter tracts include the interhemispheric transcallosal, the posterior interhemispheric approach through the medial parieto-occipital sulcus or through the or isthmus of the cingulate gyrus (described next) and the more recently described supracerebellar infra/transtentorial approach and then subsequently through the collateral sulcus.

The interhemispheric part of the parieto-occipital sulcus is related to the occipital horn rather than the trigone. A posterior approach and a corticotomy in the region of the precuneus or isthmus of the cingulate gyrus would access the trigone but for this deep approach a slack brain is desirable if not essential and the presence of a large mass may preclude its use.

Parieto-occipital interhemispheric approach The parieto-occipital interhemispheric approach to the atrium (Fig. 35.1) as proposed by Yaşargil (Yaşargil, 1996) is unique in the sense that it is the only approach which does not damage the optic radiation. Nevertheless, it is not a direct route, and the surgical corridor is rather limited by the degree of occipital retraction. The mobilization and retraction required to gain access with an interhemispheric approach may be problematic in the presence of a deep solid hemispheric mass.

Since the approach is interhemispheric along the cuneus, ideally the patient should be in the semi-sitting position, the craniotomy along the midline should extend from the lambda, which corresponds to the most distal point of the parieto-occipital sulcus, to the opisthocranion, which is the most prominent cranial point of the occipital fossa and which corresponds to the most distal point of the calcarine fissure. While the opisthocranion is usually located 3–4 cm above the inion, the lambda is usually located between 2 and 4 cm above the opisthocranion (Ribas et al., 2006).

The occipital interhemispheric approach is facilitated by the fact that the cortical parieto-occipital veins usually have an ascending course parallel to the superior sagittal sinus for a few centimetres before joining the sinus (Oka et al., 1985; Yaşargil, 1996). The access should be done between the falx-tentorium transition and the cuneal surface towards the splenium, bearing in mind that the anterior apex of the cuneus, where the parieto-occipital sulcus joins the calcarine fissure and where their respective arteries also usually meet, is located at the axial level of the splenial base. Further lateral occipital retraction can be aided by the sacrifice of small draining veins if necessary and mainly, by the opening of the parasplenial cisterns and release of CSF. The very white splenium and the vein of Rosenthal are identified and the ipsilateral isthmus of the cingulate

gyrus is easily seen wrapping around the splenium together with the precuneal base seen immediately posteriorly, which altogether constitute the site of the transcerebral approach to the atrium.

Since the atrial cavity lies laterally, such a window has to be made along a lateral and anterior orientation until the ventricular cavity is reached with the identification of the tumour or white pulvinar of the thalamus that constitute the anterior wall of the atrium, with the attached choroid plexus glomus.

The main limitation of this approach is the degree of occipital retraction and, as for any other ventricular approach, it is facilitated if there is ventriculomegaly. Since this approach requires significant brain retraction and is done through an indirect route, neuronavigation and intraoperative ultrasound are not as helpful as with other approaches, and its successful accomplishment depends on recognition of anatomical landmarks and their orientation.

Other approaches More basal temporal approaches, through a window made by the removal of the posterior part of inferior temporal gyrus and of its medially adjacent fusiform gyrus, which corresponds to the floor of the posterior aspect of the temporal horn and of the atrium, can spare both the optic radiation and the language areas within the dominant hemisphere, but are much more suitable for inferior lesions already occupying the temporal horn (Fig. 35.4). For these approaches it is important to have in mind that the inferior temporal gyrus although broad is short in height, and its exposure requires a very low temporal craniotomy. Since the fusiform gyrus lies predominantly over the superior surface of the petrous bone, the craniotomy base should include the area between the preauricular depression over the distal and superior aspect of the zygomatic arch root, and the meeting point of the horizontal parietomastoid and the posterior and ascending portion of the squamous suture located at the upper aspect of the mastoid process (Ribas and Rodrigues, 2007).

The ingenious supracerebellar approach is performed with incision of the tentorium to expose the collateral sulcus and then via a trans-sulcal approach entering the inferior aspect of the lateral ventricle 10 mm inferior to the trigone. This approach would be perfect for a lesion of an appropriate size and location. It is conceivable that a large solid mass especially with superior extension may not be adequately exposed through this approach. The medial structures including the hippocampus need to be protected with this approach.

Approaches to the temporal horn

See Chapter 81 and Figure 35.4.

Approaches to the third ventricle

Main ventricle

The initial approach is the same as the transcallosal approach to the lateral ventricle described earlier. It has to be noted that the callosotomy is to be performed at the usual place as the trajectory will still allow access to the whole third ventricle. The temptation to place the callosotomy more posteriorly not only risks damage of the underlying fornix but even if performed through the splenium of the CC can end up in the quadrigeminal cistern rather than the third ventricle. Furthermore, the visual component of posterior disconnection syndrome can have devastating effects on a patient.

Once the lateral ventricle has been entered the choice between the transforaminal and transchoroidal approach will depend on the configuration of the lesion and its relationship to, and size of, the foramen of Monro (Rhoton et al., 1981). An interforniceal approach starting with separation of the leaves of the septum pellucidum and opening the interforniceal space to gain access through the roof of the third ventricle carries a high risk of bilateral forniceal damage.

Transforaminal approach This is ideal for lesions presenting at a dilated foramen of Monro. This applies to the vast majority of colloid cysts and some other anterior third ventricular or 'dumb-bell' lesions. Surgery is facilitated in those mobile lesions that are deliverable into the lateral ventricle (Fig. 35.3). The configuration of the deep veins is variable and these have to be protected during the resection (Türe et al., 1997). Gentle traction is required to avoid avulsion of the vascular attachment at the roof of the third ventricle, which is a blind spot. Care is needed in resection of the anteroinferior aspect of the lesion to avoid hypothalamic damage.

Anatomical observations indicate that most colloid cysts arise in fact within the velum interpositum and hence are supplied by branches of the posterior medial choroidal artery and this also explains those situated cephalad within the leaves of part of the septum pellucidum through an extension of the velum interpositum (Morris and Santoreneos, 2012). In some colloid cysts especially incidental ones the anterior aspect of the taenia fornices is still intact and stretched over the capsule of the cyst. Grabbing this membrane to manipulate the cyst may result in distortion of the fornix to which it is attached and subsequent dysfunction. Therefore, under magnification incising this overlying layer renders the cyst mobile, allowing it to be delivered through the foramen of Monro and resected intact after coagulation and division of its vascular pedicle.

Transchoroidal approach Bearing in mind that the foramen of Monro is actually the anterior dilated, open portion of the choroidal fissure then a transchoroidal approach opens the space between the fornix and the thalamus posterior to the thalamostriate vein to gain access to the third ventricle (Figs. 35.3 and 35.4). This portion is covered by the choroid plexus and once this is gently delivered from the fissure it becomes apparent that it is attached superomedially to the fornix by a membrane, the 'taenia fornices', and inferolaterally to the thalamus by the 'taenia thalami'. As the later membrane may incorporate several draining veins from the thalamus to the thalamostriate vein then it is best to incise the taenia fornices, a 'transchoroidal infraforniceal' approach, rather than the taenia thalami to avoid compromise of the venous drainage of the thalamus (Rhoton, 2002). In practice, however, most lesions for which surgery is indicated are of such size that this part of the choroid fissure is 'splayed', and these membranes are stretched and easily opened. This will gain access and visualize the whole third ventricle from its anterior extent to the suprapineal recess (Ulm et al., 2009).

Blind spot

- The roof of the third ventricle and contralateral internal cerebral vein.

Anterior third ventricle

Such lesions extend from the suprasellar cisterns into the third ventricle. If these are predominantly intraventricular, then they can be approached through the transcallosal transforaminal or transchoroidal route. The others can be approached through the lamina terminalis from an anterior frontal interhemispheric or pterional craniotomy

or through an extended endonasal transplanum endoscopic route. See Chapter 27.

Posterior third ventricle

These are pineal tumours or other lesions arising in the quadrigeminal cistern and extending into the ventricle. These are best approached via the infratentorial supracerebellar approach which provides very good visualization of the third ventricular roof and allows careful dissection of the lesion from the deep veins. However caudal extension into the tectal region could represent a blind spot. Alternatively, the occipital transtentorial approach which better visualizes the caudal extent of the lesion may be used. A 'bulky' splenium may obscure the extension of the lesion along the roof of the third ventricle. See Chapter 37.

Endoscopic approaches

In addition to endoscopic procedures to obtain a biopsy and relieve CSF obstruction, there is an emerging role of endoscopic procedures to resect intraventricular lesions. Intraventricular cysts such as large symptomatic pineal or lateral ventricular arachnoid cysts or those associated with neoplasms can be endoscopically fenestrated into the ventricle and if needed a biopsy is obtained from the wall. Via a 'bipolar' fenestration of third ventricular arachnoid cysts (i.e. endoscopic fenestration of the upper dome presenting into the foramen of Monro into the lateral ventricle and through the cyst), the inferior pole is communicated to the prepontine cistern, establishes CSF circulation, and possibly decreases the risk of recurrence (Kirollos et al., 2001).

Endoscopic resection of colloid cysts is achievable in many but not all cases. Mobile cysts with contents that are easily aspirated in the presence of ventriculomegaly are favourable for the endoscopic technique (See Chapter 33).

In expert hands some solid intraventricular lesions are amenable for resection via an endoscopic route (Barber et al., 2013; Selvanathan et al., 2013).

Specific complications

Apart from technical complications described earlier with the operative technique resulting in neurovascular injuries, there are specific risks associated with surgery in this region (Hassaneen et al., 2010; Milligan and Meyer, 2010; Symss et al., 2014).

Memory dysfunction

This may occur from forniceal manipulations (Villani et al., 1997; Friedman et al., 2008).

Hypothalamic dysfunction

This may occur especially with lesions involving the floor of the third ventricle. Most commonly these are transient such as hyponatraemia or diabetes insipidus.

Visual and gaze dysfunction

This may be seen with pineal region lesions extending to the posterior third ventricle and involving the tectum. The restriction of vertical gaze can be compensated for functionally, but other dysfunctions such as skew deviation, disrupted far/near accommodation and diplopia of a dynamic nature from involvement of several pathways including the rostral medial longitudinal fasciculus have significant affection of functional outcome and quality of life (Hart et al., 2013).

Disconnection syndrome

Although classically this can result in alexia without agraphia, alien hand syndrome, tactile anomia, and left/right apraxia. However, is rarely seen in humans especially in the longer term after anterior callosotomies (Villani et al., 1997; Symss et al. 2014). The exception is in cases in which the disruption involves the splenium. In these cases, the visual consequences such as matching and comprehending objects in the different visual fields has significant implications for daily activities such as driving.

Controversies

The choice between the superior temporal and transparietal approaches to the atrium is controversial.

The posterior portion of the superior temporal sulcus is often deep and easy to identify, but on the dominant hemisphere the superior lip is the superior temporal gyrus harbouring the speech area. Hence mobilization or retraction if needed should veer on the inferior rather than the superior lip during splitting of the sulcus. Similarly, posterosuperior mobilization of the superior lip of the somewhat vertically oriented intraparietal sulcus is better undertaken to avoid excessive manipulations of the inferior parietal lobule which serves speech function located in the supramarginal and angular gyri.

With deep dissection the white matter tract encountered most superficially is the superior longitudinal or arcuate fasciculus which is oriented from the frontal lobe and its important connection regarding speech function is deep to the superior temporal sulcus (although there are possible extensions deep to the middle temporal sulcus) and to the inferior parietal lobule deep to the supramarginal and angular gyri. Therefore, the orientation of the trajectory to the trigone from either the superior temporal or intraparietal sulci should avoid severance of these important connections provided awareness of the proximity of this tract to the approach. The approach through either of these two sulci is quite away from the deeper posterior limb of the internal capsule or corona radiata. However, it is inevitable to transverse the two deeper layers which are the functionally important optic radiation and the tapetum which is without an identifiable neural deficit in case of transection. Disruption of the inferior fronto-occipital fasciculus (IFOF) may result in semantic paraphasia. At the sagittal stratum which is related to the lateral wall of the atrium the IFOF is medial to the arcuate fasciculus and lateral to the fibres of the optic radiation. More posteriorly, where the trajectory of these two approaches lies, the IFOF fibres are more splayed to reach the convexity surface of the occipital lobe, superior parietal lobe and the temporo-basal area (Martino et al., 2011).

In approaching through the superior temporal sulcus, the orientation of the optic radiation is parallel to that of the sulcus and hence a splitting dissection perhaps may separate the fibres and avoid division of a large number of tract fibres. The possible resulting superior quadrantanopia visual field defects usually have little practical impact on the patients' daily activities and these patients tend to adapt rapidly to this defect.

Conversely, through the intraparietal sulcus approach the orientation of the white matter dissection has to change orientation to keep 'in line' rather than across the optic radiation fibres. Anatomically a 'high' intraparietal approach passing superomedially to the optic radiation is advantageous as it causes minimal disruption to the white matter fibres, which are least dense on the roof of the atrium. Nevertheless, the resulting scotoma involving the inferior visual field is usually noticeable by the patient. If a large inferior quadrantanopic scotoma occurs, this may have impact on the patients' mobility and day to day activities (e.g. on descending a flight of stairs).

Although the superior temporal sulcus approach provides an early access to the choroid plexus which provides blood supply intraventricular meningiomata, nevertheless most of these lesions do not seem to be excessively vascular to impose a particular problem with bleeding by either approach.

REFERENCES

Barber, S.M., Rangel-Castilla, L., & Baskin, D. (2013). Neuroendoscopic resection of intraventricular tumours: a systematic outcomes analysis. *Minim Invasive Surg*, **2013**, 898753.

Brodal, A. (1981). *Neurological Anatomy in Relation to Clinical Medicine*, 3rd edition. New York, NY: Oxford University Press.

Duvernoy HM (1998). *The Human Hippocampus*, 2nd edition. Berlin, Germany: Springer.

Ebeling, U. & Reulen, H.J. (1988). Neurosurgical topography of the optic radiation in the temporal lobe. *Acta Neurochir (Wien)*, **92**, 26–36.

Ebeling, U. & Steinmetz, H. (1995). Anatomy of the parietal lobe: mapping the individual pattern. *Acta Neurochir (Wien)*, **136**, 8–11.

Friedman, M.A., Meyers, C.A., & Sawaya, R. (2008). Neuropsychological effects of third ventricle tumour surgery. *Neurosurgery*, **62**(6 Suppl 3), 1093–100.

Harkey, H.L., Al-Mefty, O., Haines, D.E., & Smith, R.R. (1989). The surgical anatomy of the cerebral sulci. *Neurosurgery*, **24**, 651–4.

Hart, M.G., Sarkies, N.J., Santarius, T., & Kirollos, R.W. (2013). Ophthalmological outcome after resection of tumours based on the pineal gland. *J Neurosurg*, **119**(2), 420–6.

Hassaneen, W., Suki, D., Salaskar, A.L., et al. (2010). Immediate morbidity and mortality associated with transcallosal resection of tumours of the third ventricle. *J Clin Neurosci*, **17**(7), 830–6.

Heimer, L. (1995). *The Human Brain and Spinal Cord*, 2nd edition. New York, NY: Springer Verlag.

Kirollos, R.W., Javadpour, M., May, P., & Mallucci, C. (2001). Endoscopic treatment of suprasellar and third ventricle-related arachnoid cysts. *Child's Nervous System*, **17**(12), 713–18.

Ludwig, E. & Klinger, J. (1956). *Atlas Cerebri Humani*. Basel, Switzerland: S. Karger.

Martino, J., Hamer, P.C.D., Vergani, F., et al. (2011). Cortex-sparing fiber dissection: an improved method for the study of white matter anatomy in the human brain. *J Anat*, **219**(4), 531–41.

Milligan, B.D. & Meyer, F.B. (2010). Morbidity of transcallosal and transcortical approaches to lesions in and around the lateral and third ventricles: a single-institution experience. *Neurosurgery*, **67**(6), 1483–96; discussion 1496.

Morris, T.C. & Santoreneos, S. (2012). Colloid cyst of velum interpositum: a rare finding. *J Neurosurg Pediatr*, **9**(2), 206–8.

Nagata, S., Rhoton, A.L. Jr., & Barry, M. (1988). Microsurgical anatomy of the choroidal fissure. *Surg Neurol*, **20**, 3–59.

Nieuwenhuys, R., Voogt, J., & Van Huijzen, C. (2007). *The Human Central Nervous System*, 4th edition. Berlin, Germany: Steinkopffed.

Oka, K., Rhoton, A.L. Jr., Barry, M., & Rodriguez, R. (1985). Microsurgical anatomy of the superficial veins of the cerebrum. *Neurosurgery*, **17**(5), 711–48.

Ono, M., Kubik, S., & Abernathey, C.D. (1990). *Atlas of Cerebral Sulci*. Stuttgart, Germany: Thieme.

Párraga, R.G., Ribas G.C., Welling L.C., Alves R.V., and de Oliveira E. (2012). Microsurgical anatomy of the optic radiation and related fibers in 3-dimensional images. *Neurosurgery*, **71**(1 Suppl Operative), 160–71; discussion 171–2.

Rhoton, A.L. Jr. (2003). Cranial anatomy and surgical approaches. *Neurosurgery*, **53**, 1–746.

Rhoton, A.L. (2002). The lateral and third ventricles. *Neurosurgery*, **51**(Suppl 1), 207–71.

Rhoton, A.L. Jr., Yamamoto, I., & Peace, D.A. (1981). Microsurgery of the third ventricle: part 2—operative approaches. *Neurosurgery*, **8**(3), 357–73.

Ribas, G.C. (1999). Telencéfalo. In: Meneses, M.S. (ed.) *Neuroanatomia Aplicada*, pp. 237–72. Rio de Janeiro, Brazil: Guanabara Koogan.

Ribas, G.C. & Rodrigues, A.J. (2007). The suprapetrosal craniotomy. *J Neurosurg*, **106**(3), 449–54.

Ribas, G.C., Yasuda, A., Ribas, E.C., Nishikuni, K., & Rodrigues Junior, A.J. (2006). Surgical anatomy of microneurosurgical sulcal keypoints. *Neurosurgery*, **59**(ONS Suppl4), ONS-177-ONS-209.

Ribas, G.C. (2005). *Microanatomia cirúrgica dos pontos-chave dos sulcos e giros cerebrais [tese livre-docência]*. São Paulo, Brazil: Faculdade de Medicina, Universidade de São Paulo, p. 297.

Selvanathan, S.K., Kumar, R., Goodden, J., Tyagi, A., & Chumas, P. (2013). Evolving instrumentation for endoscopic tumour removal of CNS tumours. *Acta Neurochir (Wien)*, **155**(1), 135–8.

Symss, N.P., Ramamurthi, R., Kapu, R., et al. (2014). Complication avoidance in transcallosal transforaminal approach to colloid cysts of the anterior third ventriclen: an analysis of 80 cases. *Asian J Neurosurg*, **9**(2), 51–7.

Szmuda, T., Słoniewski, P., Szmuda, M., Waszak, P.M., & Starzyńska, A. (2014). Quantification of white matter fibre pathways disruption in frontal transcortical approach to the lateral ventricle or the interventricular foramen in diffusion tensor tractography. *Folia Morphol (Warsz)*, **73**(2), 129–38.

Timurkaynak, E., Rhoton, A.L. Jr., & Barry, M. (1986). Microsurgical anatomy and operative approaches to the lateral ventricles. *Neurosurgery*, **19**, 685–723.

Türe, U., Yaşargil, M.G., & Al-Mefty, O. (1997). The transcallosal-transforaminal approach to the third ventricle with regard to the venous variations in this region. *J Neurosurg*, **87**(5), 706–15.

Türe, U., Yaşargil, M.G., Friedman, A.H., & Al-Mefty, O. (2000). Fibre dissection technique: lateral aspect of the brain. *Neurosurgery*, **47**, 417–27.

Ulm, A.J., Russo, A., Albanese, E., et al. (2009). Limitations of the transcallosal transchoroidal approach to the third ventricle. *J Neurosurg*, **111**(3), 600–9.

Villani, R., Papagno, C., Tomei, G., Grimoldi, N., Spagnoli, D., & Bello, L. (1997). Transcallosal approach to tumours of the third ventricle. Surgical results and neuropsychological evaluation. *J Neurosurg Sci*, **41**(1), 41–50.

Wen, H.T., Rhoton, A.L. Jr., Oliveira, E., et al. (1999). Microsurgical anatomy of the temporal lobe: part I: mesial temporal lobe anatomy and its vascular relationships and applied to amygdalohippocampectomy. *Neurosurgery*, **45**, 549–92.

Wen, H.T., Rhoton, A.L. Jr., & Oliveira, E. (1998). Transchoroidal approach to the third ventricle: an anatomic study of the choroidal fissure and its clinical application. *Neurosurgery*, **42**, 1205–19.

Williams, P.L. & Warwick, R. (eds.) (1980). *Gray's Anatomy*, 36th edition. Philadelphia, PA: Saunders.
Yamamoto, I., Rhoton, A.L. Jr., & Peace, D.A. (1981) Microneurosurgery of the third ventricle: part I, microsurgical anatomy. *Neurosurgery*, **8**, 334–56.
Yaşargil, M.G. (1996). *Microneurosurgery*, vol. **IVb**. Stuttgart, Germany; Georg Thieme.

RELATED LINKS TO EBRAIN

How to Do an Interhemispheric Approach for a Colloid Cyst. https://learning.ebrain.net/course/view.php?id=1260
Surgical Approaches to Tumours of the Ventricle. https://learning.ebrain.net/course/view.php?id=491

SECTION 8

Tumours and skull base—pineal

36. **Pineal tumours** *427*
Mueez Waqar, Samantha Mills, Conor L. Mallucci, and Michael D. Jenkinson

37. **Surgical management of pineal region lesions** *439*
Christoph M. Woernle, René L. Bernays, and Nicolas de Tribolet

36

Pineal tumours

Mueez Waqar, Samantha Mills, Conor L. Mallucci, and Michael D. Jenkinson

Introduction

The pineal region is located in the midline between the tectum of the midbrain and the roof of the third ventricle. Pineal tumours are rare and are more commonly seen in children than adults (Louis et al., 2016). A large variety of histological tumour types are found in the pineal region, including germ cell tumours (GCTs, 60%), pineal parenchymal tumours (PPTs, 30%) and gliomas (5%) (see **Fig. 36.1**). Other histological subtypes are rare but include papillary tumour of the pineal region (PTPR), ependymoma, meningioma, lymphoma, and metastases (Al-Hussaini et al., 2009). Historically, open surgery carried unacceptable levels of morbidity and many pineal tumours were treated with irradiation alone, without histological diagnosis. Modern neurosurgical and neuro-oncology management is determined by tumour type and includes biopsy, open surgery, fractionated radiotherapy, and chemotherapy. Most recent advances in the treatment of pineal tumours have mainly been driven by clinical trials in paediatric patients.

Presentation and preoperative workup

Patients with pineal tumours commonly present with raised intracranial pressure (87%), Parinaud's syndrome (76%) due to midbrain compression (restricted upgaze, loss of accommodation reflex, near-light dissociation, and convergence nystagmus) and cerebellar signs (52%) (Konovalov and Pitskhelauri, 2003). Contrast-enhanced magnetic resonance imaging (MRI) of the brain and whole spine is required to determine the presence of hydrocephalus, anatomy for surgical approaches, and presence of metastatic spread (Awa et al., 2014). Serum and cerebrospinal fluid (CSF) sampling for tumour markers is also necessary. Elevated β human chorionic gonadotrophin (β-HCG) and α-fetoprotein (AFP) may be diagnostic for GCT subtype without the need for biopsy. In the absence of elevated tumour markers, a tissue biopsy is required by endoscopic, stereotactic, or open approach. In the presence of hydrocephalus, CSF diversion by endoscopic third ventriculostomy (ETV) is the preferred treatment for hydrocephalus, allowing biopsy of the tumour in the same operation.

Germ cell tumours

Epidemiology

The pineal region is the most common site of intracranial germ cell tumours (Arora et al., 2012). Over 90% of cases occur before the age of 20 years with incident peaks occurring just after birth and in early adolescence. Males are more likely to be affected (Louis et al., 2016).

Pathology and genetics

Most intracranial germ cell tumours arise sporadically. These tumours may have an additional X chromosome, and there is an association with Klinefelter's syndrome. Other common chromosomal gains include 1q, 8q, and 12p, as well as less frequent losses of 11q, 13, and 18q. GCTs have been associated with Down's syndrome and neurofibromatosis type 1 (Louis et al., 2016).

Intracranial GCTs are most commonly found in the pineal region; rarely they may be suprasellar or bifocal (pineal and suprasellar concurrently). GCTs are divided pathologically into germinomatous tumours (germinomas; accounting for 70–80%) and non-germinomatous tumours (Al-Hussaini et al., 2009).

Germinomas resemble primordial germ cells, whereas non-germinomatous tumours have characteristics associated with the embryonic stage of development (e.g. the pluripotent nature of teratomas). Occasionally GCTs contain elements of both subcategories, in which case they are classified as non-germinomatous in the WHO classification (Louis et al., 2016). By convention, all GCT subtypes, except mature teratomas, are regarded as malignant.

Germinomatous tumours

Germinomas

Germinomas may seed the neuroaxis and are composed of cells with large nuclei featuring prominent nucleoli and clear cytoplasm, with a high proliferative rate and numerous mitoses (**Fig. 36.1**D). Immunoreactivity can be demonstrated to c-kit in the cell membrane and OCT4 in the nucleus (Louis et al., 2016). Germinomas with syncytiotrophoblastic giant cells can secrete low levels of βHCG (**Box 36.1**).

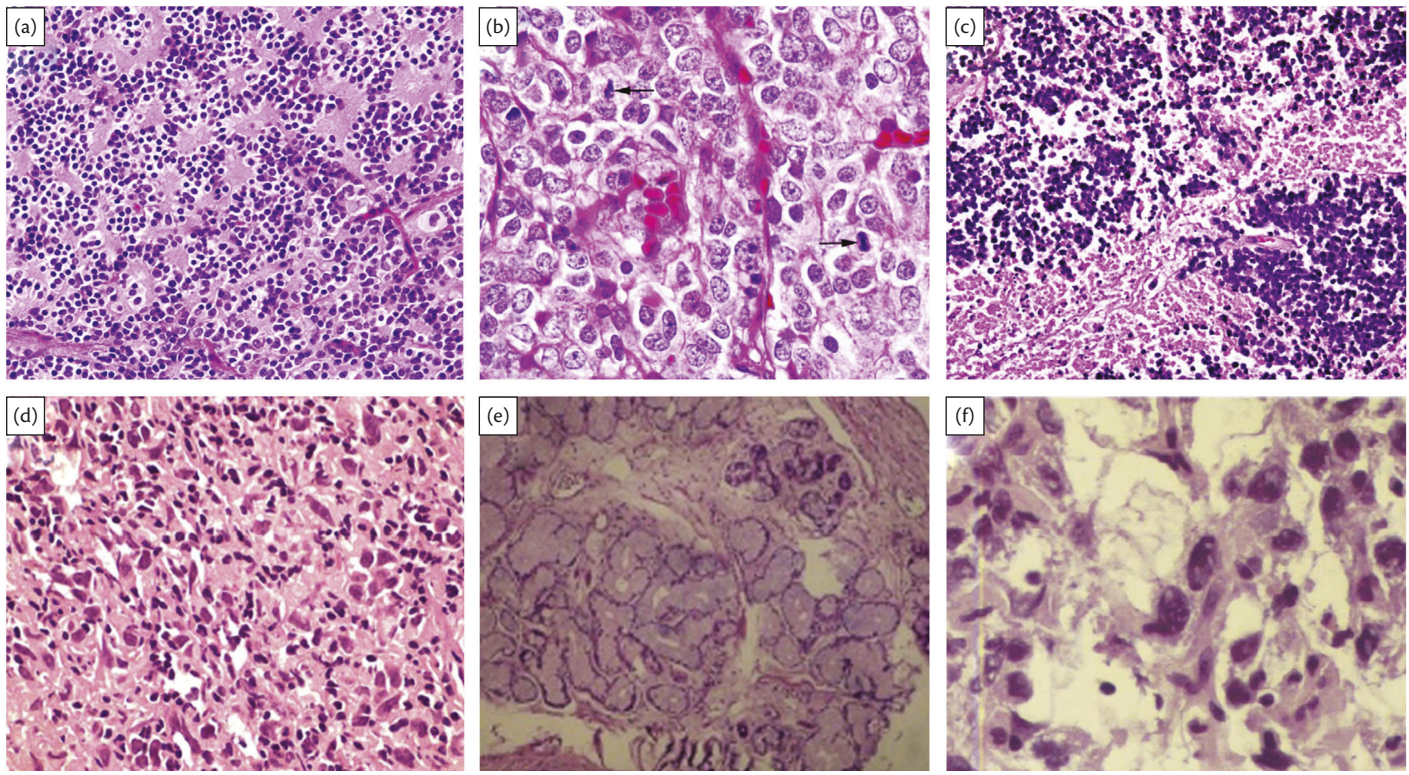

Fig. 36.1 Histopathology of pineal region neoplasms. (A) Pineocytoma: moderately cellular tumours, with well-differentiated cells that resemble pineocytes; usually cells feature a single nucleus. (B) Pineal parenchymal tumour of intermediate differentiation: although absolute diagnostic criteria are lacking, these tumours feature a moderate degree of cellularity, cellular maturity, nuclear atypia, and mitotic rate (arrows show foci of mitosis). (C) Pineoblastoma: highly cellular tumour containing primitive cells, with a high nuclear to cytoplasmic ratio and high mitotic rate. (D) Germinoma: characteristic cells with large nuclei and prominent nucleoli, and clear, glycogen-rich cytoplasm. (E) Mucous glands of a mature teratoma: these tumours can also feature several other cell morphologies. (F) Immature-looking stem cells that resemble embryonic stem cells; tumour cells are large with prominent nucleoli and abundant cytoplasm.

Non-germinomatous tumours

Non-germinomatous germ cell tumours (NGGCTs) include teratoma, embryonal carcinoma, yolk sac tumour, and choriocarcinoma. Approximately 13.5% of pineal germ cell tumours exhibit mixed histology (Al-Hussaini et al., 2009). Unlike germinomas, NGGCTs contain cytokeratin structural proteins, indicating epithelial cell lineage, a major histopathological differentiating factor between the two major GCT types.

Teratoma

Teratomas are the commonest pure NGGCT (7% of pineal GCTs) (Al-Hussaini et al., 2009). They contain elements from all three germ layers. If the elements are completely differentiated, the tumour is termed mature, while if there is any evidence of incomplete differentiation for any element, the tumour is termed immature (Figs. 36.1E and 36.1F). Rarely, somatic elements within teratomas can undergo neoplastic change, in which case the tumour is classified as teratoma with malignant transformation. Immunoreactivity depends on the tissue present in these tumours and they may stain positively for c-kit. Incompletely differentiated enteric glands in immature teratomas can also secrete AFP (Louis et al., 2016).

Embryonal carcinoma

These consist of immature-looking stem cells that resemble embryonic stem cells. Tumour cells are large with prominent nucleoli and abundant cytoplasm, which may be violaceous (eosinophilic) or clear. Cells tend to grow in sheets, gland-like patterns, or as papillary structures. Positive markers in addition to cytokeratins include PLAP, OCT4, and CD30 (Louis et al., 2016).

Yolk sac tumour

Yolk sac tumours contain cells that resemble the endodermal cells lining the yolk sac. Tumour cells are small, with non-prominent nucleoli and scant cytoplasm, which characteristically stains positive for AFP (Louis et al., 2016).

Choriocarcinoma

Choriocarcinoma contains transformed placental elements, primarily as two cells—cytotrophoblasts and synctiotrophoblastic giant cells (STGCs). Immunostaining for cytokeratins is demonstrable with both cell types, but STGCs are additionally positive for β-HCG and human placental lactogen (Louis et al., 2016).

Management pathway for germ cell tumours

An algorithm for the workup and management of suspected pineal GCTs is shown in Figure 36.2. Serum and CSF tumour markers are used to classify tumours as either secreting or non-secreting and this directly determines the treatment pathway. A lumbar puncture and spinal MRI are always indicated to identify patients with craniospinal dissemination, which may be microscopic and identified only via CSF cytology. These patients can then be treated more aggressively. ETV with endoscopic pineal biopsy is considered the

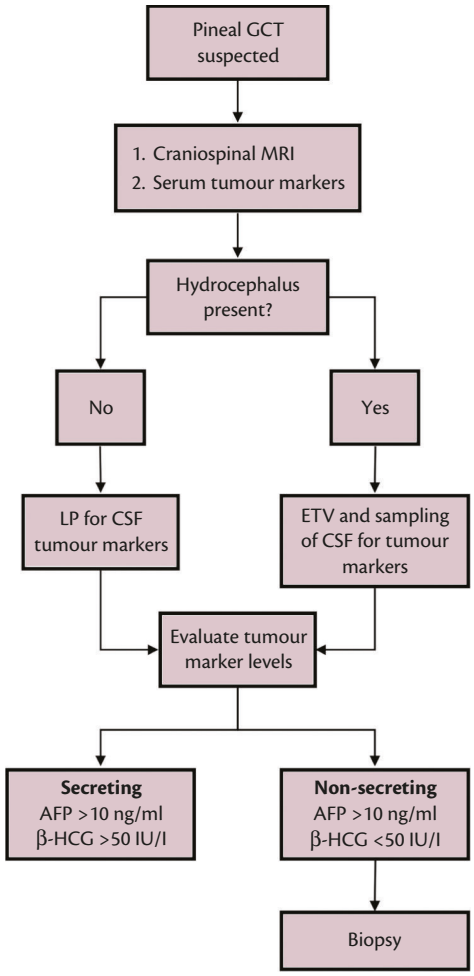

Fig. 36.2 Workup and management of pineal germ cell tumours.

optimum technique for pineal tumours with concurrent hydrocephalus and ~80% remain shunt-free (Shono et al., 2007), while minimizing the risk of iatrogenic tumour dissemination via a shunt (Kumura et al., 1986).

Tumour markers

Serum and CSF should be tested for AFP and β-HCG. The pattern of elevation serves as a guide to GCT subtype (Table 36.1). Non-germinomatous mixed GCTs may have yolk sac or choriocarcinoma components, associated with elevated AFP and β-HCG, respectively. Up to a third of germinomas (with STGCs) can secrete β-HCG causing elevations that are typically less than in non-germinomatous tumours. Tumour markers are also used to measure response to therapy and for prognostication.

Tumour biopsy

Non-secreting tumours should undergo biopsy. In patients with hydrocephalus, ETV and biopsy can be performed during the same procedure (Pettorini et al., 2013). In the absence of hydrocephalus, stereotactic biopsy can be used. Diagnostic rates favour stereotactic methods (94% vs. 81%), although reported mortality is higher (1.3% vs. 0.3%). Biopsy in the pineal region carries 4–5% risk of haemorrhage with either technique due to the proximity of the deep veins (Balossier et al., 2015a). Bifocal lesions with classical radiological features and diabetes insipidus are pathognomonic for germinoma and do not require biopsy.

Table 36.1 Tumour markers and GCT subtypes

Tumour		AFP	β-HCG	PLAP
Germinomatous	Germinoma	–	+/–[1]	+
Non-germinomatous	Mixed	+/–	+/–	+/–
	Teratoma	+/–[2]	+/–[2]	–
	Embryonal carcinoma	–	–	+
	Yolk sac tumour	+	–	+/–
	Choriocarcinoma	–	+	+/–

[1]Germinomas containing synctiotrophoblastic giant cells may secrete β-HCG. [2]Immature teratomas can rarely contain AFP or β-HCG secreting tissue; however, the differential diagnosis of mixed GCT containing yolk sac or choriocarcinoma components should also be considered.

Treatment

Germinomas

Pure germinomas can be cured with radiotherapy alone. Germinomas with high β-HCG (usually >50 IU/litre, due to presence of STGCs) have been distinguished as a subset of germinomas that may require more aggressive treatment.

- **Surgery**: Cytoreductive surgery does not improve outcomes, (Sawamura et al., 1997) however, where residual tumour remains following radiotherapy, a mixed non-germinomatous tumour with a germinoma component should be considered and surgery may be warranted (Oya et al., 2014). Pooled data from the International Central Nervous System Germ Cell Study Groups showed better outcome for germinoma patients with less than 1.5 cm^3 residual disease (recurrence rates after mean 6-years follow-up, 65% vs. 38%) (Souweidane et al., 2010). However, this data requires validation as it is contrary to the SIOP trials.
- **Radiotherapy**: Germinomas are radiosensitive. Craniospinal irradiation (CSI) achieves 5-year progression-free survival (PFS) and overall survival (OS) rates more than 90% (Bamberg et al., 1999). Radiotherapy may cause late adverse effects including neurological and cognitive impairment, secondary malignancy and endocrinopathy (Bamberg et al., 1999), especially in children. Efforts to reduce toxicity include:
  - **(1)** Decreasing volume irradiated—focal radiation is recommended for localized tumours (Rogers et al., 2005).
  - **(2)** Reducing the total dose—delivers 5-year survival rates comparable to older protocols (Bamberg et al., 1999; Calaminus et al., 2013).
  - **(3)** Induction chemotherapy with focal irradiation that includes the ventricles in order to minimize the risk of dissemination (Calaminus et al., 2013). The benefits of induction chemotherapy are being evaluated in ACNS 0232, a phase III RCT.
  - **(4)** Response-dependent decreases in radiation dose—following induction chemotherapy a reduced radiotherapy dose is administered depending on radiological response (Legault et al., 2013).
- **Chemotherapy**: The international CNS GCT studies (Table 36.2) showed that due to dismal survival rates (5-year PFS <50%),

chemotherapy cannot be used on its own (da Silva et al., 2010). The role of induction chemotherapy is still being evaluated. The International Society of Paediatric Oncology (SIOP) regimen of ifosfamide, carboplatin, and etoposide ('ICE') is used at some institutions, with platinum-based treatment consisting of carboplatin rather than cisplatin due to reduced chemotoxicity (Calaminus et al., 2013).

Non-germinomatous GCTs

Prognostically, tumours in this group can be divided into three subgroups—low-risk (mature teratoma), intermediate-risk (mixed GCTs with predominantly germinoma and teratoma elements), and high-risk tumours (embryonal carcinoma, choriocarcinoma, yolk sac tumour, mixed tumours with predominantly these elements). Ten-year OS rates for the intermediate and high-risk groups are 70% and less than 10%, respectively, highlighting the importance of accurate histological classification.

- **Surgery**: Resection of non-germinomatous tumours should be performed as follows:
  - **(1)** Mature teratomas—resection is usually curative.
  - **(2)** Postchemotherapy residuum—'second-look' surgery improves outcomes in non-germinomatous GCTs and recent trials encourage this approach (Czech et al., 2012). Residuum can represent a mature teratoma (commonly), a different non-germinomatous tumour or necrosis/scarring. Normalization of tumour markers and increasing size of the residual lesion should prompt second-look surgery.
  - **(3)** Tumours unresponsive to adjuvant therapy—these patients may benefit from surgery if they fail to respond to first and/or second-line therapy.
- **Radiotherapy**: For non-germinomatous tumours radiotherapy results in poor 5-year PFS rates of less than 50%. For disseminated disease full CSI is advised. For localized tumours, radiotherapy to the tumour and ventricles alone can be considered, however, 5-year PFS and OS rates were lower in the SIOP trial, which did not use CSI in localized tumours, versus the Children's Oncology Group trial (Table 36.2, 5-year PFS 67–69% vs. 84.3%) (Calaminus et al., 2012b; Goldman et al., 2015).
- **Chemotherapy**: Chemotherapy-only regimens produce dismal rates of survival (5-year PFS 50%, 3rd international CNS GCT trial, Table 36.2) (Marec-Berard et al., 2002; da Silva et al., 2010). The MAKEI 89 trial used sandwich chemotherapy (chemotherapy-radiotherapy-chemotherapy), and survival rates were comparable to trials withholding second chemotherapy regimens if response was adequate (Bamberg et al., 1999). Therefore, induction chemotherapy followed by radiotherapy +/– second-look surgery for residual, has become the standard of care for non-germinomatous tumours.

Outcome

Five-year PFS rates for germinomas and non-germinomatous tumours are more than 90% and 60–70%, respectively. Most disease relapse occurs intracranially and within 5 years of treatment. Patients who relapse despite first-line treatment may benefit from high-dose salvage chemotherapy and/or autologous stem cell rescue. However, patients with relapsed disease have a relatively poor prognosis, and median survival for recurrent germinomas is 48 months and for non-germinomatous tumours is 35 months (Modak et al., 2004).

Cognitive deficits are present in a substantial proportion of patients and affect working memory, processing speed, and visual memory. Neuropsychological sequelae are lower in patients with pineal GCTs compared to disseminated germ cell tumours. Patients treated with radiotherapy require long-term follow-up for late effects including cognitive impairment, endocrinopathy, and radiation-induced malignancy.

The prognostic significance of tumour markers is unclear. Some trials data have shown that elevated AFP and β-HCG do not influence survival (Kim et al., 2008). In the SIOP trial, patients with isolated β-HCG levels of more than 50–200 IU/litre +/– non-germinomatous histology (except teratoma) were shown to have 5-year OS/PFS rates of 100%, similar to 'pure' germinomas. Only those with a β-HCG of more than 200 IU/litre had survival rates closer to those expected with non-germinomatous tumours, suggesting that patients in the 50–200 group could simply be secreting germinomas (Nicholson et al., 2013). In non-germinomatous tumours AFP greater than 1000 ng/ml has been demonstrated as marker of poor prognosis and these patients need more intensive treatment regimens (Calaminus et al., 2012a).

Pineal parenchymal tumours

Epidemiology

Pineal parenchymal tumours constitute about 30% of all pineal tumours, with a median age at presentation of 21 years (Al-Hussaini et al., 2009). They affect both sexes equally. Pineoblastomas are more common in younger children, whereas lower-grade tumours are more common in older adults (Selvanathan et al., 2012).

Pathology and genetics

Most PPTs arise sporadically. Genetic alterations include gains of chromosomes 4q2 and 12, and losses of chromosomes 10 and 22 (Von Beuren et al., 2012). Pineoblastoma may rarely be associated with bilateral retinoblastoma (5–13%) and familial bilateral retinoblastoma (5–15%). PPTs are thought to arise from pineocytes and the WHO classifies four grades: pineocytomas (WHO grade I), pineal parenchymal tumours of intermediate differentiation (PPTIDs) (grade II and III) (See Box 36.2) and pineoblastomas (grade IV). The PTPR corresponds to grade II or III. PTPRs probably arise from ependymal circumventricular subcommissural organ cells and are distinct from PPTs. Histological diagnosis of primary pineal tumours is challenging and should be undertaken by experienced neuropathologists.

Pineocytoma

Pineocytomas accounts for 14–30% of PPTs and are well-circumscribed tumours that grow slowly without disseminating through the CSF (Fevre-Montange et al., 2010). These tumours have moderate cellularity and well-differentiated cells resembling pineocytes (Fig. 36.1A). Tumour cells grow in sheets or lobules and may collate around cytoplasmic processes to form characteristic pineocytomatous rosettes. Usually, cells harbour single,

Table 36.2 Contemporary trials evaluating adjuvant treatment of intracranial germ cell tumours.

Study	Arm	Tumours	Metastases	Avg age, years (range)	Group size, n	First-line adjuvant therapy			5-year actuarial survival rates	
						Radiotherapy	Chemotherapy (induction)	Chemotherapy (post-XRT)	PFS	OS
3rd international CNS GCT trial Non-randomized (Various)	Low-risk	Germinoma (β-HCG <2.2 IU/ml)	0	15 (8–24)	11	None	4 courses +/–additional based on response		27.3%[1]	88.9%[1]
	intermediate and high-risk	NGGCT or germinoma with β-HCG >2.2 IU/litre	+/–	10 (0.3–19)	14	None	Up to six courses of intensified carboplatin, cyclophosphamide, and etoposide		50.0%[1]	58.3%[1]
POG 9530 Non-randomized (USA) Response dependent irradiation doses	Low-risk	Germinoma (β-HCG <50 IU/ml)	0		8	Focal therapy CR: 30.6 Gy <CR: 50.4 Gy	2 courses Cisplatin Etoposide Vincristine Cyclophosphamide	Non	87.5%	100%
			1	15.1 (9.5–17.7)	4	+CSI as follows CR: 30.6 Gy <CR: 36 Gy		None	100%	100%
MAKEI 83/86/89 Non-randomized (German) No first-line chemotherapy	MAKEI 83/86	Germinoma (β-HCG <100 ng/μl)	NR[2]	13 (6–31)	11	CSI: 36 Gy Boost: 14 Gy	None	None	100.0%	100.0%
	MAKEI 89				49	CSI: 30 Gy Boost: 15 Gy	None	None	88.8%	92.0%
MAKEI 89- NGGCT arm	N/A	NGGCT	+/–	11 (2–24)	27	CSI: 30 Gy Boost: 20 Gy	2 courses Cisplatin Etoposide Bleomycin	2 courses Cisplatin Ifosfamide Vinblastine	74.0%	59.0%
SIOP CNS GCT 96 Non-randomized (Various) Largest reported experience of intracranial GCTs	XRT only	Germinoma (β-HCG <50 IU/litre)	0	13 (4–42)	125	CSI: 24 Gy Boost: 16 Gy	None	None	97.0%	95.0%
			0		65	40 Gy focal	2 courses Carboplatin Etoposide Ifosfamide	None	88.0%	96.0%
	Chemoradio		1		45	CSI: 24 Gy Boost: 16 Gy	None	None	100.0%	98.0%
	No mets	NGGCT (un-published data)	0	12 (0–30)	146	Focal 54 Gy	4 courses Cisplatin Etoposide Ifosfamide	None	69.0%[4]	78.0%[4]
	Mets		1		43	CSI: 30 Gy Boost: 24 Gy			67.0%[4]	70.0%[4]
Children's Oncology Group NGGCT trial Non-randomized (USA) Trial of NGGCTs	N/A	NGGCT Or Germinoma with β-HCG >50 IU/litre	+/–	12 (3–23)	102	CSI: 36 Gy Boost: 18 Gy (primary) and >9 Gy (mets)	Up to six courses Carboplatin Etoposide Ifosfamide	If no response (+/– 2nd look surgery): thiotepa and etoposide	84.3%	93.0%

[1]6-year actuarial rates, note that in the 3rd International CNS GCT trial, only event-free survival was reported and reproduced here, rather than PFS. [2]15.2% of patients had dissemination at presentation and were treated with the same protocols. [3]Event-free survival was reported rather than overall survival. [4]After median follow-up of 36–55 months.

regular nuclei, but multinucleated giant cells with bizarrely shaped nuclei may also be seen (pleomorphic subtype). Necrosis is rare and mitotic counts are low. Immunostaining can reveal neuronal (synaptophysin, neurofilaments and neuron-specific enolase) and photosensory differentiation (retinal S-antigen and rhodopsin). Interstitial cells can show positivity to glial markers (e.g. GFAP) (Louis et al., 2016).

Pineoblastoma

Pineoblastomas account for 24–50% of primary pineal tumours (Fevre-Montange et al., 2010). They are considered as primitive neuroectodermal tumours (PNET) that occur in the pineal region. The tumours are highly cellular, with immature cells with indistinct borders (Fig. 36.1C). Cells may cluster to form rosettes: Homer-Wright and Flexner-Wintersteiner (indicating retinoblastic differentiation). The mitotic rate is elevated with a high nucleus to cytoplasm ratio; they may be described as 'small blue cells' due to dominant nuclear staining over scant cytoplasm. Pineoblastomas are locally invasive, with poorly defined borders, and have a propensity to disseminate through the CSF. Immunopositivity is similar to pineocytomas (Louis et al., 2016).

Pineal parenchymal tumours of intermediate differentiation (PPTID)

PPTID accounts for 20–62% of primary pineal tumours (Fevre-Montange et al., 2010). Diagnostic criteria are poorly defined but moderate is the key word—to describe cellularity, cellular maturity, nuclear atypia, and mitotic rate (Fig. 36.1B). They can grow in a diffuse pattern (neurocytoma-like), in lobules (endocrine-like) or a mixture of both. The transitional subtype also features pineocytomatous rosettes. Tumours with elements of both pineocytoma and pineoblastoma can also be grouped in this category. Necrosis, leptomeningeal involvement, and vascular proliferation can all be present. The MIB-1 labelling index may be a more important prognostic factor than histological grading (Louis et al., 2016).

Papillary tumour of the pineal region (PTPR)

PTPRs are rare tumours characterized by epithelial and papillary features, and frequent necrotic foci. Mitotic activity and the MIB-1 labelling index are moderately raised (Louis et al., 2016). In some there is tendency for recurrence and need for repeated surgery (Santarius et al., 2008; Fauchon et al., 2013).

Diagnosis

The management algorithm is shown in Figure 36.3. Imaging features are non-specific, but they are more likely to have peripheral calcification, unlike GCTs. Pineocytomas tend to be well-circumscribed, whereas pineoblastomas have irregular margins and 15% are associated with metastases (Gaillard and Jones, 2010). PPTIDs are usually more locally invasive and heterogeneous than pineocytomas, though pathognomonic features are lacking. Multimodal imaging may aid in tumour grade prediction, but tissue is still needed for diagnosis.

Treatment

Pineocytoma

- ***Surgery***: Complete resection is curative and should be considered for symptomatic tumours. Histologically confirmed small tumours (<1 cm) grow slowly and can be monitored with serial MRI since the morbidity of surgical resection is high. Overall survival at 5 years is better following gross total resection (84%) compared to subtotal resection and radiotherapy (17%) (Clark et al., 2010b).
- ***Radiotherapy***: Guidelines by the British Neuro-Oncology Society recommend radiotherapy in the setting of residual tumour (British Neuro-Oncology Society, 2011b), though it has not been shown to influence OS/PFS (Clark et al., 2010a; Clark et al., 2010b).
- ***Stereotactic radiosurgery***: As primary therapy PFS rates are more than 85% after 30 months follow-up (Balossier et al., 2015b). Studies reporting long-term outcomes are lacking and up to 50% of tumours show no growth which may simply reflect the natural history of small pineocytomas. Its efficacy may be higher for residual tumours and a 100% 5-year PFS has been reported in this context (Mori et al., 2009).
- ***Chemotherapy***: There are no effective regimes either at diagnosis or recurrence.

Pineoblastoma

- ***Surgery***: Extent of resection (EOR) has been shown to influence patient survival (Lutterbach et al., 2002), but the data is conflicting (Lee et al., 2005; Selvanathan et al., 2012). In a systematic review, GTR was associated with significantly improved survival versus subtotal resection and biopsy—5-year OS 84% vs. 53% and 29%, respectively. The addition of radiotherapy to the STR group improved survival (5-year OS 64%), but this was still inferior to that achieved with GTR (Tate et al., 2012). Residual disease size less than 1.5 cm^3 has been shown to improve survival in PNETs in general (Zeltzer et al., 1999).
- ***Radiotherapy***: Adjuvant CSI is administered to adults and older children with pineoblastoma (British Neuro-Oncology Society, 2011a). Its use in very young children is subject to debate due to the potential for neurocognitive deficits. Inferior outcomes have been reported in studies employing chemotherapy-only protocols, albeit at normal doses (Duffner et al., 1995; Hinkes et al., 2007).
- ***Stereotactic radiosurgery***: In the absence of good quality data, stereotactic radiosurgery should not be used routinely (Balossier et al., 2015b).
- ***Chemotherapy***: Chemotherapy is associated with improved outcome. In a meta-analysis, 5-year OS rates were 45% vs. 52% for surgery/radiotherapy and surgery/radiotherapy/chemotherapy, respectively (Tate et al., 2012). Platinum-based chemotherapy regimens appear to be the most effective and phase II trials employing these in conjunction with conventional radiotherapy have reported 5-year OS rates of 71–83% (Pizer et al., 2006; Hinkes et al., 2007). High-dose chemotherapy may be useful in very young children to delay radiotherapy. Chemotherapy regimens are poorly tolerated in adults and are not recommended.

PPTID and PTPR

The optimal treatment strategy of PPTID and PTPR is not well defined and there is no prospective evidence to guide treatment decisions.

- ***Surgery***: Retrospective analyses have shown EOR to influence outcome in PPTID and PTPR. In a meta-analysis of PPTID, patients

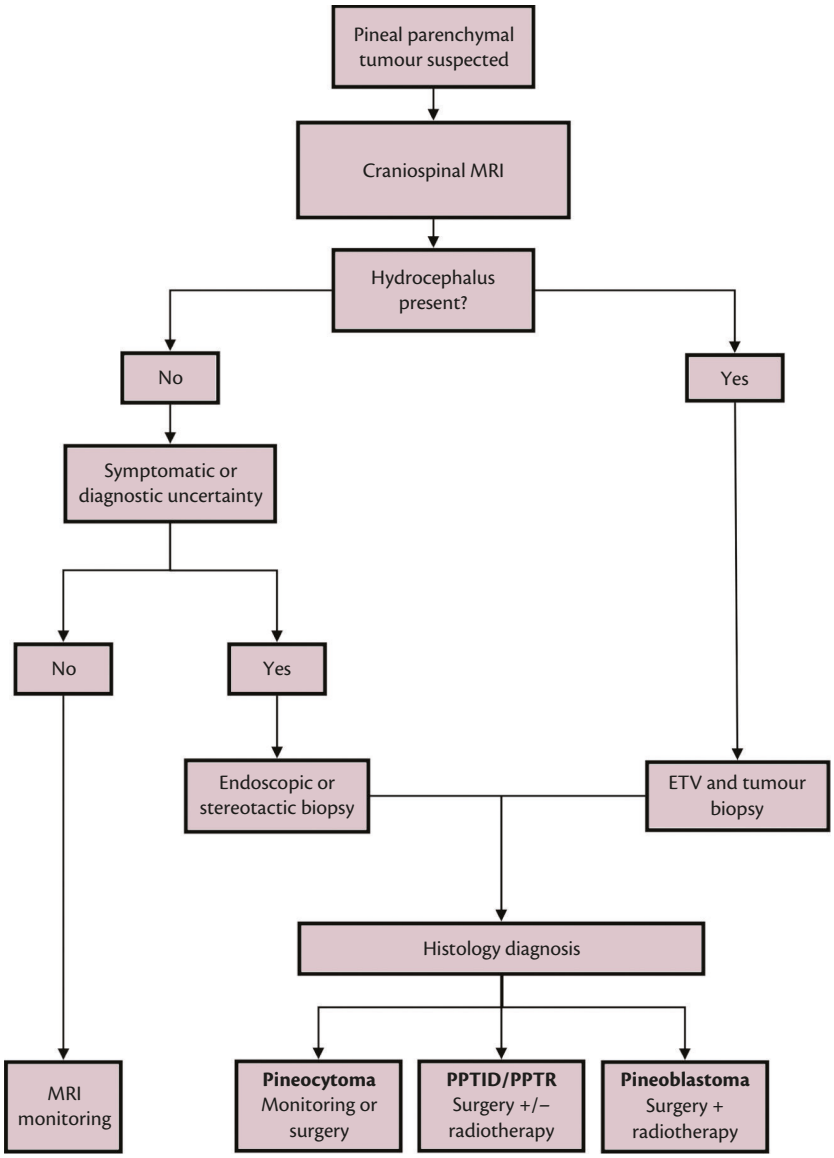

Fig. 36.3 Workup and management of pineal parenchymal tumours.

with no residual disease had a 10-year OS of 100%, compared to 40% and 15%, for those with residuals less than 50% and more than 50% in size, respectively (Lutterbach et al., 2002). PTPR has a worse 5-year OS of 73% (Louis et al., 2016).

- ***Adjuvant treatment***: Not all patients with PPTIDs receive adjuvant treatment (Villa et al., 2012). Radiotherapy may be employed in the setting of residual disease. The high rate of spinal relapse in grade III tumours would support CSI in these patients (Fauchon et al., 2000). In grade II tumours, focal radiotherapy to the tumour bed may be sufficient. The mitotic count can serve as a useful indicator to guide treatment decisions and if particularly high, then patients may be treated with protocols used for pineoblastoma (Fukuoka et al., 2012). Further prospective studies are needed on these tumours. The role of radiotherapy in PTPR has not been defined (Fauchon et al., 2013).

Outcome

Outcomes of pineal tumours are heterogeneous and depend on treatment provided. In pineocytoma, the 5-year OS in the setting of gross total resection is 84%, with no demonstrable benefit of radiotherapy (Clark et al., 2010a). Patients with pineoblastoma have a worse prognosis and reported outcomes are largely dependent on patient age. In children, 5-year OS rates of more than 70% can be achieved using contemporary radiotherapy protocols and platinum-based chemotherapy courses. The outcome for patient with PPTID and PTPR is less clear and falls somewhere between pineocytoma and pineoblastoma. A significant limitation appears to be the diagnostic criteria for these tumours, which should be made more definitive to allow appropriate patient grouping in future series and clinical trials. Non-treatment related prognostic factors identified through multivariate analysis include extent of disease, with metastases at presentation being associated with worse outcome, grade of tumour, and age of less than 5 years, particularly for higher grade PPTs (Lutterbach et al., 2002).

Surgical pearls/controversies

- MRI cannot accurately identify tumour type but is essential for surgical planning

Box 36.1 Case example 1—germinoma

A 21-year-old male presented with 6 weeks of early morning headache and diplopia. There was papilloedema but no Parinaud's syndrome. MRI revealed a homogenously enhancing pineal tumour and hydrocephalus (Fig. 36.4A). MRI of the spine was normal. Serum βHCG and AFP were normal. ETV was performed for hydrocephalus (Fig. 36.4B). CSF AFP was normal and β-HCG was only very slightly raised, prompting a stereotactic biopsy, which confirmed a germinoma. The patient received craniospinal radiotherapy and remained disease-free at 2 years (**Fig. 36.4C**).

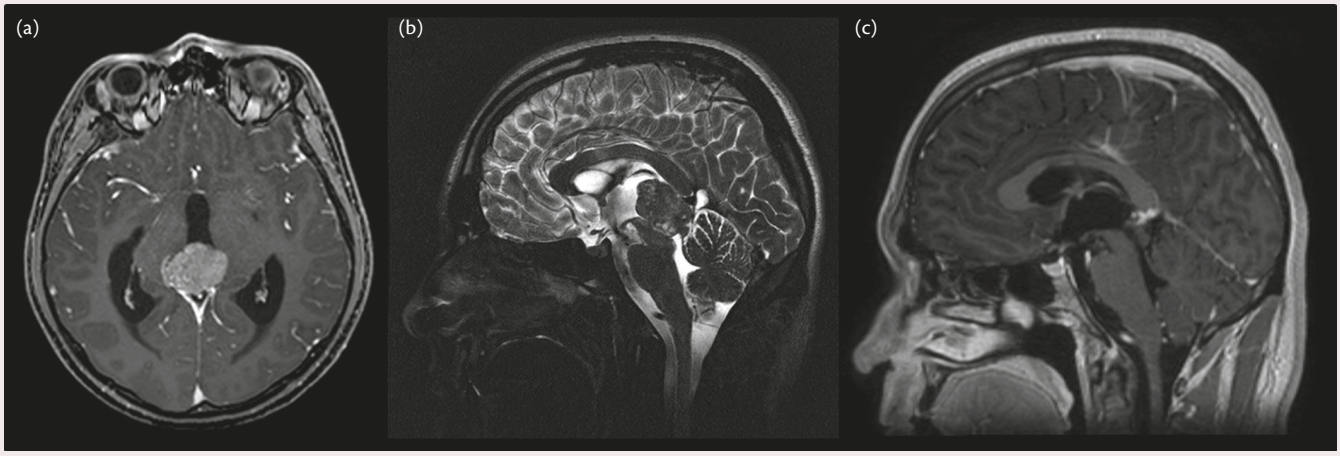

Fig. 36.4 (A) Axial T1-weighted postgadolinium MRI showing enhancing pineal tumour; (B) sagittal MRI demonstrating CSF prepontine flow following ETV; and (C) sagittal T1-weighted post-gadolinium MRI showing tumour resolution following radiotherapy.

Box 36.2 Case example 2—pineal parenchymal tumour (WHO grade II)

A 59-year-old female presented with 4 months of headache, intermittent confusion, and unsteady gait. Following a fall and head injury computed tomography (CT) revealed hydrocephalus and a pineal tumour. MRI confirmed a partly solid and partly cystic enhancing pineal tumour and hydrocephalus (**Fig. 36.5A**). MRI of the spine was normal. Tumour markers were not assessed in view of her age and gender and she proceeded to ETV and endoscopic biopsy (**Fig. 36.5B**). The pathology revealed and grade II primary pineal tumour. A complete surgical resection was performed (**Fig. 36.5C**) and the patient was referred for conformal fractionated radiotherapy.

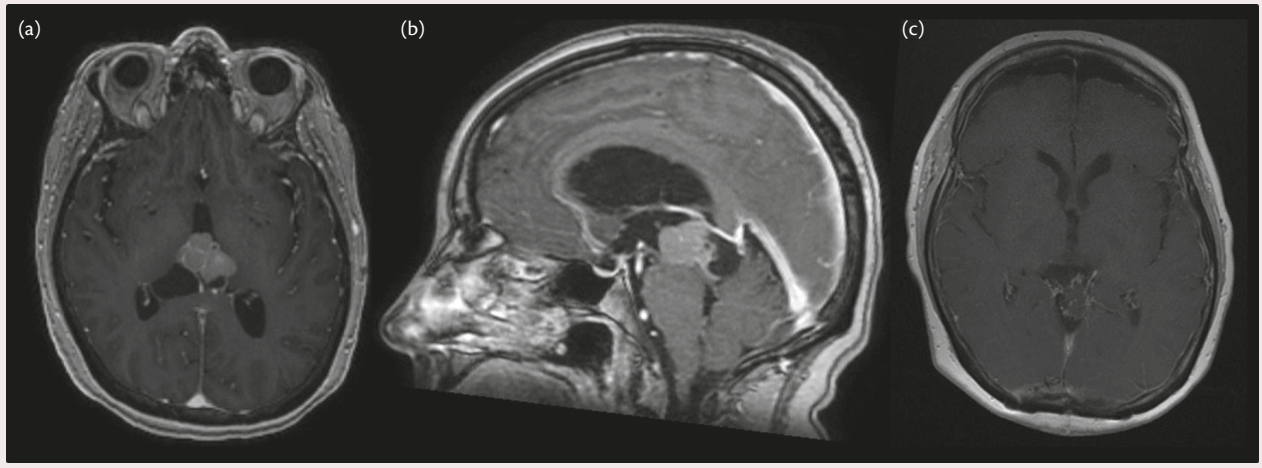

Fig. 36.5 (A) Axial and (B) sagittal T1-weighted postgadolinium MRI showing enhancing pineal tumour, and (C) axial T1-weighted postgadolinium MRI following complete tumour resection.

- ETV is the preferred method for CSF diversion and obviates the need for a shunt
- Elevated tumour markers obviate the need for biopsy and indicate a non-germinomatous germ cell tumour
- In the absence of elevated tumour markers tissue diagnosis is required to determine the correct treatment paradigm (note: a slightly elevated β-HCG may be seen in germinoma)
- EOR is prognostic for all pineal parenchymal tumours and pineocytoma can be cured with complete resection
- Non-germinomatous tumours that exhibit residual disease after chemotherapy should be offered 'second-look' surgery before radiotherapy
- The role of adjuvant radiotherapy following complete resection of PPTID and PTPR is not clearly defined

FURTHER READING

Al-Hussaini, M., Sultan, I., Abuirmileh, N., Jaradat, I., & Qaddoumi, I. (2009). Pineal gland tumors: experience from the SEER database. *J Neurooncol*, **94**, 351–8.

Arora, R.S., Alston, R.D., Eden, T.O., Geraci, M., & Birch, J.M. (2012). Comparative incidence patterns and trends of gonadal and extragonadal germ cell tumors in England, 1979 to 2003. *Cancer*, **118**, 4290–7.

Awa, R., Campos, F., Arita, K., et al. (2014). Neuroimaging diagnosis of pineal region tumors-quest for pathognomonic finding of germinoma. *Neuroradiology*, **56**, 525–34.

Bamberg, M., Kortmann, R.D., Calaminus, G., et al. (1999). Radiation therapy for intracranial germinoma: results of the German cooperative prospective trials MAKEI 83/86/89. *J Clin Oncol*, **17**, 2585–92.

British Neuro-Oncology Society (2011a). *Rare Brain and CNS Tumours Guidelines: Guidelines on the Diagnosis and Management of Adult PNETS*. https://www.bnos.org.uk/wp-content/uploads/2015/08/Adult-PNET-guidelines.pdf

British Neuro-Oncology Society (2011b). *Rare Brain and CNS Tumours Guidelines: Guidelines on the Diagnosis and Management of Adult Pineal Area Tumours*. https://www.bnos.org.uk/wp-content/uploads/2015/08/Guidelines-on-the-Diagnosis-and-Management.pdf

Calaminus, G., Frappaz, D., Kortmann, R.D., et al. (2012b). Risk adapted irradiation is feasible in intracranial non-germinomatous germ cell tumours (NGGCT): final results of SIOP CNS GCT 96. Abstracts from the 15th International Symposium on Pediatric Neuro-Oncology, 2012, Ontario, Canada. *Neuro Oncol*, **14**, i49–i55.

Clark, A.J., Ivan, M.E., Sughrue, M.E., et al. (2010a). Tumor control after surgery and radiotherapy for pineocytoma. *J Neurosurg*, **113**, 319–24.

Clark, A.J., Sughrue, M.E., Ivan, M.E., et al. (2010b). Factors influencing overall survival rates for patients with pineocytoma. *J Neurooncol*, **100**, 255–60.

Da Silva, N.S., Cappellano, A.M., Diez, B., et al. (2010). Primary chemotherapy for intracranial germ cell tumors: results of the third international CNS germ cell tumor study. *Pediatr Blood Cancer*, **54**, 377–83.

Duffner, P.K., Cohen, M.E., Sanford, R.A., et al. (1995). Lack of efficacy of postoperative chemotherapy and delayed radiation in very young children with pineoblastoma. Pediatric Oncology Group. *Med Pediatr Oncol*, **25**, 38–44.

Fevre-Montange, M., Vasiljevic, A., Champier, J., & Jouvet, A. (2010). Histopathology of tumors of the pineal region. *Future Oncol*, **6**, 791–809.

Louis, D.N., Perry, A., Reifenberger, G., et al. (eds.) (2016). *WHO Classification of Tumours of the Central Nervous System*. Lyon, France: IARC.

Lutterbach, J., Fauchon, F., Schild, S.E., et al. (2002). Malignant pineal parenchymal tumors in adult patients: patterns of care and prognostic factors. *Neurosurgery*, **51**, 44–55; discussion 55–6.

Tate, M., Sughrue, M.E., Rutkowski, M.J., et al. (2012). The long-term postsurgical prognosis of patients with pineoblastoma. *Cancer*, **118**, 173–9.

Von Bueren, A.O., Gerss, J., Hagel, C., et al. (2012). DNA copy number alterations in central primitive neuroectodermal tumors and tumors of the pineal region: an international individual patient data meta-analysis. *J Neurooncol*, **109**, 415–23.

REFERENCES

Key papers: epidemiology[$]; diagnosis[+]; management*

[$]Al-Hussaini, M., Sultan, I., Abuirmileh, N., Jaradat, I., & Qaddoumi, I. (2009). Pineal gland tumors: experience from the SEER database. *J Neurooncol*, **94**, 351–8.

[$]Arora, R.S., Alston, R.D., Eden, T.O., Geraci, M., & Birch, J.M. (2012). Comparative incidence patterns and trends of gonadal and extragonadal germ cell tumors in England, 1979 to 2003. *Cancer*, **118**, 4290–7.

[+]Awa, R., Campos, F., Arita, K., et al. (2014). Neuroimaging diagnosis of pineal region tumors-quest for pathognomonic finding of germinoma. *Neuroradiology*, **56**, 525–34.

Balossier, A., Blond, S., Touzet, G., et al. (2015a). Endoscopic versus stereotactic procedure for pineal tumour biopsies: comparative review of the literature and learning from a 25-year experience. *Neurochirurgie*, **61**, 146–54.

Balossier, A., Blond, S., Touzet, G., Sarrazin, T., Lartigau, E., & Reyns, N. (2015b). Role of radiosurgery in the management of pineal region tumours: indications, method, outcome. *Neurochirurgie*, **61**, 216–22.

*Bamberg, M., Kortmann, R.D., Calaminus, G., et al. (1999). Radiation therapy for intracranial germinoma: results of the German cooperative prospective trials MAKEI 83/86/89. *J Clin Oncol*, **17**, 2585–92.

*British Neuro-Oncology Society (2011a). *Rare Brain and CNS Tumours Guidelines: Guidelines on the Diagnosis and Management of Adult PNETS*. https://www.bnos.org.uk/wp-content/uploads/2015/08/Adult-PNET-guidelines.pdf

British Neuro-Oncology Society (2011b). *Rare Brain and CNS Tumours Guidelines: Guidelines on the Diagnosis and Management of Adult Pineal Area Tumours*. https://www.bnos.org.uk/wp-content/uploads/2015/08/Guidelines-on-the-Diagnosis-and-Management.pdf

Calaminus, G., Frappaz, D., Kortmann, R.D., et al. (2012a). Risk adapted irradiation is feasible in intracranial non-germinomatous germ cell tumours (NGGCT): final results of SIOP CNS GCT 96. Abstracts of the 2nd International CNS Germ Cell Symposium, 2012, California, USA. *Neuro Oncol*, **14**, i49–i55.

*Calaminus, G., Frappaz, D., Kortmann, R.D., et al. (2012b). Risk adapted irradiation is feasible in intracranial non-germinomatous germ cell tumours (NGGCT): final results of SIOP CNS GCT 96. Abstracts from the 15th International Symposium on Pediatric Neuro-Oncology, 2012, Ontario, Canada. *Neuro Oncol*, **14**, i49–i55.

Calaminus, G., Kortmann, R., Worch, J., et al. (2013). SIOP CNS GCT 96: final report of outcome of a prospective, multinational nonrandomized trial for children and adults with intracranial germinoma, comparing craniospinal irradiation alone with chemotherapy followed by focal primary site irradiation for patients with localized disease. *Neuro Oncol*, **15**, 788–96.

*Clark, A.J., Ivan, M.E., Sughrue, M.E., et al. (2010a). Tumor control after surgery and radiotherapy for pineocytoma. *J Neurosurg*, **113**, 319–24.

*Clark, A.J., Sughrue, M.E., Ivan, M.E., et al. (2010b). Factors influencing overall survival rates for patients with pineocytoma. *J Neurooncol*, **100**, 255–60.

Czech, T., Nicholson, J., Frappaz, D., et al. (2012). Patients with intracranial non-germinomatous germ cell tumours (NGGCT) benefit from delayed surgery after neoadjuvant chemotherapy. Final results of SIOP CNS GCT 96. Abstracts of the 2nd International CNS Germ Cell Symposium, June 2012, California, USA. *Neuro Oncol*, **14**, i49–i55.

*Da Silva, N.S., Cappellano, A.M., Diez, B., et al. (2010). Primary chemotherapy for intracranial germ cell tumors: results of the third international CNS germ cell tumor study. *Pediatr Blood Cancer*, **54**, 377–83.

*Duffner, P.K., Cohen, M.E., Sanford, R.A., et al. (1995). Lack of efficacy of postoperative chemotherapy and delayed radiation in very young children with pineoblastoma. Pediatric Oncology Group. *Med Pediatr Oncol*, **25**, 38–44.

Fauchon, F., Hasselblatt, M., Jouvet, A., et al. (2013). Role of surgery, radiotherapy and chemotherapy in papillary tumors of the pineal region: a multicenter study. *J Neurooncol*, **112**(2), 223–31.

Fauchon, F., Jouvet, A., Paquis, P., et al. (2000). Parenchymal pineal tumors: a clinicopathological study of 76 cases. *Int J Radiat Oncol Biol Phys*, **46**, 959–68.

*Fevre-Montange, M., Vasiljevic, A., Champier, J., & Jouvet, A. (2010). Histopathology of tumors of the pineal region. *Future Oncol*, **6**, 791–809.

Fukuoka, K., Sasaki, A., Yanagisawa, T., et al. (2012). Pineal parenchymal tumor of intermediate differentiation with marked elevation of MIB-1 labeling index. *Brain Tumor Pathol*, **29**, 229–34.

Gaillard, F. & Jones, J. (2010). Masses of the pineal region: clinical presentation and radiographic features. *Postgrad Med J*, **86**, 597–607.

Goldman, S., Bouffet, E., Fisher, P.G., et al. (2015). Phase II trial assessing the ability of neoadjuvant chemotherapy with or without second-look surgery to eliminate measurable disease for nongerminomatous germ cell tumors: a children's oncology group study. *J Clin Oncol*, **33**(22), 2464–71.

Hinkes, B.G., Von Hoff, K., Deinlein, F., et al. (2007). Childhood pineoblastoma: experiences from the prospective multicenter trials HIT-SKK87, HIT-SKK92 and HIT91. *J Neurooncol*, **81**, 217–23.

Kim, A., Ji, L., Balmaceda, C., et al. (2008). The prognostic value of tumor markers in newly diagnosed patients with primary central nervous system germ cell tumors. *Pediatr Blood Cancer*, **51**, 768–73.

Konovalov, A.N. & Pitskhelauri, D.I. (2003). Principles of treatment of the pineal region tumors. *Surg Neurol*, **59**, 250–68.

Kumura, E., Arita, N., Hayakawa, T., et al. (1986). Successful combination chemotherapy (cisplatinum, vinblastine, and bleomycin) against peritoneal dissemination of intracranial germ cell tumor. *Neurosurgery*, **18**, 802–4.

Lee, J.Y., Wakabayashi, T., & Yoshida, J. (2005). Management and survival of pineoblastoma: an analysis of 34 adults from the brain tumor registry of Japan. *Neurol Med Chir (Tokyo)*, **45**, 132–41; discussion 141–2.

Legault, G., Donahue, B., Dhall, G., Pollack, I.F., Zhou, T., & Allen, J.C. (2013). Neo-adjuvant chemotherapy response-based reductions in radiotherapy fields and doses for CNS pure germinoma. Abstracts of the 3rd International CNS Germ Cell Symposium. *Br J Neurosurg*, **27**, e1–e25.

*Louis, D.N., Perry, A., Reifenberger, G., et al. (eds.) (2016). *WHO Classification of Tumours of the Central Nervous System*. Lyon, France: IARC.

*Lutterbach, J., Fauchon, F., Schild, S.E., et al. (2002). Malignant pineal parenchymal tumors in adult patients: patterns of care and prognostic factors. *Neurosurgery*, **51**, 44–55; discussion 55–6.

Marec-Berard, P., Jouvet, A., Thiesse, P., Kalifa, C., Doz, F., & Frappaz, D. (2002). Supratentorial embryonal tumors in children under 5 years of age: an SFOP study of treatment with postoperative chemotherapy alone. *Med Pediatr Oncol*, **8**, 83–90.

Modak, S., Gardner, S., Dunkel, I.J., et al. (2004). Thiotepa-based high-dose chemotherapy with autologous stem-cell rescue in patients with recurrent or progressive CNS germ cell tumors. *J Clin Oncol*, **22**, 1934–43.

Mori, Y., Kobayashi, T., Hasegawa, T., Yoshida, K., & Kida, Y. (2009). Stereotactic radiosurgery for pineal and related tumors. *Prog Neurol Surg*, **23**, 106–18.

Nicholson, J.C., Alapetite, C., Kortmann, R.D., et al. (2013). HCG elevation alone in SIOP CNS GCT 96 patients treated as nongerminomatous/secreting germ cell tumours (NGGCT)—are we over-treating germinoma? Abstracts of the 3rd International CNS Germ Cell Symposium, 2013 Cambridge, UK. *Br J Neurosurg*, **27**, e1–e25.

Oya, S., Saito, A., Okano, A., Arai, E., Yanai, K., & Matsui, T. (2014). The pathogenesis of intracranial growing teratoma syndrome: proliferation of tumor cells or formation of multiple expanding cysts? Two case reports and review of the literature. *Childs Nerv Syst*, **30**, 1455–61.

Pettorini, B.L., Al-Mahfoud, R., Jenkinson, M.D., Avula, S., Pizer, B., & Mallucci, C. (2013). Surgical pathway and management of pineal region tumours in children. *Childs Nerv Syst*, **29**, 433–9.

Pizer, B.L., Weston, C.L., Robinson, K.J., et al. (2006). Analysis of patients with supratentorial primitive neuro-ectodermal tumours entered into the SIOP/UKCCSG PNET 3 study. *Eur J Cancer*, **42**, 1120–8.

Rogers, S.J., Mosleh-Shirazi, M.A., & Saran, F.H. (2005). Radiotherapy of localised intracranial germinoma: time to sever historical ties? *Lancet Oncol*, **6**, 509–19.

Santarius, T., Joseph, J.A., Tsang, K.T., O'Donovan, D.G., & Kirollos, R.W. (2008). Papillary tumour of the pineal region. *Br J Neurosurg*, **22**(1), 116–20.

Sawamura, Y., De Tribolet, N., Ishii, N., & Abe, H. (1997). Management of primary intracranial germinomas: diagnostic surgery or radical resection? *J Neurosurg*, **87**, 262–6.

Selvanathan, S.K., Hammouche, S., Smethurst, W., Salminen, H.J., & Jenkinson, M.D. (2012). Outcome and prognostic features in adult pineoblastomas: analysis of cases from the SEER database. *Acta Neurochir (Wien)*, **154**, 863–9.

Shono, T., Natori, Y., Morioka, T., et al. (2007). Results of a long-term follow-up after neuroendoscopic biopsy procedure and third ventriculostomy in patients with intracranial germinomas. *J Neurosurg*, **107**, 193–8.

Souweidane, M.M., Krieger, M.D., Weiner, H.L., & Finlay, J.L. (2010). Surgical management of primary central nervous system germ cell tumors: proceedings from the Second International Symposium on Central Nervous System Germ Cell Tumors. *J Neurosurg Pediatr*, **6**, 125–30.

*Tate, M., Sughrue, M.E., Rutkowski, M.J., et al. (2012). The long-term postsurgical prognosis of patients with pineoblastoma. *Cancer*, **118**, 173–9.

Villa, S., Miller, R.C., Krengli, M., et al. (2012). Primary pineal tumors: outcome and prognostic factors—a study from the Rare Cancer Network (RCN). *Clin Transl Oncol*, **14**, 827–34.

*Von Bueren, A.O., Gerss, J., Hagel, C., et al. (2012). DNA copy number alterations in central primitive neuroectodermal tumors and tumors of the pineal region: an international individual patient data meta-analysis. *J Neurooncol*, **109**, 415–23.

Zeltzer, P.M., Boyett, J.M., Finlay, J.L., et al. (1999). Metastasis stage, adjuvant treatment, and residual tumor are prognostic factors for medulloblastoma in children: conclusions from the Children's Cancer Group 921 randomized phase III study. *J Clin Oncol*, **17**, 832–45.

RELATED LINKS TO EBRAIN

Histopathology of Pineal Region Tumours. https://learning.ebrain.net/course/view.php?id=434

Imaging Features of Pineal Region Tumours. https://learning.ebrain.net/course/view.php?id=435

37

Surgical management of pineal region lesions

Christoph M. Woernle, René L. Bernays, and Nicolas de Tribolet

Introduction

Lesions in the pineal region are topographically located in the centre of the brain in the diencephalic-epithalamic region. An area where the brain is bounded ventrally by the quadrigeminal plate, midbrain tectum, and in-between the left and right superior colliculi, dorsally by the splenium of the corpus callosum, caudally by the cerebellar vermis and rostrally by the posterior aspects of the third ventricle. Major anatomical and surgical challenges are the vein of Galen located dorsally, the precentral cerebellar vein caudally, the internal cerebral veins anteriorly and the basal vein of Rosenthal laterally.

Most pineal region tumours can be safely removed by both approaches depending on the surgeon's experience: the occipital transtentorial approach is recommended in presence of associated hydrocephalus or a steep straight sinus and low location of the tumour and the supracerebellar infratentorial approach for posterior third ventricle tumours.

Historical review

In the beginning of the twentieth century the first contributors with fascinating reports about their surgical experiences with tumours in the pineal region were Harvey Cushing, Feudor Krause, and Sir Walter Dandy (Krause, 1926; Dandy, 1936; Cushing, 1983). Without microsurgical technique, surgery in these deep-seated and demanding anatomical regions was linked with high mortality and frowned on by some of their contemporaries (Schmidek, 1977). Today, the supracerebellar infratentorial or the occipital transtentorial approaches are performed to access these lesions in one of the most complex areas of the intracranial cavity (Ringertz et al., 1954; Poppen and Marino, 1968; Stein, 1971; Reid and Clark, 1978; Stein, 1979; Sawamura et al., 1997; Sawamura and de Tribolet, 2002).

Microsurgical anatomy of the pineal region and third ventricle

Lesions in the pineal region are located in the centre of the brain in the diencephalic-epithalamic region. Tumours growing from the pineal gland itself or from structures of the parapineal space are surrounded by critical anatomical structures (Guest and Kleriga 1979). This area is bounded ventrally by the quadrigeminal plate, midbrain tectum, and in-between the left and right superior colliculi, dorsally by the splenium of corpus callosum, caudally by the cerebellar vermis and rostrally by the posterior aspects of the third ventricle (Stein, 1971; Schmidek, 1977; Guest and Kleriga, 1979). The pineal gland is formed as an appendix of the caudal end in the midline of the diencephalon spanning the pineal recess of the third ventricle. The stem of the pineal gland is connected with the habenular commissure dorsally and the posterior commissure ventrally.

Vascularization of the pineal gland is mainly supplied by branches of the posterior cerebral artery through the medial posterior choroidal arteries. Alongside the pineal gland they supply the inferior and superior colliculi and choroidal plexus of the third ventricle. Commonly pineal tumours displace these arteries laterally in the cisterns. The posterior lateral choroidal artery supplies the pulvinar and is generally displaced laterally by pineal tumours. The superior cerebellar arteries can be considered as important arterial landmarks because they are frequently displaced inferiorly by pineal tumours. In addition, the medial occipital artery originating from the posterior cerebral artery and branching to the calcarine artery should be kept in mind (Poppen, 1966; Poppen and Marino, 1968; Page, 1977; Guest and Kleriga, 1979).

A major anatomical and surgical challenge is the Galenic venous system. The vein of Galen has several inflows: first the superior vermian vein and the precentral cerebellar vein run in the midline and into the ventrocaudal part of the vein of Galen. The internal cerebral veins and the pineal veins join ventrally. In pineal tumours, the posterior portion of the internal cerebral veins is elevated rostrally, and the veins are occasionally separated from each other. On the lateral aspect of the vein of Galen, the medial occipital veins, the third segment of the basal veins of Rosenthal, and the posterior mesencephalic veins join. The pineal veins are the draining veins of pineal tumours and drain into either the posterior portion of the internal cerebral veins or the vein of Galen. Pineal tumours can tightly adhere to the internal cerebral veins and/or the vein of Galen. Injury to the basal veins or the internal cerebral veins leads to major complications. Transection or compression of a major medial occipital vein may cause homonymous hemianopsia or visual seizures (Lazar and Clark, 1974; Guest and Kleriga, 1979; Sawamura et al., 1997; Sawamura and de Tribolet, 2002).

Symptoms and preoperative workup

Patients with symptomatic lesions in the pineal region may clinically present with varying and sometimes non-specific symptoms. Headache, gait disturbances, mental changes, pyramidal tract deficits, urinary incontinence and, less frequently, hearing disturbances can be observed.

More specific symptoms alerting for symptomatic lesions in the pineal region are signs of decompensating hydrocephalus and neuro-ophthalmologic disturbances such as Parinaud's syndrome or diplopia (Schmidek, 1977; Sawamura et al., 1997; Sawamura and de Tribolet, 2002).

Imaging

In cases of neurological symptoms, a computed tomography (CT) scan or MRI should be performed for initial work up. These modalities provide a quick overview and visualize a probable obstructive hydrocephalus or haemorrhage. In presence of these pathologies it may be necessary to perform an external ventricular drainage or endoscopic third ventriculostomy. Secondly, a contrast enhanced MRI should be performed. Some centres additionally recommend an angiography for the arterial and venous anatomy of the lesion. Three-tesla MRI and MR-angiography sequences provide excellent visualization of the vascular anatomy. In our opinion routine angiography is therefore not necessary.

Tumour markers

In lesions of the pineal region germ cell tumours can give rise to tumour markers in the serum and cerebrospinal fluid. Elevated beta-HCG is typically associated with choriocarcinoma and in 10% of cases with germinoma. An elevation of alpha-fetoprotein (AFP) can be observed in teratoma, embryonal carcinoma, and yolk sac tumours. Tumour markers can be used to follow-up the patients' treatment results and potential recurrences (see Chapter 36).

Differential diagnosis

Most pineal masses originate in the infratentorial compartment and expand into the posterior part of the third ventricle. These lesions proceed into the thalamus or inferiorly towards the quadrigeminal plate. Malignant glial tumours invade the thalamus and midbrain; this constellation ultimately determines the resectability of the tumour.

The following differential diagnosis should be considered:

Germ cell tumours: Germinoma, teratoma, embryonal tumour, yolk sac, and choriocarcinoma.

Pineal parenchymal tumours: Pineocytoma, pineal parenchymal tumour of intermediate differentiation, and pineoblastoma.

Gliomas, metastases, and cavernomas

Falcotentorial meningiomas:

Falcotentorial or velum interpositum meningioma's can be considered as pineal region tumours from the surgical point of view. Accounting for 1% of all intracranial meningiomas these are rare localizations and only 100 cases are reported in the literature.

Decision-making and surgical procedures

Germ cell tumours and malignant pineal parenchymal tumours necessitate a multimodality approach including chemotherapy, radiotherapy, and surgery (Lutterbach et al., 2002). Pure germinomas can be cured without ablative surgery with chemo and radiotherapy (see Chapter 36).

Most pineal region tumours can be safely removed by both approaches depending on the surgeon's experience, the occipital transtentorial approach is recommended when there is associated hydrocephalus or the tumour is located low in front of the vermis with a steep straight sinus. The supracerebellar infratentorial approach is recommended for posterior third ventricular tumours.

In cases of obstructive hydrocephalus with compression of the aqueduct an endoscopic ventriculocisternostomy (EVT) or external ventricular drain (EVD) placement should be performed prior to tumour resection.

Endoscopic procedures and biopsy techniques

Nowadays minimally invasive procedures for endoscopic tumour biopsy combined with endoscopic ventriculocisternostomy can be performed for tissue analysis and/or treating obstructive hydrocephalus. It is a favourable diagnostic and therapeutic tool and can be easily performed in experienced hands (Ellenbogen and Moores, 1997; Azab et al., 2014).

An endoscopic ventriculocisternostomy (EVT) can be performed in a common fashion prior to the subsequent microsurgical open tumour resection (see Chapter 33). If the burr hole is placed 2–3 cm more anterolaterally to Kocher's point an endoscopic biopsy of the lesion can be performed in the same session. Some authors use two burr holes.

The first step in combined approaches is cerebral spinal fluid (CSF) collection for tumour markers and cytology, followed by the second step with third ventriculostomy and finally the third step with biopsy of the lesion. This is performed last because blood in the CSF may obscure the optimal point for ventriculostomy between the infundibular recess anteriorly and the mamillary bodies posteriorly (Al-Tamimi et al., 2008).

Utilizing neuro-navigation and/or intraoperative MRI this is a safe and efficient procedure with a high diagnostic yield (O'Brien et al., 2006).

The endoscope-assisted infratentorial supracerebellar approach was first described by Cardia et. al in 2006. This technique was performed for detection of residual tumour and to remove blood clots from the aqueduct, to prevent postoperative obstructive hydrocephalus (Cardia et al., 2006).

Uschold et al. (2011) reported his experiences by using the endoscope solely for excision of solid tumours of the pineal region and pineal cysts. Tumours with high vascularity and infiltrative nature or crossing the midline or located above the tentorium were considered for open microsurgical procedures (Broggi et al., 2010).

Stereotactic biopsy is often associated with a limited amount of tissue. Pineal region tumours and germ cell tumours commonly display heterogeneity with different cell populations within the same lesions.

Therefore, the neuropathologist prefers as much tissue as possible for detailed diagnosis.

A recent review focusing on stereotactic biopsy for pineal region lesions reported a morbidity of 1.3% and a mortality of 8.1%. The diagnostic accuracy was 94%. Nowadays the procedure is not commonly used and has been replaced by endoscopic combined procedures (Zacharia and Bruce, 2001; Al-Tamimi et al., 2008).

Supracerebellar infratentorial approach

The supracerebellar infratentorial approach can be considered as midline approach with a direct panoramic overview through an inferior-superior corridor to the lesion. Dissecting the deep venous Galenic system and corresponding veins is the key to successful surgery without complications.

Indications for the supracerebellar infratentorial approach are lesions located in the superior part of the pineal area, posterior third ventricular tumours, midline lesions of pineal region and dorsal midbrain lesions of the quadrigeminal plate.

To avoid increased intracranial pressure during surgery an EVT or EVD placement to drain hydrocephalus can be considered.

The patient is placed in the sitting position with trunk and neck gently flexed, maintaining two fingerbreadths space between sternum and chin. In the sitting position the tentorium should be in the same plane as the floor and gravity will allow the cerebellum to fall down without retraction. Alternatively, the three-quarters prone position, semi lateral, or concorde positions are described in the literature.

Neuronavigation, sterile scrub, and preparation are performed in the usual fashion. The midline incision from the external occipital protuberance to C4 is marked. The anticipated incision can be infiltrated with local anaesthetics and adrenaline. After skin incision Raney clips are placed. It is important to stay in midline fascial plane to detach muscles from insertion at the superior nuchal line. This avoids muscle damage and minimizes blood loss.

For craniotomy, a high-speed drill is recommended. Burr holes can be placed bilaterally over the transverse sinus or one in midline above the torcular. Carefully strip sinus away from the bone flap to avoid injury of the sinuses. It is important to confirm adequate blood flow within the dural sinuses using a microdoppler probe. Wax bone edges to reduce risk of air embolism. Craniectomy should be avoided.

Before dural opening and in cases of a packed posterior fossa, give mannitol or drain CSF if an EVD is in place. The dural flap should be opened in a curvilinear fashion, starting laterally then across the midline last to control midline bleeding from the occipital sinus, which is then reflected superiorly. For additional relaxation, the cisterna magna can be opened. Midline bridging veins can be coagulated but sacrifice of lateral veins with retraction should be avoided. After dissection of adhesions and wide opening of the arachnoid the cerebellum will drop with gravity. Once the corridor between the inferior surface of the tentorium and the cerebellum is opened the important and challenging venous anatomy has to be identified. Dissection of the thick arachnoid tissue in the supracerebellar and the quadrigeminal cisterns should be performed. Pursuing the dissection symmetrically on both sides, a gentle downward retraction of the cerebellum exposes the pineal area. A further downwards retraction of the vermis can be exerted after sectioning of the superior vermian and precentral veins. A thorough dissection of all the bridging veins and of the superior vermian and precentral veins may occasionally cause venous infarction of the superior aspect of the vermis. If possible, divide and preserve the hemispheric bridging veins. For gaining a medial corridor in cases of thick bridging veins, the medial ones should be sacrificed preserving the lateral bridging veins (Fig. 37.1).

Avoid injury, tearing, or compression by retraction of the precentral cerebellar, vermian vein, internal cerebral vein, and vein of Rosenthal because of a high risk for venous congestion and infarction. If dissection or coagulation of the precentral cerebellar vein is necessary, this should be performed as far as possible from the confluence of the basal veins of Rosenthal.

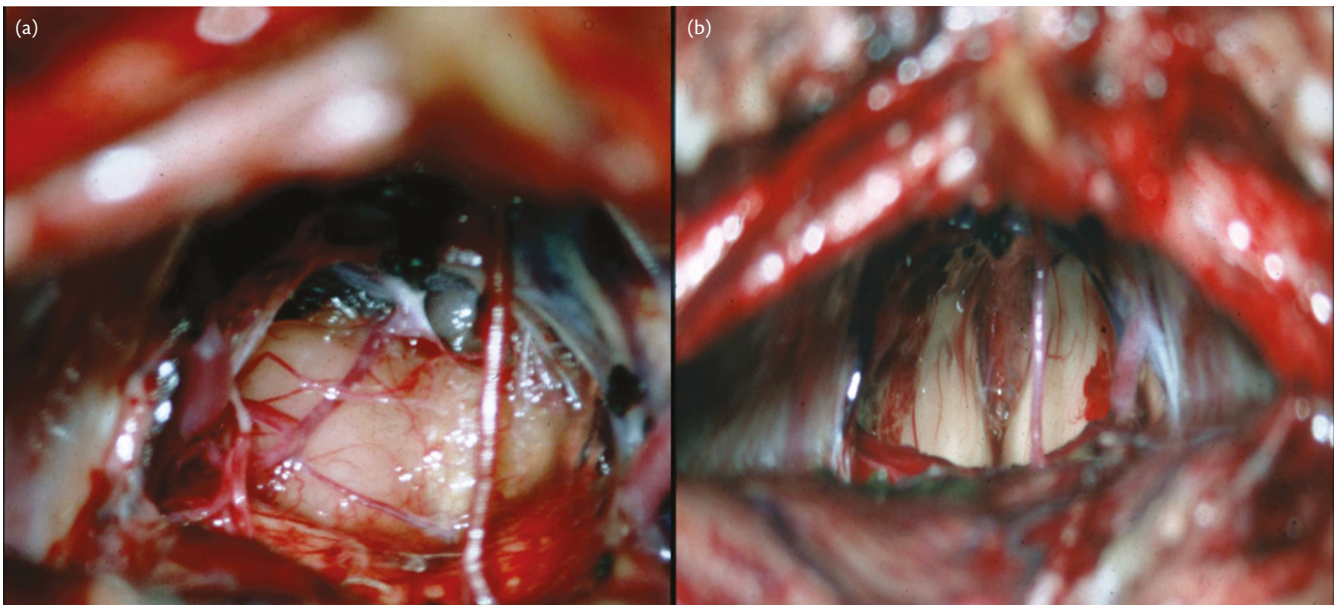

Fig. 37.1 Illustrative case for the supracerebellar infratentorial approach. (A) Panoramic midline view to the lesion with the preserved precentral cerebellar vein. (B) Panoramic midline view after total tumour resection with the preserved precentral cerebellar vein via a supracerebellar infratentorial approach.

Box 37.1 Main principles of the supracerebellar infratentorial approach

1. Sitting position
2. Dissection of thick arachnoid (CARE: the veins are behind)
3. Identify and preserve vein of Galen
4. Identify and preserve precentral cerebellar vein
5. Identify and preserve veins of Rosenthal and posterior cerebral artery lateral to the tumour
6. Internal cerebral vein is located anterosuperiorly to the tumour
7. Quadrigeminal plate is located inferior to the tumour

The infratentorial supracerebellar approach opens a view strictly through the midline that can provide an easy orientation for the complex anatomical structures around the pineal area. This approach will allow excellent identification of all the midline structures and symmetrical exposure of both walls and the roof of the third ventricle, to the foramen of Monro and dorsal midbrain lesions of the quadrigeminal plate. Under direct observation, tight tumour adhesions can be freed from the internal cerebral veins or the great veins. In some cases, however, tumour dissection from the periaqueductal tissue and the quadrigeminal plate might be more difficult using this approach than using the occipital transtentorial approach. If there is a steep inclination of the tentorium and narrow angle to the caudal and lateral side the supracerebellar infratentorial approach has its limitations.

The lateral infratentorial approach avoids retraction of the vermis and precentral vein (Kodera et al., 2011).

A watertight closure of the dura will be done with a running or single suture after the surgeon has asked the anaesthesiologist to compress the jugular veins and sealed any venous leaks. See **Box 37.1** for a summary of the main approaches.

Occipital transtentorial approach

The occipital transtentorial approach was first described by Horax in the 1937 and emphasized and modified by Poppen in 1962, and thus is now widely known by his name. The main principle of this lateral approach with an oblique view is to avoid retraction of the vermis and precentral cerebellar vein (Clark, 1983).

Indications for the occipital transtentorial approach are pineal tumours, tumours extending inferiorly, or arising in the quadrigeminal plate, posterior falcine, or tentorial meningiomas with only supratentorial components, tumours extending to the pulvinar and medial atrial wall, and intraventricular tumours of the trigone.

For positioning of the patient there are several options. The three-quarters prone position helps the medial occipital lobe to fall laterally from gravity avoiding the retraction and the increased risk of homonymous hemianopia. By approaching through the non-dominant lobe language disturbances are avoided. Alternative positioning of the patient is in prone or concorde position (Lozier and Bruce, 2003). This approach can also be performed in the sitting position, but retraction of the occipital lobe will be needed (Azab et al., 2014). The side of the approach is chosen considering the direction of tumour extension, the shape of the torcular, and the location of major occipital bridging veins, although in general, large cortical bridging veins are rarely present in the occipital area. All this taken into consideration we usually prefer approaching from the right side whenever possible.

If there is no occlusion of the aqueduct spinal drain may be helpful for brain relaxation. For anaesthesiologic and surgical principles, see the earlier section 'Supracerebellar infratentorial approach'.

Some authors recommend a U-shaped skin incision. From our point of view a 1 cm paramedian linear incision is adequate. In both incisions caution should be taken to avoid the lesser and greater occipital nerve and occipital artery. The craniotomy should be tailored according to preoperative MRI and occipital bridging veins. Placing the burr holes 2 cm and 7 cm above the torcular just off the midline on the right. Drilling should start away from the sagittal sinus and towards the sinus last. If the sinus is injured control of venous haemorrhage is more comfortable and manageable if the craniotomy is almost finished.

The dura is opened with a C-shaped or triangular leaf and reflected towards the superior sagittal sinus. Think of minimal retraction to the occipital lobe. The occipital horn of the ipsilateral ventricle can be tapped to release CSF for adequate brain relaxation. The inferior cerebral vein and vein of Labbé, both draining into the transverse sinus, must be preserved. As mentioned, no large occipital bridging veins are usually present, however when such veins are encountered, they could significantly limit the exposure. Nevertheless, they should be preserved as their sacrifice may cause a haemorrhagic venous infarction of the occipital lobe.

The surgical corridor for approaching the lesion is between the occipital lobe and falx cerebri and measures around 4–5 cm. The occipital transtentorial approach provides a good overview and is preferred for resection of tumours with inferior extension into the cerebellomesencephalic cistern. This is a blind spot during the infratentorial supracerebellar approach. Cutting the tentorium from posteriorly to anteriorly 1 cm parallel to the straight sinus offers a view to the lesion and the surrounding deep venous structures. As well as of the culmen of the vermis. The anatomical superiority of the occipital transtentorial approach is in the widest panoramic view of the supra- and infratentorial compartments (Lozier and Bruce, 2003) (**Figs. 37.2** and **37.3**).

A watertight closure of the dura is used, with a running or single suture after the surgeon has asked the anaesthesiologist to compress the jugular veins and sealed any venous leaks. See **Box 37.2** for the main principles of the occipital transtentorial approach.

Illustrative case

A 21-year-old male patient presented with GCS 15, a slight gait ataxia, and vertigo about the last months. MRI and CT scan revealed a paravermian contrast enhancing, cystic lesion (**Figs. 37.4A, 37.4B,** and **37.4C**). Microsurgical complete tumour resection was performed in the left three-quarters prone position through an occipital transtentorial approach. For brain relaxation during surgery a lumbar drain was placed. Postoperatively the patient was with GCS 15 stable, showed some vertigo and balance disturbances; these symptoms fully resolved on post-op day 8. MRI for resection control showed no residual tumour and no signs for hydrocephalus, venous congestions, or infarction. The neuropathological results reveal pilocytic astrocytoma (WHO grading I). Follow-up at 2 years showed no tumour recurrence and no signs of neurological deficits (**Figs. 37.4D, 37.4E,** and **37.4F**).

Surgery for falcotentorial Meningiomas

From a surgical point of view, falcotentorial or velum interpositum meningiomas represent challenging lesions that sum up the

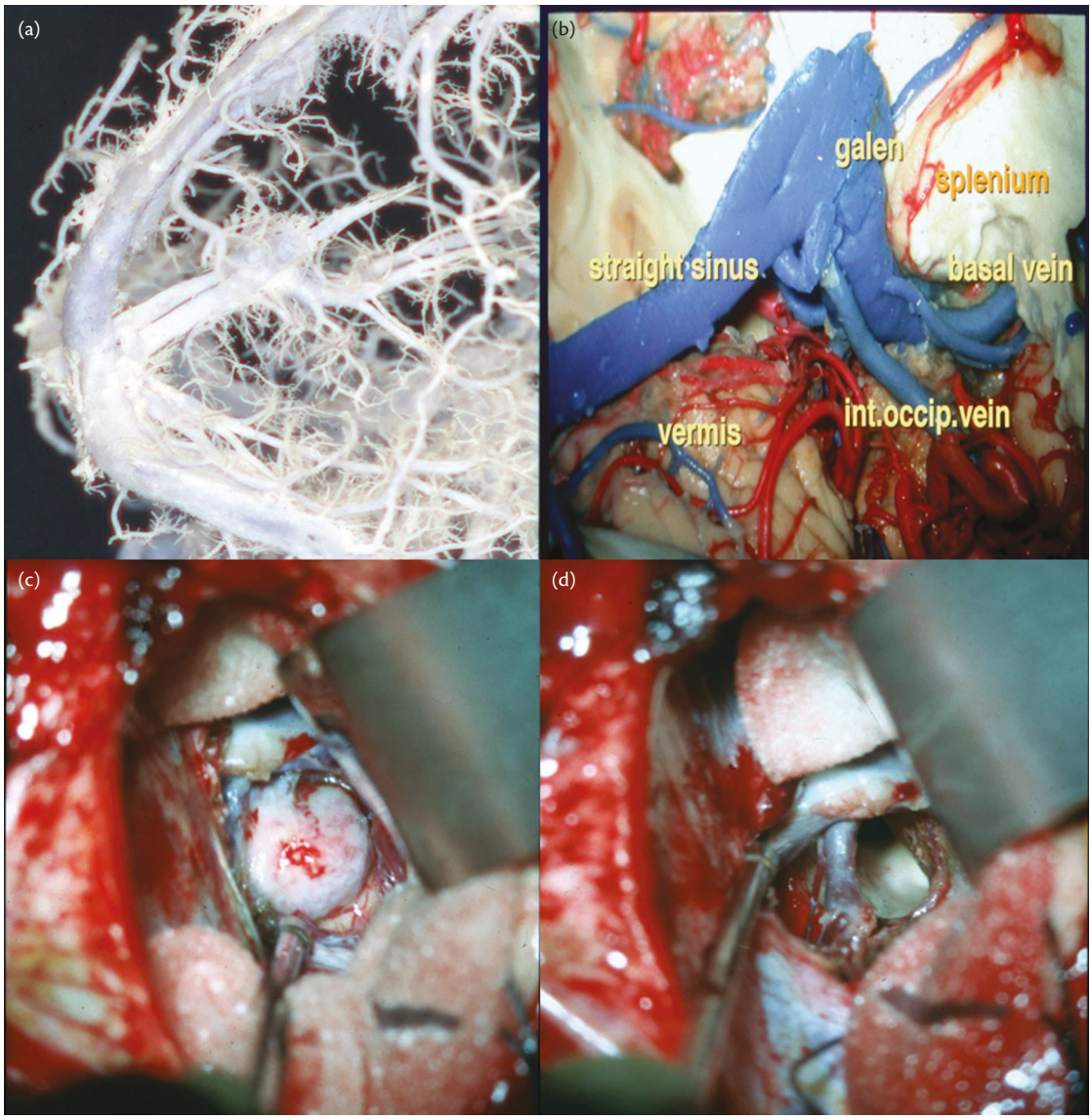

Fig. 37.2 The occipital transtentorial approach in sitting position; (A and B) venous anatomy, open corridor via an occipital transtentorial approach; (C) incised tentorium with exposure of the tumour; (D) after tumour resection, vein of Galen/precentral cerebellar vein, basal vein of Rosenthal.

Fig. 37.3 Illustrative case for the occipital transtentorial approach. (A) Preoperative lesion anterior to the quadrigeminal plate, with steep straight sinus. (B) Postoperative imaging after total tumour removal via occipital transtentorial approach.

Box 37.2 Main principles of the occipital transtentorial approach

1. Park bench position
2. Identify and preserve the internal occipital vein
3. Incision of the falx
4. Identify and preserve the culmen of vermis
5. Identify and preserve the vein of Galen
6. Identify and preserve veins of Rosenthal
7. Identify the tumour
8. Identify and preserve the internal cerebral vein
9. Identify and preserve the quadrigeminal plate

complexity of surgical approaches to the pineal region and of meningioma resection in deep locations. However, surgery is rendered more difficult by the specific features of meningiomas such as dural attachments which are here deeply located and difficult to approach as well as venous sinus invasion which here compromise the deep venous flow draining vital cerebral structures.

Some specific characteristics should be carefully attended in planning surgery for these lesions. They are attached to the dura of the falx and tentorium on both sides of the straight sinus. With consecutive partial or total compression and occlusion of the sinus.

Particular attention should be paid to the deep venous structures and the collateral channels, which have to be preserved at all costs.

The straight sinus can be excised if it is occluded but must be preserved if it is permeable, even at the cost of leaving a small piece of tumour which can be treated by radiosurgery later.

In the case of falcotentorial meningiomas, the tumour usually encases the straight sinus and the falcotentorial junction. The tentorial incision is then made laterally to the tumour and proceeds posteroanteriorly to the free tentorial edge interrupting the vascular supply. The venous channels and lakes of the tentorium can cause significant bleeding but they are usually well controlled by bipolar coagulation. However, tentorial vessels can participate in the collateral venous drainage of an already scarce venous return, therefore one should spare as much tentorial surface as possible. The tentorial flap is reflected laterally. The surgeon can then see the superior cerebellar artery and the fourth nerve running around the brain stem. In falcotentorial meningioma surgery, the falx is then incised in the same way to expose the left side of the tumour. The left side of the tentorium is then incised. At this point the posterior part of the straight sinus can be ligated and sectioned. This allows dissection of the tumour on all its faces after debulking. The most dangerous part of the dissection will be along the anterior pole where the deep veins will be in contact with the tumour. After the removal of the tumour, what is left of the vein of Galen is dissected, clipped, and sectioned. However, if the vein of Galen and the internal cerebral veins are extensively invaded, it is wiser to leave residual tumour around these veins for secondary treatment by radiosurgery.

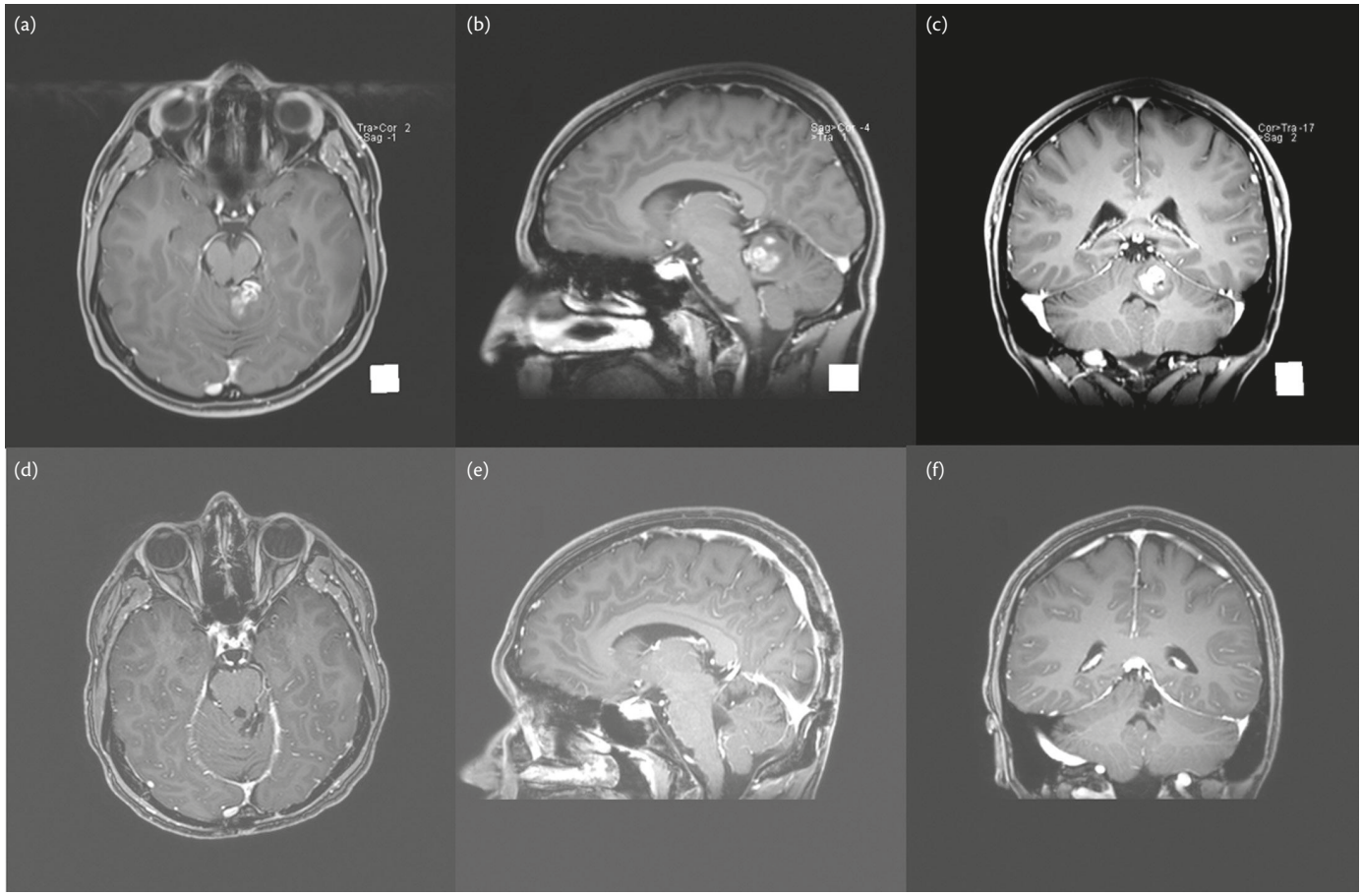

Fig. 37.4 Illustrative case for the occipital transtentorial approach. (A, B, C) Preoperative axial, sagittal, and coronal MRI planes of a symptomatic left vermian contrast enhancing lesion. (D, E, F) Postoperative 6-months follow-up after total resection via an occipital transtentorial approach of a left vermian pilocytic astrocytoma.

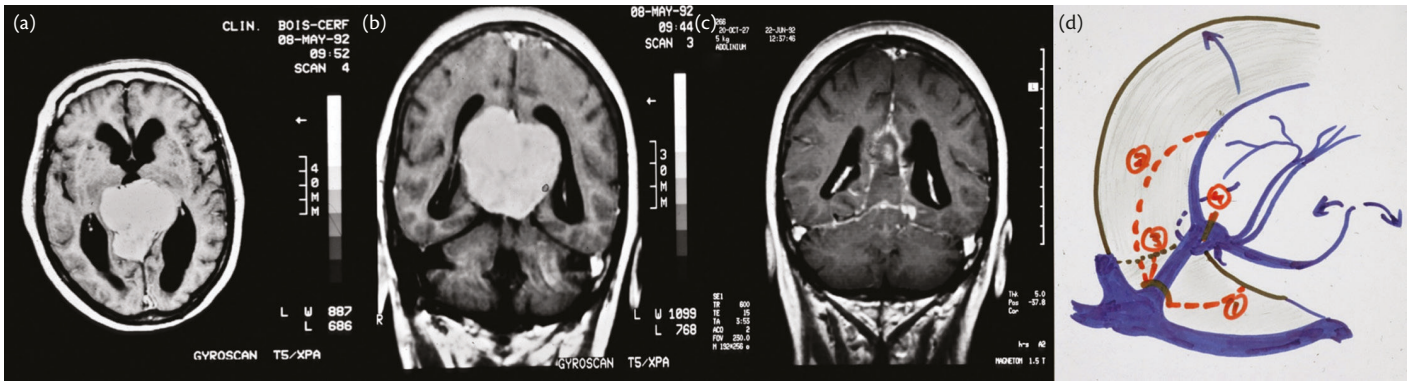

Fig. 37.5 Illustrative case with an falcotentorial meningioma. (A, B) MRI with axial and coronal planes with an falcotentorial meningioma. (C) MRI with coronal plane after total resection of an falcotentorial meningioma. (D) Illustration of the deep venous system and incision in the tentorium (1/2) and dissection/coagulation (3/4) of the straight sinus and vein of Galen.

At the end of the procedure the surgeon can inspect the splenium of the corpus callosum, the internal cerebral veins, the superior cerebellar artery, the quadrigeminal plate, and the superior and medial cerebellar peduncles (Fig. 37.5). See Box 37.3 for the main principles of the surgery of for falcotentorial meningiomas.

Combined infratentorial/supratentorial approach for falcotentorial meningioma

The combined supratentorial/infratentorial approach for large pineal region meningiomas and large pineal tumours is described in the literature. The technique consists of exposing the infratentorial and supratentorial occipital dura, the superior sagittal sinus, and the torcular as well as the transverse sinus, which is divided on the non-dominant side. The occipital lobe and the cerebellum can then be easily retracted to expose the tentorium which is divided as described earlier, to reach the tumour and the pineal region.

Postoperative procedure and results

In the first 24 hours after tumour resection the patient should be monitored in the intensive care unit. Some colleagues recommend routinely administration of Mannitol and Dexamethasone. This should be tapered over the following seven days. Within the first 48 hours MRI should be performed for resection control, infarction, or hydrocephalus. If the patient shows signs of acute hydrocephalus or neurological deterioration a CT scan should be immediately performed.

Postoperative surgery related complications include cerebellar ataxia, transitory metamorphopsia, permanent hemianopsia, transient fourth nerve palsy, and Parinaud syndrome. Homonymous hemianopsia is a rare although always transient complication of surgery for the occipital transtentorial approach. The overall mortality rate is described within 5–10% in the literature.

Box 37.3 Main principles of the surgery for falcotentorial meningiomas

1. Park bench position
2. Attachment to the dura of falx and tentorium
3. Be aware of compression and/or occlusion of the sinus
4. Identify and preserve the deep venous system
5. Tumour encases the straight sinus and falcotentorial junction
6. Incise the tentorium posteroanteriorly along the lateral edge of the tumour
7. Reflect tentorium lateral: inspect the superior cerebellar artery (SCA) and fourth central nerve
8. Incise the falx in the same way along the superior edge of the tumour to expose the other side of the tumour
9. If tumour invades anteriorly the deep veins, vein of Galen, or interior cerebral vein, then leave residual tumour

Complication management

To prevent complications during and after tumour removal it is essential to know the individual anatomy of the lesion, especially the venous anatomy. The major goal is to avoid venous infarction. Do employ pre- and intraoperative workup to prevent air embolism, with administration of antioedematous therapy and draining CSF if necessary.

There are some anaesthetic issues during surgery of pineal region lesions in the sitting position. The anaesthesiologist should use a precordial Doppler monitor and take care of the end-tidal pCO_2 to diagnose air embolism. The patient should have an arterial and central venous access to aspirate air if embolism accurse and have access to compress both jugular veins simultaneously. Dexamethasone and mannitol can be administered if necessary.

To check for postoperative neurological deterioration due to acute hydrocephalus or venous congestion or infraction, the patient should be monitored at least for 24 hours on an intensive care unit.

Management and follow-up of pineal cysts

Pineal cysts are seen in 4% of MRI and are usually regarded as incidental and benign lesions of the pineal region. Management and follow-up of pineal cysts are controversially discussed in the literature. In our point of view there is an indication for follow-up in asymptomatic cysts of +/– 2 cm of size. If MRI detects contrast enhancement of the cyst wall a neurenteric cyst as differential diagnosis is possible.

If the lesion grows or signs for compression of the aqueduct and consecutive occlusion with hydrocephalus develop, surgery should

be considered (Berhouma et al., 2015). An ETV with possible endoscopic fenestration of the cyst through the third ventricle rather than open resection can be considered in cases of hydrocephalus.

REFERENCES

Al-Tamimi, Y.Z., Bhargava, D., Surash, S., et al. (2008). Endoscopic biopsy during third ventriculostomy in paediatric pineal region tumours. *Childs Nerv Syst*, **24**, 1323–6.

Azab, W.A., Nasim, K. &, Salaheddin, W. (2014). An overview of the current surgical options for pineal region tumors. *Surg Neurol Int*, **5**, 39.

Berhouma, M., Ni, H., Delabar, V., et al. (2015). Update on the management of pineal cysts: case series and a review of the literature. *Neurochirurgie*, **61**(2–3), 201–7.

Broggi, M., Darbar, A., & Teo, C. (2010). The value of endoscopy in the total resection of pineocytomas. *Neurosurgery*, **67** 159–65.

Cardia, A., Caroli, M., Pluderi, M., et al. (2006). Endoscope-assisted infratentorial-supracerebellar approach to the third ventricle: an anatomical study. *J Neurosurg*, **104**(6 Suppl), S409–14.

Clark, K. (1983). The occipital transtentorial approach to the pineal region. In: Schmidek, H.H. & Sweet, W.H. (eds.) *Operative Neurosurgery and Techniques*, pp. 595–8. New York, NY: Grune and Stratton.

Cushing, H. (1983). *Intracranial Tumors: Notes upon a series of two thousand verified cases with surgical mortality pertaining thereto*. Springfield, IL, Charles C. Thomas.

Dandy, W.E. (1936). Operative experience in cases of pineal tumor. *Arch Surg (Chicago)*, **33**, 19–46.

Ellenbogen, R.G. & Moores, L.E. (1997). Endoscopic management of a pineal and suprasellar germinoma with associated hydrocephalus: technical case report. *Minim Invasive Neurosurg*, **40**, 13–15.

Guest, D.O. & Kleriga, E. (1979). Microsurgical anatomy of the pineal region. *Neurosurgery*, **6**, 385–90.

Kodera, T., Bozinov, O., Sürücü, O., Ulrich, N.H., Burkhardt, J.K., & Bertalanffy, H. (2011). Neurosurgical venous considerations for tumors of the pineal region resected using the infratentorial supracerebellar approach. *J Clin Neurosci*, **18**, 1481–5.

Krause, F. (1926). Operative freilegung der vierhügel, nebst beobachtungen über hirndruck und dekompression. *Zentbl Chir*, **53**, 2812–19.

Lazar, M.L. & Clark, W.K. (1974). Direct surgical management of masses in the region of the vein of Galen. *Surg Neurol*, **2**, 17–21.

Lozier, A.P. & Bruce, J.N. (2003). Surgical approaches to posterior third ventricular tumors. *Neurosurg Clin N Am*, **14**, 527–45.

Lutterbach, J., Fauchon, F., Schild, S.E., et al. (2002). Malignant pineal parenchymal tumors in adult patients: patterns of care and prognostic factors. *Neurosurgery*, **51**, 44–56.

O'Brien, D.F., Hayhurst, C., Pizer, B., & Mallucci, C.L. (2006). Outcomes in patients undergoing single-trajectory endoscopic third ventriculostomy and endoscopic biopsy for midline tumors presenting with obstructive hydrocephalus. *J Neurosurg*, **105**, 219–26.

Page, L.K. (1977). The infratentorial supracerebellar exposure of tumors in the pineal area. *Neurosurgery*, **1**, 36–40.

Poppen, J.L. (1966). The right occipital approach to a pinealoma. *J Neurosurg*, **25**, 706–10.

Poppen, J.L. & Marino, R. Jr. (1968). Pinealomas and tumors of the posterior portion of the third ventricle. *J Neurosurg*, **28**, 357–64.

Reid, W.S. & Clark, W.K. (1978). Comparison of the infratentorial and transtentorial approaches to the pineal region. *Neurosurgery*, **3**, 1–8.

Ringertz, N., Nordenstam, H. &, Flyger, G. (1954). Tumors of the pineal region. *J Neuropathol Exp Neurol*, **13**, 540–61.

Sawamura, Y., de Tribolet, N., Ishii, N., & Abe, H. (1997). Management of primary intracranial germinomas: diagnostic surgery or radical resection? *J Neurosurg*, **87**(2), 262–6.

Sawamura, Y. & de Tribolet, N. (2002). Neurosurgical management of pineal tumours. *Adv Tech Stand Neurosurg*, **27**, 217–44.

Schmidek, H.H. (1977). *Pineal Tumours*. New York, NY: Masson.

Stein, B.M. (1971). The infratentorial supracerebellar approach to pineal lesions. *J Neurosurg*, **35**, 197–202.

Stein, B.M. (1979). Supracerebellar-infratentorial approach to pineal tumors. *Surg Neurol*, **11**, 331–7.

Uschold, T., Abla, A.A., Fusco, D., Bristol, R.E., & Nakaji, P. (2011). Supracerebellar infratentorial endoscopically controlled resection of pineal lesions: case series and operative technique. *J Neurosurg Pediatr*, **8**, 554–64.

Zacharia, B.E. & Bruce, J.N. (2001). Stereotactic biopsy considerations for pineal tumors. *Neurosurg Clin N Am*, **2**, 359–66.

SECTION 9

Tumours and skull base–tumour syndromes

38. **Neurophakomatoses** *449*
Fay Greenway, Frances Elmslie, and Timothy Jones

39. **Uncommon brain lesions** *461*
Yizhou Wan, Hani J. Marcus, and Thomas Santarius

38

Neurophakomatoses

Fay Greenway, Frances Elmslie, and Timothy Jones

Introduction

The term *phakomatosis* was first used in 1920 to describe a group of multisystem disorders with common neuro-oculocutaneous findings as they all shared lens-like retinal tumours (phacomata). Others cite the Greek root *phakos*, meaning 'mother spot' or birthmark as abnormal tissue growth or tumour formation is also seen with these conditions. Three disorders were first considered phakomatoses; neurofibromatosis (NF), tuberous sclerosis complex (TSC), and von Hippel-Lindau syndrome (VHL). Other conditions such as Sturge-Weber and PHACE (posterior fossa abnormalities, haemangioma, arterial cerebrovascular anomalies, cardiac defects, eye anomalies) syndromes may also be included. Each is caused by distinct genetic defects, with some overlap in terms of protein function. They share pathogenetic mechanisms in dysfunction of a tumour suppressor gene. This chapter details phakomatoses seen in practice, paying attention to their neurological sequelae and impact on neurosurgical practice.

Neurofibromatosis type 1 (NF1)

NF1 is the most common phakomatosis with a prevalence of 1 in 3000 (Walker et al., 2006). It displays autosomal dominant inheritance and is due to a mutation in the NF1 tumour suppressor gene located on chromosome 17q11.2 (gene product neurofibromin, a regulator of the *Ras* oncogene) (Viskochil et al., 1990). Approximately 50% of cases represent new germline mutations (Jett and Friedman, 2010). Clinically heterogeneous, it is characterized by neurofibromas, café au lait spots, axillary and inguinal freckling, optic gliomas, and iris hamartomas. Neurofibromas are benign tumours composed of Schwann cells, some dissociated from axons, a proliferation of support cells (fibroblasts and mast cells) that are less well organized than normal fascicle, with a breakdown of the surrounding perineural layer.

Diagnostic criteria

NF1 is a clinical diagnosis, with two or more of the following criteria being required for diagnosis (National Institutes of Health Consensus, 1988):

- Six or more café au lait macules (>0.5 cm in children or >1.5 cm in adults)
- Two or more cutaneous/subcutaneous neurofibromas or one plexiform neurofibroma
- Axillary or groin freckling
- Optic pathway glioma
- Two or more Lisch nodules (iris hamartomas seen on slit lamp examination)
- Bony dysplasia (sphenoid wing dysplasia, bowing of long bone pseudarthrosis)
- First-degree relative with NF1

Genetic analysis may clarify the diagnosis in young children who do not meet the diagnostic criteria and is useful for affected individuals to aid reproductive decision-making.

Case history

Case 38.1

A 24-year-old woman presents with extensive cutaneous neurofibromas and 3 months of weight loss, with L3 dermatomal numbness, grade 3/5 power in her knee and brisk reflexes. MRI identified a retroperitoneal mass invading the L3 vertebral body with loss of height, canal impingement, and thecal compression. She underwent successful L1-L5 laminectomy decompression and pedicle screw fixation. Histology confirmed malignant peripheral nerve sheath tumour (**Fig. 38.1**).

Case 38.2

A 5-year-old girl presents with delayed milestones, multiple café au lait spots and increasing head circumference. MRI identified chiasmal and optic nerve lesions (**Fig. 38.2**).

Screening

Regular clinical review in childhood under the care of a paediatrician with referral to a specialist NF1 clinic when indicated is recommended. Surveillance brain imaging is not advocated. Genetic testing of the NF1 gene should be made available for affected patients as well as prenatal diagnostic genetic testing when requested (Ferner et al., 2007).

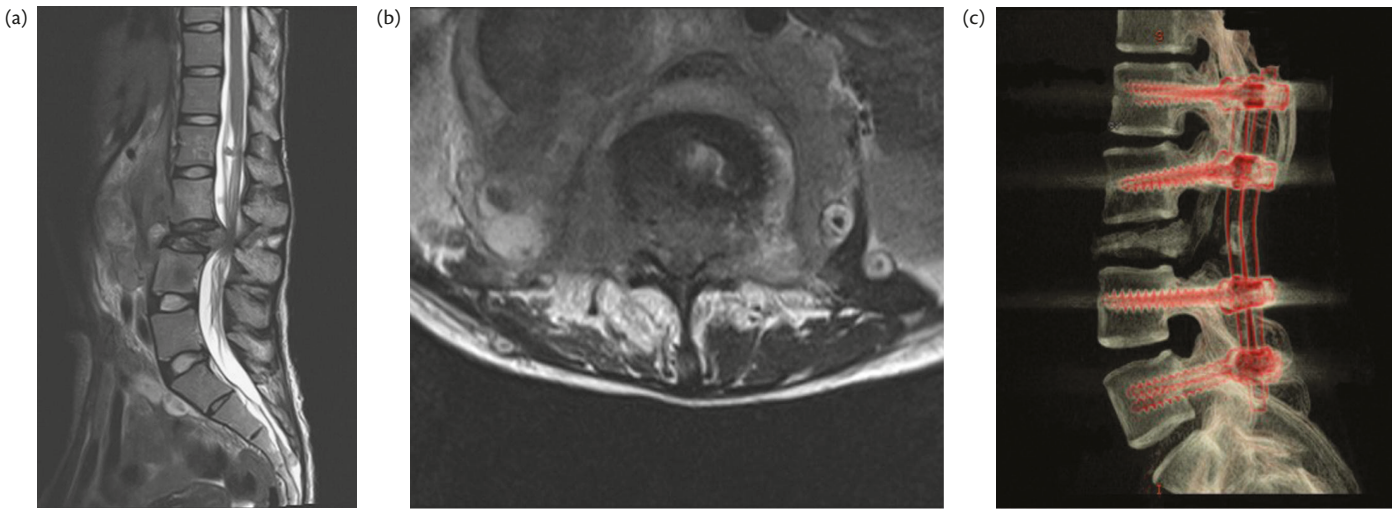

Fig. 38.1 (A) Sagittal T2-weighted MRI and (B) axial T2-weighted MRI showing retroperitoneal mass invading L3 vertebral body with loss of height, canal impingement, and thecal compression. (C) Postoperative CT reconstruction.

Clinical features

Cutaneous manifestations are typically the first sign of NF1. Café au lait spots, light brown patches on the trunk with well demarcated edges, are often present at birth, increasing in number during the first few years of life. The frequency and age of onset of NF1 clinical manifestations are shown in Table 38.1.

Neurofibromas

Neurofibromas are benign peripheral nerve sheath tumours. They may be focal cutaneous or subcutaneous, diffuse, or nodular plexiform lesions. Typically indolent, they follow a benign course, developing in the late teens and early twenties. They may cause cosmetic problems and can be removed, with risk of recurrence and hypertrophic scarring. Subcutaneous neurofibromas, evident on palpation of skin, may be tender or cause paraesthesia in the distribution of the affected nerve. They rarely undergo malignant transformation. Plexiform neurofibromas grow along the nerve length and may involve multiple nerve branches and plexi. Multiple lesions can develop on nerve trunks and can be nodular, resulting in thickened, potentially large, masses which infiltrate soft tissue and cause bone hypertrophy. When multiple spinal nerve roots are involved, patients may present with myelopathy secondary to cord compression.

Central nervous system (CNS) tumours

Pilocytic astrocytoma (WHO grade 1) is the most common paediatric brain tumour in the context of NF1, affecting up to 15% of patients. The majority are optic pathway gliomas (OPG) (Listernick et al., 2007), with 20% occurring in the brainstem. They typically follow a more indolent course than sporadic counterparts. OPG can involve the optic nerve, chiasm, or hypothalamus. They remain asymptomatic in the majority of patients but can cause visual loss, proptosis, endocrine disturbance, and are more often symptomatic in children. Gliomas of the brainstem or cerebellum occur more frequently in NF1 patients than the general population, and of those, are more frequent in NF1 patients treated with radiotherapy for OPG in childhood (Kleinerman, 2009).

Hyperintense lesions on T2 MRI (unidentified bright objects or UBOs) are seen in more than half of NF1 patients, most commonly in children aged 8–16 years. They are pathognomonic of the condition and most likely caused by aberrant myelination or gliosis.

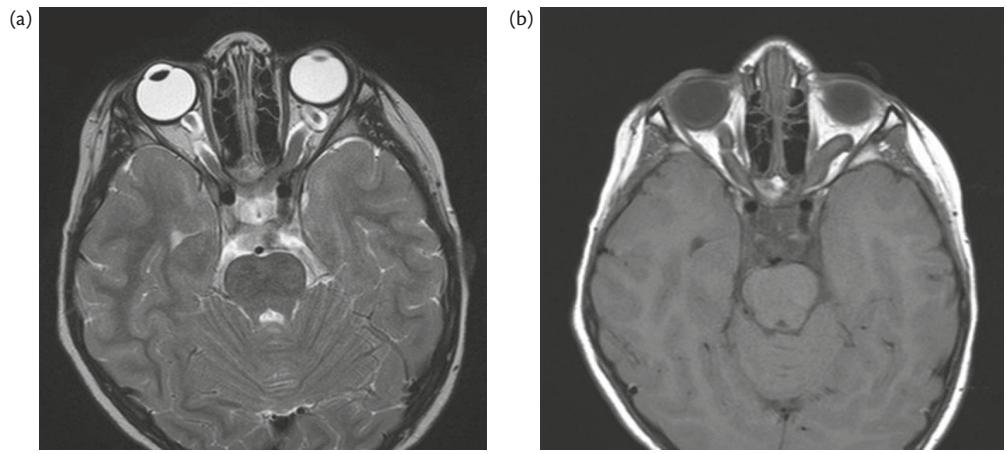

Fig. 38.2 (A) Axial T2-weighted MRI showing thickened, coiled optic nerves; high signal lesion (unidentified bright object) posterior to fourth ventricle. (B) Axial T1-weighted MRI of the orbit showing thickened, coiled optic nerves, left greater than right.

Table 38.1 Frequency and age of onset of major clinical manifestations of NF1

Clinical manifestation	Frequency (%)	Age of onset
Café au lait patches	>99	Birth to 12 y
Skin-fold freckling	85	3 y to adolescence
Lisch nodules	90–95	>3 y
Cutaneous neurofibromas	>99	>7 y (usually late adolescence)
Plexiform neurofibromas	30 (visible) – 50 (on imaging)	Birth to 18 y
Disfiguring facial plexiform neurofibromas	3–5	Birth to 5 y
Malignant peripheral nerve sheath tumours	2–5 (8–13% lifetime risk)	5–75 y
Scoliosis	10	Birth to 18 y
Scoliosis requiring surgery	5	Birth to 18 y
Pseudarthrosis of tibia	2	Birth to 3 y
Renal artery stenosis	2	Lifelong
Phaeochromocytoma	2	>10 y
Severe cognitive impairment (IQ <70)	4–8	Birth
Learning problems	30–60	Birth
Epilepsy	6–7	Lifelong
Optic pathway glioma	15 (only 5% symptomatic)	Birth to 7 y (up to 30 y)
Cerebral glioma	2–3	Lifelong
Sphenoid wing dysplasia	<1	Congenital
Aqueduct stenosis	1.5	Lifelong

Reproduced with permission from Rosalie E. Ferner et al., Guidelines for the diagnosis and management of individuals with neurofibromatosis 1, *Journal of Medical Genetics*, Volume 44, Issue 2, pp. 81–8, Copyright © 2007 BMJ Publishing Group Ltd.

Malignant peripheral nerve sheath tumours (MPNST)

MPNSTs arise from pre-existing nodular or plexiform neurofibroma; while rare (2–5% frequency), they are the most frequent malignant neoplasm associated with NF1. Patients with pre-existing plexiform neurofibromas have an 8–13% lifetime risk of MPNST, typically arising age 20 to 30 years (Evans et al., 2002). They have a poorer prognosis than sporadic cases. When they occur in children and adolescents, they tend to be of low grade, and may be difficult to distinguish from atypical plexiform neurofibromas. Pain or enlargement of a mass is a classic initial sign.

Malignancy

A recent UK study suggests that the relative risk of cancer in NF1 patients is 2.7, with an estimated overall risk of malignancy of 36% by the age of 70 (Walker et al., 2006). Of particular note is the increased risk of breast cancer (age <50 years), which has led to the recommendation of early breast screening from the age of 40 for affected women (Sharif et al., 2007).

Management

Patients with NF1 should be managed by a multidisciplinary specialist team, including neurology, paediatrics, genetics, ophthalmology, neurosurgery, plastic surgery, orthopaedics, soft tissue tumour surgery, psychiatry, dermatology, radiology, and pathology. The mainstay of management is active surveillance with age specific monitoring of disease manifestations, patient education, annual review in specialist clinic, and surgical intervention when lesions become symptomatic or show evidence of progression.

OPGs are treated with chemotherapy (vincristine and carboplatin) (Rosser and Packer, 2002), with surgery reserved usually for cosmesis or to treat corneal exposure. Radiotherapy is no longer advocated due to risks of neurovascular, endocrine, neuropsychological sequelae, and of secondary high-grade gliomas and MPNSTs (Sharif et al., 2006; Lee 2007). The decision of when to treat OPG remains challenging, with no universal agreement as to what constitutes progressive disease (radiographic progression vs. deteriorating visual acuity).

Surgery for spinal plexiform neurofibromas is performed for lesions causing neurological deficit. It can be challenging due to their vascularity and involvement of surrounding structures. They are not curable due to multiplicity so decompression (laminectomy and debulking) is advised with consideration of fusion to prevent progressive kyphosis. Surgery for MPNSTs should aim for complete resection with tumour free margins and adjuvant radiotherapy for incompletely excised tumours.

Other CNS tumours should be observed with serial MRI, with surgery reserved for focal, resectable, symptomatic tumours.

Agents which impact on the molecular pathways of tumourigenesis, such as rapamycin and everolimus, inhibitors of the Mammalian Target of Rapamycin (mTOR) pathway, may have a future role in NF1. Rapamycin has been shown in mouse models to inhibit the mTOR pathway particularly in MPNSTs and gliomas (Gottfried et al., 2010), and results of a trial of everolimus in progressive low-grade gliomas in NF1 are yet to be published (NCT01158651, 2010).

Controversy

There are several opinions as to the optimal management of OPGs (Listernick et al., 2007). These include surveillance, choice of ophthalmological test (visual acuity, visual fields, colour vision, visual evoked potentials), age limit for regular surveillance, use of surveillance imaging (MRI), frequency of review, definition of progression (both radiographic and clinical), and optimal definitive management. Evidence shows that chemotherapy with carboplatin and vincristine has good outcomes including slowed tumour progression and improved or stable visual acuity (Mahoney et al., 2000; Fisher et al., 2012; Dodgshun et al., 2015). Literature demonstrates radiotherapy to be more deleterious than beneficial, with one study reporting a threefold increase in the relative risk of secondary CNS tumour following radiotherapy for OPG, with the greatest risk being in children (Sharif et al., 2006). With such good evidence for chemotherapy available, the role of surgery is limited in OPG. It should only be considered if there is evidence of hydrocephalus due to obstruction of the third ventricle (typically hypothalamic or chiasmal lesions), or if there is significant proptosis with disfigurement, in a blind, or near-blind eye, limiting resection to partial removal of the intraorbital optic nerve.

Neurofibromatosis type 2 (NF2)

NF2 affects 1 in 25 000 individuals, with an estimated prevalence of 1 in 60 000 (Evans 2009). It exhibits autosomal dominant

inheritance due to a mutation in the NF2 tumour suppressor gene on chromosome 22q12.2 (gene product merlin, aka schwannomin, a critical regulator of contact-dependent inhibition of cell proliferation) (Rouleau et al., 1993; Trofatter et al., 1993). It has a strong genotype-phenotype correlation, and 99% penetrance by the age of 60. NF2 is characterized by bilateral vestibular schwannomas (VS) (WHO grade I, comprised of neoplastic Schwann cells). Other manifestations include meningioma (intracranial, spinal, and optic nerve sheath), schwannomas at other sites (cranial nerves, spinal cord, peripheral nerves), ocular signs (posterior subcapsular lens opacities), ependymomas, and rarely, skin manifestations (café au lait macules).

Diagnostic criteria

There have been several diagnostic criteria proposed (NIH criteria 1987, revised 1991, and Manchester criteria 1992) (Evans et al., 1992; Evans et al., 2018). In 2011, new criteria were proposed to take into account MRI and molecular genetic testing (Baser et al., 2011) but most still use the Manchester criteria for diagnosis (**Box 38.1**).

Illustrative case

Case 38.3

A 33-year-old woman presents with falls, headaches, nausea, unsteadiness, and right sided tinnitus. Examination revealed swollen optic discs and computed tomography (CT) identified enhancing mass in right cerebellopontine angle with obstructive hydrocephalus. MRI (**Fig. 38.3**) confirmed bilateral VS and meningioma, diagnosed NF2. She underwent resection of large right-side VS, with ongoing surveillance of left side VS and meningioma.

Screening

Patients with a clinical diagnosis of NF2 should be offered genetic testing. If a mutation is identified, the children of affected parents should be offered genetic testing from birth, and clinical screening of at-risk individuals commenced. There is no standard screening protocol in the United Kingdom, but a suggested guideline is shown in **Box 38.2** (Evans et al., 2005).

Box 38.1 Diagnostic criteria for NF2—Manchester criteria

A. Bilateral vestibular schwannomas

B. First-degree family relative with NF2 and unilateral vestibular schwannoma or any two* of:
meningioma, schwannoma, glioma, neurofibroma, posterior subcapsular lenticular opacities

C. Unilateral vestibular schwannoma and any two of:
meningioma, schwannoma, glioma, neurofibroma, posterior subcapsular lenticular opacities

D. Multiple meningiomas (two or more) and unilateral vestibular schwannoma or any two of: schwannoma, glioma, neurofibroma, cataract

*'Any two of' refers to two individual tumours or cataract

Reproduced with permission from Evans, DGR; Huson, SM, A Clinical Study of Type 2 Neurofibromatosis, *QJM: An International Journal of Medicine*, Volume 84, Issue 1, pp. 603–18. Copyright © 1992 Oxford University Press.

Additional groups at risk of NF2 include (Evans et al., 2005): those with a first-degree family history, patients less than 30 years with unilateral VS or meningioma (approximately 10% with an isolated meningioma in childhood will ultimately be diagnosed with NF2), and patients with multiple spinal tumours (schwannoma or meningioma) or cutaneous schwannoma. Patients with a single VS in isolation have a low risk of NF2 (<1% if age >30 years) (Mohyuddin et al., 2002). Presymptomatic genetic testing is available for affected family members. It guides clinical screening, enabling early detection of tumours and improves outcome.

Clinical features

Bilateral vestibular schwannoma typically develop by the age of 30 years in 90–95% of patients (Parry et al., 1994). They present with hearing loss, usually unilateral at the time of onset, but progressing in most patients to deafness. They may also present with vestibular symptoms; tinnitus, dizziness, and imbalance. Unlike neurofibromas, schwannomas are encapsulated tumours composed of pure Schwann cells growing around the nerve, occurring wherever there are nerves with Schwann cells. The predilection for the eighth nerve in NF2 is not understood, but schwannomas of other cranial nerves also occur.

Meningioma occur in around half of NF2 patients, are multiple in 40% of patients, and may be cranial (including optic nerve sheath) and spinal. Intradural spinal tumours, most often dorsal root schwannomas, occur in between 26 and 90% of patients depending on case series (Evans, 2009). Low-grade ependymomas and gliomas also feature in NF2, primarily in the cervical spine and brainstem. Between 60% and 80% of patients have ocular manifestations of NF2 including posterior subcapsular opacities. Cutaneous lesions and café au lait spots occur in NF2 but are fewer and subtler than in NF1.

Management

Patients with NF2 should be managed in multidisciplinary specialist units, staffed with specialists in neurosurgery, otolaryngology, neurology, genetics, audiology, paediatrics, and hearing therapy (consider teaching the patient and family lip-reading and signing at an early age). The aim of NF2 management is to preserve hearing and maximize quality of life. The natural history of NF2-VS is poorly understood making management challenging. The surgeons require experience in managing VS and auditory rehabilitation with both cochlear and auditory brainstem implants. The patient should undergo routine clinical and radiological surveillance as outlined in **Box 38.2**. Treatment should be offered if evidence of growth, progressive hearing loss, or symptomatic tumours.

Bevacizumab, a monoclonal antibody inhibitor of vascular endothelial growth factor (VEGF), demonstrated hearing improvement and VS tumour regression in 50% of NF2 patients, but little effect on NF2-related meningiomas (Plotkin et al., 2012). Trials are ongoing to further evaluate its use in children and young adults (NCT01767792, 2013), and also in NF2-associated meningioma (Nunes et al., 2013).

Stereotactic radiosurgery has a role in poor surgical candidates however, there is controversy surrounding its use and microsurgery remains the accepted primary treatment modality. NF2-VS are more difficult to treat than their sporadic counterparts—typically presenting at a younger age, tending to be larger, multifocal, and with higher risks of recurrence and facial nerve injury. Timing of surgery

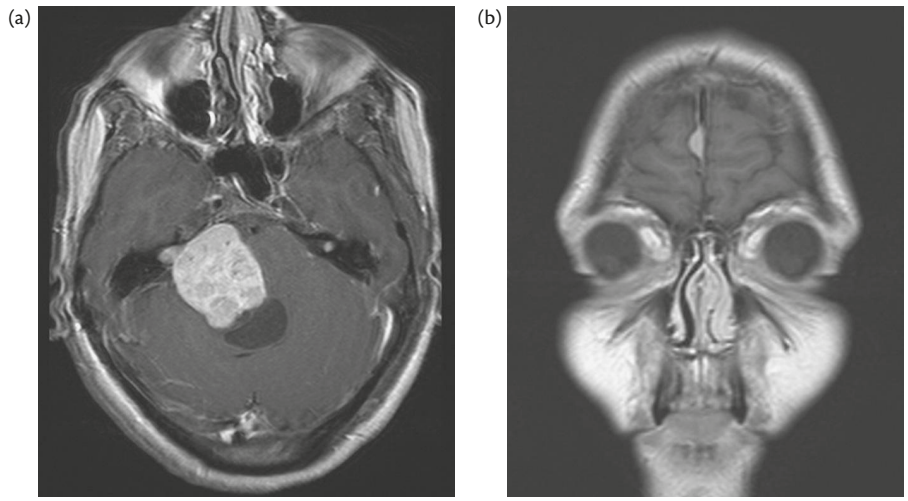

Fig. 38.3 (A) Contrast-enhanced T1-weighted MRI showing right cerebellopontine angle enhancing vestibular schwannoma and small left sided intracanalicular schwannoma. (B) Contrast-enhanced T1-weighted MRI showing enhancing durally based parafalcine meningioma.

is critical and multiple factors play a role in the decision-making process:

- Preservation of hearing and facial nerve function
- Size and growth pattern of the tumour (serial MRI can be used to assess progression)
- Hearing status and rate of deterioration

Box 38.2 Suggested screening guidelines

Initial cranial and spinal MRI age 10–12 years, unless severely affected family
Cataracts and other ocular abnormalities can affect vision in early life, and other tumours (particularly cranial meningiomas) can occur in the first 10 years of life. The initial MRI scan could be at 10–12 years of age, or earlier in severely affected families; it is rare for tumours to become symptomatic before that age.

Annual hearing test
Annual audiological tests, including auditory brainstem response, from the early teens may be useful, but all patients should be monitored with MRI as there is often tumour growth without audiological deterioration.

No tumours: MRI screening every 2 years, age <20 y, every 3 years >20 y
Surgery is unlikely to be more successful for tumours less than 6 mm in diameter than for larger tumours, but VS growth is higher in younger patients, so MRI screening every 2 years for patients less than age 20 and every 3 years for older patients should be sufficient for asymptomatic at-risk individuals without tumours.

Tumours: MRI screening every 1 year
Once tumours are present, MRI screening should be at least annual until the individual growth rate is established.

Spinal tumours are found frequently on MRI. Only 30% of patients with spinal tumours have symptomatic tumours that require a spinal operation, but a full annual neurological examination is a wise precaution, with spinal MRI every 2–3 years unless no tumours are present on the initial scan.

Reproduced with permission from DGR Evans, ME Baser, B O'Reilly, et al. Management of the patient and family with neurofibromatosis 2: a consensus conference statement, *British Journal of Neurosurgery*, Volume 19, Issue 1, 2005 © The Neurosurgical Foundation, reprinted by permission of Taylor & Francis Ltd, www.tandfonline.com on behalf of The Neurosurgical Foundation.

- Consideration of auditory rehabilitation device using either a cochlear implant or an auditory brainstem implant, and if so, when to insert (first surgery easier than revision—can be inserted even when serviceable hearing present, to be activated at later date)
- Extent of tumour resection—total removal only if the tumour yields easily (MRI can be used for surveillance of any residual tumour)

The management of other CNS tumours—meningioma, ependymoma, and other schwannoma, both cranial and spinal—follow the standard principle of active surveillance until evidence of progression or onset of symptoms when surgical resection can be considered.

Controversy

Stereotactic radiosurgery (SRS) has been proven to be an effective method of treatment for sporadic VS, with numerous studies demonstrating comparable, if not improved, results with microsurgery (tumour control rates between 92% and 98%, hearing preservation from 60% to 90%, facial nerve preservation 90% to 95%) (Golfinos et al., 2016). It is less effective in the context of NF2. Concerns surround the risks of malignant transformation, the development of secondary tumours and deleterious effect on surrounding structures (hearing loss and facial nerve damage). Although radiosurgical outcomes after treatment of sporadic VS have been studied, there remains a paucity of literature on SRS in NF2. NF2-VS are more difficult to treat due to their engulfing or infiltrating the eighth nerve more so than sporadic VS which more commonly displace and compress it; hearing and facial preservation is thus challenging whichever modality of treatment chosen. No studies directly compare microsurgical outcomes with SRS in NF2-VS. Several factors should be considered when deciding optimal management for NF2-VS.

Factors in favour of SRS include:

- Avoidance of complications of surgery—death, cerebrospinal fluid (CSF) leak, haemorrhage, meningitis, venous thromboembolism
- Tumours which may be technically difficult to surgically resect; often incomplete resection with higher risk of recurrence

- Avoidance of multiple operations in patients with multiple CNS tumours
- SRS can be performed in patients unfit for anaesthesia
- Good evidence in sporadic VS

Factors against SRS include:

- Risk of new malignant transformation of the VS.
- Theoretical risk of secondary malignancy (Plowman and Evans, 2000). Data is limited, but some suggests that this risk is very low (Rowe et al., 2007) (18 patients with >900 years of follow-up noted only two malignancies (1.7%)). Others argue (Evans et al., 2006) that most studies have short follow-up periods such that delayed presentations may be missed. One study presented a 10-fold malignancy risk in NF2 patients treated with radiotherapy (Baser et al., 2000).
- Poor long-term follow-up and outcome data.

The few studies that have looked at tumour control rates, hearing and facial preservation with SRS (Subach et al., 1999; Rowe et al., 2003; Mathieu et al., 2007; Phi et al., 2009; Sharma et al., 2010), have had variable follow-up durations (between 26 and 96 months) making comparison between studies difficult; outcomes for local control rates were between 66 and 98%, and serviceable hearing preservation between 33% and 66% (Mallory et al., 2014). No comparison has been made between the outcomes of microsurgery vs. SRS. As NF2 is a rare disease patient registration and prospective outcome collection may help define optimal treatment.

Tuberous sclerosis complex

TSC has a frequency of 1 in 6000–10 000 live births and a population prevalence of 1 in 20 000 (Sampson et al., 1989; O'Callaghan et al., 1998). It exhibits autosomal dominant inheritance due to mutations in two distinct tumour suppressor genes, TSC1 on chromosome 9q34 (Fryer et al., 1987) and TSC2 on chromosome 16p13.3 (Kandt et al., 1992), encoding hamartin and tuberin proteins. These form a complex which regulates cell growth and proliferation through the mTOR (mammalian target of rapamycin) pathway (Tee et al., 2002). TSC is characterized by hamartomas and benign neoplastic lesions affecting the CNS as well as skin, renal, cardiac, and pulmonary systems. Major CNS manifestations include cortical hamartomas (tubers), subcortical glioneuronal hamartomas, subependymal glial nodules and subependymal giant cell tumours (SGCTs). See Box 38.3.

Diagnostic criteria

See Box 38.3 for the diagnostic criteria for tuberous sclerosis complex (TSC).

Antenatal diagnosis can be made on fetal ultrasound and MRI, which show cardiac and brain lesions (Curatolo et al., 2008).

Illustrative cases

Case 38.4

A 3-year-old girl with no significant family history, was identified on fetal echocardiogram with cardiac rhabdomyoma. MRI brain at birth (Fig. 38.4A) identified lesions consistent with TSC. She had developmental delay with focal tonic seizures, simple renal cysts, a single renal angiomyolipoma, and regressing cardiac rhabdomyomas and MRI scans at age 3 showed developing features of TSC (Fig. 38.4B).

Case 38.5

A 6-year-old boy with multiple cardiac rhabdomyomas identified on antenatal 36-week ultrasound scan. Due to suspicion of TSC, neonatal MRI brain was performed which identified subependymal nodules and a large right subependymal lesion, likely SGCT (Fig. 38.5). He developed infantile spasms at 22 weeks. At 4 years he underwent resection of SGCT due to progressive enlargement on serial imaging. He has associated learning difficulties.

Screening

Individuals with suspected TSC should undergo brain imaging, EEG (in paediatric patients if seizures suspected or the patient has been diagnosed antenatally), assessment for TSC-associated neuropsychiatric disorder, renal and abdominal imaging, renal function blood tests, pulmonary function testing in adult women and symptomatic adult men, dermatology review if significant skin lesions,

Box 38.3 Diagnostic criteria for TSC

A. Genetic diagnostic criteria

The identification of either a TSC1 or TSC2 pathogenic mutation in DNA from normal tissue.
Between 10% and 25% of TSC patients have no mutation identified.

B. Clinical diagnostic criteria

Definite diagnosis: Two major features or one major feature with ≥2 minor features
Possible diagnosis: Either one major feature or ≥2 minor features

Major features

1. Hypomelanotic macules (≥3, at least 5-mm diameter) (best seen with a Woods' ultraviolet (UV) lamp)
2. Angiofibromas (≥3) or fibrous cephalic plaque (appear in 90% by age 4; hamartomas of cutaneous nerve elements typically arising in malar distribution sparing the upper lip)
3. Ungual fibromas (≥2)
4. Shagreen patch
5. Multiple retinal hamartomas
6. Cortical dysplasias*
7. Subependymal nodules
8. Subependymal giant cell tumour (SGCT)
9. Cardiac rhabdomyoma
10. Lymphangioleiomyomatosis (LAM)†
11. Angiomyolipomas (≥2)†

Minor features

1. 'Confetti' skin lesions
2. Dental enamel pits (>3)
3. Intraoral fibromas (≥2)
4. Retinal achromic patch
5. Multiple renal cysts
6. Non-renal hamartomas, e.g. hamartomatous rectal polyps

* Includes tubers and cerebral white matter radial migration lines.

† A combination of the two major clinical features (LAM and angiomyolipomas) without other features does not meet criteria for a definite diagnosis. When both are present together, other features are also required for the diagnosis.

Data from Krueger, D.A. & Northrup, H., Tuberous sclerosis complex surveillance and management: Recommendations of the 2012 international tuberous sclerosis complex consensus conference, *Pediatric Neurology*, Volume 49, Issue 4, pp. 255–65, Copyright © 2013 Elsevier.

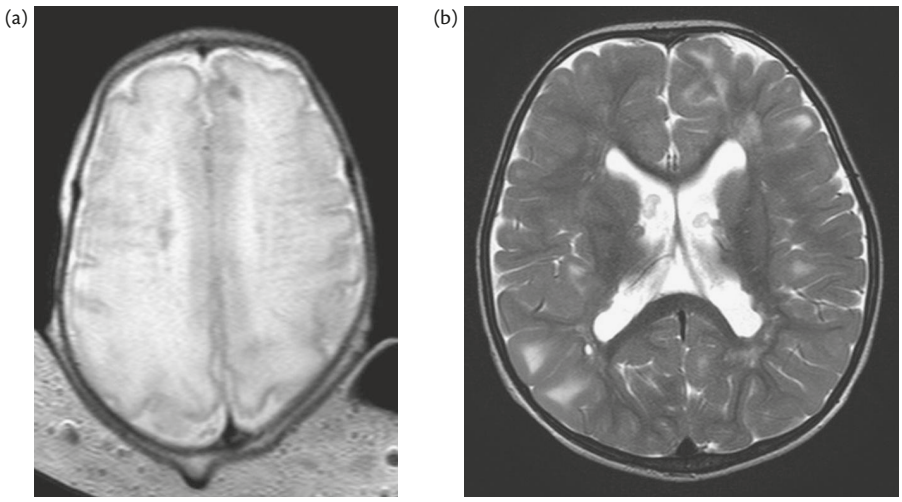

Fig. 38.4 (A) Axial T2-weighted MRI, age 3 days showing radial migration lines, left frontal (low signal) tuber. (B) Axial T2-weighted MRI, age 3 years showing multiple tubers (high signal) and scattered subependymal nodules along the lining of the lateral ventricles.

cardiac echocardiogram and electrocardiogram (ECG) in paediatric patients, ophthalmic and dental review. Once diagnosed, regular surveillance imaging and clinic review is recommended; if asymptomatic, patients should undergo brain MRI every 1–3 years from birth to age 25 years (Northrup and Krueger, 2013). The families of affected individuals should have full clinical assessment, and genetic testing and counselling should be offered.

Clinical features

Heinrich Vogt (1875–1936), a German neurologist, described a triad of three pathognomonic TSC clinical signs: seizures, learning disability, and skin lesions. This triad occurs in just 29% of patients and 6% lack all three (Schwartz et al., 2007). TSC is a multisystem disease with a wide variety of clinical features as defined in **Box 38.3**. Non-CNS lesions include cutaneous manifestations (see **Box 38.3**), renal cysts, angiomyolipomas, and renal cell carcinoma, pulmonary lymphangioleiomyomatosis, cardiac rhabdomyoma, and retinal hamartomas.

CNS lesions are identified in 90% of all TS patients (Curatolo et al., 2006):

- Cortical tubers—benign hamartomas, characterized by proliferation of glial and neuronal cells, and loss of cortical structure—large dysplastic neurons, giant cells, and bizarrely shaped astrocytes; variable in size and multiple in number.
- Subependymal nodules (SENs)—hamartomas, typically seen in the subependymal wall of the lateral ventricles; some protrude into the ventricular cavity (giving a characteristic 'candle guttering' appearance); typically calcified.
- Subependymal giant cell tumours (SGCTs) (aka subependymal giant cell astrocytoma SEGA)—WHO grade 1 tumour, displaying a mixed glioneuronal cell lineage; they are distinguished from SENs by progressive growth on serial imaging or if causing hydrocephalus; occur in approximately 10% of patients with TS.
- White matter linear migration lines—radial bands, radiating from the periventricular white matter to the subcortical region.
- Transmantle cortical dysplasia.

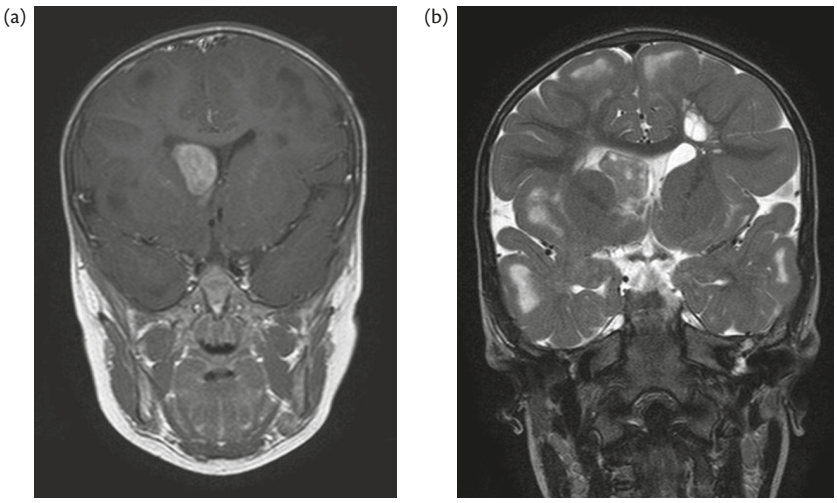

Fig. 38.5 (A) Coronal, contrast-enhanced T1-weighted MRI and (B) coronal T2-weighted MRI showing a SGCT in the right lateral ventricle as well as multiple subcortical tubers.

Management

TSC patients should be followed-up in a specialist multidisciplinary clinic with links to local services. Around 80–90% of patients have seizures; one-third will be managed successfully with medication. Those with refractory epilepsy may be suitable for surgery or vagal nerve stimulation. Surgery may be considered when a particular lesion is identified as the seizure focus. This requires thorough preoperative identification of the epileptogenic zone and consideration given to the extent of surgical resection (Fallah et al., 2015). Jansen et al. (2007) showed that 57% of children achieve seizure freedom postoperatively and another 18% experienced a reduction (>90%) in seizure frequency at one-year follow-up. Surgery should be considered for resection of tumours causing obstructive hydrocephalus, raised intracranial pressure, radiographic tumour progression, or development of new focal neurological deficits.

Controversy

The discovery of upregulation of the mTOR pathway upregulation in TSC-associated tumours presents new possibilities for treatment strategies. Sirolimus (aka rapamycin) is an immunosuppressant which binds to and inhibits the ability of mTOR to phosphorylate downstream targets. It has been approved as an immunosuppressant drug since 2001 and has been found to have application in the treatment of TSC (Jozwiak et al., 2006). Everolimus, a derivative of sirolimus, is effective in diminishing the volume of lesions in patients with renal angiomyolipomas, subependymal giant cell tumours (Franz et al., 2006) and sporadic lymphangioleiomyomatosis. It was approved by the FDA in the USA in 2010 for the treatment of TSC-associated SGCTs not amenable to surgical resection (Krueger et al., 2010). In 2013, the results of a double blind, placebo-controlled trial of everolimus to treat TSC-associated subependymal giant cell astrocytomas were published—the EXIST-1 trial (Franz et al., 2013). These also showed at least 50% reduction in the volume of the tumour as compared with placebo (Franz et al., 2013). Surgery may no longer be the treatment of choice for tumours associated with TSC.

Von Hippel-Lindau (VHL)

VHL has an estimated incidence of 1 in 36 000 live births and prevalence of 1 in 39 000–53 000 (Melmon and Rosen, 1964; Maher et al., 2011). It has autosomal dominant inheritance due to a mutation in the VHL tumour suppressor gene on chromosome 3p25 (Latif et al., 1993). The protein product regulates cell proliferation through the HIF (hypoxia inducible factor) pathway. 20% of cases arise from *de novo* mutations. VHL has marked phenotypic variability and over 90% penetrance by the age of 65 (Maher et al., 1990). It is a multisystem disorder characterized by the development of multiple haemangioblastomas (HGBs) of the central nervous system, retina, and other visceral tumours. Unlike other neurocutaneous syndromes, VHL is not typically associated with skin findings. Haemangioblastomas are composed of vascular and stromal cells.

Diagnostic criteria

See Box 38.4 for the diagnostic criteria for VHL.

In uncertain cases, genetic testing may be employed and is useful for management of the wider family. MRI brain imaging, renal ultrasound, abdominal CT, and urinary amine estimations are required to complete the evaluation.

Box 38.4 Diagnostic criteria for VHL

Confirmed family history

The presence of one single VHL tumour is sufficient for diagnosis (e.g. retinal or CNS HGB, clear cell RCC, phaeochromocytoma, pancreatic endocrine tumour, or endolymphatic sac tumour).

No family history

All of the tumours typically found in VHL disease can occur as a sporadic event.

Therefore, diagnosis requires the presence of two tumours:

either two CNS HGBs

or one CNS HGB and a visceral tumour (with exception of epididymal and renal cysts which are frequent in general population).

Reprinted from *The American Journal of Medicine*, Volume 36, issue 4, Kenneth L. Melmon, Saul W. Rosen, Lindau's disease: Review of the literature and study of a large kindred, pp. 595–617, Copyright (1964), with permission from Elsevier.

Illustrative case

Case 38.6

A 33-year-old man presented with headaches, dizziness, and unsteadiness. Imaging identified a posterior fossa lesion with local mass effect (Fig. 38.6). He underwent surgical resection; histopathology confirmed haemangioblastoma and serum VHL mutation. He also underwent cryotherapy for retinal angioblastoma, and nephrectomy for renal cell carcinoma (RCC). His pancreatic and epididymal cysts are under observation, together with ongoing CNS surveillance.

Screening

One-third of CNS HGBs are VHL-associated. VHL-HGBs tend to present 10 years earlier than sporadic lesions. Patients with a new diagnosis of CNS HGB should have a thorough family history and clinical review for VHL-associated manifestations, and whole neuro-axis imaging. If VHL is suspected, the patient should be referred to a specialist centre for further evaluation. Once the diagnosis is confirmed surveillance screening can be commenced. Screening may include annual ophthalmological assessment for retinal angioma beginning in early childhood, cranial MRI for haemangioblastoma and abdominal MRI for renal cell carcinoma and pancreatic tumours beginning in adolescence, and annual blood pressure monitoring and urinary studies for phaeochromocytoma (Maher, 2004).

Clinical features

CNS HGBs occur in 60–80% of VHL patients (Richard et al., 2000; Wanebo et al., 2003) most frequently in the cerebellum, spinal canal and, less frequently, brainstem and nerve roots. Retinal HGBs occur in more than 50% of patients, are often the earliest manifestation of the disease and can cause sudden visual loss. Other associated lesions include visceral cysts (renal, pancreatic and epididymal cystadenomas which are common but rarely compromise organ function), RCC, adrenal and extra-adrenal phaeochromocytomas, non-functioning pancreatic endocrine cancers, endolymphatic sac tumours and, occasionally, head and neck paragangliomas. RCC is the most common malignancy and cause of death, followed by CNS HGB (Maher et al., 1990).

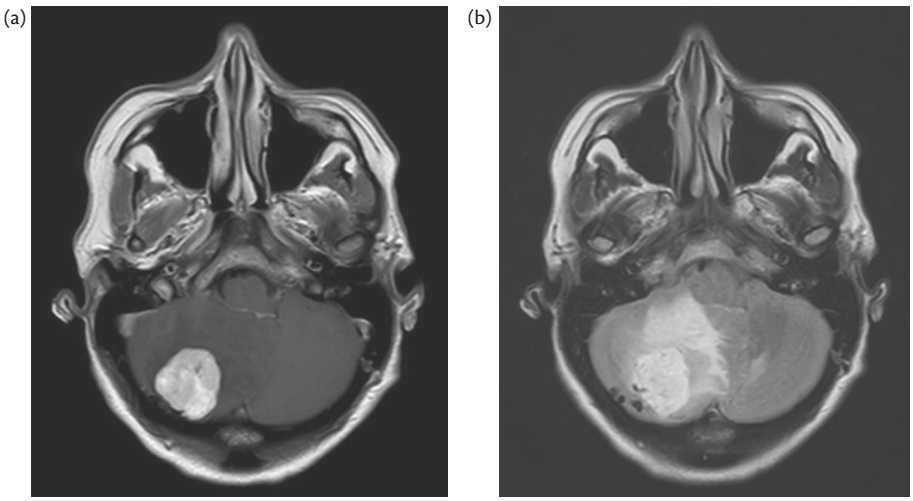

Fig. 38.6 (A) Contrast-enhanced, T1-weighted MRI showing solid enhancing HGB in right cerebellar hemisphere; (B) T2-weighted MRI showing solid lesion, associated flow voids and perilesional oedema, and local mass effect.

Management

VHL carries a lifetime risk of developing multiple organ tumours. Patients should be managed by a dedicated specialist VHL team. Surveillance should be undertaken to allow early detection and treatment of lesions. Complete surgical resection of accessible, symptomatic CNS HGBs is the mainstay of treatment. One study of 80 patients showed no recurrence after 61 months of follow-up (Jagannathan et al., 2008); others quote a recurrence rate of 17% at 53 months (Conway et al., 2001). Factors which influence the decision to proceed with surgery include neurological symptoms, evidence of growth on surveillance imaging (such that resection would be more difficult), or the presence of an enlarging cyst or syrinx (Lonser et al., 2003; Weil et al., 2003).

Preoperative work up should include MRI of the whole neuroaxis, investigation for phaeochromocytoma due to the risk of perioperative hypertensive crisis during anaesthesia, and consideration of preoperative embolization of the tumour.

When planning surgery for posterior fossa HGBs, consider external ventricular drainage and release of CSF, opening the cistern magna to further reduce CSF pressure, ultrasound-guided drainage of peritumoural or intratumoural cysts, intravenous mannitol, and/or furosemide and the use of transdural ultrasound to confirm the adequacy of bone removal for optimum exposure. The principle of resection of cystic HGBs is to remove the mural nodule in order to prevent recurrence of the cyst. The cyst wall itself does not need to be removed unless there is evidence of tumour within the cyst wall on MRI, or under direct vision at the time of surgery (Jagannathan et al., 2008). The standard principles of microsurgery should be applied to dissecting the tumour (i.e. define the plane between tumour margin and cerebellum circumferentially) and progressively dissect deeper tumour margins in layers. Vessels require coagulation and sharp division as they enter or leave the tumour capsule which is assisted by non-stick bipolar forceps. The tumour softens as the feeding supply is interrupted, and gentle retraction of the capsule becomes possible to enhance exposure and resection of the tumour.

VEGF is one of the downstream targets of the VHL protein. Sunitinib, a VEGF receptor inhibitor, is licensed for use in advanced metastatic renal cell carcinoma and has been tested for use in VHL-associated RCC. Its effect on CNS HGBs has not been proven, but research is ongoing (Jonasch et al., 2011). Stereotactic radiosurgery (SRS) may be considered for the management of surgically unresectable lesions. Few studies have yet determined the long-term safety and efficacy of the treatment (Asthagiri et al., 2010).

Controversy

SRS can be used to treat VHL-associated HGBs, less than 3cm^3 volume, tumours incompletely excised, or unresectable. It may minimize the number of surgical resections in an individual with multiple HGBs. Tumour control rates post-SRS range from 83% at 5 years, 61% at 10 years, 51% at 15 years (20 VHL patients with 44 HGBs) (Asthagiri et al., 2010) to 93% at 5 years, and 82% at 10 years (80 VHL patients with 335 HGBs) (Kano et al., 2015). Surgery, if without complication, is curative. Neurological status remains stable or improves following surgical resection (98% of patient improved at 3 months post-op cerebellar HGB resection (Lonser et al., 2003; Weil et al., 2003; Jagannathan et al., 2008).

Data from a retrospective review of 80 VHL patients showed new tumour development after SRS in 41% of patients at 67 months follow-up (rates of 7% at 1 year, 21% at 3 years, 43% at 5 years, 84% at 10 years) (Kano et al., 2015). This is comparable to new tumour formation in VHL without SRS (Wanebo et al., 2003; Ammerman et al., 2006).

As yet there are no reports of secondary malignancy or malignant transformation, but this should be considered. In a study of 186 patients with HGBs treated with SRS, only 13 (7%) developed adverse radiation effects, with one patient dying due to these side effects (Kano et al., 2015). However, this data was not defined as VHL or sporadic HGB patients. Patients with VHL are at risk of developing multiple HGBs and repeated radiotherapy is not always advisable.

Ataxia telangiectasia (AT)

AT is no longer classified as one of the neurophakomatoses. It has historically been included in neurosurgical texts due to its case report associations with some CNS tumours and with

angiographically occult capillary malformations. Unlike the other neurophakomatoses it is not associated with cutaneous or ocular manifestations, and it exhibits autosomal recessive inheritance. It is of most relevance to neurologists due to it causing cerebellar degeneration and progressive ataxia.

FURTHER READING

Evans, D.G.R. (2009). Neurofibromatosis type 2 (NF2): a clinical and molecular review. *Orphanet J Rare Dis*, **4**, 16.

Evans, D.G.R., Baser, M.E., O'Reilly, B., et al. (2005). Management of the patient and family with neurofibromatosis 2: a consensus conference statement. *Br J Neurosurg*, **19**(1), 5–12.

Ferner, R.E., Huson, S.M., Thomas, N., et al., (2007). Guidelines for the diagnosis and management of individuals with neurofibromatosis 1. *J Medical Genet*, **44**(2), 81–8.

Fisher, M.J., Loguidice, M., Gutmann, D.H., et al. (2012). Visual outcomes in children with neurofibromatosis type 1-associated optic pathway glioma following chemotherapy: a multicenter retrospective analysis. *Neuro Oncol*, **14**(6), 790–7.

Franz, D.N., Belousova, E., Sparagana, S., et al. (2013). Efficacy and safety of everolimus for subependymal giant cell astrocytomas associated with tuberous sclerosis complex (EXIST-1): a multicentre, randomised, placebo-controlled phase 3 trial. *Lancet*, **381**(9861), 125–32.

Krueger, D.A. & Northrup, H. (2013). Tuberous sclerosis complex surveillance and management: recommendations of the 2012 international tuberous sclerosis complex consensus conference. *Pediatr Neurol*, **49**(4), 255–65.

Maher, E.R., Neumann, H.P., & Richard, S. (2011). von Hippel-Lindau disease: a clinical and scientific review. *Eur J Hum Genet*, **19**(6), 617–23.

Northrup, H. & Krueger, D.A. (2013). Tuberous sclerosis complex diagnostic criteria update: recommendations of the 2012 International Tuberous Sclerosis Complex Consensus Conference. *Pediatr Neurol*, **49**(4), 243–54.

REFERENCES

Ammerman, J.M., Lonser, R.R., Dambrosia, J., Butman, J.A., & Oldfield, E.H. (2006). Long-term natural history of hemangioblastomas in patients with von Hippel-Lindau disease: implications for treatment. *J Neurosurg*, **105**(2), 248–55.

Asthagiri, A.R., Mehta, G.U., Zach, L., et al. (2010). Prospective evaluation of radiosurgery for hemangioblastomas in von Hippel-Lindau disease. *Neuro Oncol*, **12**(1), 80–6.

Baser, M.E., Evans, D.G.R., Jackler, R.K., Sujansky, E., & Rubenstein, A. (2000). Neurofibromatosis 2, radiosurgery and malignant nervous system tumours. *Br J Cancer*, **82**(4), 998.

Baser, M.E., Friedman, J.M., Joe, H., et al. (2011). Empirical development of improved diagnostic criteria for neurofibromatosis 2. *Genet Med*, **13**(6), 576–81.

Conway, J.E., Chou, D., Clatterbuck, R.E., Brem, H., Long, D.M., & Rigamonti, D. (2001). Hemangioblastomas of the central nervous system in von Hippel-Lindau syndrome and sporadic disease. *Neurosurgery*, **48**(1), 55–63.

Curatolo, P., Bombardieri, R., & Cerminara, C. (2006). Current management for epilepsy in tuberous sclerosis complex. *Curr Opin Neurol*, **19**(2), 119–23.

Curatolo, P., Bombardieri, R., & Jozwiak, S. (2008). Tuberous sclerosis. *Lancet*, **372**(9639), 657–68.

Dodgshun, A.J., Elder, J.E., Hansford, J.R., & Sullivan, M.J. (2015). Long-term visual outcome after chemotherapy for optic pathway glioma in children: site and age are strongly predictive. *Cancer*, **121**(23), 4190–6.

Evans, D.G., Huson, S.M., Donnai, D., et al. (1992). A clinical study of type 2 neurofibromatosis. *Q J Med*, **84**(304), 603–18.

Evans, D.G.R., Baser, M.E., McGaughran, J., Sharif, S., Howard, E., & Moran, A. (2002). Malignant peripheral nerve sheath tumours in neurofibromatosis 1. *J Med Genet*, **39**(5), 311–14.

Evans, D.G.R., Baser, M.E., O'Reilly, B., et al. (2005). Management of the patient and family with neurofibromatosis 2: a consensus conference statement. *Br J Neurosurg*, **19**(1), 5–12.

Evans, D.G.R., Birch, J.M., Ramsden, R.T., Sharif, S., & Baser, M.E. (2006). Malignant transformation and new primary tumours after therapeutic radiation for benign disease: substantial risks in certain tumour prone syndromes. *J Med Genet*, **43**(4), 289–94.

Evans, D.G.R. (2009). Neurofibromatosis type 2 (NF2): a clinical and molecular review. *Orphanet J Rare Dis*, **4**, 16.

Evans, D.G., King, A.T., Bowers, N.L., et al. (2018). Identifying the deficiencies of current diagnostic criteria for neurofibromatosis 2 using databases of 2777 individuals with molecular testing. *Genet Med*. doi: 10.1038/s41436-018-0384-y [Epub ahead of print]

Fallah, A., Guyatt, G.H., Carter Snead, O., et al. (2015). Resective epilepsy surgery for tuberous sclerosis in children: determining predictors of seizure outcomes in a multicenter retrospective cohort study. *Neurosurg*, **77**(4), 517–24.

Ferner, R.E., Huson, S.M., Thomas, N., et al., (2007). Guidelines for the diagnosis and management of individuals with neurofibromatosis 1. *J Medical Genet*, **44**(2), 81–8.

Fisher, M.J., Loguidice, M., Gutmann, D.H., et al. (2012). Visual outcomes in children with neurofibromatosis type 1-associated optic pathway glioma following chemotherapy: a multicenter retrospective analysis. *Neuro Oncol*, **14**(6), 790–7.

Franz, D.N., Leonard, J., Tudor, C., et al. (2006). Rapamycin causes regression of astrocytomas in tuberous sclerosis complex. *Ann Neurol*, **59**(3), 490–8.

Franz, D.N., Belousova, E., Sparagana, S., et al. (2013). Efficacy and safety of everolimus for subependymal giant cell astrocytomas associated with tuberous sclerosis complex (EXIST-1): a multicentre, randomised, placebo-controlled phase 3 trial. *Lancet*, **381**(9861), 125–32.

Fryer, A.E., Chalmers, A., Connor, J.M., et al. (1987). Evidence that the gene for tuberous sclerosis is on chromosome 9. *Lancet*, **1**, 659–62.

Golfinos, J.G., Hill, T.C., Rokosh, R., et al. (2016). A matched cohort comparison of clinical outcomes following microsurgical resection or stereotactic radiosurgery for patients with small- and medium-sized vestibular schwannomas. *J Neurosurg*, **125**(6), 1472–82.

Gottfried, O.N., Viskochil, D.H., & Couldwell, W.T. (2010). Neurofibromatosis type 1 and tumorigenesis: molecular mechanisms and therapeutic implications. *Neurosurg Focus*, **28**(1), E8.

Jagannathan, J., Lonser, R.R., Smith, R., DeVroom, H.L., & Oldfield, E.H. (2008). Surgical management of cerebellar hemangioblastomas in patients with von Hippel-Lindau disease. *J Neurosurg*, **108**, 210–22.

Jansen, F.E., van Huffelen, A.C., Algra, A., & van Nieuwenhuizen, O. (2007). Epilepsy surgery in tuberous sclerosis: a systematic review. *Epilepsia*, **48**(8), 1477–84.

Jett, K. & Friedman, J.M. (2010). Clinical and genetic aspects of neurofibromatosis 1. *Genet Med*, **12**(1), 1–11.

Jonasch, E., McCutcheon, I.E., Waguespack, S.G., et al. (2011). Pilot trial of sunitinib therapy in patients with von Hippel-Lindau disease. *Ann Oncol*, **22**(12), 2661–6.

Jozwiak, J., Jozwiak, S., & Oldak, M. (2006). Molecular activity of sirolimus and its possible application in tuberous sclerosis treatment. *Med Res Rev*, **26**(2), 160–80.

Kandt, R.S., Haines, J.L., Smith, M., et al. (1992). Linkage of an important gene locus for tuberous sclerosis to a chromosome 16 marker for polycystic kidney disease. *Nat Genet*, **2**(1), 37–41.

Kano, H., Shuto, T., Iwai, Y., et al. (2015). Stereotactic radiosurgery for intracranial hemangioblastomas: a retrospective international outcome study. *J Neurosurg*, **122**(June), 1–10.

Kleinerman, R.A. (2009). Radiation-sensitive genetically susceptible pediatric sub-populations. *Pediatr Radiol*, **39**(Suppl 1), S27–S31.

Krueger, D., Care, M.M., Holland, K., et al. (2010). Everolimus for subependymal giant-cell astrocytomas in tuberous sclerosis. *N Engl J Med*, **363**(19), 1801–11.

Krueger, D.A. & Northrup, H. (2013). Tuberous sclerosis complex surveillance and management: recommendations of the 2012 international tuberous sclerosis complex consensus conference. *Pediatr Neurol*, **49**(4), 255–65.

Latif, F., Tory, K., Gnarra, J., et al. (1993). Identification of the von Hippel-Lindau disease tumor suppressor gene. *Science (New York, N.Y.)*, **260**(5112), 1317–20.

Lee, A.G. (2007). Neuroophthalmological management of optic pathway gliomas. *Neurosurg Focus*, **23**(5), E1.

Listernick, R., Ferner, R.E., Liu, G.T., & Gutmann, D.H. (2007). Optic pathway gliomas in neurofibromatosis-1: controversies and recommendations. *Ann Neurol*, **61**(3), 189–98.

Lonser, R.R., Weil, R.J., Wanebo, J.E., DeVroom, H.L., & Oldfield, E.H. (2003). Surgical management of spinal cord hemangioblastomas in patients with von Hippel-Lindau disease. *J Neurosurg*, **98**(1), 106–16.

Maher, E.R., Yates, J.R., Harries, R., et al. (1990). Clinical features and natural history of von Hippel-Lindau disease. *Q J Med*, **77**(283), 1151–63.

Maher, E.R. (2004). Von Hippel-Lindau disease. *Curr Mol Med*, **4**(8), 833–42.

Maher, E.R., Neumann, H.P., & Richard, S. (2011). von Hippel-Lindau disease: a clinical and scientific review. *Eur J Hum Genet*, **19**(6), 617–23.

Mahoney, D.H., Cohen, M.E., Friedman, H.S., et al. (2000). Carboplatin is effective therapy for young children with progressive optic pathway tumors: a pediatric oncology group phase II study. *Neuro Oncol*, **2**(4), 213–20.

Mallory, G.W., Pollock, B.E., Foote, R.L., Carlson, M.L., Driscoll, C.L., & Link, M.J. (2014). Stereotactic radiosurgery for neurofibromatosis 2—associated vestibular schwannomas. *Neurosurg*, **74**(3), 292–301.

Mathieu, D., Kondziolka, D., Flickinger, J.C., et al. (2007). Stereotactic radiosurgery for vestibular schwannomas in patients with neurofibromatosis type 2: an analysis of tumor control, complications, and hearing preservation rates. *Neurosurg*, **60**(3), 460–8.

Melmon, K.L. & Rosen, S.W. (1964). Lindau's disease: review of the literature and study of a large kindred. *Am J Med*, **36**(4), 595–617.

Mohyuddin A, Wallace, A., Wu, C., et al. (2002). Molecular genetic analysis of the NF2 gene in young patients with unilateral vestibular schwannomas. *J Med Genet*, **39**(5), 315–22.

National Institutes of Health Consensus (1988). Neurofibromatosis. Conference statement. National Institutes of Health Consensus Development Conference. *Arch Neurol*, **45**(5), 575–8.

NCT01158651, N.C.T.C. (2010). *Study of RAD001 (Everolimus) for Children with NF1 and Chemotherapy-refractory Radiographic Progressive Low-grade Gliomas*. https://www.clinicaltrials.gov/show/NCT01158651

NCT01767792, N.C.T.C. (2013). *Phase 2 Study of Bevacizumab in Children and Young Adults With NF 2 and Progressive Vestibular Schwannomas*. https://www.clinicaltrials.gov/show/NCT01767792

Northrup, H. & Krueger, D.A. (2013). Tuberous sclerosis complex diagnostic criteria update: recommendations of the 2012 International Tuberous Sclerosis Complex Consensus Conference. *Pediatr Neurol*, **49**(4), 243–54.

Nunes, F.P., Merker, V.L., Jennings, D., et al. (2013). Bevacizumab treatment for meningiomas in NF2: a retrospective analysis of 15 patients. *PLoS One*, **8**(3), e59941.

O'Callaghan, F.J., Shiell, A.W., Osborne, J.P., & Martyn, C.N. (1998). Prevalence of tuberous sclerosis estimated by capture-recapture analysis. *Lancet*, **351**(9114), 1490.

Parry, D.M., Eldridge, R., Kaiser-Kupfer, M.I., Bouzas, E.A., Pikus, A., & Patronas, N. (1994). Neurofibromatosis 2 (NF2): clinical characteristics of 63 affected individuals and clinical evidence for heterogeneity. *Am J Med Genet*, **52**(4), 450–61.

Phi, J.H., Kim, D.G., Chung, H.T., Lee, J., Paek, S.H., & Jung, H.W. (2009). Radiosurgical treatment of vestibular schwannomas in patients with neurofibromatosis type 2: tumor control and hearing preservation. *Cancer*, **115**(2), 390–8.

Plotkin, S.R., Merker, V.L., Halpin, C., et al. (2012). Bevacizumab for progressive vestibular schwannoma in neurofibromatosis type 2: a retrospective review of 31 patients. *Otol Neurotol*, **33**(6), 1046–52.

Plowman, P.N. & Evans, D.G.R. (2000). Stereotactic radiosurgery XI. Acoustic neuroma therapy and radiation oncogenesis. *BrJ Neurosurg*, **14**(2), 93–5.

Richard, S., Marsot-Dupuch, K., Giraud, S., Béroud, C., & Resche, F. (2000). Central nervous system hemangioblastomas, endolymphatic sac tumors, and von Hippel-Lindau disease. *Neurosurg Rev*, **23**(1), 1–22; discussion 23–4.

Rosser, T. & Packer, R.J. (2002). Intracranial neoplasms in children with neurofibromatosis 1. *J Child Neurol*, **17**(8), 630–7; discussion 646–51.

Rouleau, G., Merel, P., Lutchman, M., et al. (1993). Alteration in a new gene encoding a putative membrane-organizing protein causes neuro-fibromatosis type 2. *Nature*, **363**(6429), 515–21.

Rowe, J., Grainger, A.C., Walton, L., & Radatz, M. (2007). Safety of radiosurgery applied to conditions with abnormal tumor suppressor genes. *Neurosurgery*, **60**(5), 860–3.

Rowe, J.G., Radatz, M.W., Walton, L., Soanes, T., Rodgers, J., & Kemeny, A.A. (2003). Clinical experience with gamma knife stereotactic radiosurgery in the management of vestibular schwannomas secondary to type 2 neurofibromatosis. *J Neurol Neurosurg Psychiatry*, **74**(9), 1288–93.

Sampson, J.R., Scahill, S.J., Stephenson, J.B., Mann, L., & Connor, J.M. (1989). Genetic aspects of tuberous sclerosis in the west of Scotland. *J Med Genet*, **26**(1), 28–31.

Schwartz, R.A., Fernández, G., Kotulska, K., & Jóźwiak, S. (2007). Tuberous sclerosis complex: advances in diagnosis, genetics, and management. *J Am Acad Dermatol*, **57**(2), 189–202.

Sharif, S., Ferner, R., Birch, J.M., et al. (2006). Second primary tumors in neurofibromatosis 1 patients treated for optic glioma: substantial risks after radiotherapy. *J Clin Oncol*, **24**(16), 2570–5.

Sharif, S., Moran, A., Huson, S.M., et al. (2007). Women with neurofibromatosis 1 are at a moderately increased risk of developing breast cancer and should be considered for early screening. *J Med Genet*, **44**(8), 481–4.

Sharma, M.S., Singh, R., Kale, S.S., Agrawal, D., Sharma, B.S., & Mahapatra, A.K. (2010). Tumor control and hearing preservation

after gamma knife radiosurgery for vestibular schwannomas in neurofibromatosis type 2. *J Neurooncol*, **98**(2), 265–70.

Subach, B.R., Kondziolka, D., Lunsford, L.D., Bissonette, D.J., Flickinger, J.C., & Maitz, A.H. (1999). Stereotactic radiosurgery in the management of acoustic neuromas associated with neurofibromatosis type 2. *J Neurosurg*, **90**(5), 815–22.

Tee, A.R., Fingar, D.C., Manning, B.D., Kwiatkowski, D.J., Cantley, L.C., & Blenis, J. (2002). Tuberous sclerosis complex-1 and -2 gene products function together to inhibit mammalian target of rapamycin (mTOR)-mediated downstream signaling. *Proc Natl Acad Sci U S A*, **99**(21), 13571–6.

Trofatter, J.A., MacCollin, M.M., Rutter, J.L., et al. (1993). A novel moesin-, ezrin-, radixin-like gene is a candidate for the neurofibromatosis 2 tumor suppressor. *Cell*, **72**(5), 791–800.

Viskochil, D., Buchberg, A.M., Xu, G., et al. (1990). Deletions and a translocation interrupt a cloned gene at the neurofibromatosis type 1 locus. *Cell*, **62**(1), 187–92.

Walker, L., Thompson, D., Easton, D., et al. (2006). A prospective study of neurofibromatosis type 1 cancer incidence in the UK. *Br J Cancer*, **95**(2), 233–8.

Wanebo, J.E., Lonser, R.R., Glenn, G.M., & Oldfield, E.H. (2003). The natural history of hemangioblastomas of the central nervous system in patients with von Hippel-Lindau disease. *J Neurosurg*, **98**(1), 82–94.

Weil, R.J., Lonser, R.R., DeVroom, H.L., Wanebo, J.E., & Oldfield, E.H. (2003). Surgical management of brainstem hemangioblastomas in patients with von Hippel-Lindau disease. *J Neurosurg*, **98**(1), 95–105.

39

Uncommon brain lesions

Yizhou Wan, Hani J. Marcus, and Thomas Santarius

Introduction

In this chapter we discuss neurosurgical tumours, which are uncommon and have not been covered elsewhere.

Due to their rarity this chapter reviews what is known about these conditions and primarily discusses their diagnosis. The description of management is derived largely from published case series.

Choristoma

Choristoma is a mass of heterotopic tissue (i.e. 'normal' tissue) present in an abnormal location (Lee and Roland, 2013). The presence of histologically normal tissue differentiates these lesions from hamartomas, one example of which is dysplastic gangliocytoma of the cerebellum (L'hermitte-Duclos disease). Epidermoid and dermoid tumours are the most well-known intracranial choristomas and are the subject of a separate chapter. Several rarer choristomas have been found in the nervous system, such as intracranial pancreatic (Heller et al., 2010), salivary gland (Hintz et al., 2014), and neuromuscular tissue masses (Hebert-Blouin et al., 2012). Salivary gland choristomas located in the sella have been well-described (Hintz et al., 2014). Other common locations include major peripheral nerves, such as the brachial plexus and sciatic nerve for neuromuscular choristomas (Hebert-Blouin et al., 2013).

Neural choristomas are exceedingly rare and the most commonly found in the head and neck region, especially in the nose (*nasal gliomas)*. Other areas include the trunk and back, where they usually present as isolated asymptomatic masses (Downing et al., 1997). Patients can present from early childhood onwards and the mean age of presentation for neural choristomas is approximately 10 years of age (Hebert-Blouin et al., 2012).

Pathology

Histology of choristomas depends on their tissue of origin. Neural choristomas may comprise of a disorganized population of glial cells in a fibrous background, alternatively they may represent mature neural tissue resembling cerebral or cerebellar cortex (Downing et al., 1997). Neuromuscular choristomas (NMC) are composed of an admixture of mature striated and smooth muscle cells with nerve fibres, typically the sciatic and brachial nerves, although involvement of cranial nerves such as the optic, maxillary, oculomotor, facial and vestibulocochlear nerves have also been described (Hebert-Blouin et al., 2012).

Management

Clinical presentation depends on anatomical location. For example, salivary gland choristomas in the sella can cause hormone deficits whereas suprasellar extension can cause headaches or visual disturbances (Hebert-Blouin et al., 2012). NMCs may cause pain, weakness, and sensory changes when they produce a mass effect along the course of a peripheral nerve or result in sensory or motor deficits. Intracranially they are commonly found in the acoustic meatus or cerebellopontine angle, mimicking vestibular schwannomas on imaging (Boyaci et al., 2011). Radiological findings of NMC are non-specific and may be indistinguishable from schwannomas (Boyaci et al., 2011). Preoperative imaging is important to identify any potential connections between neural choristomas and the central nervous system (Downing et al., 1997). Malignant transformation of neural choristomas has never been reported (Newman et al., 1986).

Prognosis

The rarity of these tumours means that their natural history is not well elucidated. It can generally be thought of as a 'slow-growing' lesion and treatment can be conservative (Boyaci et al., 2011). Some authors have advocated complete resection (Awasthi et al., 1991).

Hamartoma

Hamartoma is a tumour made of tissue components normally found in that anatomical site, but the tissue architecture is disorganized. Cysts and pseudocysts will be described in other chapters, this section describes other lesions found in the central nervous system including, dysplastic gangliocytoma of the cerebellum (L'hermitte-Duclos disease), cortical glioneuronal hamartomas, and hypothalamic hamartomas. Common to all these lesions are that they may represent developmental malformations, but may be mistaken for more common tumour or cystic lesions.

Epidemiology

Since the first description in 1920 more than 230 cases of L'hermitte-Duclos disease (LDD) have been described in the literature. It can present from birth to the sixth decade with no gender predilection. It has been suggested that there is a genetic association between LDD and Cowden syndrome. Cowden syndrome is an autosomal dominant hamartoma-neoplasia complex presenting with neoplasia and hamartomas of the breast, thyroid, genitourinary tract, and endometrium (Nowak and Trost, 2002).

Among the CNS manifestations of tuberous sclerosis complex (TSC), an important diagnostic criterion is the presence of cortical glioneuronal hamartomas (tubers). TSC is an autosomal dominant multisystem disorder caused by mutations in genes encoding tuberculin and harmaline, proteins involved in cell proliferation and differentiation. They cause benign non-invasive lesions in any organ system (Curatolo and Maria, 2013). It occurs at a birth rate of 1 in 6000 (Kwiatkowski and Manning, 2005).

Hypothalamic hamartomas have a prevalence of 1 in 50 000 to 1 in 100 000 (Weissenberger et al., 2001).

Pathology

LDD is characterized by regional thickening of the cerebellar folia, caused by dysplastic replacement of cerebellar Purkinje and granular cells with hamartomatous overgrowth of hypertrophic ganglion cells (Wei et al., 2014). Microscopically there are abnormal ganglion cells in the granular cell layer with thickening and hypermyelination of the molecular cell layer, and absence of the Purkinje cell layer (Ozeren et al., 2014). There may also be the presence of calcification and ectatic vessels on histopathology but no pleomorphism or mitoses (Wei et al., 2014).

In TSC *cortical tubers* are characterized by proliferation of glial and neuronal cells and the loss of the six-layer cortical structure. Within tubers a variety of abnormal cells are found, predominantly, bizarrely shaped astrocytes, giant cells, and dysplastic neurons. A further characteristic finding is that of *subependymal nodules*, hamartomas growths which can protrude into the wall of the lateral ventricle near the foramen of Monroe. These can slowly grow into *subependymal giant-cell astrocytomas* (SEGAs), the most common cerebral tumours found in TSC (Curatolo and Maria, 2013).

Hypothalamic hamartomas are developmental disorders affecting the hypothalamic area between the infundibulum and the mammillary bodies (Striano et al., 2012).

Management

Patients with LDD are initially asymptomatic, but as the tumour slowly increases in size patients usually present with vague neurological complaints related to unilateral cerebellar dysfunction for as long as 15 years (Ozeren et al., 2014). Occasionally patients can present with acute decompensation from occlusive hydrocephalus (Nowak and Trost, 2002).

MRI is fairly characteristic and can be used to diagnose LDD, especially in the context of Cowden's disease. Enlarged cerebellar folia lose their secondary folding and lead to asymmetrical widening of the cerebellar hemispheres. The lesions are non-enhancing and display a characteristic pattern of isointense bands within a discrete lesion of hypointensity on T2-weighted imaging (Fig. 39.1). This indicates widened gyri and displaced sulci structure in expanded cerebellar cortex (Nowak and Trost, 2002).

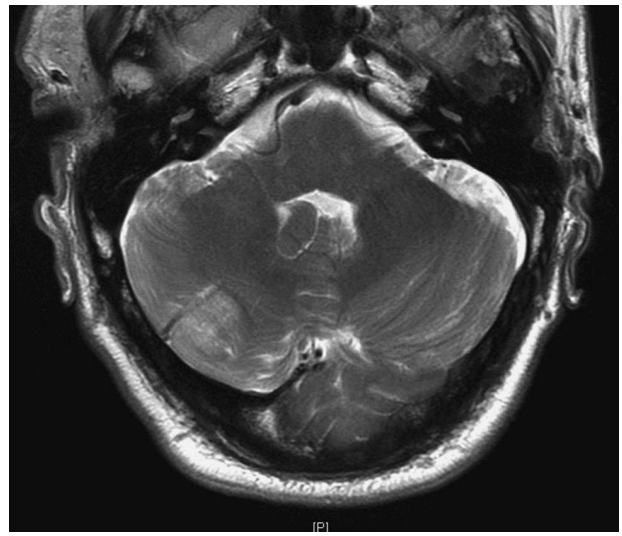

Fig. 39.1 L'hermitte-Duclos disease. Abnormal tissue involves the cerebellar cortex, appearing hyperintense on T2 with widening of cerebellar folia.

It may prove to be difficult for symptomatic LDD to be resected because the lesions blend into normal cerebellar parenchyma. Intraoperative MRI or/and intraoperative histological demonstration of a transition zone on histopathology maybe helpful.

The clinical manifestations of TSC are protean and related to the systemic effects of the condition. From a neurological perspective, the management focuses on controlling epilepsy. This generally occurs in the first year of life, evolving from focal seizures to infantile spasms. Subependymal giant-cell tumours are treated with mTOR pathway inhibitors or surgically (Franz et al., 2006).

Classically the hallmarks of hypothalamic hamartomas are gelastic seizures, developmental delay, and precocious puberty. MRI usually demonstrates a lesion with a vertical plane of attachment within the third ventricle and/or a horizontal plane of attachment on the underside of the hypothalamus (Fig. 39.2).

These lesions appear to have an intrinsic epileptogenicity (Maixner, 2006). Surgical resection has been reported to improve symptoms and seizure control (Palmini et al., 2002). Complete resection can be challenging and because it is difficult to predict the severity of a patient's epileptic course, the optimal timing of surgery is unclear (Maixner, 2006).

Prognosis

Due to the progressive growth of LDD lesions surgical resection is usually required but recurrence is common due to the difficulties in achieving a complete resection (Ozeren et al., 2014).

In TSC renal complications such as angiomyolipomas, renal cysts and renal cell carcinoma are the most frequent cause of the death (Curatolo and Maria, 2013).

Harvey et al. reported in their case series of 29 hypothalamic hamartoma patients that 15 patients achieved seizure-freedom and seven patients achieved 90% reduction in seizures over a follow-up of one to six years (mean 2.5 years). Complications of surgery included, injury to the optic tract, meningitis, communicating hydrocephalus and ischaemic infarction to the thalamus (Harvey et al., 2003).

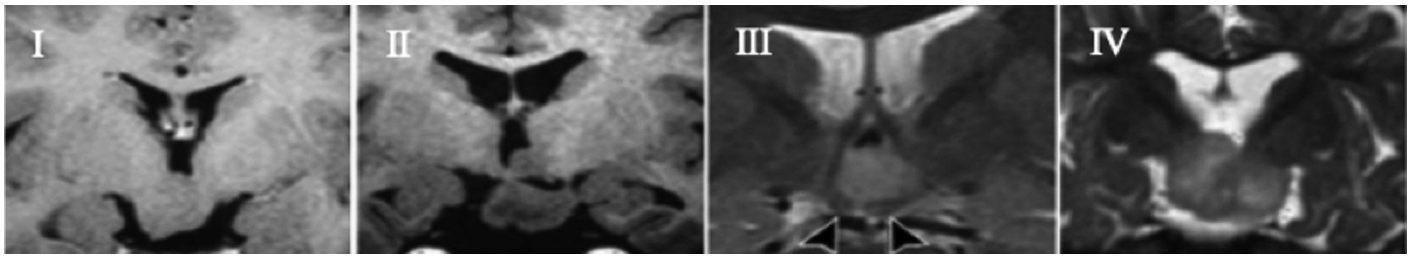

Fig. 39.2 Delalande classification of hypothalamic hamartomas: type I has a horizontal orientation; type II has a vertical orientation; type III has both a horizontal and vertical component; and type IV is a giant hamartoma.

Adapted from Endoscopic Treatment of Hypothalamic Hamartomas. *J Korean Neurosurg Soc.* 2017; 60(3): 294–300. doi: 10.3340/jkns.2017.0101.005, which is published under a Creative Commons License.

Pituicytoma, granular cell tumour (GCT), and spindle cell oncocytoma (SCO)

The 2007 WHO Classification of Tumours of the Central Nervous System describes a spectrum of benign (WHO grade I) non-adenomatous pituitary tumours including pituicytoma, GCT, and SCO (Louis et al., 2007; Covington et al., 2011).

Epidemiology

Non-adenomatous pituitary tumours are rare, with a recent meta-analysis identifying 112 cases in the literature (Covington et al., 2011). The average age at diagnosis is between 50 and 60 years, with a slight male preponderance for pituicytoma, and female preponderance for GCT and SCO (Covington et al., 2011; Pirayesh Islamian et al., 2012).

Pathology

Pituicytoma arises from pituicytes, specialized glial cells of the posterior lobe and the stalk of the pituitary gland (Zygourakis et al., 2015). Histologically, pituicytoma is characterized by elongated, bipolar spindle cells (Brat et al., 2007).

GCT arises from granular pituicytes, and are composed of polygonal eosinophilic granular cells that are strongly PAS positive due to abundant intracytoplasmic lysosomes (Orning et al., 2013). SCO also arises from pituicytes and are characterized by interlacing fascicles of spindled-to-epithelioid cells with mitochondrial accumulation seen on ultrastructural analysis (Zygourakis et al., 2015).

Management

The most common presenting symptom of patients with non-adenomatous pituitary tumours is visual disturbance (e.g. bitemporal hemianopsia) (Covington et al., 2011). Other symptoms include headache fatigue, and those related to hypopituitarism (e.g. decreased libido). Diabetes insipidus is rare.

Several features on MRI can aid diagnosis (Fig. 39.3) (Covington et al., 2011): pituicytoma may be considered if the lesion is purely intrasellar and clearly separate from the pituitary gland; GCT may be considered if the lesion is suprasellar or mixed supra- and intrasellar, and clearly separate from the pituitary gland; and SCO may be considered if the lesion is mixed supra- and intrasellar, but the mass cannot be separated for the pituitary gland. Compared to GCT and SCO, Pituicytomas more frequently demonstrate homogenous rather than heterogenous enhancement on T1-weighted images. (Covington et al., 2011).

In practice, these lesions may be difficult to distinguish from pituitary adenoma, and transsphenoidal surgical resection is generally considered safe and effective (Zygourakis et al., 2015). However, because these lesions are firm and may be highly vascular, some authors have advocated the use of preoperative embolization in

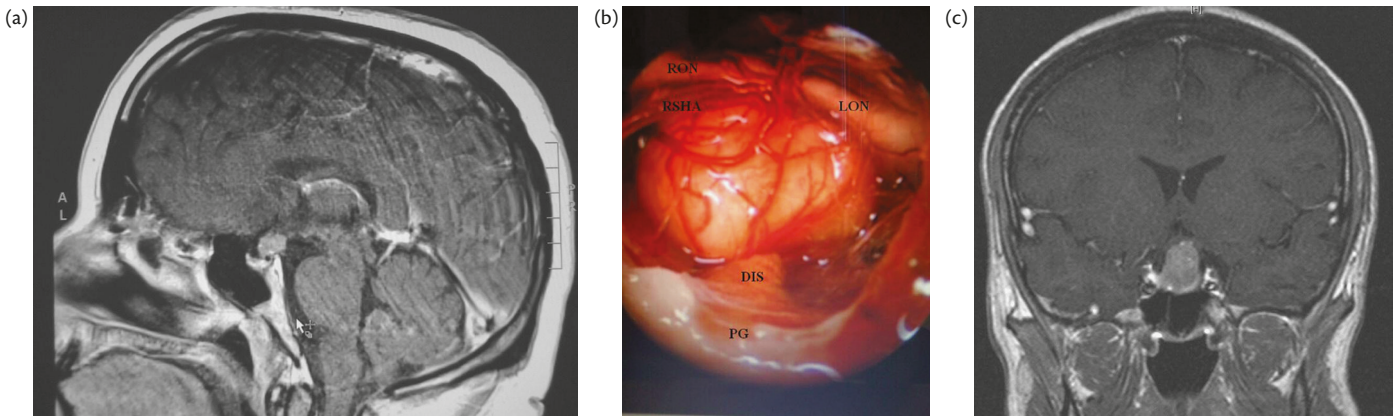

Fig. 39.3 Granular cell tumour (GCT) of the pituitary. (A) MRI (T1 with contrast) showing a GCT of the pituitary stalk. In this case the tumour is separate from the pituitary gland and the diagnosis of should be considered. (B) Transsphenoidal endoscopic approach—intraoperative photograph demonstrating the separation of the tumour from the pituitary gland as seen on the MRI. (C) Granular cell tumour of the pituitary—in this case not distinguishable from a much more common pituitary adenoma or the much rarer primary non-adenomatous pituitary gland tumours (i.e. pituicytoma and spindle cell oncocytoma, SCO).

selected cases (Wolfe et al., 2008). The role of adjuvant therapy remains unclear (Zygourakis et al., 2015).

Prognosis

Non-adenomatous pituitary tumours are generally benign and surgical resection may be curative.

Gangliocytoma

Gangliocytomas are usually considered alongside gangliogliomas as a spectrum of intra-axial tumours originating in the grey matter. Gangliocytomas differ from gangliogliomas by their noted absence of a glial component and consist of abnormal mature ganglion cells (WHO grade I).

Epidemiology

They account for 0.1–0.5% of all brain tumours and occur in children and young adults (Koeller and Henry, 2001).

Pathology

They are found in decreasing incidence in the temporal lobe, cerebellum, parieto-occipital region, frontal lobe, hypothalamus adjacent to the third ventricle and spinal cord (Koeller and Henry, 2001).

Intraoperative smear histology shows ganglion cells with vesicular nuclei and prominent nucleoli. One can differentiate between gangliocytoma and infiltrating glioma with entrapped neurons by the presence of variable-sized neoplastic ganglion cells which form clusters and have abnormal branching of apical dendrites.

Management

They present as a result of mass effect or seizures. There is possibly a long history of symptoms and it is important to consider their diagnosis because of their favourable prognosis postresection.

Non-enhanced CT demonstrates hyperattenuation and no vasogenic oedema. MRI appearances show low signal intensity on T1-weighted images and mixed signal intensity on T2-weighted images (Shin et al., 2002). These features make differentiation between gangliogliomas and gangliocytomas challenging.

Prognosis

Malignant transformation is uncommon, it is more likely to be seen with gangliogliomas and is due to the glial/astrocytic component showing increased cellularity, mitosis, and necrosis (Adesina and Rauch, 2010).

Paraganglioma

Tumours derived from chromaffin cells (themselves derived from neural crest cells) are known as paragangliomas regardless of their anatomical location. Intra-adrenal paragangliomas are called phaeochromocytomas. The most common location for extra-adrenal parasympathetic paragangliomas is in the head and neck. The most common location here is the carotid body at the bifurcation of the internal jugular and external jugular veins, where they are known as chemodectomas. Intracranially, paragangliomas occur in the region of the jugular foramen and glomus jugulare tumour is the most commonly used term to describe them. Glomus jugulare consists of one or more bodies, found in the aventitia of the dome of the jugular bulb. Glomus jugulare tumours can be found anywhere along the course of the internal jugular vein.

Epidemiology

The incidence of chemodectoma is less than 1 in 3000 (Gad et al., 2014). They are ten times more common in people living at high-altitudes (Athanasiou et al., 2007). This may be related to hypoxia-induced hyperplasia of the catecholamine-secreting chief cells (Knight et al., 2006). The mean age of onset is 45 years (Kotelis et al., 2009).

Glomus jugulare tumours are rare, comprising 0.6% of tumours in the head and neck. They are two to three times more common in women than they are in men (Lee et al., 2002).

Pathology

Chemodectomas are genetically heterogeneous. They can occur sporadically or as part of a neoplastic syndrome, such as multiple endocrine neoplasia II, neurofibromatosis I, and von Hippel-Lindau disease (Knight et al., 2006). Four different genetic susceptibility loci have been mapped in chemodectomas. They demonstrate autosomal dominant inheritance with age and hypoxia-related penetrance. Mutations in three of these genes encode for subunits of the enzyme succinate dehydrogenase complex (Knight et al., 2006).

Histology of chemodectoma demonstrates mostly chief cells, arranged in a characteristic pseudoalveolar pattern known to as 'cell balls' (Zellballen) (Athanasiou et al., 2007).

Histologically glomus jugulare tumours are composed of epithelioid or chief cells in a hypervascular stroma, surrounded by a thin capsular layer (Guild, 1953).

Management

Patients with chemodectomas typically present with a lateral neck mass, with or without involvement of the lower cranial nerves (8 to 12) (Knight et al., 2006).

Glomus jugulare tumours are slow-growing and there may be significant latency prior to diagnosis. Signs and symptoms include unilateral deafness, tinnitus, hoarseness, dysphagia, headache, and lower cranial nerve palsies (Watkins et al., 1994). In 10–20% of cases they can be multifocal and although generally benign, local invasion and metastasis to liver, lung, lymph nodes, and spleen have been reported. Preoperative workup should include MRI and CT to identify extent of bone involvement.

In contrast with phaeochromocytomas and extra-adrenal sympathetic paragangliomas, head and neck paragangliomas rarely produce significant amounts of catecholamine (Chen et al., 2010). This makes preoperative optimization of these patients less challenging from the neuroendocrine perspective.

Workup with imaging is crucial for surgical success as location renders chemodectomas technically challenging and biopsy is hazardous. Tumour enlargement typically splays the internal and external carotid arteries but does not lead to narrowing of their diameters (Wieneke and Smith, 2009). The differential diagnoses include vagal schwannomas and neurofibromas, glomus vagale tumours, and lymph node masses. Lymph nodes are not typically hypervascular, glomus vagale tumours occur more rostrally, and

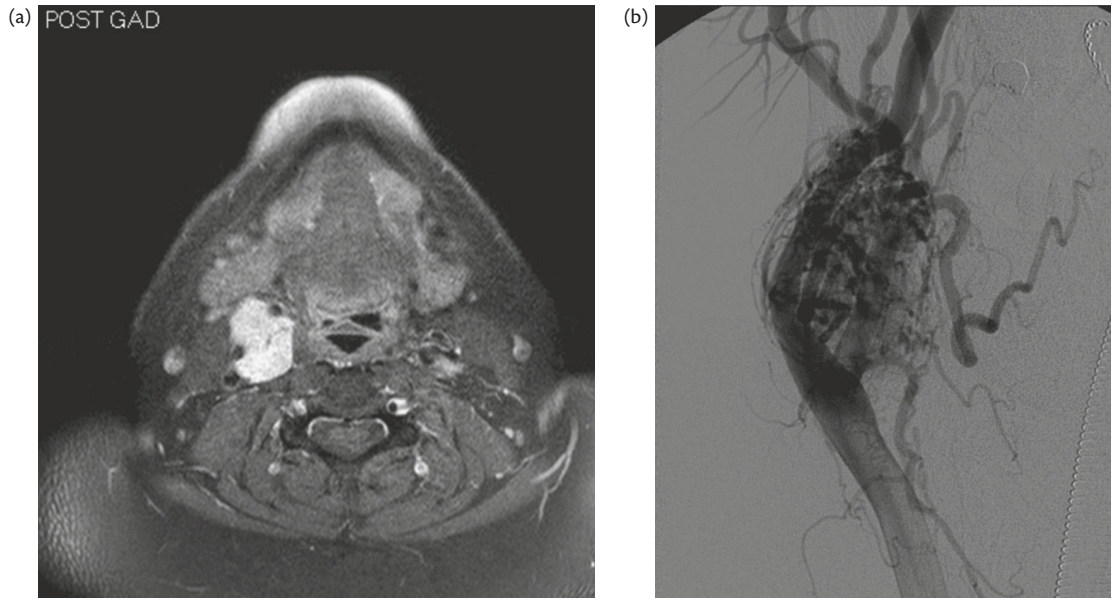

Fig. 39.4 Chemodectoma. A 59-year-old lady presented with right-sided otalgia. (A) T1W Axial MRI with gadolinium demonstrates splaying of the internal and external carotid arteries which differentiate paragangliomas from other lesions such as schwannomas and neurofibromas. (B)The lesion was resected with no complications after preoperative embolization demonstrated, extensive vascular supply from hypertrophic branches of the right ascending pharyngeal artery. ECA, external carotid artery; ICA, internal carotid artery; IJV, internal jugular vein.

vagal masses tend to displace both the carotid vessels together rather than to splay them (Fig. 39.4).

Larger tumours as much as 10 cm in diameter are more likely to encase the carotid artery. In these circumstances, neoadjuvant radiotherapy can be used to down-stage the tumours and improve resectability. Intraoperatively, internal carotid artery reconstruction with end-to-end anastomosis may be performed (Gad et al., 2014).

Historically, approaches to management of glomus jugulare tumours have been microsurgical. The median tumour doubling time has been reported to be four years or longer, but aggressive tumours exist and older patients may cope less well with its symptoms (Kemeny, 2009). Resection approaches depend on size and location and may include combined otological and neurosurgical approaches (Watkins et al., 1994).

Stereotactic radiosurgery's obvious advantages in terms of minimizing radiation damage to critical structures at the skull base have to be balanced against its limitations. Relative contraindications of radiosurgery include large tumours, typically a maximal of 3–4 cm field size and lack of radiological boundaries at the skull base. There have been no randomized control trials to directly compare radiosurgery against microsurgery but a meta-analysis of 19 retrospective studies demonstrated that radiosurgery is efficacious with 95% of a combined sample of 335 patients achieving clinical control (Guss et al., 2011).

Prognosis

The mortality and morbidity rate associated with resection of chemodectoma has been quoted at 1% and 33%, respectively (Gad et al., 2014). Cranial nerve injury, wound haematomas, and ischaemic stroke can occur. Although there is a low risk of distant metastasis, follow-up for possible lymph node metastases is indicated. Residue disease may also be controlled with radiotherapy.

Glomus jugulare tumours are typically indolent and, as the management goal is to provide long-term tumour control with low morbidity, a judicious use of stereotactic radiotherapy and modern microsurgery make achieving this goal possible (Fayad et al., 2009).

Langerhans cell histiocytosis

Langerhans cell histiocytosis (LCH), formerly known as histiocytosis X, is a heterogeneous group of tumours, typically affecting bone, characterized by a clonal proliferation of pathological cells with the characteristics of Langerhans cells (Abla et al., 2010). Langerhans cells are dendritic cells (antigen-presenting cells) that arise from the bone marrow and usually reside in the lymph nodes and skin.

The term 'eosinophilic granuloma' has been used to describe a single LCH lesion, 'Hand-Schüller-Christian disease' to describe multiple LCH lesions within one system, and 'Abt-Letterer-Siwe disease' to describe multiple LCH lesions within multiple systems (Arico et al., 2003).

Epidemiology

LCH typically occurs in children, with an estimated incidence of 4–4.5 cases per million per year (Chaudhary et al., 2013).

Pathology

The aetiology of LCH remains unclear. There are data to suggest that germ line mutations may predispose some patients to LCH. Approximately 1% of patients with LCH have an affected relative. Moreover, twin studies have found a considerably higher rate of concordance in monozygotic versus dizygotic twins (92% and 10%, respectively) (Abla et al., 2010). There are also data to suggest that viruses such as HHV6 may result in LCH, however most studies have failed to confirm this viral association (Abla et al., 2010).

Histologically the diagnosis of LCH rests on the presence of Langerhans cells within lesions, with accompanying macrophages, T-lymphocytes, eosinophils, and multinucleated giant cells. These Langerhans cells may be determined by the demonstration of CD1a on immunohistochemistry, or Birbeck granules on electron microscopy (Abla et al., 2010). The latter may now be more easily identified by immunohistochemical staining of langerin (CD207), an endocytic receptor which induces the formation of Birbeck granules (Valladeau et al., 2000).

Lesions associated with LCH are most commonly located within bone, particularly the skull. Within the central nervous system three patterns of lesions have been described (Grois et al., 2010):

1. Well-circumscribed granulomas within the brain's connective tissue with a predilection for the circumventricular organs.
2. Non-granulomatous neurodegenerative lesions mainly affecting the brainstem and cerebellum.
3. Granulomas in the pituitary stalk that invade the hypothalamus and show diffuse infiltration of the surrounding brain.

Management

The clinical symptoms and signs depend on the site and nature of LCH lesions. A single skull lesion is the most frequent presentation of LCH. Involvement of the hypothalamic-pituitary axis can result in diabetes insipidus in up to 25% of all patients (Grois et al., 2010). Non-granulomatous neurodegenerative lesions result in a highly variable presentation, ranging from mild abnormalities of the reflexes and subtle cognitive deficits, to pronounced ataxia or behavioural disturbance.

CT and MRI are indicated to investigate skull and brain lesions, respectively (Grois et al., 2010). CT of the skull may demonstrate lesions within the calvarium, with a characteristic bevelled edge. MRI of the brain may show enlargement of the pituitary stalk with potential extension to the hypothalamus (Fig. 39.5). MRI may also reveal radiological degeneration with symmetrical hyperintense signal changes on T2-weighted images and hypo- or hyperintense signals on T1-weighted images in the cerebellum, and sometimes changes in the basal ganglia and brainstem.

The evidence guiding the decision-making for LCH is limited. In unifocal skull lesions a simple curettage or even biopsy can provide diagnostic tissue and usually results in cure (Abla et al., 2010). The treatment of central nervous system lesions resulting in diabetes insipidus may include steroids or chemotherapy (Grois et al., 2010). Surgical resection and radiotherapy have also been used in lesions located in regions other than the hypothalamic-pituitary axis.

Prognosis

The prognosis of LCH is highly variable. Patients with lesions limited to a single system generally have a high chance of spontaneous remission and a favourable outcome. Patients with multiple systems affected may have a very much worse prognosis; those in whom high-risk organs (liver, spleen, or bone marrow) are involved, who fail to respond to therapy in the first 6 weeks, have a mortality rate as high as 35%.

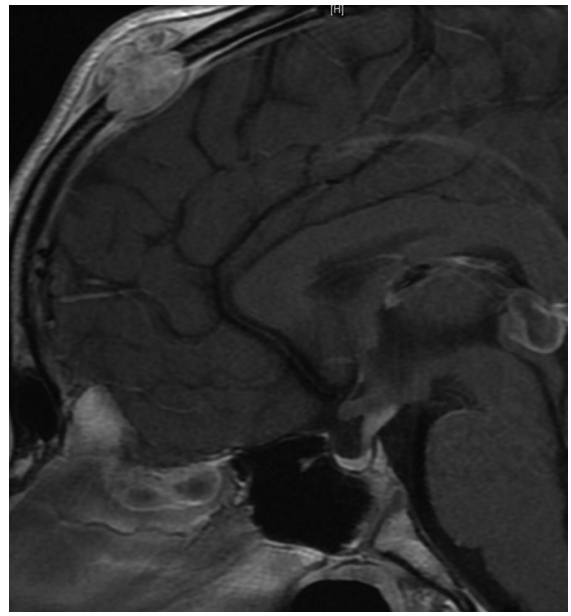

Fig. 39.5 Langerhans cell histiocytosis (LCH). A 14-year old boy presented with a lump on the forehead and chronic constipation. Subsequently diabetes insipidus and growth hormone deficiency were diagnosed and the MRI (T1 with gadolinium contrast) revealed a thickened and enhancing pituitary stalk and an enhancing lytic skull lesion. A biopsy of the skull lesion yielded a diagnosis of LCH. Further investigations uncovered involvement of the gut and chemotherapy according to LCH4 protocol was instituted.

Sarcoidosis

Sarcoidosis is a multisystem inflammatory granulomatous disease, typically affecting the lungs (Joseph and Scolding, 2007). The involvement of the central nervous system, termed neurosarcoidosis, is a rare but feared complication of the disease.

Epidemiology

The prevalence of sarcoidosis is approximately 40 per 100 000 (Joseph and Scolding, 2007). Less than 10% of patients with sarcoidosis exhibit symptoms and signs of neurological disease, though autopsy studies have suggested a significant proportion with subclinical disease. It is usually diagnosed between 20 and 40 years of age, and certain racial groups, such as Northern Europeans and West Africans, are at considerably higher risk of developing the disease.

Pathology

The aetiology of sarcoidosis remains unclear. Genetic studies have suggested that class I human leukocyte antigen (HLA)-B8 antigens and HLA class II antigens encoded by HLA-DRB1 and DQB1 alleles may predispose some patients to the disease (Vargas and Stern, 2010). Several environmental triggers have also been put forward including mould, metals, wood burning stoves, photocopier toner, and infectious agents such as mycobacterium tuberculosis and propionibacterium acnes.

Histologically sarcoidosis is characterized by non-caseating granuloma. Neurosarcoidosis most commonly affects the leptomeninges

at the base of the brain. Extension to the brain parenchyma may occur, and is usually associated with surrounding astrocyte activation and gliosis.

Management

Neurosarcoidosis presents most frequently with cranial nerve palsies, seen in 50–75% of patients. Such palsies are most commonly the result of basal meningitis, but may also be due to nerve granulomas, or raised intracranial pressure. Seizures are another common manifestation of neurosarcoidosis, often reflecting underlying mass lesions, and occur in about 10% of patients (Joseph and Scolding, 2007).

An enhanced MRI of the may show leptomeningeal enhancement with gadolinium. Multiple white matter lesions are seen in approximately 40% of patients (Joseph and Scolding, 2007). Large mass lesions may also be demonstrated, and can mimic neoplasia. Lumbar puncture may reveal raised protein (>2 g/litre), mild lymphocytosis, and possibly oligoclonal bands. Systemic investigations can also provide evidence of sarcoidosis including blood tests (elevated serum ACE, ESR, and calcium), and a chest X-ray or CT thorax (hilar and mediastinal adenopathy).

The first-line therapy for sarcoidosis are corticosteroids (Joseph and Scolding, 2007; Vargas and Stern, 2010). Long-term corticosteroid use is associated with considerable morbidity, particularly in patients with diabetes mellitus, hypertension, or osteoporosis. To this end, steroid-sparing immunosuppressive agents, including methotrexate and hydroxychloroquine, have also been used with varying success to manage sarcoidosis, though these too also carry risks of complications. In patients with drug-resistant sarcoidosis, case series have reported success with radiotherapy (Bruns et al., 2004). The role of surgery is limited to biopsy in equivocal cases, and the treatment of complications such as hydrocephalus.

Prognosis

Spontaneous remission of neurosarcoidosis has been reported but is very rare; most patients require long-term follow with therapy provided when disease exacerbation occurs.

Tumefactive multiple sclerosis

Multiple sclerosis (MS) is an autoimmune inflammatory disease affecting the central nervous system, characterized by lesions of demyelination and axonal loss. Tumefactive multiple sclerosis (TMS) describes the presence of MS lesions greater than 2 cm in diameter, often solitary, which may be mistaken for other space occupying lesions such as brain tumours on imaging (Hardy and Chataway, 2013).

Epidemiology

The prevalence of TMS has been estimated to be 1–2 per 1000 cases of MS (Hardy and Chataway, 2013). It is usually diagnosed between the ages of 20 and 40 years.

Pathology

The aetiology of TMS remains unknown. Tumefactive demyelinating lesions have been reported in diseases other than MS, including viral infections such as HIV, and as a side effect of treatment with drugs such as tacrolimus. Histologically, tumefactive demyelinating lesions are indistinguishable from other MS lesions. Active lesions consist of areas of demyelination with reactive astrocytes and myelin-containing foamy macrophages (Hardy and Chataway, 2013). Macroscopically, lesions are usually well circumscribed, with a predilection to the frontal and parietal lobes (Altintas et al., 2012).

Management

The presentation of TMS often resembles that of more sinister space occupying lesions, including symptoms and signs of raised intracranial pressure, seizures, and focal neurological deficits. Headache and vomiting are particularly common in children (Altintas et al., 2012).

An enhanced MRI brain is indicated to investigate TMS. Lesions up to 12 cm in diameter have been reported, but most range between 2 and 6 cm (Lucchinetti et al., 2008). There is usually associated cerebral oedema, though often less than that observed with malignancy. The majority of lesions enhance with gadolinium, and demonstrate a ring appearance (usually closed, but open ring is highly specific for TMS) (**Fig. 39.6**), which is thought to reflect an advancing area of active inflammation away from a more chronic non-enhancing core (Hardy and Chataway, 2013).

An unenhanced CT head may be helpful in distinguishing TMS from malignancy; regions that are hyperintense on an enhanced MRI brain, but hypodense on an unenhanced CT head, are more likely to represent TMS (Kim et al., 2009). Lumbar puncture may reveal unmatched (present in CSF but not in serum) oligoclonal bands. Systemic investigations are also important to exclude other pathologies such as vasculitis, granuloma, infection, or malignancy. These include blood tests and CT of chest, abdomen, and pelvis (Hardy and Chataway, 2013).

The treatment is with high-dose corticosteroids (Altintas et al., 2012). In patients in whom corticosteroids are ineffective, plasma

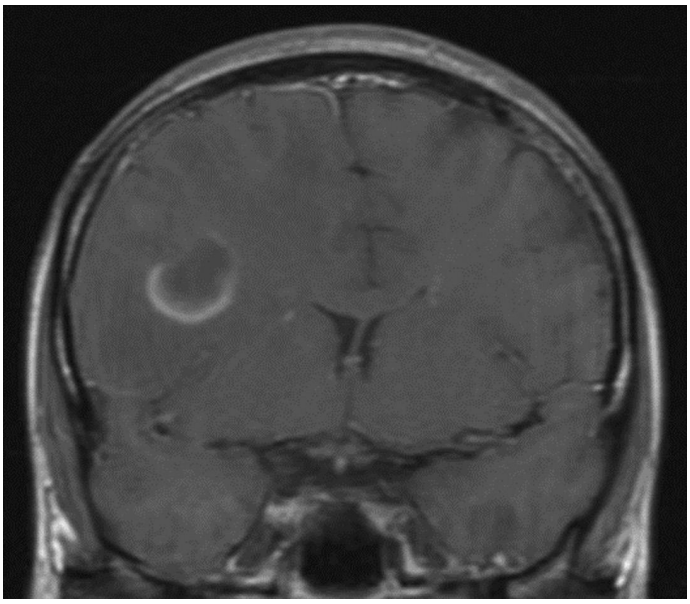

Fig. 39.6 Tumefactive MS plaque. An 'open ring sign' is relatively specific for multiple sclerosis. The enhancing component is thought to represent advancing front of demyelination, thus favouring the white matter side of the lesion. The open part of the ring will therefore usually point towards the grey matter. Stereotactic biopsy confirmed a diagnosis of MS.

Fig. 39.7 Melanocytoma. A middle-aged woman presented with headache. Dermatological and ophthalmological were unremarkable. An unenhanced CT brain showed a mixed density lesion with abnormal calcification, suggesting it was longstanding. A staging CT did not demonstrate lesions elsewhere, and she underwent a complete surgical resection. Histopathology confirmed melanocytoma and she remains well 5 years postoperatively.

exchange appears to be a reasonable second line agent. The anti-CD20 B cell monoclonal antibody rituximab has also been used with some success (Fan et al., 2012). Disease-modifying therapy such as interferon beta or glatiramer acetate may be also be beneficial in reducing the risk of recurrence, but this must be balanced against the risk of adverse events. The role of surgery is limited to biopsy in cases of diagnostic uncertainty, and the treatment of complications such as hydrocephalus.

Prognosis

Overall, the prognosis of patients with TMS does not appear to be worse than other patients with MS in general. Indeed, in the largest cohort of patients with TMS, the long-term prognosis was better than in matched controls with typical MS (Lucchinetti et al., 2008).

Primary CNS melanoma and melanocytoma

Primary melanocytic neoplasms of the CNS are a range of tumours characterized by a clonal proliferation of melanocytes of the leptomeninges, which are derived from the neural crest during early embryogenesis (Liubinas et al., 2010). These neoplasms include diffuse leptomeningeal melanocytosis (DML) or melanomatosis, melanocytoma, and primary malignant melanoma; the present discussion is limited to melanocytoma and primary malignant melanoma. As the highest concentration of meningeal melanocytes is in the spinal cord and posterior fossa and this is where these tumours occur most commonly (Goldgeier et al., 1984).

Epidemiology

The incidence of melanocytoma is approximately 1 per 10 million, and the incidence of primary CNS melanoma 1 per 20 million. The peak incidence is in the fifth decade, and there is a slight female preponderance (Liubinas et al., 2010).

Pathology

Histologically, the diagnosis of primary melanocytic neoplasms of the CNS rests on the identification of melanin in tumour cells or associated macrophages (Liubinas et al., 2010). Melanocytomas are low-grade lesions that do not invade the surrounding brain, although intermediate-grade melanocytomas are also recognized (Brat et al., 1999; Navas et al., 2009). Primary CNS melanoma is similar to melanoma arising in other sites, and may feature invasion, haemorrhage, or necrosis. Macroscopically, melanocytomas and primary CNS melanomas are solitary lesions that are generally extra-axial.

Management

The presentation of melanocytomas and primary CNS melanoma is that of other space occupying lesions, including symptoms and signs of raised intracranial pressure, seizures, and focal neurological deficits. Dermatological and ophthalmological examinations as well as CT staging must be performed to rule out a distant primary source.

Neuroimaging is indicated in suspected lesions. A CT brain often shows iso- or hyperdense lesions with or without abnormal calcification (Fig. 39.7), which enhance with contrast. An MRI brain may demonstrate lesions that are, unusually for tumours, hyperintense on T1-weighted images, hypointense on T2-weighted images, and enhance homogenously with gadolinium.

The treatment of melanocytoma and primary CNS melanoma is complete surgical resection. Radiotherapy may be indicated in incompletely resected melanocytoma, but malignant melanoma is relatively radioresistant. The role of chemotherapy is unclear, but it has been used as adjuvant therapy and in patients with recurrent disease (Cornejo et al., 2013).

Prognosis

Melanocytomas are generally benign and surgical resection curative. Primary CNS melanoma, however, is associated with a poor prognosis. Primary CNS melanoma may be prone to local recurrence or systemic spread, albeit less so than metastatic melanoma, with an average survival time approximately 6 years (Cornejo et al., 2013).

Intracranial lipomas

Epidemiology

These tumours are extremely rare with an incidence estimated at 0.06–0.46% of all intracranial tumours (Truwit and Barkovich, 1990). Older studies may however underestimate the true incidence due to

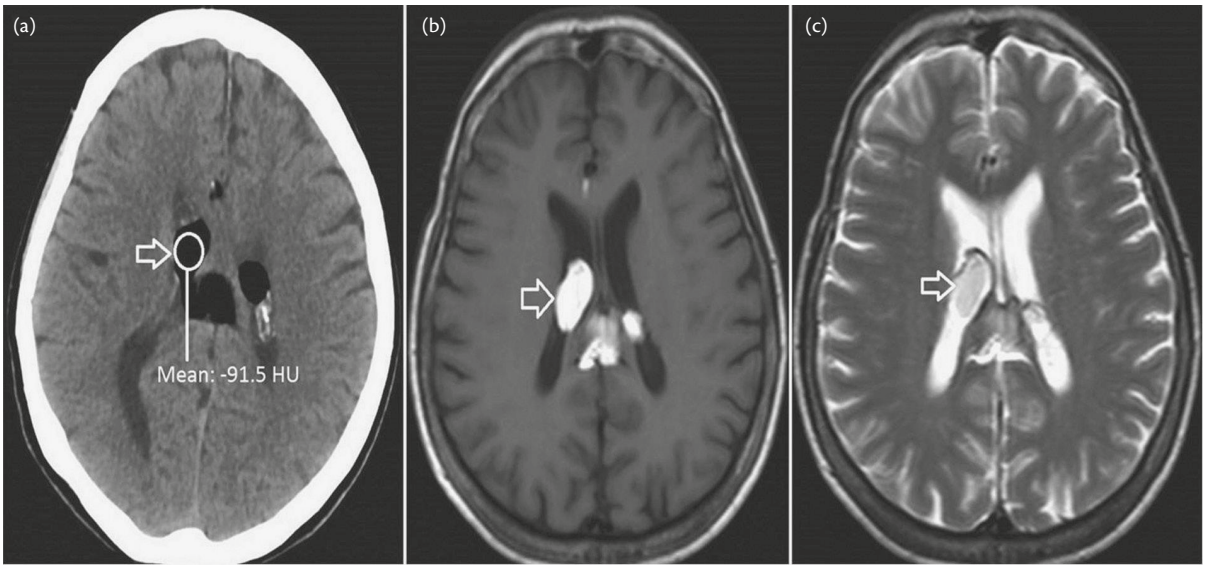

Fig. 39.8 Intracranial lipoma. (A) CT demonstrates a homogenously hypodense lesion in the lateral and third ventricle, approximately –100 Hounsfield units. (B) T1-weighted MRI showing a hyperintense mass lesion. (C) T2-weighted MRI also showing a hyperintense mass lesion.

increasingly widespread use of imaging. There does not appear to be any age or sex-differential in their distribution (Eghwrudjakpor et al., 1992). The youngest case reported is in a 3-day old child and the oldest in a 91-year-old woman (Cascino et al., 1958; Yalcin and Fragoyannis, 1966).

Pathology

Intracranial lipomas were first described by Rokitansky in 1856 following accidental discovery after an autopsy (Rokitansky, 1856). Merrill Sosman who was appointed roentgenologist to the Brigham Hospital in 1922 by Harvey Cushing made the first diagnosis in a living patient using pneumoencephalography (Sosman, 1946). These lesions are thought to be congenital malformations caused by maldifferentiation of the meninx primitiva during the development of the subarachnoid cisterns (Verga, 1929). They may interfere with cortical development near their location (Yildiz et al., 2006). Most commonly they are associated with corpus collosum dysgenesis or agenesis (Macpherson et al., 1987). Other reported abnormalities include, saccular or fusiform aneurysms, arteriovenous malformations and sagittal sinus and falcine sinus fenestrations (Futami et al., 1992; Sasaki et al., 1996). Macroscopically they do not exert a mass effect so nerves and blood vessels can run through them (Yildiz et al., 2006).

Management

In 45% of cases, lipomas are found in the interhemispheric region, in the pericallosal area. They are also frequently located in the dorsal mesencephalic area. Rarely, they have reported in the Sylvian fissure where they are associated with epilepsy (Yildiz et al., 2006). See Fig. 39.8.

Most commonly they are incidental lesions that appear hypodense on CT, hyperintense on T1-weighted images, and hyperintense on T2-weighted images. It is important to differentiate them from dermoids which frequently appear in the midline (Yildiz et al., 2006).

Prognosis

Lipomas are slowly progressing lesions so prognosis is good even with conservative management. Surgery may be considered for patients with medication-refractory seizures but tendency to adhere to surrounding neural tissue make radical resection hazardous (Yilmaz et al., 2006).

Controversies

A timely and accurate diagnosis is a guiding principle in the management of patients with brain tumours (Omuro et al., 2006). Making the diagnosis of uncommon brain lesions is inherently challenging, but this chapter has highlighted several elements that are important when investigating such lesions (Box 39.1). Considering the rarity of these lesions, their treatment is also invariably contentious. Unsurprisingly, there are no randomized controlled trials to

Box 39.1 Elements to consider when managing uncommon brain lesions

History	Onset in young adults History of subtle and transient neurological symptoms Personal or family history of autoimmune or inflammatory disease
Examination	Skin rashes Slit lamp findings
Investigations	Avoid empirical steroids unless significant mass effect MRI brain and spinal cord Lumbar puncture if not contra-indicated Anti-HIV and syphilis serology Whole-body CT scan Biopsy

guide surgical decision-making, and recommendations are therefore mostly based on case series.

FURTHER READING

Abla, O., Egeler, R.M., & Weitzman, S. (2010). Langerhans cell histiocytosis: current concepts and treatments. *Cancer Treat Rev*, **36**, 354–9.

Adesina, A. & Rauch, R. (2010). Ganglioglioma and gangliocytoma. In: Adesina, A.M., Tihan, T., Fuller, C.E., & Poussaint, T.Y. (eds.) *Atlas of Pediatric Brain Tumors*, pp. 185–94. New York, NY: Springer.

Gad, A., Sayed, A., Elwan, H., et al. (2014). Carotid body tumors: a review of 25 years experience in diagnosis and management of 56 tumors. *Ann Vasc Dis*, **7**, 292–9.

Hardy, T.A. & Chataway, J. (2013). Tumefactive demyelination: an approach to diagnosis and management. *J Neurol Neurosurg Psychiatry*, **84**, 1047–53.

Louis, D.N., Perry, A., Reifenberger, G., et al. (2016). *Acta Neuropathol*, **131**, 803.

REFERENCES

Abla, O., Egeler, R.M., & Weitzman, S. (2010). Langerhans cell histiocytosis: current concepts and treatments. *Cancer Treat Rev*, **36**, 354–9.

Adesina, A. & Rauch, R. (2010). Ganglioglioma and gangliocytoma. In: Adesina, A.M., Tihan, T., Fuller, C.E., & Poussaint, T.Y. (eds.) *Atlas of Pediatric Brain Tumors*, pp. 185–94. New York, NY: Springer.

Altintas, A., Petek, B., Isik, N., et al. (2012). Clinical and radiological characteristics of tumefactive demyelinating lesions: follow-up study. *Mult Scler*, **18**, 1448–53.

Arico, M., Girschikofsky, M., Genereau, T., et al. (2003). Langerhans cell histiocytosis in adults. Report from the International Registry of the Histiocyte Society. *Eur J Cancer*, **39**, 2341–8.

Athanasiou, A., Liappis, C.D., Rapidis, A.D., Fassolis, A., Stavrianos, S.D., & Kokkalis, G. (2007). Carotid body tumor: review of the literature and report of a case with a rare sensorineural symptomatology. *J Oral Maxillofac Surg*, **65**, 1388–93.

Awasthi, D., Kline, D.G., & Beckman, E.N. (1991). Neuromuscular hamartoma (benign triton tumor) of the brachial-plexus—case report. *J Neurosurg*, **75**, 795–7.

Boyaci, S., Moray, M., Aksoy, K., & Sav, A. (2011). Intraocular neuromuscular choristoma: a case report and literature review. *Neurosurgery*, **68**, E551–5.

Brat, D.J., Giannini, C., Scheithauer, B.W., & Burger, P.C. (1999). Primary melanocytic neoplasms of the central nervous systems. *Am J Surg Pathol*, **23**, 745–54.

Brat, D.J., Scheithauer, B.W., Fuller, G.N., & Tihan, T. (2007). Newly codified glial neoplasms of the 2007 WHO Classification of Tumours of the Central Nervous System: angiocentric glioma, pilomyxoid astrocytoma and pituicytoma. *Brain Pathology*, **17**, 319–24.

Bruns, F., Pruemer, B., Haverkamp, U., & Fischedick, A.R. (2004). Neurosarcoidosis: an unusual indication for radiotherapy. *Br J Radiol*, **77**, 777–9.

Cascino, J. P., Lake, F., Jackson, C., & Kaplan, A. (1958). Lipoma of the corpus callosum. *J Int Coll Surg*, **29**, 171–4.

Chaudhary, V., Bano, S., Aggarwal, R., et al. (2013). Neuroimaging of Langerhans cell histiocytosis: a radiological review. *Jpn J Radiol*, **31**, 786–96.

Chen, H., Sippel, R.S., O'Dorisio, M.S., Vinik, A.I., Lloyd, R.V., & Pacak, K. (2010). The North American Neuroendocrine Tumor Society Consensus guideline for the diagnosis and management of neuroendocrine tumors pheochromocytoma, paraganglioma, and medullary thyroid cancer. *Pancreas*, **39**, 775–83.

Cornejo, K.M., Hutchinson, L., Cosar, E.F., et al. (2013). Is it a primary or metastatic melanocytic neoplasm of the central nervous system? A molecular based approach. *Pathol Int*, **63**, 559–64.

Covington, M.F., Chin, S.S., & Osborn, A.G. (2011). Pituicytoma, spindle cell oncocytoma, and granular cell tumor: clarification and meta-analysis of the world literature since 1893. *Am J Neuroradiol*, **32**, 2067–72.

Curatolo, P. & Maria, B.L. (2013). Tuberous sclerosis. *Handb Clin Neurol*, **111**, 323–31.

Downing, M.T., Hamoudi, A.B., & Besner, G.E. (1997). Brain heterotopia: choristoma of the back. *Pediatr Surg Int*, **12**, 183–5.

Eghwrudjakpor, P.P.O., Kurisaka M., Fukuoka, M., & Mori, K. (1992). Intracranial lipomas: current perspectives in their diagnosis and treatment. *Br J Neurosurg*, **6**, 139–44.

Fan, X., Mahta, A., DE Jager, P. L., & Kesari, S. (2012). Rituximab for tumefactive inflammatory demyelination: a case report. *Clin Neurol Neurosurg*, **114**, 1326–8.

Fayad, J.N., Schwartz, M.S., & Brackmann, D.E. (2009). Treatment of recurrent and residual glomus jugulare tumors. *Skull Base*, **19**(1), 92–8.

Franz, D.N., Leonard, J., Tudor, C., et al. (2006). Rapamycin causes regression of astrocytomas in tuberous sclerosis complex. *Ann Neurol*, **59**(3), 490–8.

Futami, K., Kimura, A., & Yamashita, J. (1992). Intracranial lipoma associated with cerebral saccular aneurysm: case report. *J Neurosurg*, **77**, 640–2.

Gad, A., Sayed, A., Elwan, H., et al. (2014). Carotid body tumors: a review of 25 years' experience in diagnosis and management of 56 tumors. *Ann Vasc Dis*, **7**, 292–9.

Goldgeier, M.H., Klein, L.E., Klein-Angerer, S., Moellmann, G., & Nordlund, J.J. (1984). The distribution of melanocytes in the leptomeninges of the human brain. *J Invest Dermatol*, **82**, 235–8.

Grois, N., Fahrner, B., Arceci, R.J., et al. (2010). Central nervous system disease in Langerhans cell histiocytosis. *J Pediatr*, **156**, 873–81, 881 e1.

Guild, S.R. (1953). The glomus jugulare, a nonchromaffin paraganglion, in man. *Ann Otol Rhinol Laryngol*, **62**, 1045–71; concld.

Guss, Z.D., Batra, S., Limb, C.J., et al. (2011). Radiosurgery of glomus jugulare tumors: a meta-analysis. *Int J Radiat Oncol Biol Phys*, **81**, e497–502.

Hardy, T.A. & Chataway, J. (2013). Tumefactive demyelination: an approach to diagnosis and management. *J Neurol Neurosurg Psychiatry*, **84**, 1047–53.

Harvey, A.S., Freeman, J.L., Berkovic, S.F., & Rosenfeld, J.V. (2003). Transcallosal resection of hypothalamic hamartomas in patients with intractable epilepsy. *Epileptic Disord*, **5**, 257–65.

Hebert-Blouin, M.N., Amrami, K.K., & Spinner, R.J. (2013). Addendum: evidence supports a 'no-touch' approach to neuromuscular choristoma. *J Neurosurg*, **119**, 252–4.

Hebert-Blouin, M.N., Scheithauer, B.W., Amrami, K.K., Durham, S.R., & Spinner, R.J. (2012). Fibromatosis: a potential sequela of neuromuscular choristoma. *J Neurosurg*, **116**, 399–408.

Heller, R.S., Tsugu, H., Nabeshima, K., & Madsen, O.D. (2010). Intracranial ectopic pancreatic tissue. *Islets*, **2**, 65–71.

Hintz, E.B., Yeaney, G.A., Buchberger, G.K., & Vates, G.E. (2014). Intracranial salivary gland choristoma within optic nerve dural

sheath: case report and review of the literature. *World Neurosurgery*, **81**(5–6), 842.
Joseph, F.G. & Scolding, N.J. (2007). Sarcoidosis of the nervous system. *Pract Neurol*, **7**, 234–44.
Kemeny, A.A. (2009). Contemporary management of jugular paragangliomas (glomus tumours): microsurgery and radiosurgery. *Acta Neurochir (Wien)*, **151**(5), 419–21.
Kim, D.S., Na, D.G., Kim, K.H., et al. (2009). Distinguishing tumefactive demyelinating lesions from glioma or central nervous system lymphoma: added value of unenhanced CT compared with conventional contrast-enhanced MR imaging. *Radiology*, **251**, 467–75.
Knight, T.T., Jr., Gonzalez, J.A., Rary, J.M., & Rush, D.S. (2006). Current concepts for the surgical management of carotid body tumor. *Am J Surg*, **191**, 104–10.
Koeller, K.K. & Henry, J.M. (2001). From the archives of the AFIP—superficial gliomas: radiologic-pathologic correlation. *Radiographics*, **21**, 1533–56.
Kotelis, D., Rizos, T., Geisbusch, P., et al. (2009). Late outcome after surgical management of carotid body tumors from a 20-year single-center experience. *Langenbecks Arch Surg*, **394**, 339–44.
Kwiatkowski, D.J. & Manning, B.D. (2005). Tuberous sclerosis: a GAP at the crossroads of multiple signaling pathways. *Hum Mol Genet*, **14** Spec No. 2, R251–8.
Lee, J.H., Barich, F., Karnell, L.H., et al. (2002). National Cancer Data Base report on malignant paragangliomas of the head and neck. *Cancer*, **94**, 730–7.
Lee, K. & Roland, P. (2013). Heterotopias, teratoma, and choristoma. In: Kountakis, S. (ed.) *Encyclopedia of Otolaryngology, Head and Neck Surgery*. Berlin Heidelberg, Germany: Springer.
Liubinas, S.V., Maartens, N., & Drummond, K.J. (2010). Primary melanocytic neoplasms of the central nervous system. *J Clin Neurosci*, **17**, 1227–32.
Louis, D.N., Ohgaki, H., Wiestler, O.D., et al. (2007). The 2007 WHO classification of tumours of the central nervous system. *Acta Neuropathol*, **114**, 97–109.
Lucchinetti, C.F., Gavrilova, R.H., Metz, I., et al. (2008). Clinical and radiographic spectrum of pathologically confirmed tumefactive multiple sclerosis. *Brain*, **131**, 1759–75.
Macpherson, R.I., Holgate, R.C., Gudeman, S.K. (1987). Midline central nervous system lipomas in children. *J Can Assoc Radiol*, **38**, 264–70.
Maixner, W. (2006). Hypothalamic hamartomas—clinical, neuropathological and surgical aspects. *Childs Nerv Syst*, **22**, 867–73.
Navas, M., Pascual, J. M., Fraga, J., et al. (2009). Intracranial intermediate-grade meningeal melanocytoma with increased cellular proliferative index: an illustrative case associated with a nevus of Ota. *J Neurooncol*, **95**, 105–15.
Newman, N.J., Miller, N.R., & Green, W.R. (1986). Ectopic brain in the orbit. *Ophthalmology*, **93**, 268–72.
Nowak, D.A. & Trost, H.A. (2002). Lhermitte-Duclos disease (dysplastic cerebellar gangliocytoma): a malformation, hamartoma or neoplasm? *Acta Neurol Scand*, **105**, 137–45.
Omuro, A.M., Leite, C.C., Mokhtari, K., & Delattre, J.Y. (2006). Pitfalls in the diagnosis of brain tumours. *Lancet Neurol*, **5**, 937–48.
Orning, J.L., Trembath, D.G., Zanation, A.M., & Germanwala, A.V. (2013). Endoscopic endonasal approach for resection of infundibular granular cell tumor: case report and literature review. *J Case Rep Med*, **2**, 235775.
Ozeren, E., Gurses, L., Sorar, M., Er, U., Onder, E., & Arikok, A.T. (2014). L'hermitte-Duclos disease in an elderly patient: a case report and review of the literature. *Asian J Neurosurg*, **9**, 246.
Palmini, A., Chandler, C., Andermann, F., et al. (2002). Resection of the lesion in patients with hypothalamic hamartomas and catastrophic epilepsy. *Neurology*, **58**, 1338–47.
Pirayesh Islamian, A., Buslei, R., Saeger, W., & Fahlbusch, R. (2012). Pituicytoma: overview of treatment strategies and outcome. *Pituitary*, **15**, 227–36.
Rokitansky, C. (1856). *Lehrbuch der Pathologischen Anatomie*, Vol **2**. Vienna, Austria: Wilhelm Braumuller, pp. 468–8.
Sasaki, H., Yoshida, K., Wakamoto, H., Otani, M., & Toya, S. (1996). Lipomas of the frontal lobe. *Clin Neurol Neurosurg*, **98**, 27–31.
Shin, J. H., Lee, H.K., Khang, S.K., et al. (2002). Neuronal tumors of the central nervous system: radiologic findings and pathologic correlation. *Radiographics*, **22**, 1177–89.
Sosman, M.C. (1946). Discussion of Echternacht AP, Campbell JA. Midline anomalies of the brain. Their diagnosis by pneumoencephalography. *Radiology*, **46**, 119–31.
Striano, S., Santulli, L., Ianniciello, M., Ferretti, M., Romanelli, P., & Striano, P. (2012). The gelastic seizures-hypothalamic hamartoma syndrome: facts, hypotheses, and perspectives. *Epilepsy Behav*, **24**, 7–13.
Truwit, C.L. & Barkovich, A.J. (1990). Pathogenesis of intracranial lipoma: an MR study in 42 patients. *AJNR Am J Neuroradiol*, **11**(4), 665–74.
Valladeau, J., Ravel, O., Dezutter-Dambuyant, C., et al. (2000). Langerin, a novel C-type lectin specific to Langerhans cells, is an endocytic receptor that induces the formation of Birbeck granules. *Immunity*, **12**, 71–81.
Vargas, D.L. & Stern, B.J. (2010). Neurosarcoidosis: diagnosis and management. *Semin Respir Crit Care Med*, **31**, 419–27.
Verga, P. (1929). Lipoma ed osteolipomi della pia madre. *Tumori*, **15**, 321.
Watkins, L.D., Mendoza, N., Cheesman, A.D., & Symon, L. (1994). Glomus jugulare tumours: a review of 61 cases. *Acta Neurochir (Wien)*, **130**, 66–70.
Wei, G., Zhang, W., Li, Q., et al. (2014). Magnetic resonance characteristics of adult-onset Lhermitte-Duclos disease: an indicator for active cancer surveillance? *Mol Clin Oncol*, **2**, 415–20.
Weissenberger, A.A., Dell, M.L., Liow, K., et al. (2001). Aggression and psychiatric comorbidity in children with hypothalamic hamartomas and their unaffected siblings. *J Am Acad Child Adolesc Psychiatry*, **40**, 696–703.
Wieneke, J.A. & Smith, A. (2009). Paraganglioma: carotid body tumor. *Head Neck Pathol*, **3**, 303–6.
Wolfe, S.Q., Bruce, J., & Morcos, J.J. (2008). Pituicytoma: case report. *Neurosurgery*, **63**, E173–4; discussion E174.
Yalcin, S. & Fragoyannis, S. (1966). Intracranial lipoma. Case report. *J Neurosurg*, **24**(5), 895–7.
Yildiz, H., Hakyemez, B., Koroglu, M., Yesildag, A., & Baykal, B. (2006). Intracranial lipomas: importance of localization. *Neuroradiology*, **48**(1), 1–7.
Yilmaz, N., Unal, O., Kiymaz, N., Yilmaz, C., & Etlik, O. (2006). Intracranial lipomas—a clinical study. *Clin Neurol Neurosurg*, **108**(4), 363–8.
Zygourakis, C.C., Rolston, J.D., Lee, H.S., Partow, C., Kunwar, S., & Aghi, M.K. (2015). Pituicytomas and spindle cell oncocytomas: modern case series from the University of California, San Francisco. *Pituitary*, **18**, 150–8.

SECTION 10

Neurotrauma and intensive care

40. **Epidemiology of head injury and outcome after head injury** *475*
Nabeel Alshafai and Andrew Maas

41. **Pathophysiology of traumatic brain injury** *483*
John K. Yue, Hansen Deng, Ethan A. Winkler, John F. Burke, Catherine G. Suen, and Geoffrey T. Manley

42. **Intensive care management of head injury** *497*
Matthew A. Kirkman and Martin Smith

43. **Surgical management of head injury** *509*
Hadie Adams, Angelos G. Kolias, Adel Helmy, Peter J.A. Hutchinson, and Randall M. Chesnut

44. **Complications of head injury** *521*
Fardad T. Afshari, Antonio Belli, and Peter C. Whitfield

45. **Concussion and sports-related head injury** *531*
Mark Wilson

40

Epidemiology of head injury and outcome after head injury

Nabeel Alshafai and Andrew Maas

Introduction

Traumatic brain injury (TBI) constitutes a major cause of death and disability. In low- and middle-income countries the incidence of TBI is increasing, subsequent to increased motorization. It is, however, particularly vulnerable road users (pedestrians, cyclists) where the risk is greatest. In higher-income countries, children, young adults, and elderly patients have the highest rate of TBI and a substantial increase in incidence of TBI in elderly patients as a result of falls has been noted. Nevertheless, TBI is a disease that affects the population of all ages and is referred to as 'a silent epidemic'. Knowledge of the epidemiology of TBI is essential to inform healthcare planning and to target prevention campaigns appropriately.

In this chapter we will summarize global TBI epidemiological perspectives and reflect on the burden that TBI imposes on health economics and society. We will review current classification systems, outcome measures, and prognostic models for TBI.

Definition

Many different definitions have been, and continue to be, used to describe TBI. This may cause confusion and ambiguity concerning an accurate diagnosis, leading to difficulties in comparing patient cohorts. In practice, it may be difficult to distinguish between symptoms of a mild TBI and the effects of alcohol intoxication or drug abuse. In elderly patients, a fall with some bruising to the scalp may be secondary to a primary cardiac event and it may be difficult to differentiate between a temporary loss of consciousness or dizziness due to the cardiac event and a mild TBI. Furthermore, some patients may present late and the diagnosis then needs to be established on basis of the case history, introducing a subjective element. A great need exists for objective parameters to confirm or exclude a diagnosis of TBI. Various new tools, including biomarkers, studies of eye movements, balance, are showing potential, but still need to be validated in large cohorts.

WHO defines TBI as an acute injury to the brain resulting from mechanical energy to the head from external physical (Carroll et al., 2004) force excluding injuries relating to illicit drug, alcohol, or substance, medication, or caused by other treatment or injuries (Andelic et al., 2012).

TBI has also been defined as: '*an alteration in brain function, or other evidence of brain pathology, caused by an external force*' (Menon et al., 2010). TBI has replaced the old term 'head injury' as it captures the importance of the brain injury (Roozenbeek et al., 2013), in addition to injuries purely affecting the scalp, skull, and face.

Aetiology

Motorized vehicles have been described as the most persistent killers. Preventive measures have been shown to be highly effective in reducing the number of TBI related to road traffic incidents, and combined with improved trauma care saves lives (**Table 40.1**). Legislation, seat belts, air bags, and helmet use have all contributed to increased safety. Prevention campaigns should target vulnerable road users who are unaware of traffic risks (e.g. the frail, or children) as well as vehicle drivers. While road traffic incidents remain the most common cause of TBI in low and middle-income countries, in Europe, falls are now a more frequent cause of TBI (Peeters et al., 2015). **Table 40.1** provides a summary overview of the most common causes of TBI. In the United States fire arm injuries exceeded road traffic incidents for the first time in 1990. In combat situations, blast injuries due to improvised explosive devices are a frequent cause of TBI. **Table 40.2** lists methods of reducing the impact of TBI.

Incidence

When we analyse the current epidemiological incidence studies, there appear to be a number of limitations, namely, deficient standardized epidemiologic reporting, the lack of age standardized incidence rates, the lack of data specific to mild and moderate TBI and the lack of data from lower- and middle-income countries. These challenges need to be addressed in future studies. An important point to bear in mind is poly-trauma and repeated head injuries in the same patient (first time vs. recurrent head injury) which is often overlooked and is crucial to understand the late consequences of such recurrent injuries.

In a systematic review of 28 European studies published over 24 years, an aggregate incidence rate of hospital admissions was 262 cases per 100 000 people annually (Peeters et al., 2015). A recent population-based study in New Zealand shows a much

Table 40.1 Common causes of TBI

Main causes of TBI
Road traffic incidents (44–80%)
Falls[$] (12–55%)
Violence[@] (7–17%) Fire arm (>50% suicide) (Aarabi et al., 2001)
Work and sports (4%)
Others

[$] *More recently, the leading cause in northern Europe, United States, and Australia specially in young children and elderly (>75-year-old)*

[@] *Higher risk population: male, young adults, non-white (56% African-American), unemployed at the time of the injury, unmarried, history of illegal substance use, history of law enforcement encounters, poverty, and low educational level.*

higher incidence rate of 790/100 000 (Feigin et al., 2013). The discrepancy between the high incidence rate reported in this study, with complete case ascertainment, and the lower rates based upon hospital admission data indicate that the latter approach grossly underestimates the total burden of TBI. Differences in reported incidence rates between countries are unlikely to reflect real differences, but rather result from differences in case ascertainment, the use of variable definitions and in some cases a focus on subpopulations.

Prevalence

Prevalence is the total volume of living people with TBI (existing and new cases) at a given point in time (point prevalence) or in a given period (period prevalence). In a meta-analysis in 2013 of 15 prevalence studies (Frost et al., 2013) (25 134 adults), Frost et al. found that 12% had experienced a TBI with loss of consciousness (male twice as much risk as female). McKinlay et al. looked at the paediatric age group (higher risk) and showed that over 30% of people had experienced at least one TBI before they are 25 years of age (McKinlay et al., 2008) These numbers appear high compared to estimates reported by the Center for Disease Control (CDC) in the United States, that 5.3 million people are currently living with TBI in the United States today.

Mortality

For Europe, an average mortality rate of 10.5–11.7/100 000 population has been derived, with a large range identified varying from 3.0 to 21.8/100 000, mainly determined by case mix (Peeters et al., 2015; Majdan et al., 2017). Table 40.3 presents an overview of mortality rates reported in the United States and Europe. Despite a rise in the incidence of TBI worldwide, some studies claim a decrease in mortality rate from TBI secondary to implementation and adherence to evidence-based guidelines and recommendations in the developed countries (Lu et al., 2005; Gerber et al., 2013). However, improved survival was not found when comparing mortality rates reported in observational studies over the past 30 years (Rosenfeld et al., 2012).

Another important point is that 'acute mortality' is not the only concern in TBI: TBI patients have been found to have a substantially elevated long-term risk for premature mortality. This includes: suicide, subsequent injuries, and assaults, even after adjustment for socio demographic and familial factors six months after injury (Fazel et al., 2014). There is a reduced average life expectancy of nine years following inpatient rehabilitation for TBI (McMillan et al., 2011). This varies according to age and severity. It has been found that after experiencing TBI, the annual mortality remains increased, up to sevenfold, for at least 13 years (McMillan et al., 2011).

Table 40.2 Reducing the IMPACT of TBI

Reducing the IMPACT of TBI
Strict limits in blood alcohol concentration
The use of seatbelts
Separate child restraint law
Firmly enforced speed limits
Compulsory helmets for motorcycle riders
Clinical care improved with faster communication
Better trauma systems
Increased availability of CT scanning
Improved intensive care unit (ICU) facilities and care
Others

Table 40.3 Mortality rate after TBI across the world

Region	Mortality incidence/100 000	References
USA	17.1 (2010)	CDC, 2015, Rutland-Brown *et al.*, 2006
West Virginia	23.6 (1989–1999)	Adekoya and Majumder, 2004
EU	10.5–11.2	Peeters *et al.*, 2015, Majdan *et al.*, 2016
- Austria	12.6	Majdan *et al.*, 2016
- Denmark	7.3	Majdan *et al.*, 2016
- France	11.5	Masson *et al.*, 2001
- Germany	8.3	Majdan *et al.*, 2016
- Italy	7.6	Majdan *et al.*, 2016
- Norway	10.4	Sundstrøm *et al.*, 2007
- Sweden	9.2–9.5	Sundstrøm *et al.*, 2007; Majdan *et al.*, 2016
Brazil	5.1–26.2	De Almeida *et al.*, 2016; Koizumi *et al.*, 2000
China	12.99	Cheng *et al.*, 2017, Jiang *et al.*, 2019

Classification of TBI

Various approaches to the classification of TBI can be taken, these include classification by mechanism, clinical severity, burden of injury, the extent of structural damage, initial prognostic risk, and expected prognosis. Table 40.4 presents these different domains, which may be used for classification. We suggest that appropriate classification of TBI should not be restricted to a single domain but should incorporate a multidimensional perspective. Currently, no such multidimensional integrated system for classification exists, but this goal is being pursued in ongoing large-scale observational studies (Maas et al., 2017).

Mechanism of injury

Different mechanisms cause different types of injuries. In closed TBI, acceleration and deceleration forces may cause a typical picture of diffuse axonal injury in patients injured during road traffic incidents. A fall, in which the head hits a hard surface would typically result in focal contusional brain injury. Penetrating injuries caused by high velocity missiles, typically cause extensive damage along the missile track, while

Table 40.4 Different approaches to classification of TBI

Mechanism of injury	Clinical severity
• Closed • Penetrating • Crush • Blast • Combination	• GCS 3–8: Severe • GCS 9–13: Moderate • GCS 14–15: Mild
Injury burden (AIS and ISS)*	**Structural damage: CT Classification**
1: Minor **2**: Moderate **3**: Serious **4**: Severe **5**: Critical **6**: Virtually unsurvivable	• Diffuse injury I • Diffuse injury II • Diffuse injury III • Diffuse injury IV • Evacuated mass lesion • Non-evacuated mass lesion
Prognostic risk	
CRASH and IMPACT prognostic models	

** AIS per body region: external (skin), head/neck (including brain injury), thorax, abdomen/pelvic contents, spine, and extremities*
ISS: Injury Severity Score (Baker et al., 1974)

the amount of kinetic energy transferred results in substantial distant damage. In crush injuries, dynamic forces are to a large extent absorbed by the skull and not all energy is transferred to the brain. As a consequence, skull injuries may be extensive while the brain injury may be less severe. In blast injuries, several mechanisms combine in damaging the brain. These include primary injury (due to pressure waves), secondary injury (collision with debris and other objects), tertiary (being thrown down by the blast and hitting the head against an object) or quaternary (heat and toxic injury).

Clinical severity

There is a wide spectrum of clinical presentation in TBI ranging from a hit to the head with symptoms of disorientation or alteration of consciousness that quickly resolve with or without amnesia, to complete loss of consciousness and coma. The Glasgow Coma Scale (Teasdale and Jennett, 1974) (GCS) has been adopted worldwide as instrument for assessing the level of consciousness. In GCS assessments the responses observed in three components (eye, motor, verbal scale) are recorded. For purposes of classification and research, a total sum score may be derived, ranging from 3 to 15; however, on an individual basis the importance of separating out the individual domains of the GCS cannot be overemphasized. The GCS scale is made up of entirely distinct components (E, V, M) and each 'score' is qualitative and discontinuous (i.e. a change from M2 to M3 is in no way related to a change from M4 to M5, let alone E3 to E4). It should be noted that especially early after injury the GCS may change over time, following resuscitation or as part of early recovery. Accurate assessments of one or more of the components of the GCS may be confounded by prior alcohol or substance use, prehospital use of sedation, paralysis, and intubation (Balestreri et al., 2004; Stocchetti et al., 2004). Indeed, the literature review revealed over 25 different TBI severity classification systems. Notwithstanding the limitations just mentioned, based on the GCS sum score, TBI is classified as mild, moderate, or severe (Fig. 40.1).

In addition to the GCS, multiple clinical approaches to the classification of TBI severity have been proposed. Many of these address specific subpopulations, but none have been shown to be convincingly superior to the GCS. We should recognize, however, that the GCS does not provide a granular classification for mild TBI, as it is not intended to capture more subtle changes such as 'an alteration in brain function'. Subtle and transient symptoms are reported, which may overlap with symptoms due to either post-traumatic stress disorders (PTSD) and/or postconcussion syndromes. This is an area of ambiguity at the present time and further research is required to distinguish the different diagnoses and the implications on patient outcome (Maas et al., 2017).

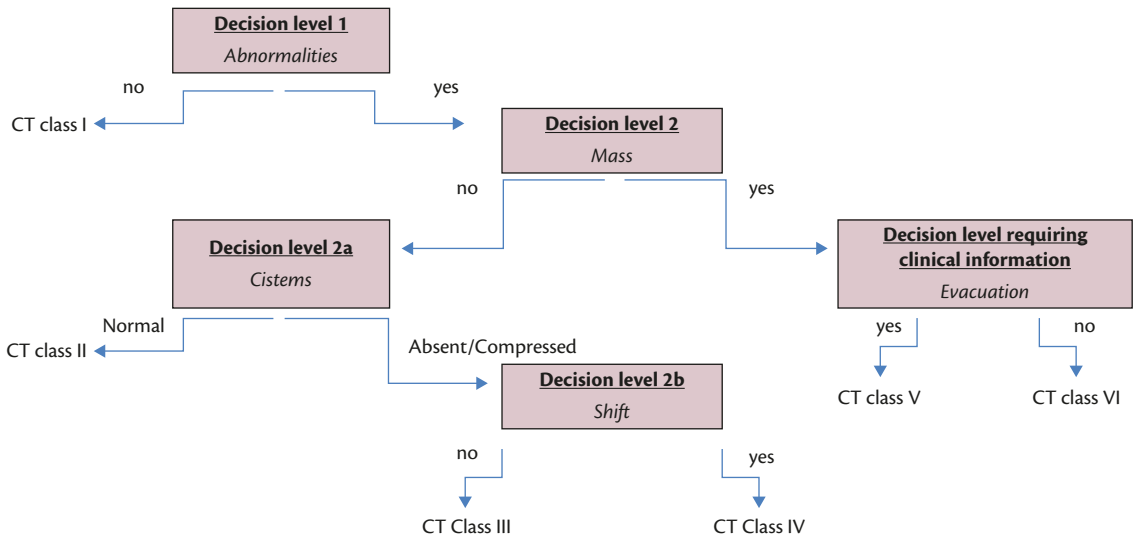

Fig. 40.1 Marshall CT classification presented in a tree structure.
Prediction of outcome in traumatic brain injury with CT characteristics: A comparison between the CT classification and combinations of CT predictors. Maas AIR, Hukkelhoven CWPM, Marshall LF, Steyerberg EW. *Neurosurgery* 2005, 57, 6, 1173–82.

Extracranial injuries (injury burden)

TBI is associated with extracranial injuries in about 35% of cases. The severity of injuries in six body regions is universally scored according to The Abbreviation Injury Score (AIS). In the AIS, severity is scored for six body regions: external (skin), head/neck (including brain injury), thorax, abdomen/pelvic contents, spine, and extremities. The severity score can range from 1 to 5 (1 is minor; 2 is moderate; 3 is serious; 4 is severe; 5 is critical; and 6 is likely unsurvivable). The Injury Severity Score (Baker et al., 1974) aims to summarize the total burden of injury by adding the quadratic scores of the three body regions with the highest score.

The extent of structural damage (CT classification)

The extent of structural damage is best assessed by neuroimaging. While MR examinations are more sensitive than computed tomography (CT), CT remains the primary procedure for diagnostic imaging because of its sensitivity for detecting intracranial hematoma and the speed, availability, and safety of examination. The extent of structural damage on the CT is commonly classified according to the Marshall Classification (Fig. 40.1) (Marshall et al., 1991). This provides a descriptive system which primarily differentiates between presence and absence of visible structural damage and differentiates between diffuse injuries (and a subclassification of these) and patients with mass lesions. Limitations of the Marshall Classification are that the scale is not ordinal, and that is does identify signs of raised intracranial pressure in patients with diffuse injury but not in those with mass lesions. Although the Marshall CT Classification was not developed from a perspective of prognosis, many studies have shown a clear association between the CT classification and outcome. The Rotterdam and Helsinki CT scores represent classification systems developed from a prognostic perspective (Maas et al., 2005; Raj et al., 2014).

Prognostic risk

A different approach to classification is by baseline prognosis. Many prognostic models for predicting risk of mortality or unfavourable outcome in patients with TBI have been developed. The two largest prognostic models, CRASH and IMPACT, have been extensively validated externally, show good performance, and aim to predict mortality and unfavourable outcome (https://www.crash2.lshtm.ac.uk and https://www.tbi-impact.org) (Perel et al., 2008; Steyerberg et al., 2008; Lingsma et al., 2013; Han et al., 2014; Majdan et al., 2014). The IMPACT models were developed on patients with moderate and severe TBI; the CRASH models also included patients with milder injuries. They were developed with data available upon admission, prior to provision of in-hospital care. They are therefore ideally suited for a baseline calculation of prognostic risk. Both approaches confirm that the largest amount of prognostic information is contained in a core set of three predictors: age, motor score, and pupillary reactivity. The IMPACT study group further evaluated the additional benefit of factors such as structural imaging (CT characteristics such as mass lesion, cerebral oedema, traumatic subarachnoid haemorrhage), secondary insults (hypoxia, hypotension) and laboratory data (glucose, haemoglobin). Additional predictive power was noted in more complex models however the model could only explain 35% of variance in outcome. Many other factors have been suggested as having prognostic importance, although not investigated within multivariate models to the rigour found in the CRASH and IMPACT models, including MRI burden of injury, comorbidities, Injury Severity Score, time to craniotomy of more than 4 hours, raised ICP, and autoregulatory indices.

Although useful for more reliably informing relatives of the anticipated outcome, it should be recognized that a prediction model is a population-based estimate and yields no more than a risk estimate with a substantial element of uncertainty, which can be expressed in the confidence interval. For this reason, the greatest application of prognostic analysis is not at the level of the individual patient, but rather at the 'group' level for quantifying and stratifying the severity of brain injury, as a reference for evaluating quality of care and for stratification and covariate adjustment in clinical trials (Maas et al., 2017).

It is worthy to add that recent studies are showing the superiority in early MR imaging as a prognostic tool in TBI, but there is still uncertainty about its discriminative predictive value and which acute phase lesion patterns correlate with long-term outcome (Haghbayan et al., 2014). Although a significant body of evidence has indicated that MRI is superior to CT in detecting most types of traumatic lesions, CT is currently used as a routine while the use of MRI is sporadic in the acute phase (Haghbayan et al., 2014).

There are several studies emphasizing the value of biomarkers as a tool for prognostications such as S100β protein and ApoE4 allele:

S100

S100β protein is a promising biomedical marker for the diagnosis, monitoring, and prognosis of TBI severity. Preoperative estimation of serum S100β in patients with TBI could be used as a prognostic predictor for postoperative survival and neurological outcome (Goyal et al., 2013) as well as being responsive to secondary insults. Measuring levels of S100β is useful in evaluating the severity of TBI and in the determination of long-term prognosis in patients presenting with moderate and severe injury (Mercier et al., 2013).

ApoE4

A current meta-analysis indicated that the ApoE4 allele might be associated with a poor prognosis in patients with severe TBI, but it may be used as a biomarker in predicting the prognosis of patients with TBI (Zeng et al., 2014). APoE4 allele presence influences recovery rate from severe TBI independent of other covariates (Alexander et al., 2007) and may also relate to the risk of subsequent cognitive decline.

Assessment of outcome: The Glasgow Outcome Scale (GOS) and beyond

Accurate characterization of outcome after TBI is essential, both from a clinical and research perspective. Historically, most TBI studies have used the Glasgow Outcome Scale or the extended version of the GOS to provide an overall global assessment of functional outcome after TBI (Table 40.5).

The GOS was initially described in 1975 as a global assessment of function following TBI (Jennett and Bond, 1975). While appropriate for more severe TBI, it was recognized that the scale was relatively insensitive at the upper levels and for this reason the Glasgow

Table 40.5 Glasgow Outcome Scale (GOS) and Glasgow Outcome Scale Extended (GOSE)

Scale	GOS	Scale	GOSE
1	Dead	1	Dead
2	Vegetative	2	Vegetative
3	Severe disability	3	Lower severe disability
	(Conscious but dependent)	4	Upper severe disability
4	Moderate disability	5	Lower moderate disability
	(Independent but disabled)	6	Upper moderate disability
5	Good recovery	7	Lower good recovery
	(Can resume normal activities)	8	Upper good recovery

GOS:
Reprinted from *The Lancet*, Volume 305, issue 7905, Bryan Jennett, Michael Bond, Assessment of Outcome After Severe Brain Damage: A Practical Scale, pp. 480–4, Copyright (1975), with permission from Elsevier.

GOSE:
Reproduced with permission from B Jennett, J Snoek, MR Bond, N Brooks, Disability after severe head injury: observations on the use of the Glasgow Outcome Scale, *Journal of Neurology, Neurosurgery & Psychiatry*, Volume 44, Issue 4, pp. 285–93, Copyright © 1981 BMJ Publishing Group Ltd.

Outcome Scale Extended (GOSE) was introduced. Alterations in major roles, independence in living and participation in social and leisure activities are assessed by the investigators and used to summarize the effects of diverse changes caused by injury. It should be recognized, however, that the GOSE remains a global approach to classifying outcome and that ceiling effects exist. TBI may cause problems in many domains: a wide variety of neuropsychiatric disturbances can be associated with functional impairments and low quality of life. Neuropsychological sequelae include: mood disturbances (Bombardier et al., 2010; Tanev et al., 2014); cognitive impairment; personality changes; and social and family effects.

An overlap may exist between sequelae of mild TBI and symptoms consistent with PTSD. The overlap of cognitive disruption between mild TBI and PTSD reflect the complex interplay of neurological, psychological, and physical factors in veterans with mild TBI and/or PTSD, and highlights the need for specialized evaluation and management (Benge et al., 2009; Brenner, 2011).

It has long been thought that quality of life measures are not appropriate for TBI as the neurocognitive sequelae might prevent accurate rating of the patient's perception of quality of life. However, this has been shown to be false. Patient-reported outcome measures in the sense of quality of life assessments are highly relevant to the field of TBI. Quality of life (QOL) measures may be generic; for example, the Short-Form-36 (SF36) or disease specific. A disease-specific measure QOL by a multidisciplinary working party and published as the Quality of Life after Brain Injury (QOLIBRI) scale. This scale provides a profile of health-related quality of life (HRQOL) in domains typically affected by brain injury. However, for more global assessments a summary measure may be preferable and as such the QOLIBRI-OS presenting a short six-item assessment was proposed. QOLIBRI was found to have moderate to strong relationships with QOLIBRI-OS, GOSE, Short-Form-36, Hospital Anxiety and Depression scale (Ware et al., 1993; Truelle et al., 2010; von Steinbüchel et al., 2010a; von Steinbüchel et al., 2010b). An important aspect is to capture the patient's own perspective on QOL (Dijkers, 2004). To date, outcome assessments have tended to be unidimensional, focusing on single domains. An alternative approach might be to combine these in multidimensional assessment scores. Much further work will however be required to determine which instruments are best suited for specific situations and to determine the weighting of different factors. Historical data on outcome differentiated by severity of injury, show that patients with severe TBI have a mortality rate of 36%, 5% are classified as vegetative, 15% have severe disability, 15–20% moderately disability, and 25% good recovery. Patients with moderate injury have been reported to have a mortality of 7%, vegetative classification of 1%, severe disability rate of 7%, moderate disability rate of 25%, and good recovery rate of 60%. Patients with mild injury have a very low mortality with a substantial majority designated as good recovery but nevertheless a high frequency of ongoing symptoms including headache, visual disturbance, dizziness, fatigue, and memory, concentration, and higher executive function impacting on family and social life and employment. With advances in treatment there is evidence that six-month outcome has improved in moderate and severely injured patients treated in specialist intensive care (increased in moderate disability and good recovery from 40.4% to 59.9%) (Patel et al., 2002).

Health economic cost

The economic cost of TBI management is tremendous and is a huge burden on society although, unfortunately, there are a paucity of studies that quantify this cost. Due to the long-term economic impact and burden of disability to family, work, and society, the average lifetime cost per person for TBI in the United States is estimated to be US$396 000. In the United States the Centre for Disease Control and Prevention estimates direct and indirect costs of TBI to be more than US$58 billion in total.

In most studies, the costs of non-hospitalized TBI were not considered at all. Feigin et al. performed a population-based TBI study and found out that 30% of cases were from non-hospitalized patients (Feigin et al., 2013). Although the cost of TBI is known to increase by severity (see **Table 40.6**), the unexpectedly large number of mild TBI in any population (95% of all TBI cases) means that the total cost of treating these cases is nearly three times that of moderate/severe TBI. The economic burden and overall outcome can be reduced by targeting both high cost injuries and population-based programmes aimed at reducing the incidence of lower cost mild injuries.

Conclusion

We have only uncovered the tip of the iceberg in TBI. There is a pressing need for further epidemiological studies with standardized criteria involving, specifically, lower income countries. This will have

Table 40.6 The cost of TBI is known to increase by severity especially with those requiring hospitalization and higher demand on rehabilitation services

TBI Grade	Mild	Moderate	Severe
Direct medical cost/person (US$)	21 160 (Farhad et al., 2013) to 35 954	25 271 (Farhad et al., 2013) to 81 153 (McGregor and Pentland, 1997)	57 637 (Farhad et al., 2013) to >100 000 (Faul et al., 2007)

a significant impact in relocating resources and better economic plans to reduce the healthcare burden on societies in the long run.

One critical area in TBI research that requires attention is the effects of risk factors and predictors of TBI outcome. Currently, a few prospective multicentre studies are undergoing. The two largest studies are the Transforming Research and Clinical Knowledge in TBI study (TRACK-TBI) to enrol 3000 patients and the Collaborative European Neuro-Trauma Effectiveness Research in TBI study (CENTER-TBI) (Maas et al., 2015) to enrol 5000 patients with controls, over the next five years, using an extensive standardized set of variables.

FURTHER READING

Butcher, I., McHugh, G.S., Lu, J., et al. (2007). Prognostic value of cause of injury in traumatic brain injury: results from the IMPACT study. *J Neurotrauma*, **24**, 281–6.

IMPACT. International Mission for Prognosis and Analysis of Clinical Trials in TBI. http://www.tbi-impact.org/

Perel, P., Arango, M., Clayton, T., et al. (2008). Predicting outcome after traumatic brain injury: practical prognostic models based on large cohort of international patients. *BMJ*, **336**(7641), 425–9.

REFERENCES

Aarabi, B., Alden, T., & Chestnut, R. (2001). Management and prognosis of penetrating brain injury—guidelines. *J Trauma*, **51**(suppl), S1–86.

Adekoya, N. & Majumder, R.R. (2004). Fatal traumatic brain injury, West Virginia, 1989–1998. *Public Health Rep*, **9–119**(5), 486–92.

Alexander, S., Kerr, M.E., Kim, Y., Kamboh, M.I., Beers, S.R., & Conley, Y.P. (2007). Apolipoprotein E4 allele presence and functional outcome after severe traumatic brain injury. *J Neurotrauma*, **24**(5), 790–7.

De Almeida, C.E.R., de Sousa Filho, J.L., Dourado, J.C., Gontijo, P.A., Dellaretti, M.A., & Costa, B.S. (2016). Traumatic brain injury epidemiology in Brazil. *World Neurosurgery*, **87**, 540–7.

Andelic, N., Anke, A., Skandsen, T., et al. (2012). Incidence of hospital-admitted severe traumatic brain injury and in-hospital fatality in Norway: a national cohort study. *Neuroepidemiology*, **38**(4), 259–67.

Baker, S.P., O'Neill, B., Haddon, W. Jr., & Long, W.B. (1974). The Injury Severity Score: a method for describing patients with multiple injuries and evaluating emergency care. *J Trauma*, **14**, 187–96.

Balestreri, M., Czosnyka, M., Chatfield, D.A., et al. (2004). Predictive value of Glasgow Coma Scale after brain trauma: change in trend over the past ten years. *J Neurol Neurosurg Psychiatry*, **75**, 161–2.

Benge, J.F., Pastorek, N.J., & Thornton, G.M. (2009). Postconcussive symptoms in OEF-OIF veterans: factor structure and impact of posttraumatic stress. *Rehabil Psychol*, **54**(3), 270–8.

Bombardier, C.H., Fann, J.R., Temkin, N.R., Esselman, P.C., Barber, J., & Dikmen, S.S. (2010). Rates of major depressive disorder and clinical outcomes following traumatic brain injury. *JAMA*, **303**(19), 1938–45.

Brenner, L.A. (2011). Neuropsychological and neuroimaging findings in traumatic brain injury and post-traumatic stress disorder. *Dialogues Clin Neurosci*, **13**(3), 311–23.

Carroll, L.J., Cassidy, J.D., Holm, L., et al. (2004). Methodological issues and research recommendations for mild traumatic brain injury: the who collaborating centre task force on mild traumatic brain injury. *J Rehabil Med*, **43**, Suppl(2), 113–25.

Centers for Disease Control and Prevention. Report to Congress on traumatic brain injury in the United States: epidemiology and rehabilitation. 2015. https://www.cdc.gov/traumaticbraininjury/pdf/tbi_report_to_congress_epi_and_rehab-a.pdf (accessed 7 august, 2019).

Cheng P., Yin P., Ning P., et al. (2017). Trends in traumatic brain injury mortality in China, 2006–2013: a population-based longitudinal study. *PLoS Med* **14**, e1002332.

Dijkers, M.P. (2004). Quality of life after traumatic brain injury: a review of research approaches and findings. *Arch Phys Med Rehabil*, **85**(4 Suppl 2), S21–35.

Farhad, K., Khan, H.M., Ji, A.B., Yacoub, H.A., Qureshi, A.I., & Souayah, N. (2013). Trends in outcomes and hospitalization costs for traumatic brain injury in adult patients in the United States. *J Neurotrauma*, **30**(2), 84–90.

Faul, M., Wald, M.M., Rutland-Brown, W., Sullivent, E.E., & Sattin, R.W. (2007). Using a cost-benefit analysis to estimate outcomes of a clinical treatment guideline: testing the Brain Trauma Foundation guidelines for the treatment of severe traumatic brain injury. *J Trauma*, **63**(6), 1271–8.

Fazel, S., Wolf, A., Pillas, D., Lichtenstein, P., & Långström, N. (2014). Suicide, fatal injuries, and other causes of premature mortality in patients with traumatic brain injury a 41-year Swedish population study. *JAMA Psychiatry*, **71**(3), 326–33.

Feigin, V.L., Theadom, A., Barker-Collo, S., et al. (2013). Incidence of traumatic brain injury in New Zealand: a population-based study. *Lancet Neurol*, **12**(1), 53–64.

Frost, R.B., Farrer, T.J., Primosch, M., & Hedges, D.W. (2013). Prevalence of traumatic brain injury in the general adult population: a meta-analysis. *Neuroepidemiology*, **40**(3), 154–9.

Gerber, L.M., Chiu, Y.L., Carney, N., Härtl, R., & Ghajar, J. (2013). Marked reduction in mortality in patients with severe traumatic brain injury. *J Neurosurg*, **119**(6), 1583–90.

Goyal, A., Failla, M.D., Niyonkuru, C., et al. (2013). S100b as a prognostic biomarker in outcome prediction for patients with severe traumatic brain injury. *J Neurotrauma*, **30**(11), 946–57.

Haghbayan, H., Boutin, A., Laflamme, M., et al. (2014). The prognostic value of magnetic resonance imaging in moderate and severe traumatic brain injury: a systematic review and meta-analysis. *Intensive Care Medicine*, **40**(1), S202.

Han, J., King, N.K., Neilson, S.J., Gandhi, M.P., & Ng, I. (2014). External validation of the CRASH and IMPACT prognostic models in severe traumatic brain injury. *J Neurotrauma*, **31**(13), 1146–52.

Jiang J.Y., Gao G.Y., Feng J., et al. (2019). Traumatic brain injury in China. *Lancet Neurol*, **18**, 286–295.

Jennett, B. & Bond, M. (1975). Assessment of outcome after severe brain damage. *Lancet (London, England)*, **1**(7905), 480–4.

Koizumi, M.S., Lebrão, M.L., Mello-Jorge, M.H., & Primerano, V. (2000). [Morbidity and mortality due to traumatic brain injury in Sao Paulo City, Brazil, 1997]. *Arq Neuropsiquiatr*, **58**(1), 81–9.

Lingsma, H., Andriessen, T.M., Haitsema, I., et al. (2013). Prognosis in moderate and severe traumatic brain injury. *J Trauma Acute Care Surg*, **74**(2), 639–46.

Lu, J., Marmarou, A., Choi, S., et al. (2005). Mortality from traumatic brain injury. *Acta Neurochir Suppl*, **95**, 281–5.

Maas, A.I., Hukkelhoven, C.W., Marshall, L.F., & Steyerberg, E.W. (2005). Prediction of outcome in traumatic brain injury with computed tomographic characteristics: a comparison between the computed tomographic classification and combinations of computed tomographic predictors. *Neurosurgery*, **57**(6), 1173–82.

Maas, A.I.R., Menon, D.K., Adelson, P.D., et al. (2017). Traumatic brain injury: integrated approaches to improve prevention, clinical care, and research. *Lancet Neurol*, **16**(12), 987–1048.

Majdan, M., Lingsma, H.F., Nieboer, D., Mauritz, W., Rusnak, M., & Steyerberg, E.W. (2014). Performance of IMPACT, CRASH and Nijmegen models in predicting six month outcome of patients with severe or moderate TBI: an external validation study. *Scand J Trauma Resusc Emerg Med*, **22**, 68.

Majdan M, Plancikova D, Brazinova A, et al. (2016) Epidemiology of traumatic brain injuries in Europe: a cross-sectional analysis based on hospital discharge statistics and death certificates in 2012. *Lancet Public Health*, **1**:e76–83.

Marshall, L.L.F., Marshall, S.B., Klauber, M.R., & Van Berkum Clark, M. (1991). A new classification of head injury based on computerized tomography. *J Neurosurg*, **75**(1), s14–s20.

Masson, F., Thicoipe, M., Aye, P., et al. (2001). Epidemiology of severe brain injuries: a prospective population-based study. *J Trauma*, **51**(3), 481–9.

McGregor, K. & Pentland, B. (1997). Head injury rehabilitation in the U.K.: an economic perspective. *Soc Sci Med*, **45**(2), 295–303.

McKinlay, A., Grace, R.C., Horwood, L.J., Fergusson, D.M., Ridder, E.M., & MacFarlane, M.R. (2008). Prevalence of traumatic brain injury among children, adolescents and young adults: prospective evidence from a birth cohort. *Brain Inj*, **22**(2), 175–81.

McMillan, T.M., Teasdale, G.M., Weir, C.J., et al. (2011). Death after head injury: the 13-year outcome of a case control study. *J Neurol Neurosurg Psychiatry*, **82**(8), 931–5.

Menon, D.K., Schwab, K., Wright, D.W., et al. (2010). Position statement: definition of traumatic brain injury. *Arch Phys Med Rehabil*, **91**(11), 1637–40.

Mercier, E., Boutin, A., Lauzier, F., et al. (2013). Predictive value of S-100beta protein for prognosis in patients with moderate and severe traumatic brain injury: systematic review and meta-analysis. *BMJ*, **346**, f1757.

Patel, H.C., Menon, D.K., Tebbs, S., Hawker, R., Hutchinson, P.J., & Kirkpatrick, P.J. (2002). Specialist neurocritical care and outcome from head injury. *Intensive Care Med*, **28**(5), 547–53.

Peeters, W., van den Brande, R., Polinder, S., et al. (2015). Epidemiology of traumatic brain injury in Europe. *Acta Neurochir (Wien)*, **157**(10), 1683–96.

Perel, P., Arango, M., Clayton, T., et al. (2008). Predicting outcome after traumatic brain injury: practical prognostic models based on large cohort of international patients. *BMJ*, **336**(7641), 425–9.

Raj, R., Siironen, J., Skrifvars, M.B., Hernesniemi, J., & Kivisaari, R. (2014). Predicting outcome in traumatic brain injury: development of a novel computerized tomography classification system (Helsinki computerized tomography score). *Neurosurgery*, **75**(6), 632–47.

Roozenbeek, B., Maas, A.I.R., & Menon, D.K. (2013). Changing patterns in the epidemiology of traumatic brain injury. *Nat Rev Neurol*, **9**(4), 231–6.

Rosenfeld, J.V., Maas, A.I., Bragge, P., Morganti-Kossmann, M.C., Manley, G.T., & Gruen, R.L. (2012). Early management of severe traumatic brain injury. *Lancet*, **380**(9847), 1088–98.

Rutland-Brown, W., Langlois, J.A., Thomas, K.E., & Xi, Y.L. (2006). Incidence of traumatic brain injury in the United States, 2003. *J Head Trauma Rehabil*, **21**(6), 544–8.

Servadei, F., Ciucci, G., Piazza, G., & Bianchedi, G. (1988). A prospective clinical and epidemiological study of head injuries in northern Italy: the Comune of Ravenna. *Italian J Neurol Sci*, **9**(5), 449–57.

Steyerberg, E.W., Mushkudiani, N., Perel, P., et al. (2008). Predicting outcome after traumatic brain injury: development and international validation of prognostic scores based on admission characteristics. *PLoS Med*, **5**(8), e165.

Stocchetti, N., Pagan, F., Calappi, E., et al. (2004). Inaccurate early assessment of neurological severity in head injury. *J Neurotrauma*, **21**(9), 1131–40.

Sundstrøm, T., Sollid, S., Wentzel-Larsen, T., & Wester, K. (2007). Head injury mortality in the Nordic countries. *J Neurotrauma*, **24**(1), 147–53.

Tanev, K.S., Pentel, K.Z., Kredlow, M.A., & Charney, M.E. (2014). PTSD and TBI co-morbidity: scope, clinical presentation and treatment options. *Brain Inj*, **28**(3), 261–70.

Teasdale, G. & Jennett, B. (1974). Assessment of coma and impaired consciousness. A practical scale. *Lancet*, **2**(7872), 81–4.

Truelle, J.-L., Koskinen, S., Hawthorne, G., et al. (2010). Quality of life after traumatic brain injury: the clinical use of the QOLIBRI, a novel disease-specific instrument. *Brain Inj*, **24**(11), 1272–91.

Von Steinbüchel, N., Wilson, L., Gibbons, H., et al. (2010a). Quality of Life After Brain Injury (QOLIBRI): scale development and metric properties. *J Neurotrauma*, **27**(7), 1167–85.

Von Steinbüchel, N., Wilson, L., Gibbons, H., et al. (2010b). Quality of Life After Brain Injury (QOLIBRI): scale validity and correlates of quality of life. *J Neurotrauma*, **27**(7), 1157–65.

Ware JE, Jr., Snow KK, Kosinski M, et al. (1993). *SF-36 Health Survey: Manual and Interpretation Guide*. Boston, MA: The Health Institute, New England Medical Center.

Zeng, S., Jiang, J., & Wang, Z.-H. (2014). Prognostic value of apolipoprotein E epsilon4 allele in patients with traumatic brain injury: a meta-analysis and meta-regression. *Genetic Testing and Molecular Biomarkers*, **18**(3), 202–10.

RELATED LINKS TO EBRAIN

Epidemiology of Head Injury. https://learning.ebrain.net/course/view.php?id=1082

Outcome after Head Injury. https://learning.ebrain.net/course/view.php?id=1081

41

Pathophysiology of traumatic brain injury

John K. Yue, Hansen Deng, Ethan A. Winkler, John F. Burke, Catherine G. Suen, and Geoffrey T. Manley

Pathophysiology of primary brain injury

Head trauma is classified into two pathophysiological stages that differ in mechanism and necessitate distinct clinical treatments. Primary trauma is due to a mechanical load that translates into deformation of cerebral tissue (e.g. neurons, glia, axons, and blood vessels), which then initiate cellular responses that lead to disturbances in autoregulation and metabolism. The first signs of trauma range from rapid, indiscrete depolarization of cortical neurons as exemplified in concussion, to focal lesions due to blunt impact, to severe damage such as diffuse shearing of axonal integrity, to acute vascular disruptions in the form of haematomas.

Secondary injuries occur across a more protracted phase and include cerebral hypoxia, hypotension, swelling, and raised intracranial pressure (ICP). In a 2007 meta-analysis of 9205 moderate to severe TBI patients as part of the International Mission for Prognosis and Analysis of Clinical Trials in TBI (IMPACT) study, McHugh and colleagues reported that hypoxia, hypotension, and hypothermia are common on admission with observed prevalence of 20%, 18%, and 10% respectively (McHugh et al., 2007). Secondary insults, particularly when in combination during acute injury and hospitalization, correlate with poor outcome, and require imperative attention, stabilization, and surgical and/or medical management.

Biomechanics of closed head injury

Closed head injuries are cases when the cranium and dura mater remain intact after impact, with patients presenting with a range of neurologic signs and symptoms. Mechanical loading to 5% gelatine in the human skull caused focal lesions to areas of indentation or fracture, and diffuse shearing throughout the subcortex occurred during rotation (Holbourn, 1944). Extensive studies in animal models, human cadavers, computational simulations, and advanced imaging have since characterized traumatic brain deformation, but direct human measurements have traditionally been challenging to obtain as part of clinical studies.

The primary phase of trauma from TBI is defined through the nature of the mechanical load, the type of induced motion, and the duration and velocity of impact. Forces along different axes produce unique modes of stress upon the head (e.g. elongation, compression, bending, shear, and torsion) (Ommaya et al., 2002). Resultant injuries in TBI cannot be attributed to any single appellation. External force generally translates into an impact or impulsive load on the head, and in the real world can include both. Head motion can be translational or rotational, depending on the alignment of two axes: the axis of force application, and the axis between the centre of gravity of the head and the atlanto-occipital joint. Whether the head is fixed or free to extend/flex by the neck is an important determinant for injury mechanism.

Impact loading

Impact loading occurs from collision typically with a short duration of 3–7 ms measured in low velocity falls. Impact can result in a skull fracture and associated extradural haematoma as well as focal cerebral lesions. Contusions known as coup (directly below impact) or contre-coup (diametrically opposite to impact) are observed. High positive pressure is observed at the coup site, and the transmission of the force vector through the brain parenchyma generates a slapping effect to the contre-coup site. At the cellular level, high negative pressure at the contre-coup site, the development and subsequent collapse of cavitation bubbles known as contre cavitations, along with the brain parenchyma bouncing against inner posterior skull are associated with the contre-coup lesions. Elastic rebounding of the skull results in significant spikes in cerebrospinal fluid (CSF) pressure and worsen tissue damage. Intracerebral haematomas are frequently associated with contusions. In the early stage after trauma, a contusion is haemorrhagic and more severe at the crest of gyrus than in the sulcus. It is associated with swelling that subsides with time though discoloration remains.

Autopsy findings show higher incidence of coup and/or contre-coup contusions in the frontotemporal and basal regions of brain, irrespective of the primary impact site. Lagrangian strain tensor fields during occipital deceleration show anatomic constraints near the frontal base of

skull that must be breached in order for the brain to compress against the occipital bone, thus predisposing these regions for injury. The contre-coup lesion is associated with temporal and occipital impacts. Cerebral rotation during impact is also thought to be a significant contributing factor to contre-coup lesions, although definitive evidence on convulsional gliding have yet to confirm this theory.

Impulse loading

Impulse loading occurs due to inertial forces during translational or rotational motion. Within normal physiological circumstances, CSF pressure provides a considerable dampening effect on brain displacement during motion, and the lack of CSF is shown to significantly increase convolutional gliding and shear strain (Pudenz and Shelden, 1946). Brain displacement lags behind that of the skull and the affixed dura mater due to the inertial force of cerebral mass, and convolutional gliding occurs in varying degrees depending on the region of brain, inducing diffuse damage to white matter tracts. Relative to the region of the skull base near the sella and suprasellar space, the brain parenchyma is more mobile. White matter is stiffer than grey matter, thus more strain is distributed at the interface. Vascular, neural, and dural elements (e.g. distal internal carotid arteries, optic nerves, olfactory tracts, oculomotor nerves, and pituitary stalk) that tether brain to the base of skull experience are most susceptible to diffuse axonal injury (DAI) due to inertial effect. The splenium of the corpus callosum and dorsolateral brainstem can experience acute DAI due to a similar trajectory to that of the skull base, relative to the more compliant cerebral cortex.

Translational and rotational motions occur simultaneously to varying degrees. Purely translational motion of the head and neck generally does not produce acute subdural haematomas (SDH), diffuse petechial haemorrhages, or injuries to the cervical cord at linear acceleration of up to 1000 g. When linear acceleration is combined with angular motion of the head and neck, the aforementioned injuries are generated. During angular acceleration, there is a higher incidence of deep-seated haematomas in the basal ganglia in addition to DAI. Rotational insults, often seen in vehicular accidents, induce shear strain as axons and vessels are stretched or compressed beyond their physiologic limits and often result in acute SDH from tearing of subdural bridging veins.

When a single inertial load combines with a minor terminal impact load as in severe extension/flexion whiplash trauma, SDH, gliding contusions, and spinal cord injuries are prevalent. During angular acceleration, the rotational axis is at either the occipital condyles or the base of the neck, amplifying the rotational load and shearing potential. This correlates with sudden vehicular impacts, when translational motion is applied at the seat to induce inertial force onto the head and neck. Rear loading occurs when an applied force from behind causes the head to rotate back at the base of the neck, while front loading occurs when an applied force from the front causes the head to rotate forward.

Static or quasistatic loading

A less common type of mechanical load is static or quasistatic loading, in which gradual compression occurs with negligible velocity and acceleration—mechanistically similar to a closing elevator door. A steady load results in skull fractures and cerebral injuries that are deeper than cortical contusions from an impact load. In comparison to blunt impact trauma with relatively shorter duration and higher velocity, energy from crushing trauma tends to be transmitted to the foraminae and hiatus of the middle cranial fossa, causing in damage to the associated cranial nerves, sympathetic nerves, and intima of blood vessels.

TBI classification by morphology

Traditional approaches to TBI classification focus on the extent of injury (focal vs. diffuse) and the anatomical location of injury with respect to the meninges (extradural/extra-axial vs. intracerebral/intra-axial). The following section proceeds via the latter classification scheme, beginning with the extra-axial layer closest to the skull and proceeding inward to intracerebral tissue.

Extra- or epidural haematoma (EDH)

EDH overlays the dura mater and typically results from a fracture of the thin squamous part of the temporal bone which lacerates the middle meningeal artery. The resulting haematoma strips the dura from the inner table of the skull forming an ovoid mass that compresses the adjacent brain. The haematoma is constrained by the periosteum, which passes through the cranial sutures so these haematomas do not cross suture lines. Venous EDH is less common and results from the disruption of the dural venous sinuses at the vertex, posterior fossa, or the anterior aspects of the cranial fossa. Although less common, EDH may also be found in the frontal region, parietal region, or the posterior fossa in 25% of cases.

EDHs are far less common than subdural haematomas and account for approximately 2% of brain injuries. Although EDHs occur in all age groups, they are far more common in patients below 50 years of age and particularly in paediatric patients where they are primarily due to meningeal and diploic vein haemorrhage and the dura mater is tightly adherent to the paediatric skull. The relatively lower venous pressure and the strong dural adhesion to the skull are responsible for the variation and occasional subacute presentation of EDH in children. Radiographic progression of EDHs can be classified into three categories on computed tomography (CT) imaging: type I (acute), type II (subacute) and type III (chronic) occurring at presentation in 58%, 31%, and 11% of cases, respectively (Zimmerman and Bilaniuk, 1982). Type I is characterized as a dense haematoma with low density 'swirl' indicative of bleeding (i.e. a hypodense zone of active bleeding from the torn vessel into a dense organizing clot). The rise in pressure eventually produces tamponade of the bleeding site and progresses to type II—a homogenous, hyperdense, and organized clot. Type III is characterized by a low density collection due to blood resorption by perivascular tissue, along with a contrast-enhanced membrane consisting of neovascularity and granulation tissue.

The classic presentation of EDH, seen in 15–20% cases, is a patient who presents following a head trauma with transient loss of consciousness, progressing to a lucid interval, before deteriorating neurologically to a coma. The lucid interval represents recovery from the concussion, during which the patient may complain of severe headache on the ipsilateral side of the lesion accompanied by nausea, vomiting, and lethargy with subsequent decompensation into unconsciousness due to increased ICP secondary to the expanding EDH. The lucid interval is not specific to an EDH and was

originally described in cases of acute SDH. Neurological deterioration after EDH may be accompanied by contralateral hemiparesis, ipsilateral oculomotor nerve paresis, decerebrate rigidity, arterial hypertension, cardiac arrhythmias, respiratory disturbances, and if uncorrected, apnoea and death.

Subdural haematoma (SDH)

SDH results from tearing of bridging veins that cross the subdural space to communicate with the venous sinuses or from disruption of superficial pial arteries on the brain surface. SDH is not limited by dural attachment and extends over the cortical surface in the typical biconcave pattern over the tentorium cerebelli or into the interhemispheric fissure. SDH is classified as acute, subacute, and chronic. Acute SDH presents as a crescent-shaped hyperdense collection. Subacute SDH is isodense with symptomatic improvement and typically presents between 7 and 21 days. Chronic SDH (CSDH, >21 days postinjury) is hypodense and may not present symptomatically until the collection has expanded significantly and signs of compression appear (Sambasivan 1997).

Acute SDH is associated with stereotypic motor disorders, impaired oculomotor reflexes, and following transtentorial herniation of the uncus of the temporal lobe, unilaterally fixed and dilated pupils. Arterial bleeds are associated with larger clots near the Sylvian fissure. Postoperative complications include reaccumulation of the haematoma and infection at the accessed site (e.g. osteomyelitis, meningitis, ventriculitis).

Acute traumatic SDH has high reported mortality rates of 22% to 66%. While a lesion surgically evacuated within four hours to reduce the risk of disability, conservative methods may be considered for patients with shallow haematomas in a good clinical state. The Brain Trauma Foundation guidelines recommend specific criteria based on thickness, midline shift, and GCS for intervention, however, these must be viewed in the context of the individual patient, their premorbid state, the length of history and any associated injuries (Chesnut, 1997). Historically, patients undergoing decompression within four hours show a 30% mortality rate, compared with 90% for patients surgically evacuated after four hours (Seelig et al., 1981). More recently series with rapid surgical intervention show a lower overall mortality rate between 8% and 10% (Bajsarowicz et al., 2015). Other predictors include extent of neurologic deficit, sex, and postoperative ICP. Rapid diagnosis and time to surgical evacuation remain of highest prognostic importance after acute SDH. The issue of decompressive craniectomy at the time of subdural haematoma evacuation is currently being investigated in a randomized control trial (RESCUE-ASDH). Currently, the decision to remove the bone flap at the time of surgery (primary decompressive craniectomy) is based on the injury burden on the brain (e.g. the presence of large contusions), the severity of injury assessed clinically and by mechanism of injury and most importantly the degree of intraoperative swelling at the time of surgery.

Chronic subdural haematoma

Chronic subdural haematoma (CSDH) can be thought of as a distinct pathological entity as it often presents in a specific demographic (elderly patients or those with cerebral atrophy) as a specific clinical syndrome. The presumed pathology is a minor head injury that leads to a small haematoma from tearing of the stretched bridging veins that span the subdural space and are therefore unsupported in those with cerebral atrophy. The initial small volume haematoma may be asymptomatic and the initial insult is often forgotten. In a subset of patients, an inflammatory neomembrane forms and potentiates ongoing haemorrhage and swelling of the enclosed haematoma by breakdown of blood products and the development of an osmotic gradient across the neomembrane. The chronicity of this process leads to a clinical presentation several weeks after the initial injury, with an SDH hypodense to brain. The haematoma may nonetheless show areas of acute haemorrhage from repeated haemorrhages, presumably from the inflammatory neomembrane.

Clinical features of CSDH are headache, hemiparesis, speech disturbance (dominant hemisphere) or behavioural disturbances (e.g. emotional outbursts, lack of concentration, manic and depressive states), and ultimately coma if large and untreated. Bilateral CSDH are more likely to progress to coma rapidly and consequently are treated at a smaller absolute volume. CSDH occur most commonly on the cerebral convexity but can occur in the interhemispheric fissure, over the tentorium cerebelli and rarely the posterior fossa.

Treatment can be with burr hole drainage (one or two to aid lavage of the haematoma), by mini-craniotomy or via closed drainage systems. The risks of intervention include infection of the subdural space, seizures, and recurrence. Proliferating microcapillaries in the capsule of SDH are implicated in bleed recurrence due to marked mitotic potential of endothelial cells and vascular permeability. There is level 1 evidence that recurrence can be reduced by the placement of a soft drain into the subdural space for 48 hours (Santarius et al., 2009).

Subarachnoid haemorrhage (SAH)

SAH is a frequent finding in closed head injuries as a result of direct damage to cortical vessels. It correlates with poorer outcome and more severe injury, although in most cases it appears be a reflection of a greater degree of violence at injury rather than being directly responsible for secondary injury. Nevertheless, in a subset of patients traumatic SAH may also contribute to secondary insults (e.g. cerebral swelling, hemodynamically significant vasospasm, and disturbances of metabolism and autoregulation due to reduced adaptive thresholds of the brain to additional physiological shifts). Posttraumatic vasospasm can be observed as early as two days postinjury and reaches maximum intensity between five to seven days (Weber et al., 1990).

Cortical SAH is associated with progression of adjacent cerebral contusions, suggestive of subarachnoid bleeding in the vault as an early sign of cortical microbleeding and significant intraparenchymal brain damage. In TBI patients matched by GCS, age, sex, and the presence of intracranial mass lesions after blunt head injuries, traumatic SAH patients spend more time in the intensive care unit (ICU), are less likely to be discharged home, and are 1.5 times more likely to die during acute hospitalization. In penetrating TBI there is a significant correlation between SAH and poor outcome.

Intraventricular haemorrhage (IVH)

IVH is found in 1.5–3.0% of all head trauma and predominantly in severe TBI. Damage to the septum pellucidum, choroid plexus, and subependymal veins in the fornix are seen in post-mortem exams in patients with primary IVH. The incidence of primary IVH, referring to isolated bleeding confined to the ventricular system, is low. An estimated 21% of patients with IVH attain functional recovery

(Glasgow Outcome Scale (GOS) moderate disability or good recovery) due to presence of concomitant intracranial injuries. In infrequent cases of isolated IVH, more improvement in GOS is possible. In general, the small sample sizes make it difficult to interpret the specific prognostic significance of IVH as opposed to the associated TBI.

Cerebral contusions

Cerebral contusions are focal or multifocal and located in cortical or subcortical regions from direct impact or an acceleration/deceleration injury. Contusions appear as a bruise to the surface from damaged small arteries, veins, or capillaries. Herniating contusions occur when tissue is displaced from one cranial compartment to another typically along the margin of the falx cerebri, the tentorium, or the foramen magnum leading to compression of the herniating tissue. Intermediary contusions are subcortical lesions affecting the corpus callosum, basal ganglia, hypothalamus, and brainstem.

Cortical impact murine models demonstrate that cerebral oedema peaks at 24 hours coincident with a marked reduction of cerebral blood flow (CBF) to contused cortex. CBF normalizes after day seven post-trauma, during which focal areas of hyperaemia appear adjacent to regions of low flow. Studies of the human brain after non-penetrating head injury show contusions being more severe in the frontal and temporal lobes and in patients who do not experience lucid intervals (Adams et al., 1985). Cellular analyses of excised contusions from emergency craniotomies corroborate necrosis as the predominant finding and apoptosis as part of the secondary injury cascade. Tumour necrosis factor increases immediately and rapidly in CSF during acute neuronal degeneration and gradually decreases within a few hours. Neutrophils and macrophages accumulate with elevated chemokines to sustain the cerebral inflammatory cascade. ICP can become elevated due to cerebral swelling and delayed haematoma formation in the pericontusional area, thus requiring ICP monitoring regardless of the need for surgical intervention. Unilateral lesions portray better prognosis while bilateral lesions can be delayed in clinical presentation. This secondary deterioration in clinical state can be delayed as long as 10 days following injury and requires careful counselling of patients and their relatives on discharge. Hyponatraemia can exacerbate this risk and serum Na must be monitored before considering discharge, as the syndrome of inappropriate antidiuretic hormone secretion can coexist in the context of TBI.

Diffuse axonal injury (DAI)

DAI is caused by angular acceleration leading to damage of axonal integrity. Diffuse brain injury is seen in up to 50% of TBIs and spans a range of outcomes from concussion to coma and vegetative state. Classically, DAI is defined as diffuse damage in the cerebral hemispheres, corpus callosum, brainstem and cerebellum (Gennarelli et al., 1982). Long-tract structures (axons and blood vessels) are especially at risk. This is graded on MR as: Grade I (parasagittal white matter of the cerebral hemisphere) Grade II (Grade I plus focal lesion in the corpus callosum), and Grade III (Grade II plus focal lesion in the cerebral peduncle) (Table 41.1). Grade I and II typically show marked improvement in GCS within 2 weeks while Grade III requires ~2 months for recovery, suggestive of prolonged loss of consciousness or coma with DAI involving the brain stem.

Strictly, a definitive diagnosis of DAI is established by immunostaining for β-amyloid precursor protein (β-APP) at autopsy and identifying axonal retraction balls in the deep white matter. *In vivo* diagnosis is challenging as it may present microscopically and in combination with one or more type of brain injuries including: contusion, anoxia, and intracerebral haemorrhage. Although there is ample data implicating DAI in moderate or severe TBI, its involvement in mTBI is difficult to prove histologically as patients rarely die from their injuries. Minor degrees of axonal injury may provide the pathophysiologic basis for deficits experienced during and after mTBI/concussion. Alternatively, functional and metabolic disturbances may be responsible with little structural axonal injury (Vespa et al., 2005).

Table 41.1 Diffuse axonal injury grading

DAI grade	Pathology
I	Grey-white matter interface (commonly parasagittal white matter of frontal lobes, periventricular temporal lobes)
II	Focal lesions in corpus callosum (commonly posterior body and splenium) in addition to Grade I lesions
III	Brainstem (commonly rostral midbrain, cerebellar peduncles, medial lemnisci, and corticospinal tracts) in addition to Grade I and II lesions

GRE: T2-weighted gradient-recalled-echo (GRE) magnetic resonance (MR) technique
SW: Susceptibility-weighted (SW) magnetic resonance (MR) technique.
Data from Tong KA, et al, Hemorrhagic shearing lesions in children and adolescents with posttraumatic diffuse axonal injury: improved detection and initial results, *Radiology*, Volume 227, Issue 7, pp. 332–9, 2003

Mild TBI/Concussion

The United States (US) Centers for Disease Control and Prevention (CDC) defines mild TBI (mTBI)/concussion as a transient neurological disturbance caused by rapid linear and/or rotational acceleration and deceleration forces, resulting in a disruption in cerebral structural or vascular physiology. The American Congress of Rehabilitation Medicine (ACRM) defines mTBI by one or more of the following: loss of consciousness (LOC), loss of memory immediately before or after the incident, alteration in mental state, or focal neurologic deficit that may or may not be transient. The U.S. Department of Veterans Affairs and Department of Defense (VA/DOD) provide similar clinical guidelines while specifying that presence of intracranial lesions classify the patient with, at minimum, moderate TBI.

An estimated 75% of TBI patients are classified as 'mild', which is likely an underestimate as most of these patients do not present to the emergency department. Current classifications of concussion centre on the impairment of neurological function, the disturbance of vision, memory, or equilibrium, alteration of consciousness (AOC), and/or LOC. The diagnosis of concussion is largely appropriate for the non-penetrating head trauma that results in one or more of the following: confusion/disorientation, LOC less than 30 minutes or post-traumatic amnesia (PTA) less than 24 hours in duration, transient focal neurological deficits, and/or seizure, with a GCS of 13–15 upon acute medical evaluation; however, multiple concussion grading scales currently exist without definitive consensus. The lack of evidence in imaging studies, perhaps due to lack of sensitivity, is a challenge to the clinical diagnosis of mTBI/concussion. Recent efforts in utilization of magnetic resonance imaging (MRI), including MR Spectroscopy, for TBI diagnosis has shown promise in identifying a subset of patients with structural changes post-mTBI.

The pathophysiology of mTBI/concussion begins with a sudden change in momentum of the head, causing mechanical stretching or compression of the partially tethered brain against the cranial vault,

initiating diffuse neuronal firing, discharge, and axonal shearing. Neurocognitive deficits tend to occur with minimal detectable pathology and can resolve over time. However, even patients with GCS score 13–15 present with acute and subacute glucose metabolic disturbances on positron emission topography (PET) and require careful assessment for postconcussive risks (Giza and Hovda, 2001). Cerebral microdialysis immediately following mTBI/concussion contains elevated levels of excitatory amino acids and ionic fluxes throughout hemispheric regions, the hippocampus, and the brainstem. Specifically, there is a sharp increase of extracellular K^+ through voltage-gated channels. Studies using electroencephalogram (EEG) demonstrated that postconcussive EEG was excitatory and epileptiform in nature comparable to generalized seizures. Likewise, during this period the sensory evoked potential was completely lost (Shaw, 2002). In early stages after mTBI/concussion, increased glucose utilization and hyperglycolysis sustain the indiscriminate neuronal depolarization and firing, but can also restore the disturbed membrane potential. Later, diffuse neuronal suppression (e.g. spreading depression) takes effect. Spreading depression is characterized by near-complete breakdown of ion gradients, loss of electrical activity, and vasoconstriction, which can trigger infarct growth and initiate cascades leading to apoptotic cell death (Dreier, 2011).

Physiological disturbances persist after mTBI/concussion and increase susceptibility to further injury. After the initial hypermetabolism, hypometabolism and reduction in CBF may persist for up to 4 weeks. Additional excitation (e.g. direct cortical stimulation or recurrent concussion) prolongs cellular recovery and induced cell death due to inability to match increased metabolic demand in part due to decoupling between neuronal activation and CBF after concussion. Dependent on the severity of impact, intracellular accumulation of Ca^{2+} also remains elevated, which impairs mitochondrial metabolism and initiates programmed cell death. In the surviving cells, reduction in cellular plasticity is associated with neurotransmission changes, particularly in subunits of *N*-methyl-D-aspartate (NMDA) receptors.

Penetrating brain injury (PBI)

Compared with blunt TBI, PBI is less prevalent and associated with worse prognosis, occurring when a non-blunt projectile breaches the cranium and dura mater. CSF leaks are common and may require surgical intervention. When a projectile also induces an exit wound, it is termed a perforating brain injury. The projectile crushes soft brain tissue in its path and generates bone fragments at impact, which can require surgical debridement. The shape and kinetic energy of projectile $E = 1/2mv^2$ (E = energy, m = mass, v = velocity) are associated with the degree of tissue damage. A high velocity projectile generates waves of compression and re-expansion (cavitation wave) and inflicts focal shearing damage, parenchymal contusions, and haematomas. CT provides clear characterization of in-driven bone fragments, missile trajectory, extent of tissue damage, haematomas, and mass effects. Cerebral angiography is recommended due to the high risk of vascular injury. High risk factors include a penetrating track crossing the ventricle, involving both hemispheres, crossing the geographical centre of the brain or associated vascular injury. Seizure control following PBI is a key part of clinical management.

Cerebral metabolism and autoregulation

The brain is responsible for the greatest overall resting energy expenditure by organ at approximately 22%, compared with the liver 21%, the heart 9%, and the kidneys 8%. The brain is 2% of overall weight while accounting for 20% of basal cardiac output and 20% of resting O_2 consumption. The cerebral metabolic rate of oxygen ($CMRO_2$) remains relatively constant in healthy adults at approximately 3.5 ml O_2/100 g/min and may be as high as 5.2 ml O_2/100 g min in children aged 3–12 years. Glucose is the primary source of ATP in the brain and approximately 50% of energy generated from cerebral metabolism is utilized for synaptic activity (i.e. neurotransmitter production, release, and uptake); 25% is for maintaining for electrochemical gradients, and the remaining 25% is for molecular transport, biosynthesis, and other processes.

Aerobic metabolism is the primary process in the brain through which glucose is efficiently converted to 36–38 molecules of ATP by glycolysis, the citric acid cycle, and aerobic oxidation. Glucose metabolism is disturbed after TBI. There is a significant increase in anaerobic glycolytic turnover and elevated level of extracellular lactate in cerebral circulation as neurons and astrocytes convert glucose to two molecules of ATP and two molecules of lactate. Hyperglycolysis contributes to prolonged elevated lactate/glucose ratio, CSF lactic acidosis, and compromised mitochondrial function via calcium-mediated interference. The duration of hyperglycolysis and lactate accumulation may reflect the extent of injury and worse prognosis. See **Figure 41.1**.

$CMRO_2$, cerebral metabolic rate of glucose (CMRG), and CBF are common measurements utilized in neurophysiology. In healthy adults, $CMRO_2$ is 3.3 ml/100 g/min, CMRG is 5.5 mg/100 g/min, and CBF is 54 ± 12 ml/100 g/min. In comatose patients with TBI, $CMRO_2$ is reduced to between 1.2 and 2.3 ml/100 g/min and is associated with GCS score and recovery outcome. Storage of glucose and oxygen by neurons and astrocytes is limited, therefore continuous CBF is essential to ensure survival. Arteries and arterioles 30–300 um in diameter can alter their resistance to control cerebral circulation. There is a linear relationship between $CMRO_2$ and CBF consistent with the notion of diffusion-limited oxygen delivery. Flow-metabolism coupling is the process by which blood flow changes in relation to the metabolic demands of cerebral tissue, largely influenced by the changes in tissue CO_2. PaO_2 does not affect CBF except in patients with drastically reduced PaO_2 below 50 mmHg. Cerebral metabolism declines after TBI with corresponding decreases in CBF.

Pressure and viscosity

The Hagen-Poiseuille law of laminar flow in a cylindrical tube is utilized to describe cerebral blood flow in relation to cerebral perfusion pressure (CPP), vessel diameter, and blood viscosity. CBF= k[CPP × d(4)]/(8 × l × v), where k is a constant, d is artery diameter, l is artery length, and v is blood viscosity. CBF is maintained at 50 ml/100 g/min in the adult to facilitate constant metabolic supply to the brain, provided that CPP is in the range of 60–160 mmHg (Cipolla, 2009). CPP is calculated as the difference between mean arterial pressure (MAP) and ICP.

CBF is also maintained via autoregulation (**Fig. 41.2**). Cerebral vasculature possesses myogenic capacity to dilate or contract to counteract deviations in wall tension (that reflect the CPP) to maintain

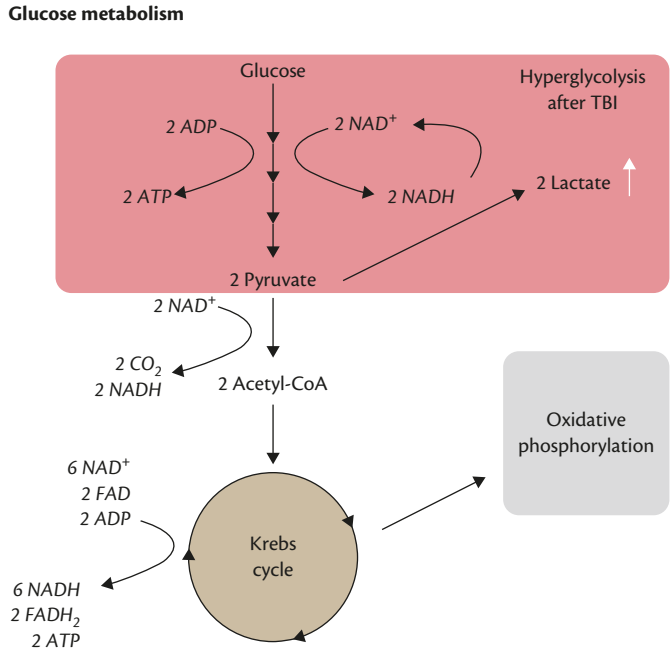

Fig. 41.1 Glucose metabolism can be divided into three distinct processes. Glycolysis is the conversion of glucose into pyruvate. This generates two ATP molecules (net) and does not require oxygen if coupled with conversion of pyruvate into lactate (anaerobic respiration). The Kreb's cycle is a circular biochemical pathway that consumes the carbon skeletons from acetyl-coenzyme A and generates reducing equivalents (nicotinamide adenine dinucleotide (NAD)-H and flavin adenine dinucleotide (FAD)-H), carbon dioxide, and two ATP molecules. The final step of oxidative phosphorylation utilizes the reducing equivalents generated in the preceding steps to generate a hydrogen ion gradient across the mitochondrial membrane which drives a proton ATPase that generates an additional 34 ATP molecules, giving a total of 38 ATP molecules per molecule of glucose (aerobic respiration).

constant flow. Outside the normal CPP 60–160 mmHg, vessels become either maximally dilated or experience forced dilation (i.e. 'pressure breakthrough'). Autoregulation is impaired or absent in the majority of severe TBI patients at some point in their clinical course. When autoregulation is lost, the brain becomes vulnerable to systemic pressure disturbances leading to secondary insults (e.g. ischaemia from reduced CBF or swelling from excess CBF). Severe TBI patients are more prone to secondary injury from low CPP. Thus, flow-metabolism and autoregulation are distinct mechanisms allowing the cerebral circulation to meet local metabolic demand and to stabilize against systemic pressure disturbances.

Changes in whole blood viscosity, largely determined by haematocrit and serum fibrinogen, affect CBF and induce an autoregulatory response under normal physiological circumstances. An increase in viscosity decreases metabolic supply to the brain and causes arterial dilation, while a decrease in viscosity increases metabolic supply and causes arterial constriction. Following acute cerebral infarction, increased haematocrit and fibrinogen are associated with reduced CBF, and that changes in blood viscosity may have important hemodynamic effects on cerebral circulation as well during acute stress.

CO_2 reactivity

CO_2 reactivity is the process by which partial pressure of arterial CO_2 ($PaCO_2$) affects CBF and the cerebral vasculature. Within the normal range of $PaCO_2$ between 20 and 60 mmHg, every 1 mmHg fluctuation results in 2% to 3% change in CBF. Hypercarbia (hypoventilation) results in vasodilation and increased CBF, while hypocarbia (hyperventilation) has the inverse effect. This is mediated through changes in pH of the perivascular space via carbonic anhydrase, and this forms the basis of the acetazolamide challenge. The normal response to acetazolamide administration (e.g. 1 g intravenous) is vasodilation and augmentation of CBF to 30–60% over

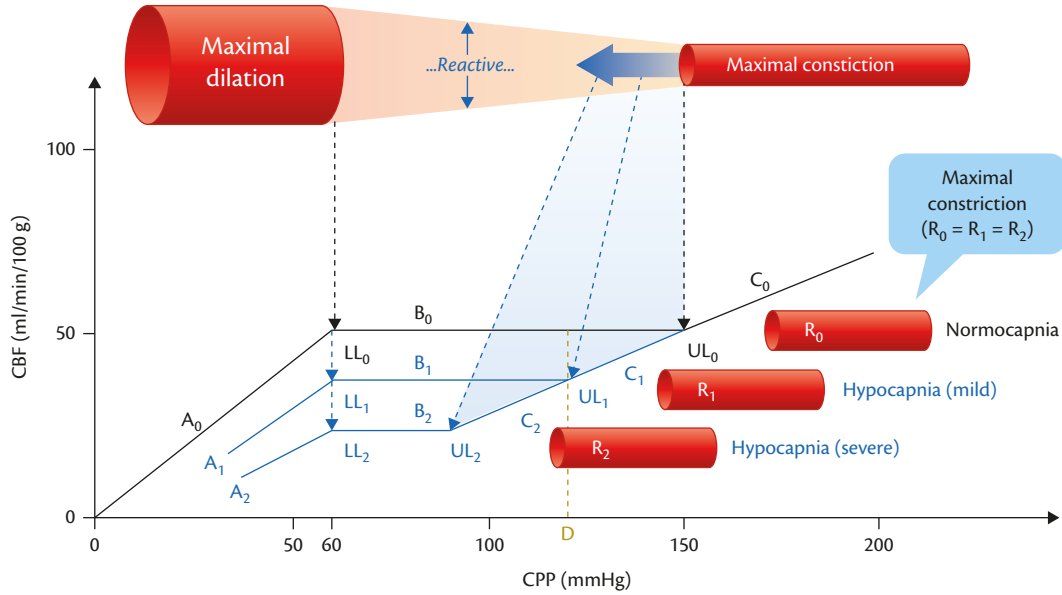

Fig. 41.2 Cerebrovascular autoregulation (A, autoregulation) is the mechanism by which a constant blood flow (B, blood flow) is maintained in the face of variations in systemic blood pressure. Over a range of blood pressures CBF is constant, however above (UL, upper limit) and below (LL, lower limit) this range the vessels are maximally vasoconstricted or vasodilated (respectively) and changes in blood pressure are transmitted as changes in CBF. This risks ischaemia below LL and exacerbates intracranial hypertension above UL.

Therapeutic hyperventilation (C_0–2) in order to reduce intracranial pressure leads to vasoconstriction (R_0–2). This has two potentially damaging effects. Firstly, CBF is reduced risking ischaemia. This can be mitigated by using a measure of intracranial oxygenation. Secondly, the autoregulatory range is reduced, making it more difficult to target an appropriate CPP. This can be mitigated by using a metric of autoregulation such as pulse reactivity index (PRx).

Reproduced with permission from Meng, Lingzhong; Gelb, Adrian W., Regulation of Cerebral Autoregulation by Carbon Dioxide, Anesthesiology, Volume 122, Issue 1, pp. 196–205, Copyright © 2015 Wolters Kluwer Health, Inc.

10–15 minutes. A failure to vasodilate in response to acetazolamide implies maximal vasodilation, usually resulting from chronic ischaemia. Hyperaemia and metabolic acidosis in CSF are associated with the acute phase of TBI, typically in the first 24 hours, and patients with persistent loss of CO_2 reactivity risk high mortality or severe neurological compromise. While CO_2 reactivity causes changes in both CBF and $AVDO_2$, autoregulation affects CBF with $AVDO_2$ maintained relatively constant. Hyperventilation and control of $PaCO_2$ are important therapeutic interventions in the management of raised ICP, however this requires cerebral oxygenation monitoring to ensure that excessive arterial vasoconstriction does not inflict ischaemia.

Secondary injury after severe head trauma

Complex neurochemical pathways after TBI disrupt cerebrovascular circulation and inflict secondary injuries that may last from minutes to weeks, and treatment of secondary injuries is essential to maximizing patient outcome. Though not all these mechanisms are fully understood, the International Mission for Prognosis and Clinical Trials in TBI (IMPACT) database identified hypoxia and hypotension to be present in 20% and 18% of TBI patients, respectively (Murray et al., 2007). Repeated investigations have consistently identified five clinical variables that are correlated with morbidity and poor outcome: arterial hypotension, reduced CPP, elevated ICP, hypoxemia, and pyrexia.

Glutamate-mediated excitotoxicity

Mitochondria play an essential role in cerebral energy metabolism, calcium homeostasis, and reactive oxygen species generation. As early as one-hour post TBI, mitochondrial oxidative phosphorylation can fail, resulting in reduction of ATP production, failed energy-dependent membrane ion pumps, and disrupted homeostasis in neural cellular metabolism. Depressed ATP production increases the rate of glycolysis, elevating lactate production, and potential accumulation in the CSF and extracellular fluid of the injured brain. High lactate levels can further contribute to neuronal dysfunction by inducing acidosis, membrane damage, altered blood brain barrier permeability, and cerebral oedema. Activation of intracellular digestive enzymes (i.e. peroxidases, proteases, phospholipases) and caspases lead to structural damage at the subcellular level, DNA degradation, and neuronal death (i.e. necrosis and apoptosis).

The relationship between excessive Ca^{2+} influx and glutamate-triggered injury is well supported, resulting in uncoupling of mitochondrial electron transfer from ATP synthesis and overactivation of calpains. Glutamate-mediated excitotoxicity activates NMDA receptors, triggering neuronal depolarization with an unchecked influx of calcium into mitochondria. Mitochondrial dysfunction becomes the main cause of energy failure of damaged tissue, as ion pumps are unable to restore membrane potentials. Experiments indicate that Ca^{2+} loading at L-type voltage-sensitive channels is non-toxic, but Ca^{2+} loading at NMDA receptors is neurotoxic. The production of toxic reactive oxygen species (i.e. nitric oxide, superoxide, and hydrogen peroxide) is also contingent on NMDA receptor activation, therefore NMDA receptors are key drivers of excitotoxicity after head injury. These cellular changes lead to cerebral oedema, elevated ICP, vascular compression, and ultimately herniation (Lucas and Newhouse, 1957). When assessing causes and treatments for ischaemia and abnormal oxygen measurements such as cerebral perfusion pressure and jugular venous oxygen saturation, mitochondrial dysfunction should be considered, as maintenance of adequate perfusion may not improve clinical outcome due to underlying mitochondrial impairment. A pragmatic definition of mitochondrial dysfunction is an inability to efficiently carry out oxidative phosphorylation of ADP in the presence of adequate oxygen and metabolic substrate.

Elevated extracellular glutamate is important in mediating both traumatic and ischaemic brain injury. Interstitial glutamate is shown to increase by several mechanisms: BBB damage and extravasation of glutamate to region of impact, membrane damage, and microporation, upregulation of complexin I and complexin II enhancing exocytosis, and glutamate transporter impairment. Beta-lactam antibiotics (e.g. ceftriaxone) are potent stimulators of glutamate transporter (GLT1), which is the astroglial protein responsible for inactivating synaptic glutamate. Beta-lactams increase brain expression of GLT1 and its functional activity, which decreases glutamate neurotoxicity to provide neuroprotective potential in ischaemic injury and neuronal degeneration (Rothstein et al., 2005). Calcium-induced mitochondrial matrix swelling and ruptured outer mitochondrial membranes uncouple the respiratory chain and further impair ATP production. The unregulated influx of calcium and membrane rupturing also induces the opening of the mitochondrial permeability transition pore (mPTP), causing an apoptotic cascade. Cyclosporin A, an immunosuppressant investigated for its ability to inhibit mPTP opening in TBI patients, has demonstrated neuroprotective effects against mitochondrial swelling, membrane breakdown, and ionic homeostatic imbalance (Okonkwo et al., 1999).

Perturbations in cerebral metabolism

TBI damages mitochondrial functionality to propagate neurodegeneration and limit neuroregeneration. Severe TBI induces a sudden shift from aerobic metabolism to hyperglycolysis/anaerobic metabolism with high glucose turnover, contributing to cerebral acidosis. Even when sufficient oxygen is present, hyperglycolysis has been demonstrated in 56% of patients through findings using PET within 1 week following TBI. Acidosis shifts the haemoglobin oxygen-dissociation curve to the right and may increase O_2 supply to injured brain tissue. Elevated CSF lactate level after TBI typically normalizes within 12 hours of injury, except following cerebral ischaemia and diffuse cerebral swelling. The hypothesized role of lactate in injured brain energetics is controversial, and has changed from metabolic waste to supplemental fuel, neuroprotection, and signalling molecule in cortical neurons. Intracerebral microdialysis catheters (Fig. 41.3) allow for biochemical analysis of changes in extracellular neurotransmitters and metabolites during the secondary stage of TBI. The microdialysis measured lactate/pyruvate ratio is a marker of anaerobic metabolism and correlates with outcome after TBI. (Timofeev et al., 2011). Increase in the lactate/pyruvate ratio can be due to cerebral ischaemia or mitochondrial dysfunction. In patients with elevated cerebral lactate/pyruvate ratio (LPR), microdialysis demonstrates that exogenous lactate therapy significantly increases cerebral glucose levels. This correlates with previous evidence that lactate is directly oxidized to pyruvate in the

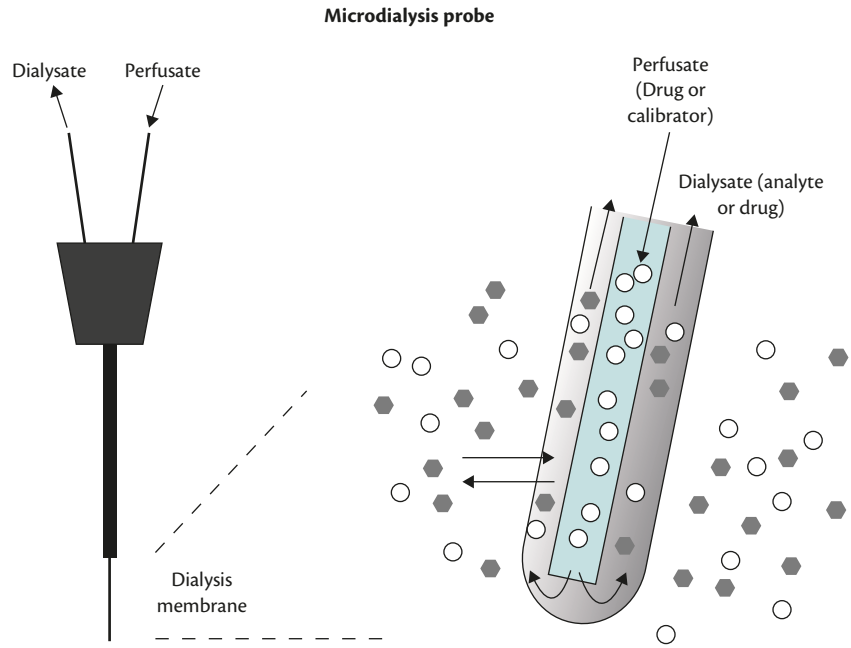

Fig. 41.3 Microdialysis is a technique for sampling the brain extracellular space. An invasive probe is inserted into the brain substance and perfused with fluid (perfusate) at ultralow flow rates (typically 0.3 μl/minute). A semipermeable membrane at the tip of the catheter allows substances to diffuse into the catheter and are recovered in the exiting fluid (microdialysate). For clinical purposes, the commonest analytes are glucose, lactate, pyruvate, glutamate (an excitotoxic neurotransmitter) and glycerol (a measure of cellular membrane breakdown). The ratio between lactate and pyruvate (LPR, lactate-pyruvate ratio) provides a measure of the balance between anaerobic and aerobic respiration (Fig. 41.1). An LPR more than 25 is regarded as pathological and correlates with poor clinical outcome in TBI.

mitochondria of neurons and astrocyte to contribute to cerebral aerobic metabolism (Lazaridis and Andrews, 2014).

Increased activity of the pentose phosphate pathway (PPP) after severe TBI contributes to elevated cerebral glucose uptake exceeding $CMRO_2$ and lactate production (Fig. 41.4). Infusion of isotype glucose after TBI increased PPP activity by 19.6% compared to 6.9% in controls. The PPP products (NADPH, ribose 5-phosphate, and erythrose 4-phosphate) that upregulate fatty acid synthesis, DNA repair and replication, and amino acid and neurotransmitter production are processes that are stimulated after brain injury (Dusick et al., 2007). NADPH is used to produce reduced forms of glutathione and thioredoxin, cofactors for glutathione peroxidases, and peroxiredoxins that combat oxidative stress after acute injury. The PPP does not use oxygen as substrate and does not produce ATP, but rather serves as an antioxidant that contributes to the shift in glucose metabolism from glycolysis to PPP in ischaemic brain tissue.

In TBI patients, 30% patients are found to have $CMRO_2$ values profoundly reduced under non-ischaemic conditions from normal value of 3.3 ml/100 g/min to 1.2–2.3 ml/100 g/min. While $CMRO_2$ after TBI correlate with GCS and is a strong predictor for neurologic outcome, reduced $CMRO_2$ does not necessarily result from ischaemia nor directly cause patient decline. Causes of patient decline include the severity of primary and secondary injuries and the level of consciousness. Studies of severe TBI with mean GCS of 6 report a 25% incidence of reduced oxidative metabolism and persistent metabolic crisis (elevated LPR >40) despite absence of ischaemia, which suggest LPR as an indicator of widespread mitochondrial dysfunction causing metabolic depression following TBI, further impairing brain capacity to meet metabolic demands in coping with secondary insults. While very low $CMRO_2$ indicates irreversible cell injury, LPR may be utilized as a sensitive marker of reversible mitochondrial dysfunction in regions with no observable tissue damage. Published studies using ^{15}O PET demonstrate a metabolism threshold of 37.6 μmol/100 ml/min resulting in irreversible injury.

Loss of autoregulation and pressure reactivity index

As previously mentioned, vascular autoregulation is a myogenic mechanism where wall tension directly results in vascular smooth muscle constriction. An increase in MAP leads to vasoconstriction within 5 to 15 seconds to decrease cerebral blood volume (CBV) and ICP, while a decrease in MAP leads to vasodilation and increase in ICP. Autoregulation may be disrupted on the days following injury with the magnitude and risk of disruption depending on the severity of injury. Quantifying vascular reactivity is clinically important after TBI when cerebral vasculature can become unreactive. Slow wave fluctuations in MAP and ICP lasting 30 seconds to several minutes are common in ventilated patients after head injury. These changes are continuously monitored and their relationship is calculated as pressure reactivity index (PRx) between –1 and +1 (Czosnyka et al., 1997). A negative correlation indicates good vasoreactivity (ICP declines as a result of arterial vasoconstriction when MAP increases) and autoregulatory protection, but a positive correlation indicates the loss of autoregulation and worse prognosis. In large series of patients, a PRx of less than 0.3 correlates with good outcome on dichotomized GOS.

PRx is frequently compromised on the first day after TBI, and the loss of autoregulation in the first 48 hours has strong indication for additional secondary injury including cerebral hypoxia and further ischaemic insults. Preserved autoregulation is a crucial protective

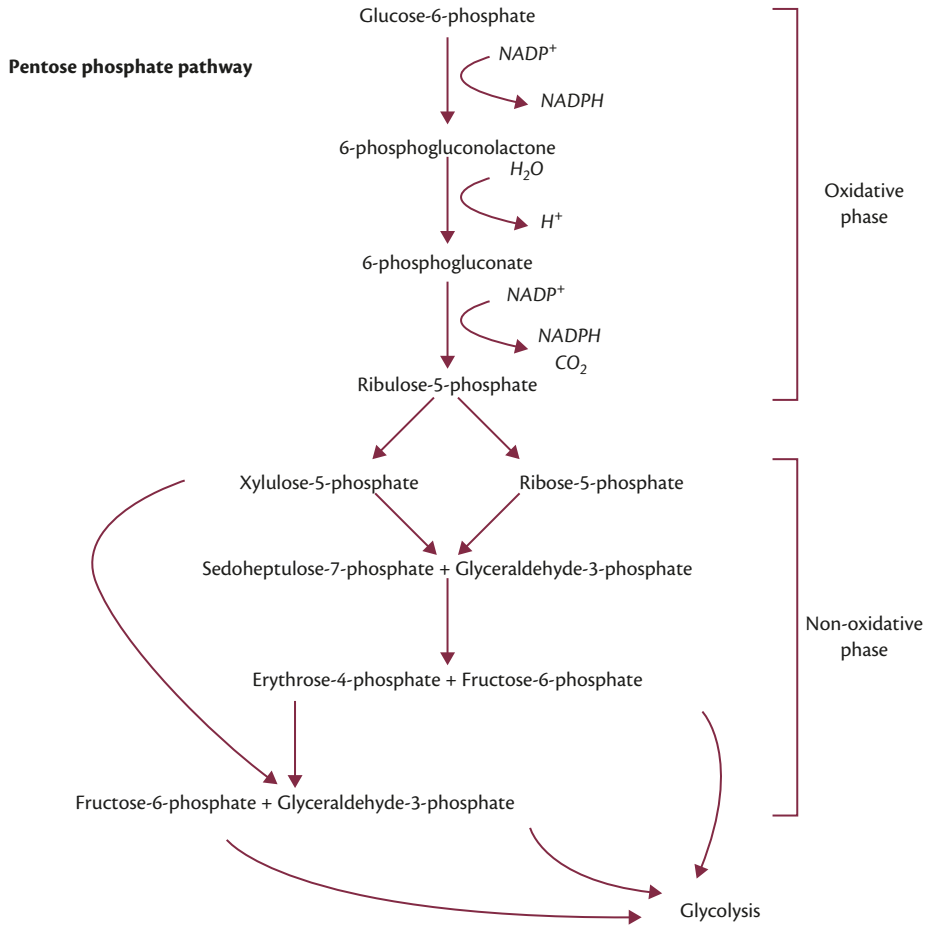

Fig. 41.4 Pentose phosphate pathway. The pentose phosphate pathway (PPP) is an alternative pathway for glucose utilization and is found to be upregulated following TBI. It provides several biochemical substrates that are potentially protective, and this is an actively explored research avenue.

mechanism against transient MAP derangements. In addition to being a strong predictor of outcome, PRx is an important clinical tool in guiding posttraumatic treatment and CPP management. PRx changes dynamically with CPP making it possible to define the CPP threshold at which PRx is minimized to maximize autoregulatory protection: this has been termed 'CPP optimal' ($CPP_{opt)}$. Continuous PRx monitoring in TBI patients determines a real-time CPP_{opt} dependent on the severity of injury, and deviation from the CPP less than CPP_{opt} appears to increase risk of mortality while CPP more than CPP_{opt} appears to discriminate between good and poor outcome on dichotomized GOS. It is yet to be determined whether targeting CPP_{opt} is a valid therapeutic target.

Raised intracranial pressure

The Monro-Kellie hypothesis explains that under normal conditions the total volume of the intracranial cavity remains constant and is formed from three main components: blood (CBV, both arterial and venous), fluid (CSF) and cerebral parenchyma. An increase in one compartment normally results in compensation in another through translocation of CSF and venous blood to maintain constant ICP. When compensatory mechanisms are exhausted, an exponential increase in ICP occurs. Patients with ICP below 20–25 mmHg have significantly better outcomes. Raised intracranial pressure (>20–25 mmHg) can induce ischaemia and hypoxia by reducing CPP (MAP–ICP); as CBF is directly proportional to CPP, the presence of hypotension, elevated ICP, and hypoxia can severely limit cerebral supply after TBI.

Oedema is common after TBI and can be attributed to three distinct mechanisms: vasogenic, cytotoxic, and osmotic. Structural damage due to breakdown of BBB endothelium causes intravascular flow of protein-rich exudate into the brain interstitium, increasing extracellular volume without cell swelling. Second, intracellular volume can accumulate without BBB disruption. Ion influxes and increased membrane permeability of neural cells cause cytotoxic oedema and cellular swelling. Cytotoxic oedema is the most common brain oedema and results in decreased interstitial volume. Third, necrotic tissue is hyperosmolar, causing osmotic-gradient driven fluid accumulation in the cell. Not surprisingly, oedema causes increased ICP and secondary ischaemic events that further exacerbate structural integrity and tissue damage.

In the management of post-traumatic cerebral oedema, hyperosmolar agents such as mannitol or hypertonic saline be administered to lower ICP. However, it is important to note that once the BBB is compromised, mannitol may exacerbate vasogenic cerebral oedema. Bolus mannitol can initiate more than 10% ICP reduction among 86% of patients with intact autoregulation, whereas ICP reduction was observed in only 35% of patients with impaired autoregulation (Muizelaar et al., 1984). When autoregulation is lost,

osmotic agents may increase CBF without compensatory vasoconstriction and thus the desired reduction in ICP may not be achieved. Other potential mechanisms of mannitol action include acting as a free radical scavenger, improving microvascular flow by dehydrating endothelial cells and reducing haematocrit as well the osmotic load. Despite intensive therapeutic measures, intractable ICP is the primary cause of 46% of TBI deaths.

Cerebral blood flow disturbances

In an uninjured brain, changes in CPP between 60 and 160 mmHg have only minor effects on CBF. Following trauma and autoregulatory impairment, CBF becomes increasingly dependent on CPP and minor fluctuations can instigate further ischaemic injury. As previously mentioned, CPP = MAP–ICP, and CBF = CPP/CVR, where CVR is cerebrovascular resistance. Secondary elevation in ICP may worsen CPP and decrease CBF. CBV is defined as millilitres of blood per 100 g cerebral tissue, and can be calculated based on measures of CBF using stable xenon and mean transit time after injection of contrast material. CBF is reflective of CBV under normal conditions, but acutely after trauma there is a dissociation between CBF and CBV due to physiological disturbances. Because metabolism decreases after severe head injury, determining $AVDO_2$ is necessary for accurate interpretation of CBF and diagnosing hypo- or hyperperfusion. CBF is generally low during the first 6 hours after injury and increase significantly in the first 24 hours. A low CBF is generally not associated with a high $AVDO_2$, and is more likely a sign of low oxidative metabolism rather than ischaemia. High CBV does not always correlate with cerebral swelling in severe TBI; other factors besides hyperaemia contribute to cerebral swelling and refractory hypertensive ICP. In patients without acute hyperaemia, CBF consistently correlates with functional recovery (i.e. the lowest CBFs exist in patients with the most severe disabilities).

More recent studies that combine oxygen 15-labelled positron emission tomography (^{15}O PET) with fluorine 18-labelled fluoromisonidazole (^{18}F FMISO) further characterize macrovascular and microvascular ischaemia in early TBI (Veenith et al., 2016). Comparison of ischaemic brain volume (IBV) and hypoxic brain volume (HBV) demonstrates that the diffusion hypoxia barrier in HBV is associated with microvascular collapse, whereas IBV represents macrovascular ischaemia and irreversible damage. Traumatic contusions show reduced CBF and $CMRO_2$, but similar CBV and oxygen extraction fraction (OEF) as controls. In pericontusional regions with no identifiable tissue dysfunction, $CMRO_2$ is lower, but CBF, CBV, and OEF are similar to the controls. Classic reasoning dictates that with reduced $CMRO_2$, OEF increase to compensate. However, recent studies using DTI showed that surrounding contusions there is a frequent rim of low diffusion coefficient consistent with cytotoxic oedema, which may explain the minimal change in OEF because of widespread microvascular failure and selective neuronal loss.

Hyperaemia

Hyperaemia, also known as vascular engorgement or luxury perfusion, results from disruption of flow-metabolism coupling when CBF exceeds $CMRO_2$ requirements. Increased CBV often indicates posttraumatic hyperaemia which in conjunction with elevated ICP portends poor recovery. While acute hyperaemia is frequently associated with hypertensive ICP (>20 mmHg), subnormal flow indicates intact flow-metabolism coupling rather than ischaemia. Hyperaemic ICP patients are often younger, present with low mean GCS (≤6), risk effacement of basal cisterns and refractory hypertension, and demonstrate gross loss of autoregulation. Of note, CBF is functionally coupled to CMRG and not $CMRO_2$, thereby luxury perfusion may be an appropriate metabolic response to hyperglycolysis after injury. Historically, hyperventilation was initiated to decrease CBF and subsequently ICP, however this approach has been tempered by the risk of inducing ischaemia. After brain injury, CBF may no longer accurately reflect CBV due to disruption in normal physiology, and in patients with acute SDH, elevated ICP, and ischaemia, CBV is half of normal value. Therefore, multiple aetiologies may contribute to intracranial hypertension and cerebral swelling after severe head trauma.

Cerebral ischaemia

Ischaemic injury consists of the infarct core and the penumbra. The core undergoes hypoxia-induced loss of cellular homeostasis and necrosis, while the penumbra's apoptotic processes can be targeted for therapeutic intervention. Cerebral ischaemia occurs when CBF does not meet cerebral metabolic demands (e.g. low CBF and high $AVDO_2$). Assuming flow-metabolism coupling is intact, jugular bulb oximetry is frequently utilized in the ICU to estimate the adequacy of CBF from its inverse relationship to $AVDO_2$. While normal $AVDO_2$ ranges from 4 to 9 ml 100 ml^{-1}, low CBF and ischaemic state increase oxygen extraction and increase $AVDO_2$. Transcranial doppler non-invasively measures the blood flow velocity of basal cerebral arteries in order to estimate CBF, with the caveat that haemorrhage can cause vasospasm which increases flow velocities irrespective of CBF. Ischaemia is often seen in acute SDH and diffuse cerebral swelling and inadequate metabolic supply to the brain after TBI is predictive of high morbidity and disability. PET has demonstrated that previous definitions of hyperaemia and ischaemia based on CBF and oxygen are inaccurate, and maintaining oxygen delivery may not be sufficient to prevent secondary injury. Mitochondrial dysfunction after TBI decreases oxygen demand, and the transition to hyperglycolysis increases lactate accumulation. Thus, decreased CBF can be misinterpreted as ischaemia, and the maintenance of adequate perfusion (CPP >70 mmHg) may not result in improvement due to impaired mitochondrial ATP synthesis.

As mentioned earlier, in normal physiology, $AVDO_2$ remains relatively constant while CBF changes in accordance to $CMRO_2$/CMRG. When autoregulation is lost in TBI and the ability of CBF to meet metabolic demands is impaired, $AVDO_2$ may increase to improve O_2 extraction in the cerebral circulation. $AVDO_2$ is capable of increasing from baseline value 6.7 ml/100 ml to a maximum 13 ml/100 ml. The normal CBF threshold at which $AVDO_2$ compensation occurs is 18 ml/100 g/min, and can rise to 20 ml/100 g/min following TBI due to decreased oxidative metabolism. ^{15}O PET shows that diffusion barrier ischaemia (increased oxygen diffusion gradient from vasculature to interstitium) is due to microvascular disturbances such a perivascular oedema surrounding traumatic lesions causing decreased partial pressure of oxygen in brain tissue (PbO_2).

In addition to caspases and other proteins directly causing neuronal death, three distinct mitogen-activated protein kinase (MAPK) inflammatory pathways contribute to ischaemic injury: extracellular signal-regulated kinase (ERK) pathway, c-Jun-N-terminal protein

kinase (JNK) pathway, and the p38 pathway. Emerging research on the use of biomarkers has yielded several markers of importance to neuronal, glial, and axonal damage. Neuron-specific enolase is a glycolytic enzyme predominantly in neurons. S100B is a calcium binding protein predominantly in astroglia. Myelin basic protein is in white matter and a marker for axonal damage. Recent studies have found these to be important biomarkers of pathological processes involved in cerebral ischaemia and neuroinflammation following TBI and reflecting the time course of secondary injury.

Cortical spreading depression and epilepsy

Cortical spreading depression (CSD) is a pervasive wave of ionic homeostasis failure that transiently interrupts cortical function. It is characterized by EEG depression, pial vasodilation, and a slow negative potential shift following severe head trauma and ischaemia (Leao, 1947). Spontaneous peri-infarct depolarizations (PID) propagate to normal cerebral tissues and take on the characteristics of CSD. Electrocorticographic (ECoG) recordings show spontaneous depressions accompanied by stereotyped CSDs spreading across the cortical mantle at 3.3 mm/min; ECoG background activity recovers spontaneously or 2 to 5 hours later (Fabricius, 2006). Propagating depolarization waves in neuronal and glial cells cause an increase in oxidative metabolism, compensated by increased CBF and metabolic activity; hence CSD does not cause neuronal injury in the normal brain when flow-metabolism is intact. Haemodynamic disruption and flow-metabolism decoupling are frequent phenomena after head injury, thus CSD may incur additional energy demand that cannot be metabolically compensated for by the injured brain.

CSD alters BBB permeability via matrix metalloproteinase (MMP) activity. MMPs consists of neutral proteases implicated in wide range of processes: the opening of the BBB; immune cell infiltration of neural tissue; shedding of cytokine and cytokine receptors; direct cellular damage; and neuronal development and plasticity. CSD increases MMP-9 activity, which leads to the breakdown of BBB and oedema formation. Neuronal expression of MMP-9 and MMP-2 is implicated in neurotoxicity after ischaemia and trauma, increasing the susceptibility to cerebral haemorrhage. CSD occurs more frequently in the younger acutely injured patients, and may be attenuated with glutamate receptor inhibitors, specifically NMDA receptor antagonists. CSD and PID contribute to the increase of final infarct volume in a step-wise fashion as part of additional secondary insults and stress-induced changes in the penumbra of primary lesions.

Seizures

Acute seizures (both convulsive and non-convulsive) are well documented secondary insults that may be due to neurochemical disarray and can exacerbate tissue damage and worsen clinical recovery. EEG monitoring demonstrates that the majority of seizures do not have overt motor manifestations and require continuous monitoring of seizure activity. ECoG recordings can distinguish the hallmark slow potential change of CSD from seizures; while CSD and seizures frequently occur together, there is no correlation between the two phenomena in regard to time, space, and intensity (Fabricius, 2006). Following moderate to severe TBI, seizures occur in more than 20% of patients in the first week; peak incidence is bimodal with an early peak at 29 hours and later peak at 140 hours, with mean duration of 2.8 minutes and a tendency to cluster. At these respective peaks for seizure activity, ICP is secondarily elevated, with the ictal ICP being higher than interictal ICP. Elevated ICP and the risk for swelling due to seizure may be attributed to prolonged increases in CBF, extracellular oedema, and glutamate accumulation in the interstitium.

Epileptiform activity is known to further stimulate glycolysis and neurochemical changes that may further stress neuronal integrity. Microdialysis LPR is higher for TBI patients with seizures (compared to without), and during the ictal periods (compared to interictal periods). Increased LPR is associated with prolonged metabolic stress, therefore seizure control is a therapeutic target for minimizing metabolic stress postinjury. Pericontusional regions, in particular in the frontotemporal region, are electrically active and capable of epileptiform activity. Patients with severe TBI are predisposed to seizures. Strong risk factors include the presence of a brain contusion and/or subdural haematoma, and early evacuations of mass lesions may be associated with reduced seizure activity (Annegers et al., 1998). Focal seizures with secondary generalization occur in 78% of reported seizures after severe TBI.

Beta-amyloid deposition and apolipoprotein E interaction

TBI is shown to trigger pathological production and accumulation of amyloid-(Aβ) peptides in the cerebral cortex, particularly localized to contusional and pericontusional regions (Roberts et al., 1991). Cleavage of amyloid precursor protein (APP) produces apolipoprotein E (ApoE) and Aβ, and the polymorphism of the ApoE gene determines the risk for plaque deposition: ApoE ε4 carries greater risk, while ApoE ε3 (more frequent) and ε2 (rare) both reduce the risk for Aβ burden. Of the three isoforms, ApoE ε4 binds the least avidly to cytoskeletal proteins that would promote neurite growth and neuroprotective effect. Rather, ApoE ε4 binds more avidly to Aβ and promotes aggregation into amyloid fibrils. Studies using intracranial microdialysis measured higher levels of Aβ in patients with DAI compared to focal injuries, and thus Aβ accumulation may also depend on the injury type. Long-term axonal degeneration and intra-axonal Aβ deposition in the brain parenchyma is likely due to continued neurodegeneration and secondary insults. *In vitro* studies support evidence of ApoE-Aβ interactions where TBI patients with ApoE ε4 allele have more Aβ deposition in the hippocampus and frontal cortex.

In the acute phase postinjury, decreased ELISA measurements of Aβ concentrations and apolipoprotein E (ApoE) in the CSF occur. Their levels gradually increase over time to correlate with improved neurologic outcome. There is reduced Aβ production immediately following neuronal trauma, and the decreased ApoE level is possibly due to increased utilization of ApoE-lipid complexes for repair as part of a coordinated response to neuronal injury. ApoE can be neuroprotective against cerebral ischaemia, and intraventricular infusion of ApoE reduced neuronal damage after ischaemia in animal models via clearance of lipid and cholesterol debris. ApoE facilitates anti-inflammatory effects through downregulation of microglia and cytokine release (Kay et al., 2003). Aβ plaques from TBI are similar to the hallmark pathology found in early stages of Alzheimer's disease. Long-term follow-up of patients with TBI also correlated with incidence of Alzheimer's disease, with ApoE isotype as a key predictor. Notably, follow-up 6 months after TBI reported 57% of patients possessing the ApoE ε4 allele to have unfavourable outcome (GOS: dead, vegetative state, or severe disability) compared to 27% of patients with the ApoE ε2 or ε3 allele.

Future directions

Successful implementation of the TBI Common Data Elements (CDEs), along with demonstration of their utility in generating novel classification approaches with robust statistical power, informed the refinement of the NIH/NINDS CDEs, version 2 (Hicks et al., 2013), and generated the impetus for the concurrent 22-nation Collaborating European NeuroTrauma Effectiveness Research in TBI (CENTER-TBI) study in the EU and 11-site TRACK-TBI study in the US (Manley and Maas 2013). These had the goals of enrolling close to 10 000 combined patients using the CDEs in order to provide novel multidimensional approaches to TBI classification, establish evidentiary benchmarks for quality of care, and generate large, well-curated TBI data repositories to enable and ensure legacy research opportunities.

Conclusion

While risk reduction of primary neurological trauma is mainly preventative in nature, understanding the sequelae of TBI in order to clinically manage and/or pre-empt secondary injuries is paramount in current neurosurgical and neurocritical care. Preventing potential complications in TBI patients who 'talk and deteriorate' emphasizes the crucial concept that a primary injury can readily induce pathophysiologic conditions for compounded secondary damage. Finally, TBI is recognized more as a disease process rather than a single event; the inherent heterogeneity of injury types and severities highlight the critical need to converge upon a classification scheme using a consensus definition of pathoanatomic injury—measurable through validated clinical, neuroimaging, and serum biomarkers similar to current standard approaches in heart disease, cancer, and diabetes. Large-scale international TBI trials using validated common data standards to accelerate advances in classification and prognosis are currently underway.

FURTHER READING

Chesnut, R.M. (1997). Guidelines for the management of severe head injury. In: Vincent, J.L. (ed.) *Yearbook of Intensive Care and Emergency Medicine*, pp. 50–67. Berlin, Heidelberg: Springer.

Lazaridis, C. & Andrews, C.M. (2014). Brain tissue oxygenation, lactate-pyruvate ratio, and cerebrovascular pressure reactivity monitoring in severe traumatic brain injury: systematic review and viewpoint. *Neurocrit Care*, **21**(2), 345–55.

McHugh, G.S., Engel, D.C., Butcher, I., et al. (2007). Prognostic value of secondary insults in traumatic brain injury: results from the IMPACT study. *J Neurotrauma*, **24**(2), 287–93.

Ommaya, A.K., Goldsmith, W., & Thibault, L. (2002). Biomechanics and neuropathology of adult and paediatric head injury. *Br J Neurosurg*, **16**(3), 220–42.

Veenith, T.V., Carter, E.L., Geeraerts, T., et al. (2016). Pathophysiologic mechanisms of cerebral ischemia and diffusion hypoxia in traumatic brain injury. *JAMA Neurol*, **73**(5), 542–50.

REFERENCES

Adams, J.H., Doyle, D., Grahma, D.I., et al. (1985). The contusion index: a reappraisal in human and experimental non-missile head injury. *Neuropathol Appl Neurobiol*, **11**(4), 299–308.

Annegers, J.F., Hauser, W.A., Coan, S.P., & Rocca, W.A. (1998). A population-based study of seizures after traumatic brain injuries. *N Engl J Med*, **338**(1), 20–4.

Bajsarowicz, P., Prakash, I., Lamoureux, J., et al. (2015). Nonsurgical acute traumatic subdural hematoma: what is the risk? *J Neurosurg*, **123**(5), 1176–83.

Chesnut, R.M. (1997). Guidelines for the management of severe head injury. In: Vincent, J.L. (ed.) *Yearbook of Intensive Care and Emergency Medicine*, pp. 50–67. Berlin, Heidelberg: Springer.

Cipolla, M.J. (2009). The cerebral circulation. *Colloquium Series on Integrated Systems Physiology: From Molecule to Function*, **1**(1), 1–59.

Czosnyka, M., Smielewski, P., Kirkpatrick, P., Laing, R.J., Menon, D., & Pickard, J.D. (1997). Continuous assessment of the cerebral vasomotor reactivity in head injury. *Neurosurgery*, **41**(1), 11–17; discussion 17–19.

Dreier, J.P. (2011). The role of spreading depression, spreading depolarization and spreading ischemia in neurological disease. *Nat Med*, **17**(4), 439–47.

Dusick, J.R., Glenn, T.C., Lee, W.N., et al. (2007). Increased pentose phosphate pathway flux after clinical traumatic brain injury: a [1,2–13C2] glucose labeling study in humans. *J Cereb Blood Flow Metab*, **27**(9), 1593–602.

Fabricius, M. (2006). Cortical spreading depression and peri-infarct depolarization in acutely injured human cerebral cortex. *Brain*, **129**(3), 778–90.

Gennarelli, T.A., Thibault, L.E., Adams, J.H., Graham, D.I., Thompson, C.J., & Marcincin, R.P. (1982). Diffuse axonal injury and traumatic coma in the primate. *Ann Neurol*, **12**(6), 564–74.

Giza, C.C. & Hovda, D.A. (2001). The neurometabolic cascade of concussion. *J Athl Train*, **36**(3), 228–35.

Hicks, R., Giacino, J., Harrison-Felix, C., Manley, G.T., Valadka, A.B., & Wilde, E.A. (2013). Progress in developing common data elements for traumatic brain injury research: version two—the end of the beginning. *J Neurotrauma*, **30**(22), 1852–61.

Holbourn, A.H. (1944). Mechanics of head injuries. *Lancet*, **243** (6293), 483.

Kay, A.D., Petzold, A., Kerr, M., Keir, G., Thompson, E., & Nicoll, J.A. (2003). Alterations in cerebrospinal fluid apolipoprotein E and amyloid β-protein after traumatic brain injury. *J Neurotrauma*, **20**(10), 943–52.

Lazaridis, C. & Andrews, C.M. (2014). Brain tissue oxygenation, lactate-pyruvate ratio, and cerebrovascular pressure reactivity monitoring in severe traumatic brain injury: systematic review and viewpoint. *Neurocrit Care*, **21**(2), 345–55.

Leao, A.A. (1947). Further observations on the spreading depression of activity in the cerebral cortex. *J Neurophysiol*, **10**(6), 409–14.

Lucas, D.R. & Newhouse, J.P. (1957). The toxic effect of sodium L-glutamate on the inner layers of the retina. *Arch Ophthalmol*, **58**(2), 193–201.

Manley, G.T. & Maas, A.I. (2013). Traumatic brain injury: an international knowledge-based approach. *JAMA*, **310**(5), 473–74.

McHugh, G.S., Engel, D.C., Butcher, I., et al. (2007). Prognostic value of secondary insults in traumatic brain injury: results from the IMPACT study. *J Neurotrauma*, **24**(2), 287–93.

Muizelaar, J.P., Lutz, H.A., Becker, D.P. (1984). Effect of mannitol on ICP and CBF and correlation with pressure autoregulation in severely head-injured patients. *J Neurosurg*, **61**(4), 700–6.

Murray, G.D., Butcher, I., McHugh, G.S., et al. (2007). Multivariable prognostic analysis in traumatic brain injury: results from the IMPACT study. *J Neurotrauma*, **24**(2), 329–37.

Okonkwo, D.O., Buki, A., Siman, R., & Povlishock, J.T. (1999). Cyclosporin A limits calcium-induced axonal damage following traumatic brain injury. *Neuroreport*, **10**(2), 353–8.

Ommaya, A.K., Goldsmith, W., & Thibault, L. (2002). Biomechanics and neuropathology of adult and paediatric head injury. *Br J Neurosurg*, **16**(3), 220–42.

Pudenz, R.H. & Shelden, C.H. (1946). The lucite calvarium; a method for direct observation of the brain; cranial trauma and brain movement. *J Neurosurg*, **3**(6), 487–505.

Roberts, G.W., Gentleman, S.M., Lynch, A., & Graham, D.I. (1991). βA4 amyloid protein deposition in brain after head trauma. *Lancet*, **338**(8780), 1422–23.

Rothstein, J.D., Patel, S., Regan, M.R., et al. (2005). β-lactam antibiotics offer neuroprotection by increasing glutamate transporter expression. *Nature*, **433**(7021), 73–7.

Sambasivan, M. (1997). An overview of chronic subdural hematoma: experience with 2300 cases. *Surg Neurol*, **47**(5), 418–22.

Santarius, T., Kirkpatrick, P.J., Ganesan, D., et al. (2009). Use of drains versus no drains after burr-hole evacuation of chronic subdural haematoma: a randomised controlled trial. *Lancet*, **374**(9695), 1067–73.

Seelig, J.M., Becker, D.P., Miller, J.D., Greenberg, R.P., Ward, J.D., & Choi, S.C. (1981). Traumatic acute subdural hematoma. *N Engl J Med*, **304**(25), 1511–18.

Shaw, N.A. (2002). The neurophysiology of concussion. *Prog Neurobiol*, **67**(4), 281–344.

Timofeev I, Carpenter KL, Nortje J, et al. (2011). Cerebral extracellular chemistry and outcome following traumatic brain injury: a microdialysis study of 223 patients. *Brain*, **134**(Pt 2), 484–94.

Veenith, T.V., Carter, E.L., Geeraerts, T., et al. (2016). Pathophysiologic mechanisms of cerebral ischemia and diffusion hypoxia in traumatic brain injury. *JAMA Neurol*, **73**(5), 542–50.

Vespa, P., Bergsneider, M., Hattori, N., et al. (2005). Metabolic crisis without brain ischemia is common after traumatic brain injury: a combined microdialysis and positron emission tomography study. *J Cereb Blood Flow Metab*, **25**(6), 763–74.

Weber, M., Grolimund, P., & Seiler, R.W. (1990). Evaluation of posttraumatic cerebral blood flow velocities by transcranial doppler ultrasonography. *Neurosurgery*, **27**(1), 106–12.

Zimmerman, R.A. & Bilaniuk, L.T. (1982). Computed tomographic staging of traumatic epidural bleeding. *Radiology*, **144**(4), 809–12.

RELATED LINK TO EBRAIN

Neuropathology of Head Injury. https://learning.ebrain.net/course/view.php?id=1088

42

Intensive care management of head injury

Matthew A. Kirkman and Martin Smith

Introduction

Traumatic brain injury (TBI) is a leading cause of death and disability in adults under 40 years of age. Outcome is determined by the severity of the primary injury and several mediators of secondary injury, including intracranial hypertension, systemic hypotension, and hypoxia, pyrexia, and hypo- and hyperglycaemia. The monitoring, prevention, and management of factors that lead to secondary brain injury are the cornerstones of the intensive care management of TBI.

Early management of head injury

The initial approach to head injury focuses on prompt and systematic assessment and management in line with standard prehospital and Advanced Trauma Life Support protocols (**Fig. 42.1**). Resuscitation and early management is a crucial stage at which mortality and morbidity after severe TBI can be influenced (Boer et al., 2012). The prevention or immediate correction of hypoxaemia and hypotension, rapid diagnosis and evacuation of an expanding intracranial haematoma, and treatment of raised intracranial pressure (ICP) are key determinants of outcome. Minimizing time to stabilization and definitive treatment is of the essence. Although airway management and ventilation are crucial interventions in comatose TBI patients and those with a deteriorating conscious level, the role of prehospital endotracheal intubation and who should perform it remains controversial (Boer et al., 2012). Unless the patient is alert and cooperative, the cervical spine should be immobilized while awaiting imaging and/or formal clinical assessment. Life-threatening extracranial injuries should be stabilized prior to transfer.

Management of polytrauma in the context of head injury

TBI is often associated with extracranial injuries, including spinal trauma (see **Chapter 64**), which can complicate brain-directed therapy. Timely and appropriate intervention to stabilize or treat extracranial injuries is critical to prevent prolonged haemorrhagic shock, systemic inflammatory response syndrome, and multiple organ failure.

A particular challenge in patients with multiple injuries is balancing the competing interests of hypotensive resuscitation and its' potential to limit ongoing blood loss and speed time to resuscitation with the risk of worsening associated brain injury. It is recommended that systolic blood pressure be maintained more than 90 mmHg at all times in patients with TBI. However, if a lower blood pressure is required during the treatment of life-threatening haemorrhage, the duration of hypotension should be as short as possible and other physiological variables optimized to maximize cerebral oxygen delivery. In particular, hypocarbia must be avoided.

ICP monitoring is recommended during multiple surgical procedures and/or prolonged sedation for extracranial injuries when the opportunity for clinical assessment is limited (Stocchetti et al., 2014).

General principles for the intensive care management of head injury

All patients with severe TBI should be managed in an intensive care unit (ICU) offering immediate access to multidisciplinary clinical neuroscience teams and other relevant specialties, supported by appropriate imaging and investigational facilities. Patients with mild or moderate TBI may also require admission to the ICU for a variety of indications (**Box 42.1**).

The intensive care management of TBI is complex and involves meticulous general intensive care support to optimize systemic physiology, and interventions targeted to the injured brain (**Table 42.1**). In addition to the continuous monitoring and assessment of cardiorespiratory functions common to all critically ill patients, several techniques are available for global and regional brain monitoring (see next).

Cardiorespiratory function

A single episode of hypoxaemia (PaO_2 <8 kPa or SpO_2 <90%) or hypotension (systolic BP <90 mmHg) is strongly associated with poorer outcomes after severe TBI, and the combination of the two is more deleterious than either insult alone (McHugh et al., 2007). Prevention or rapid reversal of hypoxia and hypotension is essential in patients with severe TBI. However, therapeutic hyperoxia is associated with adverse effects, including free radical formation

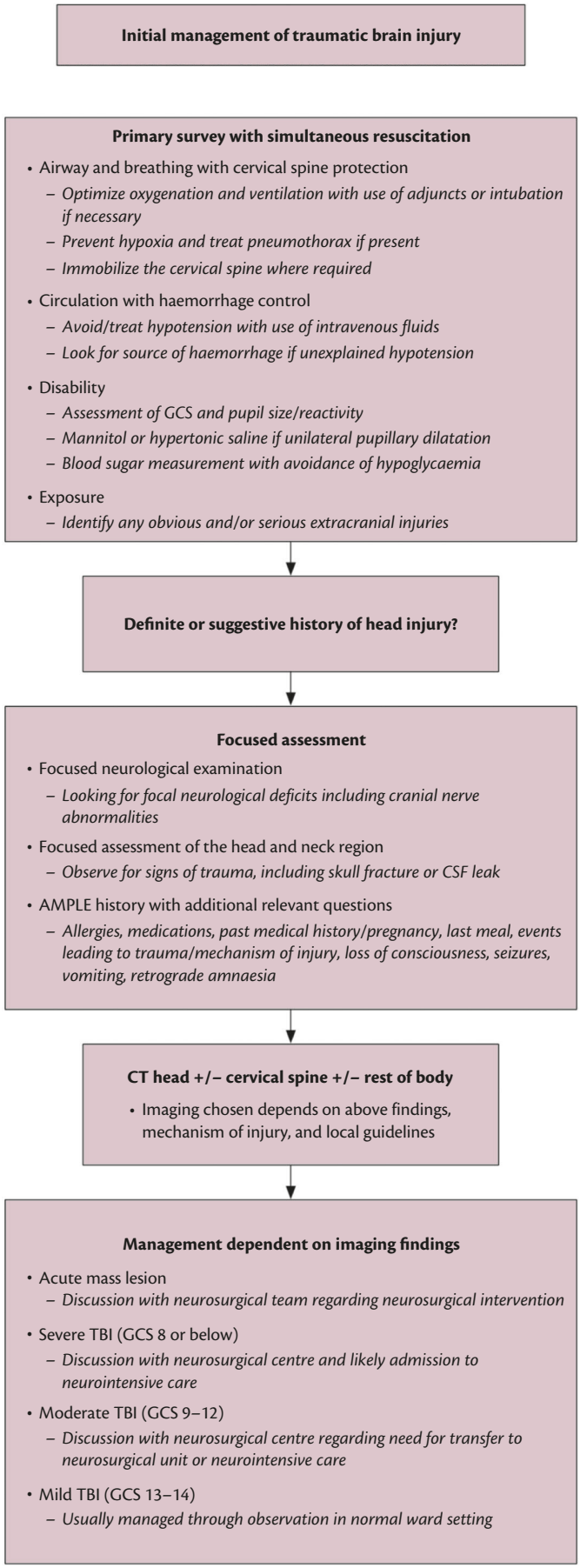
Initial management of traumatic brain injury
Primary survey with simultaneous resuscitation
• Airway and breathing with cervical spine protection
– Optimize oxygenation and ventilation with use of adjuncts or intubation if necessary
– Prevent hypoxia and treat pneumothorax if present
– Immobilize the cervical spine where required
• Circulation with haemorrhage control
– Avoid/treat hypotension with use of intravenous fluids
– Look for source of haemorrhage if unexplained hypotension
• Disability
– Assessment of GCS and pupil size/reactivity
– Mannitol or hypertonic saline if unilateral pupillary dilatation
– Blood sugar measurement with avoidance of hypoglycaemia
• Exposure
– Identify any obvious and/or serious extracranial injuries
Definite or suggestive history of head injury?
Focused assessment
• Focused neurological examination
– Looking for focal neurological deficits including cranial nerve abnormalities
• Focused assessment of the head and neck region
– Observe for signs of trauma, including skull fracture or CSF leak
• AMPLE history with additional relevant questions
– Allergies, medications, past medical history/pregnancy, last meal, events leading to trauma/mechanism of injury, loss of consciousness, seizures, vomiting, retrograde amnaesia
CT head +/– cervical spine +/– rest of body
• Imaging chosen depends on above findings, mechanism of injury, and local guidelines
Management dependent on imaging findings
• Acute mass lesion
– Discussion with neurosurgical team regarding neurosurgical intervention
• Severe TBI (GCS 8 or below)
– Discussion with neurosurgical centre and likely admission to neurointensive care
• Moderate TBI (GCS 9–12)
– Discussion with neurosurgical centre regarding need for transfer to neurosurgical unit or neurointensive care
• Mild TBI (GCS 13–14)
– Usually managed through observation in normal ward setting

Fig. 42.1 Management algorithm for immediate management of traumatic brain injury.

Box 42.1 Indications for intensive care unit admission of head-injured patients

- Severe traumatic brain injury (defined as a postresuscitation Glasgow Coma Scale score ≤8)
- Clinical or radiological evidence of raised intracranial pressure
- Need for mechanical ventilation due to:
  - Decreased conscious level
  - Evidence of brainstem dysfunction
  - Acute respiratory failure (e.g. due to neurogenic pulmonary oedema)
  - Episodes of apnoea
  - Generalized tonic-clonic seizures or status epilepticus
  - Any other cause of a compromised or threatened airway
- Cardiovascular instability requiring intensive haemodynamic monitoring and management
- Need for invasive neurological and systemic monitoring
- Management of systemic organ support such as renal and cardiac dysfunction
- Postoperatively following neurosurgical interventions
- Multisystem trauma

and pulmonary injury, and normobaric hyperoxia does not result in clinically significant improvements in brain oxygen metabolism. Although there is some evidence that hyperbaric oxygen reduces mortality, there is little evidence of improved functional outcome in survivors (Bennett et al., 2012). Routine hyperoxia beyond that which is necessary to maintain key oxygenation targets is therefore not recommended.

Hypotension should be corrected initially with intravenous fluid resuscitation, but a vasoactive agent is required if adequate blood

Table 42.1 General aspects of the critical care management of severe head injury

Ventilation	• PaO_2 >11 kPa • $PaCO_2$ 4.5–5.0 kPa • lung protective ventilation strategies (tidal volume 6 ml/kg ideal body weight, PEEP 6–12 mmHg and recruitment manoeuvres) as brain-directed therapy allows • PEEP to maintain oxygenation (PEEP (≤12–15 cm H_2O does not have adverse effects on ICP and may reduce ICP if oxygenation is improved) • ventilator 'care bundle' to minimize risk of pneumonia – head-up positioning – oral hygiene – peptic ulcer prophylaxis – venous thromboembolism prophylaxis – daily sedation holds if ICP allows
Cardiovascular	• MAP > 90 mmHg • target euvolaemia with isotonic crystalloids • vasopressors/inotropes if insufficient response to fluid
ICP and CPP targets	• CPP 60–70 mmHg • ICP <22 mmHg
Other	• normoglycaemia • normothermia • seizure control • enteral nutrition • thromboembolic prophylaxis

CPP, cerebral perfusion pressure; ICP, intracranial pressure; MAP, mean arterial pressure; PEEP, positive end-expiratory pressure.

pressure cannot be achieved with fluid resuscitation alone. Overly aggressive fluid resuscitation is detrimental, and euvolaemia is the primary cardiovascular goal (Gantner et al., 2014). Intravascular volume should be maintained with isotonic crystalloids, and 0.9% saline is a justified choice despite a lack of evidence of superiority. Albumin is associated with increased mortality, possibly secondary to an associated increase in ICP (Cooper et al., 2013). Despite interest in the use of hypertonic saline (HS) solutions for fluid resuscitation after TBI, no outcome benefits over isotonic crystalloids have been reported.

There is no reliable evidence that one vasopressor is superior to another, but norepinephrine has a predictable and consistent effect on systemic blood pressure and cerebral haemodynamics, and is widely used.

Glycaemic control

Hyperglycaemia exacerbates secondary neuronal injury and is associated with worsened outcomes after severe TBI. 'Tight' glycaemic control with intensive insulin therapy can precipitate cerebral hypoglycaemia and metabolic crises after TBI (Vespa et al., 2012). Moderate serum glucose control is therefore recommended, maintaining serum glucose concentration between 7 and 10 mmol/litre, and avoiding hypoglycaemia (serum glucose <4.4 mmol/litre) and large swings in glucose concentration (Kramer et al., 2012).

Temperature control

Pyrexia (variably defined as core body temperature exceeding 37.5°C to 38.5°C) occurs in more than 50% of TBI patients on the ICU, and is independently associated with worse outcome. Causes are multifactorial and include infection and hypothalamic dysfunction. Despite the availability of treatment options including antipyretic medications, and surface and intravascular cooling devices, high-quality evidence of outcome benefits following cooling to normothermia is lacking. Despite this, targeted normothermia or mild hypothermia (35.5–37°C)—increasingly referred to as targeted temperature management (TTM)—is often recommended in TBI management.

TTM has many potential neuroprotective actions including stabilization of the blood-brain barrier, ICP reduction, and inhibition of inflammation and intracellular calcium overload. Compelling preclinical evidence of benefit has not translated into positive outcome effects of TTM in large-scale randomized clinical trials (RCTs), although several single-centre studies have shown benefit. In contrast to previous systematic reviews, a 2014 meta-analysis including RCTs and observational studies demonstrated some evidence of benefit for TTM in terms of overall reduction in mortality and poor outcome (Crossley et al., 2014). However, the majority of included trials were of low quality and this may overestimate the effectiveness of TTM versus standard care. In particular, there is significant heterogeneity between studies in the timing of onset and duration of TTM, target temperature, and timing and rate of rewarming. Rewarming is the most dangerous phase of TTM, and must be carried out in a controlled manner (0.1–0.25°C per hour) to minimize the risk of rebound intracranial hypertension and hyperkalaemia. Disappointingly, a recent RCT failed to find a benefit of TTM over fever control alone, despite inducing TTM as soon after injury as possible, maintaining target temperature (32–34°C) for at least 72 hours, and rewarming slowly (<1°C per day) (Maekawa et al., 2015). Other adverse effects of TTM include shivering, and abnormalities in blood glucose, electrolyte levels, and fluid balance.

Moderate TTM effectively reduces raised ICP and is often incorporated into ICP management protocols (see next), despite a lack of evidence of improved outcomes. The recent international multicentre Eurotherm3235 RCT, which randomized 387 TBI patients with intracranial hypertension (ICP >20 mmHg) resistant to first-tier treatments (including mechanical ventilation, sedatives, and head of bed elevation) to either standard care or hypothermia to 32–35°C plus standard care, was suspended early because of worse functional outcomes and higher mortality rates in the hypothermia group (Andrews et al., 2015). Because this study used hypothermia as a second-tier therapy it does not address adequately whether TTM benefits refractory elevated ICP in patients with TBI. Use of stage 3 treatments (barbiturates and decompressive craniectomy) was higher in the control group (54%) than in the hypothermia group (44%), but data on the amount of mannitol and hypertonic saline used in each arm of the study were not recorded. Given these and other limitations, this trial is unlikely to significantly alter the use of TTM in TBI, although it does highlight the need for further, high-quality RCTs of TTM after TBI.

Anaemia

Around 50% of patients with severe TBI develop anaemia that can activate hypoxic cell signalling pathways and adversely affect cerebral oxygen delivery. The outcome effects of anaemia and precise haemoglobin (Hb) threshold for brain tissue injury are uncertain. However, it seems unlikely that the restrictive transfusion approaches used in general critical care can be extrapolated to patients with TBI because of the increased susceptibility of the injured brain to ischaemia. An RCT of erythropoietin and two transfusion thresholds (Hb concentrations 70 g/litre and 100 g/litre) found that neither administration of erythropoietin nor maintenance of Hb more than 100 g/litre improved neurological outcomes at six months after TBI, but the latter was associated with more adverse events particularly thromboembolism (Robertson et al., 2014). It is currently recommended that haemoglobin concentration should be maintained more than 90 g/litre in the acute phase after TBI, and aggressive transfusion practices avoided (LeRoux, 2013).

Coagulopathy

Acute traumatic coagulopathy develops in over one third of patients with isolated TBI, and is associated with worsened outcomes (Epstein et al., 2014). Both hypocoagulable and hypercoagulable states can exist, with release of large amounts of tissue factor, altered protein C homeostasis, and platelet dysfunction. Management relies on the correction of coagulation abnormalities with combinations of fresh frozen plasma and prothrombin complex concentrate according to local protocols. There are no specific guidelines for reversal of coagulopathy in TBI.

The antifibrinolytic agent tranexamic acid, when given within three hours of injury, reduces mortality in bleeding trauma patients without increasing adverse events. An ongoing prospective RCT (CRASH-3, http://www.isrctn.com/ISRCTN15088122) is investigating whether the same benefits apply after TBI.

Seizures

Seizures are common following TBI and cause elevations in ICP, cerebral ischaemia, and excessive neurotransmitter release. Post-traumatic seizures (PTS) are classified as early (occurring within 7 days) or late (after 7 days), and are associated with adverse outcomes. Prompt seizure detection and treatment improves outcome, although the use of prophylactic antiepileptic drugs (AEDs) is controversial. Some guidelines recommend a short course (7 days) of AEDs to reduce the incidence of early PTS, but there is no evidence that this improves outcomes or reduces the risk of post-traumatic epilepsy. There is also no evidence to support the use of AEDs for prophylaxis of late onset PTS, which should be managed like any new onset seizure. Phenytoin has historically been the first-line drug for prophylaxis and treatment of PTS, but levetiracetam appears to be of equal efficacy, has fewer side effects, and does not require monitoring of plasma drug levels.

Patients with TBI, particularly those with depressed skull fracture, penetrating injuries, and large cortical contusions/haematomas, are at risk of developing non-convulsive seizures (NCSz). AED prophylaxis does not prevent the development of NCSz, and the effect of treatment on outcomes remains to be elucidated. Electroencephalography (EEG) is recommended to exclude seizures in TBI patients with unexplained and persistent altered consciousness (Claassen et al., 2013).

Venous thromboembolism

Severe TBI is a significant risk factor for the development of venous thromboembolism. Graduation compression stockings or intermittent pneumatic compression stockings are recommended (unless lower limb trauma prevents their use) until the patient is ambulatory, despite no clear evidence of efficacy. Low molecular weight heparin or low dose unfractionated heparin can reduce the rates of deep vein thrombosis (DVT) and mortality respectively, but the timing of chemoprophylaxis is controversial. Concerns about associated risks of intracranial haemorrhage must be balanced against the significantly higher risk of DVT if chemoprophylaxis is withheld for seven days after injury. Based on evidence from over 5000 TBI patients, it has been recommended that chemoprophylaxis should be started after 72 h in patients at medium or high risk of haematoma expansion, and after 48 h in those with low risk of haematoma expansion and absence of expansion (Abdel-Aziz et al., 2015).

Nutritional support

TBI is associated with a hypermetabolic state and excessive nitrogen wasting, and full caloric replacement should be achieved by day five, and at the latest by day seven, postinjury (Carney et al., 2017). A recent meta-analysis found that early feeding (defined in most studies as within 48 hours of admission) was associated with a significant reduction in mortality, poor outcomes, and infectious complications (Wang et al., 2013).

Electrolyte and endocrine disturbances

Disorders of sodium homeostasis are common after TBI, and both hypo- and hypernatraemia have adverse effects on the injured brain. A systematic approach to diagnosis and treatment is essential (Table 42.2).

Endocrine failure after TBI is related to direct injury to the hypothalamic-pituitary axis (HPA), intracranial hypertension-related hypothalamic ischaemia, and inflammation-related primary gland failure. HPA dysfunction leading to adrenal insufficiency occurs in up to 50% of patients with severe TBI, and the effects can be long-lasting and affect recovery into the chronic phases of rehabilitation. Acute screening for pituitary insufficiency using standard stimulation/response tests should be considered in all at risk patients and those with unexplained hyponatraemia or hypoglycaemia, or a persisting requirement for high-dose vasopressors. The effect of hormone replacement on outcome is not well studied but hydrocortisone should be considered in the presence of refractory hypotension, and may be supplemented with a mineralocorticoid if hyponatraemia persists (Powner et al., 2006).

Non-neurological organ system dysfunction

Non-neurological organ dysfunction, particularly involving cardiorespiratory systems, is common after TBI and an independent

Table 42.2 Characteristics and treatment of sodium disturbances after head injury

Finding	SIADH	CSWS	CDI
Plasma volume	Raised	Lowered	Lowered
Sodium balance	Positive/equal	Negative	Equal
Water balance	Positive	Negative	Negative
Serum sodium	Low	Low	High
Serum osmolality	Lowered	High/normal	High
Urine sodium	High	High	Normal
Urine osmolality	High	Normal/high	Low
Management	• electrolyte-free water restriction—initially to 1000–1500 ml/day—if cardiovascular status allows • demeclocycline—inhibits renal response to ADH • ADH-receptor antagonists—inhibit binding of ADH to renal receptors	• volume and sodium resuscitation • fludrocortisone may limit sodium loss	• replace fluids to maintain normovolaemia • DDAVP if high urine output (>250 ml/h) continues

ADH, antidiuretic hormone; CDI, central diabetes insipidus; CSWS, cerebral salt wasting syndrome; DDAVP, 1-deamino-8-D-arginine vasopressin; SIADH; syndrome of inappropriate ADH secretion.

Normal values: plasma osmolality 278–305 mmol/kg; plasma sodium 135–145 mmol/litre; urine osmolality 350–1000 mmol/kg; urine sodium 20–60 mmol/litre or 100–250 mmol/24 h.

contributor to morbidity and mortality. Whether early recognition and prompt intervention improves outcomes is less clear. Systemic complications may occur because of neurogenic causes such as brain injury-related catecholamine and neuroinflammatory responses that can lead to neurogenic stunned myocardium syndrome and neurogenic pulmonary oedema, or as a complication of brain-directed therapies such as acute lung injury (ALI) secondary to cerebral perfusion pressure (CPP)-guided therapy, or TTM-related infection. Pneumonia is particularly common after TBI, occurring in up to 80% of ventilated patients. The management of systemic organ dysfunction and failure presents a significant challenge because optimum treatment for the failing systemic organ system may have potentially adverse effects on the injured brain and *vice versa*. For a detailed discussion of the aetiology and management of non-neurological complications the reader is referred elsewhere (Berthiaume and Zygun, 2006).

Intracranial and cerebral perfusion pressure monitoring and management

Monitoring and management of ICP and CPP are crucial aspects of the critical care management of severe TBI. ICP monitoring allows measurement of absolute ICP, calculation of CPP, identification and analysis of pathological ICP waveforms that predict the development of intracranial hypertension, and derivation of indices of cerebrovascular pressure reactivity. CPP is calculated as the difference between mean arterial pressure (MAP) and ICP, and is modifiable through this relationship. The Brain Trauma Foundation (BTF) recommends interventions when ICP exceeds 22 mmHg (although some centres use a threshold of >20 or >25 mmHg) and maintenance of CPP between 60 and 70 mmHg (Carney et al., 2017).

Intracranial pressure

The indications for ICP monitoring are highlighted in **Box 42.2**, which emphasizes differences between 2014 expert consensus recommendations and the 2016 BTF guidance. Stocchetti et al. (2014) advise that comatose TBI patients with normal CT scans do not require ICP monitoring whereas the latest BTF guidelines continue to recommend monitoring in such patients in the presence of specific high-risk characteristics despite the absence of high-quality evidence to support such a recommendation (Carney et al., 2017). This difference in emphasis likely relates to the fact that modern scanners are more able to identify lesions that were previously undetectable, thereby reducing the likelihood of the subsequent development of raised ICP secondary to evolution of occult lesions.

Technical aspects

ICP is most commonly measured through an intraventricular catheter or parenchymal microtransducer device. Other techniques, such as subarachnoid or epidural devices, are less accurate and rarely used. Ventricular catheters measure global ICP (cerebrospinal fluid (CSF) pressure in the lateral ventricles) and permit therapeutic drainage of CSF. There is a risk of catheter-associated ventriculitis, which increases with the length of time since catheter insertion. This can be reduced (but not abolished) by the use of antibiotic-impregnated or silver-coated catheters. Parenchymal microtransducer ICP monitoring systems are easy to insert and usually placed ~2 cm into brain parenchyma through a cranial access device or at craniotomy when they can also be sited in the subdural space. While intraventricular catheters have historically been considered the 'gold standard' for ICP monitoring, intraparenchymal devices provide equivalent pressure measurement and are safer, with lower risk of device-related complications such as haematoma and infection (Smith, 2008).

Several non-invasive ICP monitoring techniques have been developed, including transcranial Doppler (TCD) ultrasonography-derived pulsatility index and ultrasound or CT measurement of optic nerve sheath diameter. Although lacking the risks of invasive methods, these techniques currently fail to measure ICP sufficiently accurately for routine clinical use.

Management of raised intracranial pressure

The burden of intracranial hypertension (the time spent with ICP above a defined threshold—usually 20–25 mmHg) is associated with adverse outcomes after TBI. ICP-lowering strategies are usually administered in a stepwise manner, starting with first-line, safer interventions such as head-up positioning and sedation (**Fig. 42.2**). Higher risk treatment options, including hyperventilation, TTM, barbiturates and surgical decompression, are reserved for patients with multimodal brain monitoring evidence of brain hypoxia of cerebral metabolic distress, or those at imminent risk of cerebral herniation.

Sedation

Most sedative agents have beneficial effects on ICP and CPP, but there is no convincing evidence of advantage of one agent over another (Roberts et al., 2011). Propofol is widely used, usually in combination with infusion of a short acting opioid. It effectively reduces cerebral metabolic rate and ICP, and allows readily titratable sedation levels and rapid wake-up. The alpha-2 agonist dexmedetomidine has shown some promise for sedation after brain injury but there are no RCTs in patients with TBI.

Neuromuscular blocking agents do not reduce ICP, although they may prevent increases during endotracheal suctioning and other interventions. They should not be used routinely because of the increased risk of extracranial complications including pneumonia and ICU-acquired weakness.

Hyperventilation

Hyperventilation effectively reduces ICP secondary to cerebral vasoconstriction in response to reduced $PaCO_2$. It can therefore precipitate or worsen global and regional cerebral ischaemia because of critical reductions in cerebral blood flow (CBF) (Stocchetti et al., 2005). As such, hyperventilation should be used only as a temporizing measure and avoided in the first 24 hours (when CBF is often significantly reduced) and as a prophylactic intervention. Concomitant cerebral oxygenation monitoring is recommended during hyperventilation to identify impending ischaemia.

Osmotic therapy

Mannitol (0.25–1.0 g/kg) is a standard of care for the acute treatment of elevated ICP (Carney et al., 2017), but has never been subject to a randomized comparison against placebo. Side effects include initial fluid overload, subsequent hypotension, metabolic acidosis, and electrolyte imbalance, all of which can adversely affect the injured brain. Repeated administration may result in unacceptably high

Box 42.2 Indications for intracranial pressure monitoring in traumatic brain injury, from the Brain Trauma Foundation guidelines and expert consensus recommendations

Brain Trauma Foundation guidelines (2016)

- All salvageable patients with severe TBI* and an abnormal cranial CT scan
- All salvageable patients with severe TBI and a normal scan and two or more of the following:
  - age more than 40 years
  - unilateral or bilateral motor posturing
  - systolic blood pressure <90 mmHg

Note: These recommendations have been carried over from the previous (3rd) edition of the BTF guidelines, despite not being supported by current standards of evidence.

Expert consensus recommendations (2014)

- Comatose** TBI patients with an initial CT scan showing minimal signs of injury (tSAH, petechiae) that subsequently worsen (e.g. development of contusions, or compression or absence of basal cisterns)
- Comatose TBI patients with cerebral contusions when interruption of sedation to check neurologic status is dangerous, or when the clinical examination is unreliable
- Comatose TBI patients with large bifrontal contusions and/or haemorrhagic mass lesions close to the brainstem irrespective of initial Glasgow Coma Scale (GCS)
- Following a secondary decompressive craniectomy to assess the effectiveness of surgery in terms of ICP control and guide ongoing management
- After evacuation of an acute supratentorial intracranial hematoma in salvageable patients at increased risk of intracranial hypertension, including those with:
  - GCS motor score ≤5
  - pupillary abnormalities
  - prolonged/severe hypoxia and/or hypotension
  - compressed or obliterated basal cisterns
  - midline shift >5 mm or exceeds thickness of an extra-axial clot
  - additional extra-axial haematomas, parenchymal injuries (such as contusions), or swelling
  - intraoperative brain swelling
- It should also be considered in polytrauma cases as highlighted earlier
- *Not* in comatose TBI patients with a normal initial CT***

*ICP, intracranial pressure; CPP, cerebral perfusion pressure; CT, computed tomography; GCS, Glasgow coma scale; TBI, traumatic brain injury; tSAH, traumatic subarachnoid haemorrhage. * defined as a GCS score of 8 or below. ** defined as a GCS of 8 or below after haemodynamic and respiratory stabilization and in the absence of anaesthetic or paralysing agents. ***in such cases a second CT scan is recommended, urgently if the patient deteriorates neurologically.*

Reproduced with permission from Carney, Nancy; Totten, Annette M., Guidelines for the Management of Severe Traumatic Brain Injury, Fourth Edition, *Neurosurgery*, Volume 80, Issue 1, Copyright © 2016, Oxford University Press and the Congress of Neurological Surgeons (CNS).

Reproduced with permission from Nino Stocchetti, Edoardo Picetti, Maurizio Berardino et al., Clinical applications of intracranial pressure monitoring in traumatic brain injury, *Acta Neurochirurgica*, Volume 156, Issue 8, pp. 1615–22, Copyright © 2014 Springer Nature.

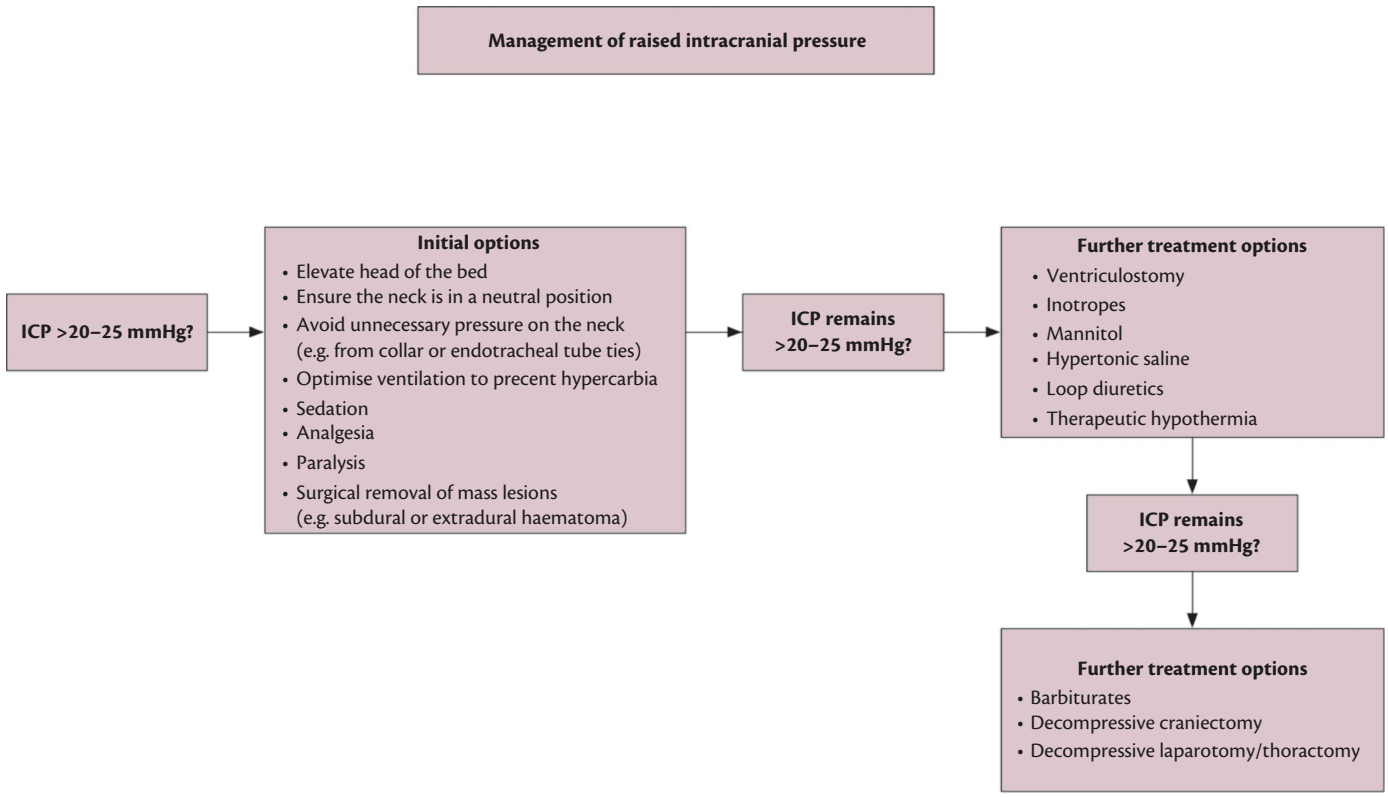
Management of raised intracranial pressure
ICP >20–25 mmHg?
Initial options
• Elevate head of the bed
• Ensure the neck is in a neutral position
• Avoid unnecessary pressure on the neck (e.g. from collar or endotracheal tube ties)
• Optimise ventilation to precent hypercarbia
• Sedation
• Analgesia
• Paralysis
• Surgical removal of mass lesions (e.g. subdural or extradural haematoma)
ICP remains >20–25 mmHg?
Further treatment options
• Ventriculostomy
• Inotropes
• Mannitol
• Hypertonic saline
• Loop diuretics
• Therapeutic hypothermia
ICP remains >20–25 mmHg?
Further treatment options
• Barbiturates
• Decompressive craniectomy
• Decompressive laparotomy/thoractomy

Fig. 42.2 Management algorithm for raised intracranial pressure.

serum osmolality (>320 mOsm/litre), neurological complications, and acute kidney injury.

HS may have a more profound and long-lasting effect on ICP compared with mannitol, but outcome benefits over mannitol have not been demonstrated (Diringer, 2013). Clinical outcome studies are inconsistent in terms of dose, concentration, frequency, and mode (bolus or continuous infusion) of HS administration, and the optimal osmolar load to lower elevated ICP is undefined. HS has multiple theoretical beneficial effects on the injured brain in addition to its osmotic action, including vasoregulatory, immunological, and neurochemical actions; it also expands intravascular volume, potentially augmenting CPP.

Although previously believed to be only a by-product of anaerobic metabolism, there is some evidence that lactate can act as a preferential fuel in the injured brain. Preliminary clinical data suggest that hypertonic lactate solutions spare cerebral glucose, improve cerebral energy metabolism, and effectively reduce elevated ICP (Bouzat and Oddo, 2014). Further data are required before its routine use can be recommended

Barbiturates

A Cochrane review has confirmed that the use of barbiturates in patients with TBI does not reduce mortality, and increases the risk of hypotension by 25% (Roberts and Sydenham, 2012). The adverse cardiovascular effects of barbiturates are likely to offset any benefit on CPP of ICP reduction. Barbiturates continue to be used in the treatment of refractory intracranial hypertension when first- and second-tier therapies have failed to control ICP, although in some centres there is a preference for decompressive craniectomy over barbiturates in this situation.

Surgery

The role of decompressive craniectomy, CSF drainage, and other neurosurgical interventions in the management of intracranial hypertension are discussed in **Chapter 43**.

Evidence for intracranial pressure monitoring and management

It is well recognized that intracranial hypertension is detrimental, but there is little evidence that monitoring and managing ICP improves outcomes. A meta-analysis of 14 studies including 24 792 patients with severe TBI concluded that ICP monitoring-guided management of intracranial hypertension had no significant mortality benefit overall compared to treatment without ICP monitoring, although mortality was lower in patients who underwent ICP monitoring in studies published after 2012 (Yuan et al., 2015). There has been only one randomized study evaluating the utility of ICP monitoring in TBI. The Benchmark Evidence from South American Trials: Treatment of Intracranial Pressure (BEST-TRIP) compared treatment guided by ICP monitoring with care based on imaging and clinical examination in the absence of ICP monitoring, and found no difference in three- or six-month outcomes (Chesnut et al., 2012). Patients in the ICP monitoring group received significantly fewer days of ICP-directed treatment (hyperventilation, HS/mannitol, and barbiturates), although the length of ICU stay was similar. This is in contrast to other (observational) studies, which have demonstrated an increased burden of brain-directed therapy in patients in whom treatment is guided by ICP monitoring,

BEST-TRIP has been criticized on several counts, but its findings reinforce the notion that assessment of ICP is integral to managing severe TBI. The evaluation and diagnosis of intracranial hypertension, whether through monitoring ICP directly, or indirectly through assessment of clinical and imaging variables, was fundamental to patient management in both groups.

Cerebral perfusion pressure

Guidelines recommend that CPP should be maintained between 60 and 70 mmHg (Carney et al., 2017), through manipulation of MAP with fluid resuscitation and vasopressors/inotropes or treatment of raised ICP, with evidence that both lower and higher values are associated with deleterious outcomes. CPP more than 70 mmHg is associated with increased risk of ALI related to overly aggressive fluid resuscitation or vasopressor therapy, and CPP less than 50 mmHg with cerebral hypoperfusion. An alternative approach, the Lund concept, targets a lower CPP (50 mmHg) to minimize increases in intracapillary hydrostatic pressure and intracerebral water content in an attempt to avoid secondary increases in ICP (Grände, 2006), but it does not have a strong evidence base and is not universally accepted. Rather than a single threshold for CPP, it is likely that 'optimal' values can be identified at the individual level using multimodality neuromonitoring (Kirkman and Smith, 2014).

Multimodality neuromonitoring

Monitoring multiple physiological variables is more accurate in the prediction of cerebral hypoxia-ischaemia than measurement of one variable alone (Bouzat et al., 2015) (**Table 42.3**). In particular, ICP monitoring should be regarded as one part of a multimodality neuromonitoring strategy rather than a monitoring modality in isolation (Kirkman and Smith, 2012).

Cerebrovascular reactivity

Cerebrovascular reactivity, a key component of cerebral autoregulation (CA), is often impaired after TBI, rendering the brain more susceptible to secondary ischaemic insults. Monitoring and correlation of spontaneous slow waves in ABP and ICP allows calculation of a pressure reactivity index (PRx) which can be used as a continuous bedside assessment of CA. A negative value for PRx, when ABP is inversely correlated with ICP, indicates normal CA, and a positive value a non-reactive cerebrovascular circulation. PRx may be used to guide therapy and identify optimal CPP after TBI (**Fig. 42.3**) (Aries et al., 2012).

An oxygen reactivity index (ORx) has also been described as the moving correlation between brain tissue oxygenation ($PbtO_2$) and ABP, as have non-invasive alternatives using the correlation between ABP and TCD-derived blood flow velocity and several near infrared spectroscopy (NIRS)-derived variables (Kirkman and Smith, 2012).

Cerebral blood flow monitoring

TCD is a non-invasive technique allowing real-time assessment of cerebral haemodynamics at the bedside. Although it measures relative changes in CBF rather than absolute values, it can be used to detect impaired CBF and assess cerebrovascular reactivity after TBI. Quantitative measurement of absolute regional CBF is possible

Table 42.3 Neuromonitoring techniques used in traumatic brain injury

Technique	Monitored variable(s)	Indications in TBI	Advantages	Disadvantages
Intracranial pressure				
Intraparenchymal or subdural microsensor	• ICP • CPP • Autoregulatory indices	• To allow CPP optimization through derivation of PRx and ORx	• Relatively easy insertion • Low procedural complication rate • Low infection risk	• *In vivo* calibration not possible • Measures localized pressure • Small zero-drift with time
Ventricular catheter	• As above	• As above, plus: • To allow therapeutic drainage of CSF	• Measures global ICP • Therapeutic CSF drainage • *In vivo* calibration possible	• More difficult insertion • Risk of procedure-related haemorrhage • Risk of catheter-related ventriculitis
Cerebral blood flow				
Transcranial Doppler ultrasonography	• Blood flow velocity • Pulsatility index • Autoregulatory indices	• May detect cerebral hypoperfusion and facilitate early goal-directed therapy	• Noninvasive • Can be used on an intermittent or continuous basis • Good temporal resolution	• Measures relative (not absolute) CBF • Operator dependent • Failure rate in 5–10% of patients (absent acoustic window) • Little evidence base in TBI
Cerebral oxygenation				
Jugular venous oximetry	• Jugular venous oxygen saturation • Arterio-venous oxygen content difference	• To evaluate the adequacy of cerebral perfusion and oxygen delivery • To supplement ICP/CPP-guided therapy • To assist titration of medical and surgical therapies to guide ICP/CPP therapy	• Global assessment of balance between CBF and metabolism	• Non-quantitative assessment of cerebral perfusion • Insensitive to regional ischaemia • Risk of extracranial contamination of samples
Brain tissue pO_2	• Brain tissue oxygen partial pressure • Oxygen reactivity	• As for jugular venous oximetry, plus: • To allow CPP optimization through derivation of ORx	• Regional assessment of balance between CBF and metabolism • Continuous • Ischaemic 'thresholds' defined	• Minimally invasive • Measures oxygenation within a small region of interest • One hour 'run-in' period limits intraoperative applications
Near infrared spectroscopy (cerebral oximetry)	• Regional cerebral oxygen saturation • Autoregulatory indices	• As for jugular venous oximetry, plus: • Detection of intracranial haematoma	• Noninvasive • Real time • Multisite measurement	• rScO2-derived 'ischaemic' threshold not defined • Readings affected by the presence of intracranial haematoma and 'contamination' of signals by extracranial tissue • Little evidence base in TBI
Cerebral microdialysis	• Glucose • Lactate, pyruvate, and LPR • Glycerol • Glutamate • Multiple biomarkers for research purposes	• To detect cerebral ischaemia, hypoxia, cellular energy failure, and glucose deprivation • To predict the development of secondary injury before it is detectable clinically or by other monitoring modalities • To optimize CPP • To assist titration of medical therapies such as systemic glucose control	• Assessment of cerebral glucose metabolism • Detection of hypoxia/ischaemia • Assessment of non-ischaemic causes of cellular bioenergetic dysfunction	• Focal measure • Thresholds for abnormality unclear • Not continuous • Labour-intensive
Electrophysiology				
EEG	• Seizures • Diagnosis-specific EEG patterns • Some evidence that detection of SDs might be possible	• To detect convulsive and non-convulsive seizures • To diagnose characteristic EEG patterns to facilitate prognostication	• Noninvasive • Detection of non-convulsive seizures • Correlates with cerebral ischaemic and metabolic changes	• Skilled interpretation required • Affected by anaesthetic and sedative agents
ECoG	• Cortical SDs	• To detect spreading cortical depolarizations	• Currently the only method to identify SDs accurately	• Highly invasive • No evidence that treatment of SDs improves outcome • Little evidence base in TBI and thus currently remains a research tool

using a thermal diffusion flowmetry probe, but clinical data using this technique are limited.

Cerebral oxygenation monitoring

Maintenance of ICP and CPP within established thresholds for normality does not guarantee against brain tissue hypoxia (Oddo et al., 2011). Cerebral oxygenation monitoring is therefore often used to assess the balance between cerebral oxygen delivery and utilization, and the adequacy of cerebral perfusion.

Jugular venous oximetry

Jugular venous oxygen saturation ($SvjO_2$) monitoring was the first bedside monitor of cerebral oxygenation, and formed the basis of our understanding of cerebral oxygenation changes after brain injury.

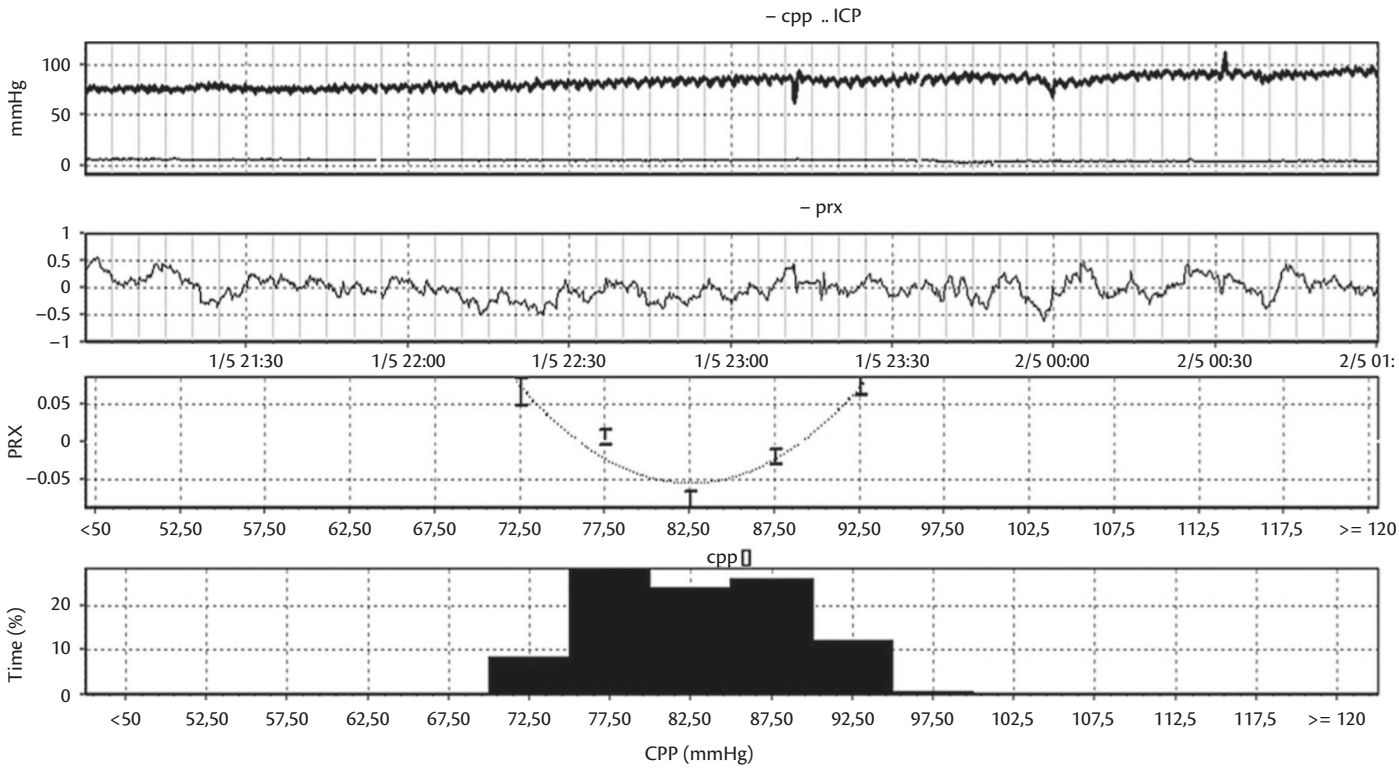

Fig. 42.3 Screenshot from ICM+ software panel (Cambridge Enterprise, Cambridge, UK) with 4 h trend charts. Determination of the PRx can guide therapy and allow identify optimal CPP at the individual level (CPPopt). *First chart*: CPP and ICP; *second chart*: PRx; *third chart*: PRx/CPP plot for evaluating CPPopt; and *fourth chart*: percentage of the 4-h time period spent within a given CPP interval.

The ICM+® brain monitoring software developed at the University of Cambridge was used to generate this image.

Reproduced with permission from Celeste Dias, Maria João Silva, Eduarda Pereira et al., Optimal Cerebral Perfusion Pressure Management at Bedside: A Single-Center Pilot Study, Neurocritical Care, Volume 23, Issue 1, pp. 92–102, Copyright © 2015 Springer Nature.

Maintenance of $SvjO_2$ more than 50% after TBI is recommended in BTF guidelines (Carney et al., 2017), but no interventional trials have confirmed a direct benefit of $SvjO_2$-directed therapy on outcome and in any case $SvjO_2$ monitoring is being superseded by other modalities.

Brain tissue oxygen partial pressure

$PbtO_2$ monitoring is considered the 'gold standard' bedside monitor of cerebral oxygenation, and recommended after severe TBI (Le Roux et al., 2014). It is a complex and dynamic variable resulting from interaction of all factors affecting cerebral oxygen delivery and demand (oxygen metabolism), the relative proportion of arterial or venous vessels in the region of interest, and tissue oxygen diffusion gradients. It is therefore a biomarker of cellular function rather than simply a monitor of hypoxia/ischaemia. $PbtO_2$ is a regional monitor and the probe is typically placed in tissue immediately surrounding a hematoma or contusion to monitor 'at risk' brain regions.

Normal brain $PbtO_2$ is reported to lie between 2.7 and 4.7 kPa (20–35 mmHg), and the ischaemic threshold usually defined as 1.33–2.0 kPa (10–15 mmHg). However, $PbtO_2$ values are best considered within a range rather than as a precise threshold and ischaemia defined by both duration and depth of hypoxia. Guidelines recommend interventions to maintain $PbtO_2$ more than 2.7 kPa (>20 mmHg) (Le Roux et al., 2014).

Observational studies suggest a potential benefit of supplementing ICP/CPP-guided management with $PbtO_2$-directed therapy after TBI (Nangunoori et al., 2012). In addition to systemic blood pressure, $PbtO_2$ is affected by several other factors including PaO_2, $PaCO_2$, and haemoglobin concentration, and which intervention or combination of interventions should be used to reverse brain tissue hypoxia is contentious. In fact, it appears that the responsiveness of brain tissue hypoxia to a given intervention is the prognostic factor, with reversal of hypoxia being associated with reduced mortality (Nangunoori et al., 2012). RCT data are urgently needed to confirm any benefits of $PbtO_2$ monitoring, and the results of the Brain Tissue Oxygen Monitoring in Traumatic Brain Injury (BOOST2) study are awaited (https://clinicaltrials.gov/ct2/show/NCT00974259).

Near infrared spectroscopy

Near infrared spectroscopy-based cerebral oximetry provides continuous and non-invasive monitoring of regional cerebral oxygen saturation ($rScO_2$), with high temporal and spatial resolution, and the possibility simultaneous measurement over multiple regions of interest. The 'normal' range of $rScO_2$ is reported as 60–75% but there is substantial intra- and interindividual variability, and $rScO_2$ values are best used as a trend monitor. There has been limited investigation of the utility of NIRS after TBI where its application is confounded by the optical complexity of the injured brain (Ghosh et al., 2012). NIRS-derived variables have been investigated as a non-invasive assessment of cerebral autoregulatory status, but its role in the broader monitoring of TBI is undefined.

Cerebral microdialysis

Cerebral microdialysis (CMD) allows bedside analysis of biochemical substances in brain tissue extracellular fluid. The catheter is usually placed in 'at risk' tissue so that biochemical changes in the area of brain most vulnerable to secondary insults can be monitored. Glucose, lactate, pyruvate, lactate:pyruvate ratio (LPR), glycerol and glutamate are the variables most commonly measured clinically, and each is a marker of a particular cellular process associated with glucose metabolism, hypoxia/ischaemia, or cellular energy failure. CMD measures the supply of substrate and its cellular metabolism, so it is a monitor not only of cerebral ischaemia but also of non-ischaemic causes of cellular energy dysfunction. It may identify cerebral compromise at the cellular level before it is detectable clinically or by other monitored variables.

Elevated lactate:pyruvate ratio (LPR) more than 40 combined with low brain glucose (<0.7–1 mmol/litre) suggests severe hypoxia/ischaemia and correlates with poor outcome after TBI (Timofeev et al., 2011). Although the clinical utility of CMD is debated, expert consensus guidance for its use has recently been published (Hutchinson et al., 2015).

Electroencephalography and electrocorticography

EEG is used to diagnose and guide therapy in patients at risk of, or having, seizures or status epilepticus. Continuous EEG (cEEG) has become more widespread with awareness that non-convulsive seizures are common after brain injury.

Spreading cortical depolarizations (SDs) are pathological near-complete, sustained depolarization of neurons and astrocytes resulting in secondary injury due to mitochondrial damage, accumulation of intracellular calcium, and excitotoxicity. They occur in 50–60% of TBI patients, and have previously been detectable only via electrode strips placed directly onto the cortical surface. Recent data suggest that standard scalp cEEG may be able to detect SDs, offering the potential for routine monitoring of this important pathophysiological manifestation of acute brain injury.

Conclusions

Understanding of the mechanisms of secondary brain injury and awareness of its adverse outcome effects has resulted in significant advances in the early and intensive care management of TBI, which focuses on the avoidance of hypoxia and hypotension, control of ICP, and maintenance of CPP. Multimodality neuromonitoring, including continuous measurement of ICP and CPP, allows individualized interventions targeted to real-time changes in cerebral physiology with the aim of improving outcomes following TBI.

FURTHER READING

Carney, N., Totten, A.M., O'Reilly, C., et al. (2017). Guidelines for the management of severe traumatic brain injury, fourth edition. *Neurosurgery*, **80**(1), 6–15.

Chesnut, R.M., Temkin, N., Carney, N. et al. (2012). A trial of intracranial-pressure monitoring in traumatic brain injury. *N Engl J Med*, **367**, 2471–81.

Gantner, D., Moore, E.M., & Cooper, D.J. (2014). Intravenous fluids in traumatic brain injury: what's the solution? *Curr Opin Crit Care*, **20**, 385–9.

Kirkman, M.A. & Smith, M. (2014). Intracranial pressure monitoring, cerebral perfusion pressure estimation, and ICP/CPP-guided therapy: a standard of care or optional extra after brain injury? *Br J Anaesth*, **112**, 35–46.

Stocchetti, N., Picetti, E., Berardino, M., et al. (2014). Clinical applications of intracranial pressure monitoring in traumatic brain injury: report of the Milan consensus conference. *Acta Neurochir (Wien)*, **156**, 1615–22.

REFERENCES

Abdel-Aziz, H., Dunham, C.M., Malik, R.J., & Hileman, B.M. (2015). Timing for deep vein thrombosis chemoprophylaxis in traumatic brain injury: an evidence-based review. *Crit Care*, **19**, 96.

Andrews, P.J., Sinclair, H.L., Rodriguez, A., et al. (2015). Hypothermia for intracranial hypertension after traumatic brain injury. *N Engl J Med*, **373**(25), 2403–12.

Aries, M.J., Czosnyka, M., Budohoski, K.P., et al. (2012). Continuous determination of optimal cerebral perfusion pressure in traumatic brain injury. *Crit Care Med*, **40**, 2456–63.

Bennett, M.H., Trytko, B., & Jonker, B. (2012). Hyperbaric oxygen therapy for the adjunctive treatment of traumatic brain injury. *Cochrane Database Syst Rev*, **12**, CD004609.

Berthiaume, L. & Zygun, D. (2006). Non-neurologic organ dysfunction in acute brain injury. *Crit Care Clin*, **22**, 753–66.

Boer, C., Franschman, G., & Loer, S.A. (2012). Prehospital management of severe traumatic brain injury: concepts and ongoing controversies. *Curr Opin Anaesthesiol*, **25**, 556–62.

Bouzat, P., Marques-Vidal, P., Zerlauth, J.-B. et al. (2015). Accuracy of brain multimodal monitoring to detect cerebral hypoperfusion after traumatic brain injury. *Crit Care Med*, **43**, 445–52.

Bouzat, P. & Oddo, M. (2014). Lactate and the injured brain: friend or foe? *Curr Opin Crit Care*, **20**, 133–40.

Carney, N., Totten, A.M., O'Reilly, C., et al. (2017). Guidelines for the management of severe traumatic brain injury, fourth edition. *Neurosurgery*, **80**(1), 6–15.

Chesnut, R.M., Temkin, N., Carney, N. et al. (2012). A trial of intracranial-pressure monitoring in traumatic brain injury. *N Engl J Med*, **367**, 2471–81.

Claassen, J., Taccone, F.S., Horn, P., Holtkamp, M., Stocchetti, N., & Oddo, M. (2013). Recommendations on the use of EEG monitoring in critically ill patients: consensus statement from the neurointensive care section of the ESICM. *Intensive Care Med*, **39**, 1337–51.

Cooper, D.J., Myburgh, J., Heritier, S., et al. (2013). Albumin resuscitation for traumatic brain injury: is intracranial hypertension the cause of increased mortality? *J Neurotrauma*, **30**, 512–18.

Crossley, S., Reid, J., McLatchie, R., et al. (2014). A systematic review of therapeutic hypothermia for adult patients following traumatic brain injury. *Crit Care*, **18**, R75.

Diringer, M.N. (2013). New trends in hyperosmolar therapy? *Curr Opin Crit Care*, **19**, 77–82.

Epstein, D.S., Mitra, B., O'Reilly, G., Rosenfeld, J.V., & Cameron, P.A. (2014). Acute traumatic coagulopathy in the setting of isolated traumatic brain injury: a systematic review and meta-analysis. *Injury*, **45**, 819–24.

Gantner, D., Moore, E.M., & Cooper, D.J. (2014). Intravenous fluids in traumatic brain injury: what's the solution? *Curr Opin Crit Care*, **20**, 385–9.

Ghosh, A., Elwell, C., & Smith, M. (2012). Review article: cerebral near-infrared spectroscopy in adults: a work in progress. *Anesth Analg*, **115**, 1373–83.

Grände, P.-O. (2006). The 'Lund Concept' for the treatment of severe head trauma—physiological principles and clinical application. *Intensive Care Med*, **32**, 1475–84.

Hutchinson, P.J., Jalloh, I., Helmy, A., et al. (2015). Consensus statement from the 2014 International Microdialysis Forum. *Intensive Care Med*, **41**, 1517–28.

Kirkman, M.A. & Smith, M. (2012). Multimodal intracranial monitoring: implications for clinical practice. *Anesthesiol Clin*, **30**, 269–87.

Kirkman, M.A. & Smith, M. (2014). Intracranial pressure monitoring, cerebral perfusion pressure estimation, and ICP/CPP-guided therapy: a standard of care or optional extra after brain injury? *Br J Anaesth*, **112**, 35–46.

Kramer, A.H., Roberts, D.J., & Zygun, D.A. (2012). Optimal glycemic control in neurocritical care patients: a systematic review and meta-analysis. *Crit Care*, **16**, R203.

Le Roux, P., Menon, D.K., Citerio, G., et al. (2014). Consensus summary statement of the International Multidisciplinary Consensus Conference on Multimodality Monitoring in Neurocritical Care: a statement for healthcare professionals from the Neurocritical Care Society and the European Society of Intensive Care Medicine. *Intensive Care Med*, **40**, 1189–209.

LeRoux, P. (2013). Haemoglobin management in acute brain injury. *Curr Opin Crit Care*, **19**, 83–91.

Maekawa, T., Yamashita, S., Nagao, S., Hayashi, N., Ohashi, Y., on behalf of the Brain-Hypothermia (B-HYPO) Study Group (2015). Prolonged mild therapeutic hypothermia versus fever control with tight hemodynamic monitoring and slow rewarming in patients with severe traumatic brain injury: a randomized controlled trial. *J Neurotrauma*, **32**, 422–9.

McHugh, G.S., Engel, D.C., Butcher, I., et al. (2007). Prognostic value of secondary insults in traumatic brain injury: results from the IMPACT study. *J Neurotrauma*, **24**, 287–93.

Nangunoori, R., Maloney-Wilensky, E., Stiefel, M., et al. (2012). Brain tissue oxygen-based therapy and outcome after severe traumatic brain injury: a systematic literature review. *Neurocrit Care*, **17**, 131–8.

Oddo, M., Levine, J.M., Mackenzie, L., et al. (2011). Brain hypoxia is associated with short-term outcome after severe traumatic brain injury independently of intracranial hypertension and low cerebral perfusion pressure. *Neurosurgery*, **69**, 1037–45; discussion 1045.

Powner, D.J., Boccalandro, C., Alp, M.S., & Vollmer, D.G. (2006). Endocrine failure after traumatic brain injury in adults. *Neurocrit Care*, **5**, 61–70.

Roberts, D.J., Hall, R.I., Kramer, A.H., Robertson, H.L., Gallagher, C.N., & Zygun, D.A. (2011). Sedation for critically ill adults with severe traumatic brain injury: a systematic review of randomized controlled trials. *Crit Care Med*, **39**, 2743–51.

Roberts, I. & Sydenham, E. (2012). Barbiturates for acute traumatic brain injury. *Cochrane Database Syst Rev*, **12**, CD000033.

Robertson, C.S., Hannay, H.J., Yamal, J.M., et al. (2014). Effect of erythropoietin and transfusion threshold on neurological recovery after traumatic brain injury: a randomized clinical trial. *JAMA*, **312**, 36–47.

Smith, M. (2008). Monitoring intracranial pressure in traumatic brain injury. *Anesth Analg*, **106**, 240–8.

Stocchetti, N., Maas, A.I.R., Chieregato, A., & van der Plas, A.A. (2005). Hyperventilation in head injury: a review. *Chest*, **127**, 1812–27.

Stocchetti, N., Picetti, E., Berardino, M., et al. (2014). Clinical applications of intracranial pressure monitoring in traumatic brain injury: report of the Milan consensus conference. *Acta Neurochir (Wien)*, **156**, 1615–22.

Timofeev, I., Carpenter, K.L., Nortje, J. et al. (2011). Cerebral extracellular chemistry and outcome following traumatic brain injury: a microdialysis study of 223 patients. *Brain*, **134**, 484–94.

Vespa, P., McArthur, D.L., Stein, N., et al. (2012). Tight glycemic control increases metabolic distress in traumatic brain injury: a randomized controlled within-subjects trial. *Crit Care Med*, **40**, 1923–9.

Wang, X., Dong, Y., Han, X., Qi, X.-Q., Huang, C.-G., Hou, L.-J. (2013). Nutritional support for patients sustaining traumatic brain injury: a systematic review and meta-analysis of prospective studies. *PLoS One*, **8**, e58838.

Yuan, Q., Wu, X., Sun, Y., et al. (2015). Impact of intracranial pressure monitoring on mortality in patients with traumatic brain injury: a systematic review and meta-analysis. *J Neurosurg*, **122**, 574–87.

RELATED LINKS TO EBRAIN

Cerebral protection strategies in head injury. https://learning.ebrain.net/course/view.php?id=1096

Early Phase Care of Moderate and Severe Head Injuries. https://learning.ebrain.net/course/view.php?id=1090

Nutrition and Fluid Balance in the Head Injured Patient. https://learning.ebrain.net/course/view.php?id=1098

43

Surgical management of head injury

Hadie Adams, Angelos G. Kolias, Adel Helmy, Peter J.A. Hutchinson, and Randall M. Chesnut

Introduction

Traumatic brain injury (TBI) is a significant cause of preventable morbidity and mortality in the United Kingdom and across the world, leading to disability and loss of productivity (Maas et al., 2008). The estimated incidence of TBI in Europe is on average 235 per 100 000, ranging of 150–300/100 000 per year (Tagliaferri et al., 2006). The Glasgow Coma Scale (GCS) is often used to classify the severity of TBI, with patients scoring 8 or less being classified as severe, 9–12 as moderate, and scores of 13–15 as mild (CDC, 2015a). Mild TBI is the most common form of head injury, and the incidence of TBI is the highest in young adult males (Nguyen et al., 2016). In Western countries the major causes of TBI-related hospitalizations are falls, assaults, and motor vehicle traffic collisions (Lawrence et al., 2016). Indications for surgery following TBI include mass lesions (extradural, acute subdural and intracerebral haematomas and contusions), depressed skull fractures, and decompressive craniectomy for diffuse injury). North-American trauma registries demonstrated that craniotomies were performed in 3.6% of all TBI patients (Esposito et al., 2005). The European Brain Injury Consortium survey showed that 69% of TBI patients with a mass lesion (>25 ml) and/or radiological signs of raised intracranial pressure (ICP) underwent emergency cranial surgery (Compagnone et al., 2007). Acute subdural haematomas were the most frequent evacuated mass lesions, contributing to approximately two-third of all emergency cases, followed by extradural haematoma and contusions/intracerebral haematomas.

Intracranial pressure monitoring

Severe TBI patients in need of neurointensive care in the acute phase are often sedated and paralysed to facilitate endotracheal intubation and for control of intracranial pressure. This limits the utility of neurological examinations, and therefore computed tomography (CT) scanning and monitoring of intracranial pressure (ICP), remain the primary methods to guide treatment in a neuro-intensive care setting (Le Roux et al., 2014; Brain Trauma Foundation, 2016). Control of ICP remains the central tenet of management of moderate-severe TBI to maintain adequate perfusion and oxygenation of the brain and to avoid or mitigate secondary insults (Valadka and Robertson, 2007; Brain Trauma Foundation, 2016). The Brain Trauma Foundation (BTF) guidelines recommends management of severe TBI patients using ICP monitoring to reduce in-hospital and 2-week postinjury mortality (Brain Trauma Foundation, 2016). ICP monitoring is routinely used in the developed world, and observational studies have demonstrated repeatedly that ICP crises can lead to adverse outcomes (Forsyth et al., 2015). This is discussed further in Chapter 42 (Intensive Care Management of Head Injury). Ultimately, if left untreated, the pressure within the intracranial compartment can rise above a critical threshold, causing damage to neuronal structures, and eventually herniation, and brain death.

It important to be aware of intracranial pressure gradients within the brain parenchyma, especially in patients with space-occupying lesions. This group is prone to develop ICP gradients, since the supporting dural folds, namely the falx cerebri, and the tentorium cerebelli divide the intracranial cavity into compartments that normally protect against excessive movement. Pressure differences between the cerebral hemispheres have been described greater than 10 mmHg in the context of acute subdural haematoma (Chambers et al., 1998). This has underpinned the argument for intraventricular probes for measurement of ICP as, with a patent ventricular system, the pressure can equilibrate between the CSF spaces to a degree (Brain Trauma Foundation, 2016). In practice, the risks associated with prolonged ventricular drainage (both infectious and procedural) limit this approach in many units in favour of parenchymal probes.

Advanced cerebral monitoring combines ICP monitoring with other cerebral monitoring techniques, including cerebral autoregulation monitoring, microdialysis monitoring of brain chemistry, brain tissue oxygen ($PbrO_2$) monitoring, and jugular bulb monitoring of arteriovenous oxygen content difference (AVDO2) (Valadka and Robertson, 2007; Le Roux et al., 2014; Brain Trauma Foundation, 2016; Makarenko et al., 2016). These monitoring methods allow for individualized management of secondary cerebral insults by assessing brain metabolic needs and the response to therapeutic intervention. Some cranial access devices allow for multiple catheters and sensors to be transmitted into the brain parenchyma to facilitate continuous multimodality monitoring at the bedside (Hutchinson et al., 2000).

Ventriculostomy

The role of CSF drainage and the optimal draining techniques (continues vs. intermittent) in TBI patients has not been firmly established (Nwachuku et al., 2014; Brain Trauma Foundation, 2016). An external ventricular drain (EVD), or ventriculostomy, is a rapid method of controlling ICP by reducing the intracranial CSF volume, even in the absence of hydrocephalus (Kerr et al., 2001; Timofeev et al., 2009; Brain Trauma Foundation, 2016). Its use has been described as a secondary ICP-lowering manoeuvre as part of protocol-driven management of elevated ICP. Physiological improvements have been reported following CSF drainage, however in a significant proportion of patient's ICP fails to be controlled if not used alongside other ICP-lowering treatments (Timofeev et al., 2009). Ventriculostomies are also associated with complications, include the risk of EVD-related infections, haemorrhages during insertions, and subsequent shunt-dependency.

An EVD connected to a pressure transducer can measure ICP in a closed position (see section on ICP monitoring), and drain CSF when opened. There is no consensus on the optimal drainage technique in TBI patients (Nwachuku et al., 2014; Brain Trauma Foundation, 2016). Practice patterns seem to vary significantly, and shown to be influenced by physician and departmental preferences and resources. Management of CSF drainage in TBI patients also appears to be related to the patient's age (Shore et al., 2004; Nwachuku et al., 2014). Continuous CSF drainage has been more commonly described in the paediatric TBI population. It is important to note that while intermitted drainage can allow for real-time visualization of ICP, the patient can be exposed to detrimental elevations of ICP between drainage periods. Continuous drainage allows for more stable ICP control, however, this risks overdrainage with subsequent collapse of the ventricles. In this circumstance, the EVD can no longer be reliably employed as a method of gauging ICP as it relies on a continuous column of fluid between the site of the transducer and the intraventricular cavity.

Craniotomy for mass lesions

Surgical intervention is aimed at mitigating injuries to the brain caused by (expanding) haematomas and their sequelae (Bullock et al., 2006a; Bullock et al., 2006b; Bullock et al., 2006c). An initial assessment of neurologic deficits, pupil abnormalities, degree of midline shift, hematoma volume, and the presence/severity of associated trauma is required to determine the necessity for emergent cranial surgery. For neurosurgeons one of the most difficult decisions to make is whether or not moderate-sized mass lesions should be evacuated or observed. As surgical interventions might not always be necessary, there is a risk with conservative management of neurological deterioration with possible secondary insults to the brain that may negatively impact the patient's outcome. Current guidelines and recommendations are available, but are limited to expert consensus with limited quality of evidence (Bullock et al., 2006a; Bullock et al., 2006b; Bullock et al., 2006c). It is worth emphasizing that although guidelines necessarily incorporate specific metrics that guide surgery, the whole clinical picture incorporating the clinical state (GCS, pupillary function) of the patient, the trajectory of deterioration, other causes of neurological compromise (such as metabolic, drug induced, hypoxia or hypotension), associated injuries, and comorbidities all influence the speed and manner of intervention (Bullock et al., 2006a; Bullock et al., 2006b; Bullock et al., 2006c).

Extradural haematomas

Extra (or epi-) dural hematomas (EDH) usually develop in young adults following traffic-related accidents, falls, and assaults (Bullock et al., 2006b). In TBI patients the incidence of surgical and non-surgical EDH cases has been estimated to be between 2.7 to 4% (Bullock et al., 2006b) EDH are thought to result from a direct blow to head and are usually found on the same side impacted by the blow. Typically, the source of bleeding is arterial, following a fracture in the region of the pterion with subsequent tearing of the middle meningeal artery and hematoma formation in the middle cranial fossa. Extradural hematomas may occur in any anatomical location including in the frontal, occipital, and vertex regions and can be associated with the anterior ethmoidal artery, transverse or sigmoid sinuses, and superior sagittal sinus, respectively. EDHs originating from venous sources are thought to expand more slowly compared to their arterial counterparts (Nalbach et al., 2012). EDH specific mortality has been described to be around 10% in adult patients (Bullock et al., 2006b). The role of surgery is to prevent irreversible brain injury or death caused by hematoma expansion, raised ICP, and herniation of the brain. Patients presenting with (progressive) focal neurologic signs or symptoms and/or hematoma growth, have to be considered as an emergency case. Evidence and expert-based recommendations for evacuations of EDH recommend surgery for all adult patients with a hematoma volume more than 30 cm^3 (>30 ml) regardless of the GCS score, and comatose patients (GCS <9) with pupillary abnormalities (Bullock et al., 2006b). Evacuation should be performed through a craniotomy window fashioned according to the location of the haematoma, and providing adequate access to the hematoma margins. If the brain appears tight it is important to inspect the subdural space for additional clots. When the bone flap is replaced several tenting sutures should be placed to obliterate the epidural space both circumferentially and over the centre of the craniotomy. Bone flaps are not left out for isolated EDH with no parenchymal injuries as these are typically injuries with a fracture haematoma rather than a brain injury *per se* that is prone to swelling. Close observation and conservative management are appropriate for patients with no focal neurologic deficits, with a small hematoma (<30 cm^3), a clot thickness less than 15 mm, and midline shift less than 5 mm on imaging (Bullock et al., 2006b).

Acute subdural hematomas

Acute subdural hematomas (aSDH) usually develop following motor vehicle accidents (MVA), falls, or assaults (Bullock et al., 2006c). In younger patients (18–40 y) 56% of the ASDH were caused by MVA and only 12% were caused by falls. Unlike young patients, those aged 65 years and older had in 22% of the cases an MVA and 56% had a fall (Bullock et al., 2006c). The mechanism of bleeding varies depending on the age of the patient and the amount of force applied. Typically, in elderly patients with relative brain atrophy, the source of bleeding is usually venous caused by torn bridging veins with a modest degree of force. In younger patients or with a greater degree of violence, the brain surface itself is badly contused

and arterial bleeding sources reported for approximately 20% to 30% of aSDH cases (Gennarelli and Thibault, 1982; Zumkeller et al., 1996; Koc et al., 1997; Servadei et al., 1998; Maxeiner and Wolff, 2007; Ryan et al., 2012). Mortality for aSDH patient requiring surgery has been described to be between 15% and 60% (Haselsberger et al., 1988; Hatashita et al., 1993; Zumkeller et al., 1996; Kok et al., 1997; Servadei et al., 1998; Bullock et al., 2006c; Ryan et al., 2012). Evidence and expert-based recommendations for evacuations of aSDH recommend surgery for all adult patients with a haematoma thickness more than 10 mm, midline shift more than 5 mm, GCS score decreased by 2 points or further from injury to hospital admission, and/or patients presenting with pupillary abnormalities (Bullock et al., 2006c). As advanced age has been associated with increased rates of adverse outcome, age should be considered when deciding whether surgery will change the natural history of the disease. TBI patients presenting with an aSDH are frequently accompanied by significant parenchymal injury and swelling on imaging (Zumkeller et al., 1996; Bullock et al., 2006c; Li et al., 2012). Patients with aSDHs that require surgery to remove the clot are treated either with a craniotomy or a decompressive craniectomy (DC). However, there is often uncertainty as to whether the bone flap should be replaced or not (Kolias et al., 2012). The RESCUE-ASDH trial has recruited aSDH patients and aimed to compare craniotomy versus DC for adult patients undergoing evacuation of an aSDH (Protocol 14PRT/6944). The results of this trial will inform surgical decision making in the management of aSDH patients. Close observation and conservative management are appropriate for patients that are neurologically stable, hematoma thickness less than 10 mm, midline shift less than 5 mm, no pupillary abnormalities, and no intracranial hypertension on ICP monitoring (Bullock et al., 2006c). Conservatively managed aSDHs resolve gradually and are usually absorbed over weeks, although in a proportion of patients may form a chronic subdural hematoma.

Intracerebral haematomas/contusion

Traumatic intracerebral haemorrhage (ICH) is also referred to as traumatic intraparenchymal haemorrhage and (haemorrhagic) contusion. Post-traumatic contusions are usually multiple and are located in the basal surface of the frontal and temporal lobes (Bullock et al., 2006a). In the acute stages, the ICH consists of a (semi-)liquid mass of blood with surrounding oedema. These mass lesions evolve over days and change consistency while oedema begins to recede. Mortality secondary to traumatic ICH is related to the location and size of the lesion(s) (Bullock et al., 2006a). Surgical interventions are aimed at preventing secondary damage, brainstem compression, and herniation of the brain. Unfortunately, the only trial investigating the role of early surgery versus initial conservative treatment to anticipate and prevent secondary damage in traumatic ICH was halted early (Gregson et al., 2012; Mendelow et al., 2015). Although the evidence is limited due to the low sample size resulting from premature termination, it appears that the STITCH(Trauma) Trial observed reduced mortality with early surgery (Mendelow et al., 2015). However, it is important to note that patients in this trial were mostly recruited in resource-limited settings where ICP monitoring was not usually available. Current evidence and expert-based recommendations for evacuations of traumatic ICH involving the cerebral hemispheres recommend surgery for patients with focal lesions and the following indications; progressive neurological deterioration, medically refractory raised ICP, a hematoma volume more than 50 cm^3 (>50 ml), GCS score of 6 to 8 in a patient with a frontal or temporal haemorrhage more than 20 cm^3 (>20 ml) with either midline shift of more than 5 mm and/or cisternal compression on CT scan (Bullock et al., 2006a). Patients with diffuse injuries developing medically refractory post-traumatic cerebral oedema and intracranial hypertension may be considered for a bifrontal DC (Bullock et al., 2006a). DCs may also be considered for patients with refractory intracranial hypertension and diffuse injuries with clinical and radiographic evidence for transtentorial herniation. Evacuation of a traumatic ICH in the posterior fossa is recommended when there is evidence of neurologic dysfunction/deterioration and significant mass effect on the basal cisterns, fourth ventricle, or signs of obstructive hydrocephalus (Bullock et al., 2006d). Intensive monitoring and serial imaging are appropriate for patients with no focal neurologic deficits, and non-significant mass effect on imaging.

Decompressive craniectomy

Management of refractory raised ICP following severe TBI consist of medical and surgical treatments (Stocchetti et al., 2008; American College of Surgeons, 2015). DC is generally considered a surgical treatment for patients with diffuse brain swelling or expanding contusions/haematomas refractory to medical treatment and impending herniation (Bohman and Schuster, 2013; Kolias et al., 2013). In recent years, the role of DC has been discussed as a primary treatment in the acute phase, leaving out the bone flap after evacuation of a mass lesion, or as a second- or third-tier therapeutic measure for diffuse brain injury and oedema, commonly named secondary or protocol-driven DC. The expansion of a swollen brain outside the skull, can potentially lead to a reduction in ICP and risk of herniation. The physiological improvements described in severe TBI patients after DC, include improvement in brain tissue oxygenation, cerebral perfusion, and neurochemistry (Yamakami and Yamaura, 1993; Stiefel et al., 2004; Ho et al., 2008; Jaeger et al., 2010; Bor-Seng-Shu et al., 2012; Lazaridis and Czosnyka, 2012). The risk of complications should also be considered as early or delayed complications can occur after DC (Kolias et al., 2013). Expansion of (contralateral) mass lesions, wound infections, and healing problems, subdural or subgaleal collections, hydrocephalus, syndrome of the trephined, and complications related to the subsequent cranioplasty have been recognized as DC-related complications (Flint et al., 2008; Stiver, 2009; Nalbach et al., 2012). As the risk of severe disability and death in severe TBI remains relatively high, several trials have explored the use of DC to improve patient outcomes (Protocol 14PRT/6944; Hutchinson et al., 2006; Cooper et al., 2011). However, defining the indications, timing, techniques, and optimal outcome measures for DC has proven to be difficult, and good quality evidence linking efficacy to outcome is lacking (Kolias et al., 2013).

Decompressive craniectomy methods

Decompressive craniectomy is an umbrella term for a group of procedures in which part of the skull is removed. In severe TBI the most frequently described DC procedures in adults are bifrontal DC and unilateral frontotemporoparietal craniectomy, also termed hemi(spheric)-craniectomy or unilateral DC (Kjellberg and Prieto, 1971; Guerra et al., 1999; Kolias et al., 2013). For unilateral pathologies

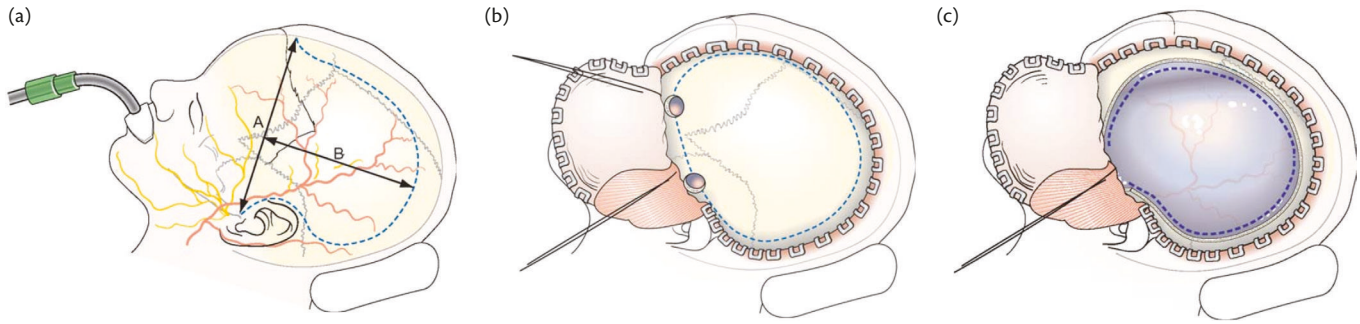

Fig. 43.1 Unilateral decompressive craniectomy. (A) The dotted line represents the usual skin incision made during unilateral decompressive craniectomy. To preserve adequate vascular supply, the length of the incision (distance B) should not exceed its width (distance A). (B) A myocutaneous flap is reflected. The dotted line represents the usual extent of the craniectomy. (C) The dotted line on the dura mater represents our preferred method for opening the dura. The dura is opened in a C-shaped fashion with its base along the sphenoid ridge. The dural incision is kept 5–10 mm away from the craniectomy edges to minimize the risk of injury to the protruding brain.

Reproduced with permission from I. Timofeev, T. Santarius, A.G. Kolias et al., Decompressive craniectomy—operative technique and perioperative care, *Advances and Technical Standards in Neurosurgery*, Volume 38, pp. 115–36, Copyright © 2012 Springer Nature.

with midline shift and (potential) swelling (e.g. aSDH with parenchymal injuries), a hemi-craniectomy can be useful (Fig. 43.1). Evidence and expert-based recommendations for adequate hemicraniectomies suggest that the bone flap should be large with a minimum anteroposterior diameter of 11–12 cm (Li et al., 2012; Tagliaferri et al., 2012) in order to achieve an adequate reduction of ICP and also reduce the risk of transcalvarial herniation that is associated with parenchymal injuries and cortical venous occlusion at the bone edge (von Holst et al., 2012; Li et al., 2013). Bifrontal DC is a treatment option for diffuse (bihemispheric) injuries with medically refractory intracranial hypertension (Fig. 43.2) (Kolias et al., 2013). A bifrontal DC extends from the floor of the anterior cranial fossa to the coronal suture posteriorly and to the temporal floor bilaterally. A widely opened dura mater is required to allow the brain to sufficiently expand. Different techniques have been described for the dura (left open with onlay of haemostatic material, pericranium, or temporalis fascia, or closure with dural expansion grafts) (Whitfield et al., 2001; Timofeev and Hutchinson, 2006; Guresir et al., 2011) and sagittal sinus sectioning or sparing (Bohman and Schuster, 2013). Studies have also described bilateral hemi-craniectomies as an approach for patients with diffuse injuries, although an improvement over the bifrontal DC approach has not been investigated (Guerra et al., 1999). For patients with temporal lesions or oedema causing brainstem compression, extension of the DC to the floor of the middle cranial fossa is essential.

Evidence base for DC in TBI

The DECRA trial failed to find an improvement in functional outcome by performing early bifrontal DC over medical management for patients with diffuse TBI (Cooper et al., 2011). The study showed that patients treated with DC had shorter duration of ventilation

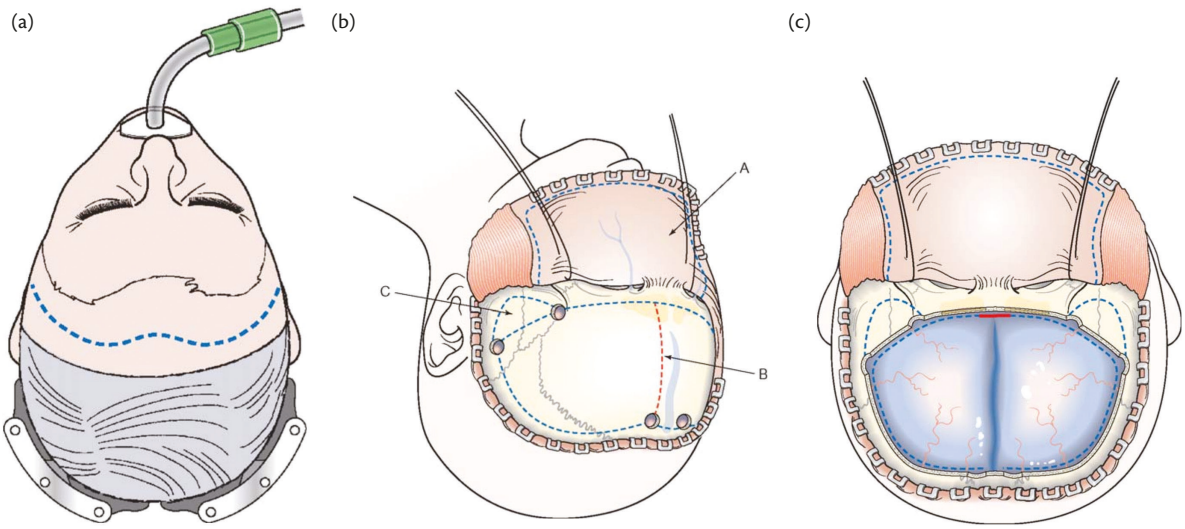

Fig. 43.2 Bifrontal decompressive craniectomy. (A) The dotted line represents the usual skin incision for bifrontal decompressive craniectomy, which should be kept behind the hairline. (B) A bicoronal myocutaneous flap is reflected anteriorly. The dotted line on the skull represents the usual extent of the craniectomy. Subtemporal decompression is optional. (C) The bone flap has been removed. The dotted line on the dura mater represents our preferred method for opening the dura. The dura is opened on either side of the midline in a C-shaped fashion with its base along the superior sagittal sinus. Division of the superior sagittal sinus anteriorly and of the falx (red line) is optional.

Reproduced with permission from I. Timofeev, T. Santarius, A.G. Kolias et al., Decompressive craniectomy—operative technique and perioperative care, Advances and Technical Standards in Neurosurgery, Volume 38, pp. 115–36, Copyright © 2012 Springer Nature.

and length of stay in the intensive care unit. The RESCUEicp trial aimed to examine the clinical and cost effectiveness of secondary DC (unilateral or bifrontal DC) for severe TBI patients with refractory intracranial hypertension as a last-tier therapy. 408 patients with raised and refractory ICP (threshold 25 mmHg >1–12 hours despite standard medical therapy) were randomised to ongoing medical therapy (plus optional barbituartes) or secondary decompressive craniectomy (Hutchinson et al., 2006). The results showed that decompressive craniectomy resulted in a marked reduction in mortality, increase in vegetative state, increase in lower (dependent) and upper (independent at home) with similar rates of moderate disability and good recovery. Outcome improved between 6 and 12 months with a significant proportion of patients in the surgical arm being upper severe disability or better. In contrast to the aforementioned trials, the RESCUE-ASDH trial is a randomised trial comparing primary unilateral DC to craniotomy (bone flap out versus bone flap replaced) for patients with aSDH (Protocol 14PRT/6944). Information from these studies will define the role of secondary and primary DC in future TBI treatment guidelines. On the basis of the current available evidence, neurosurgeons and neurointensivists must weigh the potential risks and benefits faced by their individual patients when deciding to perform a DC.

Surgical management of depressed skull fractures

Skull fractures most frequently involve the parietal bone, followed by the temporal, occipital, and frontal bones (Cooper and Golfinos, 2000). TBI patients usually present with linear fractures, and less frequently with depressed and skull base fractures. The force of the trauma to the skull required to cause fractures is significant, therefore patients are at significant risk of underlying brain injury. Evidence and expert-based recommendations for skull fractures recommend elevation and washout for patients with open skull fractures depressed more than the thickness of the cranium or more than 5 mm below the adjacent inner table (Bullock et al., 2006e). The rationale is reducing the risk of infection for these cases with early surgery, especially in the presence of dural tears, pneumocephalus, frontal sinus involvement, or contaminated wounds. Emergent surgery is also indicated for fractures with an underlying (expanding) hematoma. Elevation of the fracture will also improve cosmesis for cases with significant displacement of the bone. Reconstruction can usually be achieved by using the bone fragments; if this is not feasible, implants can be used to cover the skull defect (Marbacher et al., 2008). Antibiotics are usually administered to patients with open skull fractures; currently routine prophylaxis for all skull fractures is not supported by the available evidence (Ali and Ghosh, 2002; Bullock et al., 2006e; Ratilal et al., 2015).

Management of skull base fractures

Skull base fractures can involve the anterior, middle, and posterior cranial fossae, or a combination thereof. This section will focus on fractures of the petrous temporal bone and frontal sinus fractures.

Petrous temporal bone fractures are traditionally classified according to the orientation of the fracture line in relation to the long axis of the petrous temporal bone (i.e. line from petrous base to apex). Longitudinal fractures are parallel to the long axis of the petrous bone and their most frequent complications are ossicular injury, tympanic membrane rupture, and conductive hearing loss. Transverse fractures are perpendicular to the long axis of the petrous bone and they are thought to carry a higher risk of sensorineural hearing loss and facial nerve injury compared to longitudinal ones (Zayas et al., 2011). In reality, many fractures are mixed and therefore, a new classification system based on whether the otic capsule is involved or not may be clinically more meaningful (Dahiya et al., 1999). The so-called otic capsule–violating fractures involve the labyrinth (i.e. cochlea, vestibule, or semicircular canals) and patients were found to be twice as likely to develop facial paralysis, four times more likely to have a CSF leak, and seven times more likely to develop profound hearing loss (Dahiya et al., 1999).

The onset of palsy (immediate versus delayed) and the degree of palsy are factors that are typically taken into account when managing patients with petrous fractures and facial nerve palsy. However, in reality, it is often difficult to ascertain the timing of onset and the severity of paresis, as many patients have impaired consciousness, are sedated and ventilated, or are undergoing treatment for life-threatening injuries (Nash et al., 2010). Steroids are often used for patients with facial nerve palsy but a recent systematic review identified only low-quality evidence with lack of controlled studies (Nash et al., 2010). Surgical decompression of the nerve in its canal is usually reserved for patients with immediate onset of serious facial nerve palsy that does not improve with steroids. The timing of surgery remains controversial (Nash et al., 2010). In terms of natural history, of 189 patients managed with observation, who were included in a recent systematic review, 66% had an outcome equivalent to House-Brackmann (HB) I, one-quarter had HB II-V, and only two patients had an HB VI score (Nash et al., 2010).

The frontal sinuses are involved in up to 15% of facial fractures (Echo et al., 2010). Overall, recent years have seen a shift towards conservative management, especially with the advent of endoscopic techniques. Fractures involving the anterior wall do not usually require intervention, unless they are open or depressed. Fractures involving the posterior wall carry a higher risk of CSF leak. The indications for intervention for posterior wall fractures are controversial but in general persistent CSF rhinorrhoea or significant displacement of the posterior wall are accepted indications for intervention (Echo et al., 2010). This typically requires a bicoronal incision, repair of any dural defects if present, and cranialization of the sinus. Cranialization of the sinus aims to reduce the risk of mucocoele formation and intracranial infection; it involves removal of its posterior wall, stripping of the mucosa, and packing the frontonasal ducts. A pericranial flap positioned across the anterior cranial fossa floor, reinforced with a dural sealant, can help prevent a CSF leak. The LeFort type of fractures are usually managed by the maxillofacial surgeons; LeFort I fractures involve the maxilla and pterygoid plates; LeFort II have a pyramidal shape and involve the orbital floor, medial orbital wall, and nasofrontal suture; LeFort III involves the zygomatic arches, frontozygomatic and nasofrontal sutures, and orbital floors, resulting in craniofacial dislocation.

Surgical management of penetrating head trauma

All traumatic brain injuries that are not caused by a blunt mechanism are defined as penetrating brain injury (PBI) (Esposito and Walker, 2009). The incidence of PBI is lower than closed TBI, but PBI has been associated with more adverse outcomes. Most PBIs are caused by gunshot wounds to the head (GSWH), which are the typically lethal, as more than 90% of GSWH have a fatal outcome (Maas et al., 2008). The incidence of PBI is increasing, especially in the United States, due to the use of firearms in violence-related injuries. In addition, worldwide, armed conflicts are causing more brain injuries (No authors, 2001; Maas et al., 2008).

Since the majority of PBIs are caused by missiles or projectiles, and understanding of ballistics is required. Primary injury from GSWH is determined by the ballistic properties (kinetic energy, mass, velocity, shape, and so on.) of the projectile and any secondary projectiles, such as bone or metallic fragments (Ordog et al., 1984). Projectile and possible secondary metal or bone fragments travel through brain parenchyma creating a permanent track of injury. Higher velocity projectiles will cause temporary cavitation, which is a kinetic energy and velocity-related phenomenon (Aarabi, et al., 2001). This results from the transmission of the kinetic energy of the projectile to the surrounding tissue as the projectile slows down. Subsequently, this temporary cavity collapses and expands in wave-like pattern causing further shearing forces to surrounding tissues resulting in haemorrhages and neuronal injuries (Ordog et al., 1984; No authors, 2001).

A non-contrast CT of the head is the recommended modality in the radiological evaluation of PBI cases, since it is quick and provides identification of bone and metallic fragments, characterization of the projectile trajectory, evaluation of the extent of brain injury, detection of intracranial haemorrhages, and possible mass effect (Aarabi, et al., 2001; Tsuei et al., 2005). A formal digital subtraction angiogram is recommended, in particular when the projectile trajectory is near the Sylvian fissure, the supraclinoid carotid artery, the vertebrobasilar vessels, the cavernous sinus region, the major dural venous sinuses, or if a delayed hematoma or SAH develops (No authors, 2001; Offiah and Twigg, 2009). The common vascular complications following PBI include traumatic intracranial aneurysms, arteriovenous fistulas (AVFs), SAH, and vasospasm (No authors, 2001).

Surgical management of PBI entails a superficial debridement and watertight dural closure as a standard of care, but in patients with small entry wounds, simple wound closure may be considered (Maas et al., 2008). In the case of significant mass effect, necrotic brain tissue and bone fragments should be removed, but routine bone or projectile removal in the eloquent areas is not recommended (No authors, 2001). Additionally, any significant intracerebral haemorrhages with significant mass effect should be evacuated. PBI patients are at high risk of CNS infection since contaminated foreign bodies are driven into the brain tissue along the projectile track, hence prophylactic broad-spectrum antibiotics are recommended, and should be started as soon as possible (No authors, 2001; Maas et al., 2008).

Surgical management of CSF leaks

In TBI patients it is estimated that CSF leaks occur in approximately 2% of patients (Mendizabal et al., 1992; Brodie and Thompson, 1997; Friedman et al., 2001). Fractures carrying a high risk of CSF leaks are those involving the frontal or ethmoidal sinuses, and the petrous temporal bone (Mendizabal et al., 1992; Ommaya, 1996). The majority of CSF leaks are self-limiting and resolve spontaneously within days (Chandler, 1983; McGuirt and Stool, 1995; Brodie and Thompson, 1997). Surgical interventions are aimed at reducing the symptoms and risk of infection in cases with persistent CSF leaks or fistulae. Studies have reported infection rates between 7% and 30% for TBI patients with CSF leaks, with each day of leakage increasing the risk of ascending intracranial infection (Leech and Paterson, 1973; Spetzler and Wilson, 1978; Brodie and Thompson, 1997; Savva et al., 2003; Nyquist et al., 2013; Mathias et al., 2016). Lumbar drainage has been recognized as a treatment option for TBI patient with CSF leaks, in order to relieve CSF pressure aiding spontaneous and surgical repairs, while also facilitating a route to administer intrathecal fluorescein for diagnostic purposes (Shapiro and Scully, 1992; Mathias et al., 2016). However, lumbar drainage in the presence of a patent CSF fistula risks entraining intracranial air with a consequent risk of intracranial infection. The relative importance of antibiotic prophylaxis as well as the selection of the high-risk candidates for surgical intervention remain to be defined (Rimmer et al., 2014). However, the Centre for Disease Control and Prevention recommends either the pneumococcal conjugate vaccine (PCV13) or the pneumococcal polysaccharide vaccine (PPSV23) for patients with CSF leaks (CDC, 2015b). In the United Kingdom, the National Institute of Clinical Excellence recommends pneumococcal vaccination for all skull base fractures.

Investigation and management of carotid or vertebral dissection

Post-traumatic dissection of the internal carotid (ICA) or vertebral artery (VA) is most prevalent in young TBI patients (Rubinstein et al., 2005). Mechanisms include motor vehicle accident, falls, hangings or sport accidents, and may lead to a stroke in an acute or delayed fashion from acute vessel occlusion or thromboembolism (Geddes et al., 2016). The mechanism of injury can be direct compression of the arteries against bony structures owing to flexion, extension and rotational head movements or acceleration/deceleration that results in shearing forces to the vessel endothelium. The VA is commonly dissected at the C1–C2 level by rotational forces or directly due to a fracture or dislocation of facet joints or transverse processes, whereas the ICA can be compressed between the spine and mandible (Blacker and Wijdicks, 2004). Clinically, dissections can present as TIA, stroke, or SAH. There is often a silent period between the injury and onset of neurological symptoms. Patients with polytrauma with impaired consciousness due to the head injury itself or the use of sedatives, can make the clinical diagnosis difficult (Blacker and Wijdicks, 2004). Prognosis is variable, as dissections can vary from being asymptomatic to causing profound neurological deficits and death (Mohan, 2014).

Dissections are initiated with a tear on the innermost intimal layer or the media layer of the blood vessel wall. Extravasation of arterial blood under pressure can extend the dissection between intima and tunica media creating luminal narrowing or occlusion. A subintimal dissection may result in an intramural hematoma with consequent luminal stenosis. Dissection within the intracranial cavity may also

lead to aneurysmal dilatation and haemorrhage into subarachnoid space. Rupture of an artery with subsequent encapsulation of the extravascular hematoma may or may not produce luminal narrowing (Yamaura, 1994). Distal embolization occurs due to platelet aggregation stimulated by exposed surfaces or dislodged thrombus. It may also cause reduced distal flow due to occlusion of lumen due to thrombosis or mural haematoma (Mohan, 2014).

Prompt recognition and diagnosis is paramount. Cerebral ischaemia related to ICA most commonly affects the middle cerebral artery territory, whereas VA dissections affect the brainstem, cerebellum, and occipital lobes. Infarctions or haemorrhages can be visualized with CT imaging, however CT angiogram (CTA) or catheter angiography alone can demonstrate luminal stenosis, fusiform dilatations, occlusions, intimal flaps, proximal beading, double lumen signs, or a kinked appearance of vessels (Kitanaka et al., 1994; Eastman et al., 2006; Geddes et al., 2016). Magnetic resonance imaging angiogram is generally not considered as accurate as CTA or catheter angiography.

Intracranial lesions with SAH can be treated endovascularly or microsurgically (Halbach et al., 1993; Pham et al., 2011), however, in modern practice surgical management is rarely warranted. Dissecting aneurysms may be fusiform and cover a long segment that precludes microsurgical clipping or endovascular stenting, and in this circumstance may be candidates for occlusion of the VA proximal to the basilar artery. Balloon test occlusion of the dominant VA is recommended since some patients might not tolerate total occlusion (Mohan, 2014). Other surgical techniques described include a combination of VA clipping with vascular bypass, resection accompanied with autogenous interposition vein graft, usage of fusiform-type clipping, and wrapping (Arimura and Iihara, 2016). Extracranial dissections are managed medically, and this includes antiplatelet therapy or anticoagulation for a total of 6 months (CADISS trial investigators, 2015).

Surgical management of post-traumatic hydrocephalus

Post-traumatic hydrocephalus (PTH) is a complication of TBI and studies have reported clinical improvement after permanent CSF diversion (Guyot and Michael, 2000). Patients who suffered TBI and under active follow-up are usually monitored for PTH, which can present as worsening neurological status or lack of improvement associated with pressure related headaches or the normal pressure hydrocephalus syndrome. Late CSF leak is also suspicious for PTH. It is important to recognize and treat PTH, since it could both impact morbidity and mortality if left untreated (Paoletti et al., 1983; Tribl and Oder, 2000; Low et al., 2013). The incidence of PTH has been reported to range between 0.7% and 51.4% (Bontke and Boake, 1991; Guyot and Michael, 2000; De Bonis et al., 2010). However, it is often difficult to determine whether ventriculomegaly observed post-TBI is related to atrophy or hydrocephalus; computerized CSF infusion studies have been reported to be useful in distinguishing between the two different processes (Marmarou et al., 1996; Czosnyka et al., 2005). Selection of patient benefiting from permanent CSF diversion is important, since shunting is also associated with significant complications. No clear guidelines exist for PTH treatment, however adjustable or flow-regulated ventriculo-peritoneal shunts are most commonly described as the preferred choice of shunting to reduce the risk of overdrainage. PTH has been reported as a relative contraindication to endoscopic third ventriculostomy (Singh et al., 2008), however this notion has been challenged by others (De Bonis et al., 2013). It is difficult to predict the response of CSF diversion in PTH, since these patients often have comorbidities and significant underlying brain injury. Studies have also suggested that DC is a risk factor for hydrocephalus (De Bonis et al., 2010; Kolias et al., 2013) whereas others do not support this hypothesis (Rahme et al., 2010). Hydrocephalus has been described in TBI patients undergoing DC, ranging in case series between 0% and 88.2% (Ding et al., 2014). It is thought that CSF malabsorption or obstructed flow are the cause of post-DC hydrocephalus. However, the current case series are limited by their design and heterogeneity of criteria used to diagnose hydrocephalus.

Cranioplasty

Cranioplasty is the surgical reconstruction of a bone defect after a previous operation, usually DC, or due to skull injury (**Fig. 43.3**). A cranioplasty is recommended for both protection of the underlying brain that is left vulnerable to damage with a skull defect and also for restoring the skull contour that might have psychological and social consequences for the patient (Kolias et al., 2013). The cranioplasty can also facilitate neurological rehabilitation and may also improve neurological function, as observed in patients with syndrome of the trephined (Segal et al., 1994; Di Stefano et al., 2012; Bender et al., 2013; Honeybul et al., 2013). However, this procedure is associated with challenging complications; the most common are wound-healing problems and implant related infections (Gooch et al., 2009; Honeybul and Ho, 2011; Wachter et al., 2013). The wide range of techniques, graft materials (autologous bone, metal or synthetic) and timing of reconstruction (1–12 months) discussed in the literature reflects the lack of consensus and good quality evidence (Liang et al., 2007; Beauchamp et al., 2010; Yadla et al., 2011; Glover et al., 2012; Schuss et al., 2012; Bender et al., 2013; Klinger et al., 2014). There main controversy in relation to timing revolves around whether performing the cranioplasty early increases the risk of infections or not and whether it can independently improve neurological outcome. A recent systematic review of available studies (all retrospective), including 528 patients, concluded that cranioplasty may improve neurological outcome, and earlier cranioplasty may enhance this effect (Liang et al., 2007; Beauchamp et al., 2010; Yadla et al., 2011; Glover et al., 2012; Schuss et al., 2012; Bender et al., 2013; Malcolm et al., 2018). In terms of materials, the patient's own bone is the most commonly used one, as it fulfils many of the requirements of an ideal material (i.e. it has a low cost and ideal contour and additionally is biocompatible, strong, and radiolucent). However, a few reports in recent years have shown a high failure rate due to resorption or infection; this was confirmed by a recent single-centre RCT of autologous cranioplasty versus titanium cranioplasty which found that of the 31 patients with an autologous cranioplasty, 7 patients (22%) had complete bone resorption (Honeybul et al., 2017). Acrylic cranioplasty, in the form of polymethylmethacrylate, is cheap, malleable, and lightweight. However, the fragility of the plates that can lead to fractures and the risks associated with exothermic reaction are concerns (Aydin et al., 2011). Hydroxyapatite has

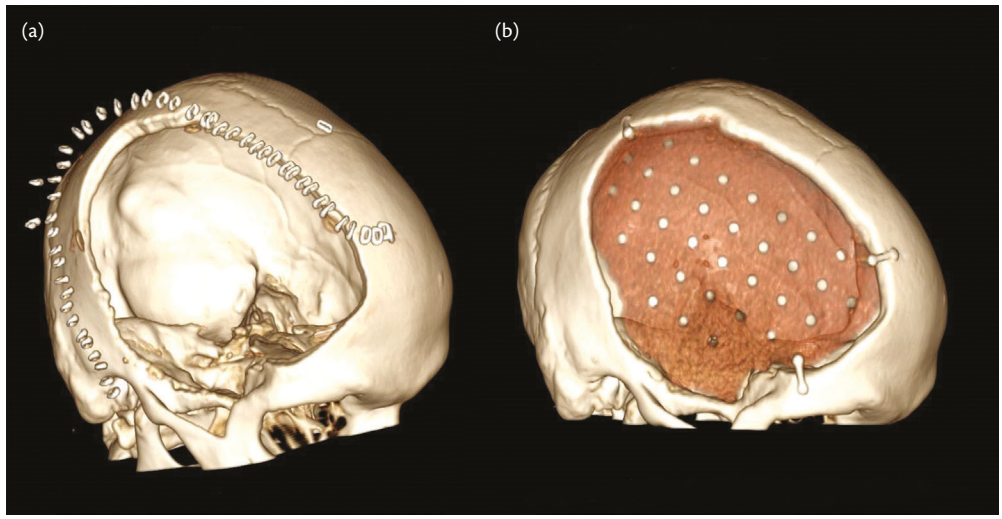

Fig. 43.3 Cranioplasty. (A) Postoperative computed tomography (CT) three-dimensional (3D) reconstructions of the head demonstrating a large calvarial defect following unilateral decompressive craniectomy for an evacuation of an acute subdural haematoma with significant intraoperative swelling. (B) Postcranioplasty CT 3D reconstructions following repair of the bony defect with customized PEEK prosthesis. Preoperative CTs were used for production of a tailored flap.

become popular in recent years, as it offers good osseointegration. Nevertheless, its cost remains high and there have been reports that the material can fracture following trauma. Titanium remains a widely used and relatively cheap option but leads to artefact on imaging. A recently published single-centre RCT of hydroxyapatite versus titanium found that the reoperation rate at 6-months (26.9% vs. 29.2% respectively) was similar, with a lower number of infections for hydroxyapatite (7.7% vs. 20.8%) but higher number of epidural haematomas (34.6% vs. 8.3%) (Lindner et al., 2017). Several other materials or combinations of materials for cranioplasty exist; detailed description of all options is beyond the scope of this chapter. Key steps of the surgical technique include careful dissection of the scalp from the dura, closure of any dural tears, exposure of bone margins circumferentially, and secure fixation of the autologous bone or artificial implant. In cases of an infection, the plate is usually removed and the wound debrided; it is important to wait until the underlying infection is clear, a process which can take up to 1 year, prior to re-inserting a plate in order to minimize the risk of further implant infection.

REFERENCES

[No authors] (2001). Part 1: guidelines for the management of penetrating brain injury. Introduction and methodology. J Trauma, **51**(2 Suppl), S3–6.

Aarabi, B., Alden, T.D., Hunter Downs III, J., et al. (2001). Neuroimaging in the Management of Penetrating Brain Injury. *J Trauma Acute Care Surg*, **51**(2), S7–S11.

Ali, B. & Ghosh, A. (2002). Antibiotics in compound depressed skull fractures. *EMJ*, **19**(6), 552–3.

American College of Surgeons (2015). TQIP Best Practices in the Managment of Traumatic Brain Injury. https://www.facs.org/quality-programs/trauma/tqip/best-practice

Arimura, K. & Iihara, K. (2016). Surgical management of intracranial artery dissection. *Neurol Med Chr (Tokyo)*, **56**(9), 517–23.

Aydin, S., Kucukyuruk, B., Abuzayed, B., Aydin, S., & Sanus, G.Z. (2011). Cranioplasty: review of materials and techniques. *J Neurosci Rural Pract*, **2**(2), 162–7.

Beauchamp, K.M., Kashuk, J., Moore, E.E., et al. (2010). Cranioplasty after postinjury decompressive craniectomy: is timing of the essence? *J Trauma*, **69**(2), 270–4.

Bender, A., Heulin, S., Röhrer, S., et al. (2013). Early cranioplasty may improve outcome in neurological patients with decompressive craniectomy. *Brain Inj*, **27**(9), 1073–9.

Blacker, D.J. & Wijdicks, E.F. (2004). Clinical characteristics and mechanisms of stroke after polytrauma. *Mayo Clin Proc*, **79**(5), 630–5.

Bohman, L.E. & Schuster, J.M. (2013). Decompressive craniectomy for management of traumatic brain injury: an update. *Curr Neurol Neurosci Rep*, **13**(11), 392.

Bontke, C.F. & Boake, C. (1991). Traumatic brain injury rehabilitation. *Neurosurg Clin N Am*, **2**(2), 473–82.

Bor-Seng-Shu, E., Figueiredo, E.G., Amorim, R.L.O., et al. (2012). Decompressive craniectomy: a meta-analysis of influences on intracranial pressure and cerebral perfusion pressure in the treatment of traumatic brain injury. *J Neurosurg*, **117**(3), 589–96.

Brain Trauma Foundation (2016). *Guidelines for the Management of Severe Traumatic Brain Injury*, 4th edition. https://braintrauma.org/uploads/03/12/Guidelines_for_Management_of_Severe_TBI_4th_Edition.pdf

Brodie, H.A. & Thompson, T.C. (1997). Management of complications from 820 temporal bone fractures. *Am J Otology*, **18**(2), 188–97.

Bullock, M.R., Chesnut, R., Ghajar, J., et al. (2006a). Surgical management of traumatic parenchymal lesions. *Neurosurgery*, **58**(3), S2–25–S2–46.

Bullock, M.R., Chesnut, R., Ghajar, J., et al. (2006b). Surgical management of acute epidural hematomas. *Neurosurgery*, **58**(3 Suppl), S7–15; discussion Si–iv.

Bullock, M.R., Chesnut, R., Ghajar, J., et al. (2006c). Surgical management of acute subdural hematomas. *Neurosurgery*, **58**(3 Suppl), S16–24; discussion Si–iv.

Bullock, M.R., Chesnut, R., Ghajar, J., et al. (2006d). Surgical management of posterior fossa mass lesions. *Neurosurgery*, **58**(3 Suppl), S47–55; discussion Si–iv.

Bullock, M.R., Chesnut, R., Ghajar, J., et al. (2006e). Surgical management of depressed cranial fractures. *Neurosurgery*, **58**(3 Suppl), S56–60; discussion Si–iv.

CADISS Trial Investigators (2015). Antiplatelet treatment compared with anticoagulation treatment for cervical artery dissection (CADISS): a randomised trial. *Lancet Neurol*, **14**(4), 361–7.

Centers for Disease Control and Prevention (CDC) (2015a). *Report to Congress on Traumatic Brain Injury in the United States: Epidemiology and Rehabilitation*. National Center for Injury Prevention and Control; Division of Unintentional Injury Prevention. Atlanta, GA. https://www.cdc.gov/traumaticbraininjury/pdf/tbi_report_to_congress_epi_and_rehab-a.pdf

Centers for Disease Control and Prevention (CDC) (2015b). *Vaccines and Immunizations. Centers for Disease Control and Prevention*. Atlanta, GA. http://www.cdc.gov/vaccines/vpd-vac/pneumo/vacc-in-short.htm

Chambers, I.R., Kane, P.J., Signorini, D.F., Jenkins, A., & Mendelow, A.D. (1998). Bilateral ICP monitoring: its importance in detecting the severity of secondary insults. In: Marmarou, A., Bullock, R., Avezaat, C., et al. (eds.) *Intracranial Pressure and Neuromonitoring in Brain Injury: Proceedings of the Tenth International ICP Symposium*, pp. 42–3, Williamsburg, VA, 25–29 May 1997. Vienna, Austria: Springer Vienna.

Chandler, J.R. (1983). Traumatic cerebrospinal fluid leakage. *Otolaryngol Clin N Am*, **16**(3), 623–32.

Compagnone, C., Murray, G.D., Teasdale, G.M., et al. (2007). The management of patients with intradural post-traumatic mass lesions: a multicenter survey of current approaches to surgical management in 729 patients coordinated by the European Brain Injury Consortium. *Neurosurgery*, **61**(1 Suppl), 232–40; discussion 40–1.

Cooper, D.J., Rosenfeld, J.V., Murray, L., et al. (2011). Decompressive craniectomy in diffuse traumatic brain injury. *N Engl J Med*, **364**(16), 1493–502.

Cooper, P.R. & Golfinos, J.G. (2000). *Head Injury*, 4th edition. New York, NY: McGraw-Hill, Medical Pub. Division, p. 598.

Czosnyka, Z., Czosnyka, M., Owler, B., et al. (2005). Clinical testing of CSF circulation in hydrocephalus. *Acta Neurochir Suppl*, **95**, 247–51.

Dahiya, R., Keller, J.D., Litofsky, N.S., Bankey, P.E., Bonassar, L.J., & Megerian, C.A. (1999). Temporal bone fractures: otic capsule sparing versus otic capsule violating clinical and radiographic considerations. *J Trauma*, **47**(6), 1079–83.

De Bonis, P., Pompucci, A., Mangiola, A., Rigante, L., & Anile, C. (2010). Post-traumatic hydrocephalus after decompressive craniectomy: an underestimated risk factor. *J Neurotrauma*, **27**(11), 1965–70.

De Bonis, P., Tamburrini, G., Mangiola, A., et al. (2013). Post-traumatic hydrocephalus is a contraindication for endoscopic third-ventriculostomy: isn't it? *Clin Neurol Neurosurg*, **115**(1), 9–12.

Di Stefano, C., Sturiale, C., Trentini, P., et al. (2012). Unexpected neuropsychological improvement after cranioplasty: a case series study. *Br J Neurosurg*, **26**(6), 827–31.

Ding, J., Guo, Y., & Tian, H. (2014). The influence of decompressive craniectomy on the development of hydrocephalus: a review. *Arquivos de neuro-psiquiatria*, **72**(9), 715–20.

Eastman, A.L., Chason, D.P., Perez, C.L., McAnulty, A.L., & Minei, J.P. (2006). Computed tomographic angiography for the diagnosis of blunt cervical vascular injury: is it ready for primetime? *J Trauma*, **60**(5), 925–9; discussion 9.

Echo, A., Troy, J.S., & Hollier, L.H. Jr. (2010). Frontal sinus fractures. *Semin Plast Surg*, **24**(4), 375–82.

Esposito, D.P. & Walker, J.B. (2009). Contemporary management of penetrating brain injury. *Neurosurgery Quarterly*, **19**(4), 249–54.

Esposito, T.J., Reed, R.L., 2nd, Gamelli, R.L., & Luchette, F.A. (2005). Neurosurgical coverage: essential, desired, or irrelevant for good patient care and trauma center status. *Ann Surg*, **242**(3), 364–70; discussion 70–4.

Flint, A.C., Manley, G.T., Gean, A.D., Hemphill, J.C., 3rd, & Rosenthal, G. (2008). Post-operative expansion of hemorrhagic contusions after unilateral decompressive hemicraniectomy in severe traumatic brain injury. *J Neurotrauma*, **25**(5), 503–12.

Forsyth, R.J., Raper, J., & Todhunter, E. (2015). Routine intracranial pressure monitoring in acute coma. *Cochrane Database Syst Rev*, **11**, CD002043.

Friedman, A.J., Ebersold, J.M., & Quast, M.L. (2001). Post-traumatic cerebrospinal fluid leakage. *World J Surg*, **25**(8), 1062–6.

Geddes, A.E., Burlew, C.C., Wagenaar, A.E., et al. (2016). Expanded screening criteria for blunt cerebrovascular injury: a bigger impact than anticipated. *Am J Surg*, **212**(6), 1167–74.

Gennarelli, T.A. & Thibault, L.E. (1982). Biomechanics of acute subdural hematoma. *J Trauma Acute Care Surg*, **22**(8), 680–6.

Glover, L.E., Tajiri, N., Lau, T., Kaneko, Y., Van Loveren, H., & Borlongan, C.V. (2012). Immediate, but not delayed, microsurgical skull reconstruction exacerbates brain damage in experimental traumatic brain injury model. *PLoS One*, **7**(3), e33646.

Gooch, M.R., Gin, G.E., Kenning, T.J., & German, J.W. (2009). Complications of cranioplasty following decompressive craniectomy: analysis of 62 cases. *Neurosurg Focus*, **26**(6), E9.

Gregson, B.A., Rowan, E.N., Mitchell, P.M., et al. (2012). Surgical trial in traumatic intracerebral hemorrhage (STITCH(Trauma)): study protocol for a randomized controlled trial. *Trials*, **13**, 193.

Guerra, W.K., Gaab, M.R., Dietz, H., Mueller, J.U., Piek, J., & Fritsch, M.J. (1999). Surgical decompression for traumatic brain swelling: indications and results. *J Neurosurg*, **90**(2), 187–96.

Guresir, E., Vatter, H., Schuss, P., et al. (2011). Rapid closure technique in decompressive craniectomy. *J Neurosurg*, **114**(4), 954–60.

Guyot, L.L. & Michael, D.B. (2000). Post-traumatic hydrocephalus. *Neurol Res*, **22**(1), 25–8.

Halbach, V.V., Higashida, R.T., Dowd, C.F., et al. (1993). Endovascular treatment of vertebral artery dissections and pseudoaneurysms. *J Neurosurg*, **79**(2), 183–91.

Haselsberger, K., Pucher, R., & Auer, L.M. (1988). Prognosis after acute subdural or epidural haemorrhage. *Acta Neurochir (Wien)*, **90**(3–4), 111–16.

Hatashita, S., Koga, N., Hosaka, Y., & Takagi, S. (1993). Acute subdural hematoma: severity of injury, surgical intervention, and mortality. *Neurol Med Chir (Tokyo)*, **33**(1), 13–18.

Ho, C.L., Wang, C.M., Lee, K.K., Ng, I., & Ang, B.T. (2008). Cerebral oxygenation, vascular reactivity, and neurochemistry following decompressive craniectomy for severe traumatic brain injury. *J Neurosurg*, **108**(5), 943–9.

Honeybul, S. & Ho, K.M. (2011). Long-term complications of decompressive craniectomy for head injury. *J Neurotrauma*, **28**(6), 929–35.

Honeybul, S., Janzen, C., Kruger, K., & Ho, K.M. (2013). The impact of cranioplasty on neurological function. *Br J Neurosurg*, **27**(5), 636–41.

Honeybul, S., Morrison, D.A., Ho, K.M., Lind, C.R., & Geelhoed, E. (2017). A randomized controlled trial comparing autologous cranioplasty with custom-made titanium cranioplasty. *J Neurosurg*, **126**(1), 81–90.

Hutchinson, P.J., Corteen, E., Czosnyka, M., et al. (2006). Decompressive craniectomy in traumatic brain injury: the randomized multicenter RESCUEicp study (www.RESCUEicp.com). *Acta Neurochir Suppl*, **96**, 17–20.

Hutchinson, P.J., Hutchinson, D.B., Barr, R.H., Burgess, F., Kirkpatrick, P.J., & Pickard, J.D. (2000). A new cranial access device for cerebral monitoring. *Br J Neurosurg*, **14**(1), 46–8.

Jaeger, M., Dengl, M., Meixensberger, J., & Schuhmann, M.U. (2010). Effects of cerebrovascular pressure reactivity-guided optimization of cerebral perfusion pressure on brain tissue oxygenation after traumatic brain injury. *Crit Care Med*, **38**(5), 1343–7.

Kerr, M.E., Weber, B.B., Sereika, S.M., Wilberger, J., & Marion, D.W. (2001). Dose response to cerebrospinal fluid drainage on cerebral perfusion in traumatic brain-injured adults. *Neurosurg Focus*, **11**(4), 1–7.

Kitanaka, C., Tanaka, J., Kuwahara, M., et al. (1994). Nonsurgical treatment of unruptured intracranial vertebral artery dissection with serial follow-up angiography. *J Neurosurg*, **80**(4), 667–74.

Kjellberg, R.N. & Prieto, A.J. (1971). Bifrontal decompressive craniotomy for massive cerebral edema. *J Neurosurg*, **34**(4), 488–93.

Klinger, D.R., Madden, C., Beshay, J., White, J., Gambrell, K., & Rickert, K. (2014). Autologous and acrylic cranioplasty: a review of 10 years and 258 cases. *World Neurosurg*, **82**(3), e525–e30.

Koc, R.K., Akdemir, H., Oktem, I.S., Meral, M., & Menku, A. (1997). Acute subdural hematoma: outcome and outcome prediction. *Neurosurg Rev*, **20**(4), 239–44.

Kolias, A.G., Belli, A., Li, L.M., et al. (2012). Primary decompressive craniectomy for acute subdural haematomas: results of an international survey. *Acta Neurochir (Wien)*, **154**(9), 1563–5.

Kolias, A.G., Kirkpatrick, P.J., & Hutchinson, P.J. (2013). Decompressive craniectomy: past, present and future. *Nat Rev Neurol*, **9**(7), 405–15.

Lawrence, T., Helmy, A., Bouamra, O., Woodford, M., Lecky, F., & Hutchinson, P.J. (2016). Traumatic brain injury in England and Wales: prospective audit of epidemiology, complications and standardised mortality. *BMJ Open*, **6**(11), e012197.

Lazaridis, C. & Czosnyka, M. (2012). Cerebral blood flow, brain tissue oxygen, and metabolic effects of decompressive craniectomy. *Neurocrit Care*, **16**(3), 478–84.

Le Roux, P., Menon, D.K., Citerio, G., et al. (2014). The International Multidisciplinary Consensus Conference on Multimodality Monitoring in Neurocritical Care: evidentiary tables: a statement for healthcare professionals from the Neurocritical Care Society and the European Society of Intensive Care Medicine. *Neurocrit Care*, **21** Suppl 2, S297–361.

Leech, P.J. & Paterson, A. (1973). Conservative and operative management for cerebrospinal-fluid leakage after closed head injury. *Lancet*, **1**(7811), 1013–16.

Li, L.M., Kolias, A.G., Guilfoyle, M.R., et al. (2012). Outcome following evacuation of acute subdural haematomas: a comparison of craniotomy with decompressive craniectomy. *Acta Neurochir (Wien)*, **154**(9), 1555–61.

Li, X., von Holst, H., & Kleiven, S. (2013). Decompressive craniectomy causes a significant strain increase in axonal fiber tracts. *J Clin Neurosci*, **20**(4), 509–13.

Liang, W., Xiaofeng, Y., Weiguo, L., et al. (2007). Cranioplasty of large cranial defect at an early stage after decompressive craniectomy performed for severe head trauma. *J Craniofac Surg*, **18**(3), 526–32.

Lindner, D., Schlothofer-Schumann, K., Kern, B.C., Marx, O., Muns, A., & Meixensberger, J. (2017). Cranioplasty using custom-made hydroxyapatite versus titanium: a randomized clinical trial. *J Neurosurg*, **126**(1), 175–83.

Low, C.Y., Low, Y.Y., Lee, K.K., Chan, S.P., & Ang, B.T. (2013). Post-traumatic hydrocephalus after ventricular shunt placement in a Singaporean neurosurgical unit. *J Clin Neurosci*, **20**(6), 867–72.

Maas, A.I., Stocchetti, N., & Bullock, R. (2008). Moderate and severe traumatic brain injury in adults. *Lancet Neurol*, **7**(8), 728–41.

Makarenko, S., Griesdale, D.E., Gooderham, P., & Sekhon, M.S. (2016). Multimodal neuromonitoring for traumatic brain injury: a shift towards individualized therapy. *J Clin Neurosci*, **26**, 8–13.

Malcolm, J.G., Rindler, R.S., Chu, J.K., et al. (2018). Early cranioplasty is associated with greater neurological improvement: a systematic review and meta-analysis. *Neurosurgery*, **82**(3), 278–88.

Marbacher, S., Andres, R.H., Fathi, A.R., & Fandino, J. (2008). Primary reconstruction of open depressed skull fractures with titanium mesh. *J Craniofac Surg*, **19**(2), 490–5.

Marmarou, A., Foda, M.A., Bandoh, K., et al. (1996). Posttraumatic ventriculomegaly: hydrocephalus or atrophy? A new approach for diagnosis using CSF dynamics. *J Neurosurg*, **85**(6), 1026–35.

Mathias, T., Levy, J., Fatakia, A., & McCoul, E.D. (2016). Contemporary approach to the diagnosis and management of cerebrospinal fluid rhinorrhea. *Ochsner J*, **16**(2), 136–42.

Maxeiner, H. & Wolff, M. (2007). Pure subdural hematomas: a postmortem analysis of their form and bleeding points. *Neurosurgery*, **61**(1 Suppl), 267–72; discussion 72–3.

McGuirt, W.F., Jr. & Stool, S.E. (1995). Cerebrospinal fluid fistula: the identification and management in pediatric temporal bone fractures. *Laryngoscope*, **105**(4 Pt 1), 359–64.

Mendelow, A.D., Gregson, B.A., Rowan, E.N., et al. (2015). Early surgery versus initial conservative treatment in patients with traumatic intracerebral hemorrhage (STITCH[Trauma]): the first randomized trial. *J Neurotrauma*, **32**(17), 1312–23.

Mendizabal, G.R., Moreno, B.C., & Flores, C.C. (1992). Cerebrospinal fluid fistula: frequency in head injuries. *Revue de laryngologie—Otologie—Rhinologie*, **113**(5), 423–5.

Mohan, I.V. (2014). Current optimal assessment and management of carotid and vertebral spontaneous and traumatic dissection. *Angiology*, **65**(4), 274–83.

Nalbach, S.V., Ropper, A.E., Dunn, I.F., & Gormley, W.B. (2012). Craniectomy-associated progressive extra-axial collections with treated hydrocephalus (CAPECTH): redefining a common complication of decompressive craniectomy. *J Clin Neurosci*, **19**(9), 1222–7.

Nash, J.J., Friedland, D.R., Boorsma, K.J., & Rhee, J.S. (2010). Management and outcomes of facial paralysis from intratemporal blunt trauma: a systematic review. *Laryngoscope*, **120** Suppl 4, S214.

Nguyen, R., Fiest, K.M., McChesney, J., et al. (2016). The international incidence of traumatic brain injury: a systematic review and meta-analysis. *Can J Neurol Sci*, **43**(6), 774–85.

Nwachuku, E.L., Puccio, A.M., Fetzick, A., et al. (2014). Intermittent versus continuous cerebrospinal fluid drainage management in adult severe traumatic brain injury: assessment of intracranial pressure burden. *Neurocrit Care*, **20**(1), 49–53.

Nyquist, G.G., Rosen, M.R., Friedel, M., et al. (2013). Management of cerebrospinal fluid leaks of the anterior and lateral skull base. *J Neurol Surg B Skull Base*, **74**(Suppl 1), A046.

Offiah, C. & Twigg, S. (2009). Imaging assessment of penetrating craniocerebral and spinal trauma. *Clin Radiol*, **64**(12), 1146–57.

Ommaya, A. (1996). *Neurosurgery*, 2nd edition. New York, NY: McGraw-Hill.

Ordog, G.J., Wasserberger, J., & Balasubramanium, S. (1984). Wound ballistics: theory and practice. *Ann Emerg Med*, **13**(12), 1113–22.

Paoletti, P., Pezzotta, S., & Spanu, G. (1983). Diagnosis and treatment of post-traumatic hydrocephalus. *J Neurosurg Sci*, **27**(3), 171–5.

Pham, M.H., Rahme, R.J., Arnaout, O., et al. (2011). Endovascular stenting of extracranial carotid and vertebral artery dissections: a systematic review of the literature. *Neurosurgery*, **68**(4), 856–66; discussion 66.

Protocol 14PRT/6944. *Randomised Evaluation of Surgery with Craniectomy for patients Undergoing Evacuation of Acute Subdural*

Haematoma (RESCUE-ASDH)—ISRCTN873705452015. http://www.thelancet.com/doi/story/10.1016/html.2015.08.14.2280

Rahme, R., Weil, A.G., Sabbagh, M., Moumdjian, R., Bouthillier, A., & Bojanowski, M.W. (2010). Decompressive craniectomy is not an independent risk factor for communicating hydrocephalus in pa tients with increased intracranial pressure. *Neurosurgery*, **67**(3), 675–8; discussion 8.

Ratilal, B.O., Costa, J., Pappamikail, L., & Sampaio, C. (2015). Antibiotic prophylaxis for preventing meningitis in patients with basilar skull fractures. *Cochrane Database Syst Rev*, **4**, CD004884.

Rimmer, J., Belk, C., Lund, V., Swift, A., & White, P. (2014). Immunisations and antibiotics in patients with anterior skull base cerebrospinal fluid leaks. *J Laryngol Otol*, **128**(7), 626–9.

Rubinstein, S.M., Peerdeman, S.M., van Tulder, M.W., Riphagen, I., & Haldeman, S. (2005). A systematic review of the risk factors for cervical artery dissection. *Stroke*, **36**(7), 1575–80.

Ryan, C.G., Thompson, R.E., Temkin, N.R., Crane, P.K., Ellenbogen, R.G., & Elmore, J.G. (2012). Acute traumatic subdural hematoma: current mortality and functional outcomes in adult patients at a Level I trauma center. J Trauma Acute Care Surg, **73**(5), 1348–54.

Savva, A., Taylor, M.J., & Beatty, C.W. (2003). Management of cerebrospinal fluid leaks involving the temporal bone: report on 92 patients. *Laryngoscope*, **113**(1), 50–6.

Schuss, P., Vatter, H., Marquardt, G., et al. (2012). Cranioplasty after decompressive craniectomy: the effect of timing on postoperative complications. *J Neurotrauma*, **29**(6), 1090–5.

Segal, D.H., Oppenheim, J.S., & Murovic, J.A. (1994). Neurological recovery after cranioplasty. *Neurosurgery*, **34**(4), 729–31.

Servadei, F., Nasi, M.T., Cremonini, A.M., Giuliani, G., Cenni, P., & Nanni, A. (1998). Importance of a reliable admission Glasgow Coma Scale score for determining the need for evacuation of posttraumatic subdural hematomas: a prospective study of 65 patients. *J Trauma*, **44**(5), 868–73.

Shapiro, S.A. & Scully, T. (1992). Closed continuous drainage of cerebrospinal fluid via a lumbar subarachnoid catheter for treatment or prevention of cranial/spinal cerebrospinal fluid fistula. *Neurosurgery*, **30**(2), 241–5.

Shore, P.M., Thomas, N.J., Clark, R.S., et al. (2004). Continuous versus intermittent cerebrospinal fluid drainage after severe traumatic brain injury in children: effect on biochemical markers. *J Neurotrauma*, **21**(9), 1113–22.

Singh, I., Haris, M., Husain, M., Husain, N., Rastogi, M., & Gupta, R.K. (2008). Role of endoscopic third ventriculostomy in patients with communicating hydrocephalus: an evaluation by MR ventriculography. *Neurosurg Rev*, **31**(3), 319–25.

Spetzler, R.F. & Wilson, C.B. (1978). Management of recurrent CSF rhinorrhea of the middle and posterior fossa. *J Neurosurg*, **49**(3), 393–7.

Stiefel, M.F., Heuer, G.G., Smith, M.J., et al. (2004). Cerebral oxygenation following decompressive hemicraniectomy for the treatment of refractory intracranial hypertension. *J Neurosurg*, **101**(2), 241–7.

Stiver SI (2009). Complications of decompressive craniectomy for traumatic brain injury. *Neurosurg Focus*, **26**(6), E7.

Stocchetti, N., Zanaboni, C., Colombo, A., et al. (2008). Refractory intracranial hypertension and 'second-tier' therapies in traumatic brain injury. *Intensive Care Med*, **34**(3), 461–7.

Tagliaferri, F., Compagnone, C., Korsic, M., Servadei, F., & Kraus, J. (2006). A systematic review of brain injury epidemiology in Europe. *Acta Neurochir (Wien)*, **148**(3), 255–68; discussion 68.

Tagliaferri, F., Zani, G., Iaccarino, C., et al. (2012). Decompressive craniectomies, facts and fiction: a retrospective analysis of 526 cases. *Acta Neurochir (Wien)*, **154**(5), 919–26.

Timofeev, I., Dahyot-Fizelier, C., Keong, N., et al. (2009). Ventriculostomy for control of raised ICP in acute traumatic brain injury. In: Steiger, H.J. (ed.) *Acta Neurochirurgica Supplements*, pp. 99–104. Vienna, Austria: Springer Vienna.

Timofeev, I. & Hutchinson, P.J. (2006). Outcome after surgical decompression of severe traumatic brain injury. *Injury*, **37**(12), 1125–32.

Tribl, G. & Oder, W. (2000). Outcome after shunt implantation in severe head injury with post-traumatic hydrocephalus. *Brain Inj*, **14**(4), 345–54.

Tsuei, Y.-S., Sun, M.-H., Lee, H.-D., et al. (2005). Civilian gunshot wounds to the brain. *J Chinese Med Assoc*, **68**(3), 126–30.

Valadka, A.B. & Robertson, C.S. (2007). Surgery of cerebral trauma and associated critical care. *Neurosurgery*, **61**(1 Suppl), 203–20; discussion 20–1.

von Holst, H., Li, X., & Kleiven, S. (2012). Increased strain levels and water content in brain tissue after decompressive craniotomy. *Acta Neurochir (Wien)*, **154**(9), 1583–93.

Wachter, D., Reineke, K., Behm, T., & Rohde, V. (2013). Cranioplasty after decompressive hemicraniectomy: underestimated surgery-associated complications? *Clin Neurol Neurosurg*, **115**(8), 1293–7.

Whitfield, P.C., Patel, H., Hutchinson, P.J., et al. (2001). Bifrontal decompressive craniectomy in the management of posttraumatic intracranial hypertension. *Br J Neurosurg*, **15**(6), 500–7.

Yadla, S., Campbell, P.G., Chitale, R., Maltenfort, M.G., Jabbour, P., & Sharan, A.D. (2011). Effect of early surgery, material, and method of flap preservation on cranioplasty infections: a systematic review. *Neurosurgery*, **68**(4), 1124–30.

Yamakami, I. & Yamaura, A. (1993). Effects of decompressive craniectomy on regional cerebral blood flow in severe head trauma patients. *Neurol Med Chir*, **33**(9), 616–20.

Yamaura, A. (1994). Nontraumatic intracranial arterial dissection: natural history, diagnosis, and treatment. *Contemporary Neurosurgery*, **16**(5), 1.

Zayas, J.O., Feliciano, Y.Z., Hadley, C.R., Gomez, A.A., & Vidal, J.A. (2011). Temporal bone trauma and the role of multidetector CT in the emergency department. *RadioGraphics*, **31**(6), 1741–55.

Zumkeller, M., Behrmann, R., Heissler, H.E., & Dietz, H. (1996). Computed tomographic criteria and survival rate for patients with acute subdural hematoma. *Neurosurgery*, **39**(4), 708–12; discussion 12–3.

RELATED LINKS TO EBRAIN

Carotid and Vertebral Artery Dissection. https://learning.ebrain.net/course/view.php?id=126

Evacuation of a Chronic Subdural Haematoma. https://learning.ebrain.net/course/view.php?id=1100

Insertion of an Intracranial Pressure Monitor. https://learning.ebrain.net/course/view.php?id=1103

Management of Depressed Skull Fractures. https://learning.ebrain.net/course/view.php?id=1102

Performing a Decompressive Craniectomy for Traumatic Brain Injury. https://learning.ebrain.net/course/view.php?id=1107

Performing a Cranioplasty. https://learning.ebrain.net/course/view.php?id=1108

Performing a Trauma Craniotomy. https://learning.ebrain.net/course/view.php?id=1105

Surgical Management of Head Injuries. https://learning.ebrain.net/course/view.php?id=1099

44

Complications of head injury

Fardad T. Afshari, Antonio Belli, and Peter C. Whitfield

Introduction

Complications following head injury can be classified according to the timing of the complication—early (within 1 week) or late (beyond 1 week). Complications can also be considered according to the underlying pathological process (e.g. cerebrospinal fluid (CSF) leak, vascular complications, epilepsy, CSF leak, and hydrocephalus). In addition, many rehabilitation needs are commonly identified following head injury. In the early phase, these focus around medical care (e.g. chest physiotherapy, avoidance of contractures, nutrition, and communication). In the later phases, patient-centred goal-directed therapy is of increasing importance. In this chapter we describe several early complications. Consideration is then given to delayed complications although it is recognized that classification by timing is an inexact science and there is considerable overlap between early and late complications.

Early complications of head injury

Vascular injuries

Traumatic brain injury may be associated with vascular injuries. Most of these occur as early sequalae directly related to the transmission of operant forces caused by the trauma. Rarely a vascular injury can occur as a result of penetrating injury (e.g. low velocity bullet) but is more commonly associated with bony injuries to the cervical spine and/or skull base.

Traumatic subarachnoid haemorrhage

Traumatic subarachnoid haemorrhage is the most common cause of subarachnoid blood on CT head. One-third of patients with moderate to severe head injury present with evidence of subarachnoid blood on CT head (Eisenberg et al., 1990; Servadei et al., 2002). The volume of traumatic subarachnoid haemorrhage on initial CT is associated with a worse outcome (Paiva et al., 2010).

Although vasospasm can occur following traumatic subarachnoid haemorrhage, this complication is not as common as vasospasm following aneurysmal subarachnoid haemorrhage. A systematic review found no evidence to suggest nimodipine improves outcomes in patients with traumatic subarachnoid haemorrhage (Vergouwen et al., 2006).

Carotid and vertebral artery dissection

Carotid dissection is the most frequent vascular injury and usually occurs in the extracranial or skull base segments at points of tethering or fracture (Fig. 44.1). Similarly, vertebral artery dissection occurs in the V2 and V3 segments where the artery enters and exits the foramen transversarium. Trauma to the carotid or vertebral arteries can cause an intimal tear resulting in a dissection with an associated false lumen. Expansion of this false tract can lead to occlusion of the parent vessel causing downstream infarction. Localized trauma to a vessel can lead to formation of mural thrombus and partial or total occlusion in the absence of dissection. A thrombus in a partially occluded vessel can cause distal emboli typically affecting watershed areas of the brain. Rarely a traumatic injury may cause a pseudoaneurysm that can cause a spontaneous post-traumatic intracranial haemorrhage. CT angiogram, MR angiogram and digital subtraction cerebral angiography are the most sensitive studies in the investigation of vascular injuries in traumatic brain injury. Antiplatelet therapy is the main mode of treatment for dissection injuries, although consideration must be given to concomitant intracranial or extracranial haemorrhagic injuries. Endovascular treatment is an option in some cases; however, most traumatic dissections tend to heal spontaneously in a matter of weeks. Wherever possible, the management of a traumatic dissection should involve neurosurgery, stroke medicine, and interventional radiology in a multidisciplinary fashion.

Arteriovenous fistulae

Although rare, arteriovenous fistulae can form following traumatic brain injury. These may present in the first week or may have a delayed appearance. The most common location for fistula formation is between the cavernous portion of carotid artery and the cavernous venous sinus. The incidence of carotico-cavernous fistulae (CCF) following head trauma is 0.2–0.3% (Fabian et al., 1999). These direct fistulae are true connections between a ruptured intracavernous carotid artery and the surrounding venous channels within the cavernous sinus and are therefore high flow and likely to be symptomatic (see Chapter 49). Clinically this condition can present with the triad of pulsatile proptosis, conjunctival injection, and bruit. The management of such fistulae is predominantly endovascular and aims to preserve ocular function and prevent cortical venous reflux and its haemorrhagic sequelae. Indirect CCF do not typically occur

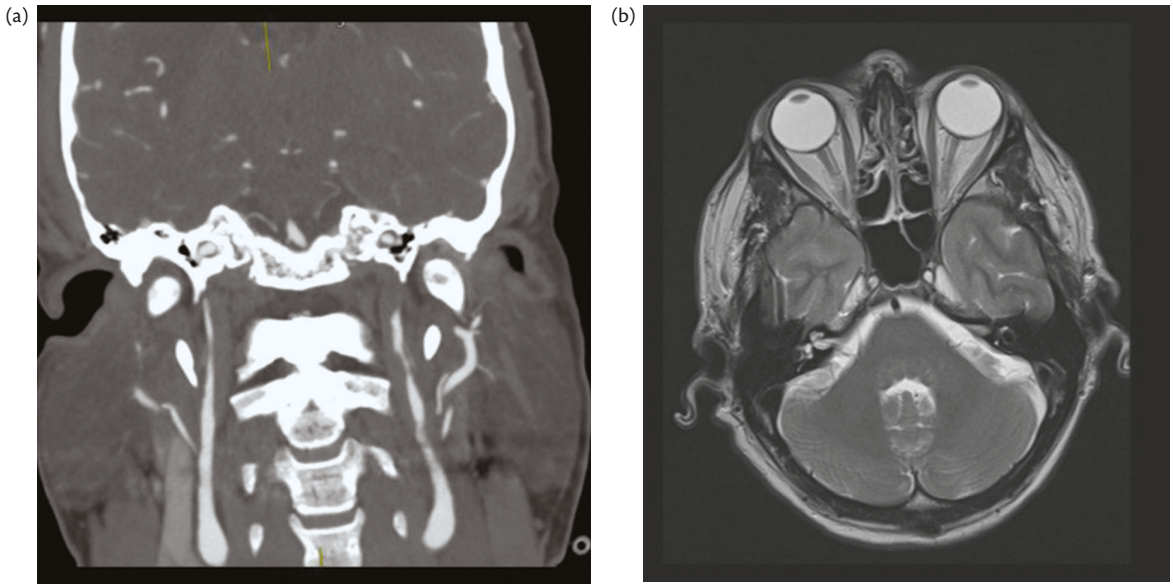

Fig. 44.1 Bilateral carotid dissection. (A) CT angiogram showing bilateral tapering of internal carotid indicative of dissection. (B) T2-weighted MRI demonstrating high signal within carotids. Normally the major vessels demonstrate flow voids (low signal such as in the basilar artery), however this is lost with carotid occlusion.

acutely following trauma, although, if identified in a patient with trauma, they can be managed less acutely and sometimes spontaneously regress.

Cranial nerve injuries

Cranial nerve injuries are common following head injury. Although they are almost always present as an early post-traumatic complication, it is not until the rehabilitation phase that the effects of a palsy become prominent. Cranial nerve palsies may result from traumatic disruption of cranial nerves, particularly at the interface with the exiting skull foraminae. They may also occur consequential to the effects of raised ICP (e.g. third nerve palsy, sixth nerve palsy, and seventh nerve palsy). Damage to the olfactory nerve is common, with or without anterior skull base fractures, as the delicate olfactory nerves are easily injured as they pass through the cribriform plate. The olfactory nerves can slowly recover in some cases, but the sensory loss is usually permanent; in addition, loss of smell can affect the sensation of taste due to overlapping perception of taste and olfaction.

Optic nerve transection or compression due to facial and orbital bone fractures typically presents with unilateral visual loss. A relative afferent pupillary defect is normally present. Visual impairment after trauma always warrants urgent radiological investigation and an ophthalmological consultation. Diplopia following head injury is common and can occur due to damage to oculomotor, trochlear, or abducent nerves and should be differentiated from non-neural, mechanical mechanisms of diplopia such as an orbital wall fracture or damage to the trochlear sling within the lateral orbit.

Temporal bone fractures can cause a range of deficits, particularly if they involve the otic capsule. Historically, these were divided into longitudinal fractures (along the long access of the petrous temporal bone) or transverse fractures. Transverse fractures being less common but more likely to cause sensorineural hearing loss and facial palsy. The involvement of the otic capsule is now recognized as the pre-eminent factor that influences cranial neuropathy. The deficits include facial nerve palsy, hearing loss, and CSF leak. Facial nerve palsies can recover over time, but the cornea must be protected if exposed. Evidence to justify the use of corticosteroids in the treatment of traumatic facial nerve palsy is weak. Early involvement of speech and language therapy and physiotherapy is recommended. Facial nerve reanimation techniques can be considered for permanent disabling deficits.

Hearing loss is a common presentation following head injury associated with temporal and petrous bone fractures. Hearing deficits may be conductive or sensory in nature. Conductive hearing loss is due to occlusion of the auditory meatus with blood, damage to tympanic membrane, or disruption of the ossicular chain. The latter may be amenable to surgical treatment and should be investigated with a high resolution fine-cut CT scan. Otological input is advised to guide further investigation and treatment. Sensorineural deafness can occur due to damage to the cochlear structures or the cochlear nerve itself. This can arise from fracture of the petrous temporal bone or secondary to nerve ischaemia caused by raised ICP.

Lower cranial nerve palsies can occur individually or in combination. These are usually secondary to occipital bone fractures extending to the jugular foramen. Different syndromes associated with lower cranial nerve palsies have been documented in the context of both tumour and trauma and are summarized in Table 44.1.

Depressed skull fractures

Traumatic brain injury is commonly associated with depressed skull fractures. Depressed fractures should be identified on the initial CT imaging and can be well visualized with volumetric reconstructions. Depressed skull fractures may be associated with underlying brain contusions, extradural, or subdural haematoma. In addition, they may be associated with a dural breach, increasing the risk of delayed infection, seizure, meningitis, or empyema. Absolute indications for elevation of a depressed skull fracture include treatment of an

Table 44.1 Jugular foramen syndromes

Syndrome	IX	X	XI	XII	Sympathetic
Villaret	Yes	Yes	Yes	Yes	Yes
Collet-Sicard	Yes	Yes	Yes	Yes	No
Vernet	Yes	Yes	Yes	No	No
Schmidt	No	Yes	Yes	No	No
Tapia	No	Yes	No	Yes	Yes/No
Jackson	No	Yes	Yes	Yes	No

open fracture that necessitates debridement of bone fragments and, in some cases, dural repair. Pericranium or temporalis fascia is the preferred material for dural repair. Relative indications for repair include significant fragment depression (+/- haematoma) causing mass effect, depression greater than the width of the bone and cosmetic defects. Any depressed fractures overlying the venous sinuses should be managed cautiously due to the risk of catastrophic haemorrhage following fracture elevation.

Early CSF leak

CSF rhinorrhoea and otorrhoea are common complications of skull base fractures and indicate breach of the dura. CSF rhinorrhoea can occur from complex ethmoidal fractures breaching the anterior fossa dura. CSF rhinorrhoea can also occur as a result of CSF egress via the aerated portion of the temporal bone, into the middle ear then through the Eustachian tube into the nasopharynx. CSF otorrhea can occur from a temporal bone fracture that is associated with a perforated ear drum. Up to 90% of these CSF leaks resolve spontaneously within 2 weeks. The remainder of the patients may continue to have persistent leak or develop delayed CSF leak. Antibiotic prophylaxis is not indicated, but antibiotic treatment should be instigated without delay if signs of meningitis develop. Antipneumococcal vaccination is also recommended in all skull base fractures or proven or suspected CSF leakage (Phang et al., 2016). For those patients with persistent CSF leak beyond 2 weeks, there is some contention as to the best subsequent treatment. CSF drainage by lumbar drain is very effective for minimizing the flow through the site of leak and therefore promoting healing. However, if the fistula is large, this may entrain air into the intracranial cavity, and caution must be used in any patient with presumed raised intracranial pressure to avoid tonsillar descent.

Although CSF rhinorrhoea or otorrhoea may be clinically evident, there are occasions that CSF leak post injury maybe difficult to distinguish from nasal discharge. In such cases, manoeuvres such as leaning the head forward may accentuate the CSF leak and further suggest CSF rhinorrhoea. Alternatively, if a CSF sample can be collected, it can be tested for beta-transferrin which is found at high levels in CSF. Glucose testing is unlikely to be helpful as nasal secretions may also contain glucose (Baker et al., 2005). **Figure 44.2** shows an algorithm for the management of a suspected CSF leak.

Pneumocephalus

Pneumocephalus (air within the cranial cavity) can occur following head trauma in association with calvarial or skull base fractures. The incidence of pneumocephalus secondary to head injury is between 0.5% and 1%. Air within the subarachnoid space indicates a breach of the dura. Patients with pneumocephalus are at high risk of CSF leak and should be closely monitored and managed as mentioned. Although small volumes of air within the cranium do not pose any danger, large amounts of air particularly when under pressure can act as a mass lesion causing midline shift. Pneumocephalus can cause a reduced level of consciousness, seizures, or focal neurological signs. The appearance of a large amount of air anterosuperior to both frontal lobes in the supine patient on axial CT scan is termed 'mount Fuji sign' owing to double peak appearance of the compressed frontal lobes (Michel, 2004). At times this can manifest as a tension pneumocephalus mandating emergency treatment. Pneumocephalus is normally managed with high-flow oxygen to reduce the partial pressure of nitrogen and encourage absorption of air from the intracranial space. Rarely, in cases of severe midline shift and tension pneumocephalus, urgent burr holes may be required to allow air egress from the subdural space.

Late complications of head injury

Seizures

Although seizures can present early after a traumatic brain injury, late seizures are of prime concern to recovering patients. Overall, seizures can occur in up to 30% of severe traumatic brain injury patients. In the early phase, seizures resulting in increased metabolic demand, excitotoxicity and raised intracranial pressure, and may cause severe secondary brain damage. Such issues also exist in the late phase although antiepileptics usually afford a degree of control over these processes.

The risk of seizure post head injury depends on several factors. The classical work of Bryan Jennett (pre-CT) defined the following: severity of injury, duration of PTA, presence of depressed skull fracture, and intracerebral haematoma/contusion. Patients who sustain a seizure within the first week are an increased risk of late epilepsy. Annegers et al. have defined the risk according to severity of injury, albeit also using data predominantly acquired pre-CT. Severe injury is characterized by brain contusion, intracranial haematoma, loss of consciousness, or post-traumatic amnesia for more than 24 hours. The 5-year cumulative probability of post-traumatic seizure is 10% and 30-year cumulative probability is 16.7%. Christensen's et al. study in children and young adults showed the risk of epilepsy was increased after a mild brain injury (RR 2.22, 95% CI 2.07–2.38), severe brain injury (7.40, 6.16–8.89), and skull fracture (2.17, 1.73–2.71). Overall, the risk of developing late epilepsy reduces with time, but nevertheless for patients at greatest risk, this remains above the baseline risk of the general population for 10–15 years (Jennett, 1973; Jennett, 1975; Annegers et al., 1998; Christensen et al., 2009).

There is currently class I evidence available that use of antiepileptics can lead to reduction in seizure frequency in early phase following head injury (first 7 days) but has no effect on the incidence of late onset seizures (Temkin et al., 1990). The use of prophylactic antiepileptics has no effect on mortality or neurological disability when used in the early or late phases post head injury (Schierhout and Roberts, 2001).

Traditionally phenytoin has been used as a first-line agent for seizure control in head injury patients. Recent prospective randomized studies have demonstrated that levetiracetam and phenytoin are

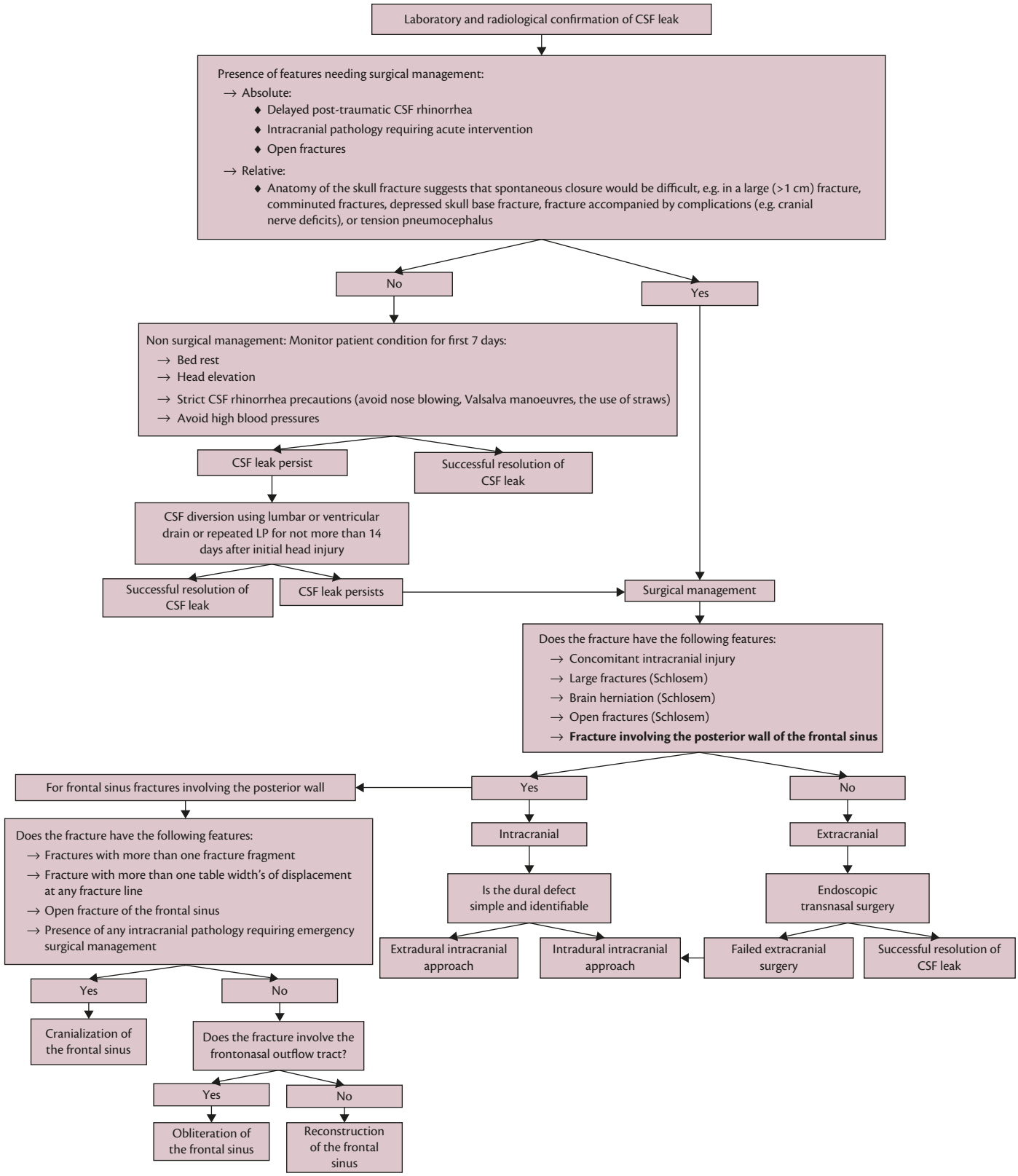
Laboratory and radiological confirmation of CSF leak
Presence of features needing surgical management:
→ Absolute:
♦ Delayed post-traumatic CSF rhinorrhea
♦ Intracranial pathology requiring acute intervention
♦ Open fractures
→ Relative:
♦ Anatomy of the skull fracture suggests that spontaneous closure would be difficult, e.g. in a large (>1 cm) fracture, comminuted fractures, depressed skull base fracture, fracture accompanied by complications (e.g. cranial nerve deficits), or tension pneumocephalus
No
Yes
Non surgical management: Monitor patient condition for first 7 days:
→ Bed rest
→ Head elevation
→ Strict CSF rhinorrhea precautions (avoid nose blowing, Valsalva manoeuvres, the use of straws)
→ Avoid high blood pressures
CSF leak persist
Successful resolution of CSF leak
CSF diversion using lumbar or ventricular drain or repeated LP for not more than 14 days after initial head injury
Successful resolution of CSF leak
CSF leak persists
Surgical management
Does the fracture have the following features:
→ Concomitant intracranial injury
→ Large fractures (Schlosem)
→ Brain herniation (Schlosem)
→ Open fractures (Schlosem)
→ Fracture involving the posterior wall of the frontal sinus
For frontal sinus fractures involving the posterior wall
Yes
No
Does the fracture have the following features:
→ Fractures with more than one fracture fragment
→ Fracture with more than one table width's of displacement at any fracture line
→ Open fracture of the frontal sinus
→ Presence of any intracranial pathology requiring emergency surgical management
Intracranial
Extracranial
Is the dural defect simple and identifiable
Endoscopic transnasal surgery
Extradural intracranial approach
Intradural intracranial approach
Failed extracranial surgery
Successful resolution of CSF leak
Yes
No
Cranialization of the frontal sinus
Does the fracture involve the frontonasal outflow tract?
Yes
No
Obliteration of the frontal sinus
Reconstruction of the frontal sinus

Fig. 44.2 Algorithm for investigation of CSF leaks.

Reproduced with permission from See Yung Phang, Kathrin Whitehouse, Lucy Lee, et al., Management of CSF leak in base of skull fractures in adults, *British Journal of Neurosurgery*, Volume 30, Issue 6, pp. 596–604, Copyright © 2016 The Neurosurgical Foundation, reprinted by permission of Taylor & Francis Ltd, www.tandfonline.com on behalf of The Neurosurgical Foundation.

both effective as seizure prophylaxis agents in head injury with no significant difference in seizure control rates (Szaflarski et al., 2010). Levetiracetam has therefore become the favoured option given that treatment is effective, with a low risk of symptomatic side effects, no impact on cognition, and is relatively low cost (Eddy et al., 2011).

Patients with head injury and seizures should be informed about risks of swimming and working on open machinery. They should be advised to refrain from driving and to inform the appropriate driving regulatory agency.

The decision to stop antiepileptic medication in the longer term, once a patient has been seizure free for a period of time, is a difficult one. The risk of seizures is likely to decline as time progresses from the initial injury, however no specific guidelines exist. A decision on stopping antiepileptics needs to balance the complications and risks of prolonged therapy against the risk of a further seizure that can risk injury and lead to further limitations in driving and independence.

Hydrocephalus

Hydrocephalus can occur both in acute or late phase following head injury. Acute hydrocephalus is rare following head injury and tends to be associated with intraventricular haemorrhage. In some units, ventricular drainage is performed as an adjunct in the management of raised ICP. This is normally a temporary measure and is not usually indicative of hydrocephalus. Late phase hydrocephalus following head injury appears to be a separate pathophysiological entity. The incidence of post-traumatic brain injury hydrocephalus is variable depending on the criteria used in the studies. Kammersgaard et al. reported post-traumatic hydrocephalus in 14.2% of patients with majority of patients presenting during the rehabilitation (Kammersgaard et al., 2013). Many patients present with a plateau in their recovery, often in association with the triad of symptoms associated with idiopathic normal pressure hydrocephalus (gait disturbance, cognitive decline, and urinary urgency or incontinence). The exact mechanism underlying late phase hydrocephalus after head injury is not fully understood. Imaging normally demonstrates communicating hydrocephalus and lumbar puncture may demonstrate normal opening pressures. Patients with delayed hydrocephalus can however present with reduced level of consciousness and drowsiness even following a long period of recovery. Patients with hydrocephalus benefit from CSF diversion procedures such as a ventriculoperitoneal shunt. Uncertainty concerning the diagnosis is however a confounding issue: the differential diagnosis of ex-vacuo dilatation of the ventricles following post-traumatic cerebral atrophy should be considered, as, in this case, CSF diversion will not help and may risk overdrainage with the risk of subdural collections. ICP monitoring studies and CSF infusion studies may be helpful adjuncts in the investigation of these patients.

Pituitary dysfunction

In recent years pituitary dysfunction has been increasingly recognized as a previously overlooked delayed complication of traumatic brain injury. Traumatic brain injury may be associated with pituitary dysfunction, which may contribute to long-term physical, cognitive, and psychological disability. Pituitary dysfunction can be broadly divided into anterior or posterior pituitary dysfunction and can be detected either in early or delayed phase (>6 months) following head injury. In a study by Bondanelli, anterior pituitary dysfunction was reported to be 37.5%, 57.1%, and 59.3% in mild, moderate, and severe traumatic brain injury patients, respectively but in a small cohort of patients (Bondanelli et al., 2004). Other studies have reported rate of anterior pituitary dysfunction at 20–25% following traumatic brain injury (Agha et al., 2007; Alavi et al., 2016). The most common alterations in anterior pituitary hormones appear to be deficiency of gonadotrophins and growth hormone, followed by ACTH and thyrotropin. Symptoms of pituitary dysfunction, such as fatigue, depression, and sexual dysfunction, overlap with postconcussional symptoms; therefore, post-traumatic pituitary insufficiency can remain undiagnosed unless specifically investigated with specific endocrinology tests. Tests in the acute phase do not accurately predict long-term dysfunction and it is important to monitor symptomatic patients in the first year after injury. The notable exception is cortisol insufficiency, which can appear very early on and is potentially a life-threatening emergency: requiring immediate hydrocortisone replacement.

Posterior pituitary dysfunction can also lead to major complications following head injury. Abnormalities of this axis can occur in both the early and late phases. The syndrome of inappropriate antidiuretic hormone secretion (SIADH), diabetes insipidus, and cerebral salt wasting are three conditions that can lead to electrolyte imbalance following head injury. Clinical assessment of patient fluid status and measurement of plasma and urine sodium and osmolality are crucial in delineating the cause of electrolyte imbalance in these patients.

SIADH is the most common posterior pituitary/hypothalamic dysfunction syndrome and is reported to affect 33% of patients with head injury. Uncontrolled release of antidiuretic hormone (ADH) can lead to excessive fluid resorption resulting in serum hyponatraemia and reduced plasma osmolality. The patient is also in a state of relative fluid overload. This should be differentiated from hyponatraemia secondary to cerebral salt wasting: this is related to brain natriuretic peptide causing excessive sodium excretion in conjunction with a reduction in total body water.

Diabetes insipidus is associated with impaired release of ADH leading to excess diuresis and dehydration in association with hypernatraemia. Replacement therapy with DDAVP nasal spray may be required.

The British Neurotrauma Group has published guidance for the screening and management of pituitary dysfunction following traumatic brain injury in adults (Tan et al., 2017).

Delayed CSF leak

Although the majority of CSF leaks post head injury resolve within 2 weeks of injury, there are cases where persistent otorrhoea or rhinorrhoea continue and require surgical intervention (Phang et al., 2016). Fractures of the posterior wall of the frontal sinus are one of the most common injuries where persistent CSF leaks occur. In addition to persistent CSF leak since the time of injury, delayed CSF leakage sometimes occurs years following the injury, which may be due to re-opening of the fistula or coexistent hydrocephalus. Thin-slice cranial CT scan with 3D reconstruction provides the necessary anatomical detail to delineate the site of CSF leak. Due to the serious infective complications associated with CSF leaks, a systematic approach to the management of patients with skull base fractures is advisable. An algorithm for management is provided in **Figure 44.3**.

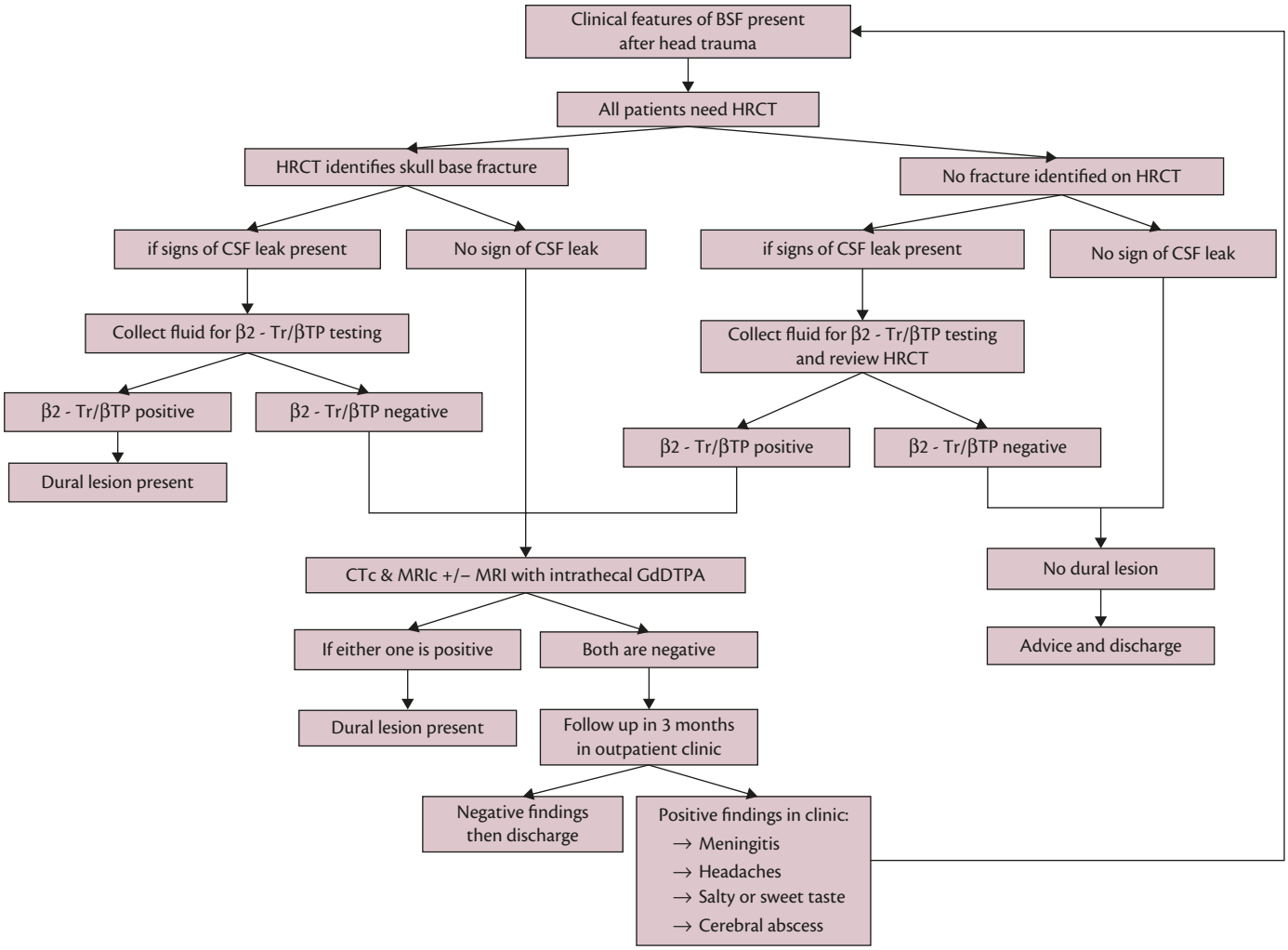
Clinical features of BSF present after head trauma
All patients need HRCT
HRCT identifies skull base fracture
No fracture identified on HRCT
if signs of CSF leak present
No sign of CSF leak
if signs of CSF leak present
No sign of CSF leak
Collect fluid for β2 - Tr/βTP testing
Collect fluid for β2 - Tr/βTP testing and review HRCT
β2 - Tr/βTP positive
β2 - Tr/βTP negative
β2 - Tr/βTP positive
β2 - Tr/βTP negative
Dural lesion present
CTc & MRIc +/– MRI with intrathecal GdDTPA
No dural lesion
If either one is positive
Both are negative
Advice and discharge
Dural lesion present
Follow up in 3 months in outpatient clinic
Negative findings then discharge
Positive findings in clinic:
→ Meningitis
→ Headaches
→ Salty or sweet taste
→ Cerebral abscess

Fig. 44.3 Algorithm for the investigation and treatment of a skull base fracture (HRCT, high resolution CT).

Reproduced with permission from See Yung Phang, Kathrin Whitehouse, Lucy Lee, et al., Management of CSF leak in base of skull fractures in adults, *British Journal of Neurosurgery*, Volume 30, Issue 6, pp. 596–604, Copyright © 2016 The Neurosurgical Foundation, reprinted by permission of Taylor & Francis Ltd, www.tandfonline.com on behalf of The Neurosurgical Foundation.

Formal skull base repair of troublesome CSF leaks is challenging. At the anterior skull base, a bicoronal flap can be raised and the pericranium delivered through an anterior 'letterbox' at the inferior extent of the craniotomy in order to provide a vascularized flap to cover the site of leak either extradurally or intradurally. This is a significant surgical undertaking and risks anosmia. Alternatively, endonasal endoscopic repair with a nasoseptal flap provides a much less invasive approach providing there is accurate localization of the leak. This approach may be augmented with the use of soft tissue (such as fascia lata graft or a vascularized nasoseptal flap), tissue glues, and lumbar CSF drainage with good effect. The leak can be identified using fine-cut bone kernel CT scan, contrast-enhanced CSF studies on CT/MRI (iodinated contrast or gadolinium delivered via the lumbar cistern), or fluorescein instillation into the lumbar cistern to allow intraoperative localization. Lateral skull base leaks can be more challenging and may require surgical approaches such as middle cranial fossa craniotomy, transmastoid or combined procedures (Phang et al., 2016). Ultimately, blind sac closure (obliteration of the Eustachian tube) can address the final common pathway for these leaks but at the cost of hearing.

Infections post CSF leak and skull fracture

Skull fractures or persistent CSF leaks following head injury can increase the risk of subsequent meningitis or delayed subdural empyema. Patients with penetrating trauma or gunshot wounds are at highest risk due to contamination and breach of the dura. Management of patients with contaminated wounds requires debridement, washout, and dural repair. Intravenous antibiotics are indicated for such contaminated or infected open fractures.

Skull base fractures associated with CSF leak pose a high risk of meningitis and delayed infection, and require specific attention. The incidence of meningitis post severe head injury ranges from 0.2 to 17.8% (Helling et al., 1988). The use of prophylactic antibiotics in patients with CSF leak is not supported by current literature. A Cochrane review of randomized controlled trials concluded that there is no evidence for prophylactic antibiotic use in patients with skull base fractures, whether there is evidence of CSF leakage or not (Ratilal et al., 2015). Pneumococcal vaccination is recommended for all skull base fractures given that *Streptococcus pneumoniae* is a common pathogen, although the evidence based for this treatment

is poor. In persistent cases of CSF rhinorrhoea or otorrhoea, repairing the defect is advocated to prevent delayed risk of infection.

Growing skull fractures

Skull fractures in paediatric population (particularly below age 3), when associated with dural tear, can progress to enlarging skull defect over time and are termed growing skull fractures. Interposition of a fold of arachnoid between the edges of the fracture transmits CSF pulsation into this space and can lead to progressive expansion of the defect with subsequent herniation of the neural elements. The herniated brain and the formation of cystic arachnoidal elements is called a leptomeningeal cyst. The incidence of growing skull fracture is reported to be between 0.05% to 1.6% (Muhonen et al., 1995). This normally occurs in the weeks to months following a fracture. Therefore, monitoring skull fractures in the paediatric population, particularly below age 3, is recommended. Treatment of leptomeningeal cysts involves craniotomy and exposure of the dural tear. Following repair of the dural tear, the bone flap is replaced to cover any bony defect. In advanced cases, extensive reconstructive surgery or ventriculoperitoneal shunting is required to allow correction of brain herniation and the bony defect.

Chronic subdural haematoma

Chronic subdural haematomas are generally considered to develop as a delayed complication of a minor traumatic brain injury. In clinical practice many patients have no recollection of trauma so other mechanisms of pathogenesis may exist. The incidence of chronic subdural is 5 per 100 000 in general population with increasing incidence linked to an ageing population (Santarius and Hutchinson, 2004; Whitehouse et al., 2016). Chronic subdural haematomas classically occur following a long delay after head injury. This delay can range from weeks to months. An initial minor head injury, which may go unnoticed by the patient, can lead to tears in bridging veins leading to low flow bleeding and acute subdural haematoma. Liquefaction of the haematoma over time leads to progressive compression of the underlying brain. Patients may present with headaches, reduced level of consciousness, seizures, or focal neurological deficits. Symptomatic chronic subdural haematomas can be managed surgically using burr hole evacuation. Cases complicated by recurrence or significant membranes may be managed with mini-craniotomy to allow better access to vascularized membranes that may occur over the clot. The role of steroids in management of chronic subdural haematoma remains controversial with no reported randomized trials reported in the literature. Randomized trials assessing the efficacy of steroids in chronic subdural haematoma are currently underway

Postcraniectomy complications

Following craniectomy, several specific problems can occur that require special consideration. Focal neurological deficits related to the area of brain below the craniectomy defect are termed the 'syndrome of the trephine'. This may relate to venous congestion due to kinking of the draining veins at the edge of the craniectomy or due to deranged cerebral blood regulation. These deficits may reverse following reconstitution of the integrity of the skull cavity.

Hydrocephalus in the context of a craniectomy can be difficult to assess as with an open craniectomy defect, the pressure that normally accumulates within a closed skull to drive the passive resorption of CSF, is absent. Ventriculoperitoneal shunting in the presence of a craniectomy defect is susceptible to overdrainage and sinking of the craniectomy flap. In this case, if the skull integrity can be reconstituted with cranioplasty this can sometimes aid CSF resorption, and if there are further concerns about hydrocephalus, this is a better juncture to consider CSF diversion.

Post-traumatic encephalopathy and dementia pugilistica

Post-traumatic encephalopathy can develop many years after a traumatic brain injury (TBI). Evidence from contact sports such as boxing and rugby suggests that repeated head trauma can lead to neuropathological changes including accumulation of beta-amyloid, neurofibrillary tangles, cerebellar degeneration, gliosis, and cortical atrophy. Patients may present with a wide range of symptoms including affective disorders, gait disturbance, cognitive decline, and parkinsonism. This chronic traumatic encephalopathy is sometimes referred to as punch drunk syndrome, or dementia pugilistica (McKee et al., 2009). This syndrome has been reported in association with a single severe injury or repeated concussion over a long period of time, such as sustained by contact sport players, and combat personnel. The pathophysiology is complex as it does not occur in every instance, and may reflect a genetic predisposition towards tau deposition in vulnerable individuals. There are currently no therapies available for this condition.

Neurorehabilitation following head injury

Rehabilitation is the process of facilitating the recovery of the patient postinjury and aims at maximizing quality of life and the patient's ability to participate in activities of daily living, work, and leisure.

Traumatic brain injury is a heterogeneous condition and the consequences of head injury are wide depending on the location of the injury and severity of head injury.

The neurorehabilitation service should be delivered by a multidisciplinary team involving medical, nursing, occupational therapy, speech and language therapy, neuropsychology, physiotherapy, social work, and psychiatry.

The process of rehabilitation starts with assessment of the patient to determine the nature of cognitive, emotional, and behavioural impairment, and to identify the functional consequences. A patient-centred goal setting process is then undertaken identifying short-term and long-term goals. This is a dynamic process depending on patient's changing needs (Holliday et al., 2007).

Neuro-rehabilitation has both acute and postacute and community components. Acute phase rehabilitation places a significant focus on the medical condition of the patient. Physiotherapy in the acute setting aims at optimizing chest function and oxygenation. This involves attention to positioning of the patient, chest physiotherapy, manual chest techniques of sputum expectoration, regular suctioning with pre- and post-treatment hyperoxygenation.

Speech and language therapy, in the acute phase is normally focussed upon difficulties with swallowing. The incidence of swallowing disorders following TBI is unknown. Post-traumatic impairment in the level of consciousness and tracheostomy can lead

to dysphagia. Many of these patients are at increased risk of aspiration, particularly if there is any coexistent gastroparesis. Early assessment of swallowing allows an appropriate route of feeding to be established, preventing unnecessary weight loss and malnutrition. Once swallowing reflexes resume an appropriately textured diet can commence.

Occupational therapy in the acute phase focuses on reduction of impairment and the prevention of complications to maximize long-term function. This involves evaluation of cognitive, motor, sensory skills of the patient allowing appropriate and meaningful goals to be established. Cognitive assessment establishes the level of awareness in this group of patients and facilitates their interaction with the environment. Motor and sensory assessment allows appropriate management and provision of equipment such as splints, seating, wheelchairs and various specialized positioning aids and orthoses to allow maximal function and prevention of long-term complications of muscle disuse (Whitfield, 2009).

Acute neuropsychological input aims at dealing with large array of behavioural and psychological issues caused by TBI. Neuropsychologists develop individualized behavioural management programmes and make recommendations to health professionals and staff about modifying approaches to provide the patient with the optimum environment for rehabilitation (Wilson and Zangwill, 2003). In addition, neuropsychological input can provide education to patients' families allowing a better understanding of the patient's behaviour and therefore enabling better coping and adaptation strategies to maximize the function of the patient.

Following acute rehabilitation of the patient, the long-term and community phases of rehabilitation ensue. This phase aims at maximizing the function of the patient on the path of recovery and is composed of similar components seen in acute phase albeit with a greater focus on promoting recovery of function, adaptation to dysfunction, and insight into psychological components with development of long-term compensatory strategies. The interaction of the patient with their environment and others is a crucial consideration in development of rehabilitation goals during this phase of care.

Physiotherapy at this stage aims at optimizing and maximizing limb function. Spasticity following head trauma is common and can have detrimental effects on patient's limb function. A long period of immobility may also have led to fixed deformities which further limit the functional recovery of the patient. Active and passive stretching of muscles aims to prevent contracture formation. Prolonged stretching of muscles is achieved by casting to reduce spasticity (Conine et al., 1990). Further control of spasticity can be achieved by use antispasmodics such as baclofen or use of botulinum toxin. In addition, physiotherapy aims to enhance proprioceptive input by moving the patient in different positions to allow better efferent control of muscles (Allum et al., 1998).

Speech and language therapy plays an important role at this stage of rehabilitation as it aims to maximize communication and interaction of the patient with others. Both verbal and non-verbal communication is impaired frequently post head injury. Although in many cases this is due to linguistic processes of language generation, in others difficulty is due to cognitive communication disorders. Patients with cognitive deficits such as impaired concentration and attention exhibit poor communication and language skills. The speech and language therapist in conjunction can identify the communication aspects that are most disabling and employ techniques aiming at resolving issues. In refractory cases, compensatory and adaptive techniques are used to assist the patient and their communication skills: technological aids may be helpful in these cases (Evans et al., 2009).

Occupational therapy during this phase focuses on functional performance and improving independence to allow patient independence in as many daily activities as possible. This is achieved by relearning basic skills such as activities of daily living including personal hygiene, dressing, meal preparation, and shopping. In addition, occupational therapy provides aids and adaptive equipment, such as specialized seating and wheelchairs to support independent living. Restorative or adaptation techniques developed by occupational therapists involve tailoring individual treatment programmes to introduce activities that the patient normally enjoys performing and to optimize their functional capacity in living independently and in regaining their role in society. Occupational therapy therefore plays an extremely important role in transition of care from hospital to community to allow ongoing holistic recovery of the patient (Evans et al., 2009).

Cognitive and neuropsychological rehabilitation is pivotal to this stage of recovery. Patients with TBI may suffer from impairments of memory, attention, executive functioning/planning, language, or perception. Various training models for improving memory, attention, executive functioning, and visuospatial function are currently under investigation and being applied that have the potential to improve our approach to cognitive rehabilitation of patients post head injury (Whyte et al., 2009).

FURTHER READING

Kammersgaard, L.P., Linnemann, M., & Tibaek, M. (2013). Hydrocephalus following severe traumatic brain injury in adults. Incidence, timing, and clinical predictors during rehabilitation. *NeuroRehabilitation*, **33**, 473–80.

Phang, S.Y., Whitehouse, K., Lee, L., Khalil, H., McArdle, P., & Whitfield, P.C. (2016). Management of CSF leak in base of skull fractures in adults. *Br J Neurosurg*, **30**, 596–604.

Santarius, T. & Hutchinson, P.J. (2004). Chronic subdural haematoma: time to rationalize treatment? *Br J Neurosurg*, **18**, 328–32.

Schierhout, G. & Roberts, I. (2001). Anti-epileptic drugs for preventing seizures following acute traumatic brain injury. *Cochrane Database Syst Rev*, **4**, CD000173.

Wilson, B.A. & Zangwill, O.L. (2003). The future of neuropsychological rehabilitation. In: Wilson, B. (ed.) *Neuropsychological Rehabilitation: Theory and Practice*, pp. 293–301. Exton, PA: Swets & Zeitlinger Publishers.

REFERENCES

Agha, A., Phillips, J., & Thompson, C. J. 2007. Hypopituitarism following traumatic brain injury (TBI). *Br J Neurosurg*, **21**, 210–16.

Alavi, S.A., Tan, C.L., Menon, D.K., Simpson, H.L., & Hutchinson, P.J. (2016). Incidence of pituitary dysfunction following traumatic brain injury: a prospective study from a regional neurosurgical centre. *Br J Neurosurg*, **30**, 302–6.

Allum, J.H., Bloem, B.R., Carpenter, M.G., Hulliger, M., & Hadders-Algra, M. (1998). Proprioceptive control of posture: a review of new concepts. *Gait Posture*, **8**, 214–42.

Annegers, J.F., Hauser, W.A., Coan, S.P., & Rocca, W.A. (1998). A population-based study of seizures after traumatic brain injuries. *N Engl J Med*, **338**, 20–4.

Baker, E.H., Wood, D.M., Brennan, A.L., Baines, D.L., & Philips, B.J. (2005). New insights into the glucose oxidase stick test for cerebrospinal fluid rhinorrhoea. *Emerg Med J*, **22**, 556–7.

Bondanelli, M., De Marinis, L., Ambrosio, M.R., et al. (2004). Occurrence of pituitary dysfunction following traumatic brain injury. *J Neurotrauma*, **21**, 685–96.

Christensen, J., Pedersen, M.G., Pedersen, C.B., Sidenius, P., Olsen, J., & Vestergaard, M. (2009). Long-term risk of epilepsy after traumatic brain injury in children and young adults: a population-based cohort study. *Lancet*, **373**, 1105–10.

Conine, T.A., Sullivan, T., Mackie, T., & Goodman, M. (1990). Effect of serial casting for the prevention of equinus in patients with acute head injury. *Arch Phys Med Rehabil*, **71**, 310–12.

Downey, B., Jackson, T., Fewings, J., et al. (2009). Acute rehabilitation of the head-injured patient. In: Whitfield, P.C., Thomas, E.O., Summers, F., Whyte, M., & Hutchinson, P.J. (eds.) *Head Injury: A Multidisciplinary Approach*, pp. 233–61. Cambridge, UK: Cambridge University Press.

Eddy, C.M., Rickards, H.E., & Cavanna, A.E. (2011). The cognitive impact of antiepileptic drugs. *Ther Adv Neurol Disord*, **4**, 385–407.

Eisenberg, H.M., Gary, H.E., Jr., Aldrich, E.F., et al. (1990). Initial CT findings in 753 patients with severe head injury. A report from the NIH Traumatic Coma Data Bank. *J Neurosurg*, **73**, 688–98.

Evans, J.J., Whyte, M., Summers, F., et al. (2009). Post-acute and community rehabilitation of the head-injured patient . In: Whitfield, P.C., Thomas, E.O., Summers, F., Whyte, M., & Hutchinson, P.J. (eds.) *Head Injury: A Multidisciplinary Approach*, pp. 233–61. Cambridge, UK: Cambridge University Press.

Fabian, T.S., Woody, J.D., Ciraulo, D.L., et al. (1999). Posttraumatic carotid cavernous fistula: frequency analysis of signs, symptoms, and disability outcomes after angiographic embolization. *J Trauma*, **47**, 275–81.

Helling, T.S., Evans, L.L., Fowler, D.L., Hays, L.V., & Kennedy, F.R. (1988). Infectious complications in patients with severe head injury. *J Trauma*, **28**(11), 1575–7.

Holliday, R.C., Ballinger, C., & Playford, E.D. (2007). Goal setting in neurological rehabilitation: patients' perspectives. *Disabil Rehabil*, **29**, 389–94.

Jennett, B. (1973). Epilepsy after non-missile head injuries. *Scott Med J*, **18**, 8–13.

Jennett, B. (1975). *Epilepsy After Non-missile Head Injuries*. London, UK: William Heinemann.

Kammersgaard, L.P., Linnemann, M., & Tibaek, M. (2013). Hydrocephalus following severe traumatic brain injury in adults. Incidence, timing, and clinical predictors during rehabilitation. *NeuroRehabilitation*, **33**, 473–80.

McKee, A.C., Cantu, R.C., Nowinski, C.J., et al. (2009). Chronic traumatic encephalopathy in athletes: progressive tauopathy after repetitive head injury. *J Neuropathol Exp Neurol*, **68**, 709–35.

Michel, S.J. (2004). The Mount Fuji sign. *Radiology*, **232**, 449–50.

Muhonen, M.G., Piper, J.G., & Menezes, A.H. (1995). Pathogenesis and treatment of growing skull fractures. *Surg Neurol*, **43**, 367–72; discussion 372–3.

Paiva, W.S., De Andrade, A.F., De Amorim, R.L., et al. (2010). The prognosis of the traumatic subarachnoid hemorrhage: a prospective report of 121 patients. *Int Surg*, **95**, 172–6.

Phang, S.Y., Whitehouse, K., Lee, L., Khalil, H., McArdle, P., & Whitfield, P.C. (2016). Management of CSF leak in base of skull fractures in adults. *Br J Neurosurg*, **30**, 596–604.

Ratilal, B.O., Costa, J., Pappamikail, L., & Sampaio, C. (2015). Antibiotic prophylaxis for preventing meningitis in patients with basilar skull fractures. *Cochrane Database Syst Rev*, **4**, CD004884.

Santarius, T. & Hutchinson, P.J. (2004). Chronic subdural haematoma: time to rationalize treatment? *Br J Neurosurg*, **18**, 328–32.

Schierhout, G. & Roberts, I. (2001). Anti-epileptic drugs for preventing seizures following acute traumatic brain injury. *Cochrane Database Syst Rev*, **4**, CD000173.

Servadei, F., Murray, G.D., Teasdale, G.M., et al. (2002). Traumatic subarachnoid hemorrhage: demographic and clinical study of 750 patients from the European brain injury consortium survey of head injuries. *Neurosurgery*, **50**, 261–7; discussion 267–9.

Szaflarski, J.P., Sangha, K.S., Lindsell, C.J., & Shutter, L.A. (2010). Prospective, randomized, single-blinded comparative trial of intravenous levetiracetam versus phenytoin for seizure prophylaxis. *Neurocrit Care*, **12**, 165–72.

Tan, C.L., Alavi, S.A., Baldeweg, S.E., et al. (2017). The screening and management of pituitary dysfunction following traumatic brain injury in adults: British Neurotrauma Group guidance. *J Neurol Neurosurg Psychiatry*, **88**(11), 971–81.

Temkin, N.R., Dikmen, S.S., Wilensky, A.J., Keihm, J., Chabal, S., & Winn, H.R. (1990). A randomized, double-blind study of phenytoin for the prevention of post-traumatic seizures. *N Engl J Med*, **323**, 497–502.

Vergouwen, M.D., Vermeulen, M., & Roos, Y.B. (2006). Effect of nimodipine on outcome in patients with traumatic subarachnoid haemorrhage: a systematic review. *Lancet Neurol*, **5**, 1029–32.

Whitehouse, K.J., Jeyaretna, D.S., Enki, D.G., & Whitfield, P.C. (2016). Head injury in the elderly: what are the outcomes of neurosurgical care? *World Neurosurg*, **94**, 493–500.

Whyte, M., Summers, F., Herbert, C., et al. (2009). Neuropsychology and head injury. In: Whitfield, P.C., Thomas, E.O., Summers, F., Whyte, M., & Hutchinson, P.J. (eds.) *Head Injury: A Multidisciplinary Approach*, pp. 233–61. Cambridge, UK: Cambridge University Press.

Wilson, B.A. & Zangwill, O.L. (2003). The future of neuropsychological rehabilitation. In: Wilson, B. (ed.) *Neuropsychological Rehabilitation: Theory and Practice*, pp. 293–301. Exton, PA: Swets & Zeitlinger Publishers.

RELATED LINKS TO EBRAIN

Cranial nerve and vascular complications of head injury. https://learning.ebrain.net/course/view.php?id=1109

CSF leak and intracranial infection following head injury. https://learning.ebrain.net/course/view.php?id=1115

Hydrocephalus, seizures and pituitary dysfunction following head injury. https://learning.ebrain.net/course/view.php?id=1113

Neuropathology of Head Injury. https://learning.ebrain.net/course/view.php?id=1088

Neuropsycology and Head Injury. https://learning.ebrain.net/course/view.php?id=1116

45

Concussion and sports-related head injury

Mark Wilson

Introduction

Interest in concussion and sports-related injury has intensified in recent years for three main reasons: (1) it is a preventable form of brain injury; (2) there is increasing evidence that repeated injury can result in long-term neurocognitive loss; and (3) as a result there are potential medicolegal costs to organizations that, possibly inadvertently, allow this form of brain injury to occur within their sport. The long-term effects of boxing resulting in dementia pugilistica have been appreciated for some time, however the results of repeated mild head injury in other sports is now under focus.

The definition of concussion has changed over time. Traditionally sports concussion occurred if there was immediate and full loss of consciousness (LOC) of variable duration accompanied by post-traumatic amnesia at least for the event. The requirements of LOC were dropped and the Congress of Neurological Surgeons defined concussion (and it has subsequently been applied to sports concussion) as:

> *A clinical syndrome characterized by immediate and transient impairment of neural function, such as alteration of consciousness, disturbance of vision, equilibrium etc due to mechanical forces.* (Gurdjian and Volis, 1966)

Others have defined concussion as:

> *A biomechanically induced brain injury characterized by the absence of gross anatomic lesions.* (Signoretti et al., 2011)
>
> *Concussion is recognized as a clinical syndrome of biomechanically induced alteration of brain function typically affecting memory and orientation, which may involve loss of consciousness (LOC).* (The American Association of Neurology)

Concussion can have short, medium, and long-term sequelae. In the immediate period an assessment and decision on return to play is required. In the medium term, managing postconcussion syndrome and the risk of second impact syndrome should be recognized, with the longer-term risks managed at an organizational or union level.

Recently there has been a call to 'retire' the term concussion, which, as can be seen from the evolving and different definitions, is confusing. Replacing it with a term that reflects it as being on the traumatic brain injury spectrum (e.g. mild traumatic brain injury), a term that is commonly used interchangeably with concussion anyway, is probably most appropriate (Sharp and Jenkins, 2015). However, for the purposes of this chapter, the term concussion will continue to be used.

Postconcussion syndrome

Common symptoms that occur after mild traumatic brain injury (TBI) include headache, dizziness, fatigue, irritability, reduced concentration, sleep disturbance, memory impairment, anxiety, heightened sensitivity to noise and light, blurred vision, and depression. The majority of these symptoms resolve within 3 months, although in approximately one-third of patients they persist beyond 6 months.

Impact brain apnoea

Although rarely considered, early descriptions of concussion specifically mention respiratory changes and apnoea occurring (Koch and Filehne, 1874). John Hughling Jackson (1835–1911) knew that concussion if severe enough could be fatal through cardiovascular and respiratory failure and at autopsy, the brain in such cases could be normal/near normal. The animal literature reports that apnoea after relatively mild brain injury is common, and the greater the impact the longer the apnoea (Atkinson et al., 1998). These phenomena occur with very little or no visible structural defect on imaging or at post-mortem. Although not the focus of this chapter, this phenomenon should receive greater focus as it may account for a significant proportion of TBI-related death.

History and sport-related injury

The Persian physician Razes (854–925 AD) used the term concussion to describe an abnormal physiological state of the brain, separate from severe traumatic brain injury. In the thirteenth century Lanfrancus subsequently separated commotio cerebri (transient disruption due to brain shaking) from *contusio cerebri* (brain injury with bruising). In the early twentieth century, many accepted the theory that explained cerebral concussion and contusions were caused by deformation of the shape of the skull causing an anaemia of the brain.

In more modern times, concussion has become commonly associated with sport. In 1893 a shoemaker fabricated a leather helmet for an American football player who had had repeated head injuries. In 1905 the American College Football season suffered 18 deaths and 159 serious injuries which came to the attention of President Roosevelt. He ushered in rules to make the game safer. The use of leather helmets increased and in 1935 these became mandatory at the high school level and in 1939, mandatory at the college level. Between 1931 and 1940 the number of football fatalities dropped from 33 to 11. In 1950s the outer plastic rigid shell of the helmet was invented, however this enabled the head to be used as a battering ram—the protective equipment becoming a weapon. With this, fatalities increased (244 between 1961 and 1970) 75% of which were from cerebral haemorrhages. Alteration of rules and increased awareness of this between 1987 and 2008 has resulted in direct football fatalities for all levels of play in the single digits per year (Mueller and Cantu, 2011). Following a high-profile brain injury, Washington and many other states now have the Zackery Lystedt Law (named after the individual who had the TBI). In this the key provisions are: (1) education for parents, athletes, and coaches; (2) immediate removal from play during game or practice after a suspected concussion with no return to play until (3); (3) written clearance by a concussion expert for return to play; and (4) uniformity of rules for all schools who use public land (Ellenbogen, 2014).

Sport-related brain injury was historically the domain of neurosurgeons. For example, in 1941 Walter Dandy patented the first protective baseball cap insert liner (Fox, 1984). However, recent decades have seen intense interest from emergency medicine, sports physicians, and other health professionals, each bringing important aspects of diagnosis and management to this field. Despite this, the regular management of all forms of TBI by neurosurgeons provides a unique experience into the patterns of parenchymal injury and their likely sequelae. Neurosurgeons have a role to lead and be accountable in this field.

The association of concussion with sport has resulted in a definition specific to sport-related concussion. The International Symposia on Concussion in Sport define sports concussion as: *A complex pathophysiological process affecting the brain, induced by traumatic forces.* Several common features include:

1. Can be caused by direct blow to head, face, neck, or elsewhere with impulsive force transmitted.
2. Usually results in rapid onset of short-lived functional neurological impairment.
3. While neuropathological changes can occur, acute symptoms are neurological functional impairment rather than structural.
4. Can be graded and may or may not involve LOC.
5. Grossly normal neuroimaging studies.
6. Occasionally symptoms are prolonged.

There is nothing specific that separates sport-related concussion from concussion due to other mechanisms (e.g. falling off a bike) hence again this separate definition and classification only adds more confusion.

Of course, some sports can result in considerably more injury than mild TBI or concussion. For example, the forces involved in motorsport are more likely to result in immediately life-threatening injuries.

The pathophysiology of concussion

Aetiology of head injury in sport

The results of brain injury in sport have to reflect a combination of laws of physics with the specifics of neuroanatomy (and the function of the areas affected). The head can undergo sudden acceleration/deceleration events causing shearing between intracranial structures. This occurs at high velocity such as in motor-racing and horse riding in which there is external force applied to the individual. Slower velocities result where the head hits the floor or other players during tackles in contact sports such as rugby, American football and soccer, and similarly causes shearing forces. While these may often be milder, they are more likely to recur resulting in cumulative injuries.

In contrast to acceleration/deceleration of the head, other sports have a propensity to cause focal injuries where objects strike a (relatively) stationary head. This can occur with hard balls for example in golf and cricket. The type of injury can be quite different.

Concussion causes a temporary disturbance of proper functioning of the brain. If allowed to return to play, he/she may appear to play normally (especially if a regular player) with relative preservation of cerebellar and motor reflex actions. However, questioning may reveal confusion or disorders of memory.

John Hughling Jackson described an intermediate or 'middle' centre which would correlate with a midbrain-diencephalic region including the upward projections of the reticular activating system and thalamocortical projections that maintain arousal and alertness. It is likely that LOC occurs with transverse shearing forces (produced by angular accelerating rather than linear forces) specifically disrupting this area.

British Neurologists Derek Denny-Brown (1901–1981) and W. Ritchie Russell (1903–1980) demonstrated that acceleration/deceleration induced concussions in cats and monkeys caused stunning without macroscopic or microscopic lesions. Holding the head rigid when the blow was delivered reduced concussion (Denny-Brown and Ritchie Russell, 1940). Shortly after this, it was demonstrated that nerve cell loss and chromatolysis within the brainstem reticular activating system occurred in primate concussion (Gurdjian, 1975).

Sabina Strich (a British neurologist) characterized extensive white matter axonal injury in those severely concussed (Strich lesions). These patients survived because of improved immediate critical care. It became apparent that neuronal disruption not previously appreciated was occurring. Bryan Jennet (1926–2008) understood that this diffuse concussional injuries could have cumulative effects such as those that occur in boxing.

Ayub Ommaya tested Holbourn's hypothesis that annular (rotational) acceleration was more damaging through shearing forces than linear acceleration and impact forces which caused less harmful compressive and tensile (pulling) forces. Non-impact isolated translational linear acceleration had a much greater threshold to produce concussion and resulted in predominantly focal lesions (Ommaya and Gennarelli, 1974).

In the 1950s and 1960s, Richard Schneider's group extensively investigated concussion and patterns of injury in monkeys visualizing the brain through a transparent clear lexan calvarium surgically replacing skull. He suggested that instantaneous respiratory or cardiac arrest may be secondary to compression of the vertebral arteries

between the occipital condyles and C1; or direct transaxial transmission of force to the skull, cervicomedullary junction and high cord, or shear force damage caused by the tethering of the upper cervical cord by the dentate ligaments (Schneider et al., 1970).

Functional vs. structural injury

Traditionally concussion has been thought of as a 'functional' injury because of the lack of macroscopic pathology demonstrated on imaging such as CT scanning. However, there is increasing evidence that there is microstructural injury underlying the functional impairment. While not detectable on CT, injury can often be seen using advanced MRI techniques such as susceptibility weighting and diffusion tensor imaging. Advanced MRI techniques taken before and after a single season of college hockey suggest the presence of scattered cerebral microhaemorrhages and white matter injury in those who experienced concussion (Helmer et al., 2014; Pasternak et al., 2014; Sasaki et al., 2014).

At a cellular level, biomechanical injury results in potassium efflux, sodium and calcium influx, depolarization (and hence indiscriminate glutamate release), and a diffuse 'spreading depression-like' state that may account for acute postconcussive symptoms (Katayama et al., 1992). To correct this cellular ionic imbalance, adenosine triphosphate (ATP)-requiring membrane ion pumps work excessively causing hyperglycolysis, depleting ATP, and increasing ADP. In the setting of reduced cerebral blood flow this leads to metabolic insufficiency. The energy crisis results in free radical generation and more damage or possibly underlie susceptibility to further injury. It has been suggested that following the hyperglycolysis period, a state of impaired metabolism occurs lasting 7 to 10 days and is associated with some postconcussive memory symptoms (Giza and Hovda, 2014).

At a cytoskeletal level, microstructures such as dendritic arbours and astrocytic processes can be disrupted and calcium influx can result in neurofilament side arm phosphorylation and collapse breaking down axons. Axonal stretch disrupts microtublues that alters bidirectional axonal transport altering synaptic neurotransmitter release.

Diffuse axonal injury has axonal disconnection and microhaemorrhages resulting in 'moderate' and 'severe' TBI. Stretching and bending of axons as may occur in mild TBI or concussion can disrupt axonal microstructure. Axolemmal permeability increases after experimental TBI (Pettus et al., 1994). Fluid percussion models injuring the white matter tracts of the corpus callosum demonstrate unmyelinated axons are more vulnerable to injury (Reeves et al., 2005). This, in addition to anatomical factors altered shearing forces may explain greater susceptibility of some brain areas to injury. There is evidence that TBI results in altered glutamate (N-Methyl-D-aspartate) receptor subunit composition altering neurotransmission, calcium influx and both intra and extracellular cell signalling (Atkins et al., 2009). This could have functional (e.g. memory) consequences. There is a dropout of hilar GABAergic interneurons following lateral fluid percussion injury in rats (Zanier et al., 2003). All of these micropathologies could explain slowed cognition.

Inflammatory changes also occur in mild TBI with up-regulation of cytokines and inflammatory genes as well as microglial infiltration. The latter is associated with damage to the substantia nigra with implications specifically for TBI-related parkinsonism (Hutson et al., 2011). The location of these injuries clearly influences functional symptomatology (hippocampus → memory; amygdala → fear/anxiety).

Markers of concussion

The chronic sequelae of repeated concussions are classically seen in boxers, but they are becoming attributed to other contact sports as well. Aggregated tau protein is considered the pathological hallmark of 'chronic traumatic encephalopathy'. While human studies indicating a dose–response correlation are lacking, there is little doubt that boxers develop hippocampal atrophy and ventriculomegaly, strongly implying that cell death has occurred. This appears to be accelerated in elderly TBI.

N-acetylaspartate (NAA), a brain-specific compound may be surrogate marker of post-traumatic biochemical damage, and monitor concussion recovery being detectable through proton magnetic resonance spectroscopy. NAA levels are reduced in the frontal lobes of concussed adults, returning to normal over 30 days except where second injury occurs delaying return for 45 days (Vagnozzi et al., 2008).

Genetic vulnerability

Channelopathies, such as the CACNA1A mutation which is associated with familial hemiplegic migraine is also associated with an exaggerated response to mild TBI (Kors et al., 2001) and may underlie different postconcussive response to injury, or even susceptibility to second impact syndrome.

In animal studies, transgenic animals (3×TG-ApoE4) show increased tau protein accumulation after TBI (Tran et al., 2011). The role of ApoE4 in TBI and Alzheimer's is gradually becoming apparent (Wilson and Montgomery, 2007).

Imaging concussion

Standard MRI techniques can falsely reassure that there is no structural injury. Gradient Echo and susceptibility weighted imaging can demonstrate small microbleeds (**Fig. 45.1**). Diffusion tensor imaging can demonstrate specific white matter tract disruption. While these have previously been mainly research techniques, they should now be considered clinically for those with persisting concussion symptoms. Positron emission tomography imaging can be used to demonstrate B-amyloid and tau pathology which may be of clinical use in the future.

Symptoms of concussion

The classification of concussion has evolved since the first mild, moderate and severe grades proposed by Thorndike in 1948 (Thorndike, 1948). Many others including Schneider (Schneider and Kriss, 1969) and Kelly (Kelly et al., 1991) have proposed other systems with the most recent being a revised version by Cantu (**Table 45.1**) (Cantu, 2001).

Grading concussion on the duration of LOC and amnesia, does not truly reflect the nature or severity of the underlying injury, though on average on a population basis, longer unconsciousness probably reflects greater injury.

Management of concussion

Figures vary, but concussion usually resolves for most patients within a few weeks of injury.

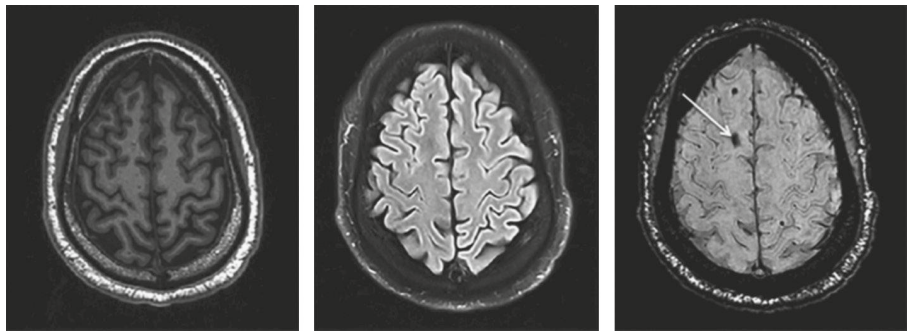

Fig. 45.1 A microbleed is clearly identified on susceptibility weighted MRI, but not seen on standard T1 of fluid attenuated inversion recovery.

Immediate management

Removal from play

Prior to removal from play, a sports club should undertake preseason planning (specific to sport and venue), assessment and education such that removal (or not removal) from play decisions are not made without forethought. Planning comprises immediate and long-term plans incorporating emergency management of immediately life-threatening head injuries. Assessment of individuals requires a comprehensive history of previous concussions and preexisting conditions that can modify concussion (e.g. migraine, depression, and anxiety).

Sideline assessment

The most universal assessment tool is the Sport Concussion Assessment Tool, or SCAT (3rd edition) (http://bjsm.bmj.com/content/47/5/259.full.pdf). This is the accepted tool for many organizations such as FIFA and the Olympic committee. It is suitable for those over 13 (there is a Child SCAT for those under). Within the initial assessment, if the player lost consciousness, has balance or incoordination issues, is disorientated or confused, has memory loss, or looks blank or vacant, then they should be withdrawn from play and not return for the day. There is a Glasgow Coma Scale (GCS) and Maddocks score component. Beyond this is a symptom evaluation including cognitive assessment (orientation, memory, and concentration), neck, balance, and coordination examinations.

Return to play

At the 4th International Conference on Concussion in Sport (2012), it was unanimously agreed that no return to play on the day of concussive injury should occur (McCrory et al., 2013). This is in agreement with American Academy of Neurology guidelines (Giza et al., 2013). Current guidelines suggest a stepwise supervised programme increasing from no activity (day one), to light aerobic exercise, sport specific exercise, non-contact training, full contact practice before return to normal play with at least 24 hours between each of these stages.

Table 45.1 Revised classification of concussion by Cantu

Grade I	No loss of consciousness, posttraumatic amnesia/ postconcussion signs or symptoms <30 mins
Grade II	Loss of consciousness <1 minute or posttraumatic amnesia >30 min but <24 hours, or postconcussion signs or symptoms >30 min but <7 days
Grade III	Loss of consciousness ≥1 minute or post-traumatic amnesia ≥24 hours, postconcussion signs or symptoms >7 days

Reproduced from Cantu, R. C., Guidelines for Return to Contact Sports After a Cerebral Concussion. *The Physician and Sportsmedicine*, 1986, Vol. 14 No. 10, p. 75–83 with permission from Taylor and Francis.

Second impact syndrome

Second impact syndrome, thought to represent malignant brain swelling following an injury without recovery from previous concussion, was put forward as a concept by Schneider in 1973. If real, it appears that the risk of second impact syndrome seems greatest in first 10 days postinjury. This may relate to the energy crisis and cellular vulnerability described. It may be that some second impact injuries are just coincidental severe injuries in people who, because of their sport, regularly suffer brain injury.

Management in the following weeks

Evaluating some of the cognitive aspects over the following few weeks after injury can be performed with tests such as the mini-mental state examination or Addenbrooke's Cognitive Examination.

The commonest issue for families of patients with mild TBI is their loved one's agitation and short-tempered nature with lack of insight into the issue. Indeed, many patients are insistent that they are fine. The best management comprises spending time with the patient and their family, explaining that this is real and common and normally resolves over a few weeks to months. There are pharmacological treatments for some symptoms. For cognitive dysfunction, lack of concentration, anger, and aggression, methylphenidate or amantadine can be useful. Donepezil (used in Alzheimer's) may also have a role. For depression, selective serotonin reuptake inhibitors are preferred (sertraline, citalopram). For headache, non-steroidal anti-inflammatory drugs, triptans, propranolol, and amitriptyline can be used, the latter being good if insomnia is also an issue.

Dizziness occurs in approximately 80% and can persist. Benign paroxysmal positional vertigo is the most common type. It can be diagnosed with a Hallpike test and often treated with repositioning manoeuvres. Referral to a specialist is recommended if prolonged symptoms do not respond.

Summary

Concussion is a common condition following relatively mild TBI, and mild TBI may be a better term to describe it as we begin to understand that it is associated with structural injury (even if microscopic). Mild TBI can have very significant consequences both for the patient and their family and labelling the condition as concussion that usually gets better on its own, may do a disservice those affected. It is important to recognize postconcussive symptoms and investigate and manage further those in whom they persist.

FURTHER READING

Giza, C.C., Kutcher, J.S., Ashwal, S., et al. (2013). Summary of evidence-based guideline update: evaluation and management of concussion in sports: report of the Guideline Development Subcommittee of the American Academy of Neurology. *Neurology*, **80**(24), 2250–7.

McCrory, P., Meeuwisse, W.H., Aubry, M., et al. (2013). Consensus statement on concussion in sport: the 4th International Conference on Concussion in Sport held in Zurich, November 2012. *Br J Sports Med*, **47**(5), 250–8.

Signoretti, S., Lazzarino, G., Tavazzi, B., & Vagnozzi, R. (2011). The pathophysiology of concussion. *PM & R*, **3**(10 Suppl 2), S359–68.

Sport Concussion Assessment Tool (3rd edition) *Br J Sports Med* 2013, **47**, 259. http://bjsm.bmj.com/content/47/5/259.full.pdf

REFERENCES

Atkins, C.M., Falo, M.C., Alonso, O.F., Bramlett, H.M., & Dietrich, W.D. (2009). Deficits in ERK and CREB activation in the hippocampus after traumatic brain injury. *Neuroscience Letters*, **459**(2), 52–6.

Atkinson, J.L.J., Anderson, R.E.R., & Murray, M.J.M. (1998). The early critical phase of severe head injury: importance of apnea and dysfunctional respiration. *J Trauma*, **45**(5), 941–5.

Cantu, R.C. (2001). Posttraumatic retrograde and anterograde amnesia: pathophysiology and implications in grading and safe return to play. *J Athl Train*, **36**(3), 244.

Denny-Brown, D.E., & Ritchie Russell, W. (1940). Experimental cerebral concussion. *J Physiol*, **99**, 153.

Ellenbogen, R. (2014). Concussion advocacy and legislation: a neurological surgeon's view from the epicenter. *Neurosurgery*, **75**(Suppl 4), S122–30.

Fox, W.L. (1984). *Dandy of John Hopkins*. Baltimore, MD: Williams and Wilkins.

Giza, C.C., & Hovda, D.A. (2014). The new neurometabolic cascade of concussion. *Neurosurgery*, **75**(Suppl 4), S24–33.

Giza, C.C., Kutcher, J.S., Ashwal, S., et al. (2013). Summary of evidence-based guideline update: evaluation and management of concussion in sports: report of the Guideline Development Subcommittee of the American Academy of Neurology. *Neurology*, **80**(24), 2250–7.

Gurdjian, E.S., & Volis, H.C. (1966). Congress of Neurological Surgeons Committee on head injury nomenclature: glossary of head injury. *Clin Neurosurg*, **12**, 386–94.

Gurdjian, E.D. (1975). *Impact Head Injury: Mechanistic, Clinical and Preventive Correlations*. Springfield, IL: Thomas.

Helmer, K.G., Pasternak, O., Fredman, E., et al. (2014). Hockey Concussion Education Project, part 1. Susceptibility-weighted imaging study in male and female ice hockey players over a single season. *J Neurosurg*, **120**(4), 864–72.

Hutson, C.B., Lazo, C.R., Mortazavi, F., Giza, C.C., Hovda, D., & Chesselet, M.-F. (2011). Traumatic brain injury in adult rats causes progressive nigrostriatal dopaminergic cell loss and enhanced vulnerability to the pesticide paraquat. *J Neurotrauma*, **28**(9), 1783–801.

Katayama, Y., Tamura, T., Becker, D.P., & Tsubokawa, T. (1992). Early cellular swelling during cerebral ischemia *in vivo* is mediated by excitatory amino acids released from nerve terminals. *Brain Res*, **577**(1), 121–6.

Kelly, J.P., Nichols, J.S., Filley, C.M., Lillehei, K.O., Rubinstein, D., & Kleinschmidt-DeMasters, B.K. (1991). Concussion in sports. Guidelines for the prevention of catastrophic outcome. *JAMA*, **266**(20), 2867–9.

Koch, W., & Filehne, W. (1874). Beltrage zur experimentellen chirurgie. *Arch Klin Chir*, **17**, 190–231.

Kors, E.E., Terwindt, G.M., Vermeulen, F.L., et al. (2001). Delayed cerebral edema and fatal coma after minor head trauma: role of the CACNA1A calcium channel subunit gene and relationship with familial hemiplegic migraine. *Ann Neurol*, **49**(6), 753–60.

McCrory, P., Meeuwisse, W.H., Aubry, M., et al. (2013). Consensus statement on concussion in sport: the 4th International Conference on Concussion in Sport held in Zurich, November 2012. *Br J Sports Med*, **47**(5), 250–8.

Mueller, F.O. & Cantu, R.C. (2011). *Football Fatalities and Catastrophic Injuries 1931–2008*. Durham, NC: Carolina Academic Press.

Ommaya, A.K., & Gennarelli, T.A. (1974). Cerebral concussion and traumatic unconsciousness. Correlation of experimental and clinical observations of blunt head injuries. *Brain*, **97**(4), 633–54.

Pasternak, O., Koerte, I. K., Bouix, S., et al. (2014). Hockey Concussion Education Project, part 2. Microstructural white matter alterations in acutely concussed ice hockey players: a longitudinal free-water MRI study. *J Neurosurg*, **120**(4), 873–81.

Pettus, E.H., Christman, C.W., Giebel, M.L., & Povlishock, J.T. (1994). Traumatically induced altered membrane permeability: its relationship to traumatically induced reactive axonal change. *J Neurotrauma*, **11**(5), 507–22.

Reeves, T.M., Phillips, L.L., & Povlishock, J.T. (2005). Myelinated and unmyelinated axons of the corpus callosum differ in vulnerability and functional recovery following traumatic brain injury. *Exp Neurol*, **196**(1), 126–37.

Sasaki, T., Pasternak, O., Mayinger, M., et al. (2014). Hockey Concussion Education Project, part 3. White matter microstructure in ice hockey players with a history of concussion: a diffusion tensor imaging study. *J Neurosurgery*, **120**(4), 882–90.

Schneider, R.C., & Kriss, F.C. (1969). Decisions concerning cerebral concussions in football players. *Sports Med Train Rehabil*, **1**(2), 165–71.

Schneider, R.C., Gosch, H.H., Norrell, H., Jerva, M., Combs, L.W., & Smith, R.A. (1970). Vascular insufficiency and differential distortion of brain and cord caused by cervicomedullary football injuries. *J Neurosurg*, **33**(4), 363–75.

Sharp, D.J., & Jenkins, P.O. (2015). Concussion is confusing us all. *Pract Neurol*, **15**(3), 172–86.

Signoretti, S., Lazzarino, G., Tavazzi, B., & Vagnozzi, R. (2011). The pathophysiology of concussion. *PM & R*, **3**(10 Suppl 2), S359–68.

Thorndike, A. (1948). *Athletic Injuries: Prevention, Diagnosis and Treatment*, 3rd edition. Philadelphia, PA: Lea and Febiger.

Tran, H.T., Sanchez, L., Esparza, T.J., & Brody, D.L. (2011). Distinct temporal and anatomical distributions of amyloid-β and tau abnormalities following controlled cortical impact in transgenic mice. *PloS One*, **6**(9), e25475.

Vagnozzi, R., Signoretti, S., Tavazzi, B., et al. (2008). Temporal window of metabolic brain vulnerability to concussion: a pilot 1H-magnetic resonance spectroscopic study in concussed athletes, part III. *Neurosurgery*, **62**(6), 1286–95; discussion 1295–6.

Wilson, M., & Montgomery, H. (2007). Impact of genetic factors on outcome from brain injury. *British Journal of Anaesthesia*, **99**(1), 43–8.

Zanier, E.R., Lee, S.M., Vespa, P.M., Giza, C.C., & Hovda, D.A. (2003). Increased hippocampal CA3 vulnerability to low-level kainic acid following lateral fluid percussion injury. *J Neurotrauma*, **20**(5), 409–20.

SECTION 11

Vascular neurosurgery

46. **Normal cerebrovascular physiology and vascular anatomy** *539*
Diederik O. Bulters and Andrew Durnford

47. **The pathophysiology of aneurysms** *559*
Federico Cagnazzo, Giuseppe Lanzino, and Neal F. Kassell

48. **The pathophysiology of subarachnoid haemorrhage** *567*
Jason McMillen

49. **Management of subarachnoid haemorrhage** *575*
Roberto Rodriguez Rubio, Brian P. Walcott, and Michael T. Lawton

50. **Cerebral arteriovenous malformations and dural arteriovenous fistulae** *591*
Michael Morgan

51. **Carotid artery disease and cerebral ischaemia** *615*
Kieron Sweeney, A. O'Hare, and Mohsen Javadpour

52. **Extracranial-intracranial bypass for cerebral ischaemia** *627*
Mathew R. Guilfoyle and Peter J. Kirkpatrick

53. **Giant aneurysms and bypass surgery** *633*
Mario Teo, Omar Choudhri, and Michael Lawton

54. **Spontaneous intracranial haematoma** *643*
Berk Orakcioglu and Andreas W. Unterberg

55. **Cavernomata and angiographically occult lesions** *651*
Janneke van Beijnum and Hiren Patel

46

Normal cerebrovascular physiology and vascular anatomy

Diederik O. Bulters and Andrew Durnford

Vascular anatomy

Embryology and the circle of Willis

The cerebrum receives blood from two sets of paired arteries, the carotid and vertebral arteries, representing anterior and posterior circulatory systems. The circle of Willis, described by Sir Thomas Willis in 1664, refers to the branches of the internal carotid and basilar arteries of these systems which anastomose, forming a stellate appearance within the suprasellar cistern. Functionally, with occlusion of one supplying vessel, the circle affords a degree of collateral circulation. Typically, during initial embryological development, the internal carotid artery supplies the anterior, middle, and posterior cerebral arteries. Later, the posterior communicating artery (PComA) atrophies, with the basilar artery supplying the posterior cerebral artery (PCA). However, if the PComA remains larger than the ipsilateral P1, this is termed a fetal PComA (approximately 25% individuals). In the majority of individuals, a completely intact circle of Willis is not present, with other common variants including PComA hypoplasia or absence, A1 hypoplasia, and anterior communicating artery (AComA) absence. Embryonic connections between the carotid and basilar arteries exist and can persist into adulthood. Most common is a persistent primitive trigeminal artery, arising from the precavernous internal carotid lateral to the dorsum sellae, to join the basilar artery. A persistent primitive hypoglossal artery can also connect the internal carotid to the basilar, thereby representing a single artery supplying the brainstem and cerebellum. Both variants are associated with an increased incidence of cerebral aneurysms.

Structure of cerebral vessels

Cerebral arterial vessels progressively divide into smaller arteries, arterioles, penetrating arterioles, and ultimately parenchymal arterioles and capillaries. Pial vessels, surrounded by cerebrospinal fluid, form penetrating arterioles. As these arterioles become intracerebral, a small extension of the subarachnoid space exists surrounding them, termed the Virchow-Robin space. These parenchymal vessels become encased by astrocytic end-feet.

The walls of cerebral arterial vessels are comprised of three concentric layers termed, from out to in, the tunica adventitia, tunica media, and tunica intima. The tunica adventitia is predominantly made up of collagen and fibroblasts. In the small parenchymal arterioles and capillaries, the associated astrocytic end-feet connect them to astroglia. The tunica media contains mostly smooth muscle, the larger arteries having a generally greater number of layers. The tunica intima is composed of one layer of endothelium and a layer of elastic tissue, the internal elastic lamina, separating it from the tunica media. Structural differences exist between cerebral and other arteries. Cerebral arteries have a thinner adventitia which contains no external elastic lamina and the tunica intima correspondingly has a more developed internal elastic lamina.

The cerebral veins have thin walls and unlike systemic veins do not contain valves, have minimal smooth muscle, and less closely follow the course of the arterial system.

The internal carotid artery (ICA) and its branches

The origin of the ICA is variable, but is typically between C3 and C5. The carotid sinus (or bulb) is a fusiform dilatation at its origin that functions as a major baroreceptor. Alongside is the carotid body, a chemoreceptor influencing respiratory regulation.

Multiple classifications of the ICA segments exist. The simplest divides it into four segments—cervical, petrous, cavernous and supraclinoid (cerebral) (Gibo et al., 1981). An alternative classification describes seven segments (Bouthillier et al., 1996):

1. Cervical
2. Petrous (horizontal)
3. Lacerum
4. Cavernous
5. Clinoid
6. Ophthalmic (supraclinoid)
7. Communicating (terminal)

The extradural ICA

The cervical segment usually has no branches. Angiographically if tortuous, a 'tonsillar loop' may be visualized. It enters the skull base through the carotid canal in the petrous portion of the temporal bone, runs near horizontally and medially before it turns upward on the foramen lacerum and then passes under the petrolingual

ligament to enter the cavernous sinus. The petrous portion has several small branches, not visible angiographically:carotico-tympanic (to the inner ear) and mandibulovidian. The lacerum segment, considered by some a redundant classification, has no branches.

The cavernous segment begins as the artery enters the posterior part of the sinus, where it runs forwards. It is surrounded by sinus endothelium and supported by trabeculae and typically contains two important branches. The first, the meningohypophyseal trunk, has three branches; the inferior hypophyseal artery supplying the posterior pituitary lobe, the dorsal meningeal artery, and the tentorial artery (artery of Bernasconi and Cassinari) supplying the tentorium. The second branch of the cavernous segment is the inferolateral trunk, which supplies the cavernous sinus cranial nerves. Angiographically, the U-shaped section of the ICA, formed from mostly the cavernous portion, is termed the carotid siphon.

The ICA exits through the dural covering of the sinus termed the proximal dural ring, which forms the roof of the sinus and is in continuity with the dura covering the adjacent anterior clinoid process. The clinoid segment is a transitional segment between the cavernous sinus before the ICA exits through the distal ring and enters the subarachnoid space (Rhoton, 2002). Clinically this region is important as the distal dural ring differentiates aneurysms that cause subarachnoid haemorrhage versus those that cause carotico-cavernous fistulae. It is therefore unfortunate that the distal ring is not visible radiologically and its location can only be estimated. Surgically understanding of this region is important as access to proximal aneurysms at or near the origin of the ophthalmic artery will require an anterior clinoidectomy. The distal dural ring sits inclined posterior-medially and is continuous medially with the falciform ligament and with the dura overlying the superior-medial aspect of the anterior clinoid process. While the two rings are fused posteriorly, they are variably separated anteriorly, giving rise to two regions medially and laterally. The lateral region may be considered to be extradural and extracavernous. On the medial side, the space between a redundant portion of distal dural ring and ICA is termed the carotid cave. Although usually extradural, rupture of carotid cave aneurysm extending superiorly out of the cave may result in subarachnoid haemorrhage.

The ophthalmic segment—ophthalmic and superior hypophyseal arteries

The ophthalmic segment gives rise to the ophthalmic artery, with its origin just beyond the distal dural ring, inferior to the optic nerve and anterior clinoid process. It enters the orbit through the optic foramen. Ophthalmic artery aneurysms arise at the origin of the artery and project dorsally or dorsomedially. The small and variable superior hypophyseal arteries arise distal to the ophthalmic artery from the medial ICA to surround the pituitary stalk. Of note, aneurysms within the clinoid, ophthalmic and hypophyseal region are frequently termed 'paraopthalmic' aneurysms, reflecting the difficulty in their angiographic localization.

Two important variants of the ophthalmic artery origin exist. It can arise from the extradural clinoid complicating surgical access. It may also rarely arise from the external carotid artery risking blindness from inadvertent sectioning (Geibprasert et al., 2009). A meningo-ophthalmic artery arising from the middle meningeal artery and entering the orbit through the superior orbital fissure may replace the ophthalmic artery and poses a risk if sacrificed at surgery or during endovascular procedures.

The communicating segment—posterior communicating and anterior choroidal arteries

The communicating segment extends from the posterior communicating artery (PComA) origin to the ICA bifurcation. The PComA arises from the dorsolateral aspect of the ICA, and connects after approximately 1 cm, to the posterior cerebral artery, thereby connecting the anterior to the posterior circulation. Its course is in close proximity to the oculomotor nerve explaining why typical posterolaterally projecting aneurysms can cause a surgical (involving the pupil) third nerve palsy. Small branches commonly arise from the PComA supplying the genu of the internal capsule and thalamus, the largest branch termed the premamillary artery. The anterior choroidal artery (1–3 mm distant to the PComA origin) usually arises from the posterior aspect of the ICA, prior to its termination at the circle of Willis and can arise as several (1–5) separate trunks. This must be recognized in surgery for ICA origin aneurysms. It is of surgical importance as inadvertent injury can lead to significant neurological deficits and is well documented from early studies of ligation of the artery for Parkinson's disease where a significant proportion of patients developed hemiparesis, hemianaesthesia, and hemianopia. It can be divided into cisternal and intraventricular segments. The cisternal segment crosses the optic tract running along its lateral aspect towards the medial temporal lobe, passes the cerebral peduncles to reach the lateral geniculate body before entering the choroidal fissure and becoming the intraventricular segment. Its supply includes the optic pathways, posterior limb of the internal capsule, basal ganglia, and choroid plexus of the temporal horn of the lateral ventricle. At the ICA bifurcation the middle cerebral artery (MCA) typically projects posterolaterally, with the bifurcation therefore best viewed angiographically with an oblique projection which separates it from the anterior cerebral circulation (Figs. 46.1A–C). Of note blister aneurysms typically arise from the dorsomedial wall of non-branching parts of the ICA, although more rarely they may arise at other anterior and posterior circulation sites.

The anterior cerebral artery (ACA)

Although wide anatomical variability exists, the typical description of the ACA is of two arteries, each with A1 and A2 segments, divided by the anterior communicating artery (AComA) (MacDonald, 2009). The A1 segment arises at the ICA bifurcation, crosses over the optic tract anteromedially, and sits in close proximity with its counterpart A1 segment, linked by the AComA. The A1 segment is sometimes referred to as the precommunicating or horizontal segment. The relationship of the A1 to the ICA, optic nerve, and MCA, having performed a classical pterional approach with splitting of the Sylvian fissure, is shown schematically in **Figure 46.2A** and in part intraoperatively in **Figure 46.2B–C**.

There are many variants of this region. The A1 segment may be hypoplastic, with supply from the contralateral A1 via the AComA and can be duplicated. An unpaired or azygous ACA, where a single A2 segment continues distal to the A1 confluence, may be recognized as well as duplicated or fenestrated AComA segments (Yasargil, 1987).

Medial (lenticulo)striate branches typically arise from the inferoposterior aspect of the A1 segment and supply the globus pallidus and medial putamen (**Fig. 46.3**) through the anterior perforated substance. The A2 segment extends from distal to the AComA

(a)

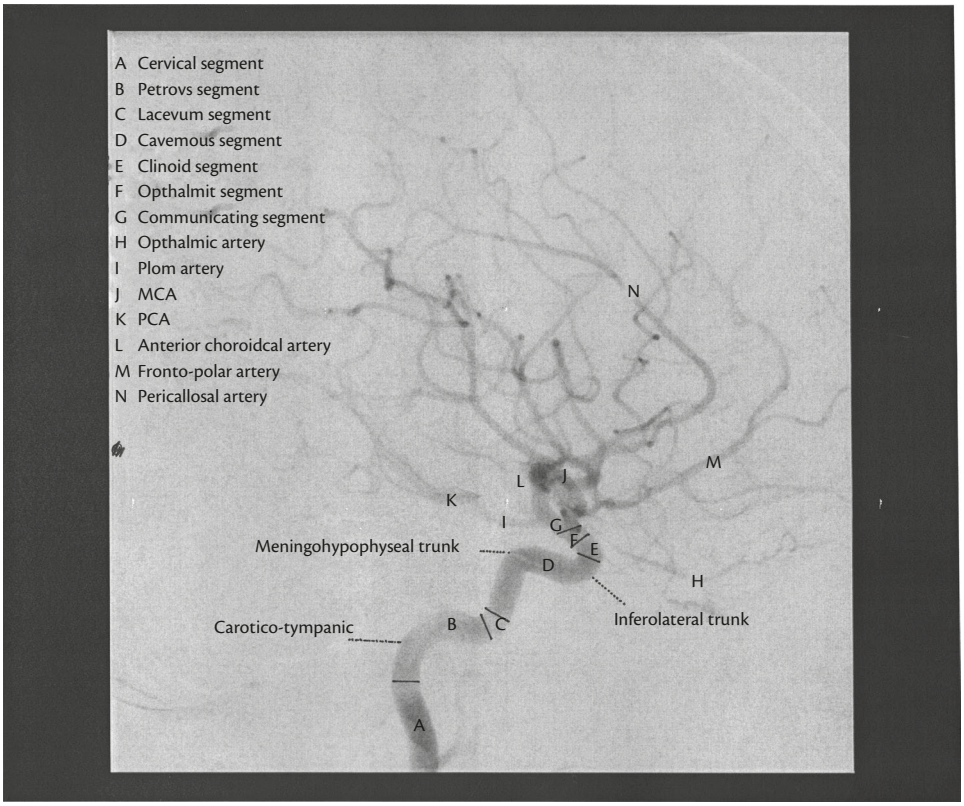

(b)

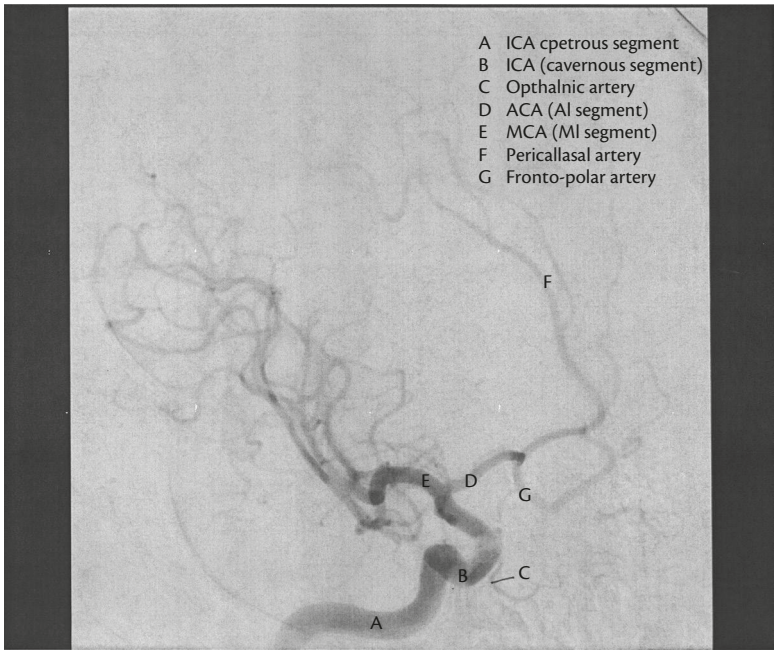

Fig. 46.1 (A) Lateral projection digital subtraction angiogram following internal carotid artery injection. Note the absent callosal marginal artery and corresponding unusually prominent frontopolar artery. The dotted lines mark the approximate origins of the angiographically invisible branches of petrous and cavernous ICA segments. At the MCA bifurcation at the base of the insula, the pattern of branching varies considerably, but typically contains an anterior (superior) and posterior (inferior) trunk which lie deep within the fissure. The angiographic appearance is termed the middle cerebral candelabra. The anterior trunk branches, including the precentral, central (Rolandic) and operculofrontal arteries, generally supply frontal and parietal regions, including the middle and inferior frontal gyri, precentral and postcentral cortex. The posterior trunk typically has three branches. The posterior parietal and posterior temporal arteries supply a significant portion of the temporal and occipital convexities. Finally, the angular artery, which courses the entire length of the insula, supplies the superior temporal gyri and parts of the parietal and occipital lobes. (B) Oblique projection digital subtraction angiogram following internal carotid artery injection. (C) Anteroposterior projection digital subtraction angiogram following internal carotid artery injection. Note cortical branches (M4) will anastomose with ACA branches over the medial convexity. (D) Lateral projection digital subtraction angiogram following external carotid artery injection. The main branches, in ascending order, are the superior thyroid artery, ascending pharyngeal artery, lingual artery, facial artery, occipital artery, posterior auricular artery, maxillary artery, and superficial temporal artery. Note in particular the occipital artery is not opacified in this image.

(c)

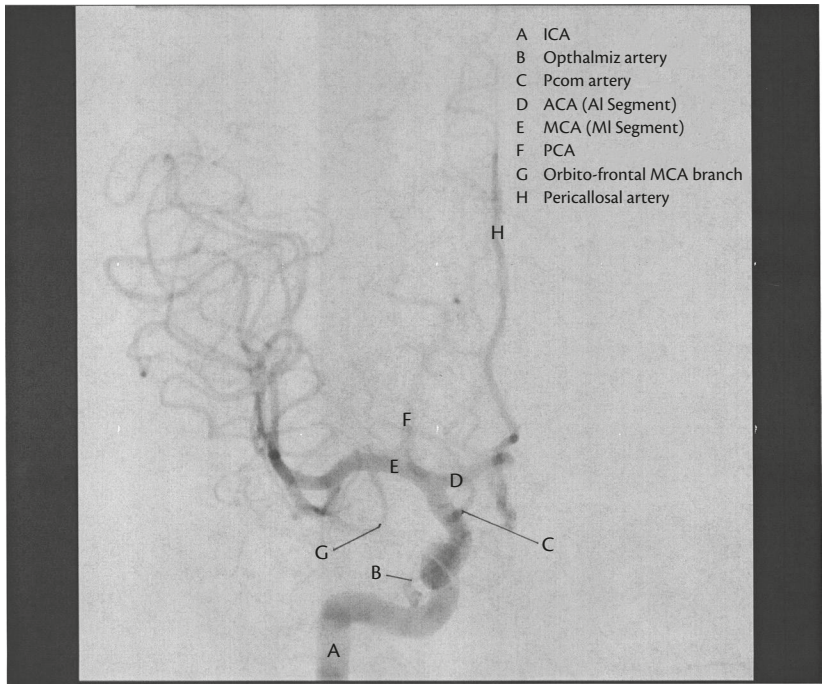

(d)

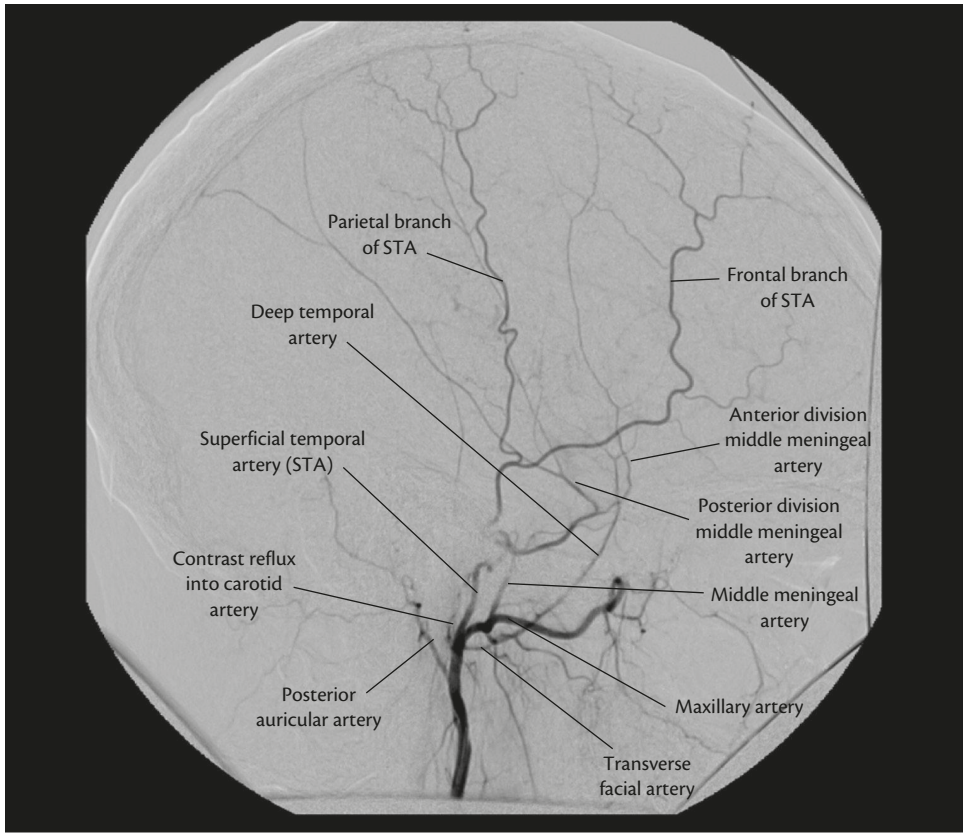

Fig. 46.1 Continued

and ends with the formation of the callosomarginal and pericallosal arteries, at the genu of the corpus callosum. Branches of the A2 include the orbitofrontal artery (typically the first cortical branch) supplying the inferior part of the frontal lobe, and the frontopolar artery supplying the anterior part of the superior frontal gyrus.

The anterior communicating artery (AComA)

This artery lies within the cistern of the lamina terminalis and is important due to its high incidence of aneurysm formation. It is short, measuring up to 3 mm in length. Its perforating branches vary in number but can be classified as subcallosal,

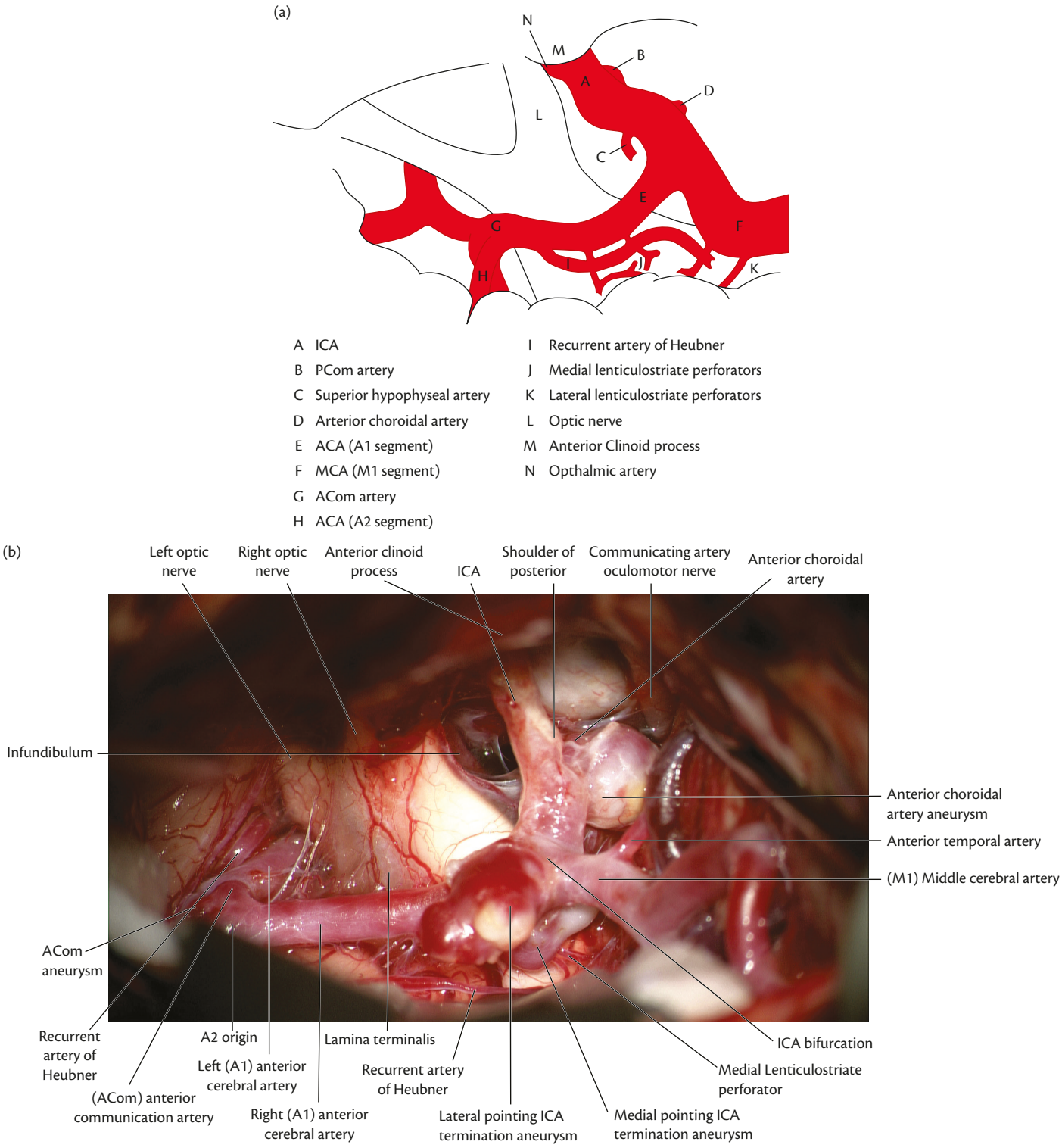

Fig. 46.2 (A) Schematic Sylvian fissure split following pterional craniotomy showing major arterial vessels at base of brain. (B and C) Intraoperative photographs following Sylvian fissure split demonstrating exposure of the ICA, optic nerve, ACA, MCA, and multiple aneurysms (a) and in the same patient with the anterior choroidal artery aneurysm gently retracted exposing the basilar termination and its branches (b). Note the direction of the PCom is deep to the ICA and therefore not seen in these views. The anterior choroidal artery is difficult to visualize as it is closely adherent to the aneurysm dome. The right recurrent artery of Heubner origin at the A1/A2 junction is obscured and the infundibulum is poorly visualized.

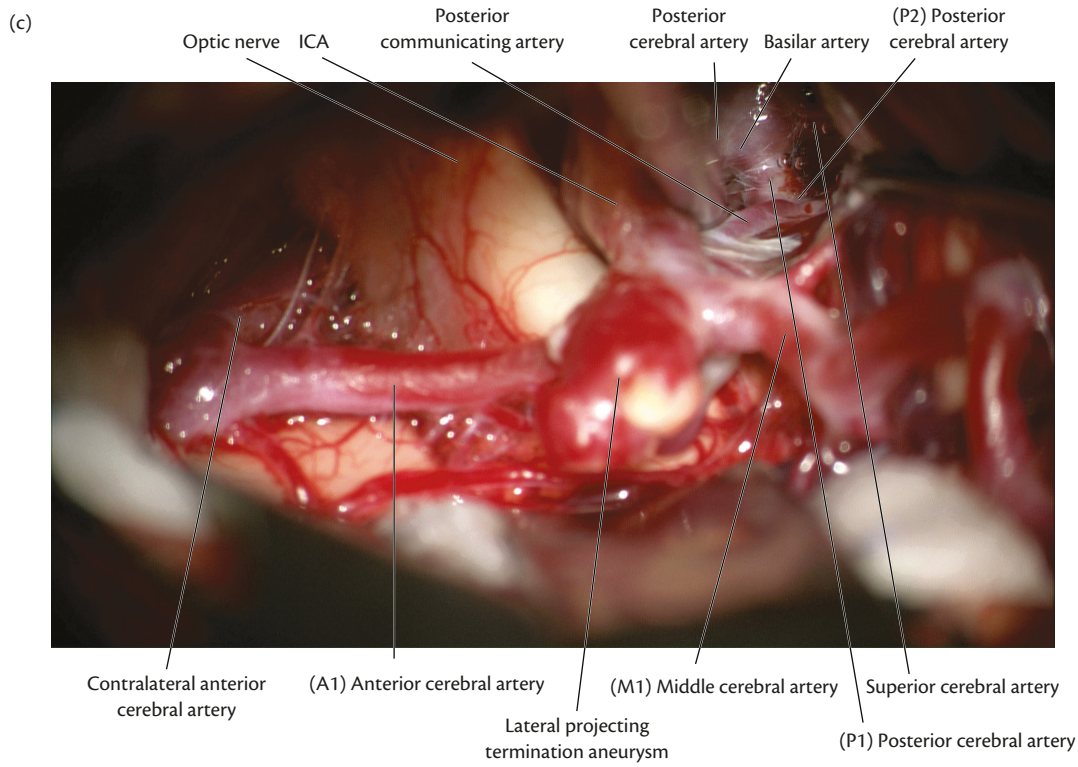

Fig. 46.2 Continued

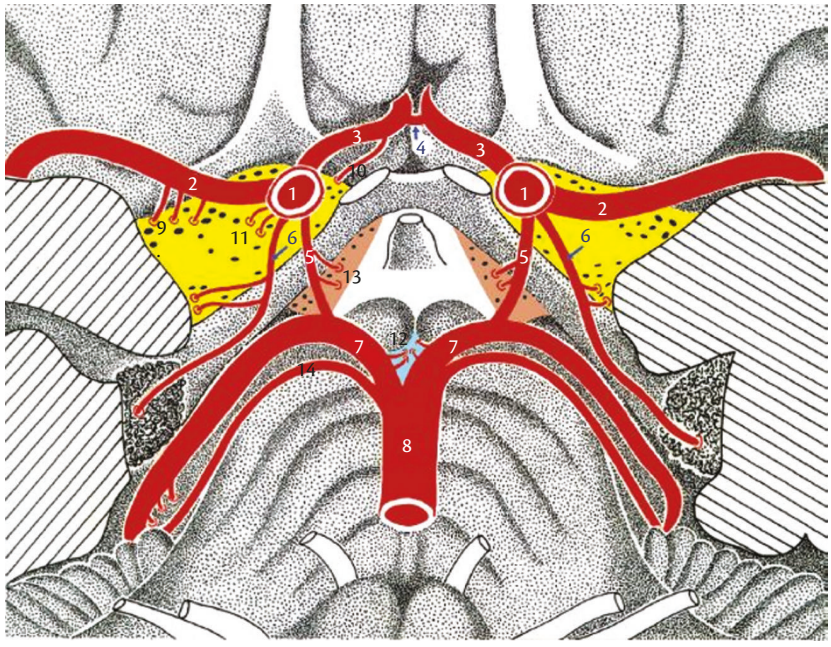

1. Internal carotid artery
2. Middle cerebral artery
3. Anterior cerebral artery
4. Anterior communicating artery
5. Posterior communicating artery
6. Anterior choroidal artery
7. Posterior cerebral artery
8. Basilar artery.
9. Lateral lenticulostriate perforators
10. Recurrent artery of Heubner
11. Medial lenticulostriate perforators (from proximal A1)
12. Thalamoperforating arteries
13. PCOM perforators
14. Superior cerebellar artery

Fig. 46.3 The perforating branches of the cerebral arteries entering through the anterior (yellow), posterior (blue) and lateral (orange) perforated substances.

Reproduced from Bo Norrving, *Oxford Textbook of Stroke and Cerebrovascular Disease*, Oxford University Press, Oxford, UK, Copyright © 2014. By permission of Oxford University Press.

hypothalamic, or chiasmatic according to their regions of blood supply.

The recurrent artery of Heubner

This artery is the largest of the perforating branches of the ACA, typically it arises from the proximal A2 segment near the A1/A2 junction, but can also arise from the A1. Its course generally follows the A1 laterally and supplies the anterior limb of the internal capsule and parts of the caudate nucleus and globus pallidus.

The callosomarginal and pericallosal arteries

The pericallosal (trunk) artery is considered a continuation of the ACA and closely follows the corpus callosum. Its branches supply the corpus callosum and its splenium, the septum pellucidum, fornix, and precuneus cortex. The cortical branches anastomose with the branches of the MCA and posterior cerebral artery. A callosomarginal artery is present in approximately 50% of cases (Butler et al., 2012). It supplies the superior frontal gyrus through various branches, taking a course through the cingulate sulcus. It terminates as the paracentral artery supplying the paracentral lobule.

The middle cerebral artery (MCA)

The MCA is the largest branch of the ICA. Its proximal segment (M1) ends at the MCA bifurcation as the distal (M2) segment. The M1 runs laterally in the anterior (or sphenoidal) compartment of the deep component of the Sylvian fissure, between the frontal and temporal lobes. A variable number of lateral striate (or lenticulostriate) arteries arise from the posteroinferior part of the M1, travel backwards along its course and penetrate the lateral portion of the anterior perforated substance. They supply the basal ganglia, internal capsule, and caudate nucleus. Clinically, these arteries are the frequent source of hypertensive intracerebral haemorrhage. The M1 bifurcates at its genu, turning upwards at a right-angle, at the anteroinferior aspect of the insula. The only large branches of the M1 are usually the anterior temporal artery and temporopolar branch.

The vertebrobasilar (posterior) system and its branches

The vertebral arteries arise as the first branch from the subclavian artery and enter the cranial vault through the foramen magnum, traversing anterolateral to the medulla before joining at the pontomedullary junction to form the basilar artery (Figs. 46.4A–B). Significant branches arise prior to their unification. Each vertebral artery gives off a posterior spinal artery that descends along the posterior aspect of the spinal cord. The second, and usually largest branch, is the posterior inferior cerebellar artery (PICA). It can sometimes arise below the foramen magnum (~15% individuals). If hypoplastic, there is characteristically a corresponding increase in the calibre of the anterior inferior cerebellar artery (AICA). A further variation is that one vertebral artery may form a PICA directly. The PICA courses around the medulla from its origin where it is closely related to the hypoglossal nerve passing around the inferior aspect of the medullary olive—termed the anterior medullary segment (Table 46.1). Next the lateral medullary segment curves beside the medulla and the tonsillomedullary segment courses around the caudal half of the cerebellar tonsil, forming the caudal loop visible on lateral angiography. The telovelotonsillar segment passes in a cleft between the tela choroidea and medulla, travelling superiorly to form a cranial loop at its apex. A cortical segment overlays the cerebellar surface (Lister et al., 1982). Branches of the PICA supply the medulla, fourth ventricle choroid plexus, and inferior and posterior cerebellum. Finally, prior to the vertebral arteries forming the basilar artery, two very short branches unite to form the descending anterior spinal artery.

The pattern of arterial supply to the midbrain, pons, and medulla from the superior cerebellar arteries (SCA), AICA and PICA is via short and long circumflex perforators to the anterior and posterolateral parts with the long circumflex branches travelling over the lateral surface. In addition, there are more direct anterior branches from the proximal segments of these vessels and the basilar trunk.

The basilar artery

The basilar arises at the pontomedullary junction and travels along the anterior surface of the pons in the pontine cistern and terminates, at the midbrain, into the two posterior cerebral arteries. Typically, small perforators supply the pons throughout its length. The paired anterior inferior cerebellar arteries arise from the basilar in close proximity to the abducens nerve. Each AICA traverses the cerebellopontine angle, closely related to the facial and vestibulocochlear nerves, to supply the anterior and inferior cerebellum (Table 46.1). The AICA usually gives rise to the labyrinthine artery, although it can also arise direct from the basilar or elsewhere. It accompanies the vestibulocochlear nerve and traverses the internal acoustic meatus to supply the cochlea and vestibular apparatus. Prior to the basilar bifurcation, the two paired SCA arise, running laterally around the midbrain in the ambient cistern. They pass below the oculomotor nerve, which separates them from the posterior cerebral arteries. The SCA approaches the midline in the quadrigeminal cistern, to supply the superior cerebellar hemispheres, peduncles, and vermis. The SCA is anatomically subdivided from proximal to distal (Table 46.1) but may also be described radiographically, as prepontine, ambient, and quadrigeminal segments. The SCA may be duplicated in approximately one-third of cases. Overall, the three neurovascular complexes of the posterior fossa are summarized in Table 46.2 (Rhoton, 1994).

The posterior cerebral artery (PCA)

From its origin, the first segment of the PCA, the P1 (or horizontal segment), sits within the interpeduncular fossa before anastomosing with the PComA. Varyingly with the PComA, perforating vessels arise from the posterior-superior surfaces of the P1 and supply the internal capsule and thalamus. A single large thalamoperforate branch is occasionally seen angiographically, often referred to as the artery of Percheron and can supply both thalami and the midbrain. Occlusion can result in a paramedian thalamic syndrome with a triad of altered conscious state, vertical gaze palsy, and impaired memory. The P2 segment formed distal to the PComA, then traverses around the oculomotor nerve, in the ambient cistern, to sit above the tentorium, before the P3 segment starts at the quadrigeminal cistern. The P2 is divided into P2A (anterior) and P2P (posterior) segments, with their junction at the most lateral aspect of the cerebral peduncle. The P2 segment has multiple perforating branches including the thalamogeniculate and lateral posterior choroidal arteries. The lateral posterior choroidal artery enters the ventricle adjacent to the lateral geniculate nucleus through the choroid fissure. The medial posterior choroidal artery arises from the proximal P2 or from the P1 segments in the ambient cistern and passes beneath the splenium of the corpus callosum to enter the roof of the third ventricle in the velum interpositum. Branches of the P2 also contribute to cerebral

(a)

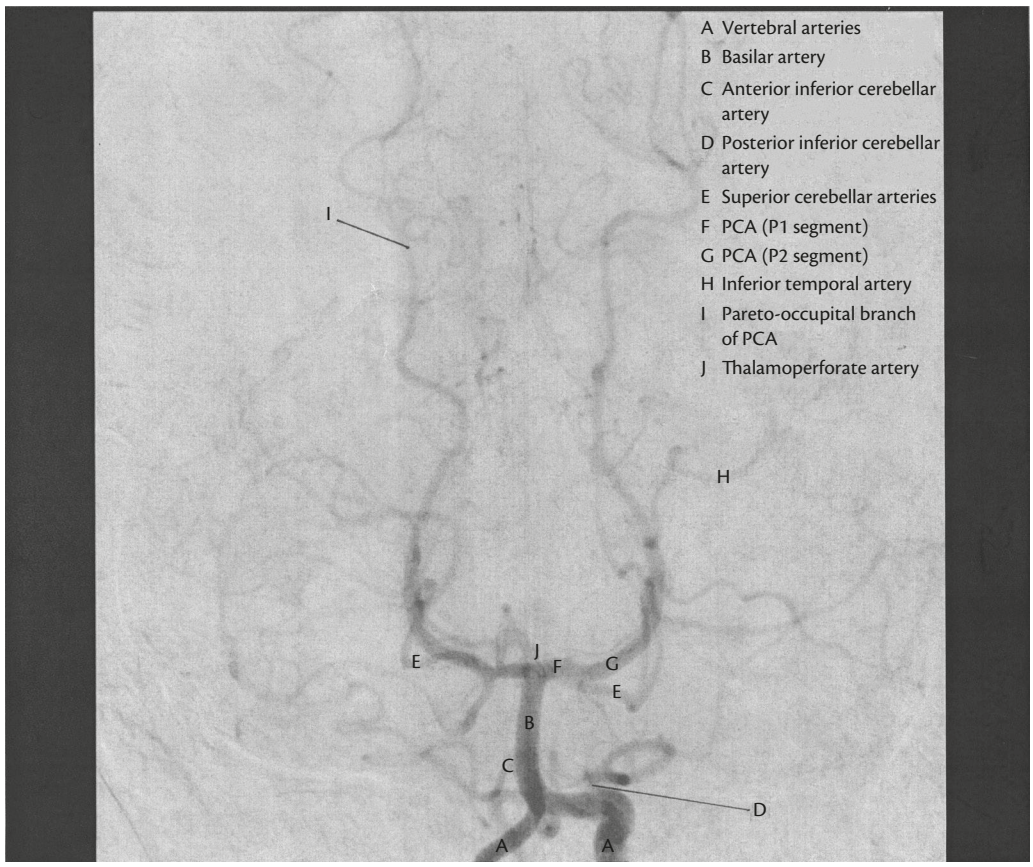

(b)

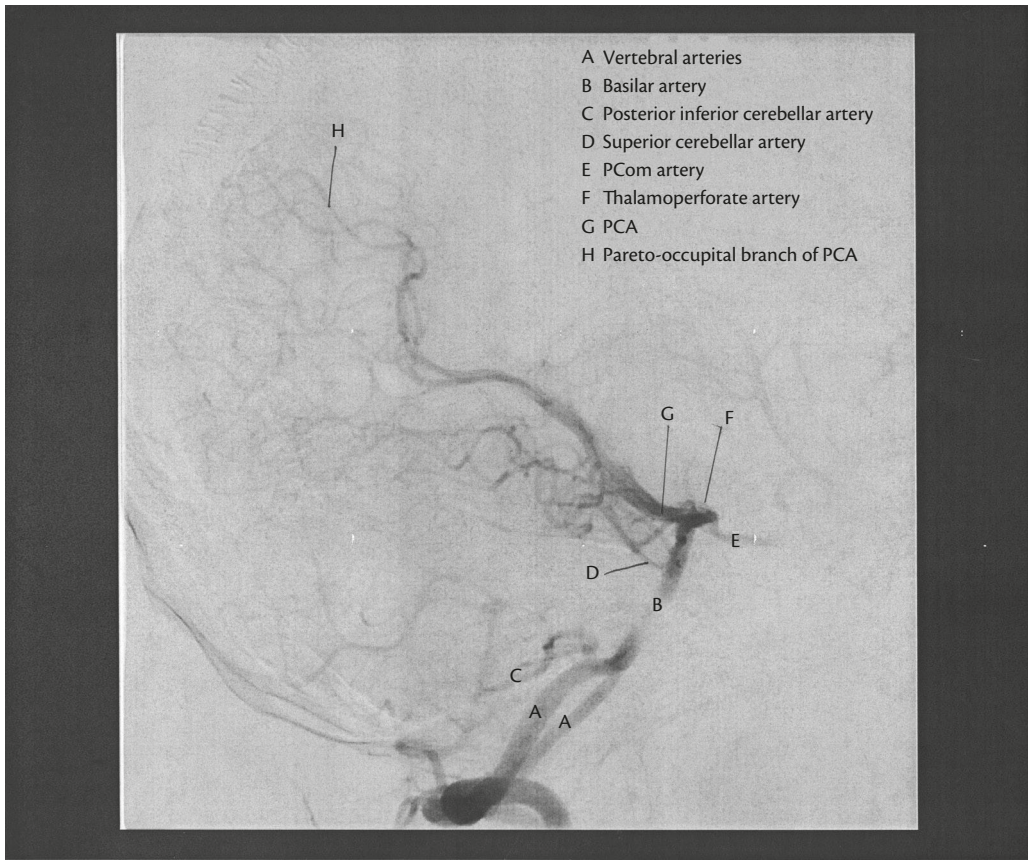

Fig. 46.4 Anteroposterior (A) and lateral (B) digital subtraction angiograms following vertebral artery injection. Note the asymmetry in the level of origin of the left and right PICA.

Table 46.1 Vascular segments of posterior fossa arteries

Artery	Subdivisions: proximal to distal				
SCA	Anterior pontomesencephalic	Lateral pontomesencephalic	Cerebellomesencephalic		Cortical (superior surface)
AICA	Anterior pontine	Lateral pontomedullary	Flocculonodular		Cortical (petrosal surface)
PICA	Anterior medullary	Lateral medullary	Tonsillomedullary	Telovelotonsillar	Cortical (suboccipital surface)

peduncle and quadrigeminal plate supply. Additional P2 branches to the temporal and parietal lobes have relevance to arteriovenous malformations (AVM) surgery. The temporal-occipital area receives blood inferiorly from the posterior inferior temporal artery and anteriorly from branches of the MCA. Notably, the P2, in the presence of high intracranial pressure, can be compressed against the tentorium resulting in occipital lobe infarcts. The P3 segment traverses along the inferomedial aspect of the temporal lobe, with associated cortical perforating branches, before bifurcating into the parieto-occipital and calcarine arteries. The calcarine artery principally supplies the visual cortex in the medial occipital lobe. Cortical PCA branches anastomose with MCA branches over the lateral surfaces of the occipital and temporal lobes. In approximately, 20% of cases the P1 segment is absent, with the PCA supplied via the PComA by the ICA (Harnsberger and Macdonald, 2006).

The external carotid artery (ECA)

The ECA typically arises at the level of C4 and initially lies anteromedial to the ICA. Classically eight branches are described (Fig. 46.1D)—although in practice this can vary considerably. Several anastomoses exist between ECA branches and both ICA and vertebral artery branches. Ascending pharyngeal artery branches anastomose with cavernous ICA branches and meningeal vertebral artery branches; the facial artery with branches of the ophthalmic artery and the occipital artery with vertebral artery branches (and also superficial temporal artery branches). Dural supply from ECA branches have relevance to dural fistula diagnosis and management, for example, ascending pharyngeal artery and occipital artery supply to the posterior fossa dura or middle meningeal and accessory meningeal branches of the maxillary artery supplying supratentorial dura.

Vascular territories in the brain

An overview of the arterial supply to the brainstem, cerebellum, and cerebrum is shown in Figure 46.5. The cerebral vascular territories supplied, despite traditional textbook reports, can vary considerably. This can be due to arterial anatomical variation and also individual variation in the area of cortex supplied by a given arterial branch (van der Zwan et al., 1992). Recent MRI flow studies have confirmed this variability but also showed that it can be related to anatomical variability of the circle of Willis (van Laar et al., 2006). It may also vary between hemispheres within the same patient.

Venous anatomy

The cerebral venous system is comprised of both superficial and deep cerebral veins and the dural venous sinuses.

The superficial system

The superficial venous system is made up of numerous and variable superficial cortical veins, which typically accompany arteries travelling within the cerebral sulci. These drain into a number of larger named veins, which subsequently drain into the venous sinuses:

- Superficial middle cerebral vein—drains into the cavernous (or sphenoparietal) sinus
- Great anastomotic vein (of Trolard)—drains the superficial middle cerebral vein into the superior sagittal sinus
- Posterior anastomotic vein (of Labbé)—drains superficial middle cerebral vein into the transverse sinus. There is often a reciprocal arrangement between the two anastomotic veins with Labbé larger in the dominant hemisphere and Trolard in the non-dominant.

The deep system

The deep venous system drains the deep white and grey matter surrounding the lateral and third ventricle and basal cisterns. The great cerebral vein (of Galen) is found below the splenium of the corpus callosum and is a short, single midline vessel. It is formed by joining of the two internal cerebral veins, and also receives the two basal veins (of Rosenthal) as well as the occipital veins draining the medial and inferior occipital lobes. It runs to the venous confluence where it is joined by the inferior sagittal sinus to form the straight sinus. The basal veins (of Rosenthal) arise at the anterior perforated substance on the medial aspect of the temporal lobe and run posteriorly and medially. They travel laterally around the midbrain through the ambient cistern and drain the hypothalamus, midbrain, and medial and inferior portions of the frontal and temporal lobes, including the insula and operculum. The internal cerebral veins, situated in the velum interpositum (roof of the third ventricle), are formed by the union of the choroidal and thalamostriate veins. The choroidal vein drains the choroid plexus of

Table 46.2 Rhoton's three neurovascular complexes in the posterior fossa

Complex	Vessel	Brainstem region	Fissure	Cranial nerve	Cerebellar peduncle	Surface of cerebellum
UPPER	Superior cerebellar	Midbrain	Cerebellomesencephalic	III, IV, V	Superior	Tentorial
MIDDLE	Anterior inferior cerebellar	Pons	Cerebellopontine	VI, VII, VIII	Middle	Petrosal
LOWER	Posterior inferior cerebellar	Medulla	Cerebellomedullary	IX, X, XI, XII	Inferior	Suboccipital

Source data from Rhoton, A. L., JR. 1994. The three neurovascular complexes in the posterior fossa and vascular compression syndromes (honored guest lecture). *Clin Neurosurg*, 41, 112–49.

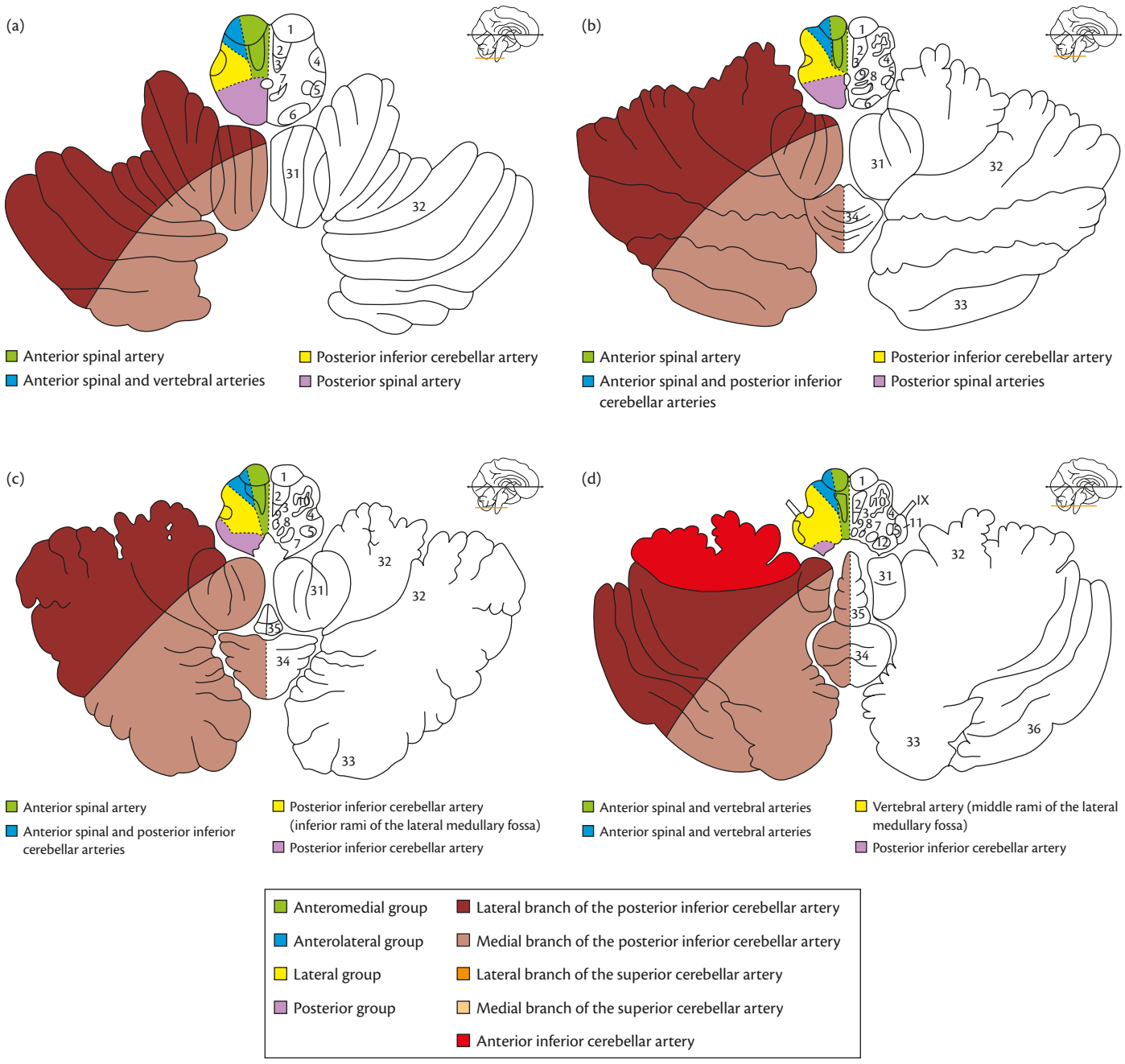
(a)
Anterior spinal artery
Anterior spinal and vertebral arteries
Posterior inferior cerebellar artery
Posterior spinal artery
(b)
Anterior spinal artery
Anterior spinal and posterior inferior cerebellar arteries
Posterior inferior cerebellar artery
Posterior spinal arteries
(c)
Anterior spinal artery
Anterior spinal and posterior inferior cerebellar arteries
Posterior inferior cerebellar artery (inferior rami of the lateral medullary fossa)
Posterior inferior cerebellar artery
(d)
Anterior spinal and vertebral arteries
Anterior spinal and vertebral arteries
Vertebral artery (middle rami of the lateral medullary fossa)
Posterior inferior cerebellar artery
Anteromedial group
Anterolateral group
Lateral group
Posterior group
Lateral branch of the posterior inferior cerebellar artery
Medial branch of the posterior inferior cerebellar artery
Lateral branch of the superior cerebellar artery
Medial branch of the superior cerebellar artery
Anterior inferior cerebellar artery

Fig. 46.5 Arterial vascular territories to the brainstem, cerebellum, and cerebrum.

Reproduced from Bo Norrving, *Oxford Textbook of Stroke and Cerebrovascular Disease*, Oxford University Press, Oxford, UK, Copyright © 2014. By permission of Oxford University Press.

the lateral ventricle. Tributaries draining into the thalamostriate vein include the transverse caudate veins, anterior terminal vein (draining the ventricular surface of the caudate nucleus) and septal vein (draining the corpus callosum and deep frontal white matter).

Dural venous sinuses

Dural sinuses are valveless, venous channels formed from dural folds. The principal dural sinuses are the superior sagittal, transverse, sigmoid, straight, superior, and inferior petrosal, cavernous, and sphenoparietal sinus. The superior sagittal sinus typically arises at the crista galli and ends at the torcular Herophili. It can also divide prior to the torcula, where it usually meets the transverse sinuses, leading clinically to misdiagnosis of superior sagittal sinus thrombosis. The smaller inferior sagittal sinus lies in the free margin of the falx cerebri, drains tributaries from the corpus callosum and cingulate gyrus, and itself drains into the straight sinus at the venous confluence. It is typically not visible radiologically. The transverse sinuses are commonly asymmetric, usually with a dominant right side which receives the majority of the blood from the superior sagittal sinus at the torcula. They become the sigmoid sinuses at the posterior petrous edge, which then continue to the jugular bulb. The sigmoid sinus can vary in size compared to the transverse sinus, particularly when receiving large flow from the posterior anastomotic vein (of Labbé) into its proximal part.

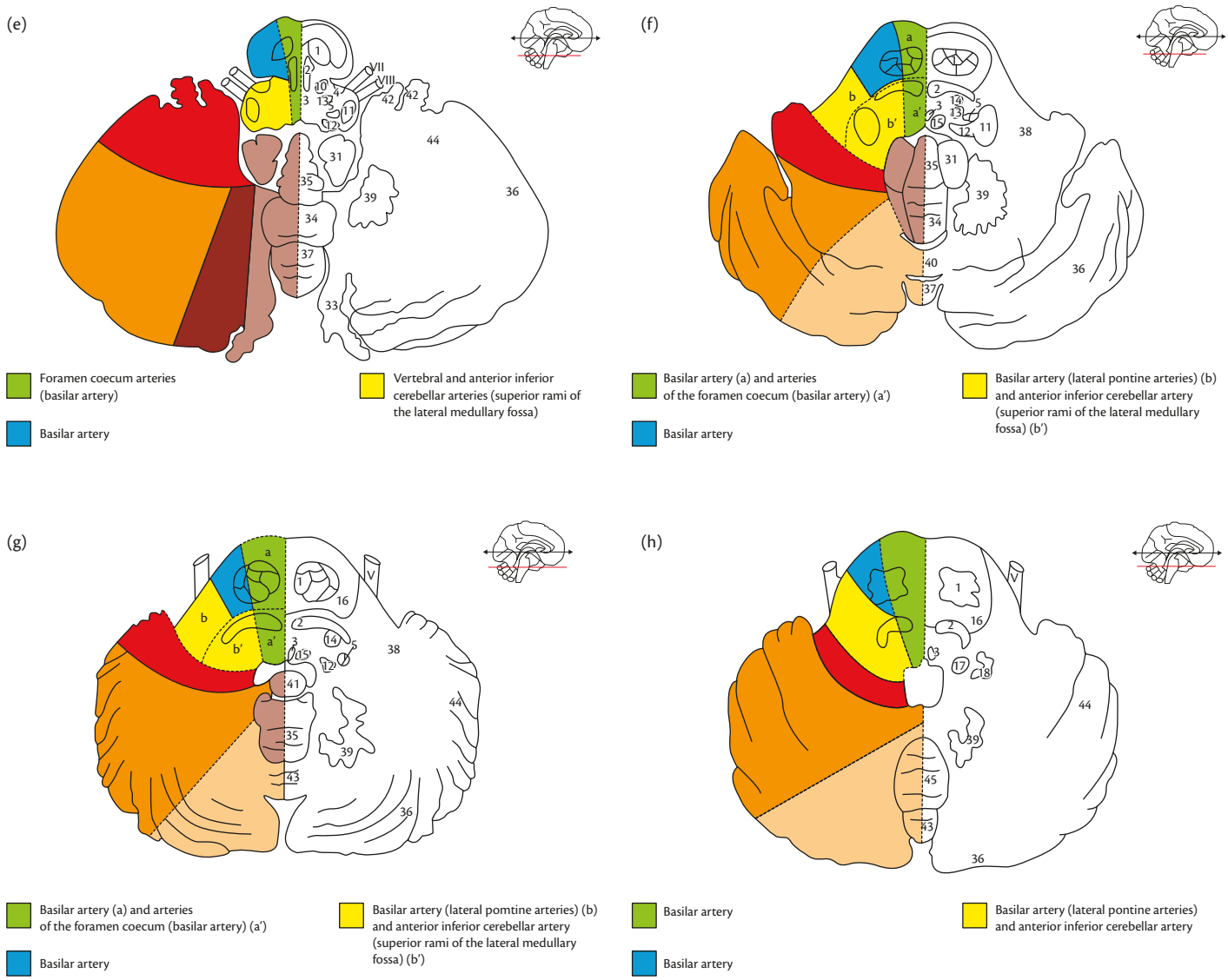
(e)
Foramen coecum arteries (basilar artery)
Basilar artery
Vertebral and anterior inferior cerebellar arteries (superior rami of the lateral medullary fossa)
(f)
Basilar artery (a) and arteries of the foramen coecum (basilar artery) (a')
Basilar artery
Basilar artery (lateral pontine arteries) (b) and anterior inferior cerebellar artery (superior rami of the lateral medullary fossa) (b')
(g)
Basilar artery (a) and arteries of the foramen coecum (basilar artery) (a')
Basilar artery
Basilar artery (lateral pomtine arteries) (b) and anterior inferior cerebellar artery (superior rami of the lateral medullary fossa) (b')
(h)
Basilar artery
Basilar artery
Basilar artery (lateral pontine arteries) and anterior inferior cerebellar artery

Fig. 46.5 Continued

The cavernous sinus typically receives flow from the superficial middle cerebral (Sylvian) veins, ophthalmic veins, and sphenoparietal sinus (itself sometimes draining the Sylvian veins). Outflow from the cavernous sinus is through the superior and inferior petrosal sinuses (connecting to the sigmoid sinus and jugular foramen respectively) and also the contralateral cavernous sinus and the pterygoid and clival venous plexuses. Varyingly present, and more common in children, an occipital sinus may run from the torcula in the midline to the foramen magnum and can be the source of significant bleeding in an otherwise straightforward midline posterior fossa approach. The dural venous sinuses also communicate with the extracranial venous system through valveless emissary veins, which can serve as a route for the introduction of intracranial infection (Fig. 46.6).

The cerebellum and brainstem

There is considerable variation in the venous system draining the cerebellum and brain stem. The superficial cerebellar hemispheres drain into the nearest of the sigmoid or transverse sinuses. The (superior and inferior) vermian veins are the exception, which run along the vermis in the midline. The anterior cerebellum drains into the superior or inferior petrosal sinuses. In the brain stem, the veins are small and networks widespread. The lateral mesencephalic vein, which is contiguous with the petrosal vein, is commonly present and runs along the lateral aspect, connecting superiorly the basal vein (of Rosenthal) with the superior petrosal sinus. The superior petrosal vein or Dandy's Vein, represents the large vein, extending from the lateral surface of the pons that drains into the superior petrosal sinus. It drains a large area, including the anterior cerebellum, lateral and posterior medulla, and anterior pons. The vein running longitudinally on the anterior aspect is termed the anterior mesencephalic, pontomedullary, or spinal vein depending on its most adjacent structure. The precentral (or cerebellar) vein is an unpaired vein running posterior to the brainstem, draining into the superior vermian vein or great vein (of Galen) and is of note as its inferior aspect marks the upper border of the fourth ventricle. It predominantly drains the cerebellum.

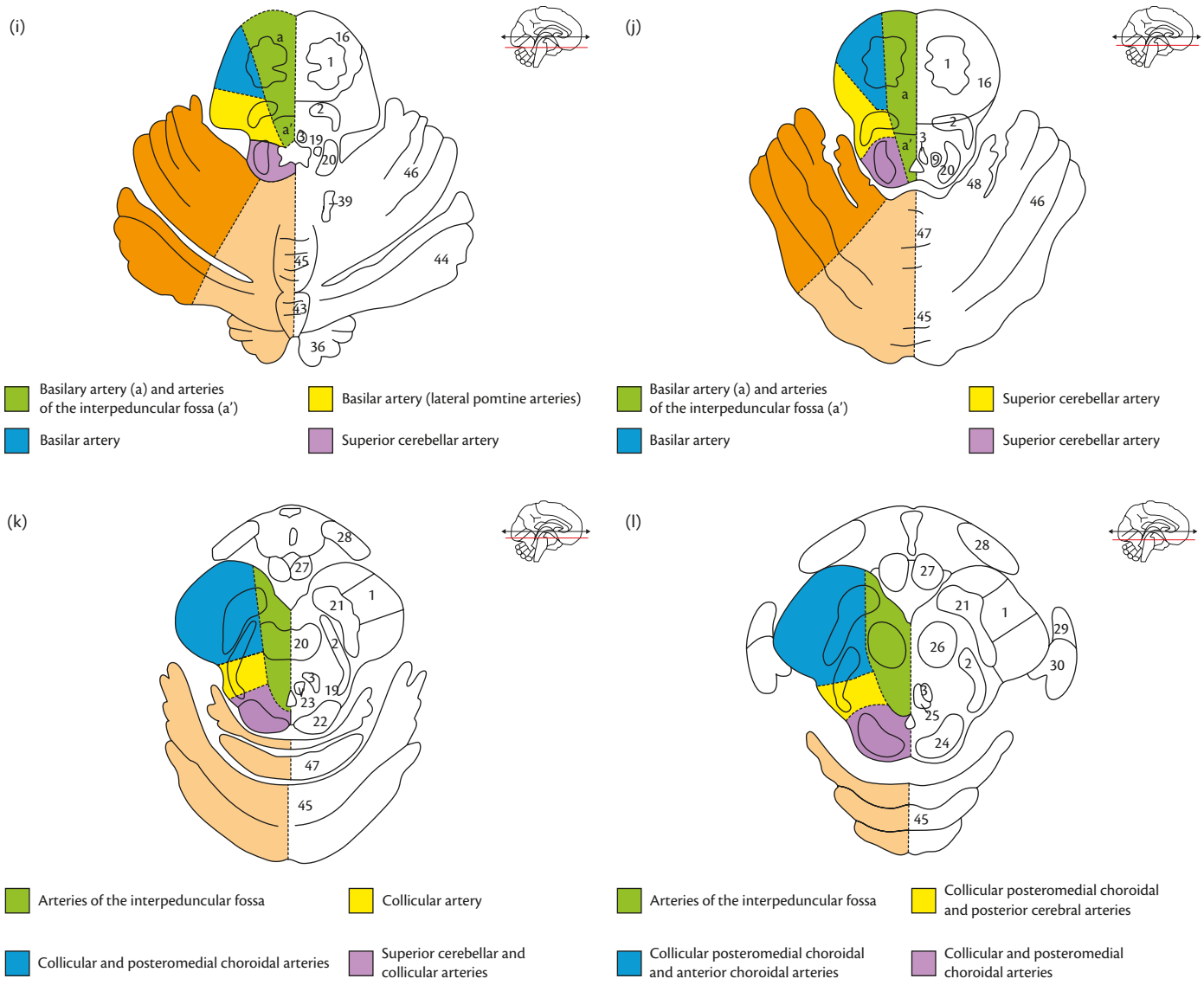

Fig. 46.5 Continued

Anatomical considerations for AVM surgery

As arterial feeders to the AVM nidus arise from normal cortical and deep arterial branches, understanding the anatomical location of these vessels based on angiographic studies is imperative for safe planning of AVM treatment. These are somewhat predicted by the lobar location of the AVM as regards the cortical arterial supply and by their deep location or extension regarding recruitment of deep perforator branches. Large AVMs straddling more than one lobe would naturally be supplied by feeders from the adjacent vascular territory as well: 'watershed' regions. This is of importance when studying angiograms (DSA) as awareness of the existence of further feeders from another vascular territory will avoid underestimation of the extent of the lesion.

Lateral hemisphere AVMs

On the lateral hemisphere AVMs are divided into frontal, temporal, parietal, occipital, and peri-Sylvian locations. Extension towards the superior frontal lobe or to the frontal pole attracts supply from distal ACA branches such as the frontopolar artery anteriorly, the fronto-orbital artery basally, and the callosomarginal artery superiorly. Extension of the surgical exposure to the medial or basal aspects of the frontal lobe is necessary to access these vessels for proximal control. M4 branches from the superior M2 trunk of the MCA extend to the cortical/subcortical surface of most of the frontal and central (the pre- and postcentral gyri) lobes with probable *en passant* vessel supply to the motor and speech areas. Corresponding vessels from the inferior M2 trunk feed AVMs located in the temporal and parietal lobes and extend to the lateral surface of the occipital lobe as well. Peri-Sylvian AVMs predominantly involve the frontal or temporal operculum with feeders arising from the opercular (M3), the M2, or the distal M1 segments. Deep extension, including to the insula, involves feeders from the lenticulostriate perforators. The short perforators supply the insular cortex while the long perforators supply the internal capsule and corona radiata. Proximal access to MCA feeders is through splitting of the Sylvian fissure. Frequently temporal AVMs

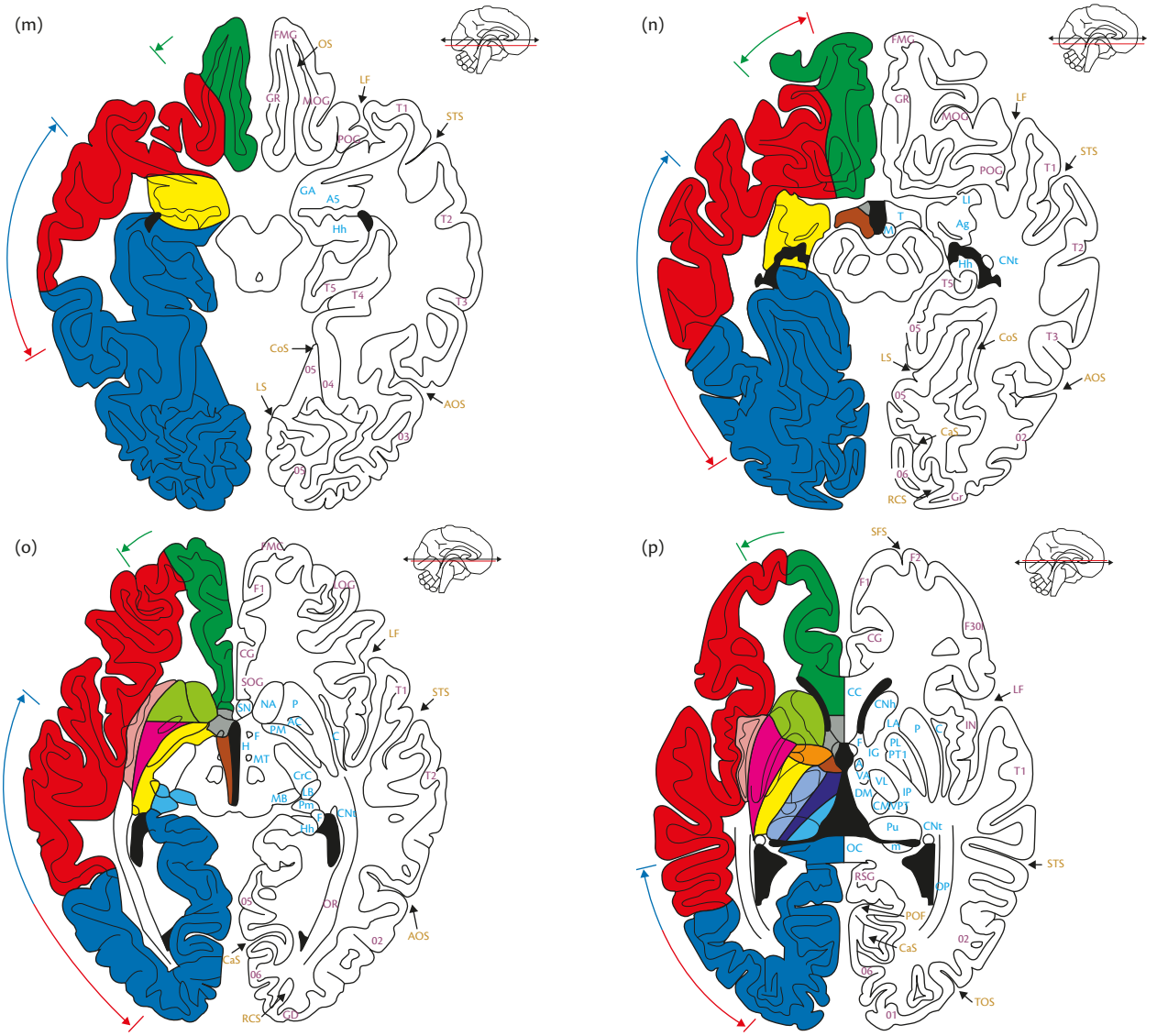
(m)
(n)
(o)
(p)
Leptomeningeal branches of the anterior cerebral artery (ACA)
Perforating branches of the anterior cerebral artery (ACA)
Leptomeningeal branches of the middle cerebral artery (MCA)
Perforating branches of the middle cerebral artery (MCA)
Insular zone
Leptomeningeal branches of the posterior cerebral artery (PCA)
Thalamoperforating branches
Thalamogeniculate branches
Posterior choroidal arteries (PChA)
Anterior choroidal artery (AChA)
Anterior communicating artery (ACoA)
Perforating branches of the posterior communicating artery (PCoA)
Perforating branches of the internal carotid artery (ICA)

Fig. 46.5 Continued

extend inferiorly and onto the basal tentorial surface. In this case a proportion, if not the predominant feeders, are from the anterior, middle, or posterior temporal branches of the P2 segment of the PCA and these are encountered as they arise proximally at the ambient cistern and over the tentorial edge and a subtemporal approach provides access to these.

Provided there are no significant deep extensions, the majority of AVMs on the lateral hemisphere drain via superficial veins to the superior sagittal or transverse sinus and those in a central location may involve the veins of Trollard or Labbé. Temporal AVMs extending on the tentorial surface may partially drain via tributaries of the vein of Rosenthal to the deep system.

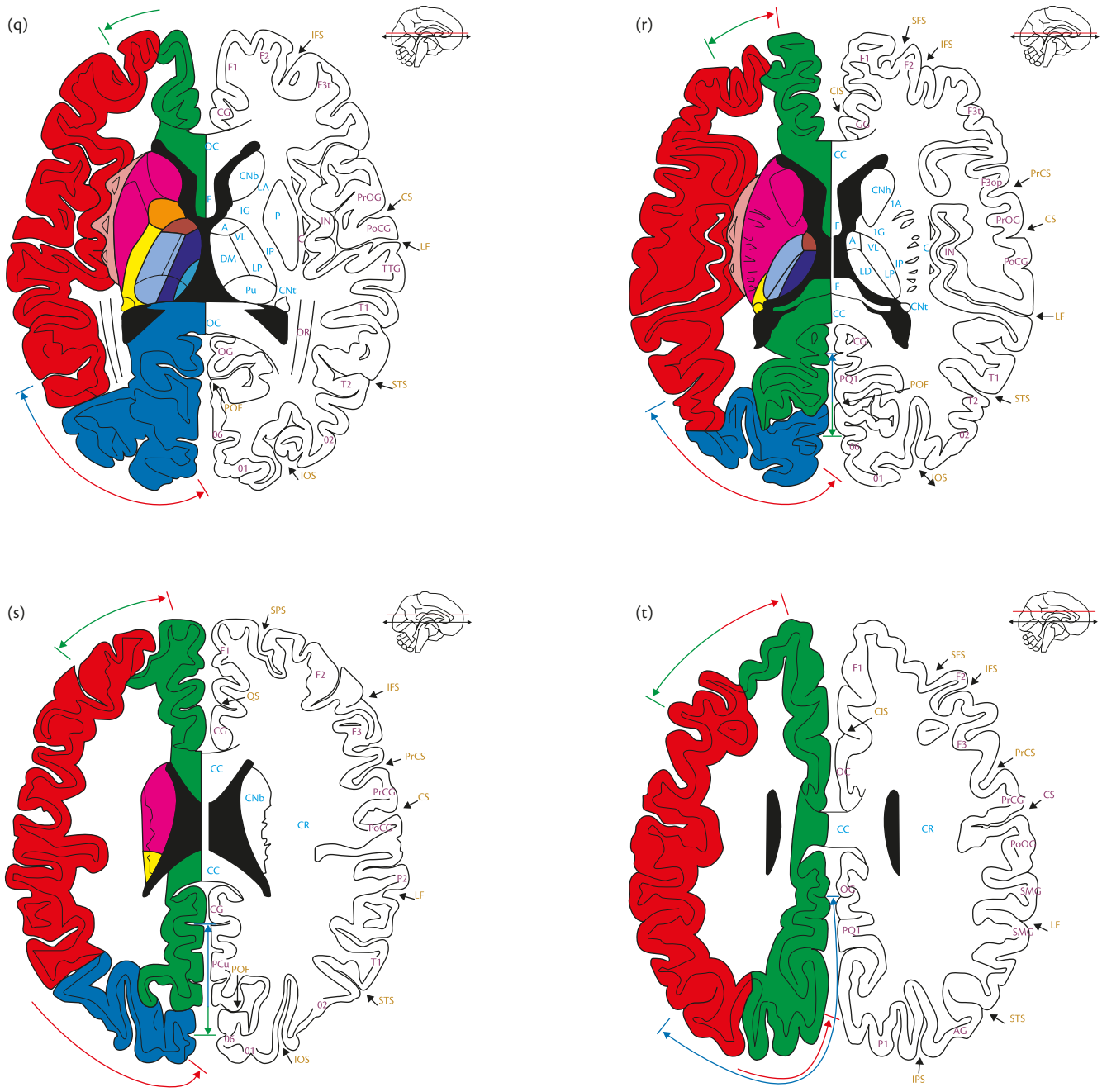

Fig. 46.5 Continued

Medial hemisphere AVMs

Anteriorly these AVMs are fed by branches arising from the callosomarginal anteriorly superiorly and the pericallosal arteries inferiorly adjacent to the corpus callosum and the frontopolar artery at the frontal pole. Cortical disruption or ischaemia in this region may result in a transient superior mesenteric artery (SMA) syndrome. The distal pericallosal (A3 and A4) arteries supply to the paracentral lobule should be maintained. AVMs on the medial parietal lobe and those adjacent to the splenium are fed by distal ACA or PCA as one of the terminal branches of the PCA is located in the medial parieto-occipital sulcus. The other terminal branch of the PCA is located in the calcarine fissure and medial occipital AVMs adjacent to the visual cortex in the cuneus and lingual gyrus are fed by its branches. These AVMs drain to the superior sagittal sinus and those involving the ventricle, splenial, or medial occipital lobe may drain to the vein of Galen via ependymal, splenial, and calcarine tributaries. Access to these feeders are through interhemispheric approaches.

Deep supratentorial AVMs

Subcortical deep extensions of some AVMs recruit deep perforator feeders such as the lenticulostriate from the MCA, A1 perforators, and Heubner's artery from the ACA. Access to these and

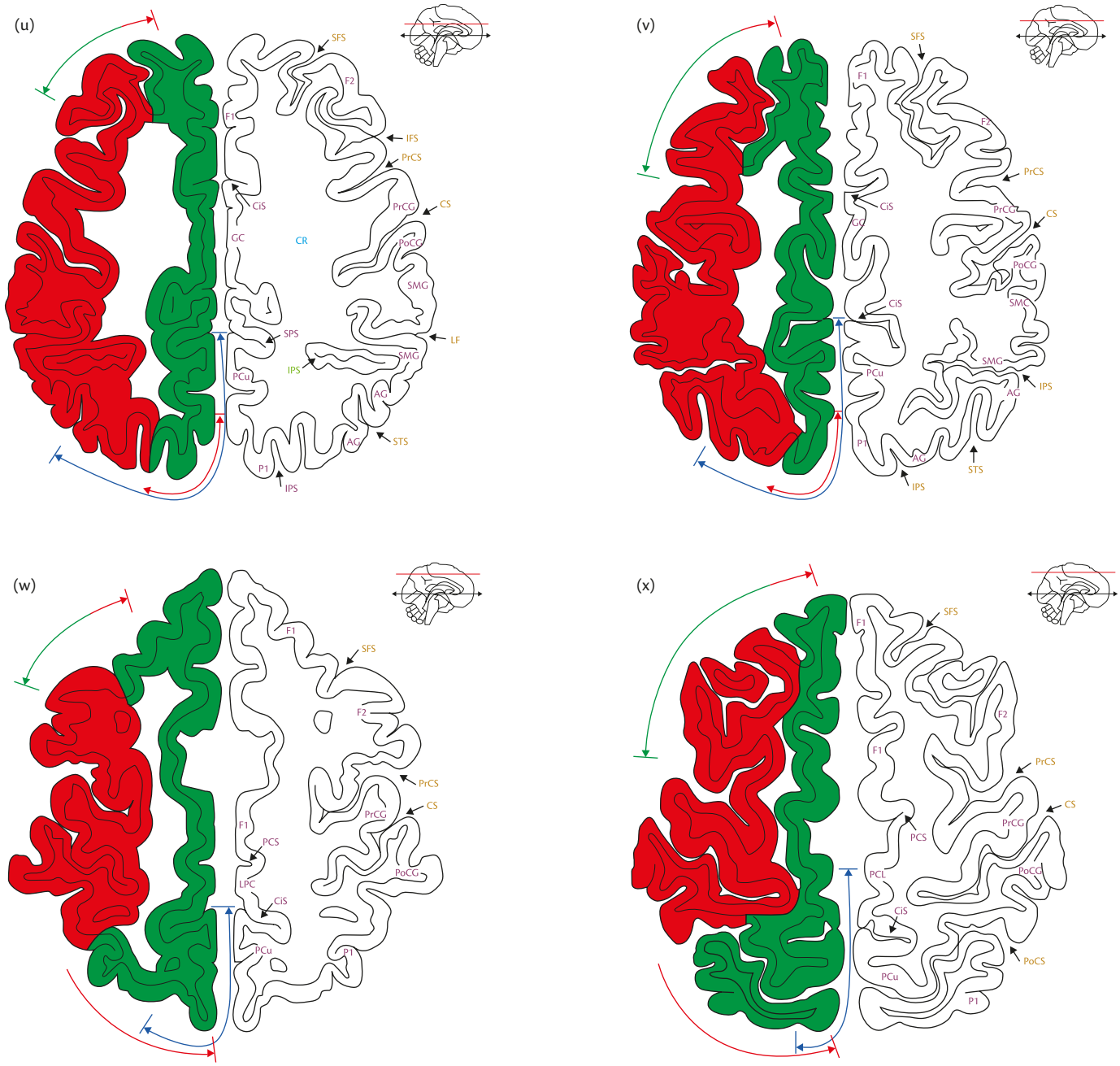

Fig. 46.5 Continued

deep dissection of the nidus can potentially disrupt the white matter tracts such as the superior longitudinal, arcuate, uncinate fasiculi, IFOF, corona radiata, and optic radiation with a resulting neurological deficit, which in contrast with cortical lesions which demonstrate plasticity, are likely to be permanent. Deep perforators also indicate that the nidus involves the basal ganglia. Frequently AVMs extend in a cone-like fashion towards the ventricles and are expected to have deep ependymal feeders even though these are not identified on the preoperative angiogram. Extensive intraventricular extension can be anticipated by demonstrating supply from choroidal arteries on angiography. Those in the temporal horn are fed by distal anterior choroidal artery or the lateral posterior choroidal artery. This extends to the choroid plexus protruding from the foramen of Monro and involved in supplying AVMs in these regions. Thalamic involvement by the AVM can be predicted by identifying the 'flame-like' appearance of the perforators adjacent to the superior basilar artery and proximal P1/P2 on angiography. Anteriorly these perforators are thalamoperforators from P1 and more posteriorly are thalamogeniculate branches from P2. Venous drainage is to the deep system.

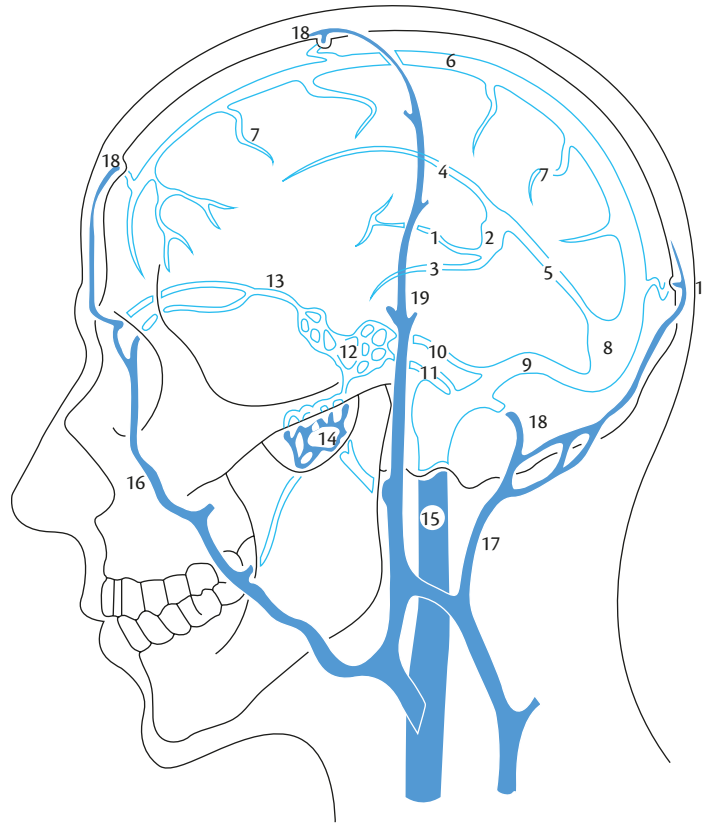

1. Internal cerebral vein
2. Great cerebral vein
3. Basal vein
4. Inferior sagittal sinus
5. Straight sinus
6. Superior sagittal sinus
7. Cortical vein
8. Torcular herophilii
9. Lateral sinus
10. Superior petrosal sinus
11. Inferior petrosal sinus
12. Cavernous sinus
13. Ophthalmic vein
14. Pterygoid plexus
15. Internal jugular vein
16. Facial vein
17. Occipital vein
18. Emissary vein

Fig. 46.6 Dural venous sinuses, major deep cerebral veins, and their connection with the extracranial venous system.

Reproduced from Bo Norrving, *Oxford Textbook of Stroke and Cerebrovascular Disease*, Oxford University Press, Oxford, UK, Copyright © 2014. By permission of Oxford University Press.

Cerebellar AVMs

Depending on their location cerebellar AVMs are supplied by cortical branches of one or more of the three branches namely SCA, AICA, and PICA. Those on the suboccipital surface and paravermian location are fed by PICA branches beyond the 'tonsillar' loop and with the fourth ventricular extension, also its choroidal branches. Proximal control at the tonsil or through a telovelar approach is straightforward. Frequently flow-related aneurysms are seen on the feeding branches proximal to the nidus. Superiorly on the suboccipital and tentorial surfaces the AVMs are fed by distal SCA branches which in fact are the predominant supply to the cerebellum. Proximal control of these is through a supracerebellar infratentorial approach and the more proximal segment can be identified at the tentorial hiatus and adjacent to the fourth nerve. Superiorly and near the midline a deep branch through the cerebellum supply the dentate nucleus which lies in a deep paravermian location. AVMs located at the petrosal cerebellar surface near the CPA may have feeders from the cortical branches of the AICA and are in relationship to the VII—XII cranial nerves. It is important to recognize that not only the premeatal but also the postmeatal segment of the AICA gives perforating blood supply to the pons and brainstem and hence only the feeders and not the main artery should be obliterated. The apex of the loop is related to the internal auditory meatus. The venous drainage is to the transverse, straight (which contrary to supratentorially located AVMs this does not constitute deep drainage for posterior fossa AVMs in the Spetzler-Martin classification) and sigmoid sinuses. Near the deep surface, venous drainage is to the Galenic deep system.

Vascular physiology

Autoregulation and the control of cerebral perfusion

Despite its small relative size, the brain requires around 14% of cardiac output and is critically dependent on adequate cerebral blood

flow. Impairment can trigger unconsciousness within one minute and irreversible neuronal tissue damage can occur if ischaemia is prolonged over four minutes (although surgically much longer vascular occlusion times may be tolerated due to collateral pathways). Autoregulation of cerebral blood flow is the ability of the brain to regulate its blood flow despite changes in systemic blood pressure (Cross and Plunkett, 2008). Cerebral perfusion pressure (CPP) is classically defined as:

CPP = MAP—(ICP + CVP)
MAP mean arterial pressure
ICP intracranial pressure
CVP central venous pressure

Early studies with baboons demonstrated that ICP represented the effective cerebral venous outflow pressure and importantly the sagittal sinus pressure did not change within a range of ICP, reflecting the rigid nature of dural sinuses compared to parenchymal veins (Johnston and Rowan, 1974). CVP is normally low, approximately 2–5 mmHg. Clinically, CVP is therefore often omitted from the equation, giving:

$$CPP = MAP - ICP.$$

As per the Monro-Kellie hypothesis, when the intracranial volume rises, compensatory mechanisms can initially maintain ICP at normal or near normal levels (ICP <20 mmHg) (**Fig. 46.7**). The volume of cerebrospinal fluid (CSF) is reduced through movement of CSF into the spinal canal and increased absorption into the venous circulation. In addition, there may be partial compression of venous sinuses. At a critical level, compensatory mechanisms are overwhelmed and a small change in intracranial volume results in a significant rise in ICP. Pathophysiologically, this rise in ICP is associated with a reduction in CPP and cerebral blood flow.

Cerebral blood flow

Cerebral blood flow (CBF) is approximately 700 ml per minute (50 ml per 100 g per minute). Grey matter has considerably greater requirements than white matter, receiving 70 ml per 100 g per min compared to 20 ml per 100 g per min. Overall, the level of CBF is critical to prevent ischaemia. Electroencephalographic changes are noted when blood flow falls below 20 ml per 100 g per minute and irreversible cerebral infarction below 10 ml per 100 g per minute (Yentis et al., 2013). An autoregulatory range exists within which a relatively constant CBF is maintained over a range of mean arterial pressure, between approximately 50 and 150 mmHg (Phillips and Whisnant, 1992) (**Fig. 46.8A**). The autoregulatory range is increased in hypertensive individuals. At low or high mean arterial pressures outside this range, CBF increases passively with rising arterial pressure.

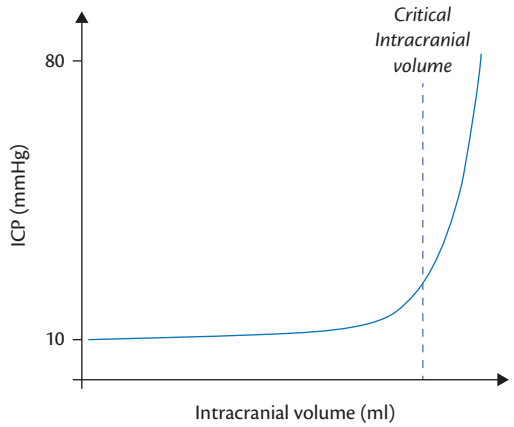

Fig. 46.7 Relationship between intracranial volume and pressure.
Reproduced from Catherine Spoors and Kevin Kiff, *Training in Anaesthesia*, Oxford University Press, Oxford, UK, Copyright © 2010. By permission of Oxford University Press.

Mechanisms of cerebral blood flow regulation

The mechanisms responsible for the autoregulation of CBF are not fully understood. Certain methodologies exist for the measurement and study of CBF. To measure total blood flow, the Fick principle can be applied following the inhalation of an inert gas (e.g. N_20), while the detection of radioactive 133-xenon, positron emission tomography, functional magnetic resonance imaging, and Doppler probes have all been utilized to measure regional blood flow. Three principle theories have been proposed to describe the mechanism of autoregulation; myogenic, metabolic, and neurogenic regulation. The calibre of vessels that mediate autoregulation may span the range of 40–300 μm but typically less than 100 μm.

Myogenic regulation

The maintenance of a relatively constant CBF across a range of CPP is thought to involve the myogenic response of cerebral smooth muscle in vessel walls, particularly at higher pressures within the autoregulatory part of the curve. Classical studies have shown that isolated vessels constrict in response to raised pressure and dilate to reduced pressure.

Neurogenic control of CBF—extrinsic and intrinsic control

The cerebral vasculature receives sympathetic innervation from the superior cervical ganglion. Extraparenchymal vessels are thought to be regulated by the autonomic nervous system. However, it is not thought to play a major role in the physiological regulation of intraparenchymal vessel tone, largely due to evidence from denervation studies. However, it may play a role when blood pressure rises above the normal limits of autoregulation through resetting or modulation of the normal autoregulatory curve. This represents an important physiological mechanism that prevents significant rises in CBF and any associated breakdown in the blood-brain barrier that would otherwise be expected from acute surges in blood pressure. The cerebrovascular system also receives parasympathetic supply, but it is thought to have little role under normal physiological conditions. Some evidence from chronic denervation studies suggests a potential role in maintaining CBF during periods of low perfusion pressure and thereby reducing ischaemia and infarction. Intrinsic or central neural regulatory pathways have also been investigated to establish their autoregulatory role, with neuronal nitric oxide implicated and so-called neurovascular units, comprised of neurons separated from microvessels by perivascular ganglia and basement membrane (Talman and Nitschke Dragon, 2007). Their exact contribution remains unclear.

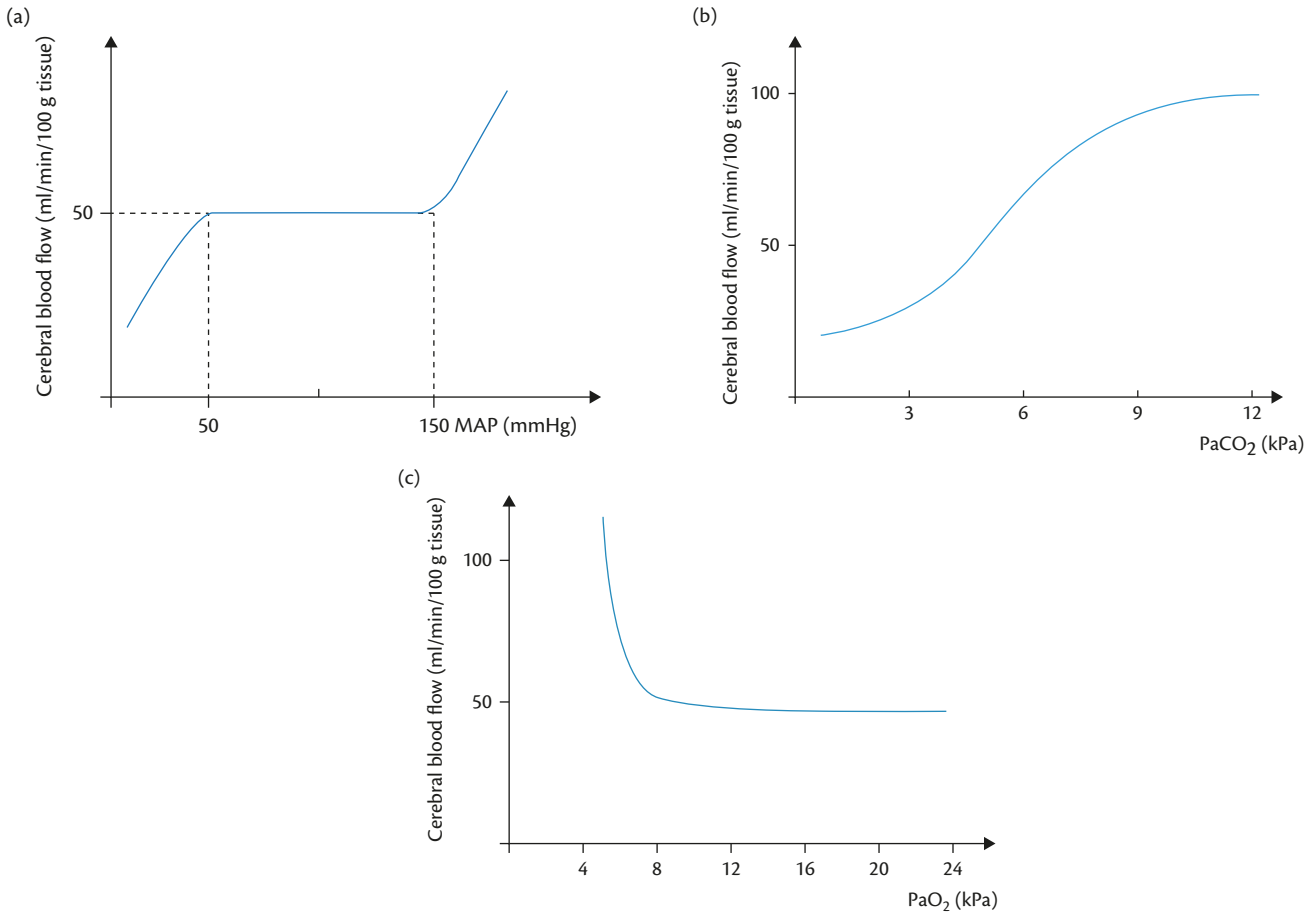

Fig. 46.8 (A) Relationship between CBF and MAP. (B) Relationship between CBF and PCO_2. (C) Relationship between CBF and PO_2.
Reproduced from Catherine Spoors and Kevin Kiff, *Training in Anaesthesia*, Oxford University Press, Oxford, UK, Copyright © 2010. By permission of Oxford University Press.

Metabolic regulation and the control of blood vessel diameter

Metabolic regulation is thought to be most influential at low perfusion pressures. When CBF falls to levels outside the autoregulatory range, there is a compensatory rise in oxygen extraction from blood. Regional increases in neuronal activity are associated with corresponding regional increases in cerebral metabolic rate. Mechanisms are likely to involve hypoxia, intrinsic neural pathways, and associated release of metabolic factors.

Arterial PCO_2 and PO_2 can affect CBF (Figs. 46.8B and 46.8C), through changes in cerebral vessel diameter. CO_2 has a marked and reversible effect on CBF. Hypercapnia causes significant dilation of cerebral arteries and arterioles, with a resulting increase in CBF, while hypocapnia causes the reverse. Following hypocapnia, detectable changes in pial artery diameter and CBF occur after 30 seconds. Due to the curvilinear relationship, outside the physiological range of PCO_2, reductions cause a marked reduction in CBF. After a period of 24–48 h, due to physiological buffering, hypocapnic reduction in CBF may not be maintained. At values beyond 10 kPa, near maximal vasodilation is achieved therefore increases in PCO_2 have a modest effect on CBF. The mechanism of hypercapnic vasodilation is not fully understood but is thought to involve the direct effect of H^+ on cerebral vascular muscle (Kontos et al., 1977). Finally, hypocapnia is known to improve cerebral pressure regulation while hypercapnia impairs it.

Hypoxia is also a profound vasodilator to ensure adequate oxygenation of brain tissue. At levels above 8k Pa, changes in PO_2 have a very minimal effect on CBF, with CBF near constant. Below 6.7 kPa, CBF increases rapidly with increasing hypoxia. Again, the mechanism of hypoxic related cerebral vasodilation is not fully understood. Mechanisms are thought to include reduction in adenosine triphosphate (ATP) levels opening potassium channels on cerebral smooth muscle and local changes in nitric oxide and adenosine production.

Controversy: Mannitol and cerebral blood flow

The blood haemocrit level and therefore viscosity of blood can affect CBF. Increases in CBF due to reduced haematocrit and viscosity may be counterbalanced by reduced and suboptimal oxygen delivery. At haematocrit levels below 30%, increases in CBF can be attributed to low arterial PO_2 and may result in cerebral ischaemia. Mannitol is known to reduce ICP, but its mechanism of action is disputed. Traditionally mannitol has been suggested to reduce ICP through a direct osmotic action and subsequent reductions in cerebral oedema (Nath and Galbraith, 1986; Donato et al., 1994). However, evidence including its speed of action, is more consistent

with an autoregulatory cerebral vasoconstriction and reduction in intravascular volume in response to a rapid increase in peripheral intravascular volume and hence cerebral perfusion (Rosner and Coley, 1987). It is also postulated the perfusion and autoregulatory cerebral vasoconstriction occurs due to a reduction in blood viscosity (due to changing red blood cell rheology) (Burke et al., 1981; Muizelaar et al., 1983). However, more recent studies in head-injured subjects have not demonstrated a fall in cerebral blood flow following mannitol administration (Diringer et al., 2012) and others have suggested it has a direct effect not on pressure but as a neuroprotectant. For example, it is thought to act as a free radicle scavenger. Studies have also suggested that prolonged usage may be detrimental through subsequent increases in ICP and recent studies have focused on hypertonic saline which may similarly lower ICP but without such rebound rises (Castillo et al., 2009; Rickard et al., 2014). In summary, although mannitol acutely reduces cerebral volume and ICP, its exact mechanism of action remains unclear (Sakowitz et al., 2007).

FURTHER READING

Geibprasert, S., Pongpech, S., Armstrong, D., & Krings, T. (2009). Dangerous extracranial-intracranial anastomoses and supply to the cranial nerves: vessels the neurointerventionalist needs to know. *AJNR Am J Neuroradiol*, **30**, 1459–68.

MacDonald, R.L. (2009). *Neurosurgical Operative Atlas. Vascular Neurosurgery*, 2nd edition. New York, NY: Thieme.

Rhoton, A.L., Jr. (2002). The supratentorial arteries. *Neurosurgery*, **51**, S53–120.

Rickard, A.C., Smith, J.E., Newell, P., Bailey, A., Kehoe, A., & Mann, C. (2014). Salt or sugar for your injured brain? A meta-analysis of randomised controlled trials of mannitol versus hypertonic sodium solutions to manage raised intracranial pressure in traumatic brain injury. *Emerg Med J*, **31**, 679–83.

Yasargil, M.G. (1987). *Microneurosurgery.* Stuttgart, Germany/ New York, NY: Georg Thieme Verlag, Thieme Medical Publishers.

REFERENCES

Bouthillier, A., Van Loveren, H.R., & Keller, J.T. (1996). Segments of the internal carotid artery: a new classification. *Neurosurgery*, **38**, 425–32; discussion 432–3.

Burke, A.M., Quest, D.O., Chien, S., & Cerri, C. (1981). The effects of mannitol on blood viscosity. *J Neurosurg*, **55**, 550–3.

Butler, P., Mitchell, A.W.M., & Ellis, H. (2012). *Applied Radiological Anatomy.* Cambridge, UK/New York, NY: Cambridge University Press.

Castillo, L.B., Bugedo, G.A., & Paranhos, J.L. (2009). Mannitol or hypertonic saline for intracranial hypertension? A point of view. *Crit Care Resusc*, **11**, 151–4.

Cross, M.E. & Plunkett, E.V.E. (2008). *Physics, Pharmacology and Physiology for Anaesthetists: Key Concepts for the FRCA*. Cambridge, UK/New York, NY: Cambridge University Press.

Diringer, M.N., Scalfani, M.T., Zazulia, A.R., Videen, T.O., Dhar, R., & Powers, W.J. (2012). Effect of mannitol on cerebral blood volume in patients with head injury. *Neurosurgery*, **70**, 1215–18; discussion 1219.

Donato, T., Shapira, Y., Artru, A., & Powers, K. (1994). Effect of mannitol on cerebrospinal fluid dynamics and brain tissue edema. *Anesth Analg*, **78**, 58–66.

Geibprasert, S., Pongpech, S., Armstrong, D., & Krings, T. (2009). Dangerous extracranial-intracranial anastomoses and supply to the cranial nerves: vessels the neurointerventionalist needs to know. *AJNR Am J Neuroradiol*, **30**, 1459–68.

Gibo, H., Lenkey, C., & Rhoton, A.L., Jr. (1981). Microsurgical anatomy of the supraclinoid portion of the internal carotid artery. *J Neurosurg*, **55**, 560–74.

Harnsberger, H.R. & MacDonald, A.J. (2006). *Diagnostic and Surgical Imaging Anatomy: Brain, Head & Neck, Spine.* Salt Lake City, UT: Amirsys.

Johnston, I. H. & Rowan, J.O. (1974). Raised intracranial pressure and cerebral blood flow. 4. Intracranial pressure gradients and regional cerebral blood flow. *J Neurol Neurosurg Psychiatry*, **37**, 585–92.

Kontos, H.A., Raper, A.J., & Patterson, J.L. (1977). Analysis of vasoactivity of local pH, PCO2 and bicarbonate on pial vessels. *Stroke*, **8**, 358–60.

Lister, J.R., Rhoton, A.L., Jr., Matsushima, T., & Peace, D.A. (1982). Microsurgical anatomy of the posterior inferior cerebellar artery. *Neurosurgery*, **10**, 170–99.

MacDonald, R.L. (2009). *Neurosurgical Operative Atlas. Vascular Neurosurgery*, 2nd edition. New York, NY: Thieme.

Muizelaar, J.P., Wei, E.P., Kontos, H.A., & Becker, D.P. (1983). Mannitol causes compensatory cerebral vasoconstriction and vasodilation in response to blood viscosity changes. *J Neurosurg*, **59**, 822–8.

Nath, F. & Galbraith, S. (1986). The effect of mannitol on cerebral white matter water content. *J Neurosurg*, **65**, 41–3.

Phillips, S.J. & Whisnant, J.P. (1992). Hypertension and the brain. The National High Blood Pressure Education Program. *Arch Intern Med*, **152**, 938–45.

Rhoton, A.L., Jr. (1994). The three neurovascular complexes in the posterior fossa and vascular compression syndromes (honored guest lecture). *Clin Neurosurg*, **41**, 112–49.

Rhoton, A.L., Jr. (2002). The supratentorial arteries. *Neurosurgery*, **51**, S53–120.

Rickard, A.C., Smith, J.E., Newell, P., Bailey, A., Kehoe, A., & Mann, C. (2014). Salt or sugar for your injured brain? A meta-analysis of randomised controlled trials of mannitol versus hypertonic sodium solutions to manage raised intracranial pressure in traumatic brain injury. *Emerg Med J*, **31**, 679–83.

Rosner, M.J. & Coley, I. (1987). Cerebral perfusion pressure: a hemodynamic mechanism of mannitol and the postmannitol hemogram. *Neurosurgery*, **21**, 147–56.

Sakowitz, O.W., Stover, J.F., Sarrafzadeh, A.S., Unterberg, A.W., & Kiening, K.L. (2007). Effects of mannitol bolus administration on intracranial pressure, cerebral extracellular metabolites, and tissue oxygenation in severely head-injured patients. *J Trauma*, **62**, 292–8.

Talman, W.T. & Nitschke Dragon, D. (2007). Neuronal nitric oxide mediates cerebral vasodilatation during acute hypertension. *Brain Res*, **1139**, 126–32.

Van Der Zwan, A., Hillen, B., Tulleken, C.A., Dujovny, M., & Dragovic, L. (1992). Variability of the territories of the major cerebral arteries. *J Neurosurg*, **77**, 927–40.

Van Laar, P.J., Hendrikse, J., Golay, X., Lu, H., Van Osch, M.J., & Van Der Grond, J. (2006). *In vivo* flow territory mapping of major brain feeding arteries. *Neuroimage*, **29**, 136–44.

Yasargil, M.G. (1987). *Microneurosurgery.* Stuttgart, Germany/New York, NY: Georg Thieme Verlag, Thieme Medical Publishers.
Yentis, S.M., Hirsch, N., Ip, J.K., & Smith, G.B. (2013). *Anaesthesia and Intensive Care A-Z: An Encyclopaedia of Principles and Practice.* Edinburgh, UK/New York, NY: Churchill Livingston/Elsevier.

RELATED LINK TO EBRAIN

Normal Vascular Radiological Neuroanatomy. https://learning.ebrain.net/course/view.php?id=700

47

The pathophysiology of aneurysms

Federico Cagnazzo, Giuseppe Lanzino, and Neal F. Kassell

Introduction

Cerebral aneurysms are pathological acquired dilatations of the arterial wall (Sforza et al., 2009). Approximately 80–90% of intracranial aneurysms (IAs) are saccular or berry aneurysms (Wiebers et al., 2004) and in this chapter, unless otherwise specified, we will refer to this specific aneurysm type. Intracranial aneurysms are found in 1–2% of people undergoing imaging studies while autopsy studies indicate a prevalence in the adult population between 1% and 5%. Intracranial aneurysms are responsible for about 80–85% of all cases of non-traumatic subarachnoid haemorrhage (SAH). The commonest age of presentation of aneurysms is in the fifth decade of life, with a slight female preponderance of 3:2.

Theories regarding aneurysm formation and development

The pathophysiology of IAs is controversial, most likely multifactorial and related to interactions between haemodynamic forces, biology of the vessel wall, genetic predisposition, and external modifiable factors (Sforza et al., 2009).

Vessel wall biology

Intracranial aneurysms are often located at bifurcation points where there are more collagen than elastin fibres, and where the muscular layer is less developed. Smooth muscle–cell (SMC) apoptosis and elastin/collagen fibre–reconstitution mechanisms which occur as part of vascular wall remodelling may be implicated in the weakening of the vessel wall, with subsequent aneurysm formation (Hara et al., 1998). Kondo et al. (Kondo et al., 1998) examined the role of medial layer smooth muscle cell (SMCs) apoptosis during development and growth of IAs. In this experimental study, IAs were induced through ligation of the left common carotid artery combined with renal hypertension. Progressive apoptotic changes in the SMCs appeared in the medial layer as the experimental aneurysms formed. In the late stages, most medial SMCs had disappeared and the aneurysm wall consisted mostly of connective tissue. Electron microscopic studies confirmed progressive SMCs apoptotic changes such as chromatin condensation and fragmentation of the cytoplasm and nucleus. Moreover, the aneurysmal dome showed late characteristics of apoptosis (advanced nuclear and cytoplasmic condensation, and formation of apoptotic bodies). This study supports the theory that aneurysm formation can result from complex remodelling of the wall which induces apoptosis of the media layer.

Vascular extracellular matrix enzymes such as gelatinase, elastase (Chyatte and Lewis, 1997), or matrix metalloproteinase (Bruno et al., 1998) may also be implicated in this process.

Genetic factors

Genetic factors are implicated in the genesis of intracranial aneurysms. Intracranial aneurysms are more prevalent in siblings of patients with a history of IAs in another first-degree relative. Many studies have focused on the isolation of genetic loci correlated with IAs and several potential candidate genes have been identified (Table 47.1).

Haemodynamic factors

The role of haemodynamic factors in the genesis of IAs is suggested by the observation of an increased risk of aneurysm formation in situations of increased haemodynamic stress such as an 'unbalanced' anterior communicating artery (Acom) complex (dominant A1 segment of the anterior cerebral artery on one side with hypoplasia of the contralateral one), in patients with low-pressure shunts such as high-flow arteriovenous malformations, and along the collateral pathway after spontaneous or iatrogenic carotid occlusion (Matsuda et al., 1983; Kayembe et al., 1984; Redekop et al., 1998).

More recently, sophisticated computer-generated flow modelling has suggested a potential role of wall shear stress and other local haemodynamic factors in the genesis, growth, and possibly rupture of IAs. However, most of these models are flawed by the fact that such calculations are based on comparisons between ruptured and unruptured IAs which are two fundamentally different pathological processes.

Environmental (modifiable) factors

Several longitudinal and case-control epidemiological studies have been conducted to identify a possible correlation between various modifiable (external) factors and development or rupture of IAs. Convincing evidence exists only for cigarette smoking and hypertension. The HUNT study, prospectively conducted in Norway (Koskinen and Blomstedt, 2006) between 1983 and 1986, showed that current smokers (hazard ratio (HR) 6.1) and, to less extent former smokers (HR 2.7), have a higher incidence of aneurysmal SAH than

Table 47.1 Most common heritable disorders associated with intracranial aneurysms

Disorder	Inheritance pattern	Gene	Gene product	Prevalence
ADPKD	AD	PKD1	Polycystin 1	>1/1000
EDS	AD	COL3A1	Collagen type III	1–9/100 000
MfS	AD	FBN1	Fibrillin 1	1–5/10 000
NF 1	AD	NF1	Neurofibromin	1–5/10 000
PXE	AD and AR	ABCC6	ATP binding cassette	1–9/100 000

ADPKD, autosomal dominant polycystic kidney; disease; EDS, Ehlers-Danlos syndrome; Marfan's syndrome; NF1, neurofibromatosis type 1; PXE, pseudoxanthoma elasticum.

those that have never smoked. The reason for this association is not completely understood. It is possible that smoking triggers an inflammatory response through various mechanisms resulting in aneurysm formation and/or rupture (Chalouhi et al., 2012).

Systolic blood pressure is another modifiable risk factor associated with IAs. In the HUNT study, the risk of aneurysmal SAH was significantly higher in people with systolic blood pressure between 130 and 139 mmHg than in the reference population (<130 mmHg systolic). Furthermore, a HR of 3.3 was present in people with systolic blood pressure more than 170 mmHg (Koskinen and Blomstedt, 2006). It is interesting how hypertension and smoking combined have an additive interaction: in a prospective study, the hazard ratio for aSAH was 13.3 times higher for smokers with hypertension than subjects without any of these two factors (Lindekleiv et al., 2012). The association between other modifiable factors (including alcohol consumption, hormonal factors, and so on) with aneurysm formation and rupture is more controversial.

Location

Saccular aneurysms arise typically at branching points of arteries forming the circle of Willis. Rhoton introduced (Rhoton et al., 1979) three basic rules about the location of saccular aneurysms: (1) aneurysms arise at branching sites of the parent artery (e.g. PComA, middle cerebral artery (MCA) bifurcation, basilar bifurcation); (2) aneurysms arise from a turn or curve of the artery; and (3) the dome lays in the direction of the maximal haemodynamic flow. Non-branching aneurysms (located at non-branching sites of the artery) are less common and often are not berry aneurysms.

About 90% of saccular aneurysms are located in the anterior cerebral circulation and their relative distribution in relation to various specific locations varies across different populations and is different between ruptured and unruptured aneurysms. Among ruptured aneurysms, anterior communicating complex aneurysms are the most frequent (30–35%) followed by internal carotid aneurysms (including PComA, 30%) and MCA aneurysms (20%). In the posterior circulation, the basilar bifurcation is the most common site.

Size and morphology

Size of an aneurysm is very important because it correlates with the risk of aneurysm rupture and with the risk of treatment. Conventionally IA are classified in three groups based on the maximum diameter of the dome: Small (up to 10 mm in diameter); Large (between 11 and 25 mm), and Giant (larger than 25 mm).

A saccular aneurysm is composed of a neck (the portion of the aneurysm connected to the parent artery) and a fundus or sac. With the development of endovascular techniques, determination of the size of the neck has become especially important. Aneurysms with a neck larger than 4 mm are considered wide-neck aneurysms. The neck/dome ratio is another important morphological feature affecting endovascular treatment.

With computational fluid dynamic studies, several other morphological aspects of IAs have been analysed particularly as they relate to the risk of rupture. These morphological features include the aspect ratio (aneurysm cranio-caudal dimension divided by transverse diameter) and the aneurysm angle (Fig. 47.1).

The presence of irregularities and secondary outpouching (also known as blebs, 'daughter sacs', or lobulations) is not uncommon. In ruptured aneurysms, these daughter sacs often identify the point of rupture (Fig. 47.2). These daughter sacs are commonly located on the dome opposite to the point of maximal inflow. In unruptured aneurysms, such irregularities may be associated with an increased risk of rupture (Cebral et al., 2010) and their presence or absence is one of the important factors in deciding whether or not to treat.

Familial IA and associated conditions

Familial aneurysms

The risk of harbouring an IA is increased in relatives of patients with IAs with or without history of aneurysmal SAH (Thompson et al., 2015). The risk is increased in first-degree relatives, in the presence of hypertension and/or smoking, and in people with two or more relatives affected the risk is increased 15-fold. Screening of family members of patients with aneurysmal SAH without additional affected relatives is controversial. Screening of family members older than 30 is recommended if two or more relatives are affected in a given family (Thompson et al., 2015). Before screening, counselling

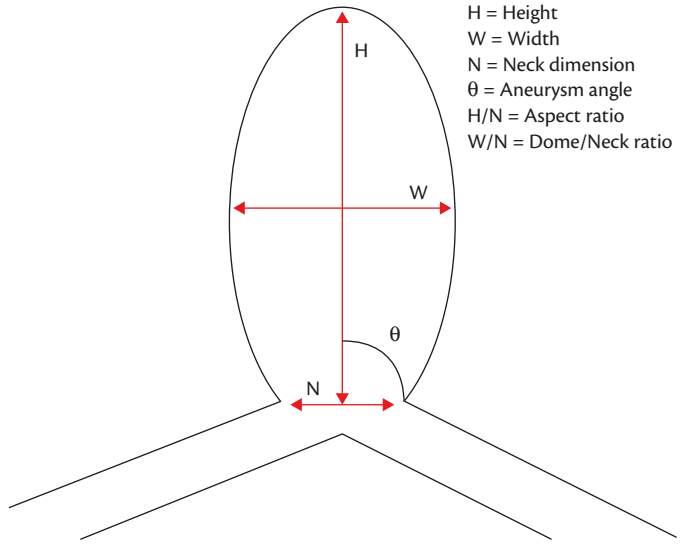

Fig. 47.1 Schematic illustration of a cerebral aneurysm and morphological parameters.

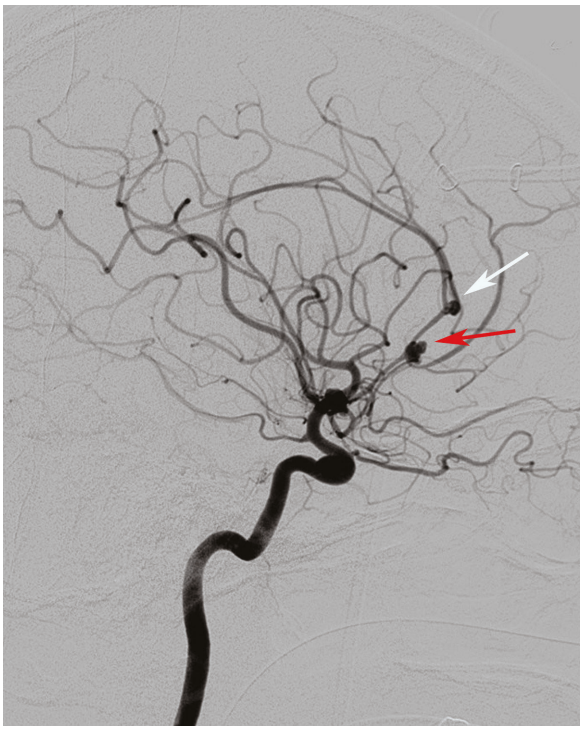

Fig. 47.2 Patient with acute subarachnoid haemorrhage (SAH). Arterial phase lateral angiogram of the left internal carotid artery (ICA) shows two distal anterior cerebral artery aneurysms (red and white arrows). The daughter sac (red arrow) identifies the point of rupture.

regarding the implications of a diagnosis of IAs is indicated since not all unruptured aneurysms warrant treatment.

There is a large spectrum of hereditable and non-hereditable pathological conditions which have been associated with IAs (Table 47.1). Some of these conditions include:

- *Autosomal dominant polycystic kidney disease (ADPKD)*: monogenetic pathology present with renal and visceral cysts associated with a spectrum of vascular abnormalities including cerebral aneurysms (often multiple). Cerebral aneurysms are found in 25% of patients with this condition and screening is recommended in patients with polycystic kidney disorder and a family history of IAs. ADPKD increases the risk of IA by 10–20-fold depending on whether there is also a family history of IAs. In ADPKD coexistent hypertension may further facilitate the formation of IAs. A recent study showed that ADPKD patients with IAs had higher blood pressure parameters (especially those older than 45 years of age), compared with ADPKD patients without IAs. Patients with ADPKD and hypertension should therefore be screened for IAs (Niemczyk et al., 2014).
- *Collagenopathies (such as Ehlers-Danlos, Type IV)*: anomalies in type III collagen with fragile skin and hypermobile joints, vascular fragility, disposition of supra-aortic vessel dissections, carotid–cavernous fistulas, and intracranial aneurysms. Although rare, it is important to recognize this condition since these patients are at very high risk of complications from intravascular diagnostic and therapeutic catheterizations because of their vascular fragility.
- *Marfan's syndrome*: abnormalities of the cardiovascular system caused by a disorder of fibrillin (the major glycoproteic component of elastic tissues). Patients are often tall with arachnodactyly and hypermobile joints, and present a higher risk of intra- and extracranial aneurysms development.
- *Aortic coarctation*: narrowing or constriction of the lumen of the aorta most commonly located distal to the origin of the left subclavian artery, near the insertion of the ligamentum arteriosum. IAs are found more often in patients with aortic coarctation (10.3% in an MR angiography series of 117 patients with aortic coarctation) (Curtis et al., 2012).
- *Fibromuscular dysplasia*: idiopathic, segmental, non-atherosclerotic, non-inflammatory vascular disease that mainly affects renal, extracranial carotid, and vertebral arteries. Intracranial fibromuscular dysplasia is rare. The most common clinical manifestations of fibromuscular dysplasia are related to steno-occlusive disease of major arteries. The incidence of IAs is higher in patients with fibromuscular dysplasia compared with the general population (7.3% in a meta-analysis performed by Cloft et al.) (Cloft et al., 1998).

Intracranial aneurysm progression and risk of rupture

Aneurysm growth is reflected in radiological (macroscopic) change and structural wall variations (microscopic) at the molecular levels. Aneurysms progression depends on a balance between wall repair and wall destruction which can be accelerated in patients who smoke or have arterial hypertension (Etminan and Rinkel, 2016). In a recent meta-analysis of nearly 13 000 IAs, Brinjikji et al. found that the overall proportion of growing aneurysms was 3% per aneurysm-year. The most important risk factors for growth included age older than 50 years, female sex, smoking history, and non-saccular shape. Aneurysm growth appears to be associated with a high risk of rupture (rupture rate of 3.1% per year compared with 0.1% per year for stable IAs) (Brinjikji et al., 2016). Similarly, Villablanca et al. found that the annual rupture rate was 12 times higher in growing compared with non-growing IAs (Villablanca et al., 2013), whereas Mehan et al. found that IAs growth was associated with an OR 55.9 for rupture on a multivariate analysis (Mehan et al., 2014).

Special situations

Traumatic aneurysms

Traumatic aneurysms (TAs) account for less than 1% of all intracranial aneurysms, although their true incidence is unknown and many may go undetected. Traumatic aneurysms are the second most common type of aneurysm encountered in children and adolescents (5–15% of all aneurysms in children) and are more prevalent in men. Traumatic aneurysms can be subdivided into 'true' TAs composed of all of the three layers of the vessel wall. Usually, they are caused by direct blunt trauma or by indirect forces and represent a 'bulge' in the vessel. 'False' TAs are the result of a direct interruption of the continuity of a vessel with formation of a perivascular haematoma. The wall of false TAs is composed only of fibrin tissue surrounding a partially organized haematoma.

All major intracranial arteries can be involved, and the vessels affected are a function of the mechanism of injury. The most common locations are the internal carotid artery (ICA) (46%), the MCA (25%), and the anterior cerebral artery (ACA) (22%).

The natural history of untreated TAs is not well understood. The risk of rupture can be high especially if progressive enlargement is documented on serial imaging studies. A low index of suspicion is important for adequate diagnosis and in high-risk cases, repeating another vascular imaging study after a negative first one may be indicated, since TAs may become visible a few days after the trauma. Iatrogenic pseudoaneurysms are a special subcategory of traumatic aneurysms and have been reported after a variety of surgical procedures including trans-sphenoidal surgery, craniotomy for tumours and vascular lesions, third ventriculostomy, and even after external ventricular catheter placement.

Dissecting aneurysms

Dissecting intracranial aneurysms are becoming increasingly recognized and are a potential, albeit less common, source of SAH. They originate from a dissection, which corresponds to a tear through the intima and internal elastic lamina in which blood accumulates between the different layers of the vessel wall. Often called pseudoaneurysms or false aneurysms (i.e. on histological section, they lack the normal three layers of vessel wall), these lesions contain the basic components of the normal vessel wall and therefore a more appropriate definition would be dissecting aneurysms.

Dissecting aneurysms are more commonly located in the extracranial vertebral or carotid artery but can also involve intracranial arteries. Intracranial dissecting aneurysms have been described to involve virtually any intracranial vessels although by far the most common localization is the intracranial vertebral artery where they characteristically involve the V4 segment of the vessel. Location in the anterior circulation is more typical in children and young adults. Unlike dissecting aneurysms involving the extracranial vessels which do not cause haemorrhage, intracranial dissecting aneurysms can be asymptomatic, present with ischaemic symptoms, headache, or frank haemorrhage (Fig. 47.3).

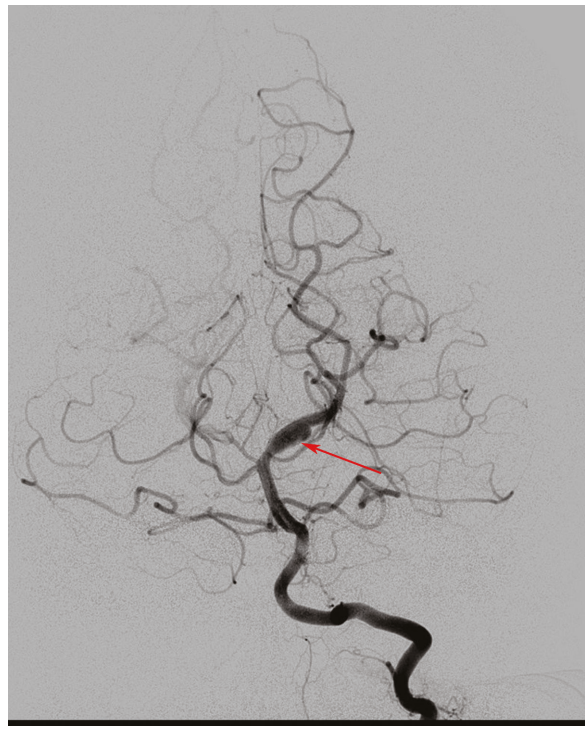

Fig. 47.3 Left vertebral artery angiography shows a dissecting aneurysm involving the proximal left posterior cerebral artery.

Blister-like aneurysms

Over time, the term *blister-like aneurysms* has been misused to indicate very small saccular aneurysms at branching sites of the circle of Willis. However, the term applies only to small dilatations, hemispherical-shaped and bulging, from non-branching sites of the dorsal wall of the supraclinoid ICA opposite to the origin of the PCom and the anterior choroidal arteries (Fig. 47.4). It is controversial whether all blister-like aneurysms represent focal dissections of the ICA or whether there are two distinct types: true blisters which represent a hole in the wall of the vessel and dissecting pseudoaneurysms of the ICA. They represent about 1% of all ruptured aneurysms and are characterized by a very fragile wall which makes treatment challenging. Typically diagnosed after a bleed, blister-like aneurysms can be difficult to identify on the first catheter angiogram and become more evident only at follow-up.

Fusiform aneurysms

The term fusiform aneurysm refers to a dilatation of the arterial wall which involves at least 270° of the vessel wall. Fusiform aneurysms are more commonly seen in the posterior circulation, in patients older than 60 years and have a male predominance. The pathophysiology is unknown, some may be related to prior dissections and it is therefore possible that the umbrella term of 'fusiform' aneurysms includes dilatations of the vessel wall of different aetiology. A particular type of fusiform aneurysm is the so-called dolicoectactic aneurysm characterized by the uniform pathological dilatation of an entire vessel segment often in association with tortuosity of the vessel itself (Fig. 47.5). Fusiform aneurysms can be incidental (in which case have often a fairly benign natural history), but they can also present with ischaemic symptoms, symptoms related to mass effect, and haemorrhage.

Mycotic aneurysms

The term 'mycotic aneurysms' implies the presence of infection and destruction of the walls of the vessels. The most common source of the infection is infective endocarditis. Mycotic aneurysms typically involve distal branches and can occur away from branch points. Antibiotic therapy targeting the offending agent is the main treatment of mycotic aneurysms and all patients should undergo appropriate antibiotic therapy based on the sensitivity of the microbial agent. In some clinical situations, antibiotics can be initiated empirically based on the original infection and standard guidelines. Monitoring of systemic infection should be made through serial blood cultures. Therapy must be continued for 4–6 weeks or until cultures become negative. Endovascular or surgical treatment can be considered in specific situations (Kannoth and Thomas, 2009).

Multiple aneurysms

Multiple IAs (MIAs) are reported with variable incidences in different studies: 13.9% in the UCAS Japan study (Morita et al., 2012), and 35% in the ISUIA study (Wiebers et al., 2003). In patients

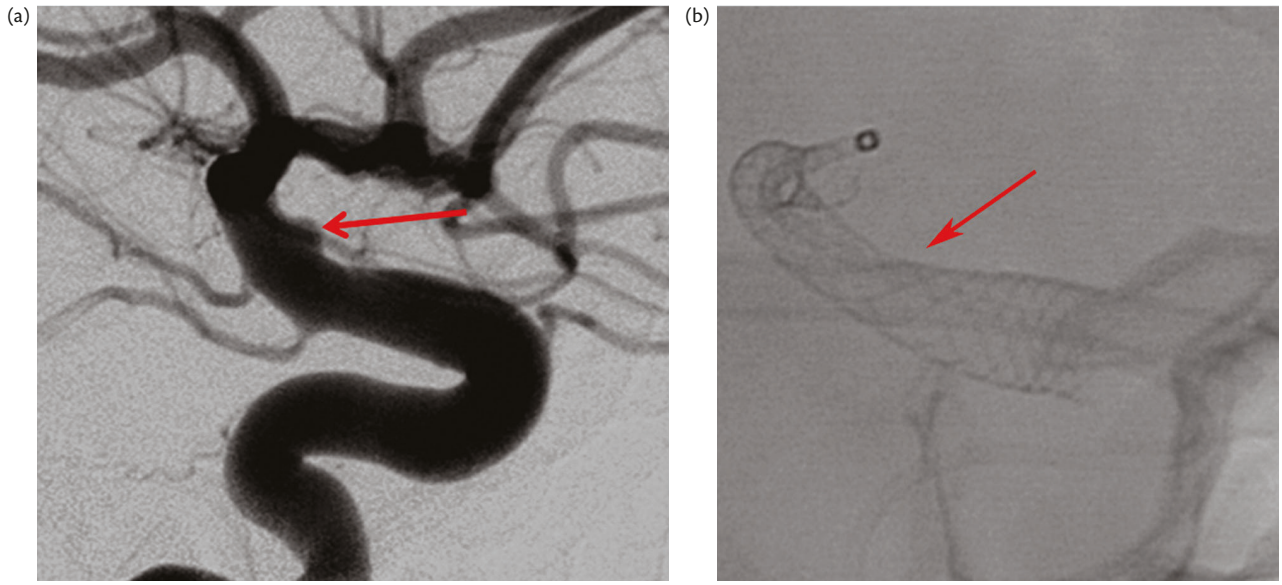

Fig. 47.4 This 30-year-old woman presented with diffuse SAH. Catheter angiography shows a blister-like aneurysm (a) involving the supraclinoid portion of the right ICA (arrow). (B) The blister-like aneurysm was treated with a flow diverter (arrow).

presenting with SAH, MIAs are found in 15–45% of patients. In patients with MIAs, each aneurysm is not at increased risk of rupture, but the cumulative risk of rupture is higher than in patients with only one aneurysm (Morita et al., 2012). The exact mechanism of MIAs' formation is not completely understood. Studies have suggested an association between MIAs and cigarette smoking, hypertension, age, and female sex (Juvela, 2000; Ellamushi et al., 2001; Lu et al., 2013). However, the correlation between MIAs and these risk factors remains controversial. Ostergaard and Hog (Ostergaard and Hog, 1985), in a series of 737 patients with IAs (in which 18% harboured MIAs), found that hypertension and female sex were independent risk factors for MIAs, whereas age had no influence. Qureshi et al. (Qureshi et al., 1998) reported that cigarette smoking and female sex, but not hypertension, correlated with MIAs in a series of 419 patients, of which 30% had multiple IAs. Recently, Lu et al. (Lu et al., 2013) reported the association between risk of rupture from MIAs and age, size, and location. In this study, middle age (45–65 years), ACom site, and increasing aneurysm size correlated with a higher risk of rupture.

Fig. 47.5 Dolichoectatic aneurysm of the vertebrobasilar system.

Screening for intracranial aneurysms

Screening for intracranial aneurysms is controversial but for certain familial conditions there is sufficient evidence to recommend screening (Steiner et al., 2013). These include a strong family history (two or more first-degree relatives with intracranial aneurysms), ADPKD and coarctation of the aorta (see earlier). Screening should start at an age 10 years younger than the age of presentation of the index family member. There are no clear guidelines on the frequency and mode of screening, particularly in ADPKD as they have a high incidence of late *de novo* aneurysm formation (1.4% per patient year) (Cagnazzo et al., 2017). Both CT and MR angiography techniques have developed to a high degree of sensitivity and the choice will depend on age (cumulative radiation burden of CT) and the preference of individual centres. Before starting on a course of screening, patients must be carefully counselled as there is a large, cumulative, psychological burden associated with multiple scans and on identifying small aneurysms that may not require immediate intervention.

Table 47.2 Factors analysed in the UIATS study (for clinical decision-making in the management of the unruptured IAs), and PHASES study (for the prediction of 5-year risk of rupture)

Factors analysed	UIATS	PHASES
Patients factors		
Age	Yes	Yes
Previous SAH from another IA	Yes	Yes
Familial IAs or SAH	Yes	No
Ethnicity	Yes	Yes
Smoking	Yes	No
Hypertension	Yes	Yes
ADPKD	Yes	No
Drug and Alcohol abuse	Yes	No
Clinical symptoms related to IA	Yes	No
Aneurysms multiplicity	Yes	No
Reduced quality of life due to fear of rupture	Yes	No
Life expectancy (for chronic or malignant disease)	Yes	No
Neuropsychiatric disorders	Yes	No
Coagulopathies	Yes	No
Aneurysm factors		
Size	Yes	Yes
Morphology	Yes	No
Location	Yes	Yes
Evolution	Yes	No
Treatment-related factors		
Risks of treatment related to age, size, and complexity of the IA	Yes	No

Controversies

Management of unruptured aneurysms

With widespread utilization of non-invasive imaging, unruptured IAs are being diagnosed with increasing frequency. Management of unruptured IAs is very controversial. While the vast majority of small IAs will remain quiescent for life, a very small number will go on to rupture with potentially disastrous consequences. There is a paucity of true natural data history on IAs because even in the two largest studies conducted so far, the ISUIA study (Wiebers et al., 2003) and the Japanese study (Morita et al., 2012), many patients were treated with either surgery or endovascular treatment based on physician and patient preference. Thus, these studies which are often incorrectly labelled as natural history studies are prospective cohorts of untreated patients. Because of this controversy and the conflicting data, treatment of an unruptured IA continues to be art more than science. In general, small aneurysms (<7 mm) in diameter have an exceedingly low risk of rupture as long as they are asymptomatic and a purely incidental finding. Factors such as location, presence of lobulations, and other risk factors for aneurysm rupture affect the risk of rupture and must be taken into account when deciding between active or conservative management. Treatment recommendations must also take into account the risk of treatment and the patient's degree of anxiety about the knowledge of the IA.

Several studies have tried to come up with algorithms of treatment based on information available (PHASES) (Greving et al., 2014) or a consensus of experts (UIATS) (Etminan et al., 2015) (Table 47.2). Additional controversy clouds the issue about the best treatment modality: surgical versus endovascular. In general, surgery achieves higher rates of complete angiographic occlusion, but it is more invasive. The converse is true for endovascular treatment. There are no studies which have studied this issue directly in unruptured IA. If a patient with an unruptured IA is managed conservatively with no intervention, the question arises about the need, frequency, and type of follow-up. There are no guidelines and follow-up must be individualized in these cases. In general, we recommend repeating a follow-up non-invasive study (usually MRA since no radiation is involved) 6–12 months after the diagnosis. If no interval growth is demonstrated, then further imaging is individualized based on factors such as patient age, risk factors, and aneurysm size and location.

FURTHER READING

Cebral, J.R., Sheridan, M., & Putman, C.M. (2010). Hemodynamics and bleb formation in intracranial aneurysms. *AJNR Am J Neuroradiol*, **31**, 304–10.

Etminan, N., Brown, R.D., Jr., Beseoglu, K., et al. (2015). The unruptured intracranial aneurysm treatment score: a multidisciplinary consensus. *Neurology*, **85**, 881–9.

Koskinen, L.O. & Blomstedt, P.C. (2006). Smoking and non-smoking tobacco as risk factors in subarachnoid haemorrhage. *Acta Neurologica Scandinavica*, **114**, 33–7.

Thompson, B.G., Brown, R.D., Jr., Amin-Hanjani, S., et al. (2015). Guidelines for the management of patients with unruptured intracranial aneurysms: a guideline for healthcare professionals from the American Heart Association/American Stroke Association. *Stroke*, **46**, 2368–400.

REFERENCES

Brinjikji, W., Zhu, Y. Q., Lanzino, G., et al. (2016). Risk factors for growth of intracranial aneurysms: a systematic review and meta-analysis. *AJNR Am J Neuroradiol*, **37**, 615–20.

Bruno, G., Todor, R., Lewis, I., & Chyatte, D. (1998). Vascular extracellular matrix remodeling in cerebral aneurysms. *J Neurosurg*, **89**, 431–40.

Cagnazzo, F., Gambacciani, C., Morganti, R., & Perrini, P. (2017). Intracranial aneurysms in patients with autosomal dominant polycystic kidney disease: prevalence, risk of rupture, and management. A systematic review. *Acta Neurochir (Wien)*, **159**, 811–21.

Cebral, J.R., Sheridan, M., & Putman, C.M. (2010). Hemodynamics and bleb formation in intracranial aneurysms. *AJNR Am J Neuroradiol*, **31**, 304–10.

Chalouhi, N., Ali, M.S., Starke, R.M., et al. (2012). Cigarette smoke and inflammation: role in cerebral aneurysm formation and rupture. *Mediators Inflamm*, **2012**, 271582.

Chyatte, D. & Lewis, I. (1997). Gelatinase activity and the occurrence of cerebral aneurysms. *Stroke*, **28**, 799–804.

Cloft, H.J., Kallmes, D.F., Kallmes, M.H., Goldstein, J.H., Jensen, M.E., & Dion, J.E. (1998). Prevalence of cerebral aneurysms in patients with fibromuscular dysplasia: a reassessment. *J Neurosurg*, **88**, 436–40.

Curtis, S. L., Bradley, M., Wilde, P., et al. (2012). Results of screening for intracranial aneurysms in patients with coarctation of the aorta. *AJNR Am J Neuroradiol*, **33**, 1182–6.

Ellamushi, H.E., Grieve, J.P., Jager, H.R., & Kitchen, N.D. (2001). Risk factors for the formation of multiple intracranial aneurysms. *J Neurosurg*, **94**, 728–32.

Etminan, N., Brown, R.D., Jr., Beseoglu, K., et al. (2015). The unruptured intracranial aneurysm treatment score: a multidisciplinary consensus. *Neurology*, **85**, 881–9.

Etminan, N. & Rinkel, G.J. (2016). Unruptured intracranial aneurysms: development, rupture and preventive management. *Nat Rev Neurol*, **12**, 699–713.

Greving, J.P., Wermer, M.J.H., Brown, R.D., et al. (2014). Development of the PHASES score for prediction of risk of rupture of intracranial aneurysms: a pooled analysis of six prospective cohort studies. *Lancet Neurol*, **13**, 59–66.

Hara, A., Yoshimi, N., & Mori, H. (1998). Evidence for apoptosis in human intracranial aneurysms. *Neurol Res*, **20**, 127–30.

Juvela, S. (2000). Risk factors for multiple intracranial aneurysms. *Stroke*, **31**, 392–7.

Kannoth, S. & Thomas, S.V. (2009). Intracranial microbial aneurysm (infectious aneurysm): current options for diagnosis and management. *Neurocrit Care*, **11**, 120–9.

Kayembe, K.N., Sasahara, M., & Hazama, F. (1984). Cerebral aneurysms and variations in the circle of Willis. *Stroke*, **15**, 846–50.

Kondo, S., Hashimoto, N., Kikuchi, H., Hazama, F., Nagata, I., & Kataoka, H. (1998). Apoptosis of medial smooth muscle cells in the development of saccular cerebral aneurysms in rats. *Stroke*, **29**, 181–8; discussion 189.

Koskinen, L.O. & Blomstedt, P.C. (2006). Smoking and non-smoking tobacco as risk factors in subarachnoid haemorrhage. *Acta Neurologica Scandinavica*, **114**, 33–7.

Lindekleiv, H., Sandvei, M.S., Romundstad, P.R., et al. (2012). Joint effect of modifiable risk factors on the risk of aneurysmal subarachnoid hemorrhage: a cohort study. *Stroke*, **43**, 1885–9.

Lu, H.T., Tan, H.Q., Gu, B.X., et al. (2013). Risk factors for multiple intracranial aneurysms rupture: a retrospective study. *Clin Neurol Neurosurg*, **115**, 690–4.

Matsuda, M., Handa, J., Saito, A., Matsuda, I., & Kamijyo, Y. (1983). Ruptured cerebral aneurysms associated with arterial occlusion. *Surg Neurol*, **20**, 4–12.

Mehan, W.A., Jr., Romero, J.M., Hirsch, J.A., et al. (2014). Unruptured intracranial aneurysms conservatively followed with serial CT angiography: could morphology and growth predict rupture? *J Neurointerv Surg*, **6**, 761–6.

Morita, A., Kirino, T., Hashi, K., et al. (2012). The natural course of unruptured cerebral aneurysms in a Japanese cohort. *N Engl J Med*, **366**, 2474–82.

Niemczyk, M., Pilecki, T., Gradzik, M., Bujko, M., Niemczyk, S., & Paczek, L. (2014). Blood pressure and intracranial aneurysms in autosomal dominant polycystic kidney disease. *Kidney Blood Pressure Res*, **39**, 630–5.

Ostergaard, J.R. & Hog, E. (1985). Incidence of multiple intracranial aneurysms. Influence of arterial hypertension and gender. *J Neurosurg*, **63**, 49–55.

Qureshi, A.I., Suarez, J.I., Parekh, P.D., et al. (1998). Risk factors for multiple intracranial aneurysms. *Neurosurgery*, **43**, 22–6; discussion 26–7.

Redekop, G., Terbrugge, K., Montanera, W., & Willinsky, R. (1998). Arterial aneurysms associated with cerebral arteriovenous malformations: classification, incidence, and risk of hemorrhage. *J Neurosurg*, **89**, 539–46.

Rhoton, A. L., Jr., Saeki, N., Perlmutter, D., & Zeal, A. (1979). Microsurgical anatomy of common aneurysm sites. *Clin Neurosurg*, **26**, 248–306.

Sforza, D.M., Putman, C.M., & Cebral, J.R. (2009). Hemodynamics of cerebral aneurysms. *Ann Rev Fluid Mech*, **41**, 91–107.

Steiner, T., Juvela, S., Unterberg, A., et al. (2013). European Stroke Organization guidelines for the management of intracranial aneurysms and subarachnoid haemorrhage. *Cerebrovasc Dis*, **35**, 93–112.

Thompson, B.G., Brown, R.D., Jr., Amin-Hanjani, S., et al. (2015). Guidelines for the management of patients with unruptured intracranial aneurysms: a guideline for healthcare professionals from the American Heart Association/American Stroke Association. *Stroke*, **46**, 2368–400.

Villablanca, J.P., Duckwiler, G.R., Jahan, R., et al. (2013). Natural history of asymptomatic unruptured cerebral aneurysms evaluated at CT angiography: growth and rupture incidence and correlation with epidemiologic risk factors. *Radiology*, **269**, 258–65.

Wiebers, D.O., Piepgras, D.G., Meyer, F.B., et al. (2004). Pathogenesis, natural history, and treatment of unruptured intracranial aneurysms. *Mayo Clinic Proc*, **79**, 1572–83.

Wiebers, D.O., Whisnant, J.P., Huston, J., 3rd, et al. (2003). Unruptured intracranial aneurysms: natural history, clinical outcome, and risks of surgical and endovascular treatment. *Lancet*, **362**, 103–10.

RELATED LINKS TO EBRAIN

Familial Intracranial Aneurysms. https://learning.ebrain.net/course/view.php?id=151

Unruptured Intracranial Aneurysms. https://learning.ebrain.net/course/view.php?id=152

48

The pathophysiology of subarachnoid haemorrhage

Jason McMillen

Subarachnoid haemorrhage

Spontaneous subarachnoid haemorrhage (SAH) is due to a rupture of an intracranial aneurysm in the majority of cases (85%). In some patients, no underlying cause is identified and approximately 60% of these cases have a perimesencephalic distribution of blood. Other non-aneurysmal SAH aetiologies include pial arteriovenous malformations, tumours, anticoagulants, vascular dissections, and vasculitides.

Perimesencephalic SAH is a specific non-aneurysmal SAH syndrome with a characteristic pattern of haemorrhage on CT scan. Haemorrhage is centred in the prepontine and perimesencephalic cisterns with some extension to the adjacent cisterns, but not distally into the interhemispheric and Sylvian fissures, and without extensive intraventricular extension.

Aneurysmal SAH usually occurs as a consequence of spontaneous rupture of the wall of a saccular intracranial aneurysm. The aetiology of the changes in the arterial wall that predispose to formation, growth, and eventual rupture of an aneurysm are multifactorial, involving changes in the structure and composition of the vessel wall, as well as haemodynamic stresses imposed upon the vessel.

Mortality and morbidity resulting from subarachnoid haemorrhage is common, and an understanding of the mechanisms of the physiological insults resulting from this condition can assist with improving management and outcomes. The main complications of aneurysmal SAH are rebleeding, delayed ischaemia, and hydrocephalus.

Pathophysiology of subarachnoid haemorrhage and brain injury

The precise details of aneurysm formation are poorly understood, but they are thought to arise secondary to an imbalance between local haemodynamic forces and arterial wall integrity, most commonly at vessel bifurcations. No single model explains all aspects of aneurysm formation, growth, and rupture, and there seem to be multiple factors involved in their pathogenesis, including congenital, acquired, and environmental influences.

When aneurysms form, they tend to follow Rhoton's rules for aneurysm formation. They arise from a branch point of a parent artery, and arise from the convex side of turns or curves, where wall shear stresses are greatest. The aneurysms also tend to point in the direction that blood would flow if the turn or curve was not present.

Aneurysm rupture may occur spontaneously, but may also occur with activities such as straining or coitus. In addition to the classical symptoms of headache and meningism, patients may present with changes to sensorium or coma, reflecting early brain injury. Rupture of an aneurysm is accompanied by an acute increase in intracranial pressure secondary to extravasation of blood into the subarachnoid space or the brain parenchyma, as well as a vasodilatory cascade. A reduction of cerebral perfusion pressure may manifest as loss of consciousness. Subsequent acute global ischaemia and cerebral oedema may contribute to the early brain injury after SAH. Less favourable outcomes associated with higher Fisher Grade SAH result from the greater volume of haemorrhage and more severe early brain injury. Intracerebral haemorrhage may cause direct injury to the brain parenchyma with consequent focal deficits.

A complex interaction of pathologies injurious to the brain occur subsequent to the acute global ischaemic insult of SAH (Budohoski et al., 2014). Cell death mechanisms are initiated within 24 hours, including necrosis, autophagy, and programmed cell death. Breakdown of the blood brain barrier and inflammatory mechanisms commence, including release of proinflammatory cytokines and migration of inflammatory cells. As well as direct brain injury, this is associated with cerebral vasospasm. Oxidative stress resulting from release of free radicals results in altered mitochondrial function and other disorders of cellular metabolism, and is associated with increased cell death after SAH. Cerebrovascular autoregulation is impaired, which may exacerbate ischaemia that may otherwise have been avoided by the usual physiological compensatory mechanisms. Electrophysiological abnormalities are associated with severe cerebral metabolic dysfunction, including seizures and cortical spreading depolarization. These may result in hypoperfusion, hypoxia, and may precede delayed ischaemic deficits, even in the absence of later vasospasm. Microthrombi in parenchymal vessels result from an early increase in procoagulant activity, and may exacerbate ischaemia associated with spasm of both larger and microvessels.

Hydrocephalus after SAH is common, and may result in progressive neurological impairment or death. The radiological criteria for the diagnosis of post SAH hydrocephalus vary, but it is thought to be

present in up to 20% of SAH patients on presentation. Approximately half of these patients will show signs of impaired consciousness, and may require acute treatment. A similar number may develop chronic hydrocephalus and may be candidates for permanent cerebrospinal fluid (CSF) diversion.

Hydrocephalus after SAH occurs due to impairment of CSF bulk flow and absorption via its normal physiological and anatomical pathways. Intraventricular blood clot may obstruct CSF flow through the usual circulation pathways such as the cerebral aqueduct of Silvius, resulting in obstructive hydrocephalus. Cellular blood components as well as elevated protein and blood breakdown products such as fibrin can impair CSF outflow and absorption through the arachnoid villi, and cause communicating hydrocephalus.

Acute symptomatic hydrocephalus is typically managed with ventriculostomy and temporary external CSF drainage. The acute change in transmural pressure in an unsecured aneurysm resulting from acute CSF drainage may be associated with an increased risk of rebleeding, and consideration should be given to maintaining a higher intracranial pressure (ICP) than would otherwise be targeted in order to reduce this risk until the aneurysm is secured. Other temporary measures to reduce hydrocephalus include serial lumbar punctures or lumbar CSF drainage. Intraoperative measures during surgical clipping of a ruptured aneurysm to minimize the risk of chronic hydrocephalus include CSF toilet and third ventriculostomy with fenestration of the lamina terminalis. However, despite these measures, some patients will have persistent hydrocephalus necessitating a ventriculoperitoneal shunt. Elevated cell and protein concentrations in CSF following SAH can impact on the function of ventriculoperitoneal shunt hardware, contributing to premature shunt failure. It may be necessary to continue temporary CSF diversion until these parameters reduce before implantation of a ventriculoperitoneal shunt.

Epidemiology and Incidence of aneurysms and risk factors for rupture

The overall incidence of unruptured aneurysms is difficult to determine accurately due to the asymptomatic nature of most of these lesions unless they rupture. Screening large populations accurately with cerebrovascular imaging is costly and not without risk from invasive procedures and radiation, although the numbers of asymptomatic aneurysms being detected are increasing with greater use of increasingly sensitive non-invasive imaging modalities. Both imaging and autopsy studies suggest an incidence of unruptured intracerebral aneurysms ranging from 1% to 9%. An increased incidence of aneurysms has been noted in the Finnish and Japanese populations, females, as well as with increasing age and certain medical conditions (Rinkel et al., 1988).

Subarachnoid haemorrhage from aneurysm rupture is the most devastating complication of intracranial aneurysms, often resulting in morbidity or death. Determining the risk of aneurysm formation, growth, and rupture is critical to balancing this prognostic risk against the risks of intervention.

The baseline incidence of aneurysmal subarachnoid haemorrhage in the general population has been reported to be 6–11 per 100 000 individuals per year. Of more clinical relevance is the risk of rupture and haemorrhage in patients diagnosed with an unruptured intracranial aneurysm. Several factors need to be considered when calculating the risk of subarachnoid haemorrhage. Patient-related factors such as increasing age, female gender, ethnicity, and family history have all been shown to influence the risk of subarachnoid haemorrhage. The presence of multiple aneurysms or a previous aneurysmal haemorrhage also confers greater future risk above the additive risk of more than one aneurysm—so-called type 2 aneurysms in the ISUIA studies discussed later. Modifiable risk factors have been recognized in numerous studies, including tobacco smoking and hypertension. Numerous aneurysm related variables have also been demonstrated to influence the risk of rupture, including anatomical location of the aneurysm, size, morphological characteristics, and demonstrated growth with serial imaging or development of new symptoms related to growth.

The most important studies attempting to quantify these risks are the ISUIA studies (Wiebers et al., 1998; Wiebers et al. 2003). While not without their critics, these prospective multicentre studies have provided useful information to prognosticate aneurysm rupture risk based on anatomical location and size. They determined that small (<7 mm) anterior circulation aneurysms have low rupture rates, as do small type 1 aneurysms of the posterior circulation. Higher rates of rupture were noted for all posterior circulation aneurysms and aneurysms larger than 7 mm in diameter. Earlier suggestions that aneurysms less than 10 mm in diameter have a near-zero risk of haemorrhage are unlikely to be correct.

Studies of the high-risk Finnish and Japanese populations (Juvela et al., 2000; Morita et al., 2012) and others have determined overall annual rupture rates to be between 0.95% and 1.3%. High risk factors identified in these studies in addition to size and location included advanced patient age, smoking, and the presence of a daughter sac. Conflicting findings between studies may be due to methodological differences and different populations.

A more recent investigation pooling the data of several previous large studies was able to generate a statistical tool to assist with prediction of rupture risk according to the variables found to be of clinical significance (Greving et al. 2014). The PHASES score (**Table 48.1**) predicts that patients from Japan and Finland (population), hypertension, age more than 70 years, aneurysm size, a history of earlier subarachnoid haemorrhage, and the aneurysm's anatomical site are all significant risk factors for haemorrhage. Smoking and female gender were not found to reach statistical significance as risk variables.

Some connective tissue and other disorders have been associated with a greater incidence of intracranial aneurysms and aneurysm rupture with subarachnoid haemorrhage. These include autosomal dominant polycystic kidney disease (ADPKD), Ehlers-Danlos syndrome type IV, Marfan's syndrome, fibromuscular dysplasia, and coarctation of the aorta. Aneurysms may occur in as many as 20% of patients with fibromuscular dysplasia, and up to 30% of patients with ADPKD. Familial aneurysms have been recognized, and these are thought to rupture at a smaller size and younger age than sporadic aneurysms.

Overall, it appears that the overall annual risk of rupture of a previously unruptured intracranial aneurysm is approximately 1%. Each patient's individual risk factors for aneurysm rupture need to be assessed and weighed against the risks of treatment in their own institution in order to make a balanced decision about surgical or endovascular management.

Table 48.1 Risk factors for aneurysm rupture

PHASES significant risk factors	P—Population—Japanese or Finnish H—Hypertension A—Age > 70 years S—Size of aneurysm E—Earlier subarachnoid haemorrhage from another aneurysm S—Site—anatomical location of aneurysm
Other postulated risk factors	Female gender Tobacco smoking Familial aneurysms Growth on serial imaging Symptomatic aneurysm

Reprinted from *The Lancet Neurology*, Volume 13, issue 1, Jacoba P Greving et al., Development of the PHASES score for prediction of risk of rupture of intracranial aneurysms: a pooled analysis of six prospective cohort studies, pp. 59–66, Copyright (2014), with permission from Elsevier.

Vasospasm

Vasospasm is one of the most devastating complications of aneurysmal subarachnoid haemorrhage, and is the leading preventable cause of neurological morbidity and mortality in patients who present for medical care. It may lead to death in as many as 7%, and cerebral infarction in 26% of patients with SAH.

By definition, vasospasm is narrowed arterial calibre demonstrated on vascular imaging. This results in delayed or diminished arterial filling distal to the spasm, and resultant ischaemia of the vascular territory supplied by those vessels—delayed ischaemic neurological deficits. The radiological appearances of vasospasm can be detected in 50–90% of patients following SAH, but only half of those patients will show clinical signs of vasospasm such as ischaemic deficits. Conversely, ischaemia can be demonstrated in patients in arterial territories that do not display radiological vasospasm, indicating that other mechanisms are contributing. Additional evidence for this is found in the beneficial action of nimodipine, which has been proven to improve neurological outcomes, but affords little improvement in arterial vasospasm. Conversely, pharmacological reversal of vasospasm with drugs such as endothelin-1 antagonists, have resulted in limited improvement in functional outcomes. It is therefore clear that arterial luminal narrowing is not the sole mechanism of cerebral ischaemia. Additional factors may include tissue inflammation, microvascular thrombosis, and mitochondrial dysfunction. However, from the clinical perspective, vascular narrowing and ischaemia are closely correlated, and strategies to prevent delayed ischaemic neurological deficits are largely based on treatment of the vasospasm.

Vasospasm pathology

Vasospasm appears to occur in intracerebral arteries that have been encased in blood clot, usually within the subarachnoid space. The pathological mechanisms underlying vasospasm are complicated and poorly understood. Oxidation of oxyhaemoglobin to produce methaemoglobin, the formation of superoxide anion radicals, and the release of endothelin 1 have all been implicated. Three main changes that narrow the vessel lumen have been observed. Vascular wall smooth muscle contraction occurs in two phases—an acute phase that is dependent on calcium and adenosine triphosphate (ATP), and a chronic and less reversible phase that is less dependent on calcium and energetic mechanisms. Prolonged muscle contraction is associated with structural damage to the layers of the vessel, including endothelial cell damage, elastic lamina damage, and myonecrosis. The second major change occurs in the endothelium, with loss of synthesis of the vasodilator nitric oxide and increased production of the vasoconstrictor peptide endothelin 1. The final changes result from activation of inflammatory mechanisms within the vessel wall, with increased activity of cytokines and intercellular adhesion molecules leading to remodelling of the vessel wall extracellular matrix and smooth muscle, and direct release of inflammatory cells.

Histological changes in the vessel wall include vacuolization of endothelial cells, and loss of their tight junctions. Breaches in the internal elastic lamina have been noted, as well as necrosis of the smooth muscle of the tunica media. Inflammatory cells and an increase in the extracellular matrix occur in the adventitia. With chronic vasospasm, smooth muscle cells may proliferate in the tunica intima, resulting in intimal thickening.

Incidence

While radiological evidence of vasospasm can be detected in over half of patients with SAH, clinical signs of ischaemia secondary to vasospasm are less common. Delayed ischaemic neurological deficits (DIND) occur in 30–40% of patients with SAH, and seem to occur during the same period post haemorrhage that radiological vasospasm is maximal.

Vasospasm is more common with increased blood volume in the subarachnoid space. The Fisher radiological grade is closely correlated with the frequency of vasospasm, with increasing rates of radiological spasm from Grade 1 (no subarachnoid blood on CT) to Grade 2 (diffuse subarachnoid blood or vertical layers <1 mm thick), and maximal rates of radiological and clinical vasospasm in Fisher Grade 3 (>1 mm vertical layer of subarachnoid blood; 23/24 patients in Fisher's original series developed DINDs). In Fisher Grade 4 (intracerebral or intraventricular blood, with diffuse or no subarachnoid blood) the rate of vasospasm is low.

Increased rates of vasospasm are also reported in higher clinical grades of SAH. Other risk factors may include increasing age, hypertension, and the presence of hydrocephalus.

Time course and natural history

Cerebral vasospasm rarely becomes clinically evident before the third day post ictus, although radiological spasm may be evident earlier than this. The clinical onset is insidious in most cases, but occasionally may become abruptly evident. The peak incidence of onset is between days six and eight post SAH, but may occur as early as day three, or as late as the third week. Clinical signs of vasospasm usually resolve before the radiological signs of vasospasm, which may persist for three to four weeks. The changes of vasospasm are felt to resolve eventually, but if left untreated during their peak may leave a permanent legacy of ischaemic neurological deficits.

Clinical presentation

In the awake patient, changes in neurological status are early signs of clinical vasospasm. The onset of changes can be gradual and subtle, and may include increased headache, slight confusion, agitation or somnolence, or diminished attention and altered cognition. Focal neurological deficits may be difficult initially to detect, and may

progress from a subtle pronator drift or word finding difficulties to more severe deficits if clinical vigilance is not maintained. These clinical changes may have other potential causes such as seizure, rebleeding, hyponatraemia, or hydrocephalus, which may need to be excluded with laboratory and radiological investigations.

Vasospasm affecting large vessels may present with a cluster of signs that reflect the territory of the affected vessel, and may result from the initial distribution of the subarachnoid blood. Anterior cerebral artery vasospasm is the most common. This predominantly affects the frontal lobe, with signs including confusion or agitation, somnolence, abulia, urinary incontinence, and motor weakness in the lower limb. Middle cerebral artery involvement may cause aphasia, monoparesis or hemiparesis, and apraxias. Vertebrobasilar vasospasm is more likely to present with a reduced level of consciousness than with focal deficits.

Other less specific systemic signs of vasospasm include peripheral leucocytosis and pyrexia, which may occur early at the onset of the condition.

In the comatose or intubated patient, clinical signs of vasospasm may be difficult to detect, and the diagnosis of vasospasm is more reliant on ancillary investigations and a high level of vigilance.

Investigation

Other causes of neurological deterioration should be excluded, including electrolyte abnormalities and hydrocephalus or haemorrhage. A positive response to initial vasospasm management, including induced hypertension, is highly suggestive of a diagnosis of vasospasm.

Diagnostic modalities specific for vasospasm measure arterial luminal narrowing, either directly or indirectly by measuring cerebral blood flow and velocity. Transcranial doppler monitoring may detect increased blood flow velocity in large intracranial vessels before the onset of clinical symptoms (Fig. 48.1). While inexpensive and non-invasive, this technique is very operator dependent, and will only detect spasm in large anterior circulation arteries. For example, a flow velocity more than 150 cm/s is considered indicative of vasospasm in the middle cerebral artery (MCA), with a value greater than 200 cm/s indicative of severe vasospasm. As flow velocity is dependent on cardiac output, the Lindegaard ratio (LR) which is the ratio of MCA mean flow velocity to extracranial internal carotid artery mean flow velocity, can be utilized. A LR of more than 3 designates vasospasm, while a LR more than 6 designates severe vasospasm.

Direct radiological measurements of cerebral blood flow can be made with CT perfusion studies (Figs. 48.2A–F), SPECT, or xenon enhanced CT. Cerebral ischaemia or infarction can be diagnosed early using diffusion weighted MRI. Direct imaging of intracerebral vessels is achieved with CT angiography, or catheter digital subtraction cerebral angiography. Catheter angiography is invasive and labour intensive, and is associated with some procedural risk. However, it is the most sensitive modality for detecting both small and large vessel spasm, and interventions such as intra-arterial vasodilator therapies or balloon angioplasty may be instigated in conjunction with the diagnostic procedure.

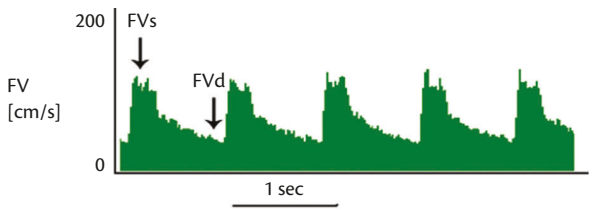

Fig. 48.1 Transcranial Doppler. Indicative waveform from insonation of the middle cerebral artery using transcranial Doppler. The systolic and diastolic flow velocites (FV) are marked. The FVs is used to gauge the progression of vascular spasm or to quantify the Lindegaard ratio (see text).

Invasive measures of cerebral perfusion, oxygenation, and hypoxic cell injury include direct cerebral oxygenation monitoring and microdialysis. These have been used in the critical care setting to detect vasospasm. The techniques only provide information about a focal region of the brain, which may limit their usefulness without appropriate targeting. Other uncommon intensive care techniques include continuous electroencephalography (EEG) monitoring, which may predict the onset of vasospasm.

Monitoring for vasospasm

Early detection and treatment of cerebral vasospasm is important to allow rapid initiation of treatment measures to prevent ischaemic deficits. Treatment of vasospasm is not without associated morbidity, so treatment should be reserved for patients in whom the condition has been proven. Radiological spasm may be detectable before the onset of clinical symptoms, and may be the only way of detecting spasm in the unconscious patient, allowing more focussed treatment on those most at risk.

The detection of vasospasm relies heavily on a number of imaging modalities, all of which have different advantages and disadvantages. Transcranial doppler is non-invasive and relatively economical, but it may not be available in every institution, the operator dependent variability may limit its utility and it is anatomically limited with the best acoustic window limited to the MCA artery. Catheter angiography is available in most neurosurgical centres, but is more labour intensive, costly, and indiscriminate use may not be justified due to procedural risks. No evidence exists to determine a single approach to investigation of vasospasm, therefore a protocol for vasospasm investigation and management should be developed in each institution, taking into account the varying resources and expertise available.

Vasospasm prevention and treatment

No single treatment or prevention strategy is entirely effective against the adverse impacts of cerebral vasospasm following SAH. Prevention of neurological deficits relies predominantly upon ensuring adequate cerebral perfusion by avoiding hypovolaemia and hypotension. Three litres of intravenous maintenance fluids should be administered per day. Blood transfusions can be given if the patient is anaemic. Hyperdynamic therapies to prevent vasospasm have not been shown to be of benefit, and hypertension in unsecured aneurysms may increase the risk of rebleeding. Blood pressure should therefore be targeted from normotension to permissive mild hypertension, strictly avoiding hypotension. Close monitoring is mandatory, including blood pressure, fluid balance, and neurological observations.

The calcium channel blocker nimodipine has been shown to be of benefit in the prevention of neurological deficits secondary to cerebral vasospasm following SAH (Pickard et al., 1989). It is administered intravenously or orally, with a dose of 60 mg every four

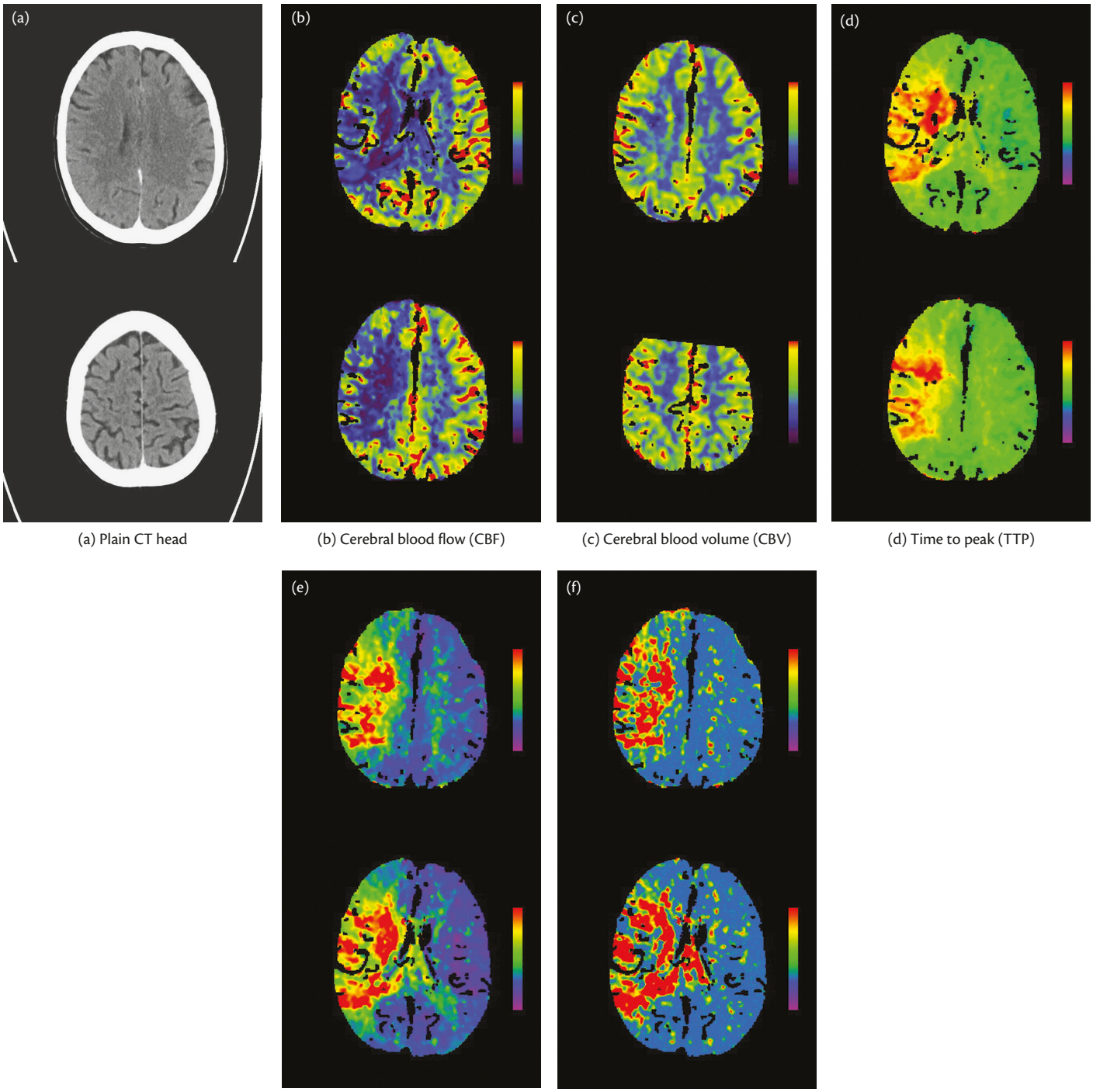

(a) Plain CT head (b) Cerebral blood flow (CBF) (c) Cerebral blood volume (CBV) (d) Time to peak (TTP)

Fig. 48.2 CT perfusion assessment of vascular spasm. Illustrative CT perfusion scan of patient with Right MCA territory vasospasm. (A) The plain CT head shows no abnormality, while (B) the cerebral blood flow (CBF) map shows reduced flow with maintained cerebral blood volume (CBV), representing ischaemia. A reduced CBV (C) is thought to result from cellular swelling, and compression of the microvasculature indicative of infarction. (D) The time to peak (TTP) map shows the delay in accumulation of contrast caused by the reduced vessel calibre. (E) The TTP map shows the overall delay in exit of contrast from the cerebrovascular bed after the TTP has been reached, typical of vasospasm. (F) The mean transit time (MTT) map demonstrates the mean transit time, the averaged time for transit of contrast through the tissues, with delays being secondary to vasospasm. The colour maps are such that the abnormality is obvious on this parameter map.

hours. It can contribute to hypotension, in which circumstance the dosing can be reduced or changed to a different regime of 30 mg every two hours.

If cerebral vasospasm is diagnosed, early treatment in a neurocritical care unit should be initiated to prevent DIND. The goal of vasospasm treatments is to improve cerebral perfusion by improving blood flow through the narrowed vessel lumen, or increasing the size of the vessel lumen directly. 'HHH' therapy consists of hypertension, hypervolaemia, and haemodilution, and aims to increase cardiac output, improve blood rheology, and improve

cerebral perfusion pressure. Intravascular volume is expanded with intravenous fluids, which also result in haemodilution. Fluid supplementation is titrated to the patient's clinical response, up to a central venous pressure of 8–10 mmHg. Further fluid loading beyond this may not offer further benefit, and may increase the risk of adverse effects such as cardiac pump failure and acute pulmonary oedema. Of most utility is the use of inotropes or vasopressor agents to induce arterial hypertension, similarly titrated to a level that improves the patient's neurological symptoms. Induced hypertension has fewer adverse effects and greater benefits than hypervolaemia and haemodilution.

Other treatment modalities for cerebral vasospasm are aimed at remodelling the arterial lumen to improve cerebral perfusion. Endovascular options include direct intra-arterial injection of vasodilator agents such as verapamil, which may be performed concurrently with diagnostic angiography once vasospasm has been demonstrated. More durable arterial remodelling may be achieved with transluminal balloon angioplasty. Neither of these treatments should be attempted in the presence of an unsecured aneurysm due to the risk of rebleeding.

Early surgical or endovascular interventions to secure the ruptured aneurysm may assist with vasospasm prevention and treatment. Surgical toilet of arachnoid cisterns and evacuation of intracerebral clot may reduce the risk of cerebral vasospasm by removal of spasmogens. Additionally, securing the aneurysm reduces the rebleeding risk and affords greater opportunity for safe use of hyperdynamic therapies and hypertension, as well as endovascular arterial remodelling. There is some evidence that lumbar drainage may also reduce the risk of vasospasm by drawing putative spasmogens into the lumbar cistern (Al-Tamimi et al., 2012), however, this remains controversial.

Outcomes following subarachnoid haemorrhage

Aneurysmal subarachnoid haemorrhage is a serious condition, associated with high rates of morbidity and mortality, even with treatment. As many as 25% of patients with ruptured aneurysms die before reaching medical care. The natural history of untreated ruptured aneurysms is not benign, with the greatest risk of death being associated with secondary rupture and rebleeding. The greatest risk of rebleeding is encountered in the first 24 hours post ictus, with a rate of 4% on day one. Subsequent daily risk of rebleeding is 1.5% per day. Approximately 20% of unsecured aneurysms will re-rupture in the first two weeks, and 50% within the first six months, resulting in an overall late mortality rate of 60%. Even after six months, untreated ruptured aneurysms remain dangerous, with a persistent annual rebleed rate of 3% per annum. It is because of these high rates of adverse outcome in untreated aneurysms that timely treatment is recommended to occlude these lesions.

Even with treatment, mortality rates remain high. Death rates have diminished over recent decades to 5–10% of admissions. Rebleeding can occur prior to aneurysm obliteration, with death rates from rebleeding reportedly as high as 70–90%. Other major causes of death associated with subarachnoid haemorrhage are vasospasm, neurosurgical complications such as hydrocephalus and hyponatraemia, as well as systemic complications including neurogenic pulmonary oedema and neurogenic stunned myocardium (Takotsubo cardiomyopathy, named after the Japanese octopus trap 'Tako-tsubo' which mimics the apical left ventricular ballooning seen on echocardiography). Rates of these complications are decreasing as treatment regimens improve. Electrocardiogram (ECG) changes observed after SAH include dysrhythmias, ST segment changes and tented or 'neurogenic' T waves. These are postulated to be secondary to the effect of excess circulating catecholamines released as a result of hypothalamic insult from SAH on the repolarization phase of the ECG. In severe cases a degree of subendocardial ischaemia which may be detected through measurement of cardiac enzymes occurs as well.

Neurological morbidity is common following aneurysm rupture. The initial haemorrhage, vasospasm-induced ischaemic neurological deficits, and hydrocephalus may all result in neurological damage. Rates of cerebral infarction are as high as 26% at six weeks post ictus. Vasospasm is a major cause of delayed neurological morbidity. Approximately one-third of survivors suffer from moderate to severe disability, and two-thirds of patients who have undergone successful aneurysm clipping never return to their premorbid quality of life, despite the majority of patients surviving with Glasgow Outcome Scores of 4 or 5. Of those that survive with a good neurological outcome, less quantifiable deficits result in only one in four returning to employment at one year.

Predictors of poor outcomes include clinical factors, patient-related variables, and radiological factors. Higher World Federation of Neurosurgical Societies (WFNS) and Hunt and Hess grades (see Chapter 49) on admission are associated with increased mortality and neurological morbidity. Similarly, a higher Fisher radiological grade on the presentation CT is associated with increased rates of vasospasm, and subsequently increased complication rates. Patient age is an independent risk factor for poor outcome, with patients over 70 years suffering significantly higher mortality rates and lower rates of favourable outcome.

Controversies—seizures, their prevention and management

Seizures are common following SAH, usually occurring in the first days following the ictus. The risk of seizures in the acute illness after SAH is approximately 3%. The reported overall long-term incidence of seizures ranges from 5% to 27%, with the ISAT researchers noting a seizure incidence of 5–10% over five years. Risk factors include younger age, ruptured middle cerebral artery aneurysms, intracerebral haematoma, subdural haematoma, and poor clinical or radiological grades. Additionally, surgical treatment of ruptured aneurysms is associated with a higher incidence of seizures than endovascular coiling.

Mechanisms suggested for seizure pathogenesis include acute intracranial hypertension resulting from SAH, vasospasm, and cortical dysfunction, early spreading cortical depolarization, and temporal lobe cortical injury. Adverse effects on the brain during a seizure may result secondary to acute raised intracranial pressure, and haemodynamic and airway instability. There is decreased oxygen utilization by the brain, and metabolic derangements such

as acidosis. A seizure in the setting of an unsecured ruptured aneurysm may be associated with devastating consequences such as rebleeding. All of these secondary adverse effects are associated with negative outcomes, supporting the treatment of seizures when they occur, and raising the option of seizure prevention strategies.

Because of the relatively low rate of seizures in the acute illness following SAH, the use of antiepileptic drugs (AEDs) to prevent seizures after SAH is controversial, with no consensus on their use. AEDs such as phenytoin can be associated with significant side effects that may outweigh their benefits. Agents such as levetiracetam may offer superior anticonvulsive properties with fewer adverse effects, and should be considered as an alternative if seizure prophylaxis is indicated. If prophylactic AEDs are utilized, they should be administered for one week postsurgery. Other strategies to reduce the risk of seizures include prevention of vasospasm and cortical ischaemia, and maintenance of normal metabolic parameters.

Treatment of seizures includes haemodynamic and airway support, and pharmacotherapy to terminate persistent seizure activity. AED use is indicated if a seizure has occurred, and carries a relatively low risk in the acute illness following SAH. As with prophylaxis regimes, the choice of drug should take into consideration its efficacy and side effects.

FURTHER READING

Budohoski, K.P., Guilfoyle, M., Helmy, A., et al. (2014). The pathophysiology and treatment of delayed cerebral ischaemia following subarachnoid haemorrhage. *J Neurol Neurosurg Psychiatry*, **85**, 1343–53.

Greving, J.P., Wermer, M.J., Brown, R.D. Jr., et al. (2014). Development of the PHASES score for prediction of risk of rupture of intracranial aneurysms: a pooled analysis of six prospective cohort studies. *Lancet Neurol*, **13**(1), 59–66.

Morita, A., Kirino, T., Hashi, K., et al. (2012). The natural course of unruptured cerebral aneurysms in a Japanese cohort. *N Engl J Med*, **366**(26), 2474–82.

Pickard, J.D., Murray, G.D., Illingworth, R., et al. (1989). Effect of oral nimodipine on cerebral infarction and outcome after subarachnoid haemorrhage: British aneurysm nimodipine trial. *BMJ*, **298**, 636–42.

Wiebers, D.O. & the ISUIA Investigators (2003). Unruptured intracranial aneurysms: natural history, clinical outcome, and risks of surgical and endovascular treatment. International Study of Unruptured Intracranial Aneurysms Investigators. *Lancet*, **362**, 103–10.

REFERENCES

Al-Tamimi, Y.Z., Bhargava, D., Feltbower, R.G., et al. (2012). Lumbar drainage of cerebrospinal fluid after aneurysmal subarachnoid hemorrhage: a prospective, randomized, controlled trial (LUMAS). *Stroke*, **43**, 677–82.

Budohoski, K.P., Guilfoyle, M., Helmy, A., et al. (2014). The pathophysiology and treatment of delayed cerebral ischaemia following subarachnoid haemorrhage. *J Neurol Neurosurg Psychiatry*, **85**, 1343–53.

Greving, J.P., Wermer, M.J., Brown, R.D. Jr., et al. (2014). Development of the PHASES score for prediction of risk of rupture of intracranial aneurysms: a pooled analysis of six prospective cohort studies. *Lancet Neurol*, **13**(1), 59–66.

Juvela, S., Porras, M., & Poussa, K. (2000). Natural history of unruptured intracranial aneurysms: probability of and risk factors for aneurysm rupture. *J Neurosurg*, **93**(3), 379–87.

Morita, A., Kirino, T., Hashi, K., et al. (2012). The natural course of unruptured cerebral aneurysms in a Japanese cohort. *N Engl J Med*, **366**(26), 2474–82.

Pickard, J.D., Murray, G.D., Illingworth, R., et al. (1989). Effect of oral nimodipine on cerebral infarction and outcome after subarachnoid haemorrhage: British aneurysm nimodipine trial. *BMJ*, **298**, 636–42.

Rinkel, G.J., Djibuti, M., Algra, A., & van Gijn, J. (1988). Prevalence and risk of rupture of intracranial aneurysms: a systematic review. *Stroke*, **29**, 251–6.

Wiebers, D.O. & the ISUIA Investigators (1998). Unruptured intracranial aneurysms: risk of rupture and risks of surgical intervention. International Study of Unruptured Intracranial Aneurysms Investigators. *N Engl J Med*, **339**, 1725–33.

Wiebers, D.O. & the ISUIA Investigators (2003). Unruptured intracranial aneurysms: natural history, clinical outcome, and risks of surgical and endovascular treatment. International Study of Unruptured Intracranial Aneurysms Investigators. *Lancet*, **362**, 103–10.

RELATED LINKS TO EBRAIN

Aetiology and pathophysiology of subarachnoid haemorrhage. https://learning.ebrain.net/course/view.php?id=163

Vasospasm. https://learning.ebrain.net/course/view.php?id=155

49

Management of subarachnoid haemorrhage

Roberto Rodriguez Rubio, Brian P. Walcott, and Michael T. Lawton

Medical management of subarachnoid haemorrhage

Subarachnoid haemorrhage resulting from a ruptured cerebral aneurysm requires advanced medical and surgical care to maximize patient outcomes. In the acute period, care is focused on rapid diagnosis and excluding the aneurysm from the circulation with either clipping or coiling to prevent further haemorrhage. In the days to weeks that follow, the focus shifts to optimizing cerebral perfusion in order to prevent delayed ischaemia. While controversy exists over various treatment modalities and management protocols, widespread advances in surgical and endovascular techniques and vasospasm care continue to decrease morbidity and mortality associated with this challenging disease.

Preoperative

Clinical presentation of subarachnoid haemorrhage

Subarachnoid haemorrhage (SAH), or bleeding surrounding the surface of the brain in the subarachnoid space, can be due to traumatic and non-traumatic aetiologies. While trauma is the most frequent cause of subarachnoid haemorrhage overall, the most common aetiology of non-traumatic (spontaneous) SAH is a ruptured cerebral aneurysm. Other causes of non-traumatic subarachnoid haemorrhage include Call-Fleming syndrome, dural arteriovenous fistulae, arteriovenous malformations, and leptomeningeal metastases, among other conditions. This chapter will focus on the management of subarachnoid haemorrhage resulting from aneurysm rupture, with an emphasis on treatment techniques to prevent aneurysm rebleeding and prevention of neurological and medical complications.

Aneurysmal SAH can be a devastating event, and the presence of a brain aneurysm is often not known (or symptomatic) until it ruptures. An estimated one-third of patients do not survive to reach medical attention, and among survivors of the initial event, there are high rates of morbidity and mortality (van Gijn and Rinkel, 2001). For these reasons, understanding the clinical presentation of SAH and arriving at a rapid diagnosis is essential to prevent or mitigate the secondary insults that can follow.

The most common initial manifestation of a ruptured aneurysm is sudden onset of severe headache, which patients will usually refer to as 'the worst headache of my life'. Occasionally, the headache may be submaximal in intensity, or it may soon dissipate and the patient may not seek rapid medical attention. Other signs and symptoms include nausea, vomiting, meningism, photophobia, and even depressed levels of consciousness (Suarez et al., 2006). Occasionally, focal neurological deficits may be present due to local mass effect from a giant aneurysm, parenchymal brain haemorrhage, subdural haematoma, or a large localized subarachnoid clot. In addition, third and sixth cranial nerve palsies may be present due to aneurysmal compression of the oculomotor nerve or globally increased intracranial pressure, respectively. Seizure activity may also result from aneurysmal SAH (Rhoney et al., 2000). Assessment of a patient's clinical condition with aneurysmal SAH is standardized with the use of the Hunt & Hess grading scale, which is largely of historical interest. This scale is one of the most widely used and classifies the initial manifestations of SAH into five grades. The grade 1 represent an entirely asymptomatic patient, or with slight clinical manifestations such as a minimal headache or nuchal rigidity. Grade 2 relates to a patient with moderate symptoms with no neurological deficit apart from cranial neuropathy. In grade 3, the patient has mild loss of consciousness with a focal neurological deficit. Grade 4 constitutes a moderate loss of consciousness (i.e. stupor), deep focal deficit, or early stages of a vegetative disturbance. Finally, grade 5 which is a patient in a deep coma or clinical evidence of decerebration (data from Hunt & Hess, 1968). Another popular grading scale is the more modern World Federation of Neurologic Surgeons grading scale (**Table 49.1**), which can be used for risk assessment and prognostication (Rosen and Macdonald, 2005). Initial presentation grades are determined after a ventriculostomy is placed when acute hydrocephalus is present.

Investigations and workup

The initial steps in the investigation of a patient with suspected aneurysmal SAH focuses on a variety of radiological assessments with or without spinal fluid analysis. Based on a concordant clinical history, it is important to confirm the presence of subarachnoid haemorrhage.

Table 49.1 World Federation of Neurological Surgeons subarachnoid haemorrhage grading scale

Grade	GCS	Motor deficit
I	15	–
II	14–13	–
III	14–13	+
IV	12–7	±
V	6–3	±

GCS, Glasgow Coma Scale.

Reproduced with permission from G M Teasdale, C G Drake, W Hunt, N Kassell, K Sano, B Pertuiset, J C De Villiers, A universal subarachnoid hemorrhage scale: report of a committee of the World Federation of Neurosurgical Societies, *Journal of Neurology, Neurosurgery & Psychiatry*, Volume 51, Issue 1, p. 1457. Copyright © 1988 BMJ Publishing Group Ltd.

While spinal fluid analysis (obtained via puncture of the lumbar cistern) has historically been the first step in the work up, the availability and speed at which a non-contrast head computed tomography (CT) scan can be obtained has shifted practice patterns in this direction.

Acute haemorrhage in the subarachnoid space appears as areas of hyperdensity in the basal cisterns, cerebral sulci, or ventricles, and exceeds a sensitivity of 95% in detecting subarachnoid haemorrhage in the first 24 hours (Fig. 49.1). The non-contrast head CT is also useful in determining the presence of acute hydrocephalus if cerebrospinal fluid absorption is impaired as a result of the haemorrhage, as well as excluding a mass lesion that may preclude safe lumbar puncture. The pattern of the haemorrhage on the CT scan can also help to direct attention to particular anatomical regions of interest during subsequent neurovascular imaging (Fig. 49.2).

If the non-contrast CT scan is negative for haemorrhage, in a patient with a classic aneurysmal SAH presentation history, it is necessary to perform further investigation with spinal fluid analysis to maximize diagnostic sensitivity. Spinal fluid analysis is particularly useful in cases of delayed presentation, where the patient experienced the first onset of symptoms several days prior to medical evaluation. In these instances, the sensitivity of a CT scan is decreased (70% after 48 hours, 50% after 7 days) and the presence of xanthochromia in the spinal fluid may help to support the presence of a recent haemorrhage. Xanthochromia can be evaluated with either visual inspection or, ideally, spectrophotometry (which measures light absorbance in the spectrum of oxyhaemoglobin and bilirubin) and its presence can be detected from six hours to three weeks following a subarachnoid haemorrhage. Potential confounders that limit the specificity of xanthochromia are high bilirubin levels, high protein levels, and a traumatic lumbar puncture.

If SAH is confirmed, the next step in the workup is to determine the source, whether it is from a ruptured cerebral aneurysm or other aetiology. Practice patterns vary according to institutional preferences, but neurovascular imaging is generally either obtained via CT angiography or catheter angiography. CT angiography with three-dimensional (3D) reconstruction has the benefit of being rapid, with

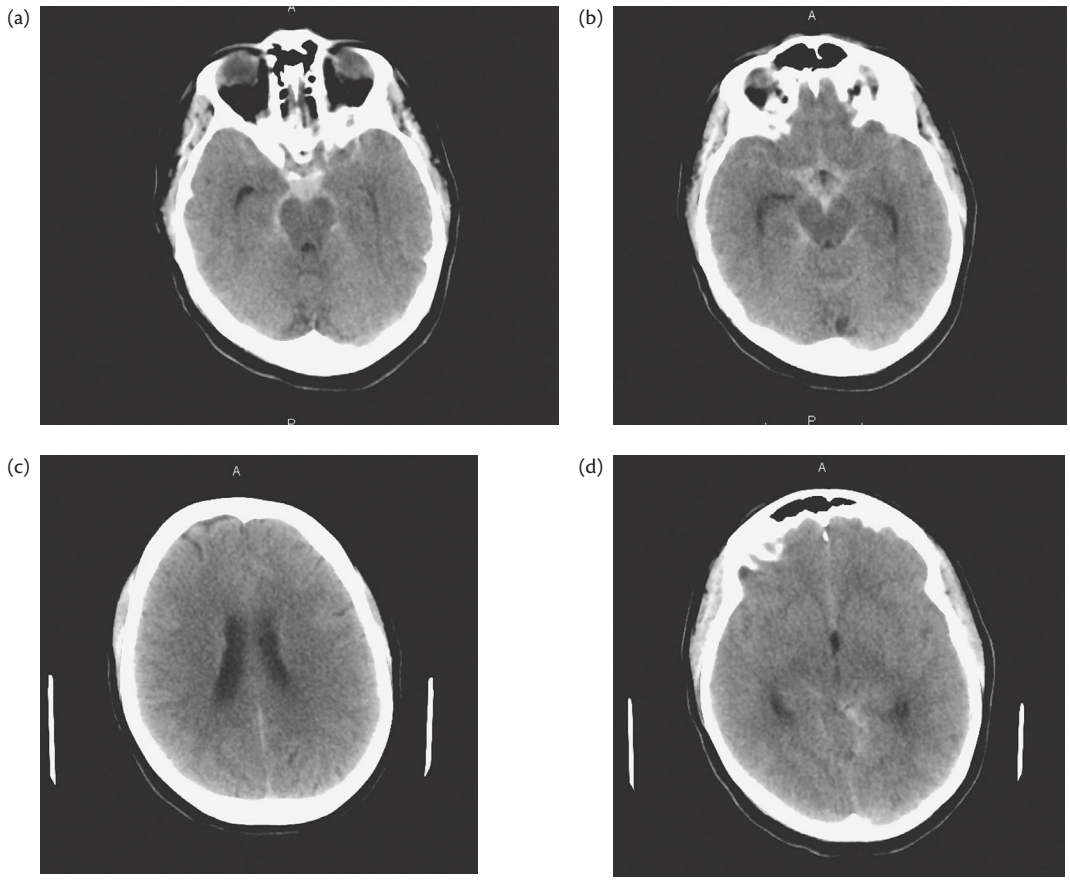

Fig. 49.1 Computed tomography scan of aneurysmal subarachnoid haemorrhage. Non-contrast axial head computed tomography of a patient who experienced an aneurysmal subarachnoid haemorrhage where blood extended into the distal Sylvian and interhemispheric fissures. Representative images are demonstrated in sequence from A to D in their inferior to superior location.

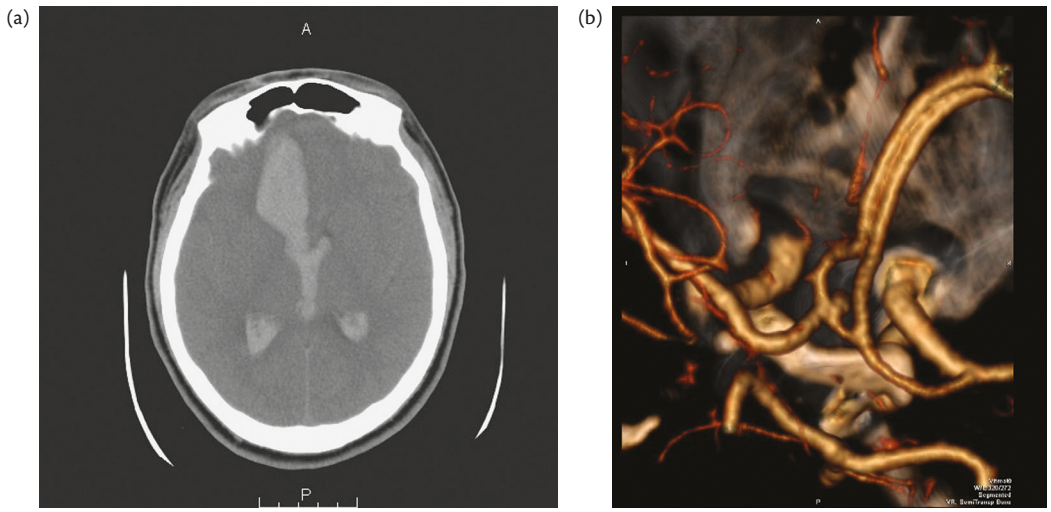

Fig. 49.2 Clip obliteration of aneurysm and haematoma evacuation for comatose patient. A 35-year-old male presented with loss of consciousness while at work in an office. He was found to have hydrocephalus, intraventricular haemorrhage, mild scattered subarachnoid haemorrhage, and a large intraparenchymal haemorrhage of the inferior frontal lobe. This is a characteristic haemorrhage pattern for an anterior communicating artery aneurysm. CTA revealed a 5 mm anterior communicating artery aneurysm in a 'windsock' configuration, pointing anteriorly and inferiorly. He was taken to the operating room emergently for successful haematoma evacuation and clip obliteration of his aneurysm.

a sensitivity and specificity that exceeds 95% in detecting aneurysms 2 mm in diameter or greater. Catheter angiography, also known as digital subtraction angiography (DSA), remains the gold standard for detection of intracranial aneurysms and has a higher sensitivity and specificity than CT angiography. DSA can identify small aneurysms and also demonstrate the surrounding normal blood vessels with better clarity. The limitations of DSA are provider availability, vasospasm preventing adequate contrast filling and a very small risk of procedure-related complications, such as cerebral ischaemia and groin haematoma.

MRI is an additional, supplemental imaging technique that is useful for the investigation of large or giant aneurysms. It can give information about adjacent brain structures such as the optic nerve or brainstem and their relationship to the aneurysm, as well as the degree to which the aneurysm contains thrombosed blood.

Preoperative management

Management of patients with aneurysmal SAH should be in specialized centres. Care delivered by a multidisciplinary team consisting of neurosurgeons, neurointerventional radiologists, neurointensivists, and neurologists, all specializing in neurovascular disease has been shown to improve outcomes (Bardach et al., 2002). The definitive treatment of a ruptured brain aneurysm is the exclusion of the aneurysm from the circulation in order to prevent it from bleeding again. Prior to this, we manage our patients in an intensive care unit in order to immediately institute measures aimed at prevention of aneurysm rerupture, while also optimizing cerebral perfusion.

Central to the core of all resuscitation protocols across many acute central nervous system disease phenotypes is an emphasis on maintenance of airway protection, ventilation, and circulation. Patients presenting in a comatose state require intubation to prevent aspiration, ensure oxygenation, and optimize gas exchange to control potential intracranial hypertension. We recommend that patients have continuous systemic blood pressure monitoring (typically via radial artery catheterization), with maintenance of systolic blood pressure under 140 mmHg in order to prevent aneurysm rebleeding (Connolly et al., 2012). In addition to titratable infusions to lower blood pressure, pain and anxiety can make a substantial contribution and should simultaneously be addressed via non-pharmacologic interventions. If acute hydrocephalus is present, controlled cerebrospinal fluid drainage via a ventriculostomy should be performed in order to reduce intracranial pressure.

Once the diagnosis of aneurysmal SAH has been made, additional evaluation of cardiac function should be obtained with electrocardiography and echocardiography. While most cardiac disturbances are self-limiting, it is important to recognize any potential impairment prior to the supraphysiologic challenges of surgery and potentially vasospasm treatment protocols. Cardiac abnormalities are common in the first 48 hours after SAH; electrocardiographic changes including tall peaked T-waves or cerebral T-waves, ST segment depression, and prolonged QT segments. Cardiac enzymes are often mildly elevated and arrhythmias are very common, but typically benign in nature. Acute neuro-cardiogenic injury or Takotsubo cardiomyopathy can also be seen, with significant left ventricular systolic dysfunction resulting from excessive catecholamine release from sympathetic nerve terminals that mimics myocardial ischaemia (van der Bilt et al., 2014).

Other medical management concerns that take priority during the initial hours following a subarachnoid haemorrhage include optional administration of antiepileptic medication for seizure prophylaxis and administration of the calcium channel blocker nimodipine for prevention of vasospasm (Barker and Ogilvy, 1996). In exceptional circumstances, if definitive aneurysm treatment is not available for several days, antifibrinolytic therapy can be administered.

Non-aneurysmal perimesencephalic subarachnoid haemorrhage

When spontaneous SAH occurs without an aneurysmal source, haemorrhage patterns can be dichotomized into one of two patterns. Firstly, the perimesencephalic pattern (Fig. 49.3), where blood is

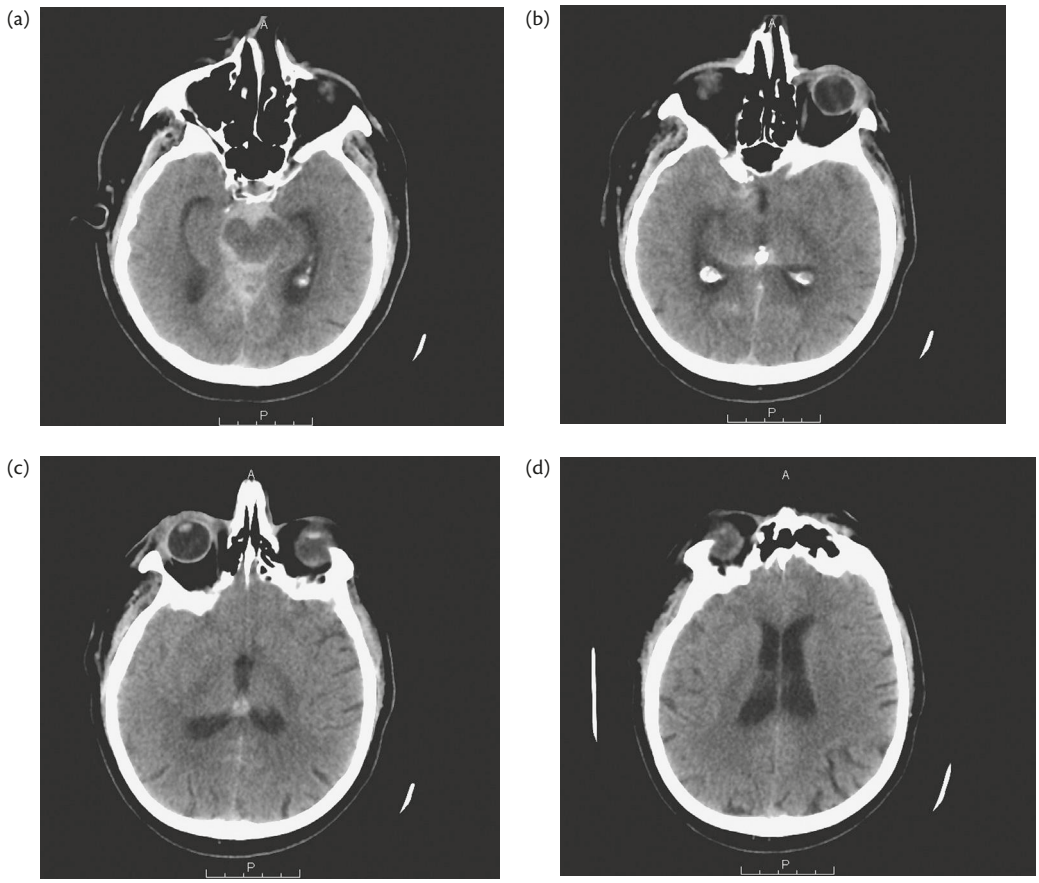

Fig. 49.3 Perimesencephalic haemorrhage pattern. Non-contrast axial head computed tomography of patient who experienced a non-aneurysmal subarachnoid haemorrhage confined to mainly the basal cisterns surrounding the midbrain. Representative images are demonstrated in sequence from A to D in their inferior to superior location.

confined mainly in the basal cisterns surrounding the midbrain and constrained by Liliequist's membrane, but can include the proximal part of the Sylvian fissure. Secondly, diffuse, where blood extends into the distal Sylvian or interhemispheric fissures.

While non-aneurysmal haemorrhage has typically been associated with a benign course, recent evidence has suggested that hydrocephalus, vasospasm, and stroke can all occur, particularly with diffuse haemorrhage patterns (Walcott et al., 2015). Although catheter-based angiography has excellent sensitivity in detecting haemorrhage aetiology, it is certainly not 100% sensitive. Follow-up catheter angiography at intervals of one and six weeks from the time of the haemorrhage has been shown to improve the sensitivity for detecting a vascular lesion when the initial catheter angiogram is negative (Grannan et al., 2014), particularly if there is a high clinical index of suspicion. The exact timing and modality of repeated neurovascular imaging is not supported by prospective trials, and recommendations are based mainly on experience from high-volume centres. An unrecognized aneurysm could have devastating consequences and vigilance must be maintained during the investigation of these patients.

Definitive management of the aneurysm

Endovascular coiling of aneurysms

Endovascular coil embolization is a relatively contemporary means of aneurysm obliteration. The first coiling procedures were used to treat human patients with cerebral aneurysms in the early 1990s (Guglielmi et al., 1992). Compared with microsurgical clipping, there is less cumulative experience and less long-term follow-up. However, both methods have been shown to be effective at the ultimate primary goal of aneurysm treatment—to safely eliminate blood flow into the aneurysm (Molyneux et al., 2015). A recent analysis of the total aneurysm surgical practice in the United States provides strong evidence for the popularity of both techniques, with over half of all aneurysms now treated with endovascular coiling. Certain adjuncts can assist with coiling, such as intraluminal stent devices and balloon assistance. Endovascular therapy with flow-diverting stents, with or without adjunctive coiling, is also an emerging treatment option. With these methods, many previously 'uncoilable' or even 'untreatable' aneurysms are now amenable to endovascular treatment.

Coil embolization

Indications

Most aneurysms can be treated with either microsurgical clipping or coil obliteration. Treatment recommendations are usually made after thorough evaluation of anticipated risks and benefits of the different treatment methods for the same unique aneurysm. This involves evaluation of patient specific factors and aneurysm specific factors. These factors generally relate to the intrinsic aneurysm configuration. Classically, a neck-to-dome ratio of 2:1 (aspect ratio) identifies aneurysms that are likely to be treatable with a coil. Other

considerations include the neck size (<5 mm, favourable) and close relationship to a neighbouring artery (unfavourable). Other factors that generally favour endovascular treatment include aneurysm location (vertebrobasilar circulation) and patient age (older). These generalizations must be considered in the context of all patient and aneurysm specific characteristics on a case-by-case basis. Optimally, review by a multimodality provider capable of performing coiling and clipping allows for a thorough evaluation of each unique clinical scenario and aneurysm configuration.

Technique

The patient is positioned supine then placed under general anaesthesia. Alternatively, the procedure can be done awake in compliant patients if they are able to hold breathing during fluoroscopy and keep still. Both groin sites are prepped in a sterile fashion and the femoral artery (usually right side) is punctured. Next, a sheath is introduced with a Seldinger technique, and this sheath is then connected to an irrigation system consisting of heparinized saline to prevent thromboembolic complications. A guide catheter, also connected to a continuous heparinized flush, is navigated over a 0.35" or 0.38" curved or j-shaped guide wire, from the groin to the aortic arch under fluoroscopic guidance into either internal carotid artery (ICA) or vertebral artery, depending on the target aneurysm location.

Three-dimensional angiography (rotational angiography) is often obtained to better characterize the aneurysm size, configuration, and adjacent neurovascular structures. A microcatheter is chosen according to the desired stiffness or profile, and then navigated the remaining distance between the guide catheter and its final destination, the aneurysm. The size and shape of the first coil to be deployed is determined by the shape and measurements of the aneurysm. Usually the first coil is used to create a framework, which fits well into the aneurysm and can be filled with subsequent coils. Intermittent super-selective angiography before and after coil placement allows confirmation of coil location inside the aneurysm dome and provides information regarding any residual filling of the aneurysm. When the operator is satisfied with coil placement, it is detached, and the decision to proceed with further packing coil placement is made.

Visual-haptic biofeedback during coil deployment, failure to deploy a small coil, packing density of the aneurysm, and any residual filling of the aneurysm are some indicators used to judge when to stop coiling. After coiling is finished, the microcatheter may be removed and a final angiographic run is performed (Fig. 49.4). All catheters are subsequently removed and the groin puncture arteriotomy may be closed with a period of manual pressure or with a vascular closure device.

Balloon-assisted coiling procedure

Indications

Primary coiling can be challenging with wide-necked aneurysms, small aneurysms with a high risk of intraprocedural rupture, bifurcation aneurysms, and aneurysms with a branch vessel originating from the neck of the aneurysm. In these settings, using inflatable balloon techniques can mitigate these factors by remodelling the neck, protecting a parent vessel/side branch, or doing both. It can also help to keep a microcatheter in the aneurysm sac and reduce 'kickback' during coil deployment, potentially resulting in a greater packing density.

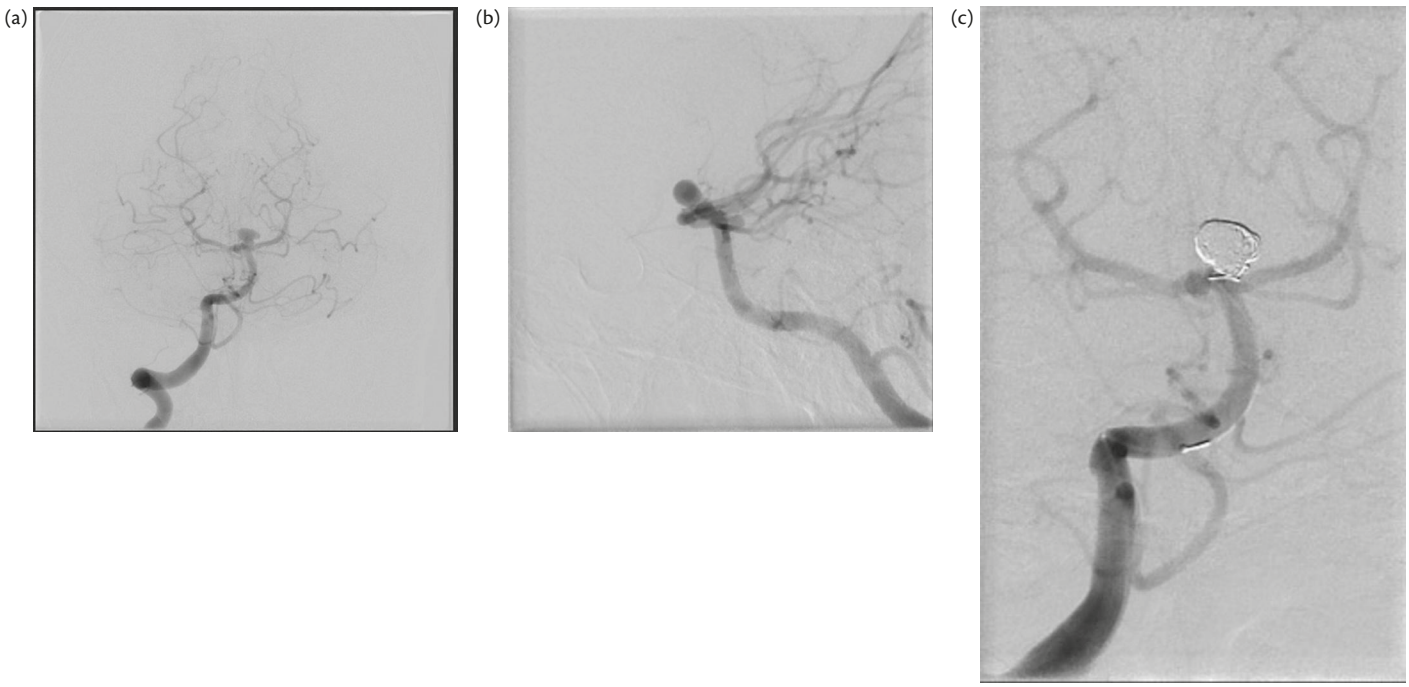

Fig. 49.4 Endovascular coiling of basilar apex aneurysm. A 60-year-old female presented with the 'worst headache of her life' and diffuse subarachnoid haemorrhage. She was found to have a 7 mm basilar artery apex aneurysm (A, B) and smaller superior cerebellar and middle cerebral artery aneurysms. In the context of haemorrhage with a diffuse pattern, it can be predicted that the irregular, largest aneurysm was the source. The basilar apex aneurysm was obliterated with coils (C) and the patient made a full recovery.

Technique

For patients with subarachnoid haemorrhage, heparinization is initially withheld, in comparison with unruptured aneurysms. Once one or two coils are deployed into the aneurysm, then heparin can be administered. The balloon catheter is introduced into the proximal end of the guide catheter, along with the microcatheter (through the side port). When the coil is nearing the aneurysm, the balloon is filled to the appropriate volume with 100% contrast. Subsequent coils can then be delivered, mindful of distal ischaemia time while the balloon is inflated.

Somatosensory evoked potentials and motor evoked potentials can be useful monitoring techniques, particularly in anesthetized patients. When changes occur, the balloon can be deflated. Once the coil mass is delivered, the balloon is deflated to assess the stability of the coil mass. If the coil mass does not herniate out of the aneurysm, then the microcatheter is removed and the device is withdrawn from the guide catheter.

Double-microcatheter technique

Indications

While wide-necked aneurysms can be treated with stent-assisted coiling or balloon-assisted coil delivery and remodelling, these methods have specific risks associated with thromboembolic complications. With stent-assisted coiling, patients require long-term antiplatelet therapy, which can be problematic during the initial management of a ruptured aneurysm. The double-microcatheter technique is a useful alternative in these situations to help achieve a safer and denser coil delivery without the need for antiplatelet therapy.

Technique

Two microcatheters are advanced through the guide catheter and into the aneurysm sac. Since a single microcatheter may deploy coils that herniate back through a wide neck and into the parent artery, a second microcatheter is also placed in the aneurysm to deploy an additional coil prior to detachment of the first framing coil. By doing this, the coils can be thought of as 'locking' onto each other if they are deployed sequentially, or 'weaving' into each other if they are deployed concurrently. One of the coils is then detached. For all subsequent coil deployments, one of the catheters retains a deployed coil that is not detached, thereby acting as a brace since it is connected to the pusher wire. Embolization is continued through the available catheter until aneurysm obliteration is complete. This technique increases the coil stability greatly and allows for coiling of some wide-necked aneurysms without stent placement.

Major complications of endovascular coil embolization

Endovascular coil embolization of ruptured aneurysms is associated with low, but recognized complication rates of thromboembolism resulting in stroke (4–5%), intraprocedural aneurysm rupture (7%) (Fig. 49.5), coil migration, incomplete aneurysm obliteration, aneurysm recurrence (20%), aneurysm rebleeding after treatment, contrast nephropathy, and groin haematoma (Owen et al., 2015; Molyneux et al., 2015; Spetzler et al., 2015; Stapleton et al., 2015a).

As coil embolization has become the accepted first line treatment for ruptured aneurysms, there is an increasing need to consider late retreatment (endovascular and possibly surgical) of recurrent aneurysms. Factors that influence recurrence after coiling include aneurysm size, aspect ratio, absolute neck width, aneurysmal thrombus, smoking, length of follow-up, familial predisposition, quality of coil packing/occlusion and presentation with haemorrhage. Indications for treatment are not well established but may include extent and rate of recurrence, age, rehaemorrhage, and clinician/patient choice.

Microsurgical clipping of aneurysms

Aneurysm clipping is the longest standing method for treatment of cerebral aneurysms. Since the first intracranial aneurysm clipping was performed by Dandy in 1937, and the introduction of microscopic techniques by Yasargil, clipping of aneurysms has developed into a refined and delicate procedure with low rates of complications and proven durability. The recent evolution of endovascular treatments is typified by advances in device technology and technique, and microsurgery is no different. The evolution of new techniques and intraoperative imaging has made open aneurysm surgery less invasive, more appealing to patients, and has progressively lowered procedural risk. Clipping treatments are especially efficacious for complex aneurysms with unfavourable configurations or for those failing endovascular therapy (Davies and Lawton, 2014).

Approaches to aneurysms are determined primarily by the aneurysm location. The majority of aneurysms in the anterior circulation (anterior communicating artery aneurysm, posterior communicating artery aneurysm, middle cerebral artery bifurcation aneurysm) can be accessed through a pterional craniotomy, with slight variations tailored to individual aneurysm anatomy. For aneurysms arising from the distal anterior cerebral artery (A2 segment and beyond), a bifrontal craniotomy and interhemispheric approach is commonly used. For aneurysms arising from the upper basilar trunk (basilar apex aneurysm, superior cerebellar artery aneurysm), a pterional craniotomy with additional removal of the orbitozygomatic unit allows for the wide trans-Sylvian dissection necessary to lessen the working depth needed to reach these lesions safely. Other aneurysms of the posterior circulation, such as the posterior inferior cerebellar artery aneurysm, are classically approached through a far lateral craniotomy, whereas aneurysms of the vertebrobasilar junction can be accessed through a retrosigmoid craniotomy. The full armamentarium of microsurgical approaches includes subtemporal, presigmoid, transpetrosal, suboccipital, supraorbital, transpalpebral, and combinations or variations thereof. The craniotomy type is selected to allow an adequate line of sight to the aneurysm anatomy, while minimizing the need for any brain retraction.

Pterional craniotomy for the trans-Sylvian approach

The frontal-temporal-sphenoidal craniotomy, better known as the pterional craniotomy, is the most common craniotomy type for an aneurysm surgeon, since the majority of aneurysms occur in the anterior circulation. It allows for exposure of the frontoparietal operculum and opening of the Sylvian fissure to access the circle of Willis. In brief, the patient is placed in skull fixation, with the head rotated 15–20 degrees away from the side of the aneurysm. The head

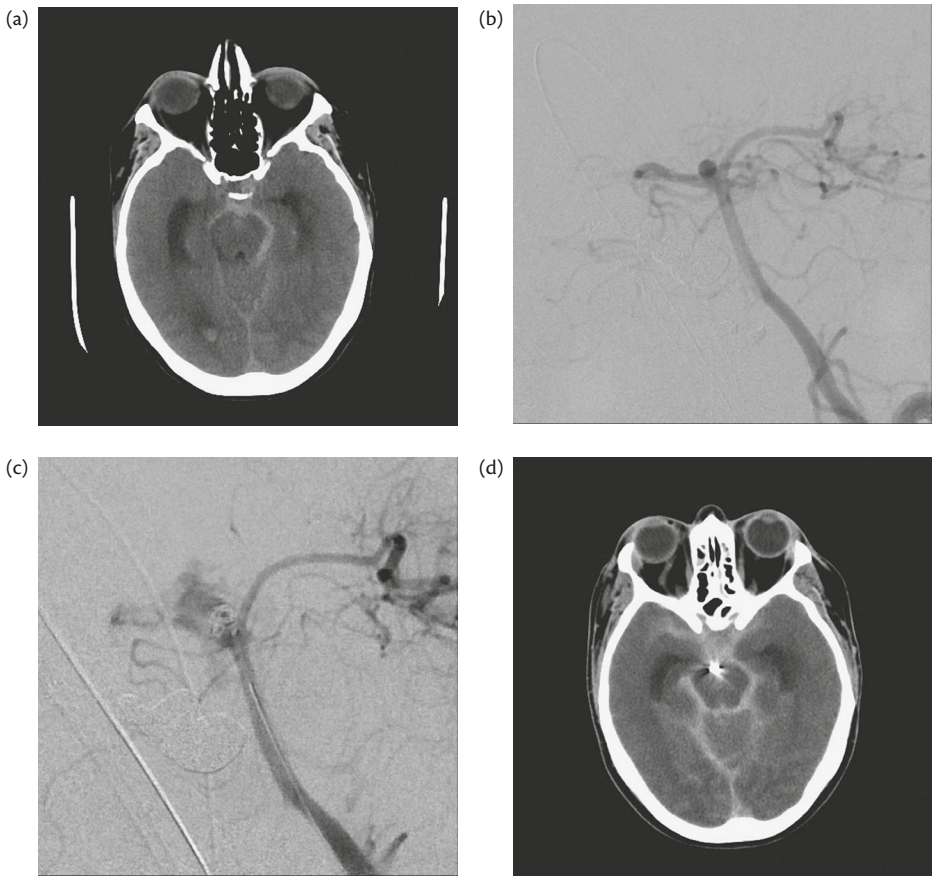

Fig. 49.5 Intraprocedural rupture during coiling of a basilar apex aneurysm. (A) Axial CT image showing SAH from a ruptured basilar apex aneurysm. (B and C) Right anterior oblique catheter angiograms obtained in the same case showing a ruptured basilar apex aneurysm (B) and active contrast extravasation (C) following intraprocedural rupture during coil embolization. (D) Axial CT image showing increased SAH and subarachnoid contrast following intraprocedural rupture of the basilar apex aneurysm.

is extended approximately 20 degrees, making the malar eminence the high point in the surgical field. The head is then lifted above the level of the heart, out of a dependent position. A curvilinear skin incision begins at the zygomatic arch 1 cm anterior to the tragus and curves to the midline, just behind the hairline at the widow's peak. The scalp is elevated only enough to expose the zygomatic root posterior-inferiorly and the keyhole anteriorly. The superficial fat overlying the temporalis fascia should not be entered because the frontalis branch of the facial nerve lies in this tissue plane and can be injured with additional elevation of the scalp flap. The temporalis muscle is incised from the zygomatic arch to the superior temporal line along the skin incision, then anteriorly to the keyhole, running 1 cm below the superior temporal line. The temporalis is flapped anteriorly, leaving a cuff of fascia and muscle along the superior temporal line to suture the muscle to during closure for improved cosmetic outcome. Next, a burr hole is placed below the superior temporal line posteriorly and a frontal-temporal craniotomy is made using a high-speed drill. After bone flap removal, the drill is used to remove the pterion and the lesser wing of the sphenoid medially, all the way to the superior orbital fissure. Bone removal is adequate when there is a flat surface over the orbit connecting the anterior and middle cranial fossa. The dura is opened with a semicircular incision, hinging anteriorly. Multiple stay sutures flatten the dural flap. At the conclusion of the exposure, there should be direct visualization of the frontal and temporal lobes on either side of the Sylvian fissure, permitting an unobstructed view along the dural flap into the carotid cistern.

Bifrontal craniotomy for an anterior interhemispheric approach

Bifrontal craniotomy is a standardized technique to facilitate an interhemispheric approach to distal anterior cerebral artery aneurysms, such as pericallosal artery aneurysms. These aneurysms are typically located in the midline, but deep to the falx. Therefore, the exposure only needs to be on one side. The bifrontal nature (with only a small portion of the craniotomy crossing over to the contralateral side) allows for sutures to retract the superior sagittal sinus, permitting a straight line of view to the aneurysm. The patient is positioned supine with the head in neutral position, or for more distal aneurysms the head can be placed in a lateral position with a 45-degree tilt away from the ground. For right sided approaches, the incision begins at the right zygoma and ends at the contralateral superior temporal line because the craniotomy is eccentric to the right side. The scalp is then pulled forward to expose supraorbital frontal bone from the ipsilateral superior temporal line to the contralateral glabella. The temporalis muscle should be undisturbed. A rectangular craniotomy is made that is two-thirds in front of the coronal suture and just across the midline to the contralateral side. Care

must be taken to strip the dura from the undersurface of the skull to prevent venous sinus injury. The dura is then opened in a semicircular flap with its hinge point being the superior sagittal sinus. The interhemispheric fissure is then in view and subarachnoid dissection can continue down to the aneurysm.

Orbitozygomatic craniotomy for a trans-Sylvian approach

The orbitozygomatic (OZ) approach dramatically enhances the standard pterional craniotomy increasing exposure, minimizing retraction, and improving manoeuvrability for large, giant, or complex anterior circulation aneurysms, and for aneurysms of the upper basilar trunk. Deep bypass procedures benefit from the additional working room of this approach. Removing the orbital walls completely and depressing the eye with the dural flap, along with zygoma resection gives the neurosurgeon a wide sweep of surgical trajectories ranging from supraorbital to trans-Sylvian to pretemporal to subtemporal. The surgical trajectory can then be tailored to the exact aneurysm location. A modified orbitozygomatic approach can be used when the zygoma resection would not meaningfully add to the exposure, and it can be left intact.

Far lateral craniotomy for anterior pontomedullary approaches

The far lateral craniotomy provides an excellent corridor to access most posterior inferior cerebellar artery aneurysms. The patient is placed in a modified park-bench or three-quarter prone position with the lesion side upward. The dependent arm hangs over the end of the table, cradled in a padded sling. Three manoeuvres are then used to position the head: (1) flexion in the anteroposterior plane until the chin is one finger's breadth from sternum; (2) rotation 45 degrees away from the side of the lesion, (bringing the nose down toward the floor); and (3) lateral flexion 30 degrees down toward the floor. These manoeuvres put the clivus perpendicular to the floor, allowing the neurosurgeon to look down the axis of the vertebral artery. The ipsilateral mastoid process becomes the highest point in the operative field. The patient's ipsilateral shoulder is retracted using cloth tape to open the cervical-suboccipital angle. Although variations exist, a classical 'hockey-stick' incision is made beginning in the cervical midline over the C4 spinous process, extending cephalad to the inion, coursing laterally along the superior nuchal line to the mastoid bone, and finishing inferiorly at the mastoid tip. The myocutaneous flap is mobilized inferolaterally as a whole to expose the occipital bone and foramen magnum. Next, a C1 laminectomy is performed all the way laterally to the sulcus arteriosus. Next, a suboccipital craniotomy is extended unilaterally from the foramen magnum in the midline, up to the muscle cuff at the level of the transverse sinus, as far laterally as possible, and then back around to the foramen magnum. After the craniotomy, the foramen magnum is opened up more widely with rongeurs and a high-speed drill, and the suboccipital craniotomy is extended past the midline. Finally, the posteromedial two-thirds of the occipital condyle are drilled away. The anterior extent of the condylar resection is defined either by the condylar emissary vein or by the dura that begins to curve anteromedially, giving a tangential view along this dural plane. Condylar resection enables the dural flap reflected against the condyle to be completely flat, and is analogous to the purpose of pterional flattening in a pterional craniotomy.

The dural incision curves from the cervical midline, across the circular sinus, to the lateral edge of the craniotomy. When completed, the exposure offers a view of the path of the intradural vertebral artery and provides adequate working space in the angle between the lateral medulla and inferior cerebellum (Rodríguez-Hernández and Lawton, 2011).

Intracranial surgical technique

The process of clipping an aneurysm is much more complex than performing a craniotomy and placing a clip across the neck of the aneurysm. There are many nuances to surgery, such as subarachnoid dissection techniques and crisis management, which all can correspond to successful patient outcomes (Lawton, 2011).

During aneurysm surgery, an emphasis must be placed on careful, extensive subarachnoid dissection. By opening up the subarachnoid spaces under high-powered magnification, corridors to the arterial system can be exposed without violating or harming the brain. The technique consists of three basic manoeuvres: cutting with microscissors, spreading with bipolar forceps, and probing with a slightly curved blunt dissector (such Rhoton #6). By opening up these natural cisterns, the frontal and temporal lobes separate, spinal fluid is drained, and the aneurysm can be approached without excessive manipulation or fixed brain retraction. As an example, anterior communicating artery aneurysms are approached by first dissecting the Sylvian fissure, then progressing from the carotid to chiasmatic to lamina terminalis cisterns.

As the surgeon approaches the final dissection of the aneurysm, the orderly sequence exposing afferent arteries, efferent arteries, and the aneurysm neck is often complicated by the presence of the aneurysm dome and difficulty with exposing perforating arteries. During this time, temporary clipping may be used in selected cases to give the surgeon more confidence in the final dissection, soften the aneurysm dome, and allow for better visualization of perforating arteries. Barbiturates to achieve electroencephalography (EEG) burst suppression and raising the systemic blood pressure can help to provide protection from ischaemia, but surgeon efficiency and highly selective use are the most important aspects of temporary clipping.

When ready, permanent clipping can take place under complete visualization from start to finish. Various types of clip configurations have been stereotyped: simple clipping, multiple intersecting clips, stacked clips, overlapping clips, and permutations of these exist. Tandem clipping, with a fenestrated clip to close the distal aspect of the aneurysm neck, followed by a shorter clip to close the proximal portion of the aneurysm neck not covered by the fenestration is also a very effective technique. Tandem clipping exploits a physical characteristic that the force of a fenestrated clip is greatest at the distal end of the clip tines. This allows for an even distribution of force to be applied across the entire aneurysm neck, preventing refilling.

Uncontrolled intraoperative bleeding from an aneurysm is one of the most feared complications in neurosurgery, and knowing what to do during this crisis can be the difference between life and death. The technical response to intraoperative rupture should proceed in a calm and orderly fashion: tamponade, suction, proximal control with temporary clipping, and permanent aneurysm clipping. A small piece of cotton can be placed over the rupture site, and pressure and suction can be applied to clear the surgical field of blood. Proximal control then slows the bleeding and is often

sufficient to finish dissecting and apply permanent clips. After any permanent clip application, whether in the setting of intraoperative rupture or otherwise, the surgeon must spend time inspecting the result. It is important to check for aneurysm occlusion, patency of the parent artery and efferent branches, patency of the perforating arteries, and to determine if any aneurysm neck is remaining. We routinely use intraoperative indocyanine green videoangiography during this inspection process, although some centres continue to use intraoperative catheter-based angiography (Raabe et al., 2005).

Specific aneurysm considerations and locations

Anterior communicating artery aneurysms are among the most challenging. The H configuration of A1 and A2 branches must be identified intraoperatively to ensure that none of the branches are compromised on clip application. During dissection, consideration must be given to the safe corridors of vascular dissection in relation to the dome of the aneurysm. For an anteriorly projecting aneurysm, dissection proceeds as follows: the outer border of the ipsilateral A1 and ipsilateral A2, then the contralateral A1 and A2. In contrast, for an inferiorly projecting aneurysm, the order changes to ipsilateral A1 and A2 then contralateral A2 as the contralateral A1 is obscured by the aneurysm fundus. This aneurysm configuration is at risk of premature rupture with injudicious mobilization of the frontal lobes if adherent to the optic chiasm (see Chapter 46 for anatomical details).

For a superiorly projecting dome, the order changes to both ipsilateral and contralateral A1s to achieve proximal control before identifying both A2s. These aneurysms are potentially the most difficult configuration to clip and often require a fenestrated clip around the ipsilateral A2 to avoid leaving a neck remnant. On occasions, anterior communicating artery aneurysms require trapping of the whole anterior communicating artery, although this risks sacrifice of the associated perforating arteries.

For ICA aneurysms (posterior communicating and anterior choroidal), the degree of head rotation during positioning depends on the projection of the aneurysm fundus. For a posteriorly projecting fundus, a greater degree of head rotation is required to reveal the neck of the aneurysm from behind the ICA. For a laterally projecting fundus, care must be taken with temporal lobe mobilization as it may be adherent to the aneurysm and risks premature rupture. The anterior choroidal artery branches may be duplicated and closely related to the aneurysm neck. It is important to identify and preserve all these branches. Preservation of the posterior communicating artery is most important with a fetal configuration which often occurs in association with aneurysm formation. For ICA bifurcation aneurysms careful identification and dissection of the medial and lateral lenticulostriate perforators is required to avoid incorporation into the aneurysm clip. Aneurysm clips at this location are particularly at risk of kinking the parent vessels.

Middle cerebral artery (MCA) aneurysm clipping requires extensive dissection of the entire fundus as variation in the number of M2 branches is common. These aneurysms may require 'clip reconstruction' (i.e. use of multiple clips to obliterate the entire neck without compromising the distal branches).

Pericallosal aneurysms are a challenge as the aneurysm fundus will be encountered before the parent vessels are identified and controlled. However, the flow through the pericallosal artery is substantially lower than for the large arteries at the base of the circle of Willis and intraoperative rupture is more easily controlled. Image guidance is a useful adjunct in order to plan both the craniotomy and trajectory to the aneurysm.

Advanced techniques for complex lesions

There is no standard definition of what constitutes a difficult aneurysm, although one could consider any aneurysm that could not be treated with straightforward clipping or coiling to be complex. Complex aneurysms have also been described as those more than 10 mm in greatest diameter, or those that have intraluminal thrombosis, were previously coiled, were heavily calcified, or have a fusiform or true blister morphology (Fig. 49.6). Treatment for these lesions often requires advanced techniques or adjunctive devices.

Advanced endovascular techniques

Intracranial stents to assist coiling

The use of stents to support coil placement in the aneurysm dome is required for some wide-necked aneurysms. By 'jailing' the coil mass in the aneurysm, the stent wires prevent prolapse of the coils into the parent vessel (Fig. 49.7). Since endoluminal devices such as stents are prone to thromboembolic complications, patients are typically treated with dual antiplatelet therapy for a period of several months, with at least some form of antiplatelet therapy continuing indefinitely. Newer generations of stents are now available with 'low profile' configurations (use of a braided design) that may provide superior conformability and parent artery apposition, as well as a more reliable and uniform neck bridging than previous neurovascular stents. 'Baby' stents are also under evaluation for use in the coiling of distal intracranial circulation aneurysm.

Endoluminal flow diversion

Flow diverting stents are a relatively new paradigm treatment for brain aneurysms, where intraluminal flow is redirected to the distal parent vessel, rather than into the aneurysm. This is accomplished by using a stent with a low porosity mesh weave. Adjunctive coils are also sometimes placed into the aneurysm to provide immediate aneurysm closure and prevent delayed haemorrhage from a 'ball-valve' haemodynamic effect that has been hypothesized to occur following a small percentage of treatments. Some of the best preliminary results for flow diverting stents have been reported for aneurysms in the cavernous and paraclinoid segments of the carotid artery (Brinjikji et al., 2013). Redirection of parent vessel flow has been associated with perforator artery ischaemia and this has been the major limitation to the widespread application of this treatment in other vascular territories.

Intrasaccular flow disruption devices

Another relatively new endovascular treatment paradigm is intrasaccular flow diversion, where a device is placed inside the aneurysm sac itself (Woven Endovascular Bridge 'WEB' device) which then provides a flow diverting barrier across a wide neck, eventually reconstructing the parent vessel and induces thrombosis and occlusion of the aneurysm. This device has been used mostly for wide-necked bifurcation aneurysms, such as those at the carotid terminus, basilar apex, and MCA bifurcation with promising preliminary results (Lubicz et al., 2013). However, there is still limited clinical experience with this device and it remains under investigational regulation in many countries, such as in the United States.

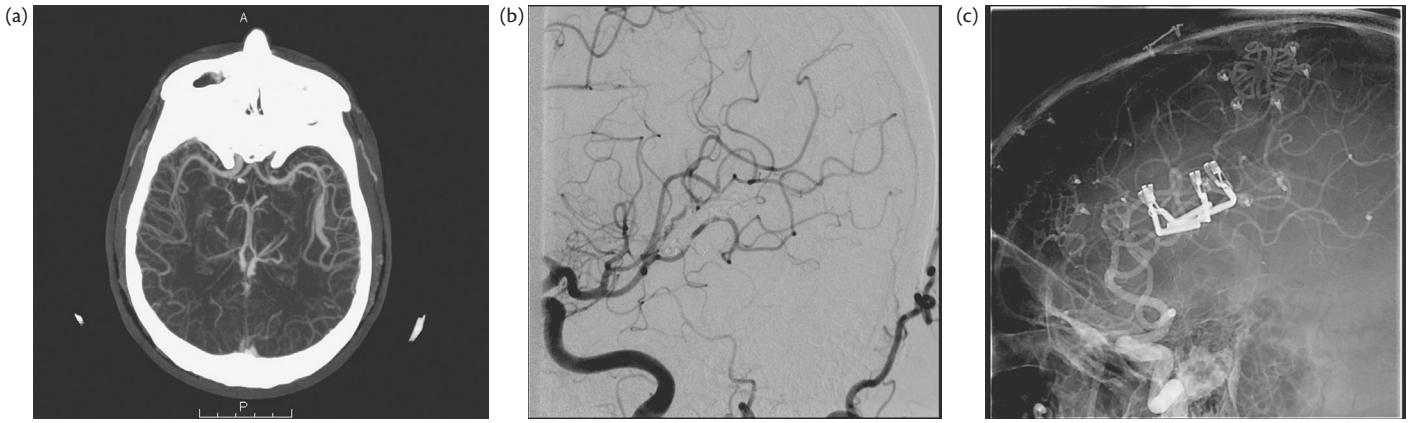

Fig. 49.6 Complex vessel reconstruction of dissecting fusiform aneurysm. A 37-year-old male presented to the emergency room with the 'worst headache of his life'. He was discovered to have subarachnoid haemorrhage resulting from a dissecting, fusiform aneurysm of the left middle cerebral artery. (A) He was taken to the operating room for vessel reconstruction with possible extracranial-to-intracranial bypass. Fenestrated, right-angle aneurysm clips were successfully placed sequentially to reconstruct the wall of the vessel. The patient made a full recovery and has done well since. A two-year follow-up angiogram is shown (B, C) demonstrating no residual aneurysm along the reconstructed M2 segment.

High-flow bypass surgery

For some aneurysms, direct clip reconstruction is not possible. Examples of these situations are relatively infrequent, but can be seen with giant fusiform MCA aneurysms that incorporate multiple MCA branches, blister or dissecting aneurysms, and giant paraclinoid ICA segment aneurysms that extend into the cavernous segment, among others. For these lesions, it is necessary to exclude the aneurysm from the circulation and also to preserve vital blood flow to

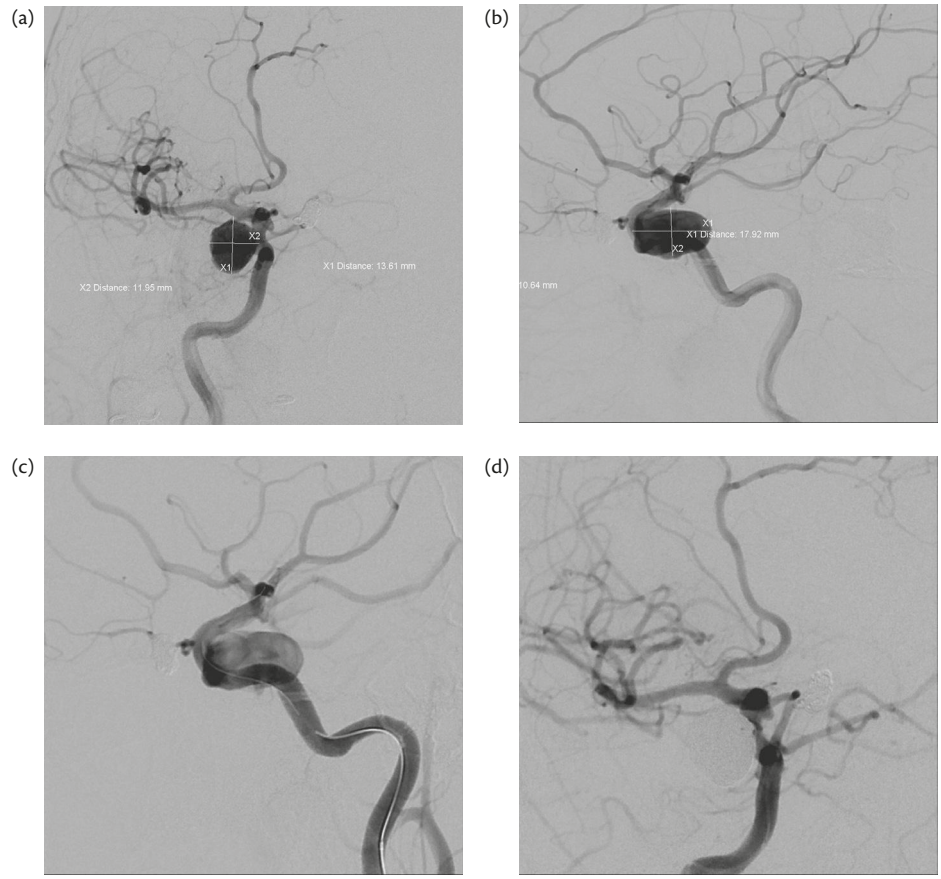

Fig. 49.7 Stent-assisted coiling of a carotid artery aneurysm. Pretreatment angiographic imaging (A and B) revealed a saccular wide-necked cavernous segment aneurysm that would be difficult to treat with standalone coiling. (C) A neuroform stent was successfully navigated, deployed, and subsequent coiling was performed. Immediate post-treatment results (D) demonstrated occlusion of the aneurysm. An additional supraclinoid aneurysm was also coiled.

the distal branches. This can be accomplished with aneurysm trapping and cerebrovascular bypass. By anastomosing a vessel distal to the aneurysm with a donor artery, one replaces the blood flow of the native circulation pattern. Historically, donor artery blood flow has been obtained from the external carotid artery (such as the superficial temporal artery or from the cervical external carotid artery via an interposition graft) and an anastomosis is performed to the intracranial circulation. More recently, intracranial-to-intracranial bypass has been developed as a viable treatment option in many cases, eliminating the need for any interposition grafts and shortening the bypass length (Sanai et al., 2009; Abla and Lawton, 2014; Davies and Lawton, 2014) (Fig. 49.8). As technology evolves and expands the endovascular armamentarium, indications for bypass are expected to decrease but not vanish. For example, many giant

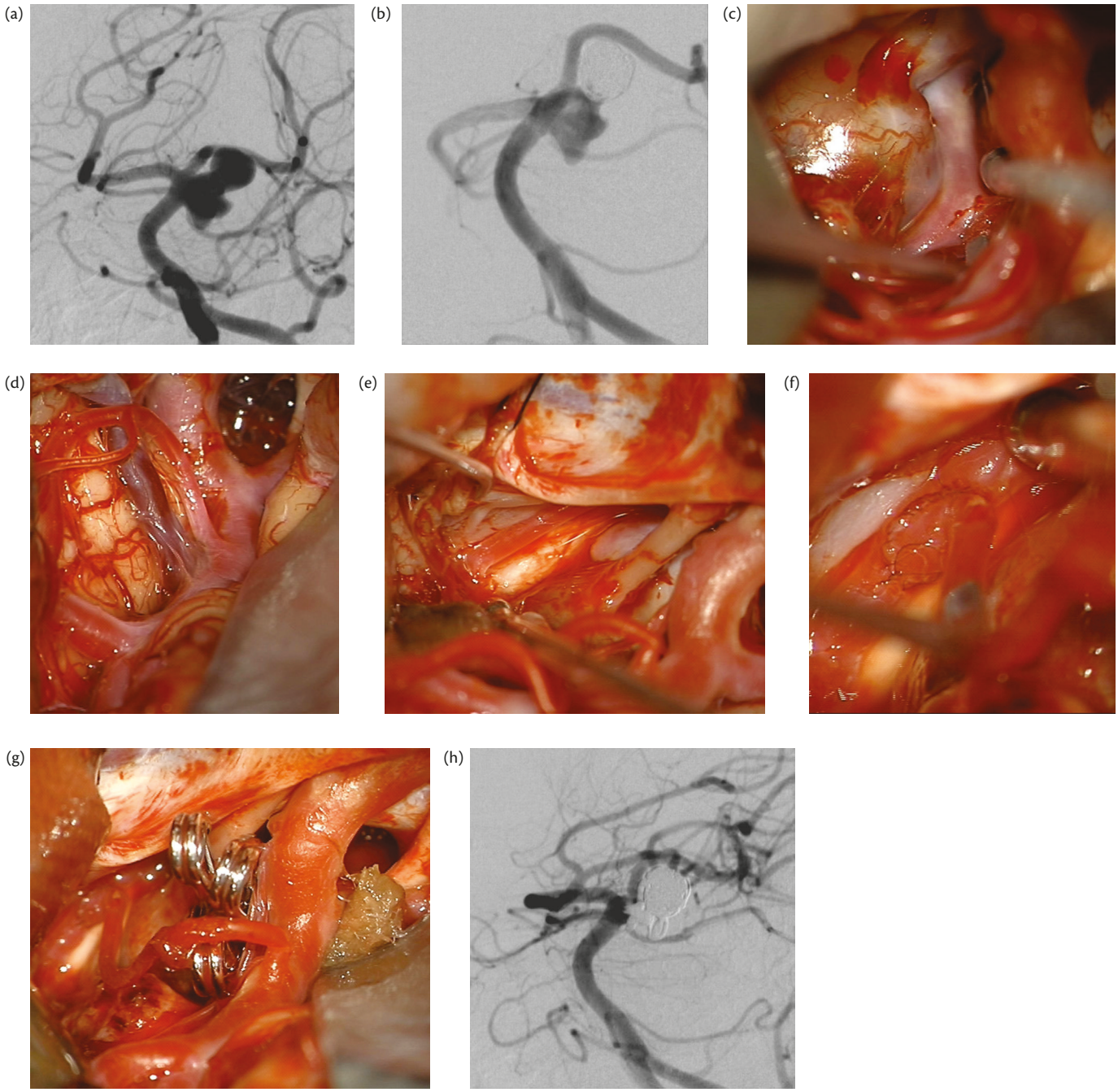

Fig. 49.8 Microsurgical treatment of incompletely coiled complex superior cerebellar artery (SCA) aneurysm with clipping and intracranial-to-intracranial bypass. (A) This ruptured, multilobulated SCA aneurysm (right vertebral artery injection, anterior oblique view) was unable to be completely coiled (B) and then referred for clipping. (C) The coil mass and adherent oculomotor nerve made the aneurysm appear to be unclippable, and a bypass/trapping strategy was pursued. (D) The anterior temporal artery (ATA) branch of the M1 middle cerebral artery was used as a donor artery to the s2 segment of the SCA, (E) which was exposed through an incision in the tentorial edge. (F) An end-to-side anastomosis created an ATA-SCA bypass (G) and the aneurysm neck was clipped successfully with only partial occlusion of the SCA origin. (H) Postoperative angiography demonstrates complete obliteration of the aneurysm with preserved flow through the SCA. Note the washout of contrast on the S2 SCA as the unopacified blood flow from the anterior circulation joins the SCA flow via the bypass.

paraclinoid segment ICA aneurysms are now being treated with flow diverting stents. Therefore, bypass proficiencies should be maintained and advanced, since the need for increasingly complex surgical solutions is growing as a function of the less complex lesions being treated with endovascular techniques, as well as the growing entity of aneurysm recurrences following prior endovascular treatment (Owen et al., 2015).

Medical management of subarachnoid haemorrhage

Vasospasm/delayed cerebral ischaemia

For those that survive the early period following subarachnoid haemorrhage and have their aneurysms treated, cerebral vasospasm can result in impaired cerebral blood flow and is the major cause of delayed ischaemia and stroke (Kassell et al., 1985). Vasospasm is defined as new intracranial arterial narrowing (mild, moderate, or severe) identified on catheter or CT angiography, and is thought to occur as a result of blood product interaction with the vascular smooth muscle of the intracranial arteries. The Fisher scale (**Table 49.2**) is the classical radiographic grading scale that provides a prediction of vasospasm development based on the initial subarachnoid blood pattern and amount following an aneurysm rupture. While many patients develop vasospasm, less than half of these become symptomatic, defined as neurological symptoms referable to a region of radiographic or sonographic vasospasm in the absence of alternative explanations. The only medical therapy in widespread use to prevent vasospasm is oral nimodipine, and it is typically administered for a total of 21 days (Barker and Ogilvy, 1996).

Currently available means of vasospasm detection rely on serial clinical examination, in addition to non-invasive imaging, either with ultrasound or computed tomography angiography (CTA). Perfusion based imaging modalities have also been shown to be useful detecting clinically significant alterations in cerebral blood flow. Additionally, catheter-based digital subtraction angiography can be used to diagnose vasospasm. The purpose of any imaging surveillance for vasospasm is to identify changes in vessel calibre or blood flow prior to neurological deterioration. Knowledge of these changes allows for the rapid institution of medical therapies, including systemic hypertension and intra-arterial vasodilator therapy (**Fig. 49.9**), if patients go on to become symptomatic in order to prevent permanent deficits (Athar and Levine, 2012).

Table 49.2 Fisher Scale

Grade	CT findings
1	No evidence of haemorrhage
2	Subarachnoid haemorrhage less than 1 mm thick
3	Subarachnoid haemorrhage more than 1 mm thick
4	Subarachnoid haemorrhage of any thickness with intraventricular haemorrhage or parenchymal extension

Reproduced with permission from Fisher, C.M.; Kistler, J.P., Relation of Cerebral Vasospasm to Subarachnoid Hemorrhage Visualized by Computerized Tomographic Scanning, *Neurosurgery*, Volume 6, Issue 1, pp. 1–9, Copyright © 1980 Oxford University Press and the Congress of Neurological Surgeons (CNS).

While practice patterns vary, surveillance for vasospasm can be accomplished with daily transcranial Doppler ultrasonography and repeated neurological examinations. CTA should then be performed on patients with elevated or rising transcranial Doppler values or with a change in neurological status thought to be attributed to vasospasm. Catheter angiography with or without pharmacologic or mechanical intra-arterial vasodilation should then be performed on patients with CTA vasospasm or on patients in whom there was a high clinical suspicion for vasospasm despite a negative CTA or in the absence of the same. All patients with vasospasm should receive systemic hypertensive therapy prior to initiation of endovascular intervention. For comatose patients, we routinely obtain a surveillance post haemorrhage day 4–7 catheter angiogram since their clinical examination is less sensitive to detect impending ischaemia.

Hydrocephalus

Hydrocephalus is a relatively common complication of subarachnoid haemorrhage, with an overall incidence of 20–30%. In the acute phase, hydrocephalus can result in coma, decreased cerebral perfusion, and even life-threatening central brainstem herniation syndrome. Emergent treatment with external ventriculostomy drainage corrects this condition, and removes hydrocephalus as a confounder during the initial neurological assessment period.

Eventually, patients with external cerebrospinal fluid drainage systems require an attempt to determine their continued reliance, and attempts to clamp these systems should be immediate rather than gradual (Klopfenstein et al., 2004). For patients that fail a clamp trial, ventriculoperitoneal shunting is the most common method of re-establishing cerebrospinal fluid dynamics (15–20% of SAH patients).

All patients, regardless of whether they required ventriculostomy drainage during their initial hospitalization or not, should be monitored for clinical signs of progressive hydrocephalus in the weeks that follow subarachnoid haemorrhage. The factors that influence the shunt rate include the extent of the SAH, opening of lamina terminalis intraoperatively and ventriculitis following external ventricular drain (EVD) placement.

Serum sodium and volume balance

Hyponatraemia is a common electrolyte disorder in the setting of aneurysmal subarachnoid haemorrhage (Sherlock et al., 2006). Sometimes, this can be attributed to the syndrome of inappropriate antidiuretic hormone secretion (SIADH). SIADH results in impaired water excretion. Any central nervous system disorder, such as SAH, can enhance antidiuretic hormone release (see **Chapter 25**). The retention of water and development of hyponatraemia can have profound effects on the clinical course of patients following aneurysmal haemorrhage. Hyponatraemia can lead to increased cerebral oedema and subsequent increased intracranial pressure and consequent cerebral ischaemia.

Another, less common, cause of hyponatraemia following aneurysm rupture is cerebral salt wasting, and it often heralds the onset of cerebral vasospasm. In this condition, natriuretic peptides are released that result in excessive salt excretion and, critically, relative hypovolemia. In the critical care setting, proper diagnosis and intense control of serum sodium levels and volume status are necessary to optimize outcomes.

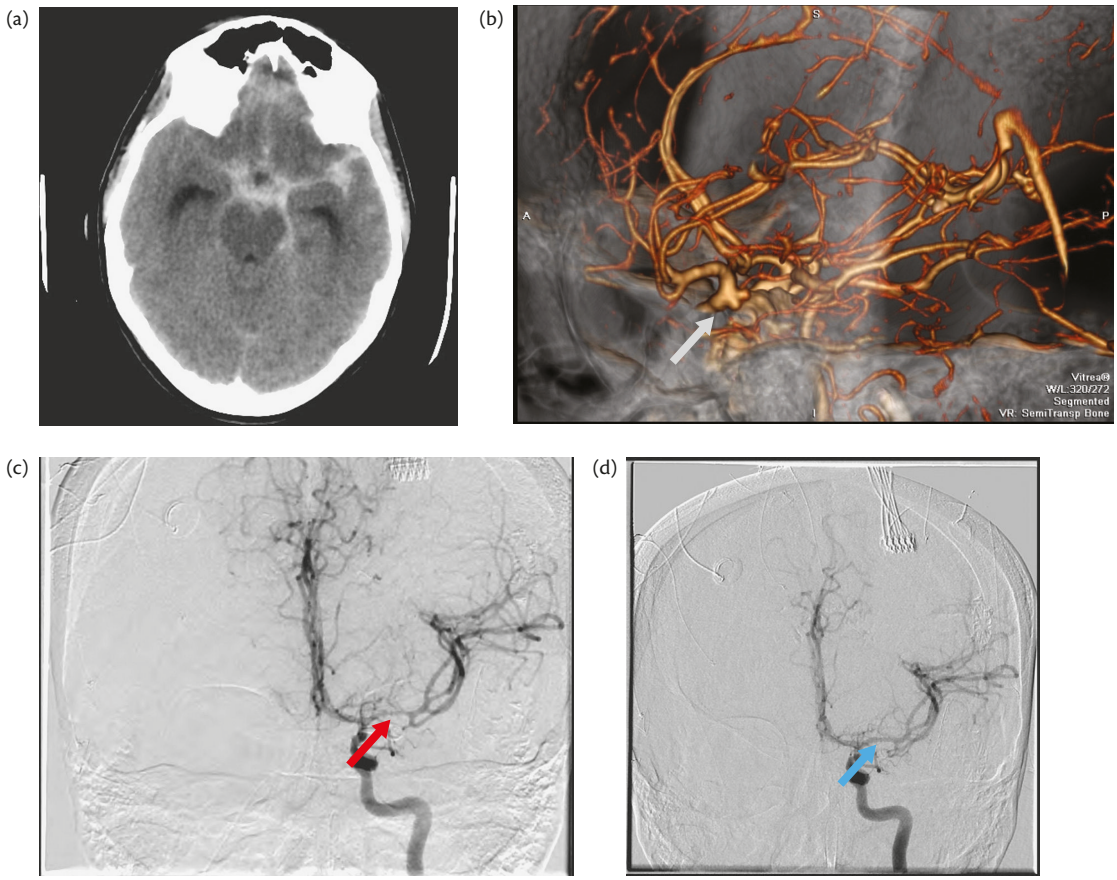

Fig. 49.9 Subarachnoid haemorrhage and vasospasm. (A) Initial non-contrast, axial head computed tomography demonstrated diffuse subarachnoid haemorrhage, and (B) 3D reconstruction of computed tomography angiogram demonstrated an internal carotid artery aneurysm (grey arrow) as the source of the subarachnoid haemorrhage. (C) Four days following presentation, the patient developed motor weakness in the right upper extremity and word finding difficulty. Digital subtraction angiography demonstrated severe vasospasm (red arrow), with narrowing of the left M1 segment of the middle cerebral artery. (D) The patient was treated with intra-arterial nicardipine with resolution of radiographic vasospasm (blue arrow). Alternative agents include intra-arterial verapamil. While balloon angioplasty has a more durable treatment effect, it is associated with a higher procedural complication risk and therefore we reserve it for vasospasm that is focal, proximal, and refractory to intra-arterial medication. All neurological symptoms in this patient resolved following treatment. Treatment of vasospasm can be effective if instituted before infarction occurs, and patients should be treated on an emergent basis if new neurological deficits are present.

Treatment of both these conditions in the context of subarachnoid haemorrhage consists of hypertonic saline, enteral salt repletion, and mineralocorticoids. Fluid restriction is typically not used to normalize serum sodium in critical, symptomatic patients for fear of exacerbating hypovolemia and increasing the risk of cerebral ischaemia.

Outcome from subarachnoid haemorrhage

The primary brain injury from a ruptured aneurysm can be severe, and dictate the overall clinical course (Stapleton et al., 2015b) (Fig. 49.10). Patients with large haematomas, who are elderly in age, or who present in a deep coma are likely to have poor outcomes, regardless of any intervention to prevent aneurysm rerupture. On the other hand, patients with good initial clinical grades may go on to develop vasospasm and suffer profound delayed cerebral ischaemia. The mortality of SAH is approximately 35% but includes patients that never present to hospital or a neurosurgeon. Overall, most patients that survive the initial haemorrhage event will go on to have good functional outcomes (~2/3) (Hop et al., 1997; Vergouwen et al., 2011). Despite this, many patients will show subtle cognitive deficits (~1/2) and emotional problems that impact on their day-to-day living (~1/2 are dissatisfied with life) and prevent their return to employment (only 1/3 return to their previous employment). Despite SAH only accounting for 5% of haemorrhagic stroke a similar number of life years are lost as from ischaemic stroke and intracerebral haemorrhage. Efforts to develop screening protocols for high-risk patients to detect aneurysms prior to haemorrhage, refinements in treatment techniques, and improved management of vasospasm will continue to better outcomes in the future.

Controversy

The longest ongoing controversy in the management of ruptured aneurysms is the decision to treat via either clipping or coiling. Two major trials have addressed this, the International Subarachnoid Aneurysm Trial (ISAT) (Molyneux et al., 2015) and the Barrow

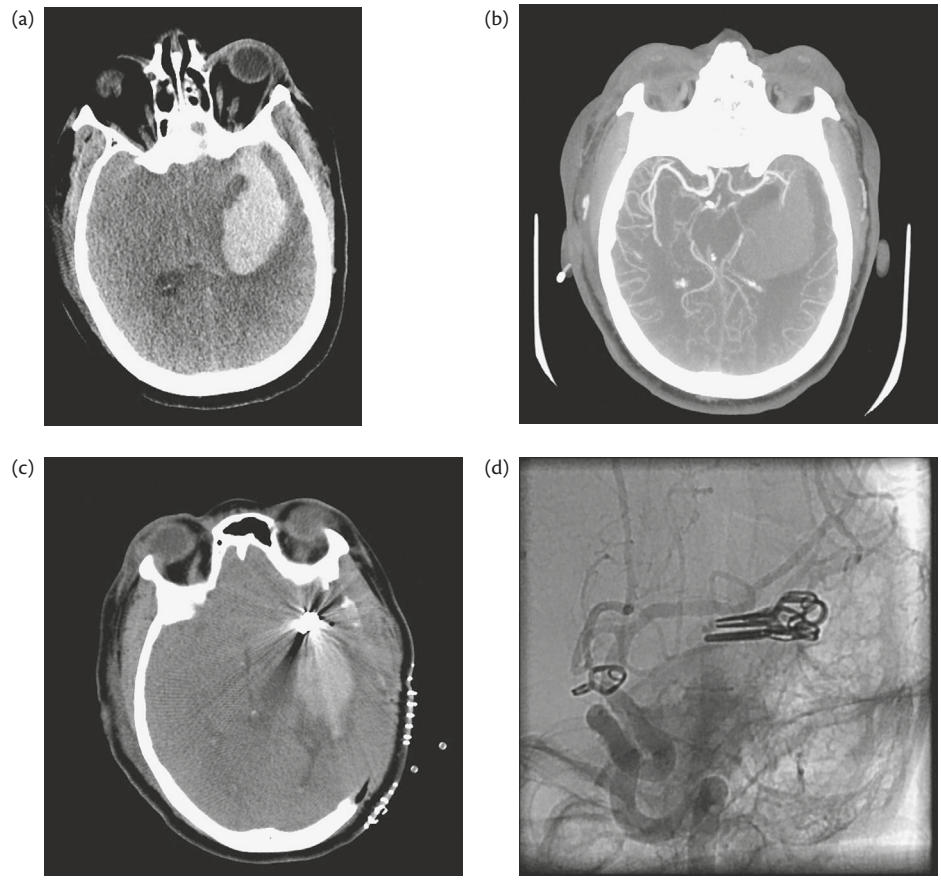

Fig. 49.10 Ruptured brain aneurysm with large Sylvian fissure haematoma. (A) Non-contrasted computed tomography (CT) of the head image showing acute subarachnoid haemorrhage with a large left frontotemporal and Sylvian fissure haematoma. (B) Maximum intensity projection of a CT angiogram of the head demonstrating a left middle cerebral artery (MCA) bifurcation aneurysm. (C) Postoperative head CT demonstrating clip artefact, partial haematoma evacuation, and decompressive craniectomy for control of intracranial pressure. (D) Left internal carotid artery digital subtraction angiogram showing complete MCA aneurysm occlusion after microsurgical clipping. An incidental anterior communicating artery aneurysm was also clipped at the time of surgery.

Ruptured Aneurysm Trial (BRAT) (Spetzler et al., 2015). The eventual long-term follow-up of the ISAT group demonstrated that the probability of dependency was not different between the clip or coil groups, although there was a greater rate of death with the neurosurgical group. However, a meta-analysis of three randomized trials (including ISAT) was unable to show a significant difference between endovascular treatment and neurosurgical clipping in terms of mortality (Lanzino et al., 2013).

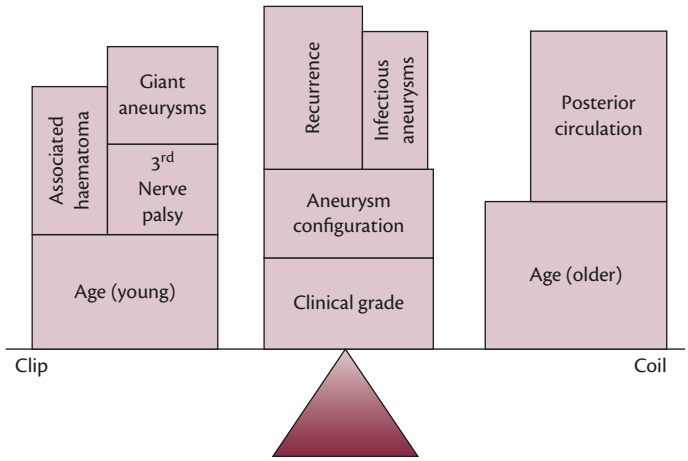

Fig. 49.11 Factors influencing the decision to clip or coil. Many factors must be considered when evaluating a treatment modality for intracranial aneurysms. In the centre of the balance are factors that can influence the decision to clip or coil either way. Farther from the centre are factors that strongly favour one treatment modality over the other. These generalizations must be considered in the context of all patient and aneurysm specific characteristics, in addition to those not shown here.

The BRAT trial, while only providing six years of follow-up, demonstrates little difference between treatment modalities for anterior circulation aneurysms, but a significant advantage of coiling over clipping for vertebrobasilar circulation aneurysms. Selection bias, provider skill set and proficiency, external validity concerns, and crossover between treatment groups have complicated the interpretation of these results.

'To clip or to coil' is at the fulcrum of aneurysm treatment planning (**Fig. 49.11**). Patients are best served by a multimodality team that can weigh the risks and benefits of treatment based on aneurysm characteristics, clinical scenario, best available evidence, and provider skill level.

FURTHER READING

Brinjikji, W., Murad, M.H., Lanzino, G., Cloft, H.J., & Kallmes, D.F. (2013). Endovascular treatment of intracranial aneurysms with flow diverters a meta-analysis. *Stroke*, **44**, 442–7.

Connolly, E.S., Rabinstein, A.A., Carhuapoma, J.R., et al. (2012). Guidelines for the management of aneurysmal subarachnoid hemorrhage a guideline for healthcare professionals from the American Heart Association/American Stroke Association. *Stroke*, **43**, 1711–37.

Lawton, M.T. (2011). *Seven Aneurysms: Tenets and Techniques for Clipping*. New York, NY: Thieme.

Spetzler, R.F., McDougall, C.G., Zabramski, J.M., et al. (2015). The Barrow Ruptured Aneurysm Trial: 6-year results. *J Neurosurg*, **123**, 609–17.

Walcott, B.P., Stapleton, C.J., Koch, M.J., & Ogilvy, C.S. (2015). Diffuse patterns of nonaneurysmal subarachnoid hemorrhage originating from the basal cisterns have predictable vasospasm rates similar to aneurysmal subarachnoid hemorrhage. *J Stroke Cerebrovasc Dis*, **24**, 795–801.

REFERENCES

Abla, A.A. & Lawton, M.T. (2014). Anterior cerebral artery bypass for complex aneurysms: an experience with intracranial-intracranial reconstruction and review of bypass options: clinical article. *J Neurosurg*, **120**, 1364–77.

Athar, M.K. & Levine, J.M. (2012). Treatment options for cerebral vasospasm in aneurysmal subarachnoid hemorrhage. *Neurotherapeutics*, **9**, 37–43.

Bardach, N.S., Zhao, S., Gress, D.R., Lawton, M.T., & Johnston, S.C. (2002). Association between subarachnoid hemorrhage outcomes and number of cases treated at California hospitals. *Stroke*, **33**, 1851–6.

Barker, F.G. & Ogilvy, C.S. (1996). Efficacy of prophylactic nimodipine for delayed ischemic deficit after subarachnoid hemorrhage: a metaanalysis. *J Neurosurg*, **84**, 405–14.

Brinjikji, W., Murad, M.H., Lanzino, G., Cloft, H.J., & Kallmes, D.F. (2013). Endovascular treatment of intracranial aneurysms with flow diverters a meta-analysis. *Stroke*, **44**, 442–7.

Connolly, E.S., Rabinstein, A.A., Carhuapoma, J.R., et al. (2012). Guidelines for the management of aneurysmal subarachnoid hemorrhage a guideline for healthcare professionals from the American Heart Association/American Stroke Association. *Stroke*, **43**, 1711–37.

Davies, J.M. & Lawton, M.T. (2014). Advances in open microsurgery for cerebral aneurysms. *Neurosurgery*, **74**, S7–S16.

Grannan, B.L., Yanamadala, V., Walcott, B.P., Stapleton, C.J., & Ogilvy, C.S. (2014). Repeated neurovascular imaging in subarachnoid hemorrhage when initial studies are negative. *J Clin Neurosci*, **21**, 993–6.

Guglielmi, G., Viñuela, F., Duckwiler, G., et al. (1992). Endovascular treatment of posterior circulation aneurysms by electrothrombosis using electrically detachable coils. *J Neurosurg*, **77**, 515–24.

Hop, J.W., Rinkel, G.J., Algra, A., & Van Gijn, J. (1997). Case-fatality rates and functional outcome after subarachnoid hemorrhage a systematic review. *Stroke*, **28**, 660–4.

Hunt, W.E. & Hess, R.M. (1968). Surgical risk as related to time of intervention in the repair of intracranial aneurysms. *J Neurosurg*, **28**(1), 14–20.

Kassell, N., Sasaki, T., Colohan, A., & Nazar, G. (1985). Cerebral vasospasm following aneurysmal subarachnoid hemorrhage. *Stroke*, **16**, 562–72.

Klopfenstein, J.D., Kim, L.J., Feiz-Erfan, I., et al. (2004). Comparison of rapid and gradual weaning from external ventricular drainage in patients with aneurysmal subarachnoid hemorrhage: a prospective randomized trial. *J Neurosurg*, **100**, 225–9.

Lanzino, G., Murad, M., D'Urso, P., & Rabinstein, A. (2013). Coil embolization versus clipping for ruptured intracranial aneurysms: a meta-analysis of prospective controlled published studies. *Am J Neuroradiol*, **34**, 1764–8.

Lawton, M.T. (2011). *Seven Aneurysms: Tenets and Techniques for Clipping*. New York, NY: Thieme.

Lubicz, B., Mine, B., Collignon, L., Brisbois, D., Duckwiler, G., & Strother, C. (2013). WEB device for endovascular treatment of wide-neck bifurcation aneurysms. *Am J Neuroradiol*, **34**, 1209–214.

Molyneux, A.J., Birks, J., Clarke, A., Sneade, M., & Kerr, R.S. (2015). The durability of endovascular coiling versus neurosurgical clipping of ruptured cerebral aneurysms: 18 year follow-up of the UK cohort of the International Subarachnoid Aneurysm Trial (ISAT). *Lancet*, **385**, 691–7.

Owen, C.M., Montemurro, N., & Lawton, M.T. (2015). Microsurgical management of residual and recurrent aneurysms after coiling and clipping: an experience with 97 patients. *Neurosurgery*, **62**, 92–102.

Raabe, A., Nakaji, P., Beck, J., et al. (2005). Prospective evaluation of surgical microscope-integrated intraoperative near-infrared indocyanine green videoangiography during aneurysm surgery. *J Neurosurg*, **103**, 982–9.

Rhoney, D., Tipps, L., Murry, K., Basham, M., Michael, D., & Coplin, W. (2000). Anticonvulsant prophylaxis and timing of seizures after aneurysmal subarachnoid hemorrhage. *Neurology*, **55**, 258–65.

Rodríguez-Hernández, A. & Lawton, M.T. (2011). Anatomical triangles defining surgical routes to posterior inferior cerebellar artery aneurysms: clinical article. *J Neurosurg*, **114**, 1088–94.

Rosen, D.S. & MacDonald, R.L. (2005). Subarachnoid hemorrhage grading scales. *Neurocrit Care*, **2**, 110–18.

Sanai, N., Zador, Z., & Lawton, M.T. (2009). Bypass surgery for complex brain aneurysms: an assessment of intracranial-intracranial bypass. *Neurosurgery*, **65**, 670–83.

Sherlock, M., O'Sullivan, E., Agha, A., et al. (2006). The incidence and pathophysiology of hyponatraemia after subarachnoid haemorrhage. *Clin Endocrinol*, **64**, 250–54.

Spetzler, R.F., McDougall, C.G., Zabramski, J.M., et al. (2015). The Barrow Ruptured Aneurysm Trial: 6-year results. *J Neurosurg*, **123**, 609–17.

Stapleton, C.J., Walcott, B.P., Butler, W.E., & Ogilvy, C.S. (2015a). Neurological outcomes following intraprocedural rerupture during

coil embolization of ruptured intracranial aneurysms. *J Neurosurg*, **122**, 128–35.
Stapleton, C.J., Walcott, B.P., Fusco, M.R., Butler, W.E., Thomas, A.J., & Ogilvy, C.S. (2015b). Surgical management of ruptured middle cerebral artery aneurysms with large intraparenchymal or sylvian fissure hematomas. *Neurosurgery*, **76**, 258–64.
Suarez, J.I., Tarr, R.W., & Selman, W.R. (2006). Aneurysmal subarachnoid hemorrhage. *N Engl J Med*, **354**, 387–96.
Van Der Bilt, I., Hasan, D., Van Den Brink, R., et al. (2014). Cardiac dysfunction after aneurysmal subarachnoid hemorrhage: relationship with outcome. *Neurology*, **82**, 351–8.
Van Gijn, J. & Rinkel, G. (2001). Subarachnoid haemorrhage: diagnosis, causes and management. *Brain*, **124**, 249–78.
Vergouwen, M.D., Etminan, N., Ilodigwe, D., & Macdonald, R.L. (2011). Lower incidence of cerebral infarction correlates with improved functional outcome after aneurysmal subarachnoid hemorrhage. *J Cereb Blood Flow Metab*, **31**, 1545–53.
Walcott, B.P., Stapleton, C.J., Koch, M.J., & Ogilvy, C.S. (2015). Diffuse patterns of nonaneurysmal subarachnoid hemorrhage originating from the basal cisterns have predictable vasospasm rates similar to aneurysmal subarachnoid hemorrhage. *J Stroke Cerebrovasc Dis*, **24**, 795–801.

RELATED LINKS TO EBRAIN

Assessment and Emergency Management of Subarachnoid Haemorrhage. https://learning.ebrain.net/course/view.php?id=162
Definitive Management of the Aneurysm: Radiology. https://learning.ebrain.net/course/view.php?id=147
Definitive Management of the Aneurysm: Surgery. https://learning.ebrain.net/course/view.php?id=458
Medical Management of Subarachnoid Haemorrhage. https://learning.ebrain.net/course/view.php?id=159
Cerebral Revascularisation. https://learning.ebrain.net/course/view.php?id=157
Radiological Investigation of Subarachnoid Haemorrhage. https://learning.ebrain.net/course/view.php?id=161
The Diagnosis and Management of Spontaneous Subarachnoid Haemorrhage. https://learning.ebrain.net/course/view.php?id=103

50

Cerebral arteriovenous malformations and dural arteriovenous fistulae

Michael Morgan

Pathophysiology, classification, epidemiology, genetics, and natural history of brain AVMs

Pathophysiology

Arteriovenous malformations of the brain (bAVM) are intraparenchymal clusters of abnormal connecting blood vessels containing elements of both artery and vein but no capillaries. The abnormal cluster is connected to the normal arterial and venous circulations. This creates a rapid transit of blood within the bAVM between normal arterial and venous circulations (conventionally known as a 'shunt') because of a reduction in the normal impedance to blood flow within the vascular bed. Most of the clinical and pathological consequences of bAVM relate to this arteriovenous shunt. BAVM have no predilection for specific central nervous system locations and are distributed proportionately with brain mass.

The physiological consequences of an arteriovenous shunt in the brain can best be illustrated with a profile of pressures along the length of the vascular system (Fig. 50.1). Because of the reduced impedance (or resistance) to flow, the pressure within arteries directly contributing to the bAVM (feeding) will be less than that of a corresponding normal artery without a bAVM. Similarly, the veins receiving flow from the bAVM (draining) have a greater pressure than for a corresponding normal vein without a bAVM. Furthermore, the branch arteries and tributary veins of these feeding arteries and draining veins will be impacted by this pressure profile. Considering that the collateral circulation is continuously adapting in response to changes in shear stress (in response to pressure gradient change). The pathological changes of the vasculature are proportionate to the physiological changes. The dilatation of the vasculature and disproportionate thinning, and in places degeneration, of vessel walls are associated with greater than normal shear stress, lower than normal local arterial pressures, higher than normal local venous pressures and dampened pulsatility (in comparison to similar vessels in the absence of a bAVM). This is due to the low impedance circulation induced by bAVM. These responses are mediated through up-regulation of eNOS and down-regulation of endothelin along with the remodelling vasculogenesis factors (e.g. vascular endothelial growth factor, VEGF). Because of the consequent transition from normal to abnormal vasculature, there is usually no sharply identifiable point where bAVM can be said to begin or end, rather there is a transition zone reflecting the pathological response to the physiological perturbations. What is called bAVM is often assigned on a pragmatic basis as the central nest of abnormal vessels and is termed 'nidus'. In reality, the surgeon, pathologist, or radiologist can state what is abnormal and what is normal. However, there is often a transition zone that is often ignored because this zone reflects abnormalities of physiology that are difficult to evaluate by direct visual observation.

Several pathophysiological processes follow from the prolonged presence of a bAVM leading to the clinical manifestations. These include:

1. Rupture into the brain parenchyma or subarachnoid space due to failure of integrity of vessels involved in the bAVM caused by wear-and-tear of this high flow system. As a consequence of shear stress and consequent vascular wall degeneration: aneurysms may develop within the interstices of the bAVM (intranidal aneurysms), or on the proximal arteries leading to the aneurysm [associated proximal intracranial aneurysms (APIA)]; and varices and webs can develop in the venous system. The weakened vessel may then rupture at some point in time. A precipitating event for this rupture may be a sudden increase in pressure within the bAVM because of increasing venous outflow stenosis or at a time of venous of thrombosis.
2. The combination of lower than normal pressure in the adjacent parenchymal arteries and greater than normal venous pressure in corresponding veins ('steal') can result in neurological deficits and seizures.
3. Haemoglobin extravasation can result in iron deposition that can lead to epileptic foci.
4. Complex migraines may develop because of fluctuations in calibre of the feeding arteries and or ischaemia induced spreading depression.
5. Headaches may develop from stretching of large veins or their thrombosis leading to stretching of venous walls, raised intracranial pressure or haemorrhage, or be associated with migraine (as mentioned earlier).

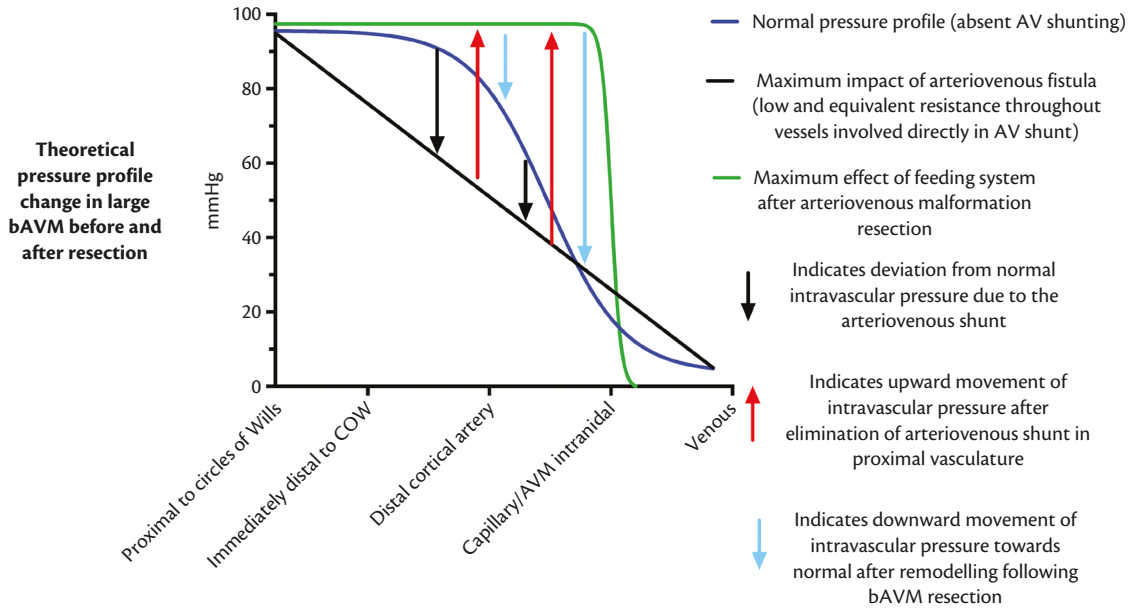
Theoretical pressure profile change in large bAVM before and after resection
mmHg
100
80
60
40
20
0
Proximal to circles of Wills
Immediately distal to COW
Distal cortical artery
Capillary/AVM intranidal
Venous
Normal pressure profile (absent AV shunting)
Maximum impact of arteriovenous fistula (low and equivalent resistance throughout vessels involved directly in AV shunt)
Maximum effect of feeding system after arteriovenous malformation resection
Indicates deviation from normal intravascular pressure due to the arteriovenous shunt
Indicates upward movement of intravascular pressure after elimination of arteriovenous shunt in proximal vasculature
Indicates downward movement of intravascular pressure towards normal after remodelling following bAVM resection

Fig. 50.1 A hypothetical pressure profile along the vasculature system of the brain containing a bAVM from the arteries proximal to the circle of Willis to the venous outflow. Blue represents the normal profile demonstrating that the majority of resistance in in the smaller arteries and arterioles. When resistance is reduced with the introduction of an arteriovenous shunt, the pressure profile moves towards the black line. This results in reduced pressure in arteries and increased pressure in the veins. On sudden removal of the shunt, when the vasculature is significantly dilated, the pressures overshoot (green line) the normal pressures due to the lower resistance resulting from the larger radii arteries and veins that exist before remodelling. After remodelling of the arteries and veins, the pressure profile returns to normal.

6. Intracranial hypertension and papilloedema may occasionally occur when pressure is elevated within the venous sinuses.
7. Cardiac failure with pulmonary hypertension can occur in neonates and infants.

Epidemiology

There is a congenital origin for at least some cases of bAVM as seen in the occasional metameric involvement of certain tissues related to embryological development (Bonnet-Dechaume Blanc syndrome or Wyburn-Mason syndrome) (Morgan et al., 1985). However, although often regarded as congenital, the evidence for this can be challenged (Stapf and Mohr, 2000; Jeffree and Stoodley, 2009; Davidson and Morgan, 2011) and reports of de novo bAVM occurring late in life confirm that there is a spectrum of age at onset (Bulsara et al., 2002). However, most are likely to be present from early childhood. BAVM are resilient lesions and although spontaneous disappearance has been reported, such occurrence is uncommon (Patel et al., 2001). For the most part, bAVM, unless intentionally obliterated, develop early and remain present throughout life. BAVM are detected in 0.9–1.5 per 100 000 head of population per year (Al-Shahi et al., 2003; Stapf et al., 2003) from a reported prevalence in adults of between 10 and 100 per 100 000 (Morris et al., 2009).

Genetics

BAVMs are usually sporadic (except for those that classify the lesions of hereditary haemorrhagic telangiectasia as bAVM or capillary malformation—AVM). Three models of brain AVM development have been proposed: failure of regression of primitive arteriovenous connections during development; dilation and a primary disorder of venules; and Notch4 induced arteriovenous shunt development from capillaries (Murphy et al., 2014).

As the pathological manifestation of bAVM is a physiological response to the arteriovenous shunting, the disease itself may not be a single disease but a number of genotypes with a common phenotype. This is consistent with hereditary haemorrhagic telangiectasia (HHT), an autosomal dominant disorder with a similar phenotype to bAVM (manifested by arteriovenous shunting with venules and telangiectasia present in skin, mucosal surfaces, lung, liver, and the central nervous system). For HHT, several mutations in two genes have so far been identified that are important in angiogenesis, affecting activin receptor-like kinase-1 (Alk-1) on chromosome 12 (responsible for HHT2) and its coreceptor, endoglin on chromosome 9 (underlying HHT1 – the most common type).

A further closely related familial disorder, the autosomal dominant capillary malformation (AVM) that presents with skin capillary malformations and AVM of the brain, limb, or face (no intra-abdominal or intrathoracic organ involvement) has been described with a RASA1 mutation (Eerola et al., 2003).

Natural history and clinical presentations.

Clinical presentation with haemorrhage occurs in approximately 50% (Stapf et al., 2003; Wedderburn et al., 2008; Gross and Du, 2013; Korja et al., 2014). There are no sex or age predilections for presentation. The annual rate of future haemorrhage is 1–3% for unruptured bAVM and 4–6% for bAVM presenting with recent rupture (Gross and Du, 2013; Kim et al., 2014; Mohr et al., 2014). BAVM specific factors also influence the future risk of rupture. Two factors with the most evidence supporting an increased risk are intracranial aneurysms (Brown et al., 1988; Redekop et al., 1998; Stapf et al., 2002; Da Costa et al., 2009) and deep venous drainage (or exclusive deep venous drainage) into the Galenic system (Gross and Du, 2013). The presence of associated aneurysms in unruptured bAVM increases

the risk to approximate that of ruptured bAVM (Brown et al., 1988; Redekop et al., 1998; Stapf et al., 2002; Da Costa et al., 2009). However, due to the presence of aneurysms or exclusive deep venous drainage occurring in significantly fewer than half of all unruptured bAVM, and the uncommon detection of bAVM cases, the use of more precise estimate of risks should be used with caution.

Although the reported outcome from rupture has a wide variation, it is reasonable to approximate the consequences of rupture to be major morbidity or mortality in 40% of cases. The discrepancy between the low risk of 10% and the high risk of 89% reported in the literature may be largely explained by case identification and whether or not a short follow-up after a single haemorrhage or a long follow-up after multiple haemorrhages is reported (Drake, 1979; Fults and Kelly, 1984; Crawford et al., 1986; Brown et al., 1988; Ondra et al., 1990; Laakso et al., 2008; Da Costa et al., 2009; Van Beijnum et al., 2009; Kano et al., 2014).

Non-haemorrhagic presentations (% incidence of presentations) include seizures (25%), headache (16%), neurological deficits not caused by haemorrhage (8%), intracranial hypertension (1%) and high output cardiac failure (<1% and confined to infants) (Hayashi et al., 1996; Galletti et al., 2011; Gross and Du, 2013; Bervini et al., 2014). The presentation and cause for these presentations are explained earlier.

Approximately 25% of patients that do not experience a haemorrhage will have a decline in function within a 10-year period (Brown et al., 1988). This is likely to be confined to larger bAVM and be due to seizure or progressive neurological deficits.

Diagnosis, grading, and workup

Diagnosis

Definitive diagnosis can best be made on digital subtraction angiography (DSA). This allows both the involved vasculature to be anatomically defined and also the rapid transit of shunted arteriovenous blood to be verified (Fig. 50.2). The appearance of a non-ruptured bAVM by non-contrast CT scan will be of a slightly hyperdense mass with a sharp border with the surrounding normal brain. A small focus of calcification may be present. The appearance of non-ruptured bAVM by non-contrast MRI in T1 and T2 is consistent with vascular flow voids with the dilated arteries and veins often recognized as consistent with bAVM (Fig. 50.2). Ruptured bAVM may be obscured by the haematoma in non-contrast CT scan and may obscure the identification of bAVM on MR. MRI angiography and CT angiography both can define the anatomical appearance while the dynamic sequencing may demonstrate venous filling during the arterial phase, confirming the arteriovenous shunting. However, if treatment is to be considered, DSA is necessary as it clearly identifies the complete arterial contribution (and this may include an external carotid contribution), the venous drainage and angioarchitectural features such as diffuseness, the presence of aneurysms, and venous stenosis. These angioarchitectural features may impact upon the anticipated natural history and the risks of treatment for the patient.

A differential diagnosis of proliferative angiopathy, a response to infarct or intracerebral haemorrhage (ICH) (particularly in the young), should be considered in diffuse vascular lesions that may resemble bAVM but lack the very early venous drainage pattern of bAVM. These are not bAVM and do not share the same propensity to haemorrhage.

Grading

Useful grading systems are the Spetzler-Martin Grading system (Spetzler and Martin, 1986), the Lawton-Young grading system (Lawton et al., 2010), and the Pollock-Flickinger score (Pollock and Flickinger, 2008). The first two of these predict the risk of surgery and the third, the likelihood of obliteration without deficit from focused irradiation (Table 50.1). The five-tier Spetzler-Martin grades can be condensed into Spetzler-Martin grades 1 and 2 combined, Spetzler-Martin grade 3, and Spetzler-Martin grades 4 and 5 combined into Spetzler-Ponce classes A, B, and C, respectively (Spetzler and Ponce, 2011).

Workup

The workup is influenced by demographic, bAVM-related factors, and clinical presentation. The workup may be limited to a diagnostic MRI or CTA because either no further intervention is anticipated (e.g. an elderly patient with an unruptured bAVM) or because of the urgency of intervention is necessary (e.g. patient presenting with a life-threatening brain haemorrhage). However, when such definitive interventions are not immediately apparent, further investigations are appropriate. From the history, a family history of HHT, intracerebral haemorrhage, brain abscess, or lung lesions

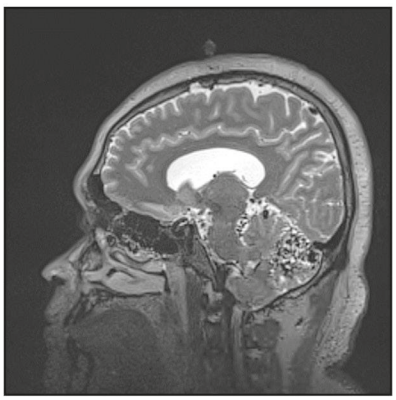

T2 MRI demonstrating typical flow voids in cerebellum of bAVM

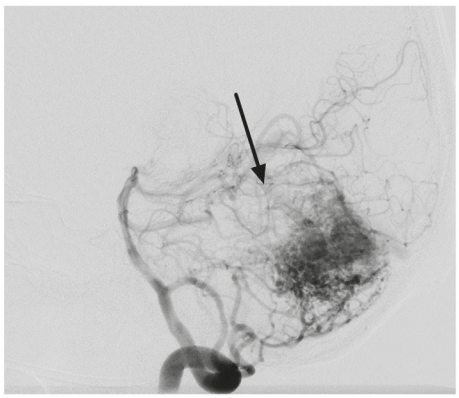

Early arterial DSA demonstrating typical filling of bAVM with early draining vein (arrow). Left vertebral artery injection (lateral on left, AP on right)

Fig. 50.2 Typical appearance of a bAVM on MRI (T2) and DSA. The early draining vein is characteristic of bAVM (arrow).

Table 50.1 Cerebral arteriovenous malformation grading systems

Grade (reference)		Base score	Additional scores	Range of scores	Implication
Spetzler-Martin grade (Spetzler and Martin., 1986).	Surgical risk ordinal categories	1 = size* <3 cm; 2 = size 3–6 cm 3 = size >6 cm	1 for deep venous drainage** and 1 for eloquent***	1–5	See below for implication
Lawton-Young scale (Lawton et al., 2010).	Surgical risk ordinal categories	Spetzler-Martin grade + 1 for age <20 years; 2 for age 20–40 years; 3 for age >40 years	1 for non-haemorrhagic presentation and 1 for diffuse bAVM	2–10	10%, 20%, 25%, 40%, and 65% adverse outcome risk for Lawton-Young score of 4, 5, 6, 7, and 8, respectively
Spetzler-Ponce scale (Spetzler and Ponce., 2011).	Surgical risk ordinal categories	Simplifies Spetzler-Martin grades (SMG): A = SMG 1 or 2 B = SMG 3 C = SMG 4 or 5		A, B, or C	Risk of <10% adverse outcome rate for SPC A, 20% for SPC B and greater than 30% for SPC C (46). In certain series, the long-term adverse outcome risk for SPC A is no greater than 4% (5, 7, 49, 50, 51)
Pollock-Flickinger score (Pollock and Flickinger., 2008).	Predict radiosurgery obliteration without deficit	= 0.1 x Volume**** (ml) + 0.02 x Age (years)	0.5 if located in basal ganglia, thalamus, or brainstem	Continuous score from <1 to >2	Risk of no obliteration or adverse outcome 10% for ≤1; 30% for Scores >1 and ≤1.5; >40% for Scores >1.5

* size is maximum diameter size in cm

** deep venous drainage includes drainage that communicates with the Galenic system

***eloquent is bAVM located in or adjacent to primary motor or sensory cortices, language cortex, internal capsule, diencephalon, brainstem, cerebellar peduncles, or cerebellar peduncles.

****volume can be approximated by dividing three orthogonal maximal diameters (cm) and dividing by 2.

a: Source data from Spetzler RF, Martin NA: A proposed grading system for arteriovenous malformations. *J Neurosurg* 65:476–483, 1986.

b: Reproduced with permission from Lawton, Michael T.; Kim, Helen, A Supplementary Grading Scale for Selecting Patients with Brain Arteriovenous Malformations for Surgery, *Neurosurgery*, Volume 66, Issue 4, pp. 702–13, Copyright © 2010 Oxford University Press and the Congress of Neurological Surgeons (CNS).

c: Source data from Spetzler RF, Ponce FA: A 3-tier classification of cerebral arteriovenous malformations. *J Neurosurg*. 2011; 114:842–849.

d: Reproduced with permission from Pollock, Bruce E.; Flickinger, John C, Modification of the Radiosurgery-Based Arteriovenous Malformation Grading System, *Neurosurgery*, Volume 63, Issue 2, pp. 239–43, Copyright © 2008 Oxford University Press and the Congress of Neurological Surgeons (CNS).

should raise the possibility of a differential diagnosis of HHT. This may be supported by a history of recurrent nose-bleeds and inspection of mucosal membranes and fingers, confirming evidence of vascular telangiectasia. Furthermore, in cases of metameric bAVM cutaneous or retinal examination may reveal arteriovenous fistulae (e.g. Bonnet-Dechaume Blanc syndrome) (Morgan et al., 1985). However, these clinical observations are not present in most cases of bAVM. From the CTA and MRA, size, location and likelihood of deep venous drainage should allow for the grade to be estimated (although may be altered slightly after DSA). If treatment might be considered, DSA is the appropriate gold-standard investigation (being mindful of renal function).

If the bAVM is small and diffuse (characteristic of HHT), a lung CT is appropriate to investigate whether pulmonary arteriovenous fistulae exist. Pulmonary arteriovenous fistulae may present the greatest risk for the patient with HHT because of their association with the development of brain abscess (and other infected emboli).

Treatment

Surgery

The principles of surgical excision are to eliminate all arteriovenous shunting while minimizing the damage to normal functional brain, avoiding the rupture from the abnormal vasculature during this process (Hernesniemi et al., 2010). This is achieved by, assessing preoperatively the functional brain adjacent to the planned resection margins to establish a safe zone, and staying within the safe zone wherever possible. In the process of eliminating the arteriovenous shunt, the physiological and pathological responses need to be considered. The following principles should be adopted:

1. Minimize collateral brain damage with:
   a. anaesthesia aimed at controlling mean arterial and pulsatile pressure, encouraging brain relaxation and protection from ischaemia;
   b. patient positioning to ensure optimize brain relaxation, retraction can be minimized, and brain herniation on the craniotomy edge is prevented;
   c. craniotomy appropriately positioned and sized for the bAVM and proximal artery exposure (including access across the midline), and allowing for alternate approach if a catastrophe should occur;
   d. retraction minimized on the brain because of the potential for shunt induced ischaemia combined with the low blood pressure associated with the anaesthesia (although retraction is reasonable on the bAVM providing that there is no associated venous outflow compromise);
   e. in the case where critical arterial blood flow continues from feeding arteries to normal brain, inspection of arteries must be made transitioning from normal to abnormal and back to normal.
2. All feeding arteries must be controlled before the venous drainage is disturbed by:
   a. controlling superficial feeding arteries early (including the use of temporary clips until definitive division site is established);

b. controlling deep feeding arteries early by a sulcal dissection and corticotomy to the deepest part of the nose-cone early in surgery along a very limited margin, before the usual corkscrew circumferential dissection that is encouraged for tumour resection;

It should be remembered that although lenticulostriate and choroidal arteries are anatomically considered to be deep, the superficial system also contributes to deep supply. This is because of the high shear stress leading to widening of the angle of flow between arteries and vein. This causes some superficial arteries to dive into the depths of the sulci at some distance from the bAVM to enter the bAVM at a deep location.

c. to prevent injury to the main draining vein, the artery immediately deep to this vein (the usual anatomical arrangement not only present in bAVM but observed where arteries and veins are juxtaposed throughout the body) should be the last artery dissected and secured, often after delivery of the bAVM on its venous umbilicus;

d. control transdural arterial supply, when present, by incising the dura at a distance from the bAVM, completing an island of dura on the bAVM, to prevent tension placed upon these arteries;

The dura should be incised at some distance from the vascular connection point between dura and bAVM. This may best be achieved by approaching from the opposite side of the involved dura when the falx cerebri is involved.

e. in order to minimize haemorrhage when turning the bone flap, in cases where transosseous supply is present, the bone opening can be performed in many narrow strips, enabling bleeding to be controlled at each step.

3. Veins must be left until all arteries have been controlled. Important considerations are:

a. small arterialized vessels connected to the bAVM within the white matter are normally veins;

These veins leave and return to the cluster of vessels of the bAVM due to vascular remodelling aimed at minimizing haemodynamic work caused by higher than normal shear stress and angular momentum. The vast majority of these vessels do not require ligation but should be swept back onto the margin of the bAVM with bipolar and sucker. As perivascular space is only large around small arteries (and not veins) the absence of cerebral spinal fluid (CSF) surrounding these vessels may be a clue to differentiate arteries from veins. Given that the veins are superficial within the bAVM, the cumulative effect of dividing these vessels will be to compromise venous drainage in the bAVM deep nose-cone, making the deep nose-cone tense and prone to problematic bleeding. By eliminating the deep arterial supply early and minimizing the loss of the marginal venous drainage by preserving the veins that sweep in and out of the white matter, the deep component of the bAVM will be more easily resected.

b. the last major vein should be divided after the mass of the bAVM is delivered on its venous umbilicus to ensure that all feeding arteries have been divided.

4. Ligation of vessels is more difficult than usual because of the thinner walls for comparative radii vessels. The ligation technique varies from whether these are within sulci or as part of the corticotomy by:

a. small vessel division within the sulci achieved with fine bipolar or microclips;

i. Bipolar should be fine, with absolutely clean mirror-surfaced points and on low setting (to ensure that the vessel wall does not explode before thrombosis has arrested flow within the vessel). The length of diathermy occlusion needs to be longer than would normally be considered when dealing with other pathologies.

ii. Microclips are a useful adjunct to bipolars, capable of arresting flow in very thin-walled vessels, diathermy of which might lead to bleeding rather than thrombosis (see earlier) (Sundt and Kees, 1986). Furthermore, on a long length of a small critical brain artery with multiple branches terminating in the bAVM, microclips placed at the origin of these terminating branches may cause less endothelial injury to the critical artery than diathermy.

b. small vessel division within the corticotomy achieved with a broader, insulated bipolar utilizing adjacent tissue to assist the reinforcement of the wall to be included in the diathermy target.

5. Suction should be fine (e.g. #3 or 4) utilizing the lowest suction necessary to clear CSF and blood. This reduces the accidental disruption of fine thin-walled vessels during the resection. A separate suction system with larger suckers should be immediately available for use if problematic bleeding occurs.

6. The bed of the bAVM should be free of bleeding before closure. Because of the thin-walled arteries associated with bAVM, there will be minimal vasoconstriction that normally occurs in most resection beds associated with other pathologies. Therefore, all bleeding points need to be arrested and no bleeding point should be covered by material. The later may lead to catastrophic intraparenchymal bleeding. If the bleeding point cannot be easily arrested with bipolar or microclip, the source of the bleeding needs to be followed into the brain to achieve a point where the vessel can be secured. This may be facilitated by utilizing two fine suckers by the surgeon, one for sucking the bleeding point and the second for dissecting around this point. Vascular anatomical details relevant to bAVMs at specific locations are included in Chapter 46.

Radiosurgery

Performed with either Gamma Knife, a linear accelerator, or proton beam radiotherapy, the focusing of the generated radiation to a focal point covering the bAVM sets in place a reaction of the vasculature that leads to the thrombosis of the bAVM over a one to four-year period. A marginal dose, around the nidus of the bAVM, of 18 Gy or more has a high probability of eliminating all shunting (Flickinger et al., 2002). This is an effective treatment modality achieving obliteration over time with a low risk of treatment and an occlusion rate dependent upon both the marginal dose delivered (which is dependent upon bAVM volume and location) and patient age. Because the time delay to obliteration may be considerable, consideration needs to be made of the natural history risk of bAVM haemorrhage during this latent period. The smaller the volume of bAVM irradiated the steeper the fall off in dose of radiation delivered to the surrounding brain

with respect to distance. This is important given that some brain may be adversely affected with doses above 12 Gy (e.g. optic nerves). Volumes are precisely calculated on the radiological assessment generated at the time of radiosurgery planning. However, an approximation can be gained multiplying the three orthogonal largest diameters (in cm) and dividing this by 2. The likelihood of incident free effective treatment can be derived from the Pollock-Flickinger score (PFS) given as (and summarized in Table 50.2):

$$= [0.1 \times \text{Volume(ml)}] + [0.02 \times \text{Age(years)}] + [0.5 \times \text{location}]$$

Location = 0 superficial (hemispheric/corpus callosum/cerebellar)
Location = 1 deep (basal ganglia/thalamus/brainstem).

The timeframe for obliteration resembles a sigmoid curve. Fitting a sigmoid curve to data provided by reports specifically for SPC A and B bAVM (and incorporating into the sigmoid curve generation the assumptions that there is no obliteration in the first 6 months following radiosurgery and there is no further obliteration beyond 5 years), produces an obliteration rate as illustrated in Figure 50.3 (Flickinger et al., 2002; Kano et al., 2014). The 50% cumulative obliteration rate is approximately 2 years 9 months for the smaller bAVM and 3 to 3 years 6 months for larger bAVM. During the latency period (between treatment and complete obliteration), the rate of haemorrhage is similar to that of the natural history without treatment. By incorporating the natural history of future haemorrhage into the obliteration rate curves allows a generation of predicted haemorrhage rate (Fig. 50.4). Therefore, it is unusual to recommend large bAVM for radiosurgery. However, strategies to perform planned staged volumetric treatment by radiosurgery, proton beam or fractionated delivery of radiotherapy are used for these larger bAVM (Karlsson et al., 2005; Huang et al., 2012; Kano et al., 2012a; Ding et al., 2014; Hattangadi-Gluth et al., 2014). Despite such strategies, evidence supporting this rationale is minimal. A prospective, intention to treat, cohort series of this management strategy had fewer cases cured than died from haemorrhage (Kano et al., 2012a). Therefore, it is difficult to find support for radiosurgery strategies for cases that are unlikely to respond to a single treatment.

Embolization

Embolization by the selective catheterization and endovascular occlusion of bAVM is commonly performed for bAVM treatment as: an adjunct to surgery to attempt to reduce the risk of intraoperative bleeding; an adjunct to radiosurgery to reduce bAVM target volume; an adjunct to radiosurgery or conservative management by eliminating regions of the bAVM or proximal vasculature (e.g. aneurysms) that is deemed to be the site of greatest risk of haemorrhage; or as the sole and definitive ablative management. The bAVM is most commonly accessed by the antegrade selective catheterization of arteries (although retrograde access through the veins is possible) (Kessler et al., 2011; Perreira et al., 2013). Currently, the most common agent employed for the purpose of occlusion is ethylene vinyl alcohol copolymer embolization (EVACE) that has the advantage over previous glue agents as having greater control with release due to its non-adhesive properties.

Table 50.2 Expected outcomes from radiosurgery based upon Pollock-Flickinger score calculated by (Pollock and Flickinger., 2008)
$= [0.1 \times \text{Volume (ml)}] + [0.02 \times \text{Age (years)}]$
$+ 0.5$ (if basal ganglia, thalamus or brainstem)

Pollock-Flickinger score	Incident free effective treatment at 70 months	mRS decline in neurological function (95% confidence interval range)
≤1	90%	0–10%
>1 and ≤1.5	70%	10–20%
>1.5 and ≤2	60%	15–30%
>2	<50%	25–50%

Defining specific roles for embolization in management of bAVM is particularly difficult due to the variety of strategies to which it is put, in contrast to surgery and radiosurgery in which ablation is usually the single goal. As a primary treatment to achieve complete occlusion, there is limited data. This is due to the potential for treatment to commence with embolization with a number of possible outcomes (complete obliteration, prepared for radiosurgery, or prepared for surgery). This shifting approach to intention of treatment is appropriate but frustrates the analysis of outcomes. From what information we have with regards agents prior to EVACE, permanent morbidity occurred in 8%, mortality in 1% and a cure rate of 5% (Frizzel and Fisher, 1995). For EVACE, disabling morbidity, mortality, and urgent surgery occurred in 6.6% of cases and complete ablation of arteriovenous shunting in 27% (Morgan et al., 2013). In a prospective, multicentre study, morbidity was reported in 5.1%, mortality in 4.3% and bAVM obliteration in 23.5% (Pierot et al., 2013). From what information that we have, EVACE of SPC A bAVM selected for planned cure is possible and commonly performed in some centres. An obliteration rate of 98% with a 3% combined mortality and morbidity for SPC A has been reported for those selected to be treated in this way (Saatci et al., 2011). However, selection bias is an important consideration when analysing these data from cohort series as cases may be found unsuitable for embolization because of concerns with regards agent reflux or access and not included in the analysis of results.

A more common role for embolization, than achieving complete bAVM obliteration, is in a sequential preparatory treatment prior to surgery or radiosurgery. The beneficial outcomes of embolization for the surgeon may include: a targeted ablation of difficult to access feeding arteries; a reduction in blood flow; a reduction in intraoperative haemorrhage; assistance with intraoperative identification of feeding vessels; the production of limited perinidal infarction of adjacent brain facilitating easy blunt dissection; and the treatment of feeder artery aneurysms subject to an increase in pressure upon AVM ablation (i.e. reducing the risk of aneurysm rupture at the time of surgery).

The benefits of preoperative embolization in the reduction of haemorrhage during surgical resection is well accepted but difficult to quantify. However, the overall management morbidity, mortality and success may not be improved with this approach as compared with surgery alone (Morgan et al., 2013; Bervini et al., 2014; Korja et al., 2014) and the subsequent radiosurgery is less likely to obliterate residual volume bAVM than equivalent volumes of bAVM treated by radiosurgery without prior embolization (Andrade-Souza et al., 2007).

The myriad of subtle variations in surgical and endovascular techniques compounded by operator dependent factors for a variety of lesions of different complexity make it impossible to quantify the contribution of embolization to the management of bAVM without

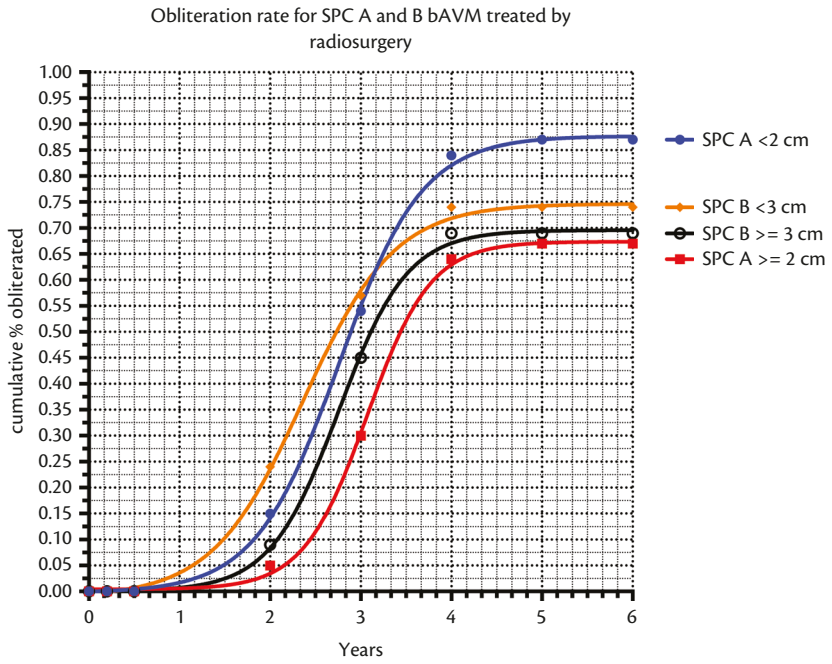

Assumptions:
1 No obliteration rate in first 6 months.
2 No further obliteration beyond 5 years.
3 Oblieration rate is best represented by sigmoid curve fit

Data derivation:
Kano 2012 (for SPC A) and Kano 2014 (for SPC B).

Fig. 50.3 Anticipated obliteration rates for SPC A and SPC B bAVM treated by radiosurgery extrapolated from a report by Kano and colleagues. They also identified that bAVM of small diameters were more likely to obliterate within each of these two groups.

Data from Kano H, Flickinger JC, Yang H-C, et al., Stereotactic radiosurgery for Spetzler-Martin Grade III arteriovenous malformations, *Journal of Neurosurgery*, Volume 120, Issue 4, pp. 973–81, 2014; and Kano H, Lunsford LD, Flickinger JC, et al., Stereotactic radiosurgery for arteriovenous malformations, Part 1:management of Spetzler-Martin Grade I and II arteriovenous malformations, *Journal of Neurosurgery*, Volume 116, Issue 1, pp. 11–20, 2012.

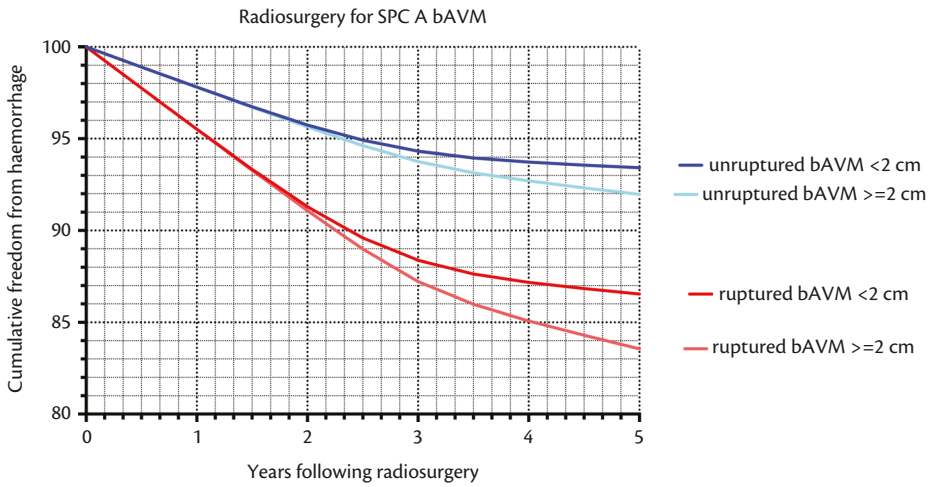

Fig. 50.4 The cumulative freedom from haemorrhage following radiosurgery for SPC A bAVM is extrapolated from combining the natural history of haemorrhage after diagnosis derived from a meta-analysis, with the proportion that is not obliterated as reported from Kano and colleagues.

Data from Gross B, Du R, Natural history of cerebral arteriovenous malformations: a meta-analysis, *Journal of Neurosurgery*, Volume 118, Issue 2, pp. 437–43, 2013; and Kano H, Lunsford LD, Flickinger JC, et al., Stereotactic radiosurgery for arteriovenous malformations, Part 1:management of Spetzler-Martin Grade I and II arteriovenous malformations, *Journal of Neurosurgery*, Volume 116, Issue 1, pp. 11–20, 2012.

knowing the institutional outcomes and place this within its correct context. Therefore, in order to plan a management pathway, both the whole-of-management outcomes as well as the individual procedure outcomes need to be understood for the institution responsible for treating a patient with bAVM. When a fluid approach to management occurs and the individual procedural outcomes are known but the whole-of-management outcomes are not known, there is a risk of hyperbolic discounting by those making the treatment decisions in that the risks of the first procedure loom larger than risks of subsequent procedures. With regards understanding this bias, the role of embolization in the outcomes of unruptured bAVM in the RCT, ARUBA, deserves some reflection (Mohr et al., 2014). The conservative arm had a better outcome at 33 months than the treatment arm. Of the three treatment modalities in the treatment arm, radiosurgery was used as an intervention in 48% (and as a single modality in 32%), embolization was used as an intervention in 44% (and as single modality in 31%), and surgery in 18% (and as a single modality in 5%) of cases. Given the brief duration of follow-up, one would not expect that radiosurgery contributed significantly to the inferiority of treatment over conservative management of unruptured bAVM. Given the small proportion of cases undergoing surgery alone, this does suggest that the treatment strategy of embolization prior to further treatment, or embolization alone, most likely contributed to the inferiority of treatment. Therefore, embolization may be inappropriate in the management of most unruptured bAVM.

In the management of ruptured bAVM, it is sometimes evident that the source of haemorrhage is from an associated proximal intracranial aneurysm or an intranidal aneurysm. In such cases, it is reasonable to consider targeted embolization of the feeding artery or intranidal aneurysm particularly if definitive obliteration of the BAVM will be delayed or not possible.

Combined management

The case for multimodality treatment may be made for individual cases but the evidence that this is appropriate for most cases is, so far, not extant. The fluid management strategy, where the next intervention is not determined until after a previous intervention, has a risk of hyperbolic discounting bias with respect to assessing risk (*vide supra* embolization). To avoid this bias, it is important to have planned the subsequent course (or potential courses) of treatments and account for the complication and likely outcomes from total management. The decision to embark on combined treatments is highly nuanced requiring a clinician with significant experience and expertise in bAVM management.

Complications of management

Surgical complications that occur with any craniotomy such as infection, subdural haemorrhage and peripheral thrombotic disorders occur with surgical resection of bAVM (Morgan et al., 1993). The incidence of these complications is often related to how intensely they are sought and, although are serious and provide management challenges, they often do not impact upon the ultimate outcome modified Rankin scale score (mRS). Microsurgery for bAVM have specific complications that relate resection of functional brain and to haemodynamic perturbations that arise in response to elimination of the arteriovenous shunt. These may be interactive and dependent upon size, location, and the magnitude of the arteriovenous shunt. To reduce the potential for direct brain damage from a resection margin containing functional brain, judgement needs to be made by the surgeon as to the site along these arteries feeding the bAVM, beyond the last branch to normal brain, that can be safely ligated without the proximal feeding artery rupturing or other complication related to arterial-capillary-venous hypertensive syndrome (ACVHS) (Morgan et al., 1999; Morgan and Winder, 2001; Morgan et al., 2003). ACVHS is haemorrhage (or oedema) occurring during or after resection caused by the physiological response of arteriovenous shunt ablation. With the resection of bAVM in a dilated arterial and venous bed, a predictable physiological response occurs that requires remodelling of the vessels (that may take approximately 10 days) or thrombosis to reduce this risk. Because it is a physiological response to the degree to arteriovenous shunting, this complication is not expected in small bAVM. It is seldom, if ever seen, in SPC A bAVM (Morgan et al., 2003). The site of vascular disruption responsible for ACVHS can be from unrecognized residual bAVM with occluded outflow (this cannot always be discerned by DSA as there may be no inflow if there is no outflow), venous occlusion ('occlusive hyperaemia') (Al-Rodhan et al., 1993), microcirculation autoregulation incompetence (normal perfusion pressure breakthrough) (Spetzler et al., 1978; Sekhon et al., 1997), or proximal thin-walled small dilated artery wall disruption (Drake, 1979; Sekhon et al., 1997). The unifying disrupting force is the proximal arterial pressure projected distally into regions of prior low pressure (see **Fig. 50.1**). This is particularly pronounced where the proximal vasculature is markedly dilated and unable to respond by vasoconstriction that should normally follow a dramatic reduction in shear stress (inhibiting eNOS expression) and increase in pulsatility (increasing the release of endothelin-1) (Faraci et al., 1995; Mazzuca and Khalil, 2012). The exaggerated increased pressure is also facilitated by the very low resistance in the dilated proximal vasculature because of the radius size of these vessels. The projected pressure is transmitted to the point of occlusion and therefore, many proximal vascular regions may be vulnerable to this sudden elevation in pressure until such time as the arterial remodelling removes this threat. This is in accord with the Poiseuillie's equation given as:

$$Flow \propto \frac{Pressure\ gradient \times radius^4}{length\ of\ tube}.$$

Where the flow equals zero after bAVM ligation the pressure gradient between the artery and outflow must equal zero.

SPC A bAVM have little risk for ACVHS unless there is extensive redundant venous drainage over a considerable surface of the brain (predisposing to the risk of propagated venous occlusion and venous infarction, or occlusive hyperaemia). In such cases, when the risk of postoperative bleeding in bAVM bed is minimal, judicious use of anticoagulant or antiplatelet therapy could be considered. For more complex bAVM this regimen of antiplatelet or anticoagulant therapy is inappropriate. The cornerstone of preventing and managing ACVHS is blood pressure control. For SPC A and SPC B less than 4 cm preventing high blood pressure is essential (e.g. prevention of systolic pressure rise above 140 mmHg). However, for large SPC B or SPC C, lowering of blood pressure may be desirable. Maintaining a cerebral perfusion pressure of at least 50 mmHg and a mean blood pressure (at the brain level) less than 70 mmHg appears successful in

Table 50.3 Management protocol and prevention of arterio-capillary-venous hypertensive syndrome (ACVHS)

Strategy	Approach	Possible agents	Limitation of use	Amelioration of potential adverse effects
Avoiding sudden elevations in blood pressure	Seizure and pain prevention to reduce momentary episodes of raised blood pressure		Induced constipation may potentiate GIT problems	
Lower mean blood pressure	Moment to moment titration of blood pressure to ensure safe perfusion of brain (e.g. cerebral perfusion pressure >50 mmHg) with mean pressures <70 mmHg	Nitroprusside for continuous titration control and other baseline agents (e.g. ACE inhibitors and beta-blockade)	Cumulative high dose toxic; Straightens the autoregulation curve making vulnerable normal brain at lower blood pressure	Addition of other antihypertensive to minimize the dose needed for moment to moment blood pressure reduction
Reduce rate of upstroke of systolic pressure	Due to the greater pulsatility in the dilated proximal redundant vasculature, dampening of the upstroke in systole is appropriate	Beta-blockade	Reducing pulse rate will increase stroke volume that might be counterproductive	Mild (but safe) reduction in cardiac output may assist
Reduction in cardiac output	Mild reduction in cardiac to reduce stroke volume	Barbiturates	Need to ensure adequate end-organ perfusion and induced coma increases the complexity of management including monitoring of intracranial pressure (ICP) and protection against immunosuppression. Prolonged use will accumulate considerable reservoir of barbiturates in fat storage leading to a considerable time of ventilator support	Fluid retention may require the addition of diuresis; ICU management; Vigilant assessment of infection status; altered metabolism of many drugs

reducing the risk of catastrophic ACVHS (Morgan et al., 2003). By a combination of lowering blood pressure, dampening the systolic peaks, reducing the rate of upstroke in the systolic wave, and reducing cardiac output (if necessary), the risks of ACVHS can be minimized (Table 50.3). However, it is critical that at all times, ischaemia is not therapeutically induced in normal brain.

Preserving normal functioning brain is critical to avoiding complications. This requires: preservation of arterial supply to, and venous drainage from, functioning brain; minimization of trauma (e.g. judicious use of retraction and dissection respecting the maximum preservation) to functional brain; avoidance of evolving haematoma concealed by cottonoids or other haemostatic material (it is best to allow haemorrhage direct access to the cavity); and avoidance of venous infarction and brain contusion from inappropriate head positioning resulting in herniation of brain over the craniotomy margin.

The major complication of radiosurgery is the development of adverse radiation effects (ARE) in approximately 7–10% of cases due to inflammatory response occurring 4 to 40 months after treatment (Boothe et al., 2013; Kano et al., 2014). The risk of this developing is related to bAVM size and complexity and is far less common for SPC A bAVM (Kano et al., 2012b). ARE relates to the volume of brain receiving 12 Gy. ARE results in oedema and neurological deficits and usually resolves. However, ARE may be life-threatening and permanently disabling. Treatment of this condition may include corticosteroids, vitamin E, phosphodiesterase inhibitors and VEGF inhibitors (Boothe et al., 2013). In addition, late cyst formation can occur in 2% of cases up to 18 years after treatment that may require surgical intervention (Kano et al., 2014). The combined morbidity and mortality following treatment by radiosurgery (including the natural history of rupture during the latency period) is given in Fig. 50.4.

The major complications from embolization include haemorrhage (from premature occlusion of outflow vein and wire perforation of the arterial wall) and occlusion of arteries supplying critical brain. Occasionally, complications related to arterial access problems (femoral artery occlusion, dissection, false aneurysm formation), embolic complications (from femoral, iliac, aortic, and cervical arterial catheterization) and arterial dissection occur. The risk of this occurrence will depend upon the complexity and number of embolization procedures performed on each patient. Therefore, risks will vary considerably between institutions because the distribution of shared responsibility for treatment varies between surgery, radiosurgery, and embolization. From large series of treatment by EVACE, in which the goal is likely to be aggressive role for embolization, the risks of major morbidity and mortality averages 7% (range 1% to greater than 10%) (Morgan et al., 2013).

Outcomes/Prognosis

For a summary of the outcomes for various management pathways, see Table 50.4. Surgical risk for SPC A bAVM is reported to be 6–10% and has been reported to be less than 3% (Gross and Du, 2013; Korja et al., 2014). This risk is likely to be generalizable to all SPC A as a group (Korja et al., 2014). The risk of surgery for SPC B is significantly worse in older patients, unruptured bAVM and diffuse bAVM (Kim et al., 2015). The Lawton-Young scale allows stratification of risks for SPC B around these factors (Table 50.4) (Kim et al., 2015). Surgical treatment for SPC C is seldom warranted in those of 20 years of age and older because of risk and usually precluded in patients under 20 years unless there is a highly nuanced reason.

Table 50.4 Comparison of management of bAVM (source reference in brackets)

Management pathway	Modifying factors	Adverse outcome leading to permanent neurological deficit (mRS >1) from treatment	Annual risk of rupture (references)	Approximate cumulative rupture rate projected for 5 years	Time to 50% of case obliteration	Obliterated on delayed studies at 5 years, % (references)
Untreated	Presentation with haemorrhage	NA	3.7–5.9% (Gross and Du., 2013., Kim et al., 2014)	20%	NA	NA
	Unruptured	NA	1–2.7% (Gross and Du., 2013., Kim et al., 2014)	10%	NA	NA
	Unruptured with aneurysm	NA	Similar to ruptured (Gross and Du., 2013., Brown et al., 1990)	>10%; <20%	NA	NA
Radiosurgery	Unruptured SPC A or B <2 cm	<3%	Unchanged until obliterated	7%	2.5 to 3.0 years	85% (Kano et al., 2014., Kano et al., 2012b)
	Unruptured SPC A or B >2 cm	<3%	Unchanged until obliterated	8%	3.0 to 3.5 years	70% (Kano et al., 2014., Kano et al., 2012b)
	Ruptured SPC A or B <2 cm	<3%	Unchanged until obliterated	14%	2.5 to 3.0 years	85% (Kano et al., 2014., Kano et al., 2012b)
	Ruptured SPC A or B >2 cm	<3%	Unchanged until obliterated	16%	3.0 to 3.5 years	70% (Kano et al., 2014., Kano et al., 2012b)
Surgery	SPC A	6–10% (34); possibly <3% (Korja et al., 2014; Spetzler and Ponce, 2011)	<1%	<1%	NA	>99%
	SPC B: 1) any <20 years of age; 2) 20 to 40 years of age ruptured or compact (not both).	10–24% (Spetzler and Ponce., 2011).); possibly closer to 20% (Korja et al., 2014; Kim et al., 2015)	<1%	<1%	NA	97%
	Other SPC B (Lawton-Young grades >6)	>39% (Kim et al., 2015)	<1%	<1%	NA	97%
	SPC C	>50% (Korja et al., 2014)	<1%	<1%	NA	96%

Combined morbidity and mortality is reported to be greater than 20% for SPC C bAVM cases (Korja et al., 2014). However, given that these are from highly selected cases, they do not represent a generalizable risk for these cases and it is reasonable to suggest that the risk of surgery for SPC C is at least 50% (with half of the adverse outcomes leading to an mRS >2).

The outcomes of radiosurgery are dependent upon the dose of radiation received by the bAVM and the dose of radiation received by the brain (*vide supra*).

Overlaying the risks of surgery with that of the natural history and that of radiosurgery (including the anticipated risk of haemorrhage in the latency period between treatment and obliteration) allows a comparison between treatment options (Fig. 50.5). It would appear that if a 10-year time horizon is considered, surgery and radiosurgery appear to be favourable options in comparison to natural history for SPC A. A distinct advantage of surgery over that of radiosurgery is apparent for ruptured SPC A bAVM. It is likely that unruptured SPC B bAVM are likely best treated by radiosurgery providing there is a high expectation of obliteration. For surgery to be appropriate for SPC B bAVM, a time horizon considerably longer than 10 years needs to be considered. Although the selection of treatment modalities should best be answered by a randomized control trial, and one has been done (Mohr et al., 2014), the external validity is questioned limiting its interpretation (*vide supra* under embolization) (Korja et al., 2014).

Dural arteriovenous fistulae

Pathophysiology, classification, and natural history of AV fistulae

Dural arteriovenous fistulae (DAVF) form part of a spectrum of arteriovenous abnormalities with bAVM (*vide supra*). BAVM have the fistula point within the venous system before the bridging veins whereas DAVF locate their fistula beyond this point. DAVF comprise one or more fistulae centred either on the bridging vein (bridging between the leptomeningeal veins and dural venous sinus) as well as fistulae within the wall of veins contained within dura (including dural venous sinuses). They are usually acquired but may be congenital (e.g. some types of vein of Galen aneurysms; see Johnston et al., 1987). DAVF are detected at a rate one-third that of bAVM (Satomi and Satoh, 2008).

The aetiology of DAVF is likely to be venous thrombosis (Houser et al., 1972; Morales et al., 2010). That the dural venous stenosis/occlusion is aetiological rather than an epiphenomenon is supported by the finding that some patients (although a minority) have been identified with acquired or genetically determined prothrombotic disorders (Kraus et al., 2002; Wenderoth and Phatouros, 2003; Saito et al., 2008; Wysokinska et al., 2008; Pasi et al., 2014; Hwang, 2015). However, prothrombotic states constitute no more than 30% of cases of DAVF (Izumi et al., 2007; Wysokinska et al., 2008).

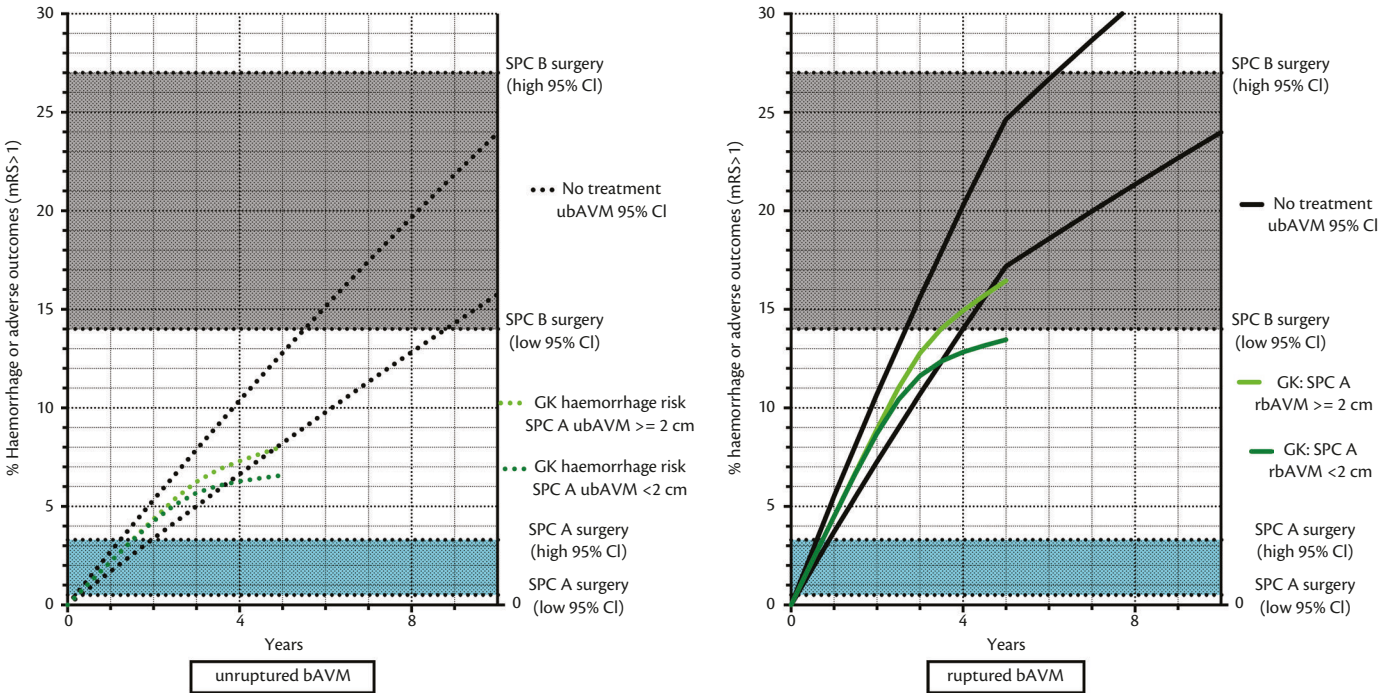

Surgery outcomes include sensitivity analysis for unoperated cases (11)
Radiosurgery outcomes derived from series classified by Spetzler-Martin grade (21, 39) incorporating natural history of haemorrhage derived from Gross and Du (12).
Natural history of rupture (12) assumed to return to that of uruptured after 5 years.

Fig. 50.5 Overlaying the risks of surgery that result in complications leading to a permanent mRS greater than 1 (the blue band representing the 95% confidence interval range for surgery on SPC A and the grey band representing the 95% confidence interval range for surgery on SPC B) (data from with the time-dependent outcomes of haemorrhage without treatment, black line) (data from or following radiosurgery, dark green <2 cm diameter; light green >2 cm) (see Fig. 50.4).

Data from Korja M, Bervini D, Assaad N, Morgan MK, The role of surgery in the management of brain arteriovenous malformations: A prospective cohort study, *Stroke*, Volume 45, Issue 12, pp. 3549–55, 2014; and Gross B, Du R, Natural history of cerebral arteriovenous malformations: a meta-analysis, *Journal of Neurosurgery*, Volume 118, Issue 2, pp. 437–43, 2013; and Kano H, Flickinger JC, Yang H-C, et al., Stereotactic radiosurgery for Spetzler-Martin Grade III arteriovenous malformations, *Journal of Neurosurgery*, Volume 120, Issue 4, pp. 973–81, 2014; and Kano H, Lunsford LD, Flickinger JC, et al., Stereotactic radiosurgery for arteriovenous malformations, Part 1: management of Spetzler-Martin Grade I and II arteriovenous malformations, *Journal of Neurosurgery*, Volume 116, Issue 1, pp. 11–20, 2012.

DAVF may induce venous stenosis. The production of endothelial growth factors from the high shear stress may induce subsequent dural venous sinus wall changes. Arterial levels of shear stress within veins may predispose to venous intimal hyperplasia (Fitts et al., 2014). The formation and progression of dural arteriovenous fistulae may be mutually interdependent (Casa et al., 2015). A cycle of veno-occlusive disease predisposing to the development of a DAVF predisposing to veno-occlusive disease suggests a very dynamic disease process that can change with time and, in at least 13% of cases, spontaneously occlude (Gross and Du, 2012).

The most feared consequence of DAVF is intraparenchymal (or occasional spontaneous acute subdural) haemorrhage (Duffau et al., 1999). Haemorrhage is recognized to occur only in the presence of cortical venous drainage and when present has an annual risk of haemorrhage of approximately 4–11% (Davies et al., 1997a; Davies et al., 1997b). Furthermore, when either exclusive cortical venous drainage or cortical venous drainage with strain (ectasia or extensive cortical venous ramification) is present, the risk of haemorrhage is significantly higher than in their absence (Baltsavias et al., 2015). In the case where cortical venous drainage is associated with ectasia, the annual risk is at least 10% and may approach 50% (Butlers et al., 2012; Gross and Du, 2012). The time to next haemorrhage is highest shortly after haemorrhage necessitating an urgency to definitive management (Butlers et al., 2012). Mortality from haemorrhage is reported to be 40% (Gross and Du, 2012). It is possible for venous drainage patterns to change with time, warranting surveillance on those deemed to pose a low risk of haemorrhage. Sites of DAVF more commonly associated with exclusive retrograde leptomeningeal venous drainage are usually deep median or paramedian locations such as anterior skull base in the ethmoidal region, tentorial edge, anterior straight sinus, and petrosal sinus. Whereas, cavernous and transverse sigmoid sinus locations are less likely to have (although may still have) retrograde leptomeningeal venous drainage.

The non-haemorrhagic venous hypertensive syndromes can be focal or generalized venous hypertensive encephalopathy due to leptomeningeal venous hypertension; generalized venous sinus hypertensive syndromes (resulting in intracranial hypertension); and focal venous sinus hypertensive syndromes (the most notable being cavernous sinus syndrome with a threat to eye health). Occasionally, deep venous variceal development may lead to hydrocephalus from aqueduct obstruction. The incidence of presentation with neurological deficits is similar in proportion to that of haemorrhage and occurs in patients with a similar pattern of venous drainage (Gross and Du, 2012).

Clinical presentation, diagnosis, classification, and workup of AV fistulae

The mode of clinical presentation of DAVF can vary considerably. A list of these and their underlying cause are included in Table 50.5.

Useful classifications of DAVF are based upon the angioarchitectural relationships of venous drainage patterns and the presence of venous ectasia and thus, reflect their natural history (Borden et al., 1995; Cognard et al., 1995; Baltsavias et al., 2015). Three useful classification systems are described and compared in Table 50.6.

The workup for those suspected of harbouring a DAVF reflects the clinical presentation. The diagnosis may be made on MRI/A and CT/CTA (Figs. 50.6 and 50.7). Of importance is the identification of retrograde cortical venous drainage (and whether there exists ectasia of the venous system) (Fig. 50.6). Although this may be apparent from dilatation of the cortical venous system, it may not be easily seen and it should be excluded by DSA. The DSA requires the external carotid circulation to be included and should be bilateral as the arterial contribution may be bilateral and more than one fistula may be present (Fig. 50.6).

In addition to establishing the angioarchitecture of the arteriovenous fistula, an assessment of the prothrombotic predisposition, if any, should be made. In the case of very young patients, an assessment of the impact of the fistula on the heart should also be made (see section on paediatrics).

Table 50.5 Clinical presentation of DAVF

Clinical presentation	Clinical nuance	Explanation
Bruit	This is typically localized to the ear on affected side of a transverse sigmoid sinus. However, it may be on the contralateral ear to the fistula where the sigmoid sinus is occluded. The bruit may be very loud and keep the patient awake at night. It may even be audible to those close to the patient when quiet. The bruit peaks in systole but is often continuous through diastole. It is audible with a stethoscope and compression of the ipsilateral internal jugular vein may suppress the bruit	Arising from turbulence or high flow within the sigmoid sinus.
Pulsatile mass	Palpated behind mastoid processes in course of occipital artery	Dilation feeding arteries (e.g. occipital artery).
Headaches	Certain considerations need to be made	1. recruitment and dilatation of meningeal vessels. 2. thrombosis within dural venous sinus 3. trigeminal neuralgia from dilatation of superior petrosal vein. 4. intracranial hypertension (see below). 5. coincidental.
Neurological deficits	1. Focal neurological deficits of the brain 2. Global cognitive neurological deficits 3. Walking difficulty from cord venous hypertensive encephalopathy or hydrocephalus 4. Cavernous sinus syndrome or cranial nerve deficits (partial or complete)	1. Focal venous hypertensive encephalopathy. This may lead to fleeting, fluctuating, or progressive focal neurological deficits. This is due to cortical venous hypertension resulting in ischaemia. 2. Generalized venous hypertensive encephalopathy. This causes generalized cognitive decline and coma. DAVF with deep retrograde venous drainage into the internal cerebral veins or bilateral cortical veins that are impeded from superior sagittal sinus drainage are the usual cause. In such cases, there is usually significant impediment to intracranial venous outflow such as bilateral transverse venous sinus stenoses. 3. Compression or ischaemia of cranial nerves. This is a common mode of presentation with cavernous sinus DAVF. This may be related to the interaction of cavernous sinus thrombosis (total or partial) with venous hypertension within the cavernous sinus. In addition, dilated draining veins within the subarachnoid space may lead to cranial nerve compression and be responsible for, as an example, hemifacial spasm. 4. Hydrocephalus from venous variceal obstruction to aqueduct of Sylvius. 5. Venous hypertensive myelopathy from intracranial DAVF predominant drainage to the spinal cord (which may be manifest from conus involvement typical of cord DAVF).
Haemorrhage	Usually intraparenchymal but may be spontaneous acute subdual haemorrhage	See natural history.
Seizures	Focal or generalized	Occur only in the presence of supratentorial retrograde leptomeningeal venous drainage.
Intracranial hypertension, with papilloedema and headache	May occur with large DAVF	Occurs as a consequence of an increase in pressure within the venous sinuses. Due to the maintenance of the subarachnoid space pressure-venous sinus pressure gradient that drive CSF absorption.
High output cardiac failure in infants	Infants with large fistula	Direct shunts into bridging veins in the absence of venous outflow obstruction can develop a very significant proportion of the cardiac output in infants and neonates. When present in neonates, they may present as a primary cardiac problem as the high output flow to the intracranial fistula may be typical of congestive cardiac failure with pulmonary hypertension (81).

Table 50.6 Useful classifications of DAVF revolve around the association with risk of intracranial haemorrhage venous hypertensive encephalopathy

Pathology	Borden-Wu-Shucart Classification (Borden et al., 1995)	Cognard et al. modification of Djindjian and Merland Classification (Cognard et al., 1995)	DES system (direct leptomeningeal venous drainage; Exclusive leptomeningeal venous drainage; leptomeningeal venous Strain) n = not/no (Baltsavias et al., 2015)	Presentation	Sex and two most common sites	% of group presentating with haemorrhage or neurologic deficit (excluding cranial nerve deficits) (Baltsavias 4)	Prognosis (Gross and Du 2012)
Direct into dural venous sinus or meningeal veins antegrade venous flow only and no retrograde cortical venous drainage	I	I	nD, nE, nS	bruit	Female predilection; transverse sigmoid sinus or cavernous sinus	0%	Unlikely to haemorrhage
Direct into dural venous sinus or meningeal veins with retrograde dural venous outflow and no retrograde cortical venous drainage	I	IIa	nD, nE, nS	bruit	Female predilection; transverse sigmoid sinus or cavernous sinus	0%	Unlikely to haemorrhage
Direct into dural venous sinus or meningeal veins with both retrograde venous sinus outflow and retrograde drainage into cortical veins that do not exhibit ectasia	II	IIa and IIb	nD, nE, nS	Bruit, venous hypertensive encephalopathy, haemorrhage, intracranial hypertension	Female predilection; transverse sigmoid sinus or cavernous sinus	0%	6% annual risk
Direct into dural venous sinus or meningeal veins with both retrograde venous sinus outflow and retrograde drainage into cortical veins that exhibits ectasia	II	IIa and IIb	nD, nE, S	Bruit, venous hypertensive encephalopathy, haemorrhage, intracranial hypertension	Female predilection; transverse sigmoid sinus or cavernous sinus	66%	6% annual risk
Direct into dural venous sinus or meningeal veins with exclusive retrograde drainage into cortical veins that do not exhibit ectasia	II	IIb	nD, E, nS	Bruit, venous hypertensive encephalopathy, haemorrhage, intracranial hypertension	Female predilection; transverse sigmoid sinus or cavernous sinus	15%	6% (95% CI: 0.1 to 19%) annual risk
Direct into dural venous sinus or meningeal veins with exclusive retrograde drainage into cortical veins that exhibits ectasia	II	IIb	nD, E, S	Bruit, venous hypertensive encephalopathy, haemorrhage, intracranial hypertension	Female predilection; transverse sigmoid sinus or cavernous sinus	90%	6% (95% CI: 0.1 to 19%) annual risk
Direct into bridging vein and both retrograde cortical venous drainage and venous sinus drainage	Not defined	Not defined	D, nE, nS	venous hypertensive encephalopathy, haemorrhage, intracranial hypertension			
Direct into bridging vein and only retrograde cortical venous drainage without venous ectasia	III	III	D, E, nS	venous hypertensive encephalopathy, haemorrhage,	Male predilection; tentorial and petrosal	75%	10% (95% CI: 4 to 20%) annual risk;
Direct into bridging vein and only retrograde cortical venous drainage with cortical venous ectasia	III	IV	D, E, S	venous hypertensive encephalopathy, haemorrhage	Male predilection; tentorial and petrosal	>90%	21% (95% CI: 4 to 66%) annual risk
Perimedullary venous drainage (spinal)		V					

CTA sagittal plane of DAVF located within the straight sinus tentorial edge border, Borden type III presenting with gobal cognitive impairment and absence of straight sinus filling.

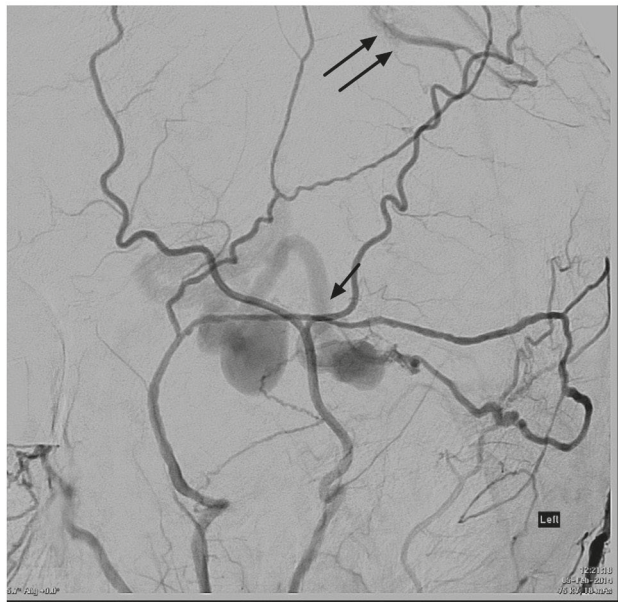

External carotid arterial DSA demonstrating retrograde parenchymal venous drainage (arrow). A second fistula is identified associated with the falx (double arrow).

Fig. 50.6 CTA and external carotid DSA demonstrating the features of a DAVF with retrograde leptomeningeal venous drainage. This adult male patient in his sixties presented with global cognitive decline. There was a second small DAVF associated with the falx communicating with the superior sagittal sinus.

Treatment

Treatment should normally only be recommended when there is the presence of retrograde cortical venous drainage (because of the risk of haemorrhage in these patients), venous sinus hypertension (causing intracranial hypertension) or cavernous sinus syndrome (causing a threat to eye health). However, occasionally treatment is aimed at palliating symptoms (e.g. audible bruit). It should be remembered that there may be alternative ways of palliating

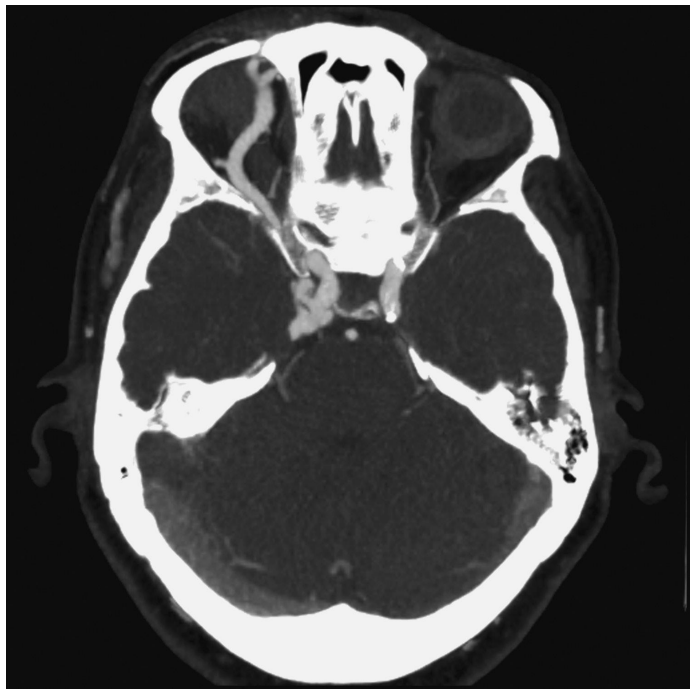

Fig. 50.7 CTA demonstrating a right cavernous DAVF by the evidence of the enlarged superior ophthalmic vein filling during the arterial phase (note: the transverse sinus is less opacified, making it possible to state that the superior ophthalmic vein is filling early).

symptoms (e.g. sleeping with background white noise) and with time, DAVF may spontaneously thrombose. When palliating a bruit, it is important to keep in mind that cure may not be necessary to alleviate the symptoms and it is critical that a benign fistula is not converted to a sinister DAVF by altering venous drainage.

Surgery

Two general approaches can be considered surgically. The first is the disconnection of the retrograde cortical venous drainage from the DAVF leaving the DAVF intact but without any cortical venous reflux. This removes the danger from haemorrhage. The second approach is to remove the DAVF itself. In this procedure, it is critical that the sinus resection does not interfere with normal cortical venous drainage.

1. *Disconnection of cortical venous drainage.* This can be applied for all locations providing that retrograde flow is established and is the optimal treatment in most situations. This is similar for both spinal dural AVF and cranial DAVF. The smallest approach possible, with a clip applied as close to the entry of the vein to the dura, will obliterate the risk of haemorrhage. However, some difficulties in performing this must be considered:
   a. Because the arterialized vein may have tributaries close to the exit point from the dura, the clip placement must be close enough to the dura to prevent continued shunting.
   b. When closing the clip at this point, it is important not to tear the draining vein exiting the dura (made possible because of the fixed venous circumference in the relatively rigid dura). Therefore, slow closure of the clip blades is important to allow the tense vein to slide within the clip blades to avoid excess wall tension.
   c. The grossly dilated and tense arterialized veins may extensively obstruct the approach to the clip target point. Consideration of this access obstruction needs to be made in planning the surgical approach. As an example, when the entry of the superior petrosal vein is the target, this might be more readily achieved by a supratentorial subtemporal approach with division of the tentorium from medial to lateral to expose the superior petrosal vein from above without the vein itself obstructing the approach.
2. *Venous sinus resection involved in the DAVF.* This approach is rarely required since the introduction of liquid embolic agents and intravenous sinus temporary balloon protection of the venous sinus lumen. However, for completeness, if the involved venous sinus is no longer functioning with normal venous drainage (i.e. it is thrombosed, or the involved segment contains no important tributaries from the brain and collateral venous drainage exists) the DAVF with the venous sinus can be excised. Although rarely performed if an endovascular or simple disconnection procedure is available, it may still have an occasional place in management. This approach was first proposed by Dr Sundt in the management of transverse sigmoid sinus DAVF (Sundt and Piepgras, 1983; Eftekhar and Morgan, 2013). Careful consideration must be made of veins that must be included within the excised segment to ensure they do not carry normal antegrade blood flow.

Embolization

The key to curing DAVF is to obliterate the 'foot of the vein' involved in the DAVF. This can be achieved with liquid embolic agents either from a transarterial or a transvenous route. A number of approaches may be taken to obliterate arteriovenous shunting by embolization including transarterial as well as transvenous routes. The transarterial route is similar to that for obliterating bAVM. However, there are additional concerns that need to be considered. Chief among these are ischaemia of the scalp and reflux into collateral supply to normal brain. Although most meningeal branches make no contribution to the brain, this is not always the case and of particular concern is reflux backward into a brain-supplying artery. Furthermore, cranial nerves may be supplied by meningeal arteries. Therefore, careful consideration of potential collateral supply (and the potential impact upon future management, such as a surgical approach) needs to be made prior to endovascular intervention. The transvenous route, although reasonable, may be complicated by the DAVF feeding into channels running parallel to a normal venous sinus. This may make obliteration of the sinus potentially non-curative. Stenting of the sinus (pinning the feeding arteries into the sinus) or balloon inflation of the sinus during embolization may allow protection of functioning venous sinuses. An important consideration while conducting the transvenous ablation is to avoid causing venous hypertensive encephalopathy during the procedure by increasing the outflow into the cortical venous drainage without having reduced the arterial inflow. This may precipitate haemorrhage or exacerbate neurological deficits (e.g. **Fig. 50.8**). When performing liquid embolic embolization of the venous foot of the DAVF, in the presence of a patent venous sinus, there is a risk for sinus occlusion. This can be prevented by concurrent balloon inflation within the venous sinus during the injection of the liquid embolic agent. However, the balloon may impede normal venous drainage during the period of inflation and should be reserved for the more aggressive DAVF when the goal is to cure the fistula rather than the lesser goal of palliation of symptoms.

Focused irradiation

Although yet to be validated for DAVF treatment, it has been reported to be successful when combined with embolization in some cases of transverse sigmoid sinus DAVF (Loumiotis et al., 2011). This may prove to be an important component of management for disabling symptomatic bruits when there is no retrograde leptomeningeal venous drainage (and therefore no immediate threat of haemorrhage). For such cases, the role of particulate arterial embolization to reduce the bruit followed by radiosurgery offers a very low risk and promising treatment for transverse sigmoid sinus DAVF (Loumiotis et al., 2011).

Conclusion with regards management of DAVF can be seen in a decision-making algorithm illustrated in **Figure 50.9**.

Complication management

The most frequent complications common to both surgical and endovascular management are:

1. *Haemorrhage at the time of treatment.*
   a. Haemorrhage may occur due to retraction in the presence of venous hypertension. When venous hypertensive encephalopathy is present great care must be taken in manipulating the brain before retrograde cortical venous drainage is eliminated. On opening the craniotomy, relaxation may be difficult due to venous hypertension. However, the additional

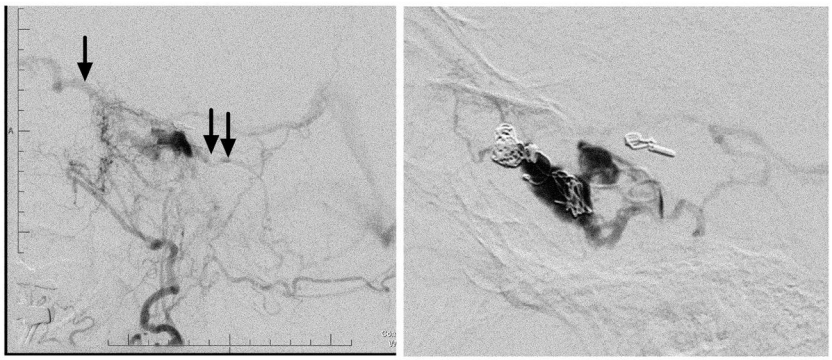

Left external carotid injection (left) demonstrating cavernous DAVF with filling of the superior ophthalmic vein (arrow) and retrogrde parenchymal venous drainage to the posterior fossa (double arrow). During the embolisation procedure via a venous transpetrosal access (right), the superior ophthalmic vein was occluded early with consequent DAVF flow entirely retrograde into the posterior fossa cortical veins (before finally occluding this outflow). Aneurysm clip placed on coincidental ICA aneurysm.

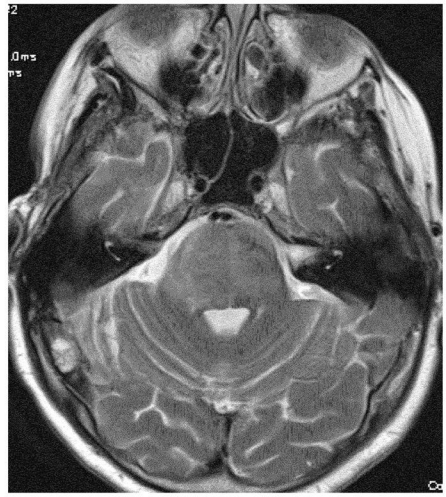

T2 MRI demonstrating hyperintensity and swelling of pons from venous hypertensive encephalopathy due to the redirection of outflow into the cortical veins of the posterior fossa during embolisation. Patient had a prolonged loss of consciousness and awoke with a hemiparesis.

Fig. 50.8 DAVF of the left cavernous sinus presenting with orbital congestion and eye threatening secondary glaucoma. The external carotid arterial injection (left) demonstrates the characteristic enlargement of the superior ophthalmic vein (arrow) with the sinister venous outflow from the inferior petrosal sinus into the prepontine veins (double arrow). This was treated by the transvenous catheterization and coil occlusion of the cavernous sinus initially packing anteriorly near the superior ophthalmic vein. Retrograde flow into the pontine venous system followed until this was eventually occluded (middle image). Slow to awake and eventually awakening with a hemiparesis, it can be seen by MRI (right image) that an episode of significant venous hypertension resulted in the clinical and radiological features (hyperintensity and swelling of pons on T2).

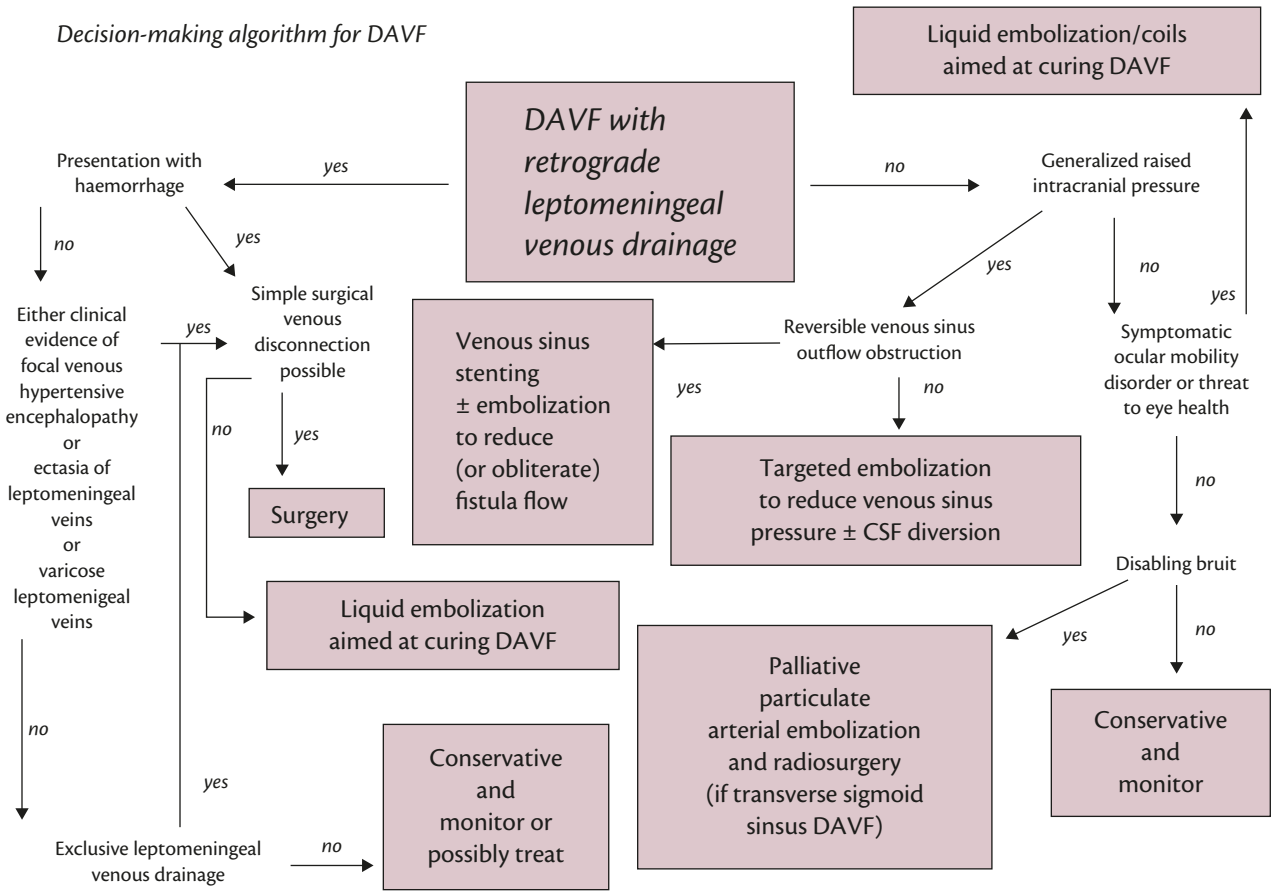

Fig. 50.9 DAVF decision-making algorithm for management.

venous obstruction that may result from retraction can result in venous infarction and haemorrhage. This is particularly the case in surgery of the torcula where the addition of a prone position accentuates the problem and a sitting position may result in herniation of brain through the craniotomy. Retraction should be kept to a minimum when venous hypertension is significant.

   b. With regards the risk of haemorrhage associated with endovascular repair, this most likely occurs with venous occlusion in which there is a momentary rise in pressure in the retrograde cortical venous outflow (e.g. in the distribution of the vein of Labbe) occurring before complete occlusion has been achieved.

2. *Venous infarction*. This arises with loss of normal antegrade flowing veins due to inadvertent occlusion or from propagated venous thrombosis. It is essential that only veins draining retrogradely can be safely disconnected.
3. *Venous hypertensive encephalopathy*. This occurs on the same basis as haemorrhage. An example can be seen in Figure 50.7.
4. *Propagated venous sinus thrombosis* (particularly at points of venous stenosis). Progressive venous sinus occlusion may occur with the reduction of flow. Particularly vulnerable are sinuses with multiple stenoses. When this is extended to, but not beyond, the next normal tributary inflow, no clinical consequences will occur. However, if this propagation extends beyond this point (e.g. across the torcula, catastrophic consequences may ensue). Monitoring the thrombosis in the post-treatment period with CT scan with and without contrast will assist in evaluating this risk. Furthermore, prophylaxis against venous thrombosis is important to consider especially as a prothrombotic state may exist (*vide supra*).
5. *Deep venous thrombosis.* Due to the propensity for some patients with DAVF to have a prothrombotic state, prophylaxis, and vigilance for deep venous thrombosis (DVT) is appropriate.

In addition, surgery carries a risk of:

6. *Pseudomeningocele formation.* This occurs with the excision of superficial sinuses (superior sagittal sinus and the transverse sigmoid sinuses) and the subsequent problem of dural closure. This will usually resolve after a period of weeks (to months) unless there is associated CSF circulation disorder.
7. *Poor wound healing.* Wound healing may be problematic if scalp artery embolization preceded surgery. This can be avoided with embolization confined to meningeal vessels.

Outcomes

Both surgery and endovascular repair have a high rate of success with a low risk (e.g. Eftekhar and Morgan, 2013). Due to the variety of approaches and the limited number of large series, quantification of risks is difficult. In the case of surgery aimed at simply excluding the cortical venous drainage from the DAVF, the limited approach of clipping the arterialized vein, reduces the surgical complexity, and therefore reduces the potential for complications. From the limited case series, treatment is likely to be superior to the natural history for DAVF in which retrograde cortical venous drainage with ectasia is present.

Carotico-cavernous fistulae (CCF)

Pathophysiology, classification, and natural history of CCF

The underpinning pathophysiology for the clinical consequences of all carotico-cavernous fistula (CCF) is elevated intracavernous venous sinus pressure. This is likely to also lead to retrograde venous drainage to the eye by the superior ophthalmic vein (Fig. 50.7). Because of the interconnections between the two cavernous sinuses, contralateral eye involvement is common. Occasionally, due to occlusion of the superior ophthalmic vein by anterior intracavernous thrombosis, the clinical presentation may only occur contralateral to the fistula.

The natural history for the eye and vision is poor in the extreme case. Threats to vision can arise from secondary glaucoma and the extreme exophthalmos with consequent corneal damage. In the case of indirect CCF, the clinical manifestations may be due to the combination of a cavernous sinus thrombosis and DAVF. In such cases, an extremely small DAVF may be responsible for extreme clinical manifestations. In the case of direct CCF, retrograde flow in the ophthalmic artery may occur contributing to retinal ischaemia that, when combined with the high venous pressure, may lead to immediate permanent loss of vision.

Problems other than that with the eye can occur. Retrograde cortical venous drainage may be present (middle cerebral veins or pontine venous tributaries to the inferior petrosal sinus). When present, the considerations discussed with DAVF (see earlier) need to be considered.

CCF can be direct or indirect. The Barrow classification is used by some authors and divides CCF into four types (A—direct, B—indirect with internal carotid supply, C—indirect with external carotid supply, D—indirect with internal and external carotid supply) (Barrow et al., 1982).

1. Indirect CCF are DAVF and can be considered with the aforementioned discussion. DAVF account for the vast majority of CCF. They are located in the wall of the cavernous sinus and may (on occasions) be associated with retrograde cortical venous drainage (Davies et al., 1997a; Davies et al., 1997b).
2. Direct CCF may be spontaneous or traumatic. These fistulae usually have a dramatic and profound onset due to a potentially very high flow that may include contributions from the internal carotid artery (ICA) (both antegrade and retrograde) ophthalmic artery and the posterior circulation through the posterior communicating artery. Therefore, depending on the size of flow and the circle of Willis competence various brain regions as well as vision can be threatened with ischaemia. Due to their size, and the interconnection between cavernous sinuses, both eyes can be affected equally, making lateralization of the offending artery difficult (also keeping in mind that bilateral fistulae may occur in traumatic cases).
   a. Spontaneous direct CCF is caused by ruptured intracavernous ICA aneurysms. These include both berry aneurysms and fungal mycotic aneurysms (Lu et al., 2014). Ruptured berry aneurysms are the most common cause of spontaneous direct CCF but are rare in comparison to DAVF as a cause

for CCF. Fungal mycotic aneurysms are far less common than berry aneurysms but when they occur they can be devastating, not only because of the large CCF occurring, but also because of the sheet of infection that tends to progress (without respecting boundaries) with the potential for brain infection. The occurrence of such aneurysms in the cavernous sinus is due to the proximity to the ethmoid sinus as well as the potential for propagated infected thrombus to the cavernous sinus from the face. This should be considered in immunocompromised patients, diabetics with poor control, and those with suspected long-standing sinusitis.

b. Traumatic CCF may be due to either rupture or dissection of the ICA. Direct CCF may be associated with fracture or erosion into the ethmoid sinus and catastrophic epistaxis may occur. They can be associated with transsphenoidal surgery for pituitary tumours. In the case of traumatic origin from head injury or ICA dissection, bilateral ICA damage is present in a significant proportion of cases (Mokri et al., 1988; Mokri, 1990). Therefore, rapid assessment of both ICAs is of importance. Clinical clues may assist, such as a Horner's syndrome. However, making a diagnosis of Horner's syndrome in the presence of a contralateral cavernous syndrome, is extremely challenging but when made should raise immediate concerns that the clinical situation may be very unstable.

Clinical presentation, diagnosis, and workup of CCF

The high venous pressure may produce a swollen red eye from venous engorgement, secondary glaucoma with the potential for vision loss, exophthalmos, and restrictive globe movement. In the case of direct CCF, the onset is dramatic, and the clinical presentation is extreme. However, when an intracavernous aneurysm is responsible for a direct CCF after rupture, there may have been a preceding sixth nerve palsy and pain prior to the development of the florid cavernous sinus syndrome (in the case of berry aneurysms) or a cavernous sinus syndrome from thrombosed sinus (in the case of fungal mycotic aneurysms). For indirect CCF, the onset may be gradual and may become extreme but is, generally, subtle at the onset. Furthermore, preceding cavernous sinus thrombosis may have been clinically apparent. Failure to improve with a known cavernous sinus thrombosis may herald the presence of a DAVF. CCF can be confirmed clinically as there is often an audible bruit detected with stethoscope placed over the closed eye.

The clinical setting may make the diagnosis difficult. For head injured patients, fractures adjacent to the ICA course should undergo a CTA. A delayed onset of the development of a sudden onset of chemosis and proptosis after head injury should immediately raise suspicion of a direct CCF.

Diagnosis can be confirmed by CT or MRI by identification of enlargement of the superior ophthalmic vein (**Fig. 50.8**). Contrast compared with non-contrast studies are useful, not only to more readily identify the dilated superior ophthalmic vein, but also to assess whether there is thrombosis within the cavernous sinus and retrograde cortical venous drainage.

In the case of suspected indirect CCF, the rush to treatment should be informed by the health of the eye as there is a greater than 10% chance of spontaneous resolution of the CCF (Gross and Du, 2012). Workup must include an evaluation by an ophthalmologist regarding state of vision, pressures, and adequacy of eye protection. If it is clear that vision or the eye is threatened or progressively worsening, or there is evidence of retrograde cortical venous drainage, DSA is appropriate with consideration to treatment.

DSA confirms the diagnosis. In the case of direct CCF, workup needs to be urgent and proceed to DSA with a potential for intervention at this time. Both internal carotid and external carotid vessels need to be examined to assess contributions. For direct CCF without retrograde arterial flow in the distal ICA, establishing the potential for adequate collaterals to the ICA should be made. This might be evident by retrograde ICA flow distal to the intracavernous ICA breach. A balloon test occlusion at the time of the DSA should be considered when antegrade distal ICA flow is present and the test is safe to perform. Indirect CCF may only be evident on external carotid angiography and may be contralateral to the eye clinically involved. Therefore, bilateral external and internal carotid DSA should be performed for indirect CCF (cavernous DAVF) (**Fig. 50.7**) to ensure an accurate diagnosis and for direct CCF to assess adequacy of potential superficial temporal arteries if bypass is considered.

Treatment

Indirect CCF management

Management of indirect CCF needs to be coordinated with an ophthalmologist. Unless there is an imminent threat to vision or the eye, a conservative approach is reasonable (providing there is no retrograde cortical venous drainage with ectasia) as there is greater than a 10% chance of spontaneous resolution. Earlier consideration should, however, be given to treatment when both eyes are affected.

When a decision has been reached that intervention is appropriate, endovascular treatment is preferred. The surgical option of opening the cavernous sinus and packing with material promoting thrombosis is of historical interest only. In the case where the outflow is exclusively into the middle cerebral veins, consideration can be given to surgical disconnection of the arterialized veins as they enter the cavernous sinus. Given that, for the most part, only the eye is at risk, surgical intervention with bypass is inappropriate.

The endovascular repair is usually transvenous, either accessing the cavernous sinus by the superior ophthalmic vein (via the superior eyelid) or by the inferior petrosal sinus. The aim is to occlude the sinus in a way that obliterates retrograde flow into either the superior ophthalmic vein, contralateral cavernous sinus, cortical veins through the middle cerebral vein or the pontine veins through the inferior petrosal sinus. Access may be difficult due to partial thrombosis of the sinus and a single approach may prove to be insufficient.

Direct CCF management

Direct CCF can be managed either by reconstructing (endovascularly) or occluding (either endovascularly or surgically) the ICA. In the case of reconstruction, flow diverter stents, covered stents, detachable balloons or coiling the point of breach with stent deployment can be performed (Lu et al., 2014). Transvenous routes are more problematic than with DAVF because of the greater flow. However, they may be used following stenting of the ICA if the transarterial route has failed to completely close the fistula (Lin et al., 2015). The choice of procedure depends upon the health of the arterial wall. Placing coils into a false aneurysm may be problematic and unless

healing of the artery is anticipated occluding the ICA may be the preferred option. When endovascular reconstruction has been performed, delayed studies are important to exclude the development of false aneurysms.

Direct CCF treatment by occlusion can be performed having established the adequacy of collaterals. In the event that existing collaterals are assessed to be inadequate, high flow or low flow bypass should be considered prior to artery occlusion. This may also influence the technique of occlusion. If bypass is considered unnecessary, occlusion can be readily achieved by endovascular means at the time of the DSA. It is critical that the point of arterial rupture is included in the territory occluded. Proximal occlusion may result in exacerbation of retrograde flows in the ophthalmic artery or ICA and consequent ischaemia. Where bypass is necessary, a low flow bypass by STA-MCA is reasonable if there is confidence that minimal additional flow is required. An example of such a scenario is when there is no clinical problem during the test balloon occlusion but there is significant delay in capillary or venous filling of the targeted hemisphere on contralateral DSA (delayed cross flow). In the case where the ICA flow needs to be replaced because of clinical indicators, test balloon occlusion, or DSA, high flow bypass is appropriate. To supply a minimum 150 cc/min to replace ICA flow and prevent infarction, interposition saphenous vein, or radial artery bypass graft is appropriate. High flow bypass has a considerably greater procedural risk than STA-MCA bypass but have similar long-term patency after the first week (Sia et al., 2011).

Complication management

Ophthalmological supervision and management are of paramount importance to assess and manage secondary glaucoma and corneal protection.

Indirect CCF complication management

For cavernous DAVF managed by transvenous approach, the complications applicable to the earlier section on DAVF are relevant. The most typical relates to a cavernous sinus syndrome (causing venous insufficiency of the orbit and globe until collaterals develop) and venous hypertension of the brain during the procedure before complete occlusion is achieved that may result in a venous hypertensive encephalopathy of brain (usually pontine) or haemorrhage within the same brain region (**Fig. 50.7**).

Direct CCF complication management

For direct CCF, managed by preserving the ICA, several complications need to be considered and avoided (or managed). Among the most feared are:

1. *Embolization.* Due to the rarity of these lesions no large series of treatment can address the incidence of embolization. However, extrapolation from the treatment of aneurysms is appropriate. Silent embolization is a relatively common phenomenon following the endovascular treatment of aneurysms and has been documented to be evident on as many as half of brain MRI scans in the event of complex aneurysm repair such as stent-assisted coiling (Hahnemann et al., 2014). However, few of these events result in adverse clinical outcomes and following flow diverter stent deployment, this incidence may be 1–5% (Saatci et al., 2012; McDonald et al., 2015). This can arise during the procedure of deploying stents and coils or shortly thereafter. Preloading with antiplatelet medications and continuing these for up to 6 months is appropriate prophylaxis against emboli. However, even with this prophylaxis, the proceduralist must be prepared to check for emboli and retrieve or dissolve them. There is a significant incidence of inadequate response to the initial recommended clopidogrel management in approximately 25% of cases (Oran et al., 2015). Therefore, attention to individual patient specific responses to the loading may decrease the embolization rate.
2. *Recurrence of the aneurysm (or false aneurysm).* Due to the rarity of these lesions no large series of treatment can address recurrence. However, extrapolation from the treatment of aneurysms is appropriate. For aneurysm management, inadequate or recurrent aneurysm may occur in 10–40% of aneurysms with flow diverters (McAuliffe et al., 2012; Saatci et al., 2012; Toma et al., 2013; Fischer et al., 2014).
3. *Occlusion of the ICA.* Although occlusion may be an effective treatment of these lesions catastrophic consequences may ensue when this is inappropriate, is unplanned, or it has been established that occlusion will not be tolerated. Emergency revascularization is possible and may prevent catastrophic stroke if performed early enough (see section on stroke). Because of the likely preloading with clopidogrel and aspirin, surgical revascularization with high flow bypass is less desirable than an endovascular solution. As for endovascular treatments, time is of the element and if revascularization cannot be achieved within 6 hours of the occlusion, attempted revascularization may do more harm than good.
4. *Remote haemorrhage.* Documented distal haemorrhage has been reported following flow diverter stent deployment. The mechanism for this may be as a consequence of embolization or from alterations of the arterial wall stiffness with the consequent failure to dampen the arterial pressure wave in the circle of Willis.

For direct CCF managed by occlusion. Having established that the ICA can be sacrificed without a risk of haemodynamic-induced stroke, either from DSA evidence (e.g. retrograde flow in the ICA without neurologic deficit) or test balloon occlusion, sacrifice of the ICA at the point of ICA breach can be performed. However, consideration should be given to the following complications:

1. *Embolization.* Propagated thrombosis from the point of occlusion will be expected to progress to the next most significant branch point. This is normally the ophthalmic artery. However, if there is insufficient flow induced shear stress in the distal ICA arising as a result of the continued supply of the ophthalmic artery, thrombus propagation may cross the ophthalmic artery and progress. This process may continue to incorporate clinically important arteries, together with the ophthalmic artery, including the anterior choroidal artery and the terminal ICA. At a point where collateral flow to the ICA supply enters the ICA (i.e. the posterior communicating artery) or the termination of the ICA (i.e. the anterior cerebral artery) and provides normal antegrade flow to the distal vasculature, the thrombus-flow interface may provide a source of embolus. The prevention of this requires the use of antiplatelet prophylaxis and the maintenance of, at least, normal blood pressure. Embolization, if small, may be managed

by anticoagulation but if large is not easily treated by clot retrieval in the presence of the proximal occlusion. In experienced hands, and if time to procedure is short, catheter access to the site of embolization by the anterior communicating artery or posterior communicating artery (without compromising the collateral flow for significant periods of time) may allow clot lysis.

2. *Recanalization of the fistula.* Incomplete occlusion or recanalization should be suspected with recurrence or failure to improve visual symptoms. A CT scan showing a continued enlargement of the superior ophthalmic artery may confirm this suspicion. A DSA to confirm and plan management is necessary when recanalization is suspected.
3. *Haemodynamic ischaemia.* Although the test balloon occlusion is reliable, it is possible that it may have been interpreted inaccurately (due to technical issues or clinical threshold error of what is deemed to be a failure) and the patient does not tolerate subsequent occlusion. Removal of the occluding agent may be inadvisable because of thrombus embolization if reversal of the occlusion is attempted after more than a short period of time. Haemodynamically induced ischaemia should be recognized quickly with blood pressure elevation commenced as an emergency. If this fails to rapidly reverse the ischaemia, induced barbiturate coma (with normal to high blood pressure maintained at all times) and revascularization with superficial temporal to middle cerebral artery bypass should immediately follow. High flow bypass in this scenario is potentially dangerous due to the time required to revascularize and the potential for hyperaemia and haemorrhagic conversion of stroke in this clinical scenario (Sia et al., 2011).
4. *Late aneurysm formation* following occlusion without flow replacement bypass. ICA occlusion can be associated with contralateral ICA, ipsilateral PCA (posterior communicating and anterior communicating) artery aneurysm development from increase shear stress (Roski et al., 1981). This important complication, though uncommon, deserves long-term surveillance for those treated by occlusion without bypass.

For direct CCF managed with bypass, there is a considerable difference in the complexity of surgery between superficial temporal to middle cerebral artery bypass and high flow bypass (with radial or saphenous vein as a conduit between the extracranial circulation and either the ICA or MCA). The complication rate for high flow bypass is 5 to 13% compared with 0.5 to 5% for superficial temporal to middle cerebral artery bypass (Sia et al., 2011). Managing these complications is very complex and normally involves rapid recognition and urgent surgical revision and for this reason treatment should be in a centre with considerable expertise in cerebrovascular surgery.

Outcomes

Indirect CCF outcomes

Clinical assessment of the eye, in most cases is an accurate way of evaluating arteriovenous fistula ablation. The exception is when the eye improves but fistula persists with retrograde cortical venous drainage or petrosal drainage and, the reverse, where the eye remains injected because of concomitant inferior ophthalmic vein obstruction. However, collateral venous capacity generally improves with time with a gradual subsequent improvement in eye problems. Most patients rapidly improve and recurrence is uncommon.

Direct CCF outcomes

Direct CCF have a number of outcomes to consider. These include the eye, the local arterial site, the distal ICA supply, the direct or indirect contralateral arterial systems and concomitant structural damage when trauma or infection is involved (including cranial nerve and potential for CSF leak). When the ICA is preserved, healing of the artery needs to be followed and seen to have occurred. For trauma or any pseudoaneurysm, it is difficult to predict the chance of healthy healed artery. There is less concern with regards healing of the local site when direct CCF are treated by occlusion, but there are greater concerns with regards potential for distal ischaemia. There is a small risk of aneurysm formation in the posterior communicating artery or anterior communicating artery due to increased flow and sheer stress. A consideration for both direct and indirect CCF elimination is that the eye symptoms and signs may commence to improve quickly but then fail to continue to resolve. This can sometimes be explained by the development of cavernous sinus thrombosis. It can take some time for the venous insufficiency from cavernous sinus thrombosis to resolve and for the eye to recover.

Patients with direct CCF treated with ICA occlusion and bypass have, in addition to eye outcomes, outcomes related to their bypass. The most common reason for adverse outcome for the high flow bypass is acute occlusion of the bypass (occurring in approximately 7% of cases). That this would be responsible for significant morbidity is not surprising, given that these cases have either failed a test balloon occlusion, or there was clinical or radiological evidence that identified an inability to tolerate ICA occlusion. Patency of superficial temporal to middle cerebral artery bypass in experienced hands is expected to be 98% (Sia et al., 2011). Having survived the first week, the long-term patency is excellent for both high flow bypass and superficial temporal bypass and these patency's are similar (Sia et al., 2011).

FURTHER READING

Gross, B. & Du, R. (2013). Natural history of cerebral arteriovenous malformations: a meta-analysis. *J Neurosurg*, **118**, 437–43.

Kano, H., Flickinger, J.C., Yang, H-C., et al. (2014). Stereotactic radiosurgery for Spetzler-Martin Grade III arteriovenous malformations. *J Neurosurg*, **120**, 973–81.

Korja, M., Bervini, D., Assaad, N., & Morgan, M.K. (2014). The role of surgery in the management of brain arteriovenous malformations: a prospective cohort study. *Stroke*, **45**, 3549–55.

Mohr, J.P., Parides, M.K., Stapf, C., et al. (2014). Medical management with or without interventional therapy for unruptured brain arteriovenous malformations (ARUBA): a multicenter, non-blinded, randomized trial. *Lancet*, **383**, 614–21.

Spetzler, R.F. & Ponce, F.A. (2011). A 3-tier classification of cerebral arteriovenous malformations. *J Neurosurg*, **114**, 842–9.

REFERENCES

Al-Rodhan, N.R.F., Sundt, T.M. JR., Piepgras, D.G., Nichols, D.A., Rufenacht, D., & Stevens, L.N. (1993). Occlusive hyperemia: a theory for the hemodynamic complications following resection of intracerebral arteriovenous malformations. *J Neurosurg*, **78**, 167–75.

Al-Shahi, R., Bhattacharya, J.J., Currie, D.G., et al. (2003). Prospective, population-based detection of intracranial vascular malformations in adults: the Scottish Intracranial Vascular Malformation Study (SIVMS). *Stroke*, **34**, 1163–9.

Andrade-Souza, Y.M., Ramani, M., Scora, D., Tsao, M.N., Terbrugge, K., & Schwartz, M.L. (2007). Embolization before radiosurgery reduces the obliteration rate of arteriovenous malformations. *Neurosurgery*, **60**, 443–52.

Baltsavias, G., Spiessberger, A., Hothorn, T., & Valvanis, A. (2015). Cranial dural arteriovenous shunts. Part 4. Clinical presentation of the shunts with leptomeningeal venous drainage. *Neurosurg Rev*, **38**, 283–91.

Barrow, D.L., Fleischer, A.S., Hoffman, J.C. (1982). Classification and treatment of spontaneous carotid-cavernous fistulas. *J Neurosurg*, **62**, 248–56.

Bervini, D., Morgan, M.K., Ritson, E.A., et al. (2014). Surgery for unruptured arteriovenous malformations of the brain is better than conservative management for selected cases: a prospective cohort study. *J Neurosurg*, **121**, 878–90.

Boothe, D., Young, R., Yamada, Y., Prager, A., Chan, T., & Beal, K. (2013). Bevacizumab as a treatment for radiation necrosis of brain metastases post stereotactic radiosurgery. *Neuro Oncol*, **15**, 1257–63.

Borden, J.A., Wu, J.K., & Shucart, W.A. (1995). A proposed classification for spinal and cranial dural arteriovenous fistulous malformations and implications for treatment. *J Neurosurg*, **82**, 166–79.

Brown, R.D. Jr., Wiebers, D.O., Forbes, G., et al. (1988). The natural history of unruptured intracranial arteriovenous malformations. *J Neurosurg*, **68**, 352–7.

Bulsara, K.R., Alexander, M.J., Villavicencio, A.T., & Graffagnino, C. (2002). De novo cerebral arteriovenous malformation: case report. *Neurosurgery*, **50**, 1137–41.

Butlers, D.O., Mathad, N., Culliford, D., Millar, J., & Sparrow, O.C. (2012). The natural history of cranial dural arteriovenous fistulae with cortical venous reflux—the significance of venous ectasia. *Neurosurgery*, **70**, 312–19.

Casa, L.D., Deaton, D.H., & Ku, D.N. (2015). Role of high shear rate in thrombosis. *J Vasc Surg*, **61**, 1068–80.

Cognard, C., Gobin, Y.P., Pierot, L., et al. (1995). Cerebral dural arteriovenous fistulas: clinical and angiographic correlation with a revised classification of venous drainage. *Radiology*, **194**, 671–80.

Crawford, P.M., West, C.R., Chadwick, D.W., & Shaw, M.D.M. (1986). Arteriovenous malformations of the brain. *J Neurol Neurosurg Psychiatry*, **49**, 1–10.

Da Costa, L.B., Wallace, M.C., Ter Brugge, K.G., O'Kelly, C., Willinsky, R.A., & Tymianski, M. (2009). The natural history and predictive features of hemorrhage from brain arteriovenous malformations. *Stroke*, **40**, 100–5.

Davidson, A.S. & Morgan, M.K. (2011). The embryologic basis for the anatomy of the cerebral vasculature related to arteriovenous malformations. *J Clin Neurosci*, **18**(4), 464–9.

Davies, M.A., Saleh, K., Terbrugge, K., Willinsky, R., & Wallace, M.C. (1997a). The natural history and management of intracranial dural arteriovenous fistulae. Part 1: benign lesions. Interventional *Neuroradiology*, **3**, 295–302.

Davies, M.A., Saleh, K., Terbrugge, K., Willinsky, R., & Wallace, M.C. (1997b). The natural history and management of intracranial dural arteriovenous fistulae. Part 2: aggressive lesions. *Interv Neuroradiol*, **3**, 303–11.

Ding, D., Yen, C-P., XU, Z., Starke, R.M., & Sheehan, J.P. (2014). Radiosurgery for low-grade intracranial arteriovenous malformations. *J Neurosurg*, **121**, 457–67.

Drake, C.G. (1979). Cerebral arteriovenous malformations: considerations for and experience with surgical treatment in 166 cases. *Clini Neurosurg*, **26**, 145–208.

Duffau, H., Lopes, M., Janosevic, V., et al. (1999). Early rebleeding from intracranial dural arteriovenous fistulas: report of 20 cases and review of the literature. *J Neurosurg*, **90**, 78–84.

Eerola, I., Boon, L.M., Mulliken, J.B., et al. (2003). Capillary malformation-arteriovenous malformation, a new clinical and genetic disorder caused by RASA1 mutation. *Am J Hum Genet*, **73**, 1240–9.

Eftekhar, B. & Morgan, M.K. (2013). Surgical management of dural arteriovenous fistulas of the transverse-sigmoid sinus in 42 patients. *J Clin Neurosci*, **20**(4), 532–5.

Faraci, F.M., Brian, J.E. Jr., & Heistad, D.D. (1995). Response of cerebral blood vessels to an endogenous inhibitor of nitric oxide synthase. *Am J Physiol*, **269**, H1522–7.

Fischer, S., Perez, M.A., Kurre, W., Albes, G., Bazner, H., & Henkes, H. (2014). Pipeline embolization device for the treatment of intra- and extracranial fusiform and dissecting aneurysms: initial experience and long-term follow-up. *Neurosurgery*, **75**, 364–474.

Fitts, M.K., Pike, D.B., Andreson, K., & Shiu, Y-T. (2014). Hemodynamic shear stress and endothelial dysfunction in hemodialysis access. *Open Urol Nephrol J*, **7** (suppl 1 M5), 33–44.

Flickinger, J.C., Kondziolka, D., Maitz, A.H., & Lunsford, L.D. (2002). An analysis of the dose-response for arteriovenous malformation radiosurgery and other factors affecting obliteration. *Radiother Oncol*, **63**, 347–54.

Frizzel, R.T. & Fisher, W.S. III. (1995). Cure, morbidity, and mortality associated with embolization of brain arteriovenous malformations: a review of 1246 patients in 32 series over a 35-year period. *Neurosurgery*, **37**, 1031–40.

Fults, D. & Kelly, D.L. Jr. (1984). Natural history of arteriovenous malformations of the brain. *Neurosurgery*, **15**, 658–62.

Galletti, F., Sarchielli, P., Hamam, M., et al. (2011). Occipital arteriovenous malformations and migraine. *Cephalgia*, **31**, 1320–4.

Gross, B.A. & Du, R. (2012). The natural history of cerebral dural arteriovenous fistulae. *Neurosurgery*, **71**, 594–603.

Gross, B. & Du, R. (2013). Natural history of cerebral arteriovenous malformations: a meta-analysis. *J Neurosurg*, **118**, 437–43.

Hahnemann, M.L., Ringelstein, A., Sandalcioglu, I.E., et al. (2014). Silent embolism after stent-assisted coiling of cerebral aneurysms: diffusion-weighted MRI study of 75 cases. *J Neurointervent Surg*, **6**, 461–5.

Hattangadi-Gluth, J.A., Chapman, P.H., Kim, D., et al. (2014). Single-fraction proton beam stereotactic radiosurgery for cerebral arteriovenous malformations. *Int J Radiat Oncol Biol Phys*, **89**, 338–46.

Hayashi, T., Ichiyama, T., Nishikawa, M., et al. (1996). A case of large neonatal arteriovenous malformation with heart failure. Color Doppler sonography, MRI and MR angiography as early non-invasive diagnostic procedures. *Brain Dev*, **18**, 236–8.

Hernesniemi, J., Romani, R., Lehecka, M., et al. (2010). Present state of microneurosurgery of cerebral arteriovenous malformations. *Acta Neurochirurgica Suppl*, **107**, 71–6.

Houser, O.W., Baker, H.L. Jr., Rhoton, A.L. Jr., & Okazaki, H. (1972). Intracranial dural arteriovenous malformations. *Radiol*, **105**, 55–64.

Huang, P.P., Rush, S.C., Donahue, B., et al. (2012). Long-term outcomes after staged-volume stereotactic radiosurgery for large arteriovenous malformations. *Neurosurgery*, **71**, 632–44.

Hwang, S.-K. (2015). A case of dural arteriovenous fistula of superior sagittal sinus after tamoxifen treatment for breast cancer. *J Korean Neurosurg Soc*, **57**, 204–7.

Izumi, T., Miyachi, S., Hattori, K., Nakane, Y., & Yoshida, J. (2007). Thrombophilic abnormalities among patients with cranial dural arteriovenous fistulas. *Neurosurgery*, **61**, 262–9.

Jeffree, R.L. & Stoodley, M.A. (2009). Postnatal development of arteriovenous malformations. *Pediatr Neurosurg*, **45**, 296–304.

Johnston, I.H., Whittle, I.R., Besser, M., & Morgan, M.K. (1987). Vein of Galen malformation: diagnosis and management. *Neurosurgery*, **20**, 747–58.

Kano, H., Flickinger, J.C., Yang, H-C., et al. (2014). Stereotactic radiosurgery for Spetzler-Martin Grade III arteriovenous malformations. *J Neurosurg*, **120**, 973–81.

Kano, H., Kondziolka, D., Flickinger, J.C., et al. (2012a). Stereotactic radiosurgery for arteriovenous malformations, part 6: multistaged volumetric management of large arteriovenous malformations. *J Neurosurg*, **116**, 54–65.

Kano, H., Lunsford, L.D., Flickinger, J.C., et al. (2012b). Stereotactic radiosurgery for arteriovenous malformations, part 1: management of Spetzler-Martin Grade I and II arteriovenous malformations. *J Neurosurg*, **116**, 11–20.

Karlsson, B., Lindqvist, M., Blomgren, H., Wan-Yeo, G., & Soderman, M. (2005). Long-term results after fractionated radiation therapy for large brain arteriovenous malformations. *Neurosurgery*, **57**, 42–9.

Kessler, I., Riva, R., Ruggiero, M., Manisor, M., Al-Khawaldeh, M., & Mounayer, C. (2011). Successful transvenous embolization of brain arteriovenous malformations using Onyx in five consecutive patients. *Neurosurgery*, **69**, 184–93.

Kim, H., Abla, A.A., Nelson, J., et al. (2015). Validation of the supplemented Spetzler-Martin Grading system for brain arteriovenous malformations in a multicenter cohort of 1009 surgical patients. *J Neurosurg*, **76**, 25–33.

Kim, H., Al-Shahi Salman, R., Mcculloch, C.E., Stapf, C., & Young, W.L. (2014). Untreated brain arteriovenous malformation. Patient-level meta-analysis of hemorrhage predictors. *Neurology*, **83**, 1–8.

Korja, M., Bervini, D., Assaad, N., & Morgan, M.K. (2014). The role of surgery in the management of brain arteriovenous malformations: a prospective cohort study. *Stroke*, **45**, 3549–55.

Korja, M., Hernesniemi, J., Lawton, M.T., Spetzler, R.F., & Morgan, M.K. (2014). Sacrifice of cerebrovascular neurosurgery at the altar of randomized controlled trial. Lancet, Letter 2014. *Lancet*, **384**, 27–8.

Kraus, J.A., Stuper, B.K., Muller, J., et al. (2002). Molecular analysis of thrombophilic risk factors in patients with dural arteriovenous fistulas. *J Neurol*, **249**, 680–2.

Laakso, A., Dashiti, R., Seppanen, J., & Juvela, S. (2008). Long-term excess mortality in 623 patients with brain arteriovenous malformations. *Neurosurgery*, **63**, 244–53.

Lawton, M.T., Kim, H., Mcculloch, C.E., Mikhak, B., & Young, W.L. (2010). A supplementary grading scale for patients with brain arteriovenous malformations for surgery. *Neurosurgery*, **66**, 702–13.

Lin, L.M., Colby, G.P., Jiang, B., Pero, G., Boccardi, E., & Coon, A.L. (2015). Transvenous approach for the treatment of direct carotid cavernous fistula following pipeline embolization of cavernous carotid aneurysm: a report of two cases and review of the literature. *J Neurointerv Surg*, **7**(8), e30.

Loumiotis, I., Lanzino, G., Daniels, D., Sheehan, J & Link, M. (2011). Radiosurgery for intracranial dural arteriovenous fistulas (DAVFS): a review. *Neurosurg Rev*, **34**, 305–15.

Lu, X., Hussain, M., Ni, L., et al. (2014). A comparison of different transarterial embolization techniques for direct carotid cavernous fistulas: a single center experience in 32 patients. *J Vasc Interv Neurol*, **7**, 35–47.

Mazzuca, M.Q. & Khalil, R.A. (2012). Vascular endothelin receptor type B: structure, function and dysregulation in vascular diseases. *Biochem Pharmacol*, **84**, 147–62.

McAuliffe, W., Wycoc, V., Rice, H., Phatouros, C., Singh, T.J., & Wenderoth, J. (2012). Immediate and midterm results following treatment of unruptured intracranial aneurysms with the pipeline embolization device. *AJNR Am J Neuradiol*, **33**, 164–70.

Mcdonald, R.J., McDonald, J.S., Kallmes, D.F., Lanzino, G., & Cloft, H.J. (2015). Periprocedural safety of pipeline therapy for unruptured cerebral aneurysms: analysis of 279 patients in a multihospital database. *Int Neuroradiol*, **21**, 6–10.

Mohr, J.P., Parides, M.K., Stapf, C., et al. (2014). Medical management with or without interventional therapy for unruptured brain arteriovenous malformations (ARUBA): a multicenter, non-blinded, randomized trial. *Lancet*, **383**, 614–21.

Mokri, B. (1990). Traumatic and spontaneous extracranial internal carotid artery dissection. *J Neurol*, **237**, 356–61.

Mokri, B., Piepgras, D.G., Houser, O.W. (1988). Traumatic dissections of the extracranial internal carotid artery. *J Neurosurg*, **68**, 189–97.

Morales, H., Jones, B.V., Leach, J.L., & Abruzzo, T.A. (2010). Documented development of a dural arteriovenous fistula in an infant subsequent to sinus thrombosis: case report and review of the literature. *Neuroradiology*, **52**, 225–9.

Morgan, M.K. (2013). AVM and embolization. *J Neurosurg*, **118**, 967–8.

Morgan, M.K., Davidson, A.S., Koustais, S., Simons, M., & Ritson, E.A. (2013). The failure of ethylene-vinyl alcohol copolymer embolization to improve outcomes in AVM management: case series. *J Neurosurg*, **118**, 969–77.

Morgan, M.K., Johnston, I.G., & De Silva, M. (1985). Treatment of ophthalmofacial hypothalamic arteriovenous malformations (Bonnett–Dechaume–Blanc syndrome management by surgery and embolisation). *J Neurosurg*, **63** (5), 794–6.

Morgan, M.K., Johnston, I.H., Hallinan, J.M., & Weber, N. (1993). Complications of surgery for arteriovenous malformations of the brain. *J Neurosurg*, **78**(2), 176–82.

Morgan, M.K., Sekhon, L.H.S., Finfer, S., & Grinnell, V. (1999). Delayed neurological deterioration following resection of arteriovenous malformations of the brain. *J Neurosurg*, **90**, 695–701.

Morgan, M.K. & Winder, M. (2001). Haemodynamics of arteriovenous malformations of the brain and consequences of resection. A review. *J Clin Neurosci*, **8**, 216–24.

Morgan, M.K., Winder, M., Little, N.S., Finfer, S., & Ritson, E.A. (2003). Delayed hemorrhage following resection of an arteriovenous malformation in the brain. *J Neurosurg*, **99**(6), 967–71.

Morris, Z., Whiteley, W.N., Longstreth, W.T. Jr, et al. (2009). Incidental findings on brain magnetic resonance imaging: systematic review and meta-analysis. *Br Med J*, **339**, b3016.

Murphy, P.A., Kim, T.N., Huang, L., et al. (2014). Constitutively active Notch4 receptor elicits brain arteriovenous malformations through enlargement of capillary-like vessels. *PNAS*, **111**, 18007–12.

Ondra, S.L., Troupp, H., George, E.D., & Schwab, K. (1990). The natural history of symptomatic arteriovenous malformations of the brain: a 24-year follow-up assessment. *J Neurosurg*, **73**, 387–91.

Oran, I., Cinar, C., Bozkaya, H., & Korkmaz, M. (2015). Tailoring platelet inhibition according to multiple electrode aggregometry decreases the rate of thrombotic complications after intracranial flow diverting stent implantation. *J Neurintervent Surg*, **7**, 357–62.

Pasi, M., Nappini, S., Salvadori, E., Mangiafico, S., Limbucci, N., & Pantoni, L. (2014). Rapidly progressive cognitive impairment in a patient with high flow dural arteriovenous fistulas, cerebral sinus thrombosis and protein S deficiency. *J Clin Neurosci*, **21**, 1654–6.

Patel, M.C., Hodgson, T.J., Kemeney, A.A., & Forster D.M. (2001). Spontaneous obliteration of pial arteriovenous malformations: a review of 27 cases. *Am J Neuroradiol*, **22**, 531–6.

Perreira, V.M., Marcos-Gonzalez, A., Radovanovic, I., et al. (2013). Transvenous embolization of a ruptured deep cerebral arteriovenous malformation. A technical note. *Int Neuroradiol*, **19**, 27–34.

Pierot, L., Cognard, C., Herbreteau, D., et al. (2013). Endovascular treatment of brain arteriovenous malformations using a liquid embolic agent: results of a prospective, multicentre study (BRAVO). *Eur Radiol*, **23**, 2838–45.

Pollock, B.E. & Flickinger, J.C. (2008). Modification of the radiosurgery-based arteriovenous malformation grading system. *Neurosurgery*, **63**, 239–43.

Redekop, G., Terbrugge, K., Montanera, W., & Willinsky, R. (1998). Arterial aneurysms associated with cerebral arteriovenous malformations: classification, incidence, and risk of hemorrhage. *J Neurosurg*, **89**, 539–46.

Roski, R.A., Spetzler, R.F., & Nulsen, F.E. (1981). Late complications of carotid ligation in the treatment of intracranial aneurysms. *J Neurosurg*, **54**, 583–7.

Saatci, I., Geyik, S., Yavuz, K., & Cekirge, H.S. (2011). Endovascular treatment of brain arteriovenous malformations with prolonged intranidal Onyx injection technique: long-term results in 350 consecutive patients with completed endovascular treatment course. *J Neurosurg*, **115**, 78–88.

Saatci, I., Yavuz, K., Ozer, C., Geyik, S., & Cekirge, H.S. (2012). Treatment of intracranial aneurysms using the pipeline flow-diverter embolization device: a single-center experience with long-term follow-up results. *Am J Neuroradiol*, **33**, 1436–46.

Saito, A., Takahashi, N., Furuno, Y., et al. (2008). Multiple isolated dural arteriovenous fitulas associated with antithrombin III deficiency. Case report. *Neurol Med Chir (Tokyo)*, **48**, 455–9.

Satomi, J. & Satoh, K. (2008). Epidemiology and etiology of dural arteriovenous fistula. *Brain Nerve*, **60**, 883–6.

Sekhon, L.H.S, Morgan, M.K., Spence, I., & Weber, N.C. (1997). Normal perfusion pressure breakthrough: the role of capillaries. *J Neurosurg*, **86**(3), 519–24.

Sia, S.F., Davidson, A.S., Assaad, N.N., Stoodley, M., & Morgan, M.K. (2011). Comparative patency between intracranial arterial pedicle and vein bypass surgery. *Neurosurgery*, **69**, 308–14.

Spetzler, R.F. & Martin, N.A. (1986). A proposed grading system for arteriovenous malformations. *J Neurosurg*, **65**, 476–83.

Spetzler, R.F. & Ponce, F.A. (2011). A 3-tier classification of cerebral arteriovenous malformations. *J Neurosurg*, **114**, 842–9.

Spetzler, R.F., Wilson, C.B., Weinstein, P., Mehdorn, M., Townsend, J., & Telles, D. (1978). Normal perfusion pressure breakthrough theory. *Clin Neurosurg*, **25**, 651–72.

Stapf, C. & Mohr, J.P. (2000). New concepts in adult brain arteriovenous malformarions. *Curr Opin Neurol*, **13**, 63–7.

Stapf, C., Mast, H., Sciacca, R.R., et al. (2003). The New York Islands AVM study: design, study progress and initial results. *Stroke*, **34**, e29–e33.

Stapf, C., Mohr, J.P., Pile-Spellman, J., et al. (2002). Concurrent arterial aneurysms in brain arteriovenous malformations with haemorrhagic presentation. *J Neurol Neurosurg Psychiatry*, **73**, 294–8.

Sundt, T.M. Jr. & Kees, G. (1986). Miniclips and microclips for surgical hemostasis. *J Neurosurg*, **64**, 824–5.

Sundt, T.M. Jr. & Piepgras, D.G. (1983). The surgical approach to arteriovenous malformations of the lateral and sigmoid dural sinuses. *J Neurosurg*, **59**, 32–9.

Toma, A.K., Robertson, F., Wong, K., et al. (2013). Early single centre experience of flow diverting stents for the treatment of cerebral aneurysms. *Br J Neurosurg*, **27**, 622–8.

Van Beijnum, J., Lovelock, C.E., Cordonnier, C., Rothwell, P.M., Klijn, C.J.M., & Al-Shahi Salman, R. (2009). Outcome after spontaneous and arteriovenous malformation-related intracerebral haemorrhage: population-based studies. *Brain*, **132**, 537–43.

Wedderburn, C.J., Van Beijnum, J., Bhattacharya, J.J., et al. (2008). Outcome after interventional or conservative management of unruptured brain arteriovenous malformations: a prospective, population-based cohort study. *Lancet Neurol*, **7**, 223–30.

Wenderoth, J.D. & Phatouros, C.C. (2003). Incidental discovery of a dural arteriovneous fistula in a patient with activated protein C resistance. *Am J Neuroradiol*, **24**, 1369–71.

Wysokinska, E.M., Wysokinska, W.E., Brown, R.D., et al. (2008). Thrombophila differences in cerebral venous sinus and lower extremity deep venous thrombosis. *Neurology*, **70**, 627–33.

RELATED LINKS TO EBRAIN

Cranial Dural Arteriovenous Fistulae. https://learning.ebrain.net/course/view.php?id=149

Embolisation of Arteriovenous Malformations. https://learning.ebrain.net/course/view.php?id=586

Stereotactic Radiosurgery for Arteriovenous Malformations. https://learning.ebrain.net/course/view.php?id=146

Surgery for Arteriovenous Malformations. https://learning.ebrain.net/course/view.php?id=154

51

Carotid artery disease and cerebral ischaemia

Kieron Sweeney, A. O'Hare, and Mohsen Javadpour

Introduction

Due to the high incidence carotid artery disease and cerebral ischaemia, accurate and timely diagnosis and treatment is required to reduce the significant morbidity and mortality associated with these conditions. Here, we discuss the epidemiology, pathophysiology, clinical presentation, investigation, and treatment of these conditions. We also discuss the current evidence for medical, interventional, and surgical treatment options.

Cerebral ischaemia and stroke/infarction

Aetiology

Cerebral ischaemia and stroke can occur due to a heterogeneous number of pathological processes. These pathological processes can affect either large or small vessels and can be broadly classified into thrombotic, embolic, or occlusive causes. The most common cause of thrombotic ischaemic is due to atherosclerosis (discussed next). The most common cause of embolic ischaemia is cardiogenic due to atrial fibrillation followed by extracranial atherosclerosis of the aorta or carotids. Both of these causes can affect both the large and small vessels. Occlusive diseases such as fibrinoid necrosis or lipohyalinosis principally affected the small vessels leading to lacunar strokes or white matter disease due to thickening of the tunica media. Lacunar strokes are also due to atheroma plaques on the parent vessel occluding the origins of the penetrating small vessels.

All these processes share common risk factors. Common non-modifiable risk factors include age, sex, race, family history, and genetics. Common modifiable risk factors include, hypertension, smoking, diabetes, dyslipidaemia, and diet.

Rare causes of thrombotic stroke include cerebral venous sinus thrombosis (Ferro and Canhao, 2014) or hypercoagulopathic states (inherited and acquired), traumatic occlusion due dissection of vessels or traumatic space occupying lesions leading to mass effect and therefore subfalcine herniation which may lead to anterior cerebral artery (ACA) infarction or transtentorial herniation causing posterior cerebral artery (PCA) infarction, vasogenic occlusive causes such as migraine or vasospasm, inflammatory vasculitides, and other occlusive disease processes such as the delayed effects of radiation, Moya fibromuscular dysplasia, cerebral amyloid angiopathy, and CADASIL (Caplan, 2015).

Incidence

Ischaemic stroke accounts for approximately 87% of all cerebrovascular accidents (CVA). Globally, there is wide variation in the incidence of ischaemic stroke as there is wide variation in risk factors such as age, smoking, and diet. The Global Burden of Disease working group have published their findings regarding ischaemic stroke. This systematic review compares reported incidence in various countries globally and stratifies them according to income (Bennett et al., 2014). From 1990 to 2010 there has been a reduction in the incidence of ischaemic stroke in high income countries while there has been persistently high incidence in low-to middle income countries. Western Europe had an incidence of 127.65/100 000 dropping to 102.39/100 000 in 2010. Sub-Saharan central Africa had an incidence of 136.36/100 000 in 1990, increasing to 166.69/100 000 in 2010. This has been attributed to rates of smoking and increasing life expectancy.

Pathophysiology of cerebral ischaemia and stroke

The brain is one of the most metabolically active organs in the human body. Comprising only 2% total body weight, it demands 15–20% of the cardiac output and 20% of total oxygen consumption. Unlike other organs the brain has limited energy reserves and relies exclusively on blood supply (Clarke and Sokoloff, 1999). The functional unit of the brain is the neuron. Neuronal metabolism is heavily dependent on aerobic mitochondrial metabolism expending large amounts of energy for the ion pump systems to maintain membrane potentials and participate in action potentials. The substrates for neuronal aerobic metabolism are glucose, lactate, and ketone bodies while the end-products of neuronal activity are extruded into the extracellular environment. These are K+ and glutamate, among others. Astrocytes act as metabolic sensors for the neuron (↑K+, ↑glutamate, ↓glucose, ↓lactate) which in turn is coupled to the microvascular endothelium allowing alteration of local blood flow related to local neuronal activity (regulation of cerebral blood flow (CBF) is discussed elsewhere). There are regional differences in metabolic demand with grey matter and cortex more metabolically

active than white matter tracts. On average CBF is approx. 50 ml/100 g of white matter 20 ml/100 g and 70 ml/100 g of grey matter.

Cerebral ischaemia is the reduction in blood flow and therefore oxygen and glucose to the cerebral tissues. Infarction is the irreversible death of cerebral tissue. When CBF drops to 30 ml/100 g/minute neurological symptoms can occur. Further drop in CBF to 15–20 ml/100 g/minute will lead to reversible injury or 'electrical failure'. This can only be tolerated for a few hours. CBF rates of 10–15 ml/100 g/minute cause irreversible neuronal damage. Within 2 minutes of this, ATP levels are depleted, and subsequent failure of the Na/K ATPase pump occurs. This prevents restoration of the normal membrane potential and the cell depolarizes with an influx of Ca. This depolarization spreads out leading to an ischaemic cascade with release of glutamate. Neuronal death is triggered by apoptosis.

The penumbra model of ischaemia is the most widely used model. This model consists of an irrigating artery or arteriole with a core of irreversibly damaged cerebral tissue (neurons, astrocytes/oligodendrocytes) around which there is an area of hypoperfused tissue that can be salvaged. The main factors that influence the volume of penumbral tissue salvaged is quality of collateral circulation and time to reperfusion (Jung et al., 2013). Collateral circulations include the circle of Willis, leptomeningeal connections between adjacent arterial territories, and anastomoses between the external carotid and internal carotid circulations.

Clinical presentation of vertebrobasilar and carotid insufficiency syndromes

Ischaemic stoke is defined as the abrupt onset of neurological symptoms producing a permanent deficit and can be classified according to aetiology and clinical symptoms (TOAST—Trial of Org 10172 in Acute Stroke Treatment) or vascular territory and presenting symptoms (OCSP—Oxford Community Stroke Project classification). The signs and symptoms of presentation correspond to the vascular territory affected.

Anterior circulation signs and symptoms

Anterior cerebral artery stroke symptoms

ACA territory infarcts are infrequent and account for only 1.3% of strokes (Arboix et al., 2009). The ACA is divided into three segments. A1 gives rise to the medial lenticulostriates and occasionally the recurrent artery of Heubner. Occlusion of the A1 segment tends to be less severe than distal occlusions due to cross flow via the anterior communicating artery and can result in any of the five lacunar stroke syndromes: pure motor, pure sensory, mixed motor-sensory, ataxic hemiparesis, and clumsy hand dysarthria. The distal segments supply the anterior corpus callosum, medial frontal, and parietal lobes, The A2 can sometimes give rise to the recurrent artery of Heubner. Therefore, an occlusion from A2 distally can result in a lacunar stroke syndrome, disconnection syndrome, urinary incontinence, hemiparesis affecting the contralateral lower limb, hemisensory loss affecting the contralateral lower limb, and apraxia.

Middle cerebral artery (MCA) stroke symptoms

MCA territory infarcts are by far the most common type of stroke. The MCA is divided into four segments and supplies the majority of the cerebral convexity cortex and subcortical white matter of the frontal, parietal, and temporal lobes, majority of the basal ganglia and anterior and posterior internal capsule. M1 gives rise to the lateral lenticulostriate vessels and occlusion of these can give result in a lacunar stroke syndrome (see earlier). M2 bifurcates into superior and inferior divisions. Occlusion of the inferior division results in a visual field loss such as a contralateral homonymous hemianopia or upper quadrantanopia. In the dominant hemisphere it results in a receptive dysphasia and in the non-dominant hemisphere it results in constructional apraxia. Occlusion of the superior division results in a contralateral hemiparesis with arm and face more affected than the leg, hemisensory loss, and expressive dysphasia in the dominant lobe and hemineglect in the non- dominant lobe. Occlusion of the superior M4 branches to the dominant inferior parietal lobe can result in Gerstmann syndrome, which is agraphia, acalculia, left-right confusion, and finger agnosia.

However, M1/stem occlusion can result in malignant MCA syndrome, in which the infarcted tissue swells over 2–5 days leading to progressive mass effect with subfalcine and uncal herniation. This results in compression of the mesencephalon and may compromise ACA and PCA territories which will further exacerbate the condition. Untreated, this condition has an 80% mortality rate. The role of decompressive craniectomy in this condition is discussed later.

Posterior circulation signs and symptoms

Posterior cerebral artery (PCA) stroke symptoms

PCA occlusion accounts for 5–10% of all ischaemic strokes. The PCA can be divided into four segments. P1: occlusion of the paramedian perforators give rise to thalamomescencephalic infarction characterized by hypersomnolence, cognitive deficits, and vertical oculomotor paresis. When there is a single dominant thalamic perforator, a rare variant, this artery is referred to as the artery of Percheron, occlusion of which leads to bilateral medial thalamic infarction. When the blood supply to the cerebral peduncles arises from perforators of the P1 segment, infarction results in hemiplegia or hemiparesis. P2: occlusion of the thalamogeniculate arteries causes severe contralateral hyperesthesia and ataxia. If the infarction causes hemisensory loss and hemi-body pain the syndrome is referred to as thalamic pain syndrome or Dejerine–Roussy syndrome. Infarction of the ventromedial midbrain involving the oculomotor fascicle and/or nucleus, along with cerebral peduncle (corticospinal and/or corticobulbar tracts) leading to ipsilateral oculomotor nerve and contralateral hemiparesis is referred to as Weber syndrome. When the infarction involves the midbrain dorsal tegmentum including the oculomotor nucleus, red nucleus, brachium conjunctivum, or decussation of the fibres of the superior cerebellar peduncle resulting in oculomotor palsy and contralateral cerebellar ataxia, it is known as Benedikts's syndrome. When the extent of the infraction within the midbrain tegmentum also involves the cerebral peduncle resulting in oculomotor, contralateral hemiparesis, and contralateral cerebellar ataxia, the stroke syndrome is Claude's syndrome. These syndromes may feature symptoms of Parkinson's disease due to involvement of the substantia nigra (Ruchalski and Hathout, 2012). Occlusion of the posterior choroidal arteries with involvement of the lateral geniculate body results in sectoranopia, a wedge, or sector-shaped visual field defect. P3 and P4 supply the occipital cortex (calcarine, cuneus), parietal lobe (percuneus), parts of the temporal lobe (uncus, anterior

fusiform gyrus, inferior temporal gyrus) and splenium of corpus callosum. Occlusion of these vessels can produce an array of visual symptoms from visual field loss such as homonymous hemianopia with or without macular sparing (collateral from MCA), visual agnosia, prosopagnosia, and alexia with or without agraphia. Anton (-Babinski) syndrome is visual anosognosia (cortical blindness with confabulation) where the patient denies that they are blind due to bilateral PCA infarcts. Balint syndrome involves optic ataxia, simultaneous and loss of voluntary but not reflexive eye moments due to bilateral parieto-occipital lobe infarction (Cereda and Carrera, 2012; Ruchalski and Hathout, 2012).

Vertebrobasilar stroke symptoms (rostral to caudal)

The rostral portion of the basilar artery gives rise to the P1s. Therefore, occlusion at this point leads to ischaemia in mesencephalon, thalamus, temporal, and occipital lobes and can give rise to a constellation of signs referred to as top of the Basilar syndrome. These include disturbances of consciousness, hypersomnia, and vertical gaze palsy, with quadriplegia being uncommon (Caplan, 1980).

The superior cerebellar artery (SCA) can be divided into four segments (prepontine, ambient, quadrigeminal, and cortical). Perforating branches from the proximal SCA supply the pons, mesencephalon, and inferior colliculus and therefore proximal occlusion can give rise to a combination of rostral brainstem, such as ipsilateral Horner's syndrome, contralateral pain, and temperature sensory loss and contralateral trochlear nerve palsy (superior lateral tegmentum of pons), and cerebellar signs such as ipsilateral limb dysmetria, dysarthria, and ataxia.

The anterior inferior cerebellar artery (AICA) arises from the middle to caudal third of the basilar artery and supplies the inferior lateral tegmentum of the pons (trigeminal, facial, vestibular, cochlear nuclei, and the spinothalamic tract), middle cerebellar peduncle, and flocculus. Occlusion can give rise to vertigo, vomiting, tinnitus, dysarthria, facial paralysis, hearing loss, Horner's syndrome, loss of pain, and temperature, ipsilateral conjugate gaze palsy (due to flocculus) and dysmetria. When all these symptoms and signs are found together, the syndrome is referred to as lateral pontine syndrome or Marie-Foix syndrome.

The basilar artery is formed by the union of the vertebral arteries and ends in the bifurcation of the P1s. It gives off median perforating pontine branches which supply medial basis pontis (corticospinal tracts); paramedian perforating pontine branches which supply medial pontine tegmentum (including the floor of the fourth ventricle, abducens nucleus, medial longitudinal fasciculus, and paramedian pontine reticular formation; short circumferential pontine branches which supply lateral basis pontis and tegmentum); and finally the long circumferential pontine branches which supply the most lateral part of the pontine base and tegmentum. The other branches of the basilar artery, SCA, and AICA are discussed earlier. Occlusion of the perforators can give rise to ataxic hemiparesis characterized by contralateral weakness and contralateral ataxia. Occlusion of paramedian and short circumferential branches can cause contralateral hemiparesis, ipsilateral facial weakness, and ipsilateral lateral gaze palsy. This is known as inferior medial pontine syndrome or Foville syndrome (Kataoka et al., 1997). If the face is spared the syndrome is referred to as the ventral pontine syndrome/Raymond syndrome. If the gaze palsy is due to abducens palsy, then it is called ventral pontine syndrome/Millard–Gubler syndrome. Locked-in syndrome results from bilateral damage to basis pontis and sparing of the tegmentum of the pons resulting in damage to the corticospinal and corticobulbar tracts with preservation of the supranuclear ocular motor pathways and the reticular formation leaving vertical eye movements, blinking, and consciousness intact.

The intracranial vertebral artery or V4 segment gives rise to two main groups of branches. The medial group comprise the anterior spinal artery (which supplies the medial medulla oblongata), and branches to the foramen caecum (which lies at the pontomedullary junction and supply as far back as tegmentum and the floor of the fourth ventricle). The lateral group comprise the posterior inferior cerebellar artery (PICA) and circumferential branches to the inferior cerebellar peduncle, lateral medulla, and the olivary structures (Akar et al., 1994). PICA is divided into four segments and supplies the lateral medulla, posteroinferior cerebellar hemisphere, and inferior vermis. Occlusion of the anterior spinal artery can result in contralateral hemiparesis, contralateral hemisensory loss, and ipsilateral hypoglossal weakness, also known as medial medullary syndrome or Dejerien syndrome. Occlusion of PICA can result in a constellation of signs and symptoms referable to the lateral medulla, which includes caudal trigeminal nucleus, vestibular nucleus, nucleus ambiguus, spinothalamic tracts, descending sympathetics) and cerebellum (restiform body). These include ipsilateral pain and temperature loss of the face, ataxia, nystagmus, vertigo, hoarseness, dysphagia, Horner's syndrome, and contralateral hemisensory loss. This is known as lateral medullary syndrome or Wallenberg syndrome.

Investigation of cerebral ischaemia and stroke

Evaluation of the acute stroke patient can be considered in two phases. The emergent evaluation consists of clinical scoring using a system such as NIHS scale (see **Table 51.1**) and imaging investigations. The imaging modality may be dictated by the treatment facilities available such as access to endovascular interventional therapies and rapid access to advanced imaging modalities. Non-emergent evaluation includes workup for the 'metabolic syndrome'.

The standard imaging modality is non-contrast CT (see **Fig. 51.1**). This is used as a screening tool to exclude ischaemic stroke mimics such as haemorrhagic strokes or space occupying lesions. Other information obtainable from a non-contrast CT is evidence of early ischaemia in the MCA territory allowing calculation of the Alberta Stroke Programme Early CT Score (ASPECTS) (see **Table 51.2**; **Fig. 51.2**), overt hypodensity and its volume, and the hyperdense artery sign. In centres with neurovascular intervention, CT angiography (CTA) can provide information regarding location of occlusion, quality of collateral supply, and stenosis of vessels (see **Figs. 51.3** and **51.4**). If the CTA incorporates the aortic arch and neck vessels, important information is obtained regarding aetiology of stroke and technical difficulty for intervention. CTA was used in four of the main endovascular trials, ESCAPE, MR CLEAN, EXTEND-IA, and SWIFT. CT perfusion provides information regarding the volume of infarct core via cerebral blood flow or cerebral blood volume, volume of penumbra rescuable via MTT or Tmax and ratio of penumbra to infarct via a mismatch ratio. MR imaging modalities such as MRA, DWI, and MR perfusion provide similar information to

Table 51.1 NIHS scale

Instructions	Scale definition
1a: Level of consciousness (LOC)	0 = Alert 1 = Not alert but rousable with minor stimulation 2 = Not alert; requires repeated painful stimulation 3 = Unresponsive
1b: LOC questions—two orientation questions	0 = Answers both correctly 1 = Answers one correctly 2 = Answers neither question correctly
1c: LOC commands—two-stage commands	0 = Performs both correctly 1 = Performs one correctly 2= Performs neither correctly
2: Best gaze	0 = Normal 1 = Partial gaze palsy 2 = Forced deviation
3: Visual	0 = Visual loss 1 = Partial hemianopia 2 = Complete hemianopia 3 = Bilateral hemianopia
4: Facial palsy	0 = Normal 1 = Minor paresis 2 = Major paresis 3 = Complete paralysis
5: Motor arm 5a: Left 5b: Right	0 = No drift 1 = Drift 2 = Some effort against gravity 3 = No effort against gravity 4 = No movement UN/X = untestable
6: Motor leg 6a: Left 6b: Right	0 = No drift 1 = Drift 2 = Some effort against gravity 3 = No effort against gravity 4 = No movement UN/X = untestable
7: Limb ataxia	0 = Absent 1 = Present in one limb 2 = Present in two limbs UN/X = untestable
8: Sensory	0 = Normal 1 = Mild-to-moderate loss 2 = Severe-to-total sensory loss
9: Best language	0 = No aphasia 1 = Mild-to-moderate aphasia 2 = Severe aphasia 3 = Mute global aphasia
10: Dysarthria	0 = Normal 1 = Mild-to-moderate dysarthria 2 = Severe dysarthria UN/X = Untestable
11: Extinction and inattention	0 = No abnormality 1= Visual, tactile, auditory, spatial, or personal inattention 2 = Profound hemi-inattention or extinction to more than one modality

Reproduced with permission from T Brott, HP Adams, CP Olinger, JR Marler, WG Barsan, J Biller, J Spilker, R Holleran, R Eberle, V Hertzberg, Measurements of acute cerebral infarction: a clinical examination scale, *Stroke*, Volume 20, Issue 7, pp. 864–70. Copyright © 1989 Wolters Kluwer Health, Inc.

CTA and CT perfusion. However, there are still considerable logistical issues regarding the use of MRI in acute stroke workup such as out of hours access, scan time, and monitoring of unstable patients (Menon et al., 2015; Na et al., 2015).

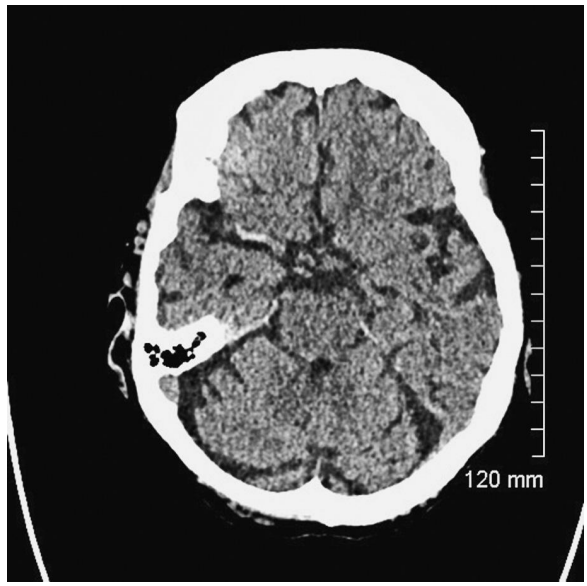

Fig. 51.1 Non-contrast CT brain demonstrating a right hyperdense middle cerebral artery (MCA).

Medical management of cerebral ischaemia and stroke

The goal of treatment is prompt restoration of blood supply by recanalization of the occluded vessel to rescue the penumbra and systemic measures to support perfusion of the penumbra, pending recanalization, by avoiding hypotension, hyperthermia, and strict glycaemic control. For effective treatment outcomes, correct and timely patient selection is imperative. In hypertensive patients who are candidates for reperfusion treatment lowering the systolic BP to less than 185 mmHg or diastolic BP to below 110 mmHg and after treatment maintain systolic BP below 180 mmHg or diastolic BP below 105 mmHg is essential using labetalol, nicardipine, or sodium nitroprusside (Jauch et al., 2013). After reperfusion therapy, patients should also undergo workup and treatment for aetiological factors.

Table 51.2 ASPECTS score for determining degree of severity of MCA infraction. Starting with an initial score of 10, one point is deducted for each structure or territory involved at two standard axial CT levels, ganglionic and supraganglionic. A score <=7 denotes a poor outcome

CT level	
Ganglionic level	Caudate, putamen, Internal capsule, insular cortex, M1 (frontal operculum/anterior MCA cortex), M2 (anterior temporal pole/cortex lateral to insular ribbon), M3 (posterior temporal pole/posterior MCA cortex
Supraganglionic level	M4 (anterior MCA territory immediately superior to M1), M5 (middle MCA territory immediately superior to M2), M6 (posterior MCA territory immediately superior to M3)

Reprinted from *The Lancet*, Volume 355, Issue 9216, Philip A Barber, Andrew M Demchuk, Jinjin Zhang, Alastair M Buchan, Validity and reliability of a quantitative computed tomography score in predicting outcome of hyperacute stroke before thrombolytic therapy, pp. 1670–74, Copyright (2000), with permission from Elsevier.

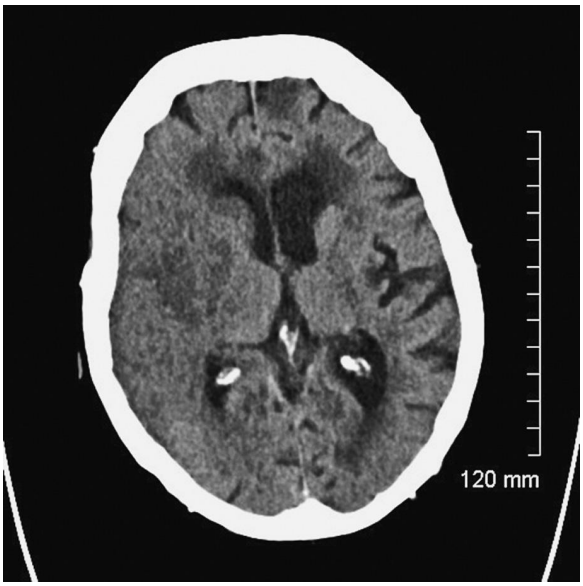

Fig. 51.2 Non-contrast CT brain at the ganglionic level demonstrating ASPECTs score of 7.

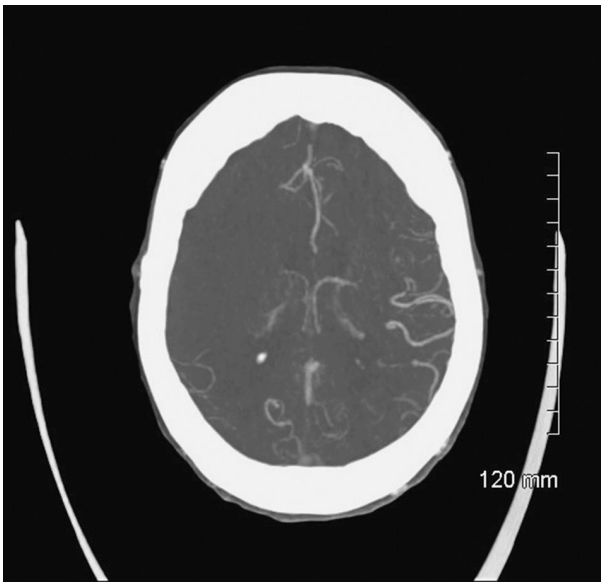

Fig. 51.4 CT angiogram of intracranial vessels demonstrating reduced and asymmetric distal filling in the right MCA territory.

Thrombolysis

The use of intravenous (IV) thrombolysis using recombinant tissue plasminogen activator (rt-PA) was established with the landmark paper published by NIND in 1995. This trial randomly assigned 600 patients into treatment and placebo groups. A single dose of rt-PA at 0.9 mg/kg (max 90 mg) was administered within three hours of symptom onset. The treatment group demonstrated improved outcomes in all outcome measures, NIHSS, Barthel index, GOS, and mRS, with acceptable increase in intracerebral haemorrhage. The recent ECASS-III trial has increased the time window to 4.5 hours (see Table 51.3 for inclusion and exclusion criteria for patient selection for IV rt-PA). This time window may be pushed out further with the use of perfusion imaging to select patients with salvageable penumbras beyond 4.5 hours (Burton et al., 2015). However, administering IV rt-PA outside the 4.5 h time window is associated with a higher SICH rate. Recanalization rates for IV rt-PA is reduced in large vessel occlusion such as internal carotid artery (ICA) and proximal MCA.

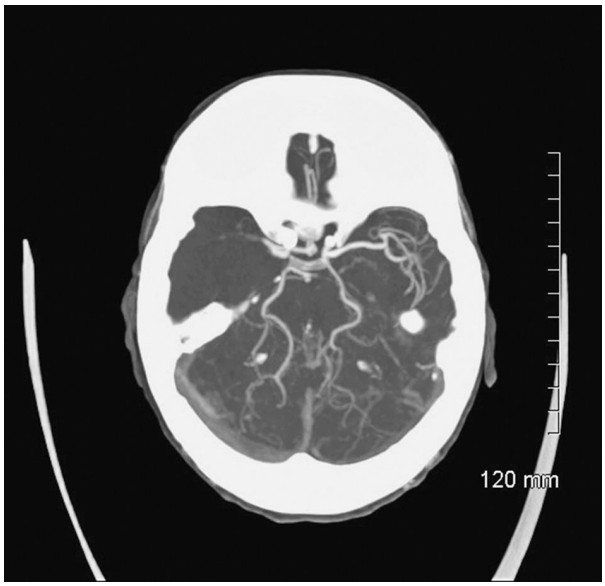

Fig. 51.3 CT angiogram on intracranial vessels (maximum intensity projection 5 mm) demonstrating a filling defect in the right MCA.

Operative and interventional management

Intra-arterial (IA) thrombolysis is a neurovascular interventional procedure where there is direct delivery of the thrombolytic agent to the site of occlusion. To date, only one trial has been published, the PROACT II trial. It established the efficacy of IA recombinant prourokinase up to 6 hours from symptom onset, despite increased SICH rates. This drug has not received Food and Drug Administration (FDA) approval and the results have been extrapolated to rt-PA.

Thrombectomy has been made possible with the development of various devices such as the coil retriever-MERCI and the stent retrievers such as TREVO® from Stryker and Solitaire FR™ from Covidien. Stent retrievers have been demonstrated to be superior to coil retrievers. Numerous recent randomized clinical trials have demonstrated improved outcomes of thrombectomy up to 6 hours from symptom onset against standard medical management with IV r-tPA. These randomized trials include MR CLEAN, ESCAPE, SWIFT PRIME, EXTEND-IA, REVASCT, and THRACE (Ding, 2015). All these trials demonstrated statistically significant improvement in mRS (0–2) at 90 days and were halted prematurely due to their efficacy in the treatment of large arterial occlusion against best medical management with and without IV r-tPA. Current recommendations are that thrombectomy, with a stent retriever, should be performed (up to 6 h) as an adjunct to thrombolysis (given within 4.5 h) for large artery occlusions. If thrombolysis is contra-indicated, then thrombectomy alone is recommended for large artery occlusion (see Fig. 51.5).

Table 51.3 Indications, relative contraindications, and absolute contraindications for r-tPA administration

Indications	Relative contraindications	Absolute contraindications
Age: >18 y	Major surgery or serious trauma within the past 14 days	Evidence of intracranial haemorrhage
Diagnosis of ischaemic cerebrovascular accidents CVA		History of intracranial haemorrhage
Time from onset 3–4.5 h	Blood glucose <2.7 mmol/litre or >22.2 mmol/litre	Intraspinal surgery, serious head trauma, or previous stroke within the past 3 months
	Platelet count <100 000	Clinical presentation suggestive of a subarachnoid haemorrhage, even with normal CT
	Coagulopathy: INR >1.7 aPTT> 40s	Active internal bleeding or acute trauma, such as a fracture
	Recent gastrointestinal (GI) or urogenital (GU) bleed within 3 weeks	Arterial puncture at a non-compressible site within the past 7 days
	Recent myocardial infarction (MI) within 3 months	Known atrioventricular malformation (AVM), neoplasm, or aneurysm
		Systolic BP > 185, diastolic >110 mmHg
		Seizure in acute setting
		Known AVM, tumour, or aneurysm

Data from Demaerschalk, B.M., et al., Scientific Rationale for the Inclusion and Exclusion Criteria for Intravenous Alteplase in Acute Ischemic Stroke: A Statement for Healthcare Professionals from the American Heart Association/American Stroke Association. *Stroke*, volume 47, Issue 2, pp. 581–641. 2016.

Patient's ineligible to receive thrombolytic and/or thrombectomy should receive antiplatelet therapy immediately. In these patients systolic BP exceeding 220 mmHg or diastolic BP more than 120 mmHg should be treated. Those patients that received reperfusion therapy should wait a minimum of 24 h and after a follow CT or MRI before antiplatelet therapy is commenced.

Decompressive craniectomy for stroke

Supratentorial

Malignant MCA syndrome (discussed earlier) accounts for 5–10% of all ischaemic strokes and can have up to 80% mortality. The natural history of malignant MCA stroke can follow one of three clinical courses (i) rapidly progressive deterioration within 96 hours; (ii) progressive deterioration over days; (iii) initially worsening course followed by a plateau then improvement. There are several reported predictors of the development of malignant MCA syndrome, NIHS score above 20 for dominant, 15 for non-dominant, elevated WBC, serum markers such as elevated serum S100B or MMP-9, early involvement (within 48 h) of more than 50% of the MCA territory on CT, more than 4 mm pineal shift, or 7.5 mm anteroseptal shift within 96 h, MRI DWI volume more than 80 cm^3 at 6 hours, or more than 145 cm^3 at 14 hours and symptoms of raised ICP such as nausea and vomiting (Staykov and Gupta, 2011; Wijdicks et al., 2014). To date there have been approximately seven RCTs published (Hatefi et al., 2014). Decompression for malignant MCA syndrome unequivocally reduces mortality. By reducing mortality, it not only increases the number of patients with good outcome (mRS 1–3) but also those with poor outcome (mRS >3). There remains controversy surrounding functional outcomes of the surviving patients. Functional outcomes in the majority of studies published to date used basic measures such as mRS. This neglects patient-orientated factors such as neuropsychological outcomes, quality of life, and financial burden. The decision to proceed with decompression should remain a multidisciplinary team decision made jointly with the patient's family.

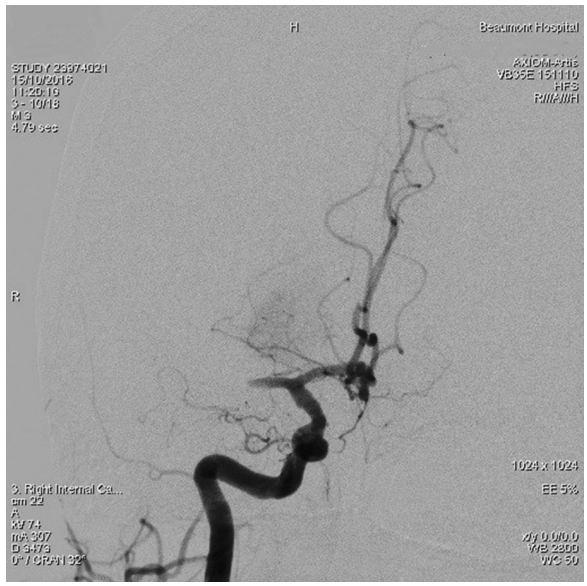

Fig. 51.5 Digital subtraction angiogram with a right internal carotid injection demonstrating a filling defect in the right MCA.

Procedure

This involves a standard question mark or T-incision. The frontotemporoparietal craniectomy should extend to a minimum 12 cm anteroposteriorly. In the coronal plane, the craniectomy should reach the mid-pupillary line superiorly, and should come down inferiorly to the floor of the anterior and middle cranial fossa, a minimum of 10 cm. The dura is opened widely and may be augmented with a graft.

Infratentorial

Unlike decompressive craniectomy for supratentorial stroke, there have been no RCTs for infratentorial decompression and current

recommendations are based on case series, observational, and retrospective studies. This is probably due to the fact that most published series have reported significant reduction in mortality with good functional outcomes. Signs and symptoms of posterior circulation stroke are discussed earlier. It is important, as ever, that a through neurological exam is performed on presentation to establish if the ischaemic territory involves the cerebellum only or brainstem and cerebellum. The mass effect from cytotoxic oedema of the infarcted cerebellum can efface the fourth ventricle, causing obstructive hydrocephalus and/or brainstem compression. This process can evolve over 1–7 days with peak at 72 hrs. The possibility of deterioration has been reported to range from 7% to 32% of cases. Current recommendations are that if a patient's deterioration is due to mass effect, then surgical intervention is appropriate. Two surgical strategies have been proposed (i) external ventricular drain (EVD) first and if patient fails to improve then suboccipital decompression; (ii) suboccipital decompression with preoperative right frontal EVD or intraoperative posterior parietal EVD. The EVD is usually set at 15–20 cm H_2O to prevent upward herniation. Published series of patients who were initially treated for clinical deterioration and radiological evidence of hydrocephalus with an EVD, demonstrate that between 20% and 30% went on to require a suboccipital craniectomy (Amar, 2012; Wijdicks et al., 2014).

Procedure

This involves a standard midline incision and exposure of the external occipital protuberance to C1, wide craniectomy with removal of the posterior arch of C1, and a Y-shaped durotomy with duroplasty. Some authors recommend resection of the infarct tissue.

Neuroprotective medical and anaesthetic strategies

These are similar to those of traumatic brain injury (TBI) protocols. See Chapter 41.

Transient ischaemic attacks (TIAs) and carotid endarterectomy

Preoperative

Atherosclerosis

Atherosclerosis is a chronic condition of the tunica intima of arteries. It is principally driven by three interdependent mechanisms; namely inflammation, oxidative stress, and dysfunction of the renin angiotensin system which leads to endothelial dysfunction. This in turn leads to subendothelial accumulation of lipids, fibronectin, and calcium, producing an atheromatous plaque, which causes gradual stenosis of the vessel. As the plaque progresses, the overlying endothelium may ulcerate, leading to activation of platelets and the clotting cascade with resultant thrombus formation. Depending on the calibre of the vessel and the degree of stenosis, this could result in occlusion at the site of the plaque or detach to cause thromboembolism distally (Tousoulis et al., 2011; Husain et al., 2015).

The risk factors associated with atherosclerosis are encompassed in metabolic syndrome or Syndrome X. There are various definitions of metabolic syndrome. However, they all share common processes such as (i) hyperglycaemia due to either insulin resistance, glucose intolerance, or type 2 diabetes; (ii) weight measurements such as increased BMI, central obesity, or race and gender waist measurements; (iii) dyslipidaemia with raised triglycerides and reduced high-density lipoproteins; and (IV) hypertension, defined as BP exceeding 140/90 (or 130/85 for the International Diabetes Federation). Other criteria include microalbuminaemia, disorders of uric acid metabolism, and serum markers of inflammation (ESR, CRP). Central to the definition is disorders of glucose regulation (van Rooy and Pretorius, 2015).

TIAs present as temporary neurological deficits that resolve fully without evidence of infarction. The signs and symptoms are discussed earlier for the various arterial territories and resolve due to collateral supply to the area of ischaemia. As most TIAs last less than 5 minutes, the patient may have recovered by the time they are reviewed. The patient may report symptoms of weakness in the arm, leg or face, unsteadiness, nausea, vertigo or dizziness, confusion, or amnesia (Markus et al., 2013). The 90-day risk of developing an ischaemic stroke after a TIA is approximately 17% with the majority occurring within 48 hrs making it imperative to diagnose and treat urgently (Giles and Rothwell, 2007; Gupta et al., 2014). The use of scoring systems such as $ABCD^2$ help predict the likelihood of subsequent stroke (see **Table 51.4**:>=4 high risk, =<3 low risk).

Investigation of TIAs usually begins with the non-contrast CT. This helps exclude TIA mimics. MRI with DWI with in 24 hrs helps establish that the presentation was due to ischaemia with 97% of diffusion restricted lesions corresponding to infarction (Souillard-Scemama et al., 2015). Vascular imaging should include the Aortic arch and neck vessels as well as the intracranial vessels assessing for evidence of atherosclerotic stenosis or occlusion. MRA, CTA, ultrasound (US), and catheter angiography all have high sensitivity and specificity in detecting carotid artery disease and estimating severity of stenosis. MRA may provide additional information regarding plaque characteristics which may predict future risk of events (Mono et al., 2012; Zhao et al., 2013). ECG and cardiac echo are used to assess for cardiogenic causes of emboli. The remaining investigations centre on the metabolic syndrome and include fasting glucose, glucose tolerance test, HbA1C, BP measurements, weight measurements, and lipid prolife.

Management depends on aetiology and modifying risk factors. If the source is cardiogenic due to atrial fibrillation (continuous or paroxysmal) the patient is commenced on long-term anticoagulation, otherwise the patient is commenced on antiplatelet therapy such as dipyridamole with aspirin. Target BP <=140/90 mmHg or 130/85 for diabetics. Dyslipidaemia is treated with a statin with goal low-density lipoprotein (LDL) less than 2.59 mmol/litre. Hyperglycaemia is treated with dietary modification or oral hypoglycaemic agents. Smoking cessation and exercise are encouraged. Current recommendations for carotid revascularization include symptomatic stenosis more than 50% or asymptomatic stenosis more than 70%. Whether to perform a carotid endarterectomy (CEA) or carotid angioplasty and stenting (CAS) depends factors such vascular and plaque anatomy as well as patient comorbidities.

Operative

Carotid endarterectomy

The evidence behind carotid endarterectomy is based on several well-designed international RCTs for both symptomatic

Table 51.4 ABCD[2]

Risk factor	Score
Age >= 60 y	 1
Blood pressure Systolic >=140 mmHg or diastolic >=90 mmHg	 1
Clinical features of TIA Unilateral weakness with or without speech impairment Speech impairment without unilateral weakness	 2 1
Duration TIA duration >= 60 minutes TIA duration 10–59 minutes	 2 1
Diabetes	1

Reprinted from *The Lancet*, Volume 366, Issue 9479, PM Rothwell, MF Giles, E Flossmann, CE Lovelock, JNE Redgrave, CP Warlow, Z Mehta, A simple score (ABCD) to identify individuals at high early risk of stroke after transient ischaemic attack, pp. 29–36, Copyright (2005), with permission from Elsevier.

and asymptomatic carotid artery disease. The North American Symptomatic Carotid Endarterectomy Trial (NASCET 1991 and 1998) and the European Carotid Surgery Trial (ECST 2003) enrolled 659 and 1807 patients, respectively. Not only did each trial established the efficacy of CEA over best medical management (antiplatelet therapy and risk factor reduction) in secondary prevention of ischaemic events, pooled analysis helped formulate current treatment recommendations. In symptomatic patients (TIA, amaurosis fugax, or non-disabling stroke) with above 70% stenosis of the ipsilateral carotid artery CEA should be performed within 2 weeks. In patients with 50–69% stenosis, CEA is only recommended in high volume centres with a complication rate less than 6%. For stenosis less than 50%, CEA is not recommended. In patients with ipsilateral stenosis more than 70% and near-total or a total occluded contralateral carotid artery, CEA on the ipsilateral side is still recommended, despite the higher risk of operative morbidity.

The Asymptomatic Carotid Artery Study (ACAS 1995) and the Asymptomatic Carotid Surgery Trial (2004) compared the efficacy of best medical management (antiplatelet therapy and risk factor reduction) to best medical management and CEA in asymptomatic patients with carotid artery disease. The benefit of CEA was less apparent and the degree of stenosis less influential. The numbers needed to treat in asymptomatic patients to achieve a 5-year risk reduction were significantly higher when compared to symptomatic patients and the influence of perioperative morbidity and mortality becomes more influential. Therefore, selection of asymptomatic patients for CEA should be based on the patient's comorbidities and complication rates of the centre (Brott et al., 2011).

Technique

The procedure can be performed under local (LA) or general (GA) anaesthesia (Link et al., 2014). An intravascular shunt can be used to maintain cerebral blood flow during the procedure. Alternatively, one of several methods (awake patient under LA, EEG, SSEP, TCD, or stump pressures), can be used for monitoring during carotid clamping, with selective shunting if there is an indication of hypoperfusion.

Position: Supine with ipsilateral shoulder roll with neck extended and head turned to contralateral side.

Incision: Curvilinear just behind the anterior border of sternocleidomastoid, extending from 1 cm below the mastoid tip to 1 cm below angle of mandible (avoiding the parotid) to 1 cm above the sternoclavicular joint.

Approach: Platysma is divided, exposing the cervical fascia, external jugular vein and the greater auricular nerve as it exits lateral border of sternocleidomastoid to supply sensation to the earlobe. The sternocleidomastoid muscle (SCM) is mobilized and retracted laterally to expose the carotid sheath which is then entered. The common facial vein serves as a landmark to the carotid bifurcation and is ligated. The vagus and hypoglossal nerves are identified and protected. Ansa cervicalis is also identified and may be sacrificed if necessary.

Endarterectomy: Intravenous heparin is administered. Careful exposure of the common carotid and ICA follows (see **Fig. 51.6**). The superior thyroid artery, ICA, and common carotid artery (CCA) are controlled in that order. A shunt should be used if there is ipsilateral change in the EEG, SSEP, or TCD. An arteriotomy is made in the mid-portion of the CC and continued cranially with Potts scissors. Normal tuncia intima is identified from CC to ICA. The plaque is dissected distally up the ICA from the intima with gentle dissection. The external carotid artery (ECA) is everted allowing dissection of the plaque. After removal of any loose debris the site is irrigated with heparinized saline. Any intimal flap is secured to the surgical bed with 7-0 prolene in an inside to outside fashion. The arteriotomy is closed either primarily or with a patch (either autologous vein, PTFE, or woven polyester) with 5-0 prolene. Antegrade and retrograde flushing manoeuvres are performed to remove debris before final sutures are placed. The ICA is back-bled to purge any remaining air or debris and then reclamped while the ICA and CCA are released to direct any debris up the ECA.

Closure: Patency of the vessels can be assessed with intraoperative doppler. A wound drain maybe placed. The wound is closed in layers.

Endovascular management of carotid disease

Endovascular options include CAS with embolic protection device. The Stenting and Angioplasty with Protection in Patients with High Risk for Endarterectomy (SAPHIRE) trial randomized high-risk symptomatic and asymptomatic patients into CEA and CAS groups. High risk patients were defined based on a combination of comorbidities and surgical anatomical factors and was defined as having one or more of the following: NYHA III or IV heart failure; COPD; more than 50% contralateral stenosis; contralateral recurrent laryngeal nerve palsy; prior carotid revascularization; previous radical neck surgery or radiotherapy; and prior carcinoma of the gall bladder (CAGB). In this study, there was better outcomes in asymptomatic patients with high surgical risk in the CAS group when compared to the CEA group. There has been no demonstration of superior efficacy of CAS over CEA in all other groups based on symptoms and risk (Ooi and Gonzalez, 2015). With improvement in endovascular techniques this may change.

Complication management

Postoperatively, blood pressure control is necessary to prevent hyperperfusion injury. Any new postoperative deficit requires emergent stroke workup to exclude ICA acute occlusion or embolic phenomenon. Lastly, the development of a neck haematoma is an emergency requiring prompt securing of the airway and evacuation

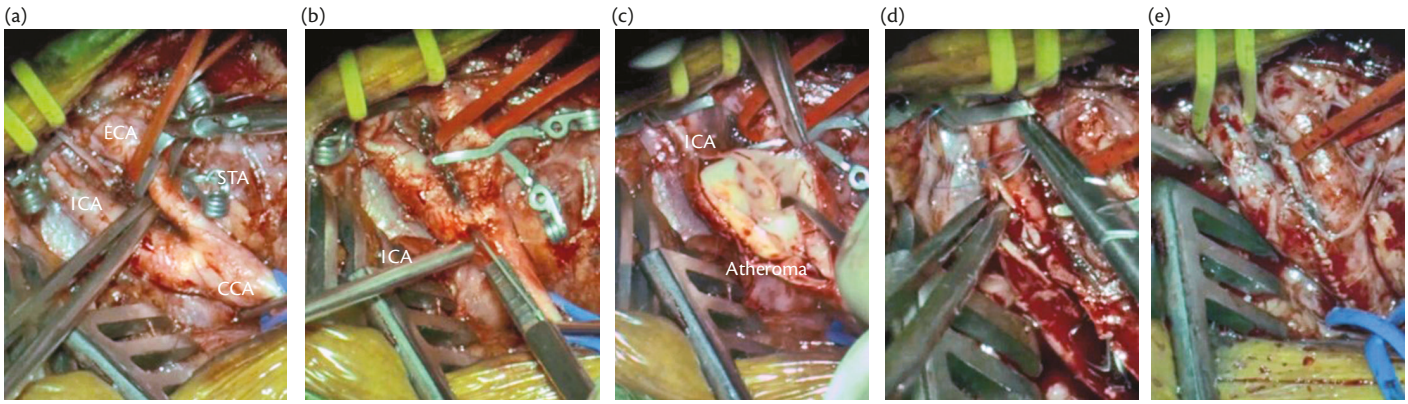

Fig. 51.6 Carotid endarterectomy. The intraoperative pictures illustrate the steps in a carotid endarterectomy. (A) The carotid bifurcation is widely exposed and slings are placed around the internal carotid artery (ICA), external carotid artery (ECA), and common carotid artery (CCA). Following the administration of intravenous heparin, vascular clips are placed on the ICA, CCA, ECA and the first ECA branch: superior thyroid artery (STA). (B) A knife is used to incise the midpoint of the ICA, over the carotid bulb into the CCA exposing the full extent of the atheromatous plaque. (C) A dissector is used to identify the plane between the atheromatous plaque and the vessel media. The atheroma is circumferentially dissected from the ICA and CCA, and a stump is followed into the ECA and amputated. Any intimal flaps (particularly distally into the ICA) are tacked down with a fine suture. (D) The vessel is closed with a continuous prolene suture from distal to proximal ensuring there is no kinking or narrowing of vessel calibre. (E) Unclamping of the STA can be used to back bleed into the endarterectomy site and exclude air before the final suture is tied. Vascular clamps are opened in a specific order in order to avoid embolic material from entering the intracranial circulation: ECA, CCA, ICA.
Courtesy of Dr Kirkpatrick, Department of Neurosurgery, Addenbrookes's NHS Trust, Cambridge, UK.

of the clot. Ear, nose, and throat (ENT) colleagues should be notified immediately in case endotracheal intubation fails and a tracheostomy is necessary.

Controversy

Decompressive hemicraniectomy for malignant MCA infarction

Decompression for malignant MCA infarction (MMCAI) unequivocally reduces mortality. By reducing mortality, it not only increases the number of patients with good outcome (mRS 1–3) but also those with poor outcome (mRS>3). We shall try to explore some of the controversy surrounding this topic with respect to age and functional outcomes.

Age and survival

It is well established that decompressive hemicraniectomy increases survival in patients younger than 60 years. Recently with DESTINY II, this trend has been confirmed in patients 61–80 years.

Age and functional outcome

Functional outcome appears to be on the most contentious issue surrounding DHC for MMCAI. Using a broad, non-specific metric such as the modified Rankin Scale, has led to significant criticism for two main reasons. Firstly, the mRS is a seven-point scale measuring motor function and the survivor's ability to look after their bodily needs. It neglects other factors such as neuropsychological, quality of life, burden on caregivers, and healthcare systems. Secondly, what constitutes a good or bad outcome using this scale. This is an important issue as all primary and secondary outcome measures dichotomize at this point. Studies demonstrating an increase in good outcomes from DHC have used a mRS of 0–4 as a good outcome and mRS 5–6 as poor outcome. If an MRS of 0–3 is used as a good outcome, then there appears to be no significant difference between treatment and control groups. This is due to the fact that there is an increase in survivors with major disability in the surgical group (mRS of 4) (Yang et al., 2015). mRS of 4 is defined as unable to attend to own bodily needs without assistance, and being unable to walk unassisted.

What is suggested by recent meta-analysis and RCTs is that there may be a direct relationship between age and survivors with major and severe disability—and that using chronological age alone, which neglects patient biological factors and comorbidities, may be as contentious as the mRS (Juttler et al., 2014).

FURTHER READING

Amar, A.P. (2012). Controversies in the neurosurgical management of cerebellar hemorrhage and infarction. *Neurosurg Focus*, **32**(4), E1.

Brott, T.G., Halperin, J.L., Abbara, S., et al. (2011). ASA/ACCF/AHA/AANN/AANS/ACR/ASNR/CNS/SAIP/SCAI/SIR/SNIS/SVM/SVS guideline on the management of patients with extracranial carotid and vertebral artery disease. A report of the American College of Cardiology Foundation/American Heart Association Task Force on Practice Guidelines, and the American Stroke Association, American Association of Neuroscience Nurses, American Association of Neurological Surgeons, American College of Radiology, American Society of Neuroradiology, Congress of Neurological Surgeons, Society of Atherosclerosis Imaging and Prevention, Society for Cardiovascular Angiography and Interventions, Society of Interventional Radiology, Society of NeuroInterventional Surgery, Society for Vascular Medicine, and Society for Vascular Surgery. *Circulation*, **124**(4), e54–130.

Hatefi, D., Hirshman, B., Leys, D., et al. (2014). Hemicraniectomy in the management of malignant middle cerebral artery infarction: lessons from randomized, controlled trials. *Surg Neurol Int*, **5**, 72.

Na, D.G., Sohn, C.H., & Kim, E.Y. (2015). Imaging-based management of acute ischemic stroke patients: current neuroradiological perspectives. *Korean J Radiol*, **16**(2), 372–90.

Wijdicks, E.F., Sheth, K.N., Carter, B.S., et al. (2014). Recommendations for the management of cerebral and cerebellar infarction with swelling: a statement for healthcare professionals from the American Heart Association/American Stroke Association. *Stroke*, **45**(4), 1222–38.

REFERENCES

Akar, Z.C., Dujovny, M., Slavin K.V., Gomez-Tortosa, E., & Ausman, J.I. (1994). Microsurgical anatomy of the intracranial part of the vertebral artery. *Neurol Res*, **16**(3), 171–80.

Amar, A.P. (2012). Controversies in the neurosurgical management of cerebellar hemorrhage and infarction. *Neurosurg Focus*, **32**(4), E1.

Arboix, A., Garcia-Eroles, L., Sellares, N., Raga, A., Oliveres, M., & Massons, J. (2009). Infarction in the territory of the anterior cerebral artery: clinical study of 51 patients. *BMC Neurol*, **9**, 30.

Bennett, D.A., Krishnamurthi, R.V., Barker-Collo, S., & Global Burden of Diseases and Risk Factors Study Stroke Expert Group (2014). The global burden of ischemic stroke: findings of the GBD 2010 study. *Glob Heart* **9**(1), 107–12.

Brott, T.G., Halperin, J.L., Abbara, S., et al. (2011). ASA/ACCF/AHA/AANN/AANS/ACR/ASNR/CNS/SAIP/SCAI/SIR/SNIS/SVM/SVS guideline on the management of patients with extracranial carotid and vertebral artery disease. A report of the American College of Cardiology Foundation/American Heart Association Task Force on Practice Guidelines, and the American Stroke Association, American Association of Neuroscience Nurses, American Association of Neurological Surgeons, American College of Radiology, American Society of Neuroradiology, Congress of Neurological Surgeons, Society of Atherosclerosis Imaging and Prevention, Society for Cardiovascular Angiography and Interventions, Society of Interventional Radiology, Society of NeuroInterventional Surgery, Society for Vascular Medicine, and Society for Vascular Surgery. *Circulation*, **124**(4), e54–130.

Burton, K.R., Dhanoa, D., Aviv, R.I., Moody, A.R., Kapral, M.K., & Laupacis, A. (2015). Perfusion CT for selecting patients with acute ischemic stroke for intravenous thrombolytic therapy. *Radiology*, **274**(1), 103–14.

Caplan, L.R. (1980). 'Top of the basilar' syndrome. *Neurology*, **30**(1), 72–9.

Caplan, L.R. (2015). Lacunar infarction and small vessel disease: pathology and pathophysiology. *J Stroke*, **17**(1), 2–6.

Cereda, C. & Carrera, E. (2012). Posterior cerebral artery territory infarctions. *Front Neurol Neurosci*, **30**, 128–31.

Clarke, D.D. & Sokoloff, S. (1999). Circulation and energy metabolism of the brain. In: Siegel, G.J., Agranoff, B.W., Albers, R.W., et al. (eds.) *Basic Neurochemistry: Molecular, Cellular and Medical Aspects*, Chapter 31. Philadelphia, PA: Lippincott-Raven.

Ding, D. (2015). Endovascular mechanical thrombectomy for acute ischemic stroke: a new standard of care. *J Stroke*, **17**(2), 123–6.

Ferro, J.M. & Canhao, P. (2014). Cerebral venous sinus thrombosis: update on diagnosis and management. *Curr Cardiol Rep*, **16**(9), 523.

Giles, M.F. & Rothwell, P.M. (2007). Risk of stroke early after transient ischaemic attack: a systematic review and meta-analysis. *Lancet Neurol*, **6**(12), 1063–72.

Gupta, H.V., Farrell, A.M., & Mittal, M.K. (2014). Transient ischemic attacks: predictability of future ischemic stroke or transient ischemic attack events. *Ther Clin Risk Manag*, **10**, 27–35.

Hatefi, D., Hirshman, B., Leys, D., et al. (2014). Hemicraniectomy in the management of malignant middle cerebral artery infarction: lessons from randomized, controlled trials. *Surg Neurol Int*, **5**, 72.

Husain, K., Hernandez, W., Ansari, R.A., & Ferder, L. (2015). Inflammation, oxidative stress and renin angiotensin system in atherosclerosis. *World J Biol Chem*, **6**(3), 209–17.

Jauch, E.C., Saver, J.L., Adams, H.P., Jr., et al. (2013). Guidelines for the early management of patients with acute ischemic stroke: a guideline for healthcare professionals from the American Heart Association/American Stroke Association. *Stroke*, **44**(3), 870–947.

Jung, S., Gilgen, M., Slotboom, J., et al. (2013). Factors that determine penumbral tissue loss in acute ischaemic stroke. *Brain*, **136**(Pt 12), 3554–60.

Juttler, E., Unterberg, A., Woitzik, J., et al. (2014). Hemicraniectomy in older patients with extensive middle-cerebral-artery stroke. *N Engl J Med*, **370**(12), 1091–100.

Kataoka, S., Hori, A., Shirakawa, T., & Hirose, G. (1997). Paramedian pontine infarction. Neurological/topographical correlation. *Stroke*, **28**(4), 809–15.

Link, M.J., Flemming, K.D., & Meyer, F.B. (2014). Carotid endarterectomy. In: Winn, H. (ed.) *Youmans Neurological Surgery*, pp. 3621–31. Philadelphia, PA: Saunders.

Markus, H.S., van der Worp, H. B., & Rothwell, P.M. (2013). Posterior circulation ischaemic stroke and transient ischaemic attack: diagnosis, investigation, and secondary prevention. *Lancet* Neurol, **12**(10), 989–98.

Menon, B.K., Campbell, B.C., Levi, C., & Goyal, M. (2015). Role of imaging in current acute ischemic stroke workflow for endovascular therapy. *Stroke*, **46**(6), 1453–61.

Mono, M.L., Karameshev, A., Slotboom, J., et al. (2012). Plaque characteristics of asymptomatic carotid stenosis and risk of stroke. *Cerebrovasc Dis*, **34**(5–6), 343–50.

Na, D.G., Sohn, C.H., & Kim, E.Y. (2015). Imaging-based management of acute ischemic stroke patients: current neuroradiological perspectives. *Korean J Radiol*, **16**(2), 372–90.

Ooi, Y.C. & Gonzalez, N.R. (2015). Management of extracranial carotid artery disease. *Cardiol Clin*, **33**(1), 1–35.

Ruchalski, K. & Hathout, G.M. (2012). A medley of midbrain maladies: a brief review of midbrain anatomy and syndromology for radiologists. *Radiol Res Pract*, **2012**, 258524.

Souillard-Scemama, R., Tisserand, M., Calvet, D., et al. (2015). An update on brain imaging in transient ischemic attack. *J Neuroradiol*, **42**(1), 3–11.

Staykov, D. & Gupta, R. (2011). Hemicraniectomy in malignant middle cerebral artery infarction. *Stroke*, **42**(2), 513–16.

Tousoulis, D., Kampoli, A.M., Papageorgiou, N., et al. (2011). Pathophysiology of atherosclerosis: the role of inflammation. *Curr Pharm Des*, **17**(37), 4089–110.

van Rooy, M.J. & Pretorius, E. (2015). Metabolic syndrome, platelet activation and the development of transient ischemic attack or thromboembolic stroke. *Thromb Res*, **135**(3), 434–42.

Wijdicks, E.F., Sheth, K.N., Carter, B.S., et al. (2014). Recommendations for the management of cerebral and cerebellar infarction with swelling: a statement for healthcare professionals from the American Heart Association/American Stroke Association. *Stroke*, **45**(4), 1222–38.

Yang, M.H., Lin, H.Y., Fu, J., Roodrajeetsing, G., Shi, S.L., & Xiao, S.W. (2015). Decompressive hemicraniectomy in patients with malignant middle cerebral artery infarction: a systematic review and meta-analysis. *Surgeon*, **13**(4), 230–40.

Zhao, H., Zhao, X., Liu, X., et al. (2013). Association of carotid atherosclerotic plaque features with acute ischemic stroke: a magnetic resonance imaging study. *Eur J Radiol*, **82**(9), e465–70.

RELATED LINKS TO EBRAIN

Acute Stroke Treatment. https://learning.ebrain.net/course/view.php?id=135

Neuroradiological Investigations in Carotid and Vertebral Artery Stenosis. https://learning.ebrain.net/course/view.php?id=130

Performing a Carotid Endarterectomy. https://learning.ebrain.net/course/view.php?id=131

Stroke Aetiology. https://learning.ebrain.net/course/view.php?id=139

Stroke Clinical Features and Classification. https://learning.ebrain.net/course/view.php?id=138

Surgical Management of Carotid Stenosis. https://learning.ebrain.net/course/view.php?id=132

The Pathology of CNS Ischaemia and Infarction. https://learning.ebrain.net/course/view.php?id=129

52

Extracranial-intracranial bypass for cerebral ischaemia

Mathew R. Guilfoyle and Peter J. Kirkpatrick

Introduction

Symptomatic stenosis or occlusion of the cervical (C1) internal carotid artery (ICA) is best addressed surgically with direct endarterectomy or thrombectomy procedures. This strategy is not usually possible for more distal lesions, and restoring brain perfusion requires diversion of blood from the extracranial to intracranial circulation with a variety of indirect and direct bypass techniques. However, despite five decades of experience and technical refinement, extracranial-intracranial (EC-IC) bypass for cerebral ischaemia remains contentious and there are conflicting bodies of evidence and opinion regarding how best to select patients for surgery, and whether there is meaningful clinical benefit.

Types of EC-IC bypass

Direct bypass

In contrast to the high-flow bypasses that permit the ICA (or vertebral artery) to be sacrificed to exclude complex aneurysms or excise tumours, revascularization for ischaemia is intended to supplement rather than replace the native circulation. Flow rates of the order of 30–50 ml/min are sufficient to augment perfusion above ischaemic thresholds and into the autoregulatory range. By far the most common direct 'low-flow' EC-IC bypass involves anastomosis of either the posterior (parietal) or anterior (frontal) branch of the superficial temporal artery (STA) to a cortical (M3 or M4) branch of the ipsilateral middle cerebral artery (MCA). The surgical technique is described in detail later. Direct bypass to the posterior circulation using the STA or occipital artery in situations of vertebrobasilar insufficiency is possible, but very rarely indicated.

Indirect bypass

Several related techniques have been advanced that essentially facilitate collateralization of cerebral blood flow from the external carotid circulation. The ischaemic brain strongly expresses angiogenic growth factors (Lanfranconi et al., 2011) and the aim of indirect bypass is to remove physical barriers to encourage neovascularization that bridges the extracranial and intracranial circulations. These procedures are most common in children, or adults where donor and recipient vessels are too small to fashion a direct anastomosis.

Pial synangiosis involves dissecting several centimetres of one or both STA branches and then suturing the adventitial cuff of the artery to the pia, such that it is in direct contact with the cortical surface. Alternatively, the STA can be sutured to the free edges of the durotomy and laid over the brain surface (encephaloduroarteri osynangiosis, EDAS), or the richly vascular temporalis muscle can be dissected on its vascular pedicle and flapped on to the cortical surface (encephalomyosynangiosis, EMS); these options are often combined as an encephalomyoarteriosynangiosis (EMAS). To encourage collateralization of larger areas of cortex, including posterior and anterior cerebral territories, drilling multiple burr holes and opening of the dura can be a simple but effective procedure.

The maximal benefit of an indirect bypass may not be apparent for up to a year following surgery and therefore patients with a relatively acute presentation or progressive symptomatology are not suitable for solely indirect revascularization. A combined procedure fashioning a STA-MCA anastomosis together with some form of indirect bypass is advocated by many surgeons.

Indications and patient selection

In the majority of patients, stenosis or occlusion of the distal ICA, or its terminal divisions, is either a consequence of atherosclerosis or moyamoya disease (MMD); rarer aetiologies include chronic dissections, penetrating trauma, or iatrogenic injury.

Crucial to determining the need for EC-IC bypass is an understanding of the natural history of the underlying disease process and the estimated future risk of stroke. Irrespective of aetiology, truly asymptomatic patients in whom vascular changes are discovered incidentally have a low risk of ischaemic events and, as a general rule, prophylactic surgery is not indicated. This group of patients should have vascular risk factors addressed and be monitored for the development of symptoms, at which time intervention may become necessary. At the contrasting end of the spectrum, patients who present with large established strokes involving entire vascular territories, without significant remaining tissue at risk, are also not appropriate for revascularization.

Atherosclerotic steno-occlusive disease

Following the initial introduction of the STA-MCA bypass procedure by Yasargil in the late 1960s (Yasargil et al., 1970), the technique rapidly gained widespread popularity for the treatment of patients at high risk of stroke from severe atherosclerotic stenosis or occlusion of the ICA or MCA. Series of several hundreds of patients suggested the procedure was both durable and safe: five-year graft patency was reported to be more than 95% and the incidence of perioperative death or major disability under 5% (Chater, 1983; Sundt et al., 1985).

To rigorously address the question of whether revascularization reduced the risk of future stroke compared to medical treatment alone, the EC-IC Bypass Study Group undertook a multicentre randomized controlled trial involving 71 North American, European, and Japanese centres (Group, 1985). Eligible patients had occlusion or severe stenosis of the distal ICA or M1-MCA segment, with clinical evidence of a transient ischaemic attack (including amaurosis fugax) or minor stroke within the preceding three months. A total of 1377 patients were recruited, all received aspirin and aggressive hypertension control, and 663 were randomly allocated to receive a STA-MCA bypass. Methodologically the study was well conducted and the surgery was technically very successful with a high graft patency rate of around 96% achieved both at high and low volume units. The principal finding of the trial striking: there was significantly higher incidence of stroke in patients who received a bypass compared with those who had medical treatment alone. On average the excesses risk was estimated at 14%, although most of the events occurred early following surgery and the cumulative number of strokes at five-years following randomization was similar between the two groups. Multiple subgroup analyses failed to identify any patients with specific clinical features that fared better with revascularization. Although critics of the trial questioned the generalizability of the study to the wider population as large numbers of patients at participating centres were treated outside the study, the number of EC-IC bypass procedures sharply declined following its publication in 1985.

In response to the EC-IC bypass trial there was renewed focus on improving patient selection for surgery by quantifying cerebrovascular reserve and reactivity using techniques including single photon emission computed tomography, positron emission tomography (PET), magnetic resonance perfusion, Xenon CT, and contrast-enhanced CT perfusion (Schmiedek et al., 1994; Grubb et al., 1998a; Patel et al., 2010). In essence, all these modalities involve measuring basal cerebral perfusion and then repeated following a vasodilatory challenge such as hypercapnia or intravenous acetazolamide. In patients with a critical stenosis, the autoregulatory capacity of the distal vascular bed is already exhausted at baseline as vessels maximally dilate to expand cerebral blood volume, preserve flow, and maintain tissue oxygenation. In response to the vasodilatory challenge the relative blood flow decreases in the affected territory as it is either unable to vasodilate further, in contrast to the hyperaemia in surrounding regions, or the increased flow into the adjacent brain induces a 'steal' effect from the ischaemic territory and the blood flow and transit times deteriorate further (**Fig. 52.1**). Using PET, the oxygen extraction fraction (OEF) of the tissue can also be quantified and as this increases it implies increasingly severe steal effect and ischaemia. A loosely defined grading system has been proposed progressing from Grade I, in which there is loss of vasodilatory capacity but no significant steal, 'severe' Grade I and Grade II where there is significant steal effect and/or increased OEF, and Grade III where there is frank ischaemia that cannot be compensated by increased OEF (Grubb et al., 1998a).

Collective analysis of perfusion imaging studies suggested that for patients with evidence of significant steal effect in response to a vasodilatory challenge the annual risk of stroke is in the region of 10–20% (Grubb et al., 1998b; Garrett et al., 2009). Moreover, STA-MCA bypass measurably improved cerebrovascular reserve and reactivity, and reduced the risk of stroke by around two-thirds (Garrett et al., 2009).

These promising findings suggested a subgroup of patients who might benefit from revascularization could reliably be identified. The Carotid Occlusion Surgery Study (COSS) was a randomized controlled trial comparing STA-MCA bypass with best medical management alone in patients with atherosclerotic ICA occlusion, an ischaemic event within the preceding 120 days, and increased OEF in the ipsilateral hemisphere on PET imaging following acetazolamide (Powers et al., 2011). Of 194 patients randomized, 97 were allocated to receive a bypass and 93 ultimately had surgery. COSS was terminated early due to futility and the results closely correspond to those of the earlier EC-IC bypass trial, again demonstrating that despite excellent graft patency rates (>96%) there was significantly increased risk of ipsilateral stroke within 30 days in the surgical arm (14.4% vs. 2.0%); the cumulative stroke risk at two years postoperatively was no different between groups (21.0% vs. 22.7%) (Powers et al., 2011; Grubb et al., 2013).

The Japanese EC-IC Bypass Trial (JET) was a study with similar methodology to COSS randomizing 196 patients with steno-occlusive disease and impaired reactivity to best medical management with or without EC-IC bypass. At an interim analysis there was a suggestion of a marginally significant reduction in further strokes among the 98 patients who received a bypass, but the full outcomes and details of the trial have never been published (JET Study Group, 2002).

It is useful to note that a randomized trial of endovascular stenting for patients similar to those enrolled to the original EC-IC bypass trial (i.e. angiographic intracranial arterial stenosis with an ischaemic attack within the previous 120 days) also failed to show a benefit of the intervention over best medical therapy (Chimowitz et al., 2011). Among a total of 451 patients the 30-day risk of stroke was 14.7% in those who received a stent, compared with 5.8% without.

Collectively, these trials clearly indicate that the majority of patients with atherosclerotic intracranial arterial stenosis are best managed medically. Nonetheless, there exists a minority of patients who fail to develop adequate collaterals and continue to have transient ischaemic events, or remain symptomatic with disabling physical and cognitive deficits as a consequence of cerebral hypoperfusion, despite optimal medical therapy. This group of patients should be carefully assessed for potential EC-IC bypass to prevent further stroke and provide symptomatic relief.

Moyamoya disease

MMD patients presenting with ischaemic events have a risk of the order of 15–50% of further stroke within 12 months; the clinical course of patients presenting with haemorrhage is more aggressive still. For symptomatic MMD patients, current opinion thus favours surgical intervention to reduce the risk of further stroke or

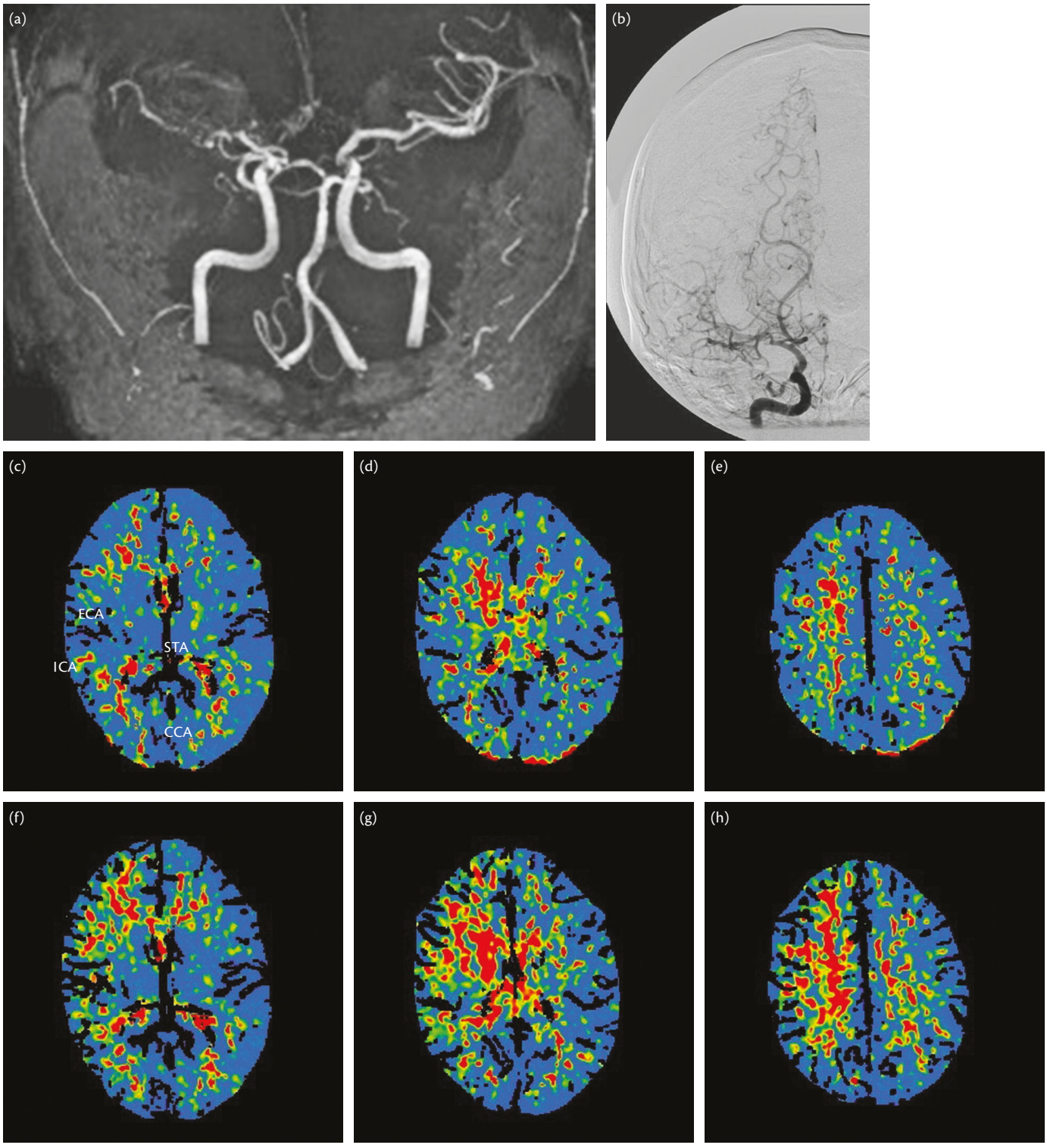

Fig. 52.1 Imaging of intracranial stenosis and cerebrovascular reserve. (A and B) Magnetic resonance angiogram and digital subtraction angiogram showing stenosis of the M1 segment of the right middle cerebral artery (arrow). (C–E) Baseline mean transit time (MTT) parameter maps of contrast-enhanced CT-perfusion imaging; minor degree of delayed perfusion within right MCA territory. (F–H) Corresponding MTT maps following administration of acetazolamide showing worsening delayed perfusion throughout the right MCA territory, indicative of exhausted cerebrovascular reserve and steal phenomenon.

haemorrhage. There are no randomized controlled trials comparing the effect of direct or indirect EC-IC bypass on further ischaemic events in MMD patients and the preferred revascularization technique remains unclear. Indirect bypass has been presumed to be the safer option but published case series suggest that the combined risk of ischaemic or haemorrhagic stroke is equivalent for both direct and indirect techniques at around 5.5%; perioperative mortality is under 1% (Kazumata et al., 2014). In contrast, the STA-MCA procedure

has superior results to indirect bypass in terms of angiographic outcomes, assessed as the extent of MCA territory that is revascularized, and is more effective at reducing the risk of recurrent stroke over the medium-term (3.5% vs. 11.2%) (Kazumata et al., 2014).

A recent small randomized controlled trial examined the efficacy of direct EC-IC bypass for the prevention of recurrent haemorrhagic events in MMD disease (Miyamoto et al., 2014). Eighty patients who had suffered a bleed within the preceding year were randomized to medical management or bilateral STA-MCA bypass. The annual risk of rebleed episodes was lower in the surgical arm (2.7% vs. 7.6%), in accordance with the findings of larger prospective observational series (Jiang et al., 2014; Miyamoto et al., 2014).

STA-MCA bypass technique

Preoperative workup

All patients should be thoroughly evaluated by a stroke physician or neurologist to confirm the diagnosis and ensure that medical management has been optimized. CT or MRI is required to establish the extent of established infarction, together with perfusion imaging sequences and acetazolamide challenge to confirm dynamic vascular steal. Catheter angiography is performed to localize the location of the stenosis/occlusion, or the grade the severity of MMD. Identifying concomitant aneurysms and other vascular malformations is imperative prior to any consideration of revascularization. It is mandatory to obtain selective external carotid injections, to assess both the degree of existing collateralization to the intracranial circulation and the patency and calibre of the STA; a minimum diameter of 1 mm is generally required. The suitability of donor and recipient arteries seen on the angiogram will influence whether a direct or indirect bypass is attempted, although the final decision is usually left until the vessels are directly inspected intraoperatively. Patients are in general recommended to continue their antiplatelet therapy perioperatively to reduce the risk of early graft occlusion.

Operative procedure

During induction of general anaesthesia there should be continuous intra-arterial monitoring to ensure a normal blood pressure is maintained; even mild hypotension may result in critical cerebral ischaemia in these vulnerable patients.

The patient is placed supine on the operating table with the head on a horseshoe head rest; a three-pin fixator can be used if preferred but is not obligatory. The course of the STA branches should be palpated or identified with a Doppler probe to plan the skin incision. A linear incision beginning in front of the tragus in the line of the main STA vessel can be used but our preference is for a Y-shaped incision with each limb following the approximate course of the STA and its terminal branches (Fig. 52.2A). It is imperative to avoid adrenaline infiltration of the planned incision as this will constrict the donor vessel; plain local anaesthetic should be carefully injected within the subcutaneous layer only.

The skin is incised and the subgaleal plane in which the STA courses is developed. The vessel is most superficial proximally at the zygoma, but it is usually preferable to identify a branch more distally in the first instance. Once the artery is identified it is dissected proximally, retaining a cuff of connective tissue, and dividing minor branches several millimetres from the vessel (Fig. 52.2B). The anterior or posterior division is chosen as the donor based on calibre and length of vessel available, and the other branch is then divided as distally as possible to allow the STA to be mobilized, retracted to one side, and protected. The intended donor vessel is maintained in continuity until the anastomosis is performed.

The temporalis is then incised and reflected, and a small craniotomy performed over the distal sylvian fissure. Under the operating microscope the cortical vessels are inspected and an appropriate recipient selected—generally the largest calibre vessel with fewest branches that affords sufficient length to allow temporary clips to be applied. The arachnoid is incised with a diamond knife and branches from the intended recipient vessel are coagulated and divided such that a segment of around 15 mm is prepared.

A contrasting piece of card is passed beneath the cortical vessel to facilitate suturing (Fig. 52.2C). Intravenous heparin (5000 IU) is administered and then the donor STA branch is divided. Good flow is confirmed and the artery is skeletonized for a few millimetres and its end and brought to the recipient vessel, ensuring it has been well mobilized to avoid tension. The STA is temporarily clipped and the anastomotic site is trapped with microclips on the recipient vessel (Fig. 52.2D). An arteriotomy is performed with the diamond knife, approximating the calibre of the STA. The end to side anastomosis is then fashioned with interrupted 10-0 nylon sutures, first inserting anchoring sutures at each corner of the arteriotomy and then completing both sides in turn with three to five sutures (**Fig. 52.2**E–H). Patency of the recipient vessel is confirmed periodically with a blunt probe. A continuous suture can be used but interrupted provides greater precision, is more easily revised if necessary, and it is better suited to adjusting for a degree of mismatch in calibre of the donor and recipient vessel.

Once the anastomosis is complete the temporary clips are sequentially removed from the cortical vessel and STA and the anastomosis is inspected. A small amount of bleeding is controlled with a haemostatic agent and gentle pressure, or if required an additional 10-0 suture can be placed. Patency and antegrade flow are confirmed with the Doppler probe and intraoperative indocyanine green angiography. A bolus of 200 ml 20% mannitol is administered to improve blood flow while the graft establishes and is monitored for 10–15 minutes prior to closure. If there is concern that either vessel or the anastomosis is occluded the unused STA branch can be employed as a vent to assess antegrade flow from the STA and retrograde flow from the cortical vessel.

The dura is approximated and the bone flap carefully replaced, ensuring the STA is not compressed as it passes over the edge of the craniotomy. Temporalis fascia, skin, and galea are closed in routine fashion.

Postoperative care

Close monitoring and control of fluid balance and blood pressure is recommended over the first 12–24 hours following surgery to avoid postoperative hypotension and ischaemia, and to try and minimize the risk of hyperaemia and brain swelling. Graft patency can be checked at regular intervals with Doppler ultrasound. Additional instructions should include strict avoidance of any pressure over the graft from, for example, elastic face masks.

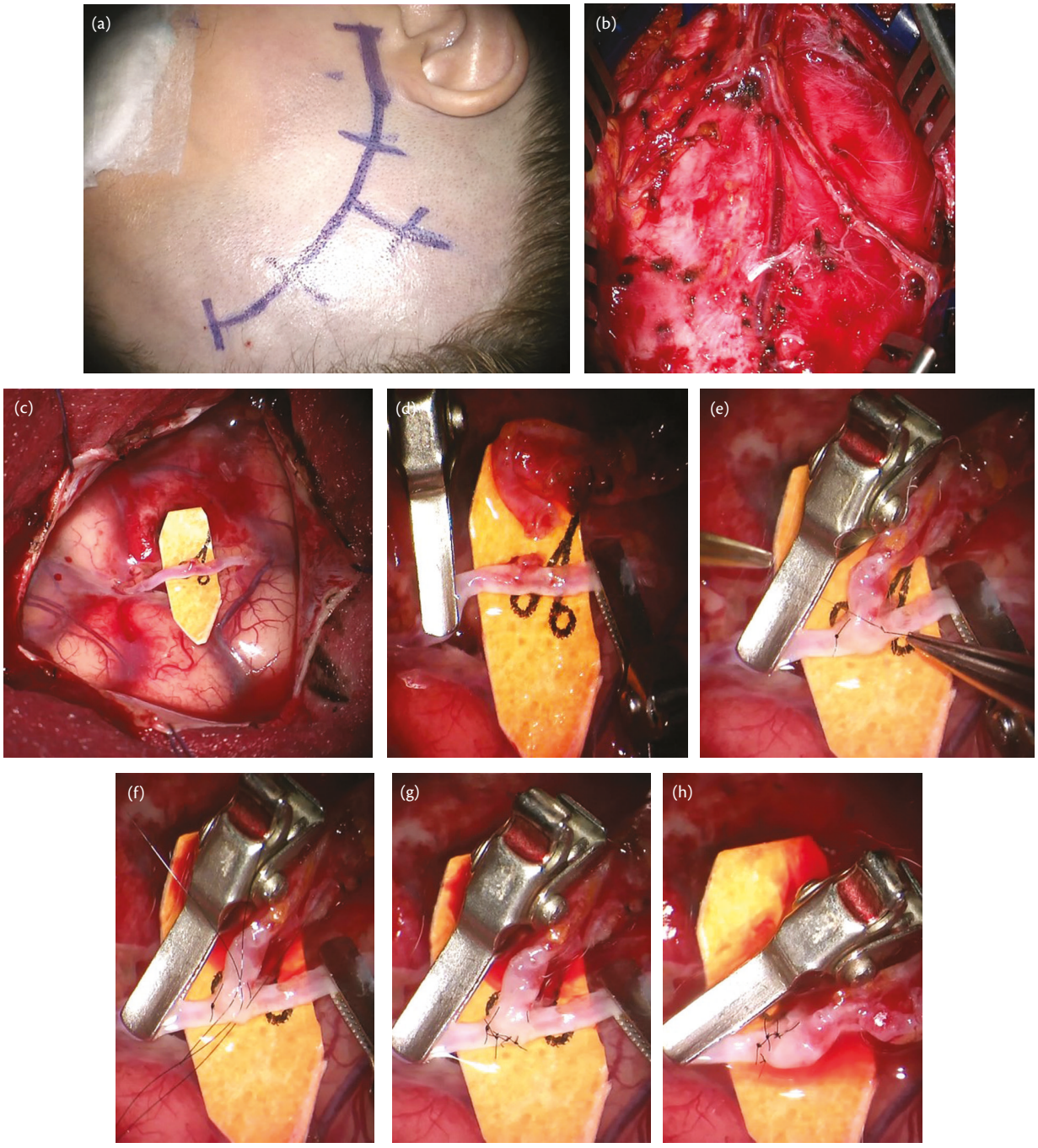

Fig. 52.2 STA-MCA anastomosis technique. (A) Skin incision along course of superficial temporal artery (STA). (B) STA branches dissected, posterior (parietal) division labelled. (C) Following craniotomy a recipient vessel is dissected and prepared. (D) Skeletonized end of STA brought alongside cortical artery and clips applied. Arteriotomy marked with dashed line. (E) Anchoring sutures at each end of the anastomosis with 10-0 nylon. (F–G) interrupted sutures placed along one side and then tied. (H) Same procedure repeated on the back wall of the anastomosis.

Conclusion

The majority of patients with atherosclerotic intracranial arterial stenosis are best managed medically but for selected patients with refractory symptoms, and demonstrable hypoperfusion on imaging, revascularization with a direct EC-IC bypass remains an important treatment option. For patients with symptomatic MMD, direct or indirect bypass effects a significant reduction in the risk of recurrent ischaemic attacks and haemorrhage. Surgery is not indicated for patients with asymptomatic stenosis due to atherosclerosis or MMD.

REFERENCES

Chater, N. (1983). Neurosurgical extracranial-intracranial bypass for stroke: with 400 cases. *Neurol Res*, **5**(2), 1–9.

Chimowitz, M.I., Lynn, M.J., Derdeyn, C.P., et al., 2011. Stenting versus aggressive medical therapy for intracranial arterial stenosis. *New Engl J Med*, **365**(11), 993–1003.

Garrett, M.C., Komotar, R.J., Starke, R.M., et al. (2009). The efficacy of direct extracranial-intracranial bypass in the treatment of symptomatic hemodynamic failure secondary to athero-occlusive disease: a systematic review. *Clin Neurol Neurosurg*, **111**(4), 319–26.

EC/IC Bypass Study Group (1985). Barnett study: failure of extracranial-intracranial arterial bypass to reduce the risk of ischemic stroke. *N Engl J Med*, **313**, 1191–200.

Grubb, R.L. Jr., Powers, W.J., Clarke, W.R., et al. (2013). Surgical results of the Carotid Occlusion Surgery Study. *J Neurosurg*, **118**(January), 25–33.

Grubb, Jr, R.L., Derdeyn, C.P., Fritsch, S.M., et al. (1998a). Importance of hemodynamic factors in the prognosis of symptomatic carotid occlusion. *JAMA*, **280**(12), 1055.

JET Study Group (2002). Japanese EC-IC Bypass Trial (JET Study). *Surgery for Cerebral Stroke*, **30**(6), 434–7.

Jiang, H., Ni, W., Xu, B., et al. (2014). Outcome in adult patients with hemorrhagic moyamoya disease after combined extracranial-intracranial bypass. *J Neurosurg*, **121**(5), 1048–55.

Kazumata, K., Ito, M., Tokairin, K., et al. (2014). The frequency of postoperative stroke in moyamoya disease following combined revascularization: a single-university series and systematic review. *J Neurosurg*, **121**(2), 432–40.

Lanfranconi, S., Locatelli, F., Corti, S., et al. (2011). Growth factors in ischemic stroke. *J Cell Mol Med*, **15**(8), 1645–87.

Miyamoto, S., Yoshimoto, T., Hashimoto, N., et al. (2014). Effects of extracranial-intracranial bypass for patients with hemorrhagic moyamoya disease: results of the Japan Adult Moyamoya Trial. *Stroke*, **45**(5), 1415–21.

Patel, H.C., McNamara, I.R., Al-Rawi, P.G., & Kirkpatrick, P.J. (2010). Improved cerebrovascular reactivity following low flow EC/IC bypass in patients with occlusive carotid disease. *Br J Neurosurg*, **24**(2), 179–84.

Powers, W.J., Clarke, W.R., Grubb, R.L. Jr., et al., (2011). Extracranial-intracranial bypass surgery for stroke prevention in hemodynamic cerebral ischemia: the Carotid Occlusion Surgery Study randomized trial. *JAMA*, **306**(18), 1983–92.

Schmiedek, P., Piepgras, A., Leinsinger, G., Kirsch, C.M., & Einhüpl, K. (1994). Improvement of cerebrovascular reserve capacity by EC-IC arterial bypass surgery in patients with ICA occlusion and hemodynamic cerebral ischemia. *J Neurosurg*, **81**(2), 236–44.

Sundt, T.M., Whisnant, J.P., Fode, N.C., Piepgras, D.G., & Houser, O.W. (1985). Results, complications, and follow-up of 415 bypass operations for occlusive disease of the carotid system. *Mayo Clin Proc*, **60**(4), 230–40.

Yasargil, M.G., Krayenbuhl, H.A., & Jacobson, J.H., 1970. Microneurosurgical arterial reconstruction. *Surgery*, **67**(1), 221–33.

53

Giant aneurysms and bypass surgery

Mario Teo, Omar Choudhri, and Michael Lawton

Introduction

Giant intracranial aneurysms are defined as lesions with the largest diameter of 2.5 cm or more, according the Cooperative Study of Intracranial Aneurysms and Subarachnoid Haemorrhage, and constitute 2–5% of all cerebral aneurysms (Locksley, 1966; Sughrue et al., 2011). They remain among the most difficult cerebrovascular lesions to treat.

The natural history of giant aneurysms is universally poor. Drake reported a mortality of 68% at 2 years and 80% mortality at 5 years in his series of giant aneurysms treated conservatively (Drake, 1979). Therefore, a conservative strategy is not appropriate in the majority of cases, particularly in the younger age group. In older series, direct surgical clipping or clip reconstruction was favourable in up to 30% and 50% of patients with posterior and anterior circulation giant aneurysms, respectively. With improvement in skull base approaches, microsurgical techniques, and neuroanaesthesia, contemporary series showed that up to two third of giant aneurysms can be directly clipped or clip reconstructed (Darsaut et al., 2011; Sughrue et al., 2011). Furthermore, steady advances in endovascular techniques have allowed endovascular treatment of giant aneurysms, with or without adjunctive techniques such as stents or balloon assistance, and more recently with flow diversion devices.

Despite significant progress, currently the best data and reported outcomes for the safe and complete obliteration of giant aneurysms remain those from surgical series (**Table 53.1**, from Sughrue et al., 2011).

Pathology and pathophysiology

Saccular aneurysms are the most common subtype of giant aneurysm, with approximately 60–70% in the anterior circulation (in the cavernous, paraclinoid, and carotid bifurcation regions of the internal carotid artery (ICA), the proximal MCA portion, the anterior cerebral artery (ACA)/anterior communicating artery (ACoA), in decreasing frequency.) Posterior circulation aneurysms are located at the basilar apex, midbasilar artery, vertebral artery, vertebrobasilar junction, and rarely on the posterior inferior cerebellar artery (PICA) and anterior inferior cerebellar artery (AICA). Other types of giant aneurysms include fusiform or serpentine subtype, with dissection as the postulated aetiology, and infectious subtype. The rupture rate for fusiform aneurysms is believed to be low and their angiographic progression is unpredictable.

The pathological basis for intracranial aneurysm formation is poorly understood, and is covered elsewhere. After giant aneurysm formation, pulsatile and irregular blood flow within the aneurysm exerts force on the diseased wall, causing the aneurysmal sac to distend, thin out, and grow. Thrombus formation and remodelling of the luminal surface of the endothelium occurs in an attempt to repair the aneurysm. However, ongoing chronic, irregular, pulsatile flow impairs the healing process and results in disorganized collagen deposition, atherosclerotic degeneration of the wall, thrombus formation of varying ages, and dystrophic calcification. Consequently, giant aneurysms are dynamic lesions with cyclical cascades of thrombus formation and resolution.

Clinical presentation

Unlike small cerebral aneurysms, patients with giant aneurysms frequently (60–80%) present with thromboembolic events or symptoms related to neurovascular compression caused by mass effect, which is especially true of posterior circulation aneurysms that occupy the small volume of the posterior fossa. Aneurysmal rupture causing subarachnoid or intraparenchymal haemorrhage is a less likely presentation (20–30% of cases), with a worse outcome than mass effect (Hamburger et al., 1992). Rapid aneurysmal growth (frequently caused by acute thrombosis) can present with severe headaches resembling an acute bleed. Other presentations that occur more rarely include seizures (usually caused by MCA aneurysm) and hemiparesis.

Table 53.2 correlates the symptoms of mass effect with giant aneurysm location.

Investigations and pretreatment workup

Historically, plain skull radiography was used to diagnose giant aneurysms as they are calcified (20% of cases), and can remodel the skull base including the sella (Pia and Zierski, 1982). Computed tomography (CT) and CT angiography allowed for measurement of aneurysm size, parent vessel calibre, assessment of its relation with skull base anatomy, and visualization of thrombosed and calcified aneurysmal contents.

Table 53.1 Published experiences with surgical and endovascular treatment of giant aneurysms.

Author	Year	Patients n	Complete Occlusion n	Complete Occlusion %	Bypass n	Bypass %	Excellent/ Good %	Fair/ Poor %	Mortality %	Morbidity %	F/U (y)	Retreatment %	Rehemorrhage %
Endovascular coiling													
Higashida[39]	1990	39	24%	62	0/39	NA	NA	NA	NA	NA	0.5	NA	NA
Gobin[1]	1966	9	5/9	56	0/9	100	0	0	11	0.5	33	0	
Tateshima[45]	1999	28	17/28	61	0/28	73			18	3.3	82	4	
Hallacq[46]	2002	5	1/5	20	0/5	60	20	20	20	1.0	0	0	
Sluzewski[44]	2003	29	5/29	17	0/29	75	4	21	10	3.1	55	7	
Henkes[38]	2004	47	10/47	21	0/47	NA	NA	NA	NA	NA	NA	NA	
Kolasa[20]	2004	7	4/7	57	0/7	85	14	0	NA	NA	NA	NA	
Murayama[48]	2006	33	19/77	25	0/33	NA	NA	NA	NA	NA	NA	NA	
Jahromi[40]	2008	39	14/39	36	0/39	63	8	29	20	1.3	54	5	
Shi[43]	2009	9	9/9	100	6/9	78	11	11	11	1.0	0	0	
Lylyk[41]	2009	8	4/6	67	0/8	NA	NA	NA	0	0.5	0	0	
Mircorsugical clipping													
Peerless, Drake[47]	1990	118	97/ 118	82	0/118	58	26	14	NA	NA	NA	NA	
Kodama, Suzuki[48]	1982	49	NA	NA	NA	61	16	22	NA	NA	NA	NA	
Yasargil[37]	1984	30	26/30	87	6/30	67	23	10	NA	NA	0	0	
Hosobuchi[49]	1985	82	80/82	98	15/82	84	9	7	38	10.0	0	0	
Heros[50]	1986	25	25/25	100	NA	72	12	16	NA	NA	NA	NA	
Sundt[51]	1990	315	310/ 315	98	81/315	80	6	15	NA	NA	NA	NA	
Ausman[31]	1990	62	62/62	100	23/62	84	11	5	NA	NA	NA	NA	
Tamaki[29]	1991	4	4/4	100	0/4	100	0	0	0	NA	NA	NA	
Lawton, Spetzler[6]	1995	136	132/ 136	97	40/136	85	9	6	11	2.2	1	0	
Shibuya, Sugita[36]	1996	29	NA	NA	NA	84	7	8	NA	NA	NA	NA	
Kattner[19]	1998	29	29/29	100	1/29	87	10	3	20	7.0	0	0	
Samson[26]	1999	44	NA	94	NA	NA	NA	NA	NA	0.5	0	0	
Lawton[22]	2002	28	28/28	100	1/28	75	11	14	5	1.6	0	0	
Jafar[18]	2002	29	29/29	100	29/29	93	3	3	10	5.0	0	0	
Lozier[23]	2004	19	6/16	38	2/19	36	47	16	89	7.4	0	0	
Gonzales[32]	2004	8	8/8	100	1/8	63	38	0	50	1.0	0	0	
Kolasa[20]	2004	13	13/13	100	0/13	76	23	0	NA	NA	NA	NA	
Krisht[21]	2007	11	11/11	10	0/11	88	12	2	27	0.5	0	0	
Hauck[17]	2008	62	56/62	90	9/62	68	32	15	42	1.0	0	3	
Sharma[28]	2008	181	106/ 118	90	11/181	86	5	9	12	NA	0	0	
Cantore[15]	2008	99	99/99	10	41/99	89	3	8	3	8.5	1	1	
Xu[30]	2009	51	51/51	100	0/51	84	14	2	NA	0.5	NA	NA	
Sano[27]	2010	109	109/ 109	100	0/109	63	16	22	4	NA	0	0	
Sughrue (current study)	2010	140	118/ 140	84	52/140	80	7	13	10	1.9	1	1	
Combined endovascular-surgical treatment													
Hacein-Bey[16]	1998	5	4/5	80	1/5	80	20	0	0	1.9	0	0	
Arnautovic[14]	1998	8	8/8	10	0/8	87	13	0	13	2.0	0	0	
Ponce[25]	2004	8	NA	NA	5/8	76	0	25	38	1.5	0	0	

[a]F/U, follow-up; NA, not available.

Reproduced with permission from Sughrue, Michael E.; Saloner, David, Rayz, Vitaliy L.; Lawton, Michael T. Giant Intracranial Aneurysms: Evolution of Management in a Contemporary Surgical Series, *Neurosurgery*, Volume 69, Issue 6, pp. 1261– 70, Copyright © 2011 Oxford University Press and the Congress of Neurological Surgeons (CNS).

Table 53.2 Aneurysm location and symptoms caused by mass effect

Aneurysm location	Presenting mass-effect symptoms and signs
Anterior circulation	Visual deficits
Cavernous ICA	Retro-orbital headache
	Diplopia
	Facial sensory loss
	Hypopituitarism (occasional)
	Epistaxis (rarely)
Ophthalmic or paraclinoid ICA	Ipsilateral retro-orbital headache
	Decreased visual acuity
	Asymmetric visual field defects
Carotid bifurcation	Visual field defects (Homonymous hemianopia)
	Hemiparesis
	Seizures
	Hypopituitarism (rarely)
MCA	Seizures
	Hemiparesis
ACA-ACoA	Visual field defects (bitemporal hemianopia)
	Decreased visual acuity
	Hormonal changes (hypothalamic compression)
	Personality changes
Basilar trunk	Diplopia
Vertebrobasilar junction	Facial sensory loss
PICA	Speech, swallowing difficulty
	Lower cranial nerve deficit
	Gait instability
	Cerebellar symptoms
	Long tract signs

Source data from Kalani MYS, Spetzler RF. Giant Aneurysm. In: Spetzler RF, Kalani MYS, Nakaji P. 2015. Neurovascular Surgery. 2nd Edn. Thieme Publishers.

MRI on the other hand, visualizes the giant aneurysm and its relationship with brain parenchyma and associated perilesional oedema that can be caused by rapid aneurysmal growth or acute thrombosis. The characteristic onion-ring appearance of laminated, intervening layers of hemosiderin and methaemoglobin can also be appreciated within the thrombus of a giant aneurysm.

Six vessel digital subtraction angiography is the gold standard for obtaining anatomical information including parent vessel anatomy, aneurysm morphology, associated perforating vessels, feasibility of vessel occlusion, evaluation of bypass options, and both intracranial—intracranial and extracranial—intracranial collaterals. To assess for vascular reserve, balloon test occlusion (BTO), including Allcock's test (ipsilateral carotid compression during vertebral artery injection) and hypotensive challenge, can be incorporated as required. Hypotensive challenge consists of lowering mean arterial pressure with nitroprusside drip by 20 mmHg, or 25% of mean arterial pressure, whichever is greater.

Taking into account of all these informative radiological studies and including the patient's neurological condition, medical comorbidities, predicted treatment risks, local expertise, and preferences of the patient and family, the best treatment strategy can be made on an individual basis in conjunction with the multidisciplinary team, which includes endovascular surgeons, interventional neuroradiologists, and neurovascular neurologists.

Surgical strategies

For surgical patients not suitable for direct clipping of the aneurysm neck, it is necessary to use other techniques to exclude the aneurysm. A good strategy is to induce flow reversal by sacrificing the diseased vessel either proximal or distal to the aneurysm, while providing a bypass graft to revascularize the distal territory (**Figs. 53.1** and **53.2**). In general, high-flow bypass is used in patients who fail BTO, and low-flow bypass for patients who fail BTO after hypotensive challenge. *In situ* bypass strategies are used for aneurysms in specific locations without the need to redirect flow from the extracranial circulation. Such techniques have been reported in the paired ACA and PICA vessels, as well as the *in situ* temporal artery to M2 bypasses for treatment of giant aneurysms in the corresponding locations (Bederson and Spetzler, 1992; Sanai et al., 2009).

Procedures such as deep hypothermic circulatory arrest for clipping of giant basilar apex and MCA aneurysms are associated with high risk and have given way to safer alternative approaches such as adenosine arrest (transient AV blockade), rapid ventricular pacing and proximal occlusion with bypass (Sughrue et al., 2011). Both adenosine and rapid ventricular pacing cause transient hypotension that decreases the tension in the aneurysm allowing safe manipulation and clipping.

Extracranial-intracranial bypass surgery

Choosing the type of graft

In general, when major parent vessel occlusion is anticipated, 'low-flow' vessels (which typically provide flows of 25–30 ml/min) such as the superficial temporal artery (STA) or occipital artery (OA) are not sufficient to revascularize a whole hemisphere. In this situation, 'higher flow' vessels such as radial artery (50–150 ml/min) or saphenous vein (100–200 ml/min) are required. Apart from flow requirement, the graft selection also depends on graft availability, size of the recipient vessels, and the preference of the surgical team.

Radial artery grafts are prone to severe vasospasm, but this problem can be overcome by the judicious use of pressure distention and soaking in papaverine (Mohit et al., 2007). The advantages of the radial artery graft include less of a size mismatch between the graft and the recipient vessel, and therefore it is an easier anastomosis technically and causes less turbulent flow at the anastomotic site (Houkin et al., 1999; Mohit et al., 2007; Kocaeli et al., 2008).

Saphenous vein graft (SVG), on the other hand is easier to harvest, supports greater flow, and is not prone to significant spasm. However, the size mismatch and the fragile endothelium could cause a more challenging distal anastomosis. Reversal of the vein graft with disruption of the venous valvar system can mitigate against size mismatch however it risks thrombosis secondary to endothelial disruption.

Choice of donor vessel

Generally, in high-flow bypass, the external carotid artery (ECA) distal to the carotid bifurcation is the preferred donor vessel.

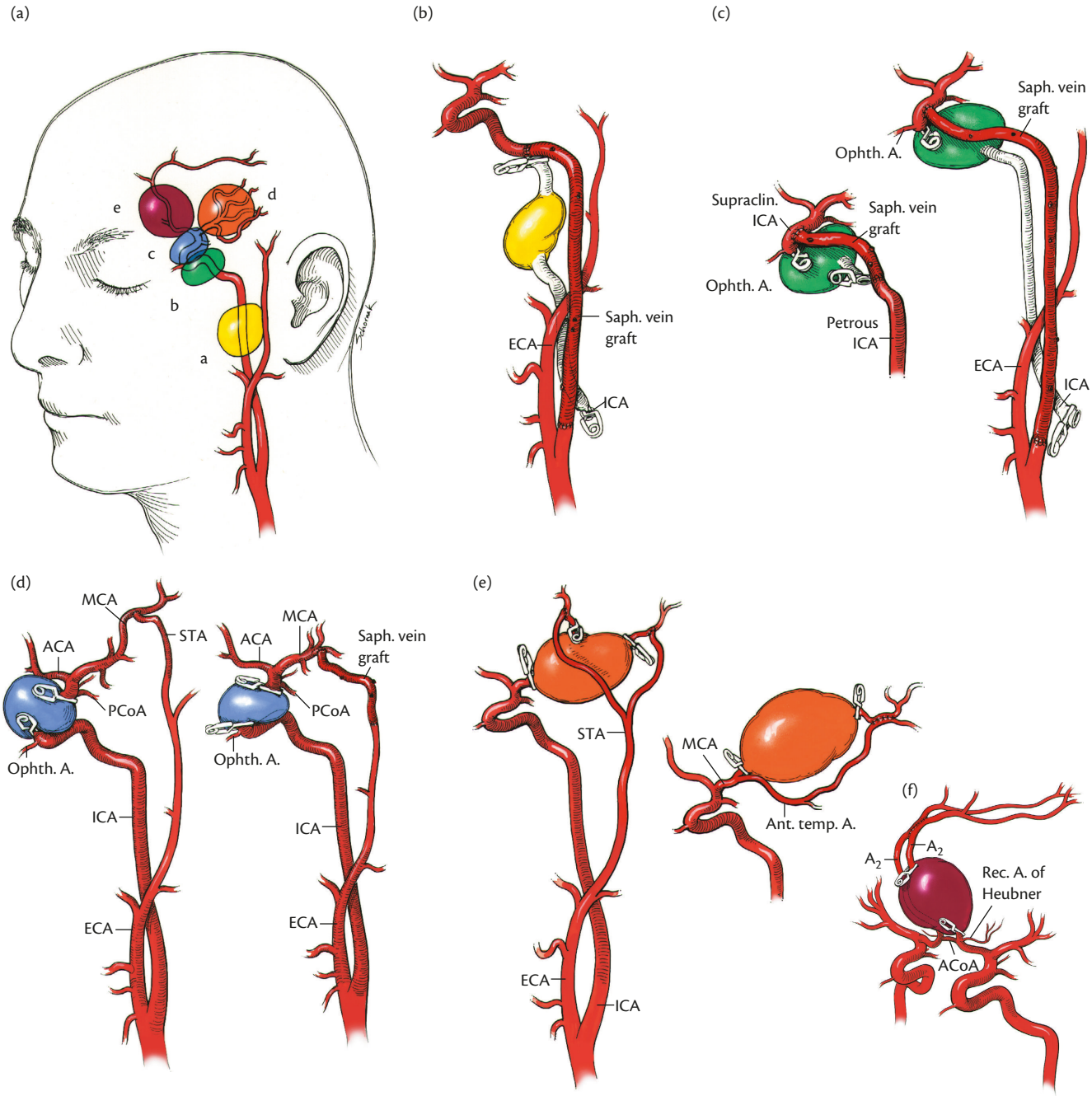

Fig. 53.1 (A) Schematic drawings of techniques for revascularization of the anterior circulation. (B) Internal carotid artery (ICA) aneurysms at the cranial base can be trapped and revascularized with a cervical-to-petrous carotid bypass using a saphenous vein graft. (C) Cavernous ICA aneurysms can be trapped with a petrous-to-supraclinoid (C3-C5) carotid bypass using a saphenous vein graft or, alternatively, a cervical-to-supraclinoid carotid bypass. (D) Supraclinoid ICA aneurysms can be trapped with a superficial temporal artery-to-middle cerebral artery (STA-MCA) bypass. An alternative strategy is to use an STA-MCA bypass with a saphenous vein interposition graft. (E) MCA aneurysms can be trapped and revascularized with a double-barrel STA-MCA bypass. Alternatively, an anterior temporal artery-to-MCA *in situ* bypass may be used for select aneurysms. (F) Anterior cerebral artery aneurysms can be trapped and revascularized with an A2-A2 *in situ* bypass. ACA, anterior cerebral artery; ACoA, anterior communicating artery; Ant. temp. A., anterior temporal artery; ECA, external carotid artery; MCA, middle cerebral artery; Ophth. A., ophthalmic artery; PCoA, posterior communicating artery; Rec. A. of Heubner, recurrent artery of Heubner; Saph., saphenous; supraclin., supraclinoid.
Courtesy of Barrow Neurological Institute, reprinted with permission.

Avoiding the ICA is important because clamping the ICA during anastomosis can cause cerebral ischaemia, particularly in patients who have already failed BTO and therefore do not tolerate ICA occlusion. If the ECA cannot be used due to anatomical variations or inaccessibility, a common carotid artery anastomosis might be necessary that permits ECA-to-ICA collateral flow during the anastomosis.

In low-flow bypass, depending on the proximity of the recipient vessels, the choices include STA vessel (frontal or parietal branch), OA, and posterior auricular artery (PAA).

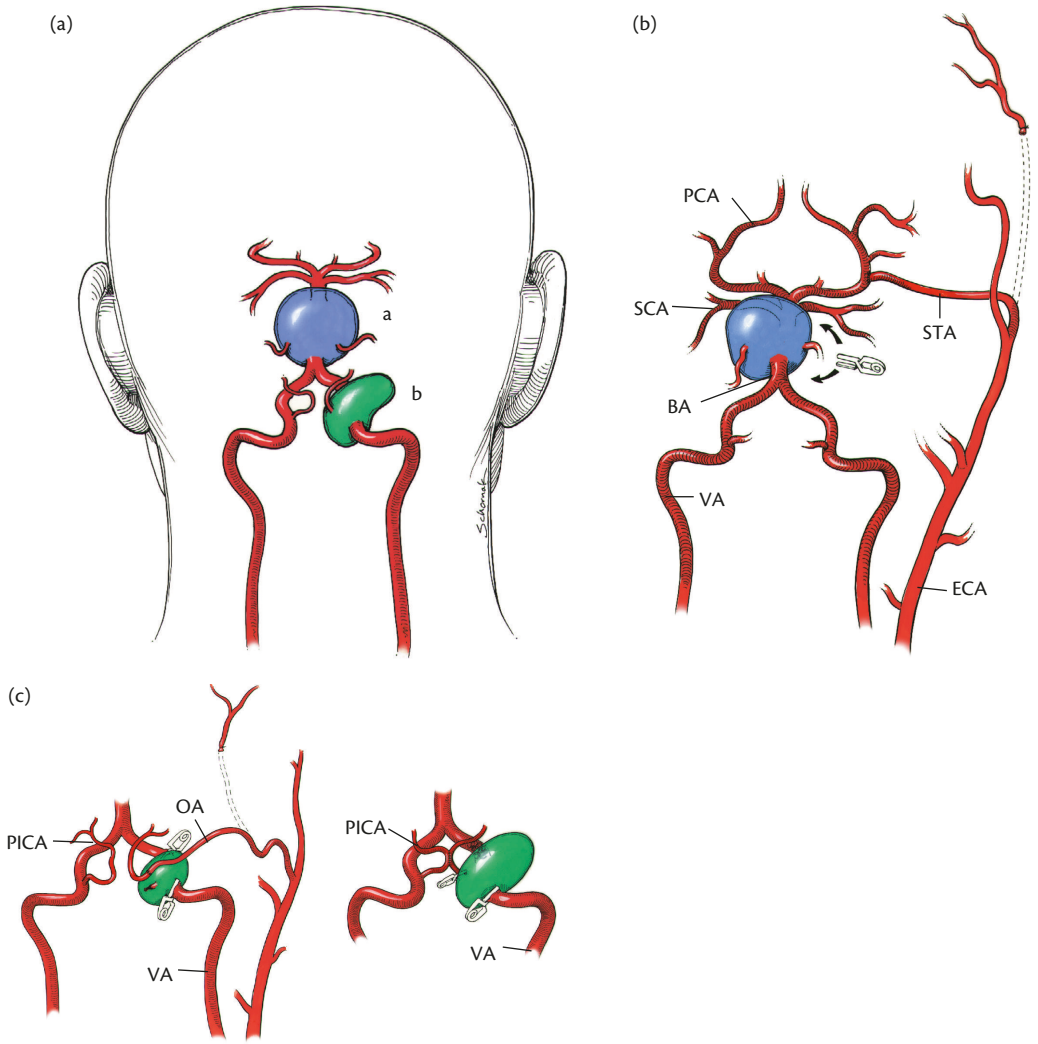

Fig. 53.2 (A) Schematic drawings of techniques for revascularization of the posterior circulation. (B) The midbasilar artery can be occluded proximally or distally to the aneurysm and revascularized with a superficial temporal artery (STA)-to-posterior cerebral artery (PCA) bypass or an STA-to-superior cerebellar artery (SCA) bypass. We prefer to occlude the basilar artery in the perforator-free zone below the SCAs. In select cases a double-barrel bypass using the STA as a donor to PCA and SCA may be used to revascularize the brainstem. (C) Vertebral artery aneurysms can be trapped by placing clips on the proximal vertebral artery and at the origin of the posterior inferior cerebellar artery (PICA). Endovascular coils can be placed distally in the vertebral artery. A PICA-PICA *in situ* bypass is used for revascularization of the distal territories. Alternatively, an occipital artery (OA)-to-PICA bypass can be performed. BA, basilar artery; ECA, external carotid artery; OA, occipital artery; PCA, posterior cerebral artery; PICA, posterior inferior cerebellar artery; SCA, superior cerebellar artery; VA, vertebral artery

Courtesy of Barrow Neurological Institute, reprinted with permission.

High-flow extracranial-intracranial bypass for the anterior circulation

The technical aspects of low-flow bypass are covered elsewhere, therefore we will concentrate on high-flow bypass in this section, and illustrate the surgical steps with a case example (Fig. 53.3).

The operation is performed under general anaesthesia with neuromonitoring, mild hypothermia (33–34°C), urinary catherization, central and arterial line (to ensure optimal fluid management).

The patient is supine, head fixed in Mayfield head holder, shoulder roll placed under the ipsilateral shoulder, and head rotated to the contralateral side to ensure the cranial operative field lies parallel to the floor.

Cranial exposure

A pterional craniotomy is fashioned after curved hairline incision with myocutaneous scalp flap, and flattening of the sphenoid wing. The dura is then tacked up and opened based on the sphenoid wing. Under microscopic guidance, the Sylvian fissure is split widely to identify an M2 branch of the MCA, as the M1 branch is generally avoided to minimize injury to lenticulostriate perforating arteries. The appropriately sized M2 segment is chosen as the recipient vessel, and the vessel dissected free of arachnoid adhesions. A piece of high-visibility background material is passed beneath the recipient vessel. We typically utilize suction microtubing under the background material to keep the field clear of irrigation and bleeding (Fig. 53.3A).

Cervical exposure

A transverse neck crease incision at the level of the hyoid bone is made to expose the carotid bifurcation. Alternatively, a longitudinal incision along the anterior border of sternocleidomastoid can be used, especially where the carotid bifurcation is difficult to expose. Medial to the sternocleidomastoid, the deep cervical fascia and carotid

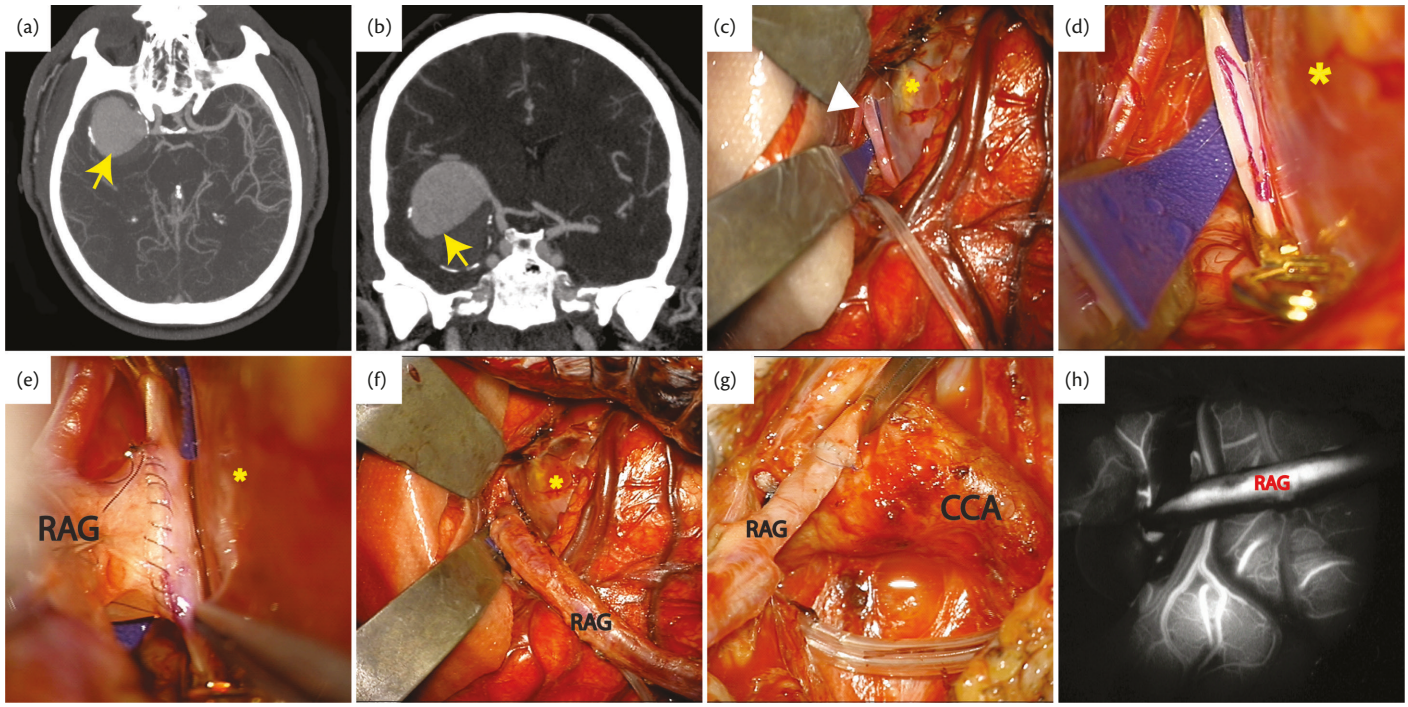

Fig. 53.3 Anterior circulation high-flow ECA-RAG-MCA bypass. A 36-year-old male presented with subarachnoid haemorrhage from a giant partially thrombosed right MCA aneurysm as seen on axial and coronal computed tomography angiography (CTA) reconstructions (yellow arrow in image A and B). (C) A right pterional craniotomy was completed followed by a trans-Sylvian approach to expose the M2 branch outflow vessel (white arrowhead) and the aneurysm dome (yellow asterisk). (D) Magnified right trans-Sylvian view showing the M2 branch arteriotomy being prepared as recipient vessel for radial artery graft (RAG). (E) Anastomosis suture line between RAG and M2 within the Sylvian fissure. (F) Trans-Sylvian dissection showing the RAG in relation to aneurysm dome (yellow asterisk). (G) Proximal anastomosis suture line in the neck between external carotid artery and RAG. Common carotid artery (CCA) is seen proximal to the bifurcation. (H) Intraoperative Indocyanine Green Angiography (ICG) following completion of bypass demonstrates filling of RAG and MCA territory. The aneurysm was subsequently trapped and dome thrombectomy completed.

sheath are opened to expose the carotid artery, and up to 2 cm of the ECA beyond the carotid bifurcation to prepare for an end to side anastomosis of donor graft to ECA. This allows for enough room to create the bypass after the application of temporary vascular clamps.

Donor graft harvest

In harvesting the SVG, we routinely check that the patient does not have varicosities or previous surgery that have compromised the saphenous vein. At the time of surgery, the vein is dissected from the ankle (medial malleolus) to the knee for 20–25 cm. Alternatively, the femoral artery is identified in the groin and the femoral vein is found medial to it, from which the saphenous vein is located. It can then be dissected distally towards the knee to harvest a long interposition graft. During the mobilization procedure all side branches are ligated or clipped, ensuring that this does not stenose or compromise the lumen. After the cranial and cervical sites are fully exposed, prepared, and haemostasis ensured, the SVG is ligated, divided, and flushed with heparinized saline. This serves to clear the lumen of blood clots and serves as a pressure test for the ligated side branches. The adventitia and connective tissue are cleaned for approximately 1–2 cm on either end of the SVG to facilitate for anastomosis. The valves in the graft are broken down by passing a series of disc dissectors, and the patency of SVG confirmed by heparinized saline flush in both directions. Alternatively, the direction of the graft can be reversed (ankle or knee end for proximal cervical anastomosis) to ensure that flow courses in the direction of the valves, which eliminates the need for valvulotomies that might damage the intimal lining and are thrombogenic.

Radial artery harvest

Radial artery graft (RAG) is an excellent option as an interposition graft given good size match with the donor and recipient vessels. While an endoscopic technique has been described, we prefer an open approach. An important prerequisite before proceeding to use a RAG, is to complete a modified Allen's test to assess ulnar collateral circulation in the hand. A curvilinear skin incision 1 cm proximal to wrist crease and 1 cm distal to elbow crease is used, centred over the radial pulse by palpation or hand-held Doppler. Brachioradialis and flexor carpi radialis muscles with their fascia form the space for the radial artery. The fascia is divided to expose the radial artery in loose areolar tissue. Once the fascial plane of the radial artery is entered, the dissection is carried proximal to distal. The artery is dissected as a pedicle along with its venae comitans. A sponge soaked in papaverine is laid over the segment of the radial artery (RA) not being addressed. The radial artery is harvested below the take off for the recurrent radial artery and proximal to the take off for the superficial palmer artery distally. The side branches encountered are managed with Weck clips and electrocautery and handling of the RA is minimized. The graft is marked with blue ink to indicate the proximal and distal ends. Once dissected the radial artery is ligated proximally and distally with a heavy silk tie and transected. The proximal radial artery is then flushed with heparinized solution (2500 U of heparin in 250 cc saline and 60 mg papaverine) using an olive tipped syringe cannula as a pressure test.

Pre- or postauricular tunnel

This should be created early on to allow subcutaneous ooze to settle, by passing a pair of Roberts forceps in the pre- or postauricular tunnel.

We routinely use a chest tube passed with a Kelly clamp from the craniotomy opening to the cervical opening. The graft is then passed through the chest tube to protect it from stretching or kinking. The chest tube conduit is then removed once the graft is passed. Enough subcutaneous dissection is required to avoid graft compression. The bypass graft is delivered after cranial anastomosis, but prior to temporary clip removal. The deflated graft is delivered with enough tension to ensure no redundant intracranial loop, and no graft kinking or twisting.

Anastomoses

Prior to applying the temporary clips to the MCA vessel, MAP is raised slightly to 90 mmHg (to optimize flow in the collateral circulation), hypothermia of 33–34°C is maintained, and propofol is titrated to achieve burst suppression. Arteriotomy is made in the recipient MCA (Fig. 53.3B), and the lumen is flushed with heparinized saline. The graft and recipient vessels are tinted with indigo-carmine or a sterile marking pen to better visualize the arteries during the microanastomosis. Monofilament sutures (10-0 or 9-0) are used to anchor the apices of the incision, heel stitch first, followed by the toe stitch. The side walls of the anastomosis are sutured in a continuous or an interrupted fashion, also using 10-0 monofilament sutures (Fig. 53.3C). We prefer a continuous technique to allow improved apposition and size match corrections.

Sutures should be passed from outside the donor to inside the recipient or outside the recipient to inside the donor, and then tied on the outer surface of the anastomosis. Great care must be taken not to catch the back wall of the vessel while suturing the anastomosis. The clamp time for the creation of microanastomosis should be as short as possible. Once the anastomosis is complete, the temporary clips on the recipient artery are released, with expected minor blood leakage around the anastomotic site.

Back bleeding of the graft is important to perfuse the graft endothelium to minimize the effects of ischaemia. After this, heparinized saline is introduced into the free end of the graft and irrigation provided while an aneurysm temporary clip is applied close to the MCA anastomosis site.

Following that, the ECA anastomosis is performed with continuous or interrupted (9-0 prolene) suture in an end to side fashion on the ECA (Fig. 53.3D). Artery slings can be used to present the ECA more favourably into the wound as the depth of the vessels increases the surgical challenge for anastomosis. After applying temporary clips on the proximal and distal ECA, an oval arteriotomy is created. The SVG is cut to size (to minimize excessive kinks and redundant loops), fish mouthed, and the anastomosis proceeds as described for the intracranial stage.

After completion of the bypass, the temporary clip on the distal graft is released to reconfirm back filling, followed by ECA clamps removed to establish anterograde flow in the graft. Adequacy of treatment and patency of parent vessels is analysed intraoperatively using intraoperative angiography, indocyanine green fluorescence videoangiography, Charbel Transonics flow probe, and/or Doppler flow measurements (Fig. 53.3E).

Closure and postoperative care

Multilayer wound closure of both cranial and neck wound proceeds with meticulous attention to haemostasis, and graft patency is monitored during bone flap replacement, temporalis opposition, and final skin closure. Postoperatively external bypass graft compressions from facemask elastic need to be avoided, and the patient managed in the ICU with strict instructions for euvolaemia and normotension. The graft is monitored regularly with hand-held Doppler.

The patient would then have occlusion of the ipsilateral parent vessel endovascularly either under the same anaesthesia, with angiographic confirmation of bypass graft patency or in a delayed manner within a few days. Long-term surveillance of bypass graft and the underlying giant aneurysm should follow a local management guideline.

High-flow extracranial to intracranial bypass in the posterior circulation

Posterior circulation giant aneurysms can be particularly challenging given their difficult access. While clip reconstruction can be used in some selected giant posterior circulation aneurysms, surgical revascularization with trapping may often be needed (Patel and Kirkpatrick, 2009). The posterior cerebral artery (PCA), superior cerebellar artery (SCA), and PICA are the usual recipient vessels, and STA or OA is used as a donor for many of these bypasses. While the OA is a robust donor vessel, it may not have sufficient flow to supply the entire posterior circulation. In addition, the length afforded by the OA may not be enough to reach the depths of the posterior fossa. Pisapia et al. examined the contemporary literature on posterior circulation bypasses and found 34 cases of high-flow bypasses for posterior circulation complex aneurysms. Twelve of these cases were done using RAG while the remaining 22 using SVG (Pisapia et al., 2011). Vertebral artery V3 segment and ECA were the most common donor vessels and over the long term, the reported graft patency rate was 95%. For some of the giant dolichoectatic posterior circulation aneurysms, flow reversal or flow reduction therapies with EC-IC and IC-IC bypasses may provide the best therapy, with the MCA-PCA bypass with a RAG being the preferred technique for revascularizing the distal basilar circulation (Lawton et al., 2016) (Fig. 53.4).

Outcome of surgical treatment

Comparing the outcome of surgical series for the treatment of giant intracranial aneurysms, the most recent literature have reported improved patient outcomes (Table 53.1), and an increasing use of bypass techniques plus indirect giant aneurysm occlusion. In the senior author's own experience, during a 13-year period, 140 patients with 141 giant aneurysms were treated surgically. One hundred aneurysms (71%) were located in the anterior circulation, and 41 aneurysms were located in the posterior circulation. 46% of the aneurysms were treated directly with neck clipping, and 51% were treated indirectly with parent artery occlusion, and bypass was used in 38% of cases. 108 aneurysms (77%) were completely occluded, 14 aneurysms (10%) had minimal residual aneurysm, and 16 aneurysms (11%) were incompletely occluded with reversed or diminished flow. Surgical mortality was 13%, and 9% permanent neurological morbidity. Bypass-related complications resulted from bypass occlusion (7 patients), aneurysm haemorrhage due to incomplete aneurysm occlusion (4 patients), or aneurysm thrombosis with perforator or branch artery occlusion (4 patients). Overall, with a mean follow-up of 2 years, good outcomes were observed in 114 patients (81%), and 109 patients (78%) were improved or unchanged after therapy (Sughrue et al., 2011).

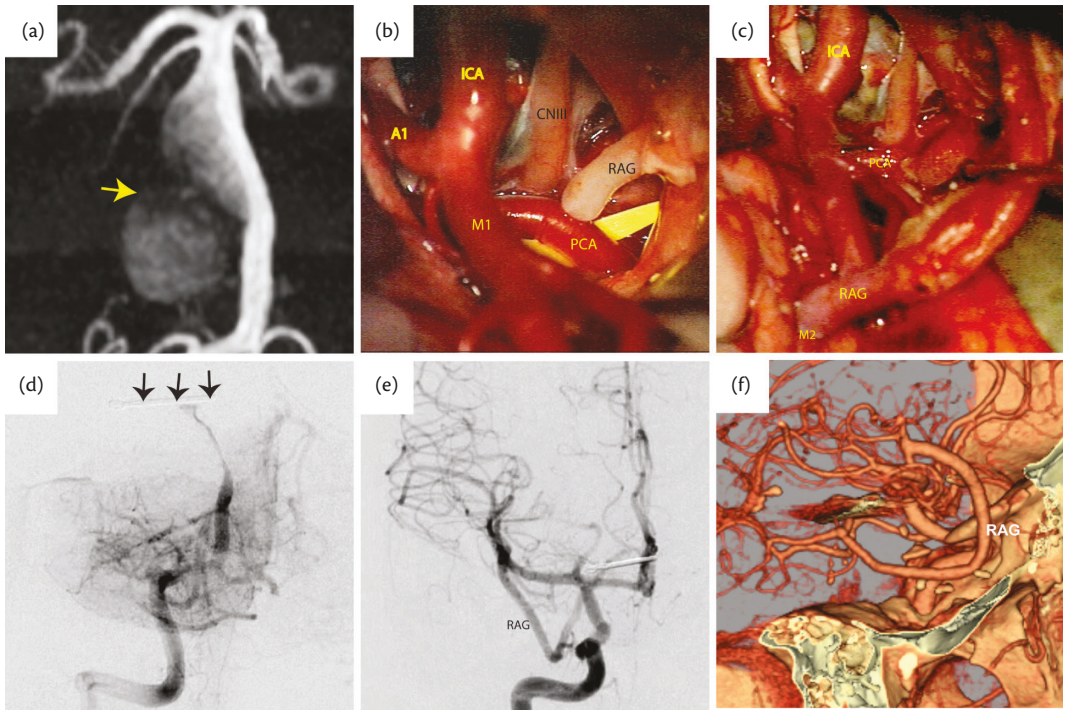

Fig. 53.4 Posterior circulation high-flow MCA-RAG-PCA bypass. A 44-year-old male presented with a giant partially thrombosed basilar trunk aneurysm (arrow in A). The patient was treated with a right orbitozygomatic craniotomy followed by an MCA to PCA bypass using a radial artery interposition graft (RAG) and aneurysm outflow occlusion proximal to SCA origin. (B) A right trans-Sylvian exposure with expansion of the carotid oculomotor triangle and anastomosis between PCA and RAG completed. Structures in the surrounding such as ICA, A1, M1 and oculomotor nerve (CNIII) can be identified. (C) Another view of the right Sylvian fissure showing RAG anastomosis with M2 and PCA. (D) An anteroposterior (AP) view of the right vertebral artery angiogram postoperatively showing filling of proximal vertebrobasilar circulation, clip occlusion of aneurysm outflow and no filling of aneurysm secondary to thrombosis from flow redirection. (E) An AP view of the right carotid circulation showing patency of the MCA-RAG-PCA bypass feeding the posterior circulation. (F) An oblique lateral postoperative 3D reconstruction CT Angiogram demonstrating filing of the radial artery bypass and obliteration of the giant basilar aneurysm.

Outcome of bypass treatment

As shown in Table 53.3, high-flow EC-IC bypass can be performed safely and successfully to allow for parent vessel occlusion in patients with complex giant intracranial aneurysms, resulting in good patient outcome and aneurysm obliteration in a large proportion of patients. Bypass graft patency rate is 90% or higher, with 5–20% of surgical morbidity reported, which included postop ischaemic stroke or haemorrhage, graft occlusion, or infectious complications. In the earlier series, 30-day surgical mortality was higher, but remained low at 1% or less in the more contemporary surgical series. In one of the largest bypass surgical series that included 93 patients with giant intracranial aneurysm (46% involving ICA, 32% MCA, 18% posterior circulation), the bypass patency rate was 96%, and long-term excellent or good outcome was observed in 94% of patients at a mean follow-up of 3 years (Shi et al., 2015).

Outcome of endovascular treatment

Giant aneurysms have not been favourable lesions for endovascular therapy (Table 53.1), as they are frequently wide-necked with intraluminal thrombosis, and the anatomy of parent and branch arteries at the base are distorted. These anatomical factors make giant aneurysms unfavourable for coiling to achieve complete obliteration. Furthermore, there is a very high likelihood of aneurysm recurrence needing multiple retreatments, and occasional rehaemorrhages, and neurological deterioration from progressive aneurysm enlargement. Techniques like stent or balloon assistance, which are frequently employed for GIA, increases intraprocedural risks (Lylyk et al., 2009). In one of the largest endovascular experiences with 39 giant aneurysms, Jahromi et al. (2008) reported a complete occlusion rate of 36%, stent assistance in 66%, and an average of two sessions to treat each aneurysm. Cumulative treatment morbidity occurred in 12 patients (32%), and treatment mortality occurred in 6 patients (16%). Overall, 11 patients died at late follow-up (29%). Despite advancement in endovascular techniques, the same group published their subsequent result from 2007 to 2012, and showed 31% procedure related mortalities, and 46% permanent neurological morbidity or death at last follow-up (Dumont et al., 2014).

Flow diverting stents have recently gained approval for treatment of proximal ICA aneurysms (from the petrous to superior hypophyseal segment) (Lylyk et al., 2009; Nelson et al., 2011; Fischer et al., 2012). They enable blood flow diversion into the native direction of blood flow, and over time neoendothelialization of the diseased vessel and exclusion of the aneurysm, thereby inducing thrombosis within the aneurysmal sac. Flow diverters have been shown to preserve flow to covered perforators in some cases, but complications including late in-stent thromboses, delayed haemorrhage and perianeurysmal oedema were not infrequent (Alderazi et al., 2014). The results of the Pipeline for Intracranial Treatment of Aneurysms (PITA) and Pipeline for

Table 53.3 Summary of published experience of bypass surgery for giant intracranial aneurysms

Study	Study period	Patient no.	Indication	Bypass type	Graft patency (%)	Operative complications			Clinical outcome at latest follow-up	
						Mortality (%)	Morbidity (%)	Mean F.U (year)	Excellent/ Good (%)	Fair/Poor (%)
Hacein-Bey et al. (1997)	1992–1997	9	ICA GIA	High and low flow	89		11	1.8	100	
				ECA-SVG-M2						
				STA-M2						
Houkin et al. (1999)	1989–1998	43	ICA GIA	High flow	95		4	7.2	N/A	
				ECA-RAG-M2						
Jafar et al. (2002)	1990–1999	30	ICA GIA	High flow	93	3	6	5.2	N/A	
				ECA/CCA-SVG-MCA						
				ECA/CCA--SVG-ICA						
Van Doormaal et al. (2006)	1999–2004	34	ICA GIA	High flow	100	6	12	4.4	79	
				ECA-SVG-ICA	(17% revision rate)					
Cantore et al. (2008)	1990–2004	41	ICA GIA	High flow	93	10	5	8.5	85.4	
			PC GIA	ECA/ICA-SVG-M2						
Patel et al. (2010)	2005–2007	9	ICA GIA	High flow	88	0	22	N/A	100	0
			ICA dissection	ECA-SVG-M2	(22% revision rate)					
Kalani et al. (2013)	1983–2011	16	MCA GIA	High and low flow	94	0	19	4.9	94	6
				STA-MCA (13)						
				ECA-SVG/RAG-MCA (3)						
Ishishita et al. (2014)	1996–2011	38	ICA GIA	High flow	95	0	5	3.9	100	0
				ECA-RAG/SVG-M2						
Shi et al. (2015)	2004–2013	93	ICA GIA	High and low flow	96	1	5	3.0	94	5
			MCA GIA	ECA/IMA-RAG/SVG-MCA/PCA						
			PC GIA	STA-MCA						
				OA-PICA/AICA						

Abbreviations: ACA, anterior cerebral artery; ACoA, anterior communicating artery; AICA, anterior inferior cerebellar artery; BA, basilar artery; CCA, common carotid artery; ECA, external carotid artery; GIA, giant intracranial aneurysm; ICA, internal carotid artery; MCA, middle cerebral artery; OA, occipital artery; PC, posterior circulation; PCA, posterior cerebral artery; PCoA, posterior communicating artery; PICA, posterior inferior cerebellar artery; RAG, radial artery graft; STA, superficial temporal artery; SVG, saphenous vein graft; VA, vertebral artery; N/A, not available.

Uncoilable or Failed Aneurysms (PUFS) trials for the use of these devices in the proximal anterior circulation have been promising (Nelson et al., 2011). However, the results of their use in posterior circulation are less promising (Siddiqui et al., 2012). This is particularly true for giant holobasilar fusiform dolichoectatic basilar aneurysms having layered thrombus, where multiple overlapping short flow diverters were employed. This led to high morbidity from perforator occlusion and delayed ruptures. Furthermore, the added risk of dual antiplatelet with flow diverters make them less ideal in the setting of SAH.

Nevertheless, the currently approved flow diversion devices are not designed for use at arterial bifurcations, or for fusiform aneurysms involving the MCA and basilar artery (BA) with perforating vessels, which could lead to devastating complications from perforator infarcts.

Conclusion

Giant aneurysms are uncommon but highly challenging lesions with a poor natural history. Therefore, treatment to minimize morbidity and mortality is paramount. A proportion of giant aneurysms can be treated with primary clipping, clip reconstruction, or coiling, however, some patients still need the use of complex revascularization and flow reversal techniques. With the ongoing development in endovascular techniques, an increasing number of these lesions may be treated successfully without open surgery in the future. In the meantime, ongoing problems with endovascular reconstruction, aneurysm recurrence after coiling, and uncertain outcomes with the use of flow diverters outside of the cavernous and paraclinoid carotid artery segments make surgical treatment the preferred treatment for patients with giant aneurysms.

FURTHER READING

Hanel, R.A. & Spetzler, R.F. (2008). Surgical treatment of complex intracranial aneurysms. *Neurosurgery*, **62**(6 Suppl 3):1289–97; discussion 1297–9. Review.

Patel, H.C. & Kirkpatrick, P.J. (2009). High flow extracranial to intracranial vascular bypass procedure for giant aneurysms: indications, surgical technique, complications and outcome. In: Pickard, J.D., Akalan, N., Di Rocco, C., et al. (eds.) *Advances and Technical*

Standards in Neurosurgery, vol. **34**, pp. 61–83. New York, NY: Springer Wein New York.

Spetzler, R.F., Nakaji, P., Rhoton, A.L. Jr., & Kawahima, M. (2014). *Color Atlas of Cerebral Revascularization: Anatomy, Techniques, Clinical Cases*. New York/Stuttgart/Delhi/Rio de Janeiro: Thieme Publishers.

Spetzler, R.F., Kalani, M.Y.S., & Nakaji, P. (2015). *Neurovascular Surgery*, 2nd edition. New York/Stuttgart/Delhi/Rio de Janeiro: Thieme Publishers.

Sughrue, M.E., Saloner, D., Rayz, V.L., & Lawton, M.T. (2011). Giant intracranial aneurysms: evolution of management in a contemporary surgical series. *Neurosurgery*, **69**(6), 1261–70; discussion 1270–1.

REFERENCES

Alderazi, Y.J., Shastri, D., Kass-Hout, T., Prestigiacomo, C.J., & Gandhi, C.D. (2014). Flow diverters for intracranial aneurysms. *Stroke Res Treat*, **2014**, 415653.

Bederson, J.B. & Spetzler, R.F. (1992). Anastomosis of the anterior temporal artery to a secondary trunk of the middle cerebral artery for treatment of a giant M1 segment aneurysm. Case report. *J Neurosurg*, **76**(5), 863–6.

Cantore, G., Santoro, A., Guidetti, G., Delfinis, C.P., Colonnese, C., & Passacantilli, E. (2008). Surgical treatment of giant intracranial aneurysms: current viewpoint. *Neurosurgery*, **63**(4 Suppl 2):279–89; discussion 289–90.

Darsaut, T.E., Darsaut, N.M., Chang, S.D., et al. (2011). Predictors of clinical and angiographic outcome after surgical or endovascular therapy of very large and giant intracranial aneurysms. *Neurosurgery*, **68**(4), 903–15; discussion 915.

Drake, C.G. (1979). Giant intracranial aneurysms: experience with surgical treatment in 174 patients. *Clin Neurosurg*, **26**, 12–95

Dumont, T.M., Levy, E.I., Siddiqui, A.H., Snyder, K.V., & Hopkins, L.N. 3rd (2014). Endovascular treatment of giant intracranial aneurysms: a work in progress. *World Neurosurg*, **81**(5–6), 671–5.

Fischer, S., Vajda, Z., Aguilar Perez, M., et al. (2012). Pipeline embolization device (PED) for neurovascular reconstruction: initial experience in the treatment of 101 intracranial aneurysms and dissections. *Neuroradiology*, **54**(4), 369–82.

Hacein-Bey, L., Connolly, E.S. Jr., Duong, H., et al. (1997). Treatment of inoperable carotid aneurysms with endovascular carotid occlusion after extracranial-intracranial bypass surgery. *Neurosurgery*, **41**(6), 1225–31; discussion 1231–4.

Hamburger, C., Schonberger, J., & Lange, M. (1992). Management and prognosis of intracranial giant aneurysms. A report on 58 cases. *Neurosurg Rev*, **15**, 97–103.

Hanel, R.A. & Spetzler, R.F. (2008). Surgical treatment of complex intracranial aneurysms. *Neurosurgery*, **62**(6 Suppl 3):1289–97; discussion 1297–9.

Houkin, K., Kamiyama, H., Kuroda, S., Ishikawa, T., Takahashi, A., & Abe, H. (1999). Long-term patency of radial artery graft bypass for reconstruction of the internal carotid artery. Technical note. *J Neurosurg*, **90**, 786–90.

Ishishita, Y., Tanikawa, R., Noda, K., et al. (2014). Universal extracranial-intracranial graft bypass for large or giant internal carotid aneurysms: techniques and results in 38 consecutive patients. *World Neurosurg*, **82**(1–2), 130–9.

Jafar, J.J., Russell, S.M., & Woo, H.H. (2002). Treatment of giant intracranial aneurysms with saphenous vein extracranial-to-intracranial bypass grafting: indications, operative technique, and results in 29 patients. *Neurosurgery*, **51**(1), 138–44; discussion 144–6.

Jahromi, B.S., Mocco, J., Bang, J.A., et al. (2008). Clinical and angiographic outcome after endovascular management of giant intracranial aneurysms. *Neurosurgery*, **63**(4), 662–74; discussion 674–5.

Kalani, M.Y., Zabramski, J.M., Hu, Y.C., & Spetzler, R.F. (2013). Extracranial-intracranial bypass and vessel occlusion for the treatment of unclippable giant middle cerebral artery aneurysms. *Neurosurgery*, **72**(3), 428–35; discussion 435–6.

Kocaeli, H., Andaluz, N., Choutka, O., & Zuccarello, M. (2008). Use of radial artery grafts in extracranial-intracranial revascularization procedures. *Neurosurg Focus*, **24**, E5.

Lawton, M.T., Abla, A.A., Rutledge, W.C., et al. (2016). Bypass surgery for the treatment of dolichoectatic basilar trunk aneurysms: a work in progress. *Neurosurgery*, **79**(1), 83–99.

Locksley, H.B. (1966). Natural history of subarachnoid hemorrhage, intracranial aneurysms and arteriovenous malformations. Based on 6368 cases in the cooperative study. *J Neurosurg*, **25**(2), 219–39.

Lylyk, P., Miranda, C., Ceratto, R., et al. (2009). Curative endovascular reconstruction of cerebral aneurysms with the pipeline embolization device: the Buenos Aires experience. *Neurosurgery*, **64**(4), 632–42; discussion 642–3.

Mohit, A.A., Sekhar, L.N., Natarajan, S.K., Britz, G.W., & Ghodke, B. (2007). High-flow bypass grafts in the management of complex intracranial aneurysms. *Neurosurgery*, **60**, ONS 105–22; discussion ONS 122–3.

Nelson, P.K., Lylyk, P., Szikora, I., Wetzel, S.G., Wanke, I., & Fiorella, D. (2011). The pipeline embolization device for the intracranial treatment of aneurysms trial. *AJNR Am J Neuroradiol*, **32**(1), 34–40.

Patel, H.C. & Kirkpatrick, P.J. (2009). High flow extracranial to intracranial vascular bypass procedure for giant aneurysms: indications, surgical technique, complications and outcome. In: Pickard, J.D., Akalan, N., Di Rocco, C., et al. (eds.) *Advances and Technical Standards in Neurosurgery*, vol. **34**, pp. 61–83. New York, NY: Springer Wein New York.

Patel, H.C., Teo, M., Higgins, N., & Kirkpatrick, P.J. (2010). High flow extra-cranial to intra-cranial bypass for complex internal carotid aneurysms. *Br J Neurosurg*, **24**(2), 173–8

Pia, H.W. & Zierski, J. (1982). Giant cerebral aneurysms. *Neurosurg Rev*, **5**(4), 117–48.

Pisapia, J.M., Walcott, B.P., Nahed, B.V., Kahle, K.T., & Ogilvy, C.S. (2011). Cerebral revascularization for the treatment of complex intracranial aneurysms of the posterior circulation: microsurgical anatomy, techniques and outcomes. *J Neurointerv Surg*, **3**(3), 249–54.

Sanai, N., Zador, Z., & Lawton, M.T. (2009). Bypass surgery for complex brain aneurysms: an assessment of intracranial-intracranial bypass. *Neurosurgery*, **65**(4), 670–83; discussion 683.

Shi, X., Qian, H., Fang, T., Zhang, Y., Sun, Y., & Liu, F. (2015). Management of complex intracranial aneurysms with bypass surgery: a technique application and experience in 93 patients. *Neurosurg Rev*, **38**(1), 109–19; discussion 119–20.

Siddiqui, A.H., Abla, A.A., Kan, P., et al. (2012). Panacea or problem: flow diverters in the treatment of symptomatic large or giant fusiform vertebrobasilar aneurysms. *J Neurosurg*, **116**(6), 1258–66.

Spetzler, R.F., Nakaji, P., Rhoton, A.L. Jr., & Kawahima, M. (2014). *Color Atlas of Cerebral Revascularization: Anatomy, Techniques, Clinical Cases*. New York/Stuttgart/Delhi/Rio de Janeiro: Thieme Publishers.

Spetzler, R.F., Kalani, M.Y.S., & Nakaji, P. (2015). *Neurovascular Surgery*, 2nd edition. New York/Stuttgart/Delhi/Rio de Janeiro: Thieme Publishers.

Sughrue, M.E., Saloner, D., Rayz, V.L., & Lawton, M.T. (2011). Giant intracranial aneurysms: evolution of management in a contemporary surgical series. *Neurosurgery*, **69**(6), 1261–70; discussion 1270–1.

van Doormaal, T.P., van der Zwan, A., Verweij, B.H., Langer, D.J., & Tulleken, C.A. (2006). Treatment of giant and large internal carotid artery aneurysms with a high-flow replacement bypass using the excimer laser-assisted nonocclusive anastomosis technique. *Neurosurgery*, **59**(4 Suppl 2), 1411–18.

54

Spontaneous intracranial haematoma

Berk Orakcioglu and Andreas W. Unterberg

Pathophysiology, epidemiology, incidence, and risk factors for spontaneous ICH

Epidemiology/incidence

Spontaneous intracerebral haematoma (ICH) accounts for up to 20% of all strokes with a slight predominance in males. Incidence increases with increasing age and anticoagulant or antithrombotic treatment. Due to demographic changes, the incidence is likely to increase by 35% by 2050 (Stein et al., 2012). There is an association with ethnic origin: among Caucasians it is 20/100 000 compared to 60/100 000 in Japan. Mortality rates in the first week and first year after ictus range from 31% to 34% and 53% to 59%, respectively (Flaherty et al., 2006).

Classification

ICH can be classified in various means: bleeding source, anatomical localization of the clot, presence of haematoma components in other compartments (i.e. ventricle). A descriptive anatomical classification allows the main haematoma localization to be defined as lobar, basal ganglia, thalamic, brain stem, or cerebellar, with or without extension into the subarachnoid space or ventricle. An ICH necessarily involves brain parenchyma, however with respect to these locations typical or atypical haematoma can be diagnosed. Typical ICH can be found in the basal ganglia or thalamus in younger patients. Lenticulostriate or thalamic arterioles are the putative rupture site and are closely related to episodes of acute or chronic arterial hypertension. In elderly patients, lobar haematomas are termed atypical and are often related to amyloid angiopathy. In younger patients atypically located haematomas raise the suspicion of a vascular malformation or tumour as a bleeding source that requires extended vascular workup.

Risk factors

The main risk factors for ICH are arterial hypertension in basal ganglia haematoma and amyloid angiopathy in the elderly population with cortical bleeds. Between 5% and 10% of ICH occur during heparin or vitamin K-antagonist (most commonly warfarin) administration. Anticoagulation with vitamin K-antagonists is associated with a 0.5–1% cerebral haemorrhage risk per year and in only half of these patients is overdosage present. Patients with oral anticoagulant (OAC) treatment are exposed to a higher risk for spontaneous ICH and mortality is higher if reversal of OAC medication is not undertaken (Kuramatsu et al., 2015).

Other known risk factors are cardiac diseases, diseases related to the haematopoietic system, coagulopathies (haemophilia, von Willebrand syndrome), thrombocytopenia, leukaemia, and disseminated intravascular coagulopathy.

Unlike ischaemic stroke, diabetes, hypercholesterinaemia, and smoking are not risk factors for ICH, whereas low level of cholesterol may double the risk of ICH. Cerebral vein thrombosis furthermore may induce ICH in various localizations.

Pathophysiology

One of the most important characteristics of ICH is that early progression of haematoma size or oedema (**Fig. 54.1**) can lead to secondary neurological worsening of patients.

Whereas haematoma enlargement is likely to occur in the first 24 h after onset, inflammatory processes begin soon after onset and oedema development may last up to weeks after ICH (**Fig. 54.2**) (Xue and Del Bigio, 2000).

Analyses of serial CT-angiography in ICH patients have found that the early 'spot-sign' (within 6 hours) is a strong predictor for bad outcome (Mayer et al., 2009; Demchuk et al., 2012). 'Spot sign' refers to contrast extravasation within the haematoma in the early phase after onset of the disease. In theory, with increasing haematoma volumes there is an increased risk of increased intracranial pressure (ICP) and consequent decrease in CBF and $P_{br}O_2$ leading to local or global ischaemia. Whether cytotoxic and/or vasogenic oedema plays a key role in perihaemorrhagic pathophysiology remains a question of debate (Butcher et al., 2004). These secondary brain tissue changes could be the most important factors that impact on patient outcome. The role of the pathophysiological factors during the first hours after the initial event, is not well understood (Kirkman and Smith, 2013).

Haematoma degradation products and coagulation factors initiate a secondary neuronal damage cascade which are mainly based on thrombin and iron toxicity. Alongside inflammatory processes and disturbance of the blood brain barrier promote oedema formation in the perihaemorrhagic tissue (Nakamura et al., 2006; Xi et al., 2006).

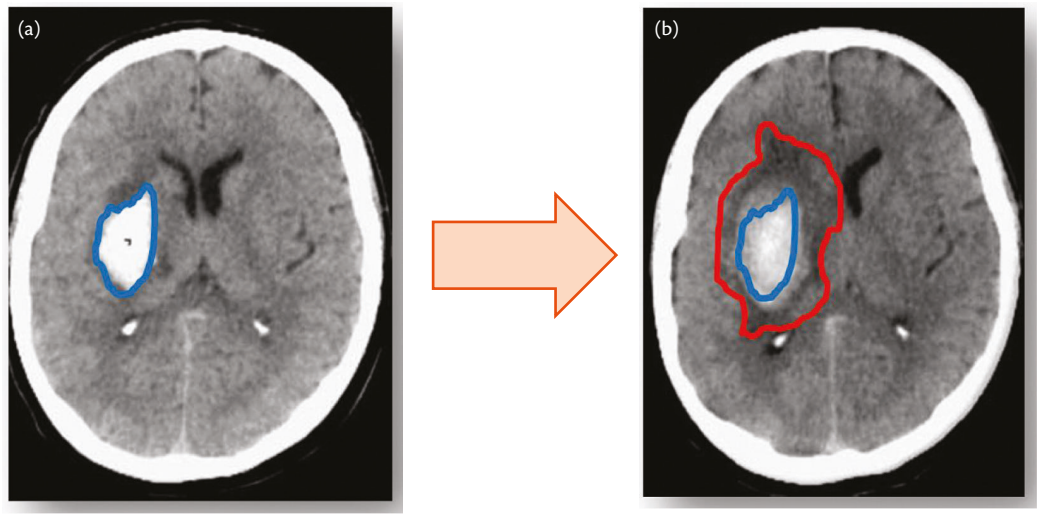

Fig. 54.1 Putaminal haemorrhage with mild space occupying effect (A); subsequent oedema development around the primary lesion leads to compression of midline structures (B).

As well as these vasogenic oedema promoting factors, metabolic contributors are discussed as a cause of late deterioration. Mechanical compression of surrounding vessels by haematoma was thought to induce ischaemia with cytotoxic oedema. However, most authors have found reduced perfusion, but no frank ischaemia in the perihaemorrhagic zone. Mitochondrial dysfunction seems to play a role, though its origin is still unclear (Kim-Han et al., 2006). New experimental data suggests that mitochondrial dysfunction induced ischaemia is more likely to occur in larger haematomas (Orakcioglu et al., 2015).

The other leading cause of ICH (15%, with an increasing tendency due to demographic changes) is cerebral amyloid angiopathy (CAA). In these patients, amyloid can be found within the medial and adventitial layers of cerebral arteries located in the cortex. These changes predispose for lobar haematomas and amyloid deposition increases with older age.

The Boston criteria summarize the diagnostic criteria for CAA. For definite diagnosis histopathological examinations are mandatory. However, the Boston criteria help to clinically classify lobar haematomas in the absence of histological correlates (see **Box 54.1**).

Clinical presentation and workup

Depending on the location, size, and dynamics of the haematoma patients clinically present in various ways. **Box 54.2** summarizes symptoms going along with certain locations. However, with increasing size of the haematoma clinical deterioration is probable and stroke unit or neurointensive care should be available in the early phases after the ictus.

Generally, ICH should be regarded as an acute life-threatening event. Even if presenting symptoms appear mild at onset, haematoma progression may lead to rapid neurological deterioration. The key aspects of acute management of ICH are: (1) identifying and treating an underlying source of bleeding (e.g. AVM);

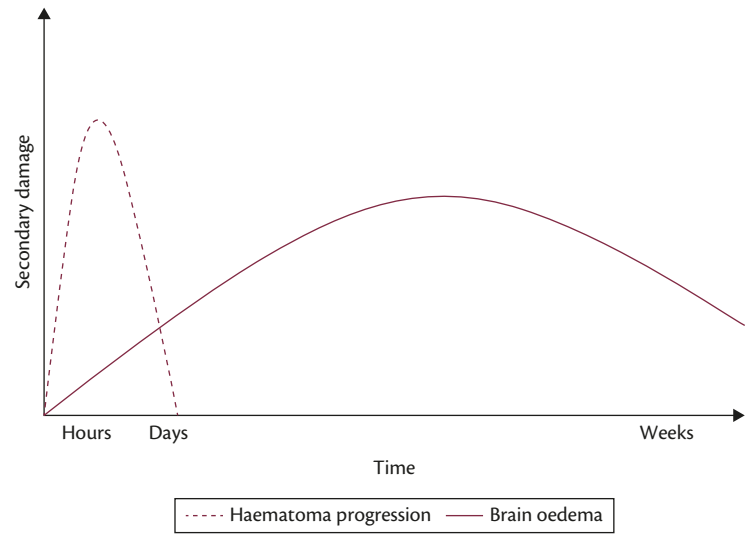

Fig. 54.2 Timeline of haematoma progression and oedema development after primary ICH.

Box 54.1 Boston criteria for cerebral amyloid angiopathy (CAA)

Certain CAA

Post-mortem histological findings showing

- lobar, cortical, or corticosubcortical haematoma
- severe CAA with associated vasculopathy
- missing other causes

Probable CAA with supporting pathology

Clinical data and pathological findings show

- lobar, cortical, or corticosubcortical haematoma
- a certain degree of CAA in histology
- missing other causes

Probable CAA

Clinical and radiological findings show

- multiple haematomas mainly lobar, cortical, or corticosubcortical (incl. cerebellum)
- age ≥55 years
- missing other causes

Possible CAA

Clinical and radiological findings show

- singular lobar, cortical, or corticosubcortical haematoma
- age ≥55 years
- missing other causes

Reproduced with permission from Steven M. Greenberg, G. William Rebeck, Jean Paul G. Vonsattel, et al., Apolipoprotein E ε4 and cerebral hemorrhage associated with amyloid angiopathy, *Annals of Neurology*, Volume 38, Issue 2, Copyright © 2004 John Wiley and Sons.

Box 54.2 Typical symptoms of ICH in relation to localization

Putamen

- contralateral hemiparesis
- conjugate gaze deviation to lesion side
- homonymous hemianopia
- aphasia if ICH on the dominant side

Thalamus

- contralateral sensory symptoms
- initial reduced conscious state progressing to coma
- hemiparesis
- hemiataxia (up to 20%)
- oculomotor symptoms caused by pressure to the midbrain (i.e. Parinaud's syndrome)
- neuropsychological deficits

Caudate nucleus

- hemiparesis
- often intraventricular involvement with meningism

Pons

- initial reduced conscious state progressing to coma
- tetraparesis
- abnormal flexion- or extension
- bilateral cranial nerve deficits in medial lesions
- tegmental localization: internuclear ophthalmoplegia, dilated pupil, and contralateral hemiparesis

Midbrain

- initial reduced conscious state progressing to coma
- Parinaud's syndrome

Cerebellum

- initial reduced conscious state progressing to coma
- ataxia
- dizziness
- gaze palsies
- signs of elevated ICP

(2) general intensive care to secure vital functions; (3) specific neurointensive measures to control elevated ICP; (4) specific treatments to limit haematoma progression; and (5) evaluation whether operative treatment options exist (i.e. EVD, operative removal of large clots).

Investigation

Computed tomography (CT) remains the gold standard for diagnostic imaging in ICH as it is widely available, cheap, and can be performed quickly on admission. Sensitivity and specificity in detecting a clinically significant ICH is close to 100% and once an ICH has been found additional contrast-enhanced sequences (CT angiography, CT venography) may add valuable information on the underlying aetiology. In atypical haematomas in young patients these additional methods are essential to exclude underlying vascular abnormalities such as aneurysms. Haematomas are classified as atypical if subarachnoid haematoma (aneurysmal SAH) or intraventricular rupture of a periventricular haematoma (AVM) are seen. Underlying calcifications and clot components in different stages (cavernous haemangioma) also lead to the suspicion of an atypical clot that requires further workup.

Gradient echo- and T2*-susceptibility-weighed magnetic-resonance imaging (MRI) are comparable to CT in terms of sensitivity and specificity in diagnosing ICH (Masdeu et al., 2006). MRI including MR-angiography can also be used to detect ICH in the early phase. However, there is a lower availability of scanners, higher technical complexity, and cost, as well as longer examination times. Sedated and ventilated patients should be managed by specialized neurointensive care units and physicians in the MRI scanner. One advantage of MRI is its sensitivity to detect cerebral microbleeds that hint towards the diagnosis of CAA.

The clot volume should be determined once ICH is seen with regard to prognosis. A well-established method to estimate ICH volume is the a*b*c/2 formula (Kothari, 1996). Clot volumes of 30 cc and below are likely to go along with an acceptable functional outcome, whereas clot volumes larger than 60 cc are often associated with a poor functional prognosis and dependency.

Recent reports have highlighted the importance of the previously defined 'spot-sign'. Patients showing a positive spot sign in early CT-A are likely to have haematoma expansion and subsequently worse prognosis. However, lobar haematomas in CAA patients rarely have a positive spot sign. Whether or not the presence of this sign will influence therapeutic stratification remains a matter of debate (Evans et al., 2010).

Typical hypertensive haematomas are not routinely investigated with contrast-enhanced CT. However, if there is sufficient clinical suspicion of an atypical haematoma at least CT-A is advocated to rule out true vascular pathologies such as aneurysms or arteriovenous malformations.

Digital subtraction angiography is indicated in selected cases in which neither CT nor MR-based imaging has demonstrated the

bleeding source in atypical cases. It is also used if vasculitis is suspected or if there is the suspicion of an underlying AVM, where it is superior to non-invasive angiography.

Medical management

The key goals of a conservative treatment regimen are maintenance of vital functions, optimization of cerebral perfusion and oxygenation, and control of the main risk factors for subsequent haematoma progression. In larger haematomas ICP-control measures may be necessary to achieve these goals.

Blood pressure management

Studies on the prognostic value of elevated blood pressure following spontaneous ICH have shown inconclusive results. Most of the studies indicate that a markedly elevated blood pressure is associated with poor clinical outcome. Most patients with acute ICH present with highly elevated blood pressure and in a high percentage these have a positive history of arterial hypertension. As a physiological reaction to elevated ICP, blood pressure may be increased, even in patients without positive history of arterial hypertension. Theoretically, elevated blood pressure may drive haematoma expansion and progressive oedema development and thereby cause worse results. Therefore, specific and aggressive blood pressure lowering measures should be undertaken in the acute management of ICH. The results of the INTERACT II Study confirm it is safe to lower systolic blood pressure to a target of less than 140 mmHg. Although the study authors could demonstrate that haematoma progression could be lowered significantly, a relevant effect on outcome was not be observed (Anderson et al., 2013). Taking into account these findings the new guidelines for the management of ICH of the European Stroke Organisation (ESO) recommend high normal to mild hypertensive systolic blood pressure levels in the acute setting (Steiner et al., 2014).

Seizure treatment

With an incidence rate of 7.5% epileptic fits are seen more often in ICH than in other stroke subtypes (Passero et al., 2002) and seizures in ICH are negative predictors for good outcome. In most cases seizures are seen within the first 3 days and in association with lobar bleeds and may be the presenting symptom. Importantly, non-convulsive seizures are a cause of unexplained deterioration in ICH patients. EEG or continuous EEG-monitoring should be used promptly if there is a suspicion of seizure. Late onset seizures are also described and are related to lobar haematoma, microbleeds and alcohol abuse trigger (Rossi et al., 2013; Madžar et al., 2014).

For the acute management of epileptic seizures benzodiazepines are favoured and for ongoing treatment in the acute setting, phenytoin, levetiracetam, and valproic acid are commonly used antiepileptics.

Treatment of anticoagulation, antiplatelet therapy, and coagulopathies

In almost 40% of all patients with ICH progressive haematoma expansion is seen within 24 hours (Box 54.3). The above-mentioned

Box 54.3 Info box 1

Correction of anticoagulation and aggressive blood pressure control constitute the basis for any intensive care or operative treatment of acute ICH.

Surgical management

The key factors in selecting appropriate surgical candidates are haematoma size, patient age, comorbidity, location (lobar vs. deep), and the clinical course of the patient.

Rationale for surgical treatments

As mentioned earlier, ICH is a volume related primary space occupying lesion. With subsequent toxic and metabolic processes perihaemorrhagic oedema is likely to occur in the border between the solid clot and brain parenchyma (Butcher et al., 2004). Experimental data suggest that local mechanical effects of the clot restrict perihaemorrhagic perfusion and thereby promote secondary neuronal injury (Orakcioglu et al., 2014). These secondary changes and concomitant tissue swelling may continue over several days and often lead to neurological deterioration. Once secondary deterioration occurs late surgical measures for haematoma reduction may miss the therapeutic window for achieving a better prognosis. In the STICH II trial 21% of initially conservatively treated patients developed oedema related deterioration and crossed-over to surgical treatment. Compared to initially surgical patients this subgroup had a worse final outcome. Subgroup analysis of STICH II suggests that patients with a GCS of 9–12 without clinical signs of cerebral herniation should be evaluated for surgical treatment.

The theoretical considerations related to the haemorrhage and pathophysiological mechanisms already mentioned here suggest early surgical removal of intracerebral clots. However, despite impressive postoperative radiological results, two large randomized controlled multicentre studies (STICH I and II) have not delivered evidence that an early policy of haematoma removal is clinically beneficial (Mendelow et al., 2005; Mendelow et al., 2013).

Individualized surgical treatments have not been studied in both STICH I and II and because of that modern operative minimally invasive techniques remain a promising treatment option. In the randomized controlled MISTIE II study, evidence could be found that the stereotactic placement of catheters into the clot with consecutive rt-PA facilitated clot reduction significantly reduced perihaemorrhagic oedema (Mould et al., 2013). MISTIE III comparing endoscopic clot reduction and lysis versus "standard medical care" did not reveal significant beneficial effects on outcome either (Hanley et al., 2019).

Other minimally invasive options comprise endoscopic treatments using navigated burr hole approaches. Experienced Asian centres have recently reported a retrospective study that found minimally invasive endoscopic haematoma evacuation can be associated with reduced early mortality thus enabling functional improvement in patients with medium- to large-sized haematomas. This may be mainly attributed to the sophisticated surgical approach including neuronavigation and modern endoscopic equipment. Prospective randomized controlled clinical trials comparing this treatment modality with conventional hematoma evacuation through craniotomy and with conservative treatment alone are needed to investigate effects on long-term mortality and functional outcome.

ICH in the posterior fossa have not been studied in randomized controlled studies comparing conservative and operative management. Only one study compared two surgical techniques in infratentorial haematoma removal, showing that a mini-craniectomy is beneficial over large decompressive surgery (Tamaki et al., 2004). From retrospective case series it is apparent that the pathophysiology is different to supratentorial ICH and surgery is more likely to be utilized in large haematomas due to the limited space in the posterior fossa. The indications for surgery are obliteration of the fourth ventricle regardless of clinical symptoms or ICH size,

GCS score is less than 14, haematoma diameter above 30 mm and not less than 7 mm (Da Pian et al., 1984; Mathew et al., 1995; Kirollos et al., 2001). However, the ESO guidelines from 2014 conclude that there is insufficient evidence from RCTs to make definitive recommendations about how, when, and for whom surgical evacuation should be performed in adults with infratentorial ICH.

Controversy section

ICH patients should be transferred to specialized neuro-ICU or stroke units whenever possible. Careful evaluation of patient-specific characteristics (i.e. age, risk factors, haematoma location and size, and so on), neurological and premorbid condition, coagulation disorders, and diagnostic workup including vascular protocols are mandatory to individually decide for best possible treatments. Whether or not to perform surgery not only depends on these factors, but also on the availability of specific techniques such as endoscopic removal and other minimally invasive procedures. Once an operative approach to remove the clot is favoured after careful discussion neuronavigation or stereotactic methods should be used to limit approach related morbidity and thereby help improving outcome. The following surgical measures exist to treat ICH patients:

- ventriculostomy and external drainage (EVD) in cases of suspected elevated intracranial pressure (ICP) or intraventricular involvement;
- navigated/stereotactic burr hole trephination and catheter placement along the long axis of the clot with consecutive and repetitive rt-PA clot lysis and aspiration (MISTIE procedure);
- navigated/stereotactic burr hole trephination and endoscopic clot removal along the long axis;
- navigation assisted small craniotomy and microneurosurgical clot removal;
- decompressive hemicraniectomy in selected cases (i.e. ICH in sinus-vein thrombosis).

Most controversy exists in younger patients with relatively large haematomas in the deep basal ganglia. As valuable indicators for secondary neurological deterioration are still missing uncertainty remains to whether surgery should be undertaken or not. If surgery is not favoured in the first instance secondary brain swelling and oedema can progress, and delayed surgery may become the only option. In STICH II 21% of conservative patients received delayed surgery of which most had a secondary deterioration. Ideally these patients could have undergone surgery before neurological and radiological worsening, but selection criteria remain unclear:

Box 54.4 Case presentation

A 35-year-old Asian female suffered sudden headaches with consecutive right-sided hemiplegia and facial paralysis. CT revealed a large basal ganglia ICH secondary to severe hypertension (Fig. 54.3A). There was an initial GCS of 14 but early deterioration to GCS of 8 followed, with significant haematoma progression that indicated an endoscopic approach for haematoma removal. Postoperatively the patients recovered quickly to a moderate hemiparesis, and early GCS of 15 before rehabilitation. Postoperative MRI on day 3 (Fig. 54.3B) showed haematoma removal and limited oedema development going along with normal ICP during the early postoperative course.

The case in Box 54.4 illustrates the need for interdisciplinary decision-making between neuro-intensivists, neurologists, and neurosurgeons. Even if optimal medical treatment was initially favoured due to the patients' early good clinical condition, the GCS of 14 at presentation may have increased the likelihood of subsequent deterioration. For this reason even mild changes in the clinical status of the patients should lead to re-evaluation of the above-mentioned surgical options.

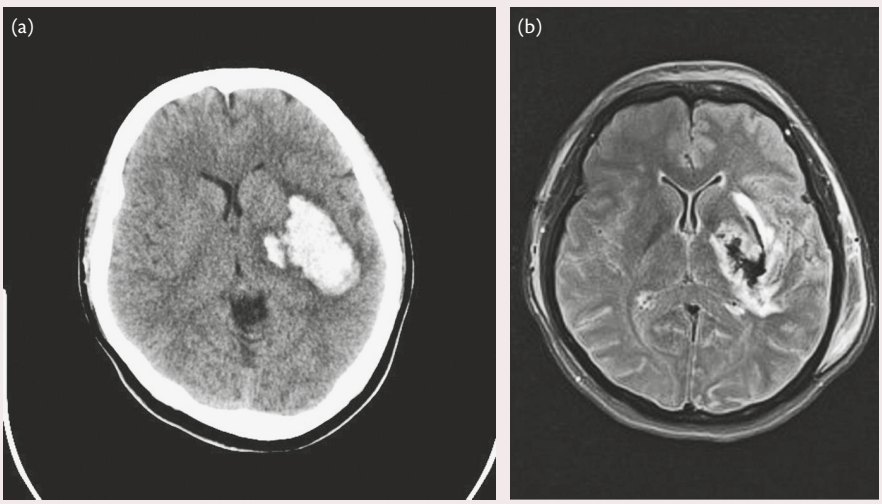

Fig. 54.3 (A) CT showing a large basal ganglia ICH secondary to severe hypertension. (B) Postoperative MRI showed haematoma removal and limited oedema development continuing with normal ICP during the early postoperative course.

medical measures (i.e. blood pressure lowering) to reduce haematoma expansion are necessary to limit secondary neurological deterioration. Point of care diagnostics are now widely available in order to rapidly assess coagulopathies, antiplatelet drug degree of efficiency, and help to accelerate coagulation management (Beynon et al., 2013; Beynon et al., 2014). If thrombolytic dysfunction is proven, then administration of tranexamic acid, desmopressin, or fresh-frozen plasma should be considered, although, there is no evidence-based data to support this practical treatment recommendation (Campbell et al., 2010; Sprigg et al., 2014).

Following the guidelines in traumatic brain injury new data have shown that OAC or NOAC (new oral anticoagulant) associated ICH should be treated by stopping anticoagulation, administering vitamin K, and considering specific reversal (e.g. prothrombin complex concentrates, PCC) to limit haematoma expansion (Le Roux et al., 2014). Among patients with OAC-associated ICH, reversal of INR less than 1.3 within 4 hours and systolic BP under 160 mmHg at 4 hours were associated with lower rates of haematoma enlargement, better outcome, and resumption of OAC therapy was associated with lower risk of ischaemic events (Kuramatsu et al., 2015).

FURTHER READING

Anderson, C.S., Heeley, E., Huang, Y., et al. (2013). Rapid blood-pressure lowering in patients with acute intracerebral hemorrhage. *N Engl J Med*, **368**, 2355–65.

Kuramatsu, J.B., Gerner, S.T., Schellinger, P.D., et al. (2015). Anticoagulant reversal, blood pressure levels, and anticoagulant resumption in patients with anticoagulation-related intracerebral hemorrhage. *JAMA*, **313**, 824–36.

Mendelow, A.D., Gregson, B.A., Fernandes, H.M., et al. (2005). Early surgery versus initial conservative treatment in patients with spontaneous supratentorial intracerebral haematomas in the International Surgical Trial in Intracerebral Haemorrhage (STICH): a randomised trial. *Lancet*, **365**, 387–97.

Mendelow, A.D., Gregson, B.A., Rowan, E.N., et al. (2013). Early surgery versus initial conservative treatment in patients with spontaneous supratentorial lobar intracerebral haematomas (STICH II): a randomised trial. *Lancet*, **382**, 397–408.

Mould, W.A., Carhuapoma, J.R., Muschelli, J., et al. (2013). Minimally invasive surgery plus recombinant tissue-type plasminogen activator for intracerebral hemorrhage evacuation decreases perihematomal edema. *Stroke*, **44**, 627–34.

Smith, E.E. &, Greenberg, S.M. (2003). Clinical diagnosis of cerebral amyloid angiopathy: validation of the Boston criteria. *Curr Atheroscler Rep*, **5**, 260–6.

Steiner, T., Al-Shahi Salman, R., Beer, R., et al. (2014). European Stroke Organisation (ESO) guidelines for the management of spontaneous intracerebral hemorrhage. *Int J Stroke*, **9**, 840–55.

REFERENCES

Anderson, C.S., Heeley, E., Huang, Y., et al. (2013). Rapid blood-pressure lowering in patients with acute intracerebral hemorrhage. *N Engl J Med*, **368**, 2355–65.

Beynon, C., Jakobs, M., Rizos, T., Unterberg, A.W., & Sakowitz, O.W. (2014). Rapid bedside coagulometry prior to urgent neurosurgical procedures in anticoagulated patients. *Br J Neurosurg*, **28**, 29–33.

Beynon, C., Sakowitz, O.W., & Unterberg, A.W. (2013). Multiple electrode aggregometry in antiplatelet-related intracerebral haemorrhage. *J Clin Neurosci*, **20**, 1805–6.

Butcher, K.S., Baird, T., MacGregor, L., Desmond, P., Tress, B., & Davis, S. (2004). Perihematomal edema in primary intracerebral hemorrhage is plasma derived. *Stroke*, **35**, 1879–85.

Campbell, P.G., Sen, A., Yadla, S., Jabbour, P., & Jallo, J. (2010). Emergency reversal of antiplatelet agents in patients presenting with an intracranial hemorrhage: a clinical review. *World Neurosurg*, **74**, 279–85.

Da Pian, R., Bazzan, A., & Pasqualin, A. (1984). Surgical versus medical treatment of spontaneous posterior fossa haematomas: a co-operative study on 205 cases. *Neurol Res*, **6**, 145–51.

Demchuk, A.M., Dowlatshahi, D., Rodriguez-Luna, D., et al. (2012). Prediction of haematoma growth and outcome in patients with intracerebral haemorrhage using the CT-angiography spot sign (PREDICT): a prospective observational study. *Lancet Neurol*, **11**, 307–14.

Evans, A., Demchuk, A., Symons, S.P., et al. (2010). The spot sign is more common in the absence of multiple prior microbleeds. *Stroke*, **41**, 2210–17.

Flaherty, M.L., Haverbusch, M., Sekar, P., et al. (2006). Long-term mortality after intracerebral hemorrhage. *Neurology*, **66**, 1182–6.

Hanley, I.F., Thompson, R.E., Rosenblum, M. et al. (2019). MISTIE III investigators. Efficacy and safety of minmally invasive surgery with thrombolysis in cerebral hemorrhage evacuation (MISTIE III): randomised, controlled, open-labeled, blinded end point phase III trial. *Lancet*, **393**, 1021–32.

Kim-Han, J.S., Kopp, S.J., Dugan, L.L., & Diringer, M.N. (2006). Perihematomal mitochondrial dysfunction after intracerebral hemorrhage. *Stroke*, **37**, 2457–62.

Kirkman, M.A. & Smith, M. (2013). Supratentorial intracerebral hemorrhage: a review of the underlying pathophysiology and its relevance for multimodality neuromonitoring in neurointensive care. *J Neurosurg Anesthesiol*, **25**, 228–39.

Kirollos, R.W., Tyagi, A.K., Ross, S.A., van Hille, P.T., & Marks, P.V. (2001). Management of spontaneous cerebellar hematomas: a prospective treatment protocol. *Neurosurgery*, **49**, 1378–86; discussion 1386–7.

Kothari, M.T.B. (1996). The ABCs of measuring intracerebral hemorrhage volumes. *Stroke*, **27**, 1304–5.

Kuramatsu, J.B., Gerner, S.T., Schellinger, P.D., et al. (2015). Anticoagulant reversal, blood pressure levels, and anticoagulant resumption in patients with anticoagulation-related intracerebral hemorrhage. *JAMA*, **313**, 824–36.

Le Roux, P., Pollack, C.V., Milan, M., & Schaefer, A. (2014). Race against the clock: overcoming challenges in the management of anticoagulant-associated intracerebral hemorrhage. *J Neurosurg*, **121**, Suppl 1–20.

Madžar, D., Kuramatsu, J.B., Gollwitzer, S., et al. (2014). Seizures among long-term survivors of conservatively treated ICH patients: incidence, risk factors, and impact on functional outcome. *Neurocrit Care*, **21**, 211–19.

Masdeu, J.C., Irimia, P., Asenbaum, S., et al. (2006). EFNS guideline on neuroimaging in acute stroke. Report of an EFNS task force. *Eur J Neurol*, **13**, 1271–83.

Mathew, P., Teasdale, G., Bannan, A., & Oluoch-Olunya, D. (1995). Neurosurgical management of cerebellar haematoma and infarct. *J Neurol Neurosurg Psychiatr*, **59**, 287–92.

Mayer, S.A., Davis, S.M., Skolnick, B.E., et al. (2009). Can a subset of intracerebral hemorrhage patients benefit from hemostatic therapy with recombinant activated factor VII? *Stroke*, **40**, 833–40.

Mendelow, A.D., Gregson, B.A., Fernandes, H.M., et al. (2005). Early surgery versus initial conservative treatment in patients with spontaneous supratentorial intracerebral haematomas in the International Surgical Trial in Intracerebral Haemorrhage (STICH): a randomised trial. *Lancet*, **365**, 387–97.

Mendelow, A.D., Gregson, B.A., Rowan, E.N., et al. (2013). Early surgery versus initial conservative treatment in patients with spontaneous supratentorial lobar intracerebral haematomas (STICH II): a randomised trial. *Lancet*, **382**, 397–408.

Mould, W.A., Carhuapoma, J.R., Muschelli, J., et al. (2013). Minimally invasive surgery plus recombinant tissue-type plasminogen activator for intracerebral hemorrhage evacuation decreases perihematomal edema. *Stroke*, **44**, 627–34.

Nakamura, T., Keep, R.F., Hua, Y., Nagao, S., Hoff, J.T., & Xi, G. (2006). Iron-induced oxidative brain injury after experimental intracerebral hemorrhage. *Acta Neurochir Suppl*, **96**, 194–8.

Orakcioglu, B., Kentar, M.M., Schiebel, P., Uozumi, Y., Unterberg, A., & Sakowitz, O.W. (2015). Perihemorrhagic ischemia occurs in a volume-dependent manner as assessed by multimodal cerebral monitoring in a porcine model of intracerebral hemorrhage. *Neurocrit Care*, **22**, 133–9.

Passero, S., Rocchi, R., Rossi, S., Ulivelli, M., & Vatti, G. (2002). Seizures after spontaneous supratentorial intracerebral hemorrhage. *Epilepsia*, **43**, 1175–80.

Rossi, C., De Herdt, V., Dequatre-Ponchelle, N., Hénon, H., Leys, D., & Cordonnier, C. (2013). Incidence and predictors of late seizures in intracerebral hemorrhages. *Stroke*, **44**, 1723–5.

Smith, E.E. &, Greenberg, S.M. (2003). Clinical diagnosis of cerebral amyloid angiopathy: validation of the Boston criteria. *Curr Atheroscler Rep*, **5**, 260–6.

Sprigg, N., Renton, C.J., Dineen, R.A., Kwong, Y., & Bath, P.M.W. (2014). Tranexamic acid for spontaneous intracerebral hemorrhage: a randomized controlled pilot trial (ISRCTN50867461). *J Stroke Cerebrovasc Dis*, **23**, 1312–18.

Stein, M., Misselwitz, B., Hamann, G.F., Scharbrodt, W., Schummer, D.I., & Oertel, M.F. (2012). Intracerebral hemorrhage in the very old: future demographic trends of an aging population. *Stroke*, **43**, 1126–8.

Steiner, T., Al-Shahi Salman, R., Beer, R., et al. (2014). European Stroke Organisation (ESO) guidelines for the management of spontaneous intracerebral hemorrhage. *Int J Stroke*, **9**, 840–55.

Tamaki, T., Kitamura, T., Node, Y., & Teramoto, A. (2004). Paramedian suboccipital mini-craniectomy for evacuation of spontaneous cerebellar hemorrhage. *Neurol Med Chir (Tokyo)*, **44**, 578–82; discussion 583.

Xi, G., Keep, R.F., & Hoff, J.T. (2006). Mechanisms of brain injury after intracerebral haemorrhage. *Lancet Neurol*, **5**, 53–63.

Xue, M. & Del Bigio, M.R. (2000). Intracerebral injection of autologous whole blood in rats: time course of inflammation and cell death. *Neurosci Lett*, **283**, 230–2.

RELATED LINKS TO EBRAIN

Aetiology and Pathophysiology of Spontaneous Intracerebral Haemorrhage. https://learning.ebrain.net/course/view.php?id=168

Management of Spontaneous Intracerebral Haemorrhage. https://learning.ebrain.net/course/view.php?id=166

55

Cavernomata and angiographically occult lesions

Janneke van Beijnum and Hiren Patel

Introduction

Cerebral cavernous malformations (CCMs), known in addition as cavernomata or cavernous (haem)angiomata, are vascular malformations consisting of abnormally enlarged capillary cavities without intervening parenchyma (see section on capillary telangiectasia, this chapter) or arterial feeders with venous drainage (see arteriovenous malformations, Chapter 50). About 10–20% of CCMs are associated with a developmental venous anomaly (DVA, see later in this chapter), which is an extreme variation of the normal venous anatomy. CCMs can occur as result of an underlying genetic disorder, and genetic analysis is recommended in patients with a positive family history or multiple lesions. A conservative approach for asymptomatic CCMs seems justified in the large majority of cases and follow-up imaging is only needed if patients become symptomatic. Indications for surgical treatment are multiples haemorrhages, CCMs with mass effect causing symptoms, and patients with intractable epilepsy with an identified epileptogenic focus. Stereotactic radiosurgery can be considered in exceptional cases with a very high surgical risk.

Pathology

Histological description

On macroscopic examination, CCMs appear as mulberry-like malformations which can vary in size from just a few millimetres to several centimetres. Evidence of haemorrhage in different stages within the CCM and haemosiderin staining of surrounding brain are visible. At a microscopic level, they consist of tightly packed single layer endothelial-lined caverns. The cavern walls are composed of connective tissue lacking organized collagen and a distinct muscular layer which is present in normal vessels and arteriovenous malformations. Additionally, tight junctions between the endothelial cells lining the caverns are missing. This may contribute to the small, repetitive bleeds which are typical for CCMs. Characteristic haemosiderin depositions are present in the basal lamina and intervening neural tissue is absent, which differentiates them from capillary telangiectasia (Wong et al., 2000; Haasdijk et al., 2012).

Theories of pathogenesis, genetics, and familial syndromes

The pathogenesis of CCMs has been partly unravelled by studying the genes implicated in familial CCMs. Familial occurrence of CCMs has been reported in nearly 20% of patients although some of the sporadic cases may represent autosomal dominant inheritance with variable expression and incomplete penetrance. In Hispanic-American patients of Mexican descent, the proportion of familial cases may be as high as 50% due to a shared mutation in the KRIT1 (k-rev interaction trapped protein 1) gene (Q455X) (Haasdijk et al., 2012).

Mutations in three known genes have been associated with CCMs which are outlined in **Table 55.1**. Proteins encoded by these CCM genes are implicated in junction formation between endothelial cells in vessels. Therefore, loss-of-function mutations may result in abnormal blood vessels with gaps between these endothelial subunits.

Although CCMs are vascular lesions, in-situ hybridization studies have demonstrated expression of KRIT-1, MGC4607, and PDCD10 in astrocytes, neurons, and various epithelial cells. Therefore, CCMs could also be the consequence of faulty signalling between endothelial and neural cells and raises the question whether the primary defect in CCMs is of vascular or neuronal origin (Haasdijk et al., 2012).

Furthermore, familial CCMs are less likely to be associated with DVAs than sporadic CCMs, which are associated with a DVA in almost half of the cases. This suggests that a different underlying pathogenic mechanism exist for CCM development (Petersen et al., 2010).

Mutations associated with CCM1 are most common, followed by CCM2, and CCM3 being much more rare. Almost all CCM patients with at least one affected relative will have a mutation in one of the CCM genes, whereas this is the case in 60–80% of patients with multiple lesions, but without affected relatives (Denier et al., 2006; Haasdijk et al., 2012) Although the number of affected relatives is generally lower in CCM3 families, the clinical course appears to be more aggressive in comparison to the CCM1 and CCM2 phenotypes, in both familial and sporadic cases with a greater number of lesions, more frequent haemorrhage and presentation in childhood (Denier et al., 2006; Shenkar et al., 2015).

Table 55.1 Genetics of CCMs

	Chromosome	Possible function(s)
CCM1 KRIT1	7q11.2-21	Cell adhesion (ICAPα), cell spreading (malcavernin), direction of endothelial cell migration (HEG1), tumour suppressor gene (RAP1a)
CCM2 MGC4607 malcavernin	7p13	Lumen formation (PDCD10), vascular permeability (Rac1), migration (kinases in p38 MAPK signalling cascade)
CCM3 PDCD10	3q26.1	Apoptosis (malcavernin), direction of endothelial cell migration (SSTK24)
Unspecified gene	3q26.3-27.2	

Abbreviations: HEG1, heart of glass 1 receptor; ICAP1α, α isoform of the β1-integrin regulator integrin cytoplasmic adaptor protein 1; KRIT1, k-rev interaction trapped protein 1; PDCD10, programmed cell death 10; STK24/25, serine/threonine protein kinase.

Adapted with permission from Remco A Haasdijk, Caroline Cheng, Anneke J Maat-Kievit, Henricus J Duckers, Cerebral cavernous malformations: from molecular pathogenesis to genetic counselling and clinical management, *European Journal of Human Genetics*, Volume 20, Issue 2, pp. 134–40, Copyright © 2011 Springer Nature.

Recommendation

- Genetic analysis is advised in patients with a family history of CCMs or multiple lesions.

Clinical presentation and radiological investigation

Clinical presentation

The incidence of CCMs varies between 0.17 and 0.56 per 100 000 population per year (Brown et al., 1996; Al-Shahi et al., 2003). In the latter prospective population-based study more than half of the CCMs were incidental findings at either autopsy (11%) or imaging (46%; see Al-Shahi et al., 2003). The lower incidence is reported from a retrospective study performed between 1965 and 1992 (Brown et al., 1996) and could therefore be hypothesized as a direct result of the increasing availability of MRI scanners since the 1980s.

CCMs most frequently present in the fourth and fifth decade, and there may be small preponderance in women (58%). Roughly half of patients with CCMs are asymptomatic whereas about a quarter of patients present with either single or multiple epileptiform phenomena. Patients who have experienced a first seizure are extremely likely to develop long-term epilepsy, as only 6% will be isolated. Almost half of the CCM patients become two years seizure-free within 5 years following the diagnosis of epilepsy (Josephson et al., 2011). Additionally, patients can present with either haemorrhage (~12%) or focal deficits (~15%) (Al-Shahi Salman et al., 2012).

Radiological investigation

CCMs are not visible on an angiogram, and therefore can be referred to as angiographically occult lesions, or cryptic vascular malformations. Although a CCM can be diagnosed on a CT-scan by virtue of brain haemorrhage or calcifications, the diagnosis is usually made on MRI imaging (see **Figs. 55.1–55.5**). CCMs can exhibit a heterogeneity in signal characteristics on MR scan, and classically they appear as 'popcorn'-like lesions surrounded by a low-signal rim due to haemosiderin deposition after repeated micro-haemorrhages (on T2(*)-weighted sequences, see **Figs. 55.1–55.3**). Radiologically, CCMs can be categorized into four types (**Table 55.2**), with gradient-echo sequence (GRE) (see **Figs. 55.4** and **55.5** compared to **Figs. 55.2** and **55.3**, respectively) demonstrating CCMs far better than T2, on account of haem causing a susceptibility artefact (Zabramski et al., 1994; Lanzino and Spetzler, 2007).

The most common location for CCMS to occur is lobar (67%), followed by infratentorial (brainstem 14% and cerebellum 13%). Deeply located cavernomata are relatively rare (6%) (Al-Shahi Salman et al., 2012).

Recommendation

- Haem-sensitive MRI sequences such as GRE or susceptibility-weighted sequences should be used in the detection of multiple CCMs.

Natural history of cavernomata

As with arteriovenous malformations, reliable data regarding the natural history of CCMs is scarce. The majority of natural history studies are biased because they describe either selected patients who did not receive treatment for some reason and a short untreated follow-up of those who did receive treatment. Moreover, the large majority of those studies are hospital-based and have not looked at the population in general.

It is generally accepted that the overall annual risk of first-ever CCM-related haemorrhage is low (0.4–0.6% per year) and that the risk of a subsequent haemorrhage is much higher (3.8–23% per year), although this risk decreases over time (Al-Shahi Salman

Table 55.2 Radiological classification of CCMs

Type		T1	T2
I	Signs of (sub)acute haemorrhage with extralesional extension	Hyperintense haemorrhage focus	Hyper- or hypointense bleeding focus which extends through hypointense rim in *type IA* CCMs and without extension in *type IB* CCMs
II	Subacute haemorrhage	Reticulated mixed core	Reticulated mixed core with hypointense rim (typical 'popcorn' lesion)
III	Chronic resolved haemorrhage Usually seen in familial CCMs	Iso- or hypointense lesions	*Standard T2*—hypointense lesions with hypointense rim *GRE*—greater magnification in comparison to T2
IV	Typically seen in familial occurrence of CCMs	Usually not visible	*Standard T2*—usually not visible *GRE*—small punctate hypointense lesions

Source data from Zabramski JM, Wascher TM, Spetzler RF, Johnson B, Golfinos J, Drayer BP, Brown B, Rigamonti D, Brown G. The natural history of familial cavernous malformations: results of an ongoing study. *J Neurosurg* 1994;80:422–32.

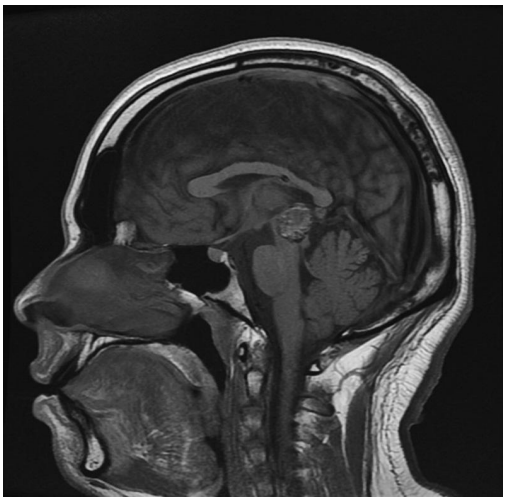

Fig. 55.1 Sagittal T1 MR image of a cavernoma in midbrain.

Fig. 55.2 Axial T2 fast spin echo (FSE) MR image of a pontine cavernoma.

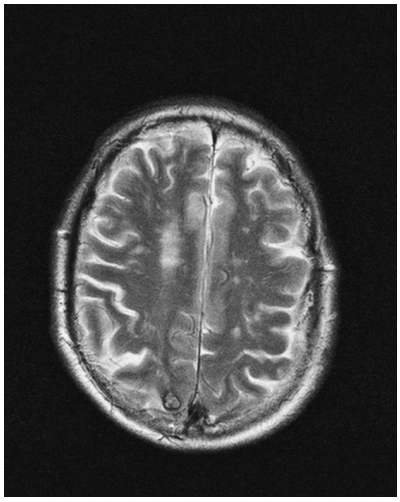

Fig. 55.3 Axial T2 FSE MR image of small cavernoma.

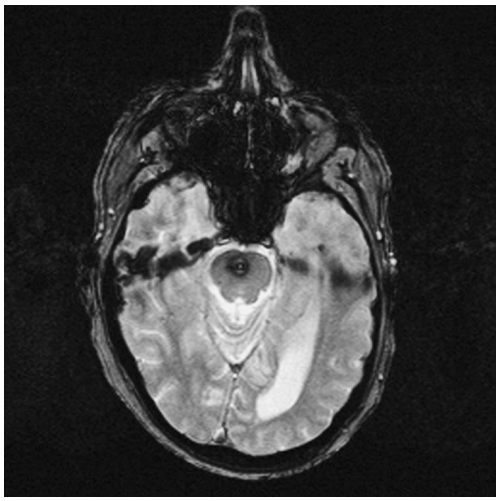

Fig. 55.4 Axial T2 gradient echo (GRE) MR image demonstrating the pontine cavernoma far better due to susceptibility artefact.

et al., 2012; Flemming et al., 2012). Data from a large retrospective hospital-based study reported a variable annual haemorrhage rate of 6.2% in patients who presented with a bleed, 2.2% in patients presenting with non-haemorrhage related symptoms and 0.33% in patients with incidental CCMs. A prospective population-based study showed that the cumulative 5-year re-bleeding risk is almost 30% in patients who initially presented with haemorrhage, whereas the 5-year risk of a first-ever haemorrhage was only 2.4% (Al-Shahi Salman et al., 2012). Presentation with haemorrhage, male sex and multiplicity of lesions can increase the haemorrhage risk (Flemming et al., 2012).

When interpreting the data about CCMs and haemorrhage rate, it is important to note that CCMs can cause symptoms without a recent overt haemorrhage. Moreover, there is a tendency of microscopic leaking of blood resulting in the typical radiological MR appearances of CCMs. This necessitates the need for a clear definition

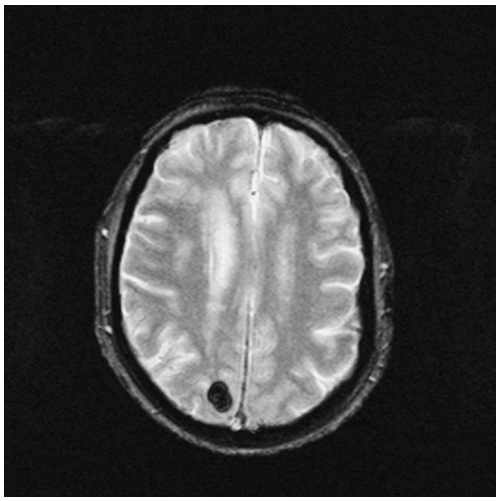

Fig. 55.5 Axial T2 GRE MR image demonstrating cavernoma more clearly compared to Figure 55.3.

of CCM-related haemorrhage. Currently, the definition stands as thus: a clinical event with acute/subacute onset of symptoms with radiological, pathological, surgical or CSF evidence of either recent extralesional or intralesional haemorrhage (Al-Shahi Salman et al., 2008).

Management strategies and outcomes

There are currently no randomized control trials comparing treatment modalities either against each other, or with conservative management. Moreover, there are no observational studies comparing microsurgical resection with radiosurgery (Samarasekera et al., 2012). One population-based cohort study compared surgical and conservative management and concluded that surgery is associated with a worse short-term functional outcome due to early complications after CMM resection. Other predictors of poor outcome following surgery are location of CCM in the brainstem, increasing age, and male sex. Additionally, the risk of symptomatic haemorrhage or new focal neurological deficit was higher after resection in comparison to conservative management. Mortality was comparable; one patient (4.0%) in the surgical group died after a seizure whereas in the conservative group four patients (3.7%) experienced CCM-related deaths (Moultrie et al., 2014).

Conservative management

In all patients, the balance between risk and benefit has to be carefully assessed before considering any intervention. Recent studies show that risks of CCM treatment cannot be disregarded and CCM resection can be associated with a poor short-term outcome when compared to conservative management (Moultrie et al., 2014; Poorthuis et al., 2014). A systematic review showed that the overall incidence of death, haemorrhage or new/worsened permanent deficit after resection or stereotactic radiosurgery (SRS), is approximately 6 per 100 person-years. The surgical risks were lower if patients presented with haemorrhage or in patients with CCMs outside the brainstem (Poorthuis et al., 2014). This suggests that for incidentally discovered CCMs strong consideration should be given to conservative treatment unless a clinical haemorrhage or symptomatic growth occurs during follow-up. Additionally, conservative management should be considered in patients with symptomatic CCMs that are associated with high treatment risks, such as those in eloquent locations (e.g. brainstem).

Surgical resection

Indications for resection are generally previous haemorrhage and/or growth with associated symptoms and signs.

Surgical risks should be weighed against the natural history in every patient, on a case-by-case basis. In general, the threshold for resection should be higher for patients with CCMs in eloquent or surgically inaccessible areas in comparison to patients with CCMs in non-eloquent areas. Surgical experience is key to this decision-making, especially for brainstem CCMs. When considering resection of brainstem CCMs, the cavernoma should reach the pial or ependymal surface, in order to minimize operative neurological deficits. Relatively safe entry zones in the brainstem are summarized in the following paragraph (Giliberto et al., 2010). However, the use of intraoperative electrophysiological monitoring is recommended given the grave consequences if critical structures are damaged.

Safe entry zones in the dorsal midbrain are located just above and below the lamina quadrigemina, and in the lateral mesencephalic sulcus. In the floor of the fourth ventricle, safe entry zones include the median sulcus, the suprafacial triangle (just above the facial colliculus), the infrafacial triangles (just below the facial colliculus). Specifically, with regards to the medial sulcal approach, care must be taken at or above the level of the facial colliculus as the medial longitudinal fasciculus may be encountered resulting in internuclear ophthalmoplegia. In this case an anterolateral approach is more appropriate. In the medulla, the posterior median fissure, posterior intermediate sulcus, and posterior lateral sulcus can be used for relatively safe access. Ventral entry zones include the corridor between SCA and PCA, the 'peritrigeminal area' between the fifth and seventh nerve, the retro-olivary sulcus, and the anterolateral sulcus (Giliberto et al., 2010).

This decision-making process approach is demonstrated by Kivelev et al., who reported outcomes according to a grading scale that their group had developed. In this scale, points are allocated for location (supratentorial 1 point; 2 points if infratentorial, basal ganglia, or spinal) and pre-existing neurological deficit (1 point if present). A good functional outcome (Glasgow outcome score 5: normal activities, minor neurological deficits) was achieved in 87%, 79%, and 46% of patients with grades 1, 2, and 3, respectively (Kivelev et al., 2011).

Most studies looking at resection of CCMs associated with seizures are also limited and lack rigorous definition criteria for epilepsy and subsequent outcome measures (von der Brelie and Schramm, 2011). Seizure freedom in CCM patients with medically refractory epilepsy can be allegedly achieved approximately 88%. Surgery may require more extensive resections in order to accomplish better seizure control. In this series, seizure freedom was achieved in 80% of patients with chronic epilepsy due to CCMs and 91% CCM patients with sporadic seizures (von der Brelie et al., 2013). The surgical procedure will undoubtedly vary with both CCM location and preferred approach.

Preoperative counselling is extremely important in order to inform patients about natural history, benefits (preventing future haemorrhage with related morbidity and mortality) and risks of surgery (including postoperative haemorrhage, infection, focal neurological deficits, CSF leak, epilepsy, and risk to life). The postoperative course after brainstem CCMs resection is likely to be associated with at least a degree of temporary neurologic deterioration, prolonged admission to intensive care with even the possibility of tracheostomy and/or percutaneous endoscopic gastrostomy (PEG) along with subsequent requirements for rehabilitation.

In pooled analyses, the risk of postoperative complications (composite of death within 30 days, symptomatic haemorrhage, new or worsened focal neurological deficit) was estimated at 7.7% (95% CI 5.2–11) for studies looking at resection of predominantly supratentorial CCMs and at 50% (95% CI 37–64%) for resection of brainstem CCMs (Moultrie et al., 2014).

In selecting the appropriate operative approach, preprocedural tri-plane MRI can be helpful. A key principle in approaching a CCM is to find the shortest trajectory which minimizes neural injury, (particularly in spinal cord or brainstem CCMs) and avoiding 'blind-spots' along the surgical corridor. The two-point method can

help to select a surgical approach, utilizing an extended line to the skull that incorporates one point in the centre of the CCM and a second point at where the CCM manifests at the pial surface (or alternatively, at a safe entry point into the brain/spinal cord).

Although intraoperative surgical landmarks such as yellow discoloration can guide the surgeon to the pial or subependymal entry point to identify the CCM, frameless navigation can be of great benefit. Intraoperative monitoring may also be useful, particularly when resecting CCMs in eloquent locations (Lanzino and Spetzler, 2007; Nader et al., 2014).

The general technique of CCM resection involves circumferential dissection of the glial plane in non-eloquent CCMs, emptying of the caverns to achieve internal debulking with subsequent facilitation of resection, by rolling it away from the glial plane. Ideally, an *en-bloc* resection should be attempted, since this minimizes the risk of incomplete resection.

Removal of eloquent CCMs requires an entirely different approach. Essentially, an 'inside-out' dissection is preferable, which is done by entering and emptying the CCM to make it collapse on itself. This is followed by careful dissection of the plan between capsule and eloquent brain tissue to minimize surrounding brain injury.

If the CCM is associated with a DVA, the latter should be preserved during resection as it represents part of the normal venous system. Only small branches of the DVA can be cauterized but sacrifice of the main trunk(s) may lead to venous infarction with potentially disastrous consequences (Lanzino and Spetzler, 2007; Nader et al., 2014).

Stereotactic radiosurgery

The aim of SRS of CCMs is the prevention of haemorrhage by inducing thrombosis-obliteration in the cavernoma. As CCMs are angiographically occult lesions, the effectiveness of SRS cannot be assessed by imaging as in AVMs, but relies solely on the basis of occurrence of haemorrhage during follow-up period (Nagy and Kemeny, 2013). As the risk of recurrent intracranial haemorrhage declines over time (Al-Shahi Salman et al., 2012; Flemming et al., 2012) it is questionable if the reduced haemorrhage risk after SRS that some studies have described can be attributed to this treatment. Therefore, SRS should be restricted to either highly eloquently or surgically inaccessibly areas, such as basal ganglia and brainstem (where the cavernoma does not present at the surface).

Morbidity related to SRS includes both post-treatment haemorrhages and adverse radiation effect. Around 7% of patients were found to have persisting neurological decline resulting from post-SRS haemorrhages. With treatment doses between 12 and 15 Gy and defining the CMS target within the haemosiderin ring, the radiation-related complications are generally between 1% and 7%. A number of SRS studies treating CCM patients with medical refractory epilepsy reported that about 40–50% of patients were seizure-free at follow-up (Nagy and Kemeny, 2013). A comparative study including patients with epileptogenic cavernomata demonstrated 87% of patients were without seizures after surgery compared to 64% after SRS (Hsu et al., 2007).

Recommendations

- Given the major limitations with respect to the evidence guiding management of CCMs only limited recommendations can be made.
- Decision-making regarding patients with CCMs should be done on a case-by-case basis (Samarasekera et al., 2012).
- A conservative approach for asymptomatic CCMs seems justified in the large majority of cases.
- Follow-up imaging is only indicated when patients develop symptoms.
- Resection of CCMs can be considered after recurrent haemorrhage, in patients with CCMs causing mass effect that results in either (progressive) neurological signs or symptoms and in CCM patients with intractable epilepsy. In the latter group, patients should undergo preprocedural evaluation, in order to identify the epileptogenic focus.
- In cases of eloquently located CCMs, the threshold for surgery is raised given the considerably higher morbidity and mortality, but may be considered after repeated extralesional haemorrhages and neurological decline.
- SRS can be considered in exceptional cases, for example recurrent haemorrhages in brainstem cavernomata which do not reach the pial surface and are therefore associated with very high surgical risk.

Other angiographically occult malformations

Developmental venous anomalies

DVA are extreme variations of the normal venous system. They are usually asymptomatic although DVAs may give symptoms due to increased inflow, compromised venous outflow, or remote arteriovenous shunt with increased venous pressure. Haemorrhage may occur but this is usually due to an associated CCM (Osborn, 1994; Pereira et al., 2008). DVAs are thought to develop in compensatory response to incidents during embryogenesis, thereby recruiting and dilating pre-existing transmedullary veins (Pereira et al., 2008).

DVAs can be diagnosed on both CT and MRI as either a curvilinear enhancing structure or flow void with enhancement of the dilated medullary veins ('caput medusae'). Their detection rate is approximately 0.43 (0.31–0.61) per 100 000 patients per year and includes a combined CCM/DVA in at least one-fifth of cases (Al-Shahi et al., 2003; Meng et al., 2014). Additionally, DVAs with three or more medullary veins in the same MRI section, infratentorial lesions, and multiple DVAs were more likely to be associated with a CCM (Meng et al., 2014). The venous phase of angiogram demonstrates the caput medusae aspect of transmedullary veins draining into the venous collector vein, which in turn drains into either the superficial or deep venous system (Osborn, 1994).

Recommendation

- In most patients, DVAs are normal variants that do not require treatment. If a DVA diagnosed during investigation of intracerebral haemorrhage (ICH), one should exclude an associated CCM.

Capillary telangiectasia

A capillary telangiectasia consists of nests of dilated capillaries without smooth muscle or elastic fibres in their walls. The presence of intervening brain parenchyma distinguishes a capillary telangiectasia from a CCM. The most frequent location is the Pons.

Multiplicity is common and they are usually incidental findings on MR or at autopsy. Often they can be found in conjunction with CCMs. Akin to CCMs, capillary telangiectasias are usually not visible on angiogram, but racemose type lesions may show a faint blush and can manifest as a curvilinear area of enhancement on MRI. On T2 or GRE sequences they can be seen as multiple hypointense foci.

It is important to realize that *brain* capillary telangiectasia is *not* a part of hereditary haemorrhagic telangiectasia (HHT). HHT is an autosomal dominant neurocutaneous disorder characterized by *mucocutaneous* capillary telangiectasia and arteriovenous malformations and fistulae in lungs, liver, brain, and spine (Osborn, 1994).

Controversy

The role of SRS in the management of CCMs is debatable. The literature is limited to single centre case series, and expert opinions vary greatly.

Some regard SRS in CCMs as effective as that for AVMs, whereas others consider it only as salvage treatment, or even not at all (Lanzino and Spetzler, 2007; Lunsford and Sheehan, 2009; Nagy and Kemeny, 2013; Lu et al., 2014; Nader et al., 2014; Mouchtouris et al., 2015). As the effect of SRS on CCMs can only be assessed by comparing the incidence of haemorrhage, current publications have therefore been limited to comparing pre- and post-SRS bleeding rates (Samarasekera et al., 2012). A meta-analysis of five retrospective Class III studies, reported a reduced haemorrhage rate after SRS of brainstem CCMs in four of these but a non-significant, slightly increased haemorrhage rate in one. Twelve per cent (12%) of patients experienced new neurological deficits after SRS and 2.2.% died after CCM haemorrhage. Unfortunately, no attempts to assess any kind of bias were made (Lu et al., 2014).

Moreover, as the risk of recurrent intracranial haemorrhage declines over time (Al-Shahi Salman et al., 2012; Flemming et al., 2012), it is questionable as to whether or not the reduced haemorrhage risk after SRS seen in some studies can be attributed to SRS, or may merely represent the natural history of CCMs.

In one handbook on intracranial stereotactic radiosurgery, a conclusion is proffered that the decrease in haemorrhage risk following SRS is limited, whereas the risk of complications is high. The use of SRS for CCMs should thus be limited until a class I randomized controlled trial provides evidence to the contrary (Lunsford and Sheehan, 2009).

FURTHER READING

Al-Shahi Salman, R., Hall, J.M., Horne, M.A., et al. (2012). Untreated clinical course of cerebral cavernous malformations: a prospective, population-based cohort study. *Lancet Neurol*, **11**, 217–24.

Flemming, K.D., Link, M.J., Christianson, T.J., & Brown, R.D. Jr. (2012). Prospective hemorrhage risk of intracerebral cavernous malformations. *Neurology*, **78**, 632–6.

Giliberto, G., Lanzino, D.J., Diehn, F.E., Factor, D., Flemming, K.D., & Lanzino, G. (2010). Brainstem cavernous malformations: anatomical, clinical, and surgical considerations. *Neurosurg Focus*, **29**, E9.

Lanzino, G. & Spetzler, R.F. (2007). *Cavernous Malformations of the Brain and Spinal Cord*. New York, NY: Thieme Medical Publishers.

Moultrie, F., Horne, M.A., Josephson, C.B., et al. (2014). Outcome after surgical or conservative management of cerebral cavernous malformations. *Neurology*, **83**, 582–9.

REFERENCES

Al-Shahi, R., Bhattacharya, J.J., Currie, D.G., et al. (2003) Prospective, population-based detection of intracranial vascular malformations in adults: the Scottish Intracranial Vascular Malformation Study (SIVMS). *Stroke*, **34**, 1163–9.

Al-Shahi Salman, R., Berg, M.J., Morrison, L., Awad, I.A.; Angioma Alliance Scientific Advisory Board (2008). Hemorrhage from cavernous malformations of the brain: definition and reporting standards. Angioma Alliance Scientific Advisory Board. *Stroke*, **39**, 3222–30.

Al-Shahi Salman, R., Hall, J.M., Horne, M.A., et al. (2012). Untreated clinical course of cerebral cavernous malformations: a prospective, population-based cohort study. *Lancet Neurol*, **11**, 217–24.

Brown, R.D. Jr., Wiebers, D.O., Torner, J.C., & O'Fallon, W.M. (1996). Incidence and prevalence of intracranial vascular malformations in Olmsted County, Minnesota, 1965 to 1992. *Neurology*, **46**, 949–52.

Denier, C., Labauge, P., Bergametti, F., et al. (2006). Genotype-phenotype correlations in cerebral cavernous malformations patients. *Ann Neurol*, **60**, 550–6.

Flemming, K.D., Link, M.J., Christianson, T.J., & Brown, R.D. Jr. (2012). Prospective hemorrhage risk of intracerebral cavernous malformations. *Neurology*, **78**, 632–6.

Giliberto, G., Lanzino, D.J., Diehn, F.E., Factor, D., Flemming, K.D., & Lanzino, G. (2010). Brainstem cavernous malformations: anatomical, clinical, and surgical considerations. *Neurosurg Focus*, **29**, E9.

Haasdijk, R.A., Cheng, C., Maat-Kievit, A.J., & Duckers, H.J. (2012). Cerebral cavernous malformations: from molecular pathogenesis to genetic counselling and clinical management. *Eur J Hum Genet*, **20**, 134–40.

Hsu, P.W., Chang, C.N., Tseng, C.K., et al. (2007). Treatment of epileptogenic cavernomas: surgery versus radiosurgery. *Cerebrovasc Dis*, **24**(1), 116-20; discussion 121.

Josephson, C.B., Leach, J.P., Duncan, R., et al. (2011). Seizure risk from cavernous or arteriovenous malformations: prospective population-based study. *Neurology*, **76**, 1548–54.

Kivelev, J., Laakso, A., Niemelä, M., & Hernesniemi, J. (2011). A proposed grading system of brain and spinal cavernomas. *Neurosurgery*, **69**, 807–13.

Lanzino, G. & Spetzler, R.F. (2007). *Cavernous Malformations of the Brain and Spinal Cord*. New York, NY: Thieme Medical Publishers.

Lu, X.Y., Sun, H., Xu, J.G., & Li, Q.Y. (2014). Stereotactic radiosurgery of brainstem cavernous malformations: a systematic review and meta-analysis. *J Neurosurg*, **120**, 982–7.

Lunsford, D. & Sheehan, J.P. (2009). *Intracranial Stereotactic Radiosurgery*. New York, NY: Thieme Medical Publishers.

Meng, G., Bai, C., Yu, T., Wu, Z., Liu, X., Zhang, J., & Zhao, J. (2014). The association between cerebral developmental venous anomaly and concomitant cavernous malformation: an observational study using magnetic resonance imaging. *BMC Neurol*, **14**, 50.

Mouchtouris, N., Chalouhi, N., Chitale, A., et al. (2015). Management of cerebral cavernous malformations: from diagnosis to treatment. *ScientificWorldJournal*, **2015**, 808314.

Moultrie, F., Horne, M.A., Josephson, C.B., et al. (2014). Outcome after surgical or conservative management of cerebral cavernous malformations. *Neurology*, **83**, 582–9.

Nader, R., Gragnaniello, C., Bert, S.C., Sabbagh, A.J., & Levy, M. (2014). *Neurosurgery—Tricks of the Trade—Cranial*. New York, NY: Thieme Medical Publishers.

Nagy, G. & Kemeny, A.A. (2013). Stereotactic radiosurgery of intracranial cavernous malformations. *Neurosurg Clin N Am*, **24**(4), 575–89.

Osborn, A.G. (1994). Diagnostic Neuroradiology. St. Louis, MO: Mosby.

Pereira, V.M., Geibprasert, S., Krings, T., et al. (2008). Pathomechanisms of symptomatic developmental venous anomalies. *Stroke*, **39**, 3201–15

Petersen, T.A., Morrison, L.A., Schrader, R.M., & Hart, B.L. (2010). Familial versus sporadic cavernous malformations: differences in developmental venous anomaly association and lesion phenotype. *AJNR Am J Neuroradiol*, **31**, 377–82.

Poorthuis, M.H., Klijn, C.J., Algra, A., Rinkel, G.J., & Al-Shahi Salman, R. (2014). Treatment of cerebral cavernous malformations: a systematic review and meta-regression analysis. *J Neurol Neurosurg Psychiatry*, **85**, 1319–23.

Samarasekera, N., Poorthuis, M., Kontoh, K., et al. (2012). *Guidelines for the Management of Cerebral Cavernous Malformations*. https://www.guidelinecentral.com/summaries/guidelines-for-the-management-of-cerebral-cavernous-malformations-in-adults/#section-society

Shenkar, R., Shi, C., Rebeiz, T., et al. (2015). Exceptional aggressiveness of cerebral cavernous malformation disease associated with PDCD10 mutations. *Genet Med*, **17**, 188–96.

von der Brelie, C. & Schramm, J. (2011). Cerebral cavernous malformations and intractable epilepsy: the limited usefulness of current literature. *Acta Neurochir (Wien)*, **153**, 249–59.

von der Brelie, C., Malter, M.P., Niehusmann, P., Elger, C.E., von Lehe, M., & Schramm, J. (2013). Surgical management and long-term seizure outcome after epilepsy surgery for different types of epilepsy associated with cerebral cavernous malformations. *Epilepsia*, **54**, 1699–706.

Wong, J.H., Awad, I.A., & Kim, J.H. (2000). Ultrastructural pathological features of cerebrovascular malformations: a preliminary report. *Neurosurgery*, **46**(6), 1454–9.

Zabramski, J.M., Wascher, T.M., Spetzler, R.F., et al. (1994). The natural history of familial cavernous malformations: results of an ongoing study. *J Neurosurg*, **80**, 422–32.

RELATED LINK TO EBRAIN

Principles in Managing Cavernomas. https://learning.ebrain.net/course/view.php?id=1297

SECTION 12

Spinal surgery—principles

56. **Surgical principles in spinal surgery** *661*
Simon Thomson, Chris Derham, and Senthil Selvanathan

57. **Spinal stability** *669*
Peter R. Loughenbury and Richard M. Hall

58. **Spinal physiology** *679*
Sadaquate Khan, Kevin Tsang, and Lamia Nayeb

59. **Medical pathologies of the spinal cord** *687*
Chris McGuigan, Karen O'Connell, Eavan McGovern, and Iain McGurgan

56

Surgical principles in spinal surgery

Simon Thomson, Chris Derham, and Senthil Selvanathan

Preoperative considerations

Patient selection

There are many spinal conditions where the outcomes from surgical and non-surgical management are similar and it is critically important to appreciate the multifactorial nature of back and neck pain. Surgery is effective at dealing with some tissue derived pain inducers, but it has no effect on factors related to secondary gains and can often make these worse. As surgery is frequently only one of many options for a patient, factors such as comorbidities, outstanding litigation, or personality type can significantly change whether surgery is the best way forward. Conversely, in some patients, where for example, there is progressive myelopathy with tight stenosis then even quite severe comorbidities should be tolerated in the decision to treat surgically.

Some patients may choose not to have surgery despite strong indications, this is a legal right and has to be respected. Other patients, however, may want surgery where there is very little indication for it, this may need to be challenged, the surgeon is not obliged to perform surgery in this situation but a second opinion should usually be offered. The assessment of risk versus benefit in spinal patients can be marginal and very challenging, to do it well requires considerable experience, but it is a skill that is as important as any technical skill relating to how a procedure is performed.

Consent and preoperative education

Consent, at least in United Kingdom, is too often thought of as a purely legal process but it should not just be reduced to a discussion of the risks, benefits, and alternatives. Patients need information about many other things including length of stay, post-op activity, and the expected time to return to work. Managing expectations is important, for example, a patient who expects their neck pain to be resolved by an anterior cervical discectomy is highly likely to be disappointed and a patient who expects to stay for 5 days postoperatively will not be keen to mobilize early. However, it should be noted that while informing and educating patients has been extensively studied, mostly in hip and knee surgery, somewhat surprisingly, it has not been shown to improve postoperative anxiety or surgical outcome (McDonald et al., 2014).

Anticoagulation medication

Most medication will continue unchanged during a spinal procedure but anticoagulation and antiplatelet therapy may need to be addressed.

Warfarin should be stopped and anticoagulation will usually reverse in up to five days. Bridging therapy with high dose low molecular weight heparin can be considered depending on the indication for warfarin therapy. High dose low molecular weight heparins will also need to be stopped and the anticoagulation effect will reverse over 24 hours. Rivaroxaban is a newer factor Xa inhibitor, used in place of warfarin. For the surgeon it is important to note that unlike warfarin, the anticoagulant effect is not immediately reversible, but it wears off faster in around 2 days. This is covered further in Chapter 5.

Whether to stop antiplatelet drugs before elective spinal surgery is controversial. Antiplatelet drugs include aspirin, the phosphodiesterase inhibitor dipyridamole, and the adenosine diphosphate (ADP) receptor inhibitors clopidogrel (irreversible) and tricagrelor (reversible). Non-steroidal anti-inflammatory drugs also inhibit platelets but unlike aspirin this effect is only while they are in the circulation and the antiplatelet activity therefore rapidly wears off when the drugs are stopped.

Aspirin works by irreversibly blocking cyclo-oxygenase enzymes. Platelets have no nucleus and cannot replace enzymes. Platelets survive for an average of 10 days, thus if aspirin is stopped it takes 10 days for the entire platelet population to be renewed. However, normal haemostasis can be demonstrated with as few as 20% normal platelets and studies show that reversing the effects of aspirin may take as little as 2–4 days. Furthermore, there is now increasing evidence for a platelet rebound phenomenon with a relative prothrombotic state when aspirin is stopped (Gerstein et al., 2012).

In a large study published in 2011, patients taking antiplatelet drugs for any indication and having elective, non-cardiac surgery were randomized to placebo or aspirin from 10 days preoperatively. There was no difference in major thrombotic or bleeding events (Mantz et al., 2011). With regards to spinal surgery, a non-randomized study was published in 2015 in patients with cardiac stents, having orthopaedic spinal surgery. Those continuing aspirin where compared with those stopping aspirin at least 5 days preoperatively. There was no difference in bleeding related complications between the groups (Cuellar et al., 2015).

Some patients with cardiac stents, especially drug eluting stents are at high risk if their antiplatelet drugs are stopped within a year of the stent being inserted. Discussion with cardiologists before stopping antiplatelet drugs is advised in these cases. Conversely intradural spinal procedures carry a high risk of adverse events if haemorrhage occurs and, in these cases, antiplatelet drugs would normally be stopped.

Operative considerations

Patient positioning

Spinal procedures are performed prone, supine, lateral, or occasionally in a lithotomy position. Correct patient positioning is critically important.

Prone positioning is used for all posterior spinal approaches. When operating on the posterior cervical spine, patients will usually be placed in head pins (Mayfield or Sugita). The chin is flexed down and the head lifted up to maximize the space between the back of the shoulders and the occiput. It is important to ensure that the chin is not resting on the operating table and is clear of the head frame. The operating table will normally be placed in a head-up position. The arms are usually beside the patient. Placing the patient head up improves venous return and therefore helps to reduce intraoperative bleeding.

Prone positioning for lumbar or thoracic spine procedures may be on a frame or spinal operating table that flexes the patient's lumbar spine. It is important to get the width of the supports correct—too close together and the abdomen will be compressed, raising venous pressure; too far apart and the patient will be inadequately supported. Alternatively, the knee elbow position is used by some surgeons which does drop venous pressure very effectively, but care needs to be taken to avoid nerve palsies.

When positioning prone ensure the neck is not overextended, especially if the knee elbow position is used. The axillae should not be compressed, the shoulders must be in a comfortable position and male external genitalia must not be compressed. The eyes are the organs most at risk, the corneas should be protected from pressure and skin prep running round from the back of the neck. Pressure on the eyes can cause blindness and extreme care should be taken to check the eyes in every case.

Supine positioning is used for anterior cervical spine surgery. The head will usually be held on a ring or horseshoe. A rolled towel or other support behind the shoulders helps in getting the right degree of neck extension. Some surgeons will elect to use traction but extreme care should be taken with patients with large cervical disc prolapses where neck extension and traction can cause spinal cord injury. The eyes should be padded to reduce the risk of an inadvertent injury.

Lateral positioning is used for extreme lateral interbody fusion (XLIF) procedures. The positioning of the patient is one of the most fundamental parts of performing safe and effective surgery. It is vital that true lateral and antero-posterior views are obtained using fluoroscopy once the patient is positioned and secured, thus minimizing the risk of parallax errors and reducing the risk of placing the cage obliquely. Depending on the level of surgery being undertaken, the operating table is sometimes 'broken' to allow lateral bending, hence opening up the disc space, particularly at the L4/5 level. The surgical working plane is perpendicular to the sagittal plane allowing the visceral contents to fall forwards upon entering the peritoneal cavity and reducing the risk of injuring its contents. Neuromonitoring assessment is recommended for the XLIF approach especially when approaching the L4/5-disc space in a transpsoas fashion due to the risk of injuring the lumbar plexus. Contra-indications to performing the XLIF approach include anomalous vascular anatomy, peritoneal scarring on both sides and spondylolisthesis greater than grade II.

The anterior lumbar interbody fusion technique (ALIF) allows better surgical access to the L5/S1 disc segments as the iliac crest does not interfere with access to this region as would occur with an XLIF approach. Positioning for the ALIF approach is more straightforward than that for the XLIF, and can be undertaken in a simple supine position with the hips and knees partially flexed and the surgeon approaching from the lateral or lithotomy position. The L5/S1 disc segment is approached as compared to the L4/5 segment due to the configuration of the vascular anatomy. Complications that may arise during the ALIF approach, other than obvious vascular injury, include visceral damage, retrograde ejaculation, and sympathetic dysfunction.

The use of X-rays and checking levels

X-rays are used extensively in spinal surgery to assess bone positions, screw trajectories, and to count levels. X-rays are ionizing radiation and their use is controlled to protect both the public and staff. Nevertheless, failing to use X-rays sufficiently is also a risk.

When using X-rays there is a risk of parallax errors. This occurs, for example if a marking needle is too far from the bones and the X-ray machine is not square to the patient. The risk can be minimized by keeping needles close to the structure that is being marked and ensuring that the X-ray machine is correctly positioned. Images can usually be checked by looking at the end plates or on anteroposterior (AP) views at the pedicles.

Performing surgery at the wrong level is a constant risk in spinal surgery. There are many pitfalls to be cautious of including lumbarization of S1, sacralization of L5, klippel-feil anomalies in the cervical spine, congenital fusion of C2 and C3, and abnormal numbers of vertebrae. The highest risk area is probably the thoracic spine. Various techniques are used to check levels including counting up from the sacrum, counting down from C2, and counting from T12 on the AP view. It is advised that counting is done by two people independently to minimize risk. Preoperative skin marking has been used but it is not very accurate. If this method is used the patient should be X-rayed with the arms in the same position as they will be on the operating table. A preoperative injection of methylene blue dye has also been used successfully to mark levels.

Intraoperative X-rays once the pathology has been reached will help confirm the level. In obese patients, even in experienced hands, it is relatively easy to go up or down a level between the skin incision and reaching bony landmarks.

Operating microscopes and image guidance

Operating microscopes are now widely available in neurosurgical theatres. The lighting and magnification of these instruments allows for smaller wounds and more precise surgery.

Image guidance is also widely available in neurosurgical departments because of its applications in cranial neurosurgery. When

used in the spine it confers some benefits over multiple X-rays. The radiation dose for the patient and theatre staff is reduced and visualization in any plane is possible with image guidance. This is particularly useful when the anatomy is not quite typical.

Image guidance registration in the spine relies on a reference being anchored to an adjacent vertebra. The vertebra of interest is then registered from multiple points on the spinous process and lamina or by using X-ray. Screw trajectories can then be assessed based on the preoperative computed tomography (CT) scan images.

Intraoperative neurophysiology in spinal surgery

Somatosensory evoked potentials (SSEPs) are measured percutaneously from the scalp over the sensory cortex. A stimulus is applied, usually using bipolar electrical stimulation over a peripheral nerve such as the median nerve at the wrist or the posterior tibial nerve at the ankle. The signal is carried in the dorsal columns.

The signal from a single stimulus is too small to be detected and gets lost in the background brain electrical activity. A technique called signal averaging is used where between 100 and 1000 signals are averaged, this results in a better signal to noise ratio. Averaging this number of signals, however, takes several minutes so SSEPs do not give immediate feedback on spinal cord function.

Motor-evoked potentials (MEPs) are measured from a muscle after a stimulus is given to the motor cortex. Signal averaging is not required for MEPs but the patient may 'jump' so surgery should be stopped briefly when the stimulus is applied, for this reason MEPs cannot be run continuously like SSEPs. The motor signal is carried in the corticospinal tracts which are more anterior in the cord. The anaesthetist should not use paralysing anaesthetic agents and total intravenous anaesthesia is usually required. Thus, SSEP and MEPs are complementary tests and will frequently be used together.

During SSEP monitoring, a 10% increase in latency from baseline, or a 50% reduction in amplitude are suggestive of a dorsal column insult in the spinal cord and this can be used to prevent further cord injury during surgery. The situation is different for the MEP response. Any significant change in morphology, amplitude or a disappearance would suggest pathological disruption to the anterior cortico-spinal tracts and some neurophysiologists may view this an all or nothing response (i.e. a non-reversible insult to the cord has occurred when this is registered). It is important to recognize that although the aforementioned changes are sensitive, they are not specific for cord injury and not uncommonly there can be false positives. Other factors such as change in temperature, blood pressure, use of volatile anaesthetics, and muscle relaxants can also affect the readings.

Neurophysiology is now routinely used in scoliosis surgery as an alternative to the 'wake up test'. It has become more commonly used in other areas of spinal surgery especially in intramedullary tumour surgery. In some countries neurophysiology is a routine part of monitoring the patient for all spinal procedures, but this is not standard practice in all parts of the world.

Fusion in spinal surgery

All metal work will eventually fail if bony fusion does not occur. In patients with malignant spinal cord compression the construct has to be longer than in patients with a traumatic spinal injury because the former is not likely to fuse while the latter usually will.

Fusion rates in the cervical spine are over 90% for anterior cervical discectomy procedures but the lumbar spine does not fuse as readily (Fraser and Härtl, 2007). Although failure of fusion can occur at either site, it is much more common in the lumbar spine. Fusion failure most commonly presents as spinal pain, especially on movement. It is best confirmed with dynamic X-rays or a CT scan.

Fusion can be promoted during an operation by decorticating bone surfaces, by adding autograft, usually taken from the iliac crest or by using several different surgical products including allogeneic cancellous or cortical bone, demineralized bone matrix, or synthetic calcium phosphate-based bone-graft substitutes. All of these provide a scaffold along which osteoblasts can migrate (**Fig. 56.1**).

Recombinant bone morphogenetic protein 2 (rhBMP-2) promotes osteoblast differentiation and is effective in promoting spinal fusion. Recent data has raised significant safety concerns with BMP2 including life-threatening events. Complications include implant displacement, subsidence, infection, urogenital events, retrograde ejaculation, radiculitis, ectopic bone formation, osteolysis, and poorer global outcomes (Carragee et al., 2011).

A review examining whether non-steroidal anti-inflammatory drugs inhibit bone fusion concluded that there is a pooled odds ratio of 3.0 for non-union in patients taking NSAIDs but that this becomes non-significant when only high-quality studies are used (Dodwell et al., 2010). Smoking also inhibits spinal fusion (Bydon et al., 2014).

Spinal surgery implants

The use of internal fixation started in the appendicular skeleton (limbs) before being used in the axial skeleton (spine). These implants can be utilized in the correction of deformity (scoliosis and kyphosis) and stabilization (fracture, dislocations, malignant, infective, and degenerative pathologies). Various implants have been used over the decades including hooks and wire-rod constructs but these relied on the presence of a lamina and are now little used. The major advance in spinal instrumentation came about following the introduction of the screw-rod fixation systems. These systems utilize pedicles and lateral masses as fixation points, the advantage being that these structures are strong fixation points in the spine. Furthermore, the screw-rod system allows instrumentation of the sacrum and can be combined with a laminectomy. Modern systems are non-ferrous to permit MRI scanning.

Screws consists of two parts (i.e. the section that contains the thread (shaft) and the head which consists of the housing where the rod sits). The variation of the different types of screws is based on the type of head, the type of interface between the screw head and shaft, whether the shaft is fully threaded/partially threaded and finally if the shaft is fenestrated.

An important aspect of screw design is the interface between the screw head and shaft. This interface provides freedom between the screw head and shaft, there are two main types; monoaxial and polyaxial screws.

Monoaxial screws (**Fig. 56.2**) do not allow movement between the screw head and the shaft. This is ideal for deformity correction however rod contouring can be difficult. Polyaxial screws on the other hand have a joint with a spherical head enclosed in a housing which allows the screw head to move in relation to the shaft. The advantage of polyaxial screws is that they allow the surgeon some flexibility in connecting screws to the rods. Polyaxial screws also have a safety

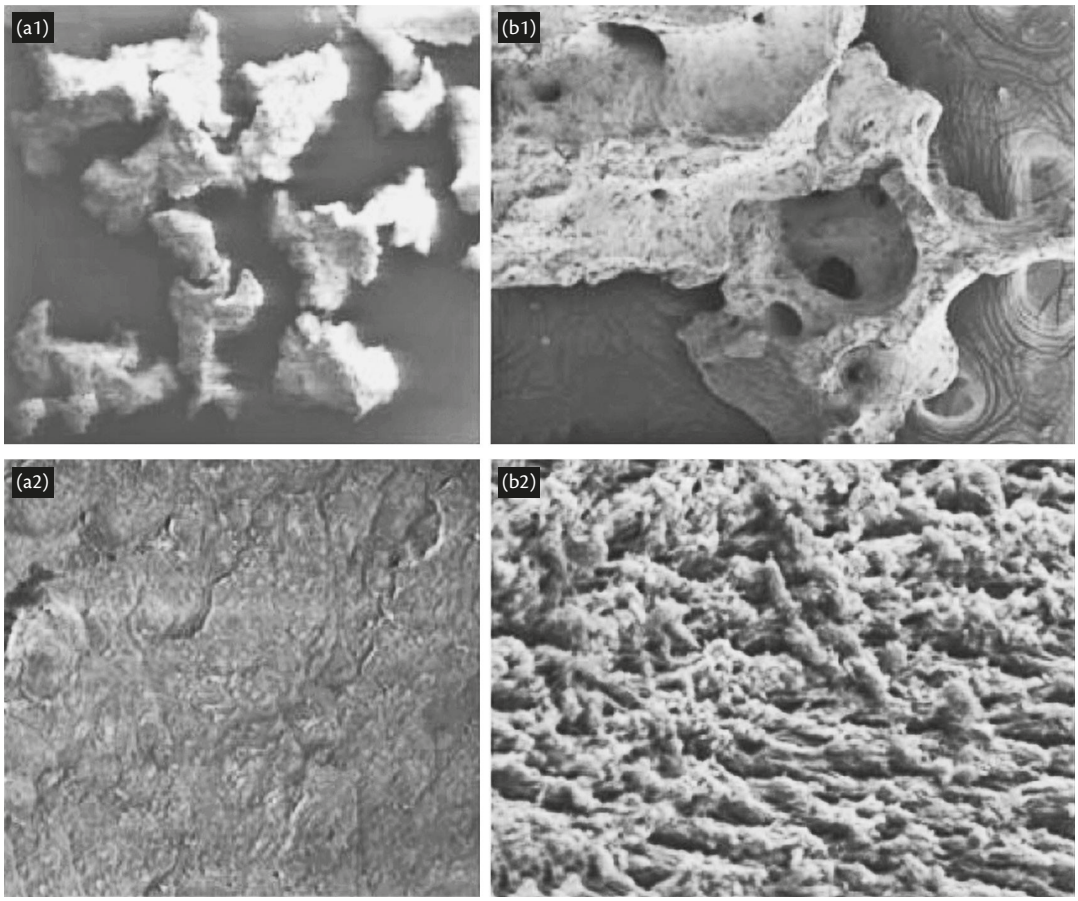

Fig. 56.1 Scanning electron microscope images of the synthetic bone substitute NanoBone® (a1, a2), whereas b1 and b2 show the characteristics for xenogenic material Bio-Oss®. (upper row: ×25 magnification, scale bar = 1 mm; lower row: ×2000 magnification, scale bar = 20 μm) (see Ghanaati et al., 2013).

benefit of failing at the head–shaft interface rather than along the screw shaft or rod.

Polyaxial screws (Fig. 56.3) can be further divided into uniplanar and multiplanar types. Uniplanar or uniaxial screws allow movement in the cranial/caudal plane only. This is useful in scoliosis cases where the polyaxial element helps in the siting of the rods and the absence of medial/lateral movement enables rotation of the vertebra.

Multiplanar polyaxial screws may be non-biased or have a biased or favoured angle. The non-biased angled polyaxial screw offers up to 30° of angulation in each direction (i.e. 60° conical movement). In biased angle polyaxial screws the offset angle of the screw head, will allow angulation of up to 55° in one direction. This high degree of angulation enables the screws to be placed in their best anatomical position at the same time avoiding the need for difficult rod contouring.

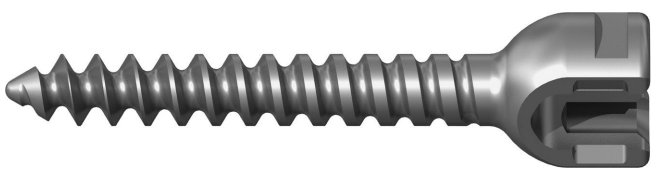

Fig. 56.2 Monoaxial screw with a fixed head.

There are also variations in the shaft designs. There are fully threaded or smooth shank screws. Smooth shank screws have a 10 mm unthreaded segment and are used in the C1 lateral mass where the smooth shank is designed to prevent the thread irritating the C2 nerve root. Another type of smooth shank screw is a lag screw which also has an unthreaded segment and a distal half that is threaded. This is used in fixation of peg fractures where the thread is in the odontoid peg and the smooth shaft in the C2 vertebral body, tightening the screw compresses the fracture and therefore enhances bony fusion. A major difference between the lag screw and the smooth shank screw is that the screw head in the lag screw is flat to enable it to sit flush with the prevertebral fascia, while the smooth shanked C2 screw has a head that can accommodate a rod.

Some screws are fenestrated with a hole down the middle of the screw. This enables K-wires to guide placement of the screw or insertion of cement into the vertebral bodies through the screws.

The pitch of the screw is the distance travelled by the screw in one 360 degree turn. A fine pitched screw travels a short distance in one turn, is used in cortical bone and generally has a higher pull out strength, while a course pitch screw travels further with each turn requires less force to insert and is used in cancellous bone. There is an outside or nominal diameter and a core diameter. The length is measured from the base of the head to the tip. Where a screw has a poor hold a rescue screw may be used—it will usually have a wider

Fig. 56.3 Polyaxial screw showing how the head can move on the shaft.

diameter and coarser pitch than the conventional screw it is used to replace.

Screw tips may be rounded requiring the drilling of a pilot hole and the hole will need tapping to start the screw off. A second type of screw tip is self-tapping—it has cutting flutes at the tip but still requires a pilot hole. Finally, self drilling screws are sharp and do not require a pilot hole at all.

Anterior vertebral constructs frequently utilize plates. These may be either locking or non-locking/dynamic plates. In locked plates the screw is held in the plate so that the angle of the screw to the plate is fixed. Conversely, dynamic plates allow some movement as the fracture 'settles'. Most plate/screw systems also have a method of stopping the screws from backing out of the plate over time. It is important to appreciate that the screw/plate and screw/rod constructs primarily resist distraction forces, while a cage primarily resists compression forces hence combining the two systems is likely to give the best stability.

Artificial disc replacement was first tried in 1966 (Fenstrom) and then abandoned in the cervical spine. Subsequently especially in the last 20 years, however, it has been developed further both in the lumbar and the cervical spine. There is now 10 year follow up data on lumbar disc arthroplasty showing an improvement in Oswestry Disability Index (ODI) (Le et al., 2004). Several different disc designs are available made of metal, polyurethane, or ultra-high-molecular-weight polyethylene (UHMWPE) (Fig. 56.4). The spine is expected to flex approximately 100 million times in a lifetime, and this puts high demands on artificial disc replacements. Surgical precision in placing these exactly in the midline is important. Problems that have been noted with these discs include implant movement, joint fusion, dysphagia (in the cervical spine) and implant fracture.

Fig. 56.4 ActivC cervical arthroplasty made from cobalt-chrome-molybdenum and high molecular polyethylene.

Minimally invasive spine

Spinal surgery frequently involves large incisions and extensive muscle dissection, consequently postoperative pain, infection, and wound problems are sometimes problematic. Minimal access surgery is a collection of techniques designed to minimize the size of the incision and muscle injury but permit the surgeon to perform the same decompression and/or fusion. The specific techniques are covered elsewhere, the general principles are explained here.

Open minimal access surgery requires that the wound is correctly positioned, and that appropriate retractors and long-handled instruments are used. The operating microscope is essential, not just for its optical magnification but also for the lighting that is designed to run parallel with the line of vision. Tubes have been developed that can act as access ports and are inserted over a series of dilators. Tubes provide excellent access for decompression procedures such as lumbar discectomy, laminectomy, and cervical foraminotomy. The extreme lateral interbody fusion technique provides a good example of how it is possible to perform extensive surgery through a 2 cm incision.

Instrumentation can also be inserted using minimal access techniques, pedicle screws are inserted through stab incisions then a rod can be rotated down into the screw heads. The main problem with this approach is that bony fusion is more difficult to promote. The technique is therefore probably best suited to malignant spinal cord compression cases.

The benefits of minimal access surgery are less pain, less analgesia requirements, and shorter lengths of stay. The disadvantages are that these operations may be more difficult than the open alternatives, risks of incorrect port placement, more X-ray exposure, inability to fuse bones, and the equipment is often expensive.

Infection prevention

Neurosurgical perioperative infection prevention, including the use of systemic antibiotics is covered in Chapter 95. Only factors specific to spinal surgery will be considered here.

Skin hair removal is usually unnecessary in the spine and there is no evidence that it reduces infection rates. If hair has to be removed then using razors as opposed to clippers has been found to increase the risk of surgical site infections (NICE, 2008).

In a large but unrandomized study, topical gentamicin applied on a collagen sponge reduced postoperative discitis. In this study

neither the treatment or placebo group had systemic antibiotics (Rohde et al., 1998).

Lamina flow theatres have been recommended for use in all orthopaedic implant surgery, however, the evidence for this comes from joint replacement surgery, there are no randomized studies in spinal surgery and recent work has suggested that lamina flow may even be a risk factor for surgical site infection as a result of patient hypothermia or poorly positioned theatre staff (Gastmeier et al., 2012).

Preoperative showering, double gloving and maintaining normothermia are also factors relevant to spinal surgery recommended by the UK National Institute for Clinical Excellence (NICE, 2008).

Postoperative considerations

Analgesia

Posterior spinal, transthoracic, and transabdominal approaches can cause significant postoperative pain. Analgesics like paracetamol, opioids, and non-steroidal anti-inflammatory drugs are widely used. The non-steroidal anti-inflammatory drugs may prevent fusion and can cause gastric problems, asthma, cardiac, and renal impairment. Local anaesthetic in the wound may help as part of a balanced analgesic regime and is often used with adrenalin before the skin incision is made to reduce bleeding from the skin edges. Paravertebral blocks are sometimes used in transthoracic surgery and there is randomized evidence to show benefit from perioperative single dose epidural fentanyl in lumbar surgery (Guilfoyle et al., 2012).

Venous thromboembolism (VTE)

Early mobilization, good hydration, and compression stockings and/or boots should be standard practice to minimize the risk of venous thromboembolism.

Low molecular weight heparins are widely used but there is little agreement on whether they should be started preoperatively or how long postoperatively (Bono et al., 2009). The incidence of deep vein thrombosis in spinal surgery is estimated as anywhere between 0.29% and 31% and is very dependent on the screening method used. There is evidence that low molecular weight heparins reduce the risk of VTE in spinal surgery but there is also evidence that they are underutilized because of concern about postoperative compressive extradural haematomas even though the reported incidence of this complication is only between 0% and 1% (Hamidi and Riazi, 2015).

Physiotherapy

Physiotherapy is widely utilized following spinal surgery—it has five main themes as follows; mobilizing patients; spinal range of motion exercises; stability exercises; neural mobility exercises; and advice and education.

In a recent review there is some low-quality evidence that physiotherapy improves outcome after surgery (Gillmore et al., 2015). Which of the physiotherapy themes is most important, the role of preoperative physiotherapy, and whether inpatient or outpatient physiotherapy should be used is not clear, however. There is considerable variability in referral to outpatient physiotherapy and in the degree of physiotherapy intervention that is provided.

FURTHER READING

Bydon, M., De la Garza-Ramos, R., Abt, N.B., et al. (2014). Impact of smoking on complication and pseudarthrosis rates after single- and 2-level posterolateral fusion of the lumbar spine. *Spine (Phila Pa 1976)*, **39**(21), 1765–70.

Cuellar, J.M., Petrizzo, A., Vaswani, R., Goldstein, J.A., & Bendo, J.A. (2015). Does aspirin administration increase perioperative morbidity in patients with cardiac stents undergoing spinal surgery? *Spine (Phila Pa 1976)*, **40**(9), 629–35.

Dodwell, E., Latorre, J.G., Parisini, E., et al. (2010). NSAID exposure and risk of nonunion: a meta-analysis of case–control and cohort studies. *Calcif Tissue Int*, **87**(3), 193–202.

Fraser, J.F. & Härtl, R. (2007). Anterior approaches to fusion of the cervical spine: a meta-analysis of fusion rates. *J Neurosurg Spine*, **6**(4), 298–303.

NICE (2008). *Surgical Site Infections: Prevention and Treatment*. Clinical guideline [CG74]. https://www.nice.org.uk/guidance/cg74/chapter/guidance

REFERENCES

Bono, C.M., Watters, W.C., Heggeness, M.H., et al. (2009). An evidence-based clinical guideline for the use of antithrombotic therapies in spine surgery. *Spine J*, **9**(12), 1046–51.

Bydon, M., De la Garza-Ramos, R., Abt, N.B., et al. (2014). Impact of smoking on complication and pseudarthrosis rates after single- and 2-level posterolateral fusion of the lumbar spine. *Spine (Phila Pa 1976)*, **39**(21), 1765–70.

Carragee, E.J., Hurwitz, E.L., & Weiner, B.K. (2011). A critical review of recombinant human bone morphogenetic protein-2 trials in spinal surgery: emerging safety concerns and lessons learned. *Spine J*, **11**(6), 471–91.

Cuellar, J.M., Petrizzo, A., Vaswani, R., Goldstein, J.A., & Bendo, J.A. (2015). Does aspirin administration increase perioperative morbidity in patients with cardiac stents undergoing spinal surgery? *Spine (Phila Pa 1976)*, **40**(9), 629–35.

Dodwell, E., Latorre, J.G., Parisini, E., et al. (2010). NSAID exposure and risk of nonunion: a meta-analysis of case–control and cohort studies. *Calcif Tissue Int*, **87**(3), 193–202.

Fraser, J.F. & Härtl, R. (2007). Anterior approaches to fusion of the cervical spine: a meta-analysis of fusion rates. *J Neurosurg Spine*, **6**(4), 298–303.

Gastmeier, P., Breier, A.C., & Brandt, C. (2012). Influence of laminar airflow on prosthetic joint infections: a systematic review. *J Hosp Infect*, **81**(2), 73–8.

Gerstein, N.S., Schulman, P.M., Gerstein, W.H., Peterson, T.R., & Tawil, I. (2012). Should more patients continue aspirin therapy perioperatively? *Ann Surg*, **255**(5), 811–19.

Ghanaati, S., Barbeck, M., Lorenz, J., et al. (2013). Synthetic bone substitute material comparable with xenogeneic material for bone tissue regeneration in oral cancer patients: first and preliminary histological, histomorphometrical and clinical results. *Ann Maxillofac Surg*, **3**(2), 126–38.

Gillmore, S.J., McClelland, J.A., & Davidson, M. (2015). Physiotherapeutic interventions before and after surgery for degenerative lumbar conditions: a systematic review. *Physiotherapy*, **101**, 111–18.

Guilfoyle, M.R., Mannion, R.J., Mitchell, P., & Thomson, S. (2012). Epidural fentanyl for postoperative analgesia after lumbar canal decompression: a randomized controlled trial. *Spine J*, **12**(8), 646–51.

Hamidi, S. & Riazi, M. (2015). Incidence of venous thromboembolic complications in instrumental spinal surgeries with preoperative chemoprophylaxis. *J Korean Neurosurg Soc*, **57**(2), 114–18.

Le, H., Thongtrangan, I., & Kim, D. (2004). Historical review of cervical arthroplasty. *Neurosurg Focus*, **17**(3), E1.

McDonald, S., Page, M.J., Beringer, K., Wasiak, J., & Sprowson, A. (2014). Preoperative education for hip or knee replacement. *Cochrane Database Syst Rev*, **5**, CD003526.

Mantz, J., Samama, C.M., Tubach, F., et al. (2011). Impact of preoperative maintenance or interruption of aspirin on thrombotic and bleeding events after elective non-cardiac surgery: the multicentre, randomized, blinded, placebo-controlled, STRATAGEM trial. *Br J Anaesth*, **107**(6), 899–910.

NICE (2008). *Surgical Site Infections: Prevention and Treatment*. Clinical guideline [CG74]. https://www.nice.org.uk/guidance/cg74/chapter/guidance

Rohde, V., Meyer, B., Schaller, C., & Hassler, W.E. (1998). Spondylodiscitis after lumbar discectomy. Incidence and a proposal for prophylaxis. *Spine (Phila Pa 1976)*, **23**(5), 615–20.

RELATED LINKS TO EBRAIN

Advanced Microsurgical Skills. https://learning.ebrain.net/course/view.php?id=93

Intraoperative Imaging Techniques. https://learning.ebrain.net/course/view.php?id=89

Intraoperative Neurosurgical Electrophysiological Monitoring. https://learning.ebrain.net/course/view.php?id=489

The Modern Theatre Environment. https://learning.ebrain.net/course/view.php?id=97

The Operating Microscope. https://learning.ebrain.net/course/view.php?id=94

Use of Standard Neurosurgical Equipment. https://learning.ebrain.net/course/view.php?id=70

X-ray Development, Physics, Uses, Risks and Regulation. https://learning.ebrain.net/course/view.php?id=788

57

Spinal stability

Peter R. Loughenbury and Richard M. Hall

Anatomy of the vertebral column

The vertebral column is a series of bones that connect the head to the pelvis. In humans, this has become highly specialized to allow for an upright posture and bipedal gait, so that the column stands as a vertical rod held in position by ligaments and muscles. There is a unique mechanical arrangement of structures within the spine and a complex relationship between the vertebral column and the skull and pelvis. Vertebral bodies increase in size from cranial to caudal to resist increasing compressive forces placed upon them. At the craniocervical junction a large proportion of the weight of the skull passes through the vertebrae leading to less developed postvertebral muscles with a smaller area of attachment. Whereas, the increased weight transferring to the pelvis leads to a large fused sacrum and more efficient transfer of weight to the lower limbs.

The vertebral column is comprised of 24 mobile vertebrae (7 cervical, 12 thoracic, 5 lumbar), 4–5 fused sacral vertebrae, and 4 fused coccygeal vertebrae. Between the mobile presacral vertebrae motion is limited by the intervertebral discs, paired posterior synovial facet joints, intervertebral ligaments, and the paraspinal muscles. The interaction of these various elements is essential for normal spinal biomechanics and function. In adults the length of the column is 72–75 cm with one-quarter of this length being due to the intervertebral discs. Approximately 40% of overall height is due to the vertebral column and differences in height reflect differing limb lengths rather than the variation in the length of the column. In addition, diurnal variations in height of around 2 cm have been reported and there is a clear loss of height with increasing age due to dehydration of the intervertebral discs.

The primary roles of the vertebral column are to protect the spinal cord, provide both stability and mobility, and to control the transmittance of movement to the upper and lower extremities. The column is adapted to perform these functions with complex articulations that allow movement and provide stability at each level and globally over the whole spine. In the sagittal plane there is an anterior convexity in the lumbar and cervical regions (lordosis) and a posterior convexity in the thoracic and sacral regions (kyphosis). This pattern develops during the early years of growth as an individual begins to ambulate. The curve seen in the sacrum is permanent as these segments are fused, but the rest of the spine is mobile and the magnitude of these curves can vary to maintain posture. In the upright position the anterior column (consisting of the vertebral bodies and intervening intervertebral discs) is responsible for the majority of load transfer in the spine. The posterior elements protect the spinal canal and include the facet joints, which both permit and limit rotation, flexion, extension, lateral bending, and translation. A typical articulation between two adjacent presacral vertebrae (excluding between the first two cervical vertebrae) consists of two posterior intervertebral facet joints, between the inferior and superior articulating facets, and the intervertebral disc. This creates three points of articulation between each vertebra.

Vertebral anatomy and regional variation

Although there is regional variation in bony anatomy of the vertebrae there is a general trend for the width, depth, and height of the vertebral bodies to increase from cranial to caudal levels. This correlates with the increased compressive strength of the vertebra in response to the greater axial loads experienced in more caudal segments. The vertebral body consists of cancellous bone with an outer shell of cortical bone. The microarchitecture of the cancellous bone is adapted so that the trabeculae are orientated along the lines of application of load. This arrangement provides resistance to dynamic loading.

The C1 (atlas) vertebra (**Fig. 57.1A**) is atypical, as it has no vertebral body. There is an anterior arch, with the odontoid peg directly behind it, and a flattened posterior arch with a small midline posterior tubercle. The articular processes are medially orientated to permit both flexion/extension and rotational movements. C2 (axis) (**Fig. 57.1A**) is a more typical cervical vertebra and includes the odontoid peg, a superior bony extension of the vertebral body that lies behind the arch of C1. The largest spinous process in the spine is located at C2. There is a uniform morphology of cervical vertebrae from C3 to C7 (**Fig. 57.1B**), often called the subaxial spine. In this region the uncinate processes on the superior anterolateral aspects of the vertebral bodies articulate with a corresponding articulation of the vertebral body above. This articulation (the uncovertebral joint) aids rotation in the cervical spine. Thoracic spine vertebrae also exhibit a uniform morphology (**Figs. 57.1C** and **57.1D**) with long, inferiorly angulated spinous processes and facet joints that are vertically orientated. There are costovertebral joints from T1 to

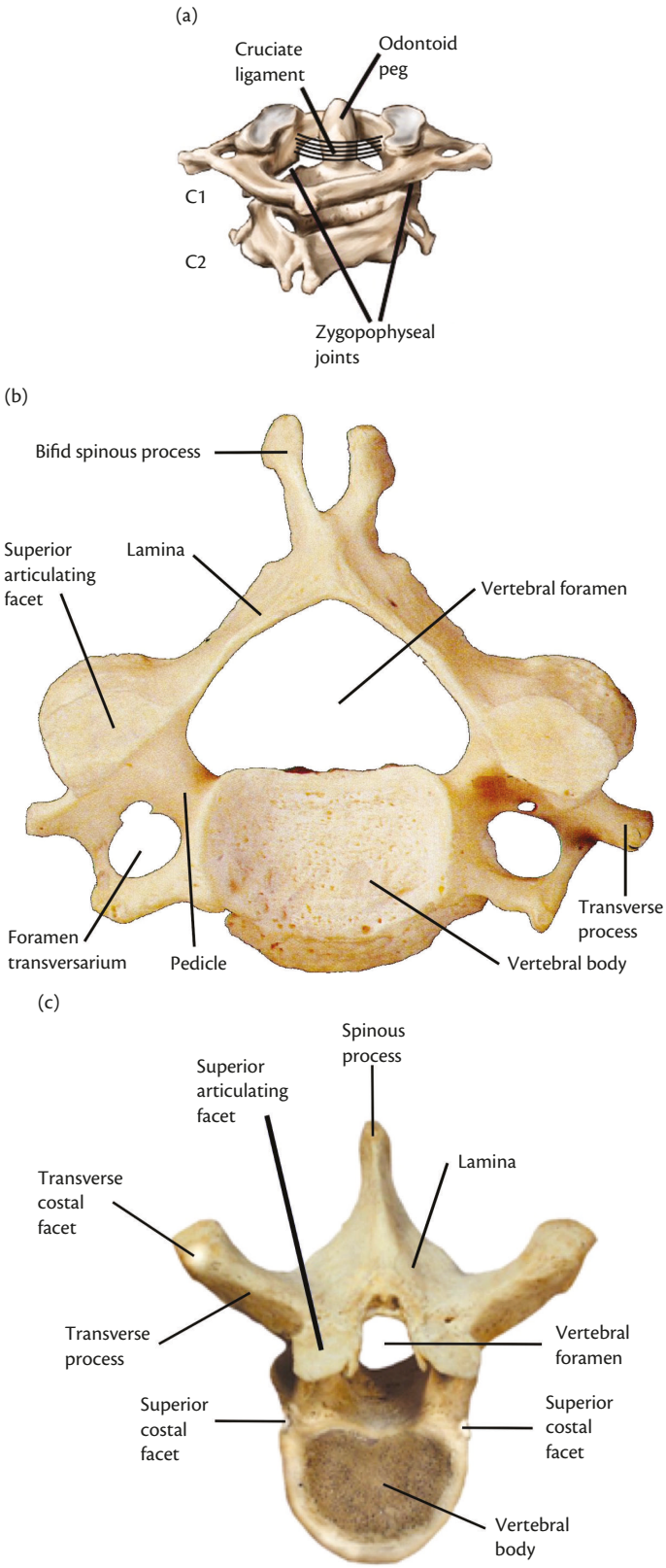

Fig. 57.1 Vertebral anatomy of (A) C1/C2 articulation; (B) axial view of a typical cervical vertebra; (C) axial view of a typical thoracic vertebra; (D) lateral view of a typical thoracic vertebra; (E) axial view of a typical lumbar vertebra; and (F) lateral view of a typical lumbar vertebra.

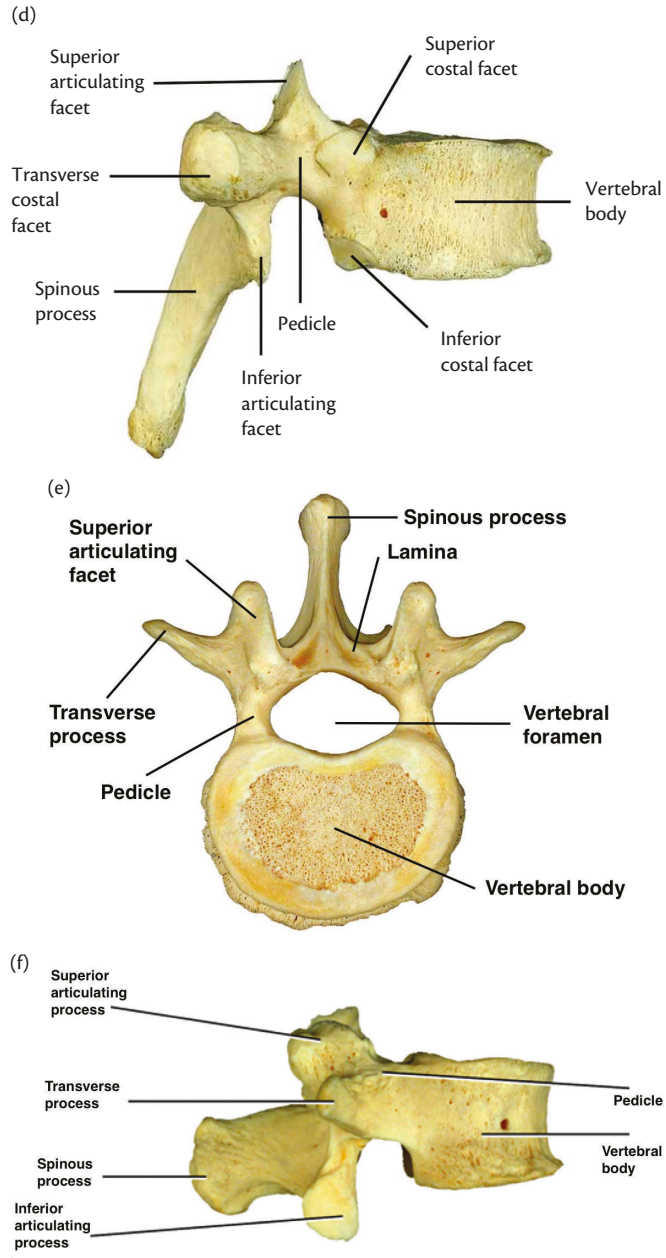

Fig. 57.1 Continued

T12 that provide an articulation between the vertebral body and the corresponding rib. There are also rib articulations on the transverse processes from T1 to T10. In this region the ribs, sternum, and intercostal structures provide extra stability. Lumbar vertebrae (Figs. 57.1E and 57.1F) have a stout, kidney-shaped body, straight spinous processes, and facet joints that are orientated in the sagittal plane.

Intervertebral disc

The intervertebral disc lies between the inferior end plate of the vertebra above and the superior endplate of the vertebra below. It is a composite structure with a central nucleus pulposus surrounded by a multiple layered annulus fibrosus (Fig. 57.2). It acts to transmit load,

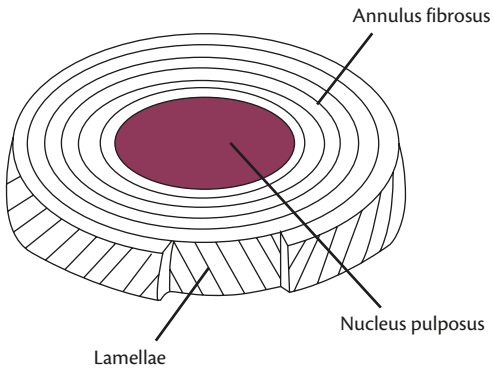

Fig. 57.2 Structure of the intervertebral disc.

allow movement, and provide stability. Axial load is transmitted effectively due to the structure of the disc. The nucleus is comprised mostly of water (80–90%), type 2 collagen, and multiple hydrophilic proteoglycans. The interaction between the annulus fibrosus and these proteoglycans leads to a unique hydrostatic structure. When the nucleus is loaded in compression water seeps out and the height of the disc is reduced, but the turgidity of the nucleus allows transmission of the force to the obliquely orientated fibres in the multiple layers (lamellae) of the annulus. The collagen fibres (type 1 collagen) are orientated at 60–70° to the vertical and this orientation alternates between each concentric layer. Fibres are connected to the cartilaginous vertebral endplates and to the cortical bone of the vertebral body walls (Sharpey's fibres). As the complex is loaded the fibres are placed under tension and this arrangement allows a multidirectional distribution of the tensile force and prevents formation of a cleavage plane through which the nucleus could herniate. The disc is poorly innervated and supplied by only sensory (mainly nociceptive) and postganglionic sympathetic (vasomotor efferent) nerve fibres.

The ability of the disc to resist axial compression decreases with age. The proteoglycan content of the nucleus changes and there is a decrease in the volume of water retained. Loss of disc height is observed alongside changes in the chemical composition of the nucleus due to sclerotic endplates impeding nutrient transfer. The orientation of the annular fibres resists tensile forces and is also effective at resisting rotation. However, they do not resist direct compression and as a result disc bulging is often seen on the concave side of a physiological or pathological curve of the spine. Asymmetric loading of the disc in a curved spine also leads to migration of the nucleus pulposus towards the convex side. Within a normal lumbar lordosis flexion therefore causes anterior compression of the annulus and a posterior migration of the nucleus pulposus. Disc bulges occur due to annulus compression and are often seen on magnetic resonance images of the spine. They should not be confused with a disc herniation where the nucleus pulposus is displaced from its normal anatomical location through a tear in the annulus to lie within the canal.

Posterior elements

The posterior elements include the laminae, spinous process, and bilateral facet joints. The posterior bony arch is formed by the laminae and provides protection for the neural elements within the canal. In the midline, the spinous processes provide a large surface area for ligamentous and tendinous attachments. The muscles and ligaments that attach onto the posterior elements act to move the spine and to provide global stability for the vertebral column. The spinous processes generally have a caudal orientation and this angulation increases in the cervical and upper thoracic spine. Less caudal angulation is seen in the thoracolumbar and lumbar regions. The spinous processes of C3-C6 are typically bifid.

The facet joints (apophyseal or zygapophyseal joints) are synovial plane joints between superior and inferior articulating processes on two adjacent vertebrae. The orientation of the joints varies in different regions of the spine and has a significant impact on the regional biomechanics. In the cervical spine the facet joints are orientated in the coronal plane. This produces the increased range of flexion-extension, lateral bending, and rotation observed in the cervical spine. In the lumbar region the orientation is in the sagittal plane and as such there is significant resistance to rotation but flexion-extension and lateral translation movements are still possible. There is an intermediate orientation in the thoracic spine providing multidirectional resistance to movement in this region. At the lumbosacral joint (L5/S1) the facet joints have a more coronal orientation and this is a factor in the lower incidence of anterior subluxation at this level. In the presence of intact facet joints, despite the vertical orientation of the disc space at L5/S1 a degenerative spondylolisthesis is more common at L4/5. During extension movements of the spine there is greater transfer of compressive load across the facet joints.

The size of the spinal canal varies throughout the column. It is most narrow in the thoracic spine with the T7 level showing the smallest cross-sectional area in most anatomical studies. The lumbar and cervical levels are more capacious. There can be a reduction in the canal diameter as a result of either pathological processes or normal ageing, processes that are more common in the cervical and lumbar spine due to the greater range of movement observed in these areas. Bulging of the annulus due to dehydration, overgrowth of facet joints due to osteoarthritis and folding in of the ligamentum flavum due to loss of disc height can narrow the canal in the lumbar spine. This can lead to the characteristic 'trefoil' appearance of the canal associated with lumbar spinal stenosis.

Anterior and posterior bony elements are connected by the pedicles. Variation in pedicle size and orientation is seen throughout the column and knowledge of this variation is critical in understanding the process of transpedicular instrumentation. Pedicle size is smallest at T4. On the lateral aspect of the column the transverse processes arise at the junction of the pedicle and the lamina. They provide points of attachment for the paraspinal muscles and therefore contribute to the control of movement and stability. Variation is seen in their angle of projection from the spine although this is largely in line with the orientation of the facet joints. The foramen transversarium lies in the transverse processes of the cervical vertebrae, and in C1 to C6 transmit the vertebral artery and vein. The foramina are present at C7 but the vertebral arteries lie outside of the foramen at this level.

Spinal ligaments and musculature

There are a large number of ligaments that provide stability to the spine including the interspinous ligaments, anterior and posterior longitudinal ligaments, ligamentum flavum, intertransverse ligaments, and capsular ligaments. The interspinous ligaments pass between the spinous processes at each level and provide significant

resistance to flexion due to their distance from the axis of rotation. The anterior longitudinal ligament (ALL) is a large ligament that runs from the skull base to the sacrum on the anterior aspect of the vertebral bodies. It has a strong attachment to the vertebral bodies but a weak attachment to the intervertebral discs. It is anterior to the axis of rotation and therefore resists extension. The posterior longitudinal ligament (PLL) is much smaller and passes from the clivus to the coccyx. It is significantly weaker than the ALL and provides limited resistance to flexion. It is considered to include two distinct layers (superficial and deep) and, in contrast to the ALL, it has a strong widened attachment at the level of the intervertebral disc and a loose attachment to the vertebral body. The tectorial membrane is a cranial extension of this ligament. The PLL acts as a constraint to herniation of the nucleus pulposus.

The ligamentum flavum extends from C2 to S1. It lies close to the axis of rotation and although it is has significant tensile strength, it offers relatively weak resistance to flexion of the spine. It is named after its yellow colour that occurs as a result of the high concentration of elastin. This prevents the ligament becoming lax in extension and buckling to narrow the canal diameter. It is deficient in the midline with a cleavage plane that allows safer access to the canal during midline decompression. The capsular ligaments also play a significant role in the maintenance of spinal stability, particularly in the cervical spine. The dura is anchored to surrounding structures throughout the spine by several epidural ligaments that appear to provide stability for the neural structures within the canal (Hoffman's ligaments) (Wadhwani et al., 2004).

The axial bones and the skull base are reinforced by several ligaments in addition to the ALL and PLL. The cruciate ligament consists of a small vertical portion running from C2 to the skull base and a more significant transverse portion that runs between the inside faces of the C1 lateral masses. This passes behind the odontoid peg and is essential for preventing C1/2 subluxation. The apical ligament is a weak ligament that runs from the tip of the odontoid peg to the skull base. It is thought to be of little functional significance but may contain notochord remnants. The alar ligaments run from the side of the odontoid peg to the skull base. These resist side movements of the head and limit rotation. Posteriorly the atlanto-occipital membrane runs from C1 to the skull base and the atlantoaxial membrane runs from C1 to C2. These membranes take the place of the ligamentum flavum in the axial spine.

Congenital variation in spinal anatomy

Congenital spine anomalies can be as a result of failure of segmentation or a failure of formation (McMaster and Ohtsuka, 1982). These are often seen alongside genitourinary, cardiac, or dysraphic anomalies, and can lead to development of a spinal deformity as the vertebral column grows. The resulting deformity can be three-dimensional, leading to a lateral deviation and rotational deformity (scoliosis), or an abnormal profile in the sagittal plane, leading to a hyperkyphosis or hyperlordosis. During growth, deformity can occur without congenital abnormalities and often there is no clear cause (idiopathic spinal deformity). Spinal deformity is covered in more detail in later chapters.

In the cervical spine multiple fused segments can be seen as a result of Klippel-Feil syndrome. This occurs either due to failure of formation or a failure of segmentation of the cervical somites at 3–8 weeks of gestation. Patients may present with the classic clinical triad of a low posterior hairline, short 'webbed' neck, and limited cervical range of movement (Kim, 2013). There may also be associated renal disease, congenital cardiac disease, brainstem anomalies, congenital cervical stenosis, and cervical scoliosis. Sprengel's deformity (an undescended scapula often associated with scapula winging, hypoplasia and omovertebral connections) is seen in 30% of patients with Klippel-Feil syndrome. Conservative treatment of any neck discomfort is the mainstay of therapy and surgical treatment is reserved for cases of spinal instability or neurological deterioration. Those affected with Klippel-Feil need to avoid collision sports and frequently develop degenerative cervical conditions in adult life.

Spinal biomechanics

Spinal biomechanics is the study of the structure and function of the spine when subjected to forces and displacements (Benzel, 2001). The functions of the spine can be static (protection of the spinal cord) or dynamic (provision of stability and mobility, and to control transmittance of movement to the upper and lower extremities). This section considers the normal movements of the spine and how the anatomical structures are adapted to balance stability and mobility as the spine is loaded.

Normal spinal movements

Flexion and extension occur primarily in the subaxial cervical and lumbar spine. There is approximately 15° permitted at C0/C1, 10° at C1/2, 7° at each level of the upper cervical spine and 20° in the lower cervical spine. In the lumbar spine the range of movement increases moving caudally to around 20° at L5/S1. In the thoracic spine flexion/extension movements are limited due to the splinting effect of the ribs. This increased range of flexion/extension seen in the cervical and lumbar spine is responsible for the higher rates of degenerative disease observed in these regions. Rotation is primarily in the cervical spine with 45° observed at C1/2. Between 7° and 10° of rotation is seen at each level from C2/3 down to T8/9. There is no rotation at C0/1 and very little in the lower thoracic and lumbar regions. Lateral flexion is more evenly distributed in the spine with approximately 5° at each level. C1/2 is the exception as there is no lateral flexion at this level.

Intrinsic stability

The interplay of anatomical structures within the spine confers intrinsic stability so that, despite the multisegmental structure, the vertebral column is relatively stable and can be held erect with only a small amount of muscle activity. The intervertebral disc does not permit a large amount of movement between levels and this is the case whether loaded or not, as the hydrophilic nature of the nucleus provides a 'preloading' effect with continuous tension on the fibres of the annulus. The resulting increase in disc height also has the effect of putting the longitudinal ligaments under tension. The mobile nature of the nucleus pulposus makes this a dynamic system where asymmetric loading produces migration of the nucleus away from the side loaded towards the convexity of the disc. These forces are also balanced by the posterior elements, particularly in flexion and extension movements. Given this inherent stability the most basic mechanical model for a spinal articulation is as a first-class lever; balanced forces around a fulcrum without

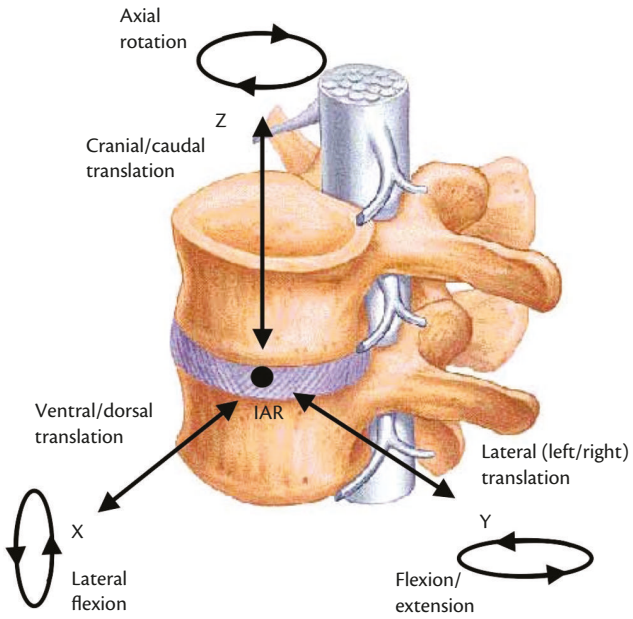

Fig. 57.3 Functional spinal unit showing the instantaneous axis of rotation and Cartesian coordinate system used to describe movement with six degrees of freedom.

gain in mechanical advantage. A lever may be considered as a simple rigid bar and the fulcrum is the point around which a lever rotates. In this model the fulcrum would be the apophyseal joints about which the elastic properties of the posterior ligaments and intervertebral discs are balanced.

Functional spinal unit

The functional spinal unit (FSU or motion segment) consists of two adjacent vertebrae with the intervening disc and associated ligaments (Fig. 57.3). It is the smallest anatomical spinal segment that can be considered to exhibit the biomechanical characteristics of the whole spine (White and Panjabi, 1990). Biomechanical testing of vertebrae has allowed us to understand the load and motion of individual FSUs and then whole spinal segments during normal activities and in pathological processes. Lumbar intervertebral discs are subject to 1–2.5 times body weight during normal walking (Huang et al., 2005). In the upright position approximately 80% of bodyweight is transferred through the anterior spine with the remainder being transferred through the posterior elements. Load transfer through the anterior spine is increased by flexion, while in extension load transfer increases in the posterior elements. During standing and loading of the column the anterior elements are compressed and the posterior elements provide anterior-posterior translational stability due to the vertical orientation of the facet joints in the lumbar spine. Spinal movements occur when an unbalanced force is applied to the FSU producing the basic movements of flexion, extension, lateral bending, and rotation.

Instantaneous axis of rotation

When forces act on an FSU a bending moment is produced and this causes a rotation or tendency to rotate about an axis. In the spine this is termed the instantaneous (helical) axis of rotation (IAR) and is defined as the point in space about which the vertebral body appears to rotate. The location of this is variable and depends on the vertebral level and motion of the spine. It generally lies posterior to the midline and inferior to the superior endplate. To describe movements around the IAR a standard Cartesian coordinate system is used with three axes—x, y, and z (Fig. 57.3). To consider this system in anatomical terms we identify these three axes as cranial/caudal, anterior/posterior (ventral/dorsal for neurological structures) and left/right. Both translation and rotation can occur about these axes and this produces 12 possible movements about the IAR, or six possible paired movements—'six degrees of freedom'. During spinal movements, the IAR of each spinal segment moves in a way analogous to movements of the nucleus pulposus—when an anterior bending moment is applied to an FSU the IAR moves in a posterior direction.

Load/deformation relationships

The mechanical models outlined earlier make the assumption that solid structures are rigid. In reality, no solid structure is truly rigid and this is certainly true for biological tissues. Hooke's law states that for small displacements the size of deformation is proportional to the force applied. This relationship occurs in the elastic phase of deformation for a material, where strain (change in length) totally recovers when the stress (force applied over an area) is removed. For larger displacements the elastic limit (yield point) of the material is reached and past this the linear relationship ceases to exist. This is termed the zone of plastic deformation and results in permanent change to the structure of the material so that strain would not fully recover when the stress is removed. This relationship is demonstrated in the stress-strain curve shown in Figure 57.4. Testing the structure to the point of failure will reveal the ultimate strength and the area under the curve is proportional to the energy absorbed before failure.

Bone, ligaments, and tendons all demonstrate a stress-strain relationship similar to that seen in Figure 57.4. However, they are also *viscolelastic* materials and so this relationship is both rate and time dependent. At lower loads application of a constant load results in viscous behaviour with progressive deformation over time, while at higher loads elastic behaviour is seen and progressive deformation does not occur. Viscoelasticity is apparent in the material properties of creep (progressive deformation over time when a constant load is applied) and stress-relaxation (progressive decrease in stress when a constant strain is applied). In addition, repeated loading can lead to different stress-strain curves with a net loss of energy (as heat), a property known as hysteresis.

Coupled movements

Movements in the spine are often coupled so that movement along one axis is linked to movement about another. This is mostly due to the orientation of the facet joints and is apparent in the cervical spine where lateral bending results in rotation of the spinal processes away from the concavity of the curve. The reverse is seen in the lumbar spine where lateral bending produces rotation of the spinous processes towards the concavity. This is an important concept to consider when understanding movements of the spine but is also key to the development of scoliotic deformities in the growing or degenerative spine. Here, lateral deviation leads to an obligatory rotation of the vertebral body creating the three-dimensional deformity which is seen clinically.

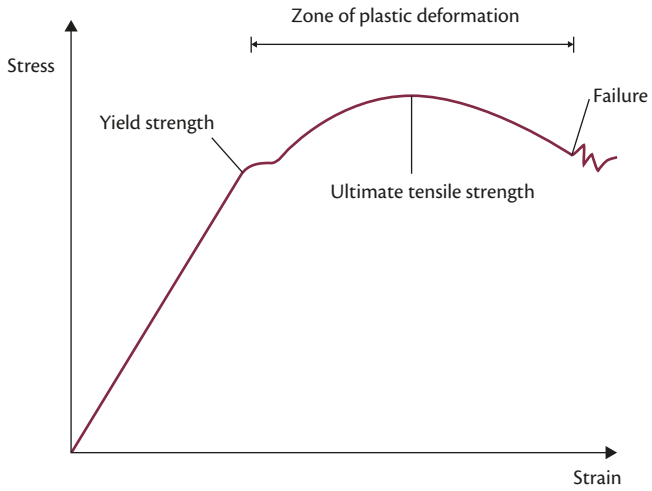

Fig. 57.4 Typical stress-strain curve for biological tissue.

Spinal stability

Clinical stability of the spine was described by White and Panjabi (1990) as 'the ability of the spine under physiological loads to limit patterns of displacement so as not to damage or irritate the spinal cord or nerve roots, and in addition to prevent incapacitating deformity or pain due to structural changes'. The application of this definition to clinical scenarios can lead to significant debate and this highlights the fact that varying degrees of stability can be seen depending on the mechanical or clinical situation. Panjabi (1992) also introduced the concept of the neutral zone for an individual FSU, the initial portion of the range of intervertebral motion during which there is minimal internal resistance. Within this range movement is not limited by the intrinsic stability at that vertebral level. When movement passes outside of this range the intrinsic stability leads to an increased stiffness and motion is limited. As clinicians, we are more often concerned with defining instability as this identifies situations where intervention might lead to improved outcomes.

Column theories

Identification of acute stability in a clinical setting has traditionally involved considering the spine as a series of columns. In 1963, Holdsworth described a two-column model to describe spinal fractures with an anterior column (vertebral bodies, intervertebral discs, ALL and PLL) that supported compressive loads and a posterior column (posterior elements) that resisted tension. In this series involvement of the posterior column suggested instability that might require stabilization. Prior to this, fractures had been described in terms of mechanism of injury. Denis developed the concept of a three-column theory in 1983, where the anterior column described by Holdsworth was divided into a middle column (posterior vertebral body, posterior annulus fibrosus and PLL) and an anterior column (anterior vertebral body, anterior annulus fibrosus, and ALL). He noted that consideration of the middle column was most useful in identifying the mechanism of injury and assessing stability (Holdsworth, 1963; Denis, 1983). More recent classification systems have further subdivided fractures according to the mechanism of injury and structures involved, and scoring systems have been developed to help identify where instability is present. These are discussed in detail in chapter 67.

Acute and chronic instability

An alternative method of categorizing instability is to consider the timescale over which instability occurs. There are no precise definitions for this but, as with most conditions, instability can be described as acute or chronic. Acute instability is most often seen following trauma but may also be seen where there is advanced degenerative disease, neoplasia, or infection. It can be further divided into overt, where there is a loss of integrity of all columns of the spine, and limited, where there is loss of integrity of the anterior or posterior columns in isolation. White and Panjabi (1990) developed a scoring system for acute clinical instability in the cervical, thoracic, and lumbar spine (Tables 57.1–57.3). Points are gained for both radiological loss of integrity and clinical evidence of pain or neurological compromise. A score of 5 or more indicates clinical instability. The system is comprehensive but complicated and is rarely used in clinical practice. In clinical practice we understand that there is a risk of delayed acute instability when muscle spasm occurs and the muscles act as an active stabilizer in the acute phase. When this spasm resolves at 10–14 days following an injury, instability may develop. This is apparent in the high risk of instability (10–45%) seen if patients receive long term follow up after cervical laminectomy. Almost all cervical injuries must be followed up with dynamic imaging for at least six weeks to ensure the spine remains stable.

Chronic instability is more difficult to define and usually involves a gradual progression of deformity that leads to physiological loading conditions causing undue pain or neurological irritation. This slow process can be described as 'glacial instability' with gradual progression of global deformity. Where there is excessive degeneration at a single level (due to degeneration, tumour, or infection) the affected level can be considered as a 'dysfunctional motion segment' and this contributes to chronic instability.

Table 57.1 Scoring system for acute instability in the cervical spine

Element	Point value
Anterior elements destroyed or unable to function	2
Posterior elements destroyed or unable to function	2
Positive stretch test	2
Radiographic criteria A. Flexion/extension X-rays 1. Sagittal plane translation >3.5 mm or 20% (2 points) 2. Sagittal plane rotation >20° (2 points) OR B. Resting X-rays 1. Sagittal plane displacement >3.5 mm or 20% (2 points) 2. Relative sagittal plane angulation >11° (2 points)	4
Abnormal disc narrowing	1
Developmentally narrow spinal canal 1. Sagittal diameter <13 mm OR 2. Pavlov's ratio <0.8[a]	1
Spinal cord damage	2
Nerve root damage	1
Dangerous loading anticipated	1

[a] Ratio of the spinal canal to the width of the vertebral body.

Table 57.2 Scoring system for acute instability in the thoracic and thoracolumbar spine

Element	Point value
Anterior elements destroyed or unable to function	2
Posterior elements destroyed or unable to function	2
Disruptions of costovertebral articulations	1
Radiographic criteria 1. Sagittal plane displacement >2.5 mm (2 points) 2. Relative sagittal plane angulation >5° (2 points)	4
Spinal cord or cauda equina damage	2
Dangerous loading anticipated	1

Source data from Panjabi, M., White, A., Basic Biomechanics of the Spine, *Neurosurgery*, Vol 7, No.1, (July 1980), pages 76–93.

Global spinal alignment

The inherent stability of each motion segment confers a global stability on the vertebral column as a whole and allows the head to remain balanced above the pelvis with minimal muscle activity. Debousset (1994) described a 'conus of economy'—a narrow range in which the trunk remains balanced with minimal muscle action. Outside this range increased muscle activity is required to maintain an upright posture and this can lead to muscle fatigability and discomfort during standing and locomotion. In order to maintain a comfortable upright posture, the centre of gravity should fall between the feet while maintaining a horizontal gaze. This may not be the case where there is coronal or sagittal imbalance and over the last two decades interest in these concepts has increased dramatically.

The global sagittal alignment of the spine can be assessed using the sagittal vertical axis (SVA). This is the horizontal offset from a plumbline dropped from the C7 body to the postero-superior corner of the sacral dome (Jackson and McManus, 1994). SVA should be within 5 cm of this point. Imbalance is considered to be positive if the plumbline falls anterior to the sacral dome and negative if it falls posterior. The SVA provides a simple and quick measure of global sagittal balance but is highly sensitive to changes in posture and does not take into account the position of the pelvis. Assessment of coronal imbalance can be achieved in the same way by measuring the offset of the C7 plumbline to a line that bisects the sacrum in the coronal plane. Other measures of global sagittal balance have been described (spino-sacral angle, T1-pelvic angle, and the T1 and T9 spino-pelvic inclinations) and sagittal imbalance has been linked with poor clinical outcomes after spinal fusion surgery (Bess et al., 2016).

The relationship of the spine to the pelvis is more difficult to describe and there is considerable variation in pelvic morphology between individuals. Understanding this relationship is vital when attempting surgical correction of sagittal balance. The pelvic incidence defines the relative orientation of the sacrum with respect to the pelvis and is constant parameter during adult life (Duval-Beaupere et al., 1992). It is intimately related to the pelvic tilt and angle of slope of the sacrum (Fig. 57.5), following the formula:

$$\text{Pelvic Incidence (PI)} = \text{Pelvic Tilt (PT)} + \text{Sacral Slope (SS)}.$$

As PI is constant in adult life, changes in the SS due to global sagittal imbalance can be compensated by altering the PT but this affects the biomechanics of the lower limbs and can make standing uncomfortable. In asymptomatic adults the mean PI is 52 +/–10°, the mean PT is 13 +/–6°, and the mean SS is 41 +/–8° (Vialle et al., 2005). The pelvis should be considered to be a critical link between the spine and lower extremities and efforts to correct sagittal imbalance should include an assessment of these parameters and an attempt to restore the normal relationship of the spine and pelvis.

Table 57.3 Scoring system for acute instability in the lumbar spine

Element	Point value
Anterior elements destroyed or unable to function	2
Posterior elements destroyed or unable to function	2
Radiographic criteria A. Flexion/extension X-rays 1. Sagittal plane translation >4.5 mm or 15% (2 points) 2. Sagittal plane rotation >5° at L1–2, L2–3, and L3–4; >20° at L4–5; > 25° at L5-S1 (2 points each) OR B. Resting X-rays 1. Sagittal plane displacement >4.5 mm or 15% (2 points) 2. Relative sagittal plane angulation >22° (2 points)	4
Cauda equina damage	3
Dangerous loading anticipated	1

Source data from Panjabi, M., White, A., Basic Biomechanics of the Spine, *Neurosurgery*, Vol 7, No.1, (July 1980), pages 76–93.

Bone diseases affecting spinal stability

Osteoporosis is a skeletal disease characterized by low bone mass per unit volume and deterioration of the microarchitecture of bone tissue, leading to enhanced bone fragility and a consequent increase in fracture risk (Consensus Development Conference, 1993). Diagnosis is made by estimating bone mineral density (BMD) using dual-energy X-ray absorptiometry (DEXA) scanning. Estimated density is compared to the mean for a healthy population and normal BMD is within 1 standard deviation of this mean. Osteopenia is considered 1–2.5 standard deviations below the mean, and osteoporosis is greater than 2.5 standard deviations below. Typically, two scores are given—a 'T score' where density is compared to a sex and race-matched healthy young adult population, and a 'Z score' where density is compared to an age, sex, and race-matched population.

Risk factors for developing osteoporosis include lifestyle factors (smoking, excess alcohol intake, low levels of physical activity, and

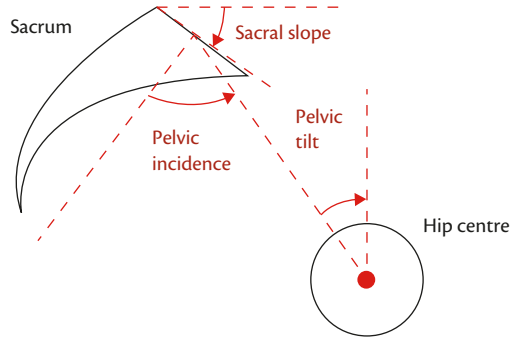

Fig. 57.5 Pelvic parameters affecting global spinal alignment.

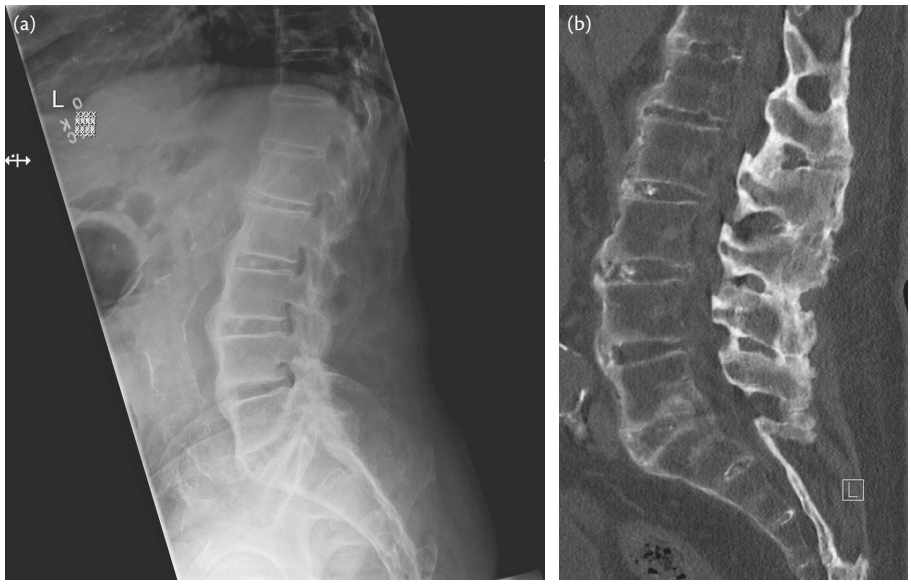

Fig. 57.6 (A) Lateral radiograph of the lumbar spine in a patient with ankylosing spondylitis showing the radiological features of vertebral squaring and vertical syndesmophytes and progressing to (B) midsagittal computed tomography (CT) scan in the same patient three years later showing almost complete ankylosis.

low body weight), family history, certain genetic polymorphisms, low calcium intake, low vitamin D levels, and medical history (corticosteroid use, thyroid conditions, malabsorption syndromes, chronic disease, e.g. rheumatoid arthritis, chronic liver and kidney disease, sarcoidosis, type 1 diabetes mellitus, and chronic obstructive pulmonary disease). Initial treatment should begin with lifestyle modification to reduce these risk factors and be focused on preventing fragility fractures, which can be associated with significant morbidity and mortality. Calcium and vitamin D levels should be checked and supplements taken if required. There are also several pharmacologic agents that have been shown to increase bone mineral density and reduce the risk of fragility fractures including bisphosphonates, conjugated oestrogen-progestin hormone replacement (HRT), oestrogen only replacement, and teriparatide.

In order to help guide which patients should be taking supplementation and pharmacologic agents the World Health Organization Collaborating Centre for Metabolic Diseases at Sheffield University developed the FRAX (Fracture Risk Assessment Tool) which includes the clinical risk factors and BMD at the femoral neck (Kanis et al., 2009). This score is available online and can be used to estimate the risk of a patient developing an insufficiency fracture. Medical treatment is recommended for postmenopausal women and men aged over 50 with:

- Hip or vertebral fractures
- T score between –1.0 and –2.5 PLUS
  - 10-year risk of hip fracture of 3% or more
  - 10-year risk of major osteoporosis fracture of 20% or more
- T score below –2.5

Ankylosing spondylitis

Ankylosing spondylitis is a spondyloarthropathy characterized by a positive HLA-B27 and a negative rheumatoid factor (RF) titre. Males are more commonly affected at a ratio of 4:1 and presentation is usually in the third decade of life. There is a genetic predisposition but the mode of inheritance is unclear. Back pain is a predominant feature from early in the disease and, as the clinical course progresses, spinal flexion deformity is seen with characteristic radiographic changes (squaring of the vertebrae, vertical syndesmophytes) (Fig. 57.6). An ascending ankylosis of the spine develops and the entire spine can become rigid. Advanced deformity in the cervical spine can lead to a 'chin-on-chest' appearance in this region and fractures are associated with a high rate of neurological injury and a high mortality rate.

FURTHER READING

Benzel, E.C. (2001). *Biomechanics of Spine Stabilisation*. New York, NY: Thieme.

Panjabi, M.M. (1992). The stabilizing systems of the spine. Part II: neutral zone and instability hypothesis. *J Spinal Disord*, **5**, 390–7.

White, A.A. & Panjabi, M.M. (1990). *Clinical Biomechanics of the Spine*, 2nd edition. Philadelphia, PA: Lippincott Williams and Wilkins.

REFERENCES

Benzel, E.C. (2001). *Biomechanics of Spine Stabilisation*. New York, NY: Thieme.

Bess, S., Prosopsaltis, T.S., Lafage, V., et al. (2016). Clinical and radiographic evaluation of adult spinal deformity. *Clin Spine Surg*, **29**(1), 6–16.

Consensus Development Conference: diagnosis, prophylaxis, and treatment of osteoporosis (1993). *Am J Med*, **94**, 646–50.

Debousset, J. (1994). Three-dimensional analysis of the scoliotic deformity. In: Weinstein, S. (ed.) *Paediatric Spine Principles of Practice*, pp. 479–96. New York, NY: Raven Press.

Denis, F. (1983). The three-column spine and its significance in the classification of acute thoracolumbar spine injuries. *Spine*, **8**, 817–31.

Duval-Beaupere, G., Schmidt, C., & Cosson, P. (1992). A barycentremetric study of the sagittal shape of spine and pelvis: the conditions required for an economic standing position. *Ann Biomed Eng*, **20**, 451–62.
Holdsworth, F.W. (1963). Fractures, dislocations and fracture-dislocations of the spine. *J Bone Joint Surg (Br)*, **45B**, 6–20.
Huang, R.C., Wright, T.M., Panjabi, M.M., & Lipman, J.D. (2005). Biomechanics of non-fusion implants. *Orthop Clin N Am*, **36**, 271–80.
Jackson, R.P. & McManus, A.C. (1994) Radiographic analysis of sagittal plane alignment and balance in standing volunteers and patients with low back pain matched for age, sex, and size. A prospective controlled clinical study. *Spine*, **19**, 1611–18.
Kanis, J.A., Oden, A., Johansson, H., Borgström, F., Strom, O., & McCloskey, E. (2009). FRAX ® and its implications to clinical practice. *Bone*, **44**, 734–43.
Kim, H.J. (2013). Cervical spine anomalies in children and adolescents. *Curr Opin Paediatr*, **25**(1), 72–7.
McMaster, M.J. & Ohtsuka, K. (1982). The natural history of congenital scoliosis: a study of two hundred and fifty-one patients. *J Bone Joint Surg (Am)*, **64A**, 1128–37.
Panjabi, M.M. (1992). The stabilizing systems of the spine. Part II: neutral zone and instability hypothesis. *J Spinal Disord*, **5**, 390–7.
Vialle, R., Levassor, N., Rillardon, L., Templier, A., Skalli, W., & Guigui, P. (2005). Radiographic analysis of the sagittal alignment and balance of the spine in asymptomatic subjects. *J Bone Joint Surg Am*, **87**, 260–7.
Wadhwani, S., Loughenbury, P., & Soames, R. (2004). The anterior dural (Hoffman) ligaments. *Spine*, **29**(6), 623–7.
White, A.A. & Panjabi, M.M. (1990). *Clinical Biomechanics of the Spine*, 2nd edition. Philadelphia, PA: Lippincott Williams and Wilkins.

RELATED LINKS TO EBRAIN

Anatomy of the Spinal Column and Spinal Stability. https://learning.ebrain.net/course/view.php?id=817
Principles of Surgical Treatment of Spinal Injuries. https://learning.ebrain.net/course/view.php?id=780

58

Spinal physiology

Sadaquate Khan, Kevin Tsang, and Lamia Nayeb

Spinal tract anatomy

Overview

Extending from the foramen magnum as a continuation of the medulla oblongata to the superior lumbar region, the spinal cord is a broadly cylindrical highly organized collection of central nervous tissue and associated glial cells, enclosed by the protective vertebral canal. It is enlarged in the cervical and lumbar regions owing to the density of grey matter responsible for the motor function of the upper and lower limbs. The length of the cord is approximately 45 cm in males and 43 cm in females, and its terminal conus medullaris typically ends between the first and second lumbar vertebrae in adults, although this can vary (T12 to L3) (Saifuddin et al., 1998). During development, the spinal canal outgrows the spinal cord and hence the conus ascends from around L3–4 in newborns to the adult location by 10 years of age (Patten, 1996). From the apex of the conus medullaris extends a thinner fibrous band of modified pia mater, the filum terminale, which stabilizes the spinal cord via its coccygeal attachment. The spinal dura is a continuation of the meningeal layer of the cranial dura and this extends to cover the spinal cord and cauda equina. This whole structure is further stabilized at every vertebral level by dentate ligaments bilaterally. Functionally, the cord can be divided into 31 segments, each giving rise to bilaterally paired spinal nerves.

Blood supply to the spinal cord is via three arteries. The anterior spinal artery, arising from the two vertebral arteries, supplies the anterior cord, and receives input along its course from anterior segmental medullary arteries. Two posterior spinal arteries supply the posterior cord, typically arising from the vertebral arteries at the level of the medulla but occasionally arising from the posterior inferior cerebellar artery. They also receive supply from segmental medullary arteries. The artery of Adamkiewicz is the largest of the anterior segmental arteries to contribute to the anterior spinal artery, usually arising from the left side between the ninth to twelfth thoracic levels. Vascular spinal cord anatomy is covered in more detail in Chapter 64.

Cross-sectional architecture

In contrast to the organization of cranial nervous tissue, the grey matter of the spinal cord is centrally located, while white matter forms an external longitudinal layer (**Fig. 58.1**). When viewed in cross-section at any level, the grey matter resembles an H or butterfly-shaped region, bridged in the midline by the grey commissure with the central canal at its centre. This region can be divided into three 'grey columns': the anterior, posterior, and lateral columns. This grey matter has also been subdivided into a system of ten cytologically distinct layers known as Rexed laminae, progressing from lamina I to XII in a posterior to anterior direction. Rexed laminae X (the grey commissure and substantia gelatinosa centralis) corresponds to a pericentral canal of grey matter extending along the entire length of the spinal cord (Patestas and Gartner, 2016).

The anterior projection of grey matter is termed the ventral horn and conveys motor efferent information. It consists of large alpha motor neurons innervating extrafusal muscle fibres (namely Rexed lamina IX), smaller gamma neurons innervating intrafusal muscle fibres and a minority group of small interneurons (Rexed lamina VIII). Within Rexed lamina IX, motor neurons supplying extensor muscles are organized more anterior to those supplying flexor muscles.

The posterior projection (i.e. dorsal horn) receives sensory afferent information and is subdivided into several Rexed laminae (I to VI) specific to the nature of sensory information received. Most importantly, lamina II (substantia gelatinosa of Rolando) is the site of synapse between the first and second order neurones of the spinothalamic tract; lamina V deals with information from the cutaneous, muscle, joint, and visceral nociceptors, while lamina VI is involved in the simple spinal reflex of withdrawal from pain. Together, the neurons of these laminae (IV, V, and VI) constitute the spinothalamic tract.

The lateral column is a posterolateral projection of the anterior grey column present between the levels of T1 and L2 only and is concerned with preganglionic sympathetic autonomic activity. A less well-defined lateral column also reappears between the S2 and S4 segments, where it relays preganglionic parasympathetic autonomic activity.

Spinal cord tracts

These are the ascending and descending fibre tracts forming the white matter of the spinal cord. The major pathways are the sensory spinothalamic tract and dorsal (medial-lemniscal) columns and the motor corticospinal and extrapyramidal tracts.

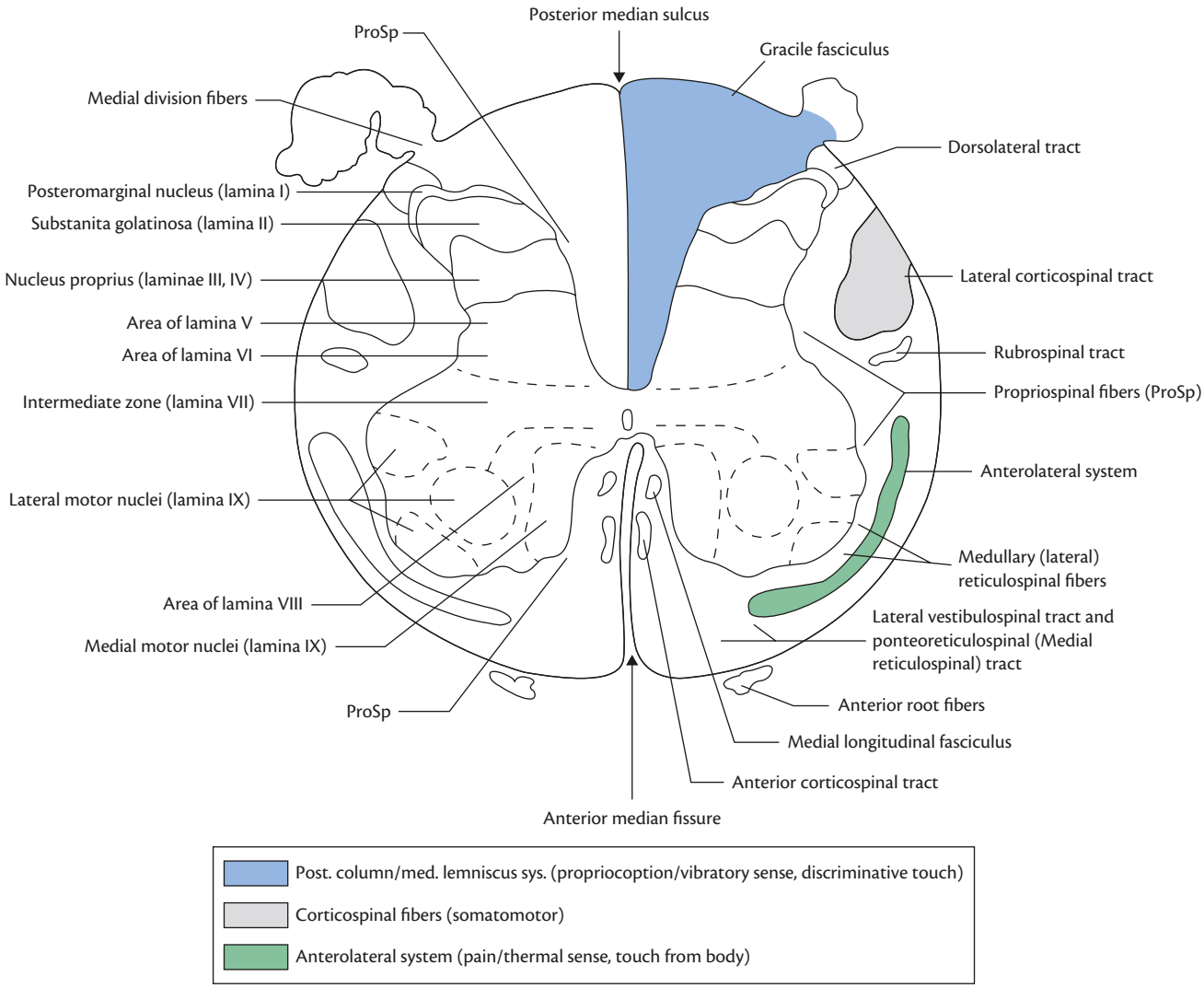

Fig. 58.1 Cross-sectional area of the thoracic spinal cord demonstrating the Rex lamina, ascending and descending tracts.
This image comes from: Figure 5.2, page 86, Haines DE, *Neuroanatomy: An Atlas of Structures, Sections and Systems*, 6th Edition, Lippincott Williams & Wilkins.

Spinothalamic tracts

Sensory information from the skin regarding pain and temperature is conveyed by the first order sensory axons of peripheral afferent neurones entering the cord within the dorsal roots. These axons enter the spinal cord via *Lissauer's tract* near the entry point of the posterior nerve roots where they ascend one to two segments to synapse with second order neurones in the substantia gelatinosa of Rolando (Rexed laminae II). These second order neurones decussate via the anterior commissure, within one or two spinal nerve segments above, to the anterolateral region of the contralateral spinal cord and ascend as the *lateral spinothalamic tract* via the rostral ventromedial medulla. They synapse in turn with axons of third order neurones in the ventral posterolateral nucleus (VPL) of the thalamus which relays information mostly to the sensory cortex in the postcentral gyrus.

An adjacent pathway, the *anterior spinothalamic tract*, conveys information regarding crude touch and pressure; the second order axons of this pathway also decussate through the anterior commissure to the anterior region of the contralateral spinal cord.

Pain and temperature sensation from the face is conveyed via the cranial nerves to the spinal trigeminal tract in the upper cervical spine, which is continuous with Lissauer's tract. The second order neurones involved decussate and ascend along with the lateral spinothalamic tract as the *trigeminothalamic (or quintothalamic) tract* to the ventral posteromedial (VPM) nucleus of the thalamus before synapsing with third order neurones that relay this information to the sensory cortex.

Within the substantia gelatinosa of the spinothalamic tract, which is continuous with the trigeminal nucleus, the sensation of pain is modulated further due to the many interactions that occur between second order afferent sensory neurones and other afferent neurones, interneurons, and descending neurones. Activation of thicker afferents conveying non-nociceptive sensation (light touch, vibration, and pressure) impedes transmission of painful stimuli via nociceptive afferents (A delta and smaller unmyelinated C fibres), through activation of inhibitory interneurons in the substantia gelatinosa (McCance and Huether, 2009). This interaction constitutes the basis of the gate theory of pain, which was proposed to explain why rubbing

a sore area can provide relief, and which is utilized by transcutaneous electrical nerve stimulation (TENS) devices. Spinothalamic tract fibres transmit information to the periaqueductal grey (PAG) in the midbrain via the *spinomesencephalic tract* which projects enkephalin-releasing neurones to the nucleus raphe magnus (NRM) in the midbrain. Serotonin neurotransmitter released from the NRM activates inhibitory interneurons within the substantia gelatinosa resulting in release of endogenous opioids (enkephalin or dynorphin); these bind to the mu-opioid receptors of nociceptive A delta and C afferent neurones. Occupation of mu-opioid receptors reduces release of substance P, and hence inhibits pain transmission (Patestas and Gartner, 2016).

Dorsal (medial-lemniscal) tract

The sensations of fine touch, vibration, and proprioception are conveyed from skin, muscles, and joints via first order axons of peripheral afferent neurones. The axons of these neurones ascend in the ipsilateral dorsal spinal cord uninterrupted as two tracts, the *fasciculus cuneatus* laterally (sensory information from the upper limbs) and the *fasciculus gracilis* medially (sensory information from trunk and lower limbs), to the lower medulla. There they synapse with axons of the second order sensory neurones of the nucleus cuneatus and nucleus gracilis, respectively. These axons decussate in the medulla as the *internal arcuate fibres* to form the *medial lemniscus*, which relays information to the VPL nucleus of the thalamus. There they synapse in turn with third order axons that project to the somatosensory cortex in the postcentral gyrus.

Corticospinal (pyramidal) tracts

Upper motor neurons (UMN) descend uninterrupted predominantly from the motor cortex (precentral gyrus) to the spinal cord. The majority (80–90%) of these decussate in the lower medulla at the level of the superior aspect of the C1 vertebral body before continuing on as the *lateral corticospinal tract.* The lateral corticospinal tract fibres primarily innervate the limb musculature.

Those fibres that do not decussate form the *anterior corticospinal tract* and cross through the anterior commissure at or a few levels above their functional level. This tract is present only in the upper cord, disappearing completely by the mid thoracic region. The anterior corticospinal tract carries fibres that innervate proximal and trunk muscles.

The fibres of both of these tracts innervate the lower motor neurons (LMN) of the contralateral ventral horn, usually known as the anterior horn cell, which gives rise to axons innervating the muscles of the trunk and upper and lower limbs.

Ascending *dorsal* and *ventral spinocerebellar tracts* fine-tune motor function further via proprioceptive sensory information from muscle spindles, Golgi tendon organs, and tactile and pressure receptors. These transmit information via primary afferent neurones terminating in the dorsal horn, which synapse with second order neurones conveying information directly to the cerebellum. The origin of the dorsal spinocerebellar tract primary neurones is known as Clarke's column (or nucleus dorsalis, Rexed lamina VII) at the T1 to L3–4 levels; from here, second order neurones ascend ipsilaterally to the cerebellum via the inferior cerebellar peduncle, whereas those of the ventral spinocerebellar tract decussate twice to reach the ipsilateral cerebellum via the superior cerebellar peduncle. The dorsal spinocerebellar tract processes information from the lower limbs. An analogous *cuneocerebellar tract,* consisting of axons rostral to Clark's column, which pass via the inferior cerebellar peduncle to the cuneate nucleus in the medulla, conveys information from the upper limbs (Latash, 2008).

Extrapyramidal tracts

The midbrain and brainstem give rise to other descending motor tracts which are modulated by the cerebral cortex, basal ganglia, and cerebellum.

Axons from the red nucleus in the rostral midbrain decussate immediately in the ventral tegmental decussation and descend as the *rubrospinal tract* in the lateral funiculus, ventrolateral to the lateral corticospinal tract, to terminate in the cervical spine. It receives afferents from both the cerebellum via the red nucleus and the cerebral motor cortex to modulate muscle movement and tone. Stimulation results in limb flexion and inhibition of limb extension (Snell, 2010).

The *medial* and *lateral reticulospinal tracts* arise in the reticular formation of the pons and medulla respectively and influence reflexes and motor function at all spinal levels. The reticular formation receives input from the red nucleus, vestibular nucleus, and basal nuclei, which are in turn influenced by the cerebellum. Axons of the former tract descend ipsilaterally to synapse upon alpha and gamma motor neurones, facilitating voluntary movement and increasing tone. Axons of the latter tract descend bilaterally to achieve the opposite, inhibiting movement and reducing tone.

The *medial vestibulospinal tract* receives input from the ipsilateral medial vestibular nucleus and descends as an extension of the medial longitudinal fasciculus to the cervical and upper thoracic cord only, influencing head movement and posture. It also stimulates lower motor neurones of the spinal accessory nerve. Ultimately it facilitates appropriate orientation in response to postural and balance changes. Largely under cerebellar control, the *lateral vestibulospinal tract* receives axons from the lateral vestibular (Deiter's) nucleus and descends ipsilaterally to terminate on alpha and gamma neurones at all spinal levels to modulate extensor motor function, in addition to contributing to the maintenance of posture through stimulation of lower limb extensors and inhibition of flexor muscles (Sengul and Watson, 2012).

The *tectospinal tract* is thought to influence posture in response to visual stimulation of the contralateral superior colliculus of the midbrain. Its axons project from the superior colliculus, decussate in the dorsal tegmental decussation, and descend to terminate in the cervical spinal cord (Rexed lamina VI, VII, and VIII).

Spinal autonomic function

Spinal autonomic function is divided into sympathetic outflow from T1–L3 and parasympathetic outflow from the S2–S4 segments (**Fig. 58.2**). Parasympathetic afferent and efferent pathways in the cranial nerves will not be covered in this section. Spinal autonomic outflow is essential in maintaining normal visceral function, including bowel, bladder, and sexual function, as well as homeostasis (**Figs. 58.3** and **58.4**).

Sympathetic nervous system

Sympathetic preganglionic axons exit the spinal cord from T1 to L3 to synapse in either the paravertebral ganglia at the same or adjacent

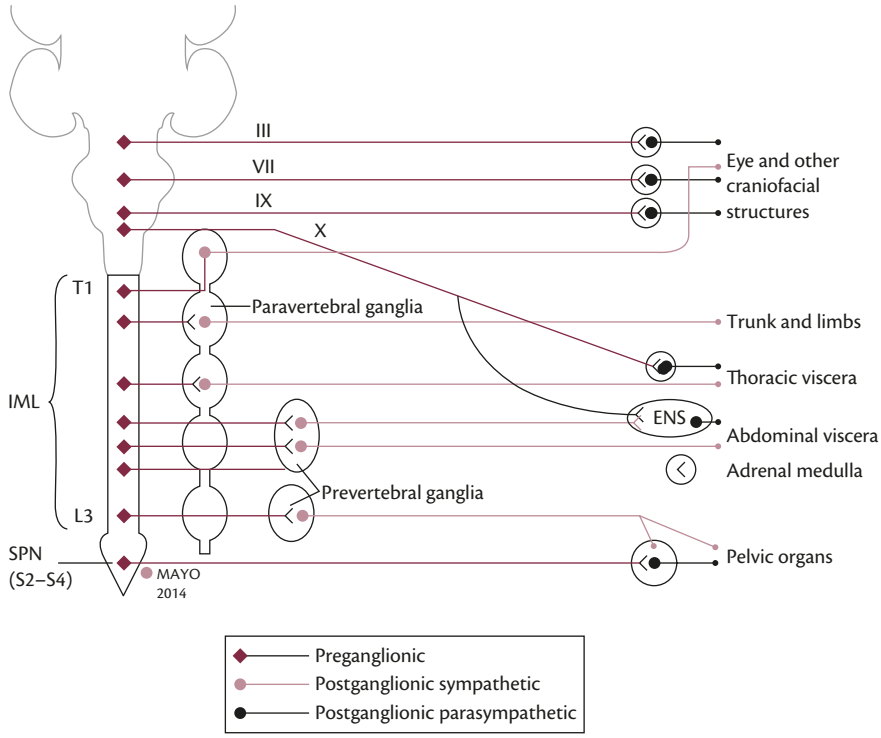

Fig. 58.2 The autonomic nervous system. IML, intermediolateral nucleus; SPN, sacral parasympathetic nucleus; ENS, enteric nervous system.
Adapted from Benarroch EE. *Basic Neurosciences with Clinical Applications*. Philadelphia [PA]: Butterworth Heinemann/Elsevier; 2006. Chapter 20, Peripheral autonomic control of visceral organs; pp. 679–720. Used by permission of Mayo Foundation for Medical Education and Research.

levels of the sympathetic chain or pass through the sympathetic chain to innervate the prevertebral ganglia and the adrenal medulla.

The paravertebral sympathetic postganglionic efferents innervate the face, trunk, limbs, and thoracic viscera. The prevertebral postganglionic sympathetic efferents innervate the abdominal and pelvic viscera. Preganglionic sympathetic neurons are cholinergic, postganglionic sympathetic neurons, except those innervating sweat glands are adrenergic.

Parasympathetic nervous system

The spinal parasympathetic outflow originates in the sacral parasympathetic nucleus (SPN), located between the levels of S2 to S4 and innervates the bladder, rectum, and sexual organs. Preganglionic and postganglionic parasympathetic neurons are cholinergic (Benarroch, 2006).

Spinal control of bladder function

The normal control of bladder function requires a contribution from the pontine micturition centre, which is in turn modulated by input from multiple supratentorial regions predominantly in the frontal lobes. This includes the anterior cingulate gyrus, preoptic hypothalamus, amygdala, bed nucleus, stria terminalis, and septal nuclei. The pontine micturition centre, via parasympathetic, sympathetic, and somatic afferent and efferent neurones coordinates the function of normal urinary storage, as well as micturition. Disruption in any of these pathways results in disturbed bladder function (Fig. 58.3).

Parasympathetic innervation of the bladder

Efferent preganglionic parasympathetic fibres originating from the S2–S4 roots synapse in the hypogastric plexus, where postganglionic fibres originate and go on to innervate the detrusor muscle and internal sphincter. The postganglionic parasympathetic innervation releases large amounts of acetylcholine at the onset of voiding that results in detrusor contraction and internal sphincter relaxation.

Afferent parasympathetic fibres, via the pudendal nerve convey distension of the bladder wall and internal sphincter. This is transmitted in myelinated Aδ-fibres which run in the intermediolateral column of the spinal cord.

Sympathetic innervation of the bladder

Efferent preganglionic innervation of the bladder originates from T9 to L2, via the pelvic nerves, hypogastric plexus, and hypogastric nerve to the inferior hypogastric ganglion. Postganglionic fibres innervate both the detrusor and internal sphincter, where noradrenaline release results in detrusor relaxation and internal sphincter contraction during the storage phase of micturition.

There is also a small contribution from sympathetic afferents running in the hypogastric nerves, which also convey the sensation of bladder distension.

Somatic innervation of the bladder

The external, or urethral sphincter is composed of striated muscle and therefore receives somatic efferents, originating in the S2–4 anterior horn cells, the motor neurones are in Onuf's nucleus (which also contains the parasympathetic nuclei) and are transmitted via the pudendal nerve.

Coordination of voluntary voiding

The storage phase of micturition requires relaxation of the detrusor muscle and contraction of the internal sphincter, via sympathetic

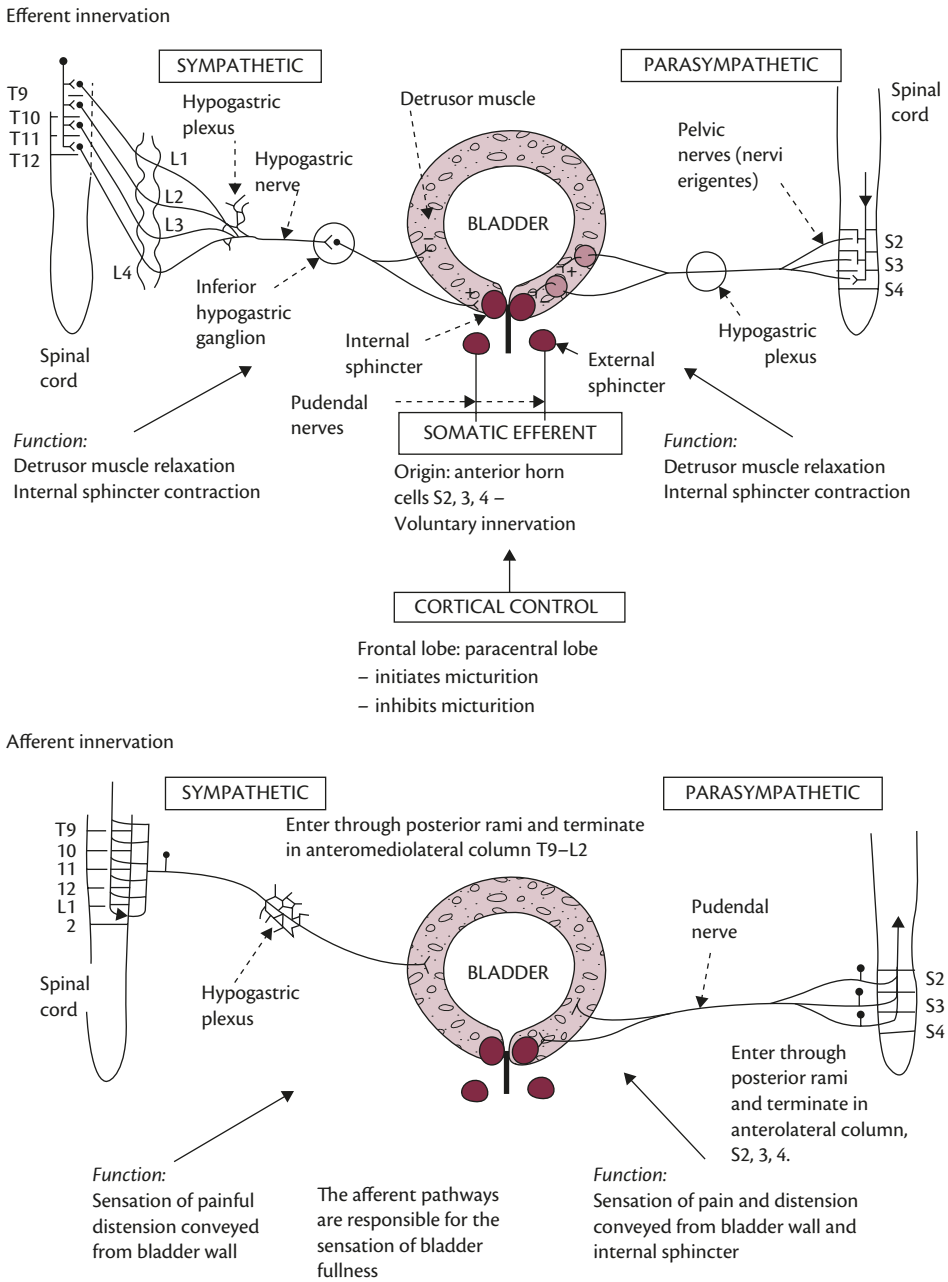

Fig. 58.3 Autonomic innervation of the bladder.

Reprinted from Kenneth W. Lindsay, Ian Bone, Geraint Fuller, *Neurology and Neurosurgery Illustrated*, Fifth Edition, pp. 429–87. Churchill Livingstone, Copyright © 2010 with permission from Elsevier.

innervation as well as conscious inhibition of micturition and contraction of the external sphincter.

The initiation of voluntary micturition involves coordination of activity between the pontine micturition centre, sacral spinal cord, detrusor muscle, and both internal and external sphincters. Micturition is preceded by relaxation of the striated muscle of the external sphincter, mediated via the pudendal nerve and relaxation of the muscle of the internal sphincter, mediated via the parasympathetic outflow from the hypogastric plexus. The parasympathetic innervation from the hypogastric plexus also causes detrusor contraction and bladder emptying.

Voluntary inhibition and initiation of micturition is controlled from the paracentral lobule of the frontal lobe, and coordination of sphincter relaxation and detrusor contraction via the pontine micturition centre (Fowler et al., 2008)

Dysfunctional voiding

Patterns of dysfunctional voiding vary depending on the level of the lesion in the pathways controlling micturition.

Suprapontine lesions can result from focal frontal lobe pathology, or global neuronal degeneration in conditions such as Parkinson's disease. As a result, there is loss of the inhibition of the pontine micturition centre, which causes symptoms of urinary urgency, frequency, and nocturia.

Spinal cord injuries above the lumbosacral level show an early and late pattern of urinary dysfunction. In the early stages with the

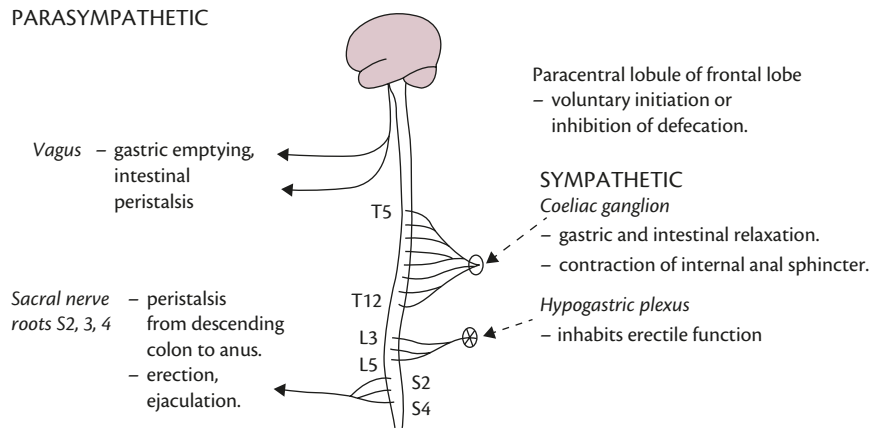

Fig. 58.4 Autonomic innervation of the bowel.

Reprinted from Kenneth W. Lindsay, Ian Bone, Geraint Fuller, *Neurology and Neurosurgery Illustrated*, Fifth Edition, pp. 429–87. Churchill Livingstone, Copyright © 2010 with permission from Elsevier.

loss of supraspinal control of voiding patients develop an areflexic bladder and urinary retention. In later stages with a return of spinal reflexes there is automatic micturition; however, due to detrusor-sphincter dyssynergy, this is an inefficient process and patients are often required to intermittently self-catheterize.

Lumbar-sacral lesions affecting the cauda equina lead to a loss of bladder tone and painless bladder dilatation but due to the intact urinary sphincter sympathetic outflow there is urinary retention and dribbling overflow incontinence (Fowler et al., 2008; Lindsay et al., 2010).

Spinal control of bowel function

The parasympathetic innervation of the gastrointestinal tract up to and including the initial two-thirds of the transverse colon is via the vagus nerve. Parasympathetic innervations of the descending colon, rectum, anus, and internal anal sphincter originate from the anterior rami of S2–4 via the pelvic splanchnic nerves and subsequently inferior hypogastric plexus. Parasympathetic efferents cause contraction of the rectum, anal canal, and relaxation of the internal anal sphincter, assisting defecation (Fig. 58.4).

Sympathetic innervation of the lower gastrointestinal tract which is derived from T11–L2 results in rectal and anal canal relaxation and internal sphincter contraction, inhibiting defecation.

The external anal sphincter consists of striated muscle and is therefore under voluntary control. It is innervated via the pudendal nerve.

With rectal distension of faeces there is a cortical awareness of the need to defecate, causing a reduction in sympathetic tone, relaxation of the internal anal sphincter and pelvic floor. This is followed by the voluntary opening of the external sphincter and subsequent parasympathetic activity resulting in peristaltic contraction of the rectum and evacuation of faeces (Lindsay et al., 2010).

Spinal control of sexual function

The control of erection and ejaculation in males and the arousal response in females results from coordinated output from parasympathetic, sympathetic, and somatic innervations of the genitals.

Parasympathetic outflow originating from S2 to S4 pass via the pelvic plexus and form the cavernosal nerves. The cavernosal nerves innervate erectile tissue in the penis and clitoris.

Sympathetic genital innervation originating from L3 to L5 passes through the hypogastric plexus and passes via the hypogastric plexus to the paired hypogastric nerves.

Afferent genital innervation is via the pelvic and pudendal nerves in the sacral region and hypogastric nerves in the thoracolumbar region.

The process of penile or clitoral erection, vaginal lubrication, and ejaculation, with simultaneous inhibition of bowel and bladder function occurs from a coordinated increase in parasympathetic outflow and reduction in sympathetic inhibition.

Spinal control of blood pressure, glucose, and temperature

Thoracic sympathetic efferents, exiting via the T1–T12 roots are divided into three groups: thermosensitive, glucosensitive, and barosensitive. Hypothermia, hyperventilation, and emotional states result in predominantly cutaneous vasoconstriction via thermosensitive efferents. Glucosensitive efferents are activated in response to hypoglycaemia and exercise and result in the release of adrenaline from the adrenal medulla.

Activation of barosensitive efferents results in systemic constriction of resistant arterioles, other than those in the skin. Barosensitive efferents to the adrenals cause release of noradrenaline and renal efferents result in increased renin secretion, increased renal sodium absorption and blood flow (Guyenet, 2006).

Patterns of spinal cord injury

Spinal cord injury (SCI) is associated with almost half of all spinal trauma and may be classified as complete or incomplete (Teufack et al., 2012). Incomplete injuries are further subdivided according to the pattern of spinal cord involvement. It is therefore important for the clinician to understand the anatomy and physiology of the spinal cord for accurate diagnosis and correct decision-making (Wheeler

Table 58.1 Patterns of spinal cord injury

Injury type	Tracts affected	Clinical presentation
Complete	All	Complete loss of motor and sensory function, including sphincter function, below the level of injury
Anterior	Corticospinal tracts Spinothalamic tracts	Paralysis with loss of pain and temperature sensation below the level of injury
Central	Corticospinal tracts	Limb weakness with arms more affected than legs
Posterior	Dorsal columns	Loss of light touch, vibration, and joint position senses
Brown-Séquard	Corticospinal tract Spinothalamic tract Dorsal column	Ipsilateral loss of motor function and light touch, vibration, and joint position senses Contralateral loss of pain and temperature

and Fok, 2003; Krishna et al., 2014). Table 58.1 outlines the classical features of each.

Complete cord injury

This implies complete loss of spinal cord function below the level of the injury (i.e. ASIA A) due to complete cord transection, severe contusion, or haemorrhage to the cord (Wheeler and Fok, 2003). The loss of sensory and motor function following such an injury may not always directly correspond to the level of spinal trauma.

There is complete motor and sensory loss starting at the level of the injury due to loss of function to all the ascending and descending tracts. The autonomic nervous system may also be affected, as described next. However, due to ascending oedema as part of the pathophysiology of the injury, the patient may also exhibit reduced function for two to three levels above the actual injury level (e.g. patients with C6/7 dislocation may have complete loss of function below C6 with weakness of the shoulders and altered sensation in the upper arms). The deficits seen above the level of injury often improve with time, unlike the complete loss of function below. There is complete loss of perineal and perianal sensation and loss of anal tone due to loss of sacral efferents. The patient, if male, may also present with priapism on admission. This is a sign of autonomic dysfunction (loss of S2–4 parasympathetic outflow to the cavernous nerves) and is a predictor for extremely poor prognosis.

Autonomic dysfunction may also present as neurogenic shock or autonomic dysreflexia. The former manifests as bradycardia and hypotension due to loss of vasomotor tone. This is related to loss of thoracic sympathetic (barosensitive) outflow. As a result, it is seen in injuries above the level of T1 (although T6 is the major efferent and therefore disruption between T1 and T6 may also result in neurogenic shock). Autonomic dysreflexia occurs most commonly when the patient urinates or defaecates, resulting in uncontrolled hypertension. The management and significance of this will be described in the following chapters.

Incomplete cord injury

This implies that some function is maintained below the level of the injury (i.e. ASIA B to D) (Krishna et al., 2014). There may be no specific pattern to this diminished function, but a few conditions have been described for specific functional losses.

Anterior cord syndrome

This is most likely due to anterior spinal artery compromise with resulting cord ischaemia and infarction. The anterior spinal artery is a single vessel, originating from both vertebral arteries, which descend on the ventral part of the spinal cord to the level of the filum terminale and supplies both the anterior and lateral corticospinal tracts and the anterior and lateral spinothalamic tracts. It is augmented by multiple radicular arteries arising from the aorta, most notably the artery of Adamkiewicz which tends to enter from the left side between T9 and T12. Disruption of the artery or the contributory vessels will lead to ischaemia and infarction of the ventral spinal cord.

The corticospinal tracts and motor nuclei in laminae X are affected most and patients present with a dense paraplegia. The spinothalamic tracts are also involved although the dorsal columns are spared and this may lead to dissociated sensory loss (i.e. loss of pain and temperature but retained light touch, vibration sense, and proprioception). Prognosis is poor with only 10–20% of patients recovering function.

Central cord syndrome

This tends to occur in elderly patients with pre-existing cervical spinal canal stenosis suffering a hyperextension injury. It is postulated that this may be due to either contusion to the spinal cord or actual haemorrhage. Either way, there is disruption to the central area of the spinal cord, affecting mainly the corticospinal tracts but also the spinothalamic tracts and dorsal columns, depending on the extent of the injury.

The corticospinal tract is arranged topographically, with the proximal fibres (upper limbs) more medially and distal fibres (lower limbs) laterally. This results in a typical loss of motor function worse in the arms than the legs. The dorsal columns, however, are arranged with the lower limb fibres medially (tractus gracilis) and the upper limb fibres laterally (tractus cuneatus) and therefore sensory loss may not follow the same pattern as the motor dysfunction.

Posterior cord syndrome

This is very rare with only case studies in the literature and is included for completeness. There are two posterior spinal arteries, arising from their respective vertebral arteries (occasionally from the posterior inferior cerebellar arteries), with good collateral from segmental arteries, hence it is uncommon to see pure posterior cord injuries and infarction. The dorsal columns (both tractus gracilis and tractus cuneatus) alone are affected and patients present with loss of light touch, vibration sense, and proprioception but retained pain and temperature sensation.

Brown-Séquard syndrome

Hemisection of the spinal cord, most likely a result of penetrating spine injury, results in this syndrome. The three main tracts affected are the corticospinal tract, spinothalamic tract, and the dorsal columns.

The corticospinal tract and dorsal columns both decussate in the medulla before descending, hence the patient would get an ipsilateral loss of motor power and light touch, vibration sense, and proprioception. The spinothalamic tract, on the other hand, decussates in the spinal cord and the patient would therefore have a contralateral loss of pain and temperature. However, the spinothalamic tract does not decussate horizontal, but rather over several levels. This means an injury at a particular level would affect the decussated fibres from two to three levels caudal, but also the non-decussated fibres at the level of injury.

FURTHER READING

Fowler, C.J., Griffiths, D. & de Groat, W.C. (2008). The neural control of micturition. *Nat Rev Neurosci*, **9**(6), 453–66.

Guyenet, P.G. (2006). The sympathetic control of blood pressure. *Nat Rev Neurosci*, **7**(5), 335–46.

Patestas, M.A. & Gartner, L.P. (2016). *A Textbook of Neuroanatomy*, 2nd edition. Hoboken, NJ: Wiley Blackwell, pp. 66–8, pp. 166–8.

Patten, J.P. (1996). *Neurological Differential Diagnosis*, 2nd edition. London, UK: Springer, p. 213.

Teufack, S., Harrop, J.A., & Sharan, A.D. (2012). Spinal cord injury classification. In: Fehlings, M.G., Vaccaro, A., Boakye, M., Rossignol, S., Ditunno, J.F. Jr., & Burns, A.S. (eds.) *Essentials of Spinal Cord Injury*, pp. 65–74. New York, NY: Thieme.

REFERENCES

Benarroch, E.E. (2006). Peripheral autonomic control of visceral organs. In: Benarroch, E.E. (ed.) *Basic Neurosciences with Clinical Applications*, pp. 679–720. Philadelphia, PA: Butterworth Heinemann/Elsevier.

Fowler, C.J., Griffiths, D. & de Groat, W.C. (2008). The neural control of micturition. *Nat Rev Neurosci*, **9**(6), 453–66.

Guyenet, P.G. (2006). The sympathetic control of blood pressure. *Nat Rev Neurosci*, **7**(5), 335–46.

Krishna, V., Andrews, H., Varma, A., Mintzer, J., Kindy, M.S., & Guest, J. (2014). Spinal cord injury: how can we improve the classification and quantification of its severity and prognosis? *J Neurotrauma*, **31**, 215–27.

Latash, M.L. (2008). *Neurophysiological Basis of Movement*, 2nd edition. Champaign, IL: Human Kinetics Europe Ltd, p. 170.

Lindsay, K.W., Bone, I., & Fuller, G. (2010). *Neurology and Neurosurgery Illustrated*, 5th edition. Edinburgh, UK: Churchill Livingstone.

McCance, K.L. & Huether, S.E. (2009). *Pathophysiology: The Biological Basis for Disease in Adults and Children*, 6th edition. St Louis, MO: Mosby.

Patestas, M.A. & Gartner, L.P. (2016). *A Textbook of Neuroanatomy*, 2nd edition. Hoboken, NJ: Wiley Blackwell, pp. 66–8, pp. 166–8.

Patten, J.P. (1996). *Neurological Differential Diagnosis*, 2nd. edition. London, UK: Springer, p. 213.

Saifuddin, A., Burnett, S.J. & White, J. (1998). The variation of position of the conus medullaris in an adult population. A magnetic resonance imaging study. *Spine (Phila Pa 1976)*, **23**(13), 1452–6.

Sengul, G. & Watson, C. (2012). Spinal cord connections. In: Jürgen, K.M. & Paxinos, G. (eds.) *The Human Nervous System*, 3rd edition, pp. 249–50. San Diego, CA: Academic Press.

Snell, R.S. (2010). *Clinical Neuroanatomy*, 7th edition. Philadelphia, PA: Lippincott Williams & Wilkins, p. 162.

Teufack, S., Harrop, J.A., & Sharan, A.D. (2012). Spinal cord injury classification. In: Fehlings, M.G., Vaccaro, A., Boakye, M., Rossignol, S., Ditunno, J.F. Jr., & Burns, A.S. (eds.) *Essentials of Spinal Cord Injury*, pp. 65–74. New York, NY: Thieme.

Wheeler, J.S. Jr., & Fok, C.S. (2003). Normal and abnormal micturition. In: Lin, V.W. (ed.) *Spinal Cord Medicine, Principles and Practice*, pp. 369–74. New York, NY: Demos Medical.

RELATED LINKS TO EBRAIN

Neural Control of the Bladder. https://learning.ebrain.net/course/view.php?id=392

Neurological Control of Sexual Function. https://learning.ebrain.net/course/view.php?id=391

59

Medical pathologies of the spinal cord

Chris McGuigan, Karen O'Connell, Eavan McGovern, and Iain McGurgan

Introduction

Medical pathologies of the spinal cord can present in an acute, subacute, or chronic manner, often mimicking neurosurgical presentations. A neurosurgical opinion may be sought prior to the involvement of a physician or neurologist and therefore it is important that neurosurgeons have knowledge of common medical conditions that can affect the spinal cord and recognize some examination findings that may assist in the diagnosis, thereby avoiding unnecessary investigations or interventions.

This chapter will discuss common symptom presentations that mimic surgical spinal pathologies including acute spastic paraparesis and acute flaccid paralysis. The chapter also covers medical disorders of anterior horn cells, nerve roots, peripheral nerves, the neuromuscular junction, or muscles which can be confused with neurosurgical disorders with focal presentations.

Section 1: Acute spastic paraparesis/tetraparesis

Acute spastic tetra/paraparesis with a medical aetiology is most commonly caused by inflammation of the spinal cord, usually referred to as transverse myelitis (TM), a term first used by Suchett-Kaye in 1948 (Suchett-Kaye, 1948) to describe a case of postinfectious myelitis. It is clinically characterized by acute or subacute motor, sensory, or autonomic spinal cord dysfunction. Transverse myelitis is often secondary to other primary neurological or systemic conditions including multiple sclerosis or neurosarcoidosis. In children, the most common cause is a postinfectious or postvaccination autoimmune phenomenon. Transverse myelitis may be idiopathic in 15–30% of cases.

The estimated incidence ranges from 1.3 to 8 cases per million (Bhat et al., 2010) with higher rates when demyelinating disorders such as multiple sclerosis are included. Prognosis is highly variable and usually dependent on the underlying cause with most of the recovery seen in the first three months, but symptoms may continue to improve for up to a year after the initial presentation. Signs of spinal shock (severe weakness, hypotonia, and areflexia) may be present at onset rather than the usual upper motor neurone signs and are associated with a poorer outcome.

Clinical findings

Transverse myelitis is an all-encompassing term and thus clinical symptoms and severity can vary, depending on the size and location of the lesion. Typical symptoms include any, or a combination of, weakness, numbness or altered sensation, pain, ataxia, and bladder or bowel dysfunction. Careful history taking often reveals that symptoms typically evolve over hours to days rather than having maximal severity at onset. In the acute phase it is often clinically indistinguishable from other causes of acute myelopathy including compressive lesions and warrants prompt urgent imaging and assessment.

Symptoms are usually bilateral but not always symmetrical; for instance in the classic Brown-Séquard syndrome with a hemi cord lesion the patient has ipsilateral motor weakness and contralateral sensory disturbance. The weakness is commonly associated with hyperreflexia and extensor plantars pointing towards a central cause. Clinicians should be mindful, however, that in the early phase of the disease there may be a flaccid paralysis and diminished deep tendon reflexes mimicking peripheral nervous system disorders such as Guillain–Barré syndrome. A well-defined sensory level is common, and can help distinguish between spinal or cerebral lesions. Often the sensory level is clinically many segments below the actual spinal lesion and this needs to be considered when ordering subsequent imaging studies, for instance, a sensory lesion at T5 may be the result of a cervical myelitis and therefore imaging of the whole cord above the sensory level should be considered. This is particularly relevant for the neurosurgeon seeking to exclude cauda equina syndrome in the patient with bladder disturbance. Neuropathic pain can present as a 'band-like' or tight sensation around the chest or abdomen offering further clues that the cause is spinal in origin.

Diagnosis and investigations

The diagnosis should be suspected when there is a clinical history of an acute or subacute onset of spinal sensorimotor or autonomic dysfunction where a compressive lesion has been ruled out. There needs to be evidence of underlying inflammation either on magnetic resonance imaging (MRI) (Fig. 59.1) or lumbar puncture (always performed after imaging) making MRI and lumbar puncture essential to establishing the diagnosis. Diagnostic criteria for idiopathic acute transverse myelitis have been proposed and are outlined in Table 59.1. Other tests are directed towards identifying the underlying cause.

Fig. 59.1 Sagittal T2 MRI of cervical spine showing short segment lesions consistent with demyelination.

Causes of transverse myelitis

Transverse myelitis can be associated with autoimmune, infectious, paraneoplastic, systemic inflammatory or multifocal neurological conditions. The paragraphs that follow outline some of the key features of the more commonly associated conditions.

Table 59.1 Criteria for idiopathic acute transverse myelitis

Inclusion criteria	Exclusion criteria
Development of sensory, motor, or autonomic dysfunction attributable to the spinal cord	History of previous radiation to the spine within 10 y
Bilateral signs and/or symptoms (though not necessarily symmetric)	Clear arterial distribution, clinical deficit consistent with thrombosis of the anterior spinal artery
Clearly defined sensory level	Abnormal flow voids on the surface of the spine c/w AVM
Exclusion of extra-axial compressive aetiology by neuroimaging (MRI or myelography, CT of spine not adequate)	Serologic or clinical evidence of connective tissue disease (sarcoidosis, Behçet's disease, Sjögren's syndrome, SLE, mixed connective tissue disorder, etc.)[a]
Inflammation within the spinal cord demonstrated by CSF pleocytosis or elevated IgG index or gadolinium enhancement. If none of the inflammatory criteria is met at symptom onset, repeat MRI and lumbar puncture evaluation between 2 and 7 days following symptom onset meet criteria	CNS manifestations of syphilis, Lyme disease, HIV, HTLV-1, Mycoplasma, other viral infection (e.g. HSV-1, HSV-2, VZV, EBV, CMV, HHV-6, enteroviruses)[a]
Progression to nadir between 4 h and 21 d following the onset of symptoms (if patient awakens with symptoms, symptoms must become more pronounced from point of awakening)	Brain MRI abnormalities suggestive of MS[a]
	History of clinically apparent optic neuritis[a]

[a] Do not exclude disease-associated acute transverse myelitis.

Reproduced with permission from Transverse Myelitis Consortium Working Group, Proposed diagnostic criteria and nosology of acute transverse myelitis, *Neurology*, Volume 59, Issue 4, pp. 499–505, Copyright © 2002 Wolters Kluwer Health, Inc.

Multiple sclerosis

Transverse myelitis may occur at any time in those with a diagnosis of multiple sclerosis (MS) or as the first ever neurological event (clinically isolated syndrome) as outlined in **Box 59.1**. The L'hermitte sign, characterized by an electric shock sensation radiating down the spine or limbs and usually brought on by neck flexion (extension of a dorsal column lesion), is considered one of the clinical hallmarks of demyelinating disease and should raise suspicion for MS or neuromyelitis optica spectrum disorder (see next). In MS, spinal lesions seen on MRI are usually short, typically spanning one vertebral segment or less (**Fig. 59.1**). They tend to be located in an eccentric, dorsal, or lateral position, and usually involve less than half the cord. The diagnosis may be also be supported by evidence of cerebral demyelination on MRI brain (**Fig. 59.2**) and positive oligoclonal bands on cerebrospinal fluid analysis.

Neuromyelitis optica spectrum disorders

Neuromyelitis optica (NMO) is an inflammatory condition affecting the central nervous system distinct from MS. It classically involves the optic nerves and spinal cord manifesting as recurrent episodes of optic neuritis and myelitis. It is associated with serum aquaporin-4 immunoglobulin antibodies. In contrast to MS, lesions are usually longitudinally extensive spanning more than three segments and are centrally located within the cord. In the acute phase there may also be evidence of cord oedema. The prognosis is usually not as good as for multiple sclerosis as individual attacks are more likely to result in permanent disability with 50% of patients requiring assistance with walking and blind in at least one eye five years from diagnosis (Wingerchuk and Weinshenker, 2003).

A proportion of patients presenting with recurrent episodes of optic nerve or spinal inflammation have a clinical phenotype consistent with neuromyelitis but is negative for aquaporin-4 IgG. The term neuromyelitis spectrum disorders (NMOSD) has been developed to encompass those with and without aquaporin-4 IgG antibodies but with a consistent clinical phenotype (Wingerchuk et al., 2015). Detection of myelin oligodendrocyte glycoprotein (MOG) antibodies accounts for approximately 20% of NMO aquaporin-4 antibody negative cases of NMOSD and tends to have a more favourable clinical course with preponderance of short segment lower spinal cord lesions on spinal MRI (Sato et al., 2014).

Box 59.1 Case 1

A 23-year-old girl with no past medical history, presented to the emergency department complaining of progressive weakness of both her legs and a numb sensation extending up her legs to her chest over the last four days. She also noticed she had difficulty passing urine. On exam she had reduced power (grade 4/5) in both her legs more marked on her right than her left, with brisk deep tendon reflexes and extensor plantar responses bilaterally. She also had reduced pinprick sensation to T6. On flexion of her neck she described an 'electric shock' sensation radiating down both arms and her back. Spinal MRI demonstrated an enhancing lesion at C6. Subsequent MRI brain showed a number of non-enhancing lesions in a typical distribution for demyelination. Lumbar puncture revealed positive unmatched oligoclonal bands. These findings supported the diagnosis of clinically isolated syndrome likely as a first presenting event of multiple sclerosis.

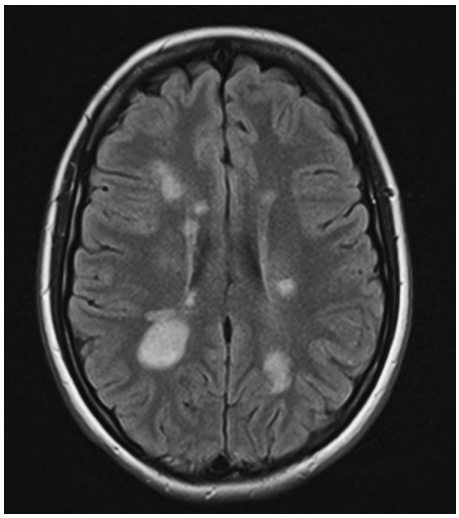

Fig. 59.2 Axial T2 FLAIR of brain showing multiple periventricular lesions consistent with demyelination, typical of multiple sclerosis.

Neurosarcoidosis

Sarcoidosis is an immune-mediated multisystem disease characterized by the presence of non-caseating granulomas. It can affect the nervous system in approximately 10% of cases. Patients usually have a prior history of systemic sarcoidosis or evidence of systemic involvement is found on subsequent investigations. Isolated neurosarcoidosis is rare. The most common manifestation is cranial neuropathies but spinal cord involvement is not uncommon and is usually associated with a worse outcome as a result of spinal cord atrophy and residual disability (Sohn et al., 2014). The most common site is the cervicothoracic spine, with most intramedullary lesions extending over three segments. In 50%, leptomeningeal enhancement is also seen (Fig. 59.3). Box 59.2 outlines a less common presentation with involvement of the cauda equina and conus medullaris. When compared to NMO onset, neurosarcoidosis is usually more gradual and patients may have coexistent radiculopathy or cranial neuropathy suggesting more diffuse central nervous system (CNS) involvement. Definitive diagnosis relies on a biopsy of CNS tissue but given associated morbidity, most patients are diagnosed with probable disease if there is pathological evidence of extraneural involvement, in combination with a compatible neurological syndrome.

Fig. 59.3 Post IV gadolinium sagittal lumbar spine MRI T1 demonstrates diffuse, nodular, leptomeningeal enhancement of the conus medullaris and cauda equina due to sarcoidosis.

Box 59.2 Case 2

A 39-year-old lady presented to the neurology service with a 6-month history of progressive walking difficulty requiring a crutch to mobilize and, recurrent urinary tract infections and constipation. She had been diagnosed with pulmonary sarcoidosis 5 years previously for which she did not require any treatment. On examination she had evidence of bilateral lower limb weakness more marked proximally (grade 4/5) and reduced pinprick sensation extending to L2 level bilaterally. Reflexes were reduced and plantar responses were flexor. She had an urgent MRI spine (Fig. 59.3), which revealed extensive leptomeningeal enhancement of the cauda equina and conus medullaris in keeping with neurosarcoidosis. She was given a diagnosis of probable neurosarcoidosis based on previous pathological evidence of pulmonary sarcoidosis in combination with her clinical and radiological findings.

Connective tissue disorders

Systemic lupus erythematous (SLE) and Sjögren syndrome may also present with transverse myelitis and should be included in the differential diagnosis. Lesions usually extend over multiple segments similar to NMO. Screening for autoantibodies including ANA, anti-Ro, and anti-La may aid diagnosis.

Paraneoplastic disorders

These are extremely rare causes of inflammatory myelitis. There will usually be diffuse CNS involvement with evidence of encephalitis, movement disorders, or seizures. Myelitis in isolation is rare and typically has a much more insidious course compared to other causes of transverse myelitis. There are a number of onconeuronal antibodies, which can be screened for, and their neurological presentation usually precedes the diagnosis of the underlying tumour.

Treatment

Patients can be treated empirically with high dose corticosteroids if they are felt to have inflammatory myelopathy. Further treatment is tailored towards the underlying cause.

Section 2: Acute flaccid paralysis

Medical conditions causing acute flaccid paralysis may be confused with cauda equina syndrome and causes of spinal shock. When assessing a patient with acute onset of limb weakness a careful history and examination can help distinguish medical and surgical causes and often an anatomical approach to localizing the level of the pathology can establish the likely cause.

Differential diagnosis based on anatomical location

Box 59.3 describes a woman presenting with acute flaccid paralysis, areflexia, and an antecedent history of a diarrhoeal illness. The most common medical cause of this presentation is Guillain–Barré syndrome (GBS) (Marx et al., 2000). The differential diagnosis for medical causes of flaccid paralysis is broad and may be considered by anatomical location (Table 59.2).

Box 59.3 Case 3

A forty-two-year-old woman was admitted to hospital with symmetrical bilateral limb weakness, ten days following consumption of undercooked chicken and a brief diarrhoeal illness. Examination revealed a sinus tachycardia (110 bpm), flaccid weakness, and areflexia of the lower limbs. There was evidence of bilateral facial weakness on assessment of the cranial nerves. Of note, there was no sensory level present on examination of pin prick sensation. Initial blood investigations were normal. MRI of the brain and spine was normal. Lumbar puncture was performed and cerebrospinal fluid (CSF) analysis demonstrated a normal cell count and glucose level, with an elevated protein concentration.

Complete or anterior spinal cord

Acute complete transverse myelitis may initially present as 'spinal shock', as discussed earlier. During this period, paradoxical motor signs present with flaccid paralysis and absent deep tendon reflexes.

It is important to consider an anterior spinal cord infarction if the flaccid paralysis is abrupt in onset and painful. Causes of this presentation include atherosclerosis of feeder vessels (artery of Adamkiewicz), aortic dissection, and aortic surgery. Rarer possibilities are thrombosis of the anterior spinal artery, vasculitis, and infective endocarditis.

Anterior horn cell

Certain viruses have a predilection for the anterior horn cell of the spinal cord and may result in a flaccid paralysis. They include enteroviruses (polio virus, enterovirus 71, group B coxsackie virus), flavivirus (West Nile virus, Japanese encephalitis), and rhabdovirus (Rabies virus) (Berger, 2012). Enteroviruses are easily spread and transmitted via respiratory and gastrointestinal secretions. West Nile virus is the most likely flavivirus to cause flaccid paralysis. It is transmitted via mosquito bite and is highly prevalent in the United States (Davis et al., 2006). Rabies virus is transmitted via bats, small animals, and dogs. One-third of infected patients present with 'paralytic rabies' and a clinical presentation of acute flaccid paralysis (Yousaf et al., 2012).

Motor neurone disease (MND) is clinically heterogeneous and is characterized by progressive degeneration of motor neurons. The typical clinical presentation is that of a progressive motor syndrome with clinical evidence of upper and lower motor neuron signs (Turner and Talbot, 2013). It can, however, present as a lower motor neuron-predominant picture. Subtypes of MND with a predilection for the anterior horn cell include progressive muscular atrophy and flail leg syndrome (Ludolph et al., 2015). Clinically, motor neurone disease can present with a foot drop or seemingly focal weakness so a thorough clinical examination looking for mixed upper and lower motor neurone signs and evidence of bulbar dysfunction should be completed. A compressive cervical myelopathy with an incidental peripheral neuropathy in the same patient may mimic mixed upper and lower motor neurone signs hence cervical spine imaging is typically performed in the diagnostic work up for MND.

Peripheral nerve

Guillain–Barré syndrome, as described in the aforementioned case, is the most common medical presentation of flaccid paralysis. If the clinical symptoms continue to deteriorate after eight weeks, one should consider chronic inflammatory demyelinating polyneuropathy. Lyme disease is transmitted by the ixodes tick and is endemic to North America, Europe, and Asia (Solomon and Shapiro, 2014) Clinically, it can cause a polyradiculopathy and may also involve the lower motor division of the facial nerve.

Certain viruses directly invade the spinal nerve roots and peripheral nerves (HIV, CMV, VZV, EBV). Porphyria, although rare, may present as a flaccid paralysis, but tends to be asymmetrical. This condition is typically preceded by abdominal and psychiatric symptoms.

Neuromuscular junction

Neuromuscular conditions such as myasthenia gravis and botulism can present with flaccid weakness. However, associated features such as fatigable weakness, cranial nerve involvement, and pupillary involvement assist in excluding neuromuscular conditions as a potential diagnosis.

Muscle

Acute myositis may present following a recent viral illness. Clinically, the weakness is associated with pain in the involved muscles and there may be an associated fever. Acute hypokalaemic periodic paralysis presents with weakness following exertion and a carbohydrate-rich meal. Frequently there is a positive family history; two-thirds of cases are autosomal dominant (Maurya et al., 2010).

Differential diagnosis based on history

An important initial step in evaluating this clinical scenario is a detailed clinical history. Questions to consider when taking the history include; recent travel history (polio-endemic areas, travel to the United States), antecedent infection (upper respiratory or gastrointestinal infective symptoms), insect or animal bites (tick or dog-bite), recent vaccination (H1N1 influenza vaccination), vascular risk

Table 59.2 Differential diagnosis of acute flaccid paralysis

Complete/Anterior spinal cord	Anterior horn cell	Peripheral nerve	Neuromuscular junction	Muscle
Transverse myelitis *(HSV, EBV, VZV, M. pneumonia)*	Enterovirus *(Polio virus, Enterovirus-71)*	Lyme disease, Tick paralysis	Botulism	Acute myositis
Vascular *(Anterior spinal artery syndrome)*	Rhabdovirus *(Rabies virus)*	Viruses *(HIV, CMV, EBV, HSV)*	Myasthenia gravis	Periodic paralysis *(Acute hypokalaemic periodic paralysis)*
	Herpes virus *(HSV2)*	Porphyria	Critical care	

factors (previous stroke/TIA) and family history (familial hypokalaemic periodic paralysis). In this case, the patient had a prodromal diarrhoeal illness and subsequently tested positive for campylobacter jejuni infection. Campylobacter jejuni is the most commonly associated infection with GBS and is observed in 30% of cases, often with onset of neurological symptoms after 10 days (Poropatich et al., 2010).

It is also important to consider symptom evolution when considering the differential diagnosis. Weakness, that is maximal at onset, without further evolution, is likely to be vascular (anterior spinal artery occlusion). Whereas, weakness that evolves gradually, over days to weeks, is more likely due to an inflammatory, immune-mediated, or an infectious process. A more slowly progressive course, evolving over months, should prompt consideration of a neurodegenerative condition, such as MND.

Differential diagnosis based on examination findings

Examination findings can provide useful clues to help to narrow the differential diagnosis further. Abnormal vital signs (increased temperature, hypotension) can assist in identifying a potential infectious cause of flaccid paralysis.

Autonomic instability, as noted in the aforementioned case, frequently presents in GBS. Patients presenting with complete transverse myelitis will have autonomic dysfunction below the level of the lesion, as described earlier. The absence of a sensory level on examination in the earlier case was useful. If present, one might consider transverse myelitis. Bladder involvement may also be observed in the latter. It is important to inspect for a rash on examination and to enquire about evidence of a preceding rash from the clinical history. Erythema migrans is the most common clinical manifestation of Lyme disease (Solomon and Shapiro, 2014). It typically appears at the site of the original tick bite, one to two weeks later. It may resemble a bull's eye with a central area of erythema, surrounded by a halo. A vesicular rash in the buccal mucosa and on the hands and feet suggests enterovirus-71, whereas, rash in a dermatomal distribution is suggestive of herpes zoster.

An additional useful finding in this case was bilateral facial weakness. The presence of bilateral facial weakness and symmetric flaccid paralysis makes a diagnosis of GBS highly likely. Involvement of the facial nerve may be also seen in Lyme disease. It is worth noting that despite flaccid paralysis being included in the diagnostic criteria of GBS, 10% of patients present with preserved or increased reflexes (Fokke et al., 2014).

Differential diagnosis based on investigatory workup

An important initial investigation is MRI of the spine to rule out an inflammatory, ischaemic, or structural cause to account for the clinical presentation. GBS may present with enhancement of the proximal nerve roots on MRI with gadolinium. A lumbar puncture can assist in narrowing the differential further. One would anticipate an albuminocytologic dissociation (high protein, normal white cell count) in GBS, as seen in this case. Meanwhile, viral aetiologies present with a lymphocytosis, high protein concentration, and a normal glucose level.

In suspected infectious cases, the diagnosis is typically confirmed by pathogen-specific serology or antigens in the cerebrospinal fluid (CSF) or serum (HSV2, VZV, Enterovirus, Borrelia Burgdoferi). When considering MND, the diagnosis is clinical, but neurophysiological tests can provide support for the presence of denervation.

Section 3: Focal presentations of medical disorders mimicking surgical pathology

Regional pain

Pain is a common early feature in several neurosurgical presentations including cord compression, where it often proceeds neurological disturbance and radiculopathies. Acute or chronic neurogenic pain is also a feature of numerous medical disorders and could be confused with surgical presentations. Central poststroke pain is a frequently encountered central neuropathic pain syndrome that may produce chronic hemi-body pain, particularly in the context of thalamic and lateral medullary infarcts, so previous history of stroke should be considered for diffuse pain syndromes.

Pain with sensory disturbance and/or weakness confined to a single limb points to a disorder of the peripheral nervous system and is often investigated initially for nerve root compression.

Complex regional pain syndrome (CRPS, formerly known as reflex sympathetic dystrophy, causalgia, or Sudeck's atrophy) produces a burning or throbbing pain in a body region (typically a limb) in its early stage. It has a strong female predominance and an inciting event such as trauma, surgery, myocardial ischaemia, cerebrovascular events, or emotional disturbance may precede episodes (Veldman et al., 1993). Signs in later stages of the condition such as soft tissue oedema, muscular atrophy, skin thickening, contracture development, and bony demineralization are useful for differentiating CRPS from differential diagnoses including radiculopathy and peripheral neuropathy, although this distinction can be more challenging at symptom onset. Examination findings at initial presentation that can help diagnose CRPS include a distribution of pain or sensory disturbance that is not in keeping with that of a nerve root, peripheral nerve, or plexus trunk. In addition, temperature or skin tone discrepancy between the affected area and the contralateral side is a useful sign. The diagnosis is made clinically; however, investigations including autonomic testing and bone scintigraphy are occasionally employed.

Herpes zoster (also known as shingles) results from the reactivation of latent varicella-zoster virus infection in the dorsal root ganglia. Burning or stabbing pain in the effected dermatome, usually thoracic and lumbar, is the most common clinical feature and occurs as a prodromal symptom prior to the development of the classical vesicular rash. In some cases, an associated myelopathy can also occur (Frohman and Wingerchuk, 2010). Diagnostic laboratory tests where the cause is uncertain include viral culture or polymerase chain reaction (PCR). The persistence of pain for more than one month after resolution of the rash is defined as postherpetic neuralgia and is thought to represent viral damage-induced hypersensitivity of the dorsal horn neurons. Unilateral neuropathic pain in the affected dermatome associated with allodynia and anaesthesia could be misinterpreted as radiculopathy and thus underlies the importance of eliciting a preceding history of skin rashes in all cases of regional pain.

Medical conditions affecting peripheral nerve plexuses can also mimic some spinal cord lesions. One of the more common

non-traumatic brachial plexopathies is brachial neuritis, also known as neuralgic amyotrophy or Parsonage-Turner syndrome. This idiopathic male-predominant condition typically presents with acute onset severe unilateral shoulder pain. Bilateral pain may occur in up to one-third of cases, but this is asymmetrical when present (van Alfen and van Engelen, 2006). This is followed usually within a few weeks of onset by the development of weakness typically in muscles innervated by the upper trunk (e.g. serratus anterior, deltoid, supraspinatus, infraspinatus). Sensory symptoms also occur in the majority of cases, with numbness or hypaesthesia found in the distribution corresponding to that of the nerves supplying the weakest muscles, and reflexes may be reduced or absent. Around half of patients report an antecedent illness or event such as viral or bacterial infection, trauma, surgery, connective tissue disorders, vaccination, or pregnancy. A hereditary (autosomal dominant) form also exists, characterized by recurrent episodes of pain with additive weakness beginning in childhood or early adulthood. The diagnosis is primarily made clinically but magnetic resonance (MR) imaging is useful to rule out compression or infiltration of the brachial plexus, and nerve conduction and electromyographic (EMG) studies can be used to rule out mononeuropathies/radiculopathies and confirm denervation, respectively. Management is largely conservative.

Sensory disturbance

Unlike the widespread causes of sensory disturbance discussed earlier, sensory loss restricted to part of a limb strongly suggests a peripheral process, as does involvement of all sensory modalities (touch, temperature, pain, vibration, and proprioception).

Symmetrical sensory loss

The differentiation of central (i.e. myelopathy) and peripheral (i.e. polyneuropathy) causes of symmetrical sensory loss can occasionally be challenging. Thorough neurological examination should aid this distinction, with increased tone, an upper motor neuron pattern of weakness (weaker upper limb extensors and lower limb flexors), hyperreflexia, and a lack of both fasciculations and severe atrophy suggesting a central cause. Disproportionate loss of proprioception and vibration sense in patients with bilateral sensory disturbance is suggestive of disorders affecting the posterior columns of the spinal cord, such as vitamin B_{12} deficiency (subacute combined degeneration of the cord), tertiary neurosyphilis (tabes dorsalis), and more rarely acquired copper deficiency, but is also a feature of demyelinating polyneuropathies (as outlined next).

The term polyneuropathy refers to a disorder of multiple peripheral nerves that is typically symmetrical and affects distal nerves most prominently. Patients usually present with symmetrical distal sensory (burning pain or numbness) or motor (weakness) symptoms. Depending on the cause, the presentation may be gradual in onset and follow a chronic clinical course, or symptoms may develop acutely and be self-limiting. Polyneuropathies are typically classified as either axonal or demyelinating and this represents a useful differentiator in terms of underlying medical pathologies, although there is considerable overlap.

Axonopathies typically involve the lower extremities first (i.e. they are length-dependent), with gradual development of sensory loss and dysaesthsias, most notably a burning pain sensation in the feet, with later involvement of the upper limbs (the so-called glove-and-stocking distribution) and motor symptoms. Examination findings include distal loss of sensation and reflexes. These most often result from metabolic and toxic disorders; however, infectious or vascular disorders can cause asymmetrical axonal polyneuropathy.

Demyelinating polyneuropathies tend to preferentially affect motor fibres, with weakness representing an early clinical presentation and later development of dysaesthesias and reduced proprioception. Generalized weakness may be elicited on examination, more noticeable in distal muscles, in association with diffuse hypo/areflexia and predominantly large-fibre (heavily myelinated) sensory disturbances (impaired proprioception and vibration sense).

Several hereditary peripheral neuropathies exist, the pathology of which can either be axonal or demyelinating. Although a wide range have been described, including many that occur as part of more widespread systemic disorders, hereditary motor and sensory neuropathy (HMSN, also known as Charcot-Marie-Tooth disease) is the most commonly occurring family of such hereditary neuropathies. Seven categories of HMSN have been described with over 30 constituent disorders recognized to date, and causative mutations in myelin genes are continually being identified (Klein et al., 2013). HMSN type 1 and 2, both usually dominantly inherited, together account for the majority of cases. HMSN 1 is a demyelinating form characterized by gross nerve hypertrophy and slow nerve conduction velocities. HMSN 2 in predominantly axonal and is associated with borderline slow/normal nerve conduction velocities. If a clear family history is not available or not present (e.g. late presentation or mild disease that has not been diagnosed in relatives), certain features of the history and examination point towards a diagnosis of an inherited peripheral neuropathy. These include a history of recurrent childhood falls, ankle sprains or fractures, a prolonged slowly progressing history, deformities such as pes cavus or an inverted champagne bottle appearance of the legs (due to leg muscle atrophy), and the presence of sensory loss without definite sensory symptoms. Diagnosis is based on clinical suspicion, electrophysiological studies, and genetic testing that can avoid the need for invasive investigation with nerve biopsy. No specific treatments for HSMN have been developed, and management is largely supportive with a large emphasis on physiotherapy.

Asymmetrical sensory loss

Sensory loss limited to part of an extremity suggests a disorder of the peripheral nerve or nerve root. Mononeuropathies and radiculopathies result from disorders of individual peripheral nerves or nerve roots, respectively. The distinction of clinical signs corresponding to either the distribution of a single nerve or to that of a nerve root (i.e. dermatome/myotome) can be difficult in some cases and nerve conduction studies and EMG may be required. Non-compressive causes of mononeuropathies and radiculopathies include infection (in particular herpes zoster and Lyme disease), diabetes, vasculitis with nerve/nerve root ischaemia, infiltration by neoplasms, granulomatous disease or amyloidosis, and demyelination.

Mononeuritis multiplex is characterized by isolated damage to at least two separate nerves causing an asymmetrical sensory and motor peripheral neuropathy. Common associated conditions include diabetes mellitus, vasculitis, connective tissue disorders, and amyloidosis, wherein inflammation-induced occlusion of the vasa nervorum

results in peripheral nerve ischaemia. Pain is typically present at onset and a foot drop is a frequent manifestation. In addition to blood tests to assess for associated conditions and nerve conduction studies/EMG, peripheral nerve biopsy (in particular of the easily accessible and frequently involved sural nerve) is useful in establishing the diagnosis prior to commencing treatment (Bennett et al., 2008).

Pathology at the level of the dorsal root ganglion can also result in asymmetrical sensory loss. Sensory neuronopathies are relatively rare disorders characterized by a degeneration of sensory neurons in dorsal root ganglia that result in a non-length-dependent distribution of almost pure sensory loss (Camdessanché et al., 2009). They may be paraneoplastic, or may be associated with Sjögren's syndrome, HIV infection, and cisplatin toxicity. The diagnosis is based on electrophysiological studies in addition to testing for the aforementioned associated disorders, and recently skin biopsy has been used to confirm non-length-dependence of small fibre degeneration.

Weakness

Localized muscle weakness is a common finding in compressive myelopathy; however, a range of medical disorders must be considered in the differential diagnosis.

As described earlier, distal symmetrical weakness, manifesting as a bilateral foot drop or decreased grip strength, for example, is commonly associated with polyneuropathy. Proximal symmetrical muscle weakness, presenting with difficulties ascending stairs, rising from a seated position, or combing one's hair, for example, is typically an indication of a myopathic rather than a neuropathic disorder, such as polymyositis, dermatomyositis, or inclusion body myositis. Metabolic disorders such as hypothyroidism, hypoparathyroidism, and drug-induced myositis (e.g. with statin treatment for lowering cholesterol) should all be considered. Other features suggestive of a myopathic process include isolated muscle weakness (absence of sensory symptoms and preserved reflexes) and delayed muscle atrophy, which in general occurs earlier with neuropathy. EMG helps to exclude primarily neurogenic processes and is a useful diagnostic adjunct, while muscle biopsy and MR scanning are often employed.

FURTHER READING

Frohman, E.M. & Wingerchuk, D.M. (2010). Clinical practice. Transverse myelitis. *N Engl J Med*, **363**(6), 564–72.

Klein, C.J., Duan, X., & Shy, M.E. (2013). Inherited neuropathies: clinical overview and update. *Muscle & Nerve*, **48**(4), 604–22.

Ludolph, A., Drory, V., Hardiman, O., et al. (2015). A revision of the El Escorial criteria—2015. *Amyotroph Lateral Scler Frontotemporal Degener*, **16**(5–6), 291–2.

Van Alfen, N. & van Engelen, B.G. (2006). The clinical spectrum of neuralgic amyotrophy in 246 cases. *Brain*, **129**(Pt 2), 438–50.

Veldman, P.H., Reynen, H.M., Arntz, I.E., & Goris, R.J. (1993). Signs and symptoms of reflex sympathetic dystrophy: prospective study of 829 patients. *Lancet*, **342**(8878), 1012–16.

FURTHER READING

Attal, N. (2012). Neuropathic pain: mechanisms, therapeutic approach, and interpretation of clinical trials. *Continuum*, **18**(1), 161–75.

Pittock, S.J. & Lucchinetti, C.F. (2006). Inflammatory transverse myelitis: evolving concepts. *Curr Opin Neurol*, **19**(4), 362–8.

Turner, M.R. & Talbot, K. (2013). Mimics and chameleons in motor neurone disease. *Pract Neurol*, **13**, 153–64.

REFERENCES

Bennett, D.L., Groves, M., Blake, J., et al. (2008). The use of nerve and muscle biopsy in the diagnosis of vasculitis: a 5-year retrospective study. *J Neurol Neurosurg Psychiatry*, **79**(12), 1376–81.

Berger, J.R. (2012). Infectious myelopathies. *Contin Lifelong Learn Neurol*, **18**(6), 1351–73.

Bhat, A., Naguwa, S., Cheema, G., & Gershwin, M.E. (2010). The epidemiology of transverse myelitis. *Autoimmun Rev*, **9**, A395–9.

Camdessanché, J.P., Jousserand, G., Ferraud, K., et al. (2009). The pattern and diagnostic criteria of sensory neuronopathy: a case-control study. *Brain*, **132**(Pt 7), 1723–33.

Davis, L.E., DeBiasi, R., Goade, D.E., et al. (2006). West Nile virus neuroinvasive disease. *Ann Neurol*, **60**(3), 286–300.

Fokke, C., van den Berg, B., Drenthen, J., Walgaard, C., van Doorn, P.A., & Jacobs, B.C. (2014). Diagnosis of Guillain-Barré syndrome and validation of Brighton criteria. *Brain*, **137**(Pt 1),33–43.

Frohman, E.M. & Wingerchuk, D.M. (2010). Clinical practice. Transverse myelitis. *N Engl J Med*, **363**(6), 564–72.

Klein, C.J., Duan, X., & Shy, M.E. (2013). Inherited neuropathies: clinical overview and update. *Muscle & Nerve*, **48**(4), 604–22.

Ludolph, A., Drory, V., Hardiman, O., et al. (2015). A revision of the El Escorial criteria—2015. *Amyotroph Lateral Scler Frontotemporal Degener*, **16**(5–6), 291–2.

Marx, A., Glass, J.D., & Sutter, R.W. (2000). Differential diagnosis of acute flaccid paralysis and its role in poliomyelitis surveillance. *Epidemiol Rev*, **22**(2), 298–316.

Maurya, P.K., Kalita, J., & Misra, U.K. (2010). Spectrum of hypokalaemic periodic paralysis in a tertiary care centre in India. *Postgrad Med J*, **86**, 692–5.

Poropatich, K.O., Walker, C.L., & Black, R.E. (2010). Quantifying the association between Campylobacter infection and Guillain-Barré syndrome: a systematic review. *J Health Popul Nutr*, **28**(6), 545–52.

Sato, D.K., Callegaro, D., Lana-Peixoto, M.A., et al. (2014). Distinction between MOG antibody-positive and AQP4 antibody-positive NMO spectrum disorders. *Neurology*, **82**, 474–81.

Sohn, M., Culver, D.A., Judson, M.A., Scott, T.F., Tavee, J., & Nozaki, K. (2014). Spinal cord neurosarcoidosis. *Am J Med Sci*, **347**, 195–8.

Solomon, C.G. & Shapiro, E.D. (2014). Lyme disease. *N Engl J Med*, **370**(18), 1724–31.

Suchett-Kaye, A.I. (1948). Acute transverse myelitis complicating pneumonia: report of a case. *Lancet*, **2**, 417.

Transverse Myelitis Consortium Working Group (2002). Proposed diagnostic criteria and nosology of acute transverse myelitis. *Neurology*, **59**, 499–505.

Turner, M.R. & Talbot, K. (2013). Mimics and chameleons in motor neurone disease. *Pract Neurol*, **13**, 153–64.

Van Alfen, N. & van Engelen, B.G. (2006). The clinical spectrum of neuralgic amyotrophy in 246 cases. *Brain*, **129**(Pt 2), 438–50.

Veldman, P.H., Reynen, H.M., Arntz, I.E., & Goris, R.J. (1993). Signs and symptoms of reflex sympathetic dystrophy: prospective study of 829 patients. *Lancet*, **342**(8878), 1012–16.

Wingerchuk, D.M., Banwell, B., Bennett, J.L., et al. (2015). *Neurology*, **85**(2), 177–89.
Wingerchuk, D.M. & Weinshenker, B.G. (2003). Neuromyelitis optica: clinical predictors of a relapsing course and survival. *Neurology*, **60**, 848–53.
Yousaf, M.Z., Ashfaq, U.A., Zia, S., et al. (2012). Rabies molecular virology, diagnosis, prevention and treatment. *Virol J*, **9**, 50.

RELATED LINKS TO EBRAIN

Clinical Introduction to Neuromuscular Diseases. https://learning.ebrain.net/course/view.php?id=338
Neuromuscular Assessment. https://learning.ebrain.net/course/view.php?id=41
Transverse Myelitis: Causes Assessment and Management. https://learning.ebrain.net/course/view.php?id=271

SECTION 13
Spinal surgery

60. **Cervical spinal disease** *697*
Navin Furtado, Georgios Tsermoulas, and Adikarige Haritha Dulanka Silva

61. **Thoracic spinal disease** *711*
Kieron Sweeney, Catherine Moran, and Ciaran Bolger

62. **Lumbar spinal disease** *719*
Christopher G. Kellett and Matthew J. Crocker

63. **Spinal tumours** *733*
John Brecknell and Boon Leong Quah

64. **Vascular lesions of the spinal cord** *751*
Daniel Walsh

65. **Spinal cerebrospinal fluid dynamics** *761*
Graham Flint

66. **Scoliosis and spinal deformity** *769*
Nigel Gummerson

60

Cervical spinal disease

Navin Furtado, Georgios Tsermoulas, and Adikarige Haritha Dulanka Silva

Pathology of degenerative cervical spinal disease

Degenerative cervical spinal disease is a broad term encompassing a number of pathologies resulting in structural changes in the joints (i.e. the intervertebral disc, facet joints and the uncovertebral joints), which potentially lead to compression of neural structures, deformity, pain, and disability. An understanding of spinal biomechanics and the pathological processes involved will aid in the treatment and management of symptomatic patients.

Degeneration of musculoskeletal tissues is a biological inevitability, but the rate of degeneration is related to loading and intensity of use over time. Additional risk factors include smoking, genetic predisposition, localized trauma, and infection, which can accelerate degenerative changes.

In the cervical spine, the intervertebral discs bear the load of the head and neck. Axial loading through the nucleus pulposus of the disc is converted to hoop stresses acting on the annulus fibrosus and vertebral endplates. This continuous mechanical loading alters the cellular composition of the nucleus pulposus with reduction in hydrophilic proteoglycans and increase in collagen (type II, III, VI, and IX) (Urban et al., 2000). Subsequently the mechanical properties of the discs change, the intervertebral height is reduced and eventually cracks and fissures appear in the annulus and vertebral end plates predisposing to nucleus pulposus herniation. Altered stresses are transferred to facet joints leading to segmental hypermobility with osteophytic spurs deposited in an adaptive remodelling process meant to confer increased stability (Galbusera et al., 2014). Histological changes observed in ligamentous hypertrophy include hyperplasia of non-fibrous cartilage, metaplasia, and capillary hyperplasia (Inamasu et al., 2006).

The commonest levels affected are C6/7 and C5/6. Below the age of 55 years, a soft disc prolapse consisting of herniated nucleus pulposus encroaches into the spinal canal or neural exit foramina causing compression of the spinal cord and/or exiting nerve roots resulting in the clinical syndromes of myelopathy and/or radiculopathy, respectively. In older patients, neural compression is more commonly caused by osteophytes and a thickened annulus (hard disc). Multilevel degenerative changes may alter normal cervical lordosis, leading to straightening or the adoption of kyphotic, hyperlordotic, or scoliotic curvatures.

Degenerative changes in the cervical spine can lead to stenosis of the spinal canal and myelopathy results if the reduction in the cross-sectional area is greater than 30% (Yu et al., 1986). A normal cervical spinal canal measures approximately 18 mm in the anteroposterior plane and the normal cervical spinal cord measures 10 mm in diameter.

There are various pathophysiological mechanisms that contribute to cord injury in degenerative cervical myelopathy. Static compression in canal stenosis results in direct trauma and chronic cord ischaemia with dynamic compression resulting from excessive translational movements (>3.5 mm). A neuroinflammatory response triggers a cascade of cellular events causing demyelination of the corticospinal tracts, central grey matter degeneration with loss of interneurons, anterior horn cell atrophy and gliosis (Kalsi-Ryan et al., 2013).

Clinical presentation and investigation

There is heterogeneity in clinical presentation with variable severity and speed of progression. Patients with myelopathy tend to have symmetrical involvement of motor and sensory tracts within the spinal cord. Bilateral weakness below the affected level (paraparesis or quadriparesis), paraesthesia, numbness, tingling, and sensory loss with a discrete sensory level can be seen. Clinical examination reveals signs including increased tone, brisk and pathological reflexes (Hoffman's and Babinski sign). There may be symptoms of difficulty with sphincter control. The onset of symptoms can be insidious and a steady deterioration in hand control especially with fine tasks may be noted progressing to increased clumsiness, unsteadiness of gait, and recurrent falls.

It is more common for degenerative cervical spinal disease to present clinically with features of radiculopathy. Radiculopathy from compression of a nerve root can lead to motor and sensory deficits with reduced deep tendon reflexes in the distribution of the involved nerve root. Pain, with associated reduced movements in the cervical spine, is the predominant symptom radiating from the neck into the arm as brachialgia. Sensory symptoms especially pins and needles are found in the distribution of the nerve. Positive root compression tests can reproduce pain.

MRI imaging of the cervical spine is used to confirm the diagnosis. Further dynamic cervical spine radiographs may assist in

identifying instability which can affect surgical planning. In a few cases a computed tomography (CT) scan of the cervical spine may be useful for assessing the degree of osteophytosis and the extent of foraminal stenosis. Oblique cervical spine films can occasionally demonstrate foraminal narrowing. Myelography has excellent sensitivity for detecting spinal cord compression but may miss very lateral nerve root foramen stenosis.

Treatment

An individualized treatment approach should be adopted, accounting for ventral versus dorsal compression, sagittal alignment, focal versus diffuse disease, presence or absence of radiculopathy, significant axial cervical pain, age, comorbidities, and surgical familiarity with an approach.

Surgical decompression is advocated in most patients with cervical myelopathy because the majority (80%) deteriorate over time with spontaneous regression being uncommon. The timing of surgery is more controversial in patients with mild features of myelopathy or asymptomatic cord compression. Patients should be counselled with regard to the risk of cord injury secondary to degenerative disc disease in the context of trauma.

Earlier intervention in symptomatic cervical myelopathy is associated with improved outcomes. Chronic neurological deficit is unlikely to improve. The risks of surgical intervention versus the benefits of surgery need to be discussed with the patient.

For cervical radiculopathy, randomized studies have shown that surgery results in rapid improvement of symptoms compared to non-operative measures like physiotherapy, but in the long term both methods are equally effective (Engquist et al., 2013). Conservative management is therefore recommended as a first line of treatment. If symptoms are persistent and debilitating, then surgery can be offered.

Degenerative cervical myelopathy patients are consented with the primary aim of surgical decompression being to halt disease progression. Following surgery, 60–70% of myelopathic patients improve with another 30% having stable disease and 10% continue to progress. For patients with radiculopathy, up to 90% have improvement in their arm symptoms.

Ossification of posterior longitudinal ligament (OPLL) and ossification of ligamentum flavum (OLF)

OPLL is more prevalent in Japan (2–4%) compared to Western countries (0.1–1.7%). The genetic basis of this geographical variation remains undetermined. Non-insulin dependent diabetes mellitus, impaired glucose tolerance, excessive weight gain, hypoparathyroidism, and hypophosphataemic rickets have all been implicated. Ectopic bone forms within the ligaments, the histological characteristics of OPLL and OLF include ossification, ligamentous hyperplasia, cell proliferation, and vascular ingrowth.

OPLL has been classified into four types as follows: (a) continuous type with ossification spreading over a number of vertebral levels; (b) segmental type with ossification localized posterior to the vertebral bodies; (c) mixed type (combination of continuous and segmental features) and (d) localized/circumferential type (ossification is confined to the disc space).

OPLL impacts on the choice of operative approach owing to different segmental kinematics and the loss of tissue planes. This complicates anterior surgical decompression and dramatically increases the risk of intraoperative durotomy. When ossification bridges the disc spaces, segmental mobility is reduced, and the posterior longitudinal ligament fuses with the thecal sac. A posterior approach is usually indicated but if adopting an anterior approach more extensive vertebrectomy decompressions are frequently required.

OLF also has a higher prevalence in Japan, affecting women more than men and typically becomes symptomatic over the age of 50 years. Ossification is within the layers of the ligamentum flavum and noted to originate from the lamina in a contiguous manner.

Rheumatoid arthritis (RA)

Rheumatoid arthritis is a systemic autoimmune disease (1% of adults in Europe and the United States) that can affect the cervical spine. Advances in disease modifying antirheumatic drugs and biological agents have reduced the number of patients presenting with RA-related cervical spinal disease (Kaito et al., 2013). The use of modern therapeutic agents when started early can prevent the destructive joint pathology from occurring but are unable to prevent progression of cervical spine lesions if already present.

The pathobiology of RA involves novel antigenic expression by synovial cells leading to persistent cellular activation and immune complex production (rheumatoid factor-IgM). Cytokine-mediated (IL-1, IL-6, TNF-α) chronic inflammation is initiated. This results in granulation tissue deposition within the synovium (rheumatoid pannus), which in itself produces proteolytic enzymes capable of destroying adjacent cartilage, ligaments, tendons, and bone (Reiter and Boden, 1998).

Within the cervical spine, destructive synovitis leads to ligamentous laxity and bony erosions with subsequent instability and subluxation of the vertebrae. Compression of neural structures can result from instability or direct compression from pannus formation. The upper cervical articulations at occiput/C1 and C1/C2 are primarily affected because the normal ligamentous structures surrounding the occipito-atlantoaxial region that confer a significant proportion of strength and stability are degraded as part of the disease process. The most common cervical spine pathologies in RA are C1/2 instability (65%), basilar invagination (20%), and subaxial subluxation (15%) (Kim et al., 2015).

Subaxial subluxation results from facet and uncovertebral joint instability. Translational movement of the vertebrae in the sagittal and coronal planes with or without rotation can occur. Abnormal alignment may include spondylolisthesis, kyphosis, scoliosis, or a 'staircase' deformity. Surgical decompression and arthrodesis may be necessary in cases of instability and canal compromise with cord compression and neurological dysfunction.

Craniocervical pathologies

Atlantoaxial subluxation

C1-C2 instability (atlantoaxial subluxation) results from destruction of the transverse, apical, and alar ligaments, for example, from rheumatoid pannus. It also occurs in ankylosing spondylitis, achondroplasia, Down's syndrome, Morquio's syndrome, and secondary

to trauma. It is becoming less common as steroid sparing drugs have allowed patients with rheumatoid arthritis to be managed with much lower doses of steroids.

The subluxation can be seen on dynamic cervical spine radiographs or kinematic MRI as excessive translational movements of C1 on C2. The normal anterior atlanto-dental interval is less than 3 mm (<5 mm in a child), as measured from the posterior aspect of the anterior arch of C1 to the anterior aspect of the dens. Surgical stabilization has been advocated in asymptomatic patients when this interval is more than 8 mm and in all patients with myelopathy. Neck pain is a feature of cervical instability in these patients. Surgical outcomes are good in the absence of preoperative myelopathy so early C1/2 fusion surgery is usually advocated. However, it is not uncommon to see RA patients who are neurologically intact with significant C1/2 subluxation and use of the anterior atlanto-dental interval has been shown to correlate poorly with neurological outcomes. The posterior atlanto-dental interval is measured from the posterior aspect of the dens to the anterior aspect of the C1 lamina and should be more than 14 mm and it correlates better with neurological outcome.

Rotatory atlantoaxial subluxation

Atlantoaxial rotatory subluxation is most common in children and is covered in Chapter 85.

Basilar invagination

Basilar invagination occurs from erosion of occiput/C1 and C1/2 joints such that the dens, migrates into the foramen magnum. It may present with hydrocephalus, syringomyelia, or progressive myelopathy. A number of radiographic measurements have been described for identifying basilar invagination (Fig. 60.1). Chamberlain's line extends from the hard palate to the opisthion (back of the foramen magnum) and the tip of the dens should be =<3 mm above this line. McGregor has modified this for when the opisthion cannot be identified. McGregor's line extends from the hard palate to the most caudal point of the occipital curve and the dental tip should by less than 4.5 mm above this line. The simplest line, however, is McRae's line drawn from the basion (front of the foramen magnum) to the opisthion. The superior tip of the dens is normally 5 mm below but should not be cephalad of this line. McRae's line is also used to diagnose Chiari 1 malformations where the cerebellar tonsils, which should normally be above this line, are seen to descend more than 3mm in children and 5 mm in adults. It may be difficult to identify the dens due to erosion and pannus. In this situation, it is possible to use the position of the anterior C1 arch in relation to the C2 body. A severe abnormality is identified when the anterior arch of C1 is adjacent to the lower third of the C2 body.

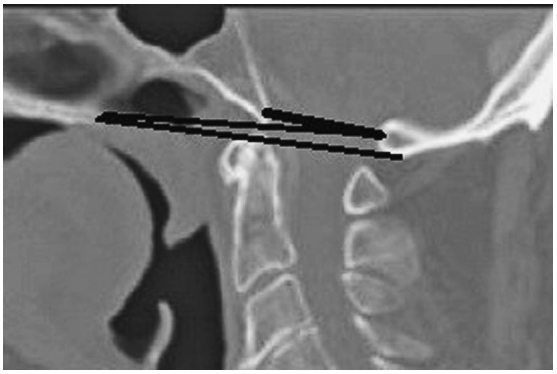

Fig. 60.1 McRae's line runs across the foramen magnum from the basion to the opisthion, Chamberlain's line runs from the back of the hard palate to the posterior margin of the foramen magnum (opisthion). McGregor's line is similar running from the palate to the lowest visible part of the occiput. The tip of the dens should be =<3 mm above Chamberlain's line, less than 4.5 mm above McGregor's line and usually 5 mm below but not above McRae's line.

Some authors differentiate this radiological appearance when it is caused by softening of the bones at the skull base and term it 'basilar impression'. In this case, there is dislocation superiorly of the upper spine onto the foramen magnum with brainstem compression as a result of skeletal anomalies of the basi-occiput and condylar segment of the occipital bone leading to infolding of the foramen magnum vs. 'basilar invagination' which involves upward migration of the dens into the foramen magnum from pathological ligamentous disruption.

The most common cause of basilar invagination is rheumatoid arthritis, but other causes include Klippel-Feil, osteogenesis imperfecta, achondroplasia, Chiari malformations, cleidocranial dysostosis, Schwartz-Jampel syndrome 2, Morquio's syndrome, hyperparathyroidism, osteomalacia, rickets, and Paget's disease.

Different procedures have been used to treat basilar invagination either on their own or in combination including traction, anterior decompression, and craniocervical fusion with or without foramen magnum decompression. There is little consensus on the best way to treat these patients. The location of the vertebral arteries must be considered. The presence of ventral tissue contraction may make an anterior approach essential. When there are no cranial nerve palsies a posterior fusion is usually adequate, preoperative traction may help to predict whether adequate reduction can be achieved intraoperatively. Where cranial nerve palsies exist or where traction is considered unsafe then an anterior transnasal or transoral resection of the odontoid peg should be considered. In some cases C1 and C2 will already have fused but in others surgical C1/2 fusion will be required either anteriorly or with a combined posterior approach. Most authors recommend performing the anterior decompression first followed by the posterior fusion, but a few authors do recommend the reciprocal.

Platybasia

Platybasia is described as flattening of the skull base and is usually asymptomatic unless associated with other anomalies. The skull base angle is formed by a line joining the nasion with the centre of the pituitary fossa and a line joining the anterior border of the foramen magnum with the centre of the pituitary fossa. Platybasia is present if this angle is more than 143°, basilar kyphosis is present if it is less than 125°. Platybasia is associated with basilar invagination and achondroplasia, Down's syndrome, Chiari malformations, craniocleidodysostosis, craniofacial anomalies, osteogenesis imperfecta, Paget's disease, osteomalacia, rickets, fibrous dysplasia, and hypoparathyroidism.

Seronegative spondyloarthropathies

These include a number of inter-related chronic inflammatory conditions of unknown aetiology; ankylosing spondylitis, Reiter's

syndrome, psoriatic arthritis, arthritis of inflammatory bowel disease and undifferentiated spondyloarthropathies.

Ankylosing spondylitis is the commonest and is associated with the HLA-B27 genotype seen in 80–98% of affected patients. Systemic inflammatory processes lead to an enthesopathy (inflammation at the insertion of tendons and ligaments into the bone) with subsequent bridging syndesmophyte (bone spur) formation. The cervical spine manifestations are typically stiffness from joint and ligament ossification, and kyphosis which when severe, manifests as a 'chin-on-chest' deformity. The chin-brow vertical angle is measured using standing whole spine radiographs and/or clinical photographs to assess overall spinal deformity and balance. Correction of cervical deformity should only be entertained if concomitant abnormalities of the thoracolumbar spine and hip/knee joints have been excluded. Osteopaenia occurs as part of the disease process and affects surgical planning involving instrumentation.

Diffuse idiopathic skeletal hyperostosis (DISH)

Also known as Forestier disease, DISH has an overall incidence of 6–12% and is more common in patients over the age of 50 years. It is characterized by the presence of non-marginal syndesmophytes at three successive levels (involving four contiguous vertebrae) and appears radiologically as flowing anterior ossification of the anterior longitudinal ligament with disc space preservation. The disease process differs from ankylosing spondylitis in that there is an absence of facet joint ankylosis, sacroiliac joint erosion, sclerosis, or intra-articular osseous fusion, and there is usually no osteopaenia.

Symptoms include stiffness and pain. Associated degenerative changes in the disc with osteophytes can lead to myeloradiculopathy. The stiff cervical spines seen in ankylosing spondylitis and DISH are more prone to fracture in minor to moderate trauma. Most cases are treated if canal stenosis results in symptomatic myeloradiculopathy. With large anterior syndesmophytes, dysphagia, stridor, and hoarseness of voice may also, rarely, be surgical indications.

Anterior cervical approaches

Anterior cervical spine approaches have been used since the 1950s (Cloward, 1958) to decompress the spinal cord and nerve roots.

Anterior techniques for decompression include discectomy and corpectomy. Following decompression, a decision is made either to fuse the joint (arthrodesis) or to preserve motion (arthroplasty). In fusion, autograft (e.g. iliac crest, fibula strut), allograft or synthetic graft may be used. This may be supplemented with anterior cervical plating.

Indications for an anterior approach

Anterior compression of neural elements should be treated with an anterior approach. Correction of cervical kyphosis is also possible with this approach. Contraindications to an anterior approach include posterior compression and OPLL. Previous anterior cervical surgery and/or neck radiotherapy with or without vocal cord dysfunction should also be considered a relative contraindication. Asymptomatic recurrent laryngeal nerve palsy is common after anterior cervical spine surgery so redo surgery should be on the same side as the first operation unless laryngoscopy has been performed to prove that both vocal cords are working. Patients reliant on their voice (e.g. opera singers) should be counselled with regard to the risk of vocal cord injury.

Technical considerations

Extensive dorsal osteophytes extending beyond the disc space, especially if associated with OPLL may require a corpectomy for more complete decompression.

Fusion rates for a single level discectomy approach 100%, but decrease with multilevel discectomies. If multilevel discectomy is indicated, supplemental anterior plating may confer a biomechanical advantage with increased stability while fusion occurs. Smoking and non-steroidal anti-inflammatory drugs can impair fusion.

More than one-level corpectomy is associated with a higher rate of implant dislodgment and failure. Therefore, many surgeons favour multilevel discectomies or augment the anterior construct with posterior instrumented fusion, which improves biomechanical stability and fusion.

Evidence suggests that for a single level discectomy, there is no difference in outcome between decompression alone, compared to decompression with the addition of a graft. Not using a graft reduces the cost and operative time as well as avoids graft related complications such as harvest site pain. Autograft has classically been the gold standard with which other techniques are compared. However, with modern synthetic cages made of carbon fibre, titanium, polyether-ether-ketone (PEEK), the morbidity of donor site including pain, wound infection, haematoma, and peripheral nerve injury or irritation is avoided.

Supplemental anterior plating adds stability and strength in extension. It provides the strongest possible anterior surgical construct and is useful in correcting kyphosis but there is evidence that plates can increase the incidence of dysphagia.

Different plate/screw combinations are available with the major determinant being dynamic versus constrained or semi-constrained plates. Dynamic or even semi-constrained systems allow for natural settling of the vertebral body on the implant increasing load sharing between the plate and the graft which may translate to improved fusion rates.

Conclusion

In terms of long-term outcome, there appears to be no superiority of anterior cervical discectomy alone with or without a cage, over anterior cervical discectomy and fusion with instrumentation, or corpectomy and fusion with instrumentation. Each technique has its advantages and disadvantages. The optimal approach to achieve the best outcome for the patient should be based on pathological factors and the surgeon's experience. See **Box 60.1** and **Fig. 60.2**.

Anterior cervical discectomy

The patient is positioned supine on a head ring with a jellyroll or rolled towel in the midline under the shoulders. A chinstrap can also improve access. A small degree of head up tilt can help reduce venous pressure but will also angle the disc space.

Box 60.1 Case 1—multilevel anterior cervical fusion with instrumentation

This 54-year-old gentleman presented with neck pain, increasing urinary urgency, balance, and mobility problems consistent with myelopathy. An MRI demonstrated multilevel cervical spondylitic changes with a broad-based disc and osteophyte bars at C4/5, C5/6 and most marked at C6/7 with increased cervical cord signal changes. He had a three-level anterior cervical discectomy and fusion with plating (**Figs. 60.2A–C**).

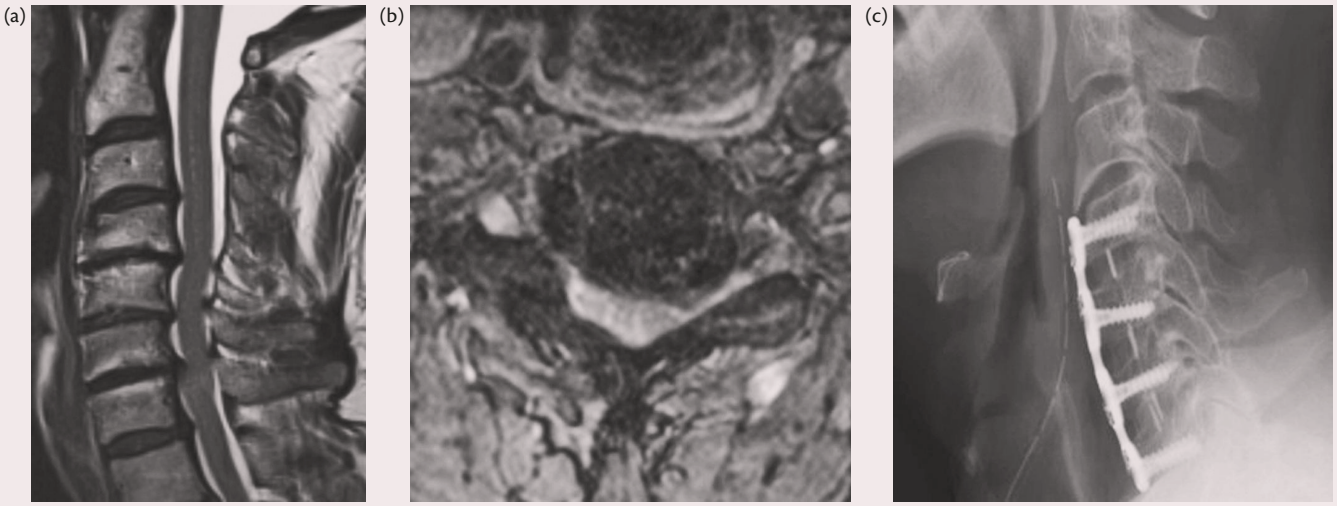

Fig. 60.2 (A) Preoperative sagittal T2W MRI. Compression from anterior primarily with C6–7 the worst affected level with subtle myelopathic signal change seen in the spinal cord. (B) Preoperative axial T2W MRI. Confirms narrow cervical canal with broad-based disc and osteophytic disc bar compressing the cord at C6–7. (C) Postoperative day 1 following surgery. Satisfactory position of screws and interbody fusion cages.

The skin incision is placed at the pathological level using surface anatomical landmarks and radiographic confirmation; C3/4 is just caudal to the hyoid bone, C4/5 is at the level of the thyroid cartilage, C5/6 is at the cricothyroid membrane and C6/7 at the level of the cricoid cartilage.

The incision is normally transverse in line with natural skin creases as this heals with less scarring or occasionally longitudinal along the anterior border of sternocleidomastoid. The approach may be from the left or right. The recurrent laryngeal nerve takes a less predictable course on the right and is more vulnerable to damage on this side while the thoracic duct on the left is at risk especially with low approaches nearer the cervicothoracic junction. Most right-handed surgeons prefer to approach from the right and vice versa.

The platysma is divided horizontally or split longitudinally and undermined superiorly and inferiorly. The superficial cervical fascia is opened and the bloodless avascular plane between the sternocleidomastoid muscle and carotid sheath laterally and the trachea and oesophagus medially are used to access the prevertebral fascia. Blunt dissection will normally achieve adequate exposure. It is important to palpate, identify, and protect the carotid sheath.

The prevertebral fascia is incised exposing vertebral bodies, discs, and the longus colli muscles. The medial border of longus colli is undermined bilaterally and elevated with diathermy. Retractors are sited underneath the muscle avoiding damage to the sympathetic chain which runs superficially along the muscle ~1 cm lateral to the medial border. A contoured spinal needle is placed into the disc space and the correct cervical level confirmed radiologically.

The disc space is incised with exposure of the uncovertebral joint, the uncinate processes defines the lateral margin of the exposure (Fig. 60.3). Disc space distraction can be achieved with caspar pins or skull traction. Anterior osteophytes are removed. The discectomy is completed with a combination of curettes, rongeurs, and a drill. Care must be taken to prevent excessive endplate removal as this predisposes to graft settling and subsidence.

The cranio-caudal orientation of fibres helps identify the posterior longitudinal ligament and it is removed exposing the thecal sac. For myelopathic patients, adequate central decompression must be achieved with undercutting of dorsal osteophytes. For radiculopathy decompression of neural exit foramina is required.

Following discectomy, a graft can be inserted. If using an anterior plate, care must be taken to avoid impingement on adjacent levels. Closure is with dissolvable sutures and most surgeons will use a drain.

Anterior cervical corpectomy

For single level corpectomy, exposure is the same as for discectomy. Discectomies are performed at the rostral and caudal levels with a central channel of bone removed from the intervening vertebra. In most patients a width 15–18 mm is sufficient for decompression.

A rigid or an expandable cage filled with bone graft can be used to reconstruct and restore alignment. A plate is used. Table 60.1 shows the complications that may occur with anterior approaches to the cervical spine.

Cervical arthroplasty

Cervical arthroplasty is a recognized alternative to anterior cervical discectomy and fusion. The principle is to preserve segmental kinematics. Controversy exists regarding the implants long-term survivability and its impact on adjacent segment disease (see controversies section).

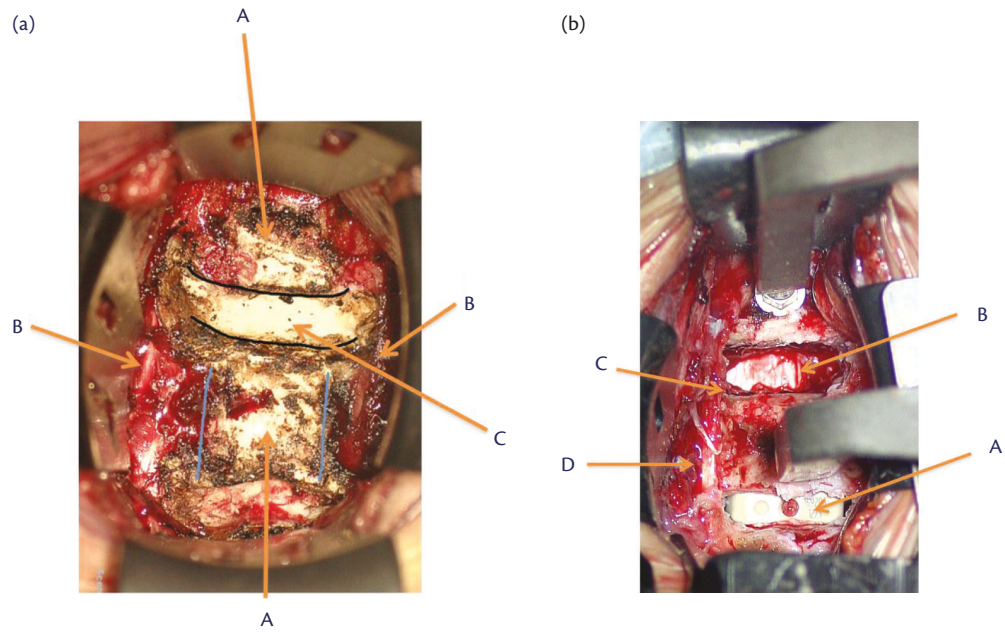

Fig. 60.3 (A) Exposure in preparation for C5/6 anterior cervical decompression. **A**—C5 (superior) and C6 (inferior) vertebral bodies visible. **B**—The right and left longus colli muscles are visualized. **C**—The C5/6 disc is visualized. The black lines demonstrate the superior and inferior endplates of the C6 and C5 vertebra respectively with the upslope of the respective uncovertebral joints which delineate the lateral margin for excision limits ('smiley face'). The blue lines demonstrate the lateral margins along the C6 vertebral body along which trenches should be drilled for vertebral corpectomy procedure.
(B) C5/6 and C6/7 Anterior cervical discectomies performed. **A**—C6/7 decompression complete with insertion of cage with bone graft within. **B**—C5/6 decompression complete with visualization of the spinal cord in the depth. **C**—the upslope demonstrating the start of the uncovertebral joint is just visible on the superior endplate of the C6 vertebral body. **D**—the right longus colli muscle is visible. Pins have been inserted into the C5 and C6 vertebra for the purposes of distraction

Table 60.1 Complications associated with anterior cervical spine approaches

Complication	Incidence	Comments
Hoarseness of voice	4%	Usually secondary to a recurrent laryngeal nerve palsy, bilateral palsies may present with complete airway obstruction. Compression is thought to occur between retractors and the cuff of the endotracheal tube (ETT) as the nerve runs in the tracheo-oesophageal groove underneath the inferior constrictor muscle. Deflating and reinflating the cuff of the ETT after positioning of the retractors might reduce the incidence of this complication
Dysphagia	10%	Risk factors include multilevel surgery, older age, high profile plates, and surgery at lower levels. Exclude implant migration
Haemorrhage	2–3%	Risk factors include absence of a postoperative drain and inadequate haemostasis (especially during exposure). Haemorrhage can precipitate airway obstruction and postoperative swelling
Dural tear	0.5%	More common in patients with OPLL (up to 25%) Perform intraoperative repair (stitches, clips, fibrin sealant)
Oesophageal injury	<1%	Risk factors include scarring from previous surgery Can be life-threatening, involve ear, nose, and throat (ENT), or upper gastrointestinal (GI) surgeons
Paralysis Worsening myelopathy	0.5% Up to 5%	Careful positioning and avoid over extension of the neck Avoid overdistraction of the disc space or excessive thecal manipulation Do a postoperative MRI early to exclude a haematoma
Horner's syndrome	<1%	Caused by excessive dissection of longus colli too laterally Usually resolves in most cases
Infection	1%	Risk factors include systemic immune suppression (e.g. diabetes), and oesophageal perforation Treat with antibiotics, implants may not require removal
Adjacent segment disease	2.9% per annum	Symptomatic disease requiring treatment is about 2.9% per annum following fusion (~25% of patients in 10 years)
Other rare complications		Extrusion of graft Vascular injury (vertebral artery, carotid artery, jugular vein) Thoracic duct injury Death (0.1%)

Arthroplasty should be considered in younger patients with predominantly soft disc herniations. Contraindications include inflammatory arthropathies (ankylosing spondylitis, rheumatoid arthritis), infectious arthropathy, OPLL, DISH, significant osteophytosis and cervical instability (translation ≥ 3.5 mm or angulation ≥ 11 degrees).

A preoperative CT and dynamic x-rays should be performed in all patients considered for arthroplasty.

The surgical technique for arthroplasty is identical to exposure and decompression for anterior cervical discectomy but care should be taken to avoid excessive decompression of the uncovertebral joints. In certain prostheses, destabilization of the uncovertebral joint may cause hypermobility of the treated segment and potential instability and implant failure. Care must be taken to minimize the amount of bone dust created during the arthroplasty procedure with the aim being to reduce the risk of postoperative osteophyte formation or heterotopic calcification. In this regard, a prosthesis that avoids drilling into the bone may be preferential. The use of non-steroidal anti-inflammatories has been documented to reduce the risk of early fusion. See **Box 60.2**.

Posterior cervical approaches

Posterior cervical decompression procedures include laminectomy or laminoplasty for myelopathy and foraminotomy or posterior cervical discectomy for radiculopathy. The indications for choosing a posterior approach include, hypertrophic ligamentum flavum and facets, multilevel disc disease, OPLL, congenital multilevel canal stenosis, and foraminal compression.

Posterior decompression may be preferable in older people where multilevel disease is more common and postoperative cervical instability is of less concern than in younger patients. Posterior approaches avoid the risks of hoarse voice, dysphagia, and adjacent segment disease. If there is evidence of instability or kyphosis, then supplemental fusion should be considered.

The surgical goal is to achieve adequate decompression of neural elements. Review studies have shown outcomes from posterior decompression comparable to anterior cervical decompression (Luo et al., 2015).

Cervical laminectomy

Cervical laminectomy is performed with the patient positioned prone with the head slightly flexed and fixed in a skull clamp. A midline exposure through the nuchal ligament minimizes blood loss. Subperiosteal muscle elevation is preferable to minimize muscle trauma. The level is confirmed with X-ray. Excessive muscle stripping and exposure of adjacent facets should be avoided to prevent instability and progressive deformity (postlaminectomy kyphosis and 'swan-neck' deformity). The incidence of instability following laminectomy is reported as being anywhere from 6% to 46% (McAllister et al., 2012).

Laminectomy can be performed *en bloc* by drilling troughs bilaterally at the lamina-lateral mass junctions. The ligamentum flavum can then be dissected away from the theca to achieve decompression. Alternative methods include use of bone nibblers and kerrison rongeurs for piecemeal removal. The medial border of the lateral masses should be the extent of the decompression. Haemorrhage from epidural venous plexuses can be troublesome and haemostasis should be meticulous. See **Box 60.3**.

Modified posterior approaches

Alternative procedures to cervical laminectomy have been developed that reduce muscle dissection and preserve the posterior cervical tension band with the aim of reducing the risk of postoperative cervical instability (**Table 60.2**).

Posterior cervical foraminotomy

Facet joint spondylosis, uncovertebral osteophytes, and foraminal disc herniation can cause nerve root compression and radiculopathy without myelopathy. Foraminotomy is used to decompress the nerve root without exposing the midline structures.

Box 60.2 Case 2—two-level cervical arthroplasty

This 41-year-old lady presented with neck stiffness and brachialgia with radicular pain affecting the C5 and C6 nerve roots. She had subtle weakness (4/5) and positive Lhermitte's sign on the left. Imaging confirmed two-level degenerative disc disease at C4/5 and C5/6. Two-level decompression with cervical arthroplasties was performed (**Figs. 60.4A–C**).

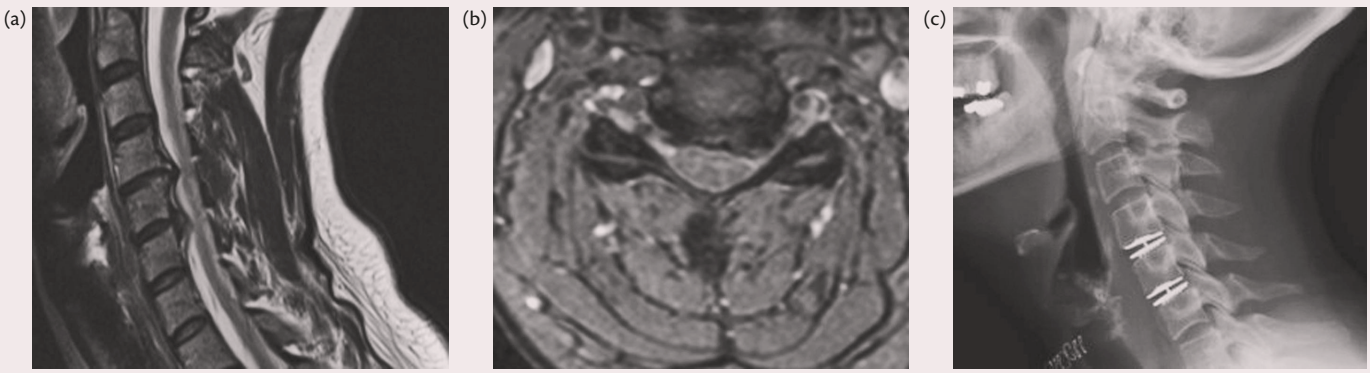

Fig. 60.4 (A) Preoperative sagittal T2W MRI. Compression from anterior at C4–5 and C5–6 with left paracentral disc prolapses. (B) Preoperative axial T2W MRI. Left paracentral disc prolapse at C4–5 with narrowing of central canal and foraminal stenosis and left C5 nerve root impingement. (C) Postoperative day 1 following surgery. Satisfactory position of disc replacements.

Box 60.3 Case 3—cervical laminectomy and lateral mass screw fixation

This 74-year-old presented with features of cervical myelopathy. Imaging confirmed severe canal stenosis and cord compression with intramedullary signal change at C3–4. A posterior approach with instrumented fusion was chosen because of atherosclerotic carotid disease and loss of cervical lordosis (Figs. 60.5A–C).

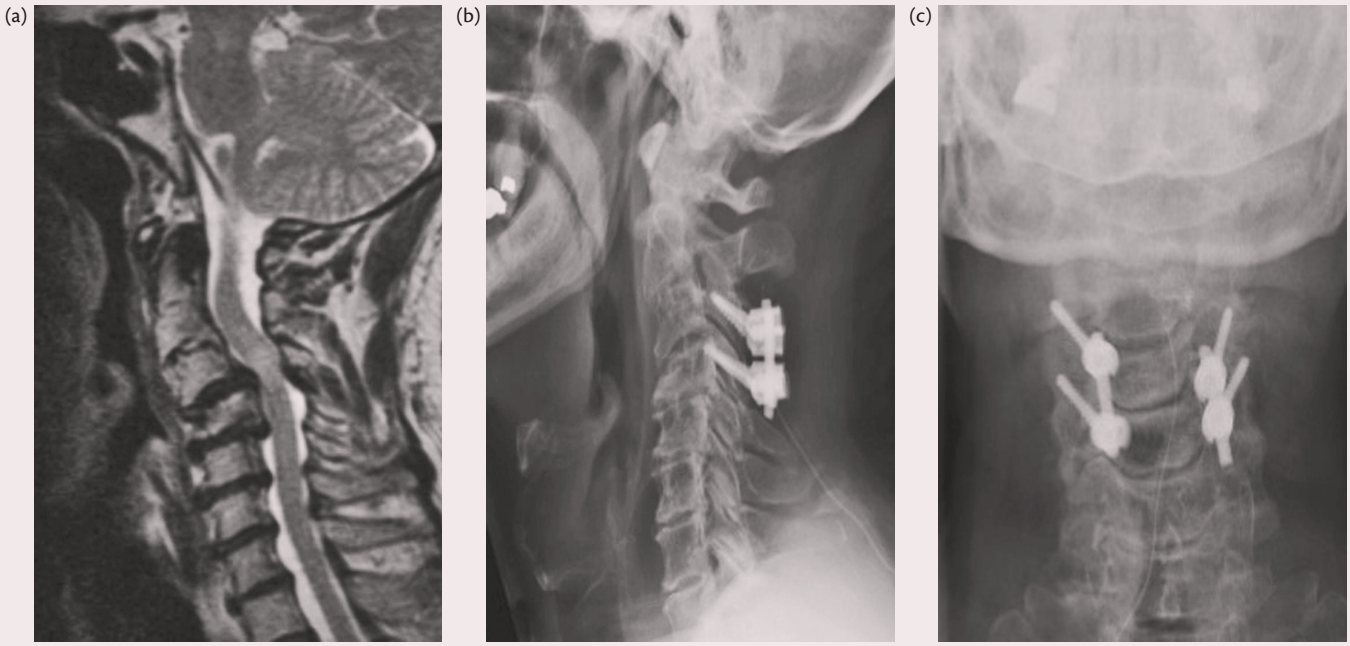

Fig. 60.5 (A) Preoperative sagittal T2W MRI. C3–4 cord compression with cord signal change secondary to spondylosis with loss of cervical lordosis and kyphosis. (B) Lateral X-rays confirming C3 and C4 lateral mass screw fixation following C3–4 laminectomy decompression. (C) Coronal x-rays demonstrating lateral mass screw fixation trajectory.

The patient positioning is as for cervical laminectomy. Exposure can involve either ipsilateral muscle stripping (open procedure) or muscle splitting (minimally invasive with tubular retractors or an endoscope). The cranial and caudal laminae and the facet overlying the exiting nerve root are exposed. The level is confirmed with intraoperative fluoroscopy. Fenestration is achieved by removing bone from the cranial and caudal lamina and undercutting of the medial facet to decompress the exiting nerve root. This can be achieved with a high-speed drill, small kerrison rongeurs or ultrasonic aspiration (Fig. 60.6D). Removal of more than half of the facet compromises shear strength of the spine and should be avoided (Raynor et al., 1985).

Table 60.2 Modified posterior cervical exposures

	Comments
Skip laminectomy	Described by Shiraishi et al. (2002), alternate standard laminectomies at selected levels allow partial preservation of midline structures. See Fig. 60.6A
Cervical laminoplasty	The spinal canal diameter is augmented by re-positioning the laminae and removing the ligamentum flavum. The two common variants are *Trap Door* (Fig. 60.6B; Hirabayashi et al., 1983) *and Double Door* (Fig. 60.6C; Kurokawa et al., 1982)

Rarely a herniated foraminal soft disc can be removed by increasing the margins of the foraminotomy inferiorly and partially removing part of the inferior pedicle. A blunt hook is passed underneath the nerve root and loose disc fragments removed. See Box 60.4.

Complications of the posterior approaches include persistent neck pain and kyphotic deformity. Careful patient selection will minimize complications. Instrumented fusion can be considered if there is concern about instability. Postoperative neurological deficit has been documented especially C5 nerve root palsy. Care must be taken during patient positioning to avoid hyperflexion and traction in myelopathic patients (Nassr et al., 2012). Overall, posterior cervical decompressions are well-tolerated, safe, and effective procedures.

Surgery for atlantoaxial subluxation

Surgical stabilization of an unstable atlantoaxial C1/2 complex (Fig. 60.8) has been performed with posterior approaches using sublaminar wiring (Gallie, Brooks-Jenkins, Dickman-Sonntag) and interlaminar clamps but these techniques are rarely used now except as an adjunct (Table 60.3). Magerl's C1/2 transarticular screw fixation or the Harms–Goel technique of posterior C1 lateral mass screws with C2 pars/pedicle screws are the two most commonly performed procedures and are described here later. Internal screw fixation is biomechanically superior to wire/clamp techniques as it directly inhibits motion at the C1/2 articular surfaces. Anterior

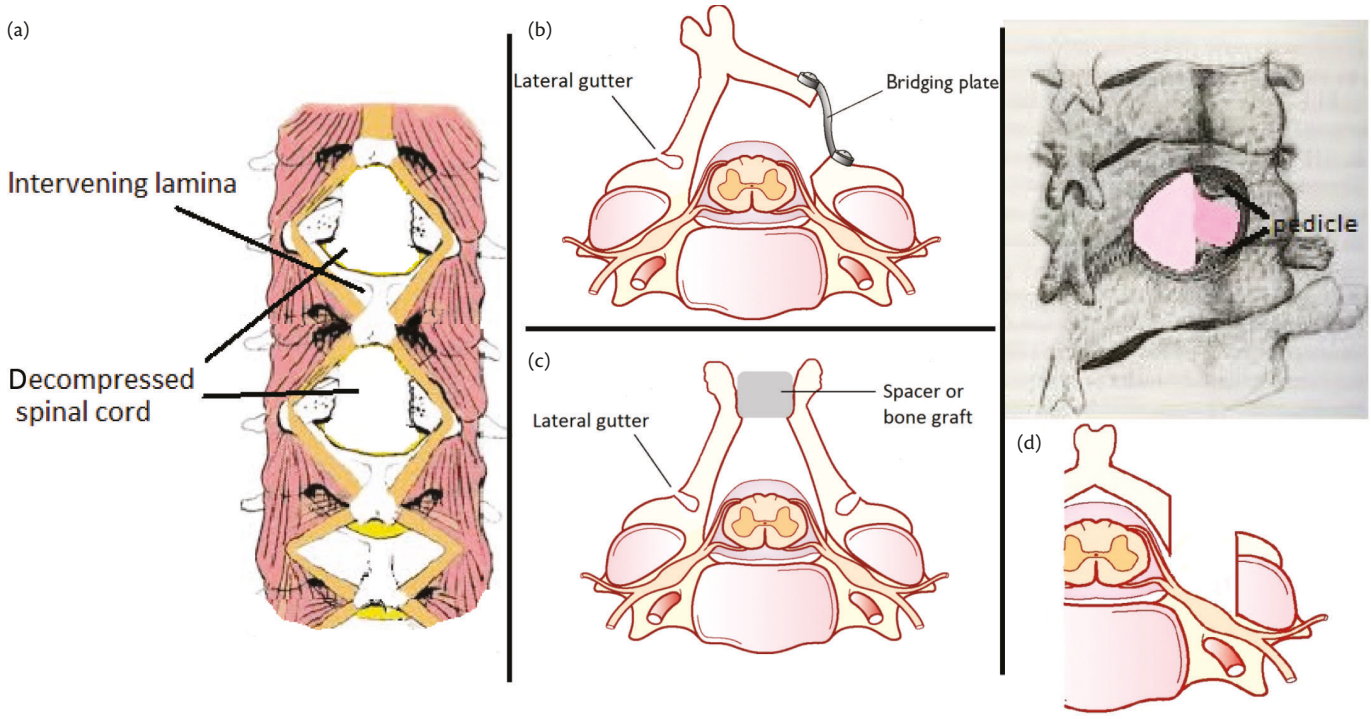

Fig. 60.6 Minimally invasive exposures for posterior cervical decompression. (A) Skip laminectomy. Removal of alternate laminae and ligamentum flavum with preservation of intervening laminae and structures. Muscles are not detached from adjacent spinous processes. (B) Trap door laminoplasty. The laminae are disconnected on one side and thinned on the other allowing for bone to be hinged outwards and held open with implants. (C) Double door laminoplasty. The spinous processes are split in the midline and the laminae are thinned bilaterally to allow for spinal canal expansion and allow undercutting of ligamentum flavum. Interposition of bone graft or spacers maintains increased canal cross-sectional area. (D) Foraminotomy. Decompression of the exiting nerve root between the adjacent pedicles by removal of overlying bone and ligaments. Adequacy is confirmed with passage of a probe.

Box 60.4 Case 4—minimally invasive cervical foraminotomy

This 41-year-old who had a previous C5/6 anterior cervical discectomy presented with right upper limb brachialgia. He had features of right C7 radiculopathy. MRI confirmed a right posterolateral C6/7 disc prolapse with impingement of the exiting right C7 nerve root. A posterior right C6/7 foraminotomy was performed with a minimally invasive technique (**Figs. 60.7A–C**).

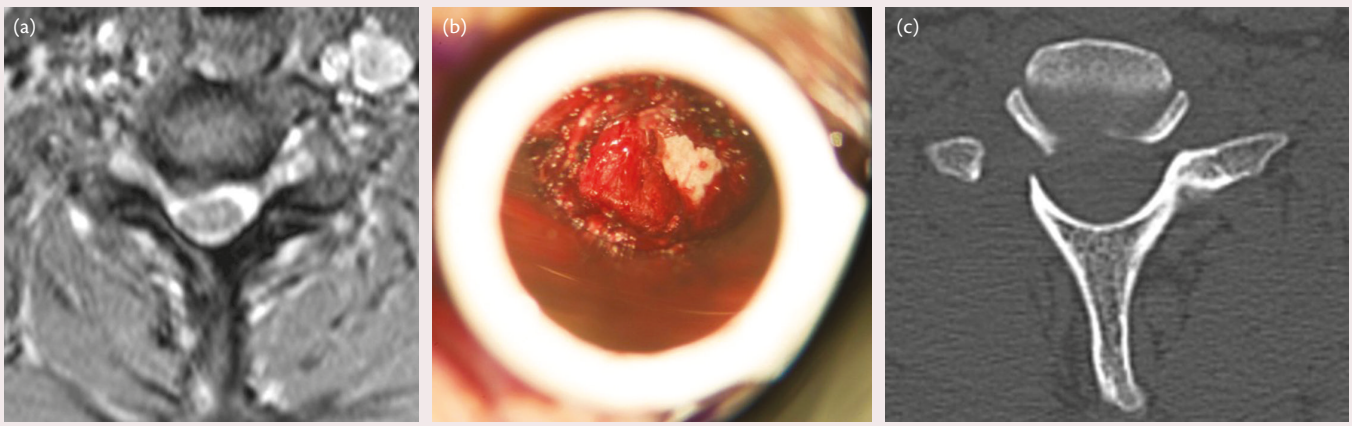

Fig. 60.7 (A) Preoperative axial T2W MRI. Right C6–7 disc prolapse with impingement of exiting right C7 nerve root with radiculopathy. (B) Intraoperative microscopic picture of right C6–7 minimally invasive foraminotomy demonstrating C7 nerve root and decompression. (C) Postoperative axial CT scan demonstrating right C6–7 foraminotomy and decompression of nerve root.

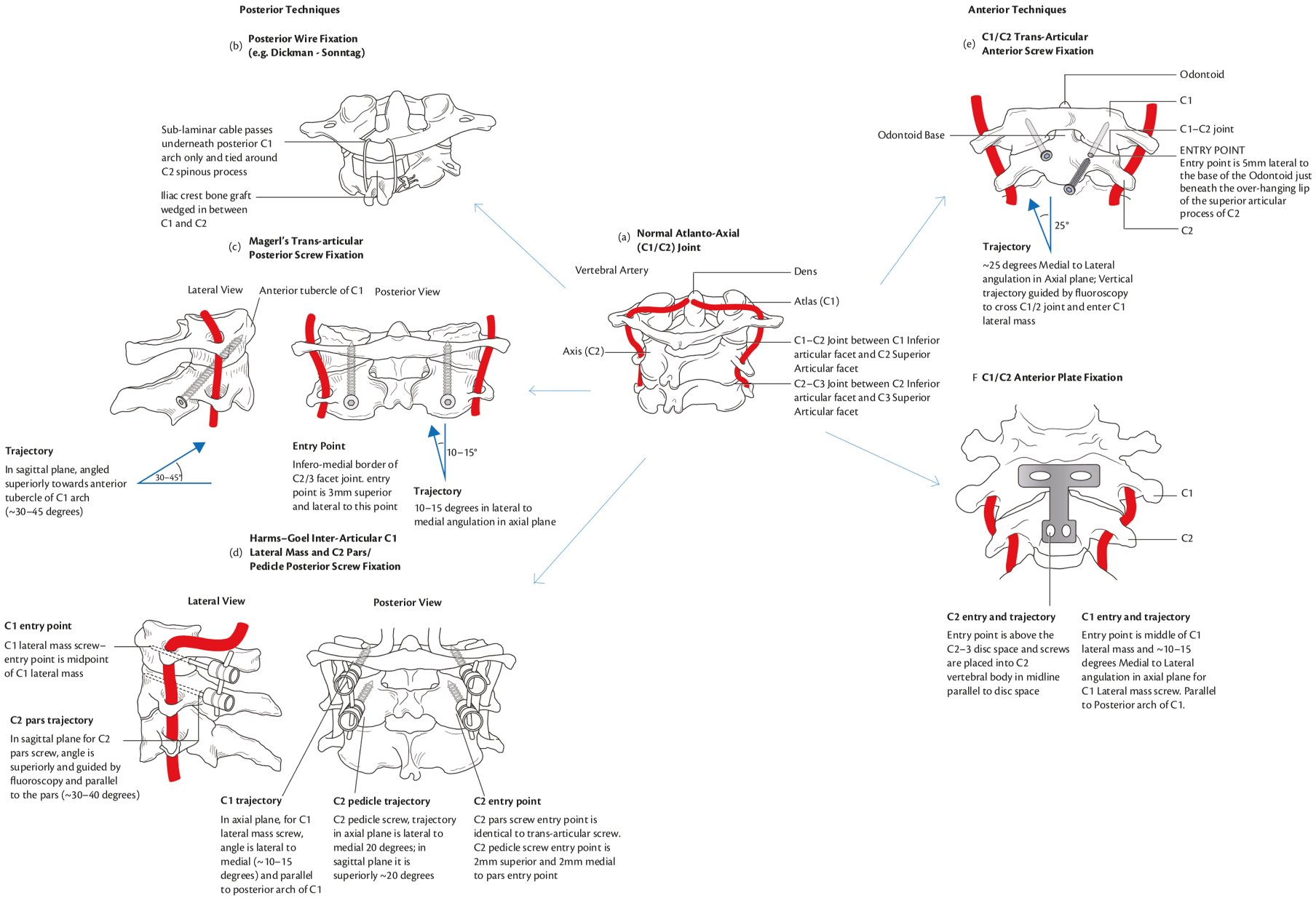
Posterior Techniques
(b) Posterior Wire Fixation (e.g. Dickman - Sonntag)
Sub-laminar cable passes underneath posterior C1 arch only and tied around C2 spinous process
Iliac crest bone graft wedged in between C1 and C2
(c) Magerl's Trans-articular Posterior Screw Fixation
Lateral View
Anterior tubercle of C1
Posterior View
Trajectory
In sagittal plane, angled superiorly towards anterior tubercle of C1 arch (~30–45 degrees)
30–45°
Entry Point
Infero-medial border of C2/3 facet joint. entry point is 3mm superior and lateral to this point
10–15°
Trajectory
10–15 degrees in lateral to medial angulation in axial plane
(d) Harms–Goel Inter-Articular C1 Lateral Mass and C2 Pars/ Pedicle Posterior Screw Fixation
Lateral View
Posterior View
C1 entry point
C1 lateral mass screw–entry point is midpoint of C1 lateral mass
C2 pars trajectory
In sagittal plane for C2 pars screw, angle is superiorly and guided by fluoroscopy and parallel to the pars (~30–40 degrees)
C1 trajectory
In axial plane, for C1 lateral mass screw, angle is lateral to medial (~10–15 degrees) and parallel to posterior arch of C1
C2 pedicle trajectory
C2 pedicle screw, trajectory in axial plane is lateral to medial 20 degrees; in sagittal plane it is superiorly ~20 degrees
C2 entry point
C2 pars screw entry point is identical to trans-articular screw. C2 pedicle screw entry point is 2mm superior and 2mm medial to pars entry point
(a) Normal Atlanto-Axial (C1/C2) Joint
Vertebral Artery
Dens
Atlas (C1)
Axis (C2)
C1–C2 Joint between C1 Inferior articular facet and C2 Superior Articular facet
C2–C3 Joint between C2 Inferior articular facet and C3 Superior Articular facet
Anterior Techniques
(e) C1/C2 Trans-Articular Anterior Screw Fixation
Odontoid
C1
C1–C2 joint
Odontoid Base
ENTRY POINT
Entry point is 5mm lateral to the base of the Odontoid just beneath the over-hanging lip of the superior articular process of C2
C2
25°
Trajectory
~25 degrees Medial to Lateral angulation in Axial plane; Vertical trajectory guided by fluoroscopy to cross C1/2 joint and enter C1 lateral mass
F C1/C2 Anterior Plate Fixation
C1
C2
C2 entry and trajectory
Entry point is above the C2–3 disc space and screws are placed into C2 vertebral body in midline parallel to disc space
C1 entry and trajectory
Entry point is middle of C1 lateral mass and ~10–15 degrees Medial to Lateral angulation in axial plane for C1 Lateral mass screw. Parallel to Posterior arch of C1.

Fig. 60.8 Surgical techniques for atlantoaxial stabilization. (A) Posterior view of the anatomy of the normal C1/C2 (atlantoaxial) joint including position of the vertebral artery. Posterior techniques demonstrated on the left (B to D) and anterior techniques on the right (E to F); the vertebral artery position is visualized in each image. (B) Posterior wire fixation technique with sublaminar wiring and bone graft in between C1 and C2. (C) Magerl's transarticular posterior screw fixation with entry point marked and the trajectories in two planes (sagittal—inferior to superior; axial—lateral to medial). (D) Harms–Goel interarticular fixation with C1 lateral mass screw and either C2 Pars or C2 pedicle screw fixation. Note the entry point varies depending on whether it is a C2 pars or C2 pedicle screw. (E) C1–C2 anterior transarticular fixation with the entry point (just beneath superior articular process of C2, 5 mm lateral from the midline at the base of the odontoid (PEG) and trajectory demonstrated. (F) C1–C2 anterior plate fixation with entry points into C1 and C2 demonstrated. Anterior fixation is much rarer compared to posterior fixation.

transoral approaches including transarticular C1/2 screws and C1 lateral mass to C2 vertebral body plate and screw fixation has also been described.

Magerl's C1/2 transarticular screws

A single screw on each side is placed through the pars interarticularis of C2 passing through the C1/2 joint directed at the lateral mass of C1 (Magerl and Seeman, 1986; Fig. 60.8). It provides the most stable and rigid fixation biomechanically of the C1/2 joint with almost complete obliteration of rotation. A major contraindication would be an anomalous high-riding vertebral artery. It is technically demanding with increased risk of vascular injury and care must be taken to avoid anterior perforation of the C1 lateral mass, which could result in injury to the pharynx, internal carotid artery, and/or lower cranial nerves.

A preoperative CT Angiogram helps define the course of the vertebral artery. Intraoperative fluoroscopy guides the screw trajectory. The patient is positioned prone in a skull clamp with neck flexion. The C1 posterior arch and lateral masses, C2 laminae, C2 pars and the C2/3 facet joints are exposed. Separate stab incisions caudally may be required to achieve the trajectory for the transarticular screw (usually 1–2 cm lateral to C7/T1 spinous process). The C1/2 joint capsule can be opened to denude the articular surface. Figure 60.8 demonstrates the entry point and trajectory. Drilling for screw placement is guided with fluoroscopy or alternatively intraoperative navigation can be used. The C1/2 transarticular screw is placed after tapping the hole. Bone graft can be sited on exposed bone surfaces to supplement the fusion. The fixation is often augmented by a Dickmann–Sonntag posterior sublaminar wire.

Harms–Goel C1 lateral mass and C2 pars/pedicle screws

Harms and Melcher (2001) and Goel et al. (2002) employed an interarticular fixation with C1 lateral mass and C2 pars/pedicle screws (Fig. 60.8) as an alternative to C1/2 transarticular fixation.

Specific advantages include that anatomic reduction of C1/2 is not essential and it can be used with a high-riding vertebral artery.

The positioning and exposure are as for the transarticular screw technique. Preservation of the C2 nerve root is optional. The entry point and trajectories are highlighted in Figure 60.8. The C1 lateral mass screw is partially threaded to reduce irritation of the C2 nerve root and subsequent neuropathic pain. Fusion rates are high.

Complications

The major complication of both procedures is vertebral artery injury (<5%), which can occur during exposure or screw placement. If arterial perforation occurs during screw preparation, the screw should be implanted for tamponade. The contralateral side is left uninstrumented and the patient should have an angiogram to assess the posterior cerebral circulation.

If C1/2 screw fixation is not possible, alternative strategies could include occipito-cervical fixation or external orthotic stabilization with a HALO. Patients should be consented for these alternatives prior to surgery.

Anterior surgical approaches to the craniocervical junction

Surgical anatomy and biomechanics

The atlanto-occipital articulation between the occipital condyle and the C1 superior facets allows about 15° of flexion and extension while the C1/C2 articulation contributes to 45° of rotation which is about 50% of the rotation occurring by the cervical spine. The stabilizing ligaments are the transverse ligament attached to a tubercle on the medial aspect of one C1 lateral mass to the other and located posterior to the dens and the alar ligaments attached from dorsolateral dens passing rostro-lateral to the medial tubercle of the occipital condyle at the anterior lip of foramen magnum. Supplementary ligaments include the apical ligament, anterior atlanto-occipital and tectorial membranes in continuity with the ALL and posterior longitudinal ligament (PLL) and also the posterior atlanto-occipital membrane and ligamentum flavum. The longitudinal fibres dorsal to the transverse ligament complete the formation of the cruciate ligament (see Chapter 57, Fig. 57.1). The transverse ligament limits flexion and anteroposterior (AP) translation of the atlantoaxial articulation. The alar ligaments limit atlanto-occipital rotation.

Open anterior approaches

Anterior transoral and transnasal approaches for C1/2 fixation are utilized when there is a need for anterior decompression and resection of the dens. These procedures may be performed open or using an endoscope. They are now rarely indicated for rheumatoid disease as rheumatoid pannus normally resolves following posterior fusion alone. Oropharyngeal infection is a contraindication.

Patients are positioned supine with biplanar intraoperative fluoroscopy available. Neuro-navigation can also be used. A decision regarding open surgery versus endoscopic surgery is made based on surgical familiarity. Two fixation techniques are available: C1-C2 transarticular screws or T-plate fixation with C1 lateral mass and C2 vertebral body screws (Fig. 60.8).

The pharyngeal mucosal incision for C1/2 transarticular screws is usually linear whereas for a T-plate a U-shaped flap is preferred. Vertebral artery injury is avoided by keeping the lateral dissection within 12 mm of the midline at the C2 vertebral body. If extended exposure is required, a transoral mandibular splitting approach is used.

The use of anterior techniques is largely confined to specialist centres. Complications include injury to viscera including the oesophagus, trachea, pharynx, tongue, internal carotid artery, internal jugular vein, and cranial nerves IX–XII.

Specifically, the potential technical complications are related to the healing of the pharyngeal mucosal flap, velopharyngeal incompetence with regurgitation and speech dysfunction from soft palate incision if needed and teeth malocclusion due to the osteotomies for transmaxillary or transmandibular approaches.

Endonasal Endoscopic Extended surgical approaches

Endoscopic odontoidectomy is considered in cases of basilar invagination. The nasopalatine line (as described by Kassam—which is a line on the midline sagittal images from the inferior tip of the nasal bone to the posterior aspect of the hard palate extended to the anterior spine) is used to indicate the lower limit of this approach. The high-riding dens found in cases of basilar invagination, allows endoscopic drilling at the base of the odontoid. Further inferior extension, if required, can be performed with a transoral endoscopic-assisted approach.

A direct incision in the nasopharyngeal wall in the midline or a flap is used to expose the lower clivus, anterior lower lip of the foramen magnum and anterior arch of the atlas. This approach avoids the need for a palatal incision. The anterior arch of the atlas is resected

Table 60.3 The evolution of surgical principles underlying sublaminar wiring and interlaminar clamping techniques

Technique	Principle	Bone graft	Advantage	Disadvantage
Gallie (1939)	Midline Sublaminar wire beneath C1 arch wrapping around C2 spinous process	Single bone graft strut abutting C1 arch and overlying C2 spinous process	Avoids sublaminar wire passage beneath C2	Non-fusion rates as high as 25% Poor rotational stability
Brooks & Jenkins (1978)	Paramedian 2 Sublaminar wires beneath C1 and C2 arches	Two bone grafts between C1 and C2 laminae	Fusion rates up to 93% Better rotational stability than Gallie	Additional risk due to sublaminar wire passage beneath C2
Dickman et al. (1991) (Fig. 60.8)	Midline Sublaminar wire beneath C1 arch and looped caudally around C2 spinous process	Single bone graft between C1 and C2 laminae	Fusion rates (with HALO) up to 97% Improved rotational stability Avoids sublaminar wire beneath C2	
Interlaminar clamps	Hooks over superior surface of C1 arch and inferior surface of C2 arch held in compression	Single bone graft between C1 and C2 laminae	Avoids sublaminar wire passage	Translation/migration of bone graft

using a high-speed drill and the base of the odontoid is drilled and 'egg-shelled' until the underlying transverse ligament and dura are reached and disconnected from the C2 body. The bone is then carefully pulled down from the foramen magnum and may require additional removal of the anterior lip of this foramen to allow sharp division of the apical and alar ligaments. The totally free odontoid bone is removed and the theca is decompressed (Fig. 60.9). The edges of the incision are approximated and do not necessarily require suturing, unless there is cerebrospinal fluid (CSF) leak. Subsequently fixation is required as this procedure makes C1/2 unstable.

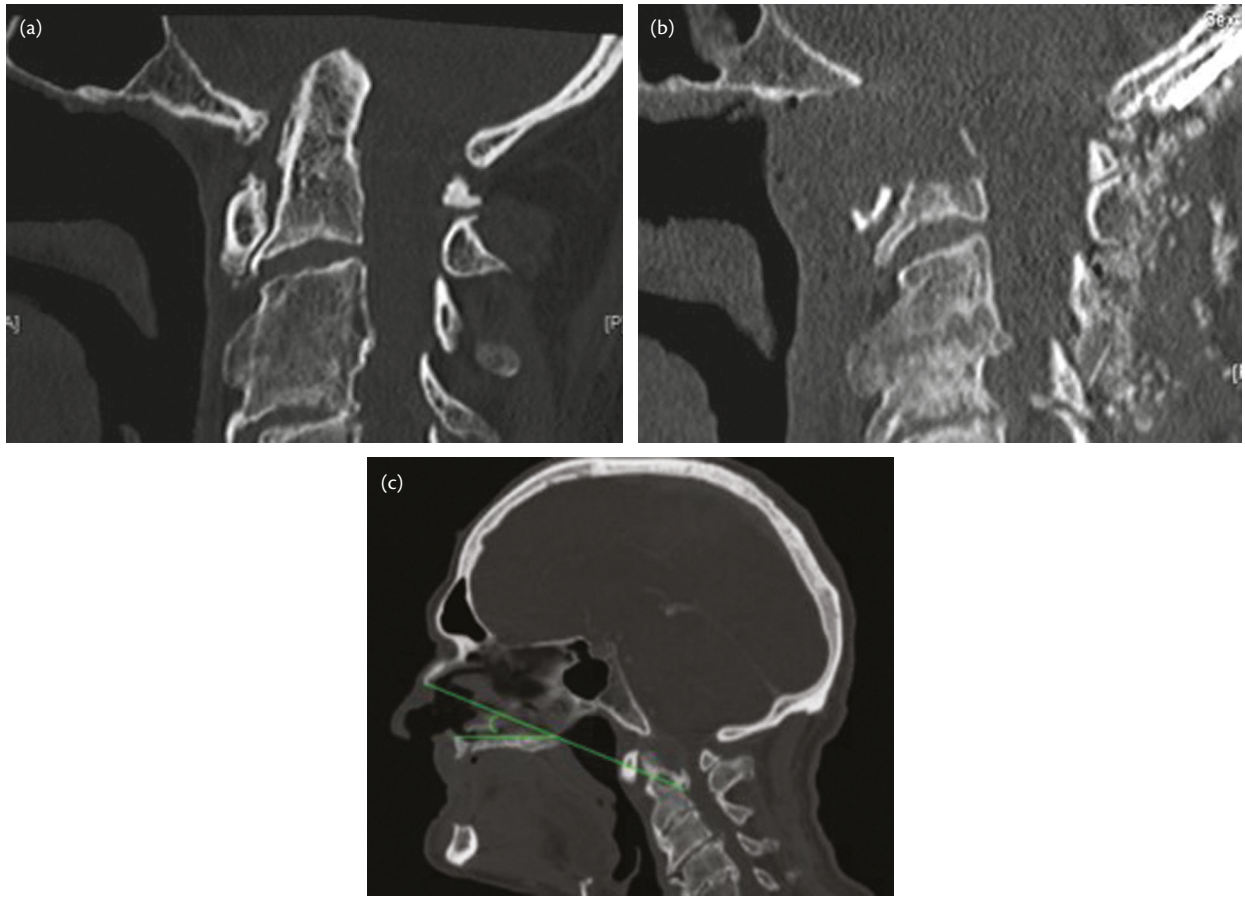

Fig. 60.9 Endonasal endoscopic odontoidectomy and craniocervical junction decompression.
(A) Preoperative midsagittal CT reconstruction demonstrating basilar invagination. (B) Postoperative midsagittal CT reconstruction following endoscopic removal of odontoid PEG. (C) Kassam's nasopalatine line demonstrated in a further patient. This demarcates the most inferior limit of the endonasal endoscopic approach.

Controversies in degenerative cervical spinal disease management

Few clinical studies provide high-class evidence to guide decision making in degenerative cervical spinal disease. Commonly debated issues include indications and timing of surgery, minimally invasive versus open techniques and anterior versus posterior approaches. There is no level I or II evidence comparing anterior versus posterior approaches and studies have shown equivalent efficacy (Fehlings et al., 2013; Lawrence et al., 2013).

Adjacent segment disease is a recognized problem in patients who have had an anterior cervical discectomy. Hilibrand et al. (1999) noted symptomatic disease requiring treatment in 2.9% per annum. Debate is ongoing about whether this is due to the arthrodesis or the natural history of the disease. Studies have demonstrated increased biomechanical strain (intradiscal pressure) and increased motion at adjacent levels following arthrodesis.

Prospective trials have examined the kinematic effect of cervical disc replacements on the spine and have compared the outcomes between arthroplasty and arthrodesis. Cervical arthroplasty has shown equivalent results compared to arthrodesis for single level discectomy (Buchowski et al., 2009) but for multilevel degenerative disc disease, there is a suggestion of reduced re-operation rates in patients with arthroplasty. Arthroplasty is more expensive. Clinical results do tend to favour arthroplasty (Ren et al., 2014). Although arthroplasty is a valid option to offer to patients being considered for anterior cervical discectomy more robust long-term outcome data are awaited.

FURTHER READING

Fehlings, M.G., Barry, S., Kopjar, B., et al. (2013). Anterior versus posterior surgical approaches to treat cervical spondylotic myelopathy: outcomes of the prospective multicenter AO Spine North America CSM study in 264 patients. *Spine (Phila Pa 1976)*, **38**(26), 2247–52.

Lawrence, B.D., Jacobs, W.B., Norvell, D.C., Hermsmeyer, J.T., Chapman, J.R., & Brodke, D.S. (2013). Anterior versus posterior approach for treatment of cervical spondylotic myelopathy: a systematic review. *Spine (Phila Pa 1976)*, **38**(22 Suppl 1), S173–82.

Ren, C., Song, Y., Xue, Y., & Yang, X. (2014). Mid- to long-term outcomes after cervical disc arthroplasty compared with anterior discectomy and fusion: a systematic review and meta-analysis of randomised controlled trials. *Eur Spine J*, **23**(5), 1115–23.

REFERENCES

Brooks, A.L. & Jenkins, E.B. (1978). Atlanto-axial arthrodesis by the wedge compression method. *J Bone Joint Surg Am*, **60**(3), 279–84

Buchowski, J.M., Anderson, P.A., Sekhon, L., & Riew, K.D. (2009). Cervical disc arthroplasty compared with arthrodesis for the treatment of myelopathy. Surgical technique. *J Bone Joint Surg Am*, **91**(Suppl 2), 223–32.

Cloward, R.B. (1958). The anterior approach for removal of ruptured cervical disks. *J Neurosurg*, **15**(6), 602–17.

Dickman, C.A., Sonntag, V.K., Papadopoulos, S.M., & Hadley, M.N. (1991). The interspinous method of posterior atlantoaxial arthrodesis. *J Neurosurg*, **74**(2), 190–8

Engquist, M., Löfgren, H., Öberg, B., et al. (2013). Surgery versus nonsurgical treatment of cervical radiculopathy: a prospective, randomized study comparing surgery plus physiotherapy with physiotherapy alone with a 2-year follow-up. *Spine (Phila Pa 1976)*, **38**(20), 1715–22

Fehlings, M.G., Barry, S., Kopjar, B., et al. (2013). Anterior versus posterior surgical approaches to treat cervical spondylotic myelopathy: outcomes of the prospective multicenter AO Spine North America CSM study in 264 patients. *Spine (Phila Pa 1976)*, **38**(26), 2247–52.

Galbusera, F., van Rijsbergen, M., Ito, K., Huyghe, J.M., Brayda-Bruno, M., & Wilke, H.J. (2014). Ageing and degenerative changes of the intervertebral disc and their impact on spinal flexibility. *Eur Spine J*, **23** Suppl 3, S324–32.

Goel, A., Desai, K.I., & Muzumdar, D.P. (2002). Atlantoaxial fixation using plate and screw method: a report of 160 treated patients. *Neurosurgery*, **51**(6), 1351–7.

Harms, J. & Melcher, R.P. (2001). Posterior C1-C2 fusion with polyaxial screw and rod fixation. *Spine*, **26**(22), 2467–71.

Hilibrand, A.S., Carlson, G.D., Palumbo, M.A., Jones, P.K., & Bohlman, H.H. (1999). Radiculopathy and myelopathy at segments adjacent to the site of a previous anterior cervical arthrodesis. *J Bone Joint Surg Am*, **81**(4), 519–28.

Hirabayashi, K., Watanabe, K., Wakano, K., Suzuki, N., Satomi, K., & Ishii, Y. (1983). Expansive open-door laminoplasty for cervical spinal stenotic myelopathy. *Spine (Phila Pa 1976)*, **8**(7), 693–9.

Inamasu, J., Guiot, B.H., & Sachs, D.C. (2006). Ossification of the posterior longitudinal ligament: an update on its biology, epidemiology, and natural history. *Neurosurgery*, **58**(6), 1027–39.

Kaito, T., Ohshima, S., Fujiwara, H., Makino, T., & Yonenobu, K. (2013). Predictors for the progression of cervical lesion in rheumatoid arthritis under the treatment of biological agents. *Spine*, **26**, 2258–63.

Kalsi-Ryan, S., Karadimas, S.K., & Fehlings, M.G. (2013). Cervical spondylotic myelopathy: the clinical phenomenon and the current pathobiology of an increasingly prevalent and devastating disorder. *Neuroscientist*, **19**(4), 409–21.

Kim, H.J., Nemani, V.M., Riew, K.D., & Brasington, R. (2015). Cervical spine disease in rheumatoid arthritis: incidence, manifestations and therapy. *Curr Rheumatol Rep*, **17**, 9.

Kurokawa, T., Tsuyama, N., & Tanaka, H. (1982). Enlargement of spinal canal by the sagittal splitting of the spinous process. *Bessatsu Seikeigeka*, **2**, 234–40.

Lawrence, B.D., Jacobs, W.B., Norvell, D.C., Hermsmeyer, J.T., Chapman, J.R., & Brodke, D.S. (2013). Anterior versus posterior approach for treatment of cervical spondylotic myelopathy: a systematic review. *Spine (Phila Pa 1976)*, **38**(22 Suppl 1), S173–82.

Luo, J., Cao, K., Huang, S., et al. (2015). Comparison of anterior approach versus posterior approach for the treatment of multilevel cervical spondylotic myelopathy. *Eur Spine J*, **24**(8), 1621–30.

Magerl, F. & Seeman, P.S. (1986). Stable posterior fusion of the atlas and axis by transarticular screw fixation. In: Kehr, P. & Weidner, A. (eds.) *Cervical Spine*, pp. 322–27. Berlin, Germany: Springer-Verlag.

McAllister, B.D., Rebholz, B.J., & Wang, J.C. (2012). Is posterior fusion necessary with laminectomy in the cervical spine? *Surg Neurol Int*, **3**(Suppl 3), S225–31.

Nassr, A., Eck, J.C., Ponnappan, R.K., Zanoun, R.R., Donaldson, W.F. 3rd, & Kang, J.D. (2012). The incidence of C5 palsy after multilevel cervical decompression procedures: a review of 750 consecutive cases. *Spine (Phila Pa 1976)*, **37**(3), 174–8.

Raynor, R.B., Pugh, J., & Shapiro, I. (1985). Cervical facetectomy and its effect on spine strength. *J Neurosurg*, **63**(2), 278–82.

Reiter, M.F. & Boden, S.D. (1998). Inflammatory disorders of the cervical spine. *Spine*, **24**, 2755–66.
Ren, C., Song, Y., Xue, Y., & Yang, X. (2014). Mid- to long-term outcomes after cervical disc arthroplasty compared with anterior discectomy and fusion: a systematic review and meta-analysis of randomised controlled trials. *Eur Spine J*, **23**(5), 1115–23.
Shiraishi, T. (2002). Skip laminectomy—a new treatment for cervical spondylotic myelopathy, preserving bilateral muscular attachments to the spinous processes: a preliminary report. *Spine J*, **2**(2), 108–15.
Urban, J.P.G., Roberts, S., & Ralph, J.R. (2000). The nucleus of the intervertebral disc from development to degeneration. *Amer Zool*, **40**(1), 53–61.
Yu, Y.L., du Boulay, G.H., Stevens, J.M., & Kendall, B.E. (1986). Computed tomography in cervical spondylotic myelopathy and radiculopathy: visualisation of structures, myelographic comparison, cord measurements and clinical utility. *Neuroradiology*, **28**(3), 221–36.

RELATED LINKS TO EBRAIN

Atlantoaxial Subluxation. https://learning.ebrain.net/course/view.php?id=1035
Inflammatory Spondyloarthropathy. https://learning.ebrain.net/course/view.php?id=805
Managing Cervical Degenerative Disease. https://learning.ebrain.net/course/view.php?id=782
Performing an Anterior Cervical Discectomy. https://learning.ebrain.net/course/view.php?id=416
Performing Posterior Cervical Decompression Procedures. https://learning.ebrain.net/course/view.php?id=415
Rheumatoid Arthritis in the Spine. https://learning.ebrain.net/course/view.php?id=810

61

Thoracic spinal disease

Kieron Sweeney, Catherine Moran, and Ciaran Bolger

Introduction

The thoracic spine occupies a unique position with respect to anatomical, biomechanical, pathological, and surgical considerations. The kyphosis of the thoracic spine is offset by the lordosis in the mobile cervical spine and the principal load bearing lumbar spine maintaining a sagittal balanced posture. The thoracic spine and its articulation with the rib cage maximizes the stability of the thoracic spine while minimizing its mobility leading to the low incidence of thoracic disc prolapse.

Incidence

The incidence is reported as 1 per 1 000 000 patient years (McInerney and Ball, 2000). Thoracic disc herniations identified incidentally on work up for other spinal pathologies are reported as frequently as 11% (Awwad et al., 1991). Between 0.2% and 4% of all symptomatic protrusions of an intervertebral disc are in the thoracic spine and thoracic disc extrusion accounts for 0.2% to 1.8% of all operations performed on symptomatic herniated discs. There is an approximate 1:1 male to female ratio and it more frequently occurs in the third to sixth decades which mimics cervical and lumbar disc herniations (McInerney and Ball, 2000). Due to the structural stability provided by the upper thoracic cage the majority of thoracic disc herniations occur below the level of T7 with the most common level being T11/T12. The majority of disc protrusions are central or centrolateral. Degeneration is the leading cause of thoracic disc herniation with only 25% due to trauma. Traumatic disc herniations usually occur in the younger age group. Some 30–70% of discs are reported to be calcified with a high incidence of calcified discs being intradural (Fig. 61.1).

Presentation

Myelopathy consisting of spastic paraparesis, sensory disturbance, bladder or bowel dysfunction and pain, and both axial back pain and radicular pain radiating around the anterior chest wall, are the most common clinical features and presenting complaints (Stillerman et al., 1998). However, there is significant variation in the presenting symptoms and signs of thoracic disc herniation from case to case. This is dependent on the spinal level, position, and size of the herniated disc and bony canal, duration of compression, and degree of neurovascular compromise and aetiology. The majority of the literature demonstrates that pain is the predominate symptom at presentation. Pain can be unilateral or bilateral and the region it radiates to depends on the level. T1/T2 discs can present with upper limb radiculopathy with pain radiating down the upper limb and weakness of the intrinsic muscles of the hand. Pain due to mid-thoracic discs can radiate across the chest wall whereas lower thoracic discs can present as abdominal or lumbar pain. There appears to be a chronological and progressive sequence of symptoms. In disc herniations due to degeneration the sequence is firstly, pain (thoracolumbar or radicular pain) followed by sensory disturbance, then motor dysfunction and bladder and bowel dysfunction (Arce and Dohrmann, 1985). In traumatic disc protrusions, pain is quickly followed by myelopathy (Arseni and Nash, 1960). However up to 25% of patients present without pain, complaining of a subtle neurological deficit or gait disturbance which can contribute to a delayed diagnosis.

Pathogenesis

Neurological signs and symptoms are due to direct neural compression and vascular insufficiency. Compression at the levels T4-T9 can have a significant impact of the spinal cord due to the vulnerable blood supply at this level.

Management

Conservative

There is little published information regarding the natural history of asymptomatic thoracic disc protrusion. The reported incidence of asymptomatic thoracic disc protrusion ranges from 15% (S&S) to as high as 37% (Wood et al., 1995). The authors reviewed the thoracic MRI from 90 asymptomatic individuals assessing for anatomical abnormalities. They then followed these individuals for a mean of 26 months with MRIs and concluded that over the follow-up period, the herniated discs remained asymptomatic but small discs tended to remain unchanged or increase in size, whereas large discs tended to decrease in size (Wood et al., 1997).

Surgical

Indications for surgery include pain refractory to medical management, evidence of myelopathy, bladder or bowel disturbance, or any long-tract signs. The main indication for surgery is neurological dysfunction in the form of myelopathy, progressive or otherwise. It

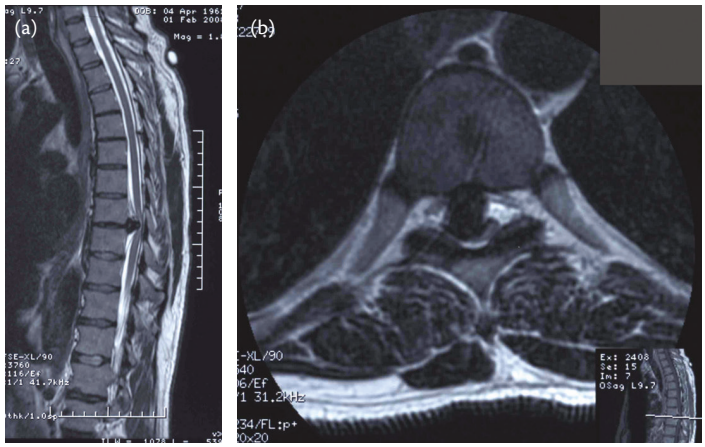

Fig. 61.1 Giant thoracic disc. Note marked cord compression on T2 images.

is the authors' experience that although patients may present with a long history of fixed neurological deficit due to delayed diagnosis, surgical decompression can still result in significant functional recovery. Cases presenting with radicular pain only, once the level is confirmed using a nerve root block, can be treated via a less extensive surgery for exiting nerve root decompression. In most cases, however, the intervention needs to be more extensive. In these cases the surgical strategy depends on the level of the disc prolapse, the position of the disc in relation to the neural structures, the consistency of the disc (soft vs. calcified) and whether or not the disc is intradural (Arts and Bartels, 2014). Of these variables, it is the level of the disc herniation and its position relative to the neural structures that dictates the optimum approach Table 61.1.

Prior to operative intervention, all cases should have a whole spine MRI, to confirm level, and a computed tomography (CT) scan of the affected area, to determine if calcification is present in the prolapsed disc.

Approaches to a thoracic disc prolapse

When considering the most appropriate surgical approach to remove a prolapsed thoracic disc the most important elements to consider prior to surgery are the location of the prolapse, central, centrolateral, or lateral, the size of the prolapse, any associated or expected deformity which may require fixation, any evidence of calcification of the prolapse which may also point to an intradural component, the size of the prolapse and the thoracic level. The historical laminectomy used for treatment of thoracic discs was associated with a morbidity of up to 60% (Fessler and Sturgill, 1998) and has no role to play in the safe management of these cases today.

Preoperative marking is recommended, marking the head of the articulating rib with dye before the surgery. Intraoperative verification with the use of C-arm or intraoperative CT scanning is essential. The use of intraoperative monitoring is optional but in the authors experience, a suitable approach which allows visualization of the prolapsed disc fragment without any manipulation of the already compromised cord is more important.

Localization of the correct level is a major consideration. The level should be localized using both anteroposterior (AP) and lateral radiographs, counting up from the sacrum and down from C2 if possible. It is essential to have a whole spine MRI on which the actual level of the prolapsed disc can be confirmed with reference to C2 and the Sacrum.

Table 61.1 Central disc herniation

Level	Approach
T1–T4	Trans-sternal
T2–T6	Right transthoracic
T6–T12	Left (or right) transthoracic

Anterior approaches: Trans-sternal

The indications for using this approach are T1-T4, central, calcified, intradural disc prolapses.

The technique is as follows. The patient is positioned supine with a shoulder bag between the scapulae to allow for slight neck and shoulder extension. An orogastric tube is placed to allow for easy identification by palpation of the oesophagus.

The incision is along the ventral border of the sternocleidomastoid muscle (SCM) to the angle of Lewis. Some authors recommend the left SCM incision as the left recurrent laryngeal nerve is more easily identifiable in the trachea-oesophageal groove. The platysma is divided along its fibres. Subperiosteal dissection of the sternal and clavicular insertion of the strap muscles, SCM, and sternohyoid, follows allowing these to be retracted. A plane is then developed by finger dissection underneath the sternum and into the upper mediastinum. The thymus may be swept laterally. The sternum can then be split with an oscillating saw and a sternal retractor is placed. The pleural is dissected and retracted laterally.

Similar to the anterior cervical approach, an avascular plane is developed by blunt dissection between the trachea and oesophagus medially and the carotid laterally. The left brachiocephalic vein and artery may be retracted inferolaterally. The plane of dissection is continued between the oesophagus and prevertebral fascia allowing identification of both longus coli muscles. At which point retractors are placed (Zengming et al., 2010). Closure is in a stepwise fashion with a chest drain and postoperative chest X-ray.

The important complications are vascular injuries, thoracic lymphatic duct injury, tracheal injury, oesophageal injury, and pleural injury/pneumothorax.

Anterior approaches: Transthoracic

The transthoracic approach gives the most anterior view of the spinal cord and disc prolapse, it is especially useful in central disc prolapses and is essential in the skill set of any surgeon treating this condition. It is the approach the author would recommend in all calcified and newly termed 'giant' disc herniations. These are defined as occupying greater than 40% of the canal on preoperative imaging (Hott et al., 2005)

The indications for this approach are T2–T12, central, calcified, intradural disc prolapses.

The technique is as follows (Figs. 61.2–61.6): The patient is positioned in a lateral decubitus position with an axillary roll. The legs are flexed with a pillow between the knees. For higher disc spaces (T2–T6) skin preparation should include the scapula and shoulder as to allow for mobilization of the scapula. A right sided approach for higher lesions allows for better visualization of the spinal surface

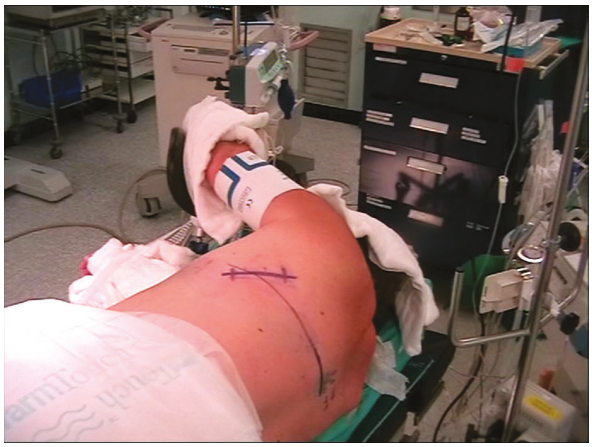

Fig. 61.2 Patient positioning and incision marked in mid-axillary line, centred over relevant disc space which was marked with AP and lateral X-ray.

as the arch and descending aorta are closely related to the left side of the vertebral bodies. A left sided approach allows for easier exposure of T8 and below as the liver and diaphragm can obscure an approach from the right. A left sided approach also minimizes the risk to the thoracic duct. A double lumen endotracheal tube is used.

An incision is made after intraoperative localization of the desired spinal and intercostal level. For a full open approach to the upper levels the incision is from the spinous process of T1 and carried medially parallel to the medial border of the scapula to the inferior angle of the scapula and continued laterally to the costal margin of the seventh rib. For lower levels, the skin incision is placed on the line of the rib to be resected. Whether a full or mini-open procedure is to be utilized, the incision should be planned so that its midpoint overlies the appropriate disc space at the level of the mid-axillary line.

The approach for higher levels includes identification and division of the dorsal shoulder girdle muscles including trapezius, latissimus dorsi, rhomboids, and serratus muscles which allow for retraction of the scapula to expose the chest wall. For lower approaches latissimus dorsi and serratus anterior are identified and divided exposing the rib. The intercostal muscles of the rib are stripped and the undersurface of the rib cleared with a periosteal elevator. The muscle

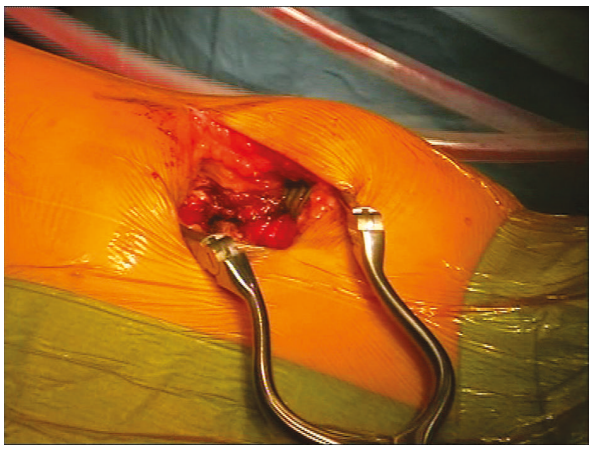

Fig. 61.3 Incision over appropriate rib.

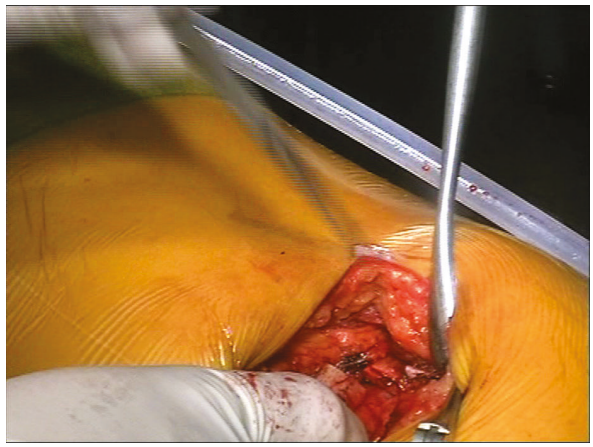

Fig. 61.4 Rib is fractured and displaced inferiorly to expose the pleura.

dissection is continued along the rib as far anteriorly and posteriorly along the rib as possible.

The rib is then cut as close to the rib head/costotransverse junction and as far anteriorly to the costal junction as possible. With mini-open approaches, the rib is not cut anteriorly, but a chest spreader is placed, and at this point the surgeon can go transpleural or retropleural. If done retropleurally, the lung should be left inflated to allow for easier dissection of the pleura and minimize pleural tears. If transpleural, the lung is deflated and the parietal pleura is incised over the desired disc space, with the flap based medially.

Careful identification of the azygous vein, aorta on the left, sympathetic plexus, intercostal bundle, and rib head is required. The intercostal artery and vein are ligated and divided close to their origin to minimize the risk of vascular compromise, at least 1 cm from the intervertebral foremen. The rib head is then removed to expose the disc space. The disc space is cleared together with a portion of the vertebral body above and below. The extent of the bony removal is dependent on the superior/inferior extent of the disc prolapse. To fully expose the prolapsed disc along its length, for very large discs, it may be necessary to partially remove the superior or inferior pedicles. The purpose is to create a cavity, anterior to the cord, into which the prolapsed disc can be delivered. The prolapsed portion of the disc is then delivered anteriorly, away from the cord.

Closure is in a stepwise fashion with repair of any dural defect, and a chest drain if a transpleural approach was used. If there is a dural defect a lumbar drain should be placed.

Complications include vascular injuries, thoracic lymphatic duct injury (right), oesophageal injury, pleural/pneumothorax injury, and sympathetic plexus injury.

Posterior-lateral approaches: Costotransversectomy

The indication for this approach is a lateral, soft disc protrusion.

The technique is as follows: The patient is positioned prone on chest rolls. A midline incision with a 'T' or paramedian straight or curvilinear incision is made, centred on the desired level.

The trapezius or latissimus dorsi is identified and divided close to the transverse process. The superficial surface of the rib is cleared from remaining muscle attachments and the undersurface of the rib cleared with a Doyan periosteal elevator. The transverse process and lamina are cleared of any remaining muscle fibres. The rib head is

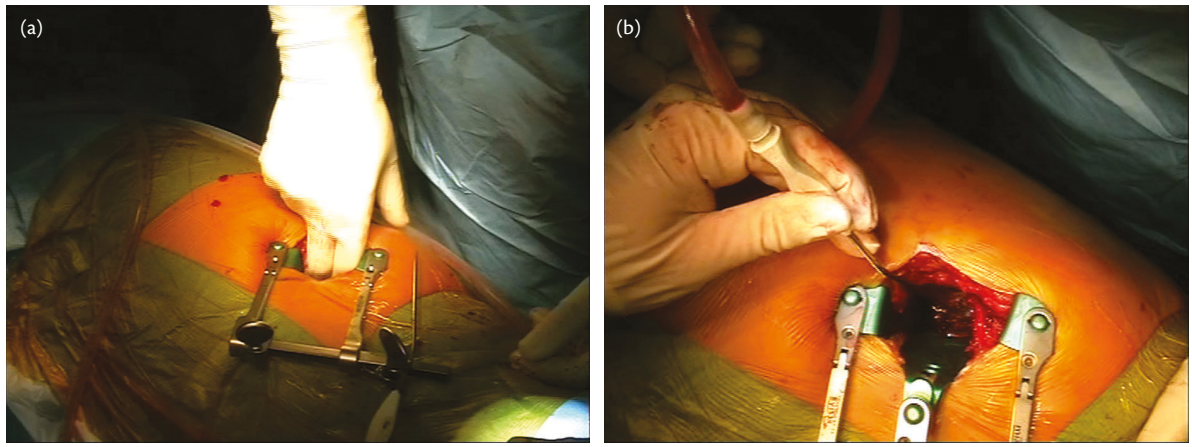

Fig. 61.5 Pleura is stripped from chest wall by blunt dissection. And deep retractor inserted on the vertebral surface.

disarticulated and the rib is cut anteriorly. This allows the rib to be disarticulated with the costotransverse process and removed completely after identification of the neurovascular bundle. The transverse process is resected exposing the pedicle. The parietal pleura is then retracted to allow resection of the pedicle. The rib removal performed in the standard procedure can be too limiting to allow for pleural retraction, and the ventral and even, lateral exposure can still be too limited. Bilateral costotranversectomies can be performed to allow for a pan-ventral exposure.

The main complications are vascular injuries, thoracic lymphatic duct injury (right), oesophageal injury, pleural/pneumothorax injury, and sympathetic plexus injury.

Posterior-lateral approaches: Lateral extra cavity

The indication for this approach is a lateral, soft disc protrusion.

The technique is as follows: The patient is positioned prone on chest rolls. The incision depends on the level either a midline incision over the spinous processes or curvilinear incision with the straight segment over the spinous process skirting along the inferior angle of scapula is used. The trapezius or latissimus dorsi is identified and divided close to the transverse process. The lateral border of the erector spinae muscles are identified and reflected medially. The superficial surface of the rib is cleared from remaining muscle attachments and the undersurface of the rib cleared with a Doyan periosteal elevator. The transverse process and lamina are cleared of any remaining muscle fibres.

The rib head is disarticulated and the rib cut greater than 12 cm laterally. The rib can then be disarticulated from the costotransverse process and removed completely after identification of the neurovascular bundle. The transverse process is resected exposing the pedicle. The parietal pleura is then retracted to allow resection of the pedicle. The level in the thoracic spine must be considered and above T4 is difficult due to the presence of the scapula. Dissection through the rhomboids and trapezius is required and carries high morbidity.

Complications include vascular injuries, thoracic lymphatic duct injury (right), oesophageal injury, pleural injury/pneumothorax, sympathetic plexus injury, dural tear, CSF leak, the need for thoracostomy, nerve root injury, and infection. The rate is quoted as

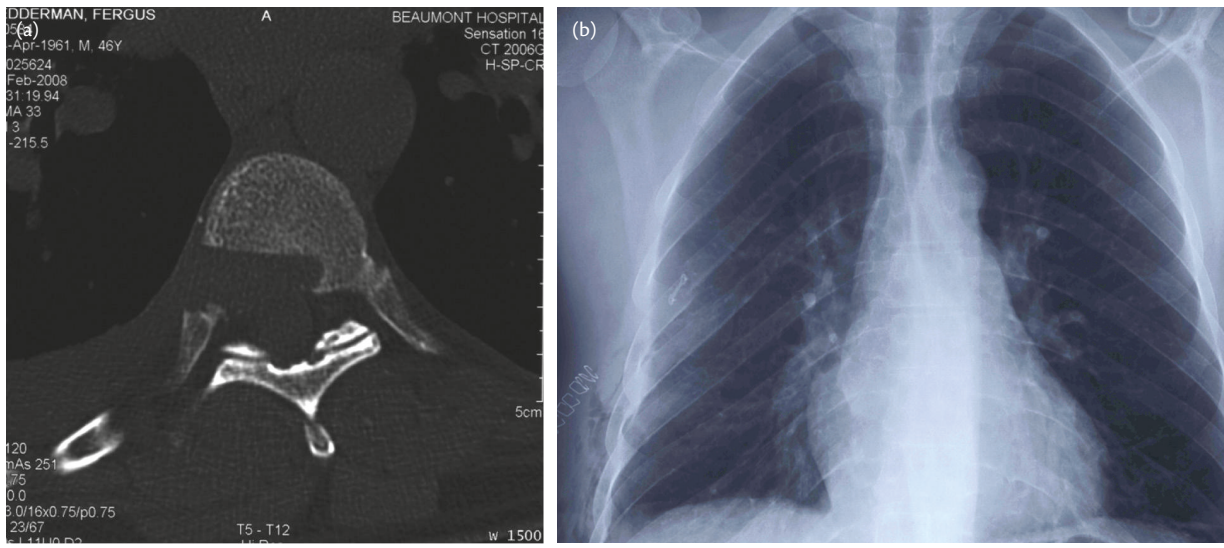

Fig. 61.6 (A) Postoperative CT shows extent of bony resection and complete removal of prolapsed disc. (B) Postoperative chest X-ray with mini plate approximating rib.

high as 53% in some series (Lubelski et al., 2012). The muscle dissection required for this exposure can result in increased blood loss, postoperative pain, and an increased hospital stay.

Posterior-lateral approaches: Transpedicular (unilateral or bilateral)

The indication for this approach is a lateral, soft disc protrusion. Bilateral approaches may achieve central disc decompression but are more destabilizing.

The technique is as follows: the patient is positioned prone on chest rolls. A midline incision is made over the spinous processes. The approach is subperiosteal dissection down along the spinous processes and lamina laterally to the facet joint. Using Kerrison's rongeurs with a small footplate a lateral laminotomy is performed to identify the nerve root and thecal sac. The inferior facet of the superior vertebra and the superior facet of the inferior vertebra along with the superior margin of the transverse process is resected exposing the caudal pedicle. The cancellous bone of the pedicle is drilled staying within the cortical bone. The superior and inferior cortical shell remaining is then resected. Cortical bone adjacent to the spinal canal is removed laterally and a partial laminectomy is then performed. A portion of the superior and inferior facets are also drilled down. The lateral disc space is incised and 'emptied' using curettes and rongeurs, gently making room medially to deliver the disc fragment in the space created.

Post-op instability is rare, thus fixation is not necessary. Complications include nerve root and spinal cord injury

Posterior-lateral approaches: Transfacet pedicle sparing

The indication for this approach is a lateral, soft disc protrusion.

The technique is as follows: The patient is positioned prone on chest rolls. A midline incision over the spinous processes is made. The approach is subperiosteal dissection down along the spinous processes and lamina laterally to the facet joint. Using Kerrison's rongeurs with a small footplate a lateral laminotomy is performed. The medial aspect of the inferior facet of the superior vertebra is resected exposing the nerve root and thecal sac. Closure is in a stepwise fashion. Complications include nerve root and spinal cord injury

Minimally invasive procedures

Minimally invasive techniques (MIT) have become increasingly popular in Neurosurgery. These techniques have been reported to reduce morbidity by reducing approach related tissue trauma, however paradoxically, have a steep learning curve which can lead to significant complications (Elhadi et al., 2015). MITs range from mini-open approaches to video-assisted thoracoscopic and endoscopic techniques. Eihadi et al. performed a systematic review comparing outcomes of MIT to conventional open approaches and concluded that soft disc herniations confined to a single level, are suitable for a minimally invasive approach but patients with calcified discs adherent to the dura would benefit from an open approach. However, their review did not include min-open approaches.

Thoracoscopic discectomy

The patient is positioned in a lateral position and is intubated using a double lumen endotracheal tube, after incisions are made for ports the ipsilateral lung is deflated. Thoracoscopic portals, 15 mm in diameter and flexible, are inserted in three different port openings for the working instruments, as well as a 1 cm port for the endoscope. The pleura is dissected from the vertebral column. The morbidity of severe postoperative neuralgia caused by muscle dissection and rib retraction, part of a large thoracotomy, is avoided. Like an open thoracotomy the head of rib and pedicle are first drilled and the spinal cord is identified clearly, a trough in the vertebral body adjacent to the prolapsed disc is drilled and the disc fragment is then slowly 'worked' into this space.

Mini-open technique

The author has previously published the mini-open retro-pleural approach. In this procedure a 4 cm incision in the mid-axillary line is performed, followed by a single rib cut, the pleura is then carefully dissected off the inside of the thoracic cavity using blunt, peanut dissectors, insertion of a long retractor may allow for the ipsilateral lung to remain inflated and negates the need for a post-op chest drain. The disc prolapse is resected as just described and the rib is reattached using a universal quick flap. For large central disc prolapses the author approaches from the left side as the more robust aorta is easier to manipulate. Various authors have reported success utilizing a mini-open approach (Moran et al., 2012; Snyder et al., 2014). Other factors to consider include surgeon experience in the various techniques (Falavigna and Piccoli Conzatti, 2013).

Prognosis

In cases where surgical intervention is indicated recovery of neurological function and pain control is seen in the majority of patients, even those with 'giant' discs (Moran et al., 2012). Historically the surgical morbidity, including postoperative neurological worsening and paralysis, was high—complications from laminectomy have been quoted as anywhere between 18 and 75% (Arseni and Nash, 1960; Fessler and Sturgill, 1998).

Clinical outcome following surgical intervention has improved dramatically since abandoning this approach and using, instead, more ventral approaches, either transthoracic or dorsolateral. However, post-thoracotomy pain syndrome has been reported in up to 50% of patients postprocedure, continuing long term in up to 30% (Karmakar and Ho, 2004).

Osteoporosis and vertebral compression fractures

Osteoporosis is a skeletal disorder resulting in an increase in fracture risk. The risk of fracture is inversely related to bone strength, which is a function of bone mineral density, bone microarchitecture and remodelling (NIH Consensus Development Panel, 2001). Bone mineral density is measured by dual X-ray absorptiometry (DXA). Factors that influence bone strength are age-related bone loss and hormonal status. It has recently been demonstrated that loss of trabecular bone can occur as early as the third decade in both men and women. However, it is not until middle age that loss of cortical bone begins for both sexes. Age-related bone loss is thought to be due to the reduced capacity of the kidney to hydroxylate vitamin D to its active form resulting in a low serum calcium and secondary hyperparathyroidism.

Hormonal related bone loss affects women more than men. With the onset of the menopause, the decline in serum levels of oestradiol and oestrone results in a mismatch between bone formation and resorption leading to progressive bone loss. The net resorption of bone leads to an increase in the level of extracellular calcium which

activates compensatory mechanism to prevent hypercalcaemia resulting in a net negative total body calcium.

In comparison, men do not experience an abrupt decline in sex hormones. Rather, there is a slow progressive decline in the bioavailability of testosterone and oestradiol due to the increase in sex hormone binding proteins (Drake et al., 2015).

Due to concerns over pharmacological replacement of oestrogen, selective oestrogen receptor modulators are licensed in the treatment of postmenopausal osteoporosis. Bisphosphonates are inorganic pyrophosphates that have a high affinity for hydroxyapatite. This forms a non-degradable barrier between osteoclast and Howship lacunae. The osteoclasts endocytose the bisphosphate leading to apoptosis.

Osteoporotic vertebral compression fractures can lead to significant morbidity due to acute or chronic pain and progressive kyphotic deformity resulting in biomechanical instability leading to falls risk or impairment of respiratory function. Therefore, screening for osteoporosis is recommend for women older than 65. For women younger than 65 or men older than 65, an analysis of individual risk factors may help predict the presence of osteoporosis. These risk factors include: female sex; White or Asian race; low body weight/body mass index; family history; early menopause; sedentary lifestyle; excessive alcohol; low calcium or vitamin D intake and inadequate sun exposure; certain medications (glucocorticoids or anticonvulsants); diseases such as rheumatoid arthritis and almost all systemic inflammatory diseases. Laboratory investigations include ESR, FBC, Ca, PO4, Alk Phos, Cr, and 24 h urinary Ca. DXA is considered the gold standard radiological investigation as it can predict fracture risk. Short tau inversion recovery (STIR) sequences on MRI scanning can help distinguish recent from long standing injuries.

Treatment of osteoporosis can be divided into non-pharmacologic and pharmacologic. Non-pharmacologic interventions include exercise and dietary modifications. Physical activity has been shown to reduce age-related bone mineral loss. A diet rich in dairy products and fish will supplement vitamin D intake. Pharmacologic therapies include bisphosphonates which reduced bone turnover in a dose-dependent manner and reduce fracture risk, hormone replacement therapy, and selective oestrogen receptor modulators.

Vertebroplasty and kyphoplasty

Vertebroplasty can be indicted in acute symptomatic osteoporotic compression fractures refractory to medical management. Under intravenous sedation with local anaesthetic or general anaesthesia. The patient is placed prone with bi-planar fluoroscopy or under CT guidance, a unilateral or bilateral approach via a small stab incision is made. An 11–13-gauge needle is passed to the anterior third or quarter of the vertebral body via a transpedicular or parapedicular route (the point of attachment of the pedicle to the vertebral body). Polymethyl methacrylate cement is then slowly injected until it approaches the posterior vertebral wall. If extraosseous cement is noted the procedure should be terminated immediately. Complications include pulmonary emboli from fat or cement, radicular pain neurological complications, and adjacent level fractures.

Kyphoplasty similarly is indicated for symptomatic osteoporotic compression fractures refractory to medical management and restoration of sagittal balance. The technique is the same except the needle is passed under the endplate at the centre of the vertebral body and a series of tools are used to create a working channel down which a bone tamp is passed. The tamp is expanded under fluoroscopic guidance with volume and pressure monitoring. Inflation is stopped when the height is restored or maximal volume/pressure is achieved in the balloon or the balloon comes within 1 mm of the cortical surface. The tamp is removed and Polymethyl methacrylate cement is then slowly injected into the cavity. Complications include pulmonary emboli from fat or cement, radicular pain, neurological complications, and adjacent level fractures.

Typical short- and long-term outcome measures for these procedures are pain scores (VAS), disability scores (ODI), complications (cement leakage, neurological injury), height of anterior vertebral body, kyphotic angle, adjacent level fractures, and length of stay. Both procedures are safe and effective with respect to all outcomes when compared to medical management. There was no difference noted in the incidence of adjacent level fracture between kyphoplasty and vertebroplasty. Both of these interventions reduced the incidence compared to conservative treatment. Kyphoplasty may have a slight advantage over vertebroplasty in restoration of the anterior vertebral height and kyphotic angle (Ma et al., 2012).

There is ongoing debate in the literature regarding the timing of vertebroplasty and kyphoplasty. The main indication for vertebroplasty is for pain control and therefore the optimum timing of vertebroplasty is uncertain with some authors suggesting that vertebroplasty can be safely and effectively performed at any time between 2 to 12 months (Nieuwenhuijse et al., 2012). As the indication for kyphoplasty is restoration of sagittal balance as well as pain control timing appears to be more important. Restoration of vertebral height is most effective in acute or subacute fractures and therefore it would appear that the accurate timing of the procedure is necessary (Crandall et al., 2004).

Controversy

Routine MRI for osteoporotic fractures

MRI may be used to assess if a fracture is acute or chronic. During the acute phase in fracture healing there may be a finding of haemorrhage and the normal fatty marrow can demonstrate significant marrow oedema that decreases over approximately three months (Brinckman et al., 2015; Piazzolla et al., 2015). This can be appreciated as a high signal intensity on T2 weighted sequences or the T1 fat suppression technique called STIR. Some recent studies have suggested that certain T1 and T2 characteristics of the acute fracture may help in predicting non-union (Tsujio et al., 2011; Takahashi et al., 2016). Other indications for using MRI in the setting of osteoporotic fractures would be if there is concern that the fracture may be a pathological fracture due to bony metastasis. This may be achieved by acquiring T1 postgadolinium and diffusion-weighted sequences (Pozzi et al., 2012).

FURTHER READING

[No authors listed] (2001). NIH Consensus Development Panel on Osteoporosis Prevention, Diagnosis, and Therapy, March 7–29, 2000: highlights of the conference. *South Med J*, **94**(6), 569–73.

Falavigna, A. & Piccoli Conzatti, L. (2013). Minimally invasive approaches for thoracic decompression from discectomy to corpectomy. *J Neurosurg Sci*, **57**(3), 175–92.

Fessler, R.G. & Sturgill, M. (1998). Review: complications of surgery for thoracic disc disease. *Surg Neurol*, **49**(6), 609–18.
Hott, J.S., Feiz-Erfan, I., Kenny, K., & Dickman, C.A. (2005). Surgical management of giant herniated thoracic discs: analysis of 20 cases. *J Neurosurg Spine*, **3**(3), 191–7.
Moran, C., Ali, Z., McEvoy, L., & Bolger, C. (2012). Mini-open retropleural transthoracic approach for the treatment of giant thoracic disc herniation. *Spine (Phila Pa 1976)*, **37**(17), E1079–84.

REFERENCES

[No authors listed] (2001). NIH Consensus Development Panel on Osteoporosis Prevention, Diagnosis, and Therapy, March 7–29, 2000: highlights of the conference. *South Med J*, **94**(6), 569–73.
Arce, C.A. & Dohrmann, G.J. (1985). Herniated thoracic disks. *Neurol Clin*, **3**(2), 383–92.
Arseni, C. & Nash, F. (1960). Thoracic intervertebral disc protrusion: a clinical study. *J Neurosurg*, **17**, 418–30.
Arts, M.P. & Bartels, R.H. (2014). Anterior or posterior approach of thoracic disc herniation? A comparative cohort of mini-transthoracic versus transpedicular discectomies. *Spine J*, **14**(8), 1654–62.
Awwad, E.E., Martin, D.S., Smith, K.R. Jr., & Baker, B.K. (1991). Asymptomatic versus symptomatic herniated thoracic discs: their frequency and characteristics as detected by computed tomography after myelography. *Neurosurgery*, **28**(2), 180–6.
Brinckman, M.A., Chau, C., & Ross, J.S. (2015). Marrow edema variability in acute spine fractures. *Spine J*, **15**(3), 454–60.
Crandall, D., Slaughter, D., Hankins, P.J., Moore, C., & Jerman, J. (2004). Acute versus chronic vertebral compression fractures treated with kyphoplasty: early results. *Spine J*, **4**(4), 418–24.
Drake, M.T., Clarke, B.L., & Lewiecki, E.M. (2015). The pathophysiology and treatment of osteoporosis. *Clin Ther*, **37**(8), 1837–50.
Elhadi, A.M., Zehri, A.H., Zaidi, H.A., et al. (2015). Surgical efficacy of minimally invasive thoracic discectomy. *J Clin Neurosci*, **22**(11), 1708–13.
Falavigna, A. & Piccoli Conzatti, L. (2013). Minimally invasive approaches for thoracic decompression from discectomy to corpectomy. *J Neurosurg Sci*, **57**(3), 175–92.
Fessler, R.G. & Sturgill, M. (1998). Review: complications of surgery for thoracic disc disease. *Surg Neurol*, **49**(6), 609–18.
Hott, J.S., Feiz-Erfan, I., Kenny, K., & Dickman, C.A. (2005). Surgical management of giant herniated thoracic discs: analysis of 20 cases. *J Neurosurg Spine*, **3**(3), 191–7.
Karmakar, M.K. & Ho, A.M. (2004). Postthoracotomy pain syndrome. *Thorac Surg Clin*, **14**(3), 345–52.
Lubelski, D., Abdullah, K.G., Mroz, T.E., et al. (2012). Lateral extracavitary vs. costotransversectomy approaches to the thoracic spine: reflections on lessons learned. *Neurosurgery*, **71**(6), 1096–102.
Ma, X.L., Xing, D., Ma, J.X., Xu, W.G., Wang, J., & Chen, Y. (2012). Balloon kyphoplasty versus percutaneous vertebroplasty in treating osteoporotic vertebral compression fracture: grading the evidence through a systematic review and meta-analysis. *Eur Spine J*, **21**(9), 1844–59.
McInerney, J. & Ball, P.A. (2000). The pathophysiology of thoracic disc disease. *Neurosurg Focus*, **9**(4), e1.
Moran, C., Ali, Z., McEvoy, L., & Bolger, C. (2012). Mini-open retropleural transthoracic approach for the treatment of giant thoracic disc herniation. *Spine (Phila Pa 1976)*, **37**(17), E1079–84.
Nieuwenhuijse, M.J., van Erkel, A.R., & Dijkstra, P.D. (2012). Percutaneous vertebroplasty for subacute and chronic painful osteoporotic vertebral compression fractures can safely be undertaken in the first year after the onset of symptoms. *J Bone Joint Surg Br*, **94**(6), 815–20.
Piazzolla, A., Solarino, G., Lamartina, C., et al. (2015). Vertebral bone marrow edema (VBME) in conservatively treated acute vertebral compression fractures (VCFs): evolution and clinical correlations. *Spine (Phila Pa 1976)*, **40**(14), E842–8.
Pozzi, G., Garcia Parra, C., Stradiotti, P., Tien, T.V., Luzzati, A., & Zerbi, A. (2012). Diffusion-weighted MR imaging in differentiation between osteoporotic and neoplastic vertebral fractures. *Eur Spine J*, **21**(Suppl 1), 123–7.
Snyder, L.A., Smith, Z.A., Dahdaleh, N.S., & Fessler, R.G. (2014). Minimally invasive treatment of thoracic disc herniations. *Neurosurg Clin N Am*, **25**(2), 271–7.
Stillerman, C.B., Chen, T.C., Couldwell, W.T., Zhang, W., & Weiss, M.H. (1998). Experience in the surgical management of 82 symptomatic herniated thoracic discs and review of the literature. *J Neurosurg*, **88**(4), 623–33.
Takahashi, S., Hoshino, M., Takayama, K., et al. (2016). Predicting delayed union in osteoporotic vertebral fractures with consecutive magnetic resonance imaging in the acute phase: a multicenter cohort study. *Osteoporos Int*, **27**(12), 3567–75.
Tsujio, T., Nakamura, H., Terai, H., et al. (2011). Characteristic radiographic or magnetic resonance images of fresh osteoporotic vertebral fractures predicting potential risk for nonunion: a prospective multicenter study. *Spine (Phila Pa 1976)*, **36**(15), 1229–35.
Wood, K.B., Blair, J.M., Aepple, D.M., et al. (1997). The natural history of asymptomatic thoracic disc herniations. *Spine (Phila Pa 1976)*, **22**(5), 525–9; discussion 529–30.
Wood, K.B., Garvey, T.A., Gundry, C., & Heithoff, K.B. (1995). Magnetic resonance imaging of the thoracic spine. Evaluation of asymptomatic individuals. *J Bone Joint Surg Am*, **77**(11), 1631–8.
Zengming, X., Maolin, H., Xinli, Z., & Qianfen, C. (2010). Anterior transsternal approach for a lesion in the upper thoracic vertebral body. *J Neurosurg Spine* **13**(4), 461–8.

RELATED LINKS TO EBRAIN

Inserting Pedicle Screws. https://learning.ebrain.net/course/view.php?id=74
Minimally Invasive Surgical Approaches to the Posterior Thoracolumbar Spine. https://learning.ebrain.net/course/view.php?id=592
Posterior Thoracic Approaches. https://learning.ebrain.net/course/view.php?id=818
Thoracic Disc Prolapse. https://learning.ebrain.net/course/view.php?id=799
Vertebroplasty and Kyphoplasty. https://learning.ebrain.net/course/view.php?id=411

62

Lumbar spinal disease

Christopher G. Kellett and Matthew J. Crocker

Introduction

Observations relating to degeneration of the lumbar spine date back to Hippocrates and Galen. It is only in the last century degenerative disc disease has become a recognized entity. In more recent years, advances in imaging and surgical technology have resulted in novel approaches to treatment, marking a renaissance in what is still an evolving field. Lumbar spinal disease is ubiquitous; it is prudent that the neurosurgeon develops a sound understanding of this challenging area.

Degenerative lumbar spinal disease

Key concepts

Three key concepts will be discussed: spinal function, the motion segment, and spinopelvic balance.

Spinal function

The spine has three principal biomechanical roles; namely load bearing, mobility, and protection of the neural elements.

Forces placed on the intervertebral disc are several times greater than the sum of the weight of body parts and supported objects. Regardless of loading pattern the healthy intervertebral disc and its hydrostatic properties, distributes load equally to the vertebral endplate. As in other diarthrodial joints, abnormal loading results in focal degeneration and pain, confirmed by discography (McNally et al., 1996).

The spinal musculature has a mechanical advantage; small changes in muscle length produce a large range of movement placing the spine under great stress. The ligamentous spine respects a tension-elongation relationship; with elongation tension increases, stability is associated with spinal tension and stiffness. There has been no conclusive evidence that translation or angular movement beyond the normal range of motion is associated with pain however anecdotally spondylolisthesis demonstrates that segmental instability results in pain.

Loss of integrity of supporting structures through the degenerative process frequently results in a mechanical and chemical insult to neural tissue. Examples include disc herniation, lumbar canal stenosis, and spondylolisthesis.

The motion segment

Schmorl and Junghanns (1971) were the first to describe the 'motion segment' consisting of two vertebrae, the intervening disc and the associated zygapophyseal (facet) joints. Segmental ligaments include longitudinal, flaval, and interspinous ligaments. The intrinsic segmental muscles (splenius, erector spinae, transversospinal) provide antagonizing actions and stability. 'The three-joint complex' was coined by Kirkaldy-Willis et al. (1978) highlighting the inextricable relationship between the intervertebral disc and facet joints. Degeneration of one component will lead to degeneration of the entire segment resulting in pain, deformity, and neural compromise. Panjabi (1992a, 1992b) describes the spine as a dynamic neuromuscular system with three subsystems (passive, active and neural with feedback subsystems) in equilibrium.

Spinopelvic balance

Optimal sagittal plane alignment allows the spine to support the weight of the body with minimal energy expenditure. Imbalance results in muscular fatigue, deformity, pain, and the psychosocial implications of kyphosis and deficient horizontal gaze. The relationship between the pelvis, spine, and overall sagittal balance is paramount when treating spinal disorders. The neurosurgeon will encounter many patients with 'failed' and 'flat back' syndrome. Obtaining full-length standing anteroposterior (AP) and lateral X-rays in these patients will allow measurement of spinopelvic geometry, reveal the magnitude of sagittal imbalance and the degree of correction required to restore balance. Discussion of spinopelvic parameters is beyond the scope of this chapter and the reader is referred to in Chapters 57 (spinal stability) and 66 (scoliosis)

Aetiology and pathophysiology

Eighty per cent (80%) of people experience an episode of low back pain in their lifetime, with 10% developing chronic pain. In the United Kingdom 8.3 million working days are lost per year secondary to musculoskeletal problems; patients are unlikely to return to work after two years of sick leave. The natural history of lumbar back pain is benign and in the majority, pain will resolve in 2–4 weeks and more than 90% are pain-free at 12 months. With the over-65 age group set to double over the next 25 years, back pain will have greater socioeconomic implications.

Degenerative disease has traditionally been linked to occupational repetitive loading. In addition, factors such as age, male gender, and smoking have been implicated. However, increasingly it is evident that genetic factors play a role. Familial degenerative disc disease is recognized and candidate-gene polymorphisms include those encoding collagen, Sox9, the vitamin D receptor metalloprotease-3, and interleukin-1.

The degenerative cascade

The degenerative process has three distinct phases (Kirkaldy-Willis et al., 1978). Instability occurs when degeneration exceeds structural changes conferring stabilization.

Firstly, dysfunction characterized by minor trauma or repetitive strain results in axial back pain secondary to segmental muscle fatigue, spasm, and inflammation. Disc degeneration manifests as circumferential annular tears and nuclear matrix changes then facet synovitis and cartilaginous degeneration occurs. Secondly instability characterized by internal disc disruption and resorption, facet capsule laxity, and subluxation. Thirdly stabilization characterized by osteophytosis and ankylosis reducing motion, thickening of the yellow ligament and circumferential encroachment with compromise of the neural elements.

Lumbar spondylosis

'Spondylosis' encompasses a group of pain disorders and clinical syndromes related to degeneration of the motion segment, the cardinal symptom being axial lower back pain. Neurological compromise and radicular pain may coexist.

Most patients with lumbar spondylosis describe non-specific back pain. A small group of patients (10–15%) present with pain related to disc or facet degeneration and instability. Degenerative findings on MRI are common in asymptomatic individuals however disc disease with associated Modic changes and significant facet degeneration is rare in younger patients. Certain clinical pointers may pinpoint specific pain generators and appropriate treatment.

Lumbar canal stenosis

Lumbar canal stenosis (LCS) and its clinical manifestations were first described in 1961 by Friedman. It affects approximately 1% of the population with patients undergoing surgery for this condition increasing eightfold over the last 30 years, predominantly in the over 65 age group. It is defined as any condition involving narrowing of the spinal canal or neural foramen. LCS may be classified as congenital (idiopathic or achondroplastic) and acquired (degenerative, spondylolytic, traumatic, or metabolic).

Congenital lumbar canal stenosis is rare and presents between 30 and 40 years of age. Degenerative lumbar canal stenosis is more common and presents predominantly in the over 60-year-old age group. The defining syndrome is neurogenic claudication: radicular leg pain, heaviness, numbness, or paraesthesia, which develops on standing and walking. The degree of radiological compression and severity of clinical symptoms reveals poor correlation. Risk factors for peripheral vascular disease should be sought; a careful history will usually differentiate vascular from neurogenic claudication.

Clinical features include back pain with associated radiation into the buttocks on walking and standing associated with heaviness and numbness. Relief of symptoms occurs with flexion of the lumbar spine and rest. Cauda equina syndrome is rare but patients may present with a chronic picture or coexisting acute disc herniation. Examination findings may be subtle and precipitated by exercise. Assessment of sagittal balance may reveal flexion of the knees and hyperextension of the hip to compensate for increased lumbar flexion.

Ligamentous thickening results in central encroachment. Shortening of the spinal column through loss of disc height and deformity causes buckling of the hypertrophied flavum, this is accentuated in lumbar extension. Olisthesis may coexist further reducing canal diameter and compromising neural content.

Claudication is hypothesized to be secondary to mechanical compression and vascular insufficiency. Longstanding compression of the cauda equina results in reduced cerebrospinal fluid (CSF) delivery, microvascular changes, and inflammation. Venous congestion impairs metabolism and nerve root arterioles lose the ability to vasodilate in response to increased metabolic demand during exercise.

In most patients, symptoms progress but a small percentage of patients improve with non-operative treatment.

Conservative management is reasonable in the presence of significant comorbidities, lack of radiological and clinical concordance, and mild or intermittent symptoms. Treatment options include non-steroidal anti-inflammatories, muscle relaxants, physiotherapy, postural education, and epidural steroid infiltration.

A direct comparison of patients undergoing surgical and conservative management of LCS is misleading due to lack of class 1 evidence and heterogeneity of the two groups. Despite this lack of evidence, it is generally accepted that surgery in patients experiencing moderate to severe symptoms is superior to non-operative management.

Progressive neurological deficit and sphincteric disturbance are absolute indications for surgery however this is rare. The surgical technique is dictated by the degree of compression, central or lateral compression, and coexisting deformity; options include laminectomy, selective decompression, laminoplasty, interspinous process distraction devices, decompression alone, or decompression and fusion (non-instrumented vs. instrumented). See **Figure 62.1**.

Laminectomy vs. selective decompression and laminoplasty

Central compression is treated surgically through laminectomy at the stenotic segment. This is favoured in severe stenosis, deformity, and when a wide lateral decompression is required. The greatest degree of compression is sublaminal where the flavum is thickest. In cases of moderate compression resection of the flavum may be performed through a unilateral approach (preserving the midline ligaments and contralateral muscles), laminotomy and an 'over-the-top' technique to decompress the contralateral canal. Moderate lateral recess and extraforaminal stenosis can be addressed using selective decompressive techniques such as laminotomy, medial facetectomy, and extraforaminal muscle splitting approaches.

Laminoplasty techniques have been described similar to those initially described in the cervical spine however, it is not commonplace in the treatment of LCS with increased operative time and no evidence to suggest benefit over other approaches.

Interspinous distraction devices

Interspinous distraction devices (ISD) require the insertion of a spacer through the interspinous ligament, maintaining the

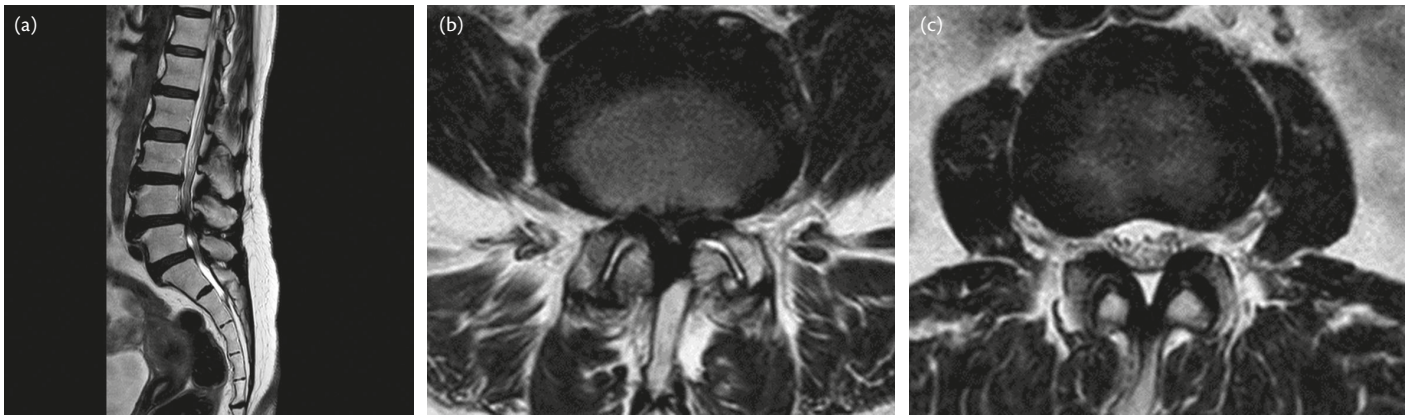

Fig. 62.1 T2 MRI. (A) Sagittal: L4/5 lumbar canal stenosis and degenerative spondylolisthesis; (B) Axial: crowding of the cauda equina secondary to a broad-based disc protrusion, facet and flaval hypertrophy; (C) Axial: non-stenotic level for comparison.

supraspinous ligament. This decreases intradiscal pressure, distracts the facets and neural foramen, unbuckles the flavum, and reduces abnormal segmental motion. They can be inserted at multiple levels, L4/5 being most common with a small S1 spinous process precluding placement at L5/S1. Contraindications include spondylolisthesis, tumours, trauma, unstable or high-grade degenerative spondylolisthesis, and osteoporosis.

Current evidence and NICE guidance (2010) suggest ISD devices are efficacious for carefully selected patients in the short and medium term, although failure may occur and further surgery may be needed. There are no major safety concerns. Therefore, these procedures may be used provided that normal arrangements are in place for clinical governance, consent and audit.

Decompression and fusion (instrumented vs. non-instrumented)

Combined decompression and fusion is recommended when there is evidence of segmental instability. This is somewhat theoretical and may be difficult to prove radiologically. It is generally accepted that fusion should be considered in cases of deformity, moderate to severe low back pain, recurrent and junctional stenosis, or when greater than 50% bilateral facetectomy is required for decompression.

Limited evidence suggests decompression and non-instrumented fusion in the context of degenerative spondylolisthesis results in significantly improved back and leg pain when comparing decompression alone. There is no evidence to suggest that instrumented fusion is superior to non-instrumented fusion in terms of clinical outcome however, instrumentation does result in higher rates of fusion. There is no evidence to suggest that interbody fusion (ALIF, PLIF, TLIF, and XLIF) improves overall outcome.

Lumbar disc herniation and cauda equina syndrome

Lumbar disc herniation (LDH) is focal displacement of disc material beyond the margin of the adjacent vertebral body. LDH and radiculopathy is the most common indication for spinal surgery. The prevalence of symptomatic LDH is approximately 3%, most commonly affecting the 30–50-year-old age group. LDH is associated with age related changes to the disc; traumatic herniation is uncommon. Occupational factors (frequent heavy lifting, twisting, and exposure to vibration) and genetic predisposition predispose to LDH. It is generally benign with most patients recovering within one month. Extruded and sequestered fragments have a greater tendency to completely resolve by six months, possibly due to engulfment by macrophages.

The location of the herniation determines which nerve root is involved (the nerve exiting or transiting the disc space, i.e. whether the protrusion is central, in the lateral recess, foraminal, or extraforaminal). LDH can be classified morphologically and whether the herniation is contained by or traverses the posterior longitudinal ligament, the following terms are used: a disc protrusion involves deformation of but not rupture of the annulus, an extruded disc breaches the annulus with nuclear continuity, a sequestered disc is a free nuclear fragment.

Radicular pain is likely secondary to a combination of mechanical and chemical irritation. Studies have suggested that radicular compression alone results in numbness but is not painful. Compression results in oligaemia, oedema, and inflammation. Reduced CSF and blood flow reduce nutritional supply and the ability to remove noxious chemicals.

A history of acute back pain may precede radicular symptoms. The possibility of a peripheral nerve lesion should be considered in cases of foot drop and disconcordant neurology.

Clinical features include dermatomal pain, paraesthesia, and numbness increased by sitting, standing, and Valsalva manoeuvres; myotomal weakness, hyporeflexia, a reduced range of motion; antalgic gait, pain on compression of the spine; a positive Lasegue sign, reversed Lasegue sign (upper lumbar compression), or crossed Lasegue sign (large discs).

MRI is the standard investigation, while high-resolution computed tomography (CT) or myelography can be used when MRI is contraindicated. Neurophysiology may help exclude peripheral nerve lesions.

In the absence of cauda equina syndrome or an acute foot drop treatment is normally conservative. Reassurance is the key, specifically a short period of bed rest (three days), optimal analgesia including anti-inflammatories followed by physiotherapy is utilized. Symptoms resolve over three months in the majority. Unrelenting severe sciatica with sensorimotor symptoms may take a different course and early surgery is reasonable. Epidural and transforaminal blockade with corticosteroid is an adjunct rather than a definitive treatment.

Absolute indications for surgery include severe paresis and cauda equina syndrome. Relative indications include non-responsive severe sciatica and persistent symptoms for greater than six weeks following optimal conservative management.

Operative techniques

Given the prevalence of asymptomatic disc herniation patient selection is paramount. Patients with concordant clinical findings unresponsive to optimal conservative management for a minimum of six weeks should be considered. Class 1 evidence supports improved short-term outcome with surgery. The efficacy of surgery in comparison to conservative treatment declines over time. Standard approaches are an interlaminar approach and lumbar microdiscectomy. Percutaneous techniques include endoscopic discectomy, chemonucleolysis, and automated percutaneous lumbar discectomy.

Interlaminar approach and microdiscectomy

The interlaminar approach uses a midline incision and bilateral or unilateral subperiosteal muscle strip to access the interlaminar space. The microdiscectomy approach is identical to the interlaminar approach. The patient is prone or placed in the lateral decubitus position with the affected side up. The standard technique used is similar to that described by Yasargil, Caspar, and Williams (**Box 62.1**).

Box 62.1 Lumbar microdiscectomy

- Following level identification a 1.5–2.5 cm incision is made just lateral to the spinous process corresponding to the disc space
- Incision of the lumbodorsal fascia lateral to supraspinatus ligament
- Subperiosteal muscle strip from the lamina
- Insertion of Williams or McCullough retractor
- Exposure of the inferior lamina: the operating microscope is brought in
- 4–5 mm high-speed burr may be used to thin the lamina and perform a medial facetectomy
- A curette may be used to detach flavum from the lamina or the flavum can be incised superficially with a number 15 blade and a Watson Cheyne dissector used to split the longitudinal flavel fibres
- A 2 or 3 mm Kerrison rongeur can then be introduced to remove the flavum and expose the epidural fat overlying the nerve root. To help identify the nerve root the pedicle can be probed with the Watson Cheyne dissector
- Once the nerve root has been delineated a nerve root retractor is introduced and gentle medial retraction is placed over the shoulder of the nerve root to expose the disc space
- Free fragments in the epidural space may be removed with a micropituitary rongeur
- Epidural veins are coagulated with bipolar on a low setting with short intermittent bursts
- The underlying posterior longitudinal ligament and annulus are incised with a number 15 blade
- Adequate discectomy is performed to decompress the nerve root
- The procedure is completed by performing a foraminotomy (removal of ligament and undercutting the superior articulating process of the facet joint)
- Haemostasis prior to closure is performed

Complications

- Recurrent disc herniation (5%)
- CSF leak
- Nerve root injury
- Discitis

Cauda equina syndrome

Cauda equina syndrome (CES) is rare with annual incidence between 1 in 33 000–100 000. CES is a major source of litigation in neurosurgical practice. It is characterized by a central or large paracentral disc herniation most commonly at L4/5 which impinges on the cauda equina, specifically, the centrally orientated sacral nerve roots. Smaller disc herniations may result in CES in the setting of a congenitally narrow canal. Presentation may be acute over hours or chronic in the context of lumbar canal stenosis.

It is important to distinguish complete from incomplete lesions according to the degree of bladder and anal sensorimotor involvement. It is hypothesized that the smaller diameter preganglionic and sensory fibres of the sacral nerves are more prone to damage from mechanical compression and inflammation.

Clinical features include severe lower back pain, bilateral radicular leg pain (pain may be absent with an inferiorly displaced sequestered L5/S1 disc fragment), disturbance of urinary function (altered urinary sensation and poor stream), myotomal weakness, and saddle and genital sensory disturbance.

Complete lesions have a poor prognosis and are defined by a neurogenic bladder (insensate and distended secondary to low tone and inability to contract and coordinate sphincter function leading to retention and overflow incontinence). Loss of anal sphincter tone resulting in faecal incontinence, complete saddle, and genital anaesthesia with loss of trigonal sensation and sexual dysfunction is usually a late finding.

The timing of surgery has generated great controversy; the clinician must be pragmatic and act in the best interest of the patient, in the absence of class 1 evidence. It stands to reason that the sooner the cauda equina is decompressed the more likely the chance of recovery. A meta-analysis of 322 patients by Ahn et al. (2000) demonstrated optimal outcome when decompression is performed within 48 hours of the onset of symptoms. Decompression as soon as possible and certainly within 24 hours of the onset of symptoms seems intuitive and is generally accepted.

The standard operative approach is a bilateral laminectomy. In experienced hands, a large disc fragment can be removed through a hemilaminectomy and medial facetectomy, or laminotomy and fenestration, the advantage being preservation of midline structures, less muscle atrophy, and proposed reduction in postlaminectomy back pain. See **Figure 62.2**.

Back pain

Eighty per cent (80%) of people experience an episode of back pain in their lifetime. The majority experience non-specific back pain (NSBP) and will have some degenerative changes on imaging. NSBP is a diagnosis of exclusion and lacks features suggestive of radicular compression or serious underlying pathology. Pain is usually diffuse and may radiate to the thigh. NSBP is a benign, self-limiting condition. Causes of specific back pain that should be excluded include neoplasia, inflammatory disorders, infection, trauma, degenerative disease, and deformity.

Management involves exclusion of serious pathology and a holistic approach addressing the patient's health beliefs, expectations, avoidance behaviour, employment issues, and potential secondary gains.

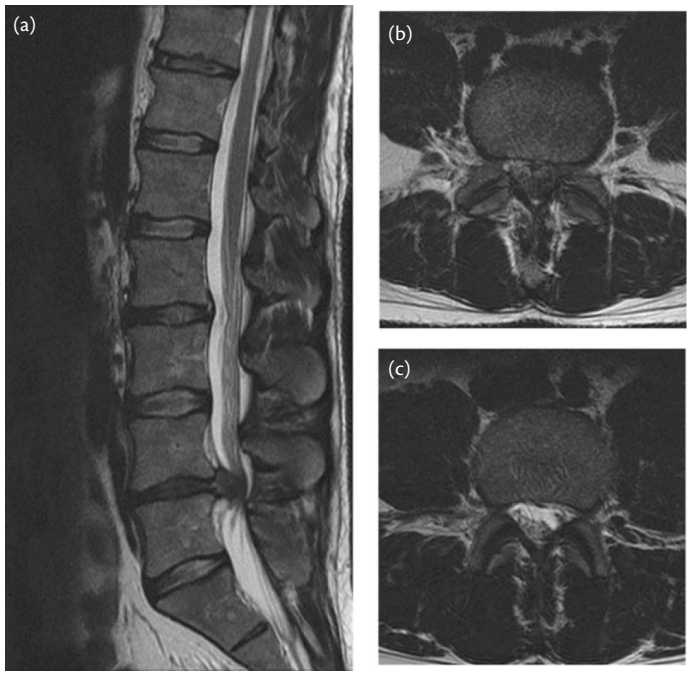

Fig. 62.2 (A) T2 sagittal: large L4/5-disc herniation and cauda equina compression; (B) T2 axial: complete obliteration of thecal CSF; (C) T2 axial: normal cross-section through lumbar canal for comparison.

Reassurance is paramount: by 12 weeks, 90% of individuals will be pain-free. Treatment is provided through a multidisciplinary approach and includes optimization of analgesia, referral to a pain specialist, regular exercise, physiotherapy, work conditioning programmes, and psychological evaluation if appropriate.

The disc, facet joints, and instability may be specific back pain generators that may respond to intervention

Lumbar disc disease

The lumbar disc supports most of the spinal load, acts as a highly efficient 'shock absorber' and withstands huge translational and rotatory forces. Mechanical failure occurs with age; a number of associated chemical and morphological changes are recognized including in the disc, loss of nuclear/annulus distinction and the ratio and distribution of type 1 to type 2 collagen changes, collagen cross-links break down which increases annular susceptibility to mechanical stress. Fissuring and deformation of the annulus, loss of sagittal/coronal disc height through deformation or resorption, nuclear matrix proteoglycan fragmentation, and disc dehydration all occur. There are reduced numbers of chondrocytes and an increased keratin/chondroitin sulphate ratio, neovascularization and neoinnervation by nerve fibres expressing substance P via hyperintensity zones, proinflammatory cytokines, increasing levels of lactate and decreased pH, which are all nociceptive.

In the vertebral end plate abnormal mechanical loading results in inflammation and Modic changes, calcification of the endplate occurs with reduction in blood supply and nutrient delivery. Increased susceptibility to mechanical stress occurs, which may be the basis for the development of Schmorl's nodes and limbus vertebrae.

Clinical features of disc disease include a deep central ache, pain referred to the anterior thigh or groin and exacerbation by loading the disc during flexion and when sitting for long periods.

MRI is the gold standard for the investigation of lumbar disc disease. In 1988 Modic classified endplate changes based on MRI signal characteristics (**Box 62.2**).

There has been renewed interest in Modic type 1 changes with infection being a potential aetiological factor for lower back pain. Albert et al. (2013) investigated the use of co-amoxiclav for 100 days in patients with back pain and Modic type 1 changes in a double-blind randomized control trial. Findings were encouraging and demonstrated a statistically significant improvement in disability indices in the antibiotic group versus the placebo group. See **Figure 62.3**.

Plain X-rays and CT are also of value demonstrating reduction in disc height, sclerosis, osteophytosis, and vacuum phenomenon. Lumbar disc stimulation may be used as an aid in selecting appropriate patients for fusion. Discs identified on MRI as potential pain generators are identified and injected. An MRI normal disc must be injected as a control during the study to ensure validity. In isolation,

Box 62.2 Modic changes

Type 1 (marrow oedema and inflammation)
- Low signal on T1 and high signal on T2

Type 2 (Fatty marrow transformation)
- High signal on T1 and T2

Type 3 (Subchondral bony sclerosis)
- Low signal on T1 and T2

Data from Modic MT, Steinberg PM, Ross JS, et al., Degenerative disk disease: assessment of changes in vertebral body marrow with MR imaging, *Radiology*, Volume 166, Issue 1, pp. 193–9, 1988 Radiological Society of North America.

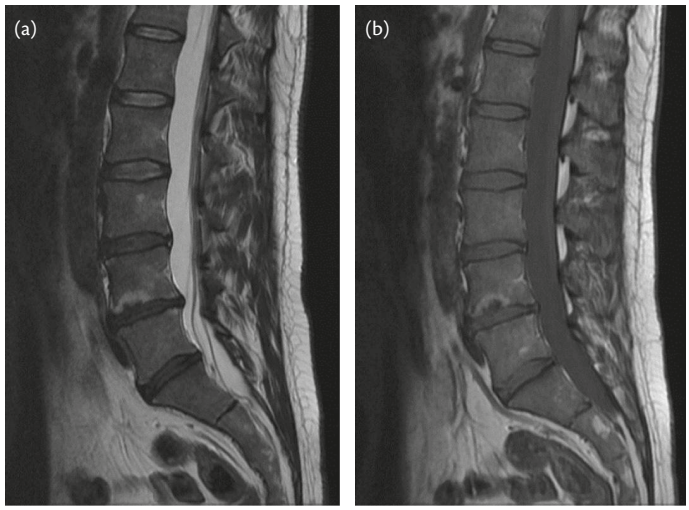

Fig. 62.3 (A) T2 sagittal MR and (B) T1 sagittal MR: type 2 Modic changes with associated Schmorl's node L4 inferior endplate.

there is poor correlation between symptoms and provocation discography. However, there is concordance with positive stimulation in the context of severe type 1 and 2 Modic changes. In addition, there is correlation between LBP and the severity of disc disruption described using the Dallas discogram scale. This is in keeping with the work by McNally et al. (1996) who demonstrated that discs with significant internal disruption transferring load solely to the annulus were painful.

Non-operative treatment options include optimal analgesia, referral to a pain specialist, physiotherapy, weight loss, regular exercise (core strengthening activities such as Pilates), and a trial of antibiotic therapy. Psychological assessment and counselling may also be appropriate.

Operative intervention is considered following failure of an adequate trial of conservative management. What constitutes an 'adequate' period of conservative management is open to interpretation and should not delay surgical intervention if it is felt that this is the best option for the patient.

Operative management of lumbar disc disease may include, non-instrumented fusion, instrumented fusion, disc arthroplasty, dynamic stabilization, intradiscal electrothermal therapy, or intradiscal delivery of biological agents and stem cell implantation.

Surgical management of lumbar disc disease

Non-instrumented fusion

Stand-alone non-instrumented fusion is rarely used today and a combination of 'bony' posterolateral fusion and pedicle screw (instrumented) fixation is recommended. In practice iliac crest is now rarely harvested secondary to the associated postoperative pain. Bone from the posterior elements and artificial bone substitute is now more commonly used. Posterolateral fusion is the gold standard procedure to which other non-fusion techniques are compared owing to its superior fusion rate and satisfactory clinical outcome (**Box 62.3**). The technique was first described in 1911 for the treatment of TB.

Posterior discectomy and interbody fusion can also be performed in combination with posterolateral fusion increasing fusion rates to almost 90% but with greater risk of neurological injury. There is no evidence to suggest anterior interbody fusion is superior to posterior approaches and has the additional risks of retrograde ejaculation and vascular injury.

Box 62.3 Posterolateral fusion: Key points

- Prone positioning with the lumbar spine in a neutral position
- Midline approach and wide subperiosteal muscle strip to expose the facet joints and transverse processes at the determined levels using fluoroscopy
- Decompression performed if necessary
- Decortication of the posterior elements as a fusion bed is achieved using a high-speed burr
- Posterior superior Iliac crest remains the graft of choice given its excellent osteogenic, osteoconductive, and osteoinductive properties. A combination of autologous bone chips harvested during decompression or bone graft substitute mixed with blood may also be used

Instrumented fusion techniques

Transpedicular fixation

Transpedicular fixation was introduced in the 1970s and has fast become the construct of choice because of its superior biomechanical stability over translaminar screws or laminar hook and clamp instrumentation (**Box 62.4**).

The technique affords the surgeon access to all three columns of the spine via the pedicle, the strongest bony structure in the spine. There is a steep learning curve but in experienced hands pedicle screws are associated with a low complication rate and, in comparison to non-instrumented fusion, provide superior fusion rates. Pedicle screws allow the surgeon to decompress widely if required without the risk of instability and the need for postoperative bracing.

Transpedicular screw fixation can be augmented with interbody fusion. Most commonly polyetheretherketone (PEEK) or carbon fibre cages are inserted following discectomy and preparation of the endplates. Iliac crest autograft and femoral ring allograft have also been described with good results. Interbody fusion can be achieved through posterior, posterolateral (transforaminal), lateral (extreme lateral) or anterior approaches. The advantages of interbody fusion are an increased fusion rate, restoration of alignment, and foraminal decompression through restoring disc space height, discectomy, and resection of endplate osteophytosis—see **Figure 62.4**.

The transforaminal approach (TLIF) involves resection of the facet and has the advantage of a unilateral approach, directly decompressing the segmental exiting and transiting nerve root with less neural retraction and blood loss. The extreme lateral approach (XLIF) is a minimally invasive transpsoas approach to the interspace with the patient in the lateral decubitus position. An interbody cage and lateral plate are used. Advantages are short operative time and minimal blood loss. This coupled with the ability to correct degenerative scoliosis make it an attractive option in older people. Intraoperative neurophysiology is mandated secondary to the risk of injury to the lumbar plexus. The L5/S1 interspace is not accessible secondary to obstruction by the ilium. The anterior approach (ALIF) has the advantage of preserving the posterior elements and maximal access and decompression with minimal risk to neural structures. Complications include increased risk of vascular injury and injury to the sympathetic chain resulting in retrograde ejaculation.

Box 62.4 Transpedicular screws: The Magerl technique

- Preoperative imaging and pedicle anatomy should be studied in detail. Vertebral anomalies may preclude screw placement (e.g. lumbar dysplasia and hypoplastic pedicles)
- The technique allows greater medialization and longer screw length than the Roy-Camille technique and therefore greater biomechanical strength
- With the patient prone and the lumbar spine in neutral alignment a midline approach and subperiosteal muscle strip is performed. A Wiltse paramidline muscle splitting technique can also be utilized which is less traumatic and results in less muscle atrophy and pain
- A wide exposure is performed to the transverse processes, allowing visualization of the pars and facet joint including the mamillary process. Care is taken to preserve facet joints at segments not involved in the fusion
- The entry point is at the intersection between a line bisecting the transverse process in the coronal plane and the inferolateral extent of the superior articulating facet in the sagittal plane
- This entry point allows a medial trajectory adjacent to the endplates
- A slightly lower entry point (lower one-third of the transverse process) and more superomedial trajectory is recommended for the upper screws of the construct so as not to impinge on the lower articulating facet of the caudal vertebrae not involved in the fusion
- The degree of medialization required increases from L1 to S1 from 15 to 30°. AP and lateral fluoroscopy should be used
- A laminotomy allows a probe to be inserted into the canal to palpate for medial breach as the screw is advanced
- Decortication as for non-instrumented fusion provides a bony fusion bed for autologous or substitute bone graft in the intertransverse trough
- Rods cut to length and contoured for lordosis are placed in-situ and secured with blockers screwed down on to the head of the screw and tightened. Polyaxiality of the screw head allows for ease of placement of the rod, regardless of angle
- Care should be taken not to trap muscle in the construct which leads to necrosis and pain

Complications

- Loss of purchase/pedicle fracture and screw breakout
- Screw misplacement
- Neurological injury
- Dural tear
- Adjacent level disease
- Vascular injury

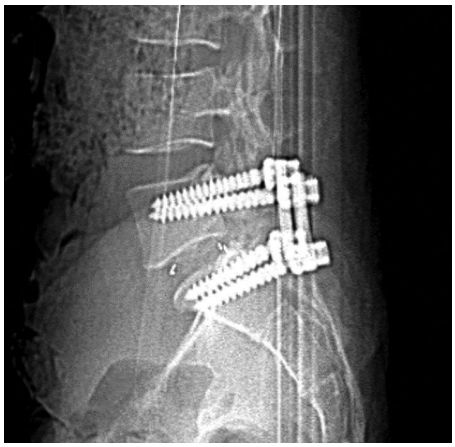

Fig. 62.4 Postoperative X-ray following posterior lumbar interbody fusion.

Disc arthroplasty

Fernstrom was the first to perform lumbar arthroplasty in the 1950s using the Fernstrom ball. The 1980s marked the development of the modern disc replacement with the SB Charité and ProDisc-L designs. The replacement is based on metal endplates sliding over a plastic ball-and-socket type core. The approach is retroperitoneal with associated complications as for ALIF. Contraindications include obesity, trauma, iatrogenic instability of the posterior elements, spondylolisthesis greater than grade 1 lytic pars osteoporosis, and trauma. Severe facet arthropathy is a relative contraindication. Level one evidence from FDA-regulated studies of Charité and ProDisc-L implants (Blumenthal et al., 2005; Zigler et al., 2007), reveals equivalent and, in some respects, superior clinical outcomes in the short to medium term when compared to fusion. David (2007) reports long-term clinical outcomes to be equivalent to fusion but with lower complication rates and a reduced incidence of adjacent segment disease. Lumbar disc arthroplasty is approved by NICE, clinicians are urged to publish their experiences. The longer-term outcome and life span of these implants is still not known.

Dynamic stabilization

Dynamic stabilization is based on off-loading the motion segment while maintaining the range of movement and reducing adjacent segment disease. Clinical outcome data remains modest and to date long-term follow-up does not exist.

Facet joint arthropathy

The facet joints support 20% of the spinal load. Segmental degeneration increases loading of the facets and arthropathy. Some evidence suggests that the more sagittal orientation of the lower lumbar facets and facet isotropy is associated with accelerated degeneration, instability, deformity, and pain. The pathological changes seen in facet degeneration include cartilaginous thinning and fibrillation, effusions, capsule laxity, joint subluxation osteophytosis, and synovial hypertrophy with cyst formation.

Facet arthropathy is best appreciated on CT. Weishaupt has devised a grading system to describe the severity of facet arthropathy based on CT and MR appearances. Single-photon emission computed tomography (SPECT) may aid in localizing active disease when MR and CT reveal multilevel degenerative changes. Facet effusions on MRI correlate with SPECT activity.

Clinical features include stiffness in the morning which improves with activity, pain is exacerbated on extension and twisting movements. Pain may be referred to the groin, buttock, or posterior thigh, and there may be localized paraspinal tenderness.

Conservative management including spinal injections performed by a pain specialist are the mainstay of treatment. Medial branch blockade (MBB) is superior to intra-articular injections. Injections should be performed on multiple occasions to increase diagnostic validity. There is some evidence to suggest that a positive response to MBB is predictive of a good response to radiofrequency ablation. Limited data suggests that radiofrequency ablation provides short- and long-term relief of facet mediated pain in selected patients.

Instability

'Instability' remains an enigmatic concept; it is the most controversial of the pain syndromes given the normal range of lumbar movement

and abnormal movement observed in asymptomatic individuals. It is more likely that abnormal movement results in abnormal loading of the annulus and vertebral endplate (pain generators) increasing demands on the spinal musculature and tendinous attachments, fatigue, and pain.

Clinical features include the back 'giving way', pain increased with sudden trivial movement and the back 'locking' and 'catching' on movement with associated muscle spasm

Anecdotal reports exist of lumbar back pain associated with instability demonstrated by abnormal translation and angulation on dynamic X-rays. Therapy is focused on improving core strength. Dynamic stabilization devices have been shown to alter the loading pattern which may explain their equivalent efficacy with fusion in the short term.

Injection therapy

Epidural Injections

Epidural corticosteroid injections are an effective adjunct for short-term relief of lumbar and radicular pain. A combination of steroid and short acting local anaesthesia is injected which address the inflammatory component of radicular pain. There is no evidence to suggest long-term efficacy. Lumbar epidural injections can be performed via an interlaminar approach above the level of interest or caudally via the sacral hiatus.

Indications for lumbar epidural injections include lumbar canal stenosis, multilevel involvement, non-specific pain, lumbar back pain with an acute annular tear and poor surgical candidates. Complications include abscess, arachnoiditis, epidural haematoma, CSF fistula, and paraparesis.

Selective nerve root block injections

Selective nerve root blockade is an effective diagnostic and therapeutic procedure used when there is lack of radiological and clinical concordance in determining or excluding a surgical target. In addition, they may be used for short-term pain relief in subacute radiculopathy in the absence of a neurological deficit. Periprocedural imaging (CT is used at the authors' institute) is essential to enter the 'safe triangle' inferior to the pedicle and superolateral to the nerve root. Complications include an increase in pain, nerve root damage, permanent neurological deficit, CSF fistula, and abscess.

Spondylolisthesis

The Greek word 'olisthanein' means to slip, and Killian coined the term 'spondylolisthesis' in 1854. Spondylolysis indicates a defect in the pars interarticularis which may lead to spondylolisthesis. Spondyloptosis refers to severe slippage and complete malalignment of the vertebral bodies. The disease was first described by the Belgian obstetrician Herbinaux in 1782, while in 1976 Wiltse, Newman, and MacNab proposed their widely accepted aetiological classification (Box 62.5).

The Meyerding classification published in 1932 describes the degree of slippage where grade 1 is 1–25%, grade 2 is 26–50%, grade 3 is 51–75%, grade 4 is 76–100%, and grade 5 is spondyloptosis.

Box 62.5 Spondylolisthesis

- **Isthmic Most common at L5/S1**
  - **Type A**—Defect in pars
  - **Type B** —Healed defect with elongation of pars
  - **Type C**—Acute bilateral fracture
- **Degenerative Most common at L4/5**
  - Disc and facet degeneration
- **Dysplasia**
  - Dysplasia of L5/S1 junction
    - Wedging of small dysplastic L5
    - Dome-shaped upper S1 vertebral border
    - Horizontal orientation of L5/S1 facets
    - Mimics isthmic type
- **Traumatic**
  - Aihara classification
- **Pathological**
  - Metabolic bone disease
  - Connective tissue disease
  - Infection
  - Neoplasia

Reproduced with permission from Leon Wiltse, P. Newman, and Ian MacNab, Classification of Spondylosis and Spondylolisthesis, *Clinical Orthopaedics and Related Research*, Volume 117, pp. 23–9, Copyright © 1976 Wolters Kluwer Health, Inc.

Isthmic spondylolisthesis (spondylolysis)

The pars interarticularis acts as a conduit connecting the neural arch to the vertebral body via the pedicle. If disconnected the vertebral body and the superior spine have the potential to drift away from the corresponding inferior articulating process and superior articulating facet of the vertebral body below. Given the enormous stress placed on the pars it is surprisingly one of the weakest bony structures in the spine.

The pars defect develops in late childhood and becomes established in adolescence or early adulthood. It most commonly occurs at the L5/S1 segment. The proposed aetiology is repeated mechanical stress resulting in fatigue and fracture of the inferomedial cortex of the pars with superolateral propagation. Isthmic fatigue fractures are well recognized in athletes and heal with conservative management. Non-union leads to the type A form with fibrous tissue spanning the fracture. Remodelling, elongation, and union results in the type B form. Less than 20% of patients with spondylolisthesis progress and develop symptoms. The isthmic type has a greater propensity to slip than the degenerative type. Some authors believe slip angle (the angle defined by the intersection of two lines drawn from the superior endplate of S1 and inferior endplate of L5) predicts progression. Clinical observation with standing lateral X-rays is recommended.

The clinical features include dull central back pain at the level of the slip exacerbated by exercise, a bony step-off at the level of the slip, increased lumbar lordosis, flattened buttocks, a waddling gait disturbance, posterior thigh pain, tightening, and spasms of the hamstrings, radicular pain (L5 most commonly secondary to compression by the isthmic fibrocartilaginous mass) but central compression, neurogenic symptoms, and cauda equina syndrome are rare. Phalen-Dixon sign presents with sciatic crisis, hamstring spasm, gait, and postural abnormality in the young patient; weakness of the extensor hallucis longus or ankle dorsiflexion are rare.

Management

Treatment options include conservative management such as optimal pain management including referral to a pain specialist, restriction of physical activity, bracing, and physiotherapy. Indications for surgical management include severe pain despite an adequate trial of conservative measures, progressive neurological deficit, and progressive slip and a high slip angle.

Surgical options include direct repair of the pars defect with a pars screw, autologous bone graft to the defect site, radical decompression of nerve roots followed by posterolateral (instrumented or non-instrumented) or interbody fusion, or wiring of the transverse processes and non-instrumented fusion with autologous bone graft.

In cases of significant radicular symptoms, decompression as described by Gill involves removal of the loose posterior elements, the hypertrophic fibrocartilaginous mass, and total facetectomy. Fusion following decompression of isthmic spondylolisthesis is recommended. Caragee (1997) reports a higher rate of pseudarthrosis and worse outcomes with decompression alone. It is controversial as to whether instrumentation in addition to fusion improves outcome but obviates the need for postoperative bracing.

In the absence of radicular symptoms decompression is not necessary and fusion can be performed through a midline approach or using the Wiltse technique: following a midline skin and fascial incision, bilateral paraspinal fascial incisions are made overlying the groove produced by multifidus medially and longissimus laterally. Using a combination of muscle splitting and sharp dissection, this plane allows access to the pars, transverse processes, and facet joints for fusion and instrumentation.

Instrumented fusion can be achieved through pedicle screw fixation or interbody fusion. Both techniques are equivalent in terms of outcome and do not reduce the rate of pseudarthrosis. Some authors believe that fusion improves radicular symptoms secondary to reduced instability and radicular irritation. Pedicle screw fixation has the additional advantage of enabling reduction of the spondylolisthesis. It is purported that reduction improves the rate of fusion but is associated with a higher rate of nerve root injury. See Figure 62.5.

Degenerative spondylolisthesis

Degenerative spondylolisthesis is seen in the middle aged and elderly population secondary to degenerative disc disease which puts additional strain on the facet joints. It is more common in females and patients of African descent. It occurs most frequently at L4/5, this may be related to the sagittal orientation of the L4/5 facets in comparison to the coronal orientation of the L5/S1 facets which resist anterior translation. Presentation is similar to that of lumbar canal stenosis and radicular pain resulting from compression of the L5 nerve roots by the slipped inferior articulating process, hypertrophied facet, and a rolling broad-based disc. Cauda equina syndrome is rare but may present subacutely with a coexisting acute disc herniation. The natural history suggests that this is a relatively benign condition, progression rates are as low as 25% with slippage rarely progressing beyond one Meyerding grade.

Non-operative treatment involves effective pain management and physiotherapy. Epidural or perineural blockade may be of use when radicular symptoms exist. Surgical management is considered in symptomatic patients following an adequate trial of optimal conservative measures. Several studies suggest superior functional and pain outcomes in surgical versus medically treated patients. See Figure 62.6.

Fig. 62.5 A and B sagittal T2 MRI. (A) Hypoplastic L5 and grade 1 isthmic olisthesis; (B) L5 isthmolysis clearly demonstrated.

The decision to decompress alone or decompress and fuse in the context of a degenerative spondylolisthesis remains controversial and should be based on individual factors such as age, comorbidities, bone quality, back pain suggestive of instability, dynamic radiographs, degree of slip, and intraoperative findings of segmental instability.

Spinal synovial cysts

These relatively rare cysts are associated with spondylosis and are most commonly an incidental finding. They most commonly occur at L4/5 but are also found in the cervicothoracic spine. It is hypothesized that abnormal movement results in myxoid degeneration and synovial hypertrophy.

Histologically, the cyst wall may or may not be lined by synovium (ganglion cyst); however, this is a purely academic point. Presentation is usually radicular in nature with small cysts causing compression in the subarticular space. Occasionally there may be an acute deterioration secondary to haemorrhage into the cyst and rarely cauda equina syndrome. They may spontaneously regress.

These cysts can usually be differentiated from other lesions according to their MR characteristics and location. The differential diagnosis includes nerve sheath tumours, a herniated disc fragment, or intradural disc fragment, a meningeal cyst, arachnoid herniation, perineural cyst, or metastatic deposit.

It is important that these cysts are recognized as they may inadvertently be drained during the surgical approach and erroneously be diagnosed as a herniated disc fragment. MR characteristics can vary according to the cyst composition and whether haemorrhage is present. Calcification of the cyst wall appears low intensity on T1 and T2, haemorrhage is hyperintense on T1. The cyst may clearly communicate with the facet joint space which differentiates it from neural associated cysts. On contrast injection the cysts may display peripheral enhancement.

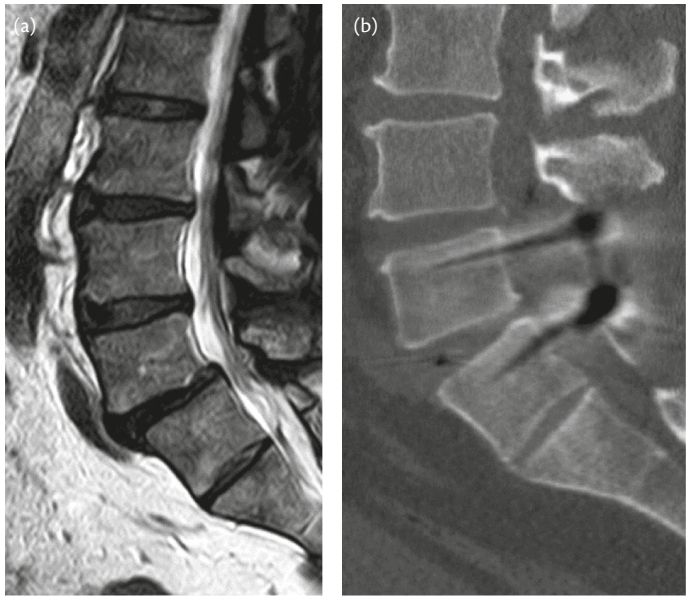

Fig. 62.6 (A) T2 sagittal MR showing a grade 1 spondylolisthesis; (B) postoperative CT in the same patient shows reduction of spondylolisthesis following posterior interbody fusion.

Management

The existing literature consists of small case series. Following an adequate trial of conservative management including optimal analgesia, facet, and targeted perineural injections, surgery is considered. The standard approach is open cyst extirpation and foraminotomy +/– fusion. The risk of recurrence is approximately 2% with decompression alone. Fusion is associated with a lower rate of recurrence and should be considered in patients who have clinical or radiological evidence of segmental instability. Minimally invasive resection and aspiration has been described but with an increased recurrence rate. See Figure 62.7.

Spinal meningeal cysts

These rare CSF containing thin walled cysts may exist as diverticulae of arachnoid, dura, or the nerve root sheath within the lumbar spine and are usually incidental findings on MRI. They can be classified according to Nabor (see Box 62.6).

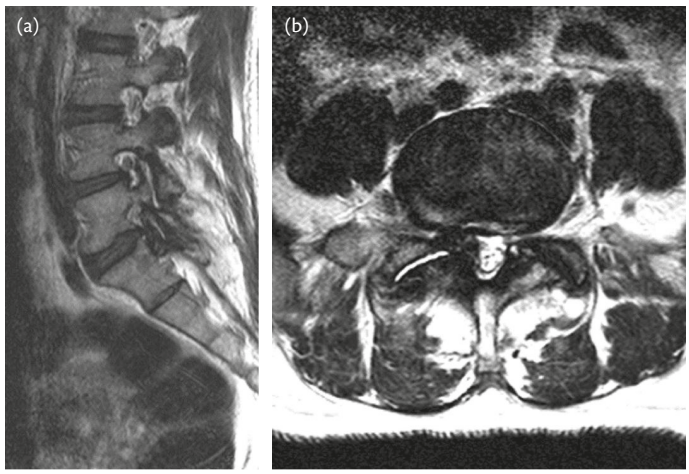

Fig. 62.7 T2 MRI sagittal (A) and axial (B) images showing right L5/S1 lateral recess stenosis secondary to a synovial cyst.

Box 62.6 Spinal meningeal cysts

- Type 1—Extradural meningeal cyst without neural tissue
  - Type 1a—Extradural spinal arachnoid cyst
  - Type 1b—Sacral meningocele
- Type 2—Extradural meningeal cyst containing neural tissue (Perineural/Tarlov cysts)
- Type 3—Intradural arachnoid cysts

Source data from Nabors MW, Pait TG, Byrd EB et-al. Updated assessment and current classification of spinal meningeal cysts. *J. Neurosurg.* 1988;68 (3): 366-77.

Tarlov cysts (Nabor type 2)

The estimated prevalence is between 5% and 9% of the population with most cysts being an incidental finding arising most commonly in association with the S2 and S3 nerve roots. There is often remodelling of the sacrum. The aetiology is unknown but is likely to incomplete obliteration of the perineural space and CSF pulsatility. They arise between the endo- and perineurium at the junction of the nerve root and the dorsal root ganglion (DRG) encompassing or invading the nerve root with compressed nerve fibres forming part of the cyst wall. There is a potential communication with the subarachnoid space in comparison to meningeal diverticulae which occur proximal to the DRG and communicate freely with the subarachnoid space. Examination with CT myelography reveals late or no filling whereas other meningeal cysts fill early.

Rarely cysts can exert mass effect and present with pain which is exacerbated by Valsalva manoeuvres. Sacral insufficiency fractures have been described secondary to scalloping of the sacrum.

While normally asymptomatic, clinical features can include progressive sacral radicular pain, numbness, and paraesthesia, poorly localized sacral, perineal, or rectal pain, and bowel, bladder, and sexual dysfunction.

Non-surgical management involves optimal pain management. Anecdotal reports suggest CSF drainage provides temporary relief of symptoms. Rarely, surgery is considered in patients with progressive symptoms despite optimal pain management. There are case reports describing CT guided injection with fibrin sealant and lumbo-peritoneal or cysto-subarachnoid shunting with good results. Definitive management involves sacral laminectomy, cyst fenestration/resection and closure with a sacrospinalis myocutaneous flap. Intraoperative electrophysiology is recommended.

Sacroiliac disease

The sacroiliac (SI) joint is a synovial and fibrous joint between the ilium and sacrum which transfers weight from the axial to appendicular skeleton. Movement involves minor rotatory and gliding movements. Ligamentous laxity commonly results in SI related pain during pregnancy. Sacroiliitis is the manifestation of a wide range of diseases and may mimic lumbar spine pathology. Common symptoms include lower back, buttock, and thigh pain, exacerbated by sitting for long periods. The New York criterion offers a grading system based on the degree of sclerosis and ankylosis on plain X-ray. Stigmata of systemic disease should be sought during history and

examination. The diagnosis is obtained through positive provocative distraction and compression manoeuvres on examination and pathognomonic changes on plain X-ray. The pattern of involvement offers clues to the underlying aetiology (symmetrical and bilateral, asymmetrical and bilateral, or unilateral). The differential includes the inflammatory athritides, infection, and neoplasia.

Management involves treatment of the underlying aetiology, effective pain management, SI joint injections, and physiotherapy. Arthrodesis is considered in patients with progressive and incapacitating pain resistant to an adequate trial of optimal conservative therapy.

Coccydynia

Coccydynia refers to pain around the region of the coccyx. It is exacerbated by sitting for long periods and on rising from a sitting position. The exact incidence is unknown, but risk factors appear to be obesity and female sex. It is sufficiently rare in males to warrant further investigation for serious underlying pathology. There is pinpoint tenderness on examination. Rectal examination allows assessment of coccygeal range of movement which may be hypo or hypermobile.

Aetiologies include osteoarthritis, local trauma, hypermobility, Infection, pelvic inflammatory disorders/chronic infection, and neoplasia (local primary bone tumours, nerve sheath tumours, direct spread from pelvic tumours or metastatic disease). Ninety per cent (90%) of cases resolve with conservative treatment. This involves non-steroidal anti-inflammatory drugs (NSAIDs), lumbar supports which encourage lordosis and specially designed cushions to reduce pressure on the area. Manipulation may reveal a dislocated coccyx and prove therapeutic.

Other options include local corticosteroid injections, caudal epidural corticosteroid injections, sympathetic blockade, or coccygectomy (variable success and should only be considered once conservative measures have been exhausted).

Failed back syndrome and management of postoperative complications

'Failed back syndrome' refers to a patient population who fail to improve to a satisfactory degree following spinal surgery. The term does not imply negligence, more that the patient has persistent pain beyond what is expected, and that this may be incapacitating and prevent return to work. When a poor surgical outcome is encountered, three questions should be asked: Was this the correct operation? For example, decompression alone in a patient with degenerative spondylolisthesis experiencing increasing back pain postoperatively. Was it the correct diagnosis? For example, performing lumbar surgery in the context of hip and knee pathology or cervical surgery in the context of shoulder pathology or coexisting ulnar or median nerve neuropathy. Medical conditions such as diabetes, vasculitis, and nutritional deficiency resulting in neurological dysfunction should always be borne in mind. Finally, was this the correct management for this particular patient? For example, it is important to assess the patient's level of motivation, expectations, psychological well-being, and be aware of potential secondary gains and litigation.

This algorithm may aid in reflective practice, however, there will be occasions when poor outcomes are beyond the control of the clinician. Recurrent or ongoing axial and radicular pain may be due to residual compression (retained disc and osteophytes), recurrent disc herniation, adjacent segment disease, peridural scar formation and fibrosis, postoperative discitis (infective and aseptic), pseudomeningocele formation, epidural haematoma, arachnoiditis, permanent nerve root injury, and operative damage following retraction or inadvertent durotomy, conjoined nerve roots (compression at an adjacent level to that operated), progressive spondylosis and instability, failure to appreciate sagittal imbalance resulting in muscular fatigue and deformity, coexisting myofascial syndrome, and complex regional pain syndrome.

It is important to ascertain the nature of pain. Burning pain is characteristic of neuropathic pain secondary to nerve damage and includes complex regional pain syndrome. This type of pain is best treated with neuropathic agents and referral to a pain specialist. Neuromodulation in the form of spinal cord stimulation may also be considered.

Sagittal imbalance (flat back/lumbar kyphosis) is corrected through the action of the back extensors and increased pelvic tilt resulting in pain and fatigue. Pain can be incapacitating, and deformity can have psychosocial implications secondary to poor self-image and deficient horizontal gaze. Correction of fixed deformity can be achieved through aggressive surgical techniques, such as the Smith–Peterson osteotomy and pedicle subtraction osteotomy.

Inadvertent durotomy and pseudomeningocele

Durotomy is a common occurrence with an incidence of approximately 15%. There is a strong association with revision surgery. In itself, it rarely results in morbidity however, there are several possible complications that may ensue including nerve root or cauda equina injury (contusion or laceration), persistent CSF leak (pseudomeningocele or CSF fistula), meningitis, arachnoiditis, and chronic headache.

It is more common during revision surgery owing to the formation of scar tissue and loss of identifiable tissue planes. The dura may be extremely thin in older people with chronic stenosis predisposing to injury. The underlying pathology may result in the dura or nerve root sleeve lying in an unexpected location. Accidental slippage of instruments and an obscured fold of dura caught in the Kerrison are common causes. The surgeon should be careful to round off any bony spikes left by the Kerrison as this can be a source of delayed CSF leak.

Management involves microscopic primary repair (e.g. with 5/0 Prolene or staples). Care should be taken to avoid lacerating or encompassing nerve roots in the suture line. If the durotomy is small, herniation of nerve roots makes it difficult to close the dura. In this case the durotomy should be lengthened and a cottonoid used to protect the nerve roots during the closure. If the durotomy is anterior the dura can be opened dorsally and an intradural repair made. Occasionally it is impossible to close the dura if the nerve root sleeve is involved or there is a large defect and closure may entrap the cauda equina. In this scenario the patient's blood, fat, or muscle can be used as graft material. The use of layered Surgicel, a crushed

muscle patty and coagulated blood, or a fibrin sealant such as Tisseel is favoured by the author.

Postoperative orders include a period of flat bed rest of usually 3–5 days. If the dural opening is small and the arachnoid remains intact with no CSF leak, then it is reasonable not to impose a period of bed rest following primary repair. The use of wound and lumbar drains is controversial and is essentially down to the surgeon's preference. Thromboembolic prophylaxis is prudent for patients on bed rest.

A contained CSF collection is termed a pseudomeningocele. Tense collections may lead to wound breakdown, CSF fistula, and infection. Symptoms include low pressure headache, back pain, and radicular symptoms. MR imaging is an essential investigation. If seroma or infection are suspected, then needle aspiration is warranted and the sample sent for MC&S. CSF can be distinguished from seroma using the beta-2 transferrin biomarker. A trial of lumbar drainage is reasonable with symptomatic pseudomeningocele. Definitive repair requires open repair as described earlier (+/– lumbar drainage). MR (fat suppression sequences), MR, CT, and digital subtraction myelography are useful when repair fails and the site of durotomy is difficult to identify. In recurrent cases plastics consultation for consideration of flap reconstruction is recommended.

Postoperative discitis

This is a rare event with an incidence of approximately 1%. Eighty per cent (80%) of cases present within the first month of surgery. Risk factors include older people, diabetes, immunosuppression, and concomitant systemic infection.

Clinical features include moderate to severe back pain and spasm, fever, a limited range of movement and point tenderness but radicular symptoms are rare and few patients will have an associated wound infection.

There are reports of aseptic or chemical discitis following surgery. The clinician should be guided by infective blood markers such as white cell count (WCC) (neutrophilia), CRP, and erythrocyte sedimentation rate (ESR) in addition to positive imaging findings. MR appearances suggestive of infection include enhancing prevertebral and epidural collections in association with disc enhancement and endplate oedema.

Blood cultures should be obtained. Needle biopsy of the disc in question provides positive microbiology in approximately 40% of cases. *Staphylococcus epidermidis* and *aureus* are most commonly implicated along with Gram-negative species and *Streptococcus*. Anaerobes, TB, and fungi are less common. Infective parameters should be followed weekly until stabilized or normal.

Positive cultures guide therapy. Intravenous (IV) antibiotics with antistaphylococcal action are administered for a minimum of 6 weeks (this can be performed in the community in some cases). If infective indices have responded a change to oral therapy (e.g. Flucloxacillin and fusidic acid) may be instituted for a further prolonged period advised by microbiology. Prior to termination of treatment a further enhanced MRI scan may be performed for comparison. In resistant cases discectomy and washout is considered. This can be performed through open or minimally invasive approaches.

Outcomes are variable according to the literature. Approximately 80% show a significant improvement in back pain, this is similar to the outcome following lumbar disc surgery.

Adhesive arachnoiditis

Arachnoiditis involves all three layers of the meninges. Inflammation results in clumping of the nerve roots. It is proposed that the adhesive process reduces blood and CSF flow to the nerve roots in addition to mechanical insult from tethering. Enhancement on MR suggests an acute process exists which should prompt further investigation and surveillance particularly if there is uncertainty regarding the underlying aetiology. Three patterns are observed on MRI namely central adhesion and the development of central cords, adherence of the nerve roots to the theca giving the appearance of an empty thecal sac and CSF is replaced by inflammatory tissue (block and 'dripping candle wax' sign on CT myelography).

It is occasionally associated with degenerative disease, and in this context is usually an incidental finding. Arachnoiditis secondary to trauma is commonly associated with the formation of syringes. The risk factors for developing arachnoiditis are inadvertent durotomy and CSF leak, the presence of blood products in the thecal sac, infection, trauma, spinal anaesthesia, previous use of oil-based contrast agents, and neoplasia.

Radicular pain related to arachnoiditis carries a poor prognosis. Treatment is aimed at symptomatic relief through a comprehensive pain management regime, physiotherapy, and psychological support. The results of surgery are disappointing and involve removal of constrictive extradural scar tissue and foraminotomies if felt beneficial.

Management of recurrent lumbar disc herniation

The strict definition of a recurrent LDH is the recurrence of pain following a minimum pain-free period of 6 months secondary to an ipsi- or contralateral disc herniation at a previously operated level. The rate of recurrence is reported as between 5% and 12%. The differential diagnosis includes progressive perineural fibrosis and arachnoiditis.

Pre- and postcontrast MR imaging of the lumbar spine provides valuable diagnostic information. Perineural scarring enhances as opposed to herniated nucleus pulposus and clues such as retraction of the theca and nerve root towards the lesion suggests fibrosis and conversely thecal displacement indicates a recurrent herniated fragment. There is no evidence to suggest whether conservative sequestrectomy or annulus incision and more aggressive discectomy at the primary operation affects recurrence rate.

A careful history should be taken and the nature of the pain clarified. Pain of a diffuse burning nature suggests neuropathic pain and does not respond to surgery. As a proposed hypothesis perineural fibrosis may result in constriction of the nerve root, chronic ischaemia, and nerve damage.

The risks of durotomy with reoperation are as great as 20% with additional increased risk of neural injury. Some authors would therefore advocate a more aggressive approach involving facetectomy ipsilateral to the disc herniation approaching from lateral and using virgin tissue planes to work medially towards the disc herniation

and area of nerve root impingement. This approach mandates instrumented fusion +/– interbody fusion with claims that this also reduces the risk of further recurrence.

The systematic review by Dower et al. (2016) concludes that there is no evidence to suggest routine fusion in the management of recurrent LDH results in improved outcome. Therefore, a pragmatic and individualized approach is recommended, if there are clinical or radiological features of segmental instability, then fusion should be considered. Likewise, intraoperatively, if fibrosis is extensive and facetectomy is considered, the surgeon should be prepared to fuse the segment.

Experience with endoscopic and minimally invasive surgery (MIS) in the spine is evolving with approaches such as endoscopic transforaminal lumbar discectomy, MIS transforaminal lumbar interbody fusion and percutaneous pedicle screw fixation. It will prove interesting to follow the long-term durability of these techniques in the future.

Degenerative spondylolisthesis with radicular symptoms: Decompression alone versus decompression and fusion (instrumented versus non-instrumented)

Progression of spondylolisthesis following decompression alone has been reported to be as great as 50% with recurrence of symptoms. Preoperative flexion-extension lateral lumbar spine X-rays do not predict instability but may occasionally demonstrate abnormal translation (greater than 4 mm). The meta-analysis by Mardjetko (1994) reported improved clinical outcomes with decompression and fusion (instrumented and non-instrumented) versus decompression alone. The meta-analysis and systematic review by Gibson and Waddell (2005), confirmed improved fusion rates, minimally superior clinical outcomes, and a higher complication with instrumentation versus non-instrumented fusion. The Spine Patient Outcomes Research Trial (SPORT) found no significant difference in outcome when comparing the various different fusion techniques.

FURTHER READING

Ahn, U.M., Ahn, N.U., Buchowski, J.M., Garrett, E.S., Sieber, A.N., & Kostuik, J.P. (2000). Cauda equina syndrome secondary to lumbar disc herniation: a meta-analysis of surgical outcomes. *Spine*, **25**(12), 1515–22.

Caragee, E.J. (1997). Single level posterolateral arthrodesis with or without posterior decompression for the treatment of isthmic spondylolisthesis in adults: a prospective, randomised study. *J Bone Joint Surg*, **79A**, 1175–80.

Kirkaldy-Willis, W.H., Wedge, J.H., & Yong-Hing, K. (1978). Pathology and pathogenesis of lumbar spondylosis and stenosis. *Spine*, **3**, 319–28.

Panjabi, M.M. (1992a). The stabilizing function of the spine. Part I. Function, dysfunction, adaption and enhancement. *J Spinal Dis*, **5**(4):383–9; discussion 397.

Panjabi, M.M. (1992b). The stabilizing funtion of the spine. Part II. Neutral zone and instability hypothesis. *J Spinal Dis*, **5**(4), 390–6; discussion 397.

REFERENCES

Ahn, U.M., Ahn, N.U., Buchowski, J.M., Garrett, E.S., Sieber, A.N., & Kostuik, J.P. (2000). Cauda equina syndrome secondary to lumbar disc herniation: a meta-analysis of surgical outcomes. *Spine*, **25**(12), 1515–22.

Albert, H.A., Sorensen, J.S., Christensen, B.S., & Manniche, C. (2013). Antibiotic treatment in patients with chronic low back and vertebral bone oedema (Modic type 1 changes): a double-blind randomised trial of efficacy. *Eur Spine J*, **22**(4), 697–707.

Blumenthal, S., McAfee, P.C., Guyer, R.D., et al. (2005). A prospective, randomised, multicentre Food and Drug Administration investigational device exemptions study of lumbar total disc replacement with the CHARITE artificial disc versus lumbar fusion. Part 1: evaluation of clinical outcomes. *Spine*, **30**, 1565–75.

Caragee, E.J. (1997). Single level posterolateral arthrodesis with or without posterior decompression for the treatment of isthmic spondylolisthesis in adults: a prospective, randomised study. *J Bone Joint Surg*, **79A**, 1175–80.

David, T. (2007). Long-term results of one-level lumbar arthroplasty: minimum 10-year follow up of the CHARITE artificial disc in 106 patients. *Spine*, **32**, 816–23.

Dower, A., Chatterji, R., Swart, A., & Winder, M.J. (2016). Surgical management of recurrent lumbar disc herniation and the role of fusion. *J Clin Neurosci*, **23**, 44–50.

Gibson, J.N. & Waddell, G. (2005). Surgery for degenerative lumbar spondylosis. *Cochrane Database Syst Rev*, **19**(4), CD001352.

Kirkaldy-Willis, W.H., Wedge, J.H., & Yong-Hing, K. (1978). Pathology and pathogenesis of lumbar spondylosis and stenosis. *Spine*, **3**, 319–28.

Mardjetko, S.M., Connolly, P.J., & Shott, S. (1994). Degenerative lumbar spondylolisthesis. A meta-analysis of literature 1970–1993. *Spine (Phila Pa 1976)*, **19**(20 Suppl), 2256S.

McNally, D., Shackleford, I.M., Goodship, A.E., & Mulholland, R.C. (1996). *In vivo* stress measurement can predict pain on discography. *Spine*, **15**, 2580–7.

Moojen, W.A., Arts, M.P., Jacobs, W.C.H., et al. (2013). Interspinous process devise versus standard conventional surgical decompression for lumbar spinal stenosis: randomised control trial. *BMJ*, **347**, f6415.

Panjabi, M.M. (1992a). The stabilizing function of the spine. Part I. Function, dysfunction, adaption and enhancement. *J Spinal Dis*, **5**(4):383–9; discussion 397.

Panjabi, M.M. (1992b). The stabilizing function of the spine. Part II. Neutral zone and instability hypothesis. *J Spinal Dis*, **5**(4), 390–6; discussion 397.

Schmorl, G. & Junghanns, S.A. (1971). *The Human Spine in Health and Disease*., New York, NY/London, UK: Grune and Stratton.

Zigler, J., Delamarter, R., Spivak, J.M. et al. (2007). Results of the prospective, randomised, multicenter Food and Drug Administration investigational device exemption study of the ProDisc-L total disc replacement versus circumferential fusion for the treatment of 1-level degenerative disc disease. *Spine*, **32**, 1155–62.

RELATED LINKS TO EBRAIN

Coccydinia. https://learning.ebrain.net/course/view.php?id=804

Diagnosis and Treatment of Back Pain. https://learning.ebrain.net/course/view.php?id=1037

Management of Lumbar Disc Prolapse and Cauda Equina Syndrome. https://learning.ebrain.net/course/view.php?id=783
Performing a Lumbar Laminectomy. https://learning.ebrain.net/course/view.php?id=1118
Performing a Lumbar Microdiscectomy. https://learning.ebrain.net/course/view.php?id=413
Sacroiliac Joint Pain. https://learning.ebrain.net/course/view.php?id=814
Spondylolisthesis. https://learning.ebrain.net/course/view.php?id=1039
Spondylolysis. https://learning.ebrain.net/course/view.php?id=811
Surgical Treatment of Chronic Low Back Pain. https://learning.ebrain.net/course/view.php?id=812

63

Spinal tumours

John Brecknell and Boon Leong Quah

Diversity

For the spinal neurosurgeon, the range of pathologies, clinical presentations and required surgical techniques included within the management of spinal neoplasia is vast, from benign lesions unchanged over a decade of observation to malignant disease that progresses over a few hours to paraplegia, and from the finest microsurgery to instrumentation over multiple spinal segments. This chapter could have a broader remit still but excludes the management of non-neoplastic masses of the spine. It will also exclude aspects of the management of spinal tumours specific to childhood.

This diversity can be rationalized to a degree by dividing spinal tumours into two broad groups: those that arise within the thecal sac and those that arise extradurally. There are very few that coexist in both compartments. The former largely represent the expression of the various types of brain tumour below the foramen magnum and are chiefly pathologically benign conditions. The latter are dominated by metastatic malignancy as well as including those tumours that have arisen from the connective and haematological tissues of the spine.

Common ground presentation

Despite the variety, there is some common ground particularly around clinical presentation and investigation. The clinical method which elucidates these aspects of each case does so before a patient with a spinal tumour receives a diagnosis.

Pain

Patients with a spinal tumour most frequently present with pain. When this is experienced locally it is the result of the effect of the tumour on nociceptors within the spine. This effect is mediated by a multitude of mechanisms including direct mechanical deformation, venous congestion, and pathological fractures of the vertebrae. Such pain is usually persistent and progressive, reflecting tumoural growth. Pain may be worse at night and in recumbency and this phenomenon is usually attributed to exacerbation of venous congestion by the distension of the epidural venous plexus, which occurs on lying down. Sudden exacerbations of pain, with a shift to worsening in erect postures and on movement, may suggest a pathological fracture.

Pain may also be experienced at a distance from the tumour and represent the compression of neural elements of the spine. Compression of one or more roots, either by tumour or distorted spinal elements is a relatively common cause of radiating pain and compression of the cauda equina can result in neurogenic claudication. Damage to the spinal cord can result in a burning dysaesthetic central neuropathic pain. While this is perhaps most associated with tumours of the spinal cord itself, it can also result from the damage caused to the spinal cord by external compression such as that from metastases.

Some 80–90% of patients with metastatic spinal cord compression have pain as their earliest symptom and 95% have pain at the point of presentation (Cole and Patchell, 2008). Over three-quarters of primary bone tumours of the spine present with pain, and about a half with no other symptoms. The authors of a large series of 438 patients attributed the majority of this local pain to tumour expansion within bone, but pathological fracture and root compression contributed (Dang et al., 2015). Just over half of patients with intradural tumours present with pain (Wu et al., 2014) but this rises to a clear majority of over 80% for tumours below the conus.

Neurological deficit

The other important symptom group arises from the dysfunction of compromised neural elements of the spine, among which the spinal cord is perhaps the most important. Although pressure on the cord can directly damage axons and lead to demyelination it seems to do most of its damage by vascular mechanisms—initially congestion and oedema from venous compression and later ischaemia and infarction from arterial insufficiency (Baptiste and Fehlings, 2006).

While metastatic spinal cord compression as a clinical syndrome is defined by neurological deficit, among all patients presenting with spinal tumours, about half have a neurological deficit, regardless of the type of tumour. Weakness, sensory deficit, loss of balance, and incontinence are reported at decreasing frequency.

Other presentations

While spinal deformity may result from the musculoskeletal destruction caused by metastases or primary bone tumours, it is rare as a dominant or isolated presenting feature. Scoliosis as the presentation of intramedullary tumours is rare but described in children.

It should also be noted that spinal tumours may be discovered incidentally. All spinal practitioners in the MR era will be aware of the common finding of vertebral haemangiomata. A pre-MR series based on pathological or plain radiological studies provided prevalence estimates for this benign vascular tumour of about 10% (Fox and Onofrio, 1993) and more recent studies of MR for other reasons have provided estimates as high as 27% in Iran (Barzin and Maleki, 2009). Series of primary bone tumours (4%, Dang et al., 2015) and intradural extramedullary tumours (4/18, Marchetti et al., 2013), have been reported including a small proportion of incidental cases. It seems as though tumours of the spinal cord itself are rarely discovered incidentally (0/89, Li et al., 2014). Metastatic spinal tumours are often discovered during the staging workup after primary diagnosis at a stage when they are asymptomatic if not entirely incidental

Differential diagnosis

Spinal pain is 'an almost universal human condition' (Hall, 2014) and a quarter of US adults, for example, report having had at least a day of back pain over the past 3 months. The lifetime prevalence of back pain may be as high as 80% and the vast majority is not attributable to any definable abnormality (Srinivas et al., 2012). It is easy then for the occasional patient with a spinal tumour, with an incidence several orders of magnitude lower than this, to be missed. Perhaps for this reason, the median time from symptom onset to diagnosis is as long as 25 months (Manzano et al., 2008) for the usually benign group of intradural tumours and even 200 days for spine metastasis presenting without a previous primary diagnosis (Quraishi et al., 2014).

There is a broad range of other pathological processes that can affect the spine and present with pain and neurological dysfunction. Infective processes can cause spinal destruction, which threatens the spinal cord and can also infiltrate the epidural space. Insufficiency fractures secondary to osteoporosis may be hard to tell apart from those secondary to tumour although the former rarely cause neurological deficit. Degenerative spine disease often presents with axial spinal pain and myelopathy, similar to extradural tumours, or with radicular pain, as may intradural extramedullary tumours. The absence of pain usually distinguishes the many neurological causes of myelopathy from tumoural causes.

Imaging

Since it became widely available in the 1990s, magnetic resonance imaging (MRI) has become the imaging modality of choice for the investigation of spinal pain and neurological deficit. While a strong case can be made for limiting the application of MRI to patients with the common complaint of spinal pain on the grounds of healthcare economics or medicalizing a normal human experience (Srinivas et al., 2012), for patients with red flags or 6 weeks of new pain it represents a non-invasive investigation without which the potentially serious diagnosis of a spinal tumour will not be made.

MRI with and without gadolinium enhancement is the modality of choice in the workup of a patient with a suspected spinal tumour. MRI provides excellent resolution of all spinal compartments, and provides enough information to differentiate blood and cystic fluid, enhancing solid tumour and spinal cord. It is particularly important to establish from the available imaging in which anatomical compartment the tumour lies and this can be achieved by the analysis of the relationship of the tumour to cord and dura (**Fig. 63.1**). Where metastatic spinal cord compression is suspected, whole spine MR within 24 hours is the gold standard.

Where MR is contraindicated, computed tomography (CT) myelography (**Fig. 63.2**) can be utilized. CT of the spine complements MR as the imaging modality of choice in assessment of bony structures, and is therefore invaluable in the imaging of the bony spine eroded or destroyed by tumour and the visualization of pathological fractures. It is also utilized in the planning of instrumentation in cases with bony collapse and instability. CT of chest, abdomen, and pelvis is widely utilized in the search for other metastatic deposits and the primary tumour and nuclear medicine bone scans also have a role in screening for other bony metastases. CT is the principle imaging modality for the guidance of percutaneous biopsies of spinal tumours, although it is unusual for this approach to be taken for intradural lesions

Plain X-ray alone is insensitive in the detection of spinal tumours and its role should be limited in contemporary practice to determining spinal level intraoperatively and the postoperative imaging of instrumentation. For highly vascular tumours such as haemangioblastoma, vertebral haemangioma, and renal metastasis, digital subtraction angiography (DSA) may prove an important investigation in identifying the spinal level of feeding vessels and imaging abnormal vasculature. It can be extended to embolization to reduce intraoperative blood loss. Ultrasound is limited to the paediatric population and intraoperative localization.

Modalities of treatment

The immediate management of patients with spinal tumours includes analgesia, the institution of antithromboembolic prophylaxis and immobilization where necessary. The instability of tumoural spinal destruction is rarely as dramatic as that following trauma and the institution of bed rest will usually suffice. Dexamethasone is a synthetic glucocorticoid with an anti-inflammatory effect that can help with analgesia and allow neurological improvement. For some haematological tumours it can have an antitumour effect affording a rapid biological decompression of the spinal cord. The rapid introduction of dexamethasone can improve the ambulatory outcome of patients with metastatic spinal cord compression (Sorensen et al., 1994) and is universally instituted prior to surgical intervention for spinal tumours with a view to improving neurological outcome through a neuroprotective effect.

Surgery

For most patients discovered to have a spinal tumour, a spinal surgical opinion is sought regarding the role of surgical intervention for diagnosis, symptomatic relief, improving prognosis, or even for cure. For some, particularly those with widespread malignancy and very limited prognosis, surgery may have nothing to offer but for many patients with intradural tumours, surgery will represent the central component of their therapy.

A sagittal image demonstrating the tumour with reference to the sacrum is a prerequisite for the planning of surgery for tumours in

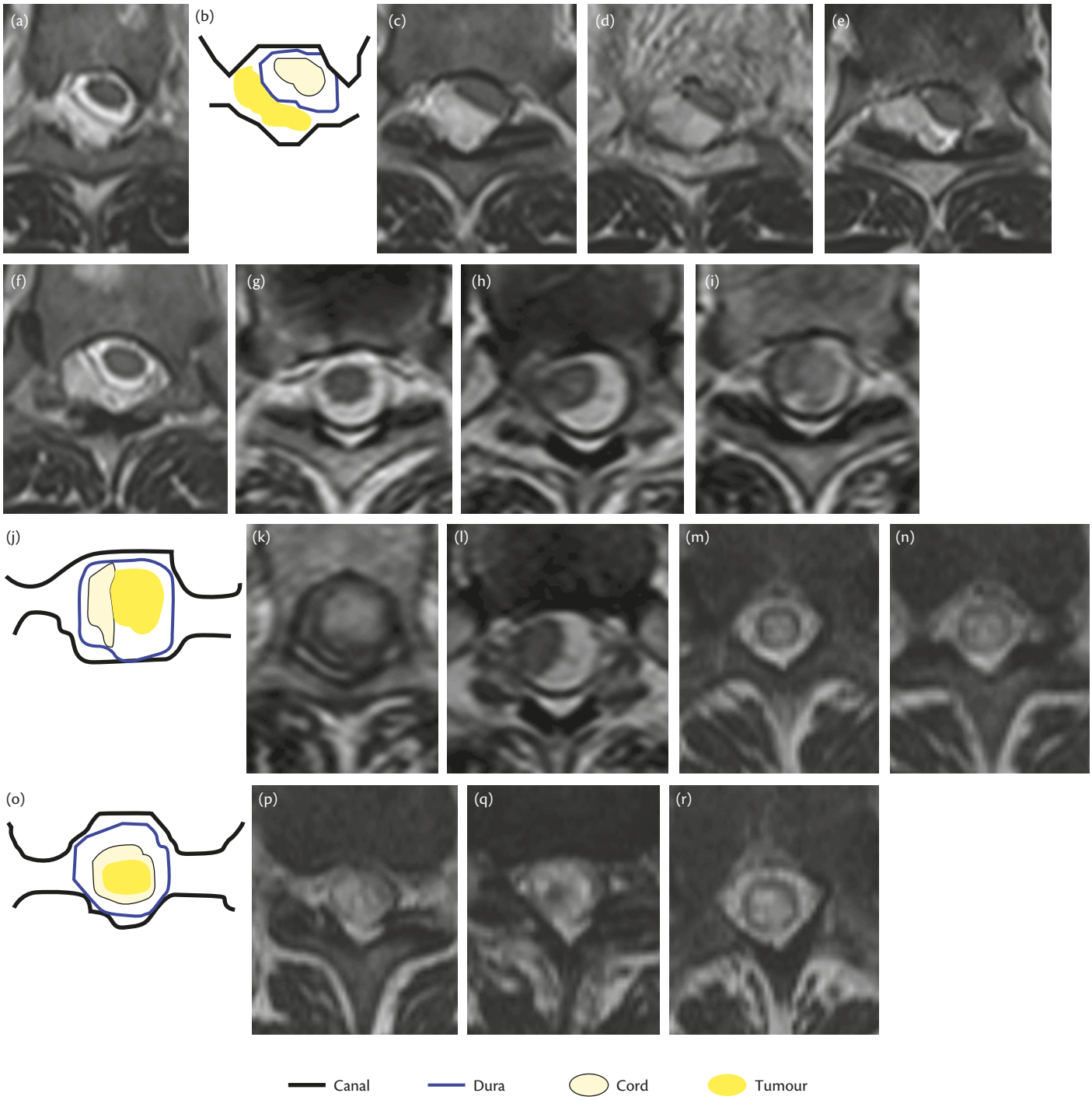

Fig. 63.1 These images show how serial axial images can help determine the compartment in which a spinal tumour lies by noting its relationship to the cord and the dura; extradural (A–F), intradural extramedullary (G–L), or intramedullary (M–R).

the sacral, lumbar, and thoracic spine. The occiput can be used as a point of reference for tumours in the cervical and uppermost thoracic spine. These preoperative images allow an image intensifier to be used intraoperatively to localize the tumour and plan a suitable incision. Careful positioning to avoid pressure damage to skin, peripheral nerves, and the face is essential. The use of a single dose of antibiotic (e.g. Cefuroxime 750 mg) on induction as prophylaxis against infection is reasonable. If a low molecular weight heparin has been introduced preoperatively for venous thromboembolism (VTE) prophylaxis in light of reduced mobility, this may be withheld for 24 hours pre- and postoperatively to reduce intraoperative bleeding and the risk of postoperative haematoma. Graduated compression stockings and intermittent calf compression are frequently used intraoperatively.

Intraspinal access

Laminectomy is the standard surgical approach employed for resection of tumours from the spinal canal. Although it affords good

Fig. 63.2 CT myelogram of a thoracic intradural, extramedullary tumour (schwannoma).

access to the canal, both intra- and extradurally, problems with postoperative pain and postlaminectomy kyphosis, especially in paediatric patients, have led some to explore alternative access procedures including laminoplasty, hemilaminectomy (Fig. 63.3), and the techniques of minimally invasive spinal surgery. Hemilaminectomy has also been applied to the decompression of the spinal cord in metastatic spinal cord compression (MSCC) without worsening stability as an alternative to the larger instrumented approaches, described next (Fig. 63.3; see also Millward et al., 2015).

Larger tumours with lateral extension may require removal of the facet joint and pedicle for adequate exposure and total resection. Although ventral access procedures have been employed for spinal tumour resection, the ventral aspect of both extra- and intradural compartments can be accessed dorsally and dorsolaterally without excessive retraction of the cord.

Intradural access

If intraoperative ultrasound imaging is available, it is advisable to check that the exposure allows access to both tumour poles prior to opening the dura. A longitudinal durotomy is usually employed. The arachnoid is then incised before the tumour is identified. The dentate ligament may be divided to allow access to tumours arising ventrally to the cord. Solid extramedullary tumours are debulked with the aid of an ultrasonic aspirator and cystic tumours drained before the peripheral tumour is dissected under microscopic control from the surrounding structures. Nerve sheath tumours with a single nerve root of origin may be able to be excised completely by division of that root above and below the tumour and surprisingly little disability usually results. When, however multiple roots, or a particularly large motor root are involved, the surgeon may elect instead to attempt to dissect tumour from root or to leave a small volume of tumour attached to each intact root. While many intradural extramedullary tumours have a good plain between them and surrounding structures and can be curatively resected, others may be densely adherent, and myxopapillary ependymomas are particularly notable in this regard.

Intramedullary access

Once the cord is exposed, the identification of the normal structures under microscopic vision aids in orientation. A large tumour or swollen cord distorts the normal anatomy and in such cases the midline dorsal vein and posterior median sulcus which guide a dorsal, midline myelotomy and the dorsal roots and posterolateral sulcus which provide the landmarks for entry through the dorsal root entry zone may be particularly difficult to identify. Once exposed, the tumour is internally debulked with an ultrasonic aspirator and a biopsy is sent for frozen section. Assessment of the interface between tumour and cord at an early stage should guide the extent of resection, and this decision may also be guided by the on-table pathology result, and intraoperative electrophysiological monitoring. While ependymomas can usually be completely resected (Fig. 63.4), astrocytomas are often less distinct from the cord.

Instrumentation

The resection of tumours from the spinal skeleton can be achieved through any number of approaches, chosen to give the best access to pathology. Neurosurgery has long been familiar with anterior approaches to the cervical spine, but the widespread application

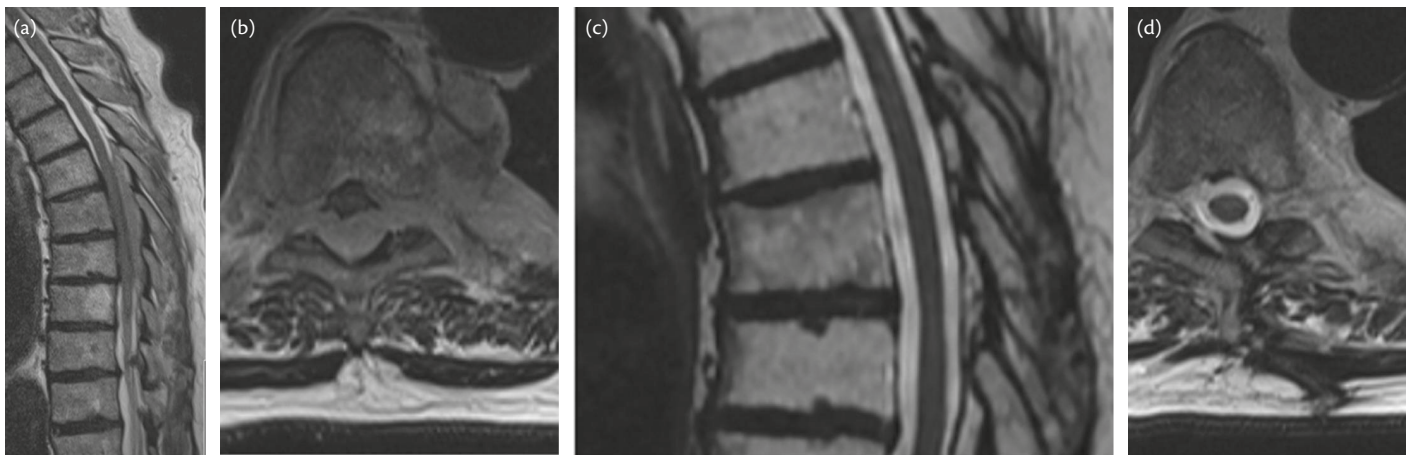

Fig. 63.3 Thoracic lymphoma. A 74-year-old man presented with progressive paraparesis and leg pain. Midsagittal T2-weighted (A) and axial gadolinium-enhanced T1-weighted (B) MRI scans demonstrating an extradural enhancing mass lesion. He had a hemilaminectomy for biopsy and decompression. Postoperative sagittal (C) and axial (D) MRI images are shown.

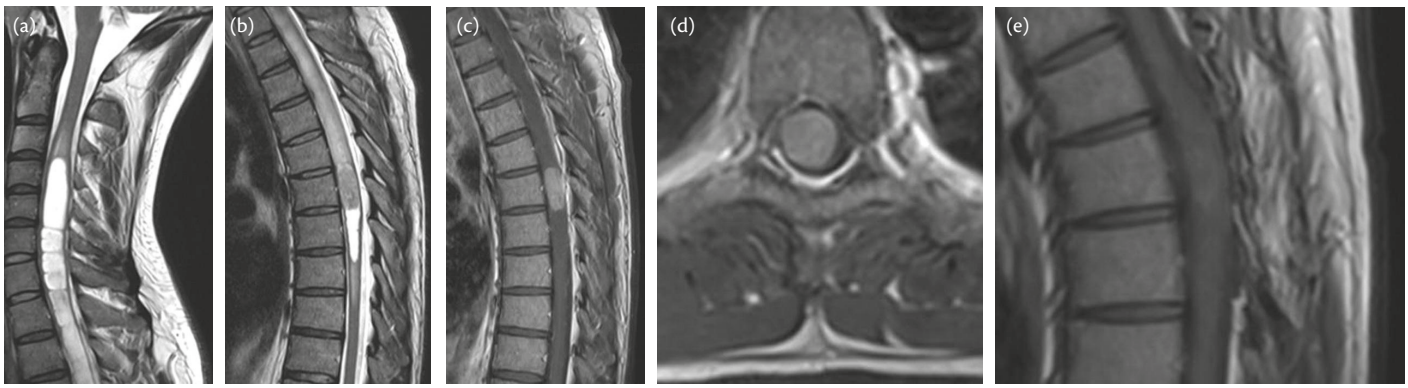

Fig. 63.4 A 30-year-old gentleman presenting with progressive paraparesis and diagnosed with an ependymoma (WHO grade 2). Note the enhancing tumour near the caudal end of the syrinx (A–D); (E) shows the MRI 4 years postresection. The patient recovered with good neurological outcome.

of trans- and extracavitary approaches to the thoracic and lumbar spines has changed the approach to tumours within the vertebral body (Young et al., 1980; *cf.* Patchell et al., 2005). Not only can destructive tumours reduce the mechanical integrity of the spine, so may the resections employed to treat them. Surgeons involved in the treatment of spinal tumours should have access to the full range of anteriorly and dorsally applied instrumentation in order to restore stability to the spine.

Over recent years there has perhaps been a shift towards posterior approaches to both metastatic spinal tumours and primary bone tumours. The contemporary generation of pedicle screw-based instrumentation allows the spine to be stabilized over a disease segment without the need for a weight-bearing element to be placed anteriorly. Minimally invasive spine surgery has been applied to both the decompression and stabilization of the spine affected by tumour (Ziari et al., 2012) again allowing a purely dorsal approach. Even total or *en-bloc* vertebrectomy, applied to solitary radiotherapy- and chemotherapy-resistant metastases, such as those from renal cell carcinoma, chordoma, and other bone tumours, can be performed through a purely dorsal surgical approach.

Surgery for spinal tumours is associated with significant risks. Table 63.1 by no means provides an exhaustive list, but rather highlights the main potential complications. These risks should be clearly emphasized during patient counselling, minimized as far as possible, and clearly explained during discussion with the patient.

Percutaneous vertebral augmentation

The percutaneous transpedicular injection of bone cement either directly into the marrow space of the vertebral body (vertebroplasty) or into a space performed by expansion of a balloon within the vertebra (kyphoplasty) are well established as options for the treatment of pain following osteoporotic vertebral collapse. Such procedures are also useful in the treatment of patients with painful vertebral metastases and myeloma deposits. Vertebroplasty can be employed

Table 63.1 Complications related to surgery for spinal tumours

Complications		
General	**Benign tumours**	**Malignant tumours**
Bleeding	DSA + embolization useful in certain tumours (e.g. haemangioblastoma, metastatic renal cell carcinoma). On the whole, surgery for malignant tumours poses a higher risk of intraoperative blood loss	
Infection	Risk increased with concomitant use of steroids, extremes of age, and other comorbidities such as diabetes mellitus	
CSF fistula +/– pseudomeningocele	Intervention only if clinically symptomatic. Surgical options include lumbar drain, surgical repair	
Tethered cord	May be reduced with pial sutures, whereas duraplasty has not been shown to be protective	
Syringomyelia	Risk increased with cord tethering at site of surgery Excision of tumour and re-establishing CSF flow usually results in decreased size, or even resolution of preoperative syrinx	
Vascular compromise	Risk increased with preoperative DSA +/– embolization procedures	
Permanent neurological worsening including tetraplegia and paraplegia	Approximately 20% of patients will experience permanent motor, sensory, sphincteric (or a combination) dysfunction; <4% risk of delayed, postoperative myelopathy. Dorsal column dysfunction seen in almost all patients with intramedullary tumours approached through a dorsal myelotomy. Useful techniques such as spinal cord monitoring give the surgeon additional information in order to reduce these risks	
Tumour recurrence	Very low in completely resected tumours. However, incompletely resected myxopapillary ependymoma is an exception	Malignant tumours almost always recur
Tumour seeding	Very rare	At site of biopsy, especially in sarcomas. The tissue surrounding the biopsy needle path should be removed during definitive sarcoma surgery
Spinal deformity	More of an issue in paediatric cases due to neurological disability caused by tumour, or following surgery	

effectively and safely, even in the presence of epidural soft tissue, for the treatment of painful metastases (Sun et al., 2014).

Oncological treatment

Despite recent evidence to support the role of surgery in the treatment of metastatic spinal cord compression, radiotherapy remains the principle modality of treatment for the majority of patients suffering from this oncological emergency. Radiotherapy is also employed in the treatment of unresectable and recurrent intradural tumours with, perhaps, modest results. For chordoma and chondrosarcoma proton beam therapy may be of benefit, where it is available.

Focused radiation, employed for over 60 years for cranial tumours through stereotactic radiosurgery, has also been applied to the spine. As a treatment for enlarging intradural extramedullary tumours, radiosurgery can achieve radiological stabilization, neurological preservation, and even improvement with the risk of cord radionecrosis rarely arising (Marchetti et al., 2013). It may have a more durable effect than conventional radiotherapy in the treatment of spine metastases and has additional benefits of efficacy in radioresistant disease and relapse after conventional radiotherapy (Gerszten et al., 2009). Chemotherapy has a limited role in the treatment of spinal tumours but for haematological malignancies, particularly lymphoma, when they affect the spine, may be curative.

Rehabilitation

Patients with spinal tumours are often understandably distressed through the course of their treatment and if pain is not appropriately managed, these patients are at risk of psychological and psychiatric disturbances such as depression, anxiety, and fatigue (Jones et al., 2003). Spinal neurorehabilitation is an integral part of management, and maximal benefits are gained with early commencement of a tailored programme at a specialized centre. Rehabilitation has also been shown to improve depression (Ruff et al., 2007).

Tumour group specifics

Intramedullary spinal cord tumours

Intramedullary spinal cord tumours (IMSCT) are rare and comprise less than 4% of central nervous system tumours and 30% of intradural spinal neoplasms. The most common tumour types are ependymomas and astrocytomas. The former outnumbers the latter in most case series with a suggestion that astrocytomas predominate in the younger age group, with ependymomas being more frequently encountered with increasing age (Manzano et al., 2008). Haemangioblastomas are less frequent, and rarer still are other miscellaneous developmental tumours and cysts such as lipomas and dermoid, epidermoid, and neurenteric cysts. Features of the more common IMSCTs are listed in Table 63.2.

It is important to note that while resection of intramedullary spinal cord tumours is compatible with both good oncological prognosis and long-term ambulation, myelotomy itself is not without morbidity. In a recently reported series of 278 patients, 61% had a worsened neurological status postoperatively, permanently so in about 20% (Klekamp, 2013).

Intradural, extramedullary spinal tumours

Intradural, extramedullary spinal tumours (IDEMs) are over twice as common as IMSCTs but still rare, accounting for 70% of the incidence of intradural tumours—between 0.8 and 1.3 per 100 000 population/year. The most common of the IDEMs are nerve sheath tumours (Fig. 63.5), followed by meningiomas and myxopapillary ependymomas (Traul et al., 2007). These tumours are usually benign and solitary; other features are listed in Table 63.3. The full range of tumours arising in this anatomical compartment is broad and includes metastatic tumours, paragangliomas, epidermoid, and dermoid cysts, lipomas, and teratomas.

Surgery is mainly indicated for progressively enlarging, symptomatic tumours. Some schwannomas, meningiomas and developmental lesions do not progress, and surveillance alone is adequate, thereby avoiding the potential surgical risks. However, the myxopapillary ependymoma behaves differently and deserves special mention.

Myxopapillary ependymoma

Myxopapillary ependymomas are almost entirely confined to the lumbar spine and usually solitary. Due to its unique location, symptoms are usually attributable to dysfunction of the conus or cauda equina. These tumours may fill the entire lumbosacral spinal canal (Fig. 63.6). Although classified as 'benign'—they are WHO grade 1 tumours—the myxopapillary ependymoma behaves aggressively with a propensity for recurrence and CSF dissemination that usually translates to multiple surgeries in the patient's lifetime (Boström et al., 2011). It may scallop bone as well as erode through dura and become densely adherent to the nerve roots of the cauda equina. The treatment of choice is complete surgical excision. Incidental, small, asymptomatic tumours may be operated on early as the chance of curative and complete excision is good at this stage reducing the risk of dissemination and progression to irresectability is reduced. In practice, an *en-bloc* excision is sometimes difficult to achieve as the tumour capsule is thin and the tumour itself is usually soft. The filum terminale should be identified early in the course of surgery, and this may be facilitated by using a nerve stimulator and EMG electrodes in the external anal sphincter.

Primary bony tumours of the spine

Primary tumours of the bony spine are again, rare, with vertebral metastases being much more common. The pathological diversity is wide and these tumours demonstrate a bimodal age distribution, affecting both young and older people. Tumours with connective tissue components as cells of origin and therefore belonging to the sarcoma group, can be classified into two broad categories, either malignant (Table 63.4) or benign (Table 63.5). Their management is the province of the supraregional specialty unit.

Malignant bone tumours

The chordoma (Figs. 63.8 and 63.9) is the most common adult primary malignant spinal bone tumour and is typically a midline tumour, found to occur commonly in the axis and lumbosacral regions. They are slowly growing but destructive lesions, with a particularly high rate of recurrence following piecemeal resection. Radical, complete, *en-bloc* resection without violation of the tumour has been shown to significantly reduce the rate of recurrence and improve survival (Fuchs et al., 2005).

The osteosarcoma is the most common primary spine sarcoma and has an especially poor prognosis (Sansur et al., 2007). Risk factors in the development of osteosarcoma include Paget's disease and

Table 63.2 Features of ependymomas, astrocytomas, and haemangioblastomas

			Tumour type					
			Ependymoma		**Astrocytoma**		**Haemangioblastoma**	
MRI features	T1WI		Variable		Hypointense		Iso- to hypointense	
	T2WI		Hypointense		Hyperintense		Iso- to hyperintense (enlarged feeding and draining vessels may be visualized)	
	Location		Central		More eccentric		Usually superficial	
	Enhancement		Homogenous		Heterogenous (none with LGG; intense in pilocytic astrocytomas and HGG)		Intense	
	Margins		Generally distinct		Poorly defined		Distinct nodule	
	Syringomyelia/Cyst		Often associated		Less common (pilocytic astrocytomas may have an associated cyst)		Very commonly associated with a cyst	
Potential for GTR			Yes		Less common		Yes	
Histology	Subtypes (commonest in bold)	WHO Grade	Subependymoma (rare) Ependymoma Anaplastic ependymoma	1 2 3	Pilocytic astrocytoma (rare) LG astrocytoma Anaplastic astrocytoma Glioblastoma	1 2 3 4	Haemangioblastoma	1
	Microscopic features of commonest subtype		Sheets of uniform cells with oval nuclei and fine cytoplasmic processes Perivascular pseudorosettes Mitoses rare/absent		Well differentiated neoplastic astrocytes within microcystic tumour matrix (No necrosis or microvascular proliferation) Mitoses: Ki-67/MIB-1 <4%		Two main components: endothelial cells and pericytes; large, vacuolated stromal cells containing lipid Rosenthal fibres in cyst and syrinx walls Mitoses usually absent (MIB-1: 0–2%)	
	Immunohistochemistry		GFAP, S-100 protein, Vimentin		GFAP Vimentin (more consistent in higher grade)		Stromal cells lack endothelial cell markers (negative in RCC) but are positive for D2–40 Ab and inhibin-A (positive in RCC), Vimentin, VEGF	
Syndromic associations			NF2 (chromosome 22q12)		NF1 (chromosome 17q11) TP53 germline mutations / Li-Fraumeni syndrome Ollier's disease		VHL (chromosome 3p25)	

Abbreviations: T1WI, T1-weighted imaging; T2WI, T2-weighted imaging; LGG, low-grade glioma; HGG, high-grade gliomas; NF1, neurofibromatosis type 1; NF2, neurofibromatosis type 2; VHL, Von Hippel-Lindau syndrome; GTR, gross total resection; Immuno, immunohistochemistry; VEGF, vascular endothelial growth factor; GFAP, glial fibrillary acid protein; RCC, renal cell carcinoma; Ab, antibody; Ollier's disease also known as inherited multiple enchondromatosis type 1.

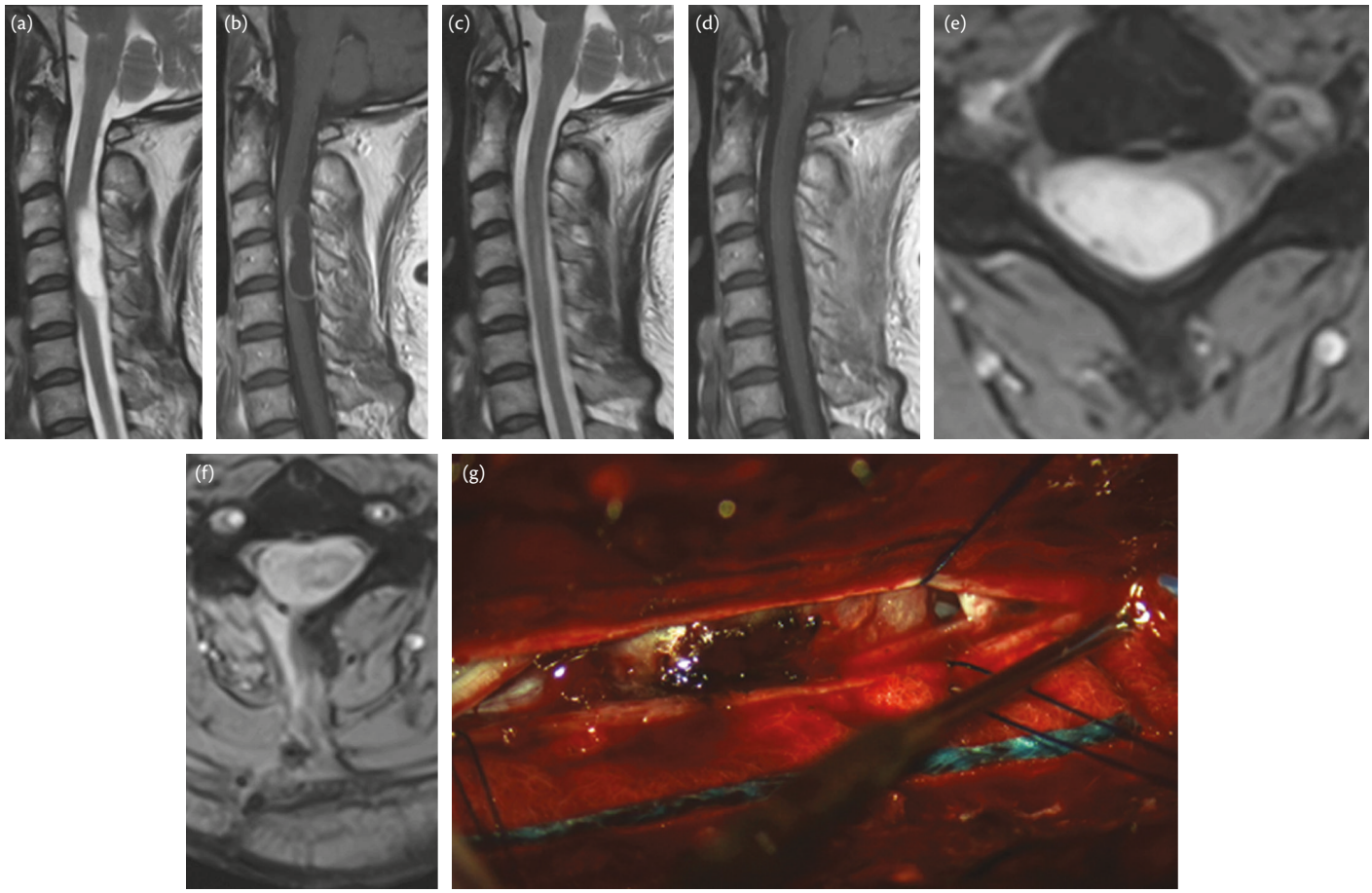

Fig. 63.5 MR images to illustrate the resection of a cervical schwannoma through a unilateral, parasagittal approach and hemilaminectomy (A–F). The postoperative image is also shown (G).

radiotherapy. Unfortunately, *en-bloc* resection is rarely achievable and despite all treatment options, the management of primary spinal osteosarcomas is palliative.

Chondrosarcoma (Fig. 63.10) has a characteristic radiological appearance including moth eaten osteolytic areas and 'rings and arcs' of calcification within the tumour matrix, which are best appreciated on CT. Extraosseous and epidural extension is common, and MR is the modality of choice in demonstrating this. Fortunately, majority of chondrosarcomas are low grade. Wide, *en-bloc* surgical resection is associated with prolonged survival and recurrence free interval, in contrast to debulking procedures (Quiriny and Gebhart, 2008).

Multiple myeloma and plasmacytoma

Multiple myeloma (MM) is a systemic haematological malignancy characterized by proliferation of monoclonal plasma cells (Fig. 63.11). It represents about 1% of all cancers worldwide and an incidence of about 5.5 per 100 000 (Ferlay et al., 2013) and is a disorder of older people with a median age at presentation of 70. Plasmacytomas are discreet, solitary lesions that are histologically identical to MM but without the systemic manifestations.

The vertebral column represents the commonest site of bony involvement. The management of symptomatic cord compression in MM remains an area of controversy. In the setting of soft tissue related cord compression, urgent local radiotherapy is the treatment of choice. Generally, surgery is reserved for symptomatic MM patients with evidence of bony or structurally related cord compression and consolidated by radiotherapy. However, Rao et al. (2006) have suggested that radiotherapy alone is an effective form of palliative treatment without surgery after reviewing a cohort of patients with MM of the cervical spine with both clinical and radiological features of instability. The bone density in this condition is notoriously low which can compromise the use of instrumentation.

Haemangioma

Vertebral haemangiomas are benign tumours and are the most common primary spinal tumours (Figs. 63.12 and 63.13). They are usually incidental lesions found on imaging; MRI characteristically demonstrates high signal on both T1- and T2-weighted imaging and these appearances allow a diagnosis to be made without the need for biopsy. Vertebral haemangiomas are rarely symptomatic, but a small proportion of these tumours may expand the bone and cause pathological fractures, or extend into the epidural space and compress neural structures. Larger lesions demonstrate the characteristic 'honeycomb' appearance or 'corduroy sign' on sagittal and coronal CT, which are prominent vertical striations of thickened trabecular bone. Treatment options for symptomatic lesions include surgical excision, vertebroplasty, endovascular embolization, and radiotherapy.

Table 63.3 Features of nerve sheath tumours, meningiomas, and myxopapillary ependymomas

			Tumour type					
			Nerve sheath tumours		**Meningioma**		**Myxopapillary ependymoma**	
MRI features	T1WI		Hyperintense		Isointense		Hypointense	
	T2WI		Hyperintense		Isointense to Hyperintense		Hyperintense	
	Location		Affecting sensory nerve root(s) Even distribution in spinal canal		Dural based; posterior / postero-lateral; Thoracic		Almost exclusively affecting filum terminale	
	Enhancement		Heterogenous		Homogenous; 'Dural tail'		Homogenous	
	Margins		Distinct		Distinct		Distinct	
	Oedema		None		Variable		Often associated	
	Cystic change		Common		None		Not uncommon; also areas of haemorrhage	
Surgical pearls	Relationship to arachnoid		Both layers of arachnoid (similar to cranial counterpart) must be opened		Clear arachnoid plane between tumour and spinal cord		Arachnoid needs to be opened to expose the tumour, which is in turn surrounded by a thin capsule	
	Surgical removal		Piecemeal. Sacrifice of sensory nerve root of origin		Piecemeal or *en-bloc* excision. Cautery or excision of overlying dura		En-bloc, total excision	
Histology	Subtypes (common in bold)	WHO Grade	Schwannoma Neurofibroma	1 1	Benign Atypical (rare) Malignant (rare)	1 2 3	Myxopapillary ependymoma	1
	Microscopic features of commonest subtype		Composed entirely of neoplastic Schwann cells in two patterns: Antoni A (cellular; spindle shaped cells, dense pericellular reticulin arranged in intertwining fascicles; characteristic Verocay bodies), Antoni B (less cellular; cells loosely arranged in myxoid stroma with scanty surrounding reticulin)		Variable, depending on subtype and grade. Common subtypes: meningothelial, psammomatous Mitotic rate (Ki–67 index) usually <4% Reticulin pattern rarely as dense as schwannoma		Encapsulated tumour; not infiltrative Clusters of tumour cells with round, monomorphic nuclei characteristically arranged in papillary pattern, enveloped in abundant mucin / myxoid stromal cores. Mitosis and necrosis rare	
	Immunohistochem		S-100: strong and diffuse expression GFAP: focal, infrequent staining Collagen IV and laminin positive: found in surface basal lamina that is present in all schwannomas		EMA, Vimentin: positive S-100 variable Cytokeratins: focal GFAP negative		GFAP, S-100, Vimentin: positive Cytokeratins: absent	
Syndromic associations			NF2 (chromosome 22q12) Carney's complex (17q23-q24) (melanotic schwannomas)		NF2 (chromosome 22q12) Previous radiotherapy Castleman's syndrome (chordoid type)		NF2 (chromosome 22q12)	

Abbreviations: T1WI, T1-weighted imaging; T2WI, T2-weighted imaging; NF1, neurofibromatosis type 1; NF2, neurofibromatosis type 2; GTR, gross total resection; GFAP, glial fibrillary acid protein; EMA, epithelial membrane antigen; Immunohistochem, immunohistochemistry.

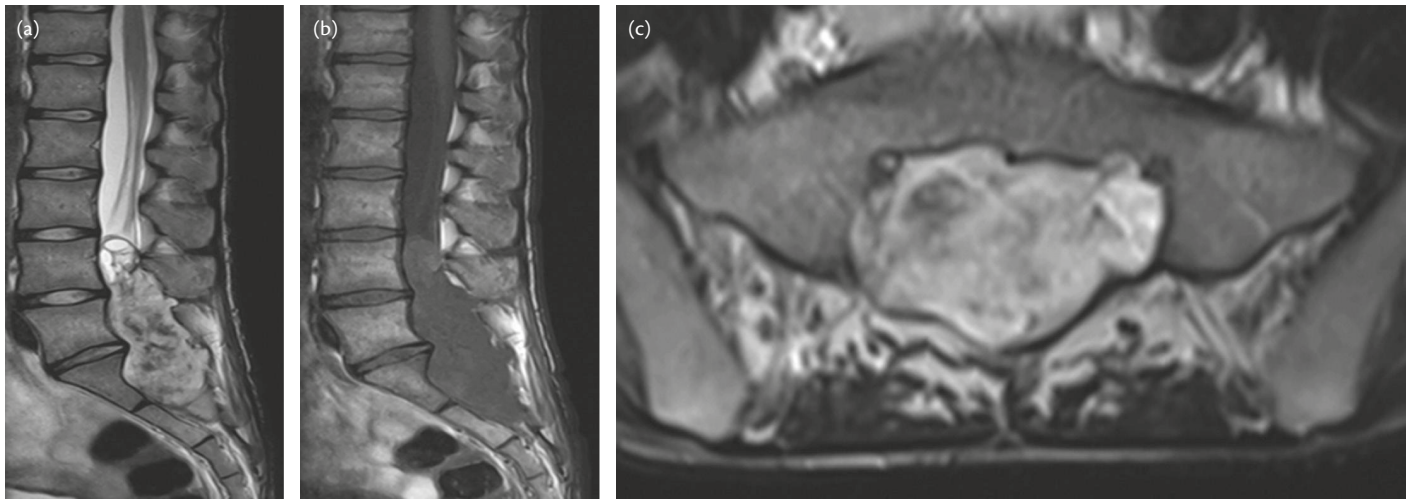

Fig. 63.6 Late presenting myxopapillary ependymoma with destruction of the posterior elements and scalloping of the sacral body (A, B). The caudal nerve rootlets and dura have been invaded by tumour, limiting resection. The wound was closed over a directly placed spinal drain as direct closure of the dura was impossible (C).

Courtesy of Dr Kieren Allinson, Department of Pathology, Addenbrooke's Hospital, Cambridge.

Spinal metastases

Among the various significant clinical entities described in this chapter, spinal metastatic malignancy is by far the most common. The spine is the most common osseous site for metastatic deposits and 40% of patients dying from cancer have spinal disease on autopsy. It is inevitable that a rise in the incidence of metastatic spinal disease will accompany the increase in survival of patients with cancer, which has accompanied more effective treatment of this group of pathologies (Sciubba et al., 2010). The commonest sources of spinal metastases are from cancers of the lung, breast (Fig. 63.14) and prostate but renal cell carcinoma, gastrointestinal malignancy, and melanoma are also common. Myeloma deposits may indeed be metastatic but have been considered here with primary tumours of bone.

When the growing tumour invades the epidural space or causes pathological fracture of a vertebral body the spinal cord can become compressed and when neurological function develops, the oncological emergency of MSCC results. Sudden onset deficits may represent cord infarction and carry a relatively poor prognosis compared to gradual onset deficit. There is an established diagnosis of malignancy in most patients but up to 20% of spine metastases represent the first presentation of the patient's disease (Cahill, 1996). The investigation of this patient group should include a myeloma screen, prostate-specific antigen in men, examination of the breasts in women and a screening CT of the chest, abdomen, and pelvis.

The spinal surgeon is often called upon to make decisions about the appropriateness of surgical intervention for MSCC. A decision is often needed promptly to facilitate rapid institution of therapy,

Table 63.4 Malignant primary osseous spine tumours

Tumour type	Age (yrs)	Location in spine	Origin	Clinical presentation	Median survival (mths)	5-year survival (%)	Metastasis	Management
Chordoma	60s	Sacrum (if occurs in C-spine, had predilection for C2)	Notochordal remnants	Pain, deformity, neurological deficit	74	50–85	Uncommon	Wide margins, *en-bloc* surgical resection, radiotherapy (insensitive to chemo)
Osteosarcoma	Two peaks: 10–30 and 50s	Sacrum, posterior elements	Bone		11	18–41	Pulmonary mets common. Malignant degeneration in Paget's disease and following radiotherapy	Wide margins, *en-bloc* surgical resection, chemo, radiotherapy (often purely palliative)
Chondrosarcoma	50s	Thoracic, posterior elements	Cartilage		26	40	Uncommon. Malignant degeneration of osteochondroma	Surgical resection (Insensitive to chemo and radiotherapy)
Ewing's sarcoma	10–30 (teens)	Sacrum, posterior elements	Small, round, blue-cell tumour		37	55–73	Commonly to lungs and bone. Rarely epidural	Surgery, chemo, radiotherapy

Table 63.5 Benign primary osseous spine tumour

Type	Age (years)	Location	Clinical presentation	Malignant degeneration	Management	Recurrence rate (%)
Haemangioma	Any age	Thoracic, body	Incidental	No	Surgical excision and/or radiotherapy for symptomatic lesions	(Low)
Osteoid osteoma	10–20	Lumbar, body	Night pain relieved by salicylates, NSAIDs <2 cm	No	Surgical excision	<4.5
Osteoblastoma	10–30	Lumbar, body	Non-specific pain; >2 cm	Yes	Surgical excision	<15
Aneurysmal bone cyst See Fig. 63.7	<20	Thoracolumbar, posterior elements	Pain, deformity, neurological deficit	No	Complete curettage and excision. High recurrence rate with incomplete excision	<30
Giant cell tumour	20–40	Sacral, body	Aggressive. High recurrence rates	Not reported. However, post-op radiotherapy associated with 10% radiation induced sarcoma	Surgical excision with wide margins. Radiotherapy not associated with improved outcomes	<40 (increased with incomplete resection and intralesional margins)
(Osteo)chondroma	30–40	C2, Posterior elements	Neurological deficits rare. Scoliosis	Yes (to chondrosarcoma)	Complete surgical excision	Paucity of data
Chondroblastoma	Adolescence	Not applicable due to rarity	Pain, neurological deficits	Not reported	Complete surgical excision. High recurrence with incomplete excision	24–100

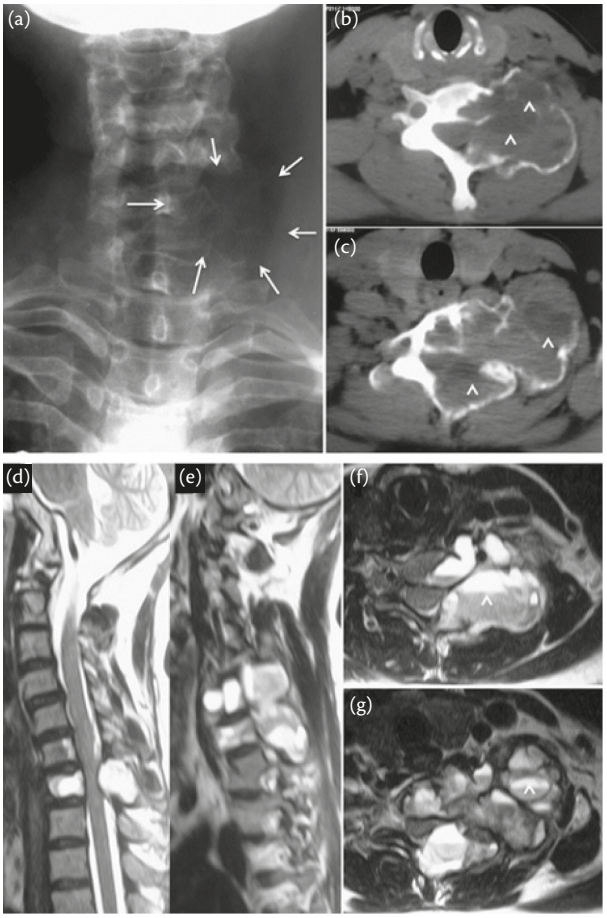

Fig. 63.7 A 47-year-old female patient with neck pain with pathological diagnosis of aneurysmal bone cyst. (A) Anteroposterior X-ray lytic destructive lesion at the left side of C6–C7 vertebra (arrows). (B, C) Fluid–fluid levels (arrowheads) demonstrated in the multilocular expansile lesion involving both the body and posterior elements on consecutive computed tomography images. Magnetic resonance imaging of the same patient. (D, E) Sagittal and (F, G) axial T2-weighted images demonstrate multiple fluid–fluid levels representing haemorrhagic elements at various ages (arrowheads).

whether it commence with surgery or radiotherapy, and should when possible be made in consultation with an oncologist familiar with the patient's case and with sight of MR imaging. Many factors need to be considered and these may be considered in four groups (Fig. 63.15). Oncological factors include the radio- and chemosensitivity of the malignancy and the patient's stage and prognosis. Neurological factors include the symptoms and deficits of neurological compression, and the presence of a radiologically compressive lesion which explains them. A complete cord lesion lasting longer than 24 hours is extremely unlikely to improve following decompression. Biomechanical factors revolve around the effect of the tumour on the structure of the spine. Mechanical pain and deformity may be indications for surgical stabilization, but the integrity of adjacent levels is required to capture spinal elements with instrumentation. Additional CT scanning may be helpful in providing this information but a patient with compromise of long segments of the spine is unlikely to become a surgical candidate. Patient factors are of primary importance and include performance status, comorbidity, age (Chi et al., 2009), and patient wishes.

Various authors such as Tokuhashi et al. (2005) have formalized consideration of some of these factors into scoring systems. They are based on actuarial survival tables to provide a guide to prognosis and can contribute to the decision-making process. The numbers should not be used blindly however and do not replace the need for careful discussion with oncologist and patient. Sciubba et al. (2010) have recommended surgical decompression and stabilization in patients with bony cord compression, rapid neurological decline, evidence of instability, radioresistant tumours, and recurrent tumours despite radiotherapy.

Controversy

There is no doubt that Patchell's landmark study, published in 2005, changed practice regarding the application of surgery to MSCC. A previous randomized controlled trial of laminectomy and

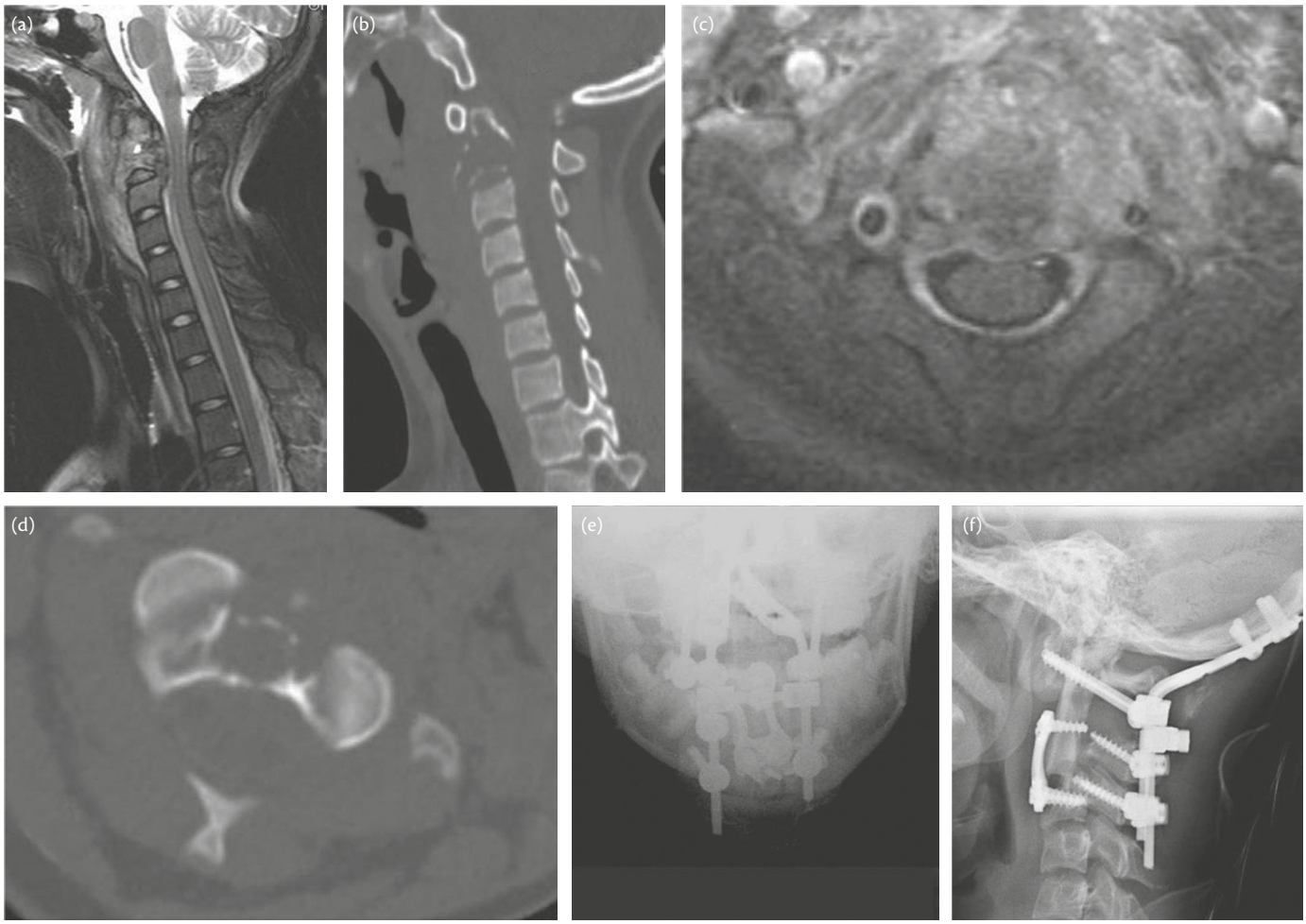

Fig. 63.8 Chordoma. Preoperative sagittal T2-weighted MRI (A) shows extensive destruction of the C2 vertebral body with prevertebral extension from the clivus to C5 (arrow). Preoperative sagittal CT reconstruction (B) shows an expansile lesion involving C2 vertebral body (arrow). Preoperative axial T2-weighted MRI (C) with gadolinium contrast enhancement shows extensive infiltration of the C2 vertebral body with tumour surrounding the vertebral arteries (arrow). Preoperative axial CT (D) shows bony involvement of C2 vertebral body (arrow). Radical extended transoral-transmandibular resection followed by posterior element resection, instrumentation, and fusion was undertaken. Postoperative anteroposterior (E) and lateral (F) radiographs were performed after total C2 resection, instrumentation, and fusion (see Walcott et al., 2012).

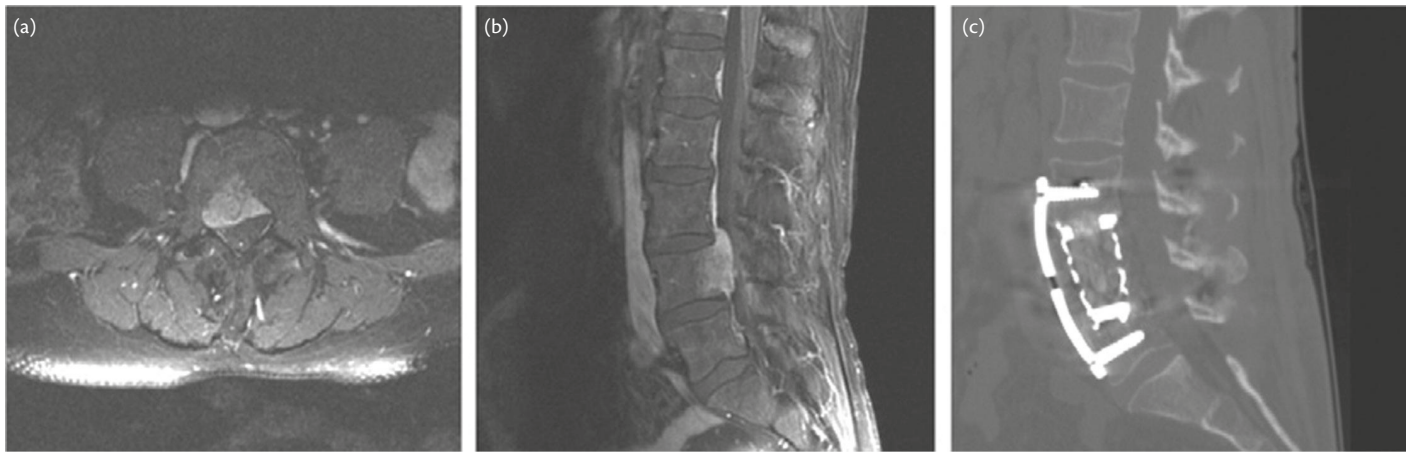

Fig. 63.9 CT and magnetic resonance images of lumbar chordoma preoperative axial magnetic resonance images of lumbar chordoma (left); preoperative sagittal magnetic resonance images of lumbar chordoma (middle); and postoperative lateral radiographs (right) (see Ozaki et al., 2002).

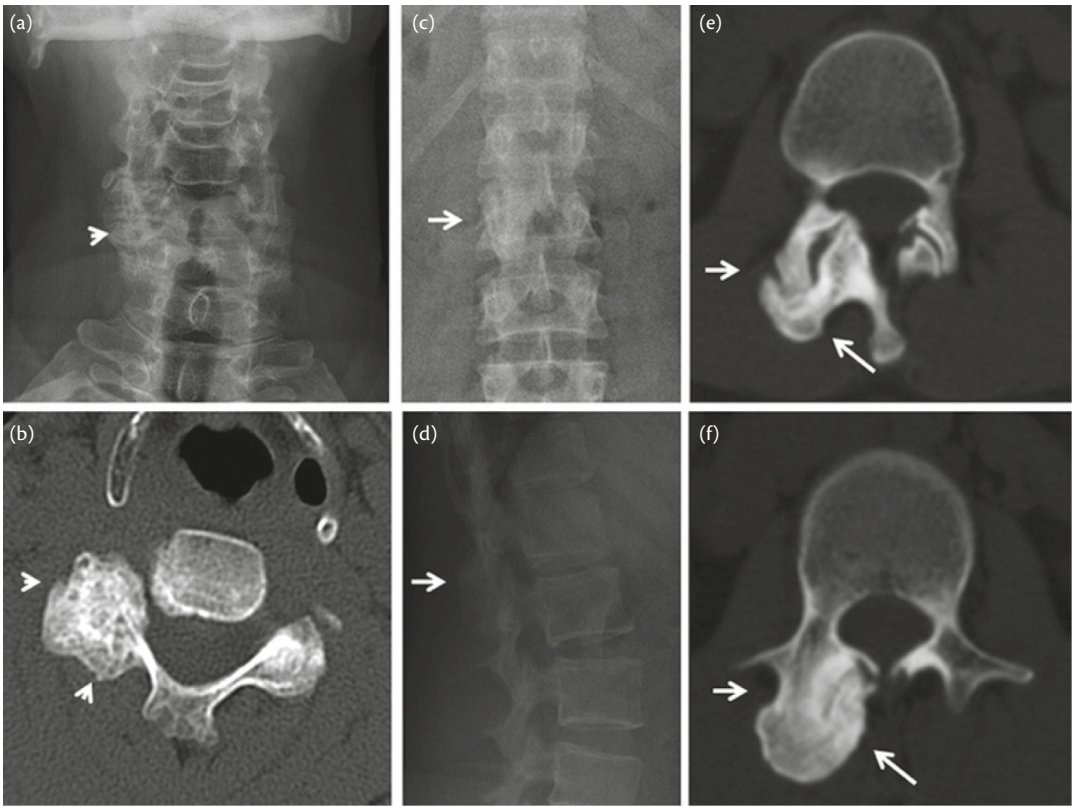

Fig. 63.10 Two different patients with osteochondromas of the spine. First patient: a 45-year-old man with an osteochondroma originating from the right C5–C6 facet joint. (A) Anteroposterior (AP) cervical X-ray; (B) axial computed tomography (CT) scan demonstrates a well-defined bone forming a tumour with lobulated contours (arrowheads). Second patient: a 36-year-old woman with back pain. (C, D) AP and lateral X-rays; (E, F) axial CT scan shows similar imaging findings at the right superior articular process of L2 vertebra (arrows) (see Anderson and Smith, 2013).

Fig. 63.11 Multiple myeloma. Sagittal images of the lumbar spine in (A) T1-weighted and (B) T2-weighted, show similar, variegated areas of abnormal signal intensity throughout the marrow of the lower thoracic and lumbar spine.

radiotherapy compared with radiotherapy alone as a treatment for MSCC had found no difference in neurological outcome between the groups (Young et al., 1980). A contemporary estimate of laminectomy morbidity of 10% together with awareness of the inefficacy of laminectomy at treating ventral cord compression from vertebral body collapse led to a surgical approach to MSCC being abandoned in favour of radiotherapy alone. Radiotherapy is efficacious in the treatment of MSCC and, for example, in one large study (Maranzano and Latini, 1995), all but 2 of 109 walkers retained the ability and of 82 patients who had lost the ability to walk but had some preserved power, 60% recovered ambulation.

Patchell et al. (2005) reported a randomized controlled trial of 101 patients with MSCC with 50 patients randomized to receive surgery followed by radiotherapy and 51 to receive radiotherapy alone. The trial was stopped early after an interim analysis. The primary outcome was ambulation and 84% of the surgical group were able to walk after treatment compared to 57% after radiotherapy alone. The study also showed a significant advantage of surgery in terms of duration of ambulation, recovery of ambulation for those patients who had lost the ability to walk preoperatively, post-treatment continence, and survival. While the evidence appears to be overwhelmingly in support of the statement that surgical treatment of MSCC has more to offer patients than radiotherapy alone, it is not unbalanced in the literature and in a larger but retrospective matched pair analysis, no significant benefit of surgery over radiotherapy alone was demonstrated (Rades et al., 2010).

If we accept that surgery does have a potential benefit over radiotherapy alone, this is not to say that all patients with MSCC should

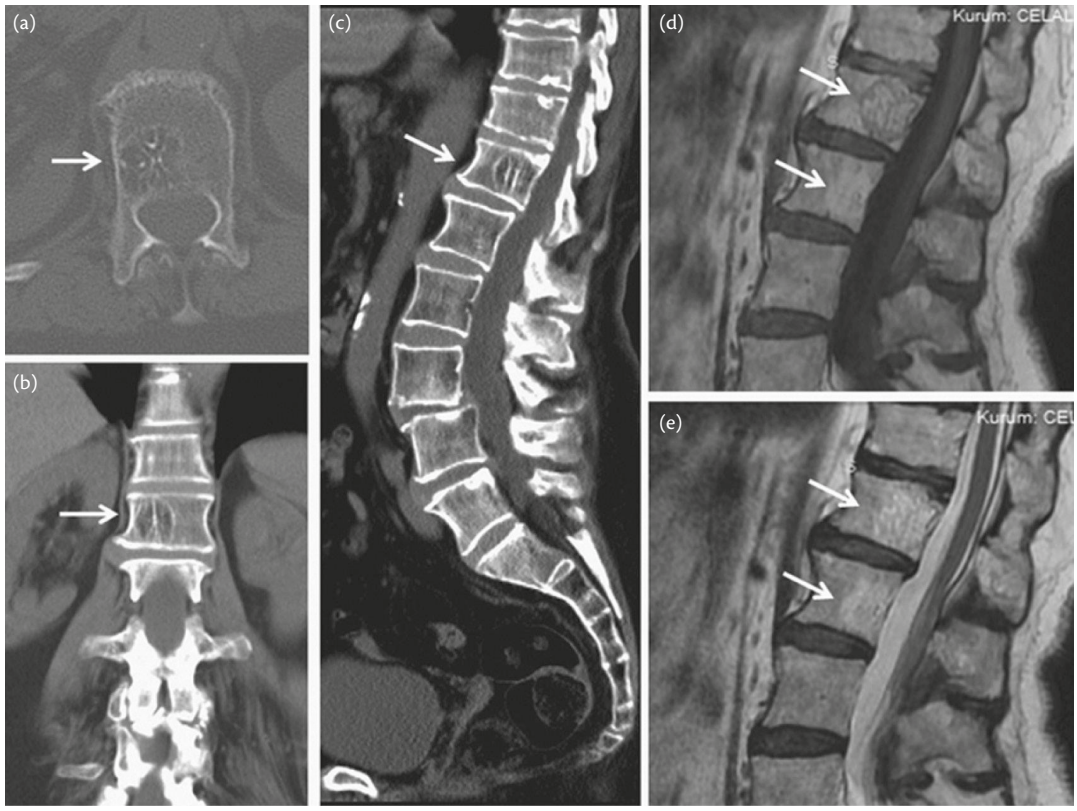

Fig. 63.12 Haemangioma. (A) Axial computed tomography (CT) scan image showing multiple punctate areas of sclerosis creating the white polka-dot sign. (B) Coronal and (C) sagittal reconstructed CT images displaying prominent vertical trabecula of corpus of the D12 vertebra resembling a honeycomb and forming the 'corduroy' sign. (D) Sagittal T1-weighted and (E) sagittal T2-weighted magnetic resonance images demonstrating two haemangiomas at the D12 and L1 vertebrae with high signal intensity (arrows).

be treated surgically. In the index study (Patchell et al., 2005), it took over 10 years to recruit the 101 patients from 7 neuro-oncology centres. This should perhaps be considered as surprising for a condition with an incidence of 5–8/100 000 (Loblaw et al., 2003) and suggests selection bias, and therefore that the treatment may be applicable to a small subgroup of patients with MSCC. Among 903 patients referred acutely for treatment for MSCC in a region of Norway during an 18-month period, only 58 (6.4%) were treated surgically (Zaikova et al., 2011).

It is thus likely then that the patients to whom the studies on the surgical treatment of MSCC apply represent a small subgroup. Anterior thoracolumbar spinal decompression and reconstruction is major surgery with reported complication rates as high as 52% and mortality as high as 13% (Dunning et al., 2012) and perhaps poorly

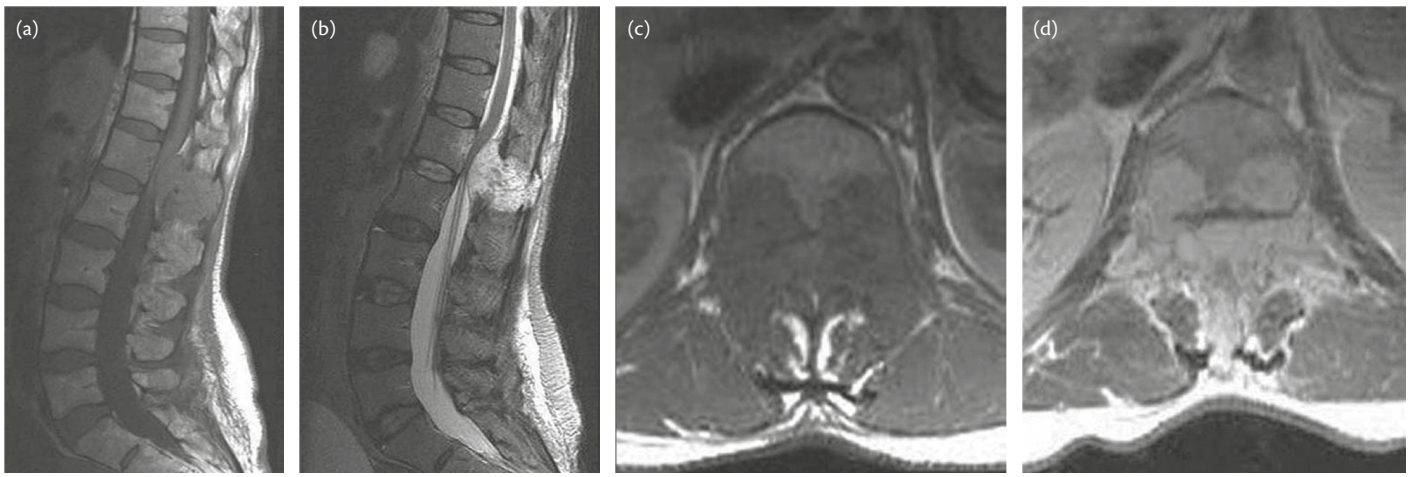

Fig. 63.13 Haemangioma. Exophytic mass affecting posterior aspect of vertebral bodies and posterior elements is shown on T1 (A) and T2 (B) sagittal MRI (arrows). Axial MRI before (C) and after (D) contrast show intense enhancement of the haemangioma with substantial compression of the thecal sac (arrows).

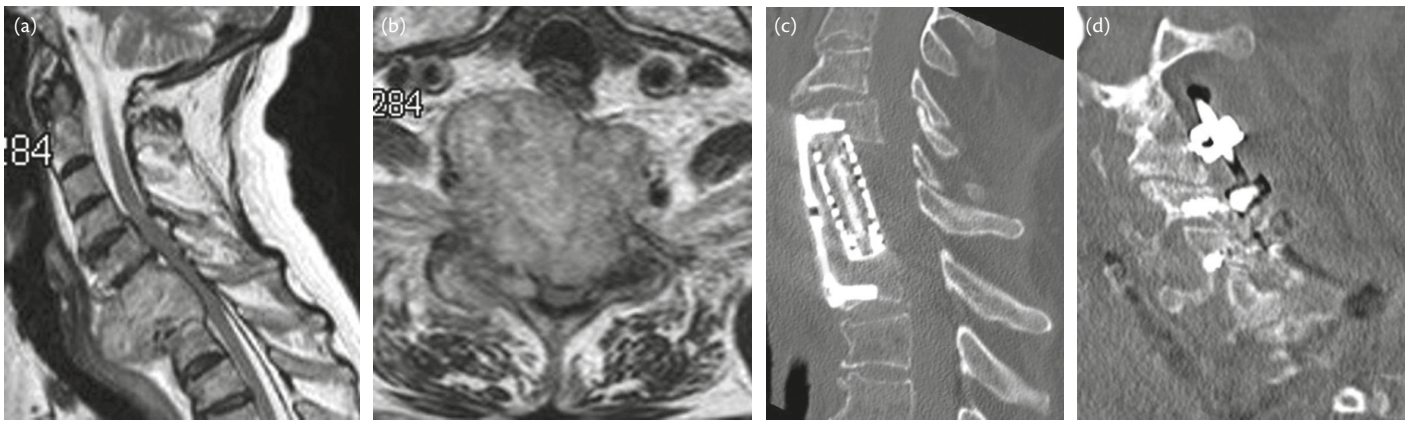

Fig. 63.14 This patient presented with progressive difficulty ambulating over a few days. They were found to have a destructive cervical lesion with cord compression on MRI, the patient was diagnosed with metastatic breast cancer at this primary presentation. She underwent a two-level vertebrectomy, followed by a posterior approach for instrumentation from C4 to T1.

suited to patients in the terminal phase of their disease. Recovery from anterior spinal surgery can be expected to last 3 months with persistent restriction of physical activity advised for as long as 6 months and symptomatic improvement possible over 18 months postoperatively (RNOH, 2018). Taken as a whole, patients with MSCC have a poor prognosis and in a population-based study, 74% had died within 3 months of admission (McLinton and Hutchison, 2006). For those patients with prognoses at or close to the anticipated rehabilitation period for the procedure, surgery is extremely unlikely to be of benefit. It is also worth noting that a subgroup analysis of the Patchell study demonstrated that the beneficial effect of surgery over radiotherapy alone is lost for patients above the age of 65 (Chi et al., 2009).

Those involved in the surgical treatment of MSCC should, while aware of the potential benefit that such therapy can bring to their patients, expect it to be applicable to only a very small proportion of patients with the condition.

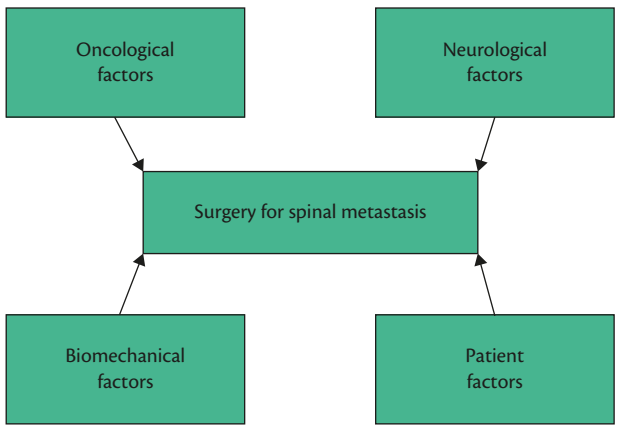

Fig. 63.15 Illustration of the many factors to be considered when advising a patient with spinal metastatic malignancy about surgical intervention.

FURTHER READING

Dang, L., Liu, X., Dang, G., et al. (2015). Primary tumors of the spine: a review of clinical features in 438 patients. *J Neurooncol*, **121**, 513–20.

Klekamp, J. (2013). Treatment of intramedullary tumors: analysis of surgical morbidity and long-term results. *J Neurosurg Spine*, **19**, 12–26.

Patchell, R.A., Tibbs, P.A., Regine, W.F., et al. (2005). Direct decompressive surgical resection in the treatment of spinal cord compression caused by metastatic cancer: a randomised trial. *Lancet*, **366**, 643–8.

Tokuhashi, Y., Matsuzaki, H., Oda, H., Oshima, M., & Ryu, J. (2005). A revised scoring system for preoperative evaluation of metastatic spine tumor prognosis. *Spine*, **30**, 2186–91.

Zaikova, O., Fossa, S.D., Bruland, O.S., Giercksky, K.-E., Sandstad, B., & Skjeldal, S. (2011). Radiotherapy or surgery for spine metastases? A population-based study of 903 patients in the south-eastern region of Norway. *Acta Orthop*, **82**, 365–71.

REFERENCES

Anderson, M.W. & Smith, S.E. (2013). *Musculoskeletal Imaging Cases*. Oxford, UK: Oxford University Press.

Baptiste, D.C. & Fehlings, M.G. (2006). Pathophysiology of cervical myelopathy. *Spine J* **6**, 190S–7S.

Barzin, M. & Maleki, I. (2009). Incidence of vertebral hemangioma on spinal magnetic resonance imaging in Northern Iran. *Pakistan J Biol Sci*, **12**, 542–4.

Boström, A., von Lehe, M., Hartmann, W., et al. (2011). Surgery for spinal cord ependymomas: outcome and prognostic factors. *Neurosurg*, **68**, 302–9.

Cahill, D.W. (1996). Surgical management of malignant tumors of the adult bony spine. *South Med J*, **89**, 653–65.

Chi, J.H., Gokaslan, Z., McCormick, P., Tibbs, P.A., Kryscio, R.J., & Patchell, R.A. (2009). Selected treatment for patients with malignant epidural cord compression—does age matter? *Spine*, **34**, 431–5.

Cole, J.S. & Patchell, R.A. (2008). Metastatic epidural spinal cord compression. *Lancet Neurol*, **7**, 459–66.

Dang, L., Liu, X., Dang, G., et al. (2015). Primary tumors of the spine: a review of clinical features in 438 patients. *J Neurooncol*, **121**, 513–20.

Dunning, E.C., Butler, J.S., & Morris, S. (2012). Complications in the management of metastatic spinal disease. *World J Orthop*, **3**, 114–21.

Ferlay, J., Soerjomataram, I., Dikshit, R., et al. (2013). GLOBOCAN 2012 v1.0, Cancer Incidence and Mortality Worldwide: IARC CancerBase No. 11. Lyon, France: International Agency for Research on Cancer. http://publications.iarc.fr/Databases/Iarc-Cancerbases/GLOBOCAN-2012-Estimated-Cancer-Incidence-Mortality-And-Prevalence-Worldwide-In-2012-V1.0-2012

Fox, M.W. & Onofrio, B.M. (1993). The natural history and management of symptomatic and asymptomatic vertebral hemangiomas. *J Neurosurg*, **78**, 36–45.

Fuchs, B., Dickey, I.D., Yaszemski, M.J., Inwards, C.Y., & Sim, F.H. (2005). Operative management of sacral chordoma. *J Bone Joint Surg Am*, **87**, 2211–16.

Gerszten, P.C., Mendel, E., & Yamada, Y. (2009). Radiotherapy and radiosurgery for metastatic spine disease: what are the options, indications, and outcomes? *Spine*, **15**(22 Suppl), S78–92.

Hall, H. (2014). Effective spine triage: patterns of pain. *Ochsner J*, **14**, 88–95.

Jones, J.M., Huggins, M.A., Rydall, A.C., & Rodin, G.M. (2003). Symptomatic distress, hopelessness, and the desire for hastened death in hospitalized cancer patients. *J Psychosom Res*, **55**, 411–18.

Klekamp, J. (2013). Treatment of intramedullary tumors: analysis of surgical morbidity and long-term results. *J Neurosurg Spine*, **19**, 12–26.

Li, T.-Y., Chu, J.S., Xu, Y.L., et al. (2014). Surgical strategies and outcomes of spinal ependymomas of different lengths: analysis of 210 patients. *J Neurosurg Spine*, **21**, 249–59.

Loblaw, D.A., Laperriere, N.J., & Mackillop, W.J. (2003). A population-based study of malignant spinal cord compression in Ontario. *Clin Oncol*, **15**, 211–17.

Manzano, G., Green, B.A., Vanni, S., & Levi, A.D. (2008). Contemporary management of adult intramedullary spinal tumors—pathology and neurological outcomes related to surgical resection. *Spinal Cord*, **46**, 540–6.

Maranzano, E. & Latini, P. (1995). Effectiveness of radiation therapy without surgery in metastatic spinal cord compression: final results from a prospective trial. *Int J Radiation Oncology Biol Phys*, **32**, 959–67.

Marchetti, M., De Martin, E., Milanesi, I., & Fariselli, L. (2013). Intradural extramedullary benign spinal lesions radiosurgery. Medium- to long-term results from a single institution experience. *Acta Neurochir*, **155**, 1215–22.

McLinton, A. & Hutchison, C. (2006). Malignant spinal cord compression: a retrospective audit of clinical practice at a UK regional cancer centre. *BJ Cancer*, **94**, 486–91.

Millward, C.P., Bhagawati, D., Chan, H.W., Bestwick, J., & Brecknell, J.E. (2015). Retrospective observational comparative study of hemilaminectomy versus laminectomy for intraspinal tumour resection; shorter stays, lower analgesic usage and less kyphotic deformity. *Br J Neurosurg*, **29**(3), 390–5.

Ozaki, T., Flege, S., Liljenqvist, U., et al. (2002). Osteosarcoma of the spine: experience of the Cooperative Osteosarcoma Study Group. *Cancer*, **94**(4), 1069–77.

Patchell, R.A., Tibbs, P.A., Regine, W.F., et al. (2005). Direct decompressive surgical resection in the treatment of spinal cord compression caused by metastatic cancer: a randomised trial. *Lancet*, **366**, 643–8.

Quiriny, M. & Gebhart, M. (2008). Chondrosarcoma of the spine: a report of three cases and literature review. *Acta Orthop Belg*, **74**(6), 885–90.

Quraishi, N.A., Ramoutar, D., Sureshkumar, D., et al. (2014). Metastatic spinal cord compression as a result of the unknown primary tumour. *Eur Spine J*, **23**, 1502–7.

Rades, D., Huttenlocher, S., Dunst, J., et al. (2010). Matched pair analysis comparing surgery followed by radiotherapy and radiotherapy alone for metastatic spinal cord compression. *J Clin Oncol*, **28**, 3597–604.

Rao, G., Ha, C.S., Chakrabarti, I., Feiz-Erfan, I., Mendel, E., & Rhines, L.D. (2006). Multiple myeloma of the cervical spine: treatment strategies for pain and spinal instability. *J Neurosurg Spine*, **5**, 140–5.

RNOH Physiotherapy Department (2018). *Rehabilitation Guidelines*. https://www.rnoh.nhs.uk/our-services/rehabilitation-guidelines

Ruff, R.L., Adamson, V.W., Ruff, S.S., & Wang, X. (2007). Directed rehabilitation reduces pain and depression while increasing independence and satisfaction with life for patients with paraplegia due to epidural metastatic spinal cord compression. *J Rehabil Res Dev*, **44**, 1–10.

Sansur, C.A., Pouratian, N., Dumont, A.S., Schiff, D., Shaffrey, C.I., & Shaffrey, M.E. (2007). Part II: spinal-cord neoplasms—primary tumours of the bony spine and adjacent soft tissues. *Lancet Oncol*, **8**, 137–47.

Sciubba, D.M., Petteys, R.J., Dekutoski, M.B., et al. (2010). Diagnosis and management of metastatic spine disease. A review. *J Neurosurg Spine*, **13**, 94–108.

Shin, S.H., Jung, K.W., Ha, J., Lee, S.H., Won, Y.J., & Yoo, H. (2015). Population-based incidence and survival for primary central nervous system lymphoma in Korea, 1999–2009. *Cancer Res Treat*, **47**(4), 569–74.

Sorensen, S., Helweg-Larsen, S., Mouridsen, H., & Hansen, H.H. (1994). Effect of high-dose dexamethasone in carcinomatous metastatic spinal cord compression treated with radiotherapy: a randomised trial. *Eur J Cancer*, **30A**, 22–7.

Srinivas, S.V., Deyo, R.A., & Berger, Z.D. (2012). Application of 'less is more' to low back pain. *Arch Intern Med*, **172**, 1016–20.

Sun, G., Li, L., Jin, P., Liu, X.-W., & Li, M. (2014). Percutaneous vertebroplasty for painful spinal metastasis with epidural encroachment. *J Surg Oncol*, **110**, 123–8.

Tokuhashi, Y., Matsuzaki, H., Oda, H., Oshima, M., & Ryu, J. (2005). A revised scoring system for preoperative evaluation of metastatic spine tumor prognosis. *Spine*, **30**, 2186–91.

Traul, D.E., Shaffrey, M.E., & Schiff, D. (2007). Part 1: spinal-cord neoplasms—intradural neoplasms. *Lancet Oncol*, **8**, 35–45.

Walcott, B.P., Nahed, B.V., Mohyeldin, A., Coumans, J.V., Kahle, K.T., & Ferreira, M.J. (2012). Chordoma: current concepts, management, and future directions. *Lancet Oncol*, **13**(2), e69–76.

Wu, Y.-L., Chang, C.-Y., Hsu, S.-S., et al. (2014). Intraspinal tumors: analysis of 184 patients treated surgically. *J Chin Med Assoc*, **77**, 626–9.

Young, R.F., Post, E.M., & King, G.A. (1980). Treatment of spinal epidural metastases: randomised prospective comparison of laminectomy and radiotherapy. *J Neurosurg*, **53**, 741–8.

Zaikova, O., Fossa, S.D., Bruland, O.S., Giercksky, K.-E., Sandstad, B., & Skjeldal, S. (2011). Radiotherapy or surgery for spine metastases? A population-based study of 903 patients in the south-eastern region of Norway. *Acta Orthop*, **82**, 365–71.

Ziari, F., Arikat, A., Allaoui, M., Marhino, P., & Assaker, R. (2012). Minimally invasive decompression and stabilization for the management of thoracolumbar spine metastasis. *J Neurosurg Spine*, **17**, 19–23.

RELATED LINKS TO EBRAIN

Imaging Features of Intramedullary Spinal Cord Tumours. https://learning.ebrain.net/course/view.php?id=784

Intramedullary Spinal Cord Tumours. https://learning.ebrain.net/course/view.php?id=1263

Malignant Spinal Cord Compression. https://learning.ebrain.net/course/view.php?id=933

Primary Bone Tumours of the Spine. https://learning.ebrain.net/course/view.php?id=809

Principles in Managing Intradural, Extramedullary Spinal Tumours. https://learning.ebrain.net/course/view.php?id=461

Radiology of Spinal Intradural Extramedullary Tumours. https://learning.ebrain.net/course/view.php?id=460

Surgical Treatment of Spinal Intradural Extramedullary Tumours. https://learning.ebrain.net/course/view.php?id=459

64

Vascular lesions of the spinal cord

Daniel Walsh

The normal vascular anatomy of the spinal cord

Arterial supply

The spinal cord is irrigated by perforating arteries which arise from a single ventral arterial axis—the anterior spinal artery (ASA)—and two dorsal arterial axes—the posterior spinal arteries (PSA). Branches of the radicular arteries reach the cord by following the dorsal and ventral roots. The anterior axis lies within the ventral spinal cleft and forms from a series of radiculomedullary arteries, while the posterior form from radiculopial vessels.

Embryogenesis

These ventral and dorsal axes themselves develop *in-utero* as paired metameric arteries. From the sixth week to the fourth month of intrauterine life fusion occurs of the anterior metameric pairs ultimately forming the ASA. Simultaneously *desegmentation* occurs with involution of many metameric arteries. Of 62 metameric vessels (31 dorsal and 31 ventral) 4–8 remain ventrally and 10–20 persist dorsally (Lasjaunias et al., 2001).

The anterior spinal axis is established first and the posterior axes mature later at approximately 15–20 weeks of fetal development. Failure of fusion accounts for the occasional fenestrations seen in the ASA.

There is great variability in the degree to which anterior metameric arteries regress, but two relatively constant remnants are named.

The artery of the lumbar enlargement (also known as the artery of *Adamkiewicz* or *arteria radciularis magna*) most often arises from the left side. In 75% of cases it arises between T9 and T12. When it arises outside of that area there is usually a second large, persisting metameric artery to be found cranially or caudally.

The artery of the cervical enlargement is reliably identified entering the C5/6 level and arises from thyrocervical and costocervical trunks. Variation is again frequent, and its direct origin from the subclavian artery has also been described (Miller, 1993).

The radicular arteries

The intrinsic supply is derived from extrinsic supply formed by each radicular artery. They reliably give radiculospinal and radiculomeningeal branches. At each level, the radiculospinal branch may divide into anterior and posterior branches entering the spinal canal with the corresponding nerve roots.

This extrinsic arterial supply is relatively well collateralized, particularly in the cervical region. Occlusion of the costocervical artery is relatively unlikely to result in anterior spinal infarction, as the deep and ascending cervical arteries will collateralize the anterior spinal axis.

The radiculomeningeal branches supply the nerve root's dural sheath and contents but do not reach the spinal cord. It is from these arteries that spinal dural arteriovenous fistulae recruit arterial supply. It is the radiculospinal branches that contribute to the intrinsic supply of the cord and from which spinal cord arteriovenous malformations and perimedullary arteriovenous fistulas recruit supply.

Arriving at the cord each radiculospinal artery contributes to the posterior and/or anterior axes via radiculopial or radiculomedullary arteries, respectively (**Fig. 64.1**).

Radiculopial arteries

The terminal branches of the radicular arteries, reaching the pia via the spinal root, form PSA. Those branches reaching the cord are termed *radiculopial* arteries and they invade the cord from the pial surface and supply the peripheral parts of the cord with a watershed region at the interface between the white and grey matter. Small branches from radiculopial and radiculomedullary systems run on the pial surface and encircle the cord. These are referred to as *vasa coronae.* These give perforating vessels into the superficial white matter of the cord as well as forming a superficial anastomosis with the anterior circulation.

Radiculomedullary arteries

The anterior axis irrigates most of the anterior grey matter of the spinal cord via radial branches of the radiculomedullary vessels as well as the anterior part of the posterior grey matter and elements of the anterior, lateral, and posterior white columns. Each radiculomedullary artery contributes a superior and inferior ramus to form the anterior arterial axis. *Sulco-commissural* arteries penetrate the cord via the ventral commissure in turn giving rise to the radially directed perforating vessels, which irrigate the cord.

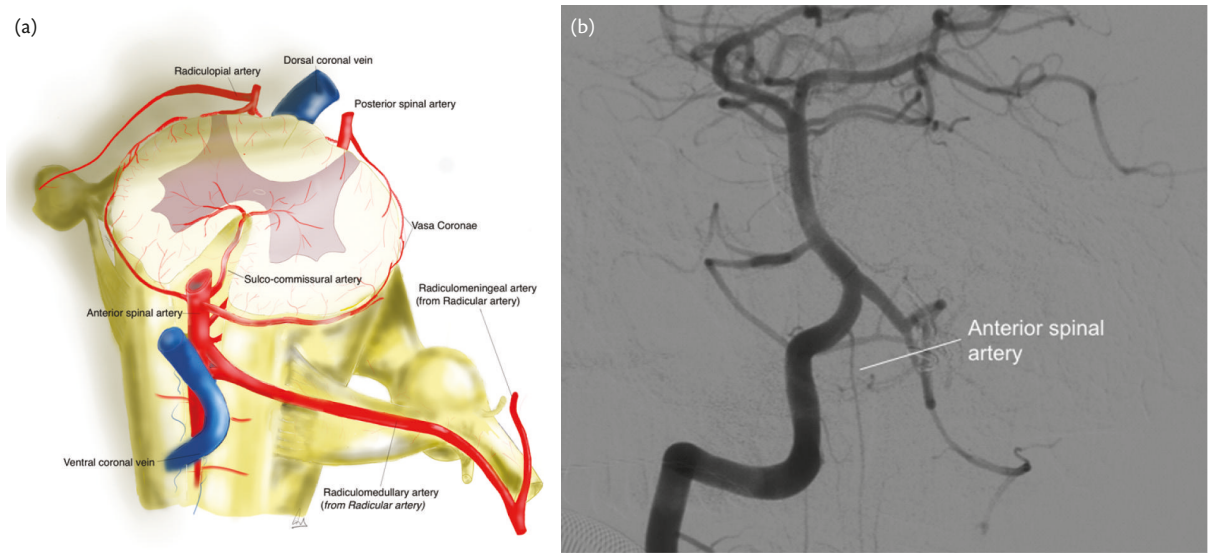

Fig. 64.1 (A) Line drawing of anterior and posterior arterial axes; (B) spinal angiogram (right vertebral artery injection).

Arterial anastomoses and the 'conus basket'

The vasa coronae and radial perforating vessels form longitudinal and segmental anastomoses along the cord. The relative contributions by the radiculopial and radiculomedullary systems vary. The cervical cord is evenly served while radiculopial vessels irrigate the thoracic cord proportionally more and less reliably although the well-known vulnerability of the thoracic cord to ischaemia may also be a function of its venous drainage as discussed next. The lumbosacral segments rely mainly on the central radiculomedullary system (Hassler, 1966).

There is an especially well-developed anastomotic channel between anterior and posterior arterial axes at the level of the conus medullaris. This is referred to as the *conus basket* (Lasjaunias et al., 2001). The ASA tapers as it runs down the anterior surface of the conus and one to two branches join it to the PSA (Martirosyan et al., 2015). The artery of the filum terminale is the terminal continuation of the anterior axis below the conus.

Venous drainage

The cord blood drains primarily via a dorsally and ventrally located coronal venous plexus each draining venous capillary networks along the length of the cord. Thron described larger veins traversing the thoracic cord particularly and facilitating communication between ventral and dorsal collectors. This results in relatively redundant venous drainage capacity in the thoracic cord perhaps rendering it vulnerable to congestion (Thron, 1988).

Spinal angiography

Catheter spinal angiography remains the gold standard for the assessment of structural vascular pathology. Sequential catheterization of each segmental arterial supply to the cord together with examination of the circle of Willis and medial sacral arteries is required. Access is usually via the femoral arteries, but brachial access may facilitate examination of the thoracic and cervical segments in the presence of severe aortoiliac disease.

A full angiographic interrogation of the cord is therefore a relatively prolonged process and may require staging or general anaesthesia to ensure the patient remains comfortable and still throughout. Physiological movement (e.g. respiration and peristalsis) may degrade imaging and are more easily controlled under general anaesthesia. Staging of the examination also allows the radiation exposure to be fractionated and the contrast load aliquoted.

At our institution specific cross-sectional imaging in the form of MR spinal angiography or CT angiography is utilized to allow targeting of catheter spinal angiography (Zampakis et al., 2006; Amarouche et al., 2015).

Neurological complications of spinal angiography are rare in experienced hands despite its technically demanding nature and that it is carried out far less frequently than cerebral angiography (Chen and Gailloud, 2011). Non-neurological complications that have been described included vascular injury, retroperitoneal haematoma, pulmonary oedema, and contrast sensitivity.

The intrinsic vessels of the cord are usually straightforward to distinguish on angiography. The veins are characteristically sinusoidal and centrally located while the arteries are straighter and the radiculomedullary vessels terminate in a characteristic 'hair-pin' morphology.

Spontaneous spinal haemorrhage

Spontaneous epidural spinal haemorrhage (SESH)

Spontaneous spinal epidural haemorrhages that are not associated with structural vascular lesions are usually the result of anticoagulant use. Such haemorrhage is responsible for up to 11.8% of non-traumatic spinal cord injury (Citterio et al., 2004). It is not presently known how the introduction of novel oral anticoagulants (NOACs) will affect its incidence.

In a systematic review of 553 reported patients with spontaneous central nervous system (CNS) haemorrhage, SESH patients were significantly younger. Some 88% underwent surgical decompression

with death and good recoveries each accounting for 21% of outcomes in an admittedly small cohort. The same authors conducted a post-mortem examination which did not identify any different cellular inflammatory responses from traumatic spinal cord injuries and suggest therefore that lessons in spinal cord protection learned from trauma can be usefully applied in SESH (Furlan et al., 2012).

Spinal aneurysm and spinal subarachnoid haemorrhage

Between 0.6 and 1% of intracranial subarachnoid haemorrhage may be caused by spinal pathology and in most of these cases a spinal vascular malformation or cavernoma is the culprit. Isolated saccular aneurysms of spinal arteries are exceptionally rare causes of subarachnoid haemorrhage (Handa et al., 1992; Massand et al., 2005).

Aneurysms of the PSAs appear to be rarer and more likely to be idiopathic. ASA aneurysms have been reported in association with mycotic infection, rheumatoid arthritis, fibromuscular dysplasia, and Behcet's disease. Most aneurysms reported have been successfully surgically treated. One case in a patient with Behcet's disease involuted with expectant management (Geibprasert et al., 2010).

There are case reports of spinal subarachnoid haemorrhage occurring in association with a variety of intradural tumours most commonly schwannomas, ependymomas, and haemangioblastomas.

Ischaemic myelopathy

Spinal cord infarction is rare and typically complicates aortic surgery or severe atherosclerotic aortic disease. Maintaining spinal cord blood flow greater than 10 ml/100 g/min (Gharagozloo et al., 1998) markedly reduces cord ischaemia during aortic cross clamping and this has led to interest in manipulating intrathecal cerebrospinal fluid pressure to potentiate the spinal cord perfusion pressure (SCPP). Animal experimental models demonstrated significant improvement in SCPP if CSF drainage was carried out before cross clamping (McCullough et al., 1988) and some have adopted it during repair of thoraco-abdominal aneurysms.

Chronic ischaemic myelopathy is most commonly encountered when caused by an arteriovenous fistula. Arterialization of the venous drainage from the cord is believed to sufficiently impair gas-transfer across the cord such that cell injury and eventually death is the result. Spinal dural arteriovenous fistula is the usual culprit but spinal vascular malformations with different architectures may also produce ischaemia.

Signs and symptoms of ischaemic myelopathy

The onset of symptoms is often insidious and delay in diagnosis common. In this author's personal series of spinal dural arteriovenous fistula (SDAVF) the median duration of symptoms before diagnosis is 18 months. Patients are more frequently male (1:1.5 ratio) and in the sixth and seventh decades of their life.

Motor and sensory symptoms tend to develop in tandem. Patients describe altered sensation and frequently a sensation of 'something crawling under the skin'. A sensory level in the later stages will be discerned. Sensory alteration typically begins distally and ascends to affect the trunk. Pain may occur mimicking lumbar radiculopathy and symptoms often deteriorate with exertion (Jellema et al., 2003). Gait disturbance has been reported to develop in between 20 to 69% of patients (Atkinson et al., 2001). Mixed upper- and lower-motor neurone findings as well as impairment of proprioception are typical. Sphincteric and sexual functions are frequently affected and are the symptoms least likely to recover after successful treatment.

A high index of clinical suspicion is necessary to prompt timely investigation and treatment. Arteriovenous shunts producing cervical cord ischaemia are relatively rare and, in our experience, more likely to be caused by Cognard type V cranial dural arteriovenous fistulae. A thorough angiographic examination of the circle of Willis and the external carotid circulation is therefore necessary in such a case.

Investigation

The appearances of cord ischaemia alone are compatible with a wide range of differential diagnoses. Where no structural vascular abnormality can be identified it is appropriate to screen for potential neuro-inflammatory and neoplastic causes and the investigation of these lies outside the scope of this chapter.

MR usually suggests the diagnosis with congestion of the cord manifesting with apparent increased volume. The middle and lower thoracic segments are affected most often and oedema of the conus medullaris observed in most cases (Muralidharan et al., 2013). There is centrally increased T2 signal and a ring of relatively low intensity peripherally thought to reflect the presence of deoxygenated blood in cord capillaries (Gilbertson et al., 1976). Where there is an associated arteriovenous shunt, the dilated coronal venous plexuses may be seen on the cord as multiple small flow voids. When prominent these make the MR appearance of a spinal dural arteriovenous fistula pathognomic (**Fig. 64.2**A). Pial shunts may mimic this appearance too although these tend to be given away by the presence of more dense conglomerations of arterialized vessels near the surface of the cord.

MR and CT angiography have both been used to characterize the architecture of spinal dural arteriovenous fistulae. Time-resolved imaging contrast kinetics MR angiography is used in our department to estimate the level of the fistula and targeted catheter angiography is carried out at that level and the immediately adjacent segments to confirm the presence of the fistula and determine if there are significant metameric arteries nearby. It does not provide particularly useful information on the architecture of polyfistulous lesions or parenchymal arteriovenous malformations in which cases catheter angiography is preferred as the index vascular imaging (Amarouche et al., 2015).

Two-dimensional (2D) angiotomography is helpful when planning surgery to lesions with complex architectures. Cross-sectional images are acquired during microcatheter angiography and allow resolution of the arterial and venous phases of the malformation while relating that to the nervous and bony structures. An example is shown in **Figure 64.3**B where the relationship of the spinal vascular malformation to the conus medullaris is better demonstrated than on axial MR or conventional angiography. This facilitated planning of the surgical approach in the illustrative case where the anatomy of the scoliotic spine was complex.

Spinal vascular malformations

In this section we will examine structural vascular malformations in more detail considering their angio-architectures, classification, and

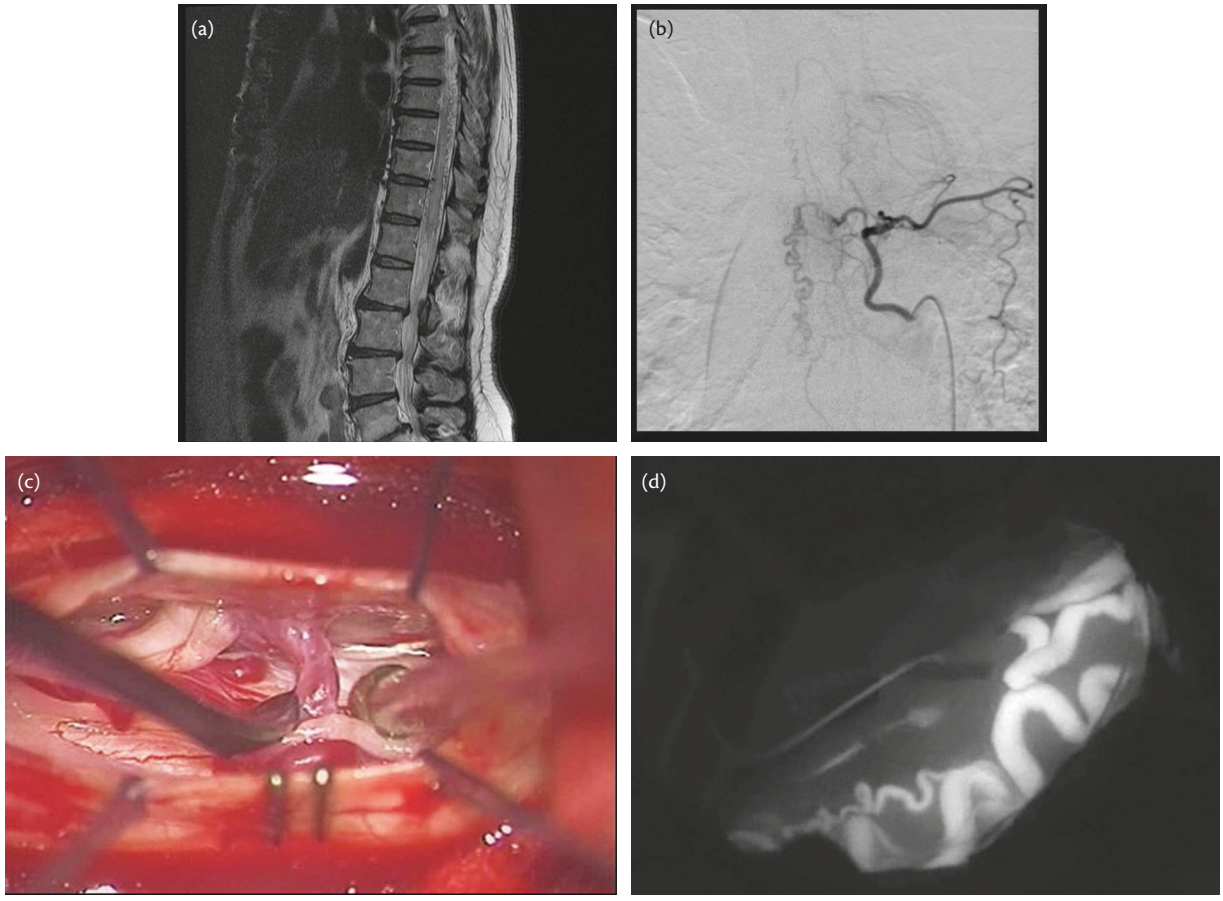

Fig. 64.2 (A) MRI of patient with spinal dural arteriovenous fistula (SDAVF); (B) angiographic appearance of SDAVF; (C) fistulous vessel draining from dural leaflet to coronal venous plexus of cord; (D) ICG-videoangiogram illustrating arterialization of dorsal coronal vein.

clinical associations. Understanding the architecture of a spinal vascular malformation (SVM) is an important step towards treating it.

Classification systems

Classification systems have proliferated over the years and the subject is intimidating when first approached. In truth there is still no universally agreed system of describing SVM and one regularly encounters lesions where there is some disagreement as to the correct terminology. Surgeons have historically tended to favour anatomically based systems while radiologists concentrate on the haemodynamics and aetiology of the arteriovenous shunt.

Essentially what one requires of a classification system are the answers to three questions:

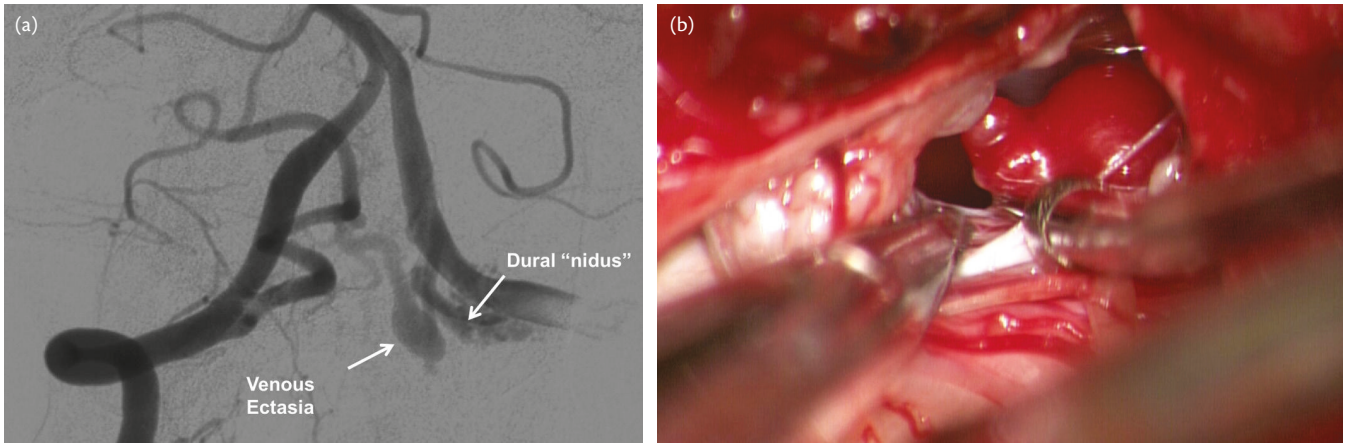

Fig. 64.3 (A) Cervical dural arteriovenous fistula with venous ectasia. This lesion presented after subarachnoid haemorrhage. (B) The venous aneurysm seen via a far-lateral approach.

1. Where is the arteriovenous shunt occurring?
2. How may I reach it?
3. Need I look for coincident pathology?

In 2002 the Hospital Bicêtre proposed a system of attractive simplicity broadly classifying spinal malformations into arteriovenous malformations and arteriovenous fistulae (Rodesch et al., 2002). They proposed assigning arteriovenous fistula (AVFs) and arteriovenous malformation (AVMs) to one of three categories, determined by their pathogenesis:

Group 1: **Genetic hereditary lesions** (e.g. associated with hereditary haemorrhagic telangiectasia)

Group 2: Genetic non-hereditary lesions which share a metameric connection. Hitherto a spinal vascular malformation affecting a variety of tissue types within one metameric segment was referred to as a *juvenile* or *metameric* AVM. Where all the tissues within the metamere were affected it was termed *Cobb's syndrome*. They may be a relatively common cause of myelopathy in CLOVES syndrome (Alomari et al., 2011). Categorization of craniofacial vascular malformations into the *cerebrofacial metameric arteriovenous syndromes (CAMS 1–3)* allows their description according to the metamere affected rather than relying on eponyms such as Wyburn-Mason syndrome or Bonnet-Dechaume-Blanc syndrome. The same system may be applied to the spinal metameres describing SAM types 1 to 31 according to the metamere affected. Polymetameric variants are possible (Bhattacharya et al., 2001).

Group 3: Solitary lesions. It is proposed that lesions in this group may represent the incomplete expression of type 1 and 2 lesions however it could also include acquired lesions meaning that the vast majority of spinal vascular malformations will fall into this latter group. It is useful to subcategorize this group accepting that the type III lesions formerly known as *juvenile* or *metameric* AVMs belong to the Bicêtre Group 2 and that there will be instances where Type IV lesions belong in Group 1 or 2 (e.g. in the *Ras*-opathy described as capillary malformation-AVM syndrome; Eerola et al., 2003; Thiex et al., 2010).

Such a system is useful because it prompts one to consider potential associated lesions with malformation of uncommon architecture or which involve more than one tissue type. For example, recognizing a group 1 lesion should prompt referral for genetic counselling and discussion with the patient regarding the potential pulmonary and central nervous system complications of hereditary haemorrhagic telangectasia (HHT). As originally described paraspinal and dural malformations are excluded, drawing criticism for making the system of limited practical application (Rodesch et al., 2002). We find it practical to include these lesions in the third group. Many paraspinal AVMs might be thought of as incomplete expressions of metameric lesions. There are examples of acquired perimedullary as well as spinal dural fistulae, and they sit comfortably together in the third group.

A system categorizing SVM into groups I-IV has endured through the years and it may be most correctly thought of as an evolving entity contributed to by a large group of clinician-scientists from France, Britain, and the United States. For that reason, some authors refer to an American–British–French connection when describing it (Black, 2006).

Box 64.1 Adapted Bicêtre Classification of Spinal Vascular Malformations

Group 1

Genetic hereditary lesions (e.g. associated with hereditary haemorrhagic telangectasia)

Group 2

Genetic Non-hereditary lesions which share a metameric connection—spinal arteriovenous metameric syndrome (SAMS)

Group 3

Solitary lesions which are acquired or represent incomplete manifestations of group 1 or 2

Paraspinal vascular malformation

Spinal dural arteriovenous fistula

- **a)** Solitary fistula
- **b)** Polyfistulous

Intramedullary AVM

Perimedullary fistula

- **a)** Solitary simple fistula, minimal venous dilation
- **b)** One to two feeding arteries, moderate venous enlargement +/– venous pouch at site of fistula
- **c)** Giant polyfistulous lesions

Reproduced with permission from Rodesch, Georges; Hurth, Michel, Classification of Spinal Cord Arteriovenous Shunts: Proposal for a Reappraisal—The Bicêtre Experience with 155 Consecutive Patients Treated between 1981 and 1999, *Neurosurgery*, Volume 51, Issue 2, pp. 374–80, Copyright © 2002 Oxford University Press and the Congress of Neurological Surgeons (CNS).

Merland proposed a useful subdivision (Gueguen et al., 1987) of the perimedullary fistulae described first by Djindjian (Djindjian et al., 1977). Heros suggested perimedullary fistulae be treated as a discrete Type IV lesion (Heros et al., 1986) while others describe them as fistulous AVMs (fistulous spinal cord arteriovenous malformations or SCAVM) because they are usually supplied mainly by the radiculomedullary arteries, considered part of the intrinsic cord blood supply.

It is perhaps best not to cling tightly to one nomenclature. Subdivisions emerge and lesions once believed distinct are discovered to have more in common than was previously understood. The remainder of this chapter utilizes the adaptation of the Bicêtre system described earlier (**Box 64.1**). The American–British–French system is summarized in **Table 64.1**. Thorough appreciation of the angio-architecture is possibly more important than the nomenclature one then applies.

Extradural (paraspinal) vascular malformations

These are rare lesions with drainage exclusively into the epidural venous plexus. These have been reported occurring autonomously (Willinsky, 1993), as a complication of trauma (Johnson et al., 1990) or in neurofibromatosis type 1 (Deans et al., 1982; Benndorf et al., 2000). These may also constitute an incomplete expression of a genetic, non-hereditary malformation as suggested by the Bicêtre group (see earlier).

Asymptomatic paraspinal malformations are occasionally encountered incidentally on cross-sectional imaging. Depending on the degree of venous engorgement they may produce symptoms when they compress the thecal sac or the nerve roots. **Figure 64.4** illustrates a paraspinal AVF presenting with a severe lumbar

Table 64.1 American–British–French classification of spinal vascular malformations

Type I	Spinal dural arteriovenous fistula • Solitary fistula • Polyfistulous
Type II	Intramedullary AVM
Type III	Juvenile or Metameric AVM (SAMS)
Type IV	Perimedullary fistula • Solitary simple fistula, minimal venous dilation • 1–2 feeding arteries, moderate venous enlargement +/– venous pouch at site of fistula • Giant polyfistulous lesions

radiculopathy. Embolization of the fistula resulted in rapid and complete resolution of the pain. Reversible myelopathy has also been reported (Willinsky, 1993).

These lesions may also present with spontaneous extradural haematomas particularly in children (Lonjon et al., 1997; Sivakumaran et al., 2016). Such haematomas are thought to result from vascular malformations in 3–18% of cases (Kubo et al., 1984; Graziani et al., 1994).

Treatment is by endovascular or surgical means and based on published case reports outcomes are usually good for symptomatic lesions.

Spinal dural arteriovenous fistulae

SDAVF account for 70–85% of vascular malformations presenting in clinical practice (Merland et al., 1980; Symon et al., 1984) and occur up to five times more frequently in males. Symptoms typically develop after the fifth decade of life. This is in contrast to other varieties of SVM which present earlier in life, usually the third and fourth decades (Djindjian et al., 1977; Rosenblum et al., 1987). SDAVF are believed to be acquired lesions although their pathogenesis is not understood.

The most common location of the fistula is in the thoracic spine. In our series this accounts for 68.5% of cases. Cervical and sacral lesions are rare accounting for less than 5% each and lumbar cases constitute 21%. Multiple fistulae have an estimated incidence of 2% (Krings et al., 2004).

Fistulation occurs within the dural leaflet near the exiting spinal nerve root. This is near where a vein normally drains blood from the radiculomeningeal artery supplying the nerve sheath and its contents. This vein becomes arterialized and is readily recognized as it penetrates the dura just caudal to the exiting nerve root. The vein typically enters directly beneath the vertebral pedicle. Careful inspection of the inside of the dura as the vein pierces it will reveal prominent arteries within feeding the fistula. Disconnection of the vein at this point will obliterate the arteriovenous shunt. Excision of the dura itself is not required to treat the fistula.

The arterialized vein connects directly to the coronal venous plexus causing congestion as described in the section on ischaemic myelopathy. Subarachnoid haemorrhage from spinal dural arteriovenous fistulae is extremely rare but has been most often reported in association with fistulae of the cervical canal. Cases of haemorrhage from lumbar and thoracic fistula have also been seen (Koch et al., 2004). Venous aneurysm and varicosity appear common in such instances.

Microsurgical treatment

The fistula is typically exposed intradurally via a (hemi)laminectomy or laminotomy. Tubular retraction systems and fibreoptic lighting allow minimally invasive approaches to be employed. The fistulous vein is identified entering the dura, diathermied, and then cut with fulguration of dura around the entry point. Extradural diathermy (or embolization) of arterial feeding vessels alone may result in transient improvement but are bound to result in the recruitment of other dural arterial vessels and recurrence of the fistula.

While arterialized the veins of the dorsal coronal plexus are engorged and slightly pink. When the shunt is closed these veins collapse and the pia-arachnoid around them becomes crenulated. This change is not always obvious to the naked eye in relatively low-flow arteriovenous shunts. Microdoppler examination (Iacopino et al., 2001) or indocyanine green videoangiography (ICG-VA) may be used to confirm normalization of flow in the vein. ICG-VA is also useful in detecting metameric vessels and distinguishing them from arterialized veins (Walsh et al., 2013). **Figures 64.2**A–D illustrate the change in flow observed on ICG-VA as the fistula is occluded.

Currently microsurgical division of the fistula is the criterion standard. A recent meta-analysis of the English Language literature

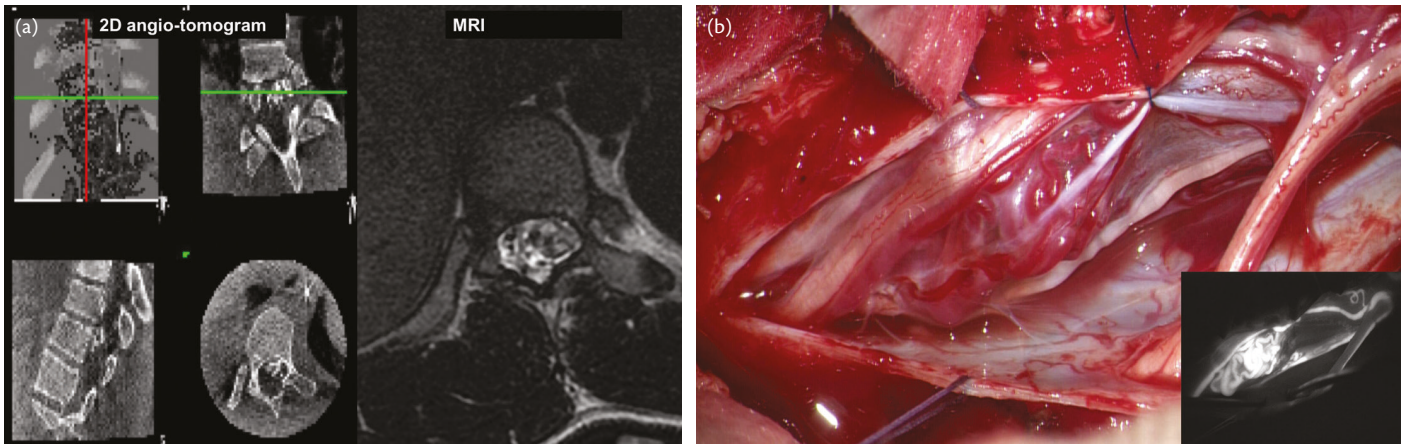

Fig. 64.4 (A) Two-dimensional (2D) angiotomograms demonstrating a compact intramedullary AVM at ventrolateral surface of conus; (B) operative view after costotransversecomy.

from 2004 onwards included 35 studies with 1112 patients. Surgery obliterated 96.6% (94.8–97.8% 95% CI) of fistulae. Endovascular treatment with N-butyl-cyanoacrylate (NBCA) glue or Onyx obliterated 72.2% (95% CI 68.1–75.9%). Late recurrence of the fistula was significantly more likely with endovascular treatment (Bakker et al., 2015).

Procedural complication rates also compare favourably. In the meta-analysis conducted by Steinmetz and colleagues a rate of 1.9% was reported for surgery and 3.7% for endovascular treatment. Both treatments are relatively safe and most morbidity minor. The 'point' disconnection possible at operation means there is little risk to the coronal vein itself.

A significant risk in surgical treatment is that the incorrect spinal level be approached. This risk is mitigated by the careful use of fluoroscopy. The deposition of an endovascular coil (Britz et al., 2004) or glue (Timo Krings et al., 2010) in the radiculomeningeal vessel aids identification of the level intraoperatively.

Endovascular treatment

To effect cure an embolic agent must reach the proximal part of the draining vein piercing the dura, replicating the 'point' disconnection of the arteriovenous shunt described earlier. Particle and coil embolization of arterial supply of the arterial inflow alone will not produce a lasting result. Liquid embolic agents such as Onyx or NCBA penetrate to the draining vein effectively when delivered transarterially. If, on control angiography, the agent has not reached the draining vein then further treatment will be required. This further procedure should not be delayed in hopes the fistula will spontaneously thrombose despite a patent draining vein. Further clinical deterioration has been described in such cases (Andres et al., 2008).

Cure rates are significantly lower than with surgical division. Some authors advocate a tentative attempt at embolization at the time of diagnostic angiography. Such a protocol should inform the patient of the small risk of retrograde coronal vein thrombosis which can result in neurological deterioration.

Treatment outcomes for SDAVF

The outcome from endovascular and surgical treatments of SDAVF are similar so long as the arteriovenous shunt is abolished. Aminoff and Logue (1974) graded deficits in the patients gait and control of micturition (Table 64.2) and this system is still commonly used to report treatment outcomes.

In a series of 154 patients treated surgically 45% of patients reported improved lower extremity strength at discharge. Some 12% reported improvement in sensation and 15% in sphincter control, while 17% reported worsened sphincter control at discharge. The majority of patients were unchanged in the short term by treatment. Utilizing the combined Aminoff-Logue gait and micturition scores as a composite index of disability, 45% of patients were found to have improved at a mean duration of follow-up of 31 months, while 34% remained at their preoperative baseline (Bakker et al., 2015). Sphincter dysfunction has an unfavourable prognosis. Steinmetz found approximately 33% of patients reported any improvement in sphincter function with 11% worsened in the longer term despite 89% of patients improving or stabilizing overall (Steinmetz et al., 2004).

Table 64.2 Aminoff-Logue grading system

Grade	Definition
Gait	
0	Normal
1	Leg weakness, abnormal gait, or stance without limitation of activity
2	Restricted activity
3	Requires one stick or similar support
4	Requires crutches or two sticks to walk
5	Unable to stand, bed-bound, or in a wheelchair
Micturition	
0	Normal
1	Hesitancy, frequency, or urgency
2	Occasional incontinence or retention
3	Permanent urinary incontinence or retention

Reproduced with permission from Aminoff, M. J.; Logue, Valentine, The Prognosis of Patients with Spinal Vascular Malformations, *Brain*, Volume 97, Issue 1, pp. 211–18, Copyright © 1974 Oxford University Press and the Guarantors of Brain.

Intramedullary arteriovenous malformations

Spinal cord arteriovenous malformations (SCAVM) are formed by shunts from the intrinsic arterial supply of the cord to its venous drainage. Some distinguish the *glomus* (or *nidal*) variety from *fistulous* AVM. Glomus (nidal) AVMs have a discrete nidus deep to the pia and are architecturally homologous to cerebral AVMs. These may be described as compact, diffuse, or of mixed types. We will consider fistulous lesions as a separate entity—perimedullary fistula (PMAVF). This distinction in the literature is confusing but illustrates the difficulty sometimes in appreciating a nidus when there is congestion of the various veno-venous and other physiological anastomoses in the cord.

These lesions may also be subdivided into 'high' and 'low' flow lesions. High-flow lesions are characterized by the remodelling of vessels: hypertrophy of arteries, and development of aneurysms and venous pouches. They are more often seen in children and patients with HHT. In their review of 155 patients, Rodesch and colleagues noted 31.6% incidence of arterial aneurysm (Rodesch et al., 2002).

Such vascular stress is associated with an increase in intramedullary or subarachnoid haemorrhage. They may also present with ischaemic myelopathy or symptoms resulting from neural compression by dilated vessels. Neuropathic pain is reported in about 30% of patients.

The natural history of incidentally discovered lesions is not known with any certainty. A pooled analysis of studies containing greater than three cases suggested an annual haemorrhage rate of 4% with approximately half these lesions first presenting with a haemorrhage. These same data showed partial treatment mitigated the risk somewhat with a recurrent rate of haemorrhage for partially treated lesions of 2–3% across all modalities (Gross and Du, 2013a).

Endovascular treatment

Endovascular treatment has an important place in the management of these lesions especially those fed primarily from the ASA. The

goals of treatment may be subtly different to cerebral AVM and there is some evidence that partial treatment may not only alleviate symptoms of ischaemia, mass-effect but may also favourably affect risk of haemorrhage. Onyx or NCBA glue are the most commonly used liquid embolic agents at present when trying to effect nidal penetration. Coils may be used to treat venous pouches, ectasia, and aneurysms.

Given considerable variation in the angio-architectures being treated, treatment outcomes vary and clearly the operator must exercise a great deal of judgement during each procedure to avoid inadvertent migration of embolic materials with resultant ischaemic injury.

In 16 studies containing 104 patients, 33% of treatments with liquid embolic agents resulted in complete obliteration of the shunt (Gross and Du, 2013a). Despite this Aminoff-Logue gait and micturition scores were similar to surgical outcomes at ten years. No re-haemorrhages were recorded in the follow-up periods. Recanalization was significantly more likely after poly-vinyl-alcohol (PVA) particle embolization (17%) compared to Onyx or NCBA glue (0–11%).

Microsurgery

Surgical extirpation is an effective treatment in selected cases, but the morbidity is determined mainly by the location of the malformation and the difficulty accessing it. Spetzler has suggested compact AVMs of the conus medullaris be considered a distinct subtype peculiarly amenable to surgical treatment (Spetzler et al., 2002).

The principles of surgical excision are similar to operating on the cranial homologue but certain nuances of technique merit comment. Firstly, as relatively low-flow lesions they may be advantageously approached from the venous side without the same fear of haemorrhage or congestion in the cord. Secondly excessive pial dissection may be avoided and elements of the shunt are divided 'in-situ' rather than attempting complete extirpation of every component of the malformation. When surgery follows endovascular embolization, it is not necessary to excise completely embolized elements of the malformation when it requires further disturbance of nervous tissue.

Most lesions are approached posteriorly or posterolaterally. Again, we have found 2D angiotomography helpful as an aid to planning the surgical approach and routinely make use of intraoperative neurophysiological monitoring, particularly of Delta waves and motor evoked potentials to detect alterations in the motor tracts anteriorly (**Fig. 64.4**A).

In Gross's analysis extirpation was achieved in 78% of cases. Long-term Aminoff-Logue gait scores were improved or stable in 93% and micturition scores the same or better in 94%. Many of these patients had significant disability however at the preoperative baseline and treatment was prompted by symptoms (Gross and Du, 2013a).

Radiosurgery

Spinal arteriovenous malformations are of such a volume as to be attractive for radiosurgical treatment. They pose challenges not encountered with their cerebral counterparts. Targeting the selected volume with highly conformal radiation while accounting for excursion of the target with respiratory movement is facilitated by modern image guidance systems.

Sinclair et al. reported their experience of treating 15 intradural AVMs using the CyberKnife™ platform. Concerned to avoid cord toxicity treatment was delivered in two to five sessions. Only one malformation was obliterated at a mean of 27.9 months of follow-up. The short follow-up of these lesions limited the conclusions that may be drawn regarding efficacy (Sinclair et al., 2006). Hida et al. reported a 10-year experience with ten patients using LINAC. Complete obliteration was not observed in any patient but with a median of 49 months follow-up, no subsequent haemorrhage was observed nor any radiation toxicity (Hida et al., 2003).

Spinal cord tolerances for radiation are still being explored. The chances of complete obliteration appear very low at present but given that partial treatment can improve outcome with other modalities, radiosurgery for these lesions merits further investigation.

Perimedullary fistula

Perimedullary arteriovenous fistulae (PMAVF) are direct communications between intrinsic arteries on the cord surface with the venous drainage. Usually arising from the anterior arterial axis, radiculopial fistulae are also occasionally encountered. They may be subclassified according to the number of arterial feeders, flow, and size (see **Box 64.1** and **Table 64.1**). In the literature they are sometimes referred to as pial arteriovenous fistulae or fistulous spinal cord AVM (SCAVM).

Most PMAVFs present with ischaemic myelopathy but haemorrhage occurs in about 32% distinguishing their clinical course from SDAVF (Gross and Du, 2013b). They may occur as isolated lesions or in association with genetic disease, for example, HHT (perimedullary macrofistulae) or CM-AVM *Ras*-opathy.

Again, reliable data on natural history are lacking since most of these uncommon lesions are discovered when symptomatic. Data on treatment is limited to relatively small case series although the published results are encouraging with obliteration rates of 93% for type A lesions and 71% for type C. Microsurgical and endovascular treatment are the mainstays of management. Type C lesions are particularly suitable for endovascular treatment as hypertrophied feeding arteries facilitate navigation. Type A and B lesions may be addressed by endovascular, surgical, or combined techniques. At our institution we have usually found PMAVF suitable for surgical treatment where endovascular treatment was not feasible (Amarouche et al., 2015).

There is little experience with radiosurgery in the literature. There is one case reported treated with CyberKnife without any outcome data. It is possible some of the Stanford series (CyberKnife) were fistulous AVMs but detail on all the architectures treated is not provided. We have treated one mid-thoracic, type A PMAVF with CyberKnife without any effect at 18 months' follow-up.

Spinal cavernoma

It may reasonably be argued that cavernomas do not belong in a discussion about vascular cord lesions. They are low-pressure, angiographically occult lesions unless associated with a deep venous anomaly (DVA). The natural history of all cavernomas is poorly understood and this is particularly the case with the rare spinal cavernomas.

The literature consists mostly of operated case series. Treatment is recommended when lesions are symptomatic. The definition of haemorrhage is problematical however in a lesion characterized by slow egress of blood products into surrounding tissues. Should overt haemorrhage be considered a less favourable predictor of subsequent disability than symptomatic microhaemorrhages?

Intramedullary cavernoma

A recent meta-analysis identified 40 studies meeting criteria for analysis and including 632 patients (Badhiwala et al., 2014). Some 376 patients had outcome data reported. The thoracic cord was the most common location accounting for 55.2% of lesions reported followed by the cervical cord (38%), cervicothoracic segments (2.4%), lumbar (2.1%), conus (1.7%), and thoracolumbar (0.6%). The annual rate of haemorrhage was 2.1%. Cerebral cavernomas and multiple cavernomas coexist in approximately 50% of cases.

The authors conclude that surgical intervention for symptomatic lesions is supported by the data. Patients who presented acutely had treatment outcomes superior to those with chronic symptoms. More than 80% of patients undergoing surgery had improved or stable symptoms at final follow-up although early postoperative deterioration was common (27%). While intervention was associated with superior outcomes it should be noted that only 10% of patients in these studies were managed conservatively.

Extradural cavernoma

Extradural spinal cavernomas are rare and occasionally require surgical attention. Purely intraosseous lesions are probably the most common but rarely become symptomatic. Epidural lesions can produce radicular pain and/or myelopathy dependent on their size and location. Surgical resection yields good results in 92% of patients (Mühmer et al., 2014).

Radiosurgery and spinal cavernoma

Surgical extirpation remains the standard of care when intervention is warranted. A single case report describes apparently successful treatment of a paraspinal cavernoma after surgery was abandoned because of bleeding (Sohn et al., 2009). Treatment of an intramedullary, mid-thoracic cavernoma has been described but with only 6 months of follow-up taken as evidence of effect (Martin et al., 2012) there remains little evidence to support such an application.

KEY REFERENCES

Lasjaunias, P., Berenstein, A., & Brugge, K. ter. (2001). *Clinical Vascular Anatomy and Variations: 1 Clinical Vascular Anatomy and Variations*. Berlin Heidelberg, Germany: Springer Science & Business Media.

REFERENCES

Alomari, A.I., Chaudry, G., Rodesch, G., et al. (2011). Complex spinal-paraspinal fast-flow lesions in CLOVES syndrome: analysis of clinical and imaging findings in 6 patients. *Am J Neuroradiol*, **32**(10), 1812–17.

Amarouche, M., Hart, J., Siddiqui, A., Hampton, T., & Walsh, D. (2015). Time-resolved contrast-enhanced MR angiography of spinal vascular malformations. *Am J Neuroradiol*, **36**(2), 417–22.

Aminoff, M.J., & Logue, V. (1974). The prognosis of patients with spinal vascular malformations. *Brain*, **97**(1), 211–18.

Andres, R.H., Barth, A., Guzman, R., et al. (2008). Endovascular and surgical treatment of spinal dural arteriovenous fistulas. *Neuroradiology*, **50**(10), 869–76.

Atkinson, J.L., Miller, G.M., Krauss, W.E., et al. (2001). Clinical and radiographic features of dural arteriovenous fistula, a treatable cause of myelopathy. *Mayo Clinic Proceedings*, **76**(11), 1120–30.

Badhiwala, J.H., Farrokhyar, F., Alhazzani, W., et al. (2014). Surgical outcomes and natural history of intramedullary spinal cord cavernous malformations: a single-center series and meta-analysis of individual patient data. *J Neurosurg Spine*, **21**, 662–76.

Bakker, N.A., Uyttenboogaart, M., Luijckx, G.J., et al. (2015). Recurrence rates after surgical or endovascular treatment of spinal dural arteriovenous fistulas. *Neurosurgery*, **77**(1), 137–44.

Benndorf, G., Assmann, U., Bender, A., Lehmann, T.N., & Lanksch, W.R. (2000). Vertebral arteriovenous fistula associated with neurofibromatosis type I misdiagnosed as a giant aneurysm. *Interv Neuroradiol*, **6**(1), 67–74.

Bhattacharya, J., Luo, C., Suh, D., Alvarez, H., Rodesch, G., & Lasjaunias, P. (2001). Wyburn-Mason or Bonnet-Dechaume-Blanc as cerebrofacial arteriovenous metameric syndromes (CAMS). *Interv Neuroradiol*, **7**, 5–17.

Black, P. (2006). Spinal vascular malformations: an historical perspective. *Neurosurgical Focus*, **21**(6), E11.

Britz, G.W., Lazar, D., Eskridge, J., & Winn, H.R. (2004). Accurate intraoperative localization of spinal dural arteriovenous fistulae with embolization coil: technical note. *Neurosurgery*, **55**(1), 252–4; discussion 254–5.

Chen, J., & Gailloud, P. (2011). Safety of spinal angiography: complication rate analysis in 302 diagnostic angiograms. *Neurology*, **77**(13), 1235–40.

Citterio, A., Franceschini, M., Spizzichino, L., Reggio, A., Rossi, B., & Stampacchia, G. (2004). Nontraumatic spinal cord injury: an Italian survey. *Arch Phys Med Rehabil*, **85**(9), 1483–7.

Deans, W.R., Bloch, S., Leibrock, L., Berman, B.M., & Skultety, F.M. (1982). Arteriovenous fistula in patients with neurofibromatosis. *Radiology*, **144**(1), 103–7.

Djindjian, M., Djindjian, R., Rey, A., Hurth, M., & Houdart, R. (1977). Intradural extramedullary spinal arterio-venous malformations fed by the anterior spinal artery. *Surg Neurol*, **8**(2), 85–93.

Eerola, I., Boon, L.M., Mulliken, J.B., et al. (2003). Capillary malformation-arteriovenous malformation, a new clinical and genetic disorder caused by RASA1 mutations. *Am J Hum Genet*, **73**(6), 1240–9.

Furlan, J.C., Hawryluk, G.W., Austin, J., & Fehlings, M.G. (2012). Spinal haemorrhage during anticoagulant regimen for thromboprophylaxis: a unique form of central nervous system haemorrhage. *J Neurol Neurosurg Psychiatry*, **83**(7), 746–52.

Geibprasert, S., Krings, T., Apitzsch, J., Reinges, M.H.T., Nolte, K.W., & Hans, F.J. (2010). Subarachnoid hemorrhage following posterior spinal artery aneurysm. A case report and review of the literature. *Interv Neuroradiol*, **16**(2), 183–90.

Gharagozloo, F., Neville, R.F., & Cox, J.L. (1998). Spinal cord protection during surgical procedures on the descending thoracic and thoracoabdominal aorta: a critical overview. *Semin Thorac Cardiovasc Surg*, **10**(1), 73–86.

Gilbertson, J.R., Miller, G.M., Goldman, M.S., & Marsh, W R. (1976). Spinal dural arteriovenous fistulas: MR and myelographic findings. *AJNR Am J Neuroradiol*, **16**(10), 2049–57.

Graziani, N., Bouillot, P., Figarella-Branger, D., Dufour, H., Peragut, J.C., & Grisoli, F. (1994). Cavernous angiomas and arteriovenous malformations of the spinal epidural space: report of 11 cases. *Neurosurgery*, **35**(5), 856–63; discussion 863–4.

Gross, B.A. & Du, R. (2013a). Spinal glomus (type II) arteriovenous malformations: a pooled analysis of hemorrhage risk and results of intervention. *Neurosurgery*, **72**(1), 25–32.

Gross, B.A. & Du, R. (2013b). Spinal pial (Type IV) arteriovenous fistulae: a systematic pooled analysis of demographics, hemorrhage risk, and treatment results. *Neurosurgery*, **73**(1), 141–51.

Gueguen, B., Merland, J.J., Riche, M.C., & Rey, A. (1987). Vascular malformations of the spinal cord: intrathecal perimedullary arteriovenous fistulas fed by medullary arteries. *Neurology*, **37**(6), 969–79.

Handa, T., Suzuki, Y., Saito, K., Sugita, K., & Patel, S.J. (1992). Isolated intramedullary spinal artery aneurysm presenting with quadriplegia. Case report. *J Neurosurg*, **77**(1), 148–50.

Hassler, O. (1966). Blood supply to human spinal cord. *Arch Neurol*, **15**(3), 302.

Heros, R.C., Debrun, G.M., Ojemann, R.G., Lasjaunias, P.L., & Naessens, P.J. (1986). Direct spinal arteriovenous fistula: a new type of spinal AVM. Case report. *J Neurosurg*, **64**(1), 134–9.

Hida, K., Shirato, H., Isu, T., et al. (2003). Focal fractionated radiotherapy for intramedullary spinal arteriovenous malformations: 10-year experience. *J Neurosurg*, **99**(1 Suppl), 34–8.

Iacopino, D.G., Giusa, M., Conti, A., Cardali, S., & Tomasello, F. (2001). Intraoperative microvascular Doppler monitoring of blood flow within a spinal dural arteriovenous fistula: a precious surgical tool. *Neurosurg Focus*, **10**(2), 1–5.

Jellema, K., Canta, L.R., Tijssen, C.C., van Rooij, W.J., Koudstaal, P.J., & van Gijn, J. (2003). Spinal dural arteriovenous fistulas: clinical features in 80 patients. *J Neurol Neurosurg Psychiatry*, **74**(10), 1438–40.

Johnson, C.E., Russell, E.J., & Huckman, M.S. (1990). Resolution of spinal epidural vascular pseudotumor following balloon occlusion of a postoperative vertebral arteriovenous fistula. *Neuroradiology*, **31**(6), 529–32.

Koch, C., Gottschalk, S., & Giese, A. (2004). Dural arteriovenous fistula of the lumbar spine presenting with subarachnoid hemorrhage. Case report and review of the literature. *J Neurosurg*, **100**(4 Suppl Spine), 385–91.

Krings, T., Mull, M., Reinges, M.H.T., & Thron, A. (2004). Double spinal dural arteriovenous fistulas: case report and review of the literature. *Neuroradiology*, **46**(3), 238–42.

Krings, T., Thron, A. K., Geibprasert, S., et al. (2010). Endovascular management of spinal vascular malformations. *Neurosurg Rev*, **33**(1), 1–9.

Kubo, Y., Nishiura, I., & Koyama, T. (1984). [Repeated transient paraparesis due to solitary spinal epidural arterio-venous malformation. A case report]. *No Shinkei Geka Neurol Surg*, **12**(7), 857–62.

Lasjaunias, P., Berenstein, A., & Brugge, K. ter. (2001). *Clinical Vascular Anatomy and Variations: 1 Clinical Vascular Anatomy and Variations*. Berlin Heidelberg, Germany: Springer Science & Business Media.

Lonjon, M.M.C., Paquis, P., Chanalet, S., & Grellier, P. (1997). Nontraumatic spinal epidural hematoma: report of four cases and review of the literature. *Neurosurgery*, **41**(2), 483–7.

Martin, A.G.R., Cowley, I.R., Taylor, B.A., Cassoni, A.M., Landau, D.B., & Plowman, P.N. (2012). (Stereotactic) radiosurgery XIX: spinal radiosurgery—two-year experience in a UK centre. *Br J Neurosurg*, **26**(1), 53–8.

Martirosyan, N.L., Kalani, M.Y.S., Lemole, G.M., Spetzler, R.F., Preul, M.C., & Theodore, N. (2015). Microsurgical anatomy of the arterial basket of the conus medullaris. *J Neurosurg Spine*, **22**(6), 672–6.

Massand, M.G., Wallace, R.C., Gonzalez, L.F., Zabramski, J.M., & Spetzler, R.F. (2005). Subarachnoid hemorrhage due to isolated spinal artery aneurysm in four patients. *AJNR Am J Neuroradiol*, **26**(9), 2415–19.

McCullough, J.L., Hollier, L.H., & Nugent, M. (1988). Paraplegia after thoracic aortic occlusion: influence of cerebrospinal fluid drainage. *J Vasc Surg*, **7**(1), 153–60.

Merland, J.J., Riche, M.C., & Chiras, J. (1980). Intraspinal extramedullary arteriovenous fistulae draining into the medullary veins. *J Neuroradiol*, **7**(4), 271–320.

Miller, D.L. (1993). Direct origin of the artery of the cervical enlargement from the left subclavian artery. *Am J Neuroradiol*, **14**(1), 242–4.

Mühmer, M., Bostelmann, R., Sarikaya-Seiwert, S., Schneiderhan, M., Steiger, H.J., & Cornelius, J.F. (2014). Clinical and radiological presentation of spinal epidural haemangiomas: clinical series in a tertiary care centre during a 10-year period. *Eur Spine J*, **23**(2), 404–10.

Muralidharan, R., Mandrekar, J., Lanzino, G., Atkinson, J.L., & Rabinstein, A.A. (2013). Prognostic value of clinical and radiological signs in the postoperative outcome of spinal dural arteriovenous fistula. *Spine*, **38**(14), 1188–93.

Rodesch, G., Hurth, M., Alvarez, H., Tadié, M., & Ph, D. (2002). Classification of spinal cord arteriovenous shunts: proposal for a reappraisal—the Bicêtre experience with 155 consecutive patients treated between 1981 and 1999. *Neurosurgery*, **51**(2), 374–80.

Rosenblum, B., Oldfield, E.H., Doppman, J.L., & Di Chiro, G. (1987). Spinal arteriovenous malformations: a comparison of dural arteriovenous fistulas and intradural AVM's in 81 patients. *J Neurosurg*, **67**(6), 795–802.

Sinclair, J., Chang, S.D., Gibbs, I.C., & Adler, J.R. (2006). Multisession CyberKnife radiosurgery for intramedullary spinal cord arteriovenous malformations. *Neurosurgery*, **58**(6), 1081–8.

Sivakumaran, R., King, A., Bodi, I., Chandler, C.L., & Walsh, D.C. (2016). Spontaneous epidural spinal haematoma in children caused by vascular malformations. *Eur Spine J*, **25**(2), 614–18.

Sohn, M.J., Lee, D.J., Jeon, S.R., & Shin, K.K. (2009). Spinal radiosurgical treatment for thoracic epidural cavernous hemangioma presenting as radiculomyelopathy: technical case report. *Neurosurgery*, **64**(6), E1202–3.

Spetzler, R.F., Detwiler, P.W., Riina, H.A., & Porter, R.W. (2002). Modified classification of spinal cord vascular lesions. *J Neurosurg*, **96**(2 Suppl), 145–56.

Steinmetz, M.P., Chow, M.M., Krishnaney, A.A., et al. (2004). Outcome after the treatment of spinal dural arteriovenous fistulae: a contemporary single-institution series and meta-analysis. *Neurosurgery*, **55**(1), 77–87.

Symon, L., Kuyama, H., & Kendall, B. (1984). Dural arteriovenous malformations of the spine. *J Neurosurg*, **60**(2), 238–47.

Thiex, R., Mulliken, J.B., Revencu, N., et al. (2010). A novel association between RASA1 mutations and spinal arteriovenous anomalies. *Am J Neuroradiol*, **31**(4), 775–9.

Thron, A.K. (1988). *Vascular Anatomy of the Spinal Cord: Neuroradiological Investigations and Clinical Syndromes*. Vienna, Austria: Springer Science & Business Media.

Walsh, D.C., Zebian, B., Tolias, C.M., & Gullan, R.W. (2013). Intraoperative indocyanine green video-angiography as an aid to the microsurgical treatment of spinal vascular malformations. *Br J Neurosurg*, **28**(2), 259–66.

Willinsky, R. (1993). Spinal epidural arteriovenous fistulas: arterial and venous approaches to embolizaiton. *AJNR Am J Neuroradiol*, **14**, 812–17.

Zampakis, P., Santosh, C., Taylor, W., & Teasdale, E. (2006). The role of non-invasive computed tomography in patients with suspected dural fistulas with spinal drainage. *Neurosurgery*, **58**(4), 686–94; discussion 686–94.

RELATED LINKS TO EBRAIN

Normal Spinal Radiological Neuroanatomy. https://learning.ebrain.net/course/view.php?id=698

Spinal Vascular Malformations. https://learning.ebrain.net/course/view.php?id=158

65

Spinal cerebrospinal fluid dynamics

Graham Flint

Pathophysiology

The column of CSF within the posterior fossa and spinal canal is subject to arterial pressure waves, about 70 times each minute, generating a 'to-and-fro' movement. It is also subject to venous pressure waves, which are less frequent and irregular in their timing but of greater amplitude, brought on by any Valsalva-like manoeuvre. Venous waves move significant volumes of fluid between the intracranial and intraspinal compartments. During any Valsalva-like manoeuvre the net flow of CSF is from the spinal theca into the head. At the end of Valsalva fluid returns to the spinal canal, distending the thecal sac once more as spinal epidural veins collapse down.

Fluid dynamics are somewhat different if there is a partial obstruction to flow at the craniovertebral junction. Fluid will still flow freely into the head, during coughing, straining, and so on. but will not flow back as readily. Instead, an extra volume of CSF is trapped, temporarily, within the head and, before it is absorbed via the arachnoid granulations, there occurs a period lasting for several seconds, during which the intracranial pressure is high. An accurate history of such pressure dissociation headaches will reveal that they develop not at the time of coughing or straining but immediately afterwards. Likewise, such headaches come on after the affected individual gets up from bending over.

Arterial pressure waves may also exert undesirable effects, if there is obstruction to free movement of CSF along the spinal canal. With normal anatomy the CSF systolic pressure wave is dissipated along the entire spinal canal. If an obstruction exists, part way along the spinal CSF channels, the same amount of energy cannot diffuse as easily and impacts, instead, upon the exterior surface of the spinal cord. Similarly, when herniated cerebellar tonsils 'punch', repeatedly, upon a column of CSF, which is effectively trapped within the spinal canal, the systolic energy waves cannot recoil freely, back into the head.

We may therefore envisage a normal state of anatomy, with rhythmic oscillation of the cerebellar tonsils, brainstem, and spinal cord within a continuous column of CSF, which rocks upwards and downwards in synchrony with the cardiac cycle. During Valsalva, the hindbrain structures will lift up, as CSF passes into the head, only to return when the straining ends. Obstruction to these movements of CSF, anywhere along the spinal canal, can cause significant disturbances of these normal flow patterns, with distortions of the normal pressure waves, generating significant symptoms and, in some cases, progressive anatomical changes.

Clinical investigations

Magnetic resonance imaging (MRI) provides the principal tool for investigating suspected disorders of spinal CSF movement. Ideally imaging should include the whole neuraxis because spinal CSF pathologies may be associated with anatomical abnormalities in the head, or may be manifested by signal changes intracranially. T2 sequences display the normal CSF channels clearly, as well as revealing abnormal accumulations of water. Moreover, a bright white signal indicates stasis of CSF whereas grey 'swirls' display turbulence. It may be difficult, at times, to distinguish presyrinx oedema of the cord from frank cavitation and T1 images my assist here. Oedema caused by an arteriovenous fistula can, potentially, be misdiagnosed as presyrinx oedema. Standard T2 may not reveal arachnoid webs but heavily weighted T2 images may do so. Contrasted scans are needed to exclude associated neoplastic lesions.

Cardiac gated phase contrast flow studies demonstrate 'to-and-fro' movement of CSF with systole and diastole. This can be useful in evaluating anatomically borderline cases of tonsillar descent. Quantitative measurements can be made in terms of volume of flow, which may be reduced, and velocity of flow, which may be increased, if there is a significant impediment to CSF movement.

Upright MRI may demonstrate subtle anatomical movements, occurring with a change from the horizontal to an upright posture. Such findings may suggest obstruction to CSF movement in an anatomically borderline case.

Ultrasonic imaging may be used intraoperatively, to help locate an abnormal collection of CSF within the spinal canal. It may also be used to determine whether an extradural decompression has effectively relieved obstruction to CSF movement at the craniovertebral junction.

Electrophysiological studies may be used as diagnostic aids. Somatosensory evoked potentials (SSEPs) may be abnormal, even when presenting symptoms do not match radiographic findings and when there are no supporting physical signs on clinical examination.

Motor evoked potentials and SSEPs have also been used as an aid for deciding, intraoperatively, whether there is a need to open the dura as part of a craniovertebral decompression.

Syringomyelia

Syringomyelia is the presence of CSF-filled cavities within the spinal cord. These are encountered in many different morphological forms (Fig. 65.1). Some authorities distinguish between hydromyelia and syringomyelia. The former are essentially dilatations of the embryonic central canal and are lined by ependyma. The later develop alongside the central canal and are lined with gliotic tissue. In either case the challenge is to explain just what causes these cavities to from and what determines how large they will become. Most cavities, of any size at least, are likely to be associated with an obstruction, somewhere along the spinal canal, to the normal movement of CSF (Box 65.1). Such obstructions are not always apparent but sequential imaging may reveal the direction in which a cavity is propagating. This will usually be away from the site of obstruction, meaning that the end of the syrinx that 'stays put' is at the site of obstruction to CSF flow.

The epidemiology of syringomyelia is imprecise. Significant geographical and ethnic differences exist and estimates have varied over time, possibly reflecting the changing make-up of populations studied. As working estimates, one may suggest an annual incidence ranging from 0.5 to 1.0 and a prevalence of between 5 and 10, per 10^5 population. Widespread application of MR imaging has led to the detection of more cases, at an earlier stage in their evolution, presenting with much less in the way of neurological disability. More cases of Chiari malformation are now detected, at least half of which do not have associated syringomyelia.

Clinical presentation

The mean age of presentation is the fourth decade of life but with a wide range, from childhood to retirement. Clinical features can be divided into those generated by the underlying pathology and those caused by the cavity itself (Box 65.2).

The classical picture of cape-distribution dissociated sensory loss, clawed and atrophied hands, covered with burns, together with lost

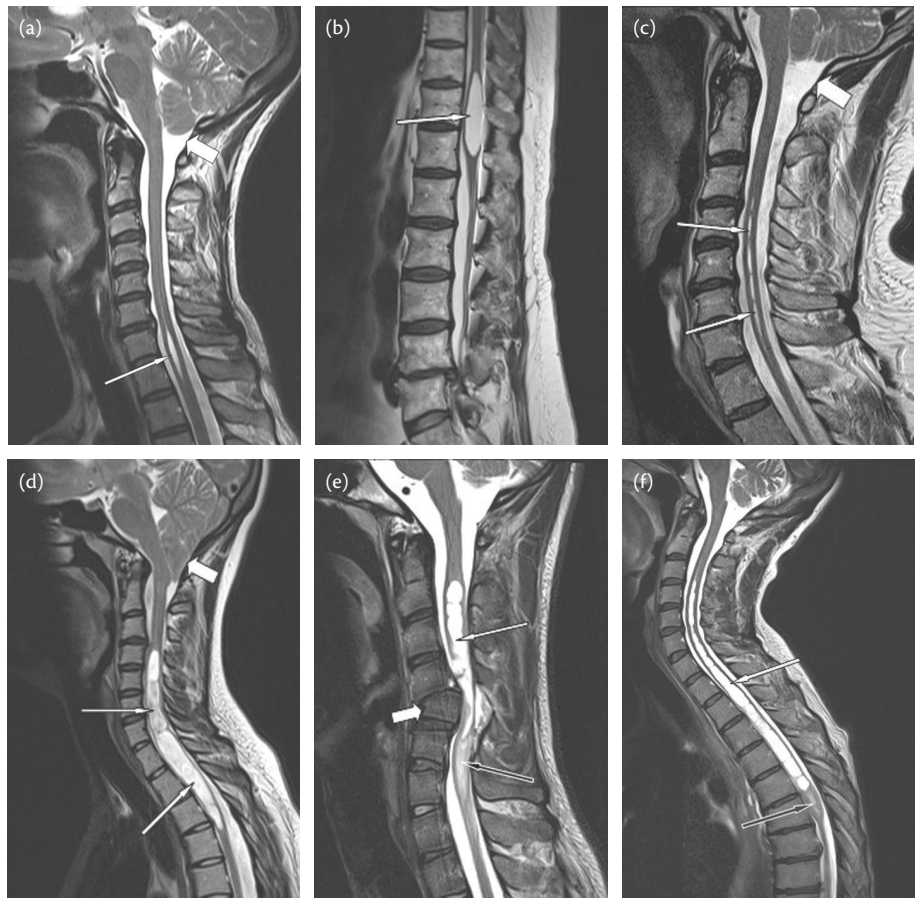

Fig. 65.1 Morphological variants of syringomyelia. T2-weighted MR images illustrating: (A) a spindle-shaped cavity, with pointed ends (long arrow). There is no obstruction to CSF movement along the spinal canal. The cerebellar tonsils are relatively low but not descended through the foramen magnum and the cisterna magna is open (short arrow); some would refer to this as Chiari type 0. (B) A short, plump CSF-filled cavity, with rounded ends (arrow), sometimes referred to as a glioependymal cyst. (C) an abnormally prominent central canal (long arrows) with a widely open cisterna magna (short arrow). (D) A large, tense syrinx (long arrows) resulting from a Chiari type 1 malformation (short arrow). (E) A post-traumatic syrinx cavity (long, white arrow) forming immediately above a C5 vertebral injury (short arrow). Below, the cord has developed presyrinx oedema (long, dark arrow). (F) An extensive syrinx cavity (white arrow), with visible haustrations, that is propagating well above an underlying intramedullary tumour (dark arrow).

Box 65.1 Classification and causes of syringomyelia

Hindbrain related

- Chiari type 1 malformation
  - Congenitally small posterior fossa
  - Craniosynostosis (e.g. Crouzon's)
  - Chronic pressure cone caused by a cerebellar mass
  - Spinal CSF leakage/lumboperitoneal shunt
  - Benign intracranial hypertension
- Chiari type 1.5 ± tethered cord
- Chiari type 2 malformations + open spina bifida
- Basal arachnoid fibrosis (posthaemorrhagic/inflammatory)
- Bone thickening or softening disorders ± basilar invagination (e.g. Paget's, rickets)

Primary spinal pathologies

- Spinal cord injuries *
- Infections—pyogenic or tuberculous *
- Subarachnoid haemorrhage—cranial or spinal *
- Arachnoid cysts or webs
- Intramedullary tumours

* Postinflammatory arachnoid fibrosis is the common element.

Idiopathic—site of obstruction to CSF flow not evident

- Chiari type 0
- Prominent central canal (hydromyelia)
- Isolated 'spindles'
- Glioependymal cysts

Box 65.2 Clinical features of hindbrain related syringomyelia

Local pressure

- Basal dura
  - Occipital headaches
- Neural elements
  - Bulbar/Lower cranial nerves
    - Diplopia/oscillopsia/nystagmus
    - Vertigo/ataxia
    - Tinnitus
    - Facial pain/numbness
    - Dysarthria/dysphonia/dysphagia
    - Sleep apnoea
    - Syncope
  - Long tracts
    - Somatic sensory disturbances
    - Subjective weakness/fatigue

Obstructed CSF flow

- Pressure dissociation headaches
  - Coughing/sneezing
  - Physical straining
  - Bending forwards
  - Blowing up balloons
- Syrinx formation
  - Central grey matter
    - Muscle wasting
    - Clawing of hands
    - Horner's syndrome
    - Scoliosis
  - Long tracts
    - Spinothalamic sensory loss
    - Central neuropathic pain
    - Lower limb spasticity
    - Autonomic disturbances (bladder, bowel, hyperhidrosis)

Occasional presentations include orthostatic hypotension, and various involuntary limb movements, which may mimic extrapyramidal syndromes.

upper limb and abdominal reflexes and with exaggerated lower limb tendon jerks, is still seen but only occasionally. More often now patients present with spinal or limb pains or somatic sensory disturbances, perhaps with clumsiness and feelings of disequilibrium. Fatigue is a common but less specific complaint. Such symptoms may be misdiagnosed as being due to fibromyalgia, causing resentment among patients when the correct diagnosis is eventually made.

True anatomical syringobulbia is rare and bulbar or lower cranial nerve features are more likely to be due to an underlying Chiari malformation. Associated skeletal abnormalities, such as Klippel-Feil, may occasionally be evidenced by a low hairline. In adolescents scoliosis is a common presentation. Very young children may present with respiratory difficulties, which may be life-threatening.

The filling mechanism

One might expect that obstruction to CSF movement in the spinal canal would lead to external hydraulic compression of the cord. This does occur but more often CSF accumulates inside the cord. Just why this comes about is still not fully explained.

Early theories suggested that, when the foramen magnum is obstructed, CSF is driven down through the obex, into the central canal of the cord, either by arterial pulsations or venous pressure waves. The advent of myelography using water-soluble contrast media revealed, however, that fluid appeared to pass from the spinal subarachnoid channels into the syrinx cavity. Experimental studies in animal models of syringomyelia have lent support to this explanation. For CSF to pass into a cavity that is itself under tension, some form of valve mechanism has to exist. When spinal CSF channels are obstructed, systolic pressure waves cannot dissipate freely so a transmural pressure develops across the cord parenchyma. This forces CSF along perivascular spaces, which presumably act as valves.

Other mechanisms may also operate. Below a point of partial obstruction to CSF flow, a Venturi effect may be created, once again resulting from arterial pressure waves. Increased velocity of CSF flow, immediately below the obstruction, creates a lower pressure outside the cord, as compared to within it. This alters the Starling forces acting across the capillary bed, leading to accumulation of interstitial fluid, initially as cord oedema, then coalescing into a fluid-filled cavity.

Thus, arterial energy seems the most likely driving force leading to syrinx formation and filling. Venous pressure waves, being of larger amplitude and longer lasting, may be responsible for subsequent propagation of syrinx cavities, by a hydraulic 'squeezing' effect.

Hindbrain related syringomyelia

Chiari type 1 malformations are the commonest cause of syringomyelia (Fig. 65.2A). They represent a heterogeneous group (Box 65.1) but most are thought to be the result of abnormal mesodermal development, where the volume of the posterior fossa is too small for the cerebellum contained within it. This probably has a genetic basis, as evidenced by the high incidence of Chiari-like malformation in

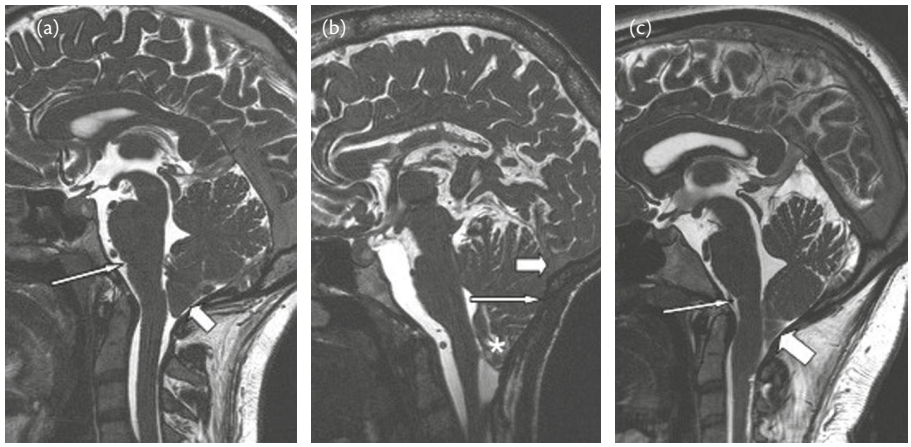

Fig. 65.2 Hindbrain hernias. MR images illustrating various types of Chiari malformation. (A) Type 1, with cerebellar tonsils that protrude through the foramen magnum, occupying the cisterna magna (short arrow). The pontomedullary junction is in a normal position (long arrow). (B) Type 2, where the medulla and a significant part of the cerebellum (asterisk) are prolapsed through a widened foramen magnum, into the upper cervical canal, as a consequence of lumbosacral spinal dysraphism. The posterior fossa is underdeveloped, the torcula (short arrow) being close to the posterior rim of the foramen magnum (long arrow). (C) Type 1.5, with features similar to type 1 but with a low pontomedullary junction (long, arrow) and a degree of tonsillar descent through the foramen magnum. The tonsillar herniation is otherwise morphologically similar to Chiari type 1 (short arrow).

certain breeds of dog. Familial clustering is also seen occasionally in humans. Posterior fossa size is the likely inheritable trait, tonsillar herniation being a secondary development. Symptoms often develop many years after skeletal growth is complete, suggesting that other factors, such as intracranial pressure, may play a role; indeed, about one in five patients with overt benign intracranial hypertension display tonsillar descent on their MRI scans.

Chiari type 2 malformations result from spinal dysraphism. Failed closure of the caudal neural tube, with consequent leakage of CSF into the amniotic sac, prevents normal development of posterior fossa structures (Fig. 65.2B).

MRI appearances intermediate between types 1 and 2 are sometimes seen, with descent of the medulla and obex, as well as the tonsils, but without spinal dysraphism or wholesale descent of the hindbrain (Fig. 65.2C)

Syringomyelia may develop with all these types of Chiari malformation but what determines whether or not this happens remains unknown. Syringomyelia may also be detected in the absence of overt hindbrain herniation and yet decompressive surgery may lead to collapse of the cavity. The term Chiari 0 is applied to such cases and the assumption is that CSF movement across the craniovertebral junction is impaired, either by a thin arachnoid web or by crowding of the cisterna magna. There is, in general, a poor correlation between the degree of anatomical descent seen on MRI and the severity of a patient's symptoms. Absolute radiological measurements of tonsillar descent are therefore of limited value in evaluating individual cases.

Clinical features of hindbrain hernias can usefully be considered in terms of those due to pressure on local structures and those caused by obstruction to CSF movement. Neuralgia and involuntary facial movements may mimic cranial rhizopathies caused by vascular compression. Sleep apnoea leads to some Chiari malformations first presenting to Ear Nose and Throat services. Drop attacks are a cause of particular concern. Once cardiac and epileptic causes have been excluded the question of medullary compression vs. non-organic causes arises. Blackouts which are clearly brought on by Valsalva-like activities certainly warrant consideration of surgery, but it may be difficult to recommend such major intervention when the cause of syncopal episodes is unclear.

The classic symptom of hindbrain hernias is the pressure dissociation headache, brought on by any Valsalva-like activity, including coughing, sneezing, laughing, shouting, straining, blowing up party balloons, or simply bending forwards.

Syringomyelia due to spinal pathology

Various pathologies can obstruct spinal CSF channels below the foramen magnum (Box 65.1). Principal among these is scar tissue formation, developing as a result of a previous episode of arachnoid inflammation, caused by infection or haemorrhage. Bleeding may have occurred intracranially or directly into the spinal canal, the latter most often the result of spinal cord injury (SCI).

Development of post-traumatic syringomyelia threatens to add to the burden already borne by SCI victims. While syringomyelia remains a relatively rare condition in the population as a whole, it is remarkably common among SCI victims, affecting 1 in 20 cases, if not more. Clinical presentation is often with increasing pain or alteration of bladder control. Other symptoms include hyperhidrosis, increased muscle spasms, loss of motor power, and ascending sensory levels. There is a wide range in the latent interval, between the original injury and the onset of symptoms, varying from a few months to many years. As with Chiari malformations, it is unclear what determines which SCI patients will go on to develop syringomyelia. Studies looking at possible predictors, including age of the victim, mechanism of injury, spinal levels involved, extent of the neurological deficit and whether initial management was surgical or conservative, have failed to provide consistent answers.

Idiopathic syringomyelia

Investigation by MRI, of almost any neurological symptoms that persist beyond a short period, has resulted in detection of many more syrinx cavities than was previously the case. Included among these are cavities for which there is no obvious underlying cause, in particular no detectable focal point of obstruction to CSF flow. Some

of these 'lesions' are no more than persisting central canals, essentially embryological remnants. The central canal is always patent in infants but reduces in size throughout life, especially during teenage years, but may still be visible on about 1% of spinal MR scans.

With other, more prominent cavities (Fig. 65.1C) three questions arise: (1) why are they present; (2) are they the cause of the patient's symptoms; (3) how should they be treated? At present there is no clear answer to the first question. Symptoms commonly consist of somatic sensory disturbances and discomforts, often characteristic of central neurogenic pain. There is no question of surgical intervention; any potential benefits are far outweighed by the likelihood of neurological deficits being produced. Standard pain clinic regimes, using neurotropic medications, TENS, acupuncture, and physiotherapy may help. If these prove ineffective a lumbar puncture and CSF drainage may be of benefit, although the physiological basis of this response is unclear.

Treatment of syringomyelia

Surgical treatment of Chiari is far from essential in most cases. Many authors advocate intervention if there is an associated syrinx cavity, but this is like shunting every case of hydrocephalus, irrespective of symptoms. Many syringomyelia cavities enter a state of hydrodynamic equilibrium and these patients require no more than observation. Deterioration is usually gradual and obvious to the patient. There is time for follow-up imaging and careful consideration of the role of surgery. Sudden deterioration is uncommon, usually following an episode of physical straining. It is, however, unnecessary to prohibit physical exercise, on the grounds that Valsalva will likely cause the syrinx to expand. Instead, the patient simply needs to be warned to avoid breath-holding during exercise.

Surgery seldom needs to be carried out urgently, at least in adults, although young children with Chiari may occasionally present in a parlous state, requiring prompt intervention. When performed, it aims primarily to halt motor deterioration. Relief of pain, control of sensory disturbances, reduction of sweating and spasms, and restoration of lost function are secondary aims. Options include opening up obstructed CSF channels, direct drainage of the syrinx cavity and lowering the overall pressure throughout the CSF pathways.

Craniovertebral decompression provides the best example of the first of these options and, provided the CSF channels are opened up adequately, the surgeon can expect syrinx cavities to collapse in at least three-quarters of cases. This may not always occur immediately and six months needs to elapse before a meaningful assessment can be made. Complications of craniovertebral decompression include chemical meningitis, CSF leakage, bacterial meningitis, hydrocephalus and, occasionally, acute cerebral swelling. An isolated fourth ventricle and brain slump are particularly difficult complications and the latter may, in fact, be the result of high pressure from above, rather than lack of support from below. Retractor damage to the greater occipital nerves can produce troublesome dysaesthesias, persisting for some time postoperatively.

Another example of creating an artificial conduit for CSF flow is laminectomy and lysis of intradural arachnoid adhesions, for post-traumatic syringomyelia. In comparison with the craniovertebral junction, the spinal canal is narrower and adhesions may reform postoperatively, with recurrent obstruction to CSF flow. Success rates for syringomyelia surgery at this level in the spine are not as good as they are following operations at the craniovertebral junction. In general, the likelihood of any surgery leading to permanent syrinx collapse is inversely proportional to the extent of any intradural arachnoid adhesions.

Direct drainage of a syrinx cavity may be appropriate when arachnoid adhesions are too extensive, for example in cases of pyogenic or post-tuberculous meningitis. Drawbacks include the need to make a myelotomy, causing some loss of dorsal column function. Drainage tubes, as with other CSF shunt systems, have a tendency to block with time and long-term efficacy is unlikely to benefit more than half of all cases. New cavities are prone to form, simply because the underlying filling mechanism has not been disabled. Receptacles for the drained syrinx fluid include the pleural cavity, the peritoneum, or the spinal theca itself. One particular form of direct drainage is transaction of the spinal cord, in patients who are completely paraplegic and in whom other measures have failed.

Beyond these manoeuvres, partial decompression of a syrinx cavity may be achieved by lowering the hydraulic pressure throughout the spinal theca, thereby reducing the amplitude of the arterial pulse waves within the spinal CSF column. Indeed, this may be a first choice of procedure if hydrocephalus is present at the time of clinical presentation. A ventriculoperitoneal shunt or even an endoscopic third ventriculostomy can reduce the intracranial pressure bearing down upon a Chiari malformation, relieve pressure dissociation headaches, and even lead to collapse of an associated syrinx. Thecoperitoneal shunts may be useful for other forms of syringomyelia, particularly if attempted creation of an artificial conduit has failed.

Even when a syringomyelia cavity has successfully been induced to collapse, following surgery, by no means will all symptoms settle in all patients. With Chiari malformations pressure dissociation headaches will usually resolve or lessen in most patients and ocular and motor symptoms tend to improve as well. Somatic pains and sensory disturbances, be these due to tonsillar pressure on long tracts or arising from a syrinx cavity, tend to persist, in up to half of all patients. Indeed, neuropathic pain remains a major challenge in the management of syringomyelia in general, often dominating a patient's life.

Extra-axial CSF collections

In addition to abnormal accumulations of CSF within the cord, we may encounter pathological collections in other planes within the spinal canal. These may be extradural or intradural and may or may not have neural elements within their walls. Their cystic nature implies that a valve mechanism must be operating, whereby they fill more readily than they empty. The resultant pressure may stimulate the adjacent meninges, producing local spinal pain. If nerve rootlets are involved radicular features may be present. Collections in the thoracic or cervical canal may cause a 'hydraulic myelopathy', producing motor, sensory, and autonomic disturbances of varying degrees.

The aetiology of these lesions remains unclear, with trauma, inflammation, and congenital defects all having been proposed. Familial clustering has been reported with some and associations have been made with various collagen disorders.

Spinal epidural cysts

Extradural collections are most often encountered in the lower thoracic spine, sited dorsally (Fig. 65.3). Their presence implies an underlying dural defect and this is most likely to be adjacent to a nerve root. If pain is intolerable or myelopathic features are prominent then surgery is justifiable. Smaller cysts may be excised but, for larger collections, multiple level laminectomies are impractical. A more limited exposure may, instead, permit sealing of the dural defect, if it can be located radiologically preoperatively. Otherwise, shunting into the peritoneum, pleural cavity, or the spinal theca may be options.

Arachnoid cysts and webs

Spinal CSF channels may be obstructed by thin diaphragms of arachnoid tissue, which can be difficult to spot radiologically. Clues as to their presence include displacement of the cord, on sagittal or axial images (Fig. 65.4). It is important then to check that the obstructing membrane is not the top of a more extensive, intradural cyst, most of which are located dorsal to the cord.

In the absence of a history of trauma, meningitis, intraspinal haemorrhage, or prior surgery, such lesions are regarded as being idiopathic. Presenting features include neuropathic pain and motor myelopathy. High lesions may cause headaches, presumably because of reduction in the compliance normally provided by the spinal theca.

Surgery is indicated if there is progressive motor deterioration. Excision is desirable, for isolated webs or short cysts. More extensive cysts may respond to fenestration manoeuvres. Neuropathic pains may, unfortunately, persist, despite an anatomically successful procedure.

Lumbar puncture, by temporarily reducing the filling pressure outside the cyst, may act as a useful test as to whether the lesion is the cause of the patient's symptoms. Alternatively, direct cyst aspiration may be performed.

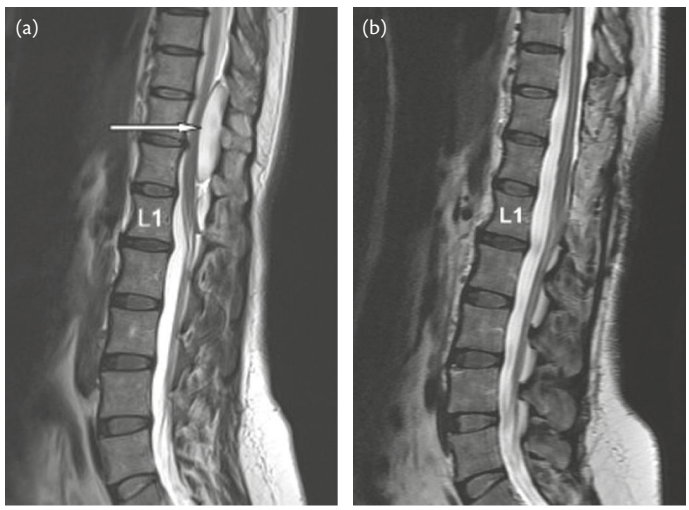

Fig. 65.3 Spinal epidural cyst. (A) T2 sagittal MRI displaying a spinal extradural, CSF-filled cyst (arrow). (B) Postoperative appearances two years later.

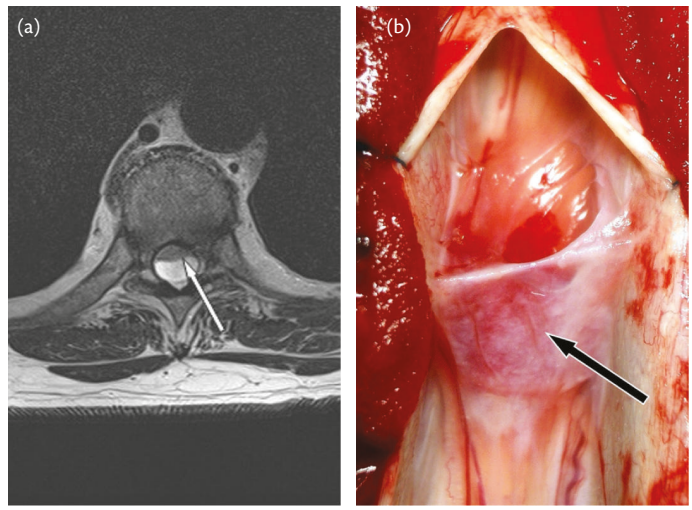

Fig. 65.4 Arachnoid web. (A) Axial T2 MRI image of the thoracic spine revealing anterior displacement and compression of the cord (arrow) caused by hydrostatic pressure built up above a spinal arachnoid web. (B) Operative appearances of an intradural arachnoid web (arrow) forming a diaphragm across the theca, dorsal and lateral to the cord.

Tarlov cysts

These perineural cysts are common incidental findings on MR scans, usually but not exclusively located in the sacral canal, and often multiple. Histologically, there are neural elements in the walls and they may generate spinal, perineal, or leg pains. They are best managed conservatively, using pain management methods. Surgical treatment may be indicated if there are clear problems with sphincter control or sexual function, caused by hydraulic pressure on the lower sacral rootlets. Dissection is difficult as the cyst walls are extremely thin and adherent to these vital structures. Various techniques are described, including fenestration, plication of the wall, and placement of shunts. Glue injection has also been used. Trial aspiration may be carried out, prior to open surgery being planned.

Spontaneous intracranial hypotension

Low pressure headaches, characteristically worse in the upright position and relieved by lying down, are a common sequel to lumbar puncture. When developing spontaneously, in the absence of any implanted CSF shunt apparatus, such headaches suggest spontaneous leakage of CSF, somewhere along the spinal canal. Causes include prior trauma, collagen disorders or dural diverticula (Fig. 65.5A) but many cases appear to be idiopathic.

Besides orthostatic headaches, symptoms may include altered hearing, diplopia, and spinal pain, although the last-mentioned is not sufficiently common for the site of leakage to be localized. Less common presentations include extrapyramidal movement disorders and altered conscious level. An interesting symptom is galactorrhoea, caused by a 'reverse Monro-Kellie' effect; reduction of the CSF volume intracranially leads to increased vascular perfusion of the intracranial contents, including the pituitary gland, with resultant increased prolactin production.

Increased blood flow is also responsible for the characteristic finding of widespread meningeal enhancement seen on contrasted

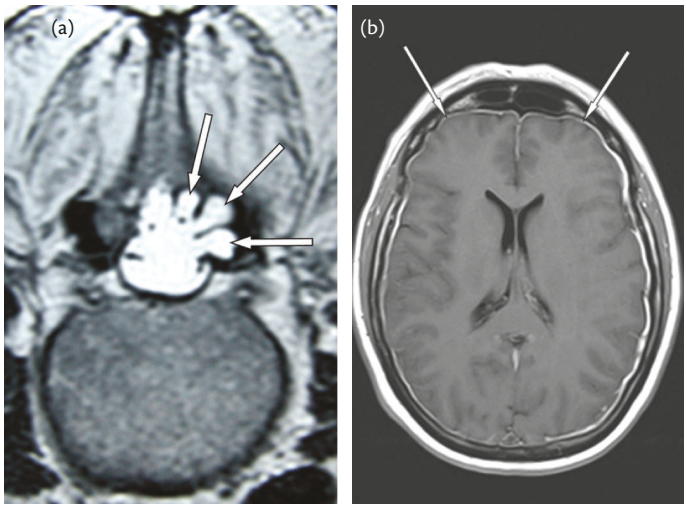

Fig. 65.5 Spontaneous intracranial hypotension. (A) Axial T2 MRI of the spine showing dural diverticula (arrows), a likely source of CSF leakage. (B) Axial T1 contrasted MRI of the head demonstrating diffuse meningeal enhancement (arrows) caused by leakage of CSF from the spinal canal.

cranial MRI (Fig. 65.5B). Brain slump and cerebellar tonsillar herniation may be seen. Occasionally subdural haematomas develop. More subtle features include distension of the transverse sinuses and collapse of the optic nerve sheaths.

Location of the site of leakage, in the spine, is often difficult. Isotope cisternography and computed tomography (CT) myelography have been used but involve a good deal of ionizing radiation. MR myelography using intrathecal gadolinium provides an alternative but it is also possible to generate T2 MR images that resemble conventional myelograms. Lumbar puncture may reveal a low opening pressure and may show a relatively low plateau pressure, if combined with an infusion study.

Treatment of spontaneous intracranial hypotension is initially conservative, with bed rest, maintenance of adequate fluid intake and simple analgesia, just as postlumbar puncture headaches are managed. The hope is that the leak will heal spontaneously. Persistent symptoms are treated with epidural blood patches, targeting the site of leakage if this can be identified but often performed 'blind' and repeated if necessary. Surgical repair would be exceptional and only when the site of leakage has been identified clearly, for example ligating dural diverticula.

Spinal cord hernias

While not a disorder of spinal CSF circulation as such, anterior spinal cord hernias produce MRI appearances similar to those generated by arachnoid webs, with anterior displacement of the cord and an increased volume of CSF dorsally. If the true nature of the lesion is missed, then inappropriate surgery may be undertaken. Phase contrast MRI or CT myelogram can be used to confirm the diagnosis of spinal cord hernia and differentiate it from a spinal arachnoid cyst.

Clinical assessment is therefore vital. Presentation, often in middle age, is that of an anterior cord syndrome, initially affecting one side of the cord. This may develop over a period, often in a stepwise manner, as the anterior columns progressively prolapse through the anterior thecal defect, most commonly encountered in the thoracic spine. The patient may display spinothalamic sensory loss in one lower limb, together with upper motor neurone deficits in the opposite leg. Dorsal column function is often spared but, if left untreated, the condition may progress to a more complete myelopathy.

Careful microsurgery can reduce the hernia, with a prosthetic barrier then being inserted between cord and dura, to prevent recurrence.

Controversies

A major area of contention, in the field of Chiari and syringomyelia surgery, concerns the best way of performing a craniovertebral decompression. Of the various methods used, the only manoeuvre they have in common is removal of bone. Beyond this, surgeons vary considerably in the extent of the dissection they perform (Box 65.3).

There is a good reason why many limit their approach because opening into the subarachnoid channels will inevitably lead to a chemical meningitis, to a greater or lesser degree. This will generate discomfort for the patient, increase the CSF pressure and, sometimes, provoke CSF leakage; this is then best treated with a lumbar drain, provided that hydrocephalus has first been excluded. On the other hand, partial or even no dural opening is less likely to lead to collapse of an associated syrinx cavity. Some surgeons advocate a limited approach, initially, with an option to return if it proves ineffective. This, however, will require the patient to go through another major and uncomfortable brain operation.

The additional measure of reducing the tonsils introduces a risk of causing cerebellar swelling, with potential obstruction of the fourth ventricle, leading to hydrocephalus. It does, however, remove the 'pistons' that have been impacting upon the trapped column of CSF within the spinal theca. While external decompression alone may open up the CSF channels, subsequent placement of a dural graft invites formation of adhesions, between it, the tonsils and the cervicomedullary junction. Spinal CSF dynamics can then become much worse than prior to surgery. Revisional surgery in these circumstances is very difficult, more hazardous, and less likely to succeed, compared to a virgin operation. Damage to the dorsal columns, with resultant loss of light touch and joint position sensation is a particular risk.

The author therefore prefers to open the dura and the arachnoid and to reduce the cerebellar tonsils, thereby creating an artificial cisterna magna into which the fourth ventricle opens freely and which itself communicates with the basal cisterns and the spinal CSF channels. There is no need for dural grafts, as it is seldom possible to make such repairs watertight. CSF will leak around and press

Box 65.3 Techniques of craniovertebral decompression

- Bony decompression alone
- Partial dural release
- Dural opening
- Arachnoid opening *
- Reduction of cerebellar tonsils
- Duraplasty
- Acrylic cranial repair

* Often inevitable, with dural opening

the graft onto the underlying neural elements, causing recurrent obstruction to CSF flow.

FURTHER READING

Flint, G. & Rusbridge, C. (eds.) (2014). *Syringomyelia: A Disorder of CSF Circulation*. Berlin, Germany; Springer.

Lee, C.H., Hyun, S.J., Kim, K.J., Jahng, T.A., & Kim, H.J. (2012). What is a reasonable surgical procedure for spinal extradural arachnoid cysts: is cyst removal mandatory? Eight consecutive cases and a review of the literature. *Acta Neurochir*, **154**, 1219–27.

Marino, D., Carluccio, M.A., Di Donato, I., et al. (2013). Tarlov cysts: clinical evaluation of an Italian cohort of patients. *Neurol Sci*, **34**, 1679–82.

Petridis, A.K., Doukas, A., Barth, H., & Mehdorn, H.M. (2010). Spinal cord compression caused by idiopathic intradural arachnoid cysts of the spine: review of the literature and illustrated case. *Eur Spine J*, **19**(Suppl 2), S124–9.

Tubbs, R.S. & Oakes, W.J. (eds.) (2013). *The Chiari Malformations*. New York, NY: Springer.

Urbach, H. (2014). Intracranial hypotension: clinical presentation, imaging findings and image-guided therapy. *Curr Opin Neurol*, **27**(4), 414–24.

White, B.D. & Tsegaye, M. (2004). Idiopathic anterior spinal cord hernia: under-recognized cause of thoracic myelopathy. *Br J Neurosurg*, **18**(3), 246–9.

RELATED LINKS TO EBRAIN

Chiari malformation. https://learning.ebrain.net/course/view.php?id=520

Disorders of the Foramen Magnum. https://learning.ebrain.net/course/view.php?id=514

Inserting or Revising a Syringopleural Shunt. https://learning.ebrain.net/course/view.php?id=518

Investigation and Treatment of Spinal Cerebrospinal Fluid Leaks. https://learning.ebrain.net/course/view.php?id=515

Management of Syringomyelia. https://learning.ebrain.net/course/view.php?id=519

Spinal Arachnoiditis. https://learning.ebrain.net/course/view.php?id=517

66

Scoliosis and spinal deformity

Nigel Gummerson

Introduction

A spinal deformity is a condition in which the spine is not the 'normal shape' because of illness, injury or because it has grown wrongly (i.e. the spine is misshapen or malformed).

In order to discuss spinal deformity, we must first consider what is normal. The spine is straight when viewed from the front or the back; there are no significant curves in the coronal plane (a slight lateral curve may be within normal limits). The sagittal profile is the shape of the spine when viewed from the side. The sagittal profile changes with growth and ageing.

At birth, the spine has a gentle C-shaped curve throughout its length. The normal cervical lordosis develops as the child gains head control and begins crawling; the lumbar lordosis begins to appear at the time of walking. There is continued development in the sagittal profile throughout growth until the normal adult pattern is achieved. The sagittal profile is never fixed, and will continue to change as the spine ages, becoming more kyphotic with advancing years.

The net effect of this normal spinal profile is to position the head and thoracic cage over the centre of the pelvis in the coronal plane. In the sagittal plane, the centre of gravity falls between the sacrum and the femoral heads. It is the relative positioning of head, shoulders, thorax, and pelvis that gives the normal body surface contour.

Traditionally, we have classified spinal deformities into scoliosis (affecting the coronal plane) and kyphosis (affecting the sagittal plane). In reality, the spine is a complex system, and changes in the coronal plane produce changes in the sagittal plane, which are accompanied by rotation (in the axial plane). Therefore, spinal deformity is a three-dimensional problem. In both the growing and ageing spine, deformities will evolve over time; the fourth dimension.

The last 30 years have brought a growing understanding of the relationship between the lumbar spine and the pelvis. Patients may tilt the pelvis to compensate for spinal deformity. There is a limit to the amount of compensation that is possible. Rotating the pelvis forwards or backwards from the normal position compromises hip function. Therefore, when considering the normal spine, we must also consider the pelvis.

Clinical assessment of spinal shape

It may be difficult to identify mild to moderate spinal deformity. Most of us spend the majority of our waking hours fully dressed and in motion. Movement and clothing obscure the subtle changes in body surface shape that spinal deformity may cause.

To assess the spinal shape clinically we must expose the patient, asking them to undress down to their underwear. The patient stands upright and still. We can observe any difference in the waist creases, trunk shift, and shoulder heights. Abnormal spinal rotation may manifest as asymmetry of the posterior chest wall or loin asymmetry. Having the patient lean forwards, bending at the waist, will usually make these asymmetries (due to rotation) more obvious. This is Adam's forward bend test. In this position, the spinal rotation (relative to the horizontal plane) may be measured with a scoliometer.

Check that the patient is able to stand upright with the hips and knees fully extended; patients with sagittal plane deformity may stand with their hips and knees flexed, allowing them to tilt the pelvis backwards and compensate for some or all of the spinal deformity.

There are several photographic techniques that may be used to generate a topographical spinal map of the back shape (e.g. ISIS 2—Integrated Shape Imaging System, Oxford, UK). This can quantify the posterior chest wall asymmetry and may be useful for monitoring scoliotic curve progression without using ionizing radiation, and for assessing the outcomes of surgery.

Radiographic assessment of spinal shape

The radiographic assessment of spinal shape is achieved with AP and lateral whole spine radiographs. These should be performed with the patient stood in a standardized position. Spinal deformities will change on standing, as the spine is loaded, so supine films (and supine MRI scans) are of limited value. Other factors, such as the position of the arms, or holding supports, will change the centre of gravity and thus change the appearance of the spine on the radiographs. The ideal radiographs will include C7, the whole rib cage, pelvis, and both femoral heads.

Radiographic assessment of the sagittal plane and pelvis

The normal spine is straight on the PA radiograph, and will have four curves in the sagittal plane. The sacral kyphosis is fixed; the sacrum is fused. The lumbar lordosis may be measured by finding the angle between the upper endplate of T12 and the endplate of S1 (normal range 40–60°). By convention, the thoracic kyphosis is measured from upper endplate of T5 to the lower endplate of T12

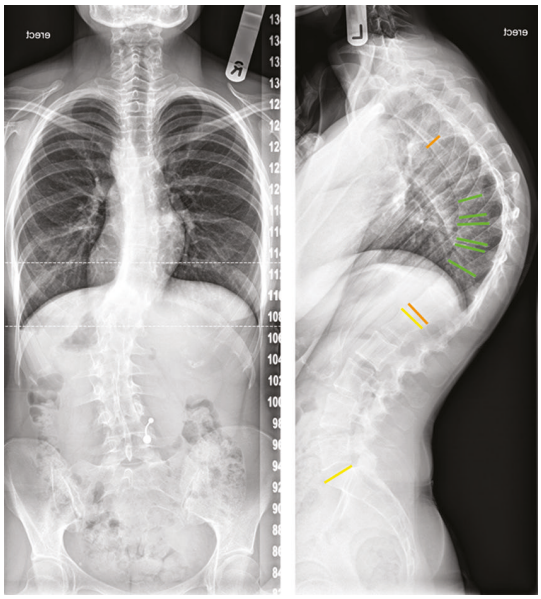

Fig. 66.1 Scheuermann's kyphosis. Increased thoracic kyphosis with wedging of at least 5° across three consecutive levels can be seen on the lateral X-ray (endplates marked in green). The AP film shows a small scoliosis, which is a common finding in Scheuermann's. In this case the lumbar lordosis (yellow) (L1–S1) measures 75° (normal range 40–60°) and the thoracic kyphosis (orange) (T5–T12) measures 96° (normal range 10–40°).

(the shoulders commonly obscure the higher thoracic levels). The normal range for T5–T12 kyphosis is 10–40°. The majority of the lumbar lordosis occurs at the lowest lumbar discs; the upper lumbar spine is relatively straight, as is the lower thoracic spine. Therefore, the segment from T10 to L2 is relatively straight (normal value 0–20° kyphosis). Pathological changes (e.g. Scheuermann's kyphosis) will disrupt the sagittal profile. See **Figure 66.1**.

It is good practice to include the pelvis on the radiographs as the anatomy and position of the pelvis has a fundamental effect on the spine; it is the foundation of the lumbar curve. The centre of gravity of the upper body should pass between the sacrum and the femoral heads. There is a concept that the spine is 'balanced' within a 'cone' of potential positions above the pelvis. Within this cone, it requires minimum muscular effort to stay standing. When the spine or centre of gravity moves outside of this cone then the spine becomes 'unbalanced' and the muscular effort required to stay standing is increased (Jean Dubousset, 'cone of economy').

We cannot easily measure the centre of gravity directly, and so substitute the relative positions of the centre of the C7 vertebral body and the posterior limit of the S1 endplate. A vertical line dropped from the C7 body should fall within 2.5 cm of the posterior limit of the S1 endplate on the lateral whole spine radiograph. This is the sagittal vertical axis.

Patients whose overall spinal balance lies outside this range are said to have decompensated sagittal deformity; this group has been shown to have lower quality of life scores.

There are three radiographic spinopelvic parameters that are commonly measured:

- Sacral slope (SS)—the slope of the S1 endplate relative to the horizontal plane (normal value 39 ± 8°).
- Pelvic tilt (PT)—the angle from the femoral heads to the midpoint of the S1 endplate relative to the vertical plane (normal value 13 ± 6°). A PT less than 25° is one of the desirable outcomes after spinal deformity surgery. See **Figure 66.2**.
- Pelvic incidence (PI)—the angle formed between a line drawn perpendicular to the S1 endplate and a line connecting the midpoint of the S1 endplate to the femoral heads. The PI changes with growth of the pelvis. Once skeletal growth is complete, the PI is fixed, and can only be changed by fractures or osteotomies to the pelvis or sacrum. The PI is equal to the sum of the sacral slope and pelvic tilt (normal value 55 ± 10.6°). Patients with a high PI tend to have a high lumbar lordosis.

A PT less than 25° and a PI within 9° of the lumbar lordosis are radiographic outcomes that statistically correlate with positive

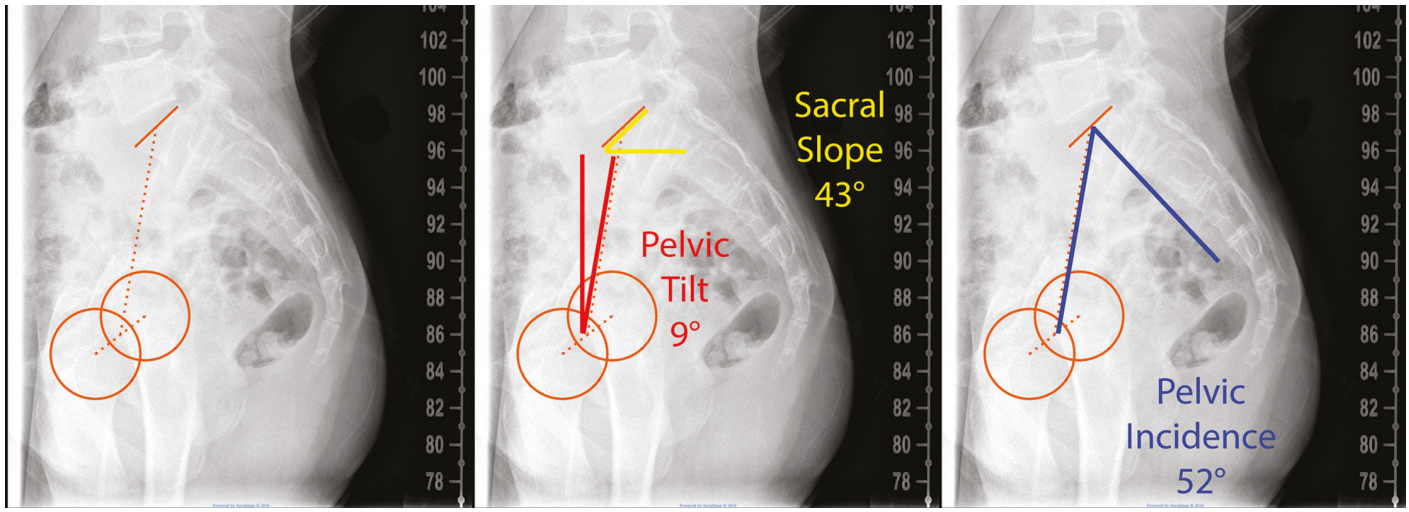

Fig. 66.2 Pelvic parameters. Outlining the femoral heads allows the centres to be identified. The S1 end plate is also marked, and a line is drawn from the midpoint of the S1 endplate to the midpoint of a line joining the centres of the femoral heads. Constructing horizontal and vertical lines allows measurement of the sacral slope (SS) and pelvic tilt (PT). The pelvic incidence (PI) is found by constructing a perpendicular line down from the midpoint of the S1 endplate. There is a fixed geometric relationship between these angles, such that: PI = SS + PT.

Table 66.1 Identification of the primary curve from the position of the apex

Curve type	Position of apex
Cervical scoliosis	C1 to the C6/C7 disc
Cervicothoracic scoliosis	C7 vertebra to T1 vertebra
Thoracic scoliosis	T1/T2 disc to T11/T12 disc
Thoracolumbar scoliosis	T12 to L1
Lumbar scoliosis	L1/L2 disc to L5

Scoliosis Research Society definitions.

outcomes after spinal deformity surgery. However, it is also important to appreciate that some patients are naturally more 'S-shaped', while others have a flatter profile: restoring a harmonious sagittal profile should be the surgical goal.

Common degenerative conditions, such as lumbar disc disease, will result in loss of anterior spinal height, while the height of the posterior elements remains unchanged. This leads to loss of lumbar lordosis and a sagittal plane deformity. Lumbar spinal fusion and decompression without restoration of the normal lumbar lordosis may improve a patient's radicular leg pain, but may leave them with a fixed sagittal deformity and a suboptimal surgical outcome.

'Whole-body' radiographs are becoming more widespread; advances in detector technology have allowed imaging of a wider field with lower dose. This has allowed researchers to examine the sagittal balance of the whole patient. The study of whole-body balance and its relationship to quality of life and outcomes after surgery is an evolving topic.

Radiographic assessment of scoliosis

The cardinal characteristic of scoliosis is a curve in the coronal plane of more than ten degrees.

Scoliotic curves may be structural or non-structural. A non-structural curve is a curve that is fully correctable. Non-structural curves may be due to posture, due to pain, due to paralysis or due to pelvic obliquity (e.g. if a curve is the result of a leg length inequality, then the curve will straighten when the patient is sitting). Structural curves have a fixed component and do not fully straighten (i.e. they do not correct to zero degrees). Non-structural curves may develop a structural component over time.

Scoliotic curves are usually described by the curve's location, direction, and magnitude. A curve can be described as having a convexity (the 'outside' of the curve) and a concavity (the 'inside' of the curve). The side of the convexity describes the side of a scoliotic curve. The position of the 'apex' of the curve is used to describe the position within the spine. The apex is the disc or vertebral body that is furthest from the midline (i.e. the most displaced from the central spinal vertical axis). See **Table 66.1**.

The magnitude of a curve is measured by finding the angle from the superior endplate of the most tilted vertebra at the cranial end of the curve to the inferior endplate of the most tilted vertebra at the caudal end of the curve. This angle is the Cobb angle.

The Cobb angle measurement is merely a two-dimensional (2D) approximation of a 3D curve. To fully describe a curve, we would need to record the number of spinal segments affected and the rotational deformity as well as the sagittal plane deformity. The Cobb angle provides a useful shorthand method for describing a curve, and is the measurement for which we know most about the natural history. See **Figure 66.3**.

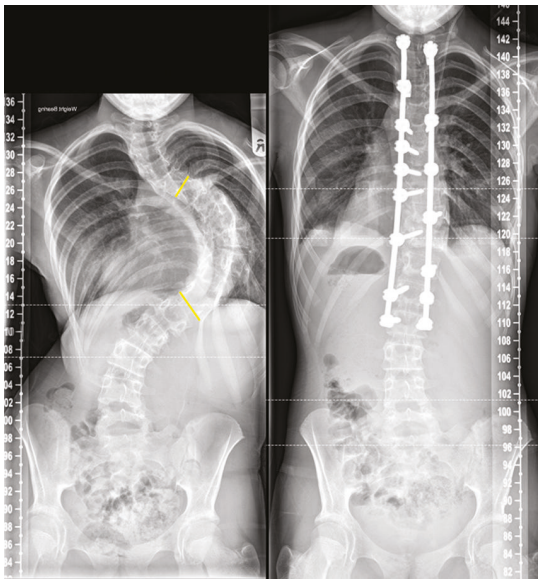

Fig. 66.3 Late onset idiopathic scoliosis (pre- and postoperative PA films). The Cobb angle is measured as illustrated. A line is drawn on the superior endplate of the most tilted vertebra at the top of the curve, and the lower endplate of the most tilted vertebra at the bottom of the curve. In this case, the Cobb angle of the thoracic curve is 108°.

Scoliosis

Scoliosis is a common, and relatively slowly evolving condition. With the exception of some neuromuscular conditions, young patients with scoliosis tend to be active and mobile. Scoliosis in children tends to present as a cosmetic problem, whereas scoliosis in adults tends to present with axial spinal pain and radicular symptoms.

Classification of scoliosis in children

Scoliosis in children may be classified by age of onset, by aetiology, or a combination of both.

Idiopathic scoliosis was traditionally divided into 'infantile' (0–3 years), 'juvenile' (4–9 years), and 'adolescent' (10–18 years). We now use the terms 'early onset scoliosis' (0–9 years) and 'late onset scoliosis' (10–18 years). The important factor here is lung development. Early onset scoliosis can lead to thoracic insufficiency syndrome.

Thoracic insufficiency syndrome is result of restricted lung growth, leading to the inability of the chest to support normal breathing. Scoliosis may restrict lung growth by limiting the height of the thoracic spine (18–22 cm of height from T1 to T12 is required for normal lung function), or because the apex of the curve rotates into the chest on the convex side, encroaching on the space available for the lung. Rib anomalies, in congenital scoliosis, may also contribute to this problem.

The details of chest and lung growth are complex, and arguments have been made for the cut-off between early and late onset at different ages. At the age of 10, the thoracic volume is 50% of its final

size. A 'late onset' scoliosis is unlikely to cause any change in lung function unless the curve becomes very large (>90 degrees).

The aetiology of a curve may be obvious, as in congenital (15%) or neuromuscular (10%) cases. In most cases there is no detectable underlying cause (idiopathic). This is the most common, with 70% of all cases of paediatric scoliosis being of the idiopathic type. A small proportion of patients with spinal deformity have an underlying syndrome.

Congenital scoliosis and kyphosis

The embryological development of the spine is described in Chapter 85. The classification of congenital scoliosis is descriptive. Congenital anomalies are divided in to defects of segmentation, defects of formation, mixed defects, and a small group of complex anomalies that defy description. This classification comes from the work of McMaster and Ohtsuka (1982), which was based largely on plain radiographs. Kawakami et al. have suggested an update to this system, analysing the 3D computed tomography (CT) appearances of the deformity. CT will reveal additional abnormalities in 50% of patients, over and above those seen on the plain films.

A 3D CT analysis allows for a better understanding of the relative (3D) position of the abnormalities, as well as providing more information regarding fusions between levels and the anatomy of the posterior elements around the abnormality.

Consideration of any associated rib anomalies is an important aspect of congenital scoliosis. Multiple rib fusions may be seen in Jarcho-Levin syndrome (spondylothoracic dysostosis). This condition causes marked reduction in thoracic growth and results in early death from thoracic insufficiency syndrome. A lesser form, spondylocostal dysostosis, causes less severe rib problems and has no appreciable effect on life expectancy. Isolated rib abnormalities may be seen in cases that do not have these syndromes, reflecting the common embryonic origin of the rib and vertebral body from the sclerotome of the somite. Non-syndromic rib anomalies are most commonly seen with unsegmented bars.

The natural history of deformity progression in congenital scoliosis is very variable. Around 50% of all cases of congenital scoliosis will progress by a significant degree, 25% do not progress, and the remainder progress only slightly or not at all. The chance of progression is dependent on the site and type of anomaly. Progression is the result of asymmetric growth.

The most benign form of congenital spinal anomaly is a block vertebra. This is the result of bilateral failure of segmentation. Block vertebrae do not cause progressive curves, but may cause shortening of the trunk when multiple block vertebrae are present.

An incarcerated or non-segmented hemivertebra has very little potential for progression. A wedged vertebra will cause only 1–2° progression per year. A single semisegmented or fully segmented vertebra will progress at 1–3.5° per year, worse at the thoracolumbar junction. Multiple hemivertebrae will progress more rapidly. Lumbosacral hemivertebrae will lead to compensatory lumbar and thoracic curves, which become stiff (and structural) over time. Early surgery is indicated to prevent this outcome.

An unsegmented bar will cause progression of between 2° and 9° per year. Again, this is worse at the thoracolumbar junction.

The most troublesome combination is the mixed defect of an unsegmented bar with a contralateral, fully segmented hemivertebra. The thoracolumbar junction is the worst location for this abnormality, where it may progress at more than 10° per year, necessitating early (prophylactic) surgical treatment when detected.

Congenital kyphosis is encountered less often than scoliosis. Kyphosis may progress at 2–7° per year. Most kyphotic anomalies are in the lower thoracic or thoracolumbar region. If left untreated, some patients with congenital kyphosis may become paraplegic.

There is a choice between continued observation and surgery in congenital deformity. Neither bracing nor physiotherapy can alter the natural history of these curves. Surgery is indicated for progressive curves. The potential for progression can be determined by a thorough work up with CT and MRI. Associated conditions should be actively sought and the possibility of an underlying syndrome considered prior to surgery. A formal assessment of pulmonary function before intervention, as a baseline, will help guide treatment and inform the prognosis.

The surgical options range from hemiepiphysiodesis (short segment anterior growth arrest over the convexity of the curve) to more complex osteotomies such as pedicle subtraction osteotomy (PSO), resection of a hemivertebra, or vertebral column resection. See **Figure 66.4**.

The choice of treatment will depend on the nature of the abnormality and the age at presentation. Techniques such as hemiepiphysiodesis rely on significant growth potential in the concavity, and are of little use in the older patient.

There is little to be gained by waiting 'to preserve growth' with a progressive deformity. Combined anterior and posterior fusion is often indicated in these cases. 'Normal' levels should be preserved where possible, but the whole curve may need to be instrumented to restore normal spinal balance.

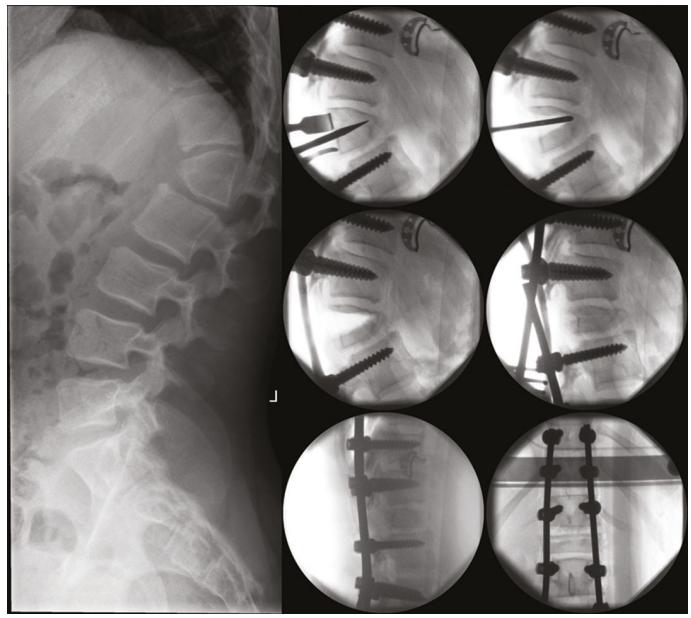

Fig. 66.4 Pedicle subtraction osteotomy (PSO) for Congenital Kyphosis. Spinal osteotomies may be required in deformity correction. In this case a wedge of bone (posterior element, pedicles, and body) has been resected, allowing the spine to be shortened posteriorly around the neural structures. This produces an angular correction with an axis of rotation at the front of the vertebral body. This osteotomy will typically produce 25–30° of correction.

Each congenital curve pattern must be assessed on its own merits but as a general rule, early surgical treatment should be considered for curves with more than one hemivertebra, a unilateral bar, or a mixed defect, as these are the curves which tend to progress.

Neuromuscular scoliosis

Disorders of the brain, spinal cord, nerves, or muscles may result in an inability to maintain normal spinal balance, leading to scoliosis. Examples include cerebral palsy, Duchenne muscular dystrophy, Friedreich's ataxia, and posttraumatic paralysis.

The frequency and severity of these curves is worse in children who cannot walk. Spinal balance is generally maintained in children who are still walking.

Neuromuscular curves are generally not painful, but they do cause problems with seating and hygiene. Poor sitting balance may mean that the child has to use an arm to help balance, depriving them of the use of that arm.

Early onset neuromuscular curves may lead to thoracic insufficiency syndrome. Patients with neuromuscular disorders are under the care of a multidisciplinary team. Non-operative treatment is appropriate for many patients with a neuromuscular curve. There is physiotherapy for all and seating modification for non-ambulators.

Operative treatment (typically posterior instrumented spinal fusion) is indicated when conservative treatment has failed. The goal is to prevent curve progression and to restore sitting balance.

Syndromic scoliosis

There are many syndromes which may cause scoliosis. Examples include neurofibromatosis, Marfan's syndrome, Ehlers–Danlos syndrome, osteogenesis imperfecta, and a very long list of others. A detailed discussion of these rare conditions is outside the scope of this article, but it is useful to examine patients very carefully for clinical signs which may suggest an underlying syndrome. If there is suspicion of an underlying syndrome, then an opinion from clinical genetics is indicated.

It is important to be aware of some of the common pitfalls in syndromic scoliosis, these are many, and vary by syndrome. The complication rate for surgery in this group is higher than in idiopathic scoliosis.

Idiopathic scoliosis

Idiopathic scoliosis is a structural curve in the absence of any other underlying problem. By definition, the deformity is self-generating, and the underlying cause is yet to be established, although there are many theories with regard to aetiology.

Early onset idiopathic scoliosis (EOIS)

EOIS is rare (1% in the United States, ~5% in Europe). It is typically a left-sided curve, which develops after birth, but is not present at birth. It is more common in boys (M:F = 3:2). EOIS is strongly associated with other conditions such as talipes equinovarus, developmental dysplasia of the hips, torticollis, and inguinal herniae. The classification of EOIS is descriptive, with useful discriminating features being the curve size, the rib-vertebral-angle difference (at the apex) and the appearance of the rib heads.

In EOIS, 90% of cases will resolve spontaneously. Interestingly and inexplicably, girls with a right-sided curve have a much poorer prognosis than those with left-sided curves. Progressive EOIS is associated with thoracic insufficiency syndrome and a consequent reduction in life expectancy.

It is likely that the historical descriptions of this group of patients included many who had an underlying cause for their scoliosis. Some 22% of patients with presumed EOIS with curves less than 20° have an underlying neural axis anomaly (i.e. they were not truly idiopathic). In one series, eight out of ten patients with a neural axis anomaly required neurosurgical intervention.

For prognostic purposes, it is useful to differentiate curves according to the RVAD (rib-vertebral-angle difference). See **Figure 66.5**. This measurement was defined by Mehta (1972) and is the difference between the right and left sides in the magnitude of the angle measured from the long axis of the rib and a line drawn perpendicular to end plate of the vertebra at the apex of the curve. Mehta showed that if this difference in the angles was less than 20°, then there was an 85–90% chance that the curve would resolve spontaneously. She went on to describe a second feature: the phase of the rib head on the convex side at the apex. A 'phase 1' rib head does not overlap the vertebral body and is associated with resolution in 84–98% of cases. A 'phase 2' rib head does overlap the vertebral body and is associated with progression in 84–97% of cases. Double curves are more likely to progress than single curves.

It has been suggested that EOIS is the result of intrauterine moulding; the counter to this suggestion is the fact that EOIS is rarely seen at birth. Others argue that it is the result of 'body moulding' from the positioning of the child. If the infant lies in the lateral decubitus position a curve will develop; this is supported by the observation of plagiocephaly in this group.

Most spinal surgeons agree that serial casting is a reasonable non-operative treatment option for progressive EOIS. Rigid braces are of

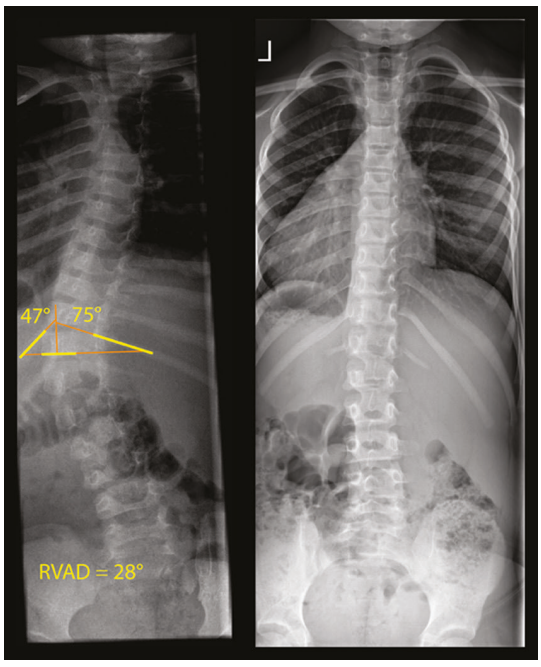

Fig. 66.5 Rib-vertebral-angle difference. In this case the RVAD at presentation (9 months old) was 28°—a marker for likely progression. The curve was progressive, and was treated with serial plaster casts (EDF casts). The curve has all but resolved by the age of 6 years.

little use, due to the rapid growth rate of the child, but serial plaster casts such as those popularized by Cotrel and used to good effect by Mehta (elongation derotation flexion, or EDF casts) can be moulded to control small, progressive curves.

Large curves (greater than approximately 50° Cobb angle) are best treated surgically. The dilemma is that early spinal fusion will prevent thoracic growth and this in turn will lead to thoracic insufficiency syndrome, respiratory failure, and reduced life expectancy. Therefore, the goal of surgical treatment is to control the curve, while maintaining growth. Many techniques have been tried.

The generally favoured technique is a dual rod growing system. Here, the curve is instrumented proximally and distally (usually two levels at each end), but the centre of the curve is left undisturbed. Rods are used on each side to connect the proximal and distal instrumentation. Traditional rods had to be lengthened every four to six months to allow growth, and this necessitated repeated surgical procedures. Complications such as wound infection or rod breakage were encountered in all of these cases eventually, due to repeated extension of instrumentation through the same scar. A rod with an intrinsic magnetic motor that allows telescoping has recently entered clinical use and offers the possibility of repeated lengthening using an external magnet in the outpatient clinic, obviating the need for repeated surgery.

Another possible solution is to selectively inhibit growth on the curve convexity. This technique is still somewhat experimental and not widely adopted.

Late onset idiopathic scoliosis (LOIS)

Late onset idiopathic scoliosis is a relatively common condition. Small curves are more common than large curves. The prevalence of curves greater than 10° is 2%; for curves greater than 30°, the prevalence is 0.2–0.3%. Overall, only 6 in 10 000 children will require treatment for LOIS.

The gender ratio approaches 1:1 for curves of 10° although for curves greater than 20°, the male:female ratio is 1:5. Small curves do not present clinically. The data on small curves originates from school screening programmes (Glassman et al., 2005). School screening programmes have largely been abandoned, as there is no reliable treatment that we can offer to children with small curves that would alter the natural history of the curve.

The development of a late onset curve is an insidious process. It is unsurprising that small curves go unnoticed by parents.

Classification of late onset idiopathic scoliosis

We have yet to find the ideal classification system for this multidimensional problem. Currently, the most widely used classification is that of Lenke et al. (2001). This has provided us with a useful tool, which allows reproducible descriptions of LOIS curves, can guide treatment, and promotes research. The Lenke classification is based on static erect and supine bending radiographs. There are three components: curve pattern, lumbar modifier, and sagittal thoracic modifier.

This classification is two-dimensional and addresses both the sagittal and the coronal plane. The rotational deformity is not classified. Work continues to find a truly 3D classification. These classification systems do not address the problems of which the patients complain—their cosmesis.

Aetiology of late onset idiopathic scoliosis

Idiopathic—arising spontaneously or from an obscure or unknown cause.

There are many theories regarding the aetiology of LOIS, but much remains unknown. Endocrine, neurological, muscular, and skeletal causes have all been postulated. It is more common in tall and slim (exomorphic) females. The deformity is lordosis with scoliosis, or lordo-scoliosis. The rotation of the curve as the spine deforms may give the appearance of kyphosis on the standard lateral radiograph, but a derotated view will give a more accurate assessment. One theory is that excess anterior spinal growth relative to posterior growth reduces the stability of the thoracic kyphosis, which then buckles, to produce a scoliosis.

Between 8% and 20% of patients with LOIS will have a first degree relative with the condition. The search for the genes responsible continues. It is likely that scoliosis is the result a complex interaction between multiple genes.

Natural history of late onset idiopathic scoliosis

The main driver of progression in late onset curves is growth. Indicators of remaining growth help predict curve progression. These indicators of remaining growth may be chronological, endocrine, or skeletal markers of maturity.

Age alone is a crude guide to remaining growth potential. Age of menarche adds further information. Girls grow rapidly for 18 months before and 18 months after menarche. A formal assessment of bone age using an X-ray of hand and wrist is also useful. The Risser grade is the degree of fusion of the iliac apophysis as seen on an anteroposterior (AP) radiograph. At grade 0 the apophysis has yet to appear. At grade 5 it is fully fused. Grades 1–4 represent progressive fusion of the apophysis to the iliac blade from lateral to medial. Age, pubertal stage, and bone age can be used to help predict the risk of progression (Table 66.2).

Even with significant remaining growth, small curves are unlikely to progress. Data for curves of 5–19° shows that 22% progress if the child is Risser grade 0–1, and only 1.6% progress if the child is Risser grade 2–4. (Note that a curve of 5° is below the current accepted threshold (10°) for a diagnosis of scoliosis.)

In the long term, LOIS patients have a normal life expectancy. The incidence of back pain is no higher than the general population, but when painful episodes do occur they may be a little more severe and last a little longer than the average. Unexplained back pain in this

Table 66.2 Predicting the risk of curve progression

Risk factor	Risk of progression (> 5°)
Age <10	88%
Age >15	29%
Premenarche	53%
Postmenarche	11%
Risser grade 0	68%
Risser grade 3–4	18%

Data from Lonstein JE, Carlson JM., The prediction of curve progression in untreated idiopathic scoliosis during growth, *The Journal of Bone and Joint Surgery Am*, Volume 66, Issue 7, pp. 1061–71, 1984.

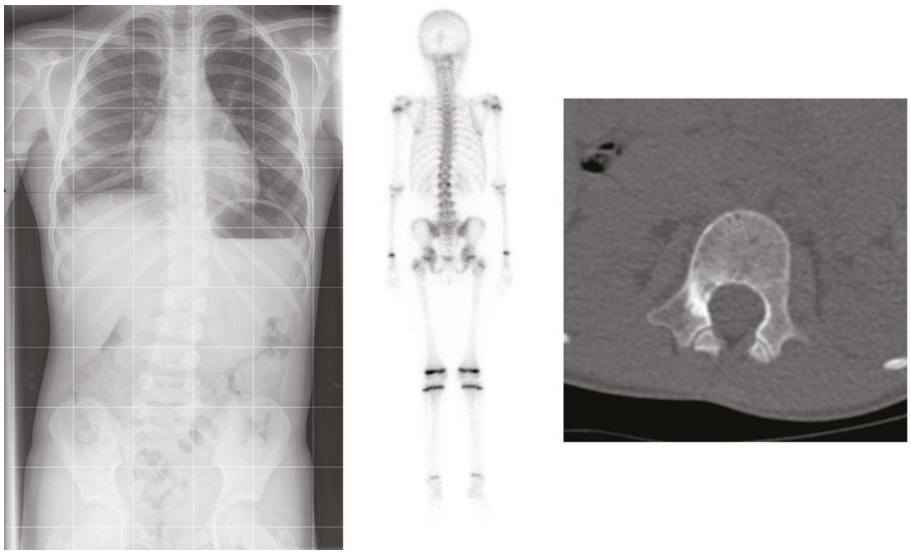

Fig. 66.6 Osteoid osteoma. This patient presented with a painful scoliosis which was investigated further with an isotope bone scan. Increased uptake can be seen in the pedicle of L2 on the bone scan. The axial CT scan shows a nidus with surrounding sclerosis.

group should prompt a search for other possible causes, especially pathologies that cause painful scoliosis such as osteoid osteoma or spondylolysis. See **Figure 66.6**.

There is an increased awareness of body image in this group, and there is certainly a psychological effect of the deformity. Girls with LOIS have a higher incidence of eating disorders and a lower BMI (body mass index).

LOIS does not cause significant cardiopulmonary compromise unless the curve is very large. A curve size of 90° is often quoted as a threshold for such compromise, although in truth some degree of measurable pulmonary dysfunction may be seen across all curve sizes. In contrast, severe pulmonary dysfunction is much more common in EOIS. The important distinction is where pulmonary dysfunction becomes *clinically* significant. Patients with a curve of more than 50° may have symptoms of exertional dyspnoea.

There is long term data to suggest that all curves progress a little, even after skeletal maturity. This progression is approximately 0.5° per year on average. Progression is more rapid in larger curves (>50°).

A number of LOIS patients will again present to spinal surgeons as adults with progression and degeneration in the curve, with symptoms of pain and possibly nerve root compression.

Treatment of late onset idiopathic scoliosis

Physiotherapy can be helpful for those children who develop back pain. There is no good evidence that physiotherapy can alter the underlying curve.

Bracing may play a role in the treatment of small curves with the aim of preventing curve progression, not correcting the curve. Bracing needs to be for 17 or more hours a day to be successful. Bracing has potentially significant physical and psychological morbidity. Ideally, bracing needs to be commenced before the growth spurt, and requires significant commitment from both patient and healthcare staff. Dynamic (elasticated) braces have been developed, and are still being evaluated.

Surgery can change the underlying spinal shape and the cosmetic appearance. A curve of less than 40° is unlikely to require surgical treatment on the grounds of dyscosmesis. The aims of scoliosis surgery are to prevent progression and leave a stable and well-balanced spine with the maximum safe cosmetic correction, preserving as many motion segments as possible. Cosmetic correction equates to level shoulders, centralization of the trunk with balanced waist creases and correction of spinal axial rotation to reduce the rib or loin prominence.

To identify fusion levels, the simple rule, followed in the majority of cases, is to identify the end vertebrae (i.e. the vertebrae with endplates that are most tilted from the horizontal plane and fuse all structural curves from the upper end vertebra to the lower end vertebra). The highest level should be chosen to ensure that the shoulders become or remain level and there should be a normal sagittal profile at the junction from fused to unfused. The lowest level should be selected based on the neutral and stable vertebra on the standing film, as well as examining the correction achieved across the disc spaces on the bending films.

Flexible curves make correction relatively straightforward. Stiff curves need some release to achieve the optimum correction. All facets joints are released as a means of achieving interfacetal fusions. Facets and the ligamentum flavum can be removed, as can the intervertebral discs, giving additional flexibility. Rigid curves require a more extensive osteotomy or complete resection of the vertebral column.

There is a decision to be made regarding the approach taken and which levels to fuse. The majority of scoliosis surgery is performed via a posterior approach. Anterior surgery may be indicated for larger, stiffer curves and is usually combined with posterior fixation. Choices regarding the precise levels of fusion will be determined by the choice of approach and the philosophy of correction.

Spinal deformity surgery is a major undertaking and carries significant risks. These risks can be managed and reduced with a systematic approach to the care of these patients. This involves any

number of protocols, including preoperative planning, patient blood management (tranexamic acid and cell salvage) and spinal cord monitoring using somatosensory evoked potential (SSEP) and motor-evoked potentials (MEPs) (see Chapter 56). 'Wake up' tests may be indicated if the electrophysiology shows persistent abnormalities.

Scheuermann's kyphosis

This condition has been given many names, but is commonly known as Scheuermann's disease or Scheuermann's kyphosis. Scheuermann first described the condition as the development of painful fixed kyphosis in teenagers. Radiographs show vertebral wedging with compression of the anterior vertebral borders.

Sorensen refined the diagnostic criteria, requiring more than 5° of anterior wedging in at least three adjacent vertebral bodies with abnormal kyphosis.

The incidence has been reported to be between 0.9% and 30%, although a figure of between 1% and 6% is more reasonable. Some studies have found that the condition is more common in boys, although others have found no gender difference.

The cause is unknown, although there are many theories. Among these theories, it has been suggested that the anterior vertebral body may have an abnormal blood supply, or that there may be abnormal ossification below the vertebral endplates.

Physiotherapy and extension exercise can be helpful for these patients. Bracing also has a role for patients with flexible curves (less than 65°), and may help patients back pain.

Surgery is indicated for unacceptable cosmesis (curves >70°) and disabling pain if conservative measures have failed. The aim of surgery is to correct the kyphosis to the upper limit of the normal range. Overcorrection may cause adjacent level junctional problems. Correction is achieved by shortening the posterior column, with multilevel osteotomies.

Spinal deformity in adults

Most adult spinal deformity patients present with a *de novo* degenerative scoliosis. We will all develop degenerative changes within the spine, but unfavourable degenerative changes such as stenosis, spondylolisthesis, lateral-listhesis, and loss of the lumbar lordosis may lead to symptoms. It is worth considering whether or not there is an underlying metabolic bone condition, such as osteoporosis, in this group of patients. Osteoporosis may be a factor in curve progression, and it will be a consideration if the patient should come to surgical treatment.

A smaller number of adult spinal deformity patients have developed degenerative change and curve progression within an adolescent idiopathic curve.

Unlike the paediatric patients, adult patients present with pain and radicular symptoms. The coronal plane deformity is relatively unimportant. It is the sagittal plane and pelvic parameters that have the biggest clinical impact. Focal subluxation, loss of lumbar lordosis, and global spinal imbalance have been correlated with disability.

With our ageing population there is an increasing number of potential candidates for adult deformity surgery. However, enthusiasm for deformity correction must be tempered by realistic goals, and an awareness of the significant potential for complications in this type surgery. Medical comorbidities may mean that some patients are not fit enough for the magnitude of surgery that is required.

A simple decompression (leaving the deformity uncorrected) may relieve radicular symptoms, but a 'small fusion' may leave the patient in a worse sate, if the problems of lost lordosis and global spinal balance are not addressed. In many cases the choice is to do nothing or a small decompressive procedure, or to consider a bigger operation and correction of the deformity, a procedure which will usually require an osteotomy or multiple intervertebral cages.

If the deformity is to be addressed, then the correction goals are restoration of the patient's sagittal vertebral alignment.

Be wary of the adult deformity patient whose deformity appears when they stand or walk, but disappears when they lie down. This may be camptocormia, which is an axial muscle myopathy associated with Parkinson's disease.

Kyphosis

Destructive pathologies such as trauma, tumour, and infection can all produce localized kyphosis. In some cases, there is sufficient flexibility across the uninvolved adjacent spinal segments for a normal global spinal balance to be maintained. In other cases, the localized destruction may result in a global sagittal spinal imbalance, which should be considered when treating the patient.

The treatment of trauma, tumours, and infections are discussed in more detail elsewhere within this text (see the chapters within Section 10, 'Neurotrauma and intensive care').

FURTHER READING

Glassman, S.D., Bridwell, K., Dimar, J.R., Horton, W., Berven, S., & Schwab, F. (2005). The impact of positive sagittal balance in adult spinal deformity. *Spine*, **30**(18), 2024–9.

Lenke, L.G., Betz, R.R., Harms, J., et al. (2001). Adolescent idiopathic scoliosis: a new classification to determine extent of spinal arthrodesis. *J Bone Joint Surg*, **83**(8), 1169–81.

McMaster, M.J. & Ohtsuka, K. (1982). The natural history of congenital scoliosis. A study of two hundred and fifty-one patients. *J Bone Joint Surg Am*, **64**(8), 1128–47.

Mehta, M.H. (1972). The rib-vertebra angle in the early diagnosis between resolving and progressive infantile scoliosis. *J Bone Joint Surg Br*, **54**(2), 230–43.

REFERENCES

Glassman, S.D., Bridwell, K., Dimar, J.R., Horton, W., Berven, S., & Schwab, F. (2005). The impact of positive sagittal balance in adult spinal deformity. *Spine*, **30**(18), 2024–9.

Lenke, L.G., Betz, R.R., Harms, J., et al. (2001). Adolescent idiopathic scoliosis: a new classification to determine extent of spinal arthrodesis. *J Bone Joint Surg*, **83**(8), 1169–81.

McMaster, M.J. & Ohtsuka, K. (1982). The natural history of congenital scoliosis. A study of two hundred and fifty-one patients. *J Bone Joint Surg Am*, **64**(8), 1128–47.

Mehta, M.H. (1972). The rib-vertebra angle in the early diagnosis between resolving and progressive infantile scoliosis. *J Bone Joint Surg Br*, **54**(2), 230–43.

RELATED LINKS TO EBRAIN

Adolescent Idiopathic Scoliosis. https://learning.ebrain.net/course/view.php?id=802
Congenital Scoliosis. https://learning.ebrain.net/course/view.php?id=800
Degenerative Scoliosis. https://learning.ebrain.net/course/view.php?id=816
Early Onset Scoliosis (Thoracic Insufficiency). https://learning.ebrain.net/course/view.php?id=813
Kyphosis. https://learning.ebrain.net/course/view.php?id=806
Neuromuscular Scoliosis. https://learning.ebrain.net/course/view.php?id=808
Principles of Surgical Scoliosis Correction. https://learning.ebrain.net/course/view.php?id=410

SECTION 14

Spinal trauma

67 **Managing spinal cord trauma** *781*
Saksith Smithason, Bryan S. Lee, and Edward C. Benzel

68 **Cervical spine injuries** *789*
Calan Mathieson, Chris Barrett, and Likhith Alakandy

69 **Thoracic and lumbar spine injuries** *801*
Bedansh Roy Chaudhary and Shiong Wen Low

70 **Spinal cord injury rehabilitation** *813*
Fahim Anwar, Wail Ahmed, Tamara Tajsic, Damiano G. Barone, and Harry Mee

67

Managing spinal cord trauma

Saksith Smithason, Bryan S. Lee, and Edward C. Benzel

Introduction

Spinal cord injury (SCI), either traumatic or non-traumatic in aetiology, leads to temporary or permanent damage to the spinal cord function. Significant efforts have been directed towards the elucidation of the underlying pathophysiology of SCI. Both primary and secondary mechanisms of SCI exist, leading to immediate and often irreversible cell damage. Immediate treatment and adequate management in the setting of acute SCI are essential, preservation of even a small amount of functional neuronal tissue can permit ambulation.

SCI is associated with a prolonged hospital stay, rehabilitation stay, and often associated with enormous monetary costs. Neurological recovery after SCI is largely dependent on the extent of injury. The management of SCI and the determination of the role and timing of surgical decompression remain crucial and yet controversial. Further epidemiological research and studies are warranted in order to enhance healthcare planning and cost-effectiveness.

Epidemiology

Incidence, prevalence, gender, and geographic distribution.

The annual incidence of SCI is 15 to 40 cases per million people throughout the world, and 11.5 to 53.4 per million in the developed countries (Botterell et al., 1975). There are 12 000 new cases of paraplegia and quadriplegia as a result of SCI in the United States, and of these cases, 4000 die prior to reaching the hospital and 1000 during hospitalization (Sances et al., 1984). The incidence of SCI patients who survived and reached a hospital was 50 per million people per year. The prevalence of acute SCI is, however, varied. A study conducted in a single county reported the prevalence of SCI to be 583 per million, whereas a number reported from multinational studies ranged from 130 to 1125 per million (Griffin et al., 1985). Age distribution peaked in the second and third decades in most countries. Regarding gender ratios, males have been consistently found to be at higher risk for traumatic SCI. The actual ratio of men to women is approximately 3–4:1, and two-thirds of new SCI cases are found to occur in young individuals of less than 30 years of age (Griffin et al., 1985). The mean age and the proportion of older individuals, however, have been shown to increase with time (Sekhon and Fehlings, 2001). Regarding geographic distribution, a Canadian study reported that the incidence of SCI among rural residents was twice that of urban residents (Dryden et al., 2003). Motor vehicle collisions (MVC), falls, sports, and violence are the leading causes.

Economic impact

As SCI is often associated with a prolonged hospital and rehabilitation stay, there are often enormous monetary costs associated with treatment. The estimated management cost of SCI in the United States was $4 billion in 1990 (Stripling, 1990). From a national study in 1992, SCI patients was associated with an average hospitalization course of 171 days in the first two years postinjury, and initial hospital expenses averaged nearly $100 000. (Harvey et al., 1992). Today, the costs are far greater. In addition, there are significant expenditures for medical services, supplies, equipment, therapy, and rehabilitation (Harvey et al., 1992). Lifetime medical expenses can range from $50 000 in incomplete injuries to $2 million in cases of high cervical tetraplegia (Harvey et al., 1992).

Pathophysiology

Primary vs. secondary injury

The primary mechanism of acute SCI is generally considered to be irreversible; caused by rapid and violent spinal cord compression and distortion from displacement of normally protective structures due to traumatic fracture or dislocation (Fehlings and Tator 1995). Secondary mechanisms involve a cascade of injury mechanisms such as hypoxic-ischaemic injuries, electrolyte derangements, and lipid peroxidation—all initiated by primary injury mechanisms (Fehlings and Tator, 1995). A cascade of events occurs within minutes of the primary injury leading to subsequent cell death via hypoxia, ischaemia, ionic shifts, lipid peroxidation, free radical formation, protease activation, and prostaglandin-causing apoptosis (Fig. 67.1) (Carlson et al., 1998). A secondary injury with associated vascular compromise causing cellular necrosis, with the subsequent death of initially survived cells is hypothesized (Tator and Koyanagi, 1997). The secondary injury, however, has been suggested to account for only 10% of the total pathology after SCI from atomic absorption

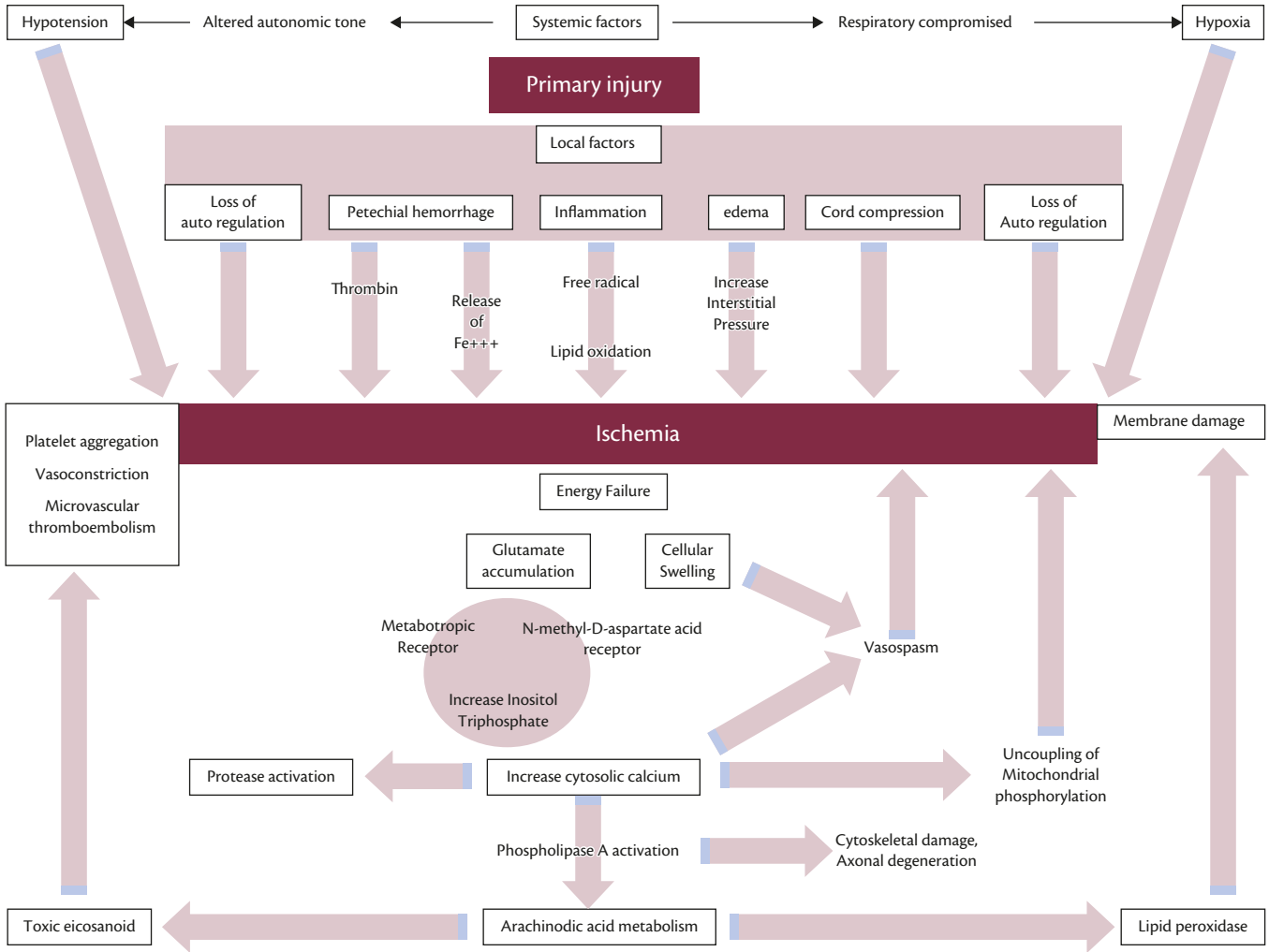

Fig. 67.1 Pathophysiology process underlying traumatic spinal cord injury.

spectroscopy (Young et al., 1982). Vascular mechanisms involved in SCI include changes in spinal cord blood flow, with the ischaemia persisting and worsening at least for 24 hours in animal models (Rivlin and Tator, 1978). Although mechanisms of such ischaemia remain unclear, vasospasm from mechanical damage, endothelial oedema, damage via focal haemorrhages with thrombosis, and the involvement of excitatory amino acids are some of the possible mechanisms (Sekhon and Fehlings, 2001).

Histological findings

Histological findings from the traumatized spinal cord specimens in the acute stage (3–5 days postinjury) demonstrated severe haemorrhages, predominantly in the grey matter This was likely related to damage to the anterior sulcal arteries. The surrounding white matter also demonstrated multiple lesions, including disrupted myelin and axonal oedema (Tator and Koyanagi, 1997). Although there were no findings of complete occlusion of major arteries, intramedullary veins were found to be occluded in the degenerated posterior white columns. It was concluded that the occlusion of such intramedullary veins from the initial mechanical stress or secondary injury likely produced the white matter lesions (Tator and Koyanagi, 1997).

Management of spinal injury

Prehospital phase, primary survey, and resuscitation

At the scene of trauma, the patient should be managed via advance trauma life support guidelines (ATLS) (Kortbeek et al., 2008). Initially, the patient should be carefully immobilized using devices such as the Kendrick extrication device, along with a rigid cervical collar, especially during extrication following a motor vehicle accident. Cervical spine immobilization must be maintained by stabilizing both the torso and the head during transfer to the nearest trauma centre, and vasopressors are recommended to maintain the systolic blood pressure above 100 mmHg (Gondim et al., 2004). Prehospital management is critical. Some 25% of prehospital fatalities are aggravated after the initial event (Bernhard et al., 2005).

Hospital phase and secondary survey

A rigid spinal board should be removed soon after the patient arrives in the emergency department to prevent pressure ulcers. Respiratory status must be monitored, since one-third of patients will require intubation in the first 24 hours. High cervical injuries

paralyse the diaphragm and intercostal muscles, whereas lower cervical injuries affect the intercostal muscles only. Paradoxical abdominal movement with respirations is often observed in patients with spinal cord injury above C5. Therefore, intubation is recommended in patient with vital capacity less than 1 litre (Ball, 2001). During the secondary survey, an entire evaluation of the spine is required since many injuries may not be obvious while the patient is kept in the supine position. It is recommended that a combination of low-molecular-weight heparin, rotating beds, adjusted dose heparin, or pneumatic compression stockings be used as prophylaxis for deep venous thrombosis. The first step is to define whether the injury is complete or incomplete. The bladder and bowel function must be assessed before one declares the presence of a complete injury. In order to accurately and consistently assess neurological function following SCI, the American Spinal Injury Association (ASIA) impairment scale is widely used due to its simplicity and similarity to the previously used Frankel scale (Fig. 67.2) (Kirshblum et al., 2011).

Methylprednisolone sodium succinate (MPSS) was extensively studied in five human SCI trials. Three multicentre, randomized, double-blinded National Acute Spinal Cord Injury Studies (NASCIS) had significant impact on the practice of spine trauma care in the United States (Bracken et al., 1990). MPSS was established as an effective neuroprotective agent for SCI on the basis of a NASCIS trial. Various dosage and administration recommendations were made over the course of the studies. However, some pitfalls have been identified in NASCIS II and III. It was alleged that conclusions were derived on the basis of non-standardized experimental design and statistical artefacts (Sayer et al., 2006). Despite all the conflicting data associated with MPSS in SCI, its known complications, and lack of proven efficacy, MPSS continues to be in widespread use for acute SCI in the United States, and many centres still resort to its use in order to avoid any possible legal repercussions (Hurlbert, 2000).

Imaging

The unconscious or uncooperative patient in the trauma setting should be assumed to have a spinal injury until proven otherwise. Helical CT was observed to identify 99.3% of all fractures of the cervical, thoracic, and lumbar spine, and those injuries missed by helical CT required minimal or no treatment (Brown et al., 2005). Magnetic resonance imaging (MRI) of the spine provides the best imaging of neurologic structures, ligaments, and discs. MRI is not routinely used in the evaluation of the polytrauma patient because of the time required. MRI is most useful in patients whose CT results do not explain the neurological status, most commonly seen in the neurologically impaired victim with an unremarkable CT. MRI may be used to exclude the presence of an associated extruded disc before or after a reduction manoeuvre in patients with cervical facet subluxations or dislocations.

Cervical traction

Halo application has been advocated in polytrauma patients given, its ability to facilitate further necessary diagnostic evaluations and emergent surgical treatment of associated injuries in the polytrauma patient. The benefit of closed cervical reduction and traction is controversial. Cervical traction can be used with a reported 80% success rate and 80% rate of improved neurological function, and worsening neurologic status from disc herniation after cervical traction may also occur. It is emphasized that such a strategy is not universally employed.

Cervical spine clearance

Issues with cervical spine clearance in polytrauma patients remains controversial. Coronal and sagittal reformatted CT scanning facilitates the visualization of bony injury. MRI is required if definitive evaluation of the soft tissues is indicated. MRI is used to confirm and quantify the anatomy of the lesion. The extent of spinal cord compression, swelling and parenchymal haemorrhage seen on MRI predicts adverse outcome after SCI (Miyanji et al., 2007). In order to definitively declare spinal stability after blunt trauma, both clinical and radiographic evidence must be thoroughly and systematically reviewed.

Mortality

Mortality after SCI has improved from 38% in 1970 to 15.8% during 1997–2000. (Bilello et al., 2003). Death at the scene is related to high-level SCIs, cardiovascular instability, or respiratory compromise. Mortality rates are highest immediately following and within the first hours after injury. It then drops precipitously after admission to the hospital (Evans et al., 2013). Odds of early death after traumatic SCI are increased by the following: older than 20 years of age, male gender, one or more comorbidities, concomitant systemic injury (Injury Severity Scale [ISS] >15), and concomitant traumatic brain injury (Varma et al., 2010).

Prognosis

Admission ASIA Impairment Scale (AIS) grade predicted neurological recovery at 1-year postinjury with a correlation between severity and expected level of recovery. Ten to fifteen per cent (10–15%) of individuals will convert from AIS grade A to an incomplete injury and only 2% will convert from AIS grade A to AIS D (Tator et al., 1999). For AIS grade C patients, the mean ASIA motor recovery score at 1-year postinjury is approximately 43 points for quadriplegic patients, with approximately 70% converting to AIS grade D or E (Kirshblum et al., 2011). Cervical SCIs demonstrate a 9.6-point increase in ASIA motor score compared to a 2.6-point average improvement seen in thoracic and lumbar complete lesions (Kirshblum et al., 2011). The chances of walking at 1 year after complete paraplegia is 5%, and 0% in complete quadriplegics (Wilson et al., 2012; Wilson et al., 2013).

Completed trials

GM1 ganglioside (Sygen)

The largest prospective randomized clinical SCI trial, enrolled more than 750 patients, involved the study of GM1 Ganglioside (Sygen). There is Class III clinical evidence that suggests the improvement of clinical outcome via optimization of spinal cord perfusion (Hurlbert, 2006). Such results, however, were not reproduced in long-term follow-up. As such, it is not in clinical use currently.

INTERNATIONAL STANDARDS FOR NEUROLOGICAL CLASSIFICATION OF SPINAL CORD INJURY (ISNCSCI)

Patient Name _____ Date/Time of Exam _____

Examiner Name _____ Signature _____

RIGHT

MOTOR KEY MUSCLES		SENSORY KEY SENSORY POINTS Light Touch (LTR)	Pin Prick (PPR)
	C2		
	C3		
	C4		
Elbow flexors	C5		
Wrist extensors	C6		
Elbow extensors	C7		
Finger flexors	C8		
Finger abductors (little finger)	T1		
	T2		
	T3		
	T4		
	T5		
	T6		
	T7		
	T8		
	T9		
	T10		
	T11		
	T12		
	L1		
Hip flexors	L2		
Knee extensors	L3		
Ankle dorsiflexors	L4		
Long toe extensors	L5		
Ankle plantar flexors	S1		
	S2		
	S3		
	S4-5		
RIGHT TOTALS			
(MAXIMUM)		*(50)*	*(56)*	*(56)*

UER (Upper Extremity Right)

LER (Lower Extremity Right)

Comments *(Non-key Muscle? Reason for NT? Pain?):*

(VAC) Voluntary Anal Contraction (Yes/No) ☐

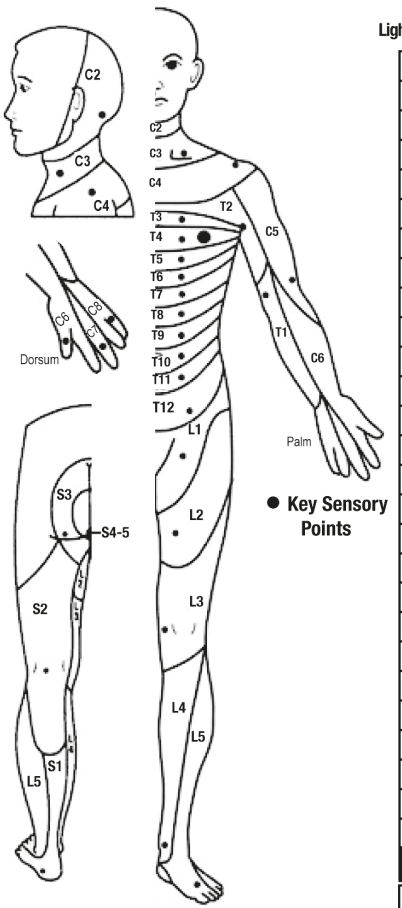

● **Key Sensory Points**

LEFT

SENSORY KEY SENSORY POINTS Light Touch (LTL)	Pin Prick (PPL)	MOTOR KEY MUSCLES	
		C2	
		C3	
		C4	
		C5	*Elbow flexors*
		C6	*Wrist extensors*
		C7	*Elbow extensors*
		C8	*Finger flexors*
		T1	*Finger abductors (little finger)*
		T2	
		T3	
		T4	
		T5	
		T6	
		T7	
		T8	
		T9	
		T10	
		T11	
		T12	
		L1	
		L2	*Hip flexors*
		L3	*Knee extensors*
		L4	*Ankle dorsiflexors*
		L5	*Long toe extensors*
		S1	*Ankle plantar flexors*
		S2	
		S3	
		S4-5	
		LEFT TOTALS	
(56)	*(56)*	**(MAXIMUM)**	*(50)*

UEL (Upper Extremity Left)

LEL (Lower Extremity Left)

MOTOR ***(SCORING ON REVERSE SIDE)***

0 = total paralysis
1 = palpable or visible contraction
2 = active movement, gravity eliminated
3 = active movement, against gravity
4 = active movement, against some resistance
5 = active movement, against full resistance
5 = normal corrected for pain/disuse*
NT = not testable

SENSORY ***(SCORING ON REVERSE SIDE)***

0 = absent *2 = normal*
1= altered *NT = not testable*

(DAP) Deep Anal Pressure (Yes/No) ☐

MOTOR SUBSCORES

UER ☐ + UEL ☐ = *UEMS TOTAL* ☐ — *MAX (25)* *(25)* *(50)*

LER ☐ + LEL ☐ = *LEMS TOTAL* ☐ — *MAX (25)* *(25)* *(50)*

SENSORY SUBSCORES

LTR ☐ + LTL ☐ = *LT TOTAL* ☐ — *MAX (56)* *(56)* *(112)*

PPR ☐ + PPL ☐ = *PP TOTAL* ☐ — *MAX (56)* *(56)* *(112)*

		R	L
NEUROLOGICAL LEVELS *Steps 1-5 for classification as on reverse*	*1. SENSORY*	☐	☐
	2. MOTOR	☐	☐

3. NEUROLOGICAL LEVEL OF INJURY (NLI) ☐

4. COMPLETE OR INCOMPLETE? ☐
Incomplete = Any sensory or motor function in S4-5

5. ASIA IMPAIRMENT SCALE (AIS) ☐

(In complete injuries only)
ZONE OF PARTIAL PRESERVATION
Most caudal level with any innervation

	R	L
SENSORY	☐	☐
MOTOR	☐	☐

This form may be copied freely but should not be altered without permission from the American Spinal Injury Association.

REV 11/15

Muscle Function Grading

0 = total paralysis

1 = palpable or visible contraction

2 = active movement, full range of motion (ROM) with gravity eliminated

3 = active movement, full ROM against gravity

4 = active movement, full ROM against gravity and moderate resistance in a muscle specific position

5 = (normal) active movement, full ROM against gravity and full resistance in a functional muscle position expected from an otherwise unimpaired person

5* = (normal) active movement, full ROM against gravity and sufficient resistance to be considered normal if identified inhibiting factors (i.e. pain, disuse) were not present

NT = not testable (i.e. due to immobilization, severe pain such that the patient cannot be graded, amputation of limb, or contracture of > 50% of the normal ROM)

Sensory Grading

0 = Absent

1 = Altered, either decreased/impaired sensation or hypersensitivity

2 = Normal

NT = Not testable

When to Test Non-Key Muscles:

In a patient with an apparent AIS B classification, non-key muscle functions more than 3 levels below the motor level on each side should be tested to most accurately classify the injury (differentiate between AIS B and C).

Movement	Root level
Shoulder: Flexion, extension, abduction, adduction, internal and external rotation **Elbow:** Supination	**C5**
Elbow: Pronation **Wrist:** Flexion	**C6**
Finger: Flexion at proximal joint, extension. **Thumb:** Flexion, extension and abduction in plane of thumb	**C7**
Finger: Flexion at MCP joint **Thumb:** Opposition, adduction and abduction perpendicular to palm	**C8**
Finger: Abduction of the index finger	**T1**
Hip: Adduction	**L2**
Hip: External rotation	**L3**
Hip: Extension, abduction, internal rotation **Knee:** Flexion **Ankle:** Inversion and eversion **Toe:** MP and IP extension	**L4**
Hallux and Toe: DIP and PIP flexion and abduction	**L5**
Hallux: Adduction	**S1**

ASIA Impairment Scale (AIS)

A = Complete. No sensory or motor function is preserved in the sacral segments S4-5.

B = Sensory Incomplete. Sensory but not motor function is preserved below the neurological level and includes the sacral segments S4-5 (light touch or pin prick at S4-5 or deep anal pressure) AND no motor function is preserved more than three levels below the motor level on either side of the body.

C = Motor Incomplete. Motor function is preserved at the most caudal sacral segments for voluntary anal contraction (VAC) OR the patient meets the criteria for sensory incomplete status (sensory function preserved at the most caudal sacral segments (S4-S5) by LT, PP or DAP), and has some sparing of motor function more than three levels below the ipsilateral motor level on either side of the body.
(This includes key or non-key muscle functions to determine motor incomplete status.) For AIS C – less than half of key muscle functions below the single NLI have a muscle grade ≥ 3.

D = Motor Incomplete. Motor incomplete status as defined above, with at least half (half or more) of key muscle functions below the single NLI having a muscle grade ≥ 3.

E = Normal. If sensation and motor function as tested with the ISNCSCI are graded as normal in all segments, and the patient had prior deficits, then the AIS grade is E. Someone without an initial SCI does not receive an AIS grade.

Using ND: To document the sensory, motor and NLI levels, the ASIA Impairment Scale grade, and/or the zone of partial preservation (ZPP) when they are unable to be determined based on the examination results.

ASIA
AMERICAN SPINAL INJURY ASSOCIATION

INTERNATIONAL STANDARDS FOR NEUROLOGICAL CLASSIFICATION OF SPINAL CORD INJURY

ISCOS
INTERNATIONAL SPINAL CORD SOCIETY

Steps in Classification

The following order is recommended for determining the classification of individuals with SCI.

1. Determine sensory levels for right and left sides.
The sensory level is the most caudal, intact dermatome for both pin prick and light touch sensation.

2. Determine motor levels for right and left sides.
Defined by the lowest key muscle function that has a grade of at least 3 (on supine testing), providing the key muscle functions represented by segments above that level are judged to be intact (graded as a 5).
Note: in regions where there is no myotome to test, the motor level is presumed to be the same as the sensory level, if testable motor function above that level is also normal.

3. Determine the neurological level of injury (NLI)
This refers to the most caudal segment of the cord with intact sensation and antigravity (3 or more) muscle function strength, provided that there is normal (intact) sensory and motor function rostrally respectively.
The NLI is the most cephalad of the sensory and motor levels determined in steps 1 and 2.

4. Determine whether the injury is Complete or Incomplete.
(i.e. absence or presence of sacral sparing)
*If voluntary anal contraction = **No** AND all S4-5 sensory scores = **0** AND deep anal pressure = **No,** then injury is **Complete.** Otherwise, injury is **Incomplete.***

5. Determine ASIA Impairment Scale (AIS) Grade:

Is injury Complete? **If YES, AIS=A** and can record ZPP (lowest dermatome or myotome on each side with some preservation)

NO ↓

Is injury Motor Complete? **If YES, AIS=B**

NO ↓ (No=voluntary anal contraction OR motor function more than three levels below the motor level on a given side, if the patient has sensory incomplete classification)

Are at least half (half or more) of the key muscles below the neurological level of injury graded 3 or better?

NO ↓ **AIS=C** **YES** ↓ **AIS=D**

If sensation and motor function is normal in all segments, AIS=E
Note: AIS E is used in follow-up testing when an individual with a documented SCI has recovered normal function. If at initial testing no deficits are found, the individual is neurologically intact; the ASIA Impairment Scale does not apply.

Fig. 67.2 International Standards for Neurological Classification of Spinal Cord Injury.

© 2011 American Spinal Injury Association. Reprinted with permission.

Thyroid-releasing hormone (TRH), gacyclidine, nimodipine, and dynormin

A thyroid-releasing hormone (TRH) trial demonstrated improvements in the NASCIS and Sunnybrook scales in incomplete SCI patients. There, however, this study was criticized for a type I error (attrition with only 20 patients analysed) (Pitts et al., 1995). The gacyclidine trial, although of insufficient statistical power, demonstrated benefit in the treatment group, but this benefit did not persist at 1-year follow-up (Hirbec et al., 2006). The nimodipine trial compared nimodipine and MPSS to placebo (NASCIS II protocol). Neither agent showed benefit (Hall, 2011). Dynormin A, an endogenous opioid, administration showed no benefit in the NASCIS II trial, as well (Bracken et al., 1990).

Ongoing trials

Newer trials on traumatic SCI model are being investigated in two capacities: (1) neuroprotective agents to limit the secondary injury; and (2) neuroregenerative agents aiming at promoting and supporting repair and regeneration of axons (Fig. 67.3).

Neuroprotective capacity: Cerebrospinal fluid drainage, electrical field, hypothermia, and riluzole

Cerebrospinal fluid (CSF) drainage via a lumbar intrathecal line is under investigation in SCI patients, given the evidence of similar strategies reducing the incidence of paraplegia during thoracic aortic aneurysm surgery (Coselli et al., 2002). Generating an electrical field along the spinal axis to promote axonal growth has also shown improvement. (Shapiro et al., 2005). Adapting the protective effects of hypothermia during cardiac arrest to the animal SCI models has been shown to be associated with variable results (Kwon et al., 2008). Recent trials with patients systemically cooled to 33°C (91.4°F) demonstrated a beneficial effect of cooling (Levi et al., 2010). However, current evidence is insufficient to support the use of therapeutic hypothermia as a standard guideline. Riluzole, a sodium blocker and an antiseizure medication, in combination with MPSS, showed a protective effect even administered at 10 days after injury in animal SCI model. (Wang et al., 2004).

Neuroregenerative capacity

Attention has been focused on cell replacement therapy. Activated autologous macrophage transplants have shown promising results in a phase I trial, but the multicentre phase II trial was suspended due to financial problems (Knoller et al., 2005). Schwann cells play is known to play an important role in facilitating regeneration of the peripheral nerve. Olfactory ensheathing cell transplantation is safe and feasible, with up to 1 year follow-up. However, long-term follow-up results are variable (Lima et al., 2006). A trial of autologous human bone marrow stromal cells, combined with granulocyte macrophage colony stimulating factor, revealed benefit in acute SCI patients, but not in chronic SCI patients (Park et al., 2005). Human embryonic stem cell transplantation showed promising results in a rat SCI model. However, the FDA placed the human trial on hold due to the risk of tumourigenesis (Keirstead et al., 2005). Rho is an axon growth inhibitor protein that results in neuronal growth cone collapse, neurite retraction and cell body rounding,

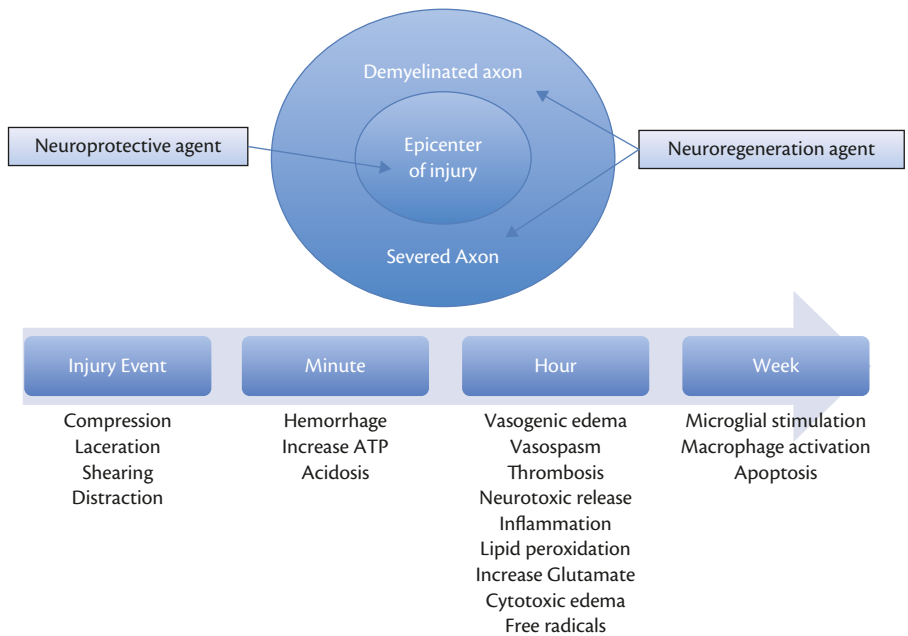

Fig. 67.3 Primary and secondary mechanisms of injury determining the final extent of spinal cord damage. The primary injury event starts a pathobiological cascade of secondary injury mechanisms that unfold in different phases within seconds of the primary trauma and continue for several weeks thereafter.

and rho associated kinase inhibitor and C3 transferase demonstrated effective cortical neuron regeneration in an *in vitro* study (Dergham et al., 2002). Local injection of activated autologous macrophages that are preincubated with sciatic nerve or skin has demonstrated a decreased synthesis of neurotoxic tumour necrosis factor (TNF-alpha), thereby promoting neuroprotective and neuroregenerative strategies (Bomstein et al., 2003).

Conclusions

SCI is a global problem with an enormous impact on financial, social, and personal cost. Treatment of the primary injury has proven amenable at present. Efforts have been made, with some success, to prevent and reduce the incidence of SCI. Secondary injury involves multiple pathophysiologic processes. Clinical guidelines have been established to minimize secondary injury. Newer pharmacological and biological agents are currently under investigation to mediate secondary mechanisms. With lessons learned from the completed trials in the past, a more effective management of SCI will obviously require multiple treatment modalities. Targeted to minimize initial damage, preserve residual function, and enhance recovery. It is hoped that a collaboration of multispecialist scientists and clinicians, will accomplish neural restoration after SCI in our lifetime.

Controversy

Early decompression surgery for spinal cord injury

Animal spinal cord injury models have demonstrated benefit from early decompression (Dimar et al., 1999). Benefit, however, is less clear in humans, especially in polytrauma patients. The first randomized prospective study regarding timing of surgery revealed no significant benefit when cervical spinal cord decompression after trauma is performed less than 72 hours after injury, as opposed to waiting longer than 5 days (Cadotte et al., 2010). The first randomized prospective trial, Surgical Treatment of Acute Spinal Cord Injury Study (STASCIS) demonstrated improved neurologic outcome, defined as at least an improvement by two grades on the AIS in patients who were decompressed prior to 24 hours after SCI (Fehlings et al., 2012).

Violent extension injury to a pre-existing degenerated compromised spine (with spinal stenosis) often results in the classic central cord injury. Poor outcome after early decompression for central cord syndrome has been published (Schneider et al., 1954). It, henceforth, has been recommended to avoid early surgery for central cord injury. Controversy has arisen when subsequent studies demonstrated benefit from early surgery. (Aito et al., 2007). Much remains unknown regarding the management of central cord syndrome. Therefore, practice patterns have often relied on clinical experience rather than scientific evidence.

Reports of mechanism of injury, the level of injury, and the timing of decompression on functional outcome from thoracic SCI are limited. A retrospective registry study compared recovery and outcome data in three groups: a control group (n = 93), an early surgery group receiving treatment within 72 hours (n = 156), and a late surgery group receiving treatment after 72 hours (n = 49). It showed the early surgery group fared significantly better than the late surgery group with regard to ventilator dependence, ICU stay, hospital length of stay, mortality, and pulmonary failure (Schinkel et al., 2006).

FURTHER READING

Dimar, J.R., Glassman, S.D., Raque, G.H., Zhang, Y.P., & Shields, C.B. (1999). The influence of spinal canal narrowing and timing of decompression on neurologic recovery after spinal cord contusion in a rat model. *Spine*, **24**(16), 1623.

Hurlbert, R.J. (2000). Methylprednisolone for acute spinal cord injury: an inappropriate standard of care. *J Neurosurg Spine*, **93**(1), 1–7.

Kortbeek, J.B., Al Turki, A.S., Ali, J., et al. (2008). Advanced trauma life support, the evidence for change. *J Trauma*, **64**(6), 1638–50.

Sekhon, L.H. & Fehlings, M.G. (2001). Epidemiology, demographics, and pathophysiology of acute spinal cord injury. *Spine (Phila Pa 1976)*, **26**(24 Suppl), S2–S12.

Tator, C.H., Fehlings, M.G., Thorpe, K., & Taylor, W. (1999). Current use and timing of spinal surgery for management of acute spinal surgery for management of acute spinal cord injury in North America: results of a retrospective multicenter study. *J Neurosurg*, **91**(1 Suppl), 12–18.

REFERENCES

Aito, S., D'Andrea, M., & Werhagen, L. (2007). Neurological and functional outcome in traumatic central cord syndrome. *Spinal Cord*, **45**(4), 292–7.

Ball, P.A. (2001). Critical care of spinal cord injury. *Spine (Phila Pa 1976)*, **26**(24 Suppl), S27–30.

Bernhard, M., Gries, A., Kremer, P., & Böttiger, B.W. (2005). Spinal cord injury (SCI)--prehospital management. *Resuscitation*, **66**(2), 127–39.

Bilello, J.F., Davis, J.W., Cunningham, M.A., Groom, T.F., Lemaster, D., & Sue, L.P. (2003). Cervical spinal cord injury and the need for cardiovascular intervention. *Arch Surg*, **138**(10), 1127–9.

Bomstein, Y., Marder, J.B., Vitner, K., et al. (2003). Features of skin-coincubated macrophages that promote recovery from spinal cord injury. *J Neuroimmunol*, **142**(1), 10–16.

Botterell, E.H., Jousse, A.T., Kraus, A.S., Thompson, M.G., Wynne Jones, M., Geisler, W.O. (1975). A model for the future care of acute spinal cord injuries. *Can J Neurol Sci*, **2**(4), 361–80.

Bracken, M.B., Shepard, M.J., Collins, W.F., et al. (1990). A randomized, controlled trial of methylprednisolone or naloxone in the treatment of acute spinal-cord injury: results of the Second National Acute Spinal Cord Injury Study. *N Engl J Med*, **322**(20), 1405–11.

Brown, C.V., Antevil, J.L., Sise, M.J., & Sack, D.I. (2005). Spiral computed tomography for the diagnosis of cervical, thoracic, and lumbar spine fractures: its time has come. *J Trauma Acute Care Surg*, **58**(5), 890–6.

Cadotte, D.W., Singh, A., & Fehlings, M.G. (2010). The timing of surgical decompression for spinal cord injury. *F1000 Medicine Reports*, **2**, 67.

Carlson, S.L., Parrish, M.E., Springer, J.E., Doty, K., & Dossett, L. (1998). Acute inflammatory response in spinal cord following impact injury. *Exp Neurol*, **151**(1), 77–88.

Coselli, J.S., LeMaire, S.A., Köksoy, C., Schmittling, Z.C., & Curling, P.E. (2002). Cerebrospinal fluid drainage reduces paraplegia after thoracoabdominal aortic aneurysm repair: results of a randomized clinical trial. *J Vasc Surg*, **35**(4), 631–9.

Dergham, P., Ellezam, B., Essagian, C., Avedissian, H., Lubell, W.D., & McKerracher, L. (2002). Rho signaling pathway targeted to promote spinal cord repair. *J Neurosci*, **22**(15), 6570–7.

Dimar, J.R., Glassman, S.D., Raque, G.H., Zhang, Y.P., & Shields, C.B. (1999). The influence of spinal canal narrowing and timing of decompression on neurologic recovery after spinal cord contusion in a rat model. *Spine*, **24**(16), 1623.

Dryden, D.M., Saunders, L.D., Rowe, B.H., et al. (2003). The epidemiology of traumatic spinal cord injury in Alberta, Canada. *Can J Neurol Sci*, **30**(2), 113–21.

Evans, L.T., Lollis, S.S., & Ball, P.A. (2013). Management of acute spinal cord injury in the neurocritical care unit. *Neurosurg Clin N Am*, **24**(3), 339–47.

Fehlings, M.G. & Tator, C.H. (1995). The relationships among the severity of spinal cord injury, residual neurological function, axon counts, and counts of retrogradely labeled neurons after experimental spinal cord injury. *Exp Neurol*, **132**(2), 220–8.

Fehlings, M.G., Vaccaro, A., & Wilson, J.R. (2012). Early versus delayed decompression for traumatic cervical spinal cord injury: results of the surgical timing in acute spinal cord injury study (STASCIS). *PLoS One*, **7**(2), e32037.

Gondim, F.A.A., Lopes, J., Oliveira, G.R., et al. (2004). Cardiovascular control after spinal cord injury. *Curr Vasc Pharmacol*, **2**(1), 71–9.

Griffin, M.R., O'Fallon, W.M., Opitz, J.L., & Kurland, L.T. (1985). Mortality, survival and prevalence: traumatic spinal cord injury in Olmsted County, Minnesota, 1935–1981. *J Chronic Dis*, **38**(8), 643–53.

Hall, E.D. (2011). Antioxidant therapies for acute spinal cord injury. *Neurotherapeutics*, **8**(2), 152–67.

Harvey, C., Wilson, S.E., Greene, C.G., Berkowitz, M., & Stripling, T.E. (1992). New estimates of the direct costs of traumatic spinal cord injuries: results of a nationwide survey. *Paraplegia*, **30**(12), 834–50.

Hirbec, H., Gaviria, M., & Vignon, J. (2006). Gacyclidine: a new neuroprotective agent acting at the N-methyl-D-aspartate receptor. *CNS Drug* Rev, **7**(2), 172–98.

Hurlbert, R.J. (2000). Methylprednisolone for acute spinal cord injury: an inappropriate standard of care. *J Neurosurg Spine*, **93**(1), 1–7.

Hurlbert, R.J. (2006). Strategies of medical intervention in the management of acute spinal cord injury. *Spine (Phila Pa 1976)*, **31**(11 Suppl), S16–S21; discussion S36.

Keirstead, H.S., Nistor, G., Bernal, G., et al. (2005). Human embryonic stem cell-derived oligodendrocyte progenitor cell transplants remyelinate and restore locomotion after spinal cord injury. *J Neurosci*, **25**(19), 4694–705.

Kirshblum, S.C., Burns, S.P., Biering-Sorensen, F., et al. (2011). International standards for neurological classification of spinal cord injury (revised 2011). *J Spinal Cord Med*, **34**(6), 535–46.

Knoller, N., Auerbach, G., Fulga, V., et al. (2005). Clinical experience using incubated autologous macrophages as a treatment for complete spinal cord injury: phase I study results. *J Neurosurg Spine*, **3**(3), 173–81.

Kortbeek, J.B., Al Turki, A.S., Ali, J., et al. (2008). Advanced trauma life support, the evidence for change. *J Trauma*, **64**(6), 1638–50.

Kwon, B.K., Mann, C., Sohn, H.M., et al. (2008). Hypothermia for spinal cord injury. *Spine J*, **8**(6), 859–74.

Levi, A.D., Casella, G., Green, B.A., et al. (2010). Clinical outcomes using modest intravascular hypothermia after acute cervical spinal cord injury. *Neurosurgery*, **66**(4), 670–7.

Lima, C., Pratas-Vital, J., Escada, P., Hasse-Ferreira, A., Capucho, C., & Peduzzi, J.D. (2006). Olfactory mucosa autografts in human spinal cord injury: a pilot clinical study. *J Spinal Cord Med*, **29**(3), 191–203.

Miyanji, F., Furlan, J.C., Aarabi, B., Arnold, P.M., & Fehlings, M.G. (2007). Acute cervical traumatic spinal cord injury: MR imaging findings correlated with neurologic outcome—prospective study with 100 consecutive patients. *Radiology*, **243**(3), 820–7.

Park, H.C., Shim, Y.S., Ha, Y., et al. (2005). Treatment of complete spinal cord injury patients by autologous bone marrow cell transplantation and administration of granulocyte-macrophage colony stimulating factor. *Tissue Engineering* **11**(5–6), 913–22.

Pitts, L.H., Ross, A., Chase, G.A., Faden, A.I. (1995). Treatment with thyrotropin-releasing hormone (TRH) in patients with traumatic spinal cord injuries. *J Neurotrauma*, **12**(3), 235–43.

Rivlin, A.S. & Tator, C.H. (1978). Regional spinal cord blood flow in rats after severe cord trauma. *J Neurosurg*, **49**(6), 844–53.

Sances, A., Myklebust, J.B., Maiman, D.J., Larson, S.J., Cusick, J.F., & Jodat, R.W. (1984). The biomechanics of spinal injuries. *Crit Rev Biomed Eng*, **11**(1), 1–76.

Sayer, F.T., Kronvall, E., & Nilsson, O.G. (2006). Methylprednisolone treatment in acute spinal cord injury: the myth challenged through a structured analysis of published literature. *Spine J*, **6**(3), 335–43.

Schinkel, C., Frangen, T.M., Kmetic, A., Andress, H.-J., & Muhr, G. (2006). Timing of thoracic spine stabilization in trauma patients: impact on clinical course and outcome. *J Trauma*, **61**(1), 156–60.

Schneider, R.C., Cherry, G., & Pantek, H. (1954). The syndrome of acute central cervical spinal cord injury. *J* Neurosurg, **11**(6), 546–77.

Sekhon, L.H. & Fehlings, M.G. (2001). Epidemiology, demographics, and pathophysiology of acute spinal cord injury. *Spine (Phila Pa 1976)*, **26**(24 Suppl), S2–S12.

Shapiro, S., Borgens, R., Pascuzzi, R., et al. (2005). Oscillating field stimulation for complete spinal cord injury in humans: a phase 1 trial. *J Neurosurg Spine*, **2**(1), 3–10.

Stripling, T.E. (1990). The cost of economic consequences of traumatic spinal cord injury. *Paraplegia News*, **8**, 50–4.

Tator, C.H. & Koyanagi, I. (1997). Vascular mechanisms in the pathophysiology of human spinal cord injury. *J Neurosurg*, **86**(3), 483–92.

Tator, C.H., Fehlings, M.G., Thorpe, K., & Taylor, W. (1999). Current use and timing of spinal surgery for management of acute spinal surgery for management of acute spinal cord injury in North America: results of a retrospective multicenter study. *J Neurosurg*, **91**(1 Suppl), 12–18.

Varma, A., Hill, E.G., Nicholas, J., & Selassie, A. (2010). Predictors of early mortality after traumatic spinal cord injury: a population-based study. *Spine (Phila Pa 1976)*, **35**(7), 778–83.

Wang, S.-J., Wang, K.-Y., & Wang, W.-C. (2004). Mechanisms underlying the riluzole inhibition of glutamate release from rat cerebral cortex nerve terminals (synaptosomes). *Neuroscience*, **125**(1), 191–201.

Wilson, J.R., Cadotte, D.W., & Fehlings, M.G. (2012). Clinical predictors of neurological outcome, functional status, and survival after traumatic spinal cord injury: a systematic review. *J Neurosurg: Spine*, **17**(1), 11–26.

Wilson, J.R., Forgione, N., & Fehlings, M.G. (2013). Emerging therapies for acute traumatic spinal cord injury. *CMAJ*, **185**(6), 485–92.

Young, W., Yen, V., & Blight, A. (1982). Extracellular calcium ionic activity in experimental spinal cord contusion. *Brain Res*, **253**(1–2), 105–13.

RELATED LINKS TO EBRAIN

Initial Management of Spinal Injury and Spinal Shock. https://learning.ebrain.net/course/view.php?id=1041

Preoperative Assessment and Anaesthetic Management of Patients with Spinal Cord Injuries. https://learning.ebrain.net/course/view.php?id=1042

Principles of Surgical Treatment of Spinal Injuries. https://learning.ebrain.net/course/view.php?id=780

68

Cervical spine injuries

Calan Mathieson, Chris Barrett, and Likhith Alakandy

Introduction

The management of cervical spine fractures is a complex and fascinating topic. A multitude of descriptive terminologies and classification systems have been developed over the years in an attempt to better understand this heterogenous group of patients. Despite this however, there is often little consensus with regards to the best way to manage this population. This chapter will predominantly discuss the decision-making process involved in the management of cervical spine fractures.

The goal of the spine surgeon in managing patients with acute cervical spine injury is to prevent secondary neurological injury, deformity, and pain by re-establishing stability if necessary. Assessing how to achieve this goal can be very challenging. The surgeon will be faced with many questions. Which patients should undergo surgical intervention? Which operation will best stabilize the spine? Which patients should be treated with a collar or a halo vest? Does the injury require reduction with traction initially? There are also questions of timing. When should the surgeon plan the proposed procedure?

Cervical spine fracture incidence

The incidence of cervical spine fractures is estimated to be 9.2–12/100 000/year (Hu et al., 1996; Brolin and von Holst, 2002). There is a male predominance and the incidence is commonly reported as having two peaks, the first between age 15–45 years and the second 65–80 years. The mechanism of injury differs between these two groups, with the older population most commonly fracturing the C2 odontoid process in simple falls. The younger population is more likely to injure their cervical spine as a result of higher velocity injuries (Blizzard et al., 2016). Overall, approximately 10% of cervical spine fractures will be associated with neurological injury.

The association of cervical spine injuries with head injuries is well established. The reported incidence of cervical spine trauma in head injured patients ranges from 4% to 14% (Nazir et al., 2012). Those patients with moderate to severe head injuries are at the highest risk of concomitant cervical spine injury. The NICE guidelines advise a CT scan of the cervical spine in any head injury patient who fulfils the criteria for a head CT.

Assessment of the patient with a potential cervical spine injury

Assessment of potential cervical spine injuries requires careful history, examination, and investigation. Clearly a good history and examination will require a fully conscious patient. In fully conscious patients with no neck pain or tenderness, normal neurological function, and no distracting injuries (and no intoxication), the cervical spine can be cleared without the need for radiological assessment. The NEXUS group (National Emergency X Radiography Utilization Study) showed that significant bony cervical spine injury could be excluded when applying these rules (Eyre, 2006).

However, trauma patients who are not fully conscious or have distracting injures or are intoxicated will require radiological assessment. Three view radiography (lateral, open-mouth odontoid and anteroposterior (AP) X-rays of the cervical spine) and CT scans can all be utilized if necessary. Flexion/extension films are not recommended in the acute setting. MRI scans are helpful to assess damage to the posterior ligamentous complex and disc structures. They will provide significant information regarding the contents of the spinal canal. MRI is usually used, when necessary, and following a CT scan.

Trauma patients who fulfil the criteria for a head CT scan should also have a cervical spine CT scan. Patients with moderate or severe head injuries may be neurologically unassessable for several weeks. In these circumstances the author will remove the collar if the fine cut CT scan demonstrates no bony injury and no malalignment. The risk of missing a ligamentous injury with a normal modern CT scan is very low indeed and the risk of pressure sores around the cervical spine area secondary to a cervical collar is not insignificant (Eastern Association for the Surgery of Trauma, 2015). If the patient subsequently improves neurologically to the level required for clinical assessment, the cervical spine should be assessed again.

Every care should be taken to maintain alignment during the assessment period to minimize secondary injury. Special attention should be paid to the ankylosing spondylitis patient. These patients are particularly vulnerable to cervical spine fractures, often in low velocity impacts. A high degree of suspicion is required in these patients to make the diagnosis of a cervical fracture. Care should be taken when immobilizing such patients as it is not sensible to position these patients completely flat if the shape of their cervical spine precludes this position. They should be immobilized in their

preinjury flexed position and not forced into supine. A high degree of suspicion should also be given to patients who have a dangerous (i.e. high velocity) mechanism of injury and the elderly population (Clinical Effectiveness Committee, 2010).

Assessment of cervical spine trauma

Having made a diagnosis of a cervical spine fracture, the patient should continue to be treated appropriately to reduce the risk of secondary neurological injury. Careful immobilization should continue. Catheterization, placement of a nasogastric tube, prescribing low molecular weight heparin and a proton pump inhibitor may be necessary in those with spinal cord injury. Further information should then be sought that will enable the surgeon to make appropriate decisions about definitive management of the fracture.

When assessing a cervical spine injury, one must consider many important factors. These can be broadly subdivided into those obtained by history, examination, and investigation. One cannot make a sensible decision about how best to manage a cervical spine injury purely on radiological assessment.

When taking a history, the age of the patient, presence of underlying conditions such as ankylosing spondylitis or osteoporosis, and the velocity and mechanism of injury (is this a flexion or extension injury with axial loading?) must all be assessed. A history of tingling or weakness in the limbs at any time following the injury is important, the presence of other injuries should be recorded.

The patient should be examined to look for neurological signs, tenderness, increased distance between spinous processes, bruising around the spine, or deformity.

Investigations will frequently include X-rays, CT, and sometimes MRI scanning.

Classification systems

Classification systems are used by many clinicians and academics to aid communication, understanding, and decision-making about subsequent management. Over the years, there have been many different classification systems proposed to simplify and categorize cervical spine injuries. Criticism of these systems broadly falls into two categories, namely that the system is too complicated to be widely adopted or that it is an oversimplification of a varied and heterogenous group. A working understanding of some of these systems is advantageous as they highlight key elements of the information required to make sensible decisions about subsequent management.

Classification systems use different aspects of the aforementioned. The earlier systems tended to focus on the mechanism of injury while the newer classifications have favoured radiological and neurological status.

Allen's classification

In 1982, Allen et al. (1982) published a classification system based on the mechanism of injury. Subcategories included compressive flexion, vertical compression, distractive flexion, compressive extension, distractive extension, and lateral flexion. Each subcategory was further subdivided depending on the radiological severity of the injury. Commonly used phrases such as a burst fracture would be roughly equivalent to a moderately severe compression flexion injury. The importance of the posterior longitudinal ligament complex was commented on with more severe extension injuries demonstrating complete disruption of this important structure. The authors demonstrated the chance of neurological injury increased as the type and severity of the spinal column injury increased.

A full description of this system can be found elsewhere. The subcategories, although still useful today, are all based on plain X-rays. Modern imaging modalities with CT and MRI scans have led to newer classification systems being developed.

The subaxial injury classification (SLIC)

The anatomy of the C1 ring and C2 are very different to the anatomy of the remaining five vertebrae in the cervical spine (Vaccaro et al., 2007). The subaxial spine can be regarded as any level of the cervical spine below the inferior border of the C2 vertebral body. The subaxial injury classification score derives a score from morphological, ligamentous, and neurological information. See Table 68.1

Disruption of the ligamentous complex can be considered likely in the presence of facetal malalignment, abnormal widening of the anterior disc space, kyphosis over a motion segment or high signal on a STIR MRI sequence.

The Cervical Spine Injury Severity Score (CSISS)

This system can be used to grade the instability of fractures (Anderson et al., 2007). It supposes a four-column model of the cervical spine (the anterior, posterior, right lateral, and left lateral). The system uses a scoring system, where zero to five points are awarded based on the severity of the injury to bone and ligamentous structures in the four spinal columns. The scores are added together to give a final CSISS score.

Assessment using this system has proven to have a good interobserver coefficient, ranging from 0.75 to 0.98, with an average of 0.88. It is claimed that this grading system can predict the need for surgery. This however was only true for those patients with a score greater than seven (all of whom underwent surgical treatment) compared to 4 of 20 patients who scored less than seven.

The authors would advise using these scoring systems to become familiar with them. Prior to calculating the score however, one should think about all aspects of the patient's case and make a decision about their best management. The scoring systems are guides and should not be followed in all cases. For example, it may not be appropriate to manage an elderly patient surgically if the risks of anaesthesia preclude this. Other patients may simply refuse surgery. Some patients will require strict bed rest for a period of time due to

Table 68.1 The subaxial injury classification score

Morphology	Discoligamentous complex	Neurological injury
0 No abnormality 1 Compression 2 Compression with burst 3 Distraction 4 Translation rotation	0 Intact 1 Indeterminate 2 Disrupted	0 Intact 1 Root injury 2 Complete cord injury 3 Incomplete cord injury 4 Cord compression +1 in the setting of a neurological deficit

Reproduced with permission from Alexander Vaccaro, R Hulbert, Alpesh Patel, et al., The Subaxial Cervical Spine Injury Classification System: A Novel Approach to Recognize the Importance of Morphology, Neurology, and Integrity of the Disco-Ligamentous Complex, *Spine*, Volume 32, Issue 21, pp. 2365–74, Copyright © 2007 Wolters Kluwer Health, Inc.

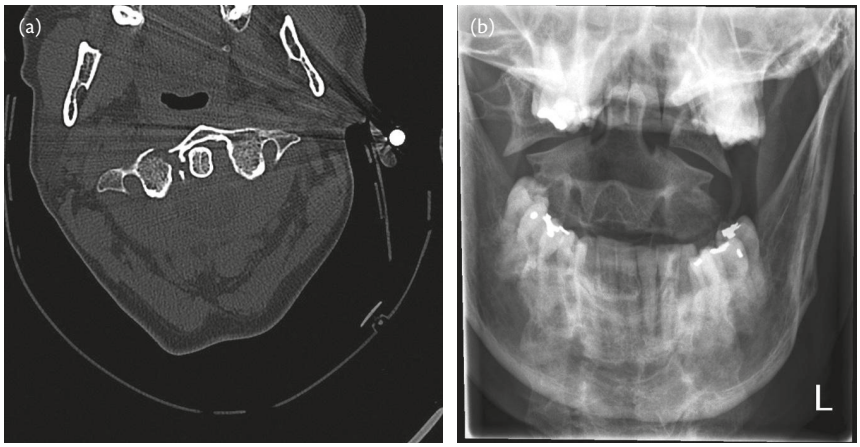

Fig. 68.1 (A) Anterior arch fracture of atlas. (B) Displaced lateral masses following C1 ring fracture and rupture of transverse ligament.

other injuries. This may mean that some fractures could be managed conservatively with bed rest when the aforementioned scores would suggest operative management.

Management of common eponymous cervical spine fractures

Jefferson's fracture

This eponymous fracture is a burst fracture affecting the C1 ring. It was originally used to describe a four-point fracture of the C1 bone, with two fractures noted to affect the anterior arch and two fractures of the posterior arch. Other patterns of bony injury are also often seen in the C1 ring. Examples are provided in Figure 68.1. Approximately 30% of C1 fractures will be associated with C2 fractures.

Isolated C1 fractures are only rarely associated with neurological injury as the bony elements tend to move outwards, away from the neural elements. The typical mechanism of injury is axial loading. It is important to assess for injury to the transverse ligament which can be indirectly assessed by measuring the atlantodental interval on a CT scan. This is usually less than three millimetres in adults and less than five millimetres in children. Sometimes a fleck of bone may be seen on an axial CT scan where the ligament has been avulsed for the medial side of the C1 lateral mass. When the transverse ligament is ruptured the lateral masses of C1 move outwards. On a transoral PEG view or coronal CT reconstruction the distance between the lateral edge of C1 and the lateral edge of C2 can be measured. Spence's rule of seven states that if the sum of the two sides is more than 7 mm then the transverse ligament is ruptured. Only very rarely is surgical intervention required for treatment of C1 fractures. If the transverse ligament is damaged, they are usually managed in a halo, if the transverse ligament is intact a collar is adequate.

Hangman's fracture

Hangman's fracture is a traumatic spondylolisthesis of the axis. See Figure 68.2. Although historically these fractures were noted following judicial hangings, the mechanism of injury most commonly associated with this pattern of fracture is road traffic accident.

Hangman's fractures have their own specific classification systems. The Effendi classification system later modified by Levine and Edwards has been used in 12 further papers assessing management of these injuries (Li et al., 2006). See Table 68.2.

A recent meta-analysis (Li et al., 2006) stated that 62.5% of publications advocated that primary therapy for Hangman's fractures should be conservative. The results of the metanalysis indicate that surgical intervention is not necessary in most type I, Effendi type II, and Levine-Edwards type II fractures. Patients with Levine-Edwards Type IIa and III fractures should be considered for surgical management. These are more likely to be associated with injury to the C2/3

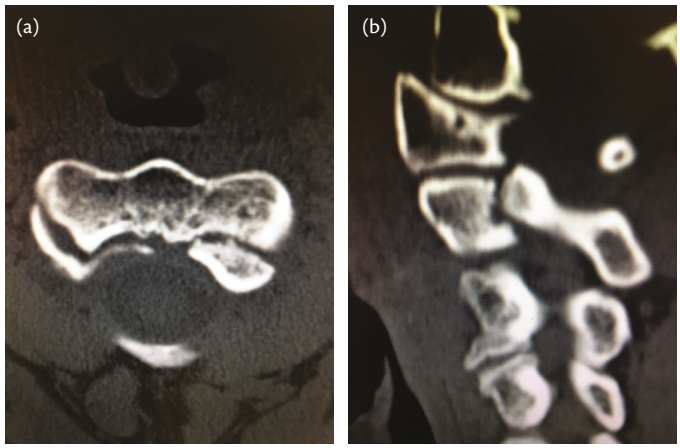

Fig. 68.2 Axial and sagittal image of Hangmans' fracture.

Table 68.2 Levine and Edwards Classification (OrthopaedicsOne, 2012)

Type I	Minimal translation (<3 mm) without C2–C3 angulation; stable
Type II	Significant C2–C3 angulation and translation (>3 mm); disc disruption, unstable
Type IIa	More angulation than type 2, without translation; unstable due to flexion-distraction injury
Type III	Severe C2–C3 angulation and translation; sometimes uni-/bilateral facet dislocation; unstable

Reproduced with permission from A Levine and C Edwards, The management of traumatic spondylolisthesis of the axis, *Journal of Bone & Joint Surgery*, Volume 67, Issue 2, pp. 217–26, Copyright © 1985 Wolters Kluwer Health, Inc.

Table 68.3 Anderson and D'Alonzo classification

Type I	Fracture of the tip of odontoid above the transverse ligament Caused by avulsion of the alar ligament
Type II	Fracture across the base of the peg, beneath the transverse ligament
Type III	Fracture in the C2 vertebral body such that the odontoid peg is detached from the rest of the vertebral body

Reproduced with permission from Lewis Anderson and Richard D'Alonzo, Fractures of the Odontoid Process of the Axis, *Journal of Bone & Joint Surgery*, Volume 56, Issue 8, pp. 1663–74, Copyright © 1974 Wolters Kluwer Health, Inc.

disc, thus making the resulting overall injury less likely to heal well without surgical fusion. Conservative management is normally with a halo.

Anterior and posterior approaches are described to treat Hangman's fractures. The authors favour an anterior approach with a C2/3 anterior cervical discectomy and fusion. This can be approached via a submental incision to gain access to the appropriate level of the spine.

Odontoid peg fractures

Odontoid peg fractures (Fig. 68.3) are most common in elderly patients, following a fall but can also occur in younger patients following cervical hyperflexion or hyperextension injuries. This injury accounts for 10–15% of all cervical spine fractures. There are three types of fracture as described by Anderson and D'Alonzo (Table 68.3).

It is important to differentiate os odontium which is benign, chronic, and thought possibly to relate to longer term non-union of an old fracture or a failure of ossification of the dens during development.

Type I fractures are very rare but require no treatment except analgesia. Type III fractures are generally quite likely to fuse with conservative management in a halo (or a collar for elderly patients unable to tolerate a halo).

The treatment of type II fractures, however, remains controversial. They are associated with higher rates of non-union (20–30%) when compared to the type I and type III fractures. Some patients, especially older people, with type II odontoid peg fractures but without transverse ligament disruption will develop fibrous non-union and may remain asymptomatic. In others however, there can be pain, stiffness, myelopathy, and chronic instability. Non-operative treatment with cervical braces or a halo vest do not achieve rigid immobilization and are known to be associated with a higher risk of non-union than surgical techniques. Halos in particular are very poorly tolerated by elderly patients where a collar may be the only option.

The usual surgical techniques used for odontoid peg fractures are either anterior odontoid peg screw fixation or posterior C1/C2 fusion using either transfacetal screws or Harms technique. A rescue technique is craniocervical fixation without fusion where the metal work can be removed once the peg fracture has fused.

The anterior approach has the advantage of preserving motion and should therefore be considered as the surgical treatment of choice for type II fractures (Apfelbaum et al., 2000). However, not all patients are appropriate for direct anterior fixation of the fracture. Patients should carefully be evaluated with CT and MRI scans for the integrity of transverse ligament of the atlas and those with disruption of the transverse ligament should be treated with posterior C1/C2 fixation. The morphology of the fracture is also an important consideration. Comminuted fractures or fracture lines that do no enable the screw to be placed adequately should not be considered for this procedure. Similarly, fractures that cannot be easily reduced to a satisfactory position with gentle extension of the spine may also not be suitable. Large patients or patients with barrel chests may pose difficulty in obtaining an optimum trajectory for screw placement. Poor bone quality is a relative contraindication due to the risk of the screw 'cheese wiring' through the distal fracture fragment. The chance of achieving bony union is significantly lower in non-acute fractures and in such cases with instability, posterior C1/C2 fixation should be considered. Single-screw anterior odontoid fixation is associated with a relatively low complication rate and a high fusion rate and should be the technique of choice (Subach et al., 1999; Lee et al., 2004).

Facet fracture dislocations

Uni (Fig. 68.4) and bifacetal (Fig. 68.5) fracture dislocations are the most common significant injuries in the subaxial spine. They occur as a result of flexion and distraction commonly following sporting or vehicle accidents.

Unifacet fracture dislocations occur when the superior facet which is normally behind the inferior facet 'jumps' onto the anterior surface of the inferior facet on one side. This produces a rotational

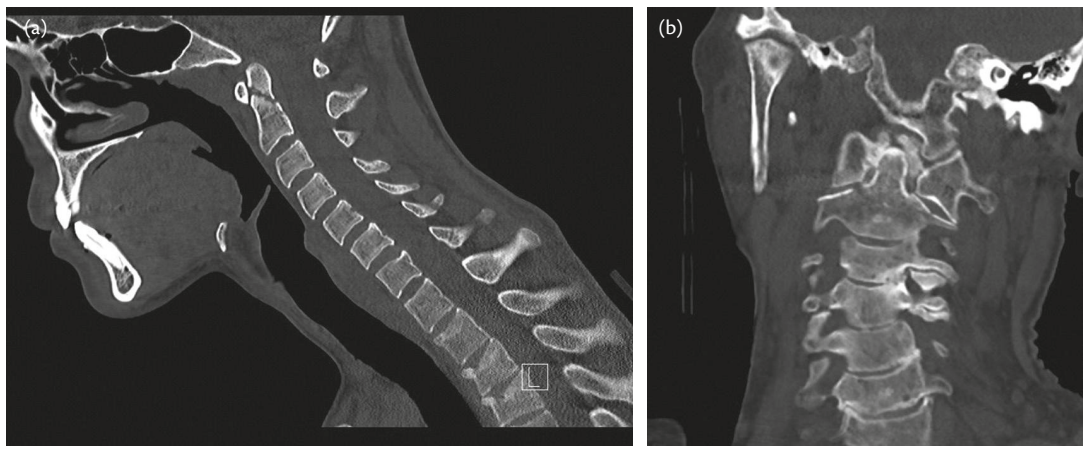

Fig. 68.3a (A) Type 2 peg fracture. (B) Type III peg fracture.

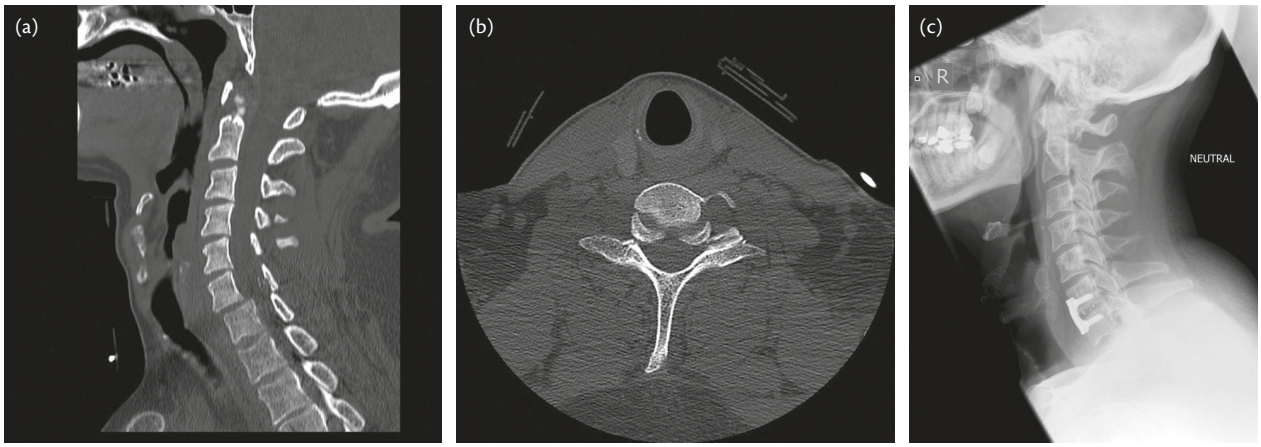

Fig. 68.4 Unifacetal dislocation at C6/7. (A) 25% dislocation on midsagittal CT scan. (B) Left-sided jumped facet shown on axial CT scan. (C) Postoperative X-ray showing reduction and anterior cervical discectomy and fusion.

malalignment which when viewed on a lateral X-ray appears as a 25% anterior subluxation of the superior vertebral body. The spinal cord is rarely affected but the nerve root exiting at that level may be compromised and radiculopathy may occur. A dislocation without a fracture can occur and a partial dislocation or perched facet is also sometimes seen. The C7/T1 level may be affected, thus a lateral X-ray may only be considered adequate if it shows the top of T1.

Bifacetal fracture dislocations are usually accompanied by spinal cord injury with complete spinal cord injury being common. These injuries are not rotational, they are true anterior subluxations, a lateral X-ray will show 50% or more subluxation.

The management of these fractures is covered in the controversy section of this chapter.

Other subaxial fractures

Patients may present with undisplaced cervical spine fractures of the lamina, pars interarticularis, or spinous processes, for example, the clay shoveler's fracture (spinous process avulsion fracture, most commonly C7), is well described (see Fig. 68.6). For the most part these fractures can be managed non-operatively, usually with just a collar, but careful observation is required as a small proportion will subsequently progress. This seems to be particularly true of fractures affecting the pars interarticularis where some authors do recommend early surgical intervention or halo immobilization.

Tear drop fractures from hyperextension injuries are fractures through the inferior, anterior portion of the vertebral body and are easily dismissed as insignificant (see Fig. 68.7). When a tear drop fracture is seen, and MRI confirms disc and/or ligament injuries, then surgery is the most definitive treatment. These being ligamentous injuries, they tend not to heal and most authors recommend surgical fusion.

Management options when treating cervical spine fractures

Cervical collar

A well-fitting rigid cervical brace is an effective way of restricting movements in the cervical spine, especially flexion and lateral flexion. In the surgical setting they are commonly used to immobilize a relatively stable spine injury during healing and often to provide additional support to the spine following surgical fixation.

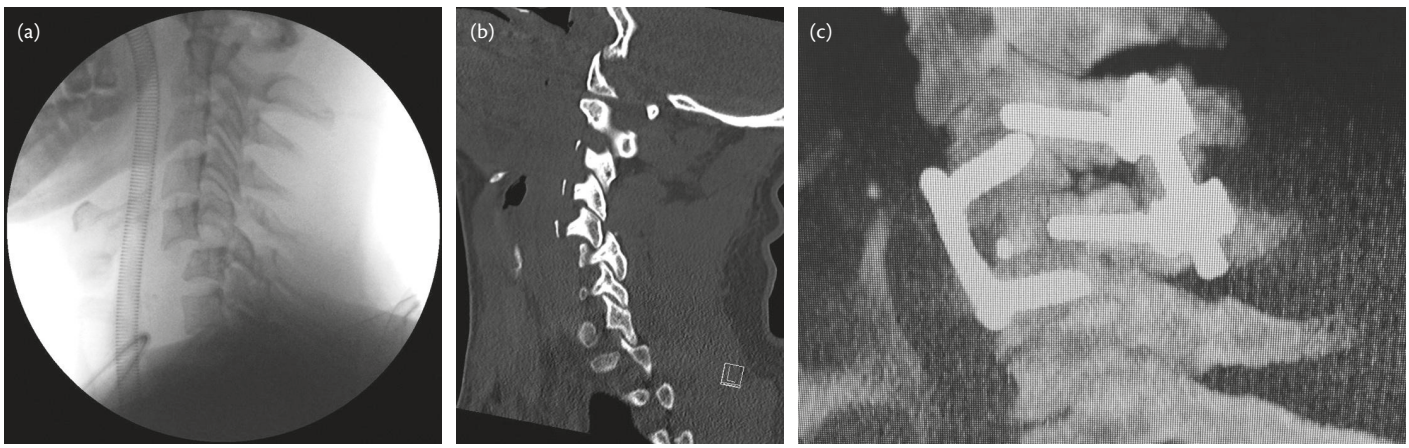

Fig. 68.5 (A) Bifacetal dislocation, shown on X-ray and (B) parasagittal reconstructed CT scan. (C) Sagittal reconstructed CT post anterior and posterior fixation at C4/5.

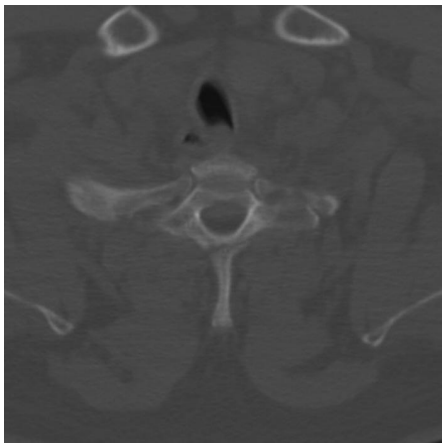

Fig. 68.6 Clay shovelers' fracture on axial CT image.

A collar is also used frequently by emergency personnel as an adjunct to spinal immobilization in patients who have sustained or are suspected to have sustained cervical spine injuries to prevent secondary spinal cord injuries. Less commonly they are also used for comfort and symptom relief following less serious soft tissue injuries. The effectiveness of immobilization diminishes in the lower cervical and cervicothoracic levels, where extensions to the cervical brace to incorporate the chest wall or halo immobilization may be necessary.

Fitting instructions

A range of rigid collars by various manufacturers are available. The typical design is a two-piece hard shell secured with straps and lined with removable soft padding. In addition to minimizing the risk of pressure related complications, a comfortable and well-fitting collar also improves patient compliance. When applying a collar in a patient with an unstable spine it is essential that the head and neck are kept in proper alignment throughout the procedure. The back piece of the collar is first carefully slid underneath the neck, and then the front piece is placed snugly against the patient's neck and secured with straps. In more stable cases the collar can be applied with the patient in an upright position. Once the collar is in place, it is important to ensure that the support extends from the mandible to the sternal notch and the pressure points are well padded. The tracheal opening and midline vents should be in the midline.

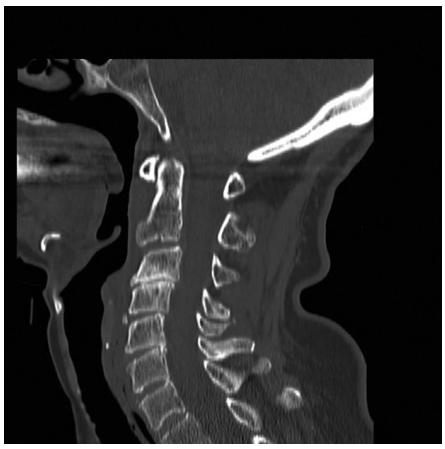

Fig. 68.7 Teardrop fracture of C2.

Complications

The main complication associated with a cervical collar is development of pressure ulcers. This risk of collar related skin problems includes minor erythema to serious ulcers and up to 10% of patients develop these complications with prolonged usage.

Cervical traction

Cervical spine fractures and traumatic subluxations/dislocations are generally treated by considering the principles of reduction, decompression, and stabilization. The aim is to achieve skeletal reduction and, if possible, decompression of the spinal cord. Stabilization self-evidently cannot be achieved by traction alone.

Cervical spine traction, which ultimately is a form of closed reduction, may be used in advance of, or occasionally as an alternative to, open reduction. In this context, if a good re-alignment can be achieved, and if patient factors preclude early surgery to stabilize the spine, the patient may be placed in temporary or definitive external immobilization (halo vest or Minerva cast).

The most effective methods of applying traction utilize tongs or a halo ring which are directly pinned to the skull. Systems which use slings or straps should be avoided: pressure sores on the chin are an extremely likely outcome and it is more difficult to apply the force in a precise direction. The ring or arc is then connected to vertically placed weights via a rope or cord which passes through a pulley, minimizing friction, and ensuring that the horizontal component of the force is directly pulling on the skull.

Tongs such as the Gardner-Wells tongs rely on two pins only. They are relatively easy to apply, especially if the clinician has limited assistance out of hours. An external, visible pin 'pops-out' usefully indicating when the skull pins have been tightened to the correct torque.

A halo ring (usually but not always an incomplete ring or C-shape) relies on a minimum of four-point skull fixation. It is slightly more difficult to apply than tongs and is often more uncomfortable for the patient as it can be difficult to achieve adequate local anaesthesia for the posterior or parietal pin sites in particular. It has, however, the distinct advantage that once adequate reduction is achieved there is an option to fit a temporary or permanent halo vest more easily.

Once the tongs or halo ring have been applied to the skull the rope is connected and passed through the pulley. By adjusting the angle of the pulley, force can be applied in the desired direction. It is important not to overly flex in an attempt to reduce the fracture as respiratory deterioration has been reported (Harrop et al., 2001). Gradually the weight can be increased, which requires good nursing care, often with careful analgesia and occasional judicious use of benzodiazepines. Regular lateral X-rays and careful patient observation for new or worsened neurological symptoms are necessary.

Various rules of thumb exist regarding the appropriate weight, which are generally dependent on the cervical spine level involved. Starting with a weight of 2 lbs per level that the fracture is distant from the occiput is reasonable (i.e. to reduce a C5 injury), a starting weight of 10 lbs is required. It is important to emphasize that often far greater weights are required to achieve reduction but these are

gradually added, with careful clinical and radiological observation, as described earlier. If neurological deterioration occurs the weight should be reduced or removed completely and an X-ray performed. Often full reduction using closed methods is not possible and general anaesthesia and open reduction are required.

In addition to neurological and respiratory deterioration as described, cervical traction is also subject to the pin site complications of the halo ring, although often traction is not of sufficient duration for such complications to occur, usually being in place for a matter of hours up to a day or two prior to definitive surgery. Prior to traction placement, an MRI should be performed. This is most important in situations of intact or partial neurological deficit, where, for example, a large disc fragment or haematoma can make closed reduction dangerous.

Halo immobilization

A halo is a more rigid and more invasive method of immobilization of the cervical spine. It consists of a ring secured to the outer table of the skull using pins, connected via adjustable metal rods to a fitted hard vest or jacket with a padded lining (Lind et al., 1988). This enables the patient to be mobile, while providing a considerably better degree of immobilization than a cervical brace. The adjustable rods provide precise control of the position that the cervical spine needs to be immobilized in. The halo crown and vest immobilization may also be used to provide stability during preoperative transfer, and also on occasions to supplement surgical fixation.

When applying the halo crown and vest, it is essential that the head and neck are kept in proper alignment throughout the procedure. The halo is typically fixed to the skull by four pins, two in the frontal region, one centimetre above the orbital rim and two in the posterior parietal region, posterior to the ears. The pins are inserted under local anaesthesia, with the eyes closed when applying the frontal pins. A torque wrench is used to prevent overtightening. The vest, which is formed by separate anterior and posterior components is then positioned and secured with straps. The metal rods are secured to the vest and connected to the halo crown. These versatile rods afford flexibility when positioning the spine. When all the rods are secured, the position of the cervical spine is confirmed with X-rays. The halo should be checked at regular intervals, during which the hardware is retightened and the pins inspected for loosening or infections. The position of the spine should also be checked radiographically. The duration of halo treatment is dependent on individual biology, but three months' duration is sufficient for most fractures.

Most patients tolerate a halo crown and vest well, although some may have difficulty mobilizing or sleeping with the halo fixator in the initial days. Pin loosening is often characterized by pain and can be visibly evident (Vertullo et al., 1997). This is avoided by inspecting the pin sites at regular intervals, more frequently in the initial period. Pin site infections are usually superficial and reported in 10–20% of patients. This may require repositioning of the pins and antibiotics. More serious infections like osteomyelitis of the skull and intracranial abscess secondary to skull penetration have been reported, but are exceedingly rare (Rizzolo et al., 1993; Van Middendorp et al., 2009). A pressure sore or localized skin breakdown can be caused by direct pressure from the vest or halo. Patients with respiratory difficulties may find it hard to tolerate the vest.

Surgical techniques

Subaxial posterior cervical fixation (C3–C7)

Posterior cervical fixation is indicated where instability is already present or is likely to result as a direct consequence, either immediate or delayed, of surgical decompression. Specific indications include trauma with bony or ligamentous instability, discitis/osteomyelitis with instability and kyphosis, degenerative spine disease with kyphosis or anterolisthesis, and where decompression is required (most commonly for myelopathy).

It is extremely important to add that any fixation, no matter how expertly constructed, will ultimately fail unless bony fusion or indeed fracture union is achieved. It is therefore incumbent upon the surgeon to fuse the spine after fixation and decompression have been undertaken. This involves the standard process of decortication of the graft recipient site followed by placement of autologous bone graft, either locally or remotely procured (e.g. bone removed following laminectomy or iliac crest graft).

A number of possible techniques exist, and these have gradually evolved over the years. Posterior cervical wiring and transfacet screws are best considered as salvage techniques where other methods are not possible or have failed.

Case series of cervical pedicle screws are reported in the literature. The pedicles in the lower cervical spine (C6 and C7) may have pedicles of sufficient calibre to present a useful surgical target, the mid-cervical spine less so. Nevertheless, the authors would contend that the presence of the vertebral artery in the foramen transversarium from C6 upwards, presents a specific, additional possible complication such that lateral mass screw placement remains the gold standard technique for posterior cervical fixation (Yoshihara et al., 2013).

Preoperative workup should include general considerations such as fitness for anaesthetic, in the context of lying prone for several hours. Specific considerations include the possibility of osteoporosis. While not an absolute contraindication to surgery, caution is required if the bone quality is extremely poor the screws may not gain an adequate hold. In such situations, there may be no alternative to lateral mass fusion without fixation with postoperative placement in a halo vest.

Standard preoperative workup is likely to include both CT and MRI and possibly dynamic imaging, either plain radiography or CT. The reconstructed CT scan is often the most useful test as it is possible to estimate screw size and trajectory and spot common pitfalls. These would include an extremely small lateral mass, often at C3, making screw placement difficult or an aberrant vertebral artery course, as indicated by the foramina transversaria. If the surgeon has specific concerns about the course of the vertebral artery, CT angiography of the neck vasculature is indicated.

Under general anaesthesia, the patient is placed prone on a suitable mattress and table in a reverse Trendelenburg position. The authors would strongly advocate the use of skull pins (e.g. Mayfield clamp) as opposed to a foam headrest or pillow. This allows more accurate positioning with intraoperative adjustment as required. It also avoids any pressure on the face or eyes and affords the anaesthetist good access at all times.

Once the patient has been positioned, lateral screening using the image intensifier should be undertaken, both to plan the skin

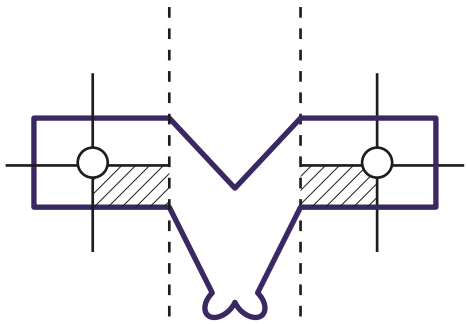

Fig. 68.8 Surgeon's view of the exposed lateral masses. The entry point is generally in the midpoint of the square or just inside the inferomedial quadrant (shaded).

incision and assess the cervical spine contour: a slight degree of flexion will improve access and exposure but fixation in an unduly flexed position should be avoided.

A midline incision is made and the avascular midline raphe is followed to the level of the spinous processes after which bilateral muscle stripping to expose fully the laminae and lateral masses is undertaken. Further lateral screening is required to confirm the levels to be instrumented.

Reduction of facet dislocations from the back can usually be carried out under direct vision of the dislocation, sometimes the inferior facet may need to be drilled off before reduction will occur. Care should be taken to avoid damage to the nerve root.

The surgeon should carefully define the lateral, superior, and inferior edges of each lateral mass: the medial edge of the lateral mass is at the point where the lamina, sweeping downwards, ends, and there is a distinct change of contour.

The lateral mass itself now presents a square to the surgeon. The entry point is effectively in the midpoint of this square or perhaps very marginally in the inferomedial quadrant (Fig. 68.8). A high-speed drill with burr is used to break the cortex.

The two primary considerations at this point are to aim the hand drill laterally enough to avoid the vertebral artery in the foramen transversarium and to aim superiorly enough to avoid the exiting nerve root in the neural foramen (Fig. 68.9). Several different screw angulations are described. Generally speaking an angle of around 20° in both the axial and sagittal planes should be sufficient. An instrument placed in the adjacent facet joint can give a useful indication of the screw trajectory in the sagittal plane, which in any regard should be confirmed and guided by radiographic screening or image guidance. Often the correct trajectory in both planes involves the drill resting on the spinous process immediately inferior to the level which is being instrumented.

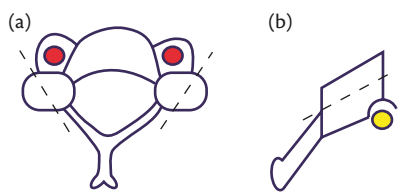

Fig. 68.9 Schematic diagram demonstrating the appropriate screw trajectory on the axial (A) and sagittal (B) planes. On the axial plane, the surgeon must aim laterally enough to avoid the vertebral arteries (red) and on the sagittal plane, superiorly enough to avoid the exiting nerve root (yellow).

After drilling has been completed and the drill tract has been carefully assessed for possible breaches using a ball-tipped probe, a 3.5 mm diameter screw of requisite length is placed (often around 14–16 mm if unicortical fixation is planned, slightly longer if bicortical). Once all the screws are positioned in a similar fashion, 3 mm diameter rods, cut and contoured to the desired length and shape are placed within the polyaxial screw heads on both sides. After appropriate final tightening, final X-ray screening is performed. Washout, fusion, and wound closure are then undertaken in the standard fashion.

Posterior C1/C2 fusion

This technique is covered in Chapter 58.

Craniocervical fixation

Craniocervical fixation is used if there is occipitocervical dislocation or a grossly unstable C1 fracture where this surgical option is preferred. Fixing from the occiput to C2 or the subaxial cervical spine is a morbid procedure, which patients find disabling, rendering the occipitoatlantal +/– the atlantoaxial joints completely immobile. It should only be utilized where other methods will not suffice (i.e. in circumstances of severe instability; see Bhatia et al., 2013).

Careful intraoperative positioning to ensure as 'anatomical' a position as possible is vital: an overly flexed position can make it extremely difficult to swallow; an overly extended position makes it difficult to walk due to an inability to see one's feet and an alteration of sagittal balance.

Once the patient is adequately positioned, prepared, and draped an incision is made from the external occipital protuberance inferiorly (the lower limit depending upon the planned lower limit of the fixation). The muscles are stripped to expose the occipital bone and the laminae and lateral masses. The techniques of C1, C2, and subaxial screw insertion is as described elsewhere.

Various occipital plates exist, most aim to utilize the naturally thickened keels of bone in the occipital region, the superior nuchal line (with certain transversely oriented plates) or more commonly, the midline from the external occipital protuberance to the foramen magnum (vertically oriented plates). In all cases, it is vital to carefully plan preoperatively (including CT scanning +/– contrast) with particular attention to any venous anomalies which would prevent safe screw placement.

The midline occipital keel thins gradually as it approaches the foramen magnum. Bicortical fixation is preferred. The inner and outer tables must be drilled and tapped to allow screw placement. If the dura is breached, bleeding or a cerebrospinal fluid (CSF) leak can often be plugged by placing the screw in the hole. It is frequently necessary to contour the plate and/or smooth the irregularities of the occipital bone to allow the plate to sit securely and snugly without rocking.

Once the plate and the chosen cervical instrumentation is in place, the rods must be placed to connect the two. The surgeon can contour a straight rod to fit or alternatively, prebent rods exist, which may need little further contouring and thus are stronger but it is almost always necessary to trim both ends to fit. Rod placement, which intuitively seems simple, can often be more awkward and time-consuming than the other parts of the procedure.

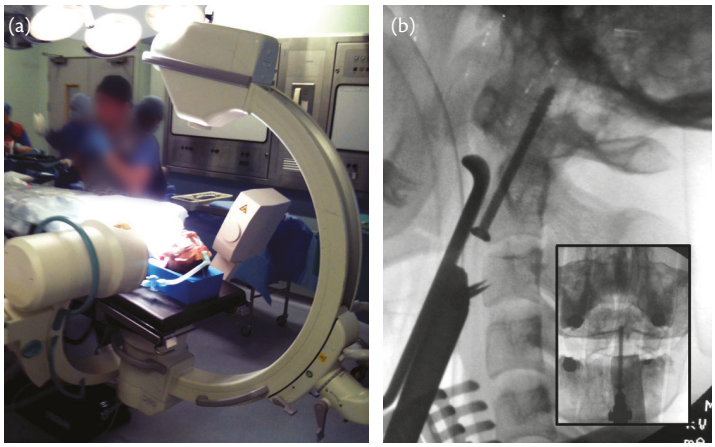

Fig. 68.10 (A) Two image intensifiers set up to obtain simultaneous images of the odontoid peg in both planes and the extended position of the cervical spine. (B) Intraoperative lateral and AP radiograph showing the position of the retractor, screw guide, and a single lag screw in position.

If one is carrying out occipito-cervical fixation for trauma, it is vitally important to decorticate all available bony surfaces and pack with bone graft material and/or synthetic bone substitutes. All metalwork will fail in the long run if fusion does not occur and the head presents a large mechanical lever arm relative to the cervical spine. It is often necessary to carry on with external immobilization postoperatively for a number of weeks until one is confident that fusion is occurring.

Cervicothoracic fusion

Using the techniques described earlier and thoracic pedicle screws (see Chapter 67), unstable junctional fractures that require extending the cervical construct to the upper thoracic spine can be treated. Cranio-cervicothoracic fixation, while possible, is an extremely morbid intervention for the patient and should be avoided if at all possible (Tanouchi et al., 2014).

Anterior odontoid screw fixation

Under general anaesthesia, the patient is positioned supine with the neck in slight extension. Biplanar radiographs should be used, with the second image intensifier positioned to obtain an open-mouth peg view. The mouth is kept open with a radiolucent mouth-gag and the endotracheal tube positioned to one side to ensure an adequate view of the odontoid peg (**Fig. 68.10**A).

The skin incision is marked by projecting the intended screw trajectory on the surface using a lateral X-ray, this typically is at the C5/6 disc level. Using a standard anterior cervical approach, the plane between the carotid sheath and the trachea and pharynx is developed down to the prevertebral space. Lateral self-retaining retractor blades are placed under the partially separated longus colli. An angled retractor blade is then used to extend the approach cephalad up to the C2/3 disc space under lateral X-ray guidance, while remaining within the prevertebral space. This blade is then attached to the lateral blades. A K-wire is inserted into the inferior lip of the C2 vertebral body slightly incorporating the anterior annulus of C2/3, and advanced partly into the body of C2 using biplanar imaging. An outer sleeve is passed over the K-wire with fixation pins anchored to the body of C3 to act as the guide for the inner drill guide and the drill. The superior edge of the annulus of the C2/3 disc and cortex of C2 is bored using a wider bore cannulated drill to create a space to countersink the screw head. The K-wire is removed once the outer sleeve is secured firmly in place. A power drill using a 3 mm drill bit is used to drill a pilot hole along the trajectory marked by the K-wire, using the outer sleeve as the guide. If necessary, the head of the patient or the partially drilled body of C2 can be manipulated, and the distal fragment reduced to achieve a suitable anatomical position. The drill is then advance into the distal fragment, taking it just past the outer cortex of the odontoid peg into the apical ligament. This hole is then tapped with a 4-mm tap through the outer sleeve. At the end of this step, the length of the screw can be measured using the markings on the tap. The screw is undersized by the distance between the fracture fragments, to account for the final compression of the fragments. A partly threaded 4.0 mm titanium lag screw is inserted into the pilot hole using biplanar imaging and tightened ensuring that the fracture fragments are well compressed, and the screw head is counter sunk (**Fig. 68.10B**).

There is evidence to suggest that early operative intervention results in a lower rate of non-union (Apfelbaum et al., 2000; Rao and Apfelbaum, 2005). Elderly patients and patients with osteoporosis have a significantly higher risk of screw failure. Loosening and back out of the screw can occur, where there is failure of bony union resulting in persistent stress at the fracture site. Elderly patients undergoing this procedure have been reported to have an increased incidence of swallowing difficulties, as the oesophagus is more fibrotic and thus less tolerant of retraction (Vasudevan et al., 2014). This may be compounded by the potential for injury to the superior laryngeal nerve, which supplies the cricothyroid muscle and provides sensory innervation to the mucosa of the larynx, it pierces the thyrohyoid membrane at approximately the C3/4 level.

Anterior cervical fusion

Anterior cervical discectomy and fusion or anterior cervical corpectomy are both commonly performed procedure in managing cervical spine injuries. These will provide two column stability with a very high fusion rate. Following removal of the affected disc(s), the surgeon will place either autologous bone graft or a cage filled with bone fragments, followed by an anterior cervical plate. Many surgeons feel it is unnecessary to incise the posterior longitudinal ligament in trauma cases where the aim is stabilization alone. A description of the techniques may be found in Chapter 58.

Internal reduction of a unifacet fracture dislocation may be carried out from the front, after the disc has been removed, by rotating one vertebra on the other using pins in the vertebral bodies, while applying traction. However, if surgery is delayed more than two to three weeks after the injury the facets may partially fuse and reduction from the front will become much more difficult.

Controversy: Unifacetal and bifacetal fractures

In cervical spine surgery, often the diagnosis is clear. The difficult decisions are related to management: conservative or surgical; anterior, posterior, both (360 degree); two, three, or more levels?

Such decisions ultimately come down to clinical judgement. Generally speaking, there are certain principles which can be used to at least guide management. Features which point towards more extensive surgery being required include evidence of gross displacement, multilevel involvement, bilaterality, evidence of ligamentous disruption on MRI and spinal cord injury.

Using these principles, one could consider the case of a unifacetal fracture. Most patients with such an injury do not have a significant spinal cord injury, although they may have a radiculopathy and root compromise, often unilateral. The contralateral facet joint may be intact, the injury confined to a single level, with no evidence of gross ligamentous disruption on MRI. In such circumstances, there may not be any requirement for surgery at all, if a reasonable reduction is achieved, the position could be maintained in halo and vest for sufficient time to allow fracture healing.

Should the position be lost or depending on patient preference, surgery may be required but this would not necessarily require anterior and posterior surgery. If the alignment is good, excellent reduction, fusion, and stability can be achieved from anterior cervical fusion or posterior cervical fusion alone. This avoids a lengthy procedure or indeed a second operation. Some surgeons, however, feel that the extra security of a 360-degree fusion is warranted.

Conversely a bifacetal fracture/dislocation is a very different injury. Often such patients have a complete neurological injury and gross ligamentous disruption on MRI. By its very nature, such an injury is bilateral and involves gross displacement.

Given the much more unstable nature of such an injury, more surgeons would consider anterior and posterior fixation to restore stability, facilitate fusion, and allow neurological rehabilitation. Other surgeons, however, would consider that this injury can also be managed with just an anterior or just a posterior fusion procedure. In the authors' opinion, the best initial procedure is often posterior reduction and fixation, followed by an anterior fusion except where the neurology is incomplete and there is a large anterior disc prolapse. In this case, posterior reduction as a first procedure could make the situation worse. Other surgeons would routinely do an anterior procedure first before doing the posterior part. If reduction cannot be managed from the front, then an anterior, posterior, anterior procedure may even be utilized. There is little consensus on which technique is best.

FURTHER READING

Anderson, P., Moore, T., Davis, W., et al. (2007). Cervical spine injury severity score. *J Bone Joint Surg Am*, **89**(5), 1057–65.

Clinical Effectiveness Committee (2010). *The College of Emergency Medicine. Guideline on the Management of Alert, Adult Patients with Potential Cervical Spine Injury in the Emergency Department*. http://www.resusme.em.extrememember.com/wp-content/uploads/2011/02/CEM5718-cervical-spine-full-guideline.pdf

OrthopaedicsOne (2012). *C2–C3 Traumatic Spondylolisthesis (Hangman's Fracture)—Levine-Edwards Classification*. OrthopaedicsOne Articles. In: OrthopaedicsOne—The Orthopaedic Knowledge Network. Created 23 May 2012. Last modified 23 May 2012. http://www.orthopaedicsone.com/x/RYEXBQ

Vaccaro, A., Hulber, J., Fisher, C., et al. (2007). The sub-axial Cervical Spine Injury Classification System (SLIC). A novel approach to recognise the importance of morphology, neurology and integrity of the disco-ligamentous complex. *Spine*, **32**(21), 2365–74.

REFERENCES

Allen, B.L., Ferguson, R.L., Lehman, T.R., & O'Brien, R.P. (1982). A mechanistic classification of closed, indirect fractures and dislocations of the lower cervical spine. *Spine (Phila Pa 1976)*, **7**(1), 1–27.

Anderson, P., Moore, T., Davis, W., et al. (2007). Cervical spine injury severity score. *J Bone Joint Surg Am*, **89**(5), 1057–65.

Apfelbaum, R.I., Lonser, R.R., Veres, R., & Casey, A. (2000). Direct anterior screw fixation for recent and remote odontoid fractures. *J Neurosurg*, **93**(2 Suppl), 227–36.

Bhatia, R., Desouza, R.M., Bull, J., Casey, A.T. (2013). Rigid occipitocervical fixation: indications, outcomes, and complications in the modern era. *J Neurosurg Spine*, **18**(4), 333–9.

Blizzard, D.J., Miller, C.P., Blizzard, S.T., & Grauer, J.N. (2016). Incidence and demographics of cervical spine fractures over a 10-year period at a level 1 trauma centre. *The Duke Orthop J*, **6**(1), 21–5.

Brolin, K. & von Holst, H. (2002). Cervical injurues in Sweden, a national survey of patient data from 1987 to 1999. *Inj Control Saf Promot*, **9**, 40–52.

Clinical Effectiveness Committee (2010). *The College of Emergency Medicine. Guideline on the Management of Alert, Adult Patients with Potential Cervical Spine Injury in the Emergency Department*. http://www.resusme.em.extrememember.com/wp-content/uploads/2011/02/CEM5718-cervical-spine-full-guideline.pdf

Eastern Association for the Surgery of Trauma (2015). Cervical spine collar clearance in the obtunded adult blunt trauma patient. *J Trauma*, **78**(2), 430–41, February 2015.

Eyre, A. (2006). Overview and comparison of NEXUS and Canadian C-spine rules. *Am J Clin Med*, **3**(4), 12–15.

Harrop JS, Vaccaro A, & Przybylski GJ (2001). Acute respiratory compromise associated with flexed cervical traction after C2 fractures. *Spine (Phila Pa 1976)*, **26**(4), E50–4.

Hu, R., Mustard, C.A., & Burns, C. (1996). Epidemiology of incident spinal fracture in a complete population. *Spine (Phila Pa 1976)*, **21**, 492–9.

Lee, S.C., Chen, J.F., & Lee, S.T. (2004). Management of acute odontoid fractures with single anterior screw fixation. *J Clin Neurosci*, **11**(8), 890–5.

Li, X.-F., Dai, L.-Y., Lu, H., & Dong Chen, X. (2006). A systematic review of the management of hangman's fractures. *Eur Spine J*, **15**(3), 257–69.

Lind, B., Sihlbom, H., & Nordwall, A. (1988). Halo-vest treatment of unstable traumatic cervical spine injuries. *Spine (Phila Pa 1976)*, **13**(4), 425–32.

Nazir, M., Khan, S.A., Raja, R.A., Bhatti, S.N., & Ahmed E. (2012). Cervical spinal injuries in moderate to severe head injuries. *J Ayub Med Coll Abbottabad*, **24**(3–4), 100–2.

OrthopaedicsOne (2012). *C2–C3 Traumatic Spondylolisthesis (Hangman's Fracture)—Levine-Edwards Classification*. OrthopaedicsOne Articles. In: OrthopaedicsOne—The Orthopaedic Knowledge Network. Created 23 May 2012. Last modified 23 May 2012. http://www.orthopaedicsone.com/x/RYEXBQ

Rao, G. & Apfelbaum, R.I. (2005). Odontoid screw fixation for fresh and remote fractures. *Neurol India*, **53**(4), 416–23.

Rizzolo, S.J., Piazza, M.R., Cotler, J.M., Hume, E.L., Cautilli, G., & O'Neill, D.K. (1993). The effect of torque pressure on halo pin complication rates. A randomized prospective study. *Spine (Phila Pa 1976)*, **18**(15), 2163–6.

Subach, B.R., Morone, M.A., Haid, R.W. Jr., McLaughlin, M.R., Rodts, G.R., & Comey, C.H. (1999). Management of acute odontoid fractures with single-screw anterior fixation. *Neurosurgery*, **45**(4), 812–19.

Tanouchi, T., Shimizu, T., Fueki, K., Ino, M., Toda, N., & Manabe, N. (2014). Adjacent-level failures after occipito-thoracic fusion for rheumatoid cervical disorders. *Eur Spine J*, **23**(3), 635–40.

Vaccaro, A., Hulber, J., Fisher, C., et al. (2007). The sub-axial Cervical Spine Injury Classification System (SLIC). A novel approach to recognise the importance of morphology, neurology and integrity of the disco-ligamentous complex. *Spine*, **32**(21), 2365–74.

Van Middendorp, J.J., Slooff, W.B., Nellestein, W.R., & Oner, F.C. (2009). Incidence of and risk factors for complications associated with halo-vest immobilization: a prospective, descriptive cohort study of 239 patients. *J Bone Joint Surg Am*, **91**(1), 71–9.

Vasudevan, K., Grossberg, J.A., Spader, H.S., Torabi, R., & Oyelese, A.A. (2014). Age increases the risk of immediate postoperative dysphagia and pneumonia after odontoid screw fixation. *Clin Neurol Neurosurg*, **126**, 185–9.

Vertullo, C.J., Duke, P.F., & Askin, G.N. (1997). Pin-site complications of the halo thoracic brace with routine pin re-tightening. *Spine (Phila Pa 1976)*, **22**(21), 2514–16.

Yoshihara, H., Passias, P.G., & Errico, T.J. (2013). Screw-related complications in the subaxial cervical spine with the use of lateral mass versus cervical pedicle screws: a systematic review. *J Neurosurg Spine*, **19**(5), 614–23.

RELATED LINKS TO EBRAIN

Application of a Halo or Traction to the Cervical Spine. https://learning.ebrain.net/course/view.php?id=398

Atlanto-axial Cervical Spine Fractures. https://learning.ebrain.net/course/view.php?id=1043

Fusing C1 to C2. https://learning.ebrain.net/course/view.php?id=396

Performing a Posterior Cervical Fusion. https://learning.ebrain.net/course/view.php?id=395

Subaxial Cervical Spine Fractures. https://learning.ebrain.net/course/view.php?id=1044

69

Thoracic and lumbar spine injuries

Bedansh Roy Chaudhary and Shiong Wen Low

Introduction

Trauma to the thoracic and lumbar spine may be classified using the Magerl's or Thoracolumbar Injury Classification and Severity Score (TLICS) classifications. Management may be conservative with analgesia and bracing or surgical with posterior, transthoracic, or circumferential spinal fusion.

In this chapter the classification of these injuries and their management will be discussed. The techniques to insert pedicle screws and the role of minimally invasive techniques will be explained.

Fracture classification

Older thoracolumbar trauma classification systems include those of Holdsworth, which emphasizes the mechanism of injury; Whitesides, which defines the two-column concept being analogous to a construction crane; Punjabi and White, who developed stability scoring systems; and Denis with a mechanistic classification based on instability pertaining to three columns of the spine.

In 1994, Magerl and colleagues devised a morphological classification system based on a review of over 1400 consecutive TL fractures presenting to their institution (Magerl et al., 1994). It was the most thorough classification based on fracture morphology at the time. The classification divided the injuries into three broad categories—compression, distraction, and axial torque—then labelled them as fracture types A, B, and C, respectively. The severity of injury progressed from A to C and within each group are several subdivisions.

The comprehensive nature of the Magerl classification resulted in 55 different subdivisions of TL fractures, a significant logistical hurdle even to those working in the specialty and its complexity has thus been considered impractical for day-to-day clinical use. In addition, isolated transverse or spinous process fractures were not considered in the AO Magerl classification.

To address these criticisms, the AO Spine Classification group embarked upon developing a consensus for an updated AO Spine TL injury classification system that would provide a reliable, relevant, simple, and robust clinical and academic tool for global application and would embody as many of the ideals of a TL classification system as possible. This resulted in the development of the TLICS published in 2005 (Vaccaro et al., 2005).

In 2013 Vaccaro et al. published an AO Spine Thoracolumbar spine injury classification system (**Fig. 69.1**), which incorporated clinical modifiers (Vaccaro et al., 2013). The AO Spine Thoracolumbar spine injury classification system is based on the evaluation of three basic parameters: fracture morphology, neurological injury, and clinical modifiers.

Morphology type A are compression injuries and are generally the mildest injury group affecting the vertebral body but without tension band involvement. Vertical fractures of the lamina may be present but do not constitute a tension band failure. There are five subtypes termed A0–A4. A0 are non-structural fractures that do not compromise the structural integrity of the spinal column such as fractures of the transverse or spinous processes. A1 are wedge-compression fractures of a single endplate without involvement of the posterior wall of the vertebral body. A2 fractures are split fractures of both endplates without involvement of the posterior wall of the vertebral body. A3 are incomplete burst fractures with involvement of the posterior wall but only a single endplate is fractured. Finally, A4 are complete burst fractures and have involvement of the posterior wall and both endplates.

Morphology type B are distraction injuries and have failure of the tension band which might be the posterior tension band, the anterior longitudinal ligament, or the bony component. There are three subtypes termed B1–B3. B1 is a pure transosseous tension band disruption or chance fracture, which is a monosegmental osseous failure. B2 fractures are posterior tension band disruptions with bone and/or ligament failure of the posterior tension band usually combined with a morphology type A fracture. B3 is a hyperextension injury through the disc or vertebral body leading to a hyperextended position of the spinal column. Anterior structures, especially the anterior longitudinal ligament, are ruptured.

Morphology type C describes displacement or dislocation. There are no subtypes because as a consequence of the dissociation between the cranial and caudal segments various configurations are possible in different images. Morphology type A fractures may also be present.

Neurological status at the moment of admission should be scored according to the following scheme: N0 neurologically intact; N1 transient neurologic deficit, which is no longer present; N2 radicular

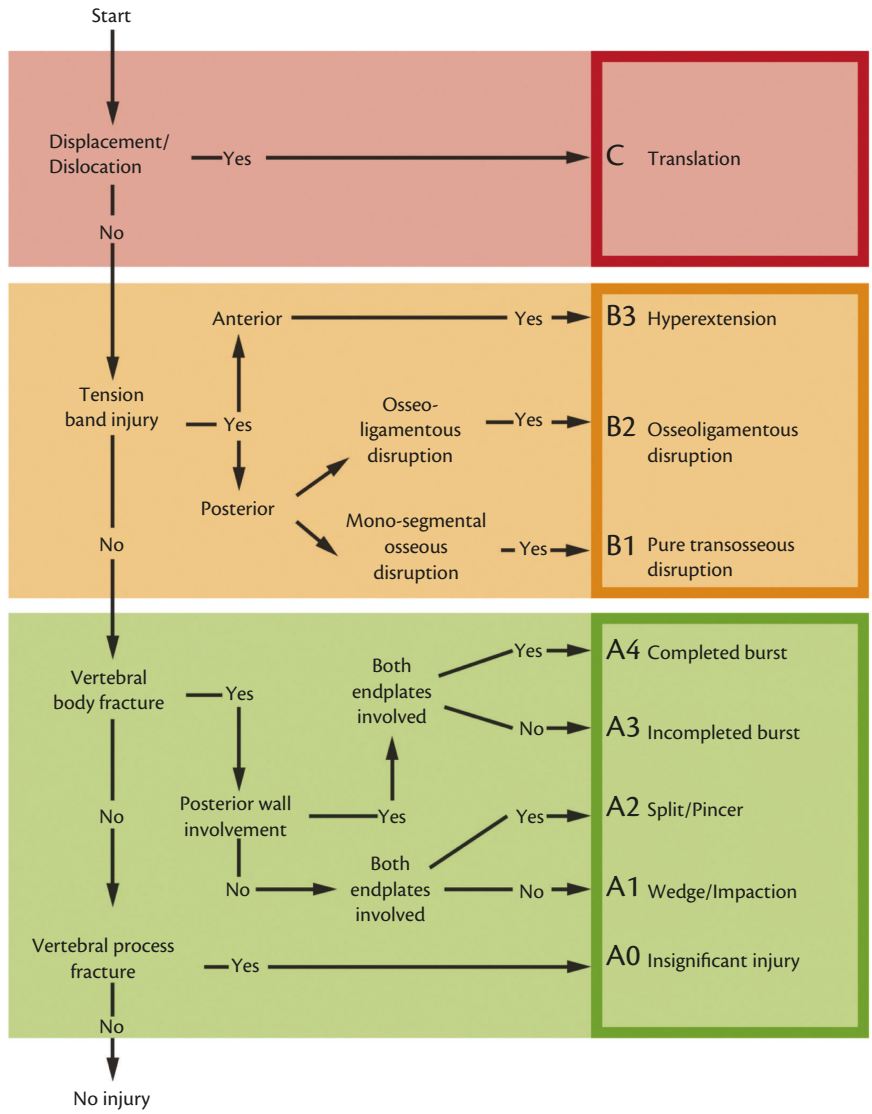

Fig. 69.1 Algorithm for morphological classification of thoracolumbar fractures.

Reproduced with permission from Maximilian Reinhold, Laurent Audigé, Klaus John Schnake et al, AO spine injury classification system: a revision proposal for the thoracic and lumbar spine, *European Spine Journal*, Volume 22, Issue 10, pp. 2184–01, Copyright © 2013 Springer Nature.

symptoms only; N3 incomplete spinal cord injury or any degree of cauda equina injury; N4 complete spinal cord injury; and NX neurologic status is unknown due to sedation or head injury.

There are two defined clinical modifiers, which can be used. The M1 modifier is used to designate fractures with an indeterminate injury to the tension band based on spinal imaging with or without MRI. This modifier is important for designating those injuries with stable injuries from a bony standpoint for which ligamentous insufficiency may help determine whether operative stabilization is a consideration. The M2 modifier is used to designate a patient-specific comorbidity, which might be a factor either for or against surgery for patients with relative surgical indications. Examples of an M2 modifier include ankylosing spondylitis or burns affecting the skin overlying the injured spine.

In 2015, Kepler (Kepler et al., 2015) published the AO Spine Injury Score which allocates scores to features of the injury so that a calculated total can be used to guide whether patients should be managed conservatively or surgically (Table 69.1).

The surgical management of thoracic and lumbar fractures

Patients with spinal injuries should be managed according to the advanced trauma life support guidelines as covered in Chapter 65. Spinal cord injury is also covered elsewhere. In this chapter only the specific surgical indications and techniques relevant to thoracolumbar spinal fractures will be addressed.

X-rays have a limited role in the assessment of spinal injury in acute major trauma although they are used in assessing patients with osteoporotic crush fractures. All patients will need a computed tomography (CT) scan of the whole spine with reconstructions so that the images can be examined in all three plains. The CT scan should be studied to look at the fracture morphology, soft tissue swelling, and adjacent or other injuries in the spine or body organs. The CT also gives information relevant to surgical planning such as the size of the pedicles and can be used in an image

Table 69.1 AO Spine Injury Score

Fracture type		Neurological		Clinical modifiers	
A0	0	N0	0	M1	1
A1	1	N1	1	M0	0
A2	2	N2	2		
A3	3	N3	4		
A4	5	N4	4		
B1	5	NX	3		
B2	6				
B3	7				
C	8				
Score 0–3 Score 4–5 Score 6–13		Manage conservatively Can be managed surgically or conservatively Manage surgically			

Reproduced with permission from Christopher K. Kepler, Alexander R. Vaccaro, John D. Koerner et al, Reliability analysis of the AOSpine thoracolumbar spine injury classification system by a worldwide group of naïve spinal surgeons, *European Spine Journal*, Volume 25, Issue 4, pp. 1082–6, Copyright © 2015 Springer Nature.

guidance system. However, the CT scan does not exclude a ligamentous injury.

All patients with persisting neurological symptoms and most other patients with a significant spinal injury on CT will also be investigated with MRI scanning. MRI should include T1, T2, and short tau inversion recovery (STIR) sequences. T1 and T2 will demonstrate spinal cord or root compression, the STIR sequence is especially useful for detecting fractures, disc, and ligament injuries.

Where indicated, the aim of surgery is to achieve neurological decompression, biomechanical stability, and restoration of alignment but there is a wide variation in clinical practice with regards to which spinal injuries should be operated on.

Neurological symptoms

Surgical spinal decompression and fusion is considered the first line treatment for most patients with persisting neurological compression. Spinal cord injury can be thought of as a primary mechanical insult that then triggers a secondary chain reaction that includes haemorrhage, vasospasm, ischaemia, oedema, excitotoxicity, inflammation, and further apoptosis of neurons.

The twin aims of surgery, therefore, are firstly to decompress, removing mass lesions and preventing secondary neural apoptosis by restoring normal perfusion to the spinal cord and secondly to fuse thus preventing further damage to the neural elements which might be incurred during movement and to allow early aggressive mobilization.

Patients who only have nerve root compression should be assessed for surgery based on the nature of the biomechanical stability of their injury and not purely on their neurological injury.

Fracture stability

In the absence of a neurological injury, fractures that are unstable and risk displacement and late neurological compromise should undergo surgical stabilization. The challenge for the surgeon is to determine which fractures are stable and can therefore be reliably treated conservatively as compared to which ones require fixation.

Over the years, no single fracture has created more controversy than the treatment of neurologically intact thoracolumbar burst fractures (Anderson et al., 1991; Miyanji et al., 2006; Aleem and Nassr, 2016; Vaccaro et al., 2016). Even a recent Cochrane review determined that contradictory evidence exists and that no conclusions can be drawn with respect to a patient's pain or functional outcome (Koller et al., 2008). The presence of a retropulsed fragment is of limited clinical relevance. There is an increased risk of complication, revision surgery, and increased cost in the surgical group.

A survey of 483 surgeons from around the world has recently been performed by Vaccaro et al. (2016) where surgeons were presented with a series of clinical cases and asked about their preferred management. While significant regional practice differences existed, the following generalization can be made with respect to A type fractures. Surgery was not favoured for A1 or A2 fractures, surgery was not favoured for A3 (incomplete burst) or A4 (complete burst) fractures so long as the posterior ligamentous complex was intact and the patient was neurologically intact. Patients with A3 or A4 type fractures and radiculopathy were generally considered to be surgical candidates, A3 or A4 fractures with an indeterminate injury to the tension band (M1 modifier) were also generally considered surgical candidates.

Patients with burst fractures who are neurologically intact should have an MRI to assess the posterior ligamentous complex (PLC). If the PLC is intact, non-operative treatment is recommended. In patients with an indeterminate PLC, surgery might be considered. In cases where there is frank disruption of the PLC, the fracture should be reclassified as B2 and surgical treatment is recommended. Burst fractures accompanied by radiculopathy can be considered for decompression and fixation.

Type B fractures (Fig. 69.2) are generally treated surgically but there has been some literature to suggest that bony chance fractures (B1) which are well aligned and have appropriate bony contact can be treated in an extension brace and go on to uneventful healing (Kim and Lenke, 2005; Lakshmanan et al., 2009; Wood et al., 2015). This can be considered in patients with less than 10 degrees of focal kyphosis, no neurological compromise, and with the ability to comply with a close follow-up schedule.

Type C injuries, which are translational or rotational injuries, are considered biomechanically unstable by definition. They are normally managed with surgical reduction and fixation (Fig. 69.3).

The level of a fracture can predict stability. High or mid thoracic fractures are supported by the rib cage and sternum and are relatively stable while fractures at the cervicothoracic or thoracolumbar junctional zones are relatively unstable. A high velocity injury is much more likely to be unstable than a low velocity injury with the same radiological characteristics. Ankylosing spondylitis is frequently complicated by osteoporosis so that chance fractures are much more common. The long lever arm created by multiple fused segments makes these fractures massively less stable than chance fractures in normal individuals. Surgical intervention across multiple levels should normally be undertaken. Osteoporosis and patient comorbidities may also be relative contraindications to surgery.

Over the last decade, it has become increasingly clear that sagittal spine balance plays a key role in predicting both surgical as well as patient outcomes. While this maxim has been intensely studied in

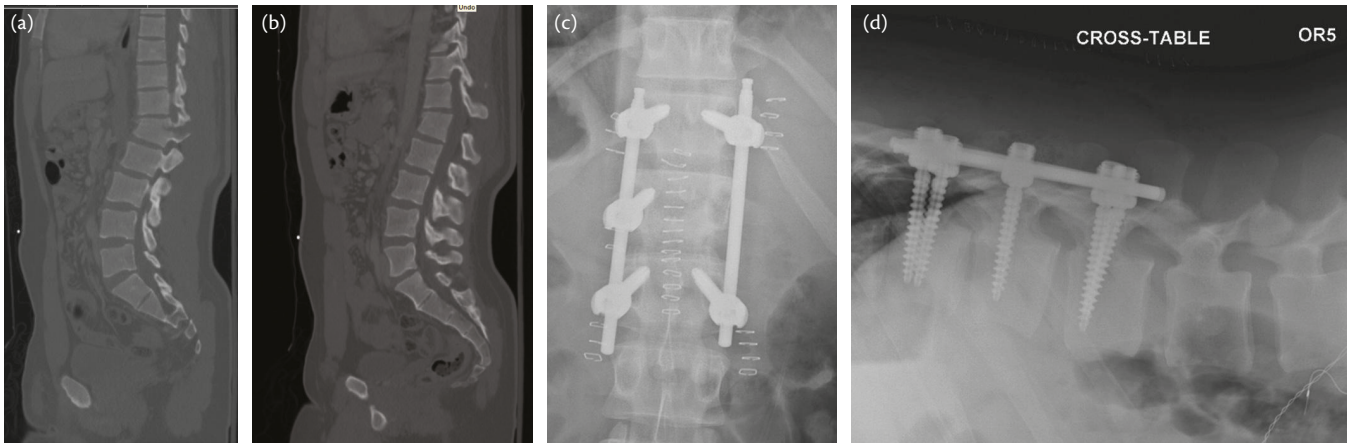

Fig. 69.2 A 23-year-old male was a restrained driver in a high-speed single vehicle motor accident. He presented with this isolated injury. He was neurologically intact. There is significant kyphosis with disruption of the interspinous and supraspinous ligaments as evident from the interspinous widening, as well as the facet disruption on the contralateral side. He had a percutaneous fixation consisting of one level above and one level below the injured level, as well as a limited open interspinous fusion. A pedicle screw was placed within the uninjured pedicle on the right.

deformity surgery, its role in trauma is less well defined, and is considered more controversial.

Koller et al. studied the role that post-traumatic deformity plays in long-term patient reported outcomes after a thoracolumbar burst fracture. They followed 21 patients treated conservatively for an average of 9.5 years. They determined that patients who suffered from greater focal kyphosis and loss of lumbar lordosis after their injuries had worse outcomes as measured by SF-36 and Visual Analogue Scale-spine scores (Koller et al., 2008). They concluded that patients with more severely crushed burst fractures, correction and maintenance of the kyphosis should be considered.

The challenge for the treating surgeon is that posterior instrumentation alone has not proven to be effective in preventing kyphosis. Lakshaman et al. (2009) have demonstrated that in burst fractures, while kyphotic deformity can be corrected initially with posterior instrumentation and positioning, there is often a 'settling' of the fracture in long term follow-up back to its baseline deformity. They concluded that posterior treatment of burst fractures to correct moderate kyphosis as a primary surgical goal without other compelling indications, such as instability or neurological deficit, is of unclear benefit (Vaccaro et al., 2016).

Wood et al. similarly performed a prospective randomized controlled trial that included 47 patients with a stable thoracolumbar burst fracture. At their final follow-up period (ranging from 16 to 22 years), there was no difference in kyphosis angle (Miyanji et al., 2006) between the operative and non-operative groups in those treated with posterior fixation only.

Pekmezci et al. in their paper instead focused on performing a minimally open corpectomy and percutaneous posterior short segment fixation in the treatment of single level traumatic lumbar burst fractures. They reported on 12 patients with an average of 38 months follow-up. They were able to effectively hold their correction, and had good patient reported outcomes (Fig. 69.4).

It is therefore the authors' opinion that severe kyphosis as a result of a thoracolumbar burst facture may be considered as an indication for surgery in the appropriate patient, especially in those

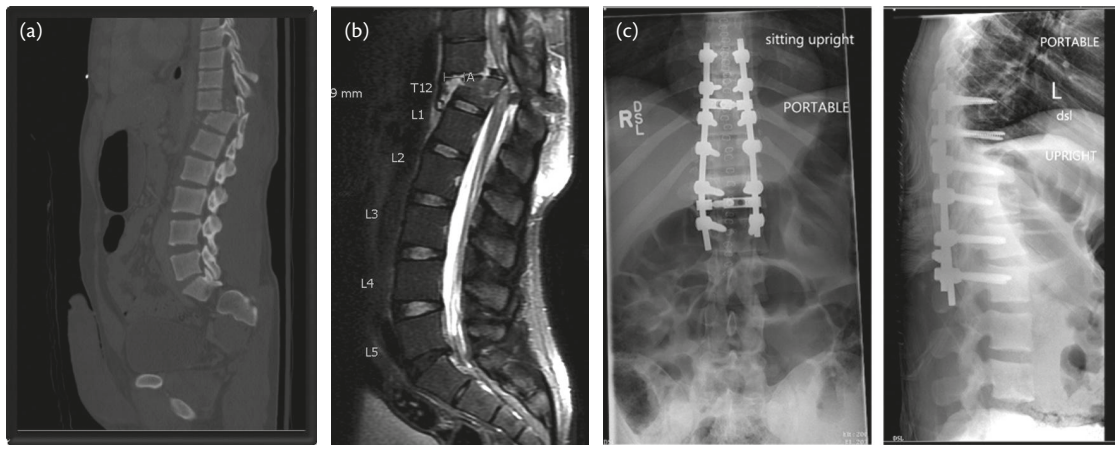

Fig. 69.3 A construction worker had a heavy object pin him onto the stairs. A T11–T12 fracture dislocation is evident on the CT scan. The patient was intubated at the scene of the accident and not clinically examinable, therefore an MRI was obtained to assess the neural elements. This type C injury was treated with an open reduction and posterior instrumented fusion as well as a decompression of the spinal cord. Postoperatively, the patient regained some sacral sparing and partial voluntary control of his bowel and bladder.

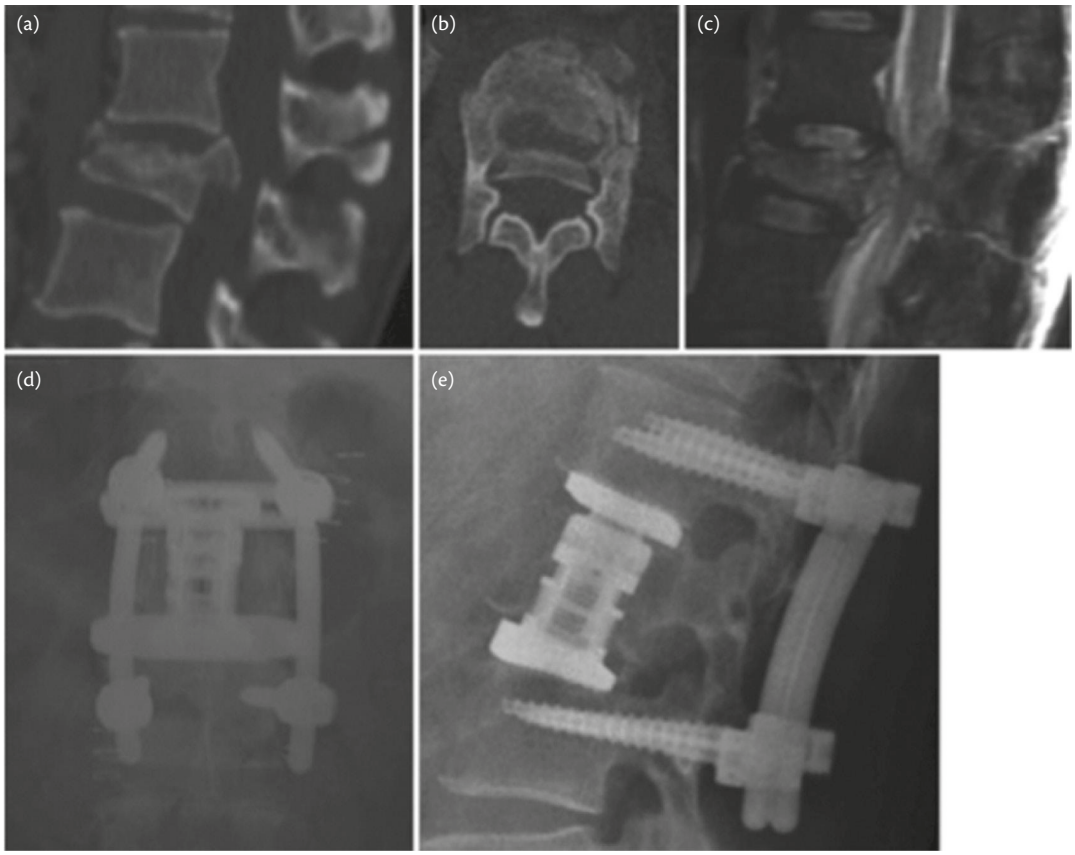

Fig. 69.4 Radiographic images of a 48-year-old man who sustained an L1 burst fracture (A–C) without neurological deficits after falling 15 feet. His fracture was stabilized with short segment posterior pedicle screws placed percutaneously and anterior decompression and stabilization. The construct shows no sign of loss of correction at the 12-month postoperative visit (D–E).

who acquire a significant mismatch between their lumbar lordosis and their pelvic incident. In order to maintain the correction, anterior column support is often required in addition to posterior instrumentation.

Bracing

Thoracolumbosacral orthoses (TLSO) are external rigid spinal braces that span the thoracic, lumbar, and sacral spine to limit motion, correct deformity, or improve the function of certain segments of the body. A TLSO brace limits motion and stabilizes injured structures resulting in reducing pain, enhanced stability, healing, and prevention of progression of deformity. These orthoses are used for spinal stabilization when surgery is not needed, after surgery, or in patients where surgery cannot be attempted safely.

The Jewett Hyperextension Orthosis reduces flexion in the lower thoracic and lumbar spine. It works through posteriorly directed pressure from the anterior sternal and suprapubic pads, with anteriorly directed pressure from the posterior thoracolumbar pad. It is indicated for fractures of the lower thoracic and thoracolumbar regions. The contraindications for the Jewett orthosis are unstable or burst-type fractures.

A custom fabricated TLSO, sometimes referred to as a clam-shell orthosis, provides rigid exterior bracing to the thoracic and lumbar spine with an effective range from T3 to L4. It is moulded from polypropylene or plastic to fit the patient. It covers anteriorly from the sternal notch to the pubic symphysis and posteriorly from the scapula to the coccyx. There is soft padding between the moulds for the patient's comfort, with Velcro straps to provide a snug fit.

The TLSO brace offers the maximum amount of external stabilization in all planes of motion. The TLSO is commonly used to provide non-operative spinal stabilization for fractures from T3-L4. These fractures include burst, compression, and chance fractures. Postoperative use of the TLSO is to limit mobility and increase bony fusion rates.

Prefabricated TLSO braces of various sizes are available. This has the advantage of immediate usage. However, they may have fitment issues and therefore may result in less stabilization of the spine and less patient comfort. The contraindications to TLSO bracing are morbid obesity, the need for increased lateral stability, presence of a chest tube, colostomy, or large wounds within the area being braced. The most common complication of external bracing are skin and soft tissue pressure sores at the contact points of the brace to the wearer's body.

A lumbar corset wraps around the abdomen, usually fastened with Velcro straps and contains posterior steel plates. The corset provides anterior and lateral trunk containment. This assists by elevating intra-abdominal pressure. The steel plates at the posterior restrict flexion and extension of the lumbar spine. This provides the weakest stabilization compared to the other orthoses. Its use is mostly limited to low back pain from prolapsed lumbar intervertebral discs, lumbar

muscle spasms, or stable single-column compression-type lumbar fractures.

Posterior thoracolumbar fusion techniques

There are generally three different methods of inserting pedicle screws. The first is done free hand, with X-ray guidance and reference to anatomical landmarks, to obtain start points and a trajectory. The second is done percutaneously, with the use of intraoperative fluoroscopy for guidance on start points and trajectory of the cannulated screws, and the last is done with the use of computer-assisted navigation.

In all cases the surgeon needs to study the CT scan preoperatively to note the patient's pedicle size, trajectories, and to look for anatomical variants. A detailed plan should be brought to the operating theatre.

The most important part of performing freehand pedicle screws is the ability to select the appropriate start point. Anatomical landmarks differ for varying levels of the thoracic spine. In general, we use the anatomical method described by Kim and Lenke (2005). In order to facilitate memorization of the start points, we group thoracic vertebra in groups of three. See **Figure 69.5**.

Thoracic Vertebra Group	
T1–T3, midpoint of the transverse process and in line with the lateral pars of the level above.	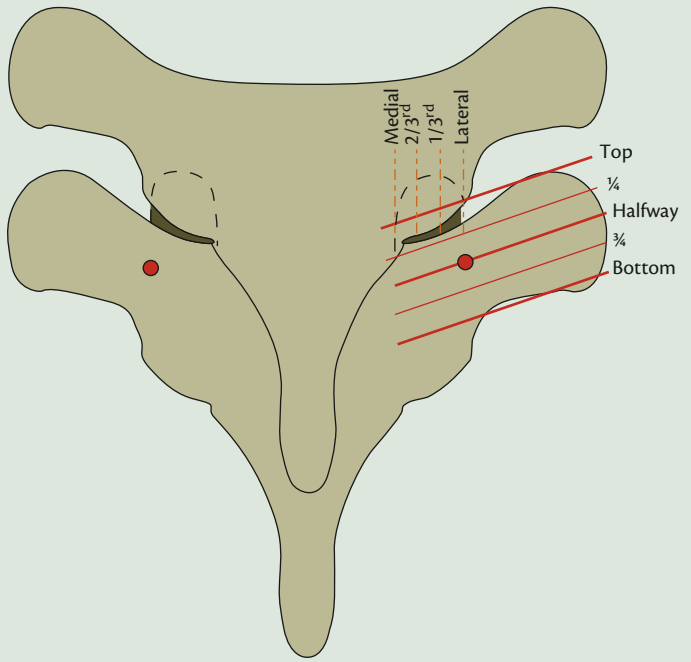
T4–T6, the lateral third of the facet, and on the superior ridge of the transverse process, which is usually one-quarter of the way from the superior edge of the transverse process.	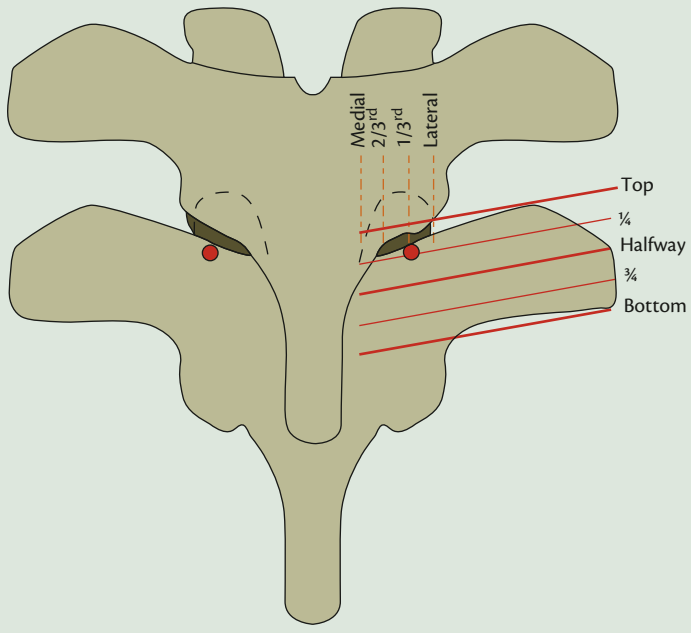

Fig. 69.5 Thoracic vertebra groups.

Thoracic Vertebra Group	
T7–T9, the most proximal and medial of all thoracic start points, are located at the lateral third of the facet and in line with the superior border of the transverse process.	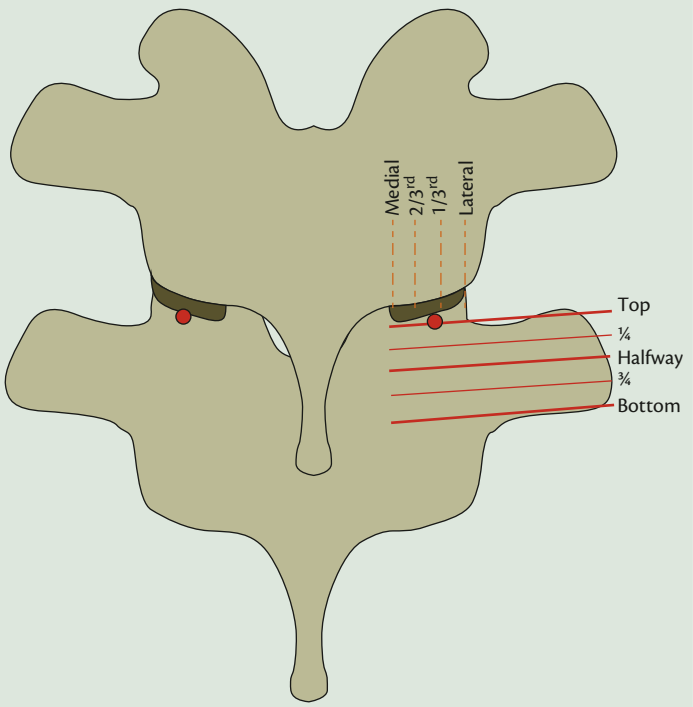
T10–T12 start points return to a more inferior and lateral aspect, similar to the T1–3 start points. They are in line with the midpoint of the transverse process, and on the lateral aspect of the pars.	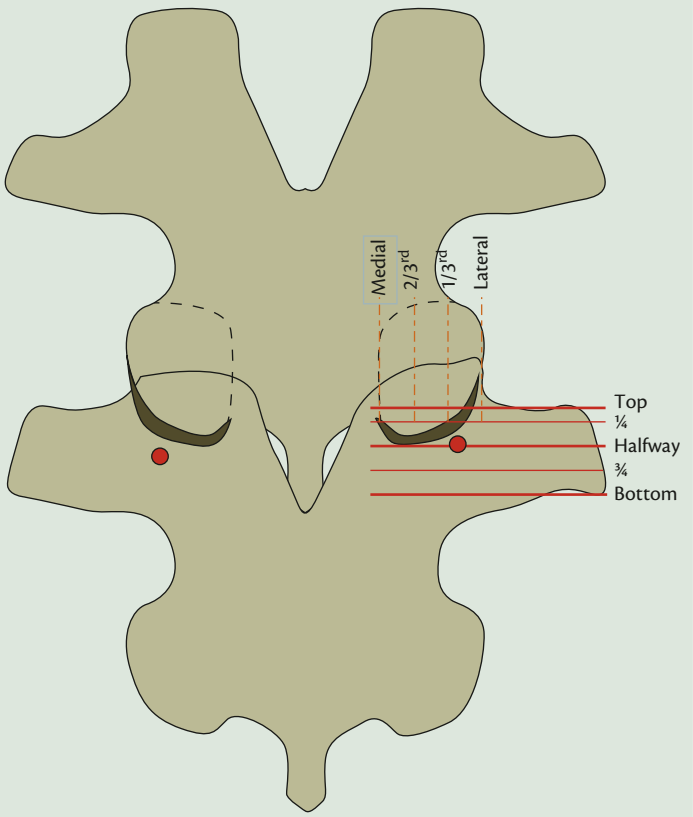

Fig. 69.5 Continued

Thoracic Vertebra Group	
Lumbar pedicle start points are located at the intersection of the midpoint of the transverse process, and with the lateral aspect of the pars.	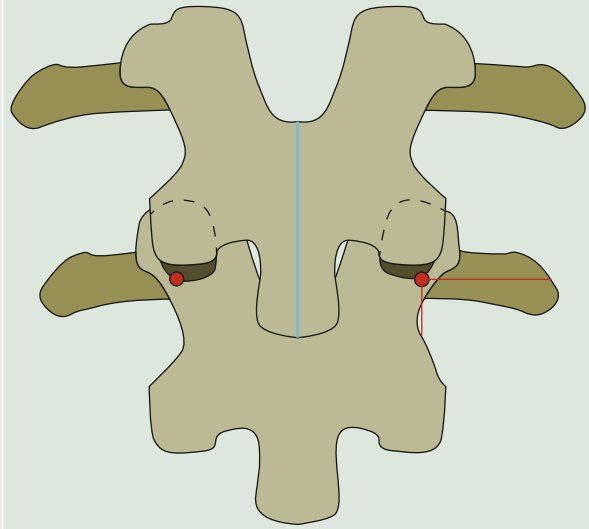

Fig. 69.5 Continued

Freehand screw placement

A radiolucent operating table is used. Great care should be exercised in ensuring that the facet capsule, supraspinous and intraspinous ligaments at the superior and inferior aspects of the last instrumented levels are not stripped of muscle in order to prevent junctional kyphosis. After appropriately exposing the spine to identify anatomical landmarks, the starting point is identified by referencing the articular facet, the transverse process, and the pars. anteroposterior (AP) X-rays can be used to identify the pedicles and must be aligned carefully as described next. Once the starting points are identified, an awl or high-speed burr is used to create a shallow pit for the start point through the outer cortex. This prevents slipping while using the pedicle probe. The medial aspect of the transverse process may need to be removed to allow the screw head to sit correctly in the thoracic spine. In the lumbar spine, the facet may need to be reduced in size. The curved pedicle probe is then used to cannulate the pedicle. A combination of AP and lateral X-rays can be used to monitor the progress of the probe, the probe should not cross the medial wall of the pedicle, as seen on the AP X-ray until it is in the vertebral body as seen on the lateral X-ray. The curved pedicle finder is typically used, with the curve pointing away from the spinal canal for the first 20 mm. Once that depth has been reached, it is then rotated 180 degrees and reinserted. A gentle 'wiggling' motion is performed while constant forward pressure is applied. A sound is then used to palpate four walls and the floor of the pedicle. The sound is often marked at the anticipated depth of the pedicle, to prevent it being inserted too deeply if a floor is not felt. The pedicle path is then tapped, often intentionally using a tap which is undersized by 1 mm as compared to the final screw. Once the tap is removed, the pedicle is then once again sounded to ensure that a new trajectory was not inadvertently tapped. Again, four walls and a floor should be felt. The appropriate screw is then inserted, taking great care to be colinear with the previously tapped trajectory and using X-ray guidance.

Cannulated fluoroscopic technique

The second method of inserting pedicle screws described here involves using intraoperative radiographs and a cannulated pedicle screw system. The key to this technique lies in obtaining proper radiographic views for each vertebra that is to be fused.

A proper radiographic view for insertion of a pedicle screw ensures that the beam of the C-arm is parallel to the endplates of the vertebra, and that the spinous process bisects the centre of the body between the two pedicles. The start points for the pedicle screws are located at the 3 o'clock for the right pedicle and the 9 o'clock position for the left pedicle. See **Figure 69.6A**.

Trochars are then inserted, advancing them slowly with a mallet and stopping prior to crossing the medial wall of the pedicle. In order to avoid a medial breach, it is important to confirm on a lateral X-ray that the trochar has entered the vertebral body BEFORE it crosses the medial wall of the pedicle on the AP view. See **Figure 69.6B**.

A lateral X-ray is then obtained to demonstrate that the trochar has entered the vertebral body before it crossed the medial wall. It can then safely be advanced further. Note that advancing the trochar further will now give the AP radiograph the appearance of having breached the medial wall. See **Figure 59.6C**.

The inner core of the trochar is then removed, and a guidewire is advanced. The floor of the vertebra is palpated. Note that since the anterior wall of the vertebra is convex, the wire may strike the anterior wall before appearing to reach the apex on the lateral radiographic view of the spine. The trochar is then removed ensuring that the guidewire stays in position. The cannulated tap is then advanced over the wire. Lateral radiographs are obtained to ensure that the wire does not bind to the tap and inadvertently advance past the anterior wall of the vertebra. Lastly, the cannulated screw is advanced over the wire, again using lateral radiographs to ensure that the wire does not bind as may happen if the tap or the screw are not properly aligned with the wire as they are advanced.

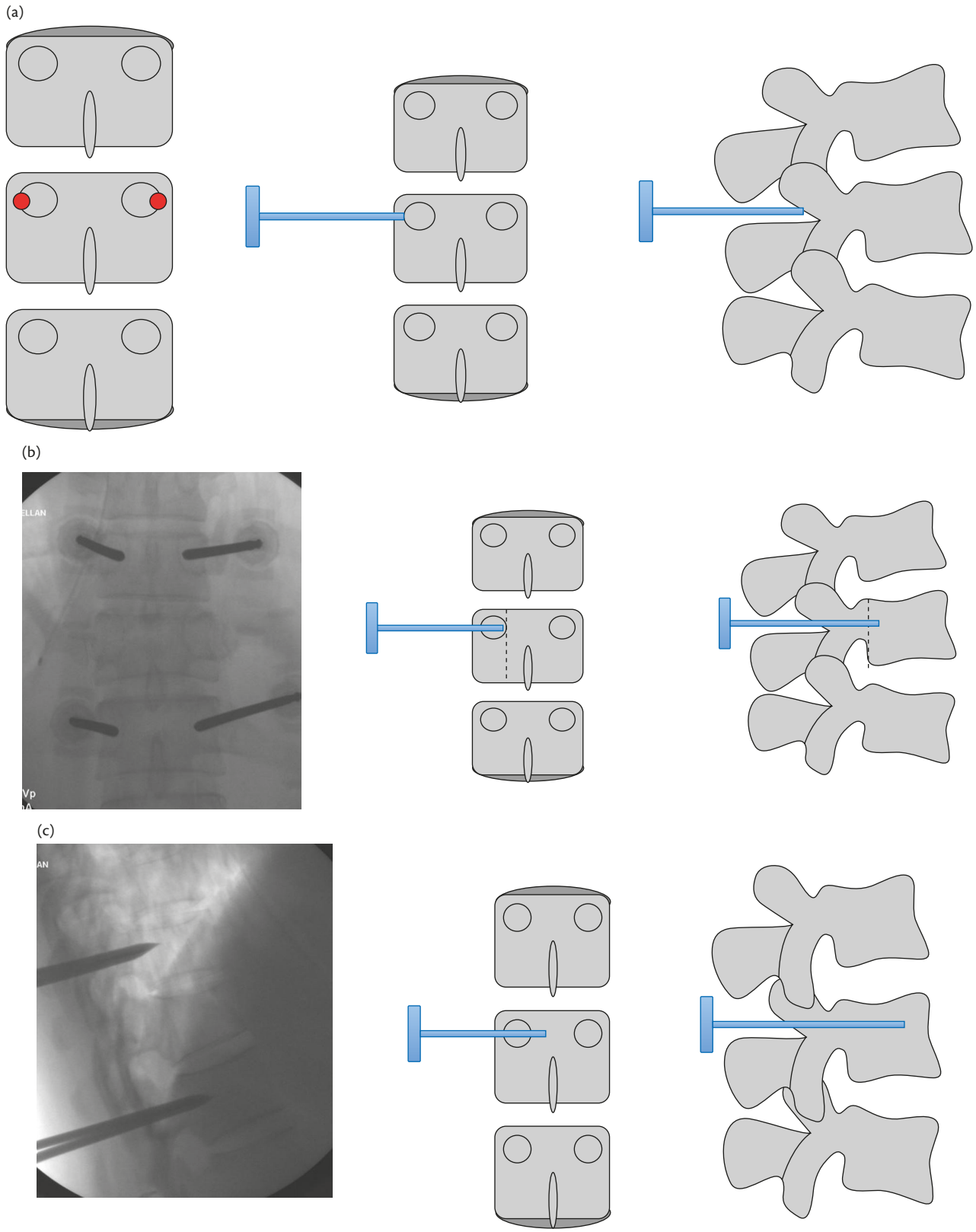

Fig. 69.6 Technique for inserting pedicle screws. The end plates must be square with the spinous process in the middle (A). Anteroposterior (AP) (B) and lateral (C) views allow the surgeon to position the screw in the pedicle. On AP views the screw should not traverse the medial wall until the screw tip is seen to have entered the vertebral body.

Image guided pedicle screw insertion

Pedicle screws can be inserted using image guidance rather than X-ray. Screws may be cannulated (to facilitate percutaneous techniques) or non-cannulated to be used with open techniques.

The neuronavigation system reference has to be securely attached to a spinous process of the vertebra and registered using anatomical landmarks from the back of the laminar or by an X-ray system for minimally invasive cases.

Image guidance reduces X-ray exposure, allows three-dimensional visualization which is especially useful in patients with abnormal anatomy. It is at least as accurate as the other techniques described.

Complications of pedicle screw insertion include breach of the pedicle wall in up to 20% although less than half will be symptomatic and require revision. The breach may be medial where there is a threat to the spinal cord or cauda equina, lateral where the great vessels are located or inferiorly where the nerve root may be compromised. Postoperative radicular pain is most commonly caused by a screw breaching the pedicle wall. The incidence of pedicle wall breach can be reduced by feeling the walls and floor with a pedicle feeler prior to inserting the screw, by neurophysiological monitoring, by careful interpretation and positioning of the X-ray machine, using neuronavigation, or with an impedance device that can detect breach of the pedicle.

Pedicle fractures occur when a screw of too great a diameter is inserted into the pedicle. The complication can be avoided by using the correct screw size and by inserting the screw slowly, so that the pedicle has time to accommodate it.

Screw pull out or screw fracture will occur if there is a failure of fusion. As with all internal fixation techniques, the metal construct will fail if the bones fail to fuse. The patient must be encouraged to stop smoking, NSAIDs should be avoided, while decortication during surgery and the use of bone graft are all helpful in promoting fusion.

Postoperative follow-up

Whether managed surgically or conservatively patients require physiotherapy and rehabilitation. Postoperative CT scanning is performed by some surgeons to assess screw and fracture positions, but it is not mandatory. X-rays should be taken at intervals over 3–6 months or until fusion occurs to monitor for progressive kyphosis or instability.

FURTHER READING

Kepler, C.K., Vaccaro, A.R., Koerner, J.D., et al. (2015) Reliability analysis of the AOSpine Thoracolumbar spine injury classification system by a worldwide group of naïve spinal surgeons. *Eur Spine J*, **25**(4), 1082–6.

Magerl, F., Aebi, M., Gertzbein, S.D., Harms, J., & Nazarian, S. (1994). A comprehensive classification of thoracic and lumbar injuries. *Eur Spine J*, **3**, 184–201.

Vaccaro, A.R., Lehman, R.A. Jr,, Hurlbert, R.J., et al. (2005). A new classification of thoracolumbar injuries: the importance of injury morphology, the integrity of the posterior ligamentous complex, and neurological status. *Spine (Phila Pa 1976)*, **30**, 2325–33.

Vaccaro, A.R., Oner, C., Kepler, C.K., et al. (2013). AOSpine thoracolumbar spine injury classification system: fracture description, neurological status, and key modifiers. *Spine (Phila Pa 1976)*, **38**, 2028–37.

REFERENCES

Aleem, I.S. & Nassr, A. (2016). Cochrane in CORR (®): surgical versus non-surgical treatment for thoracolumbar burst fractures without neurological deficit. *Clin Orthop Relat Res*, **474**(3), 619–24.

Anderson, P.A., Henley, M.B., Rivara, F.P., & Maier, R.V. (1991). Flexion distraction and chance injuries to the thoracolumbar spine. *J Orthop Trauma*, **5**(2), 153–60.

Kepler, C.K., Vaccaro, A.R., Koerner, J.D., et al. (2015) Reliability analysis of the AOSpine Thoracolumbar spine injury classification system by a worldwide group of naïve spinal surgeons. *Eur Spine J*, **25**(4), 1082–6.

Kim, Y.J. & Lenke, L.G. (2005). Thoracic pedicle screw placement: free-hand technique. *Neurol India*, **53**(4), 512–19.

Koller, H., Acosta, F., Hempfing, A., et al. (2008). Long-term investigation of nonsurgical treatment for thoracolumbar and lumbar burst fractures: an outcome analysis in sight of spinopelvic balance. *Eur Spine J*, **17**(8), 1073–95.

Lakshmanan, P., Jones, A., Mehta, J., Ahuja, S., Davies, P.R., & Howes, J.P. (2009). Recurrence of kyphosis and its functional implications after surgical stabilization of dorsolumbar unstable burst fractures. *Spine J*, **9**(12), 1003–9.

Magerl, F., Aebi, M., Gertzbein, S.D., Harms, J., & Nazarian, S. (1994). A comprehensive classification of thoracic and lumbar injuries. *Eur Spine J*, **3**, 184–201.

Miyanji, F., Fisher, C., Keynan, O., Wing, P., Boyd, M., & Dvorak, M. (2006). Flexion-distraction injuries of the thoracolumbar spine: health-related quality of life and radiographic outcomes. *Topics in Spinal Cord Injury Rehabilitation*, **12**(1), 58–69.

Vaccaro, A.R., Lehman, R.A. Jr,, Hurlbert, R.J., et al. (2005). A new classification of thoracolumbar injuries: the importance of injury morphology, the integrity of the posterior ligamentous complex, and neurological status. *Spine (Phila Pa 1976)*, **30**, 2325–33.

Vaccaro, A.R., Oner, C., Kepler, C.K., et al. (2013). AOSpine thoracolumbar spine injury classification system: fracture description, neurological status, and key modifiers. *Spine (Phila Pa 1976)*, **38**, 2028–37.

Vaccaro, A.R., Schroeder, G.D., Kepler, C.K., et al. (2016). The surgical algorithm for the AOSpine thoracolumbar spine injury classification system. *Eur Spine J*, **25**(4), 1087–94.

Wood, K.B., Buttermann, G.R., Phukan, R., et al. (2015). Operative compared with nonoperative treatment of a thoracolumbar burst fracture without neurological deficit: a prospective randomized study with follow-up at sixteen to twenty-two years. *J Bone Joint Surg Am*, **97**(1), 3–9.

RELATED LINKS TO EBRAIN

Anterior Approaches to the Lower Lumbar Spine. https://learning.ebrain.net/course/view.php?id=803

Fractures of the Spine. https://learning.ebrain.net/course/view.php?id=1045

Inserting Pedicle Screws. https://learning.ebrain.net/course/view.php?id=74
Minimally Invasive Surgical Approaches to the Posterior Thoracolumbar Spine. https://learning.ebrain.net/course/view.php?id=592
Posterior Thoracic Approaches. https://learning.ebrain.net/course/view.php?id=818
Sacral Fractures. https://learning.ebrain.net/course/view.php?id=819
Thoracolumbar Trauma. https://learning.ebrain.net/course/view.php?id=820

70

Spinal cord injury rehabilitation

Fahim Anwar, Wail Ahmed, Tamara Tajsic, Damiano G. Barone, and Harry Mee

Spinal cord injury rehabilitation in the acute phase

The importance of spinal cord injury rehabilitation

Rehabilitation is rather an educational process aimed at disabled people enabling them to achieve and sustain their optimal physical, intellectual, psychological, and social functional levels (World Health Organization, 2011). The importance of spinal cord injury rehabilitation stems from the fact that the establishment of specialist SCI rehabilitation units have improved the life expectancy of tetraplegics from approximately one month to almost normal life expectancy.

Understanding the diagnosis and pathophysiological changes in the acute phase

A prerequisite for rehabilitation is to have an understanding of the diagnosis by taking a history, conducting thorough general and neurological examinations, and reviewing relevant investigations (e.g. radiological images). More importantly, correlating the history, examination and radiological findings can help identify certain patterns of spinal syndromes such as central cord, anterior cord, or cauda equina syndromes. Furthermore, identifying associated injuries in the context of poly-trauma and recognizing their impact on additional functional impairments and rehabilitation needs is imperative to guide the process and direction of rehabilitation. For instance, it is reported that acute spinal cord injury occurs in 5–15 % of patients with severe head injury (Michael et al., 1989). Therefore, comprehensive assessment of the severity of head injury and specialist brain injury rehabilitation takes priority over specialist spinal cord injury rehabilitation in these cases.

Recognizing common pathophysiological changes associated with acute spinal cord injuries such as neurogenic shock, spinal shock, and postural autonomic dysfunction is important for the rehabilitation team to make the necessary and relevant interventions. In the acute phase of spinal shock following SCI, the neurogenic type of bladder and bowel dysfunction is primarily areflexic (and atonic) as opposed to the reflexic (and spastic) dysfunction, which is the predominant feature in the chronic phase. Consequently, the nursing management and care are also different. Another example occurs in postural autonomic dysfunction, where in addition to the medical treatment, physiotherapy treatment will concentrate on gradually adapting the patient's autonomic response to their new physiology using a tilt table.

Determination of the neurological level of injury and classification of the SCI

The standard practice across major trauma and spinal injury rehabilitation services is to use the International Standards for Neurological Classification of Spinal Cord Injury (ISNCSCI, 2015) to document the examination findings. This is a widely used international chart designed and reviewed on a regular basis by the American Spinal Injuries Association (ASIA) and the International Spinal Cord Society (ISCoS) since they joined forces in 1992 (Kirshblum et al., 2011; Kirshblum and Waring, 2014).

The main aim of the neurological examination in the context of SCI is to determine whether there is a sensory or motor level of injury and hence determine the neurological level of injury (NLI). The sensory level is the most caudal, intact dermatome for both pinprick and light touch sensation. The motor level is defined by the lowest key muscle function that has a grade of at least 3 (on supine testing), providing the key muscle functions represented by the segments above that level are judged to be intact (graded as a 5). The neurological level of injury is the most cephalad of the sensory and motor levels (Kirshblum et al., 2011; Kirshblum and Waring, 2014; ISNCSCI, 2015). If a patient has weakness in all four limbs but no sensory level (i.e. intact pinprick and light touch sensation in all dermatomes), then the injury is likely to be supraspinal as opposed to SCI.

The other aim is to determine the classification of the SCI using the ASIA Impairment Scale (AIS). By definition, an injury is classified as complete SCI (AIS A) if no sensory or motor function is preserved in the sacral segments S4 and S5. If there is any S4 or S5 sensory or motor function then the injury is classified as incomplete SCI (AIS B, C, or D). AIS B is sensory incomplete where sensory but not motor function is preserved below the neurological level and includes the S4 and S5 sacral segments (light touch or pinprick or deep anal pressure) and no motor function is preserved more than three levels below the motor level on either side of the body. AIS C is motor incomplete where motor function is preserved at the most caudal sacral segments for voluntary anal contraction or the patient meets

the criteria for sensory incomplete and has some sparing of motor function more than three levels below the ipsilateral motor level on either side of the body including non-key muscles. For AIS C, less than half of the key muscle functions below the single NLI have a muscle grade of 3 or more. AIS D is motor incomplete (as defined in AIS C) with at least half (or more) of the key muscle function below the single NLI having a muscle grade 3 or more. The importance of defining the NLI and AIS is to establish the SCI diagnosis as well as predict long-term possible functional outcomes.

Recumbent rehabilitation versus active mobilization

It remains controversial whether early decompression following a SCI conveys benefit in neurological outcome when compared to late decompression or no surgery at all. No randomized clinical trials are available on this subject, but several case-controlled studies found that surgery does not convey improved neurological outcome. What early surgery allows for is earlier mobilization thus reducing the rate of pulmonary complications such as pneumonia or atelectasis and effectively decreasing the length of stay and overall hospital costs (Donovan, 1994; Fehlings and Perrin, 2006).

Autonomic and cardiovascular system interventions

Patients with severe acute SCI are at risk of developing life-threatening cardiovascular instability and respiratory insufficiency. Primary spinal cord injury triggers several secondary injury mechanisms involving vascular compromise leading to reduced blood flow, loss of autoregulation, loss of microcirculation, vasospasm, thrombosis, and haemorrhage. Acute SCI also causes systemic vascular alteration such as bradycardia (associated more frequently with cervical injuries), cardiac arrhythmias, reduced mean arterial pressure, reduced peripheral vascular resistance, and compromised cardiac output. Systemic hypotension with concomitant loss of autoregulation reduces spinal cord perfusion and worsening ischaemia. Life-threatening cardiovascular instability may be recurrent in the first 7–10 days after injury. Several clinical series of human patients with acute SCI managed in an aggressive fashion with attention to blood pressure, oxygenation and hemodynamic performance report no deleterious effects and suggested improved neurological outcome (Hawryluk et al., 2015). The American Association of Neurological Surgeons guidelines and Congress of Neurological Surgeons recommendations (AANS and CNS, 2002) are highlighted in Table 70.1.

Chest and ventilation interventions

Respiratory insufficiency and pulmonary dysfunction are common after traumatic spinal cord injury, particularly when the injury occurs at cervical spinal cord levels (Reines and Harris, 1987; Como et al., 2005; Berlly and Shem, 2007). These are most likely to happen in the first 7–10 days after the injury (Berney et al., 2010a; Berney et al., 2010b). AANS and CNS (AANS and CNS, 2002) guidelines recommend that all patients with high cervical cord (C4 or higher) injury should be intubated immediately, and those with lower cord injuries should be evaluated on a case-by-case basis. However, in the acute setting, respiratory mechanics will be disrupted with any spinal cord lesion above T11.

Table 70.1 Summary of AANS and CNS Guidelines for management of SCI

1	Management of patients with acute SCI in an intensive care unit or a similarly monitored setting where cardiac, haemodynamic, and respiratory monitoring can be used to detect cardiovascular dysfunction and respiratory insufficiency.
2	Avoid systemic hypotension (defined as systolic blood pressure <90 mmHg) and correction as soon as possible.
3	Maintenance of mean arterial blood pressure at 85–90 mmHg for the first seven days following acute SCI to improve spinal cord perfusion.

Reproduced with permission, Guidelines for Management of Acute Cervical Spinal Injuries, *Neurosurgery*, Volume 50, Issue suppl 3, p. S1, Copyright © 2002 Oxford University Press on behalf of the Congress of Neurological Surgeons.

Critically ill mechanically ventilated patients experience impaired airway clearance due to an ineffective cough and impaired secretion mobilization (Hassid et al., 2008). Early tracheostomy in patients with lesions above C5 may reduce the number of ventilator days and the incidence of ventilator-associated pneumonia (Como et al., 2005). A diaphragmatic pacer may be useful in very selected patients. Cough augmentation techniques, including mechanical insufflation-exsufflation (MI-E), manually assisted cough, and lung volume recruitment, improve cough efficiency (AANS and CNS, 2002).

Gastrointestinal system interventions

Paralytic ileus usually accompanies severe acute SCI, and when prolonged, the resulting abdominal distension leads to splinting of the diaphragm which can affect ventilation, particularly in tetraplegics. IV fluids should be prescribed for at least 48 hours postinjury and a nasogastric tube should be inserted. All acute spinal cord injured patients will benefit from receiving chemical prophylaxis for stress ulceration. The duration of treatment is ill-defined but should be continued until risk factors are no longer present (Anwar et al., 2013).

Bowel management interventions

Neurogenic bowel dysfunction results from loss of extrinsic innervations arising from the spinal cord including pelvic splanchnic (S2–S4; parasympathetic), superior and inferior mesenteric (T9–T12; sympathetic), hypogastric (L1–L3; sympathetic), and pudendal (S2–4; somatic) innervations.

Generally, neurogenic bowels can be classified into upper motor neuron or reflex bowel resulting from a suprasacral cord injury and lower motor neuron or areflexic bowel, resulting from a complete injury at the sacral segments and/or the cauda equina.

The purpose of bowel care is to have a regular, predictable, and complete evacuation of the bowel contents (No authors listed, 1998). History taking, general and neurological examinations including assessment of the sacral segment's (S4–S5) sensory, motor, and reflex function is essential prior to prescribing a bowel care regime.

Bladder management interventions

In the initial stage of spinal shock, the resultant neurogenic bladder is flaccid and areflexic leading to urine retention with overflow incontinence. The aim of bladder management at this stage is to decompress the bladder to prevent vesicoureteric reflux and urinary tract infection. This is done by inserting an indwelling urethral catheter.

Using a closed drainage system, proper fixation of the catheter and regular catheter changes are important to avoid catheter-associated infections (Consortium for Spinal Cord Medicine, 2006).

Pressure sores prevention

Pressure ulcers are a serious secondary complication of SCI. The primary cause is felt to be externally applied pressure for a prolonged period over bony prominences, such as the sacrum and ischial tuberosities. This leads to ischaemia of overlying soft tissues, which ultimately can lead to necrosis. Muscle is believed to be even more sensitive to ischaemia caused by pressure then skin and soft tissues. Pressure sores can be life-threatening as a source of overwhelming sepsis. Pressure ulcers are staged according to the degree of tissue damage observed. The *National Pressure Ulcer Advisory Panel (NPUAP)* staging system is widely used for this purpose (Haesler, 2004).

Pressure ulcer prevention is paramount in SCI patients, and it should start in the acute setting as soon as practically possible after injury, continues into the chronic recovery phase and is lifelong for a great proportion of SCI patients. Pressure relief measures involve weight shifts or repositioning, mechanical reclining, and tilting. Optimal pressure relief should be performed every 15–30 minutes for 30–120 seconds depending on the technique used. In the chronic phase a forward leaning position, leaning side to side, having the wheelchair tipped back by 65° or more or doing a pressure relief lift for an appropriate length of time (i.e. 2 minutes) were found to be the most effective pressure relief techniques.

Nutrition interventions

Protein catabolism is common after acute, severe SCI. Changes in the body mass, resulting from muscle atrophy, leads to huge nitrogen losses, prolonged negative nitrogen balance, and rapid weight loss, especially in the first two weeks. However, the marked hypermetabolic response is blunted in SCI patients, by the flaccidity of denervated musculature after SCI. Indirect calorimetry is the recommended technique to assess energy expenditure in both the acute and chronic settings (AANS and CNS, 2002). Nutritional support of the SCI patient to meet caloric and nitrogen needs, not to achieve nitrogen balance, is safe and may reduce the deleterious effects of the catabolic, nitrogen-wasting process which occurs after acute spinal cord injury (AANS and CNS, 2002). It appears that early enteral nutrition (initiated within 72 hours) is safe, but has not been shown to affect the neurological outcome, the length of stay, or the incidence of complications in patients with acute SCI (Rowan et al., 2004). There has been no report assessing the mix or composition of nutritional supplementation for SCI patients. The literature on nutritional support for head injury patients supports a protocol beginning with high nitrogen enteral or parenteral solutions containing at least 15% of the calories as protein, no greater than 15% glucose or dextrose, a minimum of 4% of total energy needs to be as essential fatty acids and vitamins, essential elements, and trace minerals should be added (AANS and CNS, 2002).

Multidisciplinary rehabilitation team interventions

Early involvement by the multidisciplinary rehabilitation team (led by a consultant trained in rehabilitation and spinal cord medicine) is essential to improve function, prevent complications, and avoid further deterioration. The initial assessment by the team would lead to the formulation of an individualized rehabilitation plan in the acute phase. The main focus of physiotherapy is to maintain the full range of movement in all joints, help with bed mobility, improve physical capacity, and prevent secondary complications such as contractures in the muscles by providing splints. A seating and posture plan is implemented as soon as the patient can tolerate the seated position. The tilt table may help to improve autonomic control, fatigue, and exercise tolerance in the acute phase. Pulmonary interventions in the acute phase include chest physiotherapy, postural drainage, breathing exercises, and use of cough assist.

An Occupational therapist helps with upper extremity stretching and splinting, posture in the wheelchair, and oedema management. Early speech and language therapy involvement will help to establish augmentative communication, use of assistive technology to promote independence and assessment of swallowing.

Psychological interventions

Accepting the disability caused by the spinal cord injury is a lifelong process. In the acute stage of spinal cord injury acute stress reaction is very common, which if left untreated may lead to post-traumatic stress disorder. It is, therefore, essential that psychological interventions start early in the acute stage to reduce the impact of these psychological conditions and improve the quality of life. The psychological interventions that may be helpful include providing emotional support, facilitating the process of adjustment, early identification and management of anxiety and depression and interventions encouraging self-care, independence, and psychological well-being.

Prognosis and family support

The diagnosis of SCI is very devastating for patients and their families. They usually ask for the prognosis soon after the injury. Neurological recovery sometimes occurs at the level adjacent to the normal level and below the level of the injury. Neurological recovery is more common in patients with initial ASI Impairment Scale (AIS) C or D status. Patients who present with initial ASI C (age <50 years) and ASI D are expected to be walking (with or without assistive devices) on discharge from rehabilitation (Burns et al., 1997). Consultant led rehabilitation teams play a vital role in explaining prognosis and supporting the families through the acute phase of SCI.

Spinal cord injury rehabilitation in the chronic phase

Medical management of complications

Autonomic dysreflexia

Autonomic dysreflexia is a potentially dangerous clinical syndrome in SCI resulting in acute uncontrolled hypertension, leading to seizures, retinal haemorrhage, pulmonary oedema, renal failure, myocardial infarction, cerebral haemorrhage, and death. It develops due to an overactive autonomic nervous system which results in the abrupt onset of excessively high blood pressure in SCI patients with a neurological level of injury at T6 and above (Krassioukov et al., 2009). Between 48% and 90% of SCI patients with cord injury T6

and above will suffer from autonomic dysreflexia and is more likely in complete than incomplete SCI.

Any noxious or non-noxious stimuli from the intact peripheral nerves below the level of the injury produces strong sympathetic activity from the sympathetic nerves. This leads to vasoconstriction and hypertension. The brain responds to this by initiating descending inhibitory signals to shut down the sympathetic system. These signals fail to pass through the injury level at T6 and above. At the same time, the brain tends to activate parasympathetic system through the intact vagus nerve and produces bradycardia. The reflex sympathetic activity resolves as soon as the stimulus is removed. See **Table 70.2**.

Early recognition is paramount to prevent dangerous complications. A management algorithm (Acute Management of Autonomic Dysreflexia, 2001; Krassioukov et al. 2009) is shown in **Figure 70.1**.

Venous thromboembolism (VTE)

Thromboembolic disease is a common occurrence in patients who have sustained a cervical spinal cord injury and is associated with significant morbidity (AANS and CNS, 2002). Low molecular weight heparin in combination with pneumatic compression stockings or electrical stimulation is recommended as a prophylactic treatment strategy. There are multiple reports of the beneficial effects of prophylaxis therapy for 6–12 weeks following spinal cord injury (AANS and CNS, 2002). A 3-month duration of prophylactic treatment for deep vein thrombosis and pulmonary embolism is recommended in severe cervical SCI. Vena cava filters are not recommended as a routine prophylactic measure but are recommended for selected patients who fail anticoagulation or who are not candidates for anticoagulation and mechanical devices (AANS and CNS, 2002).

Spasticity management

Spasticity is defined as a motor disorder characterized by a velocity-dependent increase in tonic stretch reflex (muscle tone) with exaggerated tendon reflexes resulting in hyperexcitability of the stretch reflex, as a component of the upper motor neuron syndrome (Feldman et al., 1980). Spasticity affects 70% of patients with spinal cord injury (Johnson et al., 1998; Noreau et al., 2000).

The pathophysiology of spasticity in spinal cord injury is multifactorial. A relative overexcitation of the alpha motor neuron due to the absence of descending inhibitory signals is considered as the main pathophysiological explanation. In spinal cord injured individual, this overexcitation mainly is due to the inability of the inhibitory impulses to reach the alpha motor neuron. However, more recently it is documented that there is increased afferent input to the spinal motor neurons due to an increase in the sensitivity of muscle spindles as well as changes in the intrinsic properties of the spinal motor neuron leading to hyperexcitability of the motor neuron causing self-sustained firing in response to stretch (Nielsen et al., 2007). Similarly, there are changes in the intrinsic properties of the muscles leading to the physiological changes in the muscle fibre and tendon compliance contributing to spasticity (Friden and Lieber, 2003).

Spasticity is not always harmful and in some situations spinal cord injured patients may use it to their advantage to transfer, mobilize, or perform activities of daily living. In the lower limbs, it also helps to aid circulation and help prevent oedema and decreases the risk of deep vein thrombosis (Ashworth, 1964). The harmful effects of spasticity include functional deterioration, difficulties in activities of daily living and hygiene, postural abnormalities, contractures, pressure ulcers, and pain.

Complete multidisciplinary clinical assessment of spasticity is essential to plan any treatment. There are several clinical scales to quantify spasticity. The most widely used scale in clinical practice is the Ashworth and the Modified Ashworth Scale.

Several factors exacerbate spasticity such as infections, pressure ulcers, menstrual pain, in-growing toenails, and renal tract calculi. It is therefore imperative that these exacerbating factors are looked for and treated before treating the spasticity itself. Spasticity can be focal, multifocal, regional, or generalized. Physical modalities are the first-line treatment for spasticity. Sustained passive stretching of the muscles throughout the normal range of movement of the joint helps to reduce spasticity. The 'range of movement' exercises should be performed regularly to help prevent the development of spasticity. Well maintained posture in the wheelchair and positioning in the bed can aid in prolonged stretching of spastic muscles. Various orthoses and devices can be used, both in bed and in a wheelchair, to help maintain proper positioning.

Oral medications are used in multifocal, regional, and generalized spasticity. The most commonly used oral medication is baclofen. It is a gamma-aminobutyric acid (GABA) analogue and reduces spasticity by inhibiting monosynaptic and polysynaptic spinal reflexes. The maximum dose is 100 mg per day in three to four divided doses.

Table 70.2 Causes, signs, and symptoms of autonomic dysreflexia

Examples of triggers for autonomic dysreflexia	Symptoms of autonomic dysreflexia	Signs of autonomic dysreflexia
• Bladder distention or irritation; urinary infections, calculus, epididymitis, or scrotal compression • Bowel distention due to faecal impaction • Bowel instrumentation—colonoscopy • Haemorrhoids • Anal fissure • Gallstones • Pressure sores • Fractures • Deep vein thrombosis/pulmonary embolism • Burns • In-growing toenail • Pregnancy esp. labour • Menstruation • Sexual intercourse	• Bilateral pounding headaches • Blurred vision • Nasal congestion • Restlessness • Anxiety • Flushing of the skin above injury level	• Hypertension • Bradycardia • Dilated pupils • Goose bumps below the level of injury • Excessive sweating above the level of injury • Dry skin below the level of injury • Arrythmias, atrial fibrillation

Step 1
• Check Blood Pressure (BP)
• If elevated sit the patient up
• Loose any constrictive devices and clothing
Step 2
• Look for any triggers, starting with the urinary system
• Catheterise the patient if no indwelling catheter is in situ
• If catheter is in situ, check for a kink, fold, constriction or obstruction
• If catheter is blocked, initiate gentle irrigation with normal saline at body temperature
• If catheter is not draining, remove and replace the catheter
Step 3
• If bladder is draining and the symptoms persists, consider faecal impaction
• Check the rectum for stool with a lidocaine jelly (if the BP is less than 150 mm Hg systolic)
• If rectum is impacted, consider gentle manual evacuation
• Check pulse and BP every 2 to 5 minutes until BP normalises.
Step 4
• If BP is at or above 150 mm Hg, consider pharmacological management
• Use rapid onset and short acting anti-hypertensive agents
• Common agents used are Nifedipine (10 mg sublingual) or Glycerile Trinitrate spray (1–2 doses under the tongue)
• Diazepam is used to control intractable spasms or seizures
• Monitor the patient for symptomatic hypotension
Step 5
• Consider less frequent causes if the episode of dysreflexia continues
• Once patient is stabilised, initiate close monitoring for 2 hours (watch for recurrence)
• Review the cause and devise an appropriate care plan
• Other pharmacological agents used in autonomic dysreflexia include captopril, hydralizine and betablockers (used in specialist settings with monitoring)

Fig. 70.1 Management algorithm for autonomic dysreflexia.

Common side effects are nausea and sedation. Abrupt termination of baclofen may lead to withdrawal symptoms like epileptic seizures and psychosis.

Tizanidine is used if baclofen is not tolerated or ineffective. It is a centrally acting α2 adrenergic agonist. It reduces spasticity by decreasing the release of excitatory neurotransmitters at the spinal interneuron level. It is well tolerated; the maximum dose is 36 mg per day in four to five divided doses. It has the potential of causing reversible liver damage and therefore strict monitoring of liver function is required during its usage.

Dantrolene is a skeletal muscle relaxant and reduces spasticity by inhibiting the release of calcium from the sarcoplasmic reticulum. The maximum dose is 400 mg per day in three divided doses. Like tizanidine, it also affects the liver and monitoring of liver function is required. As it is a peripherally acting medication, it does cause sedation.

Benzodiazepines (diazepam and clonazepam) have also been used to treat spasticity and painful spasms as they bind to GABA receptors. Prolonged use of benzodiazepines is associated with sedation and cognitive impairment and is therefore not recommended.

Gabapentin has also been used in spasticity and can be useful in combination with other oral medications. It also helps to relieve painful muscle spasms. Common side effects are sedation and weight gain. Similarly, clonidine can be useful in reducing spasticity, but its use in clinical practice is limited due to its side effects.

For focal spasticity, targeted botulinum toxin injections can be very effective. It weakens the muscle by inhibiting the release of acetylcholine from the presynaptic nerve terminal. The effects of botulinum toxin last for three to six months and repeat injections are needed. The effects can be enhanced by localizing the muscle under electromyography (EMG) or ultrasound guidance. Phenol nerve and motor point blocks are a useful alternative to botulinum toxin injections. Phenol is a neurolytic agent and can be used in 3–7% aqueous solutions. Needle electric stimulation is required to localize the nerve and the motor points. The effects of phenol last for more than six months and can be repeated as required. Side effects of phenol include bruising, swelling, bleeding, and neuropathic pain. Phenol and botulinum toxin injections can also be combined to treat multifocal or regional spasticity.

Generalized spasticity in spinal cord injured patients can be treated successfully by intrathecal administration of baclofen through a pump. The patient should respond to a test dose of intrathecal baclofen before the pump is implanted. The dose of baclofen can be adjusted with a hand-held programmer with the ability to give boluses at specific intervals. The pump needs refilling regularly. Pump failure or catheter problems may lead to baclofen withdrawal symptoms. For intractable lower limb spasticity, intrathecal phenol is an option. However, it should only be used in patients with no bladder, bowel, or sexual functions, and where an effective bladder and bowel management plan is already in place. Cannabis products are not recommended for spasticity treatment because of their narrow therapeutic range and risk of dependence (Karst et al., 2010).

Definitive bowel management

The aim of bowel management in the chronic phase is to ensure compliance with the regular bowel care regime and manage complications. Following emergence from spinal shock, SCI patients will either end up with complete or incomplete reflexic bowel function, complete or incomplete areflexic bowel function, mixed bowel function (conus lesions), or normal bowel function if they recover neurologically. The severity of neurogenic bowel dysfunction depends on the level and completeness of the SCI. The higher the SCI level and AIS grade, the more severe the dysfunction.

To maintain predictable stool consistency laxatives (bulkers, osmotics, softeners) should regularly be taken while stimulants (such as Senna) should be taken only before planned evacuation of the stool as they increase bowel activity leading to movement of stool into the sigmoid colon and rectum.

Other more invasive options of neurogenic bowel management include transanal irrigation, antegrade continence enemas, colostomy (and percutaneous endoscopic colostomy), sacral anterior nerve root stimulator (SARS) and sacral nerve stimulator.

The management of the neurogenic bowel (No authors listed, 1998; Multidisciplinary Association of Spinal Cord Injured Professionals, 2012) is outlined in **Figure 70.2**.

Definitive bladder management

Following the stage of spinal shock (weeks to months), the extent of neurogenic bladder dysfunction depends on the level (supraspinal versus conus versus cauda equina lesion) and scale (complete versus incomplete) of SCI. Therefore, clinical history (including using frequency/volume charts) general examination and neurological examination (including sacral segments motor, sensory and reflex function) all play an important role in the management of the neurogenic bladder. Supraspinal lesions would usually result in a reflex neurogenic bladder (neurogenic detrusor overactivity, NDO) leading to bladder spasms which manifest as urinary leakage around a urethral or suprapubic catheter or between intermittent self-catheterizations. Occasionally, suprasacral lesions (above the sacral spinal cord) resulting from spinal cord infarction (e.g. from T6 down to the conus) can result in an areflexic bladder similar to the conus or cauda equina lesions which manifest as urinary retention with overflow incontinence.

Suprasacral lesions resulting from spinal cord injury interrupt the neural pathways between the 'pontine micturition centre' and the 'sacral micturition centre' (Blaivas et al., 2008). This usually results in detrusor external sphincter dyssynergia (DESD) which is characterized by involuntary contractions of the striated musculature of the urethral sphincter during an involuntary detrusor contraction (Blaivas et al., 2008).

The management of the neurogenic bladder usually starts early with intermittent clamping of the indwelling urinary catheter to train the bladder. This could be achieved using a flip-flow valve between the catheter and urinary bag to allow closure of the catheter. This is usually coupled with administration of oral anticholinergic medication to relax the bladder in patients with a complete (AIS A) or sensory incomplete (AIS B) spinal cord injury. Over a period of 1–2 weeks, bladder training is usually done by increasing the hours of catheter closure during the day up to three to four hours or until the patient gets the urge to empty their bladder. Patients who develop bladder sensation (or urge to empty) during bladder training may have a chance of success in emptying their bladder voluntarily following a trial without catheterization. Consistent and repeated readings of postvoid residual urine volume, using an ultrasound, of less than 100 ml is usually considered normal. Patients who fail to empty their bladder or empty their bladder incompletely (high postvoid residual urine volume) should have catheter drainage to maintain a safe low-pressure system. For patients with good hand dexterity (paraplegics and some low tetraplegics), the ideal way to manage the bladder is to learn how to do clean intermittent self-catheterization (CISC) every 4 to 5 hours depending on oral intake. For those with impaired hand dexterity, a long-term indwelling suprapubic catheter is preferred to a urethral catheter to avoid genital complications (ulcerations, urethral tears, hypospadias) and recurrent infections.

Video-urodynamic studies are particularly useful in determining the intravesical pressures, diagnosing vesicoureteric reflux, and detecting the severity of DESD. They are not a means to determine the best option of bladder management for a particular patient.

In severe DESD, intravesical botulinum toxin injection can be very effective in managing NDO symptoms of spastic urinary incontinence. Other methods include surgical bladder augmentation, neuro-modulation, neuro-stimulation and sacral anterior root stimulation (SARS).

Sexual function management

Sexual dysfunctions following spinal cord injury are common and may affect males and females in very different way. Females with spinal cord injury may experience a change in perineal sensation, delayed orgasm, and require more stimulation to achieve orgasm. Similarly, the lack of vaginal lubrication can lead to vaginal irritation during intercourse. Use of water-based lubrication agents helps to prevent this. For females, body image may be a significant factor in sexual dysfunction and accepting the impairments can lead to a happy and satisfying sexual relationship. In the acute phase, there is a loss of menstrual cycle, this spontaneously resumes between three to six months after the injury. Once the menstrual cycle becomes regular, then childbearing is usually not affected. Pregnancy following spinal cord injury is managed by a multidisciplinary team of professionals.

In males, T11 and above complete injury will lead to loss of psychogenic erection but patients can still achieve reflexogenic erection. Ejaculation may be possible in less than 10% of patients in this group (Subbarao and Garrison, 2016). Conversely, T12 and below complete injuries can cause loss of reflexogenic erection with a possibility of preserved psychogenic erection but ejaculation is usually

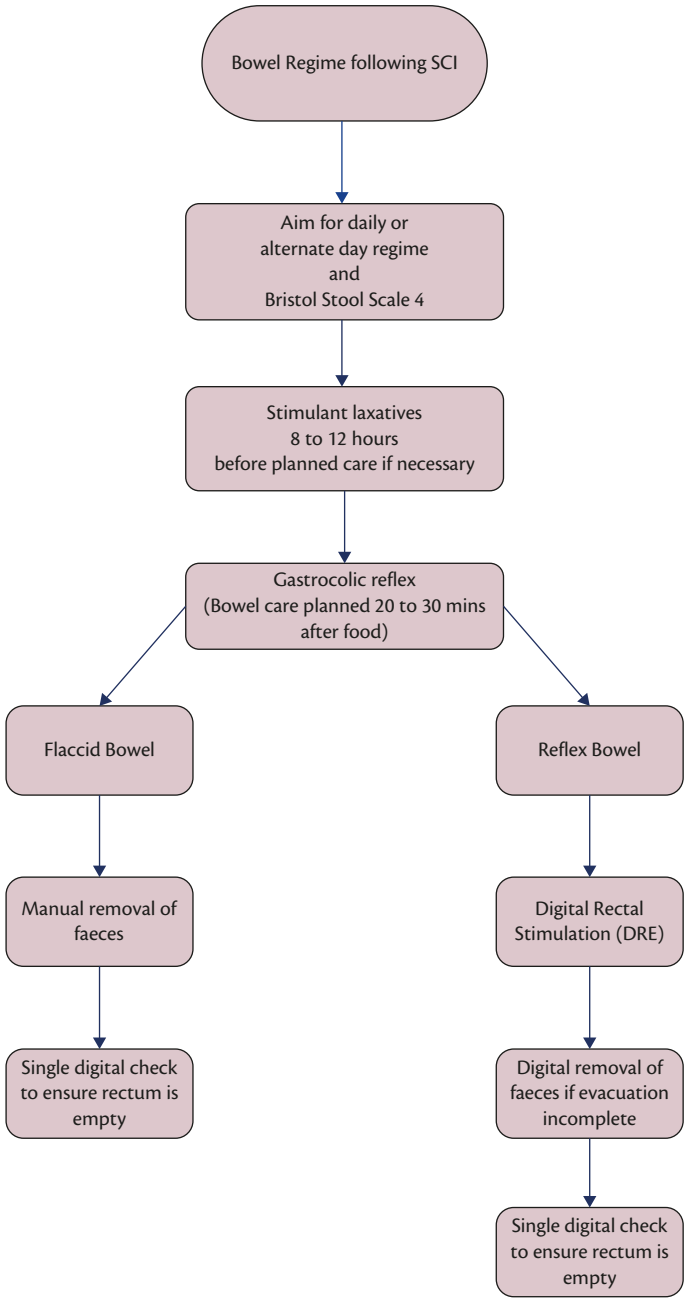
Bowel Regime following SCI
Aim for daily or alternate day regime and Bristol Stool Scale 4
Stimulant laxatives 8 to 12 hours before planned care if necessary
Gastrocolic reflex (Bowel care planned 20 to 30 mins after food)
Flaccid Bowel
Reflex Bowel
Manual removal of faeces
Digital Rectal Stimulation (DRE)
Single digital check to ensure rectum is empty
Digital removal of faeces if evacuation incomplete
Single digital check to ensure rectum is empty

Fig. 70.2 Management of neurogenic bowel.

Data from https://www.mascip.co.uk/wp-content/uploads/2015/02/CV653N-Neurogenic-Guidelines-Sept-2012.pdf; also Neurogenic Bowel Management in Adults with Spinal Cord Injury, *Journal of Spinal Cord Medicine*, volume 21, issue 3, pp. 248–93. © 1998 Taylor and Francis.

not possible (Subbarao and Garrison, 2016). Male fertility issues after spinal cord injury are common and mainly related to lack of ejaculation. This is managed by either electroejaculation, intrauterine insemination, or by *in vitro* fertilization.

Heterotopic ossification

Heterotrophic ossification (HO) is the formation of bone in ectopic sites such as soft tissues. It occurs in 20–30% of patients with spinal cord injury (Snoecx et al., 1995). The aetiology and pathogenesis of heterotrophic ossification is not known. In spinal cord injuries, muscle trauma (tears, ruptures, bleeding) is thought to trigger heterotrophic ossification (van Kuijk et al., 2002). The most common site of HO is at the hip (Sullivan et al., 2013) (Fig. 70.3) but it can occur around the elbows, shoulders, hands, and knees.

In the acute phase, raised alkaline phosphatase may raise the suspicion of HO. An isotope bone scan and MRI scan in the acute phase are sensitive in diagnosing HO. In the early stages X-ray would not show HO due to insufficient deposition of calcium.

Non-steroidal anti-inflammatory drugs (NSAIDs) have been used successfully to treat HO. However, their use is limited due to their side effects as well as their ability to inhibit bone healing after fractures (Johnson and Lanig, 1996). Treatment of established HO

Fig. 70.3 Heterotrophic ossification around the hip joint.

aims to stop the process of HO, maintain range of movements of the affected joint and prevent pain. There are very few pharmacological agents which have been tried to treat HO. Studies have been mainly on the use of indomethacin and etidronate, these agents are most helpful when given earlier, as preventative measures. Etidronate has been shown to prevent secondary HO formation, but the length of treatment is unclear, and there is a risk of osteomalacia.

Surgery is considered when HO is interfering with the quality of life or causing secondary complications. Surgical resection is considered once HO has matured as in the acute stages there is a risk of excessive bleeding. Etidronate, NSAIDs, or radiation therapy is indicated after surgery to reduce the risk of recurrence.

Neuropathic pain management

Pain following spinal cord injury may interfere with active rehabilitation and also have a negative impact on the quality of life and activities of daily living. The cause of pain after spinal cord injury is unknown. There are two distinct types of pain after spinal cord injury; neuropathic (secondary to damage to the spinal cord) and musculoskeletal (as a consequence of the spinal cord injury). Clinically neuropathic pain can be divided into three categories (Cardenas et al., 2002); spinal cord injury pain (below the level of the lesion), transition zone pain (bilateral at the level of the lesion), radicular pain, and visceral pain. Taking a detailed history and performing a physical examination followed by a focused investigation helps to make a diagnosis and also differentiate conditions like syringomyelia.

It is important to know that chronic pain following a spinal cord injury is difficult to treat. The aim of treatment is to manage the pain and improve the quality of life. The psychological factors impacting on the perception of pain should be explored and managed appropriately to improve the outcome of treatment. Pain is managed with a wide variety of therapeutic modalities such as physical therapy, cognitive behaviour therapy, self-management strategies, biofeedback, acupuncture, transcutaneous electric nerve stimulation, mindfulness, and pharmacological intervention. A comprehensive pain management plan includes a combination of all of these modalities.

Non-steroidal anti-inflammatory medications (NSAIDs) and acetaminophen are often used as first-line treatment for pain in spinal cord injury patients with variable efficacy. Prolonged use of NSAIDs is associated with a risk of gastric ulceration and acute renal damage.

Neuropathic pain is treated with antidepressants and anticonvulsants. Tricyclic antidepressants (amitriptyline, nortriptyline, and imipramine) are effective in treating neuropathic pain but anticholinergic side effects can limit their use. However, a randomized controlled trial failed to show significant pain relief from these agents in mixed neuropathic and nociceptive pains in the SCI population (Cardenas et al., 2002).

Anticonvulsants (gabapentin, pregabalin, lamotrigine) are calcium channel modulators and have been studied in spinal cord injury patients. Gabapentin (300–3600 mg per day) can cause drowsiness and weight gain limiting its use but it is effective in reducing neuropathic pain in paraplegics with complete injuries (Levendoglu et al., 2004). Pregabalin (50–600 mg per day) is better tolerated than gabapentin and has a better side-effect profile. It is also effective in reducing pain and improving sleep in both complete and incomplete spinal-cord injured patients (Siddall et al., 2006). Lamotrigine in a randomized controlled trial failed to show a statistically significant effect in the whole sample but in patients with incomplete injury, it significantly reduced pain at or below the level of the injury (Finnerup et al., 2002). Serotonin noradrenaline reuptake inhibitors such as duloxetine and venlafaxine have not been studied in spinal cord injury pain but are usually very effective in neuropathic pain.

Opioids have been used to treat pain following SCI with varying efficacy but only tramadol has a positive effect on pain. Prolonged use of opioids may lead to serious side effects particularly drowsiness, constipation, respiratory depression, endocrine abnormalities, tolerance, addiction, and opioid-induced hyperalgesia. Intrathecal drug administration should be considered only in intractable pain conditions where the oral administration has not been tolerated or effective. A combination of morphine and clonidine has been used in one clinical trial with good effect (Siddall et al., 2000). The long-term efficacy and safety of spinal cord stimulation, deep brain stimulation, and dorsal root entry zone lesions have not been evaluated clinically.

Role of tendon transfer surgery

In incomplete cervical cord injuries, tendon transfer surgery may help the patients to achieve independence by restoring some useful function in the hand. However, this type of surgery is complicated, requires experience and is not offered until the neurological examination has stabilized, and the patient has undergone an extensive rehabilitation programme.

A thorough clinical assessment is required to plan tendon transfer surgery. The aim of the tendon transfer surgery is either to restore elbow flexion or extension, wrist flexion or extension, or to improve grip.

Postoperative extensive upper limb rehabilitation helps to improve the outcome of the surgery. It is imperative to note that during the rehabilitation phase patients may lose the ability to use the limb or hand for 12 weeks as the tendon transfer heals.

Musculoskeletal interventions following spinal cord injury

Musculoskeletal interventions following SCI commence once the patient is medically stable and able to tolerate therapy. The musculoskeletal interventions may vary depending on the type and location of the SCI. The three main principals of interventions are to increase strength, prevent, and treat contractures, and improve the performance of a motor task. SCI patients respond to strength training programmes. For the upper limb, the aim of strength training programmes is to help the SCI patients lift themselves up from the floor to a wheelchair, achieve effective and safe transfers, and engage in functional tasks. Strength training in the lower limbs may help to achieve walking with aids or the ability to do standing transfers.

Passive movements are vital to prevent contractures and stretching can be used to treat contractures. The optimal quantity and duration of passive movements and stretches remains unknown and should be tailored according to the SCI level as well as to the patient's needs. Repetitive practice is used to improve the motor task following a SCI and is based on the principles of motor learning. A recent clinical trial suggested that intensive physiotherapy following SCI improves strength and gait in people with AIS C and D lesions even three years after the injury (Jones et al., 2014).

Recent advance in exoskeletal systems may change the outlook of musculoskeletal interventions after SCI in the near future.

Stem cell implantation

Stem cell therapy in SCI is a major research interest area, and several stem cells have been tested in animal SCI models. These cell types include embryonic stem cells (pluripotent), and mesenchymal cells (multipotent) harvested from the fat, bone marrow, umbilical cord, lining of the nasal cavity and tooth pulp. Although embryonic stem cells are pluripotent and have the ability to differentiate into any tissue when implanted, their use is limited due to ethical issues and the fact that the patients require immunosuppression. Mesenchymal cells, on the other hand, are multipotent and do not require immunosuppression. However, recent research does not give insight into their ability to differentiate and repair nerve cells. Recently induced pluripotent stem cells have been developed. These are mature cells genetically manipulated to become nerve cells. These are harvested from a patient's tissue and therefore do not require immunosuppression. Their use is limited in the acute phase of spinal cord injury due to the time involved in genetic manipulation (Doulames and Plant, 2016). There is also a theoretical risk of random mutations with the genetic manipulation.

The use of stem cell therapy is limited due to the severe risks that the newly implanted cells can pose in the spinal cord environment. Large randomized controlled trials are needed to ensure safety and efficacy of stem cell treatment in SCI. There are several ongoing clinical trials in the United States and Europe using neural stem cells, mesenchymal stem cells, and embryonic stem cells (Scope, 2018).

Neural-machine interfaces in SCI

The future of spinal cord injury rehabilitation relies on the research into neural-machine interface (also known as brain-computer interface, BCI, or brain-machine interface, BMI). A neural interface is a direct connection between the nervous system and a reading/stimulating electrode, in turn connected to an external hardware. The electrodes can be either penetrative or superficial. The former can be placed in deep cerebral structures (few centimetres) or in substance of large nerves, an example being deep brain stimulators used for Parkinson's disease; cortical penetrative devices (micrometres to millimetres) are also used and they allow a greater neuronal discrimination. On the other hand, superficial electrodes can be placed on the cerebral cortex (electrocorticography, ECoG) or on the scalp (electroencephalography, EEG). Neural interface electrodes can be implanted anywhere in the nervous system (brain, spine, peripheral nerves) and the myoelectric organs (muscles), potentially enabling a direct communication between any two parts of the system (or with any external neuro-prosthetic device). BCIs can be used to restore function following SCI, by stimulating and recording from either the motor, sensory, and/or autonomic systems and completely bypassing the site of the injury. A well-known example is the Utah array, which has been used in non-human primate experiments and phase 1 human studies to connect the motor and sensory cortex to either muscles or an external neuroprosthetic device in chronic SCI patients.

The priority for functional restoration depends on many factors including the level of the SCI, ASI classification and personal preference (Anderson, 2004; Snoek et al., 2004). For tetraplegic individuals, the priority is some functional recovery of the arm and hand whereas restoration of bladder and bowel function is necessary for SCI at any level. Walking and standing ability is viewed as an improvement in the quality of life for the SCI population (Collinger et al., 2013a).

The most basic form of neural-machine interface is functional electric stimulation (FES), which helps to stimulate weak muscles after SCI. FES can be applied through either surface electrodes or penetrative devices. The surface electrodes tend to stimulate the muscle itself whereas the implanted devices can target the muscles or the nerve innervating a particular group of muscles. Theoretically, FES can aid in improving upper limb function, standing, and walking following SCI. Several external FES systems are being used in clinical trials to improve grasp in SCI patients (Collinger et al., 2013b). Implantable FES systems require skills and extensive surgical interventions before they can be of any use.

Epidural and intraspinal stimulation of the spinal cord, to improve walking in incomplete SCI, is based on the fact that there are central pattern generators in the spinal cord capable of providing rhythmic movements of the legs without requiring any sensory feedback (Collinger et al., 2013b). A few clinical trials are looking at epidural spinal cord stimulation to improve walking in people with incomplete SCI (Herman et al. 2002; Huang et al., 2006).

Neural-machine interface has also been used to improve bladder control following SCI. Sacral anterior root stimulation, through an implanted pacemaker, can help to achieve continence and improve quality of life. The stimulation is beneficial for a selected group of complete SCI patients where conservative management of detrusor overactivity has failed. The commercially available stimulation system consists of an external part and an implanted device. The external stimulator is placed over the implanted device to achieve general stimulation of the anterior sacral root. The stimulation is usually combined with dorsal rhizotomy to prevent reflex bladder and sphincter contractions. SARS with dorsal rhizotomy is also helpful in treating autonomic dysreflexia and DESD (Martens and Heesakkers, 2011). However, dorsal rhizotomy limits the use of SARS in incomplete SCI as it will lead to loss of other pelvic

sensations (Martens and Heesakkers, 2011). Most recently afferent pudendal nerve stimulation is gaining momentum as an alternative to SARS and dorsal rhizotomy. This is useful in patients where reflex pathways for bladder control are intact. It is a relatively simple procedure and does not require a combination of dorsal rhizotomy. Further research is ongoing in creating closed-loop system targeting both afferent and efferent pathways to the bladder and providing a semi-independent system (Chew et al., 2013).

There are several other projects that are currently in preclinical trials including intracortical microstimulation to restore sensations, electroencephalographic (EEG) based brain-computer interfaces, brain-computer interface (neural signals decoded to operate a device and also provide feedback to the user about the brain activity), brain-computer interface using ECoG activity (recorded through subdural or epidural electrodes for precise functional localization). Advances in computer technology, in future, will translate into implants and devices that are easy to use, implanted without major complications, and cosmetically acceptable for patients.

FURTHER READING

Chhabra, H.S. (2015). *ISCoS Textbook on Comprehensive Management of Spinal Cord Injuries*. New Delhi, India: Wolters Kluwer (India).

Grundy, D. & Swain, A. (2002). *ABC of Spinal Cord Injury (ABC Series)*, 4th edition. Wiley-Blackwell.

Harrison, P. (2006). *Continuing Care: Managing the Long-term Care Needs of People with SCI in the Community (Managing Spinal Cord Injury)*. Spinal Injuries Association. https://www.sth.nhs.uk/services/a-z-of-services?id=277&page=191

Lin, V.W., Bono, B., Cardenas, D.D., et al. (eds.) (2010). *Spinal Cord Medicine, Principles and Practice*, 2nd edition. New York, NY: Demos Medical.

Sabharwal, S. (2013). *Essentials of Spinal Cord Medicine*. New York, NY: Springer Publishing Company.

REFERENCES

[No authors listed] (1998). Neurogenic bowel management in adults with spinal cord injury. *J Spinal Cord Med*, **21**(3), 248–93.

Acute Management of Autonomic Dysreflexia: Individuals with Spinal Cord Injury Presenting to Health-Care Facilities (2001). *Consortium for Spinal Cord Medicine Clinical Practice Guidelines*. http://www.pva.org/media/pdf/cpg_autonomic%20dysreflexia.pdf

American Association of Neurological Surgeons (AANS) and the Congress of Neurological Surgeons (CNS) (2002). Section on disorders of the spine and peripheral nerves of the American Association of Neurological Surgeons and the Congress of Neurological Surgeons: 2002. Guidelines for management of acute cervical spinal injuries. *Neurosurgery*, **50**(Sup 3), p.s1.

American Spinal Injury Association (2015). *International Standards for Neurological Classification of Spinal Cord Injury (ISNCSCI)*. American Spinal Injury Association. https://asia-spinalinjury.org/wp-content/uploads/2016/02/International_Stds_Diagram_Worksheet.pdf

Anderson, K.D. (2004). Targeting recovery: priorities of the spinal cord-injured population. *J Neurotrauma*, **21**(10), 1371–83.

Anwar, F., Al-Khayer, A., El-Mahrouki, H., & Purcell, M. (2013). Gastrointestinal bleeding in spinal injuries patient: is prophylaxis essential? *Br J Med Pract*, **6**(1), 607.

Ashworth, B. (1964). Preliminary trial of carisoprodol in multiple sclerosis. *The Practitioner*, **192**, 540–2.

Berlly, M. & Shem, K. (2007). Respiratory management during the first five days after spinal cord injury. *J Spinal Cord Med*, **30**(4), 309–18.

Berney, S.C., Gordon, I.R., Opdam, H.I., & Denehy, L. (2010a). A classification and regression tree to assist clinical decision making in airway management for patients with cervical spinal cord injury. *Spinal Cord*, **49**(2), 244–50.

Berney, S., Bragge, P., Granger, C., Opdam, H., & Denehy, L. (2010b). The acute respiratory management of cervical spinal cord injury in the first 6 weeks after injury: a systematic review. *Spinal Cord*, **49**(1), 17–29.

Blaivas, J. Chancellor, M., Weiss J., & Verhaaren, M. (eds.) (2008). Neurogenic bladder: the effect of neurologic lesions on micturition. In: *Atlas of Urodynamics*, 2nd edition, pp. 145–51. Hoboken, NJ: Wiley-Blackwell.

Burns, S.P., Golding, D.G., Rolle, W.A. Jr., Graziani, V., & Ditunno, J.F. Jr. (1997). Recovery of ambulation in motor-incomplete tetraplegia. *Arch Phys Med Rehabil*, **78**, 1169–72.

Cardenas, D.D., Warms, C.A., Turner, J.A., Marshall, H., Brooke, M.M., & Loeser, J.D. (2002). Efficacy of amitriptyline for relief of pain in spinal cord injury: results of a randomized controlled trial. *Pain*, **96**, 365–73.

Chew, D.J., Zhu, L., Delivopoulos, E., et al. (2013). A microchannel neuroprosthesis for bladder control after spinal cord injury in rat. *Sci Transl Med*, **5**(210), 210ra155.

Collinger, J.L., Boninger, M.L., Bruns, T.M., Curley, K., Wang, W., & Weber, D.J. (2013a). Functional priorities, assistive technology, and brain-computer interfaces after spinal cord injury. *J Rehabil Res Develop*, **50**(2), 145–60.

Collinger, J.L., Foldes, S., Bruns, T.M., Wodlinger, B., Gaunt, R., & Weber, D.J. (2013a). Neuroprosthetic technology for individuals with spinal cord injury. *J Spinal Cord Med*, **36**(4), 258–72.

Como, J.J., Sutton, E.R., McCunn, M., et al. (2005). Characterizing the need for mechanical ventilation following cervical spinal cord injury with neurologic deficit. *J Trauma*, **59**(4), 912–16.

Consortium for Spinal Cord Medicine (2006). Bladder management for adults with spinal cord injury: a clinical practise guideline for health-care providers. *J Spinal Cord Med*, **29**(5), 527–73.

Donovan, W.H. (1994). Operative and nonoperative management of spinal cord injury. A review. *Paraplegia*, **32**, 375–88.

Doulames, V. & Plant, G. (2016). Induced pluripotent stem cell therapies for cervical spinal cord injury. *Int J Mol Sci*, **17**(4), 530.

Fehlings, M.G. & Perrin, R.G. (2006). The timing of surgical intervention in the treatment of spinal cord injury: a systematic review of recent clinical evidence. *Spine*, **31**(11), s28–s35.

Feldman, R.G., Young, R.R., Koella, W.P., et al. (1980). *Spasticity, Disordered Motor Control*. Miami, FL; Chicago: Symposia Specialists; distributed by Year Book Medical Publishers.

Finnerup, N.B., Sindrup, S.H., Bach, F.W., Johannesen, I.L., & Jensen, T.S. (2002). Lamotrigine in spinal cord injury pain: a randomized controlled trial. *Pain*, **96**, 375–83.

Friden, J. & Lieber, R.L. (2003). Spastic muscle cells are shorter and stiffer than normal cells. *Muscle Nerve*, **26**, 157–64.

Haesler, E. (2004). *Prevention and Treatment of Pressure Ulcers*. Quick Reference Guide ed., pp. 1–75. https://www.npuap.org/wp-content/uploads/2014/08/Updated-10-16-14-Quick-Reference-Guide-DIGITAL-NPUAP-EPUAP-PPPIA-16Oct2014.pdf

Hassid, V.J., Schinco, M.A., Tepas, J.J., et al. (2008). Definitive establishment of airway control is critical for optimal outcome in lower cervical spinal cord injury. *J Trauma*, **65**(6), 1328–32.

Hawryluk, G., Whetstone, W., Saigal, R., et al. (2015). Mean arterial blood pressure correlates with neurological recovery after human spinal cord injury: analysis of high frequency physiologic data. *J Neurotrauma*, **32**(24), 1958–67.
Herman, R., He, J., D'Luzansky, S., Willis, W., & Dilli, S. (2002). Spinal cord stimulation facilitates functional walking in a chronic, incomplete spinal cord injured. *Spinal Cord*, **40**, 65–8.
Huang, H., He, J., Herman, R., & Carhart, M.R. (2006). Modulation effects of epidural spinal cord stimulation on muscle activities during walking. *IEEE Trans Neural Syst Rehabil Eng*, **14**(1), 14–23.
Johnson, K.M.M. & Lanig, I.S. (1996). Promotion and maintenance of sexual health in individuals with spinal cord injury. In: Chase, T.M., Butt, L.M., Hulse, K.L., et al. (eds.) *Practical Guide to Health Promotion After Spinal Cord Injury*, pp. 171–202. Gaithersburg, MD: Aspen Publications.
Johnson, R.L., Gerhart, K.A., McCray, J., Menconi, J.C., & Whiteneck, G.G. (1998). Secondary conditions following spinal cord injury in a population-based sample. *Spinal Cord*, **36**, 45–50.
Jones, M.L., Evans, N., Tefertiller, C., et al. (2014). Activity-based therapy for recovery of walking in individuals with chronic spinal cord injury: results from a randomized clinical trial. *Arch Phys Med Rehabil*, **95**(12), 2239–46.e2.
Karst, M., Wippermann, S., & Ahrens, J. (2010). Role of cannabinoids in the treatment of pain and (painful) spasticity. *Drugs*, **70**(18), 2409–38.
Kirshblum, S. & Waring, W., III (2014). Updates for the International Standards for Neurological Classification of Spinal Cord Injury. *Phys Med Rehabil Clin N Am*, **25**(3), 505–17.
Kirshblum, S.C., Burns, S.P., Biering-Sorensen, F., et al. (2011). International standards for neurological classification of spinal cord injury (Revised 2011). *J Spinal Cord Med*, **34**(6), 535–46.
Krassioukov, A., Warburton, D.E., Teasell, R., Eng, J.J.; Spinal Cord Injury Rehabilitation Evidence Research Team (2009). A systematic review of the management of autonomic dysreflexia after spinal cord injury. *Arch Phys Med Rehabil*, **90**(4), 682–95.
Levendoglu, F., Ogün, C.O., Ozerbil, O., Ogün, T.C., & Ugurlu, H. (2004). Gabapentin is a first line drug for the treatment of neuropathic pain in spinal cord injury. *Spine*, **29**(7), 743–51.
Martens, F.M.J. & Heesakkers, J.P.F.A. (2011). Clinical results of a Brindley procedure: sacral anterior root stimulation in combination with a rhizotomy of the dorsal roots. *Adv Urol*, **2011**(4), 1–7.
Michael, D.B., Guyot, D.R., & Darmody, W.R. (1989). Coincidence of head and cervical spine injury. *J Neurotrauma*, **6**(3), 177–89.
Multidisciplinary Association of Spinal Cord Injured Professionals (2012). *Guidelines for Management of Neurogenic Bowel Dysfunction in Individuals with Central Neurological Conditions*. https://www.mascip.co.uk/wp-content/uploads/2015/02/CV653N-Neurogenic-Guidelines-Sept-2012.pdf
Nielsen, J.B., Crone, C., & Hultborn, H. (2007). The spinal pathophysiology of spasticity? from a basic science point of view. *Acta Physiologica*, **189**(2), 171–80.
Noreau, L., Proulx, P., Gagnon, L., Drolet, M., & Laramée, M.T. (2000). Secondary impairments after spinal cord injury: a population-based injury. *Am J Phys Med Rehabil*, **79**, 526–35.
Reines, H.D. & Harris, R.C. (1987). Pulmonary complications of acute spinal cord injuries. *Neurosurgery*, **21**(2), 193–6.
Rowan, C.J., Gillanders, L.K., Paice, R.L., & Judson, J.A. (2004). Is early enteral feeding safe in patients who have suffered spinal cord injury? *Injury*, **35**(3), 238–42.
Scope (2018). *Spinal Cord Outcomes—Scope—Partnership Endeavor*. http://scope-sci.org/trials/
Siddall, P.J, Cousins, M.J., Otte, A., Griesing, T., Chambers, R., & Murphy, T.K. (2006). Pregabalin in central neuropathic pain associated with spinal cord injury. *Neurology*, **67**, 1792–800.
Siddall, P.J., Molloy, A.R., Walker, S., Mather, L.E., Rutkowski, S.B., & Cousins, M.J. (2000). The efficacy of intrathecal morphine and clonidine in the treatment of pain after spinal cord injury. *Anesth Analg*, **91**, 1493–8.
Snoecx, M., De Muynck, M., & Van Laere, M. (1995). Association between muscle trauma and heterotopic ossification in spinal cord injured patients: reflections on their causal relationship and the diagnostic value of ultrasonography. *Paraplegia*, **33**, 464–8.
Snoek, G.J., IJzerman, M.J., Hermens, H.J., Maxwell, D., & Biering-Sorensen, F. (2004). Survey of the needs of patients with spinal cord injury: impact and priority for improvement in hand function in tetraplegics. *Spinal Cord*, **42**(9), 526–32.
Subbarao, J.V. & Garrison, S.J. (2016). Heterotopic ossification: diagnosis and management current concepts and controversies. *J Spinal Cord Med*, **22**(4), 273–83.
Sullivan, M.P., Torres, S.J., Mehta, S., & Ahn, J. (2013). Heterotopic ossification after central nervous system trauma. *Bone & Joint Res*, **2**(3), 51–7.
van Kuijk, A.A., Geurts, A., & van Kuppevelt, H. (2002). Neurogenic heterotopic ossification in spinal cord injury. *Spinal Cord*, **40**(7), 313–26.
World Health Organization (2011). *ICF: International Classification of Functioning, Disability and Health*. Geneva, Switzerland: World Health Organization. https://www.who.int/classifications/icf/en/

RELATED LINKS TO EBRAIN

Aetiology and Management of Pressure Sores. https://learning.ebrain.net/course/view.php?id=532
Autonomic Dysfunction. https://learning.ebrain.net/course/view.php?id=534
Clinical Gait Analysis in Rehabilitation Medicine. https://learning.ebrain.net/course/view.php?id=545
Maintaining Activities of Daily Living. https://learning.ebrain.net/course/view.php?id=554
Management of Spasticity and Associated Features. https://learning.ebrain.net/course/view.php?id=787
Orthotics and the Avoidance and Management of Contractures. https://learning.ebrain.net/course/view.php?id=546
Role of Occupational Therapy in Neurorehabilitation. https://learning.ebrain.net/course/view.php?id=556
The Management of Posture and Mobility. https://learning.ebrain.net/course/view.php?id=786
Vocational Rehabilitation Following Neurological Trauma or Illness. https://learning.ebrain.net/course/view.php?id=541

SECTION 15

Peripheral nerve surgery

71. **Electrodiagnostics** *827*
Alan Forster and Robert Morris

72. **Entrapment syndromes** *839*
Grainne Bourke and Mobin Syed

73. **Supraclavicular brachial plexus and peripheral nerve injuries** *847*
Jonathan Perera and Marco Sinisi

74. **Peripheral nerve tumours** *855*
Rikin Trivedi and Vincent Nga

71

Electrodiagnostics

Alan Forster and Robert Morris

Introduction

Clinical neurophysiology provides valuable information in neurosurgery, serving as: a diagnostic tool that can quantify type and severity of damage to the central and peripheral nervous system, a means of monitoring the safety of structures within and around the surgical site, and a method to map structures. As such it aids in identifying structures (e.g. finding sacral nerve roots within a spinal lipoma or nuclei within the thalamus), assessing functional integrity (e.g. motor pathways from cortex to any relevant accessible muscle), and monitoring their function while surgery occurs near to structures (e.g. VII while retracting during trigeminal microvascular decompression, and in scoliosis surgery) providing guidance for technical operative steps (e.g. for selective dorsal rhizotomy).

Intraoperative monitoring is not new, though the advances in equipment and technique of recent years have seen an explosion in the useful ways that neurophysiology can aid the neurosurgeon and protect the patient. The development of techniques to localize epileptic foci and map eloquent cerebral cortex in the 1950s (Penfield and Jasper, 1954) produced major scientific advances as well as revolutionizing epilepsy surgery. Since the 1960s Tasker in Toronto, and Gillingham in Edinburgh, were recording from microelectrodes in the human thalamus to guide movement disorder surgery. Pioneers such as Møller have extended the applications of neurophysiological monitoring in skull base surgery (Møller et al., 1981; Møller et al., 1982; Møller and Jannetta, 1983).

This chapter describes neurophysiological mapping and monitoring, and the different tools that are useful in different situations.

Normal neuron physiology–basic principles

Neurons consist of a neuronal body, dendrites, and an axon. The dendrites and body process information from other neurons, while the axon initiates self-propagating electrical signals (the action potential) in response to such information, which cause the release of neurotransmitters at the synapse. The synapse is the junction where two neurons in close proximity are able to transfer information. The basics of normal neuron physiology are shown in **Figure 71.1**.

Action potential/membrane potentials

An action potential occurs when the cell membrane is depolarized to a threshold value. The resting membrane potential is around –60–70 mV. This potential is caused by differences in ion concentration between intra- and extracellular fluid. Membrane potential fluctuates in response to external stimuli which alter permeability to specific ions. Such stimuli can consist of electrical current across the membrane, or the action of neurotransmitters in the extracellular fluid. These stimuli cause the opening of specific ion channels, increasing the permeability of the membrane to that ion and driving the membrane potential towards the equilibrium potential for that ion.

Neurotransmitters that increase membrane permeability to sodium or calcium cause depolarization (membrane potential moves towards 0 mV), while increased permeability to potassium or chloride causes hyperpolarization (membrane potential moves away from 0 mV). The threshold value for an action potential is around –60 to –50 mV. At this threshold, a cascade of voltage gated sodium channel activation leads to a sudden increase in sodium permeability causing a rapid change in membrane potential which propagates along the membrane at speeds of up to 100 m/s in myelinated axons. An action potential can also be generated if a current is applied externally; spontaneous and externally generated volleys of nerve impulses are both useful in clinical testing.

Synaptic function

The synaptic cleft measures around 20 nm. When an action potential arrives at the presynaptic membrane, neurotransmitters are released into the synaptic cleft and bind to receptors on the postsynaptic membrane, opening ion channels, and triggering a change in voltage across the membrane. Thus, electrical changes in the presynaptic membrane can bring about changes in the postsynaptic membrane. Gamma aminobutyric acid (GABA) is the most common inhibitory neurotransmitter. GABA binds to GABA A receptors which open chloride channels, hyperpolarizing the postsynaptic membrane, or GABA B receptors which are linked through G-proteins to potassium channels that act to hyperpolarize the postsynaptic membrane. Glutamate is an excitatory neurotransmitter which binds to the N-methyl-D-aspartate (NMDA) receptor, AMPA receptor, and kainite receptors. These receptors open cation channels that allow sodium, potassium, or calcium ions in to the postsynaptic neuron,

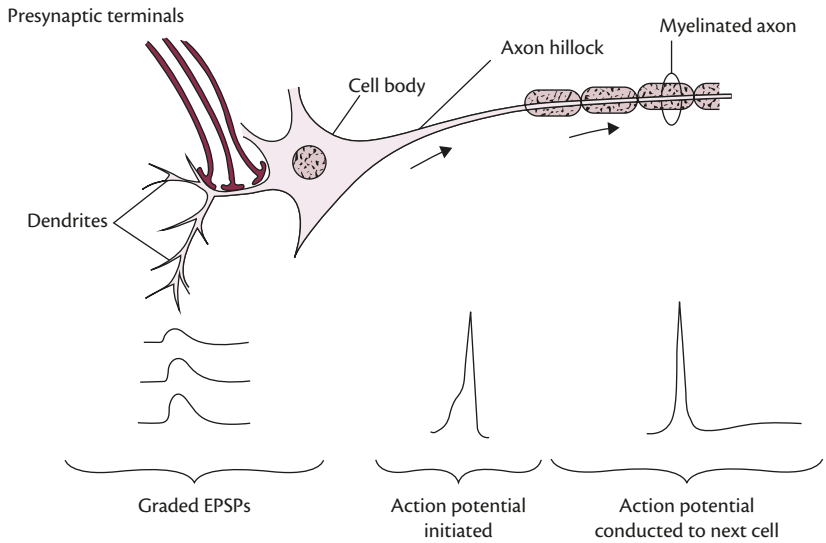

Fig. 71.1 Neuronal electrical activity from its initiation by excitatory postsynaptic potentials (EPSPs) to its transmission as an action potential to another area.

Reproduced with permission from Devon, Rubin & Daube, *Clinical Neurophysiology*, 4E, Oxford University Press, Oxford, UK, Copyright © 2016. By permission of Oxford University Press.

causing membrane depolarization. The neurones can be activated or inhibited by input from dentrites of other neurons.

Classification of types of nerve fibres

Peripheral nerve fibres are classified based on diameter, conduction velocity, and myelination state. The A fibres are larger diameter and myelinated, and have high conduction velocity (10–100 m/s). They are subdivided into:

A alpha fibres in muscle spindles and Golgi tendon organs.
A beta fibres in cutaneous mechanoreceptors, and as secondary muscle spindle receptors.
A gamma fibres are motor neurons controlling muscle spindle activation.
A delta fibres conduct fast painful stimuli as free nerve endings.

B fibres have smaller diameter and are myelinated. They are autonomic nerves with a conduction velocity of up to 15 m/s. C fibres are small and unmyelinated. Conduction velocity is hence lower, up to 2 m/s. They transmit slow pain signals and temperature.

Principles of neurophysiology relevant to neurosurgery

Electroencephalogram

The electroencephalogram (EEG) records variations in electrical activity from different areas of the head, and can be recorded through the scalp, from the cortical surface using, for example, subdural strips or grids (electrocorticography, ECoG) or from depth electrodes within the brain (stereoencephalography, SEEG). It represents a compound electrical field that originates mainly from postsynaptic potentials. The electric field is measured in the form of a voltage difference between two points, and each channel of an EEG represents the difference between two specific sites. These can be averaged to a single common reference point or measured between EEG electrodes. The '10–20' system is commonly used but does not always provide adequate anterior temporal coverage and so is often supplemented with additional electrodes.

Figure 71.2 shows the surface EEG from an adult patient who presented with seizures: standard 10–20 electrode positions used—odd numbers left, even right: F = frontal, Fp = frontopolar, P = parietal, O = Occipital, T = Temporal X1-X2—spare channel, used here for electrocardiogram (ECG) lead 1. Normal 'alpha' rhythm seen, for example, in channel 16 (T5-O1): the slow activity in channels 9, 10, and 11 is the result of damage from an underlying glioma in this region. The 'compressed spectral density' top right here does show the location of the slow activity—measured at position of green line in this trace—but such frequency maps can be misleading at times with surface EEG recordings.

Scalp EEG records mainly from cortical gyri and does not give details of deep brain structures such as the hippocampus and basal ganglia, though slow activity can overly tumours (Fig. 71.2), and frontal slow activity in particular can reflect deep midline damage. It can show the location of areas of abnormal function such as seizure foci or space occupying lesions, or show the degree of abnormal function. Spatial resolution is low, and changes often non-specific, but time resolution is superior to functional imaging. Scalp EEG can be a guide to depth of anaesthesia, and is used in intensive care. Head injured patients may show subclinical seizures. In one study, of 144 monitored head injured children, 30% showed seizure activity correlating with duration of ITU stay (O'Neill et al., 2015).

EEG can also monitor some vascular procedures such as in aneurysm surgery and carotid endarterectomy. Continuous EEG shows immediate asymmetries produced by ischaemia and although somatosensory evoked potential (SSEP) can be more sensitive, nevertheless with SSEP it takes time for averaging to record the warning changes. EEG 'raw' or processed 'cerebral function analysing monitor' (CFAM) showing an acute drop in activity can be a sensitive guide for the need of shunt insertion during carotid

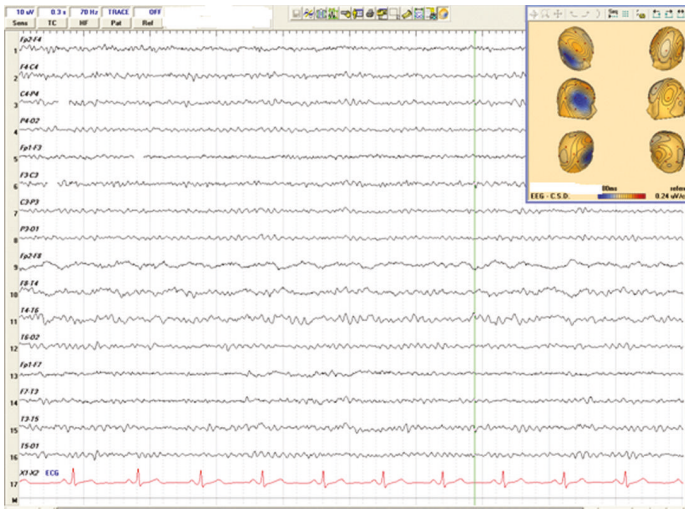

Fig. 71.2 Surface EEG from an adult patient who presented with seizures.

endarterectomy. As the CFAM displays the previous two seconds of processed EEG continuously, the response is almost immediate. EEG or cerebral function monitor can give a guide to the establishment of satisfactory burst suppression if barbiturates are used to reduce cerebral activity.

Electrocorticography (ECoG) and stereo electroencephalography (SEEG) is used for defining epileptogenic foci in the workup for, and during, epilepsy surgery. Recording seizure onset and spread during video telemetry guides the planning of surgery, and at times in theatre may be used to guide extent of resection. In addition to recording through such electrodes, stimulation can be performed to map cortical function or provoke seizures (Cossu et al., 2012). Single pulse electrical stimulation (SPES) can be used as an active technique to demonstrate areas of cortical excitability (Valentín et al., 2002). Use of such techniques is used to guide surgery in complex epilepsy cases.

Evoked potentials

An evoked potential (EP) is an electrical signal generated in response to an external stimulus. This should be contrasted with the spontaneous potentials recorded during investigations such as EEG and electromyography (EMG). These can test a huge range of pathways including motor evoked potentials (MEP), somatosensory evoked potentials (SSEP), visual evoked cortical potentials (VEP), brainstem auditory evoked potentials (BSAEP), and electroretinography (ERG). Most are attenuated or blocked completely by anaesthetic agents, with the best results in theatre being obtained by total intravenous anaesthetic with propofol and remi-fentanyl. Muscle paralysis blocks MEPs and EMG, although if paralysis is administered during intubation it has usually worn off by the time monitoring is required.

Motor evoked potentials (MEP)

MEPs can be recorded wherever distal muscle is accessible, down to the level of S3, and can be used in patients under general anaesthesia to reduce risk of damage to corticospinal tracts during cranial (and spinal) surgery (Fig. 71.3). Responses are recorded in theatre with a contralateral 'homunculus of needles', preferentially using muscles with the largest cortical representation. A representative scheme comprises:

- Mentalis
- Deltoid or biceps
- Extensor digitorum communis
- Abductor pollicis brevis
- Abductor digiti minimi
- Vastus medialis
- Tibialis anterior
- Abductor hallucis

Recordings are commonly from paired needles in the muscles supplied by the relevant pathways, or from along the motor pathway distal to the motor stimulus—termed D waves (direct waves) recorded directly from the spinal cord with electrodes placed in the subarachnoid or the epidural space. D waves are usually elicited with single transcranial stimuli in anaesthetized subjects and they are the most reliable guide to damage to the corticospinal pathways in spinal surgery, but if electrodes move false positive results can occur (Ulkatan et al., 2006).

Stimulation used includes transcranial electrical or magnetic stimulation, direct cortical, subcortical, corticospinal tract (including intraspinal) and peripheral nerve stimulation. Magnetic stimuli can be used preoperatively to map motor and speech areas. During anaesthesia trains of electrical stimuli are normally employed. A 'train of 5' is commonly used, consisting of five pulses with an interpulse interval of 2–4 ms. Taniguchi described stimulation of primary motor cortex with these high frequency (300–500 Hz) pulses to map motor cortex with a monopolar probe, and monitor the corticospinal tract under anaesthesia—usually from a subdural strip electrode contact on the cortex (Taniguchi et al., 1993). In awake procedures the cathode is better located in an anaesthetized area of scalp (e.g. the vertex). Motor tract monitoring under anaesthesia is also feasible during insular glioma resection—first locating motor cortex using SEP phase reversal with a subdural strip, then using contact over the motor cortex to stimulate (as anode—a scalp electrode as frontal cathode). Motor responses can be evoked during resection, allowing therapeutic action to be taken (rest, irrigation, papaverine) if MEPs deteriorate during surgery (Neuloh et al., 2007a). Stimulation of the facial colliculi with a probe gives recordable responses in the face and tongue and may be used to navigate the floor of the fourth ventricle if it is distorted, and to define the midline and safe entry zones to brainstem tumours (Sala et al., 2007). In spinal surgery motor responses from corticospinal tract stimulation can indicate medial pedicle breach: or adjacent corticospinal pathways in intramedullary tumour procedures.

Somatosensory evoked potentials (SEPs)

Peripheral stimulation evokes a response that can be recorded proximally within the nervous system (Fig. 71.4). For example, stimulation of the median or posterior tibial nerves can be recorded at the nerve roots, over the spinal cord, in the brainstem, and the sensory cortex. Median somatosensory response (SEP) is elicited by electrical stimuli—about 200 stimuli applied at the wrist—giving responses normally detectable by averaging at Erb's point, over the cervical spine, and cortex. Latency increases and reduced amplitude of responses indicate pathology at all levels of wrist-cortex.

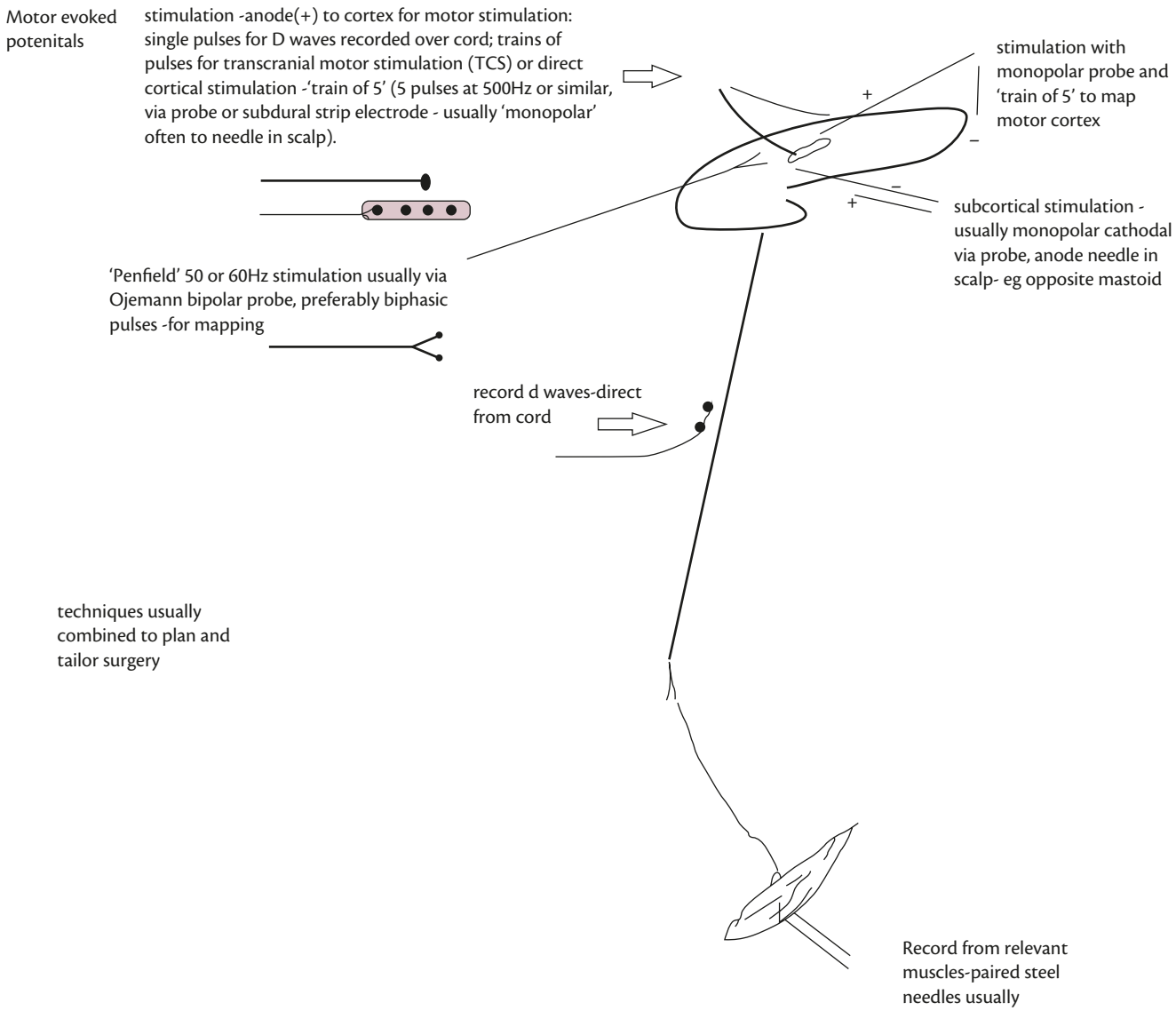
Motor evoked potenitals
stimulation -anode(+) to cortex for motor stimulation: single pulses for D waves recorded over cord; trains of pulses for transcranial motor stimulation (TCS) or direct cortical stimulation -'train of 5' (5 pulses at 500Hz or similar, via probe or subdural strip electrode - usually 'monopolar' often to needle in scalp).
stimulation with monopolar probe and 'train of 5' to map motor cortex
+
–
–
+
subcortical stimulation - usually monopolar cathodal via probe, anode needle in scalp- eg opposite mastoid
'Penfield' 50 or 60Hz stimulation usually via Ojemann bipolar probe, preferably biphasic pulses -for mapping
record d waves-direct from cord
techniques usually combined to plan and tailor surgery
Record from relevant muscles-paired steel needles usually

Fig. 71.3 Motor evoked potentials—stimulus can be transcranial: usually magnetic for preoperative mapping, electrical transcranial 'train of 5' in theatre for monitoring entire pathway. Applied via a subdural strip or probe direct to cortex when accessible: localization of motor areas at cortical and subcortical levels via probe stimulation. Recording distally can be over cord (D waves) or more usually muscle (MEPs): for spinal work recording from a muscle above the surgery acts as a control.

The response from sensory cortex, a negative waveform at 20 msec (N20), like the EEG, localizes sensory cortex, and is an indicator of cortical function. The N20 can be lost with ischaemia from vascular spasm (e.g. in aneurysm or insular surgery). In the ITU if the median SSEP cortical response is lost, but the subcortical (e.g. cervical N13) response present, it suggests cortical function is compromised and a poor outcome probable. The equivalent cortical response from posterior tibial stimuli at the ankle gives a cortical P40 response. Posterior tibial responses travel in the gracile fasciculus; recording this response over the cord from left and right ankle stimuli gives a guide to the midline of the cord and can be useful to find safe entry if anatomy is distorted over intramedullary tumours. This is mainly used to monitor posterior column function in the cord in spinal procedures rather than motor function. Stimulation over the back of the cord, can give sensory responses at ankle and scalp (and motor in leg muscles), as an alternative technique (Quinones-Hinojosa et al., 2002; Yanni et al., 2010).

Loss of responses during cord or cortical surgery must be appropriately interpreted and does not always predict loss of function. Changes may occur due to retraction, vascular events, or dislodged stimulating or recording electrodes. Pressure due to poor limb positioning can result in plexus palsies, also detected by loss of response, reversible with adjustment of the relevant limb.

Recording below and above the surgical site aids interpretation. As several roots are stimulated single root damage might not be detected by SSEPs. In brachial plexus surgery two level lesions can occur. If stimulation of a proximal nerve stump can elicit a cortical SSEP, there must be continuity of some contributing fibres at root level indicating that all roots cannot be avulsed.

Brainstem auditory evoked potentials

Intraoperatively click stimuli are applied via an insert earpiece. About 1000 EEG responses are averaged, with electrodes normally placed at the mastoid and vertex. The normal response gives five

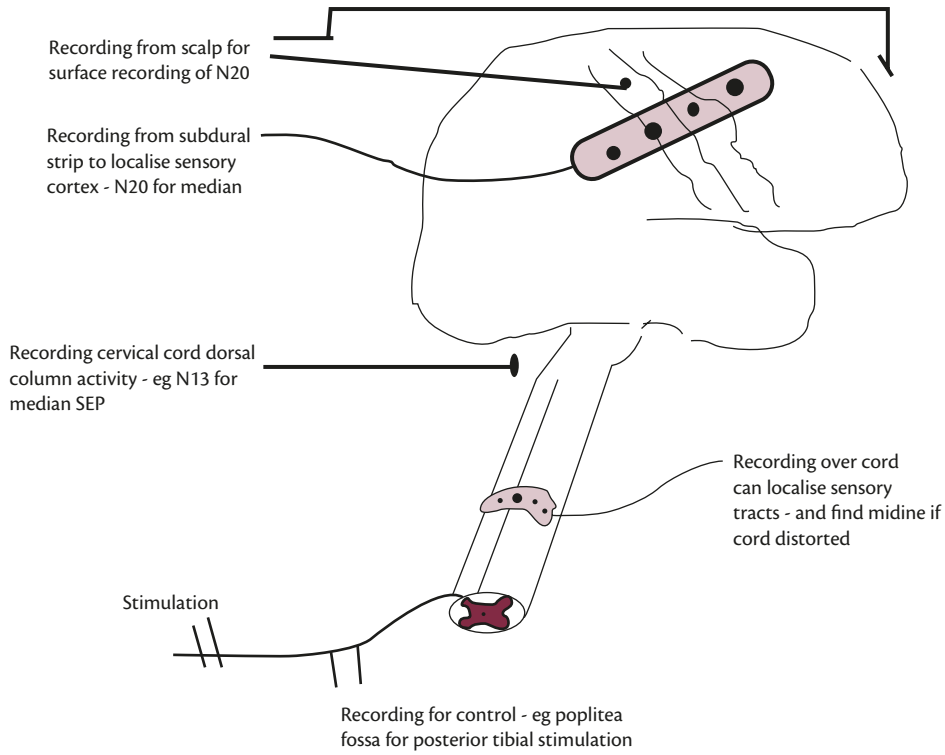
Recording from scalp for surface recording of N20
Recording from subdural strip to localise sensory cortex - N20 for median
Recording cervical cord dorsal column activity - eg N13 for median SEP
Recording over cord can localise sensory tracts - and find midine if cord distorted
Stimulation
Recording for control - eg poplitea fossa for posterior tibial stimulation

Fig. 71.4 SSEP. Peripheral nerve stimulation (commonly median or posterior tibial). Visible twitch confirms stimulation: control recording a useful check (e.g. cubital fossa or erbs for median, popliteal fossa commonly for posterior tibial): recording possible over cord, in brainstem, any accessible locations to cortex, where a negative response on the posterior bank of the Rolandic sulcus coupled with a positivity on the motor bank can be used to locate somatosensory cortex by a phase reversal when recorded from subdural strip. It is also worth noting that recording over cord: stimuli to cord here can generate both sensory responses at ankles, or cortical responses, to localize midline.

early waves with III and V often the clearest. Potentially damaging manipulations or retraction of the auditory nerve increases the latency of waves III and V. V increase more than 0.9 ms gives a measurable alteration of audiogram: 50% amplitude loss and 1 mSec latency shift of wave V normally is considered likely to show postoperative hearing deficit. Reducing retraction or resting usually allows the response to recover.

The main applications of BAEPs are in cerebellopontine angle procedures such as trigeminal neuralgia, acoustic neuroma, and hemifacial spasm surgery. A direct response to a 500 Hz tone can be recorded directly in theatre and locate auditory fibres within an acoustic neuroma (Butler et al., 1995). Click stimuli can also be recorded with electrodes directly on the nerve in theatre to localize and assess function.

In head injury, longer latency auditory evoked responses are good indicators of outcome (Fischer et al., 2008).

Nerve conduction studies (NCS)

Measurement of conduction velocity along a peripheral nerve can test motor, sensory, and reflex pathways. NCS should always be interpreted in the appropriate clinical context.

Components of the study include:

1. The motor component (M wave), measured by stimulation of a peripheral nerve and recording from a muscle innervated by that nerve (e.g. abductor pollicis brevis for the median nerve). Measurements include latency (time from stimulation to recording) and amplitude, and are affected by lesions in the anterior horn cell body, axon, Schwann cells, neuromuscular junction, or the nerve itself.
2. The sensory component, measured by recording from another point on the nerve rather than from muscle. Sensory amplitudes are smaller than motor amplitudes.
3. The F-wave results from an antidromically conducted action potential in the motor axon which, on arrival at the spinal cord, causes the anterior horn cells to fire and cause a late muscle contraction. The F-wave latency measures conduction between limb and spine, rather than within a segment of the limb, and both afferent and efferent action potentials are carried in the motor axon.
4. The H-reflex study is another form of late response that effectively measures the muscle stretch reflex. For example by stimulating the tibial nerve in the popliteal fossa and recording over soleus, can be used to distinguish L5 (H-reflex present) and S1 (H-reflex absent) radiculopathies.

The amplitude of an orthodromic sensory nerve action potential (SNAP) gives a measure of the number of functioning sensory axons. Thus, the ulnar SNAP is reduced not only with ulnar problems at the elbow, but also with any other postganglionic damage to C8 fibres (e.g. generalized diabetic neuropathy or thoracic outlet syndrome). Findings must be interpreted in the clinical context. In brachial plexus injury, sensory amplitudes are a guide to severity, root level, and pre- or postganglionic location. It should be noted that the distal part of a severed nerve still functions for about a week before Wallerian degeneration occurs. Responses recorded the day

after injury must not be misinterpreted. Cervical problems usually give abnormality proximal to the ganglion, so despite a numb hand, sensory potentials are preserved.

Conduction block will occur with pressure on a nerve (e.g. ulnar or peroneal neuropathy). Changes with increasing pressure will initially give conduction block, then localized slowing: as axons die, amplitudes reduce with sensory axons affected before motor.

Motor conduction studies (Fig. 71.5) give responses (compound motor action potentials—CMAPs) from muscles, where amplitude reflects the number of axons/muscle fibres activated. Small responses are seen in axon loss and muscle wasting while latency from distal stimulation point increases with local demyelination (e.g. carpal tunnel syndrome, Guillain Barre, and reinnervating fibres after nerve section).

Repetitive stimulation stresses the neuromuscular junction and can be used to look for myasthenia and related conditions (Kimura, 2001).

NCS aids diagnosis of entrapment neuropathies such as carpal tunnel syndrome (CTS). Local entrapments of nerves commonly produce localized slowing of conduction (see Fig. 71.5). Clinical diagnosis can be misleading in CTS, with accuracy of clinical referral about 50%, and nerve conduction studies should be performed prior to offering surgery. Severity depends on the degree of median nerve slowing compared to the equivalent ulnar velocity across the wrist (Fig. 71.5). Sensory velocity slowing is the most sensitive finding, with motor latency only increased in more severe disease (Bland, 2016).

For ulnar nerve compression localization, reduced motor velocity around the elbow and amplitude drop (50% drop = conduction block), and the 'inching' technique can localize ulnar entrapment preoperatively (Kimura, 2013). The latter technique used intraoperatively has shown the location of localized slowing, and improved outcomes (Kim et al., 2003).

Electromyography (EMG)

Electromyography (EMG) measures the electrical activity of muscle membranes from surface electrodes or needle electrodes. Voluntary muscle contraction recruits motor units with good activation giving a full 'interference pattern' (Fig. 71.6A). If there is axonal loss within a nerve, full voluntary muscle contraction will generate fewer units, or even a single unit, firing at high rates due to abnormal recruitment (Fig. 71.6B).

In nerve injury, the presence of even a single firing unit confirms the presence of at least one axon in continuity with the muscle. This is valuable in assessment of plexus injuries, or as evidence that reinnervation is occurring. With complete denervation lasting for around three weeks, the muscle membrane develops 'denervation hypersensitivity' and recordings will show spontaneous activity such as fibrillation and positive sharp waves (Fig. 71.6C). Spontaneous discharges can also occur in pathologies including myotonia and myositis. The variation of firing of different muscle fibres within a motor unit gives a measure of the 'jitter'. This increases with unstable end plates (e.g. in myasthenia, or with reinnervating unstable terminal axons). The distribution of abnormal muscles on EMG, in conjunction with the clinical and nerve conduction findings, can distinguish and localize pathologies such as radiculopathy, entrapment, and peripheral neuropathy, motor neurone disease, and multifocal conduction block.

EMG can prove useful in theatre when a motor nerve that supplies an accessible muscle is at risk of injury. A free running EMG can display activity in both visual and audible form so irritation to a nerve will alert the surgeon. For example, a pair of needles in a facial muscle will record a discharge when the facial nerve is irritated during acoustic neuroma resection. The response is not linear, so initial discharges may be brief while further insults may give longer lasting discharges for many minutes. Type of discharge varies, and correlates with severity of nerve insult-in facial nerve monitoring during vestibular schwannoma resection the detection of the A train (a pattern of high frequency and homogenous appearance) in muscles supplied by the facial nerve, is a reliable indicator of facial nerve paresis postoperatively (Prell et al., 2007).

Intraoperative monitoring

Intraoperative single cranial nerves monitoring

CN II

The optic nerves and visual pathways may be monitored by flash stimuli giving visual evoked responses that can be recorded from the occipital cortex (Sasaki et al., 2010). Responses can be recorded from optic tracts in anaesthetised patients. In the awake patient stimulation of the optic tract causes phosphenes, while visual pathway stimulation within association cortex can elicit formed visual memories.

CN III, IV, V, VI, VII, IX, X, XI

These cranial nerves may be monitored with free running and stimulated EMG, using both monopolar or bipolar probe stimulation. For the third, fourth, and sixth nerves, the needles are inserted into the extraocular muscles.

Trigeminal nerve EMG is normally recorded from masseter, but free running and stimulated EMG only assesses the motor component of the mandibular division. The blink reflex can test sensory pathways—single stimuli awake, in theatre monitored by trains of stimuli. In the cavernous sinus, V1 and V2 can be detected by stimulation from a probe intraoperatively, recording from facial muscles (Al Masri et al., 2014): trains of stimuli may best elicit the R1 blink reflex response here.

The facial nerve can be localized using stimulation before it is visible during vestibular schwannoma surgery. However, if the nerve is severed, stimulation distal to the injury will still give a response. In addition, spread of excessive stimulation—'current jump'—can be misleading, or conversely stimulus applied to pooled saline may result in current shunting and a failure of stimulation.

In trigeminal microvascular decompression for trigeminal neuralgia VIII is at risk—mainly from retraction—thus the auditory evoked response is the main nerve monitored.

In hemifacial spasm the irritation that produces the spasm alters the 'lateral spread' of a response like an F-wave (e.g. stimulation of the facial zygomatic branch giving responses in the mandibular branch supplied muscle mentalis until the irritating vessel is removed). When this is lifted from the seventh nerve, the 'lateral spread response' is modified and usually vanishes. The response resolving suggests a good outcome likely. As in trigeminal neuralgia, retraction on the eighth nerve can affect hearing—the BAEP is thus often monitored here.

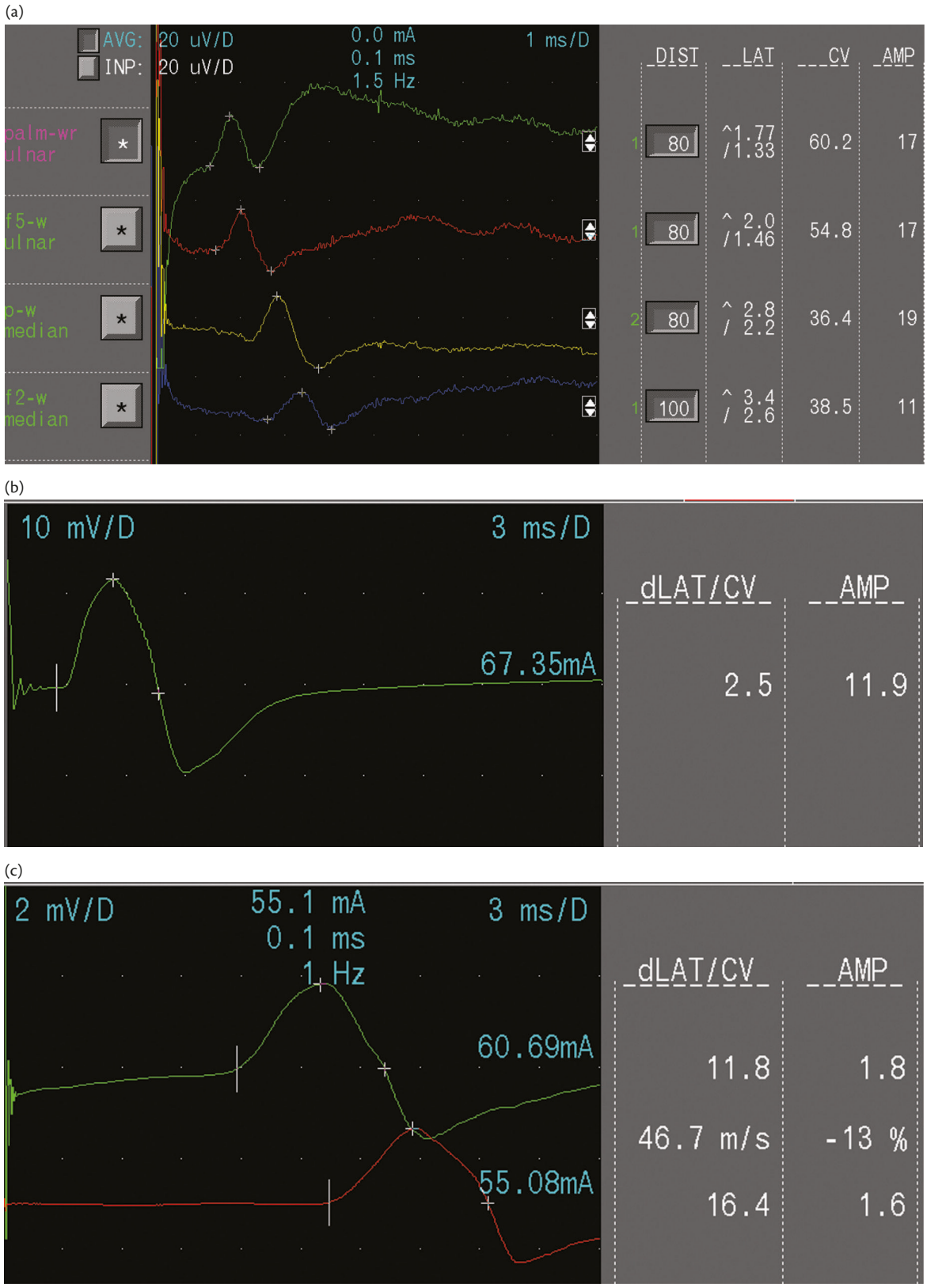

Fig. 71.5 (A) Palm to wrist velocity of 36.4 M/Sec significantly slower than the equivalent ulnar value of 60.2 M/Sec, and finger to wrist median value at 38.5 M/Sec also significantly slower than ulnar at 54.8 M/Sec. (B) With normal median distal motor latency (ii) (wrist to abductor pollicis brevis) this is a mild carpal tunnel syndrome. (C) This subject has median motor response delayed at 11.8 mSec from stimulation at wrist—more severe carpal tunnel syndrome. Second response, from stimulation at elbow, permits median motor conduction to be checked elbow to wrist. (Note other nerves tested gave normal responses -i.e. not part of a generalized problem.)

Fig. 71.6 (A) Normal EMG interference pattern in biceps. (B) Severe reduction of interference pattern to a discrete unit. (C) Fibrillations and positive sharp waves in a largely denervated abductor pollicis brevis, suggesting a postganglionic C8/T1 lesion.

VIII nerve may be monitored with BSAEP in very small acoustic neuroma tumours: direct recording from auditory fibres also possible. Responses are often unrecordable with compromised hearing on the affected side. If the tumour is larger brainstem may be monitored by BSAEP from the other ear, and long tracts by SSEPs.

Transcranial motor stimulation can give responses from cranial nerve supplied muscles, conforming continuity of their cranial nerves: stimulation artefact is a problem—long latency responses recorded from throat muscles (e.g. cricothyroid, vocalis, hypoglossus, palate) can be easier to record than the direct response—some may reflect part of speech pathways, possibly swallowing. Single stimuli of same intensity are used as controls, as high current levels may activate distal portions of peripheral nerves (i.e. response not transcranial, activating nerve distal to procedure). For some muscles (e.g. vocalis) special fine 'hookwire' electrodes are useful, and less easy to dislodge during long theatre cases. Surface EMG recordings can have specific uses (e.g. laryngeal electrodes applied via surface of an endotracheal tube pick up response from vagal innervated throat muscles), but surface recordings are less able to demonstrate high frequency irritable discharges.

Cortical mapping including awake craniotomy

Cortical mapping is mainly performed to assess motor and speech function. In tumour surgery near eloquent cortex mapping and monitoring of motor function can be assessed in anaesthetised or awake patients, speech function is monitored during awake craniotomies. Mapping motor and speech areas can also be performed preoperatively with functional imaging and magnetic stimulation, which can be combined with intraoperative localization for best outcomes in surgery on/near eloquent cortex (Bello et al., 2008).

Mapping to find safe entry zones, and continuously monitoring motor pathways and locating corticospinal tracts subcortically can be of value both to guide surgery and detect spasm of perforating vessels. To confirm main motor area, 50 or 60 Hz electrical stimulation was used by Penfield and Jasper (1954)—either with bipolar or monopolar stimuli—but most now prefer the 'train of 5' method as described by Tanaguchi and Schramm in 1993.

Motor cortex stimulation normally uses five anodal pulses at 500 Hz. A probe with 2 mm ball at end as the anode is held on cortex and the cathode as a separate electrode such as a needle inserted into the forehead, or vertex as in Figure 71.3). This short high

frequency train appears less likely to induce seizures, and a lower charge is required, than the 50 Hz method. Responses to stimuli can be recorded with paired steel needles inserted into a 'homunculus' of muscles contralaterally and the best responses are commonly seen from muscles with largest cortical representation, that is, typically abductor pollicis brevis, abductor digit minimi (or first dorsal interosseous). We commonly employ these, with mentalis, deltoid, or biceps, extensor digitorum communis, vastus medialis, tibialis anterior, abductor hallucis. In subcortical (including spinal) dissection a probe is used to give cathodal stimulation, with other electrode as anode, for direct stimulation of corticospinal tracts.

This is a simple reliable technique that can show main motor areas in an anaesthetised or awake patient. The motor cortex can be localized by SSEPs showing the Rolandic sulcus (phase reversal, usually from contralateral median stimuli), and motor area localization is confirmed by direct stimulation. SSEP gives a negativity 20 msec after stimulation over the sensory posterior bank of the Rolandic sulcus and a positivity over the anterior bank, localizing the motor cortex. A four-contact (or longer six- or eight-contact) strip electrode placed across the Rolandic sulcus thus can be used to localize motor and sensory cortex. Further mapping can be performed with stimuli from a probe where appropriate. The strip is left in this area and a contact over the motor cortex is stimulated repeatedly to give monitoring of motor tracts throughout. This method developed by Neuloh et al. (2007b) gave excellent results in insular tumours—where vascular spasm may compromise motor pathways. Some 44% of his cases showed deterioration in MEP responses. If these were lost rest, irrigation, and papaverine, restored responses in 29%, but if they did not return, a neurological deficit occurred.

Where a tumour dissection runs below motor areas, mapping of tracts with subcortical stimulation is useful using cathodal, monopolar probe, train of five stimulation. Cathodal stimuli can also be used to localize corticospinal tracts from within spinal tumours (Quinones-Hinojosa et al., 2002).

Awake surgery gives the best patient feedback, and is useful for speech, vision, higher function, and motor monitoring, but it is not suitable for all patients. Motor evoked responses also seen with 'Penfield' 50–60 Hz stimulation—usually with an Ojemann bipolar stimulator in awake procedures, for speech and motor localization (Szelényi et al., 2011). This is more likely to give seizures than 'train of 5', though either can, particularly if stimulation is excessive. These can be treated by irrigation with cold saline/ringer on the cortex. Train of five motor stimulation for an awake patient is as described earlier and a lower current is required. This does not usually cause distress if the cathode is placed in an anaesthetised area (e.g. vertex). Several papers now show significantly better outcomes in awake surgery when tumours are in eloquent areas (Sacko et al., 2011) with more complete excision and with fewer deficits. Large stimuli produce a visible contraction, but smaller stimuli can give easily recordable responses via the needles. When testing a positive response is sought first, giving a threshold before trusting 'negative' stimulation sites. If possible, EEG should be assessed to detect after discharges and detect seizures early. If mapping performed with too high a current there is increased risk of seizures, and the stimulus spread may result in excessive caution and incomplete tumour removal. The seizure risk overall is 4.9% (Serletis and Bernstein, 2007), treatment in this situation normally being by irrigation with cold saline on the seizing cortex. Excessive chemical seizure control from the anaesthetist can render the awake patient too drowsy to cooperate with the awake procedure.

Some speech pathways may be detected in asleep patients by 'train of 5' stimuli eliciting long latency responses in cricothyroid (Deletis et al., 2011), and similar responses may be seen in the palate and tongue.

Supplementary motor area damage gives profound weakness which in general resolves spontaneously over a period of days or weeks. Damage to this area can be detected by inability to perform planned motor tasks (Nakajima et al., 2015), for example, opposing specific digits: this can affect ipsilateral as well as contralateral hands. In theory, if the motor responses are intact from cortical stimulation recording directly from contralateral muscles, and voluntary activation fades, the supplementary motor cortex is being excised. Motor recovery should occur in about a month. Premotor motor area surgery can leave permanent deficit—cortical and subcortical stimulation in awake subjects can again minimize deficit (Rech et al., 2017).

Visual pathways can be located in awake subjects by stimulation eliciting flashes, colours, or visual field changes. In asleep subjects, flashes of light can evoke responses from visual pathways recorded with microelectrodes from optic tract below globus pallidum during deep brain stimulation surgery.

Huge variation exists in areas relevant for speech (Ojemann, 1979). Speech arrest with 50 Hz stimuli is the simplest test, but picture recognition and verb generation test other important components of speech (procedures reviewed in Rofes et al., 2017).

Thus, train of five stimuli give fewer seizures, and are more effective in most situations

Neurophysiology for functional procedures and microelectrode recording

Deep brain stimulation 'DBS' has now evolved to become a major area of neurosurgery. The physiological mechanism responsible for the effects of DBS remain unclear, and different patterns of stimulation have different effects at different targets. Stimuli modulate the activity of adjacent cells or fibres. McIntyre at el suggest depolarization blockade, synaptic inhibition, synaptic depression, and stimulation-induced modulation of pathological network activity' as the four general hypotheses of the effects (McIntyre et al., 2004).

Electrodes implanted, usually with four contacts, can provide a variable stimulus leading to the function at the target area being disrupted with currents passing in various ways between these implanted electrodes. Variable frequencies and currents can be programmed in to modify the effects.

Currently the main targets for movement disorder surgery are the thalamus (mainly for tremor), the globus pallidus (mainly for dystonias or Parkinson's disease), the subthalamic nucleus (for Parkinson's disease) and the more recent pedunculopontine nucleus (again for Parkinson's disease). For Neuropathic pain, targets include VPL of thalamus and periventricular grey matter. Stimulation of the PVG gives a sensation of warmth in the affected region, while VPL gives paraesthesia. Motor cortex stimulation for pain targets the motor cortex and also the anterior cingulate gyrus (Boccard et al., 2014). Numerous other targets include the nucleus accumbens for obsessive compulsive disorder and the hypothalamus for eating disorders.

Neurophysiology can be involved in accurate definition of the targets and in the correct placing of electrodes. Functional procedures

are frequently performed in awake subjects. Stimulation is employed as a means of localization of the target, determining the therapeutic window and determining the proximity of adjacent structures and avoidance of stimulation-induced side effects such as proximity to internal capsule from thalamus giving muscle contraction. In addition, impedance measurement or microelectrode recordings can be considered for guidance of tissue traversed by the electrodes.

Microelectrodes give information about the activity of the target area, but the location of the target electrode is what is critical requiring good imaging, and good targeting technique with either microelectrode or impedance methods. Extracellular microelectrodes are mainly used during DBS surgery to record action potentials from adjacent neurons. White matter shows only occasional spikes, while grey matter shows more continuous activity with patterns that vary from one location to another. This is a useful technique to determine the precise location of targets such as the subthalamic nucleus (STN) in surgery for Parkinson's disease (Fig. 71.7). Spontaneous discharges with frequencies at about 40 Hz which are normally recorded from the STN are increased in Parkinson's disease and reduced in Huntington chorea. The increased firing rate of excitatory glutamatergic STN neurones are responsible for the increased firing in inhibitory GABA-ergic output of GPi resulting in inhibiting thalamic or brainstem targets and thus reduced motor activity in Parkinson's disease. For dystonia, the globus pallidus is often targeted with the subject asleep, as vigorous movement gives technical difficulties. GPi recording in dystonia shows diminished spontaneous discharges evident as change from a tonic to a phasic pattern of the pallidal neurones discharges. This in turn results in reduced inhibition of the thalamus and increased activity in the motor and premotor cortex. The discharge pattern of the advancing activating electrode changes with its location from the putamen, GPe and GPi. Flashes of light can evoke responses from visual pathways and can be recorded with the microelectrode from the optic tract below globus pallidum. Thalamic recordings from Vim may show tremor related rhythmic burst activities.

These neurophysiological techniques were essential to locate targets when imaging technology was not able to demonstrate them clearly. Advances in imaging have resulted in successful DBS implantations without neurophysiological information, although such methods remain controversial (Ashkan, 2008).

Motor and sensory monitoring in spinal surgery

For spinal surgery 'multimodal' monitoring is best practice (Kothbauer et al., 1997). Motor, somatosensory, and EMG techniques are commonly combined. Since the 1970s SSEPs were used in scoliosis surgery (Nash et al., 1977), but could not reliably predict damage to motor pathways. 'Mulimodality monitoring' with motor evoked potentials recorded from peripheral muscles or from the back of the cord (D waves), SEPs, and free running and stimulated EMG. These techniques are considered particularly useful for intramedullary tumours, also being applied in extramedullary tumours, and even for simple decompressive surgery (Ney et al., 2015).

In spinal and conus surgery, again single peripheral nerves can be at risk. EMG activity from irritation of the supplied muscles, and response to a stimulating probe, is currently the main guidance available to the surgeon, but transcranial stimulation is also useful to confirm continuity, and monitor cord function.

Conus tumours and cauda equina surgery can be complex. In complex spinal lipoma surgery neurophysiology is a 'sine qua non' (Pang, 2015). The concentric stimulating probe is recommended with 10/sec stimuli, 0.3–3 mA for roots, or up to 2 mA on the cord. In addition, peroneal and posterior tibial SSEP recording, multiple muscles for EMG and MEP, particularly including sphincters, which are also used for the bulbocavernosus reflex monitoring (Skinner and Vodušek, 2014).

Pedicle screws insertion may risk breaching the pedicle wall. If the screw track is close to the nerve roots, stimulation applied along this track or through the inserted screw can generate a muscle twitch from the stimulated root, or lower segmental levels if the breach is medial and cord is stimulated. Monitoring requires reliable stimulation, and reliable muscle recording. The muscle must be innervated from the tested root and nerve and muscle must function. Recording can be tricky in obese patients if the muscle cannot be easily accessed with the paired recording needles. It is particularly a problem in thoracic levels.

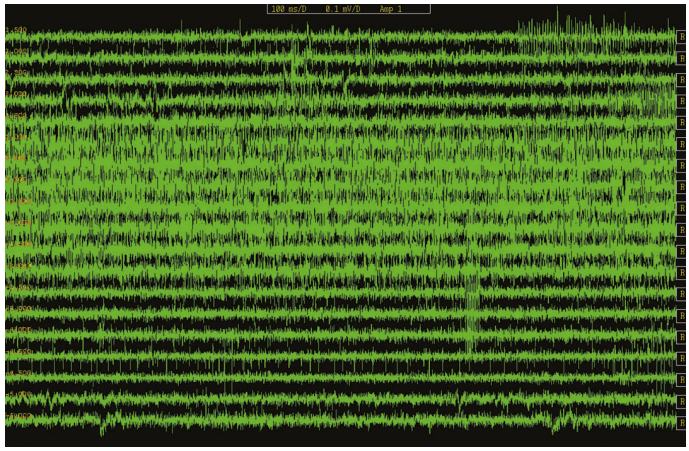

Fig. 71.7 Multicellular activity as recorded with a microelectrode passing through the subthalamic nucleus (STN). Each trace is recorded in sequence as the electrode descends, thus top traces originate deep to STN, with some regular firing cells (top right) probably arising from substantia nigra: increasing activity in the centre where rapidly firing STN cells make a sound through the amplifiers like 'ripping velcro'. Deep brain stimulating lead should be positioned to straddle this zone.

REFERENCES

Al Masri, O.A., Brown, E.E., Forster, A., Kamel, M.H. (2014). Trigeminofacial reflex: a means of detecting proximity to ophthalmic and maxillary divisions of the trigeminal nerve during surgery. *J Neurosurg*, **121**(5), 1271–4.

Bello, L., Gambini, A., Castellano, A., et al. (2008). Motor and language DTI Fiber Tracking combined with intraoperative subcortical mapping for surgical removal of gliomas. *Neuroimage*, **39**(1), 369–82.

Bland, J. (2016). Carpal-Tunnel.net. 2016. *Home Page*. http://www.carpal-tunnel.net/

Boccard, S.G., Pereira, E.A., Moir, L., et al. (2014). Deep brain stimulation of the anterior cingulate cortex: targeting the affective component of chronic pain. *Neuroreport*, **25**(2), 83–8.

Butler, S., Coakham, H., Maw, R., & Morgan, H. (1995). Physiological identification of the auditory nerve during surgery for acoustic neuroma. *Clin Otolaryngol Allied Sci*, **20**(4), 312–17.

Cossu, M., Schiariti, M., Francione, S., et al. (2012). Stereoelectroencephalography in the presurgical evaluation of focal epilepsy in infancy and early childhood. *Neurosurg Pediatr*, **9**(3), 290–300.

Deletis, V., Fernández-Conejero, I., Ulkatan, S., Rogić, M., Carbó, E.L., & Hiltzik, D. (2011). Methodology for intra-operative recording of the corticobulbar motor evoked potentials from cricothyroid muscles. *Clin Neurophysiol*, **122**(9), 1883–9.

Fischer, C., Dailler, F., & Morlet, D. (2008). Novelty P3 elicited by the subject's own name in comatose patients. *Clin Neurophysiol*, **119**(10), 2224–30.

Kim, D.H., Han, K., Tiel, R.L., Murovic, J.A., & Kline, D.G. (2003). Surgical outcomes of 654 ulnar nerve lesions. *J Neurosurg*, **98**(5), 993–1004.

Kimura, J. (2001). *Electrodiagnosis in Diseases of Nerve and Muscle: Principles and Practice*. New York, NY: Oxford University Press.

Kimura, J. (2013). *Electrodiagnosis in Diseases of Nerve and Muscle: Principles and Practice*. Oxford, UK: Oxford University Press.

Kothbauer, K., Deletis, V., & Epstein, F.J. (1997). Intraoperative spinal cord monitoring for intramedullary surgery: an essential adjunct. *Pediatr Neurosurg*, **26**(5), 247–54.

McIntyre, C.C., Savasta, M., Kerkerian-Le Goff, L., & Vitek, J.L. (2004). Uncovering the mechanism(s) of action of deep brain stimulation: activation, inhibition, or both. *Clin Neurophysiol*, **115**(6), 1239–48.

Møller, A.R., Jannetta, P.J., Bennett, M., & Møller, M.B. (1981). Intracranially recorded responses from the human auditory nerve: new insights into the origin of brainstem evoked potentials (BSEP). *Electroencephalogr Clin Neurophysiol*, **52**, 18–27.

Møller, M.B., Møller, A.R., & Jannetta, P.J. (1982). Brainstem auditory evoked potentials in patients with hemifacial spasm. *Laryngoscope*, **92**, 848–52.

Møller, A.R. & Jannetta, P.J. (1983). Monitoring auditory functions during cranial nerve microvascular decompression operations by direct recording from the eighth nerve. *J Neurosurg*, **59**, 493–9.

Nakajima, R., Nakada, M., Miyashita, K., et al. (2015). Intraoperative motor symptoms during brain tumor resection in the supplementary motor area (SMA) without positive mapping during awake surgery. *Neurol Med Chir (Tokyo)*, **55**(5), 442–50.

Nash, C.L. Jr., Lorig, R.A., Schatzinger, L.A., & Brown, R.H. (1977). Spinal cord monitoring during operative treatment of the spine. *Clin Orthop Relat Res*, (126), 100–5.

Neuloh, G., Pechstein, U., Cedzich, C., & Schramm, J. (2007a). Motor evoked potential monitoring with supratentorial surgery. *Neurosurgery*, **61**(1 Suppl), 337–46; discussion 346–8.

Neuloh, G., Pechstein, U., & Schramm, J. (2007b). Motor tract monitoring during insular glioma surgery. *J Neurosurg*, **106**(4), 582–92.

Ney, J.P., van der Goes, D.N., & Nuwer, M.R. (2015). Does intraoperative neurophysiologic monitoring matter in noncomplex spine surgeries? *Neurology*, **85**(24), 2151–8.

Ojemann, G.A. (1979). Individual variability in cortical localization of language. *J Neurosurg*, **50**(2), 164–9.

O'Neill, B.R., Handler, M.H., Tong, S., & Chapman, K.E. (2015). Incidence of seizures on continuous EEG monitoring following traumatic brain injury in children. *J Neurosurg Pediatr*, **16**(2), 167–76.

Pang, D. (2015). Total resection of complex spinal cord lipomas: how, why, and when to operate? *Neurol Med Chir (Tokyo)*, **55**(9), 695–721.

Penfield W., & Jasper, H. (1954). Epilepsy and the Functional Anatomy of the Human Brain. Boston, MA: Little, Brown.

Prell, J., Rampp, S., Romstöck, J., Fahlbusch, R., & Strauss, C. (2007). Train time as a quantitative electromyographic parameter for facial nerve function in patients undergoing surgery for vestibular schwannoma. *J Neurosurg*, **106**(5), 826–32.

Quinones-Hinojosa, A., Gulati, M., Lyon, R., Gupta, N., & Yingling, C. (2002). Spinal cord mapping as an adjunct for resection of intramedullary tumors: surgical technique with case illustrations. *Neurosurgery*, **51**(5), 1199–206; discussion 1206–7.

Rech, F., Duffau, H., Pinelli, C., et al. (2017). Intraoperative identification of the negative motor network during awake surgery to prevent deficit following brain resection in premotor regions. *Neurochirurgie*, **63**(3), 235–42.

Rofes, A., Mandonnet, E., Godden, J., et al. (2017). Survey on current cognitive practices within the European Low-Grade Glioma Network: towards a European assessment protocol. *Acta Neurochir (Wien)*, **159**(7), 1167–78.

Sacko, O., Lauwers-Cances, V., Brauge, D., Sesay, M., Brenner, A., & Roux, F.E. (2011). Awake craniotomy versus surgery under general anesthesia for resection of supratentorial lesions. *Neurosurgery*, **68**(5), 1192–8.

Sala, F., Manganotti, P., Tramontano, V., Bricolo, A., & Gerosa, M. (2007). Monitoring of motor pathways during brain stem surgery: what we have achieved and what we still miss? *Neurophysiol Clin*, **37**(6), 399–406.

Sasaki, T., Itakura, T., Suzuki, K., et al. (2010). Intraoperative monitoring of visual evoked potential: introduction of a clinically useful method. *J Neurosurg*, **112**(2), 273–84.

Serletis, D. & Bernstein, M. (2007). Prospective study of awake craniotomy used routinely and nonselectively for supratentorial tumors. *J Neurosurg*, **107**(1), 1–6.

Skinner, S.A. & Vodušek, D.B. (2014). Intraoperative recording of the bulbocavernosus reflex. *J Clin Neurophysiol*, **31**(4), 313–22.

Szelényi, A., Senft, C., Jardan, M., et al. (2011). Intra-operative subcortical electrical stimulation: a comparison of two methods. *Clin Neurophysiol*, **122**(7), 1470–5.

Taniguchi, M., Cedzich, C., & Schramm, J. (1993). Modification of cortical stimulation for motor evoked potentials under general anesthesia: technical description. *Neurosurgery*, **32**(2), 219–26.

Ulkatan, S., Neuwirth, M., Bitan, F., Minardi, C., Kokoszka, A., & Deletis, V. (2006). Monitoring of scoliosis surgery with epidurally recorded motor evoked potentials (D wave) revealed false results. *Clin Neurophysiol*, **117**(9), 2093–101.

Valentín, A., Anderson, M., Alarcón, G., et al. (2002) Responses to single pulse electrical stimulation identify epileptogenesis in the human brain *in vivo*. *Brain*, **125**(Pt 8), 1709–18.

Yanni, D.S., Ulkatan, S., Deletis, V., Barrenechea, I.J., Sen, C., & Perin, N.I. (2010). Utility of neurophysiological monitoring using dorsal column mapping in intramedullary spinal cord surgery. *J Neurosurg Spine*, **12**(6), 623–8.

RELATED LINK TO EBRAIN

Intraoperative Neurosurgical Electrophysiological Monitoring. https://learning.ebrain.net/course/view.php?id=489

72

Entrapment syndromes

Grainne Bourke and Mobin Syed

Introduction

Peripheral nerve entrapment syndromes are common (Table 72.1). In the upper limb, carpal tunnel syndrome (CTS) accounts for about 90% of entrapment neuropathies. It has an annual incidence of 0.1–0.35% and a reported prevalence between 1% and 7% in the European population (Bongers et al., 2007; Dang and Rodner, 2009). This is far greater than the incidence of ulnar nerve syndromes (0.03%), radial nerve syndromes (0.003%) or meralgia paresthetica (4.3 per 10 000 person-years) (Nordstrom et al., 1998; van Slobbe et al., 2004; Latinovic et al., 2006). Due to the prevalence of CTS in the working population age group the economic effects are significant (Foley et al., 2007).

Pathophysiology

All nerves glide through specific pathways as they pass peripherally to their target organ. It is these pathways composed of bone, ligament, fibrous tunnels, muscle origins and insertions that not only enable effective nerve movement and gliding but also are the potential source of nerve compression. For example, it is the cubital tunnel 'pulley system' (intermuscular septum, arcade of Struthers, epicondylar groove and origin of the flexor carpi ulnaris) that allows for effective movement of the ulnar nerve about the elbow with excursion of 9.8 mm and 14.5 mm in the forearm during flexion and extension of the elbow (Wilgis and Murphy, 1986). However, it is these same structures which we divide to relieve nerve compression.

Anatomical deformity secondary to pressure and alteration of epineural blood flow inducing nerve ischaemia have both been shown experimentally to be induced by nerve compression. The changes seen are dependent on the duration and degree of applied pressure. Early changes induce endoneural oedema altering intraneuronal transport. The increased endoneural pressure disrupts micro-neural circulation resulting in dynamic ischaemia of the nerve. Clinically these microanatomical changes correlate with intermittent paraesthesia and increased sensory thresholds (Ochoa et al., 1972; Rempel et al., 1999; Mackinnon, 2002).

Progressive compression leads to localized demyelination resulting in persistent paraesthesia, numbness, and changes in dexterity. Further prolonged pressure progresses to diffuse demyelination with axonal degeneration manifesting clinically as muscle wasting, permanent sensory abnormalities, and pain (Rempel et al., 1999).

Connective tissue elements, both within and surrounding each nerve, increase where each nerve crosses a joint. This change can contribute to the symptoms of compression as alteration in blood flow to this surrounding sleeve can lead to fibrosis and thickening thus promoting nerve compressive symptoms and interfering with the natural intraneural and extraneural gliding mechanisms (Rempel et al., 1999; Mackinnon, 2002).

Double crush

The double crush concept, first proposed by Upton and McComas in 1973, involves compression along the course of the nerve, insufficient to cause symptoms but leaving the nerve more susceptible to a secondary site of compression. It is then this two-level compression that then yields symptoms. Relieving the nerve compression at one of the sites might be enough to provide symptomatic relief and traditionally the more distal site is addressed first (Upton and McComas, 1973).

Carpal tunnel syndrome

Aetiology

In most patients, the aetiology of CTS remains idiopathic. Histologically these patients have been shown to have increased oedema and fibrous thickening with little inflammation. The compression being greatest at 1 cm distal to the distal wrist crease corresponding to the thickest point of the transverse carpal ligament (Ikeda et al., 2006). Several other local aetiologies which can potentially increase the pressure inside the carpal tunnel have been reported; lipomata, ganglia, haemangiomata, and anatomical anomalies such as a proximal lumbrical origin, Palmaris brevis, or persistent median artery.

Systemic conditions such as diabetes mellitus, rheumatoid arthritis, hypothyroidism, acromegaly, and chronic renal failure predispose patients to carpal tunnel syndrome. In children,

Table 72.1 Entrapment neuropathies of the upper limb with sites of compression (sites listed distal to proximal)

Nerve affected	Location: compression syndrome	Anatomical entrapment
Median	Wrist: carpal tunnel	Under the transverse carpal ligament
	Proximal forearm: pronator syndrome	Compression between the two heads of Pronator Teres or fibrous arch of flexor digitorum superficialis
Anterior Interosseous nerve	Proximal forearm: anterior interosseous nerve	Compression between the two heads of pronator teres or fibrous arch of flexor digitorum superficialis
Ulnar	Wrist	Guyon's canal
	Distal arm/elbow: cubital tunnel	Between the two heads of flexor carpi ulnaris, ligament of Osborne, arcade of Struthers
Radial	Forearm\ Elbow: posterior interosseous entrapment	Arcade of Froshe, between the heads of supinator

muco-polysaccharidosis should be excluded. Pregnancy remains a transient cause with up to 45% of women being affected during the third trimester.

Anatomy of the carpal tunnel

The carpal tunnel is an osseofascial tunnel bounded by the carpal bones and the transverse carpal ligament. This strong fascial structure takes origin from the hamate and triquetrum on ulnar side and tubercle of trapezium and scaphoid on the radial side. The median nerve along with the deep and superficial flexor tendons to the digits and flexor pollicis longus travel through it from forearm to hand. Knowledge of the variation in the anatomy of the median nerve is important during surgical decompression. Considerable variations in the anatomy of the motor branch and palmar cutaneous branch have been reported with extra ligamentous pattern of motor branching being most common (46–90%) while the other less common patterns being subligamentous (31%) and transligamentous (23%).

Clinical presentation

A diagnosis of CTS is established on the evaluation of clinical symptoms, signs, and provocative tests (Table 72.2). Classical symptoms include night time wakening with numbness, tingling in the median nerve distribution and weakness in the thenar muscles. Similar symptoms are reproduced on actions which alter the pressure\volume ratio of the carpal canal such as holding a steering wheel while driving or holding a book while reading. Consensus expert agreement on the clinical diagnostic criteria has been validated by Graham et al. in 2006 (Graham et al., 2006) (Box 72.1).

Perhaps the most commonly used sign is that of Tinel-Hoffmann. This clinical sign describes the tingling felt in the sensory distribution of an injured nerve on percussion. The sensitivities for this sign are poor while the specificity is high for identifying CTS (i.e. a patient is likely to have CTS if they have both a positive Tinel's sign and a history suggestive of CTS), however a negative Tinel's does not exclude the diagnosis (Davis and Chung, 2004). Other

Table 72.2 List of common provocative tests

Nerve	Site of entrapment	Provocative test and explanation of positive test
Median	Carpal tunnel	Tinel-Hoffman's sign: percussion over the carpal ligament produces sensory symptoms in median nerve distribution (circa 1915) Phalen's sign: flexing of the wrist while the forearm is vertical induces symptoms in less than a minute (1966) Reverse Phalen's: extension of the wrist induces symptoms in less than 1 minute Durkan's: direct compression over CT for 30 s with appearance of symptoms in any of the radial digits-sensitivity of 89% and specificity of 96% when performed with calibrated device (1994)
	Proximal Forearm	Pronator teres: onset of symptoms on resisted pronation with elbow in extension Lacertus fibrosus: symptoms on resisted elbow flexion Flexor digitorum superficialis arch: symptoms on resisted middle finger flexion
Ulnar	Guyon's canal	Pressure proximal to Guyon's canal Reverse phalens: extension of the wrist induces symptoms in less than 1 minute
	Cubital tunnel	Tinel's sign: tapping over the Cubital tunnel produces sensory symptoms in ulnar innervated digits Flexion of elbow Pressure proximal to cubital tunnel

provocative tests include Phalen's, reverse Phalen's and Durkan's (Table 72.2). Threshold sensory testing using Semmes-Weinstein filaments and assessment of two-point discrimination are also useful sensory tools (Gelberman et al., 1983). These may demonstrate sparing of the palmar skin as this is supplied by the palmar cutaneous branch which does not travel through the carpal canal.

Investigation

Investigations should be modelled around excluding differential diagnoses including cervical radiculopathy and peripheral neuropathy and evaluating predisposing conditions such as hypothyroidism, diabetes, and inflammatory arthritis. These include blood tests, electrodiagnostic studies, and imaging modalities.

Electrodiagnostic tests can support clinical diagnosis. However, they are only positive if there is demyelination or axonal loss. Those cases where there is intermittent ischaemia and a reversible conduction block will not produce abnormal nerve conduction values. In diabetic patients nerve conduction values are more abnormal.

Neurophysiological grading scales for CTS have been described. Nerve conduction findings correlate with a score for clinical characteristics. Other correlations that were demonstrated included those between the severity of disease and older age groups, mild disease was more common in young females (Padua et al., 1997; Bland, 2000).

In practice nerve conduction evaluation is used for cases where the combination of history and clinical assessment is inconclusive but suggestive of CTS. They are also used for cases of recurrent CTS again to confirm the diagnosis.

Box 72.1 Final list of unweighted clinical diagnostic criteria

Numbness and tingling in the median nerve distribution
Nocturnal numbness
Weakness and/or atrophy of the thenar musculature
Tinel's sign
Phalen's test
Loss of two-point discrimination
Ameliorating/exacerbating factors*
Improvement by splinting and/or steroid injection
Worsening with activities such as driving and strenuous hand use
Coexisting medical conditions*
Pregnancy
Diabetes
Hypothyroidism

**These factors did not contribute significantly to the logistic regression model.*
Reprinted from *The Journal of Hand Surgery*, Volume 31, issue 6, Brent Graham, Glenn Regehr, Gary Naglie, James G. Wright, Development and Validation of Diagnostic Criteria for Carpal Tunnel Syndrome, pp. 919.e1–7, Copyright (2006), with permission from Elsevier.

Ultrasound to determine the cross-sectional area, elasticity, local tissue kinematics, and Doppler studies to study flow characteristics have been proposed as non –invasive modalities. Sensitivities of up to 97.9% have been described which are comparable if not better than those ascribed to nerve conduction studies (85%) (McDonagh et al., 2015).

Anatomical MRI may be indicated to evaluate abnormal median nerve or carpal canal anatomy, including intraneural and extraneural tumours, and vascular anomalies. The role of MRI diffusion tensor imaging is currently under evaluation and as yet is not defined.

Treatment

Non-operative

Modification of the underlying disease such as inflammatory arthritis can relieve symptoms for some patients. CTS resolves in the majority of cases when associated with acromegaly once the condition is successfully treated and has been reported to occur mostly within 6 weeks.

Non-operative strategies such as wrist splints are effective in relieving symptoms and are useful in pregnancy and in early presentation of symptoms in young women. However, evidence supporting night splinting and the comparable benefit of splints compared to other treatment modalities is lacking (Page et al., 2012).

There is evidence to show that methylprednisolone injection has benefit in relieving symptoms up to 10 weeks postinjection but in a randomized placebo-controlled study 75% of patient went on to surgical decompression after steroid injection within 1 year (Atroshi et al., 2013).

Certain other non-surgical treatments have been trialled which include laser therapy, iontophoresis, electroconvulsive therapy, heat therapy, diuretics, and non-steroidal anti-inflammatories; there is however insufficient evidence in support of these.

Injection technique

This is a sterile procedure. The median nerve sits between and deep to the flexor carpi radialis and the palmaris longus just proximal to the wrist crease. The palmar cutaneous branch leaves the nerve on the radial side and travels adjacent to the nerve and does not enter the carpal tunnel (Fig. 72.1).

A combination of one millilitre of steroid and one millilitre of local anaesthetic is used. Triamcinolone acetonide 10 mg per millilitre is most commonly used. Insert the fine bore needle through the skin, directed at 30°, at the level of the wrist crease and just ulnar to the palmaris longus tendon. Draw back on the syringe to confirm the needle is not located intravascularly. There should be no resistance while injecting the fluid. Ask the patient to tell you if they are experiencing tingling or pain, as this means the needle location could be intraneural and should be withdrawn. Complications of injection include intraneural and intravascular placement of the steroid mixture, both of which have serious sequelae.

Operative

This is indicated when non-surgical treatments have failed or when the presentation is with advanced nerve compression (i.e. with loss of sensation or motor deficit). Surgery involves release of the transverse carpal ligament which can be done either open or as an endoscopic carpal tunnel decompression.

Open carpal tunnel decompression is the most commonly practised technique. It is a local anaesthetic procedure in adults and can be performed with or without adrenaline. In the later a tourniquet is needed to ensure good visibility of structures.

An incision is made over the carpal ligament in line with the radial border of the flexed ring finger, parallel to the thenar crease extending proximally to the distal wrist crease. The skin and soft tissues are retracted using self retaining retractors as the carpal ligament is divided under direct vision (Fig. 72.2). This enables the identification of any anatomical variations and avoids injury to the motor branch. A single layered skin closure is performed with absorbable sutures. A simple dressing is applied to enable full mobilization of the hand although it is usual to provide some local pressure over the operation site with advice to elevate the hand for the next 48 hours.

Endoscopic carpal tunnel release was first described by Chow using two ports in 1989. The benefits were immediately apparent: rapid recovery, decreased scarring, and lower postoperative pain (Chow, 1989). Agee modified the access using a single incision technique to view the plane between the flexor synovium and the carpal ligament. This later technique aids in visualization of the deep surface of the carpal ligament (Agee et al., 1994). It can be performed under local anaesthetic, but regional anaesthesia is probably more common.

Carpal tunnel release—open or endoscopic

Both the techniques are practised extensively. There is still controversy in the literature about which technique is best. The key factors to consider in deciding the most appropriate for each healthcare system include complications, time to return to work, cost of equipment, and theatre time and technical expertise.

Historical evidence supports an increased incidence of neurovascular complications and a steeper learning curve in endoscopic carpal tunnel release. A recent multicentre systematic review and meta-analysis did not concur with the higher complication rate (Vasiliadis et al., 2015). Patients having an endoscopic carpal tunnel release have an earlier return to work with less scar tenderness and greater grip strength. They do however have more transient

Fig. 72.1 The median nerve (yellow) sits between and deep to the flexor carpi radialis and the palmaris longus just proximal to the wrist crease. The palmar cutaneous branch 9 purple) leaves the nerve on the radial side and does not enter the carpal canal.

postoperative neurological symptoms. At 6 months the outcomes are no different to open carpal tunnel decompression (Sayegh and Strauch, 2015).

Studies have not shown a substantial difference between the procedural cost of the techniques provided the cost of equipment is disregarded for endoscopic carpal tunnel release (Sayegh and Strauch, 2015). However, for the employed group there is a statistical difference in the time to return to work (8 days earlier in the endoscopic group), which does have a cost advantage for industry (Saw et al., 2003). Thus endoscopic carpal tunnel release should be considered in patients keen on early return to work if appropriate equipment and technical expertise are available.

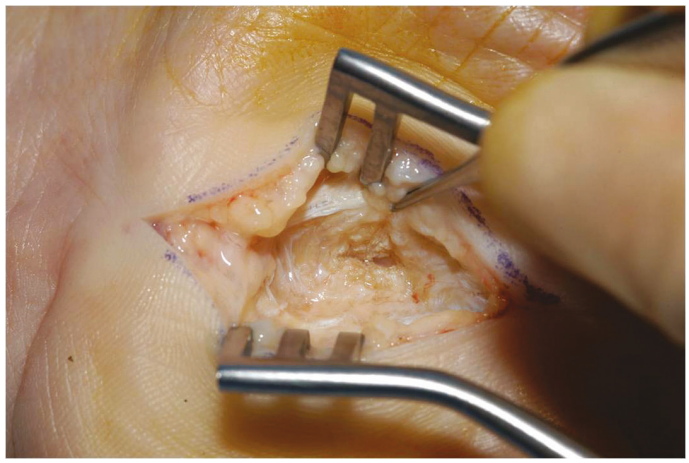

Fig. 72.2 The skin and soft tissues are retracted using a self-retaining retractor as the carpal ligament is divided under direct vision. Layers from superficial to deep; skin, subcutaneous fat, palmaris longus fascial extension, carpal ligament and, at the base, a small opening showing the contents of the carpal canal.

Outcomes and complications

Overall surgical release has good outcomes in 75% but 8% of patients are worse. Patients who have steroid injections have a 70% initial response rate but can relapse with time. A further steroid injection can be equally effective (Bland, 2007). In those over 70 years release does not result in complete relief of symptoms or recovery of function but patient-reported outcomes were statistically better (Leit et al., 2004).

The most common complication with open carpal tunnel decompression is pillar pain reported in about 25% of patients. This is followed by stiffness and swelling. Other reported specific complications include injuries to the motor branch, the palmar branch, or the main trunk of the median nerve and tendon adhesions. Recurrence of symptoms is noted in about 20% of the patients.

Cubital tunnel syndrome

Aetiology

Cubital tunnel syndrome is the second most common compression neuropathy after CTS. It is the most common entrapment neuropathy at the elbow, and it is more common in men. It has an incidence of 20.9 cases per 100 000 person-years (Mondelli et al., 2005). Cigarette smoking is a risk factor probably related to its pathophysiological effects on the micro circulation rather than the mechanical effects of elbow motion to enable the smoking action (Bartels and Verbeek, 2007). Retro epicondylar compression is seen more commonly in young administrative workers, while compression due to the humeroulnar aponeurosis is seen in manual workers (Omejec and Podnar, 2016). Predisposing systemic conditions are similar to those described for CTS.

Anatomy

The most proximal site of compression is the arcade of Struthers which is a condensation of the deep brachial fascia extending onto the medial intermuscular septum about 8 cm proximal to the medial

Fig. 72.3 The ulnar nerve travelling between the flexor and extensor compartments of the arm, traversing the epicondylar grove where the roof has been removed for visibility. The ulnar nerve is seen entering the forearm between the heads of the flexor carpi ulnaris.

epicondyle. The cubital tunnel has as its roof a thick fascial condensation extending from flexor carpi ulnaris (FCU) to the arcuate ligament of Osborne while the ulnar collateral ligament forms the floor. The nerve tunnel continues between the two heads of FCU and the deep flexor pronator aponeurosis (Fig. 72.3).

Clinical presentation

The symptoms include tingling or altered sensation in the little and ulnar border of the ring finger and the dorsum of the ulnar aspect of the hand. Patients complain of numbness on wakening and exacerbation of symptoms with elbow flexion. Late presentations are in the form of loss of sensation of the ulnar innervated digits and wasting of the intrinsic muscles. The later differentiating proximal compression at the elbow from distal compression at the wrist in Guyon's canal. The diagnosis is clinical with confirmation by provocation tests (Table 72.2).

Investigations

Investigations to exclude underlying systemic conditions are as described for CTS mentioned earlier. Imaging modalities that can be helpful include X-ray, ultrasound, and MRI. These are helpful not only in defining the anatomy of the nerve itself but also in excluding bone deformity, tumours, and other soft tissue anomalies that predispose to compression.

A combination of short segment nerve conduction studies combined with ultrasound can localize the area of compression to retroepicondylar or within the humeroulnar aponeurotic arcade (Omejec and Podnar, 2016).

Treatment

Non-surgical treatments

Non-operative strategies include splinting, physiotherapy, and activity modifications. This is the treatment of choice in the absence of muscle wasting or persistent numbness. Half the patients treated will have relief of symptoms (Dellon, 1989).

Surgical

Patients with muscle weakness, persistent numbness, or those with significant symptoms, who have failed to improve with non-operative strategies should be offered surgery.

The surgery is performed with the aid of a tourniquet under local or regional anaesthesia. Surgical options include simple decompression (open or endoscopic), anterior transposition (submuscular or subcutaneous) and medial epicondylectomy.

Common to all techniques is the rearrangement of the nerve's anatomical tunnel to allow easier gliding and eliminate areas of potential or actual compression. The nerve is released from proximal to distal as follows: ligament of Struthers; ligament of Osborne; and the FCU fascia. The nerve is dissected free along its entire length in the tunnel ensuring protection of the branches to FCU and medial and posterior cutaneous nerves of forearm.

There is significant controversy regarding the techniques and between *in situ* release versus transposition and the plane of transposition (submuscular, intramuscular, or subcutaneous). Where transposition is considered studies suggest equivalent results with *in situ* release itself. If the nerve has a propensity to subluxation in flexion following the release than transposition can be considered as more than 90% success has been reported with *in situ* decompression alone with transposition reserved for patients with unresolved symptoms.

Endoscopic decompression

Endoscopic cubital tunnel release has been reported using a small incision approach with outcomes and complications similar to open approach while avoiding a larger scar with the added benefit of early return to work. There are however no larger randomized studies relating to this approach.

Medial epicondylectomy

This is a technique originally described by King and Morgan for post-traumatic ulnar neuritis and subsequently extrapolated to patients with cubital tunnel syndrome. The philosophy behind this approach is that it allows for some degree of anterior transposition while avoiding significant dissection to mobilize the ulnar nerve. Cadaveric studies have a shown significant reduction in strain on the ulnar nerve with epicondylectomy as compared to *in situ* release alone (Hicks and Toby, 2002). Overzealous resection can result in an unstable medial elbow especially if a portion of the medial collateral ligament is resected (Efstathopoulos et al., 2006). The procedure involves following an *in situ* release of the tunnel, subperiosteal exposure of the epicondyle and osteotomizing the apical portion

(about 20%) ensuring the attachment of the medial collateral ligament is maintained. Persistent elbow pain has been reported in up to 45% of patients undergoing medial epicondylectomy.

Meralgia paresthetica

Aetiology

Entrapment of the lateral cutaneous nerve of the thigh as it passes from the pelvis to the lateral thigh is called meralgia paresthetica. It is more common in men. and overweight patients.

It may be related to anatomical variability of the nerve as it passes through the fascial tunnel leaving it susceptible to compression with variation of movement. It has also been associated with prone positioning in spinal surgery and as a complication of bone graft harvesting from the iliac crest and anterior pelvic procedures.

Clinical presentation

Patients present with pain, tingling, and paraesthesia in the anterolateral thigh. The lateral cutaneous nerve does not have any motor component, so the symptoms and signs are only sensory. Symptoms are aggravated by external compression with clothing or belts, hyperextension of the hip, and standing for prolonged periods.

Provocative tests reproduce the tingling and pain; for example, Tinel-Hoffman, which is pressure over the nerve as it passes adjacent to the anterior superior iliac spine. A helpful diagnostic test is to inject some local anaesthetic into the site of the positive Tinel-Hofmann's test. If the patient then experiences relief of symptoms and associated numbness in the distribution of the nerve, then the diagnosis is confirmed.

Investigations

The diagnosis is clinical. However, nerve conduction studies and ultrasound are the most useful investigative tools were the clinical evaluation is inconclusive. Other imaging modalities such as MRI are helpful to exclude the differential diagnoses of proximal spinal nerve compression, intraneural and extraneural tumours.

Non-operative

Non-operative strategies include removal of external compressors such as tight clothing or belts, losing weight, and anti-inflammatory medication.

Ultrasound can not only be used for diagnosis but also as a treatment modality. Ultrasound-guided steroid injection can be performed either directly or indirectly (Onat et al., 2016).

Operative

Surgery for meralgia paresthetica is indicated for those cases that have failed non-operative strategies but where significant symptoms persist. It is also useful for those cases with symptoms after previous pelvic surgery.

Surgery has a dual role in both diagnosis and treatment. Exploration and neurolysis is effective. In cases where the nerve is tethered or embedded in scar tissue options for importing normal tissue with the potential for nerve gliding should be considered.

Historical evidence in the literature suggest that neurectomy can be as effective if not more effective that neurolysis in some cases (de Ruiter and Kloet, 2015).

Other entrapment neuropathies

Other entrapment neuropathies that are seen within clinical practice include compressions of the radial nerve (radial tunnel syndrome, posterior interosseous nerve palsy), median nerve at the elbow (pronator syndrome) and compression of the ulnar nerve at Guyon's canal (Kumar and Bourke, 2016). More proximal nerves such as the suprascapular nerve and long thoracic nerve can also be subject to entrapment around the shoulder girdle. These entrapments can be more difficult to diagnose as there are no cutaneous sensory components to assess and patients present with pain aggravated by movement of the shoulder. Detailed discussion about these less common entrapment syndromes is beyond the scope of this chapter.

Summary

Nerve entrapment syndromes such as carpal tunnel and cubital tunnel syndrome are common. They can affect all age groups. They do have financial implications as they effect the working population and require time off work for rehabilitation and recovery after surgical release.

The diagnosis of nerve entrapment is based on evaluation of clinical symptoms and signs and reproduction of these with provocative manoeuvres. Ultrasound is probably the most useful imaging modality in current practice as it allows dynamic assessment during movement. Electrodiagnostic tests are also valuable but are best used as an adjunct to clinical examination.

FURTHER READING

Agee, J.M., McCarroll, H.R., & North, E.R. (1994). Endoscopic carpal tunnel release using the single proximal incision technique. *Hand Clin*, **10**, 647–59.

Bland, J.D. (2000). A neurophysiological grading scale for carpal tunnel syndrome. *Muscle Nerve*, **23**, 1280–3.

Graham, B., Regehr, G., Naglie, G., & Wright, J.G. (2006). Development and validation of diagnostic criteria for carpal tunnel syndrome. *J Hand Surg Am*, **31**, 919–24.

Kumar, S.D. & Bourke, G. (2016). Nerve compression syndromes at the elbow. *Orthopaedics and Trauma*, **30**(4), 355–62.

MacKinnon, S.E. (2002). Pathophysiology of nerve compression. *Hand Clin*, **18**, 231–41.

REFERENCES

Agee, J.M., McCarroll, H.R., & North, E.R. (1994). Endoscopic carpal tunnel release using the single proximal incision technique. *Hand Clin*, **10**, 647–59.

Atroshi, I., Flondell, M., Hofer, M., & Ranstam, J. (2013). Methylprednisolone injections for the carpal tunnel syndrome: a randomized, placebo-controlled trial. *Ann Intern Med*, **159**, 309–17.

Bartels, R.H. & Verbeek, A.L. (2007). Risk factors for ulnar nerve compression at the elbow: a case control study. *Acta Neurochir (Wien)*, **149**, 669–74; discussion 674.

Bland, J.D. (2000). A neurophysiological grading scale for carpal tunnel syndrome. *Muscle Nerve*, **23**, 1280–3.
Bland, J.D. (2007). Treatment of carpal tunnel syndrome. *Muscle Nerve*, **36**, 167–71.
Bongers, F.J., Schellevis, F.G., Van Den Bosch, W.J., & Van Der Zee, J. (2007). Carpal tunnel syndrome in general practice (1987 and 2001): incidence and the role of occupational and non-occupational factors. *Br J Gen Pract*, **57**, 36–9.
Chow, J.C. (1989). Endoscopic release of the carpal ligament: a new technique for carpal tunnel syndrome. *Arthroscopy*, **5**, 19–24.
Dang, A.C. & Rodner, C.M. (2009). Unusual compression neuropathies of the forearm, part I: radial nerve. *J Hand Surg Am*, **34**, 1906–14.
Davis, E.N. & Chung, K.C. (2004). The Tinel sign: a historical perspective. *Plast Reconstr Surg*, **114**, 494–9.
De Ruiter, G.C. & Kloet, A. (2015). Comparison of effectiveness of different surgical treatments for meralgia paresthetica: results of a prospective observational study and protocol for a randomized controlled trial. *Clin Neurol Neurosurg*, **134**, 7–11.
Dellon, A.L. (1989). Review of treatment results for ulnar nerve entrapment at the elbow. *J Hand Surg Am*, **14**, 688–700.
Efstathopoulos, D.G., Themistocleous, G.S., Papagelopoulos, P.J., Chloros, G.D., Gerostathopoulos, N.E., & Soucacos, P.N. (2006). Outcome of partial medial epicondylectomy for cubital tunnel syndrome. *Clin Orthop Relat Res*, **444**, 134–9.
Foley, M., Silverstein, B., & Polissar, N. (2007). The economic burden of carpal tunnel syndrome: long-term earnings of CTS claimants in Washington State. *Am J Ind Med*, **50**, 155–72.
Gelberman, R.H., Szabo, R.M., Williamson, R.V., & Dimick, M.P. (1983). Sensibility testing in peripheral-nerve compression syndromes. An experimental study in humans. *J Bone Joint Surg Am*, **65**, 632–8.
Graham, B., Regehr, G., Naglie, G., & Wright, J.G. (2006). Development and validation of diagnostic criteria for carpal tunnel syndrome. *J Hand Surg Am*, **31**, 919–24.
Hicks, D. & Toby, E.B. (2002). Ulnar nerve strains at the elbow: the effect of *in situ* decompression and medial epicondylectomy. *J Hand Surg Am*, **27**, 1026–31.
Ikeda, K., Osamura, N., & Tomita, K. (2006). Segmental carpal canal pressure in patients with carpal tunnel syndrome. *J Hand Surg Am*, **31**, 925–9.
Kumar, S.D. & Bourke, G. (2016). Nerve compression syndromes at the elbow. *Orthopaedics and Trauma*, **30**(4), 355–62.
Latinovic, R., Gulliford, M.C., & Hughes, R.A. (2006). Incidence of common compressive neuropathies in primary care. *J Neurol Neurosurg Psychiatry*, **77**, 263–5.
Leit, M.E., Weiser, R.W., & Tomaino, M.M. (2004). Patient-reported outcome after carpal tunnel release for advanced disease: a prospective and longitudinal assessment in patients older than age 70. *J Hand Surg Am*, **29**, 379–83.
MacKinnon, S.E. (2002). Pathophysiology of nerve compression. *Hand Clin*, **18**, 231–41.
McDonagh, C., Alexander, M., & Kane, D. (2015). The role of ultrasound in the diagnosis and management of carpal tunnel syndrome: a new paradigm. *Rheumatology (Oxford)*, **54**, 9–19.
Mondelli, M., Giannini, F., Ballerini, M., Ginanneschi, F., & Martorelli, E. (2005). Incidence of ulnar neuropathy at the elbow in the province of Siena (Italy). *J Neurol Sci*, **234**, 5–10.
Nordstrom, D.L., Destefano, F., Vierkant, R.A., & Layde, P.M. (1998). Incidence of diagnosed carpal tunnel syndrome in a general population. *Epidemiology*, **9**, 342–5.
Ochoa, J., Fowler, T.J., & Gilliatt, R.W. (1972). Anatomical changes in peripheral nerves compressed by a pneumatic tourniquet. *J Anat*, **113**, 433–55.
Omejec, G. & Podnar, S. (2016). What causes ulnar neuropathy at the elbow? *Clin Neurophysiol*, **127**, 919–24.
Onat, S.S., Ata, A.M., & Ozcakar, L. (2016). Ultrasound-guided diagnosis and treatment of meralgia paresthetica. *Pain Physician*, **19**, E667–9.
Padua, L., Lo Monaco, M., Padua, R., Gregori, B., & Tonali, P. (1997). Neurophysiological classification of carpal tunnel syndrome: assessment of 600 symptomatic hands. *Ital J Neurol Sci*, **18**, 145–50.
Page, M. J., Massy-Westropp, N., O'Connor, D., & Pitt, V. 2012. Splinting for carpal tunnel syndrome. *Cochrane Database Syst Rev*, **7**, CD010003.
Rempel, D., Dahlin, L., & Lundborg, G. (1999). Pathophysiology of nerve compression syndromes: response of peripheral nerves to loading. *J Bone Joint Surg Am*, **81**, 1600–10.
Saw, N.L., Jones, S., Shepstone, L., Meyer, M., Chapman, P.G., & Logan, A.M. (2003). Early outcome and cost-effectiveness of endoscopic versus open carpal tunnel release: a randomized prospective trial. *J Hand Surg Br*, **28**, 444–9.
Sayegh, E.T. & Strauch, R.J. (2015). Open versus endoscopic carpal tunnel release: a meta-analysis of randomized controlled trials. *Clin Orthop Relat Res*, **473**, 1120–32.
Upton, A.R. & McComas, A.J. (1973). The double crush in nerve entrapment syndromes. *Lancet*, **2**, 359–62.
Van Slobbe, A.M., Bohnen, A.M., Bernsen, R.M., Koes, B.W., & Bierma-Zeinstra, S.M. (2004). Incidence rates and determinants in meralgia paresthetica in general practice. *J Neurol*, **251**, 294–7.
Vasiliadis, H.S., Nikolakopoulou, A., Shrier, I., Lunn, M.P., Brassington, R., Scholten, R.J., & Salanti, G. (2015). Endoscopic and open release similarly safe for the treatment of carpal tunnel syndrome. A systematic review and meta-analysis. *PLoS One*, **10**, e0143683.
Wilgis, E.F. & Murphy, R. (1986). The significance of longitudinal excursion in peripheral nerves. *Hand Clin*, **2**, 761–6.

73

Supraclavicular brachial plexus and peripheral nerve injuries

Jonathan Perera and Marco Sinisi

Introduction

Injury to the supraclavicular brachial plexus (SBP), is very rare and normally associated with traumatic injury. SBP injury (SBPi), causes significant physical impairment, but also psychological and stigmatic problems.

Epidemiology

The incidence of traumatic brachial plexus injury (BPi), is extremely difficult to ascertain due to worldwide variance, under-reporting, and the lack of recognition of milder injuries. Goldie and Coates (1992) showed that approximately 500 cases of brachial plexus injury take place in the United Kingdom each year principally as a result of road traffic collisions.

As road safety in general is improving, as shown by Keep in 2013, the amount of high-energy accident survivors in the United Kingdom is increasing. Between 1990 and 2012 there has been a 66% decrease in the number of people killed in road traffic accidents and a 62% decrease in severe injury. Most SBPis are caused in motor vehicle collisions with most series quoting upwards of 60% (Allieu and Cenac, 1988; Azze et al., 1994; Doi et al., 2000). Reviewing the statistics available SBPis are predominately caused in high-energy polytrauma motorcycle accidents in young men and are associated with long-bone fractures and head injuries. Even though motorcyclists only account for 1% of road users in the United Kingdom, they account for 20% of all road fatalities and serious injuries, with approximately 7000 serious injuries per year (Clarke et al., 2003; Rhee et al., 2011; Keep and Rutherford, 2013). Even though the number of these incidents is high, SBPi accounts for only 1% of polytrauma patients, the incidence has been reported by Allieu in 1988 to be between 0.3 to 6.3 cases/100 000/year.

Narakas's rule of sevens

There are seven '70% statistics' regarding BPis, namely 70% of cases involve road accidents, 70% of these accidents are motorcyclists, 70% of these patients present with combined injuries, 70% of these lesions are supraclavicular, 70% of these lesions involve at least one nerve root avulsion, 70% of these avulsions involve a C7, C8, or T1 level nerve root, and 70% of patients with avulsions develop chronic pain (Narakas, 1985).

Mechanism of injury

As with all medical diagnoses, SBPi types and severity can be diagnosed with an accurate history. It is vitally important to understand the mechanics leading to the injury. Important factors are the anatomy, the magnitude of the force and the vector of the force. Stretching of more than 12% of a nerve or more than 8 hours of ischaemia will result in severe nerve injury. The force required to avulse cervical nerve roots is as little as 200 newtons. The nerve root exiting angles are very important, as different forequarter positions at the time of impact will result in differing force vectors and therefore differing injury. A typical injury would be the arm and head or neck being pulled away from each other, with the arm being pulled below horizontally resulting in an upper plexal injury, versus the arm being pulled above horizontally and a resultant lower plexal injury.

A dislocated shoulder is a significant injury and can be a risk factor for supra or infraclavicular brachial plexus, (ICBP), injuries. Injury is usually to the upper trunk affecting predominately the suprascapular and axillary nerves. Many of those who get combined injuries also have an abnormal band of fascia connecting the pectoralis minor to the thoracic wall. This effectively narrows the space for the exiting SBP into the ICBP and means these patients are more susceptible to injury. Using an average male of 70 kg as an example and a deceleration period over 1 second, it is easy to calculate the starting speeds to generate the force described. In order to avulse a nerve root starting speeds of only 5 mph would be required, if the force is imparted on the SBP.

Anatomy and injury classification

The brachial plexus is formed by five spinal nerves C5 to T1. The nerve roots exit from the spinal cord and emerge in the posterior

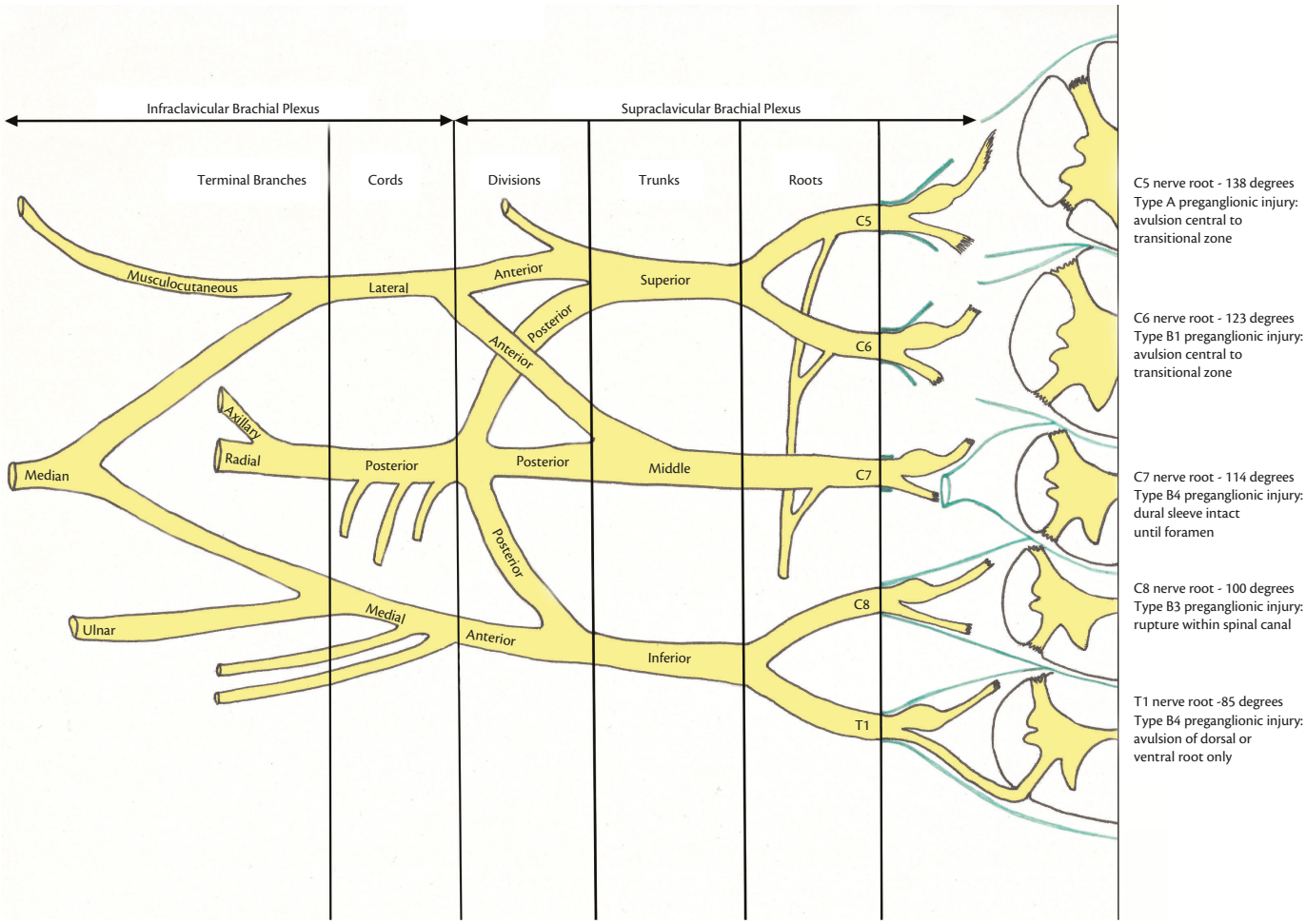

Fig. 73.1 Schematic drawing of the brachial plexus and nerve roots in addition to the root angles and the differing types of preganglionic nerve avulsion.

Courtesy of Mr Jonathan R. Perera.

triangle of the neck where they then form the upper (C5–C6), middle (C7), and lower trunks (C8–T1); see Figure 73.1. Sometimes a contribution from C4 can be present and therefore the plexus is named 'prefixed' sometimes a contribution from T2 is present and therefore is named 'postfixed'.

The SBP lies superior to the clavicle, and includes the roots, trunks, and divisions of the brachial plexus. It does not include the cords and branches, which is the ICBP. SBPi also include those injuries from further proximal and therefore can also be subdivided into pre- and postganglionic injuries, proximal and distal to the dorsal root ganglion (DRG).

The preganglionic injuries have been further classified by Birch in 2011 into five types, namely A, which is an avulsion central to the transitional zone, (TZ); B1, which is distal to TZ; B2, which has an intact dural sleeve; B3, which is root rupture within the spinal canal without DRG displacement or dural rupture; and finally B4, which is avulsion confined to dorsal or ventral roots (Fig. 73.1).

With avulsion injuries the DRG remains intact and therefore no Wallerian degeneration of the sensory nerve takes place and these patients will not have a positive Tinel's sign (Tinel, 1915). Direct and indirect nerve injury has been subdivided by the Seddon Classification (Seddon, 1942), as shown in Box 73.1. This classification applies to axonal injury, not injury of the whole nerve. The Sunderland Classification (Sunderland, 1951) defines first- to fifth-degree injuries by splitting Seddon Class III into three further divisions: preservation of the perineurium, preservation of the epineurium, and complete nerve transection.

Box 73.1 Classification of nerve injury

Class I: Neuropraxia—interruption of conduction without loss of axonal continuity and preserved supportive structures.
Prognosis: normally rapid and complete (days, weeks).

Class II: Axonotmesis—disruption of axonal continuity and its myelin with intact endoneurium.
Prognosis: variable, generally good, with worse prognosis for proximal injuries and injuries that do not re-implant in the muscle.

Class III: Neurotmesis—disruption of all nerve layers. Recovery is not possible without appropriate surgical intervention. It is a total severance or disruption of the entire nerve.

Prognosis: poor especially without intervention; normally incomplete.

Reproduced with permission from H. J. Seddon, A Classification of Nerve Injuries, *The BMJ*, Volume 2, issue 237, Copyright © 1942 BMJ Publishing Group Ltd.

Erb's point is the site where C5 and C6 form the upper trunk of the brachial plexus. It occurs halfway along the posterior border of the sternocleidomastoid muscle, from which all the cutaneous branches of the cervical plexus exit superficially (lesser occipital, greater auricular, transverse cervical, and supraclavicular nerves). This is clinically particularly important as it is at this location where forces applied to the upper forequarter and head and neck of a patient converge, commonly causing SBPi. Total plexal injury and especially those SBPi affecting the lower plexus are often associated with a Horner's syndrome (ptosis, miosis, anhidrosis, and enophthalmos). This is due to the simultaneous injury of the sympathetic trunk with preganglionic injury as well as direct spinal, head, or vascular injuries as described by Rhee in 2011. Other injuries that can sometimes worsen the presentation, confuse the diagnosis, or be initially missed are: arterial injury to the axillary; subclavian and vertebral vessels; fractures, dislocations, and muscle injuries of the forequarter.

Clinical presentation

There are three separate distinct patterns of injury that may occur in isolation or combination, namely: SBPi with preganglionic injury, SBPi with postganglionic injury, and ICBPi.

Preganglionic or avulsion injuries classically present with severe, crushing, unremitting, shooting pain in an insensate arm. The pain is usually along the dermatome of the injured spinal nerve. Kato in 2006 described a cohort where more than 50% of avulsion patients had significant pain occurring by 24 hours and 90% by 6 weeks postinjury. Patients with a preganglionic injury have a negative Tinel's test. Other signs of preganglionic injury will be injury to nerves branching at or around the root level (long thoracic, dorsal scapular, and phrenic nerves) and dysfunction of the associated muscles.

Conversely patients with an SBPi, postganglionic injury will have a positive Tinel's test, no Horner's syndrome, no serratus anterior, rhomboid, diaphragmatic dysfunction and will have absent sensory nerve action potentials, (SNAPs) on nerve conduction studies. Erb's palsy or upper brachial plexopathy (C5, C6) leaves a characteristic posture referred to as the 'waiter's tip' position, namely, shoulder adduction and medial rotation, elbow extension, and forearm pronation. Klumpke's palsy or lower brachial plexopathy (C8, T1) results in elbow flexion, forearm supination, extreme wrist extension, and clawing of the hand as a result of weakness in the small muscles of the hand. Both Erb's and Klumpke's palsy have been described as a result of birth injury from forceful depression or elevation of the shoulder, respectively, however they also occur in adults from a similar mechanism of injury.

Investigations

The main imaging investigations of choice for SBPi are magnetic resonance imaging (MRI), computed tomography (CT), and myelography.

Magnetic resonance imaging scans of the SBP and the cervical spine are extremely useful in SBPi but interpretation of the SBP portion can be challenging with conventional MRI. Since the 1990s two new magnetic resonance sequences have been discovered and implemented namely magnetic resonance neurography (MRN) as described by Filler et al. in 1993 (Filler et al., 1993) and magnetic resonance myelography (MRM) as demonstrated by Ramsbacher in 1997 (Ramsbacher et al., 1997). These sequences can be used to assess both pre- and postganglionic nerves in the SBPi. MRN requires MRI machines of 3-Tesla or more. MRN can provide an excellent form of non-invasive imaging of any peripheral nerve. MRM is useful to assess the preganglionic SBP, which is also non-invasive and just as efficient as traditional myelography in detecting injuries at this level. MRM does not require contrast medium injection into the spinal canal or radiation. Combining these two imaging modalities together can revolutionize the diagnosis and management of SBPi, especially in non-specialist centres.

CT and CT angiography are very important imaging modalities, especially when imaging polytrauma patients. Most trauma units will have quick, easy access to these scans near to the accident and emergency department. Once the patient has been stabilized, they can be safely scanned for life and limb threatening injuries. Vascular injury and/or haematomas, which are common in SBPi, will cause a significant fibrotic reaction around the SBP. This, on top of the initial injury, can be enough to cause a permanent conduction block, without surgical intervention.

Traditional myelography using fluoroscopy and CT myelography both require intradural injections. Myelography is a very useful imaging modality for assessing nerve root avulsions and to look for subsequent meningoceles or pseudomeningoceles. The lower nerve roots of the SBP can be difficult to distinguish due to the artefact created by the lower cervical and upper thoracic spinal vertebrae.

Plain X-rays

Plain X-rays are a quick and easy imaging technique, for example, a chest X-ray may show a raised hemi-diaphragm indicating a phrenic nerve injury as well as demonstrating thoracic trauma. Cervical spine X-rays may show transverse process fractures indicating nerve root avulsion injuries. Forequarter X-rays may reveal humeral, scapula, clavicular fractures, and shoulder girdle injuries, which are associated with SBPi and ICBPi.

Electrodiagnostic testing

In SBPi electrodiagnostic testing is an excellent adjunct to a thorough sensory and motor examination and imaging. Like other test modalities, electrodiagnostics require an experienced clinician to perform the testing and interpret it correctly. The tests used are predominately electromyography (EMG) and nerve conduction studies (NCS) as summarized in **Table 73.1**. EMG is used to evaluate the electrical activity of muscle during rest and during activity. Denervated muscle changes can be seen as early as 1 week after an injury (Dumitru and Zwarts, 2005) and the speed with which this change can be detected is inversely related to the nerve length. The longer the axons, the longer the Wallerian degeneration will take and so the proximal muscles will show EMG changes sooner, with the distal muscles taking 3–6 weeks to demonstrate denervation. When significant nerve injury has taken place, there will be EMG changes immediately but only a skilled Neurophysiologist will be able to detect this. EMG and NCS can both be used to demonstrate an injured nerve segment, but they will not show axonal transection. SNAPs and motor unit action potentials (MUAPs), are both important for distinguishing pre- and postganglionic nerve injuries. SNAPs are preserved in lesions proximal to the dorsal root ganglion

Table 73.1 Approximate EMG and NCS findings in nerve injury

	Conduction velocity	MUAPs	CMAPs	SNAPs	To be aware
Neuropraxia	Maintained	None	Normal Slight reduction proximally	Reduced	Permanent conduction slowing due to thinner internodes
Axonotmesis	Reduced	None	Reduced proportional to axonal loss	Reduced	Positive sharp waves and fibrillations
Neurotmesis	Nil	None	Reduced proportional to axonal loss	Absent	

therefore preganglionic injuries will have normal SNAPs with abnormal MUAPs (Table 73.1).

Histamine test

This test is not routinely performed due to the improvements in BPi imaging and diagnosis. An intradermal injection of histamine will normally cause a triple response as follows, a red reaction due to direct capillary dilatation followed by a wheal due to fluid extravasation from increased permeability of vessels and a flare of redness in the surrounding area which is caused by arteriolar dilatation mediated by the axon reflex in the sensory nerve distribution.

The histamine test can be used to distinguish between pre- and postganglionic lesions. In a preganglionic lesion the afferent axons remain intact therefore a normal triple response with flare will be seen. In a postganglionic lesion the sensory cell body and axon are not connected, and the afferent axons are degenerated therefore only the initial redness and the wheal are seen, the flare response is absent.

Management

While open SBPi needs to be dealt with urgently, there are differing opinions on when to operate in the management of a closed SBP injured patient. The benefits of early intervention include pain relief and improved outcomes although occasionally a delay in going to theatre can help to allow the inflammation to settle down (Kato et al., 2006; Birch, 2011; Birch, 2015; Hems, 2015). There have always been two main trends of thought with regards to SBPi operating, one operating early, and the other delayed until all acute problems have settled (Birch, 2015; Hems, 2015). The middle period is affected by the inflammatory phase of the original injury and tends to give poorer outcomes (Hems, 2015). Late phase repairs can also improve outcomes after the inflammatory phase had settled down (Hems, 2015). The main aims of reconstruction are to achieve the best forequarter function and relieve pain. Kato et al. (2006) found that the earlier that an operation is performed, the greater the patient's pain relief, partly due to the functional recovery which reduces pain in early surgery (Fig. 73.2).

Much like with an open injury, a vascular injury also needs to be operated on immediately. Bleeding, infection, and haematoma formation will cause significant fibrosis. This can be so severe that the normal tissue planes can disappear and the whole plexus can form a wall of scar tissue making surgery impossible. The history of the injury is very important as the level of energy imparted upon the SBP relates to the injury severity and its likely recovery. All complete lesions require exploration, as they are extremely unlikely to recover spontaneously. Pain, which occurs in many patients, is a debilitating problem that can impair their subsequent rehabilitation with physiotherapy and occupational therapy.

Distraction therapy with employment or regular exercise regimes can provide extremely effective pain relief and the more normal the routine the better (Birch, 2015). It can be clearly seen that patients returning to work earlier tend to have less pain and better outcomes with the same injuries (Kato et al., 2006; Birch, 2011). The severity of the pain predicts whether avulsion has taken place (Parry, 1980; Kato et al., 2006; Birch, 2011).

The operation

Position and skin incision

The patient is positioned in a beach chair position using a head ring with the head slightly extended about 5–10° and tilted approximately 10° to the contralateral side. The head position is very important in order to gain enough exposure of the brachial plexus, particularly at the root level, which is unattainable without this head extension. The thorax must be elevated to 30°, by tilting a split table. See Figure 73.3.

In order to achieve a complete exposure of the brachial plexus at the supraclavicular region we think that it is enough to perform a Langer's line neck incision starting 1–2 cm above the medial clavicle and extending posteriorly for about 10–15 cm, (Langer, 1861). This can avoid an incision along the sternocleidomastoid muscle and gives enough space for dissection of the plexus from the root level to the divisions of the trunks.

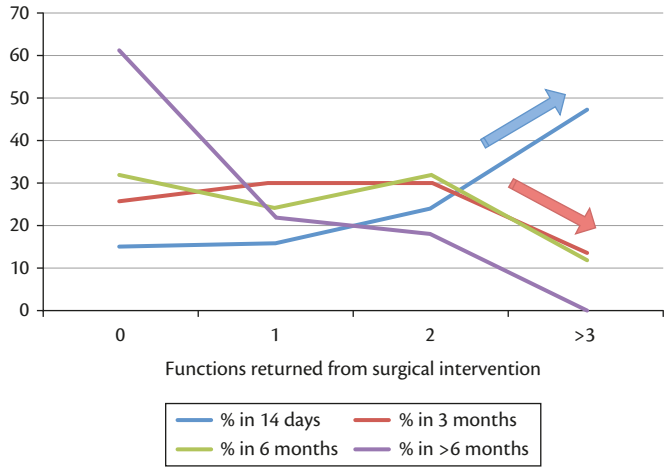

Fig. 73.2 Graph drawn with data from Birch and the Royal National Orthopaedic Hospital Peripheral Nerve Injury Unit which shows clear differences in outcome when operating within 14 days of SBPi compared to waiting more than 6 months.

Data from Birch R; 2011; Peripheral Nerve Injury Unit, Royal National Orthopaedic Hospital.

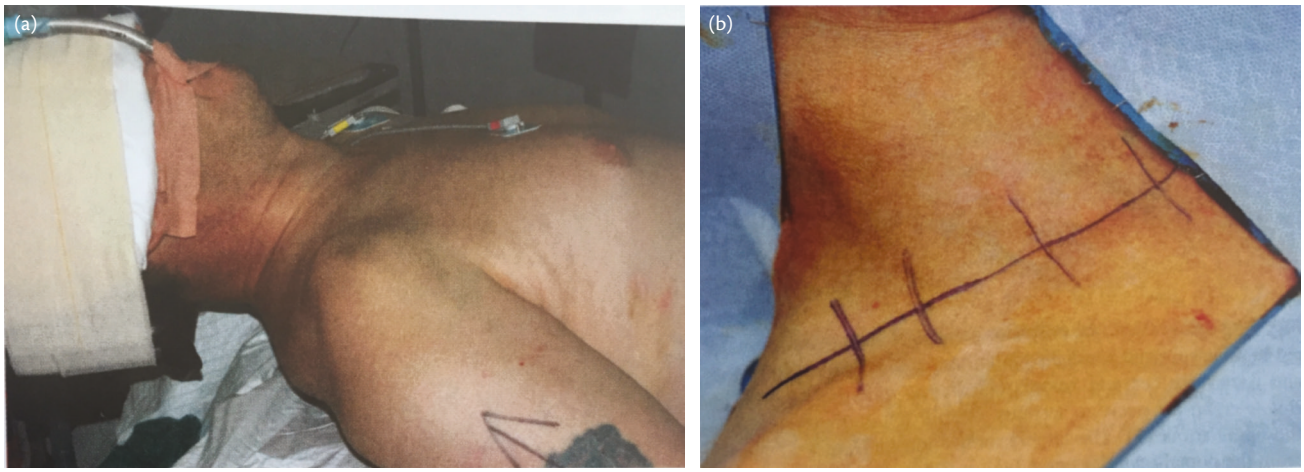

Fig. 73.3 Patient positioning for the transverse supraclavicular approach to the brachial plexus with overall position and marked incision line.
Reproduced with permission of Medtronic, Inc.

The dissection must be carried out by sectioning the platysma and by identifying the anterior surface of the sternocleidomastoid muscle medially, the supraclavicular branches of the cervical plexus, external jugular vein laterally, and the greater auricular nerve superiorly. At the end of this dissection a Joll's thyroid retractor can be used to keep the operative field open.

Dissection between sternocleidomastoid muscle and external jugular vein is carried out to mobilize the vein and retract it laterally. Sometimes mobilization, ligation, and division of the vein is required. Going deeper with the dissection between these structures the next to be identified is the omohyoid muscle. This is the only transverse muscle in this region and has to be dissected free from surrounding structures. It is then sutured with an absorbable strong suture, in order to repair it at the end of the operation. The fat pad and transverse cervical vessels have to be divided and reflected. These vessels are thin walled and can only be cauterized. Occasionally these vessels are much bigger, particularly if stasis is present.

The next step is to identify the phrenic nerve, which lies on the anterior surface of the scalenus anterior. Sometimes in a traumatic injury to the brachial plexus, particularly after many months from the injury, there is a lot of fibrosis here and the dissection is difficult. The dissection of the phrenic nerve leads to the C5 nerve root.

In a few cases, a C6 contribution to the phrenic nerve may be present. The root of C5 just after its exit from the foramen gives a branch posteriorly, which is the dorsal scapular nerve supplying the rhomboid muscles and 1–2 cm from its origin it joins C6 to constitute the upper trunk. On the lower surface of C6 there is the long thoracic nerve, which runs obliquely through the middle scalene muscle, and is constituted by branches from C5, C6, C7, and occasionally C8.

After dissecting the C5 and C6 roots, the upper trunk can be demonstrated posterolaterally and just before the anterior and posterior divisions the suprascapular nerve is identified. After this dissection inferior dissection is carried out to identify the middle and lower trunks. Between the upper trunk and the middle trunks runs the dorsal scapular artery with a transverse direction, relative to the plexus.

The middle and lower trunks are found inferior and slightly anterior to the upper trunk. To identify the trunks up to the level of the roots it is often required to divide part of the anterior scalene. It is very important to trace the subclavian artery, especially when there is a lot of scar tissue after significant traumatic injury. The subclavian vein at this level lies anterior to the scalenus anterior and inferior to the subclavian artery and all the veins passing transversely regarding the brachial plexus have their origin here. Therefore, it is vitally important never to pull too much on these veins otherwise they can be damaged as they enter the subclavian vein and even the subclavian vein itself may be traumatized.

The dissection of the three main trunks will reveal all the anterior and posterior divisions. The anterior divisions of the upper and middle trunk gather to form the anterolateral cord, the anterior division of the lower trunk constitutes alone the anteromedial cord and all the posterior divisions together give the posterior cord.

Reconstruction

Common reconstructive techniques for SBPi are direct repair, nerve transfers, and nerve grafting to give major forequarter function back to the patient. Ultimately either a working nerve or working fascicles are transferred to the nerves that do not function. There are many options for nerve transfer, but the options are limited by locations of donor and recipient nerves. After nerve transfer patients are expected to gain at least grade 3 power Medical Research Council (MRC, 1976).

Common nerve transfers include the spinal accessory nerve to the suprascapular or axillary nerves, the radial nerve fascicle to the axillary nerve, the ulnar nerve, and/or median nerve fascicle to the musculocutaneous nerve and the intercostal nerves to the musculocutaneous, axillary, radial, median, or ulnar nerves. Common nerve donors include the medial cutaneous nerve of the arm and or forearm and the sural nerve.

Nerve root reimplantation should be done within four weeks of the injury. As most of the injuries will be traumatic avulsions the roots themselves will be damaged so severely that direct repair cannot take place without fascicular grafting. Grafting is usually performed using fibrin glue or the nerve is sutured to the pia mater. The muscle power expected is weaker than prior to the injury, more than power 3 on the MRC grading scale may take over a year to achieve. However, the further distal the muscles the weaker they are. There

have been cases where great results have been seen with near normal wrist and hand function attained (Htut et al., 2007).

Free functional muscle transfer is a rare operation where a muscle free flap, along with its arterial supply, venous drainage, and motor nerve supply, are harvested and re-implanted into a new location. A common donor muscle would be gracilis and in brachial plexus injury it is used for regaining elbow flexion or finger flexion (i.e. replacing biceps or flexor digitorum profundus). This procedure is usually performed by plastic surgeons and requires micro-anastomosis of the vessels as well as the nerve repair. It requires careful planning and patient selection due to the risks involved. If successful it can provide useful function and grade 4 power to the patient (Doi et al., 1998).

Peripheral nerve injuries

Peripheral nerve palsies are common and the management of them can be simple as long as your clinical examination and subsequent diagnoses is accurate. They are generally related to acute and chronic compressions or traumatic injuries. Sometimes described as distal brachial plexal injuries, with the most common being median and ulnar nerves but radial and common peroneal nerve palsies being important as well. The general functions and findings of these nerves can be summarized in Table 73.2.

Once the diagnosis has been established then the appropriate treatment can then be commenced. Sometimes this can be fairly easy, with good outcomes, and others not.

Surgery is often required especially if there is a non-advancing positive Tinel's sign at the sight of the nerve entrapment. Surgical decompression is the easiest and if done correctly has the best outcome, carpal tunnel decompression being the most obvious. An extremely important factor in a good outcome is having excellent allied health professionals (occupational therapists and physiotherapists), who can assess and rehabilitate the patients afterwards.

Repair is performed using a microscope or loupes with fine nylon suture material and fibrin glue. Either an epineural repair or fascicle group repair are utilized. Peripheral nerves cannot be repaired under tension as this will fail. In these situations, nerve grafts are required and commonly sural or antebrachial cutaneous nerves, as they are cutaneous nerves only. If there is no chance at direct repair or the distance too long there are innumerable nerve and tendon transfers which can be undertaken to provide useful limb function.

Table 73.2 Summary table of the important nerve compressions in both the upper and lower limbs

Nerve	Common site of palsy	Muscles affected	Sensation	Key examination
Median nerve (C5–T1)	Delto-pectoral fascia; Supracondylar Process + Ligament of Struthers; Carpal Tunnel;	**L**umbricals 1&2 **O**pponens pollucis **A**bductor pollucis brevis **F**lexor pollucis brevis Wasting thenar bulk	Radial predominately volar 1st three webspaces	Thenar wasting Phalen's and Durkin's tests
AIN (C5-T1) from median	Kiloh-Nevin; superficial arch of FDS; lacertus fibrosus; superficial head of pronator teres	Flexor digitorum profundus radial half; pronator quadratus; flexor pollicis longus	n/a	Unable to make OK sign; weak resisted pronation
Ulnar nerve (C8–T1)	Cubital tunnel syndrome (5 sites); Guyon's canal	Lumbricals 3 and 4 All interossei Adductor pollicis Deep head of Flexor pollicis brevis Wasting hypothenar bulk	Ulnar/4th webspace	Froments test Hypothenar + 1st DIO wasting Wartenberg's and Jeanne's sign
Radial nerve (C5–T1)	Accessory subscapularis-teres-latissimus muscle; subscapular artery; triangular interval; lateral intermuscular septum;	Triceps brachii Aconeus Brachioradialis Extensor carpi radialis longus/brevis Supinator Entire posterior compartment, extensors, and abductor pollicis longus	Lateral/posterior upper arm and elbow and hand—radial dorsal predominately 1st three webspaces	Classical wrist drop depends on level
PIN from radial	Radial tunnel syndrome	Extensor carpi radialis brevis (normally from radial nerve) Extensor digitorum communis Extensor digiti minimi Extensor carpi ulnaris Supinator Abductor pollicis longus Extensor pollicus brevis Extensor pollicus longus Extensor indicis proprius	Sensory fibres to dorsal wrist capsule, no cutaneous	Pain Finger metacarpal extension weakness Wrist drop
Common peroneal nerve (L4–S2)	Above knee; fibula neck; below knee	**Deep:** Anterior compartment: Tibialis anterior extensor Halluces longus extensor Digitorum longus Peroneus tertius **Superficial:** Lateral compartment: Peroneus brevis and longus	Lateral sural nerve (L2–3) upper lateral-calf/knee Superficial peroneal (L4–S1) calf and dorsum of foot—lateral border Deep peroneal (L4/5) 1st webspace only	Foot drop TA, EHL, and extensor digitorum longus (EDL) weakness in varying degrees

Conclusion

SBPi is a significantly disabling diagnosis, normally affecting young healthy adult patients. Urgent referral, assessment, and intervention are often required for the best outcomes. Nerve injury has previously been seen as irreversible but with modern swift intervention this is not the case. It is always advisable therefore to refer the patient as soon as possible to a peripheral nerve specialist.

FURTHER READING

Birch, R. (2011). *Surgical Disorders of the Peripheral Nerves*, 2nd edition. London, UK: Springer UK.

Birch, R. (2015). Timing of surgical reconstruction for closed traumatic injury to the supraclavicular brachial plexus. *J Hand Surg Eur*, **40**(6), 562–67.

Doi, K., Hattori, Y., Kuwata, N., et al. (1998). Free muscle transfer can restore hand function after injuries of the lower brachial plexus. *J Bone Joint Surg Br*, **80**(1), 117–20.

Filler, A.G., Howe, F.A., Hayes, C.E., et al. (1993). Magnetic resonance neurography. Lancet, **341**(8846), 659–61.

Narakas, A.O. (1985). The treatment of brachial plexus injuries. *Int Orthop*, **9**(1), 29–36.

Seddon, H.J. (1942). A classification of nerve injuries. *Br Med J*, **2**(4260), 237–9.

Sunderland, S. (1951). A classification of peripheral nerve injuries producing loss of function. *Brain*, **74**(4), 491–516.

Tinel, J. (1915). Le signe du 'fourmillement' dans les lésions des nerfs périphériques; *Press Méd*, **47**, 388–9.

REFERENCES

Allieu, Y. & Cenac, P. (1988). Is surgical intervention justifiable for total paralysis secondary to multiple avulsion injuries of the brachial plexus? *Hand Clinics*, **4**(4), 609–18.

Azze, R.J., Mattar, R. Jr., Ferreira, M.C., Starck, R., & Canedo, A.C. (1994). Extraplexual neurotization of brachial plexus. *Microsurgery*, **15**(1), 28–32.

Birch, R. (2011). *Surgical Disorders of the Peripheral Nerves*, 2nd edition. London, UK: Springer UK.

Birch, R. (2015). Timing of surgical reconstruction for closed traumatic injury to the supraclavicular brachial plexus. *J Hand Surg Eur*, **40**(6), 562–67.

Clarke, D.D., Ward, P., Truman, W., Bartle, C. (2003). *Motorcycle Accidents: Preliminary Results of an In-Depth Case Study Using Police Road Accident Files; Behavioural Research in Road Safety 2003*: thirteenth seminar; Department for Transport, England 2003–2009; pp. 153–64.

Doi, K., Hattori, Y., Kuwata, N., et al. (1998). Free muscle transfer can restore hand function after injuries of the lower brachial plexus. *J Bone Joint Surg Br*, **80**(1), 117–20.

Doi, K., Muramatsu, K., Hattori, Y., et al. (2000). Restoration of prehension with the double free muscle technique following complete avulsion of the brachial plexus. Indications and long-term results. *J Bone Joint Surg Am*, **82**(5), 652–66.

Dumitru, D., & Zwarts, M.J. (eds.) (2005). Needle electromyography. In: Dumitru, D., Amato, A.A., & Zwarts, M.J. (eds.) *Electrodiagnostic Medicine*, pp. 257–92. Philadelphia, PA: Hanley & Belfus.

Filler, A.G., Howe, F.A., Hayes, C.E., et al. (1993). Magnetic resonance neurography. Lancet, **341**(8846), 659–61.

Goldie, B.S. & Coates, C.J. (1992). Brachial plexus injury: a survey of incidence and referral pattern. *J Hand Surg*, **17**(1), 86–8.

Hems, T.E. (2015). Timing of surgical reconstruction for closed traumatic injury to the supraclavicular brachial plexus. *J Hand Surg Eur*, **40**(6), 568–72.

Htut, M., Misra, V.P., Anand, P., Birch, R., & Carlstedt, T. (2007). Motor recovery and the breathing arm after brachial plexus surgical repairs, including reimplantation of avulsed spinal roots into the spinal cord. *J Hand Surg*, **32E**(2), 170–8.

Kato, N., Htut, M., Taggart, M., Carlstedt, T., & Birch, R. (2006). The effects of operative delay on the relief of neuropathic pain after injury to the brachial plexus: a review of 148 cases. *J Bone Joint Surg Br*, **88**(6), 756–9.

Keep, M. & Rutherford, T. (2013). *Reported Road Accident Statistics*. House of Commons Library; SN/SG/2198. http://researchbriefings.files.parliament.uk/documents/SN02198/SN02198.pdf

Langer, K. (1861). Zur Anatomie und Physiologie der Haut. Über die Spaltbarkeit der Cutis. *Sitzungsbericht der Mathematisch-naturwissenschaftlichen Classe der Wiener Kaiserlichen Academie der Wissenschaften*, **44**, 19–46.

Medical Research Council (MRC) (1976). *Aids to Examination of the Peripheral Nervous System*. Memorandum no. 45. London, UK: Her Majesty's Stationery Office

Narakas, A.O. (1985). The treatment of brachial plexus injuries. *Int Orthop*, **9**(1), 29–36.

Parry, C.B. (1980). Pain in avulsion lesions of the brachial plexus. *Pain*, **9**, 41–53.

Ramsbacher, J., Schilling, A.M., Wolf, K.-J., Brock, M. (1997). Magnetic resonance myelography (MRM) as a spinal examination technique. *Acta Neurochirurgica*, **139**(1), 1080–4.

Rhee, P.C., Pirola, E., Hébert-Blouin, M.N., et al. (2011). Concomitant traumatic spinal cord and brachial plexus injuries in adult patients. *J Bone Joint Surg Am*, **93**(24), 2271–7.

Seddon, H.J. (1942). A classification of nerve injuries. *Br Med J*, **2**(4260), 237–9.

Sunderland, S. (1951). A classification of peripheral nerve injuries producing loss of function. *Brain*, **74**(4), 491–516.

Tinel, J. (1915). Le signe du 'fourmillement' dans les lésions des nerfs périphériques. *Press Méd*, **47**, 388–9.

74

Peripheral nerve tumours

Rikin Trivedi and Vincent Nga

Introduction

Peripheral nerve sheath tumours (PNSTs) encompass a spectrum of well-defined clinicopathologic entities, ranging from benign tumours to high-grade malignant peripheral nerve sheath tumours (MPNSTs). While the majority of PNSTs arise sporadically, there are well known inherited conditions that predispose an individual to developing PNSTs such as neurofibromatosis type 1 (NF1), neurofibromatosis type 2 (NF2), schwannomatosis, and Carney complex (Rodriguez et al., 2012).

The neurosurgeon is often consulted to diagnose and manage tumours involving the peripheral nerves of the extremities and trunk. Most tumours involving the peripheral nervous systems encountered would be that of benign tumours of the nerve sheath. This chapter focuses on the pathology, diagnosis, management, and outcome of benign and malignant peripheral nerve sheath tumours.

Classification

PNSTs may be divided into benign and malignant variants. Several distinct benign subtypes have been well recognized, including that of schwannoma (neurilemmoma, neurinoma), neurofibroma, and perineurioma. Several changes have been made to the WHO classification of tumours of the nervous system in 2016 (**Table 74.1**) (Louis et al., 2016). These includes classifying melanotic schwannoma as a distinct entity, incorporating hybrid nerve sheath tumours, as well as designating two subtypes of MPNST: epithelioid MPNST and MPNST with perineurial differentiation.

The aetiology of PNSTs is unknown. The tumours may arise sporadically or in association with hereditary disorders, notably neurofibromatosis type 1 (NF1) and neurofibromatosis type 2 (NF 2). Both of these disorders are inherited in an autosomal dominant fashion, with NF1 being a mutation on chromosome 17 and NF2 a mutation on chromosome 22. NF1 patients in particular are predisposed to multiple neurofibromas and MPNSTs. NF2 on the other hand predominantly affects the spine and the cranial nerves.

Schwannoma

Schwannoma are benign neoplasms of Schwann cell origin. The gross appearance is characterized by well encapsulated spindle cell tumours with distinct Antoni A areas (compact spindled) and Antoni B components (hypocellular and microcytic), hyaline vessel walls, and nuclear palisading. Unlike neurofibromas, schwannomas arise within the nerve sheath and displace the fascicles as opposed to enveloping them. Tumour cells are strongly immunopositive for S-100 protein with abundant pericellular collagen type IV. Recent described markers frequently positive in schwannomas include podoplanin (Jokinen et al., 2008), calretinin (Fine et al., 2004), and SOX10 (Nonaka et al., 2008).

The schwannoma variants include that of conventional, cellular, plexiform, and melanotic schwannomas. Cellular schwannoma, although relatively uncommon, is an important variant to recognize because of its high cellularity, fascicular growth pattern, increased mitotic activity, and occasional locally destructive behaviour. Important clues to the diagnosis include a well-formed capsule containing lymphoid aggregates, presence of foamy histiocyte aggregate, and diffuse strong S100 protein and pericellular collagen IV expression. Of note, diffuse S100 protein expression is exceedingly uncommon in spindled MPNST. Cellular schwannoma may have higher local recurrence (5–40%) but for practical purposes lack malignant potential and never metastasize. Plexiform schwannoma is a distinctive subtype that usually occurs in superficial locations and is defined by an intraneural nodular pattern of growth. More problematic are the rare plexiform schwannomas that arise in deep anatomic locations as they demonstrate increased cellularity and mitotic activity. The presence of widespread S100, collagen IV immunoreactivity is reassuring. Melanotic schwannoma is a rare, distinctive, potentially malignant neoplasm, characterized by epithelioid cells with marked accumulation of melanin. The presence of psammoma bodies is associated in approximately half the cases with Carney complex (Carney, 1990).

Comparative genomic hybridization (CGH) analysis of sporadic and NF2-associated schwannomas has shown that the loss of 22q sequences is the most frequent imbalance. The NF2 tumour suppressor gene codes for schwannomin (merlin), a cell membrane protein that functions in the intercellular signalling pathway and helps mediate growth arrest.

Neurofibromas

Neurofibromas are benign unencapsulated tumours composed of spindle cells dispersed in fibromyxoid stroma. They appear tan-white

Table 74.1 2016 WHO Classification of peripheral nerve sheath tumours

Benign peripheral nerve sheath tumours	Malignant peripheral nerve sheath tumours
Schwannoma Cellular schwannoma Plexiform schwannoma Melanotic schwannoma Neurofibroma Atypical neurofibroma Plexiform neurofibroma Perineuroma Hybrid nerve sheath tumours	Epithelioid MPNST MPNST with perineurial differentiation

Reprinted from *WHO Classification of Tumours of the Central Nervous System*, Revised. Fourth Edition, Edited by Louis DN, Ohgaki H, Wiestler OD, Cavenee WK, International Agency for Research on Cancer, France, Copyright (2016).

with a glistening cut surface in gross specimens. A crucial histological feature that distinguishes them from schwannomas is that the tumour involves the cross section of the nerve fascicle; hence it lacks a surgical cleavage plane between the normal nerve fibres and the tumour. Their growth pattern is either as a well-demarcated intraneural type or through diffuse infiltration of soft tissue at extraneural sites. They are relatively common, particularly at superficial cutaneous sites, where they present as localized, pedunculated growths. The proportion of S-100 positive cells is variable.

Three specific clinicopathological subtypes based on architectural growth patterns have been described, namely localized, diffuse, and plexiform neurofibromas. The localized cutaneous neurofibroma is the most common and occurs sporadically in most cases. Diffuse neurofibromas are characterized by a plaque-like enlargement and usually occur in the head and neck region. Approximately 10% of cases are ultimately proven to be associated with NF1. The plexiform neurofibroma represents the rarest form and is almost always associated with NF1. It is defined by the involvement of numerous adjacent nerve fascicles and often shows an admixture of areas resembling localized and diffuse-type neurofibromas microscopically. It has a potential for malignant degeneration and is a recognized precursor for MPNST in NF1 patients. The mutation in the *NF1* gene is located at 17q11.2 locus and codes for neurofibromin, an intracellular signalling protein that contributes to inactivating the Ras-GTP signalling cascade and upregulates the cyclic adenosine monophosphate (cAMP) levels. The absence of functional neurofibromin increases cell proliferation and survival.

Perineuriomas

Perineuriomas are benign neoplasms with advanced perineural differentiation. Two distinct types are recognized; intraneural and soft tissue. Intraneural perineuriomas are characterized by the solitary expansion of peripheral nerves, due to involvement of one of more nerve fascicles. Histologically, they show 'pseudo-onion bulbs', which are composed of complex perineural cell proliferation extending into the endoneurium and concentrically surrounding the individual nerve fibres and endoneural capillaries. Soft tissue perineuriomas in contrast almost always lacks an associated nerve, are usually well circumscribed, and may have a capsule. Typical histological findings are slender cells with very delicate, overlapping elongated cellular processes, arranged in loose fascicles. The neoplastic cells express vimentin and epithelial membrane antigen but are negative for S-100 protein, desmin, muscle-specific actin, and CD34.

Hybrid nerve sheath tumours (HNSTs)

HNSTs are a recently recognized entity in the 2016 WHO classifications of peripheral nerve tumours. These include neurofibroma/perineurioma, schwannoma/perineurioma, and neurofibroma/schwannoma hybrid tumours. In the reported cases, the tumour locations are almost exclusively in the digits and extremities. The tumours tend to be solitary in nature, and located in the dermis and subcutis. Atypical sites such as the colon have been previously reported (Lang et al., 2012).

Malignant peripheral nerve sheath tumours (MPNSTs)

MPNSTs are malignant tumours arising from a peripheral nerve or in extraneural soft tissue and showing nerve sheath differentiation. Malignant spindled tumours in NF1 patients should be considered MPNST until proven otherwise. MPNSTs may also arise in the postirradiation setting. Frequent histologic findings include fascicles of alternating cellularity, whorls, palisades, or rosette-like arrangements, perineural and intraneural spread when the tumour is associated with a nerve, subendothelial accentuation of tumour cells, and large areas of geographic-like necrosis (Hruban et al., 1990).

The S-100 protein is expressed in 50–70% of these tumours and most cases are immunopositive for TP53. Although MPNSTs lack a distinctive cytogenetic signature that allows for a specific diagnosis, molecular alterations (including epidermal growth factor receptor (EGFR) amplification and deletions of NF1 or CDKN2A) are supportive of the diagnosis in the appropriate setting.

Epithelioid MPNST is a distinctive, rare subtype of MPNST that is characterized by a predominance of large epithelioid cells. These tumours are more common in superficial sites and in contrast to conventional MPNSTs, express S100 protein strongly, and are typically diffuse. The great majority of MPNST arising within pre-existing schwannomas are of epithelioid type.

Plexiform neurofibromas, in particular, are the main recognizable benign precursors to MPNST in NF1. Malignant transformation into MPNSTs of schwannomas is a much rarer phenomenon, and usually takes the form of epithelioid change, angiosarcoma, or a tumour with a primitive small cell component. MPNSTs may also rarely arise in ganglioneuromas or ganglioneuroblastomas and even less commonly in phaeochromocytomas.

The CGH data indicates that gain in distal 17q and loss of 13q14-q21 is common in MPNST. Additional frequent changes reported are gain of 5p, 7, 8q, and loss of 9p sequences.

Clinical presentation

All ages and both sexes may be affected by PNSTs. Sporadic MPNSTs are most common between 40 and 50 years of age. While those occurring in association with NF1 are diagnosed 10 years earlier. MPNSTs account for approximately 5–10% of all soft tissue sarcomas. Although rare in the general population, MPNSTs arise in 5% to 42% of patients with NF1.

Patients with PNSTs usually present with a visible or palpable mass, pain, weakness, sensory alterations, or sometimes a mass is found

as an incidental finding on imaging studies, but most peripheral nerve tumours are first noticed as asymptomatic lumps. Palpation of the mass might elicit dysesthesia or paraesthesia. Involvement of motor nerves might produce weakness or more commonly subtle functional impairment with fine motor tasks. Autonomic dysfunction may manifest as changes in texture, colour, and temperature of the skin or in the amount of sweat produced. The patient should be examined specifically for stigmata of NF1 (café au lait spots, neurofibromas, Lisch nodules, optic glioma, axillary/inguinal freckling, distinctive skeletal abnormalities, and family history).

Any rapid increase in size or rapid symptom progression should raise the suspicion of cyst formation, haemorrhage or malignant transformation, and the patient will need to be investigated accordingly.

Investigation

Historically, the diagnosis of peripheral nerve tumours was based on history, clinical examination, and electrophysiological studies. While computed tomography (CT) is able to demonstrate intrinsic calcifications and secondary skeletal changes, MRI has emerged since the 1980s as the gold standard for imaging peripheral nerve tumours. MRI permits detailed visualization of soft tissue at high resolution and can demonstrate the presence of a mass, the anatomy of the involved peripheral nerves and their relationship to adjacent major structures such as blood vessels. High-resolution MR neurography (MRN) offers improved resolution and contrast that facilitates identification of the precise location, shape, size, and resectability of peripheral nerve tumours.

MRI also provides clues to the nature of the tumour and can help distinguish benign and malignant lesions. Benign nerve sheath tumours are often isointense or slightly hyperintense on T1, hyperintense on T2 (Fig. 74.1) and heterogeneously enhancing. The majority of neurofibromas and a portion of schwannomas display increased central and decreased peripheral T1 signal intensity (termed 'target sign') and an opposite pattern on T2 signal intensity. In contrast, MPNSTs tends to heterogeneously enhance, are less discrete, and more likely to have areas of haemorrhage or necrosis. A rapid increase in tumour size on serial imaging suggests malignant transformation.

Metabolic imaging using ^{18}fluorodeoxyglucose (^{18}FDG) positron emission tomography (PET) can add valuable information regarding the tumour grade. ^{18}FDG PET/CT is currently the most efficient imaging modality in the detection of MPNST in NF1 patients. An SUV_{max} (maximum standardized uptake value) ratio greater than 1.5 provides a 98.8% negative predictive value, and a 61.5% positive predictive value. However, in view of the false positives rate, it is not specific enough to make an NF1 related MPNST diagnosis (Combemale et al., 2014). A recent study of 26 NF1 patients with suspected MPNST, who underwent stereotactic PET/CT (tumour/liver binding ratio SUV_{max} ratio greater than 1.5) core biopsy technique, has shown a diagnostic accuracy rate of 96% (Brahmi et al., 2015).

Electrophysiological studies such as electromyography (EMG) and nerve conduction studies (NCS) are often obtained in patients with peripheral nerve tumours. EMG studies and NCS may assist in localization, detect subclinical deficits, and document baseline function for future comparison. These studies are especially useful in plexus level tumours involving multiple nerves to the extremities.

Management

As benign PNSTs are usually slow growing, intervention is not warranted until symptoms appear. The indications for surgical resection include that of pain, neurologic symptoms, concern for malignancy, cosmesis, and for histological diagnosis. Plexiform neurofibromas should be monitored closely for changes in size or development of symptoms. Tumours with imaging findings suggestive of benign PNSTs do not require biopsy unless there are unusual clinical features.

Histological diagnosis should be sought when diagnostic uncertainty arises. Because of the elevated risk of malignant transformation in NF1, there should be a low threshold for percutaneous biopsy when there is rapid tumour growth or rapid onset of pain. Tissue sample can be obtained via fine-needle aspiration or with needle core biopsy. Performing the biopsy with PET/CT stereotactic

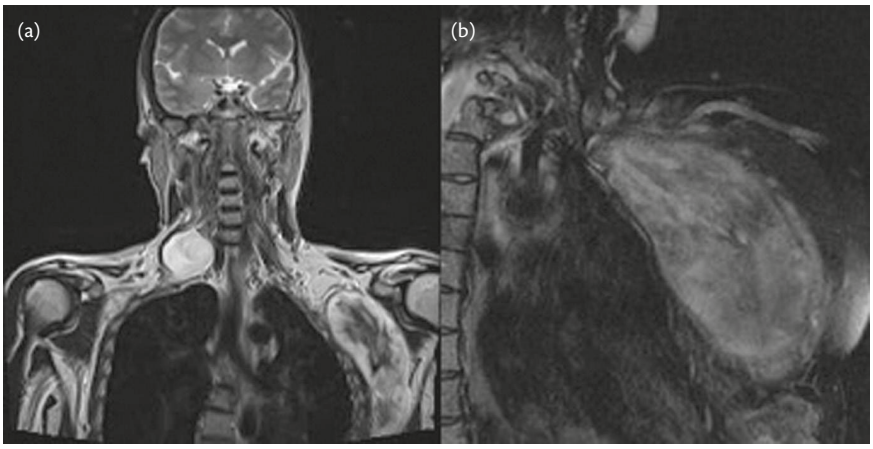

Fig. 74.1 (A, B) T-2 weighted MRI showing a large left infraclavicular plexus nerve sheath tumour as well as right supraclavicular plexus tumour in a 28-year-old woman with NF1.

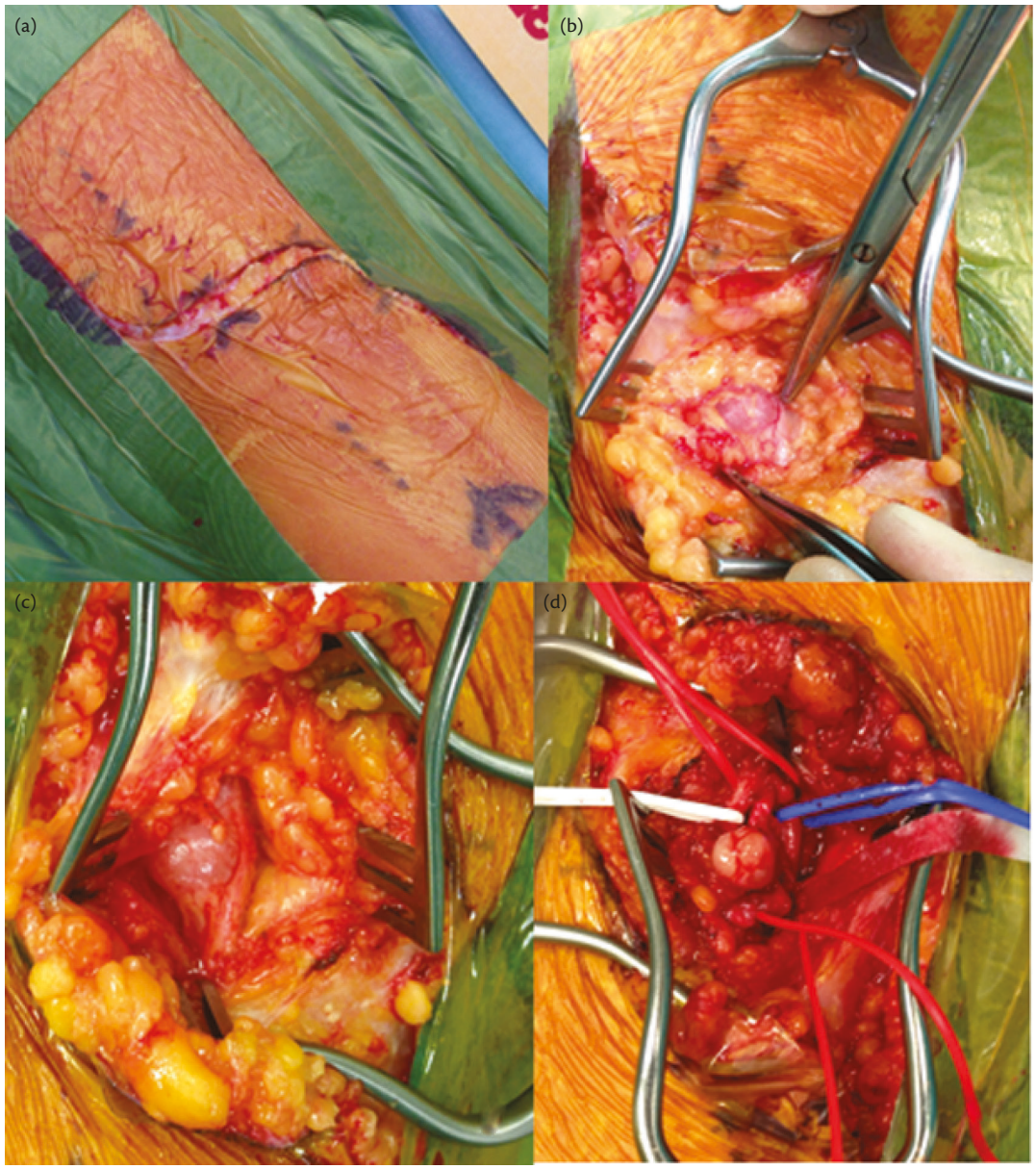

Fig. 74.2 Posterior tibial nerve schwannoma. (A) Curvilinear incision over left popliteal fossa. (B) Sharp dissection to expose tumour. (C) Isolation of *en passant* fascicles. (D) Identification of fascicles of origin.

guidance should be considered in order to reduce the false negative rate of suspicious lesions.

Surgical excision of a PNST can be performed under general, regional, or local anaesthesia (**Figs. 74.2, 74.3,** and **74.4**). Use of muscle relaxants must be avoided because these agents prevent intraoperative neurophysiological monitoring and stimulation. The patient is positioned to provide maximal exposure of the peripheral nerve in question. The skin incision is made over the course of the nerve beginning 2–4 cm proximal and extending 2–4 cm distal to the tumour. Dissection is performed though the subcutaneous tissues to expose the underlying lesion with meticulous haemostasis. Exposure of the nerve begins within an area of normal anatomy and extends into the area of tumour. It is important to identify the normal proximal and distal limits of the tumour. Loupe magnification or an operating microscope is often required to delineate the tumour, which may require internal neurolysis to identify the fascicles coursing over the tumour.

A nerve stimulator is applied to help identify afascicular entry points. An afascicular dissection plane is established by gently elevating and separating the fascicles from the tumour capsule. Internal debulking of the tumour with ultrasonic aspirator may facilitate dissection in very large tumours. Intraoperative EMG recordings provide feedback alerting the surgeon to overaggressive fascicle manipulation.

Non-functioning (as determined by stimulation) single fascicles seen entering and exiting a schwannoma may need to be divided to remove the tumour. Most schwannomas can be rolled out of their capsule and removed *en bloc*. It is not necessary to remove the tumour capsule of schwannomas as it is not associated with tumour recurrence. In contrast, fascicles enlarged by neurofibromas are often

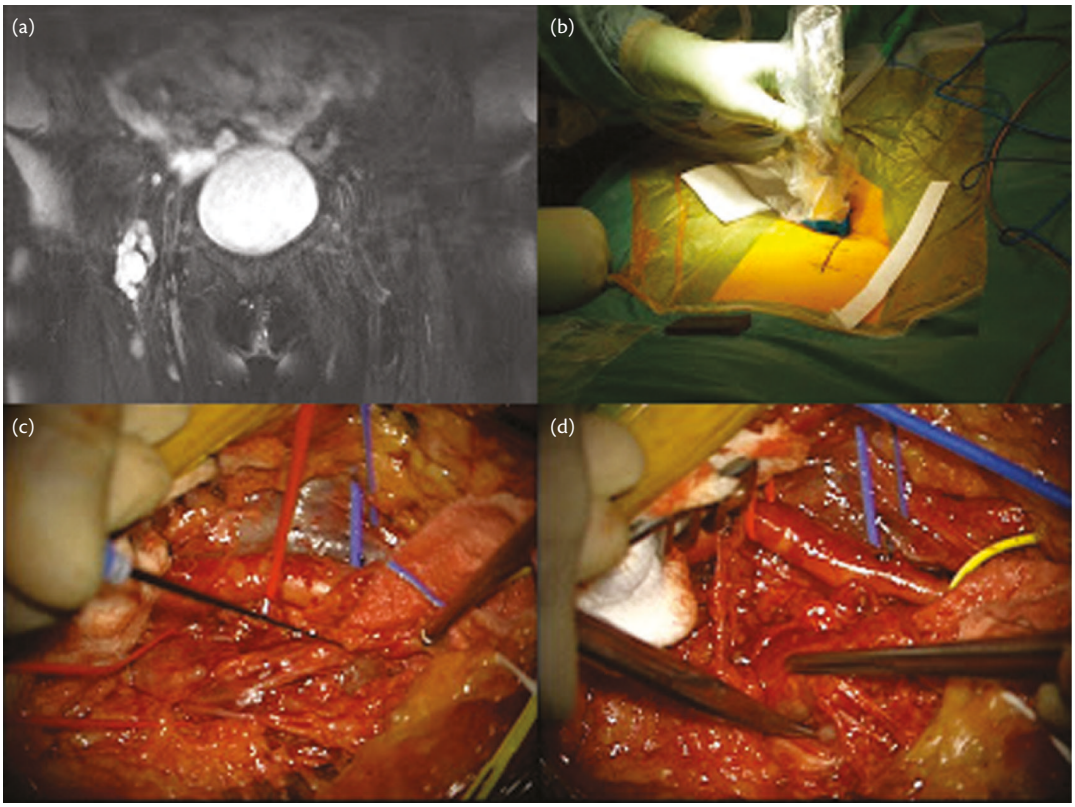

Fig. 74.3 Right genitofemoral nerve sheath tumour. (A) T1-weighted magnetic resonance imaged showing a contrast enhancing well-circumscribed tumour arising from the right genitofemoral nerve. (B) Intraoperative ultrasound to confirm location of the tumour. (C) Femoral nerve, artery, and vein identified. Nerve stimulator applied to identify afascicular plane. (D) Excision of the tumour performed using sharp dissection and microsurgical techniques.

still functioning and removal of the tumour inevitably requires sacrifice of one or more fascicles. Nerve grafting should be considered on occasions when a significant fascicle is sacrificed. The sural nerve commonly serves as the donor nerve; alternatives include the medial antebrachial cutaneous nerve or the sensory radial nerve. The surgical goal in extensive plexiform neurofibroma is often debulking to alleviate symptoms caused by neural compression. Frozen sections should be obtained to determine if a malignancy is present. Wound closure is then performed in layers with care taken not to entrap nerves in a tight compartment.

In MPNSTs with localized disease, complete surgical extirpation with clear margins is the treatment of choice. This is crucial even in large, non-extremity malignant tumours, as often seen in NF1 patients, for which extensive gross total resection would be associated with significant morbidity. Data supports the independent prognostic importance of complete surgical excision (Dunn et al., 2013). In most cases of large (>5 cm) high-grade extremity sarcomas, adjuvant radiation is advocated to reduce local recurrence. This however needs to be carefully discussed with all NF1 patients in view of the heightened risk of radiation-induced sarcoma. Although there are

Fig. 74.4 Right median nerve schwannoma. (A) T1-weighted MRI showing a contrast enhancing nerve sheath tumour arising from the right median nerve. (B) Sharp dissection performed to isolate the tumour and the median nerve. (C) Nerve stimulator applied to identify an afascicular plane prior to excision of the tumour.

no randomized trials examining adjuvant chemotherapy specifically in MPNST, adjuvant chemotherapy remains a consideration for motivated patients. The recently reported SARC006 phase II trial conducted by the Sarcoma Alliance for Research (SARC) evaluated the role of chemotherapy with doxorubicin, ifosfamide, and etoposide in 48 locally advanced metastatic MPNST patients. It revealed encouraging disease stabilization rates with responses accruing from neoadjuvant chemotherapy, that rendered subsequent local therapy feasible, in most patients with localized disease (Widemann et al., 2013).

Tumours of the brachial plexus represent an unusual disease, involve unfamiliar surgical territory for many neurosurgeons and hence present as a clinical challenge. The management of these tumours requires not only an understanding of the complex anatomy of the brachial plexus but also an appreciation of the appropriate surgical approach to the various tumours that may be encountered. The surgical recommendation is to use an anterior supraclavicular approach to treat tumours on most of the roots and trunks. The infraclavicular approach is used for lesions involving the cords and distal plexal elements. A posterior approach is utilized for tumours involving spinal nerves at the intraforaminal level, the C8-T1 roots, and the lower trunk. The posterior approach is also recommended in patients who present with residual or recurrent tumour or who have undergone radiotherapy.

Regardless of the approach selected, the operative steps for resection of most neural sheath tumours are similar. Briefly, the proximal and distal extent of the tumour is identified, and the tumour is isolated from the surrounding neurovascular structures. Involved and uninvolved fascicles at both the proximal and distal poles are identified by interfascicular dissection, intraoperative stimulation, and recording. These techniques are used to distinguish functional from dysfunctional fascicles so that non-functional fascicles may be sacrificed. The tumour is gradually dissected away and adherent but displaced fascicles and then lifted off the residual nerve. Finally, the capsule is sharply trimmed away from the remaining fascicles (Das et al., 2007).

Outcomes

Most benign PNSTs are amenable to complete excision and recurrence is infrequent. Unless a benign PNST is massive or has been previously operated on, complete excision can be achieved with little or no injury to the parent nerve.

MPNSTs are known to have high metastatic potential and poor prognosis. Reported long-term outcomes vary widely across multiple series, with 5-year survival ranging from 15% to 50%. Large tumour size at presentation (>5 cm) has been the most consistent adverse prognostic factor across all series. Other reported factors include tumour grade, surgical margin status, local recurrence, truncal location, and heterologous rhabdomyoblastic differentiation. While nuclear p53 expression, AKT, and TOR pathway activation, and MET activation have been associated with inferior outcome, to date there remains no well-defined or widely reproducible molecular prognostication factors (Farid et al., 2014)

The risk of MPNSTs in NF1 is estimated to be between 8% and 13% over a patient's lifetime and they are known to be one of the most frequent causes of death in patients with NF1. Several large series have reported significantly worse outcomes for MPNST arising in the setting of NF1 compared to sporadic tumours, with poorer responses to cytotoxic chemotherapy and 5-year survival up to 50% worse. A meta-analysis of several European studies, however, has suggested that while NF1 may have been a negative prognostic factor in studies before year 2000, this effect was subsequently lost possibly because of overall better surveillance and more rapid intervention at earlier stages of the disease in patients with NF1, and from improvements in imaging and diagnostic techniques (Kolberg et al., 2013).

In the setting of advanced or metastatic MPNST, outcomes are generally poor. The Response Evaluation Criteria in Solid Tumours (RECIST) response rate was reported to be 21% in a multi-institution retrospective study pooling MPNST patients from across multiple soft tissue sarcoma trials (Kroep et al., 2011).

FURTHER READING

Das, S., Ganju, A., Tiel, R.L., & Kline, D.G. (2007). Tumors of the brachial plexus. *Neurosurg Focus*, **22**(6), E26. Review.

Kolberg, M., Høland, M., Agesen, T.H., et al. (2013). Survival meta-analyses for 1800 malignant peripheral nerve sheath tumor patients with and without neurofibromatosis type 1. *Neuro Oncol*, **15**(2), 135–47.

Kroep, J.R., Ouali, M., Gelderblom, H., et al. (2011). First-line chemotherapy for malignant peripheral nerve sheath tumor (MPNST) versus other histological soft tissue sarcoma subtypes and as a prognostic factor for MPNST: an EORTC soft tissue and bone sarcoma group study. *Ann Oncol*, **22**(1), 207–14.

Louis, D.N., Perry, A., Reifenberger, G., et al. (2016). The 2016 World Health Organization Classification of Tumors of the Central Nervous System: a summary. *Acta Neuropathol*, **131**(6), 803–20.

Rodriguez, F.J., Folpe, A.L., Giannini, C., & Perry, A. (2012). Pathology of peripheral nerve sheath tumors: diagnostic overview and update on selected diagnostic problems. *Acta Neuropathol*, **123**(3), 295–319.

REFERENCES

Brahmi, M., Thiesse, P., Ranchere, D., et al. (2015). Diagnostic accuracy of PET/CT-guided percutaneous biopsies for malignant peripheral nerve sheath tumors in neurofibromatosis type 1 patients. *PLoS One*, **10**(10), e0138386.

Carney, J.A. (1990). Psammomatous melanotic schwannoma. A distinctive, heritable tumor with special associations, including cardiac myxoma and the Cushing syndrome. *Am J Surg Pathol*, **14**, 206–22.

Combemale, P., Valeyrie-Allanore, L., Giammarile, F., et al. (2014). Utility of 18FFDG PET with a semi-quantitative index in the detection of sarcomatous transformation in patients with neurofibromatosis type 1. *PloS One*, **9**, e85954.

Das, S., Ganju, A., Tiel, R.L., & Kline, D.G. (2007). Tumors of the brachial plexus. *Neurosurg Focus*, **22**(6), E26. Review.

Dunn, G.P., Spiliopoulos, K., Plotkin, S.R., et al. (2013). Role of resection of malignant peripheral nerve sheath tumors in patients with neurofibromatosis type 1. *J Neurosurg*, **118**(1), 142–8.

Farid, M., Demicco, E.G., Garcia, R., et al. (2014). Malignant peripheral nerve sheath tumors. *Oncologist*, **19**(2), 193–201.

Fine, S.W., McClain, S.A., & Li, M. (2004). Immunohistochemical staining for calretinin is useful for differentiating schwannomas from neurofibromas. *Am J Clin Pathol*, **122**, 552–9.

Hruban, R.H., Shiu, M.H., Senie, R.T., & Woodruff, J.M. (1990). Malignant peripheral nerve sheath tumors of the buttock and lower extremity. A study of 43 cases. *Cancer*, **66**, 1253–65.

Jokinen, C.H., Dadras, S.S., Goldblum, J.R., van de Rijn, M., West, R.B., & Rubin, B.P. (2008). Diagnostic implications of podoplanin expression in peripheral nerve sheath neoplasms. *Am J Clin Pathol*, **129**(6), 886–93.

Kroep, J.R., Ouali, M., Gelderblom, H., et al. (2011). First-line chemotherapy for malignant peripheral nerve sheath tumor (MPNST) versus other histological soft tissue sarcoma subtypes and as a prognostic factor for MPNST: an EORTC soft tissue and bone sarcoma group study. *Ann Oncol*, **22**(1), 207–14.

Lang, S.S., Zager, E.L., Coyne, T.M., Nangunoori, R., Kneeland, J.B., & Nathanson, K.L. (2012). Hybrid peripheral nerve sheath tumor. *J Neurosurg*, **117**, 897–901.

Louis, D.N., Perry, A., Reifenberger, G., et al. (2016). The 2016 World Health Organization Classification of Tumors of the Central Nervous System: a summary. *Acta Neuropathol*, **131**(6), 803–20.

Nonaka, D., Chiriboga, L., & Rubin, B.P. (2008). Sox10: a pan- and melanocytic marker. *Am J Surg Pathol*, **32**, 1291–8.

Rodriguez, F.J., Folpe, A.L., Giannini, C., & Perry, A. (2012). Pathology of peripheral nerve sheath tumors: diagnostic overview and update on selected diagnostic problems. *Acta Neuropathol*, **123**(3), 295–319.

Widemann BC, Reinke, D.K., Helman, L.J., et al. (2013). SARC006: phase II trial of chemotherapy in sporadic and neurofibromatosis type 1 (NF1)-associated high-grade malignant peripheral nerve sheath tumors (MPNSTs). *J Clin Oncol*, **31**, 10522.

SECTION 16

Functional neurosurgery

75. **Principles of deep brain stimulation** *865*
Erlick A.C. Pereira, Alexander L. Green, and Tipu Z. Aziz

76. **Movement disorders** *873*
Keyoumars Ashkan and Ismail Ughratdar

77. **Spasticity** *885*
John Goodden, Catherine Hernon, and Brian Scott

78. **Pain pathophysiology and surgical management** *895*
Richard Mannion and Rokas Tamosauskas

79. **Cranial nerve vascular compression syndromes** *909*
Marc Sindou and George Georgoulis

80. **Neurosurgical interventions for psychiatric disorders** *929*
Chris Bervoets, Bart Nuttin, and Loes Gabriëls

75

Principles of deep brain stimulation

Erlick A.C. Pereira, Alexander L. Green, and Tipu Z. Aziz

Introduction

The notion that illness can be ameliorated by electrical stimulation predates both Sir Victor Horsley's and Harvey Cushing's early twentieth century establishment of neurological surgery as a discipline and Benjamin Franklin's late eighteenth century discovery of static electricity and its effects upon muscle. First accounts date back to the ancient Roman empire when a freed man of Emperor Tiberius with painful gout stepped upon a torpedo fish. The electrocution administered relieved his gout considerably, leading the local physician Scribonius to recommend the treatment for painful gout and headache (Kellaway, 1946; Gildenberg, 2005). Not until nineteenth century animal experiments elicited movement by electrical stimulation of the brainstem and cerebral cortex did electrical brain stimulation became a noteworthy scientific endeavour (Flourens, 1824; Fritsch and Hitzig, 1870; Morgan, 1982). Horsley, the father of British neurosurgery, was first to apply electrical stimulation directly onto the human brain in the 1880s, using the technique to identify eloquent cortex and guide tumour resections (Vilensky and Gilman, 2002).

Alongside pioneering neurostimulation techniques, Horsley's other great advance enabling deep brain stimulation (DBS) was his invention, together with Clarke, of apparatus enabling stereotaxis (Horsley and Clarke, 1908). Stereotaxis uses a frame fixed to the head to localize cerebral structures with reference to a brain atlas via an external coordinate system calculated in relation to skull or brain landmarks. In 1947 Spiegel and Wycis adapted the Horsley-Clarke apparatus to humans for stereotactic neurosurgery (Spiegel et al., 1947). While irreversible lesioning surgery by chemical injections or thermocoagulation soon became the norm, many pioneers favoured reversible DBS during surgery to confirm they were on target (Hassler et al., 1960; Spiegel, 1982).

DBS emerged as a clinical tool from a nexus of translational research initiatives. Implantable neurostimulatory devices were developed by engineers such as Roger Avery and Thomas Mortimer in collaboration with surgeons and industry (Sweet and Wepsic, 1968; Mortimer et al., 1970). Intraoperative stimulation was used to produce functional maps of the sensory thalamus and other deep brain structures (Tasker et al., 1982). Knowledge of the functional anatomy of deep brain structures was increased by animal research and empirical observations from ablative neurosurgery in humans (Gildenberg, 2005; Gildenberg, 2006; Pereira and Aziz, 2006). Intermittent DBS was successfully trialled first for cancer pain in the 1950s and 1960s (Heath and Mickle, 1960; Gol, 1967) then for trigeminal neuralgia and other chronic pain syndromes targeting the thalamus, internal capsule and periaqueductal grey matter in the 1970s (Adams et al., 1974; Hosobuchi et al., 1973; Hosobuchi et al., 1977; Richardson and Akil, 1977). Throughout the last four decades, DBS for pain has continued to be undertaken by experienced specialists, its indications expanding to include stroke, amputation, multiple sclerosis, plexopathies and failed back surgery syndrome among others (Pereira and Aziz, 2014).

Despite its intraoperative use throughout the epoch of the 1950s to 1970s for localization during lesional and resective surgery for epilepsy (Spiegel et al., 1950), and movement disorders with observations of improvement in Parkinsonian tremor and dyskinesia (Hassler et al., 1960; Alberts et al., 1965; Bechtereva et al., 1975), therapeutic DBS did not promulgate to these indications until the late 1980s. Key factors obviating its use were the success of drug treatments for these conditions—phenytoin, carbamazepine, and valproate for epilepsy and levodopa for Parkinson's disease (PD) (Cotzias et al., 1967), established efficacy and surgeon experience with ablative and resective surgery in both PD and epilepsy (Cooper, 1956; Svennilson et al., 1960; Jensen, 1975), and cumbersome early neurostimulator models both less reliable and at greater risk of damage and infection than current technologies (Mullett, 1987).

Over a decade after its first use in pain (Hosobuchi et al., 1973), implantable DBS of the thalamus was performed to suppress tremor in PD refractory to drug treatments (Benabid et al., 1987). Primate-based research identified the subthalamic nucleus, a basal ganglia structure, as a putative brain target for both ablation and DBS (Bergman et al., 1990; Aziz et al., 1991). Alongside the resurgence of thalamic and globus pallidus internus lesional surgery (Narabayashi et al., 1984; Laitinen et al., 1992), together with advances in the miniaturization and reliability of neurostimulator technology, the scientific discoveries from primate research cultivated a renaissance in neurosurgery for PD in the 1990s and in particular for the popularization of DBS over the last decade as the neurosurgical therapy of choice for medically refractory PD with several other disorders of movement, pain, and affect becoming candidates for treatment. **Table 75.1** summarizes current indications for DBS and their anatomical targets.

Table 75.1 Indications for deep brain stimulation and popular deep brain structures targeted

Indication	Deep brain targets
Parkinson's disease	Globus pallidus interna, subthalamic nucleus
Dystonia	Globus pallidus interna
Tremor	Ventralis intermedius thalamic nucleus, zona incerta
Depression	Subgenual cingulate cortex, anterior limb of internal capsule
Obsessive-compulsive disorder	Anterior limb of internal capsule
Tourette's syndrome	Ventromedial thalamus, anterior limb of internal capsule, globus pallidus interna
Epilepsy	Anterior thalamic nucleus, centromedian thalamic nucleus
Cluster headache	Posterior hypothalamus
Chronic pain	Ventroposterior thalamus, periventricular and periaqueductal grey matter

Stereotactic surgery

Horsley and Clarke invented stereotaxis as 'a means of producing lesions of the cerebellar nuclei which should be accurate in position, limited . . . in extent, and involving as little injury as possible to other structures' (Horsley and Clarke, 1908). Legend has it that while gazing up at the stars and contemplating his place in them, Clarke conceived an apparatus through which probing intracranial instruments could be inserted that could be clamped to an animal's head by laterally placed skull pins, bars attached to plugs inserted into the external auditory meatus and further bars resting upon the nose and orbital margins, fixing it to a Cartesian coordinate system. They coined the term 'stereotaxic' from the Greek words 'stereos' meaning 'solid' and 'taxis' meaning 'arrangement'. 'By this means every cubic millimetre of the brain could be studied and recorded' (Horsley and Clarke, 1908; Pereira et al., 2008).

Stereotactic surgery has three fundamental concepts. Firstly, that the brain is a geometric volume in a (usually Cartesian) coordinate system, secondly that suitable reference points (such as the commissures) can be defined within this volume to calculate surgical targets and thirdly that appropriate surgical instruments can navigate the coordinate system to operate upon such targets.

Geometry and reference points

Any point in the head can be described in space by considering the head as fixed in three orthogonal planes intersecting at a given reference zero point. Thus, the distance lateral to the zero (x), anterior to it (y), and vertically above it (z) can be quantified in mm.

Visible targets in the brain can be described in terms of their distance from the zero reference point in x, y, and z directions when the head is fixed into a stereotactic frame (or frameless system). These include the subthalamic nucleus and globus pallidus interna targets for Parkinson's disease with modern MRI imaging. Invisible targets such as the ventral intermediate thalamus can be grossly targeted either in terms of their known distance from deep brain landmarks such as the mid-commissural point or using stereotactic atlases. The use of the anterior and posterior commissures (AC-PC) as part of a completely intracerebral reference framework was first described by Jean Talairach (Talairach et al., 1957). Stereotactic atlases are compiled from multiple fixed brain specimens sliced parallel to the reference planes and stained to highlight deep brain nuclei or fibres of passage. Schaltenbrand's atlas compiled from brains sliced orthogonal or in parallel with the AC-PC line is most commonly used (Schaltenbrand and Wahren, 1977). It can be helpful to some surgeons if either direct or indirect targeting is combined either with clinical assessment of the awake patient intraoperatively or electrophysiological recording by multiple microelectrodes or from the DBS 'macroelectrode' lead to increase efficacy.

Instruments

Most stereotactic systems comprise a coordinate frame and targeting device. The frame has a rigid, metallic 'base-ring' platform fixed to the skull to prevent displacement, usually by four pins penetrating its outer table. Common frames in usage are the Cosman-Roberts-Wells (CRW) (Fig. 75.1) which has its zero in the centre of the frame and Leksell which has its zero in the upper, posterior, right hand corner with 100, 100, 100 mm being its x, y, z centre. Onto the platform, a localizing system can be placed before a computed tomography (CT) or MRI is performed. The position of the head relative to the frame can then be calculated by computer software (and also manually with the Leksell frame) to transform the brain structures of interest into 'stereotactic space', the coordinate system of the frame. N-shaped bars on the localizer enable calculation of z.

Fig. 75.1 CRW Precision™Arc System on its phantom target to check targeting coordinates.

Arc radius, polar, and focal point coordinate systems can be used for stereotactic instruments. Focal point systems brought the patient's head to the framed probe and are hardly used now outside of radiosurgery. Polar coordinate systems solely used by the first stereotactic frames (such as Clarke's modified Horsley-Clarke frame, the Spiegel-Wycis frame, and the Riechert-Mundinger frame still popular in Europe) define probe trajectory in terms of angles and depth. While the target point is defined by Cartesian coordinates, the entry point through the skull chosen when planning gives the azimuth and declination of the probe carrier to target. With target and entry point fixed, the probe trajectory is the straight line between them passing through the arc of the stereotactic frame to a depth fixed by the frame. In modern, commonly used, arc radius systems, the trajectory can be defined by two angles (the arc and ring) and a linear magnitude (the radius or depth). In commonly used arc radius frames (such as CRW and Leksell), a fixed radius semicircular arc can move freely in a Cartesian coordinate system, pivot through 180° anteroposteriorly and its probe holder can translate along the arc in the frontal plane. Thus, the target can be hit from any trajectory as long as the target coordinates and depth remain fixed.

Cartesian phantom target systems (such as that of CRW) contain a pointer that mimics the target and provide a safety check to reduce human error and confirm that the frame is set to the correct target point before it is placed on the head and a probe passed to the intracranial target (Fig. 75.1). Such phantom systems were more important when stereotactic frames used polar coordinates as they provided a safety check between the intersecting angles of the probe carrying frame and the Cartesian target of the phantom—a concomitant error in both is highly unlikely.

Many DBS surgeons use CRW frames and algorithmically fuse stereotactically acquired CT scans to preoperative MRI to reduce spatial distortion of tissue representation by MRI (Fig. 75.2). Others use MRI-compatible CRW or Leksell frames to directly target from a stereotactic MRI, with spatial distortion being less of an issue in modern higher resolution scanners. A few practitioners continue to use CT alone or even ventriculography for DBS and some use computerized frameless systems and even robots that automate the whole process.

DBS hardware

The most regularly used current DBS electrode is quadripolar, having four electrical contacts, each 1.5 mm long and separated by 0.5 mm of insulation. Several stimulation parameters can be altered in DBS. Commonly, stimulation can be monopolar (with the distant pulse generator case acting as the anode) or bipolar over any combination of the four contacts of each electrode and multiple contacts can be specified as anodes or cathodes. Voltage can typically be altered from 0 to 10 v, frequency from 2 to 300 Hz, and width of the square wave pulse from 60 up to 500 μs. Stimulation may be either continuous or cycled between on and off states each of at least 0.1 s duration.

The DBS electrode is secured to the skull and connected to a lead that is tunnelled to the chest or abdomen where a pulse generator (pacemaker) containing the power source is implanted under the skin (Fig. 75.3). Some pacemakers can be transcutaneously recharged.

DBS mechanisms

The prevailing dogma surrounding DBS mechanisms is that high frequency DBS inhibits neuronal firing within its target brain structure and that low frequency DBS excites neurons to fire. The evidence for high frequency 'jamming' comes largely by analogy with lesional surgery such as pallidotomy and thalamotomy which can have similar clinical outcomes. The low frequency driving theory arises from the observation that low frequency DBS worsens some Parkinsonian symptoms and the suggestion that low frequency DBS of the pedunculopontine nucleus in freezing of gait and periaqueductal grey in chronic pain can drive motoric and analgesic

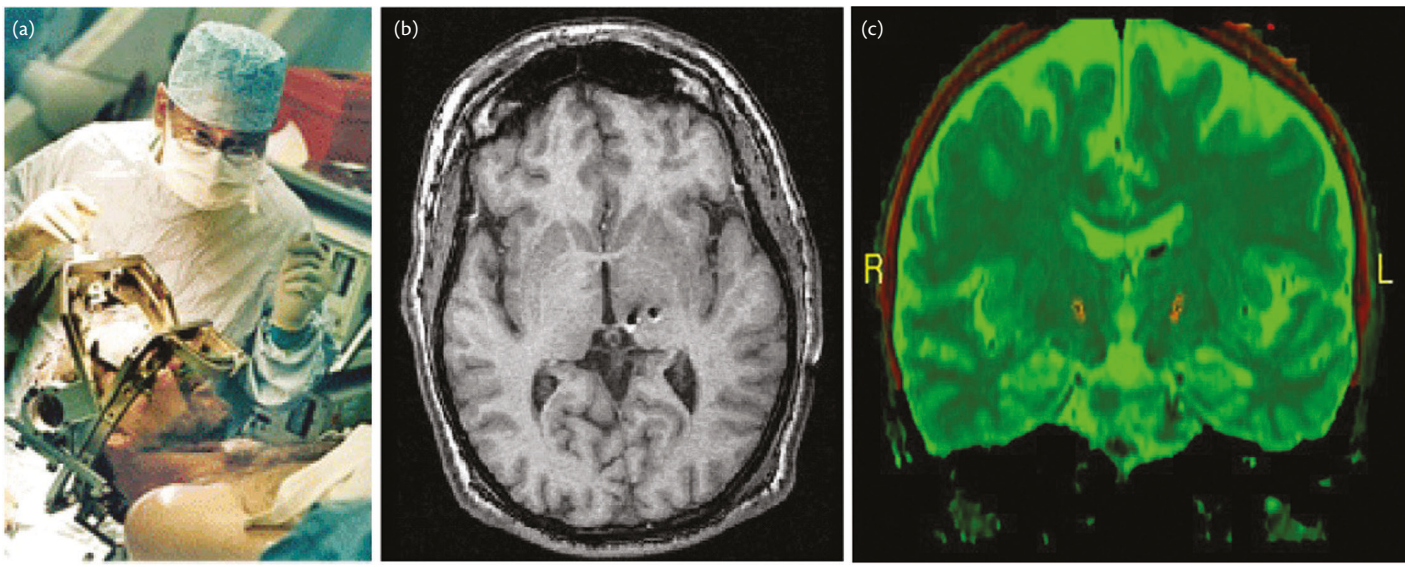

Fig. 75.2 (A) Intraoperative awake deep brain stimulation; (B) axial MRI of deep brain stimulators for pain *in situ*; (C) fused coronal CT and MRI showing subthalamic nuclei targeted in deep brain stimulation for Parkinson's disease.

Fig. 75.3 A DBS electrode, tunnelled extension lead, and implantable pulse generator *in situ*.
Reproduced with permission of Medtronic, Inc.

neural circuits, respectively. Electrophysiological experiments in humans and non-human primates, however, suggest that both low and high frequency DBS can excite target nucleus afferent and efferent neuronal axons as well as fibres of passage (McIntyre et al., 2004).

More fundamental underlying principles of DBS include firstly its effects on the neuron and its components in terms of the electrical activities generated, secondly how those effects propagate through the relevant neural circuitry such as the basal ganglia, thalamus, and cortex, and finally how DBS influences modulatory monoamine and other neurotransmitters in the brain. Here we focus upon the direct electrical effects of DBS upon neuronal physiology as the latter principles of synaptic neurotransmitter release and modulation of neuroanatomic circuits can be considered secondary to this effect.

Local electrical effects

DBS generally excites action potentials in surrounding neuronal tissue (Kringelbach et al., 2007; Montgomery and Gale, 2008). Effective DBS is reliant upon exciting sufficient action potentials in the desired target tissue while limiting spread of electric current to excite action potentials in unintended adjacent structures. Greater current intensity or volume improves outcome but increases likelihood of untoward side effects. Strategies to electrophysiologically tailor the DBS electrical field to each patient are therefore desirable. Varying stimulation parameters such as amplitude and pulse width can also alter the population of neural elements stimulated. Axonal terminals have the lowest threshold, followed by axons, dendrites, and finally neuronal cell bodies. Larger axons respond more to narrower pulse widths of stimulation. Therefore when considering which neurons are activated by DBS, general principles are firstly that neurons further away from the brain electrode are less likely to be stimulated, secondly that axons will be stimulated to give rise to an action potential at lower DBS amplitudes than neuronal cell bodies, thirdly that larger axons will respond to lower stimulus amplitudes than will smaller axons and finally that axons with branching processes will also be activated at lower stimulus amplitudes. The orientation of the neuron relative to the DBS field is also relevant. Those oriented with the voltage gradient are more likely to reach threshold than those lying orthogonal to it. Also interesting is that neurons nearest the DBS cathode are more likely to be activated than those close to the anode, hence the designation of the pulse generator case as anode in monopolar DBS.

Future developments

Currently, most pacemakers deliver stimulation continuously at a fixed rate, in what is a rather simple but nevertheless effective therapy. However, constant stimulation can incur unwanted side effects by spreading to other fibre tracts or by disrupting normal brain signals embedded in pathological activity. Alteration of such 'normal' signals may affect emotion or cognition, for example. By targeting stimulation specifically to abnormal oscillations, it may be possible to apply stimulation intermittently and thus allow normal signals to re-emerge. Indeed, there is evidence that symptom suppression may be better with such intermittent stimulation than with continuous stimulation (Little et al., 2016). Other prospects include a pacemaker with telemetric capabilities, which could aid the identification of pathological markers in various disorders. Pacemakers that respond to posture could also reduce side effects, as in the case of spinal cord stimulation where lower levels of stimulation may be required in the supine position than in the upright position. Such pacemakers use directional accelerometers to determine movement and position.

A good clinical response is sometimes limited by the proximity of the contacts to structures adjacent to the target. An electrode may be placed in the subthalamic nucleus, for example, but if it is too close to the capsule, stimulation will induce side effects within the therapeutic window. To overcome this problem, technology companies have produced alternative electrode configurations, such as splitting the ring contacts into two or three, or even arranging 32 contacts in an array resembling a fish-scale (**Fig. 75.4**). Experimentally, the latter has been shown to offer directionality in the primate (Martens et al., 2011), as well as in a clinical case series in which it was also possible to record local field potentials from multiple contacts for better localization (Bour et al., 2015).

At present, structural MRI is usually used for targeting electrodes. Although not yet fully evaluated, the use of diffusion tensor imaging may improve results by allowing specific parts of a nucleus that are connected to another region or possibly part of a network to be targeted, rather than just the nucleus itself. As demonstrated in tumour surgery, diffusion tensor imaging can be used to identify fibre tracts that, if stimulated, would induce side effects, so that these can be avoided. It is also possible to somatotopically identify the best electrode position within homogeneous structures such as the thalamus (Hyam et al., 2012).

In the realm of molecular and cellular therapies, much translational research is being undertaken but few treatments have demonstrated comparable safety and efficacy to DBS. Clinical trials of neurotrophic factors, stem cells and fetal cell transplants have all been undertaken with limited success (Astradsson and Aziz, 2016).

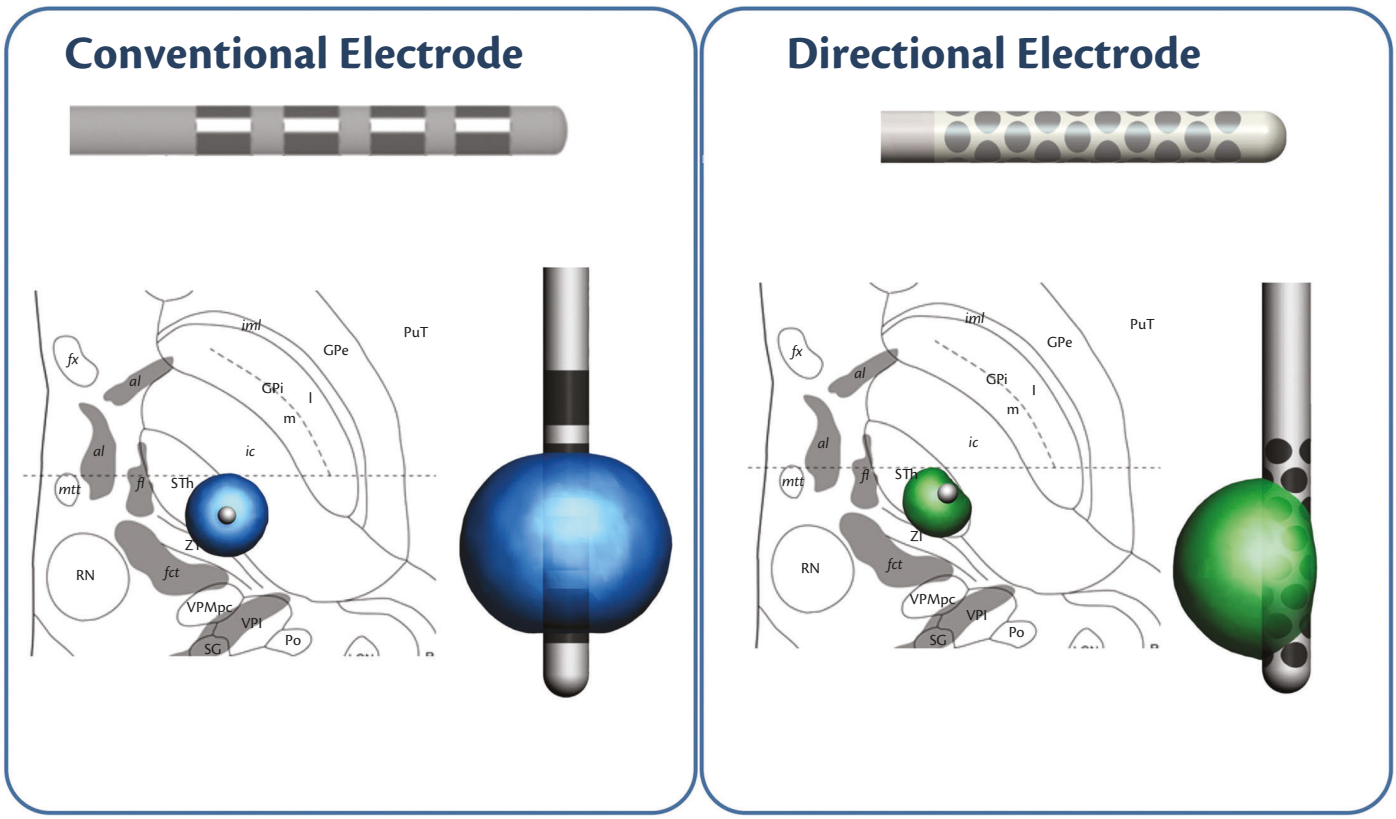

Fig. 75.4 Multicontact array directional electrode enabling optimization of brain nucleus stimulated by DBS. STN, subthalamic nucleus (common Parkinson's disease DBS target); ic, internal capsule.
Reproduced with permission of Medtronic, Inc.

Unilateral DBS does however provide an elegant potential control surgery for contralateral biological therapy implantation (Rowland et al., 2015).

Lesional surgery

Lesional procedures using radiofrequency ablation have been largely replaced by DBS due to its greater safety and its reversibility, but under certain conditions pallidotomy, thalamotomy, and even subthalamotomy remain useful alternatives, especially in the resource limited setting where DBS may not be economically feasible and clinical follow-up might be a challenge (Pereira and Aziz, 2013). Other specific indications include chronic infection complicating past DBS, metal allergies, risk to implanted DBS hardware from falls or obsessive-compulsive head banging or palliative procedures if limited lifespan such as cingulotomy for cancer pain or pallidotomy in severe, advanced Parkinson's disease (Bulluss et al., 2013; Viswanathan et al., 2013). Radiofrequency thermocoagulation of brain tissue with an electrical lesion generator is most commonly performed but requires a burr hole and passage of a rigid probe through the brain to the target to be lesioned. Alternative non-invasive lesioning modalities are gamma knife radiosurgery that has the disadvantage of several months for onset of efficacy and magnetic resonance–guided high frequency focused ultrasound for which there is promising initial clinical evidence (Elias et al., 2013; Witjas et al., 2015).

Conclusions

DBS requires accurate brain electrode placement which usually utilizes a stereotactic frame fixed to the head, although frameless and robotic alternatives exist. For all DBS targets, the relative contributions of local interactions and wider functional neuroanatomical circuitry are yet to be fully elucidated. However, the general principle is that pulsed current passed from an implanted battery generates a local field potential which in turn causes a surrounding population of neurons to individually either reach their thresholds for action potential generation or to hyperpolarize. Such neurons may release neurotransmitters from their synapses and alter deep brain neural circuitry functions controlling movement, seizures, or other behaviours such as reduced pain perception or tics. Alternatives to DBS include lesions by radiofrequency thermocoagulation, gamma knife radiosurgery, or focused ultrasound. Future developments include advances in imaging such as diffusion tensor MRI, fields made steerable by directional electrodes, segmented electrodes, 'smart' adaptive DBS, and the use of stereotactic neurosurgery to deliver molecular and cellular therapies such as gene therapy, neurotrophic factor drug delivery, fetal and stem cell transplants.

FURTHER READING

Aziz, T.Z., Peggs, D., Sambrook, M.A., & Crossman, A.R. (1991). Lesion of the subthalamic nucleus for the alleviation of

1-methyl-4-phenyl-1,2,3,6-tetrahydropyridine (MPTP)-induced parkinsonism in the primate. *Mov Disord*, **6**, 288–92.
Benabid, A.L., Pollak, P., Louveau, A., Henry, S., & De Rougement, J. (1987). Combined (thalamotomy and stimulation) stereotactic surgery of the VIM thalamic nucleus for bilateral Parkinson disease. *Appl Neurophysiol*, **50**, 344–6.
Bulluss, K.J., Pereira, E.A., Joint, C., & Aziz, T.Z. (2013). Pallidotomy after chronic deep brain stimulation. *Neurosurg Focus*, **35**, E5.
Horsley, V. & Clarke, R.H. (1908). The structure and functions of the cerebellum examined by a new method. *Brain*, **31**, 45–124.
Laitinen, L.V., Bergenheim, A.T., & Hariz, M.I. (1992). Leksell's posteroventral pallidotomy in the treatment of Parkinson's disease. *J Neurosurg*, **76**, 53–61.

REFERENCES

Adams, J.E., Hosobuchi, Y., & Fields, H.L. (1974). Stimulation of internal capsule for relief of chronic pain. *J Neurosurg*, **41**, 740–4.
Alberts, W.W., Feinstein, B., Levin, G., Wright, E.W. Jr., Darland, M.G. & Scott, E.L. (1965). Stereotaxic surgery for parkinsonism. Clinical results and stimulation thresholds. *J Neurosurg*, **23**, 174–83.
Astradsson, A. & Aziz, T. (2016). Parkinson's disease: fetal cell or stem cell derived treatments. *BMJ*, **352**, h6340.
Aziz, T.Z., Peggs, D., Sambrook, M.A., & Crossman, A.R. (1991). Lesion of the subthalamic nucleus for the alleviation of 1-methyl-4-phenyl-1,2,3,6-tetrahydropyridine (MPTP)-induced parkinsonism in the primate. *Mov Disord*, **6**, 288–92.
Bechtereva, N.P., Bondartchuk, A.N., Smirnov, V.M., Meliutcheva, L.A., & Shandurina, A.N. (1975). Method of electrostimulation of the deep brain structures in treatment of some chronic diseases. *Confin Neurol*, **37**, 136–40.
Benabid, A.L., Pollak, P., Louveau, A., Henry, S., & De Rougement, J. (1987). Combined (thalamotomy and stimulation) stereotactic surgery of the VIM thalamic nucleus for bilateral Parkinson disease. *Appl Neurophysiol*, **50**, 344–6.
Bergman, H., Wichmann, T., & Delong, M.R. (1990). Reversal of experimental parkinsonism by lesions of the subthalamic nucleus. *Science*, **249**, 1436–8.
Bour, L.J., Lourens, M.A., Verhagen, R., et al. (2015). Directional recording of subthalamic spectral power densities in Parkinson's disease and the effect of steering deep brain stimulation. *Brain Stimul*, **8**, 730–41.
Bulluss, K.J., Pereira, E.A., Joint, C., & Aziz, T.Z. (2013). Pallidotomy after chronic deep brain stimulation. *Neurosurg Focus*, **35**, E5.
Cooper, I.S. (1956). *The Neurosurgical Alleviation of Parkinsonism*. Springfield, IL: Charles C. Thomas.
Cotzias, G.C., Van, W.M., & Schiffer, L.M. (1967). Aromatic amino acids and modification of parkinsonism. *N Engl J Med*, **276**, 374–9.
Elias, W. J., Huss, D., Voss, T., et al. (2013). A pilot study of focused ultrasound thalamotomy for essential tremor. *N Engl J Med*, **369**, 640–8.
Flourens, P. (1824). *Recherches experimentales sur les proprietes et les fonctions du systeme nerveux, dans les animaux vertebres*. Paris, France: J.-B. Balliere.
Fritsch, G. & Hitzig, E. (1870). Uber die elektrische Erregbarkeit des Grosshirns. *Arch Anat Physiol Wiss Med*, **37**, 300–32.
Gildenberg, P.L. (2005). Evolution of neuromodulation. *Stereotact Funct Neurosurg*, **83**, 71–9.
Gildenberg, P.L. (2006). History of electrical neuromodulation for chronic pain. *Pain Med*, **7** Suppl 1, S7–S13.
Gol, A. (1967). Relief of pain by electrical stimulation of the septal area. *J Neurol Sci*, **5**, 115–20.
Hassler, R., Riechert, T., Mundinger, F., Umbach, W., & Ganglberger, J.A. (1960). Physiological observations in stereotaxic operations in extrapyramidal motor disturbances. *Brain*, **83**, 337–50.
Heath, R.G. & Mickle, W.A. (1960). Evaluation of seven years' experience with depth electrode studies in human patients. In: Ramey, E.R. & O'Doherty, D.S. (eds.) *Electrical Studies on the Unanaesthetized Brain*, pp. 214–47. New York, NY: Paul B. Hoeber.
Horsley, V. & Clarke, R.H. (1908). The structure and functions of the cerebellum examined by a new method. *Brain*, **31**, 45–124.
Hosobuchi, Y., Adams, J.E. & Linchitz, R. (1977). Pain relief by electrical stimulation of the central gray matter in humans and its reversal by naloxone. *Science*, **197**, 183–6.
Hosobuchi, Y., Adams, J.E., & Rutkin, B. (1973). Chronic thalamic stimulation for the control of facial anesthesia dolorosa. *Arch Neurol*, **29**, 158–61.
Hyam, J.A., Owen, S.L., Kringelbach, M.L., et al. (2012). Contrasting connectivity of the ventralis intermedius and ventralis oralis posterior nuclei of the motor thalamus demonstrated by probabilistic tractography. *Neurosurgery*, **70**, 162–9; discussion 169.
Jensen, I. (1975). Temporal lobe surgery around the world: results, complications, mortality. *Acta Neurol Scand*, **52**, 354–73.
Kellaway, D. (1946). The William Osler Medical Essay. The part played by electric fish in the early history of bioelectricity and electrotherapy. *Bull Hist Med*, **20**, 112–37.
Kringelbach, M.L., Jenkinson, N., Owen, S.L., & Aziz, T.Z. (2007). Translational principles of deep brain stimulation. *Nat Rev Neurosci*, **8**, 623–35.
Laitinen, L.V., Bergenheim, A.T., & Hariz, M.I. (1992). Leksell's posteroventral pallidotomy in the treatment of Parkinson's disease. *J Neurosurg*, **76**, 53–61.
Little, S., Beudel, M., Zrinzo, L., et al. (2016). Bilateral adaptive deep brain stimulation is effective in Parkinson's disease. *J Neurol Neurosurg Psychiatry*, **87**(7), 717–21.
Martens, H. C., Toader, E., Decre, M. M., et al. (2011). Spatial steering of deep brain stimulation volumes using a novel lead design. *Clin Neurophysiol*, **122**, 558–66.
Mcintyre, C.C., Savasta, M., Walter, B.L. & Vitek, J.L. (2004). How does deep brain stimulation work? Present understanding and future questions. *J Clin Neurophysiol*, **21**, 40–50.
Montgomery, E.B., Jr. & Gale, J.T. (2008). Mechanisms of action of deep brain stimulation (DBS). *Neurosci Biobehav Rev*, **32**, 388–407.
Morgan, J.P. (1982). The first reported case of electrical stimulation of the human brain. *J Hist Med Allied Sci*, **37**, 51–64.
Mortimer, J.T., Shealy, C.N., & Wheeler, C. (1970). Experimental nondestructive electrical stimulation of the brain and spinal cord. *J Neurosurg*, **32**, 553–9.
Mullett, K. (1987). State of the art in neurostimulation. *Pacing Clin Electrophysiol*, **10**, 162–75.
Narabayashi, H., Yokochi, F., & Nakajima, Y. (1984). Levodopa-induced dyskinesia and thalamotomy. *J Neurol Neurosurg Psychiatry*, **47**, 831–9.
Pereira, E.A. & Aziz, T.Z. (2006). Surgical insights into Parkinson's disease. *J R Soc Med*, **99**, 238–44.
Pereira, E.A. & Aziz, T.Z. (2013). Reincarnating the oxford cingulectomy in the epoch of stereotaxy and resurrecting lesions in the era of deep brain stimulation. *Stereotact Funct Neurosurg*, **91**, 262–3.
Pereira, E.A. & Aziz, T.Z. (2014). Neuropathic pain and deep brain stimulation. *Neurotherapeutics*, **11**, 496–507.
Pereira, E.A., Green, A.L., Nandi, D., & Aziz, T.Z. (2008). Stereotactic neurosurgery in the United Kingdom: the hundred years from Horsley to Hariz. *Neurosurgery*, **63**, 594–606; discussion 606–7.

Richardson, D.E. & Akil, H. (1977). Long term results of periventricular gray self-stimulation. *Neurosurgery*, **1**, 199–202.

Rowland, N.C., Starr, P.A., Larson, P.S., Ostrem, J.L., Marks, W.J., Jr., & Lim, D.A. (2015). Combining cell transplants or gene therapy with deep brain stimulation for Parkinson's disease. *Mov Disord*, **30**, 190–5.

Schaltenbrand, G. & Wahren, W. (1977). *Atlas for Stereotaxy of the Human Brain*, Stuttgart, Germany: Thieme.

Spiegel, E.A. (1982). *Guided Brain Operations.* Basel, Switzerland: Karger.

Spiegel, E.A., Wycis, H.T., Marks, M., & Lee, A.J. (1947). Stereotaxic apparatus for operations on human brain. *Science*, **106**, 349–50.

Spiegel, E.A., Wycis, H.T., & Umlauf, C.W. (1950). Electroencephalographic studies before and after thalamotomy. *Monatsschr Psychiatr Neurol*, **120**, 398–411.

Svennilson, E., Torvik, A., Lowe, R., & Leksell, L. (1960). Treatment of parkinsonism by stereotatic thermolesions in the pallidal region. A clinical evaluation of 81 cases. *Acta Psychiatr Scand*, **35**, 358–77.

Sweet, W.H. & Wepsic, J.G. (1968). Treatment of chronic pain by stimulation of fibers of primary afferent neuron. *Trans Am Neurol Assoc*, **93**, 103–7.

Talairach, J., David, M., Tournoux, P., Corredor, H., & Krasina, T. (1957). *Atlas d'Anatomie Stereotaxique*. Paris, France: Masson.

Tasker, R.R., Organ, L.W., & Hawrylshyn, P.A. (1982). *The Thalamus and Midbrain of Man. A Physiological Atlas Using Electrical Stimulation*. Springfield, IL: Charles C. Thomas.

Vilensky, J.A. & Gilman, S. (2002). Horsley was the first to use electrical stimulation of the human cerebral cortex intraoperatively. *Surg Neurol*, **58**, 425–6.

Viswanathan, A., Harsh, V., Pereira, E.A., & Aziz, T.Z. (2013). Cingulotomy for medically refractory cancer pain. *Neurosurg Focus*, **35**, E1.

Witjas, T., Carron, R., Krack, P., et al. (2015). A prospective single-blind study of Gamma Knife thalamotomy for tremor. *Neurology*, **85**, 1562–8.

76

Movement disorders

Keyoumars Ashkan and Ismail Ughratdar

Introduction

Movement disorders encompass a broad range of neurological disorders which primarily affect speed, fluency, ease, and quality of movement. They can be broadly categorized (Table 76.1) into those with excess spontaneous movement (hyperkinetic disorders) or those with absent or reduced ability to perform purposeful movement (hypokinetic disorders). Abnormal movements may be rhythmical (e.g. essential tremor) or slow and sustained (e.g. Parkinson's disease). In most cases, the irregular movements cannot be consciously controlled or suppressed.

Clinical assessment and appropriate investigation must be considered carefully as variations from the typical and overlap in presentations between diagnoses can affect treatment modality and success of surgery. A detailed history and directed examination should confirm the diagnosis in the majority, with augmentation as required utilizing electrodiagnostic studies and structural imaging.

In the present chapter the clinical assessment, pathogenesis, and medical therapy of the common movement disorders will be reviewed. A brief description of the surgical management, outcomes, and controversies is also described.

Parkinson's disease

Parkinson's disease (PD) is a chronic, progressive neurodegenerative disorder characterized by bradykinesia, rigidity, rest tremor, and postural instability. It is usually initially unilateral, insidious in onset and is associated with disabling non-motor symptoms such as depression, fatigue, and sleep disorders.

Classification

The term parkinsonism encompasses the motor syndrome described earlier and is classified into four subtypes according to the aetiology:

a. Primary/idiopathic/Parkinson's disease—the commonest form
b. Secondary/acquired (infection, drugs, trauma, vascular)
c. Hereditary parkinsonism (rare)
d. Parkinson plus syndromes—disorder occurs as a secondary effect of another primary neurological disorder (e.g. multiple system atrophy)

Epidemiology

PD is one of the most common neuro-degenerative disorders, second only to Alzheimer's disease. In the United Kingdom, the crude incidence rates range between 8–18/100 000 population/annum and prevalence rates around 108–164/100 000. Both incidence and prevalence are markedly affected by an increase in age. The onset of PD before 50 years of age is rare, but escalates dramatically over the age of 60 affecting approximately 1% of the population. This is likely to increase with an ageing population. With the ever-growing ageing population, the number of people with PD worldwide is projected to double to at least 8.7–9.3 million by 2030 (Dorsey et al., 2007).

Studies have also shown PD to be more common in males than females (1.3:1, prevalence and incidence). Crude prevalence studies suggest that PD is more common in Caucasians in Europe and North America and lowest in African races, though ascertainment bias may account for these differences. For reasons unknown, cigarette smoking and drinking beverages containing caffeine are reported to be protective against PD (Goetz and Pal, 2014).

Pathogenesis

The basic mechanism responsible for the development of PD consists of cellular degeneration of dopaminergic cells within the substantia nigra pars compacta (SNc) resulting in biochemical deficiency of dopamine (Dauer and Przedborski, 2003). There are three pathological hallmarks of PD:

- Lewy bodies—eosinophilic intraneuronal inclusions considered to be markers of neuronal degeneration
- Dopaminergic neuronal death in the SNc is an essential feature of PD and leads to loss of neuromelanin and depigmentation of this structure at post-mortem
- Removal of neuromelanin from dead cells by microglia

Understanding how this relatively selective loss of dopamine leads to parkinsonism requires a detailed understanding of the functional anatomy and neurocircuitry of the basal ganglia. In essence, the pathway 'flows' from the premotor cortex through the striatum and then back to the supplementary motor cortex. Activity in this loop is modulated by the SNc which acts as an accelerator and the subthalamic nucleus (STN) which acts as a brake. In PD, the SNc fails to work and thus the patient slows down and loses motor control.

Clearly, this model represents a gross oversimplification of the pathophysiology of PD. At a more complex level, the STN and SNc

Table 76.1 Classification of movement disorders

Hypokinetic disorders	
Parkinson's disease/ parkinsonism	Idiopathic, secondary (drugs, toxins, infection, trauma, vascular) Bradykinesia, tremor, rigidity, and postural instability
Progressive supranuclear palsy	Vertical gaze dysfunction, extrapyramidal symptoms, and frontal lobe dysfunction
Multiple system atrophy	Parkinsonism, cerebellar, and autonomic dysfunction Rapidly progressive
Stiff person syndrome	Progressive rigidity and stiffness of truncal muscles associated with spasms
Hyperkinetic disorders	
Restless legs syndrome	Irresistible urge to move limbs secondary to unpleasant sensations
Essential tremor	Action/postural tremor Autosomal dominant
Tics/Tourette's syndrome	Sudden, repetitive, non-rhythmic movements (motor) and utterances (vocal) that involve discrete muscle groups
Dystonia	Sustained muscle contractions causing twisting and repetitive movements or abnormal postures
Hemifacial spasm	Involuntary movement of one side of the face
Huntington's disease/ Chorea	Cognitive, movement, and psychiatric disorders
Torticollis	Dystonia leading to asymmetrical position of head/neck
Blepharospasm	Abnormal contraction of both eyelids
Writer's cramp	Task-specific (e.g. writing) focal hand dystonia

functions are mediated via a direct and an indirect pathway (Fig. 76.1). The direct pathway arises from a set of neurons that projects monosynaptically to neurons in GPi and SNr, whereas the indirect pathway arises from a different set of neurons that projects to GPe which is reciprocally linked with the STN. In PD, dopamine deficiency results in increased activity in striatopallidal GABAminergic fibres which inhibits the GPe neurones to the STN. Thus the glutaminergic STN projection to the GPi is stimulated which increases firing to the thalamus (Calabresi et al., 2014).

However, these models do not explain several findings from laboratory or clinical studies and thus in the last decade, theories relating to the pathophysiology of PD have moved from focussing on altered discharge rates to altered discharge patterns and now to excessive synchronization of activity across populations of neurons. In particular, when the brain is aroused and actively engaged in mental activities, it generates beta-waves. Excessive synchronization of basal ganglia neuronal activity in the beta-frequency band at 20 Hz has been implicated in PD (Little et al., 2012). The latter can be detected as undulations of the local field potential and recorded through the macroelectrodes used for therapeutic deep brain stimulation (DBS).

Diagnosis

The diagnosis of PD is usually based upon clinical impression. The UK PD Society Brain Bank criteria (Hughes et al., 1992) (Box 76.1) for diagnosis of probable PD states that bradykinesia must be present alongside one other cardinal symptom (rigidity, rest tremor, postural instability). In addition, an excellent response to dopaminergic therapy is an important criterion for the diagnosis. The response to dopaminergic therapy in other parkinsonian syndromes is reduced or absent compared with the response in PD.

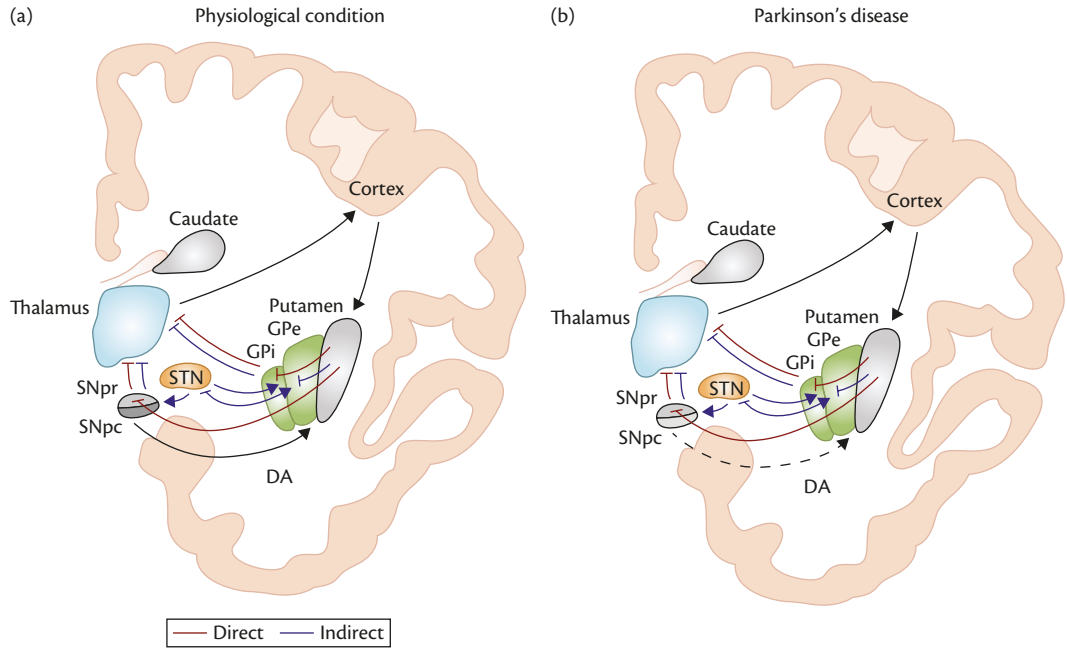

Fig. 76.1 (A) In the physiological condition, dopamine (DA) arising from the SNc is thought to activate D1-expressing striatal MSNs of the direct pathway (red lines) and to inhibit D2-expressing striatal neurons of the indirect pathway (blue lines). The output nuclei GPi and SNr project to the thalamus, which in turn sends efferents that complete the cortico-basal ganglia-thalamo-cortical loop. (B) In Parkinson's disease, degeneration of nigral neurons reduces dopamine receptor stimulation in striatal MSNs. The imbalance between direct and indirect pathways results in the abnormal activation of output nuclei and overinhibition of thalamic neurons projecting to the cortex.

Reproduced with permission from Paolo Calabresi, Barbara Picconi, Alessandro Tozzi, Veronica Ghiglieri, Massimiliano Di Filippo, Direct and indirect pathways of basal ganglia: a critical reappraisal, *Nature Neuroscience*, Volume 17, Issue 8, pp. 1022–30, Copyright © 2014 Springer Nature.

Box 76.1 UK PD Society Brain Bank criteria for diagnosis of probable Parkinson's disease

Inclusion criteria

Bradykinesia (slowness of initiation of voluntary movement with progressive reduction in speed and amplitude of repetitive actions); and at least one of the following:

- Muscular rigidity
- 4–6 Hz rest tremor
- Postural instability not caused by visual, vestibular, cerebellar, or proprioceptive dysfunction.

Exclusion criteria

- History of repeated strokes with step-wise progression of parkinsonian features, repeated head injury, or definite encephalitis
- Oculogyric crises
- Neuroleptic treatment at onset of symptoms
- More than one affected relative
- Sustained remission
- Strictly unilateral features after 3 years or symmetrical at onset
- Supranuclear gaze palsy
- Cerebellar signs
- Early severe autonomic involvement
- Early severe dementia with disturbances of memory, language, and praxis
- Babinski sign
- Presence of cerebral tumour or communication hydrocephalus on imaging study
- Negative response to large doses of levodopa in absence of malabsorption
- MPTP exposure

Supportive (prospective) criteria

Three or more required for diagnosis of definite Parkinson's disease in combination with Step 1.

- Unilateral onset
- Rest tremor present
- Progressive disorder
- Persistent asymmetry affecting side of onset most
- Excellent response (70–100%) to levodopa
- Severe levodopa-induced chorea
- Levodopa response for 5 years or more
- Clinical course of 10 years or more

Reproduced with permission from AJ Hughes, SE Daniel, L Kilford, AJ Lees, Accuracy of clinical diagnosis of idiopathic Parkinson's disease: a clinico-pathological study of 100 cases, *Journal of Neurology, Neurosurgery & Psychiatry*, Volume 55, Issue 3, pp. 181–4, Copyright © 1992 BMJ Publishing Group Ltd.

Neuroimaging is usually non-diagnostic in the evaluation of suspected PD, however magnetic resonance imaging (MRI) of the brain should be performed to exclude specific structural abnormalities and exclude other conditions. In early PD, positron emission tomography may demonstrate decreased tracer uptake in the mid- and posterior putamen of patients although the clinical use is still under debate.

Dopamine transporter (DAT) imaging using single photon emission computed tomography (SPECT) usually reveals reduced radiotracer uptake in the putamen (Fig. 76.2) and to a lesser extent the caudate (often asymmetrically). By contrast, uptake is normal in controls, patients with essential tremor, and drug-induced parkinsonism. Striatal DAT SPECT differentiates between clinically probable PD and essential tremor with a sensitivity of 79–100% and specificity of 80–100% (Vlaar et al., 2007). However, it cannot differentiate PD and most parkinsonian syndromes from one another.

Clinical assessment

A detailed neurological history and examination (Fig. 76.3) is vital to ensure the correct diagnosis and subsequent management. Alternative conditions (e.g. essential tremor), coexisting conditions and reversible causes of secondary parkinsonism (e.g. medications) need to be carefully elicited and thus these patients are best reviewed by neurologists with a specialist interest in movement disorders. Sensory examination tends to be normal and a skin examination maybe recommended given the debate on the possible increased risk of melanoma (Bertoni et al., 2010). Many of the cardinal symptoms will usually be present on examination and should be evaluated thoroughly. Additionally, focus should also be given to non-motor symptoms (Chaudhuri et al., 2006).

Several clinical rating scales are used to measure the severity, monitor progression, and response to intervention. While detailed consideration of these scales is beyond the scope of this book, some of these are commonly used by functional neurosurgeons:

- UPDRS (Unified Parkinson's Disease Rating Scale). This is the most commonly used scale in the clinical assessment of PD and is used to follow the longitudinal course. It comprises six sections assessed using a combination of interview and clinical observations. UPDRS-III is a clinician-scored motor evaluation. Recently a modification by the Movement Disorder Society, MDS-UPDRS has been published with additional emphasis on assessing non-motor aspects of the condition.
- A modified Hoehn and Yahr staging scale is used to describe symptom progression and stage the disease.

Medical therapy

The range of pharmacological treatments available for PD is broad and dependent of careful individualization of patient specific factors (e.g. stage of disease, degree of disability). Most therapies are symptomatic in nature and do not slow/reverse the natural course of the disease. However, several potential neuro-protective agents have shown some promise in animals and/or early human studies and are undergoing further investigation (Stocchi and Olanow, 2003). Non-pharmacologic management of PD, including education, support, exercise, physical/occupational/speech therapy, and nutrition are also helpful to provide holistic care.

The decision to initiate medical therapy in patients with PD is determined by the degree to which symptoms affects the patient's activities of daily living or interferes with work. The main drugs available for the treatment of PD motor symptoms include:

- **Levodopa (L-dopa)** is the most effective drug for the symptomatic treatment of PD and is the drug of first choice, particularly for bradykinesia. Tremor and rigidity can also respond to levodopa therapy, however, postural instability is less likely to do so. Levodopa is combined with a peripheral decarboxylase inhibitor (carbidopa, benserazide) to block its conversion to dopamine in the systemic circulation before it crosses the blood-brain barrier.

A significant number of patients develop levodopa-induced complications such as motor fluctuations, dyskinesia, and dystonia. These

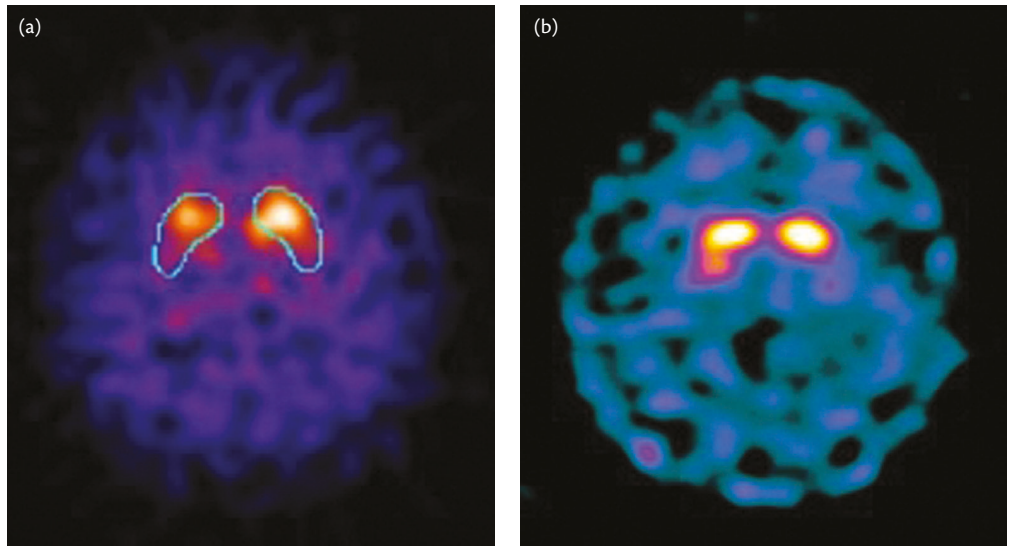

Fig. 76.2 DAT scan showing normal symmetrical (A) versus Parkinson's disease asymmetrical update (B).

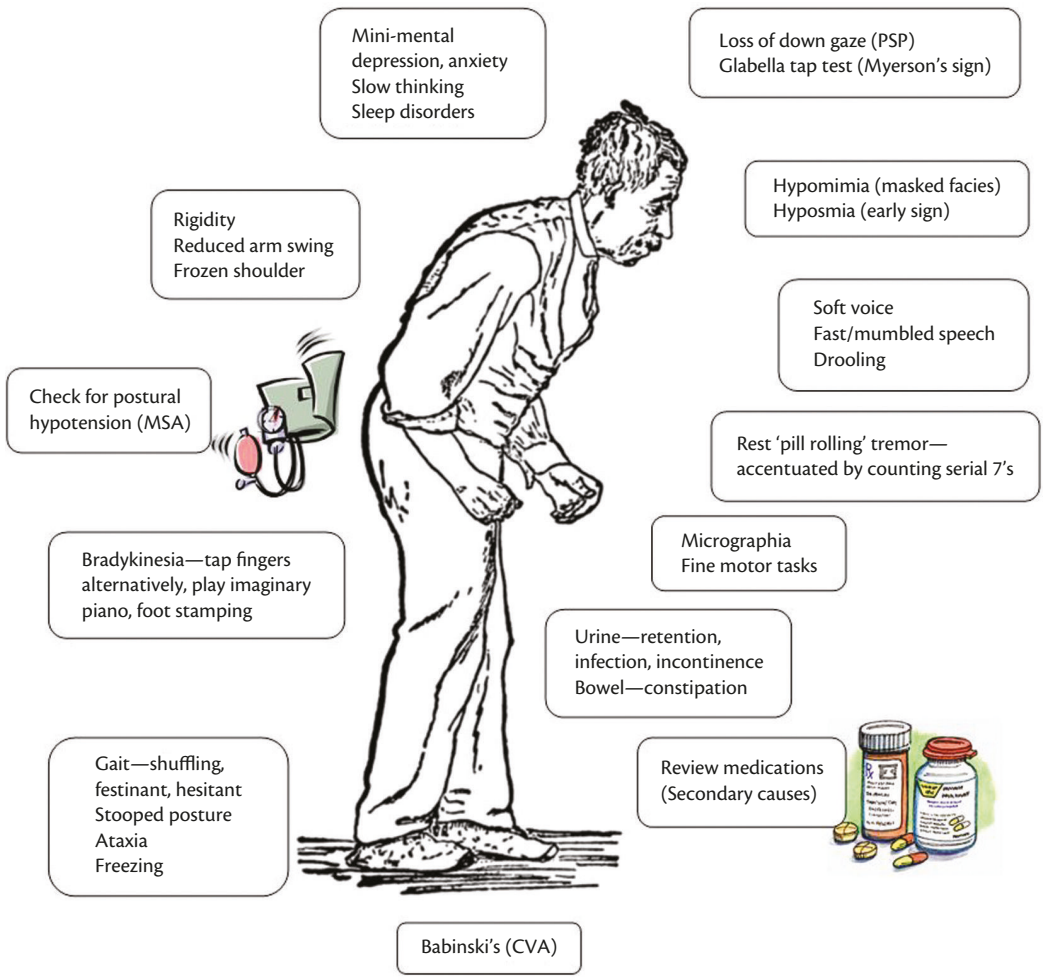

Fig. 76.3 Detailed focused neurological examination for parkinsonism.
Reprinted from *A Manual of Diseases of the Nervous System*, W.R. Gowers, 1886, London J.& A. Churchill.

are estimated to occur in at least 50% of patients after 5 to 10 years of treatment (Schrag and Quinn, 2000).

- **Dopamine agonists** (e.g. pramipexole, ropinirole, rotigotine, and injectable apomorphine) may be employed either as monotherapy in early PD or in combination with other drugs for treatment of advanced disease. While dopamine agonists possibly delay the need to initiate levodopa therapy, their use is associated with impulse control disorders (hypersexuality, pathologic gambling) (Weintraub et al., 2006). As dopamine agonists may be associated with fewer motor fluctuations than levodopa, and the evidence suggests that there is a higher incidence of levodopa-related dyskinesia in young-onset PD, it is argued to be reasonable to start therapy with a dopamine agonist in younger patients (age <65 years) after appropriate counselling.
- **MAO-B inhibitors** (e.g. selegiline, rasagiline) are modestly effective as symptomatic treatment for PD, though monotherapy does not produce a functionally significant benefit in many patients. Uncertainty remains about the relative risks and benefits of MAO-B inhibitors, as few trials compared them with other antiparkinsonian medications. Adverse effects include nausea, headache, insomnia, and confusion, especially in older adults (Riederer and Laux, 2011).
- **Anticholinergic drugs**—In PD, dopamine depletion produces a state of cholinergic sensitivity, so that cholinergic drugs exacerbate and anticholinergic drugs improve parkinsonian symptoms. They are most useful as monotherapy in patients under 70 years of age with disturbing tremor who do not have significant bradykinesia or gait disturbance. They also may be useful in patients with more advanced disease who have persistent tremor despite treatment with levodopa or dopamine agonists. Use in older or demented individuals and those without tremor is strongly discouraged.
- **Amantadine** is an antiviral agent with relatively weak antiparkinsonian effect with low toxicity that is most useful in treating younger patients with early or mild PD and also later when dyskinesia becomes problematic. Adverse effects include livedo reticularis, ankle oedema, confusion, hallucinations, nightmares, abnormalities of liver function, and cognitive changes.
- **COMT inhibitors** (e.g. entacapone) are ineffective when prescribed alone, though they may prolong and potentiate the levodopa effect and thus are useful as levodopa extenders. They are predominantly used to treat patients with motor fluctuations who are experiencing end-of-dose wearing 'off' periods.
- **Oestrogen**—Low-dose oestrogen was suggested to be helpful as adjunctive therapy in postmenopausal women with motor fluctuations on antiparkinsonian medication (Liu and Dluzen, 2007). In practice, this is rarely ever used.

Essential tremor

Tremor is an involuntary movement characterized by rhythmic and oscillatory movement of a body part about a fixed point. Essential tremor (ET), previously referred to as benign essential tremor, is the most common neurologic cause of postural or action tremor and commonly affects the finger, hands and arms though may also extend to affect other body parts such as the head and vocal cords. It is distinct from PD but can be misdiagnosed as such.

Epidemiology

ET is thought to affect 0.4–4% of the population with men and women equally affected (Benito-Leon and Louis, 2006). However, head tremor may be more frequent in women, and postural hand tremor may be more severe in men. Approximately 50% of ET cases are familial with an autosomal dominant inheritance pattern.

The prevalence of ET increases with age with bimodal peaks of the age of onset—one in late adolescence to early adulthood and the second in older adulthood. At presentation, the mean age is between 35 and 45 years, though usually manifests by age 65 years and virtually always by age 70 years. Tremor amplitude also slowly increases over time, however, tremor frequency decreases with increasing age. An 8–12 Hz tremor is seen in young adults, and a 6–8 Hz tremor is typically evident in elderly individuals. Although ET is progressive, no association has been found between age of onset and severity or disability. Rare cases of ET have been reported in newborns and infants.

Pathogenesis

The precise pathophysiology of ET remains an enigma with no consistent pathological findings. Various hypotheses from postmortem and imaging studies point either to a cerebellar-brainstem-thalamo-cortical circuit dysfunction or an abnormally functioning central oscillator located in the Guillain Mollaret triangle near the brainstem and involving the inferior olivary nucleus (Helmich et al., 2013).

Genetics

ET is commonly quoted to be familial in at least 50–70% of cases with transmission demonstrating incomplete penetrance in an autosomal dominant fashion. More accurate studies however report anywhere between 17 and 100% of cases being familial and thus due to methodological variations such as ascertainment bias, true figures for familial link may be difficult to determine (Deng et al., 2007). Some cases are sporadic with unknown aetiology.

Clinical presentation

ET is usually described as trembling or quivering movement or sensation and is typically a distal symmetrical postural tremor of the upper limbs, usually of low amplitude with a fairly rapid frequency of 8–10 Hz. Initially it may be transient but usually progresses to become persistent. Factors predicting likely progression include asymmetric tremor and unilateral onset of the initial tremor. The neck muscles may be involved, causing tremor of the head (about 30% of cases), and voice, face, and jaw muscles may also be involved. The frequency of the tremor tends to remain constant, but amplitude is highly variable depending on emotional and physiological state. It does not occur during sleep and the majority report improvement following alcohol ingestion. It may be difficult to distinguish from exaggerated physiological tremor, that caused by hyperthyroidism/fever or tremor due to medications; these causes should always be borne in mind before diagnosing ET.

The tremor can become disabling over time, interfering with a patient's activities of daily living including feeding, dressing, and personal hygiene, thus leading to depression, anxiety states, social handicap, or alcoholism. A small proportion of sufferers may be severely disabled by the condition, affecting their employment and social prospects (Lorenz et al., 2011).

Diagnosis

Like most movement disorders, diagnosis remains largely clinical (Box 76.2). Biochemical investigations (thyroid function, ceruloplasmin) and imaging studies (MRI) are useful to screen for alternative diagnoses. SPECT imaging can support a diagnosis of parkinsonism, hence decreasing the misdiagnosis of ET as Parkinson's disease. Other features to differentiate the tremor of PD and ET are shown in Table 76.2.

Table 76.2 Other features to differentiate the tremor of PD and ET

Clinical features	Parkinson's disease tremor	Essential tremor
Age at onset	>50	Bimodal 2nd and 6th decade
Gender	M ≥ W	M = W
Family history	<10%	>50%
Asymmetry	Unilateral onset	Bilateral
Frequency	4–6 Hz	4–10 Hz
Character	Rest, rarely kinetic	Postural, kinetic
Distribution	Hands, legs, chin, tongue	Hands, head, voice
Associated features	Bradykinesia, rigidity, gait difficulty, postural instability	Nil
Response to: **- Alcohol** **- Levodopa** **- Primidone/ Propranolol**	 No Yes No	 Improves No Yes

Medical therapy

Beta-blockers and in particular propranolol between 60 and 320 mg/day, if tolerated, is the most commonly used medication for the treatment of ET. Side effects include syncope, light-headedness, fatigue, impotence, and bradycardia, which occurred in 12 to 66% of patients in clinical trials (Zesiewicz et al., 2005). Propranolol may be contraindicated in the presence of heart block, asthma, or type 1 diabetes mellitus.

The *anticonvulsant* primidone is also equally effective as propranolol for the treatment of ET. Side effects from primidone are typically more severe at treatment initiation, and include sedation, drowsiness, fatigue, nausea, vomiting, ataxia, malaise, dizziness, unsteadiness, confusion, vertigo, and an acute toxic reaction. Coadministration of a beta-blocker and primidone may provide useful additive therapeutic benefits if side effects are tolerated. Other anticonvulsants that reduce tremor include gabapentin and topiramate.

Alcohol has long been known to ameliorate ET. The use of small amounts of alcohol before meals or social events is not unreasonable and is commonly practised. However, prolonged use can lead to tolerance, with a need for increasingly larger amounts of alcohol to achieve the same effect which can be complicated by the superimposed withdrawal tremor when alcohol is omitted or the risk of liver disease. Concerns for an increased incidence of alcohol addiction in patients with ET are under debate.

Benzodiazepines are reserved as late-line choice for ET due to the potential for abuse, as well as the potential for drug discontinuation to cause withdrawal symptoms and exacerbation of tremor. Furthermore, their efficacy is limited.

Botulinum toxin (BTX) injections have a limited role to play in the management of ET. Modest benefit for limb tremor is associated with dose-dependent hand weakness, while for voice tremor, the side effects may include breathlessness, hoarseness, and swallowing difficulty.

Box 76.2 Movement Disorder Society on tremor

Classic essential tremor (ET) inclusion criteria

- Bilateral, largely symmetrical postural, or kinetic tremor involving hand and forearms that is visible and persistent
- Additional or isolated tremor of the head may occur but in the absence of abnormal posturing

Classic ET exclusion criteria

- Other abnormal signs of tremor, including dystonia
- The presence of known causes of enhanced physiological tremor, including current or recent exposure to tremorogenic drugs, or the presence of a drug withdrawal state
- Historical or clinical evidence of psychogenic tremor
- Convincing evidence of sudden onset or evidence of step-wise deterioration
- Primary orthostatic tremor
- Isolated voice tremor
- Isolated position-specific or task-specific tremors, including occupational tremors and primary writing tremor
- Isolated tongue or chin tremor
- Isolated leg tremor

Reproduced with permission from Kailash P. Bhatia, Peter Bain, Nin Bajaj, et al., Consensus Statement on the classification of tremors. from the task force on tremor of the International Parkinson and Movement Disorder Society, *Movement Disorders*, Volume 33, Issue 1, pp. 75–87, Copyright © 2017 John Wiley and Sons.

Dystonia

Dystonia is defined as a clinical syndrome characterized by involuntary sustained muscle contractions that usually produce twisting and repetitive movements or abnormal postures. Herman Oppenheim in 1911 was the first to describe the condition (Klein and Fahn, 2013). It is a heterogeneous disorder with many presentations and various causes and thus can affect a multitude of functions including movement, speech, posture, visual performance, and mobility. Typically, the abnormal postures are not fixed and slow writhing movements (athetosis) can occur. Living with the condition can be painful and very debilitating.

Classification

Classification systems for dystonia are complex with several systems in place. Early systems divided dystonias into primary for idiopathic and secondary for dystonia associated with another disorders (e.g. cerebral palsy). This system has undergone many iterations with a consensus now classifying dystonia on two axes, clinical and aetiological (Box 76.3) and without the potentially confusing terminology of primary and secondary dystonias (Albanese et al., 2013).

Box 76.3 Classification of dystonia

Axis I. Clinical characteristics

Age at onset

- Infancy (birth to 2 years)
- Childhood (3–12 years)
- Adolescence (13–20 years)
- Early adulthood (21–40 years)
- Late adulthood (>40 years)

Body distribution

- Focal (e.g. writer's cramp, blepharospasm)
- Segmental (involving two or more contiguous regions, craniocervical dystonia)
- Multifocal (two or more non-contiguous regions)
- Generalized (+/– leg involvement)
- Hemidystonia

Temporal pattern

- Disease course
- Static
- Progressive
- Variability
- Persistent
- Action specific
- Diurnal
- Paroxysmal

Associated features

Isolated dystonia or combined with another movement disorder

- Isolated dystonia
- Combined dystonia

Occurrence of other neurological or systemic manifestations

- List of co-occurring neurological manifestations

Axis II. Aetiology

- Nervous system pathology
- Evidence of degeneration
- Evidence of structural (often static) lesions
- No evidence of degeneration or structural lesion
- Inherited or acquired
- Inherited
- Autosomal dominant
- Autosomal recessive
- X-linked recessive
- Mitochondrial

Acquired

- Perinatal brain injury
- Infection
- Drug
- Toxic
- Vascular
- Neoplastic
- Brain injury
- Psychogenic

Idiopathic

- Sporadic
- Familial

Reproduced with permission from Alberto Albanese, Kailash Bhatia, Susan B. Bressman, et al., Phenomenology and classification of dystonia: A consensus update, *Movement Disorders*, Volume 28, Issue 7, Copyright © 2013 John Wiley and Sons.

Epidemiology

There is estimated to be approximately 70 000 adults and children in the United Kingdom who suffer with some form of dystonia, which equates to a prevalence of 1 in 900. Though difficult to quantify accurately, according to minimum prevalence estimates, primary dystonia should be considered the third most frequent movement disorders after ET and Parkinson's disease.

Genetics

Genetic forms of the disease are important to recognize clinically and also provide valuable information about possible pathogenic mechanisms within the wider disorder. Hereditary dystonia is classified either by the gene underlying the condition or by reference to an ever-expanding list of dystonia loci, of which there are currently over 20. The DYT loci system were assigned in chronological order based on appearance of reports in the medical literature and in theory once the underlying genetic cause was known, the locus was supposed to be removed. However, in practice this has not occurred and thus dystonia loci and gene names appear interchangeably (e.g. DYT1/TOR1A) (Charlesworth et al., 2013).

DYT1/TOR1A is responsible for early onset dystonia and is inherited in an autosomal dominant fashion with reduced penetrance. The offspring of an affected individual or an asymptomatic individual known to have a TOR1A mutation have a 50% chance of inheriting the disease-causing mutation and 30–40% chance of developing symptoms.

Pathogenesis

The underlying pathogenesis for dystonia remains unclear. Interestingly in DYT1 dystonia most of the studies report no overt neurodegeneration or cell loss. One study has described ubiquitin and torsin A-positive inclusions within the brainstem. Functional MRI studies have implicated the pedunculopontine nucleus as part of dystonia 'metabolic network'.

In secondary dystonias the pathology is linked to basal ganglia structures, though several studies point to a cerebellar outflow problem. While progress has been made to pin down the exact pathophysiology much work remains to be done to refine these hypotheses.

Diagnosis

Though diagnosing dystonia can be difficult due to its variability in presentation, wide aetiology, and overlap with other movement disorders, it is a clinical diagnosis and thus best assessed by a neurologist with a special interest in movement disorders. Family history is important as up to 44% of patients have relatives with similar movement disorders. A careful drug history to rule out secondary causes is also vital.

Blood tests including liver function, ceruloplasmin, copper studies may be appropriate. Neuroimaging is useful to exclude structural causes and where appropriate to study the anatomy for potential deep brain stimulation. Genetic screening for DYT and other mutations and genetic counselling are vital for patients with early onset primary dystonia or a relative affected with condition.

Assessment for dystonia is usually performed using one of several validates rating scales:

- BFM-DRS (Burke-Fahn-Marsden Dystonia Rating Scale) is a 120-point rating scale used to test the severity of dystonia in nine body regions. This scale takes into account the severity and frequency of the dystonic movements. A higher score means greater impairment.
- CDIP-58 (Cervical Dystonia Impact Profile) includes 58 evaluative items forming eight scales. High scores indicate worse health.
- TWSTRS (Toronto Western Spasmodic Torticollis Rating Scale) is another commonly used rating scale for cervical dystonia. This exam consists of three sections: severity (range 0–30), disability (range 0–30), and pain (range 0–40).

Medical therapy

Depending on the severity of symptoms, a multidisciplinary approach to the management of dystonia is required comprising a combination of medications, allied healthcare (physiotherapy, psychological therapy, speech, and occupational therapy) and where appropriate surgery.

The use of rehabilitative physiotherapy for focal dystonias can be very effective with an aim to restore and maintain as much independence as possible. Cognitive behavioural therapy, autogenic training and counselling have an important role in the management of depression and anxiety which are often associated with the condition. Muscle spasms and abnormal posturing can cause significant pain and may require referral to pain management programmes. Where speech difficulties are present, referral to a speech and language therapist should be offered.

Medications are commonly utilized to provide symptomatic relief, though there is no one drug that is the definitive medication of choice and often a combination of several drugs is required to enable effective management.

- Levodopa—in primary dystonia, a trial of levodopa is vital to rule out dopa-responsive dystonia which can be managed in the long term on levodopa.
- Trihexyphenidyl—is usually the first line of management, though anticholinergic side effects need to be monitored.
- Baclofen is useful but can cause drowsiness, drooling, and droopiness of the trunk.
- Benzodiazepines—limited by respiratory depression and addiction.
- Clonidine—can cause somnolence.
- Gabapentin—may have additional benefit in stabilizing mood and sleep quality.
- Botulinum toxin A injection—especially useful for focal dystonia (e.g. blepharospasm, writer's cramp). It can be injected EMG/ultrasound assisted. Used off-licence in children, it is often used to treat pain and spasm in specific muscle groups.
- Intrathecal baclofen—this can prove effective for regional and total body dystonia with less risks of somnolence associated with oral baclofen.

Other support that may be considered includes dietary support, occupational therapy input, podiatry (especially for gait), genetic counselling, and social support.

Surgical management

Surgical approaches to movement disorders are an important consideration in the management of medically refractory cases. Increasingly, given their potential to avoid long-term complications of the disorder (e.g. deformity and contractures in dystonia), surgery is being used at earlier stages in the disease process. Contemporary functional neurosurgical techniques trace their origins to Dr Irving Cooper when he inadvertently ligated the anterior choroidal artery in a patient with PD resulting in serendipitous improvement in tremor and rigidity (Cooper, 1953). This was largely superseded by specific lesioning techniques which conferred beneficial results. However, concerns about irreversibility and complications associated with ablation, especially when done bilaterally, has resulted in high-frequency DBS becoming the gold standard surgical procedure for movement disorders.

Lesioning

This procedure involves acquiring stereotactic images and then passing an insulated radiofrequency electrode to basal ganglia nuclei coagulating a small area within the target nucleus. The effects are usually immediate. These techniques have largely been superseded by DBS due to concerns over irreversibility. Its use has dwindled over the decades; however, this ablative procedure is still a useful procedure in the armamentarium of a functional neurosurgeon. It has the advantage of being cheap, having a low infection profile, is relatively safe, and avoids repeated visits for adjustment of stimulation parameters or battery changes.

The recent introduction of the high-intensity focused ultrasound (HIFU) technology, allowing incision-less lesioning of target nuclei under the guidance of real time MRI thermometry, is likely to further improve the safety profile of lesioning surgery.

Stimulation

DBS involves identification of basal ganglia target nuclei utilizing high-resolution imaging, especially MRI, and subsequent implantation of permanent electrode leads using stereotactic techniques. The procedure is usually performed under local anaesthetic to allow for neuro-physiological and clinical confirmation of optimal electrode placement. The leads are then connected subcutaneously via extension wires to an implantable pulse generator (IPG) which is implanted in the chest/abdominal wall. The IPG serves both as a battery and a programming device, amenable to adjustment externally to alter the electrical output from the leads.

Transplantation

Transplantations and restorative therapies for PD have a long history, dating to the 1970s, but are still only in use as part of clinical trials. In a randomized study of 40 patients with severe PD receiving either a transplant of human embryonic dopamine-neurons or a sham surgery, it was shown that the transplanted cells survived and resulted in some clinical benefit in younger but not older patients. Furthermore, clinical benefit and graft viability were sustained up to 4 years after transplantation and the imaging changes reliably correlated with clinical outcome over the post-transplantation time

course. In contrast, in another prospective 24-month double-blind placebo-controlled trial of fetal nigral transplantation in 34 patients with advanced PD, a slight treatment effect in patients with milder disease was observed. Some 56% of the transplanted patients however developed off-phase dyskinesia (Olanow et al., 2003). These dyskinesias were also described by other groups and can persist up to 11 years. Currently neural transplantation remains as an experimental therapy. Further studies are necessary to obtain objective evidence of benefit, define target patient population, determine the optimal cells for transplant and the exact brain target area for transplantation.

Surgical outcomes

Parkinson's disease

There is good long-term evidence on effectiveness of DBS to improve motor symptoms in advanced PD with significant benefits in tremor, rigidity, and bradykinesia. Typically, improvements in general motor state as measured by UPDRS-III of 50%, reduction in off-periods during the day by 70%, and prolongation of periods with good mobility of approximately 20% are expected (Alamri et al., 2015). Overall, tremor and rigidity show better long-term improvement than bradykinesia. Axial symptoms that respond to the Levodopa usually also improve. Furthermore, medication-related complications like motor fluctuations and dyskinesias decrease by 60–70% after STN DBS. Despite these benefits, the natural neurodegenerative course of PD does not appear to be altered by DBS and, thus in the long term, worsening of axial symptoms and akinesia should be expected. Cognitive decline is also unchanged reflecting the natural course of the disease. Nevertheless, a consistent marked motor improvement especially of tremor, rigidity, motor fluctuations, and dyskinesias have been reported in studies up to 5–10 years after STN DBS. Levodopa equivalent dose of parkinsonian daily medications can be reduced by 40–60% which is maintained after 5 years.

Recently it has been shown that motor improvements after STN DBS is not limited to patients with advanced PD. The randomized, prospective multicentre EARLYSTIM trial demonstrated favourable outcomes in the neurostimulation group. Given these results, especially early at the onset of disabling motor fluctuations, DBS has been advocated at an earlier stage in the disease process than the current practice. However, long-term outcome in this cohort is awaited (Schuepbach et al., 2013).

Non-motor symptoms (NMS) are common in PD patients and can have dramatic impact on patients' quality of life. Though DBS literature has primarily focused on motor symptoms, evidence indicates that STN DBS can improve NMS in selected patients (Witt et al., 2008).

Essential tremor

The short- and long-term benefits of DBS have been repeatedly demonstrated with significant resolution of upper extremity tremor reported in up to 90% of patients. Several studies have compared the clinical outcomes and complications related to DBS and thalamotomy in ET. Both methods produce near complete resolution of contra-lateral upper extremity tremor in approximately 60–90% of patients (Zhang et al., 2010). Long-term benefits are similar between both methods, with significant lasting improvement seen in the majority of patients although with both therapies, over time there may be a reduction in benefit in some patients. The primary difference between the two therapies is an increase in serious neurological complications associated with thalamotomy compared to DBS. Thalamotomy is currently only considered in selected patients with medication resistant disabling tremor who would not be good candidates for DBS either for medical issues precluding tolerance of the DBS hardware, known need for repeated MRI scanning, inability to comply with follow-up appointments for DBS programming and costs. In rare cases, an ET patient may not be able to tolerate DBS or thalamotomy due to increased surgical risk secondary to other medical conditions. In these cases, radiosurgical thalamotomy may be considered.

Dystonia

Ablative stereotactic surgery to treat dystonia has been performed in both the thalamus and the GPi. Outcomes have been difficult to assess due to lack of standardization of inclusion criteria, assessments, and surgical technique. Nevertheless, results of thalamotomy for primary and secondary dystonia have shown 25–100% improvement in 10/20 idiopathic cases and 25–100% improvement in 68% of 29 patients with secondary dystonia. However, significant side effects (15% hemiparesis and up to 56% dysarthria/dysphonia) have limited the use of this procedure. Buzaco has reported almost the same efficacy of pallidotomy compared to thalamotomy but less frequent complications with subsequent reports, confirming the efficacy of pallidotomy in alleviating the dystono-dyskinetic symptoms in patients with primary or secondary dystonia. No long-lasting complication is documented in any of these reports (Speelman et al., 2010).

The GPi is currently the target of choice for DBS surgery in dystonia, though thalamic and subthalamic nucleus stimulation have also been utilized. In primary generalized dystonia, a significant improvement of the motor and disability scores of the BFMRS has been reported (range 40–80%). Similar results have been described in patients with segmental dystonia. With a follow-up as long as 10 years, the pallidal DBS therapeutic effects appear stable. Patients with secondary dystonia represent a heterogeneous population and though it is accepted that, in general, secondary dystonia does not respond to DBS as well as primary dystonia, several reports showed satisfactory clinical outcome in many secondary dystonia, such as tardive dystonia. The discrepancy in the post DBS outcomes in this patient population when using validated movement disorder scales versus those measuring the quality of life/patient-reported outcomes, has encouraged the increasing use of the latter.

Controversies

DBS has been firmly established as an effective intervention for movement disorders for nearly three decades and thus controversies chiefly relate to differences in surgical technique rather than the efficacy:

- General vs. local anaesthesia—good outcome from DBS relies on accurate lead position within a very small, deep target. An awake patient allows for intraoperative macrostimulation through the

DBS lead to assess the optimal position for symptom relief and thresholds for avoiding side effects, and thus allows for immediate re-positioning of the electrode to a more effective target. However, an awake patient is required to be cognitively intact to perform mental tasks, cooperative and remain still for prolonged periods while in the 'off-state'. These latter concerns are removed with general anaesthesia; however, lead positioning is then reliant only on imaging targeting methods and intraoperative microelectrode recording. There has been no randomized controlled trial comparing outcomes for both techniques.

- Microelectrode recordings (MER)—is an electrophysiological technique of verifying the borders of a target nucleus using its firing pattern and characteristic signals. Recording is performed by inserting very fine tipped electrodes. However, MER necessitates expertise, expense, and additional operating time to an already prolonged procedure. There is also evidence that MER increases the risk of intracerebral haemorrhage. With improvements in surgical technique allowing for accurate image guided 'direct' targeting of the nuclei, the continued routine use of MER has been questioned by some surgeons.
- STN vs. GPi—The debate over whether to use GPi or STN DBS as the target for PD has stemmed from various studies that have shown varying degrees in outcome. Overall opinion over the past 10 years have been in favour of STN DBS for the majority of DBS candidates, while favouring GPi stimulation in the older patients, those with predominant dyskinesia, or those at risk of neuropsychiatric disturbance. More recent studies have shown comparable outcomes with both targets.
- Duodopa vs. DBS—Maintaining steady plasma concentrations of oral levodopa presents problems due to gastric emptying which results in fluctuating motor symptoms. With a reliable pharmacological profile and a portable delivery system, the use of intrajejunal L-dopa/carbidopa gel (Duodopa) has become an option in patients with motor fluctuations. Studies comparing Duodopa with DBS are limited, though one comparing the two interventions showed that the DBS group had significantly more improvement in dyskinesias duration and disability compared to duodopa (Merola et al., 2011). Although duodopa appears to be a promising alternative for PD patients, particularly in whom DBS is contraindicated, the large complication rates related to PEG tube insertion cannot be dismissed. The issue of costs is also an important one with duodopa being significantly more expensive than DBS.

FURTHER READING

Alamri, A., Ughratdar, I., Samuel, M., & Ashkan, K. (2015). Deep brain stimulation of the subthalamic nucleus in Parkinson's disease 2003–2013: where are we another 10 years on? *Br J Neurosurg*, **29**(3), 319–28.

Albanese, A., Bhatia, K., Bressman, S.B., et al. (2013). Phenomenology and classification of dystonia: a consensus update. *Mov Disord*, **28**, 863–73

Calabresi, P., Picconi, B., Tozzi, A., Ghiglieri, V., & Di Filippo, M. (2014). Direct and indirect pathways of basal ganglia: a critical reappraisal. *Nat Neurosci*, **17**, 1022–30.

Chaudhuri, K.R., Healy, D.G., Schapira, A.H., & National Institute for Clinical Excellence (2006). Non-motor symptoms of Parkinson's disease: diagnosis and management. *Lancet Neurol*, **5**, 235–45

Schuepbach, W.M., Rau, J., Knudsen, K., et al. (2013). Neurostimulation for Parkinson's disease with early motor complications. *N Engl J Med*, **368**, 610–22.

REFERENCES

Alamri, A., Ughratdar, I., Samuel, M., & Ashkan, K. (2015). Deep brain stimulation of the subthalamic nucleus in Parkinson's disease 2003–2013: where are we another 10 years on? *Br J Neurosurg*, **29**(3), 319–28.

Albanese, A., Bhatia, K., Bressman, S.B., et al. (2013). Phenomenology and classification of dystonia: a consensus update. *Mov Disord*, **28**, 863–73.

Benito-Leon, J. & Louis, E.D. (2006). Essential tremor: emerging views of a common disorder. *Nat Clin Pract Neurol*, **2**, 666–78; quiz 2p following 691.

Bertoni, J.M., Arlette, J.P., Fernandez, H.H., et al. (2010). Increased melanoma risk in Parkinson disease: a prospective clinicopathological study. *Arch Neurol*, **67**, 347–52.

Calabresi, P., Picconi, B., Tozzi, A., Ghiglieri, V., & Di Filippo, M. (2014). Direct and indirect pathways of basal ganglia: a critical reappraisal. *Nat Neurosci*, **17**, 1022–30.

Charlesworth, G., Bhatia, K.P., & Wood, N.W. (2013). The genetics of dystonia: new twists in an old tale. *Brain*, **136**, 2017–37.

Chaudhuri, K.R., Healy, D.G., Schapira, A.H., & National Institute for Clinical Excellence (2006). Non-motor symptoms of Parkinson's disease: diagnosis and management. *Lancet Neurol*, **5**, 235–45.

Cooper, I.S. (1953). Anterior chorodial artery ligation for involuntary movements. *Science*, **118**, 193.

Dauer, W. & Przedborski, S. (2003). Parkinson's disease: mechanisms and models. *Neuron*, **39**, 889–909.

Deng, H., Le, W., & Jankovic, J. (2007). Genetics of essential tremor. *Brain*, **130**, 1456–64.

Dorsey, E.R., Constantinescu, R., Thompson, J.P., et al. (2007). Projected number of people with Parkinson disease in the most populous nations, 2005 through 2030. *Neurology*, **68**, 384–6.

Goetz, C.G. & Pal, G. (2014). Initial management of Parkinson's disease. *BMJ*, **349**, g6258.

Helmich, R.C., Toni, I., Deuschl, G., & Bloem, B.R. (2013). The pathophysiology of essential tremor and Parkinson's tremor. *Curr Neurol Neurosci Rep*, **13**, 378.

Hughes, A.J., Daniel, S.E., Kilford, L., & Lees, A.J. (1992). Accuracy of clinical diagnosis of idiopathic Parkinson's disease: a clinico-pathological study of 100 cases. *J Neurol Neurosurg Psychiatry*, **55**, 181–4.

Klein, C. & Fahn, S. (2013). Translation of Oppenheim's 1911 paper on dystonia. *Mov Disord*, **28**, 851–62.

Little, S., Pogosyan, A., Kuhn, A.A., & Brown, P. (2012). Beta band stability over time correlates with Parkinsonian rigidity and bradykinesia. *Exp Neurol*, **236**, 383–8.

Liu, B. & Dluzen, D.E. (2007). Oestrogen and nigrostriatal dopaminergic neurodegeneration: animal models and clinical reports of Parkinson's disease. *Clin Exp Pharmacol Physiol*, **34**, 555–65.

Lorenz, D., Poremba, C., Papengut, F., Schreiber, S., & Deuschl, G. (2011). The psychosocial burden of essential tremor in an outpatient- and a community-based cohort. *Eur J Neurol*, **18**, 972–9.

Merola, A., Zibetti, M., Angrisano, S., Rizzi, L., Lanotte, M., & Lopiano, L. (2011). Comparison of subthalamic nucleus deep brain stimulation and Duodopa in the treatment of advanced Parkinson's disease. *Mov Disord*, **26**, 664–70.

Olanow, C.W., Goetz, C.G., Kordower, J.H., et al. (2003). A double-blind controlled trial of bilateral fetal nigral transplantation in Parkinson's disease. *Ann Neurol*, **54**, 403–14.
Riederer, P. & Laux, G. (2011). MAO-inhibitors in Parkinson's Disease. *Exp Neurobiol*, **20**, 1–17.
Schrag, A. & Quinn, N. (2000). Dyskinesias and motor fluctuations in Parkinson's disease. A community-based study. *Brain*, **123** (Pt 11), 2297–305.
Schuepbach, W.M., Rau, J., Knudsen, K., et al. (2013). Neurostimulation for Parkinson's disease with early motor complications. *N Engl J Med*, **368**, 610–22.
Speelman, J.D., Contarino, M.F., Schuurman, P.R., Tijssen, M.A., & De Bie, R.M. (2010). Deep brain stimulation for dystonia: patient selection and outcomes. *Eur J Neurol*, **17** Suppl 1, 102–6.
Stocchi, F. & Olanow, C.W. (2003). Neuroprotection in Parkinson's disease: clinical trials. *Ann Neurol*, **53** Suppl 3, S87–97; discussion S97–9.
Vlaar, A.M., Van Kroonenburgh, M.J., Kessels, A.G., & Weber, W.E. (2007). Meta-analysis of the literature on diagnostic accuracy of SPECT in parkinsonian syndromes. *BMC Neurol*, **7**, 27.
Weintraub, D., Siderowf, A.D., Potenza, M.N., et al. (2006). Association of dopamine agonist use with impulse control disorders in Parkinson disease. *Arch Neurol*, **63**, 969–73.
Witt, K., Daniels, C., Reiff, J., et al. (2008). Neuropsychological and psychiatric changes after deep brain stimulation for Parkinson's disease: a randomised, multicentre study. *Lancet Neurol*, **7**, 605–14.
Zesiewicz, T.A., Elble, R., Louis, E.D., et al. (2005). Practice parameter: therapies for essential tremor: report of the Quality Standards Subcommittee of the American Academy of Neurology. *Neurology*, **64**, 2008–20.
Zhang, K., Bhatia, S., Oh, M.Y., Cohen, D., Angle, C., & Whiting, D. (2010). Long-term results of thalamic deep brain stimulation for essential tremor. *J Neurosurg*, **112**, 1271–6.

RELATED LINKS TO EBRAIN

Classification and Epidemiology of Movement Disorders. https://learning.ebrain.net/course/view.php?id=327
Diagnosis and Treatment of Essential Tremor. https://learning.ebrain.net/course/view.php?id=315
Dystonia: Classification and Genetics. https://learning.ebrain.net/course/view.php?id=310
Parkinson's Disease: Definition, Pathogenesis and Pathology. https://learning.ebrain.net/course/view.php?id=326
Parkinson's Disease: Surgical Treatment. https://learning.ebrain.net/course/view.php?id=323

77

Spasticity

John Goodden, Catherine Hernon, and Brian Scott

Introduction

This chapter reviews spasticity causes and treatments in adults and children. Due to the diversity of this subject, and the age range covered, it should be noted that some treatments covered in this chapter are only applicable for a limited group of patients.

Spasticity is the term used to describe an involuntary, velocity-dependent increase in muscle tone leading to increased resistance to movement. It arises as a result of upper motor neurone lesions (UMNL), which lead to loss or diminution of descending inhibitory influence on the alpha and gamma motor neurones. This is demonstrated by changes within the reflex arc, with loss of inhibitory input, leading to an exaggerated reflex. Depending upon the cause of the UMNL, the effects of spasticity may be seen in the upper or lower limbs.

Traditional descriptions of spasticity have used terms such as hemiplegia, diplegia, and quadriplegia to describe the distribution of the spasticity and the limbs involved. However, neurorehabilitation experts recommend that these terms are not used as they falsely suggest that the other limbs are unaffected, when they actually may be mildly affected. It is therefore preferred to state the mainly affected limbs (e.g. 'spasticity mainly affecting the legs' rather than 'diplegia').

Pathophysiological basis of spasticity

The pathophysiological changes in the brain and spinal cord that lead to spasticity are incompletely understood. However, it is thought to arise mainly from injury to the reticulospinal and corticospinal/pyramidal tracts and the spinal interneurons. The injury leads to a reduction in the inhibitory input to the spinal motor circuits with a consequent exaggeration of the reflex arc. Enhanced H-M ratios and F-wave amplitudes on neurophysiology testing provide evidence of this increase in motor neurone excitability.

Within the spinal cord, changes are seen in the excitability of the motor neurones, the interneurons, and reflex arc pathways. In the healthy subject, the 1a inhibitory interneurons mediate the reflex arc, receiving descending input from the descending corticospinal pathways as part of this action. Spasticity is seen when the interneurons are damaged, as well as when the descending input is reduced.

In the affected muscles, shortening and contracture commonly develop over time, but muscle spindle sensitivity is usually unaltered.

Clinical aspects of spasticity—aetiology

The causes of spasticity are congenital (cerebral palsy, spinal cord tethering/dysraphism) or acquired (stroke, trauma, tumour, demyelinating conditions, progressive neurodegenerative diseases, infections, and hydrocephalus and syringomyelia). Since spasticity arises from an UMNL, it would not be expected to result from a spinal injury below the conus medullaris. If the patient has suffered an acute UMNL, muscle tone is usually low with a flaccid paresis initially, before progressing to spasticity.

Cerebral palsy is the commonest cause of paediatric spasticity and multiple sclerosis (MS) is the commonest in adults.

Cerebral palsy has an incidence of 1 in 500 live births. It is a non-progressive condition, with a variety of clinical manifestations, including spasticity, dystonia, dyskinesia, and ataxia. While the brain lesion is static, the effects on the musculoskeletal system are often progressive because the muscles grow more slowly than the adjacent bones and also because of an imbalance of forces across the joints. These have deleterious effects on the shape of the developing bones and joints.

Multiple sclerosis is an immune-mediated, progressive degenerative condition with a variety of courses including relapsing-remitting and gradually/rapidly progressive. It occurs principally in people of a Northern-European origin, has a peak onset around age 30, and a female:male ratio of up to 3:1. The UK incidence has recently been estimated at 9.64 per 100 000 population, with a prevalence in England and Wales of 100–140 per 100 000 population, increasing to 170 in Northern Ireland, 190 in Scotland, 295 in Shetland, and 402 in Orkney.

Investigation, assessment, and diagnosis of spasticity

Patients presenting with spasticity need referral to and workup by a skilled physician, with a thorough assessment. This includes a detailed history and examination, baseline blood tests (including FBC/

UE) and blood/urine cultures to look for infection. Family history is particularly important for children when considering neurodegenerative conditions. Specialist investigations such as cerebrospinal fluid (CSF) analysis, MRI scanning, and EMG/EEG may also be required.

When a patient presents with a sudden exacerbation of their symptoms, the clinician needs to again undertake a detailed history and examination, blood tests, and urine cultures. Common factors causing deterioration include infection (especially urine or ear), medication changes, pain, pressure sores, constipation, occult fracture, foot/orthotic problems, DVT, stress, fatigue, and even cold weather.

A careful multidisciplinary team (MDT) assessment is required, including evaluation of which muscles are overactive and how the spasticity affects the patient throughout their daily life including self-care, mobility, sleep, and employment. A variety of scoring systems have been developed to document the extent of spasticity and functional limitation. The modified Ashworth Scale is the most commonly used tool to grade the extent of spasticity (Platz et al., 2005) (Table 77.1), but others such as the Tardieu score are also used. In addition, documentation of range of movement, muscle power, quality of life, function, and gait (if relevant) are required (Haley et al., 1992; Steinbok, 2001; Platz et al., 2005; Haugh et al., 2006; O'Brien and Park, 2006; Engsberg et al., 2007; Harvey et al., 2007: Khan, 2007; Delhaas et al., 2008; Gorton et al., 2009; Akerstedt et al., 2010, Gilmore et al., 2010; Ou et al., 2010; Dasenbrock et al., 2011; Reynolds et al., 2011; Tedroff et al., 2014). These assessments should be performed ahead of any planned intervention so the effects of the intervention can be evaluated.

For children with cerebral palsy, measures such as the Gross Motor Function Classification System (GMFCS) and Gross Motor Function Measure (GMFM) are useful tools to document and summarize a child's functional capabilities. The GMFCS is graded from 1 (independent) to 5 (wheelchair-bound) (see Fig. 77.1 and Table 77.2). The GMFM is a standardized observational instrument that has been designed and validated to measure change over time, helping to summarize this with a single score that can then be compared to chart their progress.

Table 77.1 The modified Ashworth Scale

Score	Description	Examination
0	No increase	Moves freely at any velocity
1	Slight increase	Catch and release or minimal resistance at end range
1+	Slight increase	Catch and release with minimal resistance through remainder of range of motion
2	More marked increase	Moderate resistance throughout range, but joint is easily moved
3	Considerable increase	High tone is present—joint is difficult to move
4	Severe increase	Affected joints are rigid-cannot be moved from flexed or extended position

Reproduced with permission from Bohannon, Richard W.; Smith, Melissa B, Interrater Reliability of a Modified Ashworth Scale of Muscle Spasticity, Physical Therapy, Volume 67, Issue 2, pp.206–207, Copyright © 1987 by permission of Oxford University Press on behalf of the American Physical Therapy Association.

Medical management of spasticity (including rehabilitation, physiotherapy, and occupational therapy)

The MDT managing spasticity should include a rehabilitation physician, physiotherapists, occupational therapy, and a variety of surgeons (neurosurgery, plastic surgery, orthopaedic surgery) (Park and Albright, 2006; Steinbok, 2006; Abbott, 2007; Ronan and Gold, 2007). It is important to carefully balance the control of spasticity against any side effects of doing so. Spasticity may be providing a positive impact in the patient's life as well as a negative one. For example, the spastic stiffness in a patient's legs may counteract the underlying weakness and allow them to walk; removing this spasticity may render them immobile.

Functional help can be provided via communication aids, splints, customized walking frames, and customized wheelchairs. The aim is to protect function and avoid/reduce the harmful effects of the spasticity and disability as a whole. Regular physiotherapy is central to this, to maintain flexibility and avoid the progression of muscle/tendon contracture formation. Occupational therapy and orthotic reviews are necessary to protect skin, and optimize splints and supports, maximizing function, and preventing pressure sore development. Finally, good bladder care is also vital to prevent recurrent infections (urinary tract infection is very common cause of spasticity exacerbation).

A variety of medical interventions can be undertaken to help limit the deleterious effects of spasticity. These treatments aim to improve tone, alleviate spasms, control gastrointestinal effects, and control bladder function.

Commonly used antispasticity medications include baclofen, dantrolene, tizanidine, and diazepam (Papavasiliou, 2009; Quality Standards Subcommittee of the American Academy of Neurology et al., 2010; Novak et al., 2013). Their side effects are varied but can include drowsiness, weakness, fatigue, sedation, and memory impairment. For these reasons they can be unpopular, especially if patients/carers read up about them prior to taking them.

Baclofen is generally considered the mainstay of spasticity treatment, especially in cerebral palsy and spinal cord lesions. It acts via the pre- and postsynaptic $GABA_B$ receptors, reducing excitatory transmission of the α-motor neuron and decreasing nociception. It has good gastrointestinal (GI)-tract absorption but poor transfer across the blood–brain barrier. Therefore, high doses may be required before clinical effects are seen, creating a higher risk of side effects—including sedation, behavioural changes, confusion, ataxia, urinary frequency, and insomnia. Baclofen is started at low dose and gradually increased until benefits are maximized or side effects become troublesome. If it is being discontinued, this must be done gradually due to the risk of seizures, rebound hyperspasticity, or hallucinations.

Dantrolene is used for treatment of spasticity, cramps, and spasms. It acts by reducing depolarization-induced calcium influx into sarcoplasmic reticulum of striated muscle. Its GI absorption is incomplete, slow but consistent. Side effects include muscle weakness (making mobility more difficult), sedation, and hepatitis.

GMFCS E & R between 6th and 12th birthday: Descriptors and illustrations

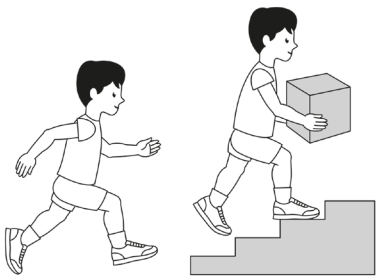

GMFCS Level I
Children walk at home, school, outdoors and in the community. They can climb stairs without the use of a railing. Children perform gross motor skills such as running and jumping, but speed, balance and coordination are limited.

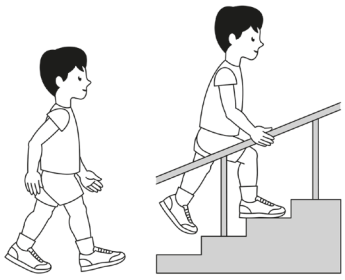

GMFCS Level II
Children walk in most settings and climb stairs holding onto a railing. They may experience difficulty walking long distances and balancing on uneven terrain, inclines, in crowded areas or confined spaces. Children may walk with physical assistance, a hand-held mobility device or used wheeled mobility over long distances. Children have only minimal ability to perform gross motor skills such as running and jumping.

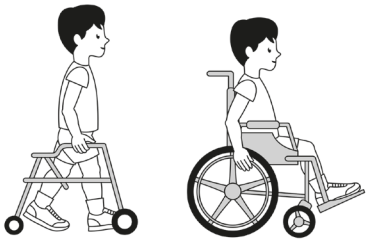

GMFCS Level III
Children walk using a hand-held mobility device in most indoor settings. They may climb stairs holding onto a railing with supervision or assistance. Children use wheeled mobility when traveling long distances and may self-propel for shorter distances.

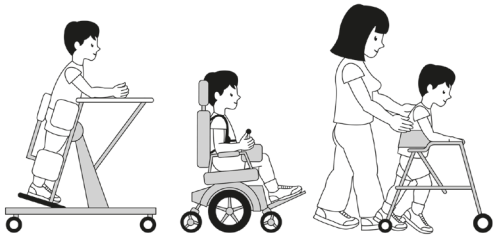

GMFCS Level IV
Children use methods of mobility that require physical assistance or powered mobility in most settings. They may walk for short distances at home with physical assistance or use powered mobility or a body support walker when positioned. At school, outdoors and in the community children are transported in a manual wheelchair or use powered mobility.

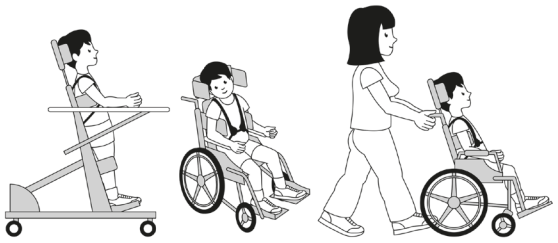

GMFCS Level V
Children are transported in a manual wheelchair in all settings. Children are limited in their ability to maintain antigravity head and trunk postures and control leg and arm movements.

Fig. 77.1 The Gross Motor Function Classification System.

Table 77.2 The Gross Motor Function Classification System

GMFCS level	General descriptor
1	Walks without limitations
2	Catch walks with limitations
3	Walks using a hand-held mobility device
4	Self-mobility with limitations; may use powered mobility
5	Transported in a manual wheelchair

Reproduced with permission from Robert Palisano, Peter Rosenbaum, Stephen Walter, et al., Development and reliability of a system to classify gross motor function in children with cerebral palsy, *Developmental Medicine & Child Neurology*, Volume 39, Issue 4, pp. 214–23. Copyright © 2008 John Wiley and Sons.

Tizanidine is a central α_2-adrenergic agonist. It is commonly used for spasticity in MS, stroke, and spinal cord injury. It is short-acting, with peak effects 1–2 h after administration; it wears off by 3–6 h. As a result, it is generally reserved for particular activities and times when relief of spasticity is most important. Its pharmacokinetics differ between different preparations and also when taken with/without food, being better when taken under fasting conditions (>3 h after food). As with other agents, its dose can be gradually increased over several days, and withdrawal should be similarly gradual.

Diazepam acts via the GABAA receptors to increase the postsynaptic inhibition of α-motor neurons, treating spasticity and muscle spasms. It is most useful in patients with complete spinal cord injuries. Doses should be increased or decreased incrementally. When used for more than one week, problems with drug-dependency can occur. Its side effects include weakness, sedation, and poor stamina. Abruptly stopping may cause depression, seizures, and an acute withdrawal syndrome.

Botulinum toxin A therapy (Criswell et al., 2006; Steinbok, 2006; Love et al., 2010; Quality Standards Subcommittee of the American Academy of Neurology et al., 2010; Williams et al., 2012; Novak et al., 2013; Cusick et al., 2015) is a neurotoxin, that permanently binds to the presynaptic terminal at the neuromuscular junction causing inhibition of acetylcholine release, functionally denervating the treated muscle. Administration is via direct injection, often with ultrasound guidance to improve accuracy and duration of effect. The effects are seen within 3–7 days and it lasts up to 16 weeks; wearing off as new neuromuscular junctions grow from sprouting nerve rootlets. If used too frequently, it can become less effective due to antibody formation. Care must be taken over the dose; the benefits can be limited if too little is used, but overdose can also occur, leading to systemic effects and widespread muscle paresis. It is licensed for use in upper limb spasticity in adults, bladder instability & overactive bladder, and cervical dystonia. It is widely used for upper and lower limb spasticity in children but is unlicensed for these purposes. It is best used in combination with stretching, serial casting, muscle re-education and strengthening, and orthotic adjustments.

Surgical procedures for spasticity

Several surgical strategies are employed to help combat the adverse effects of spasticity. These involve several different disciplines. Neurosurgical techniques include intrathecal baclofen (ITB), selective dorsal rhizotomy (SDR), percutaneous radiofrequency foraminal rhizotomy, and myelotomy. In addition to these, selective peripheral neurotomy (SPN) is offered by plastic surgeons. Orthopaedic surgery also has a major role to play due to the complex bone and joint abnormalities that can develop due to the spasticity. Constraints of space limit us to a focus on ITB, SDR, peripheral neurotomy, and an outline of orthopaedic surgery.

Intrathecal baclofen

ITB therapy is a well-established treatment for adults and children to treat both spasticity and dystonia. It was reported by Penn and Kroin in 1985 (Penn and Kroin, 1985). They postulated and then proved that direct administration of baclofen into the spinal CSF would achieve the same benefits of oral baclofen with fewer side effects due to direct administration and smaller dosage. This is because the $GABA_B$ receptors in the spinal cord are in the surface layers, allowing the baclofen to work directly. However, in the brain, the $GABA_B$ receptors are in the deeper layers, meaning there are fewer unwanted central effects.

When considering ITB therapy, a test dose is normally performed first (Albright and Ferson, 2006; Delhaas et al., 2008; Phillips et al., 2015). This is done under general or local anaesthetic, with either direct injection of 50–100 μg of baclofen via lumbar puncture, or insertion of a lumbar catheter to allow serial test doses or a test-infusion to be undertaken. The aims of the test dose are to assess the benefits of the treatment and to examine for possible side effects. Patients with dystonia, however, may not experience much benefit from the brief test dose because they tend to get more benefit from the sustained effects of prolonged infusion.

ITB therapy is delivered via an externally-adjustable programmable pump system, which contains a drug reservoir (10–40 ml), a battery, and the drug delivery mechanism. For the surgery, the patient is placed in the lateral position, right-side-up. The pump is implanted in a pocket in the right anterior abdominal wall. Left-sided ITB implants are avoided as gastrostomies are usually inserted on this side. The pump pocket is either subcutaneous, (superficial to the rectus fascia), or subfascial, (deep to the fascia of the rectus and external oblique muscles). The subfascial pocket is particularly useful for smaller, thinner children (Vender et al., 2006; Motta et al., 2007; Fjelstad et al., 2009; Ammar et al., 2012; Motta and Antonello, 2014). Once the pocket has been made, a small incision is made in the lumbar region and the intrathecal catheter is inserted via a lumbar puncture with a Toohey needle. There is debate in the literature about the catheter tip position with authors divided over whether a higher tip position is required for upper limb spasticity/dystonia or not (Grabb et al., 1999; Albright and Ferson, 2006; Dziurzynski et al., 2006; McCall and MacDonald, 2006; Motta et al., 2007; Brennan and Whittle, 2008; Sivakumar et al., 2010; Ughratdar et al., 2012; Varhabhatla and Zuo, 2012). Some studies have suggested that CSF

pulsatile flow is less in the thoracic and lumbar spine, with a consequent reduction in baclofen diffusion for catheters placed in this location (Bernards, 2006; Heetla et al., 2014). The tip position can be guided with X-ray imaging during surgery. In some cases, catheters may be inserted into the ventricle to allow intraventricular baclofen infusion (Albright, 2011; Rocque and Albright, 2011; Bollo et al., 2012; Turner et al., 2012). Once the catheter is inserted to the desired position, the catheter is tunnelled through to the abdominal pocket, secured to the pump and the system is then implanted (Fig. 77.2).

After implantation, the pump is activated and the system can start delivering baclofen immediately. The dose is gradually titrated upwards, usually with increments of 10% every 1–2 weeks. The ITB dose regime can be tailored with flexible dose programming delivering different amounts of baclofen at different times of the day. The pump reservoir needs to be emptied and refilled every 2–6 months depending on the infusion rate and the drug concentration. The system will also need surgery to replace the pump when the battery is nearing end of life.

Risks and unwanted effects of ITB therapy include the risks of the surgery itself, and risks associated with pump system failure of problems with the refill procedures (Albright and Ferson, 2006; Vender et al., 2006; Motta et al., 2007; Protopapas et al., 2007; Brennan and Whittle, 2008; Fjelstad et al., 2009; Heetla et al., 2014; Motta and Antonello, 2014).

- *Drug underdose/acute withdrawal*: Like any mechanical device, an ITB pump can fail, leading to acute baclofen withdrawal syndrome—a life-threatening condition resulting in severe rebound spasticity, rhabdomyolysis, renal failure, and death. This can also occur if the wrong drug concentration is used when refilling the system.
- *Drug overdose* can occur due to errors in programming or pump refilling. When refilling the pump, it is vital to ensure that the needle is inserted into the pump itself and has not skimmed alongside the pump, allowing the refill to be delivered to the pump pocket (a pocket-fill) rather than the pump. A pocket-fill is a life-threatening situation that requires immediate aspiration of drug from the pocket and may require supportive ventilation on intensive care unit (ICU) for the patient until the baclofen wears off.

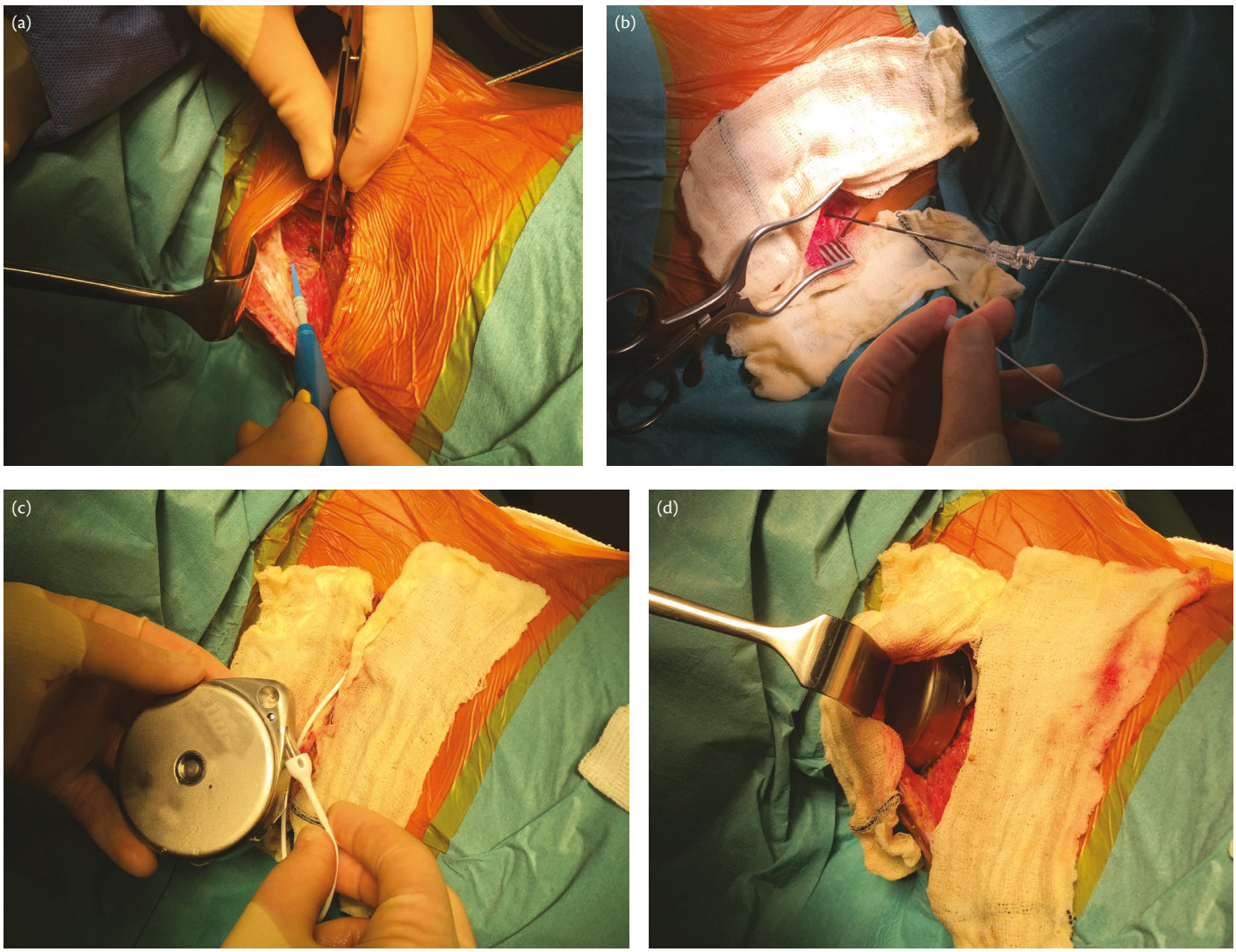

Fig. 77.2 Intraoperative photographs to illustrate insertion of an intrathecal baclofen pump. (A) A subfascial pocket is made via a right upper quadrant incision. (B) The lumbar catheter is inserted via a mid-lumbar lumbar puncture. (C) The catheter is connected to the pump. (D) The pump inserted with the catheter coiled behind.

Selective dorsal rhizotomy (SDR)

SDR is a technique for permanently reducing/removing abnormal tone in the legs. It is predominantly indicated for children rather than adults. It involves dissecting and transecting a portion of the lumbar sensory nerve roots to disrupt the abnormal reflex feedback loop. The procedure is done for cerebral palsy, where the brain injury is stable and not progressive. If SDR is performed for a progressive neurodegenerative condition, the benefits will be short-lived. It is also best performed when the only motor disorder is spasticity—if dystonia is present it will usually worsen after SDR.

The first descriptions of dorsal rhizotomy were in 1898, with Sherrington's experiments in a cat model of cerebral palsy (Sherrington, 1898). Foerster then reported the first human subjects in 1913 (Foerster, 1913). However, these two series involved complete transection of lumbar sensory roots, causing numbness and proprioceptive deficits, and hence increased mobility difficulty. Gros (Gros et al., 1967) and then Fasano (Fasano et al., 1978) investigated this further, before Peacock (Peacock and Eastman, 1981; Peacock and Arens, 1982) heralded the modern era of selective dorsal partial rhizotomy, using neurophysiology to select the most abnormal roots prior to sectioning them. The major developments since then were clarification of patient selection criteria (Peacock et al., 1987) and refining the surgery to a two-level laminectomy (Park et al., 1993), then single-level laminectomy at L1 (Park and Johnston, 2006).

Careful MDT assessment is required when considering SDR. The typical patient for SDR is a child with confirmed cerebral palsy, and dynamic spasticity predominantly affecting the legs that interferes with their mobility. They are usually GMFCS level 2–3, mobile with aids, and need adequate strength in their core muscles and leg muscles.

SDR is not usually recommended for patients with dystonia, and those with significant upper limb involvement. Its role for the more disabled GMFCS 4–5 group is under debate.

The surgery is performed via an L1 laminectomy over the conus. The L1–S1 dorsal (sensory) roots are separated from the motor roots. Each root is divided into three rootlets, tested with intraoperative neurophysiology to find the most abnormally active rootlets and then two out of every three rootlets are divided (**Fig. 77.3**). Therefore, approximately two-thirds of each sensory root is divided from L1 to S1. Anal sphincter monitoring is commonly used to help reduce risk of incontinence.

Once the spasticity is removed/reduced by SDR, the underlying muscle weakness is revealed. This requires intensive physiotherapy to build strength. After SDR, patients require 3 weeks' intensive daily physiotherapy, prior to discharge. After this, ongoing regular community physiotherapy is required and patients are encouraged to remain active.

Risks and unwanted effects of SDR include the standard risks of any neurosurgical intradural spinal procedure, and of course this includes risks of paralysis, numbness, and incontinence. However, the use of intraoperative neurophysiology helps reduce this risk to a minimum (Hays et al., 1998; Mittal et al., 2001; Steinbok et al., 2009; Turner, 2009; Fukuhara et al., 2011).

SDR outcomes have been widely studied and reported in the literature, confirming long-term benefits from this procedure both for spasticity control and also reducing rates of orthopaedic surgery requirement too (Bolster et al., 2013; Dudley et al., 2013; Hurvitz et al., 2013; Langerak et al., 2013; Steinbok, 2013; Tedroff et al., 2014; Josenby et al., 2015; Steinbok, 2015; Vermeulen and Becher, 2015). The percentage of rootlets cut in SDR is linked to the degree of

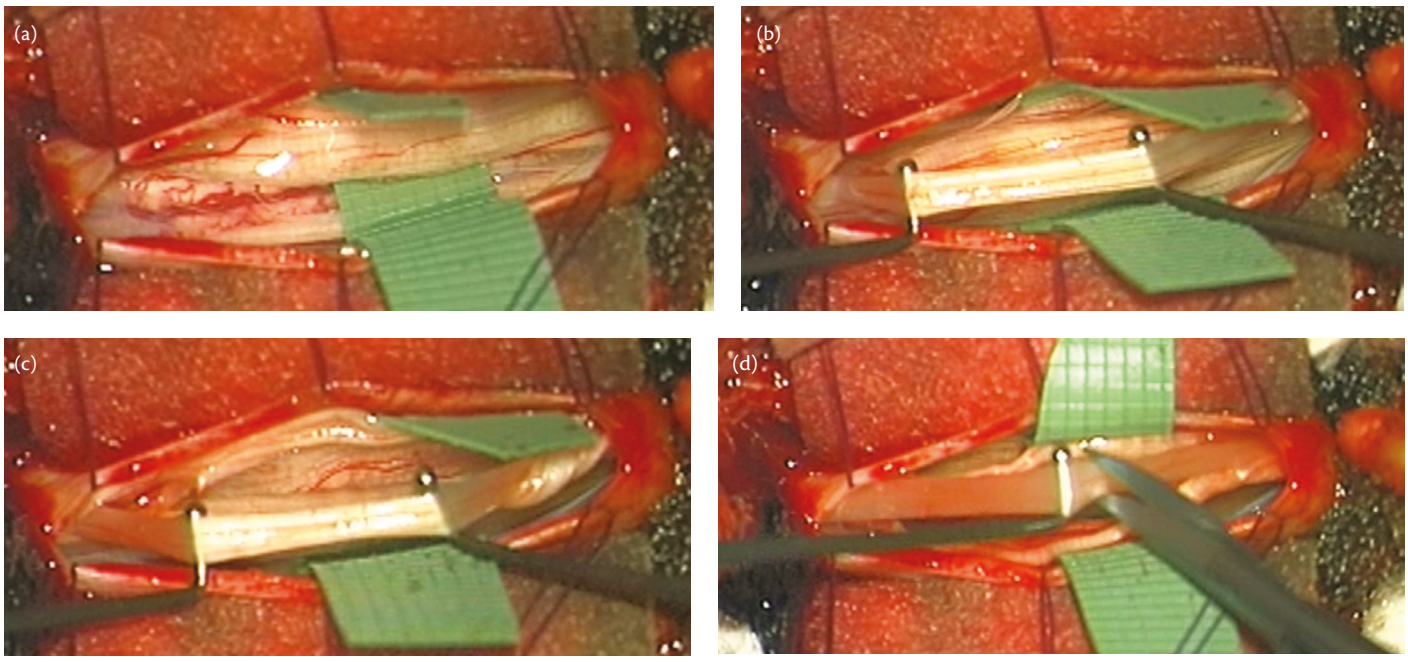

Fig. 77.3 Intraoperative photographs to illustrate the technique of selective dorsal rhizotomy via a single-level laminectomy over the conus. (A) The right-sided dorsal roots of L2-S1 have been separated from the ventral roots and placed into a green silastic sling. (B) The first rootlet of L2 is tested with bipolar stimulation via custom-made nerve hooks. (C) The second rootlet of L2 is tested. (D) The rootlet delivering the most abnormal response is divided.

spasticity control, with less than 50% rootlet section associated with increased return of spasticity.

Upper limb spasticity and selective peripheral neurotomy (SPN)

Upper limb spasticity is characterized by a combination of spastic and flaccid paralysis. Typically, there is spasticity of the flexor pronator muscles combined with flaccidity of the opposite extensor supinator muscles. This results in an adducted, internally rotated shoulder, a flexed elbow, a pronated forearm, a flexed and ulnarly deviated wrist, and a clasped hand with a thumb-in-palm deformity. The flexor pronator tonicity increases with passive stretch and is constant, except during sleep or under anaesthesia. The hypertonic muscles cocontract when the antagonists are used affecting the grasp and release ability.

MDT management aims to maintain function and range of movement. Non-operative measures of physiotherapy, splinting, tone reducing medication, and botulinum toxin should be used fully before considering surgical intervention. The surgical options include rebalancing (tendon transfers), contracture release (myofascial release, musculotendinous lengthening, joint releases), joint stabilizing procedures, and tone reducing procedures, otherwise known as SPN or selective denervation (Zancolli, 2003). SPN is only used in cases where excessive hypertonia is impeding function.

Botulinum toxin treatment mimics the potential effects of SPN on selected nerves and should be used as a preliminary treatment before considering SPN. Local anaesthetic blocks in the outpatient setting can also be used to assess the outcome of potential neurotomy.

SPN can be used in isolation or in combination with tendon transfers, releasing and stabilizing procedures. The surgery involves sectioning of both afferent and efferent pathways of the stretch reflex at the level of the neuromuscular junction. The afferent pathway, corresponding to proprioception of the muscle concerned, is lost and sectioning of the efferent pathway induces paralysis. The aim is to reduce excessive hypertonicity without suppressing useful muscular tone or impairing residual motor and sensory functions. Neurotomy should never involve a mixed nerve trunk of sensory and motor fibres as this can cause deafferentation pain. The responsible motor branches are isolated using intraoperative nerve stimulation together with the operating microscope for visualization. Variable portions (50–80%) of the isolated motor branches are resected and cauterized to prevent regrowth of fibres. The extent of partial section is dependent upon the response to electrical stimulation (Sindou et al., 2007).

SPN outcome depends upon accurately identifying the hypertonic muscles preoperatively and precisely partially denervating these muscles. Recurrence of spasticity can occur when the amount of sectioning is insufficient, however the operation can be repeated.

Orthopaedic procedures

Spastic cerebral palsy is one of the commonest conditions seen in children's orthopaedic practice.

Initially the muscles are functionally short because of spasm or contraction but with time the muscle/tendon unit becomes structurally short from contracture. This also happens to joints—after prolonged movement restriction the joint capsule becomes contracted resulting in abnormal, usually dysfunctional, postures such as fixed knee flexion. Joint instability culminating in dislocation is relatively common in children with spastic cerebral palsy, for instance grossly overpronated (flat) feet and hip subluxation and dislocation (Ounpuu et al., 2002; Pirpiris et al., 2003; Soo et al., 2006; Ross and Engsberg, 2007; Robin et al., 2009; Shore et al., 2012; Silva et al., 2012).

Antispasticity management and physiotherapy are well-established treatments during the precontracture phase but once contractures have developed orthopaedic surgery is needed to restore more normal anatomy and, hopefully, function. There are two main groups of children: those who can walk and those who cannot. The management of the latter group concentrates on prevention of hip dislocation, maintaining feet in a position to wear shoes comfortably and maintaining a comfortable seating position. The management of the former is to maintain or restore standing and walking function.

The role of orthopaedic surgery in walking children has changed following more widespread availability of SDR in the United Kingdom currently offered to those walkers with a GMFCS score of 2–3. Formerly multilevel soft tissue releases (MLSTR) was the mainstay of treatment in walking children when function was plateauing or declining as they grew taller and heavier (Gough et al., 2004; Graham et al., 2005; Khan, 2007; Gorton et al., 2009; Akerstedt et al., 2010; Harvey et al., 2012). This would be for both contraction and contracture. Typically, the child would present with a crouch or jumper's gait (hips adducted, hips and knees flexed, ankles in calcaneus or equinus), which is an energy-sapping way to stand and walk.

Children would undergo orthopaedic surgery between the ages of about 7 and 13 years but management is highly individualized. Typically, hip flexors (sartorius and psoas), knee flexors (gracilis, semitendinosus, semimembranosus medially, and sometimes biceps femoris laterally), and ankle plantarflexors (gastrocnemius or Achilles tendon) are lengthened in one session. Minimal splintage (usually a lightweight below-knee cast for four weeks) is used and early intensive rehabilitation is fundamental.

Children should be assessed in a multidisciplinary clinic and if SDR is done first the child has a further orthopaedic assessment afterwards. Often some areas of tightness will have improved so that any further orthopaedic surgery is less than would otherwise have been the case. The optimal timing of staged orthopaedic surgery is not defined except to say that if further surgery is required if it is best performed within a few months of SDR to facilitate rehabilitation.

Although there is little written, selective percutaneous myofascial lengthening ('percs') is popular method of MLSTR in the United States having advantages of smaller skin incisions and more rapid rehabilitation as well as causing less muscle scarring.

Controversy

At present, the main source of controversy in spasticity management concerns the role of SDR for children with spasticity. Concern has

been voiced because it is irreversible and can make function worse. Rigorous patient selection is therefore key.

Today, most authors accept the role of SDR for children with moderate levels of disability (GMFCS levels 2 and 3)—for whom it can improve function and mobility. Even for this group, there remains controversy. The main critique of the SDR literature is that studies are usually single-centre, small volume, and not case-controlled. This surgery is low-volume and highly specialist which makes larger, case-control studies a challenge. Some authors also cite a lack of long-term outcome data, despite there being an increasing number of reports of up to 26-year follow-up (Langerak et al., 2011; Bolster et al., 2013; Dudley et al., 2013; Hurvitz et al., 2013; Langerak et al., 2013; Steinbok, 2013; Tedroff et al., 2014; Josenby et al., 2015; Steinbok, 2015; Vermeulen and Becher, 2015). Others cite a supposed high risk of paralysis or incontinence, which has not been proven in the literature.

However, some also advocate SDR for more disabled and even wheelchair-bound children (GMFCS levels 4 and 5) as a replacement for ITB therapy (Gump et al., 2013; Ailon et al., 2015; Steinbok, 2015; Vermeulen and Becher, 2015). For this group, the indications and goals of treatment are different because these children will often not achieve independent walking. They are also more likely to have mixed spasticity and dystonia, which can make the outcome less certain. Some advocate offering SDR instead of ITB for GMFCS level 4–5 children to help with personal hygiene and ease of movement, because SDR means that they will not require the regular hospital reviews and pump refills/replacements over the subsequent years. This has not been proven to be the case, however, and is certainly an area for future clinical trial research. For this group SDR can also remove/reduce their ability to stand for transfers with associated negative consequences for quality of life.

In addition, there is interest in whether SDR could have a role in genetic conditions (Kai et al., 2014), acquired injuries (Langerak et al., 2014; Reynolds et al., 2014) (e.g. spinal trauma or postinfectious), as well as patients with hemiplegia (Oki et al., 2010; Gump et al., 2013).

Conclusions

Spasticity treatment requires carefully planned multidisciplinary assessment and treatment. Treatment strategies should be tailored around the patient's functional and physical needs, with input from allied health professionals with rehabilitation, medical, and surgical disciplines. Regular reviews are required as part of this to ensure that treatments remain suited to the individual. The treatment goals include improving tone, alleviating spasms, controlling gastrointestinal effects, and controlling bladder function, with the aim of protecting function and minimizing the deleterious effects of spasticity and their condition as a whole.

FURTHER READING

Ailon, T., Beauchamp, R., Miller, S., et al. (2015). Long-term outcome after selective dorsal rhizotomy in children with spastic cerebral palsy. *Childs Nerv Syst*, **31**, 415–23.

Fairhurst, C. (2011). Cerebral palsy: the whys and hows. *Arch Dis Child Educ Pract Ed*, **97**(4), 122–31.

Harvey, A., Rosenbaum, P., Hanna, S., Yousefi-Nooraie, R., & Graham, K.H. (2012). Longitudinal changes in mobility following single-event multilevel surgery in ambulatory children with cerebral palsy. *J Rehabil Med*, **44**, 137–43.

Novak, I., McIntyre, S., Morgan, C., et al. (2013). A systematic review of interventions for children with cerebral palsy: state of the evidence. *Dev Med Child Neurol*, **55**, 885–910.

Sindou, M.P., Simon, F., Mertens, P., & Decq, P. (2007). Selective peripheral neurotomy (SPN) for spasticity in childhood. *Childs Nerv Syst*, **23**, 957–70.

REFERENCES

Abbott, R. (2007). Editorial on 'The management of childhood hypertonia'. *Childs Nerv Syst*, **23**, 937–41.

Ailon, T., Beauchamp, R., Miller, S., et al. (2015). Long-term outcome after selective dorsal rhizotomy in children with spastic cerebral palsy. *Childs Nerv Syst*, **31**, 415–23.

Akerstedt, A., Risto, O., Odman, P., & Oberg, B. (2010). Evaluation of single event multilevel surgery and rehabilitation in children and youth with cerebral palsy--A 2-year follow-up study. *Disability & Rehabilitation*, **32**, 530–9.

Albright, A.L. (2011). Technique for insertion of intraventricular baclofen catheters. *J Neurosurg Pediatr*, **8**, 394–5.

Albright, A.L. & Ferson, S.S. (2006). Intrathecal baclofen therapy in children. *Neurosurg Focus*, **21**, e3.

Ammar, A., Ughratdar, I., Sivakumar, G., & Vloeberghs, M.H. (2012). Intrathecal baclofen therapy-how we do it. *J Neurosurg Pediatr*, **10**, 439–44.

Bernards, C.M. (2006). Cerebrospinal fluid and spinal cord distribution of baclofen and bupivacaine during slow intrathecal infusion in pigs. *Anesthesiology*, **105**, 169–78.

Bollo, R.J., Gooch, J.L., & Walker, M.L. 2012. Stereotactic endoscopic placement of third ventricle catheter for long-term infusion of baclofen in patients with secondary generalized dystonia. *J Neurosurg Pediatr*, **10**, 30–3.

Bolster, E.A.M., Van Schie, P.E.M., Becher, J.G., Van Ouwerkerk, W.J.R., Strijers, R.L.M., & Vermeulen, R.J. (2013). Long-term effect of selective dorsal rhizotomy on gross motor function in ambulant children with spastic bilateral cerebral palsy, compared with reference centiles. *Dev Med Child Neurol*, **55**, 610–16.

Brennan, P.M. & Whittle, I.R. (2008). Intrathecal baclofen therapy for neurological disorders: a sound knowledge base but many challenges remain. *Brit J Neurosurg*, **22**, 508–19.

Criswell, S.R., Crowner, B.E., & Racette, B.A. (2006). The use of botulinum toxin therapy for lower-extremity spasticity in children with cerebral palsy. *Neurosurg Focus*, **21**, e1.

Cusick, A., Lannin, N., & Kinnear, B.Z. (2015). Upper limb spasticity management for patients who have received botulinum toxin A injection: Australian therapy practice. *Aust Occup Ther J*, **62**, 27–40.

Dasenbrock, H.H., Pendleton, C., McGirt, M.J., et al. (2011). 'Fulfilling the chief of his duties as a physician': Harvey Cushing, selective dorsal rhizotomy and elective spine surgery for quality of life. *J Neurosurg Spine*, **14**, 421–7.

Delhaas, E.M., Beersen, N., Redekop, W.K., & Klazinga, N.S. (2008). Long-term outcomes of continuous intrathecal baclofen infusion for treatment of spasticity: a prospective multicenter follow-up study. *Neuromodulation*, **11**, 227–36.

Dudley, R.W.R., Parolin, M., Gagnon, B., et al. (2013). Long-term functional benefits of selective dorsal rhizotomy for spastic cerebral palsy. *J Neurosurg Pediatr*, **12**, 142–50.

Dziurzynski, K., Mcleish, D., Ward, M., & Iskandar, B.J. (2006). Placement of baclofen pumps through the foramen magnum and upper cervical spine. *Childs Nerv Syst*, **22**, 270–3.

Engsberg, J.R., Ross, S.A., Collins, D.R., & Park, T.S. (2007). Predicting functional change from preintervention measures in selective dorsal rhizotomy. *J Neurosurg*, **106**, 282–7.

Fasano, V.A., Broggi, G., Barolat-Romana, G., & Sguazzi, A. (1978). Surgical treatment of spasticity in cerebral palsy. *Childs Brain*, **4**, 289–305.

Fjelstad, A.-B., Hommelstad, J., & Sorteberg, A. (2009). Infections related to intrathecal baclofen therapy in children and adults: frequency and risk factors. *J Neurosurg Pediatr*, **4**, 487–93.

Foerster, O. (1913). On the indications and results of the excision of posterior spinal nerve roots in men. *Surg Gynecol Obstet*, **16**, 163–474.

Fukuhara, T., Nakatsu, D., Namba, Y., & Yamadori, I. (2011). Histological evidence of intraoperative monitoring efficacy in selective dorsal rhizotomy. *Childs Nerv Syst*, **27**(9), 1453–8.

Gilmore, R., Sakzewski, L., & Boyd, R. (2010). Upper limb activity measures for 5-to 16-year-old children with congenital hemiplegia: a systematic review. *Dev Med Child Neurol*, **52**(1), 14–21.

Gorton, G.E., Abel, M.F., Oeffinger, D.J., et al. (2009). A prospective cohort study of the effects of lower extremity orthopaedic surgery on outcome measures in ambulatory children with cerebral palsy. *J Pediatr Orthop*, **29**, 903–9.

Gough, M., Eve, L.C., Robinson, R.O., & Shortland, A.P. (2004). Short-term outcome of multilevel surgical intervention in spastic diplegic cerebral palsy compared with the natural history. *Dev Med Child Neurol*, **46**, 91–7.

Grabb, P.A., Guin-Renfroe, S., & Meythaler, J.M. (1999). Midthoracic catheter tip placement for intrathecal baclofen administration in children with quadriparetic spasticity. *Neurosurgery*, **45**, 833–6; discussion 836–7.

Graham, H.K., Baker, R., Dobson, F., & Morris, M.E. (2005). Multilevel orthopaedic surgery in group IV spastic hemiplegia. *JBJS*, **87**, 548–55.

Gros, C., Ouaknine, G., & Vlahovitch, B., & Frèrebeau, P. (1967). La radicotomie sélective postérieure dans le traitement neurochirurgical de lhypertonie pyramidale. *Neurochirurgie*, **13**, 505–18.

Gump, W.C., Mutchnick, I.S., & Moriarty, T.M. (2013). Selective dorsal rhizotomy for spasticity not associated with cerebral palsy: reconsideration of surgical inclusion criteria. *Neurosurg Focus*, **35**, E6.

Haley, S.M, Andrellos, P.J., Coster, W., Haltiwanger, J.T., & Ludlow, L.H. (1992). *Pediatric Evaluation of Disability Inventory (PEDI): Development, standardization and administration manual*. Boston, MA: New England Medical Centre Hospitals.

Harvey, A., Graham, H.K., Morris, M.E., Baker, R., & Wolfe, R. (2007). The Functional Mobility Scale: ability to detect change following single event multilevel surgery. *Dev Med Child Neurol*, **49**, 603–7.

Harvey, A., Rosenbaum, P., Hanna, S., Yousefi-Nooraie, R., & Graham, K.H. (2012). Longitudinal changes in mobility following single-event multilevel surgery in ambulatory children with cerebral palsy. *J Rehabil Med*, **44**, 137–43.

Haugh, A.B., Pandyan, A.D., & Johnson, G.R. (2006). A systematic review of the Tardieu Scale for the measurement of spasticity. *Disability & Rehabilitation*, **28**, 899–907.

Hays, R.M., McLaughlin, J.F., Bjornson, K.F., Stephens, K., Roberts, T.S., & Price, R. 1998. Electrophysiological monitoring during selective dorsal rhizotomy, and spasticity and GMFM performance. *Dev Med Child Neurol*, **40**, 233–8.

Heetla, H.W., Staal, M.J., Proost, J.H., & Van Laar, T. (2014). Clinical relevance of pharmacological and physiological data in intrathecal baclofen therapy. *Arch Phys Med Rehabil*, **95**, 2199–206.

Hurvitz, E.A., Marciniak, C.M., Daunter, A.K., et al. (2013). Functional outcomes of childhood dorsal rhizotomy in adults and adolescents with cerebral palsy. *J Neurosurg Pediatr*, **11**, 380–8.

Josenby, A.L., Wagner, P., Jarnlo, G.-B., Westbom, L., & Nordmark, E. (2015). Functional performance in self-care and mobility after selective dorsal rhizotomy: a 10-year practice-based follow-up study. *Dev Med Child Neurol*, **57**, 286–93.

Kai, M., Yongjie, L., & Ping, Z. (2014). Long-term results of selective dorsal rhizotomy for hereditary spastic paraparesis. *J Clin Neuroscience*, **21**, 116–20.

Khan, M.A. (2007). Outcome of single-event multilevel surgery in untreated cerebral palsy in a developing country. *JBJS*, **89**, 1088–91.

Langerak, N.G., Du Toit, J., Burger, M., Cotton, M.F., Springer, P.E., & Laughton, B. (2014). Spastic diplegia in children with HIV encephalopathy: first description of gait and physical status. *Dev Med Child Neurol*, **56**, 686–94.

Langerak, N.G., Hillier, S.L., Verkoeijen, P.P., Peter, J.C., Fieggen, A.G., & Vaughan, C.L. (2011). Level of activity and participation in adults with spastic diplegia 17–26 years after selective dorsal rhizotomy. *J Rehabil Med*, **43**, 330–7.

Langerak, N.G., Vaughan, C.L., Peter, J.C., Fieggen, A.G., & Peacock, W.J. (2013). Letter to the editor: long-term outcomes of dorsal rhizotomy. *J Neurosurg Pediatr*, **12**, 664–5.

Love, S.C., Novak, I., Kentish, M., et al. (2010). Botulinum toxin assessment, intervention and after-care for lower limb spasticity in children with cerebral palsy: international consensus statement. *Eur J Neurol*, **17** Suppl 2, 9–37.

McCall, T.D. & Macdonald, J.D. (2006). Cervical catheter tip placement for intrathecal baclofen administration. *Neurosurgery*, **59**, 634–40; discussion 634–40.

Mittal, S., Farmer, J.P., Poulin, C., & Silver, K. (2001). Reliability of intraoperative electrophysiological monitoring in selective posterior rhizotomy. *J Neurosurg*, **95**, 67–75.

Motta, F. & Antonello, C.E. (2014). Analysis of complications in 430 consecutive pediatric patients treated with intrathecal baclofen therapy: 14-year experience. *J Neurosurg Pediatr*, **13**, 301–6.

Motta, F., Buonaguro, V., & Stignani, C. (2007). The use of intrathecal baclofen pump implants in children and adolescents: safety and complications in 200 consecutive cases. *J Neurosurg*, **107**, 32–5.

Novak, I., McIntyre, S., Morgan, C., et al. (2013). A systematic review of interventions for children with cerebral palsy: state of the evidence. *Dev Med Child Neurol*, **55**, 885–910.

O'Brien, D.F. & Park, T.S. (2006). A review of orthopedic surgeries after selective dorsal rhizotomy. *Neurosurg Focus*, **21**, e2.

Oki, A., Oberg, W., Siebert, B., Plante, D., Walker, M.L., & Gooch, J. L. (2010). Selective dorsal rhizotomy in children with spastic hemiparesis. *J Neurosurg Pediatr*, **6**, 353–8.

Ou, C., Kent, S., Miller, S., & Steinbok, P. (2010). Selective dorsal rhizotomy in children: comparison of outcomes after single-level versus multilevel laminectomy technique. *Can J Neurosci Nurs*, **32**, 17–24.

Ounpuu, S., Deluca, P., Davis, R., & Romness, M. (2002). Long-term effects of femoral derotation osteotomies: an evaluation using three-dimensional gait analysis. *J Pediatr Orthop*, **22**, 139–45.

Papavasiliou, A.S. (2009). Management of motor problems in cerebral palsy: a critical update for the clinician. *EJPN*, **13**, 387–96.

Park, T.S. & Albright, L. (2006). Treatment of spasticity. *Neurosurg Focus*, **21**, E7.

Park, T.S., Gaffney, P.E., Kaufman, B.A., & Molleston, M.C. (1993). Selective lumbosacral dorsal rhizotomy immediately caudal to the conus medullaris for cerebral palsy spasticity. *Neurosurgery*, **33**, 929–33; discussion 933–4.

Park, T.S. & Johnston, J.M. (2006). Surgical techniques of selective dorsal rhizotomy for spastic cerebral palsy. Technical note. *Neurosurg Focus*, **21**, e7.
Peacock, W.J. & Arens, L.J. (1982). Selective posterior rhizotomy for the relief of spasticity in cerebral palsy. *SA Med J*, **62**, 119–24.
Peacock, W. J., Arens, L. J., & Berman, B. 1987. Cerebral palsy spasticity. Selective posterior rhizotomy. *Pediat Neurosci*, **13**, 61–6.
Peacock, W.J. & Eastman, R. (1981). The neurosurgical management of spasticity. *S Afr Med J*, **60**(22), 849–50.
Penn, R.D. & Kroin, J.S. (1985). Continuous intrathecal baclofen for severe spasticity. *Lancet*, **326**, 125–7.
Phillips, M.M., Miljkovic, N., Ramos-Lamboy, M., et al. (2015). Clinical experience with continuous intrathecal baclofen trials prior to pump implantation. *PM R*, **7**(10), 1052–8.
Pirpiris, M., Trivett, A., Baker, R., Rodda, J., Nattrass, G.R., & Graham, H.K. (2003). Femoral derotation osteotomy in spastic diplegia. Proximal or distal? *JBJS*, **85**, 265–72.
Platz, T., Eickhof, C., Nuyens, G., & Vuadens, P. (2005). Clinical scales for the assessment of spasticity, associated phenomena, and function: a systematic review of the literature. *Disability & Rehabilitation*, **27**, 7–18.
Protopapas, M.G., Bundock, E., Westmoreland, S., Nero, C., Graham, W.A., & Nesathurai, S. (2007). The complications of scar formation associated with intrathecal pump placement. *Arch Phys Med Rehabil*, **88**, 389–90.
Quality Standards Subcommittee of the American Academy of Neurology and the Practice Committee of the Child Neurology Society, Delgado, M.R., Hirtz, D., et al. (2010). Practice parameter: pharmacologic treatment of spasticity in children and adolescents with cerebral palsy (an evidence-based review): report of the Quality Standards Subcommittee of the American Academy of Neurology and the Practice Committee of the Child Neurology Society. *Neurology*, **74**, 336–43.
Reynolds, M.R., Ray, W.Z., Strom, R.G., Blackburn, S.L., Lee, A., & Park, T.S. (2011). Clinical outcomes after selective dorsal rhizotomy in an adult population. *World Neurosurg*, **75**(1), 138–4.
Reynolds, R.M., Morton, R.P., Walker, M.L., Massagli, T.L., & Browd, S.R. (2014). Role of dorsal rhizotomy in spinal cord injury-induced spasticity. *J Neurosurg Pediatr*, **14**, 266–70.
Robin, J., Graham, H.K., Baker, R., et al. (2009). A classification system for hip disease in cerebral palsy. *Dev Med Child Neurol*, **51**, 183–92.
Rocque, B.G. & Albright, A.L. (2011). Intraventricular versus intrathecal baclofen for secondarydystonia: a comparison of complications. *Neurosurgery*, **70**(2 0 0), 10.1227/NEU.0b013e31823f5cd9.
Ronan, S. & Gold, J.T. (2007). Nonoperative management of spasticity in children. *Childs Nerv Syst*, **23**, 943–56.
Ross, S.A. & Engsberg, J.R. (2007). Relationships between spasticity, strength, gait, and the GMFM-66 in persons with spastic diplegia cerebral palsy. *Arch Phys Med Rehabil*, **88**, 1114–20.
Sherrington, C.S. (1898). Experiments in examination of the peripheral distribution of the fibres of the posterior roots of some spinal nerves. Part II. *Phil Trans R Soc Lond B*, **190**, 45–186.
Shore, B., Spence, D., & Graham, H. (2012). The role for hip surveillance in children with cerebral palsy. *Curr Rev Musculoskel Med*, **5**, 126–34.
Silva, S., Nowicki, P., Caird, M.S., et al. (2012). A comparison of hip dislocation rates and hip containment procedures after selective dorsal rhizotomy versus intrathecal baclofen pump insertion in nonambulatory cerebral palsy patients. *J Pediatr Orthop*, **32**, 853–6.
Sindou, M.P., Simon, F., Mertens, P., & Decq, P. (2007). Selective peripheral neurotomy (SPN) for spasticity in childhood. *Childs Nerv Syst*, **23**, 957–70.
Sivakumar, G., Yap, Y., Tsegaye, M., & Vloeberghs, M. (2010). Intrathecal baclofen therapy for spasticity of cerebral origin—does the position of the intrathecal catheter matter? *Childs Nerv Syst*, **26**, 1097–102.
Soo, B., Howard, J.J., Boyd, R.N., et al. (2006). Hip displacement in cerebral palsy. *JBJS*, **88**, 121–9.
Steinbok, P. (2001). Outcomes after selective dorsal rhizotomy for spastic cerebral palsy. *Childs Nerv Syst*, **17**, 1–18.
Steinbok, P. (2006). Selection of treatment modalities in children with spastic cerebral palsy. *Neurosurg Focus*, **21**, e4.
Steinbok, P. (2013). Long-term effect of selective dorsal rhizotomy. *Dev Med Child Neurol*, **55**(7), 586.
Steinbok, P. (2015). Outcomes after selective dorsal rhizotomy. *Dev Med Child Neurol*, **57**, 214–15.
Steinbok, P., Tidemann, A.J., Miller, S., Mortenson, P., & Bowen-Roberts, T. (2009). Electrophysiologically guided versus non-electrophysiologically guided selective dorsal rhizotomy for spastic cerebral palsy: a comparison of outcomes. *Childs Nerv Syst*, **25**, 1091–6.
Tedroff, K., Löwing, K., & Aström, E. (2014). A prospective cohort study investigating gross motor function, pain, and health-related quality of life 17 years after selective dorsal rhizotomy in cerebral palsy. *Dev Med Child Neurol*, **57**(5), 484–90.
Turner, M., Nguyen, H.S., & Cohen-Gadol, A.A. (2012). Intraventricular baclofen as an alternative to intrathecal baclofen for intractable spasticity or dystonia: outcomes and technical considerations. *J Neurosurg Pediatr*, **10**, 315–19.
Turner, R.P. (2009). Neurophysiologic intraoperative monitoring during selective dorsal rhizotomy. *J Clin Neurophys*, **26**, 82–4.
Ughratdar, I., Muquit, S., Ingale, H., Moussa, A., Ammar, A., & Vloeberghs, M. (2012). Cervical implantation of intrathecal baclofen pump catheter in children with severe scoliosis. *J Neurosurg Pediatr*, **10**, 34–8.
Varhabhatla, N.C., & Zuo, Z. (2012). Rising complication rates after intrathecal catheter and pump placement in the pediatric population: analysis of national data between 1997 and 2006. *Pain Physician*, **15**, 65–74.
Vender, J.R., Hester, S., Waller, J.L., Rekito, A., & Lee, M.R. (2006). Identification and management of intrathecal baclofen pump complications: a comparison of pediatric and adult patients. *J Neurosurg*, **104**, 9–15.
Vermeulen, R.J. & Becher, J.G. (2015). Long-term outcome in selective dorsal rhizotomy in spastic cerebral palsy: differentiation in mobility levels is needed. *Dev Med Child Neurol*, **57**(5), 408–9.
Williams, G., Olver, J., De Graaff, S., & Singer, B.J. (2012). The use of botulinum toxin type A in the management of adult-onset focal spasticity: a survey of Australian allied health professionals. *Aust Occup Ther J*, **59**, 257–64.
Zancolli, E.A. (2003). Surgical management of the hand in infantile spastic hemiplegia. *Hand Clinics*, **19**, 609–29.

RELATED LINKS TO EBRAIN

The Management of Posture and Mobility. https://learning.ebrain.net/course/view.php?id=786
Management of Spasticity in Post Stroke Syndrome. https://learning.ebrain.net/course/view.php?id=549
Management of Spasticity and Associated Features. https://learning.ebrain.net/course/view.php?id=787
Management of Spasticity in Children. https://learning.ebrain.net/course/view.php?id=548
Managing Late Deterioration in Neurological Disability. https://learning.ebrain.net/course/view.php?id=539
Orthotics and the Avoidance and Management of Contractures. https://learning.ebrain.net/course/view.php?id=546

78

Pain pathophysiology and surgical management

Richard Mannion and Rokas Tamosauskas

Pain pathways—anatomy and physiology

Transduction and transmission of sensory input from our environment to the brain starts first in primary sensory neurons (first order neurons). This group are anatomically and functionally heterogenous, their cell bodies located in the dorsal root and trigeminal ganglia and their axons divided into a peripheral projection towards their innervation targets and a central projection into the spinal cord (**Fig. 78.1**).

Primary sensory neurons can be divided into the following: large myelinated Aβ fibre afferents responsible for conveying low-threshold mechanical sensation and vibration; thinly myelinated fibre Aδ afferents, with smaller cell bodies responsible for fast pain (e.g. pinprick); and small, unmyelinated C-fibre afferents involved in pain and temperature sensation. All these cells have peripheral terminals spread widely throughout their innervation tissue as 'free nerve endings', and transduction through highly evolved, complex processes allows the preferential detection of peripheral stimuli that is strictly regulated. Nociceptors are anatomically, functionally, and neurochemically distinct, and respond to certain stimuli through specific receptor-mediated mechanisms (Woolf and Ma, 2007). This results in predictable stimulus-response relationship within primary sensory neurons that allows reliable and reproducible coding of sensory stimuli from our environment to the brain. It is important to note, however, that these relationships are not 'hard wired'; they are continuously and actively maintained in the physiological state, and can therefore be altered in disease states, whereby primary sensory neurons can change phenotype and consequently their function in relation to coding for peripheral stimuli, that is, transduction and transmission. Indeed, they can even start to fire spontaneously in the absence of a peripheral stimulus—one of the recognized mechanisms of spontaneous (i.e. stimulus-independent) neuropathic pain (Costigan et al., 2009).

Pain transduction and transmission

In the physiological state, the sensation of physical pain results from the detection of peripheral stimuli causing potential or actual tissue damage: this is nociception. Nociceptors, that is, primary sensory neurons with the capacity to detect noxious stimuli (e.g. heat, chemical, mechanical) are the small, unmyelinated afferent fibres, with cell bodies in the dorsal root ganglia, that innervate peripheral structures such as skin, muscles, and viscera (Woller et al., 2017). Their central axons run within the dorsal root to the dorsal root entry zone where they enter Lissauer's tract in the dorsolateral white matter funiculus of the spinal cord.

As well as the usual neurotransmitters such as glutamate, nociceptors preferentially express several peptides that play a role in neurochemical transmission, such as substance P and calcitonin gene-related peptide (CGRP). Following their discovery, early excitement that these could present new therapeutic targets for pain management have not been realized, as the roles of peptide transmitters are complex, but they do play an important role in sensory transmission and have a distinct and longer lasting action on postsynaptic neurons in the dorsal horn, that works in conjunction with fast transmitters such as glutamate. In addition, these peptides can be found in the peripheral terminals of nociceptors, and anterograde action potentials from the cell body to these terminals leads to the release of peptides, that results in vasodilation, plasma extravasation and recruitment of immune cells, producing neurogenic inflammation.

Most are polymodal (i.e. they can detect more than one type of stimulus modality). Typically they have a higher activation threshold for detection of mechanical stimuli than Aβ fibres (though this nociceptive threshold may vary between tissues, e.g. cornea vs. skin). A large number of mechanically sensitive proteins including mechano-gated ion channels have been identified across different functions and species (Delmas et al., 2011; Delmas and Coste, 2013).

Thermosensitivity is thought to be mediated via a family of receptor proteins called TRPs (transient receptor proteins; Mickle et al., 2015). The TRPV1 receptor is expressed by approximately 40% of primary sensory neurons, many of which are small unmyelinated C-fibre neurons, and the ion channel opens in a temperature-sensitive manner. TRPV1 is thought to be involved in heat detection, and interestingly altered TRPV1 expression in sensory neurons has been observed experimentally in different disease models. There are several other related proteins that have been implicated cold

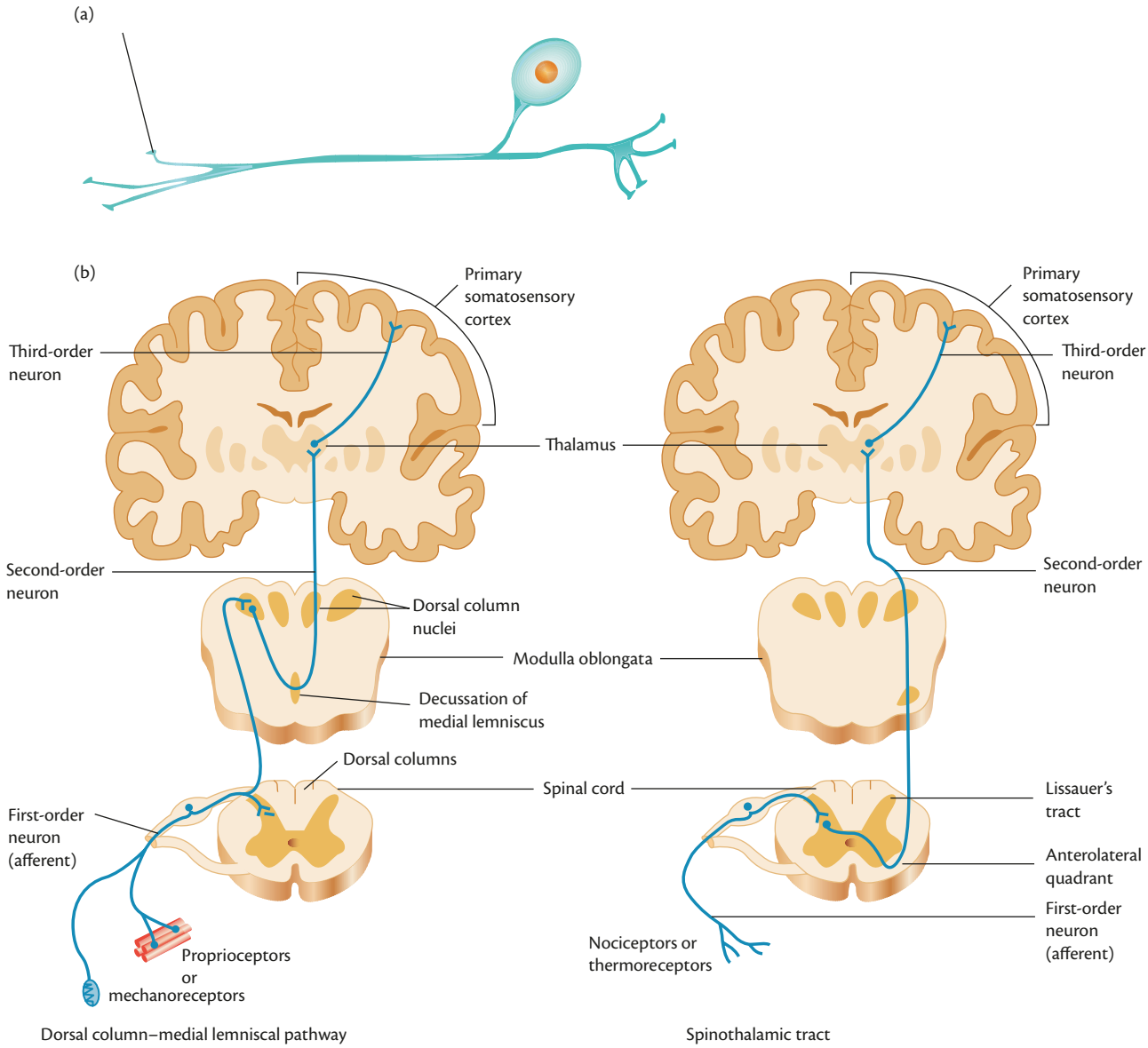

Fig. 78.1 (A) Primary sensory neurons have a single axon that leaves the cell body and divides into a long peripheral axon and a shorter centrally projecting one. (B) Cartoon showing major sensory pathways.

detection, innocuous warm detection, and noxious heat sensation in normal and diseased states (Fig. 78.2).

Different voltage gated ion channels are preferentially expressed by nociceptors versus non-nociceptive primary sensory neurons, the best characterized of which are the Na_V ion channels (1.7, 1.8, 1.9). These channels are critical to normal sensory transduction and transmission in nociceptors, and certain mutations in the genes coding for these channels are known to cause inherited chronic pain states (Cummins et al., 2007). Of note, sodium channel function changes in chronic pain states such as inflammation and following nerve injury, such that receptors are sensitized (Liu and Wood, 2011). Other ion channels implicated in nociception are the acid-sensitive ion channels, also preferentially expressed by nociceptor neurons (Dubé et al., 2009). These ion channels open at low pH, which are the conditions found in inflamed tissue where nociceptors are more sensitive and are activated at lower thresholds (Fig. 78.3).

There is a subpopulation of nociceptors which remain silent in the physiological state, not responding to any peripheral stimuli, even noxious ones, but are activated following tissue or nerve injury, when they begin to respond to mechanical and thermal stimuli. These neurons may play a role in altered pain responses during disease states such as inflammation (see Fig. 78.4).

Primary relay—the dorsal horn

Once a nociceptor is activated, action potentials pass along the axon and through the dorsal root ganglion (or trigeminal ganglion) to access the spinal cord. At the spinal levels, these fibres pass though the dorsal roots to the dorsal root entry zone (DREZ). Here, there is anatomical separation of large myelinated A-fibre axons and small, unmyelinated C fibres. A-fibre central axons pass into the ipsilateral dorsal columns to run rostrally. As they enter the white matter of the spinal cord from the DREZ, they provide a collateral axon that enters

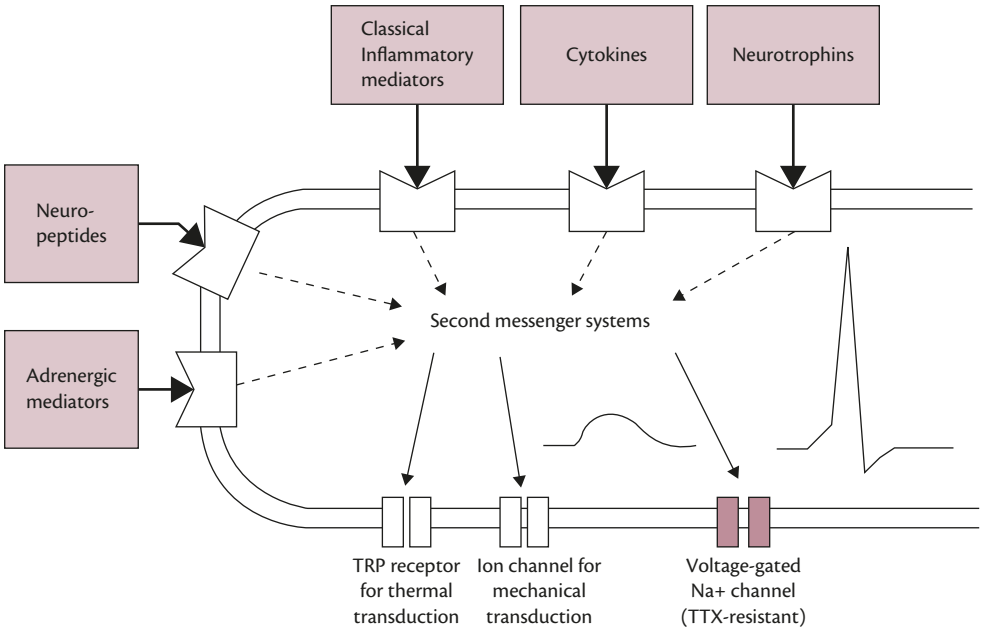

Fig. 78.2 Immunohistological TTX–resistant sodium channel expression in the dorsal root ganglion, demonstrated with immunohistochemical staining against peripherin, a protein found in larger A-fibre afferents. Note the positive cell bodies are largely the small nociceptor neurons.

Reproduced from Xi-Yao Gu et al., Dexmedetomidine inhibits Tetrodotoxin-resistant Nav1.8 sodium channel activity through Gi/o-dependent pathway in rat dorsal root ganglion neurons, *Molecular Brain*, Volume 8, Issue 15, Copyright © licensee BioMed Central. 2015.

the grey matter of the dorsal horn of the spinal cord. This axon plays a key role in sensory gating.

C fibres enter the DREZ and either pass through, to access the dorsal horn, or run a few segments rostrally or caudally in Lissauer's tract, prior to termination in the dorsal horn. These fibres are known to enter and terminate in the superficial laminae of the dorsal horn, also known as the substantia gelatinosa. Here they synapse onto the dendrites of neurons whose cell bodies lie within the dorsal horn. The majority of these cells are local interneurons involved in local anterograde and retrograde relay circuits. Some are excitatory neurons while others are inhibitory. Therefore, the superficial laminae of the dorsal horn contain a wide range of excitatory and inhibitory neurotransmitters and neuropeptide transmitters that forms a complex gating system, controlling how information is relayed from our environment (internal and external) to the brain. In addition, there are some neurons with cell bodies found in superficial dorsal horn and the deeper dorsal horn layers, that themselves have a projecting axon which crosses the spinal cord segmentally, anterior to the central canal to run in the spinothalamic tract (STT) tract (see Box 78.1).

Wide dynamic range (WDR) cells

These neurons with cell bodies located in the dorsal horn of the spinal cord, predominantly the deeper laminae, receive and respond to input from Aβ fibres, Aδ fibres and C fibres. They can respond in a graded fashion to innocuous and noxious stimuli. They are also known to have large receptive fields, whereas cells in the superficial laminae have much smaller receptive fields. It is thought that localization of a noxious stimulus is therefore encoded by populations or networks of neurons.

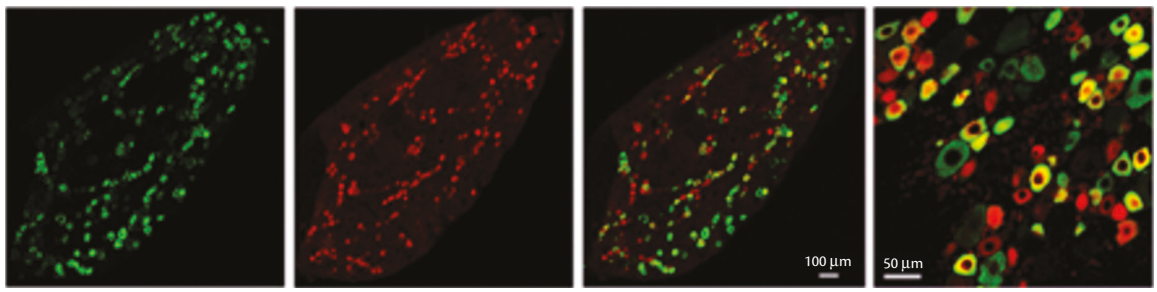

Fig. 78.3 Original model proposed by Melzack and Wall (1965). L–large/S–small sensory neurons. T–Transmission neurons. By exciting SG (substantia gelatinosa) neurons, this allow presynaptic modulation of sensory input to projection neurons via excitatory and inhibitory mechanisms, with further control superimposed from descending pathways

Reproduced with permission from Lorne Mendell, Constructing and deconstructing the gate theory of pain, *Pain*, Volume 155, Issue 2, pp. 210–16, Copyright © 2014 Wolters Kluwer Health, Inc.

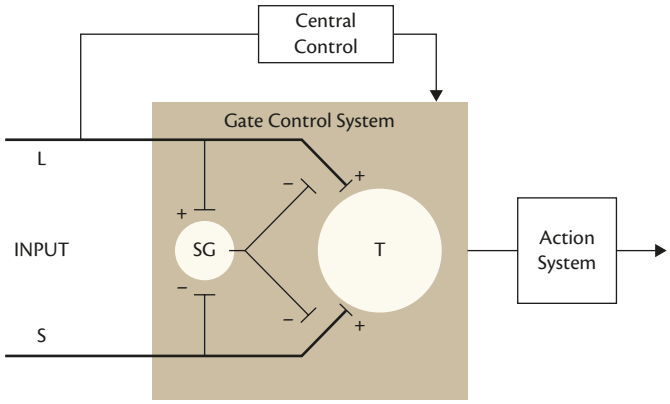

Fig. 78.4 Model of the sensory ending of a nociceptor showing ion channels for transduction of thermal and mechanical stimuli and action potential generation and metabotropic receptors subserving chemosensitivity.

Box 78.1 Gate theory

'The Gate Theory of Pain', published by Melzack and Wall in *Science* in 1965, provided a mechanism to explain how nociceptive input could be coded by the sensory system at the first sensory relay in the dorsal horn of the spinal cord. It focused on recently discovered mechanisms of presynaptic control of synaptic transmission from large and small sensory neurons, which was proposed to 'gate' incoming information, depending on the balance between these inputs (see Mendell (2014) for full review). It also incorporated other mechanisms, such as descending control pathways from the brain and the convergence of nociceptive and non-nociceptive input onto the same neurons in the spinal cord, involved in transmission to the brain. While it was later found that not all the predictions were accurate, the Gate Theory provided a catalyst for further research and understanding within the burgeoning field of pain neurobiology. It helped to change the accepted view of pain mechanisms, with a move away from fixed 'labelled line' pain pathways to the realization of both adaptive and maladaptive processes mediating physiological and pathological pain states. See Figure 78.4.

While there are complex neural arrangements involving finely balanced processes of excitatory and inhibitory transmission through anterograde projection and retrograde feedback, in the physiological state at baseline, a fixed peripheral stimulus will typically produce a predictable response. However, our experience of pain when presented with a noxious stimulus can be highly varied. It was recognized long before we developed an understanding pain anatomy and physiology that our experience of pain very much depended on circumstances (i.e. pain perception was contextual). Henry Beecher recognized in 1956 that soldiers could suffer extensive battlefield injuries yet require little or no analgesia, whereas similar injuries in civilian casualties produced much more pain (Beecher, 1956). Much of the modulation is now known to occur within the dorsal horn of the spinal cord, the first sensory relay.

Spinal gating—modulation of C-fibre input

Through mono- and poly-synaptic pathways in the dorsal horn, there is convergence of primary sensory input on to projection neurons. This allows different inputs to modulate transmission of others. Therefore, non-nociceptive inputs can inhibit nociceptive input and the appreciation of pain; for example, rubbing an injured area reduced the perception of pain. Attempts to explain observations like this led to publication of the gate control theory by Melzack and Wall in 1965 (see **Box 78.1**).

There are several different mechanisms within the spinal cord by which sensory transmission to the brain is modulated, either increased or decreased, involving local excitatory and inhibitory interneurons, and descending pathways from the brain. Direct electrical stimulation of the periaqueductal grey (PAG) produces a profound analgesia that is opioid-mediated. The PAG projects to the rostroventral medulla (RVM), with includes the raphe nuclei of the medulla, rich in serotonin. In turn, this region projects to the dorsal horn of the spinal cord where they also influence transmission from primary sensory neurons to the central nervous system. These spino-bulbo-spinal pathways are thought to form a critical loop in 'regulating the gain' in sensory processing within the primary relay. It has been suggested that one mechanism by which acupuncture may impart analgesia may be through the activation of descending pathways, a phenomenon known as diffuse noxious inhibitory control (DNIC). Further, these modulatory mechanisms are not fixed; nerve or tissue injury can alter the interplay and impact on how sensory information is relayed to the brain (D'Mello and Dickenson, 2008).

Ascending pathways

Dorsal horn projection neurons are responsible for relaying sensory information from nociceptors to the brain. This happens via a number of pathways. Some are responsible for projection to thalamus and subsequently neocortex, thought to be critical in producing a conscious response to noxious stimuli. Others are responsible for producing more complex behaviours such as avoidance (away from the noxious stimulus), autonomic responses (e.g. sympathetic activation) and emotional aspects (e.g. fear, anger, sadness). Therefore, as sensory information passes from primary sensory neurons to higher centres, there is divergence of inputs to different targets. This brings new levels of complexity to the organization of the sensory system, which hampers our understanding of the significance of each component (relative to another), and makes the process much more difficult to study scientifically. Interestingly, none of the 'pain pathways' described next are specific to noxious input; all contain cells that respond the low-threshold input, noxious input and 'wide dynamic range'.

The spinothalamic tract (STT)

This has been loosely named the ascending 'pain pathway' of the spinal cord, but this is an oversimplification. The STT runs contralaterally in the ventral and ventrolateral white matter funiculi. It has two components, lateral and ventral (anterior). The lateral STT is more heavily implicated in pain and temperature sensation, while the ventral STT is implicated in crude touch and firm pressure sensation. The STT is organized somatotopically; in the cervical spinal cord, cervical fibres are most medial and lumbosacral fibres lateral. The primary target is the ventroposterolateral (VPL) nucleus of the thalamus, part of the thalamocortical sensory coding system.

Spinoreticular tract (SRT)

This pathway also consists of axons projecting from dorsal horn projection neurons in lamina V but also deeper laminae extending into ventral horn (VII, VIII) and medial grey matter (X). Like the STT, the SRT is also located in the ventral quadrant of the spinal cord white matter, close to the lateral STT, and it projects to a number of targets including reticular formation (located in the midbrain, pons, and medulla), thalamus (lateral and dorsal reticular nuclei) and the nucleus reticularis gigantocellularis, as well as others targets.

Spinomesencephalic tract

This pathway is located ventral to the lateral STT, with projection neutron cell bodies located in superficial (I) and deep laminae of dorsal (IV, V) and ventral (VII, VIII) horns. It projects to the parabrachial nuclei and PAG; note that this region has formed a target for deep brain stimulation as a treatment of chronic pain—see next). The parabrachial limb has been implicated in emotional response to noxious stimuli, as the parabrachial region, located at the junction of midbrain and pons, part of the lateral reticular formation, and has onward projections to the amygdala as well as thalamus, hypothalamus. Is thought to contain a 'hedonic hotpot' involved in liking certain stimuli, and in addition to pain receives inputs from the gustatory portion of the solitary nucleus and is implicated in taste.

Pain pathways—pathophysiology

In the physiological state, nociceptors detect the presence of noxious stimuli and alert us to their presence. While pain is generally an unpleasant experience, it is a crucial component of our integrity and survival, by protecting us from harmful stimuli (e.g. a hand on a hot plate leading to a rapid withdrawal response), or limiting the extent of damage (swollen ankle forcing us to limit weight-bearing and allow healing). The absence of nociception leads inevitably to serious and potentially life-threatening harm; rare individuals with congenital insensitivity to physiological pain have lives that feature repetitive injury and early death; other examples are the Charcot joint in diabetic patients, or the well-recognized eye complications that can occur in patients with combined facial and trigeminal palsy.

It is important to recognize that the function in sensory pathways involving primary and secondary sensory projection neurons, interneurons of the spinal cord, brainstem and thalamus, and the descending innervation they receive, are not fixed, like a light-switch, in a passive, predetermined, hard-wired system. The phenotype of any individual neuronal cell, and therefore its function, is actively maintained by the local chemical and electrical environment. Therefore, processes that result in a change to the local neuronal environment can lead to a change in neuronal phenotype that has functional implications for the sensory system as a whole (Woolf and Salter, 2000).

To appreciate this, it is useful to consider two disease states: inflammation, and nerve injury (e.g. from trauma, compression, tumour invasion).

Inflammation

In inflamed tissue, typically non-painful stimuli (e.g. light pressure) become painful (pain hypersensitivity). As just referred to, this example of increased or abnormal pain is likely to be evolutionarily advantageous, by protecting an injured area from further harm and allowing healing. Unfortunately, however, there are many disease states where inflammation can become autonomous and serve no useful purpose (e.g. a rheumatoid joint). Under these circumstances, chronic pain becomes the disease. There is now much greater appreciation of interactions between the nervous system and immune system, resulting in reciprocal modulation of function, in both physiological and disease states (McMahon et al., 2015).

Whatever the trigger—tissue injury or auto-immune processes—inflammation is mediated by vasodilatation, plasma extravasation, tissue swelling, the recruitment of immune cells and the release of inflammatory mediators. Thermo- and chemosensitivity of nociceptors means that a change in the local environment, with an increase in inflammatory cytokines (e.g. IL-1, IL-6, TNFα), elevation in local temperature, and reduction in pH lead to altered activity patterns and increased pain. This is not simply an increase in stimulus resulting in an increased response; inflammatory cytokines can alter the processes of sensory transmission from peripheral tissue to the spinal cord, via post-translational modifications to surface receptors and intracellular signalling proteins, and transcriptional changes within the cell bodies of nociceptors. These changes of protein expression and phenotypic identity lead to an alteration in function, such that the same response results in increased gain and therefore more action potential activation. Wherever one looks at primary sensory neurons—the peripheral terminal, the axonal membrane, the cell body, or the central terminals in the spinal cord—inflammation produces changes in function, largely mediated by protein modification, itself driven by altered chemical environment and/or activity-dependent mechanisms.

The presence of inflammatory cytokines in peripheral tissue has been shown to correlate with increased pain levels and alterations in the relationship between stimulus and response. This results in phenomena such as hyperalgesia (increased pain from a noxious stimulus) and allodynia (pain from an innocuous stimulus). Furthermore, these changes can be long-lasting. Understanding these changes gives us insight into how some of the features of chronic pain states, which typically feature abnormal pain behaviour (unlike 'physiological (nociceptive) pain') may be mediated.

Nerve injury

There are many causes of peripheral nerve injury in addition to trauma or compression (e.g. from a disc prolapse), including systemic diseases causing polyneuropathy, tumour invasion, and inflammation itself. Classical lumbar or cervical radiculopathy is now understood as more than just a compression neuropathy, with the recognition of complex interplays between mechanical compression and an associated inflammatory response. Several inflammatory markers have been identified in neuropathic pain models and clinical studies, which potentially offer new pharmacological treatment targets and further revise the role of surgery for these conditions.

Of course, decompressive surgery remains an important, evidence-based treatment in the management of some patients with spinal cord or radicular compression, particularly patients with bowel or bladder impairment, or evolving neurological deficit.

Unfortunately, most patients with neuropathic pain do not have nerve compression that can be treated surgically, and symptom

Table 78.1 Examples of events observed in primary sensory neurons or their central terminals in disease states, with postulated clinical manifestations

Event	Disease state	Symptom
Peripheral sensitization	Inflammation	Pain hypersensitivity (hyperalgesia, allodynia)
Wallerian degeneration/ demyelination/axonal death	Peripheral nerve injury	Numbness/reduced sensation
Ephaptic transmission	Peripheral nerve injury	Spreading pain (increased receptive fields)
Ectopic activation—C fibres	Inflammation, nerve injury	Spontaneous burning pain (stimulus-independent)
Cell death—primary sensory neuron	Peripheral nerve injury	Numbness/reduced sensation
Cell death—dorsal horn interneurons (inhibitory)	Peripheral nerve injury	Spontaneous pain, spreading pain (increased receptive fields)
Central sensitization	Inflammation, nerve injury	Pain hypersensitivity (hyperalgesia, allodynia)

control can be extremely challenging, arguably one of the most difficult clinical problems to manage. Further, this is a huge societal problem. These patients classically have a mix of negative (sensory reduction or loss) and positive symptoms (hyperalgesia, allodynia, paraesthesia/dysaesthesia, spontaneous pain, hyperpathia). The effects of peripheral nerve injury on primary sensory neurons are widespread (Costigan et al., 2009), and critically do not confine themselves to the injured neurons, but also involve adjacent, uninjured cells and fibres. Table 78.1 details some of the pathophysiological changes that occur following peripheral nerve injury and their likely clinical manifestations.

Spinal mechanisms of chronic pain: Sensitization and disinhibition

The effects of peripheral inflammation and nerve injury on primary sensory neuron function results in changes in central nervous system sensory processing (D'Mello and Dickenson, 2008). The underlying causes are multifactorial, including activity-dependent mechanisms as well as changes in protein function (transcriptional and post-translational modifications), themselves resulting in changes in cellular activity and behaviour. These changes can be long-lasting, and can drive postsynaptic changes in activity, protein expression, and even cell death dorsal horn neurons. Changes with the spinal cord can be considered under the headings of sensitization and disinhibition.

Following nerve injury and inflammation, chronic pain often extends spatially beyond the usual dermatomal area, resulting in a zone of secondary hyperalgesia, which can become independent of the initial injury. These symptoms cannot be explained by changes in the peripheral nervous system, but instead reflect changes in spinal and supraspinal networks. Nociceptive mechanisms, whereby only physiological high-threshold stimuli caused pain, can change such that the system now results in pathological low-threshold pain hypersensitivity.

One important mechanism responsible for this change is central sensitization (Latremoliere and Woolf, 2009; see Box 78.2). Other long-lasting consequences of nerve injury include neuronal phenotypic changes due to altered gene transcription and post-translational modification of membrane proteins, and decreasing GABA-ergic and glycinergic tone in the dorsal horn. This 'disinhibition' is mediated by mechanisms such as reduced descending inhibitory control, loss of GABA-ergic or glycinergic interneurons through cell death, reduced GABA or GABA-synthesizing enzyme (e.g. glutamate decarboxylase), and altered properties of GABA receptors, glycinergic receptors, and cation-chloride cotransporters. This further contributes to central hyperexcitability and augmentation of pain pathways.

An emerging role in sensory transmission and pain processing in disease states has been identified for microglial (macrophage-like) cells, within the CNS (McMahon and Malcangio, 2009). Following nerve or tissue injury, there is a rapid morphological and functional change in microglia, which has a profound impact on sensory processing (Calvo and Bennett, 2012). These neuroimmune interactions within the CNS have identified potential targets for development of novel pain management strategies for chronic pain conditions (Scholz and Woolf, 2007).

Thus, changes in phenotype and function of primary sensory neurons, spinal interneurons, and projection neurons, as well as non-neuronal cells, can lead to profound alterations in the functional spinal relay and establishing chronic pain states that can extend well beyond the period of primary tissue injury.

Supraspinal mechanisms

Pathophysiological changes in the sensory system following peripheral tissue or nerve injury are not confined to primary sensory neurons or the spinal cord. Structural changes, changes in excitatory and inhibitory transmitters and in functional connectivity have all been detected in the brains of chronic pain patients. The challenge remains how to relate these changes to the cognitive, sensory, and emotional pain experience, understanding how much of this is cause versus effect, and whether these changes are reversible.

Box 78.2 Central sensitization

Under physiological circumstances, a fixed stimulus results in a predictable response. However, following tissue or nerve injury, where activity in primary nociceptors increases, this can lead to an increased response centrally, to the same stimulus peripherally. This is central sensitization, defined by the International Association for the Study of Pain (IASP) as the 'increased responsiveness of nociceptive neurons in the central nervous system to their normal or subthreshold afferent input'. Activity-dependent mechanisms of central sensitization include homosynaptic long-term potentiation—with exaggeration of nociceptor responsiveness—and heterosynaptic potentiation—recruiting low-threshold Aβ fibre inputs into the pain pathway, and these mechanisms may be driven and sustained by ectopic activity in the injured nerve.

Central sensitization is produced by the activation of several protein kinases by the neurotransmitter glutamate and various neuropeptide transmitters, which lead to post-translational and transcriptional changes in postsynaptic receptors (e.g. the N-methyl-D-aspartate (NMDA) receptor). That central sensitization is a major driver of neuropathic pain is supported by the action of drugs that reduce central excitability, including gabapentinoids (e.g. gabapentin and pregabalin), tricyclic antidepressants (e.g. amitriptyline), SNRIs (e.g. duloxetine), and NMDA antagonists (e.g. ketamine). Central sensitization has become a key focus for the development of new analgesics, and is the rationale behind pre-emptive analgesia (i.e. to prevent increased primary nociceptor input to the CNS).

Surgical procedures for management of chronic pain

There is a long history of ablative surgical procedures for the management of chronic pain (Loeser, 2006), though they predate a modern understanding of pain neurobiology and the likely underlying mechanisms that drive chronic pain. Of course, there is still some way to go before we fully understand these mechanisms and can identify them in individual patients, and even further from being able to offer evidence-based, effective management (von Hehn et al., 2012; Vardeh et al., 2016). Many of the current 'strategies' for managing chronic pain patients is empirically based, and we are currently unable to predict who is likely to respond to different pain interventions (e.g. with pharmacology, injection therapies, acupuncture, physical therapy, TENS, and others) nor explain the reason as to why some do respond, while others do not. Understanding sensory pathophysiology, acknowledging the profound alterations that occur in primary sensory neurons, the spinal cord, and higher centres in many ways questions the rationale for surgical management of chronic pain with, particularly for ablative/irreversible procedures which arguably might cause more maladaptive sensory plasticity than they solve. Perhaps this explains why many of these procedures only result in short-lived improvements in chronic pain, and only then in some patients, and have a recognized incidence of exacerbating neuropathic symptoms. Many of the destructive procedures have fallen from favour in recent years in most neurosurgical centres, and are now often reserved for terminal cancer patients with a short prognosis. It is also important to acknowledge the placebo effect when considering the utility and efficacy of any surgical procedure, particularly when only short term follow up is utilized (see Colagiuri et al. (2015) for review of placebo effect and underlying mechanisms, widely recognized in the field of surgery).

In carefully selected patients and in centres with high expertise, some of these procedures are still practised and considered useful (see Sindou et al., 1990 for review).

DREZ lesions

These were first attempted in the 1970s by Marc Sindou in Lyon and gained popularity thereafter. The procedure is still used, although much less frequently, for central or deafferentation pain syndromes such as brachial plexus injury, phantom limb pain, traumatic spinal cord injury, and cancer pain, as well as spasticity. Sensory axons of different diameters are mixed in the dorsal root, but organize just before they reach the spinal cord. The root divides into rootlets and the small fibres lie laterally, prior to entering Lissauer's tract, while the larger fibres enter more medially, nearer to the dorsal columns.

The procedure is done through a laminectomy or hemilaminotomy. The pia over the DREZ is opened and microsurgical lesions are made, either with the use of diathermy or radiofrequency ablation. Complications include corticospinal tract or dorsal column injury, continence issues, and worsening or persistent neuropathic pain. The procedure is now generally considered only as a last resort for patients who have failed all other less invasive management strategies.

Cordotomy

The lateral spinothalamic tract (STT) carries signals of pain, temperature, and touch from the contralateral side, therefore a destruction or interruption of the tract should lead to the analgesia and loss of sensations to heat and cold on the contralateral side. Open cordotomy was described in 1911, but the procedure was associated with significant morbidity and mortality. The development of percutaneous techniques has made the procedure less invasive and cordotomy is a recognized component of the algorithm for management of malignant unilateral pain. Computed tomography (CT)-guided techniques have allowed more precise needle positioning and lesioning. Endoscopic cordotomy techniques also have been explored.

How does it work?

The lateral STT tract is composed of fibres decussating from the contralateral side of the spinal cord. At each spinal level, a second order neural axons travel on the ipsilateral side of the spinal cord for two to five levels, before decussating to the contralateral anterolateral spinal cord where they join lateral STT. At the C1–2 level, the lateral STT has clear somatotopic organization: the anteromedial part has fibres from the upper extremity, shoulder, anterior chest, whereas posterolateral aspect contains the fibres from lower extremity, lower back, and the pelvis (Fig. 78.5).

Several techniques of percutaneous cordotomy have been described. A radiofrequency (RF) cannula is inserted via the C1–2 foramen into the anterolateral part of the spinal cord under local anaesthesia with either fluoroscopic (classical technique) or CT guidance. The aim is to penetrate the dura and enter the anterolateral spinal cord perpendicular to the sagittal plane, just anterior to the dentate ligament. Sensory stimulation should produce clear change in thermal sensations (heat or cold) with associated tingling on the contralateral side, ideally, but not necessarily overlapping the area of pain. Motor stimulation should produce ipsilateral contractions of the neck and shoulder muscles due to the stimulation of the adjacent corticospinal tract. Thermal sensation changes with stimulation on the contralateral side is considered a reliable predictor of good analgesic effect. Then, a thermal radiofrequency lesion is carried out in an incremental fashion, with continuous monitoring of motor function on the ipsilateral side. After lesioning, there should be a marked difference in sensation to pinprick between the sides.

CT guided anterior transdiscal approach has been described. Some have also advocated laser lesioning with a lateral endoscopic technique, for even better precision and accuracy.

Indications for percutaneous cordotomy

Cooperative patients who suffer unilateral nociceptive pain below C5 due to malignancy, despite appropriate palliative pharmacological and interventional management, with adequate lung function and life expectancy from 6 months to less than 1 year, can be considered for cordotomy. The best-studied groups of patients are those with malignant mesothelioma, Pancoast tumours, and metastatic lung cancer. There is some low-level evidence that cordotomy is not effective for neuropathic pain.

Evidence of efficacy

Most publications are retrospective, with some prospective case series. A recent systematic review looked at percutaneous cordotomy in the treatment of mesothelioma-related pain. In 160 patients, complete or partial pain relief was achieved immediately after the treatment in 94% of cases. Recurrence of pain is widely recognized in patients who live beyond a year.

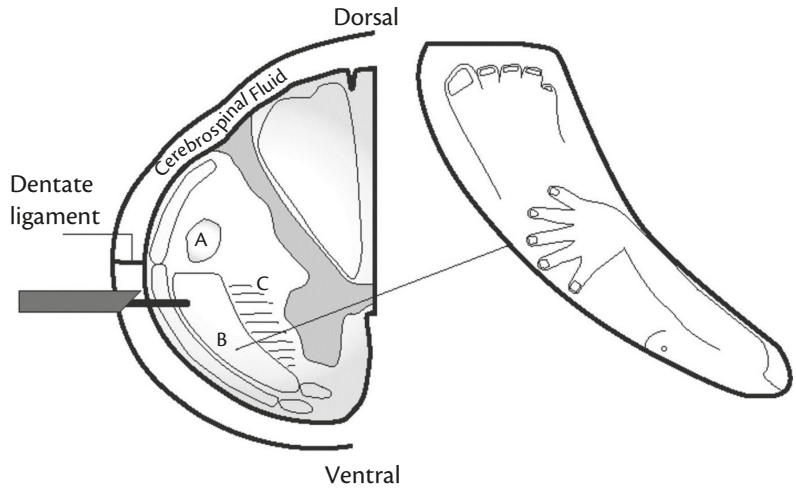

Fig. 78.5 Schematic representation of a cross-section of the spinal cord at C2.

Reproduced with permission from Alireza Feizerfan, and JHL Antrobus, Role of percutaneous cervical cordotomy in cancer pain management, *Continuing Education in Anaesthesia Critical Care & Pain*, Volume 14, Issue 1, pp. 23–6, Copyright © 2014.

Complications

In experienced hands with carefully selected patient, major complications are very rare (<1%). Procedure specific complications include transient or permanent motor weakness in the ipsilateral extremity (leg > arm), dysaesthesia, mirror pain in the ipsilateral side, and dyspnoea due to intercostal/diaphragmatic muscle weakness. General complications such as chest infection, orthostatic hypotension, urinary retention, incontinence, sexual dysfunction, confusion, and death have also been described. Lesions affecting nearby anterior spinocerebellar, reticulospinal and corticospinal tracts can produce ataxia, or disturbed autonomic and motor control.

Bilateral cordotomy

This has been used in very small numbers for bilateral cancer pain, or development of a new pain following unilateral cordotomy. There is very scant efficacy data, however, it is known that bilateral cordotomy has a much higher complication rate including ataxia, motor weakness, dysaesthesia, incontinence, respiratory depression, and death.

Practical issues

Following the arrival of long-term oral and transdermal opiate formulations (**Box 78.3**) and intrathecal drug delivery systems, the number of cordotomy procedures has been steadily declining. This is despite the growing number of malignant mesothelioma cases (anticipated to peak around 2020) and often suboptimal pain relief with pharmacological and interventional therapies. While this can be a useful method of pain relief in some patients, it may become extinct as fewer are performed and physicians become more reluctant to offer destructive and irreversible treatments.

Mesencephalic tractotomy

Like thalamotomy, this procedure has been used to treat poststroke pain and cancer pain though not in high numbers and there are few surgeons with experience. Mesencephalotomy is used for patients

Box 78.3 Opiates—kings of pain control?

Opioid receptors are the proteins that control nociceptive, hedonic, emotional, as well as autonomic, neuroendocrine, and immune responses. Gene cloning identified three receptor genes only, encoding mu, delta, and kappa receptors.

Receptor-deficient knock-out mice exhibit enhanced pain sensitivity. In models of acute pain, mu receptors modulate mechanical, chemical, and supraspinally controlled thermal nociception, while kappa receptors modulate spinally mediated thermal nociception and visceral pain. There is strong evidence for a role of delta receptors in reducing hyperalgesia in situations of inflammatory and neuropathic pain.

Endogenous opioid peptides. Met- and leu-enkephalins act on the spinal opioid receptors in lamina I and II of the dorsal horn, spinal trigeminal nucleus and periaqueductal grey (PAG). They are also present in the gastrointestinal (GI) tract and adrenal medulla. Dynorphins have actions on multiple spinal and supraspinal sites, but are considered to be weak analgesics. Multiple complex actions of beta-endorphins are largely limited to the central nervous system sites.

Spinal actions of opioids occur in tetrasynapse composed of the central terminal of primary afferent neurons, projection neurons, astrocytes, and microglia in the spinal cord dorsal horn. Opioids:

1 hyperpolarize primary afferent membrane by closing Ca ++ channels and opening K + channels, thus reducing glutamate release from nociceptive afferents (presynaptic effect); nociceptive input from the periphery is reduced;
2 reduce intracellular Ca ++ and increase K + postsynaptically thus quenching several mechanisms that would otherwise lead to hyperexcitability of second order neurons.

Supraspinal sites of opioid analgesia

There are multiple mechanisms and action sites in the brain. Opioids interact with 5-HT, GABA-ergic, and possibly other systems of central descending regulation. They move rostroventral medial medulla (RVM) output towards descending inhibition. Opioids also play an important role in regulating pain experience.

Peripheral action of opioid analgesia. Opioid receptors are also synthesized in the dorsal root ganglion (DRG) and transported down the axon into the peripheral sites. Endogenous opioid peptide synthesis can be unregulated in the DRG in inflammatory models.

with intractable pain involving the head, neck, shoulder, and arm, can be considered as a supraspinal cordotomy. The outcomes however have been mixed, and complication such as oculomotor dysfunction are widely recognized. It is rarely carried out these days, and other less invasive management strategies are usually preferred.

Spinal cord stimulation

Spinal cord stimulation (SCS) refers to direct application of electrical current to the spinal cord with the aim of achieving analgesia. Empirically, therapeutic use of electricity had been attempted at least as early as 63 BC by the ancient Greeks, who used torpedo fish as the source of electrical current in treating gout. As a modern method of chronic pain relief SCS has been in use since 1966, when Shealy applied an intrathecal monopole electrode connected to the external cardiac pulse generator for the first time and successfully palliated pain in a patient with advanced lung cancer. Shealy thought that direct electrical stimulation of large primary afferents would 'close the gate' to nociceptive signals propagating via small Aδ- and C fibres (see **Box 78.1** on Gate Theory). With the development of fully implantable spinal cord stimulation systems, SCS has become an established method of chronic pain relief (Song et al., 2014). National Institute of Clinical Excellence (NICE) in the United Kingdom recommends SCS for treatment of chronic peripheral neuropathic pain, and the FDA has approved SCS for the management of chronic pain of the trunk and extremities.

How does it work?

SCS implantable system consists of two main parts—electrode lead(s) placed in the epidural space and an implantable pulse generator (IPG) positioned in the subcutaneous pocket (**Fig. 78.6**). Electrodes can be selectively programmed to act as cathode, neutral, or anode, thus creating an electrical current and electromagnetic field which directly affect surrounding spinal structures.

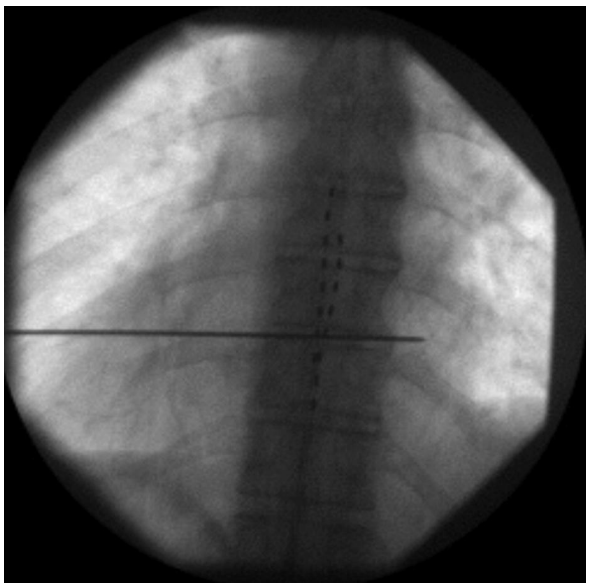

Fig. 78.6 AP view of two percutaneous cylindrical spinal cord stimulation (SCS) electrode leads placed in the lower thoracic epidural space in a in a patient with left radicular leg and bilateral low back pain.

Neurons under a cathode becomes less negatively charged and will depolarize, with resulting bidirectional action potential propagation. The anode creates localized axon hyperpolarization as the membrane becomes more negatively charged. By using different cathode-anode combinations along the lead, it is possible to create an electrical field that achieves paraesthesia in the effective dermatome(s) and concurrent analgesia. Holsheimer used computerized models to explain that stimulation efficacy is determined by several factors that include: the cathode position in relation to physiological midline; electrode polarity; cerebrospinal fluid (CSF) layer thickness under the cathode; axonal diameter and myelination; and axonal orientation within the dorsal columns, dorsal roots, and dorsal horn (anisotropism). More recently, electrical parameters of the stimulation pulse wave have been modified to allow high frequency stimulation, burst pattern stimulation, high current density stimulation, and subthreshold stimulation. Some of these novel simulation techniques do not result paraesthesiae, but still are able to achieve significant analgesic effect.

Mechanisms of action in paraesthesia-based, low frequency SCS have been investigated since the early 1970s. Data on SCS mechanisms have largely come from animal studies, and translation of preclinical data to clinical practice is challenging. While a definitive single mechanism has not yet been determined, several important factors are thought to be involved. First, activation of large diameter Aβ fibres (activating more of them appears to improve outcome), leads to inhibition of dorsal horn WDR neurons. Second, SCS induces release of neurotransmitters, some of which are inhibitory, such as GABA, but also 5-HT (serotonin), glycine, adenosine, and acetylcholine, both pre- and postsynaptically in the dorsal horn. Third, supraspinal pathway stimulation activates descending pain inhibition system resulting in a release of 5-HT and noradrenaline at the synapses with WDR neurons.

These mechanisms have some clinical validation: it is known that paraesthesia (presumably due Aβ-fibre activation) must be experienced by the patient and must overlap the patient's painful areas to result in pain relief from low frequency SCS. The necessity of overlap indicates convergence of Aβ terminal projections in the hyperexcitable regions of the dorsal horn. Also, intrathecal administration of subclinical doses of baclofen, a $GABA_B$ agonist, potentiates the effects of previously ineffective low frequency SCS, thus implicating GABA in the pain relief from traditional, paraesthesia-based SCS.

Recently, 10 kHz high frequency (HF10), paraesthesia-free SCS has been demonstrated to be statistically and clinically superior to traditional low frequency, paraesthesia-based SCS in the relief of chronic intractable back and leg pain. In contrast to low frequency SCS, patients receiving high frequency stimulation do not experience stimulation-induced sensations, and the Aβ-mediated paraesthesia-pain overlap from HF10 therapy targets appears uncorrelated to pain relief. This suggests that Aβ fibres may not play as significant a role in kHz HF-SCS mechanisms, and there is some evidence from preclinical studies that HF10 therapy engages different mechanisms to traditional low frequency SCS.

Indications and contraindications

SCS generally works very well for peripheral neuropathic pain, the most common indication being postsurgical radicular extremity pain. Its effect in treating central neuropathic pain is less

well established. Until recently, the results on low back pain have been mixed. With the introduction of high frequency stimulation and multiple contact electrode leads, it is becoming clear that some forms of low back pain appear to be responsive to SCS.

Common indications for a SCS treatment are presented as follows:

- Chronic neuropathic pain in postlaminectomy syndrome
- Complex regional pain syndrome
- Peripheral neuropathies including post-traumatic and diabetic neuropathy
- Pain due to ischaemic peripheral vascular disease
- Intractable angina
- Sacral stimulation for pelvic pain

Contraindications to SCS therapy include inability manage stimulation; cardiac pacemaker/ICD/intrathecal pump *in situ*; local or systemic infection; immunosuppression; coagulopathy. A relative contraindication is pathology otherwise amenable to surgery (nerve root or spinal cord compression, spinal instability, canal stenosis), though even this has been challenged, for example, recurrent disc prolapse, where revision surgery is known to have higher complications.

Clinical evidence for SCS

The first favourable RCT on SCS vs. reoperation for failed back pain syndrome (FBSS) patients was published by North et al. in 2005. In 2007, a prospective multicentre RCT (PROCESS) compared SCS therapy with conventional medical management (CMM) in 100 patients with FBSS. 48% patients achieved more than 50% pain control in SCS group versus 9% in a CMM group in 6 months (intention-to-treat analysis), followed by 34% and 7% at 12 months and 37% versus 2% at 24 months ($P = 0.003$). Importantly, SCS group patients reported better function with Oswestry Disability Index and quality of life with EQ-5-D questionnaire ($P < 0.0001$) (Kumar et al., 2007). Recently, a prospective multicentre non-inferiority RCT compared conventional tonic SCS with high frequency stimulation, using 10 kHz frequency at low amplitude in intractable low back and leg pain patients. 198 patients were randomized to receive either conventional or high frequency stimulation. High frequency stimulation had better responder rates than conventional SCS in both treating leg pain (78% vs. 51%) and back pain (78% vs. 51%) at 12 months (Kapural et al., 2015).

Practical considerations of SCS therapy

1. *Multidisciplinary assessment of SCS referrals*. Patients need a comprehensive assessment before recommendation for SCS trial. For SCS to be a cost-effective treatment option, careful selection of patients is the key. It is very important for patients to have realistic expectations of SCS therapy. Understanding the limitations of SCS therapy, accepting that SCS is not going to cure their condition or eliminate their pain is a prerequisite for a successful SCS. Engagement with the process of SCS assessment and education is another important predictor of successful outcome.
2. *The choice of a lead*. Electrode leads come in two versions according to their placement technique: percutaneous (cylindrical) and open (paddle) leads. The former is placed into the epidural space through a modified 14 G Tuohy needle under fluoroscopic control and can either be used for on-table testing with subsequent removal at the end of the procedure, or converted into a permanent trial lead by anchoring it to the dorsal fascia, tunnelling and extending for a 1–4-week trial. The advantages of cylindrical leads include ease of insertion and relative non-invasiveness. At the time of writing the standard array of electrodes in a cylindrical lead was 8, with one manufacturer offering a 16-electrode percutaneous lead. The disadvantages of a cylindrical lead are migration, resulting in loss of therapeutic effect, suboptimal electric current spread with stimulation of unwanted targets (e.g. ligamentum flavum) and higher electrical current demands. With the improvement in anchoring technology, migration is less prevalent. Rechargeable IPG technology has also mitigated against the premature battery drainage.

Paddle leads have one active surface and may contain up to 16 electrodes, arranged in up to three vertical rows. They have to be inserted via a small laminotomy, one to two interlaminar spaces below the target level. Wider electrode distribution within a lead may increase the likelihood of successful stimulation and reduce the chance of loss of stimulation effect. Paddle lead migration is uncommon. They also require less electrical current to stimulate the targets anteriorly, as the dorsal surface is insulated. However, placement of a paddle electrode is a more invasive procedure with slightly higher morbidity. Paddle leads occupy more of the epidural space with the risk of spinal cord compression, particularly at the cervical level.

When choosing a lead, one has to consider MR compatibility. At the time of writing most leads and IPGs are certified to be 'MRI Head and Extremity Conditional', thereby allowing patients to undergo MRI head investigations at 1.5 T. One SCS system supplier has developed a full body MRI conditional lead and IPG at 1.5 T.

3. *The choice of IPG*. Currently, all competitors of the SCS market offer rechargeable IPGs, although non-rechargeable IPGs are available. The lifespan of a rechargeable IPG depends on the number of recharge cycles, which is dependent by the stimulation parameters. IPG batteries can last 5–10 years with most available SCS devices. The longevity of an IPG is one of the important variables determining cost-effectiveness of the SCS therapy, and non-rechargeable SCS systems had least favourable cost-effectiveness and high frequency the most (McMahon and Malcangio, 2009).

Complications

Complications have been quoted as high as 34%, though most are minor and correctable. These include loss of analgesic effect with stimulation, loss of stimulation, unwanted paraesthesiae, or dysaesthesia. Causes are lead migration, epidural fibrosis, or development of tolerance, possibly due to spinal cord plasticity. Lead migration is less problematic using modern anchors, but resiting or replacing with a paddle lead may be necessary. With patient education, 'on-off duty' cycling and IPG reprogramming, target stimulation can often be re-captured. There is some data suggesting that burst pattern stimulation may reduce tolerance. Discomfort at the IPG site is common and may require repositioning. Rarely, skin erosion can occur. Other equipment related complications include lead fracture, IPG malfunction, and battery depletion.

Large trial prospective data from trials suggest infection rates as low as 2–3%, in line with other surgical prostheses rates. Percutaneous tunnelled trial, BMI more than 30, and revision surgery are risk

factors. The most common pathogen is methicillin sensitive Staph. aureus. Even superficial infections are concerning and should be treated early and aggressively to prevent neurological infection or device explant. Meticulous surgical technique with appropriate antimicrobial prophylaxis and dressing policy are mandatory.

Neurological complications of SCS therapy are very rare. Most common is inadvertent dural puncture during a lead placement. Injury to spinal cord resulting para/tetraparesis have all be reported. MRI is therefore recommended prior to implant to assess the epidural space and anticipate any potential challenges during lead placement.

Deep brain stimulation

Background

Deep brain stimulation (DBS) has been used in management of complex chronic pain states since 1954 (see Boccard et al., 2015 for review). DBS refers to a method of electrical stimulation of several neural targets thought to be a part of 'pain neuromatrix' in the brain. The hypothesis of DBS analgesic effect arose at least a decade prior to the publication of a 'pain gate' theory from animal experiments and from schizophrenia research. Heath was the first to successfully treat terminal cancer pain over several weeks with intermittent septal stimulation.

Theoretically there are several targets for DBS within a network of numerous brain nuclei, fascicles, and tracts, described as a 'pain neuromatrix'. Historically, medial septal structures were the first to be stimulated. Another important target was identified in the ventroposteromedial (VPM) and ventroposterolateral (VPL) nuclei of the thalamus, from previous data in lesioning in 1973. The periaqueductal grey and periventricular grey (PVG/PAG) were also identified as an important target for analgesia in rodents, and pain relief could be elicited from stimulating this area with DBS. More recently, there has been considerable interest in the anterior cingulate cortex for dissociating pain sensation and its affective component. It seems to work better in central poststroke pain with whole body or hemi-body pain.

How does it work?

The analgesic mechanisms of DBS are poorly understood. The understanding of complex interplay among the multiple parts of pain neuromatrix is still evolving and the hierarchical relationships within the neuromatrix have not been fully elucidated. It is believed that central pain states ultimately result in abnormal firing patterns of neural cells pertinent to pain transmission and perception. There is an ongoing debate as to how exactly neural cell electrophysiology is altered by a continuous nociceptive input. Some argue that it increases synchronous neuron firing frequency. Others, however, stipulate a different mechanism whereby the spontaneous cell firing becomes diminished. DBS either is able to synchronize and 'slow down' abnormal firing in the PAG/PVM and VPM/VPL, or it can augment a suppressed neural activity in the aforementioned structures. Interestingly, DBS of PAG does seem to affect endogenous opioid release and it has been shown that PAG appears to exert ascending modulation upon sensory thalamic nuclei.

Indications for DBS

In theory, any chronic neuropathic pain should respond to DBS. Most work, however, has been conducted with patients suffering from central neuropathic pain unresponsive to multimodal management (Box 78.4). The best results so far have been published in

Box 78.4 Managing pain with drugs—nociceptive vs. neuropathic

Chronic pain control remains a challenge in clinical practice despite improved understanding of the multiple mechanisms at play. The balance of nociceptive input and descending inhibiting output has shifted towards the former, with peripheral and central sensitization often having become major drivers of the neuropathic pain and descending inhibition mechanisms having failed to suppress hyperactivity of the somatosensory system. Pain neuromatrix activation in the brain has altered pain experience, established links with the areas of brain controlling the affect, mood, stress, and emotions. Pain is no longer a physiological nociceptive response; it has become a complex biopsychosocial phenomenon.

Main pharmacological strategies of chronic pain control include:

1. reduction of peripheral nociceptive input and peripheral sensitization;
2. reduction of central sensitization in the spinal cord and prevention of neuroplastic changes in the somatosensory system;
3. augmenting descending pain inhibition;
4. altering pain experience.

The choice of medications for chronic pain control depends of the pain mechanism. In nociceptive pain the most important strategy is the reduction of nociceptive input. non-Steroidal anti-inflammatory drugs (NSAIDs) and opioids are the most effective medication groups. NSAIDS reduce inflammation by inhibiting COX-1 and COX-2 enzymes and thus reducing pro inflammatory prostaglandin synthesis at a tissue injury site. This way peripheral sensitization is reduced. Opioids act on multiple targets in the e peripheral nervous system (PNS) and CNS and the net result reduce peripheral nociceptive input at the dorsal horn. They also reduce signal transmission via the second order neuron and enhance descending pain inhibition at the RVM. Importantly, they also alter the pain experience.

Once the changes in the somatosensory system have occurred (e.g. upregulation of TPVR1 and 2, voltage gated Na + channels, $\alpha 2\delta$ subunit of calcium channel presynaptically, activation of WDRs in the dorsal horn, activation of AMPA and NMDA receptors, glia, and astrocytes, as well as reduced activity of $GABA_A$ receptors postsynaptically, sensitization of second order neurons, inhibition of serotonergic and noradrenergic descending pain inhibition systems, and activation of pain neuromatrix in the brain) other strategies of pain control have to be used.

Peripheral desensitization can be tried with capsaicin cream or patch (acts on vanilloid receptors TPVR1 and 2 presynaptically), local anaesthetic applications (i.e. LA cream, lidocaine plaster), systemic Na + channel inhibitors (i.e. carbamazepine in TGN), gabapentinoids (i.e. gabapentin and pregabalin).

Central de-sensitization can be attempted with gabapentinoids (acting in the brain on the $\alpha 2\delta$ subunit of calcium channel and thus enhancing a descending noradrenergic pathway), serotonin and noradrenalin re-uptake inhibitors (tricyclic antidepressants, venlafaxine, duloxetine, tramadol), selective noradrenalin re-uptake inhibitor tapentadol, non-selective NMDA antagonist (ketamine, methadone), a2-agonist clonidine. Opioid agonists are not as effective in the management of central sensitization and neuropathic pain, therefore should not be the mainstay of neuropathic pain control. Over-reliance on opioid drugs may lead to development of tolerance and/or psychological dependence (addiction) that will result in dose escalation and may lead to serious iatrogenic complications (constipation, respiratory depression, opioid-induced hyperalgesia in the dorsal horn, suppression of the adrenopituitary axis, immunosuppression, cognitive deterioration).

patients with atypical facial pain, central poststroke pain, brachial plexus avulsion pain, and postamputation pain/phantom limb pain. There have been case reports on the effectiveness of DBS in spinal pain/FBSS.

Evidence of DBS efficacy

There have been two multicentre trials conducted for DBS in pain management. Both trials suffered from important design and data collection flaws as well as patient heterogeneity and high attrition rates. Neither trial was able to report more than 50% of pain relief for at least 12 months in 50% or more of the trial subjects—a primary outcome set out by FDA. As a consequence, DBS has no FDA approval in the United States. Since then there have been more publications including a randomized placebo-controlled trial. NICE in the United Kingdom has approved the use of DBS for treatment of refractory chronic pain for well selected patient group who have failed other treatments.

Complications

The clinically significant complications of DBS could be classified as surgical complications, hardware-related complications, and stimulation-dependent complications. Surgical complications of DBS surgery include intracranial haemorrhage (4%), infection (12%), electrode misplacement and, rarely, death. Hardware-related complications include electrode fracture, electrode erosion, and infection. Stimulation-dependent complications are the effect of undesired modulation of neural circuits adjacent to the targets of neuromodulation.

Motor cortex stimulation (MCS) for managing refractory central and peripheral deafferentation pain syndromes first emerged in the 1990s and has been used with some success in some small studies. The mechanism by which MCS might operate is unclear, though it is postulated it may work via activation of reciprocal pathways between motor and somatosensory cortex, that leads to sensory inhibition, or possibly through the activation of limbic pathways. There is some scepticism about its long-term benefits, but transcranial magnetic stimulation may emerge as a non-invasive screening tool for patient selection.

Conclusions

Chronic pain remains a huge problem, spanning all disciplines of medicine. The last 25 years of pain research has redefined our understanding of sensory physiology and pain biology. No longer is pain and nociception thought to be mediated via hard wired, fixed circuitry that can be 'rewired' surgically, and many of the older surgical techniques for managing chronic pain have fallen from favour. With an increased understanding of pain neurobiology and maladaptive sensory plasticity come new opportunities for effective and evidence-based interventions (Yekkirala et al., 2017). From a surgical perspective, stimulation-based techniques have produced the most optimism in recent times, and this field will continue to develop rapidly. There may still be a role for destructive techniques for well selected patients in experienced hands, but the potential for failure and the irreversibility of these techniques has made them less attractive in the current climate of medicine.

REFERENCES

Beecher, H.K. (1956). Relationship of significance of wound to pain experienced. *JAMA*, **161**(17), 1609–13.

Boccard, S.G., Pereira, E.A., & Aziz, T.Z. (2015). Deep brain stimulation for chronic pain. *J Clin Neurosci*, **22**(10), 1537–43.

Calvo, M. & Bennett, D.L. (2012). The mechanisms of microgliosis and pain following peripheral nerve injury. *Exp Neurol*, **234**(2), 271–82.

Colagiuri, B., Schenk, L.A., Kessler, M.D., Dorsey, S.G., & Colloca, L. (2015). The placebo effect: from concepts to genes. *Neuroscience*, **307**, 171–90.

Costigan, M., Scholz, J., & Woolf, C.J. (2009). Neuropathic pain: a maladaptive response of the nervous system to damage. *Annu Rev Neurosci*, **32**, 1–32.

Cummins, T.R., Sheets, P.L., & Waxman, S.G. (2007). The roles of sodium channels in nociception: implications for mechanisms of pain. *Pain*, **131**(3), 243–57.

D'Mello, R. & Dickenson, A.H. (2008). Spinal cord mechanisms of pain. *Br J Anaesth*, **101**(1), 8–16.

Delmas, P. & Coste B (2013). Mechano-gated ion channels in sensory systems. *Cell*, **155**(2), 278–84.

Delmas, P., Hao, J., & Rodat-Despoix, L. (2011). Molecular mechanisms of mechanotransduction in mammalian sensory neurons. *Nat Rev Neurosci*, **12**(3), 139–53.

Dubé, G.R., Elagoz, A., & Mangat, H. (2009). Acid sensing ion channels and acid nociception. *Curr Pharm Des*, **15**(15), 1750–66.

Kapural, L., Doust, M.W., Gliner, B.E., et al. (2015). Novel 10 kHz high frequency therapy (HF10 therapy) is superior to traditional low frequency spinal cord stimulation for the treatment of chronic back and leg pain: the SENZA-RCT randomized controlled trial. *Anesthesiology*, **123**(4), 851–60.

Kumar, K., Taylor, R.S., Jacques, L., et al. (2007) Spinal cord stimulation versus conventional medical management for neuropathic pain: a multicentre randomised controlled trial in patients with failed back surgery syndrome. *Pain*, **132**(1–2), 179–88.

Latremoliere, A. & Woolf, C.J. (2009) Central sensitization: a generator of pain hypersensitivity by central neural plasticity. *J Pain*, **10**(9), 895–926.

Liu, M. & Wood, J.N. (2011). The roles of sodium channels in nociception: implications for mechanisms of neuropathic pain. *Pain Med*, **12** Suppl 3, S93–9.

Loeser, J.D. (2006). Other surgical interventions. *Pain Pract*, **6**(1), 58–62.

McMahon, S.B., La Russa, F., & Bennett, D.L. (2015). Crosstalk between the nociceptive and immune systems in host defence and disease. *Nat Rev Neurosci*, **16**(7), 389–402.

McMahon, S.B. & Malcangio, M. (2009). Current challenges in glia-pain biology. *Neuron*, **64**(1), 46–54.

Mendell, L.M. (2014). Constructing and deconstructing the gate theory of pain. *Pain*, **155**(2), 210–16.

Mickle, A.D., Shepherd, A.J., & Mohapatra, D.P. (2015). Sensory TRP channels: the key transducers of nociception and pain. *Prog Mol Biol Transl Sci*, **131**, 73–118.

North, R.B., Kidd, D.H., Farrokhi, F., & Piantadosi, S.A. (2005). Spinal cord stimulation versus repeated lumbosacral spine surgery for chronic pain; a randomized, controlled trial. *Neurosurgery*, **56**, 98–107.

Scholz, J. & Woolf, C.J. (2007). The neuropathic pain triad: neurons, immune cells and glia. *Nat Neurosci*, **10**(11), 1361–8.

Sindou, M., Jeanmonod, D., & Mertens, P. (1990). Ablative neurosurgical procedures for the treatment of chronic pain. *Neurophysiol Clin*, **20**(5), 399–423.

Song, J.J., Popescu, A., & Bell, R.L. (2014) Present and potential use of spinal cord stimulation to control chronic pain. *Pain Physician*, **17**(3), 235–46.
Vardeh, D., Mannion, R.J., & Woolf, C.J. (2016). Toward a mechanism-based approach to pain diagnosis. *J Pain*, **17**(9 Suppl), T50–69.
von Hehn, C.A., Baron, R., & Woolf, C.J. (2012). Deconstructing the neuropathic pain phenotype to reveal neural mechanisms. *Neuron*, **73**(4), 638–52.
Woller, S.A., Eddinger, K.A., Corr, M., & Yaksh, T.L. (2017). An overview of pathways encoding nociception. *Clin Exp Rheumatol*, **35** Suppl 107(5), 40–6.
Woolf, C.J. & Ma, Q. (2007). Nociceptors—noxious stimulus detectors. *Neuron*, **55**(3), 353–64.
Woolf, C.J. & Salter, M.W. (2000). Neuronal plasticity: increasing the gain in pain. *Science*, **288**(5472), 1765–9.
Yekkirala, A.S., Roberson, D.P., Bean, B.P., & Woolf, C.J. (2017). Breaking barriers to novel analgesic drug development. *Nat Rev Drug Discov*, **16**(8), 545–64.

RELATED LINKS TO EBRAIN

Complex Regional Pain Syndrome. https://learning.ebrain.net/course/view.php?id=1139
Neuropathic Pain. https://learning.ebrain.net/course/view.php?id=100
Pain Related Anatomical Pathways and Physiology. https://learning.ebrain.net/course/view.php?id=1140

79

Cranial nerve vascular compression syndromes

Marc Sindou and George Georgoulis

Introduction

Along the last decades it has become apparent that a large number of so-called 'essential' (i.e. apparently primary) cranial nerve (CN) 'hyperactive' syndromes originate from chronic neurovascular conflict (NVC), microsurgical vascular decompression (MVD) thus being the first surgical option for these dysfunctional syndromes.

Hyperactive CN syndromes affect all CNs from third to twelfth.

- Trigeminal neuralgia (TN) is by far the most frequent syndrome. Nowadays there is a general consensus that main cause is a NVC on the sensory root of the fifth CN, classically but not always at the root entry zone (REZ). Surprisingly, the motor root is rarely affected.
- Hemifacial spasm (HFS) is also frequently observed, almost always caused by an arterial compression of the seventh CN, nearly always at REZ.
- Vago-glossopharyngeal neuralgia (VGPN), also due to a NVC but on the ninth and/or the tenth CN, is very similar to TN with regard to pain features and related treatments. Prevalence is 1% compared to TN.
- Alterations of the eighth CN—which has the longest central myelin portion of all CNs, from brainstem to internal auditory canal, may be at the origin of tinnitus (cochlear nerve) and vertigo (vestibular nerve). Both disorders are frequent and their pathophysiology various. Mechanisms are pathological insult(s), of any kind, lesions being responsible for peripheral deafferentation followed by central synaptic reorganization, similar to what can be observed at the origin of many types of neuropathic pain. A number may be related to NVC, the diagnosis of which is sometimes difficult to ascertain.
- Hyperactive syndromes of the motor CNs others than the facial nerve are infrequent. Abnormal movements of the motor ocular CNs (third, fourth and sixth) are most often in relation with causes others than NVC.
- Muscular spasms attributed to the masticatory motor root of the Vth CN have been only sporadically reported. Spasmodic torticollis, hypothesized by some to be due to NVC of the eleventh CN, should rather be classified within the frame of dystonias/dyskinesias. Origin is likely brainstem/basal ganglia dysfunction rather than accessory nerve compression. Regarding the hypoglossal CN, only one publication has reported on hemi-lingual spasm by NVC on the twelfth root.
- Vascular compression of the ventrolateral medulla, ventrally to the ninth to tenth CN REZ, has been hypothesized as a possible cause of neurogenic essential blood hypertension.
- Finally, in a few cases several CNs in the same individual can be affected by hyperactive dysfunction.

Hypotheses on neurophysiological mechanisms are summarized in **Box 79.1**.

Hemifacial spasm

Definition of hemifacial spasm (HFS) is clinical: chronic, involuntary movements on one side of the face characterized by 'twitching' spasms and synkinesis of the muscles innervated by the facial nerve. Diagnosis of primary HFS must fulfil the three following criteria: (1) not a sequela of facial palsy; (2) chronic in evolution and limiting; (3) normal investigations except for the presence of a vascular compression of the seventh CN, generally at its REZ.

Pathophysiology

There is now considerable evidence that primary HFS is related to functional changes (hyperactivity) in the facial motor nucleus, that originate from a pulsatile compression of the facial nerve at REZ (Gardner, 1962; Gardner and Sava, 1962; Møller and Jannetta, 1984; Sindou, 2005). This central hyperactivity of the nucleus would produce motor discharges that may be provoked by a variety of peripheral stimuli as well as by emotional events conveyed through the brainstem reticular formation. Such putative mechanisms are consistent with the clinical and the electrophysiological features of the spasms as well as with the imaging and the intraoperative findings of a neurovascular compression at the facial REZ. Over the last three decades microvascular decompression (MVD) has proved to be valuable to cure the disease (Barker et al., 1995). An abundant

Box 79.1 Hypotheses on neurophysiological mechanisms

Most accepted mechanisms for cranial nerve (CN) hyperactive syndromes due to NVC are several and, interestingly, rather complementary.

Chronic pulsatile compression of the root would generate ectopic stimuli that are transmitted to neighbouring fibres through focal zones of demyelination. These demyelinated zones would behave like neosynapses and be responsible for ephaptic transmission, in other words the epicentre of 'short circuits' with 'cross-talk' phenomena between fibres (Gardner, 1962). This could explain the triggered and irradiating clinical manifestations. Classically the NVC are preferentially situated at the so-called REZ (root entry/exit zone). To our knowledge there is no 'official' definition of the REZ. However, it is generally accepted that REZ corresponds to the portion of the root from brainstem to the transitional zone (TZ), which is the junction between the portion of the root with myelin of central type and the portion of the root with myelin from Schwann origin (**Fig. 79.1**). The central portion and TZ are hypothesized to be more 'excitable' structures. Actually, not all NVC are found at REZ; some are more peripherally situated. For those later NVC, observation under the operative microscope frequently showed a groove with a greyish aspect marked by the compressive vessel, namely a pulsatile artery, or also and not rarely a (non-pulsatile) vein testifying of a focal demyelination.

Mechanical pulsations and focal demyelination should not be considered as the sole source of the dysfunction. The locally generated ectopic influxes would induce, by retrograde firing of the corresponding CN nucleus (i.e. through a 'kindling-like' phenomenon), a hyperexcitability and hyperactivity of the nucleus cells. This hyperactivity generated in the central nervous system is consistent with the epileptic-like clinical manifestations of many of these CN hyperactive syndromes, as well as of their particular responsiveness to anticonvulsants.

Besides, there is no doubt that other mechanisms remain yet undiscovered. Genetic, humoral, hormonal, and also psychological factors, likely play a role in the pathogenesis of these complex—apparently essential—neurological disorders.

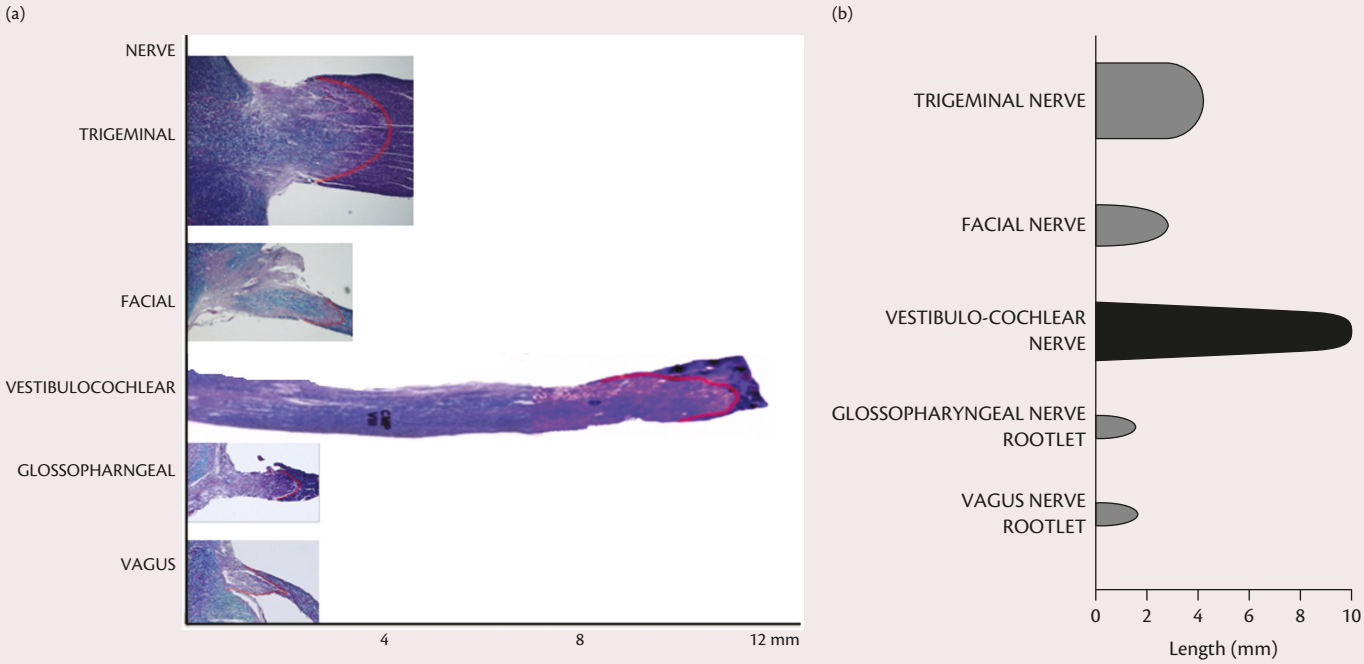

Fig. 79.1 (A) Photomicrographs of longitudinal sections stained with Luxol fast blue, of trigeminal, facial, vestibulocochlear, glossopharyngeal, and vagus roots, at same scale for comparison. The transitional zone (TZ) between central myelin portion and myelin of Schwann portion is underlined. (B) Comparative drawings of central myelin portions, obtained from mean values of the length (with diameter), of the corresponding roots.

literature has been produced on findings, techniques, and results; references can be found in the following publications (Huang et al., 1992; Sindou et al., 1997; Sauvain et al., 2001; Sindou and Keravel, 2009b; Li et al., 2016).

Diagnosis

Prevalence (in the USA) is 1/100 000. The left side is affected twice as often as the right, and women are affected twice as often as men.

In typical primary HFS, spasms usually begin as slight intermittent unilateral twitching of the orbicularis oculi muscle; lower facial muscles are involved only secondarily.

Electromyography (EMG) recordings produce a typical electrophysiological signature: clonic facial muscle contractions, synkinesis, lateral spread evoked responses.

Imaging is useful for confirming that HFS is primary in nature and due to neurovascular compression. The compressing vessel(s), generally an artery: the anterior inferior cerebellar artery (AICA), the posterior inferior cerebellar artery (PICA), and/or vertebrobasilar artery (VBA), can be reliably depicted on high-resolution MRI combined with MR-angio (MRA). 3-D T2 offers good delineation of the facial nerve. Important, there might be several false-positive images, vascular contacts with CNs being common in asymptomatic patients. The responsible artery(ies) are generally located at brainstem in ventrocaudal location to the facial REZ.

Surgical management

Pharmacological treatments show poor efficacy. The first option is repeated injections of Botulinum toxin, but when they become ineffective MVD is the only recourse.

The MVD procedure was pioneered by Gardner (Gardner, 1962), then subsequently codified and popularized by Jannetta (Jannetta et al., 1977). There may exist one or multiple arterial compressions in the same individual. In our series of 280 patients, PICA, AICA and/or vertebral artery (VBA) were the responsible vessel(s) in 61%, 56% and 27% of the cases, respectively, multiple compressions being found in as many as 40% of our patients (Marneffe et al., 2003). Missing a vessel especially at brainstem could be the source of surgical failure.

With most teams the patient is operated in the lateral decubitus position. Approach is a 'keyhole'-type retromastoid craniotomy, of 2 cm to 1.5 cm in size, posterior to the tip of the mastoid process so that the facial nerve be reached from below, inferolaterally to the cerebellar flocculus (**Fig. 79.2**). The infraflocculus route is important for two reasons. First, NVCs are generally located ventrocaudally at brainstem. Second, a lateral-to-medial retraction of the cerebellar hemisphere would exert stretching on the eighth nerve with risk on hearing. This is warned by an increase in latency of peak III and V on intraoperative BEAP recordings (Grundy et al., 1982; Møller and Møller, 1989; Sindou et al., 1992; Polo et al., 2004).

During mobilization of the compressive artery(ies), care must be taken not to avulse perforators and not to manipulate AICA as well as the labyrinthine artery. Mechanical vasospasm could be the cause of cochlear ischaemia. A warning sign is decrease in amplitude of peak I on BEAPs recordings (Sindou et al., 1992; Polo et al., 2004). The conflicting loop(s) is (are) maintained apart with a piece of material: Teflon in our practice. *('PTFE Felt' is used to make bundles or balls by stripping filaments from mattress. 'Edwards Outflow Tract Knitted PTFE' is used to make (rigid) plates for interposition. 'Sauvage Knitted Polyester' is used to make (supple) sheets for interposition. (Manufactured by Bard Peripheral Vascular, Inc. 1625 West 3rd Street, Tempe, AZ 85281 USA, https://www.crbard.com).* Attention should be brought not to exert any neocompressive effect on the facial and/or the vestibulocochlear nerve, as well as not kinking the artery(ies). Regular irrigation with (a few) droplets of 10% papaverine in normal saline solution is wise to release constrictive vasoreactions. Excessive use of concentrated solution would be toxic because of the very acid pH of papaverine.

In patients with HFS, stimulation of the facial nerve, one of its branches, gives rise to repetitive and spreading EMG responses in the facial muscles, innervated by the other branch. Intraoperative running EMG recordings of lateral spread responses (LSR) during MVD, was advocated by Møller and Jannetta to ensure that adequate decompression has been achieved (Møller and Jannetta, 1987; Mooij et al., 2001). In our series because long-term relief was obtained even in patients in whom LSR remained present at end of MVD we doubt about that reliability of LSR monitoring (Hatem et al., 2001).

Results

Long-term cure rate is reported to be 85% to 95% according to authors. Cure may be delayed by several months to one year (Goto et al., 2002; Sindou and Keravel, 2009a; Zhong et al., 2015). In our series of 280 patients, cure rate was 87% at seven years of FU, of whom in 12% cure was delayed by several months. Because of this frequency, we do not recommend early re-operation until at least one year has passed. When complete relief is obtained, recurrence is infrequent, at a rate of 1–2% according to series.

Delayed cure strongly supports that HFS is not only due to mechanical pulsations of an elongated artery against the REZ of the nerve. Demyelination of fibres and hyperactivity in the facial motor nucleus induced by the chronic vascular compression likely play a role. Delay could be explained by the time necessary for reversal of the plastic electrophysiological changes, especially those in the nucleus that are considered as having caused the symptoms (Møller and Møller, 1989; Sindou, 2005).

MVD rarely has major complications. From literature reviews, an indicative list of risks can be given as follows. Mortality was less than of 1% and cerebellar infarct or haemorrhagic complication in the order of 0.50% ± 0.30. CNs most at risk are the eighth, and the seventh, and to a lesser extent the lower CNs. Permanent hearing loss with sufficient or non—sufficient residual function occurred in the range of 2.45–15.90% and 1.18–2.60%, respectively. Permanent facial nerve palsy, of any degree, initial and irreversible, ranged between 0.8 and 5.0% according to series. A delayed facial palsy that generally occurred around the end of the first post-op week, was observed in as many as 7.30% of the patients in the reporting articles. This symptom—whose mechanism remains unknown –was totally reversible within several weeks to a few months in almost all patients. Lower CN disturbances, manifested by hoarseness, dysphagia, swallowing difficulties, were observed in 0.44% to 2.18% of the patients. Complications related to cerebrospinal fluid (CSF) leakage are: middle ear effusion, pseudomeningocele, and rhinorrhoea, with eventual meningitis. Occurrence is minimized by careful tight closure.

Trigeminal neuralgia

Definition of trigeminal neuralgia (TN) is clinical. According to the Classification Committee of the International Headache Society, TN—in its *typical presentation*—is characterized by recurrent unilateral brief electric shock-like pains, abrupt in onset and termination, limited to the distribution of one or more divisions of the trigeminal nerve, and triggered by innocuous stimuli (Headache Classification Committee, 2013). There may additionally coexist a background of continuous facial pain; this presentation is termed *atypical trigeminal neuralgia*. Whether its clinical presentation is typical or atypical, TN may develop in the absence of apparent cause (= primary) or be a result of a neurological or other disease (= secondary). When TN develops with no identifiable cause other than neurovascular compression, it is named *classical*. When it remains of unknown origin, it is considered as *idiopathic*.

Diagnosis

- *Prevalence* is 7/10 000. Incidence is five new cases per year for 100 000 population.
- *Diagnosis* relies on clinical examination. Stimulus dependence (i.e. triggered pain), is a mandatory criterion of TN. Although some mild sensory abnormalities may be found especially in longstanding TN, absence of sensory deficit is essential for the diagnosis. Noteworthy, in long-lasting classical TN with background of facial pain (i.e. atypical forms), the paroxysms may have disappeared or been masked by medical treatment. Some authors classify TN into type 1 pain, consisting of the lancinating type, and

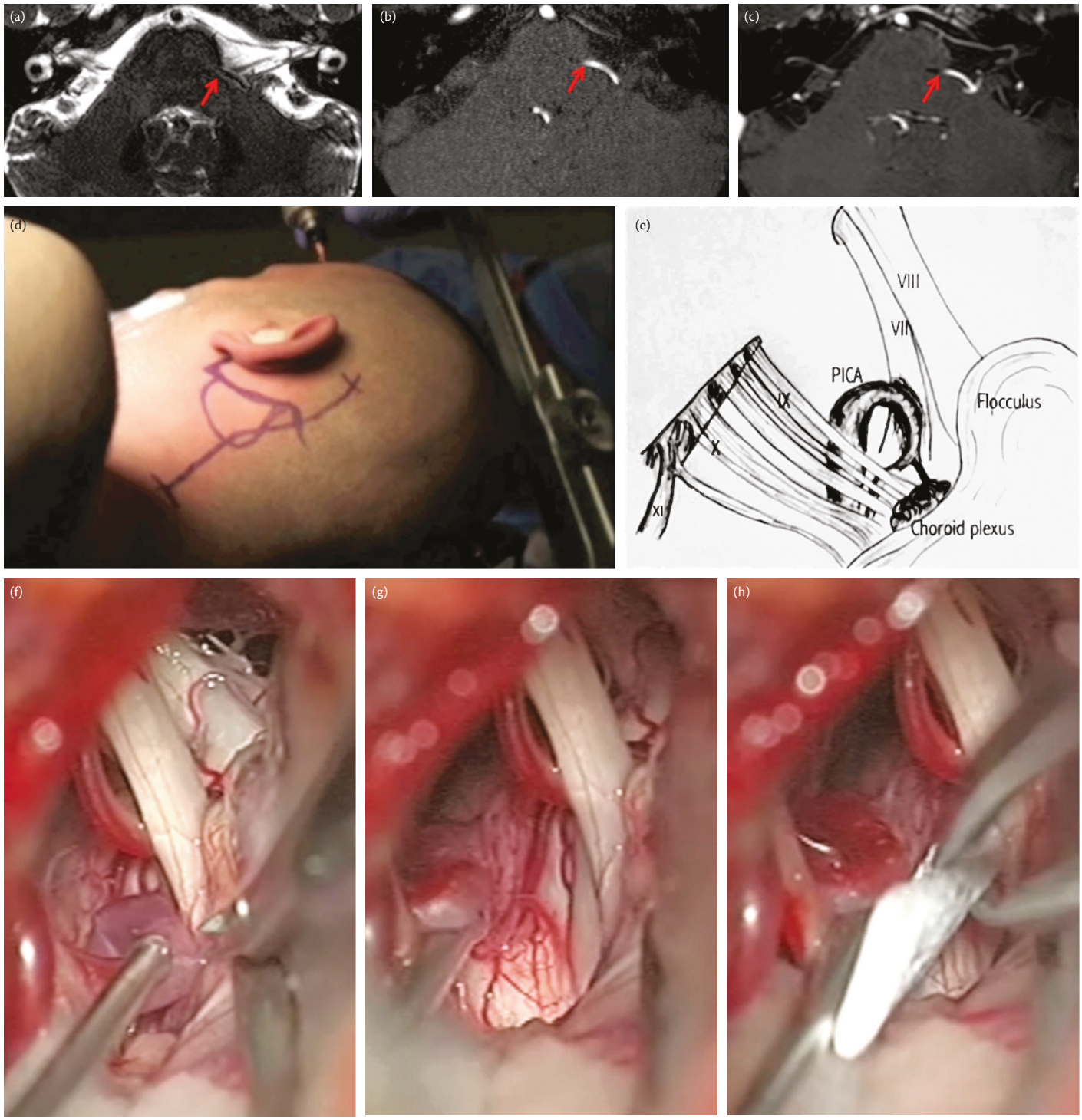

Fig. 79.2 Hemifacial spasm (HFS) on the left side.
MRI findings: Loop of posterior inferior cerebellar artery (PICA) in left facial REZ embedded in brainstem, on T2-sequence (A), clearly visible on TOF-angio sequence (B) and on T1-gadolinium sequence (C).
Surgical approach, through craniectomy performed posterior to tip of mastoid process (D), to access the facial REZ from below, that is, along the lower CNs (eleventh, tenth, and ninth) and the choroid plexus emerging through Luschka foramen at upper part of the cerebellomedullary fissure. The neurovascular conflict is located ventrocaudally to facial REZ and at adjacent brainstem (E).
Microsurgical steps: PICA loop compressing facial REZ, the later not being seen because masked by cochleovestibular nerves (F); loop detached from facial REZ (seen ventrally to the eighth nerve), with a greyish aspect (G); loop maintained away by a piece of Teflon semi-rigid material (1 cm in length, 5 mm in width) (H).

type 2 pain, which can be constant, aching, or burning (=Burchiel's classification). These two types can overlap in the same patient. It is important to exclude other facial pain syndromes such as trigeminal deafferentation pain, which may be the result of previous treatment, and SUNCT (short-lived, unilateral neuralgic headache with conjunctival injection and tearing) particularly following treatment failure and consideration of reintervention.

- *Response to anticonvulsants*—primarily carbamazepine or oxcarbazepine—at least at the onset of the disease, is an important additional criterion.
- *Multidisciplinary investigations* of the odontostomatologic, ear, nose and throat (ENT), maxillofacial, ophthalmologic and neurologic specialties are crucial to rule out secondary TN that would require specific treatment. In fact, secondary TN may remain misdiagnosed under the mask of a clinical typical presentation resembling primary TN, especially in neurologic diseases such as multiple sclerosis or cerebellopontine angle tumours.
- *Imaging* of the trigeminal root is a prerequisite for the choice of the procedure. The three following high-resolution sequences: 3D T2 high-resolution, time of flight (TOF) MR-angiography, T1 with gadolinium, in association because of their complementarity, allows—with a 1.5 Tesla machine—to depict NVC with a sensitivity of 96.7% and a specificity of 100% (Fig. 79.3A–C and Fig. 79.4A–C) (Leal et al., 2010).

The 3D–T2 sequence obtains fine images of the root. The cerebrospinal fluid has a hyperintense signal and the other structures of the cerebellopontine angle have a hypointense signal, achieving a cisternography-like exploration. Limitation is the absence of differentiation of signals between vessels and nerves. The 3D TOF-MRA if performed with a presaturation filter, visualizes only high-flow vessels (i.e. principally the arteries). The 3D-T1 sequence with gadolinium depicts arteries and veins, both being enhanced by contrast medium. Comparison of the latter two sequences allows differentiating veins from arteries.

Depicting cross-compressive veins is important (Matsushima et al., 1983; Dumot and Sindou, 2015). In our series they accounted for 39%, either separately in approximately one-fourth or in association with an elongated cerebellar artery in approximately three-quarters (Dumot and Sindou, 2015). Veins may belong to the superior petrosal venous system in the cistern (60%) or be a transverse inferior vein at exit of the root from the porus of Meckel cave (40%).

This MRI protocol also permits prediction of the degree of vascular compression, which can be: simple contact (grade I); distortion of the root (grade II); marked indentation in the root (grade III). This was possible in 84.6% of our patients (P <0.01) (Leal et al., 2010).

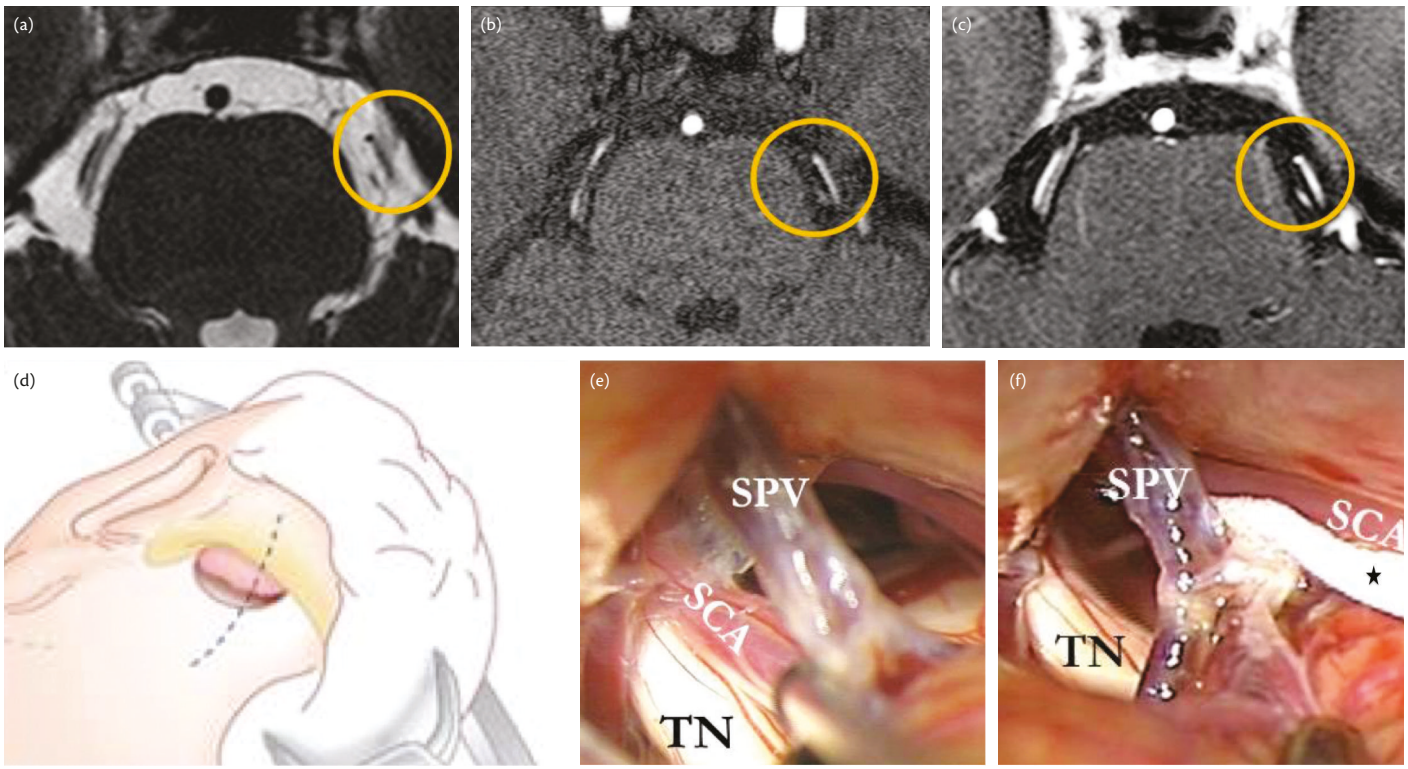

Fig. 79.3 Neurovascular conflict (left-sided TN) from the superior cerebellar artery (SCA).
(A–C) Imaging of a pure arterial compression of the trigeminal root by the SCA. (A) 3D-T2 high-resolution sequence showing the root crossed by the conflicting vessel; (B) 3D time of flight (TOF)-angio; (C) 3D-T1 sequence with gadolinium. Note that the identifiable conflicting vessel seen in T2 is not only visible in T1 + gadolinium, but also in TOF-angio, leading to conclude to a high-flow vessel (i.e. rather arterial, namely the SCA). (D–F) The microsurgical approach via an infratentorial-supracerebellar route (on the left side). The SCA is stuck to the superior aspect of the root (grade II of compression) (E). After the artery is detached and pushed away from the root, the SCA is maintained at distance by a small piece of Teflon (asterisk) (F). TN, trigeminal nerve; SCA, superior cerebellar artery; SPV, superior petrous vein. Note that the SPV and its affluents were preserved. Also note that the Teflon plate (hold by the SPV) does not touch the trigeminal root ('no neocompression').

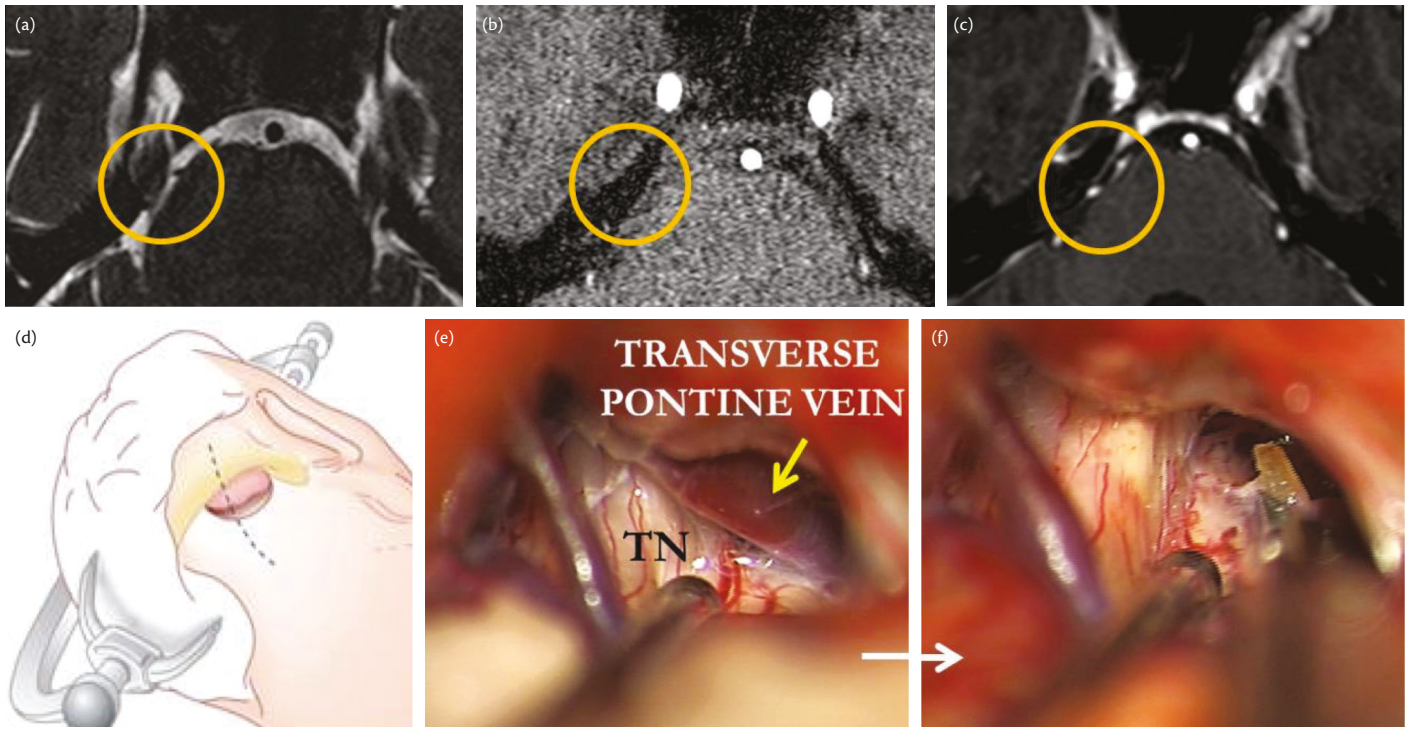

Fig. 79.4 Neurovascular conflict (right-sided TN) from pure venous compression, namely the inferior transverse vein. (A–C) Imaging of a pure venous compression by transverse (pontine) vein after exit of root from the porus of Meckel cave. High-resolution T2 axial view shows the root being crossed by the conflicting vessel. (A) The identifiable conflicting vessel on T2 is not visible in TOF-angio sequence, but apparent on T1 with gadolinium sequence, which is evocative of a pure venous conflict. Note the small size of the cerebellopontine angle cistern. (D–F) Microsurgical approach via an infratentorial-supracerebellar route (F). The transverse vein (arrow) is seen compressive to the inferior aspect of the trigeminal root as it exits from the porus of Meckel cave (E), TN: trigeminal nerve. Coagulation and division of the vein was considered indispensable for release of the trigeminal root compression (F).

With a 3 Tesla machine, images are finer and sensitivity rate even higher: 97.4% in our study, which can be useful for detection of small venous conflicts (Leal et al., 2011).

High-resolution MRI also reliably reveals morphological abnormalities of the trigeminal root, namely, global atrophy, angulation on crossing the upper petrous ridge at the porus of the Meckel cave (MC) and abnormalities of the posterior fossa, such as platybasia, Arnold-Chiari malformation, cisterns of small capacity, ….

Anatomical findings and their functional consequences

According to literature, a NVC can be found at the origin of most primary TNs, in 76.3% to 100% according to series, 90.5% on average. In our initial study on anatomical findings at surgery, a vessel was found in relation with the TR in 97% of the explored patients (Sindou et al., 2002). There was a compressive artery in 90.70% of the patients, whereas in the remaining 9.30% the conflict was found exclusively venous. The responsible elongated arteries were the superior cerebellar artery (SCA) in 88%, the AICA in 25.1%, the VBA in 37.8%, so that more than one compressive vessel was found in 37.8% of the patients. Failing to identify all conflicts at surgery could be source of failure or recurrence.

In same as well as in other personal studies (Sindou et al., 2002; Sindou et al., 2007; Dumot and Sindou, 2015), the NVC was situated at REZ as classically described in only 50% of the cases, at the midcisternal portion of the root in 40%, and more peripherally at the porus of MC in 10% (Fig. 79.5). In the latter situation the conflicting vessel, most often a transverse vein, marked a strong indentation on the root, with a greyish decoloration, typical of focal demyelination. Complete exploration of the entire root, from brainstem to porus of MC, is wise not to miss conflicts situated peripherally.

In a recent study strictly devoted to implication of veins, a clear venous compression was found in 38.7%, either alone (in one-fourth) or in association with an artery (in the other three-quarters) (Dumot and Sindou, 2015).

Determination of the degree of compression on preoperative high-resolution imaging is important as it plays a role in the outcome. In our KM study, a marked vascular compression, of grade III or II, found in 49.2% and 33.2%, respectively, was associated with a high success rate at 15 years of FU: 88% and 79%, respectively. Conversely, compression of grade I, found in 17.2%, was correlated with a 65% cure rate only (Sindou et al., 2007). The grade of compression, which can be predicted with reliability (P <0.01 for high grade of compression), should be taken into account for decision-making (Leal et al., 2010).

Anatomical abnormalities of the trigeminal root or the posterior fossa are frequently associated to vascular compression (Sindou et al., 2002; Sindou et al., 2007), (Parise et al., 2010; Parise et al., 2013). According to our observations, in 42% the TR had a significant degree of global atrophy, in the order of one to two-thirds reduction in calibre with a ruban—instead of a cylindrical—shape, testifying a coexisting neuropathy from likely degenerative origin. In 18.2%, arachnoid was thickened, with strong adhesions to the

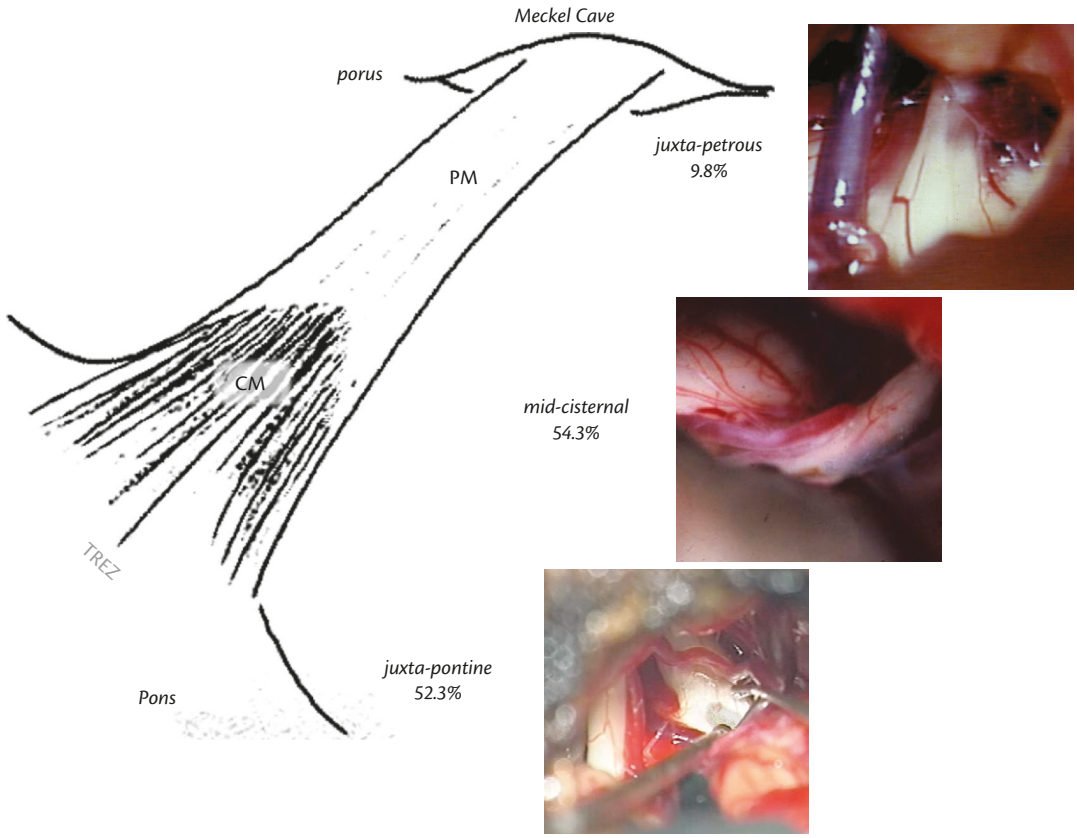

Fig. 79.5 Repartition of the neurovascular conflicts (NVC) in the patients with trigeminal nerve explored for MVD, according to respective situations at Trigeminal REZ (juxta-pontine), at mid-third of the root (midcisternal) and at exit of root from porus of Meckel cave (juxta-petrous). In 37.8% of the patients NVC were multiple in same individual. CM, central myelin, PM, peripheral myelin. Examples of operative views of NVC: Juxtapontine: right NVC inferiorly to trigeminal root entry zone (TREZ) from AICA loop (retracted with microaspirator), of grade III of compression (i.e. strong engrooving with greyish aspect of focal demyelination); Midcisternal: right NVC superiorly to midportion of the root from SCA, pushing root down (grade II of compression); Juxtapetrous: right NVC inferiorly to root at exit from porus of Meckel cave due to inferior transverse vein (grade III of compression). Note the marked greyish zone of focal demyelination.

root. In 12.6% the root had a marked angulation on crossing over the petrous ridge at exit from MC, especially when the cerebellum was atrophic, which corresponds to the so-called sagging phenomenon (Gardner et al., 1956). In 3.9% the root was compressed by being squeezed between the pons and the petrous bone within a 'virtual' cerebellopontine angle cistern due to the small size of the posterior fossa. These abnormalities must be taken into account for decision-making, as well as for the design of the surgical procedure.

Surgical methods and corresponding results

Criteria for neurosurgical indication are basically, first, investigations for eliminating a causative disease that would require specific treatment, second, neuralgia refractory to the medical treatment or intolerance due to major side effects including asthenia.

There is a variety of surgical options that the patient may be offered according to his (her) particularities, either of lesioning nature by means of percutaneous or radiosurgical techniques, or conservative with the MVD procedure.

Microsurgical vascular decompression

In 1934 Dandy, who pioneered juxtapontine rhizotomies for TN, published his observation on frequent compressions of the TR by a neighbouring elongated artery (Dandy, 1934). Surprisingly he did not reach the point to free the root from the vascular compression. It was Gardner in 1959 who performed the first decompression (Gardner and Miklos, 1959). In fact the method was really promoted by Jannetta through his famous publication of 1967 (Jannetta, 1967). In his paper the TR was accessed via the subtemporal-transtentorial approach. Tribute for the easier and safer retromastoid approach must be paid to Hardy (Provost and Hardy, 1970). The microvascular decompression (MVD) method was then codified and popularized worldwide by Jannetta through a large number of publications (Jannetta, 1976).

Operative steps for MVD are illustrated in **Figure 79.6**.

Offending vessel(s) may be more than one in the same individual, in the order of one-third of the patients (Sindou et al., 2002). For not missing multiple conflicts, the entire root must be explored from REZ at brainstem to porus of MC and freed from all arachnoid adhesions. Interposition of material to maintain the conflicting vessel away should not be 'neocompressive' (**Figs. 79.3D–F and 79.4D–F**) (Sindou et al., 2008).

Literature results are summarized in **Table 79.1**. According to the studies with a minimal average FU of 5 years and K-M analysis, MVD provides a high rate of pain relief (Tatli et al., 2008). In the largest series of 1185 patients operated on by Jannetta, probability of an excellent outcome ten years after surgery is of 70% (Barker et al., 1996).

Fig. 79.6 Microvascular decompression in patient affected with right TN due to mixed neurovascular conflicts (NVC), namely superior cerebellar artery (SCA) and vein from the superior petrosal venous (SPV) system. Illustration of patient's positioning, approach and surgery. (A) Lateral decubitus positioning with (moderate) traction on shoulder. Operating table in (slight) anti-Trendelenburg inclination to decrease cephalic extremity venous pressure. (B–D) Note 15° lateral angulation of neck/head toward contralateral side (B), 15° contralateral rotation of head (C) and landmarks of craniectomy (hatched area) below occipital crest/transverse sinus and posterior to base of mastoid process/sigmoid sinus (D). Cutaneous incision is 1 cm medial to the bisector of the angle formed by the nuchal line and the posterior aspect of the mastoid process. (E–I) MRI T1 + gadolinium sequence shows SCA loop on the ventromedial aspect of the trigeminal root and veins from the SPV system in contact with the dorsolateral aspect of the root. Drawings (F, G) and operative views (H, I) show trigeminal root before and after microvascular decompression. Asterisk, loop of SCA; V, compressive branches of SPV.

Table 79.1 Summary of results (from literature) of the various surgical methods for trigeminal neuralgias

	Immediate pain relief: Range (average)	Long-term pain relief: Range (average)	Failure and neuralgia recurrence rate mortality rate	Side effects/Complications Range (average) T = transient, P = permanent	Advantages vs. disadvantages
Thermo-rhizotomy N = 7483 pts FU: 3–26 y (9 y)	81–99% (94%)	20–93% (60.4%)	39.6% (+): 0.1% by carotid injury	Numbness (permanent): 5–98% Masticatory deficit (transient): 4–24% Corneal hypoesthesia (permanent): 5–18% (12%) Keratitis: 1–8% (5%) Trochlear palsy (transient): 1–2% (1%) Dysesthesia/anaesthesia dolorosa (permanent): 0.8–7% (3%)	• Short-lived IV anaesthesia • Selectivity • Long-lasting effect if hypoesthesia of trigger zone vs. difficult procedure, special training required
	Depending on intensity of thermolesion, and consequently degree of sensory loss				
Glycerol neurolysis N = 1310 pts FU: 1–10 y (6.5 y)	42–84% (68%)	18–59% (38.5%)	61.5% (+): none	Herpes zoster eruption: 50% Meningeal reaction: frequent Numbness ± dysesthesia (permanent): 30% Corneal hypoesthesia (permanent): 15% Keratitis: 5%	• Under local anaesthesia • Easy to perform • Low cost vs. No control of glycerol diffusion and effects
Balloon compression N = 1404 pts FU: 1–6 y (4 y)	82–100% (96%)	54.5–91.3% (67%)	33% (+): 0.2% by carotid injury	Numbness (± transient): 39% Masticatory deficit (± transient): 66% Pterygomaxillary fossa hematoma: occasional	• No numbness • No keratitis vs. • General anaesthesia • Balloon sometimes difficult to place inside the Meckel cave
Stereotactic radiosurgery N = 310 pts FU: 2–7 y (5 y)		21.8–88.9% (54%) (number of patients still under medication)	46% (+): none	Trigeminal hypoesthesia: 0–54% (32%) Corneal anaesthesia: none Trigeminal motor deficit: none	• No invasiveness vs. • Delayed effect • Long-term effect uncertain
Microvascular decompression N = 5122 pts FU: 5–15 y (7 y)	80–98% (91.8%)	62–89% (76.5%) high grade (II–III) of compression: 90% low grade (I): 65%	23.4% (arachnoiditis due to surgical exploration (P = 0.04)) (+): 0–1.2% (0.3%) cerebellar infarct	• Numbness: 2–7% (3%) • Hearing/Gait disturbances (permanent) (2.5%) • Facial palsy (permanent): 0–2% (1%) • Trochlear palsy (transient): 0–5% (1%) • Anaesthesia dolorosa (permanent): 1–3% (1.5%) • Cerebellar infarct: 1% • CSF leakage (transient): 2–17% (4%)	• Highest rate of long-term effectiveness • Keyhole surgery • Infrequent side effects vs. • Some severe complications

In our 1800 patients' series, of whom the first 362 had K-M analysis, probability of cure (i.e. no pain and no medication at 15 years of FU), is 74%; noteworthy, pain relief was equally satisfactory in atypical as in typical clinical presentations (Sindou et al., 2006).

Presence of a marked vascular compression at surgery (grade II or III) was correlated with a high success rate at 15 years of FU 79% and 88%, respectively; Conversely when the vessel was in simple contact (grade I), the probability of long-term relief amounted at only 65% (P = 0.001) (Sindou et al., 2007). Importantly, degree of compression can be predicted by imaging with high reliability (P <0.01) (Leal et al., 2010).

Advantages of MVD are its 'conservative' nature and a high rate of long-term relief when a clear-cut NVC is found. Disadvantage is the potential risk of an open surgery.

An illustration of proposed decision-making for TN is given in Figure 79.7.

Radiofrequency thermorhizotomy

Percutaneous radiofrequency thermorhizotomy (RF-ThRh) (Fig. 79.8) was introduced by Sweet as a refined version of the former electrocoagulation of the Gasserian ganglion pioneered by Kirschner in 1933 (Kirschner, 1933; Sweet and Wepsic, 1974). RF-ThRh is performed under short-lived bolus IV anaesthesia (currently with propofol) sequentially repeated as necessary. The needle electrode is driven under fluoroscopy using the *Hartel's route* through the foramen ovale, up to the immediate retrogasserian portion of the trigeminal nerve, namely the Triangular plexus where fibres have a somatotopic organization corresponding to the three trigeminal divisions. The (5 mm ± 2) uninsulated extremity of the electrode should be placed in the fibres corresponding to the pain territory, under X-ray and neurophysiological guidance, the latter based on evoked paraesthesias and muscular responses to electrical stimulation (Sindou, 1999; Tatli and Sindou, 2008). A thermolesion between 65°C and 75°C is performed to achieve a preferential, if not a totally selective analgesic effect. The lesion must not be made in the ganglion itself, but retrogasserian at the triangular plexus level to decrease the risk of trophic ulcerations by destroying the T cells of the ganglion (Sindou and Keravel, 1979). To obtain a marked hypoesthesia without important loss of tactile sensation and cover but not transpass the division(s) involved, an

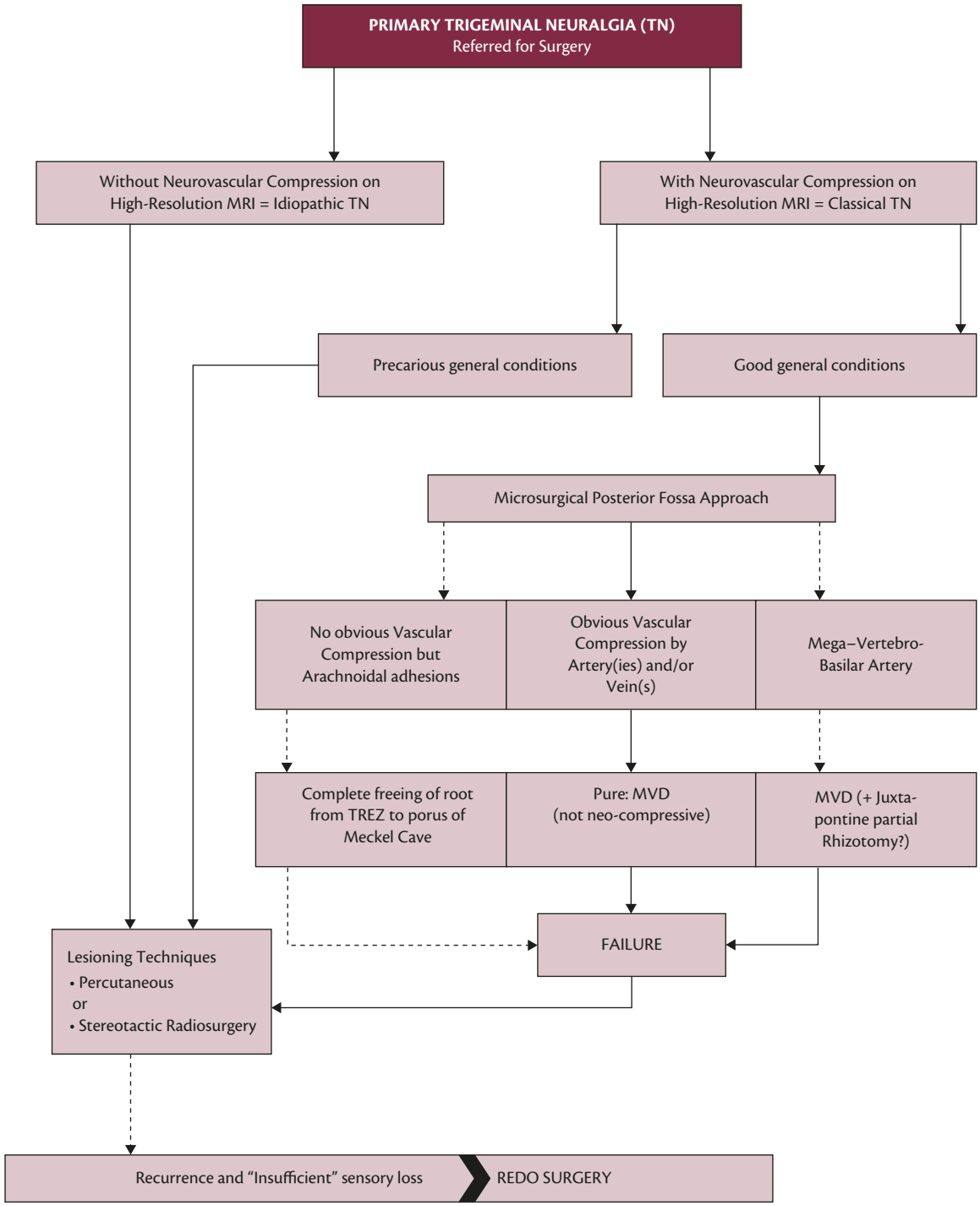
PRIMARY TRIGEMINAL NEURALGIA (TN)
Referred for Surgery
Without Neurovascular Compression on High-Resolution MRI = Idiopathic TN
With Neurovascular Compression on High-Resolution MRI = Classical TN
Precarious general conditions
Good general conditions
Microsurgical Posterior Fossa Approach
No obvious Vascular Compression but Arachnoidal adhesions
Obvious Vascular Compression by Artery(ies) and/or Vein(s)
Mega–Vertebro-Basilar Artery
Complete freeing of root from TREZ to porus of Meckel Cave
Pure: MVD (not neo-compressive)
MVD (+ Juxta-pontine partial Rhizotomy?)
FAILURE
Lesioning Techniques
• Percutaneous
or
• Stereotactic Radiosurgery
Recurrence and "Insufficient" sensory loss
REDO SURGERY

Fig. 79.7 Surgical decision-making for refractory primary trigeminal neuralgia.

accurate placement of the electrode and a gradual lesioning process are required, which is demanding and time-consuming, but of paramount importance.

Literature results are summarized in Table 79.1. In all reported series, duration of effect was proportional to the degree of the induced hypoesthesia (Sindou and Keravel, 1979). In our series, recurrence rate after FU ranging from 5 to 25 years was 7%, with the drawback that 95% of the patients had significant hypoesthesia in the pain territory. However, the resulting numbness was well-tolerated in all but 2% of the patients, these 2% suffering disabling dysesthesias (Sindou and Tatli, 2009).

Advantage of RF-ThRh is topographical selectivity. Disadvantage is the difficulty to target the proper fibres and to achieve an optimal degree of hypoesthesia. If excessive, the thermolesion may aggravate the background of burning pain in atypical TN and may also produce keratitis.

Rf-ThRh is particularly useful for patients harbouring classical TN but with precarious general condition or patients with TN due

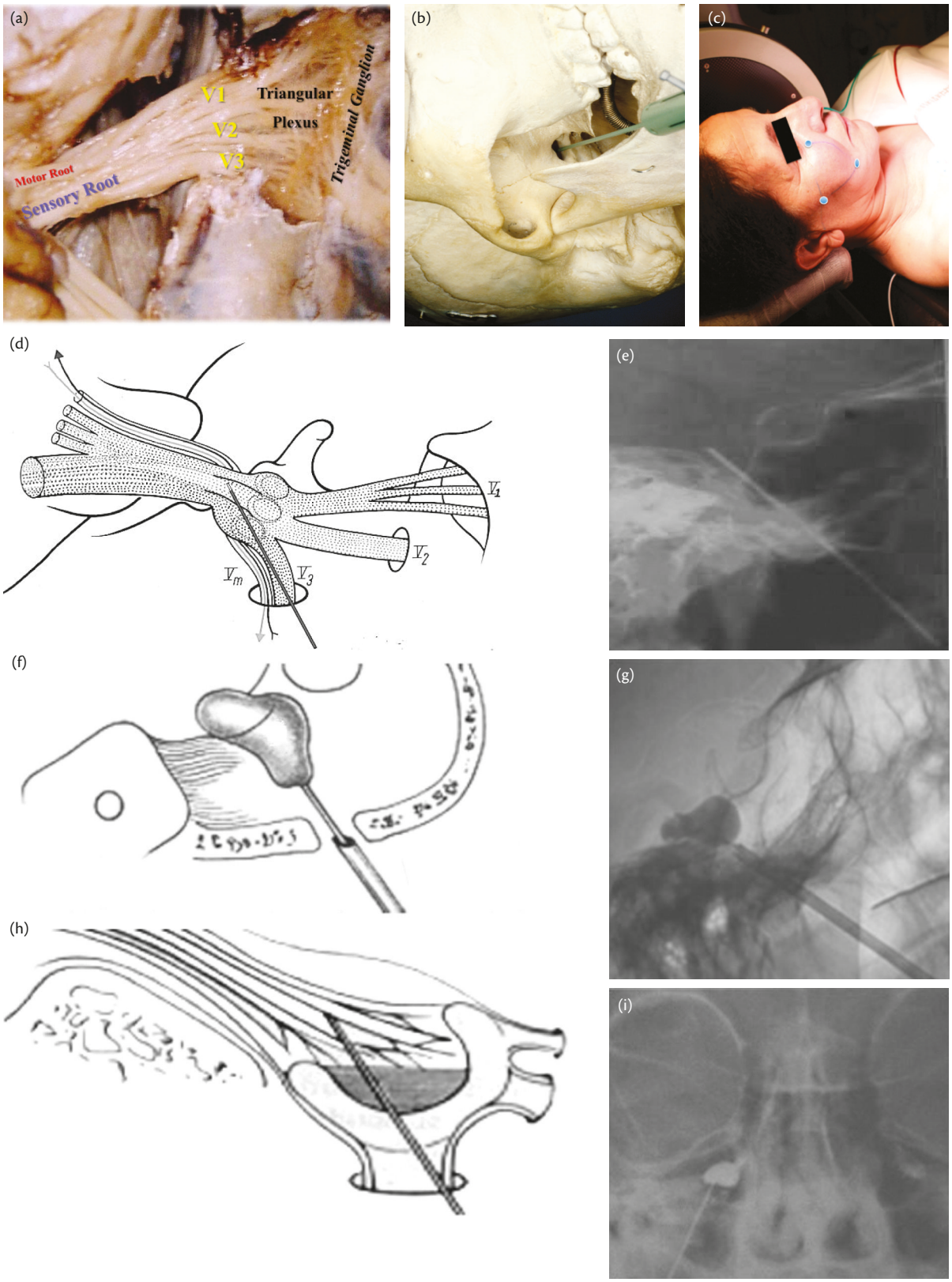

Fig. 79.8 Percutaneous lesioning techniques for tigeminal neuralgia. (A-C); Landmarks and trajectory for Hartel's transforamen ovale route (on right side). The entry point of the needle is on average at ±30mm from the labial commissure)±60mm from the middle of the intercommissural line). The foramen ovale is targeted by aiming (i) in lateral view, at 35mm anterior to the anterior wall of the external auditory meatus (tragus), (ii) in frontal view, the medial border of the pupil, (iii) the depth of the needle is guided by X-ray fluoroscopy to the level of the triangular plexus. (Tatli et al., 2008). Surgery should performed under fluoroscopy to be in accurate location (i.e., intersection of the clivus line and the upper petrous ridge) (Tatli et al., 2008). Wrong (and dangerous) trajectories would be, back to front, to jugular foramen, infrapetrosal carotid segment, carotid at foramen lacerum, orbital apex through the lower orbital fissure, then juxtaclinoidal carotid through the superior orbital fissure. (D-E): Schematic drawing and X-ray control (lateral view) for RF-Thermorhizotomy. Note the fibers from V1 division are located supero-medially, those

to multiple sclerosis (Kanpolat et al., 2001). It may also be applied to patients with secondary TN when the main component is of the paroxysmal and/or the allodynic types.

Balloon compression of gasserian ganglion

Percutaneous balloon compression (Fig. 79.8) was introduced by Mullan in the 1980s (Mullan and Lichtor, 1983). The procedure is performed under general anaesthesia with tracheal intubation and X-ray guidance of a No. 4 Fogarty catheter through the foramen ovale. Balloon should be driven inside the walls of the MC. Appropriate placement is confirmed by the pear-shaped aspect of the balloon inflated with metrizamide. Compression is maintained for approximately five ± 2 minutes according to authors. Bradycardia may happen during compression.

Literature results are summarized in Table 79.1. The method has few side effects with the exception of a high rate of (most often transient) masticatory deficits. Hypoesthesia is generally mild, especially regarding cornea (Keravel et al., 2009).

Disadvantages are effects not topographically specific and a relatively high recurrence rate. As incidence of keratitis is low, main indication is TN with involvement of the V1 territory.

Gasserian ganglion neurolysis with glycerol injection

Percutaneous gasserian ganglion neurolysis (Fig. 79.8), was developed by Håkanson in the 1980s, consists of injection of glycerol into the CSF of the trigeminal cistern, inside the MC (Håkanson, 1981). The procedure is performed under local anaesthesia with metrizamide fluoroscopic control for an accurate placement into the cistern. The technique is easy to perform but control of diffusion of glycerol outside the trigeminal cistern is somewhat hazardous.

Literature results are summarized in Table 79.1. Frequent side effects are Herpes Zoster eruption, paraesthesias and keratitis (Tatli et al., 2008).

Owing to its low cost, the method is widely performed around the world. In addition to potential complications due to its neurotoxicity, disadvantages are lack of predictability in terms of topography of effect and of long-term efficacy.

Stereotactic radiosurgery

The concept of stereotactic radiosurgery (SRS) for treating TN was introduced by Leksell as soon as the 1970s (Leksell, 1971). But the method became popular only in the last decade, when refinements in MRI allowed precise delineation of target. Irradiation is a single dose of 70–90 Gy, delivered with an isocentre at 4 mm. According to Régis's team recommendation, target should be at the retrogasserian cisternal portion of the TR, in the order of 7.5 mm from exit to porus, rather than at the trigeminal root entry zone (TREZ), to minimize brainstem irradiation (Régis et al., 2009) (Fig. 79.9).

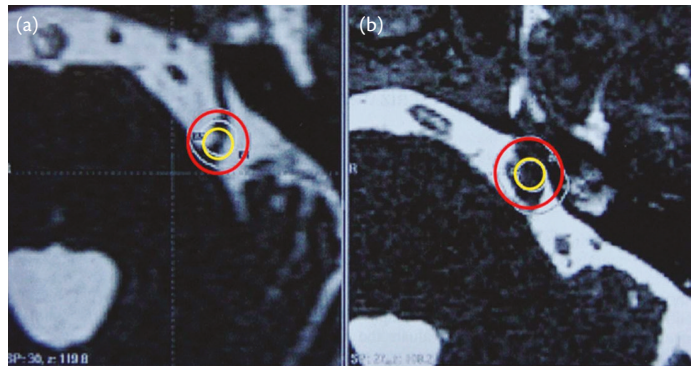

Fig. 79.9 Stereotactic radiosurgery (SRS) targets: this figure shows the two currently used targets with high-resolution T2 sequence. (A) Target at the TREZ; (B) target at the cisternal portion of the root. The target considered the least dangerous is the cisternal target, more distant from brainstem. Yellow circle, 80 Gy isodose curve; red circle, 30 Gy isodose curve.

Literature results are summarized in Table 79.1. Results significantly vary between reports, possibly because of differences in targets and doses. Furthermore, pain relief was diversely estimated among authors; in a number of publications, outcome was classified as satisfactory though patients were maintained on medication. Hypoesthesia together with subsequent numbness and paraesthesias are reported at 0–54% according to series. Although controverted by some authors, general consensus is that obtention of pain relief and its duration depend on the presence and degree of hypoesthesia ($P = 0.02$) (Pollock, 2006; Régis et al., 2016). For that reason, Pollock estimates that SRS for TN should be considered among the lesioning techniques.

Advantages of SRS are low invasiveness and low rate of complications. Disadvantage is the delay in obtaining pain relief, generally several months; however, this inconvenience is not a major problem for most patients with the exception of those referred for unbearable refractory pain.

Decision-making

Complete high-resolution MRI exploration is of extreme practical importance for decision-making as it gives the necessary anatomical bases for indicating the most appropriate procedure. There is a general consensus that MVD be considered as the first surgical option when the patient's conditions are favourable. Percutaneous lesioning techniques or stereotactic radiosurgery are most helpful for patients in whom imaging does not reveal clear-cut vascular compression;

Fig. 79.8 Continued
corresponding to V3 division infero-laterally and those corresponding to V2 division between the two. The uninsulated tip of the electrode should be located in a somatotopic way according to the trigger-zone and pain territory. Location is guided by evoking paresthesia to electrical stimulation of the root while the patient as awake and/or eliciting trigemino-facial reflexes (especially the blink-reflex) in the corresponding facial muscles (Sindou 1999). Then thermolesion is done under brief general anesthesia to provide analgesia (tested by pinprick) without complete loss of tactile sensation of skin and mucosa and decrease in corneal reflex (tested by cottonoid contact). (F-G): Schematic and X-ray control (lateral view) for balloon compression of the Gasserion ganglion and triangular plexus. Note the pear-shaped aspect of the inflated balloon, which testifies of the ideal location inside the Meckel's cave and the trigeminal cistern. (H-I): Schematic drawing and X-ray control (AP view) for Glycerol injection in the trigeminal cistern. An iodine contrast should ensure that needle is located within the trigeminal cistern; then the glycerol solution is injected with patient awake.

they also constitute an effective recourse when patients are in precarious conditions.

Comparison of the various neurosurgical methods available for TN is rather difficult because of heterogeneity between published series. The reasons for this are: heterogeneous patient selection criteria among teams; technical differences in performing surgery; disparities between authors for outcome assessment, as well as for evaluation of side effects and complications; and rarity of long-term studies with Kaplan–Meier analysis.

Vago-glossopharyngeal neuralgia

Glossopharyngeal neuralgia should rather be named vago-glossopharyngeal neuralgia, as pain frequently affects not only the ninth sensory territory of the ninth CN but also the one tributary of the vagus nerve (tenth CN). VGPN is one hundred times less frequent than TN. Definition is clinical; VGPN consists of paroxysmal, transient, severe, sharp pain in the back of the throat, the tonsillar fossa, the base of the tongue, the depth of the ear canal, the area beneath the angle of the mandible. Pain usually lasts seconds to minutes and is often triggered by swallowing, eating, chewing, coughing, yawning, talking, and so on (Headache Classification Committee, 2013). VGPN may be sometimes associated with cardiovascular manifestations, especially syncopes (Chen and Sindou, 2015), and only exceptionally with digestive manifestations (Anthérieu et al., 2016).

Aetiology and pathophysiology

VGPN can be secondarily, be due to extracranial or intracranial tumours, or various other specific pathologies. In the last decade, primary VGPNs were recognized to be most often due to ninth-tenth CN arterial compression, predominantly but not always at REZ, and named, as for TN, classical. High-resolution MR is able to depict compressive vessels with a high sensitivity and specificity, in the same way as for TN (Kawashima et al., 2010; Leal et al., 2010).

Diagnosis

Diagnosis is based on the particular features of the pain. Clinical examination does not reveal any obvious neurological deficit. ENT investigations and MRI rule out diagnoses of extracranial or intracranial tumours, vascular lesions, Chiari malformations, and others. In most patients with classical VGPN, high-resolution MRI shows a compressive elongated artery generally the PICA and/or the VBA.

Surgical management

When medical treatment, based on anticonvulsants as for TN, fails or is not tolerated, surgical treatment should be considered. Percutaneous RF-ThRh that can be performed at the foramen jugularis is rarely indicated for primary VGPN, due to the high risk of creating deficits in the motor territories of the ninth and tenth CNs (Lazorthes and Verdie, 1979; Tew et al., 1982). To be mentioned, Rf-ThRH should be rather reserved to pain of neoplastic origin. Stereotactic radiosurgery (SRS) was recently attempted with some promising results (Dhople et al., 2009; Leveque et al., 2011). For classical VGPN, MVD should be the first option because of its efficacy and its 'conservative' nature (Laha and Jannetta, 1977; Chen and Sindou, 2015).

Approach is a keyhole-type retromastoid craniectomy posterior to the tip of the mastoid process and retrocondylian, so as to follow a laterotonsilar—infraflocculare trajectory, along the cerebellomedullary fissure. Such a trajectory allows to avoid stretching of the eighth nerve and related complications (**Fig. 79.10**). The compressive vessels, generally PICA and/or VBA, lie ventrally to the ninth to the tenth REZ at adjacent brainstem. For effective decompression, the covering arachnoid membranes that are frequently thickened and adhesive to the rootlets should be widely opened and excised.

Results

Literature results have been reviewed and detailed elsewhere (Chen and Sindou, 2015). In brief the review, which included 28 publications totalizing 515 cases, shows that MVD achieved total relief in 50% to 100% of the patients according to authors, with acceptable rates of side effects or complications. In our series of 36 MVD for VGPN with a FU of more than 2 years, complete pain relief was achieved in 94.4% of the patients. There was no mortality, no general morbidity, and no wound complications. Neurological deficits consisted of some degree of (permanent) dysphonia and dysphagia in two patients.

According to recent literature, MVD proves to be an efficacious and relatively safe procedure for primary VGPN. SRS that might be promising needs more long-term evaluation to be included in the therapeutic armamentarium. Percutaneous RF-ThRh should be reserved for pain from neoplastic origin with already neurological deficits.

Tinnitus and vertigo

Tinnitus

Tinnitus is a very common symptom, mostly due to auditory deafferentation after inner ear, peripheral or central nervous system damages that result in neuronal hyperactivity and/or functional reorganization within central auditory structures (Møller, 2007; Londero et al., 2009). Origin from vascular compression is controversial; close relationships of cerebellar arterial loops with the eighth nerve in CPA cistern or the internal auditory canal are very common findings in asymptomatic patients. However, under very specific conditions, patients affected with handicapping unilateral tinnitus, with no identifiable cause other than an image of neurovascular conflict, may be candidates for eighth CN MVD (De Ridder et al., 2012; Mathiesen and Brantberg, 2015).

Criteria are both anatomical: a clear-cut arterial loop on MRI compressing the nerve at REZ or distorting its trajectory within the cistern or the auditory canal, and physiological: an increase in latency of peaks III and V at brainstem auditory evoked potentials (BAEPs) recordings. An ipsilateral vestibular hyporeflexia can be also an argument.

Reports, which are few, coincide on the fact that in spite of strict selection outcomes remain uncertain, especially when duration of tinnitus prior to surgery has been prolonged.

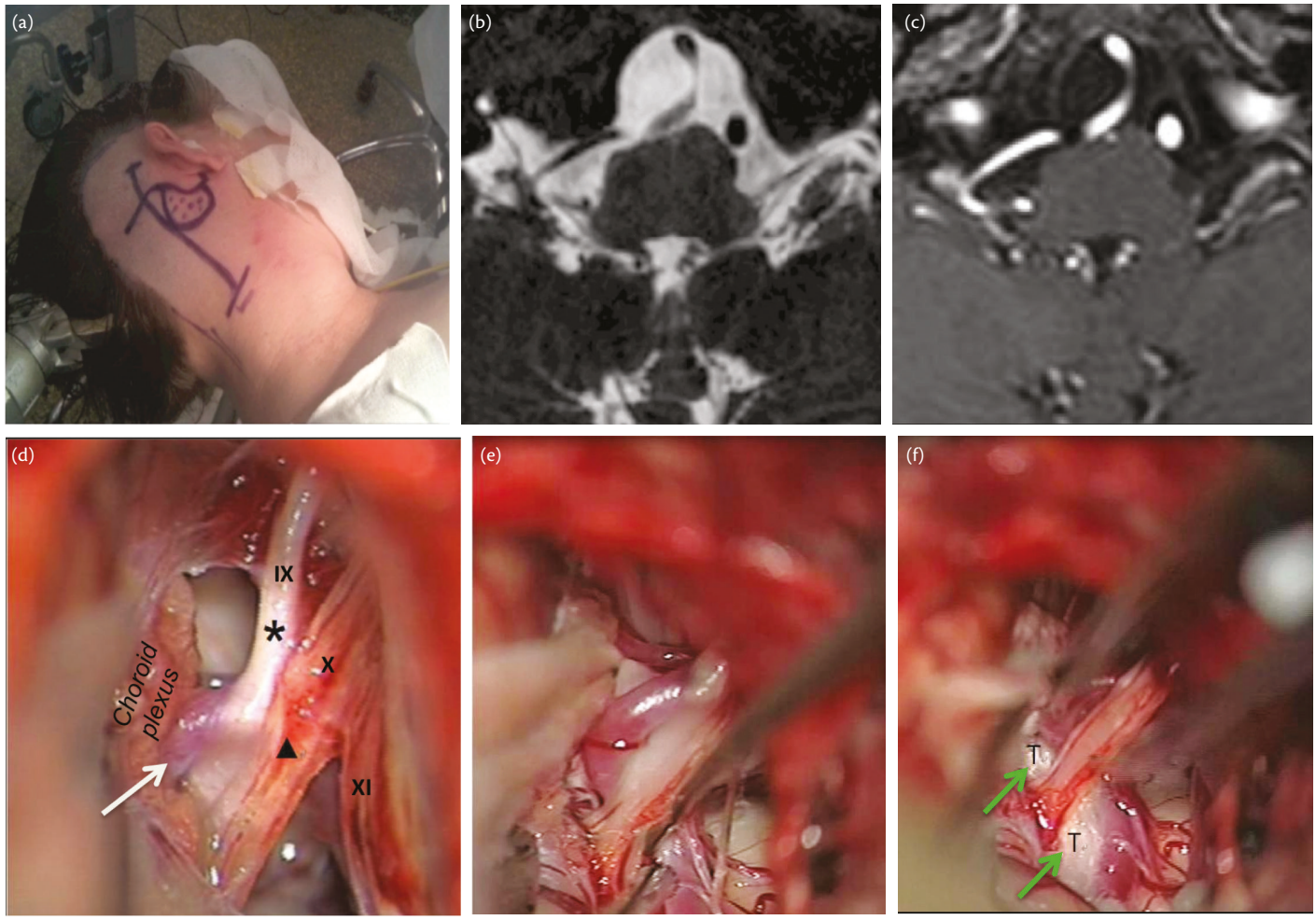

Fig. 79.10 Vasoglossopharyngeal neuralgia (on right side) due to neurovascular conflict from posterior inferior cerebellar artery (PICA), as seen on MRI with high-resolution T2 (B) and T1 + gadolinium (C) sequences. Landmarks of keyhole (retromastoid, retrocondylar, and retrosigmoid) approach for vagal and glossopharyngeal microvascular decompression (A). Infrafloccular microsurgical approach on the right side. The offending PICA is ventral to the REZ of the ninth (asterisk) and the tenth (triangle) nerves. Note the atrophic and greyish aspect of the ninth and tenth rootlets testifying of focal demyelination (D). The compressive PICA (arrow) is detached after dissection and freeing of the rootlets from arachnoid adhesions (E). The Teflon felt bundle (T) is placed so that the artery is maintained apart from REZ of ninth and tenth rootlets (F).

Vertigo

Prevalence of vestibular paroxysmia due to NVC is difficult to evaluate among the various and frequent vestibular disorders (Tilikete and Vighetto, 2009). Estimation is around 4% according to a review by Hüfner (Hüfner et al., 2008). 'Disabling positional vertigo (DPV)', as characterized by Jannetta and Møller's group, is considered as the most evocative clinical presentation of this aetiology (Jannetta et al., 1984; Møller et al., 1986).

Diagnosis and side of vascular compression are not easy to ascertain in the absence of associated auditory symptoms and signs. As a matter of fact, vascular loops in contact with the eighth CN is a common finding in many asymptomatic individuals. Unlike auditory symptoms, abnormalities found at vestibular investigations are neither specific nor reliable regarding the side or the endo- or retro-labyrinthic topography of the pathology. In ocular movement recordings, the rapid component of the nystagmus, whether spontaneous or positional, may be directed either to the affected or the normal side, indicating hyper- or hypo-excitability of the vestibular system, respectively. The same applies to the caloric test, the responses being diminished or increased according to whether the affected vestibular system is hypo- or hyper-excitable. Thus, in the absence of obvious unilateral abnormalities on the auditory investigations, namely an increase in latency of peak III and V on BEAP recordings, vestibular tests cannot be relied upon to confirm diagnosis, as well as to determine side and level of NVC.

Surgery, of any type, should be considered only for incapacitating vertigo, of a degree of 5–6 on the functional scale of the Committee on Hearing and Equilibrium (Committee on Hearing and Equilibrium guidelines for the diagnosis and evaluation of therapy in Menière's disease, 1995). When there are sufficiently solid arguments for vascular compression, MVD is the best choice because of its conservative nature (Hüfner et al., 2008). The responsible compression may be exerted by AICA or PICA at REZ or by an AICA loop in cistern or internal auditory canal. A lesioning procedure, such as vestibular neurotomy, would be only justified if preservation of auditory function is considered to be useless, that is, when tonal audiometry is less than 50 dB and vocal threshold inferior to 50% (class C–D of the Classification of the American Academy of Otorhinolaryngology

and Head and Neck Surgery) (AAOHNS) (Møller et al., 1986), (Committee on Hearing and Equilibrium guidelines for the diagnosis and evaluation of therapy in Menière's disease, 1995; Lacombe, 2009). Of course, auditory function in the contralateral side has to be verified prior to decision.

In largest published series MVD of the eighth nerve was reported as at least partially effective in approximately three-quarters of the patients in the series of Møller and Ryu (Møller et al., 1993; Ryu et al., 1998). Weakness of these reports is that patients were not systematically assessed with auditory and vestibular tests; also, functional tests were not applied. In both publications disabling complications were rare; complete hearing loss was reported at only 2% of the operated patients. However, a certain decrease in hearing was noticed in most patients.

Motor ocular syndromes

Neurogenic hyperactivity may provoke episodic spasms of one or several extraocular muscles, with a variety of clinically observable manifestations, including ocular neuromyotonia, superior oblique myokymias, ocular motor synkineses, cyclic spasms, and so on, all resulting in diplopia. Pathophysiology varies and may result from a number of diseases (Vighetto and Tilikete, 2009). Not always understood, mechanisms usually involve central rearrangement of neuronal activity in the attained nuclei. However, a proportion of apparently idiopathic cases—rather rare (three cases affecting the fourth CN and one case the third CN)—were reported in relation with a neurovascular compression (Samii et al., 1998; Mikami et al., 2005; Inoue et al., 2012; Fam et al., 2014).

To be noted, several other cases reported as NVC and treated so-called by MVD were in fact palsies by ectatic arteries.

Complex dystonic/painful manifestations

Occasionally, patients may be referred harbouring complex dystonic/painful manifestations in the face, of somewhat mysterious origin, and considered possibly related to psychogenic mechanisms. Visualization of an image of possible NVC may incite to consider MVD. As an illustration we treated one such female patient suffering from painful unilateral dystonic paroxysms of the masticatory and facial muscles on one side, accompanied with anarchic ocular revulsions, and time to time followed by falls. Symptoms were totally relieved after MVD from an AICA loop deeply embedded inside the pontomedullary junction.

Neurogenic blood hypertension

Among the hypothetic aetiologies of so-called essential hypertension (HT), one mechanism may be neurogenic dysfunction due to vascular compression of the ventrolateral (VL) aspect of medulla. Since this hypothesis was applied to humans by Jannetta and his group in the late 1970s, only few studies either clinical or experimental in baboons have been reported in the literature, although such a neurogenic mechanism might potentially concern a large number of individuals (Jannetta and Gendell, 1979; Jannetta et al., 1985; Geiger et al., 1998; Levy et al., 2001; Naraghi et al., 2001).

Surgical data

In their first clinical report Jannetta and Gendell observed a higher rate of neurovascular compression of the VL medulla predominantly on the left side in patients affected with TN or HFS when hypertension was associated (Jannetta and Gendell, 1979). To be noted, the predominant left-sided lateralization is concordant with the prevalence of left ninth to tenth nerve complex in conveying the afferences from the baroreceptors of the (left-sided) cardiac atrium.

Ever since only two surgical studies were published: one, retrospective, by Jannetta et al. with 53 patients and the other prospective, by Geiger et al. with 36 patients (Jannetta et al., 1985; Geiger et al., 1998). In both series MVD improved uncontrolled HT in 84% and 80%, respectively.

Our contribution to the field was assessment, in a prospective study, of the effects obtained on blood pressure (BP) by MVD of the ninth to the tenth REZ and adjacent VL medulla, in addition to MVD of the facial REZ, in a group of 48 patients operated on for their HFS and in whom an apparently essential HT was present (Sindou et al., 2015). In summary all enrolled patients except one had a HT of at least WHO grade I, and 18 of them an unstable form, despite appropriate medical treatment. In all, the conflicting vessel(s) found exerted compression ventrally at the REZ of the ninth to tenth CNs and at adjacent VL medulla. After MVD, at latest FU (2 to 16 years, 7 years on average), BP was found to be normalized in 28, 14 of which without the need for any antihypertensive treatment (P <0.0001). Also, at the latest FU, BP remained unstable in only 8 of the 18 patients who had unstable BP prior to MVD (P <0.02). These findings indirectly plead for an efficacy of MVD in the treatment of refractory, apparently essential, HT (**Fig. 79.11**). Regarding the side, of the 30 patients with left-sided compression 17 had BP normalized (11 of them with no need for medications), and of the 18 with right-sided compression, 11 had a normalized BP (three of them with no need for medications); however, difference was not statistically significant.

MRI findings on HT

Because not all patients with essential HT, which failed to be controlled by medications, cannot be eligible for surgery, selection should be primarily based on MRI findings, provided sufficient reliability. Most publications in literature report a higher rate of images with vascular contact/compression (vc/c) at the VL medulla in the group of patients with essential HT, compared to the group with normal BP (Sindou, 2015). Left-sided vc/c had higher rate than right-sided vc/c. However, statistical significance was absent in the prospective studies (P = 0.178) as opposed to the retrospective ones (P = 0.001).

The difficulty to discriminate whether an elongated arterial loop at the VL medulla and adjacent ninth to tenth REZ is the cause or the consequence of the increased BP is major limitation for MRI-based decision-making. Comparison of images between patients with apparent primary HT and secondary HT shows that in the latter group (secondary HT), rate of NVC at brainstem was lower than in the group with primary HT, a finding however that did not reach statistical significance.

Discussion/Conclusion

Arguments suggesting that vascular compression of VL medulla at level of ninth to the tenth REZ seem convincing enough to

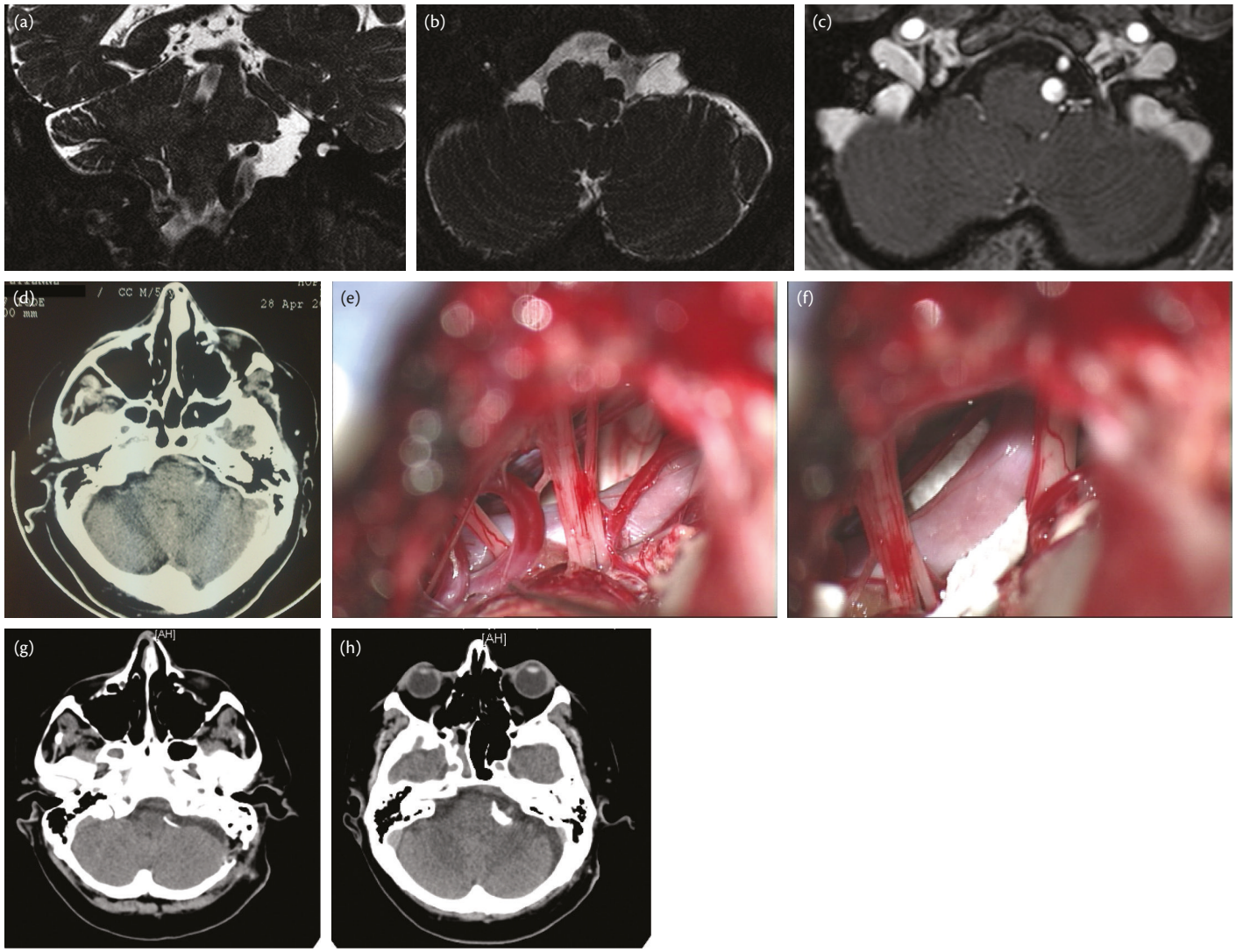

Fig. 79.11 Blood hypertension, likely from neurogenic origin due to vascular compression of ventrolateral brainstem and REZ of ninth and tenth CNs (on left side).
Imaging: Compression of VL medulla, on the left side, by a megadolicho-vertebrobasilar artery (VBA), on T2-coronal (A), T2- (B), and T1-gadolinium (C) axial views. On computed tomography (CT) axial view (D), location of megadolicho VBA is on left side.
Operative views: On the left side, at cerebellomedullary fissure, compression of VL medulla, ventral to tenth and ninth REZ and rootlets. (E) Brainstem and rootlets decompressed after interposed piece of (semi-rigid) Teflon (F). Note location of Teflon plate (hyperdense) on post-op CT axial views (G, H).

consider vascular decompression as a possible measure for the treatment of apparently essential HT likely to be of neurogenic origin (Sindou, 2015). The main problem remains patient selection, even when MRI reveals images of megalodolicho-artery(ies) likely to compress brainstem. However, it could be justified to consider decompressive surgery in the patients in whom in spite of a well-conducted medical treatment BP remains high, unstable, and thus life-threatening.

General conclusion–epilogue

Over the last decades important advances were made to identify and treat a number of so-called CN vascular compression syndromes at the origin of hyperactive functional disorders.

Indication of microvascular decompression (MVD), that must remain considered on rigorous clinical, bases may largely benefit from a battery of for neurophysiological tests and from the recently developed high-resolution imaging.

However, not all operated patients are cured. Undoubtedly, several of these (puzzling) disorders—sometimes considered from more or less psychogenic origin—arise from multifactorial mechanisms. A large amount of work still remains to be done to better understand mechanisms, accurately select patients, and improve efficacy and safety of surgical techniques.

FURTHER READING

Barker, F.G., Jannetta, P.J., Bissonette, D.J., Shields, P.T., Larkins, M.V., & Jho, H.D. (1995). Microvascular decompression for hemifacial spasm. *J Neurosurg*, **82**(2), 201–10.

Chen, J. & Sindou, M. (2015). Vago-glossopharyngeal neuralgia: a literature review of neurosurgical experience. *Acta Neurochir (Wien)*, **157**(2), 311–21; discussion 321.

Gardner, W.J. (1962). Concerning the mechanism of trigeminal neuralgia and hemifacial spasm. *J Neurosurg*, **19**, 947–58.
Headache Classification Committee of the International Headache Society (2013). The International Classification of Headache Disorders, 3rd edition (beta version). *Cephalalgia*, **33**(9), 629–808.
Keravel, Y., Gaston, A., Ciampi de Andrade, D., Mencattini, G., & Le Guérinel, C. (2009). Balloon compression for the treatment of trigeminal neuralgia. *Neurochirurgie*, **55**(2), 197–202.
Leal, P.R., Hermier, M., Froment, J.C., Souza, M.A., Cristino-Filho, G., & Sindou, M. (2010). Preoperative demonstration of the neurovascular compression characteristics with special emphasis on the degree of compression, using high-resolution magnetic resonance imaging: a prospective study, with comparison to surgical findings, in 100 consecutive patients who underwent microvascular decompression for trigeminal neuralgia. *Acta Neurochir (Wien)*, **152**(5), 817–25.
Møller, M.B., Møller, A.R., Jannetta, P.J., Jho, H.D., & Sekhar, L.N. (1993). Microvascular decompression of the eighth nerve in patients with disabling positional vertigo: selection criteria and operative results in 207 patients. *Acta Neurochir (Wien)*, **125**(1–4), 75–82.
Régis, J., Tuleasca, C., Resseguier, N., et al. (2016). Long-term safety and efficacy of Gamma Knife surgery in classical trigeminal neuralgia: a 497-patient historical cohort study. *J Neurosurg*, **124**(4), 1079–87.
Sindou, M., Mahmoudi, M., & Brînzeu, A. (2015). Hypertension of neurogenic origin: effect of microvascular decompression of the CN IX-X root entry/exit zone and ventrolateral medulla on blood pressure in a prospective series of 48 patients with hemifacial spasm associated with essential hypertension. *J Neurosurg*, **123**(6), 1405–13.
Tatli, M. & Sindou, M. (2008). Anatomoradiological landmarks for accuracy of radiofrequency thermorhizotomy in the treatment of trigeminal neuralgia. *Neurosurgery*, **63**(1 Suppl 1), ONS129–37; discussion ONS137–8.

REFERENCES

Anthérieu, P., Vassal, F., & Sindou, M. (2016). Vagoglossopharyngeal neuralgia revealed through predominant digestive vagal manifestations. Case report and literature review. *Neurochirurgie*, **62**(3), 174–7.
Barker, F.G., Jannetta, P.J., Bissonette, D.J., Shields, P.T., Larkins, M.V., & Jho, H.D. (1995). Microvascular decompression for hemifacial spasm. *J Neurosurg*, **82**(2), 201–10.
Barker, F.G., Jannetta, P.J., Bissonette, D.J., Larkins, M.V., & Jho, H.C. (1996). The long-term outcome of microvascular decompression for trigeminal neuralgia. *N Engl J Med*, **334**, 1077–83.
Chen, J. & Sindou, M. (2015). Vago-glossopharyngeal neuralgia: a literature review of neurosurgical experience. *Acta Neurochir (Wien)*, **157**(2), 311–21; discussion 321.
Committee on Hearing and Equilibrium guidelines for the diagnosis and evaluation of therapy in Menière's disease (1995). American Academy of Otolaryngology-Head and Neck Foundation, Inc. *Otolaryngol Head Neck Surg*, **113**(3), 181–5.
Dandy, W.E. (1934). Concerning the cause of trigeminal neuralgia. *Am J Surg*, **24**, 447–55.
De Ridder, D., Vanneste, S., Adriaensens, I., Lee, A.P., van de Heyning, P., & Møller, A. (2012). Vascular compression of the cochlear nerve and tinnitus: a pathophysiological investigation. *Acta Neurochir (Wien)*, **154**(5), 807–13.
Dhople, A.A., Adams, J.R., Maggio, W.W., Naqvi, S.A., Regine, W.F., & Kwok, Y. (2009). Long-term outcomes of Gamma Knife radiosurgery for classic trigeminal neuralgia: implications of treatment and critical review of the literature. *Clin Article J Neurosurg*, **111**, 351–8.
Dumot, C. & Sindou, M. (2015). Trigeminal neuralgia due to neurovascular conflicts from venous origin: an anatomical-surgical study (consecutive series of 124 operated cases). *Acta Neurochir (Wien)*, **157**(3), 455–66.
Fam, M.D., Scott, C., Forster, A., & Kamel, M.H. (2014). Microvascular decompression for superior oblique myokymia: case report. *Br J Neurosurg*, **28**(4), 552–5.
Gardner, W.J. & Miklos, M.V. (1959). Response of trigeminal neuralgia to decompression of sensory root. Discussion of cause of trigeminal neuralgia. *JAMA*, **170**, 1773–6.
Gardner, W.J., Todd, E.M., & Pinto, J.P. (1956). Roentgenographic findings in trigeminal neuralgia. *Am J Roentgenol Radium Ther Nucl Med*, **76**(2), 346–50.
Gardner, W.J. (1962). Concerning the mechanism of trigeminal neuralgia and hemifacial spasm. *J Neurosurg*, **19**, 947–58.
Gardner, W.S. & Sava, G.A. (1962). Hemifacial spasm—a reversible pathophysiologic state. *J Neurosurg*, **19**, 240–7.
Geiger, H., Naraghi, R., Schobel, H.P., Franck, H., Stenzel, R.B., & Fahlbusch, R. (1998). Decrease of blood pressure by ventro-lateral medullary decompression in essential hypertension. *Lancet*, **352**, 446–9.
Goto, Y., Matsushima, T., Natori, Y., Inamura, T., & Tobimatsu, S. (2002). Delayed effects of the microvascular decompression on hemifacial spasm: a retrospective study of 131 consecutive operated cases. *Neurol Res*, **24**(3), 296–300.
Grundy, B.L., Procopio, P.T., Jannetta, P.J., Lina, A., & Doyle, E. (1982). Evoked potential changes produced by positioning for retromastoid craniectomy. *Neurosurgery*, **10**(6 Pt 1), 766–70.
Håkanson, S. (1981). Trigeminal neuralgia treated by the injection of glycerol into the trigeminal cistern. *Neurosurgery*, **9**(6), 638–46.
Hatem, J., Sindou, M., & Vial, C. (2001). Intraoperative monitoring of facial EMG responses during microvascular decompression for hemifacial spasm. Prognostic value for long-term outcome: a study in a 33-patient series. *Br J Neurosurg*, **15**(6), 496–9.
Headache Classification Committee of the International Headache Society (2013). The International Classification of Headache Disorders, 3rd edition (beta version). *Cephalalgia*, **33**(9), 629–808.
Huang, C.I., Chen, I.H., & Lee, L.S. (1992). Microvascular decompression for hemifacial spasm: analyses of operative findings and results in 310 patients. *Neurosugery*, **30**, 53–6.
Hüfner, K., Barresi, D., Glaser, M., et al. (2008). Vestibular paroxysmia: diagnostic features and medical treatment. *Neurology*, **71**(13), 1006–14.
Inoue, T., Hirai, H., Shimizu, T., et al. (2012). Ocular neuromyotonia treated by microvascular decompression: usefulness of preoperative 3D imaging: case report. *J Neurosurg*, **117**(6), 1166–9.
Jannetta, P.J., Abbasy, M., Maroon, J.C., Ramos, F.M., & Albin, M.S. (1977). Etiology and definitive microsurgical treatment of hemifacial spasm. Operative techniques and results in 47 patients. *J Neurosurg*, **47**(3), 321–8.
Jannetta, P.J. & Gendell, H.M. (1979). Clinical observations on etiology of essential hypertension. *Surg Forum*, **30**, 431–2.
Jannetta, P.J., Møller, M.B., & Møller, A.R. (1984). Disabling positional vertigo. *N Engl J Med*, **310**(26), 1700–5.
Jannetta, P.J., Segal, R., & Wolfson, S.K. Jr. (1985). Neurogenic hypertension: etiology and surgical treatment. I. Observations in 53 patients. *Ann Surg*, **201**(3), 391–8.

Jannetta, P.J. (1967). Arterial compression of the trigeminal nerve at the pons in patients with trigeminal neuralgia. *J Neurosurg*, **26**, 159–62.

Jannetta, P.J. (1976). Microsurgical approach to the trigeminal nerve for tic douloureux. In: Krayenbuhl, H., Maspes, P.E., & Sweet, W.H. (eds.) *Progress in Neurological Surgery*, vol. **7**, pp. 180–200. Pain—Its neurosurgical management. Basel, Switzerland: Karger Publishers.

Kanpolat, Y., Savas, A., Bekar, A., & Berk, C. (2001). Percutaneous controlled radiofrequency trigeminal rhizotomy for the treatment of idiopathic trigeminal neuralgia: 25-year experience with 1,600 patients. *Neurosurgery*, **48**(3), 524–32; discussion 532–4.

Kawashima, M., Matsushima, T., Inoue, T., Mineta, T., Masuoka, J., & Hirakawa, N. (2010). Microvascular decompression for glossopharyngeal neuralgia through the transcondylar fossa (supracondylar transjugular tubercle) approach. *Neurosurgery*, **66**(6 Suppl Operative), 275–80.

Keravel, Y., Gaston, A., Ciampi de Andrade, D., Mencattini, G., & Le Guérinel, C. (2009). Balloon compression for the treatment of trigeminal neuralgia. *Neurochirurgie*, **55**(2), 197–202.

Kirschner, M. (1933). Die Punktionstechnik unf die Elektroguagulation des Ganglion Gasseri: über gezie Opereationen. *Arch Klin Chir*, **176**, 620.

Lacombe, H. (2009). Surgery for vertigo. *Neurochirurgie*, **55**(2), 268–71.

Laha, R.K. & Jannetta, P.J. (1977). Glossopharyngeal neuralgia. *J Neurosurg*, **47**, 316–20.

Lazorthes, Y. & Verdie, J.C. (1979). Radiofrequency coagulation of the petrous ganglion in glossopharyngeal neuralgia. *Neurosurgery*, **4**, 512–16.

Leal, P.R., Hermier, M., Froment, J.C., Souza, M.A., Cristino-Filho, G., & Sindou, M. (2010). Preoperative demonstration of the neurovascular compression characteristics with special emphasis on the degree of compression, using high-resolution magnetic resonance imaging: a prospective study, with comparison to surgical findings, in 100 consecutive patients who underwent microvascular decompression for trigeminal neuralgia. *Acta Neurochir (Wien)*, **152**(5), 817–25.

Leal, P.R., Hermier, M., Souza, M.A., Cristino-Filho, G., Froment, J.C., & Sindou, M. (2011). Visualization of vascular compression of the trigeminal nerve with high-resolution 3T MRI: a prospective study comparing preoperative imaging analysis to surgical findings in 40 consecutive patients who underwent microvascular decompression for trigeminal neuralgia. *Neurosurgery*, **69**(1), 15–25; discussion 26.

Leksell, L. (1971). Sterotaxic radiosurgery in trigeminal neuralgia. *Acta Chir Scand*, **137**(4), 311–14.

Leveque, M., Park, M.C., Melhaoul, A., Yomo, S., Donnet, A., & Régis, J. (2011). Gamma Knife radiosurgery for glossopharyngeal neuralgia, Marseille: experience. *J Radiosurg SBRT*, **1**, 41–6.

Levy EI, Scarrow AM, & Jannetta PJ (2001). Microvascular decompression in the treatment of hypertension: review and update. *Surg Neurol*, **55**(1), 2–10; discussion 10–11.

Li, S.T., Zhong, J., & Sekula, R.F. Jr. (2016). *Microvascular Decompression Surgery*. New York, NY: Springer Wien New York.

Londero, A. & Chays, A. (2009). Tinnitus treatment: neurosurgical management. *Neurochirurgie*, **55**(2), 248–58.

Marneffe, V., Polo, G., Fischer, C., & Sindou, M. (2003). Microsurgical vascular decompression for hemifacial spasm. Follow-up over one year, clinical results and prognostic factors. Study of a series of 100 cases. *Neurochirurgie*, **49**(5), 527–35.

Mathiesen, T. & Brantberg, K. (2015). Microvascular decompression for typewriter tinnitus-case report. *Acta Neurochir (Wien)*, **157**(2), 333–6.

Matsushima, T., Rhoton, A.L., De Oliveira E, & Peace D (1983). Microsurgical anatomy of the veins of the posterior fossa. *J Neurosurg*, **59**, 63–105.

Mikami, T., Minamida, Y., Ohtsuka, K., & Houkin, K. (2005). Resolution of superior oblique myokymia following microvascular decompression of trochlear nerve. *Acta Neurochir (Wien)*, **147**(9), 1005–6; discussion 1006.

Møller, A.R. & Jannetta, P.J. (1987). Monitoring facial EMG responses during microvascular decompression operations for hemifacial spasm. *J Neurosurg*, **66**(5), 681–5.

Møller, A.R. & Jannetta, P.J. (1984). On the origin of synkinesis in hemifacial spasm: results of intracranial recordings. *J Neurosurg*, **61**(3), 569–76.

Møller, A.R. & Møller, M.B. (1989). Does intraoperative monitoring of auditory evoked potentials reduce incidence of hearing loss as a complication of microvascular decompression of cranial nerves? *Neurosurgery*, **24**(2), 257–63.

Møller, A.R. (2007). Tinnitus and pain. *Prog Brain Res*, **166**, 47–53. Review.

Møller, M.B., Møller, A.R., Jannetta, P.J., Jho, H.D., & Sekhar, L.N. (1993). Microvascular decompression of the eighth nerve in patients with disabling positional vertigo: selection criteria and operative results in 207 patients. *Acta Neurochir (Wien)*, **125**(1–4), 75–82.

Møller, M.B., Møller, A.R., Jannetta, P.J., & Sekhar, L. (1986). Diagnosis and surgical treatment of disabling positional-vertigo. *J Neurosurg*, **64**(1), 21–8.

Mooij, J.J., Mustafa, M.K., & van Weerden, T.W. (2001). Hemifacial spasm: intraoperative electromyographic monitoring as a guide for microvascular decompression. *Neurosurgery*, **49**(6), 1365–70; discussion 1370–1.

Mullan, S. & Lichtor, T. (1983). Percutaneous microcompression of the trigeminal ganglion for trigeminal neuralgia. *J Neurosurg*, **59**(6), 1007–12.

Naraghi, F.H., Schobel, H.P., Heusser, K., Geiger, H., Fahlbusch, R., & Naraghi, R. (2001). Long-term results after microvascular decompression in essential hypertension. *Stroke*, **32**(12), 2950–5.

Parise, M., Acioly, M.A., Ribeiro, C.T., Vincent, M., & Gasparetto, E.L. (2013). The role of the cerebellopontine angle cistern area and trigeminal nerve length in the pathogenesis of trigeminal neuralgia: a prospective case-control study. *Acta Neurochir (Wien)*, **155**(5), 863–8.

Parise, M., Ribeiro, C.T., Vincent, M., & Gasparetto, E. (2010). Small cerebellopontine angle cisterns in patients with trigeminal neuralgia. *J Neurosurg*, **112**(4), 900–1; author reply 901.

Pollock, B.E. (2006). Radiosurgery for trigeminal neuralgia: is sensory disturbance required for pain relief? *J Neurosurg*, **105** Suppl, 103–6. Review.

Polo, G., Fischer, C., Sindou, M.P., & Marneffe, V. (2004). Brainstem auditory evoked potential monitoring during microvascular decompression for hemifacial spasm: intraoperative brainstem auditory evoked potential changes and warning values to prevent hearing loss—prospective study in a consecutive series of 84 patients. *Neurosurgery*, **54**(1), 97–104; discussion 104–6.

Provost, J. & Hardy, J. (1970). Microchirurgie du trijumeau: anatomie fonctionnelle. *Neurochirurgie*, **16**, 459–70.

Régis, J., Arkha, Y., Yomo, S., et al. (2009). Radiosurgery in trigeminal neuralgia: long-term results and influence of operative nuances. *Neurochirurgie*, **55**(2), 213–22.

Régis, J., Tuleasca, C., Resseguier, N., et al. (2016). Long-term safety and efficacy of Gamma Knife surgery in classical trigeminal neuralgia: a 497-patient historical cohort study. *J Neurosurg*, **124**(4), 1079–87.

Ryu, H., Yamamoto, S., Sugiyama, K., & Nuzue, M. (1998). Neuvascular compression syndromes of the eighth nerve. What are the most reliable diagnostic signs. *Acta Neurochir*, **140**, 1279–98.

Samii, M., Rosahl, S.K., Carvalho, G.A., Krzizok, T. (1998). Microvascular decompression for superior oblique myokymia: first experience. Case report. *J Neurosurg*, **89**(6), 1020–4.

Sauvain, M.O., Magistris, M.R., & de Tribolet, N. (2001). Microvascular decompression of the facial nerve. In: Spetzler, R. (ed.) *Operative Techniques in Neurosurgery*, vol. **4**, pp. 127–36. Philadelphia, PA: Saunders.

Sindou, M., Fobé, J.L., Ciriano, D., & Fischer, C. (1992). Hearing prognosis and intraoperative guidance of brainstem auditory evoked potential in microvascular decompression. *Laryngoscope*, **102**(6), 678–82.

Sindou, M., Howeidy, T., & Acevedo, G. (2002). Anatomical observations during microvascular decompression for idiopathic trigeminal neuralgia (with correlations between topography of pain and site of the neurovascular conflict). Prospective study in a series of 579 patients. *Acta Neurochir (Wien)*, **144**(1), 1–12; discussion 12–13.

Sindou, M., Keravel, Y., & Møller, A.R. (eds.) (1997). *Hemifacial Spasm. A Multidipliscinary Approach*. New York, NY: Springer Wien New York.

Sindou, M. & Keravel, Y. (1979). Trigeminal neuralgia. Percutaneous thermocoagulation of the trigeminal nerve (author's transl)). *Neurochirurgie*, **25**(3), 166–72.

Sindou, M. & Keravel, Y. (2009a). Functional neurosurgery for cranial nerve hyperactivity syndromes. *Neurochirurgie*, **55**(2), 75–292.

Sindou, M. & Keravel, Y. (2009b). Neurosurgical treatment of primary hemifacial spasm with microvascular decompression. *Neurochirurgie*, **55**(2), 236–47.

Sindou, M., Leston, J., Decullier, E., & Chapuis, F. (2007). Microvascular decompression for primary trigeminal neuralgia: long-term effectiveness and prognostic factors in a series of 362 consecutive patients with clear-cut neurovascular conflicts who underwent pure decompression. *J Neurosurg*, **107**(6), 1144–53.

Sindou, M., Leston, J., Howeidy, T., Decullier, E., & Chapuis, F. (2006). Microvascular decompression for primary trigeminal neuralgia (typical or atypical). Long-term effectiveness on pain; prospective study with survival analysis in a consecutive series of 362 patients. *Acta Neurochir*, **148**, 1235–45.

Sindou, M., Leston, J.M., Decullier, E., & Chapuis, F. (2008). Microvascular decompression for trigeminal neuralgia: the importance of a noncompressive technique—Kaplan–Meier analysis in a consecutive series of 330 patients. *Neurosurgery*, **63**(4 Suppl 2), 341–50; discussion 350–1.

Sindou, M., Mahmoudi, M., & Brînzeu, A. (2015). Hypertension of neurogenic origin: effect of microvascular decompression of the CN IX-X root entry/exit zone and ventrolateral medulla on blood pressure in a prospective series of 48 patients with hemifacial spasm associated with essential hypertension. *J Neurosurg*, **123**(6), 1405–13.

Sindou, M. (2015). Is there a place for microsurgical vascular decompression of the brainstem for apparent essential blood hypertension? a review. *Adv Tech Stand Neurosurg*, **42**, 69–76.

Sindou, M. & Tatli, M. (2009). Traitement de la névralgie trigéminale par thermocoagumation. *Neurochirurgie*, **55**, 203–10.

Sindou, M.P. (1999). Neurophysiological navigation in the trigeminal nerve: use of masticatory responses and facial motor responses evoked by electrical stimulation of the trigeminal rootlets for RF-thermorhizotomy guidance. *Stereotact Funct Neurosurg*, **73**(1–4), 117–21.

Sindou, M.P. (2005). Microvascular decompression for primary hemifacial spasm. Importance of intraoperative neurophysiological monitoring. *Acta Neurochir (Wien)*, **147**(10), 1019–26; discussion 1026.

Sweet, W.H. & Wepsic, J.G. (1974). Stimulation of the posterior columns of the spinal cord for pain control: indications, technique, and results. *Clin Neurosurg*, **21**, 278–310.

Tatli, M., Satici, O., Kanpolat, Y., & Sindou, M. (2008). Various surgical modalities for trigeminal neuralgia: literature study of respective long-term outcomes. *Acta Neurochirurgica*, **150**, 243–55.

Tatli, M. & Sindou, M. (2008). Anatomoradiological landmarks for accuracy of radiofrequency thermorhizotomy in the treatment of trigeminal neuralgia. *Neurosurgery*, **63**(1 Suppl 1), ONS129–37; discussion ONS137–8.

Tew, J.M. Jr., Tobler, W.D., & Van Loveren, H. (1982). Percutaneous rhizotomy in the treatment of intractable facial pain (trigeminal, glossopharyngeal and vagal nerves). In: Schmidek, H.H. & Sweet, W.H. (eds.) *Operative Neurosurgical Techniques*, vol. **2**, pp. 1083–106. New York, NY: Grune and Stratton.

Tilikete, C. & Vighetto, A. (2009). Vertigo treatment according to their mechanisms. *Neurochirurgie*, **55**(2), 259–67.

Vighetto, A. & Tilikete, C. (2009). Motorocular syndromes due to neurogenic hyperactivity and their treatment. *Neurochirurgie*, **55**(2), 272–8.

Zhong, J., Xia, L., Dou, N.N., et al. (2015). Delayed relief of hemifacial spasm after microvascular decompression: can it be avoided? *Acta Neurochir (Wien)*, **157**(1), 93–8; discussion 98–9.

RELATED LINKS TO EBRAIN

Diagnosis and Treatment of Non-dental Facial Pain. https://learning.ebrain.net/course/view.php?id=102

Diagnosis and Treatment of Trigeminal Neuralgia. https://learning.ebrain.net/course/view.php?id=99

Performing a Microvascular Decompression for Trigeminal Neuralgia. https://learning.ebrain.net/course/view.php?id=596

Performing a Percutaneous Trigeminal Rhizotomy. https://learning.ebrain.net/course/view.php?id=98

80

Neurosurgical interventions for psychiatric disorders

Chris Bervoets, Bart Nuttin, and Loes Gabriëls

Introduction

Psychiatric disorders are among the most prevalent illnesses worldwide and up to one-third of the general population suffers from an anxiety disorder or a depressive disorder (Kessler et al., 2005a; 2005b). Established treatments for psychiatric disorders include pharmacotherapy and psychotherapy. Various non-pharmacological, neuromodulatory strategies comprising electroconvulsive therapy, magnetic seizure therapy, vagal nerve stimulation, repetitive transcranial magnetic stimulation, and deep brain stimulation of psychiatric disorders have been investigated. Although these treatments are at various stages of clinical development, they represent a new frontier in expanding the treatment options available for individuals with psychiatric disorders, as well as contributing to a better understanding of the neurobiology for these disorders. With regard to the understanding of neurobiological aspects, there are well-validated animal models for most of the psychiatric disorders, and further progress in this field is made (e.g. van Kuyck et al., 2007). In combination with prior lesioning experience from published case reports and case series, and with additional information of neuroimaging, target selection is robustly scientifically underpinned. In addition, functional neuroimaging studies and physiological findings while using DBS in the treatment of other conditions have led to investigation of additional targets.

Reports on neurosurgical treatments for psychiatric disorders date back to 1935, with Egas Moniz and Almeida Lima reporting on a series of frontal leucotomies (later renamed 'frontal lobotomy' by Walter Freeman and James Watts) and using the term 'psychosurgery' for the first time (Feldman and Goodrich, 2001). The development of stereotactic techniques by Spiegel and Wycis in the 1940s, followed by the introduction of computed tomography and magnetic resonance imaging, provided an opportunity to perform more accurately upon lesions in the brain. Together with the growing knowledge on the link between specific brain regions and different aspects of behaviour, the development of a standardized nosological system in psychiatry, and the growing use of rating scales to evaluate treatment outcomes, this stereotactic surgery gained ground in the treatment of psychiatric disorders (Larson, 2008). Nevertheless, non-reversible lesioning of brain regions in order to alleviate severe psychiatric symptoms have often been associated with negative connotations, making lesioning procedures less acceptable as a treatment option. The development of deep brain stimulation (DBS) in the 1990s has led to renewed interest in the surgical treatment of psychiatric disorders. Building upon the fact that DBS is a reversible technique, adjustable trough manipulation of contact choice and stimulation parameters without lesioning the targeted neurocircuitry, DBS is perceived as having advantage over lesional surgery by patients. Moreover, due to the possibility to turn stimulation off, more rigorous clinical trials can be conducted in controlled conditions and with blinding of the evaluator to the stimulus condition. DBS has offered hope for patients with severe and incapacitating psychiatric disorders, although the need for large-scale studies with long-term follow-up remains paramount (Gabriëls, 2010; Luyten et al., 2016). In this chapter we will (i) provide the pathophysiological basis of psychiatric disorders with relevance to neurosurgical intervention; (ii) describe the pre- and postoperative management of the patient as well as the surgical techniques; and (iii) discuss methodological problems that hamper future development of this treatment technique in psychiatry.

Preoperative management of the patient

Patient selection

Only patients aged over 18, with a documented, otherwise treatment refractory, severe, chronic, disabling psychiatric disorder should be considered for surgical intervention. The potential benefit from an intervention must be balanced against the risks imposed by surgery (Gabriëls, 2010). Obsessive-compulsive disorder, Tourette's syndrome, and major depressive disorder might benefit from surgical intervention. In those patients, a history of personality disorder, active substance abuse or other Axis II symptomatology are (relative) contraindications for surgery. A critical issue in patient selection remains the development of solid criteria for severity, chronicity, disability, and treatment refractoriness. Severity is measured using validated clinical research instruments corresponding

to specific indicators such as a Yale-Brown Obsessive-Compulsive Scale (YBOCS) score of more than 30 for OCD or a Montgomery-Åsberg Depression Rating Scale (MADRS) of more than 30 in major depression. Disability is commonly assessed by a Global Assessment of Function (GAF) score of less than 50. Treatment refractoriness needs to be documented by the treating psychiatrist describing all appropriate treatment (specifying dose and treatment duration) according to current published guidelines (Bandelow et al., 2008). Moreover, the psychiatrist needs to provide ongoing commitment to the patient and the evaluation process, and needs to agree to take responsibility for postoperative (non-DBS related) management. The patient and their family must also agree to fully participate. It is advisable to include a family member or close relative in the evaluation process.

Presurgical screening

As a next step, a second opinion by another psychiatrist well acquainted with the disorder can be required (e.g. for surgical treatment of OCD in Belgium) and added to the application file. In Belgium, an experienced, multidisciplinary group of psychiatrists, neurosurgeons, in the presence of an ethicist conducts a thorough review of the medical records. A brain MRI is added to the evaluation, as well neuropsychological testing. Moreover, the requirements for informed consent must be fulfilled.

Surgical technique

Lesional surgery

Four procedures, anterior cingulotomy, subcaudate tractotomy, limbic leucotomy, and anterior capsulotomy, are considered safe and effective for OCD (Jenike, 1998). All procedures are usually performed bilaterally and under stereotactic conditions to allow for precise lesioning of target structures. The anterior cingulum was considered an appropriate target for surgical intervention (Fulton, 1951) in patients with intractable pain and concurrent mixed anxiety-depressive states. Currently, the surgical indications are treatment refractory major depressive disorder, chronic anxiety states, or OCD. Subcaudate tractotomy was introduced in 1964 (Knight, 1964; Knight, 1969) as one of the first attempts to restrict the size of the surgical lesion and therefore minimize the side effects seen with standard prefrontal lobotomy. The aim was to interrupt white matter tracts between orbital cortex and subcortical structures by placing a lesion in the region of the substantia innominata just below the head of the caudate nucleus. Surgical indications included major depressive illness, obsessive-compulsive disorder, and anxiety states. Limbic leucotomy (Kelley et al., 1973) combines subcaudate tractotomy with anterior cingulotomy. This procedure was designed to disconnect orbital-frontal-thalamic pathways with the former lesion and interrupt an important portion of Papez's circuit with the latter. Indications for surgical intervention included obsessional neurosis, anxiety states, depression, and a variety of other psychiatric diagnoses. The aim in anterior capsulotomy (Talairach et al., 1949) is to interrupt fronto-thalamic connections in the anterior limb of the internal capsule where they pass between the head of the caudate nucleus and the putamen. Clinical indications for capsulotomy include depression, chronic anxiety states, and obsessional neurosis.

Deep brain stimulation (DBS)

DBS produces an enduring electrical modulation of targeted deep subcortical brain structures. The lead placement depends on the condition being treated and implantation is done via burr holes in the skull using neuroimaging guided stereotactic neurosurgical techniques. Each lead consists of an electrode array containing usually four electrode contacts spanning 10–20 mm, depending on the lead type. After implantation, the leads are connected via subcutaneous extension wires to one or two subcutaneously implanted battery-operated pulse generators (IPG). The IPG is typically implanted in the subclavicular or abdominal region. Stimulation parameters (contacts used, frequency, pulse width, amplitude) are non-invasively adjusted via a physician-operated patient programmer. Clinically used parameter settings are typically in the range of 60–130 Hz, 60–450 microseconds pulse width, and 2–10 volts, either in monopolar or bipolar stimulation mode (Holtzheimer and Mayberg, 2011). Although DBS is perceived as having an advantage over lesioning procedures, it still is associated with serious risks as intracranial haemorrhage and infection and also complications associated with anaesthesia (Luyten et al., 2016). Moreover, fractures of the implanted lead or extension wire, compliance issues, and the need for frequent IPG replacements due to end of life of the battery are disadvantages that are observed with the use of DBS (Nuttin et al., 2003; Visser-Vandewalle et al., 2003; Abelson et al., 2005; Houeto et al., 2005; Machado et al., 2005; Mayberg et al., 2005). The first DBS targets for OCD were the internal capsule (with its ventral portion referred to as ventral capsule, VC, with inclusion of the bed nucleus of the stria terminalis, BST) and the ventral striatum, or VS (sometimes referred to as including the nucleus accumbens, NAcc). This selection was based on former stereotactic lesioning procedures for the same disorder (Jenike, 1998; Lippitz et al., 1999; Dougherty et al., 2002; Greenberg et al., 2003; Sturm et al., 2003). Our group reported on the use of DBS in the anterior limb of the internal capsule (Nuttin et al., 1999; Nuttin et al., 2003) and BST (Luyten et al., 2016). It is of relevance to point out that a DBS lead spanning this region is capable of influencing any of the aforementioned structures, depending on lead geometry and stimulation parameter settings (Larson, 2008). After the serendipitous finding of alleviation of OCD symptoms with stimulation of specific subdivisions of the subthalamic nucleus in patients who suffered from parkinsonism and OCD, efforts were directed to this node in the cortico-striato-thalamo-cortical circuitry. Case studies report on electrical stimulation for psychiatric disorders in different other targets, for example, in the inferior thalamic peduncle and the internal globus pallidus (GPi).

Postoperative management of the patient

In the phase of postoperative management of the patient, the neurosurgical team should work in close communication with the psychiatric team. As neurosurgery is considered a last resort treatment for patients with chronic and severe psychiatric symptoms, the postoperative psychological and emotional guidance of the patient and the family are of utmost importance. Often, early and dramatic changes in primary symptoms are noted in the patient, with impact on the whole system of surrounding close thirds. It requires counselling and time to find a new equilibrium within the family

or relation. Moreover, optimization of stimulation parameters is a complex and lengthy procedure and requires a supportive attitude from the psychiatrist and family. Moreover, parameter adjustment is best kept under the responsibility of the same physician to allow for intraindividual observation of stimulation related changes in patient's attitude and behaviour.

Future questions

Better understanding of the neurobiology of emotion through basic research may lead to better target selection and more accurate implantation. Combined with findings from further research in non-invasive techniques (e.g. transcranial magnetic stimulation, transcranial direct current stimulation) a new field of research in neuromodulation methods is currently expanding for the treatment refractory psychiatric patients. These techniques have the advantage of allowing double-blind placebo-controlled trials. This was not possible with the former lesioning procedures because of their irreversible and invasive nature. Due to this progress in scientific methodology currently used, an evidence-based statement on safety and efficacy of neurosurgical procedures for treatment refractory psychiatric disorders under investigation becomes possible. Moreover, the use of the invasive procedures is tightly linked with high standard ethical and clinical review boards.

However, we should remain cautious with regard to target selection. In DBS a multitude of targets is explored with growing methodological precision for the same psychiatric indication, and the same target is used for different psychiatric disorders. Secondly, stimulation parameters have an impact on the efficacy of DBS in a patient. At this moment we lack efficient algorithms for optimal parameter selection. Kuncel calculated that above the multiple possible anatomical targets 12 964 combinations of pulse width, frequency, and voltage and 65 combinations of electrode geometry were available within a recommended charge density limit for a given IPG (Kuncel and Grill, 2004). Maybe progress in this field can be made when mathematical models of tissue characteristics and network connectivity maps (built from diffusion tensor imaging) of the target are available to guide the clinician in selecting, improving, and optimizing stimulation parameters in individual patients (Astrom et al., 2009). Lastly, with the emerging research of non-invasive neuromodulation such as TMS, exploration of clinical efficacy of TMS should be compared to results of DBS. This will help to position both invasive and non-invasive neuromodulation in future treatment algorithms.

REFERENCES

Abelson, J.L., Curtis, G.C., Sagher, O., et al. (2005). Deep brain stimulation for refractory obsessive-compulsive disorder. *Biol Psychiatry*, **57**, 510–16.

Astrom, M.., Zrinzo, L.U., Tisch, S., Tripoliti, E., et al. (2009). Method for patient-specific finite element modeling and simulation of deep brain stimulation. *Med Biol Eng Comput*, **47**, 21–8.

Bandelow, B., Zohar, J., Hollander, E., Kasper, S., & Möller, H.J. (2008). World Federation of Societies of Biological Psychiatry (WFSBP) guidelines for the pharmacological treatment of anxiety, obsessive-compulsive and post-traumatic stress disorders—first revision. *World J Biol Psychiatry*, **9**(4), 248–312.

Dougherty, D.D., Baer, L., Cosgrove, G.R., et al. (2002). Prospective long-term follow-up of 44 patients who received cingulotomy for treatment-refractory obsessive-compulsive disorder. *Am J Psychiatry*, **159**, 269–75.

Feldman, R.P. & Goodrich, J.T. (2001). Psychosurgery: a historical overview. *Neurosurgery*, **48**, 647–57; discussion 657–49.

Fulton, J.E. (1951). *Frontal Lobotomy and Affective Behavior: A Neurophysiological Analysis*. New York, NY: WW Norton.

Gabriëls, L. (2010). Deep brain stimulation for psychiatric disorders. *Psychiatria Danubina*, **22**, Suppl 1, 162.

Greenberg, B.D., Price, L.H., Rauch, S.L., et al. (2003). Neurosurgery for intractable obsessive-compulsive disorder and depression: critical issues. *Neurosurg Clin N Am*, **14**, 199–212.

Holtzheimer, P.E. & Mayberg, H.S. (2011). Deep brain stimulation for psychiatric disorders. *Annu Rev Neurosci*, **34**, 289–307.

Houeto, J.L., Karachi, C., Mallet, L., et al. (2005). Tourette's syndrome and deep brain stimulation. *J Neurol Neurosurg Psychiatry*, **76**, 992–5.

Jenike, M.A. (1998). Neurosurgical treatment of obsessive-compulsive disorder. *Br J Psychiatry Suppl*, (35), 79–90.

Kelley, D., Richardson, A., & Mitchell-Heggs, N. (1973). Stereotactic limbic leucotomy: neurophysiologic aspects and operative technique. *Br J Psychiatry*, **123**, 133–40.

Kessler, R.C., Berglund, P., Demler, O., Jin, R., Merikangas, K.R., & Walters, E.E. (2005a). Lifetime prevalence and age-of-onset distributions of DSM-IV disorders in the National Comorbidity Survey Replication. *Arch Gen Psychiatry*, **62**(6), 593–602. Erratum in: *Arch Gen Psychiatry* (2005), **62**(7), 768. Merikangas, K.R. [added].

Kessler, R.C., Chiu, W.T., Demler, O., Merikangas, K.R., & Walters, E.E. (2005b). Prevalence, severity, and comorbidity of 12-month DSM-IV disorders in the National Comorbidity Survey Replication. *Arch Gen Psychiatry*, **62**(6), 617–27. Erratum in: *Arch Gen Psychiatry* (2005), **62**(7), 709. Merikangas, K.R. [added].

Knight, G.C. (1964). The orbital cortex as an objective in the surgical treatment of mental illness. The development of the stereotactic approach. *Br J Surgery*, **51**, 114–24.

Knight, G.C. (1969). Bifrontal stereotactic tractotomy: an atraumatic operation of value in the treatment of value in the treatment of psychoneurosis. *Br J Psychiatry*, **115**, 257–66.

Kuncel, A.M. & Grill, W.M. (2004). Selection of stimulus parameters for deep brain stimulation. *Clin Neurophysiol*, **115**(11), 2431–41.

Larson, P.S. (2008). Deep brain stimulation for psychiatric disorders. *Neurotherapeutics*, **5**, 50–8.

Lippitz, B.E., Mindus, P., Meyerson, B.A., et al. (1999). Lesion topography and outcome after thermocapsulotomy or gamma knife capsulotomy for obsessive-compulsive disorder: relevance of the right hemisphere. *Neurosurgery*, **44**, 452–8; discussion 458–60.

Luyten, L., Hendrickx, S., Raymaekers, S., Gabriëls, L., & Nuttin, B. (2016). Electrical stimulation in the bed nucleus of the stria terminalis alleviates severe obsessive-compulsive disorder. *Mol Psychiatry*, **21**(9), 1272–80.

Machado, A.G., Hiremath, G.K., Salazar, F., et al. (2005). Fracture of subthalamic nucleus deep brain stimulation hardware as a result of compulsive manipulation: case report. *Neurosurgery*, **57**, E1318.

Mayberg, H.S., Lozano, A.M., Voon, V., et al. (2005). Deep brain stimulation for treatment-resistant depression. *Neuron*, **45**, 651–60.

Nuttin, B., Cosyns, P., Demeulemeester, H., et al. (1999). Electrical stimulation in anterior limbs of internal capsules in patients with obsessive-compulsive disorder. *Lancet*, **354**, 1526.

Nuttin, B.J., Gabriëls, L.A., Cosyns, P.R., et al. (2003). Long-term electrical capsular stimulation in patients with obsessive-compulsive disorder. *Neurosurgery*, **52**, 1263–72; discussion 1272–64.

Sturm, V., Lenartz, D., Koulousakis, A., et al. (2003). The nucleus accumbens: a target for deep brain stimulation in obsessive-compulsive- and anxiety-disorders. *J Chem Neuroanat*, **26**, 293–9.

Talairach, J., Hecaen, H., & David, M. (1949). *Lobotomie prefrontale limitee par electrocoagulation des fibres thalamo-frontalis leur emergence du bras anterior de la capsule interne*. In: Proceedings of the 4th Congress Neurologique Internationale, Paris, France: Masson, p. 141.

van Kuyck, K., Gabriëls, L., Cosyns, P., et al. (2007). Behavioural and physiological effects of electrical stimulation in the nucleus accumbens: a review. *Acta Neurochir Suppl*, **97**(Pt 2), 375–91.

Visser-Vandewalle, V., Temel, Y., Boon, P., et al. (2003). Chronic bilateral thalamic stimulation: a new therapeutic approach in intractable Tourette's syndrome. Report of three cases. *J Neurosurg*, **99**, 1094–100.

SECTION 17
Epilepsy

81. **Classification of seizures and epilepsy** *935*
Andrew McEvoy, Tim Wehner, and Victoria Wykes

82. **Epilepsy—diagnosis and assessment** *945*
Richard Selway

83. **Surgical management of epilepsy** *957*
Johannes Schramm

81

Classification of seizures and epilepsy

Andrew McEvoy, Tim Wehner, and Victoria Wykes

Introduction

Epileptic seizures are frequently seen as either a presenting symptom or a comorbidity of intracranial pathology encountered by neurosurgeons. The following chapter discusses the current practical definition of epilepsy proposed by the International League against Epilepsy (ILAE) in 2014, and provides an overview of seizure manifestations, reviews two common epilepsy aetiologies amenable to surgical treatment: focal cortical dysplasia and hippocampal sclerosis, and provides an overview of the limbic system anatomy.

An epileptic seizure is a transient occurrence of signs and/or symptoms due to abnormal excessive or synchronous neuronal activity in the brain (Fisher et al., 2005). Electrographic seizures without any clinical correlate are termed 'subclinical seizures'. Clinical seizure symptoms may be divided into obvious behavioural manifestations ('positive symptoms', e.g. involuntary movements such as clonic jerks), changes in the patient's subjective experience of them self and their surroundings (aura), and impairment of cerebral functions compared to the patient's baseline ('negative symptoms'). In particular, cognitive changes as a seizure manifestation may be subtle and only apparent if the patient is adequately assessed for these. An epileptic seizure is foremost a symptom and may indicate an acute medical or neurological illness (i.e. a provoked seizure). Epilepsy has been traditionally defined as the recurrence of unprovoked seizures. To account for epidemiologic data on risk stratification after first unprovoked epileptic seizures, and to include rare clinical scenarios of similar underlying pathophysiology, the ILAE has recently proposed a practical definition of epilepsy (Fisher et al., 2014; see also **Box 81.1**). Of these, scenario 1 is by far the most common in neurosurgical practice. This definition includes an element of risk stratification. Somewhat arbitrarily, a person is thought to have epilepsy after a single unprovoked epileptic seizure if they have a 60% chance of recurrence risk over the next 10 years without treatment.

The following clinical scenarios illustrate the concepts of provoked seizures and epilepsy.

1. 'Febrile seizures in infancy'—up to 5% of children under the age of 5 years have a convulsive seizure in the setting of a febrile illness. These are considered provoked epileptic seizures that do not constitute epilepsy (even though the recurrence risk with further febrile illnesses is 40%).
2. A person with an acute central nervous system (CNS) pathology such as meningitis or encephalitis, subdural hematoma, ischaemic stroke, or traumatic brain injury may have an epileptic seizure at the onset or in the early phase (arbitrarily defined as the first seven days) of the acute illness. These seizures are considered provoked epileptic seizures. Since all cortical pathologies increase the risk for epilepsy, these patients may be at risk of developing epilepsy, however, one would not consider them to have epilepsy during the acute phase of the illness. A person who has a seizure more than 1 week after an acute CNS insult (unprovoked epileptic seizure) is thought to carry a more than 60% chance of experiencing further seizures and would thus be considered to have epilepsy even after their first seizure.
3. A person with a focal motor seizure affecting the left arm who is found to have a meningioma along the right frontal convexity meets the practical ILAE definition of epilepsy even after their first seizure. This is because the presence of the meningioma increases the risk of further seizures in this patient.

Focal and generalized seizures

Generalized seizures are conceptualized as originating at some point within and rapidly engaging bilaterally distributed networks (Berg et al., 2010).

Focal seizures are conceptualized as originating at some point within networks limited to one hemisphere (Berg et al., 2010). It may stay confined to this area, or evolve further within the same hemisphere or both hemispheres. A focal seizure may thus evolve into a bilateral convulsive seizure ('secondarily generalized seizure').

Seizure types have been traditionally classified under these two subcategories. However, the semiology (i.e. clinical manifestations) of a seizure is not specific for either subcategory. For example, atonic seizures, clonic seizures, tonic seizures, and myoclonic jerks may be generalized or focal in origin (and thus only affect one or unilateral extremities). The clinical manifestation of a typical absence seizure (brief interruption of consciousness with immediate full recovery) may be emulated by a focal seizure (e.g. arising from the frontal pole). Conversely, it is increasingly recognized that generalized tonic-clonic seizures may have focal semiological features. Epileptic

Box 81.1 Conceptual definitions of seizure and epilepsy and practical definition of epilepsy

An epileptic seizure is a transient occurrence of signs and/or symptoms due to abnormal excessive or synchronous neuronal activity in the brain.

Epilepsy is a disease of the brain defined by any of the following conditions:

1. At least two unprovoked (or reflex) seizures occurring more than 24 h apart
2. One unprovoked (or reflex) seizure and a probability of further seizures similar to the general recurrence risk (60% or more) after two unprovoked seizures, over the next 10 years
3. Diagnosis of an epilepsy syndrome

a) Reproduced with permission from Jerome Engel, Phillip Lee, Pierre Genton, et al., Epileptic Seizures and Epilepsy: Definitions Proposed by the International League Against Epilepsy (ILAE) and the International Bureau for Epilepsy (IBE), *Epilepsia*, Volume 46, Issue 4, pp. 470–2, Copyright © 2005 John Wiley and Sons.

b) Reproduced with permission from Samuel Wiebe, Masako Watanabe, Torbjörn Tomson, et al., ILAE Official Report: A practical clinical definition of epilepsy, *Epilepsia*, Volume 55, Issue 4, pp. 475–82, Copyright © 2014 John Wiley and Sons.

spasms, a common seizure type in infants with tuberous sclerosis or other gross brain pathology, have features of both generalized and focal seizures (bihemispheric EEG involvement from the onset, but in some cases amenable to surgical cure by resective neurosurgery restricted to one hemisphere (Chugani et al., 2015). The semiologic seizure classification proposed by Lüders et al. (1998), and increasingly utilized by epilepsy surgery centres around the world, classifies seizures exclusively on their phenomenology.

The vast majority of seizures and epilepsies encountered by the neurosurgeons are (primarily) focal seizures. Traditionally, these are divided into those with preserved awareness ('simple partial seizures') and those with impaired awareness ('complex partial seizures'). While alteration of consciousness often defines the morbidity of seizures (with implications for driving, employment, and leisure activities), it is not possible to infer reliably from the patient's account or their behaviour whether consciousness was preserved or impaired during a seizure.

Any seizure may cause alterations in these four domains: (1) subjective experience of self and environment; (2) awareness, cognition, and memory formation; (3) autonomic alterations; and (4) motor and behavioural manifestations. Whereas the latter are usually obvious, registration of changes in the first three domains depends on the way a person is assessed during and after a seizure. Some but not all semiological features of seizures can be reproduced during direct electrocortical stimulation of specific brain areas. These include elementary or complex visual hallucinations or blindness in the primary visual cortex, and somatosensory hallucinations (tingling) in the primary sensory cortex. Other subjective manifestations are very typical for seizures arising in the limbic system, in particular in the amygdalo-hippocampal complex of the mesial temporal lobe. These include sensations of familiarity ('déjà vu', 'déjà entendu') or alienation ('jamais vu', 'jamais entendu'), a rising sensation in the epigastrium and/or chest, and (usually unpleasant) olfactory and gustatory hallucinations, the latter often with a 'metallic' character. Some motor manifestations can be consistently reproduced during electrocortical stimulation as well. These are myoclonic or tonic contractions of the contralateral face and distal extremities in the primary motor cortex of the precentral gyrus, proximal tonic contractions in the supplementary sensorimotor area in the mesial aspect of the superior frontal gyrus, and contralateral eye and head deviation in the frontal eye fields. So-called negative motor phenomena (i.e. interruption or cessation of a movement or speech) can be reproduced during cortical stimulation of premotor areas, usually just anterior to the primary motor cortex. Observation of these symptoms and signs during a seizure suggests that the respective cortical areas are involved at a given time during the seizure. This is especially relevant since seizures with purely subjective symptoms (i.e. epileptic auras) or focal clonic or tonic contractions are often not detectable on scalp EEG. This is because the amount of cortex that needs to be ictally activated to generate these symptoms is usually smaller than the area of cortex required to generate an ictal pattern on scalp EEG. Patients with focal motor seizures of the face, arm, or leg may indeed have a completely normal ictal and interictal EEG.

On the other hand, complex movements (automatisms) such as lip smacking, chewing, hand fumbling, or grasping, leg pedalling or kicking, and whole-body rotation, cannot be reproducibly evoked during cortical stimulation, suggesting that these represent release phenomena with no specific cortical representation. In their extreme form, complex movements (the term 'complex' refers to the complexity of the movement, and not the state of consciousness) can present as 'bizarre' behaviour inappropriate for the situational context, such as jumping, rocking, thrashing, shouting, whistling, or kissing).

Alteration of awareness is a common and disabling feature of generalized and focal epilepsies arising from virtually any brain area. Alteration of awareness is thus not a symptom with localizing or lateralizing value. The commonly used term 'absence' refers to a brief (typically 5–10 seconds) generalized seizure defined by loss of consciousness with no or very subtle motor manifestations, and immediate postictal recovery, associated with generalized 3 Hz spike and wave complexes on EEG. Therefore, a focal seizure with loss of awareness is not an absence seizure.

Autonomic symptoms and signs are common in focal and generalized convulsive seizures, and usually reflect sympathetic activation (e.g. tachycardia and hyperventilation), however, bradycardia and apnoea may also occur. Gastrointestinal manifestations include ictal nausea, vomiting, and defecation. Urogenital features of seizures are incontinence, ictal or postictal urinary urge, and genital sensations. Patients may also complain of a sensation of heat or exhibit flushing. Cerebral areas involved in the generation of autonomic features are the medial prefrontal cortex, insula, amygdala, and cingulate. Generally speaking, ictal autonomic manifestations have little lateralizing or localizing value. An exception is the typical rising epigastric sensation seen in mesial temporal lobe epilepsy.

A further layer of localizing symptoms and signs in epileptic seizures stems from the correlation of ictal and postictal features with information about the seizure 'focus' using MRI, ictal EEG, and, ultimately, cessation of seizures following resective neurosurgery. Localizing and lateralizing value of common ictal symptoms and signs are summarized in Tables 81.1 and 81.2.

Epilepsy syndromes

Epilepsy syndromes combine certain clinical features, such as seizure types, the age (group) of the patient, comorbidities, and sometimes

Table 81.1 Localizing and lateralizing value of epileptic auras

Aura subtype	Symptomatogenic zone	Lateralization	Commonly associated focal epilepsy syndrome
Somatosensory (tingling, crawling sensation)	Primary somatosensory cortex	Contralateral	Parietal lobe epilepsy
	Secondary somatosensory area	Ipsilateral (if unilateral)	Parietal and temporal lobe epilepsy
	Supplementary sensorimotor area (SSMA)	Contralateral (mostly)	Frontal and parietal lobe epilepsy
Elementary visual (flashes, stars, and so on)	Primary visual cortex	Contralateral	Occipital lobe epilepsy
Complex visual (formed visual hallucinations)	Temporooccipital junction, basal temporal lobe, limbic system	Contralateral (if unilateral)	Occipital and temporal lobe epilepsy
Elementary auditory (simple sounds or deafness)	Primary auditory cortex	Contralateral (if unilateral)	Temporal lobe epilepsy
Complex auditory (noises, voices, music)	Auditory association cortex and limbic system	Contralateral (if unilateral)	Temporal lobe epilepsy
Vertiginous	Temporo-occipital junction	Not lateralizing	Temporal lobe epilepsy
Olfactory	Orbitofrontal cortex, amygdala, insula	Not lateralizing	Mesial temporal and Frontal lobe epilepsy
Gustatory	Parietal operculum and basal temporal cortex	Not lateralizing	Temporal lobe epilepsy
Abdominal	Anterior insula, frontal operculum, SSMA	Not lateralizing	Mesial temporal lobe epilepsy
Fear	Amygdala, hippocampus, mesial frontal lobe	Not lateralizing	Temporal lobe and frontal lobe epilepsy
Déjà vu, jamais vu, revocation of complex memories	Uncus, entorhinal cortex, temporal neocortex, limbic system	Not lateralizing	Temporal lobe epilepsy
Whole-body sensations	Amygdala, entorhinal cortex, secondary somatosensory area, supplementary sensorimotor area	Not lateralizing	Temporal and frontal lobe epilepsy
Autonomic (palpitations, shortness of breath, feeling hot or cold, genitourinary urge)	Amygdala, insula, anterior cingulum, medial prefrontal cortex	Not lateralizing (often non-dominant)	Temporal and frontal lobe epilepsy

Adapted from *Epilepsy & Behavior*, Volume 20, issue 2, Nancy Foldvary-Schaefer, Kanjana Unnwongse, Localizing and lateralizing features of auras and seizures, pp. 160–6, Copyright (2011), with permission from Elsevier.

Table 81.2 Localizing and lateraling value of objective seizure manifestations

Ictal sign	Common symptomatogenic area or mechanism	Lateralization	Commonly associated focal epilepsy syndrome
Myoclonus, negative myoclonus	Primary motor cortex, premotor cortex	Contralateral (if unilateral)	Frontal lobe epilepsy
Clonic jerks	Primary motor cortex, premotor cortex, SSMA	Contralateral (if unilateral)	Frontal lobe epilepsy
Tonic contractions or tonic posturing	Primary motor cortex, SSMA; activation of basal ganglia	Contralateral (if unilateral)	Frontal and temporal lobe epilepsy
Asymmetric limb posturing	SSMA, precentral area	Not lateralizing	Frontal and temporal lobe epilepsy
Immobile limb	Activation of negative motor areas or ictal exhaustion of primary or premotor cortex	Contralateral	Frontal lobe epilepsy
Automatisms	Orbitofrontal area, cingulum, opercular/insula cortex, mesial frontal area anterior to SSMA	Not lateralizing	Temporal, frontal, and parietal epilepsy
Automatisms with preserved awareness	Orbitofrontal area, cingulum, opercular/insula cortex, mesial frontal area anterior to SSMA	Non-dominant	Temporal, frontal, and parietal epilepsy
Eye and head version (sustained deviation to one side, often associated with hyperextension of the neck)	Frontal eye field, extrastriate cortex, premotor areas	Contralateral	Frontal epilepsy, also seen prior to secondary generalization of seizures arising in temporal, parietal, or occipital lobe
Ictal/postictal aphasia[1]	Anterior and posterior language areas, arcuate fasciculus	Dominant	Temporal and frontal lobe epilepsy
Ictal speech[2]	Excitation of non-dominant hemisphere or Inhibition of dominant hemisphere	Non-dominant	Temporal and frontal lobe epilepsy
Laughter	Hypothalamus, antero-mesial frontal area, basal temporal area	Not lateralizing	Temporal and frontal lobe epilepsy

SSMA, supplementary sensorimotor area.

[1] Ictal/postictal aphasia is defined as language impairment out of proportion to impairment of awareness

[2] Ictal speech is defined as intelligible speech during impaired of awareness

genetic information. While knowledge in the latter domain is rapidly expanding, this information is typically of little relevance to the neurosurgeon. Focal epilepsy syndromes are traditionally divided by anatomical localization of the epileptogenic zone (i.e. the area that is necessary and sufficient to generate seizures). It is important to note that none of the listed 'typical' seizure manifestations are absolutely specific for the given anatomical location. One reason for this is that the area of seizure origin (ictal onset zone) may be distinct from the area that generates the first seizure symptoms (symptomatogenic zone). For example, a rising epigastric sensation ('abdominal aura') is a classic symptom of mesial temporal lobe epilepsy, although this symptom can be evoked by electrocortical stimulation of the anterior insula, and can therefore occur in insular epilepsy as well.

Mesial temporal lobe epilepsy (mTLE) is the most common focal epilepsy syndrome. Common pathological substrates of mTLE are hippocampal sclerosis, cavernoma, low grade brain tumours, focal cortical dysplasia, encephalomalacia, and hamartomas. However, about 30–40% of patients have no identifiable pathology on MR imaging (Tatum, 2012). Patients with mTLE often report a history of febrile convulsions, CNS infection, or precipitating CNS injury in early childhood. There is often a latency period of 5–20 or more years prior to the onset of habitual seizures. Typical aura symptoms are a rising epigastric sensation, nausea, or unnatural and usually unpleasant olfactory or gustatory hallucinations, as well as sensations of familiarity (déjà vu, déjà entendu), or estrangement from the environment (jamais vu, jamais entendu), complex visual or auditory hallucinations, affective symptoms, or fear. These symptoms have no lateralizing value (Ferrari-Marinho et al., 2012).

In neocortical temporal lobe epilepsy (nTLE), the seizure onset tends to occur in early adulthood. Typical aura symptoms, reported by about 50–75% of patients, are simple auditory hallucinations (ringing or buzzing noises), muffled or distorted auditory perception (e.g. echoes), and a sensation of dizziness, unsteadiness, or vertigo.

Common objective symptoms of seizures arising in the temporal lobe are loss of awareness, semi-purposeful oral and manual automatisms, and dystonic posturing of contralateral limbs (Kuba et al., 2010). Some patients exhibit more complex behaviours such as wandering, drinking, or kissing, the latter two associated with non-dominant onset (Rashid et al., 2010). Autonomic features such as mydriasis, hypersalivation, vomiting, piloerection, and heart rate alterations are often seen. In TLE, symptoms tend to evolve gradually over the course of tens of seconds. The postictal period is characterized by confusion and amnesia for the seizure. Variable language impairment, ranging from global aphasia to word finding difficulties, is a common postictal symptom in seizures arising from the dominant temporal lobe.

Typical seizure features of frontal lobe epilepsy (FLE) reflect the complex functional connections within the frontal lobe and to neighbouring temporal, insular, and parietal areas. Auras in FLE are often non-specific. Patients may report or exhibit a facial expression of anxiety or fear, epigastric auras, and déjà vu (von Lehe et al., 2012), or report an ill-defined sensation of movement in the head ('cephalic aura'; see Canuet et al., 2008), sometimes associated with blurred vision (Beauvais et al., 2005). Objective behavioural manifestations of seizures involving the prefrontal areas often appear unnatural or bizarre, such as bicycling or scissoring leg automatisms, shuddering, pelvic thrusting, jumping, kicking, thrashing, crawling, and unformed vocalizations (Wehner et al., 2017). Seizures involving the supplementary sensorimotor area (SSMA) feature symmetrical or asymmetrical tonic contractions of face, throat, and limb muscles (Unnwongse et al., 2012), whereas involvement of the primary motor cortex is suggested by unilateral clonic jerking, often in a 'Jacksonian march' (i.e. sequentially involving the face, upper and lower extremity, or vice versa). Loss of postural tone (ictal atonia) may lead to head drop or falls. Awareness is often preserved in focal seizures involving the elementary motor system, even when bilateral motor features are present.

Seizure onset and offset in FLE are often abrupt, the seizures often occur repeatedly during sleep, and are typically shorter (on the order of 30 ± 15 seconds) than those seen in TLE.

The characteristic aura of seizures arising in the parietal lobe is a sensation of numbness, tingling or crawling in contralateral hemibody areas, in particular if presenting as a Jacksonian march. Other subjective symptoms are a disturbance of body image, illusions of movement, vertigo, and complex visual or auditory illusions. Objective behavioural manifestations are non-specific and may reflect ictal propagation into primary motor areas or SSMA (focal clonic activity contralateral to the side of seizure onset, tonic posturing), or the temporo-limbic system (behavioural arrest, automatisms, Wehner et al., 2017). Parietal lobe epilepsy therefore appears to be characterized by the absence of specific features (except for the somatosensory aura), and has been named the 'great imitator' among focal epilepsy syndromes (Ristic et al., 2012).

Patients with occipital lobe epilepsy (OLE) often report visual auras, ranging from flickering or flashing lights or shapes to distortions of proportions and colours, or formed visual hallucinations. Epileptic visual auras are shorter (seconds to few minutes) than visual auras reported by migraineurs (4–20 minutes, Adcock and Panayiotopoulos, 2012). Paraesthesias, epigastric sensations, and experiential symptoms suggest involvement of adjacent parietal or temporal-limbic areas (Bien et al., 2000; Jobst et al., 2010). Objective ictal manifestations in OLE are rapid eye blinking or eyelid flutter (Kun Lee et al., 2005; Tandon et al., 2009), and pursuit-like involuntary eye movements or nystagmus (Adcock and Panayiotopoulos, 2012). Depending on the seizure propagation, further signs mimic those seen in TLE (e. g. loss of contact, oral and gestural automatisms) and FLE (e.g. dystonic posturing and hyperkinetic automatisms; see Jobst et al., 2010).

Importantly, motor manifestations of epileptic seizures vary with age. Whereas myoclonic or bilateral tonic features and infantile spasms are the predominant semiology in infants and young children (Nordli, 2013), motor features and lateralizing signs tend to become more prevalent and prominent in parallel to developmental brain maturation (Fogarasi et al., 2007). In older people, secondarily generalized seizures and prolonged postictal symptoms such as confusion, memory impairment, and Todd's paresis are more common compared to younger patients (Stefan et al., 2014).

Status epilepticus

Most seizures terminate spontaneously after a few minutes. The term status epilepticus refers to the most extreme form of a seizure that does not self-terminate. The ILAE has recently revised its definition of status epilepticus as 'a condition resulting either from the failure

of the mechanisms responsible for seizure termination or from the initiation of mechanisms which lead to abnormally prolonged seizures (after time point t1). It is a condition that can have long-term consequences (after time point t2), including neuronal death, neuronal injury, and alteration of neuronal networks, depending on the type and duration of seizures' (Trinka et al., 2015). More than half of the patients with status epilepticus have an acute or remote central nervous system lesion or a systemic medical illness at the time of presentation. From a clinical perspective, generalized tonic-clonic seizures should be terminated within five minutes, and focal seizures with impaired consciousness within ten minutes. Treatment should be rapidly escalated if needed to minimize the long-term consequences.

While the clinical presentation of status epilepticus follows the same principles discussed earlier for epileptic seizures, the ictal symptoms and signs may change over a short period of time due to the highly dynamic nature of status epilepticus. Importantly, prominent motor symptoms in generalized convulsive status epilepticus tend to devolve over time, likely due to exhaustion of the underlying neuronal networks responsible for the generation of these symptoms. However, the pathological ictal activity in the brain may continue (non-convulsive status epilepticus). Therefore, non-convulsive status epilepticus needs to be considered and evaluated by EEG recordings in patients with unexplained coma or alteration of awareness, or patients who do not regain consciousness as expected following an acute brain injury.

Epilepsia partialis continua (EPC) refers to persistent regular or irregular clonic muscle twitching that affects a limited part of the body, typically distal rather than proximal body parts. The primary motor cortex is indispensably involved, and hemiparesis or other cortical based deficits are commonly associated (Bien and Elger, 2008). EPC usually has a symptomatic aetiology (most commonly vascular or inflammatory disorders, tumours, and metabolic-toxic disorders).

Structural causes of epilepsy

In neurosurgical practice, identifying a structural cause of epilepsy is important as resection of the abnormality may provide the best opportunity for seizure freedom (**Box 81.2**). Focal cortical dysplasias (FCDs) represent the commonest malformation of cortical development (MCD) encountered in epilepsy surgery. The development of a functional laminated human cerebral cortex is a multistaged process, which includes cell proliferation, differentiation, migration, synaptogenesis, and cellular reorganization. Disruption at any point during cortical lamination, neuronal migration, differentiation, and growth may result in MCD and may affect one discrete region, multiple lobes, or an entire hemisphere. In 2011, the ILAE reported a classification system incorporating histology, clinical presentation, and radiology (Blümcke et al., 2011; **Table 81.3**).

FCD types I and III result from cortical defects or injury at postmigrational stages. FCD I may be a result of severe prematurity, hypoxic ischaemic injury, head trauma, intracranial bleeding, or stroke during pre-/perinatal stages. It is considered an isolated malformation with abnormal cortical columnar disorganization in a radial (Ia; **Fig. 81.1**), tangential (Ib) or mixed (Ic) pattern. FCD III is associated with additional primary pathology that occurred early in development including hippocampal sclerosis (IIIa), tumours causing epilepsy, for example, dysembryoplastic neuroepithelial tumours (DNT: IIIb), adjacent vascular malformations (e.g. AVM, cavernoma, and other epileptogenic lesions including head injury, encephalitis, and hypoxic ischaemic injury). These lesions are typically seen on MRI, however, a causal event may not be identified.

FCD II is a result of abnormal cell development and maturation and is characterized by dyslamination and dysmorphic neurons (**Fig. 81.2**). Patients with FCD II typically exhibit medically refractory epilepsy at an earlier age, with a higher degree of cognitive decline. Balloon cells are the defining cell type of FCD IIb and may express neuronal nuclei (NeuN), glial fibrillary acid protein (GFAP), microtubule-associated protein 1B, vimentin, and nestin, suggesting that these cells are of mixed origin and retain features of immaturity. The balloon cells may also express stem cell markers including Sox2, c-Myc, and Klf4, which have been linked to enhanced mammalian target of rapamycin (mTOR) signalling pathway. Targeting the mTOR pathway with inhibitors may represent a promising novel treatment (Guerrini et al., 2015).

Box 81.2 Structural causes of epilepsy

- Focal cortical dysplasia
- Malformations of cortical development
- Hippocampal sclerosis
- Neurocutaneous syndromes
- Vascular malformations
- Hypothalamic hamartoma
- Brain tumours
- Acquired lesions
  - Abscesses
  - Inflammatory and infectious conditions
  - Ischaemic and haemorrhagic stroke

Table 81.3 Classification of focal cortical dysplasia

Focal cortical dysplasia secondary to cortical defects or injury at postmigrational stage of development	Type I Isolated dyslamination	Ia. Abnormal radial lamination Ib. Abnormal tangential lamination Ic. Abnormal radial and tangential lamination
	Type III Associated pathology	IIIa. Hippocampal sclerosis IIIb. Tumours associated with epilepsy (e.g. ganglioglioma, dysembryoplastic neuroepithelial tumour) IIIc. Vascular malformations (e.g. cavernoma) IIId. Other principal lesions during early life (e.g. head trauma, hypoxic ischaemic injury, encephalitis)
Cortical dysgenesis due to abnormal cell development and maturation	Type II Isolated dyslamination with dysmorphic neurons	IIa. Large dysmorphic neurons IIb. Large dysmorphic neurons and balloons cells

Reproduced with permission from Ingmar Blümcke, Maria Thom, Eleonora Aronica, et al., The clinicopathologic spectrum of focal cortical dysplasias: A consensus classification proposed by an ad hoc Task Force of the ILAE Diagnostic Methods Commission, *Epilepsia*, Volume 52, Issue 1, pp. 158–74, Copyright © 2010 John Wiley and Sons.

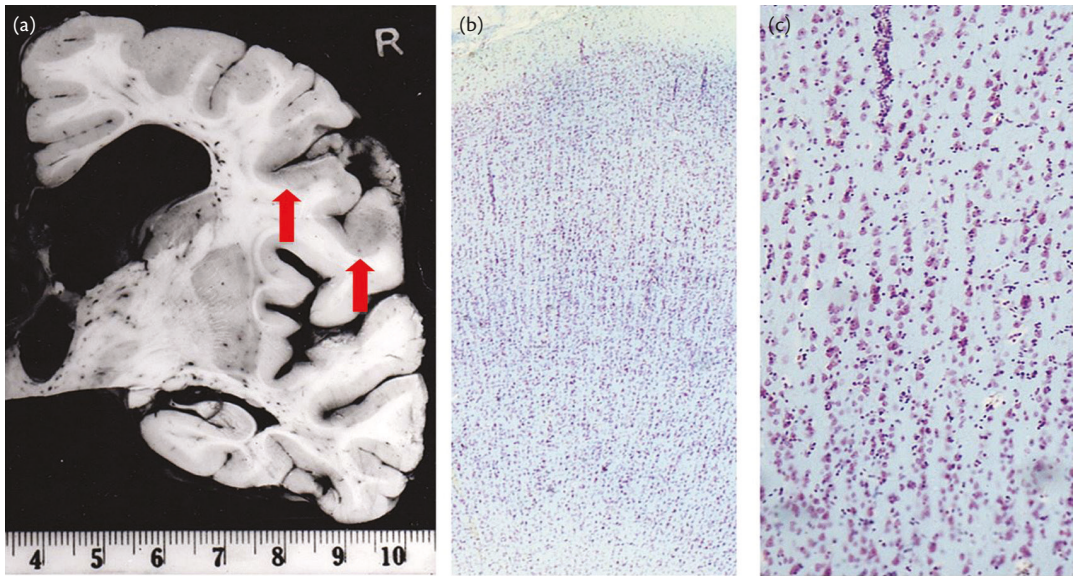

Fig. 81.1 Pathological and histological features of FCD 1a. (A) Post-mortem specimen of a 22-year-old female who died of sudden unexplained death in epilepsy (SUDEP) with history of epilepsy (generalized and partial seizures) since the age of 1 year, hemispherectomy aged 5 years in 1970s (surgical tissue not available for review). Examination of right hemisphere sections showed several regions of focal cortical dysplasia involving frontal and temporal lobe with patchy distribution. (B, C) Type FCD Ia in the ILAE 2011 classification: Nissl stain of the abnormal region highlights the preservation of the columnar architecture of the cortex with characteristic small sized neurones arranged in radial patterns (B: 10×; C: 20×)

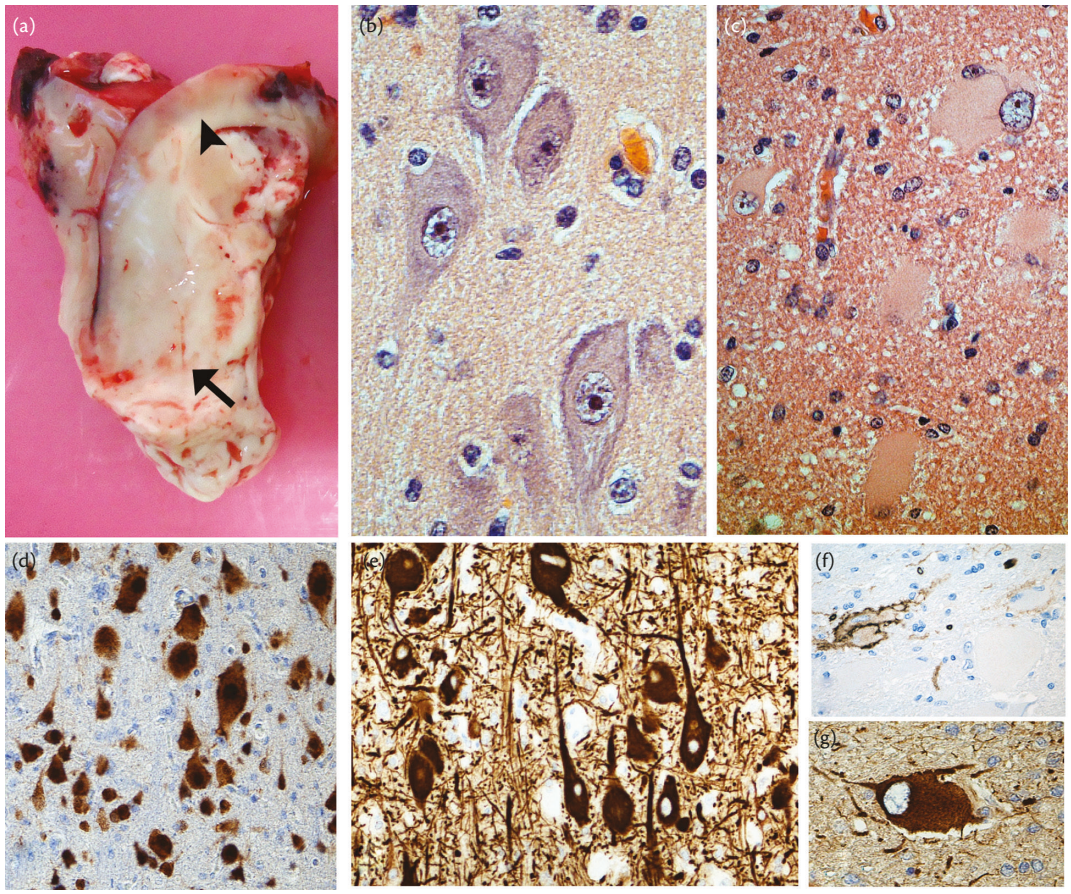

Fig. 81.2 Pathological and histological features of FCD IIb. (A) Macroscopic appearances of FCD IIb with poor demarcation between the grey and white matter (arrow) compared to adjacent well-defined cortex (arrowhead). (B) Haematoxylin and eosin staining demonstrates dysmorphic neurones populating the FCD cortex (50×), and (C) balloon cells in the white matter (20×). (D) Abnormal neurones are larger than normal neurones as shown on NeuN and with excessive labelling for neurofilament as shown in (E). (F) Balloon cells show variable labelling for CD34 and also nestin in (G).

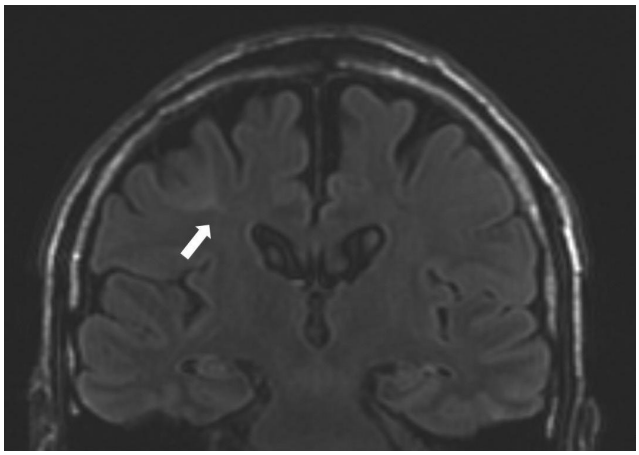

Fig. 81.3 Focal cortical dysplasia MRI characteristics. MRI FLAIR sequence demonstrating focal cortical thickening, abnormal gyral and sulcal patterns and the transmantle sign (arrow) which are most commonly seen in FCD IIb. The transmantle sign is a subcortical white matter hyperintensity extending to the ventricle.

A typical epilepsy protocol MRI at 1.5 or 3 Tesla includes T1- and T2-weighted volumetric imaging, and fluid-attenuated inversion recovery (FLAIR) images (Duncan et al., 2016). Features of FCD include cortical thickening, abnormal gyral and sulcal patterns, and the transmantle sign most commonly seen in FCD IIb (Fig. 81.3). The transmantle sign is a subcortical white matter hyperintensity extending to the ventricle, best seen on FLAIR sequence and affords better seizure control postsurgical resection than patients with FCD I (Wang et al., 2013). It is unknown whether this is related to intrinsic lower epileptogenicity or easier anatomical recognition of the epileptogenic tissue. Electrophysiological studies on balloon cells demonstrated that they are electrically 'silent', and it has been hypothesized that their presence could promote synaptic reorganization in the surrounding cortex that may result in a net increase in excitability in the tissue (Cepeda et al., 2003). An ongoing controversy is whether seizures arise within the dysplastic cortex, from the surrounding brain, or both. This is an important issue, as a significant proportion of patients remain medically refractory after surgical resection of the lesion defined by imaging only.

Within epilepsy surgical programmes for the management of medically refractory epilepsy, hippocampal sclerosis (HS) is one of the commonest pathologies ranging from 33–66% (for a review, see Thom, 2014). The 2013 ILAE classification of HS (Blümcke et al., 2013) is based on patterns of neuronal loss and gliosis as objective measures of sclerosis within the different hippocampal subfields (Fig. 81.4). In HS type 1 (previously termed classical sclerosis), neuronal loss and gliosis is found to a greater extent in subfield CA1 but also in CA4 and CA3, with sparing of CA2. This represents 60–80% of HS cases and has a common association with febrile seizures. It has the highest rates of seizure freedom postoperatively, with 70–85% seizure freedom at 2 years and 50% at 10 years. In HS type 2, the neuronal loss and gliosis is predominantly seen in CA1 subfield (5–10% of HS cases). In HS type 3, it is only present in the CA4 subfield with end folium sclerosis (3–7% of HS cases), and is associated with a dual pathology such as DNT or cavernoma. HS types 2 and 3, typically have an older age at epilepsy onset and have poorer postsurgical seizure-free outcomes in some series. Currently it is unknown why there is regional selectivity of pyramidal cell loss in different hippocampal subfields. It is likely, however, that different modulatory networks, altered excitatory pathways and inhibitory inputs, and efficacy of endogenous neuroprotective mechanisms are involved.

The aetiology of HS is still debated, however is likely to be multifactorial. Status epilepticus, repetitive generalized or partial seizures, and prolonged febrile seizures do not inevitably lead to HS. Although HS is considered a sporadic condition, there are likely to be other susceptibility factors involved. Inflammation with activation of the innate and adaptive immune system has been reported in HS, mechanisms for seizure-induced neuronal loss and an underlying abnormality in the developmental template may contribute (Thom, 2014). Imaging features of HS include hippocampal atrophy, volume loss on T1 and increased signal intensity on T2-weighted images and FLAIR (Fig. 81.5). Automated segmentation can quantify hippocampal sclerosis and is strongly recommended.

Anatomy of the limbic system

The circuit of Papez commences at the hippocampus and continues via the fornix to the mammillary bodies. Fibres are then relayed via the mammillothalamic tract to the anterior thalamic nucleus and via projections to the cingulate gyrus and back to the hippocampus. The limbic system comprises of the circuit of Papez and its associated subcortical nuclei including the amygdala, hypothalamic, and septal nuclei. It is composed of white and grey matter and phylogenetically is one of the most primitive parts of the brain involved in emotion, memory, and learning. The limbic system is one of the networks that can propagate seizure spread particularly from mesial temporal pathologies. For an anatomical review see Shah et al. (2012), and for a recently revised limbic system model incorporating tractography, see Catani et al. (2013) (also see Fig. 81.6).

The hippocampus forms the medial part of the floor of the temporal horn and rests on the subiculum, which forms the superior surface of the parahippocampal gyrus. The hippocampus is separated from the subiculum and parahippocampal gyrus by the hippocampal fissure. The white matter alveus borders the lateral ventricle and continues posteriorly as the fimbria, which gives rise to the crus of the fornix. The fornix is a projection tract connecting the hippocampus with the mamillary bodies, anterior thalamic nuclei, and hypothalamus. The crus of the fornix curves up and laterally over the pulvinar of the thalamus. It merges with the contralateral crus to form the body of the fornix beneath the splenium of the corpus callosum. The two crura of the fornices are connected by the hippocampal commissure. The body of the fornix runs forward to the anterior end of the thalamus, where the fibres of the two sides again separate and arch downwards in front of the intraventricular foramen of Monroe as the columns of the fornix. As the fibres of the fornix approach the anterior commissure, they divide. The majority forms the postcommissural portion, which terminate in the mammillary body, and a minority form the precommissural portion with connections to the septal nuclei, hypothalamus, and nucleus accumbens. Fibres then ascend to the anterior nucleus of the thalamus, forming the mammillothalamic tract. From the anterior nucleus of the thalamus, fibres merge with the fibres of the anterior limb of the internal capsule to reach the cingulate gyrus.

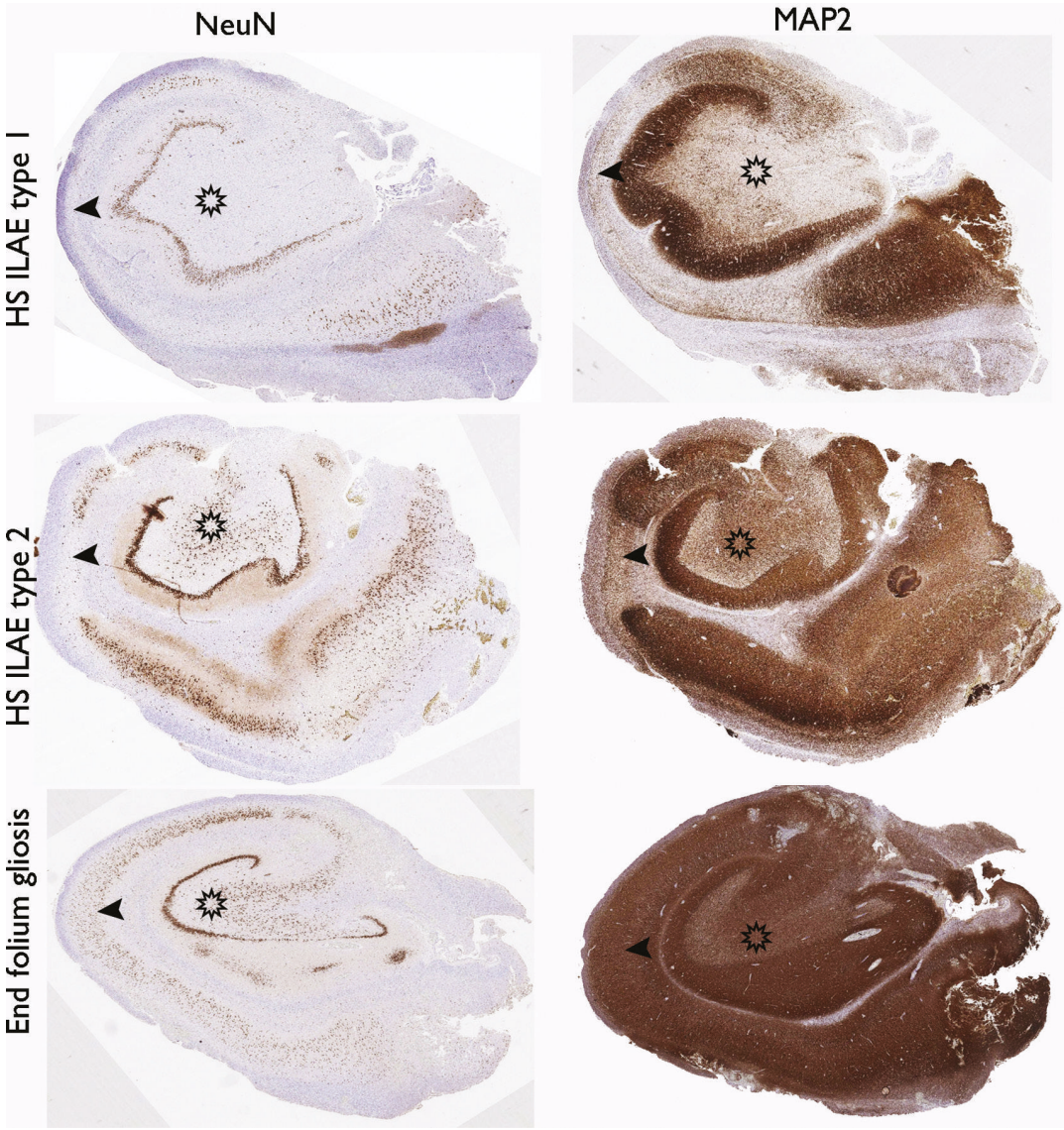

Fig. 81.4 Hippocampal sclerosis (HS) subtypes. The column on the left shows hippocampal sections stained with NeuN (neuronal nuclei) and on the right with MAP2 (neuronal cell bodies and dendrites). The asterisk shows the CA4 and the arrow the CA1. These are the main regions, which determine the patterns of HS in the 2013 ILAE classification of hippocampal sclerosis. In HS type 1, there is neuronal loss in CA4 and CA1. In type 2, the main neuronal loss is restricted to CA1. In the bottom row there is minimal loss from CA4. NB: In HS type 3, neuronal loss and gliosis is seen in CA4 only, while CA1 is preserved.

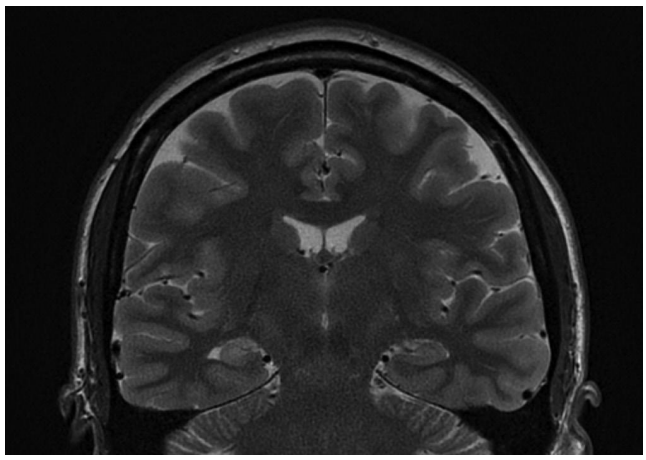

Fig. 81.5 Hippocampal sclerosis MRI characteristics. T2-weighted coronal MRI demonstrating right hippocampal sclerosis with increased signal intensity and hippocampal atrophy resulting in a more prominent ventricular temporal horn.

The cingulum is an association bundle that runs superior and parallel to the corpus callosum. Anteriorly, the fibres run below the rostrum of the corpus callosum in the subcallosal gyrus. Posteriorly, the cingulum narrows above the splenium, forming the isthmus of the cingulum. It continues below to end in the anterior parahippocampal gyrus adjacent to the hippocampus. The parahippocampal gyrus lies at the junction of the medial and inferior portions of the temporal lobe. The entorhinal area comprises the anterior aspect of the parahippocampal gyrus and contains the uncus, which contains the amygdala. However, the posterior aspect is poorly demarcated. It has many afferent and efferent connections with the hippocampus, cortical association areas, and forms an important relay centre. Laterally and anteriorly, the parahippocampal gyrus is limited by the rhinal sulcus (the anterior continuation of the collateral sulcus) and marks the lateral extent of the entorhinal area of the parahippocampal gyrus. Posteriorly, the parahippocampal gyrus is divided by the anterior calcarine sulcus into the isthmus

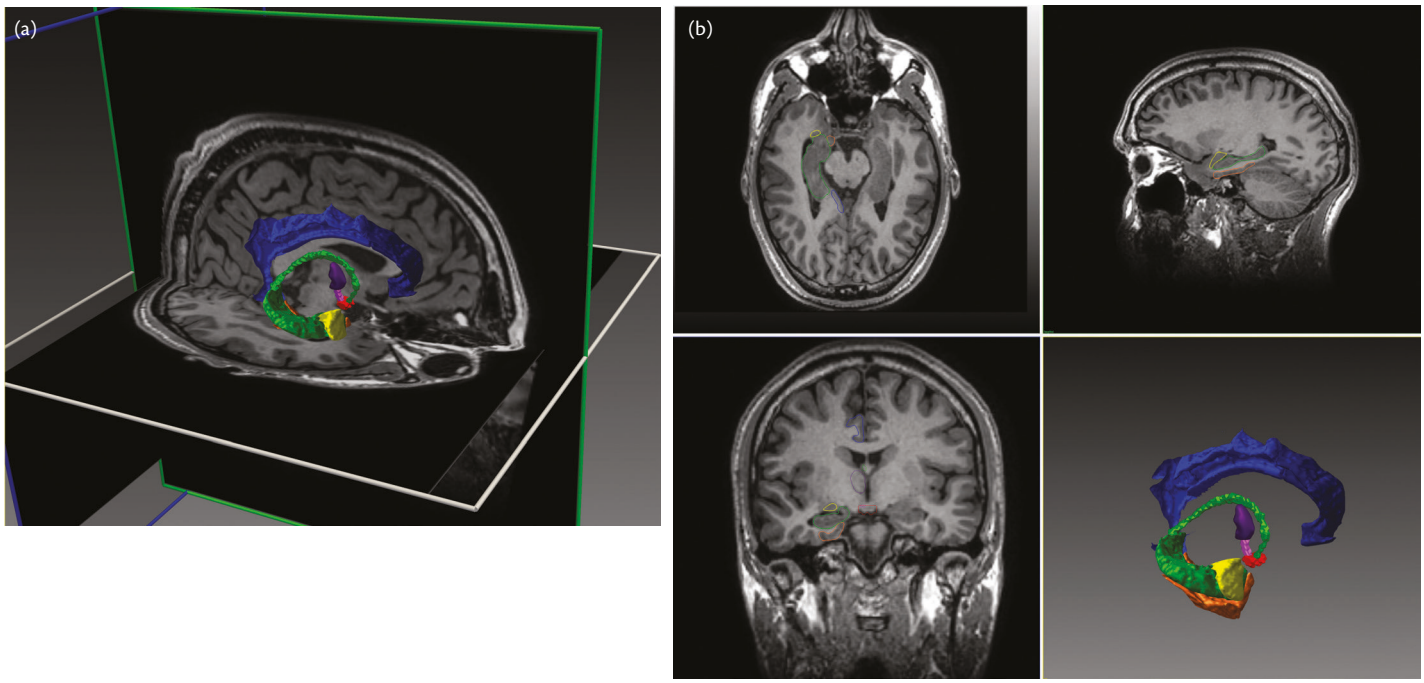

Fig. 81.6 Segmentation of the limbic pathway outlined on T1-weighted MRI: hippocampus-fornix = green, mammillary body = red, mammillothalamic tract = pink, anterior thalamus = purple, cingulum = blue, parahippocampal gyrus = orange, amygdala = yellow.

Adapted from *Epilepsy & Behavior*, Volume 20, issue 2, Nancy Foldvary-Schaefer, Kanjana Unnwongse, Localizing and lateralizing features of auras and seizures, pp. 160–6, Copyright (2011), with permission from Elsevier.

of the cingulate gyrus superiorly, which continues as the cingulate gyrus, and the parahippocampal gyrus inferiorly, which continues as the lingual gyrus. The amygdala is a complex of nuclei located entirely within the confines of the uncus. The amygdala complex gives rise to two major pathways, the stria terminalis and the ventral amygdalofugal pathway, and has widespread connections to the limbic system, thalamus, and hypothalamus.

FURTHER READING

Berg, A.T., Berkovic, S.F., Brodie, M.J., et al. (2010). Revised terminology and concepts for organization of seizures and epilepsies: report of the ILAE Commission on Classification and Terminology, 2005–2009. *Epilepsia*, **51**, 676–85.

Fisher, R.S., van Emde Boas, W., Blume, W., et al. (2005). Epileptic seizures and epilepsy: definitions proposed by the International League Against Epilepsy (ILAE) and the International Bureau for Epilepsy (IBE). *Epilepsia*, **46**, 470–2.

Foldvary-Schaefer, N. & Unnwongse, K. (2011). Localising and lateralising features of auras and seizures. *Epilepsy Behav*, **20**, 160–6.

Trinka, E., Cock, H., Hesdorffer, D., et al. (2015). A definition and classification of status epilepticus—report of the ILAE task force on classification of status epilepticus. *Epilepsia*, **56**, 1515–23.

REFERENCES

Adcock, J.E. & Panayiotopoulos, C.P. (2012). Occipital lobe seizures and epilepsies. *J Clin Neurophys*, **29**, 397–407.

Beauvais, K., Biraben, A., Seigneuret, E., Saïkali, S., & Scarabin, J.M. (2005). Subjective signs in premotor epilepsy: confirmation by stereo-electroencephalography. *Epileptic Disord*, **7**, 347–54.

Berg, A.T., Berkovic, S.F., Brodie, M.J., et al. (2010). Revised terminology and concepts for organization of seizures and epilepsies: report of the ILAE Commission on Classification and Terminology, 2005–2009. *Epilepsia*, **51**, 676–85.

Bien, C.G., Benninger, F.O., Urbach, H., Schramm, J., Kurthen, M., & Elger, C.E. (2000). Localizing value of epileptic visual auras. *Brain*, **123**, 244–53.

Bien, C.G. & Elger, C.E. (2008). Epilepsia partialis continua: semiology and differential diagnoses. *Epileptic Disord*, **10**, 3–7.

Blümcke, I., Thom, M., Aronica, E., et al. (2011). The clinicopathological spectrum of Focal Cortical Dysplasias: a consensus classification proposed by an *ad hoc* Task Force of the ILAE Diagnostic Methods Commission. *Epilepsia*, **52**, 158–74.

Blümcke, I., Thom, M., Aronica, E., et al. (2013). International consensus classification of hippocampal sclerosis in temporal lobe epilepsy: a Task Force report from the ILAE Commission on Diagnostic Methods. *Epilepsia*, **54**, 1315–29.

Canuet, L., Ishii, R., Iwase, M., et al. (2008). Cephalic auras of supplementary motor area origin: an ictal MEG and SAM(g^2) study. *Epilepsy Behav*, **13**, 570–4.

Catani, M., Dell'Acqua, F., & Thiebaut de Schotten, M. (2013). A revised limbic system model for memory, emotion and behaviour. *Neurosci Biobehav Rev*, **37**, 1724–37.

Cepeda, C., Hurst, R.S., Flores-Hernández, J., et al. (2003). Morphological and electrophysiological characterization of abnormal cell types in pediatric cortical dysplasia. *J Neurosci Res*, **72**, 472–86.

Chugani, H., Ilyas, M., Kumar, A., et al. (2015). Surgical treatment for refractory epileptic spasms: the Detroit series. *Epilepsia*, **56**(12), 1941–9.

Duncan, J.S., Winston, G.P., Koepp, M.J., & Ourselin, S. (2016). Brain imaging in the assessment for epilepsy surgery. *Lancet Neurol*, **15**, 420–33.

Ferrari-Marinho, T., Caboclo, L.O., Marinho, M.M., et al. (2012). Auras in temporal lobe epilepsy with hippocampal sclerosis: relation to seizure focus laterality and post surgical outcome. *Epilepsy Behav*, **24**, 120–5.

Fisher, R.S., Acevedo, C., Arzimanoglou, A., et al. (2014). A practical clinical definition of epilepsy. *Epilepsia*, **55**, 475–82.

Fisher, R.S., van Emde Boas, W., Blume, W., et al. (2005). Epileptic seizures and epilepsy: definitions proposed by the International League Against Epilepsy (ILAE) and the International Bureau for Epilepsy (IBE). *Epilepsia*, **46**, 470–2.

Fogarasi, A., Tuxhorn, I., Janszky, J., et al. (2007). Age-dependent seizure semiology in temporal lobe epilepsy. *Epilepsia*, **48**, 1697–702.

Foldvary-Schaefer, N. & Unnwongse, K. (2011). Localising and lateralising features of auras and seizures. *Epilepsy Behav*, **20**, 160–6.

Guerrini, R., Duchowny, M., Jayakar, P., et al. (2015). Diagnostic methods and treatment options for focal cortical dysplasia. *Epilepsia*, **56**, 1669–86.

Jobst, B.C., Williamson, P.D., Thadani, V.M., et al. (2010). Intractable occipital lobe epilepsy: clinical characteristics and surgical treatment. *Epilepsia*, **51**, 2334–7.

Kuba, R., Tyrlíková, I., Brázdil, M., & Rektor, I. (2010). Lateralized ictal dystonia of upper and lower limbs in patients with temporal lobe epilepsy. *Epileptic Disord*, **12**, 109–15.

Kun Lee, S., Young Lee, S., Kim, D.W., Soo Lee, D., & Chung, C.K. (2005). Occipital lobe epilepsy: clinical characteristics, surgical outcome, and role of diagnostic modalities. *Epilepsia*, **46**, 688–95.

Lüders, H., Acharya, J., Baumgartner, C., et al. (1998). Semiological seizure classification. *Epilepsia*, **39**, 1006–13.

Nordli, D.R. (2013). Varying seizure semiology according to age. *Handb Clin Neurol*, **111**, 455–60.

Rashid, R.M., Eder, K., Rosenow, J., Macken, M.P., & Schuele, S.U. (2010). Ictal kissing: a release phenomenon in non-dominant temporal lobe epilepsy. *Epileptic Disord*, **12**, 262–9.

Ristic, A.J., Alexopoulos, A.V., So, N., Wong, C., & Najm, I.M. (2012). Parietal lobe epilepsy: the great imitator among focal epilepsies. *Epileptic Disord*, **14**, 22–31.

Shah, A., Jhawar, S.S., & Goel, A. (2012). Analysis of the anatomy of the Papez circuit and adjoining limbic system by fiber dissection techniques. *J Clin Neurosci*, **19**, 289–98.

Stefan, H., May, T.W., Pfäfflin, M., et al. (2014). Epilepsy in the elderly: comparing clinical characteristics with younger patients. *Acta Neurol Scand*, **129**, 283–93.

Tandon, N., Alexopoulos, A.V., Warbel, A., Najm, I.M., & Bingaman, W.E. (2009). Occipital epilepsy: spatial categorization and surgical management. *J Neurosurg*, **110**, 306–18.

Tatum, W.O., 4th (2012). Mesial temporal lobe epilepsy. *J Clin Neurophysiol*, **29**, 356–65.

Thom, M. (2014). Review: hippocampal sclerosis in epilepsy: a neuropathology review. *Neuropath Appl Neurobiol*, **40**, 520–43.

Trinka, E., Cock, H., Hesdorffer, D., et al. (2015). A definition and classification of status epilepticus—report of the ILAE task force on classification of status epilepticus. *Epilepsia*, **56**, 1515–23.

Unnwongse, K., Wehner, T., & Foldvary-Schaefer, N. (2012). Mesial frontal lobe epilepsy. *J Clin Neurophysiol*, **29**, 371–8.

von Lehe, M., Wagner, J., Wellmer, J., Clusmann, H., & Kral, T. (2012). Epilepsy surgery of the cingulate gyrus and the fronto-mesial cortex. *Neurosurgery*, **70**, 900–10.

Wang, D.D., Deans, A.E., Barkovich, A.J., et al. (2013). Transmantle sign in focal cortical dysplasia: a unique radiological entity with excellent prognosis for seizure control. *J Neurosurg*, **118**, 337–44.

Wehner, T., Unnwongse, K., & Diehl, B. (2017). Focal epilepsy. In: Mills, KR (ed): *Oxford Textbook of Clinical Neurophysiology*, Chapter 28. Oxford, UK: Oxford University Press.

RELATED LINKS TO EBRAIN

The Causes of Epilepsy: Idiopathic Epilepsy. https://learning.ebrain.net/course/view.php?id=1335

Causes of Epilepsy – Symptomatic. https://learning.ebrain.net/course/view.php?id=1309

The Classification of Seizures and the Epilepsies. https://learning.ebrain.net/course/view.php?id=1336

Diagnosis of Frontal Lobe Epilepsy. https://learning.ebrain.net/course/view.php?id=1313

Diagnosis of Temporal Lobe Epilepsy. https://learning.ebrain.net/course/view.php?id=1314

Occipital and Parietal Lobe Epilepsies. https://learning.ebrain.net/course/view.php?id=1326

82

Epilepsy—diagnosis and assessment

Richard Selway

Introduction

Epilepsy was described as early as the second millennium before Christ; it was referred to in Sumerian and later Babylonian texts as the *'falling sickness'*. It is derived from the Greek word *epilambanein* which means to seize or to attack. The term *seizure* itself is of Latin origin derived from *sacire*—to claim.

Thus for much of its history, epilepsy was viewed as a paroxysmal disorder with supernatural connotations—sufferers were deemed possessed by an evil spirit notwithstanding Hippocrates' reflection in his famous fifth-century treatise on *'the sacred disease'* that the brain was the seat of epileptic attacks.

With the development of neurology as a specialty in its own rights in the nineteenth century, our understanding of epilepsy evolved. John Hughlings Jackson was instrumental in relating focal seizures to local brain disorders, beginning a long-running debate concerning the distinction between primary idiopathic epilepsy (where the brain is macroscopically normal) and secondary symptomatic epilepsy (with a defined underlying pathology) and whether one or the other represents 'true epilepsy'.

Jackson and Todd introduced the concept of abnormal electrical discharges which gained further credence following the development of the electroencephalogram by Hans Berger in 1929.

Epilepsy was now being viewed as an electromagnetic disorder, yet it never truly lost its association with alienation. For much of the nineteenth century, disorders of mood, behaviour, or personality were often labelled as epileptic in nature.

More recently, there has been an acknowledgement of the socioeconomic burden of the condition, a recognition that it still carries a significant social stigma. Furthermore, as our understanding of neural networks has improved, novel techniques of neuromodulation have been developed as an adjunct to more traditional medical and resective therapeutic measures.

What is a seizure?

A transient occurrence of signs and/or symptoms caused by abnormal, excessive, or synchronous neuronal activity within the brain.

What is epilepsy?

A disorder of the brain characterized by an enduring predisposition to generate epileptic seizures. In clinical terms, this generally implies two unprovoked seizures at least 24 hours apart.

A more practical definition was produced by the ILAE (International League Against Epilepsy) task force in 2014 *(Fisher et al., ILAE Official Report, Epilepsia 55(4): 475–82, 2014)*:

Epilepsy is a disease of the brain defined by any of the following:

1. At least two unprovoked (or reflex) seizures occurring more than 24 hours apart
2. One unprovoked (or reflex) seizure and a probability of further seizures similar to the general recurrence risk (at least 60%) after two unprovoked seizures, occurring over the next 10 years
3. Diagnosis of an epilepsy syndrome

Unprovoked refers to the absence of underlying acute conditions that can induce seizures in subjects who would not otherwise suffer attacks, for example, alcohol withdrawal, electroconvulsive therapy, encephalitis, head injury, or hypoglycaemia.

In a small proportion of patients, seizures can be triggered by specific stimuli that do not induce attacks in the general population (flashing lights, visual patterns, music, reading, intellectual activity). They are called *reflex seizures*. See Chapter 82 for a full discussion of seizure classification and definition.

Epidemiology

Epilepsy is the commonest serious neurological condition. It affects over 60 million people worldwide irrespective of gender or race, with an annual incidence of 45–50 cases per 100 000 people per year in developed countries. The point prevalence of epilepsy is 1% in both developed and developing countries with a lifetime incidence of 4–5%.

Incidence varies greatly with age (see Fig. 82.1).

There are two peaks in developed countries: young age, particularly during the first few months of life (half of all cases start in

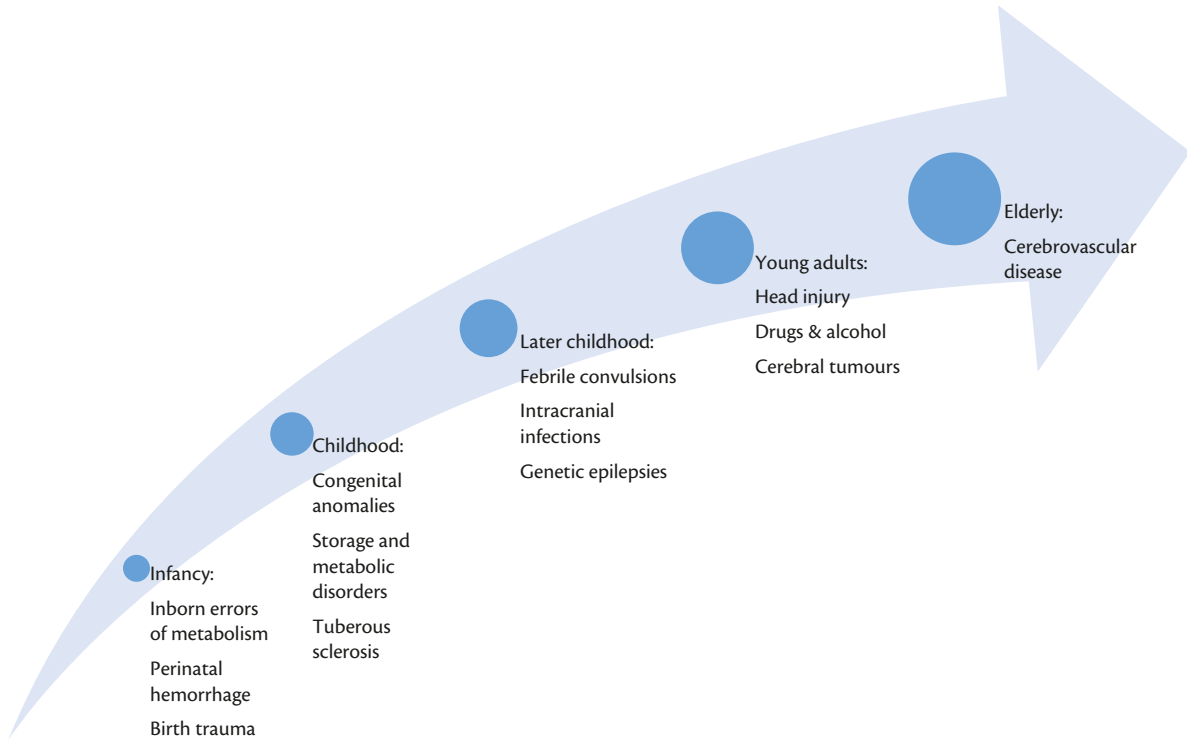

Fig. 82.1 Aetiology by age. Incidence, prevalence, cumulative incidence, and mortality for epilepsy in Rochester, Minnesota, 1935–1984.
Reprinted from Mayo Clinic Proceedings, Volume 71, issue 6, W. Allen Hauser, John F. Annegers, Walter A. Rocca, *Descriptive Epidemiology of Epilepsy: Contributions of Population-Based Studies From Rochester, Minnesota*, pp. 576–86, Copyright (1996), with permission from Elsevier.

childhood or adolescence) and in people over 65 years (due to cerebrovascular disease).

Overall, the incidence in children appears to be declining while there has been a sharp rise in older people. Indeed, old age has become the most common time of life to develop epilepsy. In developing countries, there is a third peak in young adults, which may be partially related to cerebral trauma.

Epilepsy is also the second commonest cause of mental health disability particularly in young adults. One in three patients report significant concerns about their mood. Depression, anxiety, and psychosis are common and have a significant impact on the patients' quality of life. Depression in under-recognized and often undertreated; the overall suicide rate in depressed patients with epilepsy is five times higher than that in the general population. Anxiety markedly compromises psychosocial functioning while psychosis has been reported in as many as 15% of patients with temporal lobe epilepsy.

Very few aspects of daily living remain unaffected by a diagnosis of epilepsy. It impacts on social interactions, employment, and driving, and often necessitates significant lifestyle modifications if not restrictions. Thus, it carries a significant burden over and above the clinical manifestations of the disorder although it should be noted that the incidence of seizures is not directly proportional to a patient's quality of life (Gillam, 1982).

Despite this, most patients with epilepsy do actually have a good prognosis although this is strongly dependent on the underlying cause. Many childhood epilepsy syndromes burn themselves out by the late teens or early adult years. Conversely, a significant minority suffer a relapsing-remitting course or lifelong disabling seizures. Markers of poor prognosis include a symptomatic cause, generalized epileptiform activity on an electroencephalogram (EEG), poor response to initial antiepileptic drug (AED) treatment, a concurrent psychiatric history, and a family history of epilepsy.

It is estimated that two-thirds of people with epilepsy become seizure-free on anticonvulsant drugs. The remainder suffer persistent seizures and are of particular interest to the neurosurgeon as a proportion (up to 60% depending on selection criteria) may benefit from interventions that significantly alleviate their seizure burden or even effect a cure in select cases (Brodie et al., 2012).

Sudden unexplained death in epilepsy (SUDEP)

The standardized mortality ratio (SMR = the number of observed deaths per number of expected deaths) compares mortality in a group with a specific illness to age and sex-matched controls. In patients with epilepsy, it is two to three times above that of the general population.

When deaths related to the underlying aetiology, accidents and injuries, and associated psychiatric complications are excluded, it still appears that epileptics are at risk of dying abruptly of no clear cause. SUDEP may account for up to 17% of all epilepsy-related deaths (incidence 0.35–10 per 1000 patients per year).

SUDEP is defined as 'sudden, unexpected, witnessed or unwitnessed, non-traumatic, and non-drowning death in patients with epilepsy, with or without evidence of a seizure, and excluding documented status epilepticus, in which post-mortem examination does

not reveal a toxicological or anatomical cause of death'. While some of these may be related to undetected seizures, some may also be related to cardiac dysrhythmias which can be an associated feature.

Genetic syndromes

Genetic susceptibility may be syndromic or non-syndromic with a range of aetiologies including morphological, metabolic, and vascular anomalies. Genetic screening of children with seizures should be considered where there are associated features or a family history.

Febrile convulsions

Febrile seizures are common with 5% of the general population having had one. They develop in association with fever (usually during the rapidly rising phase) with no evidence of any other cause. By definition they occur between 5 months and 5 years of age and are generally considered benign if uncomplicated although 1 in 3 children will have recurrent episodes and 5% later develop epilepsy (up to 50% of patients with mesial temporal sclerosis have a history of febrile convulsions). Such seizures occurring outside the specified age bracket should not be regarded in the same way, and carry a much worse prognosis.

The risk of developing epilepsy increases up to threefold when febrile convulsions have adverse features including a focal seizure, a seizure that last longer than 15 minutes, recurrence within 24 hours, focal neurological abnormalities, or a family history of epilepsy.

Treatment is usually symptomatic and supportive with administration of an antipyretic such as paracetamol. Tepid sponging and long-term AED treatment are not recommended in uncomplicated cases.

Diagnosis

Broadly speaking, seizures can be classified as partial (focal) or generalized. The former originate from cortical structures and, while they may become secondarily generalized, their semiology may allow seizure onset to be lateralized to a specific hemisphere or localized to a specific lobe of the brain or even a specific area within that lobe (e.g. lateral temporal neocortex vs. mesial temporal structures). By contrast, generalized seizures may be thought to originate from the deeper midline structures with simultaneous spread to both cerebral hemispheres. ('The centrencephalic theory').

In the traditional nomenclature of seizures, if awareness is maintained they are called 'simple' attacks, but with loss of awareness they are 'complex' seizures.

A seizure may be characterized by a *prodrome*, an *aura*, an *ictus*, and a *postictal period*—all of which may help to localize the seizure onset within the central nervous system.

The prodrome refers to changes in behaviour or mood which may precede an attack, sometimes by several hours. It is not regarded as part of the electrical seizure itself.

The aura describes symptoms experienced by the subject that immediately precede an attack, such as a feeling in the stomach in temporal lobe seizures. Electrically the aura is part of the seizure (a simple partial seizure, which may then spread to a wider part of the brain to produce the objective attack or ictus). Following a seizure, the patient may be disoriented or demonstrate automatisms, the so-called postictal period.

Seizure semiology

The description of an attack (the 'semiology') is the first step in localizing seizure onset and spread. While the descriptions that follow are typical seizure propagation often results in a more complex picture. For example, probably most occipital partial seizures will spread into the mesial temporal structures producing a semiology with features of both areas. A very careful history and observation of typical seizures on video may allow the site of origin and the path of propagation to be understood (Table 82.1).

Temporal lobe epilepsy

Temporal lobe epilepsies are a heterogeneous group of disorders that are anatomically broadly divided into those originating from the lateral neocortex or the medial (mesial) regions of the temporal lobe (amygdala and hippocampus).

Mesial temporal lobe epilepsy is twice as common and most often secondary to hippocampal sclerosis, hence the term *mesial temporal sclerosis*. Other causes include tumours (particularly dysembryoplastic neuroepithelial tumours or DNETs), cortical dysplasia, hamartomas, and vascular lesions such as cavernous angiomas.

Mesial temporal sclerosis

Mesial temporal sclerosis is the commonest pathology in drug-resistant temporal lobe epilepsy and one of the most distinct epileptic syndromes with defined hippocampal pathology on MRI, neuronal loss in CA1 and CA3 regions of the hippocampus, a characteristic clinical picture and, crucially, postresection surgical relief.

It probably accounts for 20% of patients with epilepsy and 65% of those undergoing a temporal lobectomy for seizure control.

Seizure onset is usually just before puberty, typically around 12 years of age although half of all patients give a history of childhood febrile convulsions. A seizure typically begins with a vegetative aura, often described as a rising sensation in the pit of the stomach although complex olfactory or gustatory sensations may also occur. This is followed by a complex partial seizure with impairment of consciousness heralded by an initial behavioural arrest and stare followed by oro-alimentary and gestural automatisms (chewing, lip smacking, fumbling, or picking at the clothes) lasting a couple of minutes which the patient does not recall. There is often contralateral dystonic posturing. Postictal confusion is common as are affective symptoms such as psychosis or anxiety. Secondary generalization is exceedingly rare.

Radiological appearances are characteristic with evidence of hippocampal atrophy on MRI and high signal on T2 or FLAIR sequences while an EEG shows anterior temporal interictal spikes. See Figure 82.2.

Table 82.1 Lateralising and localizing features of seizures

Lateralising features	
Dominant hemisphere	Ictal and postictal dysphasia
Non-dominant hemisphere	Ictal speech Preserved awareness during ictal automatisms
Ipsilateral hemisphere	Unilateral eye blinking Manual automatisms
Contralateral hemisphere	Unilateral ictal clonic (i.e. rhythmic jerks) or dystonic (sustained muscle contraction) activity Upper limb dystonia
Localizing features	
Frontal lobe	Usually brief (<2 minutes) with stereotyped features and preserved awareness Often nocturnal with clustering Prominent motor features ('hypermotor seizures') sometimes violent but coordinated may be mistaken for night terrors, sleepwalking, or rage
Primary sensorimotor cortex	Tonic, clonic, myoclonic, or atonic Jacksonian march Todd's paresis postictally
Orbitofrontal cortex	Repetitive gestural automatisms Dyscognitive features—altered awareness or responsiveness Olfactory hallucinations Autonomic signs
Frontopolar cortex	Dyscognitive features Autonomic signs Axial convulsive movements causing falls Initial ipsilateral head and eye version Forced thoughts
Dorsolateral frontal cortex	Often tonic movements Aversive with contralateral head and eye movement (frontal eye field) Forced thoughts and acts (e.g. compulsion to stare at an object) Dysphasia if dominant lobe
Cingulate cortex	Gestural automatisms at onset with loss of awareness Affective aura (e.g. fear, depression, joy, anger) Autonomic features (e.g. palpitations, urge to urinate or defecate) Gelastic automatisms (i.e. laughing)
Central (supplementary motor cortex, frontoparietal operculum, paracentral lobule)	Abrupt onset/offset of asymmetric tonic posturing lasting <60 seconds with minimal postictal confusion Extension of upper limb contralateral to hemisphere of seizure onset Flexion of ipsilateral upper limb (described as a 'sign of four' posture as the arms are held in the shape of a 4) Contralateral head and eye deviation Loud vocalization or speech arrest at onset
Opercular/Insular	Facial clonic movements Laryngeal symptoms Difficulty articulating Hypersalivation Gustatory hallucinations
Parietal lobe	Contralateral sensory aura, usually paraesthesia +/– numbness, prickling, crawling May spread in a Jacksonian march Pain, typically burning Hallucination of distortion of body shape Micro/macrosomatognosia (shrunken/swollen body part) Hyper/hyposchematica (elongated/shortened body part) Sexual sensation affecting genitalia if paracentral lobule Language impairment with difficulty reading, calculating, or writing if dominant
Occipital lobe	Visual auras in the field contralateral to the hemispheric onset Multicoloured shapes (e.g. circles or flashes) Visual loss (e.g. amaurosis, scotoma, black-out, or white-out) Visual hallucinations (these more formed visual experiences tend to involve more anterior structures into the temporal lobe) Pictures of people, animals, or scenes—static or moving Visual illusions Alteration of visuospatial perception if non-dominant parietal lobe Micro/macropsia Teleopsia (object appears small and far) Palinopsia (visual perseveration) Epileptic nystagmus Fast component away from ictal onset, slow component towards it Oculomotor features (e.g. eyelid flutter, forced eye closure)

Table 82.1 Continued

Localizing features	
Temporal lobe	Complex aura (e.g. déjà vu, often epigastric rising sensation, or auditory buzzing) Behavioural arrest—patient stops what they are doing and stares into space Loss of awareness, said to represent the spread of a temporal seizure to involve the contralateral side as well (complex partial seizure) Automatisms—oro-alimentary +/– gestural Autonomic features—pallor, palpitations Postictal confusion and headache
Mesial temporal lobe	A distinctive aura, either in isolation or followed by behavioural arrest with slowly progressive impairment of awareness and oro-alimentary and manual automatisms Rising epigastric sensation or abdominal discomfort Déjà-vu, jamais-vu Chewing, lip smacking, swallowing Autonomic features Ipsilateral pupillary dilatation Contralateral upper limb dystonia, plus head and eye version Longer duration than lateral temporal seizures
Lateral temporal neocortex	Initial aura with auditory, complex visual, illusionary, or vertiginous features Buzzing or ringing sound, if heard in only one ear, suggests onset in contralateral hemisphere Shorter aura, earlier onset of altered awareness and shorter ictus More likely to evolve to a bilateral convulsion

While most patients with hippocampal sclerosis have predominantly unilateral disease, most will also have bitemporal electrical spikes on EEG and at least 30% will have apparent bilateral ictal EEG changes on video telemetry. In 11% ictal EEG onset appears to be contralateral to the true site of onset. This may either reflect bilateral seizure foci or bilateral dysfunction from a single focus with rapid seizure spread to the contralateral side. When recording from conventional scalp EEG electrodes the electrical source is often a long way away and rapid spread to contralateral structures may then propagate to the surface first on either side. In such cases, it is often useful to establish language dominance and the memory reserve of the contralateral hemisphere before embarking on a temporal resection.

The disorder may initially respond well to AEDs but seizures tend to become drug resistant from early adulthood onwards. Surgical resection (en-bloc anterior temporal lobectomy or more selective amygdalohippocampectomy) has an excellent outcome with up to 80% of patients becoming seizure-free.

Investigations

What information does an epilepsy surgeon need? Once the notion of medical intractability is demonstrated, further investigations are aimed at localizing the seizure onset and identifying any potential underlying lesions.

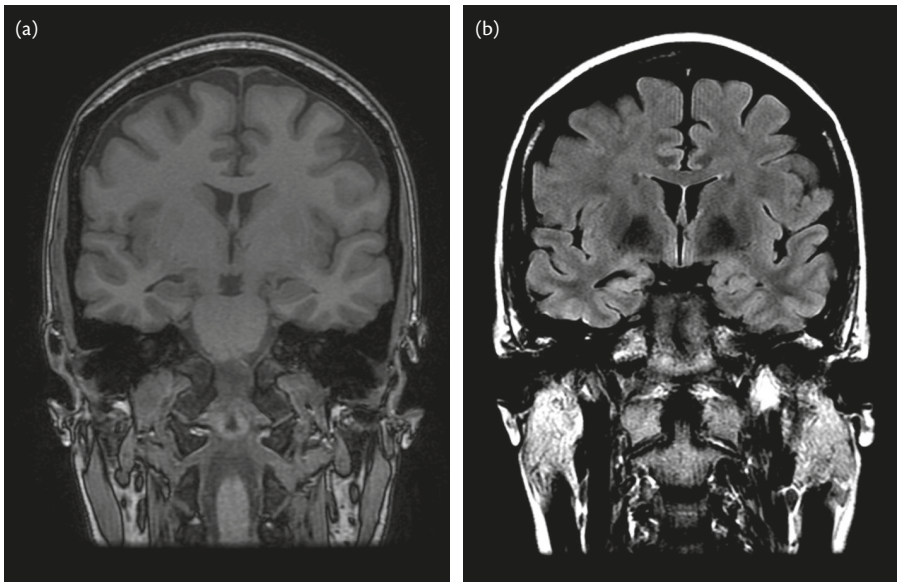

Fig. 82.2 Coronal view demonstrating volume loss, secondary dilatation of the temporal horn and signal change. Coronal SPGR (A) and FLAIR (B) MR sequences demonstrating low T2 signal and volume loss in right hippocampus.

This usually involves a combination of a high-quality MRI scan with FLAIR sequences to identify neoplastic, vascular or developmental pathologies, and scalp telemetry.

Electroencephalogram (EEG)

The EEG provides a record of electrical activity from different areas of the brain. It represents the compound electrical field generated by neuronal function (mainly from postsynaptic potentials in the cerebral cortex).

EEG recordings are usually obtained via scalp electrodes (*scalp telemetry*). *Video telemetry* allows electrical rhythms to be matched to concurrent clinical seizure activity to facilitate localization of an epileptogenic focus.

Surface electrodes are small silver discs that are placed on the patient's scalp to provide coverage of clinically relevant areas. The most commonly used convention for electrode placement is the '10–20' system where electrodes are placed and identified by letters and numbers, for example, F (frontal), T (temporal), Fp (frontopolar), with odd numbers covering the left hemisphere and lower values representing a more anterior and medial location (e.g. F7 would indicate left posterolateral frontal placement).

The EEG measures the potential difference (in millivolts) between paired electrodes. If adjacent electrode differences are displayed this is known as a bipolar montage. Alternative montages are useful to highlight particular EEG features or minimize artefact (i.e. interference) for example referential montage is used where a single specified contact is compared with all the others.

Ongoing electrical activity is called background activity. Several rhythms are identifiable varying with age, time, location, and clinical activity. Paroxysmal activity is sought as it may be epileptic in nature.

Figure 82.3 shows an EEG demonstrating a burst of alpha activity on eye closure.

Invasive EEG

Invasive EEG (iEEG), which requires surgical placement of recording electrodes intracranially, is utilized in selected cases as a stage in the work up prior to epilepsy surgery or for intraoperative monitoring during these procedures. EEG recordings from depth electrodes inserted into the brain parenchyma or within a lesion are called stereoencephalography (SEEG). EEG recordings from subdural grids or strip electrodes placed on the exposed brain surface are called electrocorticography (ECoG) which can be intra- or extraoperative. Following placement, extraoperative recording is performed off anticonvulsants for a period of typically 3–14 days, depending upon the seizure frequency, to establish the location of the epileptogenic zone.

Invasive EEG is employed whenever information from surface EEG is insufficient to allow precise targeting of the location of the seizure onset and the definition of the boundary of the epileptogenic zone. iEEG tests are valuable when there is discordance in the non-invasive investigations, or between the interictal data and the nature of the ictal episodes, in the presence of dual pathology or when the localization of the seizure onset is unclear for example, when bilateral ictal discharges are seen on EEG. Two further examples of this are the presence of bilateral independent temporal spikes on surface

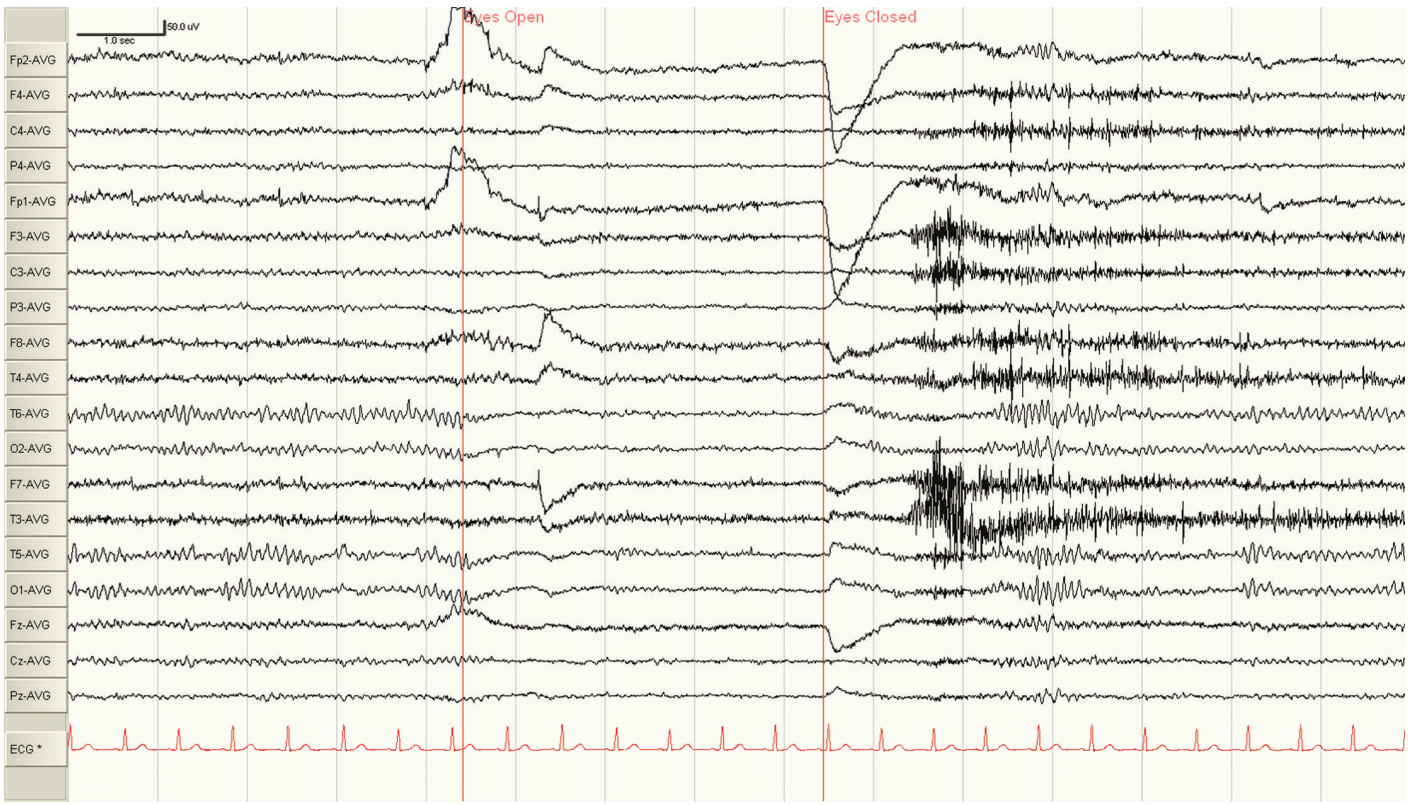

Fig. 82.3 Normal EEG demonstrating burst of alpha activity on eye closure.
Courtesy of Mr Robert Morris, Addenbrooke's Hospital, UK.

EEG and bilateral hippocampal sclerosis on MRI prior to temporal lobe epilepsy surgery. Invasive recordings are used prior to surgery for extratemporal lobe or non-lesional temporal lobe epilepsy. In addition, these electrodes can be of value to identify and delineate functional regions by using stimulation and recording of evoked responses prior to resective procedures for neocortical epilepsy near eloquent areas.

Subdural strips have electrodes in a single column while subdural grids are of different configurations and sizes with respect to the electrode arrangements. The electrodes are usually stainless steel however platinum electrodes that are non-ferromagnetic and hence MRI compatible are available but expensive. These methods only sample a limited brain region and preoperative planning is therefore important for placement of these electrodes. Depth electrodes are placed through special stylets inserted with neuronavigation or Robot-assisted techniques through burr or twist drill holes. These can have 4–10 contacts, but still record from a limited sampling area but is usually targeted to deep locations such as the insula, hippocampus, or amygdala. Bilateral placement from an occipital trajectory allows the electrodes to be orientated in line with the parahippocampal gyrus and multiple recording points are used to localize seizure activity in cases of medial temporal origin.

Subdural grids are placed via a craniotomy exposing the cortical surface with particular care used for interhemispheric or subtemporal placements due to the presence of subdural bridging veins. Grids can achieve a wider cortical coverage but provide more limited access to deep structures. Bilateral placement of subdural grids is not recommended. Although subdural strips can be placed through burr holes this is less safe than open craniotomy and misplacement is possible. SEEG and ECoG recordings can be combined by placement of both subdural grids and multiple depth electrodes in complex cases.

Nuclear imaging

When EEG, MRI, and seizure pattern are conflicting as to lateralization or lobar localization, or indeed in the presence of a normal MRI but compelling electrophysiological abnormalities, nuclear imaging in the form of an interictal FDG-PET scan or, if possible, an ictal single photon emission computed tomography (SPECT) scan can provide useful information.

FDG-PET determines regional cerebral glucose metabolism between seizures. Hypometabolism is typical of a cortical area that includes the seizure focus and left-right asymmetry can distinguish between true epileptogenic foci and regions such as both thalami which often demonstrate low glucose metabolism.

By contrast, ictal SPECT identifies cerebral hyperperfusion in seizure foci. It requires injection of a technetium tracer as early as possible after seizure onset before the seizure has spread. The tracer will fix in the brain in a concentration proportional to the blood flow at that moment. Image acquisition can be performed over the next few hours. The technical aspects of injecting a radio-labelled compound to a patient experiencing a spontaneous seizure within a few seconds of onset are extraordinarily challenging, making this a difficult and specialized investigation.

Both low-resolution studies are typically merged with an MRI to provide better resolution and anatomical localization.

Magnetoencephalography (MEG)

Magnetoencephalography is a promising technique where an array of multiple highly sensitive sensors is positioned over the scalp to detect small magnetic changes associated with the electromagnetic activity that underlies normal and epileptic EEG rhythms.

The electromagnetic dipole is calculated from numerous EEG interictal spikes and the dipole source viewed on a coregistered high-resolution MRI for anatomical correlation. Spatial resolution improves the greater the number of scalp electrodes used. The magnetic dipole is perpendicular to the EEG electrical dipole, so MEG will sometime detect activity missed on EEG such as seizures arising in the Sylvian fissure.

Medical management of seizures

See **Table 82.2** for the pharmacological properties of established anticonvulsants.

See **Table 82.3** for the pharmacological properties of newer anticonvulsants.

Phenytoin

Phenytoin was introduced into clinical practice as a non-sedating anticonvulsant in 1938 and very quickly became the drug of choice for most neurosurgeons in the treatment of acute seizures and status epilepticus largely due to its availability in intravenous form and its effectiveness in treating partial and tonic-clonic seizures. It does have a significant side-effect profile and is not effective against atonic or absence seizures.

Phenytoin exerts its action by binding to fast-inactivated sodium channels and holding them in their inactive state for longer which allows neurones to fire at moderate but not very rapid rates, limiting the generation and spread of action potentials. Phenytoin is metabolized by the liver, the first step of which process being mediated by the enzyme arene oxidase which has saturable (zero-order) kinetics within the therapeutic range. This means that the drug is eliminated at a constant rate, not related to the serum concentration. At low concentrations, phenytoin exhibits first-order kinetics where the elimination is proportional to the concentration. The concentration at which the shift in kinetics occurs varies with age. Thus, phenytoin has a narrow therapeutic range particularly at near-therapeutic doses, and any small change in dosing may result in disproportionate changes in serum concentration.

Phenytoin induces hepatic enzymes and may therefore reduce serum levels of other AEDs for instance valproate as well as lipid-soluble drugs like warfarin. Early, non-dose-related adverse effects include a skin rash in 5% of patients (this may rarely progress to a full-blown Stevens–Johnson syndrome). Neurotoxic dose-related side effects are uncommon at serum levels below 30 mg/litre. They typically present 8–12 hours after an oral dose and include asterixis, ataxia, dysarthria, nystagmus, and somnolence.

Chronic use is associated with reversible dysmorphic effects (acne, coarsening of facial characteristics, gingival hypertrophy, and hirsutism after several months) as well as osteopaenia (it antagonizes vitamin D), peripheral neuropathy, and cerebellar atrophy after years of treatment. Phenytoin is contraindicated in patients

Table 82.2 Pharmacological properties of established anticonvulsants

Drug	Primary mode of action	Indication (seizure type)	Absorption (bioavailability %)	Protein binding (% bound)	Elimination half-life (hours)	Route(s) of elimination	Target serum concentration
Carbamazepine	Sodium channel blockade	Partial, generalized	Slow (75–80)	80	24–48	Hepatic metabolism	4–12 mg/litre
Clobazam	GABAergic	Partial, generalized, epilepsy partialis continua	Rapid (90–100)	90	10–30	Hepatic metabolism	None
Phenobarbitone	GABAergic	Partial, generalized, myoclonic, status epilepticus	Slow (95–100)	50	72–144	Hepatic, 25% excreted unchanged	10–40 mg/litre
Phenytoin	Sodium channel blockade	Partial, generalized, status epilepticus	Slow (85–90)	90	24 (9–40)	Saturable hepatic metabolism	10–20 mg/litre
Sodium valproate	Multiple	Partial, generalized, absence	Rapid (100)	90	7–17	Hepatic metabolism	50–100 mg/litre

with second-degree heart block because of its lignocaine-like antiarrhythmic effect. It may also cause bone marrow suppression and an SLE-like syndrome. Its use in pregnancy is associated with the fetal hydantoin syndrome characterized by facial dysmorphism, cleft lip and palate, and cardiac defects.

Carbamazepine

Carbamazepine was first synthesized in 1953. It prevents repetitive firing of action potentials in depolarized neurones by blocking both use- and voltage-dependent sodium channels. Carbamazepine induces its own metabolism and can accelerate the hepatic breakdown of several lipid-soluble drugs, most commonly the oral contraceptive pill. Drugs that inhibit its metabolism resulting in toxicity include phenytoin and erythromycin.

It is an effective first-line agent for partial and tonic-clonic seizures, but it should be avoided in absences which it may exacerbate. It should be introduced at low doses and the dose increased very gradually to facilitate tolerance to its central nervous system side effects and to allow hepatic auto-induction to take place. Despite this, many patients do not tolerate the neurotoxic effects of the drug even at subtherapeutic doses.

Diplopia, dizziness, headache, nausea, and vomiting are the commonest signs of central nervous system (CNS) toxicity. Various idiosyncratic reactions can also happen, the commonest being a morbilliform rash seen in 5–10% of patients. Blood dyscrasias and toxic hepatitis are uncommon; a mild leukopenia is not unusual. At higher concentrations, carbamazepine has an antidiuretic hormone-like effect resulting in hyponatraemia which is usually asymptomatic. Like most anticonvulsants, carbamazepine is potentially teratogenic.

Oxcarbazepine

Functionally a prodrug, oxcarbazepine is rapidly reduced to its active metabolite in the liver. Like carbamazepine, it blocks sodium channels; it also modulates calcium and potassium channels. It has a similar spectrum of efficacy to carbamazepine and tends to be better tolerated with fewer neurotoxic side effects. A skin rash is less common but like its counterpart, it may rarely be associated with Stevens–Johnson syndrome. Hyponatraemia is more common. Oxcarbazepine does not appear to cause blood dyscrasias or hepatotoxicity. Furthermore, it has no effect on its own metabolism.

Table 82.3 Pharmacological properties of newer anticonvulsants

Drug	Primary mode of action	Indication	Absorption (bioavailability %)	Protein binding (% bound)	Elimination half-life (hours)	Route of elimination
Gabapentin	Calcium channel binding	Partial	Slow (60)	0	6–9	Not metabolized, renal excretion
Lamotrigine	Sodium channel blockade	Partial, generalized	Rapid (95–100)	55	22–36	Glucuronidation
Levetiracetam	Uncertain	Partial, generalized	Rapid (95–100)	<10	6–8	Non-hepatic hydrolysis, renal excretion
Oxcarbazepine	Sodium channel blockade	Partial, generalized	Rapid (95–100)	40	8–10	Hepatic conversion to active moiety
Pregabalin	Calcium channel binding	Partial	Rapid (90–100)	0	6	Not metabolized, renal excretion
Lacosamide	Sodium channel blockade	Partial	Rapid (95–100)	<15	13	Hepatic metabolism, 40% excreted unchanged
Zonisamide	Multiple	Partial, generalized	Rapid (95–100)	50	50–70	Hepatic metabolism, renal excretion

Gabapentin

Gabapentin was developed by adding a cyclohexyl group to GABA (gamma amino butyric acid, a major inhibitory neurotransmitter) which allows it to cross the blood brain barrier. Despite its structure, however, gabapentin does not bind to GABA receptors. Instead it binds to the alpha-2-delta subunit of the neuronal voltage-gated calcium channels, inhibiting calcium flow and neurotransmitter release from presynaptic terminals.

It is a useful adjunct in the treatment of partial seizures with or without secondary generalization and is also widely used for the treatment of neuropathic pain.

Adverse effects are mild and transient with ataxia, drowsiness, and nystagmus the commonest. Gastrointestinal symptoms such as flatulence and diarrhoea are occasionally reported and 5% of patients put on weight particularly at high doses. Gabapentin does not interact with other drugs as it is not metabolized by the liver, does not induce or inhibit hepatic enzymes, and is excreted unchanged by the kidneys.

Sodium valproate

Valproate exerts its antiepileptic action by limiting sustained repetitive firing by a use- and voltage-dependent effect on sodium channels. It also facilitates the effects of GABA. It is effective in idiopathic generalized epilepsies in particular and can be used across the complete spectrum of seizure disorders. It is metabolized by the liver but does not interfere with the hormonal component of the oral contraceptive pill. Because it does not exhibit a clear-cut concentration effect-toxicity relationship, routine therapeutic monitoring is unhelpful.

Unpleasant side effects include dose-related tremor, weight gain due to appetite stimulation, transient alopecia, and menstrual irregularities. Less commonly, thrombocytopenia and an insidious parkinsonism occur, both of which are reversible. Traditionally, patients undergoing neurosurgical intervention would have their valproate phased out prior to elective intervention because of the perceived haemorrhagic risk although this practice has now fallen out of fashion. Children under 3 years of age are at risk of hepatotoxicity, particularly when they have a concurrent metabolic disorder; rarely stupor and encephalopathy from hyperammonaemia can occur.

It should be avoided in women of childbearing age who are thinking of starting a family as it is associated with a 3% risk of neural tube defects, particularly at doses of more than 1000 mg a day.

Clobazam

Clobazam is a benzodiazepine that is a useful adjunct in the treatment of both partial and generalized seizures. It is also effective in children with Lennox–Gastaut syndrome. Like other benzodiazepines, it enhances GABA-mediated effects on chloride channels, binding to GABA-A receptors at the gamma subunit to increase the frequency of channel opening for postsynaptic inhibition. It is less sedative than diazepam. It is biotransformed in the liver to a number of metabolites.

Not all responders will maintain a worthwhile improvement in seizure control on long-term clobazam dosing because of the development of tolerance. This may be minimized with intermittent drug use. Side effects include depression, irritability, and lethargy. It may exacerbate pre-existing behavioural and mood disorders.

Phenobarbitone

The oldest anticonvulsant in common clinical practice, it was first synthesized in 1912 and enhances the effect of GABA by prolonging chloride channel opening at the GABA-A receptor, resulting in neuronal hyperpolarization.

Because of its propensity to cause sedation and behavioural problems, it has fallen somewhat out of fashion although its low cost and its effectiveness in treating seizure clusters and refractory status epilepticus ensure that it remains one of the most important AEDs in the developing world.

Phenobarbitone has a long half-life of 4 days; thus, dosing changes may take up to 3 weeks to achieve steady-state serum concentrations. It is metabolized by the liver and is a potent inducer of hepatic metabolism, accelerating the clearance of many lipid-soluble drugs. Side effects include agitation, depression, hyperactivity at extremes of age, an allergic skin rash, osteoporosis, and Dupuytren's contractures. It is teratogenic. Withdrawal seizures may occur unless it is tapered relatively slowly.

Lamotrigine

Lamotrigine is one of the most useful newer AEDs, effective across the complete range of seizure disorders. It is useful in patients with multiple seizure types, especially those with learning difficulties, possibly because its ability to reduce interictal spiking and it contributes to improved alertness.

Lamotrigine selectively blocks the slow inactivated state of the sodium channels thereby preventing the release of excitatory amino acid neurotransmitters, particularly aspartate and glutamate. It does not influence the metabolism of lipid-soluble drugs like warfarin or other AEDs.

When used as monotherapy, lamotrigine has a half-life of 24 hours. This drops to 15 hours when it is combined with enzyme-inducing agents such as phenytoin. Valproate inhibits the glucuronidation of lamotrigine, prolonging its half-life up to 60 hours. Withdrawing phenytoin therefore causes a rise in circulating concentrations of lamotrigine, while discontinuing valproate results in a fall in plasma lamotrigine levels. When used in combination with valproate, lamotrigine doses are routinely halved.

The risk of teratogenicity associated with lamotrigine monotherapy is low, making it the drug of choice in women of childbearing age wishing to conceive and unable or unwilling to discontinue AED use. Ataxia, diplopia, headache, insomnia, and tremor are sometimes reported. A self-limiting maculopapular skin rash occurs in 3% of patients on monotherapy (8% if combined with valproate). It is less likely the more gradual the drug titration regime with a reported risk of a severe skin reaction as high as 1 in 1000 adults.

Levetiracetam

Levetiracetam is an enantiomer of the ethyl analogue of piracetam whose exact mechanism of action is unknown. However, it is known to bind to synaptic vesicle protein 2A (SV2A) which is involved in synaptic vesicle exocytosis, mediating neurotransmitter release.

Its introduction represented a major breakthrough in epilepsy treatment, and it has quickly established itself as the most useful of all new AEDs. It is highly effective in all seizure types, is not

metabolized by the liver and thus has no significant drug interactions, does not require therapeutic monitoring, is often therapeutic at its starting dose and is generally well tolerated. Rare side effects include asthenia and psychosis, particularly in young males with a history of psychiatric illness and somnolence.

Status epilepticus

Status epilepticus occurs when a patient experiences continuous or repeated seizure activity without regaining consciousness for more than 30 minutes. It is most easily recognized as tonic-clonic or convulsive status epilepticus, which is a life-threatening medical emergency. A quarter of cases, however, are non-convulsive in nature, either absences or complex partial seizures that are diagnosed electrophysiologically.

Status epilepticus is most common in infants under 1 year of age and in adults over 65. The commonest causes are non-compliance with medication and withdrawal of existing anticonvulsant drugs in patients with known epilepsy. Alcohol, drug intoxication, and acute metabolic disorders are the most likely factors in patients presenting with new onset status.

Morbidity and mortality reflect the underlying cause and the physiological sequelae of prolonged convulsive activity including for example cardiac arrhythmias, circulatory collapse, hyperthermia, and hypoxia. The mortality of convulsive status epilepticus is around 10%, rising to 50% in the more physiologically challenged elderly population. Mortality is also higher the more acute the insult (e.g. acute cerebrovascular attack or trauma), while status epilepticus from alcohol intoxication or AED withdrawal carries a more favourable prognosis.

The aim of treatment is early termination to prevent neuronal damage caused by systemic and metabolic disturbances and by the direct excitotoxic effect of electrical discharges. The risk of lasting cerebral damage increases progressively if continuous convulsive status epilepticus persists for more than 30 minutes and particularly after 1–2 hours. This is because compensatory mechanisms to prevent brain damage are relatively satisfactory during the first 30 minutes but subsequently break down with increasing speed if the seizures persist unabated. Neuronal damage leads to transient or permanent neurological, epileptic, and cognitive sequelae if it does not prove fatal.

In practice, therefore, most authorities recommend emergent treatment if a seizure has lasted more than 5–10 minutes. Any delay worsens the prognosis and reduces the likelihood of seizures stopping without resorting to general anaesthesia. See Table 82.4.

Table 82.4 Treatment protocol for convulsive status epilepticus in adults

Stage (time)	Action
Stage I. 0–5 minutes *(suspected/impending status epilepticus)*	Diagnose SE or suspected SE by noting recurrent convulsive seizure activity without significant recovery of consciousness Establish and maintain airway Oxygenate (10 litre/min) Monitor vital signs Obtain IV access and start infusion (e.g. normal saline/dextrose saline) Investigate cause—draw blood for metabolic studies, AED levels, and toxic screen Consider early administration of antibiotics if infection is a possibility, thiamine in alcohol abuse or withdrawal, correct hypoglycaemia
Stage II. 5–10 minutes *(early status epilepticus)*	Administer a fast-acting benzodiazepine: 1. lorazepam 0.1 mg/kg at 2 mg/min IV OR 2. diazepam (shorter duration of action) 0.2 mg/kg at 5 mg/min IV Repeat once if seizure continues after 5 minutes Consider PR diazepam if no access—500 μg/kg to a maximum of 30 mg Consider midazolam 10 mg buccal as an alternative
Stage III. 10–30 minutes *(established status epilepticus)*	Introduce a longer acting anticonvulsant: 1. Phenytoin 15–20 mg/kg IV no faster than 50 mg/min in adults and 1 mg/kg/min in children; requires electrocardiogram (ECG) and blood pressure monitoring OR 2. Levetiracetam IV 30–70 mg/kg at 500 mg/min OR 3. Lacosamide IV 5–6 mg/kg at 40–80 mg/min
Stage IV. 30–60 minutes *(refractory status epilepticus)*	General anaesthesia in intensive care with EEG monitoring to achieve 'burst suppression' Review potential causative factors and reverse as indicated Consider intracranial imaging Consider 1. Phenobarbitone IV 20 mg/kg (100 mg/min) OR 2. Midazolam IV 0.2 mg/kg bolus followed by an infusion of 0.1–0.4 mg/kg/hour OR 3. Propofol IV 3–5 mg/kg bolus followed by an infusion of 5–10 mg/kg/hour OR 4. Thiopentone IV 2–3 mg/kg bolus followed by an infusion of 3–5 mg/kg/hour

Source data from Shorvon, S. , Baulac, M. , Cross, H. , Trinka, E. , Walker, M. and , (2008), The drug treatment of status epilepticus in Europe: Consensus document from a workshop at the first London Colloquium on Status Epilepticus. Epilepsia, 49: 1277–1285

Selecting appropriate patients for epilepsy surgery

The work up for epilepsy surgery aims to identify the relevant indications for surgery, in a stepwise fashion, such that seizures are effectively controlled with minimal resulting deficits.

- *Step 1: Confirmation of the clinical indications for surgery*

Establishment of the clinical diagnosis of epilepsy and the type seizures and in particular exclusion of pseudo-seizures is imperative. Adequate medical treatment must have been trialled and in particularly the patient must have been compliant with the medication regime. The impact of uncontrolled seizures on a patient and how much their quality of life is affected dictates whether to proceed with surgical treatment. As such the absolute frequency of seizures that necessitates surgery varies according the patient's view and their occupation. These factors require that an adequate period of time

has elapsed to establish that the seizures are sufficiently uncontrolled prior to consideration of surgery. A prolonged seizure history, on the other hand, may compromise the success of surgery as 'kindling' of further epilepsy foci may occur.

- *Step 2: Confirmation of the epileptic focus as the target for surgery*

Clinical evaluation of the semiology of the seizures, imaging, and surface EEG recordings are sufficient for the majority of cases. For mesial temporal sclerosis an MRI, ideally volumetric, in the correct coronal orientation or showing the appropriate signal changes such as on FLAIR sequences supplemented by EEG are sufficient for localization. For the latter, videotelemetry with surface EEG recordings in an inpatient setting after temporary withdrawal of anticonvulsants or even triggering of seizures is used for sufficient time to capture multiple seizures.

In cases where there is doubt regarding concordance between the imaging and electrophysiological investigations, such as interictal or ictal spikes originating from the contralateral side, then supplementary investigations are required. In practice an ictal SPECT (as described earlier) is most useful as interictal modalities can be less clear and ictal PET is impractical given the very short half-life of the radionuclide agent utilized.

More complex cases require invasive measures such as the placement of subdural grids and/or depth electrodes. These are used for extratemporal hemispheric epilepsy where the focus is accessible to a grid placed in the subdural space adjacent to the focus. Bilateral placement of depth electrodes may also be considered to capture the location or side of a seizure's origin in cases of hippocampal sclerosis. Foramen ovale (sphenoidal) electrode recordings after bilateral percutaneous placements are no longer widely used.

- *Step 3: Predicting and minimizing the resulting deficits following epilepsy focus resection*

Transfer of function away from the seizure focus does not always occur in prolonged epilepsy. There is variability in the extent of functional relocation and it will depend on the integrity of the contralateral hemisphere and alternative areas that can support the lost neurological function following resection. In cases of temporal lobe epilepsy ipsilateral to the side of speech, an amygdalohippocampectomy without neocortical resection will help preserve speech. Demonstration that memory and cognitive function can be provided by the contralateral side prior to an amygdalohippocampectomy is mandatory. f-MRI with memory algorithms will assess this prior to surgery and has largely replaced WADA testing in current practice.

Neuropsychological assessment evaluates cognitive function and helps preoperative planning to limit the deficits. It also identifies and helps to minimize the psychological impact of these procedures.

FURTHER READING

Brodie, M.J., Barry, S.J.E., Bamagous, G., Norrie, J.D., & Kwan, P. (2012). Patterns of treatment response in newly diagnosed epilepsy. *Neurology*, **78**, 1548–54.

Fisher, R.S., Acevedo, C., Arzimanoglou, A., et al. (2014). ILAE official report. *Epilepsia*, **55**(4), 475–82.

Gillam, G.L. (1982). Convulsions following birth asphyxia/birth trauma—are long-term anticonvulsants necessary? *Aust Paediatr J*, **18**(2), 90–1.

Hauser, W.A., Annegers, J.F., & Rocca, W.A. (1996). Descriptive epidemiology of epilepsy: contributions of population-based studies from Rochester, Minnesota. *Mayo Clin Proc*, **71**, 576–86.

Shorvon, S.D., Baulac, M., Cross, H., et al. (2008). The drug treatment of status epilepticus in Europe: consensus document from a workshop at the first London Colloquium on Status Epilepticus. *Epilepsia*, **49**, 2177–85.

REFERENCES

Brodie, M.J., Barry, S.J.E., Bamagous, G., Norrie, J.D., & Kwan, P. (2012). Patterns of treatment response in newly diagnosed epilepsy. *Neurology*, **78**, 1548–54.

Fisher, R.S., Acevedo, C., Arzimanoglou, A., et al. (2014). ILAE official report. *Epilepsia*, **55**(4), 475–82.

Gillam, G.L. (1982). Convulsions following birth asphyxia/birth trauma—are long-term anticonvulsants necessary? *Aust Paediatr J*, **18**(2), 90–1.

Hauser, W.A., Annegers, J.F., & Rocca, W.A. (1996). Descriptive epidemiology of epilepsy: contributions of population-based studies from Rochester, Minnesota. *Mayo Clin Proc*, **71**, 576–86.

Shorvon, S.D., Baulac, M., Cross, H., et al. (2008). The drug treatment of status epilepticus in Europe: consensus document from a workshop at the first London Colloquium on Status Epilepticus. *Epilepsia*, **49**, 2177–85.

RELATED LINKS TO EBRAIN

Acute Symptomatic Seizures. https://learning.ebrain.net/course/view.php?id=1304

Brain Imaging in Seizures and Epilepsy. https://learning.ebrain.net/course/view.php?id=1307

Choosing Antiepileptic Drugs for Focal Epilepsy. https://learning.ebrain.net/course/view.php?id=1310

Choosing Antiepileptic Drugs for Generalized Epilepsy. https://learning.ebrain.net/course/view.php?id=1311

Convulsive Status Epilepticus. https://learning.ebrain.net/course/view.php?id=1312

Diagnosis of Frontal Lobe Epilepsy. https://learning.ebrain.net/course/view.php?id=1313

Diagnosis of Temporal Lobe Epilepsy. https://learning.ebrain.net/course/view.php?id=1314

83

Surgical management of epilepsy

Johannes Schramm

Introduction

Surgical management of epilepsy is indicated in patients with drug-resistant epilepsy. As stated by the International League against Epilepsy (ILAE), drug-resistant epilepsy may be defined as failure of adequate trials of two tolerated and appropriately chosen antiepileptic drug (AED) schedules to achieve sustained seizure freedom (Kwan et al., 2010). In cases of catastrophic epilepsy of early childhood from severe brain malformations early surgery without AED trials for one or two years is possible. The aim is to resect the epileptogenic zone and a possible epileptogenic lesion. Palliative interventions aim to reduce seizure frequency.

Preoperative

History

Taking the history aims at describing seizure types (focal versus generalized), detecting loss of consciousness (simple partial versus complex partial), occurrence of auras, frequency and severity of seizures, and duration of the seizure disorder. Important hints regarding the epileptogenic zone can be obtained carefully exploring the semiology of the seizures. Precipitating events may have happened in the past history, such as early childhood febrile convulsions, brain injury, perinatal brain hypoxia, viral infections known to cause encephalitis, and need to be discussed with patient or parents. Careful history-taking is of utmost importance and the first step of presurgical evaluation.

Imaging

Imaging is primarily done by MRI, but PET and SPECT are also frequently employed. Since 'standard' cranial MRI examinations often fail to show epileptogenic lesions, it is advisable to follow a special MRI examination protocol for cases of pharmacoresistance (Wellmer et al., 2013). These authors propose six essential MRI sequences (FLAIR, T2-weighted, T1-weighted, haemosiderin/calcification-sensitive sequences). Slice thickness for T2 and FLAIR must not exceed 3 mm. T1 images should be acquired in three-dimensional technique at 1 mm isotropic voxel size. For T2 and FLAIR, at least two slice orientations each must be demanded in hippocampal angulation. If a lesion other than hippocampal sclerosis is detected, T1 weighted sequences before and after the injection of contrast are performed (Wellmer et al., 2013). The value of MRI can be enhanced by using fMRI techniques, and morphometric analysis of 3D T1 weighted images for language lateralization and visualization of functionally important whiter matter tracts (Urbach et al., 2015). SPECT is particularly useful as ictal SPECT (i.e. with the radioactive tracer injected after the start and during a seizure). Ictal SPECT identifies areas with ictal hyperperfusion, which is considered a surrogate for the epileptic zone. Depending on the timepoint of injection this technique may more show the area where the seizures propagated into, less the area where they originated from. PET using [18F] fluorodeoxyglucose demonstrates areas of glucose hypometabolism, thought to be concordant with the epileptogenic zone. The technique may be particularly useful in patients where MRI did not show a lesion but a well-defined PET-positive area in the temporal lobe (Carne et al., 2004). The WADA-test consists of an intracarotid amobarbital injection, rendering one hemisphere non-functional for 4–5 minutes, thus lateralizing language dominance. Current use is mainly in candidates for hemispherotomy and callosotomy. In the latter it serves to rule out transposition of either the motor or sensory speech area to the contralateral hemisphere which might have negative consequences if total callosotomy is planned.

Electroencephalography (EEG)

EEG recordings in surgical candidates are indispensable and are performed different from routine EEGs. Recordings with up to 68 channels are typically done in a specialized suite with continuous video surveillance in split-screen technique. Seizure semiology can thus be directly related to the EEG curves shown simultaneously on the same screen. Presurgical video-EEG is done after withdrawal of AED in order to record typical seizures, hoping to get localizing hints about seizure origin. Depending on congruent findings from MRI imaging and video-EEG it may be possible to go forward with planning a resection. In case of incongruent findings or overlap of ictal activity with eloquent cortex, the video-EEG may serve as the basis for planning the insertion of deep electrodes or subdural plate electrodes. In case the ictogenic lesion and/or the ictogenic zone is close to or overlapping with eloquent cortex the implantation of a larger grid-electrode may be necessary, since this can also

be used to map eloquent cortex extraoperatively in the awake patient. Extraoperative mapping with a grid has the advantage that not only functional cortex can be mapped but also seizures can be recorded from the same grid, whereas in awake surgery the recording of seizures cannot usually be counted on. Depth electrodes are inserted using stereotactic techniques and can reach tiny lesions at the bottom of a sulcus or in deeper parts of the cortex difficult to reach with subdural electrodes. Depth electrodes, subdural strips, and grids may be used in combination.

Epilepsy surgery

Epilepsy surgery is usually performed in an epilepsy surgery centre by an epilepsy surgery group and is the penultimate example of multidisciplinary teamwork. In most epilepsy surgery centres the presurgical evaluation is in the hands of the epileptologists and paediatric epileptologists whose main task it is to identify drug-resistant cases and within that group to identify surgical candidates. Part of the team is the neuropsychologist whose tests may point to certain areas of the brain related to cognitive deficits and the neuroradiologist. It is ideal when one neuroradiologist and one neuropathologist is specialized in dealing with the epilepsy surgery cases. Cases are finally discussed in the epilepsy surgery conference where the clinical epileptologist, the electroencephalographer, the neuroradiologist, and the neurosurgeon discuss each case with the aim of forming a hypothesis where seizures originate from, whether there is a lesion and what the significance of that lesion for this epilepsy is and finally what type of resection should be performed. Teamwork is essential as an absolute prerequisite and also for the after-care, management of side effects, the follow-up, and potential decisions on how to handle persisting seizures.

Surgical treatment of epilepsy

Epilepsy surgery comprises a spectrum of interventions, classically divided into temporal and extratemporal resections. See Table 83.1. One can also differentiate between resective and disconnective surgeries since disconnecting an epileptogenic area completely from the surrounding brain, no seizure activity can be conducted. Classic examples are callosotomy or hemispherotomy. Another group is palliative epilepsy surgery, in which complete seizure freedom can rarely be achieved, the aim being a marked reduction in seizure frequency. Palliative techniques are usually employed when resections are impossible, as in multiple subpial transections in eloquent cortex. Some palliative procedures use augmentative techniques (vagal nerve stimulation, deep brain stimulation).

Lesionectomies

Lesionectomies come in three forms: pure lesionectomy, lesionectomy with rim, and extended lesionectomy. Common lesions are vascular malformations, tumours, and focal cortical dysplasias. Whenever possible a total lesionectomy is attempted.

A pure lesionectomy is done when no seizure activity originated away from the lesion and when eloquent cortex does not allow to include a rim. A lesionectomy with rim is the preferred procedure in non-eloquent brain areas. An accepted hypothesis is that seizures originate from the cortical area which borders on the lesion. Based on this hypothesis a common resection technique for lesionectomy is to remove the lesion proper with a rim of surrounding cortex which may arbitrarily be defined (e.g. 1 cm or until next pial layer). In clinical practice a lesionectomy in non-eloquent cortex will usually be performed including the small rim of cortex around it, including deeper lying cortex around a sulcus. Occasionally this rim may be a bit more extended intraoperatively, guided by discoloration, abnormal cortex consistency, or gliotic changes in the immediate vicinity of the lesion. In cavernomas it is safe to assume that in most cases seizures will originate from the haemosiderotic cortical rim around it.

The situation is more complicated when the presurgical evaluation demonstrated an epileptogenic zone extending well beyond the immediate perilesional cortex (Fig. 83.1). How precisely could the epileptogenic zone around or close to the lesion be defined, and therefore how much epileptogenic cortex should be removed together with the lesion for an extended lesionectomy? The combination of lesionectomy plus corticectomy may consist of partial temporal lobectomy or of temporolateral lesionectomy combined with mesial amygdalo-hippocampo-parahippocampectomy. In ETL surgery an extensive variant of extended lesionectomy is a lobectomy or even a multilobar resection. In a recent large cavernoma series with pharmacoresistant epilepsy extended lesionectomies were necessary in 87% of 76 cases (von der Brelie et al., 2013). In the same series seven of 37 lateral neocortical cavernomas were resected together with mesial structures. Defining extent of resection

Table 83.1 Epilepsy surgery spectrum

Bonn University Epilepsy Surgery Group, Germany, 1989–2011

Type of procedure	Absolute numbers		Relative numbers
All therapeutic procedures	2590		100%
Temporal resections	1485		57%
AHE	715		48%
Trans-Sylvian		544	
Transcortical		77	
Subtemporal		72	
ATL	348		24%
With hippocampectomy		321	
Without hippocampectomy		39	
Lesionectomy	345		23%
With hippocampectomy		121	
Without hippocampectomy		224	
Reoperation/extension	65		4%
Extratemporal resections	456		18%
Frontal		289	
Other		167	
Disconnection:			
hemispherotomy/callosotomy	196		7.5%
MST alone	28		1.1%
(MST add-on)	108		
VNS	425		16.4%

AHE, amygdalohippocampectomy; ATL, anterior temporal lobectomy; MST, multiple subpial transection; VNS, vagus nerve stimulator implantation.

Copyright Johannes Schramm, reproduced with permission.

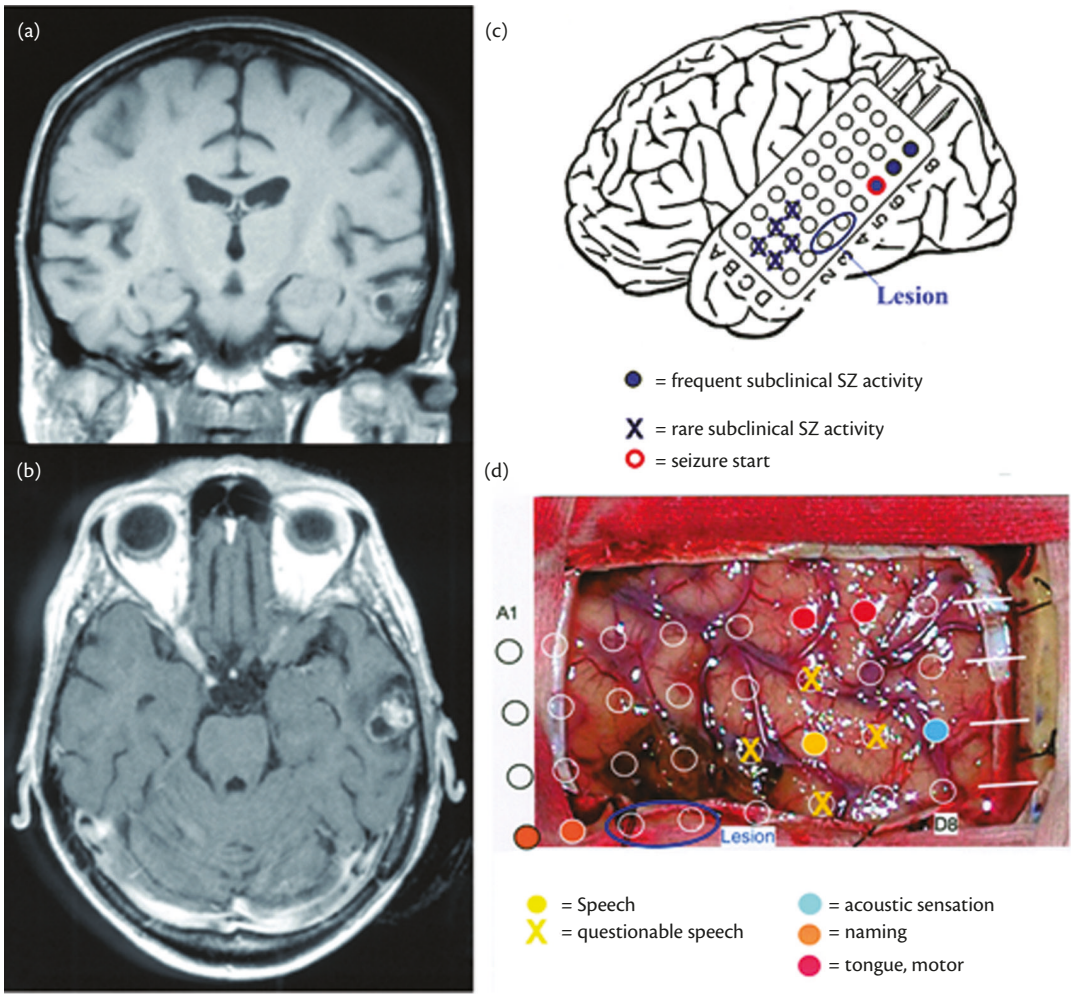

Fig. 83.1 Extended temporo-lateral lesionectomy for left-sided cavernoma. (A, B) MRI images of cavernoma in middle temporal gyrus. (C) Schematic drawing of implanted grid-electrode showing the location of frequent subclinical seizure activity in bottom row posterior to the lesion rare subclinical seizure activity in rows C and B anterior to the lesion as well as location of the seizure origin. The grid was implanted because of the proximity to the presumed speech area and the widespread ictal activity. The drawing is the result of extraoperative mapping. (D) Brain surface with position of electrode contacts shown by circles. The functional results of mapping are described next. The site of the lesion is shown by a blue ellipse and above that the dark area is the haemorrhagic cortex. Using the image from the ictal recordings in C together with the functional results from D it is clear that the seizures start well posterior from the haemorrhagic cortex and the subclinical seizure activity is also far away. The extended lesionectomy included contact B1–3, C1–5, and D1–8. The patient had no speech deficit after surgery

for extended lesionectomies frequently requires invasive presurgical evaluation with strips and grids, especially when eloquent cortex is close. Electrocorticography during surgery is used by some groups to define extent of resection, but of questionable usefulness, since no seizures are recorded, only interictal spikes. It is better to base decisions on ictal recordings (Rostomily and Silbergeld, 2006).

Temporal procedures

Choice of procedure for temporal lobe epilepsy (TLE) depends on type of TLE: mesial temporal lobe epilepsy (MTLE), lateral neocortical TLE, and temporal lobe epilepsy. Neocortical TLE is the rarest type (Walczak, 1995) and usually corresponds to a lesionectomy or an extended lesionectomy, leaving mesial structures behind. MTLE is characterized by seizures originating from the hippocampal/parahippocampal region. Temporal lobe epilepsy without further specification involves both mesial and cortical structures of the temporal lobe. Thus, temporal lobe resections come in three main versions: anterior temporal lobectomy (ATL), lateral neocortical resection, selective amygdalohippocampectomy (SAH). The pure mesial resection in SAH can be done by three approaches: transcortical (Olivier, 2000), trans-Sylvian (Yasargil et al., 1985), and subtemporal (Hori et al., 1993). See **Figure 83.2**. Many groups use ATL (synonym: anterior two-thirds lobectomy) or a combined resection of the temporal pole with extended mesial resection (synonym: cortico-(unco-)amygdalohippocampectomy) also for mesial TLE. The only prospective randomized study comparing drug treatment with surgery was performed for temporal lobectomy and proved surgery to be superior to medication treatment (Wiebe et al., 2001)

ATL is the classic resection type for TLE and by many groups used as a standard TLE procedure. It includes removal of the temporal lobe 5–5.5 cm backward from the temporal tip in the nondominant hemisphere and 4.5 cm in the dominant lobe. The extent of mesial resection can reach more posteriorly than the plane of

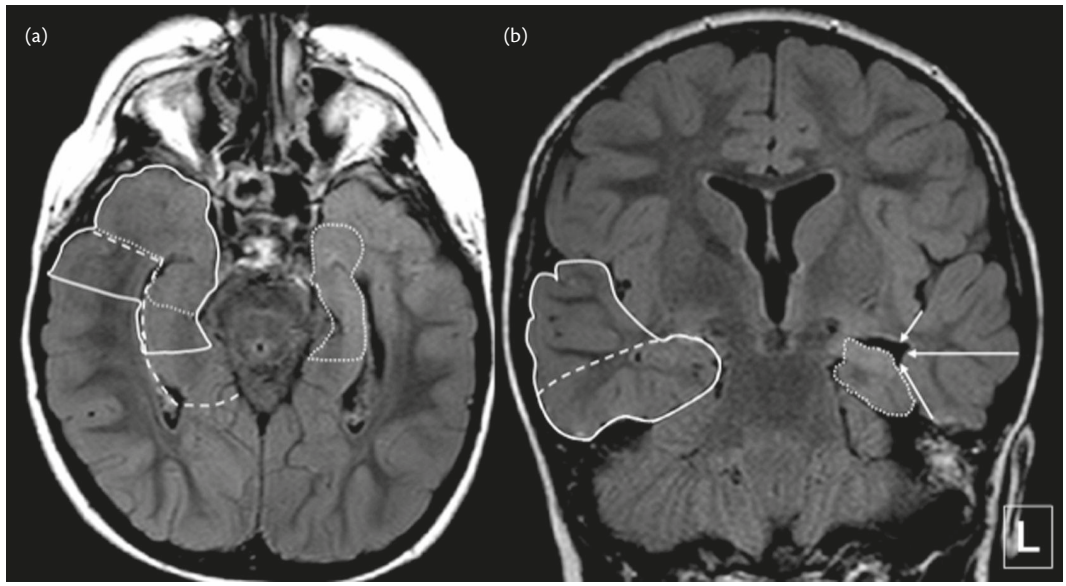

Fig. 83.2 Outline of resection types used for TLE surgery. (A) Axial MRI showing three typical resection types on the right side: Pole resection plus SAH (dotted line), pole resection combined with extensive HC-PHG resection (dashed line), standard anterior temporal lobectomy including mesial resection (solid line). In the left hemisphere the typical resection volume for SAH is outlined. (B) On the coronal MRI the outline of standard ATL is shown (solid line) and the posterior part of pole resection plus extensive amygdylohypocampectomy (AHC) (dashed line). On the right side of the MRI cut the three approaches to the mesial resection of SAH are indicated by arrows. On the left MRI side, the resection is outlined by dashed line.

neocortical resection. As a variation some groups leave the superior temporal gyrus (STG). Via a pterional craniotomy which also exposes about 2 cm of the frontal lobe and the STG and middle temporal gyrus (MTG) the distance to the resection plane is measured from the temporal tip over MTG. As the first of two steps the lateral and basal neocortical tissue block is removed first including the pole, with the second step the removal of the uncus, hippocampus, and parahippocampus. The pia is opened parallel to the Sylvian fissure over the STG and vertically down to the base (**Fig. 83.3**A). The temporal pial layer over the Sylvian fissure is not removed (**Fig. 83.3**B), when transecting the cortex and white matter of the neocortex, one will enter into the temporal horn and with the help of the cavitron ultrasonic surgical aspirator (CUSA) the temporal horn is opened anteriorly to its tip. The STG tissue between this opening and the Sylvian pial layer is removed until one reaches anteriorly the mesial arachnoid of the temporal pole. The neocortical block is still attached to the mesial structures at the base of the temporal lobe. The remaining attachment of the neocortical block is disconnected with the CUSA working laterally and parallel to the hippocampus/parahippocampal gyrus (HC-PHG) in a posterior-anterior direction until the pial cut on the mesial anterior pole area is met. Anterior to the choroidal point the amygdaloid body is bulging in a basolateral direction and can be removed with the ultrasonic aspirator. The choroidal fissure, choroid plexus, and fimbriae are easily identified. The fimbriae along the choroidal fissure are detached with a dissector. The uncus is emptied and the amygdalum removed including the tissue bridge between the head of the hippocampus and the amygdalum, which corresponds to the entorhinal cortex. The greater part of the hippocampal head can be removed, so the HC body is now detached laterally and anteriorly. When removing the amygdalum with the CUSA problems are avoided if a line drawn mentally from the choroidal point to the limen insulae is not crossed mesially. The CUSA is acting directly on the thin arachnoid layer of the mesial temporal lobe which is covering the vessels going around the brain stem, the third nerve, and the peduncle. By carefully choosing the right CUSA setting it is usually possible to not open the mesial arachnoid, except for small children.

The HC-PHG block is still attached mesially to several small arteries covered by a double layer of pia mater which enter the hippocampal sulcus from a mesial to a lateral direction. In theory it would be possible to use the CUSA and just remove the superficially located HC and the PHG below the vascular pedicle of the hippocampal sulcus. If one wants to obtain a good specimen of the hippocampal structure, *en-bloc* removal is aimed for. By elevating the fimbriae, the double layer of pia mater covering the arteries in the hippocampal sulcus can be visualized. The combined HC-PHG block can then be disconnected posteriorly using the CUSA, leaving the vessels in the hippocampal sulcus with their double pial layer as residual attachment. A final step is to open the pia mater along the choroidal fissure to gain access to the vessels which are coagulated preferably inside the hippocampal sulcus and cut. Then the lower second pial layer of the hippocampal sulcus is also cut. Mesially and mesiobasally, the layer of pia mater over the PHG is left intact and using a dissector the PHG is detached from its pia mater and mobilized in a lateral direction out of its pial bed. Usually, a 15–20 mm segment of combined hippocampus and parahippocampus can be obtained. In the majority of cases the mesial pial layer over the brainstem and the vessels can be preserved. Bipolar coagulation is only used on the small arteries in the sulcus which need to be cut a short distance away from the larger arteries going around the brainstem. Oxidized cellulose usually takes care of minor bleedings from the exposed pial layers.

A popular alternative to a standard resection for TLE is the combination of a temporal pole resection with more posteriorly extended resection of mesial structures. (synonyms: Spencer-type resection, cortico-(unco-)amygdalohippocampectomy). This approach is used

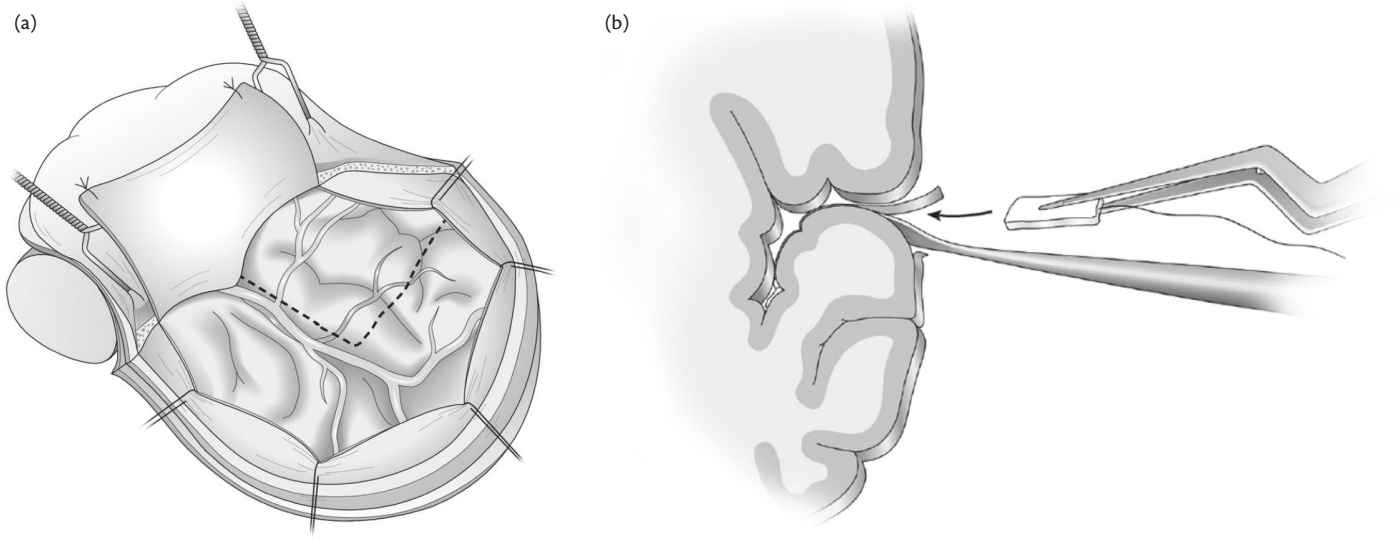

Fig. 83.3 (A) Schematic drawing of craniotomy for right-sided standard anterior two-thirds temporal lobectomy. The dotted line indicates the pial incision. (B) Schematic drawing where to develop the subpial plane on the superior temporal gyrus very close to the Sylvian fissure in order to preserve the pial layer overlying the arteries in the Sylvian fissure.
(A and B) Courtesy of Isabelle Christensen and Johannes Schramm.

in some centres as the standard approach for temporal lobe epilepsy but it also very useful if a small lesion (e.g. cavernoma or benign tumour) is located in the pole, in the amygdalum, or in the head of the hippocampus.

After a craniotomy similar to standard ATL the temporal pole is resected about 3 cm behind the polar tip. Pia is opened parallel to the Sylvian fissure and vertically down to the base. Using the CUSA one reaches the base of the temporal lobe and passing through the white matter the tip of the temporal horn is opened. Leaving the arachnoid over the middle cerebral artery intact, the uncus is emptied, and the head of the hippocampus with the amygdalum opposite is exposed. In order to reach further backward to increase extent of mesial resection, the cut surface of the temporal lobe is retracted posteriorly above the level of the opened temporal horn. The combined block of HC-PHG now needs to be mobilized laterally, posteriorly, and mesially. The anterior disconnection consists of removing the bulging major part of the amygdalum and most of the hippocampal head with the attached entorhinal cortex. The lateral disconnection is best performed by a CUSA, or bluntly with a dissector, posterior disconnection can be done with a CUSA or bipolar and suction. Mesial disconnection is achieved similar to the steps described for ATL.

Selective amygdalohippocampectomy (SAH) is considered an adequate or even ideal resection type for mesial TLE, typically caused by ammonshornsclerosis (synonym: mesial temporal sclerosis, hippocampal sclerosis). It can also be used for small lesions in these mesial structures, posterior to the choroidal point. Three approaches exist: trans-Sylvian, transcortical, and subtemporal.

A pterional craniotomy is used for trans-Sylvian SAH (Yasargil et al., 1985), which should expose about 2 cm of the frontal lobe and 3 cm of the temporal lobe. The Sylvian fissure is opened. The MCA is dissected carefully to expose the inferior circular sulcus in its first 15–20 mm behind the limen insulae (Fig. 83.4). The next step is opening of the temporal horn via an incision in the inferior circular sulcus reaching about 15 mm backward from the limen. Dissecting with bipolar coagulation through the temporal stem in a slightly basolateral fashion one should reach the ventricle after about 12–15 mm (Fig. 83.5). This opening of the ventricle is then enlarged towards the tip of the temporal horn, first working around the supero-medial bulging amygdalum. Inside the ventricle the choroidal plexus, the choroidal fissure, and the choroidal point are identified. Outside the ascending M1 can be seen and the next step is emptying the uncus, carefully leaving the mesial arachnoid intact. The fimbriae are then detached and

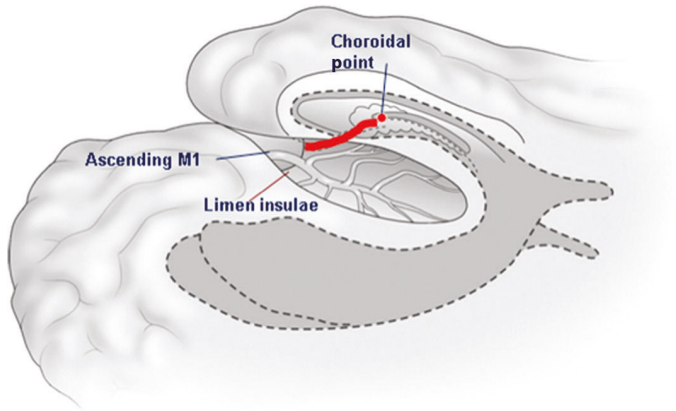

Fig. 83.4 Schematic drawing of right trans-Sylvian approach to expose insular cortex and MCA branches with projected outline of temporal horn, choroidal point, and limen insulae. The red line describes the most mesial extent of the resection, and after opening of ventricle is mentally drawn between the limen insulae and the choroidal point. Working anterolateral and along this line, no adverse effects have to be feared, resecting the amygdalum and the head of the hippocampus. This is an important landmark when dealing with small tumours in the head of the hippocampus.
Courtesy of Isabelle Christensen and Johannes Schramm.

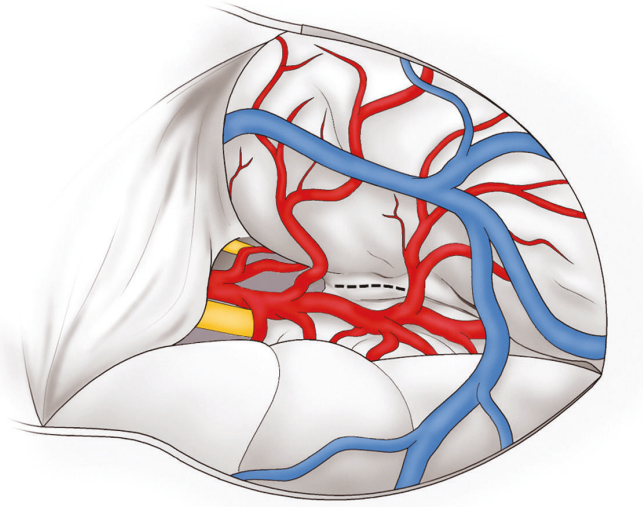

Fig. 83.5 Exposure of insular cortex and limen insulae to demonstrate entry area into temporal horn for selective amygdalohippocampectomy entry area (dotted line). Sylvian fissure has been opened in its anterior aspect, exposing the inferior circular sulcus and the ascending M1 and M2–M3 branches.
Courtesy of Isabelle Christensen and Johannes Schramm.

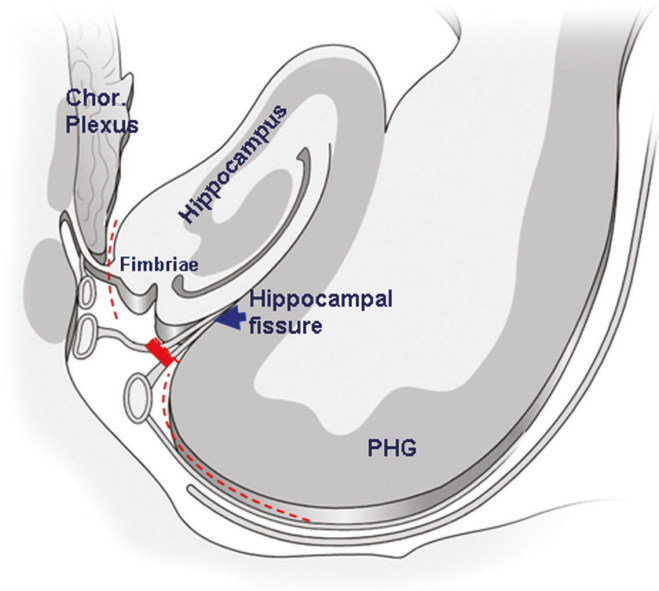

Fig. 83.6 Schematic drawing of coronal section of the mesiobasal structures of the left temporal lobe. The HC, PHG, and the hippocampal sulcus are shown, with the solid red line indicating the area where the small vessels in the hippocampal fissure are transected. The shorter dotted line shows the area where the fimbriae can be elevated with the blunt dissector and the longer dotted red line is outlining the subpial plane between the tissue of the PHG and its pial mesiobasal layer.
Courtesy of Isabelle Christensen and Johannes Schramm.

anterior to the choroidal point the bulging amygdalum is removed with a CUSA and the mesiobasal tissue bridge between the amygdaloid body and the hippocampal head is also removed with a CUSA, this disconnection leading directly into the emptied shell of the uncus. Again, one works directly on the mesial arachnoid, the CUSA setting must be appropriate. At this stage, the HC-PHG block is detached mesially. Posterior disconnection is then done with a CUSA, followed by lateral disconnection either with a dissector or a CUSA leaving the basal pia intact. The central part of hippocampal body with PHG attached can now be detached from its pial cover after having cut the two pial layers which encase the vessels and the hippocampal sulcus (see Fig. 83.6). In this way an *en-bloc* specimen of combined HC and PHG can be obtained, allowing precise histological diagnosis and analysis for scientific purposes, having obtained permission from each patient.

A lateral transcortical or trans-sulcal approach can also be used for SAH (Niemeyer, 1958; Olivier, 2000). A linear incision and a smaller craniotomy suffice. It is not easy to find the ventricle, so navigation is useful. The opening in the cortex is about 15 mm in anteroposterior (AP) direction. It is advantageous to enter the ventricle low and not to injure the roof of the temporal horn since there the fibres of Meyer's loop are located. The detachment and mobilization of the HC-PHG tissue block is performed from a different perspective but following the same principles as in trans-Sylvian SAH (i.e. leaving the mesial arachnoid intact and cutting the vessels in the hippocampal sulcus). One should also empty the uncus and remove the larger part of the amygdalum in this approach.

The third approach variant for SAH is via the subtemporal route (Hori et al., 1993; Park et al., 1996). It is usually done via a linear incision and a small very basally located craniotomy. Mesial structures can be reached via various pathways, through the fusiform gyrus, or via the PHG or via the collateral sulcus. For this the temporal lobe needs to be elevated, occasionally made difficult by basal temporal veins. In that case the basal pia of the inferior temporal gyrus is opened, and the cortex is elevated leaving the pia behind on the temporobasal dura. In rare cases a small tunnel through the ITG is created with a CUSA not higher than about 8–10 mm which significantly improves the ability to elevate the rest of the temporal lobe without damage to basal veins. It may be difficult to find the ventricular lumen and the coronal MRI will clearly show the distance the surgeon has to go underneath the temporal lobe (approximately 22–25 mm) before dissecting obliquely upwards through the cortex to reach the ventricle. Having entered into the ventricle this transcortical incision is elongated so one has a better overview over the content of the ventricle and can identify the landmarks (fimbriae, choroidal point, amygdala bulge). The HC head, the entorhinal cortex, and the amygdalum are removed with a CUSA followed by emptying the uncus. The HC-PHG block is then mobilized in a similar fashion as described for the transcortical and trans-Sylvian approach.

Lateral neocortical temporal lobe resections are usually performed for a lesion. They may be necessary as a lesionectomy with rim, or an extended lesionectomy including an area of adjacent cortex. In rare cases a larger block of lateral neocortex may be removed. The craniotomy does not need to reach above the Sylvian fissure for more than a few millimetres. A curvilinear or question-mark incision is used depending on how far posterior the lesion is located. Especially in dorsally located lesions a grid may have previously been used to map language-relevant cortex. The principle requires that all cortical tissue under the designated surface area be

removed including the cortex at the bottom of the sulcus. This can easily be done with a normal sucker or a CUSA. Dorsolateral temporal lobe lesionectomies are the only area where awake craniotomy can be helpful to locate language-relevant cortex. Larger arterial branches or the vein of Labbé need to be spared, and the resection must not extend into the white matter of the temporal lobe in order to spare the optic radiation.

Vagal nerve stimulation (VNS)

The implantation of a vagal nerve stimulator is a palliative procedure with the aim to reduce the frequency of seizures in drug-resistant patient. It is only indicated after a proper epileptological evaluation, ideally presurgical evaluation, which did not result in the detection of an operable epileptogenic lesion or zone. In case of medically refractory epilepsy and a resectable lesion, the resection should always be preferred to VNS implantation because it has the potential to cure the epilepsy. VNS is currently used for generalized and partial seizures and in many studies a greater than 50% reduction of seizure frequency in over 50% of the patients can be achieved. In some long-term studies an increase in the reduction of seizure frequency from over 50% to 70–80% has been described (Spanaki et al., 2004; Uthman et al., 2004). VNS is used in adults and the paediatric population, provided body size can accommodate the pulse generator, the current model being 45 × 32 × 7 mm. As a positive side effect, improvements in quality of life have been documented after VNS implantation (Cramer, 2001; Spanaki et al., 2004).

Extensive scarring after previous left-sided neck surgery constitutes an exclusion criterion. During surgery monopolar diathermy cannot be used, only bipolar.

A VNS set consists of a pulse generator, a lead with the helical vagus electrodes and a programming unit. A hand-held programmer covered by a sterile bag during surgery, held over the pulse generator can wirelessly set the stimulus parameters.

The patient is positioned and draped for two left-sided incisions, one at the neck below the level of the carotid bifurcation and one in the anterior-axillary line for the creation of an infraclavicular subcutaneous pocket. The left side is chosen because the left vagus nerve contains less nerve fibres going to the atrium than the right one. The vagus nerve runs with the carotid artery and jugular vein and should be freed from the connective tissue sheath for approximately 3 cm. The cervical end of the connection cable has three helical structures: two electrodes and one anchor. The highly flexible helices are placed around the vagus and anchored to deeper fascial layers with two plastic anchors, avoiding muscles which might move. See **Figure 83.7**.

A third of these anchors is used to fix the cable more superficially but underneath the platysma. From a short incision in the anterior-axillary line a subcutaneous pocket is formed over the pectoralis fascia, large enough to bury the pulse generator so that the suture line is circa 2 cm away from the pulse generator. The tunnelling instrument provided in the VNS set is used to pull the cable from the cervical incision down to the infraclavicular pocket. Cable loops should be formed and placed in the generator pocket away from the skin incision in order to avoid damage when generator replacement becomes necessary. The generator is placed with the inscription on top and fixed in the depth of the pocket with a single suture through a hole provided for that purpose. Older models of the generator may have different connector sockets and details should be looked up in the manual of the manufacturer. Before definitely closing the wound an intraoperative testing of the lead is performed, testing impedance of the electrodes and a test stimulation can be performed. The wounds are closed in two layers.

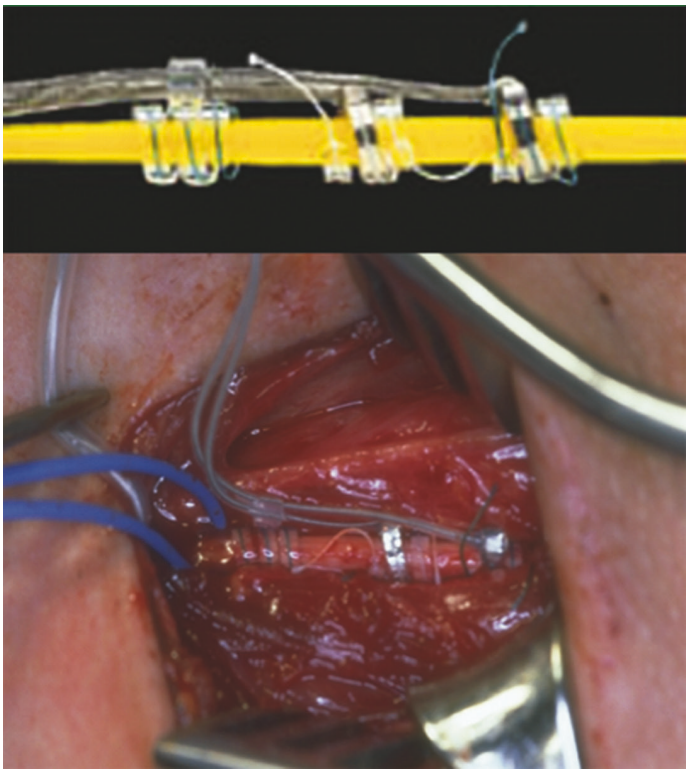

Fig. 83.7 VNS electrode sample and implant.

In rare cases a subpectoral implantation may be preferred (e.g. in patients with very little or no subcutaneous fat). Modern generator models have a battery life of 5–8 years, depending on stimulus parameters. Stimulation can begin immediately after the surgery, although many groups prefer to wait some time before stimulation is initiated. Patients are provided with a magnet which stops the stimulation when held directly over the implanted pulse generator until the magnet is removed. This may be useful for patients who have a hoarse voice during stimulation periods and want to sing or need to speak in public. The magnet can be swiped over the pulse generator to trigger an on-demand stimulation, which some patients use when they feel an aura is preceding a possible seizure. MRI head scans are possible while the generator output is programmed to 0 mA during the scan. Stimulation parameters vary but usually a short period of stimulation is followed by longer silent period. Details can be looked up in the VNS physicians' manual.

Hemispherectomy/hemispherotomy

The indication for this procedure is established for unihemispheric lesions causing intractable seizures. This hemispheric damage is usually associated with some degree of hemiparesis, frequently cognitive impairment, and hemianopia. In cases of catastrophic epilepsy in small infants where drug treatment is known to not work, very early surgery in the first months of life may be indicated. Ideally all seizures should originate in the affected hemisphere.

Classic anatomical removal of one hemisphere was largely replaced by surgery types with less tissue resection and more disconnection such as Rasmussen's functional hemispherectomy (Rasmussen, 1983). The trend to replace resection by more disconnections has evolved during the last 25 years using the terms hemispherotomy and hemispheric disconnection or deafferentation. For Rasmussen's functional hemispherectomy, functionally equivalent to anatomic resection, only a large temporal lobe resection and a large central resection is done, the rest is disconnected but remains *in situ*. The less tissue is removed the more the term hemispherotomy is justified and this includes the dorsal transcortical subinsular hemispherotomy (Delalande et al., 2007) the trans-Sylvian-transcortical-transventricular keyhole hemispherotomy (Schramm et al., 2001) and the perisylvian window technique (Villemure and Mascott, 1995), and related techniques (Shimizu and Maehara, 2000). For clarity one should restrict the term hemispherotomy for those procedures where very little brain is removed.

The advantage of the modern hemispherotomies is a marked shortening of surgery time, a significant reduction in blood loss, a reduced necessity for blood transfusion, a smaller extent of exposure with a reduced incidence of intraoperative problems. These advantages are significant in small infants and babies, but also welcome in older patients.

Common structural lesions of the hemisphere are inborn developmental defects (hemimegalencephaly, multilobar dysplasias, and others), Sturge-Weber syndrome and acquired lesions (perinatal infarctions or haemorrhages, Rasmussen's encephalitis, or post-traumatic and postencephalitic damage).

Occasional contralateral seizures or bilateral epileptogenic activity is not an automatic contraindication as satisfying rates of seizure freedom are possible (Doring et al., 1999). Indicating hemispherotomy and finding the right time-point is difficult and sometimes problematic, especially in Rasmussen's encephalitis when the dominant hemisphere is affected.

Surgical techniques

Hemispherotomies are technically demanding especially in cases of hemimegalencephaly or extensive holohemispheric dysplasia. The modern hemispherotomy procedures have in common that the callosotomy is done from within the ventricle, with ventricular access achieved by opening the Sylvian fissure or creating a window through the operculum. The disconnection of the frontal, temporal, and occipitotemporal lobe is also done through this exposure. Various modifications have been used (Devlin et al., 2003). See **Figure 83.8**. The dorsal transcortical approach is also using the transventricular route to disconnect the hemisphere from its neocortical mantel (for more detailed descriptions, see Schramm, 2002), alternative techniques, such as hemidecortication are used less commonly.

Rasmussen's functional hemispherectomy needs a large craniotomy exposing the central part of the hemisphere including all of the temporal lobe. It includes removal of the temporal lobe and a large central supra-Sylvian block of cortex (about 7–8 cm) exposing the falx and the corpus callosum. Then callosotomy is performed and the frontal and parieto-occipital lobes are disconnected from the basal ganglia block.

The trans-Sylvian keyhole technique (Schramm et al., 2001) is done via a 4–5 × 4–6 cm craniotomy placed above the Sylvian fissure, followed by exposure of the circular sulcus which is limiting the insular cortex. Next step is complete opening of the ventricle from the temporal horn all around the basal ganglia block to the tip of the frontal horn via a transcortical disconnection. The next step is a temporomesial disconnection along the choroidal fissure carried forward beyond the choroidal point to the mesial arachnoid of the uncus. To gain histology it may be appropriate to remove parts of the HC-PHG block. The next step using the transventricular approach is the mesial disconnection of the frontal and parieto-occipital lobe, including a callosotomy from within the ventricle. To start the fronto-basal disconnection a mental line is drawn from the ascending M1 to the tip of the open frontal horn, the lateral surface of the basal frontal lobe is coagulated and with the aid of the microscope the disconnection is carried through the frontal white matter with a CUSA always following the outline of M1 and later A1. This leads automatically to the interhemispheric fissure where the disconnection line is then orienting itself along the outline of the A2 which leads around the anterior part of the corpus callosum to the roof of the corpus callosum. One can then follow the pericallosal artery always transecting the callosal white matter and one will automatically end-up at the inferior rim of the falx which then turns basally into the falcotentorial margin. Thus, in the posterior half of the mesial disconnection it follows the margin of the falcotentorial rim. This will lead the surgeon through the trigone down to the temporal area meeting the initial temporo-mesial disconnection. At the end of the mesial disconnection the isolated basal ganglia block has circumferentially been disconnected. It is advisable to then remove the cortex of the insula with suction underneath the M2 branches to remove a potential source of persisting seizures. Haemostasis is usually achieved only with oxidized cellulose followed by copious irrigation. Minor branches of the M3-M4 calibre can be sacrificed but all major M2 and M3 branches are preserved, as well as the posterior cerebral artery.

Perisylvian window techniques (Villemure and Mascott, 1995; Shimizu and Maehara, 2000) follow the same principle after exposure of the insular cortex by resection of the opercula.

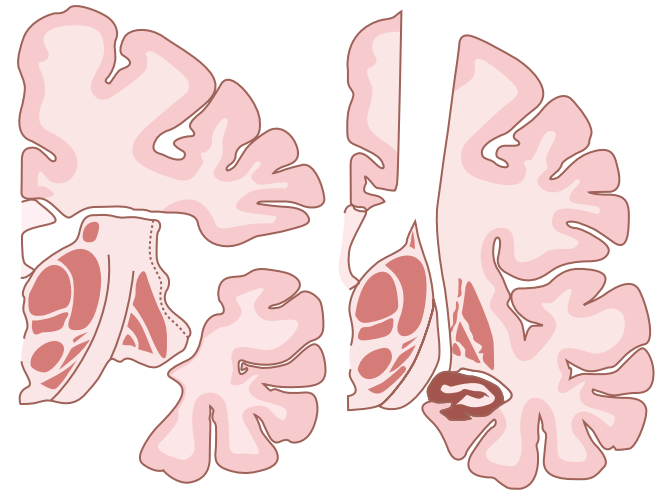

Fig. 83.8 Scheme of disconnections in trans-Sylvian keyhole (left) and dorsal transcortical hemispherotomy (right).
Courtesy of J. Schramm.

In dorsal transcortical transventricular hemispherotomy (Delalande et al., 2007), parasagittal craniotomy about 4 × 5 cm reaching about 3 cm behind the coronal suture is used. The lateral ventricle is accessed transcortically exposing the foramen of Monro and the posterior thalamus. A paramedian callosotomy is performed through this approach. A lateral disconnection is performed between the lateral border of the thalamus and the striatum from the ventricle reaching the temporal horn in the depth. Starting from the frontobasal part of the anterior callosotomy the posterior part of the gyrus rectus is removed and the transection line is extended laterally through the head of the caput caudatum and will then meet the lateral substriatal transection. Dorsally the substriatal disconnection line is connected to the posterior callosotomy line with suction, thus isolating the basal ganglia block from the hemisphere.

Both the trans-Sylvian and the dorsal transcortical hemispherotomies, have the advantage of low blood loss and small exposure with low transfusion rates. The dorsal approach preserves all of the superficial large vessels and avoids manipulation of the middle cerebral artery. The trans-Sylvian keyhole technique is ideal for patients with porencephaly or marked atrophy, suitable for near normal brain size, but for cases with hemimegalencephaly it is recommended to combine it not with opening the Sylvian fissure but with creating an opercular window similar to the perisylvian window technique.

Hemispherotomies are associated with unavoidable side effects such as completion of partial hemianopia, loss of fine pincer movement in the affected hand, sometimes deterioration in walking ability. Risks include all classical risks of craniotomy, development of hydrocephalus requiring a shunt, need for transfusions, and very rarely death. In modern series mortality rates around 1% have been described. There is also a certain risk of incomplete disconnection and of persisting seizures. All procedures are associated with a certain hydrocephalus rate varying between 5 and 30%, see discussion in (Schramm et al., 2012). Shunt rates in other series were 8%, 16%, 19%, and 23% for the modern hemispherotomies, for corticectomies up to 32% and in a large multicentre study of posthemispherectomy hydrocephalus with 690 patients the average rate was 23%. Anatomic hemispherectomy was a significant risk factor for developing hydrocephalus (Lew et al., 2013). Incomplete disconnection rates occur with every technique, even with Rasmussen's technique and incomplete resection rates between 2% and 30% have been described. Shunt rates are influenced by aetiology and surgery type. Particularly high shunt rates are observed in hemimegalencephaly patients. Shunt implantations may be necessary very late, 6–8 years after initial surgery. A recent survey of paediatric hemispherotomies described a mortality rate of 0.7% in 153 cases (Koubeissi et al., 2009).

Other operations for epilepsy

Callosotomy is a well-established procedure indicated for drop attacks, generalized tonic-clonic seizures (GTCS), atonic seizures, or Lennaux–Gastaut syndrome. By interrupting the propagation of ictal activity from one hemisphere to the other it is particularly useful to alleviate drop attacks and/or GTCS. It is frequently done limited to the anterior two-thirds or four-fifth of the corpus callosum, less frequently as a two-stage complete callosotomy (Spencer et al., 1988). Specific indications (partial vs. complete callosotomy) are less well defined than for other epilepsy resections. Among the many open questions, two are whether the anterior commissure should be transected, or whether the dorsal hippocampal commissure should be transected. Candidates for callosotomy frequently have several seizure types but the main aim is the abolition of drop attacks. It should be noted, that in about 25% of cases a temporary increase in focal seizures is observed.

In a series of 95 cases satisfactory seizure outcome (i.e. a combination of no seizures and over 75% reduction in seizure frequency was achieved in 77% of both, cases with leading drop attacks and with leading generalized tonic-chronic seizures. Anterior half callosotomy was found less effective than anterior two-thirds callosotomy (Tanriverdi et al., 2009). In the supine position an anterior unilateral frontal craniotomy, its medial border on the midline, about 6–7 cm long, 4 cm wide, allows to navigate around larger bridging veins. It is possible to sacrifice one smaller bridging vein. The non-dominant hemisphere is chosen for the interhemispheric approach. Arachnoid adhesions are carefully dissected under the microscope, especially where both hemispheres are adherent. Injury to the gyrus cinguli must be avoided, or at least restricted to one side. The corpus callosum is easy to identify, also helped by the two pericallosal arteries. These are carefully separated and covered by cottonoids. The transection of the corpus callosum can easily be done with bipolar and sucker or by CUSA at a very low setting. Some authors recommend to preserve the ependyma, but this is frequently impossible. In the supine position it is possible to reach far backward with the transection through a single frontal approach, but in case complete callosotomy is planned, some authors recommend separate frontal and parietal craniotomies. To determine the precise extent of transection one can either use a small strip of millimetre paper or intraoperative navigation. Some authors prefer the lateral decubitus position to allow the hemisphere to fall back, avoiding retractor pressure. In the lateral position it is more difficult to do a complete callosotomy through one craniotomy.

Disconnection or resection of hypothalamic hamartoma

These hamartomas may be pedunculated or broad-based and belong to the minority of lesions where seizures are generated inside the lesion. Removal is always difficult, a bit easier when using a transventricular endoscopic approach. Broad-based lesions are preferred for endoscopic disconnection. Side effects include memory deficits and considerable endocrine dysfunction (polyphagia, obesity). Alternative techniques include radiosurgery or electrocoagulation via a stereotactic electrode. Results are mixed, usually the rate of seizure freedom is well below 50%.

Multiple subpial transections (MST). MST belongs to the palliative procedures and is rarely used as a stand-alone intervention. It is mostly used as an add-on to lesionectomy or corticectomy when these areas border on motor, language, or visual cortex. To assess the effectivity of the procedure is difficult since no larger series of pure MST cases have been published (Schramm et al., 2002). Engel class I outcomes are rare, however, improvement, classified as Engel class II and III can be achieved in 45–70% of cases, somewhat depending on the definition of success for such a palliative intervention (Spencer et al., 2002). Opinions on the usefulness of MST are divided, arguments for and against have been summarized (Ojemann, 2006; Wyler, 2006). MST are based on the principle that the synchrony between groups of cortical neurons via bilateral spread within the ictogenic cortex could be weakened by interrupting the short lateral connecting fibres within the cortical layer, sparing the

efferent long fibres. Parallel cuts at 5 mm intervals are made with a blunt hook to a depth of about 5–6 mm across the superficial surface of a gyrus after inserting it into a tiny pial hole. Doing the same to the lateral banks of a gyrus is more difficult and more risky. Using the hook with the tip pointing downward appears to be a safer technique. Small bleedings are usually treated with oxidized cellulose and tamponade, larger bleedings are rare. Done in the motor cortex major deficits are exceedingly rare, some clumsiness is usually transient. Larger cortical areas may be treated in this fashion.

Deep brain stimulation is an augmentative and palliative technique. The indication is medically refractory partial seizures, including secondarily generalized seizures. In a prospective randomized study (Fisher et al., 2010) it was found that 54% of patients had a seizure reduction of at least 50% and 14 patients were seizure-free for at least 6 months. In the stimulated group 14% of participants reported depression and 13% memory problems. The procedure is not paid for in many countries, but mentioned here as an example of an augmentative modality fulfilling the criteria for successful palliative treatment. A recent review compares outcomes of different palliative procedures, including VNS versus callosotomy and MST (Fauser and Zentner, 2012).

Responsive cortical stimulator implantation

A recent randomized double-blind study (191 patients) for intractable partial epilepsy (Morrell, 2011) found after 12 weeks seizure frequency significantly reduced by 37.9% versus 19.3% in controls. Median seizure reduction increased to 44% at one year and to 53% at two years, and it ranged from 48% to 66% over postimplant years three to six (Bergey et al., 2015). Different healthcare systems will make different decisions regarding payment for implantation of these expensive palliative devices.

Box 83.1 Seizure outcome classifications

Engel outcome classification (Engel and Pedley, 2008)

- Class 1—free of disabling seizures
  - (completely seizure-free; non-disabling, simple partial seizures only; some disabling seizures, but free of disabling seizures for at least 2 years; generalized convulsion with antiepileptic drug withdrawal only)
- Class II—rare disabling seizures
  - (initially free of disabling seizures, but rare seizures now; rare disabling seizures since surgery; more than rare disabling seizures, but rare seizures for at least 2 years; nocturnal seizures only)
- Class III—worthwhile improvement
  - (worthwhile seizure reduction; prolonged seizure-free intervals amounting to more than half the follow-up period, but not less than 2 y)
- Class IV—no worthwhile improvement
  - (significant seizure reduction; no appreciable change; seizures worse)

ILAE outcome classification

1. Completely seizure-free; no auras
2. Only auras; no other seizures
3. 1 to 3 seizure days per year; ± auras
4. 4 seizure days per year to 50% reduction of baseline seizure days; ± auras
5. Less than 50% reduction of baseline seizure days; ± auras
6. More than 100% increase of baseline seizure days; ± auras

a) Reproduced with permission from Jerome Engel, Surgical treatment of the epilepsies, Lippincott Williams & Wilkins, NY, Copyright © 1993.

b) Reproduced with permission from H.G. Wieser, W.T. Blume, D. Fish, et al., Proposal for a New Classification of Outcome with Respect to Epileptic Seizures Following Epilepsy Surgery, Epilepsia, Volume 42, Issue 2, pp. 282–6, Copyright © 2003 John Wiley and Sons.

Postoperative

Outcome

Assessment of seizure outcome is not as simple as it appears. Ideally outcome should not only consider freedom from seizures but also quality of life. Ideal outcome is complete freedom of seizures including auras, including good quality of life, and full social re-integration. The most commonly used outcome scales mainly measure seizure outcome: Engel classification and the ILAE classification (see **Box 83.1**). Some seizures are severe, others hardly noticed in daily life, so seizure severity is very difficult to classify.

Minimum follow-up should be two years for outcome statistics. In general, TLE surgery outcomes are better than ETLE surgery outcomes (Engel class I between 65 and 75% for TLE, ETLE outcomes approximately 10% less), but a loss of about 1% seizure freedom per annum in the next couple of years is frequently observed. Reoperations carry success rates between 50 and 69% (Grote et al., 2016) A good discussion of outcome assessment problems and outcomes are described by Ojemann and Jung for TLE (Ojemann and Jung, 2006), and by Geller and Devinsky 2006 for ETLE (Geller and Devinsky, 2006) and Tellez-Zenteno and colleagues in 2005 (Tellez-Zenteno et al., 2005). Comparing operated with non-operated patients, Schmidt and Stavem (Schmidt and Stavem, 2009) concluded that 'the combination of surgery with medical treatment is four times as likely as medical treatment alone to achieve freedom from seizures'.

Complications

Epilepsy surgery, usually performed in younger and mostly healthy patients, carries the typical risks of cranial surgery (infection, haemorrhage, and so on), plus risks specifically associated with different epilepsy surgery types. See frequency and literature in Tanriverdi et al. (2009). Typical problems after TLE surgery include visual field defects, temporary dysphasia, and small infarcts and increased rates of depressive episodes. Cognitive side effects such as verbal memory decrease are observed after left-sided TLE surgery. Permanent morbidity rates around 2% are typically observed. Surgical complications (infection, thrombosis, and so on) are observed in 2–5% but rarely cause permanent sequelae. Mortality rates are well below 1%, in hemispherotomy series around 1%.

Controversy: Small or larger resection for TLE

This discussion is relevant only for mesial TLE. The hope is that restricted mesial resections (SAH) are associated with less cognitive side effects but similar seizure outcomes.

Evidence has been accumulating that seizure outcomes for SAH and TLR are rather similar (Schramm, 2008). In this review

most authors (6/8) found seizure outcome in SAH to be similar to that of lobectomy. There was evidence for a slightly better neuropsychological outcome for SAH in 11 of 14 studies. A meta-analysis (Josephson et al., 2013) based on 11 studies however found that 'participants were statistically more likely to achieve an Engel class I outcome after ATL compared with SAH'. The question whether a more limited mesial resection has comparable seizure outcome to TLR has not definitely been settled. The limitations of comparing studies using variable resection types have extensively been discussed (Schramm, 2008).

The question whether the mesial resection should be extended maximally in the dorsal direction is also open, since 7 of 12 studies (58%) in the first review found that seizure outcome was not related to extent of mesial resection. It is important to realize that there is only one prospective randomized study testing larger versus smaller mesial extent of resection (Schramm et al., 2011). The intent-to-treat analysis in this study with MRI volumetric determination of resection extent did not show a different seizure freedom rate for the more posteriorly reaching 3.5 cm resection group. This result remained the same when looking at volumetrically determined true resection length as compared to intended length.

FURTHER READING

Engel, J. Jr. & Pedley, T.A. (eds.) (2008). Surgical therapy, section VII. In: *Epilepsy: A Comprehensive Textbook*, 2nd edition, vol. **2**, pp. 1747–956. Philadelphia, PA: Wolters Kluwer, Lippincott Williams and Wilkins.

Miller, J.W. & Silbergeld, D.L. (eds.) (2006). *Epilepsy Surgery: Principles and Controversies*. New York, NY: Taylor and Francis.

Schramm, J. & Clusmann, H. (2008). The surgery of epilepsy. *Neurosurgery*, **62** Suppl 2, 463–81; discussion 481.

Tanriverdi, T., Ajlan, A., Poulin, N., & Olivier, A. (2009). Morbidity in epilepsy surgery: an experience based on 2449 epilepsy surgery procedures from a single institution. *J Neurosurg*, **110**, 1111–23

Wiebe, S., Blume, W.T., Girvin, J.P., & Elliasziw, M. (2001). A randomized, controlled trial of surgery for temporal-lobe epilepsy. *N Engl J Med*, **345**, 311–18.

REFERENCES

Bergey, G.K., Morrell, M.J., Mizrahi, E.M., et al. (2015). Long-term treatment with responsive brain stimulation in adults with refractory partial seizures. *Neurology*, **84**, 810–17.

Carne, R.P., O'Brien, T.J., Kilpatrick, C.J., et al. (2004). MRI-negative PET-positive temporal lobe epilepsy: a distinct surgically remediable syndrome. *Brain*, **127**, 2276–85.

Cramer, J.A. (2001). Exploration of changes in health-related quality of life after 3 months of vagus nerve stimulation. *Epilepsy Behav*, **2**, 460–5.

Delalande, O., Bulteau, C., Dellatolas, G., et al. (2007). Vertical parasagittal hemispherotomy: surgical procedures and clinical long-term outcomes in a population of 83 children. *Neurosurgery*, **60**, ONS19–32; discussion ONS32.

Devlin, A.M., Cross, J.H., Harkness, W., et al. (2003). Clinical outcomes of hemispherectomy for epilepsy in childhood and adolescence. *Brain*, **126**, 556–66.

Doring, S., Cross, H., Boyd, S., Harkness, W., & Neville, B. (1999). The significance of bilateral EEG abnormalities before and after hemispherectomy in children with unilateral major hemisphere lesions. *Epilepsy Res*, **34**, 65–73.

Fauser, S. & Zentner, J. (2012). Critical review of palliative surgical techniques for intractable epilepsy. *Adv Tech Stand Neurosurg*, **39**, 165–94.

Fisher, R., Salanova, V., Witt, T., et al. (2010). Electrical stimulation of the anterior nucleus of thalamus for treatment of refractory epilepsy. *Epilepsia*, **51**, 899–908.

Geller, E.B. & Devinsky, O. (2006). Outcomes of extratemporal epilepsy surgery. In: Miller, J.W. & Silbergeld, D.L. (eds.) *Epilepsy Surgery: Principles and Controversies*, pp. 705–20. New York, NY: Taylor and Francis.

Grote, A., Witt, J.A., Surges, R., et al. (2016). A second chance—reoperation in patients with failed surgery for intractable epilepsy: long-term outcome, neuropsychology and complications. *J Neurol Neurosurg Psychiatry*, **87**, 379–85.

Hori, T., Tabuchi, S., Kurosaki, M., Kondo, S., Takenobu, A., & Watanabe, T. (1993). Subtemporal amygdalohippocampectomy for treating medically intractable temporal lobe epilepsy. *Neurosurgery*, **33**, 50–6; discussion 56–7.

Josephson, C.B., Dykeman, J., Fiest, K.M., et al. (2013). Systematic review and meta-analysis of standard vs selective temporal lobe epilepsy surgery. *Neurology*, **80**, 1669–76.

Koubeissi, M.Z., Syed, T.U., Syed, I., Jordan, J., Alshekhlee, A., & Kossoff, E.H. (2009). Hemispherectomy-associated complications from the Kids' Inpatient Database. *Epilepsy Res*, **87**, 47–53.

Kwan, P., Arzimanoglou, A., Berg, A.T., et al. (2010). Definition of drug resistant epilepsy: consensus proposal by the ad hoc Task Force of the ILAE Commission on Therapeutic Strategies. *Epilepsia*, **51**, 1069–77.

Lew, S.M., Matthews, A.E., Hartman, A.L., & Haranhalli, N. (2013). Posthemispherectomy hydrocephalus: results of a comprehensive, multiinstitutional review. *Epilepsia*, **54**, 383–9.

Morrell, M.J. (2011). Responsive cortical stimulation for the treatment of medically intractable partial epilepsy. *Neurology*, **77**, 1295–304.

Niemeyer, H. (1958). The transventricular amygdalohippocampectomy in temporal lobe epilepsy. In: Baldwin, M. & Bailey, P. (eds.) *Temporal Lobe Epilepsy*, pp. 461–82. Springfield, IL: Charles C. Thomas.

Ojemann, G.A. (2006). Multiple subpial transections are not effective or useful. In: Miller, J.W. & Silbergeld, D.L. (eds.) *Epilepsy Surgery: Principles and Controversies*, pp. 529–32. New York, NY: Taylor and Francis.

Ojemann, G.A. & Jung, M.E. (2006). Outcomes of temporal lobe epilepsy surgery. In: Miller, J.W. & Silbergeld, D.L. (eds.) *Epilepsy Surgery: Principles and Controversies*. New York, NY: Taylor and Francis.

Olivier, A. (2000). Transcortical selective amygdalohippocampectomy in temporal lobe epilepsy. *Can J Neurol Sci*, **27** Suppl 1, S68–76; discussion S92–6.

Park, T.S., Bourgeois, B.F., Silbergeld, D.L., & Dodson, W.E. (1996). Subtemporal transparahippocampal amygdalohippocampectomy for surgical treatment of mesial temporal lobe epilepsy. Technical note. *J Neurosurg*, **85**, 1172–6.

Rasmussen, T. (1983). Hemispherectomy for seizures revisited. *Can J Neurol Sci*, **10**, 71–8.

Rostomily, R.C. & Silbergeld, D.L. (2006). Lesionectomies should be tailored based on ictal recording. In: Miller, J.W. & Silbergeld, D.L. (eds.) *Epilepsy Surgery: Principles and Controversies*, pp. 537–41. New York, NY: Taylor and Francis.

Schmidt, D. & Stavem, K. (2009). Long-term seizure outcome of surgery versus no surgery for drug-resistant partial epilepsy: a review of controlled studies. *Epilepsia*, **50**, 1301–9.
Schramm, J. (2002). Hemispherectomy techniques. *Neurosurg Clin N Am*, **13**, 113–34, ix.
Schramm, J. (2008). Temporal lobe epilepsy surgery and the quest for optimal extent of resection: a review. *Epilepsia*, **49**, 1296–307.
Schramm, J., Aliashkevich, A.F., & Grunwald, T. (2002). Multiple subpial transections: outcome and complications in 20 patients who did not undergo resection. *J Neurosurg*, **97**, 39–47.
Schramm, J., Kral, T., & Clusmann, H. (2001). Transsylvian keyhole functional hemispherectomy. *Neurosurgery*, **49**, 891–900; discussion 900–1.
Schramm, J., Kuczaty, S., Sassen, R., Elger, C.E., & Von Lehe, M. (2012). Pediatric functional hemispherectomy: outcome in 92 patients. *Acta Neurochir (Wien)*, **154**, 2017–28.
Schramm, J., Lehmann, T.N., Zentner, J., et al. (2011). Randomized controlled trial of 2.5-cm versus 3.5-cm mesial temporal resection in temporal lobe epilepsy—part 1: intent-to-treat analysis. *Acta Neurochir (Wien)*, **153**, 209–19.
Shimizu, H. & Maehara, T. (2000). Modification of peri-insular hemispherotomy and surgical results. *Neurosurgery*, **47**, 367–72; discussion 372–3.
Spanaki, M.V., Allen, L.S., Mueller, W.M., & Morris, G.L., 3rd (2004). Vagus nerve stimulation therapy: 5-year or greater outcome at a university-based epilepsy center. *Seizure*, **13**, 587–90.
Spencer, S.S., Schramm, J., Wyler, A., et al. (2002). Multiple subpial transection for intractable partial epilepsy: an international meta-analysis. *Epilepsia*, **43**, 141–5.
Spencer, S.S., Spencer, D.D., Williamson, P.D., Sass, K., Novelly, R.A. & Mattson, R.H. (1988). Corpus callosotomy for epilepsy. I. Seizure effects. *Neurology*, **38**, 19–24.
Tanriverdi, T., Olivier, A., Poulin, N., Andermann, F., & Dubeau, F. (2009). Long-term seizure outcome after corpus callosotomy: a retrospective analysis of 95 patients. *J Neurosurg*, **110**, 332–42.
Tellez-Zenteno, J.F., Dhar, R., & Wiebe, S. (2005). Long-term seizure outcomes following epilepsy surgery: a systematic review and meta-analysis. *Brain*, **128**, 1188–98.
Urbach, H., Mast, H., Egger, K., & Mader, I. (2015). Presurgical MR imaging in epilepsy. *Clin Neuroradiol*, **25** Suppl 2, 151–5.
Uthman, B.M., Reichl, A.M., Dean, J.C., et al. (2004). Effectiveness of vagus nerve stimulation in epilepsy patients: a 12-year observation. *Neurology*, **63**, 1124–6.
Villemure, J.G. & Mascott, C.R. (1995). Peri-insular hemispherotomy: surgical principles and anatomy. *Neurosurgery*, **37**, 975–81.
Von Der Brelie, C., Malter, M.P., Niehusmann, P., Elger, C.E., Von Lehe, M., & Schramm, J. (2013). Surgical management and long-term seizure outcome after epilepsy surgery for different types of epilepsy associated with cerebral cavernous malformations. *Epilepsia*, **54**, 1699–706.
Walczak, T.S. (1995). Neocortical temporal lobe epilepsy: characterizing the syndrome. *Epilepsia*, **36**, 633–5.
Wellmer, J., Quesada, C.M., Rothe, L., Elger, C.E., Bien, C.G., & Urbach, H. (2013). Proposal for a magnetic resonance imaging protocol for the detection of epileptogenic lesions at early outpatient stages. *Epilepsia*, **54**, 1977–87.
Wiebe, S., Blume, W.T., Girvin, J.P., & Eliasziw, M. (2001). A randomized, controlled trial of surgery for temporal-lobe epilepsy. *N Engl J Med*, **345**, 311–18.
Wyler, A.R. (2006). Multiple subpial transection: a review and arguments for use. In: Miller, J.W. & Silbergeld, D.L. (eds.) *Epilepsy Surgery: Principles and Controversies*, pp. 524–9. New York, NY: Taylor and Francis.
Yasargil, M.G., Teddy, P.J., & Roth, P. (1985). Selective amygdalohippocampectomy. Operative anatomy and surgical technique. *Adv Tech Stand Neurosurg*, **12**, 93–123.

RELATED LINKS TO EBRAIN

Palliative Surgical Treatments for Epilepsy. https://learning.ebrain.net/course/view.php?id=1328
The Role of EEG in the Assessment for Epilepsy Surgery. https://learning.ebrain.net/course/view.php?id=1330
Surgical Treatment of Epilepsy: Workup and Outcome. https://learning.ebrain.net/course/view.php?id=1333
Temporal Lobe Surgery for Epilepsy. https://learning.ebrain.net/course/view.php?id=1334

SECTION 18
Paediatrics

84. **Developmental disorders of the brain** *971*
Colin Ferrie, Daniel Warren, and Atul Tyagi

85. **Spinal development and spinal dysraphism** *983*
Dominic Thompson

86. **Craniofaciosynostosis: Syndromic and non-syndromic craniofacial anomalies** *993*
Federico Di Rocco, Pierre-Aurelien Beuriat, and Eric Arnaud

87. **Special considerations in paediatric head and spinal trauma** *999*
Andrew Kay, Desiderio Rodrigues, Melanie Sharp, and Guirish Solanki

88. **Paediatric brain tumours** *1009*
Jonathan Roth and Shlomi Constantini

89. **Paediatric hydrocephalus** *1023*
Matt Bailey, Chris Parks, and Conor L. Malucci

90. **Paediatric neurovascular disorders** *1037*
Helen G. McCullagh, Tufail Patankar, Tony Goddard, and Atul Tyagi

91. **Paediatric epilepsy** *1047*
Sophia Varadkar and Martin Tisdall

84

Developmental disorders of the brain

Colin Ferrie, Daniel Warren, and Atul Tyagi

Introduction

Prenatal and postnatal development of the brain is controlled by a multiplicity of genetic mechanisms. Genetic abnormalities and environmental insults are responsible for a bewildering array of developmental disorders associated with brain malformations. Classic embryology remains key to understanding these, and an appreciation of the processes of gastrulation, dorsal and ventral induction, neuronal differentiation, proliferation, histogenesis, and migration and myelination will help the neurosurgeon understand the conditions likely to be encountered in clinical practice. In this chapter the more common and many less common brain malformations are reviewed. These include anencephaly, holoprosencephaly, septo-optic dysplasia, schizencephaly, grey matter heterotopias, lissencephaly/pachygyria, polymicrogyria, porencephaly, developmental anomalies of the corpus callosum, microcephaly, hemimegalencephaly, posterior fossa malformations, and encephaloceles. The emphasis is on promoting an understanding of concepts and on clinical implications, rather than on imparting detail.

Brain development: An overview

Classic neuroembryology remains key to understanding brain development and the processes which may go wrong with it (Sarnat and Flores-Sarnat, 2013). Brain development is conventionally divided into stages, during which pathological processes (genetic and non-genetic) give rise to distinct malformations. However, it is a simplification to assume these necessarily represent discrete, time limited processes, and that one ends before the next begins.

Gastrulation

Around the third week of embryonic development so-called gastrulation occurs (Figs. 84.1 and 84.2), resulting in the formation of a three-layered structure comprising exo, meso, and endoderm. Problems during this phase gives rise to a multiplicity of conditions affecting non-nervous system (CNS) and CNS structures, including spinal cord anomalies, neurenteric, dermoid and epidermoid cysts, and anterior meningoceles

Dorsal induction

This occurs at about 3–4 weeks' gestation, with the key outcome being the formation of the neural tube. Mesoderm cells migrate rostrally towards the primitive node (formed during gastrulation), forming the notochord, and also inducing ectoderm to form neuroectoderm comprising the neural plate. This then differentiates into two layers which ultimately form the neural tube and the neural crests. Formation of the neural tube is called neurulation, and involves the neural plate rolling up and fusing. Neurulation (Fig. 84.3) is divided into primary and secondary neurulation which are key stages in the formation of the neural tube from the rostral end of the notochord to its caudal end at the L1–L2 level and the formation of the lower lumbar, sacral, and coccygeal vertebral segments, respectively.

Dorsal migration of neural crest cells is responsible for the formation of many cell populations and structures, including melanocytes, craniofacial cartilage and bone, smooth muscle, peripheral and enteric neurons, and glial cells.

Ventral induction

Ventral induction occurs between the fifth and tenth week of gestation and comprises two key processes: the formation of several vesicles, which will give rise to the brain, from the rostral end of the neural tube; and flexures which will divide the brain into different parts.

Initially three vesicles form during neuropore closure: the prosencephalon; mesencephalon; and rhombencephalon, which give rise to the fore, mid, and hind brain, respectively. Further differentiation of the prosencephalon gives rise to the telencephalon (rostrally) and diencephalon (caudally) and of the rhombencephalon to the metencephalon and myelencephalon. The cephalic flexure separates the fore from the midbrain and the cervical flexure separates the hindbrain from the spinal cord.

Diverticula of the telencephalon (the telencephalic vesicles) give rise to the cerebral hemispheres with the central cavities giving rise to the lateral ventricles. The diencephalon develops into the thalamus, hypothalamus, epithalamus, optic cups, and neurohypophysis, with the associated central cavity forming the third ventricle. Lateral out-pouchings of the telencephalon form the retinae and optic nerves. Rapid growth of the telencephalon, particularly

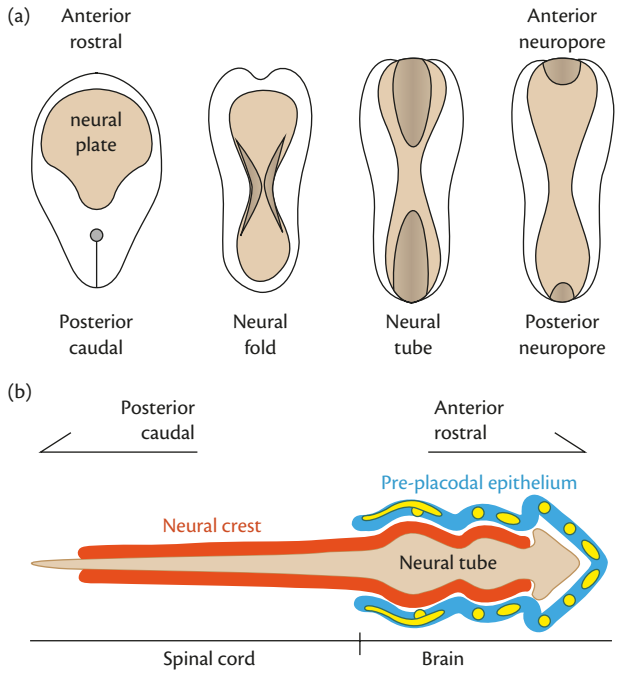

Fig. 84.1 (A) During the third week of gestation, the dorsal ectoderm forms the neural plate anterior to the node (dark circle). By the end of the third week, the neural plate has invaginated to make a neural fold, which then closes up to form a neural tube. Neural tube closure proceeds both rostrally and caudally from a starting point near the location of the future neck. Two openings, the anterior and posterior neuropores, are the last areas of the neural tube to close. (B) This cartoon shows a dorsal view of the three-vesicle embryo with rostral to the right and caudal to the left. Immediately surrounding the neural tube is neural crest, which gives rise to most of the peripheral nervous system. Within the primordial head region of the developing embryo, neuroepithelium develops into preplacodal ectoderm (blue area), which eventually populates seven bilateral pairs of placodes (yellow areas), five of which give rise to sensory neurons.

Reproduced from Peggy Mason, *Medical Neurobiology*, Oxford University Press, New York, USA, Copyright © 2012. By permission of Oxford University Press, USA.

the outer regions, cause it to cover the diencephalon, midbrain and hindbrain and ultimately gives rise to the characteristic 'C' shape of the lateral ventricles. Trapped mesenchyme between the developing cerebral hemispheres gives rise to the falx.

Development of the mesencephalon is much less dramatic than that of the prosencephalon. The mesencephalic flexure separates it from the rhombencephalon. The shrunken central cavity gives rise to the aqueduct. Cells on the dorsal side of the neural tube (the alar plate) migrate dorsally, giving rise to the tectal plate, including the superior and inferior colliculi. Others migrate ventrally to form the red nuclei and substantia nigra.

Later the pontine flexure develops separating the rhombencephalon into two parts. The myelencephalon forms the medulla oblongata and the metencephalon forms the pons and the cerebellum (with a contribution from the mesencephalon). Splaying of the rhombencephalon and stretching of the roof plate leads to the formation of the fourth ventricle.

Neural proliferation, differentiation, and histogenesis

Initially a single layer of neuroepithelial cells lines the neural tube, bounded by the internal and external limiting membranes. Proliferation of neuroepithelial cells gives rise to a pseudostratified epithelium and the outermost cells move towards the centre of the cavity of the neural tube. The innermost layer (the ventricular zone) borders the cavity and is the site of mitotic division. The future neurones (neuroblasts) subsequently migrate outwards to form the mantle zone which later becomes the grey matter. External to this is an acellular layer, known as the marginal zone. This becomes the white matter. Neurones in the mantle zone send axons into the marginal zone and outwards beyond the neural tube as motor fibres. Astrocytes and oligodendrocytes are also formed from neuroepithelial cells (glioblasts) dividing by mitosis in the ventricular zone and lastly ependymal cells are formed, covering

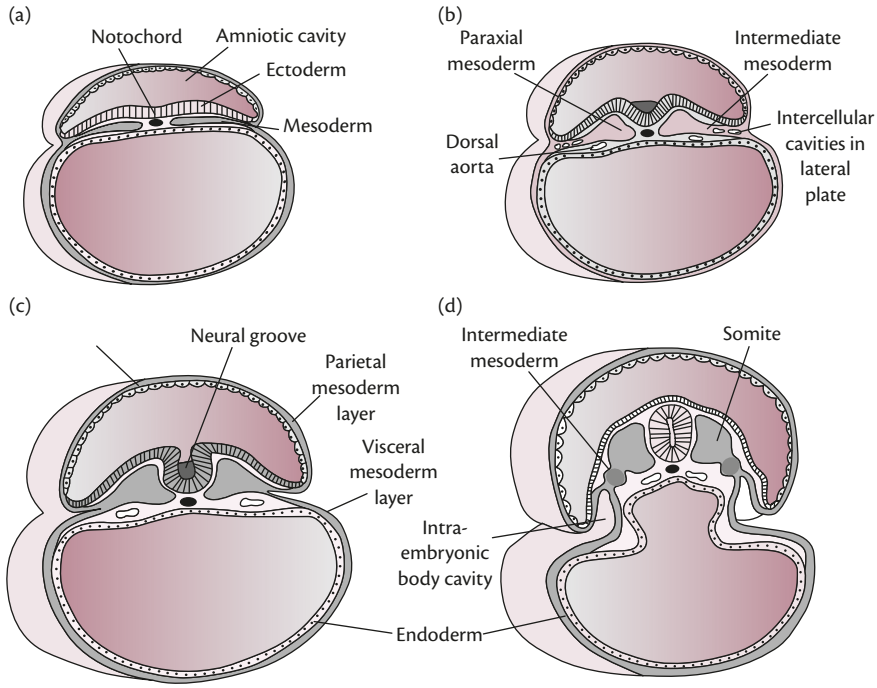

Fig. 84.2 Gastrulation.

Reproduced from Thomas W. Sadler, *Langman's Medical Embryology*, 11th edition, Wolters Kluwer. Copyright 2009, with permission. http://www.lww.com.

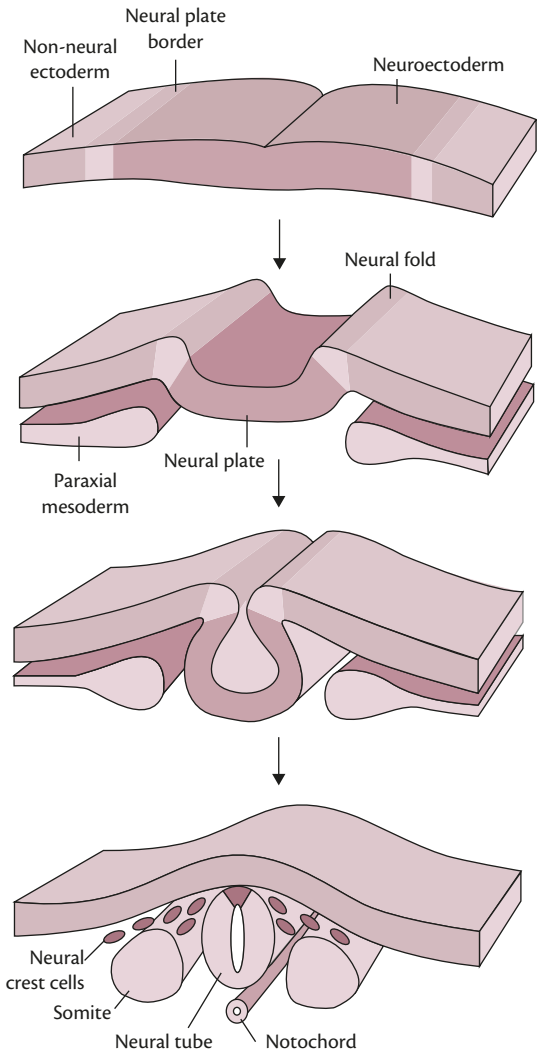

Fig. 84.3 The process of neurulation.

Reproduced with permission from Laura S. Gammill, Marianne Bronner-Fraser, Neural crest specification: migrating into genomics, *Nature Reviews Neuroscience*, Volume 4, Issue 10, pp. 795–805, Copyright ©2003 *Nature Reviews Neuroscience*.

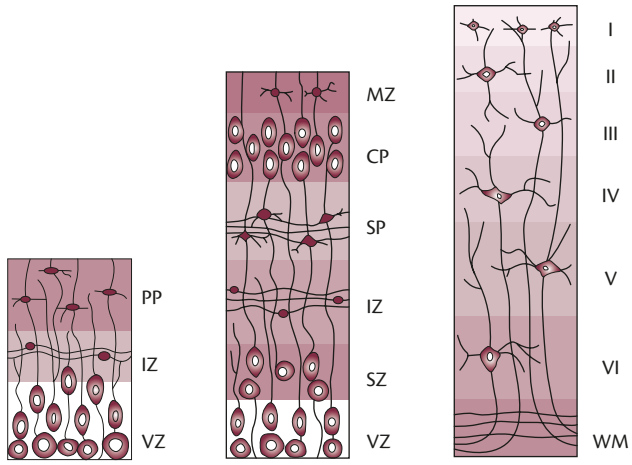

Fig. 84.4 (Left) The first neurons migrate to form the preplate (PP). (Middle) The next neurons split the PP into the marginal zone (MZ) and the subplate (SP), both transient brain structures. (Right) The mature brain has six well-developed cortical layers but none of the embryonic structures (MZ, SP, VZ). The intermediate zone (IZ) has become a mature white matter layer.

Source data from *The Fundamentals of Brain Development: Integrating Nature and Nurture* by Joan Stiles. Cambridge, MA: Harvard University Press Copyright © 2008 by the President and Fellows of Harvard College

the developing ventricular system. Microglia are derived from mesenchyme.

In the fourth week of embryonic life, proliferating neuroblasts in the mantle zone give rise to ventral and dorsal thickenings on either side of the neural tube (the basal and alar plates, respectively), separated by the sulcus limitans. The basal plate later gives rise to motor neurones and the alar plate to sensory neurones. In the brain stem the sulcus limitans separates the motor and sensory cranial nerve nuclei. Subsequent migration in various directions gives rise to the final position of the various brain stem nuclei. The margins of the alar plates (the rhombic lip) give rise to the cerebellum.

The mantle zone of the developing telencephalic vesicle is responsible for the grey matter of the cerebral hemisphere, the basal ganglia, and the hippocampi. The corpus striatum begins as a thickening of the mantle zone of the basal part of the telencephalic vesicle. It is later divided into medial and lateral parts by descending axons constituting the internal capsule. The remainder of the mantle zone of the telencephalic vesicle is thinner and is called the pallium. This becomes the cerebral cortex. In the medial wall of the pallium a thickening arises and bulges into the developing lateral ventricle. This gives rise to the hippocampus; the hippocampal sulcus separating it from the rest of the pallium

Neuronal migration

Nearly all neurones of the brain mature at sites distant form their origin. They do so as neuroblasts (rather than as neurones) but the process is conventionally known as neuronal migration (Fig. 84.4). Most neurones reach what will be the cerebral cortex (the cortical plate) by migrating along radial glial cells from the subventricular zone towards the pial surface. The cells migrating earliest become the deepest layer of the cortex, hence later migrating cells travel through earlier migrating cells. Eventually the mature six-layered cortex is formed. A minority of neurones migrate tangentially from the ganglionic eminence of the germinal matrix along axons rather than radial glial cells. These are destined to become GABAergic interneurons. Similar migratory processes are involved in the development of the cerebellar cortex and certain brain stem nuclei.

Axon sprouting begins during neuronal migration. It involves formation of short and long axons for nearby and distal targets, respectively. The dendritic tree mostly forms after migration has ceased, and is followed by synaptogenesis. Many more neurones are formed than ultimately comprise the mature brain; apoptosis is an important aspect of brain development. It generally coincides with synaptogenesis.

Myelination

Myelination begins (in the spinal nerve roots, some cranial nerves, and some longitudinal tracts of the brainstem) at 24 weeks' gestation and is mostly completed by two years of age. However, it is not until the fourth decade that the ipsilateral frontotemporal association bundle is fully myelinated.

Control of brain development

Brain development is under precise genetic control. A multiplicity of genes regulates development (Hu et al., 2014). These interact together, many only being expressed during limited periods. Some appear to only control development within the CNS, others also have roles outside the CNS. Some have different functions during different periods of development. Environmental factors are also important (Gressens et al., 2001). For example, retinoic acid (vitamin A) is important in controlling the expression of Hox genes, important in the regional control of brain development.

Many different mechanisms have been identified as important in the control of brain development (Sarnat and Flores-Sarnat, 2014). Induction refers to the influence one embryonic tissue has on another. Hence neural induction denotes the influence of non-neural tissue (e.g. the notochord) on the neural tube. Recognition molecules, adhesion molecules, cytoskeletal components, and physical barriers (such as the dorsal and ventral median septa) all play a role on the regulation of neuronal migration.

Abnormal brain development (brain malformations)

Classifications

There are numerous malformations of the brain, some relatively common others extremely rare. Bringing order involves classification. Traditionally this has been based on morphology, previously determined by pathological examination, but more recently by neuroimaging. An alternative approach has concentrated on when during developmental life various malformations have been thought to arise. Most recently classification based upon aetiology has been proposed. None of these is entirely successful. Pure morphological classification fails to take account of the explosion in our knowledge of genetics. However, non-genetic aetiologies are also important.

Combined approaches are popular (de Wit et al., 2008).

Description of selected malformations.

Anencephaly

Anencephaly, along with encephaloceles and the spina bifidas, are generally classified together as neural tube defects, as they are disorders of neurulation. In anencephaly, there is failure of the rostral neuropore to close at 24 days, resulting is an open defect (often very large), involving the skin and calvaria; a degenerate and haemorrhagic brain mass lies on the exposed basicranium. Anencephaly may occur with other neural tube defects, and also with a wide variety of extra-CNS problems. Attempts should be made to define these in case they have genetic implications.

Anencephalic foetuses often spontaneously abort. The condition is uniformly fatal in those born alive, often within minutes of birth, although survival for hours, and occasionally up to a few weeks is well recognized.

The cause of anencephaly remains poorly understood, although interplay of genetic and many environmental factors is clear. Familial recurrence is relatively common and there are associations with both young and old maternal age. There are striking geographical and secular variations in its incidence. Nutritional deficiencies, particularly of folate, appear to be important.

Anencephaly can be readily diagnosed antenatally, and therapeutic termination considered.

Holoprosencephaly

Holoprosencephaly (Fig. 84.5) is a heterogeneous group of disorders whose origins relate to pathogenic processes operating during the first four weeks of gestation. It principally affects the forebrain and face but there is also variable involvement of posterior fossa structures. Its aetiology is diverse, involving genetic and acquired mechanisms. This is reflected in it occurring as both an isolated malformation and in syndromic forms. Established teratogenic causes include maternal diabetes, retinoic acid, and alcohol. Karyotype abnormalities, especially trisomy 13 and 18, are common, and mutations of at least nine different genes affecting both dorsal and ventral patterning have been implicated (including the prosaically named sonic hedgehog gene). Recognized mutations appear to be responsible for only a tiny fraction of sporadic cases of holoprosencephaly.

Traditionally holoprosencephaly is classified as alobar, semilobar, and lobar. Alternatively, it can be divided into complete and incomplete forms. All result from failure of cleavage in the anatomic planes. In alobar holoprosencephaly there is no separation of the cerebral hemispheres, which are represented as a unified holosphere and monoventricle. In lobar holoprosencephaly there is complete separation of the hemispheres but with absent or hypoplastic olfactory bulbs and tracts (arrhinencephaly). The deep grey matter is fused to a variable extent.

Semilobar holoprosencephaly presents with intermediate changes, usually with small variably fused frontal lobes, separated occipital lobes, and a falx present posteriorly. A relatively recently identified form is characterized by separation of the frontal and occipital lobes and deep grey nuclei but fusion of the posterior frontal and parietal convexities and absence of the body (but not genu or splenium) of the corpus callosum.

Holoprosencephaly can be associated with many other brain malformations, including: agenesis of the corpus callosum (with

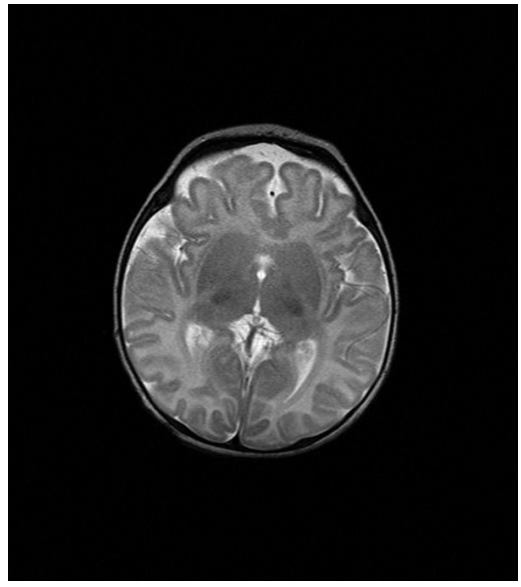

Fig. 84.5 Axial T2 of a 3 week of child with semilobar holoprosencephaly presenting with diabetes insipidus. Imaging demonstrates isolated partial frontal lobe fusion.

no Probst's bundles), fused and /or hypoplastic brain stem nuclei; abnormalities of the cerebellar hemispheres and/or vermis; Chiari 1 malformation; rhombencephalosynapsis; dorsal cysts; and hydrocephalus. Dorsal cysts are often large and lie posteriorly in the sagittal fissure or, in alobar holoprosencephaly, behind the holosphere. They sometimes represent an expansion of a single lateral ventricle, or else an extreme dilation of the third ventricle.

Hydrocephalus is often associated with the presence of a dorsal cyst, or may be a consequence of extruded germinal matrix in the ventricles. Abnormalities of neuronal migration, cortical organization, and myelination are common in holoprosencephaly. In part, these are responsible for associated developmental problems, such as learning difficulties and epilepsy.

It is said that in holoprosencephaly the face mirrors the brain, in that the more severe the facial abnormality generally the more severe the brain malformation; but there are many exceptions. The face may be normal or at the most extreme, there may be cyclopia with a single midline orbit with absent ocular structures, arrhinia (or a supraorbital proboscis), a hypoplastic or absent mandible, and otocephaly. Less severe facial abnormalities include, hypotelorism (rarely hypertelorism), nasal abnormalities, such as choanal atresia and single nostril, cleft palate or lip, and small mouth.

A majority of those with holoprosencephaly die within the first few months of age, but an increasing minority survive into early childhood and beyond. Death results from both the effects of the CNS malformation, and from associated non-CNS problems. Milder cases have a near normal life expectancy.

Most babies with holoprosencephaly are hypotonic and may remain so, but spasticity often develops. Learning difficulties are expected and, in alobar cases, are usually severe-profound. The mildest cases may have normal or near normal intelligence. Epilepsy, although not constant, is very common and is often severe and intractable.

Early, detailed MRI imaging to fully define the malformation is important. There may be difficulties distinguishing some cases from hydranencephaly and severe hydrocephalus. Vascular imaging to determine the position and configuration of the anterior cerebral arteries and dural sinuses can be helpful. Unless a teratogen is clearly implicated as the cause, a clinical genetic assessment is essential to determine if the malformation is isolated or syndromic. Endocrine and cardiac assessment is also important. Neurosurgical involvement will be required in cases with associated dorsal cysts and/or hydrocephalus.

Septo-optic dysplasia (also known as septo-optic-pituitary dysplasia complex)

This disorder is among the best known of the cerebral malformations (Fig. 84.6). Its three cardinal features—absence of the septum pellucidum, optic nerve hypoplasia, and pituitary dysfunction—can occur as isolated findings, or in any combination. There may be other associated brain malformations, which give important clues regarding likely aetiology.

Isolated absence of the septum pellucidum is not associated with detectable neurodevelopmental problem in humans, although it can lead to navigational problems in rats. Cases of partial absence of the septum are described. Anterior displacement of the fornices and septal veins may give a false impression of partial presence of the septum. In addition, cases of a wide cavum septum pellucidum are reported in association with optic nerve hypoplasia and/or pituitary problems. Optic nerve hypoplasia can be unilateral or bilateral (in which case it can be symmetrical or asymmetrical). It can be associated with anything form near normal vision to blindness. Visual field defects and restriction of peripheral vision can also occur. There may be associated optic atrophy as well as hypoplasia. Hypopituitarism can present in the neonatal period with hypoglycaemia. However, the most common presentation is with growth failure due to growth

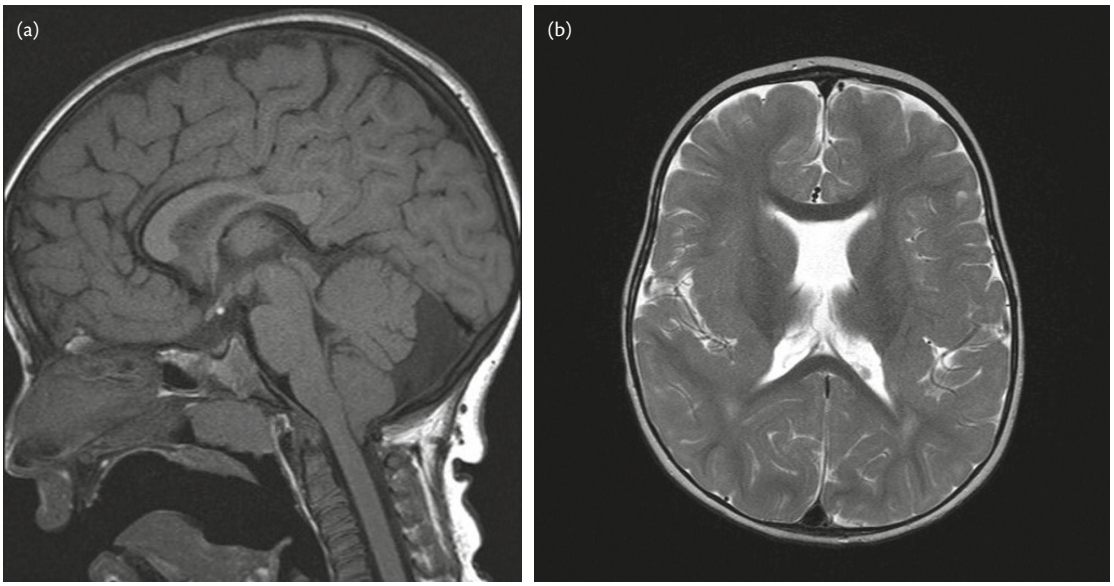

Fig. 84.6 Septo-optic dysplasia. Sagittal T1 (Fig. 84.6A) demonstrates an ectopic posterior pituitary 'bright spot' posterior to the optic chiasm, in addition to an incidental Chiari I malformation. Axial T2 (Fig. 84.6B) confirms absence of the septum pellucidum and concomitant abnormal thickening of the posterior perisylvian cortex consistent with associated perisylvian polymicrogyria.

hormone deficiency. Other pituitary hormones can be affected, and a minority of patients develop pan hypopituitarism.

The most common associated brain malformations are agenesis of the corpus callosum, lobar holoprosencephaly, schizencephaly, and focal cortical dysplasia. Hydrocephalus has been described.

The core features of septo-optic dysplasia suggest an insult during ventral induction. Young maternal age and primiparity are significant risk factors. Most cases are probably non-genetic in origin, although mutations in a multiplicity of genes are described as giving rise to various features of the condition. Various teratogens, including medicinal and non-medicinal drugs and congenital viral infections, are also implicated. A vascular pathogenesis seems probable in many cases and some of the CNS abnormalities associated with the condition may be explained by further vascular insults later in gestation.

Absence of the septum can be detected antenatally and gestational age-specific measurements of the optic nerve diameters are available. However, the condition may only be diagnosed after the possibility of therapeutic abortion is past.

Schizencephaly

This malformation is characterized by a unilateral or bilateral cleft(s) running from the ventricular margin to the pial surface (Fig. 84.7). The clefts are lined with heterotopic grey matter, usually polymicrogyria. This separates the condition from porencephaly. The sides of the cleft may be separated or apposed (open and closed lip schizencephaly). They are usually located in the region of the sylvian fissure, but may be more anteriorly or posteriorly located. Schizencephaly may be isolated or else associated with other brain malformations, including: polymicrogyria, elsewhere in the cerebrum; agenesis of the corpus callosum; absent septum pellucidum; and septo-optic dysplasia. There may also be hydrocephalus.

The clinical manifestations are very variable, and reflect the position and severity of the cleft or clefts and any associated malformations. Motor deficits (hemi or tetraplegias), learning difficulties (mild to severe) and epilepsy are common. Epileptic seizures are most often focal, but can be generalized, and are often drug-resistant.

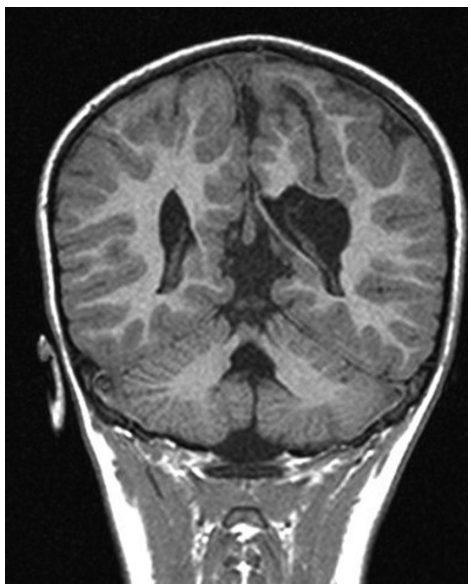

Fig. 84.7 Coronal T1 demonstrates a left hemispheric closed lip schizencephaly—note the vertical cleft extending from the lateral ventricular margin to the pial surface with the walls in near apposition and lined by abnormally thickened cortex (polymicrogyria). The midline corpus callosum is additionally absent.

Schizencephaly is a malformation arising during neuronal migration and cortical organization. A vascular aetiology is widely postulated. Familial cases are recognized and some genetic mutations are known to give rise to it. However, most cases are sporadic and drug and infective teratogens are also important in terms of aetiology. The more severe cases can be detected antenatally.

Grey matter heterotopias

Grey matter heterotopias are characterized by the presence of neurones outside the cortex (Fig. 84.8). Two main types are described: nodular, and laminar (band).

Nodular heterotopias are made up of rounded masses of normal neurones and glial cells, without laminar organization, in various positions between the ependymal lining of the ventricles and the normal cortex. They have the signal characteristics of normal grey matter, which helps distinguish them from the subependymal nodules of tuberous sclerosis. Most commonly they lie adjacent to the ependymal lining and are termed periventricular nodular heterotopias. They can be single or multiple, unilateral, or bilateral, symmetrical, or asymmetrical. Nodular heterotopias may be asymptomatic, but they frequently give rise to epileptic seizures, which may be focal or generalized. The latter suggests functional connectivity to thalamocortical circuits. Many individuals with nodular heterotopias function within the normal range intellectually and without physical difficulties. However, others, particularly those presenting in childhood, have learning and motor difficulties of variable severity. Nodular heterotopias can obstruct the aqueduct, causing hydrocephalus. Nodular heterotopias usually arise in isolation, but can be associated with other brain malformations, including Chiari II malformations.

Nodular heterotopias can be associated with cardiac, connective tissue and blood clotting abnormalities. This appears to be largely a consequence of mutations in filamin 1 (also called filamin A); screening is recommended.

Bilateral periventricular nodular heterotopia is much more common in females. This is a consequence of most cases being caused by filamin 1 mutations, which is X-linked dominant, and usually lethal in males. Non-genetic factors are thought to be responsible for most unilateral cases. They frequently occur in the posterior peritrigonal regions, which are vascular watersheds. Associated hippocampal abnormalities are frequent. Periventricular nodular heterotopias can be detected antenatally.

Band heterotopia is characterized by two layers of cortex in the cerebral hemispheres (hence, double cortex syndrome). The heterotopic layer lies in the white matter beneath the true neocortex and is unlayered. It is of variable thickness and follows the normal cortex, but is lacking in the cingulate and temporal cortex. Cases with two abnormal bands are described. The overlying cortex usually appears normal or may be thickened. Other abnormalities may include ventriculomegaly, thinning of the corpus callosum, and cerebellar vermian abnormalities. The thickness of the abnormal band correlates with the severity of the associated developmental problems. Epilepsy is expected. It usually begins in early–mid childhood, but onset can be earlier or later. Intellect varies from low

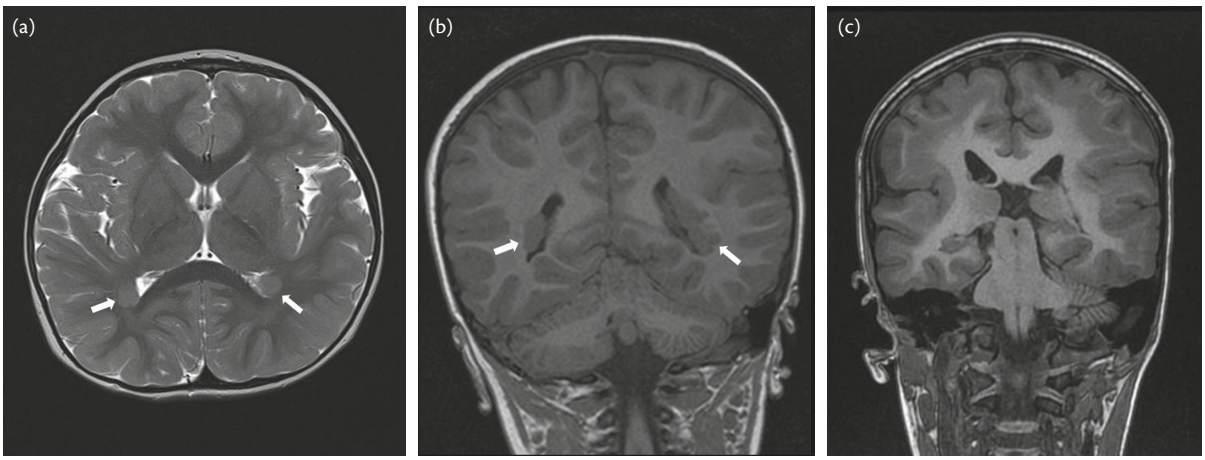

Fig. 84.8 Axial T2 (Fig. 84.8A) and coronal T1 (Fig. 84.8B) demonstrate bilateral periventricular grey matter heterotopia (white arrows) in a 4-year-old female with a complex seizure disorder; the heterotopia is iso-intense to the brain parenchyma grey matter on both T1 and T2 sequences. Figure 84.8C (coronal T1) demonstrates bilateral band heterotopia ('double cortex syndrome').

normal to severe learning difficulties. There may be motor problems as well.

Band heterotopia is a genetic disorder of neuronal migration. It is predominantly X-linked dominant, occurring in females but with lethality in males and is due to mutations of the doublecortin (*DCX*) gene. Some *DCZ* mutations are non-lethal in males, but give rise to lissencephaly, a more severe neuronal migration disorder. A small number of males are described with band heterotopia, caused by somatic *DCX* mutations.

Lissencephaly (smooth brain) and pachygyria

Classic Lissencephaly (also called type 1 lissencephaly)

Classic lissencephaly (usually shortened to just lissencephaly), is a brain malformation in which the cerebral cortex lacks (partially or completely) normal sulci (agyria) and is abnormally thick (pachygyria) (Fig. 84.9). At its most extreme, the brain presents as a figure of eight similar to that expected towards the late second trimester. The thickened cortex classically consists of only four layers. Affected individuals are often diagnosed soon after birth as a consequence of severe hypotonia and feeding difficulties. Severe-profound learning difficulties and increasing spasticity are expected. Epilepsy is usually severe. Rarely there are other associated CNS and non-CNS manifestations, depending on the genetic cause. Life expectancy is greatly reduced, with the most severely affected subjects often dying in infancy.

Lissencephaly is a genetic disorder of neuronal migration. Most cases are due to mutations on the *Lis1* gene. This gives rise to the most severe phenotype with a characteristic posterior-anterior gradient in the severity of the malformation. Some patients have a visible deletion on the short arm of chromosome 17 and a characteristic dysmorphic facial appearance known as the Miller-Dieker syndrome. The second commonest cause is X-linked lissencephaly due to *DCX* mutations, with an anterior-posterior gradient. X-linked lissencephaly can also be due to *ARX* mutations in which there is often ambiguous genitalia. Lissencephaly can also occur as a manifestation of a tubulopathy, particularly with mutations of *TUBA1A*. In this it may be associated with dysgenesis or agenesis of the corpus callosum and cerebellar hypoplasia.

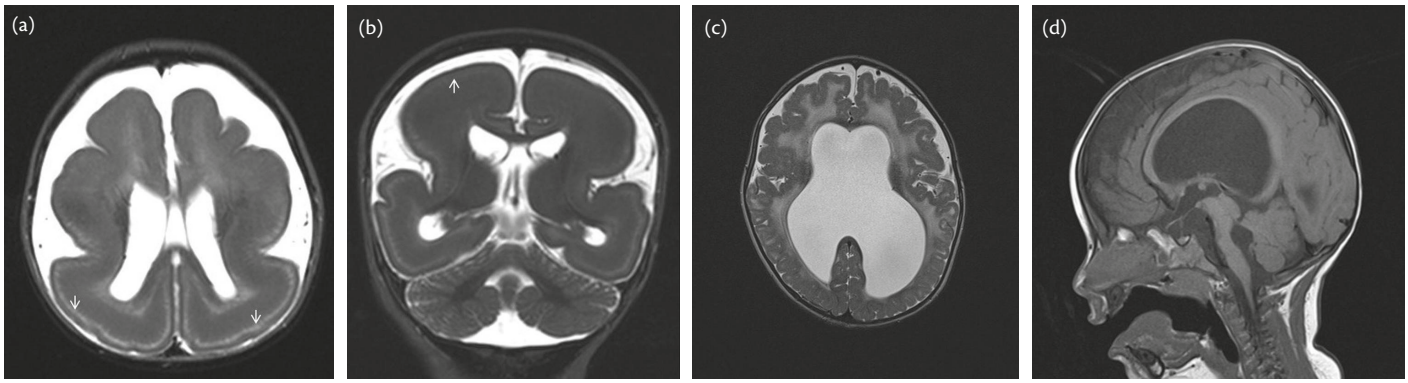

Fig. 84.9 Lissencephaly. (A, B) A 6-month-old child presenting with failure to thrive and generalized seizures. Axial T2 imaging in the axial (a) and coronal (b) plane demonstrate classic lissencephaly with a thin outer cortical layer and white matter cell sparse layer (white arrows) separated from deeper arrested neurons. Shallow sylvian fissures result in a 'figure of eight' configuration. (C and D) A 14-month-old child with confirmed Walker-Warburg syndrome. Axial T2 (C) demonstrates abnormally shallow bifrontal sulcation with delayed myelination and sagittal T1 (D) shows additional pontine hypoplasia.

An antenatal genetic diagnosis is often available in affected families. Neuroimaging can detect lissencephaly from the very late second trimester.

Cobblestone lissencephaly (also called type 2 lissencephaly)

Cobblestone lissencephaly occurs in three related disorders, all of which also feature congenital muscular dystrophy and developmental eye problems (which may be mild to severe): Walker-Warburg syndrome; Fukuyama syndrome; and muscle-eye-brain. They are alpha-dystroglycanopathies caused by deficient glycosylation of alpha-dystroglycan, due to mutations in a large number of different genes. In cobblestone lissencephaly, the surface of the brain is bumpy the glia limitans being broken, causing leptomeningeal, neuronal, and glial heterotopias. Cobblestone lissencephaly is nearly always part of a complex malformation, particularly also involving the cerebellum. Hydrocephalus is constant in Walker-Warburg syndrome, occasional in muscle-eye-brain disease, but is not a feature of Fukuyama syndrome.

Polymicrogyria

The hallmark of polymicrogyria is the presence of excessive, abnormally folded small fused gyri. On MRI its appearance is variable. Often it presents as multiple small gyri (which may be confused with the polygyria seen in some cases of hydrocephalus). Alternatively, it may appear as thickened cortex (making distinction from pachygyria difficult) with a 'bumpy' grey-white junction or as a smooth area of cortex (which if extensive may be confused with lissencephaly). The grey-white junction is often 'blurred' and the underlying white matter is often thinned. It can be unilateral or bilateral (in which case it can be symmetrical or asymmetrical), localized, or extensive. Certain distinct distributions, with aetiological implications, are recognized. These include bilateral frontal, bilateral fronto-parietal, bilateral perisylvian, bilateral parasagittal parieto-occipital, bilateral generalized, and unilateral perisylvian. There are frequently additional cerebral malformations reflecting the diverse aetiologies of polymicrogyria.

The clinical manifestations reflect a combination of the topographical distribution of the abnormal cortex, its extent, other associated malformations, and the underlying aetiology. Some cases are diagnosed shortly after birth as a consequence of severe motor problems (which may include arthrogryposis), feeding difficulties, and epilepsy. Others may only come to light as an incidental finding or following the diagnosis in a family member. Individuals with relatively subtle neurodevelopmental/neuropsychiatric disorders may be found to have polymicrogyria. Epilepsy with focal or generalized seizures is common and can present at any age. However, it is by no means constant and in contrast to when it complicates many other cerebral malformations, may be time limited, and/or responsive to antiepileptic drug medication. Because of its predilection for the peri-Sylvian regions, pseudobulbar problems are common in those with polymicrogyria.

Polymicrogyria is caused by diverse genetic and acquired insults to the developing brain. Histological features suggest many cases arise after neuronal migration is completed at around 20–24 weeks' gestation. However, other histological features suggest an earlier origin, at least in some cases, prior to the fourth month of gestation while neuronal migration is occurring. Vascular insults and *in-utero* infections (such as rubella, cytomegalovirus, and toxoplasma infection) are important acquired causes of polymicrogyria. Chromosomal abnormalities are common in polymicrogyria. Particularly important is deletions involving 22q11.2 in which perisylvian polymicrogyria is often accompanied by congenital heart defects and immune deficiency. Several specific genetic mutations have been found in familial cases of polymicrogyria, particularly but not exclusively when this is bilateral. Polymicrogyria is a feature of some metabolic disorders, including Zellweger syndrome (a peroxisomal disorder), organic acidurias, aminoacidaemias, and mitochondrial disorders. Consequently, a thorough diagnostic workup is essential.

Porencephaly

The terminology of porencephaly is confusing. A true porencephalic cyst is a focal cavity in the cerebral hemisphere which communicates with the ventricular system. It may appear to also communicate with the subarachnoid space over the cerebral convexity but nearly always there is a thin membrane separating the two. The cyst lacks internal structure and is lined with white matter. The terms congenital or clastic porencephaly are sometimes applied. Porencephaly is also sometimes applied to full thickness cysts lined with abnormal cortex (such as polymicrogyria). This can be called developmental porencephaly but the term schizencephaly is now generally preferred, as its aetiology is different (see earlier).

The clinical features of porencephaly reflect the size and position of the cyst and the underlying cause. Common problems include cerebral palsy (spastic in type, unilateral, or bilateral), learning difficulties, and epilepsy. Epilepsy occurs in around a third of affected patients and can begin from infancy to adult life. If the former it may present as an epileptic encephalopathy with apparent generalized seizure types. Later focal seizures are common. Startle-induced seizures are a well-recognized association. Rarely porencephalic cysts can expand and cause pressure effects, due to pulsation caused by the choroid plexus.

Porencephaly is generally caused by acquired insults to the brain acting from the late second trimester to the early postnatal period. Ischaemia and haemorrhage are numerically the most important aetiologies, but other causes include trauma and infection. Familial, autosomal dominant, cases can be caused by mutations in *COL4A1*, which codes for a very widely expressed collagen. Associated white matter abnormalities and calcification may help recognition. The *COL4A1* phenotype is extensive and genetic counselling essential. There is a risk of haemorrhagic stroke during childhood and adult life.

Agenesis of the corpus callosum, and other developmental anomalies of the corpus callosum

During embryogenesis, commissures connecting contralateral areas of the developing brain form. The most important of these is the lamina terminalis extending from the roof plate of the diencephalon to the optic chiasm. Others include the anterior and posterior commissures and the hippocampal commissure. Formation of the corpus callosum involves apoptosis of the lamina terminalis, allowing developing callosal fibres to project across the midline. Agenesis of the corpus callosum is caused by interference in this, with the lamina terminalis acting as a barrier rather than a facilitator. The obstructed fibres are deflected posteriorly along the medial wall of the developing hemisphere as bundles of Probst. The presence of these distinguish primary agenesis from later destructive abnormalities of the

corpus callosum. The corpus callosum forms rostral to caudal; in partial agenesis, the splenium is most likely to be absent, followed by the rostrum, with deficiency of the mid-portion the least common. Hypoplasia of the corpus callosum, in which all parts are present but abnormally thin, arises from a deficiency of nerve fibres, from whatever cause. Probst bundles are not present.

The neuroimaging features of complete agenesis of the corpus callosum include widely spaced lateral ventricles which lack the normal midline convexity, upward displacement of the third ventricle, Probst bundles lying between the bodies of the lateral ventricles above the third ventricle and often prominence of other commissures.

Agenesis of the corpus callosum can be isolated or associated with a wide variety of other developmental anomalies of the brain, particularly of midline structures. Facial dysmorphism, particularly hypertelorism, is common. Significant developmental problems are usual, including learning difficulties, ranging from mild to profound; motor problems; and epilepsy. These are often mainly a consequence of associated abnormalities. Isolated agenesis may appear asymptomatic, with other interhemispheric connections (normal and abnormal) taking over the function of the corpus callosum. However, detailed neuropsychological assessment will usually reveal visual processing, fine motor, and specific language difficulties.

Agenesis of the corpus callosum is often genetic in origin, occurring as a consequence of certain chromosomal abnormalities and single gene defects. Of particular interest are its frequent associations with X-linked hydrocephalus due to aqueduct stenosis, and agenesis of the corpus callosum with mental retardation and spasticity. Both are caused by mutations of *L1CAM*, which codes for a cell adhesion molecule. It can also arise as a consequence of various metabolic disorders and from the effects of teratogens, including alcohol.

Microcephaly and macrencephaly

Microcephaly is defined as a head circumference more than three standard deviations below the population mean. It is almost, but not quite synonymous with macrencephaly (small brain), since the brain may be small, but the head size normal. It is usual to classify it as congenital (or primary) or acquired (or secondary), depending on whether the head is a normal size at birth. The gyral pattern may be normal (microcephaly vera), simplified, thickened (microlissencephaly), or show polymicrogyria. The corpus callosum may be absent. Microscopic examination may reveal neuronal depletion, particularly in cortical layers II and III.

The causes of microcephaly are protean, encompassing most pathological processes affecting the brain. This is reflected in its diverse clinical manifestations, which range from normal to severe disability. Significant learning difficulties are the norm, but are by no means universal.

Any pathological process causing destruction of brain tissue, or interfering with brain growth, acting antenatally, or in infancy or early childhood, will result in microcephaly. Genetic microcephaly occurs with autosomal recessive, autosomal dominant, and X-linked inheritance patterns. The first of these is the most common. There are now at least six recognized genes, mutations in which give rise to autosomal recessive microcephaly. Many of the genes causing microcephaly have important roles in the regulation of neuronal proliferation and apoptosis. The study of genetic microcephaly is likely to be very helpful in aiding understanding of brain development in general (Gilmore and Walsh, 2013).

Hemimegalencephaly

This is a complex brain malformation characterized by an abnormally large cerebral hemisphere. Occasionally an abnormally small cerebral hemisphere (hemimicrencephaly) can give rise to diagnostic confusion. Although usually confined to the forebrain, the mid, and hind brains are sometime involved as well. Pathologically there is abnormal proliferation of both neurones and glial cells. The cortex tends to be abnormally thick and heterotopias are common. Ipsilateral enlargement of the lateral ventricle is usual.

Hemimegalencephaly may be associated with overgrowth of the ipsilateral face and sometimes other parts of the body. Moreover, there is a strong association with neurocutaneous disorders, including tuberous sclerosis, neurofibromatosis type I, proteus syndrome, linear sebaceous nevus syndrome, and hypomelanosis of Ito. Apart from these important associations, the embryology of hemimegalencephaly remains to be determined.

The clinical phenotype is variable. Exceptionally, those with it may be neurodevelopmentally normal. More usually they have a range of deficits which may include hemiparesis, visual field defects, learning difficulties, and epilepsy. The epilepsy may be focal or apparently generalized and is often severe and refractory to antiepileptic drugs. Hemimegalencephaly is an important cause of several severe childhood epilepsy syndromes, including Ohtahara, West, and the Lennox–Gastaut syndromes. It is one cause of epilepsy partialis continuans.

Posterior fossa malformations

Malformations of the cerebellum are not uncommon. A few of the better characterized ones are briefly described next. In addition to these, complete absence of the cerebellum, generalized cerebellar hypoplasia, cerebellar dysplasias, and macrocerebellum are all recognized. Clinically, they are usually associated with gross motor delay, various cerebellar signs, and variable general developmental delay. The term ataxic cerebral palsy is often applied. There aetiologies are diverse and encompass, Mendelian genetic disorders, chromosomal abnormalities, single gene defects, neurometabolic disorders, teratogenic damage, and other acquired insults.

Dandy-Walker syndrome comprises complete or partial absence of the cerebellar vermis, with elevation and upward rotation, and cystic enlargement of the fourth ventricle. Hydrocephalus is common. In some, but not all, of those affected there is obstruction of the exit foramina of the fourth ventricle. Dandy-Walker malformation can be an isolated finding, or can be accompanied by other malformations, particularly of the posterior fossa and agenesis of the corpus callosum, and with problems outside the CNS. Presentation with raised intracranial pressure is common. Cerebellar signs and intellectual impairment are common, but not constant.

Dandy-Walker syndrome can be a manifestation of several rare autosomal disorders, various chromosomal abnormalities, or else can be isolated. Certain specific gene mutations giving rise to it have been described in individual families.

Joubert syndrome (**Fig. 84.10**) is a genetic disorder whose most characteristic features are cerebellar vermis hypoplasia or dysplasia, prominent superior cerebellar peduncles, a deep interpeduncular fossa (giving the characteristic molar tooth appearance radiologically), and an abnormally shaped and rostrally displaced fourth ventricle. There may be an associated occipital meningocele and

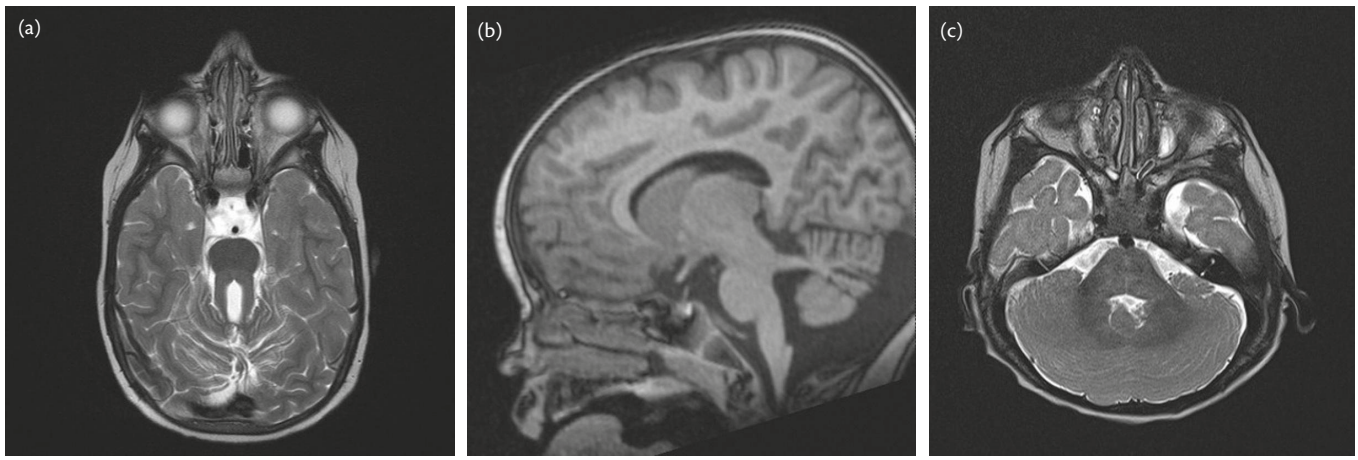

Fig. 84.10 Axial T2 (A) and Sag T1 (B) demonstrate Joubert syndrome, note the characteristic 'molar tooth' appearance on the axial T2 imaging secondary to thickening of the superior cerebellar peduncles and the rostral displacement of the fourth ventricle appreciated on the sagittal imaging, in addition to inferior vermian hypoplasia. (C) Axial T2 shows absence of the midline vermis and fusion of the medial cerebellar hemispheres consistent with rhombencephalosynapsis.

extra-CNS problems, notably retinal dystrophy and renal problems, including nephronophthisis. Affected infants are generally floppy and in early-life abnormal breathing patterns with alternating tachypnoea and apnoea is characteristic. Later oculomotor dyspraxia develops.

The disorder is usually autosomal recessive, and more than 20 mutated genes have been described as giving rise to it. These affect ciliary function, and the disorder is often classified as a ciliopathy.

Rhombencephalosynapsis is a rare malformation with congenital absence of the vermis, and fusion of the medial sides of the cerebellar hemispheres and of the dentate nuclei. It is usually an isolated malformation, but may be accompanied by other midline defects. In addition, there is an association with X-linked hydrocephalus. The clinical picture is dominated by cerebellar signs; cognitive impairment is variable. It is thought to be genetic in origin, but is usually sporadic, although Mendelian inheritance is reported.

Giant cisterna magna, seen as an incidental finding in around 1% of computed tomography (CT) and MRI brain scans, refers to non-pathological prominence of the retrocerebellar cerebrospinal fluid (CSF) space. There should be no associated cerebellar abnormalities.

Encephaloceles

An encephalocele is a herniation of neural tissue within a dural sac through a cranial defect. The failure of the neural tube to close completely is felt to be the embryological basis for this condition. The pathogenesis of encephaloceles appears to be a disturbance in the separation of neural and surface ectoderm during the final part of neural tube formation (Hoving and Vermeij-Keers, 2000). Up to 40% may have chromosomal abnormalities. The incidence is approximately 0.8–4/10 000 live births (Simpson et al., 1984).

The typical presentation is a swelling from the naso-ethmoidal to the occipital region. The subtypes are basal, sincipital (frontal), convexity, and occipital. Children may present with features of nasal obstruction, CSF rhinorrhoea, or rarely with recurrent meningitis especially with lesions in the naso-ethmoidal region or skull base. There may be associated hydrocephalus, epilepsy, neurological deficits, or developmental delay.

Antenatal ultrasound and fetal MRI can help to identify the lesion *in utero*. Postnatally, while an ultrasound can give useful information, an MRI scan is helpful in delineating sac contents and any other associated intracranial anomalies such as microcephaly, corpus callosum dysgenesis, Chiari malformation, and arachnoid cysts (Da Silva et al., 2015). The differential diagnosis for a nasal encephalocele include dermoid cyst and the rare nasal gliomas. CT scan with reconstruction is helpful in defining the bony defect.

Treatment depends upon the size, location, and contents of the sac. The key steps are defining the bony margins and the dural defect, replacing normal herniated neural content intracranially followed by repair of the dura and bony cover. Frontoethmoidal lesions may need correction of associated hypertelorism with orbital advancement techniques (Mahapatra, 2011) or other associated cranial defect/deformities besides the encephalocele. Skull base lesions are increasingly being repaired endoscopically with good results (Ma et al., 2015). Attention should be paid to the anatomy of the venous sinuses at the site of the defect as the dural venous sinuses are often closely related to the sac. Surgery may be required on an emergent basis if there is evidence of a CSF leak. Patients may need any associated hydrocephalus dealt with either before or after corrective surgery.

The anterior (i.e. frontoethmoidal) nasal encephaloceles have a much better survival as compared to the occipital lesions. Neuro disability among survivors is high with only 48% having a normal development (Lo et al., 2008). An institutional review of cephaloceles identified several risk factors on univariate tests as significant independent predictors of developmental delay (i.e. presence of associated intracranial abnormalities, hydrocephalus, seizure disorder, microcephaly, and presence of brain tissue within the malformation). Of these hydrocephalus and intracranial abnormalities carried the most cumulative predictive effect for a poor developmental outcome). Location of the lesion, however, was not a significant factor (Lo et al., 2008). In another institutional review by Da Silva et al hydrocephalus was associated with neurological deficit

in multivariate models. The location of the lesion again was not a significant factor in the incidence of hydrocephalus or neurological deficit. The presence of hydrocephalus resulted in a far worse neurological outcome in this review.

Neurosurgical considerations

Children with cerebral malformations often have complex neurodisabilities and a multidisciplinary approach is essential. Coordinating care is often most appropriately done by a neurodisability consultant. In addition, it is essential to consider if there are or may be extraneurological problems, and to involve appropriate specialists. This is exemplified by the endocrine abnormalities which accompany many midline malformations, and the cardiac problems seen in some patients with nodular heterotopias. The neurosurgeon may be involved in the management of children with brain malformations for three main reasons: to manage raised intracranial pressure; to treat epilepsy; or to help with spasticity management.

As already alluded to, many malformations are associated with hydrocephalus as a near-constant, frequent, or occasional accompaniment. Standard ventriculo-peritoneal shunting procedures are most often used. However, in some malformations, such as the Dandy-Walker malformation, cyst-peritoneal, or combined procedures are advocated by some.

For diffuse and bilateral malformations associated with epilepsy, resective surgery is never an option, but functional procedures, including corpus callosotomy, vagal nerve stimulation, and multiple subpial transections may have a role. Focal cortical dysplasias are a common reason for lobar and multilobar resections, and epileptologists have developed a distinct classification of the focal cortical dysplasias which is useful for surgical planning (Blümcke et al., 2011). Subcortical nodular heterotopias may also be candidates for respective epilepsy surgery. Hemimegalencephaly, is an important indication for hemispherectomy/hemispherectomy, which often presents in very young children as an epileptic encephalopathy. There is growing evidence that surgery may benefit cognitive development, as well as helping to control seizures.

Brain malformations are an important cause of cerebral palsy. With posterior fossa malformations, this is usually of the hypotonic or ataxic type, and is not amenable to neurosurgical interventions. Spasticity, and to a lesser extent dystonia are common in many of the other malformations and treatment with intrathecal baclofen pumps and with selective dorsal rhizotomy may have a useful role to play in carefully selected cases.

FURTHER READING

Barkovich, A.J. & Raybaud, C. (2012). *Pediatric Neuroimaging*, 5th edition. Philadelphia, PA: Lippincott Williams & Wilkins, Chapters 2 & 5.

Blümcke, I., Thom, M., Aronica, E., et al. (2011). The clinicopathologic spectrum of focal cortical dysplasias: a consensus classification proposed by an ad hoc Task Force of the ILAE Diagnostic Methods Commission. *Epilepsia*, **52**(1), 158–74.

Brodal, P. (2010). *The Central Nervous System: Structure and Function*, 4th edition. Oxford, UK: Oxford University Press.

Gilmore, E.C. & Walsh, C.A. (2013). Genetic causes of microcephaly and lessons for neuronal development. *Wiley Interdiscip Rev Dev Biol*, **2**(4), 461–78.

Gressens, P., Mesplesa, B., Sahira, N., Marretb, S., & Solac, A. (2001). Environmental factors and disturbances of brain development. *Semin Neonatol*, **6**(2), 185–94.

Mirzaa, G.M. & Paciorkowski, A.R. (2014). Brain malformations. *AJMG Part C, Seminars in Medical Genetics*, **166**(2), 117–239.

Sarnat, H.B. & Flores-Sarnat, L. (2013). Neuroembryology and brain malformations: an overview. *Handb Clin Neurol*, **111**, 117–28.

de Wit, M.C., Lequin, M.H., de Coo, I.F., et al., (2008). Cortical brain malformations: effect of clinical, neuroradiological, and modern genetic classification. *Arch Neurol*, **65**(3), 358–66.

REFERENCES

Blümcke, I., Thom, M., Aronica, E., et al. (2011). The clinicopathologic spectrum of focal cortical dysplasias: a consensus classification proposed by an ad hoc Task Force of the ILAE Diagnostic Methods Commission. *Epilepsia*, **52**(1), 158–74.

Da Silva, S.L., Jeelani, Y., Dang, H., Krieger, M.D., & Gordon McComb, J. (2015). Risk factors for hydrocephalus and neurological deficit in children born with an encephalocele. *J Neurosurg: Pediatrics*, **15** (4), 392–98.

de Wit, M.C., Lequin, M.H., de Coo, I.F., et al., (2008). Cortical brain malformations: effect of clinical, neuroradiological, and modern genetic classification. *Arch Neurol*, **65**(3), 358–66.

Gilmore, E.C. & Walsh, C.A. (2013). Genetic causes of microcephaly and lessons for neuronal development. *Wiley Interdiscip Rev Dev Biol*, **2**(4), 461–78.

Gressens, P., Mesplesa, B., Sahira, N., Marretb, S., & Solac, A. (2001). Environmental factors and disturbances of brain development. *Semin Neonatol*, **6**(2), 185–94.

Hoving, E.W. & Vermeij-Keers, C. (2000). Frontoethmoidal encephaloceles, a study of their pathogenesis. *Child's Nerv Syst*, **16**, 702–6.

Hu, W.F., Chahrour, M.H., & Walsh CA. (2014). The diverse genetic landscape of neurodevelopmental disorders. *Annu Rev Genomics Hum Genet*, **15**, 195–213.

Lo, B.W., Kulkarni, A.V., Rutka, J.T., et al. (2008). Clinical predictors of developmental outcome in patients with cephaloceles. *J Neurosurg Pediatrics*, **2**, 254–7.

Ma, J., Huang, Q., Li, X., et al. (2015). Endoscopic transnasal repair of cerebrospinal fluid leaks with and without an encephalocele in pediatric patients: from infants to children. *Childs Nerv Syst*, **31**, 1493–8.

Mahapatra, A.K. (2011). Anterior encephalocele—AIIMS experience a series of 133 patients. *J Pediatr Neurosci*, **6**(Suppl 1), S27–S30.

Sarnat, H.B. & Flores-Sarnat, L. (2013). Neuroembryology and brain malformations: an overview. *Handb Clin Neurol*, **111**, 117–28.

Sarnat, H.B. & Flores-Sarnat, L. (2014). Morphogenesis timing of genetically programmed brain. *Prog Brain Res*, **213**, 181–98.

Simpson, D.A., David, D.J., & White, J. (1984). Cephaloceles: treatment, outcome and antenatal diagnosis. *Neurosurgery*, **15**, 14–21.

85

Spinal development and spinal dysraphism

Dominic Thompson

Introduction

The term spinal dysraphism encompasses a group of disorders of spinal cord development. Within this group discrete clinical entities are recognized, these differ in their embryological origins, their clinical presentation, and their prognosis. The nomenclature of the spinal dysraphisms is apt to confuse however a simplified classification is presented, based upon the presumed point of origin in embryogenesis and serves not only to simplify terminology but also to direct appropriate investigation and management. It is important to emphasize that while detailed knowledge of embryogenesis based on animal models is available for some of the open neural tube defects this is not so for the closed spinal dysraphisms where the precise developmental defect remains a matter of hypothesis.

Development of the spinal cord

While there is an intimate association between the early development of the vertebral column (mesoderm) and spinal cord (ectoderm) it is the stages of spinal cord development that is germane to the understanding the spinal dysraphisms. For a comprehensive description of vertebral column development see Pang and Thompson (Pang and Thompson, 2010). Development of the spinal cord can be conveniently divided into three stages: gastrulation, primary neurulation, and secondary neurulation.

Gastrulation

The very primitive embryo comprises a two-layer structure, the bilaminar plate. During gastrulation the rostrocaudal polarity of the embryo is established with the formation of a midline groove, the primitive streak. Cells of the outer layer of the bilaminar plate migrate toward the primitive streak and thence between the two layers transforming it into a trilaminar structure. Thus, the three germ cell layers (endoderm, mesoderm, and ectoderm) are established. As the embryo enlarges the primitive streak regresses from head to tail leaving in its wake the notochord. The notochord is fundamental to vertebrate development maintaining not only rostrocaudal polarity but in establishing dorsoventral identity as well. For a transient period, there is a connection across the embryo, via the notochord that allows the amniotic cavity to communicate with the yolk sac, the neurenteric canal. By means of a variety of signalling processes the notochord will induce the overlying ectoderm to form the neural plate and will also begin the process of conversion of presomitic mesoderm to somitic mesoderm, a precursor to vertebral column formation.

Primary neurulation

The ectoderm, which constitutes the dorsal aspect of the early embryo will ultimately give rise to both the central nervous system and integument (skin and its adnexae). During primary neurulation, and under the influence of the notochord the ectoderm begins to fold, the lips at the edges of the fold will meet in the midline. The number of initial meeting points differs between species. A process of zipping up between these 'meeting points' then occurs thus creating the tubular structure of the central nervous system. The ectoderm lateral to the folds will be the future cutaneous ectoderm, these two derivatives of the ectoderm (neural and cutaneous) then separate in a process known as disjunction.

The neural tube formed as a result of primary neurulation will ultimately result in the brain and spinal cord, however only as far as the second sacral segment. The terminal spinal cord, conus medullaris, filum terminale, and cauda equina are formed in a different manner, known as secondary neurulation.

Secondary neurulation

In the tail bud of the embryo is a collection of pluripotent cells known as the caudal cell mass. This mass will contribute to the development of the lower genitourinary tract, the distal anorectal region, and terminal spinal cord. While the details of secondary neurulation are poorly understood in humans it is believed that cells destined to neural differentiation coalesce around a central lumen resulting in the so-called medullary cord, this will become incorporated into the more rostral spinal cord that was formed as a result of primary neurulation. Much of the spinal cord that was formed by secondary neurulation will regress (retrogressive differentiation) resulting in an apparent ascent of the conus, the filum terminale is what remains on completion of this process.

Classification of spinal dysraphism

Various classifications of spinal dysraphism appear in the literature however a classification based upon presumed developmental pathogenesis, while for the most part hypothetical serves as a useful clinical guide (Fig. 85.1). We can therefore look in turn at those dysraphic states that derive from disordered gastrulation, primary neurulation and secondary neurualtion repsectively.

Disorders of gastrulation

Establishment of the three germ cell layers is a principal feature of gastrulation, by the end of this stage the ectodermal layer will form the dorsal aspect of the embryo facing the amniotic cavity. Dysraphic disorders that have their origins in this early stage of development will therefore tend to be ventral to the neuraxis and more likely to be associated with skeletal (mesodermal) and visceral (endodermal) anomalies. In the split cord malformations, it is suggested that there has been duplication of the notochord resulting in two neural tubes. The resulting two hemicords may each lie within separate dural tubes, with an intervening bony spur (type I split cord malformation) or may be contained within a single dural tube separated by little more than a fibrous band (type II in split cord malformation or diplomyelia) (Pang, 1992; Pang et al., 1992). Congenital vertebral body fusions or malformed vertebrae commonly coexist with the split cord malformations and may result in spinal deformity.

The neurenteric canal that traverses the embryo from dorsal to ventral may persist resulting in abnormal connections between the neural and enteric derivatives in the form of neurenteric or enterogenous cysts. These may occur anywhere from the sphenooccipital synchondrosis to the lumbosacral junction but not seen beyond these limits as the neurenteric canal never extended along the full length of the embryo. Again, vertebral bony anomalies typically coexist reflecting involvement of all three germ cell layers.

Disorders of primary neurulation

Impaired primary neurulation results in classical open neural tube defects. Tubulation of the ectoderm has not occurred, the neural tissue is not covered by skin but is either completely exposed, leaking cerebrospinal fluid, or covered by rudimentary meningeal membranes. In the spine this results in myelocele or myelomeningocele. The terms are used interchangeably but are more correctly applied to situations where the neural placode is flush with the surrounding skin (myelocele) or raised up by the accumulation of cerebrospinal fluid (CSF) in the underlying subarachnoid space (myelomeningocele). Open neural tube defects are pan central nervous system (CNS) malformations, in addition to the spinal cord anomaly several structural abnormalities of the brain are usually seen encompassed by the term Chiari II malformation; hydrocephalus will also be present in approximately 80% of cases. It is important to emphasize that the Chiari II malformation and hydrocephalus are not associated with the other (closed) dysraphic conditions.

An important feature of primary neurulation is the separation of cutaneous and neural ectoderm, the process known as disjunction. Depending on whether this process occurs prematurely or incompletely a separate group of dysraphic disorders will result. If the neuroectoderm separates prematurely, before tubulation is complete then the open neural tube becomes exposed to the underlying mesoderm; according to McLone, this is the initial step in the formation of fat on the surface of the placode leading to spinal lipoma. Thus premature disjunction is thought to be the underlying mechanism responsible for dorsal lipoma. It is important to recognize that while this hypothesis is in keeping with the anatomical configuration of dorsal lipoma, it is not compatible with transitional or caudal (terminal) lipomas as these latter types of lipomas are, at least in part, attached to the conus and thus related to secondary neurulation.

If disjunction fails to occur completely then some remnant of the common origin of skin and central nervous system persists. The nomenclature for this group of disorders is particularly confusing,

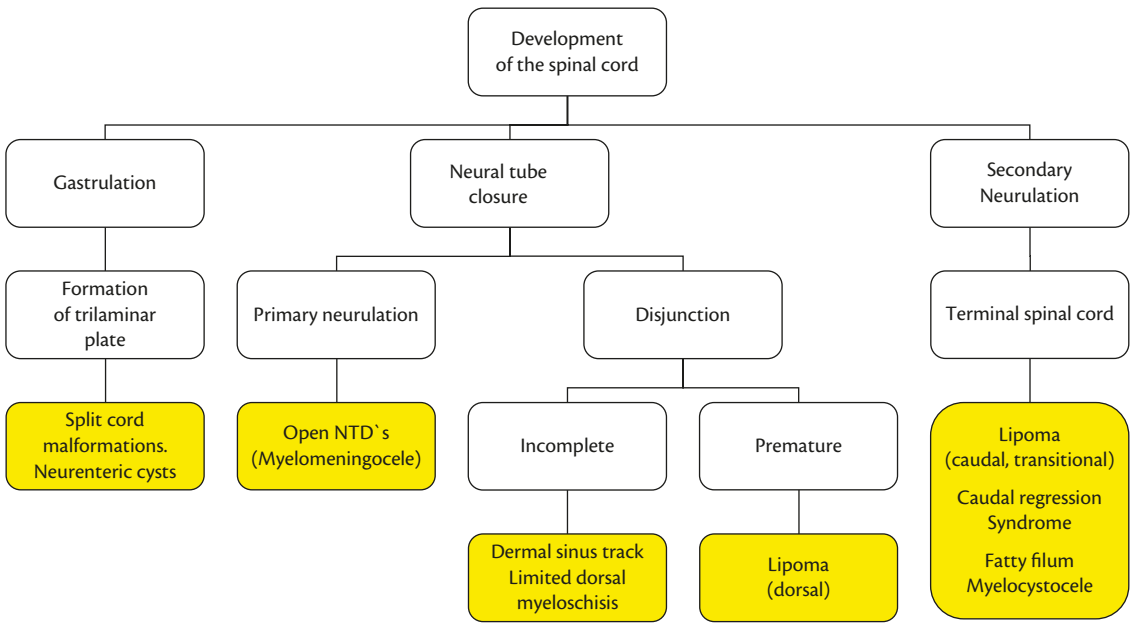

Fig. 85.1 An embryological perspective on the classification of spinal dysraphism.

terms such as meningocele manqué, true and pseudo-dermal sinus track, long and short tethering tracks and, more recently, limited dorsal myeloschisis are frequently encountered. Martínez-Lage et al., 2010; Pang et al., 2013; Thompson, 2013) It is perhaps the histological nature of the neuro-cutaneous connection that best distinguishes the different types of tethering tracks. In limited dorsal myeloschisis (LDM) a tongue of predominantly neural tissue extends from the dorsal aspect of the spinal cord to the overlying skin whereas in dermal sinus track this connection is predominantly epithelial. The distinction is more than semantic as the mode of clinical presentation and neurological differs between the two (see next).

Disorders of secondary neurulation

Many forms of spinal dysraphism involve the conus and cauda equina and thus are thought to result either from aberrant secondary neurulation or impaired regression of the medullary cord. If the medullary cord fails to involute, or does so partially the result is a thickened or fatty filum terminale, when the lipomatous component is larger this is termed a caudal or terminal lipoma, in both instances the conus tends to be functionally intact but situated at a lower level than normal. Transitional lipomas are also likely to have their origins in secondary neurulation. They are termed transitional because they are intermediate in location between the dorsal type and the caudal type, transitional lipomas are intimately related to the conus and the dorsal root entry zone of the elements of the cauda equina, as a result the surgical anatomy is the most challenging of the three lipoma types.

Some disorders of secondary neurulation have much more extensive loco-regional associations reflecting the diverse differentiation of the caudal cell mass. In such situations a variety of congenital genito-urinary abnormalities, encompassed under the term Partial UroRectal Spetal Malformations (PURSMs) including cloacal anomalies, anal atresia, rectovaginal fistula coexist with spinal dysraphism. Sometimes the associations extend beyond the caudal cell mass derivatives including foregut, cardiac, and vertebral disorders, and are grouped under various acronyms including OEIS, VATER, and VACTERL.

In caudal regression syndrome there appears to be complete absence of secondary neurulation, the conus and terminal sacral segments of the spinal cord are absent resulting in a high termination of the spinal cord (Fig. 85.2). The sacrum is dysplastic and there may be an anorectal malformation. By contrast, in the case of terminal myelocystocele the elements of secondary neurulation are present but result in a markedly expanded termination of the spinal cord. The trumpeted end of the spinal cord expands into the subcutaneous tissues resulting in a large midline swelling low in the natal cleft (Fig. 85.3).

Fig. 85.2 Sagittal T2-weighted MRI scan of a child with caudal regression syndrome. There is an absence of the conus medullaris, the terminal spinal cord has a typical truncated appearance, there is also partial sacral agenesis.

Clinical presentation

Broadly speaking there are two presentations of spinal dysraphism, the first is with a cutaneous anomaly overlying the spine, the second is with a neurological, urological, or orthopaedic deficit, the so-called neuro-orthopaedic syndrome. Of course, there is commonly overlap in these modes of presentation.

Cutaneous features of spinal dysraphism

The terms open (aperta) and closed (occulta) spina bifida require clarification. The term 'open' refers to situations in which neural tissue is exposed, often leaking CSF and is thus appropriate for myelomeningocele or rachischisis and for some severe meningoceles, where the neural tissue is covered by little more than rudimentary meningeal membranes. In all other forms of spinal dysraphism the neural tissue is not visible but hidden (occult) due to intact overlying skin. That is not to say that the overlying skin is normal, on the contrary the skin is usually abnormal in some way resulting in the so-called cutaneous stigmata of spinal dysraphism. The presence of any of these should raise suspicion of an underlying dysraphic anomaly:

i. Hairy patch. A focal area of hairy skin in the midline is the classical signature of an underlying split cord malformation and is

Fig. 85.3 Sagittal T2-weighted MRI of an infant with terminal myelocystocele. The terminal spinal cord is 'trumpeted out' due to extensive cystic dilatation of the terminal spinal cord.

easy to distinguish from constitutional hirsutism or lanugo hair of the neonate. As skeletal anomalies frequently coexist in split cord malformations (SCMs), spinal deformity such as scoliosis or kyphosis should be looked for.

ii. Subcutaneous lipoma. This represents the external component of a lipomyelomeningocele. Not infrequently there is a shallow dimple, or 'stork mark' type haemangioma in the overlying skin. Deep to the lipoma it is frequently possible to palpate a defect in the posterior bony elements of the spine. It is via this bony defect that the lipoma is connected to the low termination of the spinal cord. All or part of the lipoma invariably crosses the midline. The lipomas are often large and may vary in shape sometimes having the form of a tail like appendage. Midline lumbosacral lipomas require further evaluation even in the absence of associated neurological signs.

iii. Skin sinus. A skin punctum in the midline may represent the cutaneous end of a dermal sinus track (Fig. 85.4). Confirmatory features are course hairs protruding from the defect or a history of discharge particularly of clear fluid, an intermittent swelling or recurrent episodes of infection. These lesions predispose to intraspinal dermoid formation and infective complications such as spinal abscess or meningitis.

iv. Epithelial 'scar' An area of thinned epithelium, sometimes surround by elevated margins causing a crater like effect is the typical cutaneous feature of LDM. Another skin lesion typical of LDM is a raised dome of skin often with a broad pedicle. These are also referred to as non-saccular and saccular LDM respectively.

It is important to remember that in some instances the condition is truly occult and no external signs are evident. For example, in the case of thickened filum terminale the underlying diagnosis may only come to light once symptoms develop.

Neuro-orthopaedic syndrome

Spinal dysraphism may result in a variable combination of neurological, urological, and orthopaedic symptoms and signs, collectively referred to as neuro-orthopaedic syndrome.

Fig. 85.4 Midline cutaneous punctum typical of dermal sinus track.

Neurological symptoms include pain, which is commonly local spinal pain or exercise induced lower limb pain rather than typical radicular pain, numbness, usually around the feet and distal lower limbs and weakness. Weakness typically affects the musculature of the ankles and feet, and is usually asymmetric.

Orthopaedic manifestations of spinal dysraphism include muscle wasting, joint deformity (for example club feet) and gait disturbance. As with neurological symptoms asymmetry is common, this is particularly marked in split cord malformations where the entire limb or foot is small on the side corresponding to the smaller hemicord. Vertebral malformations including congenital fusions and hemivertebrae will increase the risk of scoliosis. Neuromuscular scoliosis may also occur in high myelomeningocele as a result of asymmetric paraspinal muscle innervation.

Urological disturbance due to involvement of the sacral nerve roots is particularly prevalent in myelomeningocele and spinal lipomas though can occur in any of the dysraphic states. Recurrent urinary tract infection, urinary dribbling, and failure to attain continence are typical clinical features. In the older child, loss of previously attained continence, urgency, or new-onset urinary infections may be indications of neurogenic bladder dysfunction. While faecal soiling due to impaired bowel control may complicate some of the more severe dysraphic states this almost invariably occurs when there is also established neurogenic bladder dysfunction. Isolated symptoms of rectal continence are rarely neurogenic in origin.

Tethered cord

The term 'tethered cord' requires some clarification. In virtually all spinal dysraphism the spinal cord lies at a lower level than normal (L1/L2) and thus might be considered from an anatomical or radiological perspective to be tethered, the exception to this is caudal regression syndrome where the termination of the spinal cord is high due to lack of secondary neurulation. However, not all children with spinal dysraphism have clinical symptoms or signs beyond a skin abnormality, the term tethered cord is therefore probably best reserved to describe the clinical features of the neuro-orthopaedic syndrome occurring in the presence of spinal dysraphism. Tethered cord implies a mechanical aetiology underlying the clinical features in contrast to neural dysplasia; in reality both mechanisms are likely to contribute to the "tethered cord syndrome".

Investigation of spinal dysraphism

Although the timing and specific details of the tests and evaluations required may differ according to the type of spinal dysraphism the general principles comprise accurate radiological definition of the disease entity, establishing a baseline for neurological and urological surveillance and putting in place a management plan that will optimize long-term functional outcome.

Ultrasound

In the first 3 months of life, before the posterior vertebral elements are ossified, it is possible to take advantage of the acoustic window to visualize the terminal spinal cord. Ultrasound can be a useful initial screening test and has been demonstrated to be sensitive to the presence of spinal dysraphism though usually MRI will be required to refine the diagnosis and for surgical planning.

MRI

MRI is the definitive imaging modality for spinal dysraphism. The level of the conus, syrinx formation, and associated vertebral anomalies are well demonstrated. In the closed dysraphic states, it is usually sufficient to image only the spine, in myelomeningocele brain imaging is required in addition to evaluate ventricular morphology and the features of the Chiari II malformation.

Urological evaluation

The two aspects of urological function that require close evaluation in cases of spinal dysraphism are firstly safety of the kidneys and upper renal tract and secondly continence, the ability to store urine and appropriately empty. Ensuring the safety and health of the kidneys is the initial priority particularly for the more severe forms of spinal dysraphism (myelomeningocele, complex lipomas, and caudal regression syndrome). A small volume, high pressure bladder, particularly in the context of urinary infection may predispose to ureteric reflux and renal damage and requires urgent treatment, this might include vesicostomy, continuous or intermittent catheterization, and prophylactic antibiotic treatment.

Achieving 'social' continence is a later priority. Many children with spinal dysraphism will have ostensibly normal bladder function in early childhood. In addition to identifying the 'hostile' bladder, early bladder function tests in infancy are used to try to identify early signs of neurogenic bladder dysfunction or to predict the likelihood of this occurring. In the precontinent child, the interpretation of bladder function and urodynamic studies can be extremely difficult and requires urological expertise.

Physiotherapy

Age appropriate recording of muscle strength is required both to provide an initial assessment of motor deficits and as a means of recording motor function over time as sequential Medical Research Council (MRC) muscle charting can help identify early signs of deterioration. Physiotherapy review is also helpful in identifying deficits in either muscle strength or gait that might be improved by orthotic aids or orthopaedic intervention.

Management of specific dysraphic entities

Myelomeningocele

Myelomeningocele differs from the rest of the spinal dysraphic disorders in being a 'pan CNS disorder'. As a result, structural brain changes and hydrocephalus commonly occur with the spinal anomalies. The characteristic brain abnormalities include downward displacement of the cerebellum, pons, and fourth ventricle, beaking of the tectum, kinking of the medulla, and low-lying hypoplastic tentorium. These features constitute the Chiari II malformation (Geerdink et al., 2012). The Chiari II malformation can be responsible for bulbar insufficiency (breathing and feeding difficulties) particularly in infancy and for high cervical myelopathy in older children. Symptoms of the Chiari II malformation may indicate evolving hydrocephalus or shunt malfunction. It is important to recognize that the Chiari II malformation is exclusive to open neural tube defects and has no association with the Chiari I malformation. Hydrocephalus is reported to occur in up to 80% of cases of myelomeningocele and may be present at birth or may develop following closure of the spinal defect. In recent years shunting rates for myelomeningocele associated hydrocephalus have fallen as in many cases ventricular dilation may stabilize with no apparent adverse consequences (Chakraborty et al., 2008).

While Caesarean section is the most commonly chosen mode of delivery for antenatally diagnosed myelomeningocele there is no clear evidence that normal vaginal delivery poses an additional infection or neurological risk. Surgery to close myelomeningocele should be performed within 48 hours of birth to reduce the risk of infection, reduce ongoing damage to the neural placode and for cosmetic reasons. Shunt placement can be performed at the time of initial closure (if there is severe hydrocephalus) or more commonly deferred until there is clear evidence of progressive hydrocephalus based on serial head circumference measurement or ultrasound.

In the case of closed spinal dysraphism urgent surgery is rarely required. Indeed the indications for surgery and the likely prognosis for many of these disorders is less clear-cut.

Closure of myelomeningocele, surgical considerations

Postnatal repair of myelomeningocele should ideally be performed within 48 hours of birth, so long as the child's clinical condition permits and there are no major contraindications to surgery such as sepsis, coagulopathy, or severe respiratory impairment.

Where there are severe comorbidities such as life threatening respiratory or cardiac conditions then it may be appropriate to consider non-operative management. However even in severe cases of myelomeningocele where the long-term functional prognosis may be poor, surgical closure is generally advised. Untreated lesions tend to become painful, chronically infected, and can present significant nursing difficulties.

Preoperative surgical evaluation

An assessment of the size of the spinal defect and quality of the adjacent skin should be made. Lesions with a diameter of more than 5 cm are unlikely to be amenable to primary closure and the possibility of a local skin flap should be considered. Plastic surgery advice should be considered in this instance. Motor evaluation is important, recording of lower limb muscle strength will indicate the functional level of the myelomeningocele and provides an important baseline for ongoing surveillance. Head circumference measurement and cranial ultrasound are undertaken to anticipate the evolution of hydrocephalus and therefore serial measurement of head circumference and ventricular size need to be instigated. A saline soaked gauze combined with a cling film wrap serves to protect the lesion from desiccation, trauma, and contamination. Prophylactic antibiotics are indicated pending surgical closure. In the absence of signs of infection these are discontinued after surgical closure.

Key surgical objectives

The principal aims of surgery are to replace the spinal cord within the spinal canal, recreate the thecal sac, and provide good quality skin closure to protect the repair and prevent leakage of cerebrospinal fluid.

Key surgical steps

The procedure is performed with the baby in the prone position, pressure areas such as the knees and face need to be protected. The operation is carried out under general anaesthesia. Specific

considerations include ensuring that the child remains warm and well perfused. Excessive blood loss is unusual but may be encountered where large skin flaps have to be raised or when a bony kyphus is removed.

The surgical incision needs to take into account the size and shape of the lesion as well as the potential need to elevate complex skin flaps. Skin laxity, underlying bone anatomy, and proximity to the anus are additional considerations. The neural placode needs to be dissected from the surrounding abnormal skin and membranes. Care needs to be taken to protect the placode, spinal cord, and any underlying nerve roots from further damage during surgical manipulation.

Each of the surgical layers requires meticulous closure in order to prevent leakage of spinal fluid, infection, or wound breakdown due to excessive tension in the skin closure.

Key anatomy

Typically the neural placode will be seen in the centre of the lesion surrounded by the myelomeningocele sac, the latter is comprised of dysplastic meningeal membranes and skin. Once the placode has been mobilized the sac is resected back to normal skin. It is important to ensure that no skin elements are left attached to the placode as these may result in implantation dermoid cysts at a later date.

The posterior vertebral elements (spinous processes and laminae) will be absent at the level of the lesion. Identification of the lowest intact lamina will aid in the identification of the normal dura at the upper end of the lesion. This is the starting point from which the new dural layer can be dissected from the inner lining of the sac.

The multilayer repair begins with neurulation of the placode, rolling up the neural tissue to recreate the terminal spinal cord, this is achieved with interrupted 8/0 monofilament suture. This step is only appropriate if it can be achieved without undue tension at the suture line as this can induce ischaemic injury to the placode. Occasionally abnormal nerve roots are encountered entering the sac these are non-functional and can be removed. A very prominent bony kyphus may have to be resected as this can compromise the skin closure. Additionally neural abnormalities that may be encountered include split spinal cord, hemi-myelomeningocele, and thickened filum.

The edges of the dura are trimmed and then approximated and closed with a continuous suture in an attempt to effect a watertight closure. Where there is concern about the integrity of the dural closure the repair can be reinforced by elevating fascial flaps from the adjacent dorsolumbar fascia.

Postoperative care

Following surgery, the child is nursed in the prone or lateral position to avoid pressure on the surgical wound. The wound should be monitored for signs of infection or CSF leakage.

The head circumference is measured daily and plotted on a head circumference chart. Serial cranial ultrasound scans are used to monitor ventricular size. Progressive ventricular enlargement or signs of raised intracranial pressure require placement of a ventricular shunt.

Urological review to assess the upper and lower urinary tracts is essential prior to discharge. Lower limb deformity, particularly ankle and foot deformities such as talipes should be evaluated and a management plan formulated by orthopaedic surgeons and physiotherapists.

More common complications include wound infection where proximity to the nappy area with risk of wound soiling increases the risk. Dressings should be changed as soon as soiled. Occlusive dressings may help protect the wound from this complication. Local necrosis and wound breakdown can occur due to excessive tension at the suture line.

CSF leakage through the surgical wound may occur due to local factors such as wound breakdown or due to the development of hydrocephalus. CSF leakage is associated with a high rate of infection and requires urgent treatment. CSF may also collect beneath the skin causing local swelling. It is more likely where there has been extensive undermining of the skin leaving a large dead space. In such a scenario a wound drain placed at surgery can help reduce this risk. Pseudomeningocele may also occur due to hydrocephalus.

At least 50% of children who have undergone myelomeningocele closure will develop hydrocephalus requiring treatment. Signs of hydrocephalus include increasing head circumference, tense fontanelle, splaying of cranial sutures, 'sunsetting' eyes or progressive ventricular dilation on ultrasound. Treatment requires placement of a ventricular shunt.

Less common complications include brainstem dysfunction. Radiological features of the Chiari II malformation can be found in most children with myelomeningocele; however, only a minority will develop symptoms of brainstem dysfunction. Bulbar symptoms and signs in the neonatal period include apnoeas, aspiration, and feeding difficulties. These findings may be precipitated by untreated or inadequately treated hydrocephalus. Hydrocephalus should be fully treated before considering hindbrain decompression.

Progressive worsening of lower limb deficits following surgical repair of myelomeningocele can be due to syringomyelia. This is a rare early complication, it can occur later in childhood as a manifestation of untreated hydrocephalus or shunt malfunction.

Lipomas

The spinal lipomas are an anatomically complex form of spinal dysraphism and perhaps the most controversial in terms of surgical management. Three types of spinal lipoma are recognized, dorsal, transitional, and caudal (terminal), based on the point of attachment to the lipoma above, at, or below the conus medullaris. A fourth, chaotic type has recently been described in which the lipoma extends ventral to the spinal cord and nerve roots. The surgical management of dorsal and caudal types of lipoma tends to be more straightforward since involvement of the conus and cauda equina is less thus reducing risk to sphincter innervation. Transitional lipomas represent a significant surgical challenge and are also the group with the highest rate of long-term morbidity (**Fig. 85.5**).

Up to one-third of cases of lipoma that present in infancy are ostensibly asymptomatic with no features of the neuro-orthopaedic syndrome, presenting solely with a lumbosacral subcutaneous mass. It is now recognized that the natural history for spinal lipomas is perhaps more benign than hitherto considered (Kulkarni et al., 2004; Pang et al., 2009; Pang et al., 2010; Wykes et al., 2012; Thompson, 2013). This has led many to question the efficacy of conventional untethering surgery, particularly in asymptomatic cases given the disappointing long-term results reported in many surgical series. The essence of the current surgical controversy surrounding lipomas is twofold; firstly, is there a role for prophylactic spinal cord tethering? and secondly, whether more recently described radical

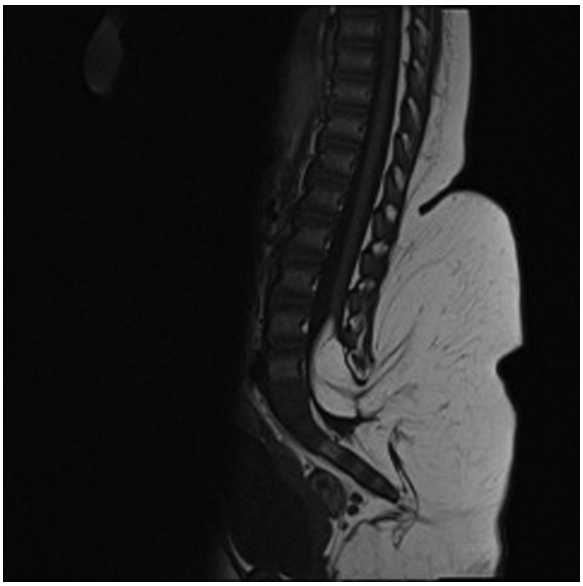

Fig. 85.5 Sagittal T1-weighted MRI of the lumbosacral spine showing a complex transitional type spinal lipoma. The spinal cord is low lying, the lipoma is continuous with a large subcutaneous component of the lipoma via a defect in the posterior sacral elements.

surgery techniques, guided by electrophysiology confer a better long-term prognosis? In attempting to resolve these controversies the following, generally accepted facts need to be taken into account.

1. Up to half of unoperated lipomas will show evidence of neurological or urological deterioration in the course of follow-up. While transitional lipomas seem to be at particular risk this is not reflected in all studies and currently there are no clear predictive features for deterioration that can be identified at the time of initial diagnosis.
2. Surgery for lipoma has a not insignificant risk. These risks include new neurological or urological deficits in at least 5%, and wounded complications such as CSF leakage in up to 20% cases.
3. Conventional untethering surgery techniques are associated with a high rate of late deterioration. The precise rate varies between series but seems comparable to the rate of deterioration in unoperated cases.
4. While pain often responds well to untethering surgery, established neurogenic sphincter disturbance is infrequently improved.
5. The precise mechanisms underlying deterioration remain unclear, specifically the relative contributions of mechanical tethering and underlying neural dysplasia.

Studies by Pang and colleagues have suggested that a more radical approach to the initial untethering is associated with long-term outcomes that are better than either natural history or conventional untethering (Pang et al., 2009; Pang et al., 2010). The principles underlying their technique are near-total resection of the lipoma guided by intraoperative electrophysiological monitoring and mapping, meticulous reconstruction of the neural placode and expansion duraplasty. Their exceptional results are yet to be reproduced in other centres but likely represent a major advance in the treatment of this condition. It is perhaps too early to recommend this technique as a standard of care particularly in asymptomatic patients. Taking the just-featured arguments into consideration our current policy is to carefully monitor asymptomatic children with regular neurological and urological evaluations reserving radical surgery for cases of new or progressive deterioration. Initial evaluations are carried out 6-monthly until urinary continence is achieved and annually thereafter. Serial MRI is not required unless there is evidence of deterioration (Fig. 85.6).

Principles of lipoma surgery

Key surgical objectives

There are three main objectives in complex lipoma surgery, firstly to detach the spinal cord and the associated lipoma from the surrounding tissues, secondly to resect the lipoma from the terminal spinal cord and finally to reconstruct the terminal spinal cord and thecal sac in such a way so as to reduce the risk of re-tethering.

Given the anatomical complexity of these lesions the risk to existing neurological and particularly urological function is not insignificant and therefore it is strongly recommended that intraoperative neuro-physiological monitoring be used. The monitoring consists of a combination of motor evoked potentials (MEP) to evaluate the integrity of the motor pathways and nerve root mapping to aid the identification and preservation of functional nerve roots particularly those to the sphincters. The muscle groups chosen for monitoring and mapping include quadriceps (L4), tibialis anterior (L5), gastrocnemius (S1), abductor hallucis (S2), and anal sphincter (S3 and S4). This ensures that each of the lumbosacral levels is monitored.

Key surgical steps

The initial step in surgery is to locate the defect in the lumbosacral fascia through which the lipoma protrudes. A paraspinal muscle reflection is now carried out to expose the intact laminae immediately rostral to the defect in the fascia. A laminectomy is performed exposing the underlying dura, the extent of the laminectomy should be sufficiently high to permit access and visualization of the normal spinal cord immediately above the attachment of the lipoma. The lipoma passes through a defect in the dura en route to its attachment to the spinal cord, this defect may be quite eccentric and further lateral bone removal is often required such that normal dura can be seen around the entire circumference of the neck of the lipoma. Under the operating microscope the dura is now opened, beginning over normal spinal cord, and continuing around the neck of the lipoma on either side. It is important to identify and protect any underlying nerve roots at this point—nerve root stimulation and mapping facilitate this. On completion of the dural opening the spinal cord and attached lipoma are now free of any surrounding attachment.

The next phase of the operation is to resect the lipoma. The dorsal root entry zone needs to be identified on each side as this will delineate the lateral extent of the lipoma resection. Using sharp dissection, the lipoma is resected from the underlying spinal cord revealing the fibrous 'white plane' at the neural placode. Repeated MEP measurements are taken during this part of the operation.

The final stage of the operation begins with neurulation of the spinal cord, this is done with 8/0 monofilament suture. The thecal sac now has to be reconstructed in such a manner as to create a generous CSF space around the terminal spinal cord. A dural graft is

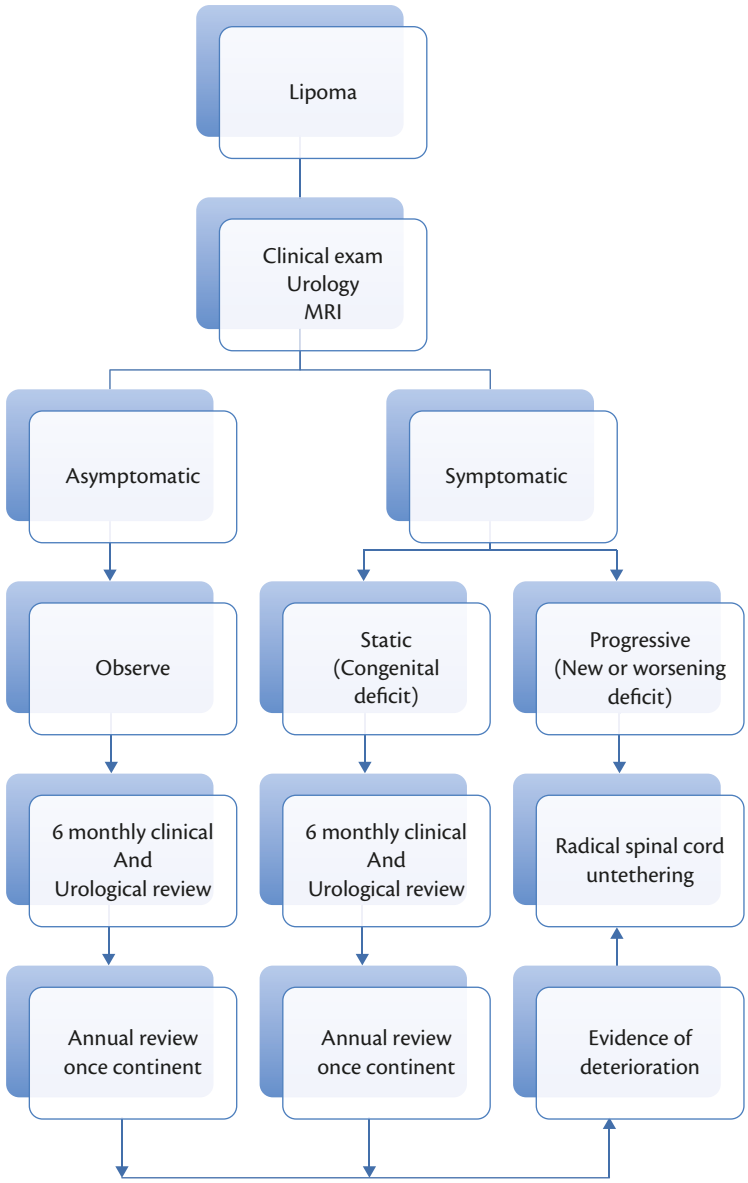

Fig. 85.6 Institutional-based algorithm for the management of spinal lipomas.

cut to the exact dimensions of the dural defect and then secured in place with a continuous non-absorbable suture to provide a watertight closure. The overlying musculofascial and skin layers are then closed meticulously to reduce the risk of any CSF leakage or wound complication.

Dermal sinus tracks and LDM

The disorders of disjunction are associated with risks of infection (spinal abscess or recurrent meningitis), inclusion cyst formation (dermoid or epidermoid) and spinal cord tethering (Thompson, 2013). The risk varies according to the specific diagnosis for example true dermal sinus tract with CSF leakage has a high rate of infection complications while LDM is more prone to neurological complications. For the child presenting with such complications, there is a clear indication for surgery. In a child presenting with a spinal abscess, usually an infected dermoid, initial surgical management is best limited to pus drainage and aggressive antibiotic treatment deferring definitive surgery until the infection is adequately treated. Even where there have been no complications, a child presenting with the typical cutaneous stigmata of dermal sinus or LDM should undergo surgery as the surgery has low risk and the long-term prognosis is good.

The operative procedure for dermal sinus or LDM entails excision of the cutaneous anomaly, identifying the underlying stalk and then tracing this through the deep tissues, into the intradural compartment, and finally excising the attachment to the spinal cord or conus. MRI may underestimate the intrathecal extent of the lesion and so intradural exploration (sometimes requiring three- or four-level laminectomy) is required in almost all cases.

Thickened filum

This is the mildest of the dysraphic anomalies and inevitably there is an overlap with normal variants. Most authorities would agree that when the filum is thickened (at least 2 mm in diameter) and when

the conus lies significantly lower than the normal level (L1/L2) there is at least the potential for damage to occur due to tractional forces as the child grows. Where there are features of the neuro-orthopaedic syndrome then the decision to operate is clear-cut, though even in asymptomatic or borderline cases since the surgical morbidity is extremely low and given the low likelihood of re-tethering prophylactic intervention can be justified.

In the young child the surgery can be performed through a simple fenestration of the ligamentum flavum without recourse to laminectomy. The filum is identified and sectioned under the operating microscope. Almost invariably there is a vessel lying within the filum, this requires explicit coagulation prior to sectioning to avoid the risk of ongoing bleeding after the cut ends have retracted out of the operative view.

Split cord malformations (SCM)

In the type I SCM (diastematomyelia) there is a bony spur lying between the two dural tubes each containing a hemi cord. Symptoms can include progressive pain, weakness or muscle wasting due to differential growth of the vertebral column and spinal cord, progressive spinal deformity is also a risk either due to tethering or by virtue of the associated vertebral anomalies (Fig. 85.7). Many of these children will require spinal orthopaedic procedures for deformity and this represents an additional indication to operate to reduce the risk of tractional damage during scoliosis correction.

The surgery for type I SCM necessitates removal of (frequently abnormal) laminae to expose the spur. The spur is then removed by the combination of rongeur and drilling. The base of the spur may be broad and care is required to avoid injury to the adjacent neural tissue. The dural sheath around the bony spur is then removed and the posterior dura reconstructed leaving the two hemicords in a single compartment. Closure of the ventral dura is not necessary.

Fig. 85.7 3D CT scan of the lumbosacral spine in a case of type I split cord malformation demonstrating the associated bony malformation. The posterior spinal elements are deficient, there are anomalies of the vertebral bodies resulting in deformity and the midline bony spur is evident.

The surgical anatomy of the type II SCM (diplomyelia) is generally more straightforward. The dura is opened along the length of the split cord to identify and remove any intervening fibrous bands. In the author's experience the type II variety may have a very indolent course and such cases can often be safely observed in the absence of symptoms.

Terminal myelocystocele

This rare complex disorder of secondary neurulation will not uncommonly occur in the context of very major urogenital and anorectal malformation. These skin-covered cystic expansions of the terminal spinal cord lie low in the natal cleft and can become extremely large making nursing care difficult and compromising the overlying skin. Early motor deterioration is well recognized in this condition and so early repair is usually recommended. Intraoperative electrophysiological mapping can help determine the lowest level of functional neural tissue, the expanded dysplastic tissue distal to this is then removed and the reconstruction both of the terminal thecal sac and overlying skin can then be performed.

Prognosis and prevention

The prognosis for spinal dysraphism varies according to the specific dysraphic entity, in general the prognosis is dependent upon on the neurological, urological, and orthopaedic status at the time of presentation, as well as the presence of coexisting congenital anomalies. Except for the most minor conditions such as thickened filum, children with spinal dysraphism are ideally followed up in the context of a multidisciplinary team as these children often have complex and changing functional needs through childhood in particular related to mobility and continence. There is often significant psychological morbidity related to issues such as self-image and sexuality, particularly in adolescents. From the neurosurgical perspective one of the main aims of follow-up is the early detection of new or progressive symptoms and signs that might herald the onset of re-tethering.

For children with myelomeningocele there is the additional burden of hydrocephalus and bulbar disturbance which will require lifelong neurosurgical surveillance.

The role of folic acid in the prevention of neural tube defects relates only to open and neural tube defects (encephalocele and myelomeningocele), there is no evidence that folic acid confers any risk reduction for closed spinal dysraphism.

Controversies

There are many controversial issues surrounding spinal dysraphism. Many of the conditions are rare which both constrains institutional experience and the ability to permit large scale clinical studies. In many instances the true natural history of the asymptomatic state is poorly documented and management is based on limited evidence. This is particularly so for spinal lipoma where the role of prophylactic intervention is far from proven. It is important that the results of radical surgical untethering are replicated in other studies. It will then be important to try and identify or risk stratify those cases that might benefit from early radical surgery.

In utero surgical repair of myelomeningocele has been demonstrated in a randomized clinical control trial to have superior outcomes to standard postnatal repair. Opponents are critical of the trial conclusions and ethical concerns are raised in respect to the maternal risk as well as to the impact on future pregnancy. It is likely that this surgery will become more widely offered and the surgery refined utilizing minimally invasive techniques.

Conclusions

Spinal dysraphism comprises a heterogeneous group of congenital spinal anomalies. Although in many cases the details are currently incomplete these disorders are best understood from an embryological perspective. Early and precise anatomical diagnosis is essential in determining prognosis and formulating and appropriate management plan.

Surgery for spinal dysraphism can be extremely complex and decision-making should be guided the principle of optimizing long-term functional outcome. Intraoperative neurophysiological monitoring and mapping are becoming indispensable tools in the surgery of these conditions.

The importance of multidisciplinary team care in the management of these lifelong conditions cannot be overstated.

FURTHER READING

Geerdink, N., van der Vliet, T., Rotteveel, J.J., et al. (2012). Essential features of Chiari II malformation in MR imaging: an interobserver reliability study—part 1. *Childs Nerv Syst*, **28**(7), 977–85.

Pang, D. & Thompson, D.N.P. (2010). Embryology and bony malformations of the craniovertebral junction. *Childs Nerv Syst*, **27**(4), 523–64.

Pang, D., Dias, M.S., & Ahab-Barmada, M. (1992). Split cord malformation: part I: a unified theory of embryogenesis for double spinal cord malformations. *Neurosurgery*, **31**(3), 451–80.

Pang, D., Zovickian, J., & Oviedo, A. (2010). Long-term outcome of total and near-total resection of spinal cord lipomas and radical reconstruction of the neural placode, part II. *Neurosurgery*, **66**(2), 253–73.

Thompson, D.N.P. (2013). Spinal inclusion cysts. *Child's Nerv Syst*, **29**(9), 1647–55.

REFERENCES

Chakraborty, A., Crimmins, D., Hayward, R.D., & Thompson, D. (2008). Toward reducing shunt placement rates in patients with myelomeningocele. *J Neurosurg Pediatrics*, **1**(5), 361–5.

Geerdink, N., van der Vliet, T., Rotteveel, J.J., et al. (2012). Essential features of Chiari II malformation in MR imaging: an interobserver reliability study—part 1. *Childs Nerv Syst*, **28**(7), 977–85.

Kulkarni, A.V., Pierre-Kahn, A., & Zerah, M. (2004). Conservative management of asymptomatic spinal lipomas of the conus. *Neurosurgery*, **54**(4), 868–75.

Martínez-Lage, J.F., Almagro, M.J., Ferri-Ñiguez, B., et al. (2010). Spinal dermal sinus and pseudo-dermal sinus tracts: two different entities. *Child's Nerv Syst*, **27** (4), 609–16.

Pang, D. (1992). Split cord malformation: part II: clinical syndrome. *Neurosurgery*, **31**(3), 481–500.

Pang, D. & Thompson, D.N.P. (2010). Embryology and bony malformations of the craniovertebral junction. *Childs Nerv Syst*, **27**(4), 523–64.

Pang, D., Dias, M.S., & Ahab-Barmada, M. (1992). Split cord malformation: part I: a unified theory of embryogenesis for double spinal cord malformations. *Neurosurgery*, **31**(3), 451–80.

Pang, D., Zovickian, J., & Oviedo, A. (2009). Long-term outcome of total and near-total resection of spinal cord lipomas and radical reconstruction of the neural placode: part I-surgical technique. *Neurosurgery*, **65**(3), 511–28; discussion 528–9.

Pang, D., Zovickian, J., & Oviedo, A. (2010). Long-term outcome of total and near-total resection of spinal cord lipomas and radical reconstruction of the neural placode, part II. *Neurosurgery*, **66**(2), 253–73.

Pang, D., Zovickian, J., Wong, S.-T., et al. (2013). Limited dorsal myeloschisis: a not-so-rare form of primary neurulation defect. *Childs Nerv Syst*, **29**(9), 1459–84.

Thompson, D.N.P. (2013). Spinal inclusion cysts. *Child's Nerv Syst*, **29**(9), 1647–55.

Wykes, V., Desai, D., & Thompson, D.N.P. (2012). Asymptomatic lumbosacral lipomas-a natural history study. *Childs Nerv System*, **28**(10), 1741–2.

RELATED LINKS TO EBRAIN

Closing a Neonatal Myelomeningocoele. https://learning.ebrain.net/course/view.php?id=408

Spinal Dysraphism. https://learning.ebrain.net/course/view.php?id=1038

86

Craniofaciosynostosis

Syndromic and non-syndromic craniofacial anomalies

Federico Di Rocco, Pierre-Aurelien Beuriat, and Eric Arnaud

Introduction

Craniosynostosis is a condition in which there is a premature fusion of one or more sutures of the skull with a modification of cranial growth and an abnormal skull shape. The shape is specific to the suture involved so the diagnosis is essentially clinical.

The genetic causes remain largely unknown. Molecular researches have identified several mutations.

Complications can result to the deformation of the skull but also abnormal facial morphology. Cerebellar tonsillar prolapse, hydrocephalus, intracranial hypertension, insufficient eye protection, respiratory obstructions, and orthodontic problems are the most common.

Several factors play a role in the surgical indications. The aim of the surgery is functional and cosmetic. Techniques have evolved from simple strip to total calvarial and supraorbital remodelling, osteogenic bone distraction, and endoscopic procedures. In all craniosynostosis, long-term follow-up is mandatory because there is a risk of secondary synostosis which exists independently from the originally affected suture.

Definitions

The term craniosynostosis (CRS) derives from *cranio:* cranium, *syn:* together and *ostosis:* bone formation. It is a condition in which there is a premature fusion of one or more sutures of the skull with a modification of cranial growth and an abnormal skull shape. Normally, skull bone growth is perpendicular to the suture, but in CRS the direction of growth becomes parallel to the suture and there is an abnormal growth of the rest of the skull to compensate for the lack of development of the affected part. Moreover, as bone growth is directly linked to brain growth, the closure of one or more sutures leads to an abnormal brain growth so that the modification of the shape is the result of both the compensatory growth but also the alteration of the brain.

CRS shape is specific to the suture involved. The elongation of the skull in a boat shape is due to the premature synostosis of the sagittal suture (scaphocephaly) (**Fig. 86.1**). A growth restriction of the frontal bones in triangular or wedge shape is due to the premature closure of the metopic suture (trigonocephaly) (**Fig. 86.2**). A skew head due to unilateral coronal or lambdoid synostosis is an anterior (**Fig. 86.3**) or posterior plagiocephaly, respectively. It is very important to differentiate, the positional posterior plagiocephaly in which the suture is still opened from a true CRS with early closure of a unilateral lambdoid suture. In positional plagiocephaly the ear on the affected side is often displaced anteriorly but remains at the same craniocaudal level whereas in case of true synostosis the ear on the affected side is deviated toward the fused suture and often tilted inferiorly. When both coronal sutures are closed (brachycephaly), there will be a lack of forward and backward growth with an impression of a short head. The term oxycephaly is used when the coronal and the sagittal sutures are closed.

CRS can also be differentiated as primary (when the closure is linked to a bony problem) or secondary (when the closure is linked to a problem in brain growth that interrupts the bony development), syndromic (when the CRS is associated to others malformations especially at the facial level) or non-syndromic cases (when the CRS is isolated) and simple (when only one suture is affected) or complex (when multiple sutures are affected) forms.

Epidemiology

The global incidence of CRS is 1:2500 births. It is the most common craniofacial malformation in humans. The most common forms are the non-syndromic CRS (NSC). They represent 80–85% of the cases (Di Rocco et al., 2009). NSC that affect only one suture represent over 70% of all CRS.

Scaphocephaly is the most common type. It represents roughly 50% of all NSC (Lajeunie et al., 1996). Trigonocephaly used to be the third most common CRS after anterior plagiocephaly but its incidence has risen in the last 20 years. It is now the second most common form of NSC. Posterior plagiocephaly is the most rare and accounts for about 3% of NSC.

The sex ratio is in favour of boys for scaphocephaly and trigonocephaly with a male-to-female ratio of 2.5:1 and 3.3:1,

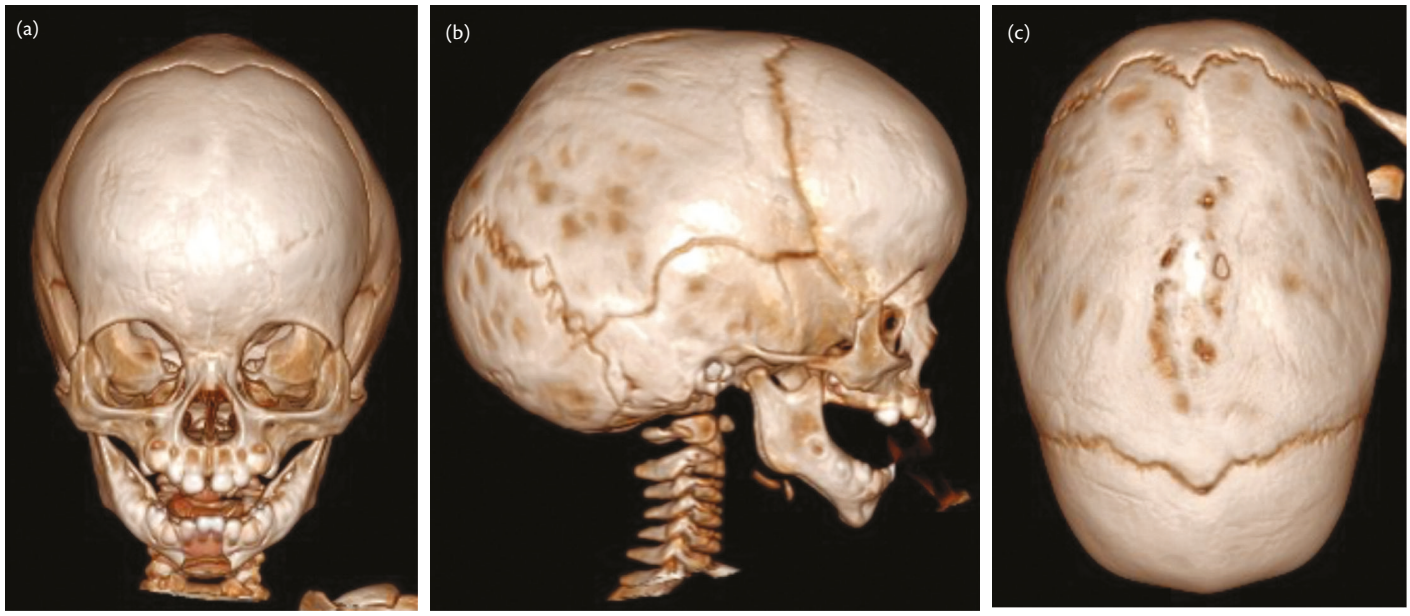

Fig. 86.1 A typical skull CT 3D reconstruction of a 6-month-old boy with scaphocephaly. Note the closure of the sagittal suture causing an anteroposterior elongation of the skull.

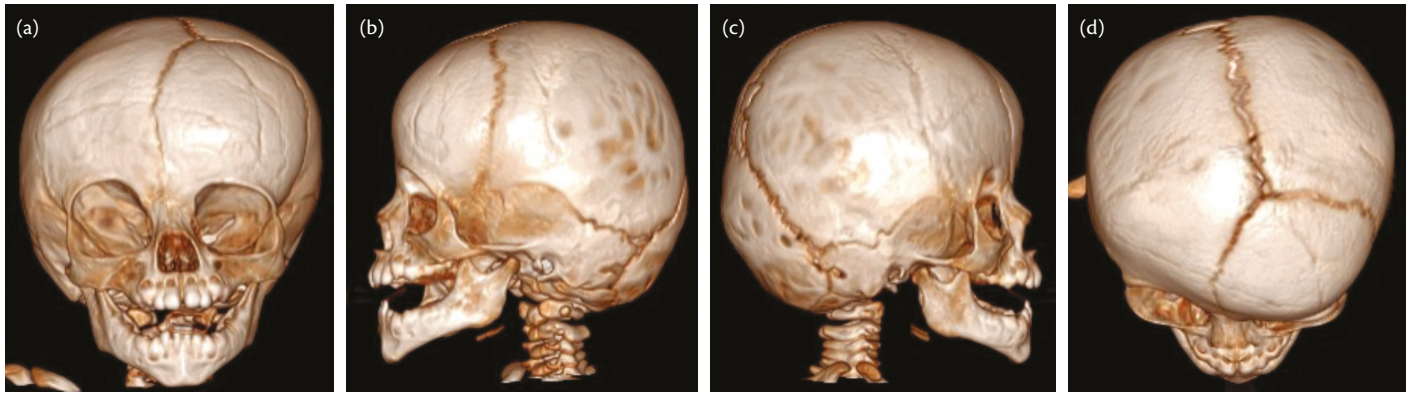

Fig. 86.2 A typical skull CT 3D reconstruction of an 8-month-old girl with a right anterior plagiocephaly. Note the closure of the right coronal suture causing a skew head.

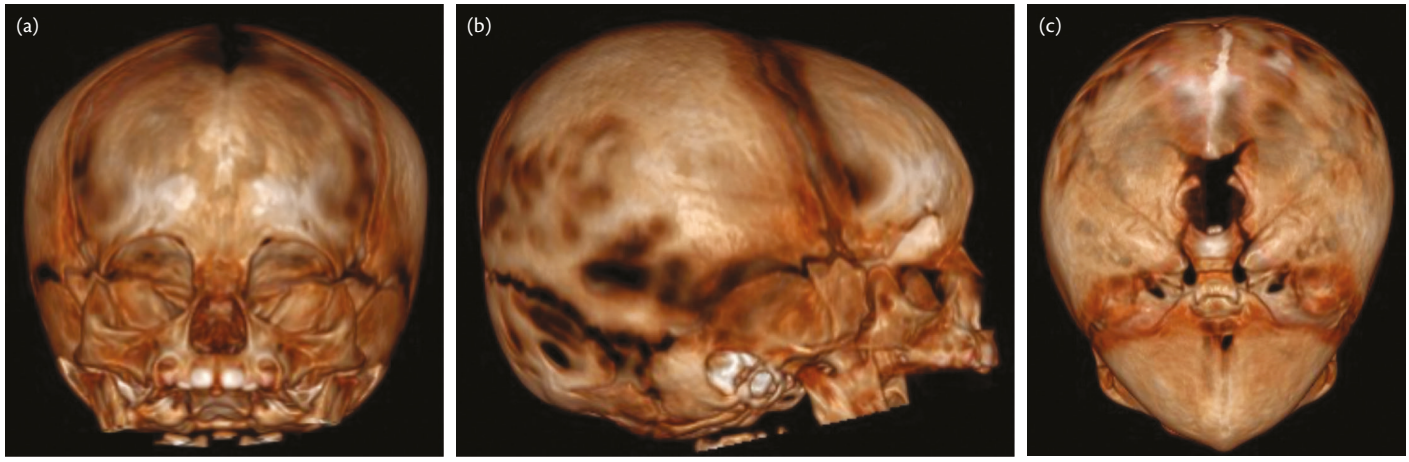

Fig. 86.3 A typical skull CT 3D reconstruction of a 7-month-old girl with a trigonocephaly. Note the closure of the metopic suture causing a triangular forehead.

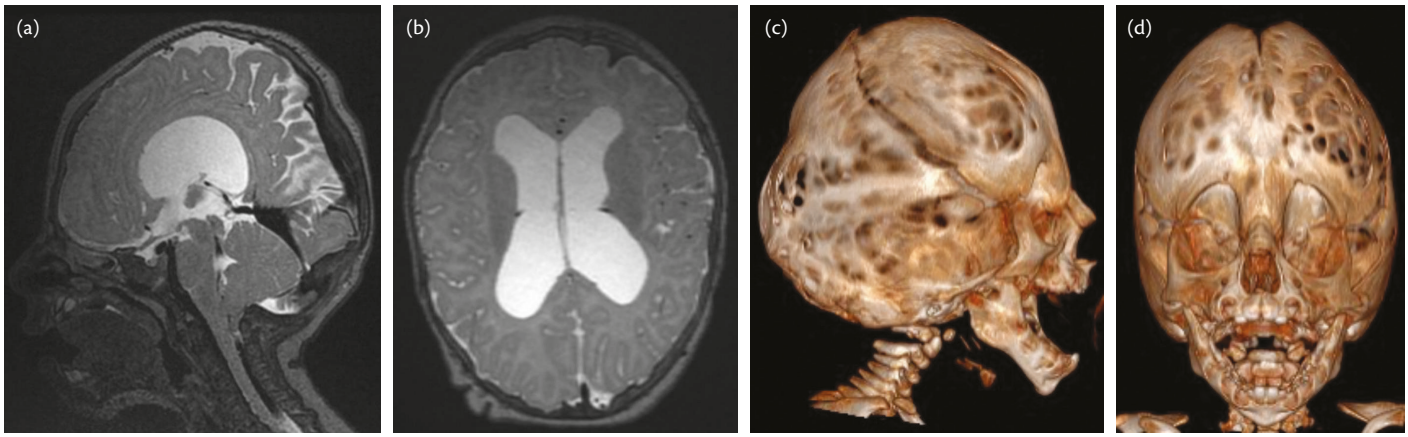

Fig. 86.4 MRI (A, B) and skull CT 3D reconstruction (C, D) of a 19-month-old boy with Crouzon syndrome. Note on the MRI the tonsillar prolapse and the ventricular dilatation. On the skull CT, note the copper beaten skull.

respectively (Lajeunie et al., 1996) while plagiocephaly is more frequent in girls (male-to-female ratio of 1:2.3) (Lajeunie et al., 1996).

Most of the time, NCS are sporadic cases but familial histories may be found in any type of synostosis (Lajeunie et al., 1996).

Syndromic CRS (SCRS) represent 15–20% of all CRS. There are more than a hundred different syndromes but the most common are the Crouzon (Figs. 86.4 and 86.5), Pfeiffer, Apert, Saethre–Chotzen, and Muenke syndromes (Table 86.1).

Aetiology and physiopathogenesis

The genetic causes remain largely unknown. Molecular research has identified several mutations in CRS which involve mostly three of the four fibroblast growth factors (FGFRs) but other genes have been identified such as *TWIST 1, ERF, TCF 12*, and *EFBN1* which are found mostly in SCRS. Mutations are mostly autosomal dominant and a great phenotypic variability exists. Different phenotypes can result from the mutation of a single gene. Appearance can be very different from one patient to another, from subnormal to extremely abnormal. On the contrary similar phenotypes can be generated by several gene defects (Heuzé et al., 2014). In NSC, mutations are rarely found (Wilkie et al., 2007). Other factors, including environmental ones (intrauterine fetal constraint, unhealthy prenatal maternal lifestyles, perinatal hypoxemia) are considered to favour the development of a CRS.

From a functional point of view, many complications can result from a CRS. They are more common in the SCRS where several sutures are involved. Not only the deformation of the skull but also the abnormal facial morphology may lead to complications making collaboration between plastic, craniomaxillofacial, and neurosurgeons essential in the management of these complex pathologies.

From the neurosurgical point of view, one of the most common brain malformations is cerebellar tonsillar prolapse (CTP) (sometimes referred to as Chiari I malformation). CTP is considered the consequence of a disproportion between the small volume of the posterior fossa and the volume of the cerebellum favoured by the premature closure of the lambdoid and skull base sutures and associated hydrocephalus (Cinalli et al., 2005). CTP is very frequent in Crouzon syndrome and Pfeiffer syndromes (Cinalli et al., 2005). Though it is usually asymptomatic, sometimes a posterior decompression may be needed.

Increased intracranial pressure (ICP) is another point of concern. It is secondary to the decreased intracranial volume due to the synostosis generating a craniocerebral disproportion, to venous flow anomalies due to the stenosis of the jugular foramina and to alterations in cerebrospinal fluid dynamics leading to ventricular dilatation.

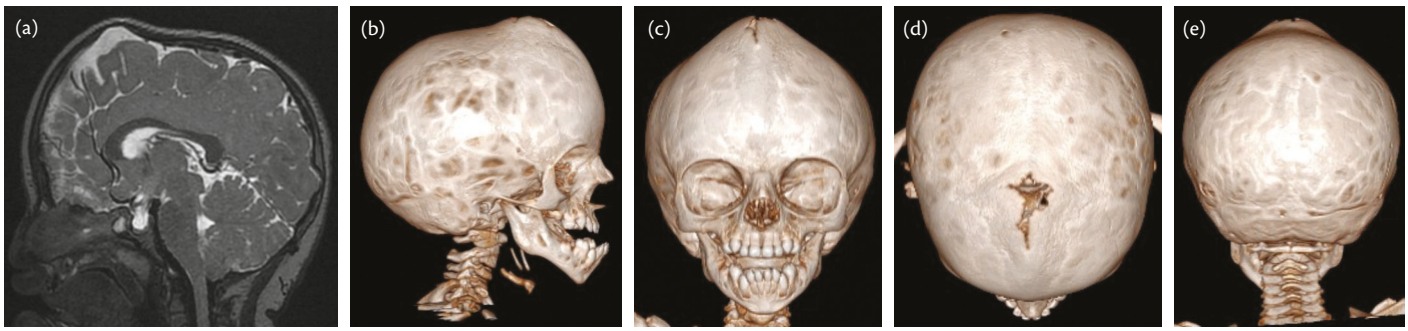

Fig. 86.5 MRI (A) and skull CT 3D reconstruction (B–E) of a 21-month-old girl with Crouzon syndrome. Note on the MRI, the absence of tonsillar prolapse and ventricular dilatation. On the skull CT, note the pansynostosis.

Table 86.1 Features of the most common craniofacial syndromes

	Clinical features	Sutures involved	Genetic findings
Crouzon syndrome	Hypertelorism Beaking nose Proptosis Midface hypoplasia	Coronals Occasional pansynostosis	Mutations in FGFR2 *De novo* or autosomal dominant inheritance
Pfeiffer syndrome	Hypertelorism Proptosis Midface hypoplasia Broad, short, great toes Broad deviated thumbs Brachydactyly	Pansynostosis Cloverleaf skull	Mutation in FGFR2 (95%) and FGFR1 (5%). *De novo* or autosomal dominant inheritance
Apert syndrome	Ocular hypertelorism, Downslanting palpebral fissures Thin upper lip Midface hypoplasia Syndactyly of the hands and feet	Pansynostosis Coronals	Mutations in FGFR2 (S252W and P253R) Mostly *de novo*
Saethre–Chotzen syndrome	Low-set hairline Parrot-beaked nose Ptosis Abnormal ears (prominent crus) Syndactyly	Coronals Metopic or sagittal sutures have been described	Mutations in TWIST1 *De novo* or autosomal dominant inheritance
Muenke syndrome	Mild midfacial hypoplasia Hypertelorism	Coronals	Mutation in FGFR3 (P250R) *De novo* or autosomal dominant inheritance

Hydrocephalus is frequent in Crouzon and Pfeiffer syndromes (Cinalli et al., 2005; Di Rocco et al., 2010). Its physiopathology is complex. It results from a combination between venous flow anomalies and CTP (Cinalli et al., 2005; Di Rocco et al., 2010).

From the craniomaxillofacial surgical point of view, the anomalies in facial morphology and facial growth of CRS may also lead to insufficient eye protection, respiratory obstructions, and orthodontic problems. Respiratory problems are the consequences of upper airway obstruction (Mathijssen et al., 2006) but also the CTP. The main problem linked to this breathing dysfunction is obstructive sleep disorder, which can worsen intracranial hypertension.

Ocular problems result from the chronically increased ICP that lead to visual impairment due to optic nerve compression, atrophy, and the complications of exorbitism (Khong et al., 2006). It is more frequent in SC.

Another very important point to stress is the intellectual, behavioural, and emotional functioning in children with CRS (Maliepaard et al., 2014). The outcome is related to the type of deformity, syndrome, and the associated brain malformation. Apert syndrome has the worst mental prognosis (Renier et al., 1996). It is rare but possible to find mental retardation in Crouzon and Saethre–Chotzen syndromes (Michael Cohen Jr., 2011). It is difficult to demonstrate whether, it is the consequences of the craniocerebral disproportion causing white matter anomalies or due to the direct effect of the genetic mutations on the brain itself (Raybaud and Di Rocco, 2007).

Diagnosis

The phenotype of CRS being specific the diagnosis is essentially clinical.

Prenatal diagnosis of many craniofacial malformations is possible but remains currently rare. The diagnosis is suspected not only on head deformity but also on brain, face, and extremities anomalies. When multiple signs are seen on the ultrasound scan, it is recommended to perform an MRI and an amniocentesis with standard karyotype and molecular genetic testing.

Investigations

After the diagnosis has been suspected by clinical evaluation, further investigations may be needed to assess the associated anomalies.

Plain X-rays, computed tomography (CT) scan, and more recently ultrasound and MR may be used to see exactly which sutures are involved. The morphological alterations of the skull and face can be clearly appreciated on CT 3D reconstructions.

Other investigations can be necessary in SCRS: MRI to evaluate the hydrocephalus, the CTP, and other potential brain malformations; ophthalmological examination to search for papilloedema and signs of raised ICP as well as complications of exorbitism; ear, nose, and throat (ENT) to evaluate the upper airways obstruction; polysomnography study because the presence of apnoea can modify the surgical procedure. The genetic testing for the patient and the family allows correct parental counselling when an underlying mutation is recognized. Finally, neuropsychological follow-up is recommended.

Surgical principles

Several factors play a role in the surgical indications: age of the patient, type of CRS, raised ICP, hydrocephalus, CTP, severity of the respiratory obstruction, degree of cranial hypoplasia, ocular problems as well as mandibular/maxillary, orthodontic, orbital, and facial morphology. The aim of surgery is dual: functional and cosmetic.

At a functional level, the aim is to treat hydrocephalus, prevent intracranial hypertension, mental delay, ocular problems, and

improve respiratory problems. At a cosmetic level, it is to correct the craniofacial dysmorphology to prevent psychological consequences.

Techniques have evolved from a simple strip to total calvarial and supraorbital remodelling. Nowadays, osteogenic bone distraction (Choi et al., 2010) and endoscopic procedures (Jimenez and Barone, 1998) represent interesting alternatives (Sanger et al., 2014). The extent, timing of surgery, and the indications are still elements of controversy. But one should remember that often NSC will undergo surgery for cosmetic reasons only (Di Rocco, 2009). Because it is not possible to predict whose patients will develop neurocognitive impairment, surgery is indicated, irrespective of the cosmetic aspect (Barritt et al., 1981) because the sooner the surgery is performed, the better the outlook is. Moreover, early surgery allows a better correction because the dysmorphism is less pronounced and the bone is more malleable, and it permits the use of the natural brain growth for passive postoperative remodelling. Therefore, these patients should be operated on before one year of age. These surgeries being associated with potentially significant blood losses (White et al., 2015), the timing of the procedure depends mostly on the type of CRS and the weight of the patient according to the planned procedure. In our practice, patients with scaphocephaly are usually operated on before the age of 6 months; for trigonocephaly and anterior plagiocephaly, between 7 and 8 months of age.

In SCRS, the surgical strategy is more complex, several surgical operations are usually necessary. The first surgical procedure to be performed depends on the presence of increased ICP, hydrocephalus, thrombocytopenia (TCP), and breathing problems. If there is a papilloedema, the surgery needs to be done as an emergency.

The classical procedures in SCRS are posterior skull expansion, fronto-orbital advancement, and facial advancement. Posterior skull expansion is usually the first step in Crouzon or Pfeiffer syndromes. Patients affected by these syndromes often suffer from progressive hydrocephalus due to the hypoplastic posterior cranial fossa with secondary crowding of the contained neurovascular structures. Ventricular CSF drainage lowers the expanding force that allows the skull to grow and favours the stenosis. Therefore, a procedure to increase the posterior cranial volume is nowadays recommended initially. It has the effect of decreasing the ICP, restabilizing CSF dynamics, and decompressing the venous structures. Sometimes when a mechanical CSF obstruction is the cause of the hydrocephalus, an endoscopic ventriculocisternostomy may be performed (Di Rocco et al., 2010). Several techniques can be used, from sole posterior craniotomy to a fixed posterior bone flap, using resorbable plates or free-floating bone flap. Another very efficient technique is to perform a posterior craniotomy and add distractors to ensure cranial expansion. Moreover, when a TCP is present, a foramen magnum decompression can be associated in order to decompress the craniovertebral junction. Further procedures will be needed to correct the anterior part of the skull. These surgeries are postponed until later in life to obtain a better and more persisting cosmetic result.

When management of the anterior part of the skull is considered fronto-orbital advancement is the gold standard procedure followed if needed by a facial advancement. The latter should be postponed as much as possible until the age of 11 or 12 years old in order to wait for the end of the last dental eruption. If the facial retrusion is severe and is creating functional (ocular, respiratory, and masticatory) or psychological problems, earlier surgery may be done.

The standard technique for fronto-orbital advancement is a horizontal tongue-in-groove advancement, including an orbital bar osteotomy and advancement. The fixation of the reconstructed elements is done with bioabsorbable plating systems.

When it comes to facial advancement, the Lefort III type described by Tessier (Tessier, 1967) is indicated. The use of a distraction technique permits a gradual expansion through an osteogenic distraction procedure (Iannetti et al., 2006).

In cases of severe exorbitism and upper airways obstruction, Tessier developed a one stage surgery with the combination of fronto-orbital and facial advancement (Tessier, 1971). Frontofacial monobloc advancement is, in most cases, associated with an osteogenic distraction procedure because it has been shown that it lowers the complications of this high-risk procedure (Arnaud and Di Rocco, 2012).

Finally, in older children and adolescents, the appearance of the patient, when facial growth is almost completed, may be further improved by cosmetic and orthognathic surgery.

In all CRS, long-term follow-up is mandatory because there is a risk of secondary synostosis which exists independently from the originally affected suture.

Controversy section: Minimally endoscopic procedures (MEP) for CRS

A controversy exists between the strip craniectomy and cranial vault remodelling in NSC.

For: As whole-vault cranioplasty is associated with important blood losses several techniques to minimize blood loss and transfusion have been designed. Among them MEP (endoscopic strip craniectomy followed by moulding cranial orthosis for several months) has been shown to have minimal blood loss (Jimenez and Barone, 2012), allow a reduced hospital stay, and be cost-effective (Chan et al., 2013). Last but not least, this procedure is possible for almost every type of single suture CRS (Jimenez and Barone, 2012).

Against: Results rely on the postoperative application of a helmet. The orthosis might reduce the cranial growth, is expensive and laborious. Incomplete remodelling is possible even with the orthosis (Sauerhammer et al., 2014). Finally, recent studies suggest that better long-term intellectual outcomes are achieved with whole-vault cranioplasty (Hashim et al., 2014).

FURTHER READING

Di Rocco, F., Arnaud, E., & Renier, D. (2009). Evolution in the frequency of nonsyndromic craniosynostosis. *J Neurosurg Pediatr*, **4**(1), 21–5.

Hashim, P.W., Patel, A., Yang, J.F., et al. (2014). The effects of whole-vault cranioplasty versus strip craniectomy on long-term neuropsychological outcomes in sagittal craniosynostosis. *Plast Reconstr Surg*, **134**(3), 491–501.

Raybaud, C. & Di Rocco, C. (2007). Brain malformation in syndromic craniosynostoses, a primary disorder of white matter: a review. *Childs Nerv Syst*, **23**(12), 1379–88.

Twigg, S.R.F. & Wilkie, A.O.M. (2015). New insights into craniofacial malformations. *Hum Mol Genet*, **24**(R1), R50–9.

REFERENCES

Arnaud, E. & Di Rocco, F. (2012). Faciocraniosynostosis: monobloc frontofacial osteotomy replacing the two-stage strategy? *Childs Nerv Syst*, **28**(9), 1557–64.

Barritt, J., Brooksbank, M., & Simpson, D. (1981). Scaphocephaly: aesthetic and psychosocial considerations. *Dev Med Child Neurol*, **23**(2), 183–91.

Chan, J.W.H., Stewart, C.L., Stalder, M.W., St Hilaire, H., McBride, L., & Moses, M.H. (2013). Endoscope-assisted versus open repair of craniosynostosis: a comparison of perioperative cost and risk. *J Craniofac Surg*, **24**(1), 170–4.

Choi, J.W., Ra, Y.S., Hong, S.H., et al. (2010). Use of distraction osteogenesis to change endocranial morphology in unilateral coronal craniosynostosis patients. *Plast Reconstr Surg*, **126**(3), 995–1004.

Cinalli, G., Spennato, P., Sainte-Rose, C., et al. (2005). Chiari malformation in craniosynostosis. *Childs Nerv Syst*, **21**(10), 889–901.

Di Rocco, C. (2009). Nonsyndromic craniosynostoses. In: Sindou, P.D.M. (ed.) *Practical Handbook of Neurosurgery*, pp. 1061–84. Berlin, Germany: Springer-Verlag Wien.

Di Rocco, F., Arnaud, E., & Renier, D. (2009). Evolution in the frequency of nonsyndromic craniosynostosis. *J Neurosurg Pediatr*, **4**(1), 21–5.

Di Rocco, F., Jucá, C.E., Arnaud, E., Renier, D., & Sainte-Rose, C. (2010). The role of endoscopic third ventriculostomy in the treatment of hydrocephalus associated with faciocraniosynostosis. *J Neurosurg Pediatr*, **6**(1), 17–22.

Hashim, P.W., Patel, A., Yang, J.F., et al. (2014). The effects of whole-vault cranioplasty versus strip craniectomy on long-term neuropsychological outcomes in sagittal craniosynostosis. *Plast Reconstr Surg*, **134**(3), 491–501.

Heuzé, Y., Martínez-Abadías, N., Stella, J.M., et al. (2014). Quantification of facial skeletal shape variation in fibroblast growth factor receptor-related craniosynostosis syndromes. *Birth Defects Res A Clin Mol Teratol*, **100**(4), 250–9.

Iannetti, G., Fadda, T., Agrillo, A., Poladas, G., Iannetti, G., & Filiaci, F. (2006). LeFort III advancement with and without osteogenesis distraction. *J Craniofac Surg*, **17**(3), 536–43.

Jimenez, D.F. & Barone, C.M. (1998). Endoscopic craniectomy for early surgical correction of sagittal craniosynostosis. *J Neurosurg*, **88**(1), 77–81.

Jimenez, D.F. & Barone, C.M. (2012). Endoscopic technique for sagittal synostosis. *Childs Nerv Syst*, **28**(9), 1333–9.

Khong, J.J., Anderson, P., Gray, T.L., Hammerton, M., Selva, D., & David, D. (2006). Ophthalmic findings in apert syndrome prior to craniofacial surgery. *Am J Ophthalmol*, **142**(2), 328–30.

Lajeunie, E., Le Merrer, M., Bonaïti-Pellie, C., Marchac, D., & Renier, D. (1996). Genetic study of scaphocephaly. *Am J Med Genet*, **62**(3), 282–5.

Maliepaard, M., Mathijssen, I.M., Oosterlaan, J., & Okkerse, J.M. (2014). Intellectual, behavioral, and emotional functioning in children with syndromic craniosynostosis. *Pediatrics*, **133**(6), e1608–15.

Mathijssen, I., Arnaud, E., Marchac, D., et al. (2006). Respiratory outcome of mid-face advancement with distraction: a comparison between Le Fort III and frontofacial monobloc. *J Craniofac Surg*, **17**(5), 880–2.

Michael Cohen Jr., M.M. (2011). Apert, Crouzon, and Pfeiffer syndromes. In: Muenke, M., Kress, W., Collmann, H., & Soomon, B.D. (eds.) *Monographs in Human Genetics*, pp. 67–88. Basel, Switzerland: Karger.

Raybaud, C. & Di Rocco, C. (2007). Brain malformation in syndromic craniosynostoses, a primary disorder of white matter: a review. *Childs Nerv Syst*, **23**(12), 1379–88.

Renier, D., Arnaud, E., Cinalli, G., et al. (1996). [Mental prognosis of Apert syndrome]. *Archives De Pédiatrie: Organe Officiel De La Sociéte Française De Pédiatrie*, **3**(8), 752–60.

Sanger, C., David, L., & Argenta, L. (2014). Latest trends in minimally invasive synostosis surgery: a review. *Curr Opin Otolaryngol Head Neck Surg*, **22**(4), 316–21.

Sauerhammer, T.M., Seruya, M., Ropper, A.E., et al. (2014). Craniectomy gap patency and neosuture formation following endoscopic suturectomy for unilateral coronal craniosynostosis. *Plast Reconstruct Surg*, **134**(1), 81e–91e.

Tessier, P. (1967). [Total facial osteotomy. Crouzon's syndrome, Apert's syndrome: oxycephaly, scaphocephaly, turricephaly]. *Annales De Chirurgie Plastique*, **12**(4), 273–86.

Tessier, P. (1971). The definitive plastic surgical treatment of the severe facial deformities of craniofacial dysostosis. Crouzon's and Apert's diseases. *Plast Reconstr Surg*, **48**(5), 419–42.

White, N., Bayliss, S., & Moore, D. (2015). Systematic review of interventions for minimizing perioperative blood transfusion for surgery for craniosynostosis. *J Craniofac Surg*, **26**(1), 26–36.

Wilkie, A.O.M., Bochukova, E.G., Hansen, R.M., et al. (2007). Clinical dividends from the molecular genetic diagnosis of craniosynostosis. *Am J Med Genet A*, **143A**(16), 1941–9.

87

Special considerations in paediatric head and spinal trauma

Andrew Kay, Desiderio Rodrigues, Melanie Sharp, and Guirish Solanki

Incidence and epidemiology of paediatric trauma

Traumatic brain injury (TBI) is the most common cause of death or disability in childhood.

It is estimated that in the United Kingdom approximately 150 000 children have a head injury but less than 14 000 attend hospital every year with TBI. The overall mortality rate is 9 per 100 000 accounting for 1% of all childhood deaths (Royal College of Surgeons, 1999).

The main mechanisms of paediatric TBI are dependent on age. In those under 2 years, non-accidental head injuries (NAI) and ground level falls are the most common. From 2 to 4 years, falls predominate. Between age 4 and teenage years, falls or road traffic collisions (RTC) are the most common. In teenagers, RTCs are the main cause of TBI.

The type of injury also differs between adult and paediatric TBI. Skull fractures and extradural haematomas are more common in paediatric patients.

Paediatric spine fractures account for a minority (1–3%) of all paediatric fractures. Around 60% are cervical spine injuries, and while only 3% of these will present with neurologic deficits, spinal cord injury (SCI) in children remains a catastrophic event and every attempt should be made at decreasing the extent and severity of the injury as well as the complications following the injury (Eleraky et al., 2000; Brown et al., 2001).

In children under the age of 8 years, as many as 87% of injuries occur at C3 or above. Injuries below C3 are more common in older children with an adult pattern of injury. With regards to age the commonest types of fracture in the very young are C1 ring and C2 (Hangman) fractures, while odontoid fractures are evenly distributed across all ages. Lumbar fractures occur in the older age group.

The causes of injury also depend on the age of the child, infants are injured by birth trauma in the neonatal period or from accidental falls from the parent's arms, cots, settees, or sofas. Children from 2 to 8 years old get spinal injuries from bicycle falls and other road traffic accidents (RTAs). It is reported as many as 25–60% follow an RTA in this age group. Older children sustain spinal injuries from falls and sports injuries.

Pathophysiology of paediatric head injury

The basic response to TBI is similar to adults but there are anatomical and physiological differences unique to the paediatric population including a disproportionately large size of the head with weak neck musculature in neonates and infants which places them at an increased risk from rotational and acceleration/deceleration injuries. Children also have greater elasticity of bone, wide subarachnoid spaces, high water content in the brain, and viscoelastic properties which increase the likelihood of a diffuse axonal injury.

Intracranial pressure (ICP) varies with age. In infants and young children, the normal ICP is under 10 mmHg. In the older child and adult, the normal ICP is 15 mmHg.

Cerebral blood flow (CBF) also shows age-related variation: in infants it is 40 ml/100 g/min, children 75–110 ml/100 g/min and adolescents, like adults 50 ml/100 g/min.

Head injury management

Early management of all TBI should follow Advanced Paediatric Life Support (APLS), Advanced Trauma Life Support (ATLS), American College of Surgeons Committee on Trauma (1997), and National Institute of Clinical Excellence (NICE) guidelines. (See 'Key references'—NICE Head injury guidelines.)

All children admitted with a head injury should be managed in a major trauma centre with Paediatric Intensive Care Unit (PICU) and paediatric neurosurgery services. Safe and timely transfer is essential.

The Glasgow Coma Score can be applied to children which allows the severity of the injury to be measured. A modified version is acceptable in preverbal children and infants (see **Table 87.1**).

Similar to adults, early head injury management is focused on prevention of secondary injury to the brain mainly from hypoxia and hypoventilation, along with cervical spine immobilization. In severe TBI (GCS less than 8) or where neurological deterioration is

predicted based on the mechanism of the injury and the scan findings, early admission to PICU is necessary.

Indications for intubation reflect those in adults, with an additional indication in uncooperative children who need a computed tomography (CT) scan. Tracheal intubation can be difficult and uncuffed tubes are used in children less than 8 years old.

Indications for ICP monitoring mirror those for adult TBI. Infant ICP can be assessed qualitatively using the anterior fontanelle. The current consensus on the threshold for active lowering of ICP in children is 20 mmHg (Adelson et al., 2003).

Management of ICP is still based on adult data, with focus on adequate oxygenation, ventilation including avoidance of hyperventilation, analgesic sedatives including opiates and midazolam with additional muscle relaxants, surgical intervention (as deemed necessary), and barbiturate coma as second-line therapies. Propofol, which is widely used in adult head injury, is an emulsion and has been associated with metabolic acidosis and high lipid levels in children.

Target cerebral perfusion pressure (CPP) values have not yet been established for infants and young children. A spectrum of 40 mmHg from infant to 70 mmHg as a teenager is considered appropriate.

To date, paediatric trials for decompressive craniectomy have been small. The largest RCT to date with 27 patients showed improved functional outcome at 6 months (Taylor et al., 2001). Longer-term outcomes have not been reviewed. As with adult decompressive craniectomy trials concerns relate to conversion of mortality to increased functional morbidity. Anecdotally the threshold for decompression remains lower among paediatric neurosurgeons in view of the unknown longer-term outcomes.

Phenytoin is more commonly used in paediatric patients with a severe TBI than in adult patients to minimize the incidence of early post-traumatic seizures. Antiepileptic medication is usually given for a 1-week course. Early seizures are much more common in young children and become less prevalent in older children. Early seizures in children are poorer predictors of post-traumatic epilepsy than in adults.

Hypothermia reduces ICP but there is limited evidence about its efficacy and safety in children (see 'Controversies in paediatric trauma' section).

A CT head scan is the scan of choice in TBI. A CT scan of the cervical spine exposes the thyroid gland to ionizing radiation and therefore is not always indicated in mild injury where X-rays may be sufficient. UK hospitals generally follow NICE guideline indications for CT scans (**Figs. 87.1** and **87.2**).

'Clearing' the cervical spine in obtunded children is less easy than in adults because the incidence of ligamentous injuries and spinal cord injury without overt radiological abnormality (SCIWORA) is much higher. MRI scanning is useful in identifying spinal cord signal change, haemorrhage, ligament, muscle, and disc injuries. Acute bone injury is well seen on short tau inversion recovery (STIR) images which can help differentiate acute from longstanding changes. Immobilization with a collar until the child is alert may be unavoidable (Lee et al., 2003).

Paediatric head injury prognosis

A significant proportion of children with TBI die before they reach hospital. The highest mortality is seen in RTA passengers and the lowest in falls (Parslow et al., 2005).

Prognosis is poor where CPP is less than 40 mmHg (highly predictive of mortality), there is bilateral absence of somatosensory evoked potentials (SSEPs) (strongly associated with severe disability and death) or a prolonged period with an ICP above 20 mmHg.

Non-accidental injury

NAI or abusive head trauma is the most common cause of serious or fatal brain injuries in children aged 2 years and younger and can be due to impact or shaking or both. Children diagnosed with NAI are five times more likely to die compared with accidentally head-injured children, yet signs and symptoms are not always obvious, and therefore the diagnosis can be overlooked (Hinds et al., 2015).

Shaking typically results in recent multifocal haemorrhages and/or large chronic subdural haemorrhages extending over both cerebral hemispheres (**Fig. 87.3**). Shaking results in tearing of bridging veins. While the volume of haemorrhage is usually small it is the pattern that distinguishes shaking from impact. There is a strong association between multiple, interhemispheric, convexity, and posterior fossa haemorrhages and NAI.

NICE National Institute for Health and Care Excellence!

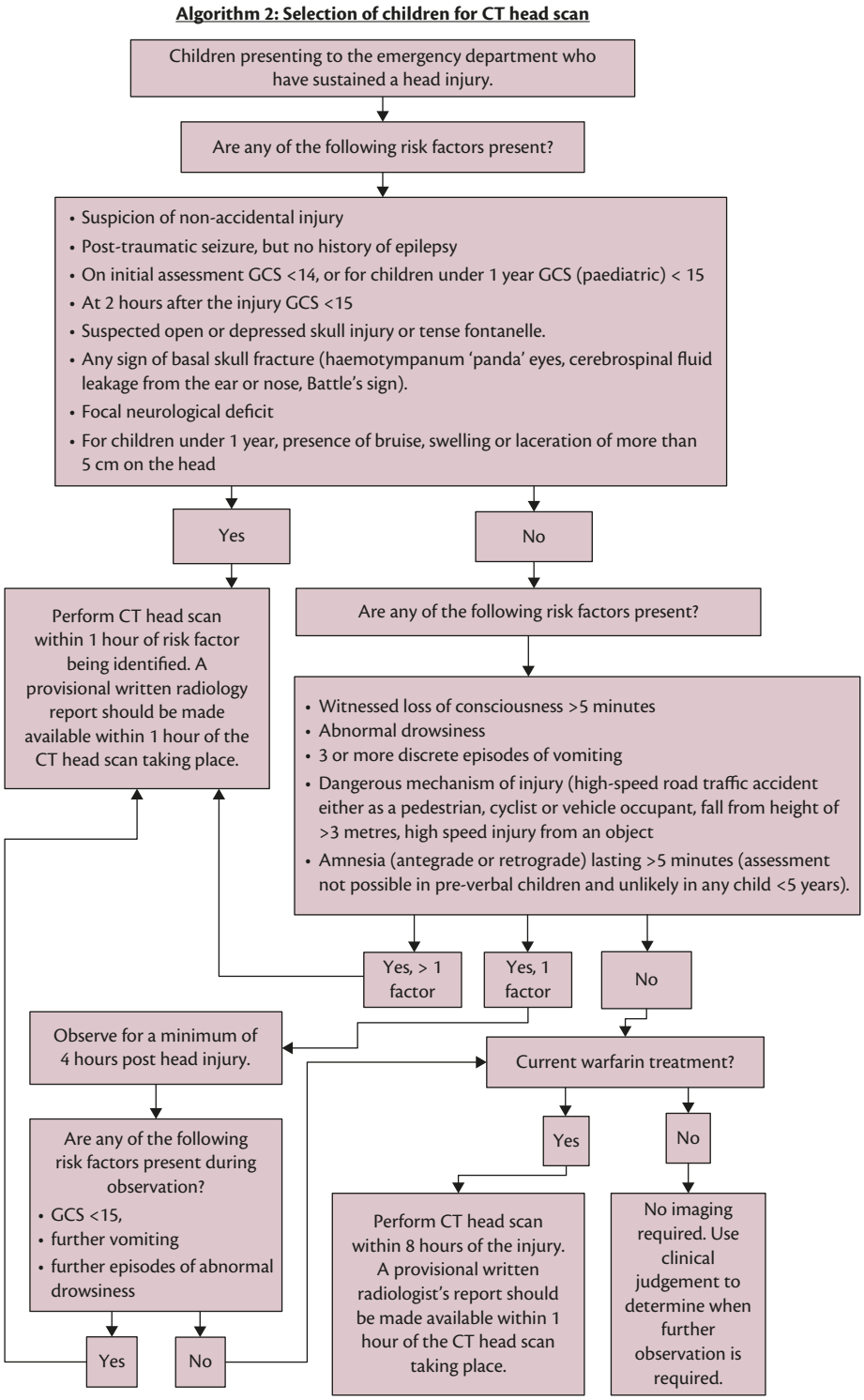
Algorithm 2: Selection of children for CT head scan
Children presenting to the emergency department who have sustained a head injury.
Are any of the following risk factors present?
• Suspicion of non-accidental injury
• Post-traumatic seizure, but no history of epilepsy
• On initial assessment GCS <14, or for children under 1 year GCS (paediatric) < 15
• At 2 hours after the injury GCS <15
• Suspected open or depressed skull injury or tense fontanelle.
• Any sign of basal skull fracture (haemotympanum 'panda' eyes, cerebrospinal fluid leakage from the ear or nose, Battle's sign).
• Focal neurological deficit
• For children under 1 year, presence of bruise, swelling or laceration of more than 5 cm on the head
Yes
No
Perform CT head scan within 1 hour of risk factor being identified. A provisional written radiology report should be made available within 1 hour of the CT head scan taking place.
Are any of the following risk factors present?
• Witnessed loss of consciousness >5 minutes
• Abnormal drowsiness
• 3 or more discrete episodes of vomiting
• Dangerous mechanism of injury (high-speed road traffic accident either as a pedestrian, cyclist or vehicle occupant, fall from height of >3 metres, high speed injury from an object
• Amnesia (antegrade or retrograde) lasting >5 minutes (assessment not possible in pre-verbal children and unlikely in any child <5 years).
Yes, > 1 factor
Yes, 1 factor
No
Observe for a minimum of 4 hours post head injury.
Current warfarin treatment?
Are any of the following risk factors present during observation?
• GCS <15,
• further vomiting
• further episodes of abnormal drowsiness
Yes
No
Yes
No
Perform CT head scan within 8 hours of the injury. A provisional written radiologist's report should be made available within 1 hour of the CT head scan taking place.
No imaging required. Use clinical judgement to determine when further observation is required.

Fig. 87.1 Algorithm published by the National Institute of Clinical Excellence on selection of children for CT head scan.

© National Institute for Health and Care Excellence, 2014. 'Head injury', NICE clinical guideline 176. London: National Clinical Guideline Centre (https://www.guidance.nice.org.uk/CG176).

NICE National Institue for Health and Care Excellance!

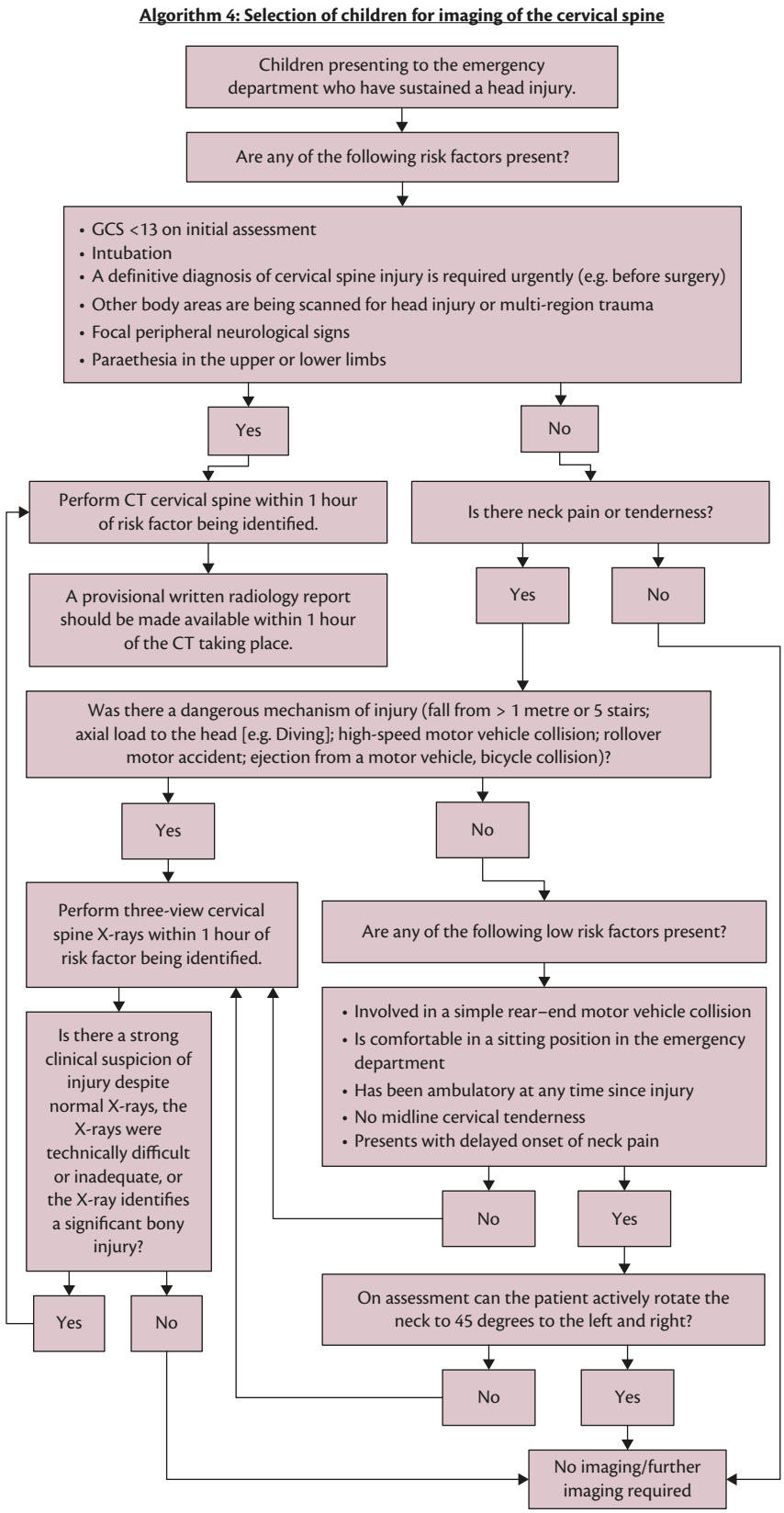
Algorithm 4: Selection of children for imaging of the cervical spine
Children presenting to the emergency department who have sustained a head injury.
Are any of the following risk factors present?
• GCS <13 on initial assessment
• Intubation
• A definitive diagnosis of cervical spine injury is required urgently (e.g. before surgery)
• Other body areas are being scanned for head injury or multi-region trauma
• Focal peripheral neurological signs
• Paraethesia in the upper or lower limbs
Yes
No
Perform CT cervical spine within 1 hour of risk factor being identified.
A provisional written radiology report should be made available within 1 hour of the CT taking place.
Is there neck pain or tenderness?
Yes
No
Was there a dangerous mechanism of injury (fall from > 1 metre or 5 stairs; axial load to the head [e.g. Diving]; high-speed motor vehicle collision; rollover motor accident; ejection from a motor vehicle, bicycle collision)?
Yes
No
Perform three-view cervical spine X-rays within 1 hour of risk factor being identified.
Are any of the following low risk factors present?
• Involved in a simple rear–end motor vehicle collision
• Is comfortable in a sitting position in the emergency department
• Has been ambulatory at any time since injury
• No midline cervical tenderness
• Presents with delayed onset of neck pain
Is there a strong clinical suspicion of injury despite normal X-rays, the X-rays were technically difficult or inadequate, or the X-ray identifies a significant bony injury?
No
Yes
On assessment can the patient actively rotate the neck to 45 degrees to the left and right?
Yes
No
No
Yes
No imaging/further imaging required

Fig. 87.2 Algorithm published by the National Institute of Clinical Excellence on selection of children for imaging of the cervical spine.

© National Institute for Health and Care Excellence, 2014. 'Head injury', NICE clinical guideline 176. London: National Clinical Guideline Centre (https://www.guidance.nice.org.uk/CG176).

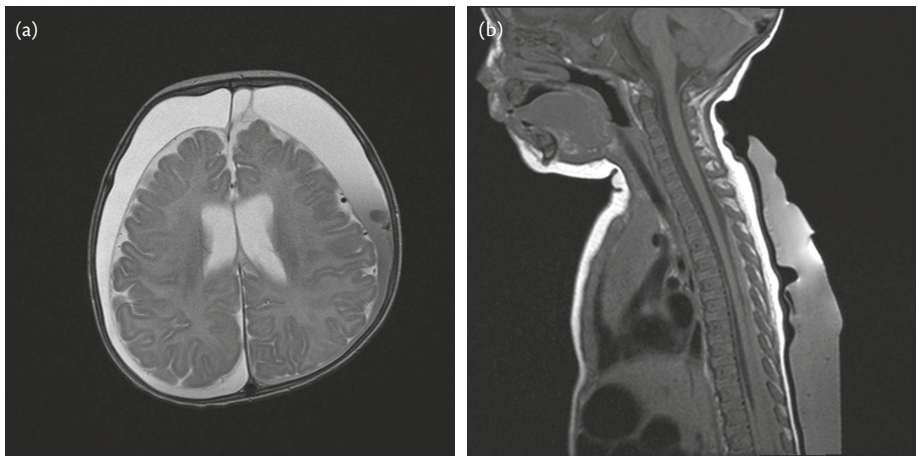

Fig. 87.3 MRI scan showing features of a child consistent with non-accidental injury. (A) shows a bilateral subdural haemorrhage, note the crossing anterior vein and lack of cortical vessels which differentiates this from external hydrocephalus. (B) A spinal subdural haemorrhage.

Subdural haematoma does occur in accidental trauma and other causes of subdural haematoma also need to be considered in this age group including birth trauma where the haematoma usually resolves by 4 weeks of age, blood clotting disorders, or rare metabolic disorders such as glutaric aciduria type I.

The association of subdural haemorrhage(s), retinal haemorrhages, and acute encephalopathy in a previously well baby constitute the so-called triad. In suspected NAI, a full skeletal survey and complete haematological workup is warranted. Neuroimaging is crucial in establishing the diagnosis of NAI as it detects occult injury in 37% of cases. Several imaging patterns are considered to be particularly associated with NAI. The presence of a subdural hematoma, especially in multiple locations, such as the interhemispheric region, over the convexity and in the posterior fossa, is significantly associated with NAI. Although CT is the recommended first-line imaging modality for suspected NAI, early MRI is increasingly used alongside CT because it provides a better estimation of shear injuries, hypoxic-ischaemic insults, and the timing of lesions. (Vázquez et al., 2014)

If NAI is suspected the case should be referred immediately to the appropriate children's safeguarding/child protection team for further investigation. The acute surgical management of suspected NAI should be discussed immediately with the regional paediatric neurosurgical unit. Management of acute encephalopathy in severe cases requires the expertise of paediatric intensive care and paediatric neurology. Management of retinal haemorrhages requires ophthalmological follow-up.

Growing fractures

A growing fracture is a rare post skull fracture phenomenon (Fig. 87.4). In addition to the skull fracture, the underlying adherent dura and arachnoid are torn and widen over time due to the cerebral pulsations and growing brain, resulting in herniation of the cerebrum through the dural and arachnoid tear.

A more rare and severe form of growing fracture is a 'burst fracture', where there is wide diastasis of the fracture and a more significant acute underlying brain injury with damaged cerebral tissue. Management consists of traumatic brain injury ICP management with subsequent surgical repair of the overlying defect.

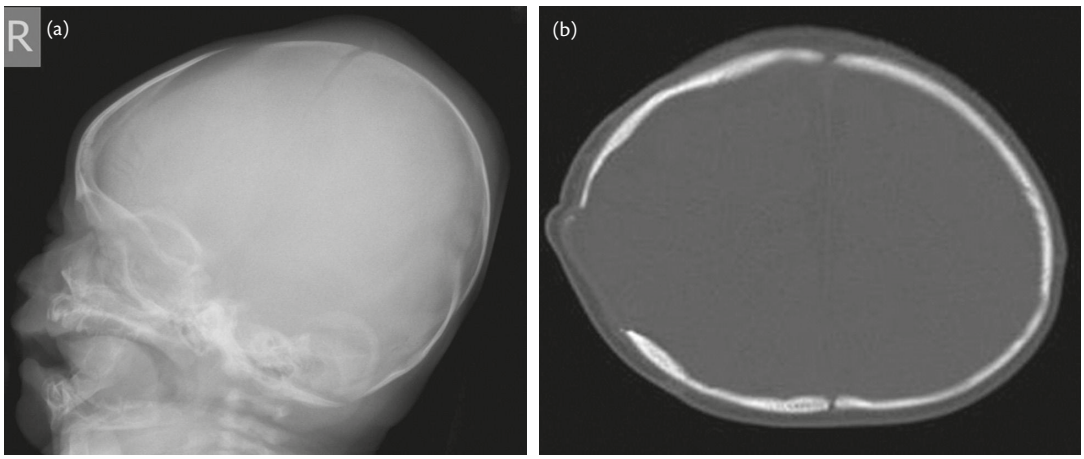

Fig. 87.4 CT scan demonstrating a growing skull fracture on days 1 (A) and 50 (B). Note how the fracture starts as a linear fracture then grows bigger as a result of cerebrospinal fluid (CSF) pulsation.

Half of children affected are under 1 year old and 90% are under 3 years old. Growing fractures usually present as a non-tender scalp swelling, most commonly in the parietal region.

Several factors indicate a potentially poorer outcome including age less than 8 years, female gender, defect less than 7 cm, a defect that crosses over the midline and a delay of more than 8 months in time to repair.

Children with a linear fracture aged less than 3 should be assessed clinically 6 weeks postinjury to look for growing fractures. Treatment of growing fractures involves either a duraplasty or split calvarial duracranioplasty.

Ping pong fractures

A 'ping pong' fracture occurs in young children and neonates. Mechanisms include birth trauma, and accidental and non-accidental injuries.

It occurs following the 'buckling' of the malleable inner table of the calvarium without a formal outer table (cortical) break in continuity. The periosteum remains intact and there is rarely an underlying brain injury (see Fig. 87.5).

The vast majority resolve naturally due to calvarial remodelling from underlying brain growth. In those with neurological deficit or in those deemed cosmetically significant (after approximately 6 months of observation), elevation can be considered.

Spinal injury in children

In trauma, 25–50% of children with a SCI will have an associated head injury. The younger the child, the more likely an upper cervical spine injury is to occur. There are several reasons for this. The integrity and alignment of the spine is maintained mainly by strong ligaments. At the craniocervical junction, several important ligaments connect the flexible craniocervical junction and permit movements between a disproportionately heavy head and a small, only partly ossified upper neck. The ligaments also secure the C1/C2 vertebrae together. Younger children possess greater ligamentous flexibility and the head to neck size ratio is greater. In older children, less flexible, stronger ligaments and heavier neck structure shift the fulcrum to the midcervical spine, where injuries are more likely to occur at C5/C6 as in adults.

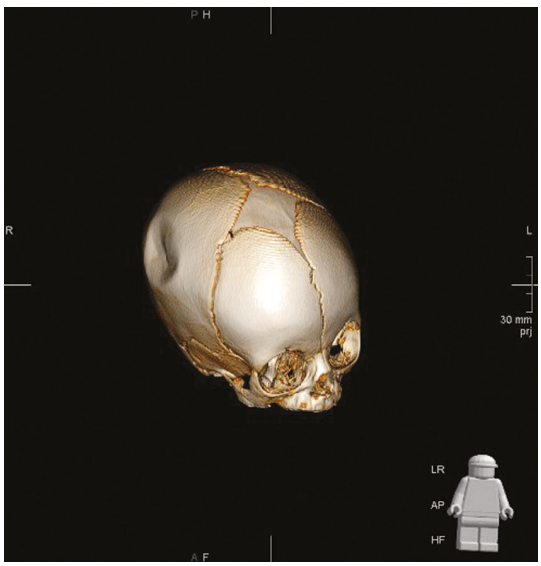

Fig. 87.5 CT scan showing a ping pong fracture. These fractures will usually remodel as the brain grows.

The cartilaginous posterior arch of the C1 ring ossifies by the age of 3 years, while the C2 body ossifies at 6 and the tip of dens at about 12 years. Under 8 years, the midline part of the C1 ring remains weak. C1 ring fractures commonly occur from rotational and compression injuries. Similarly, C2 fractures can occur. Atlantoaxial rotational injuries are very likely due to ligamentous flexibility and easier traumatic disruption at the C1/C2 level. Fracture-dislocations also commonly occur at the C1/C2 level.

The position of the facet joints is horizontal in the very young increasing the risk of horizontal subluxation, and translocation with consequent risk of spinal cord injury. SCIWORA injuries are much more common in the young and mostly occur above C3, they carry a high risk of neurological damage.

Several underlying conditions such as Down's syndrome, the mucopolysaccharidosis (Hurler's, Hurler-Scheie, Hunter's, Morquio-Brailsford, Maroteaux-Lamy), rheumatoid arthritis, and achondroplasia are specifically associated with spinal involvement. The pathology often involves ligamentous laxity (Down's syndrome) and deposition of GAGs (glycosaminoglycans). These may be deposited in the facets and atlantoaxial joints and, in the case of Maroteaux-Lamy, in the dura mater, the posterior longitudinal, and flavum ligaments. In rheumatoid arthritis there are inflammatory changes in the joints and bones. In achondroplasia, an FGFR-3 abnormality causes accelerated ossification leading to craniocervical stenosis and medullary compression. Spinal canal stenosis may occur either segmentally or diffusely over multiple segments with lateral recess impingement.

At any age, these conditions lead to variable spinal canal stenosis, atlantoaxial instability, and deformation mainly cervicothoracic and thoracolumbar kyphotic gibbus and scoliosis. The end point is spinal cord compression which if untreated will progress to myelopathic cord changes. These children are particularly exposed to a greater risk of both skeletal and neurological injury from moderate spinal trauma.

Paediatric developmental anatomy and radiology

The paediatric spine will only reach adult proportions by the age of 10–12 years. Several bones including the arch of C1 and the C2 body and lateral masses will not ossify until the age of 3 years (Munk and Ryan, 2007).

Os odontoideum was previously thought to be congenital but is now considered to be non-union of an odontoid fracture occurring before the age of 6. It can be unstable and flexion/extension X-rays should be performed. Os odontoideum should be distinguished from a persistant ossiculum terminale which is a failure of fusion of the terminal ossification centre in the dens. The ossification centre appears between 3 and 6 years, fusion normally occurs by the age of 12 (Fig. 87.6).

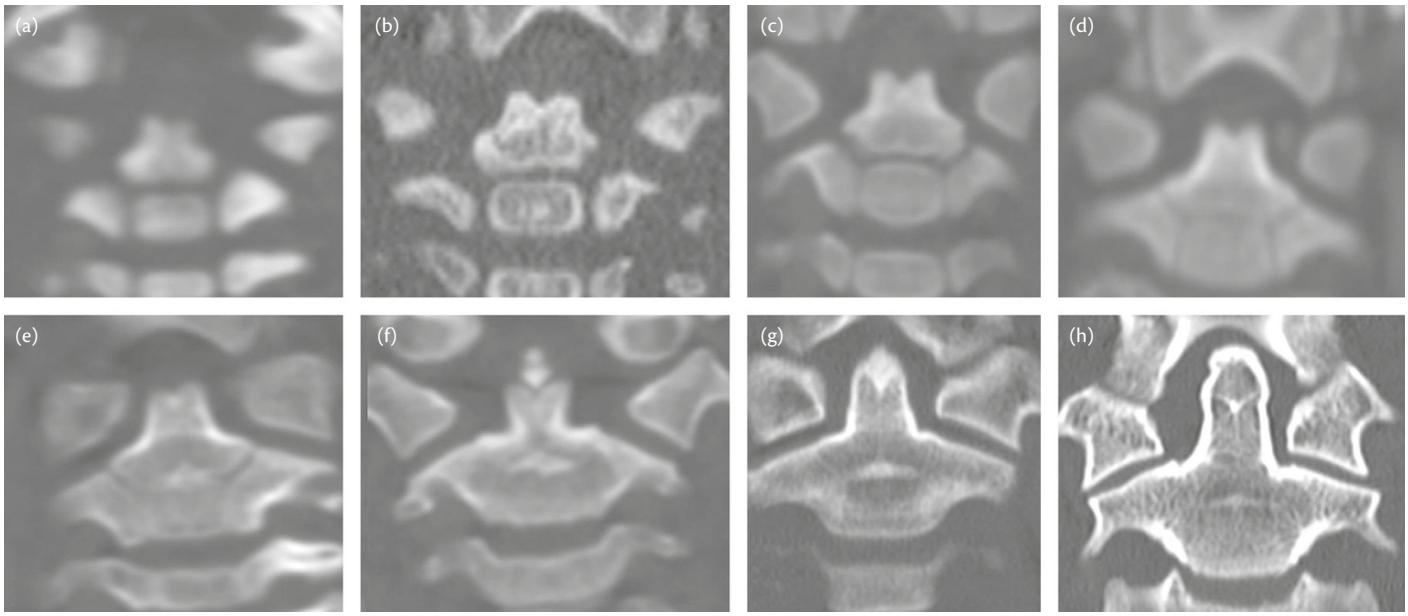

Fig. 87.6 Coronal view of ossification development of the axis. Children are of the following ages: (A) 30 days, (B) 5 months, (C) 1.5 years, (D) 2 years, (E) 3 years, (F) 5 years, (G) 8.5 years, and (H) 14 years.

Under 8 years, both C2 and C3 can show pseudo-subluxation in up to 46% and 14%, respectively. A movement of up to 4 mm or 40% may be a physiological vertebral pseudosubluxation. About one-fifth of children admitted for polytrauma may demonstrate this incidental finding which is due to incomplete ossification, hypermobility, and the fact that facets are horizontal in young children. Pseudosubluxation will reduce on extension and there should be no soft tissue swelling.

In the cervical spine neutral or dynamic views allow evaluation of the atlantodental interval (normally less than 5 mm) indicating transverse and alar ligamentous injury and horizontal instability. Trapezoidal vertebral shape, scoliosis, or offset spinous processes raise suspicion of acute injury somewhere along the spine.

Birth injuries

These may occur following mechanical repositioning of the fetus, or assisted delivery. The upper cervical and cervicothoracic junction are the most affected. These injuries are underdiagnosed mainly because of the lack of radiographic findings at birth, but the mortality for birth-related SCI is high and survivors may have a poor prognosis. Improved prenatal monitoring and obstetric techniques have helped reduce the incidence of these injuries.

Infant brachial plexus injury results from excessive force during delivery. Risk factors are difficult deliveries with the use of forceps or vacuum extraction or a breech delivery, fetal macrosomia, infant shoulder dystocia, and maternal diabetes/obesity. In brachial plexus injuries, conservative treatment with physiotherapy is recommended for the first three months as most injuries heal spontaneously. Subsequently a nerve transfer or grafting surgery may be undertaken.

Atlantoaxial injuries

Atlanto-occipital (C0/C1) and atlantoaxial (C1/C2) dislocation may occur in young children as a result of the relatively large head size in comparison to the body. These injuries are frequently fatal. Treatment in survivors requires craniocervical or atlantoaxial fusion. There is widening of the atlanto-occipital joint by more than 5 mm or the C1/C2 interspinous distance by more than 10–12 mm. These injuries are often the result of a severe RTA and occur five times more often in children than adults. Rupture of the tectorial membrane and alar ligaments in the presence of small occipital condyles and horizontally oriented atlanto-occipital joints allows for the dislocation to occur.

MRI scanning is helpful to confirm the ligament injury. Ligament injuries do not normally heal well with conservative treatment and surgery is likely to be required for more severe cases.

Atlantoaxial rotatory subluxation

Fixed rotation of C1 on C2 may occur. This is caused by subluxation or facet dislocation and it is a common cause of childhood torticollis which presents with neck pain and a fixed tilted 'wry' neck held in the cock robin position. There is a reduced range of motion, the contra-lateral sternocleidomastoid is taut, and the child may have headaches or difficulty with chewing. The diagnosis is often delayed, with average presentation occurring around 5 weeks after onset.

It may be post-traumatic but in children is also seen following retropharyngeal infectious oedema secondary to an upper respiratory tract infection leading to ligamentous laxity, known as Grisel's syndrome. Other predisposing conditions include Down's syndrome, rheumatoid arthritis, posterior fossa tumours, and congenital anomalies.

If the transverse ligament is intact, spinal canal stenosis can only occur with severe rotation and facet dislocation. However, if the transverse ligament is ruptured, the ADI (atlantodental interval) or anterolisthesis will be more than 5 mm. Spinal canal stenosis occurs with only 45 degrees rotation and vertebral arteries are at risk.

A CT is obtained with the head in a neutral position and then in maximal rotation to right and left. In rotatory subluxation the subluxation of C1 on C2 does not change. An MRI should be performed if neurological symptoms or deficits occur to rule out the differential diagnosis of a brainstem lesion.

Fielding's classification is commonly used (see Table 87.2).

Many patients probably reduce spontaneously before seeking medical attention. In subluxations present for less than 1 week, a soft collar, anti-inflammatory medications, and exercise programme can be used. If subluxation persists longer, consider manipulation under anaesthetic, muscle relaxant, and a hard collar (head halter traction and bracing are alternative choices for older children). Occasionally halo traction or C1–C2 fusion may be required.

Lumbar spine injuries in children

Depending on which combination of columns are injured, fractures are described as compression, burst, seat-belt, or fracture-dislocation injuries.

Wedge compression fractures are the most frequently seen fractures, occurring as a result of an axial compression load to the anterior vertebra in flexion. This is a stable injury without spinal canal compromise or spinal cord injury. Kyphotic angulation can occur because there is reduction in anterior vertebral height.

Hinging or seat-belt fractures are caused by extreme bending in sudden acceleration deceleration injuries. Chance fractures are commonly reported in children. The mechanics are associated with seat belts and therefore are often associated with abdominal injuries.

Burst fractures occur from axial load without flexion, and affect the anterior and middle columns. Around 15–20% of all major vertebral body fractures are of this type. There is disruption of the posterior vertebral wall, with fragments that break into the spinal canal and there may be a spinal cord injury.

Three-column injuries come from a shearing injury with sudden severe flexion and rotation. These are inherently unstable and characterized by failure of all three columns. They account for approximately 20% of all spinal injuries and are associated with the highest likelihood of SCI. Approximately 75% of patients with fracture-dislocation injuries have some neurological deficit and 50% of these have complete SCIs.

Table 87.2 Fielding Classification of rotatory atlantoaxial subluxation

Type I	Unilateral facet subluxation with intact transverse ligament	Common Mostly benign
Type II	Unilateral facet subluxation with 3–5 mm of anterior displacement. Injured transverse ligament	
Type III	Bilateral anterior facet displacement of over 5 mm. Both lateral masses are displaced	Rare Higher risk of neurologic involvement
Type IV	Posterior displacement of C1	Rare Higher risk of neurologic involvement

Reproduced with permission from JW Fielding and RJ Hawkins, Atlanto-axial rotatory fixation. (Fixed rotatory subluxation of the atlanto-axial joint), *Journal of Bone & Joint Surgery*, Volume 59, Issue 1, pp. 37–44, Copyright © 1977 Wolters Kluwer Health, Inc.

Spinal cord injury without overt radiographic abnormality (SCIWORA)

SCIWORA occurs in younger children with definite clinical neurological deficits and negative X-rays and CT scans. The MRI scan, however, is likely to show an abnormality in the cord, disc, or ligaments. The cord may be mildly to severely injured, and it is thought to occur because of the more elastic spinal column and ligamentous laxity in children, causing a sudden displacement of the spinal column back and forth, injuring the spinal cord without apparent dislocation. The neurological deficits are due to cord or vascular injury during hyperextension/hyperflexion or translocation of the spinal segment.

MRI should be performed as a haematoma compressing the cord, or ligamentous disruption and instability lead to secondary cord insults and are treatable by decompression or stabilization, respectively. These injuries are rarely identified on plain radiography or CT scanning.

Children with SCIWORA are at increased risk of recurrent and more severe injuries if left untreated. External immobilization is recommended for 6–8 weeks and if unstable consider surgical fixation.

Management of spinal cord injury

Treatment of traumatic SCI starts at the site with immediate resuscitation and transport with spine immobilization. PICU care includes improving spinal cord perfusion by maintaining adequate blood pressure with inotropes and if required supportive ventilation.

Spinal injuries in children require adequate imaging including CT and MRI for prompt and clear identification of all injuries often not seen on radiography or even CT scans. Identification of ligamentous injuries, fractures with malalignment or deformation, compressive lesions, instability, and SCI is essential. Dynamic flexion/extension views may be required.

Surgical evacuation of a compressive haematoma should be treated as urgent to avoid secondary spinal cord injury. Deformity with compression of the spinal cord may require placing a child in traction and then externally fixing in a halo-brace system once corrected. Later on, a surgical correction and fixation may be required. Cervical spine fractures without spinal cord compression can usually be treated with a halo device. It is crucial that in cases of fractures treated by immobilization, that long-term follow-up is performed as progressive deformity or instability over time does occur.

Rehabilitation of spinal cord injury

This is generally similar to adult care standards. The ASIA impairment scale is used to define and describe the extent and severity of the spinal cord injury and help determine future rehabilitation and

recovery needs (American Spinal Injury Association, 2002). It is ideally completed within 72 hours of the initial injury. Sensory and motor evaluation in children requires careful testing and re-testing. Scoliosis following SCI in children is common especially when the neurological insult occurs at a young age.

Intensive rehabilitation maximizes the potential for recovery of function or ability to function with existing deficits. Spinal rehabilitation is a multidisciplinary effort and the spinal unit should be involved at the outset with a referral within 48 hours.

Controversies in paediatric trauma

There are studies looking at the neuroprotective nature of hypothermia in children. Hypothermia effectively reduces intracranial pressure and metabolic demand but there are risks of cardiac arrhythmias and coagulation deficits. Early studies showed no increase in adverse events and a larger randomized controlled study was undertaken. This trial published in 2008 shows moderate hypothermia therapy (32–33°C), initiated within 8 hours after the injury and maintained for 24 hours, did not improve the functional outcome at 6 months or functional and neuropsychological outcomes at 3 and 12 months, length of stay in the ICU or hospital, and adverse events. (Hutchison et al., 2008). There are four other studies in children that have shown no benefit. There are 14 studies in adults with variable results. Hypothermia is now little used but still sometimes raised as a potential subject for a large clinical trial.

FURTHER READING

Adelson, D.P. (2009). Hypothermia following pediatric traumatic brain injury. *J Neurotrauma*, **26**, 429–36.

Moore, D. (2017). *Atlantoaxial Subluxation*. http://www.orthobullets.com/spine/2050/atlantoaxial-rotatory-displacement-aard

NICE (2014). *Recommendations for CT Head Imaging in Children*. https://www.nice.org.uk/guidance/cg176/resources/imaging-algorithm-pdf-498950893

REFERENCES

Adelson, D.P., Bratton, S.L., Carney, N.A. et al. (2003). Guidelines for the acute medical management of severe traumatic brain injury in infants, children and adolescents. *Pediatr Crit Care Med*, **4** (suppl), 3.

American College of Surgeons Committee on Trauma (1997). *Advanced Trauma Life Support for Doctors*, 6th edition. Chicago, IL: American College of Surgeons.

American Spinal Injury Association (2002). Guidelines for the management of acute cervical spine and spinal cord injuries. *Neurosurgery*, **50**(Suppl. 3), S1–S199.

Brown, R.L., Brunn, M.A., & Garcia, V.F. (2001). Cervical spine injuries in children: a review of 103 patients treated consecutively at a level I pediatric trauma center. *J Pediatr Surg*, **36**(8), 1107–14.

Eleraky, M.A., Theodore, N., Adams, M., Rekate, H.L., & Sonntag, V.K. (2000). Pediatric cervical spine injuries: report of 102 cases and review of the literature. *J Neurosurg*, **92**(1, Suppl.), 12–17.

Hinds, T., Shalaby-Rana, E., Jackson, A.M., & Khademian, Z. (2015). Aspects of abuse: abusive head trauma. *Curr Probl Pediatr Asdolesc Health Care*, **45**(3), 71–9.

Hutchison, J.S., Ward, R.E., Lacroix, J., et al. (2008). Hypothermia therapy after traumatic brain injury in children. *N Engl J Med*, **358**, 2447–56.

Lee, S.L., Sena, M., Greenholz, S.K., & Fledderman, M. (2003). A multidisciplinary approach to the development of a cervical spine clearance protocol: process, rationale, and initial results. *J Pediatr Surg*, **38**(3), 358–62.

Munk, P.L. & Ryan, A.G. (2007). *Teaching Atlas of Musculoskeletal Imaging*. New York, NY: Thieme Publishers.

Parslow, R.C., Morris, K.P., Tasker, R.C., Forsyth, R.J., & Hawley, C.A. (2005). Epidemiology of traumatic brain injury in children receiving intensive care in the UK. *Arch Dis Child*, **90**, 1182–7.

Royal College of Surgeons of England (1999). *Report of the Working Party on the Management of Patients with Head Injuries*. https://www.rcseng.ac.uk/services/publications/ publications/ pdf/rep_hi.pdf

Taylor, A., Butt, W., Rosenfeld, J., et al. (2001). A randomised trial of very early decompressive craniectomy in children with traumatic brain injury and sustained intracranial hypertension. *Childs Nerv Syst*, **17**, 154–62.

Vázquez, E., Delgado, I., Sánchez-Montañez, A., Fábrega, A., Cano, P., & Martín, N. (2014). Imaging abusive head trauma: why use both computed tomography and magnetic resonance imaging? *Pediatr Radiol*, **44** (Suppl 4), S589–603.

RELATED LINKS TO EBRAIN

Head Injuries in Children. http://learning.ebrain.net/course/view.php?id=1084

Non-Accidental Injury in Childhood. http://learning.ebrain.net/course/view.php?id=1085

88

Paediatric brain tumours

Jonathan Roth and Shlomi Constantini

Introduction and epidemiology

Paediatric brain tumours (PBT) are a unique entity, in children and in the overall general brain tumour population. Malignant paediatric brain tumours (MPBT) are second only to acute lymphatic leukaemia (ALL) in their incidence and during recent years, their incidence is continuing to increase. Around 30% of paediatric deaths due to cancer are caused by MPBT, three times that caused by ALL. The incidence of PBT is $4.5/10^5$ (Ostrom et al., 2015). This is significantly less than the incidence of adult brain tumours, which is $16.5/10^5$. The incidence of PBT is slightly more common in males (M:F ratio 4.5:4). White children have nearly double the incidence of black children. The reason for this discrepancy, which is maintained in other cancers too, is not known. About 50% of PBT are malignant. Age has a major impact on incidence, histological type, and outcome of PBT. Younger children (especially younger than 5 years old) have an incidence of $3.5–4/10^5$ with a 5-year survival of about 50%. Older children (10–20 years old) have an incidence of $2–2.5/10^5$ with a 5-year survival of about 75%. The 5-year survival for all paediatric patients is about 65%. This rate decreases continuously with age, down to about 23% among patients 45–54 years old.

Treatment for the paediatric population has a few goals: firstly, curing or controlling the disease and increasing long-term survival; secondly, preventing long-term complications from the various diagnostic and treatment modalities needed to treat the primary disease; and thirdly, minimizing the psychosocial impacts of the diagnosis as well as treatments on the child and the family.

Common paediatric brain tumours

Paediatric brain tumours differ from those of the adult population in several aspects, including histological (and genetic basis of the tumours), location, treatment options, and prognosis.

As opposed to adults where two-thirds of primary brain tumours are located in the cerebrum, only a quarter of paediatric tumours are located there (**Tables 88.1 and 88.2**). Nearly 30% of PBT are located in the posterior fossa (including the brainstem and cerebellum), as opposed to 7% of primary brain tumours in adults. Children have a higher rate of midline tumours (including the hypothalamic, optic pathways, pineal and pituitary regions, and the ventricular system) as opposed to adults (Ostrom et al., 2015).

Histology differs too between both populations. Certain tumours are considered 'childhood' histologies, such as pilocytic astrocytomas, medulloblastomas, and germ cell tumours. While other subtypes such as glioblastomas and meningiomas, are rare among children (Ostrom et al., 2015).

Low-grade gliomas

Low-grade gliomas in children account for about 40% of PBT, the most common subtype being WHO I pilocytic astrocytoma (PA), accounting for about half of LGG in children. Other LGG subtypes that occur more commonly in children include dysembryonal neuroectodermal tumour (DNET, WHO I), ganglioglioma (WHO I), pilomyxoid astrocytoma (WHO II), pleomorphic xanthoastrocytoma (PXA, WHO II). Diffuse astrocytoma (grade II) and oligodendrogliomas (grade II) occur too in children, but to a lesser extent compared to the adult population. These tumour subtypes are subclassified in the 2016 WHO CNS tumour classification (Louis et al., 2016).

LGG may occur at any location, although certain locations have a higher prevalence, including cerebellum, brainstem, optic pathways, hypothalamus, and temporal lobe.

Cytogenetic studies have revealed a normal karyotype in the majority of pilocytic astrocytomas examined (Sanoudou et al., 2000). Where abnormal profiles have been observed, no consistent karyotype abnormalities have been identified.

Individuals with neurofibromatosis type 1 (NF1) have an increased propensity to develop pilocytic astrocytomas, especially of the optic/hypothalamic region. As sporadic (non-NF1) pilocytic astrocytomas occasionally show loss of heterozygosity on chromosome 17q (the location of the *NF1* tumour suppressor gene), one would predict that mutations of the *NF1* gene with consequent loss of expression would be found in sporadic pilocytic astrocytomas. In fact, this appears not to be the case. In actuality, the expression of the *NF1* tumour suppressor gene in sporadic pilocytic astrocytomas is often up-regulated, perhaps as a reactive response to excessive cellular proliferation. This is in contrast to pilocytic astrocytomas arising in *NF1* patients, where loss of *NF1* expression is an obligatory

Table 88.1 Distribution of primary brain and CNS tumours by location according to age

<19 years old	Adults
Cerebellum 16%	3%
Brain stem 12%	4.3%
Ventricles 5.6%	1.8%
Cerebrum 24%	65%
Pineal 3%	–
Pituitary 8%	7%
Cranial nerves 4.6%	1%
Spinal cord 5.6%	4.2%

Data from Ostrom, Q.T., De Blank, P.M., Kruchko, C., Petersen, C.M., Liao, P., Finlay, J.L., Stearns, D.S., Wolff, J.E., Wolinsky, Y., Letterio, J.J., & Barnholtz-Sloan, J.S., Alex's Lemonade Stand Foundation Infant and Childhood Primary Brain and Central Nervous System Tumors Diagnosed in the United States in 2007–2011, *Neuro-Oncology*, Volume 16, Issue s_10, pp. x1–x36, Copyright © 2014 Oxford University Press.

finding. The precise origin of the differing contribution of the *NF1* gene product in the setting of *NF1* versus non-*NF1* pilocytic astrocytomas has yet to be elucidated.

Compared to adult LGG, mutations in tumour suppression gene *TP53*, and metabolic genes *IDH1* and *IDH2*, are exceedingly rare in childhood LGG (Chalil and Ramaswamy, 2015).

Advanced molecular analysis has shown that the most common chromosomal abnormality in PA is a gain of chromosomal region 7q34, containing the BRAF locus. This involves duplication of the BRAF oncogene, followed by insertion of one of several fusion targets. This activates the MAPK pathway, leading to tumourigenesis (Chalil and Ramaswamy, 2015).

BRAF V600E mutations are found in a small proportion of LGG, activating and causing a deregulation of the MAPK pathway. Over recent years, the MAPK pathway has become a target for chemotherapy in tumours harbouring such BRAF mutations or duplications.

Cerebellar pilocytic astrocytoma

Posterior fossa pilocytic astrocytomas are considered one of the 'classic' PBT. Often presenting with gait disturbances and increased intracranial pressure (ICP) symptoms secondary to hydrocephalus, these tumours are typically located in the cerebellar hemisphere; however, midline—vermian or tumour protruding to the fourth ventricle have been described too. These tumours often have a solid component, many times with cystic components too. The cysts may be located within the tumour, or adjacent to it, and its walls may undergo contrast enhancement on MRI.

Cerebellar pilocytic astrocytomas have a differential diagnosis with other tumours, including hemangioblastomas which may have an enhancing nodule accompanied by a cyst. It is important to acknowledge that PA may have solid components that do not undergo any enhancement, and thus other MRI modalities such as fluid attenuated inversion recovery (FLAIR) may assist defining the tumour outline. Interestingly, paediatric PA may appear like adult high-grade gliomas, composing of solid-cystic components with non-homogenous enhancements. However, HGG are rare in the paediatric population, and these are rarely diagnosed in the cerebellum.

Treatment of cerebellar PA consists of maximally safe resection. This is usually achieved using standard microsurgical techniques. Often, these tumours abate the brainstem or cerebellar peduncle; thus, judicious judgement is needed to decide when to finalize the resection.

In children, especially infants, lateral cerebellar hemispheric tissue may generally be resected with little or no long-term neurological sequala. Thus, a safe and convenient surgical corridor may be created obviating the need for significant cerebellar retraction.

One of the questions a surgeon is often faced with is the need to resect a cyst's capsule. Often the capsule undergoes contrast enhancement on MRI, thus possibly suggesting it being part of the tumour. However, we have previously shown by performing local biopsies, that if the capsule is inspected during surgery and seems transparent, with no tumoural lumps, it need not be resected (Beni-Adani et al., 2000).

The long-term recurrence rate following a gross total resection (as proved by MRI) is thought to be low. However, a recent paper showed that even in the presence of surgeon's estimation of GTR, and a clean MRI, the 5-year event free survival (no recurrence) is 95% (most occurring during first 3 years) (Dodgshun et al., 2016). Another recent study found a 19% recurrence rate following GTR of cerebellar PA over a 10-year follow-up (Kim et al., 2014). Thus, long-term follow-up even after GTR is mandatory.

Table 88.2 Distribution of primary brain and CNS tumours by histology according to age. The most common pathologies are in bold

0–14 years old	15–19 years old	Adults
Pilocytic astrocytoma **20.9%**	**14 %**	Meningioma **30.1%**
Embryonal (including medulloblastoma) **16.8%**	6.7%	Glioblastoma **20.3%**
Glioblastoma 2.8%	3.2%	Nerve sheath 8%
Other astrocytomas **10.5%**	**10.4%**	Pituitary 6.3%
Ependymoma 7%	4.6%	Astrocytoma (grades 2–3) 9.8%
Germ cell tumours 3.9%	6.8%	Oligodendroglioma 3.7%
Craniopharyngioma 3.1%	2.7%	Lymphoma 3.1%
Pituitary 0.8%	**10.1%**	Ependymoma 2.3%
Others 32%	36%	Craniopharyngioma 0.7%
		Others 14%

Data from Ostrom, Q.T., De Blank, P.M., Kruchko, C., Petersen, C.M., Liao, P., Finlay, J.L., Stearns, D.S., Wolff, J.E., Wolinsky, Y., Letterio, J.J., & Barnholtz-Sloan, J.S., Alex's Lemonade Stand Foundation Infant and Childhood Primary Brain and Central Nervous System Tumors Diagnosed in the United States in 2007–2011, *Neuro-Oncology*, Volume 16, Issue s10, pp. x1–x36, Copyright © 2014 Oxford University Press.

Brainstem tumours

Brainstem gliomas (BSG) in children include a diverse group of tumours with different presenting symptoms and tumour configurations that lead to a plethora of biological behaviours and variable prognoses. BSG represent 10–20% of all paediatric brain tumours, and about 20–30% of infratentorial tumours. BSG are diagnosed at all ages. However, they are rarely diagnosed before the age of 5 years, and their occurrence peaks at around the age of 10 years. Males and females are more-or-less equally affected.

As opposed to cerebellar and many supratentorial tumours, BSG involves super-eloquent neural tissue, and thus were previously considered inoperable. However, as has been showed by Epstein and others, in selected subgroups of tumours, and with the integration

of intraoperative mapping and monitoring, resection is feasible with reasonable neurological and oncological outcome (Constantini and Epstein, 1996). With the addition of gentle chemotherapy and modern radiation techniques, decision-making on the combination of treatment options has become more complex. Currently, there is no unified approach for BSG. Treatment is dictated by tumour location, configuration, and biological behaviour.

BSG include all WHO grades I-IV astrocytomas. Grade I tumours (also called pilocytic astrocytomas) usually present as discrete lesions, often with a cystic component; however, they may present as dorsally exophytic tectal or medullary (and cervicomedullary) tumours. They usually enhance following gadolinium, and may be associated with significant oedema (for instance, in the cervical spine). Often, the tumour includes non-enhancing components too.

WHO grade II tumours (diffuse low-grade astrocytomas) may present in any location along the brainstem. Their biological behaviour is very diverse. Tectal and exophytic tumours usually have a very indolent course. On the other hand, diffuse pontine gliomas (DPG) may also have the histological appearance of WHO II but behave aggressively. WHO grade II tumours usually do not enhance, are hypointense on T1, and hyperintense on T2 and FLAIR.

WHO grades III and IV tumours (anaplastic astrocytomas and glioblastoma multiforme) may arise in any location, more commonly in the pons (as a DPG). They are often associated with ill-defined enhancement (grade III) or a necrotic, ring-enhancing component (grade IV).

Other glial pathologies may rarely arise in the brainstem, including gangliogliomas, oligodendrogliomas, and pilomyxoid astrocytomas.

Ependymomas

Ependymomas are the third most common tumour among children, and are particularly frequent in the very young. Ependymomas are usually located at the fourth ventricle, sometimes emerging through the foramina of Luschka or Megandie and encompassing the brainstem, although they may be located at other locations.

The standard treatment of ependymomas includes gross total resection, even at the expense of the need for a tracheostomy or a gastrostomy to overcome lower brainstem injury when invaded by the tumour.

In posterior fossa ependymomas it is accepted to follow the resection with radiation therapy to the tumour bed. However, the need for radiation following complete resection of ependymomas remains controversial especially in supratentorial cases, but also in infratentorial cases (Ailon et al., 2015). The role of chemotherapy in the treatment of ependymomas remains unclear, so radiation is recommended for children even at ages below 3 years of age (Purdy et al., 2014).

Atypical teratoid rhabdoid tumour (ATRT)

ATRT are aggressive CNS tumours, often affecting infants and young children, and usually located in the posterior fossa. Prognosis is generally poor with a median survival of less than 1 year. ATRT resembles medulloblastoma, and was not recognized until the 1980s. ATRT demonstrates deletion of the long arm of chromosome 22q11.2. Further molecular studies have led to identification of the *INI1/hSNF5* tumour suppressor gene at this location. A somatic mutation in this gene predisposes children to develop ATRT. Some children with ATRT are born with heterozygous germline mutations of the *hSNF5* gene, suggesting that these children were predisposed to develop ATRT (Taylor et al., 2000). In most cases, however, these germline mutations arise *de novo*.

Medulloblastoma

Medulloblastomas are perhaps the hallmark of molecular subtyping of PBT. Until a few years ago children with posterior fossa medulloblastomas (PFMB) were dichotomized into two subgroups—average and high risk, according to age, extent of tumour residual, and metastasis. This dictated treatment algorithms and prognosis. However, over recent years PFMB have been subclassified into four subgroups based on molecular profile, each with a demographic, clinical, molecular, and prognostic pattern (Taylor et al., 2012). These groups include the WNT, SHH, and groups 3 and 4. Surgical nuances (such as brainstem infiltration), radiological (such as magnetic resonance spectroscopy (MRS)) and treatment implications differ between the various subgroups (Northcott et al., 2012). These PFMB subgroups have been implemented into the 2016 WHO CNS tumour classifications (Louis et al., 2016).

As it is anticipated that genetic tumour markers will increasingly inform the selection of adjuvant therapy for the individual patient, it is crucial to collect tumour tissue samples for genetic analysis. In addition, as it is anticipated that genetic research will continue to evolve, there is a need for multicentre cooperation. Tumour banks are being developed for ongoing and future genetic research.

Optic pathway glioma

Optic pathway gliomas (OPG) are low-grade glial tumours that originate from any location along the optic system, such as the optic nerves, chiasm, tracts, or rarely the radiation. OPG are rather rare, representing about 5% of PBT, most of which present during their first decade of life. Many OPG are associated with neurofibromatosis type I (NF1), however, about 40% are non-NF-related (Shofty et al., 2015). Pathology of OPG is usually pilocytic astrocytoma, although pilomyxoid astrocytoma is being increasingly diagnosed, especially among infants.

Much about OPG remains controversial, including classification, diagnosis, need for biopsy, indications for surgery and surgical goals, and the role and timing of chemotherapy and radiation. Thus, in the following paragraphs we will shortly overview this entity, but by no means do we intend to try and solve the many controversies associated with it.

OPG classification is generally guided by anatomical involvement; however, currently there is no good correlation between the various classification systems and the natural history of tumour progression, or to clinical aspects (especially visual prognosis).

Presenting symptoms may relate to visual function from tumour involvement or compression of the visual pathways; be related to hydrocephalus caused by extensive third ventricle with obstruction of cerebrospinal fluid (CSF) pathways; be secondary to diencephalic

compression or involvement leading to diencephalic syndrome (cachexia, microcephalus, and visual decline); or be caused by various endocrinopathies from hypothalamic—pituitary axis disturbances. Especially during infancy, visual function is difficult to accurately evaluate, posing great difficulties on clinical evaluation.

Diagnosis of OPG is often based on radiological appearance with no need for a biopsy. Optic nerve thickening, especially when also enhancing, with or without chiasmatic involvement are diagnostic. When associated with NF1, chiasmatic—hypothalamic tumours are diagnostic for OPG. Despite the importance of MRI for diagnosis of OPG, atypical cases—such as non-NF-related lesions in elder children, with no clear optic nerve origin, or with no chiasmatic swelling—should be biopsied. The biopsy technique will vary according to anatomical considerations—subfrontal for chiasmatic exposure, endoscopic for lesions involving the third ventricle causing hydrocephalus, or stereotactic biopsies. The role of biopsy is both to establish the pathology, as well as to define molecular alterations such as BRAF-KIAA 1549 fusion which have both a prognostic as well as therapeutic implication (Shofty et al., 2015).

The natural history of OPG is unpredictable. Some remain stable over years, while others grow. Often, visual decline may appear with no clear change in tumour morphology. Generally, NF-related OPG have a more indolent course compared to sporadic cases.

Treatment of OPG requires a multidisciplinary team approach, taking into account clinical (with emphasis on ophthalmological evaluation), radiological dynamics, surgical considerations, as well as oncological aspects.

Generally, stable tumours associated with stable visual exam are usually followed. However, large tumours with an extensive exophytic component extending to the subfrontal region, or those extending upward to the third ventricle causing hydrocephalus or upper brainstem compression are treated surgically. Approaches to these tumours may include a frontotemporal/subfrontal approach, or various interhemispheric/transventricular approaches. The surgical goal in never complete resection, but rather subtotal removal of the exophytic component and establishment of CSF pathways. Intraoperative imaging has been applied to assist in decision-making regarding extent of resection (Millward et al., 2015).

Ventriculoperitoneal shunts in the context of OPG have been associated with ascites (Gil et al., 2001). The reason is unclear, but shunts may need to be diverted to the atrium.

Chemotherapy is the primary treatment for most OPG. Various protocols have been advised, most starting with vincristine–carboplatin. Despite the vast use of chemotherapy for OPG, long-term visual outcome remains grim (Shofty et al., 2011). Radiation has been applied with various success rates; however, it is associated with vasculopathy (moyamoya), endocrinopathy, and secondary malignancies.

Outcome of OPG is generally favourable with about 85–90% 10-year survival. Thus, preservation of vision is the main goal treating OPG. As stated, and although debatable, the long-term visual outcome remains grim.

Environmental hazards

Infectious agents, especially certain viruses, have been associated with increased risk for certain cancers. Human polyomavirus has been associated with an increased brain tumour risk. Protein transfer from the virus to surrounding cells and secondary dysregulation of cell proliferation factors has been suggested. This may be due either to inactivation of tumour suppressor genes or to upregulating cell proliferation. Weggen et al. have found evidence of several human polyomavirus sequences in human medulloblastomas, meningiomas, and ependymomas. Currently there are no clinical implications for these findings.

Radiation has been associated with an increased risk of brain tumours. Head irradiation for treatment of children with tinea capitis has been shown to be a major risk factor for future benign and malignant tumours. This increased risk has been shown to be even higher among children with neurofibromatosis. Data suggests that even low dose radiation (such as in computed tomography (CT) scans) may induce secondary malignancies, and thus should be as low as possible. The oncogenic mechanism of radiation is to induce genetic changes, either downregulating tumour suppressor genes or upregulating oncogenic genes.

Cell phone exposure has been the focus of various epidemiological studies over the last few years. To date, no clear evidence exists to support, or disprove, the potential risk imposed by cell phones when used by children, but excessive use is discouraged. In adults, the current literature suggests that exposure to the low dose radiation emitted by cell phones does not pose additional risk for developing brain tumours.

An interesting seasonal variation in the incidence of paediatric medulloblastoma has been reported. Children born during autumn (especially during October), had an increased risk for medulloblastomas. Potential causes for this seasonal association may be related to higher levels of community infections during pregnancy and early childhood, or seasonal variation in exposure to various chemicals. However, no clear pathophysiological mechanism has been established.

Diagnosis, investigation, and preoperative considerations

History and examination

The midline location of many paediatric brain tumours results in a paucity of focal neurological signs and delay in diagnosis until the lesion has reached a significant size. Manifestations of paediatric brain tumours may be related to elevated intracranial pressure (secondary to the tumour mass or to secondary hydrocephalus), focal neurological signs, epilepsy, cognitive, and behavioural disturbances, and/or endocrine and growth disturbance. A meta-analysis reviewed childhood CNS tumour presentation (Wilne et al., 2007). Headache, nausea, and vomiting were the most common presenting symptoms, however, appeared only in 30–40% of patients (**Table 88.3**). Presenting symptoms were strongly correlated to the tumour location (**Box 88.1**).

A common complaint among children is headache. Among Swedish school children, 40% experienced a headache by the age of 7 years old, and 75% by the age of 15 years old. Approximately 20% of children in the United States have chronic headaches. Although most cases are due to benign reasons, some may be the presenting symptom of brain tumours. It is important, however,

Table 88.3 Presenting symptoms and signs of paediatric brain tumours

Among 3702 children <18 years old	Among 232 children <4 years old
• Headache (33%) • Nausea and vomiting (32%) • Abnormal gait or coordination (27%) • Papilloedema (13%) • Seizures (13%) • Unspecified symptoms of raised intracranial pressure (10%) • Squint (7%) • Changes in behaviour or school performance (7%) • Macrocephaly (7%) • Cranial nerve palsies (7%) • Lethargy (6%) • Abnormal eye movements (nystagmus, Parinaud syndrome; 6%) • Hemiplegia (6%) • Weight loss (5%) • Focal motor weakness (5%) • Unspecified visual or eye abnormalities (5%) • Altered level of consciousness (5%)	• Macrocephaly (41%) • Nausea and vomiting (30%) • Irritability (24%) • Lethargy (21%) • Abnormal gait and coordination (19%) • Weight loss (14%) • Clinically apparent hydrocephalus (bulging fontanelle, splayed sutures; 13%) • Seizures (10%) • Headache (10%) • Papilloedema (10%) • Unspecified focal signs (10%) • Unspecified symptoms of elevated intracranial pressure (9%) • Focal motor weakness (7%) • Head tilt (7%) • Decreased level of consciousness (7%) • Squint (6%) • Abnormal eye movements (6%) • Developmental delay (5%) • Hemiplegia (5%)

Reprinted from *The Lancet Oncology*, Volume 8, issue 8, Sophie Wilne, Jacqueline Collier, Colin Kennedy, Karin Koller, Richard Grundy, David Walker, Presentation of childhood CNS tumours: a systematic review and meta-analysis, pp. 685–95, Copyright (2007), with permission from Elsevier.

to recognize that not all brain tumours present with headaches, especially in the younger age groups. In one study, 18% of children younger than 5 years old, 52% between 6 and 10 years old, and 68% between 11 and 20 years old with brain tumours presented with headaches. In another study, 62% of children with brain tumours presented with headaches, and more than 50% had at least three associated symptoms, such as nausea, vomiting, visual effects, problems walking, weakness, or changes in personality, school performance, or speech. In our series of PBT, while 40% presented with headaches, only 3% had headaches alone as the sole presenting symptom.

Box 88.1 Presenting symptoms and signs according to tumour location

- Supratentorial tumours:
  - Unspecified symptoms of raised ICP (47%)
  - Seizure (38%)
  - Papilloedema (21%)
- Posterior fossa tumours:
  - Nausea or vomiting (75%)
  - Headaches (67%)
  - Abnormal gait or coordination (60%)
  - Papilloedema (34%)
- Brain stem tumours:
  - Abnormal gait or coordination (78%)
  - Cranial nerve deficits (52%)
  - Pyramidal signs (33%)
  - Headaches (23%)
  - Squint (19%)
- Centrally located tumours (area of third ventricle):
  - Headaches (49%)
  - Abnormal eye movements (20%)
  - Nausea and vomiting (20%)
  - papilloedema (also 20%? Not clear in text)

Reprinted from *The Lancet Oncology*, Volume 8, issue 8, Sophie Wilne, Jacqueline Collier, Colin Kennedy, Karin Koller, Richard Grundy, David Walker, Presentation of childhood CNS tumours: a systematic review and meta-analysis, pp. 685–95, Copyright (2007), with permission from Elsevier.

Symptoms of brain tumours in young children are often nonspecific and easily dismissed by the physician who first encounters the child. Symptoms may include 'cerebellar fits', which may be mistakenly identified as seizures but are actually acute periods of obtundation, representing incipient coning and dangerous levels of brainstem compression due to a tight posterior fossa. Visual obscurations may also indicate high intracranial pressure. Their presence heightens the urgency of surgical intervention. Symptoms may intermittently 'come and go', with the child appearing neurologically intact, giving the impression of a 'functional' cause, and thereby delaying diagnosis. Previous studies focusing on delayed diagnosis found that the median period between the first presenting symptom to diagnosis (prediagnostic symptomatic interval or PSI) was about 2 months, and was inversely related to the child's age (Kukal et al., 2009). PSI also correlated with tumour histology. High-grade tumours associated with a shorter PSI and low-grade tumours associated with a longer PSI. Kukal et al. also showed that PSI is not independently associated with the prognosis, but rather, there is an association with the tumour histology and patient age.

Head circumference is an essential component of the examination, particularly in infants, and should be recorded on a head circumference chart. Visual decline is often missed in young children until the loss is advanced, because the child does not notice or report it. Vision should be formally tested if possible. Visual fields and acuity should be recorded, particularly if there is a possibility that the lesion involves the visual pathways. Sluggish dilated pupils are a sign of severely raised intracranial pressure and are a warning sign of impending neurological deterioration. Only about 20% of children with PBTs will have papilloedema and about 50% of them will have a normal neurological exam. Therefore, taking a careful history may be more important than the actual examination (Shay et al., 2012). Hearing should be formally tested too, particularly if there is developmental delay or if the lesion is likely to involve hearing pathways.

Paediatric neurologist and paediatrician

It is helpful to involve a paediatric neurologist during the diagnostic phase, particularly if there is a complex neurological picture or epilepsy is a feature. There may be general medical problems, and/or developmental, behavioural, and family issues which require the expertise of a paediatrician. Preoperative speech pathology and physiotherapy assessments may also be relevant. Paediatric neurologists, as the gatekeepers for magnetic resonance (MR) in many Western countries, have to be trained in differentiating between important and unimportant signs of PBTs. To achieve an upward learning curve, an open line of communication must be established between paediatric neurologists, and paediatric neurosurgeons.

Neuropsychology and developmental assessment

A baseline neuropsychology assessment should be completed preoperatively for children over the age of 4 years. Some limited neuropsychological testing can even be done in some 3-year-old children. Formal developmental assessment with the Vineland Adaptive Behavior Scale can also be performed on children less than 3 years of age. Results of any neuropsychology assessment may be obfuscated by raised intracranial pressure or mood change. Nevertheless, it will be helpful in determining prognosis for recovery of cognitive function postoperatively and also has important medicolegal implications.

Endocrinology

Any child with endocrine or growth disturbance identified preoperatively, as well as any child with the possibility of endocrine complications postoperatively, should be assessed preoperatively by endocrinologists. Weight, height and, when relevant, pubertal status of the child should be documented and their nutritional state and fluid balance assessed.

Endocrinopathy is common among children with craniopharyngiomas, as well as children with optic pathway/hypothalamic gliomas. Endocrinological screening is important preoperatively, as well as postoperatively, as major endocrinopathies may follow treatment.

Epilepsy

Epilepsy should be fully characterized and preferably investigated by an electroencephalogram (EEG) or in cases of more frequent epilepsy by video-EEG monitoring. All focal seizure investigations should include MR imaging. An attempt at controlling the epilepsy should be made prior to surgery. Prophylactic anticonvulsants are usually commenced preoperatively for supratentorial pathologies; however, this remains a controversial issue (Fattal-Valevski et al., 2013).

Neuroimaging

Complete CNS imaging (including spinal imaging) is important in order to define the goals of surgery—total gross resection on one extreme, as opposed to biopsy on the other. Figures 88.1–88.4 present typical images of various paediatric brain tumours.

MR with gadolinium-DTPA contrast is superior to CT, defining the exact location and extent of the tumour, and aiding with planning the tumour resection.

MR should be obtained for all patients preoperatively. The sagittal and coronal images are particularly helpful for midline tumours, showing the tumour relationship to the brainstem, the ventricular system, and other surrounding structures, and thus aiding in the planning of surgery. When dealing with potentially metastatic tumours (such as germ cell tumours, ependymomas, and medulloblastomas), spinal screening MR should be completed along with cranial MR in order to detect spinal metastases and leptomeningeal spread before blood enters the canal during surgery and makes it more difficult to distinguish between blood and tumour. Diffusion-weighted and perfusion MR imaging may help characterize the tumour, and assess treatment response.

New white matter protocols with diffusion tensor imaging (DTI) have lately become useful in identifying functional pathways and their relation to the tumour. Especially when integrated into navigation workstations, DTI may increase surgical safety.

It is important to note that some children are diagnosed following an acute event. Thus a CT scan, which is quick to perform with greater availability than MR, is often the primary diagnostic tool. CT is superior to MR in defining skull involvement, or for demonstrating tumour related calcifications (such as in craniopharyngiomas), and is extremely important when evaluating skull base tumours that may invade the skull. However, these tumours are uncommon in children. Navigational/stereotactic techniques should be planned, and designated fiducial markers placed on the child's head prior to imaging.

A variety of other imaging tools are available, and useful within the proper context. Brain ultrasound (US), especially in small children with open fontanelles, may serve as a screening tool, but an MR is absolutely indicated for further evaluation. MRS has been used in various applications, for diagnosis, differentiation between tumour recurrence and radiation necrosis, tumour follow-up, and prognosis.

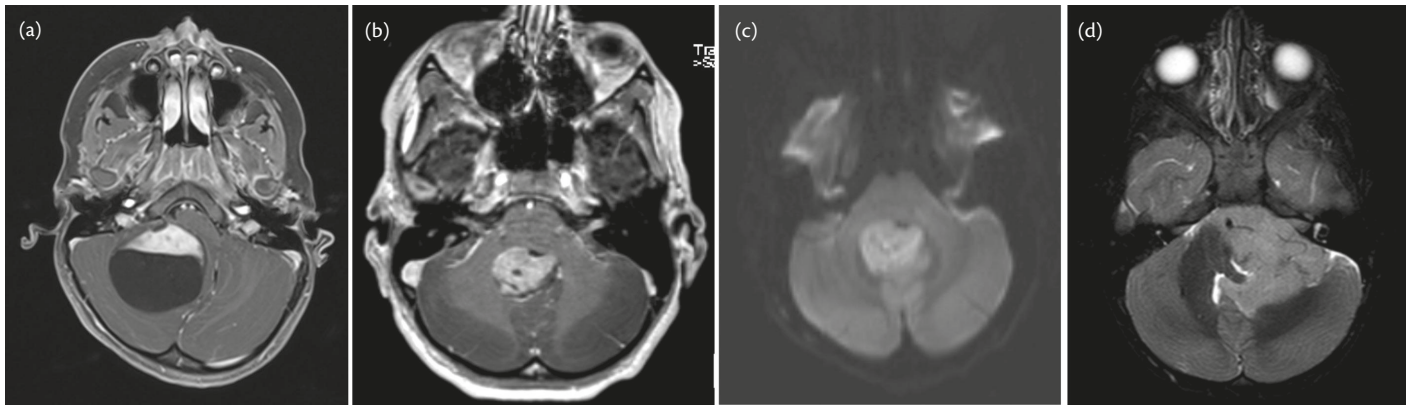

Fig. 88.1 Typical posterior fossa tumours in children: (A) pilocytic astrocytoma; (B and C) medulloblastoma; (D) ependymoma.

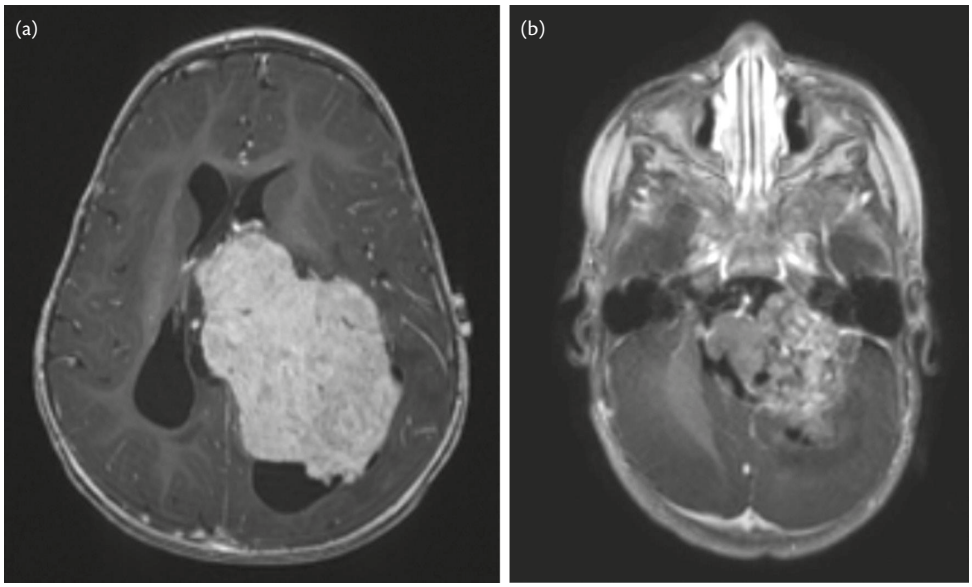

Fig. 88.2 Infantile tumours: (A) choroid plexus papilloma; (B) posterior fossa atypical terato-rhabdoid tumour (ATRT).

The sensitivity and specificity of MRS is not high, and thus MRS can only be used as a complementary tool to other studies or histological diagnosis. Nuclear medicine has a role in diagnosis and follow-up for children with brain tumours. Bone scans can be useful for showing 'hot areas' for skull-involving tumours such as Ewing sarcoma and osteosarcoma. FDG PET scans shows hypermetabolism related to tumours but this technique has a low spatial resolution and is also a complementary investigation. Similarly, SPECT scans may show increased uptake, especially in astrocytomas, but these too serve as complementary investigations.

Timing of neuroimaging

Neuroimaging is warranted whenever a new neurological deficit occurs; whether motor, cranial nerve-related, or an abnormal ophthalmological finding. Torticollis may be suggestive of a craniovertebral or a posterior fossa lesion; thus, when no other cause explains a new onset torticollis, CNS imaging is indicated. Neuroimaging is also indicated for enlarging head circumferences beyond the baseline growth curve, suggesting hydrocephalus or an intracranial mass.

New onset of a seizure disorder may be the presenting sign of a brain tumour. Yet most seizures among children are not secondary to tumours, but secondary to cortical dysplasias, trauma, and metabolic diseases. The role of MR in the workup of an unprovoked seizure in a child has been discussed in the literature. Less than 0.5% of children were shown to have a brain tumour. Currently, based on the available data, MR following an unprovoked seizure remains a recommendation. MR should be done emergently if the child remains with a focal deficit that does not resolve within several hours (such as in Todd's paresis), or in a prolonged status epilepticus not resolving within hours. A non-urgent MR is recommended following an unprovoked focal seizure (with or without generalization), or when the EEG does not suggest a benign epilepsy of childhood, or any other primary seizure syndrome, or in children under the age of 1 year.

Other investigations

Other diagnostic investigations include germ cell tumour markers such as alpha-feto-protein (αFP), beta-human-chorionic-gonadotropin (βHCG), and placental alkaline phosphatase in the serum and CSF. The presence of these markers serves in some treatment protocols as a major indicator for decision-making, as well as a baseline marker for tumour follow-up (Echevarria et al., 2008).

Dexamethasone

Steroids are often commenced several days before surgery to reduce peri-tumoural oedema. The child's condition often improves noticeably with this medication. One should avoid the cushingoid effects of prolonged high doses.

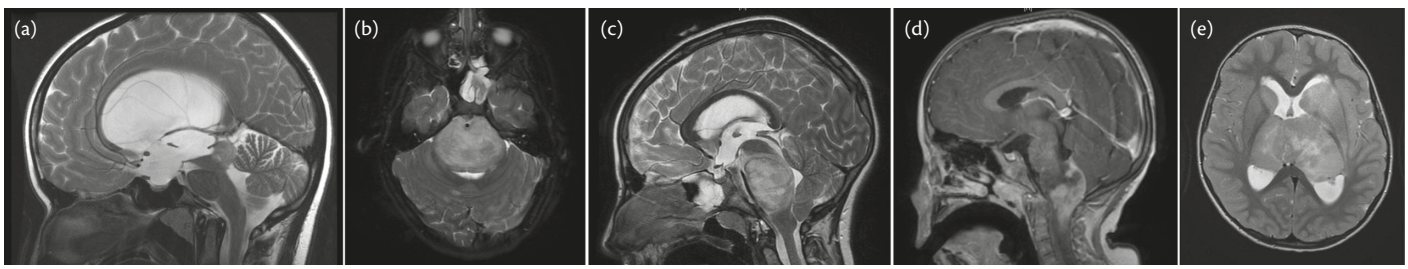

Fig. 88.3 (A) Tectal glioma; (B and C) diffuse pontine glioma (DPG); (D) cervicomedullary ganglioglioma; (E) bithalamic anaplastic astrocytoma.

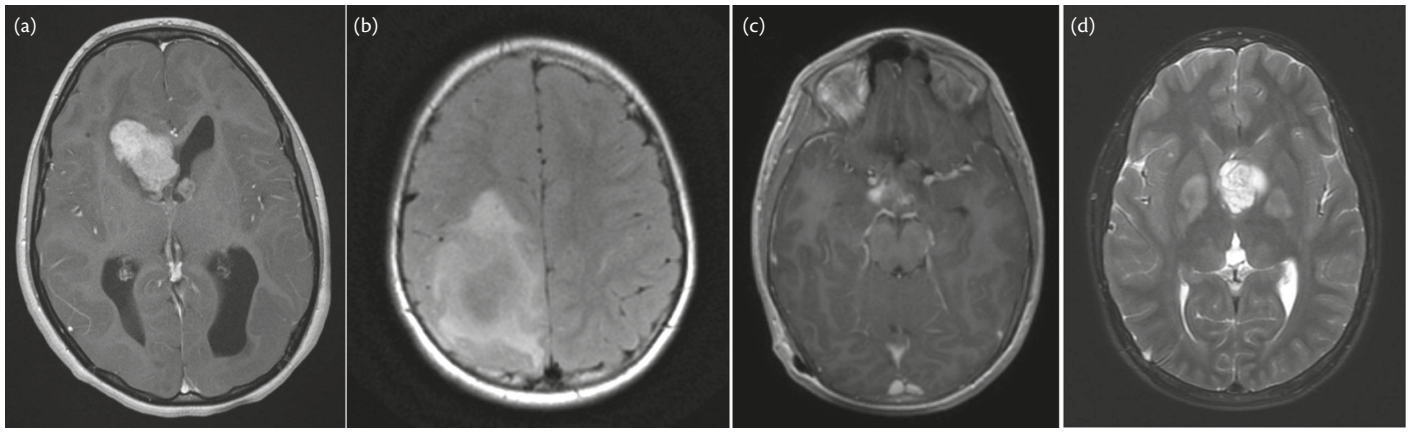

Fig. 88.4 (A) Subependymal giant cell astrocytoma (SEGA) in tuberous sclerosis; (B) glioblastoma in mismatch repair syndrome; (C and D) chiasmatic–hypothalamic glioma in neurofibromatosis type I.

Incidental brain tumours

Rising numbers of MR scans, performed during evaluations for paediatric disorders, have contributed to a significant increase in the number of incidentally found brain tumours. Currently, there is very little literature on the nature and preferred treatment of these incidental brain tumours. In a recent study, Roth et al. summarized 47 incidental tumours diagnosed at two centres (United States, Israel). Only three were eventually diagnosed as high-grade tumours. They summarize that many lesions are benign and may be closely followed (beginning with every 2–3 months); however, an individualized approach should be applied depending upon suspicion of malignancy in the imaging, changes in lesion size or enhancement, changes in neurological status, surgical risk, and parental preferences (Roth et al., 2012).

Tumours that do not need a biopsy or resection

Several paediatric brain tumours are diagnosed solely based on radiological and clinical appearance and need not go on to resection or even biopsy. These tumours may cause secondary effects such as hydrocephalus, which may need to be treated, but oncological treatments may be given with no tissue specimens. These include: classical diffuse intrinsic brainstem glioma (DIPG), classic tectal glioma, bifocal tumour (pertaining always to germinomas), optic pathway glioma (especially when associated with neurofibromatosis type 1), and subependymal giant cell astrocytoma (when associated with tuberous sclerosis).

Operative principles

The goals of surgery are to accurately define the extent of the tumour including the presence of leptomeningeal deposits, to resect as much of the tumour as can be achieved without causing further significant neurological deficit, and to correct secondary hydrocephalus and re-establish CSF pathways. Maximizing the extent of resection while minimizing morbidity is achieved using operative adjuncts such as intraoperative navigation systems, real-time imaging, and preoperative as well as real-time functional monitoring. In the following section we address the various factors that are used to achieve these goals. The goal of resecting maximal tumour is modified for specific tumour types such as germ cell tumours, which are very sensitive to adjuvant therapy. Collection of CSF for cytology and tumour markers has important prognostic implications for those tumours with a propensity to seed into the CSF pathways. Note that lumbar CSF has much better predictive value and higher positively rate than ventricular CSF (Gajjar et al., 1999).

Physiology of the child

The child is not a small adult, and the surgeon must be aware of the differences in surgical and anaesthetic techniques required for children compared to adults. This particularly relates to airway considerations, blood volume, thinness of the scalp and skull, delicacy of the tissues, surface area to weight ratio, intravenous fluid requirements, and drug metabolism. The child is easily prone to hypothermia, hypovolemia, and anaemia, all of which should be prevented. The young child needs a particularly gentle approach both in general body handling and during surgery, and the surgeon must minimize blood loss with meticulous haemostatic techniques.

In addition, the sulci and Sylvian fissure are not well developed in young children, and are not as readily used as planes of dissections or surgical corridors as in the mature brain.

Timing of surgery

The child with a posterior fossa tumour and obstructive hydrocephalus is in a parlous situation and provides a challenge for the neurosurgeon, particularly in relation to the timing and order of surgery. The hydrocephalus is usually controlled following the definitive removal of the tumour, but the conscious state is an important determinant of the timing of surgery. An obtunded patient is an urgent surgical problem requiring prompt action. Steroids may delay the urgency of surgery if the conscious state is only mildly disturbed. The

patient should be placed on the next elective list unless obtundation is present, in which case the operation should be done forthwith. Placement of a ventricular drain may be hazardous in the presence of a large posterior fossa tumour, because upward coning and secondary haemorrhage in the brainstem may occur and cause further obtundation and blindness due to the compression of the posterior cerebral arteries at the tentorial edge. The risk of upward herniation is reported to be 3% (Albright, 1983), with a higher risk for large vermian tumours. The treatment is occlusion of the drain, and immediate resective surgery. Third ventriculostomy is an alternative to an external ventricular drain.

It is preferable to proceed immediately with the definitive excision of a posterior fossa tumour rather than initially treating the hydrocephalus. Even if the patient presents obtunded, immediate placement of an external ventricular drain and resection of the tumour is advised, because the tumour itself may be causing considerable brainstem compression and contributing to the obtundation. In such a case, the ventricular drainage and pressure reduction should be minimal until the posterior fossa has been decompressed, to prevent upward herniation. If the patient has been vomiting for a prolonged period, is dehydrated with electrolyte disturbance, poorly nourished, in poor general condition, and also obtunded, it may be necessary to correct the hydrocephalus first with controlled CSF drainage. This will render the patient in a better general condition for major resective surgery. The patient must be observed very closely for any deterioration due to coning or increasing brainstem compression.

Obstructive hydrocephalus due to pineal region tumours is best managed with an endoscopic third ventriculostomy. The tumour can be biopsied at the time of the third ventriculostomy (Roth and Constantini, 2015). Tumour excision may follow as a secondary procedure if indicated (Cultrera et al., 2006). Aqueductal tumours are a unique entity that have recently been described. The surgical implications include technical nuances with the endoscopic third ventriculostomy and biopsy (Roth et al., 2015).

A controversial issue is a small tumour presenting with a seizure, with no mass effect or secondary hydrocephalus. Despite the lack of literature, it seems that the transformation of low-grade tumours to high-grade ones is extremely rare among children. It may thus be an acceptable treatment to follow intact children with small tumours that appear as low grade on the imaging and present with seizures, as long as the imaging characteristics remain stable, and their seizures are controlled medically.

Positioning

The position of the child depends essentially on the location of the tumour. The surgeon must have a direct line of sight to the tumour and comfortably reach the tumour's extremities. The prone position is commonly used for posterior fossa tumours and occipital supratentorial lesions.

The surgeon must weigh risks versus benefits when choosing the sitting position. There are some high vermis, brainstem, or pineal lesions extending predominantly infratentorially which are better suited to the sitting position compared with the prone position, but each case must be judged individually and depends on the surgeon's experience. The sitting position is not usually chosen in children under 4 years of age. The advantages of the sitting position are that the exposure of the tumour may be excellent, microscope access is improved, and haemorrhage and brain swelling are minimized. The disadvantages are that the surgeon must sit in an awkward and uncomfortable position, operating with arms elevated and extended for often prolonged periods, and may become fatigued. In addition, the patient has cardiovascular instability with a tendency to postural hypotension, and the risks of venous air embolism (VAE) and paradoxical air embolism are enhanced. The latter is rare, but its effects are disastrous. The risk of air embolism in children, as in adults in the sitting position, is 30–45%, and children are more frequently endangered by this complication than adults. A discussion of the methods of detection, clinical effects, therapy, and prevention of VAE is beyond the scope of this chapter but is developed further in the literature (Jadik et al., 2009). Pneumocephalus, intracranial hematoma, and cerebral hypoperfusion may also occur in the sitting position. The lounging position, with hips flexed and knees flexed up to near shoulder height, maintains the advantages of the full sitting position, while significantly lessening the risks of hypotension, reduced cerebral blood flow, and air embolism.

Application of three-point head fixation must be done very carefully between the ages of 18 months and 5 years, and should not be used below the age of 18 months. CSF leaks and depressed skull fractures may easily result if too much pressure is applied. A combined horseshoe and pin system has been suggested for children from 6 months to 14 years of age (Gupta, 2006).

Neuroanaesthesia

An arterial line, pulse oximeter, and urinary catheter should be placed prior to positioning the patient. Excessive neck flexion should be avoided in the prone position, and the chin should not touch the chest. The eyes need careful protection, particularly when the patient is prone. Towels should be placed and held on either side of the head to prevent any antiseptic preparation entering even fully covered eyes. Careful padding of the face, and especially the eyes, is required for the prone position on the horseshoe ring. The surgeon should check that the patient's eyes are not in close contact with the horseshoe ring itself. The surgeon should also check the peripheral cutaneous pressure points for adequate protection with soft padding. A securing adhesive plaster or silicone bar are placed under the child's buttock, to prevent the child from gliding during tilting of the operative table. Kinking of the endotracheal tube is not usually a problem in either sitting or prone position if nasal intubation is used. Once the patient is in the final position, the anaesthetist will need to check the position of the endotracheal tube to ensure that it has not entered the right mainstem bronchus.

Prophylactic broad-spectrum antibiotic cover is given at the time of induction. We currently use vancomycin and ceftriaxone, or cephalothin. Careful attention should be directed to maintenance of body temperature, particularly in the younger child, because hypothermia is a consequence of undue periods of body exposure. Further intravenous steroids are administered at induction. It is not necessary to administer anticonvulsants for a posterior fossa tumour. If the cranial contents appear tight radiologically, mannitol is administered intravenously in a dose of 0.25–0.5 g per kg at the time of the scalp incision. This helps reduce intracranial pressure and aids operative exposure. The cerebral protective effect may also

be helpful. Precordial Doppler and end-tidal CO_2 monitoring are performed when the patient is in the sitting position.

Surgical approaches

The surgeon must exercise flexibility and versatility of approach to achieve the safest and usually the most direct route to the tumour. For tumours involving the base of the skull or the basal cisterns, the same principles as apply to adult skull base surgery should be applied to the child. The aim is maximal exposure of the lesion with minimisation of brain retraction. Skull base approaches are increasingly being used in children to enable resections of tumours such as chordomas, meningiomas, and sarcomas. The transsphenoidal approach may be indicated for some selected sellar and parasellar lesions (Kassam et al., 2007). This approach is suitable for intrasellar craniopharyngiomas and those with a globular suprasellar extension (infradiaphragmatic), as well as pituitary tumours. The transnasal transsphenoidal approach using endoscopy is well suited to the child's small nasal passages (Kassam et al., 2007).

Adjuncts to operative neurosurgery

Stereotaxy

Various technical adjuncts to tumour excision are being used to increase the precision of brain tumour surgery and to decrease morbidity. Intraoperative ultrasound is a simple method for identifying larger subcortical lesions. Frameless stereotaxy is becoming an indispensable aid to brain tumour surgery, enabling the surgeon to accurately plan the trajectory, choose the entry point (enabling smaller craniotomies in many cases), and provide useful intraoperative navigation (Roth et al., 2006). Frameless stereotaxy may be used for stereotactic biopsies; however, framed stereotaxy is advisable for biopsy of small deep-seated lesions.

Neuroendoscopy

Transventricular endoscopic procedures have become commonly used for various pathologies. CSF drainage-related procedures, such as endoscopic third ventriculostomy (ETV) and septum pellucidotomy, are being widely used (Oertel et al., 2009). In addition, endoscopic resection of intraventricular tumours has been described in patients with and without hydrocephalus (Souweidane, 2008). In patients with obstructive hydrocephalus secondary to midline tumours (pineal, tectal, thalamic), the common practice is endoscopic biopsy with or without an ETV (Roth et al., 2015; Roth and Constantini, 2015). Use of fine 1–2 mm malleable fiberscopes can provide the surgeon with unparalleled views of the tumour and the tumour bed at close range and from unusual angles. This technique may enable the surgeon to minimize surgical morbidity and to improve the completeness of the excision. The endoscope and frameless stereotactic system can be combined to improve placement and navigation of the endoscope (Souweidane, 2008).

Functional magnetic resonance (fMRI) and diffusion tensor imaging (DTI)

Preoperative functional MRI (fMRI) based on blood-oxygen-level-dependent (BOLD) images can be used in cooperative children from about the age of 5 years to identify the side of speech dominance with some confidence (Hertz-Pannier et al., 2014). fMRI localization of the sensorimotor cortex can be integrated into frameless stereotactic images, correlating accurately with electrophysiological localization of the sensorimotor cortex. Coregistration of the fMRI speech cortex localization into the frameless stereotactic system can also be performed. This technique may prove useful to more confidently resect tumours which lie close to or within the language or sensorimotor cortex.

DTI has been used for imaging reconstruction of the main white matter tracts, such as the pyramidal tracts (Hendler et al., 2003). Combination of preoperative DTI with navigation may additionally aid intraoperative identification of the highly functional white matter tracts, thus assisting the surgeon during removal of intra-axial tumours situated near the pyramidal tract, such as brain stem tumours or cerebral tumours adjacent to the thalamus or motor tracts.

Resting state fMRI has emerged as a novel way for studying large scale networks by measuring connectivity. The basis for rsfMRI is spontaneous activity rather than task induced activation or BOLD. Currently rsfMRI has a low precision in identifying specific networks with potential surgical implication; however, this is an emerging tool with potential implications in the paediatric population (Hertz-Pannier et al., 2014).

Electrophysiological monitoring

Electrophysiological monitoring includes several modalities, such as motor evoked potentials (MEP), somatosensory evoked potentials (SSEP), brain stem auditory evoked responses, cortical stimulation, and cranial nerve nuclei stimulation (Sala et al., 2002). MEP and SSEP provide continuous monitoring during resection of lesions that are adjacent to the pyramidal and sensory tracts. The most common anatomical areas for these lesions are brainstem tumours. Early identification of a decrease in MEP or SSEP response alerts the surgeon to potential damage, and helps to tailor the surgery for maximum resection while also maximizing patient safety. Cortical stimulation (either in an awake patient or with the aid of EMG recording in an anaesthetised patient, without muscle relaxants) helps identify the motor strip and plan a non-eloquent corridor for surgery. In young children, while the motor thresholds are too high under general anaesthesia to obtain an accurate motor map, SSEP can be used successfully to identify the sensory cortex. SSEP or a phase reversal may be measured or defined using an electrode strip.

Cranial nerve nuclei stimulation aids in resection of brainstem tumours. Stimulation of the brainstem surface (usually the fourth ventricular floor) maps functional areas, thus again aiding in finding a non-functional corridor to the tumour (Morota et al., 1996).

Cortical mapping versus awake craniotomy

Cortical mapping is useful for resection of lesions close to or within the speech or sensorimotor cortex. It is possible to perform electrical mapping of the cortex in awake patients over the age of 8 years, but this is a very unpleasant experience for the child. In the Toronto group, out of 610 patients the youngest was also 12 years old (Serletis and Bernstein, 2007). If mapping of the speech or motor cortex is required prior to the definitive resection of a tumour in a child, we would prefer to insert cortical electrode grids, map the cortex extraoperatively, and resect the lesion at a second stage procedure. This two-staged approach is usually used when the child has

an epileptic focus and a structural lesion. The standard grids have electrode spacing of 1 cm, which does not permit accurate mapping using extraoperative stimulation. Special grids with an electrode spacing of 0.5 cm are required.

Intraoperative imaging

Real-time intraoperative imaging systems enable navigation based upon images acquired intraoperatively. These imaging systems consist of intraoperative MR (iMR) scanners, CT scanners, or ultrasound (US) systems. By obtaining intraoperative images, the navigation data set may be updated during the operation, thereby compensating for anatomical changes such as brain, tumour, or cavity shifts (Roth et al., 2006). Using iMR systems for navigational imaging and postoperative imaging alleviates the need for routinely requiring additional preoperative and early postoperative CT or MR scans. Intraoperative MR systems acquire images in a variety of sequences, such as T1 (with or without contrast), T2, and FLAIR, thereby differentiating pathological tissue from normal brain tissue and maximizing resection control. Contrast-enhanced fast FLAIR MR provides marked contrast enhancement clearly showing tumour boundaries and is a sensitive method of detecting residual or recurrent tumour (Essig et al., 1999). Note that in the paediatric population, complete resection of low-grade gliomas has been shown to be a good prognostic factor (Black, 2000; Cohen et al., 2001).

The intraoperative ultrasound (IOUS) system enables acquisition of high-resolution IOUS images. Combined with 3D reconstruction used as a basis for navigation, the new, updated images are presented simultaneously with preoperative image reconstructions in the same spatial orientation, to improve anatomic orientation. IOUS such as the SonoWand system have shown similar results differentiating normal brain tissue from glial tumours (Tronnier et al., 2001). In certain cases, the tumour to tissue resolution is even better using the IOUS system, especially when comparing high-end US equipment with low-end iMR machines (Roth et al., 2007). The IOUS system maximizes the accuracy and efficiency of neuronavigation, enabling surgeons to fine-tune the resection with optimal effectiveness.

Postoperative care

Intensive nursing is provided in the general ward or the neurointensive therapy unit, depending on the magnitude of the surgery. Any potential or manifest endocrine deficiency or hypothalamic thirst centre dysregulation will require close monitoring and management by the paediatric endocrinologist, and ongoing epilepsy may require the ongoing involvement of the neurologist.

Additional aspects that require special emphasis in the postoperative care of children following brain tumour surgery are the requirement for adequate analgesia. This may involve patient-controlled analgesia for older children, or carefully monitored opiate infusion for younger children. Postoperative neurological deficits such as cerebellar symptoms and mutism after posterior fossa surgeries, cranial neuropathy after brainstem involving procedures, and/or nausea and vomiting after procedures adjacent to the obex, all cause additional discomfort and stressful impact on the child and the family. Thus, there is often a need for rehabilitation taking place in an environment that includes specialist paediatric providers. Additionally, there is need for family counselling and support.

In the long-term, children with brain tumours have the potential for a normal quality of life (Kulkarni et al., 2013). Thus, every effort should be applied to restore function following diagnosis and treatment.

Timing of postoperative neuroimaging

Identification of residual or recurrent tumour is critical in planning therapy, determining the response to therapy, and the prognosis. Surgically induced MR-detectable contrast enhancement and extracellular methaemoglobin formation all occur within 24 hours of the completion of surgery, interfering with the detection of small amounts of residual tumour. It is often difficult to perform a scan within this time frame. It is important to perform a postoperative cranial MR within 72 hours of surgery, usually giving a good indication as to the completeness of the excision. If the tumour has a propensity to metastasize, a spinal MR scan should be included if it could not be done preoperatively, but the surgeon should be aware that blood in the spinal canal from posterior fossa surgery will obscure any pathology for several days.

Surveillance neuroimaging protocols should be developed for each tumour type to minimize the number of postoperative scans required to most likely yield a positive result based on the frequency of recurrence. Surveillance imaging timing should be tailored according to the tumour grade/malignancy, and are useful for both low- and high-grade tumours.

Reoperation or 'second look' surgery

Reoperation for residual disease may be indicated to obtain a complete clearance of tumour. This particularly applies to ependymomas or choroid plexus tumours, where complete excision is the most important factor affecting long-term survival. Several operations may be required to achieve this aim if the tumour is accessible. Intraoperative imaging will verify the total resection of the tumour, and reduce the need for second look surgery.

Interpretation of the pathology

Paediatric neuropathology is a challenging discipline because of the wide range of often uncommon tumour types with often subtle and variegated histological features. Prognostication based on paediatric neuropathology is less predictable than the adult equivalent. This is especially so in the case of gliomas with anaplastic features. Unusual tumour types have been described in children such as the desmoplastic glioblastoma of infancy (Al-Sarraj and Bridges, 1996), pleomorphic xanthoastrocytoma, the atypical teratoid/rhabdoid tumour which can be mistaken for glioblastoma and PNET tumours (Parwani et al., 2005). The teratoid/rhabdoid tumour is very aggressive in behaviour, with a poor response to chemotherapy, and should be separated from the medulloblastoma group, otherwise any analysis of results and response to chemotherapy is skewed (Squire et al., 2007). Atypical choroid plexus papilloma needs to be differentiated from both choroid plexus papilloma (CPP) and carcinoma

(CPC). The increasing emphasis on tumour markers, immunocytochemistry, proliferation indices, and cytogenetics to more accurately classify brain tumours and predict their behaviour are discussed elsewhere in this book.

Tumour seeding via shunt systems

The development of extraneural metastasis is uncommon following the placement of a ventriculoperitoneal or ventriculoatrial shunt (Pollack et al., 1994). Medulloblastoma confers the greatest risk. Pineal tumours may also metastasize this way. Children with optic pathway gliomas which harbour shunts, tend to develop ascites at higher rates compared to other pathologies.

Adjuvant treatments

The role of surgery changes according to the specific tumour type. Tumours that are treated solely by an aggressive surgical approach include some ependymomas, low-grade gliomas (including grade 1 and 2 astrocytomas), choroid plexus papillomas (including atypical), pituitary adenomas, and most meningiomas.

However, certain tumours may not be amenable to total resection without a significant associated morbidity due to their invasion of critical structures, such as the brainstem, optic tracts, and hypothalamus. Some tumours have a high recurrence rate despite 'total gross resection', this may be secondary to local invasion (such as in high-grade gliomas, CPC, and medulloblastomas), or to concurrent metastasis (e.g. medulloblastomas, ependymomas, germ cell tumours).

Thus, over the years, various adjuvant treatments have evolved, including radiation-based treatments and chemotherapeutic regimens.

Certain tumours are extremely sensitive to adjuvant treatments. When weighing the risks and benefits of the various treatments (including surgery, chemotherapy, and radiation), the logical decision for some tumours is to treat mainly by chemotherapy and/or radiation, while surgery (if at all) is applied for diagnosis only. A classic example of this approach is treating germ cell tumours. These typically midline lesions occur either in the suprasellar area or in the pineal region. These tumours are extremely sensitive to chemotherapy and radiation. Over the last few years, their diagnosis and treatment has shifted from surgical resection, to diagnosis based on serum (or CSF) markers—αFP, βHCG, and placental alkaline phosphatase. Only if all markers are negative is there an indication for a biopsy (Echevarria et al., 2008). However, when presenting with obstructive hydrocephalus from aqueductal compression, these patients are treated by an ETV and endoscopic biopsy (Shono et al., 2007).

Another example of treatment paradigm shift is in the treatment of craniopharyngiomas. This is a benign tumour, typically situated in the suprasellar region, often rising into the third ventricle. Until a few years ago, the ultimate treatment was a total gross resection. Despite a low recurrence rate, the neurocognitive and hormonal outcomes were dismal, mostly from injury to adjacent structures along the hypothalamic-pituitary axis. While surgery is still the primary treatment, with maximal resection as the goal, additional and effective adjuvant regimens enable a less aggressive surgical approach, with lower surgery associated morbidity and good tumour control. These treatments include radiation, intralesional chemotherapy (such as bleomycin or interferon), and intratumoural radiation (Puget et al., 2006).

As the focus of this chapter is the surgical aspect of paediatric brain tumours, we will only provide a brief review of the adjuvant treatments, focusing on their essentials and the major relevant tumour subpopulations.

Radiation

For many childhood CNS tumours, radiation therapy plays an essential role in treatment. For most childhood brain tumours, chemotherapy cannot eliminate all the cancer cells, thus radiation is frequently employed. Despite the beneficial oncolytic effect of radiation therapy, there are potential, mostly long-term complications. The developing immature brain is vulnerable to radiation, particularly the white matter (Kitajima et al., 2007).

Neurocognitive decline, neuroendocrinopathy, cranial neuropathy, retinopathy, vasculopathy (including secondary moyamoya disease), myelopathy, and spinal growth disturbance are all secondary to injury of the developing brain, spine, and adjacent structures.

Secondary cavernous angiomas secondary to microvascular injury may occur (Duhem et al., 2005). Secondary tumours (benign, such as meningiomas, and malignant, such as high-grade gliomas and thyroid carcinoma) occur due to various genetic insults, and may occur many years after the radiation treatment (Umansky et al., 2008). The risk of secondary tumours may be higher among syndromatic children, such as those with neurofibromatosis and nevoid basal cell carcinoma syndrome (Kleinerman, 2009).

We do not advise whole brain radiotherapy in children before the age of 3 years because of the long-lasting and often profound effects on cognitive development and neuroendocrine function.

Due to all the risks of general radiation, the improved precision of conformal radiation techniques has been increasingly utilized to treat paediatric brain tumours.

Stereotactic radiosurgery has been applied in children for treating tumours and arteriovenous malformations. The advantage of this technique is the steep target to periphery radiation exposure dose cut off. However, controversy still exists concerning the safety of radiosurgery in children in general, and for pathologies adjacent to crucial structures, such as the brainstem, cranial nerves, and hypothalamus, in particular.

Proton beam therapy is a relatively new radiation technology applied in the treatment of brain and spine tumours. Although only preliminary studies have addressed this technology in PBT, there is currently a shift in radiation technique towards proton beam especially for craniopharyngiomas. Implication of proton treatment for other PBT is under study.

Chemotherapy

Adjuvant chemotherapy has become part of the protocol for most adult brain tumours, and in some paediatric tumours too. In fact,

since in the very young population radiation therapy is associated with devastating neurocognitive and neuroendocrine sequala, the need to add adequate chemotherapy is even stronger.

Chemotherapy may be used as a neoadjuvant treatment prior to surgery especially in high risk surgical patients such as infants harbouring huge tumours, as well as children with choroid plexus carcinomas.

A subset of patients in which chemotherapy has become a valid alternative to surgery is the case with tuberous sclerosis associated subependymal giant cell astrocytomas (SEGAs). These tumours respond favourably to mTOR inhibitors (such as rapamycin and Everolimus), with about 40% of patients reducing their tumour volume by at least 50% over 6 months. mTORi have other positive effects on tuberous sclerosis patients, improving their seizures, renal tumours, rash, and even cognition, thus becoming a disease altering drug.

FURTHER READING

Kim, A.H., Thompson, E.A., Governale, L.S., et al. (2014). Recurrence after gross-total resection of low-grade pediatric brain tumors: the frequency and timing of postoperative imaging. *J Neurosurg Pediatr*, **14**, 356–64.

Roth, J., Keating, R.F., Myseros, J.S., Yaun, A.L., Magge, S.N., & Constantini, S. (2012). Pediatric incidental brain tumors: a growing treatment dilemma. *J Neurosurg Pediatr*, **10**, 168–74.

Shofty, B., Ben-Sira, L., Freedman, S., et al. (2011). Visual outcome following chemotherapy for progressive optic pathway gliomas. *Pediatr Blood Cancer*, **57**, 481–5.

Taylor, M. D., Northcott, P. A., Korshunov, A., et al. (2012). Molecular subgroups of medulloblastoma: the current consensus. *Acta Neuropathol*, **123**, 465–72.

Wilne, S., Collier, J., Kennedy, C., Koller, K., Grundy, R., & Walker, D. (2007). Presentation of childhood CNS tumours: a systematic review and meta-analysis. *Lancet Oncol*, **8**, 685–95.

REFERENCES

Ailon, T., Dunham, C., Carret, A.S., et al. (2015). The role of resection alone in select children with intracranial ependymoma: the Canadian Pediatric Brain Tumour Consortium experience. *Childs Nerv Syst*, **31**, 57–65.

AL-Sarraj, S.T. & Bridges, L.R. (1996). Desmoplastic cerebral glioblastoma of infancy. *Br J Neurosurg*, **10**, 215–19.

Albright, A.L. (1983). The value of precraniotomy shunts in children with posterior fossa tumors. *Clin Neurosurg*, **30**, 278–85.

Beni-Adani, L., Gomori, M., Spektor, S., & Constantini, S. (2000). Cyst wall enhancement in pilocytic astrocytoma: neoplastic or reactive phenomena. *Pediatr Neurosurg*, **32**, 234–9.

Black, P.M. (2000). The present and future of cerebral tumor surgery in children. *Childs Nerv Syst*, **16**, 821–8.

Chalil, A. & Ramaswamy, V. (2015). Low grade gliomas in children. *J Child Neurol*, **31**(4), 517–22.

Cohen, K.J., Broniscer, A., & Glod, J. (2001). Pediatric glial tumors. *Curr Treat Options Oncol*, **2**, 529–36.

Constantini, S. & Epstein, F. (1996). Surgical indication and technical considerations in the management of benign brain stem gliomas. *J Neurooncol*, **28**, 193–205.

Cultrera, F., Guiducci, G., Nasi, M.T., Paioli, G., & Frattarelli, M. (2006). Two-stage treatment of a tectal ganglioglioma: endoscopic third ventriculostomy followed by surgical resection. *J Clin Neurosci*, **13**, 963–5.

Dodgshun, A.J., Maixner, W.J., Hansford, J.R., & Sullivan, M.J. (2016). Low rates of recurrence and slow progression of pediatric pilocytic astrocytoma after gross-total resection: justification for reducing surveillance imaging. *J Neurosurg Pediatr*, **17**, 569–72.

Duhem, R., Vinchon, M., Leblond, P., Soto-Ares, G., & Dhellemmes, P. (2005). Cavernous malformations after cerebral irradiation during childhood: report of nine cases. *Childs Nerv Syst*, **21**, 922–5.

Echevarria, M.E., Fangusaro, J., & Goldman, S. (2008). Pediatric central nervous system germ cell tumors: a review. *Oncologist*, **13**, 690–9.

Essig, M., Knopp, M.V., Schoenberg, S.O., et al. (1999). Cerebral gliomas and metastases: assessment with contrast-enhanced fast fluid-attenuated inversion-recovery MR imaging. *Radiology*, **210**, 551–7.

Fattal-Valevski, A., Nissan, N., Kramer, U., & Constantini, S. (2013). Seizures as the clinical presenting symptom in children with brain tumors. *J Child Neurol*, **28**, 292–6.

Gajjar, A., Fouladi, M., Walter, A.W., et al. (1999). Comparison of lumbar and shunt cerebrospinal fluid specimens for cytologic detection of leptomeningeal disease in pediatric patients with brain tumors. *J Clin Oncol*, **17**, 1825–8.

Gil, Z., Beni-Adani, L., Siomin, V., Nagar, H., Dvir, R., & Constantini, S. (2001). Ascites following ventriculoperitoneal shunting in children with chiasmatic-hypothalamic glioma. *Childs Nerv Syst*, **17**, 395–8.

Gupta, N. (2006). A modification of the Mayfield horseshoe headrest allowing pin fixation and cranial immobilization in infants and young children. *Neurosurgery*, **58**, ONS-E181; discussion ONS-E181.

Hendler, T., Pianka, P., Sigal, M., et al. (2003). Delineating gray and white matter involvement in brain lesions: three-dimensional alignment of functional magnetic resonance and diffusion-tensor imaging. *J Neurosurg*, **99**, 1018–27.

Hertz-Pannier, L., Noulhiane, M., Rodrigo, S., & Chiron, C. (2014). Pretherapeutic functional magnetic resonance imaging in children. *Neuroimaging Clin N Am*, **24**, 639–53.

Jadik, S., Wissing, H., Friedrich, K., Beck, J., Seifert, V., & Raabe, A. (2009). A standardized protocol for the prevention of clinically relevant venous air embolism during neurosurgical interventions in the semisitting position. *Neurosurgery*, **64**, 533–8; discussion 538–9.

Kassam, A., Thomas, A.J., Snyderman, C., et al. (2007). Fully endoscopic expanded endonasal approach treating skull base lesions in pediatric patients. *J Neurosurg*, **106**, 75–86.

Kim, A.H., Thompson, E.A., Governale, L.S., et al. (2014). Recurrence after gross-total resection of low-grade pediatric brain tumors: the frequency and timing of postoperative imaging. *J Neurosurg Pediatr*, **14**, 356–64.

Kitajima, M., Hirai, T., Maruyama, N., et al. (2007). Asymptomatic cystic changes in the brain of children after cranial irradiation: frequency, latency, and relationship to age. *Neuroradiology*, **49**, 411–17.

Kleinerman, R.A. (2009). Radiation-sensitive genetically susceptible pediatric sub-populations. *Pediatr Radiol*, **39** Suppl 1, S27–31.

Kukal, K., Dobrovoljac, M., Boltshauser, E., Ammann, R.A., & Grotzer, M.A. (2009). Does diagnostic delay result in decreased survival in paediatric brain tumours? *Eur J Pediatr*, **168**, 303–10.

Kulkarni, A.V., Piscione, J., Shams, I., & Bouffet, E. (2013). Long-term quality of life in children treated for posterior fossa brain tumors. *J Neurosurg Pediatr*, **12**, 235–40.

Louis, D.N., Perry, A., Reifenberger, G., et al. (2016). The 2016 World Health Organization Classification of Tumors of the Central Nervous System: a summary. *Acta Neuropathol*, **131**, 803–20.

Millward, C.P., Perez, D.A., Rosa, S., et al. (2015). The role of early intra-operative MRI in partial resection of optic pathway/hypothalamic gliomas in children. *Childs Nerv Syst*, **31**, 2055–62.

Morota, N., Deletis, V., Lee, M., & Epstein, F.J. (1996). Functional anatomic relationship between brain-stem tumors and cranial motor nuclei. *Neurosurgery*, **39**, 787–93; discussion 793–4.

Northcott, P.A., Korshunov, A., Pfister, S.M., & Taylor, M.D. (2012). The clinical implications of medulloblastoma subgroups. *Nat Rev Neurol*, **8**, 340–51.

Oertel, J.M., Schroeder, H.W., & Gaab, M.R. (2009). Endoscopic stomy of the septum pellucidum: indications, technique, and results. *Neurosurgery*, **64**, 482–91; discussion 491–3.

Ostrom, Q. T., De Blank, P. M., Kruchko, C., et al. (2015). Alex's Lemonade Stand Foundation infant and childhood primary brain and central nervous system tumors diagnosed in the United States in 2007–2011. *Neuro-Oncology*, **16**, x1–x36.

Parwani, A.V., Stelow, E.B., Pambuccian, S.E., Burger, P.C., & Ali, S.Z. (2005). Atypical teratoid/rhabdoid tumor of the brain: cytopathologic characteristics and differential diagnosis. *Cancer*, **105**, 65–70.

Pollack, I.F., Hurtt, M., Pang, D., & Albright, A.L. (1994). Dissemination of low grade intracranial astrocytomas in children. *Cancer*, **73**, 2869–78.

Puget, S., Grill, J., Habrand, J.L., & Sainte-Rose, C. (2006). Multimodal treatment of craniopharyngioma: defining a risk-adapted strategy. *J Pediatr Endocrinol Metab*, **19** Suppl 1, 367–70.

Purdy, E., Johnston, D.L., Bartels, U., et al. (2014). Ependymoma in children under the age of 3 years: a report from the Canadian Pediatric Brain Tumour Consortium. *J Neurooncol*, **117**, 359–64.

Roth, J., Beni-Adani, L., Biyani, N., & Constantini, S. (2006). Classical and real-time neuronavigation in pediatric neurosurgery. *Childs Nerv Syst*, **22**, 1065–71.

Roth, J., Biyani, N., Beni-Adani, L., & Constantini, S. (2007). Real-time neuronavigation with high-quality 3D ultrasound SonoWand in pediatric neurosurgery. *Pediatr Neurosurg*, **43**, 185–91.

Roth, J., Chaichana, K.L., Jallo, G., Mirone, G., Cinalli, G., & Constantini, S. (2015). True aqueductal tumors: a unique entity. *Acta Neurochir (Wien)*, **157**, 169–77.

Roth, J. & Constantini, S. (2015). Combined rigid and flexible endoscopy for tumors in the posterior third ventricle. *J Neurosurg*, **122**, 1341–6.

Roth, J., Keating, R.F., Myseros, J.S., Yaun, A.L., Magge, S.N., & Constantini, S. (2012). Pediatric incidental brain tumors: a growing treatment dilemma. *J Neurosurg Pediatr*, **10**, 168–74.

Sala, F., Krzan, M.J. & Deletis, V. (2002). Intraoperative neurophysiological monitoring in pediatric neurosurgery: why, when, how? *Childs Nerv Syst*, **18**, 264–87.

Sanoudou, D., Tingby, O., Ferguson-Smith, M.A., Collins, V.P., & Coleman, N. (2000). Analysis of pilocytic astrocytoma by comparative genomic hybridization. *Br J Cancer*, **82**, 1218–22.

Serletis, D. & Bernstein, M. (2007). Prospective study of awake craniotomy used routinely and nonselectively for supratentorial tumors. *J Neurosurg*, **107**, 1–6.

Shay, V., Fattal-Valevski, A., Beni-Adani, L., & Constantini, S. (2012). Diagnostic delay of pediatric brain tumors in Israel: a retrospective risk factor analysis. *Childs Nerv Syst*, **28**(1), 93–100.

Shofty, B., Ben-Sira, L., Freedman, S., et al. (2011). Visual outcome following chemotherapy for progressive optic pathway gliomas. *Pediatr Blood Cancer*, **57**, 481–5.

Shofty, B., Ben-Sira, L., Kesler, A., & Constantini, S. (2015). Optic pathway gliomas. *Adv Tech Stand Neurosurg*, **42**, 123–46.

Shono, T., Natori, Y., Morioka, T., et al. (2007). Results of a long-term follow-up after neuroendoscopic biopsy procedure and third ventriculostomy in patients with intracranial germinomas. *J Neurosurg*, **107**, 193–8.

Souweidane, M.M. (2008). Endoscopic surgery for intraventricular brain tumors in patients without hydrocephalus. *Neurosurgery*, **62**, 1042–8.

Squire, S.E., Chan, M.D., & Marcus, K.J. (2007). Atypical teratoid/rhabdoid tumor: the controversy behind radiation therapy. *J Neurooncol*, **81**, 97–111.

Taylor, M.D., Gokgoz, N., Andrulis, I.L., Mainprize, T.G., Drake, J.M., & Rutka, J.T. (2000). Familial posterior fossa brain tumors of infancy secondary to germline mutation of the *hSNF5* gene. *Am J Hum Genet*, **66**, 1403–6.

Taylor, M. D., Northcott, P. A., Korshunov, A., et al. (2012). Molecular subgroups of medulloblastoma: the current consensus. *Acta Neuropathol*, **123**, 465–72.

Tronnier, V.M., Bonsanto, M.M., Staubert, A., Knauth, M., Kunze, S., & Wirtz, C.R. (2001). Comparison of intraoperative MR imaging and 3D-navigated ultrasonography in the detection and resection control of lesions. *Neurosurg Focus*, **10**, E3.

Umansky, F., Shoshan, Y., Rosenthal, G., Fraifeld, S., & Spektor, S. (2008). Radiation-induced meningioma. *Neurosurg Focus*, **24**, E7.

Wilne, S., Collier, J., Kennedy, C., Koller, K., Grundy, R., & Walker, D. (2007). Presentation of childhood CNS tumours: a systematic review and meta-analysis. *Lancet Oncol*, **8**, 685–95.

RELATED LINKS TO EBRAIN

Surgery in children. https://learning.ebrain.net/course/view.php?id=73

Principles of brain tumour management in children. https://learning.ebrain.net/course/view.php?id=425

89

Paediatric hydrocephalus

Matt Bailey, Chris Parks, and Conor L. Mallucci

Introduction

Paediatric hydrocephalus is the commonest disorder to be managed by paediatric neurosurgeons. Rather than representing a single disease process, hydrocephalus can result from a variety of different pathological processes or insults that culminate in an imbalance of CSF production and absorption. If left untreated the majority of cases are fatal (Laurence and Coates, 1962), but with appropriate surgical management most patients survive, with some leading normal lives into adulthood.

The mainstay of treatment is with CSF shunts, but with technological improvements in imaging and surgical techniques an increasing number are being successfully treated with neuroendoscopic procedures. The disorder can be complex to manage, with many patients requiring multiple surgical procedures and lifelong follow-up.

This chapter gives an overview of paediatric hydrocephalus, its causes and classification, management with shunts and endoscopy, description of surgical techniques, and the outcomes of surgical care.

Definition

The word hydrocephalus is Greek coming from the words: *hydro*, meaning water and *cephalus*, meaning head, its literal translation therefore being water in the head (Orešković and Klarica, 2011). It generally refers to a disorder of cerebrospinal fluid physiology that results in an abnormal expansion of the cerebral ventricles, typically associated with raised intracranial pressure (Kahle et al., 2015).

There is currently no universally accepted definition of hydrocephalus, although several have been proposed over the years. The following definition proposed by Rekate in 2008 has been accepted by many within the surgical community: 'Hydrocephalus is an active distension of the ventricular system of the brain resulting from an inadequate passage of cerebrospinal fluid from its point of production within the cerebral ventricles to its point of absorption into the systemic circulation' (Rekate, 2008a).

The pathophysiology of hydrocephalus is discussed in Chapter 92.

Incidence and epidemiology

The overall incidence and prevalence of hydrocephalus is difficult to ascertain as it can occur in isolation or in association with a variety of neurological disorders. The reported incidence of congenital hydrocephalus ranges from 0.6–0.8 per 1000 live births (Blackburn and Fineman, 1994; Persson et al., 2005; Persson et al., 2007; Jeng et al., 2011), however, many cases of hydrocephalus occur secondary to other disease processes (e.g. prematurity, tumour, infection, trauma). The rates of hydrocephalus are thought to be highest in developing countries, mainly due to higher rates of neonatal infection (Warf et al., 2011). In developed countries the commonest causes are posthaemorrhagic hydrocephalus of prematurity, congenital aqueduct stenosis, myelomeningocele and brain tumours (Kulkarni et al., 2013; Stone and Warf, 2014). Certain factors have been identified that are associated with an increased risk of infantile hydrocephalus: these include low birth weight, low socioeconomic status, male sex and ethnicity where lower rates are seen in those of Asian descent (Jeng et al., 2011; Tully et al., 2015).

Classification of hydrocephalus

At present there is no universally accepted classification system for hydrocephalus and there is an on-going debate on how best to classify the disorder. As hydrocephalus is not a single pathological disease but is a condition of disturbed CSF dynamics that can occur with or without an underlying disease process, its classification can be confusing and complex (Oi, 2011). Two commonly used classifications are congenital versus acquired and obstructive versus communicating hydrocephalus.

Hydrocephalus was classified into obstructive (or non-communicating) and communicating based on work by Dandy in the early 1900s (Dandy, 1919). Dandy and his coinvestigators studied hydrocephalus using ventricular and lumbar punctures. They injected dye into the ventricular system and went on to perform lumbar punctures. If the dye was found in the CSF from the lumbar puncture then the hydrocephalus was classified as being 'communicating'. If no dye was recovered from the spinal tap the hydrocephalus was considered to be 'obstructive'. This classification has stood the test of time and remains the classification by which

hydrocephalus is billed in the United States (Kahle et al., 2015). However understanding of CSF physiology has evolved and remains a matter of debate. The current most widely accepted view is that CSF circulation is via bulk flow with CSF being produced by the choroid plexus within the ventricular system, flowing into the subarachnoid space and being absorbed by the arachnoid granulations to enter the cerebral venous system. Other theories exist and are discussed in Chapter 92.

Since the introduction of modern imaging techniques including computed tomography (CT) in the 1970s and magnetic resonance imaging (MRI) in the 1980s the exact location of sites of obstruction within the CSF pathways can now often be identified. Within the surgical community, the classification system proposed by Rekate (Detwiler et al., 1999; Rekate, 2001) is commonly used as it provides a method for conceptualizing the cause of hydrocephalus in any given patient and applying potential management options (Fig. 89.1).

The identification of the specific point of obstruction allows clinicians to select an appropriate surgical technique tailored to a specific patient (see Table 89.1)

Causes of hydrocephalus in children

The causes of hydrocephalus may be congenital or acquired. Congenital causes include Chiari malformations, spina bifida, Aqueduct stenosis, Dandy-Walker anomalies, arachnoid cysts, and atresia of the foramen of Munro. Acquired causes include haemorrhage, infection, head injury, and tumours (Rekate, 2008b; Kandasamy et al., 2011; Rekate, 2011).

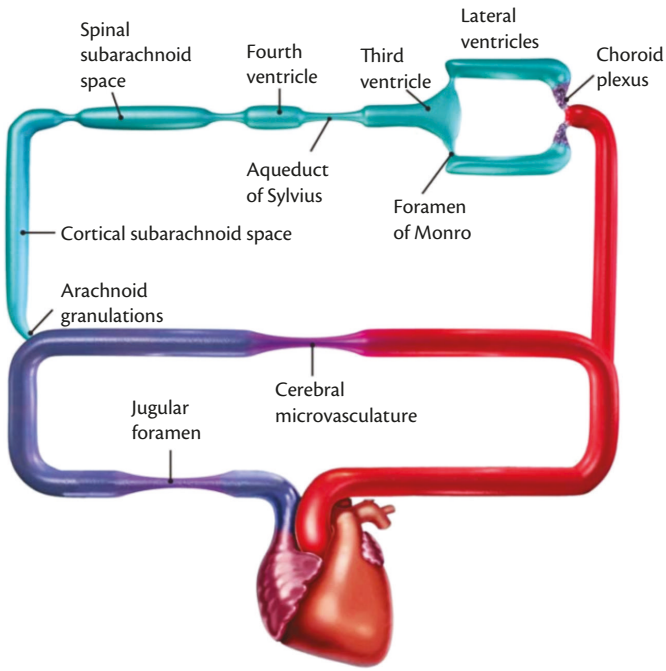

Fig. 89.1 Rekate's classification describes six potential sites where the flow of CSF may be restricted namely the foramen of Monroe; the aqueduct of Sylvius; the outlets of the fourth ventricle; the basal cisterns; the arachnoid granulations; and out flow of venous blood through the dural venous sinuses (Rekate, 2008; Rekate, 2011).

Reproduced from Rekate, H. L., The definition and classification of hydrocephalus: a personal recommendation to stimulate debate, *Cerebrospinal Fluid Research*, Volume 5, Issue 2, Copyright © 2008 Rekate; licensee BioMed Central Ltd. With permission from Barrow Neurological Institute.

Table 89.1 The treatment options for hydrocephalus caused by obstructions at different points on the CSF pathway

Point of obstruction	Differential DX	Treatments available
Foramen of Monro	Tumour	Shunt (unilateral or bilateral)
	Congenital absence	Endoscopic septum opening
	Ventriculitis	
	Functional	
Aqueduct of Sylvius	Tumour	Shunt
	Birth defect	ETV
	Secondary	
Fourth ventricle foramina	Infection	Shunt
	Tumour	ETV
	Severe Chiari	Surgical opening
Spinal to CSAS	Subarachnoid	Shunt
	Haemorrhage	ETV
	LP shunt	
Arachnoid villi	Haemorrhage or infection	VP or LP shunt
Venous hypertension	Pseudotumor	VP or LP shunt
	Congenital hydrocephalus	Clot lysis
	Sinus thrombosis	Bariatric surgery for obesity-related pseudotumor

Reproduced from Rekate, H. L., A consensus on the classification of hydrocephalus: its utility in the assessment of abnormalities of cerebrospinal fluid dynamics, *Child's Nervous System*, Volume 27, pp. 1535–41 Copyright © 2011 Rekate.

Data from the shunt design trial (Drake et al., 1998), the hydrocephalus research network (Kulkarni et al., 2013) and the UK shunt registry (Richards, 2010) give roughly similar distributions of the most common causes of hydrocephalus in children. Posthaemorrhagic hydrocephalus comprises 25%, other common causes include myelomeningocele, Chiari malformations, tumours, aqueduct stenosis, infections, trauma, and intracranial cysts.

Clinical features of hydrocephalus in different age groups

Despite the many causes of hydrocephalus, the clinical presentation is relatively similar in all pathologies. The main variation seen in presentation is related to the age of the child at presentation and whether the cranial sutures are open or closed.

The cranial sutures normally close between 12 and 18 months of age. Due to the relative dispensability of a neonate's or infant's skull before this time the signs of hydrocephalus can sometimes be subtle and can include failure to thrive, developmental delay, and poor head control. The occipitofrontal circumference (OFC) will increase disproportionately and when plotted on a centile chart will be seen to cross centile lines (Fig. 89.2). Irritability, vomiting, and poor feeding are also common. As the hydrocephalus

(a) A child with sunsetting eyes.

(b) Girl's head circumference chart that allows head growth to be plotted.

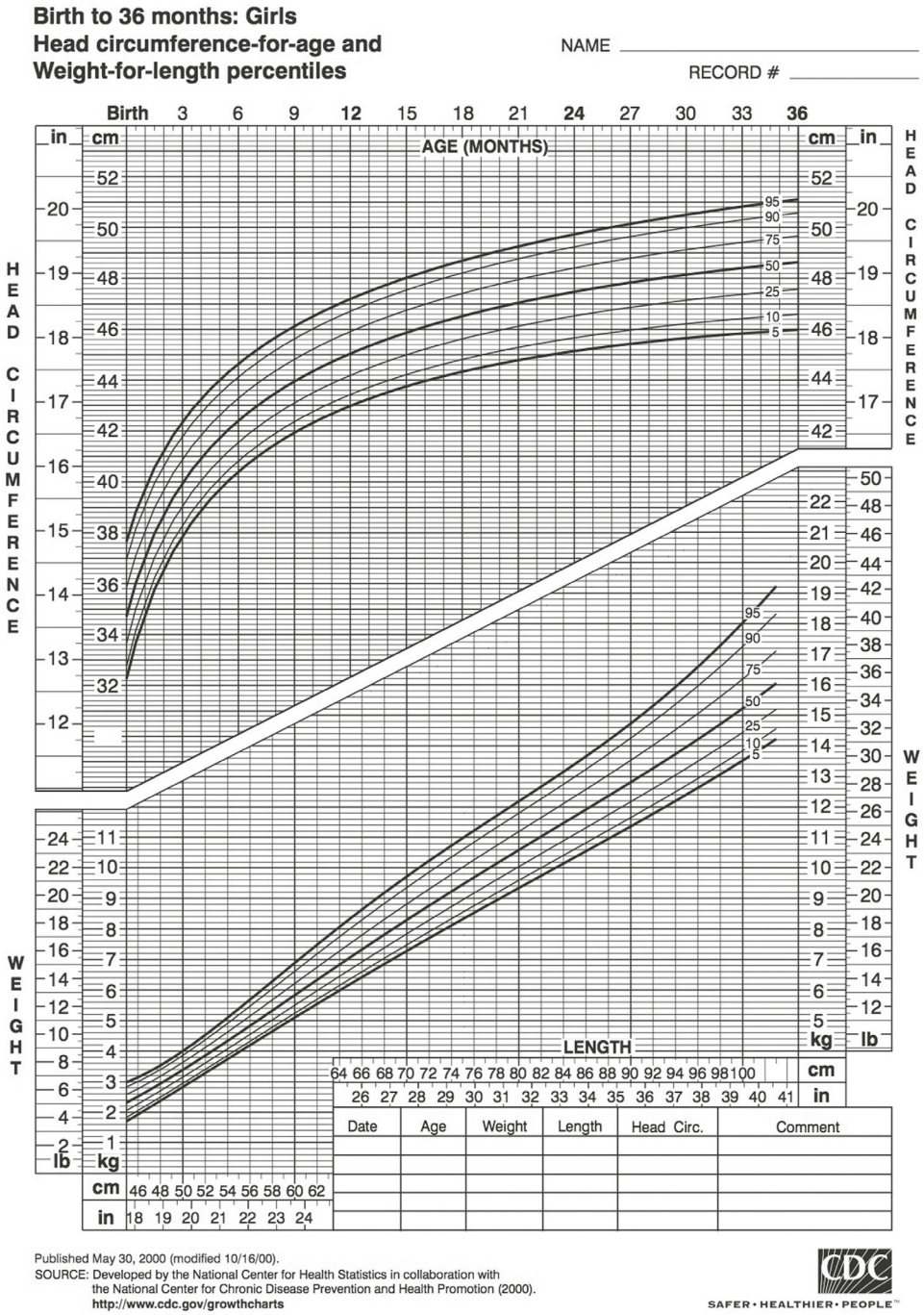

Fig. 89.2 (A) A child with sunsetting eyes. (B) Girls' head circumference chart that allows head growth to be plotted (Kandasamy et al., 2011).

progresses the cranial sutures become splayed, the anterior fontanelle bulges, and scalp veins become engorged. Some infants develop the classic 'sunsetting' appearance where upgaze is lost due to pressure of the third ventricle on the tectum. Ultimately bradycardia, desaturations, and apnoeas can occur. Seizures are not a common presenting feature of hydrocephalus alone and papilloedema is rare in this age group (Abou-Hamden & Drake, 2015). In some cases where the hydrocephalus develops slowly the signs may be few, but invariably the head circumference will have grown disproportionately.

If hydrocephalus develops after the cranial sutures have closed most patients will have a normal head circumference. Subtle signs may include headaches, deterioration performance at school, memory loss, or behavioural changes. More acutely children have symptoms and signs similar to adults with raised intracranial pressure including headaches, vomiting, papilloedema, diplopia (from a sixth cranial nerve palsy), drowsiness, and eventually coma.

The clinical features of hydrocephalus in infants and young children include irritability, impaired level of consciousness, vomiting, failure to thrive, poor feeding, developmental delay, head

circumference crossing the centiles, poor head control, tense anterior fontanelle, dilated scalp veins, sunsetting eyes, bradycardia, apnoeic spells, and seizures. In older children, headache, vomiting, drowsiness, diplopia, seizures, impaired upgaze, and papilloedema are the main features.

Imaging studies used in the investigation of hydrocephalus

Cranial ultrasound

Cranial ultrasound is very useful for imaging the brain in the first 12–18 months while the anterior fontanelle remains open and many neonatal units routinely use ultrasound for screening of preterm infants. No sedation is needed and the procedure can be repeated as often as required with no adverse effects. The size and configuration of the lateral ventricles is easily identified on ultrasound but the third and fourth ventricle, cerebral aqueduct and posterior fossa contents cannot be reliably assessed (Dinçer and Özek 2011). Therefore the precise cause of hydrocephalus is rarely confirmed by ultrasound alone and if treatment of ventriculomegaly is required additional brain imaging should be obtained (Dinçer and Özek, 2011).

Computed tomography (CT)

CT is readily available, fast, reliable, and compatible with emergency life support systems. In most cases children do not require sedation for CT as image acquisition times are short. CT demonstrates the size and morphology of the ventricles and can reveal underlying pathologies such as haemorrhage and tumours. The location of obstructions within the ventricular system may also be evidenced by significant dilatation of the ventricles proximal to the obstruction with normal sized distal ventricles (as seen, for example, in aqueduct stenosis) (Dinçer and Özek, 2011). CT is also valuable in the follow-up of patients with CSF shunts as shunt tubing is well demonstrated on CT. However, children with hydrocephalus often require many imaging studies throughout their lifetime and there are concerns about the long-term effects of exposure to ionizing radiation (Koral et al., 2012; Krishnamurthy et al., 2013). In view of this some centres are now using rapid sequence MR imaging for acute assessment and follow-up of children with hydrocephalus (Koral et al., 2012).

Magnetic resonance imaging (MRI)

MRI is the examination of choice for investigation of children with hydrocephalus.

Conventional T1 and T2 sequences are used routinely and provide excellent images of the brain parenchyma and pathological processes (such as aqueduct stenosis, tumours, and Chiari malformations), as well as evaluating the size and shape of the ventricular system. Modern sequences such as 3D CISS, turbo spin echo and cine PC have gained wide acceptance in evaluating the anatomy of the CSF pathways from the ventricles to the cortical subarachnoid spaces and CSF flow at various sites can be scrutinized (Dinçer and Özek, 2011). Fine anatomical detail of membranes within the CSF pathways, such as at the foramen of Munroe, within the cerebral aqueduct, and the outflow of the fourth ventricle can be demonstrated. Likewise, the anatomy of intracranial cysts and septations within multiloculated ventricles can be studied and can prove invaluable in determining the most appropriate surgical procedure for each patient.

Limitations of MRI include relatively long image acquisition times that often require general anaesthesia or sedation in smaller children. However, in the majority of cases there is sufficient time for children to undergo high quality MR imaging prior to surgical intervention. MRI is also extensively used in the follow-up of patients with hydrocephalus for assessment of ventricular size and to demonstrate the results of endoscopic procedures and the position of shunt catheters. Patients with programmable shunt valves may require valve reprogramming after imaging as some valves can be adjusted by the magnetic field.

Increasingly MRI is also being used in the investigation of central nervous system (CNS) abnormalities (including hydrocephalus) in the fetal period where anomalies have previously been identified on maternal ultrasound. MRI can be used to aid clinicians in prognostication.

Management of hydrocephalus in children of different ages

The following section discusses the assessment and management of children of different ages with hydrocephalus. Initially we will focus discussion on the management of hydrocephalus in preterm infants. The management of term infants and children will then be described.

Hydrocephalus in preterm infants

Preterm infants are those born before 37 weeks' gestation. The majority of cases of hydrocephalus seen in these children is secondary to intraventricular haemorrhage (IVH) related to prematurity. The pathophysiology of IVH of prematurity is discussed in Chapter 90.

Approximately 15–20% of infants with a birth weight less than 1500 g will develop IVH (du Plessis, 2009; Robinson, 2012). The lower the birth weight, the higher the risk of developing IVH (Boop, 2005). The presentation of IVH may be catastrophic with rapid neurological deterioration or progressive with reduced alertness, hypotonia and respiratory compromise, or may be clinically silent (Robinson, 2012). Therefore most neonatal units routinely screen preterm infants with cranial ultrasound (US) to detect IVH and, if present, serial cranial US is used to document progression of the haemorrhage and for monitoring of ventricular size. Imaging is used in combination with clinical features to identify those infants who may require treatment for posthaemorrhagic hydrocephalus (PHH).

Pathological studies of infants with IVH suggest that ventriculomegaly can occur in nearly half of these patients, termed posthaemorrhagic ventricular dilatation (PHVD). However, the presence of PHVD does not always represent symptomatic PHH and may be an ex-vacuo phenomenon related to loss of brain substance secondary to venous infarction or periventricular white

matter ischaemia (Boop, 2005). Clinicians must therefore use a combination of imaging and clinical findings to guide the need for potential interventions.

The clinical features of symptomatic PHH include increased rate of head growth (occipitofrontal circumference—OFC) when compared to published normal values, full anterior fontanelle, separation of the cranial sutures and progressive ventriculomegaly on imaging. Some infants also display features of raised intracranial pressure with lethargy, vomiting, apnoea, and bradycardia. By comparison, infants with ex-vacuo PHVD may have an increase in their ventricular indices, but associated with an OFC that does not cross centile lines (or may even fall across centiles), the anterior fontanelle will be soft and the cranial sutures may be overriding (Boop, 2005).

Published rates of symptomatic PHH in infants following IVH range from 22% to 29% and between 9% and 20% require permanent CSF diversion surgery (Murphy et al., 2002; Vassilyadi et al., 2009; Limbrick et al., 2010). The likelihood of infants developing PHH increases with the severity of IVH (Robinson, 2012).

Management of PHH in preterm infants

Once the diagnosis of symptomatic PHH has been made treatment should be implemented. These infants are fragile and generally of low weight. They may also be clinically unstable and many will have other medical comorbidities. It is generally accepted that ventriculoperitoneal (VP) shunts should not be used as the initial treatment strategy for symptomatic PHH in preterm infants. This is because shunt failure rates are unacceptably high in these patients, partially due to the large amount of protein and blood in the CSF increasing the risk of VP shunt blockage (Hislop et al., 1988). Additionally the skin of these babies is fragile, is at risk of breakdown and infection rates may be higher (Robinson, 2012; Whitelaw and Aquilina, 2012). In most centres VP shunts are only inserted once the infant reaches a weight of 2–2.5 kg and is of term age (Whitelaw and Aquilina, 2012; Leonard and Limbrick, 2015). In view of this there is a need to provide temporary treatment for children with symptomatic PHH.

Potential temporizing measures for these infants include serial lumbar punctures or ventricular taps or neurosurgical procedures to insert external ventricular drains, ventricular access devices, or ventriculosubgaleal shunts (VSGS).

Lumbar punctures and ventricular taps

The use of lumbar puncture for temporization of preterm PHH has been investigated extensively. Most authors describe removal of 10 ml/kg of CSF per lumbar puncture (Kreusser et al., 1985; Robinson, 2012; Leonard and Limbrick, 2015) and 20 ml/kg of CSF is considered to be the maximum volume that should be removed, as larger volumes can be accompanied by apnoea, bradycardia and desaturations (Whitelaw and Aquilina, 2012). There is no evidence that serial lumbar punctures reduce the need for shunt placement or avoid progression of hydrocephalus (Mazzola et al., 2014). Serial multiple percutaneous ventricular taps have been used in the past to temporize PHH, however due to associated complications such as 'puncture porencephaly', infection and encephalomalacia most centres have abandoned their use except as a temporizing measure in a clinically unwell child while waiting for definitive surgical management (Hudgins, 2001; Shooman et al., 2009).

Ventricular access devices (VAD), ventriculosubgaleal shunts (VSGS), and insertion technique

The goal of placing a temporary shunt or access device is to delay the insertion of a permanent shunt until the infant is older and has better nutrition and maturity (Robinson, 2012). The two commonly used options are VAD and ventriculosubgaleal shunts. VAD are made up of a length of ventricular catheter attached to a low-profile reservoir. Once *in situ* they allow percutaneous drainage of ventricular CSF through the scalp. Aspiration of 10 ml/kg of CSF can be performed to maintain a stable condition in the infant. A ventriculosubgaleal shunt is similar to a ventricular access device with the addition of a small segment of distal catheter that is coiled within a subgaleal pocket in the scalp. This has the theoretical advantage of allowing continuous CSF drainage and absorption through the subgaleal pocket and therefore sustained relief of intracranial pressure (ICP), rather than the intermittent diversion provided by access devices. We prefer to temporize infants with a ventriculosubgaleal shunt, although the principles of insertion of an access device are similar (**Fig. 89.3**).

The infant is placed supine, under general anaesthesia. Care is taken to maintain normothermia by the use of an inflatable warming mattress and blankets. A single dose of preoperative antibiotics is given. The head is supported in a neutral position on a jelly head ring (Fig. 89.3A). The scalp is palpated to identify the boundaries of the anterior fontanelle. The midline is marked. A curved skin incision is made so that a small burr hole can be placed in the posteromedial aspect of the frontal bone, just anterior to the coronal suture. The curve of the skin incision should be directed towards the midline so that if the infant were to ultimately have conversion to a VP shunt, shunt hardware would not lie immediately beneath the incision. A right- or left-sided approach can be used and is tailored to the anatomy of the patient seen on preoperative imaging. We prefer to avoid the side with a large clot within it in an attempt to reduce the chances of catheter blockage. An electrocardiogram (ECG) dot is placed in the midline at the nasion so that once the drapes are *in situ* the dot can be palpated to help with orientation (**Fig. 89.3B**).

The skin is then prepped with chlorhexidine solution. Sterile swaps are placed around the operative field and held in place with an opsite sheet to minimize contact with the skin. Surgical drapes are then attached to the opsite and swap construct thus avoiding skin contact with the adhesive on the drapes. The skin is delicate and can tear when the drapes are removed and it also protects the endotracheal tube from being accidentally dislodged when the drapes are removed at the end of the procedure (Fig. 89.3C). The shunt system is then assembled on a separate sterile trolley to that being used by the scrub nurse. A length of ventricular catheter cut to size based on measurements performed preoperatively, with the aim of targeting the catheter so that it sits within the lateral ventricle towards the foramen of Munroe, this is usually in the order of 3–4 cm in length. A piece of distal tubing is cut to a length of approximately 15 cm and four or five small holes are cut into the walls of the tubing to allow the egress of CSF. Both are then connected to a burr hole reservoir

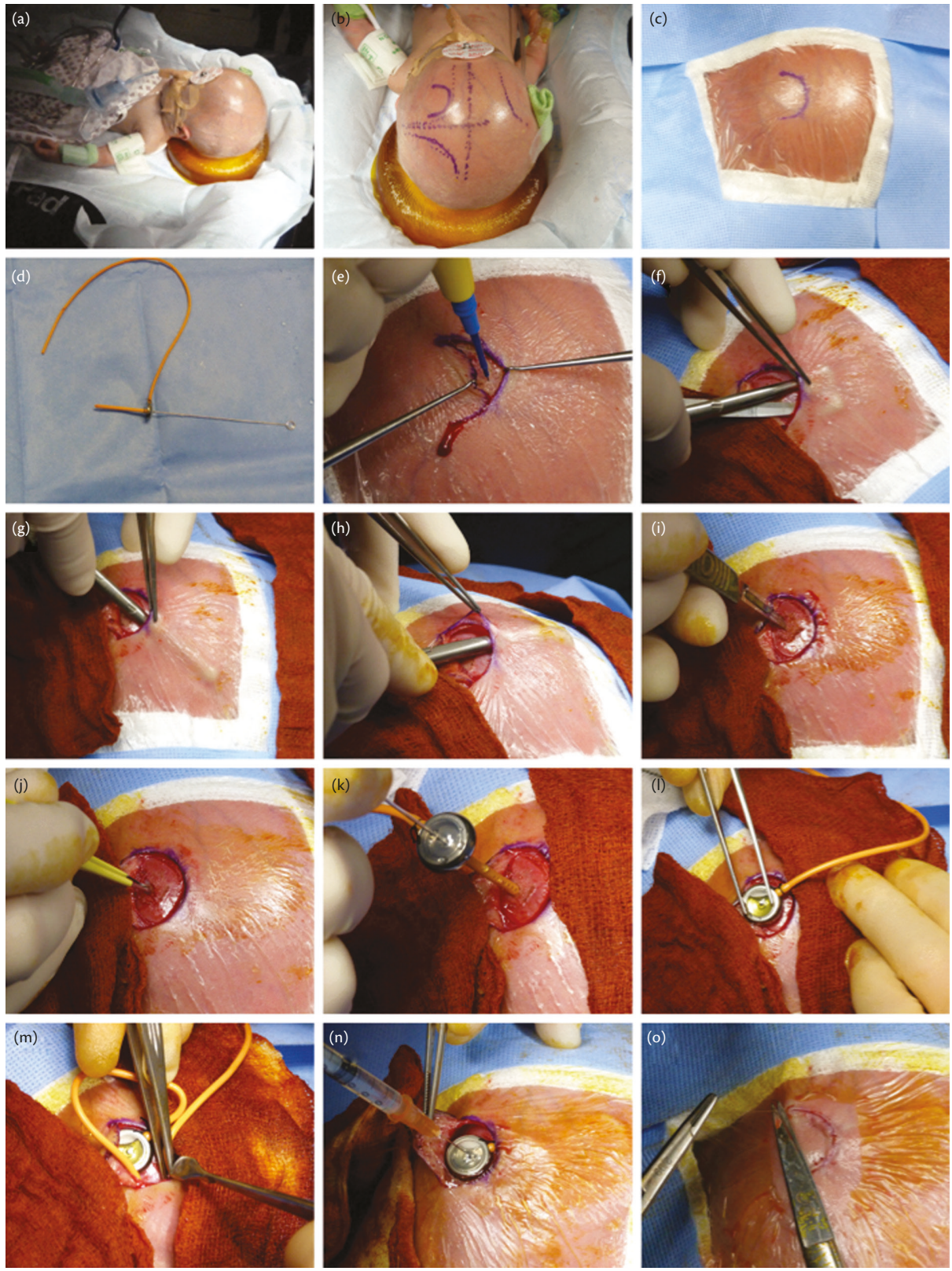

Fig. 89.3 Technique for insertion of a ventriculosubgaleal shunt or ventricular access device.

and secured with silk ties. We then pass the stylet of the ventricular catheter through the reservoir and into the ventricular catheter to facilitate placement and minimize manipulation once the ventricular catheter is *in situ* (Fig. 89.3D).

The skin is cut superficially with a scalpel and the incision is then deepened with monopolar diathermy between skin hooks to minimize blood loss (Fig. 89.3E). The incision is taken through the galea and the scalp flap is reflected and secured with a stay suture. The

pericranium overlying the frontal bone is cut with monopolar diathermy. A large pocket is then created in the subgaleal plane with scissors. Care must be taken to stay in the correct plane to ensure that the anterior fontanelle is not breached. Fibrous adhesions between the galea and the pericranium are divided until one large pocket is produced (**Figs. 89.3F–89.3H**) A 15 blade scalpel is then used in a twisting motion to develop a small burr hole in the frontal bone (**Fig. 89.3I**). This is enlarged with artery forceps. The burr hole need only be large enough to accommodate the diameter of the ventricular catheter. A small nick is made in the dura with a scalpel and the dural edges and cortex are diathermized with bipolar diathermy (**Fig. 89.3J**). The ventricular catheter is then inserted perpendicular to the skull (**Fig. 89.3K**). CSF fills the reservoir confirming entry to the ventricle normally after only a small distance. The stylet is then held still and the ventricular catheter is advanced until the reservoir comes to rest on the skull (**Fig. 89.3L**). A CSF sample is then taken from the system and sent for microbiological analysis (note the xanthochromic CSF in the example). A retractor is used to elevate the subgaleal pocket and the distal tubing is coiled within the pocket (**Fig. 89.3M**). We then instil 5 mg of intrathecal vancomycin into the system via the reservoir prior to closure. (**Fig. 89.3N**) The galea is closed with an absorbable suture (e.g. 4/0 vicryl), and the skin is closed with a similar absorbable continuous suture (**Fig. 89.3O**).

Insertion of a ventricular access device is very similar, the differences being that no distal tubing is attached to the reservoir and no subgaleal pocket is required. We favour ventriculosubgaleal shunts rather than access devices as they require less tapping than access devices (Mazzola et al., 2014) and we feel this reduces the possibility of infection. There is also some evidence that infants treated with VSGS have a reduced need for permanent CSF diversion surgery when compared to patients treated with VADs (Limbrick et al., 2010).

Immediately postoperatively the anterior fontanelle is soft and the profile of the subgaleal shunt tubing is often visible through the scalp. The subgaleal pocket quickly fills with CSF and parents and caregivers should be warned of this preoperatively as the infants often have a marked subgaleal CSF collection. The OFC is monitored daily and the pocket should be examined and palpated. A functioning VSGS will cause a full subgaleal pocket but the cranial sutures should not be splayed, the anterior fontanelle (if palpable) will be soft, and the child will be clinically well.

In infants with a functioning VSG shunt the child will be well, the fontanelle is soft, the cranial sutures are not splayed, and the head circumference should follow rather than cross the centiles. A functioning shunt will create a full, even tense subgaleal pocket; this is normal and indicates the shunt is working.

The majority of infants who have a VAD or VSGS inserted will go on to require permanent CSF diversion, normally with a VP shunt in the first instance. During the postoperative course, the OFC should be monitored and plotted against normal values and the child should be observed for signs of symptomatic hydrocephalus. The subgaleal pocket can be tapped percutaneously if additional CSF drainage is required. Once the child is over term-corrected age and above 2.5 kg they can be considered for a VP shunt if they remain symptomatic. A small proportion of children do not require permanent CSF diversion and can simply be monitored clinically in the outpatient setting. In those patients who do not need further surgery for CSF diversion we remove their subgaleal shunts as an elective procedure at around 2 months corrected age.

Assessment and management of term infants and children with hydrocephalus

Deciding when treatment is indicated

The diagnosis of hydrocephalus can be easy if children present acutely with the classic symptoms and signs of raised intracranial pressure and with ventriculomegaly present on imaging. In such cases the decision to proceed with treatment is straightforward. However, in some cases where there is 'compensated hydrocephalus' the decision to treat can be more difficult, it is not unusual for paediatric neurosurgeons to see relatively well children in clinic who have been found to have ventriculomegaly on imaging. Some patients may have subtle cognitive impairment, behavioural difficulties, or poor school performance, and the decision to intervene can be difficult. Some are seen when they are very young and cognitive impairment may be difficult to detect. Some authors believe that asymptomatic mild or moderate ventriculomegaly does not require treatment (Kalra and Kestle, 2015), but others express concern that children may not reach their developmental potential if they have untreated hydrocephalus. In such cases management strategies include serial imaging to assess for increasing ventricular size and sometimes a period of intracranial pressure monitoring is used to guide the need for intervention.

Radiological ventriculomegaly can be due to hydrocephalus or atrophy of the surrounding brain tissue. The differentiation between these conditions can be difficult. The imaging characteristics that suggest hydrocephalus rather than atrophy include enlargement of the recesses of the third ventricle, dilatation of the temporal horns, periventricular interstitial oedema, and effacement of cortical sulci (Dinçer and Özek, 2011).

Surgical options in the treatment of paediatric hydrocephalus

Since the 1890s the treatment for hydrocephalus has been surgical. In the early twentieth century Dandy and others explored extripication of the choroid plexus and attempted to bypass obstructed CSF pathways using an open craniotomy. This was initially performed through a subfrontal approach and open third ventriculostomy was performed. These early procedures carried high rates of operative morbidity and mortality (10–20%) (Warf, 2014).

CSF shunts

Sixty years ago, silastic tubing and valves were introduced, and surgical treatments shifted towards the diversion of CSF with shunts. Since then most anatomical cavities have been utilized as potential reservoirs or conduits for CSF drainage, CSF shunting has become the standard treatment for hydrocephalus. The commonest type of shunt in use today is the ventriculoperitoneal shunt but other sites are sometimes used, such as the right atrium of the heart (VA shunt) or the pleural cavity. While the introduction of shunts has made a dramatic impact on a previously devastating disease, the complications related to shunts can plague children with hydrocephalus.

External ventricular drains (EVDs) are commonly used for temporary CSF diversion, for example in the presence of infection or haemorrhage, until permanent CSF diversion can be instituted.

Endoscopic third ventriculostomy

In the 1990s improvements in endoscope design led to the development of neuroendoscopic procedures for the treatment of hydrocephalus. Endoscopic third ventriculostomy (ETV) involves the introduction of an endoscope into the frontal horn of the lateral ventricle, through the foramen of Munroe and into the third ventricle. An opening is then made in the floor of the third ventricle under direct vision. This allows CSF to pass into the prepontine cistern bypassing distal obstructions in the CSF pathways (ETV is described in Chapter 93). This technique is now routinely performed in most paediatric neurosurgical centres in high-income countries and allows some patients to be treated without the need for a shunt. ETV is also being used for patients who have previously been treated with a shunt who present with shunt failure (Chhun et al., 2015).

ETV and choroid plexus coagulation

Recently there has been renewed interest in choroid plexus coagulation (CPC) and this has been performed in combination with ETV (Warf, 2005). The technique is performed through a unilateral frontal burr hole using a flexible endoscope. An ETV is performed and then the endoscope is manipulated within the ipsilateral lateral ventricle and the choroid plexus is extensively coagulated along its entire length into the temporal horn. A septum pellucidotomy is then performed, the endoscope is introduced into the opposite lateral ventricle and coagulation of the choroid is repeated on the other side (Warf, 2005). ETV and CPC have predominantly been performed in sub-Saharan Africa but after seeing promising results there are groups in the developed world that are using the technique.

Compared with ETV alone, ETV and CPC has been reported to provide better results in infants (Warf, 2005) and has been shown to be effective in hydrocephalus due to many different aetiologies including aqueduct stenosis and neural tube defects (Warf, 2011; Warf et al., 2012). It appears that the efficacy of this procedure is proportional to the amount of choroid plexus coagulated (Warf et al., 2010). Due to its proximity to critical structures, some surgeons are concerned about the potential long-term effects of coagulation of the choroid plexus. As for many treatments of hydrocephalus knowledge of the effect on neurocognitive outcome is limited although there is some short-term data that shows that the technique has similar cognitive outcomes to VP shunting (Warf et al., 2009).

Selection of the most appropriate treatment modality

Once the diagnosis of hydrocephalus has been made treatment needs to be planned. The clinical urgency of the situation may dictate the extent of any preoperative imaging that has been performed but in the majority of cases in high-income countries it is possible to perform an MRI scan before the need for the first surgical intervention.

Careful analysis of the MRI scan usually enables an assessment of the cause of the hydrocephalus, and specifically the location of any potential obstruction to CSF flow. The presence of a mass lesion (tumour, abscess, cyst, and others) is readily identified on MRI scan and it is possible that removing the mass lesion itself may resolve the hydrocephalus.

With the increased use of endoscopic techniques appraisal of the imaging is critically important. If a point of obstruction is identified it may be possible to bypass the obstruction using an endoscopic technique, thus avoiding a shunt. Many paediatric neurosurgeons consider this to be preferable due to the long-term implications of maintenance and complications associated with shunts.

The choice between ETV and shunts is controversial and there are currently no completed randomized controlled trials that compare the two treatment options. When ETV and shunts are compared this is normally done by comparing the failure rates of each procedure, which is the time until further surgery is performed. In unselected cohorts the failure rates of ETV at 2 years is about 35% (Kulkarni et al., 2010a; Kahle et al., 2015). Prognostic factors include patient age and the aetiology of the hydrocephalus. These are included in the ETV success score which is a useful, validated tool that allows an estimation of the potential success rates of ETV in different patients (**Table 89.2**) (Kulkarni et al., 2010b). Our approach to a patient with symptomatic hydrocephalus is summarized in **Figure 89.4**.

To calculate the endoscopic third ventriculostomy success score (ETVSS), add the three component scores to get a percentage chance of an ETV being successful.

All patients should have volume imaging, normally MRI, for use with neuronavigation. Preterm infants under 2 kg are treated with ventriculosubgaleal shunts. In term infants and children where an obstruction is identified on preoperative imaging and the anatomy appears favourable for an endoscopic procedure we consider ETV.

Table 89.2 Calculation of the ETVSS score

Age	Score
<1 month	0
1–6 months	10
6–12 months	30
1–9 years	40
10 years or more	50
Aetiology	**Score**
Infection	0
Myelomengocele	20
IVH	20
Non-tectal brain tumour	20
Aqueduct stenosis	30
Tectal tumour	30
Other	30
Previous shunt	**Score**
Previous shunt	0
No previous shunt	10

Source data from Kulkarni, A.V. et al. Predicting who will benefit from endoscopic third ventriculostomy compared with shunt insertion in childhood hydrocephalus using the ETV Success Score. *J. Neurosurg. Pediatr.* 6, 310–15 (2010).

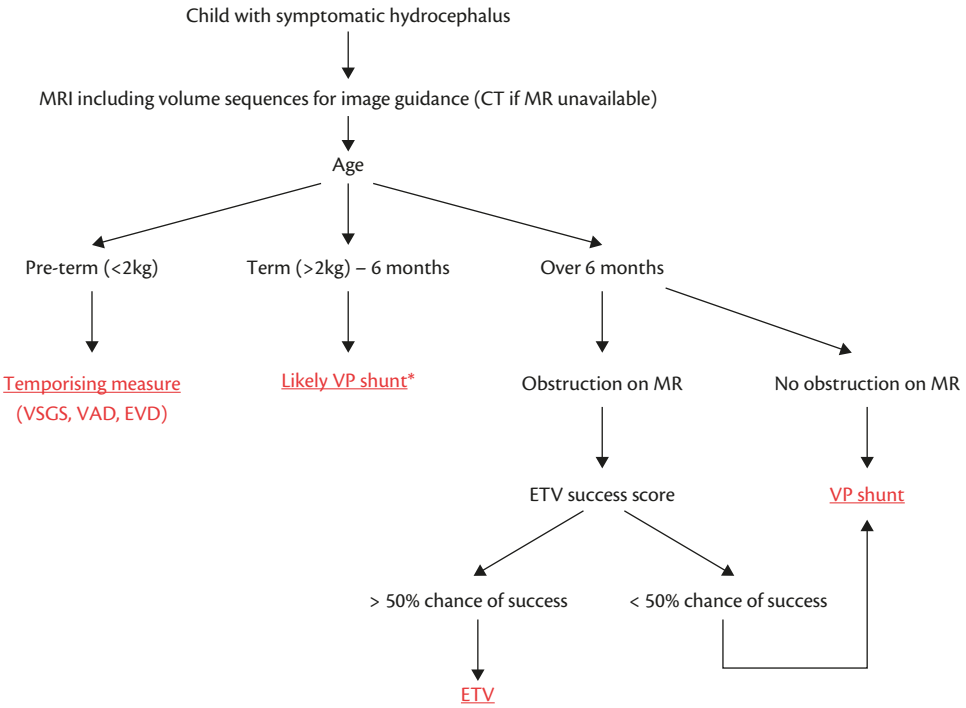

Fig. 89.4 Treatment algorithm for the management of symptomatic hydrocephalus.

Term infants over 2 kg but under 6 months of age are normally treated with a VP shunt due to the poor success rate of ETV in this age group but in some circumstances for example where children have intra-abdominal comorbidities or cranial arachnoid cysts ETV may be offered.

In those over 6 months, if evidence of obstruction is present on MR we perform an ETV success score and if the chances of success are greater than 50% ETV is performed as a primary treatment. In those where there are no obstructive features on MR or when the chance of ETV success is less than 50%, a shunt would be performed in the majority of cases. If patients represent with shunt failure in the future then ETV would be reconsidered.

Inserting a ventriculoperitoneal shunt

VP shunt insertion has one of the highest failure rates of any neurosurgical procedure and should be performed by a trained and efficient team. When a shunt actuarial survival curve is examined up to 20% of shunts are seen to fail in the first 6 months. Early shunt failures are predominantly due to infection, occlusion of catheters through suboptimal placement or migration of the shunt components secondary to disconnection. Surgeons have the opportunity to reduce the incidence of these early shunt failures, but shunt surgery is unforgiving of technical errors.

Figure 89.5, which accompanies the following description, is of a VP shunt insertion in a neonate but the steps of the procedure are similar for shunts in children of all ages. Shunt surgery should be performed by an appropriately trained team, shunts should ideally be the first case of the day and to minimize the infection risk movement around, in, and out of the operating theatre by personnel should be kept to an absolute minimum. We place signs on the doors of the operating theatre and apart from the emergency exits keep theatre doors locked (Fig. 89.5C). Current National Institute of Clinical Excellence (NICE) guidelines recommend that patients are showered or bathed with soap prior to surgery. Many studies have looked at the effectiveness of chlorhexidine-based body washes in reducing surgical site infection, currently effectiveness in reducing surgical site infection (SSI) is uncertain, although studies have demonstrated a reduction in bacterial skin levels (National Collaborating Centre for Women's and Children's Health, 2008). We treat all patients with chlorhexidine body wash and shampoo the day before and the morning of surgery and have found that since introduction of this, we have significantly reduced our surgical site infection rates.

Under general anaesthesia with endotracheal intubation and the tube directed to the contralateral side to the shunt, the patient is positioned supine on the operating table with the head supported on a jelly head ring for infants or the Mayfield horseshoe headrest for children over 2 years old. The head is turned towards the contralateral side and a roll is placed under the shoulder so that the chest wall is raised and there is a straight trajectory from the cranial incision to the abdominal incision to facilitate tunnelling (Fig. 89.5A). In neonates and infants it is often necessary to use a large chest roll to elevate the chest due to the large head size relative to the body in this age group. Patient normothermia is important, especially in neonates and infants (National Collaborating Centre for Women's and Children's Health, 2008) and we routinely use warm air flow mattresses to assist with this (Fig. 89.5A).

Intravenous antibiotics are given on induction as they reduce surgical site (National Collaborating Centre for Women's and Children's Health, 2008) and VP shunt infections (Klimo et al., 2014). A small amount of hair may be clipped at the incision sites to aid quality of closure although hair removal has not been shown to decrease the risk of infection (National Collaborating Centre for Women's and

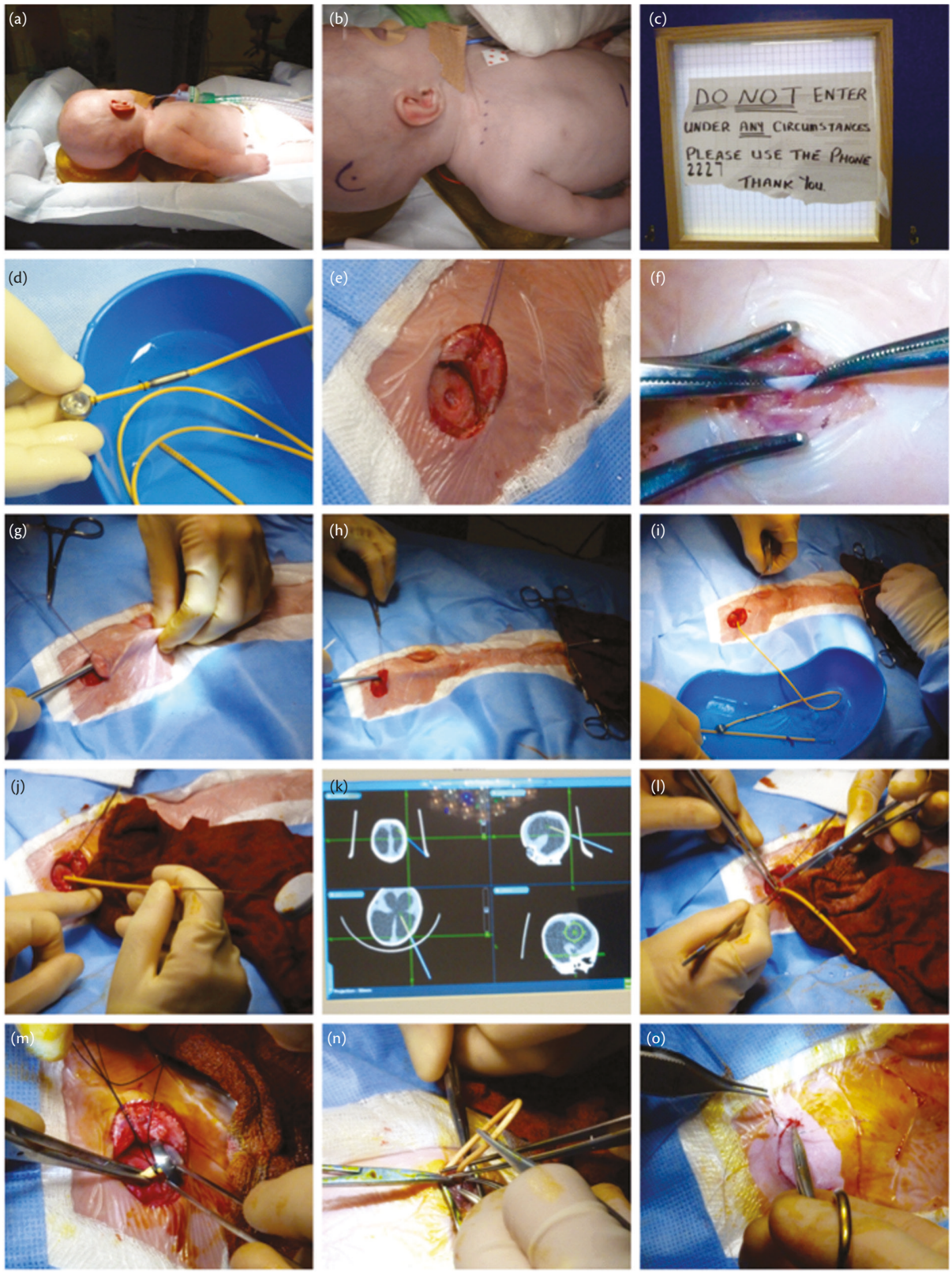

Fig. 89.5 Insertion of a ventriculoperitoneal shunt.

Children's Health, 2008). Frontal and parieto-occipital burr holes are the most commonly used entry sites for the ventricular catheter. Either route is acceptable and a recent systematic review found no evidence to recommend one route over the other (Kemp et al., 2014). Frontal burr holes are normally placed 2–3 cm off the midline 1 cm anterior to the coronal suture, parieto-occipital burr holes are placed 2–3 cm above and 2–3 cm posterior to the pinna, although if image guidance is used these entry points may vary based on the

patient's preoperative imaging. The preoperative imaging should be studied as some children with posterior fossa cysts or other malformations have transverse sinuses that are located much higher than usual, in which case a parieto-occipital entry point must be planned and adjusted accordingly. Cranial and abdominal skin incisions are marked (**Fig. 89.5B**).

The skin is meticulously prepared with an appropriate skin prep. We use a chlorhexidine-based solution in all age groups. The boundaries of the operative field are defined by large sterile swabs and an opsite cover is used to hold these in place. The surgical drapes are then attached to the swab and opsite construct, so the adhesive is not attached directly to the patient's skin. The shunt is assembled on a separate trolley to that used by the scrub nurse (**Fig. 89.5D**). There is currently no evidence that one valve design is superior to another (Baird et al., 2014). We use a low-profile fixed pressure valve as our standard valve (Miethke Paedigav) and reserve programmable valves for complex cases. Chapter 93 gives more information on valve design.

The skin incisions are opened. We score the skin with a scalpel blade and then deepen the incision through the galea with monopolar diathermy to minimize blood loss. Skin incisions should be shaped so that there is no shunt hardware immediately beneath the incision to minimize the risk of skin breakdown leading to the shunt becoming exposed. A high-speed drill is used to produce a small burr hole (**Fig. 89.5E**). The abdomen is opened simultaneously by an assistant. Various entry points in to the abdomen are described. We use a linear incision off the midline between the umbilicus and the costal margin. Dissection is taken down to the anterior rectus sheath that is opened. The fibres of the rectus muscle are split and the posterior rectus sheath and peritoneum are picked up with clips (**Fig. 89.5F**). This layer is then divided and entry to the peritoneal cavity is confirmed by the passage of a blunt instrument in to the cavity or through direct visualization of omentum or bowel.

A shunt passer is then tunnelled through the subcutaneous fat from one incision to the other (**Figs. 89.5G** and **89.5H**). Great care must be taken to ensure that the tunnelling is not taken too deep as either the chest cavity or posterior fossa can be entered. If too superficial a skin laceration can occur. A release incision is sometimes necessary in the neck if significant resistance is felt. If tunnelling to a frontal burr hole an incision behind the ear is required and tunnelling is performed in two steps. The peritoneal tubing is then passed down the shunt tunneller and the tunneller is removed from one of the incisions (**Fig. 89.5I**). The tubing is pulled and the distal end coiled in a swab soaked in aqueous betadine solution. The valve (and reservoir if used) are wrapped in a swab soaked in aqueous betadine at the cranial end while the ventricular catheter is sited.

There is evidence that ventricular catheters with resting places away from the ventricular wall and choroid plexus have a lower tendency to block and most surgeons will have experience of ventricular catheters located in suboptimal locations. Various technical adjuncts are described to improve the position of ventricular catheter placement in an attempt to improve the longevity of VP shunts including intraoperative ultrasound (Whitehead et al., 2007) and frameless stereotaxy with electromagnetic (EM) or optical guidance systems. Endoscopic placement of ventricular catheters has not been shown to improve shunt longevity (Kestle et al., 2003; Kestle, 2010). We use EM guidance for the majority of ventricular catheter placements as it improves the position of ventricular catheters (Hayhurst et al., 2010; Levitt et al., 2012) and may therefore improve shunt longevity (Hayhurst et al., 2010). For this the stylet is removed from the ventricular catheter and is replaced with the EM stylet. A small dural opening is made with a scalpel and the cortical surface is diathermized. The ventricular catheter is aligned using a navigation system (**Figs. 89.5J** and **89.5K**) and inserted along the trajectory. A 'pop' is usually felt as the catheter enters the ventricle and entry is confirmed by the free passage of CSF from the catheter. A sample of CSF is routinely taken for microbiological analysis. The ventricular catheter is then cut to a length that has been predetermined based on the preoperative imaging (**Fig. 89.5L**), and the catheter is connected to the reservoir or valve. We use a reservoir with a right-angle connection, alternatively a right-angle guide can be used with an in-line valve. It is also acceptable to simply bend the catheter, but it should be noted that in children with a thin cortical mantle the catheter may move so that it reaches an almost vertical orientation. The valve is then seated within its subgaleal pocket by gentle traction on the distal catheter from below and the ventricular catheter is secured to the reservoir with a silk tie (**Fig. 89.5M**). CSF is confirmed to be dripping from the distal tubing before the distal catheter is placed into the peritoneal cavity.

Accurate skin closure is critical as any leakage of CSF can lead to infection and increases the risk of skin breakdown. The galea and skin are closed separately. We use an absorbable suture for both. Likewise, the anterior rectus sheath and abdominal skin incision are closed with absorbable sutures. Dressings are then applied and left *in situ* for 48 hours.

In uncomplicated cases patients are observed for a period of 2–3 days before being discharged home. We do not use postoperative antibiotics routinely. If wounds require cleaning before 48 hours post-op this is performed with sterile saline. After 48 hours patients are advised to keep the wounds clean and can shower if they wish in accordance with the current NICE guidelines on surgical site infection (National Collaborating Centre for Women's and Children's Health, 2008). We see patients to check on the status of the wounds within two weeks. Outpatient follow-up is performed within 2 months along with a postoperative scan to assess the position of the ventricular catheter and the size of the ventricles. We also perform a scan between 12 and 18 months to serve as a baseline for future reference as data from the shunt design trial showed that ventricular size continues to decrease after 3 months, but stabilizes by about 14 months (Drake et al., 1998). The early postoperative scan is valuable, however, due to the high rates of shunt failure within the first year. Patients are then followed up on an outpatient basis for life, initially every 6 months, then annually, and in some cases, every two years. We do not routinely repeat imaging outside these schedules unless patients develop symptoms.

Complications of VP shunts

Parenchymal haemorrhage related to ventricular catheter insertion is reported to occur in between 1 and 4% of catheter placements (Savitz and Bobroff, 1999; Kalra and Kestle, 2015). Most of these haemorrhages are asymptomatic (Savitz and Bobroff, 1999) but they have potential to cause neurological deficit, depending upon the location of the haemorrhage.

Injury to abdominal or thoracic organs can occur during placement of a VP shunt. Shunt tubing has been reported to erode through

visceral walls, perforations of the stomach, small and large bowel, bladder, and uterus have all been reported (Wong et al., 2012).

VP shunts have high failure rates with 40% of children requiring further intervention in the first 2 years after their first shunt insertion (Kulkarni et al., 2013; Kahle et al., 2015). The majority of these failures are due to shunt obstruction. Other causes of failure are infection, disconnection, migration, fracture, and overdrainage. Failure rates are higher in younger children with patients under 2 years being at highest risk (Kalra and Kestle, 2015).

The commonest site for shunt obstruction is the ventricular catheter, accounting for 63% of cases of obstruction in one study (Di Rocco et al., 1994) although the shunt can block anywhere along its length. Proximal catheter blockages are most commonly due to the presence of choroid plexus within the ventricular catheter lumen. Valve blockages tend to occur very early after shunt insertion or revision and this is likely to be due to debris or blood from surgery (Kalra and Kestle, 2015). Patients with VP shunt failure often present with symptoms of raised ICP and imaging that demonstrates increasing ventricular size. Shunt obstruction is treated with urgent surgery to replace the blocked component. In some patients shunt failure is more subtle and a period of ICP monitoring may be indicated prior to shunt revision.

Patients who experience shunt infection have approximately twice the risk of death and undergo three times the number of shunt-related procedures as those who do not develop infection (Schoenbaum et al., 1975; Wong et al., 2012). Mortality from shunt infection is in the region of 10% and in the long term those who have suffered this complication have poorer outcomes in terms of cognition and school performance (Vinchon and Dhellemmes, 2006). Shunt infection occurs in between 3% and 12% of shunt procedures and most cases occur within 3 months of surgery (Kulkarni et al., 2001). Symptoms include pyrexia, malaise, and irritability, redness over the shunt hardware and headache. A shunt tap can confirm the diagnosis. Positive CSF analysis shows a raised white cell count with organisms seen on microscopy, and positive CSF cultures. Less commonly shunt infection can present with an abdominal pseudocyst with symptoms of shunt malfunction and abdominal pain.

The commonest pathogens in shunt infection are skin commensal organisms such as coagulase negative *Staphylococcus* and *S. aureus* species (Thompson and Hartley, 2014; Kahle et al., 2015). Infection can occur when a shunt, the CSF, or the wound becomes contaminated and this may occur at the time of surgery, through the wound in the immediate postoperative period or through direct contiguous spread such as in abdominal infection (Thompson and Hartley, 2014). If shunt infection is confirmed the majority of neurosurgeons remove the affected shunt hardware and insert an EVD. Patients are treated with intravenous and sometimes intrathecal antibiotics until the CSF is sterile at which time the shunt may be internalized or an endoscopic procedure may be considered.

Shunt overdrainage can present acutely with extra-axial fluid collections, or chronically as the slit ventricle syndrome. As the ventricles reduce in size following VP shunt insertion extra-axial fluid or blood can accumulate. This is more common in older children who have large ventricles. Programmable valves, set to a high resistance may be used to treat this or in high risk cases, to prevent it occurring. If extra-axial collections do develop management can be difficult. Strategies involve reducing the overdrainage and sometimes draining the extra-axial collections. Valve replacement with a valve with a higher opening pressure or insertion of an antisyphon device can be performed. Once the overdrainage has been reduced consideration can be given to draining the extra-axial collections through an appropriately positioned burr hole.

Slit ventricle syndrome

Headaches are common in children with VP shunts. Some children develop very small ventricles following VP shunt insertion and in association with headaches may be labelled as having slit ventricle syndrome. There is no consistent, precise definition of the syndrome in the literature but typically these children have had a shunt for several years and their ventricles have become very small (Kalra and Kestle, 2015). Slit ventricle syndrome is caused by a chronically overdraining shunt, where the skull is too small for the brain. Brain compliance is reduced and therefore raised CSF pressure does not cause ventricular dilatation.

Children may present with symptoms of chronic low-pressure headaches, or with cyclical headaches suggestive of raised intracranial pressure. Options for treating these patients are controversial and include intracranial pressure monitoring, revising the shunt or changing to a programmable or flow regulated valve, and cranial vault expansion using subtemporal decompression (Kahle et al., 2015).

Long-term outcomes for children with hydrocephalus

Most children who are treated with shunts require shunt revision at some point in their lives. One long-term study found that 32% of patients required between one and three shunt revisions, and a further 52% required four or more revisions. Some 29% of patients reported either one or two shunt infections. Up to 70% of patients reported symptoms of depression and up to 45% needed treatment. The majority of adult patients were single and only a quarter of female patients reported having children. Up to 40% of adult patients were dependent with respect to living arrangements (Gupta et al., 2007).

Cognitive outcomes in patients with hydrocephalus are predominantly dependent on the cause of the hydrocephalus and any associated brain abnormalities or primary brain injury. For example, children with isolated aqueduct stenosis have near normal cognitive profiles (Kahle et al., 2015), whereas patients with IVH of prematurity have much higher rates of impairment. Reduced intelligence, learning, memory, and executive functioning can be present (Kahle et al., 2015). Epilepsy is common and has a significant impact on quality of life for patients and their families.

FURTHER READING

Dandy, W.E. (1919). Experimental hydrocephalus. *Ann Surg*, **70**, 129–42.

Di Rocco, C., Marchese, E., & Velardi, F. (1994). A survey of the first complication of newly implanted CSF shunt devices for the treatment of nontumoral hydrocephalus. Cooperative survey of the

1991–1992 Education Committee of the ISPN. *Childs Nerv Syst*, **10**, 321–7.
Kulkarni, A.V., Drake, J.M., Kestle, J., & Malucci, C. (2010b). Predicting who will benefit from endoscopic third ventriculostomy compared with shunt insertion in childhood hydrocephalus using the ETV Success Score. *J Neurosurg Pediatr*, **6**, 310–15.
Rekate, H.L. (2011). A consensus on the classification of hydrocephalus: its utility in the assessment of abnormalities of cerebrospinal fluid dynamics. *Childs Nerv Syst*, **27**, 1535–41.
Robinson, S. (2012). Neonatal posthemorrhagic hydrocephalus from prematurity: pathophysiology and current treatment concepts. *J Neurosurg Pediatr*, **9**, 242–58.

REFERENCES

Abou-Hamden, A. & Drake, J.M. (2015). Hydrocephalus. In: Albright, A.L., Pollack, I.F., & Adelson, P.D. (eds.) *Principles and Practice of Pediatric Neurosurgery*, pp. 89–99. New York, NY: Thieme Publishers.
Baird, L.C., Mazzola, C.A., Auguste, K.I., Klimo, P., & Flannery, A.M. (2014). Pediatric hydrocephalus: systematic literature review and evidence-based guidelines. Part 5: effect of valve type on cerebrospinal fluid shunt efficacy. *J Neurosurg Pediatr*, **14** Suppl 1, 35–43.
Blackburn, B.L. & Fineman, R.M. (1994). Epidemiology of congenital hydrocephalus in Utah, 1940–1979: report of an iatrogenically related 'epidemic'. *Am J Med Genet* **52**, 123–9.
Boop, F.A. (2005). Posthemorrhagic hydrocephalus of prematurity. In: Cinalli, G., Maixner, W.J., & Sainte-Rose, C. (eds.) *Pediatric Hydrocephalus*, pp. 122–31. Milan, Italy: Springer-Verlag Italia.
Chhun, V., Sacko, O., Boetto, S., & Roux, F.-E. (2015). Third ventriculocisternostomy for shunt failure. *World Neurosurg*, **83**, 970–5.
Dandy, W.E. (1919). Experimental hydrocephalus. *Ann Surg*, **70**, 129–42.
Detwiler, P.W., Porter, R.W., & Rekate, H.L. (1999). Hydrocephalus—clinical features and mnagement. In: Choux, M., Di Rocco, C., Hockley, A., & Walker, M.L. (eds.) *Pediatric Neurosurgery*, pp. 253–74. Churchill Livingstone.
Di Rocco, C., Marchese, E., & Velardi, F. (1994). A survey of the first complication of newly implanted CSF shunt devices for the treatment of nontumoral hydrocephalus. Cooperative survey of the 1991–1992 Education Committee of the ISPN. *Childs Nerv Syst*, **10**, 321–7.
Dinçer, A. & Özek, M.M. (2011). Radiologic evaluation of pediatric hydrocephalus. *Childs Nerv Syst*, **27**, 1543–62.
Drake, J.M., Kestle, J.R., Milner, R., et al. (1998). Randomized trial of cerebrospinal fluid shunt valve design in pediatric hydrocephalus. *Neurosurgery*, **43**, 294–5.
du Plessis, A.J. (2009). The role of systemic hemodynamic disturbances in prematurity-related brain injury. *J Child Neurol*, **24**, 1127–40.
Gupta, N., Park, J., Solomon, C., Kranz, D.A., Wrensch, M., & Wu, Y.W. (2007). Long-term outcomes in patients with treated childhood hydrocephalus. *J Neurosurg*, **106**, 334–9.
Hayhurst, C., Beems, T., Jenkinson, M.D., et al. (2010). Effect of electromagnetic-navigated shunt placement on failure rates: a prospective multicenter study. *J Neurosurg*, **113**, 1273–8.
Hislop, J.E., Dubowitz, L.M., Kaiser, A.M., Singh, M.P., & Whitelaw, A.G. (1988). Outcome of infants shunted for post-haemorrhagic ventricular dilatation. *Dev Med Child Neurol*, **30**, 451–6.
Hudgins, R.J. (2001). Posthemorrhagic hydrocephalus of infancy. *Neurosurg Clin N Am* **12**, 743–51, ix.
Jeng, S., Gupta, N., Wrensch, M., Zhao, S., & Wu, Y.W. (2011). Prevalence of congenital hydrocephalus in California, 1991–2000. *Pediatr Neurol*, **45**, 67–71.
Kahle, K.T., Kulkarni, A.V, Limbrick, D.D., & Warf, B.C. (2015). Hydrocephalus in children. *Lancet*, **387**(10020), 788–99.
Kalra, R.R.S. & Kestle, J. (2015). Treatment of hydrocephalus with shunts. In: Albright, A.L., Pollack, I.F., & Adelson, P.D. (eds.) *Principles and Practice of Pediatric Neurosurgery*, pp. 100–18. New York, NY: Thieme Publishers.
Kandasamy, J., Jenkinson, M.D., & Mallucci, C.L. (2011). Contemporary management and recent advances in paediatric hydrocephalus. *BMJ*, **343**, d4191.
Kemp, J., Flannery, A.M., Tamber, M.S., & Duhaime, A.-C. (2014). Pediatric hydrocephalus: systematic literature review and evidence-based guidelines. Part 9: effect of ventricular catheter entry point and position. *J Neurosurg Pediatr*, **14** Suppl 1, 72–6.
Kestle, J.R.W., Drake, J.M., Cochrane, D.D., et al. (2003). Lack of benefit of endoscopic ventriculoperitoneal shunt insertion: a multicenter randomized trial. *J Neurosurg*, **98**, 284–90.
Kestle, J.R.W. (2010). Clinical trials in hydrocephalus: what have we learned? In: Mallucci, C.L. & Sgouros, S. (eds.) *Cerebrospinal Fluid Disorders*, pp. 488–9. London, UK: Informa Healthcare.
Klimo, P., Van Poppel, M., Thompson, C.J., et al. (2014). Pediatric hydrocephalus: systematic literature review and evidence-based guidelines. Part 6: preoperative antibiotics for shunt surgery in children with hydrocephalus: a systematic review and meta-analysis. *J Neurosurg Pediatr*, **14** Suppl 1, 44–52.
Koral, K., Blackburn, T., Bailey, A.A., Koral, K.M., & Anderson, J. (2012). Strengthening the argument for rapid brain MR imaging: estimation of reduction in lifetime attributable risk of developing fatal cancer in children with shunted hydrocephalus by instituting a rapid brain MR imaging protocol in lieu of Head CT. *AJNR Am J Neuroradiol*, **33**, 1851–4.
Kreusser, K.L., Tarby, T.J., Kovnar, E., Taylor, D.A., Hill, A., & Volpe, J.J. (1985). Serial lumbar punctures for at least temporary amelioration of neonatal posthemorrhagic hydrocephalus. *Pediatrics* **75**, 719–24.
Krishnamurthy, S., Schmidt, B., & Tichenor, M.D. (2013). Radiation risk due to shunted hydrocephalus and the role of MR imaging-safe programmable valves. *AJNR Am J Neuroradiol*, **34**, 695–7.
Kulkarni, A.V., Drake, J.M., Kestle, J.R., et al. (2010a). Endoscopic third ventriculostomy vs cerebrospinal fluid shunt in the treatment of hydrocephalus in children: a propensity score-adjusted analysis. *Neurosurgery*, **67**, 588–93.
Kulkarni, A.V., Riva-Cambrin, J., Butler, J., et al. (2013). Outcomes of CSF shunting in children: comparison of Hydrocephalus Clinical Research Network cohort with historical controls: clinical article. *J Neurosurg Pediatr*, **12**, 334–8.
Kulkarni, A.V., Drake, J.M., Kestle, J., & Malucci, C. (2010b). Predicting who will benefit from endoscopic third ventriculostomy compared with shunt insertion in childhood hydrocephalus using the ETV Success Score. *J Neurosurg Pediatr*, **6**, 310–15.
Kulkarni, A.V, Drake, J.M., & Lamberti-Pasculli, M. (2001). Cerebrospinal fluid shunt infection: a prospective study of risk factors. *J Neurosurg*, **94**, 195–201.
Laurence, K.M. & Coates, S. (1962). The natural history of hydrocephalus. Detailed analysis of 182 unoperated cases. *Arch Dis Child*, **37**, 345–62.
Leonard, J.L. & Limbrick, D.D. (2015). Ntraventricular hemorrhage and post-hemorrhagic hydrocepalus. In: Albright, A.L., Pollack, I.F., & Adelson, P.D. (eds.) *Principles and Practice of Pediatric Neurosurgery*, pp. 137–44. New York, NY: Thieme Publishers.

Levitt, M.R., O'Neill, B.R., Ishak, G.E., et al. (2012). Image-guided cerebrospinal fluid shunting in children: catheter accuracy and shunt survival. *J Neurosurg Pediatr*, **10**, 112–17.

Limbrick, D.D., Mathur, A., Johnston, J.M., et al. (2010). Neurosurgical treatment of progressive posthemorrhagic ventricular dilation in preterm infants: a 10-year single-institution study. *J Neurosurg Pediatr*, **6**, 224–30.

Mazzola, C.A., Choudhri, A.F., Auguste, K.I., et al. (2014). Pediatric hydrocephalus: systematic literature review and evidence-based guidelines. Part 2: management of posthemorrhagic hydrocephalus in premature infants. *J Neurosurg Pediatr*, **14** Suppl 1, 8–23.

Murphy, B.P., Inder, T.E., Rooks, V., et al. (2002). Posthaemorrhagic ventricular dilatation in the premature infant: natural history and predictors of outcome. *Arch Dis Child Fetal Neonatal Ed*, **87**, F37–41 (2002).

National Collaborating Centre for Women's and Children's Health (2008). *Surgical Site Infection: Prevention and Treatment of Surgical Site Infection*. Nursing standard Royal College of Nursing (Great Britain) **27**.

Oi, S. (2011). Classification of hydrocephalus: critical analysis of classification categories and advantages of 'multi-categorical Hydrocephalus Classification' (Mc HC). *Childs Nerv Syst*, **27**, 1523–33.

Orešković, D. & Klarica, M. (2011). Development of hydrocephalus and classical hypothesis of cerebrospinal fluid hydrodynamics: facts and illusions. *Prog Neurobiol*, **94**, 238–58.

Persson, E.-K., Anderson, S., Wiklund, L.-M., & Uvebrant, P. (2007). Hydrocephalus in children born in 1999–2002: epidemiology, outcome and ophthalmological findings. *Childs Nerv Syst*, **23**, 1111–18.

Persson, E.-K., Hagberg, G., & Uvebrant, P. (2005). Hydrocephalus prevalence and outcome in a population-based cohort of children born in 1989–1998. *Acta Paediatr*, **94**, 726–32.

Rekate, H.L. (2001). Hydrocephalus. In: McLone, D.G. (ed.) *Pediatric Neurosurgery: Surgery of the Developing Nervous System*, pp. 457–74. W.B. Saunders, 2001.

Rekate, H.L. (2008a). Shunt-related headaches: the slit ventricle syndromes. *Childs Nerv Syst*, **24**, 423–30.

Rekate, H.L. (2008b). The definition and classification of hydrocephalus: a personal recommendation to stimulate debate. *Cerebrospinal Fluid Res*, **5**, 2.

Rekate, H.L. (2011). A consensus on the classification of hydrocephalus: its utility in the assessment of abnormalities of cerebrospinal fluid dynamics. *Childs Nerv Syst*, **27**, 1535–41.

Richards, H. (2010). In: Mallucci, C. & Sgouros, S. (eds.) *Cerebrospinal Fluid Disorders*, pp. 494–5. Informa Healthcare USA.

Robinson, S. (2012). Neonatal posthemorrhagic hydrocephalus from prematurity: pathophysiology and current treatment concepts. *J Neurosurg Pediatr*, **9**, 242–58.

Savitz, M.H. & Bobroff, L.M. (1999). Low incidence of delayed intracerebral hemorrhage secondary to ventriculoperitoneal shunt insertion. *J Neurosurg*, **91**, 32–4.

Schoenbaum, S.C., Gardner, P., & Shillito, J. (1975). Infections of cerebrospinal fluid shunts: epidemiology, clinical manifestations, and therapy. *J Infect Dis*, **131**, 543–52.

Shooman, D., Portess, H., & Sparrow, O. (2009). A review of the current treatment methods for posthaemorrhagic hydrocephalus of infants. *Cerebrospinal Fluid Res*, **6**, 1.

Stone, S.S.D. & Warf, B.C. (2014). Combined endoscopic third ventriculostomy and choroid plexus cauterization as primary treatment for infant hydrocephalus: a prospective North American series. *J Neurosurg Pediatr*, **14**, 439–46.

Thompson, D.N.P. & Hartley, J. (2014). Shunt infections. In: Albright, A.L., Pollack, I.F., & Adelson, P.D. (eds.) *Principles and Practice of Pediatric Neurosurgery*, p. 1010. New York, NY: Thieme Publishers.

Tully, H.M., Capote, R.T., & Saltzman, B.S. (2015). Maternal and infant factors associated with infancy-onset hydrocephalus in Washington State. *Pediatr Neurol*, **52**, 320–5.

Vassilyadi, M., Tataryn, Z., Shamji, M.F., & Ventureyra, E.C.G. (2009). Functional outcomes among premature infants with intraventricular hemorrhage. *Pediatr Neurosurg*, **45**, 247–55.

Vinchon, M. & Dhellemmes, P. (2006). Cerebrospinal fluid shunt infection: risk factors and long-term follow-up. *Childs Nerv Syst*, **22**, 692–7.

Warf, B.C. (2005). Comparison of endoscopic third ventriculostomy alone and combined with choroid plexus cauterization in infants younger than 1 year of age: a prospective study in 550 African children. *J Neurosurg*, **103**, 475–81.

Warf, B.C. (2011). Hydrocephalus associated with neural tube defects: characteristics, management, and outcome in sub-Saharan Africa. *Childs Nerv Syst*, **27**, 1589–94.

Warf, B.C., Alkire, B.C., Bhai, S., et al. (2011). Costs and benefits of neurosurgical intervention for infant hydrocephalus in sub-Saharan Africa. *J Neurosurg Pediatr*, **8**, 509–21.

Warf, B.C. (2014). Three steps forward and 2 steps back. *Neurosurgery*, **61**, 105–10.

Warf, B.C., Mugamba, J., & Kulkarni, A.V. (2010). Endoscopic third ventriculostomy in the treatment of childhood hydrocephalus in Uganda: report of a scoring system that predicts success. *J Neurosurg Pediatr*, **5**, 143–8.

Warf, B.C., Tracy, S., & Mugamba, J. (2012). Long-term outcome for endoscopic third ventriculostomy alone or in combination with choroid plexus cauterization for congenital aqueductal stenosis in African infants. *J Neurosurg Pediatr*, **10**, 108–11.

Warf, B., Ondoma, S., Kulkarni, A., et al. (2009). Neurocognitive outcome and ventricular volume in children with myelomeningocele treated for hydrocephalus in Uganda. *J Neurosurg Pediatr*, **4**, 564–70.

Whitehead, W.E., Jea, A., Vachhrajani, S., Kulkarni, A.V., & Drake, J.M. (2007). Accurate placement of cerebrospinal fluid shunt ventricular catheters with real-time ultrasound guidance in older children without patent fontanelles. *J Neurosurg*, **107**, 406–10.

Whitelaw, A. & Aquilina, K. (2012). Management of posthaemorrhagic ventricular dilatation. *Arch Dis Child Fetal Neonatal Ed*, **97**, F229–3.

Wong, J.M., Ziewacz, J.E., Ho, A.L., et al. (2012). Patterns in neurosurgical adverse events: cerebrospinal fluid shunt surgery. *Neurosurg Focus*, **33**, E13.

RELATED LINKS TO EBRAIN

Aetiology and Pathophysiology of Hydrocephalus. https://learning.ebrain.net/course/view.php?id=584

Management Principles of Hydrocephalus. https://learning.ebrain.net/course/view.php?id=525

90

Paediatric neurovascular disorders

Helen G. McCullagh, Tufail Patankar, Tony Goddard, and Atul Tyagi

Introduction

The spectrum of paediatric neurovascular disorders includes several conditions like AVM, aneurysm, and cavernous malformations that occur in adults. Despite the similarity in pathology there are differences in presentation, location, and management of vascular disorders in children as compared to adults. There are disorders that are peculiar to the paediatric population like vein of Galen malformations or intraventricular haemorrhage in premature infants and others that occur predominantly in children though are seen in adults such as the Moyamoya disease.

Recent advances in endovascular therapy, radiosurgery, and multimodality management of vascular lesions have increased the options available to manage these lesions in children.

Identification of underlying gene abnormalities in cavernomas and Moyamoya disease promises to shed new light on the pathogenesis of these disorders. The common neurovascular disorders seen in the paediatric population are discussed in this chapter with the focus on those seen predominantly in children.

Intraventricular haemorrhage in preterm infants

Spontaneous intraventricular haemorrhage is a major complication of preterm birth. Large haemorrhages are associated with a high risk of disability and hydrocephalus

Aetiology

In premature infants, the site of origin of the bleeding is the subependymal germinal matrix, which is located between the caudate nucleus and the thalamus at the level of the foramen of Monro. Vessels in this region occupy border zones between cerebral arteries and the collecting zone of the deep cerebral veins and have increased permeability or germinal matrix fragility when subjected to hypoxia and or increased venous pressure, relating to changes in cerebral blood flow (CBF). Fluctuations in CBF in the preterm are associated with IVH, particularly as preterm infants have impaired autoregulation of CBF compared to term infants. Risk factors for IVH include the causes of changes in blood pressure for example during rapid infusion of fluid boluses, increases in cerebral venous pressure during labour and delivery caused by compression of the fetal head and tracheal suctioning. Causes of rapid fluctuations in CBF include hypercarbia, asphyxia, acidosis, and hypoglycaemia. Coagulation abnormalities often seen after prolonged intrapartum asphyxia and resuscitation are contributing factors also.

In term neonates IVH usually results from choroid plexus haemorrhage, deep venous sinus thrombosis, and thalamic infarction. The most common clinical symptoms are seizures and poor feeding.

Incidence

The incidence of IVH in very low birth weight infants (<1500 g) declined from 40% to 50% in the early 1980s to 20% by the late 1980s. However, in the last two decades the occurrence of IVH has remained static. In extremely premature infants weighing 500–750 g, IVH occurs in about 45% of neonates (Ballabh, 2010).

Presentation

IVH almost always occurs in the first five postnatal days with 50% occurring on the first day of life. In one study, IVH was detected in 20% within the first hour of age in babies with birth weight less than 1750 g subjected to serial cranial ultrasounds commencing minutes after birth. In the same study the overall incidence of IVH was similar between vaginal and Caesarean deliveries (Shaver et al., 1992).

Presentation is often silent with 25–50% of IVH found on routine cranial ultrasound examination of the preterm neonate. However, presentation may be with a catastrophic syndrome of rapid neurological deterioration evolving over minutes to hours with coma, flaccid tone, tonic posturing, or neonatal seizures and absence of spontaneous movements. The most common presentation is that of a subacute deterioration in alertness and spontaneous movements over hours to days often with hypotonia. Respiration may be affected.

Routine cranial ultrasound screening should be performed on all babies born with a gestational age less than 32 + 6 weeks or with a birth weight of 1.5 kg or below. In the United Kingdom, the neonatal networks suggest screening on days 0–3, repeated on days 3–5, 7–10, at 28 days and again at 36 weeks corrected gestational age or just prior to discharge from the unit for babies born between 23 and 27 + 6 weeks. Babies of any gestation who are ventilated should have routine screening scans on a weekly basis and again at discharge (Periman and Rollins, 2000).

Table 90.1 Severity and grading of IVH

Grade I	Germinal matrix only
Grade II	IVH filling 10–50% of the ventricle
Grade III	IVH filling more than 50% of the ventricle
Grade IV Periventricular haemorrhagic infarction (PVHI)	Haemorrhage in any parenchymal location in addition to a unilateral or bilateral IVH PVHI is a more precise pathophysiological definition

Reproduced with permission from Lu-Ann Papile, Jerome Burstein, Rochelle Burstein, Herbert Koffler, Incidence and evolution of subependymal and intraventricular hemorrhage: A study of infants with birth weights less than 1,500 gm, *The Journal of Pediatrics*, Volume 92, Issue 4, pp. 529–34, Copyright © 1978 Elsevier.

Grade I IVH corresponds to mild, grade II moderate, and grades III and IV severe IVH (Table 90.1). Each grade of IVH may be unilateral or bilateral with either symmetrical or asymmetrical grades of IVH.

Management

The optimal clinical management of IVH and posthaemorrhagic ventricular dilatation remains unclear. A common approach involves temporary treatment of hydrocephalus in these patients with a ventriculosubgaleal shunt (VSGS), ventricular access device (VAD), or external ventricular drain (EVD) until it becomes evident that the patient needs and can tolerate permanent CSF diversion. In a systematic review and meta-analysis of outcomes and complications, the range of outcomes was similar for VSGS, VAD, and EVD (Badhiwala et al., 2015). Posthaemorrhagic hydrocephalus (PHH) is considered in detail in Chapter 89.

Prognosis

Mortality and short-term morbidity (grades I and II) mortality of intraventricular haemorrhage. For mild IVH (grades I and II) mortality is 5% with only 7% of survivors exhibiting PHH (Murphy et al., 2002). In severe IVH (grade III and periventricular haemorrhagic infarction [PVHI]) the mortality rate is approximately 20% and 75% of survivors develop PHH. Severe IVH also increases the risk of periventricular leukomalacia (PVL) (Kusters et al., 2009)

The long-term outcome of infants with IVH who survive worsens with increasing severity of IVH and decreasing gestational age. In a prospective population-based cohort study of 1812 infants born before 33 weeks gestation the prevalence of cerebral palsy at 5 years of age increased with severity of IVH. CP was diagnosed at 5 years of age in 8% of children with grade I IVH, 11% in grade II,19% in grade III and 50% in grade IV (Beaino et al., 2010). Infants with isolated grade I–II IVH also had a higher risk of neurosensory impairment (Bolisetty et al., 2014). However, in a large longitudinal observational study in 16 centres of 1472 infants born at less than 27 weeks gestation, by follow-up at 18–22 months the neurodevelopmental outcomes of extremely low gestational age infants with grade I or II IVH were not significantly different from those without haemorrhage (Payne et al., 2013).

Controversies

There is no role for the routine use of serial lumbar punctures to reduce the need for shunt placement or to avoid progression of hydrocephalus in preterm infants

Intraventricular thrombolytic agents including tissue plasminogen activator (tPA), urokinase or streptokinase are not recommended as methods to reduce the need for shunt placement in premature infants with PHH. In one study using DRIFT (Drainage, Irrigation and Fibrinolytic Therapy) DRIFT was associated with an increased risk of secondary IVH (Whitelaw et al., 2007).

Several postnatal pharmacological prevention strategies for IVH have been studied. There is no evidence that the use of phenobarbital, indomethacin, or vitamin E confer overall benefit in terms of neurodevelopmental outcome.

Vein of Galen malformations (VGAM)

Introduction

VGAMs are rare congenital midline vascular abnormalities in the region of the cavum veli interpositi (velum interpositum). The primary pathology is considered to be an abnormal connection between the choroidal arteries and the median prosencephalic vein such that the flow through the fistula prevents normal regression of the median prosencephalic vein. These abnormalities account for 1% of the arteriovenous malformations and around 30% of the vascular malformation in the paediatric population.

Clinical presentation

VGAMs can present antenatally, in early infancy, or in childhood with signs and symptoms ranging from high-output congestive heart failure (CHF) and hydrocephalus to seizures and intracranial haemorrhage.

Imaging

Imaging shows a large midline varix in a neonate or infant within milimetres to several centimetres. The varix can vary from a few centimetres to several centimetres. Often a large varix suggests a venous stenosis and is frequently associated with ventriculomegaly and subcortical white matter calcification from chronic ischaemia. Antenatal diagnosis via ultrasonography and fetal MRI has been associated with improved outcome in survivors.

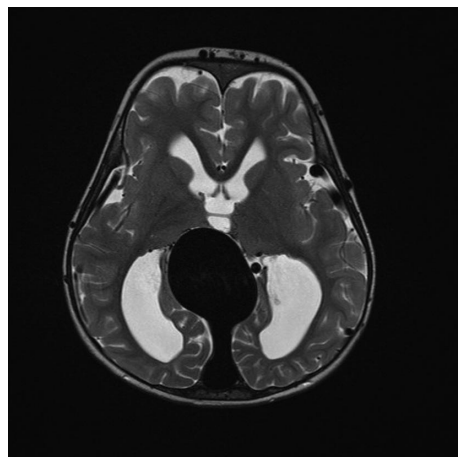

Fig. 90.1 T2 axial MRI scan image showing a venous varix in the quadrigeminal cistern with ventriculomegaly.

Differential diagnosis

VGAM resembles a persistent embryonic falcine sinus draining a single or multiple arteriovenous fistula. VGAMs are categorized based on their angioarchitecture into mural and choroidal. Multiple feeders, including choroidal, thalamoperforating, and pericallosal arteries, often supply choroidal galenic aneurysmal malformations. In contrast, mural VGAMs are often supplied by fewer feeders, including callosal and posterior choroidal arteries. Supply is usually unilateral.

The differential diagnosis for VGAM would include arteriovenous malformation with drainage into the vein of Galen or dural arteriovenous fistula. Vein of Galen aneurysmal dilatations drain into the true vein of Galen. Dural AV fistulas are high flow fistulas and are often supplied by the external carotid artery. Pial AVMs have a true nidus and are rare in children below three years.

Venous obstruction associated with VGAMs can occur at either the level of the falcine sinus or at the base of the skull.

Treatment and prognosis

Untreated vein of Galen malformations have a very poor prognosis. Treatment can be achieved by either the arterial or the venous route. Coils, onyx, and glue have been used to access and treat the fistula. The venous route is often used in patients where the arterial route cannot be approached successfully.

Younger age at first diagnosis, CHF, seizures, and choroidal angioarchitecture are predictive of an adverse clinical outcome. Poor outcomes may also be associated with hydrocephalus at presentation, and incomplete embolization.

The goals of endovascular treatment vary depending on clinical presentation. Neonates with CHF refractory to medical management are treated urgently to establish hemodynamic stability and to allow for heart and brain development. In neonates without CHF, the goal of treatment is to prevent cerebral venous hypertension, white matter damage, and the 'melting brain syndrome'. In these cases, treatment is often deferred until the child is aged 5–6 months to allow for greater cerebral maturation and enlargement of arteries. CSF shunting in VGAM is highly controversial but may be necessary in some patients with progressive ventriculomegaly especially if there are features of raised intracranial pressure.

Results

The overall survival in one series of 26 patients over 19 years was 76.9%. This included five patients who were not treated either because of minimal symptoms or severe comorbidities. Over two-thirds of treated patients had no evidence of developmental delay (Li et al., 2011).

Moyamoya disease/syndrome in childhood

Moyamoya disease (MMD) is a cerebrovascular disease of unknown aetiology characterized initially by bilateral narrowing or occlusion of the terminal internal carotid arteries (ICA) with subsequent involvement of the anterior or middle cerebral arteries. Multiple basal collateral vessels typically develop in response to the reduction in CBF. Suzuki and Takaku made the observation that collateral vessels gave the appearance of a puff of smoke on cerebral angiography and coined the term 'moya moya' in 1969.

Moyamoya syndrome (MMS) describes a similar process with unilateral or bilateral vascular changes that occur in association with conditions like Down syndrome, Neurofibromatosis type I, cranial irradiation, autoimmune disorders, meningitis, and atherosclerosis in adults.

The reduction in CBF can lead to ischaemic episodes in children usually in response to hyperventilation with activities such as crying.

Epidemiology

MMD is found in all ethnic groups but is 10 times more common in East Asian populations as compared to the west. A study conducted in California and Washington State showed that the annual incidence rate of MMD and MMS was 0.086/100 000/year, which is 4–13 times lower than incidence of MMD in Japan (Uchino et al., 2005).

All studies showed a female preponderance with twice as many females as males. Age of MMD onset follows a bimodal distribution with the two peaks between 5 and 10 years of age and during the fourth decade. A family history is noted in 10% to 15% of cases in Japan.

Genetic analysis has identified the RNF213 gene in the 17q25-ter region as an important susceptibility gene for MMD among East Asian populations (Kamada et al., 2011). A polymorphism in c.14576G>A in *RNF213* was identified in 95% of familial patients with MMD and 79% of sporadic cases. *RNF213* was correlated with early onset and severe forms of MMD (Miyatake et al., 2012).

Pathology

The pathology of stenosis in the ICA consists of intima thickened by fibrous tissue and the lamella formed by elastic fibre proliferation. Inflammatory changes are notably absent in the vascular wall. In less than 10% of cases the primary lesion starts unilaterally but becomes bilateral in 75% of cases within 3 years.

The Suzuki classification of the angiographic grades (Suzuki and Takaku, 1969), depicts the progression of vascular changes in MMS/MMD from grade I (narrowing of ICA apex); grade II (appearance of deep collateral vessels); grade III (progression of Moyamoya collateral vessels); grade IV (appearance of transdural collateral vessels from the external carotid artery—ECA); grade V (progression of transdural collateral vessels and reduction of Moyamoya vessels); to grade VI (occlusion of ICA and disappearance of Moyamoya collateral vessels).

Clinical features

The commonest presentation in children is ischaemic events unlike adults where both ischaemic events and intracerebral haemorrhage (ICH) tend to occur.

Ischaemic events may be triggered by hyperventilation due to physical or intellectual activity, dehydration, fever, and crying (Guzmann, 2009). In these patients, cortical vessels are most often maximally dilated at steady state to compensate for chronic cerebral ischaemia. Vasoconstriction in response to carbon dioxide decrease related to hyperventilation results in reduced cerebral perfusion and clinical symptoms.

Patients may present with atypical symptoms like headaches, syncope and involuntary choreiform movements (Smith and Scott, 2012).

Cognitive impairment and decline have been reported in patients without a history of stroke, suggesting that there is a deleterious effect of chronic cerebral hypoxaemia on cognitive functions, but this tended to be greater in children who have had a stroke (Kossorotoff, 2012). Bilateral disease and duration of symptoms are the main factors associated with cognitive deficits.

Intracranial bleeding is rare in children and mainly due to rupture of fragile deep collaterals with deep intraparenchymal (basal ganglia or periventricular deep white matter) or intraventricular haemorrhage. Subarachnoid haemorrhage is rare and sometimes due to the rupture of saccular aneurysms located in the circle of Willis, most often in the vertebrobasilar system.

Investigations

Digital subtraction angiography (DSA) remains the best investigation to identify the condition and visualize collaterals from the ECA (Fig. 90.2). MRI and magnetic resonance angiography (MRA) provide information on cerebral arteries, brain parenchyma, cerebral perfusion, and is being used increasingly in the diagnostic assessment and follow-up of patients (Fig. 90.3).

Fig. 90.2 DSA with common carotid artery injection showing stenosis of the terminal ICA, proximal ACA, and MCA with development of basal collaterals. There is sparing of the external carotid vessels.

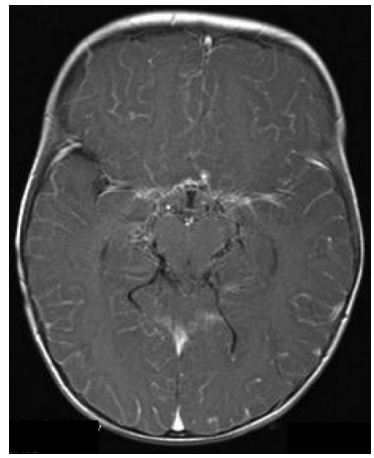

Fig. 90.3 An axial T1 postcontrast image showing the development of numerous basal collateral vessels in the chiasmatic and ambiens cistern.

MRI with MRA may be sufficient to diagnose MMD when the following criteria, which were first established on conventional angiography, are met. MR angiography showing stenosis or occlusion of the terminal portion of the ICA or proximal anterior cerebral artery (ACA) and/or the middle cerebral artery (MCA) (Fig. 90.3). Presence of abnormal vascular networks near the occlusive or stenotic lesions by MR angiography, or MR imaging demonstrating two or more flow voids in the basal ganglia in each hemisphere.

Assessment of cerebral haemodynamics by techniques such as SPECT, PET, xenon-enhanced computed tomography (CT), arterial spin-labelling MR, and CT perfusion may help to identify patients who are at risk of ischaemic events and to direct therapy. The identification of the cerebral hemisphere and region most at risk can help to target surgical revascularization.

Management

The aim of treatment is to increase CBF to the ischaemic cerebral hemisphere and reduce the incidence of ischaemic and haemorrhagic events.

General measures such as avoidance of hypotension, dehydration, and hyperventilation are recommended in order to prevent deterioration of cerebral haemodynamics. Long-term oral antiplatelet therapy, usually aspirin, is started to reduce the incidence of thromboembolic complications.

Surgical options are direct or indirect revascularization. Direct revascularization augments the blood flow by anastomosing an ECA branch to a cortical vessel resulting in an immediate increase in CBF. The most common being superficial temporal artery to a middle cerebral arterial branch (STA—MCA). Indirect revascularization is based on Moyamoya pathophysiology, which spares the ECA and its branches. The tissues supplied by ECA branches is used to augment flow to the ICA circulation over time. The development of cerebral neovascularization from the ECA branches leads to brain revascularization.

Several techniques of indirect revascularization have been developed, all based on a synangiosis procedure. During synangiosis, tissues containing ECA branches (dura mater, temporal muscle, galeal tissue, or the superficial temporal artery) are

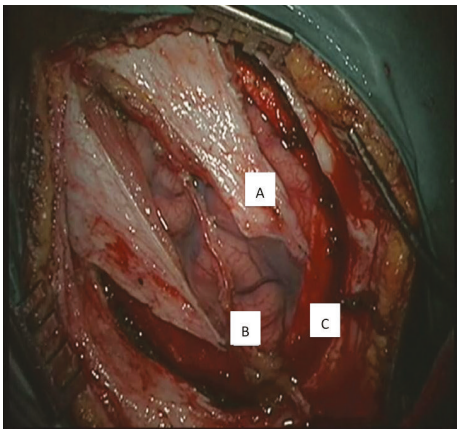

Fig. 90.4 Intraoperative image of an EDAMS procedure: (A) temporalis muscle, (B) superficial temporal artery in continuity, (C) dural margins folded over the cortex.

directly placed in contact with the surface of the ischaemic brain. Development of neovascularization from these tissues is thought to be enhanced by secretion of angiogenic factors from ischaemic brain parenchyma. This procedure does not provide immediate benefit, since efficient neoangiogenesis requires at least 3 months to develop.

Before surgical revascularization, an accurate assessment of vascular status by conventional angiography is required, to avoid disruption of pre-existing collateral vessels developed naturally from the ECA.

The common procedures used to achieve indirect augmentation of flow are encephaloduroarteriosynangiosis (EDAS), encephalodur oarteriomyosynangiosis (EDAMS, Fig. 90.4), and the multiple burr holes procedure (Oliveira et al., 2009). In EDAS the STA is dissected along with a cuff of connective tissue maintaining its continuity. The STA is placed and held on the cortical surface with pial or dural sutures. The temporalis muscle is placed in addition to the STA on the cortical surface with EDAMS.

If multiple burr holes are used, then 10–20 burr holes are made over the affected hemisphere. The dura is opened to allow vascularization from the external carotid circulation.

Results

In a comparison of symptomatic cerebral hemispheres, the 5-year risk of recurrent ipsilateral stroke was significantly greater in medically treated (65%) versus surgically treated (17%) patients. Improving blood flow to the ischaemic cerebral hemispheres could also help to improve cognitive function.

Guzman et al. (2009) reported their series of patients who were both adults and children, treated predominantly by direct surgical bypass. They reported operative morbidity and mortality rates of 3.5% and 0.7% per treated hemisphere, respectively.

Scott et al. (2004) analysed their results in children who underwent indirect revascularization via a modified EDAS technique. The reported operative morbidity was 4% per treated hemisphere.

According to experts' consensus, indirect revascularization is preferred in children because a direct bypass is technically difficult with small-diameter vessels, whereas direct bypass is preferred in adult patients (Roach et al., 2008).

Anaesthetic concerns

Maintenance of haemodynamic stability, normovolaemia, avoiding hypocarbia and hypotension are important if perioperative ischaemic complications are to be avoided.

Prognosis

The natural history of untreated symptomatic MMD in the paediatric population appears to be unfavourable. The course of the disease is variable and could go from rapid progression leading to severe disabilities to clinical silence for several years. Half of the paediatric patients who present with TIA-type symptoms continue to have these types of attacks at a mean follow-up of 7 years (Fukuyama and Umezu, 1985). Untreated MMD is associated with gradual, progressive neurological and cognitive deterioration (Kurokawa et al., 1985).

Intracranial aneurysms

Introduction

Aneurysms in children are extremely rare comprising only 0.5 to 4% of all intracranial aneurysms. In a 1966 study of 6368 ruptured aneurysms, only 41 occurred in children under 19 years of age (Locksley et al., 1966). However, they account for up to 10–15% of haemorrhagic strokes in the first two decades.

Aneurysms

Presentation is heterogeneous, patients present with subarachnoid haemorrhage (32%), headache without SAH (45%), cranial neuropathy (16%), nausea/vomiting (15%), visual symptoms (13%), trauma (13%), and seizures (4%) (Hetts et al., 2009) (Fig. 90.5).

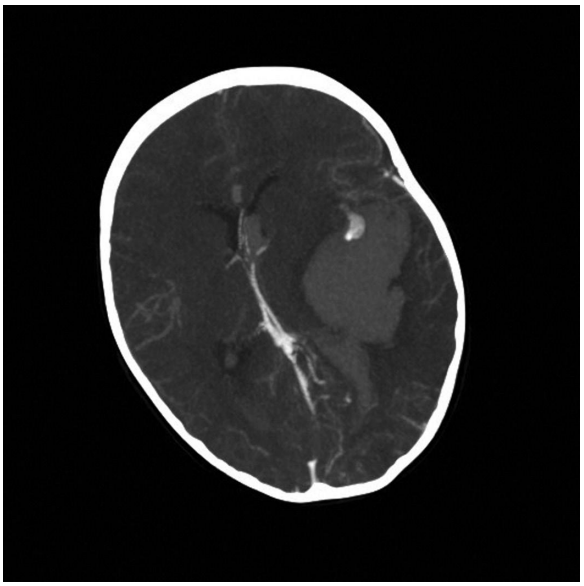

Fig. 90.5 A 27-month-old girl was admitted with sudden onset of headache followed by a drop in the GCS to 6 with a left-sided fixed and dilated pupil. She was transferred intubated and ventilated and underwent a CT and CT angiogram, which shows a left temporal ICH with an aneurysm anterior to the haematoma. A further CT scan showed good evacuation of the haematoma but an evolving infarction in the MCA territory. She had a left decompressive craniectomy which stabilized her condition. On follow-up 2 years later she is walking but has a residual left hemiparesis (arm > leg), her speech is limited to words.

Table 90.2 Lasjaunias paediatric aneurysm classification

1	Fusiform without evidence of infection or trauma
2	Saccular aneurysms without evidence of infection or trauma
3	Infectious (mycotic) aneurysms
4	Traumatic aneurysms

Reproduced with permission from Pierre Lasjaunias, Siddharta Wuppalapati, Hortensia Alvarez et al., Intracranial aneurysms in children aged under 15 years: review of 59 consecutive children with 75 aneurysms, *Child's Nervous System*, Volume 21, Issue 6, pp. 437–50, Copyright © 2005 Springer Nature.

As well as being rare, aneurysms in this population exhibit certain features not seen in the adult population:

They are more often in unusual locations such as the posterior fossa (twice the frequency than is seen in the adult population) and in association with distal vessels. Basilar trunk aneurysms are also more common than terminus aneurysms.

They are more often fusiform and giant, and occur with a slight male predominance. They have a higher rate of multiplicity, especially when associated with vasculopathies and infection (Jordan et al., 2009).

Spontaneous thrombosis has been reported in 5–10% of paediatric ruptured aneurysms but is very rare in adults. Spontaneous recanalization has been reported and thus careful imaging follow-up is required (Lasjaunias et al., 2005; Buis et al., 2006).

Aneurysms in adolescents and teenagers conform more closely to the adult phenotype.

Paediatric aneurysms have been classified into four subtypes by Pierre Lasjaunias (28) (Table 90.2). To this list other authors have added: oncologic aneurysms; haemodynamic aneurysms; and familial aneurysms, which are exceedingly rare.

Aneurysms due to haemodynamic stress may be seen in congenital vascular absence, arteriovenous malformations, and hypertension with or without aortic coarctation.

Traumatic aneurysms are much more common in the paediatric population accounting for 20% of all lesions. They are more common at points of arterial fixation at the skull base or dura with cavernous carotid and pericallosal arteries being the most common. Caroticocavernous fistula may result from cavernous carotid involvement. The majority of traumatic aneurysms even in patients with no underlying arteriopathy have a tendency to enlarge.

From a diagnostic standpoint, there has been a gradual shift towards non-invasive imaging techniques such as MRI and CT angiography with cerebral catheter angiography being reserved for treatment or treatment planning (Figs. 90.6A and 90.6B).

Haemorrhage is twice as common in saccular than in fusiform aneurysms (even in cases of infection) occurring in over 35% of cases. In paediatric patients with pure subarachnoid haemorrhage, aneurysms may be found in up to 57% of patients (Jordan et al., 2009).

A higher proportion of patients with fusiform aneurysms were likely to have an underlying predisposing condition, such as the posterior fossa malformation, haemangiomas, arterial anomalies, cardiac defect, coarctation of the aorta, eye abnormalities, and sternal abnormalities (PHACES) syndrome, tuberose sclerosis, microcephalic osteodysplastic primordial dwarfism type II, Ehlers–Danlos, osteogenesis imperfecta, or neurofibromatosis type 1.

Mycotic aneurysms comprise up to 10% of intracranial aneurysms in the first year of life (Buis et al., 2006) and are more likely to be multiple. Associated underlying conditions to consider are endocarditis, congenital and acquired immunodeficiencies (including AIDS) and meningoencephalitis. New lesions can develop during the course of the acute infection. Aneurysms associated with HIV infection are usually multifocal and morphologically are typically long proximal fusiform lesions.

We have encountered a subset of patients with aneurysms of the distal lenticulostriate arteries in association with trauma. These have been managed with careful observation only, and have a tendency to resolve without rehaemorrhage.

Management of aneurysms in the paediatric population requires a detailed medical history and supplementary investigations that may not normally be required in the adult population such as a sepsis

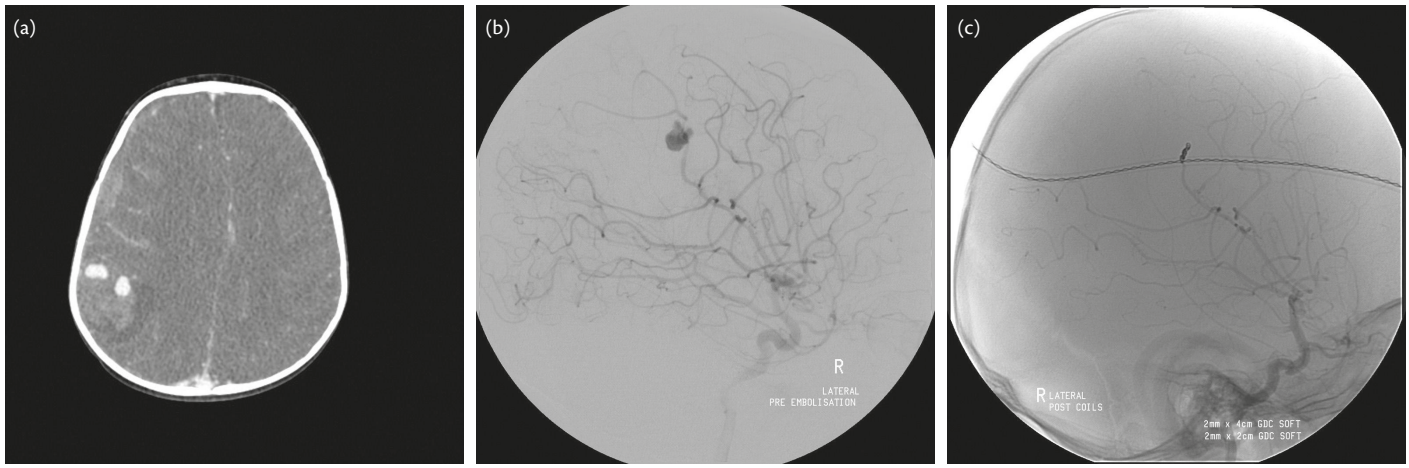

Fig. 90.6 (A) Axial source image of a CT angiogram in a 6-year-old presenting with collapse and seizure. A complex bi-lobed lesion is shown in the right parietal lobe with surrounding parenchymal haemorrhage and a subdural haematoma; (B) A lateral view catheter cerebral angiogram of the right internal carotid artery in the late arterial phase. The complex aneurysm involving a cortical branch is seen; and (C) coil embolization has occurred proximal to the main aneurysm. The microcatheter could not pass a preaneurysm stenosis. There is retrograde filling of cortical branches distal to the occlusion, but no filling of the aneurysm itself.

screen or cardiac structural studies. Additionally, it goes without saying that a multidisciplinary approach is required in all cases, involving cardiologists, paediatric neurologists, neurosurgeons, and interventional neuroradiologists.

Over the last decades, there has been a gradual shift from neurosurgical to non-invasive endovascular treatments of paediatric cerebral aneurysms (Fig. 90.6C).

Aneurysms undergoing endovascular treatment appear to have a higher retreatment rate which may be either endovascular or surgical. True recurrence is uncommon, but there may be a lower tolerance to small neck residuals.

Complex neurosurgical bypass procedures for fusiform lesions have been reported with good medium- and longer-term patency and clinical outcomes. This is particularly encouraging considering there must be tolerance to patient growth.

There is a slightly higher rate of aneurysm growth over time (up to 10%) in the paediatric population. This is due in part to a higher association with vasculopathies. The presence of multiple involved vessels limits the therapeutic options of parent artery closure whether endovascular or surgical as *de novo* aneurysm formation is a risk due to enhanced haemodynamic stress on already dysplastic vessels.

New flow-diversion devices have been utilized in the paediatric population for large and fusiform aneurysms. Such devices obviate the need for parent artery occlusion. Longer-term follow-up will determine durability. There are several sobering case series on paediatric aneurysm patients demonstrating late complications but also a higher than peer all-cause mortality into adult life. Late aneurysm rupture seems to be predominately related to the degree of initial aneurysm closure whether surgical or endovascular (Koroknay-Pal et al., 2012). Therefore, lifelong surveillance has been advocated by some authors. In one study, of 59 patients with a median time of follow-up of 34 years, 24 patients (41%) had 25 *de novo* and 11 recurrent aneurysms with 25% being symptomatic (Koroknay-Pal et al., 2013). New SAH occurred in seven patients. The annual rate of *de novo* aneurysm formation was 1.9%.

Smoking is a significant risk factor both for new aneurysm formation and subarachnoid haemorrhage. Patients with multiple and fusiform aneurysms at initial presentation are particularly prone to developing new lesions (Hetts et al., 2011).

Despite the requirement for more complex treatment strategies, the overall risks are not increased in the paediatric population. However, patients requiring combined or sequential surgical and endovascular treatment do have additive risks.

Arteriovenous malformations

Introduction

Despite the general acceptance that AVMs are developmental lesions and, unlike aneurysms are probably present soon after birth, they are very rare. However, haemorrhagic presentation is more common than in adults (Hetts et al., 2012), occurring in 86/135 (63.7%) of cases in one study (Ellis et al., 2015). Multimodality assessment and treatment are prerequisites to ensuring a good clinical outcome in these difficult conditions.

AVMs

Although the general architecture of AVMs does not differ substantially from the adult population in terms of nidus size, dural supply, or the number of draining veins, some differences are seen. These may relate to chronicity of high flow in the adult population as venous occlusion and stenosis, venous ectasia, and arterial flow aneurysms are all more common in adults. Deep venous drainage is seen more commonly in children. Additionally, paediatric AVMs are more commonly deep with lobar lesions being more common in adults. As with adults, paediatric patients with deep-seated AVMs, those with deep venous drainage and infratentorial lesions had a strong association with haemorrhagic presentation.

Clinical presentation, as stated is mostly haemorrhagic (up to 80%) (Fig. 90.7A), with 8.3% presenting with epilepsy and migrainous headaches (6.3%) (Dinca et al., 2012). Due to the young age at diagnosis, the calculated lifetime rupture risk is high and generally favours a more aggressive treatment approach.

Centres managing such patients should have at their disposal; experts in paediatric vascular neurosurgery; interventional neuroradiologists and access to modern stereotactic radiosurgery.

Neurosurgical resection, with or without targeted preoperative adjunct embolization, can achieve obliteration rates up to 90% with morbidity of 17% (mostly visual field defects) (Gross et al., 2015). Predictably, patients harbouring AVMs with lower Spetzler-Martin scores fare better. mRS at presentation also strongly influences the ultimate clinical outcome.

Stereotactic radiosurgery is an attractive treatment option for paediatric patients, even those with ruptured AVMs. Obliteration rates of 71.3% to 88% have been reported in selected series, with an annual bleeding rate between 1% and 2.2% per annum (Dinca et al., 2012; Hanakita et al., 2015). As with adult patients, smaller lesions have higher obliteration rates.

Endovascular therapy is perhaps much less tested and obliteration rates with endovascular treatment alone are unacceptably low at 20%, even though complication rates, as with aneurysms, are not high (Zheng et al., 2014).

Multimodality treatment probably offers the greatest benefit for patients (Fig. 90.7B). Combining complementary techniques to enhance obliteration rates can be achieved within large neuroscience centres with acceptable morbidity. In large lesions, the treatment may be ongoing for several years and almost always will require combination therapy. Haemorrhage risk persists until complete obliteration has been achieved. Clinical outcomes can be very good for small lesions, but there is a high risk of long-term dependency in survivors after treatment of very large lesions.

Cavernous malformations (CM)

CMs represent the most common central nervous system (CNS) vascular lesion in children, although their incidence is four times lower than that of the adult population (Acciarri et al., 2009).

A bimodal age distribution was found with a peak incidence under 4 years and another above 12 years. Patients under 6 years of age were found to have significantly more giant cavernomas (Bilginer et al., 2014).

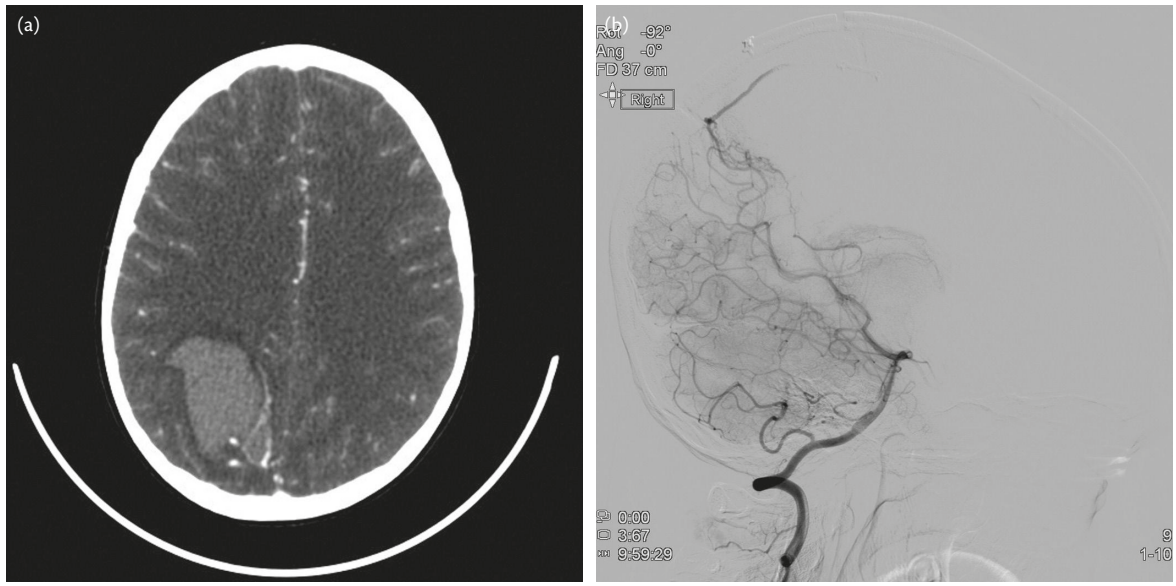

Fig. 90.7 (A) Acute cerebral haemorrhage in the right parietal lobe. CT angiography source image shows slight hypervascularity posteriorly but no definable nidus; and (B) A very small AVM is seen in the posterior right parietal lobe on catheter angiography. This was successfully managed by a combination of surgical resection and stereotactic radiosurgery.

The natural history of paediatric CMs throughout the neuraxis seems to be more aggressive than in adult patients, lesions have higher rates of growth and haemorrhage, larger dimensions, and often atypical radiological appearances at diagnosis. Beside the familial form of the disease, which is more often associated with multiple lesions and an earlier age of clinical presentation, the major risk factor for developing CMs in children seems to be cranial radiotherapy (Acciarri et al., 2009). This risk appears cumulative, the incidence of postirradiation cavernoma is 2.24%, 3.86%, 4.95%, and 6.74% within 5, 10, 15, and 20 years of irradiation. The lesions can appear from months to 20–30 years post-treatment (Strenger et al., 2008). Younger age at the time of treatment is associated with a higher cumulative risk and a shorter latency interval of formation. Conservative management is the norm for most lesions that are asymptomatic.

There is no consensus currently regarding the benefit or the interval of surveillance imaging in this group of patients.

Intracerebral haemorrhage in children

Structural lesions account for up to 50% of ICH in children. AVM's remain the commonest cause accounting for 30%, cavernomas (15%) and aneurysms (13%) are the other common structural lesions found. Other causes include Sickle cell disease, MMD, and rarely intratumoural haemorrhage. Between 10% and 30% of ICH is secondary to haematological disorders like haemophilia, thrombocytopenia, and coagulopathy secondary to vitamin K deficiency. In 25% of ICH the aetiology cannot be identified.

Presentation

Up to 45% of children may present with features of raised intracranial pressure that warrants acute management. The presentation includes severe headache, vomiting, deteriorating GCS, and seizures. Focal neurological deficits are seen in up to 50% of patients (Beslow et al., 2010).

Investigations

A CT scan is useful in identifying a bleed early. Computed tomography angiography (CTA) or MRA may be helpful in identifying an underlying structural lesion. A DSA may be necessary to identify small AVMs that may not be seen on non-invasive imaging. A DSA may need to be repeated if an underlying lesion is not identified once the haematoma has resolved.

Management

Depending upon the GCS at presentation children may need acute intervention for raised intracranial pressure (i.e. mannitol, ventricular drainage, and acute evacuation of the haematoma in up to 50% of patients). Imaging studies are helpful in identifying underlying causes and in planning the operative approach to the haematoma. The main aim of surgery is to evacuate the haematoma with or without treatment of the underlying lesion if technically feasible. Removing the underlying lesion may become necessary during haematoma removal because of uncontrolled intraoperative bleeding following evacuation of the haematoma.

Prognosis

At 3.5 months following presentation, 71% of survivors had neurological deficits and 55% had clinically significant disability (Beslow et al., 2010). The recurrence rate of ICH is 10% after 5 years.

Conclusion

Neurovascular disorders in children pose some unique challenges. They require close collaboration between multiple specialities and often combined treatment. These conditions require long-term

follow-up as these patients have many years to live with the threat of further symptoms, and disability related to both haemorrhage and treatment.

FURTHER READING

Ganesan, V. & Kirkham, F. (eds.) (2011). *Stroke and Cerebrovascular Disease in Childhood*. London International Review of Child Neurology: MacKeith Press.

REFERENCES

Acciarri, N., Galassi, E., Giulioni, M., et al. (2009). Cavernous malformations of the central nervous system in the pediatric age group. *Pediatr Neurosurg*, **45**(2), 81–104.

Badhiwala, J.H., Hong, C.J., Nassiri, F., Hong, B.Y., Riva-Cambrin, J., & Kulkarni, A.V. (2015). Treatment of posthemorrhagic ventricular dilatation in preterm infants: a systematic review and meta analysis of outcomes and complications. *J Neurosurg Pediatr*, **16**(5), 545–55.

Ballabh, P. (2010). Intraventricular hemorrhage in premature infants: mechanism of disease. *Pediatr Res*, **67**(1), 1–8.

Beaino, G., Khoshnood, B., Kaminski, M., et al. (2010). Predictors of cerebral palsy in very preterm infants: the EPIPAGE prospective population-based cohort study. *Dev Med Child Neurol*, **52**(6), e119.

Beslow, L.A., Licht, D.J., Smith, S.E., et al. (2010). Predictors of outcome in childhood intracerebral hemorrhage: a prospective consecutive cohort study. *Stroke*, **41**(2), 313.

Bilginer, B., Narin, F., Hanalioglu, S., Oguz, K.K., Soylemezoglu, F., & Akalan, N. (2014). Cavernous malformations of the central nervous system (CNS) in children: clinico-radiological features and management outcomes of 36 cases. *Childs Nerv Syst*, **30**(8), 1355–66.

Bolisetty S, Dhawan, A., Abdel-Latif, M., et al. (2014). Intraventricular haemorrhage and neurodevelopmental outcomes in extreme preterm infants. *Pediatrics*, **133**(1), 55–62.

Buis, D.R., van Ouwerkerk, W.J., Takahata, H., & Vandertop, W.P. (2006). Intracranial aneurysms in children under 1 year of age: a systematic review of the literature. *Childs Nerv System*, **22**(11), 1395–409.

Dinca, E.B., de Lacey, P., Yianni, J. et al. (2012). Gamma knife surgery for paediatric arteriovenous malformations: a 25-year retrospective study. *J Neurosurg Paediatr*, **10**(5), 445–50.

Ellis, M.J., Armstrong, D., & Vachhrajani, S. (2015). Angioarchitectural features associated with haemorragic presentation in paediatric cerebral arteriorvenous malformations. *J Neuroint Surg*, **5**, 191–5.

Fukuyama, Y. & Umezu, R. (1985). Clinical and cerebral angiographic evolutions of idiopathic progressive occlusive disease of the circle of Willis ('moyamoya' disease) in children. *Brain Dev*, **7**(1), 21–37.

Gross, B.A., Storey, A., & Orbach, D.B., et al. (2015). Microsurgical treatment of arteriovenous malformations in paediatric patients: the Boston children's hospital experience. *J Neurosurg Paediatr*, **15**(1), 71–7.

Guzman, R., Lee, M., Achrol, A., et al. (2009). Clinical outcome after 450 revascularization procedures for moyamoya disease: clinical article. *J Neurosurg*, **111**(5), 927–35.

Hanakita, S., Koga, T., Shin, M. et al. (2015). The long-term outcomes of radiosurgery for arteriovenous malformations in paediatric and adolescent populations. *J Neurosurg Pediatr*, **16**(2), 222–31.

Hetts, S., Kim, H., Cooke, D., et al. (2012). Paediatric versus adult AVM architecture: are children really just small adults? *J Neurint Surg*, **4**, A13–14.

Hetts, S.V., Narvid, J., Sanai, N. et al. (2009). Intracranial aneurysms in childhood: 27-year single institution experience. *Am J Neuroradiol*, **30**, 1315–24.

Hetts, S.W., English, J.D., Dowd, C., et al. (2011). Paediatric intracranial aneurysms: new and enlarging aneurysms after index aneurysm treatment of observation. *Am J Neuroradiology*, **32**, 2017–22.

Jordan, L.C., Johnson, S.C., Wu, Y.W., Sidney, S., & Fullerton, H.J. (2009). The importance of cerebral aneurysms childhood haemorrhagic stroke: a population-based study. Stroke, **40**(2), 400–5.

Kamada, F., Aoki, Y., Narisawa, A., et al. (2011). A genome-wide association study identifies RNF213 as the first Moyamoya disease gene. *J Hum Genet*, **56**, 34–40.

Koroknay-Pal, P., Laakso, A., Lehto, H. et al. (2012). Long-term excess mortality in paediatric patients with cerebral aneurysms. *Stroke*, **43**, 2091–6.

Koroknay-Pal, P., Niemela, M., Lehto, H. et al. (2013). De novo and recurrent aneurysms in Paediatric patients with cerebral aneurysms. *Stroke*, **44**, 1436–9.

Kossorotoff, M. (2012). Cognitive decline in moyamoya: influence of chronic cerebral hypoxia, history of stroke, or comorbid conditions? *Dev Med Child Neurol*, **54**(1), 5–6.

Kurokawa, T., Tomita, S., Ueda, K., et al. (1985). Prognosis of occlusive disease of the circle of Willis (moyamoya disease) in children. *Pediatr Neurol*, **1**(5), 274–7.

Kusters, C.D., Chen, M.L., Follett, P.L., & Dammann, O. (2009). 'Intraventricular' haemorrhage and cystic periventricular leukomalacia in preterm infants: how are they related? *J Child Neurol*, **24**(9), 1158.

Lasjaunias, P., Wuppulapatti, S., Alvarez, H., Rodesch, G., & Ozanne, A. (2005). Intracranial aneurysms in children aged under 15 years: review of 59 consecutive children with 75 aneurysms. *Childs Nerv System*, **21**(6), 437–50.

Li, A.H., Armstrong, D., & terBrugge, K.G. (2011). Endovascular treatment of vein of Galen aneurysmal malformation: management strategy and 21-year experience in Toronto. *Neurosurg Pediatr*, **7**(1), 3–10.

Locksley, H.B., Sahs, A.L., & Sandler, R. (1966). Report on the cooperative study of intracranial aneurysms and subarachnoid haemorrhage. 3. Subarachnoid haemorrhage unrelated to intracranial aneurysms and A-V malformation: a study of associate disease and prognosis. *J Neurosurg*, **24**, 1034–56.

Miyatake S, Miyake N, Touho H, et al. (2012). Homozygous c.14576G>A variant of RNF213 predicts early-onset and severe form of moyamoya disease. *Neurology*, **78**, 803–10.

Murphy, B.P., Inder, T.E., Rooks, V., et al. (2002). Posthaemorrhagic ventricular dilatation in the premature infant: natural history and predictors of outcome. *Arch Dis Child Fetal Neonatal Ed*, **87**(1), F37.

Oliveira, R.S., Amato, M.C., Simão, G.N., et al. (2009). Effect of multiple cranial burr hole surgery on prevention of recurrent ischemic attacks in children with moyamoya disease. *Neuropediatrics*, **40**(6), 260–4.

Payne, A.H., Hintz, S.R., Hibbs, A.M., et al. (2013). Neurodevelopmental outcomes of extremely low-gestational age neonates with low-grade periventricular–intraventricular hameorrhage. *JAMA Pediatr*, **167**(5), 451–9.

Periman, J.M. & Rollins, N. (2000). Surveillance protocol for the detection of intracranial abnormalities in premature neonates. *Arch Pedaitri Adolesc Med*, **154**, 822–6.

Roach, E.S., Golomb, M.R., Adams, R., et al. (2008). Management of stroke in infants and children: a scientific statement from a Special Writing Group of the American Heart Association Stroke Council

and the Council on Cardiovascular Disease in the Young. *Stroke*, **39**(9), 2644–91.
Scott, R.M., Smith, J.L., Robertson, R.L., Madsen, J.R., Soriano, S.G., & Rockoff, M.A. (2004). Long-term outcome in children with moyamoya syndrome after cranial revascularization by pial synangiosis. J Neurosurg, **100**(2 Suppl Pediatrics), 142–9.
Shaver, D.C., Bada, H.S., Korones, S.B., Anderson, G.D., Wong, S.P., & Arheart, K.L. (1992). Early and late intraventricular haemorrhage: the role of obstetric factors. *Obstet Gynecol*, **80**(5), 831.
Smith, E.R. & Scott, R.M. (2012). Spontaneous occlusion of the circle of Willis in children: pediatric moyamoya summary with proposed evidence-based practice guidelines. A review. *J Neurosurg Pediatr*, **9**(4), 353–60.
Strenger, V., Sovinz, P., Lackner, H. et al. (2008). Intracerebral cavernous haemangioma after cranial irradiation in childhood. *Strahlentherapie und Onkologie*, **184**, 276–80.
Suzuki, J. & Takaku, A. (1969). Cerebrovascular 'moyamoya' disease: disease showing abnormal net-like vessels in base of brain. *Arch Neurol*, **20**, 288–99.
Uchino, K., Johnston, S.C., Becker, K.J., & Tirschwell, D.L. (2005). Moyamoya disease in Washington State and California. *Neurology*, **65**(6), 956–8.
Whitelaw, A., Evans, D., Carter, M., et al. (2007). Randomized clinical trial of prevention of hydrocephalus after intraventricular haemorrhage in pre-term infants: brain-washing versus tapping fluid. *Pediatrics*, **119**(5), e1071–8.
Zheng, T., Wang, Q.-J., Liu, Y.-Q., et al. (2014). Clinical features and endovascular treatment of intracranial arteriovenous malformations in paediatric patients. *Childs Nerv System*, **30**(4), 647–53.

RELATED LINKS TO EBRAIN

Infantile Intraventricular Haemorrhage. https://www.ebrainjnc.com/learning/course/view.php?id=1294
Management of Vein of Galen Malformations. https://www.ebrainjnc.com/learning/course/view.php?id=148
Paediatric Vascular Neurosurgery. https://www.ebrainjnc.com/learning/course/view.php?id=164

91

Paediatric epilepsy

Sophia Varadkar and Martin Tisdall

Introduction

Epilepsy is a disease of the brain characterized by a susceptibility to recurrent spontaneous seizures (Fisher et al., 2014). Epilepsy is common, while accurate estimates of incidence and prevalence are difficult, epilepsy occurs in 0.5–1% of the population, starts in childhood in 60% and is drug-resistant in 20–25%.

Diagnosis in children

All children, young people, and indeed adults with a recent onset suspected seizure should be seen promptly by a physician with expertise in epilepsy, to avoid misdiagnosis as well as to ensure precise and early diagnosis and to recognize serious non-neurological diagnoses, especially cardiological ones (Nunes et al., 2012).

Diagnosis is made on the clinical history. An account of the event from both the child or young person and any eyewitnesses is needed and videos can be very helpful. Physical examination should look for evidence of a focal deficit, skin features of neurocutaneous syndromes and give consideration to other systems. Note should be made of developmental and educational progress.

Electroencephalography (EEG) may lend support to the diagnosis of epilepsy but it does not confirm or refute the diagnosis. EEG helps determine seizure type and the epilepsy syndrome. It should include photic stimulation and hyperventilation. Long-term video or ambulatory EEG may be useful where there is diagnostic uncertainty. Neuroimaging identifies structural abnormalities causing epilepsy and magnetic resonance imaging (MRI) is the standard. It is not routinely required after a first suspected seizure in childhood but should be undertaken in all children presenting before the age of two years and in all with a suggestion of a focal onset on history, examination, or EEG as well as in all children who do not respond to first line medication.

In all cases, advice should be given on what to do if a second seizure occurs, safety issues must be discussed, and in some cases consideration given to emergency medicine (rescue) regimes.

Epilepsy syndromes in childhood

The electro-clinical syndromes of childhood epilepsy are comprised of clinical features, signs, and symptoms that together make a distinctive, recognizable clinical disorder. Important elements include age of onset, seizure types, specific EEG characteristics and structural-metabolic causes where present (Berg et al., 2010).

In broad terms, while neonatal seizures are often reactive/symptomatic, severe early infantile onset epileptic encephalopathies (EIEE) may present any time from birth through to early childhood. EIEE is characterized by a severe seizure disorder, often with infantile spasms, a very abnormal EEG, and developmental plateau, delay, or regression in the first year of life. A structural brain abnormality should be sought although the MRI may be lesion negative. West, Ohtahara, early myoclonic epileptic encephalopathy, epilepsy of infancy with migrating focal seizures and Dravet syndrome (severe myoclonic epilepsy of infancy) are well known. Genetic evaluation of this population is revealing an expanding list of copy number variants on array comparative genomic hybridization. Genes in association with EIEE, include the monogenic *SCN1A, STXBP1, ARX, CDKL5*, and in females *PCDH19*. Potentially treatable vitamin responsive epilepsies may also present at this age including vitamin B_6 responsive epilepsies, GLUT1 deficiency syndrome, and biotinidase deficiency.

Middle childhood (4–10 years) features some more benign conditions with good developmental and educational outcomes and greater likelihood of spontaneous remission. Well-known and most common are childhood absence epilepsy and benign epilepsy with centrotemporal spikes (BECTS); less known and thus less recognized is Panayiotopoulos syndrome. However, more serious epilepsies are also seen. Lennox–Gastaut syndrome is characterized by generalized tonic-clonic seizures, absences, drops, and tonic seizures with particular EEG patterns. Epilepsy with myoclonic absences (Doose syndrome) has variable prognosis. Epileptic encephalopathy with continuous spike and wave during sleep and Landau-Kleffner (LKS) emerge.

In later childhood (10 years onward through adolescence), the common genetic generalized (previously termed idiopathic) epilepsy syndromes appear—genetic generalized epilepsy, juvenile myoclonic epilepsy, and juvenile absence epilepsy. These are lifelong syndromes. Autosomal-dominant nocturnal frontal lobe epilepsy (ADNFLE) may have manifested earlier in childhood but only now be recognized.

At any age, specific aetiologies are recognized to cause epilepsy including neurocutaneous syndromes like tuberous sclerosis, Sturge-Weber syndrome, and Neurofibromatosis as well as

other structural lesions for example tumours or polymicrogyria. Acquired lesions such as mesial temporal sclerosis, stroke, perinatal insults, infection, and trauma, which is less commonly a cause in children than in adults, can all cause epilepsy, Distinctive constellations including Rasmussen syndrome, hypothalamic hamartomata, hemiconvulsion-hemiplegia-epilepsy, and chromosomal disorders including trisomy 21 and ring 20 may also be seen.

Medical treatment

In the United Kingdom, protocols for the treatment of prolonged seizures in children and of status epilepticus are well described (Advanced Life Support Group, 2011).

With regard to daily treatment, antiepileptic drugs (AEDs) are the mainstay. Similar to adults, carbamazepine, valproate, lamotrigine, and levetiracetam are most often used. AEDs are usually introduced with slow titration aiming for the lowest effective dose. Drug side effects may differ from those in adults. AEDs are selected by seizure type and epilepsy syndrome, and here may be different to adult practice.

The management of the comorbidities of epilepsy are of great importance in children. Motor disorders, cognitive, and learning difficulties, behavioural problems, autism, attention deficit hyperactivity disorder, or psychiatric diagnoses should be actively looked for and treated.

Drug resistance is defined as a 'failure of adequate trials of two tolerated, appropriately chosen, and used antiepileptic drug schedules (whether as monotherapies or in combination) to achieve sustained seizure freedom'(Kwan et al., 2010). This is important because the chances of seizure freedom with a further medication after two drugs have failed is less than 12%. Thus, failure of a second AED should now prompt timely referral for consideration of other treatments, including epilepsy surgery, the ketogenic diet, and in children who are not candidates for resective epilepsy surgery, neurostimulation with vagus nerve stimulation (VNS) therapy.

Presurgical evaluation of a child for epilepsy surgery

Epilepsy surgery removes, disconnects, or ablates brain parenchyma assumed to generate ictal epileptic (seizure) activity with the primary aim of seizure freedom or significant improvement of seizures, without detriment to function. Careful presurgical evaluation (PSE) in a centre with expertise in epilepsy surgery for children should determine the area of seizure onset, and also minimize the risk that surgery might lead to significant impairments (**Fig. 91.1**). The 2006 International League Against Epilepsy (ILAE) subcommission for paediatric epilepsy surgery recommendations for referral and evaluation of children remain relevant, and are being updated (Cross et al., 2006). Technological advances are enhancing PSE and mean that MRI lesion-negative children are also potential candidates for surgery.

Special considerations in children

There is no minimum age for presurgical evaluation, indeed PSE should begin as early as possible to shorten the duration of disease and minimize the impact of a long-term seizure burden. Identification of potentially surgically remediable epilepsy in children may be complex. Semiology is often less helpful, especially in the younger age groups and is less lateralizing than in adults. Additionally, children presenting with apparently generalized features, such as epileptic spasms, may have a focal seizure onset zone, but with rapid spread of ictal activity. Imaging interpretation in children is complex and requires specialized paediatric neuroradiologists, well versed in the changing appearances of the paediatric brain over time. In young children under the age of 2 years, prior to the completion of myelination, lesional abnormalities may not be appreciated and repeat imaging over several years may be needed to identify surgical cases. The psychosocial effects of paediatric epilepsy are taking place against the background of changing cognitive development and the timing of surgery will therefore be influenced by developmental trajectory. Cognitive outcome will be optimized by earlier surgery and its attendant potential for drug reduction (Boshuisen et al., 2015).

Components of the presurgical evaluation

The components of an initial (now termed phase 1) PSE remain essentially unchanged from the 2006 recommendations: interictal scalp EEG (including sleep), a dedicated MRI brain epilepsy protocol, long-term ictal scalp video-EEG where possible, neuropsychology assessment and where needed functional MRI (fMRI) (Ryvlin et al., 2014). We believe neuropsychiatry and neuro-ophthalmology should also be included. Extended phase 1 investigations include positron emission tomography, magnetoencephalography (MEG), EEG-fMRI, electrical source imaging, and high-resolution EEG. Ictal and interictal single-photon emission CT (SPECT) with postprocessing analysis for ictal focal brain hyperperfusion can be useful in delineating candidate tubers in tuberous sclerosis and to localize the epileptogenic zone (EZ) in lesion-negative cases.

Underlying conditions

In 2004, the ILAE carried out a survey of international paediatric epilepsy centres. Hippocampal sclerosis, which forms a large proportion of cases in contemporary adult series, was relatively underrepresented in paediatric series whereas cortical dysplasia forms the largest group (Pellock et al., 2008). The incidence of various conditions is shown in **Table 91.1**) (Pellock et al., 2008).

Operation type

Lobar and focal resections provide the bulk of surgical procedures in most paediatric epilepsy surgery centres. However, the proportion of multilobar and hemispheric procedures is greater than in adult series. The 2004 ILAE survey demonstrates the range of procedures in paediatric centres (**Table 91.2**) (Pellock et al., 2008).

Surgical considerations

The principles of epilepsy surgery remain similar in both adult and paediatric procedures and comprise the maximum removal of presumed lesional tissue while minimizing damage to eloquent

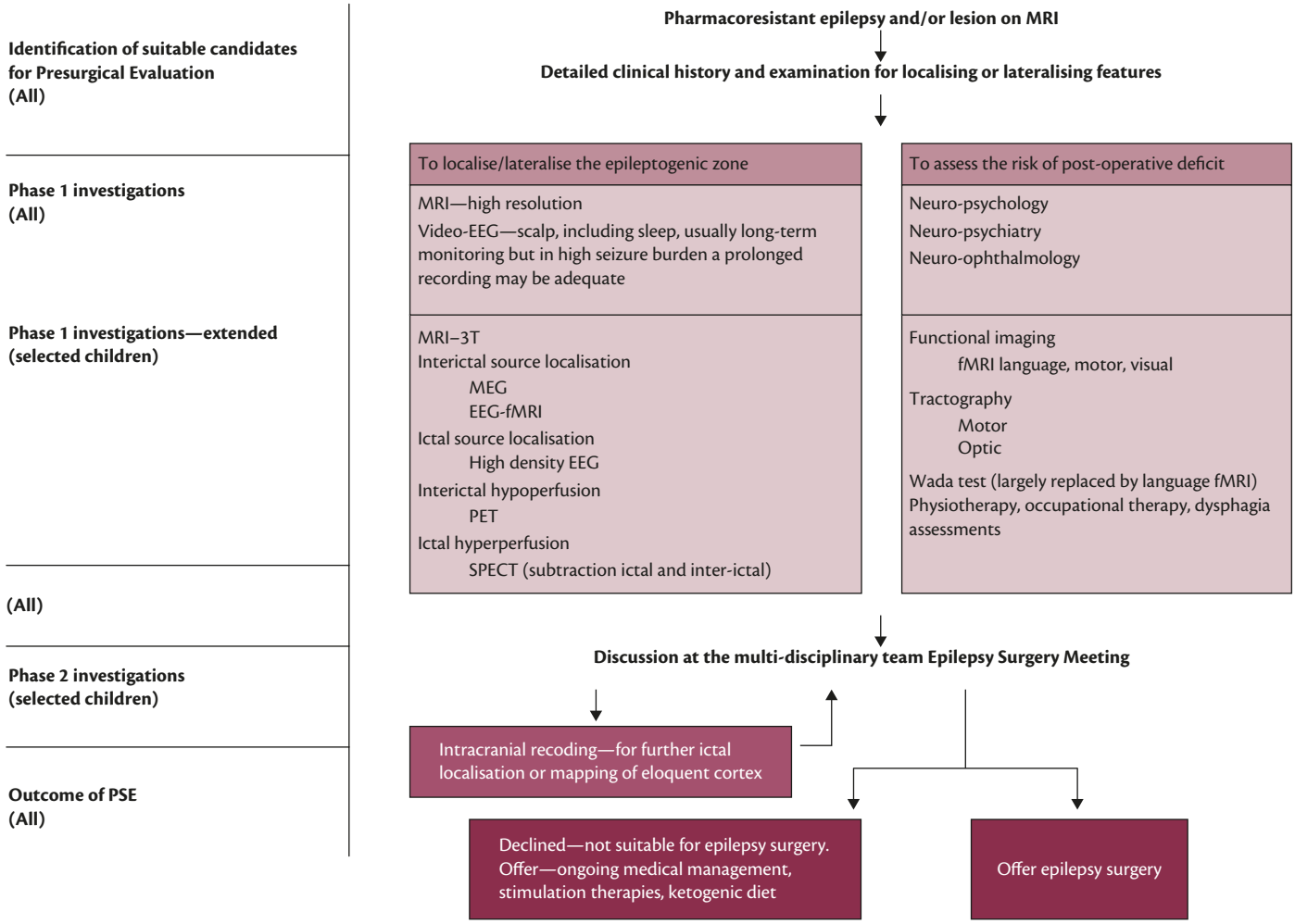
Identification of suitable candidates for Presurgical Evaluation (All)
Pharmacoresistant epilepsy and/or lesion on MRI
Detailed clinical history and examination for localising or lateralising features
Phase 1 investigations (All)
To localise/lateralise the epileptogenic zone
MRI—high resolution
Video-EEG—scalp, including sleep, usually long-term monitoring but in high seizure burden a prolonged recording may be adequate
To assess the risk of post-operative deficit
Neuro-psychology
Neuro-psychiatry
Neuro-ophthalmology
Phase 1 investigations—extended (selected children)
MRI–3T
Interictal source localisation
MEG
EEG-fMRI
Ictal source localisation
High density EEG
Interictal hypoperfusion
PET
Ictal hyperperfusion
SPECT (subtraction ictal and inter-ictal)
Functional imaging
fMRI language, motor, visual
Tractography
Motor
Optic
Wada test (largely replaced by language fMRI)
Physiotherapy, occupational therapy, dysphagia assessments
(All)
Discussion at the multi-disciplinary team Epilepsy Surgery Meeting
Phase 2 investigations (selected children)
Intracranial recoding—for further ictal localisation or mapping of eloquent cortex
Outcome of PSE (All)
Declined—not suitable for epilepsy surgery. Offer—ongoing medical management, stimulation therapies, ketogenic diet
Offer epilepsy surgery

Fig. 91.1 Presurgical evaluation pathway.

tissue. Resection is often planned to include tissue up to the next pial boundary surrounding a lesion. Dual pathology appears more prevalent in paediatric cases and especially so for temporal resections. There has therefore been less movement towards more selective resective strategies for hippocampal sclerosis than in adult practice. Seizure freedom remains the most important determinant of postoperative cognitive function (Skirrow et al., 2015) and so more extensive temporal lobe resection to include neocortical as well as mesial structures is generally thought to be beneficial as the larger volume of resection may improve seizure outcome despite removing potentially functional tissue.

In children, the brain weighs proportionally more compared to body weight than in adults. Additionally, young patients often

Table 91.1 Incidence of underlying conditions in paediatric epilepsy surgery

Aetiology	Percentage of cases
Cortical dysplasia	42%
Tumour	19%
Infection/stroke/trauma	10%
Hippocampal sclerosis	6%
Tuberous sclerosis	5%
Hypothalamic hamartoma	4%
Sturge-Weber syndrome	3%
Rasmussen syndrome	3%
Vascular lesion	1%
Other	7%

Source data from Pellock, J. et al., 2007. *Pediatric Epilepsy*, New York: Demos Medical.

Table 91.2 Procedure type in paediatric epilepsy surgery

Surgical procedure	Percentage of cases
Lobar/focal lesionectomy	48%
Hemispherotomy	16%
Multilobar resection	13%
Vagus nerve stimulator	16%
Corpus callosotomy	3%
Other	4%

Source data from Pellock, J. et al., 2007. *Pediatric Epilepsy*, New York: Demos Medical.

require large cortical resections which can be associated with significant blood loss relative to total blood volume. Great attention must be paid by both surgeon and anaesthetist to ensure adequate haemostasis and resuscitation and this highlights the need for a dedicated surgical and anaesthetic team able to predict and pre-empt operative issues.

Detailed descriptions of the principles of lesionectomy and amygdalohippocampectomy are covered in Chapter 83 and will not therefore be covered further here.

Hemispherectomy/Hemispherotomy

Hemispherectomy or hemispherotomy is a surgical procedure which aims to either resect or disconnect the entire cortex of one cerebral hemisphere. It was first introduced in 1928, by both Dandy and L'Hermitte, as a treatment for hemispheric glioma and although it did not improve prognosis in this patient group it has subsequently become an important technique in epilepsy surgery. Multiple technical variations have been proposed and these will be discussed next. For convenience, we will use the term hemispherotomy to encompass all procedures aimed at hemispheric resection or disconnection.

Indications for hemispherotomy include drug-resistant epilepsy which is hemispheric, or from multilobar pathology where less extensive resection is unsuitable, and seizures are deemed to be arising from the involved hemisphere. The contralateral hemisphere must be deemed healthy and there should be an existing hemiparesis. Over time the indications have widened and those mentioned can be considered relative. All potential cases should be discussed at an experienced multidisciplinary epilepsy surgery meeting.

Surgical decision-making will also take account of seizure burden and developmental trajectory, and 'palliative' hemispherotomy may be considered in some cases. Recent work has suggested that contralateral hemisphere MRI and EEG abnormalities may not affect prognosis in selected cases (Wyllie et al., 2007; Hallbook et al., 2010).

Pathologies in which hemispherotomy is indicated include hemimegalencephaly, migration disorders, cortical dysplasia, cerebral infarction, porencephaly, Sturge-Weber, and Rasmussen syndromes.

Functional consequences of hemispherotomy

All variants of this procedure involve interruption of the ipsilateral internal capsule and optic radiation. The inevitable consequence is contralateral hemiparesis and homonymous hemianopia. The effect of surgery depends on the preoperative functional status, age of the child, and preoperative cognitive ability. At one end of the scale a child with a hemispheric perinatal infarct with pre-existing dense hemiparesis and hemianopia will have minimal or no functional change after hemispherotomy. At the other extreme, a child with dominant hemisphere Rasmussen syndrome may have significant changes in language function, motor function, and vision. Decision-making in these latter cases is obviously complex and requires careful discussion with both patients and carers.

Technical evolution

Anatomic hemispherectomy for epilepsy was first described in 1938. In the 1960s it became apparent that the procedure was associated with a high risk of postoperative neurological deterioration secondary to superficial siderosis (secondary to recurrent haemorrhage into the surgical cavity) and hydrocephalus (Beier and Rutka, 2013). Subsequent techniques have seen a move towards cortical disconnection rather than resection. Rasmussen used the term functional hemispherectomy to describe a technique in which the central and temporal regions are resected with the frontal and occipital regions being disconnected. Further technical developments have led to a variety of hemispherotomy procedures involving little or minimal tissue resection with the aim of reducing operative time and blood loss (Villemure and Mascott, 1995; Dorfer et al., 2013). The choice of technique will depend on the surgical experience of the team and the underlying brain anatomy.

Technique

Currently two main approaches predominate, either lateral hemispherotomy centred on the insula region with the bulk of the procedure being performed through the ventricular system or alternatively a vertical parasagittal technique may be used.

Regardless of the technique used the following must be achieved; disconnection of the ipsilateral internal capsule, disconnection of mesial temporal structures, complete corpus callosotomy, and disconnection of horizontal frontal fibres.

Complications include haemorrhage, infection, postoperative non-infectious fever, aseptic meningitis, contralateral stroke, cerebral infarction, or oedema, hydrocephalus requiring a ventricular shunt in 10–15% and death in 1–3%.

Hemispherotomy outcome depends on the underlying pathology with overall seizure freedom of 70–80%. Outcome is better for acquired or progressive pathologies as opposed to those of developmental aetiology. The outcome is not affected by the surgical technique used. See **Box 91.1**.

Invasive monitoring

Invasive monitoring is a technique in which electrodes are placed either into, or over the surface of the brain, in order to record ictal and interictal activity with higher spatial resolution than is possible with a scalp EEG. Electrodes are usually left in place for approximately 7 days in order to collect sufficient data. These techniques also allow for electrical stimulation of the brain through the electrodes in order to delineate eloquent cortex or to identify epileptogenic networks. This may be especially useful in young children in whom awake craniotomy may not be an option.

Two techniques predominate: subdural grids can be placed via a craniotomy or multiple stereotactically placed depth electrodes can be placed percutaneously using neuronavigation (stereoEEG). The two methodologies have differing advantages, but in general terms subdural grids offer higher resolution mapping whereas stereoEEG gives better coverage of deep and mesial cortical areas. See **Box 91.2**.

Surgical procedures for the palliation of paediatric epilepsy

A proportion of patients with severe and medically refractory epilepsy will not be candidates for resective surgery. In this set of patients, consideration may be given to palliative surgical procedures

Box 91.1 Case study 1

A 5-month-old was referred with onset of infantile spasms at age 2 weeks. She was drug responsive at initial review and making good developmental progress other than fisting of the left hand. MRI showed a widespread malformation of cortical development affecting the right cerebral hemisphere (Fig. 91.2) and EEG revealed a chaotic pattern over the right hemisphere. Seizures recrudesced at the age of 12 months and she underwent a right hemispherotomy without complications. At 1-year follow-up she was seizure-free and making good developmental gains, with only a mild increase in tone on the left-hand side.

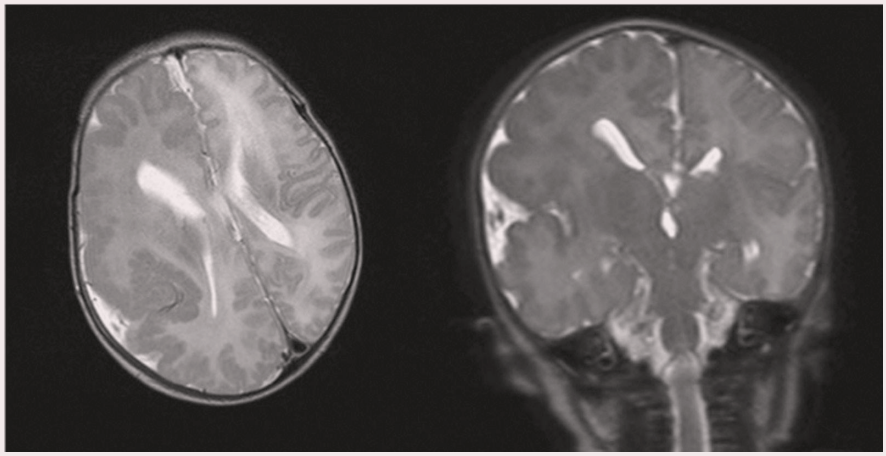

Fig. 91.2 Axial and coronal T2 MRI of a 5-month-old child showing extensive cortical malformation and polymicrogyria affecting right hemisphere.

Box 91.2 Case study 2

A 16-year-old boy had seizures with frontal lobe semiology of onset at 8 years. He had failed treatment with five AEDs. Other than some specific difficulties with memory, he had normal neurocognition. An MRI was initially felt to be lesion negative. Extended imaging identified a subtle right middle frontal gyrus lesion and after stereoEEG implantation (Fig. 91.3) he underwent successful lesionectomy. Histology was of a focal cortical dysplasia. He is seizure free and off all AEDs at 1-year follow-up.

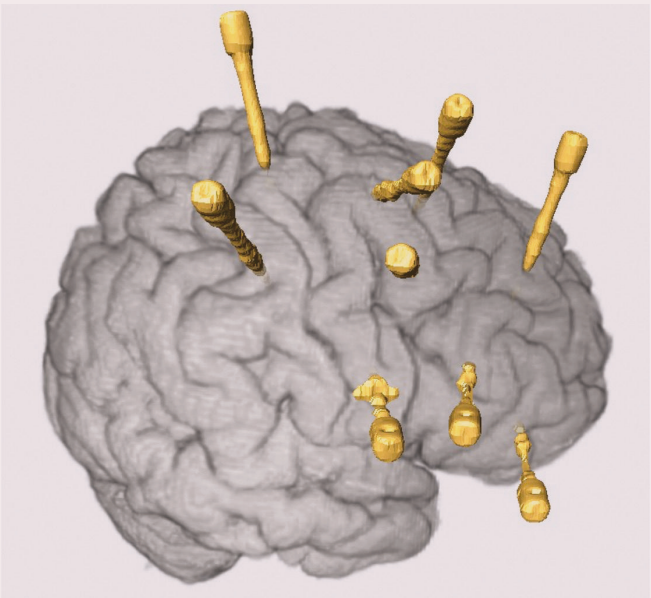

Fig. 91.3 Postoperative stereoEEG imaging demonstrating implanted electrode locations coregistered with segmented cortex.

aiming to reduce the frequency or severity of seizures with a view to improving quality of life.

Indications for palliative epilepsy surgery include generalized or multifocal seizures where there is an inability to localize the seizure source or where seizures arise from eloquent cortex where the risk to eloquent tissue is deemed unacceptably high.

Palliative epilepsy surgery techniques include corpus callosotomy, VNS, and multiple subpial transections

Corpus callosotomy

Sectioning of the corpus callosum is most effective in patients suffering with atonic (drop) seizures with lesser efficacy against tonic seizures. Complete callosotomy leads to approximately a 70% reduction in drop attacks in 70% of patients. Complete corpus callosotomy has a higher chance of seizure reduction as opposed to partial callosotomy (Kasasbeh et al., 2014). The incidence of postoperative disconnection syndrome in paediatric series is extremely low and this relates, in part, to the fact that most children in which this procedure is indicated, have significant developmental delay, and pre-existing communication impairment. In contrast to adult practice, we perform complete callosotomy in the vast majority of paediatric candidates with partial, anterior two-thirds, callosotomy reserved for children with little or no cognitive impairment.

A craniotomy crossing the midline is used and an interhemispheric approach to the corpus callosum is made. Arachnoid scarring is often encountered and great care must be taken to divide adhesions. The corpus callosum is then divided from rostrum to splenium.

Vagus nerve stimulation (VNS)

The hypothesis that vagus nerve stimulation might attenuate epileptic seizures was first proposed in 1985.

This was subsequently supported by animal studies and human clinical trials. VNS has similar efficacy to corpus callosotomy but without the attendant risks of intracranial surgery.

VNS involves implanting a stimulating electrode around the left vagus nerve (chosen to reduce the risk of cardiac effects) and connecting it to a subcutaneous stimulator placed most commonly in the pectoral region. The stimulator is set to a background discharge setting and can be triggered to an on-demand setting by swiping a magnet across the device. The latest version of the device senses heart rate and has an algorithm designed to detect seizure related tachycardia, which then automatically triggers the on-demand setting, with the aim of terminating the seizure (Schneider et al., 2015).

Multiple subpial transections (MST)

MST is a technique in which multiple transection are made at 5 mm intervals perpendicular to the gyral long axis in the presumed epileptogenic zone. The aim is to disrupt lateral cortico-cortical connections leaving cortical areas without the required critical mass required to sustain development of seizures, yet preserving the vertical cortico-subcortical pathways required for function.

MST has been used in conditions where epileptogenesis is presumed to arise from eloquent cortex and in particular gained popularity in the treatment of Landau-Kleffner syndrome. It has recently become less popular as it causes cortical damage and its efficacy has been questioned.

Choice of procedure

Corpus callosotomy and VNS may have synergistic effects. Corpus callosotomy appears to have greater efficacy in patients with atonic seizures, yet carries the risks of intracranial surgery. We would recommend corpus callosotomy as the initial surgical approach in those patients where atonic seizures predominate or where they are thought to have the greatest effect on quality of life.

Previously it was not possible to perform detailed MRI scans in patients with a VNS *in situ* however this has been addressed by modern MRI scanner design and VNS need not now preclude future evaluation for epilepsy surgery.

Controversies in paediatric epilepsy surgery

Timing of hemispherotomy surgery in dominant hemisphere Rasmussen's syndrome

Rasmussen's syndrome is characterized by refractory seizures, unilateral cortical atrophy, and associated neurological deficits. Hemispherotomy surgery remains the only cure and provides a 70–80% chance of seizure freedom (Bien and Schramm, 2009). Nevertheless, this surgical strategy has inevitable consequences of homonymous hemianopia, hemiplegia and, in patients with dominant hemisphere involvement, language dysfunction. These deficits may be present preoperatively, yet their severity, and speed of onset, varies. Cognitive decline is common, yet not inevitable, and may be heralded by the appearance of independent interictal epileptiform discharges over the contralateral hemisphere (Longaretti et al., 2012). Short duration between seizure onset and surgery is generally associated with better cognitive outcome and early surgery is, therefore, often thought to be beneficial (Jonas et al., 2004). The degree of language transfer after hemispherotomy relates primarily to age at the start of the disease process and in suitable patients may be assessed using language fMRI or Wada investigation. Controversy exists as to whether this language function transference to the contralateral hemisphere is driven best by early surgery, when neural plasticity may be retained, or whether it is best achieved by waiting for the disease process to progress in an attempt to allow function to become established naturally in the unaffected hemisphere (Hartman and Cross, 2014). Even when dominant language function remains in the affected hemisphere at the time of surgery, it is rare to produce complete aphasia (Boatman et al., 1999). Receptive function is generally retained although expressive language may be significantly reduced. Decisions around the timing of surgical treatment must be guided by the severity of seizures, and assessment of both the degree and evolution of neurological deficits (Varadkar et al., 2014). This is a challenging situation for families and clinicians and requires evaluation of the likely final outcomes of both surgical and conservative approaches.

FURTHER READING

Cataltepe, O. & Jallo, G.I. (2010). *Pediatric Epilepsy Surgery*. New York, NY: Thieme Publishing.

Chapman, K. & Rho, J.M. (2008). *Pediatric Epilepsy Case Studies*. New York, NY: CRC Press.

Lüders, H.O. (2008). *Epilepsy Surgery*. London, UK: Informa.

Pellock, J., Bourgeois, B.F.D., Dodson, E.W., et al. (2008). *Pediatric Epilepsy*. New York, NY: Demos Medical.

REFERENCES

Advanced Life Support Group (2011). *Advanced Paediatric Life Support*, 5th edition. London, UK: BMJ Books.

Beier, A.D. & Rutka, J.T. (2013). Hemispherectomy: historical review and recent technical advances. *Neurosurg Focus*, **34**(6), E11.

Berg, A.T., Berkovic, S.F., Brodie, M.J., et al. (2010). Revised terminology and concepts for organization of seizures and epilepsies: report of the ILAE Commission on Classification and Terminology, 2005–2009. *Epilepsia*, **51**(4), 676–85.

Bien, C.G. & Schramm, J. (2009). Treatment of Rasmussen encephalitis half a century after its initial description: promising prospects and a dilemma. *Epilepsy Res*, **86**(2–3), 101–12.

Boatman, D., Freeman, J., Vining, E., et al. (1999). Language recovery after left hemispherectomy in children with late-onset seizures. *Ann Neurol*, **46**(4), 579–86.

Boshuisen, K., van Schooneveld, M.M., Uiterwaal, C.S., et al., (2015). Intelligence quotient improves after antiepileptic drug withdrawal following pediatric epilepsy surgery. *Ann Neurol*, **78**(1), 104–14.

Cross, J.H., Jayakar, P., Nordli, D., et al. (2006). Proposed criteria for referral and evaluation of children for epilepsy surgery: recommendations of the Subcommission for Pediatric Epilepsy Surgery. *Epilepsia*, **47**(6), 952–9.

Dorfer, C., Czech, T., Dresslerxc, A., et al. (2013). Vertical perithalamic hemispherotomy: a single-center experience in 40 pediatric patients with epilepsy. *Epilepsia*, **54**(11), 1905–12.

Fisher, R.S., Acevedo, C., Arzimanoglou, A., et al. (2014). ILAE official report: a practical clinical definition of epilepsy. *Epilepsia*, **55**(4), 475–82.

Hallbook, T., Ruggieri, P., Adina, C., et al. (2010). Contralateral MRI abnormalities in candidates for hemispherectomy for refractory epilepsy. *Epilepsia*, **51**(4), 556–63.

Hartman, A.L. & Cross, J.H. (2014). Timing of surgery in Rasmussen syndrome: is patience a virtue? *Epilepsy Curr*, **14**(1 Suppl), 8–11.

Jonas, R., Nguyen, S., Hu, B., et al. (2004). Cerebral hemispherectomy: hospital course, seizure, developmental, language, and motor outcomes. *Neurology*, **62**(10), 1712–21.

Kasasbeh, A.S., Smyth, M.D., Steger-May, K., Jalilian, L., Bertrand, M., & Limbrick, D.D. (2014). Outcomes after anterior or complete corpus callosotomy in children. *Neurosurgery*, **74**(1), 17–28.

Kwan, P., Arzimanoglou, A., Berg, A.T., et al. (2010). Definition of drug resistant epilepsy: consensus proposal by the ad hoc Task Force of the ILAE Commission on Therapeutic Strategies. *Epilepsia*, **51**(6), 1069–77.

Longaretti, F., Dunkley, C., Varadkar, S., Vargha-Khadem, F., Boyd, S.G., & Cross, J.H. (2012). Evolution of the EEG in children with Rasmussen's syndrome. *Epilepsia*, **53**(9), 1539–45.

Nunes, V.D., Sawyer, L., Neilson, J., & Sarri, G. (2012). Diagnosis and management of the epilepsies in adults and children: summary of updated NICE guidance. *BMJ*, **344**(j2), e281.

Pellock, J., Bourgeois, B.F.D., Dodson, E.W., et al. (2008). *Pediatric Epilepsy*. New York, NY: Demos Medical.

Ryvlin, P., Cross, J.H., & Rheims, S. (2014). Epilepsy surgery in children and adults. *Lancet Neurol*, **13**(11), 1114–26.

Schneider, U.C., Bohlmann, K., Vajkoczy, P., & Straub, H.B. (2015). Implantation of a new Vagus Nerve Stimulation (VNS) Therapy® generator, AspireSR®: considerations and recommendations during implantation and replacement surgery--comparison to a traditional system. *Acta Neurochirurgica*, **157**(4), 721–8.

Skirrow, C., Cross, J.H., Harrison, S., et al., (2015). Temporal lobe surgery in childhood and neuroanatomical predictors of long-term declarative memory outcome. *Brain*, **138**(1), 80–93.

Varadkar, S., Bien, C.G., Kruse, C.A., et al. (2014). Rasmussen's encephalitis: clinical features, pathobiology, and treatment advances. *Lancet Neurol*, **13**(2), 195–205.

Villemure, J.G. & Mascott, C.R. (1995). Peri-insular hemispherotomy: surgical principles and anatomy. *Neurosurgery*, **37**(5), 975–81.

Wyllie, E., Lachhwani, D.K., Gupta, A., et al. (2007). Successful surgery for epilepsy due to early brain lesions despite generalized EEG findings. *Neurology*, **69**(4), 389–97.

SECTION 19

CSF disorders

92. **Hydrocephalus and normal CSF dynamics** *1057*
Alexander Gamble and Harold Rekate

93. **Shunt technology and endoscopic ventricular surgery** *1071*
Ian K. Pople and William Singleton

94. **Normal pressure hydrocephalus** *1083*
Nicole C. Keong

95. **Pseudotumour cerebri syndrome** *1093*
John D. Pickard and Nicholas Higgins

96. **Arachnoid cysts** *1101*
Ruichong Ma and Stana Bojanic

92

Hydrocephalus and normal CSF dynamics

Alexander Gamble and Harold Rekate

Introduction

The first investigations into the nature of CSF dynamics began in the late 1800s. These works paved the way for a renaissance in the elucidations of CSF physiology that occurred between the second and sixth decades of the 1900s. Pioneering research established the basic principles upon which rests nearly all our understanding of CSF production, circulation, and absorption. CSF physiology and hydrocephalus continues to be an active area in neuroscience research to this day. The general hydrodynamic behaviours of CSF were accurately described long ago but their underlying mechanisms have been a source of controversy in the neurosciences to this day. This chapter serves to define the most effective and robust theories governing CSF dynamics and the aetiologies behind many of the hydrocephalic states. This chapter should serve as a general review, or as a starting point to the reader whose goal is to explore the larger body of knowledge pertaining to cerebrospinal hydrodynamics.

Hydrocephalus

Hydrocephalus is a condition characterized by a dynamic imbalance between the formation (production) *and absorption* of spinal fluid resulting in an increase in the size of the ventricular spaces. In the most rudimentary sense, cerebrospinal fluid (CSF) resembles a body of water behind a floodgate. Fluid accumulates behind the closed floodgate and when a sufficient level is achieved, the excess will flow over this barrier. The volume expelled would be proportionate to its height above the barrier, automatically maintaining a constant volume in the circulating pool. Hydrocephalus would be akin to inappropriately raising the level of the floodgate with a resultant increase in the volume of fluid contained behind it. Our initial solution as neurosurgeons has been to drill a conduit from the floor of the reservoir to a point downstream of the floodgate, subverting the physics that would normally control the local environment. Even with a proper valvular mechanism to regulate flow through our artificial conduit, the laws governing flow out of the system have been reversed from a passive, self-regulating overflow mechanism to an active siphon. Although overly simplistic, this metaphor illustrates the imposition of a non-homeostatic strategy on a natural system. We can surmise that much like in our natural world, unintended consequences will arise when disrupting complex natural systems, analogous to the difficulties we encounter as neurosurgeons in the management of complex hydrocephalic patients.

CSF diversion with shunting devices remain the primary treatment option for hydrocephalus but comes with alarmingly high rates of failure and complication, sometimes with disastrous consequences. Hydrocephalus was largely untreatable and fatal until the mid-twentieth century with the advent of valve-regulated CSF shunts (Nulsen, 1951). Approximately, about 0.5–0.8/1000 infants born in developed countries will be afflicted with the condition (Garne et al., 2010; Jeng et al., 2011) and the majority will depend on a shunt. At the other end of the spectrum, it is estimated that around 700 000 individuals in the United States and 2 million in Europe suffer from normal pressure hydrocephalus (NPH) (Jaraj et al., 2014). Those responding to a shunt can enjoy an additional six quality adjusted life years, which is roughly equivalent to the benefit derived from coronary artery bypass grafting or surgery for breast cancer (Stein et al., 2006).

Role of CSF in the central nervous system (CNS)

The human brain, representing only 2% of body mass requires 15% of cardiac output, 20% of oxygen consumption, and a quarter of total body glucose utilization. The incredible complexity and energy expenditure as compared to other animals is paralleled by a commensurate increase in total CSF production and absorptive capacity. CSF fulfils multiple roles in the maintenance of brain homeostasis. It provides a buoyant force, cushioning nervous tissue within its rigid case of bone. The CSF volume serves as a capacitor to dampen the rapid fluctuations of blood volumes and pressures experienced throughout the cardiac cycle. As the arachnoid

Table 92.1 Comparison of CSF composition to plasma

Concentration (mg/100 ml^{-1})		
	CSF	Plasma
Protein	16–38	6300–8500
Glucose	45–80	80–120
Amino Acids	1.5–3	8–120
Creatinine	0.5–2.2	0.7–2
Urea	5–39	22–42
Lactate	8–25	4.7
Average electrolytes (mmol/kg^{-1})		
Sodium	147	150
Potassium	2.86	4.63
Calcium	1.14	2.35
Magnesium	1.1	0.8
Chloride	113	99
Bicarbonate	23.3	26.8
Phosphate	3.4	4.7
pH	7.3	7.4

Adapted with permission from Hladky, S.B. & Barrand, M.A., Mechanisms of fluid movement into, through and out of the brain: evaluation of the evidence, *Fluids and Barriers of the CNS*, Volume 11, Issue 1, p. 26. Copyright © 2014 Hladky and Barrand; licensee BioMed Central.

villi are capable of transferring particles on the order of a few microns into the systemic circulation, circulating CSF is able to clear not only metabolic wastes, but large proteins and cellular debris as well. A growing number of growth factors, hormones, vitamins, and micronutrients have been shown to be directly excreted into CSF for the purpose of distal delivery to their target cells via CSF pathways.

Neurons require tight regulation of their extracellular environment for optimal function. In brain parenchymal extracellular fluid (ECF) and CSF, the concentration of ions and macromolecules are effectively maintained within very narrow ranges. The blood–brain barrier (BBB) and blood CSF barrier (BCSFB) maintains disparate solute concentrations as compared to plasma as demonstrated in Table 92.1. The unique anatomical microcirculation of the brain tightly and selectively regulates passage of molecules and electrolytes. These barriers are on the order of ten times less permeable to the flow of water and at least a thousand times less permeable to the flow of organic and inorganic solutes than that of the fenestrated endothelium present in most other peripheral tissues. Although the transfer of solutes into brain ECF and CSF from plasma is an ultra-selective, active process, the movement of water between physiological compartments is passive but equally precise, as water will always follow solute concentration. The physical arrangement of endothelial cells and glial cell foot processes comprising the BBB is also able to withstand increased hydrostatic and osmotic forces far better than other organs. This serves to protect brain tissue from becoming oedematous secondary to increased filtration driven by blood pressure or low plasma oncotic pressure. Chronic hypertension or oedematous states caused by low serum protein content are well tolerated by the CNS whereas their effects elsewhere in the body may be rapidly deleterious.

Changes in CSF physiology in age and disease

CSF production decreases with age owing to fibrosis of choroid plexus and a decrease parenchymal volume as neurons and glia are lost to senescence. The total CSF volume roughly doubles from young adulthood to the seventh and eighth decades (Courchesne et al., 2000). Taken together, there is a progressive diminution in CSF turnover, reflecting a relative stagnation of CSF with advancing age. In childhood, replacement rates may be as high as 6×/day, 4×/day in young healthy individuals and drops to 3×/day or less in normal elderly individuals (May et al., 1990; Serot et al., 2012).

In NPH and Alzheimer's dementia (AD), CSF replacement is even more dramatically reduced (see Table 92.2). Animal models of both AD and NPH demonstrate beta amyloid peptide (Aβ) and tau protein accumulation in brain tissue and that specific clearance pathways for those substances are impaired. (Shibata et al., 2000; Silverberg et al., 2010). Transthyretin (TTR) is produced exclusively by choroid plexus epithelium (Sousa et al., 2007) is the main chaperone of thyroxin (T_4), binds to Aβ monomers preventing fibril formation and provides a means of amyloid excretion out of the CNS (Redzic et al., 2005). There is a clear inverse correlation between ventricular volume and CSF Aβ levels in patients with mild cognitive impairment and frank AD (Ott et al., 2010). It is entirely plausible that this correlation ultimately results from the primary disease processes and does not necessarily substantiate cause and effect. That being said, the disturbances in fluid physiology observed in senescence, AD, and NPH are difficult to ignore and may play a significant role in their pathophysiology.

There may be more overlap between AD and NPH pathologies than previously understood. Whether both diseases can exist simultaneously is highlighted by the fact that CSF markers or tissue biopsy may not clearly delineate one from the other or responsiveness to CSF diversion in any individual patient (Golomb et al., 2000; Ott et al 2010). After strengthening the suspected clinical diagnosis of NPH with a 24-hour ICP monitoring, Leinonen et al. (2010) collected frontal brain biopsies at the time of shunt placement in 219 patients. Of the 168 (77%) patients who benefited from the shunt, 52 (31%) displayed AD-related pathology and 13 (25%) of them had developed clinical AD by the end of the follow-up. Some 69% of patients did not display AD-related pathology at shunt placement, but six still (5%) developed confirmed AD. Disappointingly, a recent large, double blinded, randomized, placebo-controlled trial of low-flow ventriculoperitoneal shunting in 215 AD patients failed to show

Table 92.2 CSF changes in normal pressure hydrocephalus and Alzheimer's disease (Hladky and Barrand, 2014)

	Normal	NPH	AD
Formation (ml/min)	0.4	0.25	0.2
Volume (ml)	150	300	250
Turnover rate (vol/day)	4	1.2	1.2

Adapted with permission from Johanson, C.E., Duncan, J.A., Klinge, P.M., Brinker, T., Stopa, E.G. & Silverberg, G.D., Multiplicity of cerebrospinal fluid functions: New challenges in health and disease, *Cerebrospinal Fluid Research*, Volume 5, Issue 10 Copyright © 2008 Johanson et al; licensee BioMed Central Ltd.

any clinical benefit or a decrease in CSF tau or Aβ levels (Silverberg et al., 2008). An important caveat to these negative results is that although a shunt can drain CSF, it cannot increase CSF production. Thus, the rate of CSF replacement would be dependent on the loss of ventricular volume which is usually not observed in shunted AD or NPH patients.

Production of CSF in the CNS

Parenchymal production

The total volume of brain ECF is estimated at around 280 ml (Johanson et al., 2008) and its total contribution to CSF volume is probably around one-third. This is a best estimate as the true contribution is virtually impossible to define by today's methods. The cytoarchitecture of central nervous tissue has evolved devoid of lymphatic vessels that would normally drain the ECF that is not reabsorbed into the venous circulation. This should not be confused with the concept of terminal CSF absorption via nasal lymphatics interfacing with arachnoid at the skull base. Lymphatic drainage is a necessary physiologic process because not all of the fluid that leaves the vascular compartment into the extracellular space can be reabsorbed into the venous circulation. Generally speaking, about 1% of the plasma volume delivered to a capillary bed will enter the extracellular space at the proximal end. About 90% of this filtrate is reabsorbed into the circulation as we move to the most distal postcapillary venules. Thus, depending on the tissue, approximately 0.1% of the delivered plasma volume delivered to the end organ ultimately becomes lymph. The ECF of brain parenchyma functions similarly to lymph in other tissues. It serves as a route for removal of cellular wastes, especially those of higher molecular weights. In addition to the water generated by metabolism itself, this extracellular fluid ultimately mixes with and flows into the ventricular and subarachnoid CSF spaces. Ependymal cells are linked together by gap junctions as opposed to the tight junctions observed at the BBB, allowing for a relatively free equilibration of solute and water between extracellular and ventricular spaces. CSF derived from the choroid plexus differs from the parenchymal ECF in that it is relatively pure of metabolic and cellular wastes. These properties create a concentration gradient driving ECF solutes into ventricular CSF so that the absorptive processes that will be discussed later in this chapter may ultimately excrete them into the venous circulation.

The choroid plexus

The choroid plexus epithelium (CPe) is responsible for production of at least two-thirds of the total CSF production in humans. CPe is traditionally thought of as not possessing a blood–brain barrier like the brain parenchyma and brightly enhances on contrast-enhanced neuroimaging. This does not imply a lack of selectivity, as a very effective blood CSF barrier (BCSFB) exists in the CPe that is ultrastructurally distinct from the BBB and uniquely specialized. Tight junctions between the cuboidal epithelial cells limit the flux of ions and water. The choroid plexus is highly vascular, receiving supply from the anterior and posterior choroidal arteries at a rate of 3–4 ml per minute, ten times greater than that of grey matter. Unlike other endothelial cells in the CNS, fenestrations are large allowing access to a high volume of plasma filtrate at the basolateral membrane. The basolateral membrane contains many infoldings and the apical, ventricular facing membrane is equipped with extensive microvilli demonstrated in **Figure 92.1**. These attributes, coupled with a branching, frond-like macroscopic architecture is what allows the approximate 2 total grams of CP present in the ventricles to secrete such a large daily volume.

Mechanisms of CSF formation in the choroid plexus

Although the fluid available basolaterally to CPe cells is a plasma ultrafiltrate, the fluid produced at the apical brush border is not. Electrolyte concentrations are highly and specifically regulated. The Na^+-K^+-ATPase in CPe is localized to the apical membrane, which is the opposite configuration to that in most other tissues. This sets up the major energy-dependent electrochemical gradient driving subsequent cotransport as well as being the primary source of CSF sodium. Oubain, a potent cardiac glycoside inactivates the pump and significantly decreases CSF production. The low intracellular sodium gradients created by Na^+–K^+–ATPase drive basolateral H^+ and Na^+ exchangers (NHE1), sodium dependent Cl^- –HCO_3 exchangers and Na^+–HCO_3 cotransporters. The Na^+–HCO_3 cotransporter is inhibited by the diuretic amiloride, which also reduces CSF production. Translocation of sodium across both membranes into the ventricular lumen drives chloride transmission as well, maintaining electrochemical neutrality. In addition to high intracellular K^+, this drives apical Na^+–K^+–$2Cl^-$ (NKCC1) cotransporters that are inhibited by loop diuretics, which also decrease CSF production.

The discovery of selective water channels, or aquaporins and the potential roles they play in the regulation of brain water physiology has greatly enhanced our understanding. Aquaporin-1 (AQP-1) is expressed at high levels almost exclusively along the apical membrane of the CPe in the CNS (Longatti et al., 2004; Praetorius and Nielsen, 2006). The CPe is also devoid of AQP-4, which is expressed almost exclusively on astrocytic foot processes at the BBB. AQP-1 knock-out mice produce 20–25% less CSF and have ~50% lower mean ICP values than wild-type mice (Oshio et al., 2003; Oshio et al., 2005) Downregulation of AQP-1 has also been demonstrated in animal models of hydrocephalus (Paul et al., 2011). The discovery of AQP-1 in this location reconciles the reality of CPe's ability to translocate water through a BCSFB in volumes that violated our previous understanding of a cell membrane's capabilities. Tight regulation of net solute transport results in precise translocation of water, much like that of the BBB but amplified many fold, due to the presence of AQP-1. These insights make AQP-1 an interestingly viable molecular target for future pharmacological treatment of hydrocephalus.

The enzyme carbonic anhydrase (CA) is expressed in several isoforms, some apically and basolaterally membrane bound, and others in soluble forms functioning in the cytosol. Though not directly involved in transport, the enzyme creates bicarbonate and hydrogen from water and carbon dioxide. The CA inhibitor acetazolamide is a very effective inhibitor of CSF production by reducing the H^+ and HCO_3 available for cotransport as well as altering overall CPe physiology by increasing cellular pH. Chronic acetazolamide administration also attenuates microvilli at the apical border, significantly reducing surface area needed for excretion (Azzam et al., 1978).

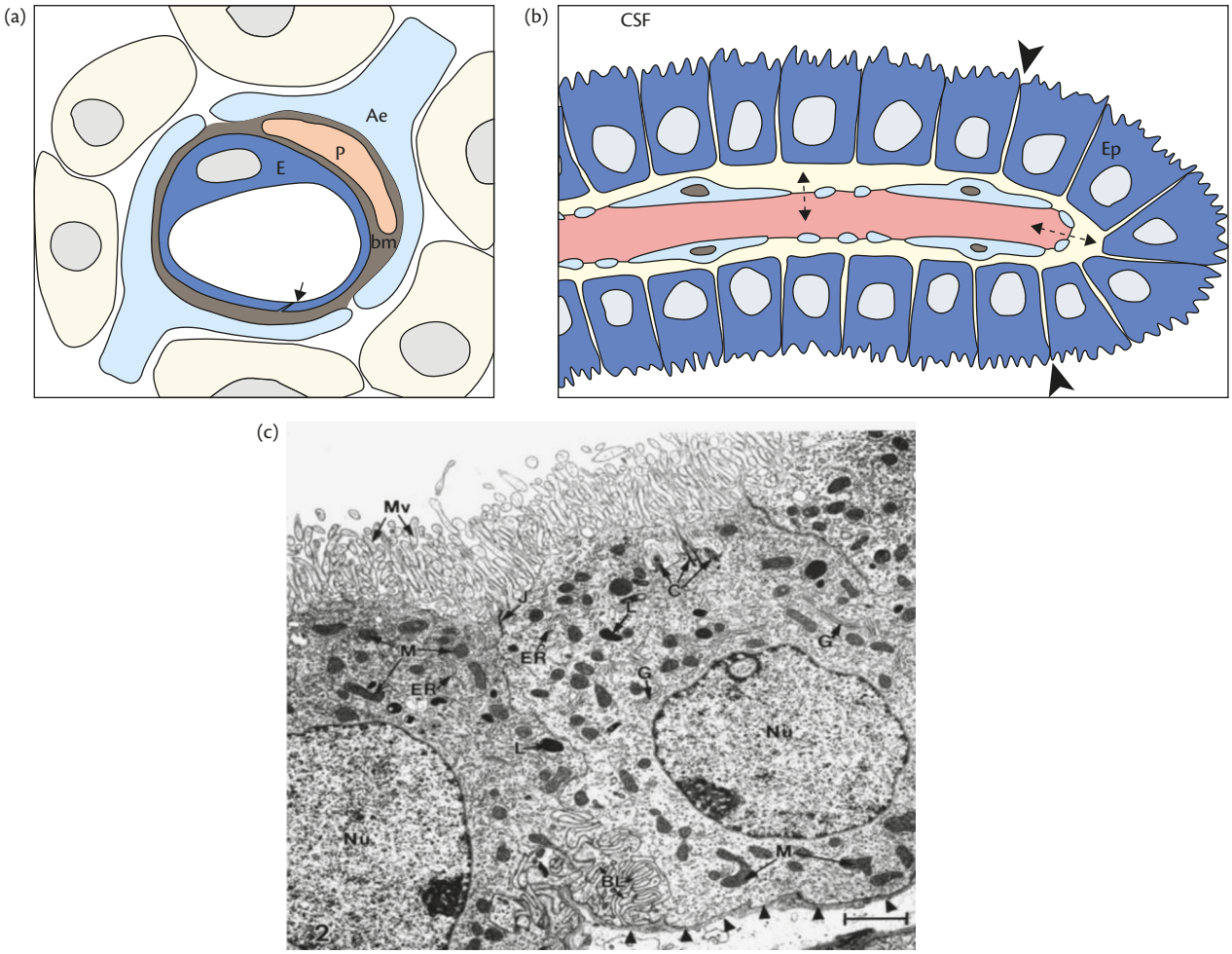

Fig. 92.1 Blood CSF and blood–brain barriers.

Schematics of the brain barriers. Barrier interfaces in the brain are indicated in blue. The primary site of the blood–brain barrier (A) is the endothelial cells of the cerebral blood vessels (E), supported by pericytes (P) and astrocytic endfeet (Ae). In the choroid plexus (B) the epithelial cells (Ep) are the barrier interface of the blood CSF barrier, as the endothelial cells in the stroma are fenestrated (Stolp et al., 2012).

(C) Ultrastructure of choroid epithelium. CP from a lateral ventricle of an untreated adult Sprague-Dawley rat was fixed for electron microscopy with OsO4. There is a profusion of apical membrane (CSF-facing) microvilli (Mv) and many intracellular mitochondria (M). J refers to the tight junction welding two cells at their apical poles. C = centriole. G and ER, Golgi apparatus and endoplasmic reticulum. Nucleus (Nu) is oval and has a nucleolus. Arrowheads point to basal lamina at the plasma face of the epithelial cell; the basal lamina separates the choroid cell above from the interstitial fluid below. Basal labyrinth (BL) is the intertwining of basolateral membranes of adjacent cells. Choroidal morphology resembles proximal tubule, consistent with both cell types rapidly turning over fluid. Scale bar = 2 μm.

(A) Reproduced with permission from Stolp, H., Neuhaus, A., Sundramoorthi, R. & Molnár, Z., The Long and the Short of it: Gene and Environment Interactions During Early Cortical Development and Consequences for Long-Term Neurological Disease, *Frontiers in Psychiatry*, Volume 3, p. 50, Copyright © 2012 Stolp, Neuhaus, Sundramoorthi and Molnár.

(B) Reprinted from *Trends in Neurosciences*, Volume 31, issue 6, Norman R. Saunders, C. Joakim Ek, Mark D. Habgood, Katarzyna M. Dziegielewska, Barriers in the brain: a renaissance?, pp. 279–86, Copyright (2008), with permission from Elsevier.

Trophic and protective function of choroid plexus

Many proteins implicated in neuronal development, maintenance and repair are produced in CPe and secreted into CSF such as: insulin-like growth factor-2 (IGF-2), members of the transforming growth factor-β (TGF-β) superfamily, bone morphogenic proteins (BMPs), fibroblast growth factors (FGFs), and retinoic acid (RA). These species have many implications in normal CNS development and injury response. CSF glucose levels approximately two-thirds that of plasma are regulated by CPe GLUT1 transporters present on the basolateral membrane. Similarly, stable concentrations of amino acids in the CSF are maintained by their respective transport mechanisms. CPe also contains specific nucleoside transporters removing purine and pyrimidine metabolites such as adenosine, which can appreciably alter neuronal function. Very high levels of the detoxifying and conjugating enzymes such as epoxide hydrolase, glutathione peroxidase, and UDP-glucuronosyltransferase among others have been measured in choroid plexus, implicating the CPe as a major site for drug metabolism in the brain (Ghersi-Egea and Strazielle, 2002). Additionally, CPe expresses high levels of solute carrier (SLC) and ATP-binding cassette proteins responsible for the active transport of drugs, toxins, and other organic proteins out of the CNS, which has many neuro-oncological implications.

Regulators of CSF production

It appears that CSF production occurs at a variable rate. Many innate factors modulating CSF production have been discovered in normal homeostasis and in pathological states. There exists a normal diurnal variation in production, which has been demonstrated in earlier invasive monitoring studies (Hayden et al., 1970) and more recently with MRI. Nighttime secretion may be twofold higher than during waking hours (Nilsson et al., 1992). It appears this phenomenon is autonomically governed as β-adrenergic antagonism abolishes this variation (Nilsson et al., 1994). The choroid plexus receives rich innervation from adrenergic, cholinergic, and peptidergic nerves, containing vasoactive intestinal polypeptide. Sympathetic innervation is inhibitory as sectioning of the superior cervical ganglion increases CSF production and intraventricularly delivered parasympathomimetic agents drastically decrease production (Lindvall and Owman, 1981).

Growing evidence exists for an innate molecular servomechanism modulating CSF production in response to rising pressures. Atrial natriuretic peptide (ANP), arginine vasopressin (AVP), angiotensin-II (AT-II), and fibroblast growth factor-2 (FGF) all appear to play pivotal roles. In animal models, intraventricular infusion of all these substances results in a diminution of CSF production. In human studies, CSF AVP and ANP levels correlate well with increasing ICP but not with ventriculomegaly observed in the absence of increased pressures (Seckl and Lightman, 1988; Tulassay et al., 1990; Yamasaki et al., 1997; Preston et al., 2003) Both also induce a higher ratio of CPe dark cells, the neuroendocrine cell implicated in longer term downregulation of CSF production and lowered chloride conductance (Johanson et al., 1999). CPe expresses receptors for AVP, suggesting a feed-forward mechanism as well receptors for ANG. In contrast to other peripheral tissues, AT-II decreases cerebrovascular resistance, and increases cerebral blood flow. Locally in the CNS, AT-II activates the sympathetic arm of the peripheral nervous system and increases vasopressin release into the blood. Its effects of lowering CSF production appear to be independent of autonomic tone and that CSF AVP promotes AT-II production, representing another positive feedback mechanism (Chodobski et al., 1998). As the BBB and BCSF render the CNS relatively impermeable to circulating AT-II, its vasoconstrictive effects are limited to the choroidal arterioles, representing an additional secondary and peripheral means of lowering CSF formation.

Although the mechanism of increased ANP synthesis and excretion into CSF is unknown, the observed proportional increases in CSF with elevated pressures and the CPe response to it is well documented. In animal models of hydrocephalus, choroidal ANP receptor expression is highly upregulated (Mori et al., 1990) and binding of ANP generates cGMP, leading to altered ion transport and the slowing of CSF production (Johanson et al., 2006). Opposite to AVP, ANP increases choroidal perfusion (Schalk et al., 1992). Taken together, the actions of ANP, AT-II, and AVP act to potently taper CSF production while maintaining CP perfusion and additionally augmenting blood flow to brain tissue at risk for ischaemia in response to elevated ICP. These mechanisms appear to play a significant role in the acute response to raised ICP and ventriculomegaly, but do not seem to be very relevant in chronic hydrocephalic states or those with comparatively lower pressures.

The ependyma

The ependyma does not produce CSF, but provides a relatively porous barrier for communication of parenchymal ECF and ventricular CSF. Ependymal cells lining the ventricular surfaces and that of the spinal central canal possess apical microvilli and motile cilia. They are joined by numerous gap junctions allowing electrochemical coupling between cells and synchrony of ciliary beating along the cranial-caudal axis. Along their luminal border, ependymal cells secrete a glycocalyx rich in sialic acid. Sialic acid is a negatively charged sugar that promotes laminar CSF flow and exerts a repulsive force against coaptation of ependymal surfaces (Jiménez et al., 2014). Micromolar injection of viral neuraminidase into the ventricles of rats, an enzyme degrading sialic acid, causes obliteration of the cerebral aqueduct within four hours (Grondona et al., 1996). This is followed by a sloughing of the majority of ependyma and ventriculomegaly of the lateral and third ventricles. In adult hydrocephalus, the ependyma is extensively thinned or lost entirely and cilia are absent (Bannister and Chapman, 1980). Ependymal denudation, loss of the germinal ependymal zone (the location of neural stem cells) and abnormal neuronal migration has been observed in human fetuses with moderate hydrocephalus and myelomeningocele (Domínguez-Pinos et al., 2005; Sival et al., 2011) A properly functional ependyma is integral to brain development and normal function throughout life and further investigations into its role in health and disease is needed.

Fluid compartments in the CNS

General hydrodynamic theory

The Scottish physicians Alexander Monro (for whom the foramen of Monro gets its name) and his pupil George Kellie are credited with the famous Monro–Kellie hypothesis popularized in the early 1800s. This is sometimes referred to as the Monro–Kellie Doctrine, but this is an erroneous conflation with the Monroe Doctrine, a nineteenth-century American foreign policy doctrine opposing colonialization by European powers. The pressure volume relationships proposed are just as alive today in medical education as they were over 100 years ago. Simply put, the skull is a compartment of fixed volume containing three major components: brain parenchyma, blood, and CSF. The parenchymal compartment consists of neurons, glia, and ECF. The vascular compartment may be divided into two general domains, the arterial and venous compartments. The intracranial subarachnoid space (SAS) can be divided into ventricular and cortical SAS, which can be further subdivided further into increasingly discrete compartments.

The ventricular system consists of the paired lateral, third, and fourth ventricles along with their respective channels of communication. These would be the paired foramen of Monro connecting the third to the lateral ventricles, the aqueduct of Sylvius connecting the third and fourth ventricles, the midline foramen of Magendie and paired lateral foramen of Lushka communicating the fourth ventricle with the cisterna magna and lateral recess of the cerebellopontine angle, respectively. From the cisterna magna in the posterior fossa the ventricular space is thus in communication with the entirety of the cisternal, cortical, and spinal SAS under normal circumstances.

We are comprised of mostly water and water is incompressible. The brain readily withstands compression in the immediate term, but will deform over time. It is evident to any clinician that significant shift of its volume is incompatible with life. In the case of an intracranial mass lesion such an expanding hematoma, CSF from the cranial compartment is shifted to the spinal compartment rapidly and venous blood in the dural venous sinuses partially empties into the systemic venous system to the right atrium. Thus, the spinal compartment acts as a capacitor for CSF volume and pressure while the absorptive mechanisms transfer CSF volume to the venous circulation. The human CNS has great absorptive capacity. CSF is absorbed into the venous circulation in a directly linear relationship with intracranial pressure over time. Eventually once the volume of the intracranial subarachnoid compartment nears exhaustion, intracranial volumes of greater resistances such as the vascular and eventually parenchymal become compromised.

Although the Monro–Kellie hypothesis is traditionally described in regards to an expanding mass lesion, the general principals apply well to the redistribution of fluid volumes in the CNS in all cases. As the volume of any particular compartment in the CNS changes, the volume of the other compartments must compensate commensurately with resistances to fluid conduction in the following order from high to low: arterial, venous, and subarachnoid. Whereas the intracranial space is of fixed volume, the spinal SAS is not. The epidural spinal space between vertebrae contains mostly fat and low-pressure venous plexuses that are quite compressible. Thus, one of the major functions of the spinal SAS is as a capacitance vessel accepting or contributing CSF volume to the cranial subarachnoid spaces.

Impaired hydrodynamics

Over each cardiac cycle, significant shifts in arterial and venous blood volumes occur with a corresponding expansion and contraction of the intracranial tissue volume in response. Thus, a major role of cerebrospinal fluid is as a buffer, shifting from spinal to cranial compartments, protecting the brain from rapid swings in pressure from systole to diastole. This normal flux is conducted through the foramen magnum. Therefore, abnormalities of the skull base and of the brain around the foramen magnum can disrupt efficient flow. Additionally, flow is affected by compartmental compliance. Significant obesity will tend to decrease spinal compliance and restriction to venous outflow from the cranial compartment will decrease compliance in the cranial compartment. Both of these phenomena are observed in idiopathic intracranial hypertension (IIH) formerly called pseudotumor cerebri to varying extents depending on the individual case. Both situations will contribute to higher peak and average ICP fluctuations in addition to higher flow velocities of CSF at the foramen magnum.

Individuals with Chiari I malformation have variable degrees of hindbrain herniation and may have a small posterior fossa. The abnormally low position of the cerebellar tonsils seen in Chiari I may represent an additional resistor in the circuit of CSF flow. This resistance is not exerted at the level of fourth ventricular outflow, but at the foramen magnum. Unimpeded flow from the ventricles to the cortical SAS is maintained and hydrocephalus should not develop unless there exists another, separate pathology driving its development. Dilation of another CSF space is commonly observed though, at the level of the central canal of the spinal cord. Heiss and colleagues have written extensively on the subject, shedding light onto the pathophysiology of syrinx formation in Chiari I (Heiss et al., 2012). High resistance at the foramen magnum to the flow of CSF between spinal and cranial compartments raises CSF flow velocity and local pressure gradients. Exaggerated local subarachnoid pressures at the foramen magnum and high cervical segments drive CSF into the spinal cord parenchyma and central canal additional to the native ependymal formation. Once a syrinx has developed, further enlargement is driven by the differential pressure gradient generated between spinal subarachnoid and central canal spaces with each heartbeat. Establishing unimpeded flow between cranial and spinal SAS will eliminate the syrinx over time and surgical failures largely result from a failure to effectively do so.

Flow of CSF through the cisternal space

An understanding of CSF flow within the cisternal spaces (see **Fig. 92.2**) is best understood beginning with the cisterna magna (CM). The CM is the conduit through which all CSF must flow and within which all CSF mixes. CSF emanating from the ventricular system flows into CM via the single, medial foramen of Magendie, and the paired lateral foramen of Lushka. Many sources have promoted the idea that from here, CSF flows downwards to the spinal SAS and then back upwards to enter the basal cisterns, which then communicate to the cortical SAS. This idea is inconsistent with the anatomy and our understanding of CSF dynamics. The CM is a mixing point connecting CSF compartments allowing equilibration of pressure and free conductance between them. Surgical decompression of the posterior fossa for Chiari 1 malformation and its multiple variations all effectively aim to achieve a similar goal: *The reconstitution of an effectively communicating cisterna magna*. Multiple pathways of outflow exist from the CM:

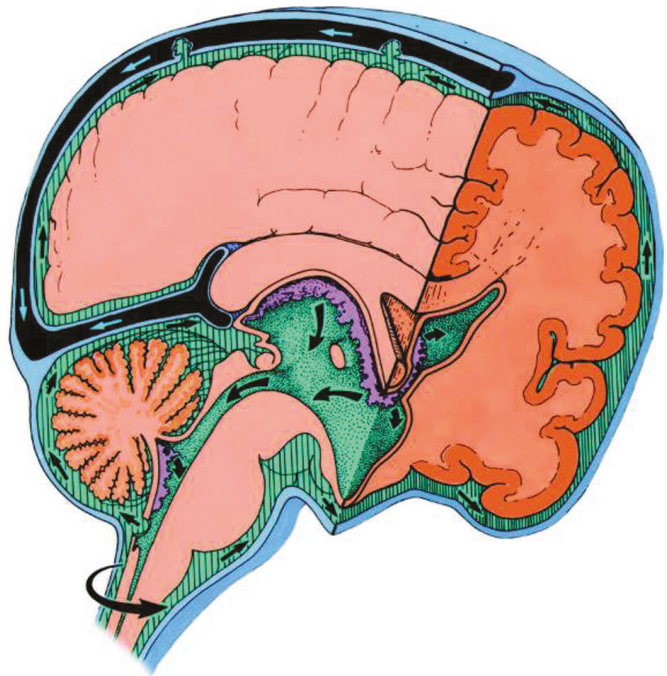

Fig. 92.2 Flow of CSF from the ventricular through the cisternal spaces.
Reproduced from Rekate, H. L., The definition and classification of hydrocephalus: a personal recommendation to stimulate debate, *Cerebrospinal Fluid Research*, Volume 5, Issue 2, Copyright © 2008 Rekate; licensee BioMed Central Ltd.

- Posterior-superiorly over the cerebellum to the quadrigeminal cistern, which then communicates anteriorly to the interpeduncular cistern via the ambient cisterns, wrapping around the midbrain.
- Anteriorly through the cerebellopontine cistern around the pons/medulla to the pontine cistern. Further flow continues superiorly to further discrete, anatomically named cisterns, and finally over the cerebral hemispheres.
- Inferiorly into the spinal SAS and the central canal of the spinal cord.

Knowledge of these cisternal spaces is especially relevant to CSF diversion. In endoscopic third ventriculostomy (ETV), a conduit is created in the floor of the third ventricle and the underlying arachnoid membrane, connecting it to the interpeduncular cistern below. The procedure is an excellent alternative to shunt placement in the case that the anatomical restriction to CSF flow is between the ventricles and the interpeduncular cistern. ETV remains the initial treatment of choice for acquired aqueductal stenosis or triventricular hydrocephalus in later life. Surgical fenestration of the lamina terminalis, the anterior-inferior limit of the third ventricle during aneurysm surgery in the setting of subarachnoid haemorrhage is commonly employed. As the anterior cerebral arteries and their communicator reside within the cistern of the lamina terminalis, access to this location is implied. The efficacy of this procedure is quite logical in that its mechanism is identical to ETV; the third ventricle is connected with a basal cistern.

CSF absorption

Our current understanding of CSF absorption stems from studies of artificial fluid infusion into the SAS performed many decades ago. Even before these experiments it had been long known that intracranial pressure exceeded venous sinus pressure, providing conceptual evidence for a gradient driving CSF absorption. The linear relationship between volumes infused and eliminated across a range of pressures was best initially characterized Weed and Mortensen in canines (Mortensen and Weed, 1934; Weed, 1935). The elimination of CSF into the venous compartment via a passive hydrostatic gradient was most clearly defined by studies carried out in goats by Pappenheimer and colleagues (Pappenheimer et al., 1962). They showed that below a certain threshold of pressure, fluid inflow perfectly matched outflow and thus no net absorption occurred. Once this threshold of pressure had been exceeded, there was a precise linear relationship between CSF pressure and absorption with a maintained total CSF volume. Furthermore, their findings supported previous claims that CSF production was independent of CSF pressure. Rubin et al. (1966) later confirmed these relationships in human adults in addition to defining a maximal elimination capacity of around 1.3 ml/min, or four times the average volume of production. Cutler et al. (Cutler et al., 1968) further corroborated these findings in children, finding an average threshold of absorption of 68 mm/H_20. Figures from their papers are often quoted and depicted in Figure 92.3.

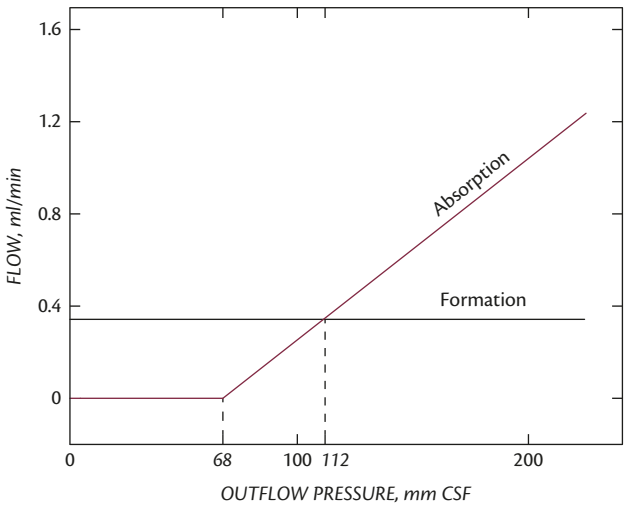

Fig. 92.3 CSF absorption in humans at various pressures.

Superimposed regression lines for CSF formation and absorption as a function of outflow pressure. The intercept at 112 mm indicates the pressure at which formation and absorption are equal. The pressure at which absorption is zero is also indicated.

Reproduced with permission from Cutler, R.W.P.; Page, L., Formation and Absorption of Cerebrospinal Fluid in Man, *Brain*, Volume 91, Issue 4, pp. 707–20, Copyright © 1968 Oxford University Press and the Guarantors of *Brain*.

The arachnoid granulations

As early as the eighteenth century, anatomists had proposed a secretory role of arachnoid granulations (AGs). These assumptions were bolstered by the observations of Luschka and Trolard that the granulations were large villi of arachnoid that protruded through the dura into the venous sinuses. Weed had published extensively in the early twentieth century that the likely mechanism of absorption occurred via an osmotic and hydrostatic gradient across semipermeable blind ended out-pouchings of arachnoid. Although Cushing had earlier proposed that these enlarged diverticulae represented biological one-way valves, it would be half a century until he was proven right. Welch and associates were the first to observe primate AG fixed while being perfused at varying pressures with the light microscope. They observed flattening of primate villi at negative pressures and a complex labyrinth of tubules, which allowed passage of particles up to several microns (Welch and Friedman, 1960; Welch and Pollay, 1961). Later, with the use of electron microscopy, unidirectional endothelial cell vacuolization leading to pore formation was demonstrated (Gómez et al., 1973; Tripathi, 1974) and that the pressure differential applied was proportional to the degree of vacuole/pore formation depicted in Figure 92.4 (Levine et al., 1982). Together, these discoveries provided the anatomical substrate to validate the absorptive behaviours of CSF documented so many years before. When taken in whole, these absorptive behaviours are analogous to the function of a slit valve. A slit valve has a set opening pressure under which no fluid flows. Once the opening pressure has been exceeded, there is a direct linear relationship to pressure and fluid outflow. The normal homeostatic arrangement allows CSF absorption to match production over time. Factors such as positional change or fluctuations in cerebral blood volume may temporarily tip the scales in one direction in a compensatory manner, but a steady circulating volume is maintained over the longer term.

Alternative routes of CSF absorption

It is traditionally taught that the AG along the superior sagittal sinus are solely responsible for CSF absorption. This appears to be only partially true. The slit valve behaviour of CSF bulk flow likely represents a combination of absorptive processes. CSF is clearly absorbed

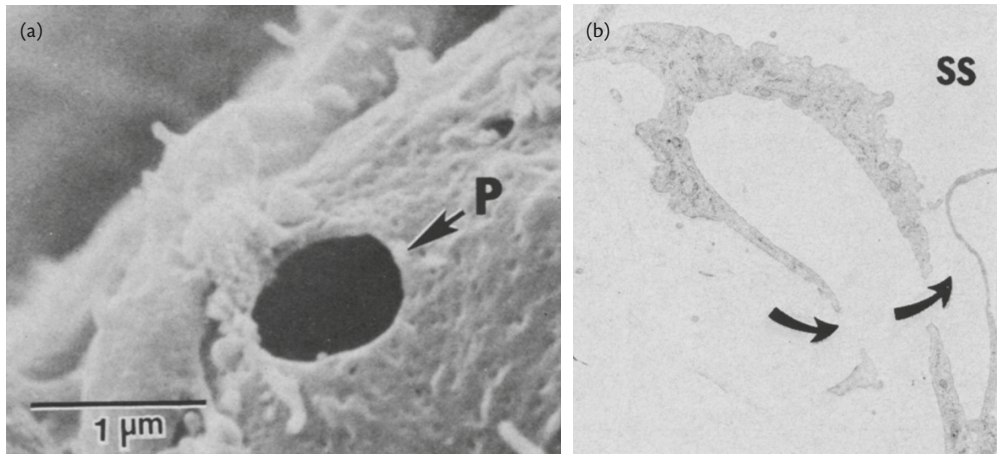

Fig. 92.4 Electron microscopy of the arachnoid granulations.
Electron micrographs showing pore formation in arachnoid villi protruding into the venous sinus under conditions of artificial CSF infusion at high pressure.

via lymphatic, spinal, and nerve root pathways in addition to the arachnoid villi. As early as 1875, Key and Retzius had documented cadaveric subarachnoid injection of trypan blue tracer accumulation in the AG as well as the cervical lymph nodes. These findings were confirmed by Weed and colleagues, and further clarified by many researchers throughout the twentieth century. These works constitute an overwhelming body of evidence supporting alternative pathways of CSF absorption other that the AG. The bulk of our knowledge arises from animal investigations. Thus, it is important to conceptualize human CSF absorption through our understanding of absorption across the animal phyla studied. Macroscopic AGs do not exist in rodents, rabbits, or cats. In larger mammals such as dogs and ruminants, they are less developed and fewer in number than in humans. Only in primates do we observe arachnoid villi of comparable size and number, albeit less than those observed in humans. In evolutionary terms, as brain size and complexity has increased, so has proportional CSF production. This is coupled with a commensurate reliance on more developed and specialized AGs. In addition to these anatomical observations, a proportional increase in CSF conductance is observed experimentally across phyla with the greatest values observed in Mann (Mann et al., 1978).

It seems that as mammalian brains have grown in size and complexity, CSF absorption has moved from primarily perineural and lymphatic routes of absorption to a strategy more dependent on excretion into the venous circulation via arachnoid villi. Although specialized AG endow humans with a great absorptive capacity, extra-arachnoidal elimination still likely plays a large role. Together, these comprise a dual outflow system. Arachnoid villi only appear microscopically around the time of birth in humans and do not contribute significantly to CSF absorption until late infancy or early toddlerhood (Gómez et al., 1982). It may be the case that during fetal development, and into early infancy a more primitive phenotype of CSF absorption is maintained. This primitive configuration at the beginning of life would rely heavily on extra-arachnoidal mechanisms of CSF absorption and much less so on AGs (Oi and Di Rocco, 2006). As the nervous system grows and matures, the adult phenotype is realized relying more heavily on arachnoid villi as shown in Figure 92.5. This phenomenon may also play a role in the high failure rate of ETV observed in the neonatal and early infantile period.

Pressure-volume curves generated over time in hydrocephalic patients as compared to normal subjects also support the dual outflow hypothesis. In a normal individual, one smooth semi-logarithmic pressure-volume curve is generated during an artificial CSF infusion study. Several published investigations have demonstrated a curve with two distinct components representing different absorptive behaviours at high or low rates of infusion likely reflecting distinct absorptive pathways (Lorenzo et al., 1970; Nelson and Goodman, 1971; Sokolowski, 1976). The presence of AV along the spinal roots has been well documented in sheep, dogs, and primates (Welch and Pollay, 1963; Gómez et al., 1974). In humans, AV are present at most levels and are juxtaposed or protrude directly into radicular veins (Tubbs et al., 2007). Upon physical separation of spinal and cranial compartments, Marmarou et al. (1975) demonstrated spinal AV in cats absorbed 15% of total CSF production and accounted for 32% of the total compliance. This number increases to about 25% of total absorption in sheep (Bozanovic-Sosic et al., 2001). In humans it has been estimated that at rest nearly 40% of absorption takes place in the spinal space and this increases to 75% with activity (Edsbagge et al., 2004). Robust evidence exists for CSF outflow via nasal lymphatics through the olfactory perineural pathway, optic nerves, and other cranial nerves in animals, but evidence is lacking in humans. There is little doubt that this absorptive pathway does function in man to some extent, but unfortunately, no method exists to date that would allow us to accurately quantify the actual contribution of perineural lymphatic drainage of CSF in humans.

Absorption of CSF via a parenchymal route is a controversial topic. There have been many recent investigations into parenchymal or glymphatic reabsorption of CSF that have some significant merit. Additionally, there are clinical observations supporting this hypothesis that are difficult to ignore. In patients with obstruction of the cerebral aqueduct, the rate of the resultant ventricular dilatation is far less than the normal CSF production (Bering and Sato, 1963) and this is supported in multiple animal models. In primates, when the cerebral aqueduct is blocked, initially the supratentorial ventricles enlarge rapidly. After some time, this enlargement slows and could not possibly reflect the total production of CSF within the ventricle (Milhorat et al., 1970). There has been much recent debate stemming from models of CSF flow obtained by cine-MRI, some of

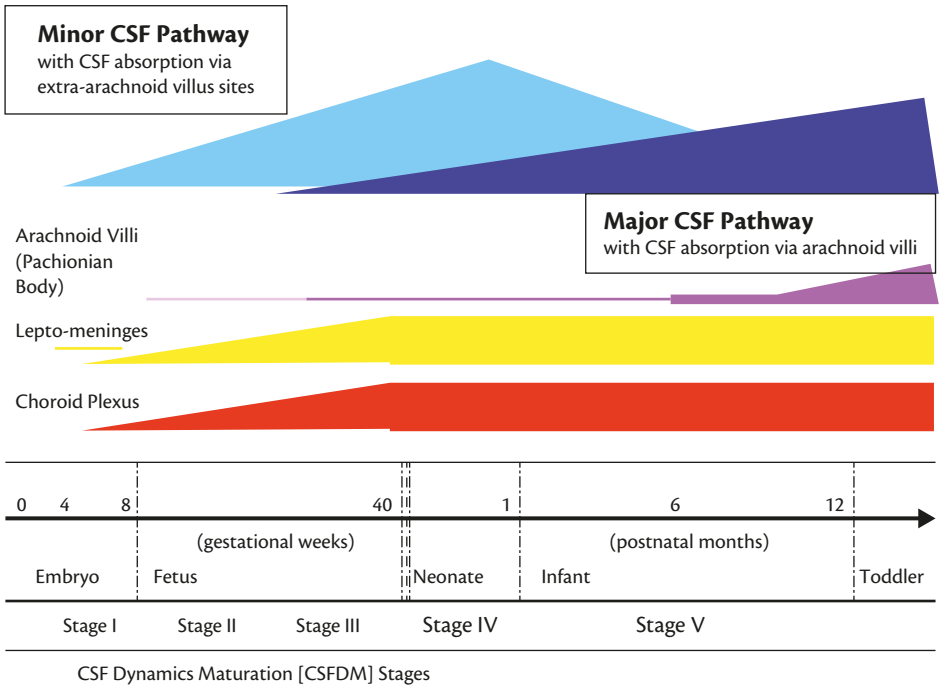

Fig. 92.5 Proposed development of CSF absorptive processes with age.

Proposed sequence of development of CSF productive and absorptive pathways in the first year of life by Oi and colleagues.

Reproduced with permission from Shizuo Oi, Concezio Di Rocco, Proposal of 'evolution theory in cerebrospinal fluid dynamics' and minor pathway hydrocephalus in developing immature brain, *Child's Nervous System*, Volume 22, Issue 7, Copyright © 2006 Springer Nature.

which demonstrate reversal of CSF flow with terminal absorption occurring within the ventricles. The findings are based on flow estimates derived from phase contrast MRI that depends on proprietary software, tight calibration, digital subtraction, precise voxel selection, and highly derived mathematical modelling. All these factors draw into question the validity of these results in addition to the lack of validation with an alternative method of flow beyond MRI.

We can accept that a substantial proportion of CSF volume, probably around one-third is derived from parenchymal ECF, although direct methods to precisely quantify this contribution have yet to be developed. There has been much recent activity in the literature attempting to characterize absorption of CSF by brain parenchyma. The ability to quantify net absorption through the interstitium, if it does become a major route, is even more problematic. Studies have demonstrated net flow of various tracer compounds from SAS through interstitial spaces via arteriolar or venular microcirculations within the Virchow-Robins spaces. Whether the transport of these tracers truly represents net or bulk flow of fluid is yet to be determined. The major thorn in the side of these theories is that they require significant violations in how we understand the blood–brain barrier. This relatively impermeable barrier tightly and actively regulates solute concentrations within the parenchymal microenvironment. Solutes are actively transported which, in turn, strictly regulate the net flow of water. We have yet to establish a mechanism of ion secretion in any direction *other* than from plasma into the CSF or interstitial space. Although extracellular fluid reabsorption at the capillary level can be enhanced by hydrostatic pressure (ICP), without a mechanism to excrete solutes out of the parenchyma, it would be impossible to maintain a net flux of water from brain tissue into the systemic circulation for more than a few minutes.

One important exception to the aforementioned physiology exists in the phenomenon of periventricular oedema observed in many hydrocephalic states, referred to as transependymal flow. Hydrostatic pressure drives water across the ependyma into the extracellular space of the white matter surrounding the ventricles, lowering its colloid osmotic pressure. This creates an osmotic gradient promoting the net flow of extracellular water into the vascular space capable of conducting a large volume of excess fluid. Aquaporin-4 (AQP-4) is heavily expressed along the astrocytic foot processes enveloping cerebral blood vessels, an integral component of the BBB. There exists a large body of research demonstrating the function of AQP-4 in animal models of hydrocephalus. AQP-4 is integral for ependymal integrity (Li et al., 2009). AQP-4 is upregulated in both multiple experimental hydrocephalus models and in hydrocephalic patients (Castañeyra-Ruiz et al., 2013; Skjolding et al., 2013). Furthermore, the experimental hydrocephalus induced in AQP-4 knock-out mice is far worse than in normal mice. Mice lacking AQP-4 have less oedema and recover better than controls in models of cytotoxic oedema such as TBI and stroke. In models of vasogenic oedema such as tumour or abscess, the knock-out mice have more oedema and fair much poorer than controls. These findings highlight the central role of AQP-4 in parenchymal water regulation. AQP-4 represents a promising pharmacological target in the treatment of a wide spectrum of neurological disorders.

Development of ventriculomegaly

Although the development or resolution of ventriculomegaly seems intuitive on a superficial level, a deeper exploration into the

mechanics governing relative compartmental sizes presents major theoretical dilemmas. If the brain and vascular volumes are to remain stable, which we can assume it must over the short term, how do we account for a major increase in the ventricular spaces? How can we account for the rapid decrease in ventricular size after ventriculostomy or shunt placement without the head becoming smaller? The answer cannot be that we are violating the law of conservation of mass.

These questions can be explained by the redistribution of the same initial volume of cerebrospinal fluid to a different location in the SAS, namely the ill-defined cortical SAS. Normally only 50–60 ml of a total 130–150 ml of CSF occupies the ventricular space. As we know, this volume can fluctuate widely in disease and with age. A rapid change in ventricular volume must be accompanied by a commensurate adjustment in the cortical and cisternal SAS if relative brain and vascular compartments are to be maintained. Volumetric changes in the cisternal and cortical SAS are difficult to appreciate with current imaging technologies. Determination of its normal volume in the absence of disease remains elusive. Thus, these relationships have been underappreciated and misunderstood by most clinicians. **Figure 92.6** demonstrates a spherical theoretical model of the ventricular and cortical SAS. An increase of only 2 mm in thickness of the cortical SAS is able to compensate for a 104 cc decrease in ventricular volume. This cryptic ability of the cortical SAS to accept CSF volume is likely further enhanced by brain sulci and the perivascular, or Virchow-Robins spaces.

Inappropriately excessive drainage of the ventricles will lead to subdural hygroma, which is in effect, a massive enlargement of the cortical subarachnoid space to compensate for overzealous shunting. If production and spinal reserves of CSF cannot match drainage, tearing of bridging veins and extravasation of blood into the hygroma, (conversion to a subdural hematoma or SDH) will account for the volume. As the ventricles present a lesser resistance to drainage then the complex multicompartmental cisternal spaces, excessive CSF removal from the lumbar spaces will behave quite similarly. This is pertinent to the discussion of hydrocephalus developing in the setting of very low to negative pressures. The missed diagnosis of spinal CSF fistulae resulting in hygroma or chronic SDH can be a disaster as progressively aggressive surgeries are carried out to drain the collection.

Similarly, progressively aggressive surgeries for shunt malfunction in a patient with an undiagnosed CSF fistula can be equally harmful. When CSF diversion was initially required as a result of high resistance to flow between ventricular and cortical SAS (i.e. 'obstructive' HCP), a CSF leak at any location will preferentially drain the cortical/cisternal SAS. A pressure gradient, denudation of cortical/cisternal SAS volume and continued ventricular CSF production will drive ventriculomegaly. This situation gives the appearance of shunt malfunction with a perfectly functional shunt; progressive ventriculomegaly is able to continue at pressures below the opening pressure of the valve. In this case, placement of a ventriculostomy catheter will yield CSF only when drained at paradoxically low or negative pressures. This rare situation is well documented in the neurosurgical literature and is definitively treated by identification and repair of the CSF leak. Further highlighting the interaction between intracranial fluid compartments, Rekate et al. (2008) have documented in multiple instances that the application of a gentle cervical tourniquet, in the form of an elastic bandage, will rapidly

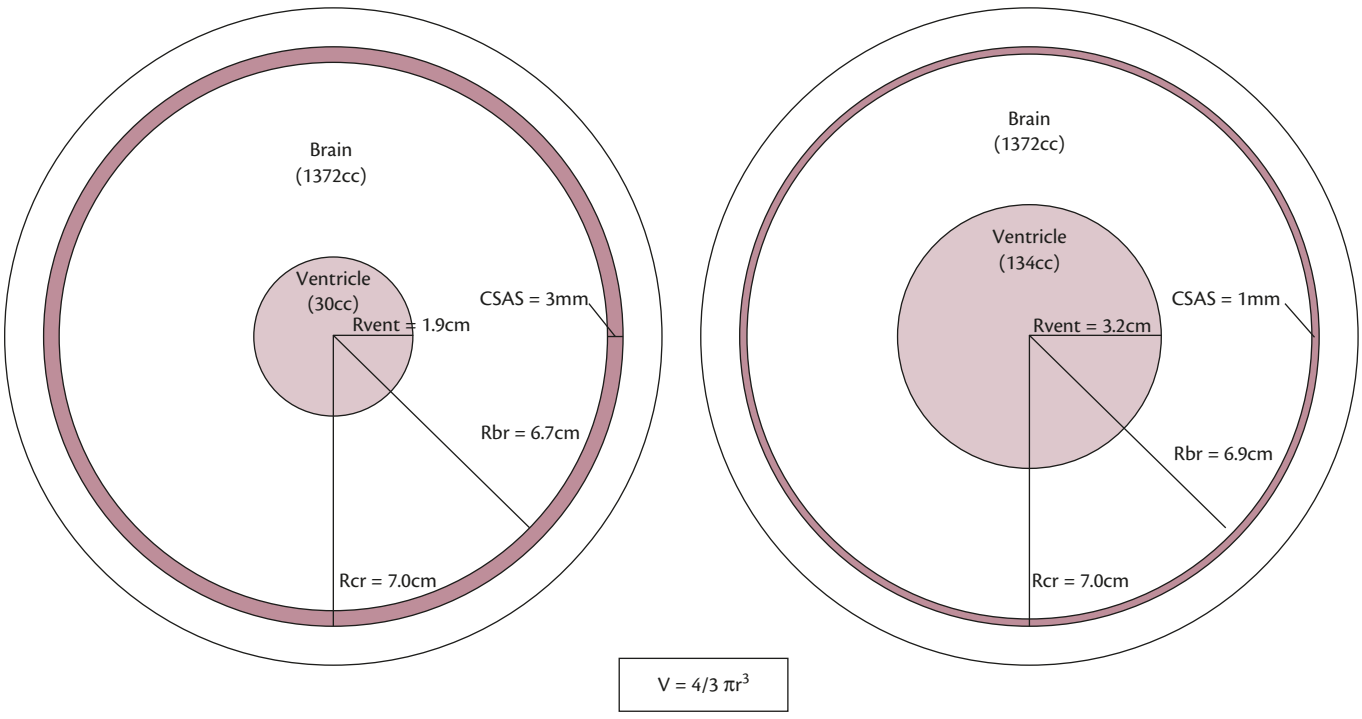

Fig. 92.6 Relationship between cortical subarachnoid and ventricular volumes.

Left: Representation of normal ventricular volume (V) in a normal or adequately shunt-treated individual. Right: Representation of the visual change in the size of the ventricular system when the thickness of the cortical subarachnoid space is decreased from 3 mm to 1 mm. In this illustration, the volume of the brain remains constant.

Reproduced with permission from Shizuo Oi, Concezio Di Rocco, Proposal of 'evolution theory in cerebrospinal fluid dynamics' and minor pathway hydrocephalus in developing immature brain, *Child's Nervous System*, Volume 22, Issue 7, Copyright © 2006 Springer Nature.

reverse ventriculomegaly and restore consciousness in cases such as these. Compression of the venous structures in the neck functioned to increase cerebral blood volume in the brain, increasing brain turgor, or stiffness. The addition of volume to the intracranial cavity and lowering of brain compliance allowed for sufficient pressure generation in excess of the shunt's opening pressure. This allowed temporary alleviation of the patient's symptoms attributable to ventriculomegaly until definitive management of the fistula could be obtained.

Classification of hydrocephalic states by point of obstruction

The traditional classification of *obstructive* or *communicating* poorly describes the pathophysiology leading to the various hydrocephalic states (see **Box 92.1**). In fact, all forms of hydrocephalus are obstructive by nature. Within the circuit of CSF flow, the location of a resistance defines the patterns ventriculomegaly observed. Here, we propose a classification based upon the location of the resistive element in the circuit from most proximal to distal in terms of CSF production and terminal absorption. The paired lateral ventricles contribute the greatest volume of CSF and contain the majority of choroid plexus shared among the four ventricles. Thus, this compartment is the driver of bulk CSF flow in its journey to more distal sites of absorption. Beginning at the most proximal, the lateral ventricles themselves can become obstructed from within. Mass effect onto the lateral ventricle by tumour, oedema, or hematoma may isolate choroid plexus, commonly in the temporal horn causing progressive enlargement of this 'trapped' ventricular portion. This can be potentially lethal, leading to uncal herniation. Scarring and loculations within the ventricular system can also create isolated CSF compartments leading to asymmetrical enlargement of portions of the ventricular system.

Several pathologies may obstruct the foramen(s) of Monro leading to progressive dilatation of only one or both lateral ventricles. A functional obstruction secondary to overdrainage of a single lateral ventricle has been described. Negative pressure draws the septum pellucidum over the ipsilateral caudate head, obstructing the foramen of Monro. The suction created by the shunt maintains isolation of the shunted ventricle and the initial pathology continues unabated, driving further enlargement of the un-shunted compartments. Another consequence of long-term overdrainage is coaptation or scarring together of ependymal linings. This may occur within the third ventricle leading to lateral ventriculomegaly or within the cerebral aqueduct, causing enlargement of all three supratentorial ventricles. Although triventricular hydrocephalus has been traditionally viewed as the *sine qua non* of aqueductal stenosis, reconstitution of the aqueduct has been demonstrated in some cases after shunting or ETV, demonstrating a functional obstruction such as compression by the enlarged posterior portions of the lateral ventricles (Rekate, 2007).

Dandy-Walker cysts or other pathologies filling the fourth ventricle actually represent an obstruction to the fourth ventricular outflow while giving the appearance of aqueductal stenosis. Fenestration of the cyst or resection of the pathology may subsequently restore a fourth ventricular space and return of flow through the cerebral aqueduct. This is one of many strategies to achieve shunt removal in a previously shunt dependent patient, or avoidance of initial shunt placement altogether. Chiari I malformation may lead to obstruction of the foramen of Magendie, but the degree of tonsillar herniation alone is not sufficient to cause obstruction of the bilateral foraminae of Lushka. Therefore, many Chiari I malformations are secondary effects of a primary hydrocephalus, not vice-versa. Conversely, Chiari II malformation causes obstruction of fourth ventricular outflow and enlargement of all ventricles. Mixing of amniotic fluid and CSF via an open neural tube defect results in dense scarring and adhesions in the basal cisterns. Combining this with a greater degree of downward herniation, ventricular spaces are functionally isolated from the spinal and cortical subarachnoid spaces as evidenced by the extremely high rate of ventricular shunting needed in this population and high failure rate of ETV. Overall, meningitis is likely the most common cause of chronic fourth ventricular outflow obstruction but is usually more amenable to ETV.

Obstruction of flow within the cisternal spaces will lead to enlargement of all ventricular spaces and is the presumed aetiology of a majority of NPH cases. Some conclusions may be drawn about the site of obstruction from the appearance of the extraventricular CSF spaces on neuroimaging. This information can be useful in selecting the right patients for the most appropriate procedure. Aneurysmal subarachnoid haemorrhage (SAH) resulting in hydrocephalus is similar in that blood products physically impede flow through the cisternal space and cause scarring over the longer term. In extremely rare situations, individual patients may produce an excessive quantity of CSF. This can occur spontaneously or in the setting of a choroid plexus papilloma. If production exceeds the absorptive capacities of the collective CSF outflow systems, ventriculomegaly may develop. Therefore, the obstruction can be viewed as occurring at the most distal point, such as the AGs.

The utility of ETV in treating NPH is unclear secondary to mixed results from multiple case series. Generally speaking, as we better define the mechanisms behind most diseases, it becomes evident that there are multiple, distinct pathophysiologies leading to a similar clinical manifestation. NPH is a perfect example of this. The disease is largely defined by ventriculomegaly disproportionate

Box 92.1 Classification of hydrocephalus by point of obstruction

Lateral ventricles
Isolation of a portion or 'trapping' of the lateral ventricle by congenital lesion, scarring, IVH, or mass

Foramen of Monroe
Colloid cyst, ventricular tumours, congenital anomalies, and functional obstruction*

Third ventricular outflow
Aqueductal stenosis, coaptation of third ventricular ependyma*, pineal tumours, focal webbing, ventriculomegaly with functional obstruction

Fourth ventricular outflow
Meningitis, Chiari 2, Dandy-Walker, tumours

Basal cisterns
NPH, SAH/IVH, arachnoid cyst, meningitis

Terminal absorption
Venous hypertension in infancy (vein of Galen malformation), choroid plexus papilloma, Hypo-vitainosis A

*Secondary to overdrainage.

to cortical atrophy with a characteristic constellation of symptoms. There is growing evidence that what we call NPH is actually a spectrum ranging from late-onset aqueductal stenosis, restrictive arachnoid membranes from within the proximal basal cisterns to the most distal cortical SAS, or progression/decompensation of an arrested infantile hydrocephalic state in late adulthood. We can deduce that some of these pathologies would respond to ETV and others would not depending on the site of restriction to flow which is consistent with the observed clinical results to date. As NPH patients are more precisely classified in regard to the nature and location of their obstruction, so will their treatments with increasing degrees of success.

Infantile hydrocephalus

The physics governing the development of hydrocephalus during the first year of life are unique. Neonates are relatively protected from elevated ICP, as their skulls are distensible. The younger an infant is, the less force is required to increase the volume of the head. As the cranial sutures become progressively interdigitated and the fontanels close, elevations in intracranial pressure have less of an effect on head size or intracranial volume. As discussed previously, CSF absorption mirrors the function of a slit valve, requiring CSF pressure to rise above a certain threshold before net absorption can occur. In newborns, with the inward force created by the cartilaginous plates that will become the bony neurocranium, scalp and ambient barometric pressure generate just enough pressure for absorption to occur. Neonatal hydrocephalus behaves as though there is an inherently higher resistance to CSF outflow, or a slit valve with a greater opening pressure. In this case, the tensile properties of the skull and atmosphere are unable to overcome the resistance to CSF absorption, resulting in distention of the intracranial compartment, or head growth. In general, brain parenchyma is probably not lost, but pushed outward and stretched mirroring the increases in cranial volume. After shunt insertion in a hydrocephalic infant, the change, or more specifically, the rate of change in ventricular size is probably best characterized by the degree of articulation of the neurocranium and the rate of brain growth. It may take many months to realize a small or normal sized ventricular system as the growth of brain tissue replaces what was excess CSF volume after a few months of life render the skull unable to collapse. Conversely, in the neonatal period and especially in the premature, sinking of the fontanel, and overlapping of the sutures can normalize ventricular volume nearly instantaneously.

Although quite controversial, the late paediatric neurosurgeon Fred Epstein reported successes in treating infantile hydrocephalus with compressive head wrapping as opposed to shunting (Epstein et al., 1974). Head compression allowed ICP to rise above the opening pressure of absorptive mechanism whereas without compression, CSF pressures never reached the levels necessary for CSF absorption. Although the neurosurgical community never adopted this treatment, Epstein claimed to have successfully treated 8/10 infants, avoiding shunt placement. ETV success is inversely related to age in infancy, with poor efficacy in patients less than 6 months of age. The same physical properties explain why the same procedure for an identical pathology, say aqueductal stenosis, tends to be successful in a 2-year-old, but more often fails in a neonate. Although a conduit for efficient CSF flow is created between the supratentorial ventricles and basal cisterns, there exists a higher resistance to CSF absorption distal to the artificial stoma. Again, the compliant neonatal cranium is unable to generate the forces required for adequate CSF absorption. Ventriculomegaly persists and pathological head circumferences continue despite a working ETV. The same anatomical arrangement also explains the hydrocephalus resultant from intracranial venous hypertension in infancy. The elevated venous pressures seen in cases of vein of Galen malformation lead to hydrocephalus in infants as CSF pressures in the cortical SAS must exceed venous ones in excess of roughly 5 cm of water. Thus, a situation that would lead to the development of IIH in an adult gives rise to macrocephaly and ventriculomegaly in the neonate.

Conclusions

We hope it is apparent to the reader that hydrocephalus is not a single disease, but actually a grouping of a myriad of conditions resulting in ventriculomegaly. The clinical decision is all too often to place a ventricular shunt without a careful consideration of an individual's unique anatomy and physiology. This is akin to the expression: 'To a hammer, everything is a nail'. We must remember that to the patient, a shunt may be a lifelong sentence. The neurosurgeon routinely consigns patients to a fate relying on mechanical devices that are destined to fail and cannot recapitulate normal physiology. The understanding of normal CSF physiology and its derangements in disease is important to the clinician to best manage and appropriate treat patients. To those of us in the neurosciences, hydrocephalus is a common problem with a seemingly limited array of management tools. It is clear that we have yet to fully appreciate the amazing complexity of the CSF dynamics. We have a responsibility to innovate in the arena CSF diversion technologies and in the development of pharmacological agents capable of modulating CSF dynamics. This is the next horizon in hydrocephalus research that our patients and their families eagerly await which is unfortunately, long overdue.

REFERENCES

Azzam, N.A., Choudhury, S.R., & Donohue, J.M. (1978). Changes in the surface of fine structure of choroid plexus epithelium following chronic acetazolamide treatment. *J Anat*, **127**(Pt 2), 333–42.

Bannister, C.M. & Chapman, S.A. (1980). Ventricular ependyma of normal and hydrocephalic subjects: a scanning electronmicroscopic study. *Dev Med Child Neurol*, **22**(6), 725–35.

Bering, E.A. & Sato, O. (1963). Hydrocephalus: changes in formation and absorption of cerebrospinal fluid within the ventricles. *J Neurosurg*, **20**, 1050–63.

Bozanovic-Sosic, R., Mollanji, R., & Johnston, M.G. (2001). Spinal and cranial contributions to total cerebrospinal fluid transport. *Am J Physiol*, **281**(3), R909–16.

Castañeyra-Ruiz, L., González-Marrero, I., González-Toledo, J.M., et al. (2013). Aquaporin-4 expression in the cerebrospinal fluid in congenital human hydrocephalus. *Fluids Barriers CNS*, **10**(1), 18.

Chodobski, A., Szmydynger-Chodobska, J., & Johanson, C.E. (1998). Vasopressin mediates the inhibitory effect of central angiotensin II on cerebrospinal fluid formation. *Eur J Pharmacol*, **347**(2–3), 205–9.

Courchesne, E., Chisum, H.J., Townsend, J., et al. (2000). Normal brain development and aging: quantitative analysis at *in vivo* MR imaging in healthy volunteers, *Radiology*, **216**(3), 672–82.

Cutler, R.W., Page, L., Galicich, J., & Watters, G.V. (1968). Formation and absorption of cerebrospinal fluid in man. *Brain*, **91**(4), 707–20.

Domínguez-Pinos, M.D., Páez, P., Jiménez, A.J., et al. (2005). Ependymal denudation and alterations of the subventricular zone occur in human fetuses with a moderate communicating hydrocephalus. *J Neuropathol Exp Neurol*, **64**(7), 595–604.

Edsbagge, M., Tisell, M., Jacobsson, L. & Wikkelsø, C. (2004). Spinal CSF absorption in healthy individuals. *Am J Physiol*, **287**(6), R1450–5.

Epstein, F., Wald, A., & Hochwald, G.M. (1974). Intracranial pressure during compressive head wrapping in treatment of neonatal hydrocephalus. *Pediatrics*, **54**(6), 786–90.

Garne, E., Loane, M., Addor, M.C., Boyd, P.A., Barisic, I., & Dolk, H. (2010). Congenital hydrocephalus—prevalence, prenatal diagnosis and outcome of pregnancy in four European regions. *Eur J Paediatr Neurol*, **14**(2), 150–5.

Ghersi-Egea, J.F. & Strazielle, N. (2002). Choroid plexus transporters for drugs and other xenobiotics. *J Drug Target*, **10**(4), 353–7.

Golomb, J., Wisoff, J., Miller, D.C., et al. (2000). Alzheimer's disease comorbidity in normal pressure hydrocephalus: prevalence and shunt response. *J Neurol Neurosurg Psychiatry*, **68**(6), 778–81.

Gómez, D.G., Chambers, A.A., Di Benedetto, A.T., & Potts, D.G. (1974). The spinal cerebrospinal fluid absorptive pathways. *Neuroradiology*, **8**(2), 61–6.

Gómez, D.G., Potts, G., Deonarine, V., & Reilly, K.F. (1973). Effects of pressure gradient changes on the morphology of arachnoid villi and granulations of the monkey. *Lab Invest*, **28**(6), 648–57.

Gómez, D.G., DiBenedetto, A.T., Pavese, A.M., Firpo, A., Hershan, D.B. & Potts, D.G. (1982). Development of arachnoid villi and granulations in man. *Acta Anatomica*, **111**(3), 247–58.

Grondona, J.M., Pérez-Martín, M., Cifuentes, M., et al. (1996). Ependymal denudation, aqueductal obliteration and hydrocephalus after a single injection of neuraminidase into the lateral ventricle of adult rats. *J Neuropathol Exp Neurol*, **55**(9), 999–1008.

Hayden, P.W., Shurtleff, D.B., & Foltz, E.L. (1970). Ventricular fluid pressure recordings in hydrocephalic patients. *Arch Neurol*, **23**(2), 147–54.

Heiss, J.D., Suffredini, G., Bakhtian, K.D., Sarntinoranont, M., & Oldfield, E.H. (2012). Normalization of hindbrain morphology after decompression of Chiari malformation type I. *J Neurosurg*, **117**(5), 942–6.

Hladky, S.B. & Barrand, M.A. (2014). Mechanisms of fluid movement into, through and out of the brain: evaluation of the evidence. *Fluids Barriers CNS*, **11**(1), 26.

Jaraj, D., Rabiei, K., Marlow, T., Jensen, C., Skoog, I., & Wikkelsø, C. (2014). Prevalence of idiopathic normal-pressure hydrocephalus. *Neurology*, **82**(16), 1449–54.

Jeng, S., Gupta, N., Wrensch, M., Zhao, S., & Wu, Y.W. (2011). Prevalence of congenital hydrocephalus in California, 1991–2000. *Pediatr Neurol*, **45**(2), 67–71.

Jiménez, A.J., Domínguez-Pinos, M.D., Guerra, M.M., Fernández-Llebrez, P., & Pérez-Fígares, J.M. (2014). Structure and function of the ependymal barrier and diseases associated with ependyma disruption. *Tissue Barriers*, **2**, e28426.

Johanson, C.E., Donahue, J.E., Spangenberger, A., Stopa, E.G., Duncan, J.A. & Sharma, H.S. (2006). Atrial natriuretic peptide: its putative role in modulating the choroid plexus-CSF system for intracranial pressure regulation. *Acta Neurochir Suppl*, **96**, 451–6.

Johanson, C.E., Duncan, J.A., Klinge, P.M., Brinker, T., Stopa, E.G., & Silverberg, G.D. (2008). Multiplicity of cerebrospinal fluid functions: new challenges in health and disease. *Cerebrospinal Fluid Res*, **5**, 10.

Johanson, C.E., Preston, J.E., Chodobski, A., Stopa, E.G., Szmydynger-Chodobska, J., & McMillan, P.N. (1999). AVP V1 receptor-mediated decrease in Cl-efflux and increase in dark cell number in choroid plexus epithelium. *Am J Physiol*, **276**(1 Pt 1), C82–90.

Leinonen, V., Koivisto, A.M., Savolainen, S., et al. (2010). Amyloid and tau proteins in cortical brain biopsy and Alzheimer's disease. *Ann Neurol*, **68**(4), 446–53.

Levine, J.E., Povlishock, J.T., & Becker, D.P. (1982). The morphological correlates of primate cerebrospinal fluid absorption. *Brain Res*, **241**(1), 31–41.

Li, X., Kong, H., Wu, W., Xiao, M., Sun, X., & Hu, G. (2009). Aquaporin-4 maintains ependymal integrity in adult mice. *Neuroscience*, **162**(1), 67–77.

Lindvall, M. & Owman, C. (1981). Autonomic nerves in the mammalian choroid plexus and their influence on the formation of cerebrospinal fluid. *J Cereb Blood Flow Metab*, **1**(3), 245–66.

Longatti, P.L., Basaldella, L., Orvieto, E., Fiorindi, A., & Carteri, A. (2004). Choroid plexus and aquaporin-1: a novel explanation of cerebrospinal fluid production, *Pediatr Neurosurg*, **40**(6), 277–83.

Lorenzo, A.V., Page, L.K., & Watters, G.V. (1970). Relationship between cerebrospinal fluid formation, absorption and pressure in human hydrocephalus. *Brain*, **93**(4), 679–92.

Mann, J.D., Butler, A.B., Rosenthal, J.E., Maffeo, C.J., Johnson, R.N., & Bass, N.H. (1978). Regulation of intracranial pressure in rat, dog, and man. *Ann Neurol*, **3**(2), 156–65.

Marmarou, A., Shulman, K., & LaMorgese, J. (1975). Compartmental analysis of compliance and outflow resistance of the cerebrospinal fluid system. *J Neurosurg*, **43**(5), 523–34.

May, C., Kaye, J.A., Atack, J.R., Schapiro, M.B., Friedland, R.P., & Rapoport, S.I. (1990). Cerebrospinal fluid production is reduced in healthy aging. *Neurology*, **40**(3 Pt 1), 500–3.

Milhorat, T.H., Clark, R.G., & Hammock, M.K. (1970). Experimental hydrocephalus. 2. Gross pathological findings in acute and subacute obstructive hydrocephalus in the dog and monkey. *J Neurosurg*, **32**(4), 390–9.

Mori, K., Tsutsumi, K., Kurihara, M., Kawaguchi, T., & Niwa, M. (1990). Alteration of atrial natriuretic peptide receptors in the choroid plexus of rats with induced or congenital hydrocephalus. *Childs Nerv Syst*, **6**(4), 190–3.

Mortensen, O.A. & Weed, L.H. (1934). Absorption of isotonic fluids from the subarachnoid space. *Am J Physiol—Legacy Content*, **108**(2), 458–68.

Nelson, J.R. & Goodman, S.J. (1971). An evaluation of the cerebrospinal fluid infusion test for hydrocephalus, *Neurology*, **21**(10), 1037–53.

Nilsson, C., Ståhlberg, F., Gideon, P., Thomsen, C., & Henriksen, O. (1994). The nocturnal increase in human cerebrospinal fluid production is inhibited by a beta 1-receptor antagonist. *Am J Physiol*, **267**(6 Pt 2), R1445–8.

Nilsson, C., Ståhlberg, F., Thomsen, C., Henriksen, O., Herning, M., & Owman, C. (1992). Circadian variation in human cerebrospinal fluid production measured by magnetic resonance imaging. *Am J Physiol*, **262**(1 Pt 2), R20–4.

Nulsen, F.E. & Spitz, E.B. (1951). Treatment of hydrocephalus by direct shunt from ventricle to jugular vein. *Surgical Forum*, **351**, 399–403.

Oi, S. & Di Rocco, C. (2006). Proposal of 'evolution theory in cerebrospinal fluid dynamics' and minor pathway hydrocephalus in developing immature brain, *Childs Nerv Syst*, **22**(7), 662–9.

Oshio, K., Song, Y., Verkman, A.S., & Manley, G.T. (2003). Aquaporin-1 deletion reduces osmotic water permeability and cerebrospinal fluid production. *Acta Neurochir Suppl*, **86**, 525–8.

Oshio, K., Watanabe, H., Song, Y., Verkman, A.S., & Manley, G.T. (2005). Reduced cerebrospinal fluid production and intracranial pressure in mice lacking choroid plexus water channel Aquaporin-1. *FASEB J*, **19**(1), 76–8.

Ott, B.R., Cohen, R.A., Gongvatana, A., et al. (2010). Brain ventricular volume and cerebrospinal fluid biomarkers of Alzheimer's disease. *J Alzheimers Dis*, **20**(2), 647–57.

Pappenheimer, J.R., Heisey, S.R., & Jordan, E.F. (1962). Perfusion of the cerebral ventricular system in unanesthetized goats. *Am J Physiol—Legacy Content*, **203**(5), 763–74.

Paul, L., Madan, M., Rammling, M., Chigurupati, S., Chan, S.L., & Pattisapu, J.V. (2011). Expression of aquaporin 1 and 4 in a congenital hydrocephalus rat model, *Neurosurgery*, **68**(2), 462–73.

Praetorius, J. & Nielsen, S. (2006). Distribution of sodium transporters and aquaporin-1 in the human choroid plexus. *Am J Physiol Cell Physiol*, **291**(1), C59–67.

Preston, J.E., McMillan, P.N., Stopa, E.G., Nashold, J.R., Duncan, J.A., & Johanson, C.E. (2003). Atrial natriuretic peptide induction of dark epithelial cells in choroid plexus: consistency with the model of CSF downregulation in hydrocephalus, *Eur J Pediatr Surg*, **13** Suppl 1, S40–2.

Redzic, Z.B., Preston, J.E., Duncan, J.A., Chodobski, A., & Szmydynger-Chodobska, J. (2005). The choroid plexus-cerebrospinal fluid system: from development to aging. *Curr Top Dev Biol*, **71**, 1–52.

Rekate, H.L. (2007). Longstanding overt ventriculomegaly in adults: pitfalls in treatment with endoscopic third ventriculostomy. *Neurosurg Focus*, **22**(4), E6.

Rekate, H.L., Nadkarni, T.D., & Wallace, D. (2008). The importance of the cortical subarachnoid space in understanding hydrocephalus. *J Neurosurg Pediatr*, **2**(1), 1–11.

Rubin, R.C., Henderson, E.S., Ommaya, A.K., Walker, M.D., & Rall, D.P. (1966). The production of cerebrospinal fluid in man and its modification by acetazolamide, *J Neurosurg*, **25**(4), 430–6.

Schalk, K.A., Faraci, F.M., Williams, J.L., VanOrden, D., & Heistad, D.D. (1992). Effect of atriopeptin on production of cerebrospinal fluid. *J Cereb Blood Flow Metab*, **12**(4), 691–6.

Seckl, J. & Lightman, S. (1988). Cerebrospinal fluid neurohypophysial peptides in benign intracranial hypertension. *J Neurol Neurosurg Psychiatry*, **51**(12), 1538–41.

Serot, J.M., Zmudka, J., & Jouanny, P. (2012). A possible role for CSF turnover and choroid plexus in the pathogenesis of late onset Alzheimer's disease. *J Alzheimers Dis*, **30**(1), 17–26.

Shibata, M., Yamada, S., Kumar, S.R., et al. (2000). Clearance of Alzheimer's amyloid-ss(1–40) peptide from brain by LDL receptor-related protein-1 at the blood–brain barrier. *J Clin Investig*, **106**(12), 1489–99.

Silverberg, G.D., Mayo, M., Saul, T., Fellmann, J., Carvalho, J., & McGuire, D. (2008). Continuous CSF drainage in AD: results of a double-blind, randomized, placebo-controlled study. *Neurology*, **71**(3), 202–9.

Silverberg, G.D., Miller, M.C., Machan, J.T., et al. (2010). Amyloid and tau accumulate in the brains of aged hydrocephalic rats. *Brain Res*, **1317**, 286–96.

Sival, D.A., Guerra, M., den Dunnen, W.F., et al. (2011). Neuroependymal denudation is in progress in full-term human foetal spina bifida aperta. *Brain Pathol (Zurich, Switzerland)*, **21**(2), 163–79.

Skjolding, A.D., Holst, A.V., Broholm, H., Laursen, H., & Juhler, M. (2013). Differences in distribution and regulation of astrocytic aquaporin-4 in human and rat hydrocephalic brain. *Neuropathol Appl Neurobiol*, **39**(2), 179–91.

Sokolowski, S.J. (1976). Bolus injection test for measurement of cerebrospinal fluid absorption. *J Neurol Sci*, **28**(4), 491–504.

Sousa, J.C., Cardoso, I., Marques, F., Saraiva, M.J., & Palha, J.A. (2007). Transthyretin and Alzheimer's disease: where in the brain? *Neurobiol Aging*, **28**(5), 713–18.

Stein, S.C., Burnett, M.G., & Sonnad, S.S. (2006). Shunts in normal-pressure hydrocephalus: do we place too many or too few? *J Neurosurg*, **105**(6), 815–22.

Stolp, H., Neuhaus, A., Sundramoorthi, R., & Molnár, Z. (2012). The long and the short of it: gene and environment interactions during early cortical development and consequences for long-term neurological disease. *Front Psychiatry*, **3**, 50.

Tripathi, R. (1974). Tracing the bulk outflow route of cerebrospinal fluid by transmission and scanning electron microscopy. *Brain Res*, **80**(3), 503–6.

Tubbs, R.S., Hansasuta, A., Stetler, W., et al. (2007). Human spinal arachnoid villi revisited: immunohistological study and review of the literature. *J Neurosurg Spine*, **7**(3), 328–31.

Tulassay, T., Khoór, A., Bald, M., Ritvay, J., Szabó, A., & Rascher, W. (1990). Cerebrospinal fluid concentrations of atrial natriuretic peptide in children. *Acta Paediatrica Hungarica*, **30**(2), 201–7.

Weed, L.H. (1935). Forces concerned in the absorption of the cerebrospinal fluid. *Am J Physiol—Legacy Content*, **114**(1), 40–5.

Welch, K. & Friedman, V. (1960). The cerebrospinal fluid valves. *Brain*, **83**, 454–69.

Welch, K. & Pollay, M. (1961). Perfusion of particles through arachnoid villi of the monkey. *Am J Physiol*, **201**, 651–4.

Welch, K. & Pollay, M. (1963). The spinal arachnoid villi of the monkeys *Cercopithecus aethiops sabaeus* and *Macaca irus*. *Anat Rec*, **145**, 43–8.

Yamasaki, H., Sugino, M., & Ohsawa, N. (1997). Possible regulation of intracranial pressure by human atrial natriuretic peptide in cerebrospinal fluid. *Eur Neurol*, **38**(2), 88–93.

RELATED LINK TO EBRAIN

Aetiology and Pathophysiology of Hydrocephalus. https://learning.ebrain.net/course/view.php?id=584

93

Shunt technology and endoscopic ventricular surgery

Ian K. Pople and William Singleton

Introduction

The management of cerebrospinal fluid (CSF) disorders is a complex clinical science, requiring a detailed understanding of CSF physiology in both the normal and diseased brain. Successful treatment requires a comprehensive knowledge of the available shunt types, their similarities, differences, and idiosyncrasies. The rapid development of endoscopic neurosurgical techniques makes treating this group of patients without a shunt often a real possibility, and arguably is now a core neurosurgical skill. In this chapter we will summarize CSF physiology in the normal state, and explain the principles of CSF diversion before going on to describe the various shunt types available. A section will be devoted to endoscopic CSF diversion techniques, including a detailed explanation of third ventriculostomy.

CSF physiology

CSF is thought to have four main functions:

1. Buoyancy: thus reducing the weight of the brain by 'floating' it in fluid
2. Removal of large and hydrophilic waste metabolites
3. Circulation and transfer of neuropeptides within the central nervous system (CNS): particularly important during fetal and early infant development
4. Maintenance of cellular homeostasis within the CNS

CSF is principally produced from choroid plexus within the ventricular system, though approximately a third of the circulating volume is thought to be produced from the pia-ependyma of the ventricular wall. With each arterial pulse wave, CSF circulates from the lateral ventricles, though the foramen of Monro to the third ventricle. It then passes to the fourth ventricle via the aqueduct of Sylvius before entering the infratentorial cisterns and spinal subarachnoid space laterally via the two foraminae of Luschka and medially through the foramen of Magendie.

Traditional teaching says that the majority of CSF absorption occurs at the arachnoid granulations located at the major venous sinuses. This is probably the case for a proportion of circulating CSF; however, there is a growing body of evidence that under normal physiological conditions, a large proportion of CSF is re-absorbed through the perivascular Virchow-Robin spaces within the brain parenchyma into draining lymphatics. Water from CSF is also actively transported into capillaries and astrocyte end-feet within the brain via aquaporin channels (Brinker et al., 2014). These discoveries explain how acute hydrocephalus is often associated with periventricular oedema/lucency on CT and MR imaging.

Normal CSF dynamics

In normal adults CSF occupies approximately 9% of intracranial space. Normal children have smaller ventricles and a smaller amount of intracranial CSF in relation to brain and blood. The pressure/dynamics of CSF circulation are controlled by three elements:

1. The rate of CSF production
2. Ventricular compliance
3. CSF absorption

In normal circumstances CSF is produced at a constant rate regardless of intracranial pressure (ICP). The elasticity of the ventricles and brain decreases as the CSF volume increases. CSF absorption or resistance to outflow (assuming that most CSF is absorbed at the arachnoid villi) is defined as the difference between the pressure of CSF at the arachnoid villi and the pressure from the arachnoid villi to the dural sinus. In the normal resting state, ICP equals CSF pressure. ICP can therefore be defined as:

$$ICP = (I_F \times R_O) + R_D.$$

Where I_F equals the rate of CSF production, R_o equals resistance to CSF absorption and R_D equals dural sinus pressure. Therefore, from a CSF dynamics perspective, ICP can rise as a consequence of increased CSF production, increased resistance to CSF absorption or an increase in dural sinus pressure. The equation explains how dural sinus occlusion has a direct effect on CSF pressure and ICP. It also shows how intracranial elastance ($\Delta P/\Delta V$) is related to

the difference between the resistance to CSF outflow and dural sinus pressure. Elastance may be reduced by anything that restricts intracranial space or decreases CSF absorption, (including ventricular or cisternal CSF obstruction). All of these will increase the amplitude of the CSF pulse wave and cause a subsequent rise in ICP (Marmarou et al., 1975; Marmarou et al., 1978; Shapiro et al., 1980).

Principles of CSF shunting and CSF diversion

Hydrocephalus is a condition characterized by an increase in the size of the CSF spaces at the expense of brain. This is often associated with a rise in intracranial pressure, which left untreated can result in death or significant disability. The principle treatment of hydrocephalus is surgical CSF diversion, most commonly with the use of a shunt device.

Shunt hydrodynamics

Familiarity with the relationship between pressure and flow is an integral part of choosing the most appropriate device when treating a patient (Chari et al., 2014). CSF flow through a shunt is dependent on various factors. These include the intraventricular pressure (IVP), the hydrostatic pressure (p), the valve's opening pressure (OPV) and the pressure within the cavity in which the shunt is placed (e.g. intra-abdominal pressure, IAP). Therefore, the pressure gradient (ΔP) through a standard ventriculoperitoneal shunt can be defined as:

$$\Delta P = IVP + p - OPV - IAP.$$

Where hydrostatic pressure (p) is the product of the height of the fluid column, the density of CSF, and the gravitational force. In any given patient, the OPV is a constant for the particular system chosen whereas IVP and IAP may fluctuate depending on posture. The main variable that contributes to hydrostatic pressure is the height of the column of fluid (i.e. length of shunt tubing), therefore shortening the distal shunt tube will affect the CSF flow.

The flow of CSF (F) through a tube is equivalent to the pressure gradient, ΔP, divided by the resistance in the tube (R_T) and valve (R_V):

$$F = \Delta P / \left(R_T + R_V\right).$$

The resistance of the tube can be calculated using Poiseuille's law and is a constant for the particular system chosen, as long as the shunt is not shortened by the surgeon. The determinants of CSF flow within a shunt will therefore be regulated by the following:

1. The underlying condition and IVP
2. The patient's position
3. The resistance provided by the shunt system

Siphoning

In normal people the difference in pressure between the arachnoid granulation and venous sinuses (the principle CSF outflow tract) is not affected by posture. However, in patients with a shunt there is a rapid increase in flow rate through the shunt when they sit/stand up as the difference between intraventricular pressure and the pressure at the distal end of the shunt increases. This will lead to siphoning of CSF from the head and overdrainage (Petrella et al., 2008; Farahmand et al., 2015). Clinically this will often present with symptoms that occur when the patient moves from a recumbent to an upright position (Table 93.1). Long-term overdrainage from a shunt system is thought to be significant risk factor in the development of slit ventricle syndrome.

Table 93.1 Symptoms/signs of shunt overdrainage

Symptoms	Signs (clinical and radiological)
Headaches and nausea on standing (resolved when recumbent)	Cranial nerve palsy (in severe cases)
Tinnitus and vertigo on standing (resolved when recumbent)	Acquired Chiari malformation
Drowsiness and coma (severe cases)	Subdural collections
	Slit-like/collapsed ventricles

Shunt types

The choice of shunt position

In its most simple form, a shunt is a surgically implanted tube that diverts CSF from the ventricular compartment to another body cavity or CSF compartment. Lumbar shunts shift CSF from the lumbar theca. Most commonly the site of drainage is the abdomen, right atrium, or pleura. Other sites of drainage are summarized in Table 93.2 along with their advantages and disadvantages. The proximal shunt catheter is most commonly placed in the ventricle through either a frontal or occipitoparietal burr hole. These two approaches are associated with several advantages or disadvantages, but are usually chosen through surgeon preference (Table 93.2). There is no randomized study to show one technique is superior to any other. The adoption of intraoperative image guidance as a routine tool in modern neurosurgery has been advocated by some surgeons to reduce the risk of misplaced or suboptimally positioned catheters within the ventricle (Flannery et al., 2014).

Valve technology

There are two main types of shunt valve: those that regulate CSF flow (flow-regulated valves), and those that activate at a set CSF pressure—differential pressure valves (Czosnyka et al., 2002). Differential pressure valves may be a simple valve that opens once the IVP equals the set opening pressure of the valve, or more sophisticated gravitational or adjustable systems. Most of the data on efficacy of various valves are reported by proponents of the device and no randomized controlled trials are available to compare these devices in full. The only randomized trial data to date did not show any clinical difference in shunt survival between three valve types; a 'normal' differential pressure valve, a differential pressure valve with an antisiphon device (Delta Valve, Medtronic) and the Orbis-Sigma (Cordis) flow-controlled valve (Drake et al., 1998). It is therefore

Table 93.2 Sites of proximal shunt position, sites of distal shunt position and their advantages and disadvantages

Shunt position	Advantage	Disadvantage
Proximal catheter		
Frontal horn	• Anatomy of ventricular catheterization more predictable (when not using image guidance): especially in patients with small ventricles. • Less choroid plexus.	• Requires an additional cranial incision for valve insertion (usually inserted in-line to the shunt behind the ipsilateral pinna) • Possible higher short-term ventricular catheter blockage rate • Often requires movement of the head intraoperatively
Occipital horn	• One surgical position during shunt insertion • Longer ventricular portion of catheter—may reduce chance of early blockage • Only requires a single cranial incision and simpler to revise	• Anatomy of ventricular catheterization more variable (when not using image guidance)
Lumbar theca	• Avoids need of ventricular shunt in patients with very small ventricles (For example in idiopathic intracranial hypertension)	• Risk of postural overdrainage and development of acquired Chiari I malformation • Requires addition of more complex gravitational valve unit.
Distal catheter		
Peritoneum	• Large cavity that absorbs fluid readily • Easy to access • Core neurosurgical skill and widely practised	• May limit shunt function in patients with high intra-abdominal pressure • Surgically challenging in patients with multiple intra-abdominal adhesions • Reduced CSF absorption in patients with a high CSF protein (CSF 'ascites')
Right atrium	• Distal shunt occlusion possibly less likely than in ventriculoperitoneal and ventriculo-pleural shunts • A good option in patients with high CSF protein, or recurrent distal shunt malfunction using the peritoneum or pleura	• Shunt nephritis • Shunt revision may be surgically challenging • Not a routine technique – requires specialist skills • Shunt infection may have significant systemic manifestations – such as endocarditis • Theoretical risk of arrhythmia
Pleura	• Easy to access surgically	• Capacity for CSF absorption through the pleura is less than in the peritoneum • Negative intrathoracic pressure during inspiration may increase risk of siphoning • Reduced CSF absorption in patients with a high CSF protein
CSF cistern (cisterna magna) 'Torkildsen shunt'	• 'Bypasses' ventricular obstruction without draining CSF away from CNS: now largely superseded by endoscopic techniques	• Technically more challenging than standard techniques (not routinely practised)
Bladder	• None in modern practice (historical technique)	• Infection • Visceral injury • Challenging revision surgery
Gall bladder	• None in modern practice (historical technique)	• Infection • Visceral injury • Challenging revision surgery

important for the treating physician to understand the properties of these shunt valves and choose the most appropriate system on an individual basis.

Flow-regulated valves

Although termed 'flow-regulated' these valve systems do not measure flow but utilize variable resistance to control the flow rate of CSF to a constant range of flow rates. One example is the Integra OSV II® system. These valves consist of a synthetic ruby pin within a moveable ring. They will work as a differential pressure valve until the ICP is high enough to displace the ruby pin downwards, reducing the outflow aperture, and thus increasing resistance to flow. This allows a constant flow rate at a range of ICP. With further increases in ICP, the moveable ring becomes displaced downwards, opening the aperture and reducing the resistance to flow (Fig. 93.1).

This type of valve may be of benefit in patients with siphoning and overdrainage problems or in those with a high risk of developing slit ventricle syndrome. Current data has shown a benefit in improving symptoms of low ICP but no difference in their revision rates compared to other types of valves (Drake et al., 1998; Hanlo et al., 2003). There is no class 1 evidence that flow regulation is superior the use of a differential pressure valve in treating hydrocephalus in children or adults (Hanlo et al., 2003; Ziebell et al., 2013).

Differential pressure valves

This type of valve utilizes a very simple concept—opening and closing pressures. When the differential pressure between IVP proximal to the valve and the pressure in the CSF distal to the valve is above the valve's opening pressure, the valve will open allowing CSF to flow. However, due to the valve's mechanisms, the closing pressure may be lower than the quoted opening pressure and symptoms of overdrainage may occur without siphoning. A large variety of these valves exist in the market and each one is subdivided according to their pressure range (high, medium, and low). They can be roughly placed into four groups according to their mechanism of actions: diaphragm valve, ball-in-cone valve, mitre valve, and slit valves (Table 93.3).

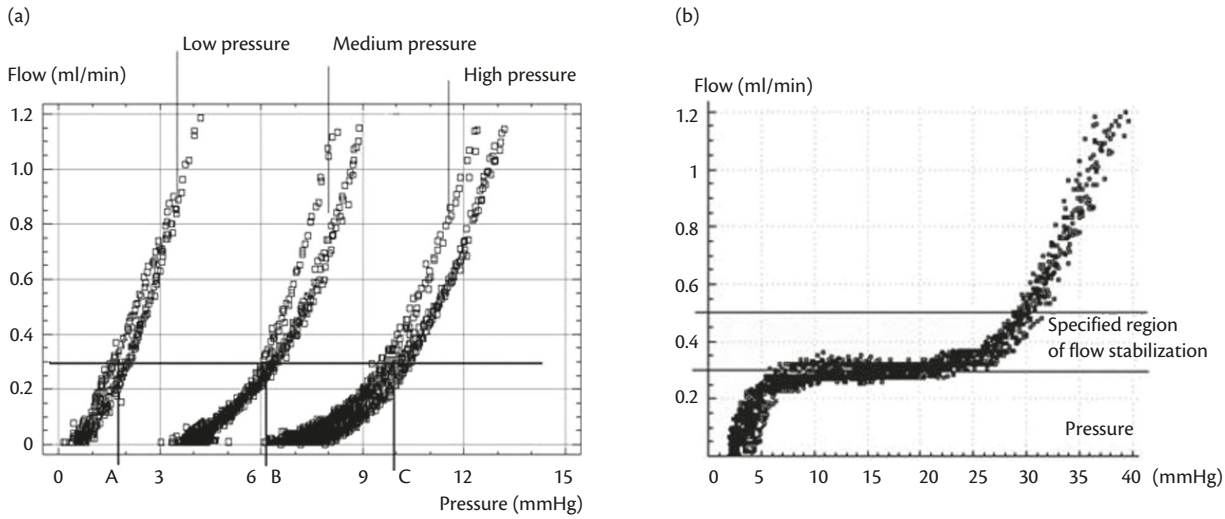

Fig. 93.1 Pressure/flow relationship in differential pressure valves at three fixed settings (A) and a flow-controlled valve (B).

(A and B) Reproduced with permission from Z. Czosnyka, M. Czosnyka, H. K. Richards et al., Laboratory Testing of Hydrocephalus Shunts—Conclusion of the U.K. Shunt Evaluation Programme, *Acta Neurochirurgica*, Volume 144, Issue 6, pp. 525–38, Copyright © 2002 Springer Nature.

Gravitational valves

This type of valve has been designed to reduce the siphoning effects of change in patient's posture by altering the opening pressure, using gravity. They are ball-in-cone differential pressure valves but with an additional gravitational unit. This is composed of a ball which would displace into the cone when the patient is upright, thus increasing resistance and reducing flow. Examples being the Integra™ H-V® valve and Mithke *Pro-Gav*® system. As with any differential pressure valve, they come in a range of different opening pressures and given this is dependent on the height of the column of fluid within the system, the choice should be based on the height of the patient. They are of particular use in lumbar shunts to reduce the common problem of postural overdrainage.

Adjustable or 'programmable' valves

These are differential pressure valves, which have a mechanism that allows adjustment of the opening pressure by the user externally. The obvious benefit is the ability to alter the opening pressure non-invasively according to the patient's symptoms and reduce the need for revision surgery in this situation. Most systems use an external magnetic field to adjust the valve—many designs exist on the market. A limitation therefore is that a strong magnetic field such as an MRI may alter the shunt opening pressure setting. It is therefore important that patients with shunts with adjustable valves know that strong magnetic fields may affect their shunt function. Equally important is that MR radiographers are aware so that shunt settings can be checked after any MRI examination (Lollis et al., 2010). Settings can usually simply be confirmed with a plain radiograph of the shunt valve, but this requires knowledge of the shunt appearance to ensure correct interpretation (Fig. 93.2).

There is no class I data to compare their efficacy to non-adjustable types of valves. Adjustable systems are, in the main, indicated in the management of idiopathic normal pressure hydrocephalus (iNPH) and have been shown to reduce postoperative overdrainage and subdural formation in these patients. They enable the stepwise reduction in valve opening pressure, and allow the titration of shunt setting against clinical response. The ability to non-invasively reduce the opening pressure over time helps to reduce the risk of developing postoperative subdural collections in patients with large non-compliant ventricles. A surgeon may also choose to use these more expensive valves in younger adults with very large ventricles or in children as a way of allowing gradual upgrading of valve pressure as the child grows taller. Whether this lowers the risk of long-term

Table 93.3 Examples of differential pressure valves and their designs

Valve design	Example	Advantage	Disadvantage
Diaphragm	• Sophysa Pulsar® • Medtronic Delta®	Simple valve. Allows ventricular CSF sampling if reservoir is proximal to valve	Silicone prone to degradation with age
Ball-in-cone	• Codman® Hakim	Less prone to ageing effects	More prone to obstruction in patients with particulate or turbid CSF
Mitre	• Integra™ Mischler Valve	Direct flow path makes obstruction less likely in patients with turbid CSF	Silicone prone to degradation with age
Slit valve	• Sophysa Phoenix® • Holter-Hausner® • Codman® Unishunt	Simple, usually cheap. Simple insertion. Small (useful in neonates). Can be placed proximally or distally	May be prone to siphoning. Do not allow shunt tapping

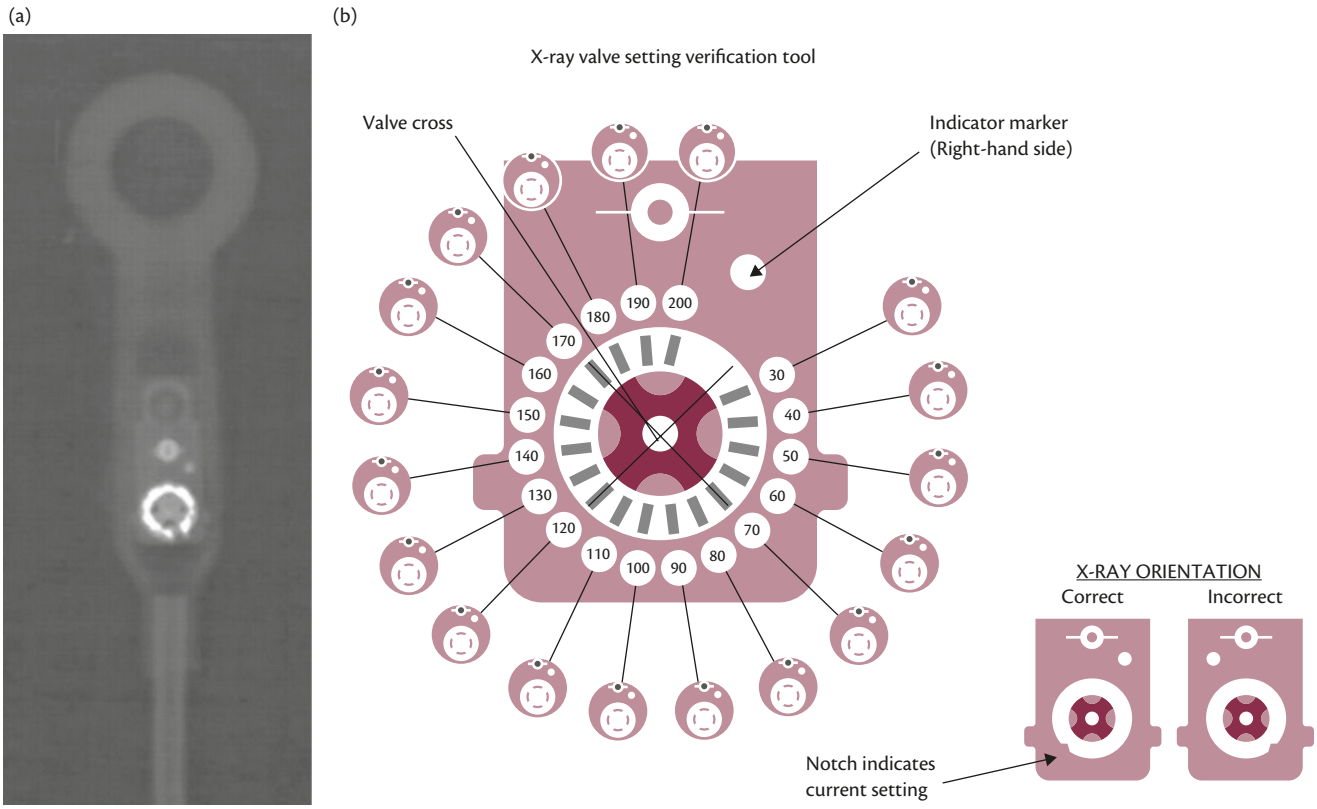

Fig. 93.2 Radiographic and diagrammatic representation of the Codman Hakim® (Depuy-Synthes) programmable differential pressure valve. Valve setting can be checked with radiograph of the valve complex and verifying the location of the notch in the valve (A) which corresponds to the valve setting (courtesy of Codman Depuy-Synthes, United Kingdom). Other valve designs use similar radiographic methods of determining valve setting.

overdrainage complications or blockage in the individual child is not yet clear from longitudinal studies.

Operative principles

External ventricular drain

Cranial CSF may be drained externally as a temporary measure through an external ventricular drain (EVD), and is often a life-saving procedure in patients with acute hydrocephalus. Temporary CSF drainage may be indicated where the CSF is contaminated with blood, when there is evidence of CSF infection, or the cause of hydrocephalus is reversible and permanent CSF diversion is not likely to be required. For the surgical technique of EVD insertion see **Box 93.1**.

Ventricular cannulation and the placement of a ventriculoperitoneal shunt

An occipitoparietal burr hole is used most commonly for the site of proximal catheter insertion, though some prefer a frontal approach, citing a reduce failure rate from choroid plexus occlusion, though this remains controversial. The use of image guidance to ensure optimum catheter position within the ventricle is become more widespread where the technology is readily available and the associated costs are reducing.

The general operative principles for shunt placement are outlined in **Box 93.2**. Whichever the preferred site of catheter entry, all efforts should be made to prevent shunt infection.

Investigation of shunt failure

In any patient with a shunt in whom shunt dysfunction is suspected, the following investigations should be performed immediately and without delay, as surgical intervention may be required urgently.

- Plain non-contrast cranial CT scan (including volume acquisition if image guidance is likely to be required for shunt revision).
- 'Shunt series' of plain radiographs to ensure shunt is in continuity. This should include radiographs that incorporate the whole shunt system: typically skull, cervical spine, chest, and abdomen in patients with a ventriculoperitoneal shunt. In patient with a known programmable valve, a dedicated radiograph perpendicular to the valve should be performed in addition to the shunt series to accurately check the valve settings.
- Laboratory tests: full blood count, coagulation, basic biochemistry as a minimum. A measure of C reactive protein is helpful if shunt infection is possible. Blood and CSF cultures should be obtained if infection is suspected.

It is vitally important old imaging is available for comparison where possible. Records should be available that describe the shunt and valve type that is implanted, though this is often made clear from the shunt series of plain radiographs. Some units are adopting a rapid MRI protocol for patients with suspected shunt failure, to limit the cranial radiation dose. This is particularly relevant in children with complex hydrocephalus that present regularly.

Box 93.1 External ventricular drain insertion technique

- Head-up position at approximately 30°. Head neutral on horse-shoe headrest (patient placed in pins if using an optical image guidance system).
- Image guidance set up and patient accurately registered to the system if being used*.
- Right-sided frontal burr hole unless contraindicated (e.g. right frontal intraventricular haematoma, asymmetric ventriculomegaly).
- Frontal hair shave and sterile preparation to allow at least 5 cm space for tunnelling of the drain.
- Drape the patient so that the tragus and ipsilateral medial canthus are visible or easily palpable.
- Place the burr hole 1–2 cm anterior to the coronal suture in the midpupillary line (Kocher's point). Plan incision so that it does not interfere with any planned surgical procedure (e.g. endoscopic ventricular surgery or pterional craniotomy for clipping anterior circulation aneurysms).
- Meticulous haemostasis—paying particular attention to bleeding bone edges (use bone wax where required), dura and pia (bipolar coagulation).
- Insert catheter perpendicular to brain surface to a depth of 5–6 cm aiming for a point that is the convergence of the ipsilateral medial canthus and tragus; this approximates the position of the foramen of Monro. If CSF does not flow at the point, then the trajectory is incorrect. Passing the catheter to a greater depth is unlikely to be successful.
- Tunnel catheter under sterile surgically prepared scalp at least 5 cm.
- Pay particular attention to securing the drain effectively without occluding it. Drains should not 'fall out' on the ward. Close and dress wound.
- Attach external drainage set under sterile conditions and set height at which CSF should be drained. Communicate this drainage height to all members of the team involved in the patients care and carefully document it in the notes.

*Image guidance (including intraoperative ultrasound) to be used at the discretion of the surgeon. It is of particular use in patients where the anatomy is abnormal (e.g. the presence of midline shift).

Shunt infection

Shunt infection is possibly the most undesirable shunt complication, and everything should be done to reduce the risk of this occurring (Di Rocco et al., 1994). The adoption of a standard departmental shunt insertion protocol addressing the multifactorial aetiology of infections has been shown to significantly reduce this risk (Kestle et al., 2011). Some shunts have been specifically designed to help prevent postoperative infection. The impregnation of catheters with antibiotics (e.g. Bactiseal®), or coating with substances that reduce bacterial adhesion (e.g. Silverline®) has been developed to reduce the rate of shunt failure from infection and have variable amounts of evidence to support their efficacy. These antimicrobial catheters do not completely eliminate the risk of infection, but provide some defence against the more common pathogens causing shunt infections, and there is currently no class 1 evidence to promote their use over cheaper systems (Klimo et al., 2014). A UK multicentre prospective randomized trial (https://www.basics.org.uk) has just completed to assess the efficacy of these different products when compared to standard shunt tubing. We await the published results with interest.

Box 93.2 Principles of ventriculoperitoneal shunt insertion: Complication avoidance

- **Preoperative considerations.** Consider chlorhexidine scalp wash the day before surgery. Ensure preoperative antibiotics are given prior to the first incision as per the hospital's antibiotic guidelines.
- **Theatre etiquette.** The number of staff present in the operating theatre should be kept to a safe minimum and traffic of personnel should be discouraged. Doors should be kept closed at all time. All staff should wear surgical masks. Laminar flow operating theatres should be used where available.
- **Patient positioning.** Ensure the anaesthetist positions the endotracheal tube away from the side of the planned surgery. Ensure that the head is positioned to allow full access to the chosen position of proximal catheter insertion. The head position should allow unhindered access to the neck and clavicle to make distal catheter tunnelling as easy and safe as possible.
- **Preparation of surgical site.** Mark planned incisions with indelible marker. Shave hair at proximal catheter insertion point and along tunnelling path. Meticulous preparation, allowing time for surgical prep to evaporate. Sterile local anaesthetic with adrenalin injected into the skin at both primal and distal incision sites. Ensure all drapes are carefully placed to maintain sterility at all times.
- **Surgical technique.** Double glove. Careful handling of tissues at all time. Make particular care not to handle wound edges. Cover all wound edges with antiseptic soaked gauze or drapes.
- **Shunt tunnelling and preparation of a pocket for the valve.** Make all efforts to ensure tunnelling tool passes over the clavicle. Some surgeons prefer to tunnel from the distal incision to make this easier. Ensure a subcutaneous pocket is fashioned that is large enough to accommodate the valve of choice without kinking the shunt tubing.
- **Handling of shunt components**. Use new gloves when handling the shunt for the first time. Always use non-toothed instruments to manipulate the shunt components. Preassemble shunt components away from the patient with new sterile gloves if possible. Open shunt components at the last minute, and keep covered and submerged in saline once opened and primed.
- **Haemostasis and wound closure.** Meticulous attention to detail to ensure haemostasis and proper wound edge apposition when closing the wound. This is of particular importance in infants.
- **Adherence to a departmental protocol.** The use of a departmental protocol for shunt insertion has been shown to drive down infection rates; irrespective of what it contains. Some may include the use of routine intrathecal antibiotics, using specific skin preparation or drapes, or using antibiotic-impregnated shunts.

Endoscopic surgery for the treatment of hydrocephalus

Over the past 20 years there has been a huge resurgence of interest in the use of endoscopic techniques to treat hydrocephalus, such as third ventriculostomy (ETV). During this period, advances in endoscope design, improved optics, and image display (including high definition and more recently 3D) has enabled these procedures to be undertaken with a greater degree of accuracy and safety. The attraction of giving children and adults the chance of escaping the numerous inherent complications of CSF shunts has led to the rapid expansion of neurosurgeons offering a neuroendoscopic alternative as a first-line treatment of hydrocephalus.

Box 93.3 Clinical indications for endoscopic third ventriculostomy

Strong indications

- Delayed-onset aqueduct stenosis
- CSF shunt obstruction in any patient with a history of obstructive hydrocephalus and large enough ventricles for endoscopy to be safe
- Older patients with spina bifida and a blocked shunt
- Obstructive hydrocephalus caused by pineal region or posterior fossa tumours; either as a primary treatment or prior to more definitive tumour resection. May be combined with endoscopic biopsy

Weaker indications

- Neonates with aqueduct stenosis or spina bifida
- CSF shunt obstruction in children or adults with a history of communicating hydrocephalus

Box 93.4 Endoscopic third ventriculostomy technique: Basic principles

- **Head-up position:** The table is tilted and the patient's neck is flexed to produce a head-up tilt of approximately 30°. This helps to prevent excessive CSF loss, which may cause pneumocephalus, subdural hematomas, and upward herniation of cerebellar tumours.
- **Siting the burr hole correctly:** It should be placed just anterior (or on) the coronal suture in the midpupillary line, which is approximately 3 cm from the midline in an adult and approximately 2 cm from the midline in a small child.
- **Using the correct trajectory and landmarks to cannulate the ventricle:** If the external auditory meatus and ipsilateral medial canthus are used for the trajectory, the tip of the cannula should lie at the foramen of Monro provided that the depth is appropriate (approximately 6 cm in an adult and approximately 4 cm in a child).
- **Perforating the floor of the third ventricle anterior to the mammillary bodies in the midline and usually at its thinnest part:** This is often halfway between the mammillary bodies and the infundibulum. The instrument used to perforate the floor should preferably be blunt-tipped but depends on the individual surgeon's preference ranging from the scope tip itself to thin unipolar wire electrodes, balloon catheters, or laser.
- **Clear visualization of the subarachnoid space after making the hole:** The basilar artery, brainstem, and clivus should be clearly seen through the stoma, which is usually enlarged with a balloon catheter. Pulsations ('flapping') of the floor of the third ventricle at the end of the procedure tend to indicate a favourable long-term outcome. Any residual Lilliquist membranes in the prepontine space should be divided if safe to do so.
- **Use of image guidance:** When the ventricular anatomy seems complex or difficult to interpret on standard scans, neuronavigation systems should be used.

Endoscopic third ventriculostomy

History

The first successful endoscopic third ventriculostomy was performed by Mixter in 1923 on a 9-month-old child with non-communicating hydrocephalus, using a small urethroscope (Mixter, 1923). Scarff advocated ETV as a rational method of treating obstructive hydrocephalus as far back as 1935 (Scarff, 1936), but reports in the literature largely comprised single cases or small series until the 1980s and 1990s, when the operation gained more widespread popularity. The indications for ETV are described in Box 93.3.

Anatomy

The standard technique for performing an ETV is described in Box 93.4, though there are various technical nuances and variations. After successful cannulation of the frontal horn of the lateral ventricle (usually the right), the foramen of Monro can be identified by following the thalamostriate or septal veins. They typically meet at the foramen, which also has choroid plexus running anteriorly in the choroidal fissure up to or through it (Fig. 93.3). After carefully passing the endoscope through the foramen (paying particular care not to damage or stretch the fornix) the typical features of the third ventricular floor can be identified. Posteriorly one should visualize the mammillary bodies, anteriorly the infundibular recess and the lamina terminalis (Fig. 93.3). In cases where the ventricular floor is very stretched and thinned, one may be able to see the basilar artery in the prepontine cistern through a thinned membrane.

Preoperative investigations

CT is often sufficient to make the diagnosis of obstructive hydrocephalus, but this should be augmented with the detail available with magnetic resonance imaging in all cases. MR imaging of the brain with midline sagittal views is useful to demonstrate the presence or absence of flow voids in the third ventricle or aqueduct. Cine-MRI may help to illustrate these flow voids. MRI is also essential to clarify the relative size of the lateral, third, and fourth ventricles, and to show the anatomy of the basilar artery and prepontine space. This will establish whether the entry of an instrument into the prepontine space is technically feasible. Volume acquisition scans should be obtained if intraoperative image guidance is going to be used. Where available, a high-resolution T2 MR scan in the midsagittal plane should be obtained, such as provided by constructive interference in steady state (CISS) sequences or equivalent. These not only give better anatomical detail but will also detect if there are any other obstructive membranes within the ventricle that may also be amenable to endoscopic treatment (Fig. 93.4).

A radiologic diagnosis of aqueduct stenosis is usually made on the basis of the sagittal MRI image but the radiologic differentiation between obstructive and communicating hydrocephalus is sometimes uncertain. CSF infusion studies through a ventricular catheter or spinal needle can be used to assess the relative compliance of the intraventricular and extracranial CSF compartments, thus giving an indirect assessment of the degree of obstruction to outward flow from the ventricles. This test has been used to select suitable candidates for third ventriculostomy, as well as shunting, though is not routine (Boon et al., 1997; Bech-Azeddine et al., 2007).

Contraindications

Clearly if the anatomy of the prepontine space has been severely distorted, for example, by a tumour, severe meningitis, or vascular abnormality, third ventriculostomy should probably not be attempted. With such a poor chance of success in premature neonates with posthaemorrhagic hydrocephalus, it is questionable whether the technique should be used routinely in these babies.

Technique

There is great variability between individual surgeons in the details of their technique, but there are certain basic principles that are vital for the success of the procedure (Box 93.4).

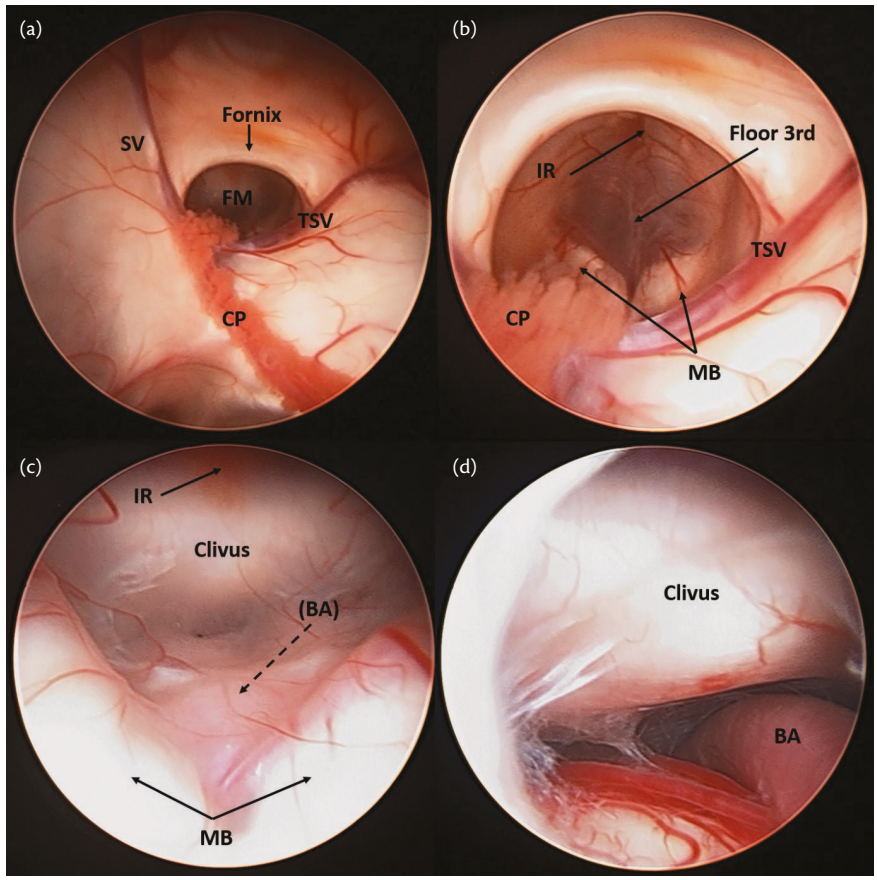

Fig. 93.3 Intraoperative neuroendoscopic images during ETV for aqueduct stenosis. SV, septal vein; TSV, thalamostriate vein; CP, choroid plexus; IR, infundibular recess; MB, mammillary bodies; BA, basilar artery; FM, foramen of Monro.
A) Foramen of Monro from a standard right frontal approach to the lateral ventricle.
B) View of the third ventricular floor through the foramen of Monro.
C) Floor of the third ventricle. In this case very thinned due to the chronic hydrocephalus. The basilar artery can be seen through the translucent floor.
D) View of the basilar artery in the prepontine cistern after third ventriculostomy. The scope is passed through the stoma to ensure there is no obstruction to CSF flow from Lilliquist membrane.

Artificial CSF should be used whenever possible for irrigation of the ventricles during ventriculoscopy because of the apparently detrimental effect of saline washouts on the brain and ependyma. Some surgeons use a temporary EVD at the end of the procedure, whereas others do not use any CSF drainage devices. The authors routinely place a subcutaneous ventricular access reservoir and have found it extremely useful in the follow-up of patients. As well as allowing immediate access to the CSF space in the case of acute life-threatening hydrocephalus due to stoma blockage, a ventricular access device also can be used to non-surgically to monitor ICP. Postoperative

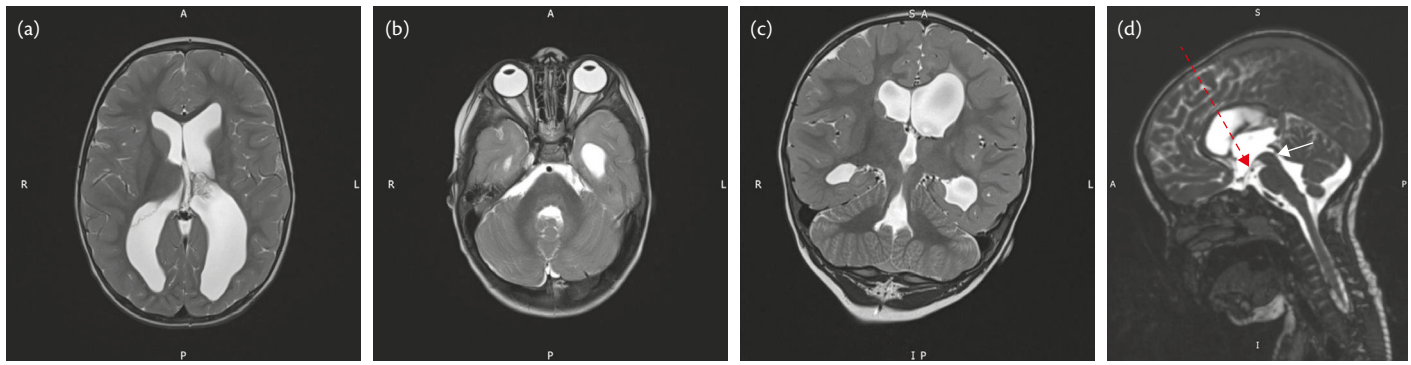

Fig. 93.4 A 2-year-old boy with asymmetric tri-ventricular hydrocephalus as shown in the axial and coronal T2-weighted MR images (A–C). Sagittal CISS MR imaging illustrated aqueduct obstruction from a web (D, white arrow). Dotted red arrow illustrates the required trajectory of the endoscope for third ventriculostomy.

analysis of CSF dynamics with the use of a constant rate infusion study can be used to predict stoma function in these patients, and can be a useful tool in patients after ETV where there is clinical doubt as to the success of the procedure (Aquilina et al., 2012).

Outcome after ETV

The possibility of achieving shunt independence in both children and adults with hydrocephalus is a tempting proposition. Indeed, in certain individuals ETV is more effective in the long term than shunting and does not carry the inevitable long-term complications associated with implanted shunt hardware. The publication of an ETV success score gives an idea of the relative probability of achieving shunt independence (Kulkarni et al., 2010b). This provides a clinician with a numerical score for a patient calculated as a function of their age, the aetiology of the hydrocephalus and whether or not they have previously treated with a shunt. The total score is approximate percentage predicted probability of a successful ETV, defined as long-term shunt freedom. Poor scores are obtained in patients less than 1 month, those with postinfectious hydrocephalus, and those that have previously been shunted. The chance of ETV success is greater in children over 10 years of age with hydrocephalus caused by obstruction at the level of the cerebral aqueduct who have not been previously treated with a shunt.

A continuation of this work has shown that ETV is less effective than shunting in the short term (less than 3 months), but more effective in the long term, that is, if the ETV is successful after 3 months postoperatively, then the risk of failure long term is better than if a shunt was used instead (Kulkarni et al., 2010a). This observation has yet to be tested in a prospective randomized trial and carries the usual inherent limitations of a retrospective study. It does however reflect the commonly held view that ETV is much more successful in older children or adults with obstructive hydrocephalus with aqueduct stenosis, than in neonates with postmeningitis or haemorrhagic hydrocephalus.

Other forms of endoscopic CSF diversion procedures

Septostomy

By Communicating both lateral ventricles with an endoscopic septostomy, CSF can bypass blockage that causes asymmetrical univentricular hydrocephalus. Hydrocephalus can then be controlled through a unilateral lateral ventricular shunt or an ETV. In the case of an isolated trapped lateral ventricle, it may be all that is required.

Multiloculated hydrocephalus

Complex multiloculated hydrocephalus is a common consequence of neonatal intraventricular haemorrhage and intracranial sepsis. Management may be through the use of multiple shunts, or shunt catheters, which creates a complex shunt system and is the nightmare case for the on call neurosurgical team when a patient presents with shunt dysfunction (**figure 93.5**). In these cases, a flexible endoscope is of particular use as it allows the surgeon to divide multiple intraventricular adhesions through as few burr holes as possible. By communicating these loculations, CSF drainage can be managed through a single shunt or ETV, providing a much more satisfactory surgical outcome.

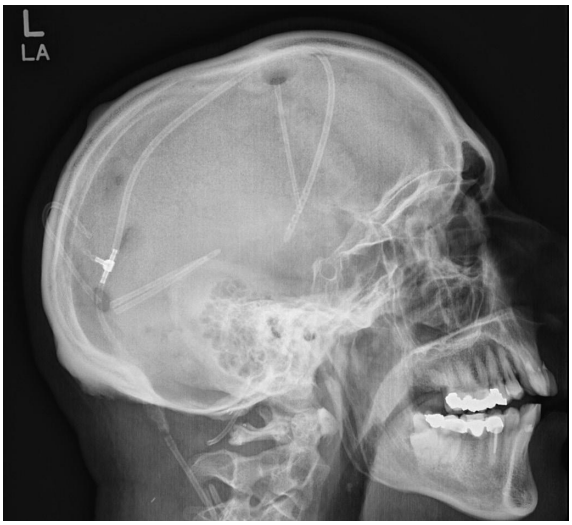

Fig. 93.5 Multiple proximal shunt catheters seen on a plain anteroposterior (AP) radiograph. The nightmare hydrocephalus case.

Aqueductoplasty

Endoscopic aqueductoplasty and aqueductal stenting as treatments for hydrocephalus caused by aqueduct stenosis are controversial techniques that are not widely practised. This is primarily because of the high risk of neurologic complications as a result of damage to midbrain structures causing disconjugate eye movements, (Parinaud's syndrome) and oculomotor or trochlear nerve palsies. Furthermore, the shape of the aqueduct, which most often depicts an S-shape in the midsagittal plane, increases the risk of midbrain trauma if rigid endoscopes or catheters are used. However, the technique does directly restore the physiologic CSF pathway and as endoscope technology evolves, is becoming increasingly possible in experienced hands to achieve without complications. In particular, endoscopic stenting of the aqueduct may have a role in the treatment of patients with an isolated obstructed fourth ventricle after shunting.

Endoscopic choroid plexus coagulation

Before the introduction of ventricular shunting procedures in the 1950s, open extirpation of the choroid plexus, first described by Dandy in 1918, was the most commonly performed operation for infantile hydrocephalus. The procedure had a high mortality rate and was largely abandoned after the introduction of shunting procedures. The introduction of endoscopic techniques to coagulate the choroid plexus led to a significant improvement in operative results, but has not established itself as a standard technique (Pople and Ettles, 1995). There is growing evidence that in combination with ETV it may be of more benefit as first-line treatment (Stone and Warf, 2014). Patients who require shunt insertion because of failure of choroid plexus coagulation to control hydrocephalus undergo fewer subsequent shunt revisions. This is probably the result of reduced rates of proximal catheter blockage by choroid plexus ingrowth. The indications for this procedure are described in **Box 93.5**.

Box 93.5 Indications for endoscopic choroid plexus coagulation

Infants with slowly progressive communicating hydrocephalus: Success rates in this group of patients as measured by shunt independence of up to 64% at 10 years of follow-up have been achieved

Hydrocephalus as a result of CSF overproduction: Choroid plexus papilloma and hyperplasia are conditions in which overproduction of CSF may result in hydrocephalus. Endoscopic choroid plexus coagulation deals directly with the pathologic cause of the hydrocephalus and may obviate the need for ventricular shunting.

Communicating hydrocephalus where shunt insertion is not feasible, such as in infants where there is persistent posthaemorrhagic hydrocephalus associated with necrotizing enterocolitis.

Intractable shunt failure: In addition to ensuring a shunt functions acutely, these patients may benefit by a reduction in proximal shunt occlusion rates

Endoscopic choroid plexus coagulation is contraindicated in obstructive hydrocephalus and in patients with rapidly progressive communicating hydrocephalus with acutely raised ICP

Endoscopic treatment of developmental posterior fossa cysts

The rapid development of intraventricular neuroendoscopy has revolutionized the treatment of hydrocephalus caused by developmental posterior fossa cystic abnormalities, such as Dandy Walker Syndrome and Blake's pouch cysts, either through aqueductoplasty, or via endoscopically fenestrating cysts to allow communication and drainage through an ETV or shunt.

Endoscopic removal/aspiration of obstructive intraventricular cysts

Arachnoid cysts

Endoscopic decompression and fenestration are most useful in intraventricular arachnoid cysts, midline septal cysts, and arachnoid cysts of the suprasellar region. The recomended treatment for middle fossa arachnoid cysts remains controversial, and fenestration, either endoscopically or by open technique, seems to have a fairly high long-term failure rate (30–50%): often a conservative approach is best. Cysts of the quadrigeminal cistern can be treated by third ventriculoscopy and fenestration of the cyst into the third ventricle, often alongside an ETV.

Colloid cyst of the third ventricle

Endoscopic removal or aspiration and coagulation of colloid cysts which are causing obstructive hydrocephalus has been used in the authors' unit since the early 1980s. The benefits of a less invasive approach to these cysts seem to outweigh the disadvantage of more frequent incomplete removal. This remains controversial, with some surgeons still advocating an open transcortical or interhemispheric transcollosal approach. However, endoscopic colloid cyst surgery is now recognized as potentially superior alternative to open surgery when in experienced hands. A successful result in terms of control of hydrocephalus, symptomatic improvement, and removal of most of the cyst has been achieved in most cases in various reported series. A second burr hole to allow passage of a reasonably large-bore suction catheter down a separate tract for aspiration of the sometimes thick viscous cyst contents may be required. When the hydrocephalus is not severe, endoscopy can be combined with stereotactic guidance into the ventricle. Indeed, Image guidance is very useful in all cases to plan the optimum scope trajectory to remove a colloid cyst as it is often different to that used in a standard ETV.

Summary

Hydrocephalus surgery is a complex clinical science. There is little clinical evidence to say whether any one of the vast range of complex shunt devices on the market are superior to another. The development of endoscopic technology and neuroimaging techniques has made the prospect of hydrocephalic patients to be managed without implanted shunt hardware a real possibility. The modern neurosurgeon needs to be aware of all the options available to make the best decisions for their patients on an individual basis.

FURTHER READING

Drake, J.M., Kestle, J.R., Milner, R., et al. (1998). Randomized trial of cerebrospinal fluid shunt valve design in pediatric hydrocephalus. *Neurosurgery*, **43**, 294–303; discussion 303–5.

Kulkarni, A.V., Drake, J.M., Kestle, J.R., Mallucci, C.L., Sgouros, S., & Constantini, S. (2010b). Predicting who will benefit from endoscopic third ventriculostomy compared with shunt insertion in childhood hydrocephalus using the ETV success score. *J Neurosurg Pediatr*, **6**, 310–15.

Marmarou, A., Shulman, K., & Lamorgese, J. (1975). Compartmental analysis of compliance and outflow resistance of the cerebrospinal fluid system. *J Neurosurg*, **43**, 523–34.

Marmarou, A., Shulman, K., & Rosende, R.M. (1978). A nonlinear analysis of the cerebrospinal fluid system and intracranial pressure dynamics. *J Neurosurg*, **48**, 332–44.

REFERENCES

Aquilina, K., Pople, I.K., Sacree, J., Carter, M.R., & Edwards, R.J. (2012). The constant flow ventricular infusion test: a simple and useful study in the diagnosis of third ventriculostomy failure. *J Neurosurg*, **116**, 445–52.

Bech-Azeddine, R., Nielsen, O.A., Logager, V.B., & Juhler, M. (2007). Lumbar elastance and resistance to CSF outflow correlated to patency of the cranial subarachnoid space and clinical outcome of endoscopic third ventriculostomy in obstructive hydrocephalus. *Minim Invasive Neurosurg*, **50**, 189–94.

Boon, A.J., Tans, J.T., Delwel, E.J., et al. (1997). Dutch normal-pressure hydrocephalus study: prediction of outcome after shunting by resistance to outflow of cerebrospinal fluid. *J Neurosurg*, **87**, 687–93.

Brinker, T., Stopa, E., Morrison, J., & Klinge, P. (2014). A new look at cerebrospinal fluid circulation. *Fluids Barriers CNS*, **11**, 10.

Chari, A., Czosnyka, M., Richards, H.K., Pickard, J.D., & Czosnyka, Z.H. (2014). Hydrocephalus shunt technology: 20 years of experience from the Cambridge Shunt Evaluation Laboratory. *J Neurosurg*, **120**, 697–707.

Czosnyka, Z., Czosnyka, M., Richards, H.K., & Pickard, J.D. (2002). Laboratory testing of hydrocephalus shunts—conclusion of the U.K.

Shunt evaluation programme. *Acta Neurochir (Wien)*, **144**, 525–38; discussion 538.

Di Rocco, C., Marchese, E., & Velardi, F. (1994). A survey of the first complication of newly implanted CSF shunt devices for the treatment of nontumoral hydrocephalus. Cooperative survey of the 1991–1992 Education Committee of the ISPN. *Childs Nerv Syst*, **10**, 321–7.

Drake, J.M., Kestle, J.R., Milner, R., et al. (1998). Randomized trial of cerebrospinal fluid shunt valve design in pediatric hydrocephalus. *Neurosurgery*, **43**, 294–303; discussion 303–5.

Farahmand, D., Qvarlander, S., Malm, J., Wikkelso, C., Eklund, A., & Tisell, M. (2015). Intracranial pressure in hydrocephalus: impact of shunt adjustments and body positions. *J Neurol Neurosurg Psychiatry*, **86**, 222–8.

Flannery, A.M., Duhaime, A.C., Tamber, M.S., & Kemp, J. (2014). Pediatric hydrocephalus: systematic literature review and evidence-based guidelines. Part 3: endoscopic computer-assisted electromagnetic navigation and ultrasonography as technical adjuvants for shunt placement. *J Neurosurg Pediatr*, **14** Suppl 1, 24–9.

Hanlo, P. W., Cinalli, G., Vandertop, W. P., et al. (2003). Treatment of hydrocephalus determined by the European Orbis Sigma Valve II survey: a multicenter prospective 5-year shunt survival study in children and adults in whom a flow-regulating shunt was used. *J Neurosurg*, **99**, 52–7.

Kestle, J.R., Riva-Cambrin, J., Wellons, J.C., 3rd, et al. (2011). A standardized protocol to reduce cerebrospinal fluid shunt infection: the Hydrocephalus Clinical Research Network Quality Improvement Initiative. *J Neurosurg Pediatr*, **8**, 22–9.

Klimo, P., Jr., Thompson, C.J., Baird, L.C., & Flannery, A.M. (2014). Pediatric hydrocephalus: systematic literature review and evidence-based guidelines. Part 7: antibiotic-impregnated shunt systems versus conventional shunts in children: a systematic review and meta-analysis. *J Neurosurg Pediatr*, **14** Suppl 1, 53–9.

Kulkarni, A.V., Drake, J.M., Kestle, J.R., Mallucci, C.L., Sgouros, S., & Constantini, S. (2010a). Endoscopic third ventriculostomy vs cerebrospinal fluid shunt in the treatment of hydrocephalus in children: a propensity score-adjusted analysis. *Neurosurgery*, **67**, 588–93.

Kulkarni, A.V., Drake, J.M., Kestle, J.R., Mallucci, C.L., Sgouros, S., & Constantini, S. (2010b). Predicting who will benefit from endoscopic third ventriculostomy compared with shunt insertion in childhood hydrocephalus using the ETV success score. *J Neurosurg Pediatr*, **6**, 310–15.

Lollis, S.S., Mamourian, A.C., Vaccaro, T.J., & Duhaime, A.C. (2010). Programmable CSF shunt valves: radiographic identification and interpretation. *AJNR Am J Neuroradiol*, **31**, 1343–6.

Marmarou, A., Shulman, K., & Lamorgese, J. (1975). Compartmental analysis of compliance and outflow resistance of the cerebrospinal fluid system. *J Neurosurg*, **43**, 523–34.

Marmarou, A., Shulman, K., & Rosende, R.M. (1978). A nonlinear analysis of the cerebrospinal fluid system and intracranial pressure dynamics. *J Neurosurg*, **48**, 332–44.

Mixter, W.J. (1923). Ventriculoscopy and puncture of the floor of the third ventricle. *The Boston Med Surg J*, **188**, 277–8.

Petrella, G., Czosnyka, M., Keong, N., Pickard, J.D., & Czosnyka, Z. (2008). How does CSF dynamics change after shunting? *Acta Neurol Scand*, **118**, 182–8.

Pople, I.K. & Ettles, D. (1995). The role of endoscopic choroid plexus coagulation in the management of hydrocephalus. *Neurosurgery*, **36**, 698–701; discussion 701–2.

Scarff, J.E. (1936). Endoscopic treatment of hydrocephalus: description of a ventriculoscope and preliminary report of cases. *Archives of Neurology & Psychiatry*, **35**, 853–61.

Shapiro, K., Marmarou, A., & Shulman, K. (1980). Characterization of clinical CSF dynamics and neural axis compliance using the pressure-volume index: I. The normal pressure-volume index. *Ann Neurol*, **7**, 508–14.

Stone, S.S. & Warf, B.C. (2014). Combined endoscopic third ventriculostomy and choroid plexus cauterization as primary treatment for infant hydrocephalus: a prospective North American series. *J Neurosurg Pediatr*, **14**, 439–46.

Ziebell, M., Wetterslev, J., Tisell, M., Gluud, C., & Juhler, M. (2013). Flow-regulated versus differential pressure-regulated shunt valves for adult patients with normal pressure hydrocephalus. *Cochrane Database Syst Rev*, **5**, Cd009706.

RELATED LINK TO EBRAIN

Performing an Endoscopic Third Ventriculostomy. https://learning.ebrain.net/course/view.php?id=523

94

Normal pressure hydrocephalus

Nicole C. Keong

Introduction

The concept of a 'symptomatic occult hydrocephalus with 'normal' CSF (cerebrospinal fluid) pressure' was described by Hakim and Adams in 1965 in their landmark paper of observations based on three cases, two post-traumatic and one idiopathic, and subsequently expanded with the support of others (Adams et al., 1965; Hakim and Adams, 1965). The term was in fact coined by Hakim for his thesis the year prior to the publication of that paper. Current guidelines and research are focused primarily on the idiopathic normal pressure hydrocephalus (iNPH) as opposed to secondary normal pressure hydrocephalus (secondary NPH), occurring following subarachnoid haemorrhage, head injury, intracranial surgery, or meningitis.

The term 'normal pressure' hydrocephalus is misleading as continuous CSF pressure measurements indicate that intracranial pressure is on average slightly higher than normal and there are waves of increased intracranial pressure, particularly during rapid eye movement (REM) sleep. Such nomenclature is also thought by some to promote an underestimation of the condition, implying a type of hydrocephalus requiring less urgent access to diagnosis and treatment. As a result, some experts prefer the term idiopathic adult hydrocephalus syndrome or chronic communicating hydrocephalus.

Pathophysiology

Theories of pathogenesis and research evidence

Many theories have been advanced to explain the underlying mechanisms by which the NPH syndrome develops. However, the basic pathophysiological processes still remain unclear. The major theory streams proposed for the pathogenesis of NPH can be loosely organized into (i) structural, (ii) cerebral blood flow, and (iii) CSF flow subgroups. The components of each theory stream are expanded in the text that follows here, although the list of studies supporting each section should be considered by no means exhaustive (see (Momjian et al., 2004; Keong et al., 2016) for detailed reviews; **Table 94.1** for an overall illustration and additional references).

Structural

Tissue distortion

Hakim and other authors have hypothesized that the starting point in the pathophysiology of NPH is tissue distortion secondary to raised intraventricular pressure (Hakim et al., 1976). Compression or stretching of both parenchyma and blood vessels produce loss of elasticity, atrophy, and/or ischaemic injury. This produces a state of normal CSF pressures that result in a reversal of the gradient of pressure and stress upon the cerebral mantle.

Interstitial fluid pressure increase

Loss of elasticity in the parenchyma results in a pressure gradient between the ventricles and periventricular tissues and/or between convexity subarachnoid spaces and the parenchyma. Fluid stagnation disrupts the balance of hydrostatic vs. osmotic pressures, resulting in reversal of interstitial fluid flow, subsequent oedema, and failure of drainage of vasoactive metabolites. Local cerebrovascular reactivity is reduced (Marmarou et al., 1980). Damage to cell and blood vessel walls causes further leakage of fluid into the interstitial space.

Biomechanical

The presence of B waves may result in intermittent raised intracranial pressures, particularly during REM sleep. This and the change in properties of ageing brain parenchyma may make the older age group susceptible to progressive ventricular enlargement (Factora, 2006). Modelling of brain deformation in chronic communicating hydrocephalus suggests that a combination of reversal of interstitial fluid flow into the parenchyma and reduced tissue elasticity occurs (Pena et al., 2002). The resultant profile of raised fluid pressure follows a U-shaped curve from the ventricular surface to the brain convexity (i.e. the minimum occurring at the middle of the cerebral mantle). This differential, also confirmed on cerebral blood flow (CBF) profiles plotted as a function of distance from the ventricles, may explain how the process of progressive ventriculomegaly affects the white matter arranged between the ventricles and cortex to varying degrees of severity (Momjian et al., 2004). This suggests that a common biomechanical process exists, causing the concurrent degradation of structural integrity within white matter, interstitial space, and cerebral vasculature.

Table 94.1 Theories of NPH pathogenesis. Images Courtesy of Dr Nicole Keong ©

	Structural	Cerebral Blood Flow	CSF Flow
	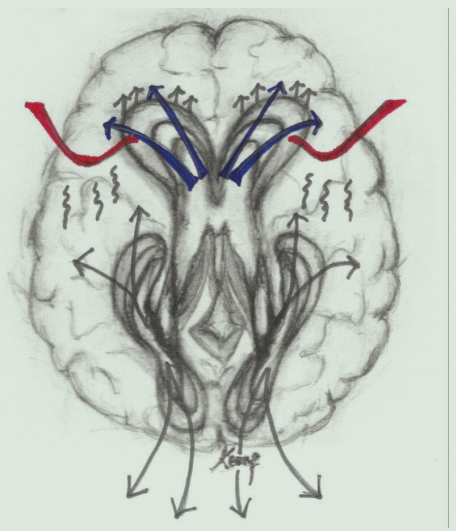	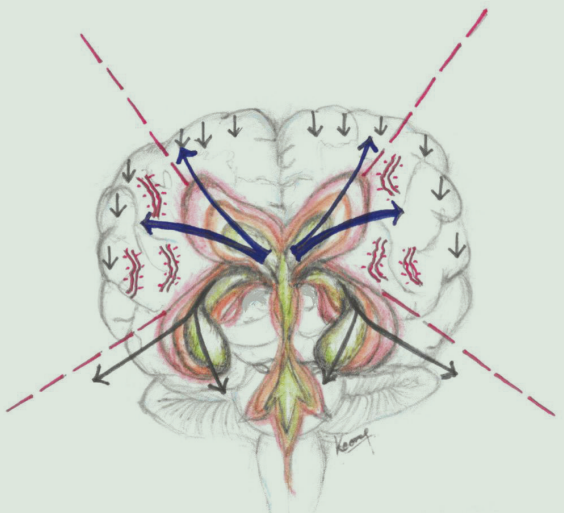	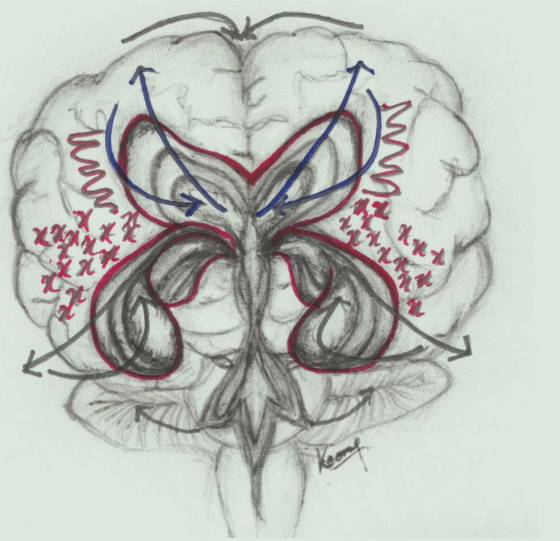
Key Concepts	• Tissue distortion • Loss of elasticity • Reversal of interstitial fluid flow = oedema • Failure of drainage of vasoactive metabolites • Brain deformation • U-shaped curve	• Ventricular expansion distorts connections and/or blood vessels between basal ganglia and frontal cortex • Deep lacunar infarctions • Loss of elasticity in parenchyma	• Adult communicating hydrocephalus • Imbalance between CSF production and reabsorption • Reduced CSF production • Resistance to CSF outflow increased • Inability to clear toxic metabolic products
Key theory streams	• *Tissue distortion* • *Interstitial fluid pressure increase* • *Biomechanical*	• *Watershed ischaemia* • *Vascular disease*	• *CSF flow disturbance* • *CSF hydrodynamics* • *Failure of drainage of vasoactive metabolites*

Cerebral blood flow

Watershed ischaemia

Positron emission tomography (PET), xenon-enhanced computed tomography (xenon-computed tomographic (CT), and single-photon emission computed tomography (SPECT) studies all indicate widespread cortical and subcortical hypometabolism and impaired global CBF (Tedeschi et al., 1995). This may result in dysfunctional regional cerebral autoregulation and watershed ischaemia occurring in the corona radiata. However, there has been a frustrating lack of congruence within the group of studies examining CBF in NPH. Only a few studies have attempted to combine CBF measurement with structural imaging coregistration to achieve a good anatomical basis for comparisons of CBF data (Owler et al., 2004).

Vascular disease

Deep white matter hyperintensities (DWMH) found on imaging in some patients with NPH have also provoked debate about cerebral small vessel disease and vascular encephalopathy. Ventricular expansion may distort the connections and/or blood vessels between the basal ganglia and frontal cortex, producing deep lacunar infarctions, or lead to loss of elasticity in the parenchyma. Ischaemia in the white matter tracts involved in frontal executive function, gait, and micturition may be implicated as a trigger for the pathogenesis of NPH. DWMH have been shown to both negatively correlate with degree of improvement (Krauss et al., 1996) and have no correlation to poor postoperative outcome (Tullberg et al., 2001). The presence of such lesions may therefore not preclude good outcome following intervention.

CSF flow

CSF flow disorder

Adult communicating hydrocephalus is thought to be a form of CSF circulation disorder, involving an imbalance between CSF production and reabsorption (Box 94.1, expanded from the original reference) (Pickard, 1982). The resulting excess accumulation of cerebrospinal fluid is thought to result in ventriculomegaly. Abnormalities of the ageing brain (loss of elasticity of the neuropil, extracellular matrix, and parenchyma) also contribute. B wave pressures behave in a 'water hammer' fashion, exerting intermittently high pressures on the parenchyma. Therefore, in addition to disturbances within the CSF circulation, an imbalance exists between the forces driving progressive ventriculomegaly and the architectural forces within the brain parenchyma that should naturally oppose this.

CSF hydrodynamics

There is physiological evidence to suggest that this imbalance exists. Czosnyka et al. examined the question of age dependence of cerebrospinal fluid pressure-volume compensation by performing CSF infusion studies on a group of patients with symptomatic hydrocephalus and normal intracranial pressures (ICP) (Czosnyka et al., 2001). They demonstrated that resistance to CSF outflow (defined as Rout or Rcsf) increased in a nonlinear fashion with advancing age and was associated with a decrease in the CSF production rate, which also occurred with increasing age. Both the pulse amplitude of the ICP waveform and the slope of the amplitude-ICP regression line increased significantly with advancing age. There was a nonlinear increase in the elastance coefficient with age and was thought to represent progressive brain parenchymal stiffness. Some have proposed a 'two-hit' hypothesis, in which adults who had 'benign external hydrocephalus' in their infancy suffer a second hit with deep white matter ischaemia due to vascular disease in late adulthood, thus starting the chain of events leading to the iNPH syndrome (Bradley et al., 2006).

Box 94.1 Disturbance of CSF regulation

Defects of flow in the subarachnoid space and CSF circulation:

Leptomeningeal inflammation
Infections
Haemorrhage
Meningitis
Carcinomatosis
Foreign matter
Tonsillar elongation/prolapse or basilar impression
Masses (neoplastic and non-neoplastic)
Subarachnoid blocks (such as those due to the above, as well as other arachnoidal or aqueductal webbing, membranes, and non-confluent CSF compartments)

Defects of absorption of CSF at the arachnoid granulations

Congenital deficiency (i.e. absence of arachnoid granulations)
Raised cerebral venous sinus pressure

Abnormalities of the CSF

Excessive production of CSF or abnormally high CSF volumes
Raised intraventricular CSF pulse pressure—for example, in the presence of a choroid plexus papilloma.
Increased CSF viscosity secondary to high protein content—for example, in the presence of spinal neurofibromas such as described in Froin's syndrome (in which CSF demonstrates a combination of elevated protein content, xanthochromia, and hypercoagulability)

Data from Pickard, J. D., Adult communicating hydrocephalus, *British Journal of Hospital Medicine*, pp. 27–40, Copyright © 1982.

Failure of drainage of vasoactive metabolites

Abnormalities in CSF production and turnover may also lead to inefficient or failed clearance of toxic molecules. An inability to clear potentially toxic metabolic products, such as amyloid ß-peptides (Aß) and tau protein, could lead to an increase in their concentration in brain interstitial fluid, creating a potentially hostile *milieu* for neuronal function and survival. The two changes noted in ageing, reduced CSF production, and increased resistance to CSF outflow, may be implicated in the pathophysiology of Alzheimer's disease and NPH. A predominance of reduced CSF production and turnover may manifest as Alzheimer's disease. Conversely, NPH may result from a predominant increase in resistance to CSF outflow. However, a prospective, randomized, double-blinded, placebo-controlled trial evaluating the safety and effectiveness of a surgically implanted shunt in subjects with probable Alzheimer's disease involving 215 subjects (Silverberg et al., 2008) did not demonstrate any benefit in low-flow CSF shunting in subjects with mild to severe Alzheimer's disease. Indeed, it may be that a sufficient level of CSF circulatory disorder is required to benefit from shunting although the threshold of Rout that is associated with improvement from shunting still continues

to provoke debate. A disease spectrum may exist, including a subset who either have both conditions or have risks of developing both even if one process is predominant.

Preoperative

Clinical presentation of classic NPH

NPH is subject to both over- and underdiagnosis because the clinical features supporting the diagnosis of NPH are commonly encountered in older age or patients with other neurodegenerative conditions (Relkin et al., 2005). This poses a diagnostic challenge as many patients with potentially curable NPH are often misdiagnosed as having Alzheimer's disease or vascular dementia and *vice versa*. As a consequence, the precise incidence and prevalence of NPH remains controversial, estimates range from as rare as 1.3 per million to as frequent as 4 per 1000 depending on the diagnostic criteria used and the sample population. The classic triad described in relation to NPH is that of a gait disturbance, dementia, and urinary incontinence. Patients frequently present with an incomplete triad, particularly if the duration of symptom onset to diagnosis is relatively short.

Gait disorder

The typical pattern is that of unsteadiness, a predisposition to falls, and a broad-based stance. Gait stride is reduced and patients may shuffle or walk as if their feet are stuck to the floor (i.e. a 'magnetic' gait). Fisher further provided the classic term of hydrocephalic ataxia-abasia to describe the overall forward leaning posture, wider sway, and imbalance that may be accentuated by eye closure (Fisher, 1977). Common observations include decreased length, height, and speed as well as *en bloc* turning. The gait disturbance may share common features with other types of frontotemporal pathologies. There are similarities with Parkinson's disease. This can be a difficult differential diagnosis if the more classic hallmarks of that degenerative condition are not obvious, such as tremor, rigidity and mask-like facies (Keong et al., 2011). There should be an absence of focal deficits, hypertonia, and hyperreflexia, which favour other neurodegenerative conditions. Standardized measures of gait examination have also been attempted (see Table 94.2).

Cognitive disturbance

Deficits are traditionally assessed at the bedside using a mini-mental state examination (MMSE). The absence of focal cortical deficits, such as agnosia or aphasia, should be confirmed. However, such approaches have significant limitations. Doubts have been raised about the reproducibility of test scores by multiple operators. Neuropsychological testing is essential to distinguish the pattern of dementia in NPH from other conditions such as age-related cognitive decline from atrophy and Alzheimer's disease (see Table 94.2). Formal neuropsychology, using a battery of focused tests, such as in the Dutch study (Boon et al., 1998), is used by relatively few groups. Yet, specific patterns of cognitive impairment, in the form of a

Table 94.2 Measures used for assessment in NPH

Assessment	(References)	Scale	Description
Gait	(Boon et al., 1997)	2–40	10 features of gait into walking score (0–20), number of steps and number of seconds for a 10-metre walk (0–20)
	(Hellström et al., 2012b)	0–100	Gait domain evaluated from means of measurements of the number of steps and seconds needed to walk 10 metres at a free pace, and an ordinal rating of the gait. This results in two sets of continuous data (11 gait categories) and two sets of ordinal data (8 rating categories).
	(Tinetti, 1986)	16 balance	
	(Podsiadlo and Richardson, 1991)	12 gait Timed in secs	Performance test of balance and gait of manoeuvres used during daily activities. Balance portion consist of nine manoeuvres graded on an ordinal scale as normal, adaptive, or abnormal. Gait portion rates seven gait characteristics as normal or abnormal. Timed 'up and go' (TU&GT)—functional mobility tested in frail elderly. Time required to rise to standing from a standard armchair, walk 3 metres, turn, walk back to the armchair and sit down.
Cognition	(Boon et al., 1997)	Test battery	Dementia scale composed of the 10-word test, digit span forward and backward, trail making, and finger tapping
	(Iddon et al., 1999)	Test battery	MMSE, Kendrick object learning test (KOLT), selected CANTAB battery (verbal fluency, memory, and attention)
	(Kubo et al., 2008)	Test battery	MMSE, frontal assessment battery, trail making test part A
	(Hellström et al., 2012a)	Combination	Grooved pegboard, the Rey Auditory Verbal Learning Task, the Swedish Stroop test
Outcome	(Stein and Langfitt, 1974)	Grade 0–IV	Grade 0 (able to work), I–II (home without or with assistance), III–IV (custodial care despite independent functioning), IV (no capacity for independent function)
	(Black, 1980)	6 grades	Excellent—Good (preillness activity without or with deficit), Fair—transient (improved), Poor—dead (poor outcome)
	(Wilson et al., 2002)	7 grades	Modified Rankin Scale (mRS) disability = 0 (no symptoms), 1–2 (no significant or slight), 3–4 (moderate to moderately severe), 5 (severe), 6 (dead)
	(Larsson et al., 1991)	Combination	Modified in use—gait = 0 (normal), 1–2 (insecure without or with cane), 3–4 (support aids), 5 (wheelchair). Living conditions = 0–1 (independent or home with assistance), 2–3 (assisted living facility), 4 (hospital)
	(Boon et al., 1997)	Combination	The Dutch NPH Scale—four clinical outcome categories but also a short neuropsychological test battery to provide a dementia scale and ten features of gait into a walking score; mRS used for assessment of disability outcome.
	(Kubo et al., 2008)	Combination	The iNPH Grading Scale—three NPH domains (cognitive impairment, gait disturbance, and urinary disturbance). Each domain is scored from 0 to 4, with higher scores indicating worse symptoms. Correlated with MMSE, Gait Status Scale (GSS), TU&GT and International Consultation on Incontinence Questionnaire—Short Form (ICIQ-SF).
	(Hellström et al., 2012b)	Combination	The European iNPH Multicentre study—comprehensive scale using assessments in four domains—gait, cognition, balance, continence. Calibrated against age-matched healthy volunteers.

subcortical frontal dysexecutive syndrome, have been demonstrated (Iddon et al., 1999). A review for the iNPH guidelines (Klinge et al., 2005) found no standardization of cognitive tests but concluded that they contributed to objective assessment of postoperative outcome.

Urinary incontinence

This is the third component of classic NPH. Such episodic or persistent urinary disturbance should not be attributable to primary urological disorders. Less commonly, both urinary and faecal incontinence are present. In the context of lower order symptoms, such as urgency, frequency, or nocturia, iNPH guidelines require that two out of three of these should be present (Relkin et al., 2005). Urodynamic studies may be helpful in distinguishing NPH urinary dysfunction vs. common comorbidities (prostatism in men, recurrent urinary tract symptoms in women or bladder dystonia/dysautonomia), as well as other conditions in the spectrum of 'neurogenic bladder syndrome'.

Complex NPH presentations

Comorbidities

The syndrome of NPH does exhibit characteristics that overlap with other neurodegenerative conditions. An early preclinical trigger is hypothesized to lead to either Alzheimer's disease or NPH (Silverberg et al., 2003) and may explain the presence of cerebral amyloid deposition in both conditions. NPH is one of the differential diagnoses in atypical Parkinson's disease and within the 'vascular parkinsonism' spectrum that also includes other types of higher-level gait disorders with cognitive disturbance. Unusual but well-recognized cognitive manifestations of NPH, including behavioural changes, low mood, paranoia, and hallucinations, may be difficult to distinguish from psychiatric conditions such as depression and schizophrenia. Urinary dysfunction may also be dependent on gait and/or cognitive status. Predominance of early urinary incontinence with delayed onset of the latter may well favour other neurological diagnoses. In patients with significant comorbidities coexisting, such as cardiac disease and vascular risk burden, the challenge, therefore, is to provide the highest level of testing possible to characterize the 'NPH' component remediable to CSF shunting, in order to facilitate a considered approach towards weighing the relative risks vs. benefits of surgical intervention.

Variations

Lethargy, loss of interest, drowsiness and visuo-spatial disturbances have been reported but the presence of these symptoms without the supporting clinical triad should indicate a need for further investigations. Other forms of hydrocephalus may also present with the NPH syndrome. Longstanding overt ventriculomegaly in adults (LOVA) is a form of hydrocephalus which develops during childhood but presents relatively late in adulthood. Patients may present anywhere in the spectrum of hydrocephalic symptoms, from subacute symptoms and signs of raised intracranial pressure to the more insidious triad of NPH, comprising gait disturbance, cognitive decline, and/or urinary incontinence (Keong et al., 2011). In this condition, adults classically present with severe ventriculomegaly involving the lateral and third ventricles, as well as obliterated cortical sulci, found on imaging. Patients may exhibit longstanding macrocephalus measuring more than two standard deviations above mean in head circumference and/or neuroradiological evidence of a significantly expanded or destroyed sella turcica. LOVA is treatable with shunting (but requires careful control with pressure-programmable valves) and endoscopic third ventriculostomy is mostly effective (Oi et al., 2000). In other hydrocephalus subgroups presenting with the NPH syndrome, aqueduct stenosis may feature but is frequently incomplete. There may be evidence of intrinsic semi-obstruction, such as webbing within the aqueduct, or external compression, for example, distortion from middle cranial fossa arachnoid cysts. As the stenosis of the aqueduct may therefore be secondary, third ventriculostomy is a possible option but ventriculoperitoneal shunting may be more effective in some cases. Detailed imaging of CSF compartments (such as additional three-dimensional T2-weighted and CISS magnetic resonance sequences) may be useful in evaluating for the presence or absence of CSF-intensity lesions to best inform surgical choices.

Investigation and differential diagnoses

Routine imaging in the form of a CT or magnetic resonance imaging (MRI) scan is the baseline required to establish the diagnosis of NPH. Important differential diagnoses to consider include the obstruction of CSF pathways due to a tumour or similar pathology (as per **Box 94.1**), significant cerebral atrophy, evidence of cerebrovascular ischaemic risk burden, and/or neurodegenerative disease. Ventricular enlargement not entirely attributable to cerebral atrophy or congenital enlargement (Evans' index ≥0.3 or comparable measure) should be present (Relkin et al., 2005). The Evans' index is defined as the maximum width of the frontal horns divided by the transverse maximum inner diameter of the skull. An alternative is the bicaudate ratio (ventriculomegaly defined by BCI ≥0.25); this is the minimum intercaudate distance divided by the brain width along the same line (see **Fig. 94.1**).

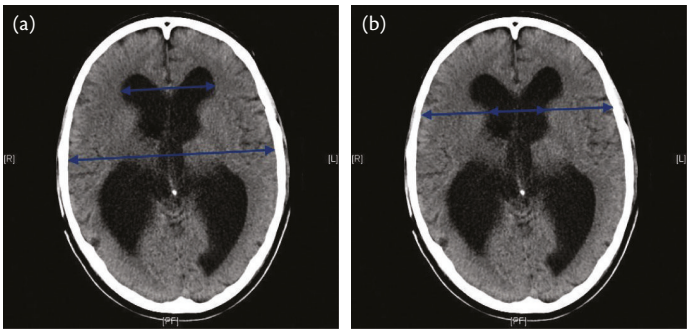

Fig. 94.1 Measurement of ventriculomegaly. (A) Evans' index/ratio: maximum width of the frontal horns of the lateral ventricles divided by the maximal internal diameter of the skull measured at the same level; axial slice in which width of the frontal horns of the lateral ventricles are maximal; significant ventriculomegaly = Evans' index of ≥0.3. (B) Bicaudate index/ratio. Minimum distance between the two caudate apices divided by the brain width along the same line of the caudate measurement: axial slice in which caudate nuclei produced the greatest amount of indentation on the lateral ventricles; significant ventriculomegaly = bicaudate index (BCI) ≥0.25.

Supplementary testing

Guidelines on this matter conclude that a single standard for the prognostic evaluation of iNPH is lacking (Marmarou et al., 2005a). A lumbar puncture 'tap test' with the withdrawal of 40–50 ml of CSF cannot be used as an exclusion test due to its low sensitivity of 26% but has a high specificity of 100%. However, a lumbar puncture is often used as a first line investigative tool to establish that the CSF pressure is within the normal range (5–18 mmHg/7–24 cm H_20) and that no biochemical or microbiological abnormalities are present. The placement of an external lumbar drain to withdraw 300 ml over 5 days has been demonstrated to have a higher sensitivity and specificity—50% and 80%, respectively (Walchenbach et al., 2002). While regarded as gold standard, this method requires an inpatient stay and carries a small risk of infection and nerve root irritation.

CSF outflow resistance measurement (Rout), involving the injection of fluid into a CSF space in the ventricles or lumbar sac (bolus or infusion) is another method of assessing the hydrodynamic state in NPH patients. CSF outflow resistance is calculated based on pressure-volume modelling and has been shown in the Dutch NPH study to have a sensitivity of 46% and a specificity of 87% at an outflow resistance of more than 18 mmHg/ml/min ((Boon et al., 1998). More recent meta analyses revealed a Rout threshold of 12 mmHg/ml/min yielded high accuracy (72.95%), high sensitivity (80.26%), and moderate specificity (46.79%) (Kim et al., 2015). The advantage of this technique is that it only requires a day attendance and can be performed through a preimplanted ventricular reservoir device (see Fig. 94.2B for an example of infusion study data).

Medical management

The option of medical therapies such as serial lumbar punctures and acetazolamide tend to produce limited clinical improvement in this condition. Therefore, surgical intervention is usually recommended on the basis of clinical findings and supportive evidence from supplementary testing.

Surgical management

The natural history of NPH is of progression without treatment, with the majority of patients demonstrating deterioration in symptoms as early as 3 months following initial assessment, although some patients may remain stable for indefinite periods of time.

Considerations for surgical intervention

These include the placement of a shunt or an endoscopic third ventriculostomy. Ventriculoperitoneal (VP) and lumboperitoneal (LP) shunts are by far the preferred options chosen over ventriculoatrial or -pleural varieties. While pressure versus flow-controlled valves may follow surgical preference, the advantage of using programmable designs is clear in the NPH population due to the need to tailor variable responses of these patients to the degree of CSF diversion (please see Chapters 92 and 93 for the technique of shunt insertion and shunt technology).

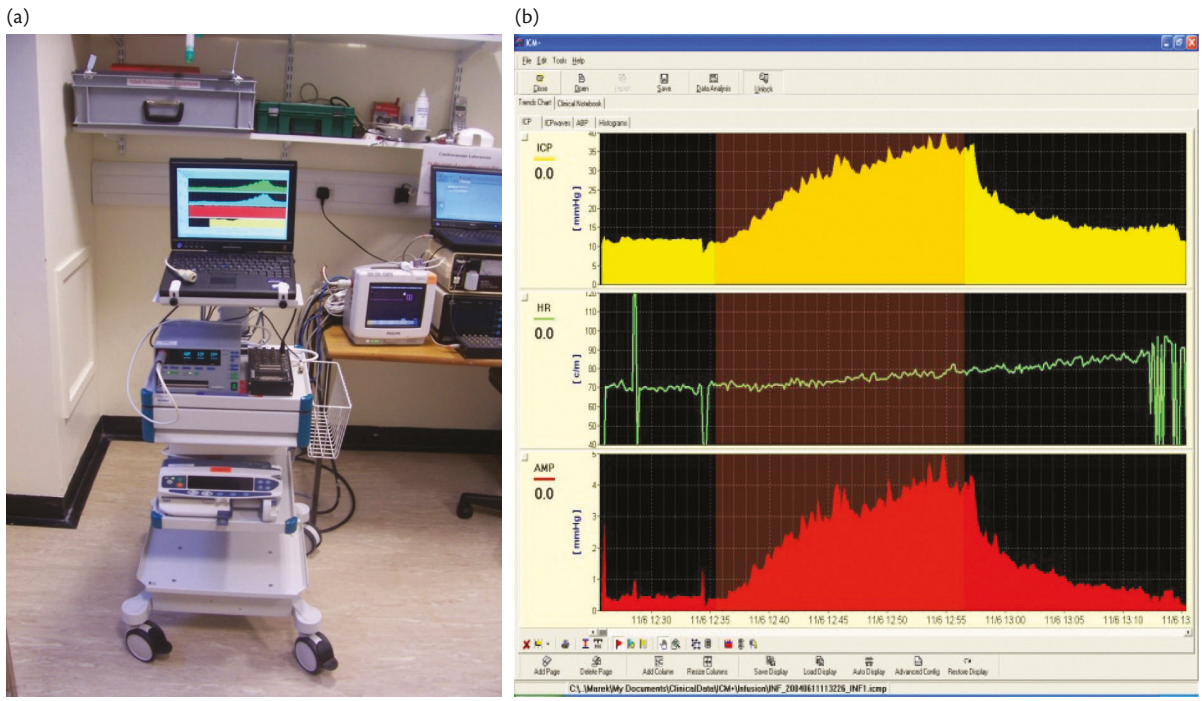

Fig. 94.2 Set-up for CSF infusion study. (A) Mobile unit stack for computerized testing (a computerized infusion test may be performed to interrogate CSF hydrodynamics and extract various parameters). (B) Example of an infusion study data capture. The resistance to CSF outflow (Rout) is calculated as the difference between the end-equilibrium CSF pressure and baseline CSF pressure (i.e. plateau-baseline ICP), divided by the infusion rate.
Courtesy of Dr Zofia Czosnyka and Dr Marek Czosnyka.

The addition of a burr hole reservoir, with the valve in-circuit, may offer the advantage of facilitating CSF interrogation while minimizing the risk of debris being drawn directly into the valve mechanism. Some patients within the NPH spectrum are found to have a form of communicating aqueduct stenosis where there is a relative mismatch between the supratentorial spaces and the fourth ventricle. Although this is a small subgroup, authors have reported good results using the endoscopic third ventriculostomy technique. In a study by Gangemi et al., 72% patients improved with a low complication rate of 4% (intracerebral haemorrhage) (Gangemi et al., 2004). Careful consideration of subgroups, including LOVA as discussed earlier, is crucial to the understanding of surgical options for the individual patient.

Image-guided navigation is not greatly advantageous over anatomical landmarks for cases of significant ventriculomegaly but may be a useful tool in cases of modest ventriculomegaly and to optimize best trajectory for tip placement and to avoid traversing vessels. Optimal placement of ventricular catheters, with or without the aid of image-guided techniques, also serves to minimize longer-term complications of shunt revision due to proximal catheter malfunction and/or blockage. Laparoscopic-guided placement of the distal catheter may minimize the incidence of pseudomeningoceles due to extraperitoneal placement or distal tip migration. This may also be the surgical approach of choice, as joint cases with general surgery colleagues, in cases of known adhesions or false compartmentalization of the abdominal cavity due to previous surgery if preferred over ventriculopleural/atrial approaches.

Risk stratification

In general, the occurrence of complications in the elderly NPH cohort, along with associated premorbidities, may translate into lengthy hospital inpatient stays and the need for rehabilitation if not managed proactively. Methodical preoperative multidisciplinary assessment may be helpful in preventing the unlikely risks of catastrophe, coma, or cardiac event while under anaesthesia by identifying patients at high risk for surgery and providing optimization as necessary. Kiefer's comorbidity index (Kiefer et al., 2006) and other cardiac/global risk scores may be useful in the risk stratification of individual patients by providing an objective assessment of NPH patients with comorbidities, in terms of concurrent vascular, cardiac, and neurodegenerative diseases (see ISHCSF review for a more comprehensive discussion of the influence of comorbidities in iNPH; Malm et al., 2013).

Managing expectations of surgical outcomes is crucial to the discussion of surgical intervention as many patients present late, only have moderate but meaningful improvement levels following lumbar drainage or have significant overlay with other conditions. Favourable predictors of shunt responsiveness include elevated Rout, positive response to external lumbar drainage or repeated lumbar punctures and impaired CBF reactivity to acetazolamide (by SPECT). While comorbidities could be considered unfavourable predictors, age itself may not be a prognostic factor (Halperin et al., 2015).

Postoperative

Complication management

The surgical intervention for NPH carries a risk of infection including meningitis, haemorrhage, seizures, CSF leak, and neurological deficit (i.e. stroke, and shunt malposition or malfunction requiring revision surgery). There is a risk of inadvertent damage to adjacent structures in the neck such as vascular injury, or to the chest, such as pneumothorax, during the tunnelling process for distal catheter placement. Iatrogenic opening of the bowel serosa or mucosa can occur during the attempt to access the peritoneal cavity for distal catheter insertion and necessitates immediate surgical repair. Contamination of the abdominal cavity would be a contraindication for distal shunt placement. The risk of catastrophe is of the order of 1–2% and there is a 3–4% risk of intracerebral haemorrhage (Black et al., 1985). Significant intraparenchymal, rather than tract haemorrhage, may require evacuation of the haematoma, removal of the shunt and insertion of an external ventricular drain but this is a rare subgroup of the overall haemorrhage risk.

More commonly, subdural effusions with or without the presence of haemorrhage are seen although the reported rates range widely from 2% to 17% (Klinge et al., 2005). This may be related to shunt overdrainage or the pre-existing cortical atrophy in some patients. Not all effusions are clinically relevant. Surgical intervention, in the form of burr hole drainage of the chronic subdural haematoma, with or without temporary shunt ligation, is required in the minority of cases. Valve adjustment to reduce drainage for a period of surveillance imaging is usually an effective strategy. Equally important is the risk of underdrainage, requiring general shunt interrogation or valve adjustment for the optimization of symptoms. Patients may also experience complete shunt blockage, breakage, or failure. This may present acutely, even in patients with previously insidious symptoms. Some patients exhibit a heightened sensitivity to shunt valve settings and a subgroup of these may benefit from elective revision to valves with more adjustment setting options. Hashimoto et al. (SINPHONI) 2010 found that, overall, there was a 3% incidence of serious events and a 20% incidence of less serious events (Hashimoto et al., 2010).

Nevertheless, patients with shunt dysfunctions still have potential to improve. Klinge et al. reported that in the European iNPH study, 11% of their unimproved patients had 'silent' shunt dysfunction but could be converted to shunt-responders following valve adjustments (Klinge et al., 2012). While this is made possible by the use of modern variable resistance valves, other options, such as the incorporation of additional antisiphon and antigravity devices into the shunt circuit, require surgical revisions. An average complication rate of 9.8%, such as reported by Marmarou (Marmarou et al., 2005b) can rise to a revision rate of 33% (McGirt et al., 2005) if optimization of surgical outcome is pursued. More strikingly, Pujari et al. found that a revision rate of 53% was still compatible with an improvement rate of 74%, further implying that such optimization was possible to achieve with surgical intervention (Pujari et al., 2008).

Management of intraoperative factors may contribute to the reduction of shunt-related infections. Theatre factors, such as restricting the flow of traffic during shunt implantation, early operative time slot, and short duration of procedure, seniority of the operating team and the use of antibiotic-impregnated catheter options, can be employed to improve surgical outcomes. The spectrum of early to late complications following shunting emphasizes the importance of maintaining regional and national shunt registries to support gaps in clinical information for patients presenting with shunt malfunction.

Outcomes

A review (Klinge et al., 2005) conducted as part of the publication on iNPH guidelines in 2005 concluded that comparisons between NPH studies were difficult due to the differences in the selection criteria for NPH patients, disparate definitions of clinical improvement, varying postoperative follow-up protocols and intervals, and substantial differences in postoperative management. Recommendations made included the following—follow-up at 3, 6, and 12 months, the careful evaluation and treatment of non-responders with regards to shunt malfunction and the use of objective scales in the measurement of improvement. Shorter-term results are more likely to be influenced by shunt-associated risks and longer-term results may be related to concomitant cerebrovascular and vascular diseases. The 1-year postshunt period was thought to be a potential determinant of shunt outcome; beyond this, studies have shown that death and morbidity related to concomitant cerebrovascular and vascular disease influence the clinical effect of shunting.

The panel found that a standard for outcome assessment of shunt treatment in idiopathic normal pressure hydrocephalus was lacking. Several scales are commonly quoted, generally functional grading based on assessments of activities of daily living (ADL) or disability, as well as rating scales for individual components of the triad (Ishikawa, 2014). Groups have also developed their own combination assessments scales, such as the 'Dutch NPH Scale' and that of the European multicentre study in iNPH (see **Table 94.2** for details). In a recent practice guideline report, authors concluded that shunting was possibly effective in iNPH, with more than 80% improvement in gait at 6 months with serious adverse event risk of 11% (Halperin et al., 2015).

Controversies—neuroimaging biomarkers

Current challenges in iNPH are centred upon refining criteria in patient selection for shunting. However, heterogeneity of available methods for grading symptomatology and comorbidities can render it difficult to reproduce the surgical results of larger published series in NPH work. Advances in the development of CSF and neuroimaging biomarkers have the potential to aid in the differential diagnosis of iNPH as well as provide much-needed prognostication and correlation to outcome. Two particular streams of neuroimaging work should be followed with great interest by any iNPH neurosurgeon as the MR techniques would be straightforward to reproduce across centres—quantitative assessments based on key structural features of NPH and diffusion tensor imaging. There is already some evidence that the former is reliable; in a prospective study of one hundred iNPH patients, SINPHONI, an MRI-based diagnosis (evidence of disproportionately enlarged subarachnoid space hydrocephalus, i.e. DESH in which tight high convexity and medial subarachnoid spaces and enlarged sylvian fissures are associated with ventriculomegaly) achieved a favourable outcome in 69–77% patients depending on which outcome grading scale was administered (Hashimoto et al., 2010).

Diffusion tensor imaging (DTI), which is already incorporated into the standard MR sequences for some pathologies, has shown some promise in the differential diagnosis of iNPH vs. other overlapping conditions such as Alzheimer's disease and characterizing the reversibility of acute hydrocephalus. Using DTI, it has been possible to demonstrate different patterns of white matter injury coexisting within NPH, and examine the relative CSF responsiveness to surgical intervention (Keong et al., 2017). Further work to elucidate white matter injury patterns would support early prognostication and prediction of shunt responsiveness. Multimodality correlations, such as with other imaging techniques to interrogate CBF, CSF dynamics, and flow, cerebrovascular reactivity, and brain elasticity, may also be useful in developing biomarkers of potential shunt responsiveness. However, adding layers of complexity to the multistage, multidisciplinary assessment of iNPH, may not always be desirable. While most imaging methods are noninvasive, none could hope to achieve the levels of sensitivity and specificity of an external lumbar drainage test. It could therefore be argued that resources could be best spent in offering this investigation option as widely and as consistently as possible in the work-up for iNPH, even at the stage of differential diagnosis, rather than focusing on analysis-heavy methods which are most likely to be confined to academic centres. Similar issues also apply to the emerging interest in CSF biochemical markers, which require further work on the interpretation of thresholds and more widespread availability as a testing modality.

The most urgent need for refocusing iNPH neuroimaging research is for a consensus of opinion as to the most likely stage in NPH pathophysiology that reversibility of injury can be recognized and the best methodological tools available to examine this in reproducible and quantifiable ways. iNPH represents a unique model of impermanent white matter damage, that if understood, could have implications for the understanding of other types of acute-on-chronic neurodegenerative diseases.

FURTHER READING

Hakim, S. & Adams, R.D. (1965). The special clinical problem of symptomatic hydrocephalus with normal cerebrospinal fluid pressure. Observations on cerebrospinal fluid hydrodynamics. *J Neurol Sci*, **2**, 307–27.

Halperin, J.J., Kurlan, R., Schwalb, J.M., Cusimano, M.D., Gronseth, G., & Gloss, D. (2015). Practice guideline: idiopathic normal pressure hydrocephalus: response to shunting and predictors of response: report of the Guideline Development, Dissemination, and Implementation Subcommittee of the American Academy of Neurology. *Neurology*, **85**, 2063–71.

Hashimoto, M., Ishikawa, M., Mori, E., Kuwana, N., & Study of INPH on neurological improvement (SINPHONI) (2010). Diagnosis of idiopathic normal pressure hydrocephalus is supported by MRI-based scheme: a prospective cohort study. *Cerebrospinal Fluid Res*, **7**, 18.

Hellström, P., Klinge, P., Tans, J., & Wikkelsø, C. (2012a). The neuropsychology of iNPH: findings and evaluation of tests in the European multicentre study. *Clin Neurol Neurosurg*, **114**, 130–4.

Keong, N.C., Pena, A., Price, S.J., Czosnyka, M., Czosnyka, Z., & Pickard, J.D. (2016). Imaging normal pressure hydrocephalus: theories, techniques, and challenges. *Neurosurg Focus*, **41**, E11.

Klinge, P., Marmarou, A., Bergsneider, M., Relkin, N., & Black, P.M. (2005). Outcome of shunting in idiopathic normal-pressure hydrocephalus and the value of outcome assessment in shunted patients. *Neurosurgery*, **57**, S40–52; discussion ii–v.

Malm, J., Graff-Radford, N.R., Ishikawa, M., et al. (2013). Influence of comorbidities in idiopathic normal pressure hydrocephalus—research and clinical care. A report of the ISHCSF task force on comorbidities in INPH. *Fluids Barriers CNS*, **10**, 22.

Marmarou, A., Bergsneider, M., Klinge, P., Relkin, N., & Black, P.M. (2005a). The value of supplemental prognostic tests for the preoperative assessment of idiopathic normal-pressure hydrocephalus. *Neurosurgery*, **57**, S17–28; discussion ii–v.

Pujari, S., Kharkar, S., Metellus, P., Shuck, J., Williams, M.A., & Rigamonti, D. (2008). Normal pressure hydrocephalus: long-term outcome after shunt surgery. *J Neurol Neurosurg Psychiatry*, **79**, 1282–6.

Relkin, N., Marmarou, A., Klinge, P., Bergsneider, M., & Black, P.M. (2005). Diagnosing idiopathic normal-pressure hydrocephalus. *Neurosurgery*, **57**, S4–16; discussion ii–v.

REFERENCES

Adams, R.D., Fisher, C.M., Hakim, S., Ojemann, R.G., & Sweet, W.H. (1965). Symptomatic occult hydrocephalus with 'normal' cerebrospinal-fluid pressure. A treatable syndrome. *N Engl J Med*, **273**, 117–26.

Black, P.M. (1980). Idiopathic normal-pressure hydrocephalus. Results of shunting in 62 patients. *J Neurosurg*, **52**, 371–7.

Black, P.M., Ojemann, R.G., & Tzouras, A. (1985). CSF shunts for dementia, incontinence, and gait disturbance. *Clin Neurosurg*, **32**, 632–51.

Boon, A.J., Tans, J.T., Delwel, E.J., et al. (1998). Does CSF outflow resistance predict the response to shunting in patients with normal pressure hydrocephalus? *Acta Neurochir Suppl*, **71**, 331–3.

Boon, A.J., Tans, J.T., Delwel, E.J., et al. (1997). Dutch normal pressure hydrocephalus study: baseline characteristics with emphasis on clinical findings. *Eur J Neurol*, **4**, 39–47.

Bradley, W.G., Jr., Bahl, G., & Alksne, J.F. (2006). Idiopathic normal pressure hydrocephalus may be a 'two hit' disease: benign external hydrocephalus in infancy followed by deep white matter ischemia in late adulthood. *J Magn Reson Imaging*, **24**, 747–55.

Czosnyka, M., Czosnyka, Z.H., Whitfield, P.C., Donovan, T., & Pickard, J.D. (2001). Age dependence of cerebrospinal pressure-volume compensation in patients with hydrocephalus. *J Neurosurg*, **94**, 482–6.

Factora, R. (2006). When do common symptoms indicate normal pressure hydrocephalus? *Cleve Clin J Med*, **73**, 447–50, **452**, 455–6 passim.

Fisher, C.M. (1977). The clinical picture in occult hydrocephalus. *Clin Neurosurg*, **24**, 270–84.

Gangemi, M., Maiuri, F., Buonamassa, S., Colella, G., & De Divitiis, E. (2004). Endoscopic third ventriculostomy in idiopathic normal pressure hydrocephalus. *Neurosurgery*, **55**, 129–34; discussion 134.

Hakim, S. & Adams, R.D. (1965). The special clinical problem of symptomatic hydrocephalus with normal cerebrospinal fluid pressure. Observations on cerebrospinal fluid hydrodynamics. *J Neurol Sci*, **2**, 307–27.

Hakim, S., Venegas, J.G., & Burton, J.D. (1976). The physics of the cranial cavity, hydrocephalus and normal pressure hydrocephalus: mechanical interpretation and mathematical model. *Surg Neurol*, **5**, 187–210.

Halperin, J.J., Kurlan, R., Schwalb, J.M., Cusimano, M.D., Gronseth, G., & Gloss, D. (2015). Practice guideline: idiopathic normal pressure hydrocephalus: response to shunting and predictors of response: report of the Guideline Development, Dissemination, and Implementation Subcommittee of the American Academy of Neurology. *Neurology*, **85**, 2063–71.

Hashimoto, M., Ishikawa, M., Mori, E., Kuwana, N., & Study of INPH on neurological improvement (SINPHONI) (2010). Diagnosis of idiopathic normal pressure hydrocephalus is supported by MRI-based scheme: a prospective cohort study. *Cerebrospinal Fluid Res*, **7**, 18.

Hellström, P., Klinge, P., Tans, J., & Wikkelsø, C. (2012a). The neuropsychology of iNPH: findings and evaluation of tests in the European multicentre study. *Clin Neurol Neurosurg*, **114**, 130–4.

Hellström, P., Klinge, P., Tans, J., & Wikkelsø, C. (2012b). A new scale for assessment of severity and outcome in iNPH. *Acta Neurol Scand*, **126**, 229–37.

Iddon, J.L., Pickard, J.D., Cross, J.J., Griffiths, P.D., Czosnyka, M., & Sahakian, B.J. (1999). Specific patterns of cognitive impairment in patients with idiopathic normal pressure hydrocephalus and Alzheimer's disease: a pilot study. *J Neurol Neurosurg Psychiatry*, **67**, 723–32.

Ishikawa, M. (2014). Normal pressure hydrocephalus grading scales. In: Rigamonti, D. (ed.) *Adult Hydrocephalus*, pp. 91–7. New York: Cambridge University Press.

Keong, N.C., Czosnyka, M., Czosynka, Z., & Pickard, J.D. (2011). Clinical evaluation of adult hydrocephalus. In: Winn, R. (ed.) *Youmans Neurological Surgery*, 6th edition, Chapter 35. Philadelphia, PA: Saunders.

Keong, N.C., Pena, A., Price, S.J., et al. (2017). Diffusion tensor imaging profiles reveal specific neural tract distortion in normal pressure hydrocephalus. *PLoS One*, **12**, e0181624.

Keong, N.C., Pena, A., Price, S.J., Czosnyka, M., Czosnyka, Z., & Pickard, J.D. (2016). Imaging normal pressure hydrocephalus: theories, techniques, and challenges. *Neurosurg Focus*, **41**, E11.

Kiefer, M., Eymann, R., & Steudel, W.I. (2006). Outcome predictors for normal-pressure hydrocephalus. *Acta Neurochir Suppl*, **96**, 364–7.

Kim, D.J., Kim, H., Kim, Y.T., et al. (2015). Thresholds of resistance to CSF outflow in predicting shunt responsiveness. *Neurol Res*, **37**, 332–40.

Klinge, P., Hellström P, Tans J, Wikkelsø C; European iNPH Multicentre Study Group (2012). One-year outcome in the European multicentre study on iNPH. *Acta Neurol Scand*, **126**, 145–53.

Klinge, P., Marmarou, A., Bergsneider, M., Relkin, N., & Black, P.M. (2005). Outcome of shunting in idiopathic normal-pressure hydrocephalus and the value of outcome assessment in shunted patients. *Neurosurgery*, **57**, S40–52; discussion ii–v.

Krauss, J.K., Droste, D.W., Vach, W., et al. (1996). Cerebrospinal fluid shunting in idiopathic normal-pressure hydrocephalus of the elderly: effect of periventricular and deep white matter lesions. *Neurosurgery*, **39**, 292–9; discussion 299–300.

Kubo, Y., Kazui, H., Yoshida, T., et al. (2008). Validation of grading scale for evaluating symptoms of idiopathic normal-pressure hydrocephalus. *Dement Geriatr Cogn Disord*, **25**, 37–45.

Larsson, A., Wikkelsø, C., Bilting, M., & Stephensen, H. (1991). Clinical parameters in 74 consecutive patients shunt operated for normal pressure hydrocephalus. *Acta Neurol Scand*, **84**, 475–82.

Malm, J., Graff-Radford, N.R., Ishikawa, M., et al. (2013). Influence of comorbidities in idiopathic normal pressure hydrocephalus—research and clinical care. A report of the ISHCSF task force on comorbidities in INPH. *Fluids Barriers CNS*, **10**, 22.

Marmarou, A., Bergsneider, M., Klinge, P., Relkin, N., & Black, P.M. (2005a). The value of supplemental prognostic tests for the preoperative assessment of idiopathic normal-pressure hydrocephalus. *Neurosurgery*, **57**, S17–28; discussion ii–v.

Marmarou, A., Takagi, H., & Shulman, K. (1980). Biomechanics of brain edema and effects on local cerebral blood flow. *Adv Neurol*, **28**, 345–58.

Marmarou, A., Young, H.F., Aygok, G.A., et al. (2005b). Diagnosis and management of idiopathic normal-pressure hydrocephalus: a prospective study in 151 patients. *J Neurosurg*, **102**, 987–97.

McGirt, M.J., Woodworth, G., Coon, A.L., Thomas, G., Williams, M.A., & Rigamonti, D. (2005). Diagnosis, treatment, and analysis of long-term outcomes in idiopathic normal-pressure hydrocephalus. *Neurosurgery*, **57**, 699–705.

Momjian, S., Owler, B.K., Czosnyka, Z., Czosnyka, M., Pena, A., & Pickard, J.D. (2004). Pattern of white matter regional cerebral blood flow and autoregulation in normal pressure hydrocephalus. *Brain*, **127**, 965–72.

Oi, S., Shimoda, M., Shibata, M., et al. (2000). Pathophysiology of long-standing overt ventriculomegaly in adults. *J Neurosurg*, **92**, 933–40.

Owler, B.K., Momjian, S., Czosnyka, Z., et al. (2004). Normal pressure hydrocephalus and cerebral blood flow: a PET study of baseline values. *J Cereb Blood Flow Metab*, **24**, 17–23.

Pena, A., Harris, N.G., Bolton, M.D., Czosnyka, M., & Pickard, J.D. (2002). Communicating hydrocephalus: the biomechanics of progressive ventricular enlargement revisited. *Acta Neurochir Suppl*, **81**, 59–63.

Pickard, J.D. (1982). Adult communicating hydrocephalus. *Br J Hosp Med*, **27, 35**, 37–8, **40**, passim.

Podsiadlo, D. & Richardson, S. (1991). The timed 'Up & Go': a test of basic functional mobility for frail elderly persons. *J Am Geriatr Soc*, **39**, 142–8.

Pujari, S., Kharkar, S., Metellus, P., Shuck, J., Williams, M.A., & Rigamonti, D. (2008). Normal pressure hydrocephalus: long-term outcome after shunt surgery. *J Neurol Neurosurg Psychiatry*, **79**, 1282–6.

Relkin, N., Marmarou, A., Klinge, P., Bergsneider, M., & Black, P.M. (2005). Diagnosing idiopathic normal-pressure hydrocephalus. *Neurosurgery*, **57**, S4–16; discussion ii–v.

Silverberg, G.D., Mayo, M., Saul, T., Rubenstein, E., & McGuire, D. (2003). Alzheimer's disease, normal-pressure hydrocephalus, and senescent changes in CSF circulatory physiology: a hypothesis. *Lancet Neurol*, **2**(8), 506–11.

Silverberg, G.D., Mayo, M., Saul, T., Fellmann, J., Carvalho, J., & McGuire, D. (2008). Continuous CSF drainage in AD: results of a double-blind, randomized, placebo-controlled study. *Neurology*, **71**, 202–9.

Stein, S.C. & Langfitt, T.W. (1974). Normal-pressure hydrocephalus. Predicting the results of cerebrospinal fluid shunting. *J Neurosurg*, **41**, 463–70.

Tedeschi, E., Hasselbalch, S.G., Waldemar, G., et al. (1995). Heterogeneous cerebral glucose metabolism in normal pressure hydrocephalus. *J Neurol Neurosurg Psychiatry*, **59**, 608–15.

Tinetti, M.E. (1986). Performance-oriented assessment of mobility problems in elderly patients. *J Am Geriatr Soc*, **34**, 119–26.

Tullberg, M., Jensen, C., Ekholm, S., & Wikkelsø, C. (2001). Normal pressure hydrocephalus: vascular white matter changes on MR images must not exclude patients from shunt surgery. *AJNR Am J Neuroradiol*, **22**, 1665–73.

Walchenbach, R., Geiger, E., Thomeer, R.T., & Vanneste, J.A. (2002). The value of temporary external lumbar CSF drainage in predicting the outcome of shunting on normal pressure hydrocephalus. *J Neurol Neurosurg Psychiatry*, **72**, 503–6.

Wilson, J.T., Hareendran, A., Grant, M., et al. (2002). Improving the assessment of outcomes in stroke: use of a structured interview to assign grades on the modified Rankin Scale. *Stroke*, **33**, 2243–6.

RELATED LINK TO EBRAIN

Normal Pressure Hydrocephalus. https://learning.ebrain.net/course/view.php?id=521

95

Pseudotumour cerebri syndrome

John Pickard and Nicholas Higgins

Introduction and classification

Following the development of the ophthalmoscope by von Helmholtz in 1851 and the technique of lumbar puncture by Quincke in 1891, Nonne coined the term pseudotumour cerebri in 1904 for cases of papilloedema and raised cerebrospinal fluid (CSF) pressure without mass lesions. The term pseudotumour cerebri syndrome (PTCS) refers to a spectrum of patients who present with raised intracranial pressure without focal neurological disturbance and without evidence on investigation of structural abnormality and who benefit from similar treatments.

The term PTCS highlights the exclusion of an intracranial mass and makes no assumptions about aetiology or mechanism. The addition by Ian Johnston of 'syndrome' to PTC is very helpful and is analogous to the distinction between Cushing's disease and Cushing's syndrome (Johnston et al., 2007). PTCS has been recommended in the recently published revised diagnostic criteria (Friedman et al., 2013).

The term benign intracranial hypertension reflects the absence of sinister intracranial pathology. However, many patients deeply resent the term—their lives are often made miserable with disabling headaches and depression, even though their vision has been preserved.

The most commonly affected group of patients are obese women of childbearing age in whom no cause has been found, hence the diagnostic label of idiopathic intracranial hypertension (IIH). Strictly speaking, IIH should only include cases where there is no known cause once a cause has been rigorously looked for. Many cases labelled as idiopathic have simply not been fully investigated so that published case series of IIH will almost always include secondary causes.

Diagnostic criteria

The diagnostic criteria for PTCS were eponymously ascribed to Walter Dandy following his detailed description of the clinical features of 22 cases in 1937. Subsequently, as a result of new knowledge, these criteria have been modified and now depend on a patient having the symptoms and signs of raised intracranial pressure, a measured increase in CSF pressure, absence of focal neurological signs except for a sixth cranial nerve palsy, normal CSF composition and normal imaging studies (including magnetic resonance venography, MRV). Small ventricles and an empty sella are allowed in the diagnostic criteria. An alternative cause for the symptoms should be excluded and the clinical course except for the effects on vision should be benign.

It is now recognized that papilloedema does not have to be present for PTCS to be diagnosed and the term idiopathic intracranial hypertension without papilloedema is used. In 2013, the diagnostic criteria were further updated and the term PTCS was recommended (**Box 95.1**) (Friedman et al., 2013).

Pathophysiology

The absorption of CSF is a passive phenomenon and, in the steady state, is described by Davson's equation (Davson et al., 1970) which has been modified to include a pulsatile component:

$$P_{csf} - P_{sss} = I_f \times R_{out} (+\text{pulsatile component}),$$

where P_{csf} is CSF pressure, P_{sss} is the pressure in the superior sagittal sinus, I_f is the CSF formation rate and R_{out} is the CSF outflow resistance. Outflow resistance may be measured in patients by measuring the change in CSF pressure as artificial CSF is infused in to the subarachnoid space using a computerized CSF infusion study.

Various mechanisms have been proposed as the basis for PTCS and more than one mechanism may be involved.

Excess CSF production

This is unlikely to be the main mechanism. A doubling of CSF production by itself, in an otherwise normal system, would only increase intracranial pressure (ICP) by 3 mmHg. The only causes of raised ICP due to excess CSF production are choroid plexus villous hypertrophy and choroid plexus papilloma where the choroid plexus is grossly enlarged. Such cases of hydrocephalus require multiple shunts and choroid plexectomy to control ICP because the excess CSF production is so severe. Enlargement of the choroid plexus is not seen in PTCS nor are such drastic procedures required to control ICP. Intracranial infection may increase CSF production but only temporarily.

Box 95.1 Diagnostic criteria for pseudotumour cerebri syndrome

1 Required for diagnosis of pseudotumour cerebri syndrome[a]
- **A** Papilloedema
- **B** Normal neurologic examination except for cranial nerve abnormalities
- **C** Neuroimaging: Normal brain parenchyma without evidence of hydrocephalus, mass, or structural lesion, and no abnormal meningeal enhancement on MRI, with and without gadolinium, for typical patients (female and obese), and MRI, with and without gadolinium, and magnetic resonance venography for others, if MRI is unavailable or contraindicated, contrast-enhanced CT may be used
- **D** Normal CSF composition
- **E** Elevated lumbar puncture opening pressure (≥250 mm CSF in adults and ≥280 mm CSF in children—250 mm CSF if the child is not sedated and not obese) in a properly performed lumbar puncture

2 Diagnosis of pseudotumour cerebri syndrome without papilledema

In the absence of papilledema, a diagnosis of pseudotumour cerebri syndrome can be made if B–E are satisfied, and in addition the patient has a unilateral or bilateral abducens nerve palsy

In the absence of papilledema or sixth nerve palsy, a diagnosis of pseudotumour cerebri syndrome can be suggested but not made if B–E are satisfied, and in addition at least three of the following neuroimaging criteria are satisfied:

1 Empty sella
2 Flattening of the posterior aspect of the globe
3 Distention of the perioptic subarachnoid space with or without a tortuous optic nerve
4 Transverse venous sinus stenosis

[a]A diagnosis of pseudotumour cerebri syndrome is definite if the patient fulfils criteria A–E. The diagnosis is considered probable if criteria A–D are met but the measured CSF pressure is lower than specified for a definite diagnosis.

Reproduced with permission from Deborah I. Friedman, Grant T. Liu, Kathleen B. Digre., Revised diagnostic criteria for the pseudotumour cerebri syndrome in adults and children, *Neurology*, Volume 81, Issue 13, pp. 1159–65, Copyright © 2013 Wolters Kluwer Health, Inc.

Cerebral oedema

This mechanism has been proposed, based on the apparently small size of the ventricles in PTCS and on the histological findings on brain biopsy. These studies are fraught with methodological artefact. Modern diffusion-weighted MR scanning has confirmed that there is no evidence of cytotoxic or vasogenic cerebral oedema in PTCS. Furthermore, the preservation of cognitive function and the depth of the cortical subarachnoid space in PTCS found at operation and on MR makes cerebral oedema an unlikely cause for this condition.

Abnormal CSF absorption

There is much experimental and clinical evidence for impairment of CSF absorption in PTCS (Johnston et al., 2007). It was Foley who provided a possible explanation for why the ventricles are not enlarged when the block to CSF absorption is at the level of the arachnoid granulations. He conjectured that, in this situation, where there is no block within the cortical subarachnoid space and free communication between it and the ventricles, excess CSF would be located in the cortical subarachnoid space. Subsequently, his concept has been supported by cisternography studies.

The measurement of CSF outflow resistance (R_{out}) in PTCS is not straightforward. This method assumes that P_{sss} remains constant as CSF pressure increases during a CSF infusion study. Recent measurements of superior sagittal sinus pressure indicate that this assumption is not valid in many patients with PTCS. CSF absorption through the intracranial arachnoid granulations may be inadequate. The spinal arachnoid granulations and other routes of absorption may be recruited in these patients but only at higher baseline pressures.

Abnormal venous drainage

The venous sinuses adjacent to infected ears have long been considered to be the link to raised ICP and otitic hydrocephalus. For example, Janny used direct pressure measurements through a burr hole to demonstrate narrowing of the superior sagittal sinus in patients with PTCS. The narrowings seen in the transverse sinuses on early MR venography studies were often dismissed as MR flow artefacts. Subsequently, meticulous methodological studies using headache-free control subjects have confirmed that these venous changes are genuine and not artefacts. The introduction of retrograde cerebral venography then demonstrated that there was often a significant pressure gradient across the narrowings of the transverse sinus seen in PTCS. Finally, venous stenting of such narrowings has helped to resolve the papilloedema in many patients (Higgins et al., 2002; Higgins et al., 2004; Pickard et al., 2008).

A key issue is the distinction between fixed stenoses and stenoses that reverse at least in part with reduction in CSF pressure after lumbar puncture. Retrograde venography has revealed that sagittal sinus pressure in obese young females with PTCS is not independent of CSF pressure but changes in step with it. Collapsible venous sinuses in PTCS have the potential to introduce a positive feedback loop into the linkage between CSF pressure, CSF absorption, and venous drainage in such a way that as ICP increases, the stenosis gets tighter, venous outflow reduces, and ICP increases even further.

One of the phenomena surrounding PTCS that remains unexplained is how a lumbar puncture may provide symptomatic relief for weeks or months despite the fact that CSF is replaced three times each day. If the narrowing of the venous sinuses is relieved by CSF drainage, the sinuses may remain open until a critical CSF pressure is again reached and this process may take weeks or months.

Steroid metabolism

Venous obstruction does not explain the relationship of PTCS to obesity nor why the CSF pressure increases to initiate the syndrome. Intriguing possibilities are emerging that link obesity to altered steroid metabolism and inflammation. For example, obesity may be linked to abnormalities of 11 beta-hydroxysteroid dehydrogenase type I that is present in both the choroid plexus and the endothelial cap of arachnoid granulations. Hypercoagulability and connective tissue disorders may alter the properties of this endothelial cap. Experimentally, administration of steroids and then withdrawal increases CSF outflow resistance. Sinclair et al. (2010a, 2010b) have

suggested that this mechanism may have dual effects in PTCS both on the choroid plexus with an increase in CSF production and on the arachnoid granulations with impaired absorption.

Clinical

Presentation

The headache of PTCS is unlike the headache of raised ICP due to a brain tumour or acute hydrocephalus which is characterized by early-morning headache made worse by bending down. The headache in PTCS may mimic migraine without aura, chronic daily headache, or tension headache. To complicate matters, many patients may have additional headache secondary to overuse of analgesics. It is instructive to assess which components of the headache are helped by removal of CSF by lumbar puncture. Headache often persists despite resolution of a patient's visual problems after treatment. A minority of patients learn that hyperventilation helps their headache. When they present with hyperventilation and carpopedal spasm, they are too often dismissed as hysterical. Headache may occur without papilloedema and vice versa.

Visual symptoms occur in over half of patients with PTCS and include blurring, obscurations of vision, and lateral diplopia. When PTCS occurs in men it is usually not associated with obesity. Men appear more likely to lose vision early.

Nausea and vomiting are common at the time of first presentation (20%).

Tinnitus is often pulsatile in nature. Pressure on the ipsilateral internal jugular vein may stop the symptom, perhaps because it raises pressure within the transverse sinus and expands an area of reversible stenosis. CSF withdrawal may also reverse such pulsatile tinnitus. If patients complain of pulsatile tinnitus, it is often instructive to compress each internal jugular vein to see whether it relieves the tinnitus temporarily. Other ear symptoms may occur and may be attributable to raised CSF pressure being transmitted to the inner ear through the cochlear aqueduct.

Nerve root symptoms in the arms and legs may occur in a minority of patients presumably due to dilatation of the root sleeves and CSF drainage may ameliorate such symptoms.

CSF rhinorrhoea may occur either spontaneously through an empty sella or via dehiscence of the tegmen tympani or superior semicircular canal. CSF leaks after skull base surgery including trans-sphenoidal pituitary surgery or foramen magnum decompression for Chiari malformations may prove refractory to reoperation until the presence of PTCS is recognized and CSF pressure lowered.

PTCS in childhood is uncommon and may be overdiagnosed if congenital abnormalities of the optic disc (e.g. drusen are not excluded and CSF pressure accurately measured under calm conditions). Children are often not overweight. Where obesity is not an issue, children must be protected against becoming anorexic.

It is important to take an accurate history and perform a general physical examination. Blood pressure should be measured to exclude malignant hypertension and neurological examination undertaken to identify any associated conditions whose treatment might help reverse PTCS (**Box 95.2**).

Box 95.2 Causes of secondary pseudotumour cerebri

Cerebral venous abnormalities
- Cerebral venous sinus thrombosis
- Head injury with fracture over the major cerebral sinuses
- Bilateral jugular vein thrombosis or ligation
- Middle ear or mastoid infection
- Right atrial hypertension
- Superior vena caval obstruction
- Giant arachnoid granulations
- Sinus meningioma
- Arteriovenous fistulae
- Reduced CSF absorption from intracranial infection or haemorrhage
- Hypercoagulable states

Medications and exposures
- Antibiotics: tetracycline, minocycline, doxycycline, nalidixic acid, sulfa drugs
- Vitamin A: hypervitaminosis A, isotretinoin, all-transretinoic acid for promyelocytic leukaemia, excessive liver ingestion
- Hormones: human growth hormone, thyroxine (in children), leuprorelin acetate, levonorgestrel (Norplant system), anabolic steroids
- Withdrawal from corticosteroids
- Lithium
- Chlordecone

Medical conditions
- Endocrine: Addison's disease, hypoparathyroidism
- Hypercapnia: sleep apnoea, Pickwickian syndrome
- Inflammatory: systemic lupus erythematous, Behçet's syndrome
- Anaemia
- Renal failure
- Turner syndrome
- Down syndrome
- Ehlers–Danlos

Others
- Familial
- Space flight

Reproduced with permission from Deborah I. Friedman, Grant T. Liu, Kathleen B. Digre., Revised diagnostic criteria for the pseudotumor cerebri syndrome in adults and children, *Neurology*, Volume 81, Issue 13, pp. 1159–65, Copyright © 2013 Wolters Kluwer Health, Inc.

For example, feeding children excess vitamin A is a cause of PTCS and treatment of iron-deficiency anaemia may reverse PTCS that has proven refractory to conservative and operative management. Inadequate screening for an underlying diagnosis is common.

While many conditions have been associated with PTCS, few studies of such associations meet the criteria for causality, namely that withdrawal of the condition results in reversal of PTCS and reintroduction causes recurrence of PTCS.

Visual abnormalities are present in most patients including papilloedema, visual field changes, reduction of visual acuity, and lateral diplopia. An expert neuro-ophthalmology review is mandatory not only to confirm the diagnosis but also to exclude congenital abnormalities and optic nerve head drusen. Ophthalmological assessment provides an objective baseline for subsequent assessment of progress although it should be noted that papilloedema may not always recur with recurrence of PTCS. If optic atrophy has supervened, even in the absence of papilloedema, patients are still at risk of losing vision.

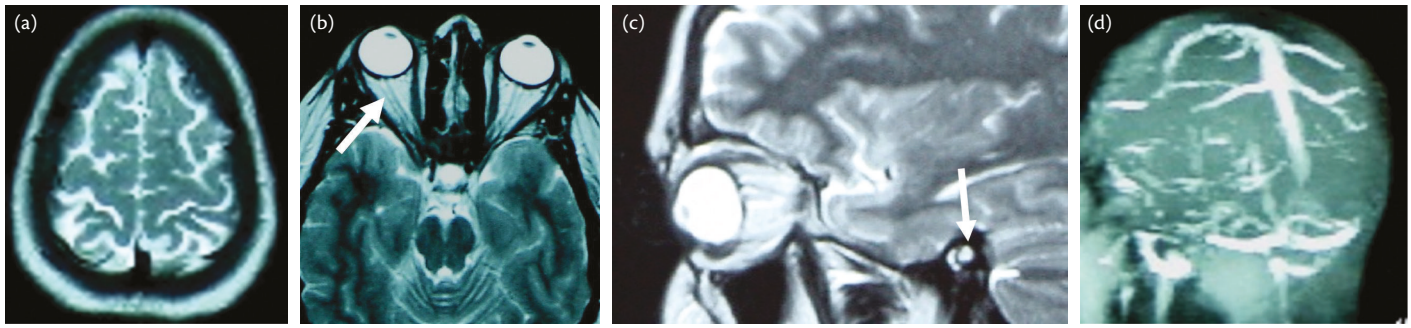

Fig. 95.1 MR features of pseudotumour cerebri syndrome. MR scan of patient with PTCS to demonstrate the various facets of 'meningeal hydrops'. (A) Excess sulcal CSF on the convexity; (B) excess CSF within the optic nerve sheath (arrowed); (C) partial empty sella (arrowed); (D) severe narrowing of the right transverse sinus on MR venography.

Investigations

Urgent computed tomography scanning will exclude a mass lesion and hydrocephalus but will not detect the subtle features of PTCS that a magnetic resonance scan will display. These include dilatation of the optic nerve sheath, with flattening of the posterior part of the globe of the eye, dilatation of the cortical sulci called meningeal hydrops, an empty sella and narrowing of the transverse sinuses (see Fig. 95.1). MRV demonstrated venous changes should not be dismissed as MR flow artefacts. Computed tomography (CT) venography (CTV) is superior to MRV in defining changes in the venous sinuses. Partial reversal of the narrowing of the transverse and other intracranial venous sinuses by CSF drainage may be documented using CTV. Angiography with retrograde venography may be indicated not only to exclude a dural fistula but also to quantify the pressure gradient across any venous sinus narrowing.

Once a mass lesion and a Chiari malformation have been excluded, it is safe to perform a lumbar puncture (LP). LPs in obese patients are often challenging and the source of much psychological trauma. Such LPs should be performed either by or under the immediate supervision of an experienced operator, preferably under X-ray control, together with electronic recording of the pressure for 20 minutes or more. Children may require sedation or general anaesthesia—hyperventilation reduces CSF pressure through lowering of arterial carbon dioxide levels. Consequentially, traumatic lumbar punctures and use of a simple manometer may underestimate the true CSF pressure.

There has been much debate about what the threshold for raised CSF pressure should be, particularly in the presence of morbid obesity and obstructive sleep apnoea. It is essential to appreciate that CSF pressure can fluctuate considerably and in various series, single lumbar puncture measurements have demonstrated pressures of 10–20 mmHg in a minority of patients with all the other features of PTCS. In these patients subsequent continuous monitoring has revealed pressures of over 20 mmHg. See Figure 95.2.

It is therefore misleading to insist on a pressure of over 25 cmH_2O (18 mmHg) in adults and 28 cmH_2O (20 mmHg) in children before making the diagnosis. If there is doubt, continuous monitoring is required aided by a CSF infusion study. The presence of waves of raised pressure during electronic recordings are also valuable indicators of raised CSF pressure. There are a small number of patients who have symptoms and signs of PTCS at CSF pressures of less than 10 mmHg. Where a Chiari malformation is present, ICP monitoring may be

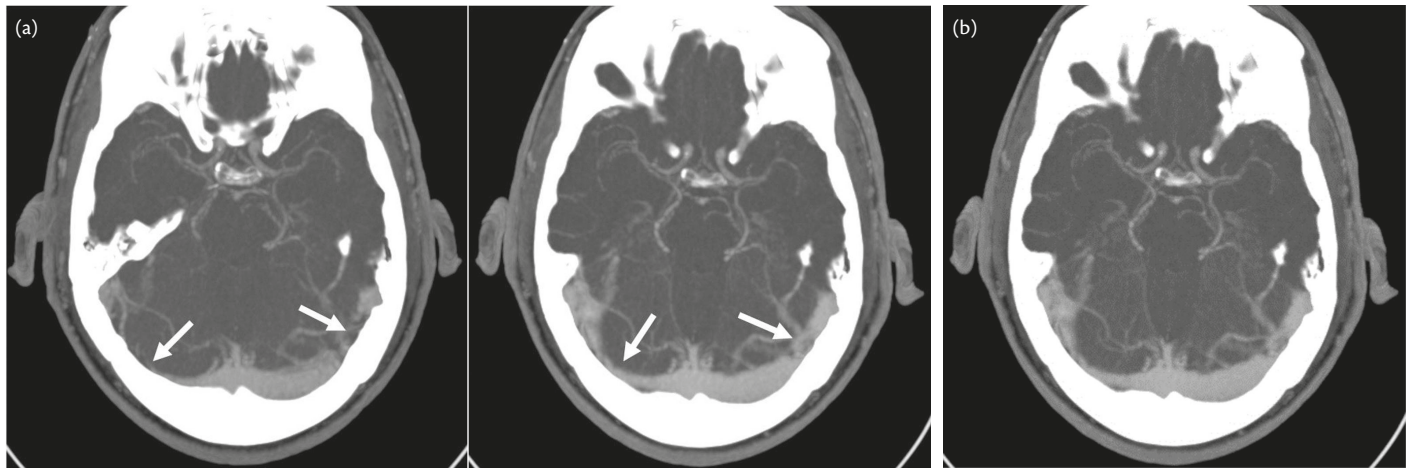

Fig. 95.2 Effect of lumbar puncture on venous sinus stenosis. CT venogram in a case of PTCS with compressible transverse sinuses showing the immediate effects of CSF withdrawal by lumbar puncture. In patients with compressible venous sinuses, this may provide a mechanism for the perpetuation of raised CSF pressures. An insult which increases CSF pressure and compresses the venous sinuses reduces the capacity for CSF resorption and further increases CSF pressure.

required to confirm the diagnosis although characteristic narrowing of the transverse sinuses on venography is indicative of raised pressure.

Protein and glucose concentrations are normal in PTCS although there is often a trend for protein levels to be slightly lower than normal. The search for PTCS-specific biomarkers in the CSF remains at the research stage.

Management

The management plan crucially depends on the rate of visual deterioration. Hence, it is essential that patients with PTCS are managed in a multidisciplinary team setting with clearly defined and carefully audited care pathways and have access to involvement in research. Frustration on the part of patients has led to the formation of specific charities devoted to PTCS/IIH both in the United States and in the United Kingdom. The combination of unsympathetic approaches to weight reduction and analgesic overuse headaches, poorly defined clinical pathways, clumsily performed multiple lumbar punctures, and overdelegation of difficult surgical procedures often leads to psychological problems. It is not surprising that litigation has sometimes followed where there appears to have been an undue delay in managing raised CSF pressure in patients with rapidly deteriorating vision.

Medical management

Causative factors should be looked for and withdrawn or treated. Effective weight reduction through dieting or bariatric surgery improves vision and reduces the severity of headaches (Sugerman et al., 1999). Many patients cannot maintain their diets long-term. A randomized controlled trial of bariatric surgery is now in progress in the United Kingdom.

Drugs

Carbonic anhydrase inhibitors (acetazolamide, topiramate) will help patients with less severe forms of PTCS but many cannot tolerate the side effects. They work by reducing CSF production but can cause renal failure and regular blood chemistry measurements should be obtained. Topiramate is milder but has the advantage of combining a modest carbonic anhydrase blocking effect with appetite suppression and antimigraine properties. It has to be used with care because of potential side effects and some patients just feel unwell on it.

The use of Furosemide has been described but conventional diuretics are little used. Because they cause weight gain, glucocorticoid steroids are now restricted to cases where there is very rapid visual deterioration and are used in combination with an urgent CSF drainage procedure. Octreotide has been used in a few cases, but great care has to be taken in supervising its administration.

Repeated lumbar punctures

Neurosurgeons are often referred patients who have been psychologically traumatized by multiple lumbar punctures, often poorly performed. Too often, only small volumes of CSF are removed. Apart from the often-increasing difficulty in performing such punctures, there is a risk of inducing arachnoiditis. The poor quality of life of patients managed by prolonged use of ineffectual drugs and multiple lumbar punctures should not be underestimated.

Interestingly, removal of large volumes of CSF through a lumbar drain as an inpatient may afford prolonged relief.

Surgical management

Surgical intervention is appropriate for rapidly deteriorating vision and where medical management has failed. Although most patients are young, there may be significant problems with wound healing secondary to smoking and obesity.

Subtemporal decompression and cranial expansion procedures

Subtemporal decompression was the first procedure to be used prior to the introduction of shunts. It has retained a small place in the surgical armamentarium until recently for the rare patient whose PTCS remains symptomatic despite other multiple failed operations (shunts and optic nerve sheath fenestration). It has to be performed with care to avoid the risk of temporal lobe epilepsy.

It should not be offered if a previous foramen magnum decompression has been performed for fear of precipitating brain slump including further tonsillar herniation, syrinx formation, and midbrain distortion.

Through a long pterional scalp flap taking care to avoid trauma to branches of the facial nerve, the temporalis muscle is split in the line of its fibres and its superior attachment preserved. The squamous temporal bone is widely removed from underneath the temporalis muscle down to the floor of the skull base. It is important to avoid making the decompression too small. The dura should not be opened but simply scored in multiple lines to allow it to expand. Anecdotally, it appears that venous stenting may avoid the need for subtemporal decompression.

CSF diversion

Shunt procedures in PTCS are notoriously challenging (Tarnaris et al., 2011). The ventricles are normal or small in size such that image guided placement of a ventricular catheter is wise. There is a tendency for ventricular catheters to intermittently block. Placing a peritoneal catheter into a grossly obese abdomen is not easy with the risk of migration of the catheter tip or variable absorption of CSF. Laparoscopic placement of the abdominal catheter is recommended by some authors. The technique of VP shunt insertion is described in Chapter 89.

Patients with PTCS are often best managed with lumboperitoneal shunts but these too may be complicated by problems with kinking and overdrainage with secondary descent of the tonsils unless a valve with antisiphon properties is used. A lumbopleural shunt that incorporates an adjustable valve and siphon control device is a further

option. This approach has the advantage of connecting two large spaces (lumbar sac and pleural cavity) with the added advantage of negative pleural pressures with each breath to keep the shunt open. A minority of patients will develop refractory pleural effusions and a careful watch has to be kept for secondary tonsillar descent.

The procedure is performed with the patient in a lateral position. As with all shunt procedures every effort must be made to minimize infection risk. This will include reducing the number of people in theatre, preventing unnecessary entry and exit of individuals, prophylactic antibiotics, and a strict sterile technique. The procedure is best performed by two surgeons.

A linear 1.5 cm incision is made through the skin at the midline in the lumbar spine. The dissection is continued down to but not deeper than the tips of the spinous processes at the level of the lumbar fascia. A Tuohy needle is used to perform a lumbar puncture, taking care to ensure that the bevel is then angled so the shunt tubing will pass in a cranial direction. The shunt tubing is inserted through the needle into the lumbar sac and advanced 5 cm. Avoid withdrawing the shunt tubing through the needle or rotating the needle once the tubing is in place, as there is a risk that the tip of the shunt will be sheared off. Once the shunt is in the lumbar sac the needle can be removed, leaving the shunt in place.

A standard open or laparoscopic approach to the abdomen may be used but in very overweight patients in a lateral position it can be surprisingly difficult to find the peritoneum. An alternative is to use the pleural cavity where the approach is just over the upper surface of the rib to avoid the intercostal bundle. The shunt is tunnelled and inserted. The wounds are closed. Postoperative X-rays are useful to confirm the correct positioning of the shunt tubing and to provide a baseline for comparison in the future.

In a patient with recurrent symptoms, detecting whether a lumboperitoneal shunt is blocked can be challenging. Bi-planar X-rays will confirm the position of a shunt and lumbar sac infusion studies may be used to assess outflow resistance but sometimes, exploring and disconnecting the shunt is the only way to definitively confirm the clinical suspicion of shunt blockage.

Optic nerve sheath fenestration

Many ophthalmic surgeons have abandoned optic nerve fenestration because of complications and because it cannot be expected to resolve headaches. Complications that have been described include ocular motility problems, optic nerve haematoma, optic disc infarcts, central branch retinal artery occlusion, sudden postoperative blindness, dacryocystitis and fibrosis (Alsuhaibani et al., 2011).

Venous stenting

Venous stenting is the logical development of the common finding of transverse sinus stenoses. The first case report was published in 2002 and attracted considerable scepticism about the potential risks. In practice and expert hands, it has proven acceptably safe when used for PTCS (Higgins et al., 2003; Ahmed et al., 2011). Stent migration, venous sinus perforation, in-stent thrombosis, and subdural haemorrhage have been described. Such complications are more likely to occur where more difficult lesions are tackled such as areas of thrombosis.

A concept is now emerging that some patients with PTCS have stenoses at the level of the jugular foramen or where the internal jugular vein is wedged between the skull base and styloid process. Some of these patients may be helped by removal of the styloid process and subsequent stenting. See **Figure 95.3**.

Prognosis

Prognosis in PTCS is variable—some patients stabilize after a single lumbar puncture, others have persistent symptoms for many years. A patient's symptoms may improve and then recur years later especially if weight has been lost and then regained again.

Acknowledgements and conflict of interest

JDP has been supported by the Cambridge NIHR Biomedical Research Centre neurosciences theme, NIHR Brain Injury Healthcare Technology Cooperative (Honorary Director) and past NIHR Senior Investigator Award. JDP receives occasional royalties from sales of the monograph *The Pseudotumor Cerebri Syndrome* that was coauthored with Ian Johnston and Brian Owler (Johnston et al., 2007).

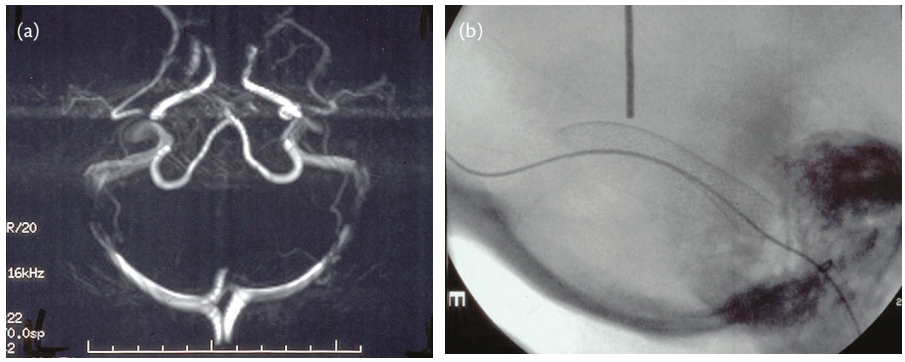

Fig. 95.3 Venous sinus stenting for PTCS patients. In cases where there is a fixed sinus stenosis, endovascular stenting has been demonstrated to alleviate symptoms of PTCS. (A) 3D phase-contrast magnetic resonance venography. Axial maximum intensity projection shows poor signal in the distal portions of both transverse sinuses implying low flow. (B) Digital subtraction angiogram postvenous stenting of the right transverse sinus, leading to improvement in patient symptoms.

FURTHER READING

Alsuhaibani, A.H., Carter, K.D., Nerad, J.A. et al. (2011). Effect of optic nerve sheath fenestration on papilloedema of the operated and the contralateral nonoperated eyes in idiopathic intracranial hypertension. *Ophthalmology*, **118**, 412–14.

Friedman, D.I., Liu, G.T., & Digre, K.B. (2013). Revised diagnostic criteria for the pseudotumor cerebri syndrome in adults and children. *Neurology*, **81**, 1159–65.

Higgins, J.N., Owler, B., Cousins, C., & Pickard, J.D. (2002). Venous sinus stenting for refractory benign intracranial hypertension. *Lancet*, **359**, 228–30.

Johnston, I., Owler, B., & Pickard, J. (2007). *The Pseudotumor Cerebri Syndrome.* Cambridge, UK: Cambridge University Press.

Sugerman, H.J., Felton, W.L., Sismanis, A., Kellum, J.M., DeMaria, E.J., & Sugerman, E.L. (1999). Gastric surgery for pseudotumor cerebri associated with severe obesity. *Ann Surg*, **229**, 634–42.

REFERENCES

Ahmed, R.M., Wilkinson, M., Parker, G.D. et al. (2011). Transverse sinus stenting for idiopathic intracranial hypertension: a review of 52 patients and of model predictions. *AJNR Am J Neuroradiol*, **3**, 1408–14.

Alsuhaibani, A.H., Carter, K.D., Nerad, J.A. et al. (2011). Effect of optic nerve sheath fenestration on papilloedema of the operated and the contralateral nonoperated eyes in idiopathic intracranial hypertension. *Ophthalmology*, **118**, 412–14.

Davson, H., Hollinsworth, J.R., & Segal, M.B. (1970). The mechanism of drainage of the cerebrospinal fluid. *Brain*, **96**, 329–36.

Friedman, D.I., Liu, G.T., & Digre, K.B. (2013). Revised diagnostic criteria for the pseudotumor cerebri syndrome in adults and children. *Neurology*, **81**, 1159–65.

Higgins, J.N., Cousins, C., Owler, B. et al. (2003). Idiopathic intracranial hypertension: 12 cases treated with venous sinus stenting. *J Neurol Neurosurg Psychiatry*, **74**, 1662–6.

Higgins, J.N., Gillard, J.G., Owler, B., et al. (2004). MR venography in idiopathic intracranial hypertension: unappreciated and misunderstood. *J Neurol Neurosurg Psychiatry*, **75**, 621–5.

Higgins, J.N., Owler, B., Cousins, C., & Pickard, J.D. (2002). Venous sinus stenting for refractory benign intracranial hypertension. *Lancet*, **359**, 228–30.

Johnston, I., Owler, B., & Pickard, J. (2007). *The Pseudotumor Cerebri Syndrome.* Cambridge, UK: Cambridge University Press.

Pickard, J.D., Czosnyka, Z., Czosnyka, M., et al. (2008). Coupling of sagittal sinus pressure and cerebrospinal fluid pressure in idiopathic intracranial hypertension—a preliminary analysis. *Acta Neurochir Suppl*, **102**, 283–5.

Sinclair, A.J., Burdon, M.A., Nightingale, P.G., et al. (2010a). Low energy diet and intracranial pressure in omen with idiopathic intracranial hypertension. *BMJ*, **341**, c2701.

Sinclair, A.J., Walker, E.A., Burdon, M.A. et al. (2010b). Cerebrospinal fluid corticosteroid levels in patients with idiopathic intracranial hypertension: a link between 11 beta-HSD1 and intracranial pressure regulation. *J Clin Endocrinol Metab*, **95**, 5348–56.

Sugerman, H.J., Felton, W.L., Sismanis, A., Kellum, J.M., DeMaria, E.J., & Sugerman, E.L. (1999). Gastric surgery for pseudotumor cerebri associated with severe obesity. *Ann Surg*, **229**, 634–42.

Tarnaris, A., Toma, A.K., Watkins, L.D., et al. (2011). Is there a difference in outcomes of patients with idiopathic intracranial hypertension with the choice of cerebrospinal fluid diversion site: a single centre experience. *Clin Neurol Neurosurg*, **113**, 477–9.

RELATED LINKS TO EBRAIN

Idiopathic Intracranial Hypertension. https://learning.ebrain.net/course/view.php?id=106

Performing a Subtemporal Decompression. https://learning.ebrain.net/course/view.php?id=522

96

Arachnoid cysts

Ruichong Ma and Stana Bojanic

Introduction

Frist described in 1831, arachnoid cysts are cerebrospinal fluid (CSF) filled spaces lined with arachnoid membrane. They account for 1% of all intracranial space occupying lesions and can also be found rarely in the spinal column. The majority of intracranial arachnoid cysts (AC) are found in the middle cranial fossa with a male predilection and a slight preponderance for the left side. With the availability of modern imaging, many more AC are being picked up incidentally in asymptomatic patients. However, symptomatic AC are predominantly found in the paediatric population with patients typically presenting with headaches, rapid head growth, developmental delay, and seizures. Treatment of patients with asymptomatic AC has typically been conservative management with surgery only considered in patients with symptoms. Surgical management remains controversial and includes open techniques, endoscopic fenestration of cyst, or shunting procedures.

Pathology

Classification and formation of arachnoid cysts

AC can be classified as congenital or acquired, secondary to intracerebral haemorrhage or meningitis. AC can be classified by their pathogenesis (i.e. primary or secondary, whether they are symptomatic, or by location). Galassi et al. produced a specific three-part classification of middle cranial fossa AC based on their anatomy and communication with the basal cisterns (**Table 96.1**, **Fig. 96.1**). True AC, however, are deemed to be primary developmental cysts that arise during fetal development. Macroscopically AC membranes look identical to normal arachnoid membranes. However, under the microscope there are several structural differences notably: (1) splitting of the arachnoid membrane at the margin of the cyst; (2) a very thick layer of collagen in the cyst wall; (3) the absence of traversing trabecular processes within the cyst; and (4) the presence of hyperplastic arachnoid cells in the cyst wall, which presumably participate in collagen synthesis (Rengachary and Watanabe, 1981). Intracranial AC are predominantly in the middle cranial fossa, posterior fossa, and frontal regions (**Table 96.2**) and are exclusively associated with normal subarachnoid cisterns. This has led authors to conclude that the formation of AC is due to an anomalous splitting of the arachnoid membrane during folding of the primitive neural tube and formation of the subarachnoid cisterns.

Pathogenesis

The mechanism behind the expansion of AC following formation is not well understood although there are several schools of thought.

Active fluid secretion

In 1964, Robinson reported that there was a difference in consistency in AC fluid as compared to normal CSF (Robinson, 1964). This was subsequently found to be due to a difference in the phosphate, protein, ferritin, and lactase dehydrogenase levels compared to CSF (Berle et al., 2010). A separate ultrastructural and cytochemical study by Go et al. showed that there were structural similarities between AC walls and the neurothelial lining of the arachnoid granulations. This is supported by more recent studies showing a genetic architecture for cyst expansion and quantitative PCR has revealed the Na-K-2Cl cotransporter as a potential mechanism for fluid transport (Helland et al., 2010).

Osmotic gradient

A separate theory suggests that the difference in composition of AC fluid and CSF leads to an osmotic gradient in which water is forced into the cyst. However, for this to have happen there needs to be an initial trigger. In secondary AC, intracerebral haemorrhage or inflammatory reactions can cause this trigger, although there is no evidence for a trigger in primary AC.

Ball and valve mechanism

Studies have shown that small to medium sized AC tend to remain fixed in size and communicate readily with the subarachnoid cisterns whereas in larger or growing cysts there may be a valve in which a unidirectional flow of CSF may occur (Galassi et al., 1982). This is supported by valve-like foldings of the AC wall or intracystic membranes observed intraoperatively.

Table 96.1 Galassi classification of middle cranial fossa arachnoid cysts

Galassi type	Description on CT cisternography	Communication to basal cisterns?
I	Small, limited to anterior middle fossa	Yes
II	Superior extension along Sylvian fissure with displacement of temporal lobe	Yes
III	Large, filling whole middle fossa with displacement of frontal and parietal lobes	No

Reprinted from *Surgical Neurology*, Volume 17, issue 5, Ercole Galassi, Francesco Tognetti, Giulio Gaist, Leo Fagioli, Franco Frank, Giorgio Frank, Ct scan and metrizamide CT cisternography in arachnoid cysts of the middle cranial fossa: Classification and pathophysiological aspects, pp. 363–69, Copyright (1982), with permission from Elsevier.

Fig. 96.1 Illustration depicting the relative size and location of middle cranial fossa arachnoid cysts based on Galassi classification. Type 1, shown in blue are small and limited to the anterior pole of the middle cranial fossa. Type 2, in yellow, extend further posteriorly and superiorly, displacing the temporal lobe, and taking the shape of a parallelogram. Type 3, in red, fill the whole of the middle cranial fossa, in a trapezoidal fashion displacing the frontal and/or parietal lobes.

Table 96.2 Relative distribution of intracranial arachnoid cysts

Location	Frequency
Sylvian fissure	49%
Cerebellar-pontine angle	11%
Supracollicular	10%
Vermis	9%
Sellar/Suprasellar	9%
Interhemispheric fissure	5%
Cerebral convexity	4%
Interpeduncular	3%

Reproduced with permission from Rengachary, Setti S.; Watanabe, Itaru, Ultrastructure and Pathogenesis of Intracranial Arachnoid Cysts, *Journal of Neuropathology and Experimental Neurology*, Volume 40, Issue 1, pp. 61–83, Copyright © 1981 Oxford University Press and the American Association of Neuropathologists.

Management options

Clinical presentation

The majority of AC, especially in adults, are asymptomatic and are picked up incidentally on imaging. Clinical symptoms in symptomatic patients will be dependent on both the age of the patient and location (Table 96.3). Patients may present following trauma with chronic subdural haematoma or hygroma if the AC wall has burst during the trauma. They can also present acutely with haemorrhage into the AC following trauma or, rarely, as a spontaneous acute subdural haematoma, presumably from the delicate vessels within the wall of the arachnoid cyst.

Middle cranial fossa

The majority of AC are located in the middle cranial fossa or Sylvian fissure (49%). The majority occur in male patients and show a predilection for the left hemisphere (Fig. 96.2A). Symptoms typically arise due to mass effect causing increased intracranial pressure or irritation of the temporal or frontal cortices. Patients can present with headaches, seizures, or contralateral motor weakness. In children, they may present with an enlarging head circumference or asymmetry of the skull/facial bones and even exophthalmos in the extremes due to abnormal development of the sphenoid ridge. Developmental delay is more common in paediatric patients with AC. There is an ongoing debate as to whether temporal AC are linked with psychiatric or neuropsychological disorders.

Posterior fossa

Infratentorial AC account for approximately 20–30% of all AC, with the majority located at the cerebellopontine angle (CPA) (Fig. 96.2B). Symptoms can include headaches from hydrocephalus or gait disturbances from cerebellar compression. Patients with CPA cysts may also develop symptoms from compression of neurovascular structures in the CPA and develop hearing loss, trigeminal neuralgia, diplopia, or bulbar symptoms. The shape of the fourth ventricle, appearance of the cerebellar vermis and the distortion of neural structures help to differentiate posteriorly located AC from an enlarged cisterna magna and Dandy-Walker malformation.

Table 96.3 Signs and symptoms seen in arachnoid cysts based on location

Location	Symptoms
Middle cranial fossa	Headaches, seizures, contralateral weakness, psychiatric or neuropsychological disorders. Children: developmental delay, rapid head growth, failure to thrive, skull/facial deformity
Posterior fossa	Headaches, ataxia, trigeminal neuralgia, hearing loss, ophthalmoplegia, bulbar dysfunction
Frontal	Pituitary dysfunction, visual disturbance, hydrocephalus, bobble-head doll syndrome
Spinal	Myelopathy, radiculopathy

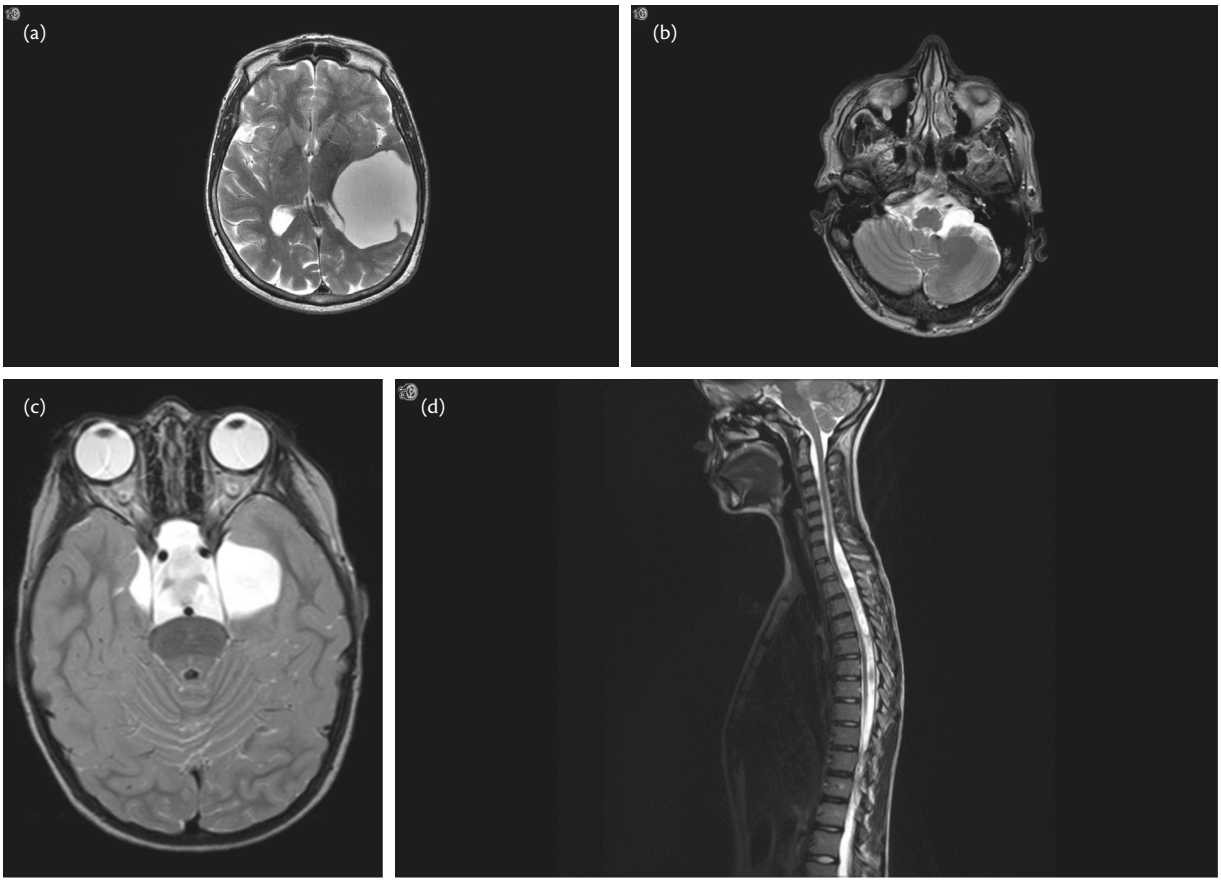

Fig. 96.2 T2-weighted MRI of patient with (A) left middle cranial fossa arachnoid cyst, (B) left cerebellopontine angle arachnoid cyst, (C) suprasellar arachnoid cyst, (D) Spinal arachnoid cysts from T1 to T3 with anterior displacement of the spinal cord.

Frontal

Sellar or suprasellar cysts arise in the basal subarachnoid space, closely approximated to the optic nerves, pituitary gland, hypothalamus, and mesencephalon (Fig. 96.2C). Thus patients may show signs of pituitary insufficiency and visual loss from compression of such structures. Occasionally, if the AC is very large, it may also cause obstructive hydrocephalus from compression of the third ventricle. In such circumstances, patients may develop a bobble-head doll syndrome showing involuntary back and forwards bobbing of the head at 2–3 Hertz.

Intra- and periventricular

The rare intraventricular AC may need high definition magnetic resonance imaging (MRI) to define the cyst wall. Suprasellar cysts compression the third ventricle anteriorly can be mistaken for a triventricular hydrocephalus with 'ballooning' of the third ventricle and be inappropriately treated by a ventriculoperitoneal (VP) shunt. Those arising within the quadrigeminal cistern similarly may compress the posterior third ventricle and aqueduct.

Spinal

Spinal AC (Fig. 96.2D) typically present with signs and symptoms of either myelopathy (ataxia, progressive spastic paralysis with a sensory level), or radiculopathy (neuralgia or localized motor-sensory deficits). This is due to compression of the spinal cord or exiting nerve roots. Occasionally, back pain can be the only presenting symptom leading to investigation.

Investigation

Patients presenting with neurological symptoms should have a detailed history and examination performed. The diagnosis of arachnoid cyst is one made on imaging, the mainstay of which is MRI. They are typically hypointense on T1 and hyperintense on T2, much like CSF. Modern phase contrast MRI and functional MRI are not only capable of showing structural abnormalities but also delineate CSF-flow patterns and any changes in functional organization of the brain. Computed tomography (CT) cisternography, where contrast is injected into the subarachnoid space with subsequent time-lapse CT scans is now reserved for the rare cases of diagnostic uncertainty. Differential diagnoses of AC are many and can be found in Table 96.4.

Asymptomatic AC are treated conservatively with serial imaging to ensure stability. Patients presenting as an emergency with acute obstructive hydrocephalus will require urgent surgical intervention. Patients with chronic subdural haematomas will require primary treatment of the haematoma but not necessarily of their underlying AC. Conversely, patients with AC and subdural hygromas at presentation do well with medical treatment with acetazolamide, avoiding the need for surgery. For symptomatic patients, treatment is usually offered in the form of surgery except if headache is the only symptom. These patients must be treated with caution, as the causes of headaches

Table 96.4 Differential diagnoses of arachnoid cysts and their differences on imaging

Differential diagnosis	Difference on imaging
Enlarged CSF space (e.g. mega cisterna magna)	Enlarged anatomically correct CSF space
Epidermoid cyst	Heterogenous signalling on MRI flair Restricted diffusion More lobulated
Cystic tumours: • **Pilocytic astrocytoma** • **Haemangioblastoma**	Intra-axial Often has enhancing component
Non-neoplastic cysts: • **Neurenteric cysts** • **Neuroglial cysts** • **Porencephalic cyst**	Intra-axial Communication with foregut derivatives (neurenteric cysts) Usually surrounded by grey matter (neuroglial cysts) or gliotic (porencephalic cysts) tissue
Infectious: • **Hydatid cyst** • **Neurocysticercosis**	Cysts in other parts of the body, e.g. liver (hydatid cysts) Usually small and multiple (neurocysticercosis)

are many-fold and all other causes of headache must be explored before surgery is offered. There is still controversy as to whether such patients receive good symptom relief from surgical management of AC.

Surgical approaches

Shunting

Much like in hydrocephalus, a shunt can be placed into the cyst to drain it into another body cavity to allow for reabsorption of the CSF. Typically, these drain either into the peritoneum or the subdural space. This is the least invasive procedure and confers the lowest perioperative risk. However, it is the least successful in the long term with a repeat operation required in 26% of patients (Helland and Wester, 2006).

Open approaches

Treatment of AC has historically been through open approaches through a craniotomy. The cyst wall can be excised or marsupialized to open up flow into the subdural space. Alternatively, most techniques revolve around fenestration of the cyst to allow CSF flow back into natural CSF spaces (i.e. the basal cisterns or ventricular system). Some surgeons would recommend fenestration of the cyst into two CSF spaces in order to allow CSF flow through the cyst in order to keep the stomata open and prevent recurrence/treatment failure.

Endoscopic approaches

More recently, endoscopic techniques have been utilized to perform endoscopic fenestration of the medial cyst wall into both the basal cisterns or ventricles (Fig. 96.3). These newer techniques reduce the size of the craniotomy required, with many operators performing surgery through a single burr hole. Some surgeons also utilize neuronavigation to help navigate through what can potentially be difficult anatomy, especially if the cyst wall is thickened. There is still ongoing debate with regards to the optimal treatment modality and this will be discussed next.

Ideally, whenever possible, a 'bipolar' fenestration, that is, a combined cystoventriculostomy in addition to a cystocisternostomy for third ventricle-associated AC ensures optimum CSF flow (Kirollos et al., 2001) (Fig. 96.3).

Management of spontaneous or post-traumatic haemorrhage with an underlying arachnoid cyst

When clinically indicated, in most cases evacuation of subdural haematomas through burr holes or less commonly by a

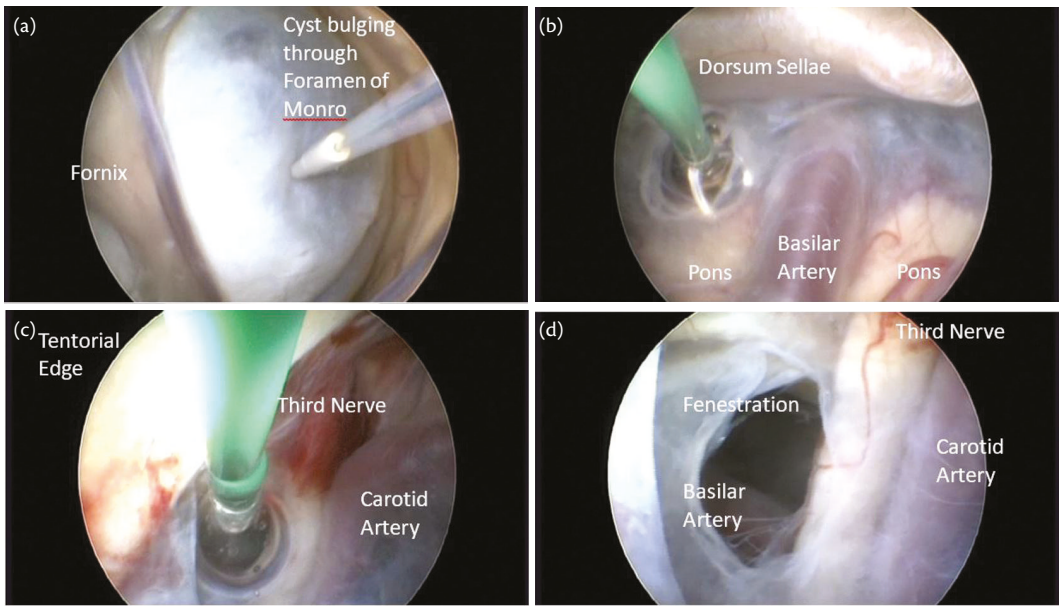

Fig. 96.3 Intraoperative view of endoscopic fenestration of a suprasellar/third ventricular arachnoid cyst. (A) Cystoventriculostomy of the cyst dome at the foramen of Monro into the lateral ventricle, (B) cystocisternostomy at the base of the cyst to the prepontine cistern just lateral to the basilar artery. Intraoperative figure of endoscopic fenestration of a middle fossa arachnoid cyst to the interpeduncular and prepontine cisterns (C) widening the fenestration using a Fogarty balloon just posterior to the third nerve, (D) a view of the basilar artery in the basal cisterns.

minicraniotomy is the initial treatment. In many reports subsequent treatment of the underlying arachnoid cyst was not necessary.

Spinal AC are treated surgically predominantly through an open dorsal approach.

Postoperative

Outcomes

Outcomes following surgery for AC are very favourable with 76–95% of patients achieving good long-term success following open techniques and up to 95% of patients following endoscopic techniques (Helland and Wester, 2006; Johnson et al., 2011). Failure rates are not significantly related to location of cyst although frontal AC tend to achieve better results, especially through endoscopic techniques. The long-term success rate for shunting procedures is lower at 74% (Helland and Wester, 2006) reflecting the long-term problems associated with shunts.

Complications

Operating on AC carries an overall complication rate of 16.9%, and a reoperation rate of 7.2% (Helland and Wester, 2006). These complications seem to almost exclusively happen in patients with temporal AC. The major complication following surgery and treatment of intracranial AC include subdural hygromas, with an incidence of 4–6% in open microsurgical techniques and 9% following endoscopic techniques for middle cranial fossa AC (Cincu et al., 2007; Johnson et al., 2011) and a 6% risk CSF leak (Pradilla and Jallo, 2007). There is a small additional risk of intraoperative haemorrhage during endoscopic techniques, which necessitates conversion to open microsurgical techniques. Although the operative risks involved with shunting procedures is thought to be lower, the immediate complication rate was not significantly lower (Helland and Wester, 2006).

Controversies

A large proportion of AC are incidental. Careful selection for treatment especially in the presence of unrelated headaches and other vague symptoms is important.

There still remains controversy among neurosurgeons regarding the optimum surgical technique for treating AC (Table 96.5). Advocates of shunting techniques state that it is a less invasive technique that conveys the lowest operative risk to the patients while providing good control of the cyst volumes through pressure-controlled systems. Data shows that resection or fenestration of AC do not confer a significantly increased risk of immediate complication and any complications arising are relatively minor or temporary (Helland and Wester, 2006). Many surgeons are now able to show extremely good long-term results from both open and endoscopic techniques with long-term success rates of up to 95% (Johnson et al., 2011) compared to 74% for shunt procedures. Many patients are children at presentation and will inevitably require multiple shunt revisions throughout their lifetime, whereas treatment of the cyst itself is potentially curative. For this reason, the majority of neurosurgeons will opt for surgical treatment of the cyst as the first line of treatment with shunting as a second line treatment.

Table 96.5 Pros and cons of various surgical techniques used to treat arachnoid cysts

Operative technique	Pros	Cons
Shunting	Minimally invasive, quick	Lower chance of long-term success, risk of shunt malfunction/infection
Open microsurgery	Low rate of recurrence	Need for craniotomy, prolonged surgical time, higher risk of infection
Endoscopic surgery	Low rate of recurrence, minimally invasive	Higher risk of intraoperative bleeding, higher risk of post-op subdural hygroma, specialist experience required

Sport participation in arachnoid cyst patients

Participation in sports is still a controversial issue in patients with AC. There are a cohort of neurosurgeons who believe that the presence of AC increases the risk of haemorrhage and brain injury following trauma and hence contact sports should be avoided. To support this, there are numerous case reports and case series in the literature of patients with AC who have sustained sports-related structural brain injury. The most common injury seen is a post-traumatic subdural hygroma thought to be due to tearing of the cyst wall creating a one-way valve. There is also an increased risk of developing subdural haematomas although bleeding directly into AC is a rare occurrence. However, it is important to recognize that all contact sports inherently carry a risk of developing traumatic brain injury even in the absence of AC, although some case reports in the literature do describe injury following low-impact trauma in patients with AC not normally associated with brain injury. In addition, patients presenting with AC-related structural brain injury tended to have a later presentation to hospital. There is an inherent publication bias with these case reports, in that in order to be publishable, the particular case typically manifest the following: (1) novel presentation; (2) surgical management; and (3) good outcomes. It is unclear how many patients presenting in a standard fashion are treated conservatively with good effect. A recent prospective cohort study of 185 children diagnosed with AC (Strahle et al., 2016) shows that 112 patients participated in 261 different sports for a total of 4410 months. In this cohort only two patients suffered from symptomatic subdural hygromas with no neurological injury. Both hygromas were treated conservatively and settled with time. However, most of these patients were young children participating in low-level, low-impact sports. It would be expected that older children and adults participating in higher-level sports will risk higher impacts and have increased rates of traumatic brain injury.

To call an activity 'safe' inherently involves a judgement call against a subjective level of acceptability, as no sport is truly 'safe' if the standard is of absolute safety (i.e. there is no risk of injury). Such a standard is not applied to the general population and should therefore not be applied to patients with AC. There is an increased risk of structural brain injury in patients with AC through participation in sports, although it is still a rare occurrence with predominantly good outcomes. Each patient should be counselled individually and the choice to continue to participate in sports should be made in partnership between the physician and patient.

FURTHER READING

Cincu, R., Agrawal, A., & Eiras, J. (2007). Intracranial arachnoid cysts: current concepts and treatment alternatives. *Clin Neurol Neurosurg*, **109**(10), 837–43.

Galassi, E., Tognetti, F., Gaist, G., Fagioli, L., Frank, F., & Frank, G. (1982). CT scan and metrizamide CT cisternography in arachnoid cysts of the middle cranial fossa: classification and pathophysiological aspects. *Surg Neurol*, **17**(5), 363–9.

Helland, C.A. & Wester, K. (2006). A population-based study of intracranial arachnoid cysts: clinical and neuroimaging outcomes following surgical cyst decompression in children. *J Neurosurg*, **105**(5 Suppl), 385–90.

Johnson, R.D., Chapman, S., & Bojanic, S. (2011). Endoscopic fenestration of middle cranial fossa arachnoid cysts: does size matter? *J Clin Neurosci*, **18**(5), 607–12.

Rengachary, S.S. & Watanabe, I. (1981). Ultrastructure and pathogenesis of intracranial arachnoid cysts. *J Neuropathol Exp Neurol*, **40**(1), 61–83.

REFERENCES

Berle, M., Wester, K.G., Ulvik, R.J., et al. (2010). Arachnoid cysts do not contain cerebrospinal fluid: a comparative chemical analysis of arachnoid cyst fluid and cerebrospinal fluid in adults. *Cerebrospinal Fluid Res*, **7**, 8.

Cincu, R., Agrawal, A., & Eiras, J. (2007). Intracranial arachnoid cysts: current concepts and treatment alternatives. *Clin Neurol Neurosurg*, **109**(10), 837–43.

Galassi, E., Tognetti, F., Gaist, G., Fagioli, L., Frank, F., & Frank, G. (1982). CT scan and metrizamide CT cisternography in arachnoid cysts of the middle cranial fossa: classification and pathophysiological aspects. *Surg Neurol*, **17**(5), 363–9.

Go, K.G., Houthoff, H.J., Blaauw, E.H., Havinga, P., & Hartsuiker, J. (1984). Arachnoid cysts of the sylvian fissure. Evidence of fluid secretion. *J Neurosurg*, **60**(4), 803–13.

Helland, C.A. & Wester, K. (2006). A population-based study of intracranial arachnoid cysts: clinical and neuroimaging outcomes following surgical cyst decompression in children. *J Neurosurg*, **105**(5 Suppl), 385–90.

Helland, C.A., Aarhus, M., Knappskog, P., et al. (2010). Increased NKCC1 expression in arachnoid cysts supports secretory basis for cyst formation. *Exp Neurol*, **224**(2), 424–8.

Johnson, R.D., Chapman, S., & Bojanic, S. (2011). Endoscopic fenestration of middle cranial fossa arachnoid cysts: does size matter? *J Clin Neurosci*, **18**(5), 607–12.

Kirollos, R.W., Javadpour, M., May, P., & Mallucci, C. (2001). Endoscopic treatment of suprasellar and third ventricle-related arachnoid cysts. *Childs Nerv Syst*, **17** (12), 713–18.

Pradilla, G. & Jallo, G. (2007). Arachnoid cysts: case series and review of the literature. *Neurosurg Focus*, **22**(2), E7.

Rengachary, S.S. & Watanabe, I. (1981). Ultrastructure and pathogenesis of intracranial arachnoid cysts. *J Neuropathol Exp Neurol*, **40**(1), 61–83.

Robinson, R.G. (1964). The temporal lobe agenesis syndrome. *Brain*, **87**, 87–106.

Strahle, J., Selzer, B.J., Geh, N., et al. (2016). Sports participation with arachnoid cysts. *J Neurosurg Pediatrics*, **17**(4), 410–17.

RELATED LINK TO EBRAIN

Pathophysiology and Management of Arachnoid Cysts. https://learning.ebrain.net/course/view.php?id=423

SECTION 20
Infection

97. **Microbiology** *1109*
Walter A. Hall

98. **Cranial infections** *1117*
Thangaraj Munusamy, Boon Hoe Tan, and Eugene Yang

99. **Spinal infection** *1129*
Nicholas Haden and Edward White

97

Microbiology

Walter A. Hall

Introduction

Infection of the central nervous system (CNS) can be due to various antimicrobial agents that include viruses, bacteria, fungi, and parasites. Several factors determine whether or not a CNS infection develops such as the virulence of the organism, the status of the host's immune system, the size of the infectious inoculum, and the presence or absence of inherent or medication-related immunosuppression (Hall, 2008). The ability to detect the presence of a CNS infection has been greatly aided by the availability of imaging techniques such as computed tomography (CT) and magnetic resonance imaging (MRI) that can demonstrate the intracranial compartment. These same radiological techniques also allow for the response to treatment to be monitored. Newer image-guided surgical approaches using neuronavigation or intraoperative-MRI allow neurosurgeons to access remote regions of the brain that harbour infection which can expedite the identification of the causative agent leading to the prompt initiation of appropriate treatment. Rapid isolation of the organism combined with surgical decompression of neural elements, if necessary, can help to improve clinical outcomes and reduce neurological morbidity and mortality. The organisms that cause infection after neurosurgery can be significantly different from the aetiologic agents found in spontaneous CNS infection. Our focus will be on those organisms that require neurosurgical intervention either for identification, the relief of brain compression causing neurological symptoms, or that are the result of having had a surgical procedure involving the CNS. The primary infectious processes that affect the CNS are meningitis (**Fig. 97.1**), encephalitis (**Fig. 97.4**), cranial epidural abscess (**Fig. 97.2**), subdural empyema (**Figs. 97.3 and 97.4**), and brain abscess (**Fig. 97.5**).

Classification

Bacteria

Bacteria are probably responsible for the majority of CNS infections for which neurosurgeons are consulted. Those bacteria that represent the patient's endogenous skin flora that leads to the majority of postoperative neurosurgical infections are *Staphylococcus aureus* and *Staphylococcus epidermidis*. Hospital-acquired pathogens that include Gram-negative bacilli and fungi are often resistant to multiple antimicrobial agents making their treatment difficult. Those bacteria that are often responsible for spontaneous meningitis are *Haemophilus influenzae* type b, *Neisseria meningitidis, Streptococcus pneumoniae*, and *Listeria monocytogenes*. Postoperative and traumatic cerebrospinal fluid (CSF) leaks are known sources for meningitis with half of the cases caused by the Gram-negative bacilli *Pseudomonas aeruginosa, Klebsiella* species (sp.), and *Escherichia coli. Mycobacterium tuberculosis* can be a cause of lepto-pachymeningitis and can also present as calcified intraparenchymal lesions representing microabscesses.

Shunt infections are most commonly due to coagulase-negative *Staphylococcus epidermidis* (Naradzay et al., 1999). Other bacteria known to cause shunt infections are *S. aureus*; the Gram-negative bacteria *Acinetobacter baumannii, Escherichia coli, Klebsiella pneumoniae*, and *Pseudomonas aeruginosa*; the diphtheroid *Propionibacterium acnes*; and anaerobes (Sacar et al., 2006). Immunocompromised patients can develop shunt infections due to *Candida* sp. Polymicrobial shunt infection can occur in 11% to 20% of cases (Grandhi et al., 2014).

Aerobic and anaerobic organisms, particularly *Streptococcus milleri*, from the paranasal and otogenic sinuses can cause cranial epidural abscesses or subdural empyemas. Staphylococci and Gram-negative bacilli can cause cranial epidural abscess and subdural empyemas after neurosurgery (Hall, 2008). Anaerobic organisms such as streptococci and *Bacteroides* sp. from an otogenic or dental source are those most responsible for the development of brain abscess. Following head trauma, brain abscess due to aerobic isolates such as *S. aureus*, streptococci, and Gram-negative bacilli are common (Hall, 2008). *Staphylococcus* sp. brain abscess are most common in intravenous drug users and after craniotomy as a result of inoculation from contaminated skin (Kim and Hall, 2014).

Viruses

Viral infections of the CNS can cause meningitis, encephalitis of the brain, and transverse myelitis of the spinal cord. Viral meningitis is relatively common and does not usually require neurosurgical intervention whereas encephalitis is much less common, far more serious, and may require neurosurgery. Although there are numerous viruses the can affect the CNS, those where neurosurgery may be consulted are limited to herpes simplex virus

Fig. 97.1 Axial CT scan of the head in a 1-month-old newborn boy showing hydrocephalus and diffuse enhancement around the brain stem indicative of meningitis that was found to be due to *Escherichia coli*.

Fig. 97.3 Axial non-contrast CT scan of the head showing a subdural empyema over the left cerebral hemisphere extending into the interhemispheric fissure with associated mass effect. The source of the infection was bilateral maxillary sinusitis due to *Streptococcus milleri*.

type 1 or 2 (HSV-1 or HSV-2), human immunodeficiency virus (HIV) type 1 or 2, and the human JC polyomavirus. Herpes simplex virus (HSV) causes 2% to 5% of encephalitis in the United States (Domachowske et al., 2014) usually due to HSV-1 in more than 90% of cases (Whitley, 2006). The virus has a predilection for the temporal lobes and subfrontal cortex which is best seen on MRI as an area of increased signal on diffusion-weighted imaging. The fact that the virus crosses the Sylvian fissure discriminates this infectious process from an intrinsic brain tumour. The

HIV causes acute viral meningitis in 5% to 10% of patients with the acquired immunodeficiency syndrome (AIDS), either when the virus is acquired or during the seroconversion phase (Fukuta and Byers, 2014). When HIV infects the brain, it can cause encephalitis and involvement of the spinal cord can result in acute transverse myelitis. In immunocompromised patients and in up to 25% of those with AIDS, the JC virus causes progressive multifocal leukoencephalopathy (PML) (Berger and Levy, 1993).

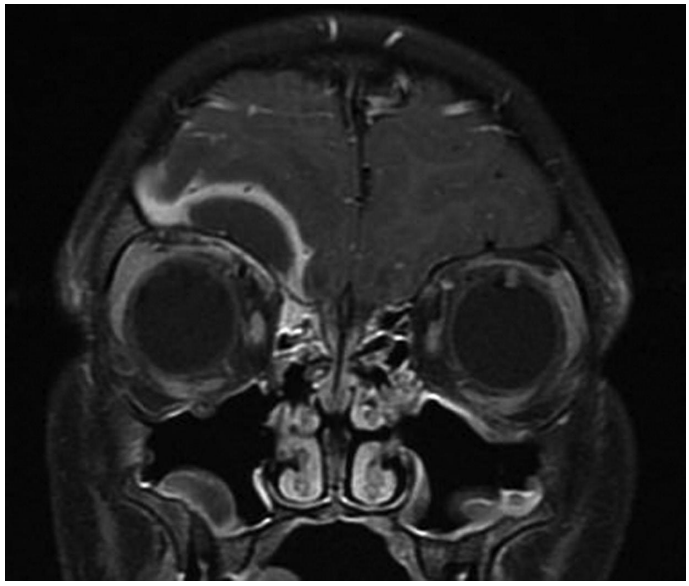

Fig. 97.2 Contrast-enhanced coronal T1-weighted MRI scan of the brain demonstrating a cranial epidural abscess due to chronic sinusitis which is also visible in a 10-year-old boy. Because of the prior administration of antibiotics before sinus cultures were obtained, the causative organism was never identified.

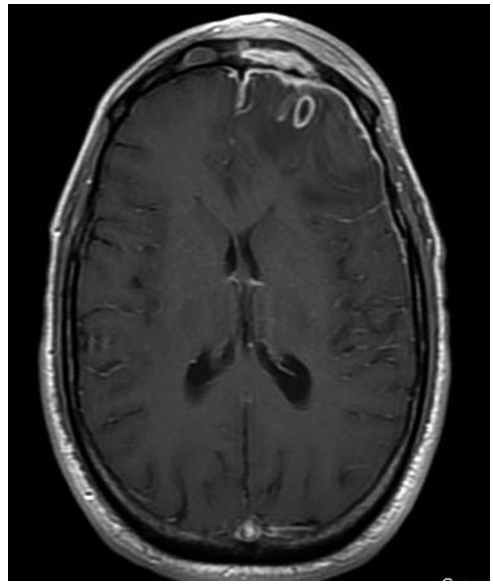

Fig. 97.4 Axial contrast-enhanced T1-weighted MRI scan of the head revealing a left frontal subdural empyema with encephalitis from frontal sinusitis which is also visible. The organism responsible for the infection was *Staphylococcus epidermidis*.

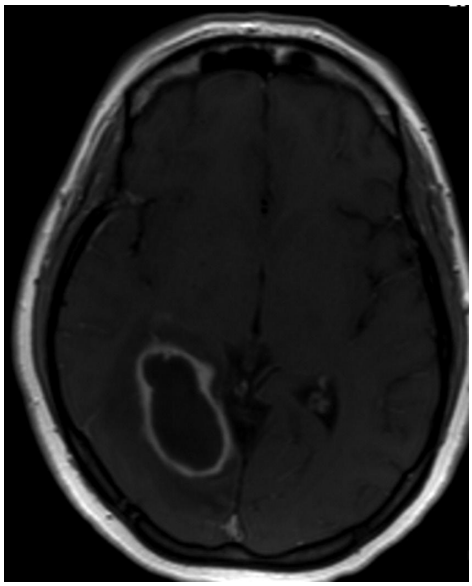

Fig. 97.5 Axial contrast-enhanced T1-weighted MRI scan of the head revealing a right occipital brain abscess. *Bacteroides fragilis* was cultured from the purulent collection that was thought to have resulted from poor dentition.

Fungi

Fungal infections of the CNS are usually manifest as meningitis or brain abscess. Clinically significant fungal infections of the CNS are usually identified in patients with altered immune function that is due to AIDS, diabetes mellitus, medication-induced immunosuppression (i.e. corticosteroids, chemotherapy, antiorgan transplant rejection medications, and broad-spectrum antibiotics), cancer, neutropenia, thermal injuries, collagen vascular diseases, hepatic disease, intravenous drug use, chronic pulmonary disease, Cushing syndrome, dehydration, ketoacidosis, anaemia, leukopenia, malnutrition, splenomegaly, chronic granulomatous disease, and prior craniotomy (Hall and Kim, 2014). Meningitis is most commonly caused by *Cryptococcus neoformans* and *Cryptococcus gattii*, whereas brain abscess is most often due to *Aspergillus* sp. Because it spreads through the bloodstream, *Candida albicans* can lead to the formation of micro- and macro-abscesses. Basilar leptomeningitis resulting in CSF obstruction and hydrocephalus is the most common form of CNS involvement by *Coccidioides immitis*. *Histoplasma capsulatum* can present either as a basilar leptomeningitis with hydrocephalus or as intraparenchymal small miliary granulomas or large histoplasmomas. Chronic meningitis or intracerebral blastomycomas are caused by *Blastomyces dermatitidis*. Vasculitis of the intracranial vasculature leading to mycotic aneurysm formation can be caused by *Candida albicans, Coccidioides immitis, Aspergillus fumigatus*, and *Mucor* sp. *Aspergillus* sp. and mucormycosis are aggressive fungal infections that usually involve the brain through the medium- and large-sized arteries resulting in the development of a mycotic aneurysm or by presenting with an intracerebral haemorrhage or ischaemic infarct from vascular occlusion (Hall and Kim, 2014). Infarcted brain tissue serves as the perfect medium for propagation of the fungus. If the proximal large arteries are invaded by fungi the clinical presentation may be a subarachnoid haemorrhage. *Scedosporium apiospermum* is the asexual form of *Pseudallescheria boydii* and usually presents as a brain abscess or rarely as meningitis (Hall and Kim, 2014).

Parasites

Parasitic involvement of the CNS is primarily due to two helminth tapeworms that cause cysticercosis and echinococcosis. Because of the worldwide increase in international travel to areas where certain parasites are endemic, these infections are becoming more commonplace. Cysticercosis is the most common parasitic disease of the CNS and is caused by the pork tapeworm *Taenia solium*. The tapeworm *Echinococcus granulosus* is responsible for the cystic form of CNS echinococcosis or hydatid disease (Akhaddar and Boucetta, 2014). Cysticerci are more commonly found in the brain parenchyma than in the subarachnoid space and cause encephalitis and seizures. Basal meningitis occurs when the meninges are involved, and hydrocephalus can result when the cysts obstruct the aqueduct of Sylvius or the fourth ventricle.

Cystic hydatidosis is the most common form of this disease to affect the brain and spine in humans. Hydatid cysts are usually solitary in the brain and the spine, where the vertebral body is more often involved in echinococcosis than in cysticercosis (Hall, 2015). In hydatid disease, symptoms due to the compression of neural elements are most commonly related to where the cyst is located in the brain or spine.

Amoebiasis is a parasitic disease caused by the protozoa *Naegleria fowleri, Acanthamoeba* sp., and *Balamuthia* sp. Free-living amoebas tend to cause encephalitis or meningoencephalitis. Cerebral amoebiasis has become a more recent concern of the medical community because it can develop in both normal and immunocompromised individuals and is generally fatal. Those conditions that are associated with the development of cerebral amoebiasis in immunocompromised individuals include AIDS, liver disease, diabetes mellitus, organ transplantation, renal failure, alcoholism, intravenous drug use, and the administration of corticosteroids or chemotherapy (Hall, 2012b).

Diagnostic techniques

Obtaining appropriate specimens is essential for determining the causative organism and assisting in the choice of effective antimicrobial therapy. Intraoperative cultures are most useful for diagnosing a hardware infection that involves neurosurgical implants although superficial cultures can be difficult to interpret because the most common offending organisms are normal skin flora (Fukuta and Byers, 2014). Ideally, the initiation of antimicrobial therapy should be delayed until adequate specimens have been collected unless the delay poses an unacceptable risk for the patient.

Cerebrospinal fluid

If postoperative meningitis is suspected, a lumbar puncture can be performed provided there is no evidence of mass effect on imaging studies that could potentially lead to a herniation syndrome. The opening pressure of the cerebrospinal fluid (CSF) can be elevated in meningitis and the colour of the fluid may be cloudy or turbid instead of being clear. The white blood cell (WBC) count can be elevated above the normal value of 0–5 mm^3 with a predominance of

neutrophils being present. A CSF glucose to blood glucose ratio of less than 0.5 is considered abnormal and the CSF protein level can be elevated. Around 1–2 ml of CSF should be sent for bacterial culture and 5–10 ml should be sent for acid-fast bacillus or fungal culture. The CSF culture is considered the diagnostic gold standard, however if prior antimicrobial therapy has already been started the chance of identifying the offending organism falls to less than 50% (Fukuta and Byers, 2014). Nucleic acid amplification tests such as the polymerase chain reaction (PCR) in the CSF may be useful for excluding bacterial meningitis or when antibiotic treatment has been started and the culture results are negative. Gram stain of the CSF will demonstrate bacteria in 50% of *L. monocytogenes* or Gram-negative bacilli cases and in up to 90% of *S. pneumoniae* cases (Fukuta and Byers, 2014). In the patient with a suspected ventriculoperitoneal shunt infection, CSF specimens obtained by valve puncture or from the ventricular catheter are more likely to yield microorganisms than CSF that is collected through a lumbar puncture. To detect the acid-fast mycobacteria in tuberculous meningitis, the Ziehl-Neelson and the Kinyoun stains are used.

In HSV encephalitis, the CSF can show a mononuclear pleocytosis, red blood cells suggestive of haemorrhagic necrosis, decreased glucose levels, and an elevated protein level (Domachowske et al., 2014). Polymerase chain reaction is the gold standard for HSV and HIV detection in CSF. Because HSV is rarely cultured from the CSF, a brain biopsy is often required to make the diagnosis. An additional role for neurosurgery in HSV encephalitis may be the performance of an emergency cranial decompression in the face of uncal herniation that occurs in a delayed manner of more than 10 days (Domachowske et al., 2014). In PML, the CSF is usually normal and the detection of the viral DNA by PCR is the diagnostic test of choice (Domachowske et al., 2014). Detection of protein 14-3-3 in the CSF is highly specific and sensitive for the diagnosis of classic Creutzfeldt–Jakob disease (CJD) (Defebvre et al., 1997).

Candida albicans can be detected in the CSF using a PCR-based test and by measuring a *Candida*-specific mannan antigen titre (Hall and Kim, 2014). Complement fixation antibodies to cryptococcal antigen, *Histoplasma* antigen, *Aspergillus* galactomannan, and *Coccidioides* sp. can identify fungal infection in the CSF. An India ink preparation can detect *C. neoformans* in the CSF and if infected brain tissue is obtained through surgery a Gomori methenamine silver stain may be used to demonstrate *Aspergillus* sp. or *Mucor* sp. (Hall and Kim, 2014).

The CSF in cysticercosis and hydatid disease is usually unremarkable and should not be sampled in the presence of significant intracranial mass effect in order to prevent a herniation syndrome. The CSF in amoebic meningoencephalitis can be haemorrhagic and demonstrate an elevated WBC count. Amoeba can be identified occasionally in the CSF on a wet mount and antibodies and PCR can be used to detect the infection in CSF (Hall, 2012b). Giemsa or Wright stains of the CSF should be used to demonstrate the trophozoites in primary amoebic meningitis (Fukuta and Byers, 2014).

Blood

C-reactive protein (CRP) can be significantly elevated in virtually all cases of intracranial infection. The erythrocyte sedimentation rate (ESR) is also usually elevated in CNS infections but not as frequently as is the CRP. The ESR and the CRP levels can also be used to follow the patient's response to antimicrobial therapy. Blood cultures can be useful in diagnosing a ventriculoatrial shunt infection although they are unlikely to be helpful in diagnosing the presence of a ventriculoperitoneal shunt infection.

Serum serology can be used to diagnose coccidioidomycosis and antigen tests for *Cryptococcus* sp. and *H. capsulatum* can establish the diagnosis in disseminated disease (Hall and Kim, 2014). Enzyme-linked immunoelectrotransfer blot is the serodiagnostic test of choice in cysticercosis with a sensitivity of 98% and a specificity of 100% although the sensitivity is only 30% in single cerebral lesions (Akhaddar and Boucetta, 2014). The serologic diagnostic test of choice for CNS echinococcosis is based on the detection of immunoglobulin G antibodies to hydatid cyst fluid-derived native or recombinant antigen B subunit on an enzyme-linked immunosorbent assay (ELISA) or immunoblot assay (Akhaddar and Boucetta, 2014).

Other tests

Herpes simplex encephalitis can demonstrate paroxysmal lateral epileptiform discharges on electroencephalography (Domachowske et al., 2014).

TORCH infections

Perinatal infections can result in congenital anomalies. Infections acquired *in utero* or during delivery can lead to fetal or neonatal mortality and early or late childhood morbidity. Five common infections with similar presenting features such as rash and ocular findings were categorized together and designated TORCH (Toxoplasmosis, Other (syphilis, enteroviruses, varicella-zoster virus, and parvovirus B19), Rubella, Cytomegalovirus (CMV), and Herpes simplex virus) infections (Stegmann and Carey 2002). Of the five virus types comprised in the TORCH acronym, CMV has emerged at the most common congenital viral infection. These infections cause mild maternal morbidity but can have serious consequences for the fetus and despite treatment of the maternal infection there is no effect on fetal outcome (Stegmann and Carey, 2002).

A high index of suspicion for perinatal infection is essential for a timely diagnosis and the rapid initiation of appropriate treatment. Clinical manifestations that are suggestive of a congenital TORCH infection can include macrocephaly, seizures, hearing loss, cataracts, rash, hydrops fetalis, congenital heart disease, hepatosplenomegaly, jaundice, and thrombocytopenia. These clinical findings are not limited to TORCH infections and can be seen in other diseases and conditions. The classic triad for congenital toxoplasmosis is chorioretinitis, hydrocephalus, and intracranial calcifications however most infants with the disease are asymptomatic without apparent abnormalities at birth. Herpes simplex virus infection in the newborn has three patterns of presentation: localization to the skin, eyes, and mouth; localization to the CNS; or widespread dissemination.

Asymptomatic infants are not routinely screened for congenital infection however they may be tested for specific pathogens based on their clinical presentation (de Jong et al., 2013). Indiscriminate screening for congenital infection by measuring TORCH titres is expensive and has a poor diagnostic yield although the identification of IgM antibodies is suggestive of infection in the newborn (Khan and Kazzi, 2000). Laboratory abnormalities such as thrombocytopenia, anaemia, elevated transaminases, and elevated serum direct and indirect bilirubin levels can be seen in congenital CMV infection. The

diagnosis of congenital CMV infection is established by isolating the virus from urine or saliva and the culture will frequently become positive after one to three days of incubation (Demmler, 1991).

Treatment of newborns with asymptomatic infection is not recommended. The use of ganciclovir to treat symptomatic CMV disease should only be considered in carefully selected cases.

Antibiotic principles

Because the brain is particularly sensitive to damage caused by inflammation, the limited immunologic responses that result from antigenic challenge is known as immunologic privilege (Nigam and Lesniak, 2014). The CNS vasculature is responsible for preventing ions and solutes from entering the brain parenchyma and for enhancing regional cerebral blood flow when needed (Nigam and Lesniak, 2014). The blood–brain barrier (BBB) consists of endothelial cells which comprise the walls of the microvasculature, pericytes, and astrocytes. The tight junctions between endothelial cells inhibit the diffusion of hydrophilic molecules into the brain. In the presence of a CNS infection, WBC will migrate across the inflamed BBB through endothelial cells by diapedesis while leaving the tight junctions intact (Engelhardt and Wolburg, 2004).

Antibiotic penetration into the CNS is variable depending on which antimicrobial agent is selected to treat the infection and to what extent the cerebral meninges are inflamed. The compromise of the BBB that occurs in the face of infection will often allow hydrophilic antibiotics to enter into the CNS and the CSF. Lipophilic drugs such as vancomycin and the fluoroquinolones cross the BBB very well. Aminoglycosides and β-lactam antibiotics do not cross the BBB easily because they are hydrophilic compounds (Kim and Hall, 2014). Antibiotics are categorized as bacteriostatic or bactericidal. The bacteriostatic antimicrobial agents require an intact immune system to kill bacteria.

The administration of intraventricular or intrathecal antibiotics usually requires the presence of an external ventricular drain or a lumbar drain, respectively, to assure adequate delivery into the CSF. Intraventricular antibiotics have been recommended for the treatment of ventriculitis and for surgical prophylaxis at the time a paediatric shunt is placed (Gruber et al., 2009). Antibiotics that are considered epileptogenic, such as the beta-lactams, should not be administered intraventricularly despite their poor penetration of the BBB.

The widespread indiscriminate use of some antibiotics has resulted in the emergence of organisms that are resistant to those agents at an alarming rate with methicillin-resistant *Staphylococcus aureus* (MRSA) being one of the more concerning bacterial strains. Vancomycin was developed to guard against the development of bacterial resistance, yet new resistant bacterial strains are emerging such as vancomycin-resistant enterococci (VRE) and vancomycin-resistant *S. aureus* (VRSA). Those bacteria that are resistant to vancomycin are now treated with linezolid, until resistance to this agent emerges. The use of handwashing and alcohol-based hand sanitizers reduce the prevalence of antibiotic-resistant bacterial strains such as MRSA in the hospital setting (Kim and Hall, 2014). In surgical cases where MRSA infection is likely, vancomycin may be a better preoperative prophylactic antibiotic than cefazolin.

Perioperative infection control

There are two specific areas where direct intervention can lead to the prevention of a postoperative neurosurgical infection that include preoperative antibiotic administration and the maintenance of a sterile surgical field. The timing of preoperative parenteral antibiotic administration is important to prevent surgical site infections (SSIs). In general, intravenous antibiotics should be administered before the surgical incision is made to assure that a bactericidal concentration of the antibiotic is present in the tissue when the skin is incised (Hall, 2015). For an antibiotic to prevent the development of an infection, the drug must be present in the tissue before the bacteria gain access to that same tissue (Kainth et al., 2014). There is no evidence that antibiotics should be continued for an extended period after surgery is concluded and extending the duration of treatment beyond 24 hours should be discouraged to prevent the development of resistant organisms. In addition, there is no evidence to support the administration of multiple doses of antibiotics versus one single dose of antibiotics for neurosurgical prophylaxis (Kainth et al., 2014). The North American Spine Society developed an evidence-based guideline for prophylactic antibiotics in complex spine surgery that called for the administration of a single dose of a broad-spectrum antibiotic that covered Gram-positive organisms and was given before the skin was incised and allowed time for adequate tissue levels of the drug to be reached (Kainth et al., 2014; Hall, 2015). Allowance was made for re-dosing the antibiotics if the surgical case was lengthy or if it was associated with significant blood loss. The continued administration of antibiotics after completion of the operative case can lead to urinary tract and gastrointestinal infections such as *Clostridium difficile* colitis due to the suppression of the normal host flora (Hall, 2015). Antibiotics that are used to treat resistant organisms should not be used for surgical prophylaxis in order to prevent the further propagation of antibiotic-resistant organisms. The antibiotic selected for prophylaxis should be effective against those organisms that are most likely to cause an infection at the parent institution.

Although parenteral antibiotic administration is the primary therapeutic modality used for neurosurgical prophylaxis, the topical administration of antibiotics has become an accepted common practice particularly when a foreign body is being implanted. Antibiotic solutions such as Bacitracin have long been used to irrigate wounds prior to surgical closure. The drug selected for the irrigation fluid should be bactericidal for the local institutional flora and should possess minimal potential toxic side effects (Kainth et al., 2014). In preparing the skin for a clean neurosurgical procedure there are several issues that must be considered. The question of whether it is necessary to remove scalp hair has been a topic of great debate. In a large Cochrane database review of 11 randomized controlled trials that included more than 5000 patients, the question of whether or not preoperative hair removal from any part of the body reduced the incidence of SSI was analysed (Tanner et al., 2008). Three independent reviewers concluded that there was no evidence that the incidence of SSI was influenced by the presence or absence of hair. However, it was found that the SSI rate was higher if a razor was used to shave the hair compared to an electric clipper or depilatory creams (Hall, 2012a).

In the face of placing an indwelling permanent foreign body such as a ventriculoperitoneal shunt, many neurosurgeons will opt to clip the hair in the hope of preventing a future shunt infection that would lead to the removal of the device even though the literature does not support hair removal in either the paediatric or adult populations (Hall, 2012a). Maintaining a patient's hair, particularly when removing a benign tumour such as a meningioma, will enhance patient satisfaction without increasing their risk for a postoperative infection.

Additional measures are necessary to assure the sterility of the skin prior to making the skin incision. In one report where the postoperative neurosurgical infection rate was 0.8% in 2111 cases, the surgical scrub included three components. Betadine surgical scrub (Purdue Pharma, Stamford, CT) was initially used to expose any bacteria located deep within the hair follicles to antimicrobial agents. Alcohol solution was next used to remove the foam associated with the preliminary scrub. Lastly, DuraPrep (3M, St. Paul, Minnesota) or ChloraPrep (CareFusion, San Diego, CA) surgical solutions were applied and allowed to dry on the surgical site before draping. In the event that the hair was not removed, DuraPrep and ChloraPrep should not be used as part of the surgical prep because the hair and the surgical site must be completely dry before beginning surgery to avoid the potential for an intraoperative fire, which can add a substantial delay to the start of the procedure.

Disinfection and sterilization of surgical instruments is essential to prevent the transmission of infectious pathogens to patients having neurosurgery. Failure to comply with established guidelines for disinfection and sterilization has led to previous outbreaks of infection. The instruments used for patient care are placed in three categories, critical, semicritical, and non-critical, based on the degree of the risk of infection that is associated with the use of those instruments (Rutala and Weber, 2004). Critical items such as the surgical instruments used to perform neurosurgery have a high risk of causing infections if they are contaminated with any microorganisms. Sterilization of critical items is essential because any contamination by antimicrobial agents will most likely result in the development of first a localized and then a potentially widespread serious infection. The critical items used in neurosurgery should be purchased sterile or steam sterilized if possible. If the critical item is heat sensitive then it should be treated with ethylene oxide, hydrogen peroxide gas plasma, or with liquid chemical sterilants (Rutala and Weber, 2004). Chemical sterilants that are used in surgery include 2.4% or over glutaraldehyde-based formulations, 1.12% glutaraldehyde with 1.93% phenol/phenate, 7.5% stabilized hydrogen peroxide, 7.35% hydrogen peroxide with 0.23% peracetic acid, 0.2% or over peracetic acid, and 1.0% hydrogen peroxide with 0.08% peracetic acid (Rutala and Weber, 2004). The exposure time for these chemical sterilants is from 3 to 12 hours except for 0.2% or over peracetic acid where the sporicidal time is 12 minutes at 50–56°C (Rutala and Weber, 2004). Instruments should be cleaned to remove any organic or inorganic material before they are either steam or chemically sterilized. Some limitations to liquid chemical sterilants include the inability to wrap sterilely the surgical instrument after it is processed which means that maintaining sterility during storage is impossible and instruments exposed to chemical sterilants should be rinsed afterwards with water which is generally not sterile (Rutala and Weber, 2004).

Prion disease

Prion disease or transmissible spongiform encephalopathy is caused by the abnormal deposition of the insoluble isoform of a cellular protein PrP^c in the CNS (Domachowske et al., 2014). There are three forms of the disease: (1) sporadic; (2) familial; and (3) iatrogenic, following exposure to the protein (Belay, 1999). The TSEs that are considered familial include familial Creutzfeldt–Jakob disease (CJD), Gersmann–Sträussler–Scheinker disease, and fatal familial insomnia (Belay, 1999). A newly recognized variant form of CJD (vCJD) was reported in young people in the United Kingdom in 1996 (Belay, 1999). Transmission of bovine spongiform encephalopathy from cows to humans is now known to be the cause of vCJD. Exposure to the protein has resulted when patients received human growth hormone prepared from human cadavers, dural grafts, corneal transplants, and exposure to contaminated neurosurgical instrumentation (Domachowske et al., 2014). Definitive diagnosis usually requires a brain biopsy with histopathological examination, immunocytochemical staining, and Western blotting to detect the PrP^c protein (Budka et al., 1995).

There are strict decontamination procedures for the neurosurgical instruments that are used in performing a brain biopsy in the patient suspected of having Creutzfeldt–Jakob disease (CJD) in order to prevent transmission of the infectious agent to other individuals having neurosurgery with the same instruments. When performing a brain biopsy in a standard operating room, cover work surfaces with disposable material that can be removed and incinerated after the procedure is completed. Ideally, the best way to ensure that there is no risk of infectivity of contaminated instruments is to discard and then destroy them by incineration (WHO, 1999). If the surgical facility has the ability to quarantine instruments until the diagnosis is confirmed than that is an acceptable alternative to the needless destruction of expensive instruments in suspected cases. If destruction of the surgical instrumentation is impractical, then they should be handled in the following manner: (1) keep the instruments moist until they are decontaminated; (2) clean instruments as soon as possible after use; (3) do not mix contaminated with non-contaminated instruments; and (4) proceed with the recommended method of decontamination (WHO, 1999).

The decontamination process for the durable instrumentation used during surgery is justifiably very involved. Two or more methods of decontamination should be combined when sterilizing against these agents. An example is the use of both heat and sodium hydroxide (NaOH) either simultaneously or consecutively. Hot alkaline hydrolysis both cleans and inactivates macromolecules. Liquids that are used for cleaning contaminated instrumentation should be decontaminated *in situ* by the addition of NaOH or sodium hypochlorite and then disposed of as routine hospital waste. Absorbent material that is used to soak up liquid spills of contaminated cleaning fluid should be incinerated after use. The recommended decontamination methods for cleaning contaminated heat-resistant instruments in the order of preference are listed in **Box 97.1**.

Controversies

Several controversial issues exist in neurological surgery that pertain to the prevention and management of CNS infections. A recent

Box 97.1 Decontamination methods for cleaning heat-resistant instruments used in performing a brain biopsy for Creutzfeldt–Jakob disease

1. Immerse in 1 Normal (N) NaOH and heat in a gravity displacement autoclave for 30 minutes at 121 degrees centigrade (°C). Clean and rinse in water before routine sterilization.
2. Immerse in 1N NaOH or sodium hypochlorite at a concentration of 20 000 ppm available chlorine for 1 hour. Transfer to water and heat in a gravity displacement autoclave for 1 hour at 121°C prior to cleaning and routine sterilization.
3. Immerse in 1N NaOH or sodium hypochlorite for 1 hour then remove and rinse in water. Transfer to an open pan and heat for 1 hour in a gravity displacement (121°C) or porous load (134°C) autoclave before cleaning and routine sterilization.
4. Immerse in 1N NaOH and boil for 10 minutes at atmospheric pressure. Clean and rinse in water before routine sterilization.
5. Immerse in sodium hypochlorite (preferred) or NaOH (alternative) at ambient temperature for 1 hour. Clean and rinse in water before routine sterilization.
6. Autoclave at 134°C for 18 minutes (WHO, 1999).

and somewhat controversial practice that has come under some scrutiny is the application of intrasite vancomycin powder (VP) to prevent SSI most notably in complex spine surgery. The rationale for using VP is to achieve high local concentrations of the drug at the location where an infection would be most likely to develop with a minimal amount of systemic redistribution. This non-Food and Drug Administration off-label use of VP has been analysed through systemic reviews and meta-analyses. A recent review of the clinical evidence for the use of in-the-wound VP to prevent infection in spinal surgery found that the odds of developing a deep infection in patients that received VP was 0.23 times the odds of experiencing an infection without VP (Bakhsheshian et al., 2014). It was estimated that VP could save up to $220 000 to $500 000 per 100 patients undergoing complex spinal surgery. Potential disadvantages to the use of VP were an increase in vancomycin resistance, an increase in hardware infections due to bacteria not covered by vancomycin, systemic side effects from the vancomycin such as hypotension, colitis, skin flushing known as red man syndrome, and Stevens-Johnson syndrome, and whether there is any influence of the drug on spinal fusion rates. The appropriate dosage of topical VP in children and adults is unknown.

FURTHER READING

Hall, W.A. (2008). Cerebral infectious processes. In: Loftus, C. (ed.) *Neurosurgical Emergencies*, 2nd edition, pp. 115–24. New York, NY: Thieme Publishers.

McClelland, S. 3rd & Hall, W.A. (2007). Postoperative central nervous system infection: incidence and associated factors in 2111 neurosurgical procedures. *Clin Inf Dis*, **45**, 55.

Rutala, W.A. & Weber, D.J. (2004). Disinfection and sterilization in health care facilities: what clinicians need to know. *Clin Inf Dis*, **39**, 702.

Tanner, J., Woodings, D., & Moncaster, K. (2008). Preoperative hair removal to reduce surgical site infection. *Cochrane Database Syst Reviews*, **2**, CD004122.

WHO (1999). WHO infection control guidelines for transmissible spongiform encephalopathies. Report of a WHO consultation. Geneva, Switzerland, pp. 23–6, March, 1999.

REFERENCES

Akhaddar, A., & Boucetta, M. (2014). Parasitic infections of the central nervous system. In: Hall, W. & Kim, P. (eds.) *Neurosurgical Infectious Diseases: Surgical and Nonsurgical Management*, pp. 81–94. New York, NY: Thieme Publishers.

Bakhsheshian, J., Dahdaleh, N.S., Lam, S.K., Savage, J.W., & Smith, Z.A. (2014). The use of vancomycin powder in modern spine surgery: systematic review and meta-analysis of the clinical evidence. *World Neurosurg*, **12**, 33.

Belay, E.D. (1999). Transmissible spongiform encephalopathies. *Annu Rev Microbiol*, **53**, 283.

Berger, J.R., & Levy, R.M. (1993). The neurological complications of human immunodeficiency virus infection. *Med Clin North Am*, **7**, 1.

Budka, H., Aguzzi, A., Brown, P., et al. (1995). Neuropathological diagnostic criteria for Creutzfeldt–Jakob disease (CJD) and other human spongiform encephalopathies (prion diseases). *Brain Pathol*, **4**, 459.

Defebvre, L., Destee, A., Caron, J., Ruchox, M.M., Wurtz, A., & Remy, J. (1997). Creutzfeldt–Jakob disease after an embolization of intercostal arteries with cadaveric dura mater suggesting a systemic transmission of the prion agent. *Neurology*, **48**, 1470.

de Jong, E.P., Vossen, A.C., Walther, F.L., & Lopriore, E. (2013). How to use neonatal TORCH testing. *Arc Dis Child Educ Pract Ed*, **98**, 93.

Demmler, G.J. (1991). Infectious Diseases Society of America and Centers for Disease Control. Summary of a workshop on surveillance for congenital cytomegalovirus disease. *Rev Infect Dis*, **13**, 315.

Domachowske, J.B., Suryadevara, M., & Hall, W.A. (2014). Viral infections of the central nervous system. In: Hall, W. & Kim, P. (eds.) *Neurosurgical Infectious Diseases: Surgical and Nonsurgical Management*, pp. 51–67. New York, NY: Thieme Publishers.

Engelhardt, B. & Wolburg, H. (2004). Mini-review: transendothelial migration of leukocytes: through to front door or around the side of the house? *Eur J Immunol*, **34**, 2955.

Fukuta, Y., & Byers, K. (2014). Microbiological diagnosis of central nervous system infections. In: Hall, W. & Kim, P. (eds.) *Neurosurgical Infectious Diseases: Surgical and Nonsurgical Management*, pp. 16–29. New York, NY: Thieme Publishers.

Grandhi, R., Harrison, G., & Tyler-Kabara, E. (2014). Implanted devices and central nervous system infection. In: Hall, W. & Kim, P. (eds.) *Neurosurgical Infectious Diseases: Surgical and Nonsurgical Management*, pp. 209–30. New York, NY: Thieme Publishers.

Gruber, T.J., Riemer, S., & Rozzelle, C.J. (2009). Pediatric neurosurgical practice patterns designed to prevent cerebrospinal fluid shunt infection. *Pediatr Neurosurg*, **45**, 456.

Hall, W.A. (2008). Cerebral infectious processes. In: Loftus, C. (ed.) *Neurosurgical Emergencies*, 2nd edition, pp. 115–24. New York, NY: Thieme Publishers.

Hall, W.A. (2012a). To clip or not to clip, that is the question? *World Neurosurg*, **77**, 291.

Hall, W.A. (2012b). Free-living amoebas: is it safe to go in the water? *World Neurosurg*, **78**, 610.

Hall, W.A. & Kim, P.D. (2014). Fungal infections of the central nervous system. In: Hall, W. & Kim, P. (eds.) *Neurosurgical Infectious Diseases: Surgical and Nonsurgical Management*, pp. 68–80. New York, NY: Thieme Publishers.

Hall, W.A. (2015). Spinal parasites. *World Neurosurg*, **83**, 39.

Hall, W.A. (2015). Vancomycin powder in spine surgery: still a work in progress. *World Neurosurg*, **83**, 1051–2.
Kainth, D.S., Terzic, D., & Haines, S.J. (2014). Neurosurgical antibiotic prophylaxis. In: Hall, W. & Kim, P. (eds.) *Neurosurgical Infectious Diseases: Surgical and Nonsurgical Management*, pp. 185–95. New York, NY: Thieme Publishers.
Khan, N.A. & Kazzi, S.N. (2000). Yield and costs of screening growth-retarded infants for torch infections. *Am J Perinatol*, **17**, 131.
Kim, P.D., & Hall, W.A. (2014). Antibiotics and the development of resistance. In: Hall, W. & Kim, P. (eds.) *Neurosurgical Infectious Diseases: Surgical and Nonsurgical Management*, pp. 30–4. New York, NY: Thieme Publishers.
Kim, P.D. & Hall, W.A. (2014). Bacterial brain abscess. In: Hall, W. & Kim, P. (eds.) *Neurosurgical Infectious Diseases: Surgical and Nonsurgical Management*, pp. 95–103. New York, NY: Thieme Publishers.
McClelland, S. 3rd & Hall, W.A. (2007). Postoperative central nervous system infection: incidence and associated factors in 2111 neurosurgical procedures. *Clin Inf Dis*, **45**, 55.
Naradzay, J.F., Browne, B.J., Rolnick, M.A., & Doherty, R.J. (1999). Cerebral ventricular shunts. *J Emerg Med*, **17**, 311.
Nigam, P. & Lesniak, M. (2014). Immunology of the central nervous system. In: Hall, W. & Kim, P. (eds.) *Neurosurgical Infectious Diseases: Surgical and Nonsurgical Management*, pp. 3–15. New York, NY: Thieme Publishers.
Rutala, W.A. & Weber, D.J. (2004). Disinfection and sterilization in health care facilities: what clinicians need to know. *Clin Inf Dis*, **39**, 702.
Sacar, S., Turgut, H., Toprak, S., et al. (2006). A retrospective study of central nervous system shunt infections diagnosed in a university hospital during a 4-year period. *BMC Infect Dis*, **6**, 43.
Stegmann, B.J. & Carey, J.C. (2002). TORCH infections. Toxoplasmosis, other (syphilis, varicella-zoster, parvovirus B19), rubella, cytomegalovirus (CMV), and herpes infections. *Curr Womens Health Rep*, **2**, 253.
Tanner, J., Woodings, D., & Moncaster, K. (2008). Preoperative hair removal to reduce surgical site infection. *Cochrane Database Syst Reviews*, **2**, CD004122.
Whitley, R.J. (2006). Herpes simplex encephalitis: adolescents and adults. *Antiviral Res*, **71**, 141.
WHO (1999). WHO infection control guidelines for transmissible spongiform encephalopathies. Report of a WHO consultation. Geneva, Switzerland, pp. 23–6, March, 1999.

RELATED LINKS TO EBRAIN

Introduction to Neurological Infectious Diseases. https://learning.ebrain.net/course/view.php?id=1144
Preparing the Operative Site. https://learning.ebrain.net/course/view.php?id=96
Prions and Neurosurgery. https://learning.ebrain.net/course/view.php?id=71

98

Cranial infections

Thangaraj Munusamy, Boon Hoe Tan, and Eugene Yang

Introduction

Cranial infections continue to be an important cause of mortality and morbidity worldwide. To understand cranial infections, knowledge of anatomy is important because it relates to both pathogenesis, complications, and functional sequelae. Microorganisms, owing to their intrinsic properties and distinct characteristics, produce relatively specific clinical syndromes in cranial infections. Definitive treatment depends on prompt microbial identification and antimicrobial treatment, reduction of microbial load, relief of excessive pressure or mass effect and modulation of the host's immune response to allow successful microbial clearance while minimizing inflammation and oedema. In this chapter, we will discuss the management of common cranial infections and their associated clinical conundrums from a neurosurgical perspective.

Brain abscess

Brain abscess is defined as a focal intracranial infection that starts as a focus of cerebritis that gradually progresses into a collection of pus with capsular formation. Brain abscesses can arise from three principal sources:

1. Direct extension of an adjacent source of infection
2. Hematogenous spread from a distant source
3. Direct inoculation into brain through a dural breach

Examples of direct extension from adjacent sources include brain abscess secondary to suppurative otitis media, mastoiditis, or anteriorly through the paranasal sinuses. These direct extensions usually affect either the temporal lobes, cerebellum, or the frontal lobes or the sellar and parasellar regions. Hematogenous spread from a distant source include septic emboli showers from infective endocarditis, as well as distant sources of infection such as an intraabdominal collection or osteomyelitis. The body's natural protective mechanism is to filter these pathogens through the capillary circulation of the lungs and in the presence of AV shunts these protective mechanisms can be bypassed, for example, congenital cyanotic heart disease or pulmonary arteriovenous malformation such as in Osler-Weber-Rendu disease (Helweg-Larsen et al., 2012; Chenran et al., 2014; Yakut et al., 2015).

Brain abscess is more commonly reported in immunocompromised patients: patients who are HIV positive, receiving chemotherapy for treatment of malignancy, receiving steroids, or immunosuppressive treatment for underlying organ transplantation or inflammatory disorders.

Direct breach of dura can form a direct portal for migration of bacteria into the intracranial cavity usually as a result of trauma, for example, depressed skull fractures and inoculation of foreign body, or as a result of neurosurgical procedures. Abscess following neurosurgery may result from the nature of the surgical procedure itself such as in implant surgery (electrodes, shunts), external ventricular drains, intracranial pressure monitors, or insertion of gliadel wafers in glioma surgery (McGovern et al., 2003).

Stages of infection

Four pathological stages of cerebral abscess formation are recognized:

1. Early cerebritis
2. Late cerebritis
3. Early capsule formation
4. Late capsule formation

The early stages of abscess formation are characterized by early cerebritis (day 1–3), which involves tissue necrosis, accumulation of neutrophils, and onset of oedema. From day 4–9, the earlier neutrophilic infiltrate progresses into a predominantly macrophage and lymphocytic infiltrate. Early capsule formation starts at day 10–13, which is thinner on ventricular side. This may lead to abscess rupture into ventricular cavity leading to ventriculitis. Late capsule formation starts after day 14, and characterized by formation of gliosis, collagenous, and granulation layers (Erdogan and Cansever, 2008).

Pathogens

The commonest organisms to cause cerebral abscess are streptococci, particularly *strep. Milleri* group, followed by anaerobic bacteria, staphylococci, and Gram-negative bacteria. Enteric Gram-negative organisms such as pseudomonas, proteus, and *E. coli* usually result from extension from otogenic or paranasal sinus foci, systemic bacteraemia, or in immunocompromised patients. Streptococci

account about 54% of cases, *Staphylococci* 15%, Gram-negative bacteria 8%, anaerobic bacteria 17%, and nocardia 2% (Helweg-Larsen et al., 2012; Chenran et al., 2014; Yakut et al., 2015).

Organism such as *Listeria monocytogenes*, and *Nocardia* should be considered in immunocompromised states such as HIV patients, patients with malignancy, transplant recipients, patient whom are on treatment with chemotherapy, or patient whom are on long-term steroid exposure.

Mortality from *Nocardia* brain abscesses is significant, with rates of 31–77% and treatment is usually with trimethoprim-sulfamethoxazole regime for a prolonged period (3 to 12 months) (Weerakkody et al., 2015).

The finding of a tuberculous brain abscess requires investigation to rule out underlying HIV exposure. Diagnostic criteria as described in 1978 by Whitener are: 1. Macroscopic evidence of true abscess formation within the brain substance (at surgery or biopsy) 2. Histological confirmation that inflammation in the abscess was composed predominantly of vascular granulation tissue containing acute and chronic inflammatory cells. 3. Positive pus culture or evidence of acid-fast bacilli. Female patients tend to be more afflicted compared to males with a mean age of 23.9 years. Incidence of tuberculous brain abscess is 4–8% of CNS tuberculosis in the absence of HIV infection (Mohindra et al., 2016).

Tuberculoma presents a diagnostic challenge, its appearance on conventional CT and MR imaging mimics multiple other entities including metastatic brain tumours, neurocysticercosis, toxoplasmosis and fungal brain abscess (**Fig. 98.1**). They are firm, avascular, spherical masses that range from 2 to 10 cm in diameter, well-circumscribed, and contain areas of caseating necrosis with tubercle bacilli. CSF evaluation in isolated tuberculoma is generally non-specific. Management is usually with medical therapy. The indication for surgery is limited as most tuberculoma responds well with adequate antibiotic treatment and steroids. Occasionally, surgical treatment is warranted to establish diagnostic certainty or to relieve significant mass effect and underlying brain compression (Chatterjee, 2011; Monteiro et al., 2013).

With the widening therapeutic use of immunosuppressive treatments (steroids, immunomodulators chemotherapy), increasing prevalence of HIV and AIDS, and organ transplant recipients, fungal infections are becoming increasingly frequent. Commonly reported organisms include CNS aspergillosis, Scedosporium, Cryptococcus neoformans and endemic mycoses (Vergara et al., 2015). Fungal brain abscess has a high mortality rate especially in immunocompromised patients.

Clinical findings

The most common symptoms are fever (60%), neck stiffness (25%), nausea or vomiting (40%), focal neurological deficits (57%), seizures (21%), and impaired consciousness (45%) (Helweg-Larsen et al., 2012). The classical triad of headache, fever, and nausea or vomiting is only present in one in five cases. The triad of headache, fever with focal neurological deficits is only seen in one in four cases.

Headaches, change in mental status with confusion and drowsiness, accompanied with symptoms of nausea and vomiting may represent the presence of increased intracranial pressure from the mass effect large abscess collection or collections and perilesional oedema.

Neck stiffness or nuchal rigidity may occur in setting of abscess rupture into the ventricular cavity leading to ventriculitis and meningitis.

Focal neurological deficits are dependent on the location of an intracranial abscess, with resultant loss of function in the corresponding location of the brain. This may manifest as hemiparesis, personality change, visual field deficits, aphasia, nystagmus, and ataxia.

Radiological features

Magnetic resonance imaging provides both diagnostic accuracy and sensitivity and is considered the diagnostic neuroimaging of choice for investigation and workup of newly diagnosed brain abscess. Classically described as a ring-enhancing lesion on contrast-enhanced T1-weighted image. MRI also provides additional information such as the surrounding enhancing rim, and degree and extent of perilesional oedema that typically occurs with abscesses (**Fig. 98.2**).

In the cerebritis stage, pyogenic brain abscesses are T1 hypointense and T2 hyperintense with minimal or non-homogenous enhancement. Tuberculous cerebritis is seen as an ill-defined, hypoattenuated

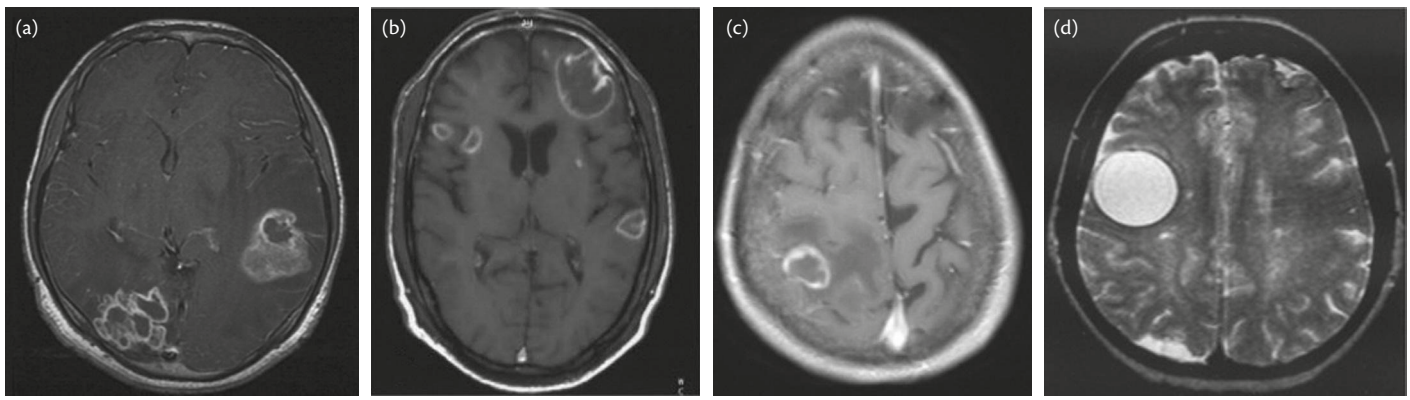

Fig. 98.1 MR imaging of CNS infections. (A) Cerebral tuberculoma (Helmy et al., 2011); (B) cerebral toxoplasmosis (Batra et al., 2004); (C) fungal brain abscess (Bagla et al., 2016); (D) cerebral hydatid cyst (Seckin et al., 2008).

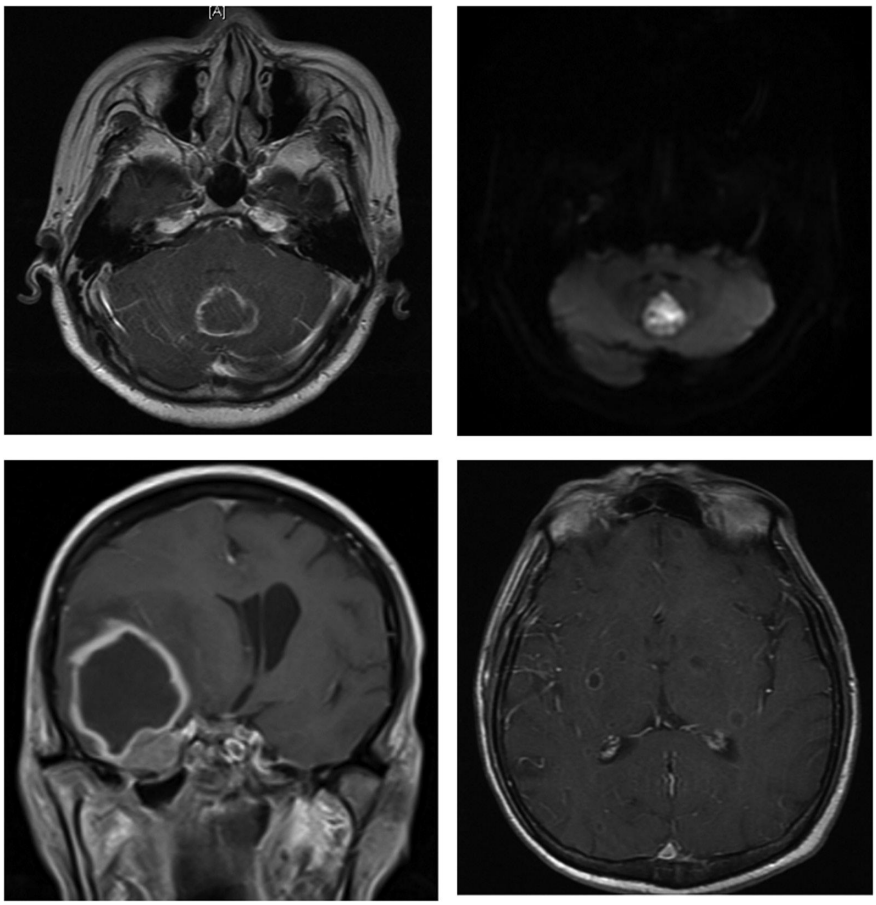

Fig. 98.2 MR imaging of pyogenic brain abscesses. (A and B) (Top row): cerebellar abscess appearing as a ring-enhancing lesion on contrast-enhanced T1-weighted image (A) and hyperintense on DWI (B). (C) (Bottom left): right temporal abscess in a patient with advanced nasopharyngeal carcinoma treated with radiotherapy. (D) (Bottom right): multiple abscesses in a patient with infective endocarditis.

areas of gyral enhancement. Fungal cerebritis is usually non-enhancing and located in the basal ganglia or deep white matter. All mature pyogenic, tubercular, and fungal abscesses demonstrate hypointensity on T1 imaging, hyperintensity on T2 imaging, and demonstrate good rim enhancement on contrast sequences. Most pyogenic and tubercular abscesses show a smooth or lobulated outer-wall. About half of fungal abscess have a creanated wall. Fungal abscesses also show intracavitary projections directed centrally from the wall without any contrast enhancement, this is not seen in other type of abscess on conventional MRI (Cartes-Zumelzu et al., 2004; Luthra et al., 2007). In immunocompromised patients, there may be relative lack of contrast enhancement which can confound diagnosis. There is a case report from 2004 of an immunocompromised patient post bone marrow transplantation which reported minimal enhancement despite fulminant cerebral toxoplasmosis (Ionita et al., 2004).

Areas of restricted diffusion are seen in pyogenic abscesses on diffusion-weighted imaging sequences (Fig. 98.2). Necrotic material is present within the abscess cavity which contains inflammatory cells, bacteria, and pus which restricts water-motion. MRI Imaging of pyogenic and tubercular abscesses will show increase signal in diffusion-weighted imaging (DWI) imaging with low apparent diffusion coefficient (ADC) values within the core of the cavity. In contrast, DWI and ADC in fungal abscess shows restricted diffusion in the projections and wall but not in the core of the abscess.

There is also some evidence to suggest the use of DWI to monitor response to medical therapy. DWI signals change from initial high signal intensity to low signal intensity, which suggest the disappearance of purulent content within the abscess core, indicating a good therapeutic response.

MR spectroscopy (MRS) in brain abscesses shows metabolites associated with hypoxia and cellular breakdown such as amino acids, lipid, lactate, acetate, and succinate in differing amounts between the various abscesses, and may help in distinguishing the subtypes of abscess (Cartes-Zumelzu et al., 2004; Luthra et al., 2007).

CT imaging with IV contrast enhancement typically reveals an area of low-density centre with rim enhancement peripherally.

MRI or CT also enables stereotactic guided abscess aspiration to facilitate microbiological diagnosis and decrease bacterial load.

Management

A multidisciplinary approach for management and treatment of cerebral abscess is required, involving a neurosurgeon, a neuroradiologist, and an infection disease specialist. The key principles to

consider is determining a microbiological diagnosis (from the abscess itself or from a potential source).

Although there is no absolute size threshold that necessitates surgical intervention, abscesses more than 2.5 cm in maximum dimension should ideally be treated surgical either through craniotomy and formal excision of the entire abscess cavity, or through needle aspiration of the abscess usually performed under stereotactic guidance. Excising abscesses in their entirety can improve radiological appearances but with additional risk, particularly of postoperative seizure. Smaller abscess can simply be needle aspirated under image guidance (Radoi et al., 2013).

Whenever an intracranial abscess is identified, the ultimate source and repository of infection must be removed to prevent recurrence. Resection of otomastoiditis, drainage of suppurative otitis media or sinus infection, drainage of distant sources of infection such as intra-abdominal collections, wound debridement of infected wound should all be considered concurrently with abscess treatment. Occasionally post-traumatic abscess may contain foreign materials such as bone chips, gun-shot pellets, bullets, or stones, and, if safe to do so, these should be removed to reduce recurrence risk.

Stereotactic aspiration of abscess has the advantage that it is simple, with less potential morbidity than craniotomy, however it is associated with increased risk of recurrences. Craniotomy and excision of the abscess has a lower incidence of recurrence, and is particularly indicated if there is a significant mass effect, if there are difficulties in the diagnosis, if the abscess is due to trauma with introduction of foreign materials, or in the posterior fossa (Ratnaike et al., 2011; Helweg-Larsen et al., 2012; Radoi et al., 2013; Aras et al., 2016).

The abscess capsule provides a physical barrier to entry of antibiotics into the abscess cavity mitigating their effectiveness, furthermore the acidic abscess environment may also inhibit the effectiveness of antibiotics.

Abscess material should be sent for microscopy and extended culture to enable identification of the offending organism. Aspiration of abscess will thus facilitate commencement of targeted antibiotic therapy based on culture sensitivity results. Commencement of empirical antibiotic therapy is dependent on several factors including—suspected bacterial involvement based on history and examination, preliminary results of Gram stain, and patterns of microbiology of the local setting.

Choice of antibiotics should take into account of the suspected source of abscess (i.e. sinusitis vs. otogenic vs. post-traumatic), pharmacokinetics of CSF penetration, duration, and route of administration (i.e. intravenous vs. intraventricular). Common empirical antibiotic regimes include use of third-generation cephalosporins with metronidazole for additional anaerobic cover especially in cases of direct adjacent source of infection (i.e. sinusitis, otogenic). In cases where there is direct inoculation such as post-trauma or post brain surgery, a combination of third-generation cephalosporins with additional Gram-positive coverage with vancomycin can be considered. Duration of antibiotic therapy is typically for 6 to 8 weeks, usually given intravenously at high dose to facilitate blood brain barrier penetration. Monitoring of treatment response requires both neuroimaging and biochemical (such as plasma C-reactive protein) markers allowing titration of antibiotic therapy duration (Cartes-Zumelzu et al., 2004; Luthra et al., 2007).

Fungal brain abscess is treated with antifungal drugs, for example, voriconazole for aspergillus infection and amphotericin B for candida and mucormycosis. External ventriculostomy may be used to deliver intrathecal antifungal drugs, however this practice is not universally accepted. Fungal brain abscess is associated with significant mortality especially in immunocompromised patients (Grannan et al., 2014; Ma et al., 2015; Gavito-Higuera et al., 2016; Patterson et al., 2016).

Corticosteroid use in brain abscess is controversial, it can reduce brain swelling with improvement of mass effect and impending herniation. However, it can also lead to a decreased host immune response to infection, and may ameliorate formation of the abscess wall leading to more destruction of perilesional viable brain tissue, and delayed containment of the abscess. Steroid treatment prior to surgery does not appear to significantly change outcome: in a retrospective study 21% treated patients versus 23% non-treated patients had GOS less than 3 at discharge (Helweg-Larsen et al., 2012). Functional outcome in patients who received steroids after surgery was also not significant with a GOS less than 3 in 25% on steroids versus 20% without steroids (Helweg-Larsen et al., 2012). In an alternative case series, use of steroids was associated with higher mortality compared to non-steroid group (15.6% vs. 3.9%) (Ratnaike et al., 2011; Radoi et al., 2013; Aras et al., 2016).

A combination of surgical and medical treatments is advocated for the management of cerebral abscess. However, this also needs to take into account of the overall picture of the patient, that is, patient factors (perioperative anaesthetic, cardiac, and respiratory risks) and pathological factors (size, number, and location of abscesses).

Neurocysticercosis and echinococcosis

Neurocysticercosis is the most common parasitic infection of the brain worldwide, with the second being echinococcosis (hydatid cyst disease). Neurocysticercosis is caused by the encysted larval stage of the tapeworm *Taenia solium*. They can present either in the parenchymal form or extraparenchymal form. The parenchymal form is the most common and usually involves the grey/white matter junction, with a more favourable prognosis compared to extraparenchymal. The extraparenchymal form shows a wider range of locations throughout the CNS and is associated with higher parasitic burden load and poorer prognosis. It can lead to arachnoiditis, inflamed meninges, entrapment of cranial nerves, and blockage of CSF flow with resultant hydrocephalus. An absolute diagnosis of neurocysticercosis if often challenging as surgery is not indicated in most cases which thereby precludes histological identification of parasites. Comprehensive neuroimaging criteria have been introduced to improve degree of diagnostic certainty (**Fig. 98.3**). Treatment consists of antihelminthic drugs such as albendazole and praziquantel, antiepileptics, and steroids to dampen down the inflammatory process. Surgery may consist of cyst extirpation or insertion of CSF diversion devices for treatment of hydrocephalus (Baird et al., 2013; Del Brutto et al., 2017; Gripper and Welburn, 2017).

Cerebral hydatid disease is a rare parasitic infestation caused by the larvae of Echinococcus tapeworm. It is endemic in the Middle East, the Mediterranean, Africa, India, Australia, and parts of South America. Intracranial echinococcosis could present either in the cystic form (*E. granulosus*) or the alveolar form (*E. multilocularis*). It most frequently occurs in the supratentorial region, mainly in the vascular territory of the middle cerebral artery. Symptoms are related

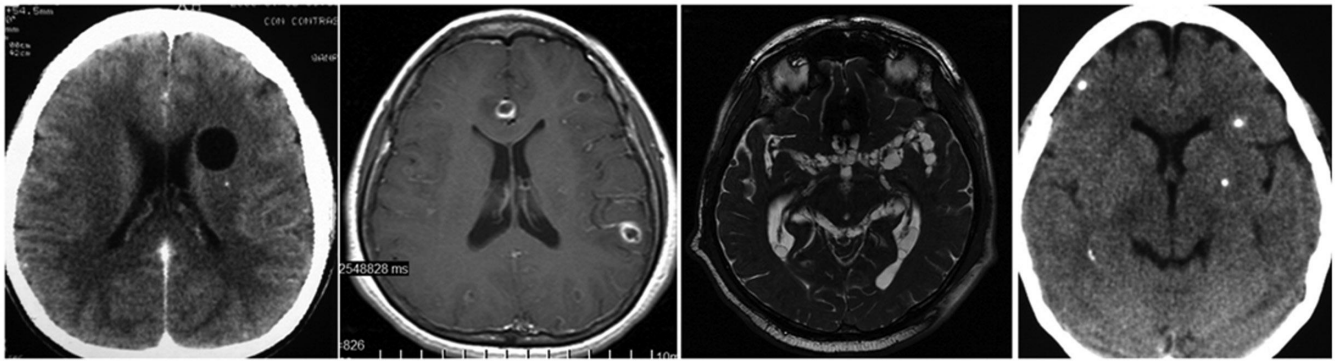

Fig. 98.3 Major neuroimaging criteria for neurocysticercosis (Del Brutto et al., 2017). Cystic lesion without discernible scolex (A), ring-enhancing lesions (B), multilobulated cysts in basal subarachnoid cisterns, (C) and typical parenchymal brain calcifications (D).

to local mass effect due to the location of the cyst or raised intracranial pressure. Computed tomography and magnetic resonance imaging are reliable diagnostic tools. Radiologically the cyst appears spherical and well-circumscribed with no enhancement, calcification, or perilesional oedema (Fig. 98.1). The alveolar form shows a well-defined multiseptated mass consisting of solid and cystic components with calcification in the solid portion. Cystic fluid is isodense or isointense with CSF. The cyst is usually solitary, although multilocular and multiple cysts in the brain have been reported. Extracranial disease is frequently absent in solitary cerebral hydatid cyst; however, it is mandatory to screen the rest of the body. Differential diagnoses include arachnoid cyst, epidermoid cyst, neurenteric cyst, cystic primary brain tumour or metastases, and brain abscess.

Surgical excision of the cyst using Dowling's method has been classically described: a wide scalp flap and dissection of the atrophic cortex, lowering the head of the operating table to benefit from gravity and the use of warm saline between the hydatid cyst and brain parenchyma to deliver the cyst. Inadvertent rupture of the cyst during manipulation may lead to spread of the parasite and anaphylactic shock (Bukte et al., 2004; Luo et al., 2013; Ulutas et al., 2015).

Extradural and subdural collection

An empyema is a collection of pus within a normal anatomical space therefore a collection in the subdural space is deemed an empyema, while a collection in the extradural space, which is only a potential space, is designated an abscess. Extradural abscesses are often located in the frontal region and are limited by sutures. Patients with extradural abscess may have subtle clinical signs and neurological deficits only occur when there is sufficient mass effect caused by the collection. If the dura mater is breached or with spread via dural venous anastomoses, empyema can progress into the subdural space or cause thrombophlebitis and cerebritis. Subdural empyema is associated with a high morbidity and mortality. As well as extension from extradural empyema it can occur secondary to haematogenous spread or as a postoperative complication.

Subdural empyema

Subdural empyema is a neurosurgical emergency associated with mortality rate of up to 20% and morbidity rate of 50% despite intervention (Le Beau et al., 1973; Nathoo et al., 1999). In immunocompetent patients, it occurs most commonly in the second decade of life and there is a marked male predominance with a male-to-female ratio of 3:1 (Osborn and Steinberg, 2007). Outcome depends on factors such as age, comorbidities, primary organism, and prompt diagnosis and treatment. Subdural empyema has the propensity to spread rapidly due to lack of fibrin capsule and anatomical barriers in the subdural space. The most common sources of infection are from otitis media and infection of the paranasal or mastoid air sinuses. Other causes include direct spread from meningitis, haematogenous spread from distant sites, surgical site infection and head trauma with skull fracture and dural tear (Munusamy and Dinesh, 2015). Concomitant intraparenchymal abscess may occur in 6–22% of cases and epidural abscess in 9–17% (Osborn and Steinberg, 2007).

Clinical presentation

Patients with subdural empyema typically present with fever, headache, and altered mental state followed by rapid neurological deterioration. The median time from the onset of symptoms to diagnosis is two days (French et al., 2014). Seizures are common and occur in up to 63% of patients (Cowie and Williams, 1983). Other presenting symptoms will depend on underlying aetiology for example sinusitis, mastoiditis, otitis media, meningitis, postoperative wound infection, systemic infection, or head trauma. Progression into an expanding mass lesion results in signs and symptoms of raised intracranial pressure. Cerebral oedema and hydrocephalus may occur secondary to disruption of cerebral blood flow or CSF flow. Thrombosis of the cortical veins or dural venous sinuses from direct spread or septic emboli result in venous hypertension and may progress to cerebral infarction.

Pathogenesis

The pathogenesis of subdural empyema is similar to that of brain abscess. The causative microorganisms vary according to the primary source of infection. They are often monomicrobial, however polymicrobial infections are not uncommon especially if the source of infection is from the paranasal sinuses (Nathoo et al., 1999). Aerobic and microaerophilic *Streptococci* are usually implicated

in subdural empyema secondary to mastoiditis or sinusitis (Miller et al., 1987). In postoperative and post-traumatic subdural empyema, *Staphylococcus aureus* is commonly isolated whereas in the immunocompromised, *Klebsiella pneumonia* is often the culprit (Greenlee et al., 2003). Other causative microorganisms that have been reported include *Escherichia coli* and *Salmonella* species (Munusamy and Dinesh, 2015). Microbiological diagnosis of subdural empyema is based on positive culture of pus or infected material taken during surgical drainage or samples taken from the primary source or infection. The success rate for culturing bacteria from surgically evacuated subdural pus ranges from 54% to 81% (Mauser et al., 1987; Nathoo et al., 1999). Low culture positivity can be explained by the use of broad-spectrum antibiotics as empirical treatment for infection before sampling and difficulties in culturing anaerobic organisms.

Radiological features

Radiological diagnosis can be made by imaging with contrast-enhanced CT or MRI. Subdural empyema appears as a crescent-shaped collection that crosses suture lines on the surface of the brain below the cranial vault or adjacent to the falx or tentorium that typically show rim enhancement with administration of contrast media. However, occasionally contrast-enhanced CT may appear normal or show subtle brain swelling especially in chronic cases where well-organized subdural pus may fail to generate peripheral enhancement (Moseley and Kendall, 1984; Munusamy and Dinesh, 2015) (**Fig. 98.4**). In this instance, MRI is more sensitive in detecting subdural empyema particularly at the skull base, in the posterior fossa, or along the falx cerebri. Subdural empyema has high signal intensity on DWI and low signal intensity on ADC maps, similar to brain abscess and ventriculitis. Thus diffusion-weighted MR imaging can reliably distinguish subdural empyema from subdural hematoma or reactive subdural effusion that may also occur after trauma, surgery, or meningitis (Wong et al., 2004).

Treatment

The principles of treatment for subdural empyema consist of surgical evacuation of pus and bacteriological identification, eradication of the primary foci of infection and adequate antibiotic therapy (Miller et al., 1987). Surgical intervention varies between burr hole, craniotomy or craniectomy and controversy exists over the procedure that is most effective (Pathak et al., 1990). Results of all three have been shown to be comparable as long as effective drainage of purulent material and relief of mass effect was achieved (Bok and Peter, 1993). In general, if the empyema is non-viscous and there are no loculated collections, evacuation via burr holes is adequate and can avoid potential surgical complications associated with longer duration or more complex surgery. However, if the pus is thick or well organized, a craniotomy is recommended to allow adequate access and drainage (Munusamy and Dinesh, 2015) (**Fig. 98.4**). In some cases, the underlying brain may be markedly swollen necessitating craniectomy. Craniectomy should also be considered in the postoperative setting if there is intraoperative suspicion of osteomyelitis of the bone flap which may act as a devascularized nidus of ongoing infection. If the source of infection is from an otologic or extracranial focus, exploration and drainage of the primary source must be performed. Initiation of empirical antibiotic therapy without delay is recommended if the patient is septic and clinically unwell from

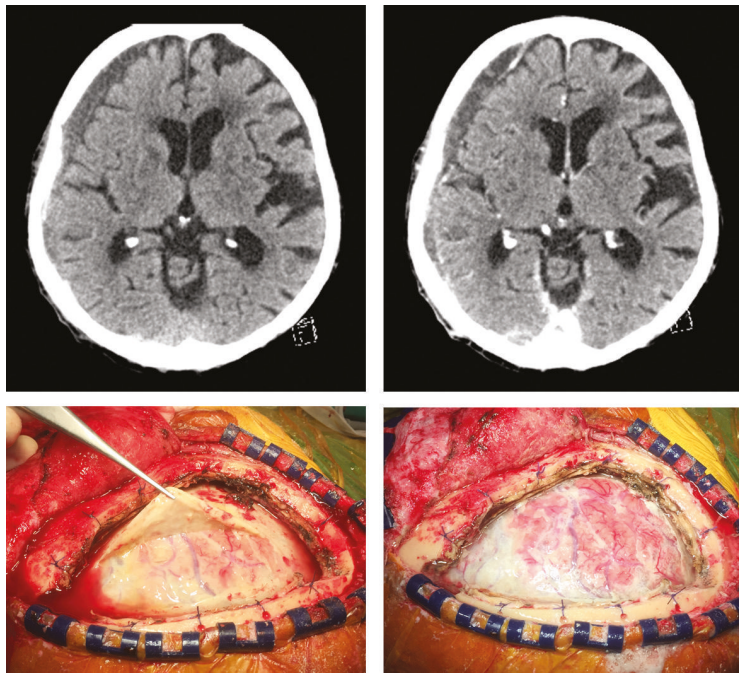

Fig. 98.4 Craniotomy and evacuation of subdural pus in a patient diagnosed with subdural empyema. (A and B) (Top row): CT scan before (A) and after (B) contrast media administration. Subtle contrast enhancement was seen in this case where the subdural pus was well organized. (C and D) (Bottom row): thick layer of subdural pus lifted off brain (C) and subdural space was irrigated with gentamicin-added saline solution. Underlying brain was hyperaemic but not swollen (D) thus bone flap was replaced, and antibiotic therapy continued.

the subdural empyema. Further antimicrobial therapy should be targeted against the causative microorganisms revealed by Gram stain or special bacterial stains, positive bacterial culture result and knowledge of the bacterial profile at the primary site of infection. Antibiotic therapy is usually continued for 4–6 weeks depending on the clinical and radiological response and expert advice from the infectious disease specialist and microbiologist should be sought at the earliest opportunity (Leys et al., 1986).

Postoperative subdural empyema has been described following craniotomy, but very rarely can be associated with burr hole drainage of chronic subdural haematoma. Presumably, the relatively simple and limited procedure minimizes tissue trauma and reduces the extent of bacterial inoculation. However, they are managed in a similar fashion where the goals of surgery are to achieve adequate decompression and evacuation of empyema. Burr holes are reopened and empyema drained however if this is insufficient conversion to craniotomy is mandatory. *Propionibacterium acnes*, a ubiquitous skin commensal can rarely be implicated with an indolent clinical presentation and course of progression (Gritchley and Strachan, 1996).

Cranial extradural abscess

Cranial extradural abscess is a suppurative infection that arises between the inner table of the skull and the dura as a result of contiguous spread from adjacent structures. It is traditionally associated with sinusitis, mastoiditis, otitis media and skull osteomyelitis (Calfee and Wispelwey, 1999). At present, the common causes are secondary to infection following neurosurgical procedures and head trauma with skull fracture and open wound. The bacteriology and pathogenesis of epidural abscess is similar to subdural empyema, but they have a sharp demarcation, slower progression rate, and an indolent course owing to the tight adherence of the dura mater to the skull. As a result it has an insidious onset and fever or headache may be the only clinical presentation. In some cases symptoms this may take weeks to develop. However, if left untreated, the infection may extend and progress to cause complications such as skull osteomyelitis, dural venous sinus thrombosis, purulent leptomeningitis, subdural empyema, and brain abscess (Pradilla et al., 2009). Contrast-enhanced CT and MRI demonstrate a lentiform-shaped enhancing lesion and a thickened dural surface that reliably distinguishes epidural abscess from sterile epidural collection. In addition, CT may also show bony destruction and fragmentation in patients with underlying skull osteomyelitis or mastoiditis. Interestingly, DWI may be an adjunct for differentiating between subdural and epidural empyemas. Subdural empyema shows high signal intensity on DWI whereas epidural empyema tends to be of low or mixed signal intensity (Tsuchiya et al., 2003). The mainstay of treatment and management of cranial epidural abscess is similar to subdural empyema. Surgical drainage of pus can be adequately performed via burr hole or craniotomy. Rarely the skull bone would need to be removed if there is severe underlying osteomyelitis (Tsai et al., 2003).

Skull osteomyelitis

Osteomyelitis of the skull usually results from spread of otogenic or odontogenic infections, head trauma with open wound or following surgical procedures involving the scalp or cranium. Patients present with fever and symptoms associated with the underlying cause. Forehead scalp swelling is seen in osteomyelitis of the frontal bone due to formation of subperiosteal abscess that was first described as Pott's puffy tumour by Sir Percivall Pott in 1760 (Kombogiorgas and Solanki, 2006). Gradenigo-Lannois syndrome is a rare complication of osteomyelitis involving the apex of the petrous temporal bone where patients present with a triad of symptoms consisting of diplopia due to abducens nerve palsy, ipsilateral periorbital or facial pain related to trigeminal nerve involvement and persistent otorrhoea associated with otitis media (Heshin-Bekenstein et al., 2014). Facial nerve or lower cranial nerves palsies may be seen in malignant otitis externa due to osteomyelitis of the skull base caused by *Pseudomonas* infection. *Aspergillus* infections have also been shown to cause skull-based osteomyelitis without any evidence of otitis externa (Pincus et al., 2009). Progression and extension of skull osteomyelitis may lead to sequelae of epidural abscess, subdural empyema, or brain abscess (Johnson and Batra, 2014). Anterior skull base osteomyelitis caused by mucormycosis is seen in many parts of the world, particularly in immunocompromised patients. The bacteriology of skull osteomyelitis depends on the site of infection and underlying cause. MRI is the diagnostic imaging modality of choice to detect changes to the diploë or cancellous bone and for detailed visualization of the skull base, cranial nerves, and soft tissues. In addition, leukocytosis and raised erythrocyte sedimentation rate (ESR) are helpful to make the diagnosis (Chang et al., 2003). Treatment of skull osteomyelitis consists of surgical debridement and biopsy or removal of infected bone flap followed by long-term antibiotic therapy directed against the responsible pathogen. Eradication of the primary source of infection is equally important to ensure successful treatment and to minimize the risk of recurrence (Pincus et al., 2009). Furthermore, there may be a role for hyperbaric oxygen therapy as an adjuvant therapy in the management of chronic refractory osteomyelitis of the skull base. Hyperbaric oxygen therapy has been suggested as an option in these cases as it enhances phagocytic oxidative killing of aerobic microorganisms and promotes angioneogenesis and osteoneogenesis (Prasad et al., 2014). Serial measurement of ESR or CRP are useful markers to monitor efficacy of treatment. Radiological follow-up with Gallium-67 bone scan can also be used to define transition from active to inactive osteomyelitis of the skull base (Chang et al., 2003). Prognosis is usually good if diagnosed and treated adequately.

Meningitis, ventriculitis, and ventriculoperitoneal shunt infections

Postoperative meningitis is a risk following neurosurgery in which the dura is breached with reported rates ranging between 0.14 to 9.2%. Patients commonly present with headache, fever, neck stiffness, change in mental status, and occasionally with nausea and vomiting. Delay in diagnosis may occur if patient symptoms such as headaches is attributed to postoperative pain, and fever symptoms are masked by the use of antipyretics. However, the clinical course of postoperative meningitis is not as fulminant as community-acquired meningitis and mortality is unusual (Srinivas et al., 2011).

Diagnosis of meningitis usually requires CSF sampling and analysis, usually via lumbar puncture. CSF examination in bacterial

meningitis reveals raised total CSF protein, low to low normal CSF glucose, and elevation of CSF white cell count associated with a neutrophilic shift. There is a higher rate of Gram-negative bacteria involvement in postoperative meningitis. In the developed world the most common causative organism is *S. aureus*. However, there are geographical variations such that in an Indian series the most common organisms were Gram-negative bacillus, pseudomonas aeruginosa, and klebsiella (Kourbeti et al., 2007; Dashti et al., 2008).

Appropriate antibiotic treatment, either intravenous or oral, is required for postoperative meningitis. In the first instance empirical antibiotic typically consists of a combination of vancomycin with third-generation of cephalosporins. If CSF sampling allows culture and sensitivity of the causative organism, antibiotic treatment should be tailored accordingly.

Ventriculitis remains a common problem in neurosurgery following temporary CSF diversion with external ventricular drains. A smaller group of patients develop ventriculitis as a result of rupture of a cerebral abscess into the ventricle. In this circumstance, the large bacterial load confers a poor prognosis.

Modern neurosurgical practice recommends antibiotic-coated or silver-lined ventricular catheters to decrease the incidence of ventriculitis (Keong et al., 2012; Athanasios et al., 2015).

Other factors that are associated with decreasing incidence of EVD infection include a standardized protocol for insertion, long subcutaneous tunnelling (>15 cm), minimal handling by both medical and nursing staff, aseptic technique for sampling of CSF, and decreasing frequency of CSF sampling (Lwin et al., 2012; Kubilay et al., 2013). Routine CSF sampling has not shown to be necessary for early detection of CSF infection (Hader and Steinbok, 2000).

Ventriculoperitoneal shunt (VP shunt) infection is defined as either early (less than 6 months) or late (more than 6 months). Patients usually present with non-specific symptoms such as fever, nausea and vomiting, irritability, change in mental states. VP shunt infection may also present as shunt malfunction. The most common pathogens involved in VP shunt infection are skin flora such as *S. epidemidis* and *S. aureus*.

The principles of treatment are removal of the infected shunt, accompanied by the use of systemic antibiotic with the use of temporary CSF diversion such as external ventricular drain, lumbar drain, or lumbar punctures. Antibiotics are continued until CSF polymorphs fall to normal allowing subsequent implantation of a new ventriculoperitoneal shunt. Pure medical treatment with antibiotics alone are less effective (James et al., 1980; Tamber et al., 2014).

Intracranial pressure monitoring and craniectomy in meningitis and encephalitis

There are no firm guidelines on the use of intracranial pressure monitoring for patients with meningitis and encephalitis. However, meningitis and encephalitis can result in severe cerebral oedema and cortical pseudolaminar necrosis with resultant raised ICP and herniation (Fig. 98.5). A recent study in Sweden compared an ICP intervention group versus a control group of patients with acute bacterial meningitis, showing significant decreased mortality in the intervention group (relative risk reduction of 68%); better neurological recovery was also seen in the ICP intervention group (Sala et al., 2009; Glimåker et al., 2014). There is also another reported case of severe cerebral oedema resulting from tuberculous meningitis which responded well with ICP monitoring and institution of ICP controlling measure, and the patient subsequently had a good neurological recovery (Trendelenberg et al., 2011).

Decompressive craniectomy in encephalitis is uncommon and may be considered in salvage situation where ICP is refractory to medical treatment. It is suggested that the long-term neurological outcome in herpes simplex encephalitis patient that received craniectomy does not differ significantly from patient which did not require craniectomy (Youenn et al., 2015; Algahtani et al., 2016).

Postoperative neurosurgical infections

Postoperative surgical site infection (SSI) is strictly defined by the Centre for Disease Control (CDC). SSI is divided into superficial incision SSI, deep incision SSI, and organ/space SSI.

Postcraniotomy SSI is a substantial cause of morbidity and mortality in postoperative neurosurgical patients. The incidence of postoperative neurosurgical SSI is between 3% and 5% depending on the series. Postcraniotomy SSI includes a wide spectrum from simple wound dehiscence and breakdown, underlying scalp infected collections, skull flap osteomyelitis, to subdural empyemas or intracerebral abscesses. The management of each individual condition are dealt with in the relevant sections.

There are several risk factors which are associated with increased risk of postcraniotomy SSI. These includes multiple operations, evidence of CSF leak, increased duration of surgery, altered sensorium, presence of comorbidities such as diabetes, and concurrent use of corticosteroids (Jiang et al., 2016). A study from Malaysia showed that patients with perioperative ASA 2 and clean contaminated wounds are significant risk factors for development of SSI (Buang and Haspani, 2012). The predominant bacteria identified in postcraniotomy SSI are *Staphylococcus aureus*, followed by *Acinetobacter* and *Enterobacter* (Buang and Haspani, 2012).

Numerous recommendations have been made for prevention of SSI, an exhaustive discussion of which is available on WHO website on Global Guidelines on the Prevention of Surgical Site Infection 2016—http://www.who.int/gpsc/ssi-prevention-guidelines/en/. Prophylactic antibiotics are widely regarded as a key preventative measure. This requires selection of appropriate antibiotic, administration within 1 hour preincision, and discontinuation within 24 hours after surgery. Other measures include the careful handling of soft tissues, good haemostasis, and a well approximated wound closure. There is some suggestion that the use of betadine irrigation decreases the risk of postop craniotomy SSI (Patel et al., 2014).

Superficial infections of the scalp are the commonest form of SSI. Typical manifestations include local erythema, swelling, and tenderness, which over time will progress to frank wound breakdown with formation of pus. Systemic symptoms such as fever, tiredness, and lethargy are generally late signs. Symptoms such as neck stiffness, altered mental status or new focal deficits warrants an investigation to ensure there is no extension of the superficial infection into the deeper structures for example subdural empyema or meningitis. In simple uncomplicated cases, treatment is predominantly with antibiotics, in particular with good Gram-positive cover. Surgical debridement of

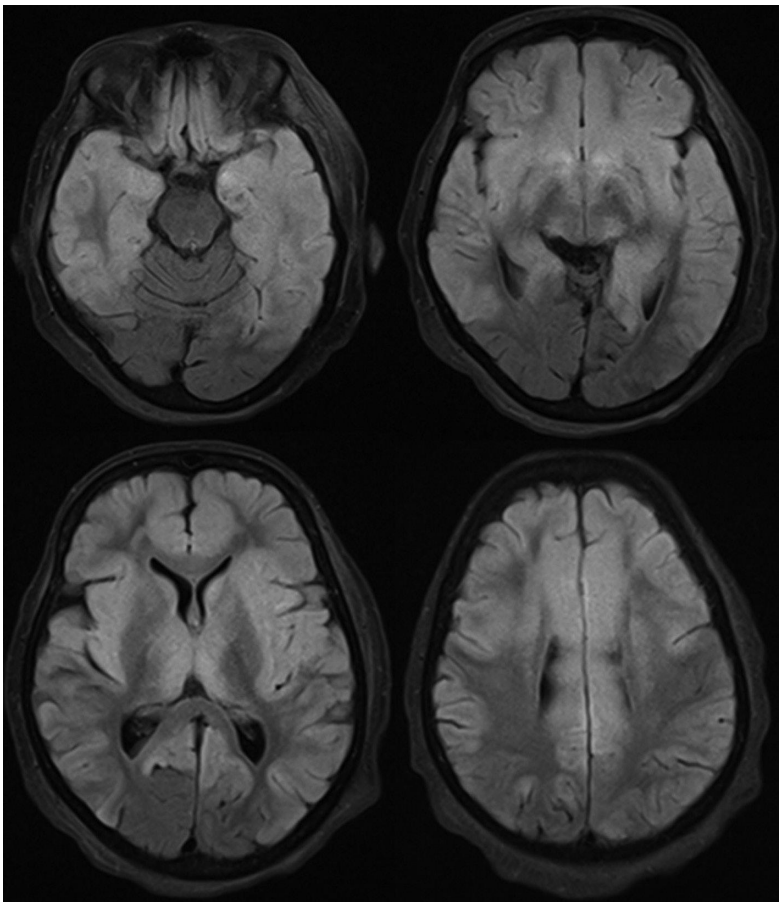

Fig. 98.5 MR imaging in herpes simplex virus (HSV) encephalitis showing extensive involvement of frontotemporal lobes and basal ganglia resulting in severe cerebral oedema and pseudolaminar necrosis (Algahtani et al., 2016).

the skin flap may be required in situations where there is an extensive infection or presence of underlying scalp collections.

FURTHER READING

Dashti, S.R., Baharvahdat, H., Spetzler, R.F., et al. (2008). Operative intracranial infection following craniotomy. *Neursurg Focus*, **24**, E10.

Kourbeti, I.S., Jacobs, A.V., Koslow, M., Karabetsos, D., & Holzman, R.S. (2007). Risk factors associated with post craniotomy meningitis. *Neurosurgery*, **60**, 317–26.

Le Beau, J., Creissard, P., Harispe, L., & Redondo, A. (1973). Surgical treatment of brain abscess and subdural empyema. *J Neurosurg*, **38**(2), 198–203.

Osborn, M.K. & Steinberg, J.P. (2007). Subdural empyema and other suppurative complications of paranasal sinusitis. *Lancet Infect Dis*, **7**(1), 62–7.

Ratnaike, T.E., Das, S., Gregson, B.A., & Mendelow, A.D. (2011). A review of brain abscess surgical treatment—78 years: aspiration versus excision. *World Neurosurg*, **76**(5), 431–6.

REFERENCES

Algahtani, H., Shirah, B., Hmoud, M., & Subahi, A. (2016). Nosocomial herpes simplex encephalitis: a challenging diagnosis. *J Infect Public Health*, **10**(3), 343–7.

Aras, Y., Sabanci, P.A., Izgi, N., et al. (2016). Surgery for pyogenic brain abscess over 30 years: evaluation of the roles of aspiration and craniotomy. *Turk Neurosurg*, **26**(1), 39–47.

Athanasios, A.A., Vardakas, K.Z., Polyzos, K.A., Tansarli, G.S., & Falagas, M.E. (2015). Antimicrobial-impregnated and -coated shunt catheters for prevention of infections in patients with hydrocephalus: a systematic review and meta-analysis. *J Neurosurg*, **122**, 1096–112.

Bagla, P., Loeffelholz, M., & Blanton, L.S. (2016). Cerebral phaeohyphomycosis by Fonsecaea monophora: report in a patient with AIDS and a ring enhancing lesion. *Med Mycol Case Rep*, **12**, 4–7.

Baird R.A., Wiebe, S., Zunt, J.R., Halperin, J.J., Gronseth, G., & Roos, K.L. (2013). Evidence-based guideline: treatment of parenchymal neurocysticercosis. *Neurology*, **80**(15), 1424–9.

Batra, A., Tripathi, R.P., & Gorthi, S.P. (2004). Magnetic resonance evaluation of cerebral toxoplasmosis in patients with the acquired immunodeficiency syndrome. *Acta Radiol*, **45**(2), 212–21.

Bok A.P. & Peter J.C. (1993). Subdural empyema: burr holes or craniotomy? A retrospective computerized tomography-era analysis of treatment in 90 cases. *J Neurosurg*, **78**(4), 574–8.

Buang, S.S. & Haspani, M.S. (2012). Risk factors for neurosurgical site infections after a neurosurgical procedure: a prospective observational study at Hospital Kuala Lumpur. *Med J Malaysia*, **67**(4), 393–8.

Bukte, Y., Kemaloglu, S., Nazaroglu, H., Ozkan, U., Ceviz, A., & Simsek, M. (2004). Cerebral hydatid disease: CT and MR imaging findings. *Swiss Med Wkly*, **134**(31–32), 459–67.

Calfee, D. & Wispelwey, B. (1999). Brain abscess, subdural empyema, and intracranial epidural abscess. *Curr Infect Dis Rep*, **1**(2), 166–71.
Cartes-Zumelzu, F.W., Stavrou, I., Castillo, M., Eisenhuber, E., Knosp, E., & Thurnher, M.M. (2004). Diffusion-weighted imaging in the assessment of brain abscesses therapy. *AJNR Am J Neuroradiol*, **25**, 1310–17.
Chang, P.C., Fischbein, N.J., & Holliday, R.A. (2003). Central skull base osteomyelitis in patients without otitis externa: imaging findings. *AJNR Am J Neuroradiol*, **24**(7), 1310–16.
Chatterjee, S. (2011). Brain tuberculomas, tubercular meningitis, and post-tubercular hydrocephalus in children. *J Pediatric Neurosci*, **6**(Suppl 1), S96–100.
Chenran, Z., Hu, L., Wu, X., Hu, G., Ding, X., & Lu, Y. (2014). A retrospective study on the aetiology, management and outcome of brain abscess in an 11-year, single-centre study from China. *BMC Infect Dis*, **14**, 311.
Cowie, R. & Williams, B. (1983). Late seizures and morbidity after subdural empyema. *J Neurosurg*, **58**(4), 569–73.
Dashti, S.R., Baharvahdat, H., Spetzler, R.F., et al. (2008). Operative intracranial infection following craniotomy. *Neursurg Focus*, **24**, E10.
Del Brutto, O.H., Nash, T.E., White, A.C., Jr. et al. (2017). Revised diagnostic criteria for neurocysticercosis. *J Neurol Sci*, **372**, 202–10.
Erdogan, E. & Cansever, T. (2008). Pyogenic brain abscess. *Neurosurg Focus*, **24**(6), E2.
French, H., Schaefer, N., Keijzers, G., et al. (2014). Intracranial subdural empyema: a 10-year case series. *Ochsner J*, **14**(2), 188–94.
Gavito-Higuera, J., Mullins, C.B., Ramos-Duran, L., Olivas Chacon, C.I., Hakim, N., & Palacios, E. (2016). Fungal infections of the central nervous system: a pictorial review. *J Clin Imaging Sci*, **6**, 24.
Glimåker, M., Johansson, B., Halldorsdottir, H., et al. (2014). Neurointensive treatment targeting intracranial hypertension improves outcome in severe bacterial meningitis: an intervention-control study. *PLoS One*, **9**(3), e91976.
Grannan, B., Yanamadala, V., Venteicher, A.S., Walcott, B.P., & Barr, J.C. (2014). Use of external ventriculostomy and intrathecal antifungal treatment in cerebral mucormycotic abscess. *J Clin Neurosci*, **21**(10), 1819–21.
Greenlee, J.E. (2003). Subdural empyema. *Curr Treat Options Neurol*, **5**(1), 13–22.
Gripper L.B. & Welburn, S.C. (2017). Neurocysticercosis infection and disease—a review. *Acta Tropica*, **166**, 218–24.
Gritchley, G. & Strachan, R. (1996). Postoperative subdural empyema caused by Propionibacterium acnes—a report of two cases. *Br J Neurosurg*, **10**(3), 321–3.
Hader, W.J. & Steinbok, P. (2000). The value of routine cultures of the cerebrospinal fluid in patients with external ventricular drains. *Neurosurgery*, **46**(5), 1149–53.
Helmy, A., Antoun, N.M., & Hutchinson, P.J. (2011). Cerebral tuberculoma and magnetic resonance imaging. *J R Soc Med*, **104**(7), 299–301.
Helweg-Larsen, J., Astradsson, A., Richhall, H., Erdal, J., Laursen, A., & Brennum, J. (2012). Pyogenic brain abscess: a 15-year survey. *BMC Infect Dis*, **12**, 332.
Heshin-Bekenstein, M., Megged, O., Peleg, U., et al. (2014). Gradenigo's syndrome: is fusobacterium different? Two cases and review of the literature. *Int J Pediatr Otorhinolaryngol*, **78**(1), 166–9.
Ionita, C., Wasay, M., Balos, L., & Bakshi, R. (2004). MR imaging in toxoplasmosis encephalitis after bone marrow transplantation: paucity of enhancement despite fulminant disease. *AJNR Am J Neuroradiol*, **25**(2), 270–3.
James, H., Walsh, J.W., Wilson, H.D., Connor, J.D., Bean, J.R., & Tibbs, P.A. (1980). Prospective randomized study of therapy in cerebrospinal fluid shunt infection. *Neurosurgery*, **7**, 459.
Jiang X et al. (2016). Neurosurgical site infection prevention: single institute experience. *Turk Neurosurg*, **26**(2), 234–9.
Johnson, A.K. & Batra, P.S. (2014). Central skull base osteomyelitis: an emerging clinical entity. *Laryngoscope*, **124**(5), 1083–7.
Keong, N.C., Bulters, D.O., Richards, H.K., et al. (2012). The SILVER (Silver Impregnated Line versus EVD Randomized trial): a double-blind, prospective, randomized, controlled trial of an intervention to reduce the rate of external ventricular drain infection. *Neurosurgery*, **71**(2), 394–403.
Kombogiorgas, D. & Solanki, G.A. (2006). The Pott puffy tumor revisited: neurosurgical implications of this unforgotten entity. Case report and review of the literature. *J Neurosurg*, **105**(2 Suppl), 143–9.
Kourbeti, I.S., Jacobs, A.V., Koslow, M., Karabetsos, D., & Holzman, R.S. (2007). Risk factors associated with post craniotomy meningitis. *Neurosurgery*, **60**, 317–26.
Kubilay, Z., Amini, S., Fauerbach, L.L., Archibald, L., Friedman, W.A., & Layon, A.J. (2013). Decreasing ventricular infections through the use of a ventriculostomy placement bundle: experience at a single institution. *J Neurosurg*, **118**(3), 514–20.
Le Beau, J., Creissard, P., Harispe, L., & Redondo, A. (1973). Surgical treatment of brain abscess and subdural empyema. *J Neurosurg*, **38**(2), 198–203.
Leys, D., Destee, A., Petit, H., & Warot, P. (1986). Management of subdural intracranial empyemas should not always require surgery. *J Neurol Neurosurg Psychiatry*, **49**(6), 635–9.
Luo K et al. 2013. Primary intracranial and spinal hydatidosis: a retrospective study of 21 cases. *Pathog Glob Health*, **107**(2), 47–51.
Luthra, G., Parihar, A., Nath, K., et al. (2007). Comparative evaluation of fungal, tubercular and pyogenic brain abscesses with conventional and diffusion MR imaging and proton MR spectroscopy, *Am J Neuroradiol*, **28**(7), 1332–8.
Lwin, S., Low, S.W., Choy, D.K., Yeo, T.T., & Chou, N. (2012). External ventricular drain infections: successful implementation of strategies to reduce infection rate. *Singapore Med J*, **54**(4), 255.
Ma, J., Jia, R., Li, J., et al. (2015). Retrospective clinical study of eighty-one cases of intracranial mucormycosis. *J Glob Infect*, **7**(4), 143–50.
Mauser, H.W., Van Houwelingen, H.C., & Tulleken, C.A. (1987). Factors affecting the outcome in subdural empyema. *J Neurol Neurosurg Psychiatry*, **50**(9), 1136–41.
McGovern, P.C., Lautenbach, E., Brennan, P.J., Lustig, R.A., & Fishman, N.O. (2003). Risk factors for postcraniotomy surgical site infection after 1.3-bis(2-chloroethyl)-1-nitrosourea (gliadel) wafer placement. *Clin Infect Dis*, **36**(6), 759–65.
Miller, E.S., Dias, P.S. & Uttley, D. (1987). Management of subdural empyema: a series of 24 cases. *J Neurol Neurosurg Psychiatry*, **50**(11), 1415–18.
Mohindra, S., Savardekar, A., Gupta, R., Tripath, M., & Rane, S. (2016). Tuberculous brain abscesses in immunocompetent patients: a decade long experience with nine patients. *Neurology India*, **64**(1), 66–74.
Monteiro, R., Carneiro, J.C., Costa, C., & Duarte, R. (2013). Cerebral tuberculomas—a clinical challenge. *Respir Med Case Rep*, **9**, 34–7.
Moseley, I.F. & Kendall, B.E. (1984). Radiology of intracranial empyemas, with special reference to computed tomography. *Neuroradiology*, **26**(5), 333–45.
Munusamy, T. & Dinesh, S.K. (2015). Delayed occurrence of *Escherichia coli* subdural empyema following head injury in an elderly patient: a case report and literature review. *J Neurol Surg Rep*, **76**(1), e79–82.

Nathoo, N., Nadvi, S.S., van Dellen, J.R., & Gouws, E. (1999). Intracranial subdural empyemas in the era of computed tomography: a review of 699 cases. *Neurosurgery*, **44**(3), 529–35; discussion 535–6.

Osborn, M.K. & Steinberg, J.P. (2007). Subdural empyema and other suppurative complications of paranasal sinusitis. *Lancet Infect Dis*, **7**(1), 62–7.

Patel KS et al. (2014). Betadine irrigation and post-craniotomy wound infection. *Clin Neurol Neurosurg*, **118**, 49–52.

Pathak, A., Sharma, B.S., Mathuriya, S.N., Khosla, V.K., Khandelwal, N., & Kak, V.K. (1990). Controversies in the management of subdural empyema. A study of 41 cases with review of literature. *Acta Neurochirurgica*, **102**(1–2), 25–32.

Patterson, T.F., Thompson, G.R. 3rd, Denning, D.W. et al. (2016). Practice guidelines for the diagnosis and management of aspergillosis: 2016 update by the Infectious Diseases Society of America. *Clin Infect Dis*, **63**(4), e1–e60.

Pincus, D.J., Armstrong, M.B., & Thaller, S.R. (2009). Osteomyelitis of the craniofacial skeleton. *Semin Plast Surg*, **23**(2), 73–9.

Pradilla, G., Ardila, G.P., Hsu, W., & Rigamonti, D. (2009). Epidural abscesses of the CNS. *Lancet Neurol*, **8**(3), 292–300.

Prasad, S.C., Prasad, K.C., Kumar, A., Thada, N.D., Rao, P., & Chalasani, S. (2014). Osteomyelitis of the temporal bone: terminology, diagnosis, and management. *J Neurol Surg B Skull Base*, **75**(5), 324–31.

Radoi, M., Ciubotaru, V., & Tataranu, L. (2013). Brain abscesses: clinical experience and outcome of 52 consecutive cases. *Chrurgia*, **108**, 215–25.

Ratnaike, T.E., Das, S., Gregson, B.A., & Mendelow, A.D. (2011). A review of brain abscess surgical treatment—78 years: aspiration versus excision. *World Neurosurg*, **76**(5), 431–6.

Sala, F., Abbruzzese, C., Galli, D., et al. (2009). Intracranial pressure monitoring in pediatric bacterial meningitis: a fancy or useful tool? A case report. *Minerva Anestesiol*, **75**(12), 746–9.

Seckin, H., Yagmurlu, B., Yigitkanli, K., & Kars, H.Z. (2008). Metabolic changes during successful medical therapy for brain hydatid cyst: case report. *Surg Neurol*, **70**(2), 186–9.

Srinivas, D., Veena Kumari, H.B., Somanna, S., Bhagavatula, I., & Anandappa, C.B. (2011). The incidence of postoperative meningitis in neurosurgery: an institutional experience. *Neurology India*, **59**(2), 195–8.

Tamber, M.S., Klimo, P. Jr, Mazzola, C.A., et al. (2014). Pediatric hydrocephalus: systematic literature review and evidence-based guidelines. Part 8: management of cerebrospinal fluid shunt infection. *J Neurosurg Pediatr*, **14** Suppl 1, 60–71.

Trendelenberg, G., Jussen, D., Grimmer, S., Jakob, W., Hiemann, N.E., & Horn, P. (2011). Invasive pressure monitoring saves from tuberculous meningitis with fulminant generalized brain edema. *Front Neurol*, **2**, 69.

Tsai, Y.-D., Chang, W.N., Shen, C.C., et al. (2003). Intracranial suppuration: a clinical comparison of subdural empyemas and epidural abscesses. *Surg Neurol*, **59**(3), 191–6; discussion 196.

Tsuchiya, K., Osawa, A., Katase, S., Fujikawa, A., Hachiya, J., & Aoki, S. (2003). Diffusion-weighted MRI of subdural and epidural empyemas. *Neuroradiology*, **45**(4), 220–3.

Ulutas, M., Cinar, K., & Secer, M. (2015). Removal of large hydatid cysts with balloon-assisted modification of Dowling's method: technical report. *Acta Neurochir (Wien)*, **157**(7), 1221–4.

Vergara, G.E., Roura, N., Del Castillo, M. et al. (2015). Cervical aspergillosis with dissemination to the central nervous system: case reports and review of the literature. *Surg Neurol Int*, **6**(Suppl 20), S524–9.

Weerakkody, R.M., Palangasinghe, D.R., Wadanambi, S., & Wijewikrama, E.S. (2015). 'Primary' nocardial brain abscess in a renal transplant patient. *BMC Res Notes*, **8**, 701.

Wong, A.M. et al. (2004). Diffusion-weighted MR imaging of subdural empyemas in children. *AJNR Am J Neuroradiol*, **25**(6), 1016–21.

Yakut, N., Kadayifci, E.K., Karaaslan, A., et al. (2015). Brain abscess due to streptococcus intermedius secondary to mastoiditis in a child. *Springerplus*, **4**, 809.

Youenn, J., Grammatico-Guillon, L., Espitalier, F., Cazals, X., François, P., & Guillon, A. (2015). Long-term outcome of severe herpes simplex encephalitis: a population-based observational study. *Crit Care*, **19**(1), 345.

RELATED LINKS TO EBRAIN

Acute Pneumococcal or Meningococcal Meningitis. https://learning.ebrain.net/course/view.php?id=1146

Diagnosing and Managing Patients with Tubercular Meningitis. https://learning.ebrain.net/course/view.php?id=1147

The Diagnosis and Management of Brain Abscesses. https://learning.ebrain.net/course/view.php?id=1167

Imaging Features of Bacterial Brain Infections. https://learning.ebrain.net/course/view.php?id=1168

99

Spinal infection

Nicholas Haden and Edward White

Introduction

Spinal infections are rare, but their incidence is rising and they are associated with significant morbidity and mortality. Delays in diagnosis and treatment initiation due to their rarity and non-specific presenting symptoms remain a significant problem. A high index of suspicion and aggressive management are critically important in optimizing patient outcomes. This chapter provides an overview of spinal epidural and paraspinal abscesses, discitis, and vertebral osteomyelitis (collectively referred to as spondylodiscitis), and post-operative spinal infections.

Spinal epidural and paraspinal abscesses

Spinal epidural abscess (SEA) is defined as a suppurative infection within the extradural space. SEA represents a significant diagnostic challenge in view of its rarity, non-specific presentation, and propensity to progress rapidly to irreversible paralysis and severe sepsis.

Epidemiology

SEA is rare with an incidence of 1.96 cases per 10 000 hospital admissions. The average age of patients diagnosed with SEA is 57.5 years and a slightly higher incidence is observed in men (Reihsaus et al., 2000). The incidence is increasing due to improved diagnostic imaging with MRI, an ageing population, the rising incidence of HIV, and intravenous drug use.

Pathophysiology

SEA arise within the epidural space in the locations containing the most epidural fat (dorsal and lateral to the dura), which due to its low vascularity is hypothesized to be susceptible to bacterial infection. The pathophysiological mechanisms underlying spinal cord dysfunction secondary to SEA are unclear. A combination of mechanical cord compression and vascular compromise are likely to be responsible and prolonged cord compression may lead to irreversible cord ischaemia.

Anteriorly placed SEA is uncommon and most often occur secondary to spondylodiscitis. SEA occur most commonly in the thoracic spine, followed by the lumbar spine and the cervical spine, although on average a SEA will extend the length of several vertebral bodies. Bacteria may gain access to the spinal epidural space via three routes, although in 30% of cases no source is identified (Darouiche et al., 1992):

Haematogenous

Haematogenous spread is responsible for approximately 50% of cases. Potential sources include:

i. Skin infection (most common)
ii. Intravenous drug use
iii. Infected vascular access
iv. Bacterial endocarditis
v. Urinary tract infection
vi. Respiratory tract infections
vii. Pharyngeal or dental abscess

Direct extension

Direct extension of infection into the extradural space is responsible for approximately one-third of cases. Potential sources include:

i. Spondylodiscitis
ii. Psoas abscess
iii. Decubitus ulcer
iv. Pharyngeal infection causing cervical SEA
v. Mediastinitis causing thoracic SEA
vi. Penetrating trauma
vii. Pyelonephritis with perinephric abscess

Intraoperative inoculation

i. Open surgical procedures

Risk factors

In common with other infections, SEA is more common in patients with diabetes mellitus, therapeutic immunosuppression, malignancy, HIV, alcoholism, and chronic renal failure, as well as in intravenous drug users. A history of trauma is observed in minority of patients and may act as a precipitant for bacterial entry into the extradural space.

Clinical features

The classical triad of back pain, fever, and a neurological deficit is observed in a minority (13%) of patients on initial presentation, although in 75% of patients there is a significant diagnostic delay (Davis et al., 2004). In a meta-analysis of 915 patients, back pain was the most common symptom associated with SEA (71%) followed by fever (66%) and a neurological deficit (63%). Less common symptoms and signs include radiculopathy (20%), focal tenderness (17%), headache (3%), and neck stiffness (3%). Postoperative SEA tends to present in a much vaguer manner as fever and neurological deficits are uncommon (Reihsaus et al., 2000). In view of the rapid and potentially irreversible progression to paralysis, a high index of suspicion is required.

Investigations

Laboratory studies

Inflammatory markers including white cell count, erythrocyte sedimentation rate (ESR) and C-reactive protein (CRP) are typically elevated. A leucocytosis is seen in 60–80% of patients and the mean CRP in a series of 25 patients was 150 mg/litre (Soehle and Wallenfang, 2002).

Imaging studies

MRI is the diagnostic study of choice as it distinguishes SEA from differential diagnoses including transverse myelitis, cord ischaemia, spinal tumours, and disc prolapses, as well as identifying concurrent osteomyelitis and discitis (Fig. 99.1). In patients in whom MRI is contraindicated, computed tomography (CT) with contrast and CT myelography are useful imaging modalities, albeit with lower sensitivity and specificity.

Microbiological studies

Identification of the causative organism is key to the management of SEA. Pus samples may be obtained following surgical drainage or CT-guided abscess aspiration in cases of non-operative management. Pus cultures are positive in 90% of cases, compared with 60% of blood cultures. The most common organism is *Staphylococcus aureus* (60%) followed by Gram-negative bacilli (including *Escherichia coli, Pseudomonas aeruginosa*, and *Klebsiella*). Infections are polymicrobial in 10% of cases (Sendi et al., 2008). The diagnostic yield of microbiological cultures is reduced if antibiotics are administered prior to sampling, although in clinical practice the benefits of identifying the causative organism must be weighed carefully against the risks of clinical deterioration, if there is a delay in obtaining pus.

Treatment

The rarity of SEA and the potentially poor outcome associated with conservative management make the conduct of a randomized controlled trial impractical and evidence is only available from several case series. Broadly speaking, treatment may be surgical drainage and targeted antibiotic therapy or antibiotic therapy alone, albeit guided by cultures. The principle difficulty associated with conservative management is that a rapid neurological deterioration may be observed in neurologically intact patients despite appropriate antibiotic therapy.

Surgical treatment is recommended unless:

i. Surgical and anaesthetic risks are prohibitive
ii. There is involvement of an extensive length of spinal cord
iii. There is complete paralysis of greater than 48 hours duration
iv. The patient is neurologically intact

If surgical decompression is not performed, CT-guided aspiration of the abscess is indicated in order to identify the causative organism and close observation is mandated to ensure that rapid neurological deterioration does not occur. Predictors of failure of conservative management include:

i. Age greater than 65 years
ii. Diabetes mellitus
iii. Bacteraemia (especially methicillin-resistant *Staphylococcus aureus*, MRSA)

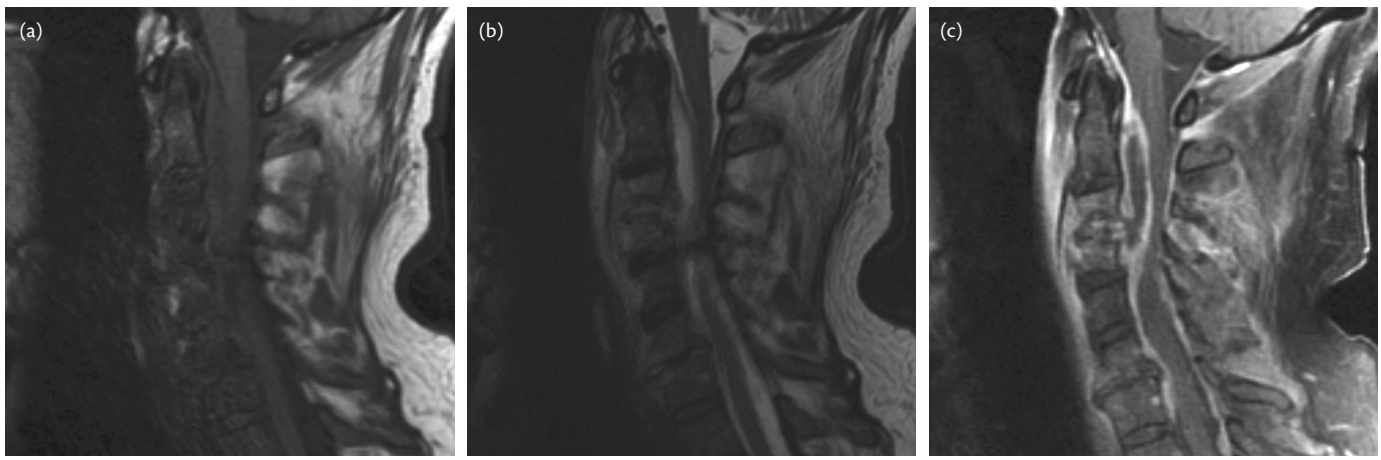

Fig. 99.1 MR imaging of spinal epidural abscesses. Sagittal cervical MRI demonstrating the characteristic features of SEA. On T1-weighted imaging (A), SEA are visible as a hypo- or isointense collection, whereas on T2-weighted imaging (B), SEA are hyperintense. Three patterns of enhancement are observed in the form of dense homogenous enhancement, inhomogeneous enhancement and rim enhancement (as seen in image C). However, in the acute stage when the collection is mainly pus without granulation tissue, little enhancement may be seen. Poor prognostic factors on MRI include (Tang et al., 2002): greater than 50% narrowing of spinal canal; peripheral enhancement; signal change within the spinal cord; SEA greater than 3 cm in length.

iv. Neurological deficits
v. White cell count greater than 12.5×10^9
vi. CRP more than 115 (Kim et al., 2014)

The goals of surgical intervention are debridement of granulation tissue and drainage of pus to alleviate cord compression and to obtain a sample for microbiological analysis. As most SEA are posterior, laminectomy or laminotomy with irrigation of the extradural space using a catheter is suitable in most cases. If the SEA is associated with an implanted spinal cord implant, explantation is mandatory. In extensive or anteriorly located SEA, osteomyelitis may be present within the vertebral body. In these cases, instability may develop after laminectomy and consideration should be made for supplemental posterior instrumented fusion and/or extracavitary approaches to the vertebral body with vertebral reconstruction using an expandable cage or strut grafting.

Typically antibiotic treatment involves a third-generation cephalosporin plus vancomycin, until MRSA is ruled out. Subsequent antibiotic therapy is modified once culture results become available. Antibiotic therapy is typically intravenous in the first instance in view of improved bioavailability compared with oral treatment and antibiotic therapy is usually necessary for a minimum of 6 to 8 weeks. Prolonged treatment may be necessary in the context of spondylodiscitis or immunosuppression.

Outcome

Spontaneous SEA is associated with a mortality of 16%, paralysis in 15%, a residual neurological deficit (excluding paralysis) in 26%, and a complete recovery in 43% (Reihsaus et al., 2000). Mortality is usually due to the consequences of paralysis or the source of infection. Poor prognostic markers include the duration and severity of the pretreatment neurological deficit, MRSA infection, steroid use, HIV, thrombocytopenia, cervical SEA, diabetes mellitus, rheumatoid arthritis, and age over 50 years.

Spondylodiscitis

There is a significant overlap between infection of the intervertebral disc (discitis) and vertebral osteomyelitis. Together these are frequently referred to as spondylodiscitis. Spondylodiscitis frequently coexists with SEA. Spondylodiscitis in the cervical spine is associated with SEA in 90% of cases, whereas thoracic and lumbar spondylodiscitis are associated with SEA in 33% and 24% of cases, respectively (Hadjipavlou et al., 2000).

Spondylodiscitis can be classified as pyogenic, granulomatous (tuberculous and fungal infections) or parasitic in nature. Pyogenic spondylodiscitis may be further classified as primary or secondary (postprocedural). Spondylodiscitis most commonly involves the lumbar spine (58%) followed by the thoracic (30%) and then cervical spine (11%) (Mylona et al., 2009).

Epidemiology

The annual incidence of spondylodiscitis has been reported as 2.4 per 100 000 and there is evidence that the incidence is rising, perhaps due to ageing population, the increasing use of spinal instrumentation and the rising prevalence of intravenous drug abuse. There is a bimodal distribution of cases, peaking in the second decade of life with a much higher peak after the sixth decade of life. Males are affected approximately twice as commonly as females in this older age group (Skaf et al., 2010).

Pathophysiology

Bacteria can infect the spine through the haematogenous route, intraoperative inoculation, or direct spread from sites of adjacent infection, which is rare. In childhood, extensive vascular anastomoses exist that extend into the intervertebral disc. Consequently, septic emboli are unlikely to cause an osseous infarcts and infection is typically localized to the disc. In the third decade of life, these anastomoses involute, creating end arteries. Septic emboli may then cause large osseous infarcts with infection involving the disc and adjacent bone. This may progress to pathological fractures and significant deformity.

In view of the comparatively poor blood supply to the posterior spinal elements, pyogenic osteomyelitis does not usually affect the lamina, pedicles, or transverse and spinous processes, and involvement of these structures should raise the possibility of tuberculous or fungal osteomyelitis.

A distant septic source is identifiable in approximately half of cases of spondylodiscitis. Sources include the urinary tract (17%), bacterial endocarditis (12%), skin and soft tissue (11%), intravascular devices (5%), gastrointestinal tract (5%), respiratory tract (2%), and oral cavity (2%) (Gouliouris et al., 2010). Direct inoculation most commonly occurs following spinal surgery, lumbar puncture and epidural anaesthesia and accounts for approximately 30% of cases.

Worldwide, tuberculosis is the most common cause of spinal infection (Pott's disease) and arises due to haematogenous spread of *Mycobacterium tuberculosis* from a primary focus. Excluding tuberculous cases, *Staphylococcus aureus* is the most frequent cause of spondylodiscitis accounting for between 32% to 67% of cases. Methicillin-resistant *S. aureus* (MRSA) spondylodiscitis remains extremely rare. The second most common cause of pyogenic spondylodiscitis are Enterobacteriaceae (most commonly *Escherichia coli*), which account for 7–33% of cases (Gouliouris et al., 2010). Streptococci and enterococci account for 5–20% of cases of spondylodiscitis and are most commonly associated with bacterial endocarditis (Mylona et al., 2009).

Risk factors

The majority of patients with spondylodiscitis have at least one of the following risk factors (Mylona et al., 2009):

i. Diabetes mellitus (24%)
ii. Intravenous drug abuse (11%)
iii. Immunosuppression (7%)
iv. Malignancy (6%)
v. Alcoholism (5%)
vi. Rheumatic disease (5%)
vii. Liver cirrhosis (4%)
viii. Renal failure (4%)
ix. Previous radiation or fracture to vertebra

Clinical features

Pain is the most common symptom of spondylodiscitis affecting more than 90% of patients. Back pain is typically unremitting and

worse at night and on movement. Fever occurs in approximately 50% of patients, although this is less frequent in patients with tuberculosis. Neurological deficits and radiculopathy occur in approximately one-third of patients (Mylona et al., 2009). The onset is usually insidious and non-specific, particularly in atypical infections, and due to the rarity of spondylodiscitis and the frequency of mechanical back pain, there is often a significant diagnostic delay. This diagnostic delay is often longer in cases of TB, which has an insidious onset, but in its later stages can lead to epidural and paravertebral collections, neurological deficits, and severe deformity.

The most common sign of spondylodiscitis is spinal tenderness and there may be associated paraspinal muscle spasm and impaired spinal movements. Rare presentations include a painful gibbus deformity, clinical features of a psoas or retropharyngeal abscess, sinus formation, and a spinal mass. Symptoms in children include irritability, refusal to move and abdominal pain (Gouliouris et al., 2010).

Investigations

Laboratory studies

The white blood cell count is elevated in 35% of cases, but is often normal in older people and immunocompromised. CRP is more sensitive, being elevated in more than 90% of cases. Approximately 70% of patients are anaemic and 50% have a raised serum alkaline phosphatase (Gouliouris et al., 2010).

Microbiological studies

In cases of suspected spondylodiscitis, blood and urine cultures should be obtained in addition to a sample from the involved disc or vertebral body. Blood cultures are positive in approximately 50% of cases and there is a concordance of 85% with disc or vertebral body culture results. This diagnostic yield is probably higher with more virulent organisms and in pyrexial patients. CT-guided, direct culture of the infected disc or vertebra, which has a diagnostic yield of around 70%, and in 24% of cases more than one organism is identified (Hadjipavlou et al., 2000). Tissue Gram stain, both aerobic and anaerobic cultures, fungal and TB cultures, and TB PCR are mandatory. Histology is also helpful in distinguishing granulomatous from pyogenic spondylodiscitis and ruling out an underlying tumour.

Imaging studies

Plain radiographs may demonstrate endplate irregularity progressing to endplate erosion, disc space narrowing, and progressive loss of vertebral height and deformity. These changes start to develop around 3–6 weeks after symptom onset. Reactive bone sclerosis starts to appear at around 8–12 weeks and may progress to exuberant osteophyte formation and spontaneous fusion. Nevertheless, the sensitivity and specificity of plain radiographs remains low with values of 82% and 57%, respectively (Modic et al., 1985). CT demonstrates these changes earlier and is invaluable in undertaking biopsies for microbiological and histological analysis.

MRI is the imaging study of choice with both high sensitivity (96%) and high specificity (92%), as well as the ability to delineate epidural and paraspinal collections (Dagirmanjian et al., 1999) (**Figs. 99.2** and **99.3**).

Radionuclide bone scanning with technetium-99m is highly sensitive (90%) in the first few days of infection, but less specific (78%), with degenerative changes resulting in false positives. In cases where there is diagnostic doubt, fluorine-18 fluorodeoxyglucose positron emission tomography (FDG-PET) is a useful adjunct as it is capable of distinguishing infection from degenerative changes.

The value of routine MRI to monitor treatment response is less certain. Radiological markers of resolution include bony restoration and loss of contrast enhancement. However, these changes often appear late and MRI scans obtained within 4–8 weeks of treatment initiation often show an increase in enhancement and marrow oedema.

Treatment

The key elements of treatment include eradication of infection, alleviation of pain, and preservation of spinal structure and function. Antibiotic therapy should be initiated after appropriate tissue samples have been obtained, although in the presence of severe sepsis or neutropenia, empirical antibiotics should be started immediately.

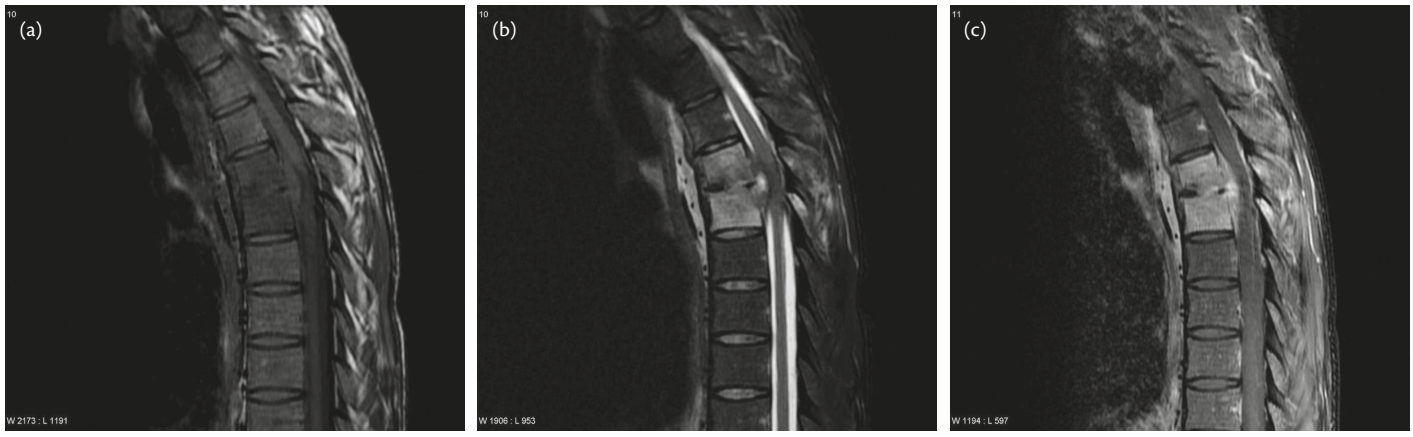

Fig. 99.2 MR imaging of spondylodiscitis. Sagittal thoracic MRI demonstrating the typical features of spondylodiscitis. Initial MR abnormalities are due to inflammation and oedema in the vertebral body and disc space. These changes are characterized by hypointensity in the bone marrow on T1-weighted imaging (A). Hyperintensity in the bone marrow and disc space is typically seen on short tau inversion recovery (STIR) and T2-weighted imaging (B). Enhancement develops initially at the end plate-disc interface and progresses into the vertebral body as bony destruction progresses (C). This enhancement improves the diagnostic utility of MRI and helps distinguish infection from modic 1 degenerative changes.

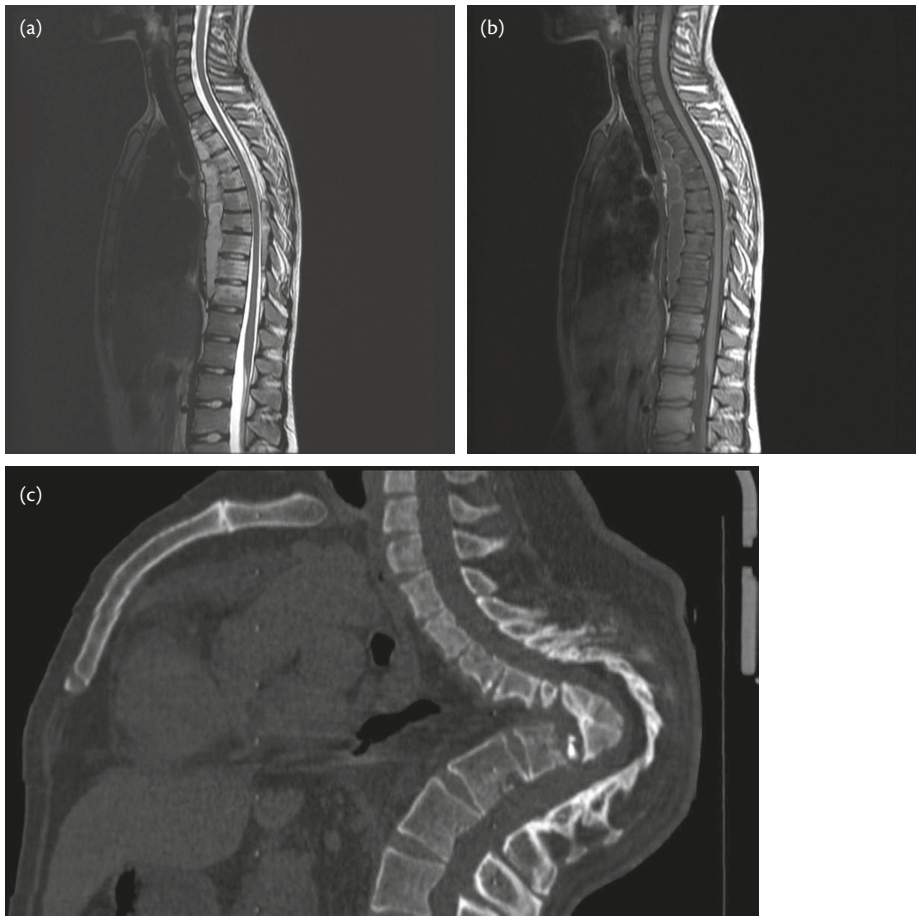

Fig. 99.3 Imaging findings in spinal tuberculosis. Sagittal T2 (A) and T1-weighted (B) MR images and sagittal CT scan (C) demonstrating typical features of spinal TB. Classically, spinal TB involves the vertebral body, sparing the posterior elements, but involving multiple levels as infection spreads in a subligamentous manner, under the anterior longitudinal ligament, potentially causing a prevertebral abscess (A, B). Consequently, irregularity of the anterior vertebral body is a characteristic early radiological sign. Progression to deformity (C) and large paraspinal collections is common.

Once the causative organism has been identified, appropriately targeted, intravenous antibiotics should be administered.

In an open-label, non-inferiority, randomized, controlled trial, Bernard et al (2015) demonstrated that 6 weeks of antibiotics (intravenous for approximately the first 14 days) was not inferior to 12 weeks of antibiotics at 1-year follow-up. Antituberculous chemotherapy for spinal TB necessitates prolonged treatment and identification of drug-resistant strains of Mycobacterium tuberculosis.

The role of spinal immobilization is less certain. If there has been significant vertebral destruction, bed rest is recommended. In cervical spondylodiscitis, a hard collar may be advisable. Once pain has settled, patients with thoracic or lumbar spondylodiscitis should be mobilized in a thoracolumbar sacral orthosis (TLSO) or a lumbar sacral orthosis (LSO).

Indications for surgical intervention include the presence of spinal instability characterized by progressive deformity or substantial bone loss, significant neurological deficits due to neural compression, failure to respond to conservative measures and intractable pain. Percutaneous drainage is often preferred to surgical drainage of large paravertebral abscesses.

A multitude of surgical techniques may be used in the management of spondylodiscitis. In the presence of a dorsally located SEA, a laminectomy may be appropriate, although due to the tendency for spondylodiscitis to involve the vertebral body and disc, this may lead to spinal instability. In the cervical spine, anterior approaches are favoured to debride infected bone. Multilevel corpectomies may be supplemented with posterior instrumentation. In the thoracic spine, the rib-cage acts to maintain stability and therefore immobilization with the use of an appropriate orthosis may negate the need for surgical stabilization. If, however, decompression and debridement are necessary, transthoracic, or posterolateral approaches may be necessary and may need to be supplemented with posterior stabilization.

Maintenance of structural integrity may be achieved using a variety of techniques including the use of autologous bone graft and titanium mesh, structural autografts such as tricortical rib and fibula, and allografts. Concerns regarding the implantation of hardware within an infected field are not borne out in the literature.

Outcome

The mortality of spondylodiscitis is approximately 5%, usually due to severe sepsis (Gouliouris et al., 2010). Approximately one-third of patients have a residual neurological deficit. The relapse rate has been reported as 14% with the majority recurring within one year. Relapse was more common in the presence of recurrent bacteraemia, chronic sinuses, and paravertebral abscesses. Risk factors for an adverse clinical outcome include a diagnosis delayed by

more than 2 months, motor weakness and a nosocomial infection (McHenry et al., 2002).

Postoperative wound infection

Postoperative surgical site infection (SSI) following spine surgery has been reported to occur in 1.2% of patients undergoing basic spinal decompression surgery and 2.4% in patients undergoing fusion surgery. This rate is even higher in patients sustaining traumatic spinal injuries where infection rates of up to 10% have been reported, perhaps due to prolonged bed rest, exposure to nosocomial infections and the development of a catabolic metabolic state following the injury (Hegde et al., 2012).

Risk factors

See **Box 99.1** for the risk factors for postoperative spinal infections.

Pathophysiology

Factors implicated in the development of SSI may be microbiological in nature or relate to the patient or surgical procedure. The most common causative organism is *Staphylococcus aureus*, although other common organisms include *Staphylococcus epidermidis, Enterococcus faecalis*, and *Pseudomonas aeruginosa* (Weinstein et al., 2000). Most commonly organisms enter the wound intraoperatively, although haematogenous spread may occur. The key elements in preventing SSI are meticulous attention to aseptic technique and the use of prophylactic antibiotics.

There are numerous patient-specific factors that have been shown to predispose to infection. Intraoperative factors that increase the likelihood of an SSI include the duration of surgery, the use of instrumentation, revision surgery, excessive staff within theatre and possibly the use of operating microscopes or loupe-magnification (Hegde et al., 2012). Potential techniques for minimizing the risks of infection include avoiding excessive use of electrocautery, regular release of retractors, debriding wounds at the end of the procedure and the use of antibiotic wound irrigation and closed suction drains.

Box 99.1 Risk factors for postoperative spinal infections

Preoperative

1. Advanced age
2. Obesity
3. Diabetes mellitus
4. Smoking
5. Previous chemotherapy or radiotherapy
6. Preoperative incontinence
7. Preoperative paralysis
8. ASA grade 3 or 4
9. Spinal trauma

Intraoperative

1. Posterior cervical surgery
2. Multilevel surgery
3. Tumour resection
4. Intraoperative transfusion

Postoperative

1. Incontinence
2. Transfusion
3. Steroid usage

Source data from Olsen et al., 2003. http://thejns.org/doi/abs/10.3171/spi.2003.98.2.0149

Clinical features

Typical features of infection include back pain, wound tenderness, erythema, and discharge. Severe infection may cause fever, hypotension, and confusion. Indolent infections from organisms such as *Propionibacterium acnes* may cause more vague symptoms of pain with possible pseudarthrosis and hardware loosening. Clinical features may also be suggestive of concurrent spondylodiscitis or SEA with associated neurological deficits.

Investigations

Laboratory tests

CRP measurements are key in evaluating patients with a suspected SSI. Normally the CRP normalizes within two weeks of surgery. White cell counts are often normal and superficial cultures are unreliable due to contamination from skin flora. Consequently, intraoperative tissue cultures are invaluable in making the diagnosis and guiding antibiotic treatment (Hegde et al., 2012). Revision spinal surgery often merits obtaining intraoperative cultures to rule out low-grade infection.

Imaging studies

CT may demonstrate implant loosening with lucency around instrumentation and evidence of discitis. Contrast-enhanced MRI is the imaging modality of choice in detecting SSI and concurrent spondylodiscitis or SEA. Nevertheless, interpreting postoperative MR imaging can be challenging due to metal artefact and the expected postoperative changes following discectomy, which include subtle enhancement within the intervertebral disc space and annulus, with endplate hypointensity on T1-weighted imaging and hyperintensity on T2-weighted imaging. Spondylodiscitis tends to produce more florid, circumferential enhancement of the intervertebral disc. Bone scans are not helpful as they will show increased uptake at sites of reactive bone formation for up to one year following surgery.

Treatment

Superficial abscesses may be managed by incision, drainage, wound debridement, and antibiotics. Indications for surgical drainage of SEA have previously been discussed. Large paraspinal abscesses may benefit from CT-guided aspiration. Infections with virulent organisms or in the immunocompromised may require multiple wound washouts.

In the context of infected fusion cases, copious irrigation, removal of loose bone graft and metalwork is mandatory. Infection can often be successfully managed in the presence of interbody cages and posterior instrumentation (Weinstein et al., 2000). When multiple wound washouts are necessary, some authors advocate implantation of antibiotic-impregnated beads into the wound (Hegde et al., 2012).

In the context of a late infection when fusion has already occurred, instrumentation removal is beneficial in clearing the infection.

Isolated postoperative discitis is effectively managed with a course of intravenous antibiotics. These may be guided by cultures obtained from a CT-guided, disc space biopsy, which has a high diagnostic yield. Bracing may be used for patient comfort. Resolution of infection is often associated with spontaneous fusion of the disc space. Rarely, in cases of failed conservative management where there is destruction of the vertebral body, progressive deformity, neurological deficits, or SEA, lumbar discectomy and interbody fusion or vertebral reconstruction may be required.

Controversy: The role of antibiotics in discogenic back pain

There is a growing body of evidence suggesting that there is an association between symptomatic disc degeneration, modic changes on MRI and disc space infection by anaerobic organisms of low virulence such as *Propionibacterium acnes and Corynebacterium propinquum* (Stirling et al., 2001). These studies are controversial as it is possible that positive cultures obtained in these studies were due to perioperative contamination with skin commensals. Nevertheless, a double-blind, randomized, placebo-controlled trial (n = 162), demonstrated a significant improvement in low back pain and leg pain in patients with a history of lumbar disc prolapse and type 1 Modic changes on MRI, following treatment with amoxicillin-clavulanate aimed at eradicating these organisms (Albert et al., 2013).

Significant questions still remain regarding the validity of the findings from this trial. Specifically, it is unclear as to the number and distribution, between treatment groups, of patients who had undergone surgery for their lumbar disc prolapse. It is conceivable that bacterial disc space contamination may have occurred during surgery, leading to a low-grade discitis, which may have subsequently been responsive to antibiotics. At 1-year follow-up, two-thirds of patients in the treatment group still had significant pain and patients treated with placebo had unusually stable measurements of pain severity and minimal placebo effect was observed. Finally, it is unclear as to whether patients were adequately blinded to their treatment.

In conclusion, there is a need for further studies evaluating whether there is a link between low-grade disc infection, modic changes, and symptomatic disc degeneration. Specifically, an appropriately designed and powered, multicentre, placebo-controlled, randomized trial is necessary to determine whether there is a role for antibiotic treatment in these patients.

FURTHER READING

Albert, H.B., Sorensen, J.S., Christensen, B.S., & Manniche, C. (2013). Antibiotic treatment in patients with chronic low back pain and vertebral bone edema (Modic type 1 changes): a double-blind randomized clinical controlled trial of efficacy. *Eur Spine J*, **22**(4), 697–707.

Bernard, L., Dinh, A., Ghout, I., et al. (2015). Antibiotic treatment for 6 weeks versus 12 weeks in patients with pyogenic vertebral osteomyelitis: an open-label, non-inferiority, randomised, controlled trial. *Lancet*, **385**(9971), 875–82.

Kim, S.D., Melikian, R., Ju, K.L., et al. (2014). Independent predictors of failure of nonoperative management of spinal epidural abscesses. *Spine J*, **14**(8), 1673–9.

Reihsaus, E., Waldbaur, H., & Seeling, W. (2000). Spinal epidural abscess: a meta-analysis of 915 patients. *Neurosurg Rev*, **23**(4), 175–204.

Weinstein, M.A., McCabe, J.P., & Cammisa, F.P. Jr. (2000). Postoperative spinal wound infection: a review of 2,391 consecutive index procedures. *J Spinal Disord*, **13**(5), 422–6.

REFERENCES

Albert, H.B., Sorensen, J.S., Christensen, B.S., & Manniche, C. (2013). Antibiotic treatment in patients with chronic low back pain and vertebral bone edema (Modic type 1 changes): a double-blind randomized clinical controlled trial of efficacy. *Eur Spine J*, **22**(4), 697–707.

Bernard, L., Dinh, A., Ghout, I., et al. (2015). Antibiotic treatment for 6 weeks versus 12 weeks in patients with pyogenic vertebral osteomyelitis: an open-label, non-inferiority, randomised, controlled trial. *Lancet*, **385**(9971), 875–82.

Dagirmanjian, A., Schils, J., & McHenry, M.C. (1999). MR imaging of spinal infections. *Magn Reson Imaging Clin N Am*, **7**(3), 525–38.

Darouiche, R.O., Hamill, R.J., Greenberg, S.B., Weathers, S.W., & Musher, D.M. (1992). Bacterial spinal epidural abscess. Review of 43 cases and literature survey. *Medicine (Baltimore)*, **71**(6), 369–85.

Davis, D.P., Wold, R.M., Patel, R.J., et al. (2004). The clinical presentation and impact of diagnostic delays on emergency department patients with spinal epidural abscess. *J Emerg Med*, **26**(3), 285–91.

Gouliouris, T., Aliyu, S.H., & Brown, N.H. (2010). Spondylodiscitis: update on diagnosis and management. *J Antimicrob Chemother*, **65** Suppl 3, iii11–24.

Hadjipavlou, A.G., Mader, J.T., Necessary, J.T., & Muffoletto, A.J. (2000). Hematogenous pyogenic spinal infections and their surgical management. *Spine (Phila Pa 1976)*, **25**(13), 1668–79.

Hegde, V., Meredith, D.S., Kepler, C.K., & Huang, R.C. (2012). Management of postoperative spinal infections. *World J Orthop*, **3**(11), 182–9.

Kim, S.D., Melikian, R., Ju, K.L., et al. (2014). Independent predictors of failure of nonoperative management of spinal epidural abscesses. *Spine J*, **14**(8), 1673–9.

McHenry, M.C., Easley, K.A., & Locker, G.A. (2002). Vertebral osteomyelitis: long-term outcome for 253 patients from 7 Cleveland-area hospitals. *Clin Infect Dis*, **34**(10), 1342–50.

Modic, M.T., Feiglin, D.H., Piraino, D.W., et al. (1985). Vertebral osteomyelitis: assessment using MR. *Radiology*, **157**, 157–66.

Mylona, E., Samarkos, M., Kakalou, E., Fanourgiakis, P., & Skoutelis, A. (2009). Pyogenic vertebral osteomyelitis: a systematic review of clinical characteristics. *Semin Arthritis Rheum*, **38**, 28–40.

Olsen, M.A., Mayfield, J., Lauryssen, C., et al. (2003). Risk factors for surgical site infection in spinal surgery. *J Neurosurg*, **98**(2 Suppl), 149–55.

Reihsaus, E., Waldbaur, H., & Seeling, W. (2000). Spinal epidural abscess: a meta-analysis of 915 patients. *Neurosurg Rev*, **23**(4), 175–204.

Sendi, P., Bregenzer, T., & Zimmerli, W. (2008). Spinal epidural abscess in clinical practice. *QJM*, **101**(1), 1–12.

Skaf, G.S., Domloj, N.T., Fehlings, M.G., et al. (2010). Pyogenic spondylodiscitis: an overview. *J Infect Public Health*, **3**, 5–16.

Soehle, M. & Wallenfang, T. (2002). Spinal epidural abscesses: clinical manifestations, prognostic factors, and outcomes. *Neurosurgery*, **51**(1), 79–85; discussion 86–7.

Stirling, A., Worthington, T., Rafiq, M., Lambert, P.A., & Elliott, T.S. (2001). Association between sciatica and Propionibacterium acnes. *Lancet*, **357**(9273), 2024–5.

Tang, H.J., Lin, H.J., Liu, Y.C., & Li, C.M. (2002). Spinal epidural abscess—experience with 46 patients and evaluation of prognostic factors. *J Infect*, **45**(2), 76–81.

Weinstein, M.A., McCabe, J.P., & Cammisa, F.P. Jr. (2000). Postoperative spinal wound infection: a review of 2,391 consecutive index procedures. *J Spinal Disord*, **13**(5), 422–6.

RELATED LINK TO EBRAIN

Discitis, Vertebral Osteomyelitis and Epidural Abscess. https://learning.ebrain.net/course/view.php?id=1169

Index

Tables, figures, and boxes are indicated by an italic *t, f,* and *b* following the page number.

Abbreviated Injury Scale 478
Abt-Letterer-Siwe disease 465
acoustic neuroma, *see* vestibular schwannomas
acromegaly 67
action potential 827
active immunotherapy 100, 158–9
acute flaccid paralysis 689–91
acute hypokalaemic periodic paralysis 690
acute spastic paraparesis/tetraparesis 687–9
adhesive arachnoiditis 730
adiposogonadal syndrome 323
adjustable valves 1074–5
adoptive immunotherapy 100, 158–9
A fibres 828
agraphia 13
AIDS-associated lymphoma 117, 119, 123, 124
airway
  intraoperative management 59–60
  preoperative assessment 57
alexia 13
Allcock's test 635
Allen's classification 790
allergies 59
Alzheimer's disease 1058–9, 1085
amantadine 877
American–British–French classification 756*b*
Aminoff-Logue grading 757*t*
5-aminolevulinic acid 49, 98, 167
amoebiasis 1111
amyloid deposition 493
anaemia 499
anaesthesia
  emergence 62
  historical development 4
  induction 59
  intraoperative events 61–2
  maintenance 61
  monitoring 60–1
  postoperative care 62–3
  preoperative evaluation 57–9
  specific neurological interventions 63–8
anaplastic ependymoma 361–2
Ancient Egypt 3, 8
Ancient Greece 3, 8
Anderson and D'Alonzo classification 792*t*
anencephaly 974
aneurysmal bone cyst 233, 743*t*
aneurysms 559–65
  anaesthesia 64–5
  associated pathologies 561, 568
  blebs (daughter sacs/lobulations) 560
  blister-like 562
  children 1041–3
  clipping 580, 587–9
  dissecting 562
  epidemiology 568
  familial 560–1
  fusiform 562
  genetics 559
  giant, *see* giant aneurysms
  hypertension 560
  intraoperative rupture 65
  location 560
  morphology 560
  multiple 562–3
  mycotic 562
  progression 561
  rupture risk 561, 568
  saccular 560
  screening 563
  size 560
  smoking 559–60
  spinal 753
  theories of formation 559–60
  traumatic 561–2
  unruptured 564
angiocentric glioma 134–5
angiogenesis 90
angiographically occult lesions 651–7
anisocoria 19
ankylosing spondylitis 676, 700
anterior capsulotomy 930
anterior cerebral artery 540, 542
  stroke 616
anterior cervical corpectomy 701
anterior cervical discectomy 700–1
anterior cervical fusion 797–8
anterior choroidal artery 540
anterior cingulotomy 930
anterior communicating artery 542
  aneurysms 583
anterior cord syndrome 685
anterior inferior cerebellar artery 545
anterior lumbar interbody fusion 662
anterior medial micro-orbitotomy 223–4
anterior odontoid screws 797
anterior temporal lobectomy 959–60
anterolateral skull base surgery 241–51
  case examples 246–51
  decision-making 243
  differential diagnosis 242
  endoscopic endonasal approach 244–5, 250
  Fisch approaches 245–6
  frontal anterior interhemispheric approach 243
  imaging 242
  interfascial dissection 242–3
  lumbar drain 242
  orbitozygomatic approach 245
  patient selection 243
  planning surgery 242–3
  positioning 242
  postoperative care 246
  preoperative workup 241–2
  reconstruction 242
  supraorbital craniotomy and minicraniotomy 243–4
antiangiogenic therapy 99, 157
antibiotics 1113, 1135
anticoagulation
  intracerebral haemorrhage 70
  intracranial haematoma 646, 648
  perioperative 69–71
  reversal 70–1
  spinal surgery 661–2
anticonvulsants (antiepileptics)
  epilepsy management 951–4, 1048
  prophylactic 62, 165
antiplatelets
  intracranial haematoma 646, 648
  perioperative 69–71
  reversal 70–1
antisepsis 4–5
Anton(-Babinski) syndrome 617
aortic coarctation 561
AO spine injury classification 801, 802*f*
Apert syndrome 996*t*
aphasia 13–14, 164
apixaban 70
apolipoprotein E 478, 493
apoptosis 90
aquaporin-1 1059
aquaporin-4 1065
aqueductoplasty 1079
arachnoid cysts 389, 1101–6
  classification 1101
  clinical presentation 1102
  differential diagnosis 1104*t*
  endoscopic removal/aspiration 1080, 1104
  frontal 1103
  intraventricular 1103
  investigations 1103–4
  middle cranial fossa 1102
  outcome 1105
  pathogenesis 1101
  periventricular 1103
  posterior fossa 1102
  postoperative complications 1105
  spinal 766, 1103
  sports participation 1105
  surgery 1104–5
arachnoid granulations 1063
arachnoiditis 730
arachnoid webs 766
arcuate fasciculus 164
arterial-capillary-venous hypertensive syndrome 598–9
arteriovenous fistula
  perimedullary 758
  traumatic brain injury 521–2
  see also dural arteriovenous fistula
arteriovenous malformations
  anatomical considerations for surgery 550–4
  children 1043
  clinical presentation 592–3
  complications 598–9
  diagnosis 593
  embolization (EVACE) 596, 598, 599
  epidemiology 592
  genetics 592
  grading 593, 594*t*
  intramedullary 757–8
  multimodal treatment 598
  natural history 592–3
  outcome 599–600
  pathophysiology 591–2
  prognosis 599–600
  stereotactic radiosurgery 595–6, 599, 600*t*
  surgery 594–5, 598–9, 600*t*
  workup 593–4
ASA status 58*t*
Ashworth Scale, Modified 886*t*
ASIA Impairment Scale 26*f*, 783, 784–5*f*, 813–14
asleep-awake-asleep technique 56
ASPECTS score 617, 618*t*
association fibres 164
astrocytoma
  desmoplastic infantile 135, 136
  diffuse 132–3
  intraventricular 385, 387
  isomorphic 133
  pilocytic 133, 1010
  spinal 738, 739*t*
  subependymal giant cell (SEGA) 387, 455–6, 462

ataxia 16
ataxia telangiectasia 457–8
atherosclerosis 621, 628
atlantoaxial injuries 1005
atlantoaxial subluxation 698–9, 704, 706*f*, 707, 1005–6
atopic disease 93
atypical choroid plexus papilloma 403, 406, 407
atypical teratoid rhabdoid tumour 354, 407, 1011
auditory brainstem implants 292
auditory brainstem responses 284
auditory examination 23
auditory monitoring, intraoperative 291
aura 937*t*, 947
autonomic dysreflexia 815–16
autonomic function
  examination 23–4
  seizures 936
  spinal 681–4
  spinal cord injury 814
autoregulation 487–9, 490–1, 554–5
autosomal dominant capillary malformation 592
autosomal dominant polycystic kidney disease 561
awake craniotomy 55–6, 66, 166, 169, 834–5, 1018–19
axonopathies 692

back pain 722–3, 1135
baclofen 886, 888–9
bacteria 1109
Balint syndrome 617
balloon-assisted coiling 579–80
balloon compression of Gasserian ganglion 917*t*, 920
band heterotopia 976–7
basilar artery 545
basilar impression 699
basilar invagination 699
Bell, Benjamin 4
Bell, John 8
Benedikt's syndrome 616
Bennett, Alexander Hughes 5
benzodiazepines 60*t*
BEST-TRIP study 503
beta-amyloid 493
bevacizumab 99, 146, 151*t*, 154–5
B fibres 828
Bicêtre classification 755*b*
bifacetal fracture dislocations 792–3, 798
bifrontal craniotomy 581–2
bipolar diathermy 50
birth injuries 1005
bladder function
  spinal control 682–4
  spinal cord injury 814–15, 818
blebs 560
blister-like aneurysms 562
block vertebra 772
blood–brain barrier 150, 1058, 1113
blood–CSF barrier 1058
Bloom syndrome 354*t*
bolus tracking 40
boron neutron capture therapy 144
Boston criteria 645*b*
botulinum toxin 878, 888
Bovie, William 6
bowel function
  spinal control 684
  spinal cord injury 814, 818
brachial neuritis 692
brachial plexus injury 847–53
  anatomy 847–9
  classification 848
  clinical presentation 849
  epidemiology 847
  investigations 849–50
  mechanisms 847
  Narakas's rule of sevens 847
  peripheral nerve injuries 852
  reconstruction 851–2
  surgery 850–2
brachial plexus tumours 860
brachytherapy 144
brachyury 190
bracing 805–6
BRAF inhibitors 157
BRAFV600 152
Bragg peak 144
brain abscess 1117–20
brain-computer interfaces 821–2
brain development 971–4
brain malformations 974–81
brain mapping 55–6, 834–5, 1018–19
brain metastases, *see* intracranial metastases
brain plasticity 76, 82
brainstem
  gliomas 390, 1010–11
  venous drainage 549
brainstem auditory evoked potentials 55, 291, 830–1
brain swelling 64
brain tissue oxygen partial pressure 504*t*, 505
BRAT study 587–9
Broca, Paul 5
Broca's aphasia 164
Brown-Séquard, Charles-Édouard 9
Brown-Séquard syndrome 686
Bruns apraxia 14
Bruns nystagmus 283
burst fractures 803–5, 1003–4
Byzantium 3

callosomarginal artery 542, 545
callosotomy 965, 1051
cancer genomics 89–91
capillary telangiectasia 655–6
carbamazepine 952, 952*t*
carbon ion therapy 194–5
Cardiac Risk Index 58*t*
cardiovascular system
  intraoperative events 61
  postoperative complications 62
  preoperative assessment 57–8
  spinal cord injury 814
  traumatic brain injury 497–9
carmustine 151*t*
  wafers 99, 155, 167
Carney complex 301
carotico-cavernous fistula 521–2, 607–10
carotid artery disease 615–25
carotid dissection 514–15, 521
carotid endarterectomy 621–3
carotid insufficiency syndromes 616–17
carpal tunnel syndrome 28*b*, 832, 839–42
cascade model 68
catheter angiography 39–40, 577
cauda equina syndrome 722
caudal lipoma 985
caudal regression syndrome 985
caudate nucleus 412
cavernoma, spinal 758–9
cavernous malformations 651–5, 1043–4
cell death 90
cellular energetics 90
Celsus 3, 8
central cord syndrome 685
central neurocytoma 387, 390–1
central sensitization 900
cephalohematoma 238
cerebellar liponeurocytoma 137
cerebellar pilocytic astrocytoma 1010
cerebellar tonsillar prolapse 995
cerebellopontine angle lesions 281–95
  anatomy 281–2
  anterior petrosal approach 286
  Kawase approach 286
  middle fossa approach 286, 290
  outcomes 290–3
  presentation 282
  presigmoid approach 285
  radiological evaluation 283–4
  retrolabyrinthine approach 285, 288, 290
  retrosigmoid approach 285, 286–7
  surgery 285–90
  transcochlear approach 285, 290
  translabyrinthine approach 285–6, 287–8
cerebellum
  assessment 16–17
  venous drainage 549
cerebral abscess 1117–20
cerebral amyloid angiopathy 644
cerebral anatomy 163–4
cerebral aneurysms, *see* aneurysms
cerebral arteries 539–47
cerebral blood flow 40–1, 555–6
  normal pressure hydrocephalus 1085
  traumatic brain injury 486, 487–8, 492, 503–4, 504*t*
cerebral cavernous malformations 651–5, 1043–4
cerebral contusions 486
cerebral function analysing monitor 828–9
cerebral ischaemia
  aetiology 615
  extracranial-intracranial bypass 627–32
  incidence 615
  investigation 617
  medical management 618–20
  pathophysiology 615–16
  penumbra model 616
  subarachnoid haemorrhage 586
  traumatic brain injury 492–3
cerebral metabolism
  imaging 41–2
  traumatic brain injury 487–91
cerebral microdialysis 504*t*, 506
cerebral oxygenation monitoring 504–5, 504*t*
cerebral palsy 885
cerebral perfusion pressure 554–5
  traumatic brain injury 503
cerebral salt wasting syndrome 63, 316, 500*t*, 586–7
cerebral veins 539, 547–9
cerebrospinal fluid (CSF)
  absorption 1063–5, 1071
  Alzheimer's disease 1058–9, 1085
  clinical investigations 761–2
  extra-axial collections 765–6
  function 1057–8, 1071
  infection diagnosis 1111–12
  normal dynamics 1071–2
  normal pressure hydrocephalus 1058–9, 1085–6
  normal volume 1058
  pathophysiology 761
  physiological changes with age and disease 1058–9
  post-head injury leaks 514, 523, 524*f*, 525–6
  primary central nervous system lymphoma 119
  production 1059–61, 1071
  pseudotumour cerebri syndrome 1093, 1094
  shunting 1029–30, 1031–4, 1072–6, 1097–8, 1104, 1124
  siphoning 1072
  ventriculomegaly development 1065–7
cerebrovascular anatomy 539–54
cerebrovascular physiology 554–7
cerebrovascular reactivity 503
cervical arthroplasty 701, 703
cervical collars 793–4
cervical laminectomy 703
cervical laminoplasty 704*t*
cervical spinal clearance 783
cervical spinal disease 697–710
  anterior cervical corpectomy 701
  anterior cervical discectomy 700–1
  cervical arthroplasty 701, 703
  cervical laminectomy 703
  cervical laminoplasty 704*t*
  clinical presentation 697
  endoscopic odontoidectomy 707–8
  individualized treatment 698
  investigation 697–8
  pathology of degenerative disease 697
  posterior cervical foraminotomy 703–4
  skip laminectomy 704*t*
cervical spine injuries 789–99
  anterior cervical fusion 797–8
  anterior odontoid screw fixation 797
  assessment 789–90
  cervical collars 793–4
  cervical traction 794–5
  cervicothoracic fusion 797
  classification 790–1
  common fractures 791–3
  craniocervical fixation 796–7
  fracture incidence 789
  halo immobilization 795

subaxial posterior cervical fixation 795–6
surgery 795–8
Cervical Spine Injury Severity Score 790
cervical traction 783, 794–5
Chamberlain's line 699
Charcot-Marie-Tooth disease 692
checkpoint inhibitors 158
chemodectomas 464–5
chemotherapy 149–61
aims 149
anterior skull base malignancies 214
chemotherapeutics 150, 151*t*
choroid plexus tumours 408
clinical trials 150
ependymomas 365
esthesioneuroblastoma 208
fractional kill 149
germinomas 429–30
glioblastoma 153–5
glomus tumours 277
haemangioblastoma 372
high-grade glioma 99, 100, 153–5
immunotherapy 99–100, 150, 153, 158–9
intracranial metastases 112
limitations 150
low-grade glioma 83, 155–7
mechanisms of action 149
molecular markers 150, 152
monitoring response 152–3
non-germinomatous germ cell tumours 430
paediatric brain tumours 1020–1
pineoblastoma 432
pituitary tumours 309
primary central nervous system lymphoma 123–4
resistance to 150
targeted molecular therapy 99, 150, 157
Chiari type 1 malformations 763–4
Chiari type 2 malformations 764
children, *see* paediatrics
chimeric antigen receptors 159
chin-on-chest deformity 700
choline-to-creatine ratio 78
chondroblastoma 743*t*
chondroma 235–6, 743*t*
chondrosarcomas 189–96
classic 190
epidemiology 189
genetics 190–1
mesenchymal 190
myxoid 190
pathology 189–90
preoperative workup and planning 191–2
prognosis 194
proton beam therapy 194
spinal 740, 742*t*
surgery 193–4
chordomas 189–96
atypical (de-differentiated) 189, 194
carbon ion therapy 194–5
chondroid variant 189
endonasal resection 195
epidemiology 189
genetics 190–1
pathology 189, 190
preoperative workup and planning 191–2
prognosis 194
proton beam therapy 194
radiotherapy 193, 194–5
seeding risk 192
spinal 738, 742*t*
surgery 192–3, 195
choriocarcinoma 428
choristoma 461
choroidal fissure 411
choroid plexus 1059–60
coagulation 1030, 1079–80
hyperplasia 406
choroid plexus tumours 388, 390, 403–10
atypical papilloma 403, 406, 407
carcinoma 403, 405, 406–7, 408
chemotherapy 408
diagnosis 405–6
embolization 407
epidemiology 403
papilloma 403, 405, 406, 408
presenting symptoms 403
radiotherapy 408
stereotactic radiosurgery 408
surgery 407–8
chromaffin paragangliomas 273
chromosomal alteration 89–90
chromosome 1p/19q deletions 94, 152
cingulum 164, 168
circle of Willis 539
clam-shell orthosis 805
Claude's syndrome 616
clay shoveler's fracture 793
Cline Jr, Mr 8
clinical assessment 11–29
clobazam 942*t*, 943
CNS–primitive neuroectodermal tumours (PNET) 353, 354, 355, 356, 358
coagulation disorders
intracranial haematoma 646, 648
perioperative management 68–71
traumatic brain injury 499
Cobb angle 771
cobblestone lissencephaly 978
coccydynia 729
cochlear implants 292
coil embolization 578–9, 580, 587–9
collagenopathies 561
Collet-Sicard syndrome 272*t*, 523*t*
colloid cysts 388–9, 393–401
conservative management 396
CSF diversion 396
endoscopic approaches 396–7, 399, 1080
epidemiology 393
imaging 395–6
incidental 399
microsurgery 397–8, 399
natural history 396
pathogenesis 393–4
pellucidotomy 396
percutaneous aspiration 396
presentation 394–5
sudden death 395
colour vision 18
column theories 674
common peroneal palsy 28*t*
complex regional pain syndrome 691
compound motor action potential 832
computed tomography (CT) 32–4
concussion 486–7, 531–5
congenital ectodermal inclusion cysts, *see* dermoid cysts
connective tissue disorders 689
conscious sedation 56
contact inhibition 90
contrast-enhanced MRA 40
contrast media 33, 36–7, 38–9
contre-coup contusions 483–4
conus basket 752
cordotomy 901–2
corneal reflex 22
corpus callosum 412–13
agenesis 978–9
callosotomy 965, 1051
corsets 805–6
cortical mapping 55–6, 834–5, 1018–19
cortical spreading depression 493, 506
cortical stimulators 966
cortical tubers 455, 462
corticospinal tracts 681
Cosman-Roberts-Wells Precision™ Arc System 52, 866
COSS trial 628
costotransversectomy 713–14
Cotugno, Domenico 4, 8
coup contusions 483–4
coupled movements 673
Cowden syndrome 131, 462
CPP optimal 491
cranial expansion 1097
cranial infections 1117–27
cranial nerve I 22
cranial nerve II 22
cranial nerve III
palsy 20
schwannomas 265
cranial nerve IV
palsy 21
schwannomas 265
cranial nerve V 22
cranial nerve VI
palsy 21
schwannomas 265
cranial nerve VII
examination 22–3
monitoring 55
vestibular schwannomas 262–3, 284–5
cranial nerve VIII 23
cranial nerve IX 23
cranial nerve X 23
cranial nerve XI 23
cranial nerve XII 23
cranial nerves
examination 20–1, 22–23
intraoperative monitoring 832, 834
traumatic brain injury 522
vascular compression (hyperactive) syndromes 909–27
craniectomy
meningitis and encephalitis 1124
stroke 620–1, 623
traumatic brain injury 511–13, 527
craniofaciosynostosis 993–8
aetiology 995–6
definitions 993
diagnosis 996
epidemiology 993, 995
investigations 996
physiopathogenesis 995–6
surgery 996–7
craniopharyngioma 313, 321–33
adamantinomatous 321, 322–3
children 323–4, 328
classification 324
clinical presentation 323–4
cyst aspiration 328
epidemiology 321
frontolateral approach 328
imaging 324
management algorithm 324*f*
molecular biology 321–3
outcome 329
papillary 321, 323
pathology 321–3
postoperative care 329
preoperative evaluation 324
radiotherapy 330, 332
surgery 325–8, 329–30
symptomatic treatment 325
transsphenoidal approach 327–8
cranioplasty 515–16
craniotomy
aneurysm surgery 580–2
awake 55–6, 66, 166, 169, 834–5, 1018–19
bifrontal 581–2
far lateral 378–80, 582
frontotemporal 222–3
minicraniotomy 243–4
orbitozygomatic 582
pterional 580–1
suboccipital 376
supraorbital 243–4
traumatic brain injury 510–11
venous thromboembolism prophylaxis 71
CRASH model 478
crocodile tears syndrome 24
Crouzon syndrome 996*t*
CRW Precision™ Arc System 52, 866
CSF, *see* cerebrospinal fluid
CT angiography 40
CT perfusion 41
CT venography 40
cubital tunnel syndrome 842–4
Cushing, Harvey Williams 5, 6–7
Cushing reflex 7
Cushing's disease 67, 311–12
cysticercosis 390, 1111, 1120–1
cytokine therapy 100
cytomegalovirus 93

dabigatran 70
Dandy, Walter 7–8
Dandy-Walker syndrome 979
dantrolene 886
daughter sacs 560
decompressive craniectomy
stroke 620–1, 623
traumatic brain injury 511–13, 527
decompressive hemicraniectomy 623
decontamination of instruments 1114, 1115*b*
DECRA trial 512–13

deep brain stimulation 835–6, 865–71
epilepsy 966
movement disorders 880, 881–2
pain relief 905–6
psychiatric disorders 929, 930, 931
deep-seated tumours 167–8
deep tendon reflexes 25
deep vein thrombosis 71, 169, 816
deep white matter hyperintensities 1085
Dejerine–Roussy syndrome 616
Dejerine syndrome 617
delayed neurological recovery 62
dementia pugilistica 527
depressed skull fractures 513, 522–3
dermal sinus tract 985, 990
dermoid cysts 197–203, 233–4, 293, 389
epidemiology 197
malignant transformation 202
pathology 197–9
radiological features 199
recurrence 202
rupture 197
surgery 199–202
surveillance imaging 202
desflurane 61*t*
desmoplastic infantile astrocytoma 135–136
desmoplastic infantile gangliogliomas 135–136
developmental venous anomalies 655
dexamethasone suppression test 306
high-dose 312
low-dose 312
overnight 312
dexamethasone therapy 97, 109–10, 123, 165, 1015
dexmedetomidine 60*t*
diabetes insipidus 316, 329, 500*t*, 525
diathermy 50
diazepam 888
DICER1 301
dietary therapies 100
differential pressure valves 1073
diffuse astrocytoma 132–3
diffuse axonal injury 486
diffuse idiopathic skeletal hyperostosis 700
diffuse low-grade glioma, *see* low-grade glioma
diffusion tensor imaging 36, 1018, 1090
diffusion-weighted imaging 35–6
digital subtraction angiography (DSA) 39–40, 577
direct compound near action potentials 291
direct electrical brain stimulation 81, 82
disc
anatomy 670–1
arthroplasty 725
artificial 665
discitis, postoperative 730
lumbar disease 723–6
lumbar herniation 721–2, 730–1
thoracic herniation 712–15
disconnection syndrome 422
disinfection of instruments 1114, 1115*b*
disinhibition 900
dissecting aneurysms 562
dizziness 262
Dolenc technique 264
Doppler ultrasound 39, 54
dorsal horn 679, 896–7
dorsal root entry zone (DREZ) 896–7
lesions 901
dorsal stream 164
dorsal tract 681
dorsal transcortical subinsular hemispherotomy 964, 965
double crush 839
double-microcatheter technique 580
double-strand break 142
DREZ lesions 901
drills 49
driver mutations 89
Dulguerov staging 206
Duodopa 882
dural arteriovenous fistula 600–7
classification 602, 603*t*
clinical presentation 602*t*
complications 605, 607
decision-making algorithm 606*f*
diagnosis 602
embolization 605
focused irradiation 605
haemorrhage risk 601
hypertensive syndromes 601
natural history 600–1
outcomes 607
palliative treatment 604–5
pathophysiology 600–1
spinal 756–7
surgery 605
workup 602
dural venous sinuses 548–9
durotomy 729
dynamic nuclear (hyper) polarization 42
dysarthria 13–14
dysdiadochokinesia 16
dysembryoplastic neuroepithelial tumours 131
dysgraphia 13
dyslexia 13
dysphonia 13, 14
dysplastic cerebellar gangliocytoma 131–2
dystonia 878–80, 881

early infantile onset epileptic encephalopathies 1047
echinococcosis 1111, 1120–1
edoxaban 70
Edwin Smith Papyrus 3, 8
electrocochleogram 291
electrocorticography 504*t*, 506, 829, 950
electroencephalogram (EEG) 828–9
epilepsy diagnosis 950–1
epilepsy surgery 957–8
traumatic brain injury 504*t*, 506
electrolytes
postoperative 63
traumatic brain injury 500
electromagnetic registration 52
electromyography 55, 832, 849–50
embolization
arteriovenous malformations 596, 598, 599
choroid plexus tumours 407
coil embolization in SAH 578–9, 580, 587–9
dural arteriovenous fistula 605
haemangioblastoma 371
meningiomas 183
embryology 539, 751, 971–4, 983
embryonal carcinoma 428
embryonal tumour with abundant neuropil and true rosettes 354
emergence from anaesthesia 62
encephalocele 980–1
endocrine system
craniopharyngioma 323–4
paediatric brain tumours 1014
pituitary tumours 305–6, 315–16
traumatic brain injury 500, 525
endoscopes 48–9
endoscopic endonasal approach
anterolateral skull base surgery 244–5, 250
chordoma 195
esthesioneuroblastoma 208
extended approaches 330, 346, 348
odontoidectomy 707–8
orbital tumours 224, 226
sellar and suprasellar tumours 344–6, 347–8
endoscopic procedures
arachnoid cysts 1080, 1104
carpal tunnel release 841–2
choroid plexus coagulation 1079
colloid cysts 396–7, 399, 1080
craniofaciosynostosis 997
cubital tunnel release 843
equipment 48–9
hydrocephalus 1076–80
intraventricular tumours 417, 422
paediatric brain tumours 1018
pineal tumours 440–1
spontaneous intracranial haematoma 646
third ventriculostomy 1030, 1077–9
endotracheal tube 59
endovascular techniques
carotid disease 622
giant aneurysms 640–1
intramedullary arteriovenous malformations 757–8
spinal dural arteriovenous fistula 757
subarachnoid haemorrhage 578–80, 583–6
entrapment syndromes 839–45
eosinophilic granuloma 231, 465
ependyma 1061
ependymomas 361–6
anaplastic 361–2
chemotherapy 365
children 1011
classic 361
epidemiology 361
intraventricular 387, 389–90
molecular genetics 362
myxopapillary 361, 738, 741*t*
NF2 patients 362
pathology 361–2
prognosis 365
proton beam therapy 365
radiotherapy 363, 365
spinal 738, 739*t*
subependymoma 361, 387, 390
surgery 362–3
epidermal growth factor receptor 152
epidermoid cysts 197–203, 233–4, 293
epidemiology 197
malignant transformation 202
pathology 197–9
radiological features 199
recurrence 202
rupture 197
surgery 199–202
surveillance imaging 202
epidural haematoma 484–5
epidural injections 726
epigenomics 91
epilepsy
associated tumours (LEATs) 129–40
aura 937*t*, 947
children 1047–53
definition 936*b*, 945
diagnosis 937, 1047
EEG 950–1
epidemiology 945–6
febrile convulsions 947
focal cortical dysplasias 939–41
frontal lobe 938
hippocampal sclerosis 941, 947
history 945
magnetoencephalography 951
medical management 951–4, 1048
mesial temporal sclerosis 938, 947, 949, 966–7
neocortical temporal lobe 938
nuclear imaging 951
occipital lobe 938
paediatric brain tumours 1014
parietal lobe 938
postictal period 947
prodrome 947
status epilepticus 938–9, 954
structural causes 939–41
sudden unexplained death 946–7
surgical treatment, *see* epilepsy surgery
syndromes 936, 938, 1047–8
temporal lobe 938
epilepsy surgery 957–68
anterior temporal lobectomy 959–60
callosotomy 965, 1051
children 1048–52
complications 966
cortical stimulators 966
deep brain stimulation 966
dorsal transcortical subinsular hemispherotomy 964, 965
hemispherectomy/hemispherotomy 963–5, 1050, 1052
hypothalamic hamartoma disconnection/resection 965–6
invasive monitoring 1050
lateral neocortical temporal lobe resection 962–3
lesionectomies 958–9

multiple subpial transections 965–6, 1052
outcome 966
patient selection 954–5
perisylvian window technique 964
presurgical evaluation 957–8, 1048
Rasmussen's functional hemispherectomy 964
selective amygdalohippocampectomy 961–2
temporal procedures 959–63, 966–7
trans-Sylvian-transcortical-transventricular keyhole hemispherotomy 964, 965
vagal nerve stimulation 963, 1051–2
essential tremor 877–8, 881
esthesioneuroblastoma 205–11
chemotherapy 208
clinical presentation 205
diagnosis 205–6
differential diagnosis 208
ectopic 205
endoscopic resection 208
epidemiology 205
histology 207
Hyams grading 207–8
immunohistochemistry 208
lymph node involvement 210
metastases 206, 210
paraneoplastic syndrome 205
prognosis 209
pseudorosettes 206
radiotherapy 208
recurrence 209–10
staging 206–7
surgery 208
ethylene vinyl alcohol copolymer embolization (EVACE) 596
etomidate 60*t*
Evan's index 1087
evoked potentials 829
brainstem auditory 55, 291, 830–1
motor 55, 663, 829
somatosensory 54–5, 663, 829–30
visual 55
Ewing's sarcoma 231–2, 742*t*
examination of patients 12–27
extended endoscopic endonasal approaches 330, 346, 348
external carotid artery 547
external ventricular drain 510, 1075, 1076*b*
extracranial-intracranial bypass 627–32, 635–9
extradural abscess 1121, 1123
extradural cavernoma 759
extradural haematoma 484–5, 510
extradural vascular malformations 755–6
extrapyramidal tracts 681
extraventricular neurocytoma 136–7
extreme lateral interbody fusion 662
eyelids 21
eye movements 20–1

facet joints 671
arthropathy 725
fracture dislocations 792–3, 798
facial nerve (CN VII)
examination 22–3
monitoring 55
vestibular schwannomas 262–3, 284–5
failed back syndrome 729
familial isolated pituitary adenoma 300
Fanconi anaemia 354*t*
far lateral craniotomy 378–80, 582
fasciculi 164
fasting 57
fat suppression 34
febrile convulsions 947
Ferrier, David 5
^{18}F-FDG PET 38
fibromuscular dysplasia 561
fibrosarcoma 232–3
fibrous dysplasia 224–5, 237–8
fiducials 52
Fielding classification 1006*t*
filum, thickened 985, 990–1
Fisch approaches 245–6
Fisch classification 274*t*
fixation 20
FLAIR 34
flexible fibreoptic endoscopes 49
flow diverting stents 583, 640–1
flow-regulated valves 1073
fluid compartments 1061–3
fluids
intraoperative 62
postoperative 63
fluorescein 49
fluorescent agents 49
fluoroscopy 32
focal cortical dysplasias 939–41
foramen magnum surgery 378–80
foramen of Munro tumours 388–9
Forestier disease 700
fornix 411
Foster–Kennedy syndrome 182
fourth ventricle
surgery 375–8
tumours 387*t*, 389–90
Foville syndrome 617
fractional kill 149
frame-based stereotactic surgery 51–2, 866
frameless stereotactic surgery 52, 1018
FRAX score 676
Fröhlich's syndrome 323
Froment's test 28*b*
frontal arachnoid cysts 1103
frontal eye fields 15–16
frontal lobe 14–16, 163
frontal lobe epilepsy 938
frontal release signs 16
frontotemporal craniotomy 222–3
Fukuyama syndrome 978
functional electric stimulation 821
functional MRI (fMRI) 36, 1018
functional networks 82
functional neuronavigation 166
functional spinal unit 673, 719
fungal infections 1111
fusiform aneurysms 562
F-wave 831

gabapentin 952*t*, 953
gadolinium-based contrast media 36–7
gait
assessment 25
normal pressure hydrocephalus 1086
Galen 3–4, 8
gamma camera 38
gamma knife 129–31, 260, 262, 308
gangliocytoma 464
dysplastic cerebellar 131–2
ganglioglioma, desmoplastic infantile 135–6
Gardner Robertson hearing classification 284*t*
Gardner's syndrome 235
Gasserian ganglion
balloon compression 917*t*, 920
glycerol neurolysis 917*t*, 920
gate theory 898
genomic instability 90
germ cell tumours 427, 429–30
germinomas 427, 429–30
germinomatous tumours 427
Gerstmann syndrome 16, 616
giant aneurysms 633–42
clinical presentation 633
endovascular treatment 640–1
extracranial-intracranial bypass 635–9
investigations 633, 635
natural history 633
outcome 639–41
pathology 633
workup 633, 635
giant cell tumour
skull 233
spine 743*t*
giant cisterna magna 980
glabellar tap 16
Glasgow Coma Score 12, 477
infants and children 1000*t*
Glasgow Outcome Scale (Extended) 478–9
Glassock–Jackson classification 274*t*
Gliadel® wafers 99, 155, 167
glioblastoma
chemotherapy 153–5
stem cells 91
glioma
angiocentric 134–5
brainstem 390, 1010–11
optic pathway 450, 451, 1011–12
see also high-grade glioma; low-grade glioma
gliomatosis cerebri 76
glomus jugulare tumours 464–5
glomus tumours 271–9
anatomical descriptions 271
chemotherapy 277
classification 271
clinical presentation 271
conservative treatment 276
drug therapy 277
epidemiology 275
genetic testing 272, 275
hereditary syndromes 275–6
histology 274
imaging 272
investigations 272
pathology 272–3
post-treatment management 277
radiotherapy/radiosurgery 277
risk factors 275–6
surgery 276–7, 278
glucagon stress test 306
glutamate-mediated excitotoxicity 489
glycaemic control
spinal involvement 684
traumatic brain injury 499
glycerol neurolysis 917*t*, 920
Godlee, Rickman 5
go/no-go test 16
Good Clinical Practice 150
Gorlin syndrome 354, 354*t*
gradient echo 34
granular cell tumours 463–4
grasp reflex 16
gravitational valves 1074
grey matter 679
heterotopias 976–7
Gross Motor Function Classification System 886, 887*f*, 888*t*
growing fracture 527, 1003, 1004
growth hormone-producing tumours 310–11
Guillain–Barré syndrome 690, 691

haemangioblastoma 367–74
cellular 368
chemotherapy 372
clinical presentation 367
cyst formation 368
embolization 371
epidemiology 367
growth patterns 368
histology 368
history 367
imaging 367–8
molecular genetics 368–9
pathology 367–9
prognosis 372–3
radiotherapy 372
recurrence 372
reticular 368
risk factors 368–9
spinal 738, 739*t*
stereotactic radiosurgery 372, 373
surgery 369, 371–2
VHL syndrome 367, 368–9, 372, 373, 456–7
haemangioma
skull 231
spinal 740, 743*t*
haemangiopericytoma 184–5
haematoma
epidural 484–5
extradural 484–5, 510
subdural 485, 510–11, 527
see also intracranial haematoma
haemostasis 6
haemostatic agents 51
hair removal 1113–14
hallmark characteristics 90, 149
Hallpike's test 23
halo immobilization 795
Halsted, William Stewart 5
hamartoma 461–3
Hand–Schüller–Christian syndrome 231, 464
handwashing 5
hangman's fracture 791–2
Hardy grading 302, 304*f*
Harms–Goel C1 lateral mass and C2 pars/pedicle screws 707

Harvey, William 4
Hayflick limit 90
headache
  craniopharyngioma 323
  intrinsic brain tumours 164–5
  vestibular schwannomas 263, 283
head injury, *see* traumatic brain injury
head-up position 45
hearing loss
  assessment 23
  traumatic brain injury 522
  vestibular schwannomas 261–2, 282–3
hemicraniectomy 623
hemifacial spasm 909–11
hemimegalencephaly 979
hemispherectomy 963–5, 1050, 1052
hemispheric anatomy 163–4
hemispherotomy 963–5, 1050, 1052
heparin 71
hereditary haemorrhagic telangiectasia 592
hereditary motor and sensory neuropathy 692
Herophilus 3
herpes simplex virus encephalitis 1110, 1112
herpes zoster 691
heterotopic ossification 819–20
HHH therapy 571–2
high-flow bypass surgery 584–6, 635–9
high-grade glioma 91–101
  aetiology 92–3
  atopic disease 93
  bevacizumab 99, 154–5
  biopsy 97–8
  carmustine wafers 99, 155
  chemotherapy 99, 100, 153–5
  chromosome 1p/19q deletions 94
  classification 91–2, 95–6
  clinical presentation 96
  conservative management 97
  cytomegalovirus 93
  development 93
  dexamethasone therapy 97
  dietary therapy 100
  epidemiology 92
  genetic risk 93
  histone H3 mutations 95
  hypoxic switch 94
  imaging 96–7
  immunotherapy 99–100
  intratumoural heterogeneity 93
  isocitrate dehydrogenase mutations 94
  layered diagnosis 95–6
  metastasis 94
  MGMT methylation 95
  molecular biology 93
  molecular biomarkers 94–5
  mutations 93
  older patients 100
  pathology 93–4
  prognosis 101
  progression 93–4
  radiotherapy 98–9, 100
  reoperation 100
  salvage therapies 100
  surgery 98, 100
  targeted molecular therapies 99
  TERT promoter mutations 95
  tumour invasion 93–4
  tumour treating fields 100
hippocampus 411
  sclerosis 941, 947
Hippocrates 3, 8
histamine test 850
histone H3 95
history of neurosurgery 3–9
history-taking 11–12
HIV
  encephalitis/meningitis 1110
  lymphoma 117, 119, 123, 124
hodotopical model 82
Hoffmann's sign 25
Holmes rebound test 16–17
holoprosencephaly 974–5
homologous recombination 142
hook effect 310
hormones, *see* endocrine system
Horner's syndrome 23
Horsley, Victor 6
Hounsfield units 32
House-Brackmann grading 263*t*, 285
H-reflex 831
Hunt and Hess scale 575
Hunter, John 4
HUNT study 559–60
Hutchinson, Jonathan 5
Hyams grading 207–8
hybrid nerve sheath tumours 856
hydatid disease 1111, 1120–1
hydrocephalus 1057
  aqueductoplasty 1079
  causes 1024
  children 1023–36, 1068
  choroid plexus coagulation 1030, 1079–80
  classification 1023–4, 1067–8
  clinical features 1024–6
  CSF shunts 1029–30, 1031–4, 1072–6
  definition 1023
  endoscopic surgery 1076–80
  endoscopic third ventriculostomy 1030, 1077–9
  epidemiology 1023
  external ventricular drain 510, 1075, 1076*b*
  imaging 1026
  long-standing overt ventriculomegaly in adults 1087
  long-term outcomes 1034
  lumbar punctures 1027
  medulloblastoma 357
  multiloculated 1079
  normal pressure, *see* normal pressure hydrocephalus
  posthaemorrhagic 1026–7
  post-traumatic 515, 525
  preterm infants 1026–9, 1037–8
  septostomy 1079
  slit ventricle syndrome 1034
  subarachnoid haemorrhage 567–8, 586
  treatment decisions 1029, 1030–1
  ventricular access devices 1027–9
  ventricular taps 1027
  ventriculoperitoneal shunts 1031–4, 1075, 1076*b*
  ventriculosubgaleal shunts 1027–9
hydroxyapatite cranioplasty 515–16
hyperactive cranial nerve syndromes 909–27
hyperaemia 492
hyperbaric oxygen 146
hyperglycemia 58
hyperkalaemia 63
hypernatraemia 63, 316
hyperostosis frontalis interna 236
hypertension
  aneurysm risk 560
  idiopathic intracranial 1093
  neurogenic 923–4
  perioperative 58
hyperthyroidism 67
hyperventilation 501
hypoglossal schwannomas 266
hypokalaemia 63
hyponatraemia 63, 316, 586–7
hypophysitis 314
hypopituitarism 316
hypotension
  intraoperative 61
  traumatic brain injury 497, 498–9
hypotensive challenge 635
hypothalamic hamartoma 462
  disconnection/resection 965–6
hypoxic switch 94

ICP, *see* intracranial pressure
idarucizumab 70
idiopathic intracranial hypertension 1093
imaging techniques 8, 31–44
immune system 90–1
immunotherapy 99–100, 150, 153, 158–9
impact brain apnoea 531
IMPACT study 478
implantation dermoids 197
incidentalomas
  children 1016
  colloid cyst 399
  meningiomas 184
  pituitary 316–18
  vestibular schwannomas 266–7
indocyanine green 49
induction of anaesthesia 59
infection
  classification 1109–11
  cranial 1117–27
  diagnosis 1111–13
  microbiology 1109–16
  perioperative control 1113–14, 1115, 1124–5, 1134–5
  pituitary gland 315
  shunts 1034, 1076, 1124
  spinal 1129–36
  spinal surgery 665–6
  TORCH 1112–13
  traumatic brain injury 526–7
inferior cerebellar artery aneurysms 583
inferior front-occipital fasciculus 164
inferior medial pontine syndrome 617
inferior petrosal vein sampling 302
inflammation
  pain and 899
  tumour-promoting 90–1
inhalational induction 59
instantaneous axis of rotation 673
insula 163–4, 168
insulin stress test 306
internal carotid artery 539–40
internuclear ophthalmoplegia 20
INTERPHONE study 258
interspinous distraction devices 720–1
interstitial laser thermal therapy 112
intervertebral discs, *see* disc
intracerebral haemorrhage
  anticoagulation-associated 70
  children 1044
  traumatic brain injury 511
intracranial aneurysms, *see* aneurysms
intracranial haematoma 643–9
  anticoagulation/antiplatelets 646, 648
  blood pressure management 646
  Boston criteria 645*b*
  classification 643
  coagulopathies 646, 648
  epidemiology 643
  investigations 645–6
  medical management 646, 648
  pathophysiology 643–4
  risk factors 643
  seizures 646
  spot sign 643, 645
  surgery 646
  symptoms 645*b*
intracranial hypertension
  idiopathic 1093
  intraoperative 61
intracranial hypotension, spontaneous 766–7
intracranial lipomas 468–9
intracranial metastases 107–16
  chemotherapy 112
  dexamethasone therapy 109–10
  epidemiology 107
  interstitial laser thermal therapy 112
  investigations 108–9
  landmark studies 114
  malignant meningitis 112–13
  management principles 108*b*
  metastatic cascade 107–8
  MR-guided focused ultrasound 112
  pathology 107–8
  prognosis 113–14
  radiotherapy 111–12
  stereotactic radiosurgery 111, 112, 114
  surgery 111, 114
  symptoms and signs 108
  treatment selection 112
intracranial pressure (ICP)
  definition 1071
  meningitis and encephalitis 1124
  traumatic brain injury 491–2, 501–3, 504*t*, 509
intradural, extramedullary spinal tumours 738, 741*t*
intramedullary arteriovenous malformations 757–8
intramedullary spinal cavernoma 759
intramedullary spinal cord tumours 738, 739*t*
intraoperative management
  airway 59–60

anaesthesia 60–2
auditory monitoring 291
imaging 52–4, 169, 1019
neurophysiological monitoring 54–6, 166, 663, 832, 834–6, 1018
surgery 165–7
intrathecal baclofen 888–9
intravenous induction 59
intraventricular arachnoid cysts 1103
intraventricular astrocytoma 385, 387
intraventricular ependymoma 387, 389–90
intraventricular haemorrhage
preterm infants 1026–9, 1037–8
traumatic brain injury 485–6
intraventricular tumours 385–92
anterior body and frontal horn 385–7, 417–19
basal temporal approach 421
classification 385–90
clinical presentation 390
complications 422
decision-making 417
endoscopic procedures 417, 422
fourth ventricle 387*t*, 389–90
lateral ventricles 385, 386*t*, 387–8, 419–21
management 390–1
meningiomas 183, 387–8, 389
parieto-occipital interhemispheric approach 420–1
posterior body–trigone 387–9
posterior temporal approach 420
preoperative planning 416
superior temporal approach 422–3
supracerebellar approach 421
surgery 411–24
third ventricle 386*t*, 388–9, 421–3, 1080
transcallosal approaches 417–19
transchoroidal approach 421
transcortical approach 419
transforaminal approach 421
transparietal approach 419–20, 422–3
tumour markers 416
intravoxel incoherent motion imaging 41
iodinated contrast media 33, 38–9
ISAT study 587–9
ischaemic myelopathy 753
ischaemic penumbra 616
isocitrate dehydrogenase mutations 80, 90, 94, 152
isoflurane 61*t*
isomorphic astrocytoma 133
isthmic spondylolisthesis 726–7
ISUIA studies 568

Jackson, John Hughlings 5
Jackson syndrome 523*t*
Jarcho-Levin syndrome 772
Jefferson's fracture 791
JET trial 628
Jewett Hyperextension Orthosis 805
Joubert syndrome 979–80
jugular foramen schwannoma 265–6, 292
jugular foramen syndromes 523*t*
jugular venous oximetry 504–5, 504*t*

Kadish staging 206
Kawase approach 286
Keen, William 5, 6
ketamine 60*t*
ketogenic diet 100
Klippel–Feil syndrome 197, 672
Knosp classification 302, 304*f*
kyphoplasty 716
kyphosis
adults 776
congenital 772–3
Scheuermann's 776

L5 radiculopathy 28*t*
lacosamide 952*t*
lactate/pyruvate ratio 489–90, 506
lamotrigine 952*t*, 953
Langerhans cell histiocytosis 231, 465–6
language areas 164
language disorders 12–14
large intraparenchymal high grade astrocytic tumours 385, 387
lateral extra cavity 714–15
lateral medullary syndrome 617
lateral neocortical temporal lobe resection 962–3
lateral orbitotomy 223, 226
lateral pontine syndrome 617
lateral positioning 662
lateral ventricle
anatomy 411–13
tumours 385, 386*t*, 387–8, 419–21
L-dopa 875, 877
LEATs 129–40
Leksell's frame 51–2
leptomeningeal cyst 239
lesional surgery 869, 880, 929, 930
lesionectomies 958–9
Letter–Siwe syndrome 231
levetiracetam 952*t*, 953–4
Levine and Edwards classification 791*t*
levodopa 875, 877
L'Hermitte-Duclos disease 131–2, 462
lids 21
Li-Fraumeni syndrome 354, 354*t*, 406–7
ligamentum flavum ossification 698
light response 19
limb examination 24–7
limbic leucotomy 930
limbic system 941–6
limited dorsal myeloschisis 985, 990
Lindegaard ratio 570
linear accelerator 308
lipoma
intracranial 468–9
intraosseous 233
spinal 985, 988–90
lissencephaly 977–8
Lister, Joseph 5
lobar examination 14–17
lobulations 560
localization theory 5–6
locked-in syndrome 617
lomustine 151*t*
long-standing epilepsy-associated tumours 129–40
long-standing overt ventriculomegaly in adults 1087
lower limb examination 24–7
lower motor neuron 22–3
low-grade epilepsy-associated neuroepithelial tumours 129–40
low-grade glioma 75–88
anaplastic (malignant) transformation 75, 77
awake surgery 82
chemotherapy 83, 155–7
children 1009–10
choline-to-creatine ratio 78
clinical presentation 76
differential diagnosis 77
direct electrical brain stimulation 81, 82
epidemiology 75
histological grading 79–80
isocitrate dehydrogenase mutations 80
molecular biomarkers 80–1
multimodal and multistaged management 84–5
prognostic factors 77–81
radiological diagnosis 76–7
radiotherapy 83–4, 141
reoperation 82–3
surgery 81–3
velocity of diametric expansion 78
low molecular weight heparin 71
lumbar canal stenosis 720–1
lumbar corsets 805–6
lumbar puncture
posthaemorrhagic hydrocephalus 1027
pseudotumour cerebri syndrome 1097
lumbar spinal disease 719–32
aetiology 719–20
back pain 722–3
canal stenosis 720–1
disc disease 723–6
disc herniation 721–2
pathophysiology 719–20
recurrent disc herniation 730–1
spondylolisthesis 726–7, 731
spondylosis 720
lumbar spine injuries 801–11
bracing 805–6
burst fractures 803–5
children 1006
fracture classification 801–2
fracture stability 803–5
imaging 802–3
neurological symptoms 803
posterior thoracolumbar fusion 806–10
postoperative follow-up 810
Luria's three-step test 16*b*
Lyme disease 690, 691
lymphocytic hypophysitis 314–15
lymphoma, *see* primary central nervous system lymphoma

Macdonald criteria 152
Macewen, William 6
McGregor's line 699
McRae's line 699
macrencephaly 979
macroprolactin 310
McCune–Albright syndrome 237, 301
Magerl's C1/2 transarticular screws 707
magnetic resonance imaging (MRI) 34–7
intraoperative 54, 169
magnetic resonance spectroscopy (MRS) 41–2
magnetoencephalography 951
maintenance of anaesthesia 61
malignant bone tumours 738, 740, 742–3
malignant meningiomas 176
malignant meningitis 112–13
malignant middle cerebral artery syndrome 616, 620, 623
malignant peripheral nerve sheath tumours 451, 856, 859–60
malignant skull base tumours 213–19
anterior skull base 213–14
histological subtypes 214*t*
lateral skull base 215
TNM system 213, 214*t*
mannitol 491–2, 501, 503, 556–7
Marfan's syndrome 561
Marie-Foix syndrome 617
Marshall CT classification 478
medial epicondylectomy 843–4
medial-lemniscal tract 681
medial medullary syndrome 617
medulloblastoma 353–60
aetiology 353
children 1011
classification 353
clinical presentation 355
familial syndromes 354*t*
fourth ventricle 390
histopathology 354–5
hydrocephalus management 357
imaging 355–6
non-surgical management 357–8
pathogenesis 353
stem cells 91
surgery 357
melanocytoma 468
melanoma 468
membrane potentials 827
MEN1/4 300–1
meningiomas 175–84
anterior cranial fossa 182
benign subtypes 176
brain invasion 176
calvarial 183
clinoidal 181
clival 182
convexity 180–1
diaphragma sellae 182
embolization 183
epidemiology 175
falcine 180
falcotentorial 442, 444–5
foramen magnum 182–3
grading 176
incidental 184
intraventricular 183, 387–8, 389
malignant 176
molecular biology 176–8
multiple 183
olfactory groove 182
parasagittal 180
pathology 175–6
petroclival 182, 292

meningiomas (*cont.*)
planum sphenoidal 182
prognosis 183–4
radiation-induced 175
radiotherapy 179–80
receptors 179
reoperation 179
Simpson classification 179
sphenoid wing 181
spheno-orbital 181
spinal 738, 741*t*
surgery 179–80
tentorial 182
tuberculum sellae 182
meningitis
ICP monitoring 1124
malignant 112–13
postoperative 1123–4
traumatic brain injury 526–7
meralgia paresthetica 844
mesencephalic tractotomy 902–3
mesial temporal sclerosis (epilepsy) 938, 947, 949, 966–7
metabolic syndrome 621
metalloproteinases 93
metastases
esthesioneuroblastoma 206, 210
high-grade glioma 94
pituitary gland 315
skull 229
spinal 742–7
see also intracranial metastases
6-methylguanine-DNA methyltransferase (MGMT) promoter methylation 95, 152
methylprednisolone sodium succinate 783
microbiology 1109–16
microcephaly 979
microdiscectomy 722
microelectrode recordings 835–6, 882
microsurgery
aneurysm clipping 580, 587–9
colloid cysts 397–8, 399
intramedullary arteriovenous malformations 758
spinal dural arteriovenous fistula 756–7
vascular decompression 909–11, 915–17, 917*t*, 922–3
vestibular schwannomas 260, 262
middle cerebral artery 545
aneurysms 583
stroke 616
middle cranial fossa arachnoid cysts 1102
mild traumatic brain injury 486–7, 531–5
Millard–Gubler syndrome 617
minicraniotomy 243–4
minimally invasive techniques 226, 665, 715
mini-open technique 715
mobile image intensifiers 52
mobile phones 258
Modic changes 723*b*
Modified Ashworth Scale 886*t*
monitored anaesthesia care 56
Moniz, Egas 8
mononeuritis multiplex 692–3
monopolar diathermy 50
Monro–Kellie hypothesis 491, 555, 1061–2
Morand, Sauveur François 4
motion segment 673, 719
motor evoked potentials 55, 663, 829
motor neurone disease 690
motor ocular syndromes 909, 923
movement disorders 873–83
moyamoya disease/syndrome 628–30, 1039–41
MR angiography 40
MRC power grading scale 25
MR-guided focused ultrasound 112
MR venography 40
Muenke syndrome 996*t*
multiloculated hydrocephalus 1079
multiple endocrine neoplasia (MEN1/4) 300–1
multiple myeloma 230–1, 740
multiple sclerosis 467–8, 688, 885
multiple subpial transections 965–6, 1052
muscle-eye-brain disease 978
mutation 89, 90
mutism 17
M-wave 831
mycotic aneurysms 562
myelination 973
myelocele 984
myelography 38–9
myelomeningocele 984, 987–8
myxopapillary ependymoma 361, 738, 741*t*

nanoparticles 42
Narakas's rule of sevens 847
nasal cavity 339
nausea and vomiting, postoperative 62–3
near infrared spectroscopy 504*t*, 505
neocortical temporal lobe epilepsy 938
nephrogenic systemic fibrosis 36
nerve conduction studies 831–2, 849–50
nerve root block injection 726
nerve sheath tumours
peripheral 855–61
spinal 738, 741*t*
neuralgic amyotrophy 692
neural-machine interfaces 821–2
neural transplantation 880, 881
neurenteric cysts 984
neuroblastoma 236
neurocysticercosis 390, 1111, 1120–1
neurocytoma 136
central 387, 390–1
extraventricular 136–7
neurofibromas 450, 855–6
neurofibromatosis type 1 (NF1) 449–51, 856, 860, 1009–10
neurofibromatosis type 2 (NF2) 176, 178, 292, 293, 362, 451–4
neurogenic bladder 814–15, 818
neurogenic blood hypertension 923–4
neurogenic bowel 814, 818
neuroimaging techniques 8, 31–44
neuromuscular choristoma 461
neuromyelitis optica spectrum disorders 688
neuronal migration 973
neuronavigation 51–2, 166
neuron physiology 827–8
neuro-orthopaedic syndrome 986
neuropathic pain 820
neurophakomatoses 449–60
neurophysiological monitoring 54–6, 166, 663, 827–37, 1018
neuroprotection 64, 786
neuroregeneration 786–7
neurosarcoidosis 314, 466–7, 689
neurovascular conflict 909
new oral anticoagulants, reversal 70–1
NICE algorithms
cervical spinal imaging in children 1002*f*
CT head in children 1001*f*
NIHS scale 617, 618*t*
nimodipine 570–1
nociception 895–6
nodular heterotopias 976
non-accidental injury 1000, 1003–4
non-chromaffin paragangliomas 273
non-germinomatous germ cell tumours 428, 430
non-homologous end-joining 142
normal pressure hydrocephalus 14, 1057, 1083–92
cerebral blood flow 1085
clinical presentation 1086–7
cognition 1086–7
comorbidity 1087
CSF physiology 1058–9, 1085–6
gait 1086
imaging 1087, 1090
investigations 1087–8
outcome 1090
pathophysiology 1083–6
postoperative complications 1089
structural disorder 1083
surgery 1088–9
urinary incontinence 1087
nuclear medicine 37–8
nystagmus 17, 20, 283

obstructive sleep apnoea 57
occipital lobe 163
occipital lobe epilepsy 938
odontoid peg fracture 792
odontoid screws 797
oligodendroglial tumours 132–3
oncogenes 89
oncology surgery 65–6
open neural tube defects 984
operating microscope 8, 46, 48
operating theatre 45–56
equipment 46, 48–51
zones 45
ophthalmic artery 540
ophthalmoscopy 19–20
opioid analgesia 63, 902*b*
optic nerve injury 522
optic nerve sheath fenestration 1098
optico-carotid recesses 339
optic pathway glioma 450, 451, 1011–12
optic radiation 413
oral glucose tolerance test 306
orbital tumours 221–7
anatomy 221
clinical presentation 221–2
complications 225–6
endoscopic endonasal approach 224, 226
keyhole approach 226
lateral corridor approaches 222–3
medial corridor approaches 223–4
surgical planning 222
orbitotomy
anterior medial micro-orbitotomy 223–4
lateral 223, 226
orbitozygomatic craniotomy 582
orbitozygomatic osteotomy 222–3
orbits 21
Osler, William 7
os odontoideum 1004
osteoblastic lesions, benign 234–5
osteoblastoma 235, 743*t*
osteochondroma 235–6, 743*t*
osteoclastoma 233
osteogenic fibroma 235
osteogenic sarcoma 232
osteoid osteoma 235, 743*t*
osteoma 234–5
osteomyelitis 1123
osteoporosis
circumscripta cranii 237
spinal stability 675–6
vertebral fractures 715–16
osteosarcoma 738, 740, 742*t*
otic capsule injury 522
oxcarbazepine 952, 952*t*
oxygen reactivity index 503

pachygyria 977
paediatrics
birth injuries 1005
brain development 971–4
brain malformations 974–81
brain tumours 1009–22
cervical spinal imaging algorithm 1002*f*
craniofaciosynostosis 993–8
CT head algorithm 1001*f*
epilepsy 1047–53
head and spinal trauma 999–1007
hydrocephalus 1023–36, 1068
neurovascular disorders 1037–46
non-accidental injury 1000, 1003–4
spinal dysraphism 983–92
Paget's disease of the bone 236–7
pain
deep brain stimulation 905–6
neuropathic 820
pathways 895–900
pharmacological strategies 905*b*
postoperative management 63
regional 691–2
spinal cord stimulation 903–5
surgical management 901–3
palmomental reflex 16
papillary craniopharyngioma 321, 323
papillary glioneuronal tumour 135
papillary tumour of the pineal region 432–3
paraganglia 272
paragangliomas 272–4, 275–6, 464–5
paralytic ileus 814
paraneoplastic disorders 205, 689
paraphasia 13
parasellar compartment 340

parasites 1111, 1120–1
paraspinal vascular malformations 755–6
parasympathetic nervous system 682
parasympathetic paragangliomas 273
parenchymal pineal tumours 430–5
parietal lobe
  anatomy 163
  assessment 16
  epilepsy 950
Parinaud's syndrome 19*b*
Parkinson's disease 873–7, 880, 881
Parsonage-Turner syndrome 692
passive immunotherapy 100, 158
Pasteur, Louis 4–5
Paulus of Aegina 8
PCV therapy 83, 99, 151*t*
pedicles 671
pellucidotomy 396
pelvic incidence 675, 770
pelvic tilt 770
penetrating brain injury 487, 514
pentose phosphate pathway 490
penumbra model 616
peptides
  pain sensation 895
  therapeutic 158
percutaneous vertebral augmentation 737–8
perfusion MRI 41
pericallosal aneurysms 583
pericallosal artery 542, 545
perimedullary arteriovenous fistula 758
perineuriomas 856
perioperative care 57–72
peripheral nerves
  brachial plexus injury 852
  cutaneous distribution 27*f*
  fibre classification 828
peripheral nerve sheath tumours 855–61
peripheral nervous system examination 24–7
perisylvian window technique 964
periventricular arachnoid cysts 1103
Petit, Jean Louis 4
Pfeiffer syndrome 996*t*
phaeochromocytomas 273
phakomatoses 449–60
phase contrast angiography 40
PHASES score 568
phenobarbitone 952*t*, 953
phenytoin 951–2, 952*t*
physiotherapy 666, 987
pilocytic astrocytoma 133, 1010
pineal cysts 445–6
pineal gland, anatomy 439
pineal tumours 389, 427–37
  complications 445
  differential diagnosis 440
  endoscopic procedures 440–1
  germ cell tumours 427–30
  occipital transtentorial approach 442
  parenchymal 430–5
  parenchymal of intermediate differentiation 432–3
  pineal cysts 445–6
  postoperative procedure 445
  preoperative workup 427
  presentation 427
  supracerebellar infratentorial approach 441–2
  surgery 440–5
  symptoms 440
  tumour markers 440
pineoblastoma 432
pineocytoma 430, 432
ping pong fractures 1004
pituicytoma 463–4
pituitary apoplexy 313
pituitary gland
  anaesthetic considerations 67–8
  anatomy 299
  hormones 305–6
  infections 315
  metastasis to 315–16
  subarachnoid haemorrhage 317, 318
  traumatic brain injury 317, 318, 525
pituitary tumours 299–319
  carinoma 305
  chemotherapy 309
  Cushing's disease 311–12
  endocrine tests 306
  epidemiology 299
  familial adenomas 300–1
  genetics 300–1
  grading 302
  granular cell tumours 463–4
  growth hormone-producing 310–11
  histopathology 303
  imaging 301–2
  immunohistochemistry 303
  incidentalomas 317
  inferior petrosal vein sampling 302
  medical management 307
  morpho-functional classification 303–4
  non-functioning adenomas 309–10
  pathology 303–5
  pituicytoma 463–4
  pituitary apoplexy 313
  postoperative endocrine management 316
  predictors of outcome 304–5
  prolactin-producing adenoma 310
  radiotherapy 307–8
  residual tumour management 317
  spindle cell oncocytoma 463–4
  sporadic 300
  stereotactic radiosurgery 308
  steroid replacement protocols 316
  surgery 306–7
  thyrotropin-releasing adenomas 312–13
plain X-rays 31
  intraoperative 52–4
plasmacytoma 740
platybasia 699
pleomorphic xanthoastrocytoma 133–4
pneumocephalus 523
Pollock-Flickinger score 594*t*, 596
polymicrogyria 978
polyneuropathy 692
porencephaly 978
positioning 45–6, 61, 67, 242, 662, 1017
positron emission tomography (PET) 37–8, 41
postconcussion syndrome 531
posterior cerebral artery 545, 547
  stroke 616–17
posterior cervical foraminotomy 703–4
posterior communicating artery 540
  aneurysms 583
posterior cord syndrome 685
posterior fossa
  anaesthetic considerations 65
  arachnoid cysts 1102
  cysts 1080
  malformations 979–80
  tumour surgery 375–81
posterior inferior cerebellar artery 545
posterior longitudinal ligament ossification 698
posterior thoracolumbar fusion 806–10
posterolateral fusion 724
posthaemorrhagic hydrocephalus 1026–7
posthaemorrhagic ventricular dilatation 1026
postictal period 947
postoperative management 62–3, 168–9
postoperative nausea and vomiting 62–3
post-traumatic encephalopathy 527
post-traumatic syringomyelia 764
potassium balance 63
Pott, Percival 4, 8
power 25–7
pregabalin 952*t*
prehospital medications 58–9, 69–70
premotor cortex 14
preoperative assessment 57–9, 165
pressure reactivity index 490–1
pressure ulcers 815
preterm infants, intraventricular haemorrhage 1026–9, 1037–8
Prévost sign 16
primary central nervous system lymphoma 117–27
  biopsy 123
  chemotherapy 123–4
  clinical presentation 117
  CSF examination 119
  debulking and excisional procedures 123
  dexamethasone 123
  diagnosis 117–21
  epidemiology 117
  eye examination 118
  histopathology 119–20
  HIV/AIDS 117, 119, 123, 124
  imaging 117–18
  immunocompromised patients 118*t*, 120–1, 124
  molecular biology 121–3
  prognosis 124
  radiotherapy 123–4, 125
primary central nervous system melanoma 468
primary motor cortex 14
primitive reflexes 16
prion disease 1114
procarbazine 151*t*
prodrome 947
programmable valves 1074–5
prolactin-producing adenoma 310
pronator drift 14
prone positioning 67, 662
propofol 60*t*
proton beam therapy 144–5, 194, 309, 365
proton spectroscopy 41
pseudomeningocele 730
pseudoprogression 146, 153
pseudoresponse 153
pseudotumour cerebri syndrome 1093–9
  clinical presentation 1095
  cranial expansion 1097
  CSF diversion 1097–8
  diagnosis 1093, 1094*b*
  investigation 1096–7
  lumbar puncture 1097
  medical management 1097
  optic nerve sheath fenestration 1098
  pathophysiology 1093–5
  prognosis 1098
  secondary 1095*b*
  subtemporal decompression 1097
  venous stenting 1098
psychiatric disorders 929–32
psychological interventions 815
pterional craniotomy 580–1
ptosis 21
pulmonary embolism 71, 169, 816
pulvinar 412
punch drunk syndrome 527
pupils 12, 19
pyramidal tracts 681

Quality of Life after Brain Injury (QOLIBRI) 479

radial artery grafts 635, 638
radiation hazards 141–2, 145–6, 175, 255, 258, 1012
radicular arteries 751
radiculomedullary arteries 751
radiculopial arteries 751
radiofrequency thermorhizotomy 917*t*, 917–18, 919*f*
radiographs 31
  intraoperative 52–4
radiomics 42
radiosurgery, *see* stereotactic radiosurgery
radiotherapy 141–8
  anterior skull base malignancies 214
  biological effects of radiation 141–2
  boron neutron capture therapy 144
  brachytherapy 144
  chordomas 193, 194–5
  choroid plexus tumours 408
  conformal external beam 143
  craniopharyngioma 330, 332
  dural arteriovenous fistula 605
  ependymomas 363, 365
  esthesioneuroblastoma 208
  germinomas 429
  glomus tumours 277
  haemangioblastoma 372

radiotherapy (*cont.*)
high-grade glioma 98–9, 100
intensity-modulated 143
lateral skull base malignancies 215
late toxicity 146
low-grade glioma 83–4, 141
malignancy induction 146, 175
meningiomas 179–80
metastases 111–12
non-germinomatous germ cell tumours 430
normal tissue necrosis 145–6
paediatric brain tumours 1020
physics of 143
pineoblastoma 432
pineocytoma 432
pituitary tumours 307–8
primary central nervous system lymphoma 123–4, 125
proton beam therapy 144–5, 194, 309, 365
pseudoprogression 146
side effects 145–6
spinal tumours 738
RANO criteria 152–3
rapid sequence induction 59–60
Rasmussen's functional hemispherectomy 964
Rasmussen's syndrome 1052
Rathke's cleft cysts 314, 333–5
Raymond syndrome 617
RECIST guidelines 152
recombinant bone morphogenetic protein 2 663
recombinant tissue plasminogen activator 619
recurrent artery of Heubner 542
reflexes
deep tendon 25
primitive 16
regional pain 691–2
registration 52
rehabilitation 527–8, 738, 813–23, 1006–7
relative afferent pupil defect 19
replicative immortality 90
RESCUE-ASDH trial 513
RESCUEicp trial 513
respiratory system
intraoperative events 61
postoperative complications 62
preoperative assessment 57
Response Assessment in Neuro-Oncology (RANO) criteria 152–3
Response Evaluation Criteria in Solid Tumour (RECIST) guidelines 152
retractors 49–50
Revised Cardiac Risk Index 58*t*
rheumatoid arthritis 698
rhombencephalosynapsis 980
Rhoton's rules 560, 567
rigid endoscopes 49
Rinne's test 23
rivaroxaban 70
Romberg's test 23, 25
rosette-forming glioneuronal tumour 135–6

S100β 478
Sabunuoglu 8
saccades 20
saccular aneurysms 560
sacral slope 770
sacroiliac disease 728–9
Saethre–Chotzen syndrome 996*t*
sagittal vertical axis 675
salivary gland choristoma 461
saphenous vein grafts 635, 638
sarcoidosis 315, 466–7, 689
scalp hair removal 1113–14
SCAT 534
Scheuermann's kyphosis 776
schizencephaly 976
Schmidt syndrome 523*t*
schwannomas, non-vestibular 263–4
facial nerve 265
fourth nerve 265
hypoglossal 266
jugular foramen 265–6, 292
peripheral nerve 855
sixth nerve 265
third nerve 265
trigeminal 264, 292
see also vestibular schwannomas
scoliosis 9, 771–6
congenital 772–3
early onset 773–4
idiopathic 771, 773–6
late onset 774–6
neuromuscular 773
syndromic 773
second impact syndrome 534
seizures
complex 947
complex partial 936
definition 945
focal 935–6, 947
generalized 935–6, 947
intracranial haematoma 646
lateralising and localizing features 937*t*, 948*t*
partial 947
semiology 947
simple 947
simple partial 936
subarachnoid haemorrhage 572–3
traumatic brain injury 493, 500, 523, 525
see also epilepsy
selective amygdalohippocampectomy 961–2
selective dorsal rhizotomy 890, 891–2
selective peripheral neurotomy 891
sellar compartment 340
sellar tumour surgery 339–49
sensation 27
sensory disturbances 692–3
sensory nerve action potential 831–2
septo-optic dysplasia 975–6
septostomy 1079
septum pellucidum 413
seronegative spondyloarthropathies 699–700
serotherapy 100
sevoflurane 61*t*
sexual function 684, 818–19
shingles 691
short Synacthen test 306
shunts and shunting 1029–30, 1031–4, 1072–6, 1097–8, 1104, 1124
Simpson classification 179
single-photon emission computed tomography (SPECT) 38
single pulse electrical stimulation 829
sinus pericranii 238
sitting position 61
Sjögren syndrome 689
skip laminectomy 704*t*
skull fixation 45
skull fractures
base 513, 525–6
depressed 513, 522–3
growing 527, 1003, 1004
skull lesions 229–40
skull osteomyelitis 1123
slit ventricle syndrome 1034
smoking 57, 559–60
snouting reflex 16
sodium balance 63, 500*t*, 586–7
sodium valproate 952*t*, 953
solitary fibrous tumours 184–5
somatic mutation 89, 90
somatosensory evoked potentials 54–5, 663, 829–30
spasticity 885–94
aetiology 885
assessment 25, 885–6
intrathecal baclofen 888–9
medical management 886, 888
orthopaedic surgery 891
pathophysiology 885
scoring systems 886
selective dorsal rhizotomy 890, 891–2
selective peripheral neurotomy 891
spinal cord injury 816–18
SPECT 38
speech and language
assessment 12–14
mapping 55
therapy 527–8
white matter tracts 164
sphenoid bone 241
sphenoid sinus 339
spinal anatomy 669–72
spinal aneurysms 753
spinal angiography 752
spinal arachnoid cysts 766, 1103
spinal astrocytoma 738, 739*t*
spinal autonomic function 681–4
spinal biomechanics 672–3
spinal canal 671
spinal cavernoma 758–9
spinal chondrosarcoma 740, 742*t*
spinal chordoma 738, 742*t*
spinal cord
anatomy 679, 751–2
autonomic function 681–4
development 983
hernias 767
infarction 753
injury, *see* spinal cord injury
intradural, extramedullary tumours 738, 741*t*
intramedullary tumours 738, 739*t*
length 679
medical pathologies 687–94
pain pathways 900
stimulation 903–5
tracts 679–81
vascular lesions 751–60
spinal cord injury
autonomic dysreflexia 815–16
autonomic system 814
bladder management 814–15, 818
bowel management 814, 818
cardiovascular systems 814
cervical spinal clearance 783
cervical traction 783
children 1004–7
classification 813–14
clinical trials 783, 786–7
complete 685
early decompression 787
economic impact 781
epidemiology 781
family support 815
gastrointestinal system 814
heterotopic ossification 819–20
histology 782
hospital management 782–3
imaging 783
incomplete 685–6
methylprednisolone sodium succinate 783
mortality 783
multidisciplinary rehabilitation 815
musculoskeletal interventions 821
neural-machine interfaces 821–2
neurological level of injury 813
neuropathic pain 820
neuroprotection 786
neuroregeneration 786–7
nutrition 815
pathophysiology 781–2
patterns 684–5
prehospital management 782
pressure ulcers 815
primary survey 782
primary vs. secondary injury 781–2
prognosis 783, 815
psychological interventions 815
rehabilitation 813–23, 1006–7
resuscitation 782
secondary survey 782–3
sexual function 818–19
spasticity 816–18
stem cell implantation 821
syringomyelia 764
tendon transfer surgery 820
venous thromboembolism 816
ventilation 814
without overt radiographic abnormality (SCIWORA) 1006
spinal deformity 769–77
spinal development 1004–5
spinal dural arteriovenous fistula 756–7
spinal dysraphism 983–92
classification 984–5
clinical presentation 985–6
cutaneous features 985–6
investigations 986–7
management 987–91
neuro-orthopaedic syndrome 986
physiotherapy 987
prevention 991
prognosis 991
tethered cord 986
urological function 987

spinal ependymomas 738, 739*t*
spinal epidural abscess 1129–31
spinal epidural cysts 766
spinal function 719
spinal haemangioblastoma 738, 739*t*
spinal haemangioma 740, 743*t*
spinal infections 1129–36
spinal instability 725–6
spinal ligaments 671–2
spinal lipoma 985, 988–90
spinal meningeal cysts 728
spinal meningiomas 738, 741*t*
spinal metastases 742–7
spinal nerve sheath tumours 739, 741*t*
spinal physiology 679–86
spinal shape assessment 769–71
spinal stability 674–6
spinal subarachnoid haemorrhage 753
spinal surgery 661–7
  anaesthesia 66–7
  analgesia 666
  anticoagulation 661–2
  artificial discs 665
  checking levels 662
  consent 661
  fusion 663
  history of 8–9
  image guidance 662–3
  implants 663–5
  infection prevention 665–6
  intraoperative neurophysiology 663, 836
  minimal access surgery 665
  operating microscopes 662
  patient selection 661
  physiotherapy 666
  plain X-rays 662
  plates 665
  positioning 662
  postoperative care 666
  preoperative education 661
  screws 663–5
  venous thromboembolism prophylaxis 71, 666
  visual loss after 67
spinal synovial cysts 727–8
spinal tumours 733–49
  differential diagnosis 734
  imaging 734
  intradural, extramedullary 738, 741*t*
  intramedullary 738, 739*t*
  malignant bone tumours 738, 740, 742–3
  presentation 733–4
  primary bony tumours 738
  radiotherapy 738
  rehabilitation 738
  surgery 734–8
spinal vascular malformations 753–9
spindle cell oncocytoma 463–4
spin echo 34
spinomesencephalic tract 899
spinoreticular tract 899
spinothalamic tracts 680–1, 898
split cord malformations 984, 991
spondyloarthropathies, seronegative 699–700
spondylocostal dysostosis 772
spondylodiscitis 1131–4
spondylolisthesis 726–7, 731
spondylolysis 726–7
spondylosis 720
spondylothoracic dysostosis 772
spontaneous epidural spinal haemorrhage 752–3
spontaneous intracranial hypotension 766–7
Sport Concussion Assessment Tool (SCAT) 534
sports
  head injury (concussion) 486–7, 531–5
  participation with arachnoid cysts 1105
spot sign 643, 645
spreading cortical depolarizations 493, 506
squamous cell carcinoma, temporal bone 215
STASCIS trial 787
status epilepticus 938–9 , 945
steady state free precession 34
stem cells 91
  implantation 821
stents, intracranial 583, 640–1
stereo electroencephalography 829, 950
stereotactic radiosurgery 143–4
  arteriovenous malformations 595–6, 599, 600*t*
  cerebral cavernous malformations 655, 656
  choroid plexus tumours 408
  glomus tumours 277
  haemangioblastoma 372, 373
  metastases 111, 112, 114
  pineocytoma 432
  pituitary tumours 309
  spinal cavernoma 759
  spinal vascular malformations 758
  trigeminal neuralgia 917*t*, 920
  vestibular schwannomas 260, 262, 452, 453–4
stereotactic surgery 51–2, 866, 1018
sterilization of instruments 1114, 1115*b*
STICH trials 646
STIR 34
stria terminalis 412
stroke
  aetiology 615
  clinical presentation 616–17
  decompressive craniectomy 620–1, 623
  incidence 615
  investigation 617
  medical management 618–20
  pathophysiology 615–16
  penumbra model 616
  thrombectomy 619
  thrombolysis 619
subarachnoid haemorrhage
  aneurysm clipping 580, 587–9
  balloon-assisted coiling 579–80
  bifrontal craniotomy 581–2
  clinical presentation 575
  coil embolization 578–9, 580, 587–9
  delayed cerebral ischaemia 586
  double-microcatheter technique 580
  endovascular techniques 578–80, 583–6
  far lateral craniotomy 582
  flow diverting stents 583
  grading scales 575
  high-flow bypass surgery 584–6
  hydrocephalus 567–8, 586
  hyponatraemia 586–7
  hypopituitarism following 317, 318
  imaging 576–7
  intracranial stents 583
  intracranial surgery 582–3
  intrasaccular flow diversion 583
  investigations 575–7
  medical management 586–7
  non-aneurysmal perimesencephalic 577–8
  orbitozygomatic craniotomy 582
  outcome 572, 587
  pathophysiology 567–73
  preoperative management 577
  pterional craniotomy 580–1
  seizures following 572–3
  spinal 753
  traumatic 485, 521
  vasospasm 569–72, 586
  workup 575–7
subaxial injury classification 790
subcaudate tractotomy 930
subdural empyema 1121–3
subdural haematoma 485, 510–11
  chronic 485, 527
subependymal giant cell astrocytoma (SEGA) 387, 455–6, 462
subependymal nodules 455, 462
subependymomas 361, 387, 390
suboccipital craniotomy 376
subtemporal decompression 1097
succinate dehydrogenase mutations 301
sucking reflex 16
sudden unexplained death in epilepsy 946–7
sulci 163
superficial temporal artery-middle cerebral artery bypass technique 630
superior cerebellar arteries 545
superior hypophyseal artery 540
superior longitudinal fasciculus 164
supine positioning 662
supplementary motor area 14
supraorbital craniotomy 243–4
suprasellar compartment 340
suprasellar tumour surgery 339–49
surgical equipment 46, 48–51
Surgical Safety Checklist (WHO) 45, 47*f*
surgical site infection 1113–14, 1115, 1124–5, 1134–5
susceptibility-weighted imaging 34, 40
swinging light test 19
Sylvian fissure 163
sympathetic nervous system 681–2
sympathetic paragangliomas 273
synapses 827–8
syndrome of inappropriate ADH production (SIADH) 63, 316, 500*t*, 525, 586–7
syndrome of the trephine 527
syndrome X 621
synthetic lethality 142
syringomyelia 762–5
systemic lupus erythematosus 689

Tapia syndrome 523*t*
targeted molecular therapies 99, 150, 157
targeted temperature management 499
Tarlov cysts 728, 766
tear drop fracture 793
temozolomide 83, 99, 151*t*
temporal bone, squamous cell carcinoma 215
temporal lobe
  anatomy 163
  assessment 16
  epilepsy 947
tendon reflexes 25
tendon transfer surgery 820
teratoma 428
terminal lipoma 985
terminal myelocystocele 985, 991
TERT promoter 95
test balloon occlusion 215
test bolus method 40
tethered cord 986
thalamic pain syndrome 616
thalamus 168, 411
theatre 45–56
  equipment 46, 48–51
  zones 45
thiopental 60*t*
third ventricle
  anatomy 413–16
  tumours 386*t*, 388–9, 421–3, 1080
thoracic spinal disease 711–17
  conservative management 711
  disc prolapse 712–15
  incidence 711
  osteoporotic vertebral compression fractures 715–16
  pathogenesis 711
  presentation 711
  surgery 711–12
thoracic spine injuries 801–11
  bracing 805–6
  burst fractures 803–5
  fracture classification 801–2
  fracture stability 803–5
  imaging 802–3
  neurological symptoms 803
  posterior thoracolumbar fusion 806–10
  postoperative follow-up 810
thoracolumbosacral orthoses 805–6
thoracoscopic discectomy 715
three-joint complex 719
thrombectomy 619
thrombolysis 619
thyrotropin-releasing adenomas 313
time-of-flight MRA 40
Tinel-Hoffmann sign 840
tinnitus 262, 283, 909, 921
titanium cranioplasty 515–16
tizanidine 888
TNM system 213, 214*t*
tone 25
top of the basilar syndrome 617
TORCH infections 1112–13
TP53 90

train of 5 829, 834–5
transconjunctival approach 223–4
transcranial Doppler 39
transependymal flow 1065
transfacet pedicle sparing 715
transient ischaemic attacks 621–3
transient receptor proteins 895
transitional lipoma 985
transpedicular fixation 724
trans-sphenoidal
hypophysectomy 345
trans-Sylvian-transcortical-transventricular keyhole hemispherotomy 964, 965
transverse myelitis 687–9
traumatic aneurysms 561–2
traumatic brain injury
aetiology 475
anaemia 499
anaesthesia 63–4
apolipoprotein E 493
arteriovenous fistula 521–2
autoregulation 487–9, 490–1
beta-amyloid deposition 493
biomarkers 478
biomechanics 483–4
cardiorespiratory function 497–9
carotid dissection 514–15, 521
cerebral blood flow 486, 487–8, 492, 503–4, 504*t*
cerebral contusions 486
cerebral metabolism 487–91
cerebral microdialysis 504*t*, 506
cerebral oxygenation monitoring 504–5, 504*t*
cerebral perfusion pressure 503
cerebrovascular reactivity 503
children 999–1004
classification 476, 484–7
clinical severity 477–8
coagulopathy 499
Common Data Elements 494
cortical spreading depression 493, 506
coup/contre-coup contusions 483–4
cranial nerve injuries 522
cranioplasty 515–16
craniotomy 510–11
CSF leaks 514, 523, 524*f*, 525–6
decompressive craniectomy 511–13, 527
definition 475
depressed skull fractures 513, 522–3
diffuse axonal injury 486
early complications 521–3
early management 497, 498*f*
economic costs 479
EEG/ECoG 504*t*, 506
electrolytes 500
endocrine disturbances 500
epidural haematoma 484–5
external ventricular drain 510
extracranial injuries 478
extradural haematoma 484–5, 510
glutamate-mediated excitotoxicity 489
glycaemic control 499
growing skull fractures 527
hearing loss 522
hydrocephalus 515, 525
hyperaemia 492
hypotension 497, 498–9
hypoxia 497–8
incidence 475–6
infections 526–7
intensive care management 497–507
intracerebral haemorrhage 511
intracranial pressure 491–2, 501–3, 504*t*, 509
intraventricular haemorrhage 485–6
ischaemic injury 492–3
late complications 523–7
Marshall CT classification 478
mechanism of injury 476–7
mild (concussion) 486–7, 531–5
mortality 476
multimodality neuromonitoring 503–6
neurorehabilitation 527–8
non-neurological organ system dysfunction 500–1
nutritional support 500
oedema 491
optic nerve injury 522
otic capsule injury 522
outcome assessment 478–9
pathophysiology 483–95
penetrating injury 487, 514
pituitary dysfunction 318, 525
pneumocephalus 523
polytrauma 497
post-traumatic encephalopathy 527
prevalence 476
prognostic risk 478
quality of life measures 479
secondary injury 489–93
seizures 493, 500, 523, 525
skull base fractures 513, 525–6
sodium disturbances 500*t*
speech and language therapy 527–8
subarachnoid haemorrhage 485, 521
subdural haematoma 485, 510–11, 527
surgical management 509–19
targeted temperature management 499
venous thromboembolism prophylaxis 71, 500
ventriculostomy 510
vertebral dissection 514–15, 521
trigeminal neuralgia 909, 911–21
anatomical findings 914–15
atypical 911
balloon compression 917*t*, 920
clinical presentation 911
decision-making 918*f*
diagnosis 911, 913–14
glycerol neurolysis 917*t*, 920
microsurgical vascular decompression 915–17, 917*t*
radiofrequency thermorhizotomy 917*t*, 917–18, 919*f*
stereotactic radiosurgery 917*t*, 920
typical 911
trigeminal schwannoma 264, 292
tuberculoma 1118
tuberous sclerosis complex 454–6, 462
tumefactive multiple sclerosis 467–8
tumour suppressor genes 89
tumour treating fields 100
Turcot syndrome 354, 354*t*

ulnar neuropathy 28*b*, 832
ultrasonic aspirators 50–1
ultrasound 39
intraoperative 54
MR-guided focused 112
uncinate fasciculus 164
unconscious patient examination 12
unfractionated heparin 71
unifacetal fracture dislocations 792–3, 798
Unified Parkinson's Disease Rating Scale (UPDRS) 875
Unterberger's test 23, 283
upper limb examination 24–7
upper motor neuron 22–3
urological function
normal pressure hydrocephalus 1087
spinal dysraphism 987

vaccines 158–9
vagal nerve stimulation 963, 1051–2
vancomycin powder 1115
vascular anatomy 539–54
vascular imaging 39–40
vascular physiology 554–7
vascular space occupancy imaging 41
vaso-glossopharyngeal neuralgia 909, 921
vasospasm 569–72, 586
vein of Galen 439
malformations 1038–9
velocity of diametric expansion 78
venous access 59
venous air embolism 65
venous stenting 1098
venous thromboembolism
neurosurgery 71, 169
spinal cord injury 816
spinal surgery 666
traumatic brain injury 500
ventral horn 679
ventral pontine syndrome 617
ventral stream 164
ventricular access devices 1027–9
ventricular taps 1027
ventriculitis 1124
ventriculomegaly 1065–7
ventriculoperitoneal shunts 1031–4, 1075, 1076*b*, 1124
ventriculostomy 510
ventriculosubgaleal shunts 1027–9
Vernet syndrome 272*t*, 523*t*
vertebral anatomy 669–72
vertebral arteries 545
vertebral dissection 514–15, 521
vertebrobasilar insufficiency syndromes 616–17
vertebroplasty 716
vertigo 262, 283, 909, 922–3
Vesalius 4
vestibular examination 23
vestibular schwannomas 255–63
aetiology 255, 258
audiometry 284
epidemiology 255
facial nerve function 262–3, 284–5
genetics 255
growth of residual tumours 259–60
headache 263, 283
hearing deficit 261–2, 282–3
incidental 266–7
ionizing radiation 255, 258
microsurgery 260, 262
mobile phone link 258
natural history 258
neurofibromatosis (NF2) 292, 293, 452, 453–4
outcomes 290–2
small lesion management 293
stereotactic radiosurgery 260, 262, 452, 453–4
symptoms 261–3, 282–3
tinnitus 262, 283
treatment goals 258–9
vertigo 262, 283
video telemetry 950
Villaret syndrome 272*t*, 523*t*
vincristine 151*t*
viruses 690, 1109–10
viscoelasticity 673
visual acuity 18
visual evoked potentials 55
visual fields 18–19
visual system examination 18–21
voltage gated ion channels 896
Von Hippel-Lindau syndrome 367, 368–9, 372, 373, 456–7
Vulpian sign 16

Walker-Warburg syndrome 978
Wallenberg syndrome 617
warfarin reversal 70
water balance 63
watershed ischaemia 1085
weakness 693
WEB device 583
Weber's test 23
Weber syndrome 616
Wernicke's aphasia 164
white matter tracts 164
WHO Surgical Safety Checklist 45, 47*f*
WHO 2016 tumour classification 389, 390, 1009, 1011
wide dynamic range cells 897–8
woven endovascular bridge 583

X-linked acrogigantism 301

yolk sac tumour 428

zone of plastic deformation 673
zonisamide 952*t*